Pediatric Cardiovascular Medicine

COMPANION WEBSITE

This book is accompanied by a companion website:

www.mollerandhoffmantext.com

The website includes:

- Interactive Multiple-Choice Questions
- Videoclips

Pediatric Cardiovascular Medicine

SECOND EDITION

SENIOR EDITORS:

James H. Moller, MD

Adjunct Professor of Medicine
Emeritus Professor and former Head of Pediatrics
University of Minnesota
Minneapolis, MN
USA

Julien I. E. Hoffman, MD, FRCP

Emeritus Professor of Pediatrics
University of California
San Francisco, CA
USA

ASSOCIATE EDITORS:

D. Woodrow Benson, MD, PhD

Professor of Pediatrics
Division of Cardiology
University of Cincinnati School of Medicine and
Cincinnati Children's Hospital Medical Center
Cincinnati, OH
USA

George F. Van Hare, MD

Professor of Pediatrics
Washington University and
St. Louis Children's Hospital
St. Louis, MO
USA

Christopher Wren, MBChB, PhD

Consultant Paediatric Cardiologist
Senior Lecturer in Paediatric Cardiology
Freeman Hospital
Newcastle upon Tyne
UK

Contents

Contents

COMPANION WEBSITE

This book is accompanied by a companion website:

www.mollerandhoffmantext.com

The website includes:

- Interactive Multiple-Choice Questions
- Videoclips

List of Contributors

Philippe Acar, MD, PhD
Pediatric Cardiology Unit
Children's Hospital
Toulouse University Hospital
Toulouse
France

Ahmad I. Alomari, MD, MSc, FSIR
Program Director, PIR Fellowship
Co-Director, Vascular Anomalies Center
Assistant Professor
Division of Vascular and Interventional Radiology
and Vascular Anomalies Center
Children's Hospital Boston
Harvard Medical School
Boston, MA
USA

Rebecca Ameduri, MD
Assistant Professor of Pediatrics
University of Minnesota School of Medicine
Minneapolis, MN
USA

Robert H. Anderson, BSc, MD, FRCPath
Visiting Professor of Pediatrics
Medical University of South Carolina
Charleston, SC
USA

Christian Apitz, MD
Staff Physician
Pediatric Cardiology
Pediatric Heart Centre
University Children's Hospital
Giessen
Germany

Jürgen Apitz, MD
Emeritus Professor of Pediatrics
Division of Pediatric Cardiology
University Children's Hospital
Tübingen
Germany

Peter J. Bartz, MD
Assistant Professor of Pediatrics
Medical College of Wisconsin
Milwaukee, WI
USA

Mary E. Bauman, RN, BA, MN, NP
Adjunct Professor, Department of Pediatrics
Program Manager, KIDClot Program
University of Alberta
Stollery Children's Hospital
Edmonton, AB
Canada

Andrea Beaton, MD
Professor of Pediatrics
Children's National Medical Center
George Washington University Medical School
Washington, DC
USA

Maurice Beghetti, MD
Professor of Pediatric Cardiology
University of Geneva
Director of Pediatric Cardiology
The University Children's Hospital of Geneva
Geneva
Switzerland

D. Woodrow Benson, MD, PhD
Professor of Pediatrics
Divisions of Cardiology
University of Cincinnati School of Medicine and
Cincinnati Children's Hospital Medical Center
Cincinnati, OH
USA

Stuart Berger, MD
Professor of Pediatrics
Medical College of Wisconsin
Childrens Hospital of Wisconsin
Milwaukee, WI
USA

Saroja Bharati, MD
Director, The Maurice Lev Congenital Heart and
Conduction System Center
The Heart Institute for Children
Advocate Hope Children's Hospital
Advocate Christ Medical Center
Oak Lawn, IL
Professor of Pathology
Rush University Medical Center
Clinical Professor of Pathology
Rosalind Franklin University of Medicine and
Science
Chicago Medical School
Visiting Professor of Pathology
University of Illinois at Chicago
Chicago, IL
USA

Bryce A. Binstadt, MD, PhD
Assistant Professor of Pediatrics
Division of Rheumatology
Department of Pediatrics and Center for
Immunology
University of Minnesota
Minneapolis, MN
USA

Philipp Bonhoeffer, MD
Former Professor of Cardiology
Great Ormond Street Hospital for Children
London
UK

Elizabeth A. Braunlin, MD, PhD
Professor of Pediatrics
University of Minnesota
Minneapolis, MN
USA

Roosevelt Bryant III, MD
Assistant Professor
Department of Surgery
University of Minnesota
Amplatz Children's Hospital
Minneapolis, MN
USA

A. Louise Calder, MD
Paediatric Cardiologist
Green Lane Paediatic and Congenital Cardiac
Service
Auckland City Hospital
Auckland
New Zealand

Charles E. Canter, MD
Professor of Pediatrics
Washington University School of Medicine
St. Louis, MO
USA

Adriano Carotti, MD
Associate in Pediatric Cardiac Surgery
Department of Pediatric Cardiology and Cardiac
Surgery
Bambino Gesù Children's Hospital
Rome
Italy

Seden Erten Çelik, MD
Associate Professor of Cardiology
Department of Cardiology
Acıbadem University Medical Faculty
Acıbadem Maslak Hospital
Maslak
Istanbul
Turkey

Alpay Çeliker, MD
Professor of Pediatrics and Pediatric Cardiologist
Department of Pediatrics
Acıbadem University Medical Faculty
Acıbadem Maslak Hospital
Maslak
Istanbul
Turkey

Frank Cetta, MD
Professor of Internal Medicine and Pediatrics
Chair, Division of Pediatric Cardiology
Department of Pediatrics
Mayo Clinic College of Medicine
Mayo Clinic
Rochester, MN
USA

Shiv Kumar Choudhary, MS, MCh
Additional Professor
Department of Cardiothoracic Surgery
All India Institute of Medical Sciences
New Delhi
India

Henry Chubb, MA, MBBS, MRCP, MRCPCH
Specialist Registrar in Paediatric Cardiology
Royal Brompton Hospital
London
UK

John M. Costello, MD, MPH
Associate Professor of Pediatrics
Feinberg School of Medicine
Northwestern University
Director, Regenstein Cardiac Care Unit
Division of Cardiology
Children's Memorial Hospital
Chicago, IL
USA

Ingo Daehnert, MD
Clinical Head of Department of Paediatric
Cardiology and Grown Up Congenital Heart
Disease
University of Leipzig – Heart Center
Leipzig
Germany

Piers E. F. Daubeney, MA, DM, MRCP, FRCPCH, DCH
Consultant Paediatric and Fetal Cardiologist
Royal Brompton Hospital
Reader in Paediatric Cardiology
Imperial College
London
UK

Joseph A. Dearani, MD
Professor of Surgery
Department of Pediatrics
Division of Pediatric Cardiology and Department
of Surgery
Division of Cardiovascular Surgery
Mayo Clinic
Rochester, MN
USA

Christoph Döhlemann, MD
Emeritus Professor of Pediatrics
Division of Pediatric Cardiology
Dr. von Haunersches Kinderspital
University of Munich
Munich
Germany

David J. Driscoll, MD
Professor of Pediatrics
Department of Pediatrics
Division of Pediatric Cardiology and Department
of Surgery
Division of Cardiovascular Surgery
Mayo Clinic
Rochester, MN
USA

Anne M. Dubin, MD
Director, Pediatric Arrhythmia Center
Lucile Packard Children's Hospital
Associate Professor of Pediatrics
Stanford University
Palo Alto, CA
USA

Bonita Falkner, MD
Professor of Medicine and Pediatrics
Thomas Jefferson University
Philadelphia, PA
USA

Per Morten Frederiksen, PT, PhD
Head of Clinical Laboratory
Section for Pediatric Heart, Lung and Allergic
Diseases
Division of Pediatrics
Women & Children's Division
Oslo University Hospital
Nydalen
Oslo
Norway

Mark K. Friedberg, MD
Associate Professor of Paediatrics
The Labatt Family Heart Center
Department of Paediatrics
The Hospital for Sick Children
University of Toronto
Toronto, ON
Canada

Helena M. Gardiner, PhD, MD, FRCP, FRCPCH, DCH
Reader and Director in Perinatal Cardiology
Department of Reproductive Biology
Division of Cancer
Imperial College London
Honorary Consultant
Queen Charlotte's and Chelsea Hospital
Royal Brompton Hospital
London
UK

Bruce D. Gelb, MD
Professor of Pediatrics and Human Genetics
Departments of Pediatrics, Genetic and Genomic
Sciences and Child Health and Development
Institute
Mount Sinai School of Medicine
New York, NY
USA

Michael H. Gewitz, MD
Physician-in-Chief
Chief Pediatric Cardiology
Maria Fareri Children's Hospital
Professor and Vice Chairman
Department of Pediatrics
New York Medical College
Valhalla, NY
USA

List of Contributors

Adriana C. Gittenberger-de Groot, PhD
Professor of Anatomy and Embryology
Department of Anatomy and Embryology
Leiden University Medical Center
Leiden
The Netherlands

Bryan H. Goldstein, MD
Instructor of Pediatrics
Division of Pediatric Cardiology
University of Michigan Health System
Ann Arbor, MI
USA

James Gossage, MD, FCCP
Professor of Medicine
Director of Pulmonary Vascular Diseases
and HHT
Medical Director of HHT Foundation
International
Department of Medicine
Section of Pulmonary and Critical Care
Medicine
Medical College of Georgia
Augusta, GA
USA

James M. Greenberg, MD
Professor of Pediatrics
Director, Division of Neonatology
Cincinnati Children's Hospital Research
Foundation
Department of Pediatrics
University of Cincinnati College of Medicine
Cincinnati, OH
USA

Paolo Guccione, MD
Associate in Pediatric Cardiology
Department of Pediatric Cardiology and Cardiac
Surgery
Bambino Gesù Children's Hospital
Rome
Italy

John T. Hambrook, MD
Assistant Professor of Pediatrics
Medical College of Wisconsin
Milwaukee, WI
USA

Robert B. Hinton, MD
Assistant Professor
Division of Cardiology
Cincinnati Children's Hospital Medical Center
University of Cincinnati School of Medicine
Cincinnati, OH
USA

Anthony M. Hlavacek MD, MSCR
Assistant Professor of Pediatrics
Cardiology
Attending Physician
Pediatric Cardiology
Medical University of South Carolina
Charleston, SC
USA

Julien I. E. Hoffman, MD
Emeritus Professor of Pediatrics
University of California San Francisco
San Francisco, CA
USA

Tim S. Hornung, MD
Paediatric and Adult Congenital
Cardiologist
Green Lane Paediatric and Congenital Cardiac
Service
Auckland City Hospital
Auckland
New Zealand

Collin John, MD, MPH
Assistant Professor of Pediatrics
Department of Pediatrics
Robert C. Byrd Health Science Center
West Virginia University School of
Medicine
Morgantown, WV
USA

Jonathan N. Johnson, MD
Assistant Professor of Pediatrics
Division of Pediatric Cardiology
Department of Pediatrics
Mayo Clinic College of Medicine
Mayo Clinic
Rochester, MN
USA

Walter H. Johnson Jr, MD
Professor of Pediatrics
Division of Pediatric Cardiology
University of Alabama at Birmingham
Alabama Congenital Heart Disease Center
Women & Infants Center
Birmingham, AL
USA

Monique R. M. Jongbloed, MD, PhD
Assistant Professor of Cardiac Anatomy and
Embryology/Cardiologist
Department of Anatomy and Embryology
Leiden University Medical Center
Leiden
The Netherlands

Vijaya Joshi, MD
Medical Director of Non Invasive Cardiology
Le Bonheur Children's Medical Center
St Jude Children's Research Hospital
Associate Professor of Pediatrics
University of Tennessee Health Science
Center
Memphis, TN
USA

Hirohisa Kato, MD, PhD, FACC
Emeritus Professor of Pediatrics
Honorary President, The Cardiovascular Research
Institute
Kurume University School of Medicine
Kurume
Japan

Beth D. Kaufman, MD
Director, Heart Failure/Cardiomyopathy
Programs
Attending Physician, Division of Pediatric
Cardiology
Assistant Professor of Pediatrics, University of
Pennsylvania School of Medicine
The Children's Hospital of Philadelphia
Philadelphia, PA
USA

Shivu Kaushik, MD
Fellow, Department of Medicine
Section of Pulmonary and Critical Care
Medicine
Medical College of Georgia
Augusta, GA
USA

James K. Kirklin, MD
Professor and Director
Division of Cardiothoracic Surgery
University of Alabama at Birmingham
Birmingham, AL
USA

Eduardo A. Kreutzer, MD
Chief Emeritus of Cardiology at Hospital de Niños
Pedro Elizalde
Director, Centro Cardiovascular Infantil
Buenos Aires
Argentina

Guillermo O. Kreutzer, MD
Ex-Chief of Cardiovascular Division
Ricardo Gutierrez Buenos Aires Children's Hospital
Ricardo Gutierrez Ex-Professor of Pediatrics
Head of Pediatric Cardiovascular Surgery
Department Clínica Bazterrica
University of Buenos Aires
Buenos Aires
Argentina

Jacqueline Kreutzer, MD, FACC, FSCAI
Associate Professor of Pediatrics
University of Pittsburgh School of Medicine
Director Cardiac Catheterization Laboratory
Children's Hospital of Pittsburgh of UPMC
Pittsburgh, PA
USA

Thomas J. Kulik, MD
Senior Associate in Cardiology
Department of Cardiology
Children's Hospital Boston
Associate Professor of Pediatrics
Harvard Medical School
Boston, MA
USA

Raman Krishna Kumar, MD, DM, FACC, FAHA
Clinical Professor and Head of Department
Pediatric Cardiology
Amrita Vishwa Vidyapeetham
Amrita Institute of Medical Sciences and Research Center
Kerala
India

Stephanie Lacey, DO
Pediatric Cardiologist
Assistant Professor of Pediatrics
Department of Pediatrics
University of Florida College of Medicine
Jacksonville, FL
USA

Bertrand Léobon, MD, PhD
Pediatric Cardiology Unit
Children's Hospital
Toulouse University Hospital
Toulouse
France

Kimberly Y. Lin, MD
Fellow, Division of Pediatric Cardiology
The Children's Hospital of Philadelphia
Philadelphia, PA
USA

Bart Loeys, MD, PhD
Center for Medical Genetics
Antwerp University Hospital
University of Antwerp
Antwerp
Belgium

Philipp C. Lurz, MD
Senior Clinical Fellow
Department of Internal Medicine/Cardiology and
Grown Up Congenital Heart Disease
University of Leipzig – Heart Center
Leipzig
Germany

Peter Lwabi, MD
Consultant Paediatrician (Cardiology)
Divisional Head
Department of Paediatric Cardiology
Deputy Director
Uganda Heart Institute
Mulago Hospital
Makerere University School of Medicine
Kampala
Uganda

Shannon M. Mackey-Bojack, MD
Anatomic and Clinical Pathologist
Jesse E. Edwards Registry of Cardiovascular
Disease
United Hospital
St Paul, MN
USA

Nitin Madan MBBS, MD
Pediatric Cardiology Fellow
Department of Pediatrics
Mount Sinai School of Medicine
New York, NY
USA

Bruno Marino, MD
Professor of Pediatrics and Director of Pediatric
Cardiology
Department of Pediatrics
"Sapienza" – University of Rome
Rome
Italy

Barry J. Maron, MD
Director, Hypertrophic Cardiomyopathy Center
Minneapolis Heart Institute Foundation
Minneapolis, MN
USA

Lisa J. Martin, PhD
Associate Professor
Divisions of Biostatistics and Epidemiology and
Human Genetics
Cincinnati Children's Hospital Medical Center
University of Cincinnati School of Medicine
Cincinnati, OH
USA

M. Patricia Massicotte, MSc, MD, MHSc, FRCPC
Professor of Pediatrics
Peter Olley Chair, Pediatric Thrombosis
Director KIDClot Program
University of Alberta
Stollery Children's Hospital
Edmonton, AB
Canada

Roxane McKay, MD, FRCS, FRCSC
600 Fourth Street SW
Rochester, MN
USA

Colin McMahon, FRCPI, FAAP
Consultant Paediatric Cardiologist
Our Lady's Children's Hospital
Crumlin, Dublin
Ireland

Alison K. Meadows, MD, PhD
Adjunct Professor of Pediatrics
and Radiology
University of California San Francisco
Director, Adult Congenital
Heart Program
Kaiser Permanente of Northern California
San Francisco, CA
USA

Shaji C. Menon, MD
Assistant Professor of Pediatrics
Adjunct Assistant Professor of Radiology
Division of Pediatric Cardiology
University of Utah
Salt Lake City, UT
USA

James H. Moller MD
Adjunct Professor of Medicine
Emeritus Professor and former
Head of Pediatrics
University of Minnesota
Minneapolis, MN
USA

Kazuo Momma, MD, PhD
Emeritus Professor of Pediatrics
Cardiology
Former Chairman of Department of Pediatric
Cardiology
Tokyo Women's Medical University
Shinjukuku, Tokyo
Japan

Charles Mondo, MD
Consultant Physician (Cardiology)
Research and Fellowship Training
Division of Cardiology
Uganda Heart Institute
Mulago Hospital
Makerere University School of Medicine
Kampala
Uganda

Tom Mwambu, MD
Consultant Physician
Division of Cardiothoracic
and Vascular Surgery
Uganda Heart Institute
Mulago Hospital
Makerere University School of Medicine
Kampala
Uganda

List of Contributors

Maryam Y. Naim, MD
Attending Physician, Pediatric Cardiac Intensive
Care
Department of Anesthesiology and Critical Care
Medicine
The Children's Hospital of Philadelphia
Philadelphia, PA
USA

William A. Neal, MD
Professor and Walker Chair of Preventive
Cardiology
Department of Pediatrics
Robert C. Byrd Health Science Center
West Virginia University School of Medicine
Morgantown, WV
USA

Jane W. Newburger, MD, MPH
Commonwealth Professor of Pediatrics
Harvard Medical School
Associate Chief for Academic Affairs
Department of Cardiology
Children's Hospital
Boston, MA
USA

Petra Opic, MSc
Researcher
Thoraxcentre
Department of Cardiology
Erasmus Medical Centre
Rotterdam
The Netherlands

Phalla Ou, MD
Head of Cardiovascular Radiology
Hôpital Necker – Enfants Malades
Université Paris V
Paris
France

Akash R. Patel, MD
Fellow, Division of Pediatric Cardiology
The Children's Hospital of Philadelphia
Philadelphia, PA
USA

Carlos A. C. Pedra, MD, PhD
Director, Catheterization Laboratory for
Congenital Heart Disease
Instituto Dante Pazzanese de Cardiologia
São Paulo, SP
Brazil

Simone R. Fontes Pedra, MD, PhD
Director, Echocardiography Laboratory for
Congenital Heart Disease
Instituto Dante Pazzanese de Cardiologia
São Paulo, SP
Brazil

Daniel J. Penny, MD, PhD
Chief of Cardiology
Texas Children's Hospital
Professor of Pediatrics
Leader of Pediatric Cardiology
Baylor College of Medicine
Houston, TX
USA

John R. Phillips, MD
Associate Professor of Pediatrics
Section of Pediatric Cardiology
Robert C. Byrd Health Sciences Center
West Virginia University College of
Medicine
Morgantown, WV
USA

Robert E. Poelmann, PhD
Professor of Cardiovascular Developmental
Biology
Department of Anatomy and Embryology
Leiden University Medical Center
Leiden
The Netherlands

Rajesh Punn, MD
Clinical Assistant Professor
Division of Pediatric Cardiology
Stanford University
Lucile Packard Children's Hospital
Palo Alto, CA
USA

**Shakeel A. Qureshi,
FRCP, MD**
Professor of Paediatric Cardiology
King's College London
Consultant Paediatric Cardiologist
Department of Paediatric Cardiology
Evelina Children's Hospital
Guy's and St. Thomas' Hospital
London
UK

Marlene Rabinovitch, MD
Dwight and Vera Dunlevie Professor of Pediatric
Cardiology
Stanford University School of Medicine
Stanford, CA
USA

Alia Rai, MD
Research Assistant Professor of
Pediatrics
Department of Pediatrics
Robert C. Byrd Health Science Center
West Virginia University School of
Medicine
Morgantown, WV
USA

Satish K. Rajagopal, MD
Assistant in Cardiology
Department of Cardiology
Children's Hospital Boston
Instructor of Pediatrics
Harvard Medical School
Boston, MA
USA

**Sivasubramanian Ramakrishnan,
MD, DM**
Assistant Professor
Department of Cardiology
All India Institute of Medical Sciences
New Delhi
India

P. Syamasundar Rao, MD
Professor of Pediatrics and Medicine
University of Texas at Houston Medical School
Director, Division of Pediatric Cardiology
Children's Memorial Hermann Hospital
Professor of Pediatrics
University of Texas MD Anderson Cancer Center
Houston, TX
USA

Andrew Redington, MD, FRCP
Professor of Paediatrics
University of Toronto
Head, Division of Cardiology
Hospital for Sick Children
Toronto, ON
Canada

Larry A. Rhodes, MD
Professor of Pediatrics
Chief, Section of Pediatric Cardiology
Robert C. Byrd Health Sciences Center
West Virginia University College of Medicine
Morgantown, WV
USA

Albert P. Rocchini, MD
Professor of Pediatrics
Division of Pediatric Cardiology
University of Michigan Health System
Ann Arbor, MI
USA

**Jolien W. Roos-Hesselink, MD,
PhD**
Professor of Congenital Cardiology
Director of Adult Congenital Heart Disease
Programme
Thoraxcentre
Department of Cardiology
Erasmus Medical Centre
Rotterdam
The Netherlands

Eric Rosenthal, MD, FRCP
Consultant Paediatric and Adult Congenital
Cardiologist
Evelina Children's Hospital
St Thomas' Hospital
London
UK

Abraham M. Rudolph, MD
Emeritus Professor of Pediatrics
University of California San Francisco
San Francisco, CA
USA

**Lindsay M. Ryerson,
MD, FRCPC**
Assistant Professor of Pediatrics
University of Alberta
Staff Physician Pediatric Cardiology and Pediatric
Critical Care
Stollery Children's Hospital
Edmonton, AB
Canada

Craig Sable, MD
Director, Echocardiography and Cardiology
Fellowship Training
Medical Director, Telemedicine
Children's National Medical Center
Professor of Pediatrics
George Washington University
Medical School
Washington, DC
USA

David E. Saudek, MD
Assistant Professor of Pediatrics
Medical College of Wisconsin
Milwaukee, WI
USA

**Pierre-Emmanuel
Séguéla, MD**
Pediatric Cardiology Unit
Children's Hospital
Toulouse University Hospital
Toulouse
France

Robert E. Shaddy, MD
Jennifer Terker Professor of Pediatrics
University of Pennsylvania School of
Medicine
Medical Director
Heart Transplant Program
Division Chief
Pediatric Cardiology
The Childrens' Hospital of Philadelphia
Philadelphia, PA
USA

Maully J. Shah, MBBS
Director, Electrophysiology Section
Division of Pediatric Cardiology
Associate Professor of Pediatrics
University of Pennsylvania School of Medicine
The Children's Hospital of Philadelphia
Philadelphia, PA
USA

Jie Shen, MD
Associate Professor
Shanghai Jiaotong University
Director of Cardiology
Cardiology Department
Children's Hospital of Shanghai
Shanghai
China

Daniel Sidi, MD
Head of Pediatric Cardiology
Hôpital Necker – Enfants Malades
Université Paris V
Paris
France

**Norman H. Silverman,
MD, DSc**
Professor of Pediatrics
The Roma and Marvin Auerback Scholar in
Pediatric Cardiology
Division of Pediatric Cardiology
Stanford University
Lucile Packard Children's Hospital
Palo Alto, CA
USA

**Jeffrey Smallhorn,
MD, FRCP**
Professor of Pediatrics
Staff Physician Pediatric Cardiology
Program Director Pediatric Cardiology
Stollery Children's Hospital
Edmonton, AB
Canada

James D. St. Louis, MD
Aldo R. Castaneda Associate Professor
Department of Surgery
Director, Pediatric Cardiac Surgery
University of Minnesota
Amplatz Children's Hospital
Minneapolis, MN
USA

Kenji Suda, MD, PhD
Associate Professor of Pediatrics
Department of Pediatrics and Child Health
Kurume University School of Medicine
Kurume
Japan

Sachin Talwar, MS, MCh
Associate Professor
Department of Cardiothoracic Surgery
Department of Cardiology
All India Institute of
Medical Sciences
New Delhi
India

Lloyd Y. Tani, MD
Professor of Pediatrics
Division of Pediatric Cardiology
University of Utah
Salt Lake City, UT
USA

**Kathryn A. Taubert,
PhD, FAHA**
Professor of Physiology
University of Texas Southwestern
Medical School
Dallas, TX
USA
Senior Science Officer
World Heart Federation
Geneva
Switzerland

**John D. R. Thomson,
FRCP, MD**
Consultant Paediatric Cardiologist
Department of Congenital Heart Disease
Leeds General Infirmary
Leeds
UK

Cécile Tissot, MD
Research Associate
Pediatric Cardiology Unit
The University Children's
Hospital of Geneva
Geneva
Switzerland

Jeffrey A. Towbin, MD
Executive Co-Director, The Heart Institute
Kindervelt-Samuel Kaplan Professor and Chief
Pediatric Cardiology
Cincinnati Children's Hospital
Cincinnati, OH
USA

James S. Tweddell, MD
The S. Bert Litwin Chair, Cardiothoracic
Surgery
Children's Hospital of Wisconsin
Professor of Surgery and Pediatrics
Chair, Division of Cardiothoracic Surgery
Medical College of Wisconsin
Milwaukee, WI
USA

Elisabeth M. W. J. Utens, PhD
Clinical Psychologist
Associate Professor, Department of Child and
Adolescent Psychiatry
Research Coordinator, Psychosocial Care
Erasmus Medical Centre
Sophia Children's Hospital
Rotterdam
The Netherlands

George F. Van Hare, MD
Director, Pediatric Cardiology
Professor of Pediatrics
Washington University
St. Louis Children's Hospital
St. Louis, MO
USA

Lut Van Laer, PhD
Center for Medical Genetics
Antwerp University Hospital
University of Antwerp
Antwerp
Belgium

Elisabeth H. M. van Rijen, PhD
Assistant Professor of Psychology
Institute of Psychology
Erasmus University Rotterdam
Rotterdam
The Netherlands

Paolo Versacci, MD
Staff Physician, Pediatric Cardiology
Department of Pediatrics
"Sapienza" – University of Rome
Rome
Italy

César Viegas, MD
Senior Associate in Cardiology
Ricardo Gutierrez Children's Hospital Buenos Aires
Director, Postgraduate Pediatric Cardiology
Subspecialty Training Course
University of Buenos Aires Medical School
Buenos Aires
Argentina

Pascal Vouhé, MD
Head of Cardiac Surgery
Hôpital Necker – Enfants Malades
Université Paris V
Paris
France

Gary D. Webb, MD
Professor of Pediatrics and Internal Medicine
University of Cincinnati
Director, Adolescent and Adult Congenital Heart
Disease Program
The Heart Institute
Cincinnati Children's Hospital Medical Center
Cincinnati, OH
USA

Paul M. Weinberg, MD
Professor of Pediatrics and Pediatric Pathology and
Laboratory Medicine
Associate Professor of Radiology
The Children's Hospital of Philadelphia
University of Pennsylvania
School of Medicine
Philadelphia, PA
USA

Kevin K. Whitehead, MD, PhD
Assistant Professor of Pediatrics
The Children's Hospital of Philadelphia
University of Pennsylvania
School of Medicine
Philadelphia, PA
USA

Christopher Wren, MBChB, PhD
Consultant Paediatric Cardiologist
Senior Lecturer in Paediatric Cardiology
Freeman Hospital
Newcastle upon Tyne
UK

Anji T. Yetman, MD
Associate Professor of Pediatrics
Director, Adult Congenital Cardiac Program
Primary Children's Medical Center
University of Utah
Salt Lake City, UT
USA

Preface

With the expansion of knowledge and methods of diagnosis and treatment of cardiac abnormalities occurring in childhood, the major textbooks on the subject have also expanded, often beyond a single volume. In our book, *Pediatric Cardiovascular Medicine*, we have attempted to be concise and focused, and publish a single volume containing contemporary knowledge of pediatric cardiology. The book is available both as a text and online for the convenience of readers who may have different needs. For readers of the textbook there is supplemental material online, including videos of cardiac images. We have focused on the international aspects of pediatric cardiology, both in content and in the selection of authors from 16 countries to contribute chapters. In this edition we have included new chapters about pediatric cardiology in the tropics and developing countries, and about rheumatic heart disease in children (a major problem in many countries with limited health resources).

The chapters are grouped according to subject matter.

The first five chapters present basic scientific information that underlies pediatric cardiology and includes cardiac development and developmental physiology, basic cardiopulmonary physiology, pulmonary vascular physiology and pathology and genetics. The subsequent eight chapters discuss the various diagnostic methods to evaluate cardiovascular problems in childhood, particularly echocardiography, advanced radiologic imaging techniques and genetic testing. Two chapters follow which discuss bypass techniques and postoperative care and three about the fetus and neonates, including fetal treatment, neonatal diagnosis and circulatory issues of small neonates.

A major portion of the book covers congenital heart disease. After chapters on epidemiology and cardiac anatomy, descriptions of individual malformations are presented primarily in the following order: left-to-right shunts, outflow and inflow tract obstruction and regurgitation, anomalies associated with a right-to-left shunt, and then vascular and situs anomalies. In most of the 25 chapters about congenital heart disease, the organization and structure of the chapters are similar, making it easier for the reader.

The final 22 chapters concern various acquired conditions affecting the cardiovascular system during childhood. The issues of adults with CHD and the quality of life after cardiac treatment are discussed in separate chapters and where relevant within individual chapters.

As editors, we sought to emphasize pathophysiologic principles or understanding to help the reader comprehend and retain the information. Each chapter contains pertinent references to enable the reader to explore the subjects further.

Since the previous edition, echocardiographic techniques have advanced significantly; interventional methods have been developed to include a wider range of abnormalities and imaging techniques, particularly with magnetic resonance which has allowed more detailed information about cardiovascular structure and function. These are being widely applied to children.

Finally, we added three Associate Editors to assist in the preparation of this expanded edition and we appreciate their careful review of chapters and editorial comments.

James H. Moller, MD
Julien I. E. Hoffman, MD, FRCP
Senior Editors

1 Normal and Abnormal Cardiac Development

Adriana C. Gittenberger-de Groot, Monique R. M. Jongbloed & Robert E. Poelmann
Leiden University Medical Center, Leiden, The Netherlands

Introduction

In this chapter, the main events of cardiac morphogenesis are discussed. We focus on morphologic descriptions and insights based on the molecular biologic approaches in animal models that have enhanced and modified our understanding of normal and abnormal cardiac development, including relevance for adult disease with a developmental background.

Advances and limitations in studying human development

The normal cardiovascular development of the human embryo in its crucial stages from 2 to 8 weeks' gestation has to be deduced from postmortem morphologic studies of abortion material [1]. In this category we are mainly dealing with spontaneous abortions and do not know whether the material reflects normal morphogenesis. Descriptions in the literature referring to normal and abnormal human development do not emphasize this aspect. An addition to early detection of human embryonic malformations, mainly providing information on disturbed genes and chromosomes, is provided by amniocentesis, chorionic villus biopsies, and subsequent FISH (fluorescent *in situ* hybridization) analysis with genetic markers. However, these are not examined within the first crucial 8 weeks of development. Fetal diagnosis is a rapidly expanding area with increasing technical possibilities of ultrasound and echo-Doppler investigations *in utero*. The earliest observations indicating normal or abnormal heart development refer to 11–12 weeks' gestation [2]. Consequently, our knowledge of detailed cardiac morphogenesis relies on describing processes in animal species, the main embryonic models being avians (chick and quail) and rodents (mouse and rat) and more recently the zebrafish. With the development of transgenic techniques, the mouse embryo has become important, and we will regularly refer to mouse embryo models when discussing certain abnormalities of cardiac development.

Knowledge about an embryonic lethal phenotype after a gene knockout and the absence of a phenotype might contribute little to the understanding of human congenital cardiac malformations [3]; 85% of the diagnosed human cardiac malformations are described as having a multifactorial origin. Epigenetic, environmental, biomechanical, and hemodynamic factors have been underestimated in research on cardiogenic programming. Their role in the development of cardiac malformations has previously been acknowledged, however, and has led to the so-called mechanistic classification [4]. There are a few recent publications linking hemodynamics to cardiovascular developmental abnormalities [5–8], but their relation to gene expression and cardiogenic patterning is unclear. A multidisciplinary approach combining clinical knowledge with basic science will lead to new insights into developmental processes.

Formation of the cardiogenic plates and the cardiac tube

The cardiac developmental program starts with the formation within the splanchnic mesoderm of the bilateral cardiogenic plates, which give rise to the myocardium and probably to parts of the endocardium (Figure 1.1). The splanchnic mesoderm at the endoderm/mesoderm interface differentiates into the vascular endothelium [9] and part of the endocardium [10,11]. The evidence for a cardiogenic plate origin of the endocardium supports a dual origin for this layer of the heart [12].
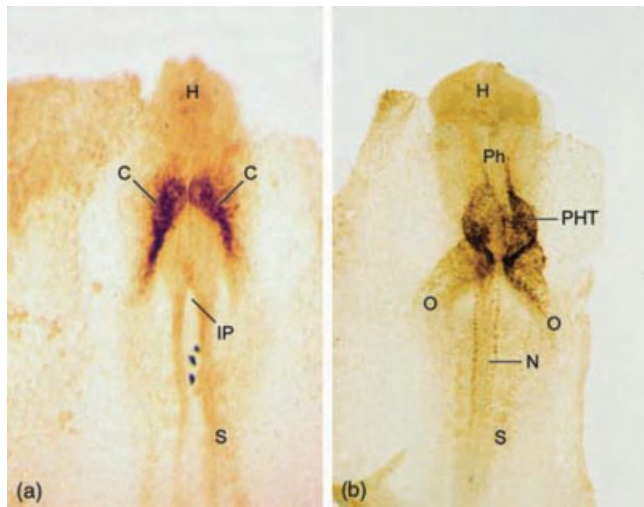
Figure 1.1 (a) Whole mount of a quail embryo (stage HH 8) viewed from the ventral aspect, showing the bilateral cardiogenic plates (C) that have not yet fused across the midline. At this stage, the staining is done by a nonspecific neurofilament antibody. (b) Whole mount of the fused primary heart tube (PHT) of a quail embryo (stage HH 10) viewed from the ventral aspect. The staining is by an anti-smooth muscle actin antibody, showing the myocardial lining of the tube. H, head region; IP, intestinal portal; N, neural tube; O, omphalomesenteric vein; Ph, pharyngeal region; S, somite. (Copyright Leiden University Medical Center.)

The bilateral asymmetric cardiogenic plates can be delineated early in embryonic life because several transcription factors and proteins are expressed. These expression patterns distinguish a first or primary heart field (PHF) laterally flanking the second heart field (SHF) component of the cardiogenic plate (Figure 1.2a). Whereas the first heart field differentiates, the secondary component remains part of the body wall mesoderm before its cells are recruited and incorporated into the poles of the cardiac tube. With formation of the cardiac tube, the pericardial coelomic cavity becomes continuous across the midline and the ventral mesocardium disappears. The cardiac tube is thereafter solely connected to the dorsal body wall or splanchnic mesoderm by the dorsal mesocardium that runs from the developing pharyngeal arches (arterial pole) to the sinus venosus (venous pole) (Figure 1.3). At this stage, the tube consists of an inner endocardial and an outer myocardial layer separated by cardiac jelly (Figures 1.2b and 1.3a).

Initially, the primitive cardiac endothelial network is remodeled into a single endocardial tube that connects the omphalomesenteric veins to the pharyngeal arch vasculature (Figure 1.1). The asymmetric cardiac jelly surrounding the endocardial tube suggests bilateral endocardial tubes, giving the wrong impression that two endocardial tubes have to fuse. From the onset, however, the endocardial tubes are connected by endocardial cells that cross the midline [13]. Real cardia bifida can occur spontaneously and can also be produced

experimentally by retinoic acid overdose in the chicken embryo [14] or in a zebrafish mutational screen [15]. Therefore, each cardiogenic plate can potentially give rise to an independent cardiac tube, implying that fusion of the cardiogenic plates is unnecessary for the onset of cardiac formation. Nevertheless, cardia bifida is lethal to the embryo as further cardiac development is hampered and no connection with the endothelium of the pharyngeal vascular system is established.

Looping of the cardiac tube

The single cardiac tube is never completely straight as both cardiogenic plates have different dimensions [12]. Normally the cardiac tube loops to the right (D-loop) (Figure 1.2). Abnormalities in looping such as L-loop or anterior-loop formation are related to ventricular inversion, which differs from laterality problems as seen in abnormalities of the atrial situs.

The mechanisms underlying the looping direction are poorly understood, but several regulating genes have been described, such as sonic hedgehog, nodal and activin receptor IIa [16]. In mouse mutants iv/iv and inv, the laterality of the heart is also affected. The iv gene has been mapped to chromosome 12 in the mouse and is syntenic to chromosome 14q in the human. In the human, this abnormality is reflected in the heart by atrial isomerism and is discussed below when considering atrial development and septation.

During looping, the outflow tract becomes more ventrally positioned, moving in front of the atrioventricular (AV) canal. The arterial and venous poles remain fixed to the dorsal body wall (Figure 1.4 and Videoclip 1.1). Both remodeling of the inner curvature (site of the disruption of the dorsal mesocardium) and asymmetric addition of SHF-derived myocardium to the primary heart tube are essential for proper looping.

Contribution of first and second heart fields

Recent mouse studies, based on various transgenic mouse models with cell tracing [17–19], have shown that the primary heart tube does not contain all components necessary for the future mature heart [20]. The first heart field provides only for the AV canal and the future left ventricle (LV), implying that the primary heart tube already has additions of the second heart field (SHF) at both poles. The primary heart tube connects the omphalomesenteric veins at the venous pole via a small atrial component, the AV canal, and a primitive LV and small outflow tract component to the aortic sac and the first pair of pharyngeal arch arteries at the arterial pole (Figures 1.2 and 1.3).
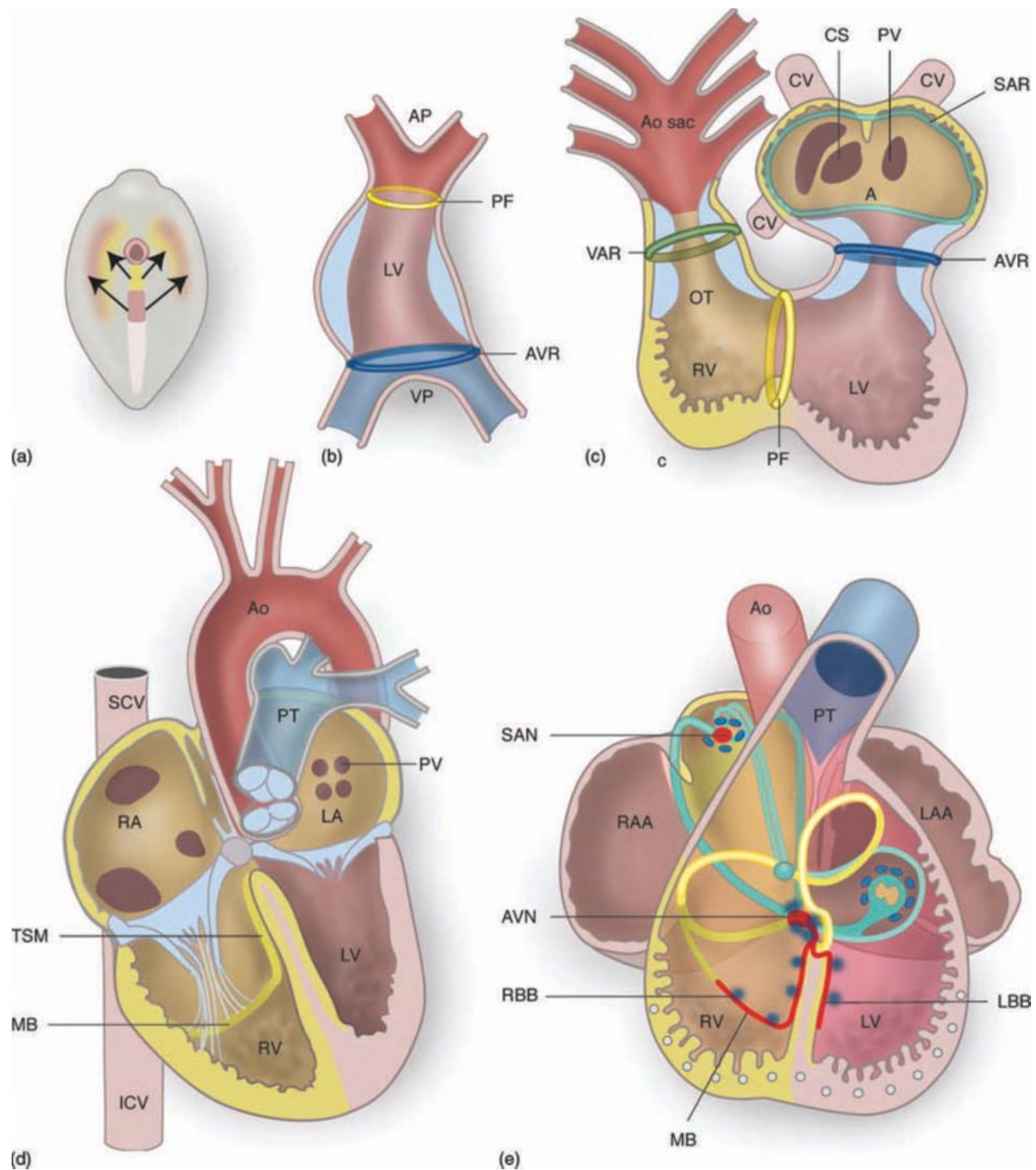
Figure 1.2 Development of the heart from the first and second heart fields. (a) In the primitive plate, bilateral fields of cardiac mesoderm are present. Progenitor cells migrate from the primitive streak to the bilateral mesoderm (arrows). Cells depicted in yellow will contribute to the second heart field-derived parts of the heart, whereas cells depicted in brown depict the primary heart fields that will contribute the primary myocardial heart tube. (b) Schematic representation of the primary heart tube, consisting of endocardium and myocardium, with myocardial jelly between the two layers. Initially the primitive heart tube consists mainly of the AV canal and the LV. (c) After looping, several transitional zones can be distinguished in the tube, namely the sinoatrial transition (light blue, SAR) in between the sinus venosus and common atrium, the AV transition (dark blue, AVR) in between the common atrium and common ventricle, the primary fold (yellow, PF) in between the primitive right ventricle (RV) and LV, and a ventriculoarterial transitional (green, VAR) zone at the outflow tract (OT) of the heart. Second heart field-derived parts of the heart are depicted in yellow. (d) The heart after completion of atrial and ventricular septation. Due to outgrowth of the RV, a remodeling of the PF has occurred, and it has divided into a lateral septal part, the trabecula septomarginalis (TSM), that contains the right bundle branch [RBB, see (e)] and continues into the moderator band (MB). (e) Part of the transitional zones will contribute to definitive elements of the cardiac conduction system, depicted in red. Bright blue dots depict neural crest cells that contribute to the network of autonomic nerve fibers surrounding the sinoatrial node (SAN) and atrioventricular node (AVN). Shaded blue dots surrounding elements of the cardiac conduction system indicate neural crest cells with an inductive role in conduction system development. A, common atrium; AP, arterial pole; Ao, aorta; Ao sac, aortic sac; CV, cardinal vein; CS, coronary sinus; ICV, inferior caval vein; LA, left atrium; LAA, left atrial appendage; LBB, left bundle branch; LV, left ventricle; PT, pulmonary trunk; PV, pulmonary veins; RA, right atrium; RAA, right atrial appendage; SCV, superior caval vein; VP, venous pole. (Copyright Leiden University Medical Center.)
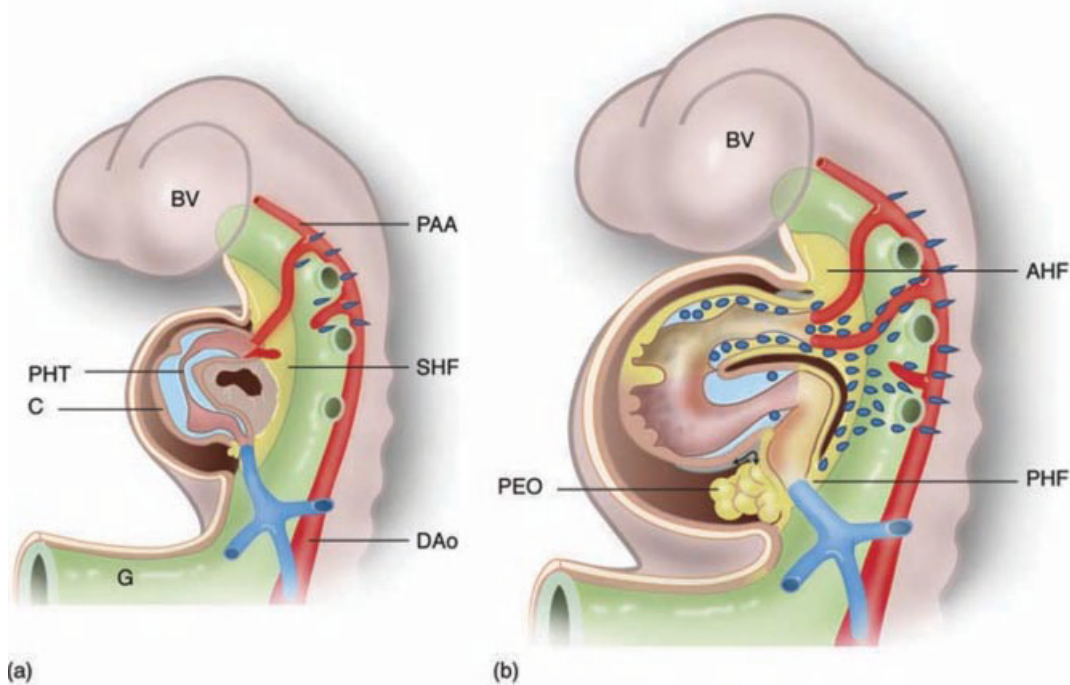
Figure 1.3 (a) Schematic representation of the primary heart tube (PHT, brown) after fusion of the bilateral plates of mesoderm. The tube is lined on the inside by cardiac jelly (blue). The mesoderm of the second heart field (SHF) is depicted by the yellow area behind the primary heart tube, and will during development contribute myocardium to both the arterial and venous poles of the heart [depicted by the yellow myocardium in (b)]. (b) The heart tube after contribution from the first and second heart fields have been made. The second heart field can be divided into the anterior heart field (AHF) and posterior heart field (PHF). The yellow lobulated structure that protrudes into the pericardial cavity at the venous pole of the heart is the pro-epicardial organ (PEO). Neural crest cells (depicted by blue dots) migrate from the neural crest along the arterial and venous pole into the heart. BV, brain ventricles; C, coelomic cavity; DAo, dorsal aorta; G, gut; PAA, pharyngeal arch arteries. (Copyright Leiden University Medical Center.)

The cardiac splanchnic mesoderm consists of so-called SHF. This precardiac mesoderm is added at both the arterial and venous poles of the heart, mainly contributing myocardium but also smooth muscle cells of connecting vessels.

The mesodermal cell population grows in a caudocranial direction [21]. Recruitment starts at the arterial pole and almost the complete myocardium of the right ventricle (RV) including the outflow tract and the larger part of the ventricular septum is derived from the SHF. The smooth muscle cells of the aortic sac are derived from this source, although probably asymmetric with respect of contribution to the pulmonary and aortic aspects. More restricted studies of the outflow tract have led to a confusing nomenclature with respect to anterior heart field [22] and secondary heart field [23], the latter often being confused with SHF that contributes to both arterial and venous poles.

At the venous pole, the myocardium lining the sinus venosus derives from SHF mesoderm referred to as posterior heart field (PHF) [24]. Incorporation of the sinus venosus implies that the myocardium of the sinoatrial node, the venous valves, the atrial septum, and the cardinal and pulmonary veins also come from this source. A further mesenchymal derivative of the SHF is the proepicardial organ (PEO), which is crucial for many aspects of differentiation of the heart (see below).

Several transcription factors and morphogenetic genes and cascades are important in the precardiac mesoderm of both first heart field and SHF [25]. Specification of the precardiac cells is accompanied by early expression of TGFβ family members, including BMP4 (bone morphogenetic protein), followed by the earliest known marker for the cardiogenic lineage – the homeobox (Hox)-containing gene Nkx2.5 (homolog to tinman in *Drosophila*) [26] and the zinc finger-containing GATA 4/5/6 cluster of transcription factors [27]. Mesp1 [28] and Mef2c [29] are also early cardiac mesoderm markers. Recently, the platelet-derived growth factor receptor (PDGFRα) was added to this list [30]. Patterning of the heart field from arterial to venous pole is accompanied by the expression of T-box gene family members Tbx1, 5 and 20, Fgf 8 and 10, and Isl1. Finally, differentiation during heart tube formation involves, for example, MLC and MHC, alpha cardiac actin and troponin I, and RhoA [31]. Mouse models in which these genes are used for cell tracing and complete or conditional knockout provide essential data on their relevance for normal and abnormal cardiac development. In some instances, such as Nkx2.5, [32] human mutations are known.
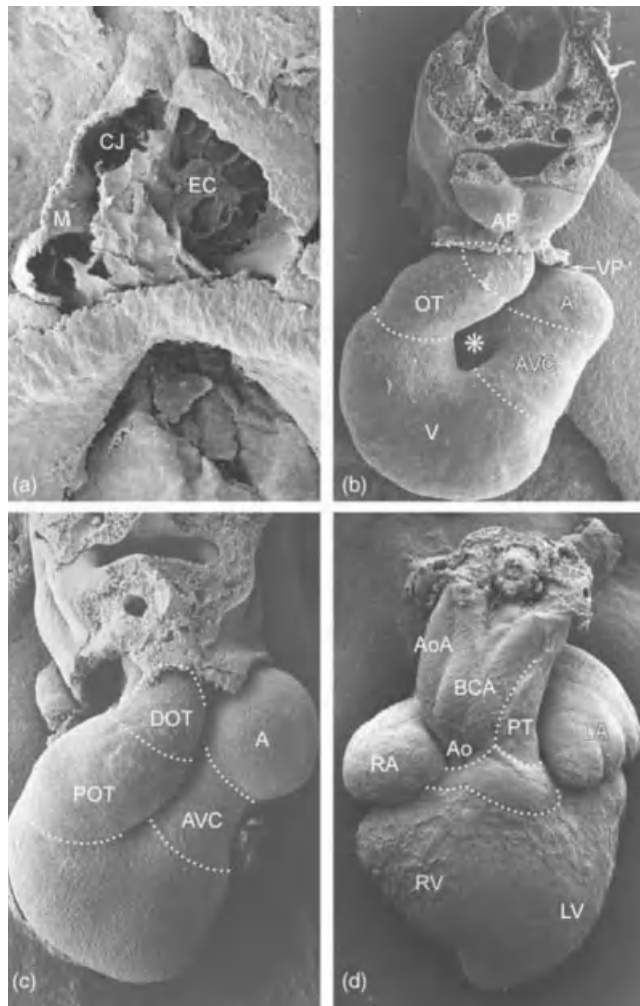
Figure 1.4 Scanning electron micrographs of the developing heart. (a) The fused heart tube (also see Figure 1.1) has been opened to show the endocardial cells (EC) inside the myocardium (M) and the cardiac jelly (CJ). (b) The heart tube normally loops to the right showing a venous pole (VP) and an arterial pole (AP) and the inner curvature (asterisk). (c) As the inner curvature tightens, the outflow tract becomes positioned in front of the venous pole. (d) With completion of the looping process, the AP is wedged in between the atrioventricular orifices that connect the right atrium (RA) to the right ventricle (RV) and the left atrium (LA) to the left ventricle (LV). A, atrium; AoA, aortic arch (right sided in birds); Ar, aortic root; AVC, atrioventricular canal. BCA, brachiocephalic arteries; DOT, distal outflow tract; OT, outflow tract; POT, proximal outflow tract; PT, pulmonary trunk; V, ventricular loop. (Copyright Leiden University Medical Center.)

Segmentation of the heart tube

The primary heart tube consists of myocardium lined on the inside by cardiac jelly and endocardium. A number of genes are expressed along the anterior/posterior axis and there is from the onset a right–left designation. Chamber outgrowth or ballooning, intricately regulated by a balance

of Tbx2 and Tbx3 transcription factor expression [33], brings out more clearly the segments (atrial and ventricular chambers) and the transitional zones. These areas stand out against the myocardial trabeculated atrial and ventricular walls. Figure 1.2b–e depicts the cardiac segments and transitional zones. Starting at the inflow at the venous pole, we can distinguish the sinus venosus, the atrium, the atrioventricular canal, the primitive LV, the primary fold, and the primitive RV that develops into a trabeculated part and a part lined by endocardial outflow tract cushions. In general, the endocardial cushion-lined transitional zones form the atrioventricular and semilunar valves and function initially as temporary valves accompanying peristaltic contractions of the cardiac tube. The myocardium of the sinus venosus (considered as a transitional zone), the AV canal, the primary fold, and the endocardial cushion-lined outflow tract are important for the formation of the future cardiac conduction system. Furthermore, these transitional zones are involved in septation.

Neural crest and epicardium contributions

For many years, the neural crest and epicardial cells were described as extracardiac contributors essential for proper differentiation of the developing heart. With new insights into the contribution of the SHF, we need to adjust their relevance.

Neural crest cells are an extracardiac source of cells that migrate from the neural crest through the mesoderm of the SHF to the cardiac tube. The main entrance site into the heart is at the arterial pole, but they also reach the venous pole of the heart [34,35] (Figures 1.3b and 1.5). These neural crest cells differentiate into smooth muscle cells of the great arteries and into the cells of the autonomic nervous system that are needed to innervate the great arteries and the coronary arteries, and for the nodes of the cardiac conduction system (Figures 1.2e and 1.5). The neural crest cells that migrate into the heart do not differentiate into a particular cardiac cell but go into apoptosis. Through release or activation of growth factors such as TGFβ they may induce myocardialization of the outflow tract septum and, at the venous pole, differentiation of the cardiac conduction system [36,37]. They are also important in the interaction with the SHF cells, mainly in the pharyngeal region, so that genetic mutations of both cell types can lead to congenital heart disease. This is best exemplified in the Tbx1-related 22q11 deletion syndrome [38].

The epicardium develops from the proepicardial organ, an epithelial derivative of the PHF at the venous pole (depicted in Figure 1.3b). These cells differentiate into smooth muscle cells and cardiac fibroblasts and migrate to many cardiac structures where their function is less known [39]. Suggestions, based on cell tracing in transgenic mouse
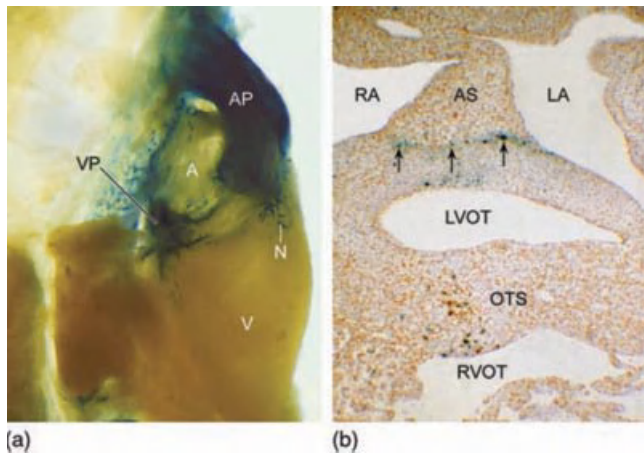
Figure 1.5 (a) Whole mount staining of a chicken heart (stage HH 35) that shows the neural crest-derived cells after a retroviral transporter gene marker containing lac-Z. The neural crest cells are present at the arterial pole (AP) as smooth muscle cells in the vessel wall and over the heart as fine nerve fibers (N). The neural crest cells also reach the venous pole (VP) of the heart, where they enter the atrioventricular region through the dorsal mesocardium. (b) A section through the inflow and outflow tract of a chicken heart in which the neural crest cells are seen in the outflow tract septum (OTS) and also at the base of the atrial septum (AS) (arrows), where they have arrived through the dorsal mesocardium. The brown staining of the outflow tract septum (OTS) neural crest cells by the TUNEL [TdT-mediated dUTP (deoxyuridine triphosphate) nick end labeling] technique detected apoptosis of these cells. A, atrium; LA, left atrium; LVOT, left ventricular outflow tract; RA, right atrium; RVOT, right ventricular outflow tract; V, ventricle. (Copyright Leiden University Medical Center.)

models, that epicardial cells can differentiate into myocardial [40] and endothelial cells [41] have been refuted.

Cardiac differentiation and development of cardiac malformations

Sinus venosus incorporation and atrial septation

The sinus venosus in the developing heart forms an intermediate transitional zone between the systemic cardiac veins and the developing atrium proper, and now receives much attention as the myocardium of the sinus venosus is derived from the PHF mesoderm, showing specific gene expression patterns. On the basis of endothelial vascular patterns, scanning electron microscopy data, and immunohistochemistry, we demonstrated that the sinus venosus is incorporated not only into the dorsal wall of the right atrium but also into the dorsal wall of the left atrium [42]. Here, it encircles the entrance of the future pulmonary veins. The sinus venosus also contributes to the posterior wall of the left atrium and pulmonary veins, as suggested for both the mouse and the human embryo [43,44], and earlier postulated by Van Praagh and Corsini [45]. Other groups, focusing on gene expression patterns, regard the pulmonary veins

(pulmonary pit lined by pulmonary ridges) as having their own origin independent of the sinus venosus [46]. All explanations have in common that the veins are connected to the cardiac tube by way of the dorsal mesocardium to the PHF mesoderm in the dorsal body wall. In the fully developed human heart, this area is demarcated by the epicardial/pericardial fold. The above morphogenesis of the sinus venosus also provides new data on the septation of the atria (Figure 1.6). The primary atrial septum is a structure that initially consists of atrial myocardium, but later becomes fibrous, and is derived from the PHF-derived myocardium. It forms an arch that runs from posterior to anterior and is lined on the inside by cushion-like tissue, called the mesenchymal cap. At this site, also PHF mesoderm, formerly referred to as spina vestibuli but now named the dorsal mesenchymal protrusion (DMP) [47], contributes to atrial and ventricular septation. The DMP provides cells to the inferior atrial septum and borders the mesenchymal cap on the right side. Fusion of the mesenchymal cap with the AV cushions is essential to close the primary atrial foramen.

The PHF mesoderm and also the derived myocardium have characteristic gene patterns that partly differ from the outflow tract. This refers to the transcription factors Tbx18, 20 [48], Shox2 [49], the functional marker HCN4 [50], and the growth factors RhoA [31] and PDGFRα [30,51]. The sinus venosus myocardium is Nkx2.5 negative before incorporation into the dorsal atrial wall and remains as such in the sinoatrial node. Transgenic mouse studies of these genes and some human mutations correlate with abnormalities in PHF-derived structures, including conduction system disturbances.

The primary atrial septum becomes perforated to form the ostium secundum that is never completely closed off by the septum secundum. The complex of the lower rim of the septum secundum and the ostium secundum is called the foramen ovale (Figure 1.6, arrow). The muscular secondary atrial septum is in its basal and dorsal part fused with the DMP. The major anterior and superior parts of the secondary atrial septum are merely a folding of the atrial wall forming the limbus fossa ovalis on the right side of the atrial septum.

Consequences for abnormal development
The above data provide new insights into abnormal pulmonary venous connections and also atrial septal defects (ASDs) and atrioventricular septal defects (AVSDs).

Abnormal pulmonary venous connection
As the plexus for forming the pulmonary veins has extensive connections to the cranial and caudal parts of the cardinal veins [52], persistent connections can lead to supracardiac and infracardiac pulmonary venous connection patterns. For cardiac abnormal pulmonary venous connection, the pulmonary veins do not grow out of the left atrial dorsal wall but
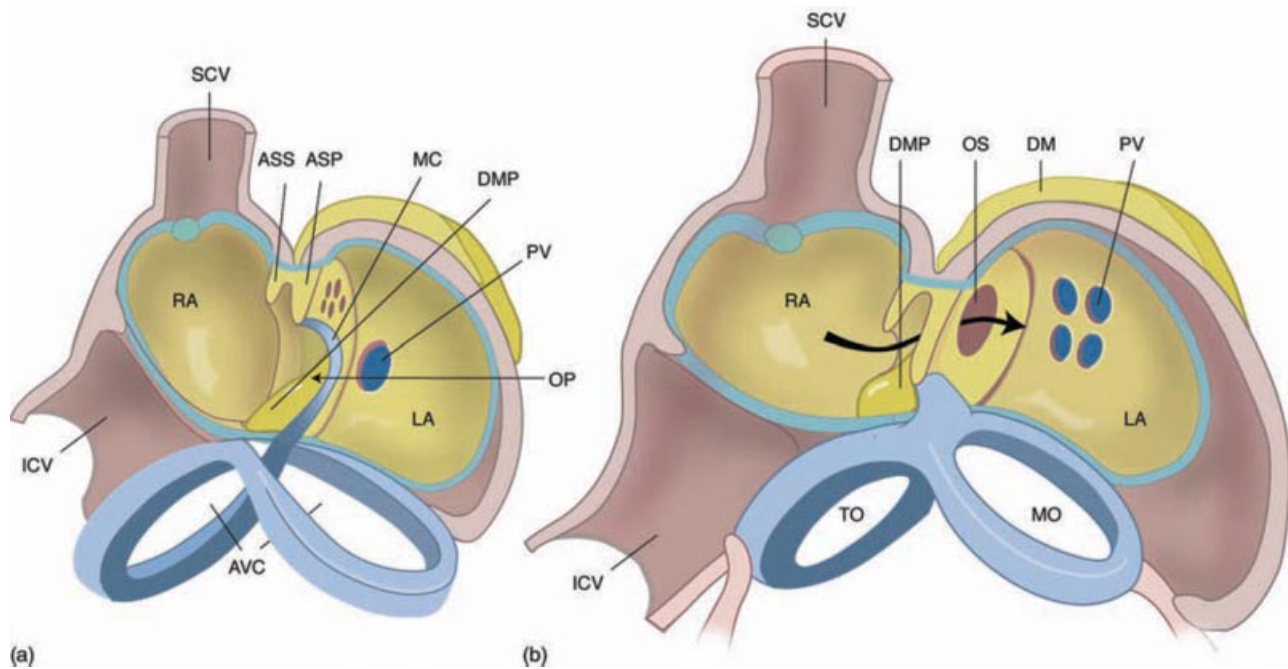
Figure 1.6 (a) Atrial septation starts out with formation of a septum primum (ASP) that grows out from the roof of the common atrium towards the AV canal (AVC). The AV cushions continue over the basal part of the primary atrial septum as the mesenchymal cap (MC). Initially, there is an opening at the basal part of the primary atrium septum, called the ostium primum (OP). Subsequently, probably by a process of apoptosis, several holes will form in the septum primum, that will eventually coalesce to form the ostium secundum [OS, see (b)]. The septum secundum (ASS) will grow out later in development from the roof of the common atrium. In between these structures, at the base, a protrusion of second heart field mesoderm called the dorsal mesenchymal protrusion (DMP) is present. (b) During further development, the ostium primum is closed by fusing the endocardial cushions with the dorsal mesenchymal protrusion. The septum secundum has grown out to form a wedge-shaped septum that during the embryologic and fetal phase will (owing to a higher pressure on the right side) allow the passage of blood towards the left side via the ostium secundum (arrow). The complex of the lower rim of the septum secundum and the ostium secundum is called the foramen ovale (FO) (arrow). After birth, the left atrial pressure rises and the FO will be functionally closed by the primary atrial septum that is being pressed to the septum secundum. The right atrium (RA) receives systemic blood via the superior caval vein (SCV), inferior caval vein (ICV), and coronary sinus (not shown). The left atrium (LA) receives pulmonary venous blood via the pulmonary veins (PV). DM, dorsal mesocardium; TO, tricuspid ostium; MO, mitral ostium. Second heart field-derived myocardium is depicted in yellow. (Copyright Leiden University Medical Center.)

are connected to the left atrial wall through incorporation of the sinus venosus. Disturbance of genes in the PHF can lead to abnormal formation of the wall of the pulmonary veins and the left atrium [53]. Familial total anomalous pulmonary venous connection (TAPVC) has been mapped to chromosome 4p13-q12 in the region near the PDGFRα gene. A knockout mouse of this gene shows TAPVC [51]. Interestingly, the DMP and mesenchymal cap are very hypoplastic in this model, leading to AVSD (see below). A recent review described the current clinical, genetic, and developmental data on pulmonary venous development and abnormalities [54]. Only pulmonary veins connected to the left atrium acquire a myocardial cuff [44]. This cuff is lacking in veins that connect to the right atrium or a spatium pulmonale.

Atrial septal defects

The most common defect is the septum secundum defect (ASD II), in which there is a discrepancy between the septum secundum (demarcated on the right side by the limbus) and the free edge of the fenestrated septum primum. In normal circumstances they overlap as two crescents (Figure 1.6) that fuse after birth. Defective development, including perforations, of the valve of the septum primum, the so-called valve of the foramen ovale, can also lead to an ASD. It is necessary to distinguish between retarded closure of the foramen ovale and a real secundum ASD.

Abnormalities in formation of the base of the atrial septum secundum can lead to so-called sinus venosus ASD, where both the inferior and superior caval veins are closely related to the defect and the pulmonary veins are often abnormally positioned [43].

Based on our new knowledge of addition of the PHF to both the atrial septal components and also the pulmonary veins, some genes are good candidates for study. We already know human mutations in Tbx5 (Holt–Oram syndrome) [55], Nkx2.5 [56], and the PDGFRα region [51] that explain the separate or combined abnormalities in atrial septation, pulmonary venous connection, and in

some patients conduction system problems particularly related to pace-making.

Atrioventricular septal defects

AVSDs are intriguing malformations with many postulated causes, including deficient differentiation of the AV valves and the endocardium lining these valves. This has been extensively studied [57] for the trisomy 21 (Down syndrome) and the syntenic trisomy 16 mouse model without resolution. In the human embryo with AVSD, however, studies of the disposition of the conduction system demonstrated a deficiency of the spina vestibuli (now DMP) and the mesenchymal cap [58], now confirmed in mouse models [47,59]. The primary ASD resulting from non-fusion with the AV cushions can now be explained by the hypoplasia of the mesenchymal cap lining the lower rim of the primary atrial septum. The deficiency of the ventricular inlet septum in humans still needs clarification [60]. The fact that the AV valve tissue in AVSD seems structurally normal confirms that abnormal AV endocardial cushion differentiation is not the primary problem.

Although the heart has two left- and two right-sided chambers, asymmetry is a dominant feature in both form and function. The ventricular asymmetry is determined during looping, whereas the atrial differences are determined by genetic regulation involving, for example, Pitx2 [61,62]. Pitx2 acts in breaking symmetry in early development, is present in the left-sided plate mesoderm only, and has subsequent roles in differentiation of the inflow and outflow segment of the heart. Pitx2 mutant mice present with right atrial isomerism, suggesting inhibition of the left program. Pitx2 mutants may present syndrome-like malformations also involving other organs, for instance the spleen, showing polysplenia in left isomerism and asplenia in right isomerism. Furthermore, DNA sequence variations close to Pitx2 have been described in patients with atrial fibrillation and atrial flutter [63]. Morphologists and clinicians are aware of the differences in the right and left atria, the most obvious being the appendage. Furthermore, the right posterior wall is trabeculated whereas the left is smooth. Usually, atrial situs correlates with bronchial anatomy (see Chapter 50). Lung lobulation, difficult to assess for the clinician, is less reliable.

Ventricular inflow tract septation and the formation of the RV inlet

The RV myocardium with all its components, including at least the right part of the ventricular septum, is derived from the anterior SHF [18]. At the border between the primitive LV and the developing RV, a myocardial ring called the primary ring or fold, previously referred to as bulboventricular fold, can be distinguished [64]. The primary fold is considered a transitional zone and attracts a great deal of attention because it forms the major part of the ventricular inlet and trabecular septum and contains precursors of the AV conduction system.

The primary fold borders on the inner curvature of the heart where it coalesces with the right side of the AV canal (Figure 1.2c). The lower part of the primary fold becomes a real septum by local condensation of the ventricular trabeculae combined with ballooning of the apices of both the LV and RV. Closure of the primary interventricular foramen between the RV and LV takes place by fusion of the inferior and superior atrioventricular cushions in combination with one of the outflow tract endocardial ridges that is connected to this superior cushion.

The role of the primary fold as progenitor of the main body of the ventricular septum deserves special attention. A proper septum is only established when a RV with the tricuspid valve and its orifice is formed. This has to be achieved during development and is important for forming the right ventricular inlet compartment. The right part of the AV canal with the adjoining part of the primary fold has to be transferred to the right side (for remodeling of the primary fold, see Figure 1.2c–e and Videoclip 1.2). Our opinion is that this is achieved by a widening in the dorsal wall of the ventricle adjacent to the primary fold. We have been able to support this developmental concept in a model for Mahaim conduction [65]. With growth of the initial minute inflow part of the RV, a new posterior wall of the right ventricle is formed. In this way, the RV consists eventually of three parts: the RV inlet, bordered by the remnants of the primary fold (trabecula septomarginalis and moderator band), the RV trabecular part (embryonic proximal ventricular outlet segment), and part of the distal ventricular outlet segment underneath the pulmonary orifice.

From an RV view, the ventricular septum is made up of three parts (Figure 1.7):

1 The inlet septum that is formed concurrently with expansion of the RV inflow.

2 This is separated from the trabecular part of the septum by the crista supraventricularis (composed of the continuum of the ventriculo-infundibular fold and the trabecula septomarginalis and also contains the outlet septum; see Figures 1.7 and 1.8), and the moderator band.

3 The muscular outflow tract "septum" or infundibulum derives its myocardium from the distal endocardial cushion-lined outflow tract or conotruncal region (see below).

Consequences for abnormal development

Isolated or multiple muscular VSDs can result from noncompaction of the myocardial trabeculae. Several mouse models present an extensive spongy myocardium that show both myocardial and epicardial differentiation problems as a basis (see below).

Tricuspid valve and orifice abnormalities

Abnormal looping of the heart tube can lead to the tricuspid valve not being optimally brought above the RV, causing a spectrum of tricuspid atresia and hypoplasia, to straddling
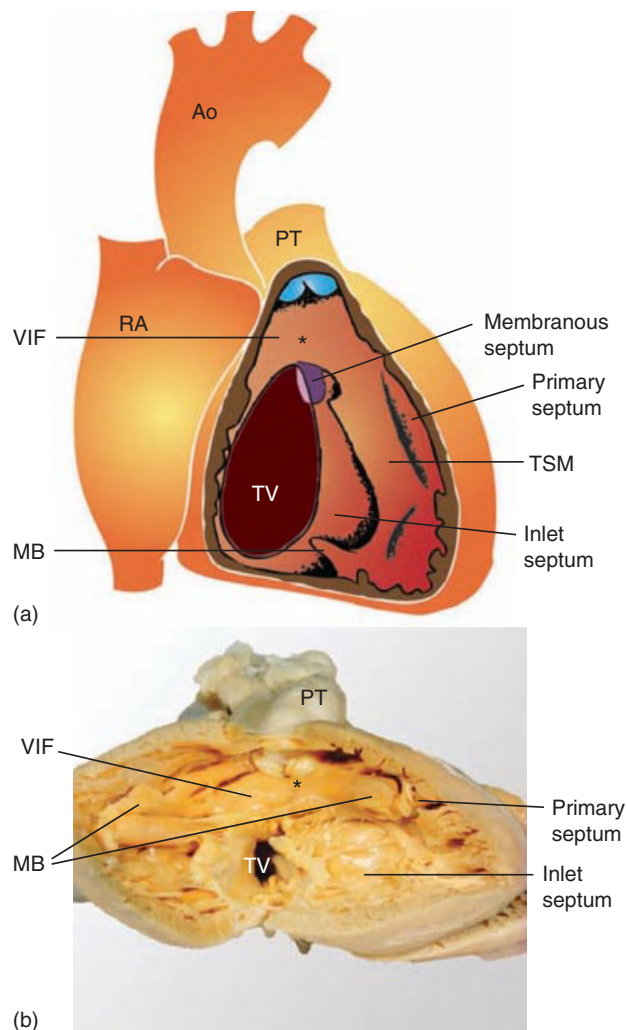
Figure 1.7 Schematic representation (a) and human specimen (b) demonstrating the elements of the ventricular septum after septation has been completed, as viewed from the right side. The ventricular inlet septum is below the tricuspid valve (TV) ostium, and separated from the primitive septum by the myocardial crista supraventricularis. The crista supraventricularis consists of the ventriculo-infundibular fold (VIF), the trabecula septomarginalis (TSM), and the outlet septum (asterisks) that in the normal heart cannot be distinguished as a separate structure. The TSM (that contains the right bundle branch) becomes continuous with the moderator band (MB). The membranous septum is part of the fibrous heart skeleton. Ao, aorta; PT, pulmonary trunk; RA, right atrium. (Copyright Leiden University Medical Center.)

tricuspid valve, and complete double inlet left ventricle. Severe deficient looping can also lead to double outlet right ventricle (DORV). In knockout mouse models with disturbed epicardial differentiation, the abnormalities result in abnormal looping, for example, the mutant RxRα [66], Sp3 [67], Ets1/2 [68], and TGFβ2 [69] mice. It is also possible that primary myocardial problems can cause these abnormalities.

Most perimembranous VSDs and also the outflow tract malalignment defects are the result of abnormal outflow tract septation (see below).

We consider the AVSD anomaly to result from abnormal fusion of the DMP, the mesenchymal cap, and the AV cushion mass [47,58].

Ventricular outflow tract septation

The myocardial contribution of the SHF, referred to as anterior [22] or secondary heart field [70], forms almost the complete RV. The relevance of neural crest cells [35] for outflow tract septation is still important but no longer unique, following studies of the 22q11 deletion syndrome in both patients and mouse models [38]. This complicated syndrome has a high incidence of outflow tract malformations, including aortic arch anomalies, persistent truncus arteriosus, and tetralogy of Fallot. Eventually, the transcription factor Tbx1 was found to be the crucial gene. This gene was not expressed in neural crest cells but in the mesoderm of the SHF. An intricate interaction between neural crest and SHF cells takes place and disturbed genes that are essential for either cell group can lead to outflow tract malformations.

We refer to the septation of the ventricular outflow tract as "separation" as in the normal heart the subpulmonary infundibular or muscular septum is mainly a free-standing sleeve of muscle in front of the vessel wall of the ascending aorta (Figure 1.8). Outflow tract separation has been described for the human embryo [71] and proved similar in animal species such as chick and mouse [64].

Outflow tract separation starts in the embryonic distal outflow tract that is lined by endocardial cushion tissue. This tissue consists of two opposing spiraling ridges. One ridge runs in a laterodorsal direction where it borders the myocardium of the primary fold at the future site of the ventriculo-infundibular fold in the full-grown heart. The other ridge runs ventroanterior to the myocardium of the primary fold as well as the superior atrioventricular cushion. This merging takes place in the bend of the inner curvature of the embryonic heart tube. The endocardial outflow tract ridges are the source of extensive nomenclature confusion. Some authors consider these ridges to consist of proximal or conal ridges (leading after septation to the conal septum) and distal or truncal ridges (leading to a truncal septum). Pexieder [72] clarified this nomenclature confusion. We indicated in a scanning electron micrograph both boundaries and ridges in their full length (Figure 1.8). It is practical to distinguish proximal and distal ridges, which are clearly visible as separate structures in the chicken embryo but are more continuous in humans and rodents (mouse and rat). The proximal ridges mainly form the muscular outflow tract septum whereas the distal ridge area is important for semilunar valve formation and the septation of the arterial orifice level.

Understanding outflow tract separation starts with acknowledging that the arterial orifice level indicated by the mesenchymal (vessel wall) joining the myocardial (outflow tract heart) boundary is not an oval or a circle in one plane but has a three-dimensional saddle shape (Figure 1.9). This
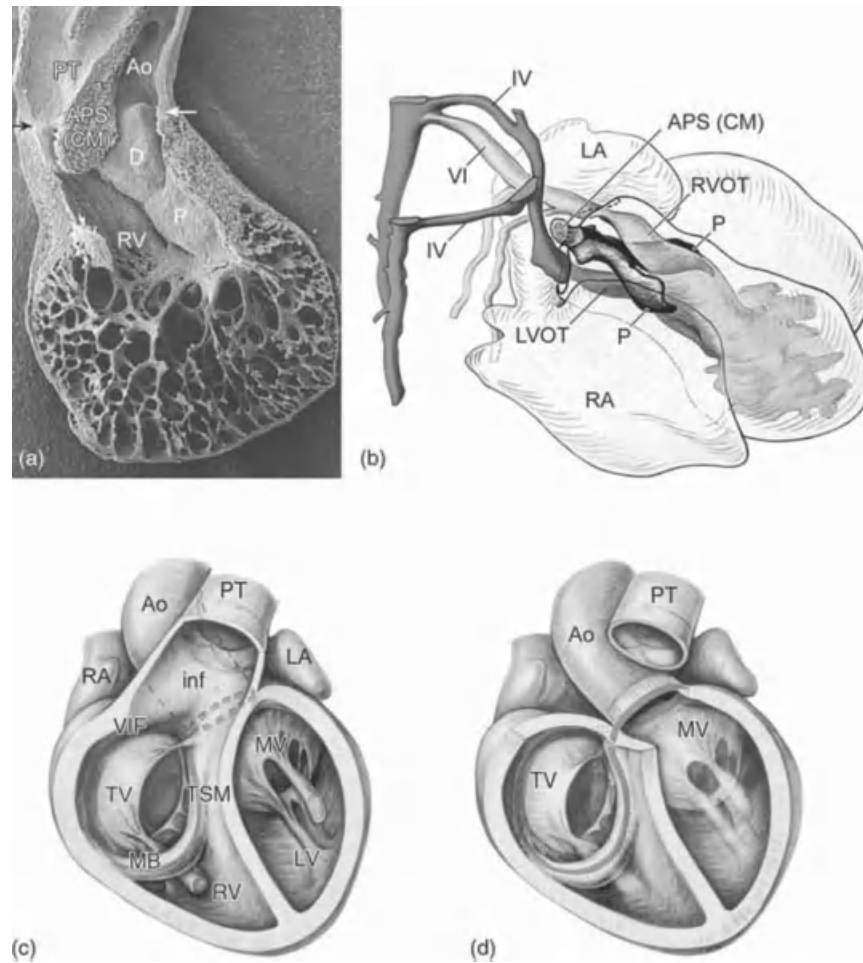
Figure 1.8 (a) Scanning electron micrograph of a preseptation chicken heart showing the proximal (P) and distal (D) outflow tract ridges. The borderline between myocardium (lined on the inside by endocardial cushions) and arterial wall is indicated by arrows. The distal cushions remodel into semilunar valves. (b) Septation of the outflow tract is achieved by fusion of the outflow tract ridges and an ingrowth of condensed mesenchyme (CM), also called the aortopulmonary septum (APS). The APS extends two prongs into the ridges. (c) After septation of the outflow tract, a muscular subpulmonary infundibulum (inf) is formed, which separates the right ventricular outflow tract (RVOT) from the outside world and the aorta (Ao). In a normal heart, the actual outflow tract septum separating the left ventricular outflow tract (LVOT) and RVOT is minimal. (d) Depiction of the difference in length of the RVOT and the relative tilted position of the aortic and pulmonary orifice. LA, left atrium; LV, left ventricle; MB, moderator band; MV, mitral valve; PT, pulmonary trunk; P, prong of CM; RA, right atrium; RV, right ventricle; TSM, trabecula septomarginalis; TV, tricuspid valve; VIF, ventriculoinfundibular fold; IV, VI, pharyngeal arch arteries. (Copyright Leiden University Medical Center.)

brings future aortic orifice more lateral and lower compared with the future pulmonary orifice. During normal looping, this orifice is brought even deeper into the heart, referred to as wedging of the aorta. We recently found (unpublished data) an asymmetric contribution of the SHF to the myocardium of the outflow tract. This Nkx2.5-expressing mesoderm differentiates into myocardium mainly confined to the subpulmonary region, explaining the relative growth of the subpulmonary outflow tract and the rotation to an anterior position with regard to the aortic orifice (see Videoclips 1.3 and 1.4). Molecular biologic experiments using retrospective clonal analysis [73] also showed a difference in subpulmonary and subaortic myocardium but did not link it to the asymmetric addition of SHF. This explains the known asymmetry in the outflow tract [74] for the human embryo. The final result is the well-known difference in position and plane of both arterial orifices.

The highest (most distal part) of the myocardium, always lined on the inside by endocardial cushion tissue, is positioned in the intersection between the sixth and fourth pharyngeal arch arteries. It is exactly at this site that the condensation of extracardiac mesenchyme takes place. The condensed mesenchyme extends two prongs that enter the endocardial cushions together differentiating into the aortopulmonary septum [64] that undergoes myocardialization. Our own chicken chimera studies and also the neural crest indicator
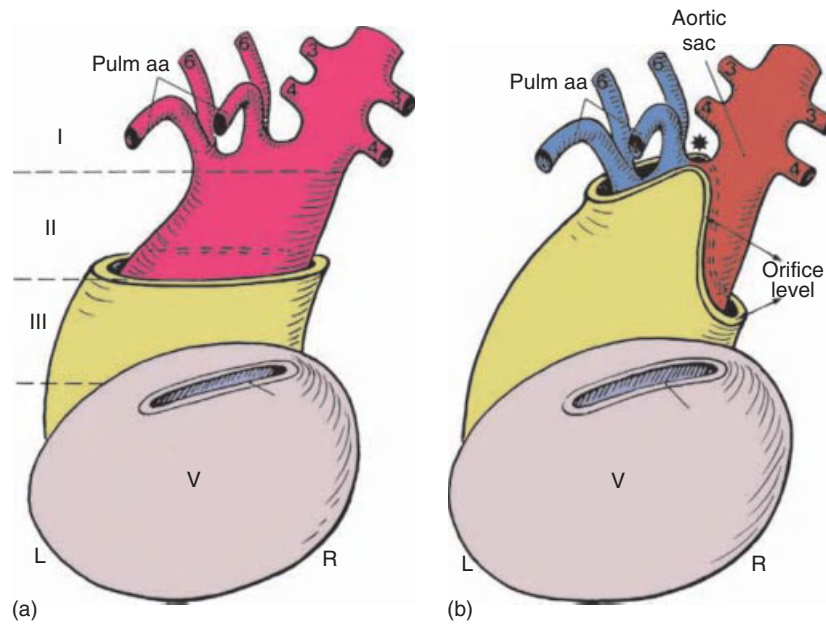
Figure 1.9 Concepts of outflow tract formation. (a) Early concept that assumed that the myocardium surrounding the aorta and pulmonary trunk was distributed symmetrically. Levels I–III indicate the supposed levels of separation, I being the great arteries, II the arterial orifices, and III the outflow tract. (b) In contrast, later work demonstrated that the myocardium in this area actually has a saddle shape, demonstrating the increase in length of the pulmonary trunk in respect to the aorta. The asterisk indicates the level of initiation of separation of the arterial pole. pulm aa, pulmonary arteries; V, ventricle. (Copyright Leiden University Medical Center.)
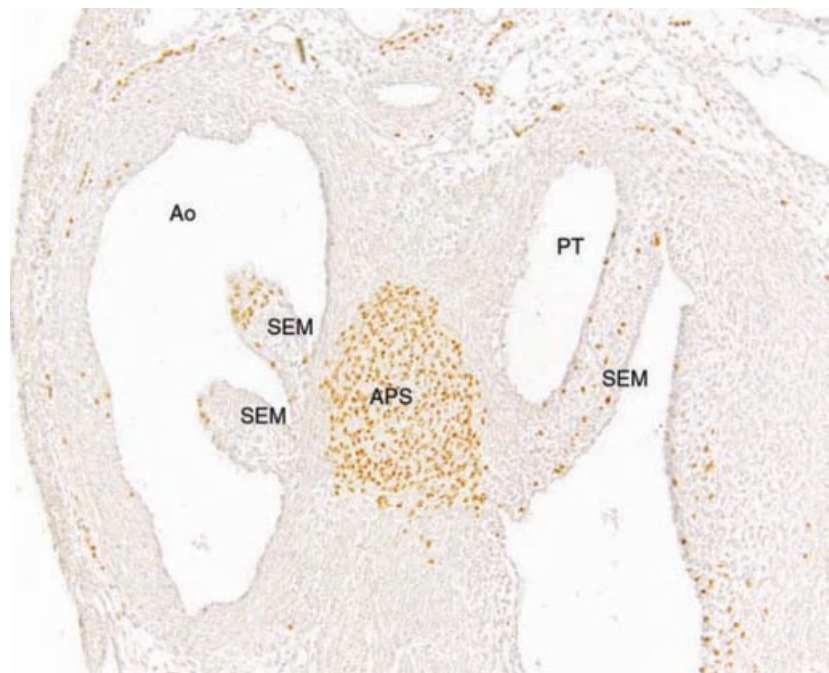
Figure 1.10 Section of the outflow tract of a chicken–quail cardiac neural crest chimera (stage HH 34). The quail cardiac neural crest cells (dark nuclei) fill almost completely the condensed mesenchyme of the aortopulmonary septum (APS). The semilunar valve leaflets (SEM) also show neural crest-derived cells. Ao, aorta; PT, pulmonary trunk. (Copyright Leiden University Medical Center.)

mouse show this condensed mesenchyme to be composed mainly of neural crest cells extending into the distal ridges and the semilunar valves and also the surrounding myocardium [75,76] (Figures 1.5 and 1.10). Staining for apoptosis reveals that most of the neural crest cells at this level have gone into apoptosis, which is particularly prominent during the stage of myocardialization of fused endocardial outflow tract ridges (Figure 1.5b). We postulate that this neural crest cell death program plays an active role in stimulating outflow tract myocardialization. This process

is much less obvious at the distal valve level, where a lump of condensed mesenchyme persists and turns into a fibrous structure (conus tendon).

In completing normal outflow tract separation, the myocardial outflow tract "septum" has merged seamlessly with the ventriculo-infundibular fold and the trabecula septomarginalis. The lower rim borders upon the anterior tricuspid orifice and is called in normal hearts the crista supraventricularis. The final result is an RV outflow tract that is long and surrounded by myocardium whereas the LV outflow tract is short and only partly surrounded by myocardium. In the normal heart, only a small stretch of musculature can really be called a septum between both outflow tracts (Figure 1.8). This situation differs markedly from specimens with disturbed outflow tract septation.

Consequences for malformations

Tetralogy of Fallot, double outlet right ventricle, malalignment defects

The main events in cardiac outflow tract septation are linked to addition of SHF and neural crest cells and their interaction. As a consequence, malformations in outflow tract septation, a major cause for CHD, are linked to disturbances of genes that are crucial for the development of both cell populations. Tbx1 is primarily expressed in the SHF mesenchyme and not in neural crest cells. Hence the phenotype of this malformation is based on a misdirection of neural crest cell contribution based on an abnormal interaction with SHF cells. Patients with solely a Tbx1 mutation have been reported to develop a 22q11 deletion phenotype [38].

van Mierop and Kutsche [77] suggested the possible impact of neural crest in outflow tract septation. Kirby *et al.* [78] were the first to show experimentally the link between outflow tract malformations and the neural crest. They ablated the neural crest in chicken embryos, ending up with a spectrum of outflow tract malformations ranging from a simple VSD to DORV and, in the extreme, a persistent truncus arteriosus (common arterial trunk).

Recent studies have refined this concept, adding specific SHF-expressed genes to the causes. Examples are semaphoring [79], TGFβ [69], and Pax3 [80] mutant mice. We recently showed a role for VEGF isoforms in development of tetralogy of Fallot in a VEGF120/120 mutant mouse [81]. There was selective apoptosis in the subpulmonary myocardium, which we know to have a distinct SHF-derived contribution that differs from the subaortic region.

Epigenetic or environmental factors also play a role, as we showed in embryos from maternal diabetic rats that presented with DORV and a too short outflow tract [82]. For the development of bicuspid aortic valve, some genes in patients have recently been described such as Notch1 [83] and Axin1 linked to endoglin [84]. This draws attention to a possible

role of hemodynamics and blood flow that has been neglected. Our studies of the chicken venous clip model showed the importance of alteration of blood flow for the development of a spectrum of outflow tract malformations, including semilunar valve abnormalities [85]. The eNOS (a shear stress responsive gene) mutant mouse showed development of a bicuspid aortic valve [86] after fusion of specific outflow tract endocardial cushions.

Transposition of the great arteries, including DORV with subpulmonary VSD (also termed the Taussig–Bing malformation), remains an enigma. Nakazawa and co-workers [87] showed that retinoic acid treatment of mouse embryos could lead to transposition of the great arteries. There seems to be a link to laterality problems during addition of SHF mesoderm at the outflow tract. In animal models with transposition, the proximal outflow tract ridges had a straighter position. This fits nicely with the morphology of the heart in human infants with transposition in which there is not simply a reverse of the great arteries but also a straighter outflow tract septum [88].

Outflow tract septation is a very vulnerable process. Abnormalities can be evoked by all key players in this area – myocardium, endocardial cushion tissue, and neural crest.

Atrioventricular and semilunar valve formation

Both valve types differentiate from the endocardial cushion tissue lining the AV canal for AV valve formation and the distal outflow tract for semilunar valve formation. The main morphologic difference is that the AV valves are connected to the ventricular wall by chordae and papillary muscles, whereas the semilunar valves do not have a tension apparatus.

The endocardial cushion tissue itself is remodeled into valve leaflets [89,90]. The chordae are also derived from the endocardial cushion tissue and are not differentiated from the papillary muscles (Figure 1.11). The endocardial cushions are formed by contributions of several cell types derived from the endocardium and myocardium in which the process of endothelial to mesenchymal transformation is very important [91]. More recent data show the addition of epicardium-derived cells (EPDCs) to the AV cushion tissue [92] (Figure 1.11). Periostin has been described as an important regulator in AV valve development [93]. Differentiation of the AV valve leaflets has not attracted much attention. Oosthoek *et al.* [89] showed for the chicken, mouse, and the human embryo expression of a number of layered differentiation markers that differ on the atrial and the ventricular side.

Semilunar valve development [94] takes place at the distal part of the outflow tract ridges on the borderline of mesenchyme and myocardium. Reconstructions of the human embryo [64] showed that the orifice level does not lie in one plane but has a saddle shape with the future aortic orifice already more dorsolateral and caudal than the
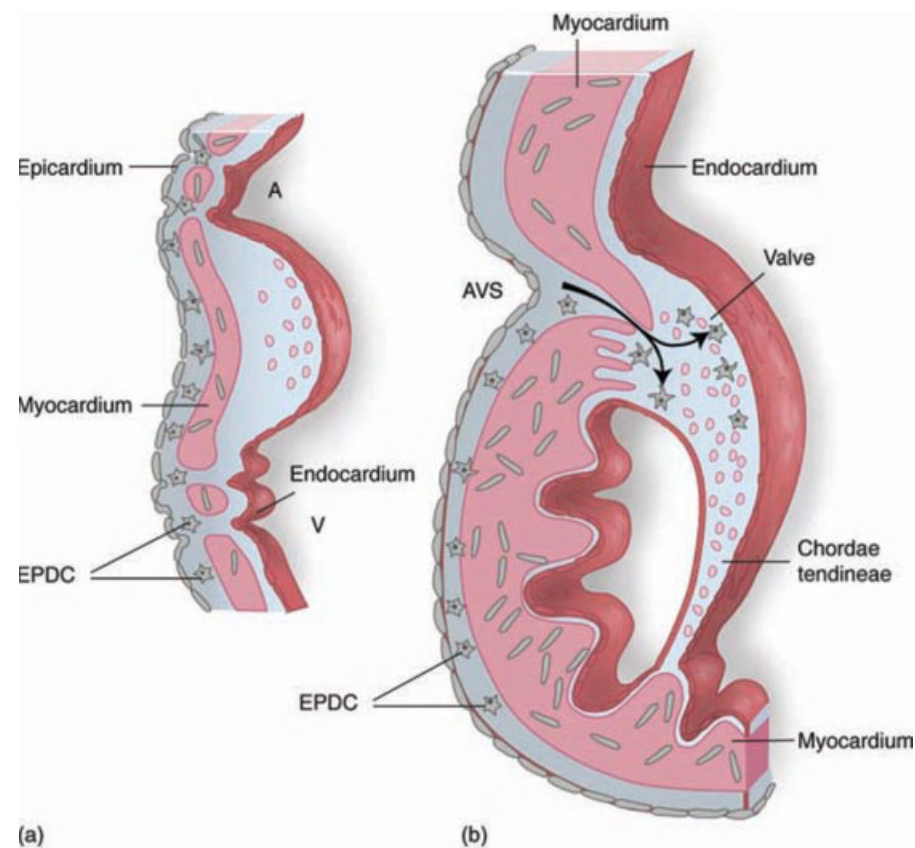
Figure 1.11 (a) The cardiac valves differentiate from the endocardial cushion tissue that is lining the AV canal for AV valve formation. AV valves are connected to the ventricular wall by chordae and papillary muscles. Both valve leaflets and the chordae are derived from endocardial cushion tissues that are remodeled from thick spongy structures into thin valve leaflets. The endocardial cushions are formed by contributions of several cell types derived from the endocardium (depicted as small circles) and myocardium. Epicardium-derived cells (EPDCs), depicted as star-shaped cells) also contribute to AV cushion formation. (b) These are derived from the epicardium and migrate towards the endocardium [arrows] once the myocardial continuity between atrium and ventricle has been disrupted by formation of the annulus fibrosis. Delamination of the valve occurs under the influence of the EPDCs, resulting in detachment of the endocardial cushion from the myocardial wall. A, atrium; AVS, AV sulcus; V, ventricle. (Copyright Leiden University Medical Center.)

pulmonary side. With septation of the outflow tract, the two main endocardial ridges are fused by the condensed mesenchyme of the aortopulmonary septum (Figure 1.8), so that four cushion masses can be distinguished, two in each orifice. To achieve three valve leaflets in each orifice, two intercalated cushion swellings are seen positioned on the far side of the facing valve cushions. In the aorta, the intercalated valve swelling develops into the noncoronary cusp. The two facing semilunar valve sinuses receive the main stems of the right and left coronary artery. For a proper attachment of the semilunar valve leaflets to the underlying myocardium and the above vessel wall, a collagen "ring" is formed [95].

Consequences for abnormal development

Atrioventricular valve abnormalities

Both in human CHD and in experimental animals, information is lacking on abnormal differentiation of the AV valve leaflets. There are reports of tricuspid valve insufficiency during fetal life which can lead to intrauterine death.

Furthermore, polyvalvar disease seems to have a genetic background [96]. As the valves are delaminated from the underlying myocardium, ventricular septation abnormalities can also lead to abnormal attachments and formation of the tricuspid and mitral valve; examples are AVSDs, straddling tricuspid and mitral valves. Studies on AV valve differentiation [97,98] provided new information on normal and abnormal papillary formation, especially with regard to the subject of parachute mitral valve in which there is usually asymmetric formation of the mitral valve rather than a real parachute. Abnormal atrioventricular valve leaflets such as seen in Ebstein's malformation are not easily explained from embryology but point towards incorrect undermining from the ventricular myocardium. The animal model using lithium treatment does not resolve the mechanism. Recently, the roles of EPDCs [99] and periostin [93] have been described. Transgenic mice (N-FATc [100] and Sox4 [101]) show specific expression in the endocardial cushion tissue. Knockouts show a spectrum ranging from absence to underdevelopment

of the mitral and tricuspid valves and also of the semilunar valve leaflets. These models are embryolethal and have not been evaluated. We postulate that absence of AV valve leaflets in the human embryo leads to early intrauterine death, as we have not seen that abnormality in humans.

Semilunar valve abnormalities

Several processes described for the AV cushions are also pertinent for the endocardial outflow tract cushions that develop into semilunar valve leaflets, with deficiencies leading to absent or very hypoplastic aortic and pulmonary valves [102]. Absence of aortic leaflets is lethal for the human fetus whereas absence of pulmonary valve leaflets is compatible with term delivery.

Extracardiac cells migrate into the developing valves, as proven for the neural crest cell population [75]. The mechanism underlying the formation of commissures and the sites of formation still need elucidation. A recent publication on the development of the bicuspid aortic valve shows beautifully the difference between a genetic Syrian hamster model and the eNos knockout [103]. Finally, hemodynamic factors [85] may play a role.

Cardiac conduction system (CCS) development

The impulse from the sinoatrial node (SAN) is propagated via Bachman's bundle to the left atrium, and via the internodal myocardium to the atrioventricular node (AVN). Although internodal tracts with specific histologic, immunohistochemical, and molecular characteristics [104–108] can be distinguished in the atria, their functionality is yet to be determined. The AVN is a compact cellular node, covered by transitional cells [109,110]. From this node, the common bundle or bundle of His supplies the ventricles (see Chapter 55).

During development of CCS, the sequence of activation changes from an immature base-to-apex activation pattern of the primary heart tube to a mature apex-to-base activation pattern, in accordance with the development of the His–Purkinje system. Pre-excitation of the ventricles can still occur after septation due to persisting myocardial AV bridges across the AV junction [111]. Insulation of the atrial myocardium from the ventricular myocardium occurs by development of the annulus fibrosis, which begins by fusion of epicardial sulcus tissue with endocardial cushion tissue at the ventricular site of the AV junctional myocardium and moves the original AV myocardium to an atrial position [90]. For this process, correct ingrowth of EPDCs is mandatory [112]. EPDCs produce in the AV annulus the extracellular matrix molecule periostin that is involved in fibrosis of the myocardium of the AV canal [112]. Fibrosis of the annulus however remains incomplete until late fetal stages [111].

In the developing and the adult heart, myocardium of the (putative) CCS can be distinguished from the surrounding working myocardium, based on histologic characteristics, and

also by the expression patterns of several immunohistologic and molecular markers [113]. Multiple genes, cells, and their interactions are involved. Furthermore, the developing CCS seems to be much more extensive than in the adult CCS. After looping of the heart has started, several *transitional zones* (Figure 1.2b–e) can be distinguished from the surrounding working myocardium [104,106,107,114]. These transitional zones are the sinoatrial transition comprising the sinus venosus segment connecting to the primitive atrium, the atrioventricular transition or primitive AV canal between the primitive atrium and primitive left ventricle, the primary fold that separates the primitive left ventricle from the primitive right ventricle, and the ventriculoarterial transition at the junction of the primitive right ventricle with the truncus arteriosus or putative outflow tract of the heart (Figure 1.2). The so-called "ring theory" hypothesizes that these transitional zones contribute to elements of the CCS [114].

Due to further looping of the primitive heart tube, the zones meet in the inner curvature of the heart where they contribute to AVN formation. During development, part of this embryonic myocardium differentiates into working myocardium. The transcription factors Tbx2/3 function as transcriptional repressors of this chamber formation process [108,115], whereas Tbx5 is required for maturation and differentiation of the CCS [116]. The latter transcription factor is also involved in molecular pathways for CCS specification, which includes the inhibitor of DNA-binding Id2 [117]. Parts of the zones that do not differentiate into working myocardium form elements of the mature cardiac conduction system (Figure 1.2).

As explained above, the first heart field contributes to the primary heart tube that includes the primitive AV canal. The myocardium at the venous pole of the heart, the sinus venosus, that includes the SAN, is incorporated later to the heart from the PHF [17,24]. This venous myocardium is characterized by the expression of several markers, including podoplanin [24] linked to RhoA [31], Shox2 [49,118], Tbx18 [119], and the functional marker HCN4 [50], and by a lack of expression of the transcription factor Nkx2.5 [24,48].

A transient left-sided SAN precedes the formation of the definitive right-sided SAN [31], making the complete embryonic sinus venosus myocardium a potential pacemaking area.

Whether the SHF also contributes to the elements of the AVN is debatable. Although a contribution from the SHF has been suggested [120], the compact part of the AVN appears to come from the primitive AV canal (first heart field derived), except from the lower part that is derived from the primary fold [121]. However, the origin of the atrial septal component of the AV conduction axis and of the transitional cells still needs to be elucidated. In addition to a direct contribution, an interaction between the tissues from the different transitional zones may also contribute to CCS formation as a

result of induction. Generally, based on histologic studies, the transitional cells are regarded as an atrial or sinus venosus contribution to the AVN [109,110]. The His bundle and bundle branches are most likely derived from the myocardium of the primary fold that undergoes extensive remodeling during development (see Videoclip 1.2). The newly incorporated SHF-derived myocardium forms the right ventricular inflow tract with expansion of the primary fold tissue, after which the medial part of the ventricular septum consists of the trabecula marginalis, containing the right bundle branch, which remains continuous with the moderator band that runs to the lateral right ventricular wall. The peripheral Purkinje fibers develop from differentiating ventricular cardiomyocytes [122] in close association with both the coronary arteries and EPDCs [92,122,123]. In the chick, EPDCs are important for inducing Purkinje fiber formation [124].

Neural crest cells also reach the venous pole of the heart, where they probably play an inducing role in CCS formation and maturation [34,37].

Consequences of abnormal development in relation to arrhythmias

Clinical arrhythmias are related to anatomic predilection sites and many of these ectopic pacemaker foci are preferentially encountered in specific parts of the right and left atrium that are related to the sinus venosus. These include the crista terminalis [125,126], the adult counterpart of the embryonic right venous valve, being related to initiating/perpetuating atrial flutter. The myocardium of the caval veins [127] and coronary sinus [128] are clinically known to initiate arrhythmias. In the left atrium, atrial fibrillation has been attributed to arrhythmogenic foci that originate from the pulmonary veins [129]. The sinus venosus myocardium, which includes the myocardium surrounding the caval and pulmonary veins, is derived from the SHF, and is characterized by specific gene expression patterns including absence of Nkx2.5 expression [24,48]. During development, the sinus venosus myocardium largely differentiates towards a chamber phenotype and acquires expression of Nkx2.5, but loses some of the characteristic early conduction system markers such as Tbx18, CCSLacZ, and Shox2 [113]. Failure of this chamber differentiation, and also re-expression of the embryonic phenotype, may explain the occurrence of clinical arrhythmias originating specifically in these areas.

AV re-entrant tachycardias are based on accessory myocardial bundles connecting atrial and ventricular tissue, thus bypassing the insulating function of the AV groove. The best known is the bundle of Kent, present in Wolff–Parkinson–White (WPW) syndrome [130]. As described above, accessory AV myocardial continuities may persist in the embryo until late stages [111]. Insulation of the annulus fibrosis requires EPDCs. In animal models in which the epicardial outgrowth is inhibited, accessory connections causing ventricular pre-

excitation, as in WPW syndrome, are observed. Valvar anomalies such as Ebstein-like malformations due to non-delamination of valves are also part of the phenotype of epicardial deficiency in avian models [99], perhaps explaining the frequent association of Ebstein's anomaly of the tricuspid valve and WPW syndrome [131]. A special form of re-entrant tachycardia is Mahaim tachycardia, during which antidromic re-entrant tachycardia occurs over an accessory bundle with AV node-like conduction properties [65]. Arrhythmias originating in the right ventricular outflow tract can be related to the ventriculoarterial transition and studies on the role of Tbx2 mutations are ongoing [115].

Whether disturbed migration and subsequent apoptosis of neural crest can be linked to human rhythm problems is uncertain. After neural crest ablation in chick embryos, there is a lack of differentiation of a compact lamellar organization by the His bundle and of (electrical) isolation from the working myocardium, and also failure of the conduction system to convert to a mature apex-to-base activation pattern [36]. Genes with differentiation abnormalities of the SHF-derived cardiac conduction system have been described but a link to human malformations has not been made with the exception of Nkx2.5 [56] and Tbx5 [117] mutations. Mutations in both genes cause ASDs and conduction disorders, explained by deficient contributions from the SHF, since both the atrial septum and elements of the CCS are SHF derived.

Development of the epicardium and the coronary vasculature

The epicardial epithelium growing out from the proepicardial organ serves as a covering layer of the myocardium. This epithelium differentiates into epicardium-derived cells (EPDCs) entering the subepicardial space and migrating into the myocardial wall where they differentiate further into the cardiac fibroblasts (also forming the annulus fibrosis) and the smooth muscle cells of the coronary vessels [39,132].

The coronary vasculature is the last part in the developing embryonic heart that is essential for its survival as a beating pump. It provides nutrients to the cardiac wall which cannot survive solely on diffusion from the cardiac lumen. In a normal human embryo at about 6 weeks of development, the coronary arteries contact the two facing semilunar sinuses of the aorta (the right and left sinus of Valsalva) [133,134].

The development of the coronary endothelial network takes place within the confinement of the subepicardial covering of the heart (see Figure 1.12) adjacent to the liver primordium. The microvasculature originates from the sinus venosus endothelial lining where it runs through the liver and enters the subepicardial space [135,136]. Patterning of the main branches of the coronary arteries is largely guided by the underlying AV sulcus (derived from EPDCs) and the position of the interventricular septum, even when abnormally positioned. Development of a peri-truncal microvascular network that remodels into arteries and veins

precedes the differentiation of these main branches [137]. The variation in the main branching pattern at the orifice level seems related to the shortest distance to the area that has to be perfused and might, therefore, depend on hypoxia-dependent gene expression.

The coronary venous drainage is through the large veins accompanying the major coronary arteries and ending in the coronary sinus. A number of small anterior veins enter the anterior part of the right atrium. The development of this system has been followed in both chicken–quail chimeras and transgenic mice. In studying the human embryo, we have been unable to find an extensive Thebesian network connecting the ventricular lumen to the coronary veins. There is evidence, however, of an extensive arteriovenous collateral network. The coronary veins have a myocardial media at their connection to the atria and only more distally is this replaced by a vascular wall containing smooth muscle cells [138].

Consequences for malformations

Cardiomyopathies

The EPDCs that enter the myocardium are essential for the development of the compact myocardial layer. Inhibition of epicardial outgrowth [139] or disturbance of the differentiation of the PHF and epicardium results in a very thin myocardium. This lack of myocardial differentiation could be the origin of cardiomyopathies such as noncompaction cardiomyopathy [39]. The important role of the epicardium for myocardial differentiation has also resulted in the use of EPDCs as cell therapy to ameliorate cardiac function after myocardial infarction [140].

Coronary vascular abnormalities

The coronary arteries grow into the aortic wall, and do not sprout from it (Figure 1.12). Why normally the two facing sinuses of the aorta harbor a coronary artery, leaving the nonfacing (noncoronary cusp) and the pulmonary sinuses empty, remains elusive. We postulate that the unequal contributions of the SHF to the aortic and pulmonary segments of the early aortic sac designates this pattern and depends in part on Tbx1. The interaction with the neural crest is shown after its ablation in the chick embryo. In persistent truncus arteriosus, the coronary arteries enter only the aortic side of the orifice [141]. For humans, this was confirmed in a pathomorphologic study [142].

An explanation for coronary fistulas, more common in the right ventricular wall, combined with diseased coronary arteries is incompletely understood. EPDCs are necessary for correct ingrowth of the coronary arteries into the aorta [68,143] and studies demonstrate transient connections between endocardium and coronary microvasculature through lacunas in the ventricular myocardium. If these connections persist, fistulas could develop. In fetal life, large fistulas are a
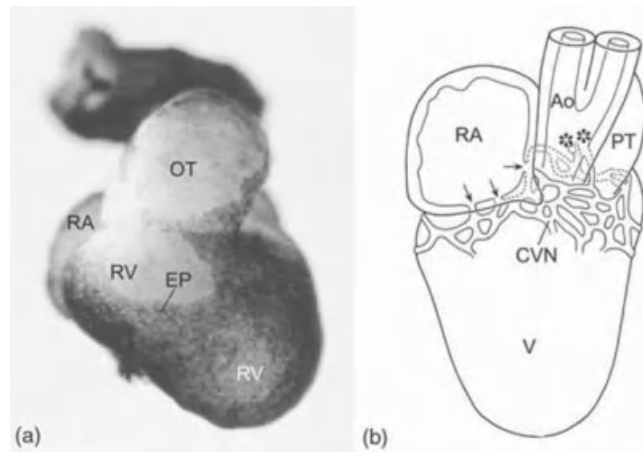
Figure 1.12 (a) Cytokeratin whole mount staining of the epicardium (EP) of a quail heart (stage HH 24). The epicardium grows out from the epicardial organ at the sinus venosus and covers the outer part of the outflow tract (OT) and the right ventricle (RV). (b) Schematic view of the coronary vascular network (CVN) at the peritruncal area underlying the epicardium. This network grows at a quail stage HH 32 into the aorta (two lumenized sprouts, asterisks) and into the anterior part (arrows) of the right atrium (RA). Ao, aorta; PT, pulmonary trunk; V, ventricle. (Copyright Leiden University Medical Center.)

primary abnormality, leading secondarily to atresia of the pulmonary orifice [144,145]. Hypoplasia of the coronary artery wall and the plasticity of coronary vessels is influenced by growth factors such as VEGF [146] and PDGF [147].

Development of the aortic arch system and pulmonary arteries

The aortic arch and its branches develop from an essentially bilaterally symmetric pharyngeal arch artery system. In the human embryo this is remodeled into a left aortic arch and prenatally a left ductus arteriosus (Figure 1.13). The first and second pairs of arch arteries are transformed into craniofacial arteries whereas the third pair provides the common stem of the carotid arteries. The fourth and sixth pairs (the fifth pair does not appear in most mammals) develop asymmetrically. The left fourth pharyngeal arch artery persists as the aortic arch, whereas the right fourth forms a small segment of the subclavian artery. The sixth pair forms a transient connection on both sides between the pulmonary trunk and the descending aorta. On the right side, the distal part of the sixth pair disappears early, leaving the left one to persist as the ductus arteriosus until birth. In human embryos, the pulmonary arteries might contact the aortic sac directly and are never inserted into the sixth arch artery. The right and left subclavian arteries have to move cranially from the seventh intersegmental level to the aortic arch. During normal development, the early left
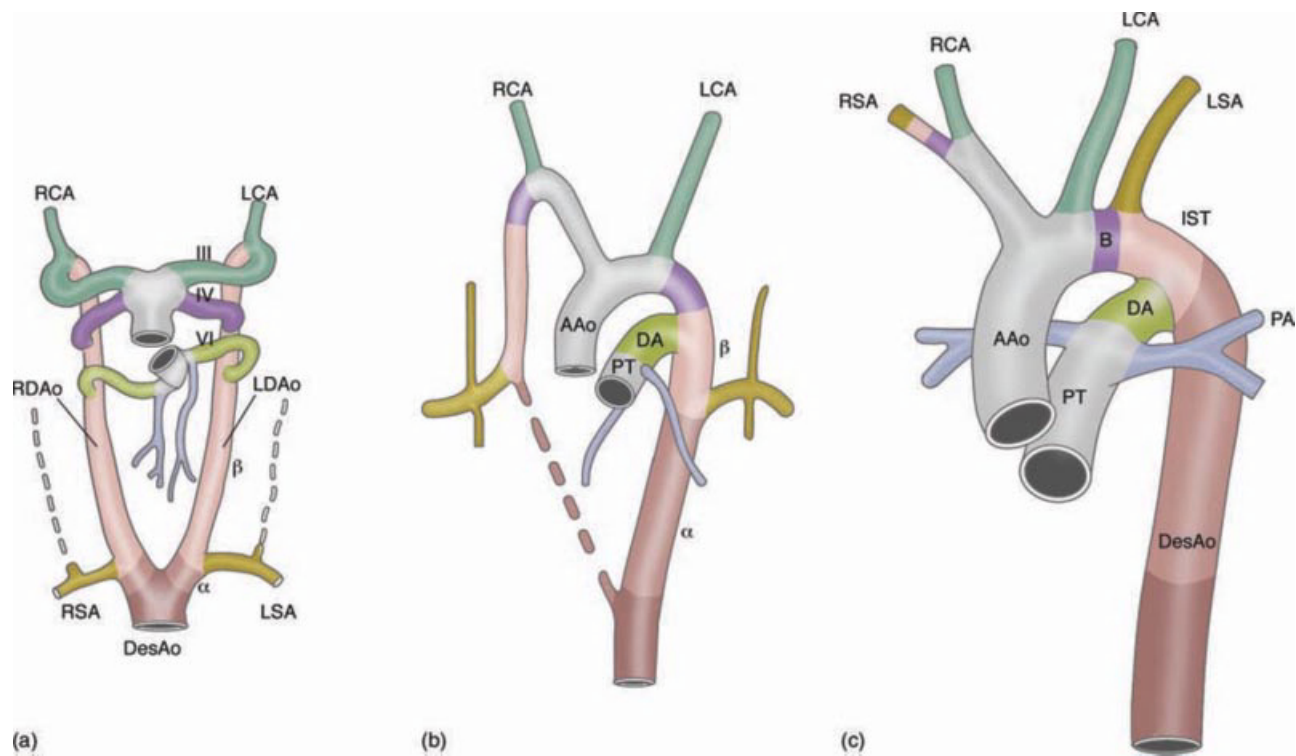
Figure 1.13 (a) Schematic view of the remodeling thoracic arterial vasculature, from an almost symmetric system with a number of pharyngeal arch arteries (depicted are III, IV, and VI) to a left aortic arch. Dashed lines represent regressing vessels. α and β indicate the aortic segments proximal and distal to the left subclavian artery. (b and c) After the left subclavian artery (LSA) has migrated into its proper position the aortic arch has an isthmus (IST) and a segment B (vulnerable in the 22q11 deletion syndrome). AAo, ascending aorta; DA, ductus arteriosus; DESAo, descending aorta; LCA, left carotid artery; LDAo, left dorsal aorta; PA pulmonary artery; PT pulmonary trunk; RCA, right carotid artery; RDAo, right dorsal aorta; RSA, right subclavian artery. (Copyright Leiden University Medical Center).

subclavian artery crosses over the ductus arteriosus entrance, thereby creating the isthmus.

The study of the pharyngeal system in the chicken and mouse shows the significance of several tissues in this region, including the neural crest, the anterior heart field, and even the foregut endoderm. The latter is involved in molecular signaling but not in cellular contributions. The significance of the cardiac neural crest, positioned between the otic placode and the third somite level, is evident as ablations of this rhombencephalic crest in chicken embryos result in abnormalities of the third, fourth, and sixth pharyngeal arch arteries and also the outflow tract of the heart. The neural crest migrates through the circumpharyngeal region and is influenced by signals from the foregut, including the sonic hedgehog and Tbx1 pathways. Next, the neural crest joins the anterior SHF area ventrally to the foregut and makes differentiation of the pharyngeal arches and the enclosed arteries even more complicated. The smooth muscle cells of the root of the ascending aorta and the pulmonary trunk derive from the anterior SHF [23], whereas the medial smooth muscle cells of the arteries come from the cardiac neural crest [148], as is true for the fibroblasts of the adventitia and for the surrounding ganglia. Vessels not populated by neural crest cells include the subclavian arteries,

the distal and intrapulmonary arteries, and the coronary arteries. The data from chicken and mouse studies cannot be simply transferred to the human embryo as reliable markers for the various vessels and the outflow tract are lacking. Note that the mouse embryo lacks the human isthmus section located between the left subclavian artery and the entrance of the ductus arteriosus (in later life a ligament).

Consequences for abnormalities

Aortic arch abnormalities

Abnormalities of the aortic arch system, including those encompassed in the 22q11 deletion syndrome (DiGeorge syndrome), show a phenotype that is paramount in certain parts of the fourth arch derived segment and also the ductus arteriosus/left pulmonary artery connection, which is sixth arch derived. The problem is mainly right sided and is probably related to the right-sided dominance of the anterior heart field-related expansion of the pulmonary trunk compared with the aortic root. The disappearance of vessel segments is accompanied by increased local apoptosis programs [149] that are at least partly governed by sonic hedgehog signaling. The postulation that hemodynamics [5,7,8] influence normal arch artery development is gaining

importance, particularly for hypoplasia and coarctation [150]. Shear stress-induced genes include Kruppel-like factor (KLF2), TGFβ and endothelin-1 [151]. The downstream mechanism is complicated, as shown by malformations including DORV, VSD, aortic arch malformations, and abnormal semilunar valves caused by rerouting the venous return in chicken embryos.

The relatively common coarctation of the aorta, localized on the border of the ductus arteriosus and the aortic arch, cannot be explained from a mouse model as this segment is missing. Interruption, hypoplasia, and local coarctation of the isthmus seem best explained by hemodynamic factors related to left ventricular outflow tract obstruction.

Acknowledgments

References

1 Sizarov A, Anderson RH, Christoffels VM, *et al*. Three-dimensional and molecular analysis of the venous pole of the developing human heart. *Circulation* 2010;**122**:798–807.

2 Haak MC, Van Vugt JM. Echocardiography in early pregnancy: review of literature. *J Ultrasound Med* 2003;**22**:271–80.

3 Yutzey KE, Robbins J. Principles of genetic murine models for cardiac disease. *Circulation* 2007;**115**:792–9.

4 Clark EB. Pathogenetic mechanisms of congenital cardiovascular malformations revisited. *Semin Perinatol* 1996;**20**:465–72.

5 Hogers B, DeRuiter MC, Gittenberger-de Groot AC, *et al*. Unilateral vitelline vein ligation alters intracardiac blood flow patterns and morphogenesis in the chick embryo. *Circ Res* 1997;**80**:473–81.

6 Hove JR, Koster RW, Forouhar AS, *et al*. Intracardiac fluid forces are an essential epigenetic factor for embryonic cardiogenesis. *Nature* 2003;**421**:172–7.

7 Wang Y, Dur O, Patrick MJ, *et al*. Aortic arch morphogenesis and flow modeling in the chick embryo. *Ann Biomed Eng* 2009;**37**:1069–81.

8 Yashiro K, Shiratori H, Hamada H. Haemodynamics determined by a genetic programme govern asymmetric development of the aortic arch. *Nature* 2007;**450**:285–8.

9 Pardanaud L, Luton D, Prigent M, *et al*. Two distinct endothelial lineages in ontogeny, one of them related to hemopoiesis. *Development* 1996;**122**:1363–71.

10 DeRuiter MC, Poelmann RE, Mentink MMT, *et al*. Early formation of the vascular system in quail embryos. *Anat Rec* 1993;**235**:261–74.

11 Wunsch AM, Little CD, Markwald RR. Cardiac endothelial heterogeneity defines valvular development as demonstrated by the diverse expression of JB3, an antigen of the endocardial cushion tissue. *Dev Biol* 1994;**165**:585–601.

12 Gittenberger-de Groot AC, Bartelings MM, DeRuiter MC, *et al*. Normal cardiac development. In: Wladimiroff JW, Pilu G, eds. *Ultrasound and the Fetal Heart*. New York: Parthenon Publishing Group, 1996: 1–14.

13 DeRuiter MC, Poelmann RE, VanderPlas-de Vries I, *et al*. The development of the myocardium and endocardium in mouse embryos. Fusion of two heart tubes? *Anat Embryol* 1992;**185**:461–73.

14 Smith SM, Dickman ED, Thompson RP, *et al*. Retinoic acid directs cardiac laterality and the expression of early markers of precardiac asymmetry. *Dev Biol* 1997;**182**:162–71.

15 Stainier DYR, Fouquet B, Chen J-N, *et al*. Mutations affecting the formation and function of the cardiovascular system in the zebrafish embryo. *Development* 1996;**123**:285–92.

16 Levin M, Johnson AL, Stern CD, *et al*. A molecular pathway determining left–right asymmetry in chick embryogenesis. *Cell* 1995;**82**:803–14.

17 Cai CL, Liang X, Shi Y, *et al*. Isl1 identifies a cardiac progenitor population that proliferates prior to differentiation and contributes a majority of cells to the heart. *Dev Cell* 2003;**5**:877–89.

18 Kelly RG. Building the right ventricle. *Circ Res* 2007;**100**: 943–5.

19 Meilhac SM, Esner M, Kelly RG, *et al*. The clonal origin of myocardial cells in different regions of the embryonic mouse heart. *Dev Cell* 2004;**6**:685–98.

20 De la Cruz MV, Castillo MM, Villavicencio L, *et al*. Primitive interventricular septum, its primordium, and its contribution in the definitive interventricular septum: *in vivo* labelling study in the chick embryo heart. *Anat Rec* 1997;**247**:512–20.

21 van den Berg G, Abu-Issa R, de Boer BA, *et al*. A caudal proliferating growth center contributes to both poles of the forming heart tube. *Circ Res* 2009;**104**:179–88.

22 Mjaatvedt CH, Nakaoka T, Moreno-Rodriguez R, *et al*. The outflow tract of the heart is recruited from a novel heart-forming field. *Dev Biol* 2001;**238**:97–109.

23 Waldo K, Kumiski DH, Wallis KT, *et al*. Conotruncal myocardium arises from a secondary heart field. *Development* 2001;**128**:3179–88.

24 Gittenberger-de Groot AC, Mahtab EAF, Hahurij ND, *et al*. Nkx2.5 negative myocardium of the posterior heart field and its correlation with podoplanin expression in cells from the developing cardiac pacemaking and conduction system. *Anat Rec* 2007;**290**:115–22.

25 Abu-Issa R, Kirby ML. Heart field: from mesoderm to heart tube. *Annu Rev Cell Dev Biol* 2007;**23**:5–68.

26 Bodmer R. Heart development in drosophila and its relationship to vertebrates. *Trends Cardiovasc Med* 1995;**5**:21–8.

27 Laverriere AC, Macniell C, Mueller C, *et al*. GATA-4/5/6, a subfamily of three transcription factors transcribed in developing heart and gut. *J Biol Chem* 1994;**269**:23177–84.

28 Saga Y, Miyagawa-Tomita S, Takagi A, *et al*. MesP1 is expressed in the heart precursor cells and required for the formation of a single heart tube. *Development* 1999;**126**:3437–47.

29 Dodou E, Verzi MP, Anderson JP, *et al*. Mef2c is a direct transcriptional target of ISL1 and GATA factors in the anterior heart field during mouse embryonic development. *Development* 2004;**131**:3931–42.

30 Bax NA, Lie-Venema H, Vicente-Steijn R, *et al*. Platelet-derived growth factor is involved in the differentiation of second heart

field-derived cardiac structures in chicken embryos. *Dev Dyn* 2009;**238**:2658–69.

31 Vicente-Steijn R, Kolditz DP, Mahtab EA, *et al*. Electrical activation of sinus venosus myocardium and expression patterns of RhoA and Isl-1 in the chick embryo. *J Cardiovasc Electrophysiol* 2010;**21**:1284–92.

32 Draus JM Jr, Hauck MA, Goetsch M, *et al*. Investigation of somatic NKX2-5 mutations in congenital heart disease. *J Med Genet* 2009;**46**:115–22.

33 Plageman TF Jr, Yutzey KE. T-box genes and heart development: putting the "T" in heart. *Dev Dyn* 2005;**232**:11–20.

34 Poelmann RE, Gittenberger-de Groot AC. A subpopulation of apoptosis-prone cardiac neural crest cells targets to the venous pole: multiple functions in heart development? *Dev Biol* 1999;**207**:271–86.

35 Waldo K, Miyagawa-Tomita S, Kumiski D, *et al*. Cardiac neural crest cells provide new insight into septation of the cardiac outflow tract: aortic sac to ventricular septal closure. *Dev Biol* 1998;**196**:129–44.

36 Gurjarpadhye A, Hewett KW, Justus C, *et al*. Cardiac neural crest ablation inhibits compaction and electrical function of conduction system bundles. *Am J Physiol Heart Circ Physiol* 2007;**292**:H1291–300.

37 Poelmann RE, Jongbloed MR, Molin DGM, *et al*. The neural crest is contiguous with the cardiac conduction system in the mouse embryo: a role in induction? *Anat Embryol* 2004;**208**:389–93.

38 Baldini A. DiGeorge's syndrome: a gene at last. *Lancet* 2003; **362**:1342–3.

39 Lie-Venema H, van den Akker NMS, Bax NAM, *et al*. Origin, fate, and function of epicardium-derived cells (EPCDs) in normal and abnormal cardiac development. *Sci World J* 2007;**7**:1777–98.

40 Zhou B, Ma Q, Rajagopal S, *et al*. Epicardial progenitors contribute to the cardiomyocyte lineage in the developing heart. *Nature* 2008;**454**:109–13.

41 Perez-Pomares JM, Carmona R, Gonzalez-Iriarte M, *et al*. Origin of coronary endothelial cells from epicardial mesothelium in avian embryos. *Int J Dev Biol* 2002;**46**:1005–13.

42 DeRuiter MC, Gittenberger-de Groot AC, Wenink ACG, *et al*. In normal development pulmonary veins are connected to the sinus venosus segment in the left atrium. *Anat Rec* 1995;**243**:4–92.

43 Blom NA, Gittenberger-de Groot AC, Jongeneel TH, *et al*. Normal development of the pulmonary veins in human embryos and formulation of a morphogenetic concept for sinus venosus defects. *Am J Cardiol* 2001;**87**:305–9.

44 Douglas YL, Jongbloed MR, den Hartog WC, *et al*. Pulmonary vein and atrial wall pathology in human total anomalous pulmonary venous connection. *Int J Cardiol* 2009;**134**:302–12.

45 Van Praagh R, Corsini J. Cor triatriatum: pathologic anatomy and a consideration of morphogenesis based on 13 postmortem cases and a study of normal development of the pulmonary vein and atrial septum in 83 human embryos. *Am Heart J* 1969;**78**: 379–405.

46 Anderson RH, Brown NA, Moorman AF. Development and structures of the venous pole of the heart. *Dev Dyn* 2006;**235**:2–9.

47 Snarr BS, Wirrig EE, Phelps AL, *et al*. A spatiotemporal evaluation of the contribution of the dorsal mesenchymal protrusion to cardiac development. *Dev Dyn* 2007;**236**:1287–94.

48 Christoffels VM, Mommersteeg MT, Trowe MO, *et al*. Formation of the venous pole of the heart from an Nkx2–5-negative precursor population requires Tbx18. *Circ Res* 2006;**98**:1555–1563.

49 Blaschke RJ, Hahurij ND, Kuijper S, *et al*. Targeted mutation reveals essential functions of the homeodomain transcription factor Shox2 in sinoatrial and pacemaking development. *Circulation* 2007;**115**:1830–1838.

50 Garcia-Frigola C, Shi Y, Evans SM. Expression of the hyperpolarization-activated cyclic nucleotide-gated cation channel HCN4 during mouse heart development. *Gene Expr Patterns* 2003;**3**:777–83.

51 Bleyl SB, Saijoh Y, Bax NA, *et al*. Dysregulation of the PDGFRA gene causes inflow tract anomalies including TAPVR: integrating evidence from human genetics and model organisms. *Hum Mol Genet* 2010;**19**:1286–301.

52 DeRuiter MC, Gittenberger-de Groot AC, Poelmann RE, *et al*. Development of the pharyngeal arch system related to the pulmonary and bronchial vessels in the avian embryo. *Circulation* 1993;**87**:1306–19.

53 Douglas YL, Mahtab EA, Jongbloed MR, *et al*. Pulmonary vein, dorsal atrial wall and atrial septum abnormalities in podoplanin knockout mice with disturbed posterior heart field contribution. *Pediatr Res* 2009;**65**:27–32.

54 Douglas YL, Jongbloed MR, DeRuiter MC, *et al*. Normal and abnormal development of pulmonary veins: state of the art and correlation with clinical entities. *Int J Cardiol* 2011;**147**:13–24.

55 Bruneau BG, Nemer G, Schmitt JP, *et al*. A murine model of Holt–Oram syndrome defines roles of the T-box transcription factor Tbx5 in cardiogenesis and disease. *Cell* 2001;**106**:709–21.

56 Benson DW, Silberbach GM, Kavanaugh-McHugh A, *et al*. Mutations in the cardiac transcription factor NKX2.5 affect diverse cardiac developmental pathways. *J Clin Invest* 1999;**104**:1567–73.

57 Barlow GM, Chen X-N, Lyons GE, *et al*. Down syndrome congenital heart disease: a narrowed region and a candidate gene. *Genet Med* 2001;**3**:91–101.

58 Blom NA, Ottenkamp J, Wenink AG, *et al*. Deficiency of the vestibular spine in atrioventricular septal defects in human fetuses with down syndrome. *Am J Cardiol* 2003;**91**:180–4.

59 Bax NAM, Bleyl SB, Gallini R, *et al*. Cardiac malformations in *Pdgfrα* mutant embryos are associated with increased expression of WT1 and Nkx2.5 in the second heart field. *Dev Dyn* 2010;**239**:2307–17.

60 Wenink ACG, Gittenberger-de Groot AC, Van Gils FAW, *et al*. Pathogenetic aspects of atrioventricular septal defects. *Acta Morphol Neerl Scand* 1984;**22**:181.

61 Franco D, Campione M. The role of Pitx2 during cardiac development. Linking left–right signaling and congenital heart diseases. *Trends Cardiovasc Med* 2003;**13**:157–63.

62 Poelmann RE, Jongbloed MR, Gittenberger-de Groot AC. Pitx2: a challenging teenager. *Circ Res* 2008;**102**:749–51.

63 Gudbjartsson DF, Arnar DO, Helgadottir A, *et al*. Variants conferring risk of atrial fibrillation on chromosome 4q25. *Nature* 2007;**448**:353–7.

64 Gittenberger-de Groot AC, Bartelings MM, DeRuiter MC, *et al*. Basics of cardiac development for the understanding of congenital heart malformations. *Pediatr Res* 2005;**57**:169–76.

65 Jongbloed MR, Wijffels MC, Schalij MJ, *et al*. Development of the right ventricular inflow tract and moderator band: a possible

morphological and functional explanation for Mahaim tachycardia. *Circ Res* 2005;**96**:776–83.

66 Jenkins SJ, Hutson DR, Kubalak SW. Analysis of the proepicardium–epicardium transition during the malformation of the RXRalpha–/– epicardium. *Dev Dyn* 2005;**233**:1091–101.

67 Van Loo PF, Mahtab EAF, Wisse LJ, *et al*. Transcription factor Sp3 knockout mice display serious cardiac malformations. *Mol Cell Biol* 2007;**27**:8571–82.

68 Lie-Venema H, Gittenberger-de Groot AC, van Empel LJP, *et al*. Ets-1 and Ets-2 transcription factors are essential for normal coronary and myocardial development in chicken embryos. *Circ Res* 2003;**92**:749–56.

69 Bartram U, Molin DGM, Wisse LJ, *et al*. Double-outlet right ventricle and overriding tricuspid valve reflect disturbances of looping, myocardialization, endocardial cushion differentiation, and apoptosis in TGFβ2-knockout mice. *Circulation* 2001; **103**:2745–52.

70 Waldo KL, Hutson MR, Ward CC, *et al*. Secondary heart field contributes myocardium and smooth muscle to the arterial pole of the developing heart. *Dev Biol* 2005;**281**:78–90.

71 Bartelings MM, Gittenberger-de Groot AC. The outflow tract of the heart – embryologic and morphologic correlations. *Int J Cardiol* 1989;**22**:289–300.

72 Pexieder T. Conotruncus and its septation at the advent of the molecular biology era. In: Clark EB, Markwald RR, Takao A, eds. *Developmental Mechanisms of Heart Disease*. New York: Futura Publishing, 1995: 227–47.

73 Zaffran S, Kelly RG, Meilhac SM, *et al*. Right ventricular myocardium derives from the anterior heart field. *Circ Res* 2004;**95**:261–8.

74 Bartelings MM, Gittenberger-de Groot AC. Morphogenetic considerations on congenital malformations of the outflow tract. Part I: common arterial trunk and tetralogy of Fallot. *Int J Cardiol* 1991;**32**:213–30.

75 Poelmann RE, Mikawa T, Gittenberger-de Groot AC. Neural crest cells in outflow tract septation of the embryonic chicken heart: differentiation and apoptosis. *Dev Dyn* 1998;**212**:373–84.

76 Sumida H, Akimoto N, Nakamura H. Distribution of the neural crest cells in the heart of birds:a three dimensional analysis. *Anat Embryol* 1989;**180**:29–35.

77 van Mierop LHS, Kutsche LM. Cardiovascular anomalies in DiGeorge syndrome and importance of neural crest as a possible pathogenetic factor. *Am J Cardiol* 1986;**58**:133–7.

78 Kirby ML, Gale TF, Stewart DE. Neural crest cells contribute to normal aorticopulmonary septation. *Science* 1983;**220**: 1059–61.

79 Brown CB, Feiner L, Lu MM, *et al*. PlexinA2 and semaphorin signaling during cardiac neural crest development. *Development* 2001;**128**:3071–80.

80 Epstein JA. Pax3, neural crest and cardiovascular development. *Trends Cardiovasc Med* 1996;**6**:255–61.

81 Van Den Akker NM, Molin DG, Peters PP, *et al*. Tetralogy of Fallot and alterations in vascular endothelial growth factor-A signaling and notch signaling in mouse embryos solely expressing the VEGF120 isoform. *Circ Res* 2007;**100**:842–9.

82 Molin DGM, Roest PA, Nordstrand H, *et al*. Disturbed morphogenesis of cardiac outflow tract and increased rate of aortic arch anomalies in the offspring of diabetic rats. *Birth Defects Res A Clin Mol Teratol* 2004;**70**:927–38.

83 McKellar SH, Tester DJ, Yagubyan M, *et al*. Novel NOTCH1 mutations in patients with bicuspid aortic valve disease and thoracic aortic aneurysms. *J Thorac Cardiovasc Surg* 2007;**134**:290–6.

84 Wooten EC, Iyer LK, Montefusco MC, *et al*. Application of gene network analysis techniques identifies AXIN1/PDIA2 and endoglin haplotypes associated with bicuspid aortic valve. *PLoS One* 2010;**5**:e8830.

85 Hogers B, DeRuiter MC, Gittenberger-de Groot AC, *et al*. Extraembryonic venous obstructions lead to cardiovascular malformations and can be embryolethal. *Cardiovasc Res* 1999;**41**:87–99.

86 Aicher D, Urbich C, Zeiher A, *et al*. Endothelial nitric oxide synthase in bicuspid aortic valve disease. *Ann Thorac Surg* 2007;**83**:1290–4.

87 Yasui H, Nakazawa M, Morishima M, *et al*. Morphological observations on the pathogenetic process of transposition of the great arteries induced by retinoic acid in mice. *Circulation* 1995;**91**:2478–86.

88 Bartelings MM, Gittenberger-de Groot AC. Morphogenetic considerations on congenital malformations of the outflow tract. Part 2: complete transposition of the great arteries and double outlet right ventricle. *Int J Cardiol* 1991;**33**:5–26.

89 Oosthoek PW, Wenink ACG, Vrolijk BCM, *et al*. Development of the atrioventricular valve tension apparatus in the human heart. *Anat Embryol* 1998;**198**:317–29.

90 Wessels A, Markman MW, Vermeulen JL, *et al*. The development of the atrioventricular junction in the human heart. *Circ Res* 1996;**78**:110–7.

91 Eisenberg LM, Markwald RR. Molecular regulation of atrioventricular valvuloseptal morphogenesis. *Circ Res* 1995;**77**:1–6.

92 Gittenberger-de Groot AC, Vrancken Peeters M-PFM, Mentink MMT, *et al*. Epicardium-derived cells contribute a novel population to the myocardial wall and the atrioventricular cushions. *Circ Res* 1998;**82**:1043–52.

93 Norris RA, Moreno-Rodriguez RA, Sugi Y, *et al*. Periostin regulates atrioventricular valve maturation. *Dev Biol* 2008;**316**:200–13.

94 Hurle JM, Colvee E, Blanco AM. Development of mouse semilunar valves. *Anat Embryol* 1980;**160**:83–91.

95 Hokken RB, Bartelings MM, Bogers AJJC, *et al*. Morphology of the pulmonary and aortic roots with regard to the pulmonary autograft procedure. *J Thorac Cardiovasc Surg* 1997;**113**:453–61.

96 Bartram U, Bartelings MM, Kramer HH, *et al*. Congenital polyvalvular disease: a review. *Pediatr Cardiol* 2001;**22**:93–101.

97 Oosthoek PW, Wenink ACG, Macedo AJ, *et al*. The parachute-like asymmetric mitral valve and its two papillary muscles. *J Thorac Cardiovasc Surg* 1997;**114**:9–15.

98 Oosthoek PW, Wenink ACG, Wisse LJ, *et al*. Development of the papillary muscles of the mitral valve: morphogenetic background of parachute-like asymmetrical mitral valves and other mitral valve anomalies. *J Thorac Cardiovasc Surg* 1998;**116**:36–46.

99 Lie-Venema H, Eralp I, Markwald RR, *et al*. Periostin expression by epicardium-derived cells (EPDCs) is involved in the development of the atrioventricular valves and fibrous heart skeleton. *Differentiation* 2008;**76**:809–19.

100 De la Pompa JL, Timmerman LA, Takimoto H, *et al*. Role of the NF-Atc transcription factor in morphogenesis of cardiac valves and septum. *Nature* 1998;**392**:182–6.

101 Schilham MW, Oosterwegel MA, Moerer P, *et al*. Defects in cardiac outflow tract formation and pro-B-lymphocyte expansion in mice lacking Sox-4. *Nature* 1996;**380**:711–4.

102 Hartwig NG, Vermeij-Keers C, De Vries HE, *et al*. Aplasia of semilunar valve leaflets: two case reports and developmental aspects. *Pediatr Cardiol* 1991;**12**:114–7.

103 Fernandez B, Duran AC, Fernandez-Gallego T, *et al*. Bicuspid aortic valves with different spatial orientations of the leaflets are distinct etiological entities. *J Am Coll Cardiol* 2009;**54**:2312–8.

104 Blom NA, Gittenberger-de Groot AC, DeRuiter MC, *et al*. Development of the cardiac conduction tissue in human embryos using HNK-1 antigen expression: possible relevance for understanding of abnormal atrial automaticity. *Circulation* 1999;**99**:800–6.

105 James TN. The internodal pathways of the human heart. *Prog Cardiovasc Dis* 2001;**43**:495–535.

106 Jongbloed MRM, Schalij MJ, Poelmann RE, *et al*. Embryonic conduction tissue: a spatial correlation with adult arrhythmogenic areas? Transgenic CCS/lacZ expression in the cardiac conduction system of murine embryos. *J Cardiovasc Electrophysiol* 2004;**15**:349–55.

107 Kondo RP, Anderson RH, Kupershmidt S, *et al*. Development of the cardiac conduction system as delineated by minK-lacZ. *J Cardiovasc Electrophysiol* 2003;**14**:383–91.

108 Hoogaars WM, Engel A, Brons JF, *et al*. Tbx3 controls the sinoatrial node gene program and imposes pacemaker function on the atria. *Genes Dev* 2007;**21**:1098–112.

109 Anderson RH, Ho SY. The morphology of the cardiac conduction system. *Novartis Found Symp* 2003;**250**:6–17.

110 Gittenberger-de Groot AC, Wenink ACG. The specialized myocardium in the fetal heart. In: van Mierop LHS, Oppenheimer-Dekker A, Bruins CLDC, eds. *Embryology and Teratology of the Heart and the Great Arteries*. Leiden: Leiden University Press, 1978: 15–24.

111 Hahurij ND, Gittenberger-de Groot AC, Kolditz DP, *et al*. Accessory atrioventricular myocardial connections in the developing human heart: relevance for perinatal supraventricular tachycardias. *Circulation* 2008;**117**:2850–8.

112 Kolditz DP, Wijffels MC, Blom NA, *et al*. Epicardium-derived cells in development of annulus fibrosis and persistence of accessory pathways. *Circulation* 2008;**117**:1508–17.

113 Jongbloed MR, Mahtab EAF, Blom NA, *et al*. Development of the cardiac conduction system and the possible relation to predilection sites of arrhythmogenesis. *Sci World J* 2008;**8**:239–69.

114 Wenink ACG. Development of the human cardiac conducting system. *J Anat* 1976;**121**(Pt 3):617–31.

115 Christoffels VM, Hoogaars WM, Tessari A, *et al*. T-box transcription factor Tbx2 represses differentiation and formation of the cardiac chambers. *Dev Dyn* 2004;**229**:763–70.

116 Moskowitz IP, Pizard A, Patel VV, *et al*. The T-Box transcription factor Tbx5 is required for the patterning and maturation of the murine cardiac conduction system. *Development* 2004;**131**:4107–16.

117 Moskowitz IP, Kim JB, Moore ML, *et al*. A molecular pathway including Id2, Tbx5, and Nkx2–5 required for cardiac conduction system development. *Cell* 2007;**129**:1365–76.

118 Espinoza-Lewis RA, Yu L, He F, *et al*. Shox2 is essential for the differentiation of cardiac pacemaker cells by repressing Nkx2–5. *Dev Biol* 2009;**327**:376–85.

119 Christoffels VM, Grieskamp T, Norden J, *et al*. Tbx18 and the fate of epicardial progenitors. *Nature* 2009;**458**:E8–9.

120 Sun Y, Liang X, Najafi N, *et al*. Islet 1 is expressed in distinct cardiovascular lineages, including pacemaker and coronary vascular cells. *Dev Biol* 2007;**304**:286–96.

121 Aanhaanen WT, Mommersteeg MT, Norden J, *et al*. Developmental origin, growth, and three-dimensional architecture of the atrioventricular conduction axis of the mouse heart. *Circ Res* 2010;**107**:728–36.

122 Gourdie RG, Mima T, Thompson RP, *et al*. Terminal diversification of the myocyte lineage generates Purkinje fibers of the cardiac conduction system. *Development* 1995;**121**:1423–31.

123 Hyer J, Johansen M, Prasad A, *et al*. Induction of Purkinje fiber differentiation by coronary arterialization. *Proc Natl Acad Sci USA* 1999;**96**:13214–8.

124 Eralp I, Lie-Venema H, Bax NAM, *et al*. Epicardium-derived cells are important for correct development of the Purkinje fibers in the avian heart. *Anat Rec* 2006;**288A**:1272–80.

125 Kalman JM, Olgin JE, Karch MR, *et al*. "Cristal tachycardias": origin of right atrial tachycardias from the crista terminalis identified by intracardiac echocardiography. *J Am Coll Cardiol* 1998;**31**:451–9.

126 Olgin JE, Kalman JM, Fitzpatrick AP, *et al*. Role of right atrial endocardial structures as barriers to conduction during human type I atrial flutter. Activation and entrainment mapping guided by intracardiac echocardiography. *Circulation* 1995;**92**:1839–48.

127 Tsai CF, Tai CT, Hsieh MH, *et al*. Initiation of atrial fibrillation by ectopic beats originating from the superior vena cava: electrophysiological characteristics and results of radiofrequency ablation. *Circulation* 2000;**102**:67–74.

128 Katritsis D, Ioannidis JP, Giazitzoglou E, *et al*. Conduction delay within the coronary sinus in humans: implications for atrial arrhythmias. *J Cardiovasc Electrophysiol* 2002;**13**:859–62.

129 Haissaguerre M, Jais P, Shah DC, *et al*. Spontaneous initiation of atrial fibrillation by ectopic beats originating in the pulmonary veins. *N Engl J Med* 1998;**339**:659–66.

130 Becker AE, Anderson RH. The Wolff–Parkinson–White syndrome and its anatomical substrates. *Anat Rec* 1981;**201**:169–77.

131 Pressley JC, Wharton JM, Tang AS, *et al*. Effect of Ebstein's anomaly on short- and long-term outcome of surgically treated patients with Wolff–Parkinson–White syndrome. *Circulation* 1992;**86**:1147–55.

132 Winter EM, Gittenberger-de Groot AC. Cardiovascular development: towards biomedical applicability: epicardium-derived cells in cardiogenesis and cardiac regeneration. *Cell Mol Life Sci* 2007;**64**:692–703.

133 Bogers AJJC, Gittenberger-de Groot AC, Poelmann RE, *et al*. Development of the origin of the coronary arteries, a matter of ingrowth or outgrowth? *Anat Embryol* 1989;**180**:437–41.

134 Waldo KL, Willner W, Kirby ML. Origin of the proximal coronary artery stems and a review of ventricular vascularization in the chick embryo. *Am J Anat* 1990;**188**:109–20.

135 Red-Horse K, Ueno H, Weissman IL, *et al*. Coronary arteries form by developmental reprogramming of venous cells. *Nature* 2010;**464**:549–53.

136 Poelmann RE, Gittenberger-de Groot AC, Mentink MMT, *et al*. Development of the cardiac coronary vascular endothelium,

studied with antiendothelial antibodies, in chicken–quail chimeras. *Circ Res* 1993;**73**:559–68.

137 Vrancken Peeters M-PFM, Gittenberger-de Groot AC, Mentink MMT, *et al*. The development of the coronary vessels and their differentiation into arteries and veins in the embryonic quail heart. *Dev Dyn* 1997;**208**:338–48.

138 Vrancken Peeters M-PFM, Gittenberger-de Groot AC, Mentink MMT, *et al*. Differences in development of coronary arteries and veins. *Cardiovasc Res* 1997;**36**:101–10.

139 Gittenberger-de Groot AC, Vrancken Peeters M-PFM, Bergwerff M, *et al*. Epicardial outgrowth inhibition leads to compensatory mesothelial outflow tract collar and abnormal cardiac septation and coronary formation. *Circ Res* 2000;**87**:969–71.

140 Winter EM, Grauss RW, Hogers B, *et al*. Preservation of left ventricular function and attenuation of remodeling after transplantation of human epicardium-derived cells into the infarcted mouse heart. *Circulation* 2007;**116**:917–27.

141 Gittenberger-de Groot AC, Bartelings MM, Bogers AJJC, *et al*. The embryology of the common arterial trunk. *Prog Pediatr Cardiol* 2002;**15**:1–8.

142 Bogers AJJC, Bartelings MM, Bökenkamp R, *et al*. Common arterial trunk, uncommon coronary arterial anatomy. *J Thorac Cardiovasc Surg* 1993;**106**:1133–7.

143 Eralp I, Lie-Venema H, DeRuiter MC, *et al*. Coronary artery and orifice development is associated with proper timing of epicardial outgrowth and correlated Fas ligand associated apoptosis patterns. *Circ Res* 2005;**96**:526–34.

144 Gittenberger-de Groot AC, Eralp I, Lie-Venema H, *et al*. Development of the coronary vasculature and its implications for coronary abnormalities in general and specifically in pulmonary atresia without ventricular septal defect. *Acta Paediatr Suppl* 2004;**93**:13–9.

145 Gittenberger-de Groot AC, Tennstedt C, Chaoui R, *et al*. Ventriculo coronary arterial communications (VCAC) and myocardial sinusoids in hearts with pulmonary atresia with intact ventricular septum: two different diseases. *Prog Pediatr Cardiol* 2001;**13**:157–64.

146 Van Den Akker NM, Caolo V, Wisse LJ, *et al*. Developmental coronary maturation is disturbed by aberrant cardiac vascular endothelial growth factor expression and Notch signalling. *Cardiovasc Res* 2008;**78**:366–75.

147 Van Den Akker NM, Winkel LC, Nisancioglu MH, *et al*. PDGF-B signaling is important for murine cardiac development: its role in developing atrioventricular valves, coronaries, and cardiac innervation. *Dev Dyn* 2008;**237**:494–503.

148 Bergwerff M, Verberne ME, DeRuiter MC, *et al*. Neural crest cell contribution to the developing circulatory system. Implications for vascular morphology? *Circ Res* 1998;**82**:221–31.

149 Molin DGM, DeRuiter MC, Wisse LJ, *et al*. Altered apoptosis pattern during pharyngeal arch artery remodelling is associated with aortic arch malformations in Tgf beta 2 knock-out mice. *Cardiovasc Res* 2002;**56**:312–22.

150 Moulaert AJ, Bruins CC, Oppenheimer-Dekker A. Anomalies of the aortic arch and ventricular septal defects. *Circulation* 1976;**53**:1011–5.

151 Gittenberger-de Groot AC, Azhar M, Molin DGM. Transforming growth factor beta-SMAD2 signaling and aortic arch development. *Trends Cardiovasc Med* 2006;**16**:1–6.

2 Genetics of Cardiovascular Disease in the Young

Lisa J. Martin, Robert B. Hinton & D. Woodrow Benson
Cincinnati Children's Hospital Medical Center and University of Cincinnati School of Medicine, Cincinnati, OH, USA

Introduction

Cardiovascular disease in the young comprises varied phenotypes, including cardiovascular malformations (CVMs), cardiac arrhythmias, cardiomyopathies, and vasculopathies. In the past two decades, there has been an explosion of relevant genomic/genetic information. In this edition, progress in understanding the genetic origins of specific cardiac disease phenotypes is provided in each chapter. Although cardiovascular genetics is still in an early phase of gene discovery, genetic testing of embryos, fetuses, children, and adults is expanding rapidly in both research and clinical settings, and Chapter 13 addresses the challenge and current utility of genetic testing. However, despite progress in the genetics of cardiovascular disease in the young, cause is still unknown in most anomalies. Because the genetic origins of cardiac arrhythmias (Chapter 55), cardiomyopathies (Chapter 58), and vasculopathies (Chapter 67) are dealt with in other chapters, the emphasis here will be on genetic etiology of CVMs.

CVMs are the most common birth defects, with an estimated incidence of 5–10 per 100 live births [1] and 20 per 100 abortuses [2]. Although there have been tremendous advances in the medical and surgical care of infants and children with CVMs [3], CVMs remain a major cause of fetal loss, infant death, and childhood morbidity [4,5]. Healthcare providers have long had an interest in elucidating the cause of CVMs, and for many families with an affected child, the cause of their child's heart disease remains an important question. Based on the increased availability of genomic/genetic information in the past decade (Table 2.1), an increasing role of genetics in the diagnostic approaches, therapeutic strategies, and outcomes of assessments of cardiovascular disease in the young can be expected.

What is the incidence of CVMs?

An estimate of 4–10 liveborn infants per 1000, 40% being diagnosed in the first year of life, is often cited as the prevalence of CVMs [2,5]. The true prevalence, however, may be much higher. For example, bicuspid aortic valve (BAV), the most common CVM, occurring in 10–20 per 1000 in the general population, is usually excluded from this estimate. When isolated aneurysms of the atrial septum and persistent left superior vena cava, each occurring in 5–10 per 1000 live births, are considered, the incidence of CVMs approaches 50 per 1000 live births. The incidence of ventricular septal defect (VSD) has also been demonstrated to be as high as 5% in two independent Israeli cohorts of 5000 serial newborns and 5000 serially studied premature infants [1]. In the light of these considerations, an incidence of CVMs of 50 per 1000 live births is a conservative estimate.

Cause of CVMs: understanding in the pregenomic era

Although early epidemiologic studies recognized environmental teratogens, such as rubella and thalidomide, as risk factors for CVMs, in the Baltimore-Washington Infant Study [6], the risk factor identified most often was a positive family history, suggesting a significant genetic component. Numerous examples of increased CVM risk in family members of affected individuals support a genetic cause of CVMs [7], as does the association of CVMs and other birth defects with chromosomal abnormalities [1]. At present, the cause of most CVMs remains unknown, however. Although only ~15% of all CVMs can currently be attributed to genetic causes [8], increasing evidence suggests that most if not all CVMs have a genetic component [9,10].

Table 2.1 Web sites with genomic/genetic information.

Source	Web site	Description
National Center for Biotechnology Information	http://www.ncbi.nlm.nih.gov/	Provides access to biomedical and genomic information
Online Mendelian Inheritance in Man (OMIM)	http://www.ncbi.nlm.nih.gov/omim/	Compendium of human genes and genetic phenotypes
Genetests	http://www.genetests.org/	Listing of US and international laboratories offering genetic testing
HapMap	http://www.hapmap.org	Characterization of common variation across major racial groups
1000 Genomes Project	http:// www.1000genomes.org	Sequence level genetic variation
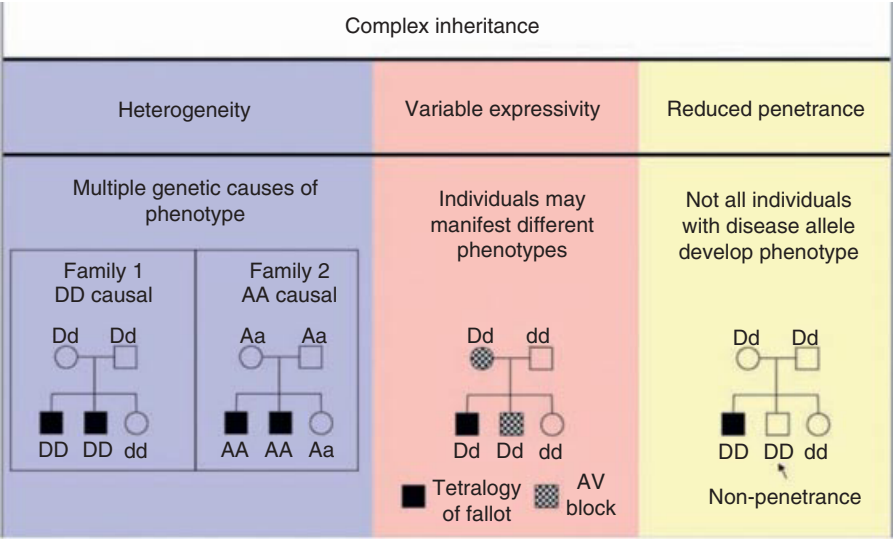
Figure 2.1 Phenomena frequently observed in genetic studies of cardiovascular disease in the young. Genetic heterogeneity, variable expressivity, and reduced penetrance are defined.

Cause of CVMs: understanding in the postgenomic era

The primary challenge in identifying additional genetic causes of CVMs may be the approach to discovery. Despite the relative rarity of CVMs that exhibit Mendelian inheritance patterns (single gene), molecular and cytogenetic studies have used family-based linkage analysis to identify a handful of CVM-causing genes (reviewed in [1]). These studies have demonstrated variable expressivity, reduced penetrance, and genetic heterogeneity (Figure 2.1), confirming that most CVMs are the result of complex inheritance. Complex inheritance occurs when multiple genes contribute to the phenotype, and different combinations of genetic variants may result in variable expressivity based on gene–gene interactions or gene–environment interactions. From developmental biology (Chapter 1), it is clear that cardiogenesis results from multiple tightly regulated processes, and dysregulation of any of these processes can result in CVMs [11]. Taken together, a mixture of genetic and environmental or epigenetic insults may result in CVMs, and identifying these combinations is challenging.

The presence of multiple genes and interactions between genes and the environment does not preclude the ability to identify genes associated with CVMs; however, complex inheritance must be considered if researchers are to continue to define the genetic underpinnings of CVMs and other forms of cardiovascular disease in the young. This approach requires careful phenotype definition, estimation of genetic effects, recruiting strategy, and integrated statistical methods. In the sections that follow, our goal is to provide an overview of these study design considerations.

Definition of the phenotype

Genetic studies have shown that the clinical taxonomy (the clinical phenotypes used by anatomists, cardiologists, and surgeons) does not precisely align with the emerging genetic taxonomy. For example, there is not a tetralogy of Fallot gene or an atrial septal defect gene, as both conditions exhibit

Table 2.2 Single gene and cytogenetic abnormalities for ASD and TOF.

Defect	Secundum atrial septal defect	Tetralogy of Fallot
Single gene defects	EVC/EVC2	FOG2
	GATA4	JAG1
	MYH6	NKX2.5
	NKX2.5	PTPN11
	PTPN11	TBX5
	TBX5	
	ZIC3	
Cytogenetic defects	Trisomy 21	Trisomy 21
	Del22q11	Del22q11

considerable genetic heterogeneity (Table 2.2). Further, individuals within a family harboring the same mutation may exhibit distinct phenotypes (i.e., variable expressivity) that cross the clinical taxonomy boundaries. Therefore, the first step of any human genetic research study is to define the phenotype precisely. Studies using too broad or too narrow a phenotype definition may fail either to find association with an existing genetic variant or to identify a pathologic variant. Hence definition of the phenotype most aligned with the underlying genetic etiology is essential for successfully identifying causative genetic variants.

Clinically, CVMs have clearly defined phenotypes and individual lesions are classified based on anatomy (e.g., atrial septal defect), physiology (e.g., left to right shunt defects), and embryology (e.g., endocardial cushion defects), with echocardiography being the gold standard for diagnosis. Although these approaches to classification have been useful, there is substantial phenotypic heterogeneity in clinically defined CVMs. For example, ventricular septal defect (VSD) is further classified into four types: conoseptal, conoventricular, muscular, and inlet (Figure 2.2). Evidence is accumulating that each VSD type has a distinct genetic basis and different developmental origins. Specifically, some conoventricular VSDs are associated with 22q11 deletion syndrome, whereas inlet VSDs are often associated with trisomy 21. Further, the second heart field and neural crest programs are expected to contribute to conoseptal and conoventricular septation but not inlet or muscular septation. In addition, in complex CVMs such as tetralogy of Fallot, defined by pulmonary stenosis, overriding aorta, and VSD, specific phenotypic details distinguish subtypes. For example, tetralogy of Fallot phenotype heterogeneity may be subclassified into variants involving aortic arch specification, pulmonary valve anatomy, and noncardiac malformations (Figure 2.2).

Recent advances in cardiac developmental biology have revealed new complexity in the genetic regulation of heart morphogenesis and may help explain CVM phenotypic heterogeneity. The cardiovascular system is the first to function in the embryo, and viability depends on the successful establishment of this organ system (Chapter 1). The cardiac crescent including the lateral plate mesoderm is a major source of cardiac progenitor cells; however, there are other extracardiac precursors derived from the second heart field,
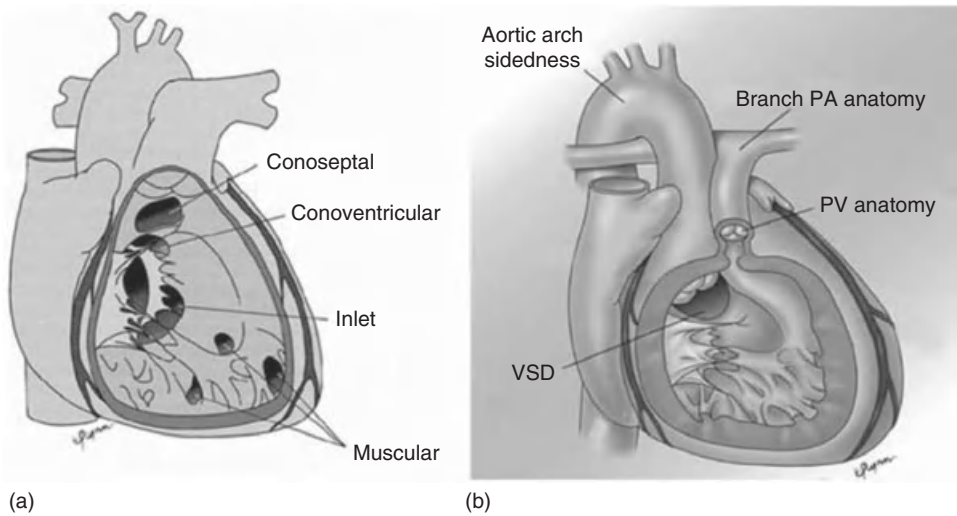
Figure 2.2 Phenotype variability. The clinical taxonomy names lesions implying specificity; however, there is significant variability in phenotypic detail. For example, ventricular septal defects may be classified as conoseptal, conoventricular, muscular, or inlet (a). In addition, complex lesions such as tetralogy of Fallot may have anatomic features that distinguish them from the group at large, for example, right aortic arch (b). These distinctions have significant implications when considering genetic etiology and the contribution of specific molecular cardiac developmental pathways. (Modified from Geva T, Powell A. Pediatric Heart Disease. In: Edelman R, ed. In Clinical Magnetic Resonance Imaging, 3rd edition. Elsevier, 2005: 1050–1059. With permission.)

cardiac neural crest, and pro-epicardium which migrate into the heart and contribute to its development. Differentiation of the progenitor cells results in spatially and temporally organized lineages, including muscle, conduction system, coronary vessels, and cardiac valves. The linear heart tube then loops, develops endocardial cushions, which ultimately contribute to valve structures, and forms chambers. Further, epigenetic factors, such as blood flow perturbations, that occur after primary cardiac morphogenesis but before birth may significantly affect and modify the ultimate phenotype [12]. Thus, CVMs result from complex interaction between multiple developmental factors, which may not be captured by the clinical nomenclature of CVMs.

Phenotypic heterogeneity may also affect the ability to detect genes and the underlying etiology of CVMs. Thus, although there are clinical definitions of specific phenotypes that are essential for establishing a diagnosis and designing a surgical treatment strategy, these definitions do not address etiology and may not be sufficient for genetic discovery. The insights gained by human genetic and molecular biology studies must be reconciled with the established clinical taxonomy to provide the most precise classification scheme for CVM. Elucidating the genetic basis of CVMs will result in a meaningful classification system that integrates the molecular basis of cardiac development with the clinical phenotype.

Evidence of genetic origins

Before conducting any gene discovery study, it is important to establish that there is a genetic basis. Researchers have long noted that CVM risk is increased in family members of affected individuals, suggesting a genetic basis [10,13]. However, given the variation in phenotype determination and the phenotypic variability of CVM, it is not surprising that there are also many reports of anomalies with no known family history [14,15]. Thus, statistical evidence of an increased occurrence of a specific CVM in family members of affected individuals compared with the general population is needed. There are two main quantitative measures of familial risk, recurrence risk and heritability.

Recurrence risk of a specific phenotype (e.g., atrial septal defect) or group of phenotypes (e.g., CVM) measures the proportion of the proband's relatives (usually defined as degree or relationship type) who are affected. CVM recurrence risk in siblings varies greatly, ranging from 0.5 to 22% [10,14,16–18]. One possible reason for the marked differences is that these estimates are specific to the study cohort and are influenced by study design (phenotype definition, ascertainment bias). Nonetheless, these studies demonstrate several interesting findings. First, there is approximately a doubling of recurrence risk on expanding the phenotype to include siblings with any type of CVM as compared with complete concordance [14,18]. This demonstrates significant

phenotypic heterogeneity with risk of one type of CVM increasing relatives' risk of a different CVM. Second, the method of evaluating relatives is important; recurrence risk estimates are higher when individuals are phenotyped with echocardiography as compared with interview [14,16,17]. Third, the definition of CVMs can influence the estimates. For example, the definition of a CVM often excludes subclinical or nonpediatric diagnoses, such as BAV, mitral valve prolapse, and left superior vena cava. Exclusion of these common CVMs results in lower recurrence estimates [14]. Recurrence risk studies support phenotypic heterogeneity and demonstrate a strong genetic component to CVMs.

Heritability estimates the proportion of a trait attributable to genetics. CVM heritability estimates are high, ranging from 49 to 95% [19,20]. Like recurrence risk, heritability is population specific and dependent on phenotyping. Importantly, some of the lower heritability estimates were based on self-reported phenotypes [18], compared with studies clinically examining all relatives [20]. Heritability was also lower when probands were defined broadly (e.g., ascertained groups of CVMs) [19,21] as compared with a specific CVM phenotype [14,15,22]. Taken together, these studies support the recurrence risk finding that there is a strong genetic basis to CVMs.

Study design for CVM gene discovery

Once the phenotype has been defined and a genetic component established, the next decision is which study design to use. Human genetic discovery research is challenging given the long lifespan, complex genetic background, and variable environmental exposures. Appropriate study design, however, helps minimize confounding. Factors that should be considered include prevalence and the timing of milestone events.

Prevalence is an estimate of how common a condition is within a population (the number of diseased individuals/ population size) and is a critical variable in genetic studies. Rare traits (prevalence <5%) have specific implications for study design. Although CVMs are the most common congenital malformation, it is a rare trait as only 5% of live births have CVMs [1]. Further, specific CVM phenotypes are even more rare and occur in <1% of live births [5]. Phenotypes that have a relatively high prevalence, such as obesity (occurring in >30% of the adult population), allow random selection of individuals from the population resulting in a large number of affected individuals. In contrast, for rare traits such as CVMs, large samples are necessary to obtain a modest number of patients. As a result, researchers often use nonrandom sampling, such as the case–control strategy.

Another factor to consider when designing a study is the timing of events. *Age of disease onset* influences potential misclassification of phenotype. Diseases with a late age of onset, such as mitral valve prolapse [23], potentially describe

individuals as "normal" or "unaffected" when they are actually affected. Additionally, diseases with late age of onset may be difficult to study using family-based data because few evaluated individuals may be affected. Conversely, CVMs unequivocally determined *in utero* should have minimal classification error. *Age of death* may bias the sample because only those who survive until sampled are included. Given the substantial mortality with some forms of CVMs, researchers must recognize this potential bias. Indeed, CVMs are responsible for a significant proportion of pre- and postnatal loss, with 20% of abortuses having a CVM [2]. For example, hypoplastic left heart syndrome (HLHS) is uniformly fatal without intervention in the newborn period. Because surgical palliation for HLHS has only been used for the past 25–30 years and interstage mortality continues to be significant (Chapter 38), identifying multiplex families may be difficult because individuals with HLHS might not have been recognized and have only survived to childbearing recently.

The next step is to determine the appropriate sampling strategy, family or population based, as sampling design affects the hypotheses that can be tested. There are two main questions in gene discovery: (1) are there genetic differences between affected and unaffected individuals, and (2) do genetic variants segregate with disease in families? The first question can be answered using *family-* or *population*-based data; however, the second question can only be tested using family-based information.

Family sampling may include trios (proband and parents), nuclear families (first-degree relatives, i.e., parents and siblings), or extended families (multiple generations). For rare traits such as CVMs, families are ascertained by a proband. Familial sampling depends on the inheritance pattern. A low recurrence risk means that a large number of family members must be sampled to find affected individuals. For CVMs with a modest to high recurrence risk, sequential sampling is effective [15]. In this approach, phenotypic information is collected on all first-degree relatives. If another affected individual is identified within the family, then all of that person's first-degree relatives are phenotyped. Sequential sampling is superior to traditional extended family sampling because it focuses on informative arms of the family.

Because CVMs are rare traits, the classic population-based sampling strategy is *case–control*. In this approach, the researcher recruits individuals with disease (cases) and unrelated individuals without disease (controls). Although this approach appears simple, the challenge is to ensure that the controls come from the same population as the cases and that controls are definitively unaffected. Differences between cases and controls can result in spurious associations. For example, in BAV, the male to female ratio is ~3:1. Thus, in a sample of BAV cases there would be more males than in a random sampling of the general population (male to female ratio ~1:1). For a case–control study of BAV, researchers should ensure that the case and control populations have similar proportions of males to minimize false associations. Further, ensuring that the controls do not have BAV requires echocardiographic assessment.

Methods for genotyping

Completion of the Human Genome Project made it clear that genetic variation is common and occurs on many different scales, ranging from gross karyotype alterations to single nucleotide changes [24,25]. The most common markers for population- and family-based studies are simple sequence tandem repeats (SSTRs, microsatellites) and point changes in nucleotides (single nucleotide polymorphisms, SNPs) (Figure 2.3). SSTRs are useful genetic markers because they tend to be highly polymorphic and therefore segregation of alleles can be traced in families. Current SSTR linkage maps contain approximately 400 markers. Limitations with SSTRs include a relatively high error rate compared with SNPs and lower density. On the other hand, there are over 3 million SNPs in the genome [26], creating data management and computational challenges. Current SNP linkage panels utilize only a fraction of those available (approximately 5000). Although less polymorphic than SSTRs, the number of SNPs available means that the information content can surpass that of SSTRs [27]. Further, the genotyping error rate is much lower in SNPs [28]. Cost and ease of automation have made SNPs the current preference [27].

Statistical approaches to gene discovery

There are two main statistical approaches to gene discovery, *linkage* and *association*. Linkage analysis tests to determine whether a variant segregates with disease in families, whereas association analysis determines whether a genetic variant occurs more often in individuals with disease than without disease. Linkage studies can be performed only in family-based studies, but association testing can be performed in population- or family-based studies. These two approaches may appear to ask the same question, but statistically they are independent tests.

Linkage
Linkage analysis is based on the assumption that the genetic marker and the disease variant are in close proximity and transmitted intact across generations [29]. Thus, markers in close proximity to the disease-causing gene segregate with disease. Evidence of linkage is determined either by consistent transmission of both the disease and the marker from parent to offspring (parametric) or by an increased proportion of alleles shared between affected relative pairs (nonparametric). Parametric linkage analyses are most powerful (e.g., a relatively small sample size can be informative) when the
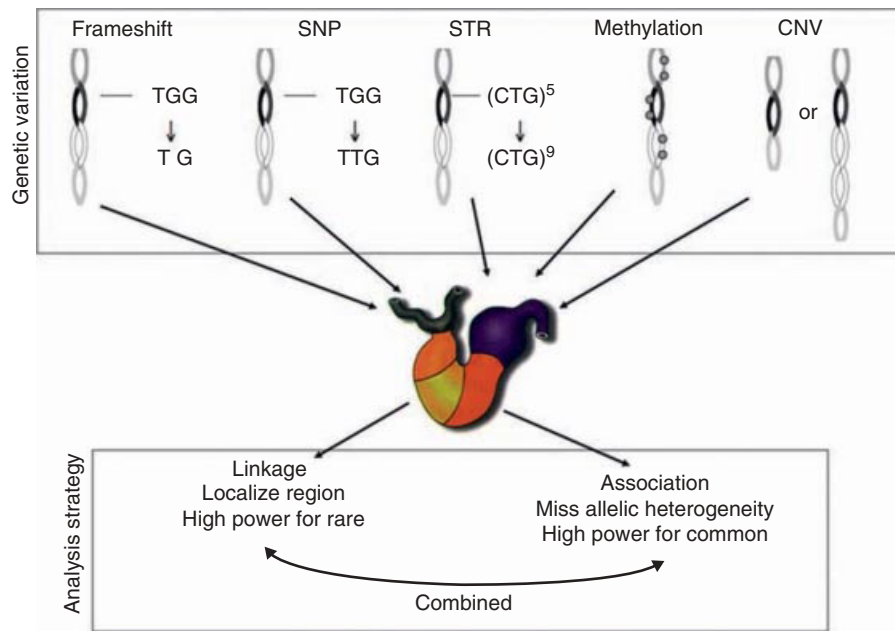
Figure 2.3 Strategy for continued CVM genetic discovery. Various markers of genetic variation (frameshift, SNP, STR, methylation, CNV) will be used to combine evidence from linkage and association. The genetic and molecular elucidation of CVMs will require complementary statistical approaches to realize discovery.

correct underlying disease inheritance model (e.g., autosomal dominant, X-linked) is specified. Specifying the appropriate model can be challenging as small pedigrees, incomplete penetrance, and complex inheritance may result in the incorrect inference. Non-parametric linkage analyses do not require a genetic model to be specified but are less powerful than a correctly specified parametric model. If the underlying model is complex or unknown, nonparametric methodology is appropriate. Linkage identifies genomic regions (i.e., loci, not genes), which often encompass hundreds of genes. Hence linkage analysis is traditionally coupled with fine mapping to identify individual variants at a particular locus.

Linkage analysis identifies genetic cause of CVMs

In this section, we provide three examples of the successful use of linkage analysis to identify genomic regions harboring rare variants with large effect. In each example, statistical analysis of the linkage data was based on the assumption of simple inheritance. However, mutations identified in all three examples exhibit reduced penetrance and variable expressivity, features typically associated with complex inheritance.

First, use of linkage analysis led to the identification of mutations in TBX5 as the cause of Holt–Oram syndrome (MIM #142900). Holt–Oram syndrome is one of the "heart–hand" syndromes, so called because of the association of skeletal abnormalities in the hand and fore limbs with varied CVMs, typically atrial septal defects. Holt–Oram syndrome is inherited as an autosomal dominant trait; to date, numerous genetic variants in *TBX5*, resulting in loss of function of this T-box transcription factor, have been identified in patients with Holt–Oram syndrome (reviewed in [30]).

Linkage analysis also led to the identification of *PTPN11* as a gene causing Noonan syndrome (MIM #163950), a constellation of findings characterized by cardiac and noncardiac abnormalities. The most common cardiac defects are pulmonary stenosis with a dysplastic valve, secundum atrial septal and atrioventricular septal defects, and/or hypertrophic cardiomyopathy. Noncardiac defects include hypertelorism and short stature. Noonan syndrome is primarily inherited as an autosomal dominant condition; however, inheritance may be heterogeneous. Mutations in *PTPN11* account for approximately 50% of Noonan syndrome patients. Studies of the related Noonan, Costello, and cardio-facio-cutaneous (CFC) syndromes led to a new concept that these clinically related disorders are caused by dysregulation of the RAS/mitogens-activated protein kinase (MAPK) pathway [31].

Linkage analysis was also successful in patients with nonsyndromic CVMs and led to the identification of mutations in the homeobox transcription factor, *NKX2.5* (MIM #600584). Heterozygous *NKX2.5* mutations are fully penetrant but exhibit variable expressivity. Progressive atrioventricular block is common. A variety of CVMs have been observed, and *NKX2.5* mutations account for 2% of all nonsyndromic CVMs. Atrial septal defects are common (~80%), but ventricular septal defects including tetralogy of Fallot and double outlet right ventricles (~30%) are also observed (reviewed in [32]).

In each example, linkage was used to identify a region that contained promising candidate genes. Successful linkage required careful broad definitions of phenotype to determine affected status. For example, identifying Noonan syndrome, rather than a specific CVM, determined affected status, and for *NKX2.5* affected status was determined by finding any

CVM or being the parent and sibling of someone with any CVM. Candidate genes were selected based on biologic insight into their function; mutational analyses of the candidate genes identified rare genetic variants predicted to alter protein function, thus supporting causation. In retrospect, even though the associated traits exhibit characteristics of complex inheritance (variable expressivity, reduced penetrance), the assumption of simple inheritance worked adequately to determine linkage, possibly due to the large size of the genetic effect.

Association

Association studies measure the statistical dependence between two or more variables. For genetic studies, association tests the hypothesis that a genetic variant occurs more or less frequently in individuals with a particular phenotype than without, and can use population- or family-based samples. A challenge for genetic association is the selection of the type of genetic variant to test [26]. The human genome organization facilitates gene localization. Instead of each variant being independent, variants close together are more likely to be inherited together. This nonrandom segregation is known as linkage disequilibrium (LD). There are blocks of high LD conserved within populations [33]. The important implication of LD blocks is that researchers can test a subset of variants for association (known as a tagging approach) and capture nearly full information about untyped common variants [34] but not rare variants [35]. Hence, if a disease is caused by a rare variant, the power to detect association using a tagging SNP approach is low. Taken together, although genetic association studies are well positioned to find common variants for common (high prevalence) traits with small effect, they are not well suited for rare variants that cause rare (low prevalence) diseases [36]. As such, the suitability of association for gene discovery in CVMs is questionable.

Association does not equal causation. Significant associations can be due to one of several misleading factors, including LD, population stratification, or random chance. Although LD can reduce the number of variants tested, it makes identifying the causal variant difficult because the causal variant will be in LD with other variants in the region. Another possible cause of spurious association is population stratification, where cases and controls are not drawn from the same population [37] To account for population stratification, researchers can test whether cases and controls differ over a large number of variants not expected to be associated with disease. If differences exist, adjustments can be made to minimize this effect. Family-based association affords protection against stratification, which is a decided advantage of family-based designs [38]. Random associations may also occur by chance. In traditional statistical testing, biomedical researchers require a p-value of 0.05. For a genome-wide chip, significance thresholds of 10^{-8} are required to control for multiple comparisons [39]. Given this level of significance, the number of samples required to obtain adequate power in a genome-wide association study (GWAS) is in the thousands for a gene with modest effect. Once significance is achieved, replication is required to ensure the validity of the results [39].

To date, a GWAS has not been published for CVMs, perhaps in part because of their rarity. A GWAS has, however, identified genes for QT interval [40] and atrial fibrillation [41]. A common feature of these traits is moderate prevalence. These successes were characterized by variants accounting for a modest proportion of variation and therefore required very large sample sizes to identify these effects. Extrapolating from GWASs performed in other disciplines, rare traits will require large sample sizes, which means that consortia with many participating centers will be required to have sufficient power to identify associations [42]. Even then, the characteristics of previously identified variants and genes for CVM (locus heterogeneity, genetic heterogeneity, rare variants) suggest that GWAS findings will be limited.

Prioritizing statistical approaches

When deciding whether to use linkage or association as a first step, researchers should consider several factors (Table 2.3). First, they need to determine the characteristics of causal genes/variants. Specifically, is the CVM expected to be due to common or rare variants? Although association is a powerful

Table 2.3 Comparison of linkage analysis and association studies.

	Linkage	Association
Sampling	Family based	Families or unrelateds (case–control)
Population stratification adjustment	Matching ethnicity unimportant	Matching ethnicity crucial
Markers required for coverage	Few: 300–400 STRs or 5000 SNPs	Many: 10^5–10^6 SNPs
Localization of region	Good for initial detection	Poor for initial detection
	Poor for fine mapping	Good for fine-mapping
Identification of common variants	Low power	High power
Identification of rare variants	High power	Very low power

method to identify common variants, association studies have low power to detect rare variants. Further, if the researcher expects multiple causal variants within a gene, linkage will be more powerful as it is designed to identify regions and not specific variants. Second, researchers need to determine what types of sampling are available for the disease of interest. For example, when multiple affected family members are not available, linkage is not feasible.

Strategies for finding genes given complex inheritance

Combined linkage-association

Because linkage and association use different information and each method has distinct strengths for gene discovery, combined linkage–association is an excellent approach for discovering CVM genes. A major benefit of linkage analysis is that it can identify regions that harbor susceptibility variants. By performing association in select regions of interest, as opposed to scanning the whole genome, researchers can minimize false positives as fewer variants must be screened. Given the same false-positive rate, the traditional case–control design is more efficient than the family-based design for detecting association. However, the family-based combined linkage–association approach is more powerful because a lower false-positive threshold can be utilized for association analysis as fewer tests are being performed [43]. With combined linkage–association, families responsible for the linkage can be identified and association analyses can be restricted to those individuals most likely affected by that locus.

Gene–gene interactions

Gene–gene interactions have been a common theme for gene discovery of CVMs. For example, the cardiac phenotype of *Nkx2.5* knockout mice differed when placed in different strains, and suggested interaction with other loci to determine phenotype [44].Although a combined linkage–association approach is useful in identifying variants with significant main effects, it will not identify interactions between loci. As secondary loci modify genetic effects [45], interactions should be considered when searching for genes. Both linkage and association analyses can incorporate statistical interactions; however, researchers must recognize that the power to detect these interactions may be low, especially when at least one of the risk variants is of low frequency.

Novel genotyping technology – moving beyond SNPs

In recent years, it has become clear that genetic variation occurs on different scales. Indeed, Mendelian inheritance of CVMs has been attributed to structural variation, such as microdeletion and microduplication, copy number variation (CNV), and also traditional mutations (nonsynonymous, frameshift, and missense). In addition, the genome may be modified by patterns of methylation. Methylation can alter gene transcription without changes to the underlying DNA sequence bed and may explain inconsistent patterns of disease segregation (Figure 2.3). Unfortunately, usually gene discovery projects are limited to genetic variants of a specific type, for example, SNPs, CNV, methylation; analytical methods to evaluate multiple genotyping techniques have been used infrequently. Increasingly, it will be useful to combine evidence from linkage, GWAS associations, and candidate gene associations (Figure 2.3). In addition, approaches such as meta-analyses may be used across multiple domains to reinforce evidence for trait loci qualitatively [46]. Novel analytical methods of this type may be required to dissect the genetics of CVMs.

Causality

Once a statistically significant association has been demonstrated, the next logical question is what the nature of this association is with respect to etiology, that is, causal or probabilistic. Determination of causality is essential in interpreting results of genetic testing. For Mendelian traits, variants are considered causal if they are sufficient (when the variant is present disease occurs). Given the phenomenon of reduced penetrance, a more inclusive definition is that the variant is probabilistic (variant increases the probability of the disease occurring) [47]. Further, determining definitively whether the variant is associated with disease can be a challenge. To demonstrate causality, statistical association should be consistent, specific, and unbiased. Further, evidence of association should be coupled with basic biologic research, for example, *in vitro* biologic (functional) effect. Sometimes the functional effect can be anticipated based on the predicted effect of the genetic variant on protein structure, for example, a nonsense mutation predicted to truncate the protein prematurely. More subtle alterations, however, may require specific assays of protein function, such as enzyme assay or patch clamp study in a heterologous expression system. In addition, with complex inheritance, this biologic evidence may be hard to obtain, as this would require concurrent functional assessment of two or more gene products. In the absence of biologic evidence, data supporting causality include biologic plausibility, coherence with previous knowledge, and experimental evidence [47]. In the postgenomic era, there are many public sources that may provide insight into biologic plausibility, including SNP/gene expression databases, categorization of putative functionality of SNPs, and gene pathway analysis (Table 2.1) [48].

Conclusion

Cardiovascular disease in the young comprises varied phenotypes, including CVMs, cardiomyopathies, vasculopathies, and cardiac arrhythmias. CVMs are a common and clinically important form of pediatric heart disease. Despite advances in diagnosis and therapy, morbidity and mortality of CVM remain significant, and there is considerable interest in understanding the causes of these clinically important birth defects. Although some progress has been made in identifying the genetic origins of CVMs, in most anomalies the cause remains unknown. The frequent observation of genetic heterogeneity, reduced penetrance, and variable expressivity indicates that a single gene does not fully explain inheritance and the occurrence of sporadic anomalies suggests that inheritance is complex. Advances in methodology to determine individual human genetic variations provide an opportunity to revolutionize discovery in individuals with CVMs. Continued genetic discovery of CVM-causing genetic variants poses challenging study design questions and suggests that complementary approaches may be required to realize discovery. Strategies to identify genetic causes of CVMs will require precise phenotype assessment and an emphasis on statistical considerations (study design).

References

1 Pierpont ME, Basson CT, Benson DW Jr, *et al.* Genetic basis for congenital heart defects: current knowledge: a scientific statement from the American Heart Association Congenital Cardiac Defects Committee, Council on Cardiovascular Disease in the Young: endorsed by the American Academy of Pediatrics. *Circulation* 2007;**115**:3015–38.

2 Hoffman JI. Incidence of congenital heart disease: II. Prenatal incidence. *Pediatr Cardiol* 1995;**16**:155–65.

3 Williams RG, Pearson GD, Barst RJ, *et al.* Report of the National Heart, Lung, and Blood Institute Working Group on research in adult congenital heart disease. *J Am Coll Cardiol* 2006;**47**:701–7.

4 Boneva RS, Botto LD, Moore CA, *et al.* Mortality associated with congenital heart defects in the United States: trends and racial disparities, 1979–1997. *Circulation* 2001;**103**:2376–81.

5 Hoffman JI. Incidence of congenital heart disease: I. Postnatal incidence. *Pediatr Cardiol* 1995;**16**:103–13.

6 Ferencz C, Rubin J, Loffredo C, Magee D. Epidemiology of congenital heart disease: The Baltimore–Washington Infant Study 1981–1989. In: Anderson R, ed. *Perspectives in Pediatric Cardiology*. Mount Kisco, NY: Futura Publishing, 1993: 359–82.

7 McKeown T, Macmahon B, Parsons CG. The familial incidence of congenital malformation of the heart. *Br Heart J* 1953;**15**:273–7.

8 Botto LD, Correa A. Decreasing the burden of congenital heart anomalies: an epidemiologic evaluation of risk factors and survival. *Prog Pediatr Cardiol* 2003;**18**:111–21.

9 Nora JJ. Multifactorial inheritance hypothesis for the etiology of congenital heart diseases. The genetic-environmental interaction. *Circulation* 1968;**38**:604–17.

10 Calcagni G, Digilio MC, Sarkozy A, *et al.* Familial recurrence of congenital heart disease: an overview and review of the literature. *Eur J Pediatr* 2007;**166**:111–6.

11 Bruneau BG. The developmental genetics of congenital heart disease. *Nature* 2008;**451**:943–8.

12 Heymann MA, Rudolph AM. Effects of congenital heart disease on fetal and neonatal circulations. *Prog Cardiovasc Dis* 1972;**15**:115–43.

13 Abbott M. *Congenital Heart Disease*. New York: Nelson, 1932.

14 Hinton RB Jr, Martin LJ, Tabangin ME, *et al.* Hypoplastic left heart syndrome is heritable. *J Am Coll Cardiol* 2007;**50**:1590–5.

15 Cripe L, Andelfinger G, Martin LJ, *et al.* Bicuspid aortic valve is heritable. *J Am Coll Cardiol* 2004;**44**:138–43.

16 Hinton RB, Martin LJ, Rame-Gowda S, *et al.* Hypoplastic left heart syndrome links to chromosomes 10q and 6q and is genetically related to bicuspid aortic valve. *J Am Coll Cardiol* 2009;**53**:1065–71.

17 Czeizel A, Meszaros M. Two family studies of children with ventricular septal defect. *Eur J Pediatr* 1981;**136**:81–5.

18 Boon AR, Roberts DF. A family study of coarctation of the aorta. *J Med Genet* 1976;**13**:420–33.

19 Lewin MB, McBride KL, Pignatelli R, *et al.* Echocardiographic evaluation of asymptomatic parental and sibling cardiovascular anomalies associated with congenital left ventricular outflow tract lesions. *Pediatrics* 2004;**114**:691–6.

20 Sanchez-Cascos A. The recurrence risk in congenital heart disease. *Eur J Cardiol* 1978;**7**:197–210.

21 Liu CY, Tong XH, Du YH. A study on the genetic epidemiology of congenital heart disease. *Zhonghua Liu Xing Bing Xue Za Zhi* 1997;**18**:224–6 (in Chinese).

22 McBride KL, Pignatelli R, Lewin M, *et al.* Inheritance analysis of congenital left ventricular outflow tract obstruction malformations: segregation, multiplex relative risk, and heritability. *Am J Med Genet A* 2005;**134**:180–6.

23 Levine RA, Slaugenhaupt SA. Molecular genetics of mitral valve prolapse. *Curr Opin Cardiol* 2007;**22**:171–5.

24 Udwadia AD, Khambadkone S, Bharucha BA, *et al.* Familial congenital valvar pulmonary stenosis: autosomal dominant inheritance. *Pediatr Cardiol* 1996;**17**:407–9.

25 Stankiewicz P, Lupski JR Structural variation in the human genome and its role in disease. *Annu Rev Med* 2010;**61**:437–55.

26 Pushkarev D, Neff NF, Quake SR. Single-molecule sequencing of an individual human genome. *Nat Biotechnol* 2009;**27**:847–50.

27 Evans DM, Cardon LR. Guidelines for genotyping in genomewide linkage studies: single-nucleotide-polymorphism maps versus microsatellite maps. *Am J Hum Genet* 2004;**75**:687–92.

28 Saunders IW, Brohede J, Hannan GN. Estimating genotyping error rates from Mendelian errors in SNP array genotypes and their impact on inference. *Genomics* 2007;**90**:291–6.

29 Bray GA, Ryan DH. Clinical evaluation of the overweight patient. *Endocrine* 2000;**13**:167–86.

30 Clark KL, Yutzey KE, Benson DW. Transcription factors and congenital heart defects. *Annu Rev Physiol* 2006;**68**:97–121.

31 Tidyman WE, Rauen KA. The RASopathies: developmental syndromes of Ras/MAPK pathway dysregulation. *Curr Opin Genet Dev* 2009;**19**:230–6.

32 Benson DW. Genetic origins of pediatric heart disease. Pediatr Cardiol 2010;**31**:422–9.

33 Morton NE. Into the post-HapMap era. *Adv Genet* 2008;**60**: 727–42.

34 Neale BM, Sham PC. The future of association studies: gene-based analysis and replication. *Am J Hum Genet* 2004;**75**:353–62.

35 Saccone SF, Bierut LJ, Chesler EJ, *et al.* Supplementing high-density SNP microarrays for additional coverage of disease-related genes: addiction as a paradigm. *PLoS One* 2009;**4**:e5225.

36 Wray NR, Goddard ME, Visscher PM. Prediction of individual genetic risk of complex disease. *Curr Opin Genet Dev* 2008;**18**: 257–63.

37 Salmela E, Lappalainen T, Fransson I, *et al.* Genome-wide analysis of single nucleotide polymorphisms uncovers population structure in Northern Europe. *PLoS One* 2008;**3**:e3519.

38 Spielman RS, Ewens WJ. The TDT and other family-based tests for linkage disequilibrium and association. *Am J Hum Genet* 1996;**59**:983–9.

39 McCarthy MI, Abecasis GR, Cardon LR, *et al.* Genome-wide association studies for complex traits: consensus, uncertainty and challenges. *Nat Rev Genet* 2008;**9**:356–69.

40 Nolte IM, Wallace C, Newhouse SJ, *et al.* Common genetic variation near the phospholamban gene is associated with cardiac repolarisation: meta-analysis of three genome-wide association studies. *PLoS One* 2009;**4**:e6138.

41 Benjamin EJ, Rice KM, Arking DE, *et al.* Variants in ZFHX3 are associated with atrial fibrillation in individuals of European ancestry. *Nat Genet* 2009;**41**:879–81.

42 Harley JB, Alarcon-Riquelme ME, Criswell LA, *et al.* Genome-wide association scan in women with systemic lupus erythematosus identifies susceptibility variants in ITGAM, PXK, KIAA1542 and other loci. *Nat Genet* 2008;**40**:204–10.

43 Borecki IB, Province MA. Genetic and genomic discovery using family studies. *Circulation* 2008;**118**:1057–63.

44 Winston JB, Erlich JM, Green CA, *et al.* Heterogeneity of genetic modifiers ensures normal cardiac development. *Circulation* 2010;**121**:1313–21.

45 Nemer G, Fadlalah F, Usta J, *et al.* A novel mutation in the GATA4 gene in patients with tetralogy of Fallot. *Hum Mutat* 2006;**27**:293–4.

46 Schunkert H, Brockel U, Kromer EP, *et al.* A large pedigree with valvuloseptal defects. *Am J Cardiol* 1997;**80**:968–70.

47 Page GP, George V, Go RC, *et al.* "Are we there yet?": deciding when one has demonstrated specific genetic causation in complex diseases and quantitative traits. *Am J Hum Genet* 2003;**73**:711–9.

48 Tatusova T. Genomic databases and resources at the National Center for Biotechnology Information. *Methods Mol Biol* 2010;**609**:17–44.

49 Geva T, Powell AJ. Pediatric Heart Disease. In: Edelmann RR, Hesselink JR, Zlatkin MB, Crues JV, eds. *Clinical Magnetic Resonance Imaging*. Philadelphia, PA: Elsevier Science, 2006: 1041–69.

3

Developmental Physiology of the Circulation

Abraham M. Rudolph

University of California San Francisco, San Francisco, CA, USA

The adult circulation is characterized by series blood flow. Blood is oxygenated in the lungs, returns through the pulmonary veins to the left atrium and ventricle, and is ejected into the arterial system to be distributed to the tissues. At the tissue site, oxygen is extracted for metabolism, and carbon dioxide is taken up by blood, which then returns through the venous system to the right atrium and ventricle, which ejects it into the pulmonary arteries.

In the fetus, oxygen uptake and carbon dioxide elimination occur in the placenta. Oxygenated blood flows to the fetus through the umbilical veins, which connect with the hepatic portal venous system and distribute blood to the liver. The ductus venosus, a connection between the umbilical vein and the inferior vena cava, allows some umbilical venous blood to bypass the hepatic vasculature and enter the central circulation directly. This well-oxygenated blood mixes with poorly oxygenated blood from the gastrointestinal tract in the portal veins or with venous blood from the lower body in the inferior vena cava. Unlike the adult, in whom there is a complete separation of oxygenated blood returning to the left side of the heart from the lungs and poorly oxygenated blood returning to the right side of the heart, there is some admixture in the fetus, and the blood distributed to the tissues is a mixture of well-oxygenated and poorly oxygenated blood.

In the fetus, the lungs do not serve the function of gas exchange as in the adult. Blood flow to the lung is limited by passage of some blood ejected by the right ventricle through the ductus arteriosus, which connects the pulmonary trunk to the descending aorta. A third connection present in the fetus is the foramen ovale, which allows blood to enter the left atrium from the inferior vena cava and right atrium without having to be ejected by the right ventricle through the pulmonary circulation. The importance of these three fetal communications is discussed below.

Course of the fetal circulation

Patterns of flow have been studied in fetal lambs *in utero*, several days after recovery from surgery to insert catheters into limb vessels. Radionuclide-labeled microspheres with different isotopic labels were injected into fetal vessels, and the specific isotopes and also their quantity could be measured in various tissues [1]. From these data, it was possible to calculate not only the patterns but also the magnitude of blood flows in cardiac chambers and major vessels.

Maternal arterial blood entering the uterine circulation has a P_{O_2} of about 100 mmHg and an oxygen saturation close to 100%. Oxygen diffuses across the placental membrane into fetal arterial blood; in the sheep, blood entering the placenta from the umbilical artery has a P_{O_2} of ~20–23 mmHg and an oxygen saturation of ~45–50%. Umbilical venous blood has a P_{O_2} of ~32–36 mmHg and an oxygen saturation of ~80–90%. This high oxygen saturation at a relatively low P_{O_2} is due to the greater affinity of fetal hemoglobin for oxygen compared with that of adult hemoglobin; the P_{50} for fetal hemoglobin is ~25–28 mmHg, compared with 35–38 mmHg in the adult. Umbilical venous blood returns to the fetus through the umbilical vein, which enters the fetal abdomen and courses to the porta hepatis. It provides several branches to supply the left lobe of the liver, after which the ductus venosus arises and passes dorsally and cephalad to connect with the left side of the inferior vena cava just below the diaphragm. The umbilical vein then arches to the right side of the porta hepatis to connect with the portal vein. The portal veins to the right lobe of the liver arise beyond this junction (Figure 3.1a).

Umbilical blood flow averages ~200 ml min⁻¹ kg⁻¹ of fetal weight in the sheep; this represents ~40% of the combined ventricular output (see below). About 50% of the
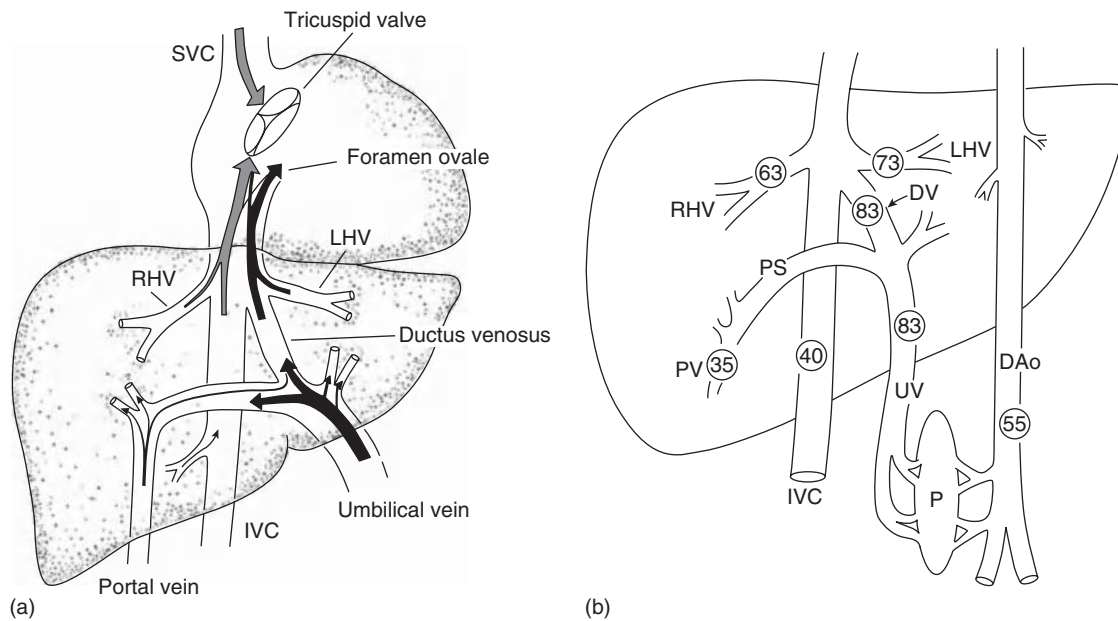
Figure 3.1 (a) Pattern of blood flow in major fetal veins. The umbilical vein provides branches to the left lobe of the liver; it then gives rise to the ductus venosus and arches to the right to join the portal vein. The ductus venosus blood is joined by left hepatic venous blood and is preferentially distributed through the foramen ovale. Portal venous blood is distributed mainly to the right liver lobe. Distal inferior vena cava blood is joined by right hepatic venous blood and passes preferentially through the tricuspid valve. Almost all superior vena cava blood is directed through the tricuspid valve. IVC, inferior vena cava; LHV, left hepatic vein; RHV, right hepatic vein; SVC, superior vena cava. (b) Blood oxygen saturations in vessels entering and leaving the liver in the fetal lamb. DAo, descending aorta; DV, ductus venosus; IVC, inferior vena cava; LHV, left hepatic vein; P, placenta; PS, portal sinus; PV, portal vein; RHV, right hepatic vein; UV, umbilical vein. (Reproduced with permission from Rudolph AM. *Congenital Diseases of the Heart*. Oxford: Wiley-Blackwell, 2009.)

umbilical venous blood is distributed to the left and right lobes of the liver, and the other half bypasses the liver through the ductus venosus [2]. Portal venous blood is almost completely distributed to the right lobe of the liver; only 5–10% passes through the ductus venosus, and none enters the left lobe of the liver. Thus, the left lobe of the liver receives almost exclusively well-oxygenated umbilical venous blood, whereas the right lobe receives umbilical venous blood and also most portal venous blood, which has a P_{O_2} of 12–14 mmHg and an oxygen saturation of 20–25%. Because of these flow patterns, left hepatic venous blood has an oxygen saturation of 70–75%, whereas right hepatic venous blood oxygen saturation is 55–65% (Figure 3.1b).

The inferior vena cava just below the diaphragm receives blood from four sources, all with different oxygen saturations, namely umbilical vein, distal inferior vena cava, and left and right hepatic veins. Distal inferior vena cava blood has a P_{O_2} of 12–15 mmHg with an oxygen saturation of 20–28%. The blood flowing from these four veins does not mix completely but shows differential streaming. The ductus venosus and left hepatic vein enter the inferior vena cava through a single orifice, which in the sheep fetus is partly covered by a thin valve-like membrane. The blood from these two veins is well oxygenated, and it streams in the posterior and left portion of the inferior vena cava in the direction of the foramen ovale to enter the left atrium

(Figure 3.1a and b). This valve-like membrane has not been identified in the human fetus. The preferential distribution of ductus venosus blood through the foramen ovale is probably related to the high velocity of blood in the ductus venosus. Color Doppler flow studied in both lamb and human fetuses indicate that the velocity of flow in the distal inferior vena cava is ~15 cm s^{-1}, whereas flow velocity in the ductus venosus is ~55 cm s^{-1}. The poorly oxygenated blood from the right hepatic vein joins blood returning from the distal inferior vena cava, and these flows stream along the anterior and right portions of the inferior vena cava towards the tricuspid valve to enter the right ventricle. Although these are the preferential patterns of flow, some of the blood derived from the ductus venosus does enter the tricuspid valve, and some blood from the distal inferior vena cava crosses the foramen ovale into the left atrium.

Blood returning to the heart through the superior vena cava has a P_{O_2} of 12–15 mmHg and an oxygen saturation of 20–30%. It is deflected by the tubercle of Lower in the right atrium in the direction of the tricuspid valve, and ~95% enters the right ventricle, whereas only ≤5% of superior vena caval blood passes across the foramen ovale into the left atrium.

The preferential streaming of the venous blood returning to the heart results in blood of higher oxygen saturation in the left atrium than in the right ventricle and pulmonary artery. The blood entering the left atrium through the
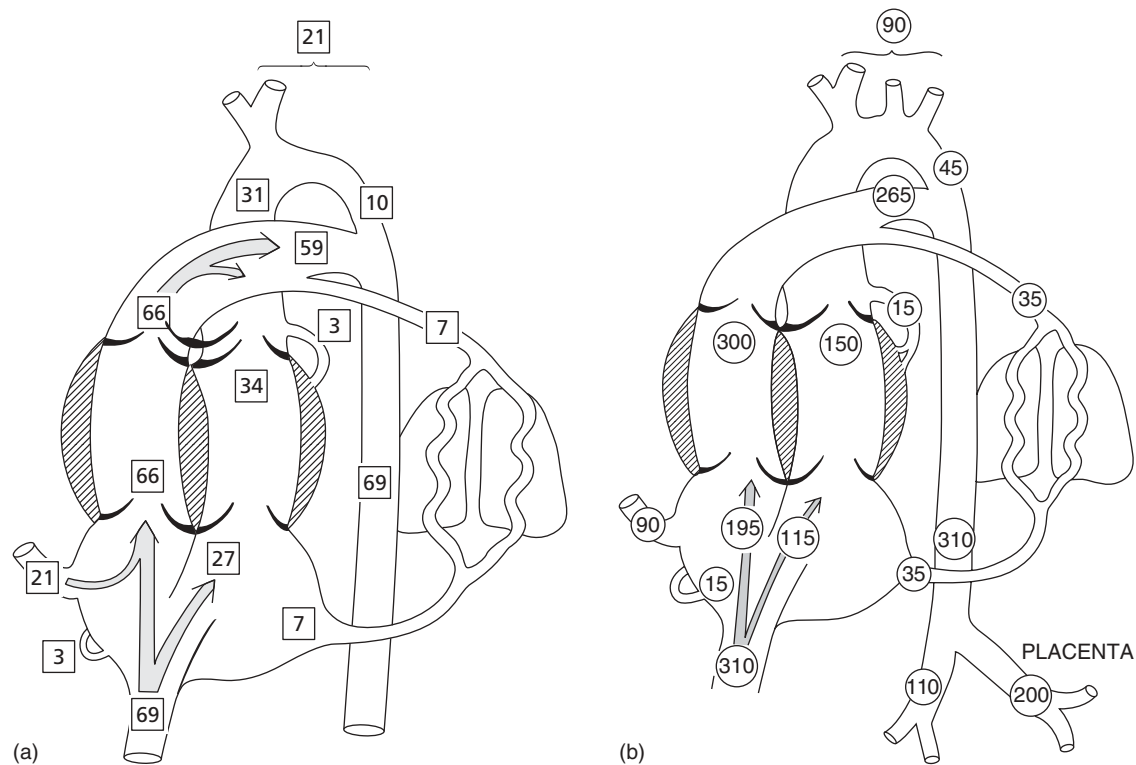
Figure 3.2 (a) Percentages of the combined ventricular output flowing through the major veins and arteries, and the proportions of blood ejected by each ventricle, are shown for the fetal lamb. (b) Volumes of blood (ml min^{-1} per kg fetal body weight) flowing through the great vessels and cardiac chambers are shown for the fetal lamb heart. (Reproduced with permission from Rudolph AM. *Congenital Diseases of the Heart*. Oxford: Wiley-Blackwell, 2009.)

foramen ovale is joined by pulmonary venous blood. In the fetus, because there is no gas exchange in the lung, the oxygen saturation of pulmonary venous blood (~50%) is slightly lower than that in the pulmonary artery. However, because pulmonary blood flow is low in the fetus and is considerably less than the volume of blood traversing the foramen ovale, the oxygen saturation of mixed blood in the left atrium and left ventricle is only moderately lower than that of ductus venosus blood (left ventricular oxygen saturation of 65–70% versus ductus venosus blood oxygen saturation of 80–90%).

Distribution of cardiac output

In the adult with a series circulation, the cardiac output is defined as the volume of blood ejected by each ventricle. These volumes are essentially similar, although small differences in left and right ventricular output may occur during short periods. The term *cardiac output* represents the volume of blood flow per unit time, through the series circulation.

In the fetus, the blood from umbilical and systemic veins mixes to some extent and enters both the left and right sides of the heart. Blood ejected by each ventricle consists of a mixture of poorly oxygenated and well-oxygenated blood.

The concept of cardiac output used for the adult circulation cannot be applied to the fetus. It has become customary to use the term *combined ventricular output* for the total volume of blood ejected by the fetal heart [3]. Combined ventricular output has been measured most definitively in fetal lambs by use of radionuclide-labeled microspheres or electromagnetic flow transducers placed around the ascending aorta and pulmonary trunk [4]. Measurements in human fetuses have been more limited, but left and right ventricular output measurements have been reported with the use of ultrasound techniques and application of the Doppler principle [5,6].

Figure 3.2a shows the proportions of the combined ventricular output returning to the heart through various veins and the proportions of blood ejected by each ventricle into the central arteries in the fetal lamb. Figure 3.2b presents the volumes of blood flowing through the cardiac chambers and great vessels. Unlike in the adult, the volumes ejected by each ventricle are different. In the fetal lamb, the right ventricle ejects ~65% of combined ventricular output, almost twice as much as the 35% of combined output ejected by the left ventricle. Combined ventricular output is fairly constant in relation to fetal body weight in the last trimester of gestation in the sheep at 450–500 ml kg^{-1} fetal body weight per minute. Hence right ventricular output is ~300–325 ml kg^{-1} min^{-1} and left ventricular output is ~150–175 ml kg^{-1} min^{-1}.

Because pulmonary vascular resistance is high in the fetus, only ~12% of blood ejected into the pulmonary trunk is distributed to the lungs; this represents ~8% of combined ventricular output or ~40 ml kg^{-1} min^{-1}. The remaining 88% of blood ejected by the right ventricle passes through the ductus arteriosus to the descending aorta. Thus, ~57% of combined ventricular output or ~265–285 ml kg^{-1} min^{-1} traverses the ductus arteriosus.

About 70% of the blood ejected by the left ventricle into the ascending aorta is distributed to the coronary circulation, the brain, the tissues of the head and neck, and the forelimbs, whereas only ~30% crosses the aortic isthmus to the descending aorta to join the blood traversing the ductus arteriosus from the pulmonary trunk. Of the 35% of combined ventricular output ejected by the left ventricle, ~22% is distributed to the forelimbs, heart, head, and brain, and only ~10% of combined ventricular output traverses the aortic isthmus to the descending aorta. This represents only ~50 ml/kg body weight per minute. This low flow explains why the aortic isthmus is the narrowest part of the aorta in the term infant and why lesions that alter ascending aortic flow in utero affect the diameter of the aortic isthmus and transverse aortic arch. The left ventricle is filled by blood returning to the left atrium from the pulmonary veins (~8% of the combined ventricular output) and through the foramen ovale (~27% of combined ventricular output).

The descending aortic flow is ~67% of combined ventricular output, or 335 ml min^{-1} kg^{-1}. The umbilical-placental circulation receives ~40% of combined ventricular output, or ~200 ml min^{-1} kg^{-1}. The lower trunk, hind limbs, and abdominal organs receive ~27% of combined ventricular output, or 135 ml min^{-1} kg^{-1}.

Human fetus

The body configuration of the human fetus differs greatly from that of the lamb; the most striking difference is in brain size. Because brain blood supply is derived from branches of the ascending aorta, left ventricular output might be expected be higher in the human.

Measurements of blood flows in various vessels and of left and right ventricular output have been made in human fetuses by ultrasound and the Doppler technique. A wide range of outputs has been reported, but in most studies right ventricular output was only 1.2–1.4 times the left ventricular output, compared with a ratio of 2:1 in the sheep. The combined ventricular output in the human fetus has been reported to be 450–500 ml kg^{-1} min^{-1}, similar to that in the fetal lamb. The greater volume of blood ejected from the left ventricle could be derived either from a higher pulmonary blood flow or by a larger flow across the foramen ovale. Although wide variations in the magnitude of pulmonary blood flows have been reported, several studies have

recorded pulmonary blood flow of 85 –100 ml min^{-1} kg^{-1} of estimated fetal weight [7,8]. This is about twice the pulmonary blood flow in fetal lambs, and it could account for most of the higher left ventricular output in human compared with lamb fetuses.

The higher pulmonary blood flow and left ventricular output in the human fetus are also associated with considerable differences in the proportions of combined ventricular output and in actual blood flows through various vessels and to various organs of the fetus. These differences are summarized in Table 3.1. Of note is the considerably smaller flow from the pulmonary trunk to the descending aorta through the ductus arteriosus and the smaller umbilical blood flow relative to fetal size.

Determinants of cardiac output

Cardiac ventricular output is the product of heart rate and stroke volume. Stroke volume is determined by the force of contraction of the ventricle, which is influenced by preload, afterload, and myocardial contractility. In the intact heart, ventricular volume at end-diastole determines the degree to which the ventricular muscle is stretched and thus the length of the cardiac myocytes and the sarcomeres immediately prior to contraction. This represents preload. The greater the length of the sarcomere, up to an optimal level, immediately before contraction occurs, the greater is the force generated during contraction. An increase in end-diastolic volume enhances the force of ventricular contraction and, in the intact heart, increases the stroke volume in the absence of other changes. Afterload, or load on the heart muscle during development of active force, determines the degree of shortening of the sarcomeres and thus the volume ejected during systole. If the ventricular contractile force is the same, a greater volume will be ejected if afterload is low and stroke volume will be lower if afterload is high. In the intact circulation, afterload is influenced by several factors, such as arterial pressure, compliance of the arterial system, and peripheral vascular resistance. Contractility is the intrinsic force of contraction of the muscle; with isolated muscle, increased contractility increases the force developed and, in the intact heart, increases the stroke volume, or developed pressure (see Chapter 4). In the intact circulation, heart rate, preload, afterload, and contractility are interrelated, and a change in one factor may modify other parameters. Therefore, changes in all factors regulating ejection must be considered when assessing the effects of alteration of one regulatory factor.

Effects of heart rate

In the adult, cardiac output is relatively constant over a wide range of heart rates. The resting heart rate is 70–80 beats min^{-1} (bpm); increasing the heart rate to 150 bpm or

Table 3.1 Comparison of the distribution of blood flows in the sheep and human fetus as percent combined ventricular output (% CVO) and as actual blood flows (ml min^{-1} kg^{-1} fetal weight)[a].

	Sheep		Human	
	% CVO	ml min^{-1} kg^{-1} fetal weight	% CVO	ml min^{-1} kg^{-1} fetal weight
Combined ventricular output	100	450	100	450
Left ventricular output	34.0	150	45.0	202
Aortic isthmus	10.0	45	8.0	36
Brain	3.5	16	24.0	107
Upper trunk, forelimbs	20.5	90	13.0	59
Right ventricular output	66.0	300	55.0	248
Ductus arteriosus	58.0	260	30.0	135
Pulmonary circulation	8.0	36	25.0	113
Descending aorta	68.0	305	38.0	171
Umbilical–placental circulation	40.0	180	26.0	112
Hepatic circulation	18.0	80	14.0	68
Ductus venosus	22.0	100	11.0	44
Lower body organs, hindlimbs	28.0	125	12.0	60
Superior vena cava	24.0	108	37.0	165
Inferior vena cava + umbilical flow	68.0	305	38.0	172
Foramen ovale	25.0	115	20.0	90

[a]The values for sheep were obtained in chronically instrumented fetuses in the latter part of gestation. The values for human fetuses were obtained by ultrasound in the third trimester; in view of the considerable variations in reported measurements, those considered most appropriate have been selected. CVO-combined ventricular output
Reproduced with permission from Rudolph AM. *Congenital Diseases of the Heart.* Oxford: Wiley-Blackwell, 2009.

decreasing it to 50 bpm does not significantly affect cardiac output, because the stroke volume changes appropriately. Cardiac output falls progressively with further increases in heart rate, because the duration of diastole is decreased and there is inadequate filling of the ventricle. As the heart rate falls, the stroke volume is increased to maintain cardiac output, but when maximum diastolic filling has been achieved, further slowing results in a decrease in ventricular output.

In studies in fetal sheep, spontaneous increases in heart rate above the resting level were associated with increases of ventricular output of up to 15–20%, and spontaneous decreases in heart rate resulted in a fall in output. It is not possible to assess whether these changes were directly related to the heart rate changes or whether the factors inducing changes in heart rate could also have altered myocardial contractility or afterload [4]. Increases in heart rate were induced in fetal lambs by electrical pacing of the left or right atrium. Pacing the right atrium at rates of 240–300 bpm induced a small increase in left ventricular output of up to 15%, with no significant change in right ventricular output. At rates above 300–320 bpm, the output of both ventricles fell progressively with increasing rate, probably as a result of inadequate filling time in diastole. Pacing the left atrium resulted in a small increase in right ventricular output, but a

decrease in left ventricular output. This deleterious effect on left ventricular output was shown to result from alteration of left atrial pressure contour, which resulted in interference in filling of the left atrium through the foramen ovale.

Effects of preload and afterload

In the intact circulation, preload and afterload are closely related, because a change in one is likely to affect the other; thus, if the stroke volume of the ventricle during systole is decreased, the residual volume will increase and, if ventricular filling is maintained, preload will be greater with the next beat. The effects of preload on cardiac output have been studied in fetal lambs. In several reports, ventricular end-diastolic or atrial pressures have been used as an index of preload; this may not be a reliable indicator of volume, because ventricular compliance may change. Studies in both isolated myocardium and intact hearts have shown that fetal myocardium is less compliant than that of the adult [9]. In newborn lambs, rapid intravenous infusions of 0.9% NaCl solution elevated atrial pressures and this was associated with a progressive increase in cardiac output as the mean atrial pressures rose to ~15 mmHg [10].

In fetal lambs, atrial pressures were decreased by reducing the blood volume by bleeding, or increased by rapid

intravenous infusion of electrolyte solution [11]. A fall in right atrial pressure resulted in a marked decrease in cardiac output. Output rose when the atrial pressure increased by 2–4 mmHg above resting levels, but further increases in pressure did not result in a greater output by the ventricles. This response is distinctly different from that in postnatal lambs. Based on these studies, it was proposed that the fetal heart is normally operating near the top of its ventricular function curve; the elevation of cardiac output associated with an increase in preload is limited because myocardial performance, or contractility, is relatively poor in the fetus. However, a decrease in atrial pressure reduces preload, resulting in a fall in cardiac output.

In these studies, the effects of rapid infusion of electrolytes on arterial pressure were not taken into consideration. Associated with the infusion, fetal arterial pressure also increased and therefore the afterload on the ventricles changed. We examined the effects of changing preload when the arterial pressure was maintained constant at various levels [12]. An increase in arterial pressure dramatically reduced the left ventricular stroke volume at all levels of mean atrial pressure. At constant arterial pressure levels, progressive elevation of the left atrial pressure increased the left ventricular stroke volume even with atrial pressures of 10–12 mmHg. This study demonstrated that the fetal heart responds to increases in preload by increasing its output. It did not, however, resolve whether the performances of the fetal and adult myocardium are comparable.

Myocardial performance

Studies of isolated myocardium from fetal and adult sheep have demonstrated that fetal myocardium develops less active tension than adult myocardium at similar muscle lengths [9]. Also, the maximum force that can be generated is considerably lower for fetal than for adult myocardium.

Several differences in morphologic and biochemical features of myocardium have been described that could account for the lesser contractility of fetal myocardium. Fetal myocardium contains fewer sarcomeres, or contractile units, in each myocyte. Another factor that may be important is the development of the sarcoplasmic reticulum, which regulates the movement of calcium ions, essential for myocardial contraction. The fetal myocardial sarcoplasmic reticulum is well developed, but the T-tubular system, representing the extension of the sarcoplasmic reticulum to provide closer relations with the contractile elements, is either poorly developed or absent in the immature myocardium. Not only are there structural differences in the sarcoplasmic reticulum, but also in studies with isolated sarcoplasmic reticulum vesicles, calcium uptake was found to be impaired in fetal myocardium [13].

Local release of norepinephrine (noradrenaline) at sympathetic nerve endings is an important mechanism for increasing myocardial contractility. Sympathetic nerve endings are sparse or even absent in fetal myocardium. The abundance of sympathetic nerve endings varies greatly during development in different species. In the guinea pig, myocardial sympathetic innervation is almost fully developed at birth [14], whereas in the rabbit and the rat there is almost no innervation at birth, but it develops within 14–21 days after birth [15]. The sheep fetus has no detectable sympathetic innervation at 75 days (mid-gestation), but innervation begins to appear at 90–100 days, and is abundant but not yet fully developed just before birth [16]. In addition to the difference in sympathetic innervation, β-adrenergic receptor concentration is lower in fetal than in adult myocardium [17]. Although these differences in sympathetic innervation and β-adrenoreceptor concentration may not be important in the resting fetal heart, they could influence the ability to respond to stress.

Regulation of the circulation in the fetus

In the adult, the systemic and pulmonary circulations are separate. The preload and afterload of the right and left ventricles are different, and their stroke volumes could differ. The Frank–Starling mechanism adjusts the outputs of the two ventricles so that over a short period the ventricles eject similar volumes. A reduction in venous return to the right atrium decreases the filling pressure and end-diastolic volume of the right ventricle, resulting in a decrease in stroke volume. Pulmonary blood flow and venous return to the left atrium and ventricle are also reduced and the stroke volume decreases. An increase in systemic arterial pressure decreases left ventricular stroke volume; the end-diastolic volume increases so that, with the next beat, greater force is generated to increase the stroke volume. In the fetus, the large foramen ovale tends to equalize right and left atrial pressures throughout the cardiac cycle. The ductus arteriosus provides a large communication between the aorta and the pulmonary artery, resulting in almost identical pressures in the two vessels. In view of the similar atrial pressures and similar aortic and pulmonary arterial pressures, differences in stroke volumes of the left and right ventricles in the fetal lamb are the result of differences in afterload. The aortic isthmus, which is narrower than the ascending and descending aorta, to some extent functionally separates the upper and lower body circulations. The left ventricle ejects into the ascending aorta and the vessels of the head and neck, a circulation that in the lamb fetus is poorly compliant and has a relatively high vascular resistance. The right ventricle ejects into the pulmonary trunk and directly through the large ductus arteriosus into the descending aorta and its branches. This circulation has a higher compliance and a lower resistance because it includes the umbilical–placental circulation.

Reflex regulation

Chemoreflexes

Previous studies have suggested that aortic and carotid chemoreceptors are relatively inactive in the fetus, but they were performed in anesthetized exteriorized fetal lambs [18]. Aortic chemoreceptors are important in the bradycardic response of the fetus to hypoxia [19]. More recent studies in fetal lambs have shown that chemoreceptors are active, at least in the last third of gestation [20]. Responses to hypoxemia are much greater to carotid than aortic chemoreceptor stimulation [21]. The chemoreceptors are stimulated by hypoxemia, and experimentally can be activated by intravascular injection of small doses of sodium cyanide [22]. The cardiovascular response dominates, with bradycardia and immediate hypotension, but respiratory gasps are noted. The bradycardia can be abolished if the lambs are pretreated with atropine, indicating that the bradycardia is induced by vagus nerve stimulation. Confirmation of the fact that the cyanide response is the result of chemoreceptor stimulation was obtained by demonstrating the loss of the cardiovascular and respiratory responses in fetal lambs after sinoaortic denervation.

In the adult, chemoreceptor stimulation results in reflex peripheral vasoconstriction. It is likely that the peripheral vasoconstriction induced by fetal hypoxemia is largely mediated by chemoreceptor stimulation. From the studies in fetal lambs, it is apparent that their chemoreflex responses are different from those in the adult. The respiratory response in the adult animal dominates, whereas chemoreceptor stimulation in the fetus causes only a minor respiratory response. There is as yet no explanation for this difference in response.

Baroreflexes

In the adult, arterial pressure is maintained over a fairly narrow range through the control of baroreceptors. An increase in arterial pressure stimulates the aortic and carotid baroreceptors, resulting in bradycardia, depression of myocardial contractility, and peripheral vasodilatation. Ablation of aortic and carotid baroreceptors, by bilateral section of the aortic and carotid afferent nerves, results in an initial increase in resting heart rate and arterial pressure, but these soon return to normal levels. However, wide swings of arterial pressure and heart rate occur around the average pressure and rate, in response to stimuli that produce only small changes in the normal animal [23].

Arterial baroreceptors are functional in the fetus relatively early in gestation, but their importance in regulating fetal arterial pressure has been questioned. In fetal lambs, baroreflex sensitivity increases with gestational age from about 80 days' gestation; near term, the bradycardia induced by increased arterial pressure is equal to that observed postnatally. In fetal lambs, sinoaortic denervation results in the same wide variations in heart rate and blood pressure as observed in adult animals [24]. It is therefore apparent that baroreflexes are also important in stabilizing arterial blood pressure in the fetus.

Changes in circulation at birth

Conversion of the fetal to the adult circulation requires eliminating the umbilical–placental circulation, an increase of pulmonary blood flow to a level necessary for adequate gas exchange, and separation of the left and right sides of the heart by closure of fetal channels. The major events occurring at the time of birth include separation of the placental circulation and establishment of rhythmic ventilation. Ventilation comprises two components: physical expansion of the lungs with gas and elimination of fluid in the alveoli, and increase in alveolar oxygen concentration associated with breathing air.

Changes in patterns of blood flow

The changes in circulation at the time of birth normally occur almost simultaneously. It has been difficult to establish the role of individual events in inducing postnatal circulatory adjustments. To examine the contribution of ventilation and elimination of the placental circulation, we chronically instrumented fetal lambs *in utero* with a tracheal tube to ventilate the fetus, a balloon occluder around the umbilical cord, and various intravascular catheters to measure blood flows with radionuclide-labeled microspheres [25,26]. The lungs were ventilated with a gas mixture of 3% oxygen, 5% carbon dioxide, and 92% nitrogen. This did not change the fetal arterial blood P_{O_2} of ~21 mmHg and P_{CO_2} of ~40 mmHg. Rhythmic ventilation resulted in a marked reduction in pulmonary vascular resistance and an increase in pulmonary blood flow (Figure 3.3). Subsequent ventilation with air or oxygen markedly increased systemic arterial P_{O_2}, and the pulmonary blood flow increased further. Individual fetuses showed considerable differences in the increase in pulmonary blood flow resulting from lung expansion alone and ventilation with oxygenation.

During ventilation with 3% oxygen, the proportion of blood ejected by the right ventricle that entered the pulmonary circulation increased, whereas the volume traversing the ductus arteriosus from the pulmonary trunk to the descending aorta fell (Figure 3.4). Although pulmonary vascular resistance fell, there was no significant fall in pulmonary arterial pressure, probably because the ductus arteriosus remained widely patent. The blood flow through the foramen ovale into the left atrium also decreased. Left ventricular output increased and right ventricular output decreased.

Ventilation with 100% oxygen produced a further fall in pulmonary vascular resistance and, with the greater rise in pulmonary blood flow, flow from the pulmonary trunk through the ductus arteriosus was negligible and there
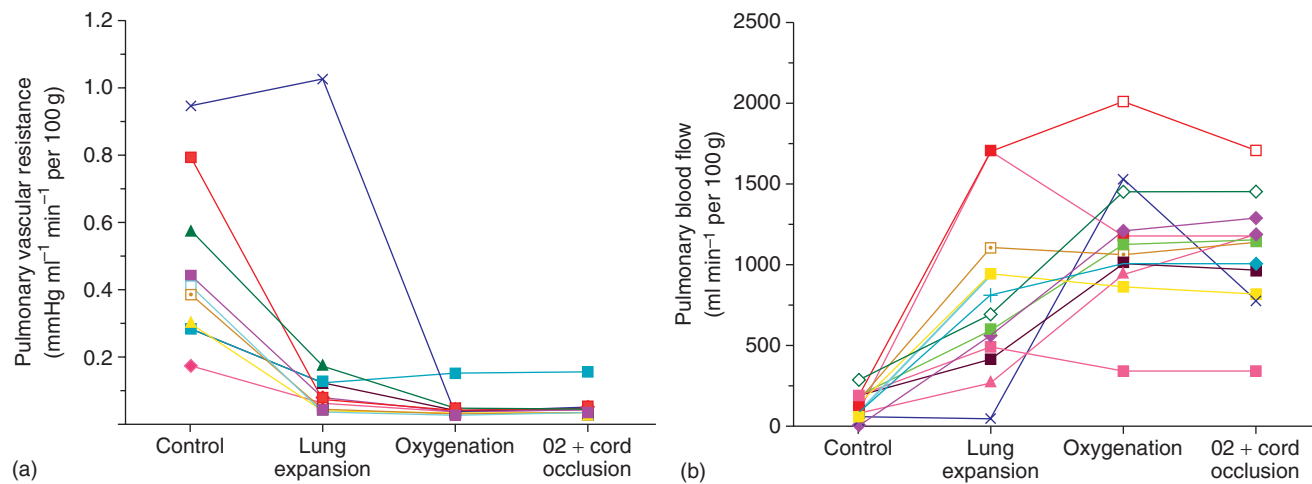
Figure 3.3 Changes in (a) pulmonary vascular resistance and (b) pulmonary blood flow are shown following physical expansion of the lung, ventilation with oxygen, and umbilical cord occlusion in fetal lambs *in utero*. (Reproduced from Rudolph AM. *Congenital Diseases of the Heart*. Oxford: Wiley-Blackwell, 2009. Original figure reproduced with permission from Teitel *et al.*, *Pediatr Res* 1987;**22**(5):557–66.)

was a small left-to-right shunt from the aorta to the pulmonary artery. Also, flow through the foramen ovale into the left atrium was abolished. The left ventricular output increased and was slightly higher than that of the right ventricle. This was the result of a small left-to-right shunt through the ductus arteriosus. In association with these changes, the left atrial mean pressure increased to levels 2–3 mmHg higher than that in the right atrium. The pulmonary arterial pressure fell slightly in the first few minutes after ventilation with oxygen and subsequently fell slowly. This was probably related to gradual constriction of the ductus arteriosus, leading to separation of the two sides of the heart.

Occlusion of the umbilical cord after ventilation with oxygen produced little further change. The systemic arterial pressure increased slightly and the left-to-right shunt through the ductus arteriosus increased slightly, but no further changes in pulmonary blood flow occurred.

Hence the changes in the circulation after birth can be accounted for largely by the onset of rhythmic ventilation with air. Even without eliminating the placental circulation, ventilation increases pulmonary flow and results in foramen ovale closure, and even though the ductus arteriosus does not close completely immediately after birth, flow from the pulmonary trunk to the aorta is almost completely eliminated.

Removal of the placental circulation abolishes umbilical venous return. Hepatic blood flow is reduced within the first few hours after birth but increases after the portal blood flow is increased in association with feeding. The elimination of umbilical venous blood flow reduces inferior vena caval return by 200 ml min^{-1} kg^{-1}. This facilitates closure of the foramen ovale and causes a small decrease in right atrial pressure.

Changes in pulmonary circulation

During fetal life, pulmonary blood flow is low owing to the high pulmonary vascular resistance. This high resistance is related to both morphologic and functional features of pulmonary vessels. Small pulmonary arteries have a thick medial layer composed predominantly of smooth muscle cells. These vessels are extremely reactive; they constrict markedly with hypoxia and dilate with an increase in P_{O_2}. Endothelial factors, such as endothelium-derived relaxing factor and nitric oxide, have an important role in regulating pulmonary vascular resistance.

The reduction in pulmonary vascular resistance after birth is associated with rhythmic ventilation and oxygenation. The mechanisms by which these events affect the pulmonary vessels have not been fully delineated. Studies in fetal lambs indicate that gaseous expansion of the lungs results in liberation of prostacyclin (prostaglandin I$_2$), a pulmonary vasodilator [27]. A rise in P_{O_2} is thought to increase endothelial release of nitric oxide, which is also a potent vasodilator. Other vasoactive agents, such as endothelin, bradykinin, and angiotensin, possibly also have a role in affecting pulmonary vascular responses after birth. Oxygen-sensitive potassium channels have recently been considered to play an important role in these changes [28]. Physiologic responses of the fetal pulmonary circulation and the mechanisms involved in the postnatal fall in pulmonary vascular resistance are discussed in Chapter 5.

After the immediate fall in pulmonary vascular resistance that follows birth, morphologic changes in the pulmonary vessels result in a permanent fall in pulmonary vascular resistance. The most striking change is a decrease in the thickness of the smooth muscle layer in the small arteries. This results in a gradual further decrease in pulmonary vascular resistance and pulmonary arterial pressure within
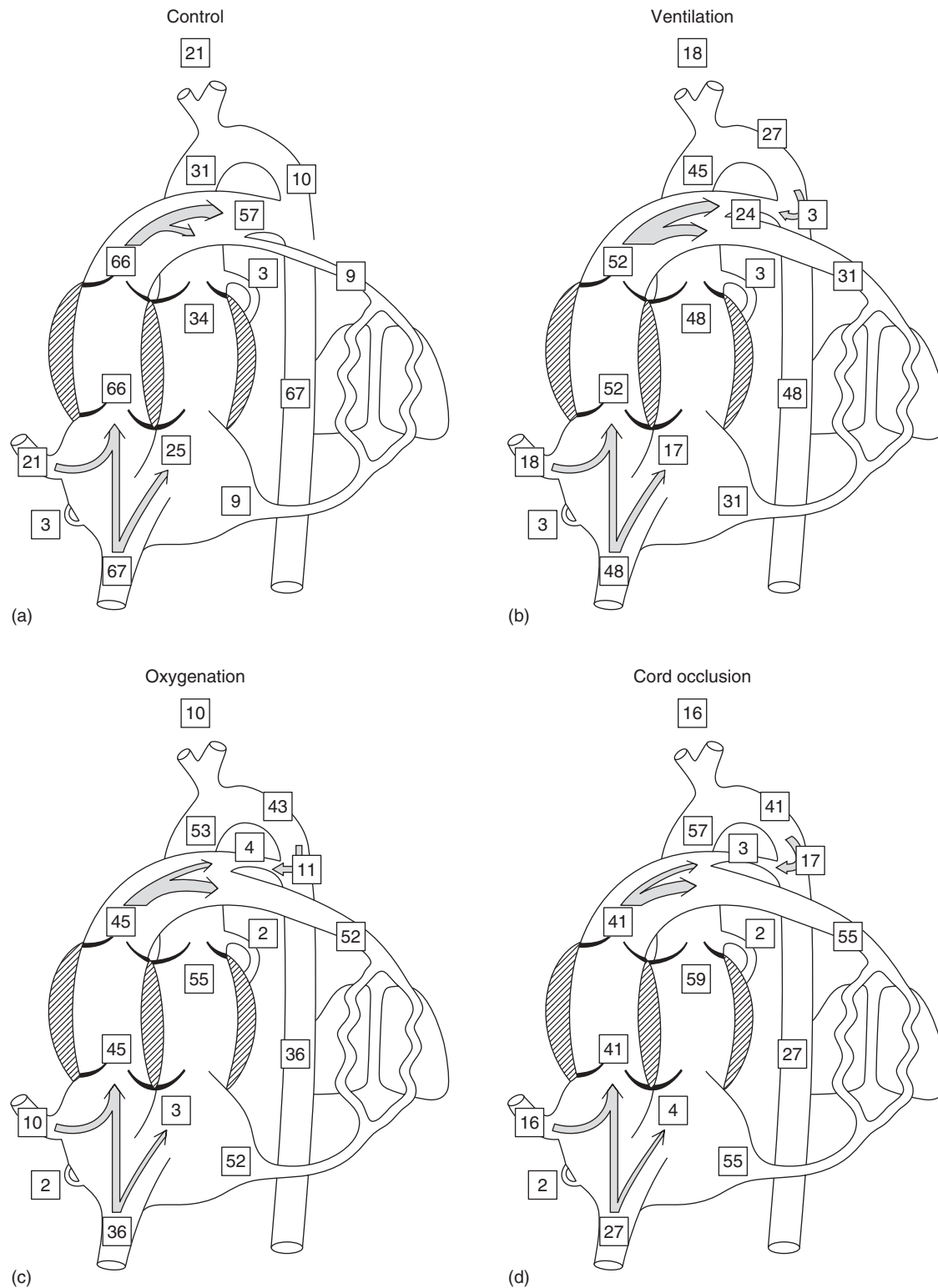
Figure 3.4 Effects of simulated birth events on the percentages of combined ventricular output flowing through great vessels and cardiac chambers are shown in late gestation fetal lambs. (a) Control fetal circulation; (b) ventilation (physical expansion of lung with no change of blood gases); (c) ventilation with oxygen; (d) occlusion of umbilical cord. (Reproduced with permission from Rudolph AM. *Congenital Diseases of the Heart*. Oxford: Wiley-Blackwell, 2009. Original figure reproduced with permission from Teitel *et al.*, *Pediatr Res* 1987;**22**(5):557–66.)

2–3 weeks after birth. The perinatal changes in morphology of the pulmonary vessels are discussed in Chapter 5.

Closure of the ductus arteriosus

The ductus arteriosus, normally widely patent in the fetus, constricts after birth. The current concept is that two factors are largely responsible for maintaining ductus patency *in utero* – the low oxygen tension of pulmonary arterial blood to which it is exposed, and the effect of circulating prostaglandin (prostaglandin E_2), which relaxes ductus arteriosus smooth muscle. Closure of the ductus after birth occurs at variable times in different species. In the lamb, it is usually closed within 1 h of birth, but in the human, complete closure may be delayed for 10–15 h. Constriction of the ductus arteriosus occurs with increase in arterial P_{O_2} associated with ventilation. After birth, there is a decrease in plasma prostaglandin E_2 concentrations. These two factors are thought to be the important mechanisms responsible for ductus constriction. Recently, oxygen-sensitive potassium channels have been demonstrated to play an important role in the contraction of ductus arteriosus smooth muscle in response to increased oxygen levels [29]. Subsequently, permanent closure of the ductus is achieved by fibrosis. The initial process is thought to be dissolution of normal smooth muscle cells by hypoxia of the muscle associated with constriction. Recently, however, the importance of platelets in effecting permanent closure of the ductus has been considered [30]. The ductus arteriosus is discussed in Chapter 24.

Congenital cardiovascular malformations and the fetal circulation

It has long been recognized that congenital cardiovascular malformations may influence the development of the fetal circulation. In recent years, ultrasound examination has provided the opportunity to assess the changes in circulatory development associated with advancing gestation. It has also become apparent that gestational changes in development and responses of the fetal circulation may affect the influence of various cardiovascular anomalies. The principal mechanisms by which congenital cardiovascular anomalies may affect fetal circulatory development are discussed in this section.
Cardiovascular malformations may

- change the volume or direction of blood flow
- obstruct blood flow
- alter the oxygen saturation of blood delivered to various organs
- cause hydrops fetalis by increasing venous pressure.

Changes in blood flow

Ventricular Development

Interference with blood flow into or out of the left or right ventricle may affect the development of chamber size. It had been suggested that restriction of the foramen ovale or mitral orifice reduces blood flow into the left ventricle and results in hypoplasia as a result of the decreased volume in the chamber [31]. Experimental reduction of inflow of blood into the left ventricle of the fetal lamb for at least several days interferes with growth of the chamber [32].

Postnatally, outflow obstruction of a ventricle reduces the stroke volume, resulting in an increased end-systolic volume, with ventricular enlargement. An increase in atrial and ventricular end-diastolic pressures enhances ventricular contractility; this helps to maintain stroke volume. If obstruction is maintained, hypertrophy ensues but ventricular volume is not significantly different from normal.

In the fetus, obstruction to the outflow of either the left or right ventricle also reduces stroke volume. However, there is no significant increase in either atrial pressure because of the large communication created by the large foramen ovale. Ventricular filling is thus not augmented and the volume ejected by the ventricle is reduced. Ventricular muscle mass increases in response to the increased pressure, but ventricular volume is reduced. The total combined ventricular output may be maintained at normal levels because the volume ejected by the unobstructed ventricle can be increased to compensate for the lower volume ejected by the obstructed chamber. Outflow obstruction of the left ventricle was induced in fetal lambs by placing a constriction around the ascending aorta; this resulted in increased left ventricular muscle mass but a substantial reduction in the size of the left ventricle within just a few days [32]. Ultrasound studies in human fetuses with aortic stenosis show that the left ventricular volume becomes progressively smaller during gestation and may result in hypoplasia of the left heart [33,34].

We produced pulmonary stenosis in fetal lambs at about 60 days' gestation by placing a band around the pulmonary trunk. The lambs were allowed to develop *in utero* and studied at about 120 days' gestation. Right ventricular muscle mass was greatly increased but, in the majority of fetuses, the size of the cavity of the ventricle, and also the diameter of the tricuspid valve, were markedly reduced. These studies confirm that reducing the volume of blood flowing into and out of a ventricle in the fetus resulted in hypoplasia of the chamber.

Ascending aorta and aortic arch development

In fetal lambs, the left ventricle ejects ~33% of combined ventricular output (CVO), and about two-thirds of blood entering the ascending aorta is distributed to the head and upper body. Thus only ~10% of CVO passes through the aortic isthmus. The relatively low blood flow through this segment is reflected by the fact that the isthmus diameter is only half that of the ascending aorta. In the human fetus, the left ventricle ejects ~45% of CVO. The volume passing through the aortic isthmus is not known, but it appears to be similar to that in the lamb and thus accounts for the fact that the isthmus diameter is ~75% of that of the ascending aorta.

The diameter of the ascending aorta is also affected by the volume of blood flowing though it. Thus in the fetus with aortic atresia, no blood enters the aorta from the left ventricle, but flow occurs retrograde from the ductus arteriosus across the arch to the ascending aorta. The flow into the ascending aorta is very low, only that passing to the coronary circulation, hence the marked hypoplasia.

In the fetus with pulmonary atresia, the right ventricle ejects no blood into the pulmonary artery. All blood returning to the right side is directed through the foramen ovale and joins pulmonary venous return to the left atrium. Thus the total CVO is ejected into the ascending aorta. In the lamb, this would represent a flow about three times normal and in the human fetus a flow about twice normal. This high flow is associated with an aortic diameter considerably greater than normal.

Ductus arteriosus size and orientation
In fetal lambs, the ductus arteriosus transports ~60% of CVO from the pulmonary trunk to the descending aorta in the fetal lamb. In the human fetus, ~30% of CVO is estimated to pass through the ductus from the pulmonary trunk to the descending aorta. Because the ductus conducts such a large volume, the diameter is large, being similar to or somewhat greater than the aortic diameter. Also, because all ductus flow is from the pulmonary artery to the descending aorta, the inferior angle between the ductus and the descending aorta is oblique.

When right ventricular output is completely or severely obstructed, as with pulmonary atresia, all blood flow in the pulmonary arteries is derived from the aorta through the ductus arteriosus. The direction of flow in the ductus induces an acute inferior angle between the aorta and the ductus. Also, because the magnitude of flow through the ductus is reduced, it may be smaller in diameter than normal.

With severe reduction of output by the left ventricle, as in fetuses with aortic atresia, the total combined ventricular output passes through the ductus arteriosus to supply the whole body. In this condition, the ascending aorta is considerably smaller than normal, whereas the ductus arteriosus diameter is increased.

Effect of obstruction
The effect of obstruction of left or right ventricular output on blood flow into and out of the ventricle and on the development of chamber size has been discussed above. Two other sites of obstruction that may affect fetal development are in the ductus arteriosus and in the aortic arch proximal to the ductus.

Ductus arteriosus obstruction and the pulmonary circulation
Pulmonary arterial and aortic pressures are similar in the fetus. Studies in fetal lambs have shown that constriction of the ductus arteriosus elevates pulmonary arterial pressure.

This may result from constriction by mechanical means; prolonged compression of the ductus arteriosus in fetal lambs induces an increase in the medial smooth muscle layer of small pulmonary arteries, resulting in increased pulmonary vascular resistance [35]. The increased smooth muscle development may interfere with the normal fall in pulmonary vascular resistance after birth and result in the clinical presentation of persistent pulmonary hypertension of the newborn.

Aortic arch obstruction and cerebral blood flow
In fetuses with aortic atresia, no blood is ejected from the left ventricle into the ascending aorta. Blood flow to the head is derived from blood traversing the ductus arteriosus and then passing retrogradely across the aortic arch to the carotid arteries. Aortic atresia is frequently associated with coarctation of the aorta adjacent to the ductus arteriosus. Infants with aortic atresia have been reported to show a high incidence of neurodevelopmental problems [36] and also cerebral lesions on imaging [37], and reduced cerebral blood flow during fetal life may be responsible [38].

Effects of changes in blood oxygen content
Oxygen saturation of blood in various fetal vessels may be modified by alterations in blood flow patterns resulting from congenital cardiovascular malformations.

Increased oxygen saturation of pulmonary arterial blood
In the normal fetus, well-oxygenated umbilical venous blood passing through the ductus venosus is preferentially directed through the foramen ovale to the left atrium and ventricle, which ejects it into the ascending aorta. However, in the fetus with aortopulmonary transposition, this well-oxygenated blood will be directed into the pulmonary artery, which arises from the left ventricle. The fetal pulmonary circulation is very reactive to changes in oxygen content of perfusing blood; thus, pulmonary vascular resistance may be lowered in fetuses with transposition. This could induce an increase in pulmonary blood flow with a greater than normal pulmonary venous return to the left atrium, resulting in a higher left atrial pressure and a reduction in the size of the foramen ovale. A restricted foramen ovale has been reported in some fetuses with transposition; they are very likely to show rapid clinical deterioration after birth, with severe cyanosis and cardiopulmonary distress [39].

A narrowed ductus arteriosus has also been reported in some fetuses with transposition. This could be related to the increase in pulmonary blood flow, so that only a small proportion of flow from the pulmonary trunk is directed through the ductus. Perhaps more important is that the ductus could be constricted by the high oxygen content of pulmonary arterial blood passing through the ductus to the descending aorta. Constriction of the ductus may result in

elevation of pulmonary arterial pressure that could induce the persistent pulmonary hypertension encountered in some neonates with transposition [40]. These concepts are presented in more detail in Rudolph AM [41].

Decreased oxygen saturation of ascending aortic blood

In the normal fetus, ascending aortic blood is derived from the left ventricle and has an oxygen saturation of ~65%. However, with aortopulmonary transposition, the aorta arises from the right ventricle and ascending aortic blood oxygen saturation will be considerably lower, probably ~45–50%. Whether this lower oxygen saturation will affect the cerebral circulation is open to speculation. Studies in fetal lambs indicated that cerebral vasodilation was able to compensate for arterial hypoxemia, thus increasing cerebral blood flow and maintaining cerebral oxygen consumption [42]. It is possible, however, that if the fetus is subjected to intrauterine stress, oxygen supply to the brain would be more readily compromised than in the normal fetus.

Hydrops fetalis and cardiac failure

The occurrence of fetal hydrops with cardiovascular malformations had been noted, but the frequency with which hydrops resulted from cardiovascular anomalies was emphasized following the introduction of ultrasound examination. The hemodynamic feature common to all instances of hydrops associated with circulatory disturbances is an increase in systemic venous pressure. The congenital cardiac lesions most likely to be associated with hydrops are those resulting in valvar insufficiency, such as Ebstein malformation and atrioventricular septal defect. Myocardial disease is also an important cause of hydrops. Factors favoring the development of edema in the fetus with elevated venous pressure are the greater permeability of the vascular system, the low plasma albumin concentration, with lower plasma colloid osmotic pressure and reduction of lymph flow from tissues. These features are discussed in Rudolph AM [38].

References

1 Rudolph AM, Heymann MA. The circulation of the fetus *in utero*. *Circ Res* 1967;**21**:163–84.

2 Edelstone DI, Rudolph AM, Heymann MA. Liver and ductus venosus blood flows in fetal lambs *in utero*. *Circ Res* 1978; **42**:426–33.

3 Rudolph AM, Heymann MA. Circulatory changes with growth in the fetal lamb. *Circ Res* 1970;**26**:289–99.

4 Rudolph AM, Heymann MA. Cardiac output in the fetal lamb: the effects of spontaneous and induced changes of heart rate on right and left ventricular output. *Am J Obstet Gynecol* 1976;**124**: 183–92.

5 Sutton MS, Groves A, MacNeill A, *et al*. Assessment of changes in blood flow through the lungs and foramen ovale in the normal human fetus with gestational age: a prospective Doppler echocardiographic study. *Br Heart J* 1994;**71**:232–7.

6 Mielke G, Benda N. Cardiac output and central distribution of blood flow in the human fetus. *Circulation* 2001;**103**:1662–8.

7 Rasanen J, Wood DC, Weiner S, *et al*. Role of the pulmonary circulation in the distribution of the human fetal cardiac output during the second half of pregnancy. *Circulation* 1996;**94**: 1068–73.

8 Rasanen J, Wood DC, Debbs RH, *et al*. Reactivity of the human fetal pulmonary circulation to maternal hyperoxygenation increases during the second half of pregnancy: a randomized study. *Circulation* 1998;**97**:257–62.

9 Friedman WF. The intrinsic physiologic properties of the developing heart. *Prog Cardiovasc Dis* 1972;**15**:87–111.

10 Klopfenstein HS, Rudolph AM. Postnatal changes in the circulation and responses to volume loading in sheep. *Circ Res* 1978;**42**:839–45.

11 Gilbert RD. Control of fetal cardiac output during changes in blood volume. *Am J Physiol (Heart Circ Physiol)* 1980;**238**: H80–6.

12 Hawkins J, Van Hare GF, Schmidt KG, Rudolph AM. Effects of increasing afterload on left ventricular output in fetal lambs. *Circ Res* 1989;**65**:127–34.

13 Mahony L, Jones LR. Developmental changes in cardiac sarcoplasmic reticulum in sheep. *J Biol Chem* 1986;**261**:15257–65.

14 Lipp JA, Rudolph AM. Sympathetic nerve development in the rat and guinea-pig heart. *Biol Neonate* 1972;**21**:67–82.

15 Friedman WF, Pool PE, Jacobowitz D, *et al*. Sympathetic innervation of the developing rabbit heart. Biochemical and histochemical comparisons of fetal, neonatal, and adult myocardium. *Circ Res* 1968;**23**:25–32.

16 Lebowitz EA, Novick JS Rudolph AM. Development of myocardial sympathetic innervation in the fetal lamb. *Pediatr Res* 1972;**6**:887–93.

17 Birk E, Tyndall MR, Erickson LC, *et al*. Effects of thyroid hormone on myocardial adrenergic beta-receptor responsiveness and function during late gestation. *Pediatr Res* 1992;**31**:468–73.

18 Jansen AH, Chernick V. Respiratory response to cyanide in fetal sheep after peripheral chemodenervation. *J Appl Physiol* 1974;**36**:1–5.

19 Dawes GS. *Foetal and Neonatal Physiology*. Chicago, IL: Year Book Medical Pynlishers, 1968.

20 Boekkooi PF, Baan J Jr, Teitel D, Rudolph AM. Chemoreceptor responsiveness in fetal sheep. *Am J Physiol (Heart Circ Physiol)* 1992;**263**:H162–7.

21 Bartelds B, van Bel F, Teitel DF, Rudolph AM. Carotid, not aortic, chemoreceptors mediate the fetal cardiovascular response to acute hypoxemia in lambs. *Pediatr Res* 1993;**34**: 51–5.

22 Itskovitz J, Rudolph AM. Cardiorespiratory response to cyanide of chemoreceptors in fetal lambs. *Am J Physiol (Heeart Circ Physiol)* 1987;**252**:H916–22.

23 Cowley AW Jr, Liard JF, Guyton AC. Role of the baroreflex in daily control of arterial blood pressure and other variables in dogs. *Circ Res* 1973;**32**:564–76.

24 Itskovitz J, LaGamma EF, Rudolph AM. Baroreflex control of the circulation in chronically instrumented fetal lambs. *Circ Res* 1983;**52**:589–96.

25 Teitel DF, Iwamoto HS, Rudolph AM. Effects of birth-related events on central blood flow patterns. *Pediatr Res* 1987;**22**: 557–66.

26 Teitel DF, Iwamoto HS, Rudolph AM. Changes in the pulmonary circulation during birth-related events. *Pediatr Res* 1990;**27**: 372–8.

27 Leffler CW, Hessler JR, Green RS. The onset of breathing at birth stimulates pulmonary prostacyclin synthesis. *Pediatr Res* 1984; **18**:938–42.

28 Mital S, Konduri GG. Vascular potassium channels mediate oxygen-induced pulmonary vasodilation in fetal lambs. *Biol Neonate* 2000;**77**:58–68.

29 Thebaud B, Michelakis ED, Wu XC, et al. Oxygen-sensitive Kv channel gene transfer confers oxygen responsiveness to preterm rabbit and remodeled human ductus arteriosus: implications for infants with patent ductus arteriosus. *Circulation* 2004;**110**: 1372–9.

30 Echtler K, Stark K, Lorenz M, *et al*. Platelets contribute to postnatal closure of the ductus arteriosus. *Nat Med* 2010;**16**:33–5.

31 Lev M, Arcilla R, Rimoldi HJA, *et al*. Premature narrowing or closure of the foramen ovale. *Am Heart J* 1963;**65**:638–47.

32 Fishman NH, Hof RB, Rudolph AM. Models of congenital heart disease in fetal lambs. *Circulation* 1978;**58**:354–64.

33 Hornberger LK, Sanders SP, Rein AJ, et al. Left heart obstructive lesions and left ventricular growth in the midtrimester fetus. A longitudinal study. *Circulation* 1995;**92**:1531–8.

34 Makikallio K, McElhinney DB, Levine JC, *et al*. Fetal aortic valve stenosis and the evolution of hypoplastic left heart syndrome: patient selection for fetal intervention. *Circulation* 2006;**113**: 1401–5.

35 Levin DL, Hyman AI, Heymann MA, Rudolph AM. Fetal hypertension and the development of increased pulmonary vascular smooth muscle: a possible mechanism for persistent pulmonary hypertension of the newborn infant. *J Pediatr* 1978;**92**:265–9.

36 Rogers BT, Msall ME, Buck GM, *et al*. Neurodevelopmental outcome of infants with hypoplastic left heart syndrome. *J Pediatr* 1995;**126**:486–98.

37 Hinton RB, Andelfinger G, Sekar P, et al. Prenatal head growth and white matter injury in hypoplastic left heart syndrome. *Pediatr Res* 2008;**64**:364–9.

38 Rudolph AM. *Congenital Diseases of the Heart*. Oxford: Wiley-Blackwell, 2009: 265.

39 Jouannic JM, Gavard L, Fermont L, *et al*. Sensitivity and specificity of prenatal features of physiological shunts to predict neonatal clinical status in transposition of the great arteries. *Circulation* 2004;**110**:1743–6.

40 Dick M II, Heidelberger K, Crowley D, *et al*. Quantitative morphometric analysis of the pulmonary arteries in two patients with D-transposition of the great arteries and persistence of the fetal circulation. *Pediatr Res* 1981;**15**:1397–401.

41 Rudolph AM. Aortopulmonary transposition in the fetus; speculation on pathophysiology and therapy. *Pediatr Res* 2007; **61**:375–80.

42 Van Bel F, Bartelds B, Teitel DF, *et al*. Effect of indomethacin on cerebral blood flow and oxygenation in the normal and ventilated fetal lamb. *Pediatr Res* 1995;**38**:243–50.

4

Basic Anatomy and Physiology of the Heart, and Coronary and Peripheral Circulations

Julien I. E. Hoffman

University of California San Francisco, San Francisco, CA, USA

This chapter summarizes the structure, actions, and interactions of components of the cardiovascular system.

Gross anatomy

Aspects of cardiac anatomy are presented in Chapters 20 through 48, but the architecture of ventricular muscle is summarized here. The left ventricle and septum of all mammalian hearts essentially have three layers (Figure 4.1) [1].

The outer subepicardial layer of the free wall and the right side of the septum (light blue) are spirals with an average angle of –60° to the equatorial axis, the middle layer (purple) is approximately in the plane of the equator (0°), and the inner subendocardial layer (red) forms a spiral with an average angle of +60° to the equator. The subendocardial spiral layer forms a right-handed helix and the subepicardial layer a left handed helix [2] (Figure 4.2).

The subendocardial helix of the free LV wall, sometimes called the descending loop, forms a vortex at the apex and continues into the subepicardial helix of the apex and septum, sometimes called the ascending loop (Figure 4.3) [3].

These spiral fibers are shown well in studies using diffusion tensor magnetic resonance imaging (Figure 4.4) [4]

These spirals develop the torsion that is essential for effective ventricular ejection and filling (see below). The 60° angulation is essential for optimal function, and when the ventricle dilates and becomes more globular, the angulation becomes 40–50° and function becomes abnormal. This is the basis of the RESTORE procedure after a myocardial infarction; the infarcted area is excised and the ventricle is changed from a globular to a more elongated form [5]. This remodeling procedure has been extended to hearts dilated from other causes. Details of the anatomy are still debated, but the main features are accepted.

Physiology and pathophysiology

Cardiovascular function is a complex interaction between the heart, an efferent arterial system, and an afferent venous system. The heart is a pump, designed to accept various amounts of venous blood (venous return) and eject a required amount of blood (cardiac output) at a desired pressure. This pump interacts with the arterial system that has compliance, resistance, and inertance. Once the blood passes through the capillaries, it is contained in a capacious venous system whose pressure, as exemplified by central venous or right atrial pressure, is one of the driving forces of the heart pump.

Cardiac function curves

The heart is a pump that responds to increased venous return by dilating and stretching its fibers (increased preload), and this by the Frank–Starling effect produces a greater output. The relationship between preload and output (Figure 4.5) is complicated by the fact that output is affected by the arterial systolic blood pressure, and also by the intrinsic contractility of the heart muscle. The input–output relation shown is therefore an overall description of cardiac function but does not distinguish between its various components.

Attempts made to separate intrinsic contractility, a function of calcium entry into the myofiber or the sensitivity of the myofibrillar apparatus to calcium, from the associated mechanical events are based on the isovolumic period of the cardiac cycle or on ejection indices. Most of them are unsatisfactory [6,7].
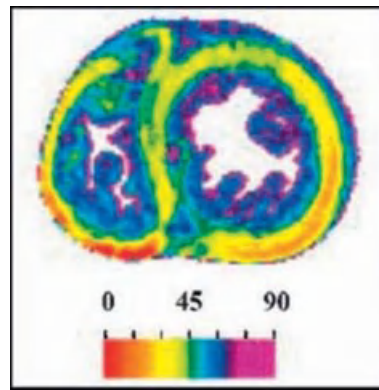
Figure 4.1 Cross-section of left ventricle (septum on left) to show three major layers of the wall defined by their fiber angles, as measured by diffusion tensor MRI. Arrow indicates papillary muscle. (Reproduced from Wu *et al.*, *Circulation* 2006;**114**:1036–45, with permission from the American Heart Association.)

Figure 4.2 Right- and left-handed spirals. The right-handed spiral is subendocardial and the left-handed spiral is subepicardial in the free wall and continues on to the right side of the septum. (Reproduced from Sengupta PP, Krishnamoorthy VK, Korinek J, *et al. J Am Soc Echocardiogr.* 2007; **20**:539–51, with permission from the American Society of Echocardiography.)

The isovolumic indices are typified by the V_{max} concept that examined the initial velocity of muscle contracting against zero load [8,9]. Unfortunately, even in isolated muscle strips it was not possible to assess the true index, that of the contractile element alone [10], and its application to the intact heart was even more tenuous. As an alternative, investigators used dP/dt_{max} (the maximal rate of change of ventricular pressure) or dP/dt at a developed ventricular pressure of 40 mmHg. These values, usually measured before the aortic valve opens, are relatively unaffected by changes in preload but are affected by changes in afterload.

Ejection indices, for example, ventricular function, examine the relationship of left ventricular diastolic pressure and stroke work such as the curve shown in Figure 4.5 except that the *y*-axis represents stroke work and not just cardiac output [11]. The curve becomes steeper with increased contractility and less steep if contractility decreases. Because stroke work is the product of flow and pressure, these curves
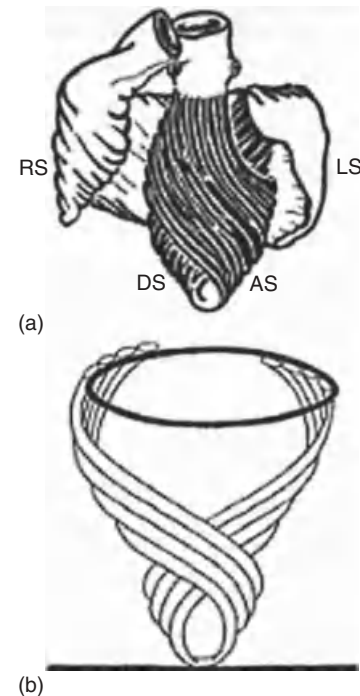
Figure 4.3 Diagrams of formation of the apical loop. (Reproduced from Ballester-Rodes *et al.*, *Eur J Cardiothorac Surg* 2006;**29**(Suppl 1):S139–44, with permission from the European Society of Cardiovascular Surgery.) (a) Exploded view of ventricle; (b) diagram of basal loop. RS, LS, DS, AS-right, left, descending and ascending segments.

did allow for aortic pressure, but because pressure work uses more energy than volume work, a given product might have different effects on cardiac function depending on the actual pressures and stroke volumes. In addition, end-diastolic pressure is not a good measure of end-diastolic fiber length because fibrosis or altered pericardial or pleural pressures changes their relationship.

A more satisfactory model is the time-varying elastance model of Sagawa [12,13] to explain how the ventricles adjust beat by beat to changes in preload and afterload; elastance = $\Delta P/\Delta V$, that is, the inverse of capacitance. The elastance approach requires simultaneous measurement of ventricular pressure and volume to produce a pressure–volume (PV) loop. Figure 4.6 shows changes in PV loops (a) when venous return increases at constant aortic pressure and (b) when aortic pressure changes at constant venous return.

In Figure 4.6a, each loop shows the phases of pre-ejection pressure increase, ejection with decreased volume, decreased pressure at a constant volume, and then filling. When venous return increases at constant aortic pressure, the ventricle dilates, and the ventricle ejects more blood (Frank–Starling law). The end-systolic pressure–volume point does not change, and the ejection fraction increases. In Figure 4.6b, if aortic pressure increases with constant venous return, the ventricle also dilates, and by virtue of the Frank–Starling law ejects the same amount of blood at a higher pressure. The
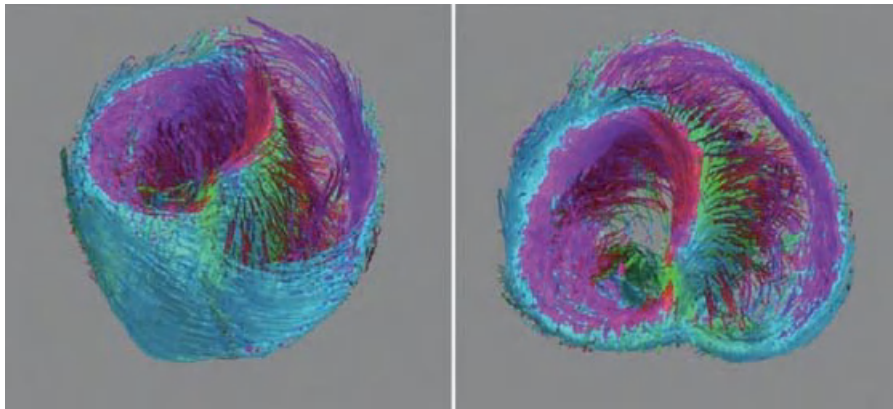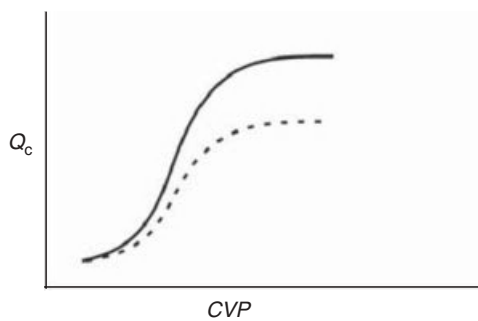
Figure 4.5 Function curve relating preload (*CVP*) to cardiac output (Q_c). The solid line is a control state, and the dashed line shows decreased function due to increased aortic pressure, decreased contractility, or reduced distensibility.

different end-systolic pressure–volume points lie on a straight line termed E_{max}. This line intersects the volume axis at V_0, the unstressed volume.

The slope E_{max} is an index of contractility, and it becomes less steep when contractility decreases (Figure 4.7a) and steeper when contractility increases (Figure 4.7b).

In Figure 4.7a, if contractility decreases from disease or decreased β-adrenergic stimulation, the loops are shifted to the right. The increased preload (end-diastolic fiber length) allows the ventricle to eject a normal stroke volume, but now the end-systolic pressure–volume points lie on a less steep E_{max} line. If preload did not increase, (absence of preload reserve [14,15]) then the ventricle would be unable to eject a normal stroke volume. Because of the elasticity of relaxed ventricular muscle, an increased preload produces a raised end-diastolic pressure that rises higher and higher as the ventricle dilates more; in addition, the ejection fraction decreases. In Figure 4.7a, because the E_{max} slope of the diseased heart is relatively flat, a slight reduction in afterload causes a relatively large decrease in end-diastolic pressure. If the stroke volume had been abnormally low because of absence of preload reserve, then reducing afterload would also have increased stroke volume. In Figure 4.7b, the

increased contractility allows the ventricle to eject a normal stroke volume in the face of increasing aortic pressures without such large increases in end-diastolic volume. The E_{max} slope is steeper.

These PV loops are not measured routinely because they are time consuming. They avoid many of the problems of sensitivity to changes in afterload and preload that makes other indexes of contractility unreliable. Glower and colleagues described a similar concept termed preload recruitable stroke work [16,17].

The maximal elastance line is often alinear and can give a negative intercept on the pressure axis [18,19]. To avoid these problems, some investigators use the values of E_{max} in the mid-range of pressures [19].

Ejection fraction and velocity of shortening also help to evaluate ventricular function, but changes in afterload must be accounted for. This can be done in adults and children [20–25] by providing normal data for the relationship between end-systolic wall stress and either velocity of shortening or ejection fraction (Figure 4.8). Because the relationship is not linear, single-point determinations are difficult to interpret [26].

Vascular hydraulics

Peripheral vascular function is characterized by flow acceleration and velocity (fastest in larger vessels), and also by vascular resistance and compliance. Vascular resistance (R) is defined as pressure drop across a vascular bed ($P_1 - P_2$) divided by flow (Q) through the bed. This relation can be further examined by the modified Poiseuille equation:

$$R = \frac{P_1 - P_2}{Q} = \left(\frac{8}{\pi}\right)\left(\frac{l}{kr^4}\right)\eta$$

where η is viscosity, l is the vessel length, r is the vessel radius, and k is the number of vessels. Because the first component $8/\pi$ is constant, and because in the second component length and vessel number are usually constant in any vascular bed at a given age and body size, the main factors
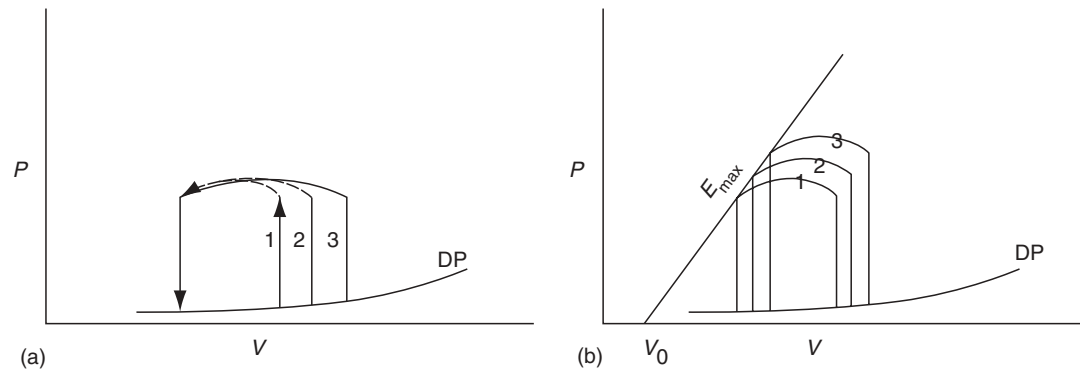
Figure 4.6 (a) PV loops at increasing venous return and (b) PV loops with increasing aortic pressure. DP, diastolic pressure; P, systolic pressure; V, volume; V_0, unstressed volume; E_{max}, slope of line connecting end-systolic pressure–volume points. Arrows show direction of pressure and volume changes.
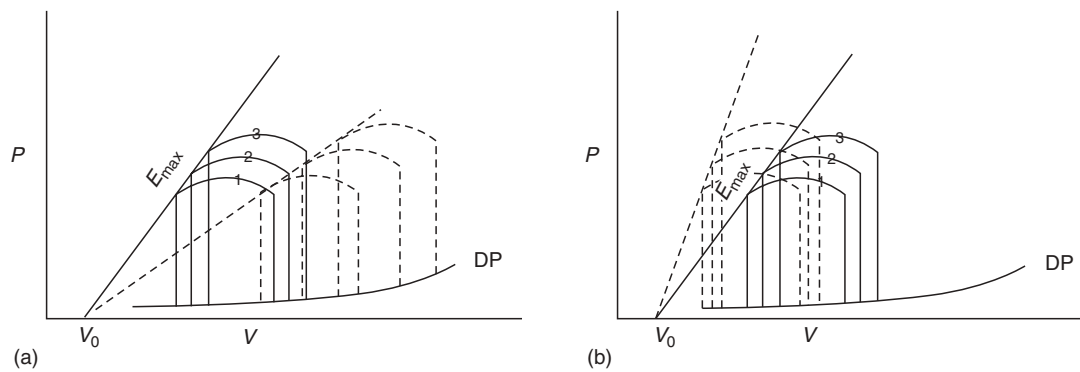
Figure 4.7 (a) Decreased contractility and (b) increased contractility. Control loops as solid lines, loops with altered contractility as dashed lines.
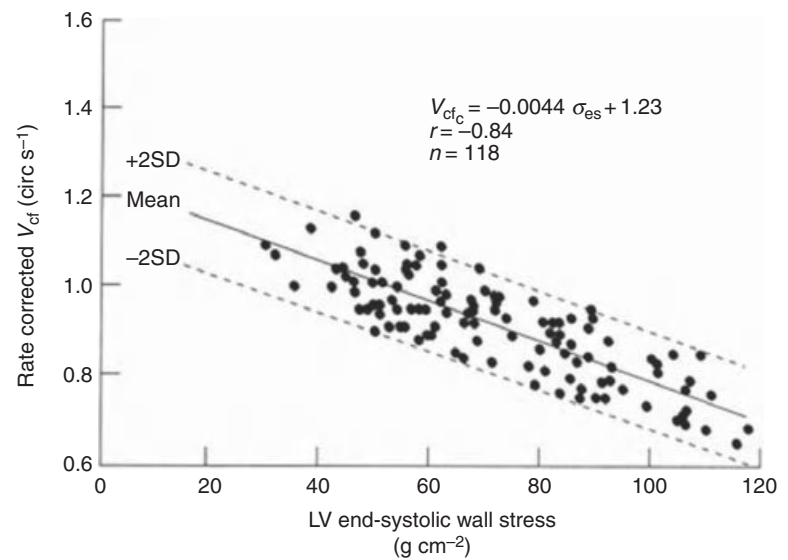
Figure 4.8 Velocity of circumferential shortening (V_{cf}) plotted against LV end-systolic wall stress. (Reproduced from Colan *et al*. *J Am Coll Cardiol* 1984;**4**:715–24, with permission from the American College of Cardiology.)

$$V_{cf_c} = -0.0044\ \sigma_{es} + 1.23$$
$$r = -0.84$$
$$n = 118$$

affecting resistance are viscosity (increased by polycythemia, decreased by anemia), and vessel radius. Because of the fourth power function, a small decrease in radius produces a disproportional increase in resistance.

Vascular compliance (C) is given by $C = \Delta V/\Delta P$, where ΔV is the change in volume and ΔP is the change in pressure.

Because an absolute volume change does not have the same meaning for a small than a large structure, specific compliance is calculated by dividing by the baseline volume. Therefore, specific compliance is $C = \Delta V/V\Delta P$. Because veins have thinner walls and are about 20-fold more distensible than arteries, most of the blood volume is in the venous system.
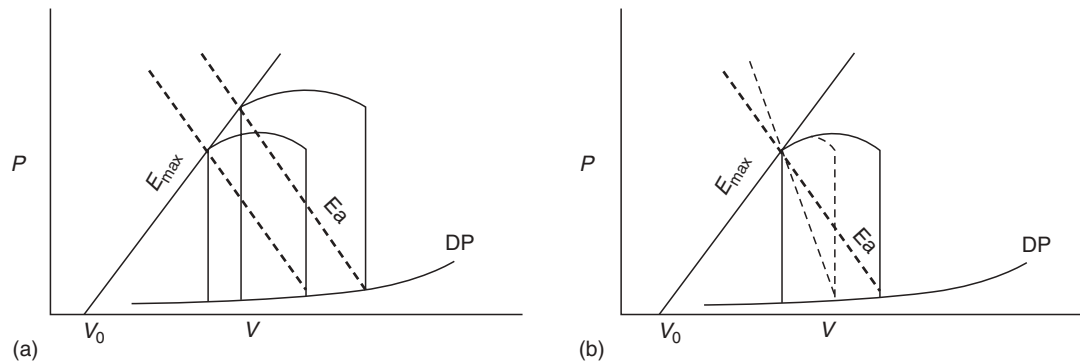
Figure 4.9 Effective arterial elastance (E_a) shown by diagonal dashed lines passing from end-diastolic to end-systolic points. The slope of this line is $\Delta P/\Delta V$, that is, the inverse of capacitance. (a) Change in PV loop at constant E_{max} does not change E_a. (b) Increased elastance – or decreased compliance – (thin dashed line) reduces stroke volume at a given pressure.
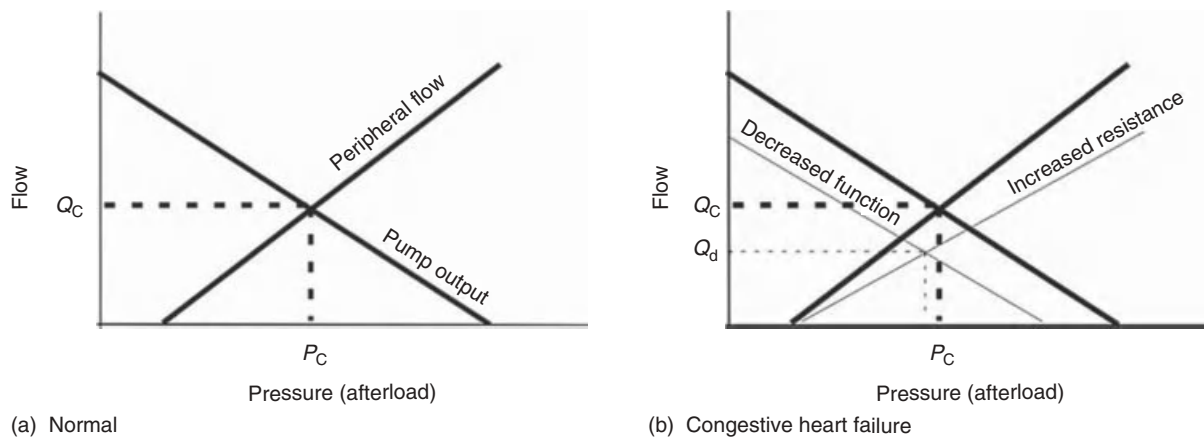
Figure 4.10 Cardiac and arterial response to aortic pressure loading. Q_c, control output; P_c, control arterial pressure; Q_d, disease output. The line showing peripheral flow is equivalent to the line showing effective arterial elastance as described above. Thick lines, control lines; thin lines, effect of disease.

Sunagawa *et al.* [27] showed that an effective arterial elastance ($\Delta P/\Delta V$) could be calculated from the pressure–volume loop as end-systolic pressure/stroke volume, as shown in the pressure–volume diagram in Figure 4.9. They showed that arterial peripheral resistance was more important than arterial compliance in changing effective elastance.

Cardiovascular coupling

The heart pumps blood into the arteries and receives blood from the veins, and all three components interact. If we disconnected (uncoupled) the heart from the rest of the circulation we could consider each component separately. Increasing the load against which the left ventricle pumps causes the output to decrease, and eventually the heart cannot eject. If we connect a mechanical pump to the aorta and change perfusing pressure, the higher the pressure, the greater is the flow through the system. For simplicity, both relationships are shown in Figure 4.10 as linear.

In the intact circulation, aortic pressure is an afterload for the ventricle and a pressure that pushes blood around the body; cardiac output and peripheral flow will be equal and

occur where the two pressure-flow lines intersect (Figure 4.10a). In disease, the heart can pump less blood at any given pressure, and peripheral resistance is usually elevated, so that the two function lines cross at a markedly reduced stroke volume, even though the arterial pressure may be fairly normal (Figure 4.10b). Therefore, treatment to reduce afterload or increase inotropy, or both, will raise the crossover point and increase stroke volume.

Now consider replacing the heart by a pump to move blood from the venous to the arterial systems (equivalent to the cardiac output); as the pump speed increases, blood is moved from the venous to the arterial side and venous pressure decreases. Eventually so much blood is transferred out of the veins that they collapse and no more blood can be moved. The pressure at which this occurs is termed the critical closing pressure. If the pump slows, more blood remains in the veins, and venous pressure increases. However, with the heart in place, an increased venous pressure causes an increase in cardiac output (Frank–Starling law). These two curves, the vascular and cardiac function curves, are shown in Figure 4.11.
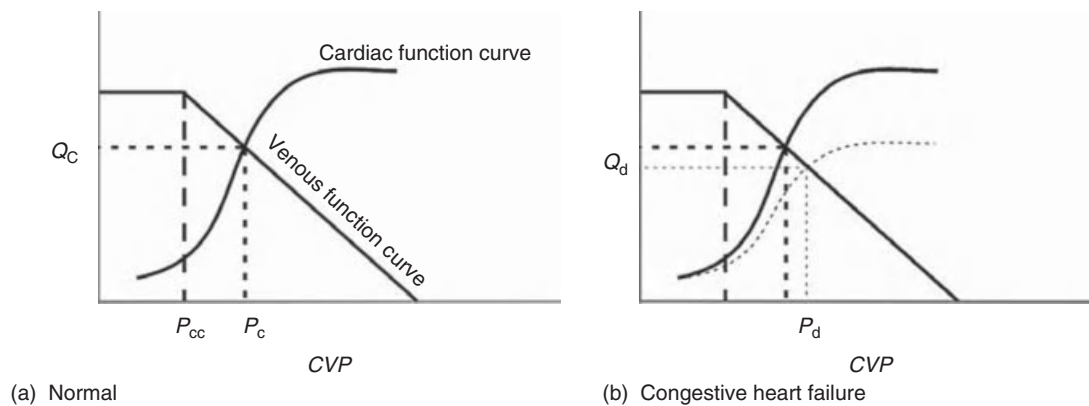
Figure 4.11 Cardiac function curve and vascular function curve relating central venous pressure (*CVP*) to cardiac output (*Q*). P_c, control venous pressure; Q_c, control, cardiac output; P_{cc}, critical closing pressure; P_d, venous pressure with congestive heart failure. (a) Normal (all thick lines) and (b) decreased cardiac function (light dashed lines).
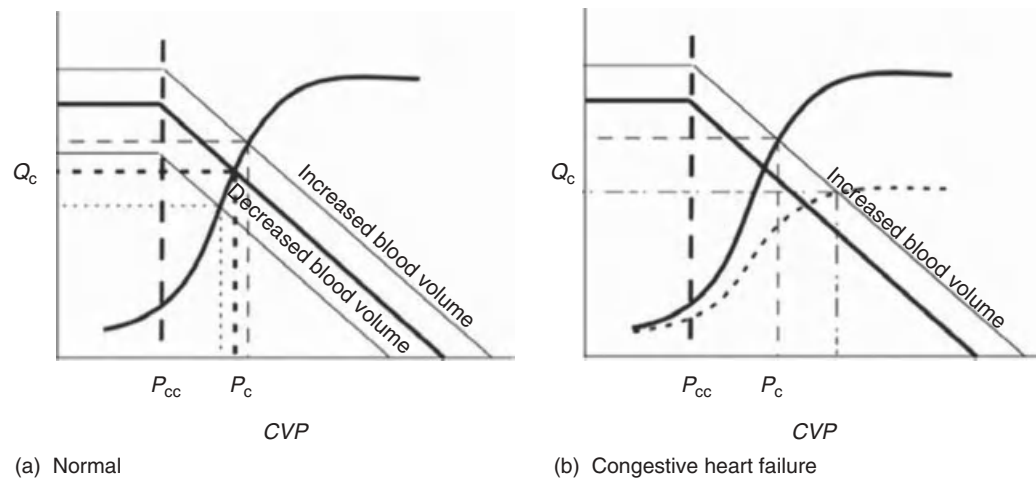
Figure 4.12 Effects of increased or decreased blood volume.

To study venous coupling in more detail, note that increases in atrial or cardiovascular pressure cause a large increase in output at first (preload effect), and then subsequently output rises less markedly because preload reserve is used up; sarcomeres have reached or passed their optimal lengths (Figure 4.11). For small increases in atrial pressure, the venous return does not change, because the atrial pressure is below critical closing pressure, but after atrial pressures of about 10–12 mmHg the venous return decreases more or less linearly as atrial pressures increase. The point at which these two curves cross is the operating point for the normal circulation; this is normally near the plateau of the venous return curve (Figure 4.11a). In the normal heart, decreasing venous return decreases cardiac output, as occurs in the brief hypotension when a person suddenly stands up. In other words, cardiac output is normally limited by venous return and not by cardiac performance. In congestive heart failure, however, the venous system is overfilled and at high pressure. The cross-over point occurs on the sloping portion of the venous

return curve because cardiac output is now determined by the depressed cardiac function and is low, and because venous pressure is high, cardiac function is not limited by venous return (Figure 4.11b).

These function curves may also be altered by changes in blood volume (Figure 4.12). In Figure 4.12a, an increased blood volume (upper thin line) moves the crossing point up and to the right, so that cardiac output and *CVP* increase even though contractility is constant (thin long dashed lines). A decreased blood volume (lower thin line) lowers cardiac output and *CVP* at constant contractility. Figure 4.12b shows what occurs commonly in congestive heart failure, namely blood volume is increased, as is *CVP*, but the cardiac output is reduced. Then reducing blood volume (by diuretics, for example) shifts the crossing point to a higher cardiac output and a lower *CVP* without any change in contractility.

Pericardial function

The parietal pericardium is a stiff membrane that surrounds the heart loosely, separated from it by a small amount of
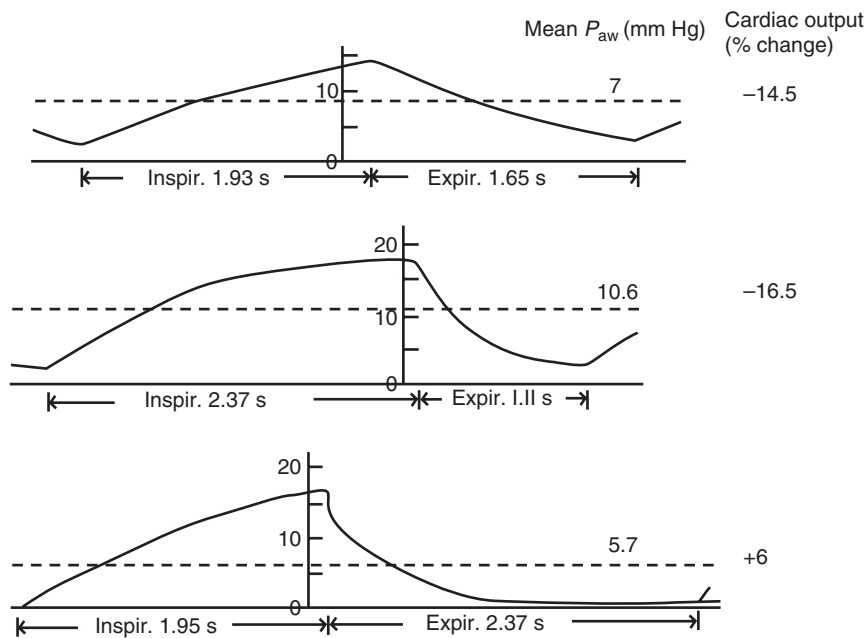
Figure 4.13 Effect of positive airway pressure on cardiac output in humans. Paw-mean airway pressure (mmHg). Percentage change compared with normal breathing. Three airway pressure curves are shown, differing in peak airway pressure and relative durations of inspiration and expiration. The effects on cardiac output are shown to the right of each curve. (Reproduced from Cournand *et al. Am J Physiol* 1947;**152**:162–74, with permission from the American Physiological Society.)

lubricating pericardial fluid. Normally, it does not affect ventricular filling and emptying. Intrapericardial fluid pressure is negative if measured by a catheter, reflecting the negative intrapleural pressure. On the other hand, the pericardium exerts a surface pressure on the heart; if the pericardium had holes in it, fluid would leak out and there would be no fluid pressure, but the heart could still be compressed, just like a fish caught in a net. This surface pressure is different in various regions, but in general is similar to right atrial pressure [28–30]. Therefore, transmural diastolic pressure across the wall of the left ventricle is not the same as left ventricular diastolic ventricular pressure, and can be estimated by subtracting right atrial from left ventricular pressure. The pericardium can tense and restrict left ventricular dilatation if there is a tense pericardial effusion (tamponade) [31] or if the ventricles enlarge because of a sudden volume load or sudden myocardial depression [32,33]. In some patients with acute myocardial ischemia, left ventricular diastolic pressure can be greatly increased without much change in ventricular volume because of tension in the pericardium. This mechanism makes it difficult to interpret changes in diastolic pressure–volume relations only in terms of myocardial stiffness [29,32,34–36].

Interaction between the ventricles

Ventricular interaction occurs in two ways. If right ventricular output decreases, filling of the left ventricle that is in series with the right ventricle is reduced so that left ventricular output decreases. Second, the left and right ventricles interact because they share the ventricular septum and are both contained by a relatively rigid pericardium. Consequently, right

ventricular distention, as in acute pulmonary embolism or congestive heart failure, pushes the septum to the left, thereby decreasing left ventricular volume and preload [37,38]. Sudden volume infusion may produce similar changes [39]. The resulting decrease in cardiac output should not be taken to indicate left ventricular dysfunction [28,38,40–42]. Volume unloading of the right ventricle under these circumstances will paradoxically increase left ventricular volume and function [43].

Cardiopulmonary interaction

The effects of pericardial restraint and ventricular interaction are important during positive pressure ventilation [44–46]. With a normal circulation, increased intrathoracic pressure with positive pressure inspiration (PPV or PEEP) reduces venous return to the right atrium, and by raising pulmonary vascular resistance may also increase right ventricular afterload [47]. Both of these actions decrease right ventricular output and therefore also reduce left ventricular output. PPV or PEEP therefore decreases transmural pressures, end-diastolic volumes, and stroke work of both ventricles. This was well shown in humans by Jellinek *et al.* [48], who noted that cardiac output was decreased by ~30% for a 10 mmHg increase in right atrial pressure secondary to positive pressure ventilation.

The reverse occurs when PPV or PPEP is lowered ("expiration"), and the net effect on the circulation depends on the ratio of inspiration to expiration [49] (Figure 4.13).

The degree to which increased airway pressure affects cardiac output depends greatly on lung compliance [48], because a stiffer lung allows less transmission of airway

(a)

(b)

(c)
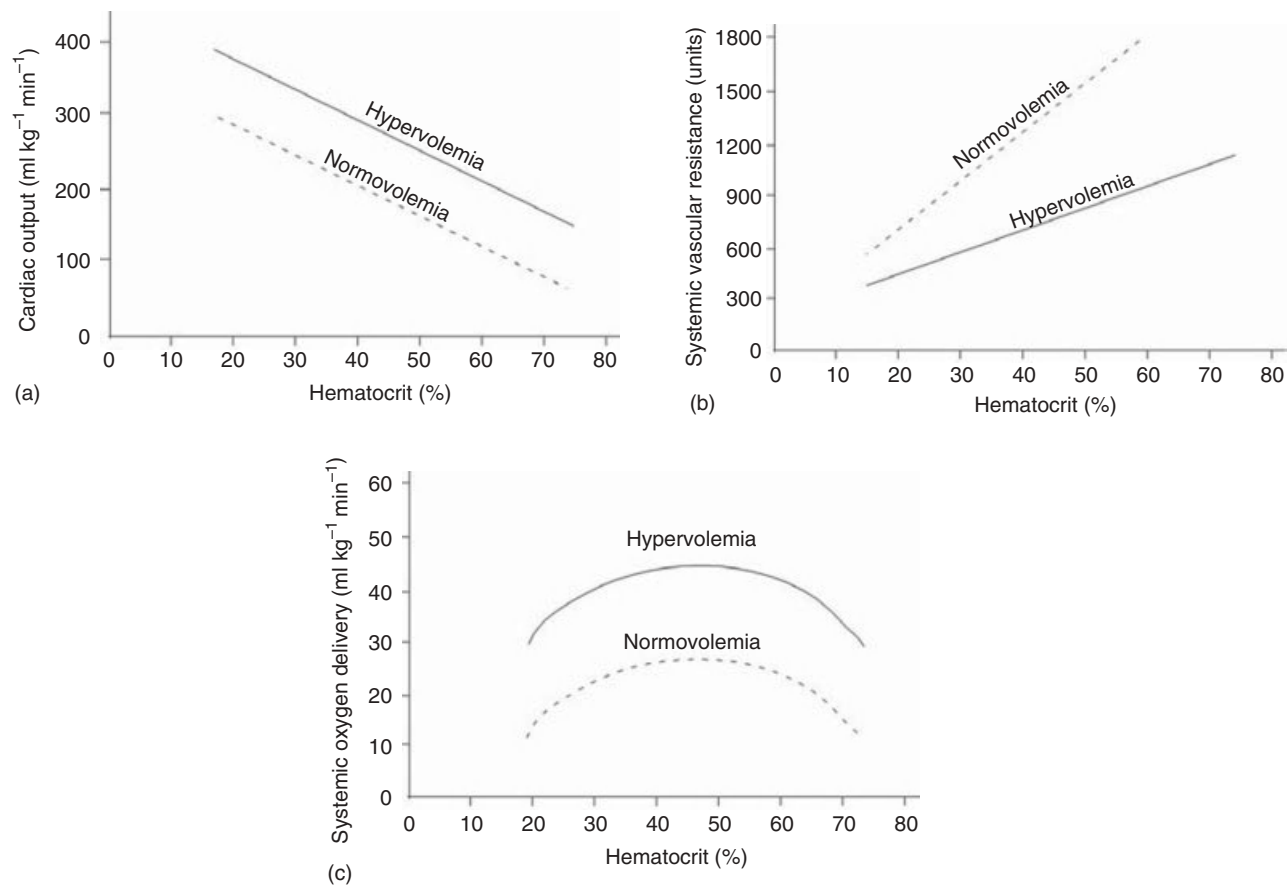
Figure 4.14 Relationships between hematocrit, cardiac output, blood volume, systemic vascular resistance, and systemic oxygen delivery. (a) As hematocrit increases, cardiac output decreases at any blood volume, but at a given hematocrit cardiac output is higher at higher blood volumes. (b) As hematocrit increases, so does systemic vascular resistance, but the resistance is lower with hypervolemia because the vessels are more dilated. Both of these panels show lines that are approximately linear, although linearity in the original data was less in (b) than in (a). (c) Systemic oxygen delivery as the product of two roughly linear relationships shows a second-order, that is, parabolic relationship to hematocrit at any blood volume. (Based on figures of Murray *et al. J Clin Invest* 1963;**42**:1150–9.)

pressure to the pericardiac region. Fuhrman [50] described the relationship of positive airway pressure to cardiovascular function as preload dependence and emphasized that the effects were exaggerated by hypovolemia.

In congestive heart failure, however, where pericardial restraint regulates total cardiac volume, increased intrathoracic pressure decreases right ventricular transmural pressure, filling, and volume, resulting in an increased left ventricular transmural pressure, end-diastolic volume, and stroke work via the Frank–Starling relationship.

Systemic oxygen delivery

Delivery of oxygen to tissues is measured by calculating systemic oxygen delivery (or transport), the product of arterial oxygen content and cardiac output. Systemic oxygen delivery is greatly influenced by hemoglobin concentration and blood volume. Patients who have heart disease frequently have anemia or polycythemia, and may have altered blood volumes. In an elegant series of experiments,

Murray and colleagues [51–55] examined factors that influence systemic oxygen delivery. Their results are summarized in Figure 4.14.

The peak of the inverted U is broad, but centered approximately at the normal hematocrit. (This centering occurs in species that have different normal hematocrits.) The curved relationship means that at low hematocrits cardiac output is increased, but not enough to compensate for the reduced amount of arterial oxygen per milliliter, and at high hematocrits the increased amount of arterial oxygen per milliliter does not compensate for the effect of increased blood viscosity in decreasing cardiac output.

To determine if systemic oxygen delivery is sufficient for tissue metabolism, we can measure mixed venous oxygen saturation to find out if oxygen extraction has increased beyond normal values, a technique often used in the intensive care unit, or can measure the lactate:pyruvate ratio that rises once systemic oxygen delivery decreases below a critical value [56]. Note that global measurements of mixed venous
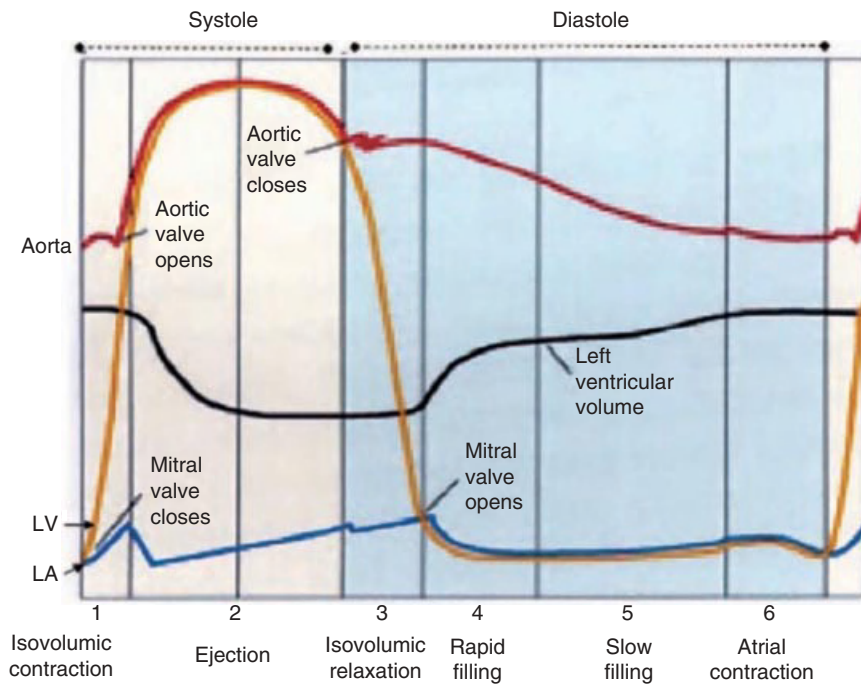
Figure 4.15 Traditional diagram of events during the cardiac cycle. (Reproduced with permission from Buckberg *et al.*, *Circulation*. 2008; **118**:2571–87.)

oxygen saturation and lactate:pyruvate ratio may be normal in the face of localized ischemia of one organ system.

Ventricular mechanics

The pressure–volume loops described above have the disadvantage that they lump all ventricular muscle into a single amorphous structure. In fact, the ventricle has a complex architecture, and this is beginning to be incorporated into physiologic understanding. The spiral muscle bands are involved in torsion of the ventricle that is essential for normal contraction. Details of ventricular contraction and relaxation are still being worked out (for reviews, see [2,57–59]), but basically the following sequence occurs (Figure 4.15).

At the onset of systole, during the isovolumic (pre-ejection period), the left ventricle narrows and lengthens, and then during ejection it continues to narrow and becomes shorter. When the aortic valve closes, in the isovolumic (pre-filling period), the ventricle lengthens, and then widens as blood fills it in later diastole. To this accepted description we now have to add information about torsion. If we look up at the heart from the patient's feet, we will notice that the left ventricle rotates around an axis passing from the apex to the middle of the aortic valve (Figure 4.16).

As shown in Figure 4.16, at the onset of the QRS complex the whole heart rotates slightly clockwise for a few milliseconds, then counter-clockwise for a few more milliseconds, after which the apex and base rotate in opposite directions; rotation in opposite directions is the definition of torsion. Note that there is more rotation of the free apex than the tethered base. During systolic torsion, the apex continues to rotate counter-clockwise but the base rotates clockwise,
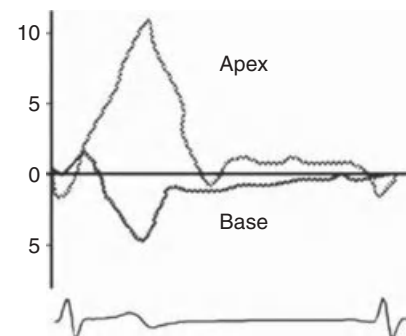
Figure 4.16 Torsion during the cardiac cycle. Clockwise rotation below the zero line, counter-clockwise rotation above it. (Reproduced with permission from Buckberg *et al.*, *Circulation*. 2008;**118**:2571–87.)

produces an action just like wringing water out of a wet towel; if there were no torsion, ejection would be inadequate. Then, once the aortic valve has closed, there is a rapid untwisting, most marked at the apex, and it is this rapid untwisting that generates a negative pressure within the ventricular cavity and enables rapid filling of the ventricle once the mitral valve opens.

The degree and velocity of torsion increase with age [60]. Torsion increases strikingly in rate and magnitude with exercise or adrenergic stimulation, and this helps rapid filling during the shortened systolic interval that accompanies tachycardia. Torsion decreases with adrenergic blockade [59,61]. Abnormal torsion may be the earliest sign of diastolic dysfunction, as shown by Stuber *et al.* [62], who compared normal subjects, athletes with left ventricular

hypertrophy, and patients with aortic stenosis. The normal subjects and athletes had almost identical torsion. The patients with aortic stenosis, however, had torsion that although greater in magnitude was unduly prolonged, so that it delayed untwisting during early diastole.

Coronary pathophysiology

Myocardial energetics

The heart requires an enormous amount of oxygen per gram per minute. At rest it uses 8–10 ml of oxygen per 100 g of tissue per minute, and 60–80 ml per 100 g min^{-1} at maximal exercise [63]. The oxygen is used to fuel the ATP cycle, the main substrates being fatty acids and glucose that are moved into the mitochondria [64–66]. Preferentially the heart gets its energy by β-oxidation of long-chain fatty acids that require carnitine to cross the mitochondrial outer and inner membranes and also to transport potentially toxic acylcarnitine esters of CoA out of the mitochondria. In infants, who have low quantities of carntine palmitoyl transferase, short-chain fatty acids are preferred [67,68]. During oxygen deprivation, the heart can turn to glycolysis, but the metabolic products that accumulate soon inhibit function and decrease contractility. Carnitine deficiency is most often inherited [69], but can occur in preterm infants [70], chronic congestive heart failure [71,72], end-stage renal failure [73], and a variety of diseases and drug exposures [74–76].

Determinants of myocardial oxygen consumption

The main determinant of myocardial oxygen consumption is peak wall stress [77–80]. An earlier index, the tension–time index (TTI) that measured the area under the left ventricular pressure curve [81], is less satisfactory because the true afterload of the left ventricle is not aortic pressure but wall stress. In an isolated muscle strip, the afterload is the force that the strip exerts in lifting a weight during contraction, but in the intact heart the best equivalent is wall stress and not arterial pressure. Based on the LaPlace law (wall stress = $Pr/2h$, where P is pressure, r is radius, and h is wall thickness), wall stress in an irregularly shaped left ventricle can be approximated by an equation derived developed by Grossman *et al.* [82]:

$$Wall\ stress = \frac{Pr}{2h}\left[\frac{1.35}{1+\frac{h}{r}}\right]$$

Therefore, if the ventricle dilates, the radius increases, the wall thins, and stress rises markedly.

Other factors that also affect myocardial oxygen consumption are stroke volume [83–87], which involves shortening of fibers, and also contractility. The best way of incorporating all of these factors is to use the pressure–volume diagram of Suga [88,89] (Figure 4.17). These components of oxygen

usage are a function of ATP breakdown and re-formation, and also calcium cycling, and were discussed in detail by Suga [88,89].

Myocardial blood flow

Definitions, units of measurement

Coronary blood flow (flow passing through the coronary arteries) and *myocardial flow* (flow entering the myocardium) are normally similar, except for a small amount of myocardial flow that comes from pericardial and mediastinal vessels. In coronary–cameral or coronary–pulmonary arterial fistulas, not all the flow entering the coronary arteries goes into the myocardium.

Myocardial oxygen consumption or uptake is the amount of oxygen used by the myocardium. It may be measured in units of milliliters or micromoles of oxygen per beat or per minute for the whole heart, the left ventricle, or per unit mass of tissue (per gram or 100 g). *Myocardial oxygen demand* is the amount of oxygen that the heart needs. Normally, myocardial oxygen consumption and demand are equal as long as myocardial oxygen supply is unrestricted, but if supply falls below demand, there will be *myocardial ischemia*. The definition of ischemia has been defined in many ways [90]. In general, ischemia represents an imbalance between oxygen supply and demand that leads to impaired myocardial oxidative metabolism and function. The impairment may be transient, causing stunning or hibernation, or permanent. If ischemia lasts more than several hours, cells die and are replaced by scar tissue.

Basic flow mechanisms

The heart has an enormous demand for oxygen at rest and on exercise (Figure 4.18).

Heart data are for the left ventricle based on sampling blood from the coronary sinus, and we know little about regional myocardial oxygen consumption in ventricles or atria, or different layers of the left ventricle. Because of its lower systolic pressure, the right ventricle normally has less oxygen consumption than the left ventricle, but the two ventricles are more alike when there is right ventricular hypertension and hypertrophy. One study [91] observed slightly greater oxygen extraction and oxygen consumption in the left ventricular subendocardial muscle than in the midwall or the subepicardial muscle. This may reflect the greater shortening and intramyocardial systolic pressure generated by the subendocardial layer during systole [92].

Flow per 100 g to the normal right ventricular myocardium is about 50–67% of that of the left ventricle [93]. The ventricular septum, although usually contracting as part of the left ventricle, has flow characteristics of both ventricles. The left side of the septum behaves like the left ventricular free wall, particularly its subendocardial region, whereas the right part of the septum has flows similar to those in the right ventricular free wall [94].

55
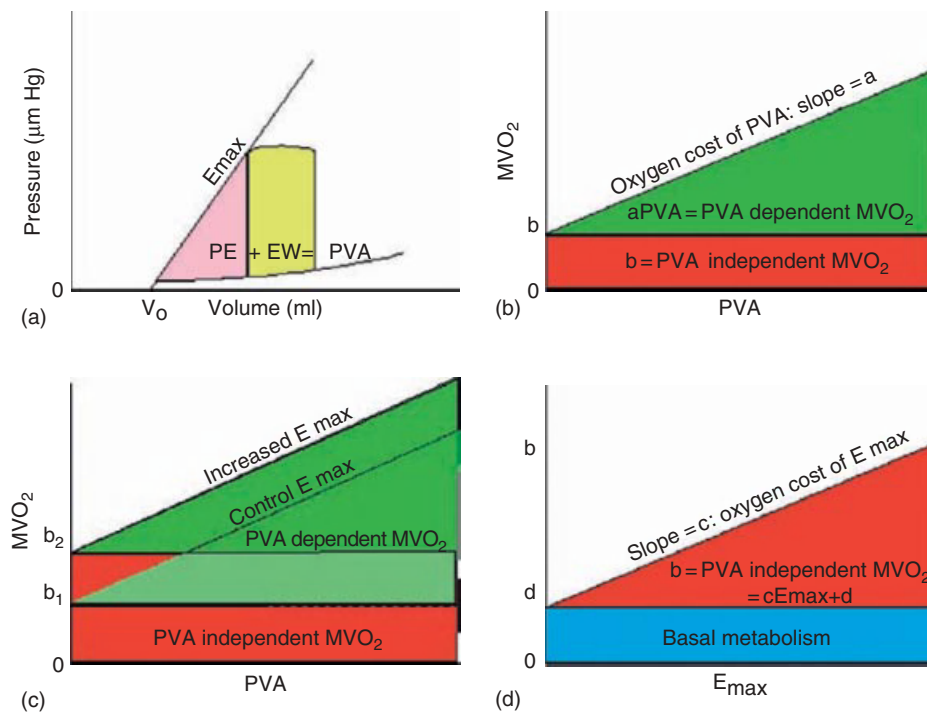
Figure 4.17 (a) The *PV* loop (*EW*) represents external work. The shaded triangular area (*PE*) represents elastic potential energy. The two areas combined make up *PVA* (pressure–volume area) that represents the total mechanical energy. (b) If *PVA* is changed and MVO_2 is measured, the relationship is a straight line with the equation $MVO_2 = aPVA + b$; *b* is the intercept on the *y*-axis, and the area between *b* and the zero baseline is independent of changes in E_{max}. The triangular shaded area above line *b* is the *PVA*-dependent MVO_2. Therefore, with increased *PVA* (equivalent to increased stroke work), MVO_2 also increases, with part of the increase proportional to the increase in *PVA* and another part that is independent of it. Panel (c) shows what happens if contractility and therefore E_{max} increase. The *PVA*-dependent portion of MVO_2 does not change (see triangle between dashed lines), but the independent part that represents basal metabolism has increased, thus accounting for the increased MVO_2. Panel (d) shows a different relationship, that between E_{max} and the value of *b*, the *PVA*-independent MVO_2. This quantity is composed of two parts. One is the basal metabolism (the hatched area below *d*) and is constant. (About 15% of total MVO_2 is used for basal metabolism – protein synthesis, transport of sodium and potassium – and about 10% in activation, related to Na⁺,K⁺-ATPase and Ca^{2+}-ATPase.) The other part that varies is the shaded triangular area above line *d*. This area represents the MVO_2 that is independent of PVA but dependent on E_{max} or, in other words, contractility. Therefore, MVO_2 is a function of basal metabolism (fixed), contractility (variable), and *PVA* that can also vary with the workload.

Flows in ventricular walls are inhomogeneous. If the left ventricular free wall is cut into concentric layers, flows tend to be less in the outermost third or quarter (subepicardial muscle) than the innermost third or quarter (subendocardial muscle), particularly in conscious animals [93]. Therefore, the LV inner:outer (or subendocardial:subepicardial) ratio of flows per gram may normally be 1.2–1.4. In addition to this regional layer inhomogeneity, there is considerable small-scale inhomogeneity within each layer [95,96]. In the right ventricle, the inner:outer flow ratio per gram is usually close to 1 [93].

What determines the regional distribution of myocardial blood flow? For a given coronary arterial pressure, flow depends upon the vascular resistance; the lower the resistance, the higher is the flow. In any region of the ventricle, there are three resistances to consider [95,97]. The first is the minimal resistance (R_{min}) of the vascular bed when it is maximally dilated and the heart is not contracting (long diastole, cardioplegia). The second is the added resistance ($R_{beating}$)

imposed when the heart beats and compresses the vessels. Finally, when the vessels have tone, this superimposes another resistance, R_{tone}.

R_{min} is lower in left ventricular subendocardium than subepicardium, so that in the arrested heart with maximally dilated vessels subendocardial flow is much greater than subepicardial flow [93,98]; the inner:outer flow ratio may be 2 or more. Within any layer, however, there is great variability of flow [95,96], presumably due to differences in the resistances of the vascular pathways to small regions of the ventricular wall. The flow patterns are not completely random. Regions with high or low flows surround other regions with high or low flows, respectively; the diameters of regions with similar flows are about 5–9 mm in the canine left ventricle.

$R_{beating}$: with increasing heart rate, subendocardial flow per minute per gram decreases roughly linearly [99]. Because of the high intramyocardial pressures in the subendocardium in systole, there is probably no systolic perfusion of the
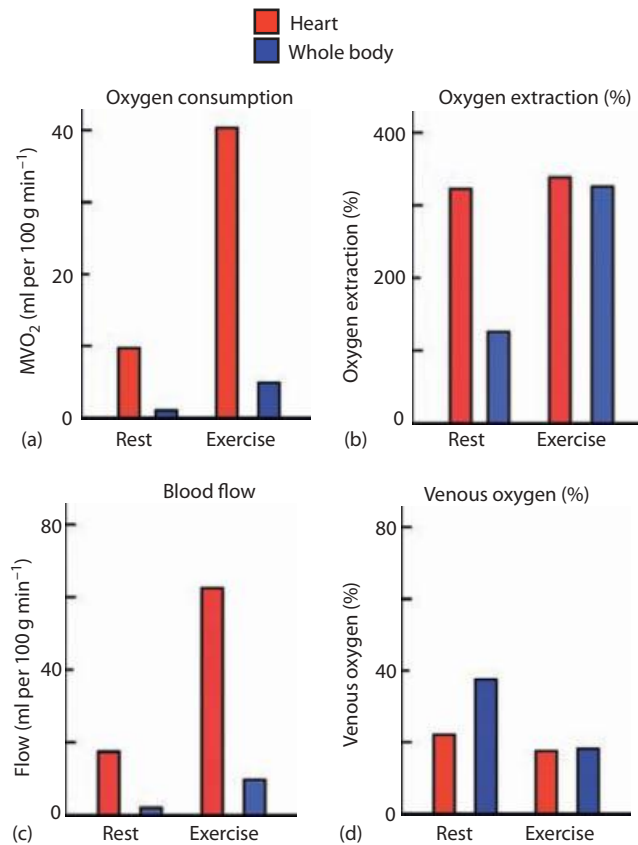
Figure 4.18 Oxygen consumption and flow at rest and severe exercise. Comparison of heart and whole body made with the same units for each. Drawn from data in humans studied by Kitamura *et al.* [12]. (a) Although the whole body's oxygen consumption increases with severe exercise, the usage per 100 g is still only about 10% of the heart's usage. (b) The high left ventricular MVO_2 is associated with a high oxygen extraction at rest, and although a little more oxygen can be extracted to meet increased oxygen demands, as with severe exercise, this amount is limited by the hemoglobin oxygen dissociation curve if tissue hypoxia is to be avoided. Therefore, the only way for the myocardium to obtain more oxygen is to increase flow. (c) The increased flow needed for maximal MVO_2 is shown. (d) During maximal exercise, the venous oxygen saturation of the body decreases to that seen normally in the coronary sinus.

subendocardial muscle. As heart rate increases, the duration of diastole per minute decreases, and therefore so does subendocardial blood flow. On the other hand, when the heart beats, subepicardial flow exceeds the flow in the arrested heart [100], for complex reasons. There are no high systolic intramyocardial pressures in the subepicardium, so that no obstruction to forward flow occurs in this region in systole or diastole. Studies performed with tiny flow transducers placed on small coronary arteries just before they enter the myocardium [100,101] have shown little, if any, forward flow in systole, particularly if contractility is increased. Therefore, although 20–25% of the coronary flow enters the origins of the left coronary arteries in systole, most or all of this merely

distends the extramural arteries and is stored there. On the other hand, microscopy of the superficial subepicardial vessels in the beating heart has shown continuous forward flow throughout the cardiac cycle [102]. The conclusion is that almost no flow enters the myocardium from the extramural vessels in systole, and that systolic subepicardial forward flow comes from blood squeezed retrograde from the subepicardial vessels [100]. These conclusions have been confirmed by direct observation of the intramyocardial vessels [103–105].

R_{tone}: when tone is added to the vessels, the flows are lower than when the vessels are maximally dilated. There is still great heterogeneity of flow, even within a layer, but no correlation exists between flows in the beating heart with and without vascular tone. The inner:outer flow ratio per gram remains about 1–1.4, but in small regions flows are determined primarily by local metabolic demands rather than by intramyocardial pressures or static minimal vascular resistances.

Autoregulation

Normally each region of the heart regulates flow to match its metabolic needs. This can be studied by cannulating the left coronary artery so that its perfusing pressure can be raised or lowered without altering left ventricular pressure or heart rate, and thus without altering myocardial oxygen consumption. When pressure is raised, flow immediately rises but then over 20–30 s returns to near its control value because the vessels constrict. When pressure is lowered, flow immediately decreases but then gradually returns to near normal because the vessels dilate. At high pressures (over about 120 mmHg mean perfusing pressure in acute studies), the flows increase persistently, presumably because high pressure has overcome vasoconstriction. Below a pressure of about 60–70 mmHg in anesthetized dogs and about 40 mmHg in conscious dogs [106], flow begins to decrease, because some vessels cannot dilate further and so can no longer compensate for a reduced perfusion pressure. These vessels are then pressure dependent, and in them any fall in pressure decreases flow, or any increase in myocardial oxygen demand at a constant pressure cannot be met by an increased flow. In either event, ischemia will occur in the territory supplied by those vessels.

The mechanisms underlying autoregulation are not fully understood, and probably involve both myogenic and chemical regulation [107].

Metabolic regulation

Myocardial oxygen demands are increased by tachycardia, increased pressure, and, to a lesser extent, volume work, and an increase in contractility. Normal hearts can tolerate very high heart rates, for example, 200–250 beats per minute, for short periods [108,109]. The tachycardia decreases the total diastolic time per minute and the proportion of diastole per cycle [110]. It also decreases stroke volume, ventricular volume, and wall stress, but increases contractility. Therefore, tachycardia increases myocardial oxygen consumption [111].
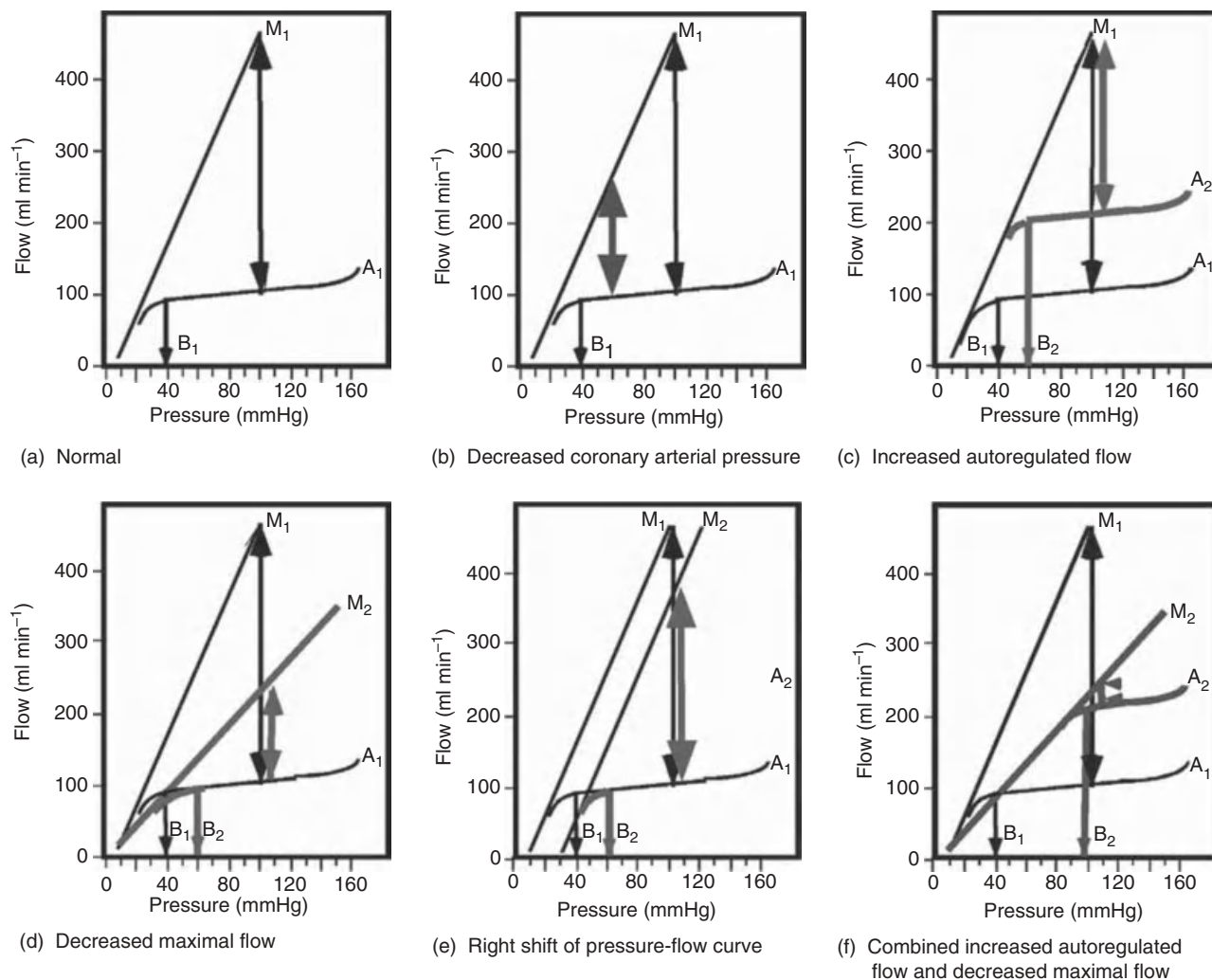
Figure 4.19 Coronary conductograms under various circumstances (see text). Abnormal CFR in thick gray lines and arrows shown by vertical lines slightly offset for clarity.

Increased wall stress due to higher pressure or volume work also increases myocardial oxygen demand, as does an increase in contractility. Even when myocardial oxygen demands are increased, however, autoregulation still occurs at the higher flow.

Coronary flow reserve [112–114]

At any given pressure, the flow when the vessels have tone is determined by the myocardial oxygen needs at that moment. When the vessels are maximally dilated, flow depends only on vascular resistance and myocardial contraction, independent of metabolism. If flow is measured at different perfusing pressures when the vessels have tone and then when they are maximally dilated, a typical coronary conductance diagram results (Figure 4.19). (Conductance is the reciprocal of resistance; the higher the conductance, the greater is the flow at any perfusion pressure.) The normal conductogram (Figure 4.19a) shows a relatively horizontal

line of autoregulated flow (A_1) between perfusing pressures of 40 and 120 mmHg; autoregulation fails outside those limits.

When the coronary vessels are maximally dilated, there is a steep pressure–flow line (M_1). The vertical difference between the two lines indicates the extra flow that can be attained at any given pressure by dilating the vessels, and is termed the coronary flow reserve (CFR) that is also measured in milliliters per minute. A dimensionless coronary flow reserve ratio is obtained by dividing maximal flow by autoregulated flow; this is particularly useful if flows or velocities cannot be related to a particular tissue mass. Note that flow reserve becomes smaller as the perfusing pressure decreases (Figure 4.19b); this occurs, for instance, with stenosis in a coronary artery.

What happens to flow reserve when, in the uncannulated preparation, aortic pressure rises? The increased pressure work increases the autoregulated flow, but the increased

Table 4.1 Causes of increased basal coronary flow.

Exercise[a]
Fever
Increased inotropy[a]
Tachycardia[a,b]
Thyrotoxicosis
Ventricular hypertrophy[a,b]
Hypoxemia
Anemia
Left shift of hemoglobin oxygen dissociation curve:
   Fetal hemoglobin
   Alkalosis
   Carboxyhemoglobin
   Abnormal hemoglobins

[a]May increase zero flow pressure.
[b]May also reduce maximal flow.

Table 4.2 Causes of decreased maximal flow.

Increased blood viscosity:
   Polycythemia
   Macroglobulinemia
Abnormal cardiovascular function:
   High right ventricular diastolic pressure[a]
   Hypertrophic cardiomyopathy
   Low aortic diastolic pressure:
     Aortic regurgitation
     Large arteriovenous fistula
   Pericardial tamponade
   Marked increase in contractility[b]
   Tachycardia[ab]
   Left ventricular hypertrophy[a,b]
   Right ventricular hypertrophy[a,b] (if acquired after early childhood)
Small vessel disease:
   Systemic lupus erythematosus
   Aortic stenosis
   Essential hypertension
   Diabetes mellitus
   Tobacco smoking
   Hyperlipidemia
   Idiopathic
Large vessel disease:
   Atherosclerosis
   Thrombosis
   Embolism
   Loss of cardiac muscle to scar tissue

[a]May increase zero flow pressure.
[b]May also increase basal flow.

coronary perfusing pressure increases maximal flow. McGinn *et al.* [115] observed in humans that increases in mean arterial pressure of ~20 mmHg increased autoregulated and maximal flows proportionally, so that the coronary flow reserve ratio was unaltered. What happens at greater pressure elevations is unknown.

Three types of changes can reduce coronary flow reserve. The first is if maximal flow remains unchanged but autoregulated flow increases (Figure 4.19c); the second is if autoregulated flow remains the same but maximal flows are reduced (Figure 4.19d); and the third is if the pressure–flow curve is shifted to the right (Figure 4.1e). The causes of these changes in flows are given in Tables 4.1, 4.2, and 4.3, respectively.

Some factors, such as tachycardia, may both increase autoregulated flow and decrease maximal flow, and some diseases such as cyanotic heart disease may elevate autoregulated flow (from hypoxemia) and decrease maximal flow (from polycythemia). Such combinations may decrease coronary flow reserve (between two horizontal arrow points) profoundly (Figure 4.19f).

Note that when coronary flow reserve is reduced, because of either an increase in autoregulated flow, a decrease in maximal flow, or a shift of the pressure–flow curve to the right, then the pressure at which autoregulation fails and pressure dependence starts shifts to the right, that is, towards higher pressures. This is a consequence of the slope of the line of maximal pressure–flow relations. As a result, autoregulation can fail at normal perfusing pressures (Figure 4.19f).

Regional coronary flow reserve

Failure of autoregulation and therefore pressure dependence occurs first in the subendocardial muscle, no matter what the cause. The loss of reserve is heterogeneous, even within a layer [116].

Table 4.3 Causes of increased zero flow pressure.

Increased left ventricular diastolic pressure[a]
Increased right ventricular diastolic pressure >12 mmHg
Pericardial tamponade[a]
Increased coronary venous pressure >12 mmHg but normal right ventricular diastolic pressure, e.g., after Fontan procedure
β-Adrenergic blockade or α-adrenergic stimulation
Left or right ventricular hypertrophy[a]
Tachycardia[a]
Some anesthetic agents, e.g., nitrous oxide

[a]May also reduce maximal flow.

Pressure–flow relations

When the coronary perfusing pressure is progressively reduced, flow ceases at a pressure of about 45 mmHg during autoregulation and at about 10–18 mmHg when the vessels are maximally dilated. The mechanism is not fully resolved [117]. Some investigators believe that there is vascular closure within the myocardium that causes this back-pressure, whereas others believe that the zero flow pressure is a mixture
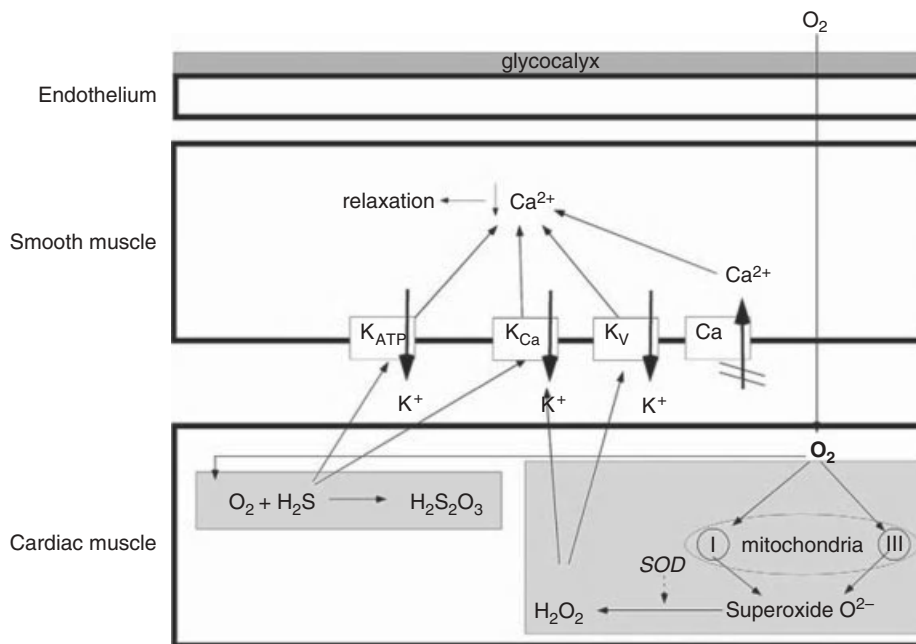
Figure 4.20 Mechanisms of small vessel vasomotion. Details of the endothelial compartment are omitted for clarity (see Figure 4.21). Ca^{2+}, calcium ion; H_2O_2, hydrogen peroxide; H_2S, hydrogen sulfide; $H_2S_2O_3$, thiosulfuric acid; SOD, superoxide dismutase; I and III, components of mitochondria

of a vascular waterfall in the epicardial coronary veins and a time factor related to intramyocardial blood volume. (In a waterfall, raising the level of the water in the river below the fall does not change flow over the lip of the fall; similarly, in a vascular waterfall, there is a discontinuity between pressure in the "waterfall" segment and more distal venous pressure, and increasing venous pressure will not alter flow in the vascular bed until it exceeds the waterfall pressure [117].)

Under some circumstances, the zero flow pressure rises and reduces the coronary driving pressure (the difference between inflow perfusion pressure and outflow or back-pressure). This can certainly occur with pericardial tamponade, and with very high right or left ventricular diastolic pressures. A rise in back-pressure, for whatever reason and mechanism, has the same effect in reducing coronary flow reserve as a decrease in perfusing pressure (Figure 4.19e).

Regulation of myocardial vascular tone

When myocardial work increases with tachycardia or exercise, coronary blood flow must increase to supply the added oxygen needed. This response is so important that many redundant systems have evolved [118,119]. Increasing myocardial blood flow involves first the dilatation of the resistance arterioles that are about 100–150 μm in diameter and then subsequent dilatation of the upstream conduit arteries and arterioles to help provide the added flow. The major mechanism of muscle relaxation is reduced calcium influx, and this follows hyperpolarization of the muscle cell when potassium leakage out of the cell through potassium channels is increased [107,120]. Other mechanisms also exist.

One mechanism for dilating resistance vessels could be autonomic nerve activity, but myocardial flow in exercise can still increase after denervation, and Duncker and Bache [119] concluded that the autonomic nervous system modulates but does not necessarily initiate the increased flow. The primary mechanisms are biochemical changes in the myocardial cells, attributed to a decrease in tissue oxygen or to products produced by increased breakdown of ATP as it generates the energy for contraction. Possible mechanisms are shown in Figure 4.20.

The first major mechanism proposed (not shown in the diagram) involved adenosine as the by-product of ATP metabolism [121]. When muscle contraction breaks down ATP, some of the adenosine monophosphate produced is degraded by 5'-nucleotidase to adenosine, a powerful coronary vasodilator. The more the muscle works, the larger is the amount of adenosine produced and the greater is the coronary vasodilatation. The increased myocardial oxygen supply therefore increases to match the demand. When muscle work increases, so does the amount of adenosine produced, and the vessels dilate to increase flow and oxygen supply appropriately. Although this mechanism has all the ingredients needed for a control system, there are some major arguments against it being the only or even the most important system. Eliminating almost all of the interstitial adenosine by infusing low molecular weight adenosine deaminase does not alter autoregulation. Even with definite ischemia, as in reactive hyperemia, infusing adenosine deaminase reduces but does not abolish the hyperemic response [122]. Furthermore, intracellular adenosine concentrations in the absence of profound ischemia are probably too low to affect vascular tone [123,124]. Finally, Saitoh *et al.* [125] pointed out that once tissue oxygen levels had been restored, the error signal responsible for the changes would disappear.
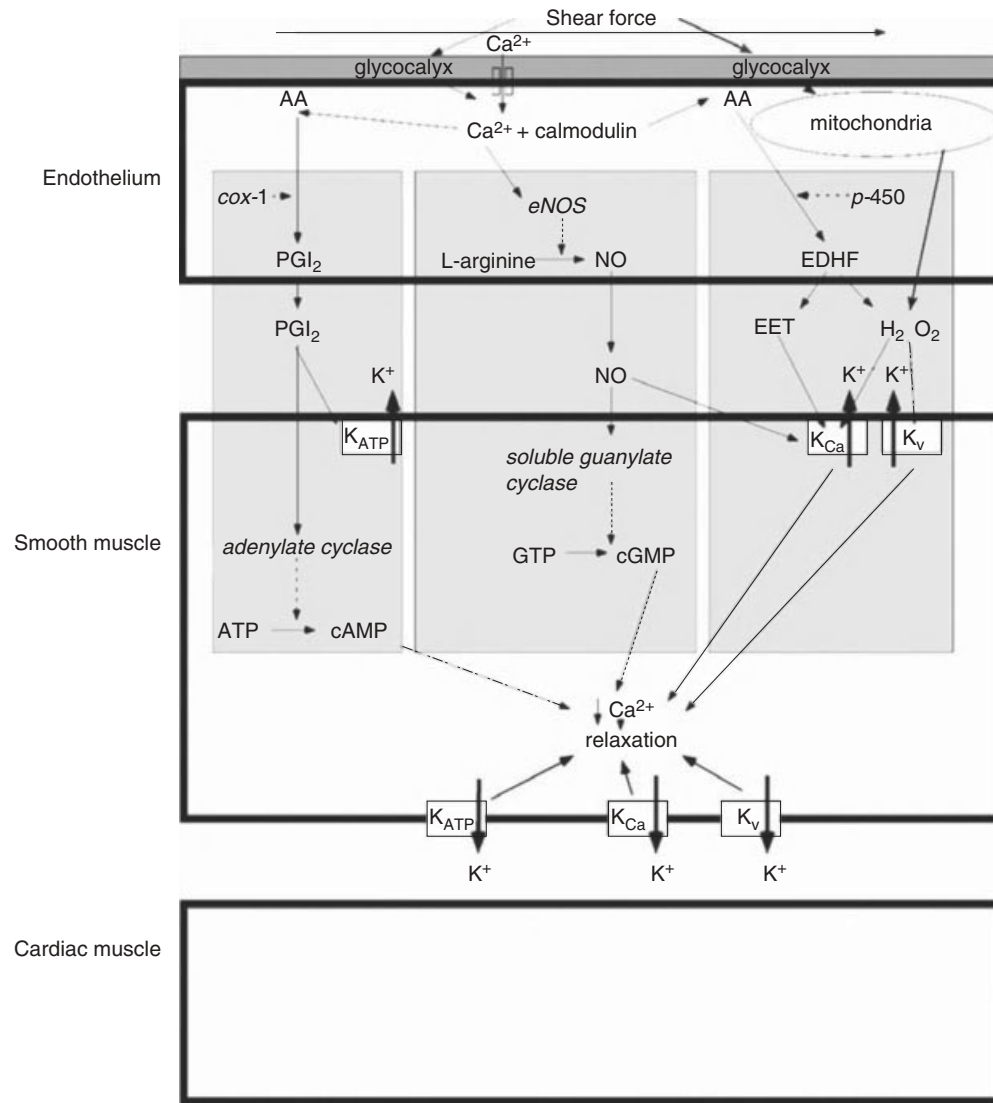
Figure 4.21 Simplified diagram of some vasomotor control mechanisms, based on studies from the laboratories of Gutterman [107,129,130], Chilian [125,131,132], and others [126,133–136]. The cardiac muscle compartment is left blank for clarity (see Figure 4.20). AA, arachidonic acid; ATP, adenosine triphosphate; cAMP, cyclic adenosine monophosphate; EDHF, endothelial-derived hyperpolarizing factor; EET, epoxyeicosatrienoic acid; eNOS, nitric oxide synthase; GTP, guanine triphosphate; cGMP, cyclic guanine monophosphate; H_2O_2, hydrogen peroxide; K, potassium; K_{ATP}, ATP-dependent potassium channel; K_{Ca}, calcium-dependent potassium channel; K_v, voltage-dependent potassium channel; NO, nitric oxide; PGI_2, prostacyclin.

The alternative mechanism associated with increased ATP metabolism is that when oxygen provides energy for the Krebs cycle, complexes I and III of the mitochondria produce superoxide anions as a by-product. These anions are converted by superoxide dismutase into hydrogen peroxide that also acts on potassium channels to hyperpolarize the smooth muscle cell and relax it.

Another possibility involves oxygen that diffuses into the muscle cell and is consumed. Hydrogen sulfide (H_2S) is constitutively produced in the cardiac muscle cell and the endothelium by the action of cystathionine-γ-lyase (CSE) or cystathionine-β-synthase (CBE) on L-cysteine [126], and via mitochondrial action H_2S is oxidized to a compound with no

vasomotor action. Calcium–calmodulin acts as a regulator for the action of CSE, just as it does for the enzymes that produce NO and CO [127]. Lack of tissue oxygen leads to excess free H_2S, a potent vasodilator that acts on potassium channels to hyperpolarize the smooth muscle cell and decrease calcium influx [128]. In support of the role of H_2S is the fact that mice with CSE knockout are hypertensive, with blood pressure decreasing in response to exogenous H_2S [127]. These mice also show reduced endothelial-stimulated vasodilatation.

The increase in flow at the level of the resistance vessels then causes a flow-mediated increase of flow in the upstream conduit vessels, with major proposed mechanisms delineated in Figure 4.21. Although the conduit vessels are also exposed

to products of myocardial cell metabolism, the thicker vessel walls limit the effects of diffusion from myocytes.

Shear forces acting on glycoproteins (integrins and others) in the glycocalyx transmit changes to the intracellular domains of these proteins, and via complex interactions affect mitochondria in the endothelial cells in addition to activating arachidonic acids in the cell membranes. The result is stimulation of the production and co-release of nitric oxide and prostacyclin, and also the generation of two important components of endothelial-derived hyperpolarizing factor (EDHF), epoxyeicosatrienoic acids (EETs), and hydrogen peroxide. These agonists act to inhibit calcium influx both by hyperpolarizing the smooth muscle cell via a variety of potassium channels and also by activating adenylate and guanylate cyclase. These same factors may play a secondary role at the small arteriolar level, with EETs predominating. With vascular disease, not only coronary artery disease but also diabetes mellitus and hypercholesterolemia, reactive oxygen species increase and inhibit the production of prostacyclin, nitric oxide, and epoxyeicosatrienoic acids (EETs), leaving hydrogen peroxide as the main dilator. Not shown in the diagram are interactions among these various agonists.

There are many other potential modulating factors, including potent vasodilators such as substance P, prostacyclin, vasoactive intestinal peptide, bradykinin, atrial natriuretic peptides, and calcitonin gene-related product (CGRP), and also vasoconstrictors such as neuropeptide Y and endothelin, the adrenergic nerves with their transmitters, and cellular PKC and MAPK. A role for carbon monoxide has been suggested [129–144]. The pathways featured in Figures 4.20 and 4.21 are currently regarded as those of greatest importance.

General considerations of causes of ischemia

When perfusing pressure decreases below the lower limit of autoregulation, the fall in flow occurs first in the subendocardium [145,146]. The changes in flow are not uniform within each layer; some pieces of muscle retain reasonable flows whereas others decrease their flow markedly [116]. Nevertheless, most low-flow regions are in the subendocardium, some are in the mid-wall, and a few are in the subepicardium. A similar pattern of selective subendocardial ischemia was shown in experiments in non-cannulated dogs in which severe supravalvar aortic stenosis, an arteriovenous fistula, or rapid ventricular pacing all reduced the inner:outer ratio per gram to very low values, even though the absolute subendocardial flow might not have been reduced. In these studies, some of the maneuvers increased myocardial oxygen demand throughout the heart, but the pathophysiologic changes prevented the appropriate increase in subendocardial blood flow [147]. Common to all these experiments is the notion that once the vessels become maximally dilated, and this always occurs first in the subendocardium, subendocardial flow becomes pressure dependent. Therefore, an inadequate perfusion pressure or a reduced diastolic perfusion time for myocardial needs either decreases subendocardial flow or leads to failure to increase flow appropriately, and leads to a lowered inner:outer flow ratio per gram and also functional and biochemical manifestations of subendocardial ischemia.

Specific cardiac lesions or abnormalities

Tachycardia

Heart rates above 250 beats per minute for extended periods may decrease the inner:outer flow ratio, due to a shorter diastolic perfusion time, lowered aortic diastolic perfusing pressure, and perhaps a rise in left ventricular diastolic pressure. Although the absolute flows rise in all layers, coronary flow reserve becomes reduced in the inner half and, at very high rates, may be absent. The subendocardial vessels become pressure dependent and ischemia may result. The absolute subendocardial flow might be above normal, but is not high enough to supply the oxygen needed to the muscle. The inner:outer flow ratio per gram in these instances is a better guide to subendocardial ischemia than the actual subendocardial flow [148]. If the ventricle is hypertrophied, then tachycardia causes subendocardial ischemia much more readily, in fact, above heart rates of 200 beats per minute [108,109]. Modest tachycardia at a rate of 200 beats per minute causes subendocardial ischemia in dogs with coronary stenosis. The tighter the stenosis, the smaller is the heart rate increase required to cause subendocardial ischemia. In infants during recovery after prolonged paroxysmal supraventricular tachycardia, the T waves may be generally inverted for several hours, and this has been attributed to subendocardial ischemia.

Ventricular hypertrophy

With ventricular hypertrophy in adult animals, muscle mass increases without a corresponding increase in arteries and larger arterioles [145,149,150]. In general, increased wall thickening tends to keep wall tension normal, so that myocardial oxygen consumption per unit mass remains at control values. However, because of a greater muscle mass, myocardial oxygen consumption per ventricle is increased in proportion to the increase in muscle mass. Flow increases to supply this increased amount of oxygen, and does so by dilating the normal-sized myocardial vascular bed. On the other hand, maximal flow per ventricle is not increased (or may even be decreased if there is associated small-vessel medial hypertrophy or intimal disease). Therefore, coronary flow reserve is reduced [151–153]. Similar results have been found in humans [151,152]. When hypertrophy is due to hypertension, the increased perfusion pressure may result in a normal coronary flow reserve, with both resting and maximal flows being increased in proportion.

Young animals, however, can increase the cross-sectional area of the right ventricular myocardial vascular bed to keep pace with the increase in ventricular muscle mass [154,155].

There is one study that suggested that this can also occur for the left ventricle [156].

Aortic stenosis

In this lesion, subendocardial ischemia and fibrosis are prominent, both in children and in adults [145,157–159]. The pressure load causes ventricular hypertrophy that normalizes the wall stress. Therefore, flow per unit mass is relatively normal but total flow is increased in proportion to the increased muscle mass. Because conducting intramyocardial coronary vessels do not increase in number or size, or do not increase enough to compensate for the increased muscle mass, coronary flow reserve is reduced, and may even be absent in the subendocardium. Because the subendocardial vessels are the first to be affected, the effort angina that these patients get is accompanied by ST depression in the left precordial leads, and often there will be substantial subendocardial fibrosis and necrosis. If there are added obstructive changes in intramural arteries, the tendency to subendocardial ischemia is more marked. With significant aortic stenosis, subendocardial ischemia occurs earlier with added stresses such as anemia, tachycardia, extramural coronary arterial disease, or anything that causes the ventricle to dilate and increase the wall stress. Injudicious use of catecholamines in treating non-cardiac disease in these patients may also be detrimental.

Aortic regurgitation

With severe aortic regurgitation, left ventricular systolic pressure is elevated and there is ventricular hypertrophy, but with the associated increase in ventricular volume the wall stress is elevated. Furthermore, the mean diastolic aortic perfusing pressure is reduced. These patients therefore have a reduced coronary flow reserve, so that angina pectoris and subendocardial ischemic damage may occur. One notable difference from aortic stenosis is that with regurgitation, tachycardia can improve cardiac function and subendocardial blood flow for at least two reasons. First, a faster heart rate reduces the time available for regurgitation and so reduces the degree of regurgitation and ventricular volume. Second, the shorter diastole raises the mean diastolic perfusing pressure. This may explain why clinically pacing about 15–20 beats per minute above the resting heart rate has produced major clinical improvements in patients with aortic regurgitation and intractable cardiac failure [160,161].

Anemia

Anemia increases cardiac output and thus myocardial oxygen consumption, and at the same time decreases the oxygen carrying capacity of the blood. This is compensated for by an increased coronary blood flow, but at the expense of reducing coronary flow reserve.

Polycythemia

Polycythemia reduces resting blood flow because of its increased oxygen-carrying capacity and viscosity. Because increased blood viscosity decreases maximal flows, coronary flow reserve is reduced. As for anemia, resting blood flow can be supplied (to a normal heart) at any hematocrit and perfusing pressure, and arterial oxygen saturation, but the demands of exercise cannot be met.

Hypoxemia

Hypoxemia increases coronary blood flow and reduces coronary flow reserve.

Coronary Arterial Stenosis

With a localized atheromatous lesion of a major branch of the left coronary artery, there is a pressure drop at rest across the obstruction because of the increased resistance that it offers to flow. This pressure drop is greater in diastole, when flow is highest, than in systole. Autoregulation causes the small intramural vessels to dilate and lower their resistance, so that myocardial oxygen demands can be met. Coronary flow reserve is, however, decreased in this distal bed. If the stenosis becomes more severe, whether acutely by spasm or hemorrhage into the plaque, or chronically by growth in volume of the plaque, then distal pressures may fall below the level at which autoregulation can compensate; coronary flow reserve will be absent. Consequently, flow decreases below the amount needed to supply myocardial oxygen needs, particularly in the subendocardium, and the patient has rest pain. Because rest pain indicates severely impaired coronary flow to a region that does not have an increased oxygen demand, it is a precursor of necrosis if it persists.

If a mild obstruction gradually increases, resting flow remains at its previous value but coronary flow reserve becomes progressively reduced. Exercise that raises myocardial oxygen needs may then exhaust flow reserve and lead to subendocardial ischemia. These features are the basis for various types of exercise tests, with or without radionuclide scans to delineate ischemic regions.

Cardiopulmonary bypass

Acute subendocardial necrosis in patients with normal coronary arteries was all too frequent in the early days of bypass surgery [162–166]. Necrosis was seen most often during prolonged normothermic ventricular fibrillation, the mechanism being the difficulty of perfusing the subendocardium in the absence of a prolonged period of relaxation equivalent to diastole [167–169]. With improved myocardial protection, this lesion is seen less often, but still occurs.

Direct and indirect measurement of coronary blood flow

Although these measurements are easy and relatively accurate in animals, they are is more difficult in humans, especially
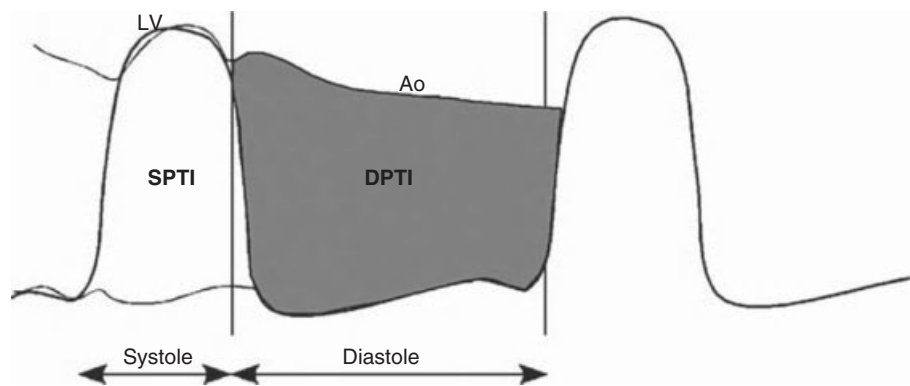
Figure 4.22 The systolic:diastolic pressure-time index.

small children. Ideally, non-invasive or minimally invasive methods should be used. Transthoracic Doppler echocardiography of the major coronary arteries has been done, and yielded results that are comparable to those found in animals [170–176]. The method can usually make repeatable measurements of flows in the left anterior descending, left circumflex, or right coronary arteries, and gives values for flow and flow reserve that match those in animal studies. Only large regions can be studied, and flow variations within a region are not obtainable. Nuclear medicine techniques with technetium or thallium can show localized deficits, but do not measure absolute flow. Positron emission tomography (PET) scanning with rubidium has better spatial resolution but is complex and expensive [177]. Inserting a Doppler flow wire (Cardiometrics, Mountain View, CA, USA) through a small catheter provides the most accurate measurements for specific coronary arteries. Just as with the echo-Doppler method, however, this does not give information about small regions.

Because none of these methods currently give information about ischemia of the subendocardium, which is the earliest region affected, an indirect index has been proposed. Based on acute animal studies, Buckberg *et al.* [147] examined the ratio of two pressure–time areas (Figures 4.22).

The rationale for the ratio is that the area under the left ventricular pressure curve in systole (SPTI) represents myocardial oxygen demand (with the caveats mentioned above about pressure and wall stress not being the same), whereas the area between the aortic and left ventricular curves in diastole (DPTI) represents the time and pressure head for perfusion of the subendocardium that, as described above, is perfused only in diastole. DPTI is directly related to flow as flow = Pressure difference/resistance. With maximal vasodilatation, subendocardial flow becomes pressure dependent, and subendocardial flow is proportional to the pressure difference per minute, which, for subendocardial muscle, is DPTI.

The DPTI:SPTI ratio thus represents a supply:demand ratio. Buckberg *et al.* [147] produced various models of heart disease in dogs, and found a good linear correlation between the DPTI:SPTI ratio and the subendocardial:subepicardial flow ratio. If the DPTI:SPTI ratio decreased to <0.8, the flow ratio decreased below its normal value of about 1. Note that these ratios do not predict absolute flows, but instead use the subepicardial flow (which is almost never jeopardized) as a normalizing value.

The concept is straightforward, and it fits many lesions in which subendocardial ischemia is known to occur [178,179]. The difficulty in using this concept is determining the critical values for the ratio. Some guidance is available. Studies done on healthy athletes immediately after the onset of a 100 m sprint showed 4 mm ST depression of classical ischemic pattern [180]. To investigate this finding, normal healthy firemen were exercised on a treadmill either with gradual increase to maximal speed or with maximal speed started immediately. The first group showed merely the expected tachycardia, whereas the second group showed initial ST depression. A rough estimate of DPTI:SPTI ratio was obtained from a brachial arterial pressure. The investigators found that ischemic changes in the electrocardiogram occurred if the DPTI:SPTI ratio decreased below 0.45. It is essential to correct the DPTI:SPTI ratio for the hemoglobin concentration [181]. This is done simply by multiplying the DPTI area by arterial oxygen content in milliliters per 100 ml of blood (normal value about 20). The critical oxygen content adjusted ratio would then be about 8–9.

It is therefore reasonable to use this cut off value for normal hearts. What happens if hearts are hypertrophied or dilated? Then the SPTI underestimates myocardial oxygen demand because either wall stress is increased or the wall is hypertrophied, and the critical value is <0.45 by some unknown amount. In a study of patients known to have aortic stenosis, lactate production detected in the coronary sinus (and by inference subendocardial ischemia) was associated with a DPTI:SPTI ratio <0.3 [182]. It is safe to state that any DPTI:SPTI ratio >0.45 (or if corrected for arterial oxygen content >9) suggests that the subendocardium is not ischemic.

Coronary flow patterns

In the left coronary artery, about 75–80% of the flow is diastolic, for reasons discussed above. A reduction of the proportion of diastolic blood flow probably reflects underperfusion of the subendocardium of the left ventricle [146].

On the other hand, systolic flow in a large branch of the left coronary artery may be reduced if excess systolic backflow from the myocardium opposes normal systolic inflow, as may occur when ventricular pressure exceeds aortic pressure in systole, as occurs with aortic stenosis. It has also been described with acute hemorrhage, a large coronary cameral fistula, and pericardial tamponade [146]. Now that it is possible to use Doppler-tipped flow wires in children, assessment of flow patterns may provide indirect information about subendocardial flow.

The flow wire has been used also to determine whether a child with some degree of coronary artery stenosis after Kawasaki disease will benefit from coronary bypass surgery [183]. This has been done by using the concept of myocardial fractional flow reserve, in which measurements are made during maximal vasodilatation of the coronary arteries of pressures in the artery proximal to the stenosis (P_a), distal to the stenosis (P_d), and a wedge as a measure of coronary venous pressure (P_v). Then myocardial fractional flow reserve (FFR_{myo}) is calculated [162–164] as

$$FFR_{myo} = \frac{P_d - P_v}{P_a - P_v}$$

A value of <0.75 suggests that there is significant stenosis. In the study by Ogawa et al. [183], there was a good relationship between the coronary flow reserve (determined by the same Doppler flow wire) and FFR_{myo}. The method has value, although questions have been raised about its value in practice [184] and even about the validity of the method [185].

Right ventricular myocardial blood flow

Right ventricular myocardial blood flow follows the general principles regarding coronary blood flow, but has differences related to the low right ventricular systolic pressure and to the fact that alterations in aortic pressure change coronary perfusing pressure without altering right ventricular pressure work. If the normal right ventricle is acutely distended, for example, by pulmonary embolism, there will eventually be right ventricular failure; the increased wall stress increases its oxygen consumption but the raised systolic pressure reduces the coronary flow, so that when supply cannot match demand there will be right ventricular myocardial ischemia [186]. Raising aortic perfusing pressure mechanically or with α-adrenergic agonists increases right ventricular myocardial blood flow, relieves ischemia, and restores right ventricular function to normal despite continued right ventricular systolic hypertension. Improved coronary flow is not the only mechanism of this improvement; the increased left ventricular afterload moves the ventricular septum towards the right ventricle and improves left ventricular performance [187]. As shown by Sonnenblick and colleagues [188] in earlier experiments, ischemia is likely to be the predominant mechanism.

If right ventricular systolic pressure is chronically elevated so that there is right ventricular hypertrophy, as in pulmonic stenosis, many forms of cyanotic congenital heart disease, and some chronic lung diseases, then right ventricular myocardial blood flow behaves in the same way as left ventricular blood flow [189–191], with one exception. If aortic pressure is lowered, left ventricular pressure also decreases, as does left ventricular work and oxygen consumption. In the right ventricle, however, the workload may not be reduced (if there is no ventricular septal defect), so that an imbalance between myocardial oxygen supply and demand may occur. The worst imbalance occurs when aortic systolic pressure is maintained but coronary perfusing pressure decreases, and this can occur in a child with tetralogy of Fallot who has too large an aortopulmonary anastomosis. The high aortic and left ventricular systolic pressures mandate an equally high right ventricular systolic pressure, but the low diastolic aortic pressure reduces coronary perfusion pressure in diastole and can cause both left and right ventricular ischemia and failure [192].

In the right coronary artery, because some of the flow perfuses the low-pressure right ventricle, about 40–60% of the flow is in systole. With increased right ventricular pressures, as in congenital pulmonic stenosis, the flow pattern resembles that of the left coronary artery [193].

References

1 Jouk PS, Usson Y, Michalowicz G, Grossi L. Three-dimensional cartography of the pattern of the myofibres in the second trimester fetal human heart. *Anat Embryol (Berl)* 2000;**202**(2):103–18.

2 Sengupta PP, Krishnamoorthy VK, Korinek J, *et al.* Left ventricular form and function revisited: applied translational science to cardiovascular ultrasound imaging. *J Am Soc Echocardiogr* 2007;**20**:539–51.

3 Torrent-Guasp F, Buckberg GD, Clemente C, *et al.* The structure and function of the helical heart and its buttress wrapping. I. The normal macroscopic structure of the heart. *Semin Thorac Cardiovasc Surg* 2001;**13**(4):301–19.

4 Zhukov L, Barr AH. Heart-muscle fiber reconstruction from diffusion tensor MRI. In: *Proceedings of the 14th IEEE Visualization Conference (VIS'03)*, 2003: 597–602.

5 Athanasuleas CL, Buckberg GD, Stanley AW, *et al.* Surgical ventricular restoration in the treatment of congestive heart failure due to post-infarction ventricular dilation. *J Am Coll Cardiol* 2004;**44**:1439–45.

6 Van den Bos GC, Elzinga C, Westerhof N, Noble MI. Problems in the use of indices of myocardial contractility. *Cardiovasc Res* 1973;**7**:834–48.

7 Parmley WW, Chuck L, Yeatman L. Comparative evaluation of the specificity and sensitivity of isometric indices of contractility. *Am J Physiol* 1975;**228**:506–10.

8 Glick G, Sonnenblick EH, Braunwald E. Myocardial force–velocity relations studied in intact unanesthetized man. *J Clin Invest* 1965;**44**:978–88.

9 Sonnenblick EH. Instantaneous force–velocity–length determinants in the contraction of heart muscle. *Circ Res* 1965;**16**:441–51.

10 Pollack GH. Maximum velocity as an index of contractility in cardiac muscle. A critical evaluation. *Circ Res* 1970;**26**:111–27.

11 Sarnoff S, Mitchell J. The control of the function of the heart. In: Hamilton WE, Dow P, eds. *Handbook of Physiology*. Washington, DC: American Physiological Society, 1962: 489–532.

12 Sagawa K. The ventricular pressure–volume diagram revisited. *Circ Res* 1978;**43**:677–87.

13 Sagawa K. The end-systolic pressure–volume relation of the ventricle: definition, modifications and clinical use. *Circulation* 1981;**63**:1223–7.

14 Ross J Jr. Afterload mismatch and preload reserve: a conceptual framework for the analysis of ventricular function. *Prog Cardiovasc Dis* 1976;**18**:255–64.

15 Ross J Jr. Mechanisms of cardiac contraction. What roles for preload, afterload and inotropic state in heart failure? *Eur Heart J* 1983;**4**(Suppl A):19–28.

16 Glower DD, Spratt JA, Kabas JS, *et al.* Quantification of regional myocardial dysfunction after acute ischemic injury. *Am J Physiol* 1988;**255**:H85–93.

17 Glower DD, Spratt JA, Snow ND, *et al.* Linearity of the Frank–Starling relationship in the intact heart: the concept of preload recruitable stroke work. *Circulation* 1985;**71**:994–1009.

18 Kass DA, Beyar R, Lankford E, *et al.* Influence of contractile state on curvilinearity of *in situ* end-systolic pressure–volume relations. *Circulation* 1989;**79**:167–78.

19 Krosl P, Abel FL. Problems with use of the end systolic pressure–volume slope as an indicator of left ventricular contractility: an alternate method. *Shock* 1998;**10**:285–91.

20 Borow KM, Green LH, Grossman W, Braunwald E. Left ventricular end-systolic stress–shortening and stress–length relations in human. Normal values and sensitivity to inotropic state. *Am J Cardiol* 1982;**50**:1301–8.

21 Borow KM, Neumann A, Wynne J. Sensitivity of end-systolic pressure–dimension and pressure–volume relations to the inotropic state in humans. *Circulation* 1982;**65**:988–97.

22 Borow KM, Propper R, Bierman FZ, *et al.* The left ventricular end-systolic pressure–dimension relation in patients with thalassemia major. A new noninvasive method for assessing contractile state. *Circulation* 1982;**66**:980–5.

23 Colan SD, Borow KM, MacPherson D, Sanders SP. Use of the indirect axillary pulse tracing for noninvasive determination of ejection time, upstroke time, and left ventricular wall stress throughout ejection in infants and young children. *Am J Cardiol* 1984;**53**:1154–8.

24 Colan SD, Borow KM, Neumann A. Left ventricular end-systolic wall stress–velocity of fiber shortening relation: a load-independent index of myocardial contractility. *J Am Coll Cardiol* 1984;**4**:715–24.

25 Franklin RC, Wyse RK, Graham TP, *et al.* Normal values for noninvasive estimation of left ventricular contractile state and afterload in children. *Am J Cardiol* 1990;**65**:505–10.

26 Banerjee A, Brook MM, Klautz RJ, Teitel DF. Nonlinearity of the left ventricular end-systolic wall stress–velocity of fiber shortening relation in young pigs: a potential pitfall in its use as a single-beat index of contractility. *J Am Coll Cardiol* 1994;**23**:514–24.

27 Sunagawa K, Maughan WL, Burkhoff D, Sagawa K. Left ventricular interaction with arterial load studied in isolated canine ventricle. *Am J Physiol* 1983;**245**:H773–80.

28 Tyberg JV, Belenkie I, Manyari DE, Smith ER. Ventricular interaction and venous capacitance modulate left ventricular preload. *Can J Cardiol* 1996;**12**:1058–64.

29 Tyberg JV, Taichman GC, Smith ER, *et al.* The relationship between pericardial pressure and right atrial pressure: an intraoperative study. *Circulation* 1986;**73**:428–32.

30 Hamilton DR, Sas R, Tyberg JV. Atrioventricular nonuniformity of pericardial constraint. *Am J Physiol Heart Circ Physiol* 2004;**287**:H1700–4.

31 Smiseth OA, Frais MA, Junemann M *et al.* Left and right ventricular diastolic function during acute pericardial tamponade. *Clin Physiol* 1991;**11**:61–71.

32 Glantz SA, Misbach GA, Moores WY, *et al.* The pericardium substantially affects the left ventricular diastolic pressure–volume relationship in the dog. *Circ Res* 1978;**42**:433–41.

33 Tyberg JV, Misbach GA, Glantz SA, *et al.* A mechanism for shifts in the diastolic, left ventricular, pressure–volume curve: the role of the pericardium. *Eur J Cardiol* 1978;**7**(Suppl):163–75.

34 Glantz SA, Parmley WW. Factors which affect the diastolic pressure–volume curve. *Circ Res* 1978;**42**:171–80.

35 Slinker BK, Glantz SA. End-systolic and end-diastolic ventricular interaction. *Am J Physiol* 1986;**251**:H1062–75.

36 Smiseth OA, Frais MA, Kingma I, *et al.* Assessment of pericardial constraint: the relation between right ventricular filling pressure and pericardial pressure measured after pericardiocentesis. *J Am Coll Cardiol* 1986;**7**:307–14.

37 Belenkie I, Dani R, Smith ER, Tyberg JV. Ventricular interaction during experimental acute pulmonary embolism. *Circulation* 1988;**78**:761–8.

38 Belenkie I, Dani R, Smith ER, Tyberg JV. The importance of pericardial constraint in experimental pulmonary embolism and volume loading. *Am Heart J* 1992;**123**:733–42.

39 Kroeker CA, Shrive NG, Belenkie I, Tyberg JV. Pericardium modulates left and right ventricular stroke volumes to compensate for sudden changes in atrial volume. *Am J Physiol Heart Circ Physiol* 2003;**284**:H2247–54.

40 Belenkie I, Smith ER, Tyberg JV. Ventricular interaction: from bench to bedside. *Ann Med* 2001;**33**:236–41.

41 Moore TD, Frenneaux MP, Sas R, *et al.* Ventricular interaction and external constraint account for decreased stroke work during volume loading in CHF. *Am J Physiol Heart Circ Physiol* 2001;**281**:H2385–91.

42 Baker AE, Dani R, Smith ER, *et al.* Quantitative assessment of independent contributions of pericardium and septum to direct ventricular interaction. *Am J Physiol* 1998;**275**:H476–83.

43 Atherton JJ, Moore TD, Lele SS, *et al.* Diastolic ventricular interaction in chronic heart failure. *Lancet* 1997;**349**:1720–4.

44 Mitchell JR, Sas R, Zuege DJ, *et al.* Ventricular interaction during mechanical ventilation in closed-chest anesthetized dogs. *Can J Cardiol* 2005;**21**:73–81.

45 Mitchell JR, Whitelaw WA, Sas R, *et al.* RV filling modulates LV function by direct ventricular interaction during mechanical ventilation. *Am J Physiol Heart Circ Physiol* 2005;**289**:H549–57.

46 Tyberg JV, Grant DA, Kingma I, *et al.* Effects of positive intrathoracic pressure on pulmonary and systemic hemodynamics. *Respir Physiol* 2000;**119**:171–9.

47 Meliones JN, Kern FH, Schulman SR, Greeley WJ. Pathophysiological approach to respiratory support for patients with congenital heart disease. *Prog Pediatr Cardiol* 1995;**4**:161–7.

48 Jellinek H, Krafft P, Fitzgerald RD, *et al.* Right atrial pressure predicts hemodynamic response to apneic positive airway pressure. *Crit Care Med* 2000;**28**:672–8.

49 Cournand A, Motley HL, Werko L. Physiological studies of the effects of intermittent positive pressure breathing on cardiac output in man. *Am J Physiol* 1947;**152**:162–74.

50 Fuhrman BP. Cardiopulmonary interactions. In: Fuhrman BP, Zimmerman J, eds. *Pediatric Critical Care*, 3rd edn. Philadelphia, PA: Mosby/Elesevier, 2006: 325–45.

51 Gold PM, Murray JF. Changes in red cell distribution, hemodynamics, and blood volume in acute anemia. *J Appl Physiol* 1969; **26**:589–93.

52 Murray JF, Escobar E. Circulatory effects of blood viscosity: comparison of methemoglobinemia and anemia. *J Appl Physiol* 1968;**25**:594–9.

53 Murray JF, Escobar E, Rapaport E. Effects of blood viscosity on hemodynamic responses in acute normovolemic anemia. *Am J Physiol* 1969;**216**:638–42.

54 Murray JF, Gold P, Johnson BL Jr. Systemic oxygen transport in induced normovolemic anemia and polycythemia. *Am J Physiol* 1962;**203**:720–4.

55 Murray JF, Gold P, Johnson BL Jr. The circulatory effects of hematocrit variations in normovolemic and hypervolemic dogs. *J Clin Invest* 1963;**42**:1150–9.

56 van der Hoeven MA, Maertzdorf WJ, Blanco CE. Mixed venous oxygen saturation and biochemical parameters of hypoxia during progressive hypoxemia in 10- to 14-day-old piglets. *Pediatr Res* 1997;**42**:878–84.

57 Buckberg G, Hoffman JI, Mahajan A, *et al.* Cardiac mechanics revisited: the relationship of cardiac architecture to ventricular function. *Circulation* 2008;**118**:2571–87.

58 Hoffman JI, Mahajan A, Coghlan C, *et al.* A new look at diastole. *Heart Fail Clin* 2008;**4**:347–60.

59 Notomi Y, Popovic ZB, Yamada H, *et al.* Ventricular untwisting: a temporal link between left ventricular relaxation and suction. *Am J Physiol Heart Circ Physiol* 2008;**294**:H505–13.

60 Notomi Y, Srinath G, Shiota T, *et al.* Maturational and adaptive modulation of left ventricular torsional biomechanics: Doppler tissue imaging observation from infancy to adulthood. *Circulation* 2006;**113**:2534–41.

61 Notomi Y, Martin-Miklovic MG, Oryszak SJ, *et al.* Enhanced ventricular untwisting during exercise: a mechanistic manifestation of elastic recoil described by Doppler tissue imaging. *Circulation* 2006;**113**:2524–33.

62 Stuber M, Scheidegger MB, Fischer SE, *et al.* Alterations in the local myocardial motion pattern in patients suffering from pressure overload due to aortic stenosis. *Circulation* 1999;**100**: 361–8.

63 Kitamura K, Jorgensen CR, Gobel FL, *et al.* Hemodynamic correlates of myocardial oxygen consumption during upright exercise. *J Appl Physiol* 1972;**32**:516–22.

64 Drake-Holland AJ. Substrate utilization. In: Drake-Holland AJ, Noble MIM, eds. *Cardiac Metabolism*. Chichester: John Wiley & Sons, Ltd, 1983: 195–214.

65 Opie LH. High energy phosphate compounds. In: Drake-Holland AJ, Noble MIM, eds. *Cardiac Metabolism*. Chichester: John Wiley & Sons, Ltd, 1983.

66 Opie LH. *Fuels: Carbohydrates and Lipids*. New York: Raven Press, 1991: 279–307.

67 Anderson PAW. Immature myocardium. In: Moller JH, Neal WA, eds. *Fetal, Neonatal, and Infant Cardiac Disease*. Norwalk, CT: Appleton & Lange, 1990: 35–71.

68 Rebouche CJ, Paulson DJ. Carnitine metabolism and function in humans. *Annu Rev Nutr* 1986;**6**:41–66.

69 Roe CR, Ding J. Mitochondrial fatty acid oxidation disorders. In: Scriver CL, Beaudet AL, Valle D, Sly WS, eds. *The Metabolic Basis of Inherited Disease*, 8th edn. New York: McGraw-Hill, 2001: 2297–325.

70 Rebouche CJ. Carnitine function and requirements during the life cycle. *FASEB J* 1992;**6**:3379–86.

71 Retter AS. Carnitine and its role in cardiovascular disease. *Heart Dis* 1999;**1**:108–13.

72 Sole MJ, Jeejeebhoy KN. Conditioned nutritional requirements: therapeutic relevance to heart failure. *Herz* 2002;**27**:174–8.

73 Hedayati SS. Dialysis-related carnitine disorder. *Semin Dial* 2006;**19**:323–8.

74 DiPalma JR. Carnitine deficiency. *Am Fam Physician* 1988;**38**: 243–51.

75 Editorial. Carnitine deficiency. *Lancet* 1990;**335**:981–2.

76 Longo N, Amat di San Filippo C, Pasquali M. Disorders of carnitine transport and the carnitine cycle. *Am J Med Genet C Semin Med Genet* 2006;**142C**:77–85.

77 McDonald RH Jr. Developed tension: a major determinant of myocardial oxygen consumption. *Am J Physiol* 1966;**210**:351–6.

78 McDonald RH Jr, Taylor RR, Cingolani HE. Measurement of myocardial developed tension and its relation to oxygen consumption. *Am J Physiol* 1966;**211**:667–73.

79 Taylor RR, Cingolani HE, McDonald RH Jr. Relationships between left ventricular volume, ejected fraction, and wall stress. *Am J Physiol* 1966;**211**:674–80.

80 Strauer B-E. Ventricular function and coronary hemodynamics in hypertensive heart disease. *Am J Cardiol* 1979;**44**:999–1006.

81 Sarnoff SJ, Braunwald E, Welch GH Jr, *et al.* Hemodynamic determinants of oxygen consumption of the heart with special reference to the tension–time index. *Am J Physiol* 1958;**192**:148–56.

82 Grossman W, Jones D, McLaurin LP. Wall stress and patterns of hypertrophy in the human left ventricle. *J Clin Invest* 1975;**56**: 56–64.

83 Rooke GA, Feigl EO. Work as a correlate of canine left ventricular oxygen consumption, and the problem of catecholamine oxygen wasting. *Circ Res* 1982;**50**:273–86.

84 Vinten-Johansen J, Barnard RJ, Buckberg GD, *et al.* Left ventricular O_2 requirements of pressure and volume loading in the normal canine heart and inaccuracy of pressure-derived indices of O_2 demand. *Cardiovasc Res* 1982;**16**:439–47.

85 Vinten-Johansen J, Duncan HW, Finkenberg JG, *et al.* Prediction of myocardial O_2 requirements by indirect indices. *Am J Physiol* 1982;**243**:H862–8.

86 Weber KT, Janicki JS. Myocardial oxygen consumption: the role of wall force and shortening. *Am J Physiol* 1977;**233**:H421–30.

87 Weber KT, Janicki JS. Interdependence of cardiac function, coronary flow, and oxygen extraction. *Am J Physiol* 1978;**235**:H784–93.

88 Suga H. Ventricular energetics. *Physiol Rev* 1990;**70**:247–77.

89 Suga H. Cardiac function. In: Moller JH, Hoffman JIE, ed. *Pediatric Cardiovascular Medicine*. New York: Churchill Livingstone, 2000: 65–77.

90 Hearse DJ. Myocardial ischaemia: can we agree on a definition for the 21st century? *Cardiovasc Res* 1994;**28**:1737–44: discussion 1745–6.

91 Weiss HR, Sinha AK. Regional oxygen saturation of small arteries and veins in the canine myocardium. *Circ Res* 1978;**42**: 119–26.

92 Spotnitz HM, Sonnenblick EH, Spiro D. Relation of ultrastructure to function in the intact heart: sarcomere structure relative to pressure volume curves of intact left ventricles of dog and cat. *Circ Res* 1966;**18**:49–66.

93 Feigl EO. Coronary physiology. *Physiol Rev* 1983;**63**:1–205.

94 Hoffman JIE, Buckberg GD, Fixler DE, Archie JP. Regional flow in the right and left ventricular free walls and septum during tachycardia, aortic constriction and arterio-venous fistulas. In: Maseri A, ed. *Myocardial Blood Flow in Man*. Turin: Minerva Medica, 1972: 65–76.

95 Austin RE Jr, Smedira NG, Squiers TM, Hoffman JIE. Influence of cardiac contraction and coronary vasomotor tone on regional myocardial blood flow. *Am J Physiol* 1994;**266**(Heart and Circulatory Physiology 35):H2542–53.

96 Hoffman JI. Heterogeneity of myocardial blood flow. *Basic Res Cardiol* 1995;**90**:103–11.

97 Klocke FJ. Coronary blood flow in man. *Prog Cardiovasc Dis* 1976;**19**:117–66.

98 Chilian WM. Microvascular pressures and resistances in the left ventricular subepicardium and subendocardium. *Circ Res* 1991;**69**:561–70.

99 Domenech RJ, Goich J. Effect of heart rate on regional coronary blood flow. *Cardiovasc Res* 1976;**10**:224–31.

100 Flynn AE, Coggins DL, Goto M, *et al.* Does systolic subepicardial perfusion come from retrograde subendocardial flow? *Am J Physiol* 1992;**262**(Heart and Circulatory Physiology 31):H1759–69.

101 Kajiya F, Hiramatsu O, Kimura A, *et al.* Blood velocity patterns in poststenotic regions and velocity waveforms for myocardial inflow associated with coronary artery stenosis in dogs. *J Biomech Eng* 1992;**114**:385–90.

102 Ashikawa K, Kanatsuka H, Suzuki T, Takishima T. Phasic blood flow velocity pattern in epimyocardial microvessels in the beating canine left ventricle. *Circ Res* 1986;**59**:704–11.

103 Kajiya F, Yada T, Hiramatsu O, *et al.* Coronary microcirculation in the beating heart. *Med Biol Eng Comput* 2008;**46**:411–9.

104 Kajiya F, Yada T, Matsumoto T, *et al.* Intramyocardial influences on blood flow distributions in the myocardial wall. *Ann Biomed Eng* 2000;**28**:897–902.

105 Toyota E, Ogasawara Y, Hiramatsu O, *et al.* Dynamics of flow velocities in endocardial and epicardial coronary arterioles. *Am J Physiol Heart Circ Physiol* 2005;**288**:H1598–603.

106 Canty JM Jr. Coronary pressure-function and steady-state pressure–flow relations during autoregulation in the unanesthetized dog. *Circ Res* 1988;**63**:821–36.

107 Liu Y, Gutterman DD. Vascular control in humans: focus on the coronary microcirculation. *Basic Res Cardiol* 2009;**104**:211–27.

108 Bache RJ, Vrobel TR, Arentzen CE, Ring WS. Effect of maximal coronary vasodilation on transmural myocardial perfusion during tachycardia in dogs with left ventricular hypertrophy. *Circ Res* 1981;**49**:742–50.

109 Bache RJ, Vrobel TR, Ring WS, *et al.* Regional myocardial blood flow during exercise in dogs with chronic left ventricular hypertrophy. *Circ Res* 1981;**48**:76–87.

110 Boudoulas H, Rittgers SE, Lewis RP, *et al.* Changes in diastolic time with various pharmacologic agents: implication for myocardial perfusion. *Circulation* 1979;**60**:164–9.

111 Graham TP Jr, Covell JW, Sonnenblick EH, *et al.* Control of myocardial oxygen consumption: relative influence of contractile state and tension development. *J Clin Invest* 1968;**47**:375–85.

112 Hoffman JIE. Problems of coronary flow reserve. *Ann Biomed Eng* 2000;**28**:884–96.

113 Hoffman JIE. Maximal coronary flow and the concept of coronary vascular reserve. *Circulation* 1984;**70**:153–9.

114 Hoffman JIE. A critical view of coronary reserve. *Circulation* 1987;**75**(Suppl I):6–11.

115 McGinn AL, White CW, Wilson RF. Interstudy variability of coronary flow reserve: influence of heart rate, arterial pressure, and ventricular preload. *Circulation* 1990;**81**:1319–30.

116 Coggins DL, Flynn AE, Austin RE Jr, *et al.* Nonuniform loss of regional flow reserve during myocardial ischemia in dogs. *Circ Res* 1990;**67**:253–64.

117 Hoffman JIE, Spaan JAE. Pressure–flow relations in coronary circulation. *Physiol Rev* 1990;**70**:331–90.

118 Vanhoutte PM. Endothelial control of vasomotor function: from health to coronary disease. *Circ J* 2003;**67**:572–5.

119 Duncker DJ, Bache RJ. Regulation of coronary blood flow during exercise. *Physiol Rev* 2008;**88**:1009–86.

120 Dick GM, Tune JD. Role of potassium channels in coronary vasodilation. *Exp Med Biol* 2010;**235**:10–22.

121 Berne RM. The role of adenosine in the regulation of coronary blood flow. *Circ Res* 1980;**47**:807–13.

122 Hoffman JIE. Coronary physiology. In: Garfein OB, ed. *Current Concepts in Cardiovascular Physiology*. New York: Academic Press, 1990: 289–349.

123 Hanley FL, Grattan MT, Stevens MB, Hoffman JIE. Role of adenosine in coronary autoregulation. *Am J Physiol* 1986;**250** (Heart and Circulatory Physiology 19):H558–66.

124 Feigl EO. Coronary autoregulation. *J Hypertens Suppl* 1989;**7**:S55–8; discussion S9.

125 Saitoh S, Zhang C, Tune JD, *et al.* Hydrogen peroxide: a feed-forward dilator that couples myocardial metabolism to coronary blood flow. *Arterioscler Thromb Vasc Biol* 2006;**26**: 2614–21.

126 Wang R. Two's company, three's a crowd: can H_2S be the third endogenous gaseous transmitter? *FASEB J* 2002;**16**:1792–8.

127 Yang G, Wu L, Jiang B, *et al.* H_2S as a physiologic vasorelaxant: hypertension in mice with deletion of cystathionine gamma-lyase. *Science* 2008;**322**:587–90.

128 Olson KR, Whitfield NL. Hydrogen sulfide and oxygen sensing in the cardiovascular system. *Antioxid Redox Signal* 2010;**12**: 1219–34.

129 Liu Y, Zhao H, Li H, *et al.* Mitochondrial sources of H_2O_2 generation play a key role in flow-mediated dilation in human coronary resistance arteries. *Circ Res* 2003;**93**:573–80.

130 Larsen BT, Gutterman DD, Sato A, *et al.* Hydrogen peroxide inhibits cytochrome p450 epoxygenases: interaction between two endothelium-derived hyperpolarizing factors. *Circ Res* 2008;**102**:59–67.

131 Brzezinska AK, Merkus D, Chilian WM. Metabolic communication from cardiac myocytes to vascular endothelial cells. *Am J Physiol Heart Circ Physiol* 2005;**288**:H2232–7.

132 Rogers PA, Chilian WM, Bratz IN, *et al.* H_2O_2 activates redox- and 4-aminopyridine-sensitive Kv channels in coronary vascular smooth muscle. *Am J Physiol Heart Circ Physiol* 2007;**292**: H1404–11.

133 Oltman CL, Kane NL, Miller FJ Jr, *et al.* Reactive oxygen species mediate arachidonic acid-induced dilation in porcine coronary microvessels. *Am J Physiol Heart Circ Physiol* 2003;**285**:H2309–15.

134 Thengchaisri N, Kuo L. Hydrogen peroxide induces endothelium-dependent and -independent coronary arteriolar dilation: role of cyclooxygenase and potassium channels. *Am J Physiol Heart Circ Physiol* 2003;**285**:H2255–63.

135 Feletou M, Vanhoutte PM. Endothelium-derived hyperpolarizing factor: where are we now? *Arterioscler Thromb Vasc Biol* 2006;**26**:1215–25.

136 Mitchell JA, Ali F, Bailey L, *et al.* Role of nitric oxide and prostacyclin as vasoactive hormones released by the endothelium. *Exp Physiol* 2010;**93**:141–7.

137 Kozma F, Johnson RA, Zhang F, *et al.* Contribution of endogenous carbon monoxide to regulation of diameter in resistance vessels. *Am J Physiol* 1999;**276**:R1087–94.

138 Loboda A, Jazwa A, Grochot-Przeczek A, *et al.* Heme oxygenase-1 and the vascular bed: from molecular mechanisms to therapeutic opportunities. *Antioxid Redox Signal* 2008;**10**:1767–812.

139 Gow AJ, Stamler JS. Reactions between nitric oxide and haemoglobin under physiological conditions. *Nature* 1998;**391**:169–73.

140 Jia L, Bonaventura C, Bonaventura J, Stamler JS. *S*-Nitrosohaemoglobin: a dynamic activity of blood involved in vascular control. *Nature* 1996;**380**:221–6.

141 Stamler JS, Jia L, Eu JP, *et al.* Blood flow regulation by *S*-nitrosohemoglobin in the physiological oxygen gradient. *Science* 1997;**276**:2034–7.

142 Cosby K, Partovi KS, Crawford JH, *et al.* Nitrite reduction to nitric oxide by deoxyhemoglobin vasodilates the human circulation. *Nat Med* 2003;**9**:1498–505.

143 Kim-Shapiro DB, Schechter AN, Gladwin MT. Unraveling the reactions of nitric oxide, nitrite, and hemoglobin in physiology and therapeutics. *Arterioscler Thromb Vasc Biol* 2006;**26**: 697–705.

144 Aamand R, Dalsgaard T, Jensen FB, *et al.* Generation of nitric oxide from nitrite by carbonic anhydrase: a possible link between metabolic activity and vasodilation. *Am J Physiol Heart Circ Physiol* 2009; **297**:H2068–74.

145 Hoffman JIE. Transmural myocardial perfusion. *Prog Cardiovasc Dis* 1987;**29**:429–64.

146 Hoffman JIE, Buckberg GD. Transmural variations in myocardial perfusion. In: Yu P, Goodwin JF, eds. *Progress in Cardiology*. Philadelphia, PA: Lea and Febiger, 1976: 37–89.

147 Buckberg GD, Fixler DE, Archie JP, Hoffman JI. Experimental subendocardial ischemia in dogs with normal coronary arteries. *Circ Res* 1972;**30**:67–81.

148 Brazier JR, Buckberg GD. Effects of tachycardia on the adequacy of subendocardial oxygen delivery in experimental aortic stenosis. *Am Heart J* 1975;**90**:222–30.

149 Hoffman JIE. Coronary circulation, cardiac hypertrophy, and myocardial ischemia: basic concepts. In: Safar ME, Fouad-Tarazi FM, eds. *The Heart in Hypertension*. Dordrecht: Kluwer, 1989: 243–51.

150 Marcus ML. *The Coronary Circulation in Health and Disease*. New York: McGraw-Hill, 1983.

151 Strauer B-E. Myocardial oxygen consumption in chronic heart disease: role of wall stress, hypertrophy and coronary reserve. *Am J Cardiol* 1979;**44**:730–40.

152 Strauer B-E. *Hypertensive Heart Disease*. New York: Springer, p980.

153 Wicker P. Coronary circulation and coronary reserve in the hypertensive heart. In: Safar ME, Fouad-Tarazi FM, eds. *The Heart in Hypertension*. Dordrecht: Kluwer, 1989: 253–69.

154 Botham MJ, Lemmer JH, Gerren RA, *et al.* Coronary vasodilator reserve in young dogs with moderate right ventricular hypertrophy. *Ann Thorac Surg* 1984;**38**(2):101–7.

155 Vlahakes GJ, Turley K, Uhlig PN, *et al.* Experimental model of congenital right ventricular hypertrophy created by pulmonary artery banding *in utero*. *Surg Forum* 1981;**32**: 233–6.

156 Tomanek RJ, Schalk KA, Marcus ML, Harrison DG. Coronary angiogenesis during long-term hypertension and left ventricular hypertrophy in dogs. *Circ Res* 1989;**65**:352–9.

157 Moller JH, Nakib A, Edwards JE. Infarction of papillary muscles and mitral insufficiency associated with congenital aortic stenosis. *Circulation* 1966;**34**:87–91.

158 Cheitlin MD, Robinowitz M, McAllister H, *et al.* The distribution of fibrosis in the left ventricle in congenital aortic stenosis and coarctation of the aorta. *Circulation* 1980;**62**:823–30.

159 Franciosi RA, Blanc WA. Myocardial infarcts in infants and children. I. A necropsy study in congenital heart disease. *J Pediatr* 1968;**73**:309–19.

160 Judge TP, Kennedy JW, Bennett LJ, *et al.* Quantitative hemodynamic effects of heart rate in aortic regurgitation. *Circulation* 1971;**44**:355–67.

161 Meyer TE, Sareli P, Marcus RH, *et al.* Beneficial effect of atrial pacing in severe acute aortic regurgitation and role of M-mode echocardiography in determining the optimal pacing interval. *Am J Cardiol* 1991;**67**:398–403.

162 Buckberg GD. Left ventricular subendocardial necrosis. *Ann Thorac Surg* 1977;**24**:379–93.

163 Buckberg GD, Towers B, Paglia DE, *et al.* Subendocardial ischemia after cardiopulmonary bypass. *J Thorac Cardiovasc Surg* 1972;**64**:669–84.

164 Ghidoni JJ, Liotta D, Thomas H. Massive subendocardial damage accompanying prolonged ventricular fibrillation. *Am J Pathol* 1969;**56**:15–29.

165 Najafi H, Henson D, Dye WS, *et al.* Left ventricular hemorrhagic necrosis. *Ann Thorac Surg* 1969;**7**:550–61.

166 Morales AR, Fine G, Taber RE. Cardiac surgery and myocardial necrosis. *Arch Pathol* 1967;**83**:71–9.

167 Hottenrott C, Buckberg GD. Studies of the effects of ventricular fibrillation on the adequacy of regional myocardial flow. II. Effects of ventricular distension. *J Thorac Cardiovasc Surg* 1974;**68**:626–33.

168 Hottenrott C, Buckberg GD, Maloney JV Jr. Effects of ventricular fibrillation on distribution and adequacy of coronary blood flow. *Surg Forum* 1972;**23**:200–2.

169 Hottenrott C, Maloney JV Jr, Buckberg GD. Studies of the effects of ventricular fibrillation on the adequacy of regional myocardial flow. III. Mechanisms of ischemia. *J Thorac Cardiovasc Surg* 1974;**68**:634–46.

170 Harada K, Tamura M, Orino T, Yasuoka K. Coronary blood flow assessed by transthoracic echocardiography in neonates. *Pediatr Cardiol* 2001;**22**:189–93.

171 Harada K, Yasuoka K, Tamura M, Toyono M. Coronary flow reserve assessment by Doppler echocardiography in children with and without congenital heart defect: comparison with invasive technique. *J Am Soc Echocardiogr* 2002;**15**:1121–6.

172 Yasuoka K, Harada K, Tamura M, *et al.* Blood flow in the left anterior descending coronary artery in children with ventricular septal defect. *J Am Soc Echocardiogr* 2002;**15**:807–13.

173 Oskarsson G. Coronary flow and flow reserve in children. *Acta Paediatr Suppl* 2004;**93**:20–5.

174 Oskarsson G, Pesonen E. Coronary flow abnormalities in neonates with aortic stenosis. *J Pediatr* 2000;**137**:875–7.

175 Oskarsson G, Pesonen E. Coronary blood flow in healthy neonates: effects of left ventricular function and mass. *Pediatr Cardiol* 2004;**25**:11–6.

176 Aburawi EH, Liuba P, Pesonen E. Coronary blood flow by transthoracic echocardiography in children with endomyocardial fibrosis. *Pediatr Cardiol* 2009;**30**:371–3.

177 Chhatriwalla AK, Prieto LR, Brunken RC, *et al.* Preliminary data on the diagnostic accuracy of rubidium-82 cardiac PET perfusion imaging for the evaluation of ischemia in a pediatric population. *Pediatr Cardiol* 2008;**29**:732–8.

178 Lewis AB, Heymann MA, Stanger P, *et al.* Evaluation of subendocardial ischemia in valvar aortic stenosis in children. *Circulation* 1974;**49**:978–84.

179 Vincent WR, Buckberg GD, Hoffman JIE. Left ventricular subendocardial ischemia in severe valvar and supravalvar aortic stenosis. A common mechanism. *Circulation* 1974;**49**:326–33.

180 Barnard RJ, Gardner GW, Diaco NV, *et al.* Cardiovascular responses to sudden strenuous exercise – heart rate, blood pressure, and ECG. *J Appl Physiol* 1973;**34**:833–7.

181 Brazier J, Cooper N, Buckberg GD. The adequacy of subendocardial oxygen delivery: the interaction of determinants of flow, arterial oxygen content and myocardial oxygen need. *Circulation* 1974;**49**:968–77.

182 Buckberg G, Eber L, Herman M, Gorlin R. Ischemia in aortic stenosis: hemodynamic prediction. *Am J Cardiol* 1975;**35**:778–84.

183 Ogawa S, Ohkubo T, Fukazawa R, *et al.* Estimation of myocardial hemodynamics before and after intervention in children with Kawasaki disease. *J Am Coll Cardiol* 2004;**43**:653–61.

184 Hoffman JIE. Do we have a gold standard yet? *J Am Coll Cardiol* 2004;**43**:662–4.

185 Spaan JA, Piek JJ, Hoffman JIE, Siebes M. Physiological basis of clinically used coronary hemodynamic indices. *Circulation* 2006;**113**:446–55.

186 Vlahakes GJ, Turley K, Hoffman JIE. The pathophysiology of failure in acute right ventricular hypertension: hemodynamic and biochemical correlations. *Circulation* 1981;**63**:87–95.

187 Belenkie I, Horne SG, Dani R, *et al.* Effects of aortic constriction during experimental acute right ventricular pressure loading. Further insights into diastolic and systolic ventricular interaction. *Circulation* 1995;**92**:546–54.

188 Brooks H, Kirk ES, Vokonas PS, Urschel CW. Sonnenblick EH. Performance of the right ventricle under stress: relation to right coronary flow. *J Clin Invest* 1971;**50**:2176–83.

189 Archie JP, Fixler DE, Ullyot DJ, *et al.* Regional myocardial blood flow in lambs with concentric right ventricular hypertrophy. *Circ Res* 1974;**34**:143–54.

190 Manohar M, Thurmon JC, Tranquilli WJ, *et al.* Regional myocardial blood flow and coronary vascular reserve in unanesthetized young calves with severe concentric right ventricular hypertrophy. *Circ Res* 1981;**48**:785–96.

191 Murray PA, Vatner SF. Reduction of maximal coronary vasodilator capacity in conscious dogs with severe right ventricular hypertrophy. *Circ Res* 1981;**48**:25–33.

192 Cooper N, Brazier J, Buckberg G. Effects of systemic-pulmonary shunts on regional myocardial blood flow in experimental pulmonary stenosis. *J Thorac Cardiovasc Surg* 1975;**70**:166–76.

193 Lowensohn HS, Khouri EM, Gregg DE, *et al.* Phasic right coronary artery blood flow in conscious dogs with normal and elevated right ventricular pressures. *Circ Res* 1976;**39**:760–6.

5

Pulmonary Vascular Pathophysiology

Marlene Rabinovitch

Stanford University School of Medicine, Stanford CA, USA

Development of the pulmonary vasculature in embryonic and fetal life

Severe pathological changes of pulmonary hypertension (PAH) are observed in the arteries accompanying the terminal respiratory unit or the acinus. The acinus is composed of the terminal bronchiole, respiratory bronchioli, alveolar ducts, and alveoli. Normally in the newborn, arteries at the level of the terminal bronchiolus are muscular, whereas those accompanying respiratory bronchioli are mostly partially muscular (surrounded by a spiral of muscle). Arteries at alveolar duct and wall levels are generally nonmuscular. The immediate postnatal period is characterized by rapid recruitment of small alveolar duct and wall arteries, which appear to be functionally and structurally closed in the prenatal period [1].

Progressive dilatation of muscular arteries also occurs postnatally – that is, the smallest muscular arteries (<250 μm) dilate, and their walls thin to adult levels within a few days; by the age of 4 months, this process has included the largest pulmonary arteries (PAs) at the hilum. With age, more distal arteries become muscularized. Although most alveolar duct arteries become partially muscularized, most alveolar wall arteries remain nonmuscular even in the adult [2]. The process of distal muscularization appears to be related to the differentiation of pericytes and recruitment of fibroblasts that also differentiate into muscle cells.

Precapillary (alveolar duct and alveolar wall) arteries proliferate through the neonatal period and early infancy, accompanying the proliferation of alveoli; the ratio of alveoli to arteries can therefore be used as a measure of numerical arterial growth. The ratio of alveoli to arteries decreases from the newborn value of 20:1 to 6:1–8:1, which is achieved first in early childhood and persists.

Experimental studies indicate that the normal adaptation to postnatal life is regulated by remodeling of the smooth muscle cell actin cytoskeleton through the Rho-kinase pathway and by changes in the production of connective tissue, especially elastin and collagen. Several groups relate lung vascular development to alterations in growth factors and extracellular matrix molecules that regulate migration, proliferation, and differentiation of endothelial, smooth muscle cells, and fibroblasts and direct the process of branching morphogenesis. Cells sense changes in extracellular matrix proteins, such tenascin-C [3],that influence the activity of growth actors, including vascular endothelial growth factor (VEGF), fibroblast growth factors (FGF-1 and FGF-2), and angiopoietins and their interaction with receptors. The balance between proteases and antiproteinases regulate the constant turnover of matrix and the cell surface expression of growth factor receptors that direct vascular cell behavior.

Recent studies have shown that VEGF coordinates alveolar and vascular development [4] and is regulated by transcription factors, such as the hypoxia inducible transcription factor [5]. The Wnt signaling pathway also plays an important role in lung vascular development [6], as do specific transcription factors [7]. Vasoactive peptides, such as endothelin, induce smooth muscle cell proliferation. This effect is balanced by nitric oxide (NO) [4], produced by NO synthase [8]. The availability of NO is also controlled by nitrites [9].

Congenital heart defects with pulmonary hypertension

Lung biopsy studies from patients with a congenital heart defect first suggested how structural alterations in the PAs lead to progressive hemodynamic changes in the pulmonary circulation [10] (Figure 5.1). The first PA abnormality detected in a patient with a congenital heart defect and high pulmonary blood flow and pressure is extension of muscle into peripheral normally non-muscular arteries (morphometric grade A) [11] (Figure 5.1). This appears to be an acceleration and exaggeration of the normal process of growth associated with differentiation
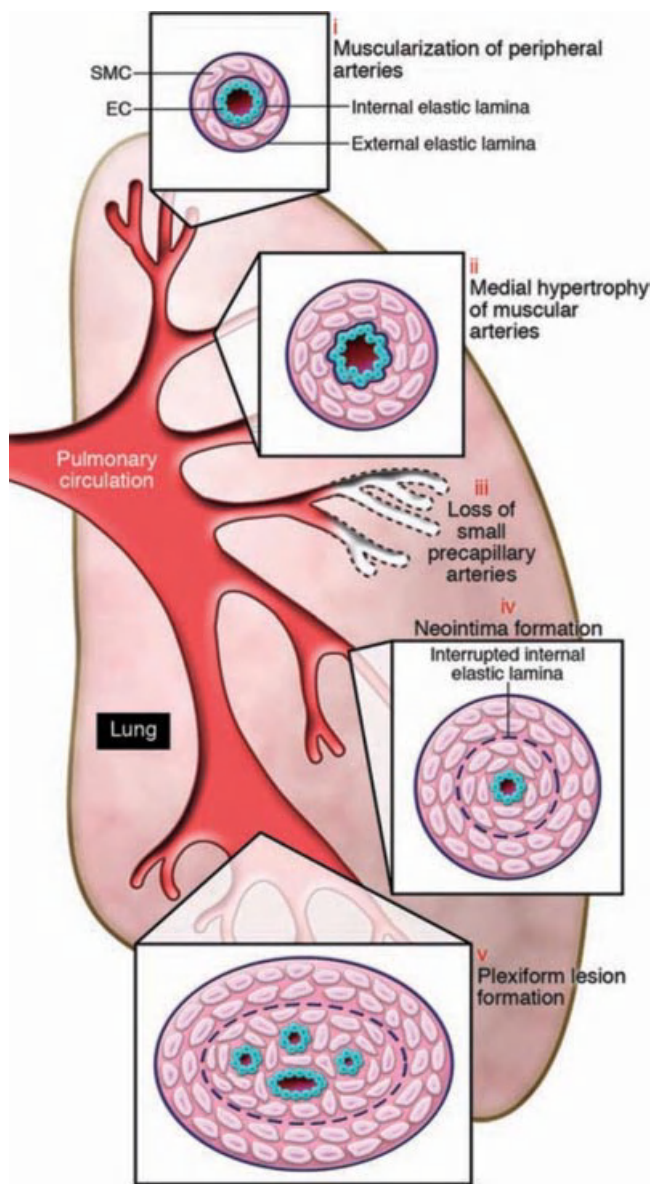
Figure 5.1 Pathobiology of PH. Schema illustrating the different vascular abnormalities compared with normal pulmonary circulation, associated with PH. This schema depicts the abnormalities throughout the pulmonary circulation, including (i) abnormal muscularization of distal precapillary arteries, (ii) medial hypertrophy (thickening) of large pulmonary muscular arteries, (iii) loss of precapillary arteries, (iv) neointimal formation that is particularly occlusive in vessels 100–500 μM, and (v) formation of plexiform lesions in these vessels. EC, endothelial cell; SMC, smooth muscle cell. (Reproduced from Rabinovitch, *J Clin Invest* 2008;**118**:2372–9, with permission.)

of pericytes into smooth muscle cells (SMCs) that subsequently proliferate and also recruitment of fibroblasts. The initial response to high flow induced experimentally from the time of birth appears to be angiogenic with high levels of VEGF and its receptors.

The second change is medial hypertrophy of muscular arteries (grade B). It always accompanies abnormal muscularization of distal arteries and is associated with high mean PA pressure. This change represents an increase in the number and size of smooth muscle cells in the muscular media of the arterial wall.

The third change, reduced arterial number (grade C), is always accompanied by muscularization of peripheral arteries and medial hypertrophy of muscular arteries, and is associated with elevated pulmonary vascular resistance. The basis for grade C is likely the failure of new vessels to develop and also "injury"-mediated loss of arteries through apoptosis of endothelial cells and pericytes. Grades A and B are refinements of Heath–Edwards grade I (medial hypertrophy). Grade C may be found with Heath–Edwards grade I, is common with grade II (cellular neointimal formation), and is invariable with grade III (occlusive neointimal formation with fibrosis). In fact, when grade III is seen, the arterial concentration is generally half of normal or less.

Progressive neointimal obliterative and plexiform lesions are associated with a progressive rise in resistance to flow that culminates in right to left shunting in the presence of a congenital heart defect. The extensive neointimal obliterative changes (Heath–Edwards grade III) are related to an expansive proliferation and migration of cells considered to be SMCs because they express α-SM actin. These cells may represent a specialized subpopulation of SMCs or they may have originated as stem cells or fibrocytes (cells that have properties of fibroblasts and leukocytes), or they may even be transformed endothelial cells (ECs).

The development of the dilatation complex and plexiform lesion (Heath–Edwards grade IV and V, respectively) is characterized by the formation of aberrant channels in the otherwise obliterated lumen of the vessel and in the adventitia. These channels may reflect clonal expansion of apoptosis-resistant ECs or they may originate from circulating endothelial progenitor cells that accumulate at sites of endothelial denudation or injury and expand locally.

In general, features of grade IIIC or more severe abnormalities, such as Heath–Edwards grade IV (dilatation complexes) or grade V (angiomata formation), that together comprise plexiform lesions, or grade VI (fibrinoid necrosis), are observed with severe elevation in pulmonary vascular resistance >8 U m^{-2} that is frequently refractory to acute vasodilation in response to oxygen, prostacyclin, or NO. A pulmonary wedge angiogram performed at the time of a catheter study can help relate the extent of pulmonary vascular disease to the calculations of pulmonary vascular resistance. A frozen section is a valuable addition to the hemodynamic data and angiogram in helping make a clinical decision with regard to operability.

Age at cardiac repair is critical in the potential for hemodynamic improvement and (presumably) resolution of the vascular pathology. For example, infants repaired under

6 months of age had normal hemodynamics as assessed at cardiac catheter study 1 year later, whereas those repaired over 2 years of age characteristically had some impairment or even progressive disease, except if the pathology was limited to muscularized arteries and medial hypertrophy (grade B) [12–14]. This is consistent with early studies showing that in a congenital heart defect, such as a ventricular septal defect with PAH, banding the PA band in infancy could substantially reverse the PA vascular pathology [15]. Regression of medial hypertrophy and muscularization of distal vessels has been shown in experimental studies following pressure off-loading. We showed that transplantation into a normal rat of a lung from a rat in which a toxin, monocrotaline, had induced severe pulmonary vascular disease resulted in regression of those abnormalities. Regression of severe pulmonary vascular disease occurred in the original lung from a PAH patient that remained after single lung transplant [16]. However, there is the possibility that the regression might have been induced by immunosuppressive agents rather than by the reduction in PA pressure. Experimentally, immunosuppressive agents can attenuate PAH. As we learn more about the genetic basis of congenital heart disease, we may uncover genes that contribute to the PA pathology independent of the hemodynamic changes.

Endothelial biology and pathobiology of PA hypertension

EC dysfunction appears to play a central role in the development of pulmonary vascular disease. Scanning and transmission electron microscopic analyses [17] revealed structural alterations in the PA ECs from patients with PAH. These were related functionally to defective von Willebrand factor, a blood glycoprotein involved in coagulation and fibrinolysis, and also to abnormal production of vasodilators and repressors of SMC proliferation.

Endothelial alterations precede the development of muscularization of PAs. Cultured PA ECs release factors, such as FGF-2, that stimulate the proliferation of PA SMCs [18]. In PA ECs from patients with idiopathic PAH (IPAH), there is an increased release of serotonin from ECs and serotonin-mediated SMC proliferation. In recent studies, we have shown that reduced production of apelin by PAH PA ECs impairs endothelial recovery from injury (survival) and derepresses PA SMC proliferation.

PA ECs from patients with IPAH produce decreased amounts of NO, a vasodilator and suppressor of SMC proliferation. The reduction in NO is thought to be related to reduced endothelial nitric oxide synthase or high arginase levels [19], because L-arginine is the substrate of NO synthase required to produce NO. The ECs from patients with PAH are highly proliferative in response to growth factors and represent expansion of apoptosis-resistant clones that exhibit high rates of glycolysis attributed to induction of hypoxia inducible factor [20]. These cells, however, appear poorly differentiated and show impaired formation of endothelial tubes in culture. This is consistent with the observation that PAH ECs fail to restore the precapillary vessels that have been occluded or lost.

There is also considerable thickening of the pulmonary adventitia and venous hypertrophy in patients with PAH. Immunohistochemical studies have revealed increased expression of transforming growth factor (TGF)-β, matrix glyoproteins and glycosaminoglycans, in addition to macrophages, and T cells, and also inflammatory mediators such as fractalkine. Our immunohistochemical studies carried out on lung biopsy tissue from patients with congenital heart defects showed that the deposition of the glycoproteins tenascin-C and fibronectin in the media and neointima increases progressively with the severity of the lesion. We related increased expression of tenascin-C to vascular smooth muscle cell proliferation and deposition of fibronectin to smooth muscle cell migration associated with neointimal formation [21]. Studies by other investigators found evidence that the neointimal lesions in PAH are accompanied by increased expression of TGF-β and procollagen. More recently, we described an increase in the expression of the calcium binding protein S100A4/Mts1 in advanced lesions from patients with congenital heart defects causing PAH or with IPAH (Figure 5.2) [22]. S100A4/Mts1 stimulates vascular smooth muscle cell migration and proliferation, is produced in response to serotonin stimulation [23], and is enhanced with increased activity of the serotonin transporter. This is in keeping with studies indicating that a polymorphism causing heightened activity of the serotonin transporter is increased in patients with PAH [24].

Counteracting the pathology of PAH with "vasodilator" therapy

The idea that the advanced pathology associated with PAH could be attenuated or reversed by vasodilator therapy originated in studies of patients with IPAH in which there was evidence of reduced circulating levels of the vasodilator prostacyclin relative to the vasoconstrictor thromboxane. This observation led to the institution of continuous intravenous prostacyclin as a therapy for PAH patients, a treatment that, despite not always reducing the pulmonary vascular resistance, has appreciably improved the quality of life and the survival of PAH patients (see Chapter 51). A recent meta-analysis, however, has questioned the survival benefit of this and other therapies for PAH in adults. A compelling need exists to find oral and improved alternatives to intravenous prostacyclin. Experimental studies in rats with hypoxia-induced pulmonary hypertension documented elevated levels of endothelin (ET), a powerful vasoconstrictor that promotes SMC proliferation and inflammation [25]. In clinical studies, an increase in ET was
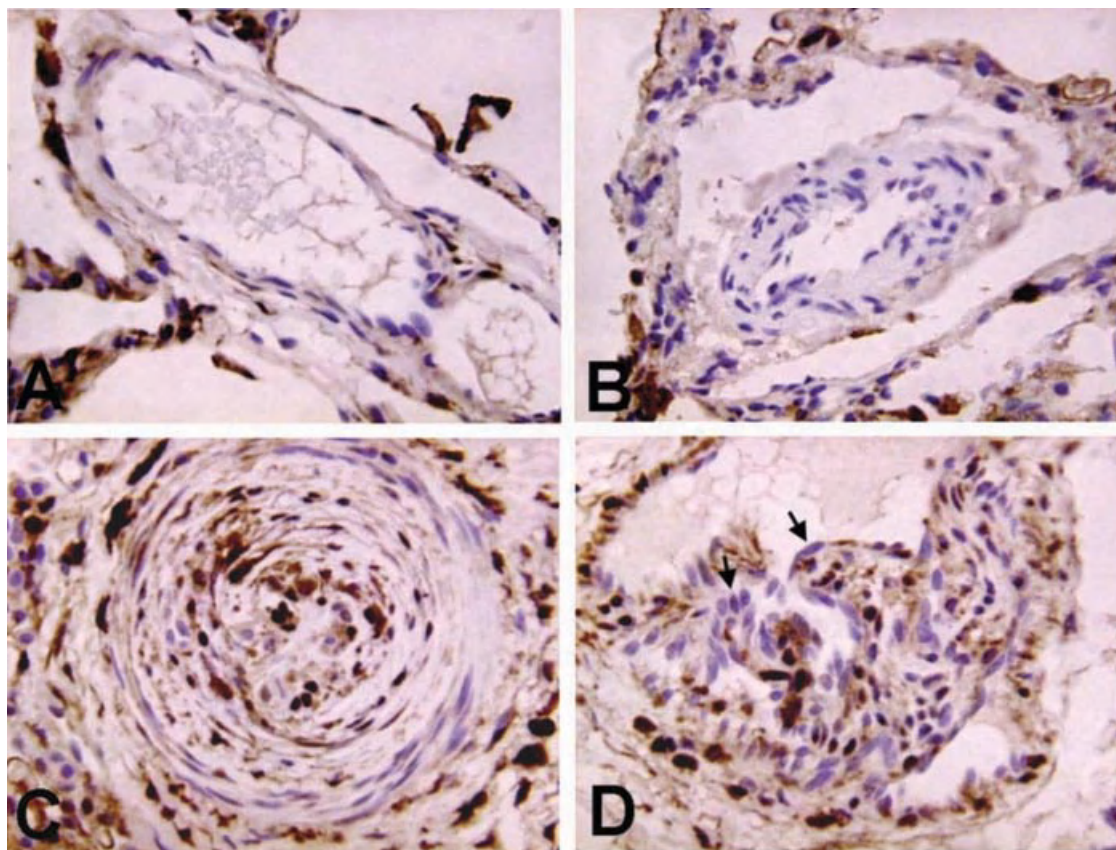
Figure 5.2 Representative photomicrographs of human lung biopsy tissue after immunoperoxidase staining for S100A4/Mts1. (a) Vessel from patient graded 0–IB showing normal pulmonary artery with no immunodetectable S100A4/Mts1. (b) Vessel showing a typical grade IB lesion with severe medial hypertrophy but without immunoreactivity for S100A4/Mts1. (c) An artery from a patient with grade IVC disease with occlusive neointimal proliferation and strong positive staining for S100A4/Mts1 particularly in the intima compared with the media of the vessel. S100A4/Mts1 was not detected in all cells and appears to be localized in a subpopulation of intimal cells. (d) A plexogenic lesion from a patient with grade IVC disease with staining of the smooth muscle cells and sparing of the endothelial cells (arrows). Immunoreactivity for S100A4/Mts1 was present in the lung parenchyma at a similar level in all grades of pulmonary vascular disease. Original magnification, ×40. (Reproduced from Greenway *et al*. *Am J Pathol* 2004;**164**:253–62, with permission.)

detected in the lungs of patients with IPAH [26]. Hence ET receptor blockade was proposed as a potential treatment for PAH. The two endothelin receptor subtypes ET_A and ET_B are found in smooth muscle cells of blood vessels and both can mediate vasoconstriction. However, ET_B receptors on ECs may mediate vasodilatation and ET clearance, particularly in microvessels. Recent results using either the dual ET receptor antagonist or a selective ET_A receptor antagonist demonstrate a reduction in symptoms and slowing of PAH progression in some patients. Studies documenting reduced expression of NO synthase, the enzyme that generates NO, suggested that phosphodiesterase V inhibitors, such as sildenafil, could prolong the NO-mediated increase in cGMP to dilate PAs effectively. Phosphodiesterase inhibitors also improve cardiac function. Recent studies showed that nitrites, molecules that produce NO in the lung, may also be of therapeutic benefit as they reverse experimental pulmonary vascular disease.

Experimental studies have also shown success in reversing PAH with other vasodilators that include adrenomedullin. Vasoactive intestinal peptide (VIP), a vasodilator and inhibitor of SMC proliferation, is a very promising agent. Transgenic mice that are null for VIP develop PAH with remodeled distal arteries. Studies in rodents showing vasodilatation and reversal of PAH by Rho-kinase inhibitors such as fasudil that disassemble the cytoskeleton suggest that these agents should be developed for clinical use. Fasudil has shown some benefit in acute testing of PAH patients. The systemic hypotensive side effects of fasudil may be reduced when it is administered via inhalation. Table 5.1 lists novel agents currently in use or in trial for treatment of pulmonary hypertension.

Table 5.1 Summary schema outlining current and future therapeutic strategies. Those with asterisks are in trial for PAH, those in bold are in trial for other indications and that in italics is in clinical use for other indications.

Elastin inhibition
Kv channel openers (DCA)
Malonyl coenzyme decarboxylase inhibitor
TRP channel suppressor
Dominant negative survivin
*Statins
VIP
*PPARγ agonists
*Growth factor inhibitors (anti-PDGF, EGF)
Adrenomedullin
*Rho-kinase inhibition
*Endothelial progenitor cells engineered with eNOS
Cyclosporine and rapamycin
Apelin
γ-Secretase inhibitors

Modified from Rabinovitch, *J Clin Invest* 2008;**118**:2372–9.

Chronic hypoxia-induced pulmonary hypertension

Chronic hypoxia induces PAH and vascular changes that, based upon experimental studies, consist of muscularization of distal vessels, medial hypertrophy of muscular arteries, and a reduced number of peripheral arteries despite the increase in capillaries from an increase in hypoxia-inducible transcription factors. These features are largely reversible with restoration of a normoxic environment. However, we have learned about the pathobiology of PAH by studying mechanisms by which chronic hypoxia causes remodeling of the PAs.

Stenmark *et al*. [27] took newborn calves to a simulated high altitude of 4300 m and observed severe PAH with right-to-left shunting from the rapid development of suprasystemic levels of pulmonary artery pressure. There was striking medial hypertrophy and remarkable proliferation of a dense adventitial sheath that, in large vessels, was sometimes seen to exhibit neovascularization. A striking increase in elastin synthesis in the pulmonary arteries of these neonatal calves [28,29] was observed but, based on studies in rats, this is likely stimulated by ongoing elastin degradation. Fibrocytes, cells having characteristics of both fibroblasts and leukocytes, appear to be key contributors to the remodeling of the pulmonary vasculature. They migrate into the vessel wall through openings in the expanding adventitia [30].

There are both direct cellular effects of hypoxia and indirect effects that are the consequence of the hemodynamic changes, that is, vasoconstriction. For example, pulmonary artery smooth muscle cells of neonatal lambs and bovine endothelial cells in culture show decreased production of prostacyclin in response to acute hypoxic exposure. Endothelin receptor blockade appears to be most selective in reversing acute hypoxia-induced pulmonary vasoconstriction and also the remodeling associated with chronic exposure. However, even without vasoconstriction, hypoxia inhibits endothelin receptor B-mediated NO synthesis and cyclic guanosine monophosphate (cGMP)-dependent activation of NO is impaired. Agents useful in treating chronic hypoxic pulmonary hypertension, at least based on experimental studies in rodents, include inhibitors of 5-lipoxygenase activating protein and also phosphodiesterase inhibitors and continuous inhalation of NO. Because potassium channels are down-regulated during hypoxia in association with an influx of calcium that promotes vasoconstriction and smooth muscle cell proliferation, activation of voltage-gated K channels (Kv 2.1) by gene transfer or a metabolic activator inhibits chronic hypoxic pulmonary hypertension. Activating metabolic pathways that positively influence mitochondrial metabolism and prevent K channel activation and SMC proliferation can also be achieved by Nfatc inhibition and by malonyl coenzyme carboxylase.

Recent studies of transgenic mice have extended our knowledge about important mechanisms in regulating both hypoxia-induced vasoconstriction and vascular remodeling. For example, in the absence of hemoxygenase 1, there is reduced production of CO and its associated vasodilatory effects [31]. Prostacyclin synthetase overexpression can protect against the hemodynamic and vascular changes in pulmonary hypertension. In the fawn-hooded rat, abnormal release of serotonin is implicated in the pulmonary hypertension observed with mild hypoxia. There are also abnormalities in mitochondrial metabolism that activate hypoxia-inducible genes [20]. Consistent with this observation, the severity of pulmonary vascular disease induced by chronic hypoxia is enhanced in mice lacking the serotonin transporter gene. Recently, Rho-kinase inhibitors and PPARγ agonists have proven effective in preventing and reversing pulmonary hypertension and structural changes associated with chronic hypoxia. Mice lacking PPARγ in either endothelial cells [32] or smooth muscle cells [33] have PAH.

Over-expression of the serotonin transporter worsens hypoxia-induced pulmonary hypertension, as does loss of function of bone morphogenetic protein receptor II (BMP-RII) (the gene that is mutant in familial and sporadic IPAH). Reduced BMP-RII in cultured smooth muscle cells and in transgenic mice makes them more sensitive to the pro-proliferative effects of serotonin or of inflammatory stimuli. Experimental studies in hypoxic rodents first suggested that vascular smooth muscle growth inhibitors may be useful in preventing PAH. Heparin infusion decreases the severity of hypoxia-induced vascular changes, presumably by binding growth factors. Calcitonin gene-related peptide administered

by gene transfer not only attenuates hypoxia-induced vasoconstriction and remodeling but also enhances the effects of phosphodiesterase inhibitors. We also showed that serine elastase inhibitors reduce chronic hypoxia-induced pulmonary hypertension.

Collagen vascular disease, inflammation, and pulmonary hypertension

Pulmonary hypertension is a frequent complication of certain collagen vascular diseases (e.g., commonly scleroderma), the CREST syndrome (calcinosis cutis, Raynaud's phenomenon, esophageal dysfunction, sclerodactyly, and telangiectasias), and, more rarely, systemic lupus erythematosus, rheumatoid arthritis, Takayasu's arteritis, polymyositis, and dermatomyositis. Although the pathological features of PAH include thromboemboli, particularly associated with the antiphospholipid syndrome, an immune/inflammatory vasculitis appears to be the initiating event. The prevailing hypothesis is that endothelial injury coupled to an immune defect leads to a peri- and intravascular inflammatory response causing vascular lesions leading to progressive PAH. In addition to high circulating levels of endothelin-1 (indicating an endothelial injury), there is increased production of autoantibodies that reflect the immune compromise. Activating antibodies to platelet-derived growth factor (PDGF) receptor could explain the proliferative response of smooth muscle cells causing vascular lesions. In an allergic model of PAH, an IL-13-mediated increase in an α-resistin-like molecule was observed and this protein can induce SMC proliferation. An increase in a similar molecule was observed in patients with scleroderma and pulmonary hypertension.

The results of therapy, including intravenous prostacyclin, have not appreciably improved long-term survival in the subset of patients with PAH associated with systemic sclerosis. These patients appear to deteriorate with lower levels of PA pressure and resistance, perhaps because of intrinsic abnormalities in the right ventricle or increased stiffness of the conduit PAs.

Severe PAH has been associated with acquired immunodeficiency syndrome, even in the absence of lung parenchymal disease, and has been reproduced experimentally [34]. Here too there is a combination of endothelial injury and immune compromise that could explain the observed pathology. The development of PAH in the subset of patients with human immunodeficiency virus infection appears to be linked to the immunogenetic background (i.e., human leukocyte antigen class II alleles) and to the injurious effect of a virus. Here the human herpesvirus 8 (HHV-8) is associated with Kaposi sarcoma virus, which is prevalent in HIV, and some patient groups with idiopathic PAH. The Kaposi sarcoma virus appears to stimulate lysosomal-mediated degradation of BMP-RII, the gene that is mutant in patients with idiopathic pulmonary hypertension that protects the vasculature, as will be discussed later in the chapter. The HIV-nef gene has been implicated in plexogenic pulmonary vascular lesions associated with PAH in HIV-infected patients and SIV-infected non-human primates.

Recently, we reported that the mouse that overexpresses S100A4/Mts1 develops extensive and severe neointimal lesions following injection of the gamma murine herpes virus-68 (the murine homolog of HHV-8). This is associated with an elevated elastase activity that we have now identified as neutrophil elastase produced by PA SMC. Overexpression of S100A4 also appears to be linked to an immune defect.

Neointimal formation associated with inflammatory processes in systemic arteries is also accompanied by an increase in serine elastase activity [35] and fibronectin production. Inflammation has been linked to the development of PAH, and both the chemokine receptor CX3CR1 and the chemokine fractalkine appear to be elevated [36]. An interesting recent study showed that loss of function of BMP-RII leads to up-regulation of IL-6, the pro-inflammatory cytokine, and we have delineated a post-transcriptional mechanism associated with up-regulation of the cytokine GM-CSF (unpublished). We have also shown that GMCSF co-distributes in PAH lesions with TNF-α and that GMCSF can aggravate hypoxia-induced PAH. Other experimental models of chronic inflammation, such as repeated injections of endotoxin and TNF-α, produce pulmonary vascular changes.

The high incidence of PAH in areas of the world endemic for schistosomiasis has resulted in several experimental studies addressing pathogenesis and pathobiology of this complication. About 10% of patients with schistosomiasis develop portal hypertension and 10% of those (1% of the total) have PAH. Chronic infection with high-dose cercariae resulted in extensive lung vascular remodeling [37]. Allergic responses to ovalbumin or to aspergillus can result in extensive vascular remodeling, although in this model of disease, as in the S100A4 over-expressing mice inoculated with virus, right ventricular systolic pressure is not elevated. A Th2 immune response characterizes both the ovalbumin and the cercariae models but not the viral model of pulmonary vascular remodeling. Here an autoimmune Th17 response may be relevant. In mice lacking prostaglandin synthase, inducing allergic inflammation with the house dust mite induces intense pulmonary vascular remodeling, changes that are reversed by administration of PGE2.

In the model of PAH in which loss of arteries is induced by combining injection of an inhibitor of vascular endothelial growth factor (VEGF) and hypoxia, depletion of T cell subsets actually worsens the pathology [38]. This adverse response has been attributed to unbalanced B cell activity resulting from impaired Treg production.

Even in patients with IPAH, with no documented immunodeficiency, there are heightened circulating levels of cytokines

and their receptors, stromal-derived factor (SDF)-1 and monocyte chemoattractant protein (MCP)-1, in addition to fractalkine [36] and its cognate receptor, which are associated with heightened SMC proliferation. Also intriguing are recent studies suggesting that heightened expression of the transcription factor NFATc2 that is associated with inflammatory cells may underlie PAH. Increased nuclear NFATc2 is observed in T cells from IPAH patients and in pulmonary vascular lesions, and this can lead to repression of Kv 1.5 channel expression. NFATc2 can be inhibited by VIVT and its nuclear translocation can be suppressed by cyclosporine. These agents can also attenuate experimentally induced PAH [39].

Toxins and pulmonary hypertension

Ingested substances associated with PAH include aminorex, which resembles epinephrine in its chemical structure, suppresses appetite, and causes symptoms of right-sided heart failure in 10% of patients within 6–12 months of initial administration, as do fenfluramine compounds, for example, dexfenfluramine, a serotonin antagonist [40]. Pathophysiologic studies have also suggested that there are similarities to IPAH. Toxic oils, such as rapeseed oil, have been implicated in the development of malignant PAH. Ingesting pyrrolizidine alkaloids, such as bush tea, causes hepatic veno-occlusive disease, and a similar compound, monocrotaline, when ingested by animals, causes severe pulmonary vascular disease. Rats that ingest the toxin monocrotaline develop pulmonary arterial changes that can be correlated with increased elastase activity. Furthermore, we demonstrated that elastase inhibitors are effective not only in reducing the pulmonary hypertension and vascular changes but also in reversing them.

Based on subsequent knowledge that the effect of elastase was critical in maintaining survival signals through the epidermal growth factor receptor (EGFR), other studies were carried out to block these receptors [41]. Reversal of progressive PAH was sustained even 1 month after cessation of treatment, but the extent of regression was not as great as with elastase inhibition. The use of a PDGF receptor blocker to reverse PAH in this experimental model [42] has prompted a report showing the successful use of a tyrosine kinase inhibitor imatinib (Gleevec) in a patient with advanced pulmonary vascular disease. Subsequent clinical trials using Gleevec in patients with PAH have shown some efficacy but perhaps only in the patients with the most severe disease.

Simvastatin has been used to reverse PAH in a monocrotaline–pneumonectomy model. In the monocrotaline model of PAH, endothelial nitric oxide synthase (eNOS) gene therapy in association with endothelial progenitor cell administration (Figure 5.3) [4,43], gene therapy with survivin, angiopoietin-1, inhibiting the serotonin transporter (SERT), adrenomedullin and the Rho-kinase inhibitor fasudil,

and gene therapy restoring K channel function or BMP-RII have all been used effectively to suppress or reverse pulmonary vascular disease in this model [44].

Unexplained pulmonary hypertension: novel insights through genetics

After all known causes of PAH have been ruled out, the diagnosis becomes that of idiopathic IPAH. This unexplained disease, in which a structural abnormality is always found either in the arteries or in the veins, occurs in both children and adults, sometimes with a familial tendency [45–47]. A mutation in the gene for BMP-RII is associated with >70% of familial PAH [45–47], but the penetrance is only ~20%, that is, 80% of family members who carry the mutation never develop PAH. Moreover, mutations in BMP-RII have been described in 20% of sporadic instances of PAH. In addition, other BMP–TGF-β receptor family members such as ALK1 and endoglin, that were first identified as mutated in hemorrhagic telangiectasia, are also occasionally mutated in patients with PAH.

Although the penetrance is low, the functional link between mutations in BMP-RII and PAH is reinforced by the fact that independent of a mutation in BMP-RII, IPAH patients have reduced BMP-RII protein expression, as do, to some extent, patients with secondary PAH. The functional consequence of reduced or absent BMP-RII in endothelial or smooth muscle cells is related to the pathological features observed in PAH. Impaired downstream signaling has been described in association with a variety of BMP-RII mutations [48,49] and there is also a newly described mutation in pSmad 8 in a patient with IPAH. Signaling through a Smad-independent, p38-mediated pathway may be abnormal when there are alterations in BMP-RII. A few studies have specifically addressed the transcription factors and genes that are subsequently up-regulated or suppressed as a result of impaired BMP-RII signaling. We have shown in smooth muscle cells that BMPs can induce PPARγ transcriptional activity to induce apoE, a suppressor of smooth muscle cell proliferation. These studies showed that the main function of BMP-RII signaling is suppression of the proliferative response of SMC when stimulated by growth factors that are induced under conditions of vascular injury. In EC, in contrast to SMCs, BMPs induce a complex between PPARγ and β-catenin to regulate genes such as apelin that have important protective paracrine and autocrine effects. BMPs suppress apoptosis of endothelial cells in response to injury and are pro-angiogenic, indicating that they may play an important role in repairing damaged microvessels. Apelin, in addition to being a factor that improves endothelial survival, can also suppress smooth muscle cell proliferation.

Interactions between the BMP-RII signaling pathway and the Notch signaling pathway led investigators to determine
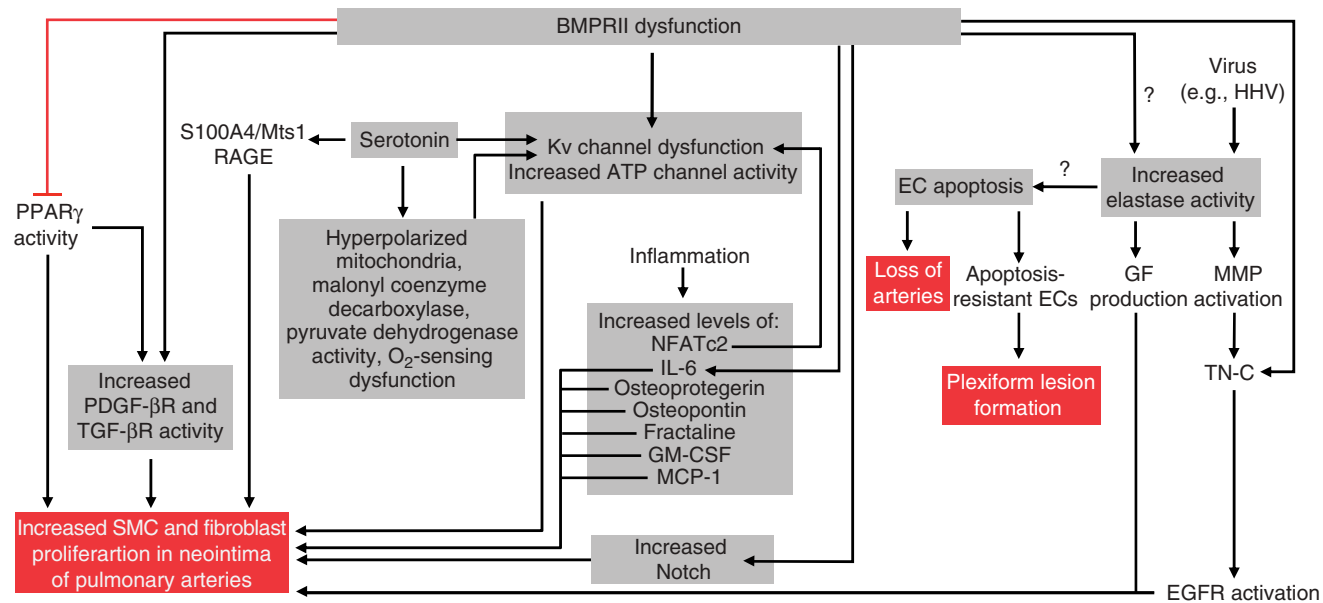
Figure 5.3 Schema outlining factors that converge in the molecular pathogenesis of PAH and how these may interact with BMP-RII dysfunction, a known genetic defect associated with PAH. This schema focuses on factors causing increased SMC and fibroblast proliferation and also apoptosis of ECs, causing an initial reduction in vessel number, followed by proliferation of apoptosis-resistant ECs in plexiform lesions. It shows multiple levels of interaction, with numerous factors related as described in the text. For example, serotonin stimulates both PDGF-mediated and S100A4/Mts1-mediated SMC and fibroblast proliferation and it also reduces Kv channel function, as does hyperpolarized mitochondria. BMP-RII dysfunction causes Kv channel dysfunction and enhances TRP channel activity, which increases intracellular calcium levels, and may (as reflected by the question marks) induce elastase activity. Viruses of the herpes family can induce elastase activity. Elastase, via activation of MMPs and tenascin C (TN-C), up-regulates growth factor (GF) receptors such as EGF receptors (EGFRs) and also triggers release of growth factors such as EGF from the extracellular matrix, all of which leads to SMC proliferation. BMP-RII dysfunction can also increase PDGF activity, increase SMC proliferation by suppressing PPARγ, and increase TGF-β activity. BMP-RII dysfunction can enhance inflammation via osteoprotegrin and IL-6. NFATc2 can suppress Kv channel function. Other inflammatory mediators such as fractalkine and MCP-1 can, in addition to osteoprotegrin and IL-6, increase SMC proliferation. BMP-RII dysfunction can lead to EC apoptosis, as can elastase activity. EC apoptosis may predispose to the development of apoptosis-resistant ECs in plexiform lesions. MCP-1, mast cell proteinase 1; TRP, transient receptor potential Ca^{2+} channels. Loss of BMP-RII also activates Notch signaling that induces smooth muscle cell proliferation. ATP, adenosine triphosphate; BMPII, bone morphogenetic protein II; EC, endothelial cell; GF, growth factor; GM-CSF, granulocyte macrophage colony stimulating factor; HHV, human herpes virus; IL6, interleukin 6; Kv, voltage gated potassium; MCP-1, mast cell proteinase 1; MMP, matrix metalloproteinase; NFATc2, nuclear factor of activated T cells c2; PDGF, platelet derived growth factor; SMC, smooth muscle cell; TGF, transforming growth factor; TN-C, tenascin C; TRP, transient receptor potential. (Modified from Rabinovitch, *J Clin Invest* 2008;**118**:2372–9.)

that in PAH there is an increase in activity of Notch. The cleavage of Notch following its interaction with a receptor on the SMC surface leads to the internalization of the Notch intracellular domain that serves as a transcription factor to induce genes that cause smooth muscle cell proliferation [50]. Blockade of γ-secretase, the enzyme that cleaves Notch, resulted in prevention and regression of experimental PAH.

Future directions

Further insights into the pathophysiology of PAH will come from genomic studies in which extensive sequencing will likely reveal additional genetic variants associated with this disease. Epigenetic studies are currently being undertaken to address whether changes in chromatin remodeling will help explain why the lung is a target organ and how environmental factors perturb the genome and can lead to further alterations in expression of a rare variant or in the genes that interact with this rare variant. High-throughput gene expression and proteomic studies are also revealing changes that reflect specific pathways that are perturbed and how environmental exposures and immune defects can interact with a vulnerable vasculature. Intense focus on aberrations in immune mechanisms ranging from disturbances in T cell subsets and autoantibody production will be important in understanding all forms of PAH. The more we learn about specific pathways, the better equipped we will be to develop new treatments for pulmonary hypertension.

References

1 Hall SM, Haworth SG. Normal adaptation of pulmonary arterial intima to extrauterine life in the pig: ultrastructural study. *J Pathol* 1986;**149**:55–66.

2 Hislop M, Reid L. Pulmonary arterial development during childhood: branching pattern and structure. *Thorax* 1973;**28**:129–35.

3 Ihida-Stansbury K, McKean DM, Gebb SA, *et al.* Paired-related homeobox gene Prx1 is required for pulmonary vascular development. *Circ Res* 2004;**94**:1507–14.

4 Zhao L, Wang K, Ferrara N, Vu TH. Vascular endothelial growth factor co-ordinates proper development of lung epithelium and vasculature. *Mech Dev* 2005;**122**:877–86.

5 Asikainen TM, Ahmad A, Schneider BK, *et al*. Stimulation of HIF-1alpha, HIF-2alpha, and VEGF by prolyl 4-hydroxylase inhibition in human lung endothelial and epithelial cells. *Free Radic Biol Med* 2005;**38**:1002–13.

6 Wang Z, Shu W, Lu MM, Morrisey EE. Wnt7b activates canonical signaling in epithelial and vascular smooth muscle cells through interactions with Fzd1, Fzd10, and LRP5. *Mol Cell Biol* 2005;**25**:5022–30.

7 Kim IM, Ramakrishna S, Gusarova GA, *et al*. The forkhead box m1 transcription factor is essential for embryonic development of pulmonary vasculature. *J Biol Chem* 2005;**280**:22278–86.

8 Balasubramaniam V, Tang JR, Maxey A, *et al*. Mild hypoxia impairs alveolarization in the endothelial nitric oxide synthase-deficient mouse. *Am J Physiol Lung Cell Mol Physiol* 2003;**284**:L964–71.

9 Zuckerbraun BS, Shiva S, Ifedigbo E, *et al*. Nitrite potently inhibits hypoxic and inflammatory pulmonary arterial hypertension and smooth muscle proliferation via xanthine oxidoreductase-dependent nitric oxide generation. *Circulation* 2010;**121**:98–109.

10 Rabinovitch M, Haworth SG, Castenada AR, *et al*. Lung biopsy in congenital heart disease: a morphometric approach to pulmonary vascular disease. *Circulation* 1978;**58**:1107–22.

11 Meyrick B, Reid L. Ultrastructural findings in lung biopsy material from children with congenital heart defects. *Am. J Pathol* 1980;**101**:527–37.

12 Taraseviciene-Stewart L, Gera L, Hirth P, *et al*. A bradykinin antagonist and a caspase inhibitor prevent severe pulmonary hypertension in a rat model. *Can J Physiol Pharmacol* 2002;**80**:269–74.

13 Rabinovitch M, Castenada AR, Reid L. Lung biopsy with frozen section as a diagnostic aid in patients with congenital heart defects. *Am J Cardiol* 1981;**47**:77–84.

14 Rabinovitch M, Keane JF, Norwood WI, *et al*. Vascular structure in lung tissue obtained at biopsy correlated with pulmonary hemodynamic findings after repair of congenital heart defects. *Circulation* 1984;**69**:655–67.

15 Dammann JF Jr, Ferencz C. The significance of the pulmonary vascular bed in congenital heart disease. III. Defects between the ventricles or great vessels in which both increased pressure and blood flow may act upon the lungs and in which there is a common ejectile force. *Am Heart J* 1956;**52**:210–31.

16 Deb S, Yun J, Burton N, *et al*. Reversal of idiopathic pulmonary arterial hypertension and allograft pneumonectomy after single lung transplantation. *Chest* 2006;**130**:214–7.

17 Rabinovitch M, Bothwell T, Hayakawa BN, *et al*. Pulmonary artery endothelial abnormalities in patients with congenital heart defects and pulmonary hypertension: a correlation of light with scanning electron microscopy and transmission electron microscopy. *Lab Invest* 1986;**55**:632–53.

18 Thompson K, Rabinovitch M. Exogenous leukocyte and endogenous elastases can mediate mitogenic activity in pulmonary artery smooth muscle cells by release of extracellular-matrix bound basic fibroblast growth factor. *J Cell Physiol* 1996;**166**:495–505.

19 Xu W, Kaneko FT, Zheng S, *et al*. Increased arginase II and decreased NO synthesis in endothelial cells of patients with pulmonary arterial hypertension. *FASEB J* 2004;**18**:1746–8.

20 Bonnet S, Michelakis ED, Porter CJ, *et al*. An abnormal mitochondrial-hypoxia inducible factor-1alpha–Kv channel pathway disrupts oxygen sensing and triggers pulmonary arterial hypertension in fawn hooded rats: similarities to human pulmonary arterial hypertension. *Circulation* 2006;**113**:2630–41.

21 Clausell N, Rabinovitch M. Upregulation of fibronectin synthesis by interleukin-1 beta in coronary artery smooth muscle cells is associated with the development of the post-cardiac transplant arteriopathy in piglets. *J Clin Invest* 1993;**92**:1850–8.

22 Greenway S, van Suylen RJ, Du Marchie Sarvaas G, *et al*. S100A4/Mts1 produces murine pulmonary artery changes resembling plexogenic arteriopathy and is increased in human plexogenic arteriopathy. *Am J Pathol* 2004;**164**:253–62.

23 Lawrie A, Spiekerkoetter E, Martinez EC, *et al*. Interdependent serotonin transporter and receptor pathways regulate S100A4/Mts1, a gene associated with pulmonary vascular disease. *Circ Res* 2005;**97**:227–35.

24 Eddahibi S, Chaouat A, Morrell N, *et al*. Polymorphism of the serotonin transporter gene and pulmonary hypertension in chronic obstructive pulmonary disease. *Circulation* 2003;**108**:1839–44.

25 Li H, Chen SJ, Chen YF, *et al*. Enhanced endothelin-1 and endothelin receptor gene expression in chronic hypoxia. *J Appl Physiol* 1994;**77**:1451–9.

26 Giaid A, Yanagisawa M, Langleben D, *et al*. Expression of endothelin-1 in the lungs of patients with pulmonary hypertension. *N Engl J Med* 1993;**238**:1732–9.

27 Stenmark KR, Fasules J, Hyde DM, *et al*. Severe pulmonary hypertension and arterial adventitial changes in newborn calves at 4,300 m. *J Appl Physiol* 1987;**62**:821–30.

28 Prosser IW, Stenmark KR, Suthar M, *et al*. Regional heterogeneity of elastin and collagen gene expression in intralobar arteries in response to hypoxic pulmonary hypertension as demonstrated by *in situ* hybridization. *Am J Pathol* 1989;**135**:1073–88.

29 Durmowicz AG, Parks WC, Hyde DM, *et al*. Persistence, re-expression, and induction of pulmonary arterial fibronectin, tropoelastin, and type I procollagen mRNA expression in neonatal hypoxic pulmonary hypertension. *Am J Pathol* 1994;**145**:1411–20.

30 Davie NJ, Crossno JT Jr, Frid MG, *et al*. Hypoxia-induced pulmonary artery adventitial remodeling and neovascularization: contribution of progenitor cells. *Am J Physiol Lung Cell Mol Physiol* 2004;**286**:L668–78.

31 Yet SF, Perrella MA, Layne MD, *et al*. Hypoxia induces severe right ventricular dilatation and infarction in heme oxygenase-1 null mice. *J Clin Invest* 1999;**103**:R23–9.

32 Guignabert C, Alvira CM, Alastalo TP, *et al*. Tie2-mediated loss of peroxisome proliferator-activated receptor-gamma in mice causes PDGF receptor-beta-dependent pulmonary arterial muscularization. *Am J Physiol Lung Cell Mol Physiol* 2009;**297**:L1082–90.

33 Hansmann G, de Jesus Perez VA, Alastalo TP, *et al*. An antiproliferative BMP-2/PPARgamma/apoE axis in human and murine SMCs and its role in pulmonary hypertension. *J Clin Invest* 2008;**118**:1846–57.

34 Gillespie MN, Hartsfield CL, O'Connor WN, Cohen DA. Pulmonary hypertension in a murine model of the acquired immunodeficiency syndrome. *Am J Respir Crit Care Med* 1994;**150**:194–9.

35 Oho S, Rabinovitch M. Post-cardiac transplant arteriopathy in piglets is associated with fragmentation of elastin and increased activity of a serine elastase. *Am J Pathol* 1994;**145**:202–10.

36 Balabanian K, Foussat A, Dorfmuller P, *et al*. CX(3)C chemokine fractalkine in pulmonary arterial hypertension. *Am J Respir Crit Care Med* 2002;**165**:1419–25.

37 Crosby A, Jones FM, Southwood M, *et al*. Pulmonary vascular remodeling correlates with lung eggs and cytokines in murine schistosomiasis. *Am J Respir Crit Care Med* 2010;**181**:279–88.

38 Taraseviciene-Stewart L, Niçolls MR, Kraskauskas D, *et al*. Absence of T cells confers increased pulmonary arterial hypertension and vascular remodeling. *Am J Respir Crit Care Med* 2007;**175**:1280–9.

39 Bonnet S, Rochefort G, Sutendra G, *et al*. The nuclear factor of activated T cells in pulmonary arterial hypertension can be therapeutically targeted. *Proc Natl Acad Sci USA* 2007;**104**:11418–23.

40 Abenhaim L, Moride Y, Brenot F, *et al*. Appetite-suppressant drugs and the risk of primary pulmonary hypertension. International Primary Pulmonary Hypertension Study Group. *N Engl J Med* 1996;**335**:609–16.

41 Merklinger SL, Jones PL, Martinez EC, Rabinovitch M. Epidermal growth factor receptor blockade mediates smooth muscle cell apoptosis and improves survival in rats with pulmonary hypertension. *Circulation* 2005;**112**:423–31.

42 Schermuly RT, Dony E, Ghofrani HA, *et al*. Reversal of experimental pulmonary hypertension by PDGF inhibition. *J Clin Invest* 2005;**115**:2811–21.

43 Zhao YD, Courtman DW, Deng Y, *et al*. Rescue of monocrotaline-induced pulmonary arterial hypertension using bone marrow-derived endothelial-like progenitor cells: efficacy of combined cell and eNOS gene therapy in established disease. *Circ Res* 2005;**96**:442–50.

44 Michelakis ED, McMurtry MS, Wu XC, *et al*. Dichloroacetate, a metabolic modulator, prevents and reverses chronic hypoxic pulmonary hypertension in rats: role of increased expression and activity of voltage-gated potassium channels. *Circulation* 2002;**105**:244–50.

45 Nichols W, Koller WC, Slovis B, *et al*. Localization of the gene for familial primary pulmonary hypertension to chromosome 2q31-32. *Nat Genet* 1997;**15**:277–80.

46 Lane KB, Machado RD, Pauciulo MW, *et al*. Heterozygous germline mutations in BMPR2, encoding a TGF-beta receptor, cause familial primary pulmonary hypertension. *Nat Genet* 2000;**26**:81–4.

47 Deng Z, Morse JH, Slager SL, *et al*. Familial primary pulmonary hypertension (gene PPH1) is caused by mutations in the bone morphogenetic protein receptor-II gene. *Am J Hum Genet* 2000;**67**:737–44.

48 Nishihara A, Watabe T, Imamura T, Miyazono K. Functional heterogeneity of bone morphogenetic protein receptor-II mutants found in patients with primary pulmonary hypertension. *Mol Biol Cell* 2002;**13**:3055–63.

49 Rudarakanchana N, Flanagan JA, Chen H, *et al*. Functional analysis of bone morphogenetic protein type II receptor mutations underlying primary pulmonary hypertension. *Hum Mol Genet* 2002;**11**:1517–25.

50 Li X, Zhang H, Leathers R, *et al*. Notch3 signaling promotes the development of pulmonary arterial hypertension. *Nat Med* 2009;**15**:1289–97.

6 Clinical History and Physical Examination

James H. Moller
University of Minnesota, Minneapolis, MN, USA

In infants and children, the clinical history and physical examination are key in the diagnostic process. After completing these two initial steps, the physician should usually have a major diagnosis or a narrow differential diagnosis and a focused approach to further diagnostic studies. For example, in requesting an echocardiogram after the history and physical examination, the physician requesting the study should indicate a tentative diagnosis and the particular anatomic and hemodynamic information being sought. In neonates, the physical examination changes with the transition from fetal to neonatal life and is often unclear so that the diagnosis often relies primarily on the echocardiographic findings.

History

The history provides four categories of information: (1) diagnostic, (2) severity assessment, (3) etiologic, and (4) effect on the child and family. In addition, while obtaining the history from the parents and the child (when it is age appropriate), the physician can allow the parents to express their concerns and questions, and can assess the level of understanding about the child's condition. The medical interview is an excellent time to provide information and allay anxiety.

Diagnostic information
The medical history, although generally not specific for a particular diagnosis, can often lead to specific diagnostic categories.

The age at onset of congestive heart failure can suggest a diagnosis. Heart failure present at birth or in a fetus is rare and caused by paroxysmal tachycardia, myocardial abnormality, or a volume load that is independent of pulmonary vascular resistance, for example, a severely regurgitant valve or a large arteriovenous fistula. Failure within the first 10 days of life is usually secondary to closure of the ductus arteriosus that unmasks a serious left-sided obstructive condition, such as hypoplastic left ventricle, aortic stenosis, coarctation of the aorta, or interruption of the aortic arch.

Cardiac failure presenting between 6 weeks and 3 months of age occurs with a shunt at either the ventricular or great vessel level. Examples are a large ventricular septal defect, patent ductus arteriosus, and truncus arteriosus. In each of these, the volume of blood shunted is inversely related to the pulmonary vascular resistance. As the pulmonary vascular resistance declines postnatally, the volume of pulmonary blood flow increases. The left ventricle is incapable of handling this excessive volume load, and failure ensues. Heart failure occurring at an older age is likely related to an acquired cardiac problem (see Chapter 70).

The age at which a murmur is first heard is important. A loud systolic murmur heard at or immediately after birth reflects either semilunar valve stenosis, atrioventricular valve insufficiency, or a small ventricular septal defect. Classically, the murmur of a large ventricular septal defect or patent ductus arteriosus is heard initially on the first examination after discharge from the nursery. Murmurs heard for the first time on preschool or school examinations are usually functional, but mild valvar stenosis, atrial septal defect, mitral valve prolapse, and hypertrophic cardiomyopathy may be recognized initially at this time.

Cyanosis, blueness, or duskiness must be carefully assessed by history, physical examination, and oximetry to distinguish central (serious) from peripheral cyanosis (see Chapter 17). The age at onset of the cyanosis is also helpful diagnostically. Complete transposition is the most common cause of cyanosis appearing during the first day of life; more severe forms of tetralogy of Fallot, pulmonary atresia, and tricuspid atresia are others. Ebstein's malformation can also result in severe neonatal cyanosis, but becomes milder as pulmonary

vascular resistance declines, allowing improved pulmonary blood flow (see Chapter 36).

Stridor or noisy breathing and dysphagia can point to a vascular ring or sling (see Chapters 47 and 49). These symptoms appear in infancy and may improve with extension of the neck. Dysphagia can develop with the introduction of solid foods.

Chest pain

In children, chest pain, a common complaint both in emergency rooms [1] and in cardiology clinics [2], is usually of musculoskeletal origin. Chest pain accounts for about 0.25% of clinic visits for children [3,4]. One study [5] reported that 0.6% of encounters in a pediatric emergency room was for chest pain with a 1:1 male to female ratio. In one study [6], the most common causes were chest wall pain (28%), pulmonary causes (19%), minor trauma (15%), idiopathic (12%), psychogenic (5%), and miscellaneous (21%), most often from referred abdominal or respiratory tract. There were no instances with myocardial ischemia. Sik and colleagues [7] wrote of the problem of atypical chest pain in athletes and indicated that it is common and, although almost always unrelated to myocardial ischemia, careful evaluation is indicated. A report by Gregory et al. [8] discusses the common occurrence of musculoskeletal problems of the chest wall in athletes.

Because chest pain in adults is often associated with cardiac disease, its occurrence in a child causes parental anxiety. Careful history of the features of the pain can usually identify its cause. Most chest pain in children and adolescents [9] originates in the chest wall and occurs from costochondritis, trauma, myositis, and precordial catch syndrome. It may be related to a chest wall deformity [10]. Such pain starts abruptly and may last for 15 min, but it usually lasts only a few seconds and is sharp and focal [11]. When asked to indicate its location, the child usually points with a finger to a small area usually lateral to the sternum. In my experience, it is usually on the left side.

Selbst [12], in a prospective study, found that pain of acute onset, abnormal physical findings, pain that awakens the child, and fever indicate an organic cause, but that chest pain in children is usually benign.

Anginal chest pain occurs rarely in children with a cardiac abnormality and is usually associated with severe valvar aortic stenosis or supravalvar aortic stenosis (in the latter, coronary arterial abnormalities may coexist), cardiomyopathy, or pulmonary hypertension. The characteristics of angina in children are similar to those in adults. The chest pain is typically substernal, pressing or constricting, of some duration, and may follow exertion. The child indicates the location by placing the palm of the hand over the midsternum. In an 11-year period, Lane and Ben-Shachar [13] found nine children and adolescents with myocardial infarction presenting to their emergency room. Each had elevation of myocardial enzymes and eight showed an electrocardiographic abnor-

mality. None had an abnormal coronary arterial abnormality, but several had left ventricular hypokinesis.

Other uncommon causes of chest pain in children include the typical pain complexes of dissecting aortic aneurysm of Marfan's syndrome, pericarditis, pulmonary embolism, spontaneous pneumothorax, pleurisy, and peptic ulcer disease.

Pneumonia and pleuritis cause chest pain by irritation of the pleura. The pain is sharp, accentuated by respiration or cough, and may be referred to the shoulder. Pneumonia, bronchitis, and other conditions associated with excessive coughing can irritate the chest wall. Gastritis and esophagitis may cause chest pain, but the history of relation to meals helps to identify these conditions.

Apley [14] has written a great deal about pain in children which is helpful, even though his focus was abdominal pain. In general, if the pain has been present for more than 6 months and there are no abnormal findings, then the pain can be considered as having no organic cause. In this regard, Driscoll et al. [4] found that the average duration from onset of symptom to presentation was 244 days, but with trauma or bronchitis it was 1–18 days.

Syncope is discussed in Chapter 56.

Information about severity of cardiac condition

Details about growth patterns, cyanosis, or congestive heart failure may provide information about severity.

Growth

Growth is often slowed by a serious cardiac malformation. Weight is more affected than is length, and head circumference is seldom affected by the severity of the cardiac anomaly [15]. An abnormally small head circumference can point to a potential cause of the cardiac malformation (e.g., a syndrome, or intrauterine growth retardation secondary to maternal viral infection).

Perhaps 20% of neonates with a cardiac malformation have a birth weight below 2500 g [16]. The frequency of low birth weight varies with the type of anomaly, being higher in ventricular septal defect and atrioventricular septal defect but rare in those with complete transposition. In fact, in complete transposition, the weight frequently exceeds 4.0 kg.

The explanation for delayed growth in utero is uncertain but could include hemodynamic effects of the anomaly on the developing fetus, the generalized effect of an etiologic agent (e.g., rubella), or the presence of an associated syndrome. Postnatal slow growth may be related to a combination of poor feeding and increased metabolic demands related to increased respiratory effort.

Congestive heart failure

The physiologic mechanisms associated with congestive heart failure are discussed in Chapter 70. The cardinal symptoms in infants are slow feeding, rapid respiration, excessive perspiration, growth failure, and frequent respiratory

infections. An infant with congestive heart failure is a "poor feeder." Although eager to eat, the infant soon tires from the fatigue of sucking (sucking is exercise to a infant). Heart failure indicates a severe cardiac malformation.

Cyanosis

Central cyanosis indicates a right-to-left shunt. The intensity of cyanosis reflects the magnitude of shunting and, when combined with knowledge of the anatomy of the malformation, allows estimation of the severity of factors influencing pulmonary blood flow or intracardiac mixing (see Chapter 17).

Etiologic factors

Although the etiology of the cardiac condition cannot be discovered in many instances of congenital or acquired heart disease, the history and physical examination may provide clues to etiology, the underlying diagnosis, and, at times, prognosis.

A careful history seeking information about siblings or other relatives with cardiac problems, neonatal deaths, sudden unexpected deaths, "blue babies," and cardiac operations during childhood may provide clues. The recurrence rate of congenital heart disease is about 3% between siblings or between parent and child, and the concurrence rate for the type of defect is about 50%. Certain conditions, such as complete transposition, seem to have a low rate of recurrence. Others, such as hypoplastic left ventricle, coarctation of the aorta, and aortic stenosis, have perhaps a 10% recurrence rate if careful screening is done to identify bicuspid aortic valves in relatives.

Many acquired conditions afflicting the heart follow Mendelian patterns of inheritance. These are discussed in Chapter 2 (genetics), Chapter 58 (myocardial disease), Chapter 67 (connective tissue disorders), Chapter 30 (aortic stenosis relative to Williams' syndrome), and Chapter 33 (pulmonary stenosis relative to Noonan syndrome).

As many as 50% of children with Down syndrome (trisomy 21) have a cardiac malformation, most commonly atrioventricular septal defect and ventricular septal defect. Less common, but occurring in equal proportions, are tetralogy of Fallot, patent ductus arteriosus, and atrial septal defect. Pulmonary vascular obstructive disease tends to develop early. Aortic stenosis and coarctation are rare. The frequency of Down syndrome increases with maternal age, being 1 per 1925 women at age 20 years and 1 per 100 women at age 40 years, and trisomy is found in age-related Down syndrome. Chromosome analysis should be performed to identify familial translocation involving chromosome 21 or mosaicism. Half of the translocations arise *de novo*, and the other half are inherited from a carrier parent.

Maternal history

A history of acute illness during pregnancy, especially within the first trimester, or a chronic condition in the mother may provide important etiologic information.

A viral infection during the first trimester may be an etiologic factor. Only rubella, which can cause the classic triad of cataracts, neurosensory deafness, and congenital heart disease (patent ductus arteriosus and peripheral pulmonary artery stenosis) [17], has been clearly identified.

Maternal diabetes mellitus has been associated with a higher (about three times) occurrence rate of cardiac malformation [18]. Diabetes mellitus during pregnancy, even of gestational origin, has been associated with asymmetric septal hypertrophy that resolves in the months after delivery. About 30% of such infants of diabetic mothers have cardiomegaly, and cardiac failure occurs in 5–10%.

Maternal systemic lupus erythematosus and other collagen vascular disease cause complete heart block from the transplacental transfer of antibodies that attack this developing conduction system (see Chapter 68).

Excessive maternal alcohol ingestion is associated with fetal alcohol syndrome, in which ventricular septal defect is common [19]. The level of alcohol intake during the first trimester of pregnancy correlates with teratogenic risk.

Maternal medications may also have a teratogenic effect. Phenytoin, trimethadione, and paramethadione have been associated with a higher rate of cardiac malformation, including congenital heart disease, although it remains controversial. Lithium use in mothers has been associated with Ebstein malformation of the tricuspid valve. Thalidomide was found 40 years ago to cause truncus arteriosus and limb abnormalities in infants born of mothers who took this agent as a sedative. Major fetal abnormalities are related to isotretinoin, including cardiovascular anomalies, and this drug must not be used in pregnant women.[20]

The American Heart Association has published two important scientific statements that review the current data about genetic and about other etiologic factors associated with cardiac malformations [21,22].

Physical examination

The patient's age and the setting of the examination determine the way in which the physical examination is performed. Most physicians who care for infants and children have developed particular techniques and sequences of the examination, so that all the necessary information is gathered and key data are not overlooked. Examination of neonates and infants receiving ventilatory assistance may be difficult because access to the patient may be limited and the ventilator noise interferes with auscultation. Often in these situations, it may be difficult to listen to the back, but this should be done if possible because cardiac murmurs may be louder or heard only over the back.

Children aged 1–3 years fear strangers. Having the child sit on the parent's lap for the examination is helpful. Begin by inspecting a child of this age and palpating the peripheral

pulses, before progressing to palpating the thorax. Auscultation should be performed last. In older children, the examination can proceed in the usual manner. Examine from the patient's right side if you are right-handed, from the left side if you are left-handed.

In all patients, length and height must be measured and plotted on a growth chart. For those younger than 3 years, the occipital–frontal circumference should be measured and plotted. In infants and children, cyanosis or cardiac failure affects growth. Weight may be severely affected, but height is affected to a lesser extent. Head circumference is usually unaffected. When head circumference, height, and weight are each low or the severity of the cardiac condition is mild, the retarded growth should be attributed to another factor, such as familial factors or a chromosome anomaly.

The body mass index (BMI) should be calculated and the resultant value compared with normal values to determine if the child is overweight or obese: BMI = weight (kg)/[height (m)]^2. The normal values are available from the Centers for Disease Control; these graphs are similar to standard growth charts showing mean and percentiles for males and for females (http://apps.nccd.cdc.gov/dnpabmi/; http://kidshealth. org/misc/body_mass_index/P_bmi_chart.html).

General appearance

Take a moment to assess the general appearance of the infant or child. Is there distress or appearance of acute or chronic illness? Is the infant or child responsive? Most infants respond to people and are happy. Infants with cyanosis or congestive cardiac failure are frequently irritable.

Skin color

Particularly in neonates and infants, the skin color can provide a clue about the cardiovascular status. Is it pale, red, blue, or mottled?

Cyanosis may be difficult to note, particularly in neonates, especially if the degree of hypoxemia is mild. The amount of ambient light, the examiner's experience, pigmentation, and other factors influence ability to detect cyanosis. Nurses or parents often use the term "dusky" to describe mild cyanosis. With the widespread availability of oxygen saturation monitors, milder degrees of hypoxemia can be detected and quantified.

Cyanosis can be detected when approximately $5\,g\,dl^{-1}$ of reduced hemoglobin is present in capillary beds. Therefore, in a patient with a normal hemoglobin concentration, cyanosis can be detected when oxygen saturation is less than 88% [23]. With polycythemia, it should be possible to detect cyanosis at a higher oxygen saturation. Conversely, anemia makes it difficult to detect even more marked desaturation.

Cyanosis has been divided into peripheral and central. In peripheral cyanosis, also called acrocyanosis, the arterial oxygen saturation is normal, but because of sluggish peripheral circulation, cyanosis appears peripherally. The classic examples are the hands and feet of neonates or infants that

appear blue when exposed to ambient temperature and the circumoral cyanosis that occurs in children who live in a cold climate or have a fair complexion. This form of cyanosis disappears with passive or active motion of the extremity or exposure to warmth. The trunk, abdomen, lips, and mucous membranes are not cyanotic. On occasion, generalized cyanosis occurs in a cardiac condition with normal arterial oxygen saturation, but a severe reduction in cardiac output that causes inadequate and slow tissue perfusion.

In central cyanosis, generalized cyanosis is present, including mucous membranes. In contrast to peripheral cyanosis, aortic oxygen saturation is reduced. Pulmonary, cardiac, and hematologic abnormalities may be associated with central cyanosis. Any condition that interferes with the transport of oxygen from the air to the pulmonary capillary bed can reduce the oxygen saturation of blood returning to the left atrium. In neonates, the respiratory conditions include choanal atresia, respiratory distress syndrome, pneumothorax, severe pneumonia, and pulmonary edema.

Methemoglobinemia can cause cyanosis [24]. Whether it is inherited or acquired, as from infant formula made with contaminated well water (with nitrates), the ferrous ion of hemoglobin is being replaced with the ferric ion. The resultant methemoglobin with the ferric ion cannot combine with oxygen, and cyanosis results. Methemoglobinemia can be suspected by finding a normal arterial P_{O_2} but reduced oxygen saturation value. Another cause of methemoglobinemia is from local anesthetic agents used during transesophageal echocardiography.

Malformations with a right-to-left shunt cause cyanosis, because some of the blood reaching the aorta has not passed through the pulmonary capillary bed. In one group, there is coexistent obstruction to pulmonary blood flow and an intracardiac shunt (e.g., tetralogy of Fallot and tricuspid atresia). In the second group, systemic and pulmonary venous returns mix within the heart (e.g., complete transposition, truncus arteriosus, and total anomalous pulmonary venous connections). A rare cause of cyanosis is pulmonary arteriovenous fistula.

In older infants and children, it is usually easy to determine from history and physical examination the organ system causing the cyanosis. In neonates, it may be difficult to identify cyanosis and determine the underlying condition by physical examination alone. In neonates, the hemoglobin is elevated, which may give a ruddy appearance. The ductus arteriosus and foramen ovale may be patent and allow an intermittent right-to-left shunt if the neonate cries or there is pulmonary disease. Finally, a serious cardiac condition may be present without a murmur to point to the heart as being an issue. With oximetry and echocardiography, the diagnosis can usually be determined

In neonates, cyanosis requires careful assessment (discussed fully in Chapter 17). Oxygen saturation should be

measured in the right arm and a lower extremity in neonates to detect differential cyanosis [25], indicating different levels of oxygen saturation in the upper and lower portions of the body. If the ductus is patent and blood flows from the pulmonary trunk to the descending aorta, the oxygen saturation is lower in the legs than the arms. This difference in oxygen saturation may be found during the first 24 h of life in a neonate without a cardiac anomaly, but is abnormal if found later. This pattern of differential cyanosis is the result of either increased pulmonary vascular resistance, due to causes ranging from pulmonary parenchymal disease to pulmonary venous obstruction (as from obstructed total anomalous pulmonary venous connection), or severe obstruction in the distal aortic arch (as from interruption of the aortic arch or coarctation of aorta). The pattern of differential cyanosis is reversed in a neonate with complete transposition and a patent ductus arteriosus, with flow of oxygenated blood from the pulmonary trunk to the descending aorta. Cyanosis in a single extremity is usually from interference to venous return, as may be associated with a vascular catheter.

Neonates may appear ruddy if hemoglobin or hematocrit is elevated, as from maternal–fetal transfusion or stripping of the umbilical cord [26]. In this situation, the arterial oxygen saturation is usually normal. Because of hypervolemia, there are tachypnea and tachycardia and the chest radiograph shows cardiomegaly and increased pulmonary vascular markings. Distinction from a cardiac malformation may be difficult without echocardiography.

Pallor or mottling of the skin indicates reduced cardiac output or cardiogenic shock. Sepsis, aortic atresia, and critical aortic stenosis or coarctation of the aorta are typical causes in neonates.

Respiration

The respiratory pattern and effort should be assessed. In neonates and infants with elevated pulmonary venous pressure and congestion, edema develops in alveoli and bronchial and interstitial tissues. This leads to increased work of breathing manifested initially by tachypnea; but as the condition progresses, it becomes associated with flaring of the alae nasi and suprasternal and intercostal retractions. Wheezing and rales may appear.

Hyperpnea is found in neonates and infants with reduced pulmonary blood flow and hypoxemia.

Tachypnea is present in infants with left heart failure because of reduced pulmonary compliance from increased pulmonary blood flow or pulmonary edema.

Features of syndromes

The more common syndromes associated with cardiac malformation are given in Table 6.1. The diagnosis of a specific syndrome often pinpoints a cardiac diagnosis or a limited set of conditions.

Thorax

Inspect the thorax for symmetry and precordial abnormalities. Usually the left side of the chest is slightly more prominent than the right. This is accentuated with cardiac enlargement. The posterior thorax is inspected throughout the respiratory cycle for size and symmetric movement with breathing. In patients with a hypoplastic lung, as in scimitar syndrome, the involved hemithorax is smaller. Scoliosis can also cause thoracic asymmetry. Scoliosis should be sought, particularly in adolescents, and it can be brought out by having the patient stand and touch their toes. Although scoliosis may be more common in children with a cardiac malformation, all adolescents should be screened for it. Other causes of thoracic asymmetry and scoliosis include a classic Blalock–Taussig shunt, Marfan's syndrome, and muscular dystrophy.

A precordial bulge signifies cardiac enlargement or right ventricular hypertrophy. In some patients, particularly with Marfan's syndrome, there may be pectus carinatum or pectus excavatum. The latter is also common in prematurely born neonates. Even if severe, it rarely causes cardiac problems. The apex impulse, however, is displaced to the left; on chest radiography, the transverse diameter of the cardiac silhouette is increased, but it is narrow on a lateral film.

Palpate the precordium for the apex impulse, heaves, or thrills. The apex impulse is the most lateral spot on the thorax where cardiac activity can be felt. Percussion may also help identify the location of the cardiac apex. The apex should be within the midclavicular line and in the fourth interspace through age 4 years and in the fifth interspace thereafter. Displacement lateral to the site indicates cardiac enlargement or mediastinal shift. Dextrocardia can be identified by palpating or percussing the heart in the right hemithorax. On palpating the precordium with the palm of the hand, an outward movement along the left sternal border reflects right ventricular hypertrophy, and at the apex, left ventricular hypertrophy.

It was Auenbrugger in 1776 who described the use of percussion to identity the position and size of organs, including the heart. His father was an innkeeper who sent his son to determine the level of wine in the casks. He did this by tapping on the barrel head, finding the point where the tap became dull, thus marking the level of the fluid [27].

Thrills should also be sought with the palm of the hand since it is more sensitive to vibration than fingertips. Thrills indicate a loud murmur, and help to identify the location of its maximal intensity. The suprasternal notch should also be palpated (with the finger tips). Murmurs originating from the base of the heart, particularly from aortic stenosis, result in a thrill in this area. Pulmonary stenosis, coarctation of the aorta, and patent ductus arteriosus are sometimes associated with a thrill at this site, but ventricular septal defect is not. Aortic notch pulsations are prominent in patients with "aortic runoff," as in significant aortic or truncal regurgitation or a large systemic arteriovenous fistula or patent ductus arteriosus.

Table 6.1 Major syndromes associated with cardiac anomalies.

Disorder	Major feature	Cardiovascular abnormality[a]	Etiology
Craniofacial syndrome			
Goldenhar syndrome (oculoauriculovertebral dysplasia, hemifacial microsomia)	Facial asymmetry and hypoplasia, microtia, eartag, cleft lip/palate, hypoplastic vertebrae	(35%) VSD, T of F	?
DiGeorge syndrome (velocardiofacial syndrome, Shprintzen syndrome, familial conotruncal disease, CATCH-22)	Hypertelorism, short philtrum, down-slanting eyes, cleft palate, hypoplastic/absent thymus and parathyroid	IAA, type B; T of F ± pulmonary atresia, right aortic arch	Chromosome 22q11 deletion
Alagille syndrome (arteriohepatic dysplasia)	Long, thin face, intrahepatic bile duct paucity, butterfly vertebrae	Peripheral pulmonary arterial stenosis	Chromosome 20p11.2
Laurence–Moon–Biedl syndrome	Obesity, retinitis pigmentosa, syndactyly, polydactyly, hypoplastic genitalia, mental retardation, diabetes mellitus	Common atrium	Autosomal recessive
Syndromes with limb defects			
Holt–Oram syndrome (see also Chapter 2)	Upper limb deficiency – absent or triphalangeal thumb	ASD	Autosomal dominant
Aase syndrome	Triphalangeal thumb, radial hypoplasia, hypoplastic anemia	CHD	?Autosomal recessive
Thrombocytopenia-absent radius (TAR) syndrome	Thrombocytopenia, absent radii	VSD	Autosomal recessive
Associations			
VATER	Vertebral defects, anal atresia, tracheoesophageal fistula, radial dysplasia, renal dysplasia	VSD	
Charge	Coloboma, congenital heart defect, choanal atresia, growth and mental retardation, genitourinary anomalies, ear anomalies	CHD	8q12 deletion
Cardiofacial syndromes			
Noonan syndrome (see also Chapters 2 and 13)	Abnormal facies, hypertelorism, low-set ears, small stature, lymphedema, mental retardation	Pulmonary stenosis (often dysplasia), peripheral pulmonary artery stenosis, ASD, hypertrophic cardiomyopathy	Autosomal dominant
Williams syndrome	Small stature, mental retardation, characteristic facies (epicanthal folds, anteverted nares, periorbital fullness), infantile hypocalcemia, stellate iris	Supravalvar aortic stenosis, peripheral pulmonary artery stenosis	Sporadic 7q23
Rubenstein–Taybi syndrome	Short stature, mental retardation, broad thumbs and toes, beaked nose, hypoplastic mandible	VSD	Microdeletion of 16p13.3
de Lange syndrome	Prenatal growth retardation, microcephaly, limb reduction anomalies, hirsutism, synophrys, anteverted nares, down-turned lips	CHD	Some partial deletion of chromosome 3
Major chromosome abnormalities			
Down syndrome (trisomy 21)	Characteristic facies, hypotonia, mental retardation, Brushfield's spots, simian crease, intestinal obstruction	40–50% AVSD, VSD; PDA, ASD, T of F, often PVOD; aortic stenosis, coarctation – rare	Trisomy 21, balanced translocation
Turner syndrome	Short stature, webbed neck, lymphedema, gonadal dysgenesis	(20%) Coarctation of aorta–bicuspid aortic valve	Monosomy 45,X (50%); other abnormalities of sex chromosomes (50%)

Table 6.1 (cont'd).

Disorder	Major feature	Cardiovascular abnormality[a]	Etliology
Edward syndrome (trisomy 18)	Low birth weight, microcephaly, micrognathia, rocker-bottom feet, closed fist with overlapping fingers	80% VSD with pulmonary hypertension	Trisomy 18
Patau syndrome (trisomy 13)	Low birth weight, central facial anomalies, polydactyly, chronic hemangiomas, low-set ears, visceral and genital anomalies	80% VSD with pulmonary hypertension, dextrocardia	Trisomy 13
Other syndromes discussed elsewhere			
Tuberous sclerosis	See Chapter 66 (cardiac tumors)		
Marfan syndrome	See Chapter 67 (connective tissue disease) and Chapter 2 (genetic disease)		
Ehlers–Danlos syndrome	See Chapter 67 (connective tissue disease)		

[a]ASD, atrial septal defect; AVSD, atrioventricular septal defect; CHD, congenital heart disease; IAA, interruption of aortic arch; PDA, patent ductus arteriosus; PVOD, pulmonary vascular obstructive disease; T of F, tetralogy of Fallot; VSD, ventricular septal defect.

Cardiac auscultation

With the attention directed to learning and applying a variety of diagnostic techniques, such as echocardiography, to evaluate the heart of children, the skills of auscultation are frequently considered to be less important. The important skills of auscultation must be learned by supervised listening to a variety of heart sounds and murmurs and maintained by frequent practice. Studies of the auscultatory skills of residents showed a disappointing ability to recognize commonly encountered findings [28]. Furthermore, studies have shown that the auscultatory ability did not improve following the third year of medical school through further training including cardiac fellowship [29]. Repetition is very important in developing the ability to identify properly murmurs and heart sounds [30,31]. The Internet can be searched for recordings of heart sounds and murmurs which are on-line. Individuals who play a musical instrument have a greater ability for auscultation [32]. It is ironic that Laennec, who is considered to have discovered the use of stethoscope, was a superb flautist [33,34].

Physical examination is a highly sensitive and specific method of screening asymptomatic subjects for valvar heart disease [35,36]. Newburger *et al.* [37] evaluated the ability of pediatric cardiologists to detect accurately a cardiac condition or a functional murmur by history and physical examination. They further determined the frequency that the initial categorization rate of abnormal or normal status was altered by subsequent investigative studies. Among 142 children considered to have a normal heart, 134 were still considered normal after further testing with electrocardiography and chest X-ray, five had a possible anomaly, and only three had a cardiac anomaly, and these were considered minor anomalies. Among the 104 initially diagnosed with a cardiac anomaly, after investigation all 104 did have an abnormality. The study concluded that an experienced pediatric cardiologist could accurately distinguish between normal and abnormal murmurs. Through training, experience, confidence in one's abilities, and a conviction that auscultation is a valuable diagnostic technique, physicians can correctly identify cardiac murmurs and avoid unnecessary costs and parental anxieties.

To gather the maximal amount of information from cardiac auscultation, particularly in neonates and infants, concerted effort, patience, and experience are required. Repeated examination may be necessary, particularly in neonates or critically ill infants and children, because of changes in cardiac rate or physiologic state. It is preferable to listen to neonates and infants when they are asleep, because the cardiac rate is slower and respirations are quieter. In the young, it is wise to listen through the clothing initially, before disturbing the infant by removal of the clothing, causing the infant to cry or have a faster cardiac rate. In 1–3 year olds, it is best to examine them while they sit on the parent's lap. Because of the natural fear of strangers in this age group, the child should be approached slowly and in a nonthreatening way. Distraction with a toy, a flash-light, blowing bubbles, or having the child view his (her) self in a mirror facilitates auscultation. In older children and adolescents, the anxiety from being examined may cause tachycardia and make auscultation more difficult.

Physicians should use their own stethoscopes rather than one available at the bedside or in the clinic. Stethoscopes can dampen and distort heart sounds and murmurs. Various types have differences in transmission of sound. The ideal stethoscope should have short (about 10 in), thick, fairly stiff tubing and snugly fitting earpieces. Even a tiny leak around

the ear pieces about five times the diameter of a human hair can reduce the sound transmission [38]. The bore of the tubing should be 1/8 in as this is the most efficient for sounds with a frequency of 40–115 cps, the range of most heart sounds [39]. The metal tubing adjacent to the earpieces can be bent to create a firm fit with the external auditory canal. The stethoscope should have both a bell and a diaphragm. I use a 1 in wide diaphragm and 3/4 in bell. It is not necessary to use a smaller sized diaphragm even when examining premature infants; a smaller diaphragm may mask some high-pitched sounds. The chest pieces should fit snugly to the thorax to avoid loss of sound.

High-pitched murmurs, clicks, and cardiac sounds are heard best with a diaphragm. Low-frequency sounds and murmurs are heard better with the bell. Do not press the bell tightly against the skin, as this stretches the underlying skin, creating a diaphragm and diminishing low-frequency sounds. The interested reader is directed to a number of articles on the stethoscope in the digital age [40–46]. A wonderful poem by Oliver Wendell Holmes describes the perils of using a new stethoscope [47]. It might amuse you.

The examination should be performed in a setting with minimal ambient noise. Auscultate both the anterior and posterior thorax for murmurs with the patient in the upright and supine positions. The back can be examined for both respiratory sounds and murmurs when the child sits, when an infant is held against the parent's chest, or when a neonate is prone. The murmurs of coarctation of aorta and peripheral pulmonary artery stenosis are heard over the back, as are murmurs from pulmonary stenosis. Frequently, I sit to the right side of the recumbent patient to perform auscultation. My head is positioned slightly above the level of the patient's head. Often I close my eyes to improve my concentration and open my mouth slightly because this improves hearing.

The examiner should develop a standard sequence to listen to the heart. Each of the four standard auscultatory areas, cardiac apex (mitral area), lower left sternal border (tricuspid area), upper left sternal border (pulmonary area), and upper right sternal border (aortic area), should be systematically listened to with both diaphragm and bell. The right anterior chest and both axillae should also be auscultated, particularly in neonates and infants in whom peripheral pulmonary artery stenosis is common. Both sides of the back should also be auscultated for transmissions of murmurs, such as pulmonary stenosis or coarctation of the aorta, which is heard well in the fourth left intercostal space between the spine and scapula. If abnormalities are noted at a particular site, further exploration should extend outwards from that site. In neonates with severe cardiac failure, auscultation over the head, liver, or other sites may identify an arteriovenous malformation. Attention must be directed to both the characteristic of the heart sounds and the features of murmurs.

The cardiac apex is a logical place to begin because at this location the first heart sound is loudest. In the pulmonary area, the second heart sound is the loudest. Identification of these two sounds allows one to identify more easily the location of murmurs and other heart sounds within the cardiac cycle.

The human ear can select desired sounds from many frequency patterns. With experience, two sounds separated by 20 ms can be distinguished. On the other hand, if a soft sound follows a very loud sound, it may not be heard. The examiner should try to develop the skill of selective auscultation by focusing only on high-pitched sounds or particular aspects of a murmur without interference from the other sounds. It is similar to the ability to listen to a symphony orchestra and pick out the music from a particular instrument to the exclusion of others. One way to help develop this skill is by making a simple line drawing of the sounds and murmurs showing their sequence, location, and loudness.

The human ear has a range of perception from 20 to 16 000 Hz (cps). The normal speech range is from 1000 to 2000 Hz. In comparison, most heart sounds and murmurs are of lower frequency. Most significant murmurs are from 600 to 1000 Hz and functional murmurs are usually below 200 Hz, as are the heart sounds. Below 200 Hz, the human threshold for audibility increases dramatically so that only a portion of the heart sounds may be heard. To be heard, a sound at 30 Hz must have an energy level thousands of times that at 1000 Hz.

Cardiac sounds

The classic work of Wiggers [48] describes the relationship between electrical events, intracardiac pressure, and flow changes during the cardiac cycle. An understanding of these relationships is invaluable in understanding cardiac sounds and in interpreting murmurs on the basis of their location within the cardiac cycle (Figure 6.1). The origin of heart sounds is uncertain, having been ascribed to valvar events, acceleration or deceleration of columns of blood, myocardial contractions, or a combination of these [49].

Although a number of mechanisms for heart sound production have been proposed, the one discussed most widely involves the generation of vibrations which are transmitted to the thoracic wall. These vibrations in the cardiovascular system are caused by (1) acceleration or deceleration of blood and (2) turbulence during rapid blood flow.

In this proposed theory, the relationship between the combined mass of the heart and its blood–volume–cardiohemic system is compared with the elasticity of the cardiac walls. As blood moves within the heart and great vessels, the momentum of the moving blood causes overstretch of the wall, which then recoils. In diastole, when the combined mass is large in comparison with the elasticity of the relaxed ventricle, low-frequency vibrations are produced. During systole, with the heart contracting, the frequency of the
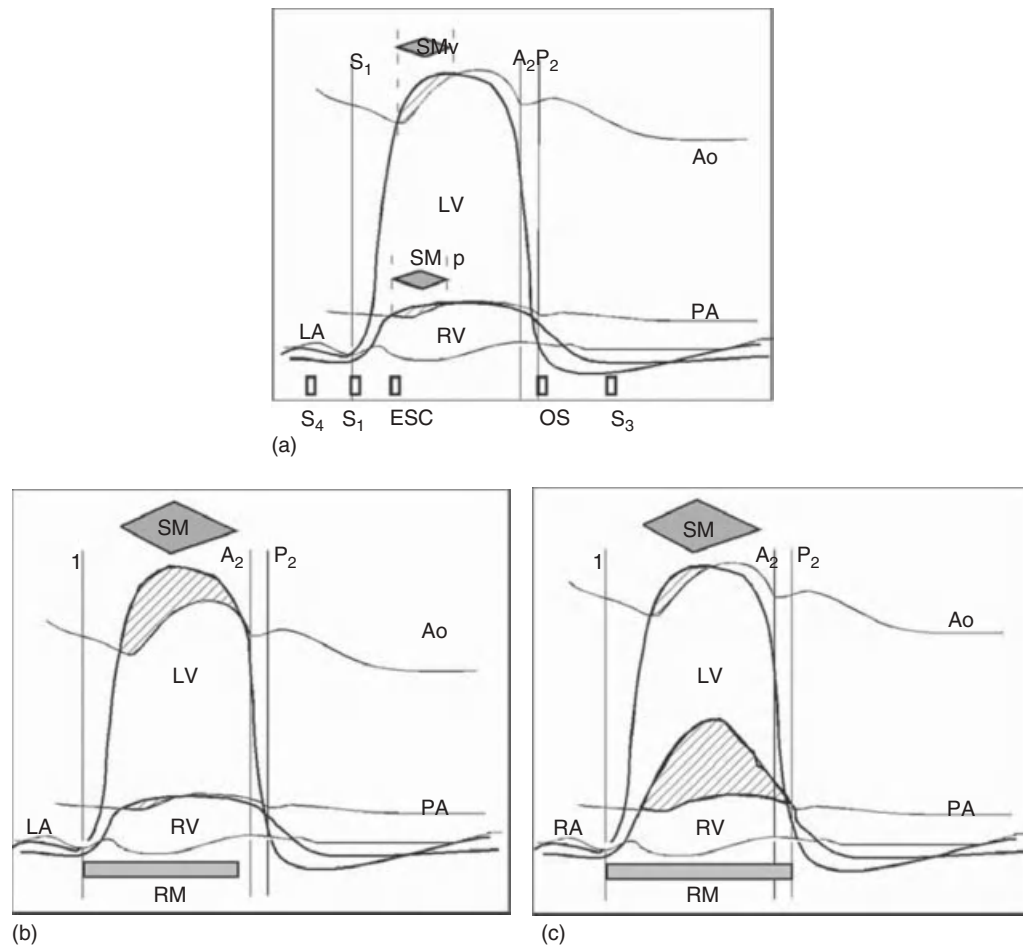
Figure 6.1 Modifications of Wigger's diagram [48]. (a) Pressure curves from right and left sides of heart and superimposed heart sounds and murmurs. Pressure curves: Ao, aorta, LA, left atrium, LV, left ventricle, PA, pulmonary artery, RA, right atrium, RV, right ventricle. Heart sounds: A_2, aortic component of second sound, ESC, ejection systolic click, OS, opening snap, P_2, pulmonic component of second sound. S_1, first sound, S_3, third heart sound, S_4, fourth heart sound. (b) Events on left side of heart. Systolic ejection murmur (SM) begins when left ventricular pressure exceeds that in aorta and extends to point where aortic pressure falls below LV pressure (A_2) Regurgitant murmur (RM) begins when left ventricular pressure exceeds left atrial pressure and extends to closure of aortic valve (A_2). (c) Events on right side of heart. Systolic ejection murmur (SM) extends to closure of pulmonary valve (P_2). Regurgitant murmur (RM) extends to point where right ventricular pressure falls below that of right atrium.

vibrations is increased. These vibrations are transmitted to the thoracic wall with sufficient intensity and high enough frequency to be audible. The sound waves are not reflected. The energy from the heart sounds is lost in the compressible lungs and dampened by fat tissue. Transmission is best through solid tissues.

First heart sound. At the onset of systole, blood is accelerated towards the AV valves before they are sealed, causing the low-pitched vibrations of the first component of the first heart sound. Once the valve has closed and the ventricular pressure is rising during systolic contraction, the movement of blood towards the valve is suddenly stopped and there is recoil towards the ventricle, causing the higher pitched second component of the first heart sound. The intensity of this component depends on the velocity and abruptness with

which it is decelerated. The sound is loudest when the valve has been widely open at the beginning of systole. A third component is heard following the opening of the semilunar valves. The inertia of the columns of blood in the great vessels opposes the acceleration of blood flow from the ventricles. This may lead to some rebound towards the ventricle. There may be a fourth component from blood flowing through the arterial trunks.

Second heart sound. At the end of systolic ejection, ventricular pressure falls rapidly and the ventricle relaxes. The column of blood in the arterial trunks rushes back towards the semilunar valves and its movement is stopped by the closed valves and recoils, causing vibrations. The difference in time between the closure of the valve and the dicrotic notch on the arterial pressure tracing and the second heart sound is

called the "hang out" interval. This interval for the aortic valve ranges from 5 to 13 ms It is longer for the pulmonary valve because of the much more compliant or distensible pulmonary circuit. This is a major factor in the splitting of the second heart sound.

Third heart sound. When the atrioventricular valves open, blood rushes into the relaxed ventricles. Its forward motion is arrested and recoil occurs, causing low-frequency vibrations because the ventricular walls are relaxed.

Murmurs. Murmurs often result from some form of obstruction to flow. Several hypotheses have been made for their production. These were outlined by Rushmer [49] as follows:

1 Eddies occurring around a jet through a restricted orifice.

2 A jet impacting a wall, which would produce vibrations from that wall.

3 Vortex shedding causing vibrations.

4 Periodic wake as sounds travel alternately around either side of an obstruction. This is unlikely.

5 Flutter. This would be produced by a Bernoulli effect. Although this phenomenon can produce sound, it is unlikely in the vascular system.

6 Cavitation. Although cavitation can be produced with high-speed jets and sound, it is unlikely to be found in the cardiovascular system.

Because both normal and abnormal heart sounds occur at approximately the same time as closure or opening of cardiac valves, it has been convenient to ascribe a causal relationship between the two, particularly in discussing cardiac auscultation as in this chapter. In 1958, Leatham [50] wrote an excellent article about cardiac auscultation. It is an extremely helpful review for understanding heart sounds and murmurs, even though it is six decades old. The information included in his paper is used extensively in the sections on heart sounds and murmurs below. This article is one of the most important publications that I read as a fellow and I have used its information throughout my career as a foundation to build upon; it can be highly recommended. Another excellent source was published by Chizner [44].

Heart sounds mark the transition of phases of the cardiac cycle (Figure 6.1). In infants and children, four distinct heart sounds may normally be heard. These include a first heart sound, the aortic component of the second heart sound, the pulmonic component of the second heart sound, and a third heart sound (about 50% of children). Below these are described first, followed by abnormal heart sounds including systolic ejection click, mid to late systolic click, opening snap, and fourth heart sound. The normal characteristics and the alterations from normal are discussed.

First heart sound (S₁)

The first heart sound occurs near the time of closure of the mitral and tricuspid valves [51,52]. Although consisting of several components, the first heart sound appears single in most infants and children. It may be split, with the initial component reflecting the earlier closure of the mitral valve. Rarely is the first heart sound split in infancy. When it is, Ebstein's malformation of the tricuspid valve must be considered strongly. Some adolescents have a split first heart sound.

The first heart sound is heard best at the cardiac apex, where it is louder than the second heart sound. If the first heart sound is heard better along the lower left sternal border, an abnormality on the right side of the heart must be suspected.

The first heart sound may be either accentuated or diminished. The first heart sound may be accentuated in four conditions:

1 *Increased blood flow across an atrioventricular valve.* In patients with either increased pulmonary blood flow from a left-to-right shunt or regurgitation of an atrioventricular valve, the first heart sound may be accentuated. The first heart sound is accentuated at the cardiac apex in patients with increased anterograde flow across the mitral valve, as in ventricular septal defect, or patent ductus arteriosus. The first heart sound is accentuated along the lower left sternal border (tricuspid area) in patients with increased anterograde flow across the tricuspid valve, as in atrial septal defect or tricuspid regurgitation.

2 *Atrioventricular valvar stenosis.* Both mitral stenosis and tricuspid stenosis are rare in children in the developed world. In areas with a high prevalence of rheumatic heart disease, however, mitral stenosis may be found in late childhood and adolescence. In such patients, a high-pressure differential exists across the mitral valve at the end of the diastole. Thus, a higher than normal ventricular systolic pressure must develop before valve closure occurs. Because of the higher closure pressure, the first heart sound is accentuated. I have heard accentuation of S1 in older children with congenital mitral stenosis but have not appreciated it in infants or young children with this condition.

3 *Short PR interval.* If the PR interval is short, as in Wolff–Parkinson–White syndrome, the interval between atrial contraction and onset of ventricular systole is also shortened. Thus, the atrioventricular valves are maximally open, so the length of excursion of leaflets to closure is great. Therefore, the first heart sound is loud.

4 *Conditions with increased cardiac output.* Increased cardiac output from conditions such as anemia and arteriovenous fistula is associated with increased anterograde flow across the atrioventricular valves, shortened diastole, and increased ventricular contractility. These factors combine to increase loudness of the first heart sound.

The loudness of the first heart sound may be diminished from three general conditions:

1 *Prolonged atrioventricular conduction.* When the interval between atrial contraction and onset of ventricular systole is prolonged, the atrioventricular valve leaflets have returned from their maximally opened position. Hence the length of

valvar excursion to closure is presumably decreased, and the first heart sound is soft. The loudness varies with atrial fibrillation [53] and with heart block.

2 *Depressed myocardial function.* In patients with depressed myocardial contractility, as in myocarditis, the first heart sound may be diminished.

3 *Moderate to severe mitral regurgitation.*

Second heart sound (S₂)

The normal second heart sound is composed of two sounds; the first, A_2, represents the earlier closure of the aortic valve, and the second, P_2, the later closure of the pulmonary valve. The second heart sounds occur at the time of the incisura of aortic and pulmonary arterial pressure tracings and are generally coincidental with the transition between the end of ejection and the onset of isovolumetric relaxation. The two components of the second heart sound are heard best in the second and third left intercostal spaces because the pulmonary valve, the most anteriorly located valve, lies immediately below this area and the aortic valve slightly lower along the left sternal border.

The term *splitting of the second heart sound* is applied to the phenomenon of hearing two components of the second heart sound. Our studies have indicated that an interval of at least 20–25 ms must be present between the two components before they can be heard as separate sounds by an experienced pediatric cardiologist. The degree of splitting normally varies with respiration, increasing with inspiration and decreasing with expiration, reflecting the variable volume of blood returning to the right ventricle with the phases of respiration. This phenomenon is termed *variable splitting.* In patients with tachycardia, particularly neonates and infants, it may be difficult to appreciate splitting or variability. Repeated auscultation when the heart rate is slower may allow clearer characterization of the second heart sound components. Considerable diagnostic information can be obtained by careful attention to details of the second heart sound. Three aspects of the second heart sound must be assessed: loudness of individual components, degree of splitting, and variations in patterns of splitting.

Loudness of the components of the second heart sound depends on the level of pressure in the great arteries, position of the aortic and pulmonary valves within the thorax, and thickness of the anterior chest wall. In infants and children, P_2 is louder than A_2 because the pulmonary valve lies immediately below the chest wall, whereas the aortic valve is located centrally within the thorax and is surrounded by cardiac structures. The difference occurs even though pulmonary arterial pressure is considerably lower than aortic pressure. In patients with transposition of the great arteries, the second heart sound is loud and single because the aortic valve, located beneath the chest wall, is closed with a high pressure and the more distant pulmonary valve being closed at a lower pressure is masked.

The loudness of a component of the second heart sound depends on the pressure level at the time of the incisura of the arterial pressure wave It reflects neither peak systolic nor diastolic arterial pressure. Because many forms of cardiac malformation are associated with pulmonary hypertension, care must be directed towards increased loudness of P_2, which reflects an elevated pulmonary arterial pressure.

The aortic valve is centrally placed in the thorax, approximately behind the sternum at the level of the fourth space and midway in the chest. The ascending aorta comes closest to the chest wall to the right of the upper sternum. Therefore, A_2 is normally heard loudest at the upper right sternal border or equally loud at the upper right and left sternal borders. If A_2 is loudest at the left sternal border, an abnormal aortic position is indicated. Thus, in tetralogy of Fallot, with a dextroposed and dilated ascending aorta, A_2 is loudest to the left of the sternum in the fourth intercostal space. In both complete and corrected transposition, A_2 is loudest to the left of the sternum in the second intercostal space, and the same may be true in a truncus arteriosus. Other forms of malposition, including dextrocardia, may also give an A_2 that is loudest at the upper left sternal border.

During the first 2 days of life, the second heart sound appears single because of the elevated pulmonary vascular resistance normally present at this stage of life and the nearly identical aortic and pulmonary arterial pressure curves. Subsequently, the second heart sound becomes split as the pulmonary vascular resistance falls. A single second heart sound beyond the immediate neonatal period indicates a serious cardiac anomaly with a single functioning semilunar valve. There may be only one semilunar valve, as in truncus arteriosus, or two valves in which one is either atretic or severely stenosic. The second heart sound is single (aortic component) in patients with pulmonary atresia, severe pulmonary stenosis, or tetralogy of Fallot. It may be single (pulmonary component) in aortic atresia or severe aortic stenosis. Unfortunately, these anomalies cause severe symptoms in the neonatal period, when S_2 normally appears single, so auscultation cannot allow their identification.

If the second heart sound is split but does not vary with respiration, the phenomenon is called *fixed splitting.* This usually coexists with wide splitting and indicates a large atrial communication, as typically occurs in patients with an atrial septal defect in which wide, fixed splitting is characteristic. Wide splitting reflects an increased volume of blood being ejected from the right ventricle and being fixed reflects an atrial communication that allows adjustment of flow distribution in the atria with phases of respiration.

In evaluating the second heart sound, attention should be directed to the degree of splitting. With experience, it is possible to identify wide splitting, indicating that this interval between the components of the second heart sound exceeds 60 ms. If the second heart sound can easily heard as split in a tachycardic neonate or infant, it should be considered widely split.

The second heart sound is widely split in patients with prolonged right ventricular ejection due to:

1 *Increased volume of right ventricular ejection.* If the volume of blood ejected by the right ventricle across the pulmonary valve is increased, P_2 is delayed. This may result from pulmonary regurgitation or an atrial level shunt, such as atrial septal defect or anomalous pulmonary venous connection.

2 *Obstruction to right ventricular outflow.* In severe pulmonary stenosis or tetralogy of Fallot, right ventricular ejection is prolonged and P_2 delayed.

3 *Complete right bundle branch block in which right ventricular depolarization is prolonged abnormally, as is right ventricular systole.* Thus, P_2 is delayed.

Delayed closure of the aortic valve can be identified by paradoxical splitting of the second heart sound. Because A_2 is delayed and may occur after P_2, the degree of splitting narrows on inspiration and widens on expiration, a pattern opposite of normal. In my experience, paradoxical splitting is rare during childhood and adolescence. Three types of conditions associated with paradoxical splitting are (1) increase in left ventricular ejection volume, as in severe aortic regurgitation or patent ductus arteriosus; (2) obstruction to left ventricular outflow, as found in patients with severe aortic stenosis; and (3) complete left bundle branch block.

Third heart sound (S₃)

A third heart sound may be heard in childhood. This low-frequency, broad sound occurs at the peak velocity of ventricular inflow and the transition between rapid and slow filling phases of diastole. This sound has been considered to arise in a ventricle from sudden deceleration of flow during rapid filling [54–59]. The normal third heart sound disappears in adulthood by the age of 40 years because the increased left ventricular wall thickness with age causes a decrease in the velocity of ventricular filling [60].

Third heart sounds may originate from either the left or right ventricle, being heard better at the cardiac apex (mitral area) or lower left sternal border (tricuspid area), respectively. This sound is prominent in patients with increased volume of ventricular filling [61–63]: increased pulmonary blood flow, valvar regurgitation, and anemia. In a patient with tachycardia from any cause, a third heart sound may become prominent and be interpreted as a gallop, a sound suggesting cardiac failure and myocardial dysfunction. In this situation, proceed carefully and reserve the term *gallop* when other findings support a diagnosis of cardiac failure.

Early systolic ejection click

An early systolic ejection click occurs shortly after the first heart sound and at the transition between isovolumetric contraction and the onset of ejection. It is recorded at or shortly after the opening of a semilunar valve. During the first 24 h of life, a click may be heard normally; but after that age, an ejection click is always abnormal and indicates dilatation of either the ascending aorta or pulmonary trunk. Dilatation may occur from either aortic or pulmonary valvar stenosis (poststenotic dilatation) or from conditions associated with an enlarged major arterial trunk, such as truncus arteriosus, Marfan's syndrome or pulmonary hypertension.

The mechanism for production of a click is unknown. It occurs at the time of maximal opening of a stenotic valve, suggesting that it may be valvar in origin. On the other hand, it may result from sudden tensing of the wall of a dilated great vessel in which elastic fibers are known to have degenerated so that the wall is supported mainly by indistensible collagen.

The characteristics of a systolic ejection click reflect the vessel of origin – pulmonary artery or ascending aorta. Pulmonary clicks are heard best with the diaphragm of the stethoscope in the pulmonary area with the patient sitting. They become louder in expiration. Aortic ejection clicks are heard best at the cardiac apex and left lower back with the patient reclining. They do not vary with the phase of respiration. They are lower pitched and may be difficult to distinguish from the second component of a split first heart sound.

Mid to late systolic click

Mid to late systolic clicks occur with mitral valve prolapse, and are sharp, high-pitched sounds heard best at the cardiac apex. They vary considerably in loudness with maneuvers that alter left ventricular volume. They are louder when the patient is standing or sitting because of the smaller left ventricle volume and become softer and later when the patient reclines or squats, resulting in a larger left ventricular volume. This click may also be heard along the left sternal border when a ventricular septal defect is being closed by a pseudoaneurysm, but it does not vary during the respiratory cycle.

Opening snap

An opening snap is a rare auscultatory finding in children and adolescents in most parts of the world. It is heard in mitral valve stenosis, which is most commonly caused internationally by rheumatic heart disease. This sound, heard better with a diaphragm at the cardiac apex or lower left sternal border, occurs shortly after the end of isovolumetric relaxation, at the time of maximum opening excursion of the anterior leaflet of the mitral valve. The mechanism for the sound production is unknown.

Fourth heart sound (S₄)

A fourth heart sound is low pitched, occurs during atrial contraction, and precedes peak atrial inflow velocity. It is associated with lesions that limit ventricular distensibility. It is a frequent finding in patients with coronary artery disease, cardiomyopathy, severe semilunar valve stenosis (either aortic or pulmonic), and hypertension (systemic or pulmonary) [64]. A fourth heart sound may be found in patients with

increased cardiac output, as in anemia or arteriovenous fistula. It can also be heard in patients with second- or third-degree heart block. Fourth heart sounds originating from the left ventricle are heard at the apex, those from the right ventricle along the lower left sternal border. These are common in adults but infrequent in children.

Cardiac murmurs

Cardiac murmurs result from turbulence of blood flow through the heart or major arteries. Reynolds' number has been used to understand the factors that cause turbulence in a system of laminar flow. Although blood flow is not necessarily laminar and homogeneous, the equation helps understand factors leading to turbulence. Reynold's number (Re) [65] indicates that turbulence arises in a Newtonian fluid of viscosity η and density ρ, flowing with a velocity V through a tube with diameter D according to the relationship $Re = DV\rho/\eta$. Reynolds' number is dimensionless, but when it exceeds a critical value, about 2000 for a viscous fluid, turbulence occurs. Turbulence could occur with a high flow velocity or low blood viscosity.

Six characteristics of a murmur should be identified and described. Each provides a specific type of information about hemodynamic and anatomic associations. These characteristics are

- loudness: reflecting severity of the anomaly
- location within the cardiac cycle: relating the murmur to hemodynamic events
- location on the thorax: relating the murmur to an anatomic site
- radiation: indicates direction of turbulent blood flow
- pitch: reflecting the pressure difference
- other characteristics meaningful to the examiner, such as "musical," "blowing."

By identifying and describing these characteristics, the examiner can gain much understanding of the underlying condition causing the murmur.

Loudness

The loudness of a murmur is described by a system of grades. These are

- grade 1/6: soft and heard after an extended period of listening
- grade 2/6: soft but immediately heard
- grade 3/6: moderately loud, unassociated with a thrill
- grade 4/6: loud, usually associated with a thrill
- grade 5/6: loud, heard with stethoscope barely off the thoracic wall
- grade 6/6: loud, heard with stethoscope off the thoracic wall.

This system is most useful to an individual examiner who has developed an internal sense of grading so that, with experience, murmurs of similar loudness receive the same grade. Even with experience, this is not always possible to achieve. I find it particularly difficult to apply grades 3/6

and 4/6 to systolic murmurs and grades 1/6 and 2/6 to diastolic murmurs.

The loudness of a murmur reflects the severity of a lesion and the amount of blood passing through the abnormal area, as in the following examples.

1 In aortic or pulmonic regurgitation, the more severe the lesion, the greater is the regurgitant volume and the louder the regurgitant murmur. If the regurgitant orifice is small, there is a pressure gradient from the artery to the ventricle throughout the whole of diastole, and the murmur is long. If the regurgitant orifice is large, pressures tend to equalize in the artery and the ventricle so that the murmur tends to end earlier during diastole.

2 When the entire cardiac output passes through an abnormal structure, as in aortic, pulmonic, or mitral valve stenosis, the more severe the stenosis, the greater is the pressure drop across the valve, the flow is more turbulent, and the murmur is louder. If the obstruction is severe enough to reduce the cardiac output, the murmur becomes softer. Furthermore, with significant aortic or pulmonic stenosis, the velocity of flow across the valve is greater and the resulting murmur is higher pitched (see below).

3 In a small ventricular septal defect, the pressure difference between the ventricles is large, and the murmur is often loud. If the defect is larger and associated with a huge left-to-right shunt through it, the murmur is also loud, even though the pressures are similar in the two ventricles. If a ventricular septal defect is associated with increased pulmonary vascular resistance (neonatal period, or after pulmonary vascular disease develops), only a small flow crosses the defect. This results in little turbulence and only a soft murmur. Similarly, when the ventricular septal defect is small, perhaps less than 2 mm in diameter, little blood crosses and the murmur is high pitched and soft.

Location in the cardiac cycle

Murmurs should be described according to when they occur in the cardiac cycle. Timing of murmurs has been described as systolic, diastolic, or continuous, each being further subdivided into more specific intervals of the cardiac cycle. In neonates, infants, and others with tachycardia, it may be difficult to categorize beyond systolic, diastolic, or continuous. Other features, such as location on the thorax or pitch, may be helpful.

Systolic murmurs

There are three types of systolic murmurs: pan(holo)systolic, ejection systolic, and late systolic.

Pansystolic murmurs

Although the prefix *pan-* suggests all of systole, these murmurs do not necessarily extend to the second heart sound, but they do begin with the first heart sound. Therefore, pansystolic murmurs include the period of isovolumetric

contraction, and make it difficult to identify the first heart sound. During isovolumetric contraction, because all cardiac valves are closed, blood should not be moving within the heart. Only three conditions allow blood to flow during isovolumetric contraction: ventricular septal defect, because the ventricles are in full communication throughout systole; mitral insufficiency; and tricuspid insufficiency. In the last two, the higher ventricular systolic pressure compared with lower atrial pressure allows blood to regurgitate from a ventricle to an atrium during isovolumetric contraction. Pansystolic murmurs are also called regurgitant murmurs, indicating regurgitation across an atrioventricular valve.

The murmur of mitral insufficiency is heard best at the cardiac apex, is high pitched, and has been described as "blowing." Tricuspid insufficiency is low pitched and heard along the lower left sternal border. In this same area, the much more frequently occurring ventricular septal defect murmur is heard and is generally high pitched.

The systolic murmur of a ventricular septal defect, located over the precordium and associated with a thrill, has been called a Roger murmur. Roger described it as "long and loud" and that "it entirely occupies the period of the normal tic-tac of the normal heart sounds" [66]. Henri Louis Roger (1809–1891) was a French pediatrician who was very interested in auscultation. He presented his observations to the French Academy of Medicine and concluded that the only explanation for such a prominent murmur was a defect in the interventricular septum. Subsequent to his initial presentation, he observed a 26-month-old child with such a murmur who died of "pulmonary mishap." The autopsy of the child showed a ventricular septal defect in the "upper portion of the interventricular septum" [67].

Ejection systolic murmurs

Ejection murmurs are limited to the ejection phase of systole. Therefore, they begin after the isovolumetric contraction phase. This point is a key distinction between the two major types of systolic murmurs. In an ejection murmur, a short period exists between the first heart sound and the onset of the murmur.

Ejection murmurs result from turbulence either into or within the aorta or pulmonary trunk. These can be caused by outflow tract obstruction, by stenosis in large central arterial vessels, or from increased volume of blood across a normal outflow tract. Respective examples are pulmonary or aortic stenosis (valvar, subvalvar, supravalvar), coarctation of the aorta or peripheral pulmonary artery stenosis, and atrial septal defect. Because there are only two outflow tracts by which blood exits the heart, the maximal location of the murmur allows identification of whether obstruction lies in the right (pulmonary area) or left (aortic area) outflow tracts.

Late systolic murmurs

Late systolic murmurs occur with mitral valve prolapse. As the left ventricular volume becomes progressively smaller during systole, the volume becomes small enough so that the posterior leaflet prolapses into the left atrium. This permits regurgitation that increases as the ventricle continues to contract to the end of systole. Hence the murmur is crescendo to the second heart sound. As discussed previously in this chapter, the murmur is introduced by a mid to late systolic click (see also Chapter 28) and its duration varies with body position as discussed above.

Diastolic murmurs

There are three types of diastolic murmurs, early, mid, and late. The first follows S_2, the second represents a widening of the S_3, and the last reaches a peak in the cardiac cycle where an S_4 would be heard.

Early diastolic murmurs

Early diastolic murmurs immediately follow the second heart sound, occupy the period of isovolumetric relaxation, and may extend beyond that period. They result from insufficiency of either the aortic or the pulmonary valve. Regurgitation occurs from flow from the higher pressure great artery to the lower pressure ventricle. They have been called regurgitant murmurs. Note that all regurgitant murmurs, whether in systole or diastole, occupy isovolumetric periods.

Mid-diastolic murmurs

Mid-diastolic murmurs occupy the period of time at the transition from rapid to slow filling phases of the cardiac cycle. They occur from increased volume of blood flow across anatomically normal atrioventricular valves. Usually, the anterograde flow must be about twice normal before a mid-diastolic murmur is heard. Mitral mid-diastolic murmurs are heard in conditions such as mitral insufficiency and shunts at the ventricular or great vessel level (ventricular septal defect, patent ductus arteriosus, truncus arteriosus). Tricuspid mid-diastolic murmurs occur in tricuspid regurgitation (as in the Ebstein's malformation) and atrial level shunts (atrial septal defect, total anomalous pulmonary venous connection). Mid-diastolic murmurs occur with mitral and tricuspid stenosis with presystolic accentuation. Because there is little diastolic pressure difference across the atrioventricular valves in these conditions, mid-diastolic murmurs are low pitched. In 1862, Austin Flint described in patients with aortic insufficiency a mid-diastolic murmur that was distinct from the high-pitched early diastolic murmur from the regurgitation [68]. Called an Austin Flint murmur, he considered it to be related to fluttering of the anterior leaflet of the mitral valve being struck by the regurgitant jet.

Late diastolic murmurs

Murmurs occurring late in diastole are also called protodiastolic or presystolic. They result from atrioventricular valve stenosis, which is usually of the mitral valve. They increase in loudness (crescendo) to the first heart sound as the gradient between the atrium and its respective ventricle increases and is accentuated by atrial contraction.

Continuous murmurs

A continuous murmur begins in systole and continues into diastole, but does not necessarily continue throughout the cardiac cycle. The murmur has the same characteristics in both phases of the cardiac cycle. It is not a separate systolic and a diastolic murmur. Continuous murmurs can be divided into two categories, depending on whether the murmur is louder in systole or in diastole.

Louder in systole

A continuous murmur, louder in systole, indicates a communication between the arterial and venous systems, usually large vessels. The classic example is patent ductus arteriosus, but others include bronchial collaterals in cyanotic patients and a peripheral arteriovenous malformation. In a neonate, a continuous murmur over the upper chest often indicates pulmonary valvar atresia, with a patent ductus arteriosus being the major or sole source of pulmonary blood flow. In a neonate, continuous murmurs are also heard from arteriovenous malformations or fistulas and are heard best over their anatomic location. In a patent ductus arteriosus, the murmur is often crescendo in late systole because of the time taken for the pulse wave to reach the ductus. The original description of the murmur by Gibson in 1900 remains as true today as it was over a century ago [69].

Louder in diastole

Continuous murmurs louder in diastole point to an abnormality of blood flow in major veins. The volume of blood returning to the right atrium is greater during diastole because of right ventricular filling. The most frequent cause is a benign venous hum, but it can occur if there is increased blood flow in the superior caval system, as in total anomalous pulmonary venous connection to a supracardiac vein or cerebral arteriovenous fistula.

Location on the thorax

A murmur is loudest closest to its anatomic origin. Murmurs should be described by their anatomic location, such as upper right sternal border, upper left sternal border, lower left sternal border, or cardiac apex, rather than by the respective terms commonly used: aortic area, pulmonary area, tricuspid area, mitral area. Because of the array of cardiac malformations, for instance the pulmonary artery and valve may not be located in the "pulmonary area," as in transposition of the great arteries, and a murmur in the "mitral area" may arise from an inverted tricuspid valve as in congenitally corrected transposition of the great arteries.

In addition to the four traditional auscultatory sites, both axillae should be auscultated (peripheral pulmonary artery stenosis), as should the back, particularly the left paraspinal area (coarctation of the aorta). In patients with normally related great arteries, murmurs heard best along the upper left sternal border and beneath the left clavicle originate from the right ventricular outflow tract, and those extending from the midsternum to the area beneath the right clavicle originate from the left ventricular outflow tract. Murmurs along the lower left sternal border commonly result from a ventricular septal defect, and less frequently from obstructive cardiomyopathy or tricuspid regurgitation.

Radiation

Other locations where the murmur is heard should be described. These secondary sites indicate radiation of the murmur and reflect the direction of turbulent blood flow. Murmurs from the right ventricular outflow tract radiate to the left upper back. The left pulmonary artery is a direct extension of the pulmonary trunk and is directed posteriorly and to the left. In tetralogy of Fallot, wherein the right ventricular outflow tract is oriented typically towards the right, the murmur is heard best over the right side of the back. Murmurs from the left ventricular outflow tract area are directed into the carotid arteries, particularly the right. In patients with a moderate or large ventricular septal defect or significant tricuspid regurgitation, radiation is towards the right sternal border and right anterior chest, reflecting the direction of turbulent flow. The murmur of mitral regurgitation classically extends to the left axilla and left lower back.

Pitch

The pitch or frequency of a murmur reflects the pressure difference creating the turbulent flow and murmur. High-pitched murmurs result when there is a large pressure difference, as in mitral regurgitation or aortic regurgitation. In contrast, the murmurs of tricuspid and pulmonary regurgitation are lower pitched because of lower right-sided cardiac pressures in normal individuals. Diastolic murmurs from anterograde flow across an atrioventricular valve, as in a left-to-right shunt, are low pitched.

The murmur of pulmonary regurgitation can be higher pitched with pulmonary hypertension. This murmur has been named Graham Steell murmur [70], after the English physician who described it. Steell lived from 1851 to 1942 and was an Assistant Physician to the Manchester Royal Infirmary when he described it. In his paper, he indicated how it could be distinguished from the murmur of aortic regurgitation which was also high pitched.

Other features

A variety of other terms are used commonly on rounds or in clinics to describe murmurs. These terms, such as harsh, blowing, musical, and to-and-fro, are less precise and perhaps are of greatest use to the individual examiner who has his or her own auditory concept of harsh, blowing, or musical.

Functional murmurs

During childhood, half of children have a murmur. These are often transient, appearing when the child has a fever or only on one examination, and occur in a structurally normal heart. Although these have been called functional or innocent murmurs, I prefer to call them "normal murmurs" when describing them to parents, to indicate that the heart is structurally and functionally normal and that these murmurs are normal phenomena.

The clinical diagnosis of a functional (normal) murmur is a two-step process. The first is to distinguish whether the patient's murmur reflects a major cardiac condition or could represent a normal murmur. This step depends on whether the murmur is associated with five features common to all children with a functional murmur:

1 There are no meaningful cardiovascular symptoms.

2 The murmur is less than grade 3/6.

3 The heart sounds are normal. Particular attention must be directed to the second heart sound.

4 The heart size is normal. This can be assessed by palpation of the cardiac apex.

5 The murmur is usually short, ending by the first half of systole.

In a study of children with an innocent vibratory or a pulmonary flow murmur and a group of children with an easily confusable mildly pathologic murmur, phono-spectrographic analysis was performed. The functional murmurs were usually below 200 Hz and with a frequency spectrum with more harmonic structure. In contrast, pathologic murmurs had both lower and higher frequencies [71].

Rosenthal, in an article about distinguishing innocent from pathologic murmurs, listed six criteria for identifying a pathologic murmur [72]:

1 all diastolic murmurs

2 all pansystolic murmurs

3 late systolic murmurs

4 very loud murmurs

5 continuous murmurs

6 associated cardiac abnormalities.

Eight distinct normal murmurs have been identified, and each must be distinguished from murmurs resulting from cardiac abnormalities that may have some similar features. One early study of children showed that 85% were Still's murmurs, 14% pulmonary flow murmurs, and 1% cardiopulmonary murmurs [73].

Pulmonary flow murmurs

This soft, short systolic ejection murmur, believed to result from turbulence in the right ventricular outflow tract and pulmonary trunk, is heard along the upper left sternal border. It is more common in adolescents and in females by a ratio of 3:1 [71]. It can appear with fever and anemia. It must be distinguished from atrial septal defect, which has a similar murmur, but the wide, fixed splitting of the second heart sound is diagnostic. Also in atrial septal defect, in contrast to a functional pulmonary flow murmur, the tricuspid valve closure is loud, and a mid-diastolic murmur is common in the tricuspid area. Mild valvar pulmonary stenosis may have a similar murmur, but it is longer, higher pitched, and preceded by an ejection click.

Vibratory, "twangy string," or still's murmur

This short, early midsystolic murmur is heard best between the lower left sternal border and the cardiac apex. Like the pulmonary flow murmur, it seldom persists beyond midsystole. It is uniform in frequency, hence its name vibratory. The origin of the murmur is uncertain. Many believe it to be related to turbulent flow in the left ventricular outflow tract and related to higher aortic flow volume and velocity [74–76]. Harris *et al.* [77], using cathode-ray oscilloscopy, found relatively dense spectrographs below 250 cps for both Still's and murmurs from other high-output states. They considered that the murmur was caused by vibrations of its natural period of some structures of the cardiac walls or great vessels. In some children, an anomalous band has been found in the left or right ventricle [78]. In one study [79], 76% of patients with this murmur had a band in the left ventricular outflow tract, compared with 14% of those without a murmur. Joffe, however, could not detect turbulence around the anomalous bands by echocardiography [80]. Others [81–85] suggested that the murmur is from the combination of a small aortic diameter and high aortic velocity. A report [86] and accompanying commentary [87] provide insight into this type of murmur as possibly originating from increased intraventricular velocities. Klewer *et al.* [88] used dopamine stress echocardiographic studies in normal subjects without a murmur to produce a Still's-like murmur when the cardiac output was increased. They found that a lower body surface area correlated with the presence of the murmur, explaining why Still's murmur is most often seen in younger ages. Subsequently, Donnerstein and Thomsen [89], using spectral analysis of Still's murmurs, found characteristic time-varying spectra related to a patient's age and cardiac dimensions rather than flow velocity. The spectral frequency decreased with age. They suggested that the disappearance of the murmur as the child grows may be related to a murmur having such a low frequency that is below the auditory threshold. The murmur is usually heard in preschool-aged children [90].

The major differentiation is from ventricular septal defect. Because most ventricular septal defects are membranous, they are heard best along the left sternal border in the third and fourth interspace. The murmur of a muscular ventricular septal defect may be heard in the same area, but it is harsher.

It was the British pediatrician, Sir George Frederick Still (1868–1941), who first described this functional murmur in an era before echocardiography. Still also described a variety of chronic polyarthritis associated with lymphadenopathy, splenomegaly, and irregular fever. Still's description of the murmur which bears his name is as follows [91]: "It is heard usually just below the level of the nipple and about half way between the left margin of the sternum and the vertical nipple line; it is not heard in the axilla nor behind, it is systolic and is often so small that only a careful observer would detect it; moreover it is variable in audibility; its characteristic is a twangy sound very like that made by twanging a piece of tense string."

Venous hum

This continuous murmur is louder in diastole and heard best along the upper right sternal border. It results from turbulent flow in the jugular venous system. Thus, there may be a thrill posterior to the sternocleidomastoid muscle over the jugular vein. The murmur is heard better when the patient is sitting and disappears or softens on reclining. The murmur varies as the patient turns the head back and forth or when gentle pressure is applied over the base of the neck.

A similar murmur can be heard in an occasional patient with total anomalous pulmonary venous connection to the left superior vena cava. It may also be heard with a cerebral arteriovenous malformation.

Carotid bruit

In virtually all children, an early systolic murmur may be heard over the bifurcation of the carotid arteries. It should not be confused with radiation of a murmur of aortic stenosis to the carotid arteries. Palpation of the suprasternal notch helps to distinguish these because with aortic stenosis, a thrill is palpated in this area.

Cardiopulmonary murmur

This noise is believed to result from compression of the lingula of the lung between the heart and anterior chest wall. I have heard a similar noise along the right sternal border. This noise is louder during mid-inspiration and mid-expiration, becoming soft or absent on full inspiration or full expiration. It is heard better when the patient is sitting.

Peripheral pulmonary artery stenosis

In some neonates, particularly those born prematurely, a midsystolic ejection murmur may be heard over both lung fields, including on the back, in the axillae, and beneath both clavicles, but not over the precordium. Present in the neonatal period, it usually disappears by 3 months of age

and is always gone by 1 year of age. In fetal life, because little flow occurs through the lungs, there is a discrepancy of size between the large main pulmonary artery and smaller branch pulmonary arteries. Postnatally the murmur disappears as the branch pulmonary arteries increase in size.

Mammary souffle

In lactating women, a low-frequency background hum due to a large increase in blood flow to the breasts through superficial blood vessels may be heard immediately over the breast. Gentle pressure over the area may diminish the loudness. Its importance is in distinguishing it from a patent ductus arteriosus or an arteriovenous fistula.

Cephalic bruit

Cephaic bruits are heard much more commonly in early school-aged children than adults, perhaps because of the higher cerebral blood flow in the young than adults. (100 ml per 100 g min^{-1} in a 5-year old versus 50 ml per 100 g min^{-1} in a 30-year-old) They are more common in those with decreased blood viscosity (anemia), increased blood flow (hyperthyroidism, cerebral arteriovenous fistula), or local narrowing of an artery.

Variant auscultatory findings

In two groups of pediatric patients, neonates and athletes, the auscultatory findings are unique.

Neonates

The first heart sound is loud at birth and decreases in intensity during the first 48 h of life. It may be split, with the second component being loud in the tricuspid area. A systolic ejection click along the left sternal border has been reported to occur in many neonates. The second heart sound is single at birth, presumably due to elevated pulmonary vascular resistance [92]. By 2 days of age, it becomes split in normal neonates.

Several studies of normal neonates have described the frequency and types of murmurs in neonates [93–102]. On careful auscultation, one-third to three-quarters of neonates have been described as having a murmur.

1 A continuous murmur in the pulmonary area heard best with the bell. In one series, this occurred in 37% of normal neonates [95], was transient, and usually disappeared by 12 h of age. Its frequency is higher in premature infants and those with asphyxia, in whom it may not disappear for several months, indicating delayed closure of the ductus arteriosus.

2 Crescendo systolic murmur in the pulmonary area. This grade 1 to 2/6 murmur is believed to be related to flow through the ductus, because in some neonates this murmur represents a transition towards closure.

3 Pulmonary systolic ejection murmur. This grade 1 to 2/6 murmur may develop during the first day of life and last up to 6 days.

A high occurrence of functional murmurs has been found in infants and, in one study, in 80% of prematurely born infants [97], most frequently at 3 months of age. Many of these have characteristics of a vibratory murmur. Other authors have described a low incidence of functional murmurs in neonates and infants [99–101].

In neonates, a significant murmur present at birth or during the first hours of life usually indicates either aortic stenosis or pulmonary stenosis (with either intact ventricular septum or a ventricular communication). Mitral and tricuspid insufficiencies, both rare conditions in a neonate, also result in a systolic murmur. A small ventricular septal defect may be heard within days of birth. Large shunts at either the ventricular or great vessel level may not be evident in the neonatal period because elevated pulmonary arterial pressure and resistance limit blood flow through the communication.

Athletes

In trained athletes, the resting cardiac rate is often low. Therefore, the stroke volume and end-diastolic volume are increased as a result of these physiologic adaptations. The peripheral pulses are strong. The pulse pressure is increased, reflecting an increase in systolic pressure from increased stroke volume and lowered diastolic pressure from prolonged diastole. The apex impulse may be slightly beyond the midclavicular line. An ejection systolic murmur is heard along the upper left sternal borders, and a third heart sound may be prominent.

Evaluation of murmurs

In a 1996 article entitled "The demise of the physical examination," Janhar [102] commented that physicians are busier and have less time for physical examination and that their examinations are often inaccurate. He also posited that doctors are uncomfortable with uncertainty and rely on technology. But technology also can be inaccurate and the results be irreproducible and filtered through the eyes and mind of the interpreter. Thus, they may be contaminated by subjectivity. There have been a number of articles about the evaluation of murmurs in children particularly because of the incidence of functional murmurs. McCrindle *et al.* [103] found that referring physicians are reasonably accurate in determining the presence of a cardiac abnormality and that a noncardiac factor often was a major factor in referral to a cardiologist. One study showed that the decision for referral to a cardiologist is based on the presumed diagnosis, confidence of the referring physician, and the level of parental anxiety [104].

In the evaluation of a child referred for evaluation of a cardiac murmur, are diagnostic studies necessary? An early study by Newberger *et al.* [37] showed that diagnostic tests of electrocardiography and chest X-rays were unlikely to change a diagnosis of either the presence of a functional murmur or a murmur of a cardiac anomaly, when evaluated by a qualified pediatric cardiologist. As echocardiography became available, the issue has become whether this relatively more expensive test should be performed. Many authors have indicated that careful clinical examination allowed the diagnosis of functional murmurs and that echocardiography was unnecessary [104–109].

The discovery of a murmur causes parental anxiety, which is lessened by parental understanding of murmurs. Consultation relieves the anxiety in most parents [110]. High parental anxiety, however, is associated with lower pediatrician reassurance and greater pediatrician practice years [111]. In one study [112], on referral only 3% of parents felt their child could have a serious cardiac condition, 19% felt there was a non-serious cardiac problem, 76% felt their child had a normal heart, and 2% felt confused. After consultation, the perception that their child had a non-serious problem increased by 30%, those who felt that their child's heart was normal decreased to 68%, and 3% were confused. None felt that there was a serious heart problem.

Pericardial friction rubs

Pericardial friction rubs are characteristic of pericarditis, but are not always present. Sometimes the rub disappears if there is coexisting effusion, but the fluid in the pericardial sac does not necessarily obliterate the rub. Friction occurs as the heart moves, and so can be present during atrial systole, ventricular systole, and ventricular diastole. Although separate rubs may occur during each cardiac phase, they often blend into a single rub. Rubs are scratchy noises that sound close to the ear and become louder as pressure is placed on the stethoscope. Usually they are heard better over the lower left sternal border and may be loudest in either phase of respiration.

Abdomen

Hepatic location and size are key components to be determined in examining an infant or child with a cardiac abnormality. Hepatic location helps identify visceral situs, which is important in understanding the nature of a cardiac malposition. Assessment of hepatic size aids in recognizing congestive cardiac failure, for in this hemodynamic state hepatomegaly is present and may change rapidly. The lower margin of the liver should be palpated and its distance from the rib margin measured in the midclavicular line. The upper margin of the liver should be assessed by percussion over the lower thorax. Therefore, the total height of the liver can be determined. Studies have shown no correlation between palpability of the lower border and the total height of the liver. This finding shows that both parameters of the size of the liver depend on the position of the organ apart from size. Thus, a child could have an enlarged liver even with a liver edge in the normal range. The upper extent of the liver is normally located in the fifth

intercostal space in the mid-clavicular line. The hepatic span is 6 cm in neonates [113]; it may be palpated as far as 3 cm below the right costal margin, and it is usually no longer palpable by 4 years. Remember that the liver edge may be easily palpable in patients with hyperexpanded lungs as it is displaced into the abdomen by the flattened diaphragms. The normal (average) liver span is 7–8 cm in the first 6 months of life, 9–10 cm until 24 months, 12 cm for preschoolers, 14 cm for 5–9 year olds and 16 cm for 10–16 year olds [114,115].

The spleen tip may be palpable in infants and is rarely enlarged in pediatric patients with cardiac failure. It may be enlarged in those with infective endocarditis.

In children with hypertension, stenosis of a renal artery can be suspected by finding a bruit over the upper or mid-abdomen.

Peripheral edema

Peripheral edema is present in many normal neonates during the first 2 days of life. It may persist longer in premature infants.

Abnormal degrees of edema are found at birth from fetal hydrops and nonpitting lymphedema, often associated with Turner's syndrome. Cardiac causes are uncommon (supraventricular tachycardia being the most common); urinary tract obstruction and hepatic cirrhosis are other causes. Observing puffy eyelids or edema over the back of a neonate may identify the edema.

Edema from cardiac causes is also uncommon after the neonatal period and is usually related to renal disease or exudative enteropathy. An unusual but important cause to recognize is constrictive pericarditis.

Skin

Hypoxemia, even mild, may be associated with digital clubbing after 6 months of age. Early in the process, there is a decrease in the angle between the base of the nail and the mantle. At this stage, there is redness or shininess of the terminal phalanx. There are often hangnails. Subsequently, widening and thickening of the distal phalanx of the toes and fingers occur, and the nails become convex like the back of a spoon. In some infants and small children with a large left-to-right shunt, the fingertips and at times the palms are unusually erythematous. Nail beds should be inspected for splinter hemorrhages in patients with suspected infective endocarditis. In cyanotic patients, the scalp veins are often dilated. The skin should be inspected for hemangiomas, particularly of the strawberry type, in patients with a clinical picture that could represent multinodular hemangiomatosis [116]. In infants with cyanosis or cardiac failure, the hair is thin and fine and the fingernails require clipping infrequently. Following relief of their condition, the hair becomes thicker and the nails need clipping much more frequently.

References

1 Lin CH, Lin WC, Ho YJ, *et al.* Children with chest pain visiting the emergency department. *Pediatr Neonatol* 2006;**49**:26–9.
2 Tunaoglu FS, Olgunturk R, Akcabay S, *et al.* Chest pain in children referred to a cardiology clinic. *Pediatr Cardiol* 1995;**16**:69–72.
3 Selbst SM, Ruddy RM, Clark BJ, *et al.* Pediatric chest pain: a prospective study. *Pediatrics* 1988;**82**:319–23.
4 Driscoll DJ, Glicklich LB, Gallen WJ. Chest pain in children. A prospective study. *Pediatrics* 1976;**57**:648–51.
5 Rowe BH, Dulberg CS, Peterson RG, *et al.* Characteristics of children presenting with chest pain to a pediatric emergency department. *Can Med Assoc J* 1990;**143**:388–94.
6 Zararas-Angelidou KA, Weinhouse E, Nelson DB. Review of 180 episodes of chest pain in 134 children. *Pediatr Emerg Care* 1992;**8**:189–93.
7 Sik EC, Batt ME, Heslop LM. Atypical chest pain in athletes. *Curr Sports Med Rep* 2009;**8**:52–8.
8 Gregory PL, Biswas AC, Batt ME. Musculoskeletal problems of the chest wall in athletes. *Sports Med* 2002;**32**:235–50.
9 Pantell RH, Goodman BW Jr. Adolescent chest pain. *Pediatrics* 1983;**71**:881–7.
10 Gokhale J, Selbst SM. Chest pain and chest wall deformity. *Pediatr Clin N Am* 2009;**56**:49–65.
11 Danduran MJ, Earing MG, Shrida DC, *et al.* Chest pain: characteristic of children/adolescents. *Pediatr Cardiol* 2008;**29**:775–81.
12 Selbst SM. Consultation with the specialist. Chest pain in children. *Pediatr Rev* 1997;**18**:169–73.
13 Lane JR, Ben-Shachar G. Myocardial infarction in healthy adolescents. *Pediatrics* 2008;**120**:e938–43.
14 Apley J. The child with recurrent abdominal pain. *Pediatr Clin North Am* 1967;**14**:63–72.
15 Linde LM, Dunn OJ, Shireson R, *et al.* Growth in children with congenital heart disease. *J Pediatr* 1967;**70**:413–9.
16 Anderson RC, Moller JH. Ten year and longer follow-up of 1,000 consecutive children with cardiac malformations. The University of Minnesota Experience. In: Engle MA, Perloff JK, eds. *Congenital Heart Disease After Surgery*. Chicago: Yorke Medical Books, 1983: 49.
17 Hardy JB. Rubella as a teratogen. *Birth Defects* 1971;**7**:64.
18 Rowland TW, Hubbell JP Jr, Nadas AS. Congenital heart disease in infants of diabetic mothers. *J Pediatr* 1973;**83**:815–20.
19 Loser H. Human alcohol embryopathy and changes in the cardiovascular system (Abstract). *Teratology* 1981;**24**:29A.
20 Stern RS, Rosa F, Baum C. Isotretinoin and pregnancy. *J Am Acad Dermatol* 1984;**10**:851–4.
21 Pierpont ME, Basson CT, Benson DW Jr, *et al.* Genetic basis for congenital heart defects: current knowledge. A scientific statement from the American Heart Association Congenital Cardiac Defects Committee, Council on Cardiovascular Disease in the Young. *Circulation* 2007;**115**:3015–38.
22 Jenkins KJ, Correa A, Feinstein JA, *et al.* Noninherited risk factors and congenital heart defects: current knowledge: a scientific statement from the American Heart Association Council on Cardiovascular Disease in the Young. *Circulation* 2007;**115**: 2995–3014.
23 Goldman HI, Maralit A, Sun S, *et al.* Neonatal cyanosis and arterial oxygen saturation. *J Pediatr* 1973;**82**:319–24.

24 Barker SJ, Tremper KK, Hyatt J. Effects of methemoglobinemia on pulse oximetry and mixed venous oximetry. *Anesthesiology* 1989;**70**:112–7.

25 Chesler E, Moller JH, Edwards JE. Anatomic basis for delivery of right ventricular blood into localized segments of the systemic arterial system. Relation to differential cyanosis. *Am J Cardiol* 1968;**21**:72–80.

26 Gatti RA, Muster AJ, Cole RB, *et al.* Neonatal polycythemia with transient cyanosis and cardiorespiratory abnormalities. *J Pediatr* 1966;**69**:1063–72.

27 Auenbrugger L. On percussion of the chest. Reprinted in *Bull Inst Hist Med* 1936;**4**:379–403.

28 Mangione S, Nieman LZ. Cardiac auscultatory skills of internal medicine and family practice trainees: a comparison of diagnostic proficiency. *JAMA* 1997;**278**:717–22.

29 Vukanovic-Criley JM, Criley S, Warde CM, *et al.* Competency in cardiac examination skills in medical students, trainees, physicians and faculty. *Arch Int Med* 2006;**166**:610–6.

30 Barrett MJ, Lacey CS, Sekara AE, *et al.* Mastering cardiac murmurs. The power of repetition. *Chest* 2004;**126**:470–5.

31 Barrett MJ, Kuzma MA, Seto TC, *et al.* The power of repetition in mastering cardiac auscultation. *Am J Med* 2006;**119**:73–5.

32 Roncevic Z. Music from the heart – in praise of auscultation. Interview by Keith Barnard. *Circulation* 2007;**116**:f81–2.

33 Markel H. The stethoscope and the art of listening. *N Engl J Med* 2006;**354**:551–3.

34 Laennec RTH. *Treatise on Mediate Auscultation*, 1st American edn. Philadelphia: James Webster, 1823.

35 Etchells E, Bell C, Rob BK Does the patient have an abnormal systolic murmur? *JAMA* 1997;**277**:564–71.

36 Rolden CA, Shively BK, Crawford MH. Value of the cardiovascular physical examination for detecting valvar heart disease in asymptomatic subjects. *Am J Cardiol* 1996;**77**:1327–31.

37 Newburger JW, Rosenthal A, Williams RG, *et al.* Noninvasive tests in the initial evaluation of heart murmurs in children. *N Engl J Med* 1983;**308**:61–4.

38 Rappaport MB, Sprague HB. The effects of improper fitting of stethoscope to ears on auscultatory efficiency. *Am Heart J* 1952;**43**:713–5.

39 Rappaport MB, Sprague HB. The effects of stethoscope bore on stethoscope efficiency. *Am Heart J* 1951;**42**:605–9.

40 Conn RD, O'Keefe JH. Cardiac physical diagnosis in the digital age: an important but increasingly neglected skill (from stethoscopes to microchips). *Am J Cardiol* 2009;**104**:590–5.

41 O'Donnell M. The world is round: salute to the stethoscope. *BMJ* 2008;**336**:1326.

42 Murphy RL. In defense of the stethoscope. *Respir Care* 2008;**53**:355–69.

43 Dolara A. The decline of cardiac auscultation: 'the ball of the matchpoint is poised on the net.' *Cardiovasc Med* 2008;**9**:1173–4.

44 Chizner MA. Cardiac auscultation: rediscovering the lost art. *Curr Probl Cardiol* 2008;**33**:326–408.

45 Grenier MC Gagnon K, Genest J Jr, *et al.* Clinical comparison of acoustic and electronic stethoscopes and design of a new electronic stethoscope. *Am J Cardiol* 1998;**81**:653–56.

46 Salomon B. What the stethoscope said. *Ann Int Med* 2001;**135**: 56–7.

47 Holmes OW. The stethoscope song; a professional ballad. Reprinted in *Texas Heart Inst J* 2005;**32**:260–1.

48 Wiggers CJ. Studies on the consecutive phases of the cardiac cycle: II. The laws governing the relative duration of ventricular systole and diastole. *Am J Physiol* 1921;**56**:439.

49 Rushmer RF. *Cardiovascular Dynamics*, 3rd edn. Philadelphia, PA: Saunders, 1970: 293–327.

50 Leatham A. Auscultation of the heart. *Pediatr Clin North Am* 1958;**5**:839–70.

51 Luisada AA, MacCanon DM, Kumar S. Changing views on the mechanisms of the first and second heart sounds. *Am Heart J* 1974;**88**:503–14.

52 Abrams J. Current concepts of the genesis of heart sounds. I. First and second sounds. *JAMA* 1978;**239**:2790–1.

53 Rytand DA. The variable loudness of the first heart sound in auricular fibrillation. *Am Heart J* 1949;**37**:187–204.

54 Vancheri F, Gibson D. Relation of third and fourth heart sounds to blood velocity during left ventricular filling. *Br Heart J* 1989;**61**:144–8.

55 Ewing G, Magundar J, Goldblatt E, *et al.* A non-invasive study of the third heart sound in children by phono- and echo-cardiography. *Acta Cardiol* 1984;**39**:241–5.

56 Pozzoli M, Febo O, Tramarin R, *et al.* Pulsed Doppler evaluation of left ventricular filling in subjects with pathologic and physiologic third heart sound. *Eur Heart J* 1990;**11**:500–8.

57 Abrams J. Current concepts of the genesis of heart sounds. II. Third and fourth sounds. *JAMA* 1978;**239**:2790–1.

58 Vancheri F, Gibson D. Relation of third and fourth heart sounds to blood velocity during left ventricular filling. *Br Heart J* 1989;**61**:144–8.

59 Owen A. The third heart sound is the result of a shock wave caused by the ventricular inflow velocity exceeding the wave velocity. *Med Hypotheses* 1996;**47**:81–3.

60 Van de Werf F, Geboers J, Kesteloot H., *et al.* The mechanism of disappearance of the physiologic third heart sound of age. *Circulation* 1986;**73**:877–84.

61 Martinez-Lopez JI. Sounds of the heart in diastole. *Am J Cardiol* 1974;**34**:594–601.

62 Mehta NJ, Khan IA. Third heart sound: genesis and clinical importance. *Int J Cardiol* 2004;**97**:163–186.

63 Reddy PS. The third heart sound. *Int J Cardiol* 1985;**7**:213–21.

64 Baracca E, Scorzoni D, Brunazi MC. Genesis and acoustic quality of the physiological fourth heart sound. *Acta Cardiol* 1995;**50**:23–8.

65 Reynolds O. An experimental investigation of the circumstances which determine whether the motion of water shall be direct or sinuous and the law of resistance in parallel channels. *Philos Trans R Soc Lond* 1883;**174**:935.

66 Roger H. Clinical researches on the congenital communication of the two sides of the hearts, by failure of occlusion of the interventricular septum. *Bull Acad Méd, 2ème Sér* 1879;**8**:1074–94.

67 Roger H. Communication concerning congenital patency of the interventricular septum. *Bull Acad Méd, 2ème Sér* 1879;**8**:1189–91.

68 Flint A. On cardiac murmurs. *Am J Med Sci* 1862;**44**:29–54.

69 Gibson GA. Clinical lectures on circulatory affections. Lecture I. Persistence the arterial duct and its diagnosis. *Edinb Med J* 1990;**8**:1–10.

70 Steell G. The murmur of high-pressure in the pulmonary artery. *Med Chron Manchester* 1888–9;182–8 and 188–9.

71 Fogel DH. The innocent systolic murmur in children: a clinical study of its incidence and characteristics. *Am Heart J* 1960;**59**: 844–55.

72 Rosenthal, A. How to distinguish between innocent and pathologic murmurs in childhood. *Ped Clin North Am* 1984;**31**:1229–40.

73 Fogel DH. The innocent systolic murmur in children: A clinical study of its incidence and characteristics. *Am Heart J* 1960;**59**:844–55.

74 Noponen AL, Lukkarinen S, Angeria A, *et al.* Phono-spectrographic analysis of heart murmur in children. *BMC Pediatr* 2007;**7**:23.

75 Gardiner HM, Joffe HS. Genesis of Still's murmurs: a controlled Doppler echocardiographic study. *Br Heart J* 1991;**66**:217–20.

76 Stuckey D. Innocent systolic murmurs of aortic origin. *Med J Aust* 1957;**1**:38.

77 Harris TN, Friedman S, Tuncaali MT. Comparison of innocent cardiac murmurs of childhood with cardiac murmurs in high output states. *Pediatrics* 1964;**33**:341–55.

78 Miao CY, Zuberbuhler JS, Zuberbuhler JR. Genesis of vibratory functional murmurs. *Am J Cardiol* 1987;**60**:1198–99.

79 Darazs B, Hesdorffer GS, Butterworth AM, *et al.* The possible etiology of the vibratory systolic murmur. *Clin Cardiol* 1987;**10**:341–4.

80 Joffe HS. Genesis of Still's innocent systolic murmur. *Br Heart J* 1992;**66**:217–20.

81 Schwartz ML, Goldberg SJ, Wilson N, *et al.* Relation of Still's murmur, small aortic diameter and high aortic velocity. *Am J Cardiol* 1986;**57**:1344–8.

82 Celebi A, Onat T. Echocardiographic study on the origin of the innocent flow murmurs. *Pediatr Cardiol* 2006;**27**:19–24.

83 Nothroff J, Suemenicht SG, Wessel A. Can fibrotic bands in the aortic arch cause innocent murmurs in childhood? *Cardiol Young* 2001;**11**:643–6.

84 Van Oort A, Hopman J, De Boo T, *et al.* The vibratory innocent heart murmur in school children: a case–control Doppler echocardiographic study. *Pediatr Cardiol* 1994;**15**:275–81.

85 Perry LW, Ruckman RN, Shapiro SR, *et al.* Left ventricular false tendons in children: prevalence as detected by 2-dimensional echocardiography and clinical significance. *Am J Cardiol* 1983;**52**:1264–6.

86 Spooner PH, Perry MP, Brandenburg RO, *et al.* Increased intra-ventricular velocities. An unrecognized cause of systolic murmur in adults. *J Am Coll Cardiol* 1998;**32**:1589–95.

87 Murgo JP. Systolic ejection murmurs in the era of modern cardiology. What do we really know? *J Am Coll Cardiol* 1998;**32**:1596–602.

88 Klewer SE, Donnerstein RL, Goldberg SJ. Still's-like innocent murmur can be produced by increasing aortic velocity to a thres-hold value. *Am J Cardiol* 1991;**68**:810–2.

89 Donnerstein RL, Thomsen VS. Hemodynamic and anatomic factors affecting the frequency content of Still's innocent murmur. *Am J Cardiol* 71994;**4**:508–10.

90 Pelech AN. Evaluation of the pediatric patient with a cardiac murmur. *Pediatr Clin North Am* 1999;**46**:167–88.

91 Still GF. *Common Disorders and Diseases of Childhood.* London: Frowde, 1909.

92 Craige E, Harned HS Jr. Phonocardiographic and electrocardio-graphic studies in normal newborn infants. *Am Heart J* 1963;**65**:180–9.

93 Braudo M, Rowe RD. Auscultation of the heart – early neonatal period. *Am J Dis Child* 1961;**101**:575–87.

94 Papadopoulos GS, Folger GM Jr. Transient solitary diastolic murmurs in the newborn. *Clin Pediatr* 1983;**22**:548–50.

95 Burnard ED A murmur from the ductus arteriosus in the newborn baby. *Br Med J* 1958;**i**:806–10.

96 Clarkson PM, Orgill AA. Continuous murmurs in infants of low birth weight. *J Pediatr* 1974;**84**:208–11.

97 Walsh SZ. The incidence of murmurs in healthy premature infants during the first 18 months of life. *J Pediatr* 1963;**62**:480–3.

98 Hallidie-Smith KA. Some auscultatory and phonocardiographic findings observed in early infancy. *Br Med J* 1960;**i**:756–9.

99 Lyon RA, Rauh LW, Stirling JW. Heart murmurs in newborn infants. *J Pediatr* 1940;**16**:310–7.

100 Taylor WC. The incidence and significance of systolic cardiac murmurs in infants. *Arch Dis Child* 1953;**28**:52–4.

101 Richards MR, Merritt KK, Samuels MH, *et al.* Frequency and significance of cardiac murmurs in the first years of life. *Pediatrics* 1955;**15**:169–79.

102 Janhar S. The demise of the physical exam. *N Engl J Med* 2006;**3354**:548–51.

103 McCrindle BW, Shaffer KM, Kan JS, *et al.* Factors prompting referral for cardiology evaluation of heart murmurs in children. *Arch Pediatr Adol Med* 1995;**149**:1277–9.

104 Pelech AN. The cardiac murmur. When to refer? *Pediatr Clin North Am* 1993;**45**:107–22.

105 Advani N, Menahem S, Wilkinson JL. The diagnosis of innocent murmurs in chidhood. *Cardiol Young* 2000;**12**:340–2.

106 Shub C. Echocardiography or auscultation? How to evaluate systolic murmurs. *Can Fam Physician* 2003;**49**:163–7.

107 Danford DA, Nasir A, Gambiner C. Cost assessment of the eva-luation of heart murmurs in children. *Pediatrics* 1993;**91**:365–8.

109 Smythe JF, Teixeira OHP, Vlad P, *et al.* Initial evaluation of heart murmurs. Are laboratory tests necessary? *Pediatrics* 1990;**86**:497–500.

109 Geva T, Hegesh J, Frand M. Reappraisal of the approach to the child with heart murmurs. Is echocardiography mandatory? *Int J Cardiol* 1988;**19**:107–13.

110 Giuffre RM, Walker I, Vaillancourt S, *et al.* Opening Pandora's box: parental anxiety and the assessment of childhood mur-murs. *Can J Cardiol* 2002;**18**:406–14.

111 Geggle RL, Horowitz LM, Brown EA, *et al.* Parental anxiety associated with referral of a child to a pediatric cardiologist for evaluation of a Still's murmur. *J Pediatr* 2002;**140**:747–52.

112 Dyck JD, Robertson MA. The innocent of innocent heart mur-murs. *Perspect Cardiol* 2003;**9**:38–46.

113 Reiff MI, Osborn LM. Clinical estimation of liver size in new-born infants. *Pediatrics* 1983;**71**:46–8.

114 Deligeoris D, Yannakos D, Doxiadis S. Normal size of liver in infancy and childhood. X-ray study. *Arch Dis Child* 1973;**48**:790–3.

115 Deligeorgis D, Yannakos D, Panaxotou P, *et al.* The normal bor-ders of the liver in infancy and childhood. Clinical and X-ray study. *Arch Dis Child* 1970;**45**:702–4.

116 McLean RH, Moller JH, Warwick WJ, *et al.* Multinodular hemangiomatosis of the liver in infancy. *Pediatrics* 1972;**49**:563.

7 Electrocardiography

Anne M. Dubin

Stanford University, Palo Alto, CA, USA

The electrocardiogram (ECG) is useful in diagnosing a variety of functional and pathological changes from arrhythmias to electrolyte disturbances or atrial and ventricular hypertrophy, in addition to their progression or regression. It aids in diagnosing several specific anomalies, such as tricuspid atresia and anomalous left coronary artery from the pulmonary artery.

Principle and technical considerations

Basic vector principles

Contracting heart muscle generates an electric current that flows in specific pathways through the heart. It is convenient to regard the current as coming from a single source in the heart, although this oversimplifies the problem. If we could place electrodes on the heart to detect the current or its associated voltage, it would be relatively simple to deduce where the current came from and where it was going. Because the electromagnetic forces are altered as they spread through the various body compartments and tissues to reach the surface, the voltages detected there are not the same as the voltages in the heart.

As in all electromagnetic phenomena, the voltage detected at the skin surface follows the inverse square law, so that for a given vector, voltages are diminished if the ventricular wall is far from the surface and exaggerated if it is very close. This explains why in some premature infants the mid-precordial leads show abnormally large voltages. Furthermore, the media through which the voltage is transmitted to the skin (blood in the chamber, pericardial fluid, air in the lung, and skeletal muscle) affect the surface voltages. Because air is a poor conductor of electricity, lung hyperinflation (airway disease, cystic fibrosis, emphysema) often decreases voltage transmission anterior and laterally but increases posterior

transmission, rotating the vector posteriorly. This may make diagnosing right ventricular hypertrophy difficult. As another example, in Pompe disease (glycogen storage disease type II), the ECG voltages are out of proportion to the degree of hypertrophy because of altered conductivity of the muscles of the chest.

Because an electric current has a voltage and a direction of flow, it can be represented by a vector, an arrow pointing in that direction with a length proportional to the voltage. Two vectors moving simultaneously in different directions produce a single resultant vector (Figure 7.1). In the heart, electrical currents may travel in different directions simultaneously, and at each moment we see the resultant vector. Thus, although the impulse spreads out from the sino-atrial node in all directions, because the sino-atrial node is at the upper right portion of the atria, the resultant vector – the P wave – passes down and to the left. In the ventricles, the initial vector normally is negative in aVF and positive in lead I, as shown by a q wave in lead aVF and no q wave in lead I, and so passes to the left and superiorly. At the apex, some impulses pass to the right in the right ventricular wall and some pass to the left in the left ventricular wall. In the neonate, the right and left ventricles are equally thick, but the right ventricular wall is closer to the anterior chest leads so that the QRS complex has a predominant R wave in V1. In the left chest leads, the left ventricular wall is closer to the leads, so that there is usually a dominant R wave in V6, although not as large as the R in V1. Because mean right vectors are greater than mean left vectors, the main frontal plane QRS axis is to the right.

With age, the right ventricular wall thins, the R wave in V1 becomes smaller and the R wave in V6 becomes larger; the main frontal plane vector moves to the left (Figure 7.2). At the end of ventricular depolarization, the vector points to

(a) (b)

(c) (d)
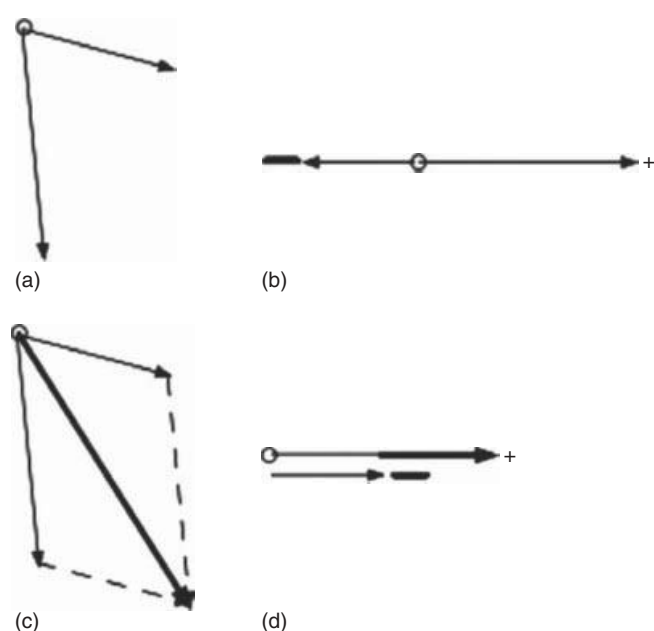
Figure 7.1 Two pairs of vectors with different directions are shown in (a) and (b), and (c) and (d) show how the resultant vectors would look (heavy arrows). It is shown in (d) that the negatively directed vector reduces the size of the resultant positive right-directed vector. The final vectors cannot indicate what the initial vectors were.

Neonate Older child
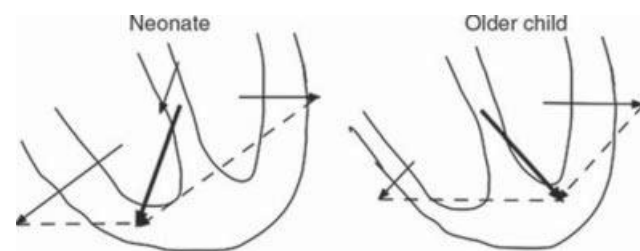
Figure 7.2 Diagram to show how right ventricular wall thickness influences main frontal plane QRS axis.

the right and superiorly, generating small negative waves in leads I and aVF. The tips of the mean vectors at each moment can be joined to form a loop (Figure 7.3). At times, analyzing the initial and terminal vectors helps in evaluating complex depolarization patterns. Although vector recordings are not used much clinically today, projection of vectors on the various leads produces the typical scalar ECG.

Vector loops can also be constructed in the horizontal plane, and can be applied to all the waves on the ECG.

Scalar ECG

The standard ECG has 12 leads recorded from 12 standard body surface positions (Figure 7.4). Electrodes must be placed accurately, and the skin cleaned with alcohol to decrease skin resistance. The patient should be quiet to eliminate motion artifact, but this may be difficult to achieve, especially in infants and small children.
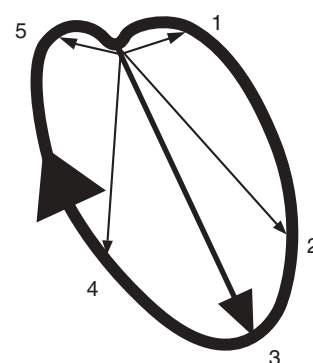
Figure 7.3 Diagram of five sequential vectors labeled 1–5. A thicker line shows the main vector 3. The tips of the vectors are joined to form a loop that here is counterclockwise.

In children, the ECG often includes three additional leads, V3R, V4R, and V7, to add right- and left-sided chest leads to determine ventricular hypertrophy.

ECGs are routinely recorded at a paper speed of $25\,mm\,s^{-1}$, but can provide speeds up to $50\,mm\,s^{-1}$ that help determine rhythm disturbances. The machine has a standard voltage gain of $1\,mV$ per $10\,mm$ in vertical deflection that can be decreased to reduce large voltages and so avoid overlap between leads.

Reading the pediatric ECG

An organized approach to reading a pediatric ECG is essential. Rate and rhythm are assessed, as are intervals: RR, PR, QRS, and QT (Figure 7.5). The P, QRS, and T wave axes are determined. Atrial and ventricular hypertrophy and also abnormalities of ventricular repolarization are sought. For each major wave, three features should be assessed: axis, amplitude, and duration. Normal intervals and voltages are age dependent. Davignon *et al.* published normal ECG measures by age in 1979 [1], standards commonly used when interpreting pediatric ECGs (Table 7.1). Any interpretation of the tracings must consider the clinical setting.

Rate and rhythm

The RR interval is commonly reported as cycle length (measured in milliseconds), and the heart rate measured by dividing the cycle length into $60\,000\,ms\,min^{-1}$. Heart rate depends on many factors, including age, autonomic nervous tone, and physical activity.

The first step in assessing the cardiac rhythm is to confirm normal AV conduction with P waves preceding each QRS. Sinus P waves have an ECG pattern indicating atrial depolarization from top to bottom and right to left (positive in leads I, II, and aVF). The normal P wave axis is 15–75° in both the frontal and horizontal (precordial lead) planes. P waves are often biphasic in lead V1, with an initial upright
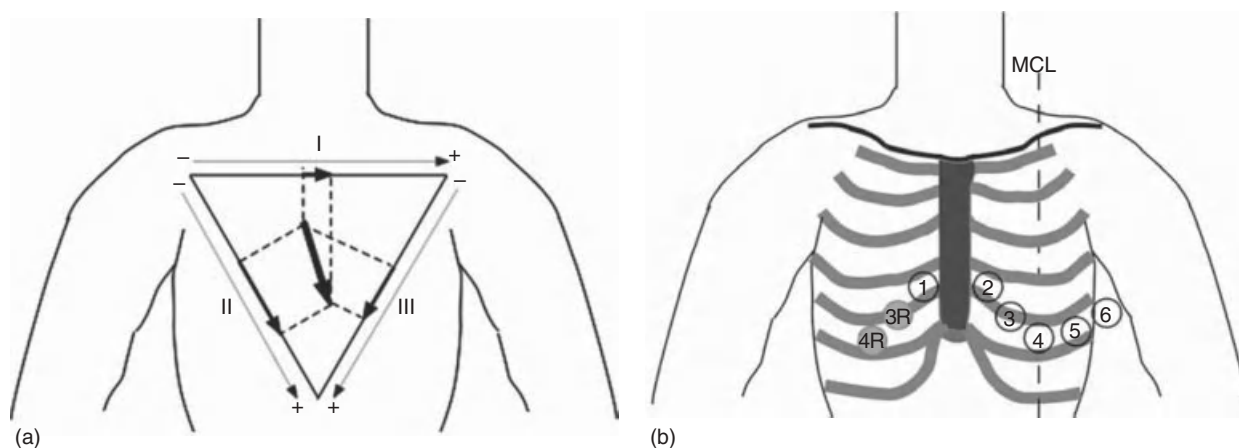
Figure 7.4 Electrode placement for standard ECG. (a) At any moment during ventricular depolarization there is a net voltage moving in a given direction. This voltage can be depicted as an arrow pointing in that direction with a length proportional to the voltage, that is, a vector. The main frontal plane vector is indicated by the thick solid line and arrowhead inside the loop. Around the vector is the Einthoven triangle, derived from the three limb leads (I, II, and III). The long, thin lines parallel to the Einthoven triangle indicate the convention for each lead, with a wave passing from negative to positive being upright. If perpendiculars are drawn from the end of the major frontal plane axis to the three edges of the triangle (dotted lines), they show how much of the voltage of the frontal plane axis will appear in each lead. These voltages are shown by the heavy lines and arrows superimposed on the triangle. The greatest voltage appears in the lead most nearly parallel to the frontal plane axis (lead II), and the smallest voltage appears in the lead most nearly perpendicular to the frontal plane axis. (b) The conventional sites for placing the unipolar V leads. V1 and V2 are in the fourth intercostal space at the right and left sternal edges, respectively. V4 is in the fifth space in the midclavicular line (MCL), and V3 is half way between V2 and V4. V5 and V6 are in the fifth interspace in the anterior and mid-axillary lines, respectively. V3R and V4R are the equivalent of V3 and V4, but in the right thorax. Sometimes V7 is placed in the fifth space in the posterior axillary line, especially if no Q wave is seen in V6.
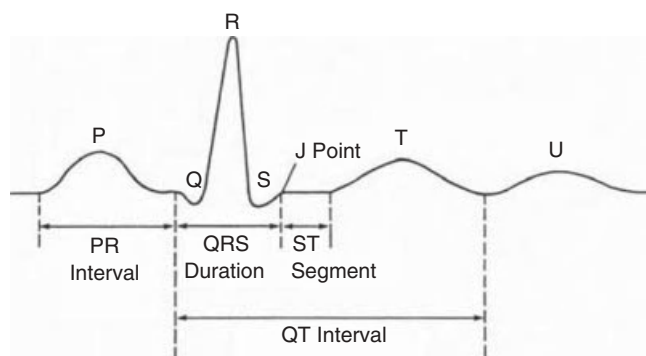
Figure 7.5 Scalar ECG showing P, Q, R, S, T, and U waves. The J point and also standard intervals including the PR interval, QRS duration, ST segment, and QT interval are shown.

deflection followed by a brief downward deflection and are upright in the left precordial leads. If the P wave does not meet these criteria, there is an ectopic atrial rhythm or cardiac malposition. The P wave vector can be used to predict the origin of the atrial pacemaker: an inverted P wave in leads I and aVL suggests a left atrial rhythm, a P wave inverted in leads I, II, and aVF suggests a low right atrial rhythm, and a P axis positive in lead aVF and negative in lead I suggests situs inversus, other cardiac malposition, or an artifact of reversal of right and left arm leads.

Conduction of the impulse slows as it passes through the atrioventricular node, producing the PR interval and allowing time for complete ventricular filling. The PR interval increases with age, and varies with activity and heart rate. Abnormally prolonged AV conduction can indicate impaired AV nodal or infranodal disease, and is classified as first- (long PR interval), second-, or third-degree AV block. A short PR interval can be seen with glycogen storage disease, tricuspid atresia, Wolff–Parkinson–White (WPW) syndrome, or a low atrial pacemaker near the AV node.

Axis

The electrical axis is the direction of the predominant vector of a waveform. In the frontal plane, it is presented on a Cartesian system with lead I as 0° (left) to 180° (right) and lead aVF as 90° (inferior) to 270° (superior), with the other limb leads corresponding to other angles in the frontal plane (Figure 7.4). The frontal plane axis should be calculated for the P, QRS, and T waves. Initially the quadrant is determined by looking at leads I and aVF. Once the quadrant is established, the most isoelectric frontal lead is identified. The axis is perpendicular to this lead in the previously identified quadrant (Figure 7.6). Frontal plane QRS axis deviation depends on the child's age and generally moves from right to left as the heart develops (see Table 7.1 for changes in axis with age).

The precordial leads essentially map a transverse plane, with right–left and anterior–posterior coordinates. In this plane, the QRS axis also shifts from right anterior in neonates to leftward in older children.

Table 7.1 Normal ECG standards for children by age. All values are 2nd to 98th percentiles (and mean, in parentheses). All amplitudes of waves are given in millimeters at full standardization [1].

Parameter	0–1 days	1–3 days	3–7 days	7–30 days	1–3 months	3–6 months	6–12 months	1–3 years	3–5 years	5–8 years	8–12 years	12–16 years
Heart rate (beats min⁻¹)	94–155 (122)	91–158 (122)	90–168 (128)	106–182 (149)	120–179 (149)	105–185 (141)	108–169 (131)	89–152 (119)	73–137 (109)	650133 (100)	62–130 (91)	60–120 (80)
Frontal plane QRS axis (°)	59–189 (135)	64–197 (134)	76–191 (133)	70–160 (109)	30–115 (75)	7–105 (60)	6–98 (55)	7–102 (55)	6–104 (56)	10–139 (65)	6–116 (60)	9–128 (59)
PR interval, lead II (s)	0.08–0.16 (0.11)	0.08–0.14 (0.11)	0.07–0.15 (0.10)	0.07–0.14 (.10)	0.07–0.13 (0.10)	0.07–0.15 (0.11)	0.07–0.16 (0.11)	0.08–0.15 (0.11)	0.08–0.16 (0.12)	0.09–0.16 (0.12)	0.09–0.17 (0.13)	0.09–0.18 (0.14)
QRS duration, V5 (s)	0.02–0.07 (0.05)	0.02–0.07 (0.05)	0.02–0.07 (0.05)	0.02–0.08 (0.05)	0.02–0.08 (0.05)	0.02–0.08 (0.05)	0.03–0.08 (0.05)	0.03–0.08 (0.06)	0.03–0.07 (0.06)	0.03–0.08 (0.06)	0.04–0.09 (0.06)	0.04–0.09 (0.07)
P wave amplitude, lead II	0.05–2.8 (1.6)	0.03–2.8 (1.6)	0.7–2.9 (1.7)	0.7–3.0 (1.9)	0.7–2.6 (1.5)	0.4–2.7 (1.6)	0.6–2.5 (1.6)	0.7–2.5 (1.5)	0.3–2.5 (1.4)	0.4–2.5 (1.4)	0.3–2.5 (1.4)	0.3–2.5 (1.4)
Q wave amplitude, aVF	0.1–3.4 (1.0)	0.1–3.3 (1.0)	0.1–3.5 (1.1)	0.1–3.5 (1.2)	0.1–3.4 (0.9)	0–3.2 (0.9)	0–3.3 (1.0)	0–3.2 (0.9)	0–2.9 (0.6)	0–2.5 (0.6)	0–2.7 (0.5)	0–2.4 (0.4)
Q wave amplitude, V6	0.1.7 (0.1)	0–2.2 (0.1)	0–2.8 (0.1)	0–2.8 (0.4)	0–2.6 (0.3)	0–2.6 (0.3)	0–3.0 (0.4)	0–2.8 (0.6)	0.1–3.3 (0.8)	0.1–4.6 (0.8)	0.1–2.8 (0.6)	0–2.9 (0.4)
R amplitude, V1	5–26 (13)	5–27 (15)	3–25 (12)	3–12 (10)	3–19 (10)	3–20 (10)	2–20 (9)	2–18 (8)	1–18 (8)	1–14 (7)	1–12 (5)	1–10 (4)
S amplitude, V1	1–23 (8)	1–20 (9)	1–17 (7)	0–11 (4)	0–13 (5)	0–17 (6)	1–18 (7)	1–21 (8)	2–22 (10)	3–23 (12)	3–25 (12)	3–22 (11)
R amplitude, V6	0–12 (4)	0–12 (5)	1–12 (5)	3–16 (8)	5–21 (12)	6–22 (13)	6–23 (13)	6–23 (13)	8–25 (15)	8–26 (16)	9–25 (16)	7–23 (14)
S amplitude, V6	0–10 (4)	0–9 (3)	0–10 (4)	0–10 (3)	0–7 (3)	0–10 (3)	0–8 (2)	0–7 (2)	0–6 (2)	0–4 (1)	0–4 (1)	0–4 (1)
R:S ratio, V1	0.1–9.9 (2.2)	0.1–6 (2.0)	0.1–9.8 (2.8)	1.0–7.0 (2.9)	0.3–74 (2.2)	0.1–6.0 (2.3)	0.1–4.0 (1.8)	0.1–4.3 (1.4)	0.03–2.7 (0.9)	0.02–2.0 (0.8)	0.02–1.9 (0.6)	0.02–1.8 (0.5)
R:S ratio, V6	0.1–9 (2)	0.1–12 (2)	0.1–10 (2)	0.1–12 (4)	0.2–14 (5)	0.2–18 (7)	0.2–22 (8)	0.3–27 (10)	0.6–30 (11)	0.9–30 (12)	1.5–33 (14)	1.4–39 (15)
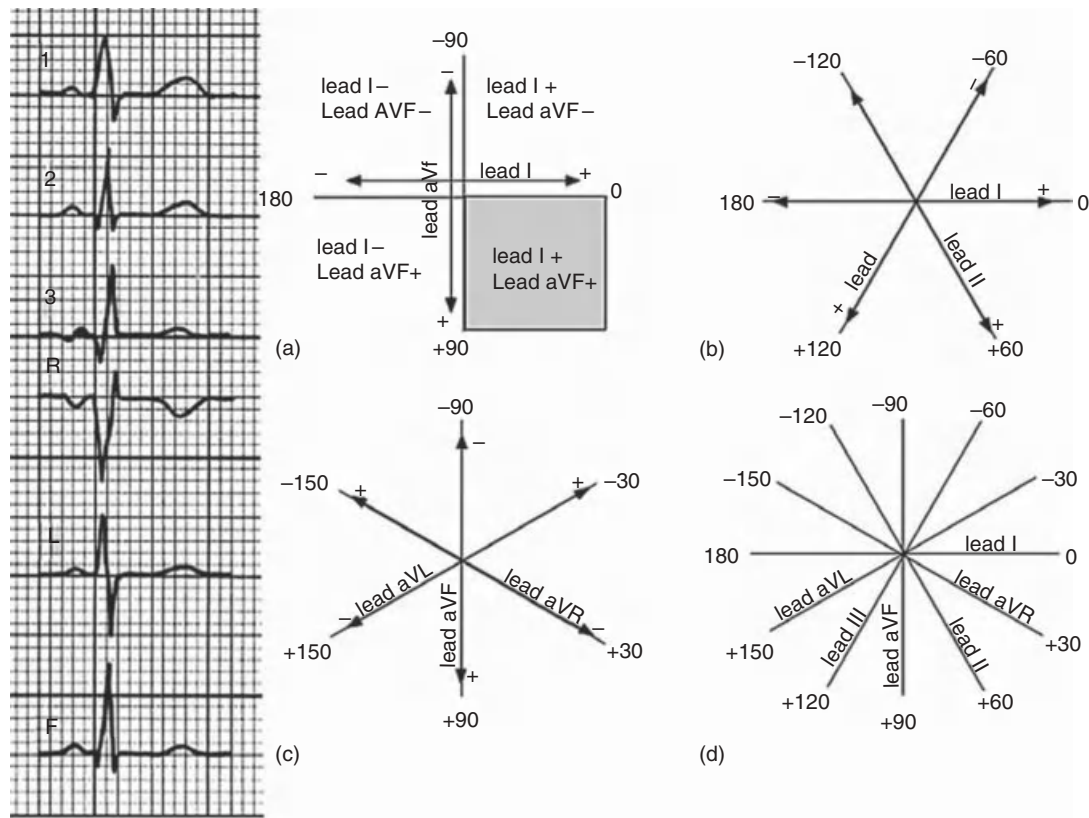
Figure 7.6 A normal electrocardiogram in an older child is shown. To calculate a frontal plane QRS axis: (a) first assign a quadrant, based on the area under the QRS deflection (positive or negative) in leads I and aVF. In the tracing shown, the left lower quadrant (shaded) is selected. (b) The three limb leads I, II, and III are inclined at 60° to each other. The + and – symbols on the arrowheads indicate the direction of each major deflection. (c) The three unipolar limb leads aVF, aVL, and aVR are also inclined at 60° to each other but at 30° to the bipolar limb leads. Because they are unipolar leads, an impulse directed towards either shoulder or the foot will give a positive deflection, as shown by the symbols over the arrowheads. (d) The two triaxial sets of lines in panels (b) and (c) can be superimposed in a hexaxial figure. This can be used to refine the calculated axis. In the accompanying example, the axis lies in the left lower quadrant, so we examine leads aVR and II. The S wave in lead aVR is similar in height to the R wave in lead II, so that the axis is between +30 and +60°. Alternatively, look for the lead with nearly equiphasic RS waves and take the perpendicular to this lead. The lead with almost equiphasic RS waves in the example is aVL, and the perpendicular to this which passes through the lower left quadrant is ~60°. Because it is actually area under the QRS rather than maximal voltage, there may be slight differences in the axis calculation made by eye. In most modern ECG machines, the axis is calculated automatically. Occasionally, some or all of the leads show almost equiphasic R and S waves so that a frontal plane axis cannot be calculated. This has no clinical significance.

Atrial enlargement

Because the normal spread of activation in the atria is from right to left, the first part of the P wave is right atrial, the last part is left atrial, and the middle has an overlap. Therefore, right atrial enlargement increases the P wave voltage but does not make the P wave wider, and left atrial enlargement makes the wave wider.

In assessing P wave amplitude, right atrial enlargement can be diagnosed by a peaked tall P wave in lead II, usually accompanied by a biphasic or tall P wave in lead V1. Left atrial enlargement shows a broad notched P wave in lead II, or a deep slurred biphasic P wave in V1 with a prominent terminal negative component and the P wave duration is 100 ms or longer. Biatrial enlargement is diagnosed when signs of both right and left atrial enlargement are seen.

Ventricular depolarization

Ventricular depolarization produces the QRS duration on the surface ECG. The QRS duration is age dependent, with a normal upper limit of 80 ms at <8 years of age, and 90 ms through childhood and adolescence. By assessing QRS duration, an abnormality of ventricular depolarization can be identified. Fairly specific conditions prolong the QRS, including bundle branch block (left or right), pre-excitation, or a ventricular pacemaker. The term intraventricular conduction delay refers to QRS prolongation that does not fit the above categories.

Bundle branch block

The distal conduction system is divided into the left and right bundle branches that depolarize the right and left ventricles, respectively. The right bundle is narrow and long, and passes

Figure 7.7 Typical right bundle branch block pattern.

Figure 7.8 Typical left bundle branch block pattern.

across the apex of the right ventricular body in the moderator band. The left bundle divides into two fan-like sheets of specialized conduction tissue, the anterior and posterior fascicles. Because of the wide distribution of the left fascicles, damage must be extensive before conduction to the left ventricle is affected. Conduction delay or block of one of these bundles, or in one of the fascicles, whether secondary to CHD surgery, medication, or ischemia, delays activation of the corresponding ventricle with a characteristic appearance on ECG.

Right bundle branch block (RBBB)
In RBBB, the QRS complex is characterized by abnormalities of its terminal portion. There is rapid initial depolarization of the left ventricle followed by a slower depolarization of the right ventricle. Complete RBBB is diagnosed when QRS exceeds upper limits of normal for age, and a terminal QRS complex is delayed and directed anteriorly, to the right, and superiorly. Characteristically there is a broad R′ wave in leads aVR, V1 and V 2 and a broad S wave in leads I, II, V5 and V6 (Figure 7.7). RBBB is common following surgical closure of ventricular septal defects. Occasionally it is familial. With RBBB, it is not possible to diagnose right ventricular hypertrophy (RVH) because criteria for ventricular hyper-

trophy are based on normal depolarization. The secondary ST and T wave abnormalities cannot be used to diagnose ischemia reliably.

Left bundle branch block (LBBB)
In LBBB, the initial portion of the QRS complex is affected. The QRS in LBBB is prolonged, slurred, and directed towards the left, posteriorly and inferiorly. LBBB is diagnosed by prolonged QRS duration because of delayed initial portions, indicated by notched slurred QRS complexes directed leftward and posteriorly (QS or rS in lead V1 and tall notched R wave in lead V6). The initial part of the QRS complex is directed towards the right rather in the normal pattern of a Q wave in leads I and V6 (Figure 7.8). LBBB is uncommon in children and results from surgery on the left ventricular outflow tract and hypertrophic cardiomyopathy. It is difficult to assess hypertrophy and ischemic changes with LBBB.
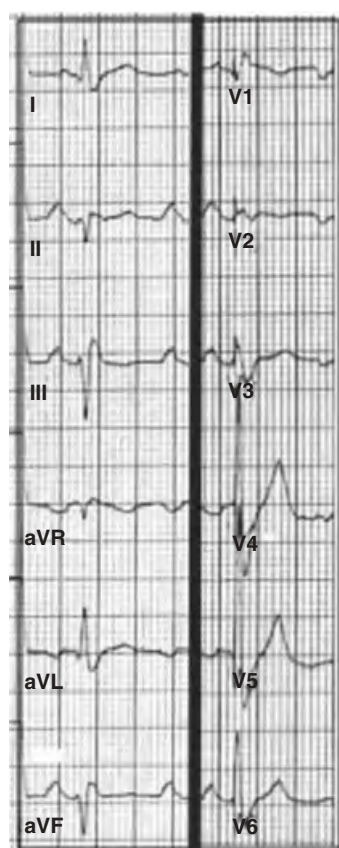
Figure 7.9 Left anterior hemiblock.

Left anterior hemiblock

The left anterior fascicle activates the anterior and superior portion of the left ventricle, and when blocked the posterio-inferior region activates first, followed by the anterior–superior aspect. This produces a marked superior left axis deviation (−30 to −90°) with an rS in the inferior limb leads (II, III and aVF) and a qR complex in leads I and aVL. The QRS is minimally prolonged (Figure 7.9). This abnormality, relatively rare, can occur after left ventricular outflow tract surgery. This diagnosis should not be made simply on the appearance of left superior axis deviation, because a similar ECG pattern is found regularly in endocardial cushion defects.

Left posterior hemiblock

The left posterior fascicle activates the posterior and inferior portion of the left ventricle, and when blocked causes antero-superior activation followed by postero-inferior activation. This produces a rightward and inferior axis (>120°). Q waves in leads II, III, and aVF are found because initial forces are directed superiorly. Isolated left posterior hemiblock is extremely rare in children but can follow a cardiac operation or myocarditis.

Bifascicular block

Bifascicular block usually refers to a left anterior hemiblock plus RBBB, as often seen after repair of tetralogy of Fallot. The ECG shows an RBBB with initial forces directed right and superiorly. When associated with PR interval prolongation, it suggests more significant conduction system disease. It may presage complete atrioventricular block, because normal conduction then depends on the one remaining fascicle.

Pre-excitation

Pre-excitation, the most common form being WPW syndrome, refers to an accessory pathway that connects atria directly to ventricular muscle, bypassing the AV node. Because of early abnormal activation of local ventricular myocardium secondary to bypassing the AV node and His–Purkinje system, in the WPW syndrome there is a short PR duration and wide QRS duration as the impulse spreads slowly through ventricular muscle. This slowly conducted wave produces a characteristic slurred upstroke of the QRS, the delta wave, which fuses with the remainder of the QRS complex resulting from normal conduction thorough the AV node. Children with this finding may have episodes of atrioventricular re-entrant tachycardia. Ventricular hypertrophy is difficult to diagnose with WPW.

Hypertrophy

Ventricular hypertrophy criteria primarily depend on QRS voltages in specific leads, compared with ECG findings of normal infants and children. Interpreting these criteria assumes that both the cardiac–torso geometry and the ventricular depolarization sequence (i.e., no bundle branch block or WPW) are normal. Think anatomically when assessing ventricular hypertrophy. The right ventricle is positioned to the right, anterior, and superior, hence increased QRS forces directed towards the right, anterior, and superior suggest right ventricular hypertrophy (RVH). The left ventricle is located to the left, inferior, and posterior, and therefore increased forces directed to the left, inferior, and posterior suggest left ventricular hypertrophy (LVH). There are many sets of criteria for diagnosing ventricular hypertrophy, each considered by the author to distinguish best abnormal from normal, because there will be overlap between the two.

Right ventricular hypertrophy

Criteria for RVH are more specific than those for LVH and include QRS voltage and repolarization criteria. These include:

1 R wave >98%tile in lead V1. This is a very specific finding for RVH outside the neonatal period.

2 S wave >98%tile in lead V6. An abnormally deep S wave in V6 is a very sensitive indicator of RVH, but is less specific than the R wave in V1. It is often seen with increased RV pressure secondary to chronic lung disease.

3 The R/S ratio is well established for different ages. If it is abnormally high in V1 or low in V6, this suggests RVH.

4 The T wave orientation changes with age. It is upright in lead V1 until 5–7 days of age, and then becomes negative until adolescence, when it reverts to upright again. An upright T wave in lead V1 after 7 days of age is a sensitive indicator of increased right ventricular systolic pressure.

5 A qR pattern in lead V1 can indicate RVH when seen, especially with a large R wave. It can also occur with l-looping of the ventricles (ventricular inversion), where it is due to reversed initial septal depolarization.

6 An RSR′ in lead V1 can be normal in children. It is also associated with right ventricular volume overload, such as in atrial septal defects, when the R′ amplitude is large and broadened.

7 Right axis deviation alone is not a criterion for RVH, but may support other findings.

8 A pattern of tall R waves and small S waves in the right precordium progressing to small R waves and deep S waves in the left lateral precordium in the child or adolescent suggests severe RVH.

Left ventricular hypertrophy

LVH criteria are based on QRS voltage and repolarization criteria (T wave axis). These include:

1 R wave >98%tile in lead V6, S wave >98%tile in lead V1. The large S wave in lead V1 is a relatively good predictor of LVH. However, LVH may have normal left-sided QRS forces and normal children may present with R waves >98%tile in lead V6.

2 A tall R wave in lead aVF can support LVH, especially with large mid-precordial voltages.

3 An adult pattern of R wave progression (the R wave increases in size from V1 to V6) in newborns strongly suggests LVH. This pattern is consistent with left ventricular dominance that is abnormal at that age.

4 T wave abnormalities are most reliable measures of LVH. The "strain" pattern consists of inverted T waves in the inferior and left precordial leads (II, III, aVF, and V5–V6). T wave abnormalities in LVH may sometimes be associated with depression of the ST segment in the same leads.

5 Left axis deviation beyond normal limits for age supports LVH, especially in infancy. A left superior axis deviation is not a feature of LVH; it usually is a feature of abnormal His bundle pathways in the ventricle, as in complete atrioventricular canal.

6 Prominent Q waves in leads V5 and V6 may be secondary to interventricular septal hypertrophy.

Biventricular hypertrophy

The diagnosis of biventricular hypertrophy (BVH) is most easily made when criteria for both RVH and LVH are met. Large R and S waves should be seen in both leads V1 and V6. Prominent mid-precordial voltages may be secondary to

proximity effects of the neonatal heart and should not be interpreted as BVH unless voltages in leads V1 and V6 are large. However, if the total voltage R plus S in lead V4 is greater than 60 mm (6 mV), BVH is likely (Katz–Wachtel criterion).

The QRS complex can be abnormally small. It should exceed 5 mm in leads I, II, and III and 8 mm. in leads V1 and V6. Small voltages occur with pericardial effusions, pneumomediastinum, myocarditis, and anorexia nervosa, where it is accompanied by marked bradycardia.

Ventricular repolarization

Repolarization is the return of the cell membrane potential to baseline following depolarization. On the single-cell level, this is relatively simple concept. However, in the entire heart, many factors account for the complexities of ventricular repolarization [2]. The subepicardium repolarizes before subendocardium, leading to ST segments and T waves that in general have the same polarity as the QRS complex. An age-dependent overlap between the end of depolarization and the onset of repolarization produces the characteristic J point elevation seen particularly in the mid-precordial leads in childhood [3], also known as "early repolarization," a normal variant in children and adolescents.

QT intervals

The QT interval is defined as the time from the onset of the Q wave to the end of the T wave. It can be difficult to measure, as the T wave can fuse with the U wave [3]. When the U wave is smaller and clearly separated from the T wave, it is not included in the QT interval. The QT interval is age, gender, and heart rate dependent. Heart rate dependency may be corrected in several ways, most commonly by Bazett's formula (QT/square root of preceding RR) to derive the corrected QT (QTc) interval. This empiric correction is inaccurate with very low or high heart rates. An alternative formula is 656/(1 + 0.1 × heart rate) [4]. The corrected QT interval is the same in boys and girls until puberty, then it becomes 20 ms shorter in males, after which it gradually increases to equalize in men and women by 60 years of age.

It is difficult to determine the corrected QT when heart rate varies, as with normal sinus arrhythmia. Garson suggested that using the shortest RR interval on a tracing to determine the QTc, and using a cut-off of 460 ms, identifies 98.4% of known long QT syndrome patients, but only 3.8% of normal controls [5]. If the QT interval is prolonged by a wide QRS, an alternative is to measure the JTc interval as JT/√RR, where J is the end of the QRS interval [6]; the upper limit of normal is ~0.34 s. Although the QT interval is automatically calculated by the ECG machine, it is often wrong. It should always be measured manually.

A prolonged QT interval can be due to a genetic abnormality that causes a channelopathy (long QT syndrome) or secondary to antiarrhythmic drugs or electrolyte imbalance (acquired long QT syndrome) [7–9]. The diagnosis of long QT syndrome can be difficult, as the significance of a prolonged QT in an asymptomatic individual can be difficult to determine, and requires a careful family history and, often, other testing. The QT interval is often long in normal neonates on the first day of life and shortens quickly. The T wave has an unusual configuration in such neonates initially.

ST segment, T waves, and U waves

ST segment

Interpreting the ST segment depends on choosing a baseline, which can be difficult with fast heart rates. ST segments exceeding 1 mm are regarded as elevated, and less than −0.5 mm are depressed. However, ST segment elevation or depression depends on age, with maximal elevation during adolescence (early repolarization or J point elevation), especially in the anterior and mid-precordial leads (V2–V4). Hence it is important to pay attention to the clinical setting when interpreting ST segments.

T waves

Ventricular repolarization (represented by the T wave) is directly influenced by ventricular depolarization. In the frontal plane, the T wave axis is normally 15–75°. The meaning of an abnormal T wave axis must be interpreted in the light of abnormalities of the QRS complex. Thus, any abnormality of ventricular depolarization (such as a bundle branch block or ventricular pre-excitation) causes an abnormal T wave, termed a secondary T wave abnormality. In contrast, primary T wave abnormalities occur with normal ventricular depolarization and reflect actual abnormalities of repolarization. Normally in the frontal plane the T axis is within 60° of the QRS axis after 3 years of age; any greater difference suggests a primary T wave abnormality. Primary T wave abnormalities generally reflect a major metabolic abnormality and not an abnormality of the myocardium.

Sometimes abnormal T waves are seen soon after a subject has swallowed something ice-cold (possibly due to local cooling of the left ventricle), after eating a large meal, or even with anxiety or hyperventilation. Repeating the ECG some hours later may reveal normal T waves.

U waves

U waves are usually seen in the mid-precordial leads (V2–V5) and often overlap the end of the T wave, resulting in T–U fusion. U waves typically are about 10% of T wave amplitude, and become more prominent at slower heart rates. Large U waves that are difficult to separate from the T wave are common with long QT syndrome.

Abnormalities of the ST segment, T wave, and U wave

Pericarditis

Pericarditis is the commonest cause of ST segment elevation in children, once early repolarization is excluded. Initially the ST segment is elevated with a normal T wave (thought to be secondary to subepicardial myocarditis) (see Figure 59.5). The ST segment then returns to normal but the T wave becomes flattened and then inverted and symmetrical. Subsequently, the T wave returns to its upright configuration. In pericarditis, these finding are seen across the entire precordium, as opposed to ischemia, where ST segment elevation is localized [10].

Myocarditis

Myocarditis can present with flattened or inverted T waves and low-voltage QRS patterns. The QT interval may be prolonged, and AV block and intraventricular conduction delays may occur, as may arrhythmias, including ventricular tachycardia and PVCs.

Ischemia

Myocardial ischemia is rare in children, except for a few congenital or acquired coronary abnormalities. Myocardial ischemia presents initially as a peaked T wave on the surface ECG in the lead near the affected myocardial segment. If the ischemia disappears, these findings resolve. If ischemia persists, the myocardium becomes injured, and ST segments elevate or depress depending on whether the injury is endocardial or epicardial. This again resolves if the ischemia disappears. If the ischemia causes infarction, there are decreased R wave voltages and abnormal Q waves facing the infarcted segment [11]. Normal Q waves are <4 mm in amplitude and commonly seen in leads V5, V6, and aVF. To diagnose a myocardial infarction, the Q wave duration should be ≥40 ms and amplitude >4 mm [11].

The most common cause of neonatal infarction is anomalous left coronary artery from the pulmonary artery. These infants have ischemia of the anterior and septal region, or the apex (the distribution of the left anterior descending coronary artery). Deep Q waves in leads I, aVL, and V3–V6 are typical. They also show failure of normal R wave progression across the precordium.

Potassium imbalance

Hyperkalemia causes symmetrical tall-peaked T waves which are generally seen at concentrations >7 mEq l⁻¹. This, however, is not a very specific or sensitive finding, as normal children tend to have more peaked T waves than adults, but they are usually asymmetric. Usually, the average height of the T wave is 20% of the average amplitude of the QRS complexes. As potassium levels increase, the T wave becomes

more peaked, and an intraventricular conduction delay prolongs both the QRS and PR intervals. At concentrations $\geq 9\,mEq\,l^{-1}$, atrial standstill, AV block, and ventricular fibrillation occur. Hypokalemia decreases T wave amplitude. As potassium levels decrease, a U wave appears and the ST segment becomes depressed [12].

Calcium/magnesium imbalance

Hypercalcemia shortens the QT interval by shortening the ST segment. It can also slow sinus rates and cause sinoatrial block. Hypocalcemia lengthens the QT interval by prolonging the ST segment. Low magnesium levels potentiate the effect of a low calcium level [12].

The normal ECG

Developmental changes

Elctrocardiograms change drastically during childhood, most notably a decreased heart rate with a concomitant increase in PR interval and QRS duration [13,14]. The right ventricular dominance of infancy shifts to a left ventricular dominant system, shown by a shift of QRS axis in the frontal plane from right to left. Furthermore, R wave progression changes over the first year of life. In infancy, tall R waves with small S waves are seen in the right precordium (V3R, V4R, and V1) and deep S waves are found in the left precordium (V6 and V7). As the left ventricle becomes dominant, the child develops a more adult-looking ECG, with deeper S waves in the right and anterior precordium and taller R waves in the left precordium. However, an R/S ratio of <1 in lead V6 is rare at any age, occurring in <5% of normal subjects, and may indicate left ventricular hypoplasia.

T waves also change characteristically with age [13,15]. In the first minutes after birth, the T wave vector is anterior and leftward (upright in V1 and V6). Over the next few hours, the T wave vector swings more rightward, inverting the T wave in the left lateral leads. Over the next 5–7 days, the T wave vector moves posterior and leftward, with an inverted T wave in V1 and upright T wave in V6. Finally, the T wave often becomes upright again in V1 after 7–8 years of age, but may remain inverted through adolescence. This should not be misinterpreted as ischemia or pericardial disease.

Premature infants

Premature infants have shorter conduction times and faster resting heart rates than term infants. The QRS duration is shorter, as are the PR and QT intervals. There tends to be less right ventricular predominance in a preterm infant, and this finding persists until 1 year of age [15].

Athletes

Athletes may have "abnormal" ECG findings in the absence of disease. Oakley and Oakley found LVH criteria by voltage, nonspecific ST and T wave changes, and Q waves suggestive of myocardial infarction in 10 athletes [16]. No underlying cardiac abnormality, however, was ever found on extensive evaluation. Balady *et al.* also found similar findings in power-trained athletes [17]. Athletes also have slower heart rates and PR and QT prolongation compared with sedentary controls [18]. Many highly trained athletes have physiologic left ventricular hypertrophy [19].

Gender and race differences

Both sex and race differences appear in the ECG as children approach adolescence [20,21]. Racial differences are seen in the pre-teen years, and sex differences occur during puberty. Teenage girls and women tend to have longer QT intervals. QRS voltages are increased in males compared with females, and blacks compared with whites, associated with differences in left ventricular posterior wall thickness [20,21].

References

1 Davignon A, Rautaharju P, Barselle E, *et al.* Normal ECG standards for infants and children. *Pediatr Cardiol* 1979/80;**1**:123–34.

2 Spach MS, Barr RC. Origin of epicardial ST-T wave potentials in the intact dog. *Circ Res* 1976;**39**:475–87.

3 Spach MS, Barr RC, Benson W, Walston A II, *et al.* Body surface low-level potentials during ventricular repolarization with analysis of the ST segment: variability in normal subjects. *Circulation* 1979;**59**:822–36.

4 Rautaharju PM, Warren JW, Calhoun HP. Estimation of QT prolongation. A persistent, avoidable error in computer electrocardiography. *J Electrocardiol* 1990;**23**(Suppl):111–7.

5 Garson A Jr. How to measure the QT interval – what is normal? *Am J Cardiol* 1993;**72**:14B–6B.

6 Berul CI, Sweeten TL, Dubin AM, *et al,* Use of the rate-corrected JT interval for prediction of repolarization abnormalities in children. *Am J Cardiol* 1994;**74**:1254–7.

7 Singh BN. When is QT prolongation antiarrhythmic and when is it proarrhythmic? *Am J Cardiol* 1989;**63**:867–9.

8 Keating M. Linkage analysis and long QT syndrome. Using genetics to study cardiovascular disease. *Circulation* 1992;**85**:1973–86.

9 Moss AJ, Schwartz PJ, Crampton RS, *et al.* The long QT syndrome. Prospective longitudinal study of 328 families. *Circulation* 1991;**84**:1136–44.

10 Spodick DH. Electrocardiogram in acute pericarditis. Distributions of morphologic and axial changes by stages. *Am J Cardiol* 1974;**33**:470–4.

11 Towbin JA, Bricker JT, Garson A Jr. Electrocardiographic criteria for diagnosis of acute myocardial infarction in childhood. *Am J Cardiol* 1992;**69**:1545–8.

12 Surawicz B. Relationship between electrocardiogram and electrolytes. *Am Heart J* 1967;**73**:814–834.

13 Rautaharju PM, Davignon A, Soumis F, *et al.* Evolution of QRS–T relationship from birth to adolescence in Frank-lead orthogonal electrocardiograms of 1492 normal children. *Circulation* 1979;**60**:196–204.

14 Walsh EP, Lang P, Ellison RC, *et al.* Electrocardiogram of the premature infant at 1 year of age. *Pediatrics* 1986;**77**:353–6.

15 Hait G, Gasul BM. The evolution and significance of T wave changes in the normal newborn during the first seven days of life. *Am J Cardiol* 1963;**12**:494–504.

16 Oakley DG, Oakley CM. Significance of abnormal electrocardiograms in highly trained athletes. *Am J Cardiol* 1982;**50**:985–9.

17 Balady GJ, Cadigan JB, Ryan TJ. Electrocardiogram of the athlete: an analysis of 289 professional football players. *Am J Cardiol* 1984;**53**:1339–43.

18 Bjornstad H, Storstein L, Meen HD, Hals O. Electrocardiographic findings in athletic students and sedentary controls. *Cardiology* 1991;**79**:290–305.

19 Roeske WR, O'Rourke RA, Klein A, *et al.* Noninvasive evaluation of ventricular hypertrophy in professional athletes. *Circulation* 1976;**53**:286–91.

20 Hashida E, Nishi T. Constitutional and echocardiographic variability of the normal electrocardiogram in children. *J Electrocardiol* 1988;**21**:231–7.

21 Rao PS. Racial differences in electrocardiograms and vectorcardiograms between black and white adolescents. *J Electrocardiol* 1985;**18**:309–13.

8

Echocardiography

Rajesh Punn[1], Mark K. Friedberg[2] & Norman H. Silverman[1]

[1]Stanford University, Lucile Packard Children's Hospital, Palo Alto, CA, USA
[2]The Labatt Family Heart Center and Department of Paediatrics, The Hospital for Sick Children and University of Toronto, Toronto, ON, Canada

Echocardiography is a diagnostic tool used by all pediatric cardiologists. This chapter describes its physical principles, strategies of anatomic and physiologic examination, limitations of the technique, and a description of some newer technologies. Features of the major congenital lesions are included in the relevant sections.

Physics

An electrical signal applied to a piezoelectric crystal makes it vibrate, transmitting ultrasound waves at its natural frequency, generally 2.5–15 MHz. Conversely, when ultrasound waves make the crystal vibrate, it emits an electrical impulse with an intensity correlated with the density of acoustic waves received. Because the instrument knows the timing of the pulse, the speed of sound in the body, when the signal returns, and how great the returning signal is, it can interpret the distance from the transducer and produce the appropriate image.

The primary mode of imaging is two-dimensional scanning, in which a sector is produced by aiming the ultrasound beam in a particular direction, sending the pulse, and receiving the echoes returning from the body. The beam is then redirected and the process repeated. This produces individual "scan lines" that are displayed on the screen to represent the image. Most instruments acquire and display a sector of 128 scan lines. A single scan line that traverses the heart perpendicularly is termed an M-mode.

Determinants of image quality

Penetration power
As ultrasound waves pass through the body, some are reflected (or echoed) back to the transducer from each tissue interface, some are reflected off at an angle (refracted) and cannot be detected by the transducer, and some are absorbed by the tissue. The degree of attenuation is inversely related to the frequency of the transducer. Higher frequency ultrasound transducers (7–10 MHz) lose significant penetration above 6–8 cm, whereas lower frequency transducers (2.5–5 MHz) can penetrate to 20 cm.

Resolution
Detail resolution is defined as the minimal separation needed for two structures to produce two separate acoustic echoes. *Axial* resolution describes the minimal distance along the direction of the beam, and depends on the physical length of the pulse. The echoes from two objects closer to each other than the length of the pulse merge and produce one long echo. The physical length of the pulse depends on its wavelength and duration. The speed (c) of electromagnetic waves in the body is constant (roughly 1560 m s^{-1}) and is expressed by the equation

$$c = f \times l$$

where f is the frequency of the wave in hertz (Hz, cycles s^{-1}) and l the wavelength in meters. Therefore, wavelength is inversely proportional to the transducer frequency. The wavelength is the absolute limit to resolution. Wavelengths for standard ultrasound transducers vary as ~0.80, ~0.30, and ~0.10 mm at a frequency of 2, 5, and 15 MHz, respectively. Most systems produce a pulse of 3–5 wavelengths. Therefore, a 5 MHz transducer with a pulse duration of three wavelengths has a physical pulse length of $3 \times 0.3 = 0.9$ mm, and two objects <1 mm apart are seen as one object. In practice, most systems produce a pulse with a physical length of 1.5 mm at any frequency, somewhat smaller for higher frequency transducers. However, an axial resolution of 1 mm serves as a rough guide for most ultrasound systems.

Lateral resolution is that perpendicular to the direction of the beam and depends upon the beam width. Two objects closer to each other than the beam width are seen as a single, broad echo. Like all waves, the ultrasound beam diverges as it passes through the tissue. Therefore, lateral resolution also depends on the depth of the tissue. Modern transducers are able to focus the beam electronically in order to narrow it at the optimum distance, or focal zone. The width of the beam in millimeters at the focal zone is expressed as

$$\text{width} = \frac{\lambda x}{d}$$

where λ is the wavelength of the wave, x the distance to the structure, and d the diameter of the transducer. Therefore, minimal beam diameter and lateral resolution are directly related to transducer frequency and depth of the structure, and inversely related to transducer size. An ideal transducer would then be of higher frequency and larger. However, because of the physics of beam formation, nearer to the focal zone (near-field) the beam has a wider diameter, and practical considerations limit the ability of large transducers to focus in the near-field. In addition, in smaller patients, a large transducer may produce rib artifacts when viewed from the parasternal planes. Therefore, in general, smaller, higher frequency transducers provide the best near-field resolution in smaller children, and larger, lower frequency transducers provide the best far-field resolution. For a standard size 5 MHz transducer, the minimal beam diameter at the focal zone is approximately 1.5 mm. In addition, better lateral resolution is achieved by using a scan plane that brings the structure closer to the transducer.

Contrast resolution, the ability to distinguish differences in tissue density, refers to the ability to distinguish faint structures next to brighter ones. The determinants of contrast resolution are similar to those for detail resolution, and axial resolution is better than lateral resolution. The manufacturer but not the operator controls these signals.

Artifacts

Artifacts, most commonly drop-out of parallel structures, side-lobing, and shadowing, degrade image quality. Images generated by waves echoed to the transducer depend upon an interface perpendicular to the ultrasound beam. Most structures are irregular so that even when nearly parallel to the beam, enough of the surface is perpendicular to generate an image. Very smooth structures parallel to the ultrasound beam generate very little echo, and therefore generate very weak signals, which can easily be lost. The best example of this is the atrial septum, which is parallel to the beam from the apical view, and often drops out. From the subcostal view, however, the septum is perpendicular and easily seen.

Side-lobing and shadows are both caused by very dense structures that produce bright echoes. These structures, such as the pericardium, reflect back a much greater proportion of the beam than do other structures. Side-lobing refers to the lateral spread of these very bright echoes, and is due to divergence of the beam in the far-field. Although we refer to beam diameter (see lateral resolution, above), the beam does not have distinct edges. Rather, the beam becomes less intense further away from the centerline. High-intensity echoes are therefore wider than less intense echoes, and can appear to extend more laterally than they actually do. This is most often seen when a bright structure, such as the pericardium, appears to extend into the lumen of a nearby vessel.

Shadows are caused when extremely bright echoes allow little of the ultrasound beam to pass through them. Thus a very bright object, such as a prosthetic valve, almost completely obscures all structures behind it.

Doppler ultrasound

The Doppler principle states that the frequency of transmitted sound is altered if the source is moving, as in the classic example of the moving train. This principle applies if either the source or the receiver of the sound is moving. The frequency is altered according to the Doppler equation:

$$f_d = \frac{2f_0 V \cos\theta}{c}$$

where f_d is the observed Doppler shift in hertz, f_0 the frequency of the source sound in hertz, V the velocity of the object (source or receiver) in meters per second, θ the intercept angle between the source and receiver in degrees, and c the velocity of sound in the body (1560 m s^{-1}). In echocardiography, the Doppler shift measures the velocity of moving blood. The frequency shift observed, usually several kilohertz, produces an audible signal. The signal is also processed and displayed graphically as the component velocities (Figure 8.1a and b). By convention, blood moving toward the transducer is shown as a signal above the baseline and that moving away as a signal below the baseline. In laminar flow, nearly all the blood streams move parallel at similar velocity, producing a musical tone and a narrow band on the graphical display (Figure 8.1b). However, with turbulent flow, the audible signal is harsher and the graphical display is "filled in". The velocity can be calculated by resolving the Doppler equation shown above for velocity:

$$V = \frac{f_d}{2f_0 \cos q}$$

Therefore, the velocity is proportional to the frequency shift, but inversely proportional to the originating frequency and the cosine of the angle of incidence, the latter the principle source of error in velocity measurements. Rarely is the blood flow parallel to the transducer beam, particularly in disturbed flow. In practice, if the angle of incidence is <20°, the error is minimal. If the angle is >20°, it should be minimized by using a different view, but also can be corrected in the instrument.

(a) (b)
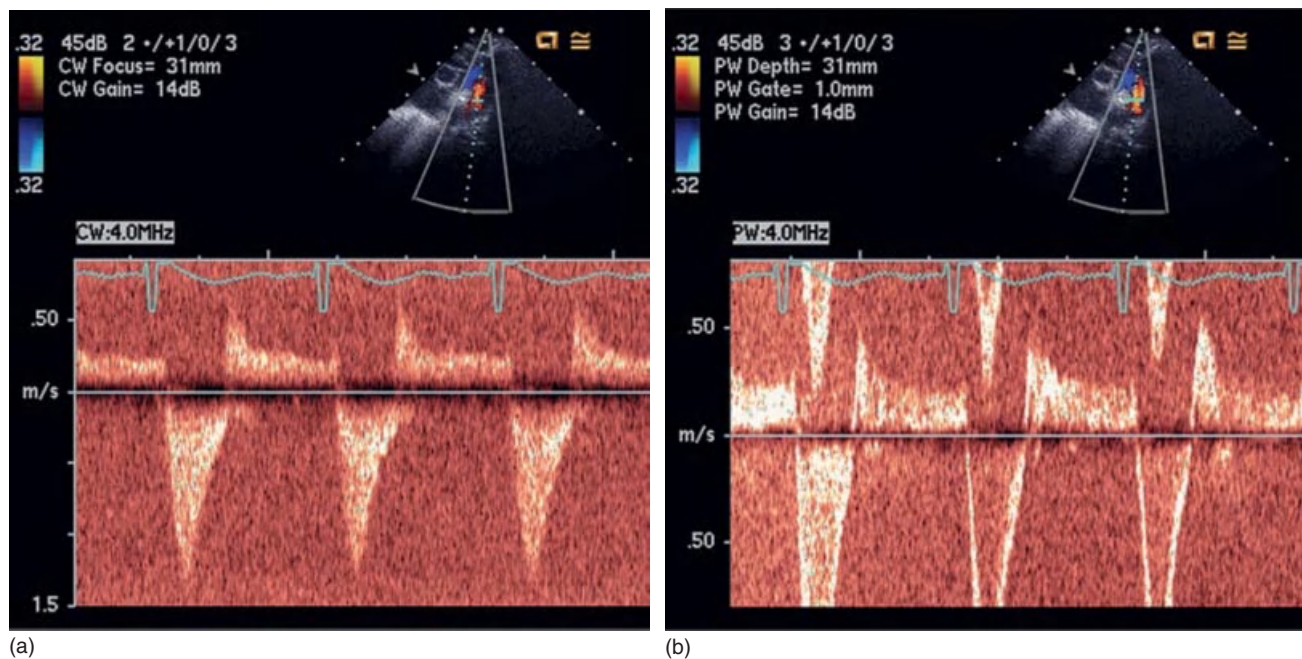
Figure 8.1 Continuous wave and pulsed wave images of the same flow signal. (a) With continuous wave Doppler, continuous sampling allows measurement of higher velocities, but because multiple samples are being taken, the result is a "filled in" signal. (b) With pulsed wave Doppler, the limited sampling frequency prevents measurement of higher velocities, which leads to aliasing (wrapping around) of the signal.

Three types of Doppler applications are commonly employed: continuous wave, pulsed, and color Doppler.

Continuous wave doppler

One crystal is used as the transmitter and the other as the receiver. Signals are sent and received continuously so that the instrument cannot calculate the depth of the returning signal, and signals are received from the entire path of the beam, which may contain multiple flows. However, Doppler shifts of any magnitude can be received. To display a signal of a given frequency, it must be sampled at least at twice that frequency. Because sampling is continuous, any frequency can be sampled (Figure 8.1a). Therefore, continuous wave Doppler is accurate at any velocity, but inaccurate with respect to location.

Pulsed doppler

In pulsed Doppler, a single crystal alternately transmits pulses, then receives echoes that can be sampled within a time window established by the desired depth of sampling. Sampling must finish before the next pulse transmission. Therefore, the location can be accurately sampled, but because the sampling frequency is limited by the pulse repetition frequency, only a limited range of frequencies, and therefore a limited range of velocities, can be sampled. This limit is the Nyquist limit. Velocities above the Nyquist limit cannot be resolved accurately, and are therefore electronically cut off and "wrapped around," or aliased (Figure 8.1b). From the previous equation, the velocity is inversely proportional to the transmitted frequency. Therefore, lower frequency transducers can resolve higher velocities for a given Doppler shift, and hence are more useful in pulsed Doppler than are higher frequency transducers. A standard 5 MHz transducer has a Nyquist limit of $1–3 \, \text{m s}^{-1}$, depending upon the depth of sampling.

Color doppler

Color Doppler is pulsed Doppler in which a mean velocity for an area is calculated and represented by a color. Color Doppler detects very small defects that are impossible to see by two-dimensional imaging alone.

Color Doppler is subject to all the advantages and limitations of pulsed Doppler, but has additional advantages and limitations. A much broader area can be sampled using color Doppler, allowing quicker determination of velocities across a larger area, but the pulse repetition frequency is much lower, as is the Nyquist limit, or maximal detectable velocity. The same 5 MHz transducer that can sample $1–3 \, \text{m s}^{-1}$ by pulsed Doppler can achieve only $0.5–1 \, \text{m s}^{-1}$ by color Doppler. Decreasing the size of the sampling volume, a feature available on most commercial systems, can increase the Nyquist limit significantly.

Effective use of ultrasound

In cross-sectional imaging, a higher frequency transducer generally produces better resolution, but a lower frequency transducer provides better penetration. In Doppler sampling,

SUPRASTERNAL – in plane of body
• sagittal & coronal cuts

PARASTERNAL
• short axis
• long axis

in plane of heart

APICAL – both long axis planes
• right angles to inlet ("four chamber")
• right angles to outlet ("two chamber")

(a)

SUBCOSTAL – in plane of body

• parasagittal & paracoronal cuts

SHORT AXIS

LONG AXIS
right angles to inlet septum–"4-chamber"
right angles to outlet septum–"2-chamber"

(b)   ORTHOGONAL PLANES OF HEART

Figure 8.2 (a) The standard echocardiographic windows on the body surface are oriented to the major axes of either the body or the heart. (b) The standard reference planes for cardiac long axis or short axis imaging. (Reproduced with permission from Silverman *et al*. *Br Heart J* 1983;**50**:421–31.)

a lower frequency transducer allows more accurate determination of velocity in spectral displays, and also provides more penetration for better color Doppler signals. The use of appropriate scan planes, particularly those bringing structures closer to the transducer, significantly increases the resolution by allowing the use of higher frequency transducers and by improving lateral resolution and penetration.

The echocardiographic examination

An echocardiographic examination is used to assess the morphology and physiology of the heart and great vessels. Because of the asymmetric position of the heart in the chest, and the sonographic interference by the lungs and thoracic
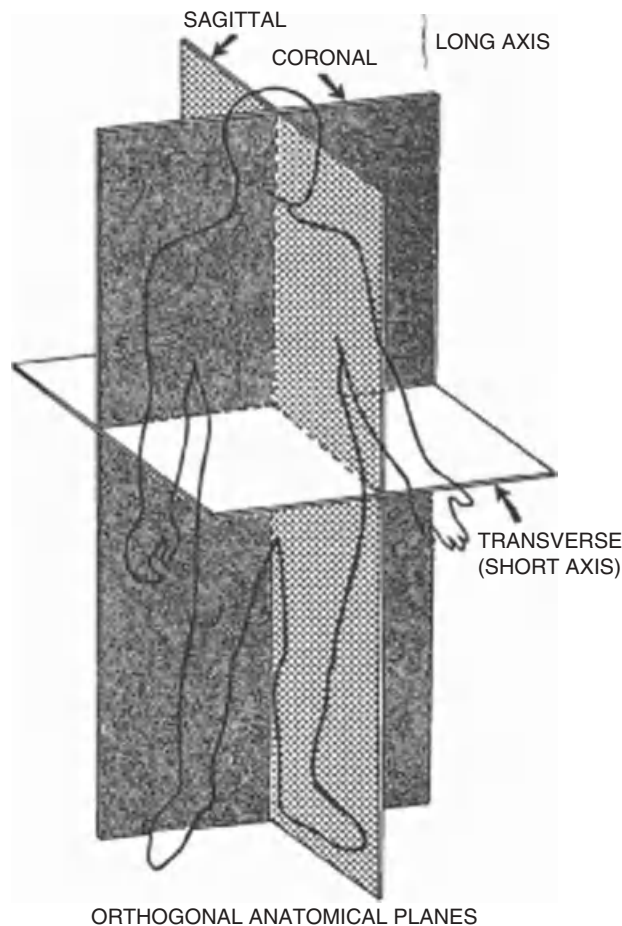
Figure 8.3 The three orthogonal planes of the body are the sagittal, coronal, and transverse planes. (Reproduced with permission from Silverman *et al. Br Heart J* 1983;**50**:421–31.)

skeleton, several standard acoustic windows are typically employed during a study: the parasternal, apical, subcostal, and suprasternal. The transesophageal route is an alternative.

Because the major cardiac axes differ from those of the body, we relate the spatial relationship of the heart and great vessels to other thoracic structures to perform an echocardiographic study or appreciate an image (Figures 8.2 and 8.3) [1]. The cardiac long axis runs from the apex to the base, approximately from the left hypochondrium anteroinferiorly through to the tip of the right scapula posterosuperiorly. Several standard echocardiographic views, such as the parasternal and apical, are oriented with respect to the cardiac axes, and orthogonal planes from these windows are described in terms of the cardiac long and short axis (parasternal) or two- and four-chamber (apical) views. Other windows, such as the subcostal and suprasternal, are more closely aligned with the major axes of the body, and are thus described in terms of coronal, sagittal, and transverse (horizontal) planes (Figures 8.2 and 8.3).

An echocardiographic examination may be performed in a sequential approach, the views being integrated to define the anatomy of the heart according to the segmental method. The morphologic information is complemented by physiologic information.

Morphologic evaluation

Cross-sectional two-dimensional echocardiography allows excellent delineation of morphology, and can be complemented with data obtained from Doppler color flow, Doppler speckle tracking, and M-mode ultrasound. Examples of morphologic evaluation in specific anomalies are discussed in later chapters discussing specific cardiac lesions, although selected examples will be given here to illustrate the capabilities of ultrasound.

Systemic veins

The relationships between the major abdominal systemic veins (inferior vena cava, hepatic veins, and azygos/hemiazygos system) and the abdominal aorta are central in determining visceroatrial situs (Figure 8.4). In situs solitus, the inferior vena cava is right-sided and to the right of the aorta, and the azygos and hemiazygos veins are more posterior in the right and left paravertebral spaces, respectively. These relationships are reversed in situs inversus. In patients with visceroatrial heterotaxy (atrial isomerism), these relationships are generally disturbed.

The positions of the abdominal systemic veins can be evaluated from the subcostal window with both transverse and sagittal views. A coronal image can also be used to identify the intrahepatic segment of the inferior vena cava and the entrance of the hepatic veins (Figure 8.5). The inferior vena cava must be imaged from below the liver to its junction with the right atrium in order to verify that it is truly the inferior cava and not a hepatic vein. With an interrupted inferior vena cava and azygos continuation, the intrahepatic segment of the inferior vena cava is absent, and the more posterior azygos vein is wider. Pulsed Doppler ultrasound and color flow mapping characterize flow patterns, helping to confirm the identity of the vessel in question (Figure 8.6).

The proximal superior vena cava, its tributaries, and both cavoatrial junctions can be imaged (Figure 8.7), and the position of the left innominate vein relative to the aortic arch can be appreciated (Figure 8.8). The azygos vein runs posteriorly and then over the right pulmonary artery to join the superior vena cava (Figure 8.9). A left superior vena cava can be identified readily (Figure 8.10). If it drains to the coronary sinus, the coronary sinus is usually enlarged and seen as a large annular structure above the mitral valve (Figure 8.11). When this occurs, a bridging vein is typically absent. The coronary sinus can be distinguished from the descending aorta by identifying the pericardium, which defines the coronary sinus as an intrapericardial structure (Figure 8.11). In addition, the coronary sinus passes anterior to the left pulmonary veins whereas the descending aorta is posterior to the left pulmonary veins.

Vascular arrangement in variations of body situs
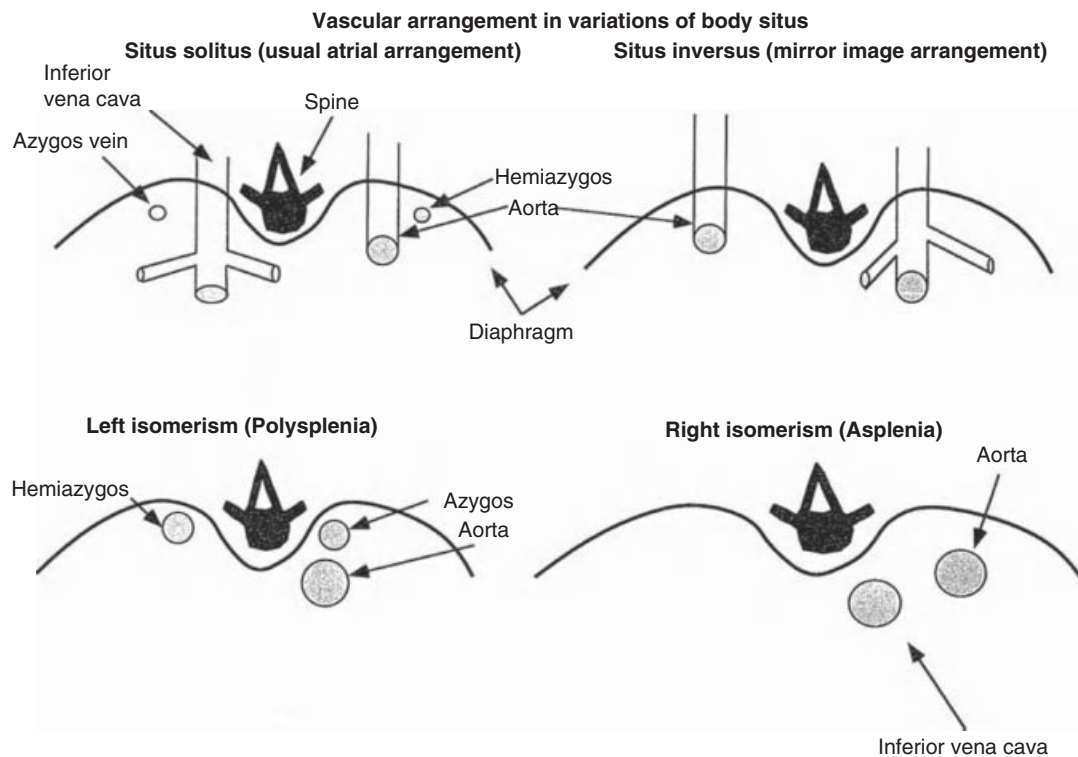
Figure 8.4 Diagrammatic representation of the probable positions of the aorta, inferior vena cava, and azygos veins in the four possible forms of atrial situs. In left isomerism, the inferior vena cava is interrupted and drainage of lower extremity venous blood continues via either the azygos or hemiazygos. Left isomerism and right isomerism are both depicted here with the aorta and azygos/inferior vena cava on the left, although the vessels may also be located on the right. (Modified from Silverman, *Pediatric Echocardiography*. Baltimore: Williams & Wilkins, 1993.)
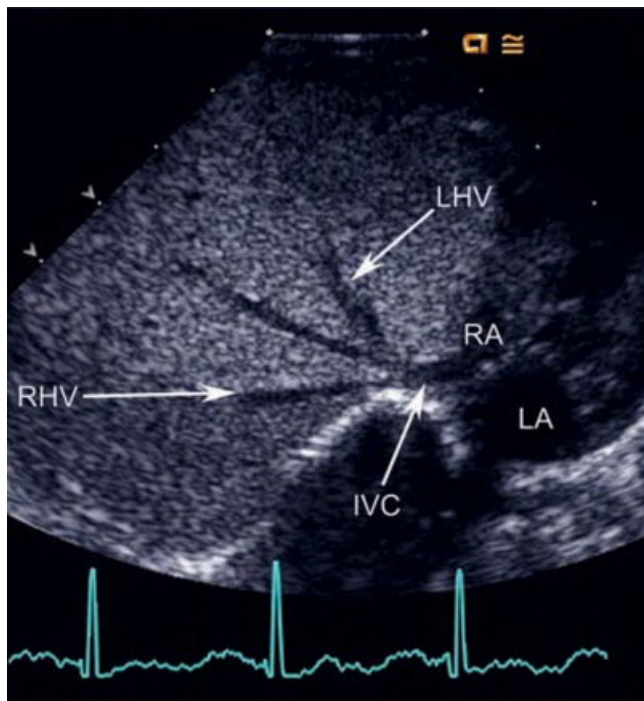
Figure 8.5 Subcostal coronal image demonstrating the confluence of the left (LHV) and right hepatic veins (RHV) with the inferior vena cava (IVC) just below the caval junction with the right atrium (RA). LA, left atrium.

Pulmonary veins

All four pulmonary veins and their venoatrial connections should be identified. With careful manipulation of the transducer, all four pulmonary veins can sometimes be seen at their confluence with the left atrium in a single plane ("crab view," Figure 8.12). It is important to remember that the descending aorta passes posterior to the left atrium between the left and right pulmonary veins, and should not be confused with the left pulmonary veins (Figure 8.13). Pulsed Doppler interrogation and color flow mapping can be used to demonstrate flow, and offer guidance regarding the anatomy of the pulmonary veins when their identity is otherwise not obvious.

Atria

The relationships of the major abdominal vessels and the connections of the systemic and pulmonary veins to the atria provide important information about atrial situs. The right atrial appendage is typically broad-based and triangular, whereas the left atrial appendage is thin and "finger-like" with a narrow base (Figure 8.14) [2]. Other typical features of the morphologic right atrium include the orifice of the coronary sinus, the limbus forming the superior border of the fossa ovalis on the right atrial aspect of the septum, and the Eustachian valve. The interatrial septum is investigated
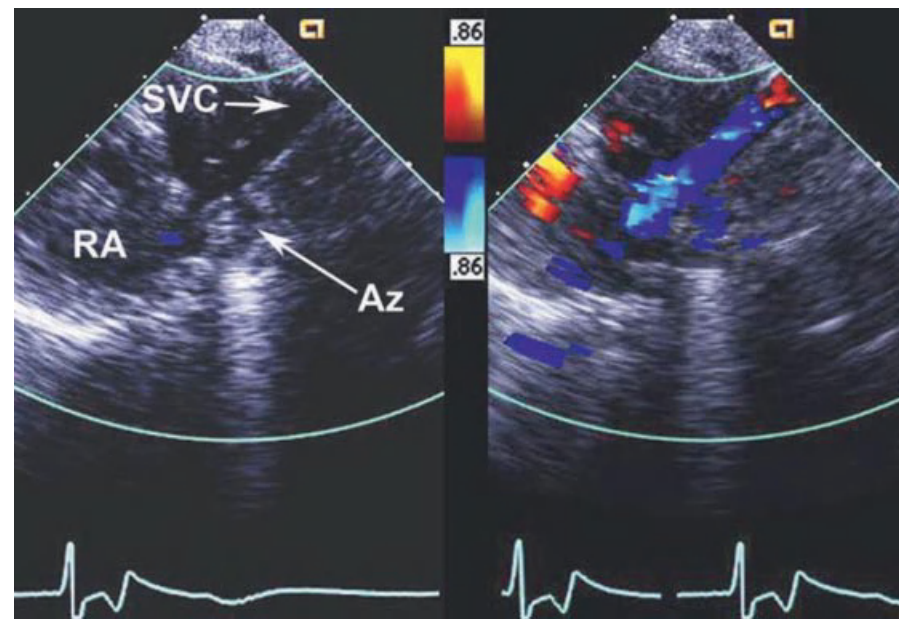
(a)

(b)

Figure 8.6 (a) Parasternal long axis view demonstrates the superior vena cava (SVC) entering into the right atrium (RA) with the azygos vein (Az) entering posteriorly. (b) Subcostal sagittal view again shows the azygos vein entering the posterior aspect of the superior vena cava. The left atrium (LA) and descending aorta (DAo) are demonstrated further posteriorly.

from multiple windows, allowing all aspects of the septum to be identified (Figure 8.9).

Atrioventricular valves

The atrioventricular valvar apparatus consists of the annulus (or basal attachment of the leaflets to the atrioventricular junction), the valve leaflets proper, the chordae tendineae, and the papillary muscles.

The mitral valve, its annulus, and tensor apparatus are well defined using multiple views. (Figure 8.15). An image plane is directed through the mitral valve orifice, allowing assessment of orifice geometry and also anomalous structures such as clefts and accessory orifices or tissue (Figure 8.16).

The tricuspid valve and subvalvar apparatus can be investigated in the plane of the valve ring. The normal

offset appearance of the mitral and tricuspid valves, wherein the atrioventricular septum separates the right atrium from the left ventricular outflow tract, can be appreciated from the apical four-chamber view (Figure 8.15b).
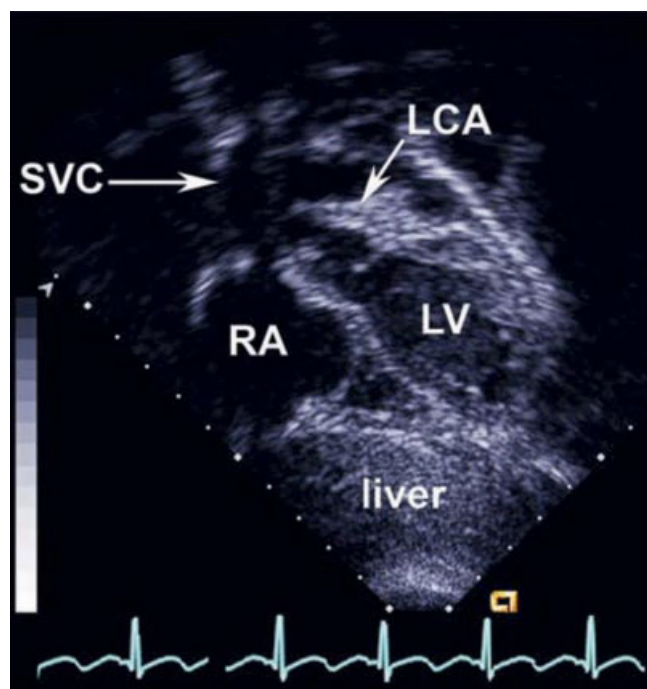
The hinge points, thickness, and chordal attachments of the septal and antero-superior leaflets are clearly shown. All three leaflets can also be examined from the subcostal window. Anomalous attachments of tricuspid chordae, such as with straddling, may be seen from various windows.

Ventricles

Ventricular morphology, size, and position, and also atrioventricular and ventriculoarterial connections, are readily delineated. The echocardiographic hallmarks of the morphologic right ventricle are septal attachment of the right atrioventricular (tricuspid) valve, the triangular shape of the ventricle, the trabecular septal surface, and the septomarginal trabeculation (Figure 8.17). The characteristic features of the left ventricle are the lack of mitral valve chordal attachments to the septum (Figure 8.15a), the smooth septal surface, conical shape of the ventricle, and aortic–mitral fibrous continuity, the last not always definable. The inlet, body, and outlet components of the left ventricle can be seen in a single plane from several windows (Figures 8.7, 8.15a, and 8.18). The inlet, body and outlet components of the right ventricle can be depicted in a single subcostal plane (Figure 8.19).

Assessment of chamber size is based on geometric models that allow volume estimation from cross-sectional measurements (Figure 8.20). In our experience, the most reliable approach in children is the biplane Simpson's rule (method of discs), which can be applied irrespective of the shape of the chamber to be measured [3]. This method requires imaging in two orthogonal planes sharing a common long axis,

Figure 8.7 The subcostal coronal view shows the superior vena cava (SVC) entering the right atrium (RA) while the left ventricle (LV) is also imaged. The left coronary artery can also be imaged from this view (LCA).
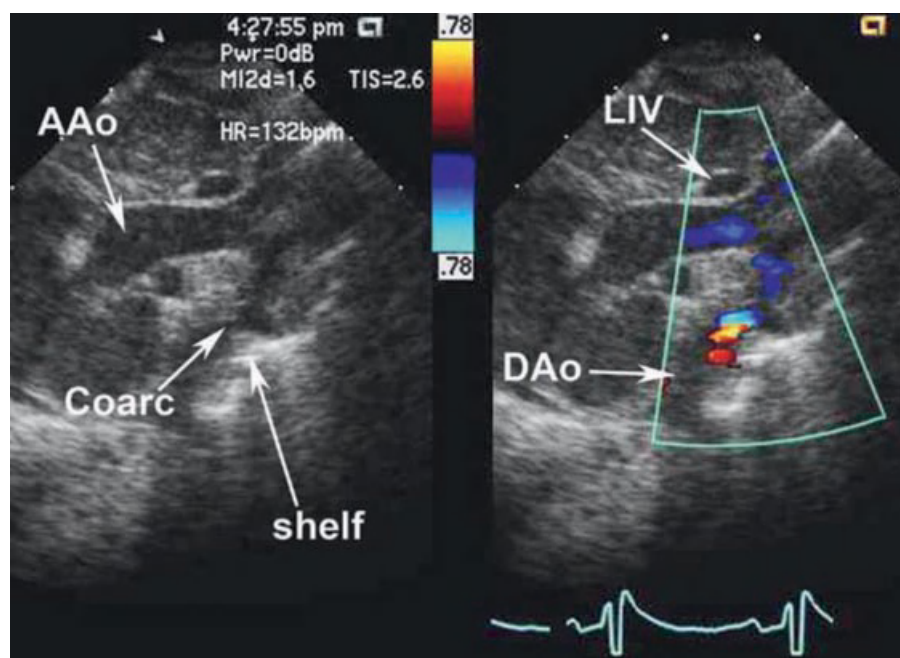
Figure 8.8 In this oblique scan from the suprasternal notch, the left innominate vein (LIV) is identified running anterior to the ascending aorta (AAo). A coarctation (Coarc) is present at the proximal descending aorta (DAo). The posterior shelf is also imaged behind the coarctation.
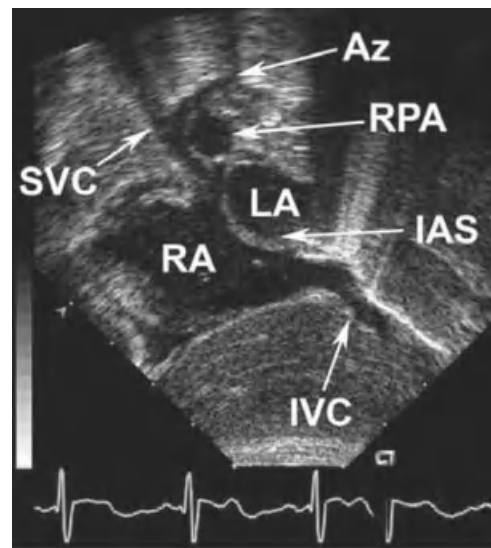
(a)
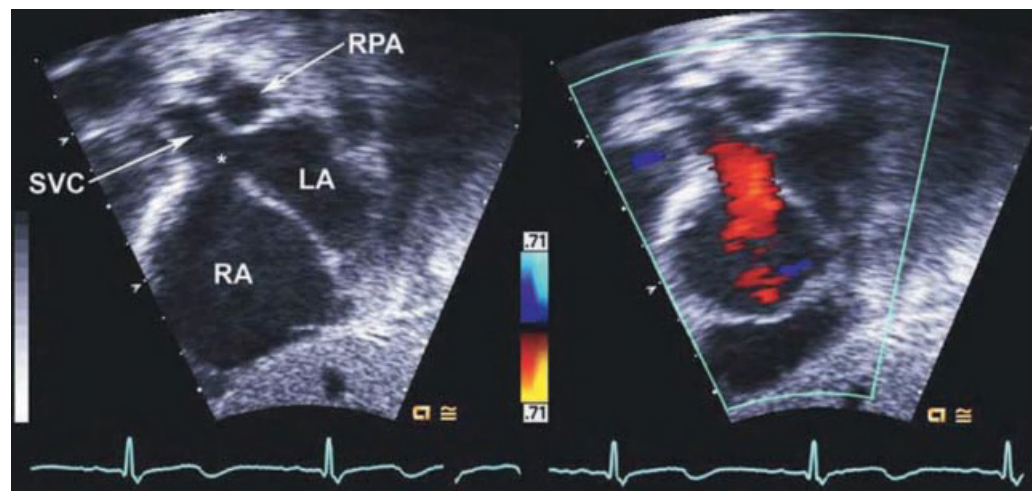
(b)

Figure 8.9 (a) This subcostal sagittal image shows both the superior vena cava (SVC) and inferior vena cava (IVC) entering into the right atrium (RA) and the interatrial septum (IAS) anterior to the left atrium (LA). The azygos vein (Az) arches over the right pulmonary artery (RPA). (b) This subcostal sagittal image demonstrates a superior sinus venosus defect (*). The superior vena cava (SVC) overrides the crest of the interatrial septum. The right and left atria are labeled (RA and LA). The right pulmonary artery (RPA) runs posterior to the superior vena cava.

and reconstructs the chamber volume from the summed volumes of multiple elliptical slices of equal thickness that are defined by the two orthogonal short axis dimensions (Figure 8.20). For calculating left ventricular volume, we use apical four- and two-chamber views as the orthogonal planes. Estimating right ventricular volume is more complex because the right ventricle has an irregular shape that fits no simple geometric model and lies very close to the chest, which makes imaging of the entire ventricular outline difficult in older children. In children, however, orthogonal views of the right ventricle can be obtained easily from the subcostal window, and Simpson's rule can be applied for volume calculation from these images by using the common long axis from

the diaphragmatic surface to the pulmonary artery and the area outlines of the right ventricle from orthogonal subcostal cuts, which may be best obtained from slightly oblique views rather than true sagittal and coronal images [4]. These measurements appear to be accurate in small children since the ventricles can be imaged well using subcostal technique. These volumes are usually within 10–15% of volumes measured by angiography or casts of the ventricles [4a, 4b].

Semilunar valves

The semilunar valves are structures that include the leaflets, annuli, sinuses of Valsalva, and sinotubular junctions. The aortic root and the hinge points of the aortic valve
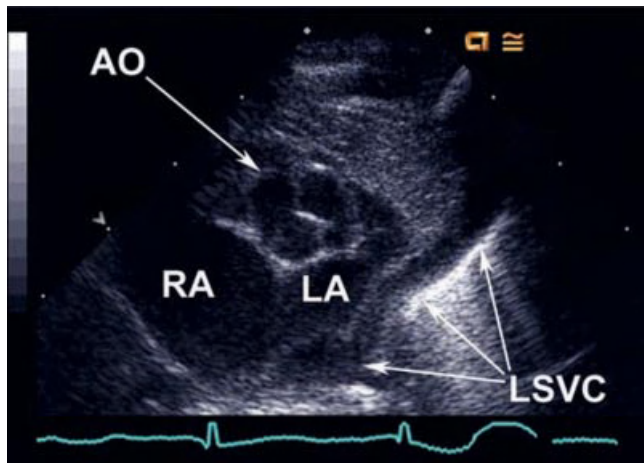
(a)
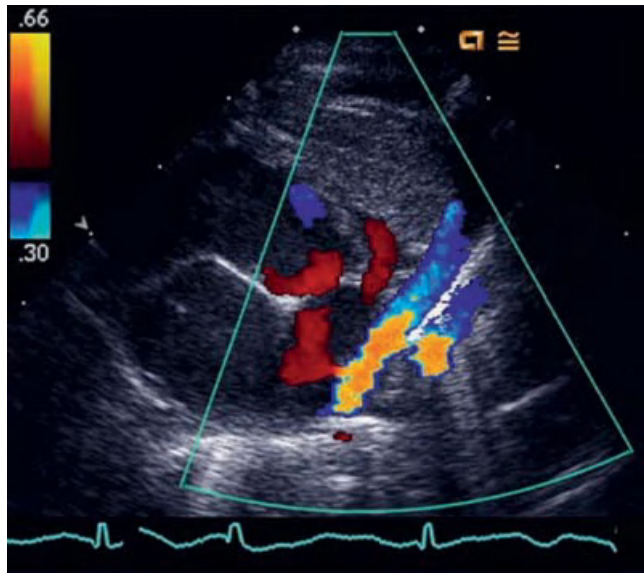
(b)

Figure 8.10 (a) This image from the high parasternal window shows a left superior vena cava (LSVC) draining via the coronary sinus to the right atrium (RA). The left atrium (LA) and aorta (Ao), are also shown. (b) Same figure with color Doppler.

Figure 8.11 Parasternal long axis view demonstrating a coronary sinus enlargement (CS) anterior to the descending aorta (DAO) in a patient with a superior vena cava–coronary sinus connection. AO, aorta; LA, left atrium; LV, left ventricle; RV, right ventricle.
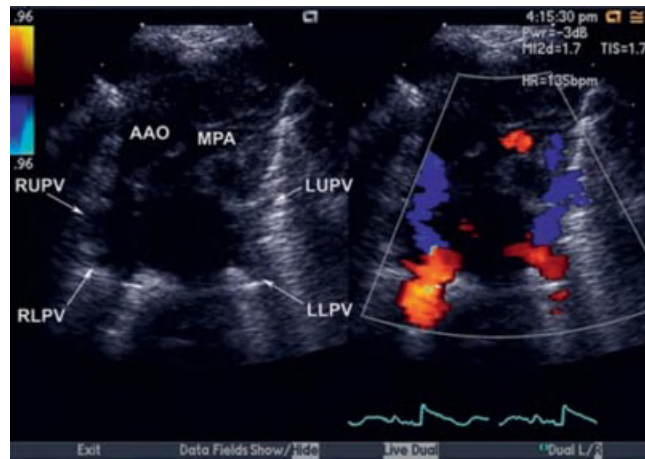
Figure 8.12 This is a suprasternal notch (SSN) coronal view showing the confluence of the right upper (RUPV), right lower (RLPV), left upper (LUPV), and left lower (LLPV) pulmonary veins entering the left atrium. The ascending aorta (AAO) and main pulmonary artery (MPA) are also seen in cross-section cranial to the left atrium. The color Doppler view is on the right.

leaflets and also their thickness can be appreciated, as can the dimensions of the sinuses and sinotubular junction (Figures 8.15a and 8.18). The morphology of the aortic valve leaflets can be distinguished clearly from the parasternal short axis, in both systole and diastole, when the imaging plane passes through the sinuses of Valsalva (Figure 8.21). The leaflets may be of unequal size. A bicuspid aortic valve, which typically results from fusion of the left coronary leaflet with either the right or non-coronary leaflet, may appear to be a normal tricuspid valve from this view, as the raphe of the fused commissure is visible. However, the motion of this leaflet differs from this normal trileaflet configuration, and an asymmetric valvar orifice is typically present during

systole and can be distinguished using two-dimensional and Doppler color flow imaging.

The pulmonary valve leaflet thickness, hinge points, and dimensions of the sinuses and sinotubular junction are evaluated in the long axis of the pulmonary artery. The pulmonary valve is at the level of the aortic valve,

(a)   (b)
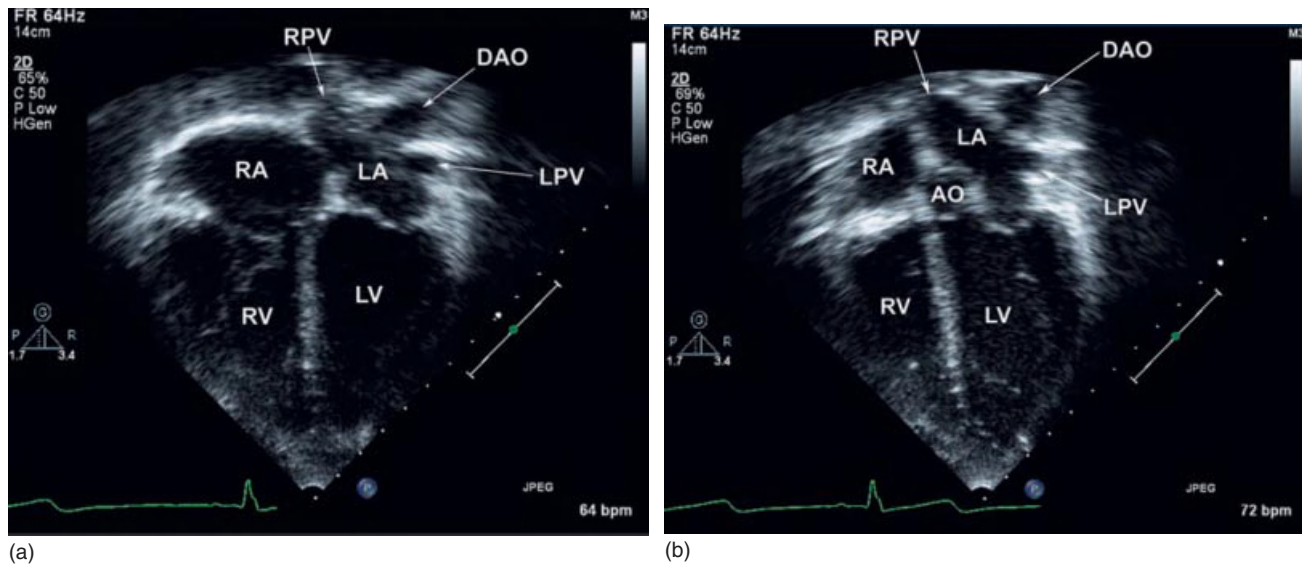
Figure 8.13 In these images from the apical view, the right and left lower pulmonary veins (RPV, LPV) can be seen entering the left atrium and straddling the descending aorta (DAO) from a 4-chamber (a) and 5-chamber view (b). Ao, aorta; LA, left atrium; LV, left ventricle; RA, right atrium; RV, right ventricle.
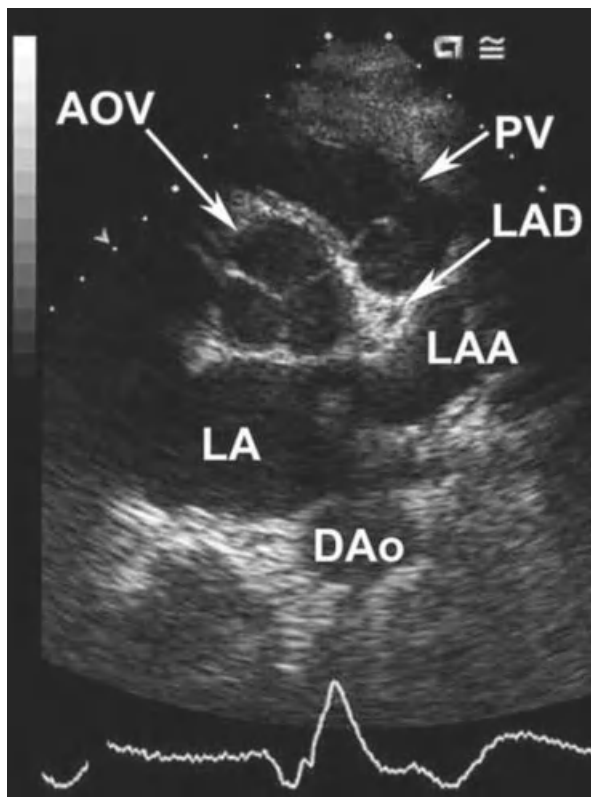
Figure 8.14 This parasternal short axis view at the level of the left ventricular outflow tract demonstrates the characteristic morphology of the left atrial appendage (LAA). The "finger-like" left atrial appendage joins the body of the left atrium (LA) with a narrow connection. Other structures identified in this plane are the aortic valve (AOV), pulmonary valve (PV), left anterior descending coronary artery (LAD) and descending aorta (DAo).

to which it is oriented almost perpendicularly (Figures 8.21c, 8.22b, and 8.23a).

Coronary arteries

Depending on the cardiac anatomy, techniques must be modified to define the coronary arteries. Because the acoustic plane remains stable while the heart shifts in position through the cardiac cycle, the coronary arteries move in and out of the image plane, and segments that are displayed during the various parts of the cycle will differ. The coronary origins and proximal arteries are most reliably identified from the parasternal short axis and with anterior angulation from the apical four-chamber view (Figure 8.23a and b). The bifurcation of the left main coronary artery into the left anterior descending and circumflex arteries can also be appreciated from these views (Figure 8.23a and b). The right coronary and circumflex arteries run in the atrioventricular grooves, and can be seen in longitudinal section (Figures 8.23a and 8.24a). A variety of planes and windows are necessary to display all the peripheral coronary branches.

Great arteries

It is important to determine size, morphologic anomalies or variations, and the ventriculoarterial connections of the great arteries. The aorta, arch vessels, and main and branch pulmonary arteries are effectively assessed from most echocardiographic windows. Characteristic features that help distinguish the aorta from the pulmonary trunk include the origins of the coronary arteries, the arch and its branches, and the bifurcation of the pulmonary trunk into two separate branch pulmonary arteries.

(a)　　　　　　　　　　　　(b)　　　　　　　　　　　　(c)
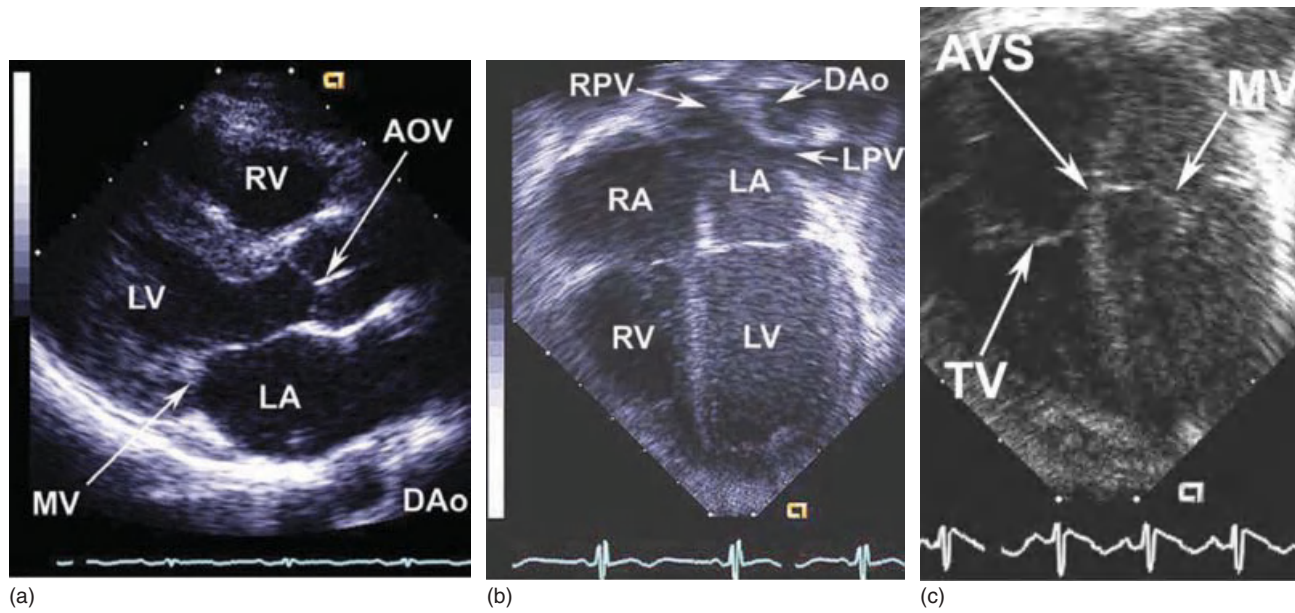
Figure 8.15 (a) This parasternal long axis view demonstrates the mitral valve between the left atrium (LA) and left ventricle (LV) during late diastole. The aortic valve (AOV) and descending aorta (DAo) are seen anterior and posterior to the left atrium (LA). The right ventricle (RV) is demonstrated anterior to the left ventricle. (b) In this image from the apical four-chamber view, both atria and ventricles (RA, RV, LA, LV) are clearly demonstrated while a right and left pulmonary vein (RPV, LPV) are visualized entering the left atrium (LA). Again the descending aorta (DAo) is noted posterior to the left atrium. (c) Another apical four-chamber view clearly delineates the normal separation between the tricuspid (TV) and mitral valves (MV) by the atrioventricular septum (AVS).

(a)　　　　　　　　　　　　　　　　　　(b)
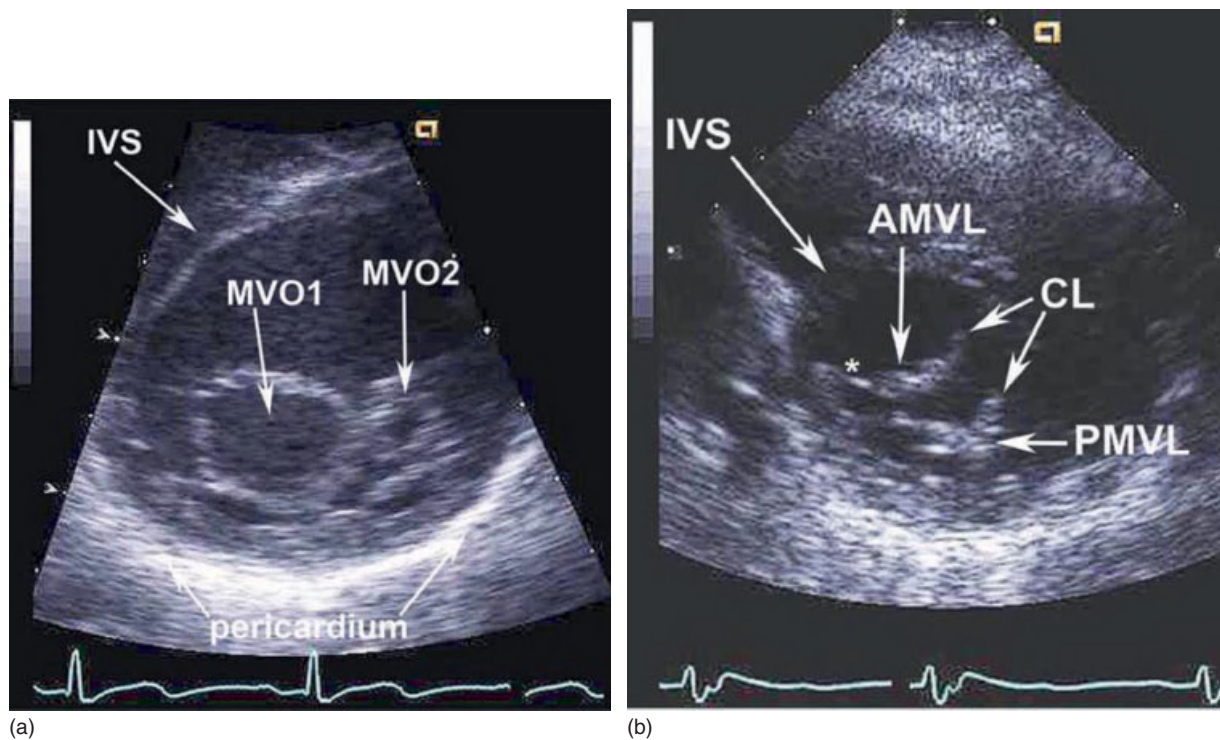
Figure 8.16 (a) This parasternal short axis view shows a double-orifice mitral valve, with two different sized openings (MVO1 and MVO2). The interventricular septum (IVS) is located anterior to the mitral valve. (b) This image of a parasternal short axis images shows a lateral cleft (CL) in the anterior leaflet of the mitral valve (AMVL). The valve is shown open during diastole and attachments to the interventricular septum (IVS) help support the mitral valve apparatus (*). The posterior mitral leaflet (PMVL) is also shown.

The left ventricular origin of the ascending aorta and its proximal course can be demonstrated (Figure 8.25), as can the full course of the arch (Figure 8.25c). The arch is always on the side opposite the innominate artery, and can be seen to course posterior and lateral to the trachea. Arch laterality can be confirmed with progressive lateral angulation from the suprasternal sagittal view, which allows the transverse arch to be followed to either the left or the right of the trachea and esophagus. The innominate, carotid, and subclavian arteries can also be identified, and their recognition is essential for confirmation of arch identity (Figure 8.25b).

The main pulmonary artery can be imaged at its origin from the right ventricle, as can the branching of the pulmonary trunk into left and right pulmonary arteries. (Figure 8.26). The branch pulmonary arteries can be followed peripherally beyond the level of the upper lobe artery origin in many patients.

Pericardium and adnexae

The pericardium is present in most views. Pericardial effusion or thickening is best appreciated from multiple windows (Figure 8.27). The parasternal short axis view is the standard view for M-mode imaging of the pericardium. The diaphragm may also be evaluated. Abdominal and mediastinal organs may be abnormal in certain forms of congenital heart disease, such as those occurring with DiGeorge syndrome and atrial isomerism, respectively, and can be evaluated during the echocardiographic examination. It is also important to be aware of the anatomic relationships between these structures and the heart and great vessels. The thymus is visible in young children in whom the thymus is typically large (Figure 8.26). The liver, stomach, and spleen can be evaluated and are important to visualize with forms of heart disease consistent with visceroatrial heterotaxy.

Figure 8.17 With cranial angulation and orientation of the transducer to concentrate on right ventricular structure, the septomarginal trabeculation (SMT) can be seen lying within the right ventricular cavity separated from the ventricular septum, a common finding with right ventricular enlargement. LV, left ventricle; RV, right ventricle.
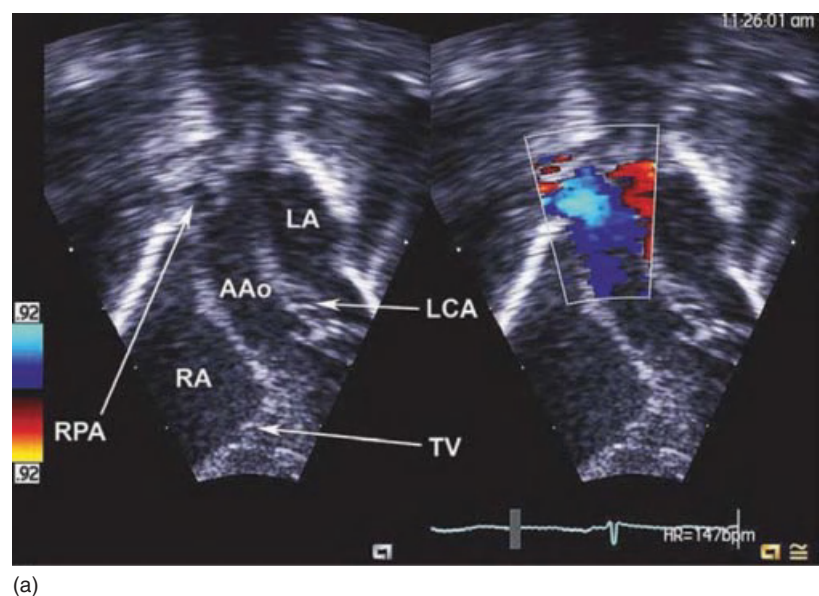
Figure 8.18 (a) In this subcostal coronal view in a patient with anomalous origin of the right pulmonary artery (RPA) from the ascending aorta (AAo), the aortic root dimensions are seen clearly. The tricuspid valve (TV), left coronary artery (LCA), and right (RA) and left (LA) atria can also be identified.

(a)

(*continued*)

(b)
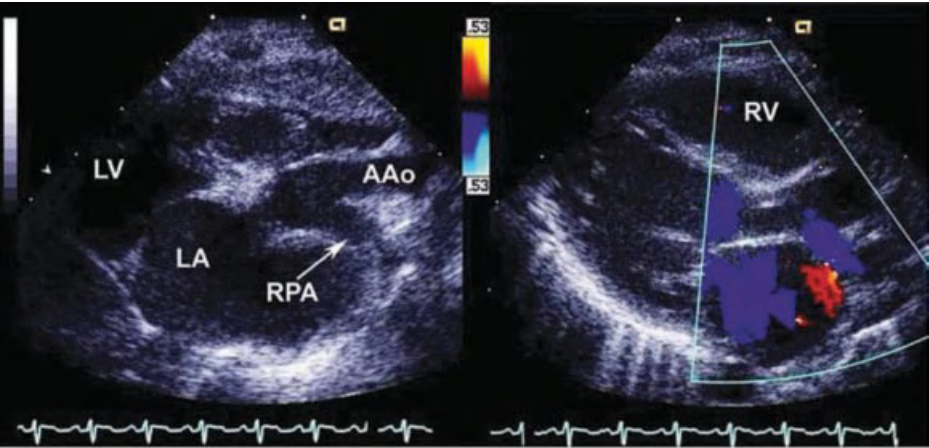
Figure 8.18 (cont'd) (b) The parasternal long axis also demonstrates the right pulmonary artery off the ascending aorta. RV, right ventricle.

(a)

(b)
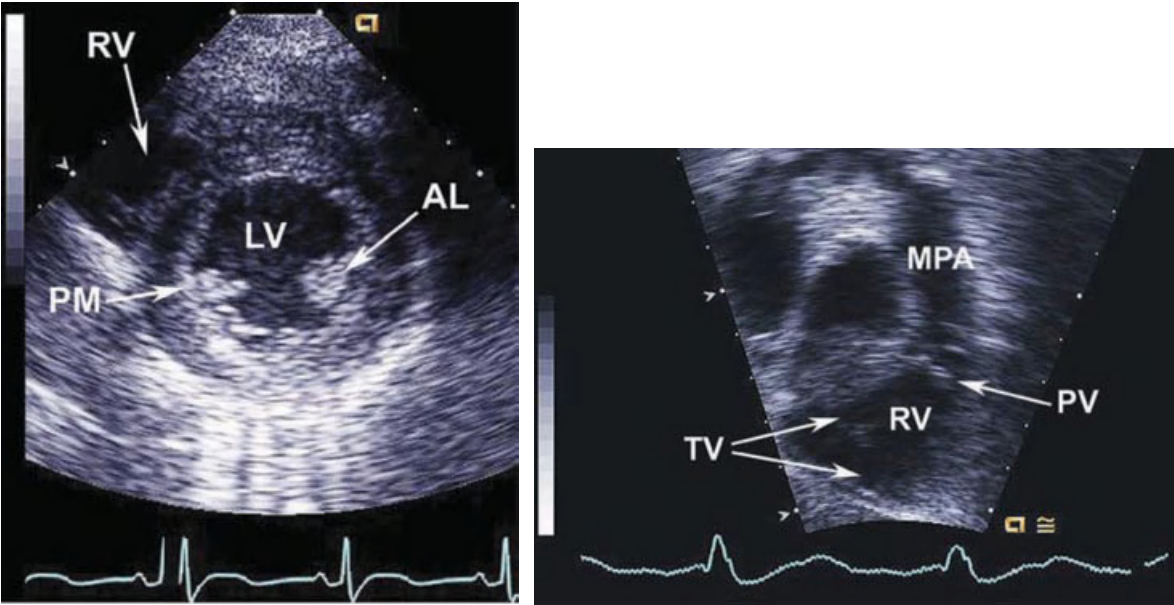
Figure 8.19 (a) From the parasternal short axis (PSAX) window, the most inferior cut is taken through the papillary muscle level and demonstrates the circular left ventricle (LV). AL, anterolateral; PM, posteromedial; RV, right ventricle. Because the transducer is oriented slightly to the left, minor rotation of the short axis occurs with the anterolateral and posteromedial papillary muscles being approximately in the 4 and 7 o'clock positions. (b) In this subcostal oblique view, the tricuspid valve (TV), right ventricle (RV), and outflow tract and main pulmonary artery (MPA) can be seen in a single plane.

ALGORITHM

I
Simpson's
rule
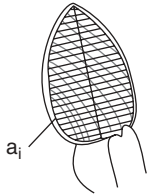
MODEL
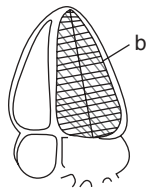
FORMULA

$$V = \frac{\pi}{4} \sum_{i=1}^{20} \alpha \; b_i - \frac{L}{20}$$

Figure 8.20 Schematic demonstration of various methods employing different geometric models to calculate chamber volumes from two-dimensional echocardiography. (I) The biplane Simpson's rule based on orthogonal views in an apical two- and four-chamber view. The volume is calculated as the sum of volumes of ellipsoidal cylinders with the major and minor axis *a* and *b* and the height *L/n*, where *L* is the common long axis and in the number of segments chosen. In the example shown $n = 20$.
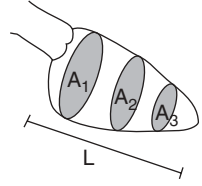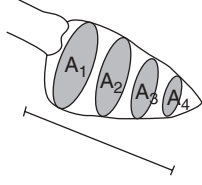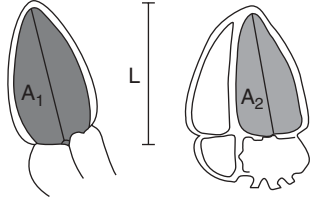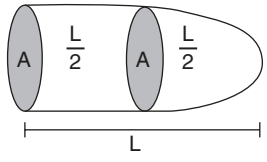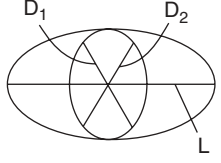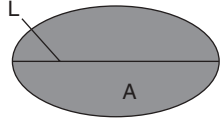
ALGORITHM   MODEL   FORMULA

II
Simpson's
rule

$$V = \left(\frac{A_1 + A_2}{2}\right)\frac{L}{3} + \left(\frac{A_2 + A_3}{2}\right)\frac{L}{3}$$
$$+ \frac{1}{3}\ A_3 - \frac{L}{3}$$

III
Simpson's
rule

$$V = \frac{L}{4}\left(A_1 + \frac{A_2 + A_3}{2} + \frac{A_3 + A_4}{2}\right.$$
$$\left. + \frac{1}{3}\ A_4\right)$$

IV
Biplane
area
length

$$V = \frac{8A_1 - A_2}{3\ \pi\ L}$$
$$= \frac{0.85 - A_1 A_2}{L}$$

V
Hemisphere
cylinder

$$V = A - \frac{L}{2} + \frac{2}{3}\ A - \frac{L}{2}$$
$$= \frac{5}{6}\ AL$$
$$= 0.83\ AL$$

VI
Biplane
area
length

$$V = \frac{\pi}{6}\ D_1 D_2 - L$$

VII
Single plane
area length

$$V = \frac{8(A)^2}{3\ \pi\ L}$$
$$= 0.85\ \frac{(A)^2}{L}$$

Figure 8.20 (cont'd) (II, III) The principle of Simpson's rule can be applied to a different method that calculates the chamber volume from three (II) or four (III) area measurements obtained in parasternal short axis; the height of the segments is taken from equivalents of the long axis measured from the apical window. The assumption, however, that all slices in the parasternal short axis are equidistant from each other and are perpendicular to the long axis is almost impossible to satisfy in practice. (IV) Using a biplane area–length method the areas A_1 and A_2 are traced in apical two- and four-chamber views; the long axis L is taken from either plane. The equation used in this calculation is that for an ellipse, which may be reasonable for the left ventricle, but not for the right ventricle. (V) The hemisphere–cylinder (or bullet) model uses a cross-sectional area of the left ventricle in a parasternal short axis at the level of the tips of the papillary muscles and a length taken from an apical view. The equation considers the chamber volume as the sum of a hemisphere and a cylinder, which also is not valid for the right ventricle. (VI) Biplane ellipsoidal method using the length L taken from an apical plane and the diameters D_1 (antero-posterior) and D_2 (lateral) taken from a parasternal short axis at the level of the tips of the papillary muscles. This model can also be used only for left ventricular volume calculation. (VII) The single area–length method is similar to the biplane area–length method (IV), but assumes both orthogonal areas to be equal; either the apical two- or four-chamber view may be used with this method. (Reproduced with permission from Silverman NH, Snider AR. *Two-Dimensional Echocardiography in Congenital Heart Disease*. Norwalk, CT: Appleton-Century-Crofts, 1982.)
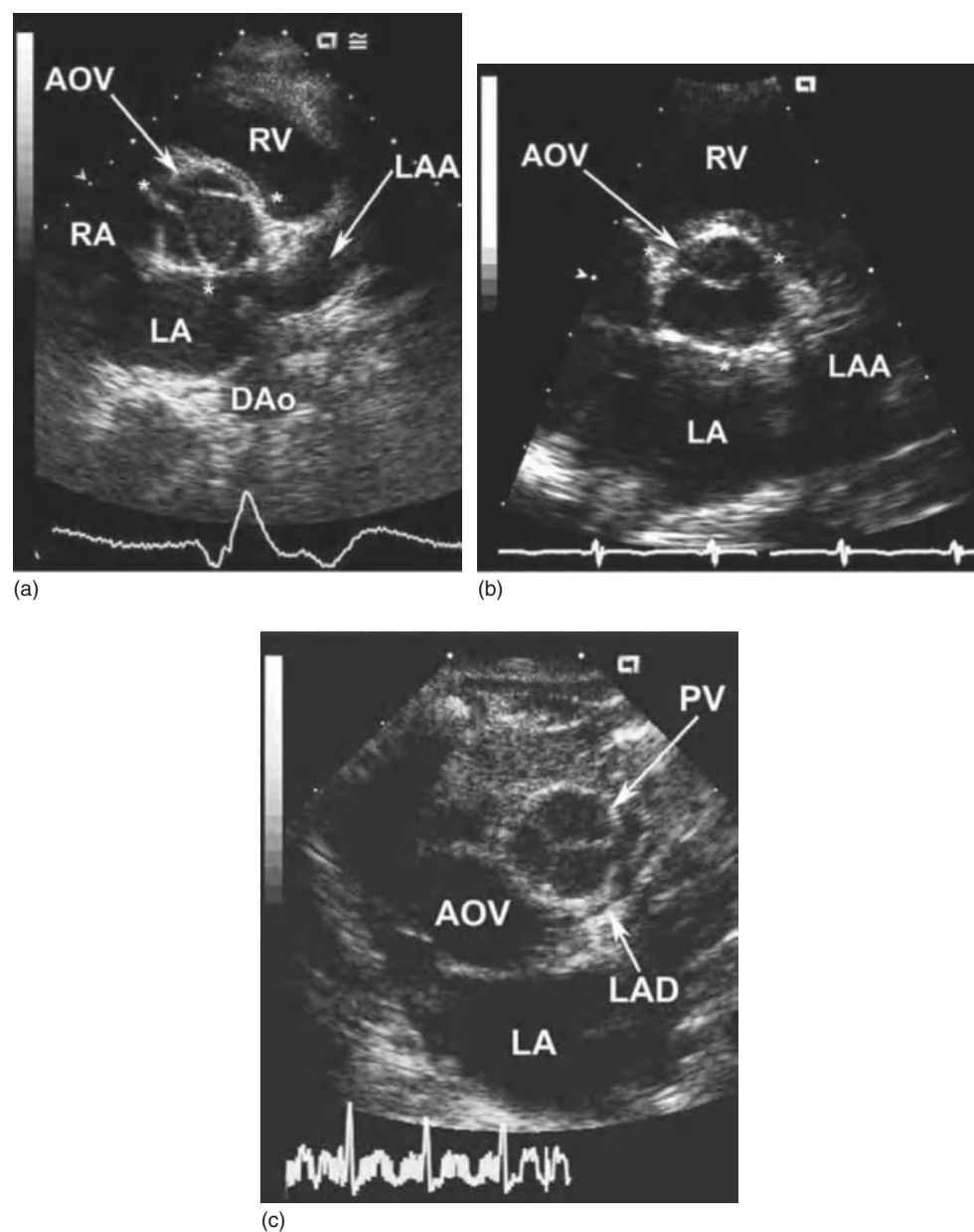
Figure 8.21 (a) These frames demonstrate the aortic valve cusps (AOV) in systole within the aortic root from the parasternal short axis view. In the top frame these are identified by asterisks (*) adjacent to the junction of the commissures. The right atrium (RA), right ventricle (RV), left atrium (LA), and left atrial appendage (LAA) are also visualized with the descending aorta (DAo). (b) This parasternal short axis shows the aortic valve in diastole with the cusps in a closed position. (c) Moving the transducer further superior from the previous view can demonstrate the pulmonary valve (PV) with three cusps in the short axis during diastole. Additionally, the left anterior descending coronary artery (LAD) is also seen. The left atrium is still visualized posteriorly (LA).

Physiologic evaluation

Spectral and color flow Doppler techniques have the most to offer in terms of characterizing blood flow patterns, and two-dimensional and M-mode show myocardial and valvar motion in addition to the anatomic substrates of flow abnormalities. Contrast echocardiography is valuable for evaluating intracardiac or intrapulmonary shunts, and also anomalies of systemic venous return and certain forms of vascular obstruction that may otherwise be difficult to image.

Ventricular physiology

Systolic ventricular function

Ventricular contraction and ejection are collectively referred to as systolic function. The shortening fraction (SF) and ejection fraction (EF) are the most often used methods of assessing function because of their simplicity. The shortening fraction is the ratio of decrease in ventricular short axis dimension relative to the diastolic
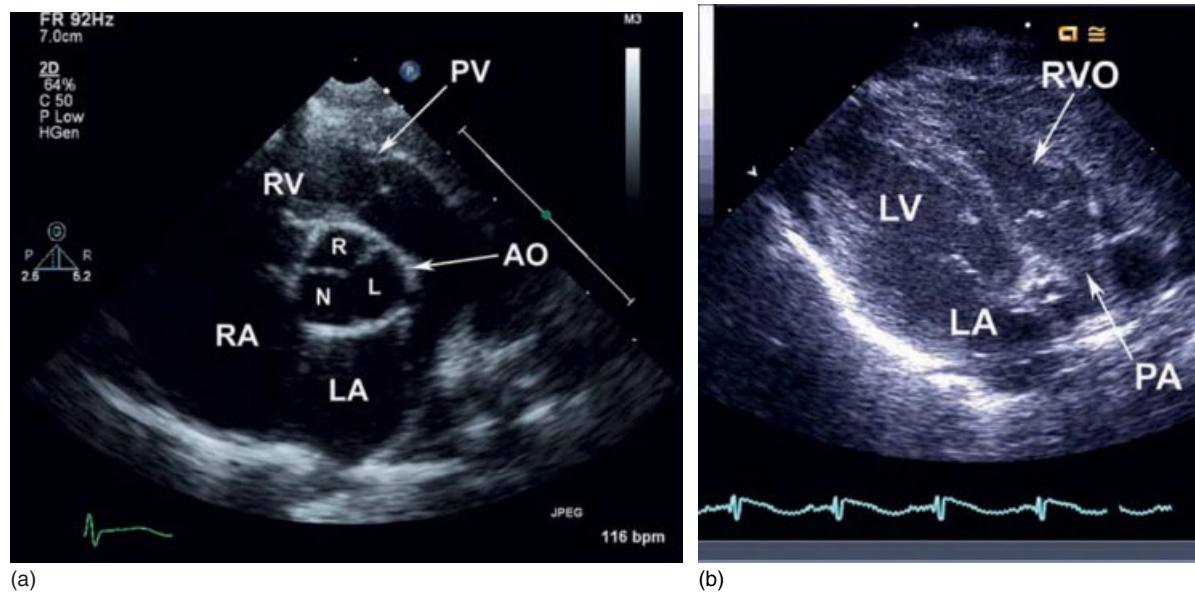
Figure 8.22 (a) In this parasternal short axis view at the level of the semilunar valve roots, the aortic root (AO) can be seen in the center of the plane. Within the aortic root, the characteristic V at the junction between the non-coronary (N) and right coronary (R) leaflets and right and left (L) coronary leaflets is shown by dense bright lines, and a faint echo is seen where the non-coronary and left coronary leaflets abut. (b) Extreme leftward angulation from the parasternal long axis shows the pulmonary valve (PV) separating the right ventricular outflow tract (RVO) from the pulmonary artery (PA). The left atrium (LA), mitral valve, and left ventricle (LV) are also shown. RA, right atrium; RV, right ventricle.
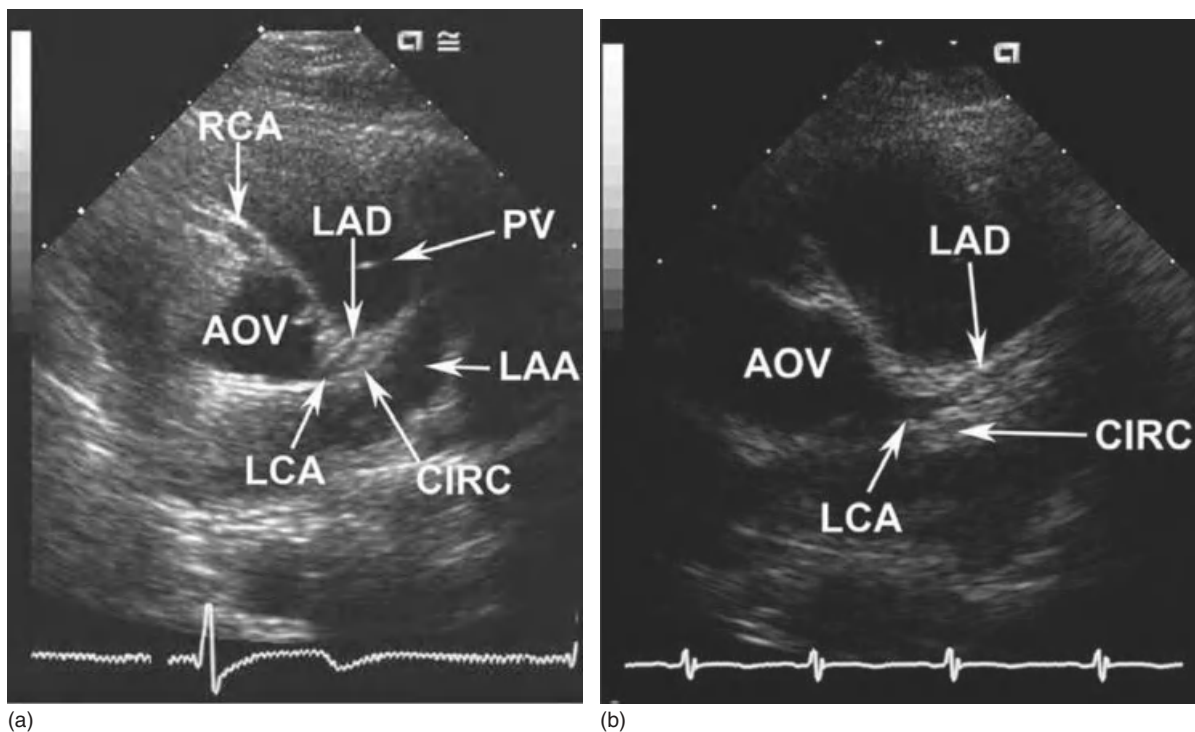
Figure 8.23 (a) Parasternal short axis view at the level of the coronary ostia shows the right (RCA) and left (LCA) coronary arteries arising from the aortic root (AOV). The bifurcation of the left coronary artery into the left anterior descending (LAD) and circumflex coronary arteries (CIRC) is also noted. The left atrial appendage is also visualized from this view (LAA). The pulmonary valve can be seen in its long axis (PV) from this view. (b) This parasternal short axis view shows the left main coronary artery (LCA) dividing into the left anterior descending branch (LAD), which then courses behind the pulmonary artery, and the circumflex (CIRC).
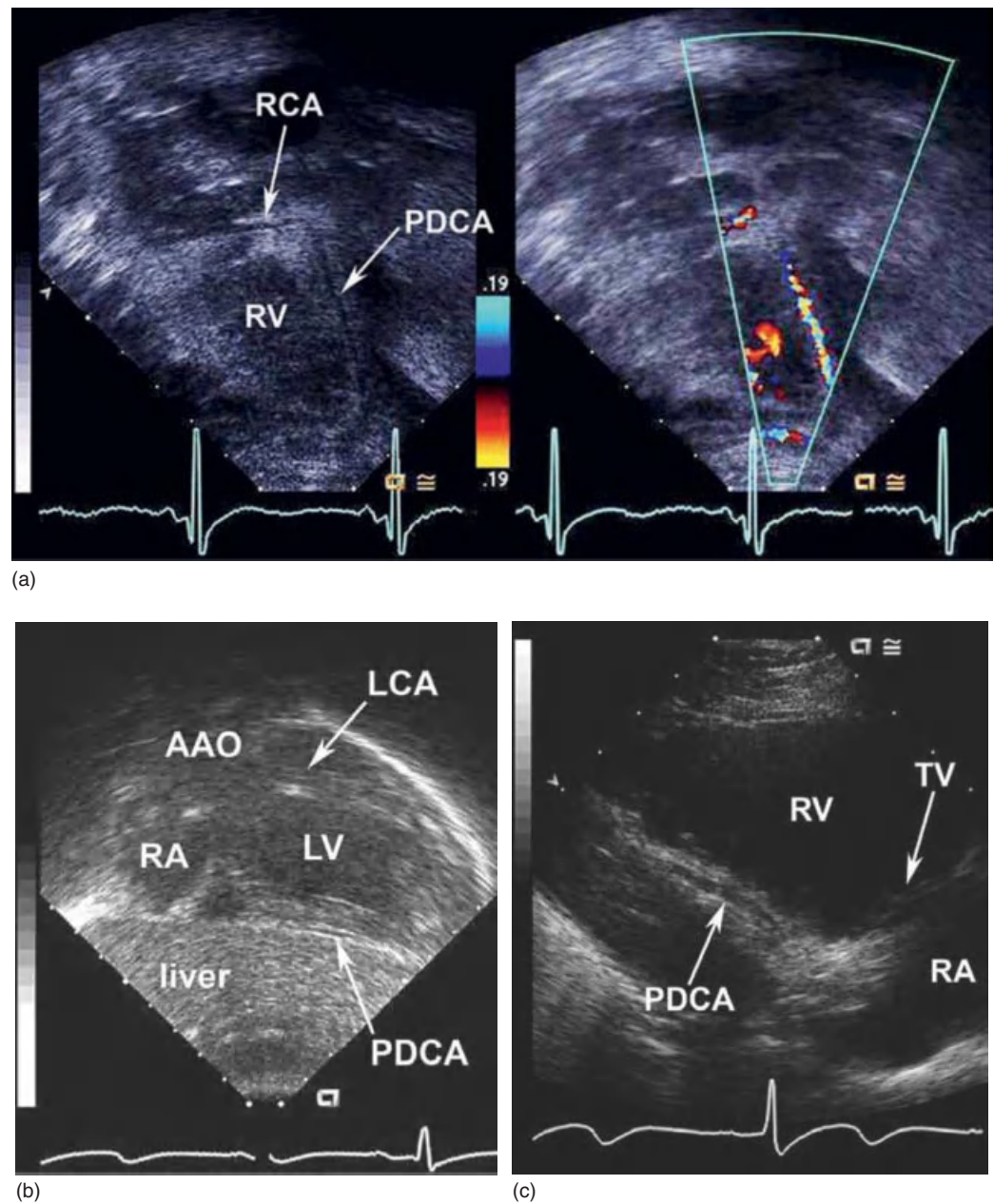
Figure 8.24 (a) This subcostal sagittal figure concentrates on the right coronary artery (RCA) lying posteriorly to the right ventricle in the right coronary groove and its extension into the posterior descending coronary artery (PDCA). (b) In this subcostal coronal cut, the posterior descending coronary artery (PDCA) can be identified. Other structures imaged in this view include the right atrium (RA), left ventricle (LV), ascending aorta (AAo), and left coronary artery (LCA). (c) The posterior descending coronary artery is also seen from the parasternal long axis tricuspid valve (TV) inflow view. The right atrium and ventricle are also displayed (RA, RV).

dimension. The ventricular end-diastolic (*EDD*) and end-systolic (*ESD*) short axis dimensions are measured in M-mode and the ratio of shortening to end-diastolic dimension is obtained:

$$SF = 100\frac{EDD - ESD}{EDD}$$

Ejection fraction is the change in ventricular volume from end-diastole to end-systole using M-mode or cross-sectional two-dimensional images. In M-mode measurements, a shape is assumed for the ventricle and a volume calculated based upon the measurements obtained for the shortening fraction. End-diastolic volume (*EDV*) and end-systolic volume (*ESV*) are measured from one or two planes, either by manual

(a)

(b)

(c)

(d)
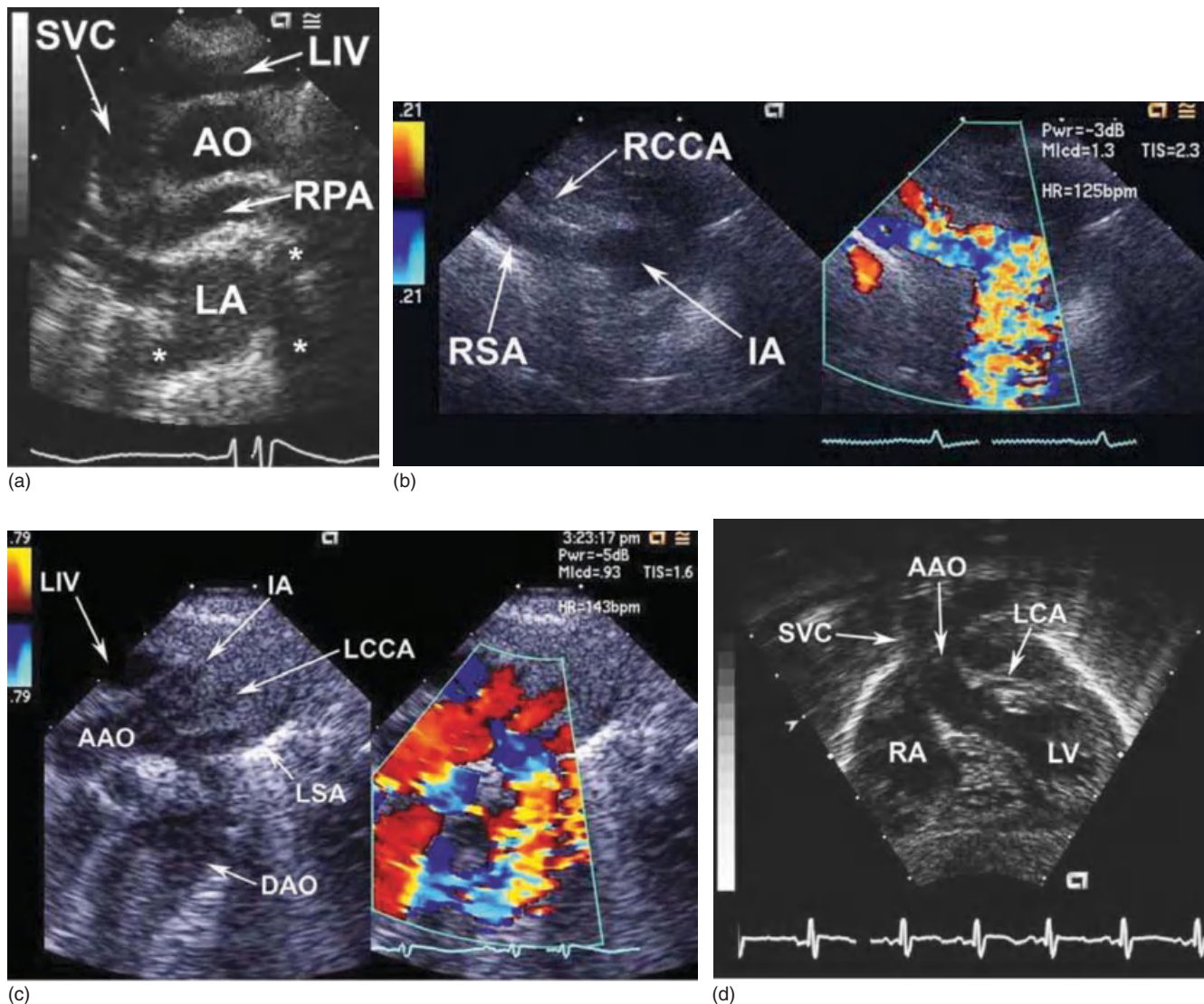
Figure 8.25 (a) Suprasternal coronal notch view shows the left innominate vein (LIV) draining in the superior vena cava (SVC). The ascending aorta (AO) is seen in the short axis while the right pulmonary artery (RPA) is in its long axis. Three pulmonary veins (*) drain appropriately into the left atrium (LA). (b) Angling the transducer more posterior provides a view of the first brachiocephalic artery or innominate artery (IA) which bifurcates rightwards into the right common carotid artery (RCCA) and right subclavian artery (RSA), indicating a left aortic arch. (c) The relationship of the ascending aorta (AAo), aortic arch, and descending aorta (DAo) can be appreciated from this suprasternal notch view. The innominate artery (IA), left common carotid artery (LCCA), and left subclavian artery (LSA) can be identified superiorly. (d) In this subcostal coronal view, the body of the left ventricle (LV) can be seen to be continuous with the ascending aorta (AAo). The position of the left main coronary artery (LCA) is clearly delineated. The superior vena cava (SVC) enters the right atrium (RA).

tracing or automated border detection, and the ejection fraction (*EF*) is obtained by dividing the volume difference (stroke volume) by end-diastolic volume and converting to a percentage:

$$EF = 100\frac{EDV - ESV}{EDV}$$

Automated border detection with integrated ultrasonic back-scatter may simplify and standardize this process for both left and right ventricular function. These indices are useful for simple estimation, but are less reliable than other methods because they depend on heart rate, ventricular preload, and assumptions of ventricular geometry. M-mode measurements of ventricular size and function can vary, due to variability both in the position of the left ventricle from which the measurements are made, and in positioning the measurement cursors. There is uncertainty about the exact position of the ventricular endocardial surface (as opposed to papillary muscles) and the timing of end-systole and end-diastole (relative to the R wave versus when the ventricle

131
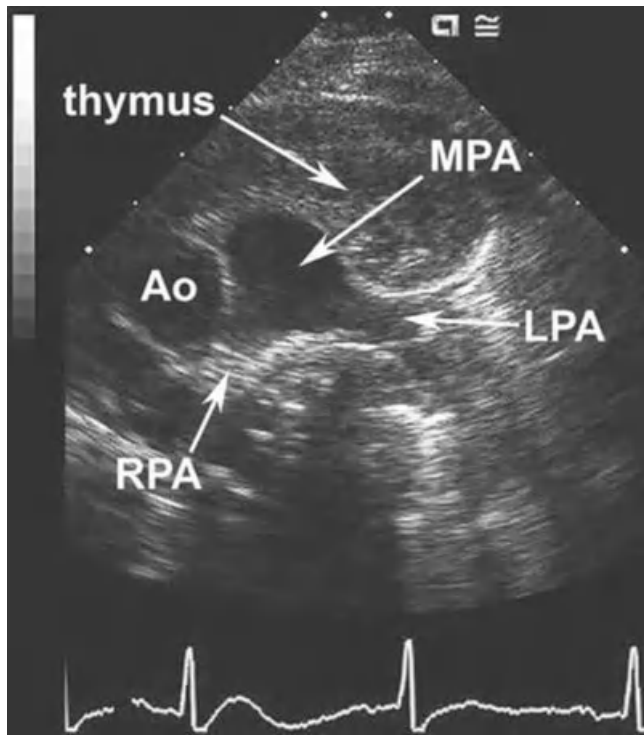
Figure 8.26 This parasternal short axis view shows the main pulmonary artery (MPA) branching into the left (LPA) and right (RPA) pulmonary arteries. The ascending aorta (Ao) is also seen. The highly echogenic mass anterior and lateral to the pulmonary artery is the thymus.

reaches its maximum or minimum). Therefore, M-mode measurements should not be viewed as absolutes. Normal standards for children can be obtained from the literature [5,6]. Although M-mode appears to be the standard, new recommendations from the American Society of Echocardiography advise making all measurements using two-dimensional echocardiography and not M-mode [7]. Standard measurements are also available using the website http://parameterz.blogspot.com/

Dividing the shortening fraction by the heart rate-adjusted ejection time

$$ET_C = \frac{\text{ejection time}}{\sqrt{\text{electrocardiogram R} - \text{R interval}}}$$

yields a rate-corrected mean velocity of circumferential fiber shortening, VCF_C. This is related to end-systolic wall stress, which is calculated as

$$ESWS = \frac{1.35D_{ES}P_{ES}}{4h\left(1 + \dfrac{h}{D_{ES}}\right)}$$

where D_{ES}=end-systolic dimension, P_{ES}=end-systolic pressure, and h=end-systolic posterior wall thickness. $ESWS$ and VCF_C are inversely related in a linear fashion in most

physiologic ranges [8,9]. In addition, they depend less upon preload and afterload than do other indices, but require rather cumbersome data acquisition.

Doppler techniques for evaluating systolic ventricular function are independent of ventricular geometry. Measurements from Doppler-derived aortic velocity curves include peak velocity, acceleration time, ejection time, isovolumic contraction time, and the velocity-time integral. Indices derived from these measures include peak and mean acceleration (Figure 8.28), which correlate with systolic performance [10,11]. The ratios of acceleration time to ejection time and of isovolumic contraction time to acceleration time are also used as indices of ventricular function. Two other Doppler-based techniques for assessing ventricular function employ the continuity equation (flow=arterial cross-sectional area × mean velocity) to determine flow through the ascending aorta and by extension stroke volume and cardiac output. The area of the vessel is calculated from the diameter, and mean systolic velocity is calculated by integrating the area under the velocity–time curve measured with spectral Doppler (velocity–time integral, VTI). The product of area and VTI is flow for one cardiac cycle, or stroke volume. This can be multiplied by the heart rate to yield cardiac output, and divided by estimated body surface area to give the cardiac index, providing an estimate of cardiac performance.

Assessment of ventricular performance by tissue velocity and deformation imaging

Most conventional methods to assess cardiac function provide a global assessment of pump function using blood pool indices such as the ejection fraction. These measures do not directly assess myocardial performance and often depend on incorrect geometric assumptions. Many of these indices are greatly influenced by preload (ventricular filling) and afterload (the resistance the ventricle must overcome to eject blood), limiting their ability to reflect intrinsic myocardial contractility.

Tissue velocities

In contrast to the low-amplitude, high-velocity blood flow captured by conventional Doppler, myocardial motion generates low-velocity, high-amplitude signals captured by tissue Doppler imaging (TDI) using appropriate low wall filters and Nyquist limits of 15–30 cm s⁻¹. Myocardial motion and velocities reflect, at least in part, myocardial contraction, thereby providing a more direct assessment of contractility. However, a segment may move because the whole heart is moving (translational motion) or because it is being passively dragged by an adjacent contracting segment (tethering), even if it itself is not actively contracting. Nonetheless, in children where segmental infarction is uncommon, TDI is useful and easily obtained
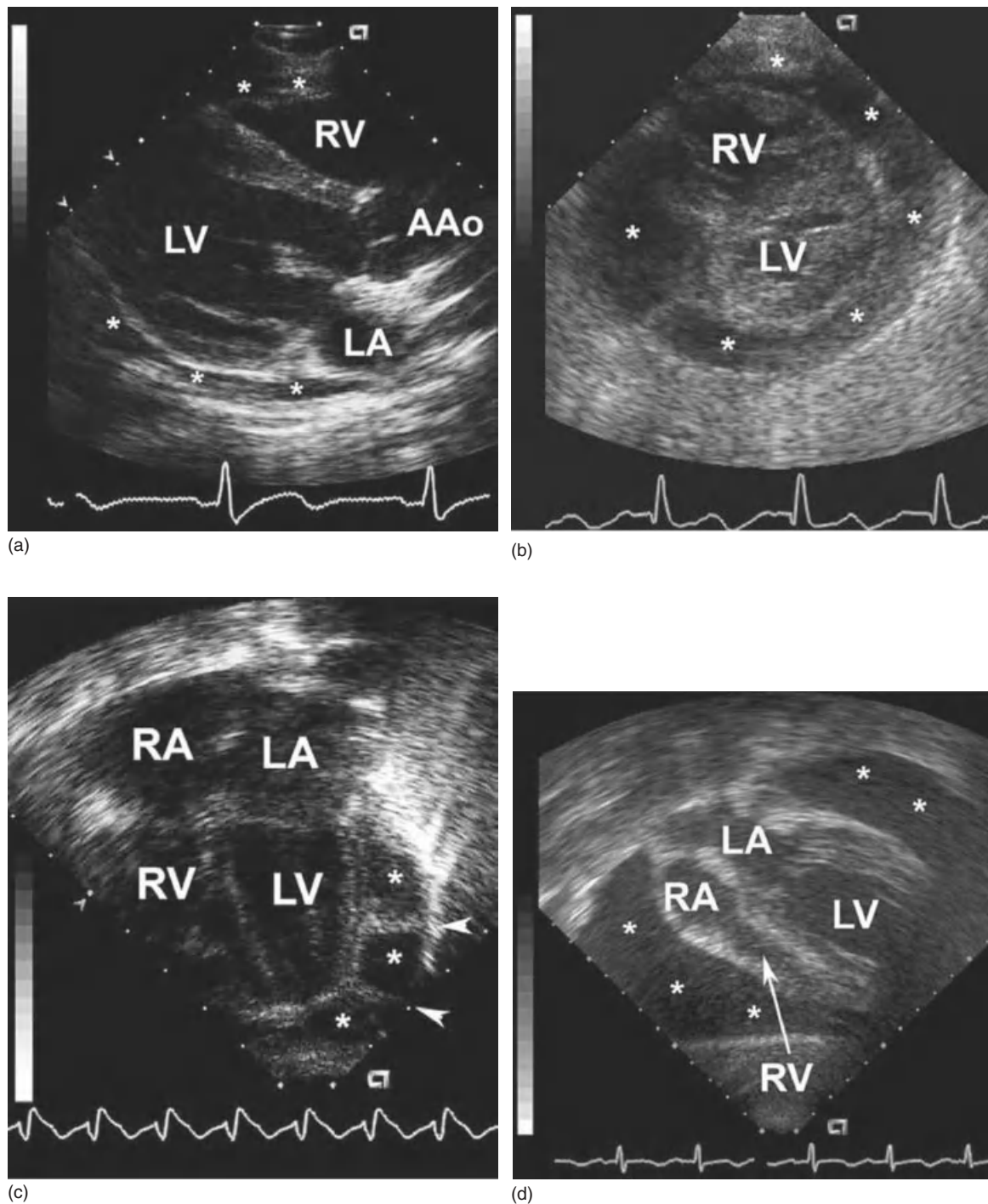
Figure 8.27 Pericardial effusion (*) can be appreciated from many views, including (a) the parasternal long axis, (b) the parasternal short axis, (c) apical four chamber, and (d) subcostal views. The arrowheads represent fibrinous material within the pericardial effusion. AAo, ascending aorta; LA, left atrium; LV, left ventricle; RA, right atrium; RV, right ventricle.

with high temporal resolution and good intra- and inter-observer reliability [12].

Peak myocardial velocities can be acquired using pulsed wave TDI, using sample sizes between 3 and 8 mm (Figure 8.29). Alternatively, color Doppler myocardial images

may be acquired and stored for on-line/off-line analysis of regional myocardial mean velocities. This allows the simultaneous quantification of myocardial velocities from multiple cardiac segments during the same cardiac cycle. Mean velocities are ~15–20% lower than peak velocities.
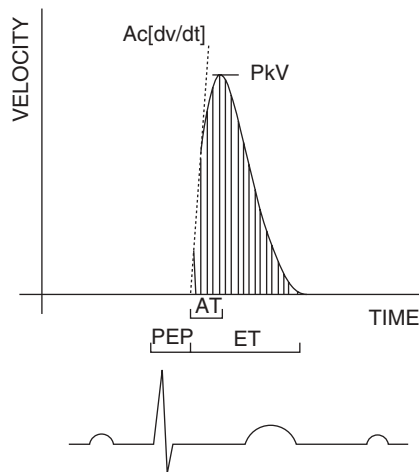
Figure 8.28 Graphic representation of an aortic velocity curve from which the peak velocity (PkV), the acceleration time (AT), the ejection time (ET), and the velocity time integral (shaded area) can be measured. Indices of systolic left ventricular function that can be derived from these measurements include the peak rate of acceleration [Ac (dv/dt)], the mean acceleration (mAc = PkV/AT), and the ratio AT/ET. With the use of the electrocardiogram, the pre-ejection period (PEP) can also be measured and the PEP/ET ratio can be calculated as another index of systolic left ventricular function. (Reproduced with permission from Silverman NH, Schmidt KG. *Cardiol Clin* 1989;**7**:265–97.)
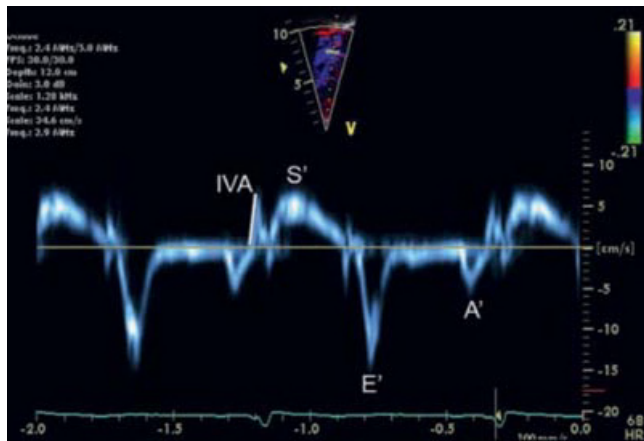
Figure 8.29 Pulsed TDI post wall. Pulsed tissue Doppler from the left ventricle showing a typical systolic (S'), early diastolic (E') and late diastolic (A') velocity. Also depicted (white bar) is the slope of the isovolumic acceleration (IVA), a relatively load-independent index of myocardial performance.

From tissue Doppler tracings, isovolumic acceleration (IVA) can be measured from the slope of the initial positive systolic wave that occurs during isovolumic contraction. IVA occurs just after onset of the ECG QRS complex and peaks before aortic valve opening.

Normal tissue Doppler velocity values have been published for children, including neonates and fetuses [13].

Deformation imaging: strain and strain rate

Deformation or strain is the percentage change in dimension of an object in response to stress (force per unit cross-sectional area). This is calculated as the instantaneous dimension minus the original dimension divided by the original dimension. For myocardium, the original dimension is the unstressed muscle dimension. However, *in vivo*, the absolute unstressed muscle length is difficult to measure and the end-diastolic length is often used. In the longitudinal and circumferential directions, strain measures myocardial lengthening or shortening, and in the radial direction thickening and thinning. Strain rate is the rate of deformation (strain over time). Deformation parameters allow a more direct assessment of myocardial contractility in that the change in muscle dimension and its rate of change are directly related to myocardial contractility and are not affected by tethering and translational motion. Although both strain and strain rate are affected by loading conditions, strain rate is less affected by loading as it peaks in early systole and has a short duration. The degree of posterior wall thickening obtained by M-mode echocardiography is an example of regional strain, albeit from a very limited scan line. Strain and strain rate from larger regions are currently obtained using one of two techniques, each with its advantages and disadvantages. Strain rate may be calculated from color tissue Doppler by calculating the instantaneous difference in myocardial velocities between two points. Strain is then derived from strain rate measurements. Advantages of color tissue Doppler include its wide availability, easy application, and high temporal resolution. Disadvantages include its low signal-to-noise ratio (especially for strain rate) and exquisite dependence on insonation angle. One such example is evaluating left ventricular basal lateral wall strain from the apical four-chamber view. The ultrasound beam is oriented laterally from the apex of the scan triangle. However, in dilated ventricles the basal curvature is exaggerated, rendering a poor insonation angle and unreliable strain values. To overcome these limitations, strain imaging from two-dimensional images has been implemented by speckle tracking and by vector velocity imaging [14] (Figure 8.30).

Although these techniques use different algorithms, both are based on computer software tracking unique ultrasound speckles caused by the tissue–sound wave interface through the cardiac cycle. This technique is independent of insonation angle but significant disadvantages include lower frame rates (lower temporal resolution) and relatively poor intra- and inter-observer reliability [15]. As compared with shortening indices, velocity and deformation indices are calculated without mathematical assumptions of ventricular geometry (although they are influenced by ventricular geometry). Therefore, tissue velocity and deformation imaging may be well suited for assessing RV function and congenital heart disease including single ventricles.
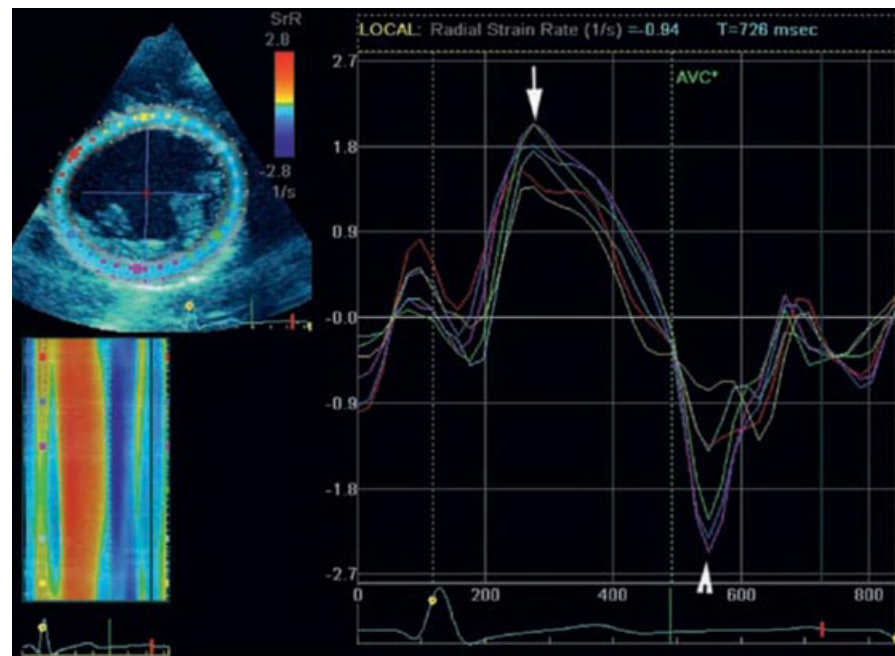
Figure 8.30 SAX strain rate normal. Left ventricular radial strain rate obtained by two-dimensional speckle tracking in a normal child. Peak systolic (arrow) and early diastolic (arrowhead) radial strain rate are depicted. At the bottom left, a color-coded M-mode display of the strain rate is depicted. The ventricle is displayed in a linear format with each color dot corresponding to the matching ventricular segment in the short axis image. Progression from left to right is through time, corresponding to the ECG display. As for Doppler flow imaging, the colors code the direction and magnitude of the strain rate. In this example, orange codes for positive radial strain rate in systole and blue codes for negative radial strain rate in diastole. Yellow and green code for lower strain rate intensities.

Furthermore, tissue velocities and deformation measure regional myocardial performance, whereas ejection and shortening fraction provide a global assessment. Regional assessment of function has been especially useful in ischemic heart disease and this is pertinent in certain congenital lesions such as anomalous left coronary artery from the pulmonary artery (ALCAPA), transposition of the great arteries after the arterial switch operation and tetralogy of Fallot (TOF). Although tissue velocities and deformation imaging measure regional function, they may correlate with measures of global function. For instance, regional RV and LV deformation or excursion correlate with stroke volume and are sometimes used to report "global" ventricular function. However, these measurements remain regional. Certain diseases are characterized by regional heterogeneity, hypertrophic cardiomyopathy being one example. Septal performance in this disease may not reflect the performance of other ventricular segments.

Velocity and deformation imaging may also be useful for detecting early ventricular dysfunction before patients develop symptoms and when shortening indices are still normal. Examples include early detection of heart graft rejection, early ventricular dysfunction in children with Duchenne muscular dystrophy, early dysfunction in aortic regurgitation, and early effects of pacing on regional myocardial performance [16–18].

In contracting, the left ventricle shortens and rotates along its long axis and thickens in the radial direction. The opposite rotation at the base and apex creates a twisting or torsional motion of the LV, akin to wringing a wet towel (Figures 8.31 and 8.32). Whereas conventional methods to assess ventricular function, such as M-mode assessment of ejection fraction, rely predominantly on the assessment of radial function, newer methods allow the quantification of myocardial motion and deformation in all vectors, providing a more comprehensive assessment of ventricular performance and the differential effects of disease. Quantifying longitudinal myocardial function may be especially important when assessing RV performance due to the predominantly longitudinal orientation of the RV myocytes.

Velocity and deformation measurements are relatively easily obtained at the bedside using standard echo systems in a relatively short period of time. There are now normal fetal [19] and pediatric [15,20] values available for reference.

Velocity and deformation imaging in CHD
Influence of volume and pressure loading on tissue velocities and deformation parameters in children.

Although the ideal index of ventricular contractility should be independent of loading conditions, volume and/or pressure loading that lead to ventricular remodeling are central to many cardiac abnormalities affecting children. Tissue velocities and
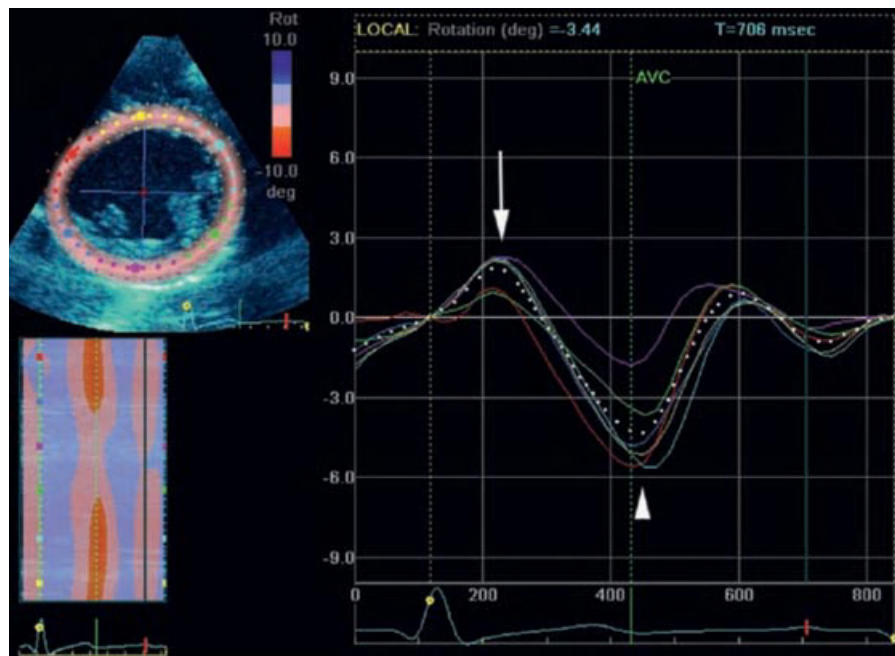
Figure 8.31 SAX rotation normal. Normal left ventricular basal rotation obtained by two-dimensional speckle tracking in a child. An initial counterclockwise rotation (arrow) is followed by a predominant clockwise rotation (arrowhead) as viewed from the ventricular apex. Together with predominant counterclockwise rotation at the apex, this rotational motion produces systolic torsion (or twist). As in Figure 8.30, a color-coded M-mode display is depicted at the bottom left. The ventricle is displayed in a linear format with each color dot corresponding to the matching ventricular segment in the short axis image. Progression from left to right is through time, corresponding to the ECG display. The colors code the direction and magnitude of the rotation. In this example, the initial counterclockwise rotation is coded in blue and the predominant clockwise rotation in red–pink (depicting the magnitude of rotation).
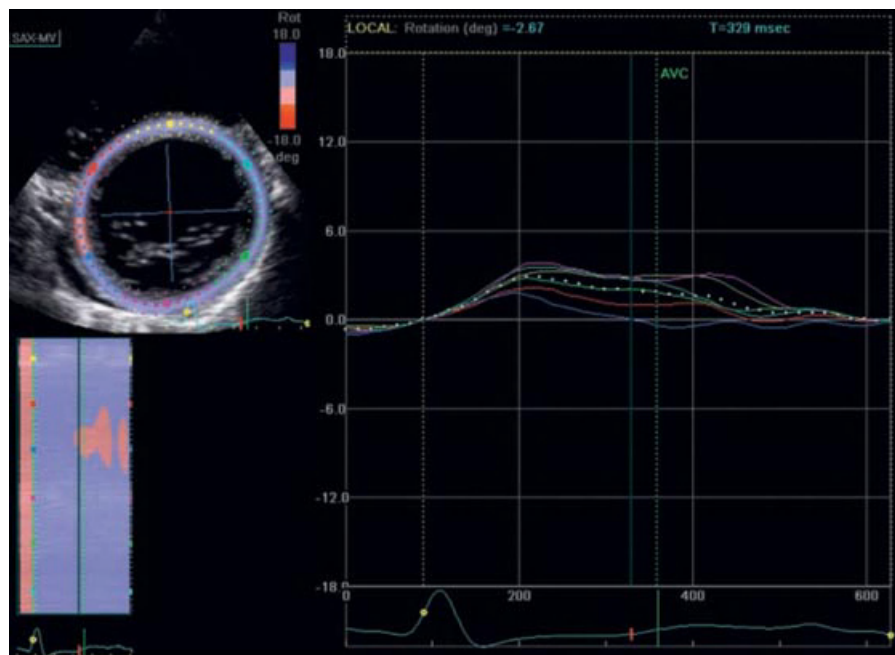
Figure 8.32 SAX basal rotation. Abnormal low and counterclockwise basal left ventricular rotation in a child with dilated cardiomyopathy. Contrast these curves with the normal rotation shown in Figure 8.31. At the bottom left the color-coded M-mode display is shown as in Figure 8.31.
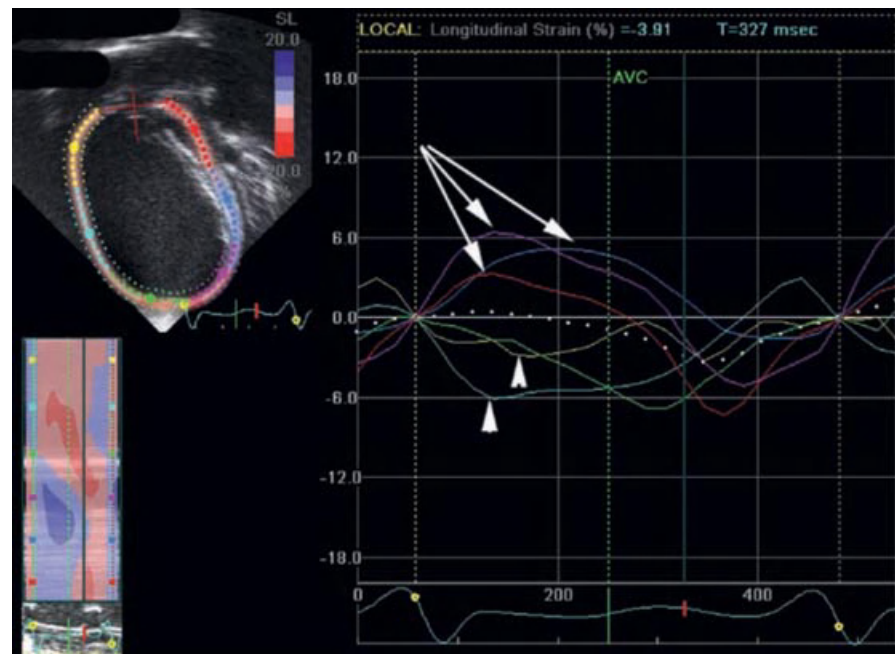
Figure 8.33 ALCAPA strain 1. Highly abnormal and dyssynchronous left ventricular longitudinal contraction in a child with severe left ventricular dysfunction secondary to anomalous left coronary artery from the pulmonary artery. Left ventricular dysfunction persists despite surgical repair. Longitudinal strain curves obtained by two-dimensional speckle tracking show early stretching of the lateral wall segments (positive strain, arrows). This occurs during early, albeit low, septal deformation (arrowheads) and increases wall stress in the delayed segments.

deformation are influenced by loading conditions, although isovolumic acceleration (IVA) and peak systolic strain rate are less dependent on loading as they occur during isovolumic contraction or early systole [21]. When interpreting loading effects, it is important to consider that acute changes affect myocardial indices differently from chronic changes, largely due to adaptive mechanisms such as hypertrophy.

When left ventricular volume loading is chronic, such as in moderate to large VSDs and patent arterial ducts, preload does not significantly influence either systolic or diastolic tissue velocities, likely due to LV myocardial adaptation [22]. This differs from mitral inflow indices, which are clearly affected by changes in volume load and atrial pressures. In contrast to chronic volume loading, increased LV afterload, such as in moderate to severe aortic stenosis, leads to reduced systolic and diastolic tissue velocities. This reduced longitudinal performance may also stem from secondary hypertrophy. Indeed, children with hypertrophic cardiomyopathy have regional reduction in deformation despite normal afterload [23].

Acute changes in loading conditions, either in the experimental setting or after ASD closure, affect peak systolic tissue velocities, but IVA remains unchanged [24]. Likewise, RV strain and strain rate are less affected by acute loading than are tissue velocities. This has been useful to demonstrate that patients who underwent device closure of an ASD had better left and right ventricular longitudinal deformation

than patients who underwent surgical closure, presumably related to the negative effects of cardiopulmonary bypass on myocardial function.

Tissue Doppler imaging has been useful for noninvasive assessment of left ventricular diastolic dysfunction and left ventricular filling pressures. In early diastolic dysfunction, impaired ventricular relaxation is characterized by a low mitral E wave (early diastolic filling), increased dependence on atrial contraction for ventricular filling and therefore reversal of the E/A ratio. With progression of diastolic dysfunction and increasing filling pressures, the E wave heightens, leading to so-called "pseudo-normalization" of the E/A ratio. However, tissue Doppler early diastolic velocities are less affected by the increased pressures and remain low. Therefore, the E/E′ ratio reflects filling pressures [25] and, in conjunction with left atrial volume, pulmonary vein Doppler, and other diastolic parameters, provides useful semiquantitative information. Although not validated in children to the same extent as in adults, in various settings the E/E′ ratio has been shown to be related to LAP [26]. However, this index likely is only useful when ventricular relaxation is impaired [25].

Velocity and deformation imaging in children may also be useful for longitudinal follow-up of ventricular function. Serial recovery of LV and RV strain after repair of anomalous coronary artery from the pulmonary artery has been demonstrated (Figure 8.33). Likewise, differences in recovery

of radial versus longitudinal function have been found after coronary re-implantation. This may be related to associated subendocardial fibroelastosis that reflects irreversible myocardial damage.

Use of tissue velocities to predict clinical outcomes in children

Reduced mitral diastolic velocity helps predict children at risk for adverse outcomes, including death and need for cardiac transplantation in dilated cardiomyopathy and left ventricular non-compaction. Likewise, the E/E′ ratio predicts adverse clinical outcomes, including death, cardiac arrest, VT, and significant cardiac symptoms in children with HCM. Reduced TV tissue velocities have also identified children with heart transplant at risk for graft failure secondary to rejection [17]. We have studied heterogeneous left ventricular contraction and relaxation (mechanical dyssynchrony) using tissue velocities and strain as predictors of outcomes in children with dilated cardiomyopathy. The timing of contraction was related to the degree of deformation in both normal children and in those with dilated cardiomyopathy [27]. Although mechanical dyssynchrony was prevalent in children with dilated cardiomyopathy, systolic dyssynchrony was not associated with need for transplant or death [28]. In contrast, diastolic dyssynchrony was associated with decreased transplant-free survival, although there were no obvious associations with other abnormalities of diastolic function [28].

Limitations of the newer techniques

Velocity and deformation imaging have important limitations. Their utility in specific clinical situations remains to be confirmed and solid validation in pediatrics is lacking. Difficulties in technical acquisition which affect data quality and interpretation, large inter- and intra-observer variability, large scatter and variation when compared with reference methods, conflicting data regarding load dependence of the various indices, standardization of what should be measured (regional versus global function, which and how many myocardial segments should be measured), which method should be used in routine practice (velocities, strain, strain rate, a combination of these), standardization within the method (peak versus mean velocities, color versus pulsed Doppler, TDI versus 2D speckle derived strain, radial versus longitudinal versus circumferential strain versus a combination of these), potential differences between data obtained from the use of systems from different commercial vendors, and long post-acquisition processing times remain issues for their use in routine clinical practice. Standardized reporting also remains a challenge.

Diastolic function

Ventricular relaxation and filling constitute diastolic function. All diastolic indices, both echocardiographic and invasive, are less developed than are their systolic
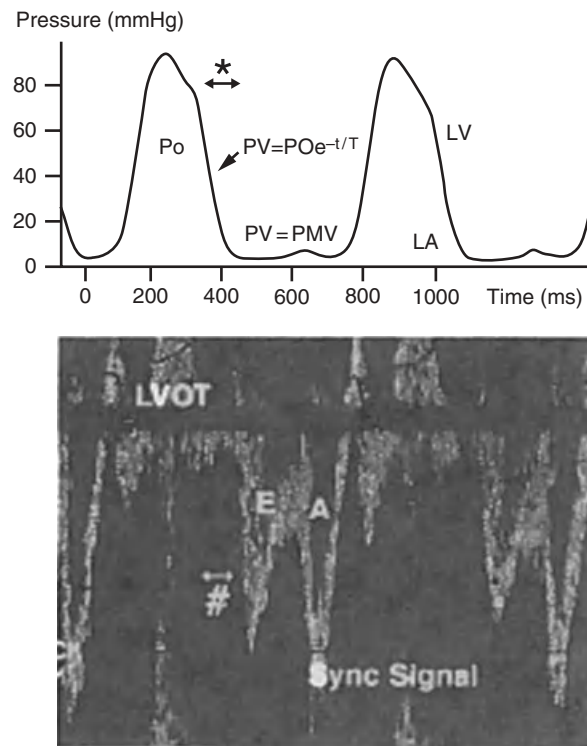
Figure 8.34 Display of left ventricular (LV) pressure and the relationship to transmitral Doppler flow patterns. Instantaneous left ventricular pressure (*PV*) follows an exponential pressure decay during early diastole (*PV = POe*$^{-t/T}$). Invasive isovolumic relaxation time (*) represents the period from peak −d*P*/d*t* (*PV = PO*) until mitral valve opening (*PV = PMV*). Doppler-derived isovolumic relaxation time (#) is the interval from the valve artifact at the end of left ventricular outflow (LVOT) until the beginning of transmitral inflow (E). LA, left atrium. (Reproduced with permission from Scalia *et al. Circulation* 1997;**95**:151–5.)

counterparts. Ventricular diastole is composed of an isovolumic relaxation phase, during which intracellular calcium is resequestered in the sarcoplasmic reticulum by energy-dependent means, and a filling phase, during which venous return passes from the atria into the ventricles. Diastolic dysfunction can manifest as either impaired isovolumic relaxation, impaired filling, or both. Isovolumic relaxation time is the interval from aortic valve closure to mitral valve opening, and can be measured using Doppler techniques (Figure 8.34) [29]. Ventricular filling may be assessed with Doppler analysis of mitral and tricuspid valve diastolic inflow patterns, composed of three phases. Early (rapid) filling is represented by Doppler as the upslope of the E wave. After the peak early filling velocity is reached, there is a transition to slow filling, represented by the deceleration of the E wave and measured as deceleration time. Atrial contraction produces late ventricular filling, represented by the A wave on the mitral/tricuspid inflow tracing. Pulmonary and hepatic venous flow Doppler velocity spectra can also provide insight into diastolic
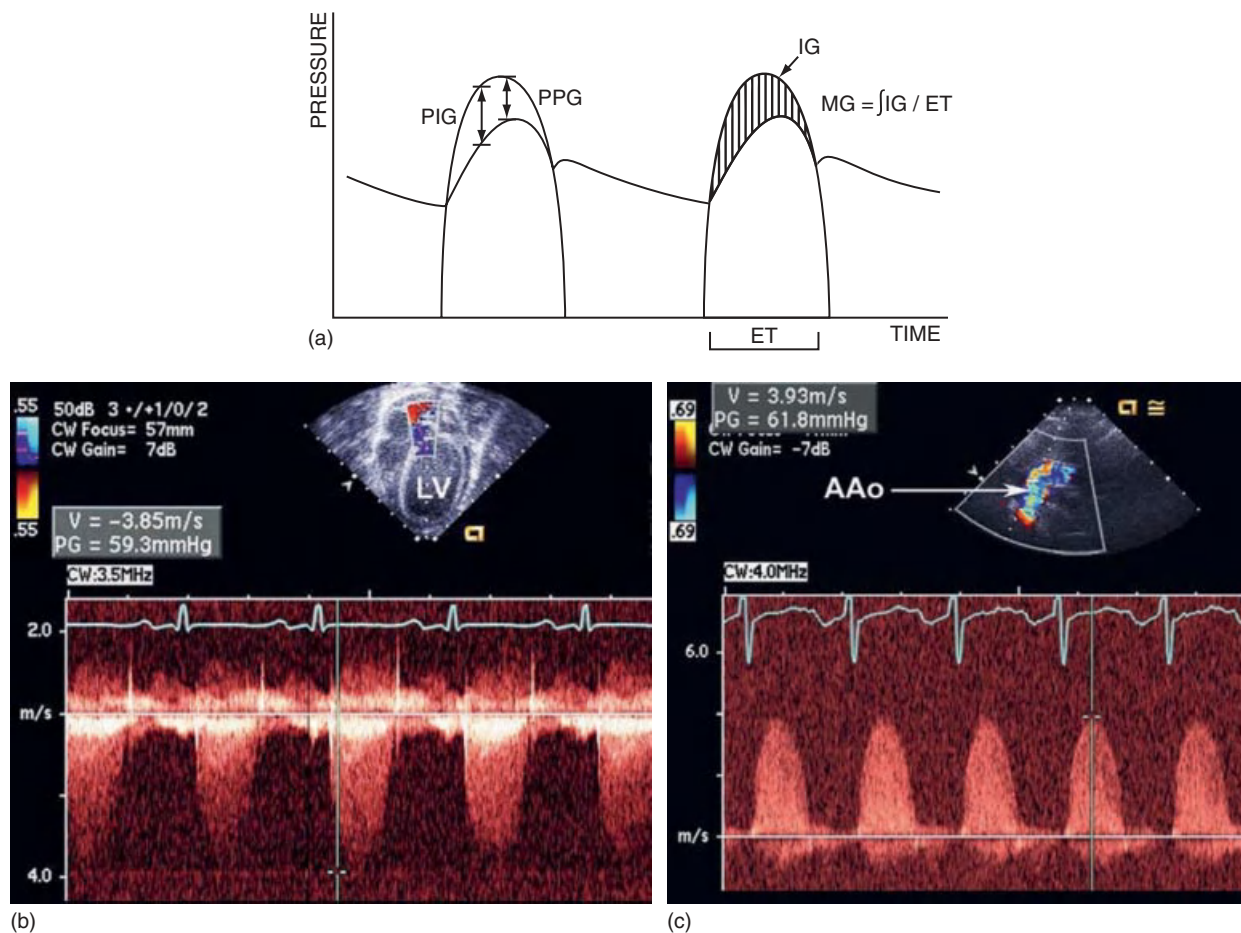
Figure 8.35 (a) Graphic representation of the relationship between the variables of pressure drop that can be measured at cardiac catheterization and/or by Doppler. The tracings represented schematically are those from ventricular and arterial pressures. Doppler measures peak instantaneous gradient (PIG), whereas it is conventional to measure the peak-to-peak gradient (PPG) at catheterization, even though peak ventricular and arterial pressures are not simultaneous. At catheterization and by Doppler, the mean gradient throughout systole (MG) is obtained by integrating the area of all instantaneous gradients (IG) and dividing by ejection time (ET). For measurement of the mean gradient, Doppler and manometric values are the same. Continuous wave (CW) Doppler tracing recorded from an apical four-chamber (b) and suprasternal notch (c) position demonstrating an increased velocity in the ascending aorta in a patient with valvar aortic stenosis, LV, left ventricle; AAo, ascending aorta. Peak velocity is approximately 3.9 m s^{-1}. Using the modified Bernoulli equation, the instantaneous pressure drop is calculated to be approximately 60 mmHg. (Part (a) reproduced with permission from Silverman, *Pediatric Echocardiography*. Baltimore: Williams & Wilkins, 1993.)

function, insofar as atrial inflow velocity is inversely related to pressure in the receiving chamber.

Isovolumic relaxation time is typically increased by impaired ventricular relaxation and decreased by a restrictive pattern. The ratio of early filling to atrial filling (E/A), normally between 1.9 and 2.5 in children, is decreased by impaired relaxation and increased by restrictive filling. Similarly, the deceleration time of the E wave is an indicator of ventricular compliance, being inversely related to the square of ventricular stiffness [30].

Ventricular relaxation during the isovolumic relaxation interval is characterized by the maximum negative slope of ventricular pressure decay ($-dP/dt$) and by the relaxation time constant (τ), which is the inverse slope of the natural logarithm of left ventricular pressure decay over time. The primary advantage of τ over isovolumic relaxation time and $-dP/dt$ as an indicator of diastolic function is its independence from heart rate and preload. Noninvasive estimates of these properties using Doppler technology correlate well with high-fidelity manometer-tipped catheter measurements [29]. More recently, color Doppler M-mode echocardiography of ventricular inflow has been proposed as a means of evaluating diastolic function, insofar as the slope of flow propagation in this mode is inversely related to $-dP/dt$ and τ (Figure 8.35) [31,32].

Tei *et al.* devised an index for assessing overall myocardial performance, including both systolic and diastolic components [33]. Using pulsed wave Doppler analysis of mitral
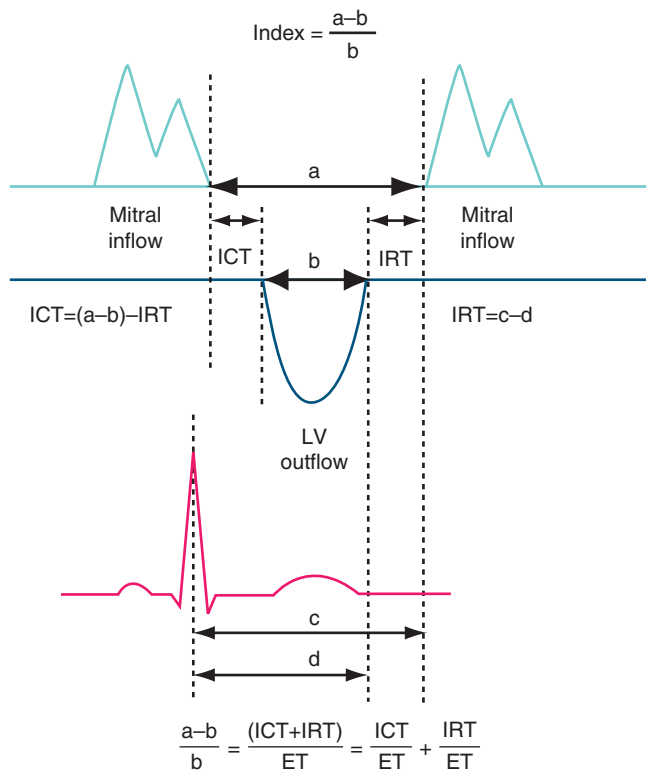
$$\text{Index} = \frac{a-b}{b}$$

a

Mitral inflow

Mitral inflow

ICT : b : IRT

$ICT = (a-b) - IRT$

$IRT = c - d$

LV outflow

c

d

$$\frac{a-b}{b} = \frac{(ICT+IRT)}{ET} = \frac{ICT}{ET} + \frac{IRT}{ET}$$

Figure 8.36 Schematic diagram of Doppler and electrocardiogram intervals used by Tei *et al.* [33] to determine a noninvasive index of myocardial performance. The index (*a* – *b*)/*b* is calculated by measuring *a* (interval between cessation of and onset of mitral inflow) and *b* [ejection time (ET) of left ventricular (LV) outflow]. The index is equivalent to the sum of isovolumic contraction time (ICT) and isovolumic relaxation time (IRT) divided by ejection time. The isovolumic relaxation time can be calculated as the difference between interval *d* (from the R wave of the electrocardiogram to cessation of left ventricular outflow) and interval *c* (from the R wave to onset of mitral inflow). Isovolumic contraction time can be calculated by subtracting isovolumic relaxation time from the quantity *a* – *b*. (Modified from Tei *et al. J Am Soc Echocardiogr* 1997;**10**:169–78.)

valve inflow and left ventricular outflow, two intervals are measured: from cessation of mitral inflow to onset of mitral inflow during the next cardiac cycle, and ejection time. The former represents the sum of isovolumic contraction time, ejection time, and isovolumic relaxation time. Ejection time is subtracted from this, and the difference is the sum of isovolumic contraction and relaxation times. The index of myocardial performance is the ratio of this duration (summed isovolumic contraction and relaxation times) to ejection time (Figure 8.36). Although this index has not been assessed in children, it correlates well with catheter-derived measurements of peak −d*P*/d*t*, +d*P*/d*t*, and τ, and is likely to prove useful in a variety of patient populations.

An additional method for establishing diastolic dysfunction is the ratio of mitral velocity to early diastolic velocity of the mitral annulus (E/E′ ratio). A measurement of >15 was

highly associated with elevated left ventricular end-diastolic pressure by cardiac catheterization [34].

Valvar physiology
Although cross-sectional methods are used to image the motion of the semilunar and atrioventricular valvar leaflets, Doppler technologies are the primary echocardiographic tools for evaluating valvar dysfunction, either stenosis or regurgitation.

Semilunar valvar stenosis
Valvar obstruction is identified with continuous or pulsed wave Doppler analysis, which shows increased flow velocity during systole when the sample volume is placed distal to the stenotic orifice. Evaluating the severity of flow obstruction is done by applying the simplified Bernoulli equation, which estimates the pressure gradient between two points as

$$P = 4\left(V_2{}^2 - V_1{}^2\right)$$

where V_1 and V_2 are the proximal and distal flow velocities, respectively. For practical application in the echocardiography laboratory, proximal flow velocity is generally negligible (<1 m s^{-1}) and this term is omitted, yielding the simplified equation $P = 4V_2{}^2$. This method is reasonably reproducible, but requires an understanding of the principles of Bernoulli's law. Viscous forces are assumed to be minimal relative to inertial forces in the system being studied, which does not occur in long-segment stenoses or mild stenoses in a patient with increased blood viscosity (e.g., polycythemia in cyanotic patients). This technique, which yields an estimate of peak instantaneous gradient, requires consistent placement of the sample volume at the vena contracta, the point of maximum velocity at the midline of the jet immediately downstream from the stenotic orifice. Continuous wave Doppler aids in minimizing variability due to sample volume placement, insofar as it detects the highest velocities as it passes axially along the jet length. The acoustic signal of the sample volume must also be aligned as closely as possible with the direction of the jet to optimize sensitivity. The sample volume is typically located with the aid of Doppler color flow mapping, which shows the direction and dimensions of the jet. The simplified Bernoulli method tends to overestimate the pressure gradient of a stenosis relative to direct catheter measurements due to methodological and physical factors [3,35,36]. Catheterization measurements are of peak-to-peak pressure gradient (non-simultaneous), whereas Doppler analysis estimates peak instantaneous gradient (Figure 8.35); pressure is lower at the vena contracta than it is at the site of pressure recovery further downstream, where catheter measurements are generally made due to the difficulty of maintaining the catheter in the center of the jet; and sedation during catheterization tends to decrease stroke

volume and hence flow velocity across the stenotic orifice. The mean systolic pressure gradient is less prone to systematic overestimation, but peak velocity measurements are less time consuming and we use this approach in our practice.

Another useful method of calculating pressure drop is to measure acceleration time (the duration from valve opening to peak flow velocity), although other physiologic conditions (such as severe mitral regurgitation and ventricular dysfunction) can also cause the gradual rise in the velocity profile characteristic of more severe stenosis. Valvar orifice area, an indirect indicator of function, can be estimated by several techniques, including planimetry, M-mode, the continuity equation, and measurement of pressure half-time. With an arterial level shunt, significant valvar obstruction may be indicated by diastolic flow reversal in the artery downstream from the affected valve. Color Doppler M-mode imaging may increase the temporal and spatial sensitivity for detecting flow disturbances and helping to break down complex outflow tract obstruction into its various components.

Valvar regurgitation

Unlike stenotic lesions, quantification of valvar regurgitation is complicated by several factors. Measuring the size of the regurgitant jet does allow gross characterization of the severity of regurgitation, but it is difficult to make fine distinctions between grades. Atrioventricular and semilunar valvar regurgitation pose different problems of quantification, due primarily to geometric features of the respective proximal and receiving chambers and to the flow dynamics in the proximal and receiving chambers.

The shape and size of a regurgitant jet are influenced by numerous factors, only one of which is the severity of regurgitation [37–40]. Pressure in the receiving chamber, atrial counterflow, and cardiac function influence the morphology of the jet. Geometric features of the proximal chamber, the valve itself, and the receiving chamber have a significant effect on the flow pattern of the jet and on the Doppler color map [37–39]. In addition, instrument settings such as color gain, transducer frequency, velocity scale, and filtration can all substantially alter the appearance of a regurgitant jet [40].

Determining semilunar valvar regurgitation severity employs both color flow and spectral Doppler imaging. The regurgitant jet is interrogated with continuous or pulsed wave Doppler at the center of the aortic or pulmonary valve. The velocity profile of the jet reflects the diastolic aorta–left ventricle (or pulmonary artery–right ventricle) pressure gradient, and the velocity decay rate ($-dV/dt$) is a function of the gradient change over time. Accordingly, more severe regurgitation is reflected by a steeper velocity decay of the jet, as the higher regurgitant volume leads to more rapid diminution of the ventriculo-arterial pressure gradient. Unfortunately, this method is not of great value in evaluating regurgitation in children. A better indication of the severity of aortic regurgitation is finding retrograde diastolic flow in the descending aorta. Pulmonary regurgitation correlates best with the width of the regurgitant jet and right ventricular size. Methods for estimating atrioventricular regurgitation according to the principles of free jet physics cannot be applied to semilunar valvar regurgitation, largely because the regurgitant volume originates as flow reversal after ejection in the restrictive confines of the great artery, which combine to create a nonideal proximal flow field. As with valvar stenosis, color Doppler M-mode imaging may be used to increase the sensitivity for detecting a regurgitant jet, whether atrioventricular or semilunar.

Vascular physiology

Vascular stenoses can be evaluated by Doppler estimation of the peak instantaneous pressure gradient. The simplified Bernoulli equation is the standard method, although it may not apply to serial or long-segment stenoses. Because pressure is estimated by measuring flow velocity at a single point, assuming that velocity proximal to the stenosis is negligible, high flow velocities distal to one stenosis and proximal to the next invalidate this assumption. Each successive stenosis must be measured separately, which is possible with continuous wave Doppler, where each separate point of acceleration is superimposed on the spectral display. In addition, with long-segment stenoses, viscous forces may exert a substantial effect on the pressure drop, but these are ignored by the simplified Bernoulli equation. Arterial flow patterns distal to the obstruction, such as damping of the pulse wave and diastolic flow reversal, may also indicate significant stenosis.

Pulmonary arterial pressures and flows can be estimated with echocardiography, although not with sufficient precision to obviate catheterization to assess the state of the pulmonary vasculature. Pressure is estimated by subtracting the right ventricle-pulmonary artery gradient (predicted with Doppler imaging and the simplified Bernoulli equation) from the estimated right ventricular pressure. Right ventricular pressure is calculated by determining the systolic right ventricle–right atrium pressure drop, estimated by applying the Bernoulli equation to the velocity of a tricuspid regurgitant jet (often present even without cardiac pathology) and assuming a right atrial pressure of 5–10 mmHg. Pulmonary arterial distensibility, estimated by measuring the diastolic–systolic diameter change, may also contribute information regarding pulmonary arterial pressure. In patients with decreased pulmonary vascular compliance, late diastolic flow reversal may be evident with Doppler analysis.

Shunt physiology

Doppler color flow mapping allows the visualization of most shunts at the cardiac or great vessel levels. The restrictiveness of a discrete anatomic shunt (such as a septal defect or patent ductus arteriosus) may be evaluated with spectral
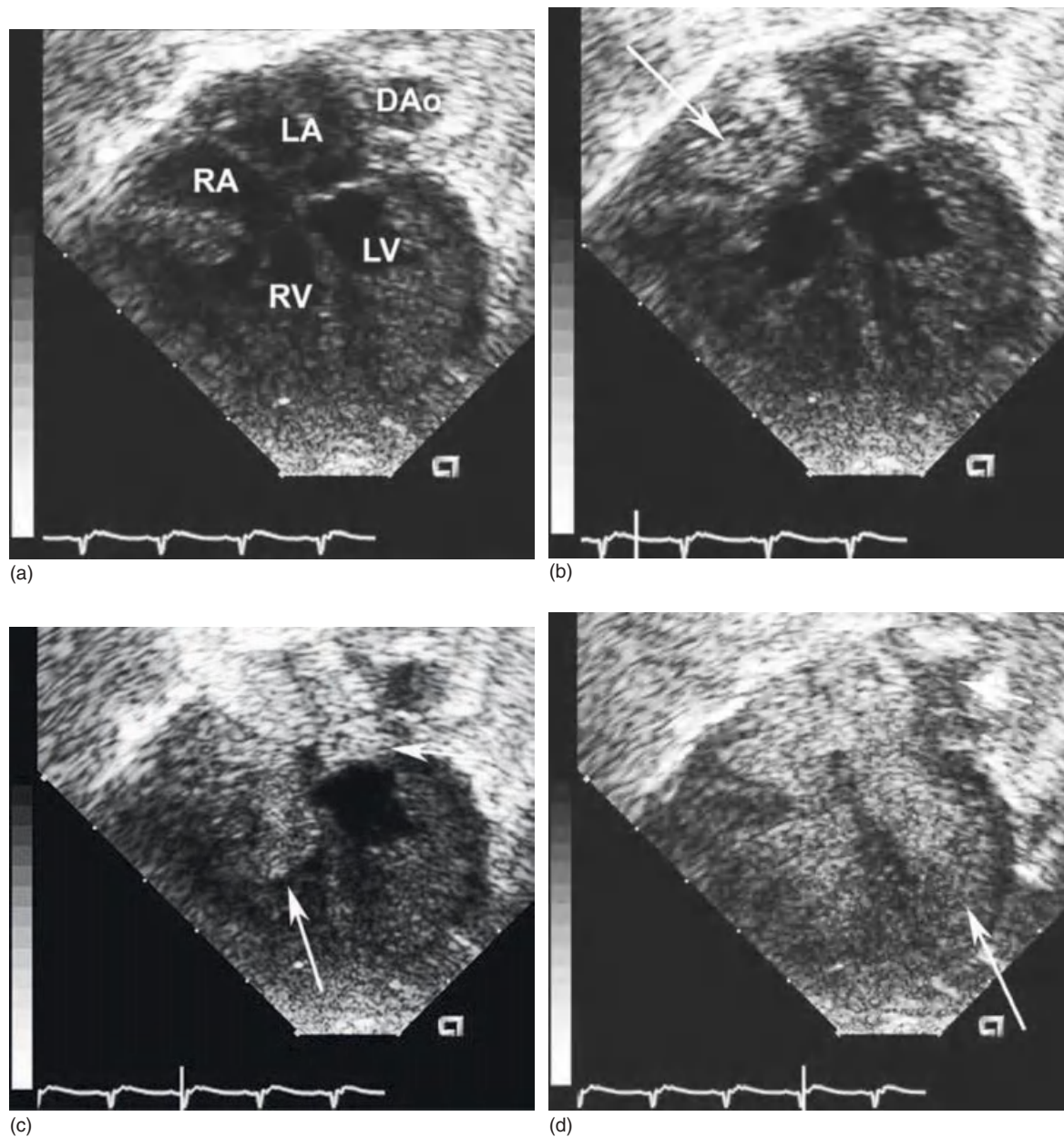
Figure 8.37 (a) Apical four-chamber view showing right atrium (RA), left atrium (LA), right ventricle (RV), left ventricle (LV), and descending aorta (DAo). After injection of agitated saline into the right arm (b), microcavitations (arrow) appear in the right atrium and enter the right ventricle and left atrium (c). This obliteration of the atrial septum indicates a right–left interatrial communication. Eventually, microcavitations appear in the left ventricle and descending aorta (d). If there had been a right-to-left ventricular communication and mitral incompetence, the microbubbles would have appeared in the left ventricle before the left atrium.

Doppler to estimate the pressure gradient from the Bernoulli principle. Shunts more difficult to image with color flow, such as those from pulmonary or systemic arteriovenous malformations or small interatrial communications, can be analyzed by contrast echocardiography. Agitated saline is injected into a systemic vein or artery, and the echogenic microbubbles pass through all vessels or cardiac defects larger than their 8–15 μm diameter, and appear downstream or in the receiving chamber (Figure 8.37) [41]. Alternatively, interchamber defects that are difficult to distinguish from valvar regurgitation with standard Doppler color flow may sometimes be clarified by increasing the color gain in the Doppler color flow mode to highlight the proximal flow convergence region approaching the low-velocity defect. The diagnosis of an arteriovenous shunt can be verified by diastolic flow reversal in the descending aorta (distal to the

shunt) in the absence of semilunar valvar regurgitation, and by identifying high levels of output and associated chamber dilatation. Shunt lesions that are most likely to be missed on echocardiography are small defects occurring with a larger, non-restrictive defect, as in multiple muscular ventricular septal defects with a nonrestrictive inlet or perimembranous defect. In these patients, there may be no pressure gradient between the chambers and no accelerative flow shown with Doppler techniques.

Special techniques

Stress echocardiography

Echocardiography can be used to assess the effect of increased workload on ventricular performance and hemodynamics (stress echocardiography). The increased workload is generated either by exercise [42] or by giving dobutamine [43]. Dobutamine is particularly useful in smaller patients who cannot exercise on demand. Stress echocardiography provides information about the coronary reserve, ventricular function under increased output demands, and the response of ventricular outlet obstruction to increased output.

The procedure is similar to that performed in adults [44]. Views of the left ventricle are obtained from the parasternal short and long axis, and from the apical two- and four-chamber views. These views allow visualization of the entire ventricular wall. Images are obtained at rest, at multiple levels of stress, and after recovery. The images are then compared for changes in regional wall motion that suggest impaired myocardial perfusion. Stress echo compares favorably with nuclear medicine studies in adults [44]. When evaluating obstructive lesions, Doppler gradients are obtained at all stress levels and compared to assess the change in degree of obstruction. Response of the obstruction to stress is variable; some patients with minimal obstruction at rest can develop severe obstruction with stress. The increased cardiac motion, particularly when combined with the motion of exercise, can make image acquisition difficult. Anterior wall segments are most affected by motion, as they are the most difficult to image even at rest. In patients with obstructions, the examiner must measure both proximal and distal velocities, because with increased output the proximal velocity may increase to significantly greater than $1\,\mathrm{m\,s^{-1}}$. When this occurs, the longer version of the Bernoulli equation ($V_2{}^2 - V_1{}^2$) must be used to account for this increase.

Children who benefit most from stress echocardiography include patients who have undergone coronary manipulation, such as after the arterial switch, Ross procedure, or Konno procedure [45]; coronary anomalies, as in Kawasaki syndrome; abnormal ventricular function, as in anthracycline cardiotoxicity [46]; and left heart obstructions, such as aortic stenosis and coarctation [47].

Transesophageal echocardiography

With the development of miniaturized transducers suitable for patients weighing <20 kg, the application of transesophageal scanning in children expanded rapidly [48–51]. These studies demonstrated the suitability of transesophageal echocardiography for monitoring intraoperative cardiac function and evaluating the adequacy of surgical repair, demonstrating accurately most forms of normal and abnormal cardiac morphology, and evaluating physiology with pulsed wave Doppler and color flow Doppler features (Figures 8.38 and 8.39).

The primary application of transesophageal echocardiography in children is intraoperative monitoring and evaluating surgical repair [50]. Transesophageal echocardiography may also be valuable in larger children, adolescents, and the few smaller children who cannot be imaged completely with transthoracic transducers, or when surgical dressings preclude noninvasive imaging. The transesophageal approach does not interrupt the surgical procedure, provides multiple imaging windows for morphologic evaluation and Doppler analysis, and avoids causing dysrhythmias, hypotension, or potential infectious complications associated with direct transducer contact with the epicardium. Aside from intraoperative studies, transesophageal echocardiography is not a substitute for precordial echocardiography. It is an invasive procedure reserved for patients in whom a thorough precordial examination has proved inadequate, or during surgical and interventional cardiac catheterization procedures.

The transducer employed for transesophageal echocardiography is mounted on a standard flexible endoscope. The pediatric transesophageal probe can be manipulated in three directions: advanced or withdrawn, anteroflexed or retroflexed, and rotated clockwise or counter-clockwise (Figure 8.39). Biplane and multiplane transesophageal echocardiography probes provide an additional control that allows lateral flexion. These scan planes differ from those of precordial imaging but the same information can be acquired, especially in infants and children, whose hearts and thoracic dimensions are small relative to the depth resolution of the ultrasound technology used. For more detailed descriptions of transesophageal echocardiography, the reader is referred to other sources [50–54].

Fetal echocardiography

Fetal echocardiography in experienced hands detects most congenital heart disease and dysrhythmias [55–63]. Detecting structural heart disease becomes especially important for cyanotic congenital heart disease or ductal-dependent lesions [56,64,65]; diagnosing lesions such as complete transposition or hypoplastic left heart disease in the fetus has led to improved outcomes [66–68]. The primary indications include suspected congenital heart disease, fetal dysrhythmia, family
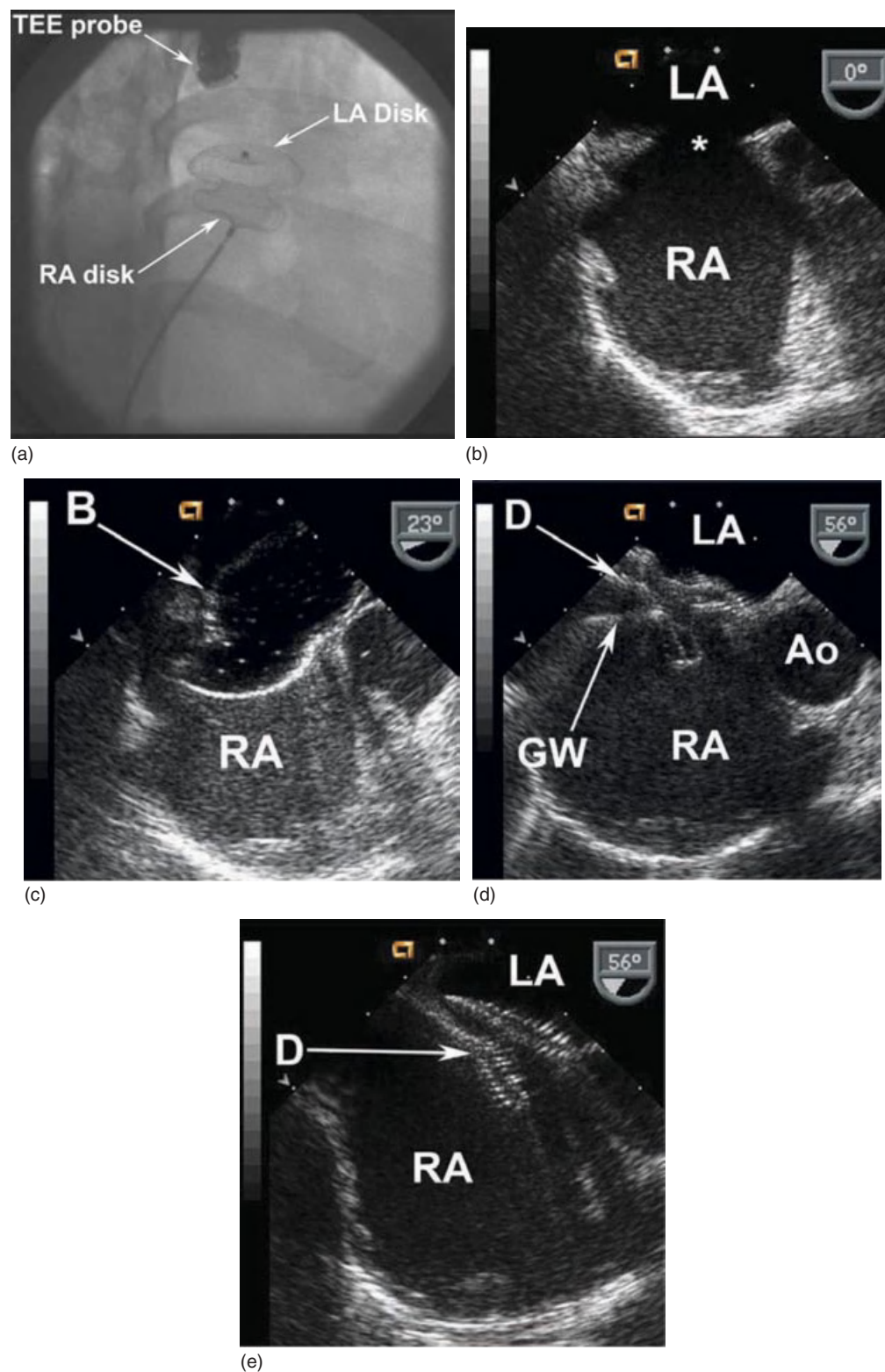
Figure 8.38 (a) This fluoroscopy image taken during transcatheter device closure of an atrial septal defect shows the catheter in the right atrium attached to the device. The left (LA) and right atrial (RA) disks are clearly demonstrated along with the end of the transesophageal (TEE) probe. (b) A transverse transesophageal image taken prior to deployment of the device; a secundum atrial septal defect is noted (*). (c) A sizing balloon (labeled B) is positioned across the defect. (d) The tip of the guide wire (GW) can be seen connected to the center of the device (labeled D). The left and right atrial disks are in the respective atria. (e) The device has been deployed across the atrial septal defect with appropriate position. Ao, aorta.
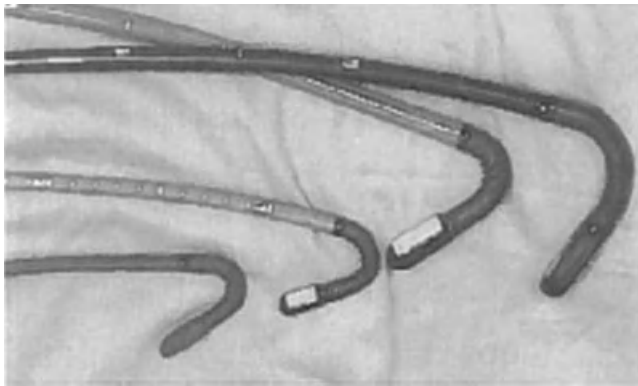
Figure 8.39 From top to bottom, this figure depicts adult omniplane, adult biplane, pediatric biplane, and pediatric single plane transesophageal ultrasound transducers. The differences in transducer diameter, which range from 13 mm for the adult omniplane transducer to 8 mm for the pediatric single plane transducer, can be appreciated, as can the increased flexion possible with pediatric transducers. The scale is indicated by the 5 cm markers on the probes.

Figure 8.40 This fetal apical four-chamber view demonstrates both atria (RA, LA) and ventricles (RV, LV) along with the descending aorta posteriorly (DAo). The left lung is identified and the apex is on the ipsilateral side, consistent with levocardia.

history of congenital heart disease, history of familial inherited disorders, maternal systemic lupus erythremotosis, maternal diabetes mellitus or phenylketonuria, increased nuchal thickening, exposure to teratogens or prostaglandin synthetase inhibitors, and *in vitro* fertilization [69–81]. Some studies suggest that a single umbilical cord or echogenic density in isolation is not an indication for a fetal echocardiogram because of the lack of associated congenital heart disease [73,74,76,81].

Approach to Fetal Morphology

Initially, the position of the cardiac mass and apex relative to the thorax is established (Figure 8.40). The cardiothoracic ratio is determined [82]. The connections of systemic and pulmonary veins to the atria are established, as are the atrioventricular and ventriculoarterial relationships. The great vessels should essentially cross each other at near right-angles (Figure 8.41).

Special anatomic considerations apply to the fetus. Both the ductus arteriosus and foramen ovale should have unobstructed right–left shunting across them, as the pulmonary blood flow is diminished *in utero*. Left–right shunting across the atrial septum represents left atrial obstruction such as mitral stenosis or atresia (Figure 8.42). A left–right shunt across the ductus arteriosus may indicate inadequate output from the right ventricle (Figure 8.43), as in tetralogy of Fallot with pulmonary atresia, severe Ebstein's anomaly, and severe pulmonary stenosis. Any obstruction to the ductus arteriosus flow may lead to significant tricuspid valve regurgitation and right ventricular dilation/failure (Figure 8.44), and subsequent pulmonary hypertension. Multiple medications and NSAIDs are known to cause ductal constriction that is, however, frequently idiopathic [83–85].
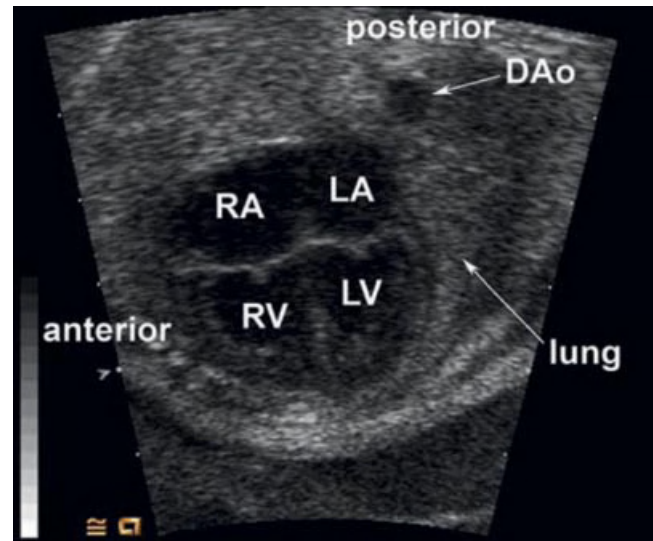
Approach to fetal rhythm

The fetal rhythm is established by M-mode, pulse wave, and tissue Doppler techniques to detect the type of ectopy, tachycardia, or bradycardia [86–89]. The absolute fetal heart rate can be established using the mitral inflow or aortic outflow. The mitral inflow and aortic outflow pulse wave Doppler indicate sinus rhythm and provide a surrogate for the PR interval for mothers with collagen vascular disorders such as lupus or Sjogren's disease [90–94] (Figure 8.45). Reference standards are available to establish prolonged atrioventricular intervals that suggest first-degree heart block [90,91,93–95]. An M-mode determination of atrioventricular association also helps to establish the fetal atrial and ventricular rates and their relationship. Second- or third-degree heart block can be determined (Figure 8.46). Multiple atrial beats compared with ventricular beats suggest atrial flutter; typically, the atrial rate measures about 400 beats per minute whereas the ventricular response is 200 beats per minute, consistent with 2:1 flutter (Figure 8.47). Orthodromic reentrant tachycardia is also highly likely when the atrioventricular relationship is 1:1 with a heart rate range of 220–300 beats per minute (Figure 8.48). The most common rhythm disturbance is premature atrial contractions (Figure 8.49), but ventricular tachycardia is exceedingly rare.

### Approach to fetal function

The systolic function of both ventricles may be evaluated qualitatively, but M-mode may be used to calculate a shortening fraction. Secondary signs of cardiac dysfunction are also useful. Makikallio *et al.* described a biophysical profile to determine fetal well-being through a scoring system [96]. This biophysical profile utilizes the presence or absence of
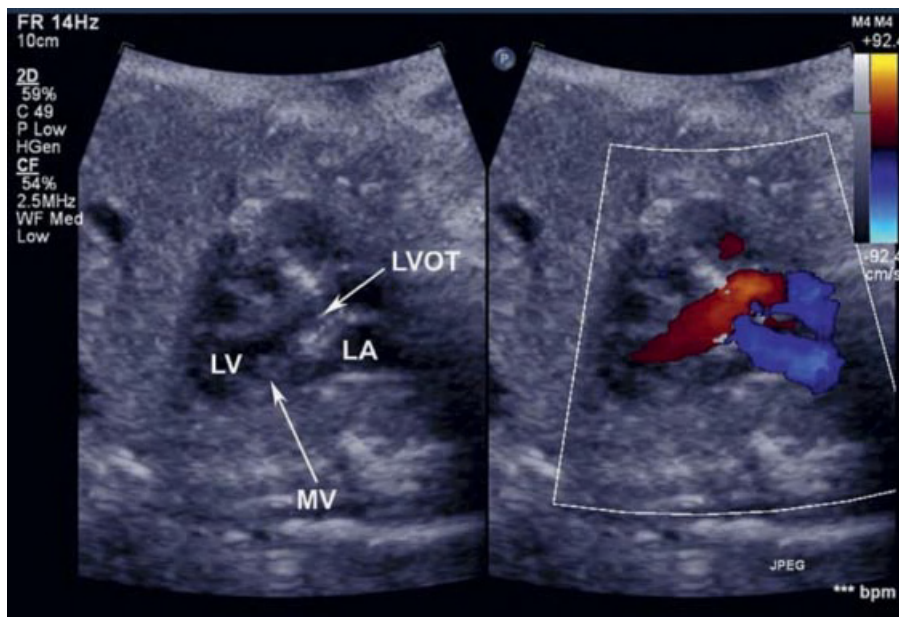
(a)
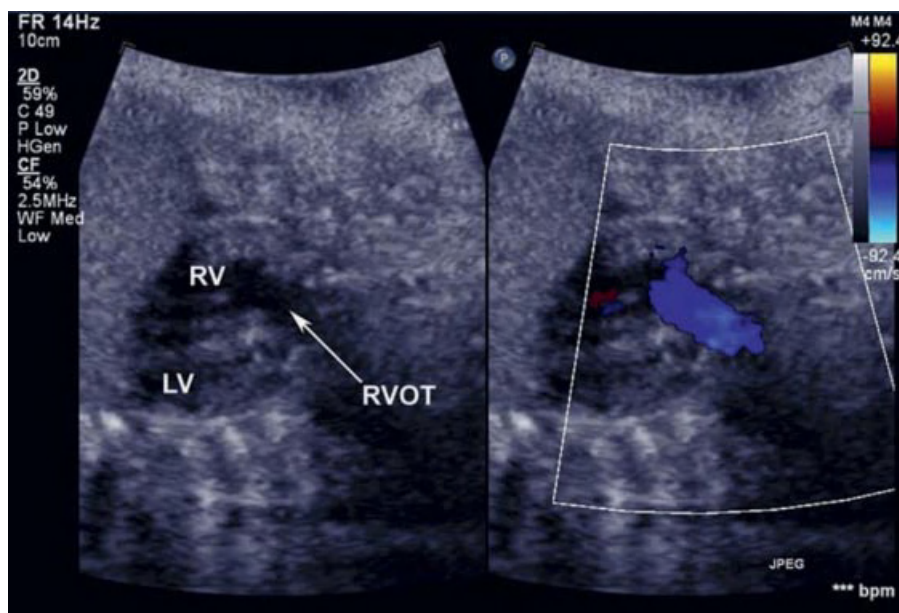
(b)
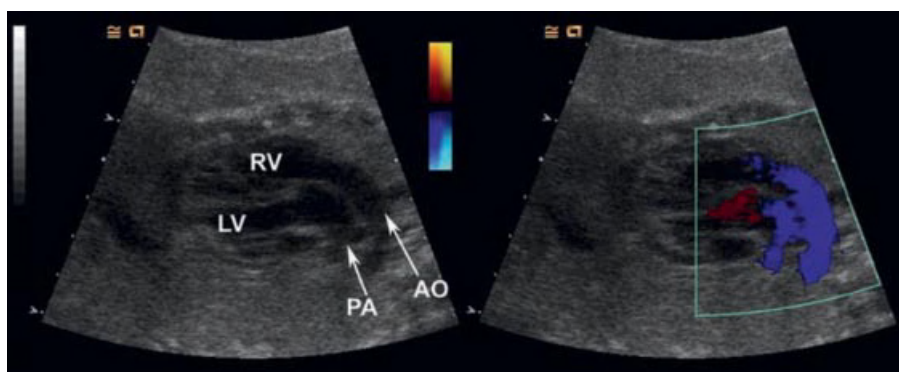
(c)

Figure 8.41 These images show normal ventriculoarterial relationships given that the left ventricle (LV) gives rise to the aorta (a) and the right ventricle (RV), in a different plane, connects to the pulmonary artery (b). This criss-cross of the great vessels can be imaged as a sweep and is essential to establish ventriculoarterial concordance. LVOT, left ventricular outflow tract; MV, mitral valve; RVOT, right ventricular outflow tract. Parallel outflow tracts and great vessels (Ao and PA) are noted in patients with complete transposition of the great vessels (c). Here the discordant ventriculoarterial relations are clear given that, in the same plane, the right ventricle (RV) gives rise to the anterior aorta (Ao) while the left ventricle (LV) gives rise to the posterior pulmonary artery (PA).

(a)   (b)
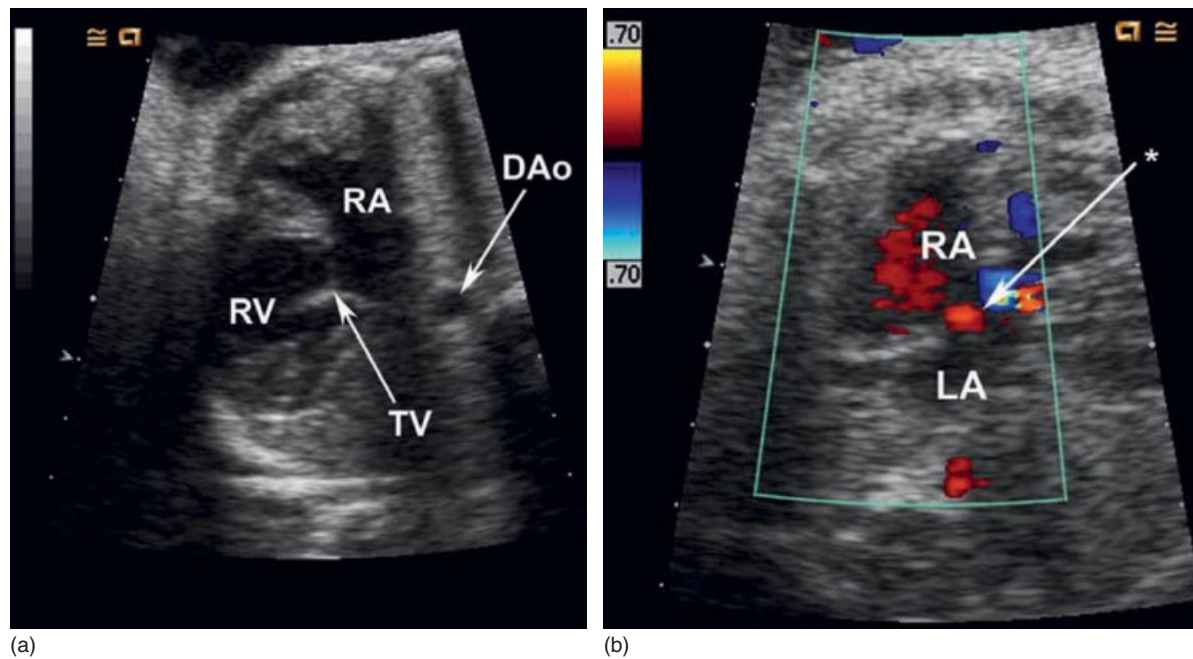
Figure 8.42 (a) The right atrium (RA) and right ventricle (RV) are visualized in the four-chamber view; however, there is no obvious left ventricle, consistent with mitral atresia and hypoplastic left heart syndrome. The tricuspid valve (TV) and descending aorta (DAo) are also demonstrated. (b) Left-right atrial shunt (*) is seen. LA, left atrium; RA, right atrium.

hydrops, atrioventricular valve regurgitation, and venous Doppler patterns. Examples of these lesions can be found in Figure 8.50.

Limitations to fetal echocardiography

Often due to maternal body habitus and fetal position, the fetal cardiologist is limited to lower frequency transducers that provide adequate depth but lack appropriate resolution. This lower resolution often leads to insufficient visualization of the ventricular septum and defects in this region may not be excluded. A patent foramen ovale and ductus arteriosus are normal in the fetus and their persistence in infancy cannot be predicted by fetal echocardiography. Given a patent ductus arteriosus, a coarctation of the aorta cannot be excluded.

Fetal cardiac intervention

See Chapter 16.

Three-dimensional echocardiography

Two-dimensional echocardiography provides an excellent evaluation of the heart in children given that high-frequency probes may often be utilized. Multiple cross-sectional images yield a complete anatomic and physiologic evaluation of the heart. However, three-dimensional echocardiography may provide a more comprehensive evaluation of this complex organ. Currently, three-dimensional echocardiography is a useful adjunct to standard transthoracic imaging. Its primary applications include determining ventricular volume, valve morphology, and ventricular synchrony. The technique relies on excellent two-dimensional images and is helpful in quantifying ventricular size and function. Ventricular volume and ejection fraction are useful in patients with corrected transposition, physiologically corrected complete transposition, and cardiomyopathy. The advantage of this technique is that a true volume is obtained; however, the frame rates of 20–30 Hz are inferior to standard echocardiographic imaging. This technique may also give a real-time view of ventricular aneurysms or wall motion abnormalities (Figure 8.51).

Atrioventricular valve assessment can be readily performed; specific lesions include double orifice mitral valve, detecting mitral valve clefts, and mitral valve ring (Figure 8.52).

A more recent application of three-dimensional echocardiography is establishing ventricular synchrony. The various segments' time to minimal volume may be used to establish the level of dyssychrony through a graphical display (Figure 8.53). The time for segments to reach minimal dimension is automatically calculated and there are reference standards for anatomically normal hearts [97,98]. As there is more ventricular dysfunction or dilation, the time for segments to reach a minimal volume disperses, consistent with dyssynchrony.
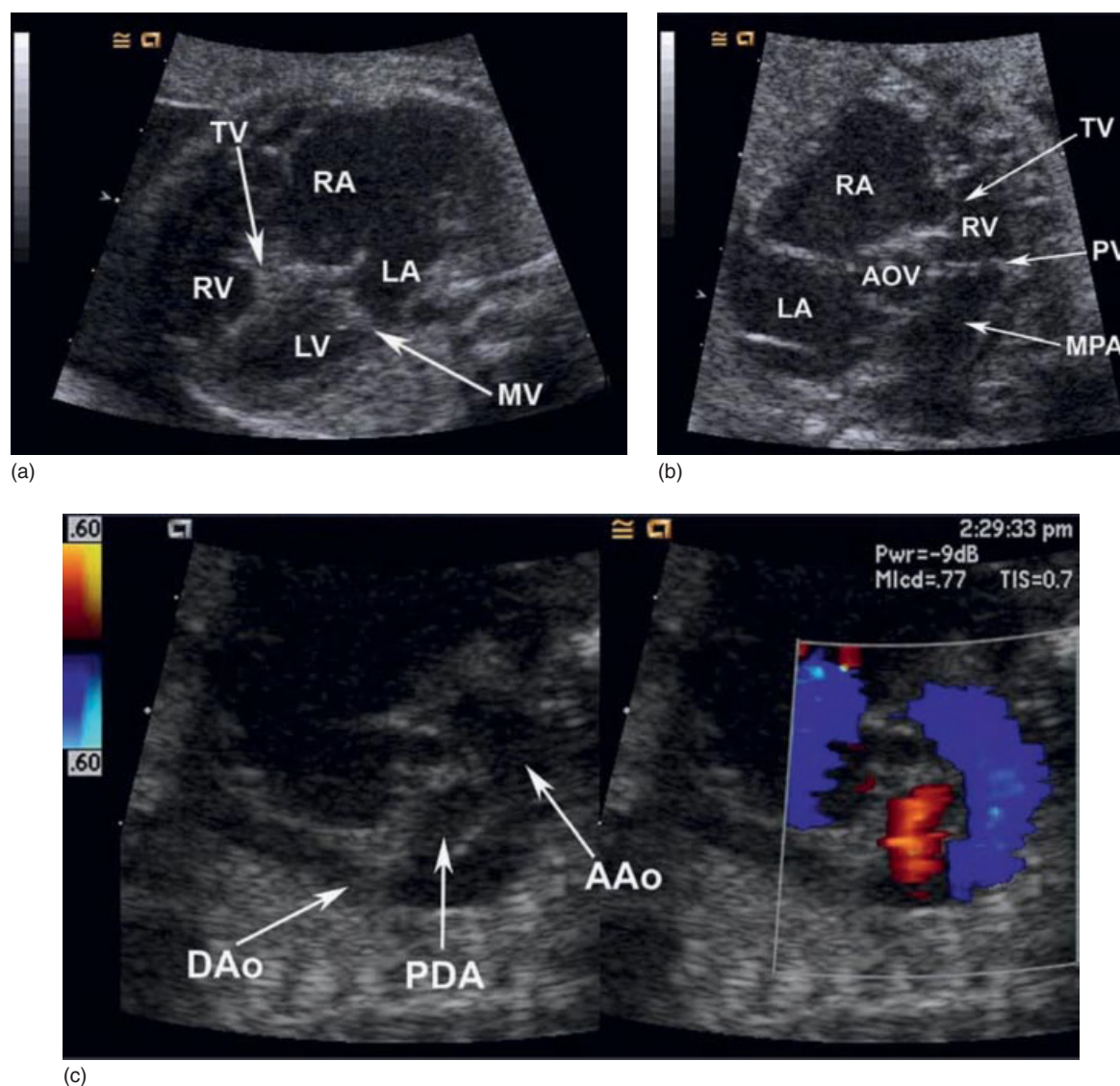
(a)

(b)

(c)

Figure 8.43 (a) This four-chamber view of the fetus shows significant apical displacement of the tricuspid valve (TV) relative to the mitral valve (MV). The right atrium (RA) is fairly large compared with the left atrium (LA). (b) The short axis view at the base of the heart shows the tricuspid valve in the right ventricular outflow tract very near the pulmonary valve (PV), consistent with marked Ebstein's anomaly. The right ventricle is fairly small as a result of this tricuspid valve displacement. (c) The patent ductus arteriosus (PDA) shunts left to right (red color) from the descending aorta (DAo) to the pulmonary artery as a result of inadequate prograde flow from the diminutive right ventricle. AAo, ascending aorta; LV, left ventricle; MPA, main pulmonary artery; RV, right ventricle.

Intravascular ultrasound

A variety of transducer configurations are mounted on the tip of an endovascular catheter. The most commonly used designs provide 360° cross-sectional imaging at right-angles to the catheter, by means of either a rotating transducer or mirror, or an array of multiple crystals encircling the catheter with phased-array technology used to produce the image. Intravascular imaging is typically performed at frequencies of 20–30 MHz, allowing for much higher resolution than with other ultrasound techniques but limiting the scanning depth substantially. As such, currently available forms of this technology are most useful for demonstrating fine detail of relatively small-caliber vessels. With decreasing catheter:lumen diameter ratio, the potential for erroneous imaging is increased. Not only does this place the catheter at a greater distance from the arterial wall where lateral resolution is decreased, but it also increases the likelihood of cross-sectional distortion due to non-coaxial orientation of the ultrasound catheter within the vessel (Figure 8.54).

Cross-sectional imaging can be used to distinguish the intimal, medial, and adventitial layers of an artery, and also calcifications, atheromatous plaques, thrombi, tumors, and

(a)

(b)

(c)
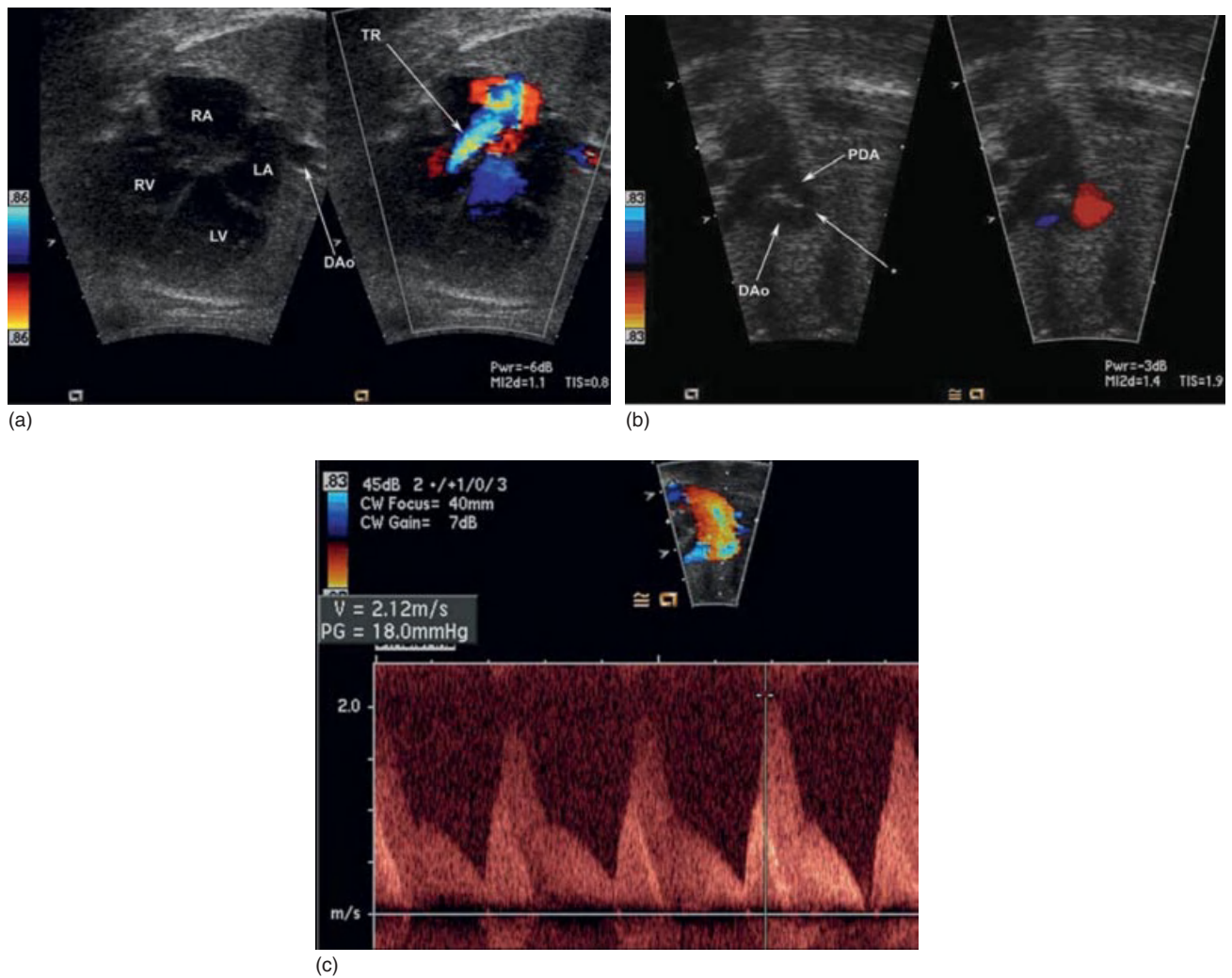
Figure 8.44 (a) This four-chamber view demonstrates severe tricuspid valve regurgitation (TR) with right atrial and right ventricular enlargement (RA, RV). LA, left atrium; LV, left ventricle. (b) The ductus arteriosus (PDA) has a focal narrowing (*) prior to its drainage into the descending aorta (DAo). (c) Spectral continuous-wave Doppler demonstrates an obstructive pattern given the extended flow into diastole and higher peak systolic velocity above 2 m s⁻¹.

(a)

(b)
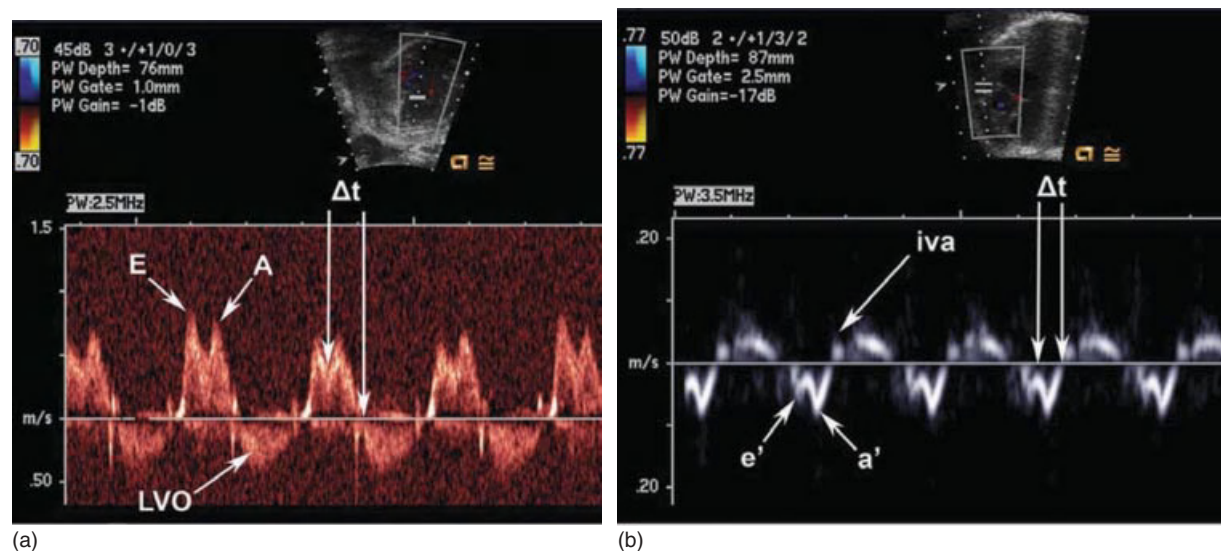
Figure 8.45 (a) Pulsed-wave Doppler at the mitral and aortic valve continuity region demonstrates mitral inflow (E, A) which is above the baseline and left ventricular outflow (LVO) which is the pattern below the baseline. The time between the onset of the A wave and the beginning of ejection (LVO) represents a surrogate for the PR interval (Δt). (b) Pulsed tissue Doppler at the tricuspid valve annular free wall yields tissue motion in systole and diastole. The diastolic motion (e' and a') represent diastole while motion above the baseline occurs during systole. The isovolumic acceleration (iva) region represents motion occurring during left ventricular isovolumic contraction. The time between the onset of the a' and the onset of the iva (Δt) is also a surrogate for the PR interval in the fetus.

149

(a)

(b)
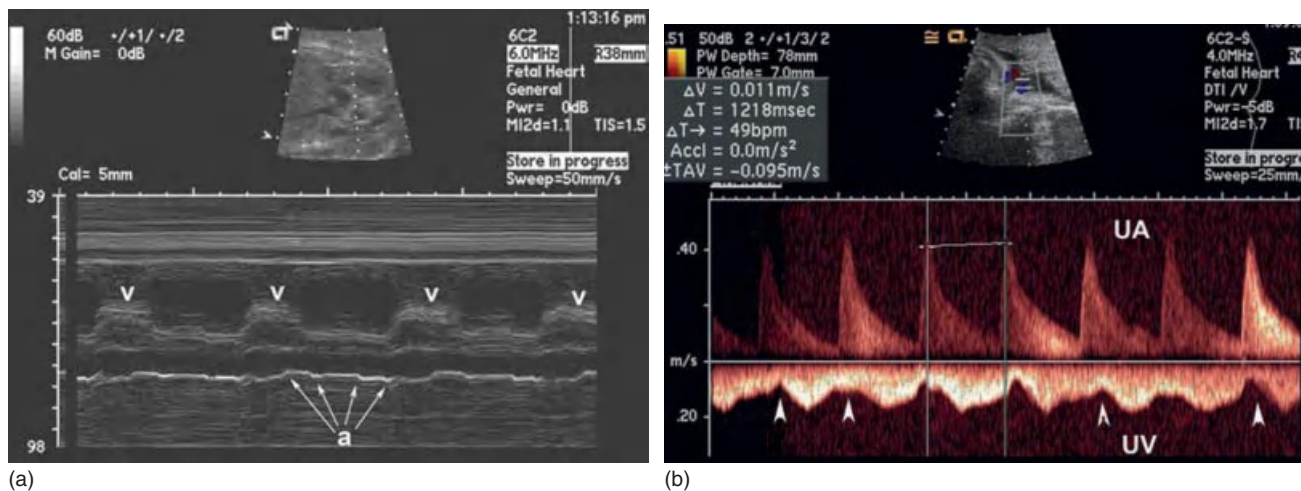
Figure 8.46 (a) An M-mode across the atria and ventricle from the short axis view of the fetal heart yields far fewer ventricular contractions (v) compared with the atrial contractions (a) with no relationship between atrial and ventricular beats, consistent with third-degree heart block. (b) Pulsed-wave Doppler of the umbilical artery (UA) and vein (UV) simultaneously shows notching (arrowheads) in the umbilical vein during systole. This phenomenon represents cannon a waves that occur with atrial contraction during a closed tricuspid valve due to the atrioventricular disassociation. The umbilical venous flow is thus blunted during these times manifesting as notching.

(a)

(b)
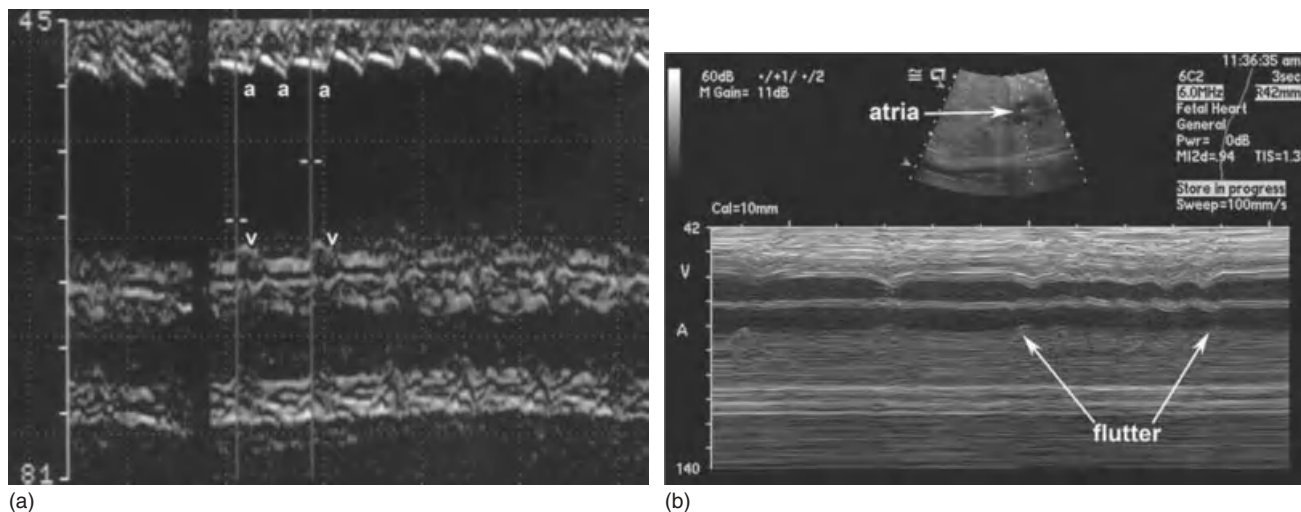
Figure 8.47 (a) M-mode of the atrial and ventricular wall demonstrates two atrial beats (a) for every one ventricular beat (v) with association, consistent with 2:1 flutter. (b) An M-mode through both atria shows the sudden onset and termination of atrial tachycardia, consistent with flutter.

(a)

(b)
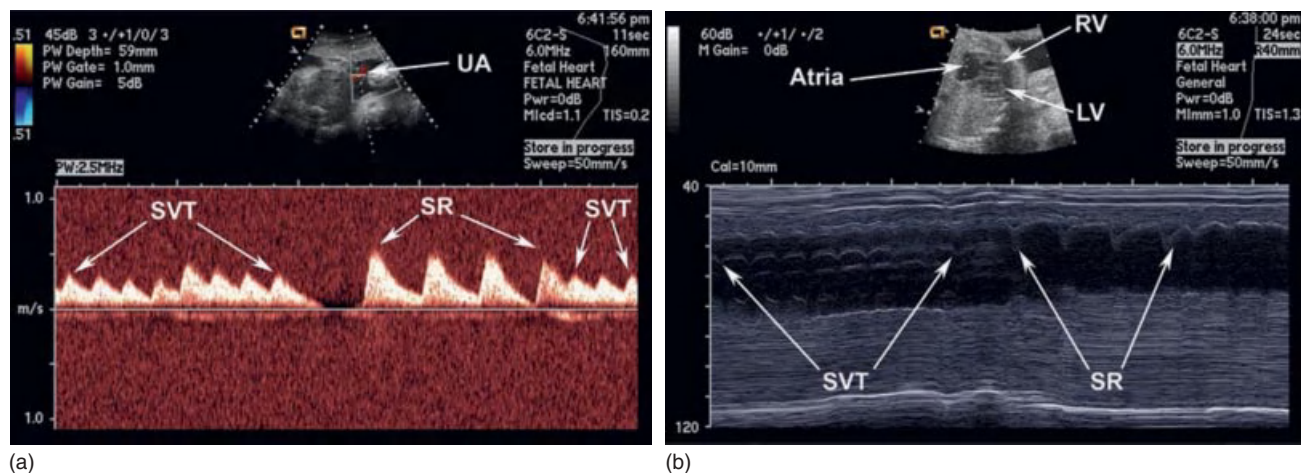
Figure 8.48 (a) The umbilical arterial Doppler shows the sudden termination and onset of supraventricular tachycardia (SVT), suggesting a reentrant mechanism. Sinus rhythm is also demonstrated (SR). (b) The M-mode through both atria again shows the sudden termination of supraventricular tachycardia in the same fetus who was diagnosed with orthodromic re-entrant tachycardia. LV, left ventricle; RV, right ventricle; UA, umbilical artery.

150

Figure 8.49 Premature atrial contractions (PAC) can be easily demonstrated by an M-mode through the atria. In this example, the atria contract regularly 'a' until a premature atrial contraction which causes a compensatory pause and a delay until the next atrial contraction (*).
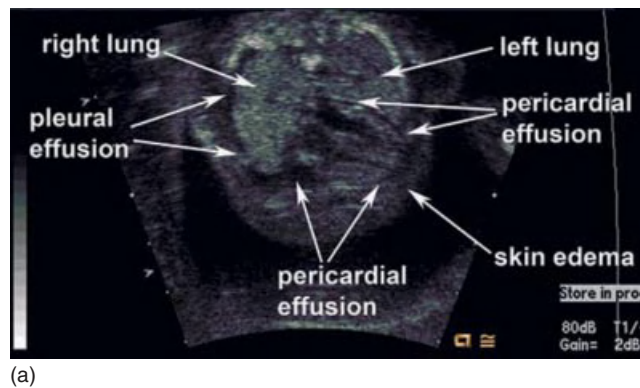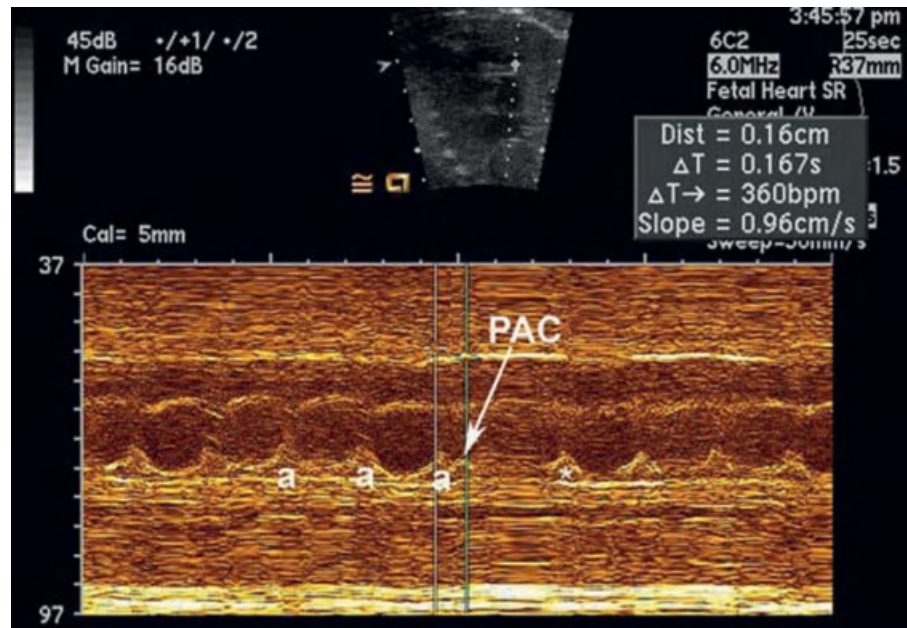
(a)
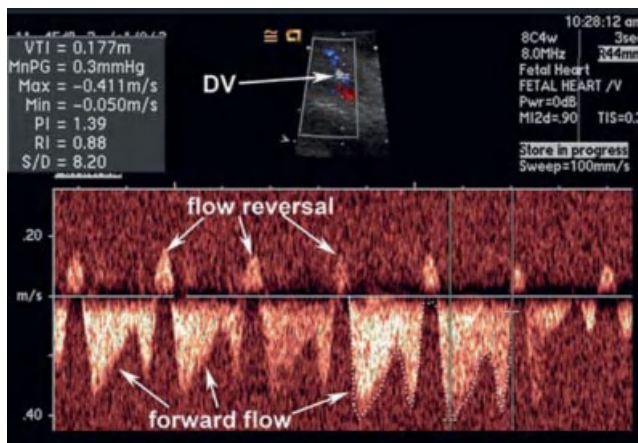
(b)
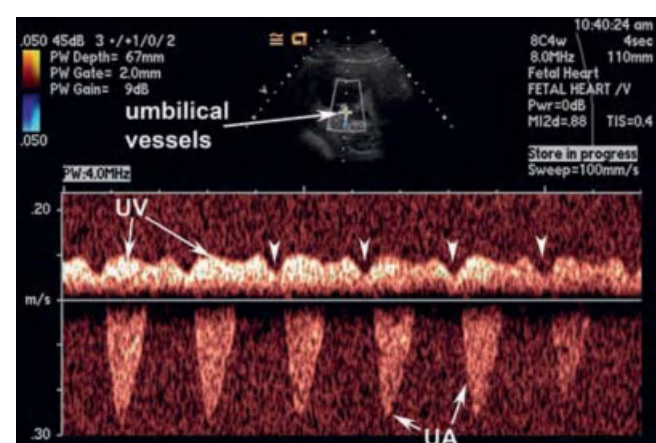
(c)

Figure 8.50 The abnormal cardiovascular profile can be used to establish overall fetal well-being. In the first example (a), there is evidence of hydrops given the presence of pleural and pericardial effusion along with skin edema. The ductus venosus (DV) should have no flow reversal in the normal fetus; however, the second example (b) clearly shows flow reversal. Doppler of the umbilical vessels is important and in this example the normal diastolic flow in the umbilical artery (UA) cannot be seen, a marker for increased placental resistance. (c) Additionally, there is evidence of notching (arrowheads) in the umbilical vein (UV) just prior to the umbilical arterial systolic flow. The notching in this example probably represents increased right ventricular end-diastolic pressure resulting in diminished umbilical venous flow during that part of the cardiac cycle.

151
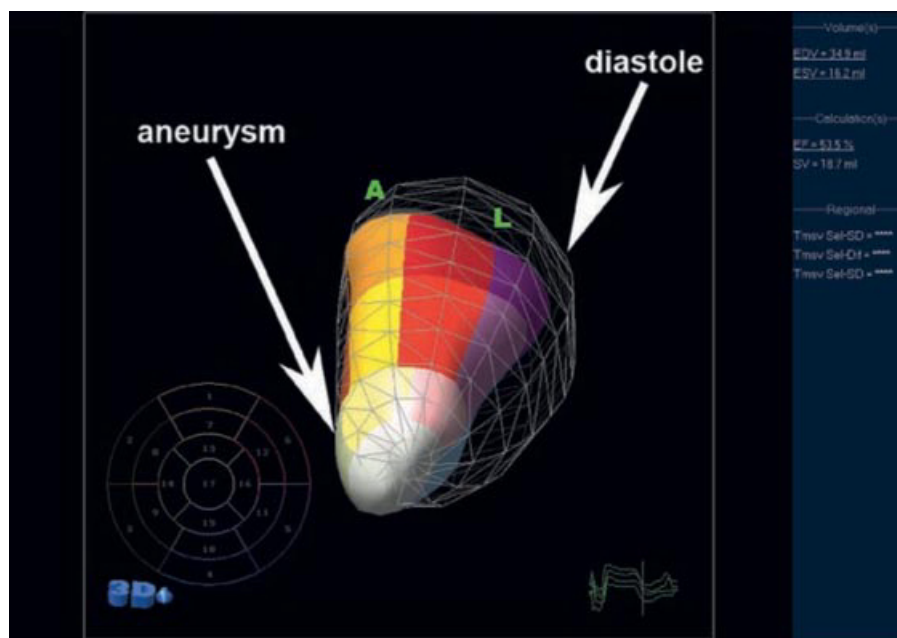
Figure 8.51 This example shows a three-dimensional rendition of the left ventricular chamber in systole by acquiring a full volume set. An aneurysm is clearly seen towards the apex. The wire frame surrounding the left ventricular model represents the position of the ventricle at end-diastole.

(a) (b)
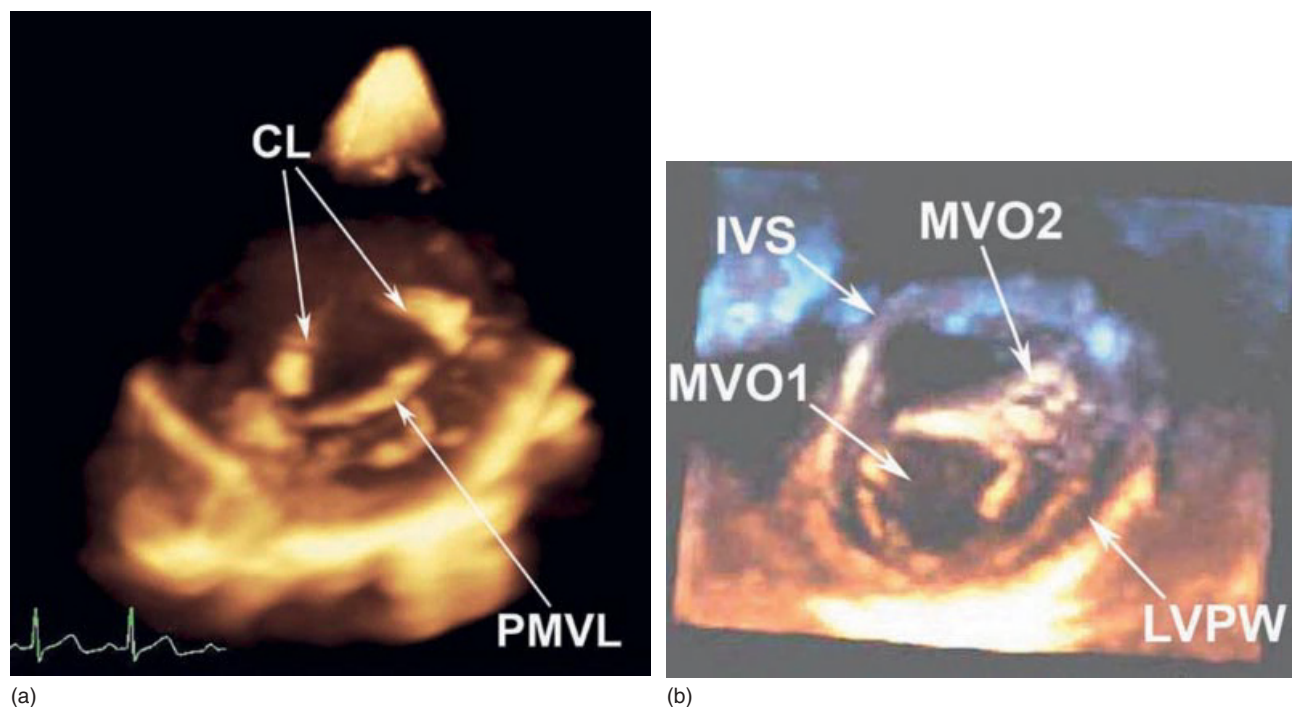
Figure 8.52 (a) This three-dimensional view shows a cleft in the anterior leaflet of the mitral valve (CL); the posterior mitral valve leaflet (PMVL) is shown posteriorly. (b) A double-orifice mitral valve can also be visualized using three-dimensional echocardiography. In this example, there is a larger orifice mitral valve (MVO1) and an accessory orifice mitral valve (MVO2). The left ventricular posterior wall (LVPW) and interventricular septum (IVS) are also demonstrated.

foreign bodies. Precise measurements of luminal area are also possible. Blood flow velocity can be measured by Doppler velocimetry, using a flexible guide wire system with a piezoelectric Doppler crystal mounted in the tip. For simultaneous cross-sectional imaging and flow velocimetry, the ultrasound catheter may either be placed alongside or introduced over the Doppler guide wire.

The widest clinical and experimental application of intravascular ultrasound has been in adult cardiology, where it is most often used to evaluate coronary arterial architecture before
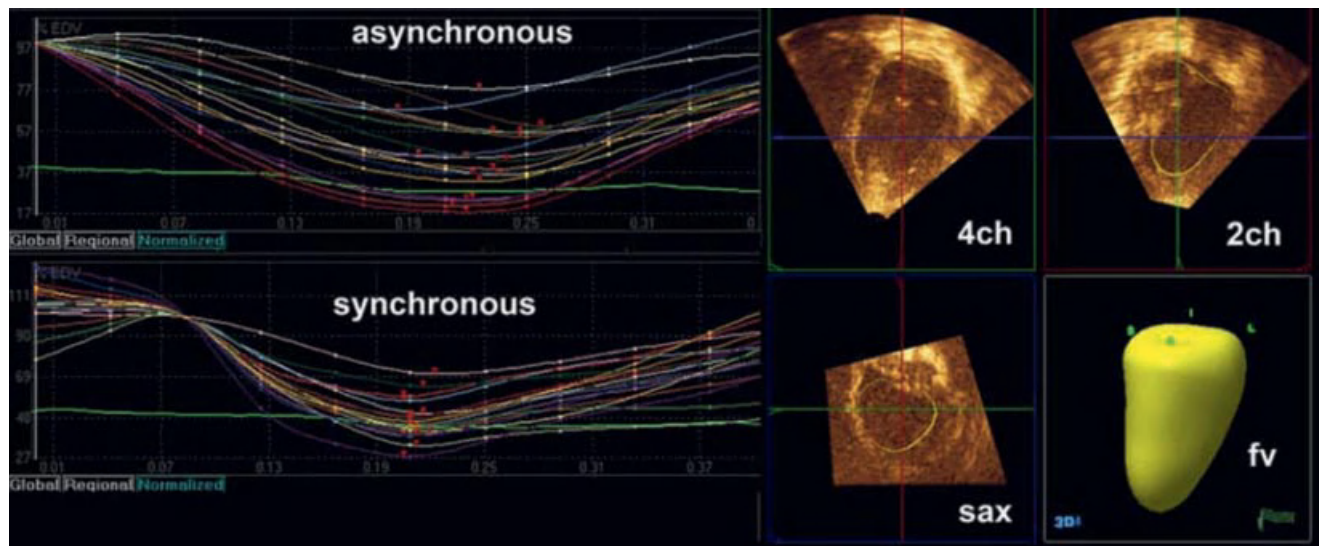
Figure 8.53 After obtaining a full volume by three-dimensional echocardiography, the individual segments can be tracked throughout the cardiac cycle. In this example, a patient underwent biventricular pacemaker optimization for a dyssynchrony and the image labeled asynchronous shows that the segments achieve minimum size (*y*-axis) at various times (*x*-axis). After determining the optimal biventricular pacemaker settings, the segments achieve minimum size at nearly the same time (graph labeled synchronous).
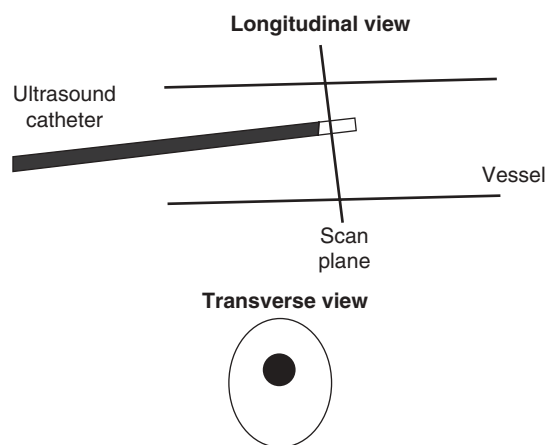

Figure 8.54 This is a diagram to represent the implications of an intravascular ultrasound catheter oriented in the vessel in a non-coaxial fashion (longitudinal view). The resulting transverse scan image appears as an ellipse rather than a circle.

Figure 8.55 Intravascular ultrasound image after balloon dilatation of a native aortic coarctation showing an echogenic intimal flap (arrow). (Reproduced with permission from Sohn *et al*. *Circulation* 1994;**90**:340–7.)

and after transcatheter dilatation, stenting, and atherectomy [99]. In children, intravascular ultrasound has had limited clinical application. For the most part, it has been used to evaluate vascular and valvar lesions treated with transcatheter dilatation when the ability to visualize clearly intimal flaps following balloon dilatation of aortic coarctation or pulmonary arterial stenosis may help to define more clearly factors associated with successful dilatation and, ultimately, to guide the interventionalist in determining further management (Figure 8.55) [100,101]. Morphologic evaluation of the intermediate pulmonary arteries and the coronary arteries may also prove useful in
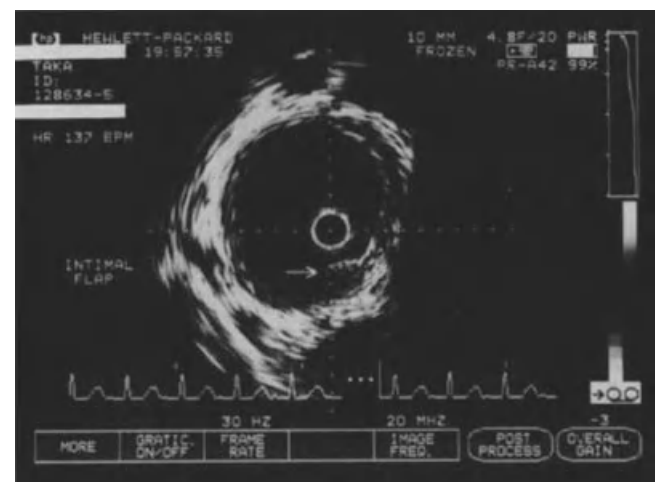
certain circumstances, such as in Williams syndrome, postoperative pulmonary atresia with unifocalized aortopulmonary collaterals, and Kawasaki disease [102,103].

References

1 Silverman NH, Hunter S, Anderson RH, *et al*. Anatomical basis of cross sectional echocardiography. *Br Heart J* 1983;**5**0:421–31.
2 Van Praagh S, Kreutzer J, Alday L, Van Praagh R. Systemic and pulmonary venous connections in visceral heterotaxy with

emphasis on the diagnosis of the atrial situs: a study of 109 postmortem cases. In: Clark EB, Takao A, eds. *Developmental Cardiology, Morphogenesis and Function*. Mount Kisco, NY: Futura Publishing, 1990: 671–727.

3 Silverman NH. *Pediatric Echocardiography*. Baltimore: Williams & Wilkins, 1993.

4 Shiraishi S, DiSessa T, Jarmakani J, *et al*. Two-dimensional echocardiographic assessment of right ventricular volume in children with congenital heart disease. *Am J Cardiol* 1982;**50**:1368–75.

5 Roge CL, Silverman NH, Hart PA, Ray RM. Cardiac structure growth pattern determined by echocardiography. *Circulation* 1978;**57**:285–90.

6 Henry WL, Gardin JM, Ware JH. Echocardiographic measurements in normal subjects from infancy to old age. *Circulation* 1980;**62**:1054–61.

7 Lopez L, Colan SD, Frommelt PC, *et al*. Recommendations for quantification methods during the performance of a pediatric echocardiogram: a report from the Pediatric Measurements Writing Group of the American Society of Echocardiography Pediatric and Congenital Heart Disease Council. *J Am Soc Echocardiogr* 2010;**23**:465–95; quiz 576–7.

8 Colan S, Borow K, Neumann A. Use of calibrated carotid pulse tracing for calculation of left ventricular pressure and wall stress throughout ejection. *Am Heart J* 1985;**109**:1306–110.

9 Colan S, Borow K, Neumann A. Left ventricular end-systolic wall stress–velocity of fiber shortening relation: a load independent index of myocardial contractility. *J Am Coll Cardiol* 1984;**4**: 715–24.

10 Isaaz K, Ethevenot G, Admant P, *et al*. A simplified normalized ejection phase index measured by Doppler echocardiography for the assessment of left ventricular function. *Am J Cardiol* 1990;**65**:1246–151.

11 Sabbah H, Khaja F, Brymer J, *et al*. Noninvasive evaluation of left ventricular performance based on peak aortic blood acceleration measured with continuous-wave Doppler velocity meter. *Circulation* 1986;**74**:323–39.

12 Eidem BW, McMahon CJ, Cohen RR, *et al*. Impact of cardiac growth on Doppler tissue imaging velocities: a study in healthy children. *J Am Soc Echocardiogr* 2004;**17**:212–21.

13 Chan LY, Fok WY, Wong JT, *et al*. Reference charts of gestation-specific tissue Doppler imaging indices of systolic and diastolic functions in the normal fetal heart. *Am Heart J* 2005;**150**: 750–75.

14 Langeland S, D'Hooge J, Wouters PF, *et al*. Experimental validation of a new ultrasound method for the simultaneous assessment of radial and longitudinal myocardial deformation independent of insonation angle. *Circulation* 2005;**112**: 2157–262.

15 Lorch SM, Ludomirsky A, Singh GK. Maturational and growth-related changes in left ventricular longitudinal strain and strain rate measured by two-dimensional speckle tracking echocardiography in healthy pediatric population. *J Am Soc Echocardiogr* 2008;**21**:1207–115.

16 Mertens L, Ganame J, Claus P, *et al*. Early regional myocardial dysfunction in young patients with Duchenne muscular dystrophy. *J Am Soc Echocardiogr* 2008;**21**:1049–154.

17 Fyfe DA, Ketchum D, Lewis R, *et al*. Tissue Doppler imaging detects severely abnormal myocardial velocities that identify children with pre-terminal cardiac graft failure after heart transplantation. *J Heart Lung Transplant* 2006;**25**:510–7.

18 Tuzcu V, Bodtke JP, Best TH. Early detection of regional myocardial dysfunction in paced children with congenital complete atrioventricular block. *Pacing Clin Electrophysiol* 2007;**30**: 764–71.

19 Di Salvo G, Russo MG, Paladini D, *et al*. Two-dimensional strain to assess regional left and right ventricular longitudinal function in 100 normal foetuses. *Eur J Echocardiogr* 2008;**9**:754–76.

20 Weidemann F, Eyskens B, Jamal F, *et al*. Quantification of regional left and right ventricular radial and longitudinal function in healthy children using ultrasound-based strain rate and strain imaging. *J Am Soc Echocardiogr* 2002;**15**:20–8.

21 Vogel M, Schmidt MR, Kristiansen SB, *et al*. Validation of myocardial acceleration during isovolumic contraction as a novel noninvasive index of right ventricular contractility: comparison with ventricular pressure–volume relations in an animal model. *Circulation* 2002;**105**:1693–9.

22 Eidem BW, McMahon CJ, Ayres NA, *et al*. Impact of chronic left ventricular preload and afterload on Doppler tissue imaging velocities: a study in congenital heart disease. *J Am Soc Echocardiogr* 2005;**18**:830–8.

23 Ganame J, Mertens L, Eidem BW, *et al*. Regional myocardial deformation in children with hypertrophic cardiomyopathy: morphological and clinical correlations. *Eur Heart J* 2007; **28**:2886–94.

24 Pauliks LB, Chan KC, Chang D, *et al*. Regional myocardial velocities and isovolumic contraction acceleration before and after device closure of atrial septal defects: a color tissue Doppler study. *Am Heart J* 2005;**150**:294–301.

25 Nagueh SF, Middleton KJ, Kopelen HA, *et al*. Doppler tissue imaging: a noninvasive technique for evaluation of left ventricular relaxation and estimation of filling pressures. *J. Am Coll Cardiol* 1997;**30**:1527–33.

26 Harada K, Tamura M, Yasuoka K, Toyono M. A comparison of tissue Doppler imaging and velocities of transmitral flow in children with elevated left ventricular preload. *Cardiol Young* 2001;**11**:261–8.

27 Friedberg MK, Slorach C. Relation between left ventricular regional radial function and radial wall motion abnormalities using two-dimensional speckle tracking in children with idiopathic dilated cardiomyopathy. *Am J Cardiol* 2008;**102**:335–9.

28 Friedberg MK, Roche SL, Mohammed AF, *et al*. Left ventricular diastolic mechanical dyssynchrony and associated clinical outcomes in children with dilated cardiomyopathy. *Circ Cardiovasc Imaging* 2008;**1**:50–7.

29 Scalia GM, Greenberg NL, McCarthy PM, *et al*. Noninvasive assessment of the ventricular relaxation time constant (tau) in humans by Doppler echocardiography. *Circulation* 1997; **95**:151–5.

30 Thomas JD, Newell JB, Choong CY, Weyman AE. Physical and physiological determinants of transmitral velocity: numerical analysis. *Am J Physiol* 1991;**260**:H1718–30.

31 Cohen GP, Pietrolungo JF, Thomas J, Klein A. A practical guide to assessment of ventricular diastolic function using Doppler echocardiography. *J Am Coll Cardiol* 1996;**27**:1753–60.

32 Takatsuji H, Mikami T, Urasawa K, *et al*. A new approach for evaluation of left ventricular diastolic function: spatial and

temporal analysis of left ventricular filling flow propagation by color M-mode Doppler echocardiography. *J Am Coll Cardiol* 1996;**27**:365–71.

33 Tei C, Nishimura R, Seward J, Tajik A. Noninvasive Doppler-derived myocardial performance index: correlation with simultaneous measurements of cardiac catheterization measurements. *J Am Soc Echocardiogr* 1997;**10**:169–78.

34 Ommen SR, Nishimura RA, Appleton CP, *et al*. Clinical utility of Doppler echocardiography and tissue Doppler imaging in the estimation of left ventricular filling pressures: a comparative simultaneous Doppler–catheterization study. *Circulation* 2000;**102**:1788–94.

35 Levine R, Jimoh A, Cape E, *et al*. Pressure recovery distal to a stenosis: potential cause of gradient "overestimation" by Doppler echocardiography. *J Am Coll Cardiol* 1989;**13**:706–15.

36 Cape E, Jones M, Yamada I, *et al*. Turbulent/viscous interactions control Doppler catheter pressure discrepancies in aortic stenosis: the role of the Reynolds number. *Circulation* 1996; **94**:2975–81.

37 Pu M, Vandervoort PM, Greenberg NL, *et al*. Impact of wall constraint on velocity distribution in proximal flow convergence zone. Implications for color Doppler quantification of mitral regurgitation. *J Am Coll Cardiol* 1996;**27**:706–13.

38 Simpson I, Valdes-Cruz L, Sahn D, *et al*. Doppler color flow mapping of simulated *in vitro* regurgitant jets: evaluation of the effects of orifice size and hemodynamic variables. *J Am Coll Cardiol* 1989;**13**:1195–207.

39 Maciel B, Moises V, Shandas R. Effects of pressure and volume of the receiving chamber on the spatial distribution of regurgitant jets as imaged by color Doppler flow mapping: an *in vitro* study. *Circulation* 1991;**83**:605–13.

40 Sahn D. Instrumentation and physical factors related to visualization of stenotic and regurgitant jets by Doppler color flow mapping. *J Am Coll Cardiol* 1988;**12**:1354–65.

41 Van Hare G, Silverman N. Contrast two-dimensional echocardiography in congenital heart disease: techniques, indications and clinical utility. *J Am Coll Cardiol* 1989;**13**:673–86.

42 Pahl E, Sehgal R, Chrystof D, *et al*. Feasibility of exercise stress echocardiography for the follow-up of children with coronary involvement secondary to Kawasaki disease. *Circulation* 1995;**91**:122–8.

43 Noto N, Ayusawa M, Karasawa K, *et al*. Dobutamine stress echocardiography for detection of coronary artery stenosis in children with Kawasaki disease. *J Am Coll Cardiol* 1996;**27**:1251–6.

44 Takeuchi M, Miura Y, Toyokawa T, *et al*. The comparative diagnostic value of dobutamine stress echocardiography and thallium stress tomography for detecting restenosis after coronary angioplasty. *J Am Soc Echocardiogr* 1995;**8**:696–702.

45 Kimball TR, Witt SA, Daniels SR. Dobutamine stress echocardiography in the assessment of suspected myocardial ischemia in children and young adults. *Am J Cardiol* 1997;**79**:380–4.

46 De Wolf D, Suys B, Maurus R, *et al*. Dobutamine stress echocardiography in the evaluation of late anthracycline cardiotoxicity in childhood cancer survivors. *Pediatr Res* 1996;**39**:504–12.

47 Cyran SE, Grzeszczak M, Kaufman K, *et al*. Aortic "recoarctation" at rest versus at exercise in children as evaluated by stress Doppler echocardiography after a "good" operative result. *Am J Cardiol* 1993;**71**:963–70.

48 Stumper O, Elzenga N, Hess J, Sutherland G. Transesophageal echocardiography in children with congenital heart disease: an initial experience. *J Am Coll Cardiol* 1990;**16**:433–41.

49 Kaulitz R, Stumper OG, Geuskens R. Comparative values of the precordial and transesophageal approaches in the echocardiographic evaluation of the atrial baffle function after an atrial correction procedure. *J Am Coll Cardiol* 1990;**16**:686–94.

50 Muhiudeen I, Roberson D, Silverman N, *et al*. Intraoperative echocardiography in infants and children with congenital cardiac shunt lesions: transesophageal versus epicardial echocardiography. *J Am Coll Cardiol* 1990;**16**:1687–95.

51 Roberson D, Muhiudeen I, Silverman N. Transesophageal echocardiography in pediatrics: technique and limitations. *Echocardiography* 1990;**7**:699–712.

52 Snider A, Serwer G, Ritter S, eds. *Echocardiography in Pediatric Heart Disease*, 2nd edn. St Louis, MO: Mosby-Year Book, 1997.

53 Muhiudeen I, Silverman N, Anderson R. Transesophageal transgastric echocardiography in infants and children: the subcostal view equivalent. *J Am Soc Echocardiogr* 1995;**8**:231–44.

54 Seward J, Khandheria B, Edwards W, *et al*. Biplanar transeosphageal echocardiography: anatomic correlations, image orientation, and clinical applications. *Mayo Clin Proc* 1990;**65**:1193–213.

55 Gembruch U, Knopfle G, Chatterjee M, *et al*. Prenatal diagnosis of atrioventricular canal malformations with up-to-date echocardiographic technology: report of 14 cases. *Am Heart J* 1991;**121**:1489–97.

56 Hornberger LK, Sanders SP, Rein AJ, *et al*. Left heart obstructive lesions and left ventricular growth in the midtrimester fetus. A longitudinal study. *Circulation* 1995;**92**:1531–8.

57 McCaffrey FM, Sherman FS. Prenatal diagnosis of severe aortic stenosis. *Pediatr Cardiol* 1997;**18**:276–81.

58 Allan LD, Sharland GK. The echocardiographic diagnosis of totally anomalous pulmonary venous connection in the fetus. *Heart* 2001;**85**:433–7.

59 McElhinney DB, Hoydu AK, Gaynor JW, *et al*. Patterns of right aortic arch and mirror-image branching of the brachiocephalic vessels without associated anomalies. *Pediatr Cardiol* 2001; **22**:285–91.

60 Perolo A, Prandstraller D, Ghi T, *et al*. Diagnosis and management of fetal cardiac anomalies: 10 years of experience at a single institution. *Ultrasound Obstet Gynecol* 2001;**18**:615–8.

61 Volpe P, Paladini D, Marasini M, *et al*. Common arterial trunk in the fetus: characteristics, associations, and outcome in a multi-centre series of 23 cases. *Heart* 2003;**89**:1437–41.

62 Kim N, Friedberg MK, Silverman NH. Diagnosis and prognosis of fetuses with double outlet right ventricle. *Prenat Diagn* 2006; **26**:740–5.

63 Taketazu M, Lougheed J, Yoo SJ, *et al*. Spectrum of cardiovascular disease, accuracy of diagnosis, and outcome in fetal heterotaxy syndrome. *Am J Cardiol* 2006;**97**:720–4.

64 Berning RA, Silverman NH, Villegas M, *et al*. Reversed shunting across the ductus arteriosus or atrial septum in utero heralds severe congenital heart disease. *J Am Coll Cardiol* 1996;**27**:481–6.

65 Rychik J, Gullquist SD, Jacobs ML, Norwood WI. Doppler echocardiographic analysis of flow in the ductus arteriosus of infants with hypoplastic left heart syndrome: relationship of flow patterns to systemic oxygenation and size of interatrial communication. *J Am Soc Echocardiogr* 1996;**9**:166–73.

66 Bonnet D, Coltri A, Butera G, *et al*. Detection of transposition of the great arteries in fetuses reduces neonatal morbidity and mortality. *Circulation* 1999;**99**:916–8.

67 Maeno YV, Kamenir SA, Sinclair B, *et al*. Prenatal features of ductus arteriosus constriction and restrictive foramen ovale in d-transposition of the great arteries. *Circulation* 1999;**99**:1209–14.

68 Michelfelder E, Gomez C, Border W, *et al*. Predictive value of fetal pulmonary venous flow patterns in identifying the need for atrial septoplasty in the newborn with hypoplastic left ventricle. *Circulation* 2005;**112**:2974–9.

69 Soslow JH, Friedberg MK, Silverman NH. Idiopathic premature closure of the ductus arteriosus: an indication for early delivery. *Echocardiography* 2008;**25**:650–2.

70 Simpson LL, Malone FD, Bianchi DW, *et al*. Nuchal translucency and the risk of congenital heart disease. *Obstet Gynecol* 2007;**109**: 376–83.

71 Albert TJ, Landon MB, Wheller JJ, *et al*. Prenatal detection of fetal anomalies in pregnancies complicated by insulin-dependent diabetes mellitus. *Am J Obstet Gynecol* 1996;**174**:1424–8.

72 Devine PC, Simpson LL. Nuchal translucency and its relationship to congenital heart disease. *Semin Perinatol* 2000;**24**:343–51.

73 Huggon IC, Cook AC, Simpson JM, *et al*. Isolated echogenic foci in the fetal heart as marker of chromosomal abnormality. *Ultrasound Obstet Gynecol* 2001;**17**:11–6.

74 Gossett DR, Lantz ME, Chisholm CA. Antenatal diagnosis of single umbilical artery: is fetal echocardiography warranted? *Obstet Gynecol* 2002;**100**:903–8.

75 Koivurova S, Hartikainen AL, Gissler M, *et al*. Neonatal outcome and congenital malformations in children born after *in-vitro* fertilization. *Hum Reprod* 2002;**17**:1391–8.

76 Wax JR, Donnelly J, Carpenter M, *et al*. Childhood cardiac function after prenatal diagnosis of intracardiac echogenic foci. *J Ultrasound Med* 2003;**22**:783–7.

77 Friedberg MK, Silverman NH. Changing indications for fetal echocardiography in a University Center population. *Prenat Diagn* 2004;**24**:781–6.

78 Prucka S, Clemens M, Craven C, McPherson E. Single umbilical artery: what does it mean for the fetus? A case–control analysis of pathologically ascertained cases. *Genet Med* 2004;**6**:54–7.

79 Rychik J, Ayres N, Cuneo B, *et al*. American Society of Echocardiography guidelines and standards for performance of the fetal echocardiogram. *J Am Soc Echocardiogr* 2004;**17**:803–10.

80 Dane B, Dane C, Kiray M, *et al*. Fetuses with single umbilical artery: analysis of 45 cases. *Clin Exp Obstet Gynecol* 2009;**36**:116–9.

81 Shanks AL, Odibo AO, Gray DL. Echogenic intracardiac foci: associated with increased risk for fetal trisomy 21 or not? *J Ultrasound Med* 2009;**28**:1639–43.

82 Paladini D, Chita SK, Allan LD. Prenatal measurement of cardiothoracic ratio in evaluation of heart disease. *Arch Dis Child* 1990;**65**:20–3.

83 Moise KJ Jr, Huhta JC, Sharif DS, *et al*. Indomethacin in the treatment of premature labor. Effects on the fetal ductus arteriosus. *N Engl J Med*. 1988;**319**:327–31.

84 Huhta JC, Cohen AW, Wood DC. Premature constriction of the ductus arteriosus. *J Am Soc Echocardiogr* 1990;**3**:30–4.

85 Hofstadler G, Tulzer G, Altmann R, *et al*. Spontaneous closure of the human fetal ductus arteriosus – a cause of fetal congestive heart failure. *Am J Obstet Gynecol* 1996;**174**:879–83.

86 Allan LD, Anderson RH, Sullivan ID, *et al*. Evaluation of fetal arrhythmias by echocardiography. *Br Heart J* 1983; **50**:240–5.

87 Kleinman CS. Prenatal diagnosis and management of intrauterine arrhythmias. *Fetal Ther* 1986;**1**:92–5.

88 Lingman G, Lundstrom NR, Marsal K. Clinical outcome and circulatory effects of fetal cardiac arrhythmia. *Acta Paediatr Scand Suppl* 1986;**329**:120–6.

89 Chao RC, Ho ES, Hsieh KS. Fetal atrial flutter and fibrillation: prenatal echocardiographic detection and management. *Am Heart J* 1992;**124**:1095–8.

90 Glickstein JS, Buyon J, Friedman D. Pulsed Doppler echocardiographic assessment of the fetal PR interval. *Am J Cardiol* 2000;**86**:236–9.

91 Andelfinger G, Fouron JC, Sonesson SE, Proulx F. Reference values for time intervals between atrial and ventricular contractions of the fetal heart measured by two Doppler techniques. *Am J Cardiol* 2001;**88**:1433–6, A1438.

92 Nield LE, Silverman ED, Taylor GP, *et al*. Maternal anti-Ro and anti-La antibody-associated endocardial fibroelastosis. *Circulation* 2002;**105**:843–8.

93 Rein AJ, O'Donnell C, Geva T, *et al*. Use of tissue velocity imaging in the diagnosis of fetal cardiac arrhythmias. *Circulation* 2002;**106**:1827–33.

94 Nii M, Hamilton RM, Fenwick L, *et al*. Assessment of fetal atrioventricular time intervals by tissue Doppler and pulse Doppler echocardiography: normal values and correlation with fetal electrocardiography. *Heart* 2006;**92**:1831–7.

95 Rosenthal D, Friedman DM, Buyon J, Dubin A. Validation of the Doppler PR interval in the fetus. *J Am Soc Echocardiogr* 2002; **15**:1029–30.

96 Makikallio K, Rasanen J, Makikallio T, *et al*. Human fetal cardiovascular profile score and neonatal outcome in intrauterine growth restriction. *Ultrasound Obstet Gynecol* 2008;**31**:48–54.

97 Kapetanakis S, Kearney MT, Siva A, *et al*. Real-time three-dimensional echocardiography: a novel technique to quantify global left ventricular mechanical dyssynchrony. *Circulation* 2005;**112**:992–1000.

98 Ten Harkel AD, Van Osch-Gevers M, Helbing WA. Real-time transthoracic three dimensional echocardiography: normal reference data for left ventricular dyssynchrony in adolescents. *J Am Soc Echocardiogr* 2009;**22**:933–8.

99 Chou TF, Fitzgerald PJ, Yock P, Sudhir K. Intravascular two-dimensional and Doppler ultrasound. In: *Cardiology*. Philadelphia: Lippincott-Raven, 1996: 893–7.

100 Sohn S, Rothman A, Shiota T, *et al*. Acute and follow-up intravascular ultrasound findings after balloon dilation of coarctation of the aorta. *Circulation* 1994;**90**:340–7.

101 Ino T, Okubo M, Akimoto K, *et al*. Mechanism of balloon angioplasty in children with arterial stenosis assessed by intravascular ultrasound and angiography. *Am Heart J* 1995;**129**:132–8.

102 Rein A, Preminger TP, Perry SB, *et al*. Generalized arteriopathy in Williams syndrome: an intravascular ultrasound study. *J Am Coll Cardiol* 1993;**21**:1727–30.

103 Sugimura T, Kato H, Inoue O, *et al*. Intravascular ultrasound of coronary arteries in children: assessment of the wall morphology and the lumen after Kawasaki disease. *Circulation* 1994; **89**:258–65.

9 Radiographic Techniques

Alison K. Meadows

University of California San Francisco, Kaiser Permanente of Northern California,
San Francisco, CA, USA

Introduction

The complexity of the anatomy and physiology of patients surviving with congenital heart disease (CHD) is increasing exponentially. The majority will survive to adulthood, and the need for reintervention is common. As such, the field is placing new demands on imaging to diagnose and plan medical management, and also to identify the need for and timing of reintervention. There are a number of imaging modalities available to the clinician and radiologist.

Echocardiography has been, and remains, a mainstay of imaging in congenital heart disease. Despite its importance in rapid diagnosis and follow-up, it has limitations. A postoperative scar, chest wall deformities, overlying lung tissue, and large body size as the patient ages often result in suboptimal transthoracic echocardiographic windows. Transesophageal echocardiography, although providing improved acoustic windows, is limited by its small field of view and more invasive nature that often requires deep sedation or general anesthesia.

Cardiac catheterization, employing X-ray fluoroscopy and contrast angiography, has an expanding role in minimally invasive interventions, but its role as a diagnostic procedure is rapidly diminishing. This is partly due to its limitation as a 2D projection imaging technique with poor soft tissue contrast and the substantial ionizing radiation exposure involved, and partly because both diagnostic and functional analysis are often better performed with noninvasive imaging techniques.

This chapter focuses on the evolving and expanding roles of other imaging modalities in diagnosing and monitoring patients with CHD, including cardiac magnetic resonance imaging (MRI), cardiac computed tomography (CT), and radionuclide scintigraphy. It finishes with a reminder that the simple chest X-ray (CXR) is still useful.

Cardiac magnetic resonance imaging

Cardiac MRI has emerged as an alternative, complementary, and frequently superior imaging modality for investigating anatomy and function in the patient with CHD. It has many advantages over other imaging modalities. It neither requires the use of iodinated contrast agents nor involves exposure to ionizing radiation. This is particularly important in patients who have been, and continue to be, exposed to large doses of contrast agent and radiation during hemodynamic and interventional catheterization. Additionally, many of these patients are children, who are more susceptible to the adverse effects of radiation. Major advances in MRI hardware and software, including advanced coil design, faster gradients, new pulse sequences, and faster image reconstruction techniques, allow rapid, high-resolution imaging of complex anatomy and accurate, quantitative assessment of physiology and function.

Cardiac MRI techniques

Cine MRI

ECG-gated gradient-echo (GRE) sequences can be employed to provide multiple images throughout the cardiac cycle in prescribed anatomic locations. Display of these images in a cine mode demonstrates the dynamic motion of the heart and vessels [1–3]. Cine MRI techniques, at a minimum, allow the assessment of anatomy, but more importantly, allow qualitative and quantitative assessment of physiology and function by quantifying chamber volumes, myocardial mass, and ventricular function. Further, cine MRI allows qualitative assessment of focal and global wall motion abnormalities,

qualitative and quantitative assessment of valve pathology including the mechanism and severity of valve regurgitation and the location and severity of valve stenoses, identification and quantification of intra- and extracardiac shunts, and visualization of other areas of flow turbulence.

MRI techniques for quantifying chamber volumes, myocardial mass, and ventricular function, both fast GRE [4–7] and balanced steady-state free precession (SSFP) imaging [1,2], have been extensively evaluated and validated [8–10]. Briefly, evaluation of function begins with obtaining a series of contiguous slices (cines) along the short axis of the ventricles, extending from base to apex. These images are played back in a cine loop and the end-systolic and end-diastolic phases are chosen. The endocardial borders are traced at both time points and the epicardial borders are traced at one of the two time points (Figure 9.1). Ventricular volumes are then calculated as the sum of the traced volumes (area times slice thickness). Myocardial mass is calculated as the myocardial muscle volume times $1.05\,\mathrm{g\,mm^{-3}}$ (density of myocardium). From these data, ventricular end-diastolic volume, end-systolic volume, stroke volume, ejection fraction, myocardial mass, and mass:volume ratio can be calculated for both the right and left ventricles. Most computer workstation software packages for cardiac MRI analysis provide semi-automated post-processing tools to maximize efficiency.

Spin-echo (black blood) imaging

ECG-gated spin-echo (SE) sequences, or black blood imaging, despite being static, have many benefits in this patient population. It allows assessment of anatomy with thin slices, high spatial resolution, and excellent blood–myocardium and blood–vessel wall contrast (Figure 9.2). Black blood techniques are superb for evaluating the spatial relationship between cardiovascular and other intrathoracic structures such as the chest wall and the tracheobronchial tree. These features hold particular relevance when delineating complicated native and postsurgical cardiac anatomy. Such techniques are also less susceptible to artifacts from metallic implanted devices, commonly seen in the CHD patient, such as stents, coils, occluder devices, clips, and sternal wires.

Flow quantification

Cardiac-gated GRE sequences with flow encoding gradients are used to quantify the velocity and flow of blood (Figure 9.3) [11]. These sequences are referred to as velocity-encoded cine (VEC) MRI or phase contrast (PC) MRI. 2D VEC MRI sequences are the most commonly used in clinical practice. They can be used to quantify cardiac output, pulmonary to systemic flow ratio (shunt), valvar regurgitation, differential lung perfusion, and coronary flow reserve. They can be used to observe the location and severity of flow obstruction. In addition, VEC MRI assessment of flow is useful for corroborating volumetric data obtained with cine imaging to assure the clinician or radiologist that the data obtained are accurate.

Newer VEC MRI sequences allow resolution of velocity vectors in three directions, with spatial and coverage of a 3D volume, temporally throughout the cardiac cycle. Such techniques have been termed 4D flow encoding [11–13] and even "7D flow" [14], and have the advantage of providing complete spatial and temporal resolution of velocity with a higher signal-to-noise ratio than 2D methods. Post-processing tools allow the construction of vector field plots that highlight the intracardiac and intravascular nature of flow. Ultimately, these techniques may shed light on the mechanism of disease and disease progression [13]. Although currently limited by long scan durations, faster imaging techniques will likely soon allow such methods to reach clinical practice.

Gadolinium-enhanced 3D angiography (3D MRA)

3D MRA sequences are typically not cardiac gated, and therefore do not allow assessment of intracardiac structures. Nevertheless, they provide excellent depiction of arterial and venous vascular structures (Figure 9.4). In a CHD patient, 3D MRA plays a significant diagnostic role. It can diagnose systemic arterial anomalies such as aortopulmonary collaterals, shunts, vascular rings, and coarctation. It is useful in diagnosing pulmonary arterial abnormalities such as focal and diffuse stenoses and abnormal distal arborization patterns. 3D MRA methods are also useful for investigating systemic and pulmonary venous abnormalities, both congenital and postoperative. Finally, 3D MRA is useful for evaluating the relation between vascular and other thoracic structures. With faster techniques and navigator pulses, time-resolved 3D MRA and also noncontrast 3D MRA are becoming alternatives [12].

Coronary artery imaging, perfusion and stress imaging, and myocardial viability

Coronary artery abnormalities, ischemia, and myocardial fibrosis (scar) are important issues to be investigated in CHD patients who commonly have congenitally abnormal or postoperatively acquired coronary artery lesions. It is not uncommon to find an anomalous origin or course of the left or right coronary artery, postsurgical coronary obstruction (e.g., after arterial switch for transposition of the great arteries), coronary artery thrombus, and abnormal fistulous connections (e.g., pulmonary atresia with intact ventricular septum and right ventricular dependent coronary circulation). Identifying such abnormalities is often critical to planning of reintervention and/or medical management. In addition, the CHD population is aging sufficiently to develop atherosclerotic coronary artery disease. There is growing evidence to indicate that myocardial delayed enhancement in a number of subsets of postoperative CHD patients predicts poor outcome [15–18]. There are a number of MRI tools available to study coronary artery anatomy and screen for ischemia or previous infarction/scar.
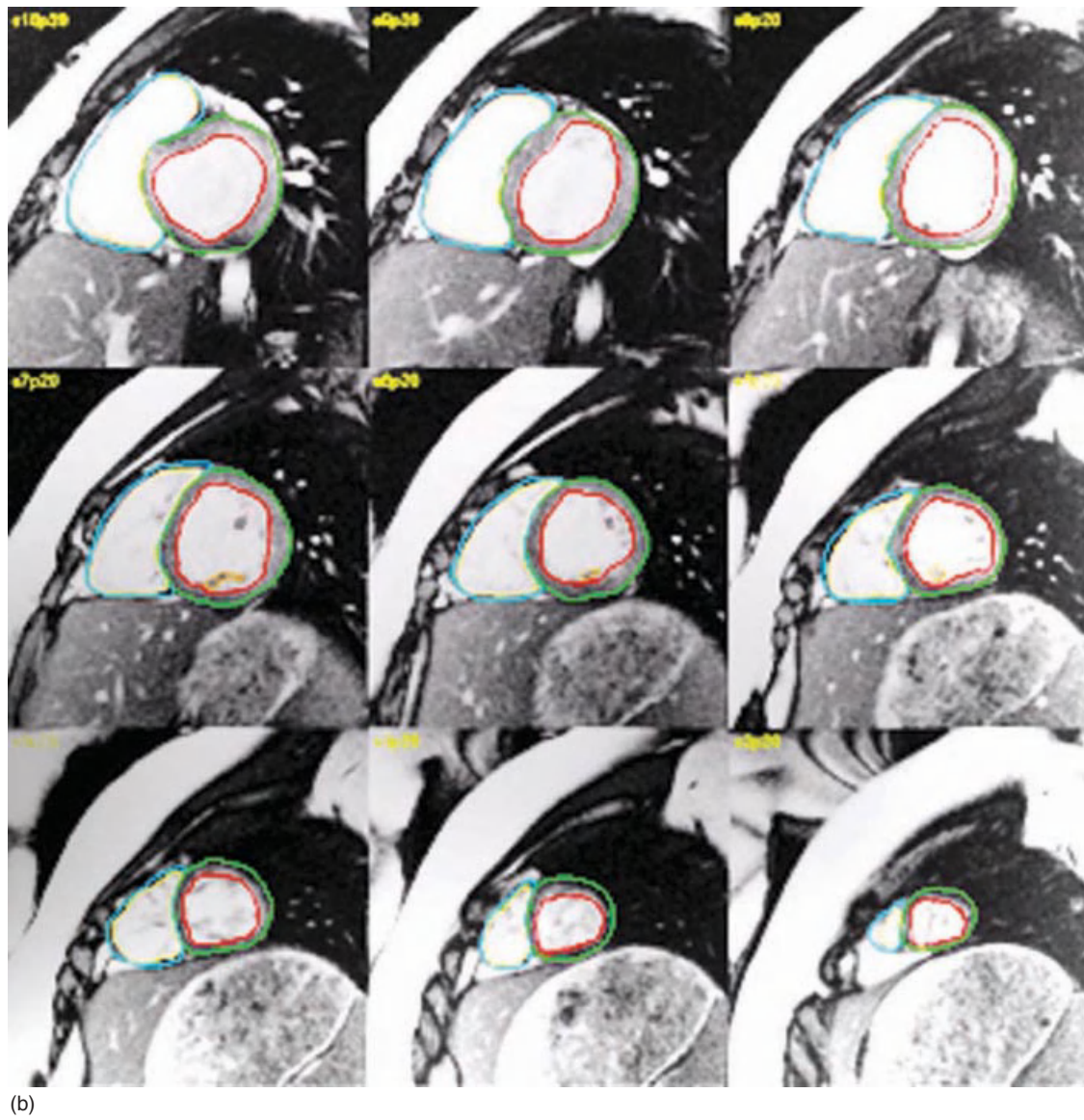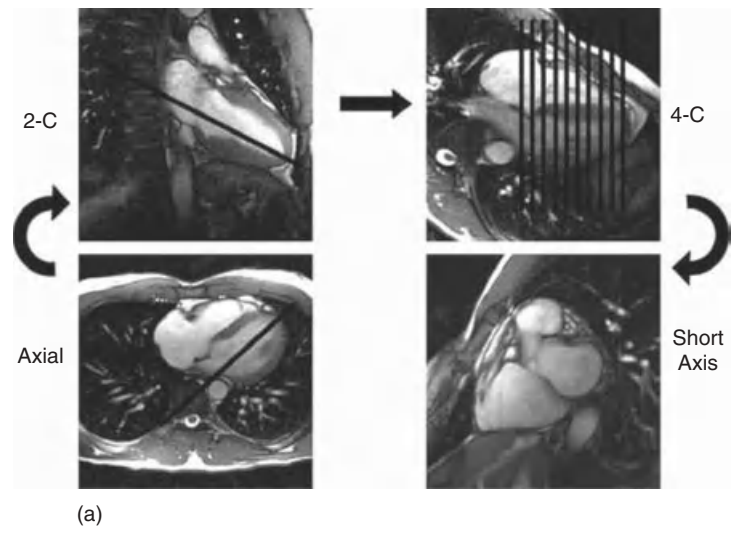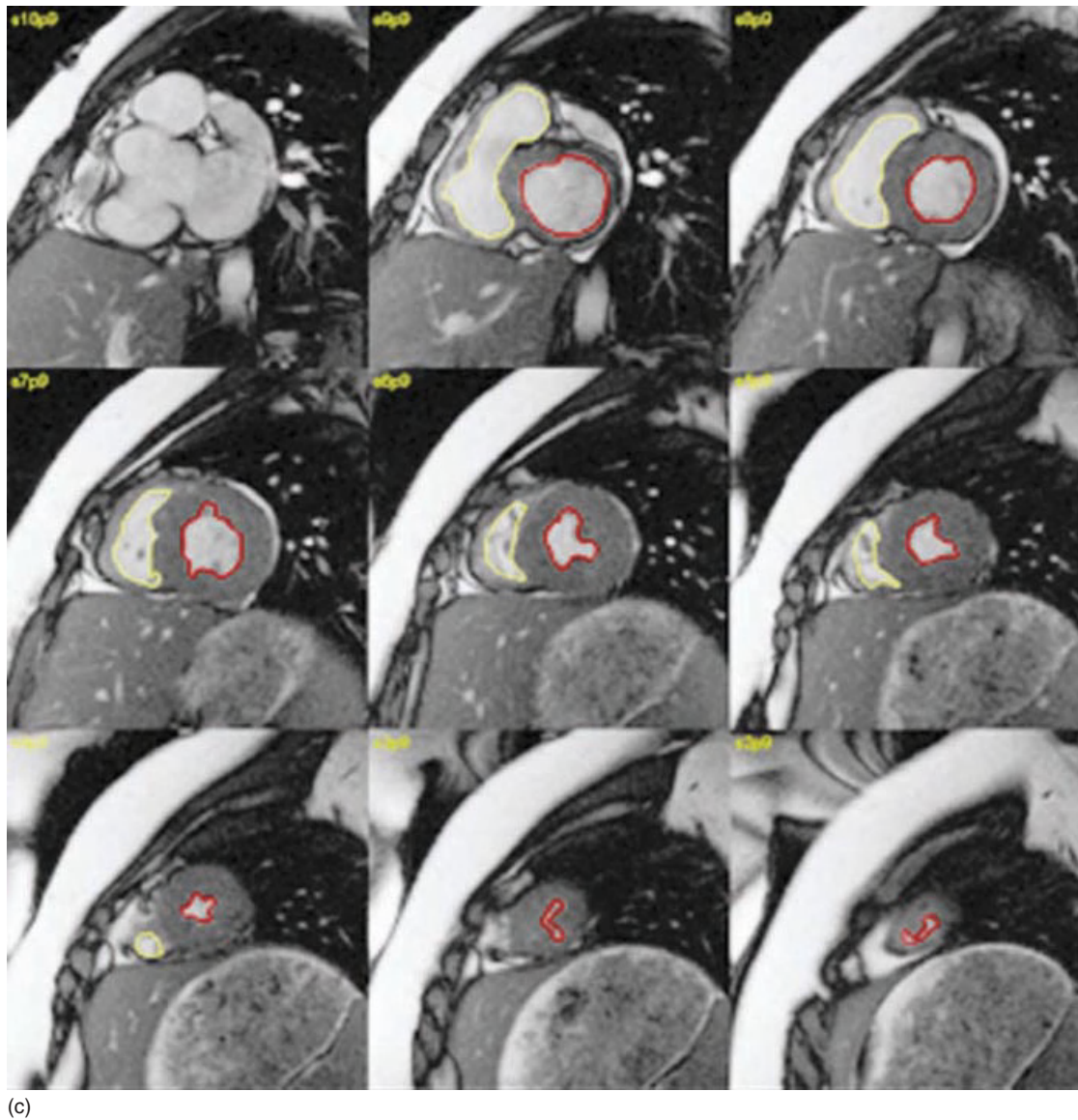
(a)

(b)

Figure 9.1 (a) To obtain a stack of short axis cine images, a two-chamber (2C) view is prescribed from an axial cine, then a four-chamber view (4C) is prescribed from the two-chamber cine, then a short-axis stack is prescribed from the four-chamber cine at end-diastole. (b) Endocardial and epicardial borders traced on a stack of short-axis cine images at end-diastole.

(c)

Figure 9.1 (cont'd) (c) Endocardial borders traced on a stack of short-axis cine images at end-systole.

Coronary artery imaging

Coronary artery imaging is performed using a 3D SSFP (steady-state free precession) imaging sequence that is both cardiac gated (to end diastole) and respiratory gated (navigator pulse). Yielded are high-resolution, nearly isotropic 3D images that demonstrate the origins and proximal courses of the coronary arteries. Although motion artifacts preclude assessment of distal stenoses, this proves a useful technique for evaluating anomalous coronary arteries.

Perfusion imaging and stress imaging

To perform perfusion imaging, pharmacologic stress with a continuous infusion of adenosine or a single bolus of dipyridamole is administered, a bolus of low-dose gadolinium contrast is given, and echo-planar (single-shot) images are collected in three short-axis planes covering the ventricular mass (base, mid, apex) to follow the contrast bolus as it makes its first pass through the heart and perfuses the myocardium. Adenosine is discontinued and, 10–15 min later, rest images are obtained with a second bolus of gadolinium. Alternatively, dobutamine stress can be performed. In this technique, rest cine images are obtained in the short-axis, vertical long-axis, and horizontal long-axis planes. Dobutamine is given in increasing doses (with an additional dose of atropine if necessary) to reach peak heart rate. Cine imaging is repeated at multiple time points as the heart rate rises and focal wall motion abnormalities are sought. In assessing atherosclerotic coronary artery disease,
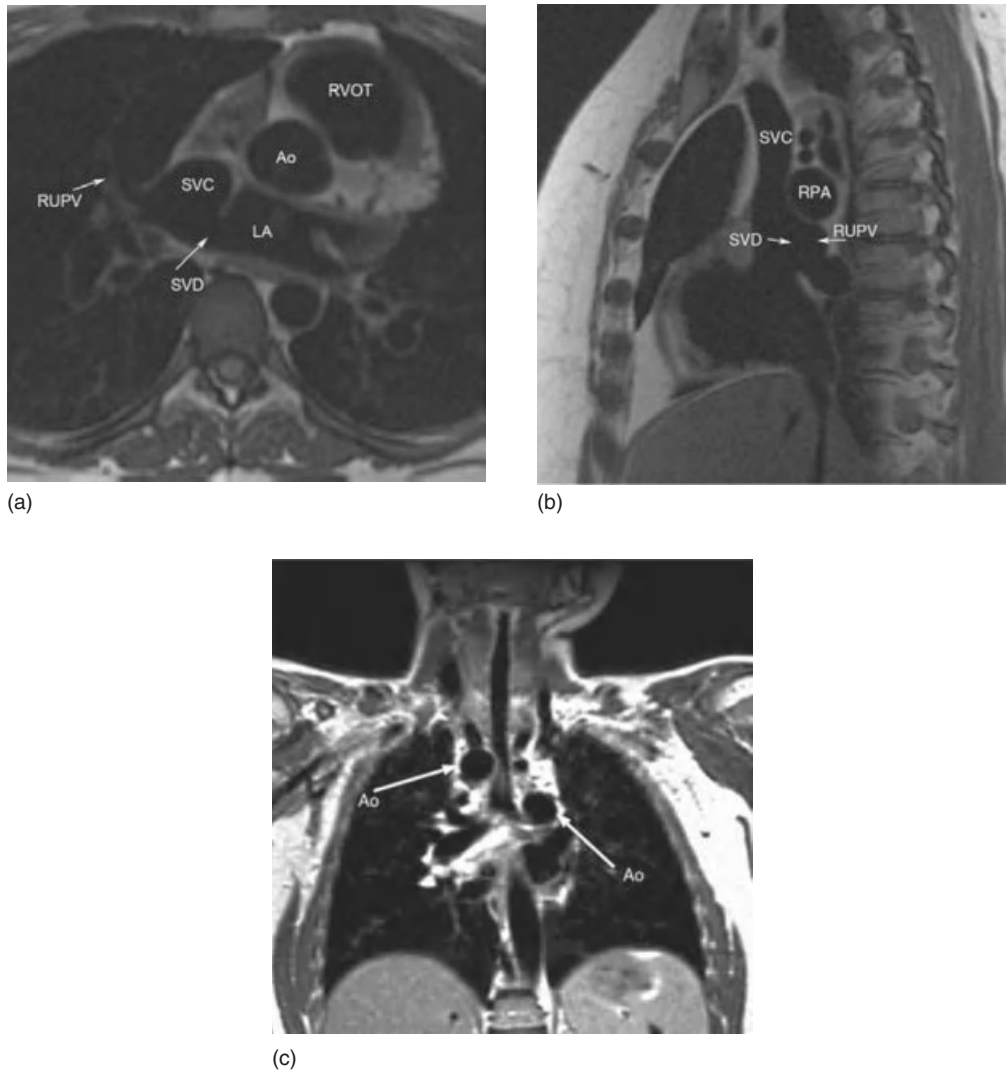
Figure 9.2 (a) Axial and (b) sagittal BB (black blood) images in a patient with a sinus venosus defect and partial anomalous pulmonary venous return. (c) Coronal BB image in a patient with a double aortic arch and airway compression, demonstrating this technique's ability to assess the relationship of airway to vascular structures. Ao, aorta; LA, left atrium; RPA. right pulmonary artery; RVOT, right ventricular outflow tract; RUPV, right upper pulmonary vein; SVC, superior vena cava; SVD, sinus venosus defect.
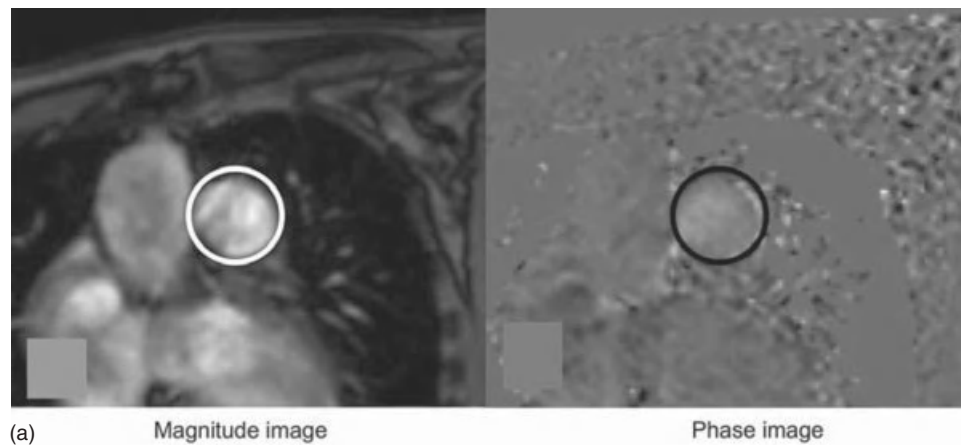
Figure 9.3 An imaging plane is chosen perpendicular to the main pulmonary artery. (a) VEC MRI is then performed in this plane to produce magnitude and phase images. A region of interest encompassing the main pulmonary artery is chosen for each image in the cardiac cycle. From these data, a net flow is obtained.
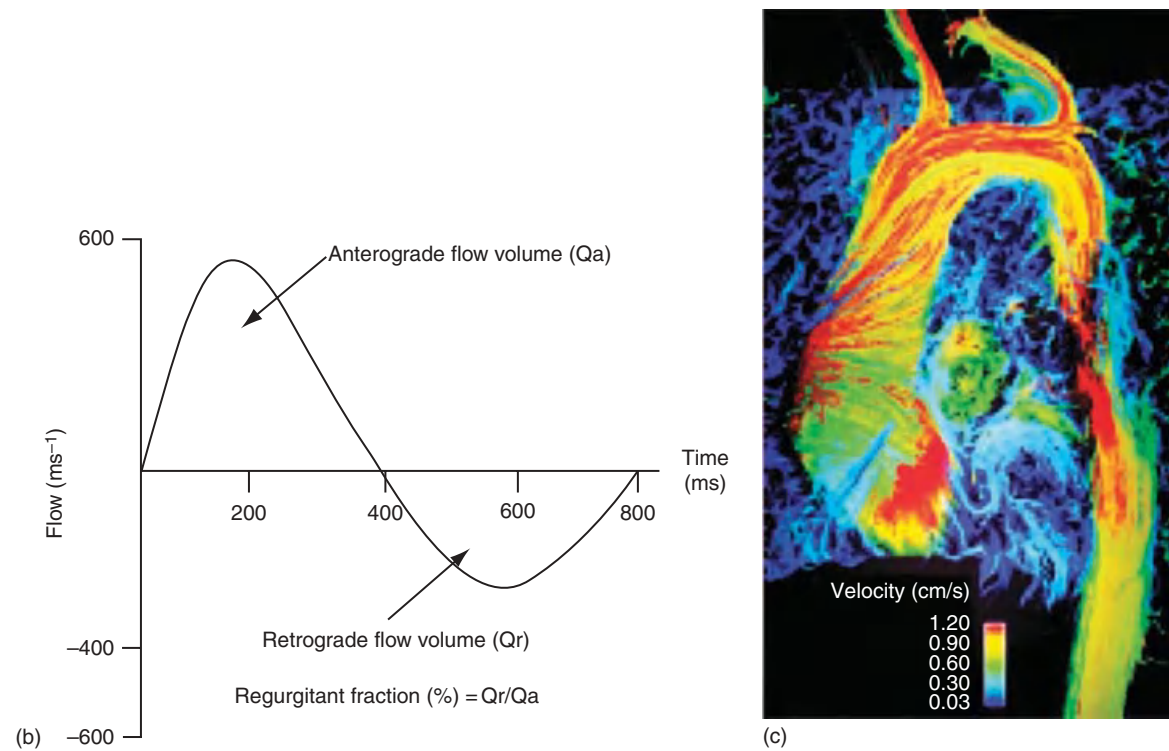
Figure 9.3 (cont'd) (b) Flow is then displayed allowing the calculation of peak velocity, net forward flow, and regurgitant fraction. (c) a "7D" flow in a patient with coarctation of the aorta.
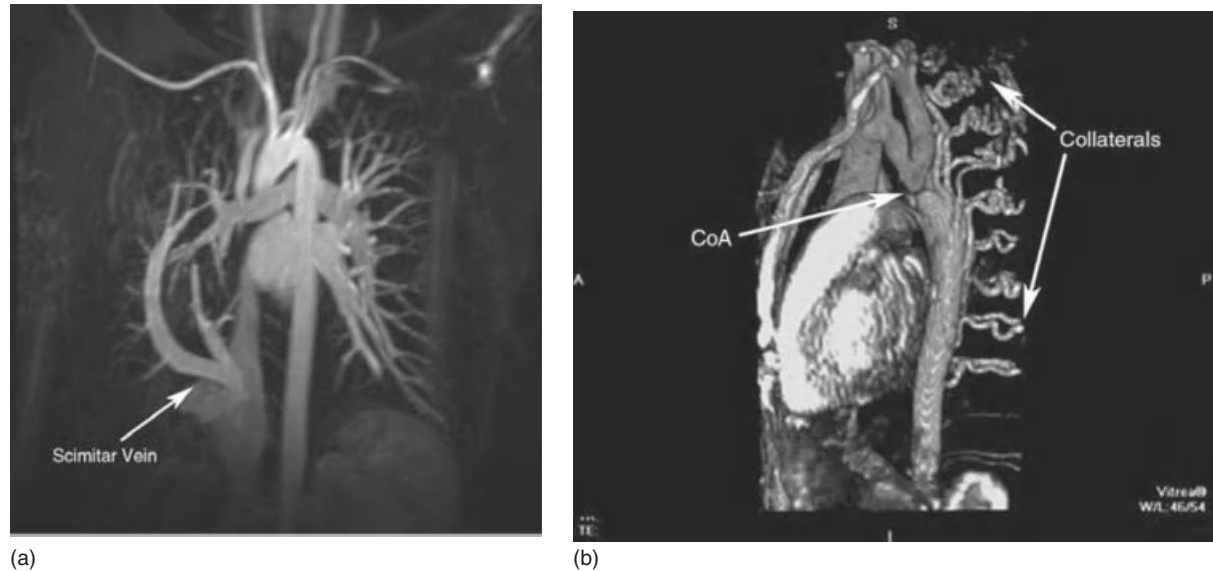
Figure 9.4 (a) MIP image of a 3D gadolinium-enhanced MRA in a patient with scimitar syndrome. (b) 3D reconstruction of a 3D gadolinium-enhanced MRA in a patient with severe native coarctation of the aorta (CoA) with significant collaterals.

adenosine MRI stress has a similar sensitivity and specificity to nuclear perfusion stress testing. Similarly, dobutamine MRI stress has similar sensitivity and specificity to dobutamine echocardiography. Finally, when combining both techniques in one cardiac MRI examination, there is added benefit in predicting poor outcomes [19–27].

The use of dobutamine MRI stress and adenosine MRI stress have been demonstrated in patients with repaired
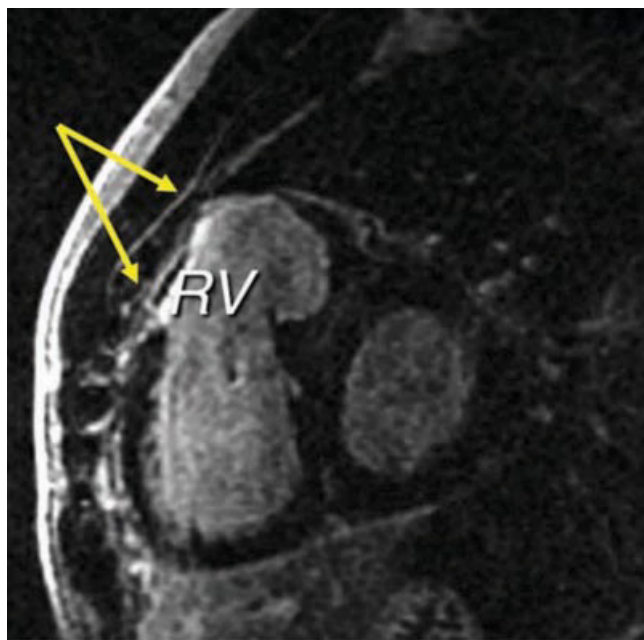
Figure 9.5 Delayed enhancement (arrows) along the RV outflow tract in a patient with tetralogy of Fallot after repair with a transannular patch. RV, right ventrical.

tetralogy of Fallot, D-transposition of the great arteries following atrial switch procedures, and single-ventricle patients following Fontan procedures [28–31]. Often these studies have focused on reporting hemodynamic changes with stress rather than coronary ischemia. These have been small studies but they have demonstrated safety, accuracy, and reproducibility. Future studies are needed to demonstrate the usefulness of this technique in routine practice.

Myocardial viability (delayed hyperenhancement)

Myocardial viability imaging utilizes a T1-weighted inversion–recovery GRE sequence in which the inversion time is chosen to null signal from the myocardium. Imaging is performed 10–15 min after gadolinium administration. Gadolinium washes out of normal myocardium, but is trapped in tissue that has an increased extracellular space (fibrosis, scar, or inflammation) (Figure 9.5).

In summary, although still not as robust as routine coronary artery angiography with X-ray fluoroscopy or cardiac-gated CT angiography at investigating distal coronary artery lesions, MRI can image proximal coronary arteries well [32–35], evaluate myocardial perfusion and viability [36–39], and allow stress testing [40,41], all noninvasively and without exposure to contrast agents and ionizing radiation.

Indications

The indications for MRI in CHD patients are evolving and expanding as MRI technology advances and this population becomes more complex. In general, MRI is indicated in this population when transthoracic echocardiography is insufficient in providing adequate diagnostic information (e.g., postoperative CHD patients, adults with CHD), as an alternative to invasive and costly diagnostic catheterization, and when the unique capabilities of MRI can be exploited. For example, cardiac MRI is fairly effective in the segmental description of complex anatomy. It can diagnose and evaluate the severity of arterial and venous anomalies. Cardiac MRI is unrivaled in the quantitative evaluation of biventricular function, particularly the right ventricle, which is so often at risk in patients with CHD. It is frequently indicated to detect and quantify shunts, valvar and vascular stenoses, and regurgitant lesions. Finally, cardiac MRI is excellent at characterizing anomalous coronary arteries and evaluating myocardial perfusion and viability.

Cardiac computed tomography

Cardiac CT has historically been very useful in evaluating vascular anatomy. With the developments in high-resolution CT with broader anatomic coverage, faster speed, lower radiation dose, and flexible ECG synchronization, CT has emerged as a useful tool for assessing intracardiac anatomy, coronary anatomy, and myocardial function in CHD [42–44]. This newest technology allows faster acquisition times (often precluding the need for sedation in the young patient), improved spatial resolution, thinner slices, and decreased motion artifacts. Although such technology is proving invaluable in cardiovascular imaging in adults, its use in the pediatric population in the assessment of CHD has only just begun [45–47]. The CT imaging techniques for CHD are not the same as those for acquired heart disease and must be tailored to the specific anatomic structures and the purpose of the study.

Non-ECG-synchronized spiral CT

Since the development of multi-slice CT, non-ECG-synchronized spiral CT has been useful for assessing extracardiac vascular abnormalities in CHD (Figure 9.6) [42,43,48]. It is unparalleled in its ability to provide spatial relationships of intrathoracic structures, including the vasculature and the airways. Multi-slice CT produces submillimeter isotropic volume data and greatly improves the image quality of the multiplanar reformatted and three-dimensional CT images. Interestingly, with these newer techniques, the origins and proximal segments of the coronary arteries are observed in as many as 80% of CHD patients on the non-ECG-synchronized spiral CT images [49].

ECG-synchronized spiral CT

The introduction of the ECG-synchronized scan with either retrospective or, more recently, prospective triggering represents a dramatic advancement for CT imaging of CHD as it freezes the heart in motion and allows accurate assessment
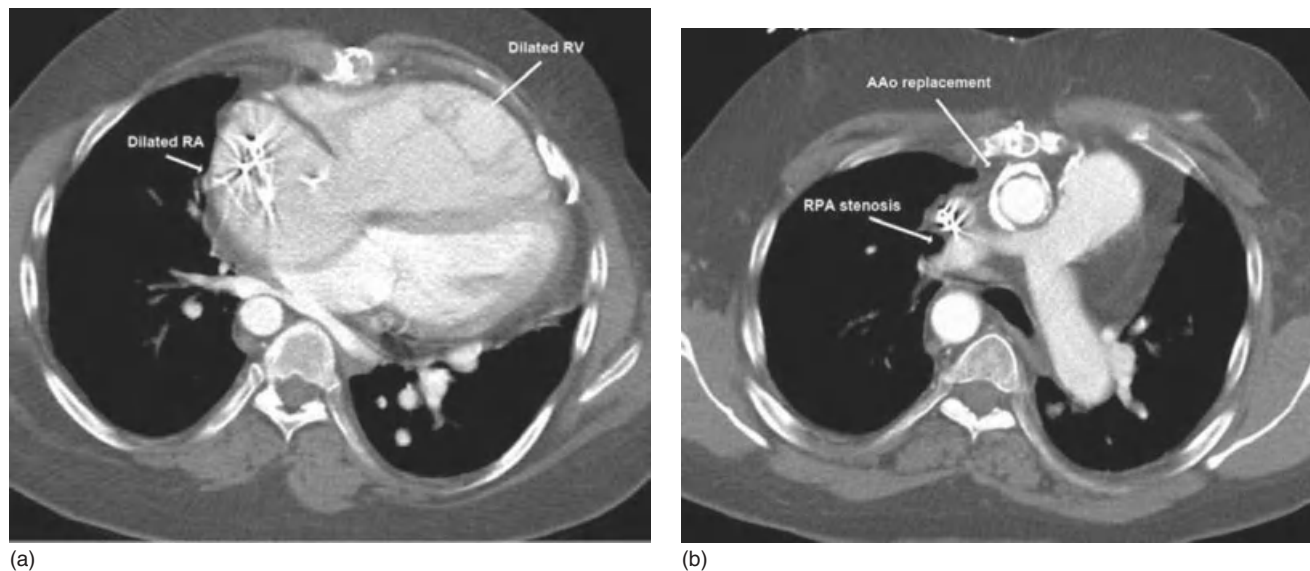
(a)   (b)

Figure 9.6 (a) CT scan in a patient with tetralogy of Fallot after repair. This CT scan revealed a dilated right atrium (RA) and right ventricle (RV). (b) It also revealed a diffusely hypoplastic right pulmonary artery (RPA) and replaced ascending aorta (AAo), the complications of a previously placed Waterston shunt.

of intracardiac, conotruncal, and epicardial structures and also ventricular volumes, wall mass, and function. [42–44,50–52].

The relatively high radiation dose of retrospective ECG-synchronized spiral scanning is primarily attributed to the low pitch that is necessary to obtain gapless ECG-synchronized spiral data. Breath-holding is usually recommended because this scan mode is relatively vulnerable to respiratory motion artifacts. The effective dose estimates of this scan mode for dual-source CT with ECG-controlled tube current modulation are 2–6 mSv [50]. Retrospective ECG-synchronized spiral scanning, however, allows image capture at multiple phases in the cardiac cycle, thus allowing the evaluation of end-systolic and end-diastolic ventricular volumes, stroke volumes, ejection fraction, and wall mass. The analysis tools are similar to those for analyzing short-axis cardiac cine MRI.

Prospective ECG-synchronized sequential scanning is a low-dose technique that can reduce the CT dose to 1–3 mSv [53,54]. Degraded ECG synchronization (stair-step artifacts) may occur with irregular heart rates with this technique. The artifacts are less pronounced in the images acquired at the end-systolic phase because the phase is relatively constant regardless of the heart rate. A limitation of this technique is the inability to perform multi-phase functional evaluation compared with retrospective ECG-synchronized spiral scanning.

Contrast delivery

Shorter scan times have reduced the amounts of iodinated contrast agent needed to provide optimal enhancement of the cardiovascular structures. A larger amount is necessary for patients with a large intracardiac or extracardiac shunt, substantial valvar regurgitation, and/or a severe chamber enlargement. The iodine delivery rate (calculated from both the iodine concentration and the injection rate) should be maximized to optimize cardiovascular enhancement. The intravenous injection site is important and it should be carefully selected in advance: for example, a leg vein is preferred for evaluating the aortic arch and a left superior vena cava; simultaneous injection of 50% diluted contrast agent through the arm and leg veins is preferred for evaluating Fontan pathways; the leg vein should not be used in patients who have undergone bidirectional cavopulmonary connection [43,44].

In addition to achieving adequate vascular enhancement, proper CT imaging of CHD, requires minimization of perivenous artifacts. A triphasic intravenous injection protocol, in which undiluted contrast agent is followed by 50–60% diluted contrast agent and then by a saline chaser, was recently developed to improve the visualization of the right heart, minimize the amount of contrast agent required, and reduce the perivenous artifacts [55,56].

Clinical indications

The clinical applications of CT for CHD are rapidly growing and evolving. Classically, the extracardiac great vessels, including the aortic arch and the pulmonary vessels, have been evaluated with CT [42,43.48]. Evaluating the patency of vascular shunts, conduits, or stents is another traditional indication for CT [57]. A dedicated reconstruction algorithm for vascular stents has recently been introduced for better evaluation of in-stent stenosis [58]. Clear evaluation of the airways is a unique advantage of CT over other imaging modalities: vascular or nonvascular narrowing, anomalies,
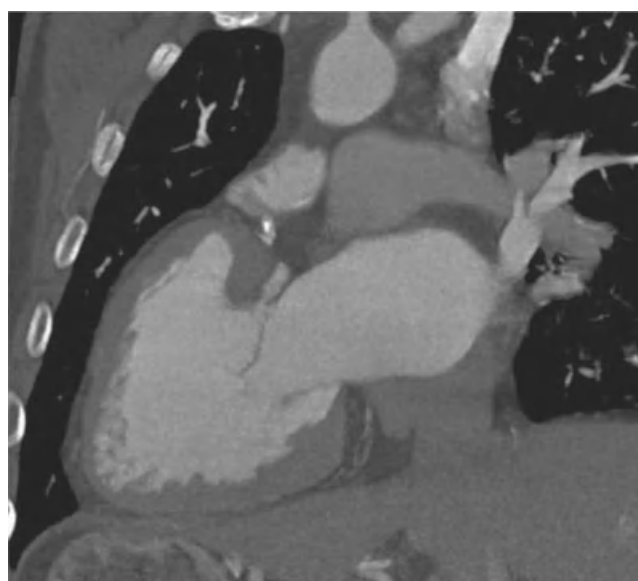
(a)

(b)

(c)

Figure 9.7 A 56-year-old man with situs inversus, dextrocardia, and L-transposition of the great arteries developed chest pain, ECG changes, and a troponin elevation. (a) CT coronary angiography demonstrated not only the location of the coronary ostia but also (b) allowed reconstruction to define the anatomic location of the coronaries in question. (c) This allowed the interventional cardiologist to locate the lesions angiographically. Two bare metal stents were placed successfully, resolving the patient's symptoms.

and dynamic airway obstruction can be accurately evaluated with CT [59–61]. The introduction of the ECG-synchronized CT scan improves the visibility of those cardiovascular structures that are greatly affected by cardiac pulsation. They include the ascending aorta, the pulmonary trunk, the coronary arteries, and the heart itself [43,44,50,51]. In fact, some argue that CT provides equal or even better image quality of the epicardial coronary vessels than even invasive angiography (Figure 9.7). CT is particularly indicated in patients with pacemakers and defibrillators in whom cardiac

MRI is precluded, or in patients with metallic implants that create unmanageable artifacts on cardiac MRI (e.g., steel coils). It also can take the place of cardiac MRI if the question is strictly vascular anatomy and not intracardiac anatomy or cardiac function, because CT can answer these questions with a rapid study, often without sedation.

Limitations

There is less temporal resolution than with cardiac MRI or echocardiography. For this reason, its ability to characterize ventricular function is limited. There are no CT techniques to quantify flow. CT contrast agents, albeit improved and less toxic, still have well-documented renal toxicity. Finally, and importantly, there is significant radiation exposure associated with CT. It is critical for the clinician to consider this when ordering a CT, particularly in the young patient and the patient who has been, and continues to be, exposed to large doses of contrast agent and radiation during hemodynamic and interventional catheterization. Furthermore, gated studies and higher resolution studies are performed with higher radiation doses [62].

Radionuclide scintigraphy

Radionuclide methods often lack sufficient resolution to characterize complex morphology in CHD precisely, but can provide an accurate and reproducible quantitative assessment of the physiologic consequences of structural heart disease, including shunts, myocardial function, and myocardial perfusion.

Shunt

The radionuclide technique for shunt quantification was established and validated in 1973 [63]. The scintigraphic technique involves the rapid injection of a bolus of radionuclide (usually ^{99m}Tc-DTPA) into the circulation while monitoring the transit through the heart and lungs with a gamma camera (4–25 frames per second). The delivery of a compact, nonfragmented bolus of activity is critical to allow accurate determination of the size of the shunt. With good technique, the success rate should be >90%. It may be necessary to sedate infants and some children because crying simulates a Valsalva maneuver, which can impede entry into the thorax and lead to fragmentation of the bolus. As mentioned, ^{99m}Tc-DTPA is most commonly used for shunt studies. Doses are $200\,\mu\text{Ci}\,\text{kg}^{-1}$ body weight, with a minimum dose of 2 mCi. The advantage of ^{99m}Tc-DTPA over other technetium-based agents is the fairly rapid renal excretion, which leads to prompt clearance of background activity. This is important if a second injection is necessary to improve the quality of the bolus. In general, no more than two sequential injections are made because of dosimetry limitations.

In the absence of shunt, the appearance of contrast follows normal flow through the heart; right atrium, right ventricle, pulmonary artery, lungs, left atrium, left ventricle, and aorta. Persistence of pulmonary activity is consistent with a significant left-to-right shunt (usually with a pulmonary-to-systemic flow ratio of >1.6:1). For a clinically significant range (1.2:1 to 3.0:1), there is good correlation with catheterization [63]. In right-to-left shunt, there is premature appearance of tracer in the ascending aorta. Other radionuclide techniques for quantifying right-to-left shunt include (1) intravenous injection of an inert radioactive gas such as ^{133}Xe or ^{81}Kr, which are entirely extracted from the blood by the lungs; persistence in the systemic arterial system demonstrates shunting, or (2) intravenous injection of ^{99m}Tc-labeled macroaggregated albumin (MAA) particles. In the absence of right-to-left shunting, all particles are trapped in the lungs. In right-to-left shunt, the particles appear in the systemic circulation in proportion to the shunt flow, lodging in the capillary and precapillary beds of systemic organs (Figure 9.8). A series of whole-body images is taken to determine the percentage of right-to-left shunt as determined by the difference between whole-body counts and lung counts. The pulmonary-to-systemic flow ratio can be calculated as the ratio of lung counts and whole body counts. Administration of particles is safe, even in admixture lesions [64]. Finally, radionuclide techniques have a unique role in characterizing complex venous and arterial streaming; particularly useful in patients with surgical shunts [65,66].

Assessment of ventricular function

Radionuclide methods are well suited for assessing ventricular size and function in congenital heart lesions. Both first-pass and gated equilibrium methods for the determination of ejection fraction have been validated in children [67,68]. Quantitative assessment of absolute ventricular volumes [69] and determination of regurgitant fraction have also been reported in children [70,71]. For infants, the imaging is optimized by using a converging collimator to improve spatial resolution and increase the sensitivity. It is feasible to measure the ejection fraction even in tiny premature infants with the use of a pinhole collimator [72]. Ventricular size and function evaluations are useful at rest and with dynamic stress in a variety of congenital lesions, both before and after surgical correction [73,74].

Assessment of myocardial perfusion

The primary abnormality leading to the onset of myocardial ischemia is inadequate myocardial blood flow to meet the metabolic demands of the heart. The heart has limited energy stores and requires constant delivery of oxygen and substrates and removal of metabolic wastes via the coronary arteries in order to function properly. Moderate narrowing or stenosis of the coronary arteries is tolerated during the resting state without reductions in coronary flow or ischemia.
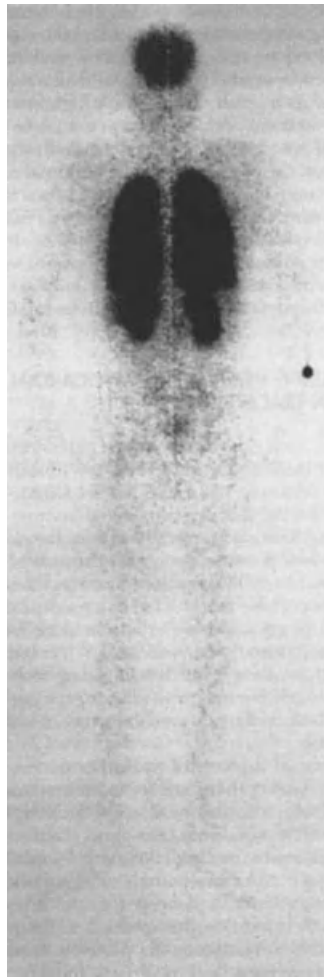
Figure 9.8 A posterior whole-body image. Technetium-labeled macroaggregated albumin particles were injected intravenously and show localization to lungs, kidneys, and brain, indicating a right-to-left shunt.

As myocardial demands are increased, such as during exercise, the resulting augmentation in blood flow in a stenotic coronary artery is often insufficient to maintain adequate perfusion. In this situation, the sequence of events is as follows: during exercise there is first a relative decrease in blood to a region of myocardium supplied by a stenotic vessel; second, a sudden decrease in contractile function due to the rapid exhaustion of energy stores and the accumulation of metabolites; third, electrocardiographic changes, including depression of the ST segments; and finally, the onset of chest pain. If normal blood flow is quickly restored, the chest pain resolves, electrocardiographic changes return to baseline, and contractile function returns. If there is some delay in restoration of flow, contractile function may remain depressed for up to weeks (stunned myocardium). If blood flow is chronically reduced at rest, resulting in a chronic state of ischemia, contractile function may remain chronically depressed (hibernating myocardium). If blood flow is not restored, irreversible damage leads to myocardial necrosis and the eventual replacement of myocytes with scar. This regional territory then has permanent functional abnormalities, and if much muscle is involved, heart dilatation and failure ensue and long-term prognosis is adversely affected. Detecting decreased myocardial perfusion by myocardial perfusion imaging, or scintigraphy, is therefore important in early prediction of these pathophysiologic changes.

Thallium

The most common agent for assessing myocardial perfusion is thallium, ^{201}Tl, which is a cyclotron-produced radionuclide with a half-life of 73 h and a predominant emission energy of 80 keV. It behaves physiologically like potassium and is transported into cells largely by the sodium–potassium ATPase pump located on cellular membranes [75]. Myocardial cells extract thallium to a high degree. On the first exposure to the heart (first pass), there is uptake of more than 85% of the dose that reaches the myocardial cells (extraction fraction). As a result, the initial distribution of thallium provides a static map of myocardial perfusion at the time of injection. Thallium extraction by the myocardium depends on the delivery of the tracer (perfusion) and viable myocytes. Ischemic myocytes retain the ability to extract thallium (provided that some degree of perfusion is present); however, when ischemia is of sufficient severity and duration to lead to loss of membrane integrity (necrosis), thallium will not be extracted [76]. Figure 9.9 provides an example in a patient with a 70% stenotic LAD lesions.

Thallium also redistributes [77]. After the initial accumulation in the heart, the intracellular concentration gradients of thallium in the heart tend to equalize. As a result, regions with high blood flow and high concentrations of thallium wash out faster than do regions with lower blood flow or low concentrations of thallium. In fact, thallium may leave the normal areas of the heart and enter the areas of low concentration (ischemic territory) over time. The resultant delayed thallium image shows a more homogeneous distribution if the initial region of reduced uptake represented ischemia in a region of viable myocytes (see Figure 9.9). If the initial region of reduced uptake represented scar, a persistent defect appears on the delayed images.

Technetium-99m-labeled tracers

Although thallium has gained widespread popularity as a useful myocardial perfusion agent, there are drawbacks. The relatively long half-life (72 h) limits the amount of activity that can be injected because of dosimetry concerns. The low energy (80 keV) of the major photon emission poses potential problems because of soft tissue attenuation. Also, thallium is cyclotron produced, which limits its availability. Relative to thallium, ^{99m}Tc has the advantage of higher energy (140 keV), leading to less attenuation, a shorter half-life (6 h), allowing the administration of larger doses, and ready availability because it is generator produced.
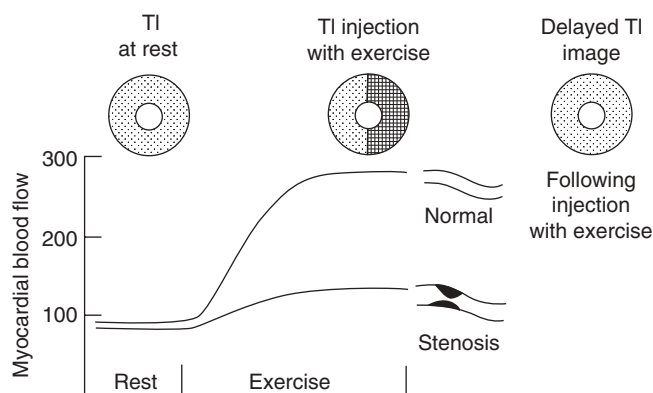
Figure 9.9 Diagrammatic illustration of the relationship between myocardial blood flow at rest and during exercise and regional myocardial ^{201}Tl uptake in zones perfused by normal and stenotic coronary arteries. When thallium is injected at rest, there is a uniform distribution of the radionuclide through the myocardium (upper left). When thallium is injected during exercise, there is a relative diminution in thallium uptake in the zone perfused by the stenotic vessel (middle). Several hours after ^{201}Tl injection with exercise, there is "redistribution" and normalization of thallium in normal and stenotic zones (top right). (Reproduced from Beller GA, in Gerson MC (ed.), *Cardiac Nuclear Medicine*. New York, McGraw-Hill, 1987, pp. 349–69, with permission from The McGraw-Hill Companies.)

A number of [99m]Tc -labeled myocardial perfusion tracers have been developed. Of these newer agents, sestamibi has been most extensively studied. ^{99m}Tc-sestamibi, or Cardiolite, is a lipophilic, cationic complex of a class of compounds called isonitriles [78]. Sestamibi, like thallium, is delivered to the myocardium in proportion to blood flow. Its uptake is different from that of thallium, however. Sestamibi passively crosses the sarcolemmal membrane, and the driving force for uptake appears to be a large electrochemical gradient provided by the largely negative charge on mitochondria. Sestamibi shows little significant redistribution within the heart [79]. Separate injections of sestamibi are required for rest and stress assessment of myocardial perfusion.

The extraction fraction of sestamibi is lower than that of thallium (65% versus 85%) [80]. As a result, sestamibi may underestimate myocardial blood flow at high flow rates ($>2\,\mathrm{ml\,min^{-1}\,g^{-1}}$) to a greater extent than does thallium [80]. In spite of this diffusion limitation, clinical results evaluating the sensitivity and specificity of thallium and sestamibi have been comparable [81]. Another property shared between sestamibi and thallium is the dependence on viable myocytes for extraction [82]. Sestamibi uptake is markedly diminished in irreversibly injured myocytes.

Application of perfusion scintigraphy in congenital heart disease

Myocardial perfusion scintigraphy has been applied extensively to adults and during recent years also to children [83]. In children, perfusion imaging has been most widely
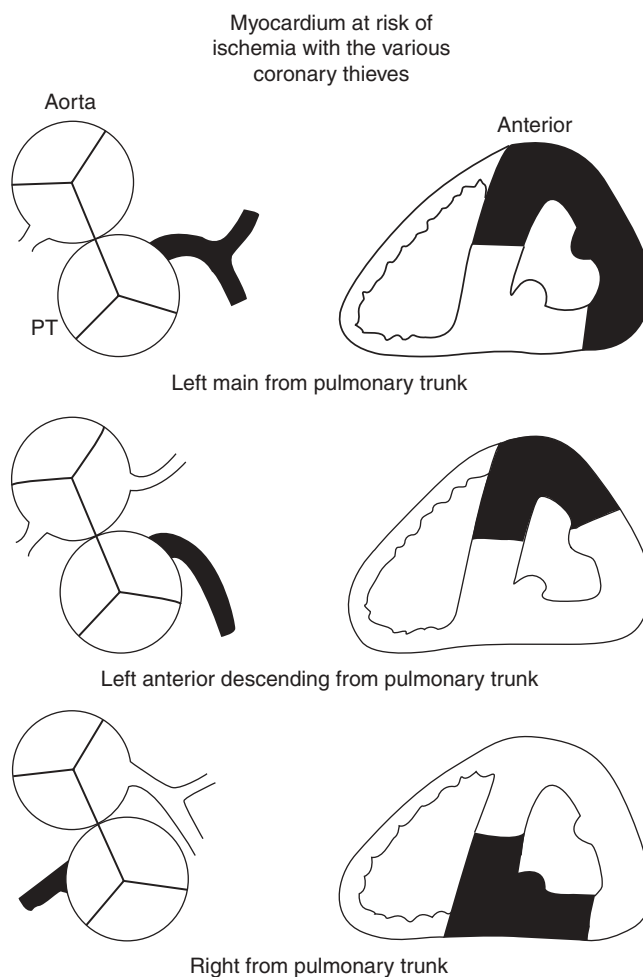

Figure 9.10 Diagram showing the portion of left ventricular myocardium at risk for ischemia or necrosis when the left main, left anterior descending, or right coronary artery arises from the pulmonary trunk. (Reproduced with permission from Roberts WC, in Roberts WC (ed.), *Adult Congenital Heart Disease*. Philadelphia, FA Davis, 1987, pp. 583–629.)

used for the noninvasive identification of an anomalous left coronary artery from the pulmonary artery [84,85], as demonstrated in Figures 9.10 and 9.11. Perfusion abnormalities have also been induced with stress in adults with a variety of anomalous origins of the left coronary artery from the right.

Another clinical condition for which perfusion scintigraphy may be useful is Kawasaki disease [86]. Before the introduction of intravenous immune globulin therapy, up to 20% of these patients developed aneurysms of the coronary arteries. With treatment, this incidence is decreased to 4%. About 30–50% of such aneurysms spontaneously regress within the first 2 years. The remaining may later thrombose, resulting in myocardial ischemia and infarction.

Evaluating the resting pattern of ventricular perfusion and function can help differentiate a segmental pathologic process related to large-vessel coronary disease from other causes,
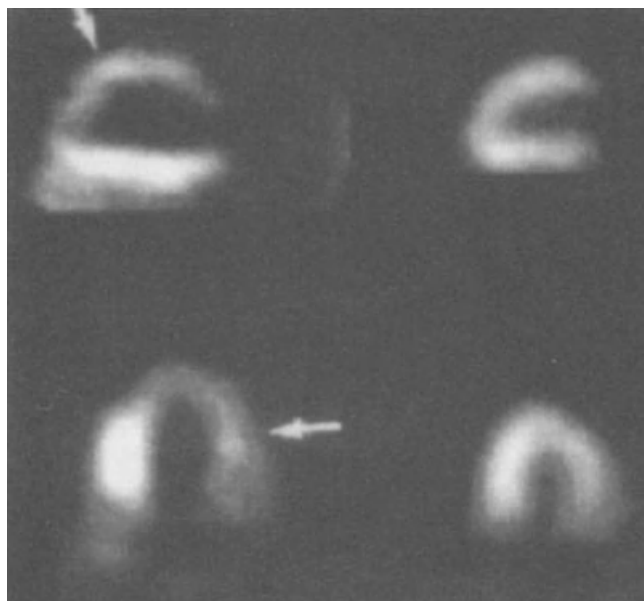
Animal studies have shown intense and uniform gallium accumulation in experimental myocarditis [92]. In addition, a high correlation between biopsy-proven myocarditis and gallium uptake has been demonstrated [93]. In nearly all reported instances of gallium uptake in myocarditis, the pattern of uptake is diffuse. even with characteristic electrocardiographic changes that mimic myocardial infarction [94]. Antimyosin antibody cardiac imaging has also shown success in detecting biopsy-proven myocarditis [95]. Antimyosin localizes to regions of myocyte necrosis in myocarditis, as opposed to the localization of ^{67}Ga to the inflammatory component. Few studies have examined thallium uptake in myocarditis; however, focal thallium uptake or perfusion defects have been reported [96]. These defects, however, tend to be in nonvascular distributions. Experimental and clinical studies have confirmed that gallium accumulates in regions of acute myocardial infarction [97,98].

Coronary artery disease in infants

Myocardial infarction in neonates is rare and associated with high mortality. It usually occurs in the absence of CHD. Congenital lesions associated with myocardial ischemia usually present with myocardial infarction in later infancy or in childhood [99]. In infants with structurally normal hearts and coronary arteries, the most common causes of myocardial infarction are perinatal asphyxia and thromboembolic occlusion.

Plain film

Plain film analysis used to be one of the most important diagnostic tools in the assessment of CHD. With the development of echocardiography, the importance of plain film findings has decreased; however, it remains a very simple, inexpensive method to obtain important information about cardiac size, pulmonary vasculature, concomitant pulmonary disease, bone abnormalities, situs, bronchomalacia, and other features. In many patients, the cardiac configuration is characteristic enough to allow a specific diagnosis. Serial radiographs are also important because changes in heart size and pulmonary vasculature have prognostic implications, particularly after an operation for the cardiac anomaly.

Technical factors

To evaluate the pulmonary vasculature, the chest radiograph must be properly exposed, neither overpenetrated nor underpenetrated. On an overpenetrated radiograph, the thoracic spine is clearly visible through the cardiac silhouette, whereas on underpenetrated X-ray films, the spine is not visible. In general, overpenetrated radiographs are interpreted as decreased pulmonary vasculature and underpenetrated radiograph as increased pulmonary vasculature.

Figure 9.11 Rest myocardial thallium uptake images by single-photon emission CT from a 2-month-old infant presenting with a left coronary artery originating from the pulmonary artery. On the left are preoperative images showing markedly decreased perfusion to the anterior and lateral walls (arrows) and dilatation of the left ventricle. Postoperative images on the right show almost complete normalization of perfusion and a dramatic reduction in the chamber size. (Reproduced with permission from Fernandez *et al.*, *Clin Nucl Med* 1992:**17**:177–9.)

including cardiomyopathy, myocarditis, and small-vessel embolization. The pattern of thallium uptake can also suggest right and left ventricular hypertrophy and suggest the diagnosis of asymmetric septal hypertrophy.

Assessment of myocardial perfusion is becoming increasingly important in evaluating and following patients with transposition of the great vessels status after an arterial switch procedure [87–89]. Concerns have been raised since the inception of the arterial switch procedure about the possibility that distortion or growth failure of the newly implanted coronary arteries may result in myocardial ischemia and possibly infarction. Some studies suggest that coronary artery manipulation and reimplantation do not cause late myocardial perfusion abnormalities, at least in those infants with successful initial results [89]. However, large perfusion abnormalities have been seen in the territories of occluded coronary arteries after the switch procedure [83].

Radionuclide assessment of inflammation

Gallium citrate (^{67}Ga) accumulates in both acute and chronic inflammatory lesions of bacterial and nonbacterial etiology [90]. Mechanisms leading to gallium uptake have been reviewed by Tsan [90]. Gallium uptake has been described in a number of causes of inflammatory heart disease, including bacterial endocarditis, myocardial abscess, and pericarditis [91].

The degree of inspiration is another technical factor affecting evaluation of pulmonary vasculature and cardiac size. During deep inspiration, the lung fields appear much darker because of the high content of air within the alveoli and are often interpreted as decreased pulmonary vasculature. In contrast, during expiration, a large amount of the air is expelled, and the lungs are denser and are often interpreted as increased vasculature or even pulmonary edema. A position of the diaphragm at the level of the ninth ribs posteriorly is considered to be an adequate respiratory effort. The degree of inspiration also has a profound influence on cardiac size. The heart is attached to the diaphragm by the cardiophrenic ligament and consequently follows diaphragmatic motion. In deep inspiration, the heart assumes a midline vertical position, giving the appearance of a small heart. In contrast, during expiration the heart assumes a more transverse position, simulating cardiomegaly.

Three features must be assessed when interpreting a chest radiograph: pulmonary vasculature, cardiac size, and cardiac contour.

Pulmonary vasculature

The pulmonary vasculature can be increased by distention of pulmonary arteries, pulmonary veins, or both. Radiographically increased arterial and increased venous pulmonary vasculature may be difficult or impossible to differentiate, but there are helpful secondary signs. If increased vascular markings are present, they are likely to be arterial because increased venous vasculature is comparatively rare in childhood. Furthermore, the appearance of increased pulmonary venous vasculature in infancy and childhood produces a very characteristic pattern that differs from that in increased arterial vasculature.

What is observed radiographically is not increased pulmonary flow but the size of the pulmonary arteries. Obviously, with enlargement of peripheral pulmonary arteries, an enlargement of the main pulmonary artery is also present, as evidenced by a prominent pulmonary arterial segment, if the great vessels are normally related (Figure 9.12).

If the peripheral pulmonary vasculature is increased and the main pulmonary arterial segment is not prominent, it may be either overshadowed by thymic tissue, common in infancy, or in an abnormal intramediastinal position, as with transposition complexes (Figure 9.13).

Increased pulmonary arterial vasculature may be difficult to diagnose in patients with a left-to-right shunt and normal pulmonary arterial pressure, as in patients with an atrial septal defect. Many young patients with an atrial septal defect have radiographically normal pulmonary vasculature but usually have right-sided cardiac enlargement.

The radiographic diagnosis of increased arterial vasculature becomes much more obvious if pulmonary hypertension is also present, as occurs with a shunt located beyond the level of the atrioventricular (AV) valves. In these conditions, enlargement

Figure 9.12 Typical left-to-right shunt with increased arterial vasculature. The arterial pattern is distinct. Numerous vessels are seen on end, suggesting tortuosity, which in turn indicates increased pulmonary artery pressure. With increased pulmonary artery vasculature, there must be enlargement of the main pulmonary artery, as seen here.
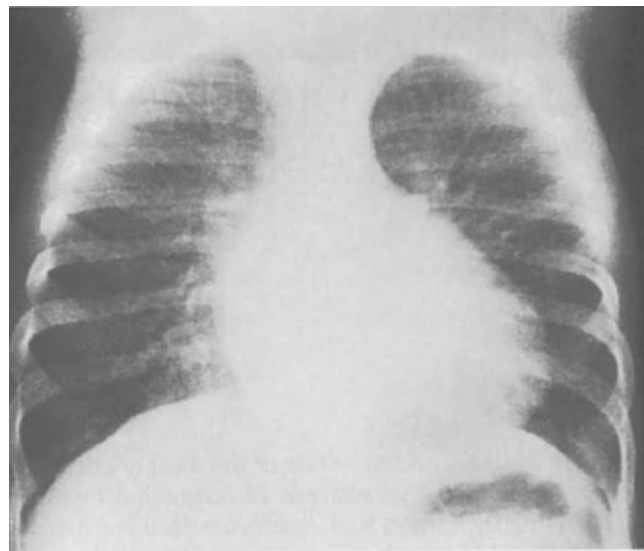

Figure 9.13 Posteroanterior radiograph showing transposition of the great arteries. The heart is enlarged and the pulmonary vasculature is increased. The main pulmonary artery, which is also enlarged, does not form a prominent pulmonary arterial segment because it is in an abnormal intramediastinal position. The mediastinum is narrow because of the small thymus.

of the pulmonary arteries occurs by both increased flow and pressure (Figure 9.12). In addition, increased pulmonary arterial pressure causes tortuosity of the pulmonary arteries, as evidenced by an increased number of arteries seen on end.
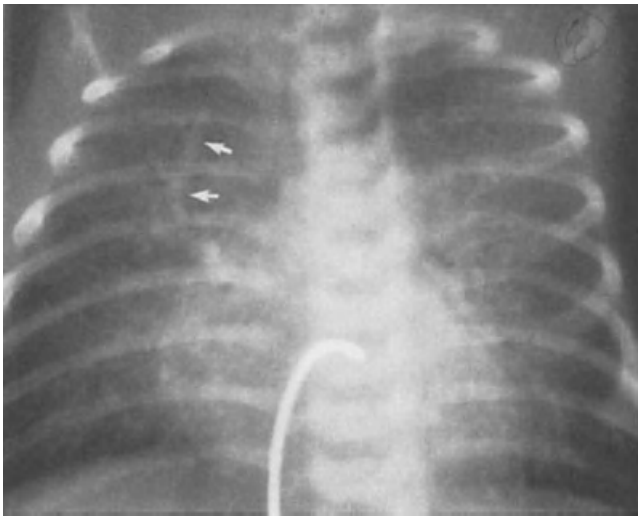
Figure 9.14 Posteroanterior radiograph of acute pulmonary venous obstruction. Diffuse haziness over both lung fields and indistinctness of the pulmonary vasculature indicate frank pulmonary edema. Marked prominence of the right upper lobe pulmonary vein (arrows) further confirms venous pulmonary obstruction.

Figure 9.15 Posteroanterior radiograph of pulmonary venous hypertension showing the redistribution of blood flow (cephalization). The upper lobe pulmonary veins are distinctly seen (arrows). The heart is not enlarged, as is typical for left-sided obstruction proximal to the mitral valve.

Increased pulmonary venous vasculature as a result of pulmonary venous occlusive disease produces a characteristic radiographic appearance, particularly in infancy. A typical example of pulmonary venous obstruction is total anomalous pulmonary venous connection below the diaphragm. This condition results in a characteristic granular pattern throughout both lung fields (Figure 9.14). This granularity is due to edema of the interlobar septa, and sometimes a small pleural effusion may be present. In general, pleural effusions caused by pulmonary venous obstruction are exceedingly rare in infants and children, in contrast to adults, who develop large pleural effusions with increased pulmonary venous pressure.

The radiographic appearance of pulmonary venous hypertension in neonates is difficult to distinguish from hyaline membrane disease. A small pleural effusion suggests venous obstruction, and pulmonary consolidation with an air bronchogram strongly favors the diagnosis of hyaline membrane disease.

In children who have chronic pulmonary venous hypertension, redistribution of blood flow occurs (see Figure 9.15). In a healthy individual, relatively little blood flows through the upper lobes because of the gravitational effect on pulmonary pressure. In pulmonary venous obstruction, preferential flow occurs through the upper lobes. The likely explanation for redistribution is increased resistance to flow through the lower lobes because of interstitial edema, alveolar hypoxia, or reflex vasoconstriction of arterioles.

Concurrently, or somewhat later, another characteristic and diagnostic finding appears, namely Kerley's B lines. These horizontal lines, best seen at the lung base and at the peri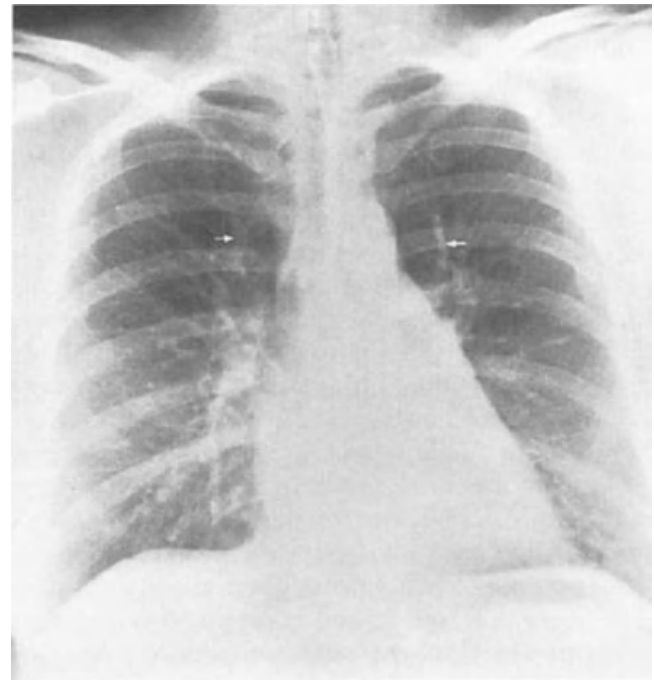phery of the lung, are caused by interstitial edema and later by fibrosis and hemosiderosis of the intralobular septa (Figure 9.16). Kerley's B lines occur when the pulmonary wedge pressure exceeds 20 mmHg. They are rarely seen in infants and young children.

Later in life, signs of pulmonary venous hypertension show a different radiographic pattern, with transudation of fluid into alveoli resulting in an indistinct fluffy appearance.

Bronchial vasculature

In patients with pulmonary atresia and ventricular septal defect, and also more complex conditions with pulmonary atresia, the lungs may be supplied with bronchial arteries that can be recognized on a plain chest radiograph. Normally, the pulmonary arteries form a characteristic shadow in the hila, but this density is absent in patients with pulmonary atresia. The pulmonary vasculature may not be decreased but has a unique appearance. In contrast to pulmonary arteries, which have a characteristic regular fan-like pattern emanating from the hila, bronchial arteries lack regularity and are much more tortuous. As a result, numerous pulmonary vessels are seen on end.

Cardiac size

The most important value of a chest radiograph is probably evaluating cardiac size. Proper interpretation requires an understanding of the technical factors and anatomy of the heart.
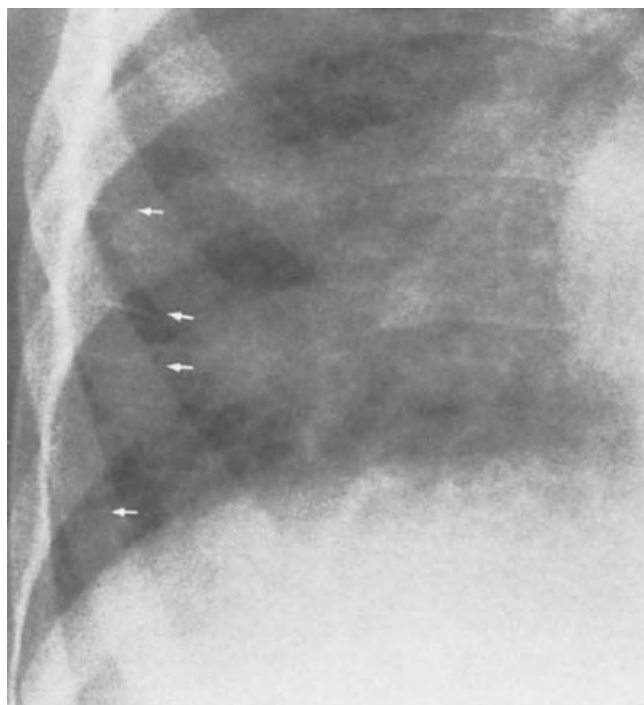
Figure 9.16 Close-up view of the right base. This shows typical horizontal lines (arrows) described as Lerley's B lines. This is good radiographic evidence for long-standing venous pulmonary hypertension with wedge pressures above 20 mmHg.

There are many causes of apparent cardiomegaly. First, a common technical problem is an anteroposterior (AP) rather than a PA projection. Because of the divergence of the X-ray beam emanating from the X-ray tube, structures that are further away from the radiographic film are magnified more than structures located closer to the film. Because the heart is located anteriorly in the thoracic cavity, it is magnified more on an AP projection than a PA projection. Because the chest of an infant is small, the projection is not as important in the evaluation of cardiac size.

Second, the divergence of the X-ray beam is more pronounced when the X-ray tube is closer to the film. By increasing the film distance to 6 ft, the divergence of the X-ray beam can be minimized and a true nonmagnified image of the chest can be obtained. Portable X-ray machines use a 40 in film distance. Therefore, a heart may appear enlarged with a portable machine.

A third factor influencing cardiac size is the patient's position. When the patient is supine, the diaphragm tends to be higher than when the patient is in the upright position. Therefore, the cardiac silhouette appears larger on a supine chest radiograph than in an upright radiographic study.

Another important factor is the degree of inspiration. The heart is attached to the diaphragm by the cardiophrenic ligament and moves with the left hemidiaphragm. On deep inspiration, the heart rotates into a left anterior oblique position, resulting in a small cardiac silhouette (Figure 9.17a). On expiration, it rotates into a right anterior oblique
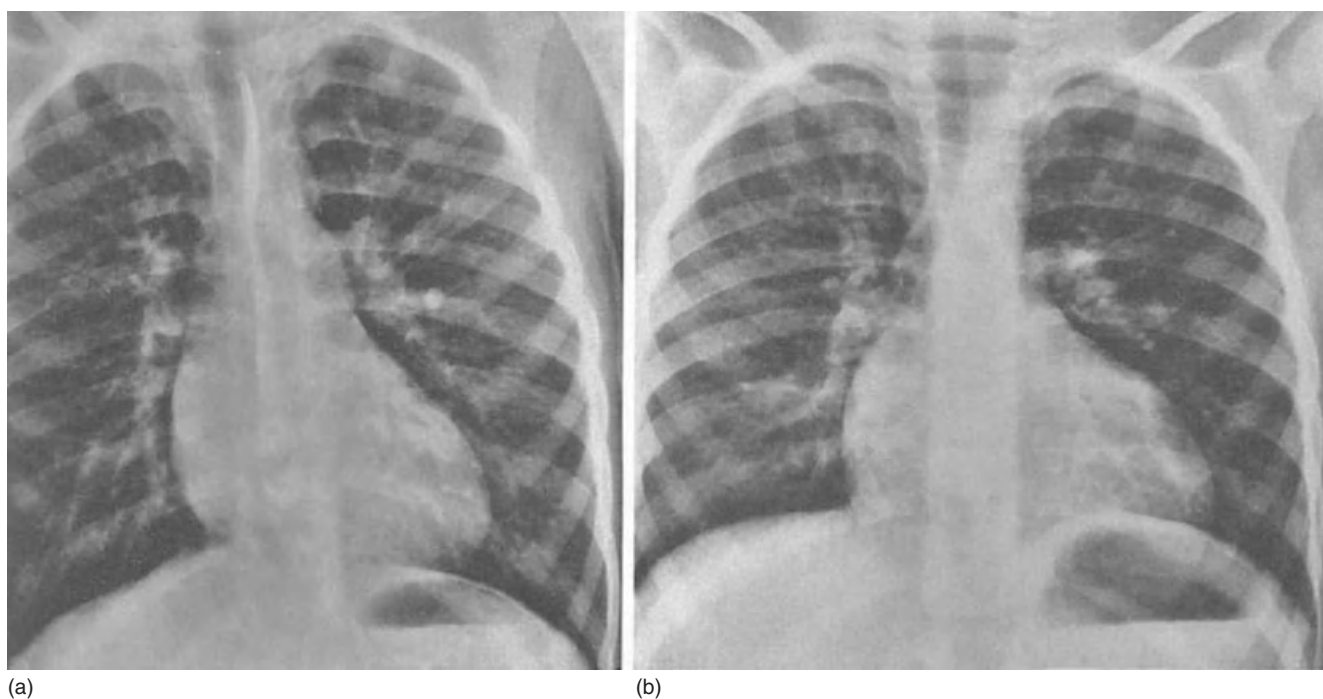
(a)   (b)

Figure 9.17 Posteroanterior radiograph of a small ventricular septal defect. (a) No significant cardiomegaly (deep inspiration); (b) during expiration, the heart assumes a transverse position.

position, resulting in an apparent enlargement of the cardiac silhouette (Figure 9.17b). Typically, an individual with a low diaphragm, for example, a patient with asthma, has a vertical heart, which is pulled down by the low diaphragm; the cardiac silhouette appears radiographically small. However, a person with an elevated diaphragm, particularly an adult patient with obesity, shows an enlarged cardiac silhouette, although the heart may be normal in size. This variation in the radiographic appearance of the cardiac silhouette is a strong argument against the use of cardiothoracic ratio, in which the transverse diameter of the heart is related to the transverse diameter of the chest to assess cardiac size.

A final concept in the evaluation of cardiac size is the position of the heart within the thoracic cavity. The long axis of the heart passes obliquely to the sagittal plane of the thorax. Therefore, on a chest radiograph the long axis is foreshortened. Normally the cardiac axis is inclined about 45° to the sagittal plane. If this angle is greater, hearts appear large on a PA view and small on lateral view (for example, an obese patient with a high diaphragms or a patient with a pectus excavatum deformity). If this angle is smaller, hearts appear small on a PA view and large on lateral view (for example, a patient with pulmonary emphysema). Consequently, cardiac size cannot be evaluated on a PA chest film alone, and the commonly used cardiothoracic ratio is inaccurate for evaluating cardiac size.

Characteristic plain film findings in CHD

A synopsis of characteristic plain film findings in various CHD lesions is presented in the relevant figures in this chapter. Emphasis is placed on the characteristic radiographic appearance.

Conclusion

The future of MRI will involve parallel processing and navigator pulses, which will decrease scan times and decrease need for sedation/anesthesia. Real-time imaging, MRI-guided interventions, myocardial tagging assessment of wall strain, and 7D flow techniques will reach the clinical armamentarium in the near future, making MRI an even more useful tool in evaluating and managing this patient population. The evolution of higher field strength scanners (3 T) may augment some MRI tools.

CT techniques are continuously evolving. Second-generation dual-source CT will decrease scan times and radiation dose [100]. Large-coverage volume CT (256–320 slices) is emerging [101]. Other innovative technical developments include dual-energy lung perfusion and ventilation scan, new tube current modulation to reduce the radiation dose to superficial radiation-sensitive tissue, and combined ECG and respiration synchronization.

Nuclear medicine techniques are additionally growing in application and scope, with new radioisotopes and new applications being explored. Finally, the plain film is not just a historic imaging technique; rather, it remains an important diagnostic tool and also an important modality to monitor progression of disease and postoperative status.

References

1 Plein S, Bloomer TN, Ridgway JP, *et al*. Steady-state free precession magnetic resonance imaging of the heart: comparison with segmented *k*-space gradient-echo imaging. *J Magn Reson Imaging* 2001;**14**:230–6.

2 Carr JC, Simonetti O, Bundy J, *et al*. Cine MR angiography of the heart with segmented true fast imaging with steady-state precession. *Radiology* 2001;**219**:828–34.

3 Weiger M, Pruessmann KP, Boesiger P. Cardiac real-time imaging using SENSE. SENSitivity Encoding scheme. *Magn Reson Med* 2000;**43**:177–84.

4 Hernandez RJ, Aisen AM, Foo TK, Beekman RH. Thoracic cardiovascular anomalies in children: evaluation with a fast gradient-recalled-echo sequence with cardiac-triggered segmented acquisition. *Radiology* 1993;**188**:775–80.

5 Furber A, Balzer P, Cavaro-Menard C, *et al*. Experimental validation of an automated edge-detection method for a simultaneous determination of the endocardial and epicardial borders in short-axis cardiac MR images: application in normal volunteers. *J Magn Reson Imaging* 1998;**8**:1006–14.

6 Bax JJ, Lamb H, Dibbets P, *et al*. Comparison of gated single-photon emission computed tomography with magnetic resonance imaging for evaluation of left ventricular function in ischemic cardiomyopathy. *Am J Cardiol* 2000;**86**:1299–305.

7 Bellenger NG, Marcus NJ, Davies C, *et al*. Left ventricular function and mass after orthotopic heart transplantation: a comparison of cardiovascular magnetic resonance with echocardiography. *J Heart Lung Transplant* 2000;**19**:444–52.

8 Lorenz CH. The range of normal values of cardiovascular structures in infants, children, and adolescents measured by magnetic resonance imaging. *Pediatr Cardiol* 2000;**21**:37–46.

9 Pennell DJ. Ventricular volume and mass by CMR. *J Cardiovasc Magn Reson* 2002;**4**:507–13.

10 Alfakih K, Plein S, Thiele H, *et al*. Normal human left and right ventricular dimensions for MRI as assessed by turbo gradient echo and steady-state free precession imaging sequences. *J Magn Reson Imaging* 2003;**17**:323–9.

11 Varaprasathan GA, Araoz PA, Higgins CB, Reddy GP. Quantification of flow dynamics in congenital heart disease: applications of velocity-encoded cine MR imaging. *Radiographics* 2002;**22**:895–905; discussion 905.

12 Zhang H, Maki JH, Prince MR. 3D contrast-enhanced MR angiography. *J Magn Reson Imaging* 2007;**25**:13–25.

13 Hope MD, Meadows AK, Hope TA, *et al*. Clinical evaluation of aortic coarctation with 4D flow MR imaging. *J Magn Reson Imaging* 2010;**31**:711–8.

14 Nielsen JF, Nayak KS. Referenceless phase velocity mapping using balanced SSFP. *Magn Reson Med* 2009;**61**:1096–102.

15 Babu-Narayan SV, Kilner PJ, Li W, *et al*. Ventricular fibrosis suggested by cardiovascular magnetic resonance in adults with repaired tetralogy of Fallot and its relationship to adverse markers of clinical outcome. *Circulation* 2006;**113**:405–13.

16 Oosterhof T, Mulder BJ, Vliegen HW, de Roos A. Corrected tetralogy of Fallot: delayed enhancement in right ventricular outflow tract. *Radiology* 2005;**237**:868–71.

17 Harris MA, Johnson TR, Weinberg PM, Fogel MA. Delayed-enhancement cardiovascular magnetic resonance identifies fibrous tissue in children after surgery for congenital heart disease. *J Thorac Cardiovasc Surg* 2007;**133**:676–81.

18 Prakash A, Powell AJ, Krishnamurthy R, Geva T. Magnetic resonance imaging evaluation of myocardial perfusion and viability in congenital and acquired pediatric heart disease. *Am J Cardiol* 2004;**93**:657–61.

19 Akhtar M, Ordovas K, Martin A, *et al*. Effect of chronic sustained-release dipyridamole on myocardial blood flow and left ventricular function in patients with ischemic cardiomyopathy. *Congest Heart Fail* 2007;**13**:130–5.

20 Jahnke C, Nagel E, Gebker R, *et al*. Prognostic value of cardiac magnetic resonance stress tests: adenosine stress perfusion and dobutamine stress wall motion imaging. *Circulation* 2007;**115**:1769–76.

21 Ingkanisorn WP, Kwong RY, Bohme NS, *et al*. Prognosis of negative adenosine stress magnetic resonance in patients presenting to an emergency department with chest pain. *J Am Coll Cardiol* 2006;**47**:1427–32.

22 Kim RJ, Chen EL, Lima JA, Judd RM. Myocardial Gd-DTPA kinetics determine MRI contrast enhancement and reflect the extent and severity of myocardial injury after acute reperfused infarction. *Circulation* 1996;**94**:3318–26.

23 Plein S, Radjenovic A, Ridgway JP, *et al*. Coronary artery disease: myocardial perfusion MR imaging with sensitivity encoding versus conventional angiography. *Radiology* 2005;**235**:423–30.

24 Nagel E, Klein C, Paetsch I, *et al*. Magnetic resonance perfusion measurements for the noninvasive detection of coronary artery disease. *Circulation* 2003;**108**:432–7.

25 Kim RJ, Fieno DS, Parrish TB, *et al*. Relationship of MRI delayed contrast enhancement to irreversible injury, infarct age, and contractile function. *Circulation* 1999;**100**:1992–2002.

26 Weinsaft JW, Klem I, Judd RM. MRI for the assessment of myocardial viability. *Cardiol Clin* 2007;**25**:35–56, v.

27 Simonetti OP, Kim RJ, Fieno DS, *et al*. An improved MR imaging technique for the visualization of myocardial infarction. *Radiology* 2001;**218**:215–23.

28 Singh GK, Greenberg SB, Yap YS, *et al*. Right ventricular function and exercise performance late after primary repair of tetralogy of Fallot with the transannular patch in infancy. *Am J Cardiol* 1998;**81**:1378–82.

29 Fratz S, Hager A, Busch R, *et al*. Patients after atrial switch operation for transposition of the great arteries can not increase stroke volume under dobutamine stress as opposed to patients with congenitally corrected transposition. *Circ J* 2008;**72**:1130–5.

30 Oosterhof T, Tulevski II, Roest AA, *et al*. Disparity between dobutamine stress and physical exercise magnetic resonance imaging in patients with an intra-atrial correction for transposition of the great arteries. *J Cardiovasc Magn Reson* 2005;**7**:383–9.

31 Helbing WA, Luijnenburg SE, Moelker A, Robbers-Visser D. Cardiac stress testing after surgery for congenital heart disease. *Curr Opin Pediatr* 2010;**22**:579–86.

32 Weber OM, Martin AJ, Higgins CB. Whole-heart steady-state free precession coronary artery magnetic resonance angiography. *Magn Reson Med* 2003;**50**:1223–8.

33 Weber OM, Pujadas S, Martin AJ, Higgins CB. Free-breathing, three-dimensional coronary artery magnetic resonance angiography: comparison of sequences. *J Magn Reson Imaging* 2004;**20**:395–402.

34 Spuentrup E, Katoh M, Buecker A, *et al*. Free-breathing 3D steady-state free precession coronary MR angiography with radial *k*-space sampling: comparison with cartesian *k*-space sampling and cartesian gradient-echo coronary MR angiography – pilot study. *Radiology* 2004;**231**:581–6.

35 Danias PG, Roussakis A, Ioannidis JP. Diagnostic performance of coronary magnetic resonance angiography as compared against conventional X-ray angiography: a meta-analysis. *J Am Coll Cardiol* 2004;**44**:1867–76.

36 Langerak SE, Vliegen HW, Jukema JW, *et al*. Vein graft function improvement after percutaneous intervention: evaluation with MR flow mapping. *Radiology* 2003;**228**:834–41.

37 Nagel E, Klein C, Paetsch I, *et al*. Magnetic resonance perfusion measurements for the noninvasive detection of coronary artery disease. *Circulation* 2003;**108**:432–7.

38 Costa MA, Shoemaker S, Futamatsu H, *et al*. Quantitative magnetic resonance perfusion imaging detects anatomic and physiologic coronary artery disease as measured by coronary angiography and fractional flow reserve. *J Am Coll Cardiol* 2007;**50**:514–22.

39 Davis CP, Liu PF, Hauser M, *et al*. Coronary flow and coronary flow reserve measurements in humans with breath-held magnetic resonance phase contrast velocity mapping. *Magn Reson Med* 1997;**37**:537–44.

40 Saeed M. New concepts in characterization of ischemically injured myocardium by MRI. *Exp Biol Med* 2001;**226**:367–76.

41 Jerosch-Herold M, Muehling O. Stress perfusion magnetic resonance imaging of the heart. *Top Magn Reson Imaging* 2008;**19**:33–42.

42 Goo HW, Park IS, Ko JK, *et al*. CT of congenital heart disease: normal anatomy and typical pathologic conditions. *Radiographics* 2003;**23**:S147–65.

43 Goo HW, Park IS, Ko JK, *et al*. Computed tomography for the diagnosis of congenital heart disease in pediatric and adult patients. *Int J Cardiovasc Imaging* 2005;**21**:347–65.

44 Leschka S, Oechslin E, Husmann L, *et al*. Pre- and postoperative evaluation of congenital heart disease in children and adults with 64-section CT. *Radiographics* 2007;**27**:829–46.

45 Goo HW. Haemodynamic findings on cardiac CT in children with congenital heart disease. *Pediatr Radiol* 2011;**41**:250–61.

46 Kawano T, Ishii M, Takagi J, *et al*. Three-dimensional helical computed tomographic angiography in neonates and infants with complex congenital heart disease. *Am Heart J* 2000;**139**(4):654–60.

47 Bean MJ, Pannu H, Fishman EK. Three-dimensional computed tomographic imaging of complex congenital cardiovascular abnormalities. *J Comput Assist Tomogr* 2005;**29**:721–4.

48 Yang DH, Goo HW, Seo DM, *et al*. Multi-slice CT angiography of interrupted aortic arch. *Pediatr Radiol* 2008;**38**:89–100.

49 Goo HW, Park IS, Ko JK, *et al*. Visibility of the origin and proximal course of coronary arteries on non-ECG-gated heart CT in patients with congenital heart disease. *Pediatr Radiol* 2005;**35**:792–8.

50 Goo HW, Seo DM, Yun TJ, *et al*. Coronary artery anomalies and clinically important anatomy in patients with congenital heart disease: multislice CT findings. *Pediatr Radiol* 2009;**39**:265–73.

51 Tsai IC, Lee T, Chen MC, *et al*. Visualization of neonatal coronary arteries on multidetector row CT: ECG-gated versus non-ECG-gated technique. *Pediatr Radiol* 2007;**37**:818–25.

52 Busch S, Johnson TR, Wintersperger BJ, *et al*. Quantitative assessment of left ventricular function with dual-source CT in comparison to cardiac magnetic resonance imaging: initial findings. *Eur Radiol* 2008;**18**:570–5.

53 Watanabe S. Diagnostic CT imaging of the heart and aorta in health and disease. *Jpn Circ J* 1981;**45**:1030–44.

54 Stolzmann P, Leschka S, Scheffel H, *et al*. Dual-source CT in step-and-shoot mode: noninvasive coronary angiography with low radiation dose. *Radiology* 2008;**249**:71–80.

55 Hopper KD, Mosher TJ, Kasales CJ, *et al*. Thoracic spiral CT: delivery of contrast material pushed with injectable saline solution in a power injector. *Radiology* 1997;**205**:269–71.

56 Litmanovitch D, Zamboni GA, Hauser TH, *et al*. ECG-gated chest CT angiography with 64-MDCT and tri-phasic IV contrast administration regimen in patients with acute non-specific chest pain. *Eur Radiol* 2008;**18**:308–17.

57 Eichhorn JG, Jourdan C, Hill SL, *et al*. CT of pediatric vascular stents used to treat congenital heart disease. *AJR Am J Roentgenol* 2008;**190**:1241–6.

58 Struffert T, Kloska S, Engelhorn T, *et al*. Optimized intravenous flat detector CT for non-invasive visualization of intracranial stents: first results. *Eur Radiol* 2011;**21**:411–8.

59 Goo HW. Evaluation of the airways in patients with congenital heart disease using multislice CT. *J Korean Pediatr Cardiol Soc* 2004;**8**:37–43.

60 Jhang WK, Park JJ, Seo DM, *et al*. Perioperative evaluation of airways in patients with arch obstruction and intracardiac defects. *Ann Thorac Surg* 2008;**85**:1753–8.

61 Goo HW, Jhang WK, Kim YH, *et al*. CT findings of plastic bronchitis in children after Fontan operation. *Pediatr Radiol* 2008;**38**:989–93.

62 The ALARA (as low as reasonably achievable) concept in pediatric CT intelligent dose reduction. Multidisciplinary conference organized by the Society of Pediatric *Radiology*. August 18–19, 2001. *Pediatr Radiol* 2002;**32**:217–313.

63 Maltz DL, Treves S. Quantitative radionuclide angiocardiography. Determination of Qp/Qs in children. *Circulation* 1973;**47**:1049–56.

64 Sty J, Starshak R, Miller J. Particle body imaging in cardiopulmonary disorders. In: Wagner HN, ed. *Pediatric Nuclear Medicine*. New York: Appleton-Century-Crofts, 1983.

65 Pruckmayer M, Zacherl S, Salzer-Muhar U, *et al*. Scintigraphic assessment of pulmonary and whole-body blood flow patterns after surgical intervention in congenital heart disease. *J Nucl Med* 1999;**40**:1477–83.

66 Holzer R, Hijazi ZM. Interventional approach to congenital heart disease. *Curr Opin Cardiol* 2004;**19**:84–90.

67 Baker EJ, Ellam SV, Tynan M, Maisey MN. First-pass measurement of left ventricular function in infants and children. *Eur J Nucl Med* 1985;**10**:422–5.

68 Baker EJ, Ellam SV, Maisey MN, Tynan M. Radionuclide measurement of left ventricular ejection fraction in infants and children. *Br Heart J* 1984;**51**:275–9.

69 Parrish MD, Graham TP Jr, Born ML, *et al*. Radionuclide ventriculography for assessment of absolute right and left ventricular volumes in children. *Circulation* 1982;**66**:811–9.

70 Parrish MD, Graham TP Jr, Born ML, *et al*. Radionuclide stroke count ratios for assessment of right and left ventricular volume overload in children. *Am J Cardiol* 1983;**51**:261–4.

71 Hurwitz RA, Treves S, Freed M, *et al*. Quantitation of aortic and mitral regurgitation in the pediatric population: evaluation by radionuclide angiocardiography. *Am J Cardiol* 1983;**51**:252–5.

72 Hannon DW, Gelfand MJ, Bailey WW, *et al*. Pinhole radionuclide ventriculography in small infants. *Am Heart J* 1986;**11**:316–21.

73 Reduto LA, Berger HJ, Johnstone DE, *et al*. Radionuclide assessment of right and left ventricular exercise reserve after total correction of tetralogy of Fallot. *Am J Cardiol* 1980;**45**:1013–8.

74 Hurwitz RA, Papanicolaou N, Treves S, *et al*. Radionuclide angiocardiography in evaluation of patients after repair of transposition of the great arteries. *Am J Cardiol* 1982;**49**:761–5.

75 Mullins LJ, Moore RD. The movement of thallium ions in muscle. *J Gen Physiol* 1960;**43**:759–73.

76 Friedman BJ, Beihn R, Friedman JP. The effect of hypoxia on thallium kinetics in cultured chick myocardial cells. *J Nucl Med* 1987;**28**:1453–60.

77 Pohost GM, Alpert NM, Ingwall JS, Strauss HW. Thallium redistribution: mechanisms and clinical utility. *Sem Nucl Med* 1980;**10**:70–93.

78 Wackers FJ, Berman DS, Maddahi J, *et al*. Technetium-99m hexakis 2-methoxyisobutyl isonitrile: human biodistribution, dosimetry, safety, and preliminary comparison to thallium-201 for myocardial perfusion imaging. *J Nucl Med* 1989;**30**:301–11.

79 Carvalho PA, Chiu ML, Kronauge JF, *et al*. Subcellular distribution and analysis of technetium-99m-MIBI in isolated perfused rat hearts. *J Nucl Med* 1992;**33**:1516–22.

80 Di Rocco RJ, Rumsey WL, Kuczynski BL, *et al*. Measurement of myocardial blood flow using a co-injection technique for technetium-99m-teboroxime, technetium-96-sestamibi and thallium-201. *J Nucl Med* 1992;**33**:1152–9.

81 Kahn JK, McGhie I, Akers MS, *et al*. Quantitative rotational tomography with Tl and [99m]Tc 2-methoxy-isobutyl-isonitrile. A direct comparison in normal individuals and patients with coronary artery disease. *Circulation* 1989;**79**:1282–93.

82 Beanlands RS, Dawood F, Wen WH, *et al*. Are the kinetics of technetium-99m methoxyisobutyl isonitrile affected by cell metabolism and viability? *Circulation* 1990;**82**:1802–14.

83 Bjorkhem G, Evander E, White T, Lundstrom NR. Myocardial scintigraphy with 201-thallium in pediatric cardiology: a review of 52 cases. *Pediatr Cardiol* 1990;**11**:1–7.

84 Finley JP, Howman-Giles R, Gilday EL, *et al*. Thallium-201 myocardial imaging in anomalous left coronary artery arising from the pulmonary artery. Applications before and after medical and surgical treatment. *Am J Cardiol* 1978;**42**:675–80.

85 Moodie DS, Cook SA, Gill CC, Napoli CA. Thallium-201 myocardial imaging in young adults with anomalous left coronary artery arising from the pulmonary artery. *J Nucl Med* 1980;**1**:1076–9.

86 Hijazi ZM, Udelson JE, Snapper H, *et al*. Physiologic significance of chronic coronary aneurysms in patients with Kawasaki disease. *J Am Coll Cardiol* 1994;**24**:1633–8.

87 Hayes AM, Baker EJ, Kakadeker A, *et al*. Influence of anatomic correction for transposition of the great arteries on myocardial perfusion: radionuclide imaging with technetium-99m 2-methoxy isobutyl isonitrile. *J Am Coll Cardiol* 1994;**24**:769–77.

88 Weindling S.N, Wernovsky G, Colan SD, *et al*. Myocardial perfusion, function and exercise tolerance after the arterial switch operation. *J Am Coll Cardiol* 1994;**23**:424–33.

89 Cohen DM. Surgical management of congenital heart disease in the 1990s. *Am J Dis Child* 1992;**146**:1447–52.

90 Tsan MF. Mechanism of gallium-67 accumulation in inflammatory lesions. *J Nucl Med* 1985;**26**:88–92.

91 Morguet AJ, Munz DL, Kreuzer H, Emrich D. Scintigraphic detection of inflammatory heart disease. *Eur J Nucl Med* 1994;**21**: 666–74.

92 Reeves WC, Jackson GL, Flickinger FW, *et al*. Radionuclide imaging of experimental myocarditis. *Circulation* 1981;**63**:640–4.

93 O'Connell JB, Henkin RE, Robinson JA, *et al*. Gallium-67 imaging in patients with dilated cardiomyopathy and biopsy-proven myocarditis. *Circulation* 1984;**70**:58–62.

94 Folger G, Eltohami E, Hajar H. Acute myocardial-infarction-like findings with myocarditis in infancy. A case report. *Angiology* 1194;**47**:737–41.

95 Dec GW, Palacios I, Yasuda T, *et al*. Antimyosin antibody cardiac imaging: its role in the diagnois of myocarditis. *J Am Coll Cardiol* 1990;**16**:97–104.

96 Tamaki N, Yonekura Y, Kadota K, *et al*. Thallium-201 myocardial perfusion imaging in myocarditis. *Clin Nucl Med* 1985;**10**:562–6.

97 Kramer RJ, Goldstein RE, Hirshfeld JW Jr, *et al*. Accumulation of gallium-67 in regions of acute myocardial infarction. *Am J Cardiol* 1974;**33**:861–7.

98 Schor RA, Massie BM, Botvinick EH, Shames DM. Gallium-67 uptake in silent myocardial infarction: a case report. *Radiology* 1978;**129**:117–8.

99 Bernstein D, Finkbeiner WE, Soifer S, Teitel D. Perinatal myocardial infarction: a case report and review of the literature. *Pediatr Cardiol* 1986;**6**:313–7.

100 Petersilka M, Bruder H, Krauss B, *et al*. Technical principles of dual source CT. *Eur J Radiol* 2008;**68**:362–8.

101 Rybicki FJ, Otero HJ, Steigner ML, Vorobiof G, *et al*. Initial evaluation of coronary images from 320-detector row computed tomography. *Int J Cardiovasc Imaging* 2008;**24**:535–46.

10 Cardiac Catheterization and Angiography

John D. R. Thomson[1] & Shakeel A. Qureshi[2]

[1]Leeds General Infirmary, Leeds, UK
[2]Evelina Children's Hospital, Guy's and St. Thomas' Hospital, London, UK

Introduction

The nature of invasive study of the heart has changed dramatically. Catheterization was initially developed to understand the anatomy and physiology of the cardiovascular circulation. For anatomic diagnosis it has largely been superseded by echocardiography, cardiac computed tomography (CT), and magnetic resonance imaging (MRI).

Equipment for cardiac catheterization in congenital heart disease

The catheterization laboratory

A number of standards have been published for the structure and contents of a modern catheterization laboratory [1,2]. The physical requirements in such a laboratory depend on the procedures to be performed. Although it is possible to perform limited studies with a mobile fluoroscopy arm outside a formal laboratory environment, this is far from ideal and should not be used as the basis for a catheterization program. At the other extreme are complex "hybrid" catheter/operating suites facilitating catheterization, surgery, or both within a single space [3]. The physical requirements for this laboratory exceed those for a standard catheter laboratory and are beyond the scope of this chapter.

Physical considerations for a catheterization laboratory include:

1 Adequate floor space: for a biplane laboratory, ideally ~30 × 24 ft (~9 × 7.5 m) can reasonably accommodate the necessary staff and equipment. The catheterization equipment and monitors need to be situated so that there is enough space to access the patient easily for both anesthetic equipment and additional imaging, such as trans-esophageal echocardiography (TEE). The lateral fluoroscopic tube must be able to be removed easily before and after the procedure for safe access to the patient.

2 High-quality biplane fluoroscopic equipment with compound angulation, and intrinsic field size capabilities to cope with all sizes of patients with congenital heart disease.

3 Adequate numbers of high-quality, real-time monitors to display biplane images and hemodynamic data (ideally with additional monitoring to show directly TEE imaging and previous CT/MRI data on the main monitor rack simultaneously). Monitors should be installed on rails for easy movement and angulation so that operators can easily see them.

4 Sterile operative environment: although not strictly necessary for many catheterization procedures, a modern catheter laboratory, intended for increasingly complex interventional procedures in congenital and structural heart disease should have clean air filtration systems ideally on a par with a modern operating theater. This is particularly important for programs intending to perform trans-catheter valve replacements or "open" hybrid interventions.

5 Anesthetic equipment: in addition to the necessary space for general anesthesia, there should be piped-in anesthetic gas and oxygen supply, suction, and scavenging systems to remove escaped anesthetic gases.

6 Adequate room lighting that can be dimmed. An additional movable, powerful, and widely adjustable light should be available to illuminate vascular access sites, ideally on a ceiling-mounted boom to minimize the use of floor space.

7 Digital storage of angiographic data, so that they are immediately archived and available for review and on-line/off-line analysis.

8 Auxiliary space: a separate room with appropriate recording facilities for hemodynamic information along with a microphone system to allow communication between the

catheterizing physician and the technician (over the noise of a busy catheter laboratory).

Catheterization laboratory staff

Minimum standards exist in many countries regarding the numbers of staff considered necessary for safe cardiac catheterization. In addition to the primary operator and a skilled assistant, we consider the following staff necessary to perform a congenital cardiac catheterization safely:

1 Dedicated cardiac technician: responsible for pressure monitoring, oxygen saturation determination, hemodynamic calculations, monitoring a continuous electrocardiogram (ECG), and maintaining the defibrillator system including remote pads where appropriate.

2 Radiographer: to minimize radiation exposure actively, ensure accurate calibration and angiographic measurements, and for the mandatory calculation of radiation exposure [a requirement of the UK mandatory Central Cardiac Audit Database (CCAD)].

3 A "running" member of staff, without other duties, but with specific knowledge of the location of equipment required in congenital cardiac catheterization.

In addition, most laboratories have a catheter scrub nurse available.

Disposable equipment

Catheterization of patients with congenital heart disease requires a large inventory of consumables. Individual clinicians and programs develop preferences for particular pieces of equipment and inventories change over the years. Therefore, the stock list of consumables varies from center to center.

A large program may carry as much as £500 000 (~$800 000) worth of disposable equipment at any one time. Therefore, it is absolutely essential that the laboratory has an efficient system for restocking disposables and is realistic about minimum numbers of items necessary for safe procedures. Catheterizing cardiologists must ensure that the correct equipment is available before commencing a study, particularly if a patient requires general anesthesia.

Diagnostic catheterization

Until the capabilities of cardiac MRI reach their full potential, diagnostic catheterization remains the most reliable technique for obtaining hemodynamic and physiologic data in patients with congenital cardiac disease. As surgical techniques have improved, so too has the ability to treat increasingly complex patients and there is a continuing need for invasive cardiac assessment for this group of patients.

Precatheterization assessment

It is unnecessary and potentially unsafe to collect large, untargeted datasets routinely during a procedure, and therefore catheterization studies should be goal oriented and guided by a thorough review of the available information, including the patient's notes and other pre-procedural imaging.

The patient should be in the best possible physical condition for an invasive procedure. This does not mean that catheterization is contraindicated in sick patients; on the contrary, it sometimes can be the only investigation that allows an appropriate management plan. However, every effort should be made to deal with treatable co-morbidity such as acidosis, anemia, and heart failure prior to catheterization, and the catheterizing cardiologist, as always, must be mindful of the balance between risk and benefit for each patient [4].

As an absolute minimum, a contemporary two-dimensional echocardiogram should be reviewed before the procedure. Not only will this help guide the catheter study but it also identifies already established information that does not need further investigation, and decreases the use of unnecessary amounts of intravenous contrast material. Anomalies of the systemic venous and arterial circulation should be noted to plan the vascular access route [5].

An ECG may be required to establish the pre-procedural rhythm. An arrhythmia may need to be controlled prior to the procedure.

We do not routinely cross-match blood for diagnostic cardiac catheterization procedures, although stocks of universal donor blood are readily available in close proximity to our catheterization laboratory suite.

Most pediatric catheterizations require either general anesthesia or sedative agents. Either method is acceptable but each requires patient preparation and appropriate monitoring. Although some investigations can be performed under general anesthesia using a laryngeal airway, this has limitations and militates against the use of trans-esophageal imaging, which cannot be performed without endotracheal intubation. Sedative agents, such as ketamine, promethazine, and morphine analogs, should be administered by practitioners familiar with their use under the guidance of local protocols. There should be anesthetic support and on-site intensive care available in the event of a problem. All catheterization laboratories should be equipped with size-appropriate cardiopulmonary resuscitation equipment and staff properly trained to use it and apply resuscitation protocols.

The environment and monitoring during cardiac catheterization

Standard monitoring for all patients should include real-time ECG (two leads minimum), peripheral oxygen saturation, and blood pressure in addition to clearly displayed data obtained during the procedure. Neonates and infants require temperature monitoring and external warming devices to maintain body temperature even for the shortest of

procedures. Ventilated patients should have appropriate anesthetic monitoring including the display of end tidal carbon dioxide and inspired concentrations of anesthetic agents. Blood gas and saturation monitoring is essential for all congenital cardiac catheterizations. Keeping track of the amount of blood withdrawn is necessary, especially for infants.

Vascular access

The percutaneous femoral route is preferred for diagnostic catheterization for most patients with congenital heart disease [6]. Vascular cut-down procedures are rarely performed in the modern era, but catheterizing cardiologists should be familiar with the technique as occasionally a cut-down may be desirable or necessary. In general, however, the best approach is the Seldinger technique, using a needle to introduce a wire into the target vessel. Almost every operator of any experience has their own preferred method for this form of vascular access. Beyond the absolute principle of understanding the external anatomy, in general familiarity through repeated practice of a particular technique should be encouraged as the best way of obtaining consistent results. Over recent years, ultrasound evaluation of target vessels has become increasingly accepted as the gold standard for central venous access [7]. Although not always necessary for every catheter procedure, all invasive cardiologists should be trained in the technique and be prepared to use ultrasound-guided access in specific circumstances. Although even relatively large sheaths can be inserted into the femoral veins of small infants (a 7Fr sheath can be inserted into the femoral vein for an atrial septostomy in babies weighing as little as 1.5 kg), the general principle of "as small as possible" should be observed, particularly in patients who are likely to require repeat studies.

The umbilical vein can usually be accessed easily in a newborn infant up to ~10 days after birth and is appropriate for a balloon septostomy, provided that the operator is familiar with negotiating the catheter through the liver [8].

Brachial, carotid, jugular, and axillary approaches can be used if the femoral route is unavailable or if the anatomy dictates an approach from above the heart. Brachial venous puncture is straightforward and, provided that the correct vessel is cannulated, usually offers a straight route towards the heart and great vessels, although the capacity of the vessel is limited in infants and smaller children, and brachial venous spasm may make catheter manipulation difficult. Brachial artery cannulation can be performed either percutaneously or via a cut-down procedure. The axillary vein can be accessed percutaneously (usually lying medial to the arterial pulsation in the distal axillary crease), but for this approach and for access to the axillary artery a cut-down procedure is preferable, allowing the direct insertion of a needle and wire into the vessel [9]. The internal jugular veins can be easily cannulated and offer an excellent alternative approach to the central venous system in patients of all sizes if the femoral vessels are occluded or an approach from above the heart is preferable. Generally, the right internal jugular is the best access approach, although at times the left vessel offers a better route to the target, but operators should always be mindful of a persistent left superior vena cava to the coronary sinus, which is common in patients with congenital heart disease. Infraclavicular access to the subclavian vein is often used. Although external landmarks are reasonably consistent, now we always use ultrasound to facilitate access of the jugular veins [7]. Vascular access is effected with lidocaine analgesia, the injection often being preceded by lidocaine cream.

Systemic anticoagulation with heparin is not performed for purely venous catheterization, but should be used in diagnostic procedures with arterial access at a dose of 50 IU kg^{-1}. If it is used, check activated clothing time every 30–60 min. Some cardiologists apply anticoagulation if a venous procedure uses guidewires or for prolonged left-sided catheterization.

Vascular complications

Although the incidence of vascular complications after pediatric cardiac catheterization has fallen over the years, probably due to both greater awareness and progressive miniaturization of catheterization equipment, some problems remain [10–12]. In a recent report of over 11 000 patients reflecting contemporary practice, complications occurred in 7.3% of patients; one-third were vascular complications and of these 20% were designated major [12]. All pediatric vascular access sites should be treated with care from the point of access to the equally important hemostasis after removing the access sheath. Although arterial access complications are clearly the more important, having the capacity to threaten both life and limb, central venous access points are also precious. There is an increasing capacity to deliver trans-catheter treatment as an alternative to surgery in complex patients, but this requires access to the central venous system.

Other complications of cardiac catheterization

Vascular and other complications during cardiac catheterization have fallen dramatically over the years [12–14]. The reasons for this are numerous: techniques have been refined, cardiologists are better trained and supervised, equipment is more suited to the needs of infants and children, improvements have been made in intravenous contrast agents, and there is greater awareness of the dangers of catheterization in sick patients. A moribund, acidotic, poorly perfused neonate who has not responded to precatheterization measures may die in spite of, rather than because of, catheterization [14]. Complications that can occur include death, cerebral or systemic embolus, cardiac perforation potentially leading to tamponade, heart block, arrhythmia (ventricular or supraventricular), hypercyanotic spells, sepsis, and vascular damage.

Angiography

Although contrast medium-enhanced fluoroscopy is no longer the mainstay of anatomic imaging in congenital cardiology, angiograms remain an essential part of interventional pediatric catheterization. A working knowledge of how images are generated and also radiation protection issues for both patients and catheter laboratory staff are essential for all catheterizing cardiologists [15,16].

Generating X-rays and images

Current systems for generating X-rays consist of a rotating rhenium–tungsten anode target and a cathode made from a tungsten filament housed in a focusing apparatus. Voltage and current from the generator heat the tungsten cathode, generating electrons that flow from the cathode to the anode (with the patient in between). The electron flow is related directly to the number of photons produced by the tube, and measured in milliamperes (mA). Current multiplied by exposure time in milliseconds gives milliampere-seconds (mAs), a measure of total exposure to X-rays. The penetrating power of each photon depends on the electrical potential across the X-ray tube and is measured in kilovolts (kV). Picture density doubles with about a 10 kV increase in voltage or a doubling of mAs. Lower energy photons that do not participate in image production are prevented from entering the patient by a thin aluminum screen. In general, increasing kV produces greater penetration of X-rays whereas increasing mA increases image sharpness and the amount of scatter. To minimize blurring, the image intensifier should be as close to the patient's chest as possible. In addition, a lead grid between the intensifier and the patient reduces the amount of scattered X-rays reaching the image receptor. The X-ray beam is attenuated by 50% by ~4 cm of tissue. To obtain adequate tissue density in larger patients or some angulated views, either the voltage must be increased by 10 kV or the exposure in mAs must be doubled.

The X-ray is automatically collimated so that the beam is directed within the confines of the image intensifier on the opposite side of the patient. Further manual collimation allows the beam to cone around the structure of interest, thus improving the quality of image by decreasing the amount of stray radiation striking the intensifier. Almost without exception, the X-ray tube is mounted such that the beam passes from under the patient to an intensifier above and from the right to left side of the patient in biplane systems. Modern equipment uses increasingly complex microprocessors both to control the delivery of energy to the X-ray tube and for the interpretation of the data generated.

The image intensifier is the key receptor in the system, increasing the brightness of the image several thousand-fold. The light produced by the image intensifier is electronically boosted and directed to a camera with an optical lens to produce the final image in analog systems. In digital systems there is no optical lens, rather a microprocessor that processes the data and facilitates the display of the final image. The relative advantages and disadvantages of digital and analog systems are hotly debated, but in reality digital fluoroscopic image generation, manipulation, and storage are here to stay, and in time analog imaging systems will become obsolete.

Radiation protection

Direct primary exposure to ionizing radiation affects the patient for limited periods of time and cumulative secondary exposure leads to risk for personnel in the catheter laboratory [15,16]. There are a number of methods for measuring radiation exposure, the most practical and commonly used being photographic film (badges) usually worn underneath the protective lead used by catheterization laboratory staff.

The units used to measure radiation are complicated by overlapping terminology, particularly as the unit of exposure (the roentgen) differs from the unit of protection that describes the absorbed dose [16]. The roentgen (R) is the ionization that the beam from an X-ray tube produces in air and is the amount of radiation that produces 2.58×10^{-4} coulombs (C) per kilogram of air. Exposure (rad and gray) and equivalent (rem and sievert) doses describe absorbed radiation and are essentially a semantic distinction as the factor to convert the former to the latter for X-rays is one. The absorbed dose describes how much heating the X-rays produce in each unit of a specified material. The unit for absorbed dose is the familiar rad, which is 100 erg of energy deposited in 1 g of tissue, with the SI unit being the gray (Gy), which is 1J kg^{-1}. The equivalent dose is the rem, which measures effective biologic radiation, and the analogous SI unit is the sievert (Sv). Equivalent doses are generally used in radiation protection as they describe the absorbed dose in biologic tissue. Fortunately, conversion between units is generally simplified in that under normal circumstances in the laboratory 1 R approximates 1 rad = 1 cGy = 1 rem = 10 mSv.

The patient is exposed to radiation directly from the X-ray beam. Only ~1% of the original X-ray beam reaches the image intensifier. Soft tissues absorb less radiation than denser tissues such as bone. Very roughly, when considering analog systems used in children, X-ray exposure has been estimated at between 50 and 1000 times that of plain chest X-ray exposure, depending on the type and length of procedure performed [17]. Radiation exposure with modern digital systems is significantly lower, and the dose savings are generally much greater for children than adults. The radiation dose is at least 10 times greater per unit time for cineangiography than fluoroscopy. Therefore, the additional advantage to the patient of a digital laboratory that obviates the need for cineangiography is self-evident.

Somatic effects of X-radiation are related to the radiosensitivities of tissues. The thyroid gland, gonads, bone

marrow, breast, and eye lens are more sensitive than are other tissues. Effects such as fibrosis, inflammation, cataracts, atrophy, ulceration, and malignancy (especially of the thyroid and involving bone marrow) have all been described [18,19].

Measures to decrease radiation effects start with the primary exposure to the patient. All equipment must be used in a specifically designed suite that contains the radiation produced. Vulnerable gonadal tissue should be protected in patients directly, where possible using lead shields. The use of the minimum amount of X-ray energy to produce the required image is important for point source reduction. Equipment must be well maintained and calibrated regularly. Magnification should be used judiciously. If a digital system is available, post-processing magnification is preferable to using a smaller intensifier. The X-ray should be collimated carefully with filters, and lead bars should be utilized to cone the beam around the area of interest. The image intensifier should be as close to the patient as possible. Importantly, every second of fluoroscopy should have a purpose, with intermittent screening providing the additional benefit of prolonging the life of the X-ray tube. Digital review of previously saved fluoroscopy scenes can significantly reduce exposure. As always, each study should be carefully planned to minimize catheter exchanges and therefore the use of catheters for multiple purposes can also help [20].

Short diagnostic angiograms are preferable to prolonged acquisitions, with the need for more than 6–8 s runs rarely indicated. Axial projections require more X-ray energy and are associated with additional radiation scatter, hence the operator must use these projections judiciously, especially during prolonged interventional procedures. Secondary exposure is caused predominantly by scatter and affects both the patient and staff. Catheterization laboratory staff are exposed to cumulative long-term permanent doses of radiation and so clear and effective policies to regulate and control radiation exposure must be in place. Shielding equivalent to 0.5 mm of lead decreases the exposure by a factor of 50; hence its use over radiation-sensitive areas with aprons, shields or collars, and glasses provides substantial protection. The protective equipment should be screened regularly for defects. Steerable lead screens for use in prolonged procedures should be available. Staff should be aware of the inverse square law (the radiation exposure decreases proportionally to the inverse square of the distance from the X-ray beam) and should step away from the field during angiography. In addition, they should understand the areas of greatest exposure to scatter.

Contrast media

Contrast agents are based on iodine and function to increase the innate contrast that exists between tissues. Blood solubility and the side effects of these compounds are to a large extent a function of their chemical properties, primarily the capacity of

a central benzene ring to bind to iodine atoms. Modern contrast agents contain benzene rings with the capacity to hold large numbers of iodine atoms and this reduces osmolality. However, these agents are more expensive than the standard higher osmolality contrast agents. Because of the higher osmolality (approximately six times that of blood), ordinary contrast agents cause far more side effects than low- or nonionic contrast agents [21–23]. The lower osmolality agents, including "nonionic" or water-soluble agents, are much safer (even though still hyperosmolar with respect to blood) and are used almost exclusively in pediatric catheterization laboratories in the developed world, particularly in patients with renal failure or ventricular dysfunction.

The incidence of major side effects with contrast agents is low, with death occurring in ~1/40 000 injections and serious but nonfatal reactions in ~1/14 000 injections [24]. Pulmonary effects include an increase in pulmonary artery pressure and edema. Systemic effects include hypotension, peripheral vasodilation, and allergic reactions. Very rarely, massive histamine release can be encountered and individuals with previous documented reactions to intravenous contrast agents require particular care. All contrast agents can lengthen the QT interval.

Safe absolute amounts of contrast agent in any patient depend on specific individual circumstances, but cumulative doses >6 ml kg^{-1} should be given with great care.

Injection techniques

Angiograms can be performed either manually (using a Luer-lock syringe) or using a power injector. Many operators prefer the tactile "feedback" of a syringe injection in smaller patients, but there is clearly a size limit beyond which a manual injection cannot opacify a vessel. Power injectors vary in design but all essentially deliver a constant pressure allowing for greater flow of contrast into the vessel. Many injectors (particularly those designed to work in modern digital systems) specifically interface with the fluoroscopy system, and so are not necessarily interchangeable with other injectors in a laboratory facility. Power injectors are set to deliver a user-defined volume of contrast agent over a period of time (in children always ml s^{-1}) and most can be programmed to give a gradual step up in pressure ("rate rise") to avoid catheter recoil, although in practical terms the physical properties of injector systems mean that a "square-wave" injection is not possible. Deciding upon the correct amount of contrast agent for any particular injection requires a mental calculation based on the chamber to be filled, the size of the patient, the presence or absence of a shunt, and the particular angiographic settings within the laboratory. Suffice it to say that this is learned with experience. The basic rule of thumb is that within a modern laboratory, in most children an injection of 1 ml kg^{-1} into a large vessel or chamber without a shunt is normally adequate. Injections into

ventricular chambers should be performed using either a pigtail or non-end hole catheter, for example, an NIH, or, if this is not possible, an end hole catheter, such as a Gensini, with sufficient side holes to deliver a large bolus of contrast agent. Other catheters can and have been used to provide satisfactory angiograms, but as is often the case in cardiac catheterization, attention to detail and applying the extra effort to execute each element of a study to the highest standards yield the best results. Before any power injection, a small test shot should be performed to ensure that the catheter is not wedged in the myocardium or entangled in another structure into which a large bolus of contrast may cause harm.

Occasionally, particularly in complex catheter interventions, to maintain position it is desirable to perform angiography over a guidewire. In these circumstances, it is preferable to use either a long sheath (e.g., a Mullins sheath, Cook Medical, Bloomington, IN, USA) with sufficient additional volume or a Multitrack catheter (NuMed, Hopkinton, NY, USA), specifically designed to provide high volumes of contrast agent over a guidewire.

Angiographic projections (Table 10.1)

Prior to the late 1960s, all angiography was performed in frontal and lateral projections (Figure 10.1a and b). Subsequently, axial angiography became valuable in cardiac malformations [25,26]. In standard nomenclature, the straight frontal projection is designated as 0°. Movement of the frontal intensifier to the left or right constitutes left or right anterior oblique projections (LAO or RAO), respectively, often further quantified by the degree of rotation. A rotation of 90° from the frontal projection designates the lateral view. The X-ray tube head can also be angulated towards either the patient's head or feet, adding additional cranial or caudal tilt, respectively.

The ventricular septum is best defined in LAO (Figure 10.1c), with the inlet moving to outlet with additional tilt to the left. LAO with cranial tilt also profiles the course of the atrial septum and the main and proximal branch pulmonary arteries. Ventriculo-arterial connections and branch pulmonary arteries are best seen in their respective axial tilts (for the normally positioned right heart in RAO and left heart in LAO) (Figure 10.1c and d). Pulmonary venous connections are variable but are again often best profiled in their respective axial angulation. Optimal angiographic projections require tailoring to each individual heart and the information required from a particular study. This is particularly true for patients with atypical cardiac position or connections. When precisely defining anatomic position, biplane angiography, particularly in "ordinary" frontal and lateral projections, is extremely useful, allowing a composite calculation in two interfacing planes (Figure 10.1a and b).

The need for complex and involved diagnostic angiography is relatively rare, being superseded by other forms of

Table 10.1 Common cineangiographic projections[a].

View	A plane (°)	B plane (°)
Posteroanterior and lateral	0	90 (LAO)
Long axial (LV and PA)	30 RAO	60 LAO
		20 cranial
Hepatoclavicular	30 LAO	120 LAO
(four-chamber LV)	40 cranial	15 cranial
Sitting up (cranial–caudal):	0–7 LAO	90 LAO
RVOT, pulmonary arteries	40 cranial	
Right bidirectional	30–40 RAO	90 LAO
cavopulmonary connection	20–30 cranial	
Atrial septal defect	30 LAO	Parked
	40 cranial	
Down-the-barrel	30 RAO	30 LAO
transposition of the great		45 caudal
arteries		
Selective biplane left	30 RAO	60 LAO
coronary artery (No. 1)		
Selective biplane left	30 RAO	60 LAO
coronary artery (No. 2)	30 cranial	25 cranial
Selective biplane left	30 RAO	90 LAO
coronary artery (No. 3)	30 caudal	
Selective biplane right	30 RAO	60 LAO
coronary artery (No. 1)		
Selective biplane right	30 LAO	Parked
coronary artery (No. 2)	30 cranial	

[a]A plane, intensifier that records posteroanterior views; B plane, intensifier that records lateral or LAO views; LV, left ventricle; LPA, left pulmonary artery; RVOT, right ventricular outflow tract; LAO, left anterior oblique; RAO, right anterior oblique.

imaging. However, every cardiologist must understand the basic axial angiographic views. Because of the sigmoid nature of the inter-ventricular septum and separation of the pulmonary artery tree, the most commonly used view for showing these structures is the LAO projection, often with additional cranial tilt, commonly known as the "sitting view" referring to earlier days when the patient, not the X-ray tube, moved to achieve the required projection) [27] (Figure 10.1e and f). Atrioventricular connections in the normally positioned and connected heart are usually obtained in LAO projection.

3D Rotational angiography

Recent advances in commercially available angiographic technology have made 3D rotational angiography a realistic prospect in modern congenital cardiac catheterization laboratories. Data sets akin to those obtainable with high resolution multi-slice CT can now be obtained within a catheterization study allowing increased diagnostic accuracy,
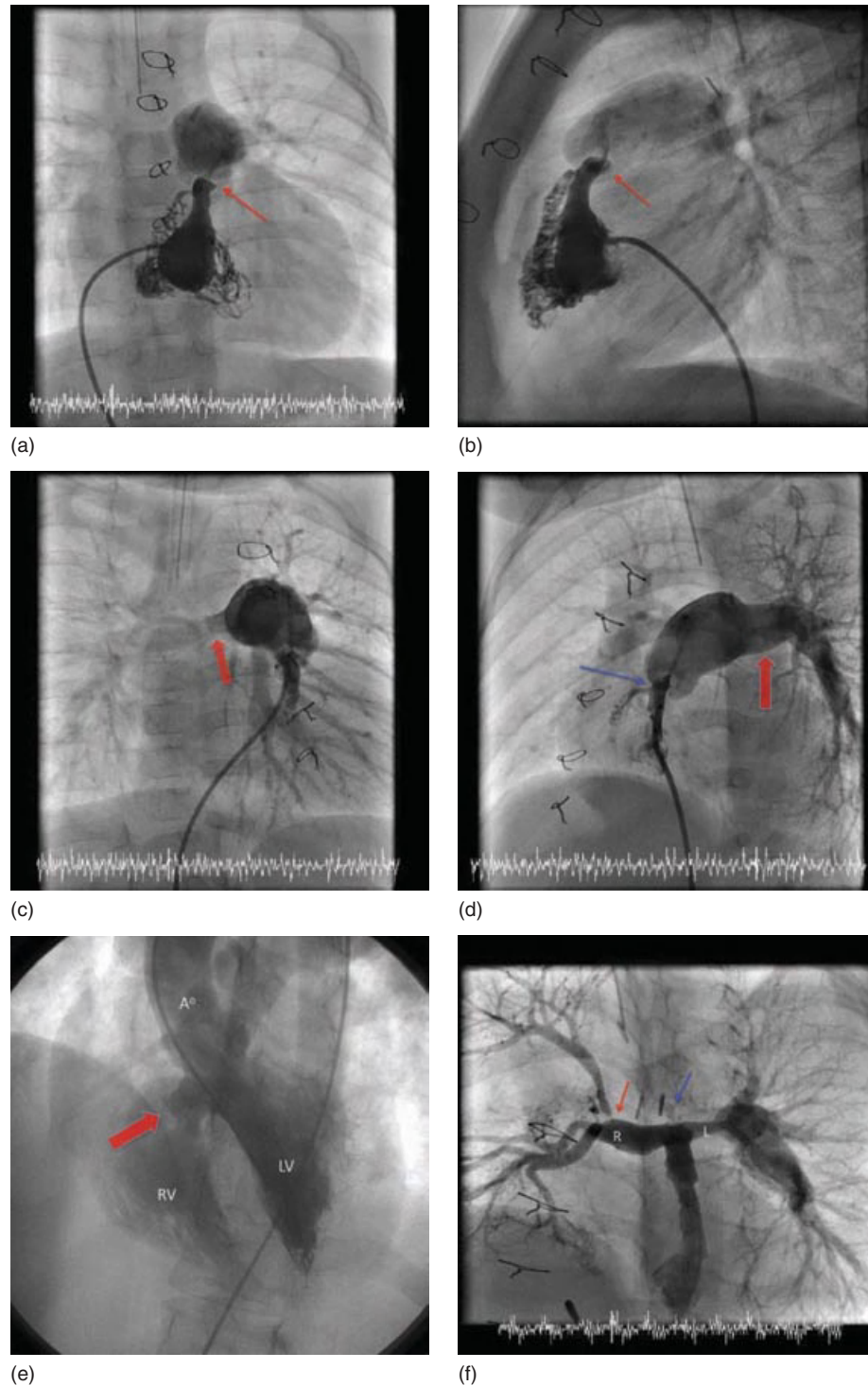
Figure 10.1 (a) Biplane right ventricular angiogram in the anteroposterior ("frontal") projection in a patient with pulmonary atresia with intact ventricular septum after ventricular decompression. Note the dysplastic pulmonary valve (thin red arrow). (b) Lateral projection [at 90° to (a)] in the same patient. (c) Pulmonary artery angiogram in the right anterior oblique projection (RAO) in the same patient. This view profiles the right pulmonary artery (RPA) (arrowed). Note the RPA appears faint because of "washout" from an aortopulmonary shunt. (d) Pulmonary artery angiogram in the same patient as in (a)–(c), but here in the LAO projection, showing the left pulmonary artery (red arrow). Note the extremely dysplastic pulmonary valve demonstrated on this angiogram (thin blue arrow). (e) Pigtail injection into the left ventricle in the left anterior oblique projection (LAO with cranial angulation) outlining the ventricular septum and the left ventricular outflow tract, here a patient with a perimembraneous ventricular septal defect (arrow). LV, left ventricle; RV, right ventricle; A°, aorta. (f) "Sitting view" (LAO with cranial angulation) showing the pulmonary artery tree in a patient after unifocalization of pulmonary arteries and connection to the right ventricle with a restrictive right ventricle to pulmonary artery conduit. Note the stenosed origins of previous aortopulmonary collaterals (red arrow) and the remnants of a previous ductal stent (blue arrow) used to maintain ductal blood flow into the native left pulmonary artery. R, right pulmonary artery; L, left pulmonary artery.

a better understanding of the relationships between structures and improved understanding of the anatomy underlying targets for therapeutic intervention. Experience is currently limited and enthusiasm for the technique needs to be viewed in the light of the increased radiation doses required, technical difficulties in image acquisition (mainly movement artifact making general anesthesia a necessity) along with the need for post processing which currently takes minutes rather than seconds. However, there is certainly the potential for rotational angiography to develop into a clinically useful technique in mainstream practice in the future [27a].

Hemodynamic calculations

Physiologic recordings

It is very difficult to measure blood flow directly within the heart and great vessels. Therefore, calculations based on surrogates are used. The most important element for hemodynamic calculations in the laboratory is the accuracy of the readings and measurements themselves, Therefore, all equipment, including pressure recording transducers and oxygen saturation measuring devices, should be thoroughly checked and calibrated before any procedure.

Shunt calculations

Although many catheter laboratories and computerized reporting systems provide automated calculations, cardiologists must understand the fundamentals of hemodynamic calculations, many of which are simple and can be roughly but readily applied and adapted during the catheterization itself [28].

Flow and shunt calculations often depend on manipulating values for oxygen in the blood, and the following information is essential:

1 Oxygen-carrying capacity of blood (ml l^{-1})=13.6 ml O_2 g^{-1}Hb L^{-1}blood.

2 Dissolved oxygen (ml l^{-1}) = 0.03 ml l^{-1} $mmHg^{-1}$ partial pressure of oxygen.

3 Oxygen saturation (%) = percentage of oxygenated hemoglobin.

4 Oxygen content of blood (ml l^{-1}) = [oxygen-carrying capacity (ml l^{-1}) × oxygen saturation] + dissolved oxygen (ml l^{-1}).

Of most practical value is the pulmonary to systemic flow ratio (Qp:Qs). This is an important index upon which many of the early indications for intervention in congenital heart disease were based. To calculate Qp:Qs, heparinized blood from the aorta (or ideally a pulmonary vein), main pulmonary artery, superior vena cava, and inferior vena cava is obtained with the patient ventilated, preferably on normal inspired FiO_2 concentrations, but not >30% inspired oxygen. The calculations should be based on samples obtained within a brief period, rather than random samples which may reflect differing hemodynamics. Patients breathing higher concentrations of oxygen are likely to have raised pulmonary artery oxygen concentrations, artificially elevating the calculated left-to-right shunt. From these measurements, the following can be calculated.

The pulmonary to systemic flow ratio (Qp:Qs) is based on the Fick principle and although the oxygen-carrying capacity of the blood and oxygen consumption (see later) are important parts of the calculation of both pulmonary and systemic flow, they cancel each other out in the final analysis to give a simple equation [28,29]:

$$Qp : Qs = \frac{Sao - Smv}{Spv - Spa}$$

where S is percentage saturation, ao = aorta, mv = mixed venous, pv = pulmonary vein, and pa = pulmonary artery, and

$$Smv = \frac{3 \times SVC + 1 \times IVC}{4}$$

where Smv is mixed venous saturation, SVC is superior vena cava, and IVC is inferior vena cava.

The IVC saturation should be taken at the level of the diaphragm to take into account hepatic venous return. Mixed venous saturation is to some extent inaccurate because of unmixed streams of blood with different oxygen saturations in the venae cavae and even in the right atrium. Because of this streaming, an increase in oxygen saturation of 7% at the atrial level, 5% at the ventricular level, and 2% at the pulmonary arterial level is needed to diagnose left-to-right shunting at that level.

Assessing pulmonary venous saturation can also be difficult. A saturation measured within the left atrium can be substituted for the pulmonary venous saturation assuming that there is no shunt at the atrial level. In most patients, it is unreasonable to perform a transeptal puncture purely to measure a pulmonary venous saturation and so frequently the pulmonary venous saturation is assumed to be 98%. Patients with a left-to-right shunt are usually fully saturated and therefore the systemic saturation is always about 98%. Under these circumstances, the shunt equation becomes even simpler and an approximation of the calculation can readily be performed mentally without even writing the figures down! The same equation allows an assessment of right-to-left shunt, but clearly in a desaturated patient, no assumptions can be made about systemic or pulmonary venous saturations.

Cardiac output, flow, and resistance

Thermodilution is the easiest technique with which to calculate cardiac output. The procedure requires introducing cold injectate of known temperature into the blood stream

and measuring the temperature further downstream, leading to a time–temperature curve that can be related to cardiac output [30]. Cardiac output determined by thermodilution is largely automated and correlates well with the Fick technique.

The dye dilution method uses indicator dye, usually indocyanine green, injected into the circulation. The concentration of the indicator is measured continuously and allows the construction of a first-pass indicator concentration curve [31]. The Stewart–Hamilton equation is then used to calculate cardiac output:

$$Q(\text{l min}^{-1}) = \frac{I(\text{mg}) \times 60}{\overline{C}(\text{mg l}^{-1}) \times t(s)}$$

where I is the quantity of dye (mg), $\overline{C}$ is the mean concentration in the absence of recirculation (mg l^{-1}), and t is the duration of the curve (s).

Both thermodilution and indicator dye techniques require training and practice to produce reliable results. However, both rely on the assumption that pulmonary and systemic flow ratios are the same, which does not occur in patients with an intracardiac shunt, invalidating the techniques in many patients with a congenital cardiac defect.

Systemic and pulmonary flow

The Fick technique for calculating cardiac output is the most reliable in patients with intracardiac shunts but relies fundamentally on measuring oxygen consumption (VO$_2$ ml min^{-1}), a highly involved (and expensive) technique in its own right with a number of inbuilt potential errors [28,32]. Many laboratories rely on assumed oxygen consumption based on the age and gender of the patient rather than a direct measurement when calculating pulmonary vascular resistance. This approach introduces a fundamental and systematic error to all subsequent calculations [32]. Studies have shown a poor correlation between assumed and calculated oxygen consumption values, which many operators believe militates against the use of assumed oxygen consumption in calculating cardiac output and also flow and resistance [32].

The Fick technique assumes that the oxygen uptake in the lungs is in equilibrium with oxygen usage in the systemic tissues. As such, the difference between arterial and venous blood oxygen concentrations across a "circuit" (either the pulmonary or systemic beds) represents tissue oxygen utilization. Pulmonary blood flow can then be determined by the following equation:

$$Qp \ (\text{l min}^{-1}) = \frac{\text{VO}_2(\text{ml min}^{-1})}{(\text{PV} - \text{PA}) \text{ oxygen content } (\text{ml l}^{-1})}$$

Where Qp is pulmonary blood flow, VO$_2$ is oxygen consumption, PV is pulmonary vein, and PA is pulmonary artery.

Table 10.2 Calculation of flows and shunts.

Parameter[a]	No shunt	Left–right shunt	Right–left shunt	Bidirectional shunt
VO$_2$ (ml min^{-1})	250	250	250	250
Cpv (ml l^{-1})	200	200	200	200
Cao (ml l^{-1})	200	200	175	175
Cpa (ml l^{-1})	150	175	125	125
Cmv (ml l^{-1})	150	150	125	100
Qp (l min^{-1})	5.0	10.0	3. 33	10.0
Qs (l min^{-1})	5.0	5.0	5.0	3.33
Qep (l min^{-1})	5.0	5.0	3.33	2.5
Qlr (l min^{-1})		5.0	–	7.5
Qrl (l min^{-1})	–		1.67	0.83

[a]C, oxygen content.

Oxygen consumption should ideally be directly measured, but if this cannot be done then oxygen consumption tables can be used [33]. Usually these values are then indexed for body surface area as this correction allows a natural progression to figures for pulmonary vascular resistance in Wood units. To perform this calculation, the calculated absolute flow is divided by body surface area. Thus in small child with a body surface area of 0.3 m^2 an absolute flow of 2l min^{-1} gives an index of 2/0.3 = 6.7 l min^{-1} m^{-2}, about double the normal resting value, but which is very low for an adult with a body surface area of 1.5 m^2, because that cardiac index is 2/1.5 = 1.3 l min^{-1} m^{-2}. The normal index is approximately 3.5 l min^{-1}. The second crucial element in the equation is the oxygen content of the blood samples; this requires a calculation based upon the hemoglobin (g l^{-1}) multiplied by 1.36. The oxygen content of each sample is then calculated by multiplying the oxygen-carrying capacity by the saturation. Using this technique, the difference between arterial and venous oxygen contents across a circuit (either pulmonary or systemic) can be readily calculated and applied to the equation above.

Systemic flow (Qs) can be calculated by substituting the difference between pulmonary venous and arterial oxygen in the equation above with those for systemic venous and arterial oxygen contents. Examples of calculations are given in Table 10.2.

If pulmonary flow exceeds systemic flow, that is, if $Qp > Qs$, then the difference $Qp - Qs$ is the amount of the left-to-right shunt. If $Qs > Qp$, then the difference $Qs - Qp$ is the amount of the right-to-left shunt. If there are both left-to-right and right-to-left shunts, then oxygen saturation in the pulmonary veins exceeds that in the aorta, and oxygen saturation in the pulmonary artery exceeds the mixed

Table 10.3 Data for calculation of multiple left-to-right shunts.

Parameter[a]	Oxygen saturation (%)	Oxygen content (ml l⁻¹)
Cpv (ml l⁻¹)	95	193.8
Cao (ml l⁻¹)	95	193.8
Cpa (ml l⁻¹)	85	173.4
Crv (ml l⁻¹)	80	163.2
Cra (ml l⁻¹)	75	153
Cmv (ml l⁻¹)	70	142.8

[a]C, oxygen content.

venous saturation. Then the concept of effective pulmonary flow (Qep), which is the amount of desaturated venous blood that is oxygenated in the lungs, is used:

$$Q\text{ep}(\text{l min}^{-1}) = \frac{\text{VO}_2(\text{ml min}^{-1})}{(\text{pulmonary vein - mixed venous})\text{oxygen content}(\text{ml l}^{-1})}$$

Then Qp – Qep is the left-to-right shunt and Qs – Qep is the right-to-left shunt. For examples, see Table 10.2.

If there are left-to-right shunts at different levels, the pulmonary blood flow at each level is calculated as if the saturation in that chamber was the final saturation entering the lungs. Consider left-to right-shunts at atrial, ventricular and pulmonary arterial levels (Table 10.3).

Assume perfect mixing in each chamber and $\text{VO}_2 = 196$ ml min⁻¹. Calculate Qs as usual:

$$Q\text{s} = \frac{196}{193.8 - 142.8} = 3.84 \text{ l min}^{-1}$$

If there had been no shunt beyond the right atrium, then the oxygen contents in the pulmonary artery and right atrium would have been the same. Therefore, Qp would have been

$$Q\text{p} = \frac{196}{193.8 - 153} = 4.80 \text{ l min}^{-1}$$

and the left-to-right shunt would have been 4.8–3.84 = 0.96 l min⁻¹. This is the shunt through the ASD.

If there been a shunt through the VSD, then Qp would have been

$$Q\text{p} = \frac{196}{193.8 - 163.2} = 6.40 \text{ l min}^{-1}$$

Then the difference 6.40–4.80 = 1.6 l min⁻¹ must have been due to the extra flow across the VSD.

If we add in the ductus shunt, then Qp becomes

$$Q\text{p} = \frac{196}{193.8 - 173.4} = 9.61 \text{ l min}^{-1}$$

The added flow comes from the ductus, so that the ductus shunt is 9.61–6.4 = 3.21 l min⁻¹.

Note that for equal increments of saturation from one level to the next the shunt becomes larger and larger. This means that a small shunt beyond a large shunt may be difficult to detect because of the variability of saturations due to streaming.

Pulmonary Vascular Resistance

The calculations for pulmonary flow as described above are in themselves not particularly useful. In most patients, these calculations are performed to derive measurements of pulmonary vascular resistance, which is of fundamental importance in decisions in many patients with congenital heart disease.

Pulmonary vascular resistance (Rp) is expressed as

$$R\text{p} = \frac{\overline{P}_{\text{PA}} - \overline{P}_{\text{LA}}}{Q\text{p}}$$

where $\overline{P}_{\text{PA}}$ and $\overline{P}_{\text{LA}}$ are mean pulmonary arterial and left atrial pressures (mmHg), respectively, and Qp is pulmonary flow (l min⁻¹).

If the left atrium cannot be accessed, then the pulmonary capillary wedge pressure can be substituted. Assuming that the pulmonary blood flow has been calculated as above and indexed correctly for body surface area, calculation of the equation becomes simple and leads to a pulmonary vascular resistance in mmHg l⁻¹ min⁻¹, commonly referred to as Wood units.

Trans-Pulmonary Gradient

Many operators prefer to use the "trans-pulmonary" gradient (the difference between the mean pulmonary artery pressure and the mean left atrial pressure) as an index of pulmonary vascular resistance, rather than Wood units. This approach removes all of the assumptions and potential inaccuracies related to the calculation of pulmonary blood flow. The normal pulmonary vascular resistance is <2 Wood units m⁻², but that is only if flow is normal. If pulmonary blood flow is increased in normal subjects, as with exercise, the pressure in the pulmonary

artery barely changes because Rp decreases. Therefore, a child with a large VSD, high pulmonary blood flow and Rp = 2 Wood units m^{-2} has abnormal resistance, because at those flows Rp should be <1 Wood unit m^{-2}. Using the transpulmonary pressure avoids this source of error.

Calculations of Rp should also consider the effect of blood viscosity. Resistance to flow of blood through a tube is a function of tube geometry (mainly length and radius) multiplied by blood viscosity. To assess the geometric factor alone, the resistance is divided by the viscosity to derive what is termed "hindrance." For constant hindrance, halving the viscosity halves the resistance, and doubling the viscosity doubles resistance. Hence in patients with polycythemia and a hematocrit of 70% the viscosity is about doubled, and Rp is correspondingly increased. To assess what Rp would be at normal hematocrit (as in a child after a successful single ventricle repair), the calculated value for Rp is divided by the relative viscosity, as determined by Figure 10.2.

Consider interpreting a pulmonary vascular resistance in the two patients illustrated in Table 10.4. Patient A with a
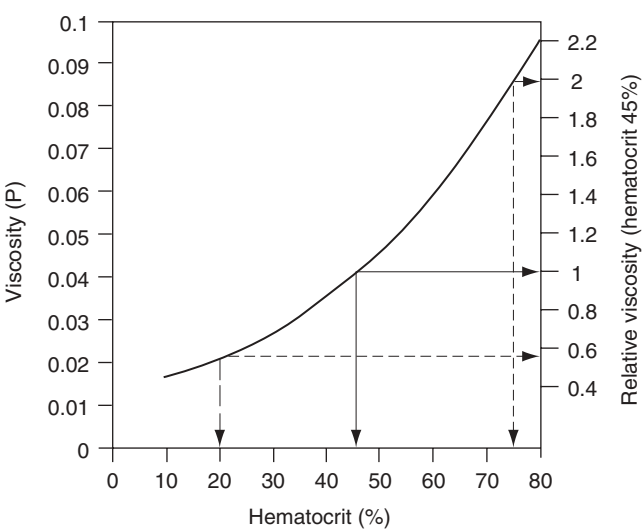
Figure 10.2 Relationship of hematocrit to changes in blood viscosity both relative to plasma and to a standard viscosity at 45% hematocrit. P, poise.

resistance of 4 Wood units m^{-2} normally would be a candidate for a Fontan repair. If, however, the preoperative hematocrit was 20% and the hindrance was actually elevated to 195, then after operation if the hematocrit returns to a normal value of 45%, with that same geometric factor (hindrance) the resistance would be ~8 Wood units m^{-2}. In patient B, a resistance of 8 Wood units m^{-2} might normally preclude a single ventricle repair. The preoperative hematocrit of 70%, however, indicates a lower hindrance and therefore favors a good outcome, because the postoperative resistance at a normal hematocrit would be ~4 Wood units m^{-2}.

Pressure measurements in chambers and vessels ideally require high-fidelity recordings that are difficult to achieve through long, narrow catheters. Catheter movement, especially in the right ventricle, may distort tracings and give a sharp, excessively large systolic peak referred to as "fling" that must be allowed for. Furthermore, formation of air bubbles in the catheter from air dissolved in the saline damps the pressure tracing, so that frequent flushing with saline is required. A discussion of damping and its determination during clinical procedures was provided by Glantz and Tyberg [34].

Important weaknesses and sources of error in physiological calculations

When carrying out a diagnostic study in which the primary objective is to calculate physiological variables, it is important to be mindful of the following:

1 Ensure that the patient is appropriately ventilated because high end tidal CO_2 and high FiO_2 can both exert a significant influence on the figures generated.

2 Ensure that the patient is stable and that there is no acidosis (check an arterial gas at the beginning and the end of the procedure).

3 Ensure that you are familiar with the techniques. Calculations of outputs and in particular measurement of oxygen consumption require considerable expertise.

4 Do not assume that pulmonary artery pressure is analogous with resistance.

Table 10.4 Effect of viscosity on Rp.

Parameter	Patient A		Patient B	
	Preoperation	**Postoperation**	**Preoperation**	**Postoperation**
Hematocrit (%)	20	45	70	45
Rp (Wood units m^{-2})	4	8	8	4
Relative viscosity	0.5	1	2.0	1.0
Hindrance (mmHg l^{-1} min^{-1} m^{-2} P^{-1})	195	195	100	100

5 Take care with calculations, particularly corrections for body surface area, which if inserted at the wrong point can invalidate the calculations.

6 Although dissolved oxygen contributes little to calculated flows when the patients are breathing air, the amount increases considerably when they are breathing 100% oxygen. At a partial pressure of 500 mmHg, there will be 15 ml of dissolved oxygen per liter of blood. Disregarding this contribution to the arteriovenous difference in oxygen content will give a falsely high value for Qp and a falsely low value for Qs.

Therapeutic cardiac catheterization

Introduction

Cardiac catheterization is also a means of treating congenital cardiac anomalies. The first attempt to perform a therapeutic catheter procedure was in 1953, when Rubio-Alvarez *et al*. tried to perforate a pulmonary valve with a wire [35]. This procedure was far before its time and was not repeated. In 1966, Rashkind and Miller performed a balloon septostomy in an infant with transposition of the great arteries, and the era of transcatheter intervention was born [36]. The 1970s saw a significant expansion of therapeutic possibilities in the catheterization laboratory. By the 1980s and 1990s, interventional cardiac catheterization had moved well beyond the "proof of concept" stage and for many lesions a transcatheter approach had achieved acceptance, either as the preferred treatment or as an acceptable alternative to surgery depending on specific clinical circumstances. The latter half of the 1990s saw the maturation of technology leading to an explosion of devices and equipment, vastly expanding treatment options in the catheterization laboratory. Current practice of cardiac catheterization in congenital heart disease bears little resemblance to that of even 15 years ago, and the drive for development shows little sign of slowing.

All therapeutic catheterization procedures need the skills of specialists who have had additional training [1,37]. The wide variety of techniques and the large inventory of equipment necessary for modern catheterization in congenital heart disease mean that these are no longer techniques that should be carried out by every pediatric cardiologist or even every unit practicing pediatric cardiology. Pediatric cardiologists performing therapeutic catheterization and congenital cardiac surgeons increasingly rely on each other to obtain the best results for patients [38]. In the modern era, neither discipline should exist in a particular cardiac unit without the availability of the other [1,37].

Balloon atrial septostomy

This is a potentially life-saving procedure in a newborn infant with transposition of the great arteries and restrictive atrial septum (~10% of these patients). These infants can be desperately sick very soon after birth from lack of mixing at atrial level, and balloon atrial septostomy is the only procedure to prevent the inevitable decline of progressive cyanosis and acidosis. In addition, there are a small number of babies with hypoplastic left heart syndrome and a restrictive atrial septum who may require a balloon septostomy. The need to relieve an inter-atrial restriction in other forms of single ventricle physiology is debated. In our opinion, there is no role for routine atrial septostomy in these patients, although the atrial septum should be carefully examined using echocardiography and the procedure performed if there are concerns.

The most commonly used balloon for atrial septostomy is the Miller–Edwards balloon (Edwards Lifesciences, Irvine, CA, USA). The balloon has changed very little since the original design attributable to William Rashkind. It is a single lumen latex balloon with an angle of approximately 30° at the distal end to facilitate passage across the atrial septum. The balloon is available in two inflation sizes (1.8 and 4 ml) and requires a 7Fr introducer sheath. The alternative to the Miller–Edwards balloon is the Z5 atrioseptostomy balloon (NuMed), a non-compliant balloon available in two sizes designed to be introduced over the wire through a 6Fr sheath.

In a neonate with simple transposition of the great arteries, a balloon septostomy, using a Miller–Edwards balloon can be safely performed either in the catheter laboratory or at the bedside using trans-thoracic ultrasound guidance [39]. Access must be from either the femoral vein or the umbilical vein, as this balloon cannot be negotiated across the atrial septum from the internal jugular route. After venous access has been established, the balloon is passed up through the inferior vena cava with the stylet inside. Once in the right atrium, the stylet is removed and the balloon passed into the left atrium using the distal tip angle. Within the left atrium, the balloon is inflated to the maximum diameter and rapidly withdrawn to the right atrium with a "jerk" or "tug" while making an effort to control the distance of the withdrawal so that the balloon does not enter the IVC. This should be repeated 2–3 times until there is a wide jet across the atrial septum on color Doppler. Potential complications of the technique are damage to the mitral or tricuspid valve (particularly if the balloon is mistakenly inflated in the left ventricle rather than the atrium), damage to the IVC if the balloon is forcibly pulled too far back, femoral vascular damage, and stroke, although generally these complications are rare [40–42].

Static balloon dilation

Although a relatively limited technique, because of the high incidence of recurrence, there are patients in whom a static "over the wire" dilation of the atrial septum with a standard angioplasty balloon can be employed. An advantage of this approach is that a much larger balloon can be used compared

with a standard septostomy catheter where only two sizes are available. Therefore, a larger opening can be created, although the technique is bedeviled by recurrence, particularly in older patients with a thick atrial septum. The procedure is relatively simple and essentially analogous to a balloon atrial septostomy except that a wire is passed across the atrial septum and positioned in one of the left pulmonary veins. A balloon, or multiple balloons, if necessary can then passed over the wire and inflated within the atrial septum. The procedure should be performed in the catheter laboratory and, because of the space constraints, generally a shorter balloon should be used.

Blade atrial septostomy

When balloon septostomy was extended to lesions other than transposition of the great arteries, particularly in infants and children older than 1 month, the results were less satisfactory and only temporary. At that age, the septum is usually too thick or tough, and the balloon stretches the existing hole only temporarily, if at all. As a nonoperative solution to this problem, the Park blade septostomy catheter was developed [43]. At the distal end of a Park catheter, a small recessed blade can be extended and retracted by a slide mechanism at the proximal end. There are three blade lengths: 1.0 and 1.34 cm in a 6Fr catheter and 2.0 cm in an 8Fr catheter. The purpose of the blade is first to create a small incision in the septum, which can then be torn further with a standard balloon atrial septostomy as described above.

The blade catheter is positioned in the left atrium through a long sheath that has been passed into the left atrium either through a pre-existing opening or by a trans-septal puncture. The blade is opened carefully in the left atrium with the tip facing either the patient's right or left, but always anteriorly. The blade is withdrawn slowly and forcefully through the septum into the right atrium. This process is repeated one or more times, changing the angle of the blade with each withdrawal. When little or no resistance to the blade pull-through is apparent, the blade procedure is followed by a balloon atrial septostomy.

Not surprisingly, complications, such as atrial perforation or damage to other cardiac structures, can occur, so blade septostomy catheters should only be used by operators who have considerable experience with the technique.

Stenting of the atrial septum

This technique has become increasingly popular over recent years, often as an alternative when blade septostomy is seen to have unacceptably high risk (very small infants) or for patients (again usually infants) who require temporary relief of atrial obstruction, usually following recurrence after standard balloon atrial septostomy. An example is infants with hypoplastic left heart syndrome who have undergone "hybrid" palliation and require completely unrestrictive flow across the atrial septum for 3–6 months before definitive

palliative surgery [38,44] The technique has also been used with some success to improve mixing in adults with uncorrectable cyanotic cardiac lesions.

Generally, patients selected for this procedure have a thicker muscular atrial septum. If there is no atrial communication, a trans-septal needle is used to perforate the septum. Once across the septum, a supportive wire is positioned in one of the left pulmonary veins and a long sheath placed in the left atrium. A balloon-mounted stent [in our experience currently either a Palmaz–Genesis (Cordis, Bridgewater, NJ, USA) or an LD Max stent (EV3, Plymouth, MN, USA)] is positioned across the septum. Clearly, the correct length of stent is critical; as a general principle, shorter lengths are preferable considering stent shortening at the desired final diameter. Using both angiography through the sheath and echocardiography to assist, the stent is positioned evenly across the septum before dilation. Complications include stent embolization and in smaller patients interference with adjacent valvar structures.

Balloon dilation procedures

Kan *et al.*, using a newly developed dilation balloon, first reported successful dilation of the pulmonary valve in 1982 [45]. This led to a number of reports in quick succession describing successful pulmonary valve dilation followed subsequently by balloon dilation of aortic and mitral valve stenosis. Many publications, including registry data of large numbers of patients, attest to the success and durability of balloon dilation procedures [46,47]. A number of commercially available balloons are suitable for valvoplasty and other forms of balloon dilation. Most are made from polyurethane or polyethylene and are noncompliant (or in some "semi-compliant") at the stated inflation diameters. A desirable characteristic in modern balloons is relatively short tapering ends. There is a trend towards smaller shafts, shorter tips, and better profiles both before and after inflation. Currently available balloons are available in diameters ranging from 2.5 to 30+ mm, and fit through sheaths as small as 3Fr and deliver circumferential pressures between 2.5 and 20 atm.

Specific descriptions of pulmonary, aortic, mitral, and tricuspid valve dilation and also coarctation angioplasty are given in their respective chapters.

Systemic venous dilation

Obstruction to superior vena caval (SVC) flow often follows scarring related to surgery or previous intravenous lines. Although these stenoses can be dilated with a balloon, usually a stent is required to reduce the risk of recurrence in the long-term [48]. Intra-atrial obstruction is relatively common after atrial switch procedures to correct transposition of the great arteries. The onset is usually gradual, giving time for the formation of collateral vessels if the obstruction is severe, so that symptoms are rare, although there have been reports

of edema, ascites, and protein-losing enteropathy. Treatment is indicated for the relief of such symptoms, or to preserve patency of the superior baffle limb in patients who may require endocardial pacing later.

Technically, balloon dilation of these stenoses is straightforward. The lesion is crossed and a stiff support wire positioned. Balloon angioplasty is then performed with an appropriately sized balloon. Acute improvement in the narrowing results, but often this is not maintained long-term. Currently, most operators advocate primary stenting rather than balloon angioplasty for these lesions [49]. Published series suggest that angioplasty alone can be effective and safe [50], but major complications have been reported [50].

Pulmonary venous dilation

Obstruction in pulmonary veins of any nature, either primary or secondary to previous surgical correction, responds only transiently to either balloon dilation or the insertion of stents [51,52]. The only exception is pulmonary venous stenosis occurring after radiofrequency pulmonary venous isolation for atrial fibrillation. These lesions occur because of fibrous scarring and may respond to cutting balloon angioplasty [53]. This indication aside, generally the technique has been abandoned by most centers.

Intravascular stents

Often following apparently successful balloon dilation of vessels, the stenosis recurs either immediately after deflating the balloon or in the subsequent weeks or months. Since the late 1980s, balloon-expandable stents have been deployed to prevent elastic recoil and dramatically improved results [54]. Most stents used to treat patients with congenital heart disease were originally designed for placement in the iliac or renal arteries, but are also effective in other vessels such as the pulmonary artery and the aorta (Figure 10.3a and b). Over recent years, stents specifically designed for use in congenital heart disease populations (e.g., the Cheatham-Platinum stent, NuMed) have become commercially available. Covered stents are also routinely used for excluding aneurysms and unwanted/abnormal vascular structures (Figure 10.3c and d).

Stenosis of systemic veins, pulmonary arteries, and coarctation of the aorta are examples of lesions that can be treated using stents with good long-term results [49,50,54,55]. In addition to long-term treatment, stents have also been used as effective short-term palliation within the right ventricular outflow tract (tetralogy of Fallot) [56] and the patent ductus arteriosus (duct-dependent congenital heart disease) [57].

Stent delivery is a more involved technical procedure than standard balloon dilation, with the addition risks of stent embolism and jailing of adjacent vessels. Stent delivery requires a mastery of specific techniques and knowledge of the technical characteristics of equipment, both of which are beyond the scope of this chapter.

Radiofrequency perforation in pulmonary atresia intact ventricular septum

A biventricular circulation can be established in patients with pulmonary atresia and intact ventricular septum provided that patients are correctly selected [58]. Transcatheter decompression of the right ventricular outflow tract is one of the most technically demanding catheter procedures. Continuity between the pulmonary artery and the right ventricle can be established using a number of approaches, although in recent years perforation of the valve plate using a radiofrequency wire has become by far the most common [59]. After thoroughly evaluating the anatomy, a guide catheter is placed in the right ventricular cavity and manipulated into the right ventricular outflow tract. The catheter must be positioned directly under the middle of the valve plate, most importantly at a right-angle. Obtaining the correct catheter position takes time and often a number of catheter shapes. Many operators prefer to pass an additional catheter or even a small snare through the ductus via an arterial approach to provide distal angiography and a target for perforation. Once in a satisfactory position, the radiofrequency wire is advanced through the guide catheter within a small coaxial catheter. When under the valve plate, a short pulse of radiofrequency energy is delivered through the wire, which should then pass easily into the pulmonary artery, provided that the positioning has been correct. Once in the pulmonary artery, the radiofrequency wire and its coaxial housing are manipulated across the ductus and into the descending aorta, using a snare if necessary. The radiofrequency wire is then exchanged for a stiff support wire and the valve is serially dilated using balloons. Most patients remain ductus dependent for some time following the procedure while the right ventricle adapts to new loading and unloading conditions. In the past, prolonged prostaglandin infusions were used, but increasingly there is interest in ductal stenting either at the time of right ventricular decompression or shortly after to avoid long-term prostaglandin infusion [57,60].

In patients with pulmonary atresia with intact ventricular septum, the direction of the main pulmonary artery is usually relatively horizontal, and the guide catheter is naturally directed more anteriorly so it is very easy to perforate the pulmonary artery and enter the pericardium, with potentially serious results. This can occur even if the catheter is only a fraction of a millimeter out of position. Recognizing and quickly treating this complication are absolutely essential as accumulation of even 10–15 ml of blood in the pericardial sac acutely leads to tamponade and hemodynamic collapse.

This procedure, when correctly applied, results in right ventricular growth and ultimately a biventricular circulation [57,61]. In some patients, when the right heart is borderline in size, a so-called "one and a half" circulation is created by an operation, in which anterograde flow through the right heart is supported by a bidirectional Glenn shunt.
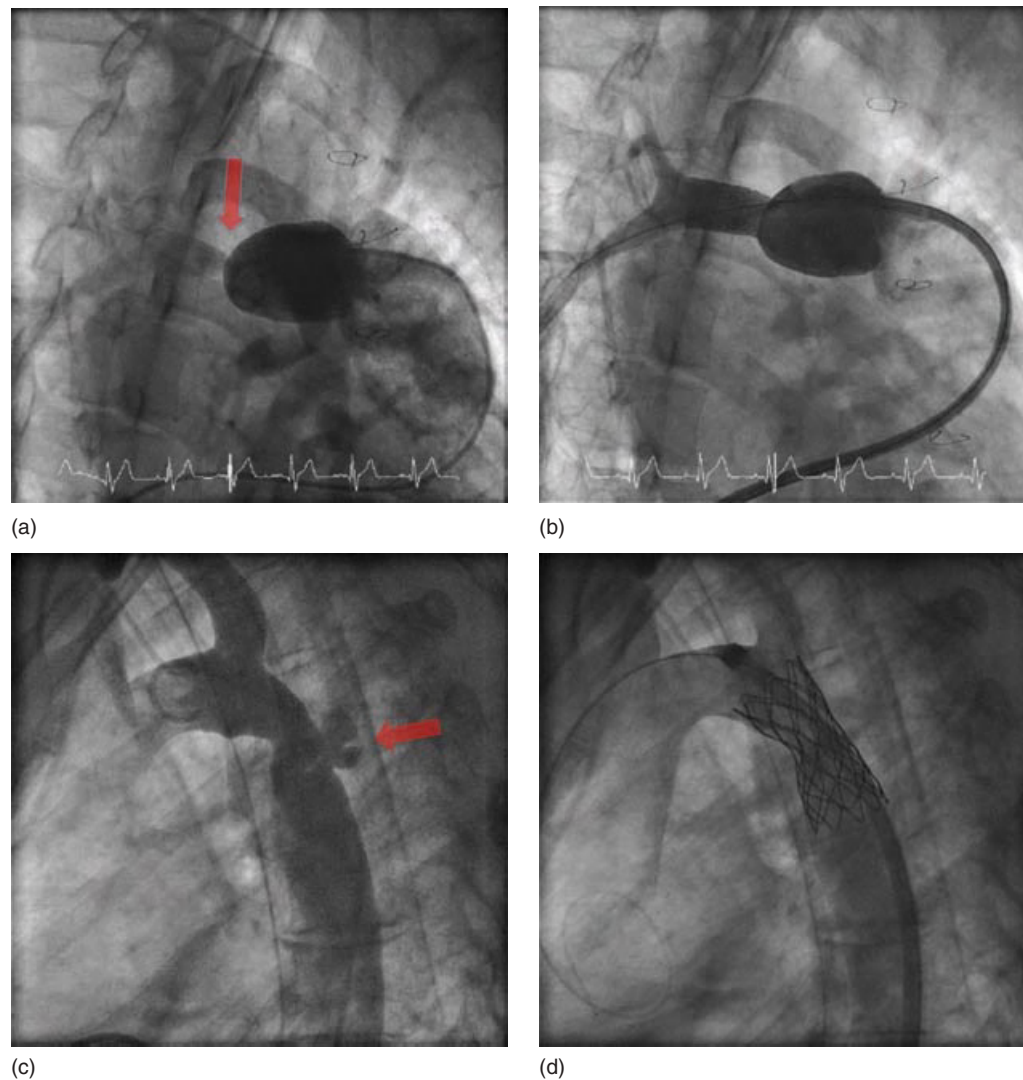
Figure 10.3 (a) Pulmonary arterial angiogram in a patient with right pulmonary artery stenosis following repair of tetralogy of Fallot. (b) Following deployment of a Max LD stent (EV3). (c) Aortogram in the lateral projection in a patient with both an aneurysm and recurrence of obstruction after surgical treatment for coarctation of the aorta. (d) Following deployment of a covered Cheatham-Platinum (CP) stent.

Percutaneous valve replacement

The first human trans-catheter valve replacement was performed in 2000, where a stent containing a bovine jugular vein was implanted into the right ventricular outflow tract of a patient with congenital heart disease [62]. The technology has the ability to reduce the need for repeated cardiac operations in a subset of patients with significant congenital heart disease by rehabilitating surgically positioned conduits. Since the original description, over 700 percutaneous pulmonary valve replacements have been performed worldwide, and the technology has sparked the development of other valve replacement procedures such as trans-catheter aortic valve replacement (TAVI). Percutaneous pulmonary valve replacement is effective in reducing the gradient and restoring pulmonary valve competence [63]. There have been concerns about stent fracture leading to valve dysfunction, but these have been resolved to some extent by the use of bare metal stents within the outflow tract to provide a rigid implantation tube [63,64]. The most commonly used valve, the Melody trans-catheter pulmonary valve (Medtronic, Minneapolis, MN, USA), can be reimplanted so a dysfunctional valve stent can "re-habilitate" itself using another valve planted within it. The other commercially available valve for use in the right ventricular outflow tract is the Edwards SAPIEN valve (Edwards Lifesciences, Irvine, CA, USA), a balloon-expandable stainless-steel stent containing a bovine pericardial valve. Experience with its use in the right ventricular outflow tract is extremely limited. It has an advantage of maintaining valve function at larger diameters than the Melody valve [65].

Although the use of these prostheses requires specific training, technically implanting percutaneous pulmonary valves is very similar to implanting any large stent into the right ventricular outflow tract. Before implantation, care must be taken to ensure that there is not a coronary anomaly that may be affected by expansion of the right ventricular outflow tract. Other potential complications include conduit rupture and vascular damage related to the large-bore venous access sheath (24Fr).

Occlusion devices

Patent Ductus Arteriosus (PDA) occlusion

Porstmann *et al*. first described a percutaneous technique for permanent closure of the ductus arteriosus in 1968 [66]. The procedure was technically complicated, unsuitable for certain types of ductal morphology, and required a large-bore sheath in the femoral artery, Therefore, this plug never achieved widespread use. The Rashkind device was the first occluder to be used in significant numbers for transcatheter ductal occlusion. It was introduced commercially in 1979. The device was associated with significant problems, including occlusion of the left pulmonary artery and a high rate of residual shunting (15–20%). These factors eventually rendered it obsolete.

Controlled release coils such as the Flipper (Cook, Bloomington, IN, USA) or one of the Amplatzer family of PDA occlusion plugs (AGA Medical, Plymouth, MN, USA) are most commonly used currently for ductal occlusion (Figure 10.4a–d). Transcatheter coils have the advantage of deliverability through a small sheath from either a transvenous or trans-arterial approach. They are inexpensive and effective, particularly in smaller ducts. In a large PDA, there is the possibility of residual shunting, which necessitates the use of more than one coil, and hemolysis is relatively common [67]. For this reason, most operators now prefer Amplatzer plugs for ductal connections more than 2.5–3 mm in diameter at the pulmonary artery end. The original Amplatzer duct plug (ADO 1) has been available for over a decade, is easy to use, and is highly effective. The shape of the plug means, by necessity, that it has to be delivered from the venous side of the ductus. This results in the potential for obstruction of adjacent vascular structures (left pulmonary artery and descending aorta), particularly when large plugs are used in smaller children. Recently, a second Amplatzer duct plug (the ADO 2) has been introduced [68]. Primarily designed for smaller ducts, this device has two retention skirts (as opposed to one in the ADO 1) and can be delivered from either the venous or arterial end of the duct, through a sheath as small as 4Fr. Because of the second retention skirt, the length of the center of the device must be considered when deploying this device. Experience with the device is limited and operators are currently assessing what this new device adds to the existing armamentarium.

In addition to Cook coils and the Amplatzer ductal plugs, other devices such as Amplatzer atrial septal occluders, muscular ventricular septal defect occluders (generally very large ducts), vascular plugs, and other types of coils have all been used to occlude ducts.

Atrial septal defect closure

In 1974, King and Mills reported the first successful transcatheter atrial septal defect (ASD) closure [69]. The device used consisted of two umbrella-like prostheses which were independently opened inside the left atrium and then snapped together. Although the system was deployed with success in five adolescent and adult patients, it never developed into routine clinical use mainly because of the complexity of deployment and the size of the delivery system (22Fr). Subsequently, Rashkind introduced an atrial septal occluder in 1987, but it was not until it had been modified into a device known as the clamshell occluder that the first device used in significant numbers for ASD closure was born. This device has undergone a number of design iterations and is still used clinically [70,71].

Although a number of ASD closure devices are currently available for clinical use, by far the most frequently implanted is the Amplatzer septal occluder (ASO) that was introduced in the mid-1990s. In common with other occluders in the Amplatzer family, the device is made of a weave of Nitinol (an alloy of 55% nickel and 45% titanium), shaped, in this model, into a design resembling two buttons joined by a central core (Figure 10.5a and b). The central core means that the device self-centers within an atrial septal defect. Deployment of this device is straightforward provided that the defect to be closed is properly selected. For successful closure, there must be a margin of at least 5 mm around the important adjacent structures, the hole should be single (multiple defects can be closed, but require very careful assessment), the defect must be <40 mm in diameter (in practical terms usually less than this), and it is only suitable for secundum defects.

Delivery is via the femoral vein (with venous occlusion, a trans-hepatic approach can be used) under both fluoroscopic and ultrasound (either trans-esophageal or intracardiac echocardiographic) control. The device is loaded into a delivery catheter and the left atrial disk extruded into the left atrium before withdrawing it back to the atrial septum. Once the left disc is engaged, the central core and then the right atrial disk are deployed before releasing the device from the delivery cable. Other self-centering devices currently commercially available include:

- Occlutech Figulla device (Occlutech, Helsingbord, Sweden) – a Nitinol wire device similar to the Amplatzer occluder (Figure 10.5c and d).
- Lifetech Cera device (Lifetech Scientific, Shenzhen, China) – a Nitinol wire device with a ceramic coating similar to the Amplatzer occluder.
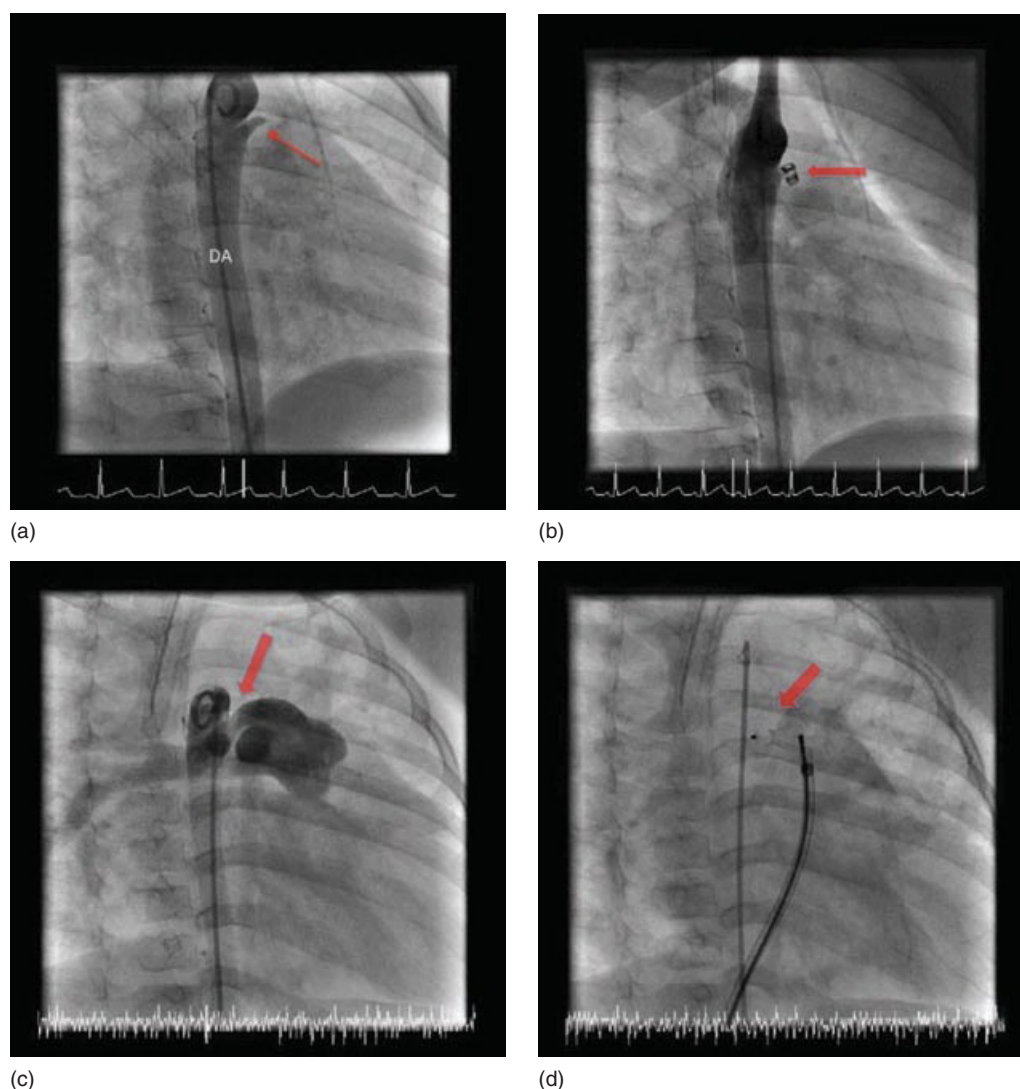
Figure 10.4 (a) Aortogram in the right anterior oblique projection (RAO) showing a small tubular patent ductus arteriosus (red arrow). (b) Repeat angiogram after occlusion with a Cook controlled-release (Flipper) coil. (c) Aortogram in the right anterior oblique projection (RAO) showing a larger ductus (red arrow). (d) After occlusion with an Amplatzer ductal occluder 1 (ADO 1). DA, descending aorta.

• Cardia Atriasept device (Cardia, Eagen, MN, USA)– the latest iteration of the Cardia family of devices with an internal Nitinol and titanium frame covered by poly(vinyl alcohol) (PVA) sails.

Non centering devices (essentially two disks but no central core) include:

• Gore Helex device (Gore Medical, Flagstaff, AZ, USA) – a single Nitinol wire frame with polytetrafluoroethylene (PTFE) patch along its length. The device cork-screws into two discs which can be deployed on either side of the atrial septum (Figure 10.5e and f).

A large amount published data attests to the safety and long-term effectiveness of percutaneous ASD closure, particularly with the Amplatzer septal occluder [72,73]. Device fracture has not been reported with the ASO but occurs with other designs, particularly where wire limbs are an integral design feature. Device closure is as effective as surgery [74]. Risks include device embolization (generally the ASO can be removed percutaneously if this happens) and, most importantly with the ASO, cardiac erosion, which although a very rare complication is potentially life threatening and thought to be related to over-sizing of the device [75].

Ventricular septal defect closure

The ventricular septum is a complex structure and device closure of any ventricular septal defect (VSD) is technically challenging. Muscular VSDs can occur in various positions in the septum and may be multiple. They are often difficult for cardiac surgeons to find and close. Although a number of
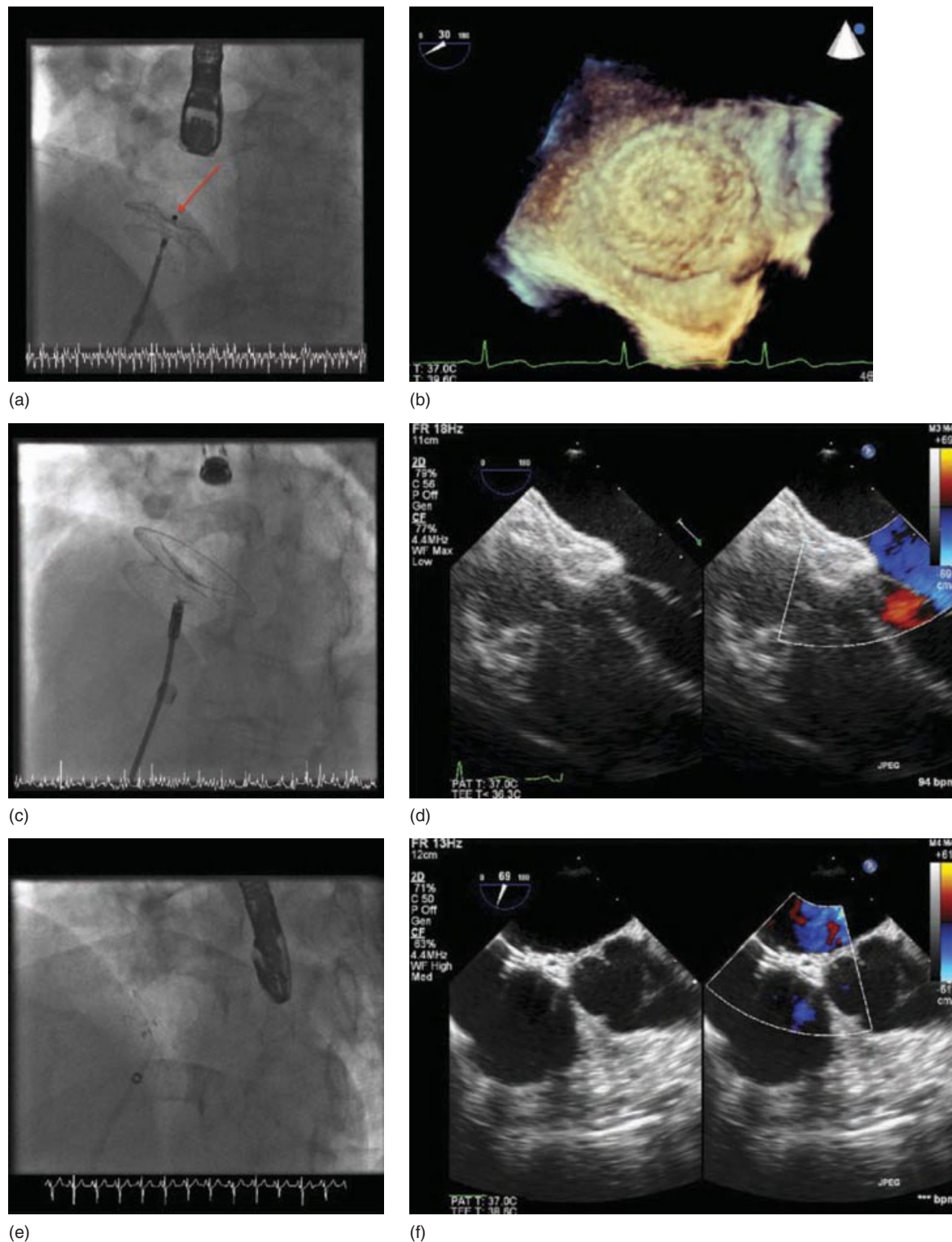
Figure 10.5 (a) Amplatzer septal occluder during atrial septal defect occlusion prior to release from delivery cable. Note the left retention nipple on the left atrial disc (arrow). (b) Three-dimensional echocardiographic view of the left atrial aspect of the Amplatzer device immediately after deployment. (c) Occlutech Figulla septal occluder during atrial septal defect occlusion prior to release from the delivery cable. Note the absence of the retention nipple on the left atrial disc and the different delivery cable allowing increased articulation of the device against the atrial septum. (d) Trans-esophageal echocardiography after release of the Occlutech device. No left-to-right shunt is seen. (e) Gore Helex occluder during occlusion of an atrial septal defect. This device is composed of an PTFE patch supported by a single Nitinol wire frame. (f) Trans-esophageal echocardiography following release of the Helex septal occluder. Note the low profile of this device compared with the Amplatzer septal occluder and the Occlutech device.

trans-catheter-delivered devices have been used to close muscular VSDs, by far the most commonly deployed is the Amplatzer muscular VSD occluder (mVSD) [76]. This device is similar in design to the atrial septal occluder (ASO) but has symmetrical and wider occlusion disks and a larger, squarer waist. It comes in eight sizes up to 18 mm with a few larger devices specifically designed for occlusion of post-myocardial infarction-related ventricular septal defect. TEE guidance is essential. The device is deployed either from the femoral vein (for defects higher up in the septum) or from the jugular vein (if the defect is positioned towards the apex). The occluder can also be delivered using a hybrid approach through the wall of the right ventricle (see later) [76]. For trans-catheter delivery, the minimum patient weight is ~10 kg. In most patients, it is very difficult to cross the defect directly from the right ventricle, so creating an arteriovenous loop is advantageous. This technique allows the defect to be crossed from the smooth left ventricular side, after which the wire is positioned in either the pulmonary artery or the superior vena cava and snared and externalized through the venous sheath. The delivery sheath is introduced through the venous sheath and guided through the VSD along the guidewire. The device is then introduced and deployed, very much in the manner of an ASD occluder, relying on the ultrasound imaging for position before release. A number of other devices have been used for muscular VSD closure, including the CardioSEAL device (NMT Medical, Boston, MA, USA), various coils, and Amplatzer vascular plugs.

Complications can occur during trans-catheter VSD closure, one of the most common being hemodynamic instability relating to entanglement of the tricuspid valve apparatus in the arteriovenous loop. This problem often occurs if an ordinary end hole catheter is used to move from the right atrium to the right ventricle. The use of a Swan–Ganz catheter makes this less likely. The only solution once this problem has occurred is to remove the guidewire, wait for stability to return, and start again. Other complications include blood loss, arrhythmia, aortic valve damage, cardiac perforation, hemolysis, and the inevitable risk of access site injury and damage [76].

The anatomic margins of perimembraneous ventricular septal defects (PMVSDs) and their proximity to conducting tissue make them a very different prospect for percutaneous closure. AGA Medical produces an occluder with a deficient rim specifically designed for PMVSD occlusion, allowing the device to occupy a defect without interfering with the function of the aortic valve. Although readily implantable, the main concern has been the occurrence of heart block, presumed to be due to pressure exerted on the atrioventricular node by a stiff occlusion device. Long-term atrioventricular block (AVB) and the need for permanent pacing after device closure of perimembraneous VSD varies in incidence from 0.23 to 8.6% in reported series [77–79], despite efforts to

ensure that over-sized devices are not used. Large registry data suggest that this complication is less frequent in the hands of an experienced, higher volume operator. In some centers, the results are comparable to the <1% heart block rate achieved in large surgical series [77]. However, of more concern than the overall incidence of AVB is the occurrence of symptomatic late heart block long after device deployment in patients without previous evidence of post-deployment dysrhythmia [79,80]. Although perimembraneous VSD closure is still performed by a number of centers with particular enthusiasm for the technique, many cardiologists, because of the unpredictable nature of this complication, have returned to surgical closure of perimembraneous VSDs.

Occlusion of other structures

Nonoperative occlusion of vascular structures can be accomplished with a number of catheter-delivered devices. Initial procedures were performed in the 1970s using Gianturco coils (segments of 0.025–0.038 in spring wire with filaments of nylon embedded and preformed into coils of diameters ranging from 2 to 15 mm), which were created for occluding bleeding end arteries but were found useful in congenital heart disease patients [81]. This technology has developed and diversified such that a huge range of vascular occlusion devices are now available, including coils of varying sizes and consistency with differing release technology, Nitinol vascular plugs, and injectable microparticles for embolizing smaller bore vascular beds.

Embolization procedures frequently performed in congenital heart disease include occluding venous collaterals (e.g., in patients with venous shunts), arteriopulmonary collaterals (e.g., in patients with pulmonary atresia), coronary artery fistulas, and bronchial arterial systems in patients presenting with hemoptysis.

Technical details depend on the anatomy and the occlusion device used and are highly varied and beyond the scope of this chapter.

Foreign body removal

Indwelling catheters for chemotherapy, in addition to therapeutic devices implanted in the catheterization laboratory, have the potential to embolize. Therefore, transcatheter removal of foreign bodies is an essential part of the armamentarium of the interventional pediatric cardiologist. Most intravascular foreign bodies originate in the systemic venous circulation and lodge in the right side of the heart or pulmonary arterial bed. A high-resolution biplane imaging system is absolutely essential for foreign body removal. The operator must be able to localize the foreign body within millimeters and in three dimensions. Without this capability, the likelihood of successful retrieval is small.

Many catheter devices are available for intravascular foreign body removal. Most have been adapted from other

specialties, particularly urology and radiology. Retrieval devices include snares, retrieval baskets, and grabber devices of various diameters and configurations. In general snare devices are most useful, but each device has a special application for different types of foreign bodies in different locations. The retrieval device needs to be deployed through a sheath large enough to accommodate the captured foreign body. In general, it is best to use a long sheath where the tip is positioned immediately adjacent to the foreign body, and the retrieval device is delivered to the foreign body through the sheath.

With the proper equipment and technique, virtually all intravascular foreign bodies should be retrievable in the cardiac catheterization laboratory without the need for operative intervention.

Hybrid procedures

A combined operative–catheter approach to treat a patient with pulmonary atresia–intact ventricular septum was described as early as 1987 [82]. Over recent years, pediatric cardiologists and pediatric cardiac surgeons have recognized the limitations of each discipline, and that to treat some complicated patients with congenital heart disease a joint approach is best. As a result, a number of new joint therapeutic strategies have developed over recent years.

Hybrid palliation for hypoplastic left heart syndrome

Small babies with hypoplastic left heart syndrome are at high risk with conventional Norwood stage 1 palliation [83]. As a result, there has been a move to reapply the principles first described by Gibbs *et al*. [84] in which pulmonary blood flow would be controlled by the application of branch pulmonary artery (PA) bands while ductal patency (and hence systemic perfusion) is maintained using a stent. The procedure is possible even in very small infants. Although initially the procedures were performed separately, recently the entire palliative procedure has been performed through a single median sternotomy [85,86]. Following bilateral PA banding using slices of a standard Gore-Tex shunt, a purse string is applied to the external main pulmonary artery. Through this a sheath is placed and a guidewire passed through the PA, across the ductus and into the descending aorta. Angiography is then performed and an appropriately sized stent is delivered into the ductus to ensure patency. An unrestrictive atrial septum is essential, so balloon septostomy may also need to be performed.

The procedure allows palliation and somatic growth in babies for a number of months, allowing the child to reach a size where both Norwood stage 1 and 2 procedures can be performed, leading to surgical creation of a neo-aorta and a

Glenn shunt to maintain pulmonary blood flow. The hybrid palliation procedure has undoubtedly expanded the repertoire of treatment for a group of patients with an otherwise poor outlook. Complications include obstruction of retrograde blood flow to the head and neck from the position of the stent and anatomic narrowing and pulmonary artery stenosis (particularly the left pulmonary artery) related to the surgically placed band.

Intraoperative pulmonary artery stenting

Percutaneous pulmonary artery stenting for branch pulmonary stenosis is accepted therapy for correctly selected patients. Occasionally the technique is limited by difficult access to the target lesion (particularly the left pulmonary artery), balloon/stent stability, vascular size, and hemodynamic stability in smaller patients. These can be overcome by a hybrid approach. Good imaging is essential for accurate sizing of the stent/balloon. The procedure requires a short period of low-flow cardiopulmonary bypass or circulatory arrest. After surgical exposure of the pulmonary artery, a J tipped guidewire is passed distally across the stenosis. A balloon-expandable stent is then deployed. If facilities are available, the result can be immediately evaluated angiographically. A number of reports, in small cohorts of patients, have described the results of intraoperative PA stenting [87–89] and showed that the procedure is technically feasible in patients as small as 2.5 kg.

Hybrid ventricular septal defect closure

Muscular ventricular septal defects (mVSDs) can be closed by direct delivery of a device through the right ventricular wall. The technique is applicable in patients who are small, have vascular access issues, in whom trans-catheter closure of a particular defect is technically unfeasible, or undergoing concomitant cardiac surgery where device closure will shorten the cardiopulmonary bypass [76].

The procedure is performed through a median sternotomy, with trans-esophageal echocardiographic control. A portion of the right ventricle directly opposite the ventricular septal defect is identified. The surgeon then places a purse string suture in this area through which a needle is passed. Under ultrasound control, a guidewire is passed from the right ventricle, across the mVSD, and into the left ventricular cavity. Over this wire a standard sheath is positioned and the device is deployed.

Although the literature shows that the procedure is effective and safe, there are potential problems and complications shared with trans-catheter mVSD closure. For mVSD it is not infrequent for the right ventricular disk of the device not to conform fully to the septum in very apical defects. Also, the heart can be perforated with either a stiff wire or sheath, but since the heart is in direct vision this is obvious and can be surgically treated. Heart block is unlikely unless a very high defect is closed.

Other hybrid procedures

Many other lesions have been treated using combined approaches, generally in small numbers of patients, so relatively limited data are available in the literature. Valvar dilation procedures have been described, including treatment of pulmonary atresia with intact ventricular septum, where the difficult angle of approach to the pulmonary valve from the right ventricle can be addressed by a hybrid approach directly through a surgically placed purse string [90]. Hybrid ASD closure and treatment of coarctation have both been described [91].

References

1 American College of Cardiology/American Heart Association Ad Hoc Task Force on Cardiac Catheterization. ACC/AHA guidelines for catheterization and cardiac catheterization laboratories. *J Am Coll Cardiol* 1991;**18**:1149–82.

2 Allen HD, Beekman RH III, Garson A Jr, *et al*. Pediatric therapeutic cardiac catheterization: a statement for healthcare professionals from the Council on Cardiovascular Disease in the Young, American Heart Association. *Circulation* 1998;**97**:609–25.

3 Cheatham JP. The ideal cardiac catheterization laboratory: not just for cardiologists anymore – it is hybrid time! In: Sievert H, Qureshi SA, Wilson N, Hijazi ZM, eds. *Percutaneous Interventions for Congenital Heart Disease,* 1st edn. Abingdon: Informa Publishing, 2007: 3–11.

4 Srouji MN, Rashkind WJ. The effects of cardiac catheterization on the acid–base status of infants with congenital heart disease. *J Pediatr* 1969;**75**: 943–5.

5 Huhta JC, Smallhorn JF, Macartney FJ, *et al*. Cross-sectional echocardiographic diagnosis of systemic venous return. *Br Heart J* 1982;**48**:388–403.

6 Takahashi M, Petry EL, Lurie PR, *et al*. Percutaneous heart catheterization in infants and children: catheter placement and manipulation with guide wires. *Circulation* 1970;**42**:1037–48.

7 Etheridge SP, Berry JM, Krabill KA, *et al*. Echocardiographic-guided internal jugular venous cannulation in children with heart disease. *Arch Pediatr Adolesc Med* 1995;**149**:77–80.

8 Sapin SO, Linde LM, Emmanouilides G. Umbilical vessel angiography in the newborn infant. *Pediatrics* 1963;**31**:946–51.

9 Greenwald BM, Notterman DA, DeBruin WJ, *et al*. Percutaneous axillary artery catheterization in critically ill infants and children. *J Pediatr* 1990;**22**:442–4.

10 Burrows PE, Benson LN, Williams WG, *et al*. Iliofemoral arterial complications of balloon angioplasty for systemic obstructions in infants and children. *Circulation* 1990;**82**:697–704.

11 Lee HY, Reddy SC, Rao PS. Evaluation of superficial femoral artery compromise and limb growth retardation after transfemoral artery balloon dilatations. *Circulation* 1997;**95**:974–80.

12 Mehta R, Lee, K-J, Chaturvedi R, *et al*. Complications of pediatric cardiac catheterization: a review in the current era. *Catheter Cardiovasc Interv* 2008;**72**:278–85.

13 Cohn HE, Freed MD, Hellenbrand WE, *et al*. Complications and mortality associated with cardiac catheterization in infants under one year. *Pediatr Cardiol* 1985;**6**:123–31.

14 Braunwald E. Cooperative study on cardiac catheterization. Deaths related to cardiac catheterization. *Circulation* 1968;**37**: III-17–26.

15 Culham JAG, Freedom RM, Mawson JB, *et al*. Physical principles of image formation and projections in angiocardiography. In: Freedom RM, Mawson JB, Yoo S, Benson LN, eds. *Congenital Heart Disease. Textbook of Angiocardiography*, Vol. 1. Futura: Armonk, NY, 1997: Chapter 3.

16 Aldridge HE, Chisholm RJ, Dragatakis L, *et al*. Radiation safety in the cardiac catheterization laboratory. *Can J Cardiol* 1997;**13:** 459–67.

17 Wu JR, Huang TY, Wu DK, *et al*. Radiation exposure of pediatric patients and physicians during cardiac catheterization and balloon pulmonary valvuloplasty. *Am J Cardiol* 1991;68:221–5.

18 Moore RJ. *Imaging Principles of Cardiac Angiography*. Aspen: Bethesda, MD, 1990: 207–39.

19 Miller SW, Castronovo FPJ. Radiation exposure and protection in the catheterization laboratories. *Am J Cardiol* 1985;**55**: 171–6.

20 Mannino SC, Scavina M, Palmer S. Modified multipurpose catheter enhances clinical utility for cardiac catheterizations. *Cathet Cardiovasc Diagn* 1994;**33**:166–70.

21 Barrett BJ, Parfrey PS, Vavasour HM, *et al*. A comparison of non-ionic, low-osmolality radiocontrast agents with ionic, high-osmolality agents during cardiac catheterization. *N Engl J Med* 1992;**326**:431–6.

22 Steinberg EP, Moore RD, Powe NR, *et al*. Safety and cost effectiveness of high-osmolality as compared with low-osmolality contrast material in patients undergoing cardiac angiography. *N Engl J Med* 1992;**326**:425–30.

23 Matthai WJ, Hirshfeld JJ. Choice of contrast agents for cardiac angiography: review and recommendations based on clinically important distinctions. *Cathet Cardiovasc Diagn* 1991; **22**:278.

24 Lalli AF, Carswell HM. Nonionic agents extend safety of invasive studies. *Diagn Imaging* 1986;**7**:70–3.

25 Puyau FA, Burko H. The tilted left anterior oblique position in the study of congenital cardiac anomalies. *Radiology* 1996;**87**:1069–73.

26 Bargeron LM, Elliott LP, Soto B, *et al*. Axial cineangiography in congenital heart disease. Section 1: concept, technical and anatomic considerations. *Circulation* 1977;**56**:1075–83.

27 Goor D, Lillehei CW, Edwards JE. The sigmoid septum. Variation in the contour of the left ventricular outlet. *AJR Am J Roentgenol* 1969;**107**:366–76.

27a Kapins CEB, Coutinho RB, Barbosa FB, *et al*. Use of rotational 3D (3D-RA) in congenital heart disease patients: experience with 53 cases. *Rev Bras Cardiol Invasiva* 2010;**18**:199–203.

28 Wilkinson JL. Haemodynamic calculations in the catheter laboratory. *Heart* 2001;**85**:113–20.

29 Miller HC, Brown DJ, Miller GA. Comparison of formulae used to estimate oxygen saturation of mixed venous blood from caval samples. *Br Heart J* 1974;**36**:446–51.

30 Freed MD, Keane JF. Cardiac output measured by thermodilution in infants and children. *J Pediatr* 1978;**92**:39–42.

31 Wood EH. Diagnostic applications of indicator-dilution techniques in congenital heart disease. *Circ Res* 1962;**10**:531–68.

32 Lundell BPW, Casas ML, Wallgren CG. Oxygen consumption in infants and children during heart catheterization. *Pediatr Cardiol* 1996;**17**:207–13.

33 LaFarge CG, Miettinen OS. The estimation of oxygen consumption. *Cardiovasc Res* 1970;**4**:23–30.

34 Glantz SA, Tyberg JV. Determination of frequency response from step response: application to fluid-filled catheters. *Am J Physiol (Heart Circ)* 1979;**236**:H376–8.

35 Rubio-Alvarez V, Limon RL, Soni J. Valvulotomias intracardiacas por medio de un cateter. *Arch Inst Cardiol Mex* 1953;**23**:183–92.

36 Rashkind WJ, Miller WW. Creation of an atrial septal defect without thoracotomy: a palliative approach to complete transposition of the great arteries. *JAMA* 1966;**196**:991–2.

37 Qureshi SA, Redington AN, Wren C, *et al*. Recommendations of the British Paediatric Cardiac Association for therapeutic cardiac catheterization in congenital cardiac disease. *Cardiol Young* 2000;**10**:649–67.

38 Bacha EA, Daves S, Hardin J, *et al*. Single-ventricle palliation for high-risk neonates: the emergence of an alternative hybrid stage I strategy. *J Thorac Cardiovasc Surg* 2006;**131**:163–71.

39 Martin AC, Rigby ML, Penny DJ, *et al*. Bedside balloon atrial septostomy on neonatal units. *Arch Dis Child Fetal Neonatal Ed* 2003;**88**:F339–40.

40 Schroeder VA, Shim D, Spicer RL, *et al*. Surgical emergencies during pediatric interventional catheterization *J Pediatr* 2002;**140**:570–5.

41 Venables AW. Balloon atrial septostomy in complete transposition of great arteries in infancy. *Br Heart J* 1970;**32**:61–5.

42 Mukherjee D, Lindsay M, Zhang Y, *et al*. Analysis of 8681 neonates with transposition of the great arteries: outcomes with and without Rashkind balloon atrial septostomy. *Cardiol Young* 2010;**20**:373–80.

43 Park SC, Neches WH, Mullins CE, *et al*. Blade atrial septostomy: collaborative study. *Circulation* 1982;**66**:258–66.

44 Rupp S, Michel-Behnke I, Valeske K, *et al*. Implantation of stents to ensure an adequate interatrial communication in patients with hypoplastic left heart syndrome. *Cardiol Young* 2007;**17**:535–40.

45 Kan JS, White RI Jr, Mitchell SE, *et al*. Percutaneous balloon valvuloplasty: a new method for treating congenital pulmonary-valve stenosis. *N Engl J Med* 1982;**307**:540–2.

46 McCrindle BW. Independent predictors of long term results after balloon pulmonary valvuloplasty. Valvuloplasty and Angioplasty of Congenital Anomalies (VACA) Registry Investigators 1994;**89**:1751–9.

47 Fawzy ME, Galal O, Dunn B, *et al*. Regression of infundibular pulmonary stenosis after successful balloon pulmonary valvuloplasty in adults. *Cathet Cardiovasc Diagn* 1990;**21**:77–81.

48 Wisselink W, Money SR, Becker O, *et al*. Comparison of operative and percutaneous balloon dilatation for central venous obstruction. *Am J Surg* 1993;**166**:200–4.

49 Bu'Lock FA, Tometzki AJ, Kitchener DJ, *et al*. Balloon expandable stents for systemic venous pathway stenosis late after Mustard's operation. *Heart* 1998;**79**:225–9.

50 Tzifa A, Marshall AC, McElhinney DB, *et al*. Endovascular treatment for superior vena cava occlusion or obstruction in a pediatric and young adult population: a 22-year experience. *J Am Coll Cardiol* 2007;**49**:1003–9.

51 Driscoll DJ, Hesslein PS, Mullins CE. Congenital stenosis of individual pulmonary veins: clinical spectrum and unsuccessful treatment by transvenous balloon dilatation. *Am J Cardiol* 1982;**49**:1767–72.

52 Cullen S, Ho SY, Shore D, *et al*. Congenital stenosis of pulmonary veins: failure to modify natural history by intraoperative placements of stents. *CardiolYoung* 1994;**4**:395–8.

53 Moak JP, Moore HJ, Lee SW, *et al*. Pulmonary vein stenosis following RF ablation of paroxysmal atrial fibrillation: successful treatment with balloon dilation. *J Interv Card Electrophysiol* 2000;**4**:621–31.

54 O'Laughlin MP, Perry SB, Lock JE, *et al*. Use of endovascular stents in congenital heart disease. *Circulation* 1991;**83**:1923–39.

55 Chessa M, Carrozza M, Butera G, *et al*. Results and mid-long-term follow-up of stent implantation for native and recurrent coarctation of the aorta. *Eur Heart J* 2005;**26**:2728–32.

56 Gibbs JL, Uzun O, Blackburn MEC, *et al*. Right ventricular outflow stent implantation: an alternative to palliative surgical relief of infundibular pulmonary stenosis. *Heart* 1997;**77**: 176–9.

57 Schranz D, Michel-Behnke I, Heyer R, *et al*. Stent implantation of the arterial duct in newborns with a truly duct-dependent pulmonary circulation: a single-center experience with emphasis on aspects of the interventional technique. *J Interv Cardiol* 2010;**23**:581–8.

58 Agnoletti G, Piechaud JF, Bonhoeffer P, *et al*. Perforation of the atretic pulmonary valve: long term follow up. *J Am Coll Cardiol* 2003;**41**:1399–403.

59 Alwi M. Management algorithm in pulmonary atresia with intact ventricular septum. *Catheter Cardiovasc Interv* 2006;**67**: 679–86.

60 Alwi M, Choo KK, Haifa AL, *et al*. Initial results and medium-term follow up of stent implantation of patent ductus arteriosus in duct-dependent pulmonary circulation. *J Am Coll Cardiol* 2004;**44**:438–45.

61 Ovaert C, Qureshi SA, Rosenthal E, *et al*. Growth of the right ventricle after successful transcatheter pulmonary valvotomy in neonates and infants with pulmonary atresia and intact ventricular septum. *J Thorac Cardiovasc Surg* 1998;**115**:1055–62.

62 Bonhoeffer P, Boudjemline Y, Saliba Z, *et al*. Percutaneous replacement of pulmonary valve in a right-ventricle to pulmonary-artery prosthetic conduit with valve dysfunction. *Lancet* 2000;**356**:1403–5.

63 McElhinney DB, Hellenbrand WE, Zahn EM, *et al*. Short- and medium-term outcomes after transcatheter pulmonary valve placement in the expanded multicenter US Melody valve trial. *Circulation* 2010;**122**:507–16.

64 Nordmeyer J, Lurz P, Khambadkone S, *et al*. Pre-stenting with a bare metal stent before percutaneous pulmonary valve implantation: acute and 1-year outcomes. *Heart* 2011;**97**:118–23.

65 Boone RH, Webb JG, Horlick E, *et al*. Transcatheter pulmonary valve implantation using the Edwards SAPIEN transcatheter heart valve. *Catheter Cardiovasc Interv* 2010;**75**:286–94.

66 Porstmann W, Wierny L, Warnke H. Closure of ductus arteriosus persistens without thoracotomy. *Fortschr Geb Rontgenstr Nuklearmed* 1968;**109**:133–48.

67 Uzun O, Veldtman GR, Dickinson DF, *et al*. Haemolysis following implantation of duct occlusion coils. *Heart* 1999;**81**:160–1.

68 Forsey J, Kenny D, Morgan G, *et al*. Early clinical experience with the new Amplatzer Ductal Occluder II for closure of the persistent arterial duct. *Catheter Cardiovasc Interv* 2009;**74**:615–23.

69 King TD, Mills NL. Non-operative closure of atrial septal defects. *Surgery* 1974;**75**:383–8.

70 Beekman RH, Rocchini AP, Snider AR, *et al*. Transcatheter atrial septal defect closure: preliminary experience with the Rashkind occluder device. *J Interv Cardiol* 1989;**2**:35–41.

71 Prieto LR, Foreman CK, Cheatham JP, *et al*. Intermediate term outcome of transcatheter secundum atrial septal defect closure using the Bard Clamshell Septal Umbrella. *Am J Cardiol* 1996;**78**:1310–2.

72 Omeish A, Hijazi ZM. Transcatheter closure of atrial septal defects in children and adults using the Amplatzer septal occluder. *J Interv Cardiol* 2001;**14**:37–44.

73 Chan KC, Godman MJ, Walsh K, *et al*. Transcatheter closure of atrial septal defect and interatrial communications with a new self expanding Nitinol double disc device (Amplatzer septal occluder): multicentre UK experience. *Heart* 1999;**82**:300–6.

74 Du ZD, Hijazi ZM, Kleinman CS, *et al*. Comparison between transcatheter and surgical closure of secundum atrial septal defect in children and adults: results of a multicenter nonrandomized trial. *J Am Coll Cardiol* 2002;**39**:1836–44.

75 Divekar A, Gaamangwe T, Shaikh N, *et al*. Cardiac perforation after device closure of atrial septal defects with the Amplatzer septal occluder. *J Am Coll Cardiol* 2005;**45**:1213–8.

76 Amin Z, Cao QL, Hijazi ZM. Closure of muscular ventricular septal defects: transcatheter and hybrid techniques. *Catheter Cardiovasc Interv* 2008;**72**:102–11.

77 Yang J, Yang L, Wan Y, *et al*. Transcatheter device closure of perimembranous ventricular septal defects: mid-term outcomes. *Eur Heart J* 2010;**31**:2238–45.

78 Knauth AL, Lock JE, Perry SB, *et al*. Transcatheter device closure of congenital and postoperative residual ventricular septal defects. *Circulation* 2004;**110**:501–7.

79 Carminati M, Butera G, Chessa M, *et al*. Transcatheter closure of congenital ventricular septal defects: results of the European Registry. *Eur Heart J* 2007;**28**:2361–8.

80 Butera G, Massimo C, Carminati M. Late complete atriovenous block after percutaneous closure of a perimembranous ventricular septal defect. *Catheter Cardiovasc Interv* 2006;**67**: 938–41.

81 Gianturco C, Anderson JH, Wallace S. Mechanical devices for arterial occlusion. *AJR Am J Roentgenol* 1975;**124**:428–35.

82 Hamilton JR, Fonseka SF, Wilson N, *et al*. Operative balloon dilatation for pulmonary atresia with intact ventricular septum. *Br Heart J* 1987;**58**:374–7.

83 Stasik CN, Goldberg CS, Bove EL, *et al*. Current outcomes and risk factors for the Norwood procedure. *J Thorac Cardiovasc Surg* 2006;**131**:412–7.

84 Gibbs JL, Wren C, Watterson KG, *et al*. Stenting of the arterial duct combined with banding of the pulmonary arteries and atrial septectomy or septostomy: a new approach to palliation for the hypoplastic left heart syndrome. *Br Heart J* 1993;**69**:479–80.

85 Akintuerk H, Michel-Behnke I, Valeske K, *et al*. Stenting of the arterial duct and banding of the pulmonary arteries: basis for combined Norwood stage I and II in repair in hypoplastic left heart. *Circulation* 2002;**105**:1099–103.

86 Galantowicz M, Cheatham JP, Phillips A, *et al*. Hybrid approach for hypoplastic left heart syndrome: intermediate results after the learning curve. *Ann Thorac Surg* 2008;**85**:2063–70.

87 Bökenkamp R, Blom NA, De Wolf D, *et al*. Intraoperative stenting of pulmonary arteries. *Eur J Cardiothorac Surg* 2005; **27**:544–7.

88 Menon SC, Cetta F, Dearani JA, *et al*. Hybrid intraoperative pulmonary artery stent placement for congenital heart disease. *Am J Cardiol* 2008;**102**:1737–41.

89 Ungerleider RM, Johnston TA, O'Laughlin MP, *et al*. Intraoperative stents to rehabilitate severely stenotic pulmonary vessels. *Ann Thorac Surg* 2001;**71**:476–81.

90 Burke RP, Hannan RL, Zabinsky JA, *et al*. Hybrid ventricular decompression in pulmonary atresia with intact ventricular septum. *Ann Thorac Surg* 2009;**88**:688–9.

91 Schmitz C, Esmailzadeh B, Herberg U, *et al*. Hybrid procedures can reduce the risk of congenital cardiovascular surgery. *Eur J Cardiothorac Surg* 2008;**34**:718–25.

11 Exercise Testing

Per Morten Frederiksen
Oslo University Hospital, Nydalen, Oslo, Norway

Introduction

Over the last 30 years, treatment of congenital heart disease has developed markedly, moving from issues of survival to quality of life and challenges to be met as adults [1,2]. Most children with congenital heart disease (CHD) experience reduced physical capacity that may affect their quality of life [3–7]. In most hospitals, consultation at a CHD center includes physical examination, cardiac ultrasound, ECG, X-ray, and conversation with the cardiologist. Recently, more centers have included an exercise test, often regarded as synonymous with testing aerobic capacity. However, physical limitations are not restricted to impaired aerobic capacity but also involve static and dynamic balance, muscle strength in arms and legs, and motor skills [8]. These functions receive little or no attention in daily medical practice, but are nonetheless important for the child's welfare. Limited motor skills and strength may restrict a child's activity level as much as reduced aerobic capacity.

Performing strenuous exercise requires transport of large amounts of oxygen to and carbon dioxide from working muscles. The maximum amount of oxygen transported before anaerobic metabolism begins (the anaerobic threshold) is termed the aerobic capacity. Maximal oxygen transport depends on:

- Excellent lung function to take in oxygen and excrete carbon dioxide.
- Excellent cardiac function that can be broken down into components via a rearranged Fick equation:

VO_2 = cardiac output × arteriovenous difference in oxygen content ($\Delta A\text{-}V_{oxygen\ content}$):

(a) cardiac output = HR × stroke volume = HR × LVEDV × EF

where HR = heart rate, LVEDV = left ventricular end-diastolic volume, and EF = ejection fraction.

(b) $\Delta A\text{-}V_{oxygen\ content} = \Delta A\text{-}V\% \times [Hb] \times 1.36$

where $\Delta A\text{-}V\%$ = arteriovenous difference in oxygen saturation and [Hb] = hemoglobin concentration. Therefore,

$VO_2 = HR \times LVEDV \times EF \times \Delta A\text{-}V\% \times [Hb] \times 1.36$

At maximal exercise in highly trained erect individuals, heart rate can triple, stroke volume can increase by 50–100%, and arterial oxygen extraction (a function of muscle perfusion and metabolism) can double. Aerobic capacity is therefore reduced if lung function is reduced, with anemia, with deconditioned (untrained) muscles, or if the heart cannot increase rate or stroke volume appropriately. An exercise test allows these components to be evaluated.

The onset of anaerobic metabolism is detected by measuring the respiratory exchange ratio (RER), the ratio of CO_2 produced to O_2 used. The RER reflects muscle metabolism and is normally 0.8; a value of 0.7 indicates that fat supplies all the energy, and a value of 1.0 indicates pure carbohydrate sources. A rise in RER from 0.8 to 1.0 reflects anaerobic glycolysis.

An aerobic exercise test gives instant knowledge about progression of the disease and is widely used to estimate timing of surgery. It may also assess the result of a surgical procedure, and determine if drug treatment is effective. An exercise test is also useful for detecting arrhythmia, particularly at higher heart rates. Perhaps the most important aspect of an exercise test is reassurance for the child and the parents about the safety of exercising. Many parents and indeed cardiologists are afraid of letting a child with CHD perform high workloads. The patients themselves may be anxious and an exercise test may allay concerns.

An exercise test of aerobic capacity is believed to be the most informative and important physical test for children

with CHD. It gives instant information about the changes in blood pressure, oxygen saturation, heart rhythm, and heart rate with exercise. The heart's ability to increase its cardiac output is the central limitation of aerobic capacity [9]. Together with spirometry, an exercise test gives extended information about a child's lung and heart status. This chapter describes different methods, protocols, and guidelines for performing an aerobic exercise test in children with CHD.

In the complex interaction between the heart and lung, a heart defect may mask a lung disease (primary or secondary to longstanding heart problem), and it may sometimes be difficult to distinguish between heart and lung disability in children with CHD. Spirometry before, during, and after the exercise test may be helpful. It is also sometimes difficult to distinguish between general deconditioning (unfitness) and heart disease. which may be distinguished by the maximal heart rate. Healthy children in poor physical shape usually show a pattern of rapidly increasing heart rate at low levels of resistance, reaching a normal heart rate maximum near 200 beats per minute. A child with a heart disease usually has maximal heart rate below 180–200 beats per minute.

Test methods

Various methods and protocols give different results. Depending on age, diagnosis, and physical ability, one should choose the method and protocol with care. The first consideration is the method that ideally should reflect the activity that the test subject normally participates in, usually bicycling, walking, or running. Bicycle and treadmill are the most extensively used methods worldwide. Both have advantages and disadvantages (Table 11.1). For sport there are several methods in use for exercise testing, for example, an ergometer for rowing, paddling, skiing, stair climbing, swimming pools with resistance, and others.

Reclining bicycle

A reclining bicycle may be used to test response to exercise, but not maximal effort. This bicycle is extensively used for measuring heart function during exercise with ultrasound while the patient's upper body is fixed in one position. The patient reclines and a tilt to the left gives good images, even during heavy exercise [9]. The exercise values are not comparable to ordinary bicycle test results because of differences

Table 11.1 Comparison between bicycle and treadmill.

Parameter	Bicycle	Treadmill [10]
Body movement	Less	More
Comfort	Patients feel safer as no risk of falling	Risk of falling may make patients hold bars, lengthening the test and reducing work load[a]
Acceptability	Good because of familiarity	Children learn more quickly than adults
BP measurement	Easier with still upper body	Less easy, but can synchronize Korotkoff sounds with R of QRS complex.
BP level	Often higher, because of continuous leg movement and holding tightly to handle bars	
Maximal VO_2	Lower because fewer muscles active, and leg fatigue might cause early cessation of exercise[b]	Higher due to more muscle activity. May be lower if patient holds bars
Onset of anaerobic metabolism	Earlier because static (isometric) contraction of muscles around ankle and arms impedes flow	
Ease of measuring ECG	Easier with still upper body	Less easy
Ease of measuring SpO_2	Finger probe may mislead because of tight grip on handle bars[c]	Reflector probe on forehead avoids problem
Power measurement (watts)	Exact	Approximate
Effect of leg length	Fixed pedal arm gives patients with longer legs an advantage, making comparisons difficult	Leg length does not affect test
Effect of obesity	Support of body weight on seat reduces work load	Full weight involved. More like daily activity

[a]Close contact between the test supervisor and the patient eliminates falls and reduces the need for holding the handle bars [11].
[b]When using a bicycle, VO_2 might increase after the ending of the test. This is caused by the high resistance when pedaling that forces the muscle to have continuous high pressure on the pedals during every cycle. This reduces the venous return. When the pressure of pedaling is released, venous return increases and as a result a rise in VO_2 occurs 30–60 s after the end of pedaling.
[c]Do not have finger probe on same arm as BP cuff; preferably use an ear oximeter or reflector probe on forehead.

in body position and heart rate. In aortic or pulmonic steno-sis, an increase in gradient may be measured. Pulmonary hypertension may be estimated with this method [9].

Test protocols

There are numerous exercise protocols for both bicycle and treadmill [12,13]. The most extensively used protocol for treadmill is the Bruce protocol with its modifications [14]. Few protocols are designed especially for children [15]. In most protocols, there are mainly two types of incremental choices, step and ramp.

Step

Most protocols traditionally increase the workload in steps by increasing speed, incline, or both periodically. If only speed is used to increase work, the patients' motor skills may hinder them from achieving a high speed [8]. An increase in incline, especially if steep, may hinder patients with less muscle mass. The initial speed and incline are crucial for the outcome of the test. Too steep an incline may cause leg fatigue and premature termination of the test, similarly to a test on a bicycle, and too high a speed may cause coordina-tion problems.

A simultaneous increase in both speed and incline often gives large steps in workload, and may lead to stopping the test prematurely. Some protocols alternate between increase in speed and incline every other step [14]. The protocols should be designed to reduce the stepwise increase in workload, as this may make it easier for patients to achieve maximal effort. The time on each step is impor-tant. Steps should exceed 2 min because the metabolism in the working muscle mass needs to reach a steady state. There is a time lag from the metabolism in the muscles to the measurement of metabolic markers at the mouth and oxygen analyzer. A protocol with too short steps will not register correct results at each step. Too long steps might tire the patient. Usually 2–3 min steps are used.

Ramp

A ramp protocol gives a continuous load during the whole protocol until fatigue occurs [16]. This has advantages in estimating ventilatory threshold. Most treadmills have a program that smoothes out a step protocol and permits the performance of a ramp protocol [17,18].

Risks

There are small risks when testing children with CHD. Some experience dizziness due to a vasovagal reaction (often due to anxiety before the test), but it is very rare (personal expe-rience: eight of 1800 tests). An abnormal cardiac rhythm

Table 11.2 Indications for terminating a test.

Parameter	Indications for terminating a test	
	Relative	Absolute
Fall in BP as workload increases (mmHg)	>10	>20
Systolic BP (mmHg)	>250	
Cardiac rhythm	Multifocal PVC, triple PVC, supraventricular tachycardia or bradycardia	Sustained ventricular tachycardia
Chest pain	Increasing	Moderate to severe angina
Other signs, symptoms		Dizziness, severe cyanosis
Electrocardiogram	ST depression >2 mm with horizontal or down-sloping curve	

is more common; however, many tests are performed to provoke arrhythmias Ventricular tachycardia is not common, and is easy to detect. Exercise testing of children with CHD is fairly safe and gives extensive information.

Despite a low risk of incidents, it is advisable for at least two persons to attend the test. A defibrillator must be avail-able. The test supervisors should receive regular training in resuscitation.

Criteria for terminating a test

The criteria for ending a test are extensively described in guidelines [10]. Experience has shown that many children may continue exercising despite reaching the target level [11]. This is a challenge for the supervisor, who should urge the patients to complete a test as near exhaustion as possible despite reaching or exceeding the predetermined criteria. If supervisors from different laboratories use the criteria as end points and do not encourage the patients to continue the test, lower values may result. In addition to the guidelines, there are relative and absolute criteria for ending a test based on medical reasons (Table 11.2).

Interpreting VO$_2$ values

In most oxygen analyzers used in exercise testing, there is a nine-plot page of significant graphs. This gives important information with regard to the heart and lung status during exercise, and is described in a book by Cooper and Storer [19]. There are, however, a few factors that are seldom described, especially the differences between tests that may

be considered significant clinically. The cardiologist should not accept as a significant change a difference of less than 10% from a previous test. There are several issues to be considered:

1 There is an error within any system independent of calibration. In most oxygen analyzers, there is a drift and error measurement of around 3–5%.

2 The values from a bicycle are on average 10% (3–18%) [20] lower than for treadmills. This may be very misleading when interpreting the results.

3 Reference values differ considerably between countries or cultures. Various cultures regard physical activity during childhood differently. Test supervisors may differ regarding the acceptability of forcing a child to exhaustion. Even though there are criteria for ending tests [10], studies show that it may be the supervisor's ability to encourage the child to fatigue that has a large effect on the results [11]. Therefore, the reference material used should be from the same geographic area as the child and preferably done by the same supervisor. All laboratories covering an extended geographic area should have their own reference material.

4 When retesting a child after one to several years, the growth and increase in body weight must be considered. Because the increase in VO_2 does not vary linearly with weight, a correction factor must be used. Several correction factors are available, the easiest being $kg^{-0.67}$ or $kg^{-0.75}$, based on theories of body size and body production of heat, respectively [21].

5 The child's motivation during the test may play an important role in the results.

Considering all these factors, several pitfalls in interpreting a test are evident. For example, if the system has drifted 3%, the reference material is for a different method or a different country, a correction factor to account for the relationship between VO_2 and body weight is not used, or the patient has not been pushed to the limit of exhaustion, the result may be adversely affected and lead to misinterpretation.

Precautions regarding some cardiac diagnoses

In most patients with simple lesions, there are few or no special precautions to be taken before an exercise test, except for those already mentioned. A few lesions, however, need special attention.

Left ventricular outflow tract obstruction

Patients with left ventricle outlet tract obstruction (LVOTO) are at increased risk of serious complications or death during an exercise test. Aortic stenosis and coarctation of the aorta are the most common causes of LVOTO. When severe,

several factors must be considered while testing. Due to the increased left ventricular systolic pressure, nerve impulses and blood flow may be hampered in the left ventricular wall. These patients are in danger of arrhythmias or complete loss of heart rhythm during strenuous physical activity. Some patients may experience pressure or pain behind sternum during heavy exercise, but others have no symptoms.

A drop in blood pressure more than 20 mmHg from one measurement to the next may be one indication of overload of the left ventricle. This occurs most often in patients with the most severe obstruction, and the blood pressure drop may be difficult to detect due to the difficulty in measuring BP during exercise. A better indication of severe LVOTO during exercise is ST depression. The development of an ST segment depression of more than 2 mm may indicate severity, especially if it occurs in leads V_{4-6}. Other symptoms of severity include dizziness and chest pain, but these are rare. The use of VO_2 as an indicator of the severity of a stenosis is often not useful in children since they maintain a nearly normal cardiac output.

Patients with severe coarctation of the aorta may develop significant upper body hypertension that may cause a subarachnoid hemorrhage during a heavy workload. Blood pressure should be evaluated carefully before an exercise test, and the workload kept lower until the coarctation has been treated. In comparison with valvar stenosis with its fixed orifice size, in muscular subaortic stenosis the obstruction becomes more stenotic with increased heart rate. If the goal in patients with aortic stenosis is to estimate the gradient, a reclining bicycle protocol with continuous ultrasound measurement is recommended because it gives instant information about the severity of a stenosis.

Fontan

Testing a patient with a Fontan circulation requires special attention. The VO_2 values in these patients mirror the cardiac output. Their severely reduced chronotropic response further affects the aerobic capacity. Their reduced pulmonary function, due to insufficient diffusing capacity, also affects the aerobic capacity [22]. An exercise test with its VO_2 values is therefore a good indicator of the functional status of the heart in Fontan patients. In general they have a limited ability to increase the cardiac output compared with patients with other cardiac lesions [23,24]. Their aerobic capacity drops significantly with age, so that this group of patients should have periodical exercise tests.

Atrial and ventricular septal defects

Patients with a small ASD usually have no limitations in their exercise activity. Those with a moderate or large ASD may be limited, but are usually not tested before the defect

is closed. Surgically corrected ASD and VSD have been considered not to be limited during vigorous exercise. Patients with pulmonary hypertension following closure of the defect [9] should have more frequent exercise testing, preferably with a reclining bicycle with ultrasound to assess the level of pulmonary hypertension.

Transposition of the great arteries

The arterial switch correction of TGA is believed to be preferable to the older atrial switch operation. It is certainly better for maintaining sinus rhythm, but the expected improvement in aerobic capacity is not evident. A study by Fredriksen *et al.* indicated that the atrial switch patients displayed a lower than normal aerobic capacity [25]. The low values may be explained by a failing systemic right ventricle. The anatomically more correct arterial switch heart should theoretically be better able to increase cardiac output with exercise, and have higher aerobic capacity values. Patients following an arterial switch group, however, also have reduced aerobic capacity. Chronotropic incompetence may be a plausible explanation. In addition, patients following both procedures show a decrease in VO_2 with increasing age. Although there are fewer older patients following an arterial switch, there are indications that their aerobic capacity declines with increasing age [26].

Conclusion

An exercise test is an important tool for assessing the functional status of children, adolescents, and adults with CHD. It provides vital information about any decline of cardiac function and also improvement following surgery, drug treatment, and exercise training. Several methods and protocols are used and these give different results. Therefore, an expert in exercise physiology should join with a cardiologist to evaluate these results. Exercise tests should not be limited to a few diagnostic groups, but rather be performed regularly in a variety of conditions to follow the patient's status across the years.

References

1 Dore A. Adult congenital heart disease: a new challenge. *Perspect Cardiol* 1999;**15**:43–51.

2 Warnes CA, Liberthson R, Danielson GK, *et al.* Task force 1: the changing profile of congenital heart disease in adult life. *J Am Coll Cardiol* 2001;**3**:1170–5.

3 Meijboom F, Szatmari A, Deckers JW, *et al.* Cardiac status and health-related quality of life in the long term after surgical repair of tetralogy of Fallot in infancy and childhood. *J Thorac Cardiovasc Surg* 1995;**110**:883–91.

4 Spijkerboer AW, Utens EM, De Koning WB, *et al.* Health-related quality of life in children and adolescents after invasive treatment for congenital heart disease. *Qual Life Res* 2006;**15**:663–73.

5 Spijkerboer AW, Utens EM, Bogers AJ, *et al.* Long-term behavioural and emotional problems in four cardiac diagnostic groups of children and adolescents after invasive treatment for congenital heart disease. *Int J Cardiol* 2008;**125**:66–73.

6 Fredriksen PM, Diseth TH, Thaulow E. Children and adolescents with congenital heart disease: assessment of behavioural and emotional problems. *Eur Child Adolesc Psychiatry* 2009;**18**: 292–300.

7 Fredriksen PM, Mengshoel AM, Frydenlund A, *et al.* Follow-up in patients with congenital cardiac disease, more complex than haemodynamic assessment. *Cardiol Young* 2004;**14**:373–9.

8 Holm I, Fredriksen PM, Fosdahl MA, *et al.* Impaired motor competence in school-aged children with complex congenital heart disease. *Arch Pediatr Adolesc Med* 2007;**161**:945–50.

9 Moller T, Peersen K, Pettersen E, *et al.* Non-invasive measurement of the response of right ventricular pressure to exercise, and its relation to aerobic capacity. *Cardiol Young* 2009;**19**:465–73.

10 American College of Sports Medicine. *ACSM's Guidelines for Exercise Testing and Prescription*, 5th edn. Baltimore: Williams & Wilkins, 1995.

11 Fredriksen PM, Ingjer F, Nystad W, Thaulow E. A comparison of VO_{2peak} between patients with CHD and healthy subjects, all aged 8–17 years. *Eur J Appl Physiol Occup Physiol* 1999;**80**: 409–16.

12 Balke B, Ware RW. An experimental study of "physical fitness" of Air Force personel. *US Armed Forces Med J* 1959;**10**:675–88.

13 Astrand PO, Rodahl K. Evaluation of physical performance on the basis of tests. In: Provenzano MD, ed. *Textbook of Work Physiology*, 3rd edn. New York: McGraw-Hill, 1986: 354–87.

14 Bruce RA, Kusumi F, Hosmer D. Maximal oxygen intake and nomographic assessment of funtional aerobic impairment in cardiovascular disease. *Am Heart J* 1973;**85**:546–62.

15 Fredriksen PM, Ingjer F, Nystad W, Thaulow E. Aerobic testing of children and adolescents – a comparison of two treadmill protocols. *Scand J Med Sci Sports* 1998;**8**:203–7.

16 Barker AR, Williams CA, Jones AM, Armstrong N. Establishing maximal oxygen uptake in young people during a ramp cycle test to exhaustion. *Br J Sports Med* 2011; Jan 24 [Epub ahead of print].

17 Myers J. A treadmill ramp protocol using simultaneous changes in speed and grade – a (ramp) step forward in exercise testing. *Med Sci Sports Exerc* 2003;**35**:1604.

18 Porszasz J, Casaburi R, Somfay A, *et al.* A treadmill ramp protocol using simultaneous changes in speed and grade. *Med Sci Sports Exerc* 2003;**35**:1596–603.

19 Cooper CB, Storer TW. *Exercise Testing and Interpretation*, 1st edn. Cambridge: Cambridge University Press, 2001.

20 Myers J, Walsh D, Sullivan M, Froelicher V. Effect of sampling on variability and plateau in oxygen uptake. *J Appl Physiol* 1990;**68**:404–10.

21 Pettersen SA, Fredriksen PM, Ingjer E. The correlation between peak oxygen uptake (VO2peak) and running performance in

children and adolescents. aspects of different units. *Scand J Med Sci Sports* 2001;**11**:223–8.

22 Matthews IL, Fredriksen PM, Bjornstad PG, *et al.* Reduced pulmonary function in children with the Fontan circulation affects their exercise capacity. *Cardiol Young* 2006;**16**:261–7.

23 Fredriksen PM, Veldtman G, Hechter S, *et al.* Aerobic capacity in adults with various congenital heart diseases. *Am J Cardiol* 2001;**87**:310–4.

24 Veldtman GR, Nishimoto A, Siu S, *et al.* The Fontan procedure in adults. *Heart* 2001;**86**:330–5.

25 Fredriksen PM, Pettersen E, Thaulow E. Declining aerobic capacity of patients with arterial and atrial switch procedures. *Pediatr Cardiol* 2009;**30**:166–71.

26 Hechter S, Webb G, Fredriksen PM, *et al.* Cardiopulmonary exercise performance in adult survivors of the Mustard procedure. *Cardiol Young* 2001;**11**:407–14.

12 Thrombosis in Congenital and Acquired Disease

Lindsay M. Ryerson, M. Patricia Massicotte & Mary E. Bauman
University of Alberta, Stollery Children's Hospital, Edmonton, AB, Canada

Introduction

Advances in medical, surgical, and interventional therapy in children with acquired and congenital heart disease have increased survival. However, most of these children have an increased risk of thrombosis, with many ultimately developing this potentially life-threatening problem [1]. As a result, antithrombotic therapy, including anticoagulation and thrombolytic therapy, now plays a major role in the management of many children in a cardiac intensive care unit. Particular problems include mechanical circulatory support, systemic to pulmonary artery shunts, bidirectional cavopulmonary anastomosis, Fontan palliation, mechanical valves, central arterial or venous line-related thrombosis, and less commonly pulmonary embolism. Concurrently, these children have a high risk of bleeding, hence the risks and benefits of the use of antithrombotic therapy must be carefully considered, with the objective of maintaining balanced hemostasis.

Hemostasis is the reparative process for damaged vasculature in a closed high-pressure circulatory system [2]. The process restoring vascular integrity is modulated by regulatory mechanisms that prevent over-compensation which could lead to thrombosis. However, if these mechanisms are overwhelmed, excessive amounts of thrombin are produced and cause thrombus formation [2]. For understanding thrombus formation, the following discussion is limited to the most salient participating hemostatic components.

Normal hemostasis

Hemostasis is maintained through vessel wall, blood composition, and blood flow. Much of our knowledge of the physiology of hemostasis has come from the study of mouse models [2].

Normal physiologic hemostasis depends upon maintaining a fine balance between thrombosis (clotting) and hemorrhage (bleeding), the fundamentals being shown in Figure 12.1. The original model of hemostasis is the cascade model [3] where procoagulant proteins present in the blood [factors (F) XII, XI, HMWK, X, IX, VIII, VII, V, and II, and fibrinogen] are activated by a stimulus (e.g., sepsis, trauma, surgery) with thrombin (FIIa) being produced. Three pathways are described: the intrinsic pathway (FXII, XI, IX, and VIII), the extrinsic pathway (tissue factor and FVII), and the common pathway (FX, V, II, and I). where these pathways converge. Sequential activation of the factors within each pathway occurs, followed by thrombin activation of fibrinogen into fibrin, the precursor of a polymerized clot. The fibrinolytic system is then activated to break down the clot. Inhibitor proteins of hemostasis (antithrombin, protein C, protein S, α_2-macroglobulin) and fibrinolysis (plasminogen activator inhibitor 1) prevent massive clot formation or clot lysis, respectively (Figure 12.1).

Hemostasis involves the complex interaction of platelets with damaged vascular endothelium followed by activation of specific proteins to produce a fibrin platelet plug that will prevent bleeding, but not result in pathologic thrombosis. The cascade model of hemostasis (coagulation and fibrinolysis) excluded important cellular involvement in coagulation [4,5], and has therefore been revised to the cell-based model (Figure 12.2), which is a more accurate reflection of *in vivo* processes [5]. The endothelium of the vessel wall plays a major role in ensuring patency of vasculature by secreting three thrombo-regulating substances, nitric oxide, prostacyclin, and ectonucleosidase or CD39, which inhibit platelet adhesion and activation.

Vessel wall damage may occur from disruption, or more subtle endothelial cell alterations as hypothesized by Sacco *et al*. [2], resulting in activation of hemostasis. When vessel wall damage occurs, initiation of platelet activation occurs
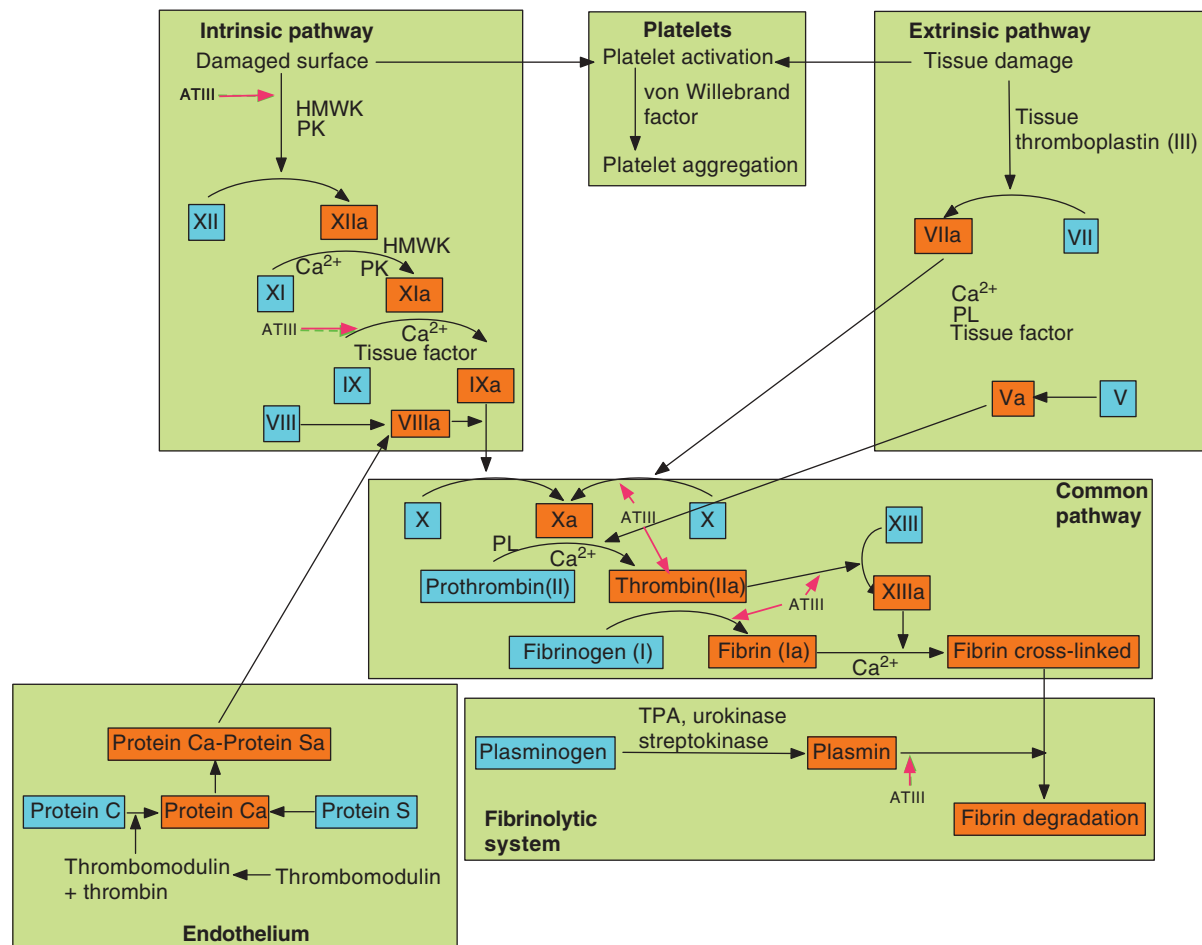
Figure 12.1 Schema of coagulation cascade. Inactive proteins in blue; activated proteins in orange. Antithrombin III (ATIII) inhibition shown by red arrows. HMWK, high molecular weight kininogen; PK, prekalikrein; PL, activated phospholipids from platelets TPA, tissue plasminogen activator. Many of these components are involved in feedback systems (not shown) that modulate the response. The platelets play two roles: (1) they are activated by tissue factors and then with von Willebrand factor are aggregated; (2) most of the reactions in the common pathway take place at the platelet surface.
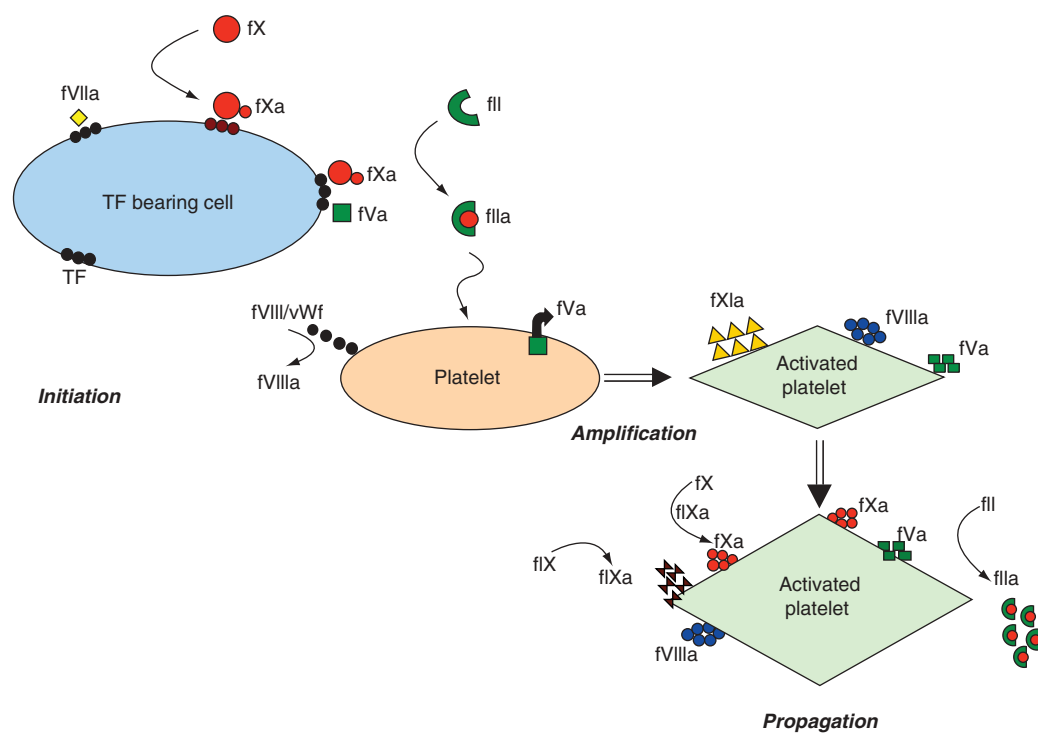
Figure 12.2 Coagulation phase of hemostasis. The coagulation phase of hemostasis occurs in three phases: initiation, amplification, and propagation. TF, tissue factor; vWF, von Willebrand factor. (Adapted from Becker *J Thromb Thrombol* 2005;**20**:65–8, with kind permission from Springer Science+Business Media.)

via two separate mechanisms, one invoked by collagen and the other by tissue factor (TF). Either or both mechanisms may predominate depending on the type of vasculature damaged or disease entity [6,7]. Exposed collagen in the subendothelial matrix interacts with platelets resulting in adhesion by two mechanisms: binding to von Willebrand factor (vWF) followed by platelet glycoprotein (GP) 1b–IX–V, and through direct interaction with platelet GPVI [8]. Shear force influences which receptor plays the foremost role in platelet tethering to the vessel wall, but GPVI and GP1b are essential for platelet adhesion [6,9,10]. Integrin $\alpha_2\beta_1$ also plays a lesser role in platelet adhesion [11,12].

Tissue factor in microparticles [13,14] circulates in its inactive form [15,16] and requires activation, which may occur through protein disulfide isomerase (PDI) released by activated endothelial cells and platelets [2,14]. Transformed TF activates FVII and FIX. The combination of FXa and FVIII, known as the tenase complex, activates FX. Activated FX (FXa) then combines with FV to form the prothrombinase complex, which in turn activates a small amount of prothrombin to thrombin. The minute amount of thrombin generated is a catalyst that activates FV and VIII to their most active cofactor forms, FVIIIa and FVa. Large amounts of thrombin are then generated as a result of the continued action of the tenase and prothrombinase complexes [17] (Figure 12.1). Thrombin activates fibrinogen to form nonpolymerized thrombus, but also activates platelets [18] (Figure 12.2) through cleaving protease-activating receptor 1 (PAR1), causing platelet granule release [adenosine diphosphate (ADP), which is stored in the dense granules, and serotonin and thromboxane A_2 which are stored in the α-granules) and further platelet activation. The compound ADP activates platelets through receptors P2Y1 and P2Y12 (Figure 12.3). Serotonin activates platelets through 5-hydroxytryptamine 2A (FHT-2A) receptors (Figure 12.3). Thromboxane A_2 activates platelets through the thromboxane receptor (TP) (Figure 12.3).

In addition to activating TF, PDI activates GP IIb IIIa ($\alpha_{IIb}\beta_3$) on platelets which binds to the ligands fibrinogen and vWF, thus promoting platelet recruitment to the thrombus and platelet–platelet interactions [19–21]. Increased affinity for the ligands occurs when platelets bound to the damaged vessel wall are activated and GP IIb IIIa undergoes a transformational change [22]. Blood flow shear rates determine the binding ligand with low and high shear rates binding with fibrinogen and vWF, respectively [8].

Microparticles circulate in the blood and carry proteins associated with their derived cell type (e.g., leucocytes, platelets, endothelial cells, smooth muscle cells, and monocytes). Activated platelets expose the protein P selectin [23] on their surface, which binds to circulating microparticles derived from monocytes that have the counter receptor displayed, P selectin glycoprotein ligand 1 (PSGL-1) [13]. Through this mechanism, TF exposed on these microparticles [13,14] is responsible for further thrombin generation and thrombus extension.

Developmental hemostasis

Children have physiologic differences in hemostasis and fibrinolysis compared with adults. Known as developmental hemostasis [24,25], the levels of activating and inhibiting proteins are decreased in both pathways (Figure 12.1). Differences include decreased levels of thrombus precursor proteins (FXII, XI, X, IX, VII, II), and inhibitor proteins protein C, protein S, antithrombin), and proteins of fibrinolysis (plasminogen and tissue plasminogen activator, tPA), and inhibitor proteins of fibrinolysis (plasminogen activator inhibitor, PAI-1). In addition, children generate less thrombin, FIIa, than do adults during hemostasis, with the composition of thrombi reflecting this. These differences affect the etiology, dosing, and management of anticoagulant and thrombolytic therapy, and also outcomes of thrombosis in children [26–28]. Understanding hemostasis and the differences in children compared with adults allows more informed antithrombotic therapeutic decisions.

Thrombophilia

Congenital thrombophilia refers to alterations in the levels of proteins that facilitate and inhibit clotting. Congenital prothrombotic disorders are relatively rare, but most commonly include FV Leiden, prothrombin gene G20210A, deficiencies of protein C, protein S, and antithrombin, FXII deficiency, and increased FVIII [17,19–25,27]. The influence of congenital thrombophilia on childhood thrombosis remains controversial. Furthermore, the need to screen for prothrombotic disorders in children with a major illness, undergoing an invasive procedure, or with a history of confirmed thrombosis, especially in the presence of clinical risk factors, remains uncertain. Most children with thrombotic abnormalities without an additional risk factor, such as central venous lines, arterial lines, prosthetic heart valves, systemic to pulmonary artery shunts, or superior or bicaval pulmonary-arterial anastamoses, do not develop thrombosis until adulthood [17].

Common measurement of hemostasis

For measurements of hemostasis, blood should be obtained peripherally, particularly if low-dose heparin is administered through a central line to maintain its patency. Test results on samples drawn from central lines may be artificially prolonged from heparin contamination.
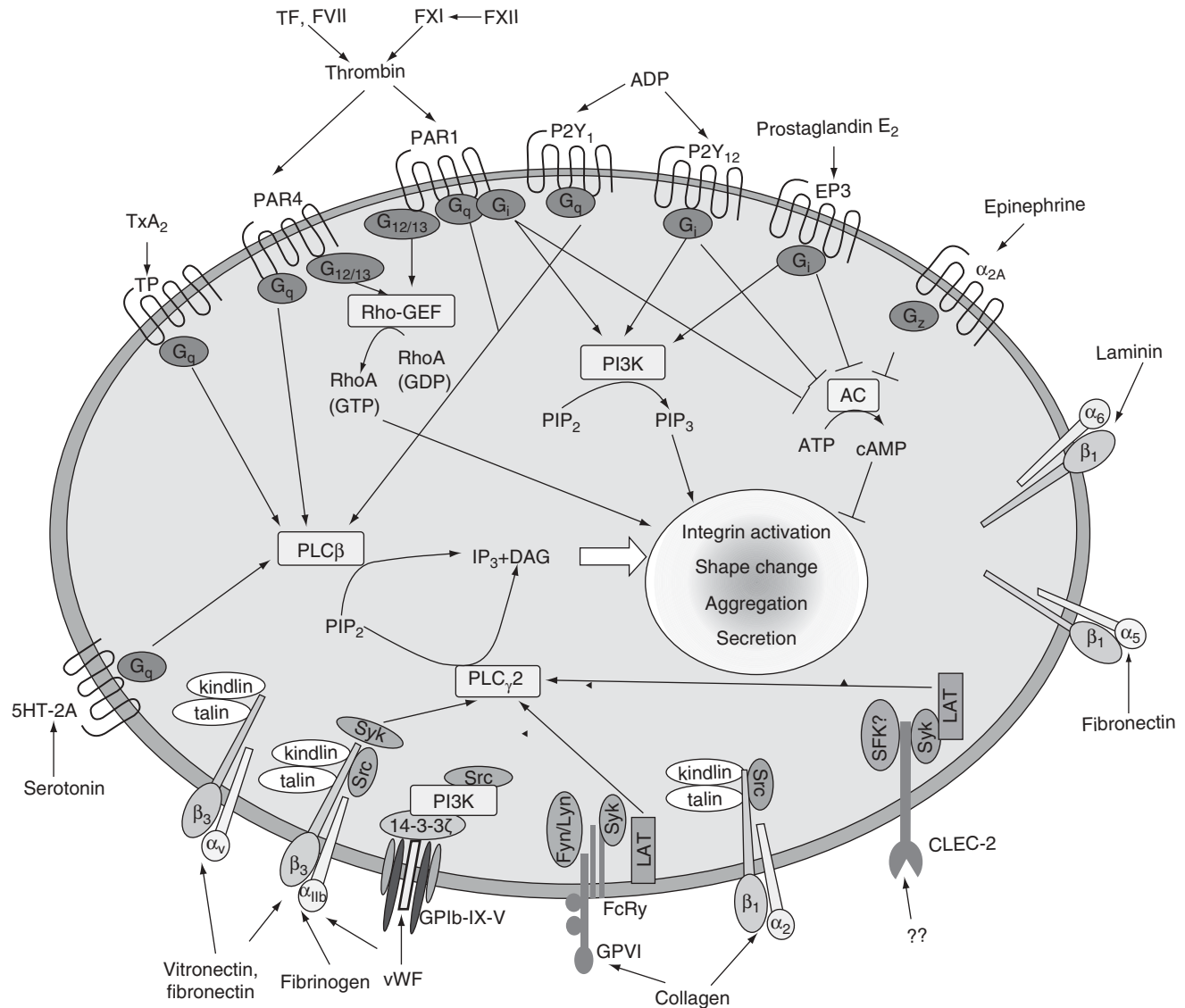
Figure 12.3 There are 2 principal pathways leading to platelet activation, adhesion and aggregation. Pathway 1: Soluble agonists [thrombin, adenosine diphosphate (ADP), thromboxane A_2 (TXA_2), serotonin] stimulate specific G protein-coupled receptors (eg. PAR, protease-activated receptor, 5HT-2A, 5-hydroxytryptamine 2A receptor, TP, TXA_2 receptor) and induce signaling pathways. Pathway 2: GPVI and C-type lectin receptor 2 (CLEC-2) trigger tyrosine phosphorylation reactions. Crosslinking of GPVI or CLEC-2 when binding to their respective ligands; collagen or unknown receptor, brings the SRc family tyrosine kinases, Fyn and Lyn, into contact with the FcRy chain starting a tyrosine phosphorylation cascade via Syk, the linker of activated T cells (LAT). These reactions result in activation of phospholipase (PL) Cy2, calcium mobilization and ultimately platelet aggregation. All platelet signaling events end in the final common pathway of platelet activation, up regulation of integrin adhesion receptors leading to stable adhesion and platelet aggregation. Integrins consist of 2 distinct chains known as α chain and β chain. TF, Tissue factor; TxA2, Thromboxane A2; TP, TxA2 receptor; PAR, protease-activated receptor; RhoGEF, Rho-specific guanine nucleotide exchange factor; PL3K, phosphoinositide-3-kinase; AC, adenylyl cyclase; PIP2, phosphatidylinositol-4, 5-biphosphate; PIP3, phosphatidylinositol-3,4,5-triphosphate;IP3, inositol-1,4,5-triphosphate; DAG, diacylglycerol. (With kind permission from Springer Science+Business Media: Stegner and Nieswandt, *J Mol Med* 2011;**89**:109–21.)

The partial thromboplastin time (PTT) and prothrombin time–International Normalized Ratio (PT–INR) are the most common tests. They are based on the cascade model of anticoagulation, and do not reflect the complexity of hemostasis. The PTT measures contact factors (FXI, XII), FII, VIII, and X, and the conversion of fibrinogen to fibrin. The PT–INR measures factors synthesized in the liver, including vitamin K-dependent factors (FII, VII, IX, X). The conversion to the use of INR is an attempt to account for different analyzers and thromboplastin reagents used in PT testing. In children and neonates, the normal PTT and PT–INR values are age-dependent secondary to hemostatic protein differences present during normal developmental hemostasis [24,25,29].

Hemostatic assessment (including preoperative or preinvasive procedure)

The laboratory tests included in the initial hemostatic work-up of a child should include the PT–INR, PTT, fibrinogen levels, and platelet count. A prolonged PTT or INR can result from several different phenomena and does not necessarily predict the clinical risk of bleeding. Furthermore, clinical bleeding may occur in a patient with normal age-appropriate test results. An example of a patient at increased risk of bleeding with normal screening hemostatic testing (INR, PTT, platelet count, and fibrinogen) occurs in congenital or acquired von Willebrand disease (vWD). Currently, unless there is a patient or family history of bleeding, vWD is not screened for preoperatively.

vWD occurs as a result of qualitative or quantitative deficiency in vWF. *In vivo*, vWF binds with FVIII as a stabilizer, protecting it from degradation, and, as discussed above, participates in platelet adhesion to damaged or altered vascular endothelium. If vWF is unable to carry out these functions, mild or major bleeding may occur. Congenital vWD has a heterogeneous phenotype ranging from mild to severe. Acquired vWD has been demonstrated to occur in situations of high shear stress, for example, mechanical heart valves and ventricular assist devices in adults. Treatment includes agents which cause either increased release of FVIII and vWF from endothelial stores (desmopressin, DDAVP) or replacement of vWF with vWF concentrates.

Prolongation of the INR or PTT requires formal evaluation to determine the etiology. These patients are sometimes felt to be "auto anticoagulated;" however, this may be a misnomer because these patients may be at risk for developing thrombosis depending on the etiology of the abnormal test. In a patient who is not anticoagulated, a number of clinical situations may prolong the INR or PTT and affect the risk for bleeding and/or thrombosis or have no effect (heparin contamination of a central line blood sample used for testing).

In adults, elevated D-dimer levels indicate active coagulation, fibrin production, and fibrinolysis. D-dimers have not been formally evaluated in children and therefore the pretest likelihood of confirmed thrombosis is unknown [30,31]. Furthermore, following cardiac surgery, D-dimers are always elevated, so the test is an unreliable measure of the presence of thrombosis. If baseline hemostatic test results are abnormal, experts in hemostasis (e.g., hematology) should be consulted for further evaluation.

Global measures of hemostasis

Global measures of hemostasis, the activated clotting time, and the thromboelastogram may be more representative of hemostasis as these tests use whole blood that includes cellular components in the test systems.

Activated clotting time (ACT)

The ACT uses activated whole blood and measures clotting time in seconds. This point of care test is used during cardiopulmonary bypass (CPB) and extracorporeal membrane oxygenation (ECMO) to monitor anticoagulation, specifically heparin effect. No well-designed studies have evaluated the safety and efficacy of ACTs to monitor anticoagulation in children. The ACT does not solely or accurately reflect the effect of heparin [32–34].

Thromboelastogram (TEG)

The TEG uses activated whole blood to measure hemostasis (formation of a clot) and also fibrinolysis (clot degradation). The most common devices used to measure thromboelastography are the ROTEM (Pentapharm, Munich, Germany) and the TEG (Haemonetics, Braintree, MA, USA). Although some normative TEG data are available in children, formal well-designed studies are required to evaluate the precision, accuracy, and application of this measure in children [35,36].

Thrombosis in children with congenital heart disease

Levels of coagulation proteins, fibrinolytic proteins, and inhibitors have been found to be abnormal in children with congenital heart disease (acyanotic and cyanotic) compared with age-matched controls. Depending on the specific coagulation abnormality, these children can bleed and/or thrombose. Decreased production of coagulation proteins (anticoagulant and procoagulant factors) have been implicated from delayed liver maturation, liver failure, and/or vitamin K deficiency. Children with acyanotic congenital heart disease achieve age-appropriate levels of their hemostatic proteins similarly to age-matched controls (1 year of age), whereas children with cyanotic congenital heart disease achieve age-appropriate levels by 4 years of age [27,28].

The following section describes the thrombotic risk in children after congenital heart surgery. The American Heart Association Guidelines [37] for antithrombotic/antiplatelet therapy are very useful.

Systemic–pulmonary artery shunts

Systemic–pulmonary artery shunts are a necessary part of first-stage palliation in neonates and infants with complex congenital heart disease. The classic Blalock–Taussig shunt (BTS) [38] has since been modified to include the use of prosthetic material. The modified Blalock–Taussig shunt (MBTS) interposes a Gore-Tex graft between the subclavian artery and ispilateral pulmonary artery. Shunt size depends primarily on patient weight, varying from 3.0 mm in smaller infants to 4.0 mm. Longer shunts have an

Table 12.1 Published incidence of systemic to pulmonary artery shunt occlusion.

Study	Year	Population	N	Occluded (%)
Al Jubair *et al.* [41]	1998	Mixed	418	6.7
Motz *et al.* [44]	1999	Mixed	46	33
Fenton *et al.* [43]	2003	Mixed	169	5.9
De Oliveira *et al.* [42]	2004	Post-Norwood	105	3.8
Li *et al.* [45]	2007	Mixed	954	10
Ahmad *et al.* [40]	2008	Mixed	22	9

increased risk of thrombosis; therefore, both size and length are important factors.

Several factors may lead to shunt occlusion. Neointimal hyperplasia, followed by platelet aggregation and adherence to the subendothelium, and then proliferation of smooth muscle cells is induced by the artificial material [39]. Turbulence may affect platelet aggregation by increasing platelet hyper-reactivity. Increased wall shear stress may lead to a prothrombotic state. The rate of shunt occlusion varies between 0 and 33% [40–45] (Table 12.1). This wide discrepancy in shunt failure may or may not be explained by different postoperative anticoagulation regimes [39,41,44,45]. The only prospective study found that patients receiving aspirin [acetylsalicylic acid (ASA)] had a lower risk of shunt thrombosis and lower rate of interstage death compared with the group without ASA [45]. Factors that increase the incidence of shunt failure include smaller conduit size [43,44], smaller patients [41], younger patients [41], and small pulmonary artery size [41]. The CLARINET trial, a randomized, double-blind, placebo-controlled trial, examined the efficacy and safety of clopidogrel and ticlopidine in neonates and infants with systemic to pulmonary artery shunt palliation (www.clinicaltrials.gov, NCT00396877). Most patients were also taking aspirin. The primary outcome was a composite end point including death, shunt thrombosis, and cardiac procedure prior to 120 days following an event considered thrombotic in nature. No difference in the composite endpoint was found between the two groups.

There are limited prospective data about direct antithrombotic management after a systemic-pulmonary artery shunt. Recommendations for infants with an MBTS as part of a Norwood procedure are similar to those for infants with an MBTS. On the other hand, the Norwood procedure with an RV–PA shunt may have a decreased rate of thrombosis because of the increased conduit diameter, but the increasing turbulence from the longer conduit may offset this. Some infants are palliated with a central shunt with a Gore-Tex graft between the ascending aorta and the main pulmonary artery. A central shunt has an advantage of being short (3.5 or 4 mm long).

Bidirectional cavopulmonary anastomosis (BCPA)

Thrombotic complications are rarely reported after BCPA [46–48]. There are no prospective data to support routine thromboprophylaxis; however, antiplatelet therapy may be considered.

Fontan procedure

Fontan palliation (total cavopulmonary anastomosis) is the final operation for children with a univentricular heart. Optimal surgical technique is unknown and includes the lateral tunnel Fontan procedure, the extracardiac conduit, or more recently the intra–extracardiac Fontan procedure. Each surgical connection has its own advantages and disadvantages, but no one technique eliminates the thrombotic risk. All three procedures expose patients to prosthetic material. The lateral tunnel Fontan procedure uses a Gore-Tex intra-atrial baffle to divert blood from the inferior vena cava to the pulmonary arteries. As such, prosthetic material is exposed to the left-sided circulation that may increase the risk of systemic embolization. The extracardiac and intra–extracardiac Fontan procedures use a 16–18 mm Gore-Tex conduit to baffle blood to the pulmonary artery. These prosthetic conduits have no growth potential. There is a theoretical risk of flow obstruction secondary to thrombus formation or the development of fibrosis and/or calcification.. Turbulence of blood and lost kinetic energy may predispose to right atrial dilation, stagnation of blood flow, and thrombosis. Hydrodynamics depend primarily on the connection geometry or, more specifically, the horizontal offset of the cavopulmonary anastomoses to avoid flow collision.

Venous thrombosis is a major cause of morbidity and mortality after the Fontan procedure [49,50]. An acquired prothrombotic state may occur secondary to increased levels of FVIII [27]. Additional hypotheses for these thromboembolic phenomena include low flow states, stasis in the venous pathway, right-to-left shunts, blind cul-de-sacs, prosthetic materials, and atrial arrhythmias. The reported incidence of thromboembolic events varies from 7 to 23% [51–55]. The incidence of intracardiac thrombus is >33% [56–58]. There is insufficient prospective evidence to anticoagulate children routinely after the Fontan procedure. McCrindle *et al.* performed a multicenter, international randomized trial of anticoagulation with aspirin versus heparin/warfarin for a 2 year period after the Fontan procedure in children [53]. Unfortunately, the study was underpowered and showed no difference in thrombosis, either intra- or extracardiac, between the two groups. Current prophylactic anticoagulation practices are based on theory and expert opinion.

Right ventricle to pulmonary artery (RV–PA) conduits

RV–PA conduits to direct pulmonary blood flow are common in patients with various forms of tetralogy of Fallot and pulmonary atresia, truncus arteriosus, aortic valve disease

following a Ross procedure, and D-transposition of the great arteries with ventricular septal defect and pulmonary stenosis. Little information is available about the thrombosis risk in these patients. There is no indication for long-term anticoagulation, but antiplatelet therapy may be considered.

Cardiomyopathies

Anticoagulation may be considered in infants and children with normal structural cardiac anatomy, but decreased ventricular function as with idiopathic, post-viral, or dilated cardiomyopathy. A left ventricular ejection fraction of <30% increases the risk for stagnant blood flow and intracardiac thrombus.

Valve replacement

A prosthetic valve is necessary when a child's native valve cannot be repaired surgically [59,60]. Biologic prosthetic valves (allograft or xenograft tissue valves) are typically placed on the right side (tricuspid or pulmonary positions). In contrast, mechanical prosthetic valves are preferred for the mitral and aortic positions, given the higher pressure and velocity of blood flow, the potential for rapid deterioration of tissue valves, and the dire consequences of valve failure in this anatomic position. Mechanical valves are generally contraindicated on the right side of the heart because of the lower blood pressure and flow velocity that may precipitate valve thrombosis and failure. Mechanical valves are sometimes used on the right side of the heart when the right ventricle is functioning as the systemic ventricle.

Long-term anticoagulation is unnecessary for tissue valves, but imperative for mechanical valves. Most studies examining mechanical prosthetic valve anticoagulation are retrospective and include small numbers of patients, hence high-grade evidence for prophylactic agent choice is unavailable. Most providers use a vitamin K antagonist with or without an antiplatelet agent. Valves placed in the mitral position pose an increased risk for thrombosis. The recommendations of the ACC/AHA Guidelines for Management of Patients with Valvular Heart Disease [37] are extremely valuable.

Intracardiac, arterial, or venous thrombosis

Symptoms of thrombosis depend upon the location of the thrombus. Intracardiac thrombus may be asymptomatic or cause congestive heart failure, pulmonary embolism, or sequelae secondary to an embolus, including stroke and organ or limb compromise. Intracardiac thrombosis is often an incidental finding for children with compromised cardiac function [56,61,62] and may be identified through echocardiogram, cardiac catheterization, angiogram, or cardiac MRI or CT.

Deep venous thrombosis in a limb commonly occurs in vessels where central catheters (venous or arterial) have been attempted or placed, including cardiac catheterization [63,64].

Symptoms include pain, swelling, skin discoloration, and altered perfusion [65,66]. The most sensitive methods for diagnosing upper system thrombosis are ultrasound for jugular venous thrombosis and venography for intrathoracic vessels. For symptomatic thrombosis of both the upper and lower system, ultrasound may be used; however, if the clinical suspicion for thrombosis is high and the ultrasound is negative, further imaging should be considered by magnetic resonance imaging (MRI) [67,68], computed tomography (CT), and/or venography of the suspicious venous or arterial system. No studies have determined the sensitivity and specificity of these imaging techniques in children, but they are commonly used.

Thromboses require rapid diagnosis and treatment to prevent thrombus extension or embolism. Management of children with venous or arterial thrombosis focuses on preventing extension, recurrence, or embolization of thrombus. The duration and intensity of therapy are based on recommendations for adults that may be excessive in children. It is reasonable to base therapy on adult recommendations [69]. Newly diagnosed thrombosis is treated with 5–7 days of heparin therapy and may be followed by continued heparin or warfarin treatment.

Anticoagulant agents

Therapeutic agents commonly used in children include heparin and oral vitamin K antagonists (warfarin). When patients are maintained within their defined therapeutic range, they will be adequately protected from the risk of thrombosis without unacceptable risk of side effects [26,70,71]. Newer agents, such as direct thrombin inhibitors, are available, although there are limited data available to support their use. Despite this, there are clinical situations, for example, in confirmed heparin-induced thrombocytopenia (HIT) [69,72,73], where these agents must be used.

Therapeutic agents (Table 12.2)

Heparin is a term that describes unfractionated heparin (standard heparin) and low molecular weight heparins (LMWH). Both are heparins with LMWH being modified using enzymes to reduce molecular size. This smaller molecular size results in a more specific inhibition of activated Xa.

Unfractionated heparin (UFH)

Unfractionated heparin (standard heparin) remains a commonly used anticoagulant agent in hospitals for children at increased risk of hemorrhage (i.e., postoperatively) or when rapid reversal of anticoagulant effect is required [69]. Heparin is not absorbed orally, so it must be administered intravenously or subcutaneously.

Table 12.2 Anticoagulant agents. Heparin (unfractionated or low molecular weight) and warfarin are commonly used in children. There is little evidence supporting the use of direct thrombin inhibitors and therefore they should be reserved for patients with HIT. Currently bivalirudin or argatroban are the agents of choice for adults with HIT. Lytic therapy should be reserved for patients where there is a risk to life, limb or organ.

Anticoagulant and mechanism of action	Properties	Indications	Contraindications	Dose	Target range	Monitoring	Side effects
Unfractionated heparin (UFH)							
Potentiates antithrombin's inhibition of factors XIIa, XIa, Xa, IIa	$t_{1/2}$ dose dependent (max. 150 min) Hepatic and renal clearance Completely reversible with protamine sulfate Poorly bioavailable, requires frequent blood monitoring Antithrombin required to achieve heparin effect. If no heparin effect achieved with high doses of heparin, determine antithrombin level as antithrombin supplement may be required	Treatment of thrombosis or increased risk of thrombosis when the risk of bleeding is considerable (i.e., postoperative period) or when the child undergoes frequent invasive procedures requiring reversal of anticoagulation	HIT (heparin-induced thrombocytopenia) Poor venous access due to parenteral administration and frequent monitoring is required	Age-dependent dosing: age <12 mo = 28 U kg^{-1} h^{-1} age ≥12 mo = 20 U kg^{-1} h^{-1}	Gold standard measure is anti-Xa 0.35–0.7 U ml^{-1} If anti-Xa not possible, then PTT 1.5–3 × baseline PTT	q 24h at minimum UFH (anti-XA) level is gold standard (0.35–0.70 U ml^{-1}) If it is necessary to use a PTT to monitor therapy, the PTT range must be determined by each hospital to correspond to UFH 0.35–0.7 U ml^{-1}	Hemorrhage reported as 1.5% (95% CI 0.0–8.3) HIT 0–2.5% May be associated with osteoporosis
Low molecular weight heparin (LMWH)							
Same as UFH, but greatest inhibition on factor Xa	$t_{1/2}$ = 5 h Highly bioavailable, "stable drug" Renally cleared Not fully reversible Low dependence on antithrombin. Requires 24h to clear anticoagulant effect	For treatment of thrombosis or as thromboprophylaxis when bleeding risk considered stable or as a bridge between heparin and warfarin postoperative or when child has poor venous access	High risk for bleeding Reversal required frequently for interventions Hold LMWH × 24h pre-procedure Renal insufficiency	Age-dependent dosing	Doses are titrated to target LMWH level (anti-Xa) of 0.5–1 U ml^{-1}	LMWH level (anti-Xa) Target 0.5–1 U ml^{-1} Dose titrated to achieve level Minimum monthly levels INR or PTT will not be affected	Hemorrhage reported as 4.8–8.1% No evaluation of risk for HIT or osteoporosis
Enoxaparin q 12h	$t_{1/2}$ = 3–6h	Stable anticoagulant effect required		Age-dependent dosing: age <3 mo = ~1.5 mg kg^{-1} per dose age ≥3 mo = ~1.0 mg kg^{-1} per dose		LMWH level 4–6h post-dose	
Tinzaparin q 24h	$t_{1/2}$ = 3–6h	Needle phobic children on long-term therapy		200 U kg^{-1} per dose		LMWH level age <5 years 2h post-dose, ≥5 years 4h post-dose	
Vitamin K antagonists (VKA)							
Warfarin VKA specifically inhibit the γ-carboxylation of the vitamin K-dependent proteins II, VII, IX, X, proteins C, S and Z	$t_{1/2}$ = 160h Oral administration Hepatic metabolism	Long-term anticoagulant therapy	Relative: <1 years of age unless mechanical valve in situ	Load: 0.2 mg kg^{-1} day^{-1} except for patients with Fontan, then 0.1 mg kg^{-1} day^{-1}. Maintenance: individualized dosing titrated to INR No studies in children evaluating warfarin dosing based on pharmacogenomics	Target INR range 2–3 Mechanical mitral valves 2.5–3.5	INR daily until therapeutic then decreased frequency when stable with minimum monthly testing Test INR with illness, medication, or diet change	Hemorrhage 0.5% per patient-year Increases with INR >8 Tracheal calcification, hair loss, decreased bone mineral density Consider administering vitamin K for INR >8

(continued)

Table 12.2 (cont'd)

Warfarin dosing nomogram^a: maintenance phase

	Target INR 2.5 (2–3)	Target INR 3 (2.5–3.5)	Dose adjustment
INR	1.1–1.4	1.1–2.0	Increase dose by 20%
INR	1.5–1.9	2.1–2.4	Dose increase by 10%
INR	2.0–3.0	2.5–3.5	No change
INR	3.1–3.5	3.6–4.0	Decrease dose by 10%
INR	>3.5–4.0	4.1–4.5	Administer one dose at 50% < maintenance dose, *then* restart at 20% < previous maintenance dose
INR	4.1–5.0	4.6–5	Hold 1 dose, *then* restart at 20% < previous maintenance dose
INR	>5.0		Hold 1 dose. Check INR next day. Consider reversal if bleeding or if high risk for hemorrhage

^aThis nomogram is intended for use once the loading phase is completed. Prior to each dose adjustment, assess the patient for medication change, illness (cold, flu), and adherence. New oral agents that inhibit either factor Xa or IIa are being tested in children and have advantages over VKA (e.g. less monitoring, no interactions). Completion of clinical studies using these agents in adults has allowed approval of many of these agents for specific clinical indications [101].

Antiplatelet therapy

Antiplatelet	Properties	Indications	Contraindications	Dose	Target range	Monitoring	Side effects
Aspirin (ASA) Inhibition of COX-1 and COX-2 activity	Oral Oral $t_{1/2}$ = 2 h Irreversible platelet inhibition Discontinue ASA 7 days preoperation to allow if full platelet regeneration required	Platelet inhibition Thromboprophylaxis of stents Shunts: Blalock–Taussig Norwood, Glenn, bi-cavopulmonary Fontan Valves: bioprosthetic mechanical in addition to oral antithrombotic therapy for patients at high risk for thrombosis Kawasaki disease	Hemorrhage Ibuprofen within 4 h of ASA dose Bleeding Varicella, fever due to risk for Reye syndrome Lack of pharmacokinetic/pharmacodynamic data	1–5 mg kg^{-1} day^{-1} Max. 81–325 mg 80–100 mg kg^{-1} day^{-1} during acute phase of illness then 3–5 mg kg^{-1} day^{-1} for additional 6–8 weeks	None studied	There are no studies that link outcome to measuring ASA effect	Bruising, confusion, vertigo, nausea, vomiting, tinnitus, abdominal pain, cramping, burning, fatigue, bleeding

Anticoagulant and mechanism of action	Properties	Indications	Contraindications	Dose	Target range	Monitoring	Side effects
Clopidogrel Inhibition of ADP-induced platelet aggregation. No effects on arachidonic acid metabolism	$t_{1/2}$ = 7 h Renal clearance Discontinue clopidogrel 7 days preoperation to allow if full platelet regeneration is required	Failure of antiplatelet therapy in select circumstances. Antiplatelet therapy in varicella or 1 week pre- and 6 weeks post-varicella vaccine in place of ASA	Lack of pharmacokinetic and pharmacodynamic data (in progress, PICOLO/ CLARINET)	0.2–1 mg kg⁻¹ day⁻¹	None studied	There are no studies that link outcome to measuring clopidogrel effect	Fatigue, vertigo, stomach upset or pain, bruising, bleeding, diarrhea
Dipyridamole Adenosine reuptake inhibitor Two mechanisms have been proposed for increase in cyclic AMP, a platelet inhibitor	$t_{1/2}$ 2–4 min or 2.5h	Ventricular assist devices	Lack of pharmacokinetic and pharmacodynamic data	1–5 mg kg⁻¹ day⁻¹ 4 mg kg⁻¹ day⁻¹ divided q.i.d. Max. 15 mg kg⁻¹ day⁻¹	None studied	There are no studies that link outcome to measuring dipyridamole effect	Chest pain, angina pectoris, headache, vertigo, ECG abnormalities
Abciximab IIb–IIIa inhibitor	Kawasaki disease (lysis of thrombosed coronary aneurysms)	Kawasaki disease in addition to standard therapy	Lack of pharmacokinetic and pharmacodynamic data	0.25 mg kg⁻¹ bolus then 0.125 µg kg⁻¹ min⁻¹ ×12 h	None studied	There are no studies that link outcome to measuring abciximab effect	Nausea, vomiting, vertigo, irritation at injection site
Anticoagulant and mechanism of action	**Properties**	**Indications**	**Contraindications**	**Dose**	**Target range**	**Monitoring**	**Side effects**
Heparinoid Danaparoid Inhibition of Xa	Renal clearance $t_{1/2}$ = 24 h	HIT treatment	Lack of pharmacokinetic and pharmacodynamic data	30 U kg⁻¹ i.v. bolus then 1.2–2 U kg⁻¹ h⁻¹	Anti-Xa 0.4–0.8 U ml⁻¹	4–6 h post-bolus or each dose change	Hemorrhage
Direct thrombin inhibitors[b] Argatroban	Hepatic clearance $t_{1/2}$ 40–50 min Not reversible	HIT	Lack of pharmacokinetic and pharmacodynamic data	Age-dependent dosing: Age 6 mo–6 years = 0.5–1 µg kg⁻¹ min⁻¹ Age 6–16 years = 1–2 µg kg⁻¹ min⁻¹ Continuous infusion (max. 10µ/kg/min)	1.5–3 × baseline PTT (not to exceed 100s	PTT 2 h post-start of infusion and each dose change	Hemorrhage 6–15% with therapeutic PTT, prolongation of baseline PT (INR)
		ECMO		ECMO 50µg kg⁻¹ per 750ml circuit prime then 100µg kg⁻¹ per bolus if not already anticoagulated, then 1–2 µg kg⁻¹ min⁻¹	ACT 180–220 or 250–300		

Table 12.2 (cont'd)

Anticoagulant and mechanism of action	Properties	Indications	Contraindications	Dose	Target range	Monitoring	Side effects
		Cardiac catheterization/coil PCI		$150\,\mu g\,kg^{-1}$ $350\,\mu g\,kg^{-1}$ per bolus then $25\,\mu g\,kg^{-1}\,min^{-1}$			
Bivalirudin (Angiomax)	Enzymatic 80% and renal 20% clearance $t_{1/2}$ 25 min Reversible	Treatment	Lack of pharmacokinetic and pharmacodynamic data	Age <6 months[c] = $0.125\,mg\,kg^{-1}$ i.v. bolus, then $1.25\,mg\,kg^{-1}\,h^{-1}$	ACT 2.5 × baseline	Activated clotting time (ACT) 5 min post-i.v. bolus	2.4% hemorrhage
		CPB		50 mg to circuit, then $1\,mg\,kg^{-1}$ i.v. bolus, then $2.5\,mg\,kg^{-1}\,h^{-1}$	ACT 400–500 s		
		PCI		$0.75\,mg\,kg^{-1}$ i.v. bolus then $1.75\,mg\,kg^{-1}\,h^{-1}$ for duration of procedure May continue infusion for 4 h post-procedure or at $0.2\,mg\,kg^{-1}\,h^{-1}$ for an additional 20 h			
Lepirudin (Refludan)	Renal clearance $t_{1/2}$ = 80 min Not reversible	HIT	Lack of pharmacokinetic and pharmacodynamic data	$0.2\,mg\,kg^{-1}$ (max. 44 mg h^{-1}) i.v. bolus, then $0.1\,mg\,kg^{-1}\,h^{-1}$ (max. $16.5\,mg\,h^{-1}$)	PTT 1.5–2 × baseline Optimal PTT <65 s	PTT 2 h post-start of therapy and each dose change	Not reported in children. In adults 17% hemorrhage 30% develop anti-lepirudin antibodies

[b]There are no pharmacokinetic, pharmacodynamic, safety, or efficacy data for direct thrombin inhibitor use in infants and children. These agents should be reserved for circumstances where no other agent can be used and the Pediatric Thrombosis Program at Stollery Children's Hospital should be consulted prior to the use of direct thrombin inhibitors.

[c]No data available for children >6 months of age.

Unfractionated heparin therapy: dosing and monitoring

Dosing of UFH in children is age dependent (Table 12.2). Heparin doses are titrated based on laboratory measure of anti-factor Xa or PTT if anti-factor Xa measures are unavailable. Anti-Xa levels are commonly referred to as "heparin levels."

The internationally accepted standard measure of UFH is the anti-factor Xa level, with a target range of 0.35–0.7 U ml^{-1} [74] to reflect a therapeutic heparin level. Using the PTT to monitor heparin in pediatric patients is likely to be invalid because normal PTTs in infants and children are increased secondary to developmental hemostasis [75–78]. Equally, children have a different response to heparin than adults; therefore, the use of the PTT to monitor heparin therapy may be inaccurate. In addition, *in vitro* and *in vivo* data demonstrate significant variations in correlation of the PTT to the anti-Xa level in children [75–78]. Unfractionated heparin has a short half-life, clearing within 4–6 h of cessation of heparin administration, and is fully reversible with protamine sulfate. Venous access is required for administration and heparin infusions should not be interrupted for medication administration or blood sampling (due to the short half-life). Daily monitoring of the PTT and anti-Xa levels is required because of the poor bioavailability of heparin.

Heparin-induced thrombocytopenia (HIT) is an immune-mediated platelet reaction response to heparin. HIT is characterized by a sudden drop in platelets by more than 50% after 5 days of first-time heparin exposure or any time after a previous heparin exposure. The incidence among children is <0.1% [79–81].

Low molecular weight heparins

Low molecular weight heparins have rapidly become the anticoagulants of choice for pediatric patients without a bleeding risk [82–87]. These heparins have increased bioavailability and result in a more stable anticoagulant effect. Adult reports show equal efficacy to the higher molecular weight UFH and a decreased risk for hemorrhage. No well-designed studies have evaluated their safety and efficacy in children. There are three commonly used LMWHs (Table 12.2).

Low molecular weight heparin: dosing and monitoring

Dosing of LMWHs is age dependent [69]. Recent publications describing enoxaparin dosing have suggested that age-dependent dose requirements [88,89] may be higher than suggested in Table 12.2.

Monitoring the LMWH effect can only be performed using an anti-factor Xa level as LMWH maximally inhibits the activation of procoagulant FX. The influence of LMWH on the activation of FII is diminutive and therefore a PTT will not measure LMWH effect. Anti-factor Xa levels should be monitored monthly and dose adjustments be made to maintain an anti-factor Xa (LMWH level) (Table 12.2) as children often outgrow their current dose or some accumulation occurs over time due to insufficient renal clearance.

Low molecular weight heparins: reversal

If anticoagulation with LWMHs needs to be terminated for clinical reasons, discontinuation of LMWH injections for 24 h usually suffices. If an immediate reversal of effect is required, protamine sulfate reverses 80% of the anti-factor Xa activity of LMWHs.

Oral vitamin K antagonists

The most commonly prescribed oral vitamin K antagonist (VKA) is warfarin. Alternatively, in Europe and South America, phenprocoumon is commonly prescribed. Target INRs are specific to the indication for anticoagulation (Table 12.2). Frequent INR monitoring is important because of the variability of INRs in children from the following challenges:

• There is no pediatric formulation available, so accurate dosing is difficult.

• Children with congenital heart disease have complex underlying health problems that may require frequent reversal for invasive procedures, multiple medication changes, or illness-effect dose requirements.

• Inconsistent nutritional intake such as breast milk which contains little vitamin K, bottled formula with varying amounts of vitamin K, and normal age-appropriate fluctuations in daily intake.

• Increased susceptibility to respiratory infections and influenza as part of childhood which interferes with VKA metabolism.

• Poor venous access limits monitoring of VKAs that have a narrow therapeutic index.

• Anxiety and needle phobias.

• The unreported use of complementary alternative medications that may interfere with VKA metabolism.

• Possibility of life-long monitoring (i.e., mechanical heart valve), which results in many more patient years of anticoagulation.

A warfarin dosing algorithm is presented in Table 12.2. There are data among adults that indicate that the therapeutic range expands by 10% without a warfarin dose adjustment and increases over time in the therapeutic range [90]. The side effects of oral anticoagulant therapy (bleeding and new or extension of thrombus) increase with poor oral anticoagulant control. The event rate of side effects in children ranges from 0 to 0.5% per patient year and from 0 to 1.3% per patient year for bleeding and thrombosis, respectively [91,92]. Long-term VKA therapy in children may be associated with osteoporosis [69].

Vitamin K antagonist: reversal

The antidote for warfarin depends whether urgent or nonurgent reversal is necessary. For children at high risk for thrombosis (i.e., with mechanical valves), bridge anticoagulant therapy using *heparin* may be considered [69].

• Non-urgent reversal requires holding warfarin for 3 days pre-procedure [93].

• For semi-urgent reversal, vitamin K may be administered at a dose of 0.5–1 mg orally depending upon patient size [69,94]. Administering vitamin K either intravenously or intramuscularly is less efficacious than orally, provided that gut absorption is not severely compromised [95].

• For urgent reversal (major bleeding or interventional procedure), FVIIa 50 U kg^{-1} i.v. or FFP 20 ml kg^{-1} is administered. Octaplex is approved for VKA reversal in adults in various countries. The composition of 20 ml of Octaplex includes the human coagulation factors FII (220–760 IU), VII (180–480 IU), IX (400–620 IU), X (360–600 IU), protein C (140–620 IU), protein S (140–640 IU), and heparin (80–310 IU) and sodium citrate (17–276 mmol l^{-1}). Although not currently evaluated or approved for use in children, dose recommendations are 40 ml i.v. for a patient of adult size/weight [70]. For further dosing guidelines, see Ansell *et al.* [70].

POC INR monitoring: a solution to VKA therapy

The use of the POC INR meter represents a solution to manage VKA therapy effectively in children [96]. The POC INR meter uses a capillary sample to determine the INR, may be performed at home, and facilitates more frequent testing. As a result, the time in the therapeutic range is better than in children using laboratory INR testing [97,98]. POC INR meter use is believed to improve quality of life.

Direct thrombin inhibitors

Heparin-induced thrombocytopenia (HIT), developing rarely in children (less than 1% of those who receive UFH) is an extremely hypercoagulable state which occurs from development of an IgG antibody to the combination of platelet factor 4, presented on the surface of activated platelets, and glycosaminoglycan units of UFH. In a child who develops the HIT antibody, all UFH must be discontinued to avoid the antigen–antibody reaction that can result in massive thrombosis. In adults with HIT, the direct thrombin inhibitors (DTIs) argatroban and bivalirudin are recommended. In children, few studies have been completed with these agents [72,73,99]; however, they are used if HIT is confirmed and anticoagulation is required. Different clearance mechanisms exist with renal and hepatic clearance for bivalirudin and argatroban, respectively. Advantages include no reactivity with HIT antibodies and short half-life (in adult volunteers, 39–51 min for argatroban and 25 min for bivalirudin). Challenges of both agents include the inability to reverse the anticoagulant effect and inaccurate monitoring methods. Both agents should be monitored by an echarin (snake venom) clotting time, but currently this test is available only in research laboratories. The agents are monitored mostly by PTT and less often by activated clotting time [100].

Thrombolytic therapy

In life-, organ- or limb-threatening thrombosis, including pulmonary embolism, thrombolytic therapy is an appropriate therapeutic choice [26]. Tissue plasminogen activator (tPA) administered intravenously activates plasminogen, which then degrades thrombus. Few prospective studies in children have examined the dosing (range 0.01–0.6 mg kg^{-1} h^{-1} for 6–24 h), safety, and efficacy of this therapy. Reports of >30% major bleeding exist in the literature, hence discussion with parents before therapy is strongly recommended with documentation of informed consent. Monitoring the fibrinogen level should be carried out with replacement if levels are less than 100 mg dl^{-1} to avoid hemorrhage. The administration of fresh frozen plasma at 10–20 ml kg^{-1} every 8–12 h during therapy will maximize thrombolysis by ensuring an adequate plasminogen level.

Antiplatelet therapy

Multiple receptors participate in platelet activation, so single-target therapeutic agents may not protect against all mechanisms of platelet activation. The most common antiplatelets used are ASA, dipyridamole, and clopidogrel.

ASA acetylates enzyme cyclooxygenase, inhibits thromboxane A2, and causes irreversible inhibition of this enzyme, thus impairing platelet aggregation until the death of the platelets. Dipyridamole inhibits platelet phosphodiesterase. Clopidogrel inhibits platelet aggregation induced by ADP.

Antiplatelet therapy: dosing

• ASA 1–5 mg kg day^{-1}
• Dipyridamole 2–5 mg kg day^{-1}
• Clopidogrel 0.2 mg kg day^{-1}.

Various methods have been used to monitor antiplatelet effect (platelet aggregation, PFA100, Accumetrics, TEG); however, none have been associated with improved safety and efficacy outcomes.

Antiplatelet therapy: reversal

• Discontinuation of therapy is sufficient to clear effect (may take up to 7 days).

• Special consideration should be given to withholding aspirin with fever or exposure to chickenpox due to the small risk of developing Reyes syndrome.

• Immunizations and injections may be administered while on antiplatelet therapy. However, firm pressure must be applied to the injection site to minimize bruising.

• The manufacturer of the varicella vaccine recommends withholding ASA for 1 week before and for 6 weeks following varicella immunization.

Conclusion

The incidence of thrombotic complications continues to increase as a result of continued advances in medical and surgical cardiac therapy. Currently, there are few properly designed clinical studies to determine the *best* prevention and treatment in children with congenital or acquired heart disease with or at risk for thrombosis.

References

1 Human DG. Living with complex congenital heart disease. *Pediatr Child Health* 2009;**14**:161–82.

2 Sacco RL, Adams R, Albers G, *et al*. Guidelines for prevention of stroke in patients with ischemic stroke or transient ischemic attack: a statement for healthcare professionals from the American Heart Association/American Stroke Association Council on Stroke: co-sponsored by the Council on Cardiovascular Radiology and Intervention: the American Academy of Neurology affirms the value of this guideline. *Circulation* 2006;**113**:e409–49.

3 Macfarlane RG. An enzyme cascade in the blood clotting mechanism, and its function as a biochemical amplifier. *Nature* 1964;**202**:498–9.

4 Davie EW, Ratnoff OD. Waterfall sequence for intrinsic blood clotting. *Science* 1964;**145**:1310–2.

5 Hoffman M, Monroe DM III. A cell-based model of hemostasis. *Thromb Haemost* 2001;**85**:958–65.

6 Dubois C, Panicot-Dubois L, Gainor JF, *et al*. Thrombin-initiated platelet activation *in vivo* is vWF independent during thrombus formation in a laser injury model. *J Clin Invest* 2007;**117**:953–60.

7 Mangin P, Yap CL, Nonne C, *et al*. Thrombin overcomes the thrombosis defect associated with platelet GPVI/FcRγ deficiency. *Blood* 2006;**107**:4346–53.

8 Ruggeri ZM. Old concepts and new developments in the study of platelet aggregation. *J Clin Invest* 2000;**105**:699–701.

9 Bergmeier W, Piffath CL, Goerge T, *et al*. The role of platelet adhesion receptor GPIbα far exceeds that of its main ligand, von Willebrand factor, in arterial thrombosis. *Proc Natl Acad Sci USA* 2006;**103**:16900–5.

10 Massberg S, Gawaz M, Grüner S, *et al*. A crucial role of glycoprotein VI for platelet recruitment to the injured arterial wall *in vivo*. *J Exp Med* 2003;**197**:41–9.

11 Holtkötter O, Nieswandt B, Smyth N, *et al*. Integrin α2-deficient mice develop normally, are fertile, but display partially defective platelet interaction with collagen. *J Biol Chem* 2002;**277**:10789–94.

12 Nieswandt B, Brakebusch C, Bergmeier W, *et al*. Glycoprotein VI but not α2β1 integrin is essential for platelet interaction with collagen. *EMBO J* 2001;**20**:2120–30.

13 Falati S, Liu Q, Gross P, *et al*. Accumulation of tissue factor into developing thrombi *in vivo* is dependent upon microparticle P-selectin glycoprotein ligand 1 and platelet P-selectin. *J Exp Med* 2003;**197**:1585–98.

14 Giesen PLA, Rauch U, Bohrmann B, *et al*. Blood-borne tissue factor: another view of thrombosis. *Proc Natl Acad Sci* 1999; **96**:2311–2315.

15 Bach R, Rifkin DB. Expression of tissue factor procoagulant activity: Regulation by cytosolic calcium. *Proc Natl Acad Sci USA* 1990;**87**:6995–9.

16 Maynard JR, Heckman CA, Pitlick FA, Nemerson Y. Association of tissue factor activity with the surface of cultured cells. *J Clin Invest* 1975;**55**:814–24.

17 Becker RC. Cell-based models of coagulation: a paradigm in evolution. *J Thromb Thrombol* 2005;**20**:65–8.

18 Stegner D, Nieswandt B. Platelet receptor signaling in thrombus formation. *J Mol Med* 2011;**89**:109–21.

19 Burgess JK, Hotchkiss KA, Suter C, *et al*. Physical proximity and functional association of glycoprotein 1bα and protein-disulfide isomerase on the platelet plasma membrane. *J Biol Chem* 2000;**275**:9758–66.

20 Chen VM, Hogg PJ. Allosteric disulfide bonds in thrombosis and thrombolysis. *J Thromb Haemost* 2006;**4**:2533–41.

21 Essex DW, Li M, Miller A, Feinman RD. Protein disulfide isomerase and sulfhydryl-dependent pathways in platelet activation. *Biochemistry* 2001;**40**:6070–5.

22 Du X, Gu M, Weisel JW, *et al*. Long range propagation of conformational changes in integrin α(IIb)β3. *J Biol Chem* 1993; **268**:23087–92.

23 Sitaru AG, Holzhauer S, Speer CP, *et al*. Neonatal platelets from cord blood and peripheral blood. *Platelets* 2005;**16**:203–10.

24 Andrew M, Paes B, Milner R. Development of the human coagulation system in the full-term infant. *Blood* 1987;**70**:165–72.

25 Andrew M, Vegh P, Johnston M, *et al*. Maturation of the hemostatic system during childhood. *Blood* 1992;**80**:1998–2005.

26 Monagle P, Chan A, Massicotte P, *et al*. Antithrombotic therapy in neonates and children: the Eighth ACCP Conference on Antithrombotic and Thrombolytic Therapy. *Chest* 2008;**133** (6 Suppl):645S–87S.

27 Odegard KC, Zurakowski D, DiNardo JA, *et al*. Prospective longitudinal study of coagulation profiles in children with hypoplastic left heart syndrome from stage I through Fontan completion. *J ThoracCardiovasc Surg* 2009;**137**:934–41.

28 Odegard KC, Zurakowski D, Hornykewycz S, *et al*. Evaluation of the coagulation system in children with two-ventricle congenital heart disease. *Ann Thorac Surg* 2007;**83**:1797–803.

29 Andrew M, Paes B, Milner R, *et al*. Development of the human coagulation system in the healthy premature infant. *Blood* 1988;**72**:1651–7.

30 Wells PS, Brill-Edwards P, Stevens P, *et al*. A novel and rapid whole-blood assay for D-dimer in patients with clinically suspected deep vein thrombosis. *Circulation* 1995;**91**:2184–7.

31 Goldenberg NA, Knapp-Clevenger R, Manco-Johnson MJ. Elevated plasma factor VIII and D-dimer levels as predictors of poor outcomes of thrombosis in children. *N Engl J Med* 2004;**351**:1081–8.

32 Chan AK, Leaker M, Burrows FA, *et al*. Coagulation and fibrinolytic profile of paediatric patients undergoing cardiopulmonary bypass. *Thromb Haemost* 1997;**77**:270–7.

33 Nankervis CA, Preston TJ, Dysart KC, *et al*. Assessing heparin dosing in neonates on venoarterial extracorporeal membrane oxygenation. *ASAIO J* 2007;**53**:111–4.

34 Green TP, Isham-Schopf B, Irmiter RJ, *et al*. Inactivation of heparin during extracorporeal circulation in infants. *Clin Pharmacol Ther* 1990;**48**:148–54.

35 Chan KL, Summerhayes RG, Ignjatovic V, *et al*. Reference values for kaolin-activated thromboelastography in healthy children. *Anesth Analg* 2007;**105**:1610–3.

36 Alexander DC, Butt WW, Best JD, *et al*. Correlation of thrombo-elastography with standard tests of anticoagulation in paediatric patients receiving extracorporeal life support. *Thromb Res* 2010;**125**:387–92.

37 Barst R, Erikson C, Bauman M, *et al*. Prevention and treatment of thrombosis in children and adults with congenital heart disease and in children with acquired heart disease. *Circulation* 2011; in press.

38 Blalock A, Taussig HB. Landmark article May 19, 1945: The surgical treatment of malformations of the heart in which there is pulmonary stenosis or pulmonary atresia. By Alfred Blalock and Helen B. Taussig. *JAMA* 1984;**251**:2123–38.

39 Centazzo S, Montigny M, Davignon A, *et al*. Use of acetylsalicylic acid to improve patency of subclavian to pulmonary artery Gore-Tex shunts. *Can J Cardiol* 1993;**9**:243–6.

40 Ahmad U, Fatimi SH, Naqvi I, *et al*. Modified Blalock–Taussig shunt: immediate and short-term follow-up results in neonates. *Heart Lung Circ* 2008;**17**:54–8.

41 Al Jubair KA, Al Fagih MR, Al Jarallah AS, *et al*. Results of 546 Blalock–Taussig shunts performed in 478 patients. *Cardiol Young* 1998;**8**:486–90.

42 De Oliveira NC, Ashburn DA, Khalid F, *et al*. Prevention of early sudden circulatory collapse after the Norwood operation. *Circulation* 2004;**110**(11 Suppl):II133–8.

43 Fenton KN, Siewers RD, Rebovich B, Pigula FA. Interim mortality in infants with systemic-to-pulmonary artery shunts. *Ann Thorac Surg* 2003;**76**:152–6; discussion 156–7.

44 Motz R, Wessel A, Ruschewski W, Bürsch J. Reduced frequency of occlusion of aorto-pulmonary shunts in infants receiving aspirin. *Cardiol Young* 1999;**9**:474–7.

45 Li JS, Yow E, Berezny KY, *et al*. Clinical outcomes of palliative surgery including a systemic-to-pulmonary artery shunt in infants with cyanotic congenital heart disease: does aspirin make a difference? *Circulation* 2007;**116**:293–7.

46 Randolph A, Wypij D, Venkataraman S, *et al*. Pediatric Acute Lung Injury and Sepsis Investigators (PALISI) Network. Effect of mechanical ventilator weaning protocols on respiratory outcomes in infants and children: a randomized controlled trial. *JAMA* 2002;**288**:2561–8.

47 Kopf GS, Laks H, Stansel HC, *et al*. Thirty-year follow-up of superior vena cava–pulmonary artery (Glenn) shunts. *J ThoracCardiovasc Surg* 1990;**100**:662–71.

48 Koutlas TC, Harrison JK, Bashore TM, *et al*. Late conduit occlusion after modified Fontan procedure with classic Glenn shunt. *Ann Thorac Surg* 1996;**62**:258–62.

49 Monagle P, Cochrane A, McCrindle B, *et al*. Thromboembolic complications after Fontan procedures – the role of prophylactic anticoagulation. *J Thorac Cardiovasc Surg* 1998;**115**:493–8.

50 Monagle P, Karl TR. Thromboembolic problems after the Fontan operation. *Semin Thorac Cardiovasc Surg Pediatr Cardiac Surg Annu* 2002;**5**:36–47.

51 Jahangiri M, Shore D, Kakkar V, *et al*. Coagulation factor abnormalities after the Fontan procedure and its modifications. *J Thorac Cardiovasc Surg* 1997;**113**:989–93.

52 Kaulitz R, Ziemer G, Rauch R, *et al*. Prophylaxis of thromboembolic complications after the Fontan operation (total cavopulmonary anastomosis). *J Thorac Cardiovasc Surg* 2005;**129**:569–75.

53 McCrindle BW, Cochrane A, Roberts R, *et al*. Factors associated with thrombotic complications in the first 2 years after the Fontan procedure: a multicentre prospective study. *Circulation* 2009;**120**(Suppl II):S591.

54 Seipelt RG, Franke A, Vazquez-Jimenez JF, *et al*. Thromboembolic complications after Fontan procedures: comparison of different therapeutic approaches. *Ann Thorac Surg* 2002;**74**:556–62.

55 Rosenthal DN, Friedman AH, Kleinman CS, *et al*. Thromboembolic complications after Fontan operations. *Circulation* 1995;**92** (Suppl):II287–93.

56 Balling G, Vogt M, Kaemmerer H, *et al*. Intracardiac thrombus formation after the Fontan operation. *J Thorac Cardiovasc Surg* 2000;**119**:745–52.

57 Buck JR, Connors RH, Coon WW. Pulmonary embolism in children. *J Pediatr Surg* 1981;**16**:385–91.

58 Shirai LK, Rosenthal DN, Reitz BA, *et al*. Arrhythmias and thromboembolic complications after the extracardiac fontan operation. *J Thorac Cardiovasc Surg* 1998;**115**:499–505.

59 el Makhlouf A, Friedli B, Oberhansli I, *et al*. Prosthetic heart valve replacement in children. Results and follow-up of 273 patients. *J Thorac Cardiovasc Surg* 1987;**93**:80–5.

60 Reiss N, Blanz U, Breymann T, *et al*. Mechanical valve replacement of the systemic atrioventricular valve in children. *ASAIO J* 2006;**52**:559–61.

61 Alioglu B, Avci Z, Tokel K, *et al*. Thrombosis in children with cardiac pathology: analysis of acquired and inherited risk factors. *Blood Coagul Fibrinol* 2008;**19**:294–304.

62 Yang JYK, Williams S, Brandão LR, Chan AKC. Neonatal and childhood right atrial thrombosis: recognition and a risk-stratified treatment approach. *Blood Coagul Fibrinol* 2010;**21**:301–7.

63 Monagle P, Adams M, Mahoney M, *et al*. Outcome of pediatric thromboembolic disease: a report from the Canadian Childhood Thrombophilia Registry. *Pediatr Res* 2000;**47**:763–6.

64 Van Ommen CH, Heijboer H, Büller HR, *et al*. Venous thromboembolism in childhood: a prospective two-year registry in The Netherlands. *J Pediatr* 2001;**139**:676–81.

65 Goldenberg NA. Long-term outcomes of venous thrombosis in children. *Curr Opin Hematol* 2005;**12**:370–6.

66 Kuhle S, Koloshuk B, Marzinotto V, *et al*. A cross-sectional study evaluating post-thrombotic syndrome in children. *Thromb Res* 2003;**111**:227–33.

67 Varnholt H. Computed tomography and radiation exposure. *N Engl J Med* 2008;**358**:852.

68 Frush DP, Goske MJ, Hernanz-Schulman M. Computed tomography and radiation exposure. *N Engl J Med* 2008;**358**:851.

69 Monagle P, Chalmers E, Chan A, *et al*. Antithrombotic therapy in neonates and children: American College of Chest Physicians Evidence-Based Clinical Practice Guidelines (8th Edition). *Chest* 2008;**133**(6 Suppl):887S–968S.

70 Ansell J, Hirsh J, Hylek E, *et al*. Pharmacology and management of the vitamin K antagonists: American College of Chest Physicians Evidence-Based Clinical Practice Guidelines (8th Edition). *Chest* 2008;**133**(6 Suppl):160S–198S.

71 Hirsh J, Dalen JE, Anderson DR, *et al*. Oral anticoagulants: mechanism of action, clinical effectiveness, and optimal therapeutic range. *Chest* 2001;**119**(1 Suppl):8S–21S.

72 Young G, Tarantino MD, Wohrley J, *et al.* Pilot dose-finding and safety study of bivalirudin in infants <6 months of age with thrombosis. *J Thromb Haemost* 2007;**5**:1654–9.

73 Young G, Yonekawa KE, Nakagawa P, Nugent DJ. Argatroban as an alternative to heparin in extracorporeal membrane oxygenation circuits. *Perfusion* 2004;**19**:283–8.

74 Hirsh J, Bauer KA, Donati MB, *et al.* Parenteral anticoagulants: American College of Chest Physicians Evidence-Based Clinical Practice Guidelines (8th Edition). *Chest* 2008;**133** (6 Suppl):141S–159S.

75 Newall F, Johnston L, Summerhayes R, *et al.* Novel interactions between UFH and TFPI in children. *Br J Haematol* 2011; **151**:376–80.

76 Newall F, Ignjatovic V, Johnston L, *et al.* Clinical use of unfractionated heparin therapy in children: time for change?: research paper. *Br J Haematol* 2010;**150**:674–8.

77 Newall F, Ignjatovic V, Johnston L, *et al.* Age is a determinant factor for measures of concentration and effect in children requiring unfractionated heparin. *Thromb Haemost* 2011; **103**:1085–90.

78 Greenway A, Ignjatovic V, Summerhayes R, *et al.* Point-of-care monitoring of oral anticoagulation therapy in children. Comparison of the CoaguChek XS system with venous INR and venous INR using an International Reference Thromboplastin preparation (rTF/95). *Thromb Haemost* 2009;**102**:159–65.

79 Newall F, Barnes C, Ignjatovic V, Monagle P. Heparin-induced thrombocytopenia in children. *J Paediatr Child Health* 2003; **39**:289–92.

80 Schmugge M, Risch L, Huber AR, *et al.* Heparin-induced thrombocytopenia-associated thrombosis in pediatric intensive care patients. *Pediatrics* 2002;**109**:E10.

81 Alsoufi B, Boshkov LK, Kirby A, *et al.* Heparin-induced thrombocytopenia (HIT) in pediatric cardiac surgery: an emerging cause of morbidity and mortality. *Semin Thorac Cardiovasc SurgPediatr Cardiac Surg Annu* 2004;**7**:155–71.

82 Dix D, Andrew M, Marzinotto V, *et al.* The use of low molecular weight heparin in pediatric patients: a prospective cohort study. *J Pediatr* 2000;**136**:439–45.

83 Kuhle S, Massicotte P, Dinyari M, *et al.* Dose-finding and pharmacokinetics of therapeutic doses of tinzaparin in pediatric patients with thromboembolic events. *Thromb Haemost* 2005; **94**:1164–71.

84 Massicotte P, Julian JA, Gent M, *et al.* An open-label randomized controlled trial of low molecular weight heparin for the prevention of central venous line-related thrombotic complications in children: the PROTEKT trial. *Thromb Res* 2003;**109**:101–8.

85 Massicotte P, Julian JA, Gent M, *et al.* An open-label randomized controlled trial of low molecular weight heparin compared to heparin and coumadin for the treatment of venous thromboembolic events in children: the REVIVE trial. *Thromb Res* 2003;**109**:85–92.

86 Michaels LA, Gurian M, Hegyi T, Drachtman RA. Low molecular weight heparin in the treatment of venous and arterial thromboses in the premature infant. *Pediatrics* 2004;**114**:703–7.

87 Young, G. New anticoagulants in children: a review of recent studies and a look to the future. *Thromb Res* 2011;**127**:70–4.

88 Bauman M, Belletrutti M, Bajzar L, *et al.* Evaluation of enoxaparin dosing requirements in infants and children. Better dosing to achieve therapeutic levels. *Thromb Haemost* 2009;**101**:86–92.

89 Malowany JI, Monagle P, Knoppert DC, *et al.* Enoxaparin for neonatal thrombosis: a call for a higher dose for neonates. *Thromb Res* 2008;**22**:826–30.

90 Rose AJ, Ozonoff A, Berlowitz DR, *et al.* Warfarin dose management affects INR control. *J Thromb Haemost* 2009;**7**:94–101.

91 Streif W, Andrew M, Marzinotto V, *et al.* Analysis of warfarin therapy in pediatric patients: a prospective cohort study of 319 patients. *Blood* 1999;**94**:3007–14.

92 Jones S, Newall F, Manias E, Monagle P. Assessing outcome measures of oral anticoagulation management in children. *Thromb Res* 2011;**127**:75–80.

93 Bauman ME, Black K, Bauman ML, *et al.* Warfarin induced coagulopathy in children: assessment of a conservative approach. *Arch Dis Child* 2011;**96**:164–7.

94 Crowther MA, Ageno W, Schnurr T, *et al.* Oral vitamin K produces a normal INR within 24 hours of its administration in most patients discontinuing warfarin. *Haematologica* 2005; **90**:137–9.

95 Crowther MA, Douketis JD, Schnurr T, *et al.* Oral vitamin K lowers the international normalized ratio more rapidly than subcutaneous vitamin K in the treatment of warfarin-associated coagulopathy. A randomized, controlled trial. *Ann Intern Med* 2002;**137**:251–4.

96 Bauman M, Conroy S, Massicotte M. Point of care INR measurement in children: what has been evaluated and future directions. *Pediatr Health* 2008;**2**:651–9.

97 Bauman ME, Black K, Kuhle S, *et al.* KIDCLOT: the importance of validated educational intervention for optimal long term warfarin management in children. *Thromb Res* 2009;**123**: 707–9.

98 Newall F, Monagle P, Johnston L. Home INR monitoring of oral anticoagulant therapy in children using the CoaguChek S point-of-care monitor and a robust education program. *Thromb Res* 2006;**118**:587–93.

99 Young G. Current and future antithrombotic agents in children. *Expert Rev Cardiovasc Ther* 2004;**2**:523–34.

100 Ansell J. New anticoagulants and their potential impact on the treatment of thromboembolic disease. *Curr Hematol Rep* 2004;**3**:357–62.

101 Mahan CE, Fanikos, J. New antithrombotics: the impact on global health care. *Thromb Res* 2011;**127**:518–24.

13 Genetic Testing

Nitin Madan & Bruce D. Gelb

Mount Sinai School of Medicine, New York, NY, USA

Knowledge concerning the genetic basis of congenital heart defects (CHDs) has expanded rapidly over the past decade and genetic testing has become an increasingly common part of clinical care for patients with CHDs. Established genotype–phenotype associations rationalize the screening of other organ systems and provide important prognostic information about clinical outcomes. Genetic information can be used to identify reproductive risks in families and recommend testing for other at-risk family members.

A wide array of genetic tests is available to assist the clinician in diagnosing genetic alterations in children with CHDs. Genomic technological breakthroughs are making today's laboratory methods outdated faster than ever. To remain current with the latest advances in this rapidly evolving field, the reader is encouraged to visit web sites that are updated regularly, such as Online Mendelian Inheritance in Man (http://www.ncbi.nlm.nih.gov/omim/) and Gene-Tests (http://www.genetests.org/), resources supported by the National Library of Medicine and the National Institutes of Health [1].

The objective of this chapter is to discuss techniques currently available for genetic testing. These include chromosomal analysis, fluorescence *in situ* hybridization (FISH), array comparative genomic hybridization (CGH) or chromosomal microarray analysis and DNA sequencing (Table 13.1). Commoner disorders with CHDs that illustrate their use are highlighted.

Chromosome analysis

In the mid-1950s, Levan and Tjio established that the diploid human genome consisted of 46 chromosomes [2]. The development of improved culture and slide preparations and the subsequent introduction of chromosomal banding techniques in the 1970s facilitated the identification of each individual chromosome. It was soon established that chromosome aberrations are present in 8–13% of neonates with CHDs [3]. Among all children with chromosomal abnormalities, at least 30% are born with CHDs with rates that vary with the specific genetic defect, ranging from that observed in the general population to nearly 100% for certain forms of aneuploidy, such as trisomy 18 [4]. Therefore, chromosomal analysis is now routine in children with various types of CHDs, especially if they have a recognizable syndrome associated with chromosomal defects.

GTG banding with metaphase chromosomes based on application of trypsin followed by Giemsa staining is the most accepted method for routine clinical settings [5]. Higher resolution banding of longer pro-metaphase chromosomes [6] has increased the number of identifiable bands in a haploid genome to over 550 (providing a resolution of ~5–10 million nucleotides). This technique better defines structural chromosomal abnormalities such as duplications, inversions, translocations, and interstitial or terminal deletions. In most laboratories, the required time for standard karyotyping is 1–2 weeks and up to 3 weeks for high-resolution banding. Postnatal chromosomal analysis is most commonly performed on peripheral blood lymphocytes. A number of other sources can be exploited, including skin fibroblasts, bone marrow, cord blood, amniotic fluid, and chorionic villi, the last two being relevant for prenatal assessments. Prior blood product transfusions are unlikely to impede chromosome testing considering the small volume of transfusion in relation to the total blood volume of the patient, especially if leukoreduced and/or irradiated blood products have been used. Many clinicians will defer testing in newborns and young infants after cardiac surgery with cardiopulmonary bypass due to the relatively larger blood volume loss and replacement.

Table 13.1 Genetic tests for congenital heart defects (CHDs).

Genetic test	Indications	Limitations
Chromosome analysis	CHD in a child with syndromic features and multiple organ system involvement	Inadequate resolution for visualizing aberrations smaller than 5–10 Mb
FISH	Specific heart defects or features suspicious for microdeletion syndromes	Limited number of probes can be used in parallel, clinical presentation must suggest area of genome to be tested, time consuming, difficult to automate
aCGH	CHD+[a], research setting towards the identification of novel loci in patients with identical malformations	Inability to detect balanced chromosomal translocations and inversions, cost, establishing the pathogenicity of identified copy number variations
DNA sequencing	Presence of CHD, particularly syndromic, previously associated with point mutations, research setting towards the identification of novel mutations causing CHD	Cost, relatively slow turnaround times, uncertain interpretation for novel sequence variants particularly missense changes

[a]CHD+: CHDs in association with other malformations.

The rate of association of CHDs with chromosomal abnormalities is higher prenatally (22–26%) than postnatally [7,8]. The likelihood of detecting aneuploidy increases with certain heart defects (e.g., atrioventricular canal defects) and if extracardiac anomalies are found [8]. Hence prenatal chromosome testing is generally indicated after detecting a fetal cardiac malformation, excluding small muscular VSDs. Amniocentesis and chorionic villus sampling (CVS) are the primary methods used to obtain cells for prenatal chromosomal diagnosis. An amniocentesis for chromosome analysis at 15–24 weeks gestation is considered optimal with respect to cell growth rates and the success rates with cell culture. CVS involves the biopsy of chorionic villi from the placenta at 10–14 weeks gestation via a transabdominal or transcervical catheter. The major advantage of CVS over amniocentesis is the ability to obtain a result earlier in pregnancy. The major drawback, however, is the relatively increased incidence of maternal cell contamination, estimated at 1–2% for CVS compared with <0.5% for cultured amniotic fluid samples [9]. Karyotyping of amniocytes and chorionic villi yields diagnostic accuracy for trisomies and sex chromosome aneuploidy of >99%. More rapid analysis to identify common aneuploidies can be accomplished in 1–2 days using interphase fluorescence *in situ* hybridization (FISH) with uncultured amniocytes or chorionic villi.

Clinical applications

Chromosomal analysis identifies structural chromosomal abnormalities, such as duplications, inversions, translocations, and interstitial or terminal deletions. Chromosome aberrations such as trisomy 21 in Down syndrome, 45,X in Turner syndrome, 47,XXY in Klinefelter syndrome, trisomy 13, and trisomy 18 are readily recognized. For certain

chromosomal abnormalities such as an unbalanced translocation, the parents should be analyzed for balanced translocations that indicate high recurrence risks.

FISH

FISH tests use fluorophore-labeled nucleic acid probes to visualize specific DNA sequences on chromosomes in metaphase or interphase. An appropriately sized probe that hybridizes specifically with the intended genomic target is tagged either indirectly with nucleotides containing haptens or directly using nucleotides containing fluorophores. Then interphase or metaphase chromosomes from the patient are prepared and attached to a substrate, usually a glass slide, and. the labeled probe is hybridized to the chromosomal DNA and visualized using a fluorescent microscope (Figure 13.1).

Subtelomeric FISH

Telomeres are thymine- and guanine-rich repetitive DNA sequences at the end of chromosomes that protect against degradation and also end-to-end fusion of chromosomes [10]. Because the adjacent subtelomeric regions are exceptionally gene rich [11], deletions, duplications, and subtle translocations involving these regions often have important phenotypic effects. Detecting abnormalities in these regions has improved significantly with the development of FISH probes for the entire set of human telomeres [12]. Subtelomeric FISH has been investigated in children with non-specific mental retardation and a normal karyotype, and detected 2.5% with submicroscopic abnormalities [13]. Of note, 50% of those defects are inherited from parents
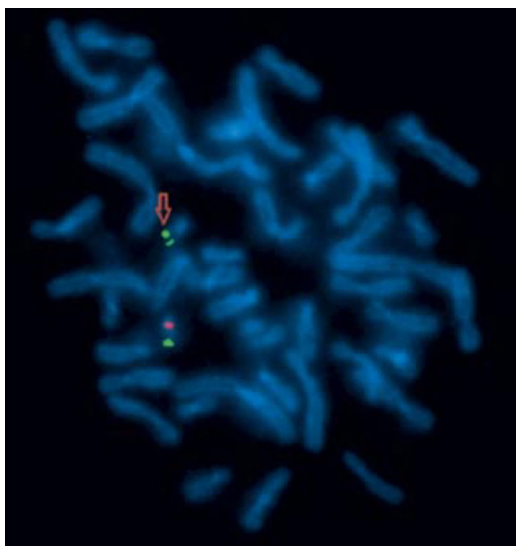
Figure 13.1 FISH for 22q11 deletion. A metaphase spread obtained from cultured chorionic villi is hybridized with *TUPLE1* from the 22q11 critical region (orange) and a control probe from elsewhere on chromosome 22 (green). Absence of orange signal on one copy of chromosome 22 (arrow) indicates a deletion causing DiGeorge or velocardiofacial syndrome.

who are carriers of a balanced translocation and, therefore, the recurrence risk in offspring is high .Children with mental retardation and CHD may have these chromosomal anomalies, but subtelomeric FISH has not been studied systematically in large cohorts of children with CHD *per se*. Array CGH is supplanting subtelomeric FISH as it detects these lesions plus others affecting other portions of chromosomes [14].

Multicolor FISH

This technique involves the simultaneous visualization of all chromosomes using different fluorophores. Routine application of such techniques to human chromosomes started in 1996 with the simultaneous use of 24 human whole chromosome painting probes in multiplex-FISH (M-FISH) [15] and spectral karyotyping (SKY) [16]. Multicolor FISH techniques are extremely useful for detecting the origin of marker chromosomes, translocations, and complex rearrangements, especially those identified in hematologic malignancies and solid tumors [17].

Clinical applications

FISH is a sensitive technique capable of detecting chromosomal abnormalities with resolution down to 1–10 kb [18,19], and is widely used clinically [20]. Increasing numbers of probes can specifically identify regions of chromosomes especially vulnerable to deletion and/or duplication. In particular, FISH testing is now commonly used to confirm many microdeletion syndromes associated with CHDs.

DiGeorge, velocardiofacial (Shprintzen), or conotruncal anomaly face syndromes (DGS/VCFS/CAFS) are clinically related syndromes with overlapping features including CHDs, the most common ones being tetralogy of Fallot, truncus arteriosus, interrupted aortic arch type B, conoventricular VSDs, and aortic arch anomalies. Cardiac involvement with DGS is seen in ≥90% of patients [21]. Deletions of 22q11 are identified using FISH testing in 88–90% of patients with DGS [22,23] and 76% of patients with VCFS [22]. The deletions constitute the second most common chromosomal cause of significant CHDs and occur in one in every 68 children born with CHDs [24,25]. Because of co-morbidities associated with these syndromes, FISH for 22q11 deletions is commonly performed for evaluating fetuses and patients with the forms of CHDs associated with them.

Most 22q11 deletions occur *de novo*, although ~6% of affected children have an undiagnosed parent who is often mildly affected. Therefore, FISH testing is frequently offered to parents of affected offspring, particularly if they possess any potentially related clinical features. Those with a deletion are counseled for a 50% recurrence risk in each successive pregnancy [25]. The high spontaneous deletion rate of this segment of the genome arises from the existence of flanking, nearly identical blocks of DNA sequences, called low-copy repeats or segmental duplications, that result in meiotic errors (non-allelic homologous recombination) [26]. With an apparently *de novo* deletion, there is a small increase in recurrence risk for siblings, resulting from rare occurrences of parental gonadal mosaicism.

Williams–Beuren syndrome (WBS) is a contiguous gene deletion syndrome characterized by distinctive clinical features corresponding to deletion of specific genes. Associated cardiovascular manifestations include supravalvar aortic stenosis (SVAS in ≤70% of patients), peripheral pulmonic stenosis, and hypertension.

In this disorder, submicroscopic deletions in the chromosomal band 7q11.23 extend across a region of 1.5 Mb and encode 26–28 genes [27]. Rarely, smaller or very large deletions in this region are associated with milder and severe clinical phenotypes, respectively [27,28]. Deletion of the elastin (*ELN*) gene at this locus is the primary cause of the cardiovascular pathology. This was established by the discovery that individuals with intragenic *ELN* deletions or *ELN* point mutations have familial SVAS syndrome, which shares the same cardiovascular involvement as WBS. FISH testing for WBS using an *ELN* probe detects deletions in 96% of WBS patients.

Most instances of WBS occur sporadically, but autosomal dominant transmission has been described occasionally [29]. The WBS critical region is flanked by low-copy repeats rendering the region vulnerable to non-allelic homologous recombination. Asymptomatic parents do not carry the deletion and their likelihood of having a subsequent child with

WBS is <1%, slightly higher than the general population due to the possibility of gonadal mosaicism [27].

Limitations

FISH testing is useful for identifying specific genomic defects, but only a limited number of probes can be applied simultaneously. Detecting abnormalities of regions beyond the subtelomeres requires specifying the most probable probe(s) to use for hybridization. As most lesions detected with FISH are *de novo*, recurrence risks for parents are near the population level, so the benefit is for the affected child, including counseling for reproductive risks.

Array Comparative Genomic Hybridization (aCGH)

aCGH overcomes these FISH limitations by interrogating the entire genome simultaneously for deletions or duplications without any prior bias as to the regions of interest. The method requires genomic DNA from the patient, usually from blood leukocytes postnatally and amniocytes or CVS cells prenatally (Figure 13.2). The patient's DNA and control DNA, generally from a pool of normal individuals, are labeled with different fluorophores [often cyanine 3 (cy3) and cyanine 5
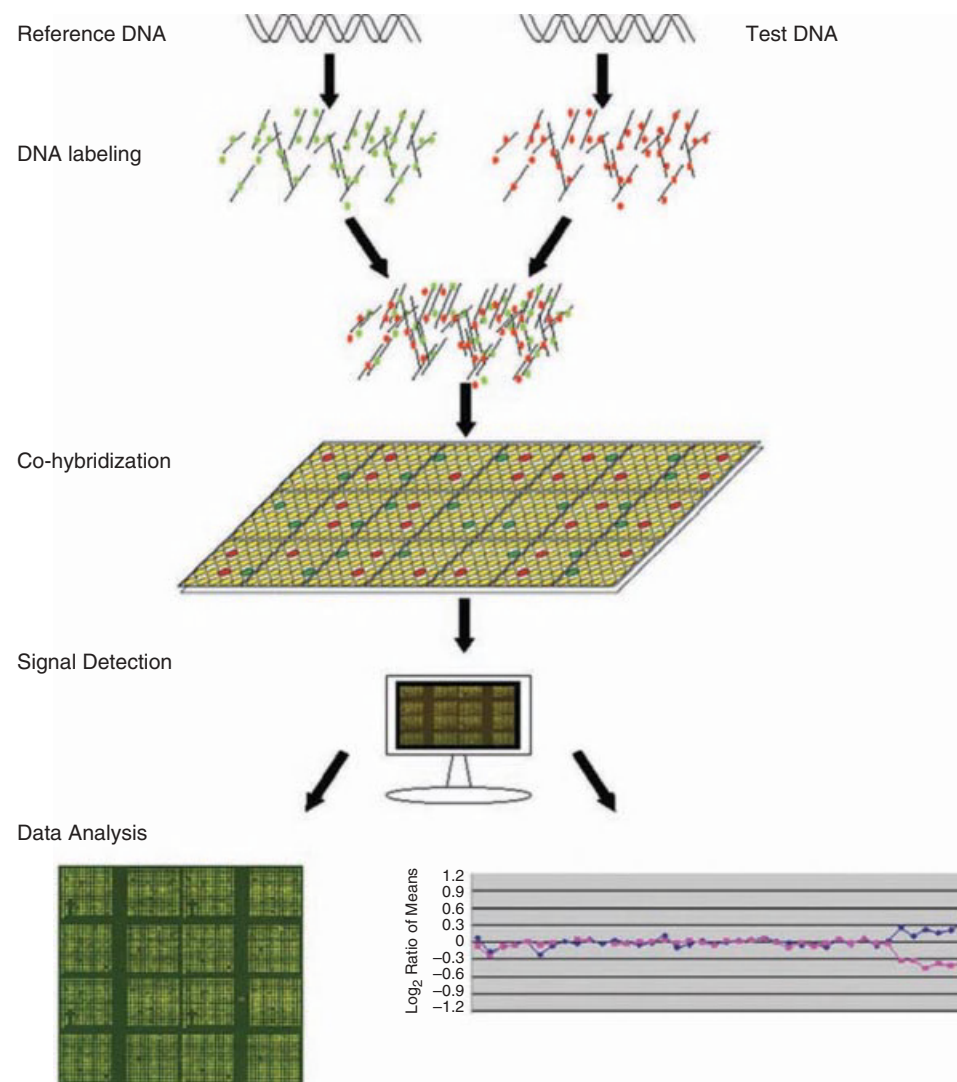
Figure 13.2 Array CGH. Genomic DNA from the patient (Test, red) and control (Reference, green) are labeled with different fluorescent colors and mixed in equal amounts. The mixture is hybridized to oligonucleotides (Target) that have been printed on to a glass slide. Computer imaging programs assess the relative fluorescence levels of each DNA for each target on the array (lower left). The ratio between control and test DNA for each clone is plotted linearly using data analysis software to visualize dosage variations, consistent with either a gain or loss of the genome (lower right), indicated by a deviation from the normal $\log_2$ ratio of zero. (Reproduced from Bejjani and Shaffer, *J Mol Diagn* 2006;**8**:528–33, with permission from the American Society for Investigative Pathology and the Association for Molecular Pathology.)

(cy5)]. The labeled DNAs are competitively hybridized to microarrays, on which oligonucleotides representing unique sequences spaced across the human genome are printed. After hybridization, the arrays are scanned to detect the fluorescence intensity at each oligonucleotide location and the cy3-to-cy5 ratio is established. Analysis then determines the genomic locations at which the cy3-to-cy5 ratios at consecutive oligonucleotides are skewed, consistent with either a gain or loss of the genome. The resolution of aCGH is determined by the number of oligonucleotides used. Current aCGH for clinical purposes relies on microarrays with 44 000–135 000 elements, providing resolution down to around 100 kb.

Applications

Clinically, aCGH detects aneuploidies, microdeletion/microduplication syndromes, and other unbalanced chromosomal rearrangements. Molecular karyotyping using aCGH also provides a platform for identifying new candidate disease genes. Examples are discussed below.

CHARGE syndrome has features that include ocular colobomata (C), heart defects (H), choanal atresia (A), retarded growth and/or anomalies of the central nervous system (R), genito-urinary defects and/ or hypogonadism (G), and ear anomalies and/or deafness (E). The estimated incidence of CHARGE syndrome ranges from 0.1 to 1.2 per 10 000 with CHDs reported in 75–80% of patients [30]. The cardiovascular malformations include tetralogy of Fallot, patent ductus arteriosus, septal defects, coarctation of the aorta, and complete and partial atrioventricular canal defects [31].

Identifying an overlapping microdeletion on chromosome 8q12 region in two affected individuals using aCGH [32] defined a critical region. Subsequently, DNA sequencing of positional candidate genes in other patients with CHARGE syndrome who were without apparent deletion led to the identification of point mutations in the chromodomain helicase DNA-binding gene (*CHD7*) as the primary cause of CHARGE syndrome. DNA sequence analysis can now reliably detect *CHD7* mutations in up to 75% of patients with the clinical diagnosis of CHARGE syndrome [30].

Congenital Heart Defects with other associated malformations

CHDs are commonly associated with dysmorphic facial features, developmental delay/mental retardation, and involvement of multiple other organ systems (sometimes called CHD+). When aCGH was performed in a cohort of children with CHD+ with normal karyotypes and no identifiable syndrome, putatively pathologic copy number variations (CNVs) were reported in 25% [33,34]. Some of these CNVs altered genes that had previously been implicated in causing CHDs.

Limitations of aCGH testing

Despite increasing use and excellent resolution, aCGH techniques are limited by their inability to identify balanced rearrangements such as translocations and inversions. In addition, genome-wide testing with aCGH uncovers numerous CNVs of unclear significance. Systematic studies have revealed large CNVs in apparently normal individuals, altering up to 12% of the human genome [35–37]. Their widespread presence can make the interpretation of clinical aCGH tests challenging. Most pathologic CNVs of interest clinically, however, are large (>500 kb), a size at which the number of benign CNVs in the general population is limited and most are robustly covered by survey studies.

A novel CNV in a patient with CHD does not necessarily indicate pathogenicity. Studying parental samples may help distinguish a pathogenic CNV from an inherited benign variation. Electronic resources that warehouse CNV data are important in establishing the clinical significance of submicroscopic aberrations detected by aCGH tests. Useful CNV databases include the Database of Genomic Variants (http://projects.tcag.ca/variation/), Children's Hospital of Philadelphia CNV (http://cnv.chop.edu/), and DECIPHER (https://decipher.sanger.ac.uk/application/).

DNA sequencing

Using DNA sequencing, the human genome sequence has been essentially decoded, identifying 20 000–25 000 genes and the regions controlling them. The Human Genome Project accomplished this using Sanger sequencing, still the primary method for sequencing-based mutation testing. Recently, new DNA sequencing techniques have been developed, which expand sequencing capacity, permitting the discovery of complex genetic traits including CHDs.

Sanger sequencing

Sanger sequencing, described in 1977, uses chain terminator nucleotides [38]. These dideoxynucleoside triphosphate (ddNTP) analogs of the normal deoxynucleoside triphosphates (dNTPs) lack a 3'-hydroxyl group, which is essential to the formation of an ester bond with an incoming nucleotide and resultant elongation of the DNA strand. In the sequencing process, fluorescently labeled ddNTP analogs of the four dNTPs (ATP, TTP, CTP, and GTP) are added to a medium containing a DNA template, a short primer, DNA polymerase enzyme, and the four dNTPs. The incorporation of a ddNTP in the elongating DNA strand results in its premature termination and formation of DNA fragments truncated to different lengths (Figure 13.3). The separation processes now use ultrathin gel and thin-walled capillary tubes, which lowers separation times by a factor of 25 relative to standard gels.

For most clinical applications, polymerase chain reaction (PCR) is used to amplify target sequences from genomic DNA prior to Sanger sequencing. Genes are comprised of variable numbers of protein-encoding exons, for example,
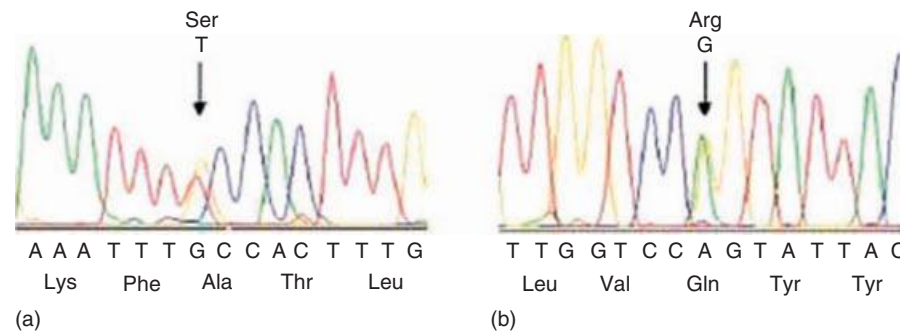
Figure 13.3 Sanger sequence analysis detecting point mutations. Shown are two examples of point mutations in exon 3 of the *PTPN11* gene causing Noonan syndrome. A G-to-T transversion (a) and an A-to-G transition (b) and the resulting changes in the amino acid sequences are indicated with arrows (note the double peaks). (Reproduced with permission from Pierpont ME, Basson CT, Benson DW Jr, *et al. Circulation*, 2007;**115**:3015–38.)

the *NKX2.5* gene has two exons whereas the *FBN1* gene has 65. DNA mutation testing of genes generally requires separate PCR and sequencing reactions for each exon with its flanking intron boundaries. Furthermore, this process is more extensive if a group of genes need to be tested, as occurs with genetically heterogeneous disorders such as Noonan and Alagille syndromes.

Clinical applications of Sanger sequencing-based techniques

Recent studies using familial linkage analysis and direct DNA sequencing identified several single-gene defects resulting in nonsyndromic CHDs. Mutations in *NKX2.5* have been identified in some familial and sporadic patients with atrial septal defects, especially associated with atrioventricular conduction abnormalities [39]. Transcription factor *GATA4* gene mutations were identified in two large families, one having multiple family members with atrial septal defects and the other with atrial septal defects, ventricular septal defects, and pulmonary valve stenosis [40].

Holt–Oram syndrome (HOS) is an autosomal dominant syndrome caused by mutations in the *TBX5* gene. Most patients have skeletal anomalies of the upper limb with preaxial radial ray malformation (e.g., triphalangeal, hypoplastic, or absent thumb and/or radial dysplasia) and 85–95% of patients have CHDs, most commonly ostium secundum atrial septal defects and muscular ventricular septal defects. Cardiac conduction disturbances ranging from asymptomatic first-degree heart block to complete heart block and sudden deaths are also important cardiovascular features [41]. Among patients who meet strict phenotypic criteria for HOS, mutation testing for *TBX5* gene reveals mutations in 54–74% of subjects [42,43]. Direct DNA sequencing of *TBX5* is available clinically.

Alagille syndrome (AGS) is an autosomal dominant disorder characterized by paucity of intrahepatic bile ducts, vertebral anomalies (butterfly vertebrae), ocular abnormalities (pigmentary retinal anomalies and anterior chamber defects,

particularly posterior embryotoxon), facial dysmorphism, renal anomalies, hematologic abnormalities (bleeding tendency), vascular anomalies, and CHDs. Cardiovascular involvement is observed in >90% patients with AGS, the most common pathology being pulmonary branch stenosis [44]. Other forms of CHD include tetralogy of Fallot, pulmonary valve stenosis, left-sided lesions, and septal defects. Point mutations in the *JAG1* gene and also large deletions or rearrangements of 20p12 which include *JAG1* have been demonstrated as pathogenic for this disorder. *JAG1* mutations can be identified in 94% of individuals with AGS [45]. Mutations in *NOTCH2* were reported in two of 11 *JAG1* mutation-negative probands [46]. *JAG1* mutations have been found in patients with a strong family history of isolated right-sided heart defects without other classic phenotypic features of AGS [47,48]. DNA sequencing of *JAG1* and *NOTCH2* is available clinically and *JAG1* FISH testing is needed to detect larger genomic events.

Limitations of Sanger sequencing techniques

Despite recent improvements, the throughput of Sanger sequencing is still limited. Read lengths of less than 1000 nucleotides are achieved in a single reaction and current sequencers can simultaneously process 30 lanes per run. The need to PCR amplify exons and their intron boundaries separately limits the number of assays that can be practically performed in parallel. Hence this approach is best for DNA mutation testing for one or two genes of modest size.

Microarray sequencing

The recent development of microarray sequencing techniques has allowed parallel sequencing, thereby immensely increasing throughputs and overcoming some of the limitations of Sanger sequencing. In clinical mutation testing, thousands of oligonucleotide probes (~18–20 nucleotides) are printed on the microarray chip followed by hybridization with the target DNA of interest prelabeled with a fluorescent

probe. The pattern of hybridization allows the target DNA sequence to be deciphered in a single analysis. Current microarray chips include more than 50 000 oligonucleotides on a 1.28 × 1.28 cm chip. The process is automated and many samples are run in parallel, generating large amounts of data rapidly.

Clinical application of microarray sequencing

Noonan syndrome (NS) is an autosomal dominant trait characterized by short stature, hypertelorism, ptosis, and CHDs. Some 80–90% of individuals with NS have valvar pulmonic stenosis and hypertrophic cardiomyopathy. Seven genes encoding proteins in the RAS signaling pathway (*PTPN11*, *KRAS*, *NRAS*, *SOS1*, *SHOC2*, *RAF1*, and *BRAF*) are causal in patients with this syndrome [49–51]. Moreover, a spectrum of disorders phenotypically related to NS, including LEOPARD, Costello, and cardiofaciocutaneous syndromes, also result from genetic alterations in this signaling pathway. In addition to mutations in some genes causing NS (*KRAS*, *BRAF)*, changes are observed in *HRAS*, *MEK1*, and *MEK2*. The proportions of these disorders accounted for by the currently known genes are variable. For instance, *HRAS* mutations are found in essentially all patients with Costello syndrome whereas the seven NS genes cover ~70% of instances of this disorder. RAS pathway mutation testing using a custom microarray chip design is available clinically. The test assesses the coding regions and splice sites of eight genes (*PTPN11*, *SOS1*, *RAF1*, *KRAS*, *BRAF*, *MEK1*, *MEK2*, and *HRAS*).

Limitations of microarray sequencing

For microarray sequencing, individual exons and their intron boundaries are still PCR amplified, limiting the number that can practically be assayed. This technique is also not robust for detecting small insertions and deletions, which is relevant for certain disorders, particularly those with loss of function.

Exome sequencing

The exome refers to the portion of the human genome formed by all of the exons that are translated into proteins and other purposeful gene products. The exome comprises 1% of the total human genome (30 million base pairs), but 85% of mutations with resultant disease-related traits occur in it. Hence exome sequencing is a potentially efficient strategy for identifying point mutations and CNVs and will drive genetic discovery of common birth defects, including CHDs.

The goal of exome sequencing required the development of two technological advances. First, generating the exon fragments for sequencing was not practical using PCR because it required nearly 200 000 separate reactions. Second, the sequencing capacity of the Sanger sequencing-based machines required impractically long periods of time

to complete this task. These problems have been overcome by the development of DNA sequence capture methods and so-called next-generation sequencing.

1 In targeted DNA sequence capture, specific DNA sequences are enriched from a larger pool of sequences by physically separating DNA fragments containing the target sequences from those that are not of interest. The process begins with oligonucleotide-based exome capture from a pool of sheared human genome. Currently available technologies use microarray chips or in-solution methods for hybridization and selection. This step of fishing through the genome requires a modest-sized sample (<10 μg) and provides an exome-specific catch of 90%. The captured DNA, to which short universal primer sequences are ligated on their ends, can be amplified simultaneously in a single PCR reaction and subsequently sequenced *en masse*. The same technology can be applied in a customized fashion for other genomic subsets (e.g., all genes known to cause CHDs).

2 Next-generation sequencing refers to novel approaches to achieve dramatically higher sequencing capacity. Currently available next-generation sequencers use various approaches to amplify DNA sequences clonally (emulsion PCR, solid-phase amplification) and then sequence the amplified clones (cyclic reversible termination, sequencing by ligation), which are then imaged with lasers. Additional approaches that avoid clonal amplification (i.e., use single-molecule templates) are approaching the market as this chapter is being written. The interested reader should consult one of the excellent reviews of this topic [52,53].

Current next-generation sequencers provide 60 million paired-end reads of 75 bp per lane, providing roughly 4.5 Gb of sequence in 9 days per machine. Using one lane per human exome results in a mean 40× coverage per base, 90% of targeted bases are read 10 or more times and 80% are read 20 or more times. These read depths are necessary in order to assure that both alleles are sequenced and to overcome the substantially higher read error rate of next-generation sequencing compared with Sanger sequencing. Recent studies using exome sequencing have demonstrated the speed, cost-effectiveness, sensitivity, and specificity of this method [54,55]. Discoveries of new gene mutations underlying human Mendelian disorders using exome sequencing have recently been published and larger numbers will emerge rapidly in the coming years.

Conclusions

In summary, cytogenetics is rapidly moving into the direction of molecular approaches and DNA sequencing capacity is dramatically increasing. These developments have improved diagnostic services as well as provided unprecedented research opportunities. The clinical indications for genetic testing for fetuses and patients with CHDs have

expanded dramatically, a trend that will continue in the years ahead. New genetic tests utilizing next-generation sequencing are likely to enter the clinical setting soon. Finally, affordable sequencing of the entire human genome appears within reach. Awareness of the wide array of genetic tests, including their utility and limitations, will assist providers caring for patients with CHDs.

References

1 Pierpont ME, Basson CT, Benson DW Jr, *et al.* Genetic basis for congenital heart defects: current knowledge: a scientific statement from the American Heart Association Congenital Cardiac Defects Committee, Council on Cardiovascular Disease in the Young: endorsed by the American Academy of Pediatrics. *Circulation* 2007;**115**:3015–38.

2 Arnason U. 50 years after – examination of some circumstances around the establishment of the correct chromosome number of man. *Hereditas* 2006;**143**:202–11.

3 Ferencz C, Neill CA, Boughman JA, *et al.* Congenital cardiovascular malformations associated with chromosome abnormalities: an epidemiologic study. *J Pediatr* 1989;**114**:79–86.

4 Goc B, Walencka Z, Wloch A, *et al.* Trisomy 18 in neonates: prenatal diagnosis, clinical features, therapeutic dilemmas and outcome. *J Appl Genet* 2006;**47**:165–70.

5 Seabright M. A rapid banding technique for human chromosomes. *Lancet* 1971;**2**:971–2.

6 Yunis JJ. Mid-prophase human chromosomes. The attainment of 2000 bands. *Hum Genet* 1981;**56**:293–8.

7 Paladini D, Russo M, Teodoro A, *et al.* Prenatal diagnosis of congenital heart disease in the Naples area during the years 1994–1999 – the experience of a joint fetal–pediatric cardiology unit. *Prenat Diagn* 2002;**22**:545–52.

8 Chaoui R, Korner H, Bommer C, *et al.* Prenatal diagnosis of heart defects and associated chromosomal aberrations. *Ultraschall Med* 1999;**20**:177–84.

9 Randolph LM. Prenatal cytogenetics. In: Gersen SL, Keagle MB, eds. *The Principles of Clinical Cytogenetics*, 2nd edn. Totowa, NJ: Humana Press, 2005: 267–321.

10 Knight SJ, Flint J. Perfect endings: a review of subtelomeric probes and their use in clinical diagnosis. *J Med Genet* 2000;**37**:401–9.

11 Saccone S, De Sario A, Della Valle G, Bernardi G. The highest gene concentrations in the human genome are in telomeric bands of metaphase chromosomes. *Proc Natl Acad Sci USA* 1992;**89**:4913–7.

12 National Institutes of Health and Institute of Molecular Medicine. A complete set of human telomeric probes and their clinical application. National Institutes of Health and Institute of Molecular Medicine collaboration. *Nat Genet* 1996;**14**:86–9.

13 Ravnan JB, Tepperberg JH, Papenhausen P, *et al.* Subtelomere FISH analysis of 11 688 cases: an evaluation of the frequency and pattern of subtelomere rearrangements in individuals with developmental disabilities. *J Med Genet* 2006;**43**:478–89.

14 Ballif BC, Sulpizio SG, Lloyd RM, *et al.* The clinical utility of enhanced subtelomeric coverage in array CGH. *Am J Med Genet A* 2007;**143**A:1850–7.

15 Speicher MR, Gwyn Ballard S, Ward DC. Karyotyping human chromosomes by combinatorial multi-fluor FISH. *Nat Genet* 1996;**12**:368–75.

16 Schrock E, du Manoir S, Veldman T, *et al.* Multicolor spectral karyotyping of human chromosomes. *Science* 1996;**273**:494–7.

17 Jalal SM, Law ME. Utility of multicolor fluorescent *in situ* hybridization in clinical cytogenetics. *Genet Med* 1999;**1**:181–6.

18 Trask BJ. Human cytogenetics: 46 chromosomes, 46 years and counting. *Nat Rev Genet* 2002;**3**:769–78.

19 Korenberg JR, Chen XN, Adams MD, Venter JC. Toward a cDNA map of the human genome. *Genomics* 1995;**29**:364–70.

20 Volpi EV, Bridger JM. FISH glossary: an overview of the fluorescence *in situ* hybridization technique. *BioTechniques* 2008;**45**: 385–409.

21 Van Mierop LH, Kutsche LM. Cardiovascular anomalies in DiGeorge syndrome and importance of neural crest as a possible pathogenetic factor. *Am J Cardiol* 1986;**58**:133–37.

22 Wilson DI, Cross IE, Goodship JA, *et al.* A prospective cytogenetic study of 36 cases of DiGeorge syndrome. *Am J Hum Genet* 1992; **51**:957–63.

23 Greenberg F. DiGeorge syndrome: an historical review of clinical and cytogenetic features. *J Med Genet* 1993;**30**:803–6.

24 Goodship J, Cross I, LiLing J, Wren C. A population study of chromosome 22q11 deletions in infancy. *Arch Dis Child* 1998;**79**:348–51.

25 McDonald-McGinn DM, Zackai EH. Genetic counseling for the 22q11.2 deletion. *Dev Disabil Res Rev* 2008;**14**:69–74.

26 Edelmann L, Pandita RK, Morrow BE. Low-copy repeats mediate the common 3-Mb deletion in patients with velo-cardio-facial syndrome. *Am J Hum Genet* 1999 ;**64**:1076–86.

27 Pober BR. Williams–Beuren syndrome. *N Engl J Med* 2010;**362**:239–52.

28 Marshall CR, Young EJ, Pani AM, *et al.* Infantile spasms is associated with deletion of the MAGI2 gene on chromosome 7q11.23-q21.11. *Am J Hum Genet* 2008;**83**:106–11.

29 Sadler LS, Robinson LK, Verdaasdonk KR, Gingell R. The Williams syndrome: evidence for possible autosomal dominant inheritance. *Am J Med Genet* 1993;**47**:468–70.

30 Blake KD, Prasad C. CHARGE syndrome. *Orphanet J Rare Dis* 2006;**1**:34.

31 Lalani SR, Safiullah AM, Fernbach SD, *et al.* Spectrum of CHD7 mutations in 110 individuals with CHARGE syndrome and genotype-phenotype correlation. *Am J Hum Genet* 2006;**78**:303–14.

32 Vissers LE, van Ravenswaaij CM, Admiraal R, *et al.* Mutations in a new member of the chromodomain gene family cause CHARGE syndrome. *Nat Genet* 2004;**36**:955–7.

33 Thienpont B, Mertens L, de Ravel T, *et al.* Submicroscopic chromosomal imbalances detected by array-CGH are a frequent cause of congenital heart defects in selected patients. *Eur Heart J* 2007;**28**:2778–84.

34 Richards AA, Santos LJ, Nichols HA, *et al.* Cryptic chromosomal abnormalities identified in children with congenital heart disease. *Pediatr Res* 2008;**64**:358–63.

35 Iafrate AJ, Feuk L, Rivera MN, *et al.* Detection of large-scale variation in the human genome. *Nat Genet* 2004;**36**:949–51.

36 Sharp AJ, Locke DP, McGrath SD, *et al.* Segmental duplications and copy-number variation in the human genome. *Am J Hum Genet* 2005;77:78–88.

37 Redon R, Ishikawa S, Fitch KR, *et al.* Global variation in copy number in the human genome. *Nature* 2006;**444**:444–54.

38 Sanger F, Nicklen S, Coulson AR. DNA sequencing with chain-terminating inhibitors. 1977. *Biotechnology* 1992;**24**:104–8.

39 Sarkozy A, Conti E, Neri C, *et al.* Spectrum of atrial septal defects associated with mutations of NKX2.5 and GATA4 transcription factors. *J Med Genet* 2005;**42**:e16.

40 Garg V, Kathiriya IS, Barnes R, *et al.* GATA4 mutations cause human congenital heart defects and reveal an interaction with TBX5. *Nature* 2003;**424**:443–7.

41 Huang T. Current advances in Holt–Oram syndrome. *Curr Opin Pediatr* 2002;**14**:691–5.

42 McDermott DA, Bressan MC, He J, *et al.* TBX5 genetic testing validates strict clinical criteria for Holt–Oram syndrome. *Pediatr Res* 2005;**58**:981–6.

43 Debeer P, Race V, Gewillig M, *et al.* Novel TBX5 mutations in patients with Holt–Oram syndrome. *Clin Orthop Relat Res* 2007;**462**:20–6.

44 McElhinney DB, Krantz ID, Bason L, *et al.* Analysis of cardiovascular phenotype and genotype–phenotype correlation in individuals with a JAG1 mutation and/or Alagille syndrome. *Circulation* 2002;**106**:2567–74.

45 Warthen DM, Moore EC, Kamath BM, *et al.* Jagged1 (JAG1) mutations in Alagille syndrome: increasing the mutation detection rate. *Hum Mutat* 2006;**27**:436–43.

46 McDaniell R, Warthen DM, Sanchez-Lara PA, *et al.* NOTCH2 mutations cause Alagille syndrome, a heterogeneous disorder of the notch signaling pathway. *Am J Hum Genet* 2006;**79**:169–73.

47 Krantz ID, Smith R, Colliton RP, *et al.* Jagged1 mutations in patients ascertained with isolated congenital heart defects. *Am J Med Genet* 1999;**84**:56–60.

48 Eldadah ZA, Hamosh A, Biery NJ, *et al.* Familial tetralogy of Fallot caused by mutation in the jagged1 gene. *Hum Mol Genet* 2001;**10**:163–9.

49 Tartaglia M, Mehler EL, Goldberg R, *et al.* Mutations in PTPN11, encoding the protein tyrosine phosphatase SHP-2, cause Noonan syndrome. *Nat Genet* 2001;**29**:465–8.

50 Schubbert S, Zenker M, Rowe SL, *et al.* Germline KRAS mutations cause Noonan syndrome. *Nat Genet* 2006;**38**:331–6.

51 Roberts AE, Araki T, Swanson KD, *et al.* Germline gain-of-function mutations in SOS1 cause Noonan syndrome. *Nat Genet* 2007;**39**:70–4.

52 Metzker ML. Sequencing technologies – the next generation. *Nat Rev Genet* 2010;**11**:31–46.

53 Voelkerding KV, Dames SA, Durtschi JD. Next-generation sequencing: from basic research to diagnostics. *Clin Chem* 2009;**55**:641–58.

54 Ng SB, Turner EH, Robertson PD, *et al.* Targeted capture and massively parallel sequencing of 12 human exomes. *Nature* 2009;**461**:272–6.

55 Choi M, Scholl UI, Ji W, *et al.* Genetic diagnosis by whole exome capture and massively parallel DNA sequencing. *Proc Natl Acad Sci USA* 2009;**106**:19096–101.

14

Practices in Congenital Cardiac Surgery: Pulmonary Artery Banding, Systemic to Pulmonary Artery Shunting, Cardiopulmonary Bypass, and Mechanical Ventricular Assist Devices

James D. St. Louis & Roosevelt Bryant III
University of Minnesota, Amplatz Children's Hospital, Minneapolis, MN, USA

Introduction

This chapter has two sections. The first deals with cardiac operations that are not specific to a particular condition but are used to palliate anomalies with hemodynamic abnormalities of pulmonary blood flow. The second focuses on issues related to cardiopulmonary bypass and the principles and techniques of ventricular assist devices,

In the section on cardiac operations, pulmonary artery banding and aortopulmonary shunts are discussed because they are applied to a variety of cardiac malformations with increased or decreased pulmonary blood flow, respectively. The general principles are discussed here and specific applications to individual lesions are presented in the respective chapters. The Glenn and Fontan operations are also used for various conditions but are discussed in Chapters 35 and 39.

Pulmonary artery band

A pulmonary artery band (PAB) is a constrictor placed around a pulmonary artery:

1 It can decrease excessive pulmonary blood flow and pulmonary arterial pressure in patients with a large left-to-right shunt, thereby ameliorating congestive heart failure and decreasing the risk of pulmonary vascular disease. The main pulmonary artery is almost always used except for banding separately the left and right pulmonary arteries in the hybrid treatment of the hypoplastic left heart syndrome.

    a. Most patients who require biventricular repair today can have it performed as a single stage in early infancy, but at one time banding was performed as a palliative first stage [1–4], with complete correction delayed until the patient was large enough. A PAB is still needed for a few patients whose correction must be deferred because of the specific lesions, for example, multiple muscular ventricular septal defects, or because of co-morbidity such as intracranial hemorrhage, sepsis, or necrotizing enterocolitis.

    b. Patients who will eventually have a single ventricle repair must be protected against any increase in pulmonary vascular resistance that would jeopardize their outcomes [5,6]. In some patients with tricuspid atresia or double inlet left ventricle, subaortic stenosis may develop after PAB and a Damus-Kaye-Stansel procedure needs to be performed [7–9].

2 Patients who are to have an arterial switch for D-transposition or congenitally corrected transposition of the great arteries but have a low-pressure, thin-walled left ventricle must have the left ventricle conditioned by raising its pressure with a PAB placed on the main pulmonary artery [10,11]. An aortopulmonary shunt is often added to prevent severe systemic hypoxemia [12].

The band is a tape made from one of a number of materials. It is difficult to gauge the degree of constriction needed because the main pulmonary artery is narrowed by the intimal folds, which adds to the obstruction in an unpredictable way. Decisions are often based on body size or changes in systemic blood pressure or oxygen saturation. Intraoperative Doppler measurement has been used to assess the degree of constriction.

Despite its uses, a PAB has many complications. Because it is usually used in very small infants, a band ideal at the time of placement becomes too small as the child grows, and may

need to be revised. Some surgeons have used bands tied with clips or sutures in such a way that the band that becomes too tight can be dilated by a balloon. Others have used a variety of bands that can be adjusted after implantation, so that the band can be tightened or loosened as required.

PABs frequently distort and scar the main pulmonary artery, and may migrate distally and obstruct a branch pulmonary artery (usually the right). They have eroded through the arterial wall so that the constriction is abolished. Occasionally there may be formation of a pseudoaneurysm or a periarterial abscess, infective endarteritis at the site of the band, or thrombosis of the main pulmonary artery. There may be thickening of the pulmonary valve leaflets, and in some patients severe infundibular hypertrophy occurs. Scarring may make debanding difficult.

A few attempts have been made to insert flow restrictors into the branch pulmonary arteries by catheter.

Systemic to pulmonary shunt

Providing an alternative source of pulmonary blood flow by a palliative procedure has been practiced for the past five decades. As with the pulmonary artery band, the systemic to pulmonary artery anastomosis has been largely supplanted by the belief that early definitive repair of complex lesions is now regarded as better than an initial palliative and a secondary corrective procedure [13], although this has been questioned [14].

The first clinical application of the systemic to pulmonary shunt was accomplished by Alfred Blalock and Helen Taussig in 1944 when they anastomosed a subclavian artery to the ipsilateral pulmonary artery [15]. This operation is usually done on the side opposite the aortic arch to avoid kinking, and the subclavian artery is tied off to avoid a vascular steal. There were sometimes deleterious effects on the affected arm due to ischemia. Furthermore, although the shunts were seldom too large, their effect was impossible to predict [16,17]. Interestingly, the development of pulmonary vascular changes was slow [17]. Therefore, although many children benefited from this procedure, alternative approaches were sought.

Other operative techniques were developed to address these issues. One modification was Pott's procedure, in which an opening was made between the descending aorta where it crossed behind the left pulmonary artery. Although improving oxygenation, pulmonary vascular disease often developed, the left pulmonary artery could be distorted, and if the patient was ultimately to have eventually a corrective operation through a sternotomy it was difficult to take down this anastomosis. Another procedure was the Cooley–Waterston shunt, in which a communication was made between the aorta and the right pulmonary artery where it passes behind the ascending aorta. Unfortunately, the

openings were either too small and the patient did not get sufficient relief or too large and the patient could develop heart failure and ultimately pulmonary vascular disease [18]. Also, blood flow could be predominantly to one lung, which then developed pulmonary vascular disease while the other pulmonary artery could become stenotic or hypoplastic. Both procedures had a moderate mortality rate. Their importance, apart from historic interest, is that some older adult patients currently seen in ACHD clinics had these procedures during childhood and may manifest their long-term complications.

Almost all of these procedures have now been replaced by the modified Blalock–Taussig shunt. Through a lateral or posterolateral thoracotomy, the surgeon places a short segment of PTFE (usually 3.4–4 mm in diameter) between the subclavian artery and the ipsilateral pulmonary artery. This anastomosis can be performed with a partial occlusion clamp and a continuous monofilament suture. Placement on the side of the aortic arch is technically easier to construct, but more difficult to take down during the next staged procedure. Although flow through this shunt is controlled by the size of the subclavian artery, the length and diameter of the prosthetic material add an additional resistance to the blood flow. Tubes with diameters of 3–6 mm are available, but those <4 mm have a higher risk of thrombosis (see Chapter 12). The advantages of the modified BT shunt include less deformation of hypoplastic pulmonary arteries, less mediastinal dissection, preservation of arterial circulation to the upper extremity, and consistent shunt flow regardless of anatomic distance between the aorta and the pulmonary arteries.

Complications include those of any thoracotomy: pericardial or pleural effusions, chylothorax, sepsis, and occasionally Horner syndrome or phrenic palsy. In addition, there can be stenosis at the anastomotic site, true or false aneurysms (sometimes years after the operation), infective endarteritis, or thrombosis of the shunt. PTFE tubes are porous and sometimes cause seromas, a collection of peritubular fluid that may sometimes compress mediastinal structures.

Cardiopulmonary bypass

Extracorporeal mechanical support in infants and children has undergone a dramatic evolution in the past five decades that has allowed both the correction of intracardiac defects in small infants and the support of the failing myocardium for extended periods of time.

The first half of the twentieth century was marred by failure to support completely the circulatory system to the extent required to have timely and accurate repair of intracardiac defects. The materials utilized to construct these early devices were the same as those that were used in various

industries. Progress was also hampered by the inability to prevent blood from coagulating on contact with an artificial surface. With the introduction of heparin and protamine, the problem of safely anticoagulating a patient and then being able quickly to reverse these effects, coagulation became less of an issue. The greatest barrier was inability to oxygenate blood and dissipate carbon dioxide during the time that the patient's heart and lungs were not functioning.

In 1952, while working in Philadelphia, John Gibbon supported the circulation of a dog while performing an extended operative intervention within the heart. The machine that he used was a heavy stainless-steel device weighing >90 kg. Blood was pumped by three crude roller heads. The oxygenator was an enclosed battery of stainless-steel screens, each 40 cm tall and 25 cm wide. Blood flowed over each side of the six screens while being exposed to oxygen. This provided a surface area of 8 m² to expose blood to oxygen. The monitoring and safety systems were very sophisticated for the period, with the ability to monitor constantly the volume and pH of the blood. In February 1952, Gibbon applied his technology to repair an atrial septal defect in a 15-month-old child. The chest was opened via a right thoracotomy, the child was placed on the machine, and the heart was opened. Unfortunately, the diagnosis was incorrect, the child rapidly deteriorated, and postmortem examination revealed a large patent ductus arteriosus. A second attempt was made in an 18-year-old college student with repeated episodes of heart failure. A cardiac catheterization confirmed an atrial septal defect. On 6 May 1953, the complete closure of this atrial level defect was achieved utilizing the heart–lung machine. The patient was on the bypass machine for 45 min and awoke within 1 h following the procedure [19]. This successful closure of an intracardiac defect marked the beginning of the surgical treatment of both acquired and congenital cardiac disease.

The cardiopulmonary bypass circuit

Although the structure of the modern cardiopulmonary bypass machines varies significantly from the early Gibbon oxygenator, the basic design is very similar. Deoxygenated blood is removed from the circulation through a cannula usually placed in the right atrial appendage or occasionally the individual venae cavae. Blood is withdrawn either passively or under vacuum assistance to a venous reservoir. The blood level in the reservoir is closely monitored and can be manipulated as desired. This blood is pumped to a membrane oxygenator that incorporates a heat exchanger, which allows the patient to be cooled and subsequently warmed at the procedure's conclusion. The oxygen-enriched blood from the oxygenator is returned to the patient through a cannula in the distal ascending aorta. A hemofilter is often placed in the circuit to ultrafilter the blood either during or at the conclusion of the operation. The liquid in the cardiopulmonary bypass circuit prior to initiating extracorporeal

support is referred to as bypass prime. Important issues about specific components of the bypass circuit and the volume utilized will be reviewed.

In a 2 kg neonate whose total blood volume may be as low as 170 ml, the prime volume at the initiation of cardiopulmonary bypass may exceed the patient's blood volume by >200%. This results in dramatic hemodilution and an abrupt fall in the circulating hemoglobin concentration. What constitutes the lowest acceptable circuiting hemoglobin during support remains debatable. Generally, the hematocrit concentration is maintained at >25% regardless of the lowest temperature used during support [20]. Some maintain a higher hematocrit, up to 35% based on improved long-term neurological outcomes [21,22]. Banked packed red blood cells are usually used to maintain an appropriate hematocrit level in the prime solution. Packed red cells, especially if a few days old [23], have higher levels of lactate and potassium. Therefore, they may contribute to and worsen inflammatory response and increase hemodynamic instability upon initiation of cardiopulmonary bypass. Some institutions wash all packed red cells before adding them to the prime solution and only use red cells <5 days from donation [24]. Fresh whole blood used in the prime solution maintains colloid oncotic pressure and increases the level of circulating clotting factors[25]. Using transfused fresh whole blood following bypass has the advantage of maintaining more appropriate hemostasis, although the current literature does not completely support this idea [26]. Fresh whole blood has a higher glucose content in the prime solution, and hyperglycemia may be a risk factor for increased neurologic injury following bypass. Systems that harvest and maintain stores of fresh whole blood are expensive and logistically difficult to maintain. Using packed red cells to achieve the desired hematocrit level by the addition of fresh frozen plasma (FFP) optimizes appropriate coagulation in the presence of the hemodilution upon initiation of CPB. In one study, the addition of FFP to the prime solution significantly limited dilutional hypofibrinogenemia, decreased the need for cryoprecipitate after bypass, and decreased patient exposure to blood products [27].

Additional components of the prime solution include variable levels of electrolytes, buffers, calcium, glucose, and lactate. Calcium levels are generally maintained at a sub-physiologic level to prevent deleterious myocardial effects of ionized calcium during periods of arrest. More controversial additives include mannitol and steroids. Steroids may reduce the inflammatory response to cardiopulmonary bypass, but recent studies have questioned this common practice [28].

Ultrafiltration is an important process that removes both water and solutes during and after cardiopulmonary bypass. Conventional ultrafiltration (CUF) during the rewarming period of cardiopulmonary bypass uses a filter connected in parallel and allows the continual removal of excess fluid from the circuit [29]. Modified ultrafiltration (MUF)

is a similar process instituted at the conclusion of cardiopulmonary bypass with the circuit connected in series, for greater efficiency of filtration and increased concentration of red cells [30]. The major drawback of CUF is that the volume of fluid removed is limited by the circuit volume, because the volume in the venous reservoir must be sufficient to maintain adequate arterial blood flow. An advantage of MUF is that greater volumes can be removed from the bypass circuit.

The evolution of our ability to support infants and neonates has improved significantly the success with repair of congenital cardiac lesions. In-hospital mortality for repair of most congenital lesions is <2%. With these achievements, a significant emphasis has shifted to the long-term neurologic sequel and outcomes. The incidence of significant neurologic injury has been reported to be between 10 and 25% [31–34]. The occurrence of minor long-term neurodevelopmental deficits is likely to be even higher. These issues are discussed in detail in Chapter 52.

Myocardial protection

The ability of a surgeon to repair accurately and effectively even the most complex intracardiac lesions has been significantly enhanced by protecting myocardial tissue during periods of controlled cardiac arrest. The neonatal myocardium is immature, both structurally and metabolically. It differs significantly from the mature adult myocardium, particularly in its response to myocardial arrest and acute ischemia. Myofibrils are organized more randomly and sarcomeres are incomplete. T tubules and the sarcoplasmic reticulum are rudimentary, so that the neonatal myocardium is exquisitely sensitive to extracellular calcium levels, often depending on serum calcium to maintain adequate function. There are fewer mitochondria and these lack well-developed cristae. These structural differences lead to reduced oxidative capacity [35]. These differences from adults become less pronounced as a child matures.

The fetal and early immature cardiac metabolism depends on the consumption and breakdown of carbohydrates [36]. This is in sharp contrast to adult myocardium, which depends on free fatty acid oxidation. This ability to utilize energy stores anaerobically allows the immature myocardium to tolerate ischemia and recover myocardial function following a brief periods without coronary blood flow.

The ability to achieve an excellent result often depends on a motionless heart. Although techniques vary, electromechanical arrest is achieved by utilizing a potassium-based cardioplegia solution. While maintaining a clear operative field, continued myocardial protection is achieved by intermittent dosing of maintenance cardioplegia solution [37].

Cardioplegia is administered in two dosing regimens. An induction dose of 30 ml kg^{-1} is used to achieve rapid electromechanical arrest while at the same time reversing any metabolic anomalies that may have occurred within the myocardium. Cardioplegia solution is generally perfused anterograde under a strictly controlled pressure >120 mmHg [38]. The initial arrest can be achieved rapidly and consistently with a potassium dose of 15–30 mequiv per liter of solution. A potassium concentration >30 mequiv l^{-1} should never be used as it injures the myocardium. Decompressing the immature heart is critical during the initial arrest, as coronary perfusion pressure is indirectly related to intraventricular pressure, with a relaxed, empty heart having the greatest coronary perfusion. Once the initial delivery of cardioplegia solution is complete and the myocardium relaxed, subsequent dosing of maintenance cardioplegia is provided either anterograde or retrograde via the coronary sinus. Blood at a 1:4 blood:crystalloid volume ratio is often added to the cardioplegia solution to increase its buffering capacity.

Preventing ischemia depends on safe maintenance of electromechanical arrest. The accumulation of injurious byproducts of hypoxia has a dramatic effect on postoperative myocardial function and must be avoided by providing a periodic oxygen supply by intermittent administration of cardioplegia with a potassium concentration of 15 mequiv l^{-1} every 20–25 min during the arrest period. Also critical to myocardial protection is reducing myocardial energy demands by lowering the temperature of the heart by a combination of systemic and local hypothermia, maintaining the electromechanical arrested state of the myocardium, and keeping blood flow to the myocardium from noncoronary sources to a minimum. Although hypothermia has been considered to have the greatest effect on the reduction in oxygen demand, a great reduction comes from maintained cardiac arrest and preventing ventricular distension [39].

There is evidence that postoperative myocardial damage is due more to reperfusion injury caused by free radicals than to ischemia *per se* [40,41], so that myocardial protection is a function of not only of how the heart is arrested, but also how it is reperfused and restarted.

Left heart bypass

The incidence of paraplegia associated with operations on the aortic arch and proximal descending aorta has been reported to be 0.2–0.4% in children [42]. The occurrence of this devastating complication may result from several factors: age, degree of aortic obstruction, lack of collateral arteries, number of previous operations on the aorta, and duration of operative interruption of distal perfusion. Each factor can contribute to the development of spinal cord ischemia [43]. The use of partial cardiac bypass during blood flow interruption to the spinal cord theoretically protects against irreversible spinal cord ischemia [44]. Because the incidence of ischemia and the resultant paraplegia is extremely low and the number of patients who would require these techniques is small, it is unlikely that an unbiased, randomized clinical study will be accomplished. Therefore, the use of partial cardiac bypass has been based on retrospective and

small case studies [44]. "Partial cardiac heart bypass" during the repair of aortic arch anomalies represents a method to bypass the area of surgical repair while maintaining distal perfusion.

The procedure is often performed through a posterior-lateral thoracotomy with the side depending on the position of the aortic arch The technique is accomplished by removing oxygenated blood from the left atrium, either through the appendage or left upper pulmonary vein, augmenting perfusion pressure with a simple bio-centrifugal pump, and perfusing it into the distal aorta. At the time of cannulation, the patient is systemically anticoagulated with 50–100 U kg^{-1} of heparin. Depending on the patient's size, the outflow end of the circuit is placed into either the distal descending thoracic aorta or the femoral artery via a separate incision. The circuit is then meticulously de-aired as there is often no inline mechanism to capture air. The pump is started and distal flow and pressure are measured appropriately. During the procedure, it is critical to realize that pulmonary support must be given by a ventilator and cerebral blood flow maintained as it would be without the adjunct use of this bypass circuit. Once the cross clamp period is finished and the repair completed, the circuit is removed. Usually, it is unnecessary to reverse the heparin effects with protamine as the duration and degree of anticoagulation are usually minimal.

The considerations for use of this technique include the patient's age, degree of aortic obstruction, and the maturity of the collateral vessels. In general, newborns with a ductus arteriosus supplying the distal systemic circulation will not require bypass support during the aortic cross clamp period. An older child with a mild gradient across a coarctation and an insufficient collateral bed often needs perfusion to the distal aorta during cross clamping. Although specific data about minimal perfusion pressure are lacking, a mean arterial blood pressure of <40 mmHg during a test clamp is usually considered an indication for augmenting distal perfusion [45].

Mechanical ventricular assistance in the failing heart

Extracorporeal membrane oxygenator (ECMO)

ECMO has been used for ~25 years to treat a variety of conditions in children, but predominately in newborns. The general application of ECMO is for conditions that are believed to resolve either naturally or by surgery or other interventions. Realistically, a patient can be maintained for >2 weeks, and occasionally even longer. However, it is a temporary management option and if longer support is required the patient is often switched to a "Berlin" heart.

Its major use has been to support neonates with respiratory failure from meconium aspiration, persistent fetal circulation, diaphragmatic hernia, hyaline membrane disease, and cardiovascular conditions such as refractory septic shock or congenial heart disease, often postoperatively for severe cardiovascular instability. Neonates must weigh >2 kg and have a gestational age >35 weeks. From the Extracorporeal Life Support Organization (ELSO) Registry Report 2004, of 29 000 patients reported to date, ~19 000 were for neonatal respiratory diseases [46]. The survival rate for neonates with pulmonary problems is ~80%, whereas in neonates with congenital heart disease it is ~40%, but one report had a 64% survival following Norwood stage I procedure [47]. For congenital heart disease, the rate of ECMO usage has remained constant at 200 per year for the decade preceding 2005 [46]. ECMO is being used more often after the Norwood stage I procedure (28%) in one series [48].

For infants and children, ECMO is used for rapid resuscitation for respiratory arrest, postoperative support for cardiac lesions, support for failing myocardium, such as from myocarditis or acute ischemia, and for patients awaiting transplantation. A study of 279 children with a cardiac anomaly found an overall survival of 42% [49]. Pre-ECMO predictors of death included single ventricle physiology, history of a Norwood stage I operation, and significant acidosis, and major complications of ECMO were associated with death [49].

ECMO requires medical, nursing, and technical staff dedicated almost exclusively to the patient. The equipment is large and complex, being the size of a pump–oxygenator. Cannulae are placed in the right carotid artery and jugular vein and blood is circulated through a membrane oxygenator. The patient, sedated and on a ventilator, is constantly monitored, especially for mixed venous oxygen level and coagulation. The major complications are infections, bleeding, and renal insufficiency. Intracranial hemorrhage is the most devastating and one reason besides size that neonates under 35 weeks' gestation do not receive ECMO, because of cerebral vascular immaturity.

Neonates who have undergone ECMO management may have significant long-term respiratory and neurologic morbidity. The pre-ECMO mortality risk and prematurity were important factors. The post-ECMO abnormalities usually do not progress after ~3 years [50]. In infants and children there is a high readmission rate, 62% in one study, These were for respiratory problems in 41% and neurologically significant causes in another 21% (the latter being epilepsy or developmental delay).

For a comprehensive review of ECMO see Pearson GA, Firmin RK, 1995 [51].

Mechanical ventricular assistance is a reliable modality as a bridge to cardiac transplantation in children with heart failure. The recent introduction into the United States of the Berlin Heart EXCOR Pediatric Ventricular Assist Device has extended our ability to support neonates, infants, and young children. Of >600 EXCOR devices placed world-wide, 270 have been in the United States. The Berlin Heart EXCOR is an extracorporeal ventricular assist device (VAD) initially used to support mechanically adult patients with heart

failure [52]. The experience with EXCOR as a bridge to cardiac transplantation or as destination therapy in adult patients with heart failure led to modifications specific for children. The EXCOR system has three primary components, and it can be implanted in either a left ventricular or biventricular configuration. The components are a *blood pump*, *cannulae* for connecting the device to the great vessels and cardiac chambers, and a *pneumatic drive unit*. The *blood pump* is made of transparent polyurethane. It has two polyurethane trileaflet valves, which allow unidirectional blood flow into and out of the pump. A pneumatic compressor-operated diaphragm separates the blood chamber from an air chamber. Multiple pump sizes allow for different body weights in pediatrics. For instance, a 10 ml pump can support infants weighing <9 kg or with a body surface area of 0.43 m², and a 25 ml pump can support patients weighing <30 kg or with a body surface area of 0.95 m² [53]. Because the device is transparent, it can be evaluated daily for clot formation. The extracorporeal position of the pump allows straightforward exchange under conscious sedation should the need arise. Silicone cannulae are designed with several internal diameters (4, 6, 9 mm) for children. A layer of Dacron velour covers the mid-portion of the cannulae. The velour bridges the skin exit site and allows for rapid tissue in-growth, preventing an ascending infection. For a left ventricular configuration (LVAD), two cannulation sites are used. Usually, the left ventricular apex is cannulated for inflow to the pump, but the left atrium is an alternative site [54]. Left ventricular apical cannulation results in lower left ventricular end-diastolic pressure (LVEDP) and consequently lowers the right ventricular afterload by 15–25 mmHg [55]. The ascending aorta is cannulated for pump outflow. For a right ventricular configuration (RVAD), the right atrium is cannulated for inflow to the device, and the main pulmonary artery is cannulated for outflow. A biventricular configuration (BVAD) involves the use of both an LVAD and RVAD. The EXCOR ventricular assist device has an electropneumatic driving unit called IKUS that uses compressed air to move the diaphragm separating the blood and air chambers. This movement provides pulsatile blood flow. A positive driving pressure of >350 mmHg can be used to compress the diaphragm to end-systole, allowing ejection of blood from the device. A negative driving pressure up to −100 mmHg is used to expand the diaphragm to end-diastole, allowing the device to fill. The high driving pressures are necessary because of the small cannula sizes [56]. The driver can function in either a left ventricular mode or a biventricular mode. The system can also function in an asynchronous mode that allows separate rates for the RVAD and LVAD when biventricular support is necessary. This asynchronous mode allows the rate of the RVAD to be less than that of the LVAD with a smaller stroke volume (blood pump) to prevent pulmonary edema. Finally, all blood-contacting surfaces are heparin coated [57].

The first successful report of a left ventricular assist device (a centrifugal flow device) was for 12 h as a bridge to cardiac transplantation in a child [58], and another report also described the use of an adult EXCOR device (50 ml blood pump) as a bridge to cardiac transplantation in an 8-year-old [59]. The disadvantages of using an adult EXCOR device in children quickly became apparent and modifications were made, including a range of blood pump and cannula sizes to meet the sizes of infants and young children.

The indications for implanting EXCOR in infants and children include progressive heart failure refractory to medical therapy, cardiac index <2.0 l min⁻¹ m⁻², development of metabolic acidosis, and signs of end organ dysfunction, such as renal insufficiency or elevation of liver enzymes. Other indications are the need for mechanical ventilation or a mixed venous oxygen saturation <40%. In many children, the goal of implantation is to provide the recipient time for end organ recovery to make the patient a better transplant candidate.

The major use of the Berlin Heart EXCOR ventricular assist device has been as a bridge to cardiac transplantation, although other uses have been for end-stage congenital heart disease, post-cardiotomy heart failure and myocarditis. In a 15 year experience with pediatric EXCOR systems, 68 patients <18 years of age were supported for a mean duration of 35 days [60]. Thirty-one (45%) received cardiac transplantation. Eleven other patients (16%) recovered. Thirty-seven (54%) of the patients were discharged home. Only four patients had neurologic injury [60]. In the largest American experience at a single center with the EXCOR pediatric ventricular assist system[61], 17 patients <18 years of age received either an LVAD (*n* = 13] or BVAD (*n* = 4). Eleven patients were transplanted, one recovered, one remained on support, and four died. When the EXCOR system was compared with extracorporeal membrane oxygenation (ECMO) as a bridge to cardiac transplantation, the survival to transplant and recovery was significantly higher in the EXCOR group (86%) than the ECMO group (57%). Despite this excellent result, 40% of the patients sustained neurologic injury [62]. A series of nine patients, each with right ventricular dysfunction, with biventricular support (BVAD) ultimately received a transplant [63]. The mean duration of support was 31 days and eight patients (89%) survived to transplant without acute neurologic injury, thromboembolic events, or hemolysis. All patients in this series had significantly elevated (>90%) panel reactive antibodies and 12 pump exchanges were performed because of fibrin deposits or clot formation in the device. Other series [64,65] reported small sets of patients in whom neurologic injury occurred and device exchanges were needed.

The EXCOR system has also been used for fulminant myocarditis [65] either to bridge the child to transplantation or until recovery from the disease. Because it may take months for the myocardium to recover in patients with fulminant myocarditis, the EXCOR system provides an

excellent means for long-term mechanical support [66]. Among its advantages are the ability to extubate the patient, give physical therapy, including ambulation, and feed the patient. Feeding enhances the integrity of the gastrointestinal tract mucosa, preventing bacterial translocation and decreasing the risk for infection.

The EXCOR system has been used in patients with hypoplastic left heart syndrome after a BDG and Fontan with mixed results [67]. Its versatility makes it ideal for children because it can be tailored to the size and needs of the patient. The Berlin Heart EXCOR ventricular assist device has become a widely accepted form of mechanical circulatory support for children in Europe and the United States. Questions remain regarding the ideal anticoagulation strategy and the neurologic outcomes. The Berlin Heart EXCOR ventricular assist use of partial cardiac bypass support during aortic arch-related surgical procedures has filled a void for the increasing number of pediatric patients with end-stage heart disease.

References

1 Ebert PA, Turley K, Stanger P, *et al*. Surgical treatment of truncus arteriosus in the first six months of life. *Ann Surg* 1984; **200**:451–6.

2 Gunthar T, Mazzitalli D, Haehnel J, *et al*. Long-term results after repair of complete atrioventricular septal defects: analysis of risk factors. *Ann Thorac Surg* 1998;**65**:754–60.

3 Pizarro C, Norwood W. Pulmonary artery banding before the Norwood procedure. *Ann Thorac Surg* 2003;**75**:1008–10.

4 Kanter K, Mahle W, Kogen B, Kirshbom P. What is the optimal management of infants with coarctation and ventricular septal defect? *Ann Thorac Surg* 2007;**84**:612–8.

5 Galantowicz M, Cheatham J, Phillips A, *et al*. Hybrid approach for hypoplastic left heart syndrome: intermediate results after the learning curve. *Ann Thorac Surg* 2008;**85**:2063–70.

6 Calderone C, Benson L, Hotby H, *et al*. Initial experience with hybrid palliation for neonates with single ventricle physiology. *Ann Thorac Surg* 2007;**84**:1294–300.

7 Sittiwangkul R, Azakiw A, Van Arsdell GV, *et al*. Outcomes of tricuspid atresia in the Fontan era. *Ann Thorac Surg* 2004; **77**:889–94.

8 Donofrio M, Jacobs M, Norwood W, *et al*. Early changes in ventricular septal defect and ventricular geometry in the single ventricle after volume-unloading surgery. *J Am Coll Cardiol* 1995; **26**:1008–15.

9 Chang Y, Lee J, Hwang S. Pulmonary artery banding before Damus–Kaye–Stansel procedure. *Pediatr Cardiol* 2006;**27**:594–9.

10 Wernovsky G, Mayer J, Jonas R, *et al*. Factors influencing early and late outcomes of the arterial switch operation for transposition of the great arteries. *J Thorac Cardiovasc Surg* 1995;**109**:289–302.

11 Gayet-Lacour F, Piot D, Zoghbi J, *et al*. Surgical management and indication of the left ventricular retraining in arterial switch for transposition of the great arteries with intact ventricular septum. *Eur J Cardiothorac Surg* 2001;**20**:824–9.

12 Jonas R, Giglia T, Sanders S, *et al*. Rapid two-stage arterial switch for transposition of the great arteries and intact ventricular septum beyond the neonatal period. *Circulation* 1989;**80** (Suppl 1):203–8.

13 Nollert G, Fischlein T, Bouterwek S, *et al*. Long term survival in patients with tetralogy of Fallot: 36 year follow-up of 490 survivors of the first year after surgical repair. *J Am Coll Cardiol* 1997;**30**:1374–83.

14 Fraser C, McKenzie D, Cooley D. Tetralogy of Fallot: surgical management individualized to the patient. *Ann Thorac Surg* 2001; **71**:1556–63.

15 Blalock A, Tausig HB. The surgical treatment of malformation of the heart in which there is pulmonary stenosis or pulmonary atresia. *JAMA* 1945;**128**:189–202.

16 Currarino G, Engle M. The effects of ligation of the subclavian artery on the bones and soft tissue of the arm. *J Pediatr* 1965; **67**:808–12.

17 Holfschire PJ, Rosenquist GC, Ruckermann RN, *et al*. Pulmonary vascular disease complicating the Blalock–Taussig anastomosis. *Circulation* 1977;**56**:124–6.

18 Norberg WJ, Tadavarthy M, Knight L, *et al*. Late hemodynamic and angiographic findings after ascending aorta-pulmonary anastomosis. *J Thorac Cardiovasc Surg* 1978;**76**:345–52.

19 Gibbon JH Jr. Application of a mechanical heart and lung apparatus to cardiac surgery. *Minnesota Med* 1954;**37**:171–85

20 Jaggers J, Underleider RM. Cardiopulmonary bypass in infants and children. In: Mavroudis C, Backer CL, eds. *Pediatric Cardiac Surgery*, 3rd edn. Philadelphia, PA: Mosby, 2003: 171–193.

21 Duebener LF, Sakamoto T, Hatsuoka S, *et al*. Effects of hematocrit on cerebral microcirculation and tissue oxygenation during deep hypothermic bypass. *Circulation* 2001;**104**(Suppl);1260–4.

22 duPlessis AJ. Higher hematocrit improves cerebral outcome after deep hypothermic circulatory arrest. *J Thorac Cardiovasc Surg* 1996;**112**:1610–21.

23 Koch CG, Li L, Sessler DI, *et al*. Duration of red-cell storage and complications after cardiac surgery. *N Engl J Med* 2008;**358**: 1229–39.

24 Dai B, Wang L, Djaiani G, *et al*. Continuous and discontinuous cell-washing autotranfusion systems. *J Cardiothorac Vasc Anesthes* 2004;**18**:210–7.

25 Gruenwald C, McCrindle B, Crawford-Lean L, *et al*. Reconstituted fresh whole blood improves clinical outcomes compared with stored component blood therapy for neonates undergoing cardiopulmonary bypass for cardiac surgery: a randomized controlled trial. *J Thorac Cardiovasc Surg* 2008;**136**:1442–9.

26 Mou S, Giroir B, Molitor-Kirch E. Fresh whole blood versus reconstituted blood for pump priming in heart surgery in infants. *Circulation* 2004;**351**:1635–44.

27 McCall M, Blackwell M, Smyre J, *et al*. Fresh frozen plasma in the pediatric pump prime: a prospective, randomized trial. *Ann Thorac Surg* 2004;**77**:983–7.

28 Pasquali S, Hall M, Li J, *et al*. Corticosteroids and outcome in children undergoing congenital heart surgery: analysis of the pediatric health information systems database. *Circulation* 2010;**122**:2123–30.

29 Huang H, Yao T, Wang W, *et al*. Continuous ultrafiltration attenuates the pulmonary injury that follows open heart surgery with cardiopulmonary bypass. *Ann Thorac Surg* 2003;**76**:136–40.

30 Bando K, Turrentine M, Vijay P, *et al*. Effect of modified ultrafiltration in high-risk patients undergoing operations for congenital heart disease. *Ann Thorac Surg* 1998;**66**:821–8.

31 Hovels-Gurich H, Konrad K, Shorzenski D, *et al*. Long-term neurodevelopment and exercise capacity after corrective surgery for tetralogy of Fallot or ventricular septal defect in infancy. *Ann Thorac Surg* 2006;**81**:958–67.

32 Hovels-Gurich, Konrad K, Skorzenski D, *et al*. Attentional dysfunction in children after corrective cardiac surgery in infancy. *Ann Thorac Surg* 2007;**83**:1425–30.

33 Mahle WT, Wernovsky G. Long-term developmental outcome of children with complex congenital heart disease. *Clin Perinatol* 2001;**28**:235–47.

34 Newburger J. Neurologic and developmental morbidity in children with complex congenital heart disease. *J Pediatr* 2003; **142**:6–8.

35 Achterberg PW, Nieukoop AS, Schoutsen B, De Jong JW. Different ATP-catabolism in reperfused adult and newborn rat hearts. *Am J Physiol* 1988:**254**:H1091–8.

36 Ascuitto RJ, Ross-Ascuitto NT, Chen V, Downing SE. Ventricular function and fatty acid metabolism in neonatal piglet heart. *Am J Physiol* 1989;**256**:H9–15.

37 Bull C, Copper J, Stark J. Cardioplegic protection of the child's heart. *J Thorac Cardiovasc Surg* 1984;**88**:287–93.

38 Baker JE, Boerboom LE, Olinger GN. Age-related changes in the myocardial protection of the isolated rabbit heart. *Surg Forum* 1986;**37**:293–5.

39 Athanasuleas CL, Buckberg GD. Myocardial protection. In: Kaiser LR, Kron IL Spray TL, eds. *Mastery of Cardiothoracic Surgery*. Philadelphia, PA: Lippincott, Williams & Wilkins, 2007: 315–25.

40 Buckberg GD. Studies of hypoxemic/reoxygenation injury: I. Linkage between cardiac function and oxidant damage. *J Thorac Cardiovasc Surg* 1995;**110**(4 Pt 2):1164–70.

41 Del Nido PJ, Mickle DA, Wilson GJ, *et al*. Evidence of myocardial free radical injury during elective repair of tetralogy of Fallot. *Circulation* 1987;**76**(5 Pt 2):V174–9.

42 Palatianos GM, Kaiser GA, Thurer RJ, Garcia O. Changing trends in the surgical treatment of coarctation of the aorta. *Ann Thorac Surg* 1985;**40**:41–5.

43 Keen G. Spinal cord damage and operations for coarctation of the aorta: etiology, practices, and prospective. *Thorax* 1987;**42**:11–8.

44 Pennington DG, Liberthson RR, Jacobs M, *et al*. Critical review of experience with coarctation of the aorta. *J Thorac Cardiovasc Surg* 1979;**77**:217–29.

45 Backer C, Stewart R, Kelle A, Mavroudis C. Use of partial cardiopulmonary bypass for coarctation repair through a left thoracotomy in children without collaterals. *Ann Thorac Surg* 2006;**82**:964–72.

46 Conrad SA, Rycus PT, Dalton N. Extracorporeal Life Support Registry Report 2004. *ASAIO J* 2005;**51**:1–10.

47 Darling EM, Kaemmer D, Lawson DS, *et al*. Use of ECMO without the oxygenator to provide ventricular support after Norwood stage I procedure. *Ann Thorac Surg* 2001;**71**:735–6.

48 Duncan BW. Mechanical circulatory support for infants and children with cardiac disease. *Ann Thorac Surg* 2002;**73**:1670–7.

49 Chan T, Thiagrajan RR, Frank D, Bratton SL. Survival after extracorporeal cardiopulmonary resuscitation in infants and children with heart disease. *J Thorac Cardiovasc Surg* 2008;**136**:984–92.

50 Jen HG, Shew SB. Hospital readmissions and survival after neonatal pediatric ECMO. *Pediatrics* 2010;**125**:1217–23.

51 Pearson GA, Firmin RK. Extracorporeal membrane oxygenation in children. In: Unger F, ed. *Assisted Circulation 4*. Berlin: Springer, 1995:310–35.

52 Jurmann MJ, Weng Y, Drews T, *et al*. Permanent mechanical circulatory support in patients of advanced age. *Eur J Cardiothorac Surg* 2004;**25**:610–8.

53 Hetzer R, Stiller B. Technology insight: use of ventricular assist devices in children. *Nat Clin Pract Cardiovasc Med* 2006;**3**:377–86.

54 Merkle F, *et al*. Pulsatile mechanical cardiac assistance in pediatric patients with the Berlin Heart ventricular assist device. *J Extra Corpor Technol* 2003;**35**:115–20.

55 Stiller B, Weng Y, Hubler M, *et al*. Pneumatic pulsatile ventricular assist devices in children under 1 year of age. *Eur J Cardiothorac Surg* 2005;**28**:234–9.

56 Hetzer R, Loebe M, Potapov E, *et al*. Circulatory support with pneumatic paracorporeal ventricular assist device in infants and children. *Ann Thorac Surg* 1998;**66**:1498–506.

57 Frazier O. Use of left ventricular assist device as a bridge to transplantation in a pediatric patient. *Texas Heart J* 1989;**16**:46–50.

58 Warnecke H, Berdjis F, Henning E. Mechanical left ventricular support as a bridge to cardiac transplantation in childhood. *Eur J Cardiothorac Surg* 1991;**5**:330–3.

59 Hetzer R, Potapov EV, Stiller B, *et al*. Improvement in survival after mechanical circulatory support with pneumatic pulsatile ventricular assist devices in pediatric patients. *Ann Thorac Surg* 2006;**82**:917–25.

60 Hetzer R, Meskishvili V, Wen Y, *et al*. Mechanical cardiac support in the young with the Berlin Heart EXCOR pulsatile ventricular assist device:15 years' experience. *Semin Thorac Cardiovasc Surg Pediatr Card Surg Annu* 2006;**9**:99–110.

61 Rockett SR, Bryant JC, Morrow WR, *et al*. Preliminary single center North American experience with the Berlin Heart Pediatric EXCOR device. *ASAIO J* 2008;**54**:479–82.

62 Imamura M, Dossey AM, Prodhan P, *et al*. Bridge to cardiac transplant in children: Berlin Heart versus extracorporeal membrane oxygenation. *Ann Thorac Surg* 2009;**87**:1894–901.

63 Gandhi SK, Huddleston CB, Balzer DT, *et al*. Biventricular assist devices as a bridge to heart transplantation in small children. *Circulation* 2008;**118**(Suppl 1):S89–93.

64 Malaisrie SC, Pelletier MP, Yun JJ, *et al*. Pneumatic ventricular assist devices in infants and children: initial Stanford experience. *J Heart Lung Transplant* 2008;**27**:173–7.

65 Stiller B, Dahnert I, Weng YG, *et al*. Children may survive severe myocarditis with prolonged use of biventricular assist devices. *Heart* 1999;**82**:237–40.

66 Jones CB, Cassidy JV, Kirk RC, *et al*. Successful bridge to recovery with 120 days of mechanical support in an infant with myocarditis. *J Heart Lung Transplant* 2009;**28**:202–5.

67 Irving CA, Cassidy JV, Kirk RC, *et al*. Successful bridge to transplant with the Berlin Heart after cavopulmonary shunt. *J Heart Lung Transplant* 2009;**28**:399–401.

15 Postoperative Problems

John M. Costello[1], Satish K. Rajagopal[2] & Thomas J. Kulik[2]

[1]Feinberg School of Medicine, Northwestern University, and Children's Memorial Hospital, Chicago, IL, USA
[2]Children's Hospital Boston and Harvard Medical School, Boston, MA, USA

This chapter covers a number of developmental abnormalities and acquired problems of the gastrointestinal and renal systems that may afflict the perioperative pediatric cardiac patient. In a few patients, therapy for these conditions needs to consider the cardiovascular status of the patient, and this is covered here.

Gastrointestinal complications

Gastrointestinal complications are associated with the gastrointestinal tract and organs supplied by the celiac, superior mesenteric, and inferior mesenteric arteries. These include the esophagus, stomach, small intestine, colon, liver, gallbladder, spleen, and pancreas. An extensive list of proposed definitions for potential gastrointestinal complications occurring following pediatric cardiac surgery has been published [1]. Although serious gastrointestinal complications following pediatric cardiac operations are relatively uncommon, precise estimates of occurrence rates are limited because of the lack of standardized nomenclature and reporting, difficulties in identifying temporal associations with operation and the assignment of causality in complex patients. Children recovering from heart transplantation are an exception, since a variety of serious early and late gastrointestinal complications, including pancreatitis, cholecystitis, recurrent abdominal infections, intestinal pneumatosis, and abdominal malignancies occur in 18% of patients [2]. This section focuses on selected gastrointestinal complications linked to congenital heart disease and its treatment. These complications include necrotizing enterocolitis (NEC), malrotation and midgut volvulus, abdominal compartment syndrome, and inability to eat.

Necrotizing Enterocolitis (NEC)

NEC is a neonatal disease in which the intestinal mucosal barrier is compromised, leading to inflammation and bacterial translocation, and sometimes to mucosal or transmural necrosis and sepsis (see also Chapter 18). The pathogenesis of NEC is multifactorial and incompletely understood. General risk factors include hypoxic–ischemic injury to the gastrointestinal tract, physiological immaturity of the gastrointestinal tract, and alterations of the normal microbiological flora of the intestines [3]. With systemic hypoperfusion in a neonate, reduced mesenteric perfusion occurs as blood is shunted preferentially to the heart and brain and away from the splanchnic circulation. Reperfusion may promote inflammation and exacerbate intestinal injury. In premature patients, compromised integrity of epithelial tight junctions and deficient intestinal IgA production may be contributory. Impaired peristalsis may facilitate bacterial overgrowth and increase the contact time between bacterial antigens and enterocytes. Finally, alteration of the normal bacterial colonization of the intestines, perpetuated by exposure to broad-spectrum antibiotics or rapid increases in volume of feedings, may predispose patients to developing NEC.

Given these physiologic considerations, it is not surprising that 90% of NEC affects premature neonates. Neonates with a complex cardiac malformation have at least a 10-fold greater risk of developing NEC than neonates without congenital heart disease [4]. The rate of NEC in neonates with critical congenital heart disease is approximately 3%, and is higher in prematures [4–6]. Neonates with a cardiac lesion with significant diastolic runoff through a ductus arteriosus or a surgically created systemic to pulmonary shunt, such as in hypoplastic left heart syndrome, are also at increased risk

[4,7]. NEC may occur before or after cardiac intervention, and mucosal ischemia and inflammation related to cardiopulmonary bypass may be contributory [8]. Preventive measures to reduce the occurrence of NEC include administering antenatal maternal corticosteroids for threatened preterm delivery and feeding with breast milk [3].

The common signs and symptoms of NEC, along with laboratory and radiographic findings, have been used to assign stages of NEC based on the modified Bell's criteria [3] (see Chapter 18, Table 18.3). Higher stages of disease have a greater risk of mortality. Potential secondary complications of NEC include short gut syndrome, stricture formation, problems related to the use of parenteral nutrition (e.g., catheter-associated bloodstream infection, cholestasis, and liver failure), prolonged hospitalization, and worse neurodevelopmental outcomes [4,9]. In addition to close monitoring and supportive care, treatment for NEC includes bowel rest and antibiotic therapy directed at aerobic and anaerobic organisms. Surgical intervention, either peritoneal drainage or laparotomy, is generally reserved for patients with intestinal perforation (Bell's stage III-B) or clinical deterioration despite maximum medical therapy [10,11]. Mortality directly attributable to NEC in neonates with congenital heart disease is approximately 10% [4,7,12].

Abdominal compartment syndrome

Abdominal compartment syndrome (ACS) may be defined as a sustained increase in intra-abdominal pressure (>17–20 mmHg in children) associated with dysfunction or failure of an organ not previously involved [13]. In children recovering from a cardiac operation, ACS often results from a combination of factors: ascites, postoperative ileus, and visceral edema from elevated central venous pressure and renal insufficiency. Intra-abdominal pressure can be measured directly via an intraperitoneal catheter or indirectly via the bladder (intravesical). Palpation of a tense abdomen may be all that is needed to make the diagnosis. Increased intra-abdominal pressure may contribute to further deterioration of cardiac, respiratory, renal, and hepatic function. Elevation of the diaphragm reduces lung compliance, which requires higher ventilator settings, exacerbates lung injury, and causes pulmonary hypertension and other adverse cardiopulmonary interactions. Renal dysfunction may be caused by direct compression of renal vessels and be exacerbated by low cardiac output. Similar hemodynamic changes may lead to hepatic dysfunction.

Management of ACS involves serial measurement or estimation of intra-abdominal pressure, maintaining adequate end-organ perfusion, and, for refractory patients, percutaneous or surgical decompression. Elevating the head of the bed and prone positioning increase intra-abdominal pressure and should be avoided. Patients with evolving ACS should be kept flat and supine. Meticulous management of fluid overload with diuretics or dialysis, and nasogastric and colonic decompression may help. Inserting a percutaneous catheter to drain ascites, air, or other fluid collections may decrease intra-abdominal pressure and remarkably increase urine output. We have observed marked improvement in ACS in some patients who had reached a critical intra-abdominal pressure threshold that was alleviated by drainage of a minimal amount of ascitic fluid. Similarly, we have observed rapid improvement in ACS following the onset of venoarterial extracorporeal membrane oxygenation (ECMO) in children recovering from a complex cardiac operation, presumably from improved cardiac output and systemic venous decompression.

Malrotation and midgut volvulus

In addition to complex cardiac malformations, children with heterotaxia syndrome often have gastrointestinal abnormalities, the most prominent being abnormalities of intestinal fixation. Early in gestation, the midgut rotates around the axis of the superior mesenteric artery such that the proximal jejunum is anchored by the ligament of Treitz to the retroperitoneum in the left upper quadrant and the cecum is anchored to the retroperitoneum in the right lower quadrant. The resultant broad-based small bowel mesentery is at minimal risk for volvulus. In patients with malrotation, there is either no rotation or reverse rotation of the midgut loop, such that the proximal jejunum and cecum are both affixed close to each other in the upper abdomen, on either the right or left. The resultant narrow-based small bowel mesentery is thereby predisposed to volvulus and potentially fatal necrosis of the entire midgut [14].

Malrotation is usually diagnosed with an upper gastrointestinal contrast study, by which the distance between the ligament of Treitz and ileocecal junction is estimated. When diagnostic uncertainty persists, a contrast enema may be useful to locate the displaced cecum [15]. The symptoms most commonly develop in the neonatal period, and 90% of patients present within the first year of life. Evaluation and treatment must be undertaken urgently in patients with signs and symptoms suggestive of midgut volvulus (e.g., bilious emesis). Definitive treatment involves an open or laparoscopic Ladd procedure, in which the malrotation is reduced, abnormally positioned bands are released, and the bowel is repositioned.

Screening all patients with heterotaxia syndrome for malrotation and performing an elective operation to prevent midgut volvulus are controversial. Volvulus occurs in only 1–7% of patients with malrotation, and between the two extremes of normal rotation and malrotation is a spectrum of rotational abnormalities, some of which may not predispose to the development of volvulus. Therefore, the potential for false-positive radiologic diagnosis, the complexity of the associated cardiac anomalies, and the risk of developing adhesions leading to bowel obstruction (up to 15%) must be considered when contemplating an elective operation. Many physicians do not screen asymptomatic heterotaxia patients for malrotation, and follow them conservatively when malrotation is diagnosed incidentally

[14,16]. Others suggest that all patients with heterotaxia syndrome be evaluated for malrotation, and that a Ladd procedure be performed in those with malrotation regardless of the presence or absence of symptoms [17].

Inability to eat

The inability to ingest adequate liquid and caloric intake is common following cardiac surgery in neonates and infants. In one prospective study, new-onset dysphagia was diagnosed by a speech pathologist in 18% of children recovering from a cardiac operation [18]. Contributing factors include innate poor suck–swallow coordination (e.g., prematurity, DiGeorge syndrome), anomalies of the oropharynx or airway (e.g., cleft lip or palate), use of transesophageal echocardiogram, prolonged intubation, gastroesophageal reflux, and central nervous system injury [18,19]. Vocal cord dysfunction associated with dysphagia contributes to aspiration risk. Vocal cord dysfunction may be caused by congenital laryngotracheal anomalies, prolonged intubation, and central nervous system anomalies. In cardiac surgery patients, however, the most likely etiology is recurrent laryngeal nerve injury in neonates following ductus arteriosus surgery or aortic arch reconstruction. It also may follow cervical ECMO cannulation.

Evaluating dysphagia may include assessment by a speech pathologist, videofluoroscopic swallowing study, upper gastrointestinal contrast study, or flexible fiber-optic laryngoscopy. Children whose postoperative course is complicated by inability to eat have increased hospitalization and prolonged hospitalization [19]. Management of children with inability to eat following cardiac surgery is guided by the underlying etiologies and expected time course for improvement. Options include thickening of feeds, nasogastric feedings, and gastrostomy tube placement with or without Nissen fundoplication.

Disorders of the liver and pancreatitis

Virtually any disease of the liver can occur in patients with congenital heart disease. This section discusses those encountered in perioperative cardiac patients. We have no data documenting their prevalence. Common neonatal conditions, such as jaundice related to ABO incompatibility, which have no notable association with congenital heart disease, are not covered.

Biliary atresia

Direct hyperbilirubinemia is common in a cardiac intensive care unit and observed in patients with long-standing reduced systemic perfusion and especially with parental nutrition (see below). Direct hyperbilirubinemia may indicate extrahepatic biliary atresia associated with the heterotaxy syndromes (especially polysplenia) [20,21]. In one study extrahepatic biliary atresia occurred in 10% of patients with left atrial isomerism (polysplenia) [22]. The relative hazard ratio for death was considerably higher for children with biliary atresia associated with cardiac malformations related to left atrial isomerism (2.76 [1.10–5.46]) than for patients without biliary atresia [22]. Biliary atresia has also been reported with hypoplastic left heart syndrome [23] and other cardiac lesions unassociated with heterotaxy. There is little information regarding the effect of biliary atresia on outcomes of cardiac surgery.

The impact of cardiac malformations on the outcomes of operations for biliary atresia or liver transplantation is also poorly defined. Davenport *et al.* [21] reported 56 children with biliary atresia associated with a splenic abnormality and noted that the 5-year *liver* survival was less favorable for patients with a splenic abnormality than for those with isolated biliary atresia. This reduction in survival was not related to congenital cardiac defect. Vazquez *et al.* [24] reported the results of *Kasai operation* in 11 patients with polysplenia syndrome, two of whom had a "cardiac malformation." One of the two patients with a "cardiac malformation" survived operation. Living donor *liver transplantation* for end-stage hepatic disease in children with a congenital cardiac defect can be undertaken with low mortality, although most of the reported patients had relatively mild heart disease [25,26].

Cirrhosis is an important risk factor in adults undergoing cardiac surgery utilizing cardiopulmonary bypass, with patients having Child–Turcotte–Pugh class C disease being at particularly high risk of postoperative complications and death [27]. Limited information is available for pediatric patients. Bacha *et al.* [28] reported open-heart operations involving four patients (aged 10 weeks–2 years) with end-stage liver disease; two had had the Kasai procedure for biliary atresia and two had Alagille's syndrome. One patient had Child's class A and three had Child's class B disease. One (Child's class B with Alagille's) died of refractory hypotension due to vasodilation postoperatively, and three were hospital survivors.

Acute liver failure

Ischemia can cause acute liver failure (ALF), the histological picture of which is confluent or multilobular necrosis [29]. Pre- and postoperative cardiac patients might be at risk for ischemic ALF because of reduced systemic oxygen delivery, systemic arterial hypotension, and increased central venous pressure, either alone or in combination. Mildly increased serum levels of liver enzymes and bilirubin are indeed common, although full-blown ALF (including hypoglycemia, clinically relevant coagulopathy, and encephalopathy) is very unusual. Postoperative Fontan patients seem more vulnerable to ALF than most, because they have acutely increased central venous pressure (2–5-fold greater than before operation), and some also have systemic arterial hypotension and reduced systemic oxygen delivery. Indeed, given the relatively high incidence of (at least transient) hypotension and low systemic oxygen delivery in most congenital cardiac patients after operation, with the very

low incidence of ALF, it seems likely that markedly increased systemic venous pressure (in concert with the other hemodynamic abnormalities) is often an important factor in the genesis of ALF.

Reports of ALF in pediatric cardiac patients are sparse [29–32]. It is difficult to know to what extent the patient's phenotype is shaped by the liver dysfunction as distinct from the coexisting severe hemodynamic disturbance. Indeed, for unknown reasons, ALF itself can reduce systemic vascular resistance and cause hypotension. Renal dysfunction often complicates nonischemic ALF [29]. It may be difficult to distinguish ALF-related encephalopathy and even cerebral edema from that caused by hemodynamic events. The effect of ALF on outcome is obscured by the fact that patients may die from a cardiac cause rather than liver disease. As the two reports [30,31] discussed below show, the Fontan procedure is associated with acute liver injury.

Jenkins *et al.* [30] reported 11 patients (aged 0.25–20 years) with ALF in the early postoperative period, six after Fontan palliation and the remainder after various reparative or palliative operations. Hepatic failure was apparent in the first or second postoperative day in seven, and between postoperative days 6 and 9 in the remainder. They had low cardiac output (cardiac index <2 l min m^{-2}), elevated central venous pressure (12–29 mmHg, mean 20 mmHg) and hepatic perfusion pressure from 29 to 56 mmHg (mean 42 mmHg). Mean systemic arterial pressure ranged from 50 to 85 mmHg at the onset of ALF, but the ages of the patients were not linked to the arterial pressure, limiting interpretation. Inotropic support (and aortic counterpulsation in two patients) was required. Acute renal failure developed in each, with seven requiring peritoneal dialysis. Six children died acutely, all of intractable cardiac failure, and two died later of their cardiac lesions; the authors did not attribute any of the deaths to hepatic failure *per se*.

In a retrospective review of early postoperative "liver dysfunction" after Fontan palliation [31], of 15 consecutive patients seven had elevated serum glutamic pyruvic transaminase (SGPT) >1000 U l^{-1} and total bilirubin and abnormal prothrombin time. Hepatic dysfunction correlated with cardiac index, urine output, systolic arterial pressure, and central venous pressure. Four of the 15 patients died before hospital discharge, but none of the deaths were attributed to liver dysfunction. The same group [32] subsequently reported that in Fontan patients, acute postoperative liver dysfunction (as measured by elevation of alanine aminotransferase and serum total bilirubin) was only weakly related to cardiac index, but strongly related to hepatic venous oxygen saturation; hepatic venous oxygen saturation less than a "critical value" of about 25% was strongly correlated with hepatic dysfunction.

Preventing ischemic ALF consists in maneuvers to maintain adequate systemic oxygen delivery and arterial pressure, while minimizing central venous pressure. Close attention should be paid to volume infusion and to judge, as best as

possible, when to switch from augmenting central venous pressure to inotropic and pressor agents to maintain adequate arterial pressure and systemic blood flow. *Therapy*, in addition to strategies to increase hepatic perfusion, is supportive: close monitoring and provision of blood glucose, monitoring and adjustment of serum electrolytes, replacement of coagulation factors as needed, lactulose to treat elevated ammonia, monitoring of central nervous system status, and responding with appropriate therapy.

Cholestasis

Any of the many causes of cholestasis can affect cardiac patients in an intensive care unit, but few occur with any frequency. Biliary atresia and acute liver failure, although very uncommon, are two causes discussed above. *Conjugated hyperbilirubinemia* is observed in neonates with chronically marginal systemic perfusion, especially if they are receiving total parenteral nutrition [33]. The cause of parenteral nutrition-related jaundice in neonates remains unknown [34].

Acute acalculous cholesystitis

Acute acalculous cholecystitis can rarely develop after cardiac surgery or cardiac catheterization [35]. Presenting signs and symptoms are fever, right upper quadrant pain, vomiting, jaundice, and right upper quadrant mass. Risk factors for acute acalculous cholecystitis include shock, sepsis, total parenteral nutrition, prolonged fasting, intravenous narcotics, and multiple transfusions – a list which explains why postoperative cardiac patients are at risk. Optimal therapy is unclear; antibiotics (only), drainage of the gallbladder, and cholecystectomy are the usual approaches [35].

Portal hypertension

Portal hypertension is very uncommon. It occurs occasionally in neonates with a cardiac lesion and umbilical venous cannulation causing portal venous thrombosis. The most common presenting signs and symptoms are splenomegaly and gastrointestinal bleeding [36].

Acute pancreatitis

Acute pancreatitis is well described in adults after cardiopulmonary bypass [37], and there are a few reports in pediatric patients after cardiotomy [38–41]. In adults, one retrospective study found that pancreatic cellular injury (hyperamylasemia with increased serum lipase or pancreatic isoamylase) occurred in 27% of post-bypass patients; 9% had abdominal signs or symptoms consistent with acute pancreatitis. Pancreatic cellular injury was associated with preoperative renal insufficiency, valve surgery, postoperative hypotension, and perioperative administration of calcium chloride.

In a report [40] of 349 patients (all >3 months old) having open-heart surgery, 46 had hyperamylasemia and 18 had "clinical pancreatitis." The "pancreatitis" was defined by increased serum amylase activity plus high output failure,

central nervous system changes, and hypocalcemia, rather than abdominal findings or pancreatic imaging. The mortality rate for patients with clinical pancreatitis was 49.2%. The patients had a variety of cardiac lesions and the inciting factor(s) for pancreatitis were unknown. A subsequent prospective study [40] from the same institution found that serum amylase was increased relative to preoperative values in 34% of patients after cardiac surgery (both closed and open); the incidence of clinical pancreatitis was not reported. In a report of four children with acute pancreatitis after open-heart surgery [38], all were hemodynamically unstable and receiving high doses of vasoactive drugs. The authors concluded that shock and pre-existing systemic disease are risk factors for this disease. In another study, acute pancreatitis occurred in four (of 40) patients soon after Fontan palliation, two of whom died in the early postoperative period [39]. *Preoperatively*, the patients with pancreatitis had a higher echocardiographic tau (suggesting decreased ventricular compliance) and lower systemic blood flow than patients who did not develop pancreatitis.

Acute Kidney Injury (AKI)

Patients with congenital heart disease have a wide range of circulatory alterations that can stress renal compensatory mechanisms and contribute to AKI. Potent physiologic derangements induced by palliative and reparative congenital heart surgery can further destabilize the cardiorenal axis. Although the responsible biologic mechanisms remain unclear, even subtle alterations in renal function are associated with increased hospitalization and mortality rates among a wide range of critically ill patients, including those recovering from heart surgery [42–45]. Hospitalization and mortality rates in children recovering from cardiac surgery increase with the severity of AKI and may approach 60% for those requiring dialysis [46–49].

Definition and diagnosis

The more than 30 definitions of AKI have hindered the epidemiologic understanding of this important postoperative complication. In 2004, the Acute Dialysis Quality Initiative developed a consensus definition and staging system for adult AKI (*RIFLE* classification) [50]. In 2007, the Acute Kidney Injury Network (*AKIN*) modified the *risk* category of the *RIFLE* classification to include patients with a serum creatinine increase of ≥0.3 mg dl⁻¹ (*AKIN* Stage 1) and eliminated the *loss* and *end-stage renal disease* categories [51]. This was based on the recognition that even a small increase in serum creatinine can be associated with hospitalization and mortality rates and that the *loss* and *end-stage renal disease* categories were outcomes of AKI, rather than descriptors [42]. In both staging systems, the criteria for AKI can be met by an increase in serum creatinine concentration or a specified degree of oliguria (Tables 15.1 and 15.2).

The *RIFLE* classification system and the closely related *AKIN* staging system have become the *de facto* definitions of AKI in critically ill adults, and are slowly becoming the standard in children also. Although creatinine concentration and urine output are the currently accepted clinical standards for assessing renal function in critically ill patients, they have limitations, including delay in the rise of the serum creatinine concentration after kidney injury, the potential uncoupling of serum creatinine and true renal function (i.e., glomerular filtration rate) related to tubular secretion of creatinine, and the dependence of creatinine on muscle mass [52,53].

There is an effort to find more accurate markers of AKI, assayable shortly after renal injury; these include measurement of cystatin c, kidney injury molecule-1, neutrophil gelatinase-associated lipocalin, interleukin-18 (IL-18), and *N*-acetyl-β-D-glucosaminidase [54]. These markers are not yet in widespread clinical use, but it appears that one (or several) will become so, forcing a change in the definition of AKI. Although the use of changes in creatinine concentration to define AKI has been more accepted in children, its use in neonates is limited. In the

Table 15.1 *RIFLE* acute kidney injury classification system.

RIFLE category	GFR criteriaª	Urine output criteriaª
Risk	Creatinine increase of 1.5 × or GFR decrease of >25%	UOP <0.5 ml kg⁻¹ h⁻¹ × 6 h
Injury	Creatinine increase of 2 × or GFR decrease of >50%	UOP <0.5 ml kg⁻¹ h⁻¹ × 12 h
Failure	Creatinine increase of 3 × or GFR decrease of >75%	UOP <0.3 ml kg⁻¹ h⁻¹ × 24 h or anuria × 12 h
Loss	Complete loss of renal function for >4 weeks	
End-stage renal disease	Need for renal replacement therapy for >3 months	

ªGFR, glomerular filtration rate; UOP, urine output.

Table 15.2 *AKIN* acute kidney injury staging system.

AKIN stage	GFR criteria[a]	Urine output criteria[a]
Stage 1	Creatinine increase of 1.5–2 × or creatinine increase ≥0.3 mg dl^{-1}	UOP <0.5 ml kg^{-1} h^{-1} × 6 h
Stage 2	Creatinine increase of >2–3 ×	UOP <0.5 ml kg^{-1} h^{-1} × 12 h
Stage 3	Creatinine increase of >3 × or need for renal replacement therapy	UOP <0.3 ml kg^{-1} h^{-1} × 24 h or anuria × 12 h

[a]GFR, glomerular filtration rate; UOP, urine output.

early neonatal period, serum creatinine concentration reflects maternal creatinine concentration, not glomerular filtration rate, rendering the diagnosis of AKI based on this measurement unreliable in this age group [55].

Incidence

Post hoc application of the *RIFLE* classification system to the limited available data regarding renal function after congenital heart surgery (CS-AKI) demonstrates an overall AKI prevalence of 20–37%. The prevalence of more than mild AKI, corresponding to the *Injury*, *Failure*, *Loss*, and *End Stage* categories, ranges from 12 to 19% [56,57]. Unpublished data from 321 patients from the Children's Hospital Boston suggest that the prevalence of any degree of AKI within 72 h of surgery is 33% (*n* = 107), with 15% (*n* = 48) in the *Injury*, *Failure*, *Loss*, and *End Stage* categories. Significant threshold variation makes the accurate determination of the prevalence of AKI severe enough to require dialysis difficult, with recently reported rates ranging from 2 to 12% [46,48].

Pathophysiology

The development of CS-AKI is the result of several complex processes that often begin well before operation. Focusing on the pre-, intra-, and postoperative periods facilitates understanding the pathophysiology of CS-AKI. Accumulating evidence suggests that pre-existing renal insufficiency is an important risk factor for AKI. The potential etiologies of preoperative renal insufficiency in pediatric patients include coexisting developmental kidney anomalies, shock-induced acute tubular necrosis in neonates with delayed recognition of ductal dependent heart disease, suboptimal hemodynamics resulting in lower renal perfusion pressure (mean arterial pressure – systemic venous pressure), cyanosis, exposure to nephrotoxic medications, diuretic-induced prerenal azotemia, and renal injury related to previous congenital heart surgery. The prevalence of preoperative renal insufficiency in children with congenital heart disease is unknown.

Several events during the operation contribute to CS-AKI by directly or indirectly causing cellular injury to the tubular epithelium, beginning with the induction of general endotracheal anesthesia. Induction can be associated with peripheral vasodilation, redistribution of blood flow away from vital organs, and occasionally hypotension causing a decrease in renal perfusion pressure and a period of relative renal ischemia. Most palliative and reparative procedures require cardiopulmonary bypass (CPB). The renal perfusion provided by CPB has complex and deleterious effects on the kidney that are likely proportional to the duration of bypass. The lack of pulsatile renal blood flow provided by both roller and centrifugal CPB disturbs kidney autoregulation and microcirculatory flow, both of which contribute to ischemia–reperfusion injury of the kidney. Mechanical hemolysis related to suction, autotransfusion, CPB cannulae, tubing, and pump trauma release iron and free hemoglobin, both of which cause renal oxidative stress injury. CPB also induces a potent and complex inflammatory response, partly by activating white blood cells and platelets, an increase in the ratio of pro-inflammatory interleukins and cytokines to anti-inflammatory proteins, and an upregulation of vascular adhesion molecules. The resultant kidney injury from this pro-inflammatory cascade is complex and incompletely understood, but likely involves direct tubular damage and acute tubular necrosis [58,59].

In almost all circumstances, congenital heart surgeons utilize some degree of hemodilution during CPB. Because of improved rheology and viscosity, hemodilution decreases blood exposure and improves perfusion through certain microvascular territories. Significant hemodilution during CPB (i.e., hematocrit <24%), however, is associated with AKI because of a reduced oxygen-carrying capacity to a level that induces renal ischemia [60–62]. The optimal degree of hemodilution to maximize clinical outcomes, including renal function, remains uncertain, but is likely above 25%.

Some degree of hypothermia is used in most on-pump congenital heart operations. The rationales for hypothermia include decreasing global tissue metabolic rate, thus allowing lower bypass flow rates, providing greater end-organ protection, and decreasing CPB-related systemic inflammation. The degree of hypothermia achieved on bypass may be associated with AKI as a result of renal cortical hypoperfusion during rewarming [63].

Cessation of CPB and a period of deep hypothermic circulatory arrest (DHCA) are often used during an operation where a completely bloodless surgical field is required (e.g., repair of obstructed total anomalous pulmonary venous connection) and in operations involving reconstruction of the aortic arch. This profoundly altered physiologic state (DHCA) has been associated with end-organ dysfunction, particularly when prolonged. Whereas most work has centered on the relationship of DHCA to neurologic injury, DHCA can be

associated with postoperative AKI, possibly from vascular endothelial dysfunction [64].

During complex congenital heart surgery, antifibrinolytics are often administered to decrease bleeding. One such medication, aprotinin, attracted much attention after a large study of adults undergoing coronary surgery demonstrated an association between aprotinin use and a twofold increase in AKI requiring dialysis. Because of the studies in adults demonstrating increased rates of both mortality and end-organ dysfunction, aprotinin is no longer marketed. The renal toxicity of aprotonin, however, remains controversial. Some clinical and basic studies support its role as a nephrotoxin, but others suggest that it may have nephro-protective effects [56,57,65,66].

Early postoperative period events are significant in AKI development because of the intraoperative stressors outlined above. Myocardial ischemia–reperfusion injury, direct myocardial injury and edema, CPB-induced systemic inflammatory response syndrome (SIRS), and residual cardiac lesions each contribute to the postoperative low cardiac output syndrome which results in decreased renal perfusion. The decrease in renal perfusion pressure can be compounded by renal afferent arteriolar vasoconstriction induced by inotropes and vasoconstrictors used to treat the low cardiac output. Furthermore, postoperative fluid overload and decreased myocardial compliance elevate central venous pressure and contribute to decreased renal perfusion pressure [58,59].

When severe, ascites resulting from a combination of capillary leak secondary to SIRS, accumulation of transudate secondary to high central venous pressure, and fluid overload related to volume administration can cause abdominal compartment syndrome, compromising kidney function [67]. Many components of the stress response to congenital heart surgery interfere with normal carbohydrate metabolism and cause hyperglycemia, an effect compounded by the frequent administration of glucocorticoids in the perioperative period during CPB. Renal mitochondrial dysfunction secondary to intracellular hyperglycemia has been suggested as a potential mechanism for hyperglycemia associated with AKI [68,69]. Finally, pre-renal states induced by diuretics and fluid restriction and the administration of directly nephrotoxic medications (e.g., nonsteroidal anti-inflammatory agents and aminoglycosides) exacerbate AKI [70].

Prevention and management

There have been many failed attempts at preventing or ameliorating CS-AKI, including the use of low-dose dopamine, diuretics, volume loading, dexamethasone, theophylline, natriuretic peptides, mannitol, calcium channel blockers, angiotensin-converting enzyme inhibitors, preoperative statin therapy, and *N*-acetylcysteine [59,71]. Two renal protection strategies, however, are promising: perioperative infusion of sodium bicarbonate (inhibits the production of oxygen radicals in the renal tubules) and infusing the

selective dopamine receptor agonist fenoldopam (renal vasodilator) [72,73].

Beyond optimizing hemodynamics to maintain renal perfusion pressure with appropriately selected vasoactive medications and minimizing residual cardiac defects surgically, two important strategies to preserve renal function are minimizing nephrotoxic medications and avoiding diuretic-induced prerenal azotemia. Both exacerbate or cause CS-AKI, particularly in a susceptible host. Evolving ascites-related abdominal compartment syndrome, characterized by abdominal distension, a fluid wave, worsening respiratory mechanics, and oliguria should be promptly recognized and relieved to avoid CS-AKI, intestinal ischemia, and progressive respiratory and hemodynamic compromise.

In patients with severe CS-AKI, renal replacement therapy (RRT) may be required, although mortality remains unacceptably high despite its use [46–48]. The common RRT modalities after congenital heart surgery are peritoneal dialysis for infants and continuous veno-venous hemofiltration for larger patients. The indications for RRT after cardiac surgery include anuria with hyperkalemia or metabolic acidosis, severe volume overload refractory to diuretics and fluid restriction, and uremic encephalopathy or platelet dysfunction. RRT has the potential to alter clinical outcomes and disease course for adults with CS-AKI. The timing, institution threshold, and intensity of RRT remain largely unresolved [74–76].

References

1 Ghanayem NS, Dearani JA, Welke KF, *et al*. Gastrointestinal complications associated with the treatment of patients with congenital cardiac disease: consensus definitions from the Multi-Societal Database Committee for Pediatric and Congenital Heart Disease. *Cardiol Young* 2008;**18**(Suppl 2):240–4.

2 Rakhit A, Nurko S, Gauvreau K, *et al*. Gastrointestinal complications after pediatric cardiac transplantation. *J Heart Lung Transplant* 2002;**21**:751–9.

3 Thompson AM, Bizzarro MJ. Necrotizing enterocolitis in newborns: pathogenesis, prevention and management. *Drugs* 2008;**68**:1227–38.

4 McElhinney DB, Hedrick HL, Bush DM, *et al*. Necrotizing enterocolitis in neonates with congenital heart disease: risk factors and outcomes. *Pediatrics* 2000;**106**:1080–7.

5 Cheng W, Leung MP, Tam PK. Surgical intervention in necrotizing enterocolitis in neonates with symptomatic congenital heart disease. *Pediatr Surg Int* 1999;**15**:492–5.

6 Lambert DK, Christensen RD, Henry E, *et al*. Necrotizing enterocolitis in term neonates: data from a multihospital health-care system. *J Perinatol* 2007;**27**:437–43.

7 Carlo WF, Kimball TR, Michelfelder EC, Border WL. Persistent diastolic flow reversal in abdominal aortic Doppler-flow profiles is associated with an increased risk of necrotizing enterocolitis in term infants with congenital heart disease. *Pediatrics* 2007; **119**:330–5.

8 Giannone PJ, Luce WA, Nankervis CA, *et al*. Necrotizing enterocolitis in neonates with congenital heart disease. *Life Sci* 2008;**82**:341–7.

9 Hintz SR, Kendrick DE, Stoll BJ, *et al*. Neurodevelopmental and growth outcomes of extremely low birth weight infants after necrotizing enterocolitis. *Pediatrics* 2005;**115**:696–703.

10 Blakely ML, Gupta H, Lally KP. Surgical management of necrotizing enterocolitis and isolated intestinal perforation in premature neonates. *Semin Perinatol* 2008;**32**:122–6.

11 Moss RL, Dimmitt RA, Barnhart DC, *et al*. Laparotomy versus peritoneal drainage for necrotizing enterocolitis and perforation. *N Engl J Med* 2006;**354**:2225–34.

12 Pickard SS, Feinstein JA, Popat RA, *et al*. Short- and long-term outcomes of necrotizing enterocolitis in infants with congenital heart disease. *Pediatrics* 2009;**123**:e901–6.

13 Carlotti APCP, Carvalho WB. Abdominal compartment syndrome: a review. *Pediatr Crit Care Med* 2009;**10**:115–20.

14 Borenstein SH, Langer JC. Heterotaxia syndromes and their abdominal manifestations. *Curr Opin Pediatr* 2006;**18**:294–7.

15 Applegate KE. Evidence-based diagnosis of malrotation and volvulus. *Pediatr Radiol* 2009;**39**(Suppl 2):S161–3.

16 Choi M, Borenstein SH, Hornberger L, Langer JC. Heterotaxia syndrome: the role of screening for intestinal rotation abnormalities. *Arch Dis Child* 2005;**90**:813–5.

17 Yu DC, Thiagarajan RR, Laussen PC, *et al*. Outcomes after the Ladd procedure in patients with heterotaxy syndrome, congenital heart disease, and intestinal malrotation. *J Pediatr Surg* 2009;**44**:1089–95.

18 Kohr LM, Dargan M, Hague A, *et al*. The incidence of dysphagia in pediatric patients after open heart procedures with transesophageal echocardiography. *Ann Thorac Surg* 2003;**76**:1450–6.

19 Sachdeva R, Hussain E, Moss MM, *et al*. Vocal cord dysfunction and feeding difficulties after pediatric cardiovascular surgery. *J Pediatr* 2007;**151**:312–5.

20 Carmi R, Magee CA, Neill CA, Karrer FM. Extrahepatic biliary atresia and associated anomalies: etiologic heterogeneity suggested by distinctive patterns of associations. *Am J Med Genet* 1993;**45**:683–93.

21 Davenport M, Tizzard SA, Underhill J, *et al*. The biliary atresia splenic malformation syndrome: a 28-year single-center retrospective study. *J Pediatr* 2006;**149**:393–400.

22 Gilljam T, McCrindle BW, Smallhorn JF, *et al*. Outcomes of left atrial isomerism over a 28-year period at a single institution. *J Am Coll Cardiol* 2000;**36**:908–16.

23 Becker DJ, Islam S, Geiger JD. Biliary atresia associated with hypoplastic left heart syndrome: a case report and review of the literature. *J Pediatr Surg* 2004;**39**:1411–3.

24 Vazquez J, Lopez Gutierrez JC, Gamez M, *et al*. Biliary atresia and the polysplenia syndrome: its impact on final outcome. *J Pediatr Surg* 1995;**30**:485–7.

25 Kimura T, Hasegawa T, Ihara Y, *et al*. Successful living related liver transplantation in a case with biliary atresia associated with corrected transposition of the great arteries. *Pediatr Transplant* 2007;**11**:540–2.

26 Concejero A, Chen CL, Liang CD, *et al*. Living donor liver transplantation in children with congenital heart disease. *Transplantation* 2007;**84**:484–9.

27 Filsoufi F, Salzberg SP, Rahmanian PB, *et al*. Early and late outcome of cardiac surgery in patients with liver cirrhosis. *Liver Transplant* 2007;**13**:990–5.

28 Bacha EA, Hardin J, Cronin DC, *et al*. Open-heart surgery in pediatric patients with end-stage liver disease. *Ann Thorac Surg* 2004;**78**:e30–3.

29 Alonso EM, Squires RH, Whitington PF. Acute liver failure in children. In: Suchy FJ, Sokol RJ, Balistreri WF, eds. *Liver Disease in Children*, 3rd edn. New York: Cambridge University Press, 2007: 71–96.

30 Jenkins JG, Lynn AM, Wood AE, *et al*. Acute hepatic failure following cardiac operation in children. *J Thorac Cardiovasc Surg* 1982;**84**:865–71.

31 Matsuda H, Covino E, Hirose H, *et al*. Acute liver dysfunction after modified Fontan operation for complex cardiac lesions. Analysis of the contributing factors and its relation to the early prognosis. *J Thorac Cardiovasc Surg* 1988;**96**:219–26.

32 Takano H, Matsuda H, Kadoba K, *et al*. Monitoring of hepatic venous oxygen saturation for predicting acute liver dysfunction after Fontan operations. *J Thorac Cardiovasc Surg* 1994;**108**:700–8.

33 Suchy FJ. Approach to the infant with cholestasis. In: Suchy FJ, Sokol RJ, Balistreri WF, eds. *Liver Disease in Children*, 3rd edn. New York: Cambridge University Press, 2007: 179–89.

34 Karpen SJ. Mechanisms of bile formation and cholestasis. In: Suchy FJ, Sokol RJ, Balistreri WF, eds. *Liver Disease in Children*, 3rd edn. New York: Cambridge University Press, 2007: 28–34.

35 Tsakayannis DE, Kozakewich HP, Lillehei CW. Acalculous cholecystitis in children. *J Pediatr Surg* 1996;**31**:127–30.

36 Alvarez F, Bernard O, Brunelle F, *et al*. Portal obstruction in children. I. Clinical investigation and hemorrhage risk. *J Pediatr* 1983;**103**:696–702.

37 Fernandez-del Castillo C, Harringer W, Warshaw AL, *et al*. Risk factors for pancreatic cellular injury after cardiopulmonary bypass. *N Engl J Med* 1991;**325**:382–7.

38 Berney T, Belli D, Bugmann P, *et al*. Influence of severe underlying pathology and hypovolemic shock on the development of acute pancreatitis in children. *J Pediatr Surg* 1996;**31**:1256–61.

39 Syed AU, Border WL, Michelfelder EC, *et al*. Pancreatitis in Fontan patients is related to impaired ventricular relaxation. *Ann Thorac Surg* 2003;**75**:153–7.

40 Leijala M, Louhimo I. Pancreatitis after open heart surgery in children. *Eur J Cardiothorac Surg* 1988;**2**:324–8.

41 Tikanoja T, Rautiainen P, Leijala M, *et al*. Hyperamylasemia after cardiac surgery in infants and children. *Intensive Care Med* 1996;**22**:959–63.

42 Lassnigg A, Schmid ER, Hiesmayr M, *et al*. Impact of minimal increases in serum creatinine on outcome in patients after cardiothoracic surgery: do we have to revise current definitions of acute renal failure? *Crit Care Med* 2008;**36**:1129–37.

43 Praught ML, Shlipak MG. Are small changes in serum creatinine an important risk factor? *Curr Opin Nephrol Hypertens* 2005;**14**:265–70.

44 Nin N, Lombardi R, Frutos-Vivar F, *et al*. Early and small changes in serum creatinine concentration are associated to mortality in mechanically ventilated patients. *Shock* 2010;**34**:109–16.

45 Zappitelli M, Bernier PL, Saczkowski RS, *et al*. A small post-operative rise in serum creatinine predicts acute kidney injury in children undergoing cardiac surgery. *Kidney Int* 2009;**76**:885–92.

46 Kist-van Holthe tot Echten, Goedvolk CA, Doornaar MB, *et al*. Acute renal insufficiency and renal replacement therapy after pediatric cardiopulmonary bypass surgery. *Pediatr Cardiol* 2001; **22**:321–6.

47 Baskin E, Saygili A, Harmanci K, *et al*. Acute renal failure and mortality after open-heart surgery in infants. *Ren Fail* 2005; **27**:557–560.

48 Pedersen KR, Hjortdal VE, Christensen S, *et al*. Clinical outcome in children with acute renal failure treated with peritoneal dialysis after surgery for congenital heart disease. *Kidney Int Suppl* 2008:S81–6.

49 Dent CL, Ma Q, Dastrala S, *et al*. Plasma neutrophil gelatinase–associated lipocalin predicts acute kidney injury, hospitalization and mortality after pediatric cardiac surgery: a prospective uncontrolled cohort study. *Crit Care* 2007;**11**:R127.

50 Bellomo R, Ronco C, Kellum JA, *et al*. Acute renal failure – definition, outcome measures, animal models, fluid therapy and information technology needs: the Second International Consensus Conference of the Acute Dialysis Quality Initiative (ADQI) Group. *Crit Care* 2004;**8**:R204–12.

51 Mehta RL, Kellum JA, Shah SV, *et al*.: Acute Kidney Injury Network: report of an initiative to improve outcomes in acute kidney injury. *Crit Care* 2007;**11**:R31.

52 Stevens LA, Coresh J, Greene T, Levey AS. Assessing kidney function – measured and estimated glomerular filtration rate. *N Engl J Med* 2006;**354**:2473–83.

53 Haase-Fielitz A, Bellomo R, Devarajan P, *et al*. Novel and conventional serum biomarkers predicting acute kidney injury in adult cardiac surgery – a prospective cohort study. *Crit Care Med* 2009;**37**:553–60.

54 Rosner MH. Urinary biomarkers for the detection of renal injury. *Adv Clin Chem* 2009;**49**:73–97.

55 Askenazi DJ, Ambalavanan N, Goldstein SL. Acute kidney injury in critically ill newborns: what do we know? What do we need to learn? *Pediatr Nephrol* 2009;**24**:265–74.

56 Manrique A, Jooste EH, Kuch BA, *et al*. The association of renal dysfunction and the use of aprotinin in patients undergoing congenital cardiac surgery requiring cardiopulmonary bypass. *Anesth Analg* 2009;**109**:45–52.

57 Guzzetta NA, Evans FM, Rosenberg ES, *et al*. The impact of aprotinin on postoperative renal dysfunction in neonates undergoing cardiopulmonary bypass: a retrospective analysis. *Anesth Analg* 2009;**108**:448–55.

58 Stafford-Smith M, Shaw A, Swaminathan M. Cardiac surgery and acute kidney injury: emerging concepts. *Curr Opin Crit Care* 2009;**15**:498–502.

59 Rosner MH, Okusa MD. Acute kidney injury associated with cardiac surgery. *Clin J Am Soc Nephrol CJASN* 2006;**1**:19–32.

60 Karkouti K, Beattie WS, Wijeysundera DN, *et al*. Hemodilution during cardiopulmonary bypass is an independent risk factor for acute renal failure in adult cardiac surgery. *J Thorac Cardiovasc Surg* 2005;**129**:391–400.

61 Swaminathan M, Phillips-Bute BG, Conlon PJ, *et al*. The association of lowest hematocrit during cardiopulmonary bypass with acute renal injury after coronary artery bypass surgery. *Ann Thorac Surg* 2003;**76**:784–91.

62 Huybregts RAJM, de Vroege R, Jansen EK, *et al*. The association of hemodilution and transfusion of red blood cells with biochemical markers of splanchnic and renal injury during cardiopulmonary bypass. *Anesth Analag* 2009;**109**:331–9.

63 Kourliouros A, Valencia O, Phillips SD, *et al*. Low cardiopulmonary bypass perfusion temperatures are associated with acute kidney injury following coronary artery bypass surgery. *Eur J Cardiothorac Surg* 2010;**37**:704–9.

64 Dittrich S, Priesemann M, Fischer T, *et al*. Circulatory arrest and renal function in open-heart surgery on infants. *Pediatr Cardiol* 2002;**23**:15–9.

65 Gagne JJ, Griesdale DEG, Schneeweiss S. Aprotinin and the risk of death and renal dysfunction in patients undergoing cardiac surgery: a meta-analysis of epidemiologic studies. *Pharmacoepidemiol Drug Saf* 2009;**18**:259–68.

66 Mangano DT, Tudor IC, Dietzel C. The risk associated with aprotinin in cardiac surgery. *N Engl J Med* 2006;**354**:353–65.

67 Shear W, Rosner MH. Acute kidney dysfunction secondary to the abdominal compartment syndrome. *J Nephrol* 2006;**19**:556–65.

68 Gunst J, Schetz M. Clinical benefits of tight glycaemic control: effect on the kidney. *Best Pract Res Clin Anaesthesiol* 2009;**23**:431–9.

69 Vanhorebeek I, Gunst J, Ellger B, *et al*. Hyperglycemic kidney damage in an animal model of prolonged critical illness. *Kidney Int* 2009;**76**:512–20.

70 Bellomo R, Auriemma S, Fabbri A, *et al*. The pathophysiology of cardiac surgery-associated acute kidney injury (CSA-AKI). *Int J Artif Organs* 2008;**31**:166–78.

71 Argalious M, Xu M, Sun Z, *et al*. Preoperative statin therapy is not associated with a reduced incidence of postoperative acute kidney injury after cardiac surgery. *Anesth Anal* 2010; **111**:324–30.

72 Haase M, Haase-Fielitz A, Bellomo R, *et al*. Sodium bicarbonate to prevent increases in serum creatinine after cardiac surgery: a pilot double-blind, randomized controlled trial. *Crit Care Med* 2009;**37**:39–47.

73 Cogliati AA, Vellutini R, Nardini A, *et al*. Fenoldopam infusion for renal protection in high-risk cardiac surgery patients: a randomized clinical study. *J Cardiothorac Vasc Anesth* 2007; **21**:847–50.

74 Elahi MM, Lim MY, Joseph RN, *et al*. Early hemofiltration improves survival in post-cardiotomy patients with acute renal failure. *Eur J Cardiothorac Surg* 2004;**26**:1027–31.

75 Bent P, Tan HK, Bellomo R, *et al*. Early and intensive continuous hemofiltration for severe renal failure after cardiac surgery. *Ann Thorac Surg* 2001;**71**:832–7.

76 Demirkilic U, Kuralay E, Yenicesu M, *et al*. Timing of replacement therapy for acute renal failure after cardiac surgery. *J Card Surg* 2004;**19**:17–20.

16 Fetal Treatment

Helena M. Gardiner

Imperial College, and Queen Charlotte's and Chelsea Hospital, Royal Brompton Hospital, London, UK

Introduction

Surgical procedures for major congenital heart disease (CHD) are performed in the first days to months after birth following the recognition that neonatal mortality is high in unoperated children and secondary myocardial damage (thought in part to be due a reduction in coronary angiogenesis) is common in children undergoing their first surgical procedure later in childhood [1]. It is likely that the substrate for damage occurs prenatally [2] and this has led to evaluation of the benefits of cardiac intervention for aortic and pulmonary stenosis in the fetus [3]. Relatively noninvasive fetal therapy for arrhythmia, with antiarrhythmic drugs given (in relatively high dosage) to the healthy mother to treat fetal tachycardia transplacentally, is already well established and usually successful [4,5]. More invasive fetal therapies include intrauterine blood transfusions for fetal anemia, insertion of pleural shunts for recurrent effusions, and laser photocoagulation of placental anastomoses to separate the circulation in monochorionic twins with twin-to-twin transfusion syndrome, and are performed by fetal medicine obstetricians [6,7]. Teams combining this fetal medicine expertise with their cardiologists have more recently introduced fetal cardiac interventional procedures: valvoplasty of the aortic and pulmonary valve, balloon atrial septostomy for restrictive or closed interatrial septum, and fetal pacing in complete heart block into this range of therapeutic options [8–10].

Assessment of therapeutic efficacy

In general, new fetal therapies are offered where the procedure is either life saving or may improve postnatal outcomes. The rapidity of progression of fetal aortic and critical pulmonary valve stenosis results in substantial ventricular damage, including impaired growth, and affected hearts are often considered to lie within the spectrum of hypoplastic left or right heart syndrome within weeks following diagnosis [3,11,12].

Several percutaneous fetal procedures, such as bladder shunting and opening of posterior urethral valves, have been evaluated and largely discarded as ineffective. Open fetal surgery for repair of diaphragmatic hernia and spina bifida has been the subject of randomized trials, [13,13a]. The approach for these procedures is more invasive and involves exteriorization of the fetus to perform surgery. Where the therapeutic efficacy of one treatment versus another, or one treatment versus no treatment, has not been established, a randomized trial is the ideal assessment tool. However, it may be difficult to obtain sufficient power for a randomized controlled trial for fetal cardiac disease for several reasons, including rarity of suitable patients, relatively poor detection rate at an early stage of the disease, compromising recruitment, and the wide diversity of cardiac morphology that may require further subgroup analysis and reduce power.

Detection of heart disease in pregnancy

The fetal heart is examined using ultrasound usually as part of a fetal anomaly scan at ~20 weeks' gestation (Videoclip 16.1). Antenatal screening tests in the first and second trimesters vary depending on health care systems and are undertaken by a variety of health professionals. Prenatal detection of cardiac defects remains disappointingly low in many countries, with only one in four affected babies detected in screening programs [14,15]. However, if fetal therapy is to be evaluated further, an improvement in antenatal detection is vital to detect fetuses with semilunar valve stenosis or

atresia in the early stages of the disease when valvoplasty is most likely to be effective by protecting the growth of the supporting ventricle and theoretically preventing the development of a hypoplastic left or right heart [11] (Videoclips 16.2 and 16.3).

History of human fetal cardiac intervention

Human fetal cardiac intervention was first attempted in the 1990s because surgical results for critical aortic stenosis in the neonate were poor and because aortic valve stenosis detected *in utero* often progressed rapidly to hypoplastic left heart syndrome, for which there was no widely available successful surgical strategy. The fetuses had advanced disease and technical success was only achieved in about half (defined as crossing the valve and achieving forward flow) and procedure-related deaths occurred in ~30% with only one long-term survivor [16,17]. Fetal valvoplasty was not developed further until more recently; the stimulus for this is not entirely clear but perhaps the development of fetal screening programs with more timely referral of cardiac malformations played a role. Early reports of technical success [8,9] stimulated others to try these techniques, but apart from one large center in the United States, there are no studies with sufficient power to evaluate efficacy. There are important criteria to consider when introducing a new therapy and any new interventional program must be able to demonstrate an improvement in outcome over current surgical techniques. Current in-hospital survival following the Norwood procedure for hypoplastic left heart syndrome or the borderline left heart size is ~70% with 2 year survival of 55% in most centers. Higher risk morphology has been identified and includes babies with an intact or restrictive interatrial septum who have only a 30% 1 month survival, even in high-volume centers, because of pulmonary lymphangiectasia and pulmonary venous damage [18,19].

Case selection, counseling, and timing

True outcomes for fetuses diagnosed with CHD are not as good as those reported in postnatal surgical series because such series do not represent the entirety of the disease. Fetuses may not be born either because of spontaneous demise or interruption of the pregnancy; babies may not be offered surgery because morphology or function are worse than anticipated from fetal scans, or because of important coexisting chromosomal defects or extracardiac malformations which occur in ~10% of patients with aortic and pulmonary stenosis or atresia [20].

Guidelines for selecting patients for left-sided procedures have been modified based on best-available but relatively

Table 16.1 Revised selection criteria and threshold score for fetal aortic valvoplasty[a].

Aortic valve	Stenosis – not atresia
LV size	LV length Z score ≥−2
Mitral valve annulus	Z score ≥−3
LV function	MR >15 or AS >10 mmHg
Threshold score ≥4 points	*(permits 100% sensitivity for BV outcome)*
LV length	Z score >0 = 1 point
LV width (short axis)	Z score >0 = 1 point
Aortic valve annulus	Z score ≥−3.5 = 1 point
Mitral valve annulus	Z score ≥−2 = 1 point
LV function	MR or AS >20 mmHg = 1 point

[a]AS, aortic stenosis; LV, left ventricular; MR, mitral regurgitation.

short-term experiences of outcome from one center (Table 16.1). Not surprisingly, the better the fetal anatomy at the time of procedure, the more likely a two-ventricle circulation is after birth. However, the ideal gestation for interventions remains unclear [8,21]. The fetus may not tolerate the procedure well below 20 gestational weeks, particularly if the procedure is lengthy or there is hydrops. There is a 10–20% risk of procedure-related death with a 5% risk of premature labor following the procedure [22]. We know that cardiac pathology worsens during pregnancy, but the risk of preterm delivery after fetal intervention must be weighed up when considering its timing as it is unlikely that the Norwood [23,24] or hybrid procedure [25] would be offered to a baby of <30 weeks gestation because of low birth weight, although radiofrequency perforation and dilatation of the pulmonary valve and surgery have been performed in low birth weight babies in some large centers [26]. As a consequence, in our interventional program we have elected not to offer emergency Cesarean section should persistent fetal bradycardia occur that is unresponsive to intracardiac atropine or adrenaline.

Patient selection

Aortic valve stenosis

Previous guidance based on one retrospective series suggested that the fetus should have a dilated left ventricle and reasonably sized mitral valve with a Z score better than −4 to be considered suitable for fetal intervention. The observation of reversed flow in the transverse aortic arch (Videoclip 16.4) was identified as an indicator of progression to hypoplastic left heart syndrome [11], but this center has subsequently revised outcomes, considering only those with the best morphology (Videoclip 16.5) to be suitable for intervention because it has become clear that a fetal intervention cannot

Table 16.2 Potential selection criteria for fetal pulmonary valvoplasty[a].

Pulmonary valve	Stenosis or membranous atresia
Tricuspid valve annulus and TV/MV ratio	Z score $\geq$−3.4; TV/MV >0.71 below 31 weeks
	Z score $\geq$−3.95; TV/MV >0.59 above 31 weeks
Predictive score[b] for BV	Selection could be based on scores worse than predictive for BV
<23 weeks (100% prediction BV; 80% UV)	TV Z score >−3.4 ; PV Z score >−1.0
<26 weeks (sensitivity 68%; specificity 72%)	Median TV Z score >−3.95
26–31 weeks (sensitivity 100%; specificity 100%)	(Median PV Z score >−2.8) + (median ratio TV/MV >0.71)
>31 weeks (AUC = 0.87)	(Median TV Z score >−3.9) + (median ratio TV/MV >0.59)
Right atrial pressure score	Tricuspid regurgitation + ductus venosus + oval foramen dynamics
	Values 0–2 per variable: score >3 predictive for BV circulation[b]
Tricuspid regurgitation	None/mild = 0; moderate = 1; severe = 2
Ductus venosus	Normal = 0; absent EDF = 1; reverse EDF = 2
Oval foramen dynamics	Normal = 0; tense $1-1.5\,m\,s^{-1}$ = 1; restrictive >$1.5\,m\,s^{-1}$ = 2

[a]AUC, area under the ROC curve; BV, biventricular circulation; EDF, end-diastolic flow; MV, mitral valve;
PV, pulmonary valve; TV, tricuspid valve; UV, univentricular circulation.
[b]Based on scoring system in Gardiner HM, Belmar C, Tulzer G, *et al*. *J Am Coll Cardiol* 2008;**51**:1299–308. [30].

alter outcome from a univentricular circulation in more severely affected patients [22] (Table 16.1).

Restrictive interatrial septum

About 6–10% of patients with aortic stenosis and hypoplastic left heart syndrome have a restrictive interatrial septum and may be considered for balloon atrial septostomy to maximize the chances of developing a normal pulmonary bed (Videoclips 16.6 and 16.7). However, the stage at which this damage occurs and when it becomes irreversible are unknown [19]. Abnormalities of lymphatic development cause lymphangiectasia and poor function and this, coupled with pulmonary venous stenoses and occlusions, proves almost universally fatal in early life. Restrictive interatrial septum may also be recognized in fetuses with simple transposition of the great arteries (ventriculo-arterial discordance). The restriction reduces left-to-right shunting at the atrial level after delivery and may result in early pulmonary venous hypertension, acidosis, and pulmonary hemorrhage with significantly increased preoperative morbidity and perinatal mortality [27]. However, as restriction usually occurs towards the end of pregnancy, a planned delivery with ready access to facilities for septostomy or early surgery is the more usual management pathway.

Pulmonary atresia with intact interatrial septum

Fetuses with critical pulmonary stenosis or membranous pulmonary atresia have also been considered for prenatal intervention. The United Kingdom and Ireland study reported a 64% 10 year survival for live-born children with pulmonary atresia with intact ventricular septum (PAIVS). Moreover only about 50% of the survivors have a two-ventricle repair, the remainder having a univentricular

"Fontan" circulation or no final pathway [28,29]. There is a spectrum of morphology in this anomaly, and clearly fetuses with minute tricuspid valves, diminutive right ventricles, and large coronary fistulas will never be suitable candidates for fetal intervention as there is no prospect of achieving a two-ventricle circulation (Videoclip 16.8). Only fetuses with membranous pulmonary atresia with an adequate right ventricle (Videoclip 16.9) are suitable for fetal valvoplasty (Table 16.2), and as only a handful of procedures have been performed there is insufficient power to assess efficacy of outcome [9,30,31]. Some children initially designated to follow a biventricular surgical pathway eventually require conversion to a Fontan circulation several years after delivery because of right ventricular failure, often associated with pulmonary regurgitation [28]. The substrate for right ventricular failure probably has its roots in fetal life and it is this that theoretically may be altered by a fetal intervention because cardiomyocyte division and maturation are severely compromised under the increased pressure load and post-mortem histopathology reveals intense mineralization, calcification, and fibrosis [21].

Fetal pacing

Complete heart block is associated with complex structural heart disease in about half of the patients (usually isomerism of the left atrial appendages) (Videoclips 16.10–16.12) and in the remainder normally connected hearts have been damaged by the transplacental transfer of anti-Ro or anti-La antibodies leading to fibrosis of the conduction tissue, myocardial calcification, and sometimes diminished cardiac function. Their mothers may be asymptomatic or have signs of connective tissue disease such as systemic lupus erythematosis or Sjorgren's syndrome [32]. There is a spectrum of fetal

presentation, the worst presenting with complete heart block and hydrops in early gestation (Videoclip 16.13) when therapeutic options are limited, usually unsuccessful, and fetal demise is common. [33] Current therapeutic strategies have included prophylactic approaches [34] (intravenous γ-globulin and maternal plasmaphoresis) to reduce or remove the antibody load early in pregnancy, and those intended to prevent progression of atrioventricular block (high-dose steroids). There is no sufficiently powered trial of any of these therapies to test their efficacy [35]. When there is no hydrops, the intrauterine course is more stable, but if the ventricular rate falls below 55 beats per minute fetal hydrops may develop and carry a high risk of intrauterine demise. Sympathomimetic drugs have been used to increase the fetal heart rate, but not always successfully as tolerance develops and higher doses of the drug are not well tolerated by the pregnant woman [36]. Fetal pacing is an alternative potential therapy [10] and was first reported in 1986 where temporary pacing was achieved in a hydropic fetus, but not sustained [37,38]. As about 75% of babies will require pacing in the first year of life, it is not known whether fetal pacing rather than earlier delivery would theoretically improve long-term outcomes as important myocardial disease coexists in ~8% and is difficult to manage. Most cardiologists try to extend the intrauterine period for as long as possible and deliver the fetus as close to term as feasible.

Interventional techniques

Fetal valvoplasty is largely performed in the same way as it was in the early 1990s, despite animal work that has explored various methods of gaining vascular access in the fetus [39] and improved imaging using fetal trans-esophageal echocardiography. Although these techniques are very attractive, they remain experimental with only isolated reports in humans [40]. They are more invasive than current percutaneous methods and lengthen the procedural time, both of which put mother and fetus at increased risk and increase the likelihood of preterm delivery due to amnionitis or rupture or separation of membranes.

Since 2000, improvements in equipment, including ultrasound imaging and development of small coronary catheters that are suitable for fetal procedures, have encouraged a reappraisal of fetal therapy. However, the development of a successful fetal therapeutic program requires an experienced team approach with the fetal medicine obstetrician key to a technically successful procedure. Most procedures have used an ultrasound-guided percutaneous technique (Videoclip 16.14) performed under local or general anesthetic [8,9]. The invasive part of the cardiac procedure takes only a few minutes once fetal lie is optimal. General anesthesia gives some procedural advantages, such as easy manipulation of the fetus into a good position for intervention, but increases the potential dangers to a pregnant woman.

Equipment and protocol

The mother is given prophylactic intravenous antibiotics to prevent amnionitis and the procedure is performed under aseptic techniques using local or general anesthesia. A 15 cm needle with a flexible stylet is introduced percutaneously by the fetal medicine obstetrician through the maternal abdominal and uterine walls and into the fetal chest. Correct alignment of the needle along the right or left outflow tract is essential for technical success and is guided by ultrasound. There is a learning curve for this, but experienced fetal medicine obstetricians already have skills in percutaneous fetal cardiac access from performing feticide for serious anomalies beyond 22 weeks by intracardiac injection of potassium chloride prior to terminating pregnancy. The percutaneous technical success rate is high in most reports, although mini-laparotomy has been required by some to gain access to the fetal heart in the early stages of their experience [8,9].

Although debate exists as to whether the fetus has the neural circuitry and developmental processes to feel pain, fetal analgesia (usually fentanyl) is usually delivered using intramuscular, intravenous, or intracardiac routes either before or just after gaining access [41]. Atropine and adrenaline are often prepared to treat sustained fetal bradycardia and may be used prophylactically upon entry into the fetal chest. The use of a paralyzing agent is not usually necessary and may be counter-productive as the fetus may then lie in a fixed, unfavorable position. Following percutaneous access, an over-the-wire short coronary balloon is used. The balloon is usually slightly larger than the diameter of the valve. An 8 mm length is the shortest balloon commercially available. A high-pressure 4 mm balloon inflated to 18 atm pressure may be suitable for creating an interatrial communication. The balloon is inflated 2–3 times across the valve if tolerated by the fetus and all equipment is removed from the fetal heart and uterus in one movement to minimize the development of pericardial effusion. A similar technique is used to cross the interatrial septum and create a patent oval foramen, and a stent has been deployed across the defect to maintain its patency. This has proved challenging and a wide variety of balloons, stents, and radiofrequency catheters have been used to create a reasonably sized and persistent communication [42,43].

Post-procedural pregnancy management and support

Women who have undergone the procedure using local anesthetic can be managed as day patients and reviewed the following morning. Those who have had a general anesthetic

or a mini-laparotomy require a longer hospital stay. The risk of premature labor associated with this type of procedure is ~5% and cervical length is usually checked before discharge. The cardiologists review the baby's cardiac function and circulation immediately after the procedure and the following day, and plan for serial evaluation locally or at the referral center depending on available expertise and family convenience.

Altering the natural history of disease

The ideal study of any disease comprises a longitudinal series of observations beginning before birth [20]. Unfortunately, the anomalies for which percutaneous fetal cardiac therapy is currently suitable are relatively rare and data are limited, and a recent audit of success in the largest series has substantially revised the acceptance criteria for fetal valvoplasty.

It is difficult to envisage a single center, or indeed a European country, having enough patients to power a study adequately to test whether the natural history has been altered by a fetal intervention. The end points of a study should ideally include preservation of a two-ventricle circulation in the short term, normal pulmonary pressures, and, for those where this has proved impossible, whether they are better Fontan candidates and experience less heart failure later in childhood or adult life [44]. Thus real benefit may only be assessed 20 years later. Centers performing fetal valvoplasty should be supported by a surgical program that includes a surgical strategy for babies with critical aortic stenosis born with a borderline left ventricle, usually including aggressive resection of endocardial fibroelastosis from the left ventricle [45]. Interestingly, neither fetal or postnatal valvoplasty nor removal of endocardial fibroelastosis were statistically significant contributors to a successful biventricular circulation in this series [46].

Conclusions

It is tempting to conclude that there is little merit in fetal therapy as only those with the very best anatomy have achieved biventricular outcomes in the largest series and we do not know whether these fetuses would have achieved this without intervention. There is still insufficient power and a lack of a large contemporaneous natural history series to be sure of its potential. However, perhaps too much emphasis is placed on the achievement of a biventricular circulation at all costs [1]. We recognize that the early surgical pathway does not always predict the final circulation because of reduced right ventricular function and progressive valvar regurgitation in some. Perhaps the success of a fetal intervention should be judged on the medium- and long-term functional outcome of either the one- or two-ventricle

circulation, reflecting the optimization of the pulmonary and myocardial development that may be achievable following successful and timely fetal intervention.

Acknowledgment

References

1 Castenada A. Congenital heart disease: a surgical–historical perspective. *Ann Thorac Surg* 2005;**79**:S2217–20.

2 Gardiner H. Response of the fetal heart to changes in load: from hyperplasia to heart failure. *Heart* 2005;**91**:871–3.

3 Gardiner HM. Progression of fetal heart disease and rationale for fetal intracardiac interventions. *Semin Fetal Neonatal Med* 2005;**10**:578–85.

4 Fouron JC. Fetal arrhythmias: the Saint-Justine hospital experience. *Prenat Diagn* 2004;**24**:1068–80.

5 Maeno Y, Hirose A, Kanbe T, *et al*. Fetal arrhythmia: prenatal diagnosis and perinatal management. *J Obstet Gynaecol Res.* 2009;**35**:623–9.

6 Deprest JA, Devlieger R, Srisupundit K, *et al*. Fetal surgery is a clinical reality. *Semin Fetal Neonatal Med* 2010;**15**:58–67.

7 Senat MV, Deprest J, Boulvain M, *et al*. Endoscopic laser surgery versus serial amnioreduction for severe twin-to-twin transfusion syndrome. *N Engl J Med* 2004;**351**:136–44.

8 Tworetzky W, Wilkins-Haug L, Jennings RW, *et al*. Balloon dilation of severe aortic stenosis in the fetus: potential for prevention of hypoplastic left heart syndrome: candidate selection, technique, and results of successful intervention. *Circulation* 2004;**110**:2125–31.

9 Tulzer G, Arzt W, Franklin RC, *et al*. Pulmonary valvoplasty for critical pulmonary stenosis or atresia with intact septum. *Lancet* 2002;**360**:1567–8.

10 Assad RS, Zielinsky P, Kalil R, *et al*. New lead for *in utero* pacing for fetal congenital heart block. *J Thorac Cardiovasc Surg* 2003;**126**:300–2.

11 Mäkikallio K, McElhinney DB, Levine JC, *et al*. Fetal aortic valve stenosis and the evolution of hypoplastic left heart syndrome. Patient selection for fetal intervention. *Circulation* 2006;**113**:1401–5.

12 Simpson JM, Sharland GK. Natural history and outcome of aortic stenosis diagnosed prenatally. *Heart* 1997;**77**:205–10.

13 Harrison MR, Keller RL, Hawgood SB, *et al*. A randomized trial of fetal endoscopic tracheal occlusion for severe fetal congenital diaphragmatic hernia. *N Engl J Med* 2003;**349**:1916–24.

13a Adzick NS, Thom EA, Spong CY, *et al*. A randomized trial of prenatal versus postnatal repair of myelomeningocele. *New Engl J Med* 2011;**362**:993–1004.

14 Bull C. Current and potential impact of fetal diagnosis on prevalence and spectrum of serious congenital heart disease at term in the UK. *Lancet* 1999;**354**:1242–7.

15 Acharya G, Sitras V, Maltau JM, *et al*. Major congenital heart disease in Northern Norway: shortcomings of pre- and postnatal diagnosis. *Acta Obstet Gynecol Scand* 2004;**83**:1124–9.

16 Maxwell D, Allan L, Tynan MJ. Balloon dilatation of the aortic valve in the fetus: a report of two cases. *Br Heart J* 1991;**65**:256–8.

17 Kohl T, Sharland G, Allan LD, *et al*. World experience of percutaneous ultrasound-guided balloon valvoplasty in human fetuses with severe aortic valve obstruction. *Am J Cardiol* 2000;**85**:1230–3.

18 Ishino K, Stümper O, De Giovanni JJ, *et al*. The modified Norwood procedure for hypoplastic left heart syndrome: early to intermediate results of 120 patients with particular reference to aortic arch repair. *J Thorac Cardiovasc Surg* 1999;**117**:920–30.

19 Rychik J, Rome JJ, Collins MH, *et al*. The hypoplastic left heart syndrome with intact atrial septum: atrial morphology, pulmonary vascular histopathology and outcome. *J Am Coll Cardiol* 1999;**34**:554–60.

20 Rasiah SV, Ewer AK, Miller P, *et al*. Antenatal perspective of hypoplastic left heart syndrome: 5 years on. *Arch Dis Child Fetal Neonatal Ed* 2008;**93**:F192–7.

21 Matsui H, Gardiner HM. Fetal intervention for cardiac disease: the cutting edge of perinatal care. *Semin Fetal Neonatal Med* 2007;**12**:482–9.

22 McElhinney DB, Marshall AC, Wilkins-Haug LE, *et al*. Predictors of technical success and postnatal biventricular outcome after *in utero* aortic valvoplasty for aortic stenosis with evolving hypoplastic left heart syndrome. *Circulation* 2009;**120**:1482–90.

23 Glatz JA, Tabbutt S, Gaynor JW, *et al*. Hypoplastic left heart syndrome with atrial level restriction in the era of prenatal diagnosis. *Ann Thorac Surg* 2007;**84**:1633–8.

24 Tabbutt S, Dominguez TE, Ravishankar C, *et al*. Outcomes after the stage I reconstruction comparing the right ventricular to pulmonary artery conduit with the modified Blalock Taussig shunt. *Ann Thorac Surg* 2005;**80**:1582–90.

25 Galantowicz M, Cheatham JP. Lessons learned from the development of a new hybrid strategy for the management of hypoplastic left heart syndrome. *Pediatr Cardiol* 2005;**26**:190–9.

26 Reddy VM, McElhinney DB, Sagrado T, *et al*. Results of 102 cases of complete repair of congenital heart defects in patients weighing 700 to 2500 grams. *J Thorac Cardiovasc Surg* 1999;**117**:324–31.

27 Bonnet D, Coltri A, Butera G, *et al*. Detection of transposition of the great arteries in fetuses reduces neonatal morbidity and mortality. *Circulation* 1999;**99**:916–8.

28 Daubeney PE, Wang D, Delany DJ, *et al*. UK and Ireland collaborative study of pulmonary atresia with intact ventricular septum. *J Thorac Cardiovasc Surg* 2005;**130**:1071–8.

29 Dyamenahalli U, McCrindle BW, McDonald C, *et al*. Pulmonary atresia with intact ventricular septum: management of, and outcomes for, a cohort of 210 consecutive patients. *Cardiol Young* 2004;**14**:299–308.

30 Gardiner HM, Belmar C, Tulzer G, *et al*. Morphological and functional predictors of eventual circulation in the fetus with pulmonary atresia or critical pulmonary stenosis with intact septum. *J Am Coll Cardiol* 2008;**51**:1299–308.

31 Tworetzky W, McElhinney DB, Marx GR, *et al*. *In utero* valvoplasty for pulmonary atresia with hypoplastic right ventricle: techniques and outcomes. *Pediatrics* 2009;**124**:e510–8.

32 Sonesson SE, Salomonsson S, Jacobsson L-A, *et al*. Signs of first-degree heart block occur in one-third of fetuses of pregnant women with Anti-SSA/Ro 52-kd antibodies. *Arthritis Rheum* 2004;**50**:1253–61.

33 Cuneo BF, Lee M, Roberson D, *et al*. A management strategy for fetal immune-mediated atrioventricular block. *J Matern Fetal Neonatal Med* 2010;**23**:1400–5.

34 Friedman DM, Llanos C, Izmirly PM, *et al*. Evaluation of fetuses in a study of intravenous immunoglobulin as preventive therapy for congenital heart block: results of a multicenter, prospective, open-label clinical trial. *Arthritis Rheum* 2010;**62**:1138–46.

35 Jaeggi ET, Fouron JC, Silverman ED, *et al*. Transplacental fetal treatment improves the outcome of prenatally diagnosed complete atrioventricular block without structural heart disease. *Circulation* 2004;**110**:1542–8.

36 Groves AM; Allan LD, Rosenthal E. Therapeutic trial of sympathomimetics in three cases of complete heart block in the fetus. *Circulation* 1995;**92**:3394–6.

37 Carpenter RJ, Strasburger JF, Garson A, *et al*. Fetal ventricular pacing for hydrops secondary to complete atrioventricular block. *J Am Coll Cardiol* 1986;**8**:1434–6.

38 Walkinshaw SA, Welch CR, McCormack J, *et al*. *In utero* pacing for fetal congenital heart block. *Fetal Diagn Ther* 1994;**9**:183–5.

39 Jouannic JM, Boudjemline Y, Benifla JL *et al*. Transhepatic ultrasound-guided cardiac catheterization in the fetal lamb. *Circulation* 2005;**111**:736–41.

40 Kohl T, Muller A, Tchatcheva K, *et al*. Fetal transesophageal echocardiography: clinical introduction as a monitoring tool during cardiac intervention in a human fetus. *Ultrasound Obstet Gynecol* 2005;**26**:780–5.

41 Derbyshire SWG. Can fetuses feel pain? *BMJ* 2006;**332**:909–12.

42 Marshall AC, Velde ME, Tworetzky W *et al*. Creation of an atrial septal defect *in utero* for fetuses with hypoplastic left heart syndrome and intact or highly restrictive atrial septum. *Circulation* 2004;**110**:253–8.

43 Quintero R, Huhta J, Suh E, *et al*. *In utero* cardiac fetal surgery: laser atrial septostomy in the treatment of hypoplastic left heart syndrome with intact atrial septum. *Am J Obstet Gynecol* 2005;**193**:1424–8.

44 Burch M, Kaufman L, Archer N, *et al*. Persistent pulmonary hypertension late after neonatal aortic valvotomy: a consequence of an expanded surgical cohort. *Heart* 2004;**90**:918–20.

45 Pigula FA, Vida V, Del Nido P, *et al*. Contemporary results and current strategies in the management of hypoplastic left heart syndrome. *Semin Thorac Cardiovasc Surg* 2007;**19**:238–44.

46 Emani SM, Bacha EA, McElhinney DB, *et al*. Primary left ventricular rehabilitation is effective in maintaining two-ventricle physiology in the borderline left heart. *J Thorac Cardiovasc Surg* 2009;**138**:1276–82.

17 Newborn Diagnosis and Management

Kazuo Momma

Tokyo Women's Medical University, Shinjukuku, Tokyo, Japan

Critical congenital heart disease: frequency of and necessity for early diagnosis

Neonates with critical congenital heart disease (CHD) frequently die within 30 days after birth if not correctly diagnosed and treated [1–3]. These diseases were documented in autopsy studies before 1960 in Toronto, Boston, and Baltimore, and are tabulated in Table 17.1. The frequency of critical CHD has not changed much since those studies [4,5].

Among those critical CHDs, hypoplastic left heart syndrome, complete transposition, and coarctation of the aorta are the most frequent conditions. They account for 60% of the neonatal deaths from critical CHD [1–3]. These neonates present in several ways: with cyanosis frequently due to a ductus-dependent pulmonary circulation, dyspnea and congestive cardiac failure due to excessive volume or pressure loads, a heart murmur, or shock with weak or absent pulses in the lower extremities or indeed in all extremities due to a ductus-dependent systemic circulation.

Advances in surgical techniques have substantially reduced the perioperative mortality for neonates with critical CHD, but early diagnosis is essential for a good surgical outcome. In the best centers, the in-hospital mortality for neonates who undergo the arterial switch operation early for simple complete transposition of the great arteries now approaches 1% [6]. In a report from Paris [6], all 68 prenatally diagnosed patients survived neonatal arterial switch operation, whereas 250 postnatally diagnosed patients had a 6% presurgical mortality and a 9% postsurgical mortality, respectively. The disadvantages of delayed diagnosis have been well described in other studies [7,8]. Delay of diagnosis is particularly serious in neonates with critical CHD. Many infants with missed or late diagnosis of critical CHD die [8–10], and most of these neonatal deaths are from hypoplastic left heart syndrome, coarctation of the aorta and interrupted arch, and transposition of the great arteries. Reports from the United Kingdom that 30–50% of neonates with critical CHD left hospital undiagnosed emphasize the need for neonatal screening [11,12].

Critical CHD: Presentations

Neonates with critical CHD are usually well nourished and developed at birth, because their cardiac malformations do not impair the circulation during fetal life [13]. In every neonate after birth, the respiration switches from the placenta to the lung, the ductus arteriosus and the foramen ovale close, and the right and the left ventricles, which worked in parallel prenatally, function in series postnatally. A neonate with critical CHD cannot adapt to the postnatal circulation brought about by these physiologic changes. Table 17.1 shows presentations of these forms of critical CHD.

In complete transposition of the great arteries, cyanosis persists after birth and increases because the parallel systemic and pulmonary circulations have little blood exchange between them [13]. The neonatal patent ductus arteriosus permits aorto-pulmonary shunting and increases pulmonary blood flow, which increases left-to-right atrial shunting and increases arterial oxygen saturation. Postnatal constriction of the ductus arteriosus increases aortic hypoxemia, which can be treated with prostaglandin E_1 (PGE_1), opening the ductus arteriosus [14–16].

In coarctation of the aorta, the aortic obstruction is mild prenatally, and increases with the constriction of the ductus arteriosus postnatally [13]. This occurs usually from 1 to 7 days after birth [13]. A careful early check may reveal

Table 17.1 Critical congenital heart disease in the neonate: frequencies (%, total 376 autopsy cases) [1–3], presentation, treatment with prostaglandin E$_1$ (PGE$_1$) [14–16], and surgical indication[a].

Critical congenital heart disease	Frequency (%)	Presentation	PGE$_1$	Surgery
Transposition of great arteries	18	Cyanosis	+	+
Ventricular septal defect	15	Murmur, dyspnea		+
Coarctation of the aorta	13	Absent pulses	+	+
Aortic and mitral atresia	13	Cyanosis, shock	+	+
Pulmonary atresia and stenosis	6	Cyanosis, murmur	+	+
Patent ductus arteriosus	5	Murmur, dyspnea		+
Tetralogy of Fallot	4	Cyanosis, murmur	+	+
Cor biloculare and triloculare	4	Cyanosis	+	+
Persistent truncus arteriosus	3	Cyanosis		+
Atrioventricularis commune	2	Murmur, dyspnea		+
Total anomalous pulmonary venous return	2	Cyanosis		+
Dextrocardia or levocardia	2	Cyanosis, murmur	+	+
Endocardial fibroelastosis	3	Dyspnea		
Miscellaneous	7	–		+

[a]Note that most of those with a ventricular septal defect died with, but not because of, the defect. Most infants with an isolated large ventricular septal defect do not develop congestive heart failure until 4–6 weeks after birth when the pulmonary vascular resistance has decreased enough to permit a large left-to-right shunt.

normal femoral pulses and right-to-left ductal shunting, resulting in low SpO$_2$ in the lower extremities but a normal SpO$_2$ in the right arm. A few days after birth, femoral pulses are no longer palpable and the SpO$_2$ is the same in the upper and lower extremities. PGE$_1$ infusion in these neonates is effective in lessening aortic obstruction and can be used as a bridge to emergency surgery [13]. Similar changes occur in the courses of neonates with interruption of the aortic arch. Some neonates with very severe coarctation or with severe aortic stenosis present with a clinical picture of shock.

In aortic and mitral atresia (hypoplastic left heart syndrome), the neonate deteriorates in the first week of life [13]. Cyanosis persists after birth because the entire systemic blood flow depends on the right ventricular output and blood flow through the ductus arteriosus [13]. Postnatal ductal constriction causes circulatory shock and death, which occurs between 3 and 7 days after birth in 70% of patients [2]. PGE$_1$ infusion [14–16] is used to dilate the ductus arteriosus as a bridge to emergency surgery.

In pulmonary atresia or severe pulmonary stenosis with intact ventricular septum, the pulmonary circulation depends entirely on the ductus arteriosus [13]. After birth, the ductus arteriosus constricts, pulmonary blood flow decreases, and cyanosis increases. A ductus-dependent pulmonary circulation is present in those critical CHDs associated with pulmonary atresia, including instances with tetralogy of Fallot, tricuspid atresia, transposition of the great arteries, or single ventricle. In such patients, cyanosis is usually mild at birth while the ductus is patent. Then cyanosis may increase progressively during the first 7–10 days, or may suddenly become severe if the ductus closes rapidly. Apart from the cyanosis, the neonate is usually asymptomatic. Only when hypoxia is severe, with arterial oxygen saturation below 45%, do symptoms, particularly tachypnea, appear [13]. Metabolic acidemia develops due to tissue hypoxia and stimulation of aortic chemoreceptors causes tachypnea and hyperpnea. Urgent treatment of the hypoxia is indicated, as discussed later in this chapter.

Diagnosis

Phenotypic signs of chromosomal anomalies [17] may be the first clue to congenital heart disease. Down syndrome is associated with CHD in 30–50% of patients, including atrioventricular septal defect and tetralogy of Fallot [17]. Chromosome 22q11.2 deletion syndrome (DiGeorge syndrome) may present with hypocalcemia in the neonate, and is associated with congenital heart disease in 80% of patients, with anomalies including tetralogy of Fallot, truncus arteriosus, and aortic arch interruption (type B) [18,19]. A heart murmur in a neonate may be the first clue to the disease [20]. It is present in valvar abnormalities, such as aortic stenosis and pulmonary stenosis, and is frequently

heard on the first day. It may be slight or absent with severe stenosis. A murmur of a small ventricular septal defect may be heard in the newborn nursery, but in a large ventricular septal defect the murmur appears some weeks later, following the decrease in pulmonary vascular resistance and the increase in shunting. An innocuous murmur [20] is frequently present in healthy neonates, and is often due to peripheral pulmonary artery stenosis, pulmonary blood flow, or a small or closing patent ductus arteriosus. The best way to determine the origin of these cardiac murmurs is from echocardiographic studies.

Peripheral pulses should be evaluated carefully. Tachycardia may be associated with heart failure. Easily palpable bounding pulses in all extremities occur in CHD associated with large aorta-to-pulmonary shunts, such as a patent ductus arteriosus and truncus arteriosus [21]. Weak or absent pulses in the lower extremities are associated with coarctation and interruption of the aortic arch.

Feeding difficulty, tachycardia, tachypnea, and peripheral cyanosis may be signs of cardiac failure.

Cyanosis is a serious sign in neonates, and one to be treated with respect. Generalized cyanosis occurring more than a few minutes after birth is associated with low cardiac output, polycythemia, methemoglobinemia, cyanotic congenital heart disease, and pulmonary diseases. When a neonate remains cyanotic after a period of oxygen therapy, the clinician must perform a rapid and systematic evaluation to determine whether a cardiac malformation is present so that potentially life-saving measures can be instituted and must determine if the patient is in an optimal hemodynamic and metabolic state to undergo an operation. Neonates suspected of cyanosis are best examined when they are quiet or sleeping under a white light, preferably daylight. Central cyanosis is noticed in the tongue, mucous membranes, and nail beds, and the extremities are usually warm. A comparison of the patient's nail beds with those of the examiner may clarify the presence or absence of cyanosis. In central cyanosis, the oxygen saturation of arterial blood is reduced.

Pulse oximetry

Pulse oximetry [8,10,22–25] measures arterial oxygen saturation and pulse rate. In the neonate, an oximeter probe is applied to the right hand and a foot. If an adequate pulse is not present, as in patients with poor perfusion due to shock, or obstruction to flow as in infants with aortic coarctation, the measurement may not be possible or may be unreliable. Measurement of arterial oxygen saturation by oximetry is more reliable at higher levels of saturation. Thus, at oxygen saturation levels >90% the saturation varies by ~2%, at levels of 70–90% the variation is 3–4%, whereas at levels <70% the variation may be 5% or even higher [13].

Normal neonatal oxygen saturation [13,23]

Every neonate is cyanotic at birth. The first breaths and increasing pulmonary circulation induce a rapid rise in pulse oximeter saturation (SpO_2). The mean preductal (right hand) and postductal (foot) SpO_2 of healthy newborns at the age of 2 min is 73% (range 44–95%) and 67% (34–93%), respectively. At 10 min of age, these values increase to 92% (65–99%) and 85% (62–99%), respectively, and both of these measurements reach 95% within 1 h except in ~5% of newborns with a delayed transitional circulation. Thereafter, the normal baseline SpO_2 is fairly stable at ~98%, except for short periods when it is lower, such as during feeding and apneic spells.

Abnormal oxygen saturation [13,22]

In complete transposition, cyanosis is associated either with a generally low level of SpO_2 (<88%) or a continuous preductal/postductal difference of at least 7%. Rarely with an associated large patent ductus arteriosus, the postductal saturation exceeds the preductal saturation. In critical CHD with a ductus-dependent pulmonary circulation such as tetralogy of Fallot with pulmonary atresia, cyanosis is associated with a generally low level of SpO_2 (<88%). In ductus-dependent obstructive left heart defects, such as coarctation of the aorta, the preductal–postductal SpO_2 difference is often at least 4–5%. In hypoplastic left heart syndrome [26] and total anomalous pulmonary venous return, mild cyanosis is associated with generally low levels of SpO_2 (<95%). A pure left-to-right shunt, such as a ventricular septal defect, does not affect systemic oxygenation and is not detectable by pulse oximetry.

Age at screening [25]

The first hour of life is not suitable for pulse oximetry screening owing to the large number of false-positive findings. Thereafter, infants can be screened at any age, but more reliably at ≥2 h. First-day screening identifies CHD and some other problems, whereas later screening is more specific for congenital heart disease. Most institutions screen between 6 and 48 h after birth [8,10,24,25].

First-day screening [22,25] is performed at ≥2 h. It is so early that even many acute or life-threatening noncardiac problems may still be asymptomatic. Many such diseases have been detected as false-positive findings during screening, most of these being respiratory problems and persistent pulmonary hypertension (discussed later). First-day screening uses a two-point cut-off to form three groups. Immediate echocardiography of all newborns with SpO_2 <90% is indicated. If the first measurement is >95%, no further action is needed [10]. Those within the 90–94% group are checked at 6-hourly intervals, including respiratory rate, heart rate, and feeding. Repeat measurements within 6 h show most of the asymptomatic newborns with an SpO_2

of 90–94% group as false positive. Later screening [22,24,25] is simple because a single measurement is sufficient but may delay diagnosis.

Probe site [22,25]

Newborns with transposition or various types of pulmonary atresia have reduced SpO_2 both pre- and postductally. Anomalies with a ductus-dependent systemic circulation exhibit higher pre- than postductal SpO_2 levels due to right-to-left shunting of unoxygenated blood to the lower body. Pulse oximetry screening is therefore most effective with postductal probe placement.

Signal quality and newborn behavior [13,24]

Technical errors are minimized by accepting only high-quality pulse oximetry signals, confirmed by a good pulse signal displayed simultaneously. The heart rate displayed by the oximeter should be within the range expected for a calm, regularly breathing newborn (~90–160 min^{-1}). The highest average stable SpO_2 value of the pulse oximetry is recorded.

Cut-off [24,25]

On the first day screening, a cut-off of 95% is adequate. On the second day or later, cut-offs of 95–96% appear high enough to make the measurement of pre- or postductal SpO_2 differences unnecessary.

Sensitivity of pulse oximetry screening [24,25]

The sensitivity of pulse oximetry screening in critical CHD is ~70%, and higher than that of clinical examination. Cyanotic CHDs can be detected by pulse oximetry more often than by the clinical examination. Defects in which murmurs are predominantly absent (total anomalous pulmonary venous connection, atrioventricular septal defect, and coarctation of the aorta) are missed clinically more often than by pulse oximetry. Pure left-to-right shunts such as ventricular septal defect or patent ductus arteriosus should not be detectable by pulse oximetry. Some of these shunts (5–17%) are screen positive, however, within the first 24 h of life, probably due to bidirectional shunting during early postnatal pulmonary hypertension.

Discharges with undiagnosed heart disease [8,10,22,24,25]

Pulse oximetry before discharge reduces the number of discharges with an unrecognized serious defect. For example, in one study six of the eight newborns in whom asymptomatic cyanotic CHD was not diagnosed on clinical examination (three with total anomalous pulmonary venous return and one each with pulmonary atresia, tricuspid atresia, and common arterial trunk), the anomaly was detected by late pulse oximetry screening.

Benefits [8,10,24,25]

Pulse oximetry screening enhances timely diagnosis of critical CHD and minimizes the risk and sequelae of delayed detection. Emergency transfer and surgery carry increased risk, not to mention parental anxiety.

Drawbacks [22,25]

Pulse oximetry does not detect left-to-right shunts or other CHDs not affecting oxygenation. Its sensitivity for most of the severe defects is good, but coarctation of the aorta is often missed. A recent study has suggested that the more accurate newest generation of oximeters reveals smaller ductal shunts than previously, allowing for more sensitive detection of coarctation of the aorta. Although false-positive results incur costs for follow-up echocardiography, they are less than those using clinical diagnosis alone, and are probably very low [26].

Further diagnosis

A full cardiac work-up usually includes blood pressure measurements (all limbs), electrocardiogram (ECG), X-rays, and oxygen tests, but only echocardiography is mandatory. B-type natriuretic peptide concentration reveals CHD causing volume or pressure overload, but its sensitivity is unknown, and neonatal reference values need to be refined.

Electrocardiography

In neonates with suspected cardiac anomalies, electrocardiography may show patterns specific to each congenital heart disease. A pattern of right ventricular hypertrophy and right axis deviation is present in normal neonates, and is indistinguishable from the pattern in neonates with critical CHD, including tetralogy of Fallot, aortic atresia, and complete transposition of the great arteries. In tricuspid atresia, left ventricular hypertrophy and left axis deviation are invariably present.

Chest radiography

In the neonate with cyanosis or dyspnea, chest radiography is essential to evaluate any pulmonary disease and also critical CHD. It may show a diaphragmatic hernia, agenesis or hypoplasia of the lungs, atelectasis, pneumonia, or other lung diseases.

Management: prostaglandin E$_1$ [14–16]

Many neonates with critical CHD become symptomatic as the ductus arteriosus closes. Four types of anomalies depend on ductal flow postnatally: (1) those in which the systemic flow is either totally through the ductus (HLHS) or partially (interruption of aortic arch); (2) those in which pulmonary blood flow depends on ductal flow (conditions with

pulmonary atresia); (3) those which depend upon ductal flow for admixture (complete transposition); and (4) those in which ductal closure makes manifest a coarctation.

Maintaining ductal patency with prostaglandin E_1 (PGE_1) is vital in preoperative management [27]. Although ductal closure is rarely immediate, nearly all infants have physiologic closure of the ductus by the fourth day of life; 20% of infants demonstrate functional ductal closure during the first day, and 80% of infants demonstrate ductal closure during the second day of life. For this reason, PGE_1 therapy [14–16] should be initiated immediately when HLHS or other ductal-dependent conditions are diagnosed or suspected. The patient's physiologic state directs initial PGE_1 dosing. For patients who present in shock with suspected ductal closure, initial doses range from 0.05 to 0.1 $\mu g\,kg^{-1}\,min^{-1}$. Once ductal patency is ensured, the infusion rate can be decreased to an effective dose of 0.01 $\mu g\,kg^{-1}\,min^{-1}$. Maintaining ductal patency with the lowest effective PGE_1 dose minimizes the most common dose-dependent side effects of PGE_1.

Hypotension associated with PGE1 necessitates volume resuscitation. The associated respiratory depression necessitates mechanical support. Intravenous caffeine or aminophylline can be used to prevent apnea. Caffeine's loading dose is 20 $mg\,kg^{-1}$ followed by a maintenance dose of 5 to 10 $mg\,kg^{-1}\,day^{-1}$. Aminophylline is given as a bolus dose of 6 $mg\,kg^{-1}$ before or during the initiation of PGE_1, and is continued at a dose of 2 $mg\,kg^{-1}$ every 8h. Patients who receive these have a decreased incidence of apnea and may not require intubation.

In complete transposition, intercirculatory mixing between the systemic and pulmonary circulations is essential for postnatal survival [13,28]. In complete transposition with intact ventricular septum, the ductus arteriosus is often widely patent after birth. At this time, when pulmonary vascular resistance is still high, there is bidirectional ductal flow. With a continuous fall in pulmonary vascular resistance, the shunt through the ductus is primarily from aorta to pulmonary artery, with an equal amount of shunted blood from the left to the right atrium [13,28]. Some patients present with a delayed fall in pulmonary vascular resistance that results in persistent pulmonary hypertension, trivial ductal shunting, and limited intercirculatory mixing. Urgent balloon septostomy will not improve the severe hypoxemia, and these neonates may need urgent support with early repair or extracorporeal membrane oxygenation [13,28]. During the brief perinatal transitional interval, there may be sufficient intercirculatory mixing to limit cyanosis and avoid severe hypoxemia. However, in most affected infants, the ductus soon constricts, with resulting increased hypoxia.

In neonates with transposition, PGE_1 infusion is instituted as a bridge to surgery as soon as feasible, including during transport to the cardiac surgical center, even before the diagnosis has been confirmed echocardiographically. If the PGE_1 infusion is not effective in improving hypoxemia, balloon atrial septostomy may be required urgently.

Pulmonary atresia and patent ductus arteriosus are associated either with an intact ventricular septum [29] or with various congenital heart diseases, including ventricular septal defect, complete transposition, single ventricle, and tricuspid atresia [30]. The pulmonary circulation depends completely on the patent ductus in most patients, but only partially in those patients associated with major aorto-pulmonary collateral arteries (MAPCAs) [30]. In those neonates with a ductus-dependent pulmonary circulation, mild cyanosis persists after birth. The timing of postnatal ductal constriction in these patients is variable, but in most patients it occurs during the first 7 days of life [2]. Infusion of PGE_1 is life-saving in such neonates, and is used as a bridge for surgery [14–16].

Constriction of the ductus arteriosus is important in the development of aortic obstruction in infants with coarctation or interruption of the aortic arch. PGE_1 is used effectively in lessening the aortic obstruction and improving left ventricular failure [13]. PGE_1 is usually effective within the first 7–10 days after birth, but has less effect later [14].

Persistent Pulmonary Hypertension of the Newborn (PPHN) [31]

This syndrome consists of persistent pulmonary hypertension leading to cyanosis and respiratory failure in a newborn [32,33]. The condition usually presents at or shortly after birth. The severity of PPHN can run the full spectrum from mild with transient respiratory distress to severe hypoxemia and cardiovascular instability requiring intensive care support. Current mortality is <10% at most tertiary care centers. Most PPHN patients have an associated pulmonary parenchymal disease, such as meconium aspiration syndrome (MAS) and respiratory distress syndrome (RDS). Some occurrences without known lung disease are termed, however, primary PPHN [32–34].

PPHN primarily affects full-term and near-term neonates with an incidence estimated to be two per 1000 live births. MAS is the most common underlining diagnosis of PPHN, followed by primary PPHN. Other diagnoses include RDS, pneumonia or sepsis, pulmonary vasoconstriction from asphyxia, and pulmonary hypoplasia secondary to congenital diaphragmatic hernia or oligohydramnios [35]. Perinatal stress, such as hemorrhage, hypoglycemia, aspiration, or hypoxia, may also cause PPHN [32].

Diagnosis [30]

PPHN should be suspected in a newborn with symptoms of respiratory distress complicated by labile oxygenation and hypoxia out of proportion to the degree of lung disease. Physical examination usually reveals tachypnea, intercostal retractions, grunting, and cyanosis. Abnormal cardiac sounds, such as a systolic murmur of tricuspid regurgitation or a prominent S_2, may be heard. The chest radiograph can be

normal in primary PPHN, but in PPHN secondary to parenchymal lung disease obvious changes are evident. An atypical course with a poor response to surfactant therapy and hypoxia that is out of proportion to the respiratory problem should lead the clinician to suspect cyanotic CHD or severe PPHN. A PaO_2 increase of >20 mmHg or a saturation increase of >10% in response to oxygen suggests that hypoxemia is secondary to lung disease or mild PPHN. Higher preductal PaO_2 and SaO_2 compared with postductal equivalents indicate a ductal right-to-left shunt which occurs in approximately half of the neonates with PPHN. Ductus-dependent critical left-sided CHDs are also associated with a right-to-left shunt at the PDA and lower postductal oxygen saturation. The response to inhaled nitric oxide (iNO) may help to differentiate PPHN from cyanotic CHD. Most neonates who have PPHN respond rapidly to iNO, with an increase in PaO_2 and SaO_2. On the other hand, neonates with severe PPHN and infants with cyanotic CHD may experience little or no increase in oxygenation with iNO. An echocardiogram is needed to make an accurate diagnosis and if ductus-dependent CHD is found then PGE_1 therapy is begun. In PPHN, echocardiography can also document right-to-left or bidirectional shunts at the level of the ductus or foramen ovale, and can estimate the pulmonary artery pressure from Doppler velocity measurement of the tricuspid regurgitation jet.

Management [31]

Neonates with PPHN require supportive care tailored to the degree of hypoxemia and physiologic instability. The approach should focus on restoring the cardiopulmonary adaptation while avoiding lung injury and adverse effects on systemic perfusion. Prolonged exposure to 100% oxygen and aggressive ventilation can be avoided by judicious application of newer therapies, such as iNO, surfactant replacement, and inotropic support. A normal PaO_2 of 60–90 mmHg is important for postnatal adaptation. There is no evidence that a PaO_2 of >100 mmHg causes a greater reduction in pulmonary vascular resistance [31].

Because PPHN is often associated with parenchymal lung disease or systemic illness, therapy should target the underlying disease. Neonates with mild and transient respiratory distress may respond well to supplemental oxygen alone or with added nasal continuous positive airway pressure. Neonates with moderate respiratory distress and hypoxemia may need ventilator support and monitoring of blood gases. Management of moderate to severe PPHN requires a comprehensive approach to optimize cardiac function and to achieve uniform lung expansion and pulmonary vasodilatation. Reversal of right-to-left extrapulmonary shunting requires a reduction in pulmonary artery pressure and maintenance of the systemic blood pressure. Sedation may be necessary to provide comfort and to decrease oxygen consumption from agitation in hypoxic neonates. Finally, neonates who fail to respond to

optimum medical management may require extracorporeal membrane oxygenation (ECMO).

Inhaled Nitric Oxide therapy (iNO) [31,34]

This is the most important therapy used as a vasodilator in PPHN. The improvement in oxygenation is usually evident within a few minutes of starting iNO. iNO improves oxygenation in ≥70% of neonates who have PPHN, with the best responses in idiopathic PPHN. The ideal starting dose for iNO is 20 ppm, with the effective dose being 5–20 ppm. Doses >20 ppm do not appear to increase efficacy and are associated with more adverse effects. iNO therapy can lead to three potential adverse events: methemoglobinemia generated by oxidation of hemoglobin by NO, exposure to nitrogen dioxide generated by reaction of NO and oxygen, and inhibition of platelet aggregation by NO. With the use of iNO at <20 ppm, these adverse effects are insignificant.

Alternatives to iNO [33,35]

These include inhibiting phosphodiesterase-5 by sildenafil to preserve cyclic GMP, activation of cyclic AMP by PGI_2, and phosphodiesterase-3 inhibition by milrinone. To date, these therapies have been tested in limited clinical trials in patients who did not respond to iNO or when iNO was not available. In the most severe PPHN, ECMO is utilized [36].

Acknowledgments

References

1 Rowe RD, Cleary TE. Congenital cardiac malformation in the newborn period: frequency in a children's hospital. C*an Med Assoc J* 1960;**83**:299–302.

2 Mehrizi A, Hirsch MS, Taussig HB. Congenital heart disease in the neonatal period. Autopsy of 170 cases. *J Pediatr* 1965;**65**:721–6.

3 Izukawa T, Lightfoot NE. Trends in neonatal heart disease. The Toronto experience. In: Freedom RM, Benson LN, Smallhorn JF, eds. *Neonatal Heart Disease*. London: Springer, 1992: 31–4.

4 Hoffman JIE, Kaplan S. The incidence of congenital heart disease. *J Am Coll Cardiol* 2002;**39**:1890–900.

5 Botto LD, Correa A, Erickson JD. Racial and temporal variations in the prevalence of heart defects. *Pediatrics* 2001;**107**:e32.

6 Bonnet D, Coltri A, Butera G, et al. Detection of transposition of the great arteries in fetuses reduces neonatal morbidity and mortality. *Circulation* 1999;**99**:916–8.

7 Brown KL, Ridout DA, Hoskote A, *et al*. Delayed diagnosis of congenital heart disease worsens preoperative condition and outcome of surgery in neonates. *Heart* 2006;**92**:1298–302.

8 de-Wahl Granelli A, Wennergren M, Sandberg K, *et al*. Impact of pulse oximetry screening on the detection of duct dependent congenital heart disease: a Swedish prospective screening study in 39,821 newborns. *BMJ* 2009;**338**:a3037.

9 Chang R-KR, Gurvitz M, Rodriguez S. Missed diagnosis of critical congenital heart disease. *Arch Pediatr Adolesc Med* 2008;**162**:969–74.

10 Meberg A, Andreassen A, Brunvand L, *et al*. Pulse oximetry screening as a complementary strategy to detect critical congenital heart defects. *Acta Paediatr* 2009;**98**:682–6.

11 Wren C, Richmond S, Donaldson L. Presentation of congenital heart disease in infancy: implications for routine examination. *Arch Dis Child Fetal Neonatal Ed* 1999;**80**:F49–53.

12 Wren C, Reinhardt Z, Khawaja K. Twenty-year trends in diagnosis of life-threatening neonatal cardiovascular malformations. *Arch Dis Childh Fetal Neonatal Ed* 2008;**93**:F33–5.

13 Rudolph AM. *Congenital Diseases of the Heart*, 3rd edn. Chichester: Wiley- Blackwell, 2009.

14 Momma K, Takao A, Sone K, Tasiro M. Prostaglandin E$_1$ treatment of ductus-dependent infants with congenital heart disease. *Int Angiol* 1984;**3**(Suppl):33–8.

15 Momma K. Ductus arteriosus and cardiovascular system in the neonate. In: Curtis-Prior PB, ed. *Prostaglandins. Biology and Chemistry of Prostaglandins and Related Eicosanoids.* Edinburgh: Churchill Livingstone, 1988: 476–89.

16 Momma K. Fetal and neonatal ductus arteriosus. In: Curtis-Prior P. ed. *The Eicosanoids*. Chichester: John Wiley & Sons, Ltd, 2004: 569–81.

17 Towbin JA, Greenberg F. Genetic syndrome and clinical molecular genetics. In: Garson A Jr, Bricker JT, Fisher DJ, Neish SR, eds. *The Science and Practice of Pediatric Cardiology.* Baltimore: Williams & Wilkins, 1998: 2627–99.

18 Momma K. Cardiovascular anomalies associated with chromosome 22q11.2 deletion. *Int J Cardiol* 2007;**114**:147–9.

19 Momma K. Cardiovascular anomalies associated with chromosome 22q11.2 deletion syndrome. *Am J Cardiol.* 2010;**105**:1617–24.

20 Park MK, Troxler RG. *Pediatric Cardiology for Practitioners*, 4th edn. St. Louis, MO: Mosby, 2001: 372–3.

21 Momma K. Tetralogy of Fallot and truncus arteriosus. In: Crawford MH, DiMarco JP, Paulus WJ, eds. *Cardiology*, 2nd edn. Edinburgh: Mosby, 2004: 1289–98.

22 Valmari P. Should pulse oximetry be used to screen for congenital heart disease? *Arch Dis Child Fetal Neonatal Ed* 2007;**92**:F219–24.

23 Toth B, Felt LR, Seelbach-Goebel B. Oxygen saturation in healthy newborn infants immediately after birth measured by pulse oximetry. *Arch Gynecol Obstet* 2002;**266**,105–10.

24 de-Wahl Granelli A, Mellander M, Sunnergardh J, *et al*. Screening for duct dependent congenital heart disease with pulse oximetry: a critical evaluation of strategies to maximize sensitivity. *Acta Paediatr* 2005;**94**,1590–6.

25 Mahle WT, Newburger JW, Matherne GP, *et al*. Role of pulse oximetry in examining newborns for congenital heart disease. *Circulation* 2009;**120**:447–58.

26 Hoffman JI. It is time for routine neonatal screening by pulse oximetry. *Neonatology* 2010;**99**:1–9.

27 Tweddell JS, Hoffman GM, Ghanyem NS, *et al*. Hypoplastic left heart syndrome. In: Allen HD, Driscoll DJ, Shaddy RE, Feltes TF, eds. *Moss and Adams' Heart Disease in Infants, Children and Adolescents*, 7th edn. Philadelphia: Lippincott Williams & Wilkins, 2008: 1005–38.

28 Wernovsky G. Transposition of the great arteries. In: Allen HD, Driscoll DJ, Shaddy RE, Feltes TF, eds. *Moss and Adams' Heart Disease in Infants, Children and Adolescents*, 7th edn. Philadelphia: Lippincott Williams & Wilkins, 2008: 1038–87.

29 Freedom RM. Pulmonary atresia and intact ventricular septum. In: Moller JH, Hoffman JIE, eds. *Pediatric Cardiovascular Medicine.* New York: Churchill Livingstone, 2000: 442–60.

30 Doyle TP, Kavanaugh-McHugh A, Graham TP. Tetralogy of Fallot and pulmonary atresia with ventricular septal defect. In: Moller JH, Hoffman JIE, eds. *Pediatric Cardiovascular Medicine*. New York: Churchill Livingstone, 2000: 391–408.

31 Konduri KK, Kim UO. Advances in the diagnosis and management of persistent pulmonary hypertension of the newborn. *Pediatr Clin N Am* 2009;**56**:579–600.

32 Rabinovitch M. Pathophysiology of pulmonary hypertension. In: Allen HD, Driscoll DJ, Shaddy RE, Feltes TF, eds. *Moss and Adams' Heart Disease in Infants, Children and Adolescents*, 7th edn. Philadelphia: Lippincott Williams & Wilkins, 2008: 1322–54.

33 Abman SH. Recent advances in the pathogenesis and treatment of persistent pulmonary hypertension of the newborn. *Neonatology* 2007;**91**:283–90.

34 Clark RH, Kueser TJ, Walker MW, *et al*. Low-dose nitric oxide therapy for persistent pulmonary hypertension of the newborn. *N Engl J Med* 2000;**342**:469–74.

35 Steinhorn RH, Kinsella JP, Pierce C, *et al*. Intravenous sildenafil in the treatment of neonates with persistent pulmonary hypertension. *J Pediatr* 2009;**155**:841–7.

36 Graves ED, Loe WA, Redmond CR, *et al*. Extracorporeal membrane oxygenation as treatment of severe meconium aspiration syndrome. *Southern Med J* 1989;**82**:696–8.

18 Noncardiac Problems of the Neonatal Period

James M. Greenberg

Cincinnati Children's Hospital Research Foundation,
University of Cincinnati College of Medicine, Cincinnati, OH, USA

Preterm birth and congenital malformations account for the vast majority of mortality and morbidity encountered during the neonatal period, typically defined as the first 28 days of postnatal life. This chapter focuses on noncardiac problems encountered by small preterm infants, problems that can have dramatic effects on approaches to the management of congenital heart disease and related problems.

Preterm birth

A preterm birth is defined as occurring prior to the 259th day (37 weeks) after the onset of the last menstrual period. More than 12% of all births in the United States are preterm, with rising rates over the past two decades. The preterm birth rate in the United States is substantially higher than those in most developed countries. Preterm birth is now considered a major public health problem and is a major contributor to the high infant mortality rates reported by the United States [1]. Although preterm birth is typically treated as a single entity in vital statistics reports, the problem is a consequence of a complex interplay among biologic, genetic, environmental, and socioeconomic factors that lead to delivery prior to 37 weeks' gestation [2]. Key factors associated with preterm birth are listed in Table 18.1.

Threshold of viability

Decisions regarding delivery room resuscitation and ongoing clinical care for extremely preterm infants remain extraordinarily challenging for parents and caregivers. Most developed countries identify gestational ages ranging from 22 to 26 weeks to define the threshold of viability [3].

Reported survival rates range from 15 to 30% among infants born at 23 weeks' gestation and rise to 30–55% among those born at 24 weeks' gestation [4,5]. At 25 weeks' gestation, 30–50% of survivors display moderate to severe long-term disabilities in the form of neurodevelopmental delay, cerebral palsy, blindness, and deafness [6]. However, even published data do not account for co-morbid conditions such as major malformations or genetic disorders. Accurate gestational age dating is imperative. Survival and outcomes improve when delivery takes place at a specialty perinatal center with on-site level III NICU facilities [7].

The late preterm infant

Infants born at 34–37 weeks' gestation are the largest proportion of preterm infants. These so-called late preterm infants may appear healthy at delivery and are frequently managed in low-acuity hospital nursery settings. Analysis of large data sets demonstrates that these newborns have a significantly higher mortality risk than their term counterparts [8]. Late preterm infants are also at higher risk for numerous complications of premature birth, including hypothermia, hypoglycemia, infection, hyperbilirubinemia, and respiratory distress requiring positive pressure ventilation (Table 18.2) [9]. Long-term follow-up studies suggest that late preterm infants are more likely to experience learning difficulties in school and attention deficit disorders [10,11].

Many maternity centers are implementing restrictions and guidelines for elective inductions and cesarean delivery with subsequent reductions in the proportion of late preterm delivery [12]. Infants with congenital malformations, including those with congenital heart disease, are more likely to experience poor outcomes when delivered prior to 39 weeks [13].

Table 18.1 Risk factors for preterm birth [2]: the complexity of preterm birth is underscored by the spectrum of risk factors – despite decades of research, the pathophysiologic mechanisms leading to premature delivery remain elusive.

Pregnancy-related conditions
Pre-eclampsia
Chorioamnionitis
Gestational diabetes
Short interpregnancy interval (<6 months)
Family history of preterm birth
Assisted reproductive technology
Polyhydramnios
Cervical dysfunction
Premature, preterm rupture of membranes

Maternal medical conditions
Asthma
Hypertensive diseases
Heart disease
Diabetes
Hyperthyroidism
Autoimmune disease
Proinflammatory states (bacterial vaginosis)

Fetal conditions
Aneuploidy
Multifetal gestation
Congenital malformations

Behavioral/psychosocial
Tobacco use
Alcohol/illicit drug use
Underweight/low BMI
Stress

Sociodemographic
African-American race
Mother <18 years old
Mother >35 years old
Low socioeconomic status
Environmental/toxin exposure
Elective delivery

Table 18.2 Common complications associated with late preterm infants: most of the problems encountered by late preterm infants resolve with timely diagnosis and treatment; however, the number of late preterm births has grown over the past two decades, and associated morbidities contribute substantially to the high aggregate cost of preterm birth.

Hypothermia/temperature instability
Respiratory distress
    Transient tachypnea
    Respiratory distress syndrome
Hypoglycemia
Feeding difficulties
Hyperbilirubinemia

Maternal considerations

Optimal neonatal management requires careful attention to maternal history. Complications of pregnancy have well-described consequences for neonatal outcomes. Diabetes during pregnancy is an excellent example. In addition to an increased risk for congenital heart disease, infants born to diabetic mothers at any gestational age have elevated risk for hypoglycemia, polycythemia, and electrolyte disturbances. Those born at or near term are often macrosomic, with an attendant risk for shoulder dystocia or birth injury.

Chorioamnionitis is associated with premature rupture of membranes and preterm delivery. Fetal exposure to proinflammatory cytokines may increase fetal susceptibility to neurologic injury [14]. Maternal chorioamnionitis may accelerate fetal lung maturation as measured by surfactant protein production, but also increase the risk for subsequent bronchopulmonary dysplasia [15–17]. Neonatal complications of pre-eclampsia include growth restriction, thrombocytopenia, neutropenia, polycythemia, and hypoglycemia. Maternal autoimmune disorders such as lupus may cause fetal heart block, and prompt early delivery.

Respiratory problems

The most common respiratory problem of preterm birth is *respiratory distress syndrome* (RDS), caused by pulmonary surfactant deficiency. Since 1990, the availability of exogenous surfactant treatment and advances in respiratory support have reduced the morbidity and mortality associated with this problem [18].

The classic risk factors for RDS include preterm delivery, maternal diabetes, perinatal asphyxia, cesarean delivery without labor, and genetic factors including male gender and surfactant protein gene deficiencies. Newborns with RDS typically present with respiratory distress characterized by retractions, tachypnea, and grunting respirations. The last symptom reflects an effort to increase end-expiratory pressure by exhalation against the resistance of a partially closed glottis.

The symptoms of RDS are due to increased surface tension within the terminal airspaces, with attendant small airway collapse and air trapping. The consequences are hypoxemia and hypercarbia that progress without treatment. The cornerstone of management of RDS is exogenous surfactant treatment. Prompt intratracheal administration reverses the surfactant deficiency and improves pulmonary compliance and gas exchange.

Some providers are now employing early continuous positive airway pressure (CPAP) support in the delivery room instead of early surfactant, with good results. Early CPAP safely distends distal airways without lung injury.

Either early surfactant administration or CPAP supports respiratory function until endogenous surfactant production suffices to reduce alveolar surface tension, usually by 2–3 days after birth [19].

Surfactant treatment is typically accompanied by positive pressure mechanical ventilation. Careful control of ventilator pressure and volumes minimizes lung injury from atelectasis or over-distension.

Bronchopulmonary dysplasia (BPD) is the most important pulmonary complication of preterm birth. Northway *et al.* first described this disorder as a complication of mechanical ventilation for RDS, resulting in chronic respiratory failure with associated characteristic chest radiographic findings of atelectasis and hyperinflation [20]. This manifestation of BPD is less common in the post-surfactant era. Instead, a "new" form of BPD is now encountered which is characterized by arrest or delay of alveolarization with subsequent progressive impairment of gas exchange [21]. Neonates born prior to 28 weeks' gestation represent the highest risk group.

The diagnostic criteria for BPD have evolved over the past three decades. The current diagnostic definition is based upon oxygen requirement at 28 days after birth and further designated as mild, moderate, or severe based upon oxygen requirement at 36 weeks' postmenstrual age. Clinical decision-making surrounding oxygen administration in the NICU remains variable and subject to interpretation [22].

Both forms of BPD can be complicated by pathologically high pulmonary artery pressures and persistent abnormalities of pulmonary function. It remains difficult to predict who will develop BPD among the at-risk population. In general, the risk of BPD varies inversely with gestational age. RDS, especially severe disease, may increase risk. Volutrauma (over-distension) from excessive tidal volume delivery during mechanical ventilation also clearly raises risk [23]. However, some preterm neonates with benign early neonatal clinical courses develop BPD.

Vitamin A treatment during the early neonatal period is the only intervention capable of reducing the risk of BPD. The effect is mild, with the number needed to treat calculated as 15 on the basis of a well-controlled clinical trial [24]. Several large clinical trials have examined early treatment with inhaled nitric oxide to prevent BPD [25,26]. None showed consistent benefit, although secondary analysis suggests other potential benefits, including reduction of neurologic morbidity and respiratory morbidity for certain subpopulations.

Treatment options for BPD are supportive and do not change important long-term outcomes such as length of stay or mortality [27]. Diuretic treatment remains popular, although only short-term improvements in pulmonary compliance and respiratory support occur. Long-term complications of BPD account for a large proportion of hospital readmissions for bronchiolitis and pneumonia in the at-risk population, even among those with mild disease. Abnormalities of pulmonary function persist throughout the first year of life and beyond. BPD is an independent predictor of poor neurodevelopmental outcome and poor somatic growth [28].

Pulmonary hypoplasia is usually a secondary phenomenon following premature preterm prolonged rupture of membranes (PPPROM) during pregnancy [29]. Other causes of decreased amniotic fluid production, such as bladder outlet obstruction and renal dysplasia, also lead to pulmonary hypoplasia. The resulting oligohydramnios blunts pulmonary development during the period of branching morphogenesis, leading to decreased surface area for gas exchange after delivery. The severity of pulmonary hypoplasia is directly related to the degree and duration of the oligohydramnios and also the extent of prematurity. Prenatal treatment with amnio-infusion accompanied by shunting procedures to relieve bladder outlet obstruction may improve outcomes [30]. Space-occupying lesions in the thorax can also cause pulmonary hypoplasia. These include congenital diaphragmatic hernia and congenital pulmonary adenomatoid malformations (CPAMs).

Whatever the precipitating cause, the clinical presentation of pulmonary hypoplasia varies as a function of severity. Subtle signs and symptoms include tachypnea and spontaneous pneumothorax. As severity increases, respiratory distress escalates, with oxygenation and ventilation affected. Elevated pulmonary vascular resistance and pulmonary hypertension complicate care, as there is usually a limited response to treatment with pulmonary vasodilators, such as nitric oxide. Many practitioners, however, offer these therapeutic interventions to reduce the potential for the development of fixed pulmonary hypertension.

Feeding and gastrointestinal problems

Difficulty with oral feedings is one of the most common problems encountered in the intensive care nursery [31]. Prematurity, congenital malformation, gastrointestinal disorders, and neurologic compromise all contribute to feeding dysfunction during the newborn period. Immature suck–swallow coordination and lower esophageal sphincter function in preterm infants resolve with maturation. Co-morbidities such as BPD with tracheomalacia invariably delay progression to oral feedings [32,33]. Chronic intubation and associated procedures such as suctioning further exacerbate the problem, with oral aversion a significant long-term issue that may persist for months to years.

Infants with congenital malformations are at particularly high risk for feeding difficulties. For example, the incidence of gastroesophageal reflux in patients with congenital diaphragmatic hernia is reported as ≥60% [34,35]. Most are refractory to therapy and require long-term gastrostomy feedings. Foregut malformations such as congenital tracheo-esophageal fistula frequently include a significant degree of

tracheomalacia and esophageal dysmotility. Careful introduction and advancement of oral feedings using cue-based strategies can optimize feeding outcomes. Experienced bedside providers working closely with NICU-based speech and occupational therapists best manage the transition to oral feedings for the at-risk population. Parents and other post-discharge caregivers should also be engaged in oral feedings to ensure a safe, timely discharge from the NICU.

Necrotizing enterocolitis (NEC) remains one of the most devastating gastrointestinal complications of the neonatal period (also see Chapter 15). The etiology of NEC remains unclear. Pathologic invasion of the intestinal mucosa by endogenous bacterial flora appears to be an important common mechanism. Affected individuals develop inflammation and, if severe, transmural necrosis of the bowel. The terminal ileum is preferentially affected, although any region of the large or small bowel may be involved.

Preterm infants are the primary at-risk population. The incidence of NEC decreases with increasing gestational age. Among very low birthweight infants (<1500 g) the incidence is ~7% [36]. The disease is occasionally encountered in term infants. Congenital heart disease or myocardial dysfunction is associated with increase risk of NEC in the late preterm and term neonatal population [37].

The presentation of NEC may be subtle or fulminant and is characterized by the acute onset of feeding intolerance, with tender abdominal distension and dysmotility. Severe disease displays hematochezia, septic shock, and respiratory

Figure 18.1 Radiographic findings in severe necrotizing enterocolitis. This plain film of the abdomen demonstrates many of the classic radiographic findings of severe, Bell stage IIIB, NEC (see Table 18.3 for a complete staging scheme). Of note there is pneumatosis intestinalis, portal venous gas, and pneumoperitoneum. Surgical intervention is indicated and may take the form of exploratory laparotomy with resection of necrotic bowel, or placement of a peritoneal drain. Mortality risk approaches 50% for stage IIIB disease.

Table 18.3 The modified Bell staging system [1,2] for necrotizing enterocolitis (NEC) guides management and provides a useful basis for clinical studies.

Stage	Systemic signs	Abdominal examination	Radiographic signs	Treatment
IA (suspected NEC)	Nonspecific temperature instability, apnea, lethargy, feeding intolerance	Normal or subtle distension	Normal or mild ileus	Bowel rest; 3 day antibiotic treatment
IB (suspected NEC)	As above with hematochezia	As above	As above	Bowel rest; decompression; 3–10 day antibiotic treatment
IIA (definite, mild disease)	As above	As above with tenderness or absent bowel sounds	Intestinal dilation, bowel wall thickening, and pneumatosis intestinalis	Bowel rest; decompression; 10 day antibiotic treatment
IIB (definite, moderate disease)	As above plus mild metabolic acidosis, thrombocytopenia	As above; tenderness more pronounced	As above; ascites may be evident	As above; may require correction of acid–base abnormalities and blood products
IIIA (severe disease with intact bowel)	As above with definite metabolic acidosis, thrombocytopenia, neutropenia, clotting abnormalities	As above with definite abdominal distension, peritonitis	As above	As above
IIIB (severe, with bowel perforation)	As above	As above	As above with pneumoperitoneum or portal venous gas	As above plus surgical intervention

failure exacerbated by compromised diaphragmatic excursion. Abdominal X-rays demonstrate distended bowel loops, bowel wall thickening, and pneumatosis intestinalis, a speckled pattern of intraluminal radiolucency caused by bacterial gas production (Figure 18.1). This X-ray finding is pathognomonic of NEC. A staging scheme described by Bell *et al.* remains useful for defining management and prognosis [38,39]. Those with Bell stage IIIB (Table 18.3) usually require surgical intervention in the form of peritoneal drain placement or exploratory laparotomy with resection of nonviable bowel. Medical management is supportive. Antibiotics, fluid resuscitation, bowel rest, and respiratory support with a focus on achieving acid–base balance are the norm. Bell stage III or IV disease has a high mortality risk approaching 40%. Long-term complications among survivors include stricture formation and complication of short bowel syndrome and also increased risk for developmental delay. Prevention strategies remain largely investigational. Pro- and prebiotics have shown promise in prospective trials [40]. Progress has been limited by variations in such preparations, availability, and safety concerns.

Hyperbilirubinemia is common in the early neonatal period, with >50% of preterm infants experiencing some degree of clinical jaundice [41,42]. Much of this is an exaggerated physiologic manifestation of the normal increase in unconjugated bilirubin levels that takes place after delivery. Bilirubin is a catabolic bile pigment byproduct of heme metabolism. Excess production from pathologic hemolysis or impaired catabolism due to hepatic dysfunction or immaturity represents a major source of elevated bilirubin levels. The overriding concern associated with hyperbilirubinemia is kernicterus, the irreversible death of central nervous system structures caused by toxic levels of unbound bilirubin crossing the blood–brain barrier.

Treatment of hyperbilirubinemia is directed towards eliminating the risk of kernicterus. In general, the risk of kernicterus increases with rising serum bilirubin levels. There is no single level of bilirubin that predicts kernicterus, especially in a preterm infant. Nomograms designed to predict peak bilirubin levels represent an important advance in clinical management [43]. In general, the rate of rise, duration of elevated levels, and etiology of bilirubin production are important variables to consider when developing a management strategy. The standard first-line treatment of hyperbilirubinemia is phototherapy, its effectiveness being a function of maximizing the area of exposed skin illuminated by an effective light source. Specialized banks of lights and fiber-optic phototherapy "blankets" are used to achieve this therapeutic goal. Recent studies demonstrate that immune-mediated hemolysis, such as that caused by ABO or rH incompatibility, also responds to reticuloendothelial blockade with intravenous immunoglobulin treatment [44]. If bilirubin levels do not decrease with phototherapy and intravenous immunoglobulin, double-volume exchange

Figure 18.2 Cranial ultrasound examinations demonstrating intraventricular hemorrhage and periventricular leukomalacia. The upper panels depict (A) coronal and (B) sagittal views of a severe, grade IV, intraventricular hemorrhage involving the right lateral ventricle. A large clot and hemorrhage extend into the surrounding brain parenchyma. There is also ventricular dilation. In (C), multiple small cystic lesions and excess echogenicity of periventricular white matter are seen over the posterior horn of the lateral ventricle. These lesions can occur without associated intraventricular hemorrhage and may not be apparent on ultrasound during the first 1–2 months after delivery. MRI imaging is more sensitive.

transfusion should be performed. This procedure carries substantially more risk than phototherapy and should be performed under careful observation by experienced providers.

Neurologic problems (also see Chapter 52)

The preterm infant is at risk for *intraventricular hemorrhage* (IVH) that arises in the germinal matrix and, in more severe forms, extends into the lateral ventricles. Staging of IVH is based upon anatomic location: grade I hemorrhage is limited to the germinal matrix, grade 2 bleeding involves the ventricle without dilatation, grade 3 IVH includes ventricular dilatation, and grade 4 IVH extends beyond the lateral ventricle into the adjacent parenchyma. The incidence of IVH has declined with more frequent transfer of high-risk mothers to specialty perinatal centers, antenatal steroid administration, and surfactant treatment for RDS.

The risk of severe (grade 3 or 4) IVH increases with decreasing gestational age, especially at <32 weeks. Most IVH occurs within the first 5 days after birth; it is very unusual to encounter new-onset IVH after 10 days of age [45]. Because IVH can be asymptomatic, at-risk infants should be screened by cranial ultrasound at 7–10 days of age (Figure 18.2). Treatment for IVH is supportive. Follow-up cranial ultrasounds should be provided for infants with IVH until the hemorrhagic process is deemed to be in the resolution stage. Obstructive hydrocephalus is the most common complication of severe IVH and may require neurosurgical intervention for intraventricular shunt placement [46].

Preterm infants are also at risk for periventricular white matter injury, also known as *periventricular leukomalacia* (PVL). Those with IVH or a history of cardiopulmonary instability are most likely to develop PVL [47,48]. Affected areas may be defined by focal necrosis (cystic PVL) or demyelination (Figure 18.2). The periventricular white matter in preterm infants is particularly sensitive to ischemia due to immature cerebrovascular pressure regulation and vascular distribution. The reported prevalence of PVL diagnosed by cranial ultrasound is estimated as 5–15% in at-risk populations. Improvements in access and protocols for MRI techniques, however, may reveal lesions in more patients, including those with congenital heart disease. Those who have undergone surgical correction appear to be at particularly high risk. The clinical and prognostic significance of PVL diagnosed by advanced imaging techniques remains an important area for future investigation. Long-term sequelae include cerebral palsy and developmental delay.

References

1 Mathews TJ, MacDorman MF. Infant mortality statistics from the 2005 period linked birth/infant death data set. *Natl Vital Stat Rep* 2008;**57**:1–32.

2 Behrman R, Butler A, eds. *Preterm Birth: Causes, Consequences, and Prevention*. Washington, DC: Institute of Medicine, National Academy of Sciences, 2007.

3 MacDonald H. Perinatal care at the threshold of viability. *Pediatrics* 2002;**110**:1024–7.

4 Wood NS, Marlow N, Costeloe K, *et al*. Neurologic and developmental disability after extremely preterm birth. EPICure Study Group. *N Engl J Med* 2000;**343**:378–84.

5 Lucey JF, Rowan CA, Shiono P, *et al*. Fetal infants: the fate of 4172 infants with birth weights of 401 to 500 grams – the Vermont Oxford Network experience (1996–2000). *Pediatrics* 2004;**113**:1559–66.

6 Vohr BR, Wright LL, Poole WK, McDonald SA. Neurodevelopmental outcomes of extremely low birth weight infants <32 weeks' gestation between 1993 and 1998. *Pediatrics* 2005; **116**:635–43.

7 Warner B, Musial MJ, Chenier T, Donovan E. The effect of birth hospital type on the outcome of very low birth weight infants. *Pediatrics* 2004;**113**:35–41.

8 Kramer MS, Demissie K, Yang H, *et al*. The contribution of mild and moderate preterm birth to infant mortality. Fetal and Infant Health Study Group of the Canadian Perinatal Surveillance System. *JAMA* 2000;**284**:843–9.

9 Escobar GJ, Clark RH, Greene JD. Short-term outcomes of infants born at 35 and 36 weeks gestation: we need to ask more questions. *Semin Perinatol* 2006;**30**:28–33.

10 Kirkegaard I, Obel C, Hedegaard M, Henriksen TB. Gestational age and birth weight in relation to school performance of 10-year-old children: a follow-up study of children born after 32 completed weeks. *Pediatrics* 2006;**118**:1600–6.

11 MacKay DF, Smith GC, Dobbie R, Pell JP. Gestational age at delivery and special educational need: retrospective cohort study of 407,503 schoolchildren. *PLoS Med* 2010;**7**:e1000289.

12 Laye MR, Dellinger EH. Timing of scheduled cesarean delivery in patients on a teaching versus private service: adherence to American College of Obstetricians and Gynecologists guidelines and neonatal outcomes. *Am J Obstet Gynecol* 2006;**195**:577–82; discussion 582–4.

13 Costello JM, Polito A, Brown DW, *et al*. Birth before 39 weeks' gestation is associated with worse outcomes in neonates with heart disease. *Pediatrics* 2010;**126**:277–84.

14 Yoon BH, Jun JK, Romero R, *et al*. Amniotic fluid inflammatory cytokines (interleukin-6, interleukin-1beta, and tumor necrosis factor-alpha), neonatal brain white matter lesions, and cerebral palsy. *Am J Obstet Gynecol* 1997;**177**:19–26.

15 Kallapur SG, Jobe AH. Contribution of inflammation to lung injury and development. *Arch Dis Child* 2006;**91**:F132–5.

16 Watterberg KL, Demers LM, Scott SM, Murphy S. Chorioamnionitis and early lung inflammation in infants in whom bronchopulmonary dysplasia develops. *Pediatrics* 1996;**97**:210–5.

17 Richardson BS, Wakim E, daSilva O, Walton J. Preterm histologic chorioamnionitis: impact on cord gas and pH values and neonatal outcome. *Am J Obstet Gynecol* 2006;**195**:1357–65.

18 Halliday HL. Recent clinical trials of surfactant treatment for neonates. *Biol Neonate* 2006;**89**:323–9.

19 Stevens TP, Harrington EW, Blennow M, Soll RF. Early surfactant administration with brief ventilation vs. selective surfactant and continued mechanical ventilation for preterm infants with or at risk for respiratory distress syndrome. *Cochrane Database Syst Rev* 2007;(4):CD003063.

20 Northway WH Jr, Rosan RC, Porter DY. Pulmonary disease following respirator therapy of hyaline-membrane disease. Bronchopulmonary dysplasia. *N Engl J Med* 1967;**276**:357–68.

21 Jobe AH, Bancalari E. Bronchopulmonary dysplasia. *Am J Resp Crit Care Med* 2001;**163**:1723–9.

22 Walsh MC, Yao Q, Gettner P, *et al*. Impact of a physiologic definition on bronchopulmonary dysplasia rates. *Pediatrics* 2004;**114**:1305–11.

23 Donn SM, Sinha SK. Minimising ventilator induced lung injury in preterm infants. *Arch Dis Child* 2006;**91**:F226–30.

24 Tyson JE, Wright LL, Oh W, *et al*. Vitamin A supplementation for extremely-low-birth-weight infants. National Institute of Child Health and Human Development Neonatal Research Network. *N Engl J Med* 1999;**340**:1962–8.

25 Kinsella JP, Cutter GR, Walsh WF, *et al*. Early inhaled nitric oxide therapy in premature newborns with respiratory failure. *N Engl J Med* 2006;**355**:354–64.

26 Ballard RA, Truog WE, Cnaan A, *et al*. Inhaled nitric oxide in preterm infants undergoing mechanical ventilation. *N Engl J Med* 2006;**355**:343–53.

27 Baveja R, Christou H. Pharmacological strategies in the prevention and management of bronchopulmonary dysplasia. *Semin Perinatol* 2006;**30**:209–18.

28 Anderson PJ, Doyle LW. Neurodevelopmental outcome of bronchopulmonary dysplasia. *Semin Perinatol* 2006;**30**:227–32.

29 Lindner W, Pohlandt F, Grab D, Flock F. Acute respiratory failure and short-term outcome after premature rupture of the membranes and oligohydramnios before 20 weeks of gestation. *J Pediatr* 2002;**140**:177–82.

30 Wu S, Johnson MP. Fetal lower urinary tract obstruction. *Clin Perinatol* 2009;**36**:377–90.

31 Burklow KA, Phelps AN, Schultz JR, *et al*. Classifying complex pediatric feeding disorders. *J Pediatr Gastroenterol Nutr* 1998;**27**:3–7.

32 Wang LY, Luo HJ, Hsieh WS, *et al*. Severity of bronchopulmonary dysplasia and increased risk of feeding desaturation and growth delay in very low birth weight preterm infants. *Pediatr Pulmonol* 2010;**45**:165–73.

33 Singer LT, Davillier M, Preuss L, *et al*. Feeding interactions in infants with very low birth weight and bronchopulmonary dysplasia. *J Dev Behav Pediatr* 1996;**17** 69–76.

34 Kieffer J, Sapin E, Berg A, *et al*. Gastroesophageal reflux after repair of congenital diaphragmatic hernia. *J Pediatr Surg* 1995;**30**:1330–3.

35 Muratore CS, Utter S, Jaksic T, *et al*. Nutritional morbidity in survivors of congenital diaphragmatic hernia. *J Pediatr Surg* 2001;**36**:1171–6.

36 Lemons JA, Bauer CR, Oh W, *et al*. Very low birth weight outcomes of the National Institute of Child Health and Human Development Neonatal Research Network, January 1995 through December 1996. NICHD Neonatal Research Network. *Pediatrics* 2001;**107**:E1.

37 McElhinney DB, Hedrick HL, Bush DM, *et al*. Necrotizing enterocolitis in neonates with congenital heart disease: risk factors and outcomes. *Pediatrics* 2000;**106**:1080–7.

38 Bell MJ, Ternberg JL, Feigin RD, *et al*. Neonatal necrotizing enterocolitis. Therapeutic decisions based upon clinical staging. *Ann Surg* 1978;**187**:1–7.

39 Walsh MC, Kliegman RM. Necrotizing enterocolitis: treatment based on staging criteria. *Pediatr Clin North Am* 1986;**33**:179–201.

40 Deshpande G, Rao S, Patole S, Bulsara M. Updated meta-analysis of probiotics for preventing necrotizing enterocolitis in preterm neonates. *Pediatrics* 2010;**125**:921–30.

41 Maisels MJ. Neonatal jaundice. *Pediatr Rev* 2006;**2**:443–54.

42 Dennery PA, Seidman DS, Stevenson DK. Neonatal hyperbilirubinemia. *N Engl J Med* 2001;**344**:581–90.

43 Bental YA, Shiff Y, Dorsht N, *et al*. Bhutani-based nomograms for the prediction of significant hyperbilirubinaemia using transcutaneous measurements of bilirubin. *Acta Paediatr* 2009;**98**:1902–8.

44 Huizing K, Roislien J, Hansen T. Intravenous immune globulin reduces the need for exchange transfusions in Rhesus and AB0 incompatibility. *Acta Paediatr* 2008;**97**:1362–5.

45 Hill A. Intraventricular hemorrhage: emphasis on prevention. *Semin Pediatr Neurol* 1998;**5**:152–60.

46 Wilson-Costello D, Friedman H, Minich N, *et al*. Improved neurodevelopmental outcomes for extremely low birth weight infants in 2000–2002. *Pediatrics* 2007;**119**:37–45.

47 Volpe JJ. Brain injury in the premature infant: overview of clinical aspects, neuropathology, and pathogenesis. *Semin Pediatr Neurol* 1998;**5**:135–51.

48 Golden JA, Gilles FH, Rudelli R, Leviton A. Frequency of neuropathological abnormalities in very low birth weight infants. *J Neuropathol Exp Neurol* 1997;**56**:472–8.

19 The Epidemiology of Cardiovascular Malformations

Christopher Wren

Freeman Hospital, Newcastle upon Tyne, UK

Introduction

Congenital malformations are the commonest cause of infant mortality in the Western world, and those affecting the cardiovascular system are the commonest type of major congenital anomaly [1,2]. Cardiovascular malformations are said to account for 6% of infant deaths and 30% of deaths due to malformation [3]. Study of the epidemiology of cardiovascular malformations is important for several reasons: we may gain insight into possible causes, we can measure the disease burden in the population, and we can use the data for planning health services and the training and provision of facilities for healthcare providers.

Definitions, inclusions, and exclusions

Most reports adopt the definition first proposed by Mitchell *et al.*: "a gross structural abnormality of the heart or intrathoracic great vessels that is actually or potentially of functional importance" [4]. Most also exclude isolated systemic venous anomalies, patent ductus arteriosus associated with prematurity, cardiomyopathies, isolated cardiac arrhythmias, and cardiac tumors. Bicuspid aortic valve without stenosis or regurgitation is another common exclusion. Its reported prevalence ranges from 0.4 to 2.25%, so it is more common than all other "congenital heart defects" [5,6].

Most congenital cardiovascular malformations are easy to define so that their clinical ascertainment should be complete. Three common exceptions to this are mild pulmonary valve stenosis, mild aortic valve stenosis, and atrial septal defect. Very few reports define Doppler velocities in valve stenosis. None defines atrial septal defect, which is a common normal finding in infancy. The frequent lack of a definition, and lack of consistency when there is one, means that there is likely to be considerable variation between studies and this leads to ascertainment bias.

In some reports, double outlet right ventricle is a relatively common diagnosis whereas in others it does not occur at all. Double outlet right ventricle defines one part of a malformation, which is important when contemplating surgical repair [7], but it does not have a constant definition [8,9] and does not define an anatomically or physiologically distinct group of malformations [8]. It includes diagnoses that may otherwise be described as transposition of the great arteries, tetralogy of Fallot, ventricular septal defect, and so on. There are other instances of methods of classification leading to apparent inconsistencies in birth prevalence of cardiovascular malformations. Pulmonary atresia with ventricular septal defect is sometimes considered as a variation of tetralogy of Fallot and is coded as such. This accounts for the apparent lack of patients having pulmonary atresia with ventricular septal defect in many US reports [10].

Description of complex malformations

Most malformations are easily described by a single term such as ventricular septal defect or coarctation of the aorta. Some common abnormalities, such as tetralogy of Fallot, are made up of more than one morphological abnormality but occur together so frequently that the pattern is universally recognized. Other malformations are complex and cannot be described by a single term or combination of terms [11]. If this occurs, sequential analysis is used to describe the total cardiac morphology and connections, beginning at the venous end of the heart and progressing to the great arteries [12].

Diagnostic hierarchy

Classification of patients with multiple cardiovascular malformations can be difficult, and most published reports have allocated each patient a single diagnosis based on the malformation which is judged to be most important. If patients with more than one diagnosis have to be given only one label, some type of hierarchy is required to decide in which category they fit best, but there is no consensus on how this is best achieved.

The main hierarchies which have been used can be described as anatomic, physiologic, embryologic, and functional, although many older series ignore the problem altogether. Many reports have adopted either the classification proposed in the New England Regional Infant Cardiac Program, which defined a hierarchy based mainly on anatomic severity [13], or that in the Baltimore–Washington Infant Study, in which priority was given to "the malformation components with the earliest embryonic disturbance" [10]. In practice, these two approaches, both of which use a broadly "anatomic" hierarchy, are similar. Reports which are institution based and which cannot define the denominator population usually adopt a "physiologic" hierarchy, taking as the most significant that abnormality which requires the earliest intervention or which causes the greatest hemodynamic disturbance.

Measures of disease frequency

The incidence of disease measures the number of new cases arising over a period of time in a population at risk. Prevalence is a measure of the disease burden in a population. Neither incidence nor prevalence in their classical definitions is directly applicable to descriptive studies of congenital malformations. Most congenital cardiovascular malformations are not immediately apparent at birth but come to notice over time. Hence the period of ascertainment has a significant effect on the measure of disease frequency.

Incidence or prevalence?

Hoffman and Kaplan have argued that the population frequency of cardiovascular malformations should be known as the incidence [6,14]. Both Ferencz and colleagues [10,15] and Daniels [16] favor the use of the term "prevalence at live birth." Because many diagnoses are made retrospectively (i.e., some time after birth), the prevalence would appear to increase with time, yet this is only due to increasing retrospective diagnosis. Open-ended ascertainment obviously gives the opportunity for further increase in the apparent

prevalence at live birth. Ferencz and colleagues therefore suggested that reported diagnoses should be made within 1 year from birth.

The definition of "prevalence at live birth" used here is *the number of patients with a cardiovascular malformation within the population present at birth and diagnosed within the first year of life*. Obviously this is not a true measure of disease occurrence or frequency. It does not consider cardiovascular malformations causing stillbirth or early fetal loss. The rates of cardiovascular malformations in stillbirths are many times higher than those in live births [17]. Prevalence at live birth also cannot take account of antenatally identified lesions that lead to termination of pregnancy, and such reports have to be made separately. This means that prevalence at live birth is the best measure we have but can never be a precise measure of total disease frequency. The total amount of disease is higher because of failure to consider cases causing death before birth, continued ascertainment in childhood and adult life, and the necessarily restrictive definition of cardiovascular malformation.

Prevalence at live birth of cardiovascular malformations

There have been many reports of the live birth prevalence of cardiovascular malformations in the last 50 years. Comparison of reports is hampered by the lack of a common method. Early studies included many unconfirmed clinical diagnoses (before ultrasound was widely available) and some more institution-based recent studies are limited by their inability to define the population from which their patients were derived. Comparisons between studies are also made more difficult by uncertainties over ascertainment and because of the different diagnostic categories and diagnostic hierarchies employed. The reported disease frequency varies considerably. Even if we limit assessment to studies which have a defined denominator population, exclude stillbirths and terminations of pregnancy, and limit ascertainment to the first year of life, there is no evidence of a significantly higher or lower number of malformations in any specific population [6]. The same applies to individual malformations.

The overall prevalence at live birth of cardiovascular malformations is around eight per 1000 live births [14]. The reported live birth prevalence has increased over time but this is probably entirely due to better ascertainment of minor malformations [18]. Figure 19.1a shows a plot of results in 84 population-based reports published in 1951–2005, and Figure 19.1b shows the relationship between smaller studies and higher reported live birth prevalence in the same 84 reports.

Ventricular septal defect is the commonest anomaly in all reports (Table 19.1), with a mean live birth prevalence of
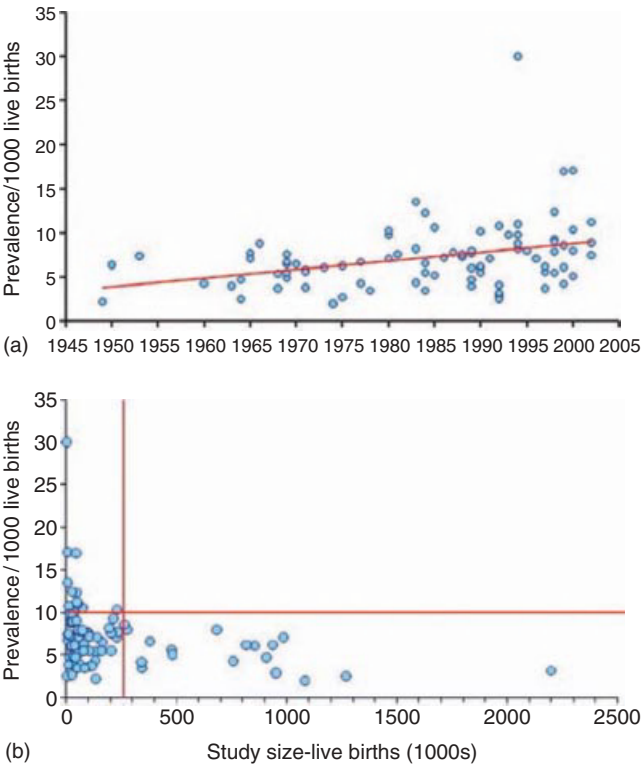
Figure 19.1 (a) Relationship between final year of data collection and reported prevalence at live birth of cardiovascular malformations. Similar results are obtained by plotting middle year of study or year of publication. (b) Relationship between study size (denominator live births) and prevalence at live birth of cardiovascular malformations.

Table 19.1 Prevalence at live birth of cardiovascular malformations – all per 100 000 live births[a].

Cardiovascular malformation[b]	Hoffman and Kaplan, 2002 [14]: median	Papers with common method [41–55]: mean
VSD	283	289
PDA	57	70
ASD	56	101
CAVSD	34	39
PS	53	62
AS	26	21
CoA	36	36
ToF	36	37
TGA	30	34
HLH	23	21
CAT	9	8
TAPVC	9	19
TA	9	10
PA (all)	8	32
DIV/SV/UVH	9	11
PA/VSD	–	11
PA/IVS	–	8
CTGA	–	5
Ebstein	4	5
All	767	620

[a]A summary of published data on the prevalence at live birth of the most common cardiovascular malformations. Data from Hoffman and Kaplan [14] are compared with a summary of data from papers [41–55] sharing a common method (having a defined birth cohort, confining ascertainment to the first year of life, excluding stillbirths and terminated pregnancies, and including only diagnoses confirmed by echocardiography, cardiac catheterization, surgery, or autopsy).

[b]AS, aortic valve stenosis; ASD, atrial septal defect; CAT, common arterial trunk; CTGA, congenitally corrected transposition of the great arteries; CAVSD, complete atrioventricular septal defect; CoA, coarctation of the aorta; DIV, double inlet ventricle; Ebstein, Ebstein's malformation of the tricuspid valve; HLH, hypoplastic left heart; PA, pulmonary atresia; PA/IVS, pulmonary atresia with intact ventricular septum; PA/VSD, pulmonary atresia with ventricular septal defect; PDA, persistent ductus arteriosus; PS, pulmonary valve stenosis; SV, single ventricle; TA, tricuspid atresia; TAPVC, total anomalous pulmonary venous connection; TGA, transposition of the great arteries; ToF, tetralogy of Fallot; UVH, univentricular heart; VSD, ventricular septal defect.

around 175 per 100 000 (but up to 5000 per 100 000 in studies which used early color Doppler echo to find very small defects). Coarctation of the aorta, complete atrioventricular septal defect, transposition of the great arteries, and tetralogy of Fallot all have a mean live birth prevalence of around 30–40 per 100,000 (Table 19.1). Data for other individual anomalies are also summarized in Table 19.1. The lack of a definition of malformations such as aortic stenosis, pulmonary stenosis, and atrial septal defect leads to marked variations in ascertainment.

Some cardiovascular malformations are more prone to ascertainment bias than other. Those, such as transposition of the great arteries and tetralogy of Fallot, have a widely accepted definition, usually occur as isolated anomalies, are little affected by prenatal diagnosis and termination of pregnancy, and almost always present in the first year of life. As expected, they have fairly constant reported birth prevalence with variations explained by sample size, that is, a wider confidence interval in smaller studies (see Figure 19.2a–d). Others, such as ventricular septal defect, atrial septal defect, coarctation of the aorta, and pulmonary valve stenosis, are affected by variable ascertainment and reporting due to

lack of a uniform definition, significant numbers being first diagnosed after infancy, variable ranking of diagnostic hierarchy in the presence of multiple malformations, and so on. This leads to significant skew when the data are plotted, as shown in Figure 19.2e and f.
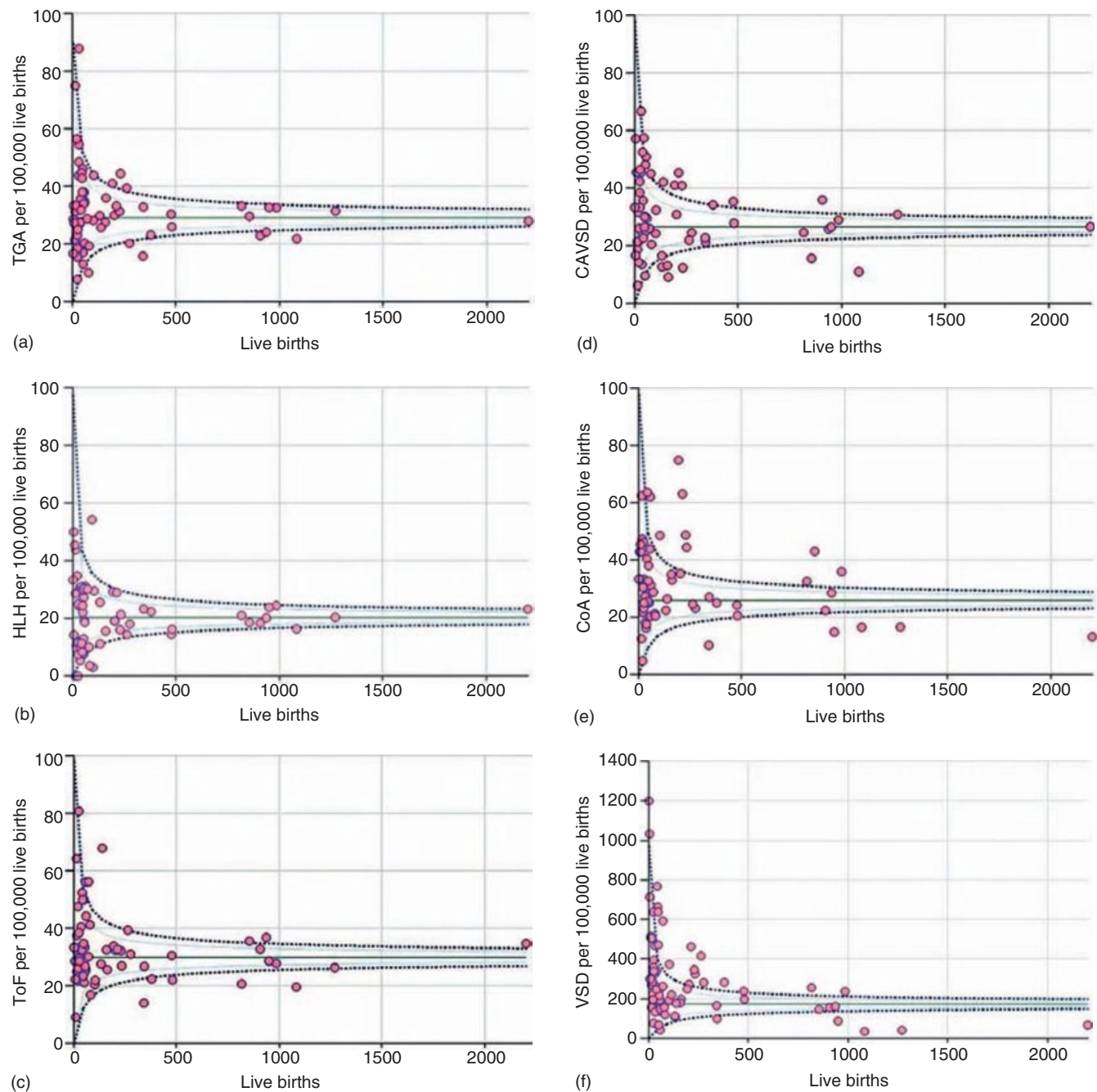
Figure 19.2 Funnel plots of the variation in reported prevalence at live birth of six common cardiovascular malformations. Each funnel plot shows the relationship between study size (thousands of live births in the denominator population) on the *x*-axis and reported live birth prevalence on the *y*-axis. Each individual study is shown by a pink circle. The green line shows the mean, the pale blue lines show two standard deviations from the mean and the dashed dark blue lines show three standard deviations from the mean. As can be seen, the variation is much wider with smaller study size. In the absence of ascertainment bias, almost all data points will lie within three standard deviations from the mean – as shown here for transposition of the great arteries (TGA) in (a) and hypoplastic left heart (HLH) in (b). There is a little more variation for tetralogy of Fallot (ToF) in (c) and complete atrioventricular septal defect (CAVSD) in (d). The results for coarctation of the aorta (CoA) in (e) and ventricular septal defect (VSD) in (f) are notably skewed and more widely scattered, providing clear evidence of ascertainment bias – see text for further explanation.

Table 19.2 Estimates of population prevalence of cardiovascular malformations.

	UK	EU	USA
2005 population	60 266 000	491 875 000	281 422 000
2005 birth rate (per 1000 population)	12.0	10.4	14.1
2005 births	723 000	5 134 000	3 940 000
New cases of CVM[a] (at 10 per 1000 live births)	7000	51 000	39 000
Hoffman *et al.* all CVM 3.9	235 000	1 919 000	1 110 000
Severe CVM 0.46	28 000	226 000	129 000
Marelli *et al.* all CVM 4.1	247 000	2 017 000	1 154 000
Severe CVM 0.38	23 000	187 000	107 000

[a]CVM, cardiovascular malformation.

Causes of cardiovascular malformations

About 10–15% of cardiovascular malformations have a chromosomal or genetic cause [19–22]. Rather fewer are known to be environmental in origin [23,24]. Most environmental causes of cardiovascular malformations occur within the fetal–placental–maternal "environment." Factors associated with increased risk include maternal illness and infection, maternal nutritional excesses and deficiencies, maternal drug exposure, and other environmental exposures.

The cause of most cardiovascular malformations remains unknown, although many more will probably be found to be caused by genetic factors. Epidemiologic studies have produced some interesting findings which offer intriguing clues. Cardiovascular malformations are more common in the offspring of diabetic mothers [25], in twins [26], and in preterm [27] and small-for-dates infants [28]. Some anomalies, such as transposition of the great arteries, hypoplastic left heart, and aortic valve stenosis, are more common in boys, whereas atrioventricular septal defects, atrial septal defects, and patent ductus arteriosus are more common in girls [29].

Population prevalence of cardiovascular malformations

The term "prevalence" measures the total disease burden in a population at any given time. Hoffman *et al.* estimated the total prevalence of cardiovascular malformations by modeling the survival of individual malformations with and without treatment over the period 1940–2002 [30]. They produced high and low estimates and predicted the range of malformations to be found within the total population. Rosamond *et al.* assumed that the true prevalence is two-thirds of the way between Hoffman *et al.*'s estimated

high and low ranges [31]. This leads to predictions that the total population prevalence of all cardiovascular malformations is 3.9 per 1000 (7.4 in children and 2.4 in adults) (Table 19.2).

Marelli *et al.* used a healthcare administration database to determine the population prevalence of severe and other cardiovascular malformations in Quebec [32]. The prevalence increased over time so that there are now more adults than children with cardiovascular malformations (Table 19.2).

The increasing number of children with cardiac malformations who now survive into adolescence and adulthood underscores the need for the healthcare community to prepare for the challenging and often complex needs of adults with congenital heart defects. The predicted number of patients graduating to adult follow-up each year is relatively small compared with the number of adults with heart disease. These patients, their families, and their cardiologists and surgeons, however, have already invested greatly in time, effort, and resources. Rapid recent advances have led to the emergence of adult congenital heart disease as a distinct subspecialty and it is important to be able to predict its future growth to ensure appropriate provision of medical manpower, facilities, and resources for the care of these patients [33–35,35a].

Predicting and measuring surgical workload

Rosamond *et al.* [31] used predictions from Moller [36] to suggest that cardiovascular malformations needing surgery or causing death in infancy occur in 2.3 per 1000 live births. The United Kingdom Central Cardiac Audit Database data for 2005–2006 showed that 2372 operations were performed in infancy – 3.3 per 1000 live births (another 1612 operations

(a) Infant deaths per 100,000 population

(b) Infant deaths per 100,000 live births
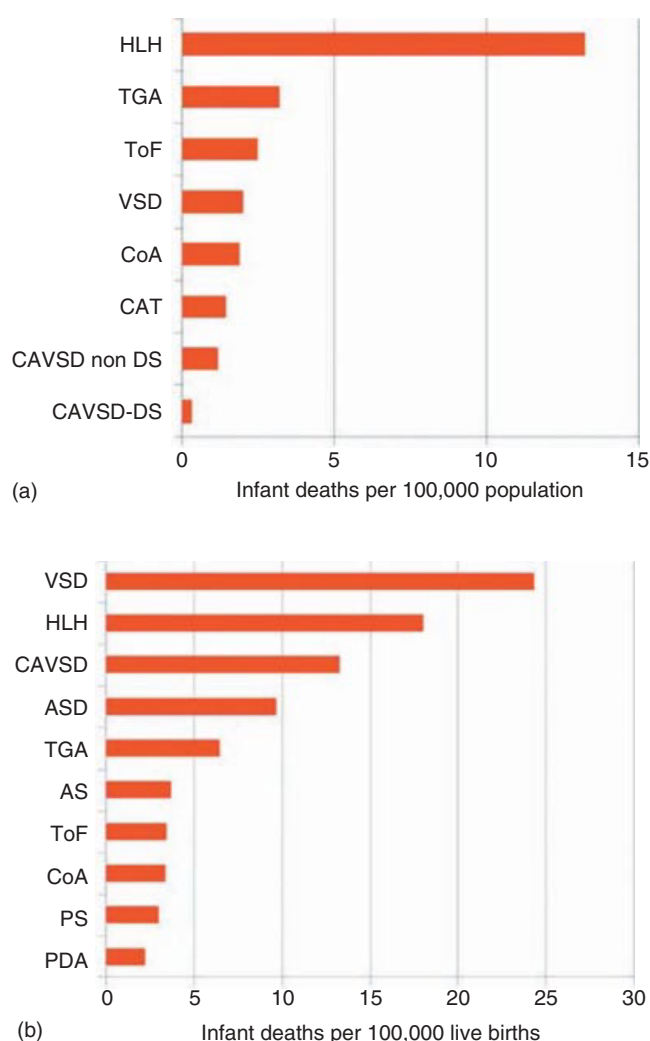
Figure 19.3 The contribution of individual diagnoses to infant mortality. (a) is redrawn from data in Boneva *et al.* [38] and shows the relative contribution of individual malformations *causing* infant mortality. (b) is redrawn from data in Wren and O'Sullivan [35] but includes malformations in all infant deaths, where the malformation was not necessarily the cause of death. This explains the much higher numbers of ventricular septal defects and atrioventricular septal defects, both strongly associated with fatal trisomies. AS, aortic valve stenosis; ASD, atrial septal defect; CAT, common arterial trunk; CAVSD, complete atrioventricular septal defect; CoA, coarctation of the aorta; DS, Down syndrome; HLH, hypoplastic left heart; PDA, patent ductus arteriosus; PS, pulmonary valve stensosis; TGA, transposition of the great arteries; ToF, tetralogy of Fallot; VSD, ventricular septal defect.

were performed in childhood) [37].There will have been more than one procedure per patient, so the number of infants requiring intervention is probably around 3–3.5 per 1000 live births. These data can be used to predict the surgical workload and show that around 2200–2500 infants per year will require intervention in the United Kingdom and 15 000–18 000 within the European Union. The prediction for the United States of 12 000–14 000 procedures is close to measured activity [31].

Cardiovascular malformations and mortality

Mortality associated with cardiovascular malformations has been assessed in several studies, although most include only surgical or postoperative deaths. Boneva *et al.* analyzed death certificate data to investigate trends in mortality associated with cardiovascular malformations in the United States in 1979–1997 [38]. Mortality decreased from 2.5 to 1.5 per 100 000 persons in the whole population. Mortality in infancy declined by 39%. In Western populations, it is estimated that 44% of all deaths from malformations are due to cardiovascular malformations [39] and that cardiovascular malformations cause around 10% of all infant deaths [40].

The contribution of individual malformations to total mortality can be derived from published data [38]. Figure 19.3a, adapted from Botto and Correa [39], shows that hypoplastic left heart made the highest individual contribution to mortality. Other data show a different picture (Figure 19.3b), with ventricular septal defect making the largest contribution to infant deaths [35].The discrepancy between these two findings is that the US study investigated the cause of death whereas the UK study looked at deaths in infants with a malformation. Most deaths in infants with a ventricular septal defects were not caused by the malformation itself but represent the total mortality in patients from associated severe noncardiac malformations or chromosomal and genetic problems, such as fatal trisomy.

References

1 Mathews TJ, MacDorman MF. Infant mortality statistics from the 2005 period linked birth/infant death data set. *Natl Vital Stat Rep* 2008;**57**:1–32.

2 Petrini J, Damus K, Russell R, *et al*. Contribution of birth defects to infant mortality in the United States. *Teratology* 2002;**66**(Suppl 1): S3–6.

3 Shultz AH, Localio AR, Clark BJ, *et al*. Epidemiological features of the presentation of critical congenital heart disease: implications for screening. *Pediatrics* 2008;**121**:751–7.

4 Mitchell SC, Korones SB., Berendes HW. Congenital heart disease in 56,109 births. Incidence and natural history. *Circulation* 1971;**43**:323–32.

5 Ward C. Clinical significance of the bicuspid aortic valve. *Heart* 2000;**83**:81–5.

6 Hoffman JIE. Incidence and natural history. In: Anderson RH, Baker, EJ, Macartney FJ, *et al.*, eds. *Paediatric Cardiology,* 2nd edn. London: Churchill Livingstone, 2002: 111–39.

7 Jacobs JP, Franklin RC, Jacobs ML, *et al*. Anatomic features and surgical strategies in double outlet right ventricle. *Circulation* 1997;**96**:1233–9.

8 Kleinert S, Sano T, Weintraub RG, *et al*. Anatomic features and surgical strategies in double-outlet right ventricle. *Circulation* 1997;**96**:1233–9.

9 Šamánek M, Voříšková M. Congenital heart disease among 815,569 children born between1980 and 1990 and their 15 year survival: a prospective Bohemia natural history study. *Paediatr Cardiol* 1999;**20**:411–7.

10 Ferencz C, Rubin JD, Loffredo CA, Magee CA. *Epidemiology of Congenital Heart Disease. The Baltimore Washington Infant Study: Perspectives in Pediatric Cardiology*, vol 4. Mount Kisco, NY: Futura Publishing, 1993.

11 Kurosawa H, Weinberg PM, Elliott MJ, *et al*. Classification of the functionally univentricular heart: unity from mapped codes. *Cardiol Young* 2006;**16**(Suppl 1):9–21.

12 Anderson RH. Terminology. In: Anderson RH, Baker, EJ, Macartney FJ, *et al.*, eds. *Paediatric Cardiology*, 2nd edn. London: Churchill Livingstone, 2002: 19–36.

13 Fyler DC. Report of the New England Regional Infant Cardiac Program. *Pediatrics* 1980;**65**(Suppl):377–461.

14 Hoffman JIE, Kaplan S. The incidence of congenital heart disease. *J Am Coll Cardiol* 2002;**39**:1890–900.

15 Ferencz C, Czeizel A, Lys A. The problem of comparative analysis of birth prevalence of congenital cardiovascular malformations. *Acta Paediatr Hung* 1990;**30**:169–89.

16 Daniels SR. Epidemiology. In: Long WA, ed. *Fetal and Neonatal Cardiology*. Philadelphia: Saunders, 1990: 425–38.

17 Hoffman JIE. Incidence of congenital heart disease: II. Prenatal incidence. *Pediatr Cardiol* 1995;**16**:155–65.

18 Wren C, Richmond S, Donaldson L. Temporal variability in birth prevalence of cardiovascular malformations. *Heart* 2000; **83**:414–9.

19 Ferencz C, Neill CA, Boughman JA, *et al*. Congenital cardiovascular malformations associated with chromosome abnormalities: an epidemiologic study. *J Pediatr* 1989;**114**:79–86.

20 Johnson MC, Hing A, Wood MK, *et al*. Chromosome abnormalities in congenital heart disease. *Am J Med Genet* 1997;**70**:292–8.

21 Lin AE, Ardinger HH. Genetic epidemiology of cardiovascular malformations. *Prog Cardiovasc Cardiol* 2005;**20**:113–26.

22 Pierpont ME, Basson CT, Benson DW Jr, *et al*. Genetic basis for congenital heart defects: current knowledge: a scientific statement from the American Heart Association Congenital Cardiac Defects Committee, Council on Cardiovascular Disease in the Young. *Circulation* 2007;**115**:3015–38.

23 Mone SM, Gillman MW, Miller TL, *et al*. Effects of environmental exposures on the cardiovascular system;prenatal period through adolescence. *Pediatrics* 2004;**113**:1058–69.

24 Jenkins KJ, Correa A, Feinstein JA, *et al*. Noninherited risk factors and congenital cardiovascular defects: current knowledge: a scientific statement from the American Heart Association Council on Cardiovascular Disease in the Young: endorsed by the American Academy of Pediatrics. *Circulation* 2007;**115**: 2995–3014.

25 Wren C, Birrell G, Hawthorne G. Cardiovascular malformations in infants of diabetic mothers. *Heart* 2003;**89**:1217–20.

26 Manning N, Archer N. A study to determine the incidence of structural congenital heart disease in monochorionic twins. *Prenat Diagn* 2006;**26**:1062–4.

27 Tanner K, Sabrine N, Wren C. Cardiovascular malformations among preterm infants. *Pediatrics* 2005;**116**:e833–8.

28 Archer J, Yeager S, Kenny M, *et al*. Distribution and mortality of serious congenital hart disease in very low birth weight infants. *Pediatrics* 2011; in press (doi:10.1542/peds.2010-0418).

29 Pradat P, Francannet C, Harris JA, *et al*. The epidemiology of cardiovascular defects, Part I: a study based on data from three large registries of congenital malformations. *Pediatr Cardiol* 2003;**24**:195–221.

30 Hoffman JI, Kaplan S, Liberthson RR. Prevalence of congenital heart disease. *Am Heart J* 2004;**147**:425–39.

31 Rosamond W, Flegal K, Friday G, *et al*. American Heart Association Statistics Committee and Stroke Statistics Subcommittee. Heart disease and stroke statistics – 2007 update. *Circulation* 2007;**115**:e69–171.

32 Marelli AJ, Mackie AS, Ionescu-Ittu R, *et al*. Congenital heart disease in the general population: changing prevalence and age distribution. *Circulation* 2007;**115**:163–72.

33 Garson A Jr. Health care policy for adults with congenital heart disease. The patient, the physician, and society. *Circulation* 1992;**86**:1030–2.

34 Skorton DJ, Garson A Jr, Fox JM, *et al*. Task Force 5: adults with congenital heart disease: access to care. *J Am Coll Cardiol* 2001;**37**:1193–8.

35 Wren C, O'Sullivan JJ. Survival with congenital heart disease and need for follow up in adult life. *Heart* 2001;**85**:438–43.

35a Moons P, Bovijn L, Budts W, *et al*. Temporal trends in survival to adulthood among patients born with congenital heart disease from 1970 to 1992 in Belgium. *Circulation* 2010;**122**: 2264–272.

36 Moller JH. *Perspectives in Pediatric Cardiology, Vol. 6. Surgery of Congenital Heart Disease: Pediatric Cardiac Care Consortium, 1984–1995.* Armonk, NY: Futura Publishing, 1998.

37 UKCCAD Congenital Heart Disease Website 2005–2006. National aggregate summary data. http://www.ccad.org.uk (last accessed 31 December 2010).

38 Boneva RS, Botto LD, Moore CA, *et al*. Mortality associated with congenital heart defects in the United States: trends and racial disparities, 1979–1997. *Circulation* 2001;**103**:2376–81.

39 Botto LD, Correa A. Decreasing the burden of congenital heart anomalies: an epidemiologic evaluation of risk factors and survival. *Prog Pediatr Cardiol* 2003;**18**:111–21.

40 Rosano A, Botto LD, Botting B, *et al*. Infant mortality and congenital anomalies from 1950 to 1994: an international perspective. *J Epidemiol Community Health* 2000;**54**:660–6.

41 Abushaban L, Al-Hay A, Uthaman B, *et al*. Impact of the Gulf war on congenital heart diseases in Kuwait. *Int J Cardiol* 2004;**93**:157–62.

42 Bolisetty S, Daftary A, Ewald D, *et al*. Congenital heart defects in Central Australia. *Med J Aust* 2004;**180**:614–7.

43 Cerboni P, Robillard PY, Hulsey TC, *et al*. Congenital heart disease diagnosed in Guadeloupe. *Bull Pan Am Health Organ* 1993;**27**:151–3.

44 Chehab G, Bittar Z. Cumulative incidence and distribution of congenital heart diseases in newborns in Beirut and its southern suburb (1999–2002). *J Med Liban* 2004;**52**:121–5.

45 Cleves MA, Ghaffar S, Zhao W, *et al*. First-year survival of infants born with congenital heart defects in Arkansas (1993–1998): a survival analysis using registry data. *Birth Defects Res A Clin Mol Teratol* 2003;**67**:662–8.

46 Ferencz C, Rubin JD, Loffredo CA, Magee CA, eds. *Perspectives in Pediatric Cardiology, Vol 4. Epidemiology of Congenital Heart Disease. The Baltimore Washington Infant Study.* Mount Kisco, NY: Futura Publishing, 1993.

47 Forrester MB, Merz RD. Descriptive epidemiology of selected congenital heart defects, Hawaii, 1986–1999. *Paediatr Perinat Epidemiol* 2004;**18**:415–24.

48 Garne E. Congenital heart defects – occurrence, surgery and prognosis in a Danish county. *Scand Cardiovasc* 2004;**38**:357–62.

49 Grabitz RG, Joffres MR, Collins-Nakai RL. Congenital heart disease: incidence in the first year of life. The Alberta Heritage Pediatric Cardiology Program. *Am J Epidemiol* 1998;**128**:381–8.

50 Grech V. Spectrum of congenital heart disease in Malta. An excess of lesions causing right ventricular outflow tract obstruction in a population-base study. *Eur Heart J* 1998;**19**:521–5.

51 Kidd SA, Lancaster PA, McCredie RM. The incidence of congenital heart defects in the first year of life. *J Paediatr Child Health* 1993;**29**:344–9.

52 Mogyorosy G, Belicza E, Karacsonyi T, *et al*. Incidence and invasive treatment of congenital heart diseases in Hajdu-Bihar county. *Orv Hetil* 2000;**141**:1287–92.

53 Robida A, Folger GM, Hajar HA. Incidence of congenital heart disease in Qatari children. *Int J Cardiol* 1997;**60**:19–22.

54 Sung RY, So LY, Ng HK, *et al*. Echocardiography as a tool for determining the incidence of congenital heart disease in newborn babies: a pilot study in Hong Kong. *Int J Cardiol* 1991;**30**:43–7.

55 Wren C, Richmond S, Donaldson L. Temporal variability in birth prevalence of cardiovascular malformations. *Heart* 2002;**83**:414–9.

20 Anatomy and Description of the Congenitally Malformed Heart

Robert H. Anderson[1], Anthony M. Hlavacek[1] & Jeffrey Smallhorn[2]
[1]Medical University of South Carolina, Charleston, SC, USA
[2]Stollery Children's Hospital, Edmonton, AB, Canada

Introduction

In the first edition of this book, the question was posed as to why a chapter needed to be devoted to the nomenclature of congenitally malformed hearts, because the lesions themselves had not changed since their initial descriptions. In fact, two chapters were included in the first edition in attempts to answer this question, as not all were agreed at that time on the best way to describe and catalog the manifold individual lesions that could coexist within the congenitally malformed heart. In this second edition, this is the only chapter specifically devoted to anatomy and nomenclature, albeit that accounts of salient anatomic features will be provided in the various chapters describing well-recognized individual lesions. The reasons why a single chapter is now considered sufficient are multiple. In the first place, it is now appreciated that many perceived differences between "schools of nomenclature" are more apparent than real. More importantly, the techniques used to demonstrate the anatomic features of the congenitally malformed heart are now sufficiently advanced that morphology can now be displayed with as much, if not more, accuracy during life as when we hold the autopsied hearts in our hands. In this chapter, therefore, we summarize the details of sequential segmental analysis, now universally accepted as the point of departure for clinical diagnosis. We show how the newly developed diagnostic techniques providing three-dimensional information during life have resolved many, if not most, of the previous controversies. We conclude the chapter with brief considerations of the morphology that underpins the understanding of septal deficiencies.

Sequential segmental analysis

All congenitally malformed hearts, like normal hearts, have three building blocks, namely the atrial chambers, the ventricular mass, and the arterial trunks (Figure 20.1). Initial approaches to description and categorization were based on the need to recognize the limited potential for variation in each of these so-called cardiac segments [1–4]. When some of us sought to modify these early approaches [5], our failure to recognize the fact that the terms concordance and discordance had been used to describe harmony or disharmony between the segments, rather than the fashion in which the components were joined, or not joined, together led to decades of ongoing controversy. The initial use of concordance and discordance to account for the relations between the topological arrangement of the segments [1,2] was reasonable, because at that time it was difficult to be sure of how, for example, the cavities of the atrial and ventricular chambers were joined across the atrioventricular junctions. The development of cross-sectional echocardiography changed all that. Thus, when the concept of sequential segmental analysis was promoted [5], attention was concentrated on the potential anatomic variations across the atrioventricular and ventriculoarterial junctions [5]. Junctional connections, of course, cannot be established without knowledge of segmental topology, so the arrangements within the segments remained the starting point for analysis.

As intimated above, the reason for subsequent dissent came because concordance and discordance were used specifically to define the feature now known as "connections," using these terms to distinguish these variants from other
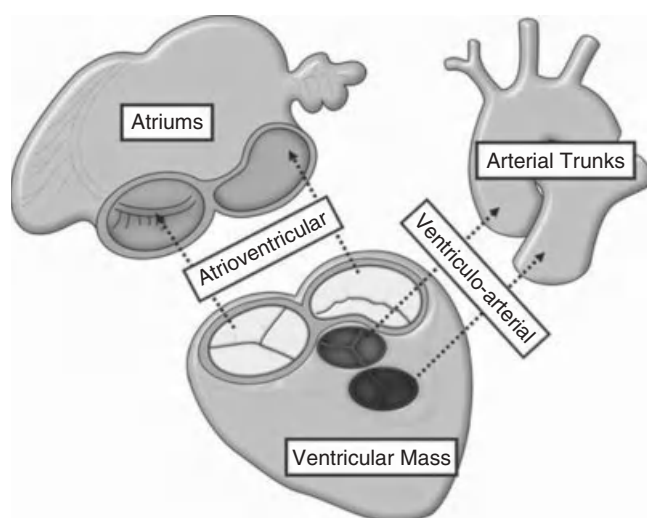
Figure 20.1 The three primary cardiac segments are delineated anatomically by the discrete atrioventricular and ventriculoarterial junctions.

arrangements such as double inlet or double outlet [5]. Within the original concept, however, patients having double inlet left ventricle within the segmental combination codified as {S,D,D} were also described as exhibiting atrioventricular concordance [1,4]. One of the fundamental differences between the usual heart (Figure 20.2a) and the heart showing double inlet left ventricle (Figure 20.2b), nonetheless, lies in the way that the atrial cavities join the ventricular cavities across the atrioventricular junctions. We now overcome these conceptual difficulties between the segmental and sequential segmental approaches by avoiding the use of "concordance" and "discordance" to describe the fashion in which cavities are joined together across the atrioventricular and ventriculoarterial junctions. Instead, we specify the existence of concordant or discordant connections.

Sequential segmental analysis, therefore, has evolved with the passage of time [5,6]. Despite the changes, it continues to follow its initial basic and simple rules. Morphology, connections, and relations of the segmental components are recognized as three individual facets of the cardiac make-up. Clarity in describing these features is considered more important than brevity. It is the desire to achieve optimal clarity that has led to the changes in descriptions made during the process of evolution. No apologies are made for these changes [7], made in response to valid criticisms, which have eradicated initially illogical points from the system to its advantage [8]. Should further illogicalities become apparent, they will similarly be extirpated.

The morphological method

Segmental analysis depends on the ability to distinguish the morphology of the individual atrial and ventricular chambers, and to recognize the nature of the arterial trunks taking origin from the ventricular mass. This is not as straightforward

as it may seem, because when the heart is congenitally malformed, these chambers or arterial trunks may lack some of the morphologic features that most obviously characterize them in the normal heart. For example, the most obvious feature of the morphologically left atrium in the normal heart is its connection to the pulmonary veins. In hearts with totally anomalous pulmonary venous connection, these veins connect to extracardiac sites, yet it is still possible to recognize the remnant of the left atrium. It was considerations of this type that prompted the establishment of the concept now used to underpin the recognition of the cardiac chambers and great arteries, which is known as the morphologic method [9,10]. The principle states that cardiac structures should be recognized in terms of their intrinsic morphology, one part of the heart not being defined in terms of other structures that are themselves variable.

When applying this concept to the atrial chambers, the connections of the great veins are immediately disqualified as markers of morphological rightness or leftness, simply because the veins do not always connect to their expected atrial chamber. Septal morphology is of little help when the septum itself is absent, and the atrial vestibule is ruled out as a marker because it is usually lacking in hearts with atrioventricular valvar atresia. Fortunately, there is another component of the atrial chambers that is almost universally present, namely the appendage. When judged on the extent of its contained pectinate muscles, this feature always distinguishes between morphologically right and left atrial appendages [11]. The morphologically right appendage has the shape of a blunt triangle and joins over a broad junction with the remainder of the atrium. The junction is marked externally by the terminal groove and internally by the terminal crest, while the pectinate muscles lining the appendage extend all around the parietal atrioventricular junction (Figure 20.3a). The morphologically left appendage, in contrast, is much narrower and tubular. It has a narrow junction with the remainder of the atrium that is marked by neither terminal groove nor muscular crest. The pectinate muscles are confined within the morphologically left appendage, with the posterior aspect of the morphologically left vestibule being smooth-walled as it merges with the pulmonary venous component (Figure 20.3b).

The morphologic method also shows its value when it is applied to the ventricular mass, which extends from the atrioventricular to the ventriculoarterial junctions. Within the ventricular mass, as thus defined, there are almost always two ventricles. Description of ventricles, no matter how malformed they may be, is facilitated if they are analyzed as possessing an inlet, extending from the atrioventricular junction to the distal attachment of the atrioventricular valvar tension apparatus, an apical trabecular component, and an outlet component, the latter part supporting the leaflets of the arterial valve. Of these three components, it is the apical trabecular component that is most universally

(a)   (b)
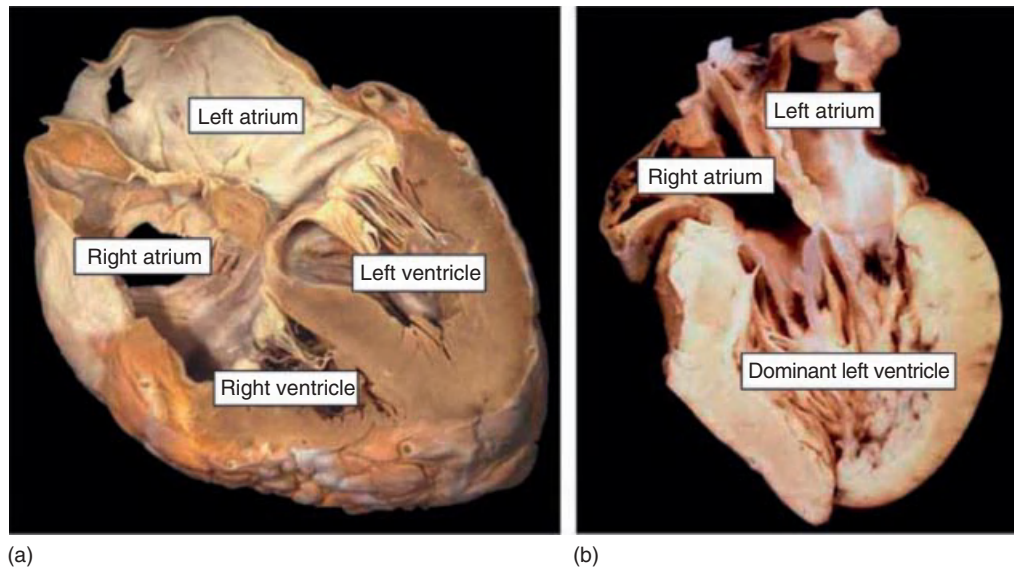
Figure 20.2 Panel (a) shows how the normal heart has separated atrioventricular junctions for the right-sided and left-sided atrial and ventricular chambers. The cavities of the chambers are connected together across these junctions. Panel (b) shows double-inlet left ventricle. The essential feature is that both atrioventricular junctions are connected to a dominant left ventricle.
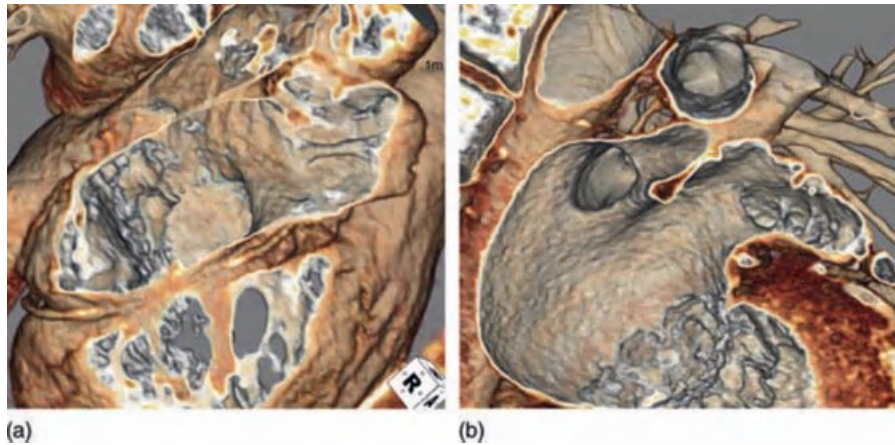
Figure 20.3 The computed tomographic reconstructions show the morphologic differences, based on the extent of the pectinate muscles, between the morphologically right (a) and the morphologically left atrial appendages (b). The pectinate muscles in the right atrium extend around the orifice of the tricuspid valve, while those in the left atrium are confined within the tubular appendage.

present in normal, and also in malformed and incomplete, ventricles. Furthermore, it is the pattern of the apical trabeculations that differentiates best the morphologically right from the left ventricle (compare Figure 20.4a and b). This remains true when the apical components exist as the basis of incomplete ventricles, which lack either an inlet or an outlet component, or sometimes both.

When the morphology of individual ventricles is identified according to the apical myocardium, all hearts with two ventricles can readily be analyzed according to the way that the inlet and outlet components are shared between the apical trabecular components. When describing the overall ventricular mass, it is also necessary to describe the way in which the two ventricles themselves are related to each other. There are two patterns, which are mirror images of

each other. They can be conceptualized in terms of the way that, figuratively speaking, the palmar surface of the hands can be placed on the septal surface of the morphologically right ventricle. In the morphologically right ventricle of the normal heart, irrespective of its position in space, it is the palmar surface of the right hand which can be placed on the septal surface such that the thumb occupies the inlet and the fingers fit into the outlet (Figure 20.5a). The palmar surface of the left hand then fits in comparable fashion within the morphologically left ventricle, but it is the right hand that is taken as the arbiter for the purposes of categorization. The usual pattern, therefore, can be described as right-hand ventricular topology [12]. The second pattern is then described as left-hand ventricular topology. It is seen in the mirror-imaged normal heart, or in the variant of

Figure 20.4 Computed tomograms showing the characteristic apical trabeculations that distinguish the morphologically right ventricle (a) from its left ventricular partner (b). Both ventricles, nonetheless, have obvious inlet and outlet components in addition to the apical component.
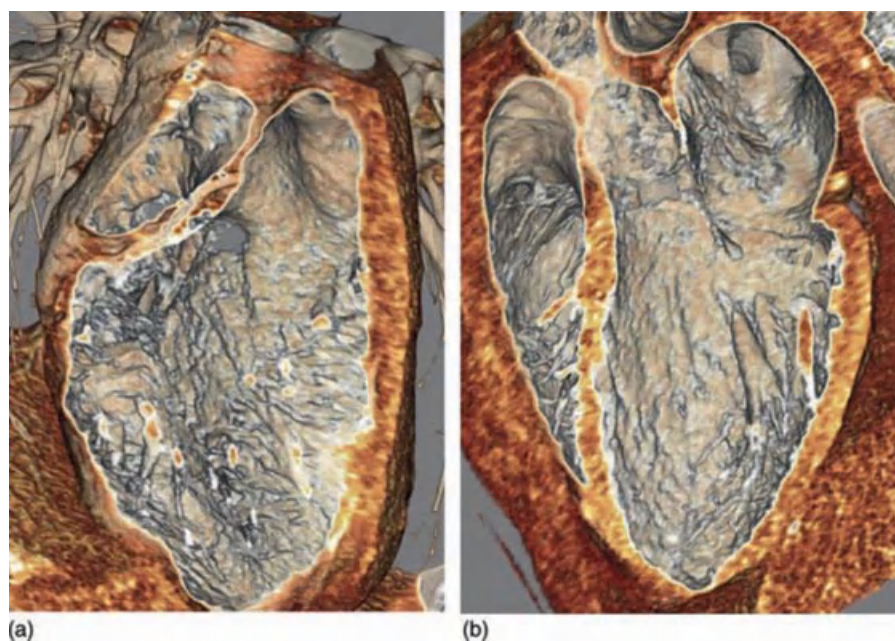
Figure 20.5 Ventricular topology is conceptualized in terms of the way in which the right (a) and left hands (b) can be placed on the septal surface of the morphologically right ventricle. All hearts with biventricular atrioventricular connections have either right-hand or left-hand topology. Panel (a) shows the normal heart and (b) shows the left-sided right ventricle in the heart from a patient with usual atrial arrangement and congenitally corrected transposition.
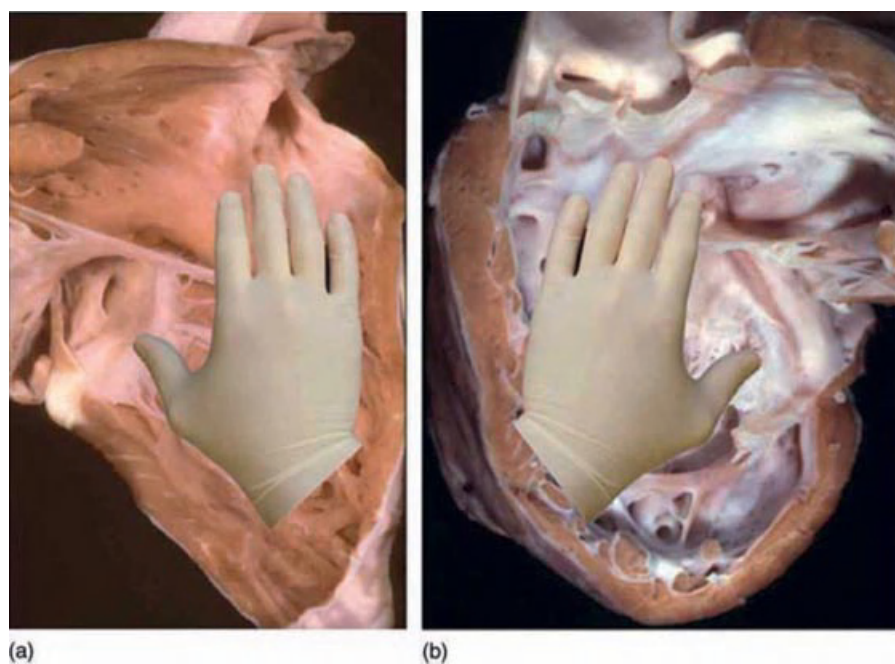
congenitally corrected transposition found with usual atrial arrangement (Figure 20.5b). With this pattern, it is the palmar surface of the left hand that fits on the septal surface of the morphologically right ventricle with the thumb in the inlet and the fingers in the outlet.

When determining the identity of the arterial trunks, there are no intrinsic features that enable an aorta to be distinguished from a pulmonary trunk, or from a common or solitary arterial trunk. The branching pattern of the trunks themselves, nonetheless, is sufficiently characteristic to permit these distinctions (Figure 20.6). Thus, the aorta gives rise to at least one coronary artery and the bulk of the systemic arteries. The pulmonary trunk gives rise directly to both, or one or other, of the pulmonary arteries. A common trunk directly supplies the coronary, systemic, and pulmonary arteries. A solitary arterial trunk exists in the absence of the intrapericardial pulmonary
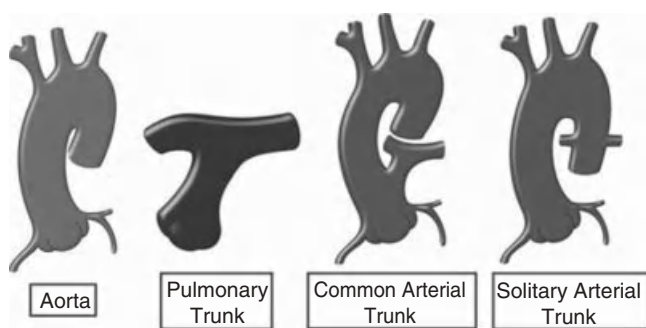
Figure 20.6 The arterial trunks can be divided into four patterns according to the nature of their branching. The solitary trunk exists in the complete absence of any intrapericardial pulmonary arteries.

Figure 20.7 The four possible arrangements of the atrial chambers based on the extent of the pectinate muscles relative to the atrioventricular junctions.

arteries. In such circumstances, it is impossible to state with certainty whether the persisting trunk is common or aortic, hence it is best described as being solitary.

Basic analysis

The system depends first on the establishment of the arrangement of the atrial chambers, or atrial situs. Next, attention is concentrated on the anatomic nature of the junctions between the atrial myocardium and the ventricular myocardial mass. This feature, which is described as a type of connection, is separate from the additional feature of the morphology of the valve or valves that guard the junctions. There are two atrioventricular valves in the normally constructed heart, each guarding a separate atrioventricular junction (Figure 20.2a), but the junction can be a common structure, guarded by a common valve, without changing the overall fashion in which the atrial myocardium is connected to the ventricular mass. Proper analysis of the atrioventricular junctions also requires identification of the structure, topology, and relationships of the chambers within the ventricular mass. When the atrioventricular junctions have been dealt with in this fashion, the ventriculoarterial junctions are similarly analyzed in terms of the arrangement of the connections of ventricles with arterial trunks, and the morphology of the arterial valves guarding them. Separate attention is directed to the morphology of the outflow tracts, and to the relationships of the great arterial trunks. A catalog is then made of all associated cardiac and, when pertinent, noncardiac, malformations. This should include such features as the location of the heart, and the arrangement of the other thoracic and abdominal organs. Each system is analyzed in its own right, and is not designated according to changes observed in other systems. When analyzed and described in this fashion, there is obviously no such thing as "situs ambiguous."

Atrial arrangement

Analysis of atrial arrangement cannot be done on the basis of venoatrial connections, because this would be a direct abrogation of the morphologic method. In the current era,
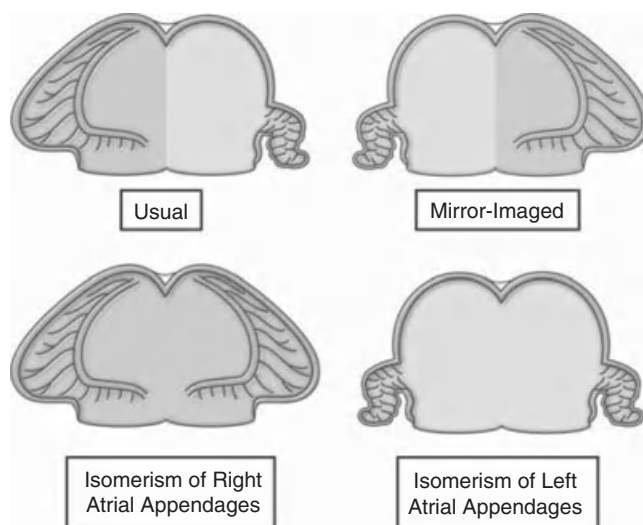
there is no problem in analyzing atrial arrangement according to the morphology of the junction of the appendages with the rest of the atrial chambers (Figure 20.3). Assessment on the basis of this myocardial morphology reveals that there are four possible patterns of arrangement. This is because all hearts have two atrial appendages, each of which can only be of morphologically right or left type (Figure 20.7). With the usual and mirror-imaged arrangements, the appendages are lateralized, the morphologically right appendage being to one side of the heart and the morphologically left appendage to the other. The two other arrangements show isomerism of the atrial appendages. Ideally, this feature should also be recognized by direct examination of the extent of the pectinate muscles around the vestibules, now possible with use of cross-sectional echocardiography, particularly in its three-dimensional format. Morphology of the appendages is also accurately displayed with magnetic resonance imaging or computed tomography (Figure 20.2).

In most clinical situations, however, it is rarely necessary to rely only on direct identification. This is because, almost always, the morphology of the appendages is in harmony with the arrangements of the thoracic and abdominal organs. In patients with usual and mirror-imaged arrangements, it is exceedingly rare for there to be disharmony between the location of the thoracic and abdominal organs. When the appendages are isomeric, there is usually so-called visceral heterotaxy. In this setting, the lungs and bronchial tree are almost always symmetric, and it is rare for the bronchial arrangement to be disharmonious with the morphology of the appendages. In suspicious circumstances, therefore, isomerism can almost always be inferred from the bronchial anatomy. The morphologically left bronchus is long, and

branches only after it has been crossed by a branch pulmonary artery, making the bronchus hyparterial. In contrast, the morphologically right bronchus is short, and is crossed by a pulmonary artery supplying the lower lobe only after it has branched, giving an eparterial pattern of branching.

Inferences similar to those provided from bronchial arrangement can also usually be obtained noninvasively by using cross-sectional ultrasonography to image the abdominal great vessels [13]. The relation of these vessels to each other, and to the spine, generally reflects bodily arrangement, although not as accurately as does bronchial anatomy. When the atrial appendages are lateralized, the inferior caval vein and aorta lie to opposite sides of the spine, with the caval vein on the side of the morphologically right appendage. When there is right isomerism, the great vessels usually lie to the same side of the spine, with the caval vein anterior. The finding of an azygos vein carrying the inferior caval venous blood on the same side, and posterior to, the abdominal aorta is a good indicator of left isomerism, albeit not always differentiating the isomeric variant from usual or mirror-imaged arrangement with interrupted inferior caval vein. Generally, right isomerism is associated with absence of the spleen, whereas left isomerism is associated with multiple spleens. Because of this association, patients with isomerism of the atrial appendages have traditionally been grouped together, from the cardiac standpoint, under the banner of the "splenic syndromes." This approach is much less accurate than describing the syndromes directly in terms of isomerism of either the right or left atrial appendages [14,15]. In reality, it is necessary to describe both the state of the spleen and the morphology of the appendages, but it is the latter feature that serves to concentrate attention on the heart.

Atrioventricular junctions

In the normal heart, the atrial myocardium is contiguous with the ventricular mass around the orifices of both the mitral and tricuspid valves (Figure 20.2a). Electrical insulation is provided at these junctions by the fibrofatty atrioventricular grooves, other than at the site of the penetration of the bundle of His. In abnormal hearts, in order to analyze the morphology of the atrioventricular junctions accurately, it is first necessary to know the atrial arrangement. Equally, it is necessary to know the morphology of the ventricular mass to establish which atrium is connected to which ventricle. With this information, it is then possible to define the pattern of the atrioventricular connections and to determine the morphology of the valves that guard the junctions.

In every heart, because there are two atrial chambers, there is the possibility for two atrioventricular connections, which will be right-sided and left-sided. This is irrespective of whether the connections are guarded by two valves or a common valve. One of the connections as thus defined may be blocked by an imperforate valvar membrane, but this does not alter the fact that, in such a setting, there are still two atrioventricular connections present. In some hearts, in contrast, this possibility is not fulfilled because one of the connections is completely absent. Then, the atrial myocardium on that side has no connection with the underlying ventricular myocardium, being separated from the ventricular mass by the fibrofatty tissues of the atrioventricular groove. This arrangement is the most common pattern producing atrioventricular valvar atresia.

When atrioventricular connections are defined in this way, all hearts fit into one of three groups. In the first group, by far the most common, each atrial chamber is connected actually or potentially, but separately, to an underlying ventricle. In the second group, only one of the ventricles, if indeed two are present, has connections with the atrial chambers. In the third, and rarest, group, one atrioventricular connection is absent, the solitary atrioventricular junction being connected to two ventricles by a straddling valve. This arrangement is uniatrial but biventricular [16].

There are three possible types of biventricular atrioventricular connections, concordant, discordant, and biventricular and mixed. The last arrangement is found in hearts with isomeric appendages, whether they are of right or left morphology. Because of the isomeric nature of the appendages, this third arrangement cannot be described accurately in terms of concordant or discordant connections. It is a discrete biventricular pattern in its own right. The mixed variant is independent of ventricular relationships and atrioventricular valvar morphologies, but requires specification of ventricular topology to make the description complete.

There are also three possible junctional arrangements that produce univentricular atrioventricular connections [17]. The first is when the cavities of right-sided and left-sided atrial chambers are connected directly to the same ventricle (Figure 20.2b). This is double-inlet atrioventricular connection, irrespective of whether the right-sided and left-sided atrioventricular junctions are guarded by two atrioventricular valves or a common valve. The other two arrangements exist when one atrioventricular connection is absent, giving absent right-sided or absent left-sided atrioventricular connections. The group of univentricular atrioventricular connections is different from the group of biventricular connections, being independent not only of ventricular relationships and valvar morphology, but also of atrial and ventricular morphologies. Hearts with concordant or discordant atrioventricular connections can exist only when usually arranged or mirror-imaged atrial chambers are each connected to separate ventricles. A heart with biventricular and mixed connections can be found only when each of two atrial chambers having isomeric appendages is connected to a separate ventricle. In contrast, double-inlet, absent right-sided, or absent left-sided atrioventricular connection can be found in the settings of usually arranged, mirror-imaged, or isomeric atrial appendages. Each type of univentricular atrioventricular connection can also be found with the atrial

chambers connected to a dominant left ventricle (Figure 20.2b), a dominant right ventricle, or a morphologically indeterminate ventricle. Hence it is always necessary to describe ventricular morphology in hearts with univentricular atrioventricular connections [8].

In the hearts with univentricular atrioventricular connections, although only one ventricle is connected to the atrial chambers, most possess a second ventricle. This second ventricle, of necessity, is incomplete, lacking at least its inlet component. It is of complementary trabecular pattern to the dominant ventricle. Most frequently, the dominant ventricle is morphologically left, and the incomplete ventricle possesses right ventricular apical trabeculations. More rarely, the dominant ventricle is morphologically right and the incomplete ventricle is morphologically left. Even more rarely, hearts will be found with a solitary ventricular chamber of indeterminate morphology, albeit that, in clinical practice, it can be difficult to distinguish the truly solitary ventricle from apparently solitary left or right ventricles in which the incomplete ventricle is too small to be demonstrated.

Description of the type of atrioventricular connection accounts only for the way in which the atrial musculature is joined to the ventricular mass. The morphology of the valves guarding the overall atrioventricular junctional area, within the constraints imposed by the connections themselves, is an independent feature. Thus, when the cavities of both atrial chambers communicate directly to the ventricular mass, the right-sided and left-sided atrioventricular connections may be guarded by two patent valves, by one patent valve and one imperforate valve, by a common valve, or by straddling and overriding valves. These arrangements can all be found with the concordant, discordant, mixed, or double-inlet types of connection. Either the right-sided or left-sided valve may be imperforate, producing atresia, but in the setting of a potential as opposed to an absent atrioventricular connection. A common valve guards both right-sided and left-sided atrioventricular connections, irrespective of its morphology. A valve straddles when its tension apparatus is attached to both sides of a septum within the ventricular mass. It overrides when its annulus is connected to ventricles on both sides of a septal structure. A right-sided valve, a left-sided valve, or a common valve can straddle, can override, or can straddle and override. Rarely, both right-sided and left-sided valves may straddle or override in the same heart. When one atrioventricular connection is absent, however, the possible modes of connection are greatly reduced. This is because there is a solitary atrioventricular valve, which is usually committed in its entirety to one ventricle. More rarely, it may straddle, override, or straddle and override. These patterns produce the extremely rare group of uniatrial but biventricular connections [16].

An atrioventricular valve that overrides has an additional influence on description, as the degree of commitment of the overriding atrioventricular junction determines the precise nature of the atrioventricular connections. Hearts with overriding valves are anatomically intermediate between those with, on the one hand, biventricular and, on the other hand, univentricular atrioventricular connections. There are two ways of describing such hearts. One is to consider the hearts as representing a special type of atrioventricular connection. The other is to recognize their intermediate nature, and to split the series depending on the precise connection of the overriding junction. Our preference is for the second option. When most of an overriding junction is connected to a ventricle that already receives the other atrioventricular connection, we designate the connection as being double inlet. If the overriding junction is connected mostly to a ventricle not itself connected to the other atrium, each atrium is categorized as though connected to its own ventricle.

When describing the atrioventricular valves, the adjectives "mitral" and "tricuspid" are strictly accurate only in hearts with biventricular atrioventricular connections having separate junctions, each guarded by its own valve. The tricuspid valve is then always found in the morphologically right ventricle, and the mitral valve in the morphologically left ventricle. In hearts with biventricular atrioventricular connections but with a common junction, in contrast, the common valve lacks mitral and tricuspid components, even when it is divided into right and left components. The essence of the left-sided component in this setting is its trifoliate, rather than bifoliate, configuration (Figure 20.8). In hearts with double inlet connection (Figure 20.2b), the two valves are again better considered right-sided and left-sided, rather than mitral or tricuspid. Similarly, when one connection is absent, although it is usually possible to deduce the presumed nature of the remaining solitary valve from concepts of morphogenesis, this is not always practical or helpful. The valve can always accurately be described as being right-sided or left-sided.

Ventricular topology and relationships

Even in the normal heart, the ventricular spatial relationships are complex. The inlet portions are more or less to the right and left, with the posteroinferior part of the muscular ventricular septum lying in an approximately sagittal plane. The outlet portions are more or less anteroposteriorly related, with the septum between them in an approximately frontal plane. The trabecular portions extend between these two components, with the apical muscular septum spiraling between the inlet and outlet components. If a short-hand term is needed to account for these complex spatial arrangements, it is provided for by the concept of ventricular topology (Figure 20.5). In persons with usually arranged atrial chambers and discordant atrioventricular connections, for example, the left ventricular mass almost always shows left-hand topologic pattern (Figure 20.5b), whereas right-hand ventricular topology is usually found with the combination of mirror-imaged atrial chambers and discordant atrioventricular
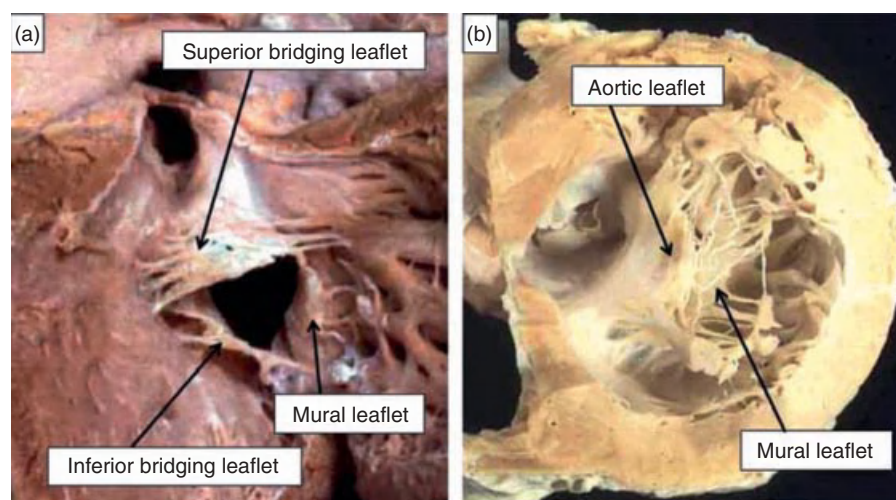
Figure 20.8 The left side of the common atrioventricular valve seen in association with atrioventricular septal defects (a) is a trifoliate structure, and bears scant resemblance to the bifoliate morphologically mitral valve (b).

connections. These topological arrangements can be modified by rotation or twisting, accounting for so-called "criss-cross" and "upstairs–downstairs" hearts. In noting such unexpected ventricular relationships as a feature independent of topology, it may be necessary to account for right–left, anterior–posterior, and superior–inferior coordinates. Should it be necessary, the position of the three ventricular components may be described separately, and relative to each other. Description of ventricular topology is also essential when accounting for the combination of isomeric appendages with mixed and biventricular atrioventricular connections. It is equally important to describe both the position and relationships of incomplete ventricles in hearts with univentricular atrioventricular connections. Here, the relationships are independent of both the connections and the ventricular morphology. For example, while the incomplete right ventricle is usually anterior and right-sided in classical tricuspid atresia, it can be anterior and left-sided without in any way altering the clinical presentation and hemodynamic findings. Similarly, in hearts with double-inlet ventricle, the position of the incomplete ventricle plays only a minor role in determining the clinical presentation. Although an argument can be made for interpreting such hearts with univentricular atrioventricular connections on the basis of presumed morphogenesis in the settings of right-hand or left-hand topologies, there are sufficient exceptions to make this approach unsuitable in the clinical setting. In accounting for the position of incomplete ventricles, therefore, it is best simply to account for their location relative to the dominant ventricle, taking note, when necessary, of right–left, anterior–posterior, and superior–inferior coordinates.

Ventriculoarterial junctions

Most previous polemics concerning the ventriculoarterial junctions have reflected the failure to distinguish between connections, relations, and infundibular morphology. It is the prerogative of those who choose to define transposition in terms of an anterior aorta to speak rightly of "double outlet with transposition." For those choosing this approach, "posterior transposition" is an impossibility. This is not so when transposition is defined on the basis of discordant ventriculoarterial connections. Such problems in the qualification of transposition, however, are dispelled when the term is not used as a descriptor for any single facet of the ventriculoarterial junctions, but rather as a combination of connections at atrioventricular and ventriculoarterial junctions, as in regular transposition or the congenitally corrected variant. It is possible also to defuse controversies concerning the role of the "bilateral conus" in the diagnosis of double-outlet right ventricle when assessing connections independently from infundibular morphology. Whenever connections, infundibular morphology, and arterial relationships are described independently, with mutually exclusive terms, there is no confusion.

There are four types of ventriculoarterial connections, specifically concordant, discordant, double outlet, and single outlet. A single outlet may take one of four forms. A common trunk exists when both ventricles are connected by a common arterial valve to one trunk that gives rise directly to the coronary arteries, at least one pulmonary artery, and the majority of the systemic circulation. A solitary arterial trunk exists when it is not possible to identify any remnant of an atretic pulmonary trunk within the pericardial cavity (Figure 20.6). The other forms of single outlet are single pulmonary trunk with aortic atresia and single aortic trunk with pulmonary atresia. These two categories are used only to describe those arrangements in which, by use of clinical techniques, it is not possible to establish the precise connection of the atretic arterial trunk to a ventricular cavity. If its connection can be established, but is found to be imperforate, the appropriate connection is described, and the imperforate valve is then categorized separately. It is also necessary in hearts with
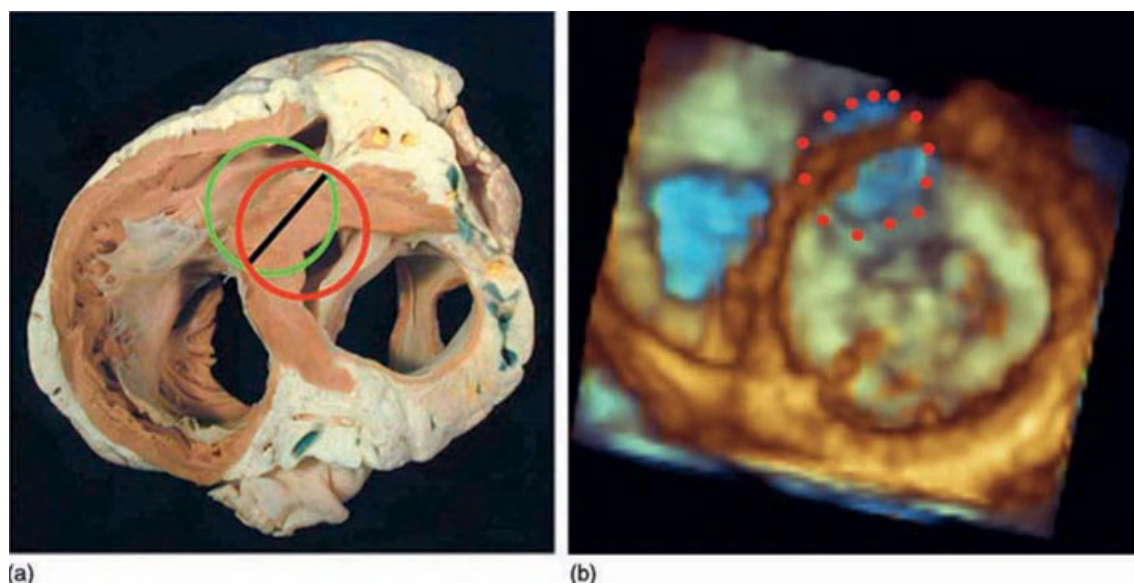
Figure 20.9 Overriding arterial valves are assigned to the ventricle supporting their greater circumference as judged relative to the cord subtended by the ventricular septum on the valvar orifice. In the examples shown in (a), a circle, representing the aortic valve, is superimposed on the normal heart as viewed from the apex in short axis. The red circle shows an aorta predominantly supported by the left ventricle, and the green circle shows an aorta supported mostly by the right ventricle. Panel (b) shows how this decision can now be made on the basis of three-dimensional echocardiography.

single outlet to describe the ventricular connection of the arterial trunk. This may be exclusively from a right or a left ventricle, but more usually the trunk overrides the septum, being connected to both ventricles.

There are fewer modes of connection at the ventriculoarterial than at the atrioventricular junctions. A common arterial valve exists only with a common arterial trunk. Straddling of an arterial valve is impossible because it has no tension apparatus. Hence the potentially variable modes of connection are two perforate valves, one or both of which may override, and one perforate and one imperforate valve. The degree of override of an arterial valve determines the precise ventriculoarterial connections. For this purpose, we allocate the overriding valve to the ventricle supporting the greater part of its circumference. For example, if more than half of an overriding pulmonary valve is connected to a right ventricle, the aorta being connected to a left ventricle, the ventriculoarterial connections are appropriately described as concordant. In contrast, if more than half the overriding aortic valve is connected to the right ventricle in this situation, there are double-outlet ventriculoarterial connections. When making this arbitration, it is best to assess the connection of the valve in its short axis, determining the proportions of the overriding junction supported by the right as opposed to the left ventricle (Figure 20.9a). This approach, now readily achievable using three-dimensional techniques for clinical diagnosis (Figure 20.9b), again avoids the need for intermediate categories.

The infundibular regions are no more and no less than the outlet components of the ventricular mass. When recognized in this fashion, and their morphology described as such, they also provide no problems in recognition and description. The morphology of the ventricular outlet portions is variable for any heart. Potentially, each ventricle can possess a complete muscular funnel as its outlet portion, and then each arterial valve can be said to have a complete infundibulum. Considered as a whole, the outlet portions of the ventricular mass in the setting of bilateral infundibulums have three discrete parts (Figure 20.10). Two of the parts form the anterior and posterior halves of the funnels of muscle supporting the arterial valves. The anterior parietal part is the free anterior ventricular wall. The posterior part is the inner heart curvature, or ventriculo-infundibular fold, which separates the leaflets of the arterial from those of the atrioventricular valves. The third part is the muscular or fibrous septum that separates the two subarterial outlets, the outlet or infundibular septum. In most hearts, some part of the infundibular musculature is effaced so that fibrous continuity occurs between the leaflets of one of the arterial valves and the atrioventricular valves. Most frequently, it is the morphologically left ventricular part of the ventriculo-infundibular fold that is attenuated, so there is fibrous continuity between the leaflets of the mitral valve and the arterial valve supported by the left ventricle. When both arterial trunks are connected to the morphologically right ventricle, the ventriculo-infundibular fold often persists in its entirety, and there is bilateral atrioventricular-arterial valvar discontinuity (Figure 20.10a). Many hearts in which both arterial valves are connected unequivocally to the right
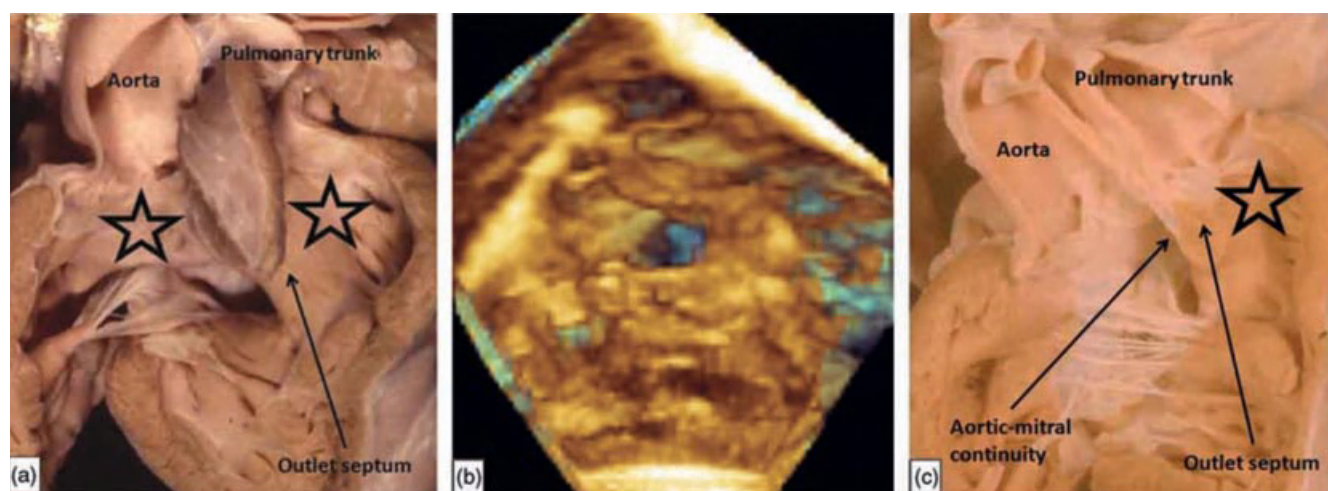
Figure 20.10 A morphologic specimen (a) and a comparable three-dimensional echocardiogram (b) revealing the location of the ventriculo-infundibular fold (star) and the muscular outlet septum in the setting of double outlet from the right ventricle when the interventricular communication is in the subaortic position and there are bilateral infundibulums. Panel (c) shows how the arterial trunks can arise exclusively from the right ventricle in this setting even when there is fibrous continuity between the leaflets of the aortic and mitral valves in the roof of the interventricular communication.

ventricle, nonetheless, have atrioventricular–arterial valvar continuity (Figure 20.10c). Such hearts unequivocally possess a double-outlet ventriculoarterial connection. The ventriculo-infundibular fold, therefore, does not need to be intact bilaterally to justify the diagnosis of double-outlet right ventricle (Figure 20.10c).

The final feature of the ventriculoarterial junctions requiring description is the relationships of the great arteries and their valves. Arterial valvar relationships are best described in terms of right–left and anterior–posterior coordinates. The positions of the arterial trunks are also important. The pulmonary trunk either spirals around the aorta as it ascends, or else the two trunks ascend in parallel. Spiraling trunks are usually associated with concordant ventriculoarterial connections, and parallel trunks with discordant or double-outlet connections, but there is no predictive value in these relationships. The arcane conditions of "anatomically corrected malposition" and "isolated ventricular discordance" are greatly simplified when it is realized that these are no more than concordant ventriculoarterial connections, but with parallel rather than spiraling arterial trunks [18]. The aortic arch itself crosses superiorly to the bifurcation of the pulmonary arteries. The side of the aortic arch is then determined by whether it passes to the right or left of the trachea, with the position of the descending aorta defined relative to the vertebral column.

Associated malformations

Most patients seen with congenital heart disease have normal intersegmental connections together with normal morphology and relations. In such settings, the associated malformation will be the major anomaly. The body of this book is concerned with describing the specific morphologic and clinical features of these anomalies. Certain anatomic principles, nonetheless, pertain to the description of all these lesions, and will be discussed briefly below. Consideration must also be given to the position within the chest of the heart itself, and of the cardiac apex, or, for that matter, identification of a heart positioned outside the thoracic cavity, so-called ectopia cordis. An abnormal position of the heart within the chest is best considered as an associated malformation, and the cardiac malposition should not be promoted as a prime diagnosis. This is not to decry the importance of cardiac malposition, if only to interpret an electrocardiogram, but knowing that the heart is malpositioned gives no information concerning its internal architecture. Full sequential segmental analysis is needed to determine this analysis, not the other way around.

Septal morphology

A majority of congenitally malformed hearts exhibit the potential for shunting through holes between the cardiac chambers or arterial trunks. Such holes are usually termed septal defects, yet not all are found within the septal components of the normal heart. Understanding of septal defects, therefore, requires an appreciation of the extent of the normal septal structures, and knowledge of the mechanisms that permit shunting outside the confines of these normal components. In the normal heart, it is possible to recognize atrial, atrioventricular, and ventricular septums. There are then additional parts of the cardiac walls that interpose
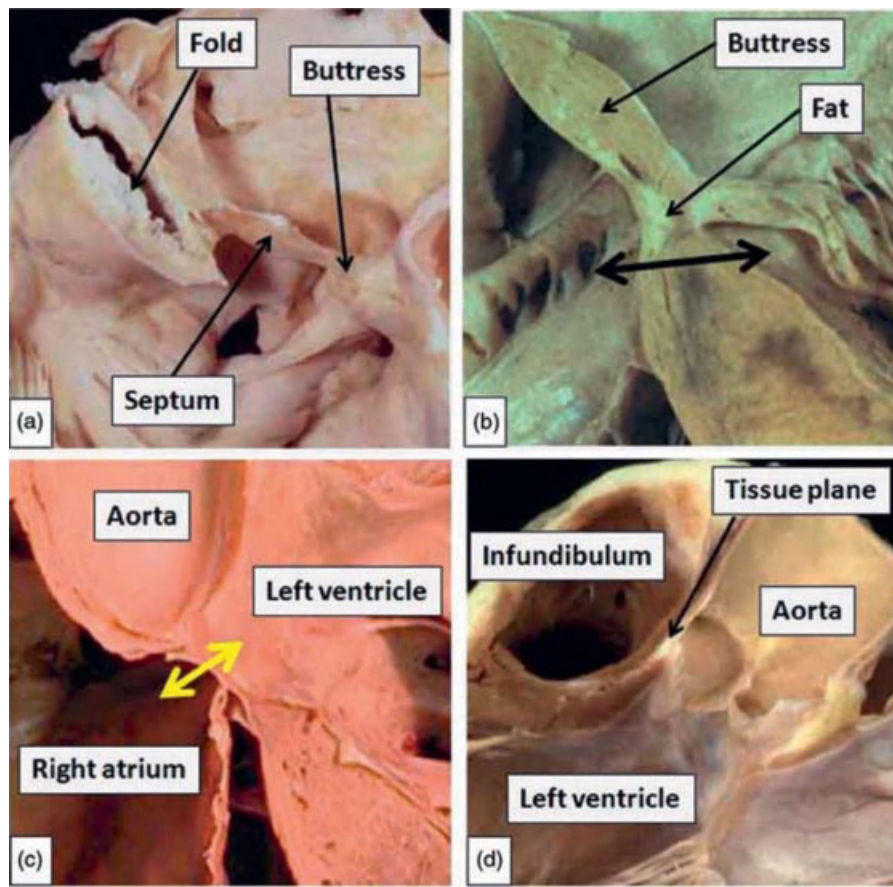
Figure 20.11 Not all of the walls that separate adjacent chambers can be removed without trespassing on extracardiac space. Four-chamber sections through the walls separating the atrial chambers (a and b) show that the superior rim of the oval fossa is a deep fold (a), whereas the extension of the atrial muscle into the vestibule of the tricuspid valve is the superior fold of an atrioventricular muscular sandwich [double-headed arrow in (b)]. A further four-chamber section (c) reveals that the only true atrioventricular septum in the normal heart is that part of the membranous septum superior to the hinge of the septal leaflet of the tricuspid valve (yellow double-headed arrow). The parasternal long axis section (d) then reveals that the "septal" aspect of the subpulmonary infundibulum is separated by a fibrofatty tissue plane from the sinuses of the aortic root.

between chambers, but in the form of folds or sandwiches, rather than as solitary walls that can be removed without compromising the pericardial space [19]. When the structures interposing between the atrial chambers are analyzed in this fashion, it is the floor of the oval fossa, and its muscular anteroinferior buttress, that qualify as septal structures (Figure 20.11a). The extensive superior rim, although often described as the "septum secundum," is the deep infolding between the attachments of the superior caval vein to the right atrium and the right pulmonary veins to the left atrium. Even though a large part of the anteroinferior buttress is also a septal structure, when this atrial musculature is traced into the septal vestibule of the tricuspid valve, it overlies the crest of the muscular septum. It is then possible to place needles through this area, the floor of the triangle of Koch, and to enter the base of the left ventricle. This area is seemingly an atrioventricular muscular septum. More rigorous analysis, however, shows that a layer of the inferior atrioventricular groove, containing extracardiac fat, interposes between the atrial and ventricular musculatures. The area, therefore, is an atrioventricular muscular sandwich, rather than a septum (Figure 20.11b). The only true atrioventricular septum in the normal heart is the small part of the fibrous septum

that interposes between the cavity of the right atrium and the subaortic outflow tract (Figure 20.11c). Part of this so-called membranous septum also interposes between the ventricular cavities. The greater part of the ventricular septum, nonetheless, is muscular. Not all of the apparently septal surface of the right ventricle, however, separated the cavities of the right and left ventricles. The apparently septal surface of the subpulmonary outlet is part of the free-standing muscular sleeve that lifts the leaflets of the pulmonary valve away from the base of the ventricular mass (Figure 20.11d). It is this feature that permits the surgeon to remove the pulmonary valve as a free-standing structure, and to use it as a prosthesis in the Ross procedure [20]. All of these anatomic features are also key to understanding the structure of the so-called septal defects.

Interatrial communications

There are several lesions that permit shunting between the atrial chambers. Not all are correctly described as septal defects, at least not when the septal structures are defined as suggested above. Only the holes within the confines of the oval fossa, so-called "secundum" defects, and the rare holes found within the substance of the anteroinferior buttress,
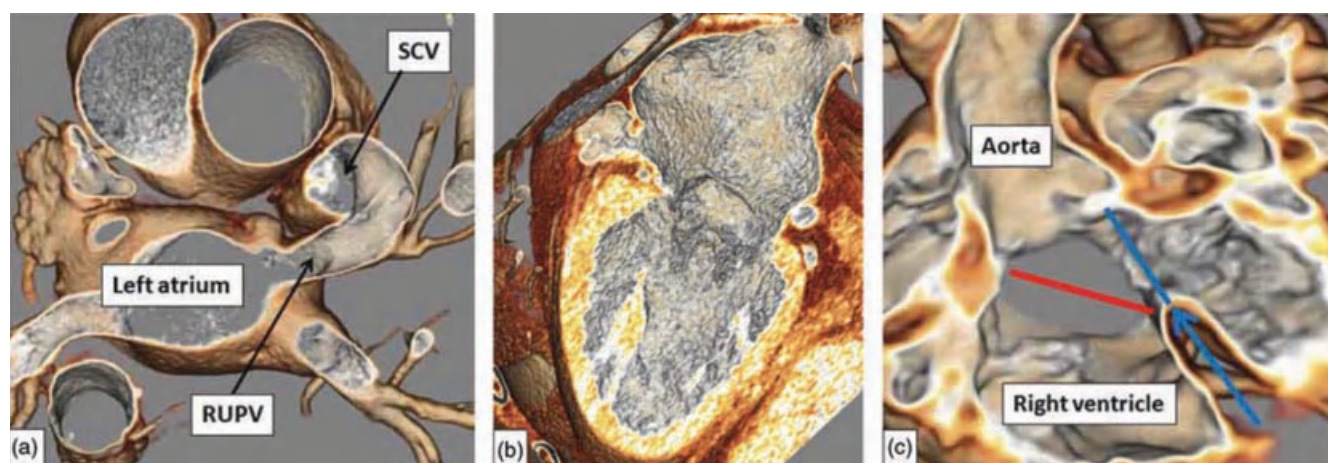
Figure 20.12 The images show features of so-called "septal defects," albeit that not all are true septal deficiencies. In (a), the so-called sinus venosus defect is seen to be a veno-venous collateral channel. Panel (b) shows the common atrioventricular junction, which is the pathognomic feature of the "ostium primum" defect, thus revealing it to be an atrioventricular rather than an atrial septal defect. Panel (c) shows the aortic valve overriding the crest of the muscular ventricular septum in the setting of tetralogy of Fallot, creating problems as to whether the right ventricular aspect of the cone of space subtended from the valvar leaflets to the crest of the septum (red line) is the ventricular septal defect, or whether this is the superior continuation of the plane of the muscular ventricular septum (blue arrow and line). The latter blue line is certainly the interventricular communication.

are true septal deficiencies. The essence of the sinus venosus defects is that they are found outside the confines of the oval fossa. These holes exist because one of more of the right pulmonary veins achieves a connection to either the superior or the inferior caval vein while retaining the expected connection with the left atrium. The lesions are veno-venous collateral channels (Figure 20.12a) rather than septal defects, albeit that they unequivocally permit interatrial shunting of blood. Shunting between the atrial chambers can also exist through the mouth of the coronary sinus when the walls that normally interpose between the cavities of the coronary sinus and left atrium are either fenestrated or absent. The so-called ostium primum defect also permits interatrial shunting, but in these instances through an atrioventricular rather than an atrial septal defect.

Atrioventricular septal defects

These holes are true septal defects, but their pathognomonic feature is the common atrioventricular junction (Figure 20.12b). It is the level of shunting across the atrioventricular septal that accounts for the variability within the lesion. In the so-called "complete" variant, defined on the basis of a common atrioventricular valvar orifice, the bridging leaflets float to varying degrees so that shunting is possible at both atrial and ventricular levels. The ostium primum defect is usually considered a "partial" form of the lesion, albeit that the atrioventricular junction is just as common as when there is a common atrioventricular valvar orifice [21]. The feature of the ostium primum defect is that a tongue of valvar tissue joins together the bridging leaflets so that there are dual valvar orifices within the

common atrioventricular junction. In most instances, the bridging leaflets, along with the connecting tongue, are firmly fused to the scooped-out crest of the muscular ventricular septum, this feature serving to confine shunting across the septal defect at atrial level. In some instances, however, there can be additional minimal shunting at ventricular level through intercordal spaces on the ventricular aspect of the bridging leaflets. Rarely, the bridging leaflets can be attached to the leading edge of the atrial septum, thus serving to confine shunting at ventricular level. It is this lesion that is the true ventricular septal defect of atrioventricular canal type. Even more rarely, although now recognized with increasing frequency, the atrioventricular septal defect itself can undergo spontaneous closure, so that there is no shunting even though there is a common atrioventricular junction [22].

Ventricular septal defects

Holes between the ventricles are the commonest congenital cardiac malformations, and form part of many other lesions, such as common arterial trunk, tetralogy of Fallot, and double-outlet right ventricle. In countries where the vernacular language is derived from Latin, these holes are often described as interventricular communications, which is in many ways a better descriptor, since as with holes between the atriums, not all the so-called ventricular septal defects are found within the confines of the normal ventricular septum. Problems also exist in defining the plane of space best defined as representing the interventricular communication, raising questions as to whether the interventricular communication is necessarily the same thing as the

ventricular septal defect. Consider the situation in the setting of tetralogy of Fallot, where one of the anatomic features is overriding of the orifice of the aortic valve (Figure 20.12c). The plane of space that is blocked by the surgeon when closing the "ventricular septal defect" is the right ventricular aspect of the cone of space subtended from the attachments of the overriding valve. The interventricular communication, in contrast, is the plane of space marked by the superior continuation of the plane of the muscular ventricular septum. Also, in double-outlet right ventricle, the interventricular communication is the hole between the ventricles, albeit that this hole is never closed by the surgeon during an operative repair, but rather is tunneled to one or other of the subarterial outlets. In most instances, nonetheless, it is the right ventricular border over which the surgeon places a patch that is considered to represent the "ventricular septal defect," and this plane is usually considered as being synonymous with the interventricular communication. Different systems still exist for describing the different types of "ventricular septal defect" as thus defined, but the differences reflect the feature used for the purposes of categorization. Unity can again be achieved if note is taken of all the pertinent clinical features. These include the size of the hole, the anatomic nature of its borders as seen from the right ventricle, the direction in which the hole opens into the right ventricle, and the additional presence of malalignment of the septal components. If all of these features are described, there should be no room for disagreement on nomenclature [23].

Conclusion

The techniques now available for the clinical diagnosis of congenitally malformed hearts are now so sophisticated that all the features of normal and abnormal cardiac anatomy can be seen with greater facility during life than in the autopsy room, with the added advantage that serial studies will now permit the establishment of the natural and unnatural history of the various lesions. It is hoped that the lessons being learned from the applications of these new techniques will resolve all of the controversies that have bedeviled pediatric cardiologists and pediatric cardiac surgeons over recent decades.

References

1 Van Praagh R, Ongley PA, Swan HJC. Anatomic types of single or common ventricle in man: morphologic and geometric aspects of sixty necropsied cases. *Am J Cardiol* 1964;**13**:367–86.

2 Van Praagh R, Van Praagh S, Vlad P, Keith JD. Anatomic types of congenital dextrocardia. Diagnostic and embryologic implications. *Am J Cardiol* 1964;**13**:510–31.

3 de la Cruz MV, Nadal-Ginard B. Rules for the diagnosis of visceral situs, truncoconal morphologies and ventricular inversions. *Am Heart J* 1972;**84**:19–32.

4 Van Praagh R. The segmental approach to diagnosis in congenital heart disease. *Birth Defects* 1972;**8**:4–23.

5 Shinebourne EA, Macartney FJ, Anderson RH. Sequential chamber localization: the logical approach to diagnosis in congenital heart disease. *Br Heart J* 1976;**38**:327–40.

6 Anderson RH, Ho SY. Sequential segmental analysis – description and categorization for the millenium. *Cardiol Young* 1997;**7**:98.

7 Anderson RH, Shirali G. Sequential segmental analysis. *Ann Pediatr Cardiol* 2009;**2**:24–35.

8 Jacobs ML, Anderson RH. Nomenclature of the functionally univentricular heart. *Cardiol Young* 2006;**16**(Suppl 1):3–8.

9 Lev M. Pathologic diagnosis of positional variations in cardiac chambers in congenital heart disease. *Lab Invest* 1954;**3**:71–82.

10 Van Praagh R, David I, Wright GB, Van Praagh S. Large RV plus small LV is not single LV. *Circulation* 1980;**61**:1057–9.

11 Uemura H, Ho SY, Devine WA, *et al*. Atrial appendages and venoatrial connections in hearts with patients with visceral heterotaxy. *Ann Thorac Surg* 1995;**60**:561–9.

12 Bargeron LM Jr. Angiography relevant to complicating features. In: Becker AE, Losekoot TG, Marcelletti C, Anderson RH, eds. *Paediatric Cardiology*, Vol 3. Edinburgh: Churchill Livingstone, 1981: 33–47.

13 Huhta JC, Smallhorn JF, Macartney FJ. Two dimensional echocardiographic diagnosis of situs. *Br Heart J* 1982;**48**:97–108.

14 Anderson C, Devine WA, Anderson RH, *et al*. Abnormalities of the spleen in relation to congenital malformations of the heart: a survey of necropsy findings in children. *Br Heart J* 1990;**63**:122–8.

15 Uemura H, Ho SY, Devine WA, Anderson RH. Analysis of visceral heterotaxy according to splenic status, appendage morphology, or both. *Am J Cardiol* 1995;**76**:846–9.

16 Anderson RH, Rigby ML. Editorial note. The morphologic heterogeneity of "tricuspid atresia." *Int J Cardiol* 1987;**16**:67–73.

17 Anderson RH, Becker AE, Tynan M, *et al*. The univentricular atrioventricular connection: getting to the root of a thorny problem. *Am J Cardiol* 1984;**54**:822–8.

18 Cavalle-Garrido T, Bernasconi A, Perrin D, Anderson RH. Hearts with concordant ventriculoarterial connections but parallel arterial trunks. *Heart* 2007;**93**:100–6.

19 Anderson RH, Brown NA. The anatomy of the heart revisited. *Anat Rec* 1996;**246**:1–7.

20 Merrick AF, Yacoub MH, Ho SY, Anderson RH. Anatomy of the muscular subpulmonary infundibulum with regard to the Ross procedure. *Ann Thorac Surg* 2000;**69**:556–61.

21 Anderson RH, Wessels A, Vettukatil JJ. Morphology and morphogenesis of atrioventricular septal defect with common atrioventricular junction. *World J Pediatr Congen Heart Surg* 2010;**1**:59–67.

22 Kaski JP, Wolfenden J, Josen M, *et al*. Can atrioventricular septal defects exist with intact septal structures? *Heart* 2006;**92**:832–5.

23 Friedman BA, Hlavacek A, Chessa K, *et al*. Clinico-morphological correlations in the categorization of holes between the ventricles. *Ann Pediatr Cardiol* 2010;**3**:12–24.

21 Atrial Level Shunts Including Partial Anomalous Pulmonary Venous Connection and Scimitar Syndrome

Carlos A. C. Pedra & Simone R. Fontes Pedra

Instituto Dante Pazzanese de Cardiologia, São Paulo, SP, Brazil

Introduction

An atrial septal defect (ASD) is an opening between the atria due to a deficiency of one or more components of the interatrial septum (IAS) [1]. The most common type of ASD is the secundum defect located in the region of the fossa ovalis [1]. It is usually single but multiple fenestrations may also be encountered. A patent foramen ovale (PFO) should not be considered an abnormal finding *per se* and occasionally may coexist with an ASD. Because of its association with paradoxical embolization, it is briefly discussed. Partial anomalous pulmonary venous connection (PAPVC) to the systemic venous circulation shares physiologic similarities with ASD and is often associated with it, and is also discussed. Defects in the inferior portion of the atrial septum, the so-called primum ASDs, represent a form of endocardial cushion defect and are discussed in Chapter 22.

An ASD of the secundum or fossa ovalis type is a common congenital heart defect (CHD), with an incidence of around 568 per million live births [2]. The true incidence may be even higher because many patients have a smaller defect that is not diagnosed until adulthood. It affects 5–10% of patients with CHD and is usually considered the fourth or fifth most common type of cardiac malformation [3]. Additionally, up to 50% of children with CHD have an associated ASD. Females are affected approximately 2–3 times more often than males. Although most secundum ASD occurs sporadically, an autosomal dominant inheritance has been reported in some families [4]. When it is associated with atrioventricular conduction defects there may be a mutation of the *NKX*-2.5 gene [4]. Also, an ASD is associated with abnormalities of the radius or radial portion of the hand (Holt–Oram syndrome). Because of its relative lack of symptoms and at times inconspicuous physical signs in childhood, it is one of the most frequent forms of CHD initially recognized in adults [1].

Anatomy

The IAS is a complex structure that develops from two separate primitive septal ridges (*septum primum* and *septum secundum*) that must migrate, coalesce with the endocardial cushions and sinus venosus, and partially reabsorb to function normally in fetal and postnatal life [5]. The septum primum appears first, growing superiorly from the junction between the inferior vena cava (IVC) and the right atrium (RA) towards the septum secundum. It normally forms the inferior portion of the atrial septum and the flap-like valve of the foramen ovale. The septum secundum is a crescent-shaped muscular ridge that invaginates from the postero-superior portion of the developing atria. It forms the anterior and posterior rims of the limbus of the fossa ovalis, which demarcates the foramen ovale, and much of the superior portion of the IAS [5]. The smooth-walled posterolateral portion of the RA is the remnant of the right horn of the sinus venosus. Abnormal incorporation of this structure into the RA produces a sinus venosus defect near the orifice of the superior vana cava (SVC) or the IVC. The AV canal septum is formed, at least in part, by the endocardial cushions and septates the outlet portion of the atria and the inlet portion of the ventricles. The normal development of the IAS results in formation of the fossa ovalis, which is bounded superiorly by the septum secundum and inferiorly by the muscular AV canal septum [5]. The superior portion of the septum primum attaches to the left atrial aspect of the septum secundum (Figure 21.1).
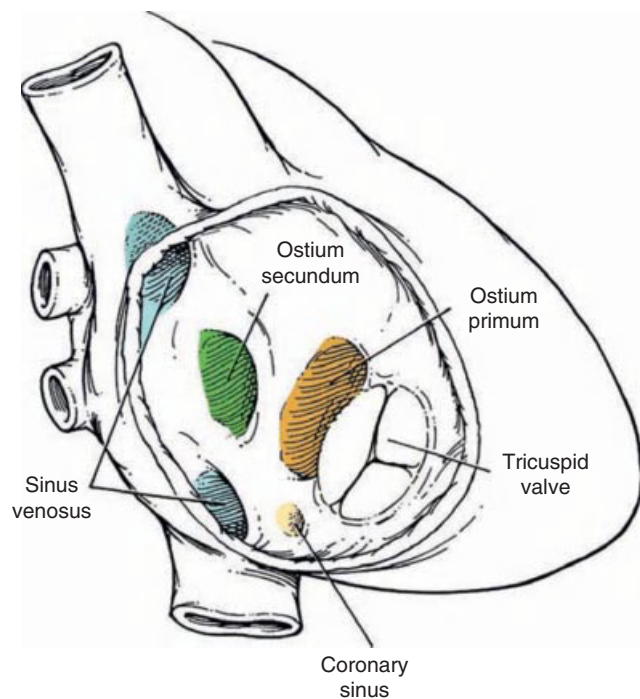
Figure 21.1 Diagram of the interatrial septum viewed from the right atrium. The locations of the different types of atrial septal defects (secundum, sinus venosus, coronary sinus and primum defects) are displayed in different colors.

A secundum ASD occurs in the region of the septum primum, which is also called the valve of the fossa ovalis (Figure 21.1) [5]. It can result from an abnormally short valve, an unusually large foramen ovale that is incompletely covered by a normal valve, fenestrations in the valve, or a combination of these factors [5]. It is by far the most common type of ASD.

The foramen ovale is an opening in the septum secundum that is covered on its left atrial side with a flap of tissue derived from the septum primum. This flap valve allows right-to-left atrial shunting during fetal life. After birth, when left atrial exceeds right atrial pressure, the flap usually seals the defect and separates the atria. However, persistent patency of the foramen ovale from incomplete fusion of the valve of the foramen ovale to the septum secundum may occur and can be found in 30% of adults at autopsy or by echocardiography [6,7]. Usually unassociated with a significant left-to-right shunt, it is considered a normal finding rather than a pathologic defect. To avoid considering a PFO as an ASD, some investigators define an ASD as having an opening of >5–6 mm in diameter associated with a dilated RA and right ventricle. On the other hand, variable degrees of right-to-left shunting may occur through the PFO and result in paradoxical embolization and neurologic events in an occasional patient. Both ASDs and PFOs may be associated with aneurysms of the atrial septum (ASA), although an ASA may occur with an intact atrial septum [1].

Sinus venosus defects comprises 3–10% of all ASDs [1,5]. They are located in the smooth-walled region of the atrium posterior to the fossa ovalis (Figure 21.1). They usually occur superiorly near the orifice of the SVC, but an inferior sinus venosus defect may also be found near the orifice of the IVC. Some 80–90% of patients with a superior sinus venosus defect also have PAPVC of the right pulmonary veins to either the RA or SVC [8,9].

PAPVC is a connection between one or more (but not all) pulmonary vein(s) with a systemic vein, right atrium, or coronary sinus. This anomaly is associated with a sinus venosus ASD in >85% of patients [9] but can also occur with an intact IAS [8]. There are several anatomic variations, with the most common types being the left upper pulmonary vein connecting to the left innominate vein [10] and one or more right-sided veins connecting to the SVC at its junction with the RA [9]. Anomalous connection of the inferior or all right pulmonary veins to the IVC is known as Scimitar syndrome [11], other features of which include hypoplasia or even absence of the right pulmonary artery, hypoplasia of right lung with secondary dextrocardia, anomalous systemic arterial supply to the right lung through collaterals usually arising from the descending aorta, pulmonary artery stenoses, and bronchial abnormalities. About 70% of these patients also have an ASD [11].

A coronary sinus septal defect is a rare type of ASD in which the coronary sinus is partially or completely unroofed, allowing communication between the coronary sinus and the left atrium (LA) with left-to-right shunt through the coronary sinus orifice [5]. When this defect is associated with a persistent left superior vena cava it is termed Raghib syndrome [12] (see Chapter 37).

Finally, a most uncommon type of ASD may be occasionally encountered especially in patients with isomerism of the right atrial appendages or heterotaxy syndrome. Due to leftward malposition of the septum primum, one or more of the right pulmonary veins may functionally drain into the RA despite being normally connected to the LA [5]. Closure of the defect eliminates the left-to-right shunt.

Associated lesions may be encountered with an ASD [13]. Occasionally, an unusually large Eustachian valve may be found with an ASD or PFO and may contribute to significant right-to-left shunting across the IAS when the patient stands up (platypnea–orthodeoxia syndrome) [14,15]. Functional abnormalities and prolapse of the mitral valve are commonly present in patients with an ASD [16–18]. It is unknown whether the prolapse is secondary to deformation of the mitral apparatus by an enlarged right ventricle, an inherent abnormality of mitral valve tissue, or reduced left ventricular volume [13]. Although it is common to record a flow-related gradient across the pulmonary valve, anatomic pulmonary valvar stenosis is found in only 5% of patients with an ASD [13]. Despite the posterior displacement and compression of the left ventricle (LV), left ventricular systolic function is

usually normal. Left ventricular diastolic distensibility, however, is often decreased, especially in older patients, and may complicate closure of the defect [19]. The right ventricle (RV) is dilated with larger shunts, but functions well [13]. Significant tricuspid regurgitation may develop with marked dilatation, especially if pulmonary hypertension coexists. Pulmonary regurgitation occurs late in patients with severe pulmonary hypertension.

Pathophysiology

The amount of shunting through an ASD depends on the relative right and left ventricular compliances [1,5,13,20]. Early after birth, flows in the pulmonary and systemic circulations equalize with expansion of the lungs and removal of the placenta from the circulation. In the neonate, compliance of the left and right ventricles is similar, atrial pressures are relatively equal, and flow through an ASD may be bidirectional with little net left-to-right or right-to-left shunt. During infancy, the RV gradually becomes more compliant than the LV because of the markedly lower pressure and resistance in the pulmonary circulation compared with the systemic circuit. Because the increasingly compliant RV more readily accepts excess volume, more blood is diverted from the LA to the RA through the ASD. Pulmonary blood flow, consisting of systemic venous return plus the volume of blood that shunts from the LA to the RA, is thus increased. The pulmonary-to-systemic flow ratio usually exceeds 1.5:1 and atrial level left-to-right flow enlarges the RA and RV after infancy. Under normal circumstances, flow through an ASD is nearly all left-to-right, but there is a phasic variation, with a small and transient right-to-left shunt occurring near the end of the QRS.

Because the volume and direction of shunting through an ASD largely depend on the relative distensibility of the right and left ventricles, patients with right ventricular hypertrophy secondary to conditions such as pulmonary stenosis or pulmonary hypertension have a smaller left-to-right shunt [1,5,13,20]. Severe right ventricular hypertrophy with an ASD or a PFO results in a net right-to-left shunt and cyanosis. In contrast, reduced left ventricular distensibility due to aging, ischemic heart disease, diabetes and systemic arterial hypertension, may cause left ventricular hypertrophy and an increase in left-to-right shunting in late adulthood.

Congestive cardiac failure in an ASD might be thought to affect only the overloaded RV, but the cardiac failure is atypical in that both ventricles have equally raised diastolic pressures, even though the LV is not dilated. The raised left ventricular diastolic pressure has been ascribed to compression of the LV by a hugely dilated RV, much as ventricular diastolic pressures are raised by pericardial tamponade [13].

With PAPVC, the degree of volume overload to the RV depends on how much of the pulmonary venous drainage in diverted to the right atrium [8]. If only one lobe drains to the right atrium, the left-to-right shunt is small (Qp/Qs < 1.5) with little or no dilation of the RV. In contrast, if two or more pulmonary lobes are draining anomalously to the RA, the left-to-right shunt is significant (Qp/Qs > 2) and produces RV enlargement. There is more flow to an anomalously connected pulmonary vein to the RA than through a similarly sized vein connected to the LA because the pressure drop across the low-resistance pulmonary vascular bed is slightly greater to the RA than to the LA [8]. Conversely, little flow passes through a pulmonary lobe if a significant stenosis is present in the anomalous pulmonary vein draining that lobe.

In patients with Scimitar syndrome, the deleterious hemodynamic effects depend on many factors, including associated complex cardiac defects, especially in infants; size of the right pulmonary artery and the amount of flow through it; possible stenoses in either or both pulmonary arteries; size, number, and possible obstruction of the anomalous pulmonary veins draining into the IVC; and the amount of flow through the collateral supply to the lung [11]. Bronchial abnormalities may be responsible for respiratory symptoms. Pulmonary arterial hypertension often occurs in infants, even without associated lesions, usually because of a large systemic-to-pulmonary flow through the collateral supply and a decreased size of the right pulmonary arterial bed. Pulmonary venous obstruction may also play a role [11].

Natural history

The deleterious effects of an ASD depend mainly on the magnitude of the left-to-right shunt. Small shunts through defects <5–6 mm in diameter produce no symptoms and few, if any, abnormal physical signs [1,5,13]. Larger shunts may cause fatigue on exertion, frequent pulmonary infections, and with increasing age pulmonary vascular disease, congestive heart failure, and atrial arrhythmias. Infective endocarditis is rare in the absence of other cardiovascular abnormalities such as mitral insufficiency [1].

Depending on its size and the age of the patient, a secundum ASD may become smaller and close spontaneously [21–28]. An echocardiographic study has suggested that a secundum ASD <3 mm in diameter in the first 3 months of life nearly always closes, and those >8 mm in diameter are unlikely to close [27]. Closure of small defects occurs frequently within the first or second year of life, with closure rates reaching 74–100% [21–28]. Although closure is much more likely with a small defect, it can also occur in patients with a relatively large ASD (>10 mm), and even in patients with congestive heart failure. Some larger defects become smaller but do not close completely. There is no substantial rate of spontaneous closure above 6 years of age. On the

other hand, an ASD can also increase in size over time [25,26,29]. The causes of this increase in size and rate of increase are unknown.

Patients with an isolated secundum ASD are generally asymptomatic through infancy and childhood. Rarely, symptoms of pulmonary overcirculation, frequent respiratory infections, and overt congestive heart failure are seen in small infants with very large defects who have no other identified cardiac abnormality [30–32]. However, associated extracardiac anomalies, chromosomal abnormalities and chronic lung disease associated with prematurity are common in such symptomatic infants and may contribute to the underlying status [33]. Patients diagnosed later in childhood often come to the cardiologist's attention because of a relatively inconspicuous murmur. Although they do not have overt symptoms, they may appear asthenic [13]. Symptoms become progressively more common after the age of 20 years and include dyspnea on exertion, fatigue, palpitations, and arrhythmias, with 90% of untreated patients having one or more of these "minor" symptoms by the age of 40 years [13]. More debilitating symptoms due to complications, such as congestive cardiac failure, pulmonary arterial hypertension, and recurrent arrhythmias develop in ~35% of the patients older than 40 years [13]. Usually pregnancy is well tolerated in untreated women but congestive heart failure may occasionally occur [1].

Mild-to-moderate pulmonary hypertension occurs in <10% of children with an ASD [1]. Although pulmonary vascular disease may occasionally be seen in young children with a large defect [34], in a few patients with a (coincidental) small ASD, pulmonary vascular resistance remains high from birth and resembles idiopathic pulmonary hypertension [13]. Pulmonary artery pressure does gradually increase with age in patients with an ASD. Approximately half of patients older than 30 years have a pulmonary artery mean pressure greater than 20 mmHg but only mild elevation of pulmonary arterial resistance [35–37]. Advanced histologic changes of the small pulmonary arteries are much less frequent and take longer to develop with an ASD than with other types of CHD with a large left-to-right shunt. As such, markedly increased pulmonary vascular resistance is uncommon in patients under the age of 20 years. Patients living at high altitudes may have pulmonary hypertension at an earlier age and progress more rapidly [38]. It is debatable whether symptoms and pulmonary hypertension are found more often and earlier with sinus venosus than with secundum ASDs [39]. Another rare cause of severe pulmonary hypertension in a patient with a large ASD is thrombosis of the large pulmonary arteries [40,41].

Atrial arrhythmias become increasingly common with advancing age. More than half of patients >45 years old have intermittent or chronic atrial fibrillation or flutter [42–49]. The onset of atrial fibrillation or flutter is a common cause of relatively rapid deterioration in a previously minimally symptomatic adult. These atrial arrhythmias are probably due to the stretched right atrium, but a distended left atrium and mitral regurgitation are contributory. A few may present with severe paroxysmal supraventricular tachycardia. Although an ASD is a potential pathway for paradoxical embolization, >90% of strokes in adult ASD patients occur in those who have atrial fibrillation [50]. In addition to these overt abnormalities in adults, many children with an ASD may have subclinical sinus node dysfunction and atrioventricular conduction abnormalities [51]. It seems that patients with sinus venosus defects do not have an increased incidence of arrhythmias preoperatively [1].

Survival of patients with a clinically detectable ASD into adulthood is expected, with >75% of patients surviving into their 30s. Campbell et al., however, estimated that ~75% of patients do not survive past the age of 50 years, and only 10% survive past the age of 60 years [52]. Because Campbell et al.'s patients were identified before the widespread availability of current sensitive diagnostic tests, these estimates may be overly pessimistic and apply accurately only to patients with a large, easily detectable ASD. There are numerous reports of patients with an ASD surviving past the age of 80 years [13].

Finally, an ASD or a PFO also allows possible paradoxical embolization of thrombus, air, or other material to the systemic circulation, resulting in stroke or ischemic damage to the extremities or major organs [53–55]. The risk of paradoxical embolization may be increased with pregnancy, especially in the peripartum period. Paradoxical embolism was inferred originally from autopsies that showed typical venous thrombi in an artery [53,54]. Several case–control studies of adults with cerebral vascular events showed that those without any known risk factors were more likely to have a PFO or an ASA that is often associated with a PFO [1,56]. Venous thrombi have also been observed straddling the foramen ovale at autopsy or on echocardiography [57]. Right-to-left shunting through these defects detected by echocardiography can occur during transient pressure reversal during the cardiac cycle or with release of a Valsalva maneuver [55]. An extensive meta-analysis of the relationship of PFO and ASA concluded that under 55 years of age both lesions were associated with ischemic strokes in patients without other likely predisposing causes [1,56]. More recently, this association has been shown to be valid in patients over 55 years of age [58]. However, in prospective, longitudinal, and observational studies in the general population, PFOs were not found to be independently associated with ischemic strokes [59,60]. As such, any form of preventive treatment in asymptomatic patients with PFOs detected incidentally appears unjustified at present [1]. Additionally, PFOs have also been associated with migraine, especially with aura, increased mortality in patients with pulmonary embolism, and central nervous system lesions in divers [1,55,61–65].

Diagnosis

Clinical history and physical examination

Because of the lack of both symptoms and an easily audible murmur, the diagnosis of an ASD is usually delayed and only made at the preschool/school age, and sometimes later in adolescence or adulthood [1,5,13]. The clinical history in most children is usually unremarkable. It may be possible to elucidate a minor difference in exercise tolerance or growth compared with siblings, but it is unusual to have failure to thrive or clearly reduced exercise tolerance. In adult patients, symptoms of overt congestive cardiac failure are more common [1,5,13]. Palpitations are a frequent complaint, and the onset of atrial fibrillation or flutter may precipitate the definitive evaluation and diagnosis. A small percentage of patients may be found to have an ASD or PFO on cardiac evaluation after a stroke [13].

The physical findings of an ASD may be relatively subtle, especially to a noncardiologist. Mild left chest prominence or bulge on inspection and a right ventricular lift or heave on palpation can be detected in patients with large left-to-right shunts. The first heart sound is usually loud at the left lower sternal border. The second heart sound at the left upper sternal border is characteristically widely split and the respiratory variation is greatly reduced, leading to the perception of fixed splitting [13]. A large, nonrestrictive ASD equalizes the respiratory influence on both right and ventricular output, with the wide split resulting from delayed emptying of the enlarged RV. The intensity of the pulmonary component is usually normal, reflecting normal pulmonary artery pressures. There is usually a grade 3 (or less) soft systolic ejection murmur at the mid-to-upper left sternal border due to the increased blood flow passing through the pulmonary valve (flow-related "relative" pulmonary stenosis). The murmur radiates to the lung fields posteriorly. Patients with a large left-to-right shunt (Qp/Qs >2:1) often have along the lower left sternal border a mid-diastolic flow rumble due to the increased diastolic flow through the tricuspid valve [3,15]. Pulmonary hypertension may accentuate the pulmonary component of the second heart sound and also normalize its respiratory variation. With severe pulmonary hypertension, murmurs of pulmonary regurgitation and tricuspid regurgitation may appear [13].

Electrocardiography

The normal regression of right ventricular dominance with age usually does not occur and a typical pattern of persistent right-axis deviation and right ventricular enlargement becomes identifiable in early childhood [5,13]. The QRS duration is at the upper limit of normal or mildly prolonged, with an rSr′ or rsR′ pattern seen in the right precordial leads in ~90% of patients. Crochetage, a notch near the apex of the R wave in inferior limb leads, occurs in ~75% of patients

with an ASD, especially if large, but in <10% of normal subjects or patients with other forms of CHD. In the occasional patient with severe pulmonary hypertension or significant pulmonary valve stenosis associated with an ASD, the electrocardiographic pattern may be more typical of pure pressure overload with an rR or tall monophasic R wave preceded by a small Q wave in lead V_1 [13].

Conduction abnormalities and arrhythmias become increasingly apparent with age [13]. Usually the PR interval is normal, in contrast with the prolonged interval found in patients with atrioventricular septal (endocardial cushion ostium primum) defects [5]. The P waves frequently become tall, peaked and slightly prolonged as the right atrium enlarges. An advanced first-degree atrioventricular block progressing to a second-degree block or a complete atrioventricular block may be seen in a familial pattern associated with secundum ASDs. Atrial fibrillation (most commonly), atrial flutter, and supraventricular tachycardia can also develop at older ages, with more than half of patients having atrial fibrillation after the fourth decade [42–49].

Chest radiography

The typical appearance is of cardiac enlargement, including the RA, RV, and MPA with a small-appearing ascending aorta. The SVC shadow is often absent in the posteroanterior view due to RA enlargement and clockwise rotation of the heart [5]. Right ventricular enlargement may be better appreciated in the lateral view with reduction in the normal retrosternal clear space. Pulmonary vascularity is increased, in proportion to the amount of shunting. With pulmonary hypertension, the peripheral pulmonary vascularity may gradually become decreased along with increasing size of the central pulmonary arteries. In adult patients with congestive cardiac failure, especially associated with atrial fibrillation or flutter, the pulmonary veins may be prominent and the left atrium may become enlarged [13]. In the occasional patient with Scimitar syndrome, the heart shadow is shifted to the right hemithorax and the right lung is hypoplastic with diminished pulmonary vascularity (also known as hypertranslucent lung). The anomalously connected right pulmonary veins form a curved line in the right lower lung field, giving an appearance of a scimitar [5].

Echocardiography

Echocardiography is the primary method of diagnosis and evaluation of ASDs. Transthoracic two-dimensional echocardiography (TTE) using standard views demonstrates the size and location of an ASD, the systemic and pulmonary venous connections, and also the expected secondary changes of right atrial and right ventricular enlargement [5,13]. Estimates of the pulmonary-to-systemic flow ratio may be obtained, although their accuracy and reproducibility are uncertain [5]. The parasternal views typically demonstrate enlargement of the RV with flattening of the left ventricle

(a)
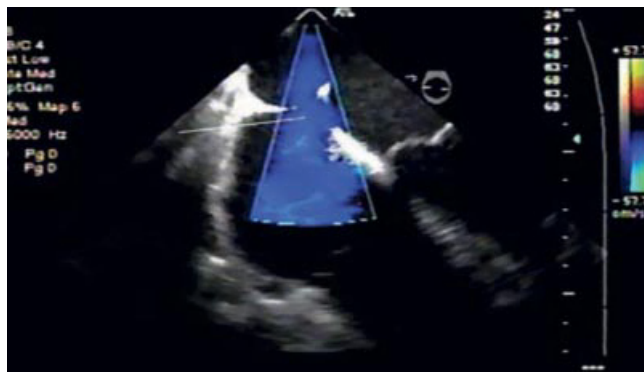
(b)

Figure 21.2 Two-dimensional echocardiograms of a patient with a relatively small secundum atrial septal defect. (a) Transthoracic echocardiogram, subcostal view. The defect is seen in the middle of the atrial septum measuring 8 mm. The right atrium is dilated. (b) Transesophageal echocardiogram, modified four-chamber view (0°). Color flow mapping shows the left-to-right shunt (in blue) across the defect.

(a)

(b)

Figure 21.3 Two-dimensional transesophageal echocardiogram of a patient with a sinus venosus ASD. (a) Modified four-chamber view shows a superior sinus venosus defect and an enlarged right upper pulmonary vein connected to the superior vena cava–right atrium junction. (b) Color flow mapping in bicaval view shows left-to-right shunting across the superiorly located defect.

in the long-axis view. Short-axis views are helpful in demonstrating that the intraventricular septum typically maintains a normal rounded contour in systole but is flattened or even concave in diastole because of the right ventricular volume overload. Secundum ASDs are seen in the central portion of the atrial septum and may extend anteriorly to the aortic root. The best views to visualize and measure an ASD are from the subxiphoid or subcostal location because the atrial septum is nearly perpendicular to the imaging axis [5,13], and measurements of the defect are most accurate and correlate with the transesophageal echocardiography (TEE) findings (Figure 21.2a and b). In contrast, a false drop-out in the middle of the septum is relatively common in the apical view because the ultrasound beam is parallel to the septum. The apical view, however, is excellent to evaluate the relative size of the right and left atria and right and left ventricles. Sinus

venosus ASDs are typically more difficult to image than secundum ASDs due to their location in the superior atrial septum near the orifice of the SVC. The finding of a sinus venosus ASD should prompt thorough evaluation of the right-sided pulmonary veins because partial anomalous drainage of one or more right-sided pulmonary veins is seen in 90% of affected patients. Complete delineation of the anatomy in such patients may be better appreciated by TEE or magnetic resonance imaging (Figure 21.3a and b). Color Doppler echocardiography is helpful in confirming flow through an apparent ASD on two-dimensional echocardiography (Figure 21.2b). Normally left-to-right flow is relatively laminar and can be easily seen. In patients with a small and restrictive ASD, the left-to-right flow may be identified as a higher velocity turbulent jet extending from the atrial septum into the right atrium. In patients with right ventricular hypertrophy from pulmonary

stenosis or pulmonary hypertension, there may be little left-to-right flow, and right-to-left flow may predominate. Contrast echocardiography using agitated saline can help to demonstrate right-to-left shunting across the inter-atrium septum at baseline and/or after a Valsalva maneuver in patients with suspected PFOs and paradoxical embolization [5]. Also, it can demonstrate the rapid appearance of contrast in the LA after injection into the left arm in patients with unroofed coronary sinus and Raghib syndrome [5].

In younger patients with good windows and une-quivocal delineation of the underlying anatomy, transtho-racic echocardiography usually suffices for management planning. However, in patients with suboptimal trans-thoracic echocardiographic windows, especially in obese adolescents and adults, TEE may be needed [1,5,13]. It is also better for patients with a sinus venosus defect and anomalies of the pulmonary veins (Figure 21.3a and b). TEE has been used frequently for screening patients who are candidates for transcatheter closure of secundum ASDs [66–68]. It provides an excellent window to assess the size and location of the defect, number of defects, septal rims, pliability and total length of the IAS, and other important nearby cardiac structures (Figure 21.4a). It also guides the procedure for balloon sizing of the defect (stretched diameter), proper device placement and assessment of residual leaks [66–69]. Some centers use intracardiac echocardiography (ICE) for these purposes with excellent imaging views and results (Videoclips 21.1 and 21.2). This technique provides better imaging of the posteroinferior portion of the IAS near the IVC and obviates the need for general anesthesia [70–73]. Whether it is associated with cost reduction is debatable [74]. The choice between ICE and TEE to guide the transcatheter procedure depends on local issues such as availability of equipment and anesthesiology, costs, and familiarity of the operators with the techniques. Recently, real-time three-dimensional TEE has been used as a new imaging tool to better understand the anatomy of the interatrial septum and secundum ASDs [75] (Videoclips 21.3 and 21.4). Although it provides superb pictures, it is debatable whether its use results in better outcomes after transcatheter treatment of the secundum ASD (Figure 21.4b). TEE has also been employed intraoperatively to assess surgical results, especially after correcting sinus venosus or other complex defects [5].

Magnetic Resonance Imaging (MRI)

Magnetic resonance imaging (MRI) is another noninvasive modality that may be useful in selected patients with a known or suspected ASD, especially adolescents and adults who have inconclusive clinical and echocardi-ographic findings due to suboptimal echocardiographic imaging windows [76]. It is an alternative to transesophageal

(a)
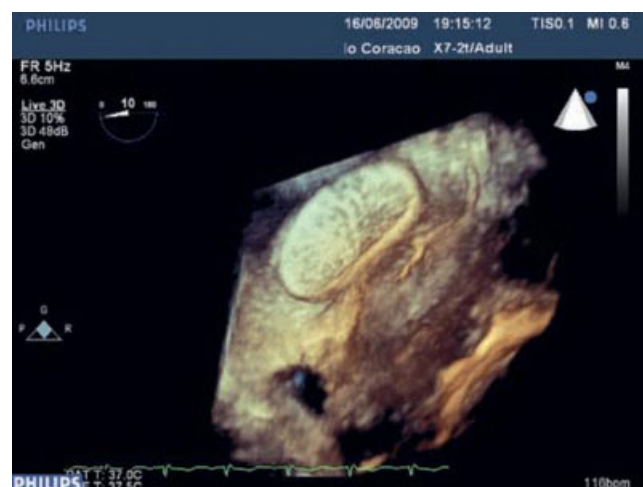
(b)

Figure 21.4 Two-dimensional transesophageal echocardiogram of a patient with a secundum atrial septal defect and an atrial septal aneurysm who underwent percutaneous closure of the defect. (a) Short-axis view shows an anterior defect and an aneurysm of the posterior portion of the interatrial septum. The septum bulges into the right atrium. Also, there is an additional and very small posterior defect. (b) Real-time three-dimensional transesophageal echocardiogram. After percutaneous closure of the defect, the left disc of the device is seen on the left side of the picture. Its anterior portion is splayed around the aorta, which was cut longitudinally.

echocardiography and diagnostic catheterization. MRI can demonstrate the size and location of the ASD and its suitability for transcatheter versus surgical closure [5]. MRI is particularly helpful in older patients with sinus venosus defect and anomalous connections of the pulmonary veins [77]. Functional assessment can also be performed to estimate the pulmonary-to-systemic flow ratio [78] and RV size and function.

Diagnostic cardiac catheterization and angiography

Diagnostic cardiac catheterization and angiography are no longer indicated in most patients with typical clinical and echocardiographic features of an ASD [5]. Catheterization may sometimes be needed to evaluate associated abnormalities such as pulmonary valvar stenosis, pulmonary hypertension, or exact sites of connection of the pulmonary veins. In older adult patients, catheterization is indicated preoperatively to exclude concomitant coronary artery disease [13].

The hemodynamic burden of an ASD can be evaluated in the cardiac catheterization laboratory [20]. Oximetry is useful in estimating the relative pulmonary/systemic blood flows (Qp/Qs) by the Fick principle, but the inability to obtain a true mixed venous saturation introduces a significant source of error in the calculations [5,13]. With a large shunt, there is considerable reflux of highly saturated blood to the SVC coming from the LA and RA. Therefore, saturations should be obtained in the high SVC or even in the proximal innominate vein. This is particularly true if there is suspicion of an anomalous connection of the right or left pulmonary vein to the normal right SVC. When there is anomalous connection of one or more left pulmonary veins to the distal innominate vein through a left vertical vein, blood samples should be taken in the left internal jugular vein or left subclavian vein. An increase in saturation of ~8–10% is found in the area of left-to-right shunting of pulmonary venous blood [20]. The estimated Qp/Qs frequently exceeds 2:1, but values as small as 1.5:1 may be associated with right atrial and right ventricular enlargement. Systemic arterial saturation is generally normal (occasionally slightly diminished), as is systemic cardiac output measured by the Fick method. Estimation of the cardiac output by thermodilution is misleading due to intracardiac shunting [5]. Right and left atrial pressures are usually similar in patients with unrestrictive moderate or large defects. Patients with significant pulmonary arterial hypertension should be assessed with regard to pressure and resistance response to vasodilators such as oxygen and nitric oxide [5]. In such patients, if the catheterization data suggest that the defect can still be closed, temporary test occlusion with a balloon or a device may be advisable [5]. When appropriate, a pulmonary arteriogram delineates the sites of pulmonary venous connection if the pulmonary veins are not entered directly or the oxygen saturation values are inconsistent [13]. In patients with severe pulmonary hypertension and vascular obstructive disease, selective pulmonary angiography with a wedge catheter typically shows enlarged proximal vessels with abrupt distal tapering. The distal vessels are tortuous and small in number. If it is necessary to delineate the secundum ASD angiographically, the catheter can generally be passed through it in the midportion of the atrial septum and an injection of contrast agent in the right upper pulmonary vein in a left anterior oblique with cranial angulation projection profiles the defect because flow from the vein is directed along the atrial septum. If there is a sinus venosus defect, the catheter passes into the left atrium near the base of the superior vena cava.

Management

Secundum ASDs

The main reasons for closing a secundum ASD (and all ASDs) is to prevent late pulmonary vascular disease, arrhythmias, and heart failure, all rare at <20 years of age [1]. Because the optimal timing for treatment has yet to be defined, the management strategy of a patient with a secundum ASD is based on multiple factors including the size and natural history of the defect, magnitude of the shunt and hemodynamic burden to the RV, age of the patient, and symptoms and/or co-morbid diseases [1,5,13]. Asymptomatic infants with a secundum ASD <8 mm in diameter should be observed expectantly [21–28]. Endocarditis prophylaxis precautions are not necessary. More than 75% of such secundum ASDs, particularly those <3–4 mm, close spontaneously before 18 months of age [21–28]. Spontaneous closure can also occur in infancy, even among patients who have signs of congestive cardiac failure [27]. If medical management fails, closure of the defect may be warranted even in children younger than 1 year [30,33]. Similarly, infants with associated co-morbid diseases, such as genetic syndromes, prematurity, diaphragmatic hernia, tracheoesophageal fistula, and chronic lung disease, may benefit from earlier closure [32,33]. Defects that are >8 mm in diameter in infancy are unlikely to close spontaneously and may even become larger with time [27]. If an infant with such a defect is asymptomatic and thriving well, closure may be deferred and carried out at 3–5 years of age, [13] provided that close surveillance is assured. Studies have shown no long-term benefit to earlier closure [79]. In older children and young adults, elective closure is recommended shortly after diagnosis if there is evidence of right ventricular enlargement. The management of an older adult patient with a secundum ASD is more controversial because of the lack of carefully conducted clinical trials on a large number of patients [1]. Despite some discussions about which patients need to have defect closure, the limited studies suggest that closure of an ASD in the older patients is warranted if the shunt is large and pulmonary vascular disease is not severe [1]. Although older patients may have a higher operative risk (especially if they have significant pulmonary hypertension with indexed PVR >7 Wood units m^{-2}, it seems that outcomes after surgery are better than those patients who are treated medically [44–50,80]. Theoretically, transcatheter treatment should further improve the beneficial effects of closure in this older age group. If the defect and

shunt are small and the right heart is not dilated, the patients can be followed, although a few will develop a larger shunt or symptoms and require closure of the defect [81].

A patient with an ASD associated with severe pulmonary hypertension and severely elevated pulmonary vascular resistance must be evaluated carefully. Operative risk is substantially increased by increased pulmonary vascular resistance (>7 Wood units m^{-2}) and is contraindicated if pulmonary vascular resistance is >15 Wood units m^{-2} [82–84]. In the latter, the ASD is probably an associated defect in conjunction with idiopathic pulmonary hypertension rather than Eisenmenger's reaction. Patients with severe idiopathic pulmonary hypertension may survive longer and have better exercise tolerance if a small ASD is present, and creation of a small ASD has even been used as a form of palliation in this situation [13,85]. Patients with a pulmonary resistance between 10 and 15 Wood units m^{-2} need expert investigation of pulmonary vascular reactivity or even lung biopsy [82–84]. Patients in this group whose defects are closed usually benefit symptomatically [82].

Closure of a secundum ASD can be performed surgically or by transcatheter means. Due to its less invasive nature, short hospital stay, no scar formation, and no need to use blood products, transcatheter closure of ASDs is indeed more appealing and has become the preferred method of treatment for selected patients in the last 5 years. Although no randomized trial has been conducted to compare both management strategies (catheter versus surgery), recent studies with contemporaneous cohorts of patients demonstrated that transcatheter closure of ASDs using either Amplatzer or Helex devices is as effective as surgery and results in less morbidity [86,87]. These studies resulted in approval of the Amplatzer and Helex devices for clinical use in the United States. Generally, 80–85% of all patients with secundum ASDs are suitable for transcatheter closure [88]. Due to evolving techniques, feasibility and indications for device implantation have expanded and now include the small child (<15 kg), those a with large defect, two or more isolated defects, a fenestrated IAS and an ASA, or only one insufficient rim (usually the retroaortic) [88–95]. Although device closure of secundum ASDs in the small child (<10–15 kg) is feasible, safe, and effective, higher rates of implantation failure, complications, and residual leaks are observed in this age group when compared with older patients [92,93]. Therefore, the indications for device closure in an asymptomatic small child who is thriving well and has no associated co-morbid conditions should be more strict and individualized. On the other side of the age spectrum, the elderly adult probably benefits the most from transcatheter closure due to anesthetic and thoracotomy issues, and other associated ailments that substantially increase the operative risks [1,95]. An occasional patient judged unsuitable for device closure may have a very large defect (>35–40 mm), defects with more than one inadequate rim,

too large a defect for the size of the patient (usually in children <10–15 kg), or a combination of these factors. These patients and those with all other types of ASDs, when indicated, should undergo surgical repair. Obviously, device closure is not indicated when a secundum ASD is associated with other cardiac lesions that require surgical correction. Although several devices have been used worldwide with varied results, only the Amplatzer septal occluder (AGA Medical, Golden Valley, MN, USA) and the Helex device (W. L. Gore and Associates, Flagstaff, AZ, USA) are approved for clinical use in the United States. In terms of costs, device closure has generally been less costly than [96,97] or similar to surgery [98], except in underdeveloped countries where the price of the devices may exceed hospital and professional costs [99].

PFOs, paradoxical embolization, and stroke

Because longitudinal studies in the general population fail to demonstrate that a PFO is a risk factor for ischemic strokes [59,60], any form of preventive treatment in asymptomatic patients with PFOs detected incidentally is unjustified at present. Therefore, patients with a PFO or a small ASD unassociated with right ventricular and right atrial enlargement do not generally require closure unless there is a high risk of paradoxical embolization with potentially life-threatening consequences (e.g., professional scuba divers) [65,100]. In this setting, the rationale of PFO closure is primary prophylaxis. On the other hand, in uncontrolled studies, percutaneous closure of the PFO in patients who had a cryptogenic stroke (i.e., unknown cause) due to presumed paradoxical embolization has abolished or markedly reduced the risk of repeat cerebral embolism (secondary prophylaxis) [55,56,101–103]. This is in contrast to the 8–16% recurrence rate in a 3–5 year follow-up in patients treated medically with antiplatelet medications or anticoagulants [104,105]. There are ongoing prospective and randomized clinical trials comparing both treatment strategies (device closure versus medical treatment) to determine whether device closure should be applied to all or some patients with a PFO with a single cryptogenic stroke. At present, most authorities and published guidelines agree that the PFO should be closed percutaneously only in cryptogenic stroke patients who had a second event while on medical treatment [106]. There are insufficient data to justify routine percutaneous closure of the PFO for such patients after the first cerebral event. Platelet antiaggregants (aspirin) are as effective as anticoagulants for secondary prevention and are associated with less bleeding [104]. Anticoagulants are indicated for recurrence prevention only if there is evidence of deep venous thrombosis or a coagulopathy [106]. Some offer transcatheter closure after the first cryptogenic stroke to patients who have unique PFOs with anatomic and/or functional characteristics considered at a higher risk for recurrences. These characteristics include large openings

(>4 mm), much mobility and redundancy of the interatrial septum, an atrial septal aneurysm, a right-to-left shunt at rest, massive right-to-left shunting after Valsalva maneuver, or a prominent Eustachian valve [102]. Probably a coagulopathy should also be included in the decision to treat [1]. Until the results of the prospective trials become available, many experts consider the issue of the best treatment strategy to be unsolved [1]. Interestingly, many studies in which the PFO or a small ASD was closed to prevent cerebral embolization reported a marked decrease in the incidence of migraine, especially migraine with an aura [61,63,64, 107–110]. Conversely, case–control studies failed to show such beneficial effect [111]. Therefore, at present, owing to the lack of well-conducted prospective and randomized trials, PFO device closure cannot be indicated as a well-established form of prophylactic treatment for patients with migraines unresponsive to medical treatment.

Sinus venosus defects

These patients have clinical findings similar to those with secundum ASDs. Essentially, all patients are referred to surgery because they usually have a significant left-to-right shunt through the defect and the commonly associated PAPVC [5,8,13]. The SVC type of sinus venosus defect should be closed using a prosthetic patch. The patch usually needs to be directed to the orifice of the SVC because of the PAPVC to this area. In some patients, the SVC needs to be enlarged with a patch or transected and relocated to the roof of the RA to ensure unobstructed drainage [5]. The rarer form of the IVC type of sinus venosus defect should also be repaired using a patch to close the defect and redirect the anomalously connected right lower pulmonary vein to the LA.

Partial Anomalous Venous Connections (PAPVCs)

These relatively common lesions have a wide anatomic variation. Usually there is an associated ASD [9]. Surgical indications and techniques should be tailored individually, considering the likelihood of operative success, expected technical difficulties, possible postoperative stenoses, and debatable benefits in an individual patient [5,8,9]. Because it does not result in a significant left-to-right shunt, PAPVC of a single small pulmonary vein does not require an operation [5]. On the other hand, PAPVC of all left pulmonary veins into a left vertical vein and then to the inomminate vein usually results in right ventricular volume overload and does require surgical treatment [5]. In this anomaly, the vertical vein is usually large and long enough to be detached from the innominate vein and anastomosed to the LA [5]. In neonates and infants, anastomosis of the small anomalous pulmonary veins to the LA may be complicated by postoperative stenosis and complete occlusion [5]. The incidental finding of a single anomalous pulmonary vein or multiple small anomalous pulmonary veins at a cardiac operation can be dealt with by simply leaving them alone [5].

Unroofed coronary sinus defects

The management strategy should be tailored to the underlying anatomy. If the mouth of the coronary sinus on the right side is small with no right ventricular enlargement, the ASD is left alone. If it is large, it should be patch closed with little practical consequence if the coronary venous blood cannot be redirected to the RA [5]. If a left SVC connected to the LA is present, it can be redirected and baffled to the RA or simply ligated if an adequate innominate vein is present [5].

Scimitar syndrome

This rare entity can be readily diagnosed based on the chest X-ray findings. Surgical treatment should be tailored based on the age of the patient, associated lesions, the amount of flow going across the right lung, and the amount of flow through the collateral supply to the lung [11]. The adult form of this disease has a more benign presentation and limited symptoms. Surgical correction is debatable because the amount of left-to-right flow shunting through the hypoplastic right lung is usually small [5]. However, if the shunt is large and results in RV enlargement, surgical redirection of the anomalous vein to the LA should be undertaken. In contrast, infants are usually more symptomatic from pulmonary hypertension and pulmonary sequestration [11]. Although the anomalous right pulmonary veins can be surgically redirected to the LA, postoperative obstruction is common at this age, causing reduction or abolition of flow to the right lung. Alternatively, the right pulmonary veins are left alone and the large aortopulmonary collaterals supplying the right lung are closed percutaneously, ameliorating symptoms and decreasing the pulmonary artery pressures [11]. Left pulmonary artery stenoses, if present, can also be dilated in the catheterization laboratory. Lobectomy or pneumonectomy may be indicated for patients with repeated pulmonary infections or hemorrhage due to abnormal bronchi [11].

Platypnea–orthodeoxia syndrome

Platypnea–orthodeoxia is a rare and poorly understood syndrome of postural hypoxemia accompanied by breathlessness [14]. The predominant symptom, dyspnea induced by upright posture, can be striking and debilitating. The precise cause of the syndrome is unclear, but patients develop right-to-left intracardiac shunting across a PFO, a small ASD, or a fenestrated septal aneurysm despite normal right-sided cardiac pressures. A persistent and unusually large Eustachian valve may be seen in some, but not all, patients. Hypothetically, standing upright could stretch the interatrial communication, thus allowing more streaming of venous blood from IVC through the defect, whether or not a persistent Eustachian valve coexists. This redirection of flow caused by an anatomic distortion of the atrial septum might also result from a variety of conditions, including cardiac

(pericardial effusion), pulmonary (emphysema, arteriovenous malformation, pneumonectomy, amiodarone toxicity), abdominal (cirrhosis of the liver or ileus), and vascular (aortic aneurysm, aortic elongation) diseases [14]. Catheter closure of the interatrial communication results in dramatic symptomatic and hemodynamic improvement [15].

Outcomes after treatment

The prognosis for patients with an ASD is generally very good, especially if the diagnosis is made early and the defect is closed [112]. Young patients who undergo uneventful ASD closure have an excellent outlook for survival for the next 30 years, but should be evaluated periodically.

Outcomes after surgery for secundum ASDs

Operative closure is accomplished by either direct suture closure or placement of a prosthetic patch over the defect with use of cardiopulmonary bypass. Direct suture is usually preferred if the defect is not too large because of concern about the possibility of thrombus formation on patch material, but no clear data exist regarding the superiority of one technique over the other [13]. Surgical techniques have improved and the use of a ministernotomy has become widespread. Other approaches, such as the submammary incision in women, lateral thoracotomy or right axillary incision, can also be used because of the potentially better cosmetic result [113–123]. More recently, techniques for video-assisted closure [124], robotic-assisted closure [125,126], and off-pump closure [127,128] have also been applied. In the modern era, the operative mortality risk in younger patients should approach zero and even in patients >30–40 years old, hospital mortality rates are usually <6.5% and indeed are often zero [43–50,79,112,129–138]. On the other hand, significant transient complications that delay discharge may occur in up to 25% of patients, including incomplete defect closure, bleeding, wound or patch dehiscence, wound infection, transient arrhythmia (including sinus node dysfunction and atrial fibrillation), pneumonia, pulmonary embolism, pleural effusion, superior vena cava obstruction, and postpericardiotomy syndrome requiring pericardiocentesis [43–50,79,112,129–138]. Despite these in-hospital complications, the average time of hospitalization for ASD closure has been reduced to 3–4 days in some institutions.

Long-term survival after operation is usually very good in children and good even in older adults [43–50,79,112, 129–138]. All the survival curves are better than the natural history curve derived from autopsy data and comparable to the population survival for the younger patients [1]. Patients under 20 years of age at the time of surgery show little decreased survival with age over a 20–30 year period, with their survival curves paralleling those for the normal population [1]. Survival curves for patients over 30 years of age at the time of operation show slightly more fall-off with age [1]. This does not mean, however, that such patients should not undergo closure of their ASD. Late operative closure may or may not lengthen survival in an individual patient but clearly results in improvement of symptoms [43–50]. In this regard, symptoms associated with a large left-to-right shunt are generally reversible even if operation is undertaken after the age of 60 years [46,139]. Children and adults who previously did not admit to symptoms often report that they can undertake more activity after the surgery. Even in those in heart failure before surgery, symptoms usually disappear [43–50,79,129–138]. Women who had surgery before becoming pregnant had a lower incidence of miscarriage, preterm delivery, and cardiac symptoms during pregnancy [140]. Exercise capacity increases in most patients, no matter the age at operation, but does not always return to normal [141–145]. Better performance has been found when defects were closed at <5 years of age [144].

Late complications and cardiovascular events may occur after surgical repair and are generally more common when the operation is performed at an older age. These include right ventricular dysfunction, residual pulmonary hypertension, symptomatic arrhythmias, need for pacemaker implantation, endocarditis, and mitral or tricuspid regurgitation requiring valvar surgery [13]. Cerebral embolism is also a threat, especially in older patients with atrial fibrillation [13]. Incomplete closure of the defect is rare and any residual defect is seldom large enough to cause problems [5].

Surgical closure of an ASD usually leads to a progressive decrease in size of the RV, usually taking 6–12 months (or even more) to attain normal dimensions [1,146–148]. In some patients, however, especially those with higher pulmonary blood flows and operated at older ages, the RV remains enlarged [1,79,146–148]. Although this residual dilatation has been termed cardiomyopathy of volume loading [1], its clinical effect on exercise performance is limited [146–149]. The left ventricular volume increases due to the shift of the septum towards the decompressed right ventricle and this plays a major role in the improved exercise response [1]. Echocardiography, computed tomography, and functional studies have shown better RV improvement in younger than older patients and those undergoing closure by interventional catheterization rather than by surgery [150–162]. Pulmonary arterial pressure usually decreases but resistance does not always return to normal [163–165]. Some may show increase in pulmonary arterial pressures during exercise [166].

Management of postoperative arrhythmias is an important issue in patients with an ASD. Persistent or newly developed arrhythmias may occur after surgical repair [1]. In general, those who already had arrhythmias before operation tended to have them postoperatively [167]. Also, the incidence of postoperative atrial arrhythmias has correlated with

increasing age of the patient, the left-to-right shunt size, and the degree of pulmonary hypertension [168]. A recent study suggested that arrhythmias are less frequent after interventional device than surgical closure [169]. In children, postoperative arrhythmias were reported in usually <10% after surgery, with most being sinus node dysfunction manifested by ectopic atrial rhythms, bradycardia, or sick sinus syndrome [1]. Relatively few had paroxysmal or sustained atrial fibrillation or needed pacemakers. In adults, however, paroxysmal or sustained supraventricular tachycardia, atrial fibrillation, or flutter are reported in up to 20–40% of patients after surgery, being increasingly frequent with aging [1,43–50,79,129–138]. The appearance of atrial fibrillation is serious because it may result in symptomatic deterioration and greatly increases the risk of stroke, which can occur late after surgery. In general, the risk of embolization is very low if the patients are <40 years of age and have normal pulmonary arterial pressures, sinus rhythm, and no history of preoperative emboli [13,43–50,79,129–138]. Although operative closure of an ASD in an older patient does not significantly reduce the incidence of late strokes because the incidence of atrial fibrillation is not reduced, this should not influence the decision to close the defect [13]. Therefore, patients should be monitored for the onset of atrial fibrillation, and if sinus rhythm does not return, anticoagulation therapy should be considered strongly [13]. On the other hand, some patients with atrial flutter revert to sinus rhythm after surgery [170]. Alternatively, surgical treatment of arrhythmias (Maze procedure) or radiofrequency ablation of atrial flutter or fibrillation have been performed successfully at the time of closing an ASD [171–174].

Outcomes after device closure of secundum ASDs

The technical aspects, feasibility of implantation, safety, and efficacy of device closure of the secundum ASD should be evaluated for each device available on the market. Because of the plethora of devices, this is beyond the scope of this chapter. The discussion is focused on the Amplatzer septal occluder (AGA Medical) and the Helex device (W. L. Gore and Associates). In short, the Amplatzer septal occluder, the most often used device worldwide, is constructed of a weave of relatively fine nitinol (nickel–titanium alloy) wire filled with thrombogenic fabric. The device can be withdrawn into a delivery catheter and resumes its intended shape as it is extruded from the catheter. The shape is that of two relatively flat, round disks connected by a central portion of large diameter that provides self-centering and stenting to maintain the device in position. It can be easily withdrawn and repositioned before release [86]. The Helex device is a non-self-centering double disk device consisting of a nitinol wire frame on which is bonded a curtain of hydrophilic ePTFE (Goretex; W. L. Gore and Associates). The nitinol is wound as two opposing spirals such that when the device is positioned it configures in two planar parallel discs that sit

on either side of the IAS. It is also repositionable and retrievable before release and even after it [87]. The success rate of implantation of such devices depends on the operator. Due to its design and easier-to-use system, the Amplatzer device results in higher rates of successful implantation, approaching 99% in experienced hands [86,88–95,175–179] (Figure 21.4b) (Videoclips 21.1–21.2). Reasons for failure include larger defects, multiple defects, inadequate rims of septal tissue, an atrial septal aneurysm, or a combination of these factors [86,88–95,175–179]. Whereas the Amplatzer septal occluder can close a broad range of ASD dimensions including the very large ones, the Helex device should be used only for the small to moderate ASD (<18 mm stretched diameter) [87,89,180,181].

Complication rates decrease with operator experience. Mortality is virtually zero. Occasionally the device embolizes immediately after release but can usually be retrieved in the catheterization laboratory and replaced. The Helex device is the easiest device to retrieve using transcatheter techniques. Sometimes surgery is needed to remove the embolized device, especially if it is stuck in the RV. Late (1 day–6 years) embolization is very unusual [182]. Occasionally there are supraventricular arrhythmias or atrioventricular block after closure, but no more than after surgical closure [183]. Older patients and oversizing of the device may be risk factors for arrhythmias. Thrombus formation on the left atrial side of all available devices has occasionally been detected immediately after placement or in the first 6 months of follow-up, and ironically may occur after closure of a patent foramen ovale to prevent paradoxical embolism [184]. The prevalence of thrombus formation is 2–3%, with the Amplatzer device being the least affected [1,184]. Treatment includes medical lysis or sometimes surgical removal. Cerebral embolism, however, is rare, perhaps no more frequent than after surgical closure of the defect. Fracture of the wire frame of the Helex device with no untoward clinical effect has been described with the larger diameter devices [185]. Probably the most feared complication is early or late erosion into the aortic root with subsequent pericardial tamponade and very rarely death or production of a fistula between the aorta and left or the right atrium [186]. This has been described with the Amplatzer device with an incidence of 0.1% [186], and also with other devices [187]. Owing to its design, flexibility, and softer characteristics, the Helex device has not resulted in perforations or erosions. Oversizing of the Amplatzer device and a higher ASD location in the IAS are risk factors for this complication [186]. Rarely, infective endocarditis occurs after device placement [188,189].

Complete closure of the defect depends on the type of device, size of the defect, and timing of evaluation. An immediate residual shunt may be seen in up to 10–30% of patients immediately after device release [86–95,175–181]. With progressive endothelialization of the devices, closure rates reach 92–99% after 1 year of follow-up, being higher

for the Amplatzer device and smaller defects [86–95, 175–181]. Because of its non-self-centering mechanism, a residual leak is more frequently observed with the Helex device [87,180,181]. Most, if not all, of these residual leaks seen with either device are trivial or small (<3–4 mm) and do not result in any hemodynamic burden to the RV. Therefore, clinical cure is achieved in virtually 100% of patients.

As with surgery, closure of the defect with a device decreases the size of the right ventricle, increases the size of the left ventricle, and improves cardiac function and exercise capacity. Improvement has occurred in children and adults without any notable age-related differences, with remodeling and cardiac function being slightly better after device closure than surgical repair [150–162,190–193].

Outcomes after surgical repair of other types of ASDs and PAPVC

Operative mortality for correcting a PAPVC with or without a sinus venosus defect is <3% [8]. After surgery, patients become asymptomatic or less symptomatic and exercise tolerance increases. Late complications such as reoperation, vena cava obstruction, pulmonary vein obstruction, and pacemaker implantation are uncommon [9]. Occasionally, the technique of repair may stenose the SVC and require balloon dilation and stent implantation [5]. Significant postoperative arrhythmias are also uncommon, although an occasional patient may show late sinus node dysfuntion due to surgical damage to the sinoatrial node [8,9].

Symptomatic infants with the Scimitar syndrome have a more guarded prognosis. Pulmonary arterial hypertension is a risk factor for operative mortality and may persist in those patients undergoing transcatheter closure of the collateral arterial supply to the right lung [11]. If surgical reimplantation of the anomalous pulmonary veins is undertaken, postoperative obstruction is common [5]. In contrast, the outcomes after surgical treatment of the adult form of this disease are much better [11]. If the right pulmonary artery and the right lung are not significantly hypoplastic, redirection of the anomalous veins to the left atrium results in symptomatic improvement and reduction of RV size. However, postoperative pulmonary vein stenosis is more common than for other types of PAPVC [11].

Future directions

In the next 10 years, we will witness the application of new technologies for the imaging, diagnosis, and treatment of ASDs. Evolving imaging technology will be applied not only for the accurate diagnosis of all types of ASDs but also for the guidance of transcatheter closure of the secundum ASD. Real-time three-dimensional intracardiac echocardiography will probably be helpful in this regard.

MRI-guided intervention is an exciting field that may have an effect on abolishing the need for radiation exposure in the catheterization laboratory for ASD closure. MRI-compatible catheters and devices should be developed to achieve this goal. Closure devices with reabsorbable materials have already been employed in clinical practice with good short-term outcomes [194–197]. Their main advantage is to allow free transseptal access to the left atrium in the future. With the rapid development of new devices to close the left atrial appendage in high-risk elderly patients with atrial fibrillation and to repair functional mitral valve insufficiency percutaneously, this is of paramount importance. Surgical approaches will also evolve and the application of less invasive, video-guided robotic surgery through small thoracic ports will be available for selected patients with ASDs.

References

1 Hoffman JIE. Atrial septal defect (secundum). In: Hoffman JIE, ed. *The Natural and Unnatural History of Congenital Heart Disease.* Oxford: Blackwell, 2009: 133–56.

2 Hoffman JIE, Kaplan S. The incidence of congenital heart disease. *J Am Coll Cardiol* 2002;**39**:1890–900.

3 Fyler DC, Buckley LP, Hellenbrand WE, *et al.* Report of the New England Regional Infant Cardiac Program. *Pediatrics* 1980;**65**(Suppl):375–82.

4 Calcagni G, Digilio MC, Sarkozy A, *et al.* Familial recurrence of congenital heart disease: an overview and review of the literature. *Eur J Pediatr* 2007;**166**:111–6.

5 Keane JF, Geva T, Fyler DC. Atrial septal defect. In: Keane JF, Lock JE, Fyler DC. eds. *Nadas' Pediatric Cardiology*, 2nd edn. Philadelphia: Saunders, 2006: 603–16.

6 Hagen PT, Scholz DG, Edwards WD. Incidence and size of patent foramen ovale during the first 10 decades of life: an autopsy study of 965 normal hearts. *Mayo Clin Proc* 1984;**59**:17–20.

7 Fisher DC, Fisher EA, Budd JH, *et al..* The incidence of patent foramen ovale in 1,000 consecutive patients. A contrast transesophageal echocardiography study. *Chest* 1995;**107**: 1504–9.

8 Hoffman JIE. Partial anomalous pulmonary venous connection with an intact atrial septum. In: Hoffman JIE, ed. T*he Natural and Unnatural History of Congenital Heart Disease.* Oxford: Blackwell, 2009: 157–60.

9 Alsoufi B, Cai S, Van Arsdell GS, *et al.* Outcomes after surgical treatment of children with partial anomalous pulmonary venous connection. *Ann Thorac Surg* 2007;**84**:2020–6.

10 Haramati LB, Moche IE, Rivera VT, *et al.* Computed tomography of partial anomalous pulmoanry venous connection in adults. *J Comput Assist Tomogr* 2003;**27**:743–9.

11 Hoffman JIE. Scimitar syndrome. In: Hoffman JIE, ed. *The Natural and Unnatural History of Congenital Heart Disease.* Oxford: Blackwell, 2009: 161–6.

12 Raghib G, Ruttenberg HD, Anderson RC, *et al.* Termination of the left superior vena cava in left atrium, atrial septal defect, and absence of coronary sinus. A developmental complex. *Circulation* 1965;**31**:906–9.

13 Latson L. Atrial septal defect. In: Moller JH, Hoffman JIE, eds. *Pediatric Cardiovascular Medicine*. New York: Churchill Livingstone, 2000: 311–21.

14 Cheng TO. Mechanisms of platypnea–orthodeoxia: what causes water to flow uphill? *Circulation* 2002;**105**:e47.

15 Guérin P, Lambert V, Godart F, *et al.* Transcatheter closure of patent foramen ovale in patients with platypnea–orthodeoxia: results of a multicentric French registry. *Cardiovasc Intervent Radiol* 2005;**28**:164–8.

16 Schreiber TL, Feigenbaum H, Weyman AE. Effect of atrial septal defect repair on left ventricular geometry and degree of mitral valve prolapse. *Circulation* 1980;**61**:888–96.

17 Suchon E, Podolec P, Plazak W, *et al.* Mitral valve prolapse associated with ostium secundum atrial septal defect – a functional disorder. *Acta Cardiol* 2004;**59**:237–8.

18 Speechly-Dick ME, John R, Pugsley WB, *et al.* Secundum atrial septal defect repair: long-term surgical outcome and the problem of late mitral regurgitation. *Postgrad Med J* 1993;**69**:912–5.

19 Ewert P, Berger F, Nagdyman N, *et al.* Masked left ventricular restriction in elderly patients with atrial septal defects: a contraindication for closure? *Catheter Cardiovasc Diag* 2001;**52**:177–80.

20 Rudolph AM. Atrial septal defect. In: Rudolph AM. *Congenital Diseases of the Heart: Clinical–Physiological Considerations*, 2nd edn. Armonk, NY: Futura Publishing, 2001: 245–81.

21 Fukazawa M, Fukushige J, Ueda K. Atrial septal defects in neonates with reference to spontaneous closure. *Am Heart J* 1988;**116**:123–7.

22 Ozcelik N, Atalay S, Tutar E, *et al.*The prevalence of interatrial septal openings in newborns and predictive factors for spontaneous closure. *Int J Cardiol* 2006;**108**:207–11.

23 Brassard M, Fouron JC, van Doesburg NH, *et al.* Outcome of children with atrial septal defect considered too small for surgical closure. *Am J Cardiol* 1999;**83**:1552–5.

24 Cockerham JT, Martin TC, Gutierrez FR, *et al.* Spontaneous closure of secundum atrial septal defect in infants and young children. *Am J Cardiol* 1983;**52**:1267–71.

25 Azhari N, Shihata MS, Al-Fatani A. Spontaneous closure of atrial septal defects within the oval fossa. *Cardiol Young* 2004;**14**:148–55.

26 Hanslik A, Pospisil U, Salzer-Muhar U, *et al.* Predictors of spontaneous closure of isolated secundum atrial septal defect in children: a longitudinal study. *Pediatrics* 2006;**118**:1560–5.

27 Radzik D, Davignon A, van Doesburg N, *et al.* Predictive factors for spontaneous closure of atrial septal defects diagnosed in the first 3 months of life. *J Am Coll Cardiol* 1993;**22**:851–3.

28 Brand A, Keren A, Branski D, *et al.* Natural course of atrial septal aneurysm in children and the potential for spontaneous closure of associated septal defect. *Am J Cardiol* 1989;**64**:996–1001.

29 McMahon CJ, Feltes TF, Fraley JK, *et al.* Natural history of growth of secundum atrial septal defects and implications for transcatheter closure. *Heart* 2002;**87**:256–9.

30 Bull C, Deanfield J, deLeval M, *et al.* Correction of isolated secundum atrial septal defect in infancy. *Arch Dis Child* 1981;**56**:784.

31 Dimich I, Steinfeld L, Park SC. Symptomatic atrial septal defect in infants. *Am Heart J* 1973;**85**:601.

32 Mahoney LT, Truesdell SC, Krzmarzick TR, *et al.* Atrial septal defects that present in infancy. *Am J Dis Child* 1986;**140**:1115.

33 Lammers A, Hager A, Eicken A, *et al.* Need for closure of secundum atrial septal defects in infancy. *J Thorac Cardiovasc Surg* 2005;**129**:1353–7.

34 Andrews R, Tulloh R, Magee A, Anderson D. Atrial septal defect with failure to thrive in infancy: hidden pulmonary vascular disease? *Pediatr Cardiol* 2002;**23**:528–30.

35 Anderson M, Moller I, Lyngborg K, *et al.* The natural history of small atrial septal defect: long-term follow-up with serial heart catheterizations. *Am Heart J* 1976;**92**:302.

36 Cherian G, Uthaman CB, Durairaj M, *et al.* Pulmonary hypertension in isolated secundum atrial septal defect: high frequency in young patients. *Am Heart J* 1983;**105**:952–7.

37 Butera G, Bossone E, Chessa M, *et al.* Range of pulmonary artery pressures in patients undergoing percutaneous atrial septal defect device closure. *Monaldi Arch Chest Dis* 2003;**60**:258–60.

38 Dalen JE, Bruce RA, Cobb LA. Interaction of chronic hypoxia of moderate altitude on pulmonary hypertension complicating defect of the atrial septum. *N Engl J Med* 1962;**266**:272–7.

39 Vogel M, Berger F, Kramer A, *et al.* Incidence of secondary pulmonary hypertension in adults with atrial septal or sinus venosus defects. *Heart* 1999;**82**:30–3.

40 Schamroth CL, Sareli P, Pocock WA, *et al.* Pulmonary arterial thrombosis in secundum atrial septal defect. *Am J Cardiol* 1987;**60**:1152–6.

41 Ishizaka N, Kage N, Iida H, *et al.* Massive pulmonary artery thrombosis, pulmonary hypertension and untreated atrial septal defect. *Cardiology* 2002;**97**:53–4.

42 Craig RJ, Selzer A. Natural history and prognosis of atrial septal defect. *Circulation* 1986;**37**:805–15.

43 Attenhofer Jost CH, Connolly HM, Danielson GK, *et al.* Sinus venosus atrial septal defect: long-term postoperative outcome for 115 patients. *Circulation* 2005;**112**:1953–8.

44 Attie F, Rosas M, Granados N, *et al.* Surgical treatment for secundum atrial septal defects in patients <40 years old. A randomized clinical trial. *J Am Coll Cardiol* 2001;**38**:2035–42.

45 Engelfriet P, Meijboom F, Boersma E, *et al.* Repaired and open atrial septal defects type II in adulthood: an epidemiological study of a large European cohort. *Int J Cardiol* 2008;**126**:379–85.

46 St John Sutton MG, Abdul MB, Tajik AJ, McGoon DC. Atrial septal defect in patients sixty years and older. Operative results and long term post operative follow up. *Circulation* 1981;**64**:402–9.

47 Vogel M, Berger F, Kramer A, *et al.* Incidence of secondary pulmonary hypertension in adults with atrial septal or sinus venosus defects. *Heart* 1999;**82**:30–3.

48 Gatzoulis MA, Freeman MA, Siu SC, *et al.* Atrial arrhythmia after surgical closure of atrial septal defects in adults. *N Engl J Med* 1999;**340**:839–46.

49 Konstantinides S, Geibel A, Olschewski M, *et al.* A comparison of surgical and medical therapy for atrial septal defect in adults. *N Engl J Med* 1995;**333**:469–73.

50 Murphy JG, Gersh BJ, McGoon MD, *et al.* Long-term outcome after surgical repair of isolated atrial septal defect: follow-up at 27 to 32 years. *N Engl J Med* 1990;**323**:1645.

51 Ruschhaupt DG, Khoury L, Thilenius OG, *et al.* Electrophysiologic abnormalities of children with ostium secundum atrial septal defect. *Am J Cardiol* 1984;**53**:1643–7.

52 Campbell M, Neill C, Suzman S. The prognosis of atrial septal defect. *Br Med J* 1957;**i**:1375–83.

53 Gazzaniga AB, Dalen JE. Paradoxical embolism: its pathophysiology and clinical recognition. *Ann Surg* 1970;**171**:137–42.

54 Loscalzo J. Paradoxical embolism: clinical presentation, diagnostic strategies, and therapeutic options. *Am Heart J* 1986;**112**:141–5.

55 Di Tullio MR. Patent Foramen Ovale: echocardiographic detection and clinical relevance in stroke. *J Am Soc Echocardiogr* 2010;**2**:144–55.

56 Overell JR, Bone I, Lees KR. Interatrial septal abnormalities and stroke: a meta-analysis of case–control studies. *Neurology* 2000;**55**:1172–9.

57 Thanigaraj S, Zajarias A, Valika A, *et al.* Caught in the act: serial, real time images of a thrombus traversing from the right to left atrium across a patent foramen ovale. *Eur J Echocardiogr* 2006;**7**:179–81.

58 Handke M, Harloff A, Olschewski M, *et al.* Patent foramen ovale and cryptogenic stroke in older patients. *N Engl J Med* 2007;**357**:2262–8.

59 Meissner I, Khandheria BK, Heit JA, *et al.* Patent foramen ovale: innocent or guilty? Evidence from a population-based study. *J Am Coll Cardiol* 2006;**47**:440–5.

60 Di Tullio MR, Sacco RL, Sciacca RR, *et al.* Patent foramen ovale and the risk of ischemic stroke in a multiethnic population. *J Am Coll Cardiol* 2007;**49**:797–802.

61 Wilmhurst PT, Nightingale S, Walsh KP, Morrison WL. Effect on migraine of closure of cardiac right-to-left shunts to prevent recurrence of decompression ilness or stroke or for haemodynamic reasons. *Lancet* 2000;**356**:1648–51.

62 Meier B, Lock JE. Contemporary management of patent foramen ovale. *Circulation* 2003;**107**:5–9.

63 Wahl A, Praz F, Tai T, *et al.* Improvement of migraine headaches after percutaneous closure of patent foramen ovale for secondary prevention of paradoxical embolism. *Heart* 2010;**96**:967–73.

64 Rigatelli G, Dell'Avvocata F, Ronco F, *et al.* Primary transcatheter patent foramen ovale closure is effective in improving migraine in patients with high-risk anatomic and functional characteristics for paradoxical embolism. *JACC Cardiovasc Interv* 2010;**3**:282–7.

65 Torti SR, Billinger M, Schwerzmann M, *et al.* Risk of decompression illness among 230 divers in relation to the presence and size of patent foramen ovale. *Eur Heart J* 2004;**25**:1014–20.

66 Hellenbrand WE, Fahey JT, McGowan FX, *et al.* Transesophageal echocardiographic guidance of transcatheter closure of atrial septal defect. *Am J Cardiol* 1990;**66**:207–13.

67 Pedra SR, Pontes SC Jr, Cassar R de S, *et al.* The role of echocardiography in the percutaneous treatment of septal defects. *Arq Bras Cardiol* 2006;**86**:87–96.

68 Boutin C, Musewe NN, Smallhorn JF, *et al.* Echocardiographic follow-up of atrial septal defect after catheter closure by double umbrella device. *Circulation* 1993;**88**: 621–7.

69 Cao Q, Radtke W, Berger F, *et al.* Transcatheter closure of multiple atrial septal defects. Initial results and value of two- and three-dimensional transoesophageal echocardiography. *Eur Heart J* 2000;**21**:941–7.

70 Hijazi Z, Wang Z, Cao Q, *et al.* Transcatheter closure of atrial septal defects and patent foramen ovale under intracardiac echocardiographic guidance: feasibility and comparison with transesophageal echocardiography. *Catheter Cardiovasc Interv* 2001;**52**:194–9

71 Koenig P, Cao QL, Heitschmidt M, *et al.* Role of intracardiac echocardiographic guidance in transcatheter closure of atrial septal defects and patent foramen ovale using the Amplatzer device. *J Interv Cardiol* 2003;**16**:51–62.

72 Luxenberg DM, Silvestry FE, Herrmann HC, *et al.* Use of a new 8 French intracardiac echocardiographic catheter to guide device closure of atrial septal defects and patent foramen ovale in small children and adults: initial clinical experience. *J Interv Cardiol* 2005;**17**:540–5.

73 Patel A, Cao QL, Koenig PR, Hijazi ZM. Intracardiac echocardiography to guide closure of atrial septal defects in children less than 15 kilograms. *Catheter Cardiovasc Interv* 2006;**68**:287–91.

74 Alboliras ET, Hijazi ZM. Comparison of costs of intracardiac echocardiography and transesophageal echocardiography in monitoring percutaneous device closure of atrial septal defect in children and adults. *Am J Cardiol* 2004;**94**:690–2.

75 Lodato JA, Cao QL, Weinert L, *et al.* Feasibility of real-time three dimensional transesophageal echocardiography for guidance of percutaneous atrial septal defect closure. *Eur J Echocardiogr* 2009;**10**:543–8.

76 Holmvang G. A magnetic resonance imaging method for evaluating atrial septal defects. *J Cardiovasc Magn Reson* 1999;**1**:59–64.

77 Ferrari VA, Scott CH, Holland GA, *et al.* Ultrafast thre-dimensional contrast-enhanced magnetic resonance angiography and imaging in the diagnosis of partial anomalous pulmonary venous drainage. *J Am Coll Cardiol* 2001;**37**:1120–7.

78 Powel AJ, Tsai-Goodman B, Prakash A, *et al.* Comparison between phase-velocity cine magnetic resonance imaging and invasive oximetry for quantification of arial shunts. *Am J Cardiol* 2003;**91**:1523–9.

79 Meijboom F, Hess J, Szatmari A, *et al.* Long-term follow-up (9 to 20 years) after surgical closure of atrial septal defect at a young age. *Am J Cardiol* 1993;**72**:1431.

80 Gatzoulis MA, Redington AN, Somerville J, *et al.* Should atrial septal defects in adults be closed? *Ann Thorac Surg* 1996;**61**:657.

81 Andersen M, Moller I, Lyngborg K, Wennevold A. The natural history of small atrial septal defects; long-term follow-up with serial heart catheterizations. *Am Heart J* 1976;**92**:302–7.

82 Steele PM, Fuster V, Cohen M, *et al.* Isolated atrial septal defect with pulmonary vascular obstructive disease; long term follow up and prediction of outcome after surgical correction. *Circulation* 1987;**76**:1037–42S.

83 Sachweh JS, Daebritz SH, Hermanns B, *et al.* Hypertensive pulmonary vascular disease in adults with secundum or sinus venosus atrial septal defect. *Ann Thorac Surg* 2006;**81**:207–13.

84 Yamaki S, Horiuchi T, Miura M, *et al.* Pulmonary vascular disease in secundum atrial septal defect with pulmonary hypertension. *Chest* 1986;**89**:694–8.

85 Barst RJ, Gibbs JS, Ghofrani HA, *et al.* Updated evidence-based treatment algorithm in pulmonary arterial hypertension. *J Am Coll Cardiol* 2009;**54**(1 Suppl):S78–84.

86 Du ZD, Hijazi ZM, Kleinman CS, *et al.*, Amplatzer Investigators. Comparison between transcathter and surgical closure of secundum atrial septal defect in children and adults: results of a multicenter nonrandomized trial. *J Am Coll Cardiol* 2002;**39**:1836–44.

87 Jones TK, Latson LA, Zahn E, *et al.* Multicenter pivotal study of the Helex Septal Occluder Investigators. Results of the US multicenter pivotal study of the Helex septal occluder for percutaneous closure of secundum atrial septal defects. *J Am Coll Cardiol* 2007;**49**:2215–21.

88 Butera G, Romagnoli E, Carminati M, *et al.* Treatment of isolated secundum atrial septal defects: impact of age and defect morphology in 1,013 consecutive patients. *Am Heart J* 2008;**56**:706–12.

89 Pedra CA, Pedra SR, Esteves CA, *et al.* Transcathter closure of secundum atrial septal defects with complex anatomy. *J Invasive Cardiol* 2004;**16**:117–22.

90 Du ZD, Koenig P, Cao QL, *et al.* Comparison of transcatheter closure of secundum atrial septal defect using the Amplatzer septal occluder associated with deficient versus sufficient rims. *Am J Cardiol* 2002;**90**:865–9.

91 Awad SM, Garay FF, Cao QL, Hijazi ZM. Multiple Amplatzer septal occluder devices for multiple atrial communications: immediate and long-term follow-up results. *Catheter Cardiovasc Interv* 2007;**70**:265–73.

92 Cardenas L, Panzer J, Boshoff D, *et al.* Transcatheter closure of secundum atrial defect in small children. *Catheter Cardiovasc Interv* 2007;**69**:447–52.

93 Diab KA, Cao QL, Bacha EA, Hijazi ZM. Device closure of atrial septal defects with the Amplatzer septal occluder: safety and outcomes in infants. *J Thorac Cardiovasc Surg* 2007;**134**:960–6.

94 Berger F, Ewert P, Abdul-Khaliq H, *et al.* Percutaneous closure of large atrial septal defects with the Amplatzer septal occluder: technical overkill or recommendable alternative treatment? *J Interv Cardiol* 2001;**14**:63–7.

95 Losay J, Petit J, Lambert V, *et al.* Percutaneous closure with Amplatzer device is a safe and efficient alternative to surgery in adults with large atrial septal defects. *Am Heart J* 2001;**142**:544–8.

96 Baker SS, O'Laughlin MP, Jollis JG, *et al.* Cost implications of closure of atrial septal defect. *Catheter Cardiovasc Interv* 2002;**55**:83–7.

97 Hughes ML, Maskell G, Goh TH, Wilkinson JL. Prospective comparison of costs and short term health outcomes of surgical versus device closure of atrial septal defect in children. *Heart* 2002;**88**:67–70.

98 Thomson JD, Aburawi EH, Watterson KG, *et al.* Surgical and transcatheter (Amplatzer) closure of atrial septal defects: a prospective comparison of results and cost. *Heart* 2002;**87**:466–9.

99 Vida VL, Barnoya J, O'Connel M, *et al.* Surgical versus percutaneous occlusion of ostium secundum atrial septal defects: results and cost-effective considerations in a low-income country. *J Am Coll Cardiol* 2006;**47**:326–31.

100 Cartoni D, De Castro S, Valente G, *et al.* Identification of professional scuba divers with patent foramen ovale at risk for decompression illness. *Am J Cardiol* 2004;**94**:270–3.

101 Anzola GP, Zavarize P, Morandi E, *et al.* Transcranial Doppler and risk of recurrence in patients with stroke and patent foramen ovale. *Eur J Neurol* 2003;**10**:129–35.

102 De Castro S, Cartoni D, Fiorelli M, *et al.* Morphological and functional characteristics of patent foramen ovale and their embolic implications. *Stroke* 2000;**31**:2407–13.

103 Nedeltchev K, Arnold M, Wahl A, *et al.* Outcome of patients with cryptogenic stroke and patent foramen ovale. *J Neurol Neurosurg Psychiatry* 2002;**72**:347–50.

104 Homma S, Sacco RL, Di Tullio MR, *et al.* Effect of medical treatment in stroke patients with patent foramen ovale: patent foramen ovale in cryptogenic stroke study. *Circulation* 2002;**105**:2625–31.

105 Homma S, Sacco RL. Patent foramen ovale and stroke. *Circulation* 2005;**112**:1063–72.

106 Messe SR, Silverman IE, Kizer JR, *et al.* Practice parameter: recurrent stroke with patent foramen ovale and atrial septal aneurysm: report of the Quality Standards Committee of the American Academy of Neurology. *Neurology* 2004;**62**:1042–50.

107 Giardini A, Donti A, Formigari R, *et al.* Transcatheter patent foramen ovale closure mitigates aura migraine headaches abolishing spontaneous right-to-left shunting. *Am Heart J* 2006;**151**:922.e1–922.e5.

108 Mortelmans K, Post M, Thijs V, *et al.* The influence of percutaneous atrial septal defect closure on the occurrence of migraine. *Eur Heart J* 2005;**26**:1533–7.

109 Reisman M, Christofferson RD, Jesurum J, *et al.* Migraine headache relief after transcatheter closure of patent foramen ovale. *J Am Coll Cardiol* 2005;**45**:493–5.

110 Schwerzmann M, Wiher S, Nedeltchev K, *et al.* Percutaneous closure of patent foramen ovale reduces the frequency of migraine attacks. *Neurology* 2004;**62**:1399–401.

111 Garg P, Servoss SJ, Wu JC, *et al.* Lack of association between migraine headache and patent foramen ovale: results of a case–control study. *Circulation* 2010;**121**:1406–12.

112 Roos-Hesselink JW, Meijboom FJ, Spitaels SE, *et al.* Excellent survival and low incidence of arrhythmias, stroke and heart failure long-term after surgical ASD closure at young age. A prospective follow-up study of 21–33 years. *Eur Heart J* 2003;**24**:190–7.

113 Ak K, Aybek T, Wimmer-Greinecker G, *et al.* Evolution of surgical techniques for atrial septal defect repair in adults: a 10-year single-institution experience. *J Thorac Cardiovasc Surg* 2007;**134**:757–64.

114 Bichell DP, Geva T, Bacha EA, *et al.* Minimal access approach for the repair of atrial septal defect: the initial 135 patients. *Ann Thorac Surg* 2000;**70**:115–8.

115 Byrne JG, Adams DH, Mitchell ME, Cohn LH. Minimally invasive direct access for repair of atrial septal defect in adults. *Am J Cardiol* 1999;**84**:919–22.

116 Chang CH, Lin PJ, Chu JJ, *et al.* Surgical closure of atrial septal defect. Minimally invasive cardiac surgery or median sternotomy? *Surg Endosc* 1998;**12**:820–4.

117 De Mulder W, Vanermen H. Repair of atrial septal defects via limited right anterolateral thoracotomy. *Acta Chir Belg* 2002;**102**:450–4.

118 Khan JH, McElhinney DB, Reddy VM, Hanley FL. A 5-year experience with surgical repair of atrial septal defect employing limited exposure. *Cardiol Young* 1999;**9**:572–6.

119 Tao L, Zeng X-J, Ma X-J, *et al.* New minimally invasive technique to occlude secundum atrial septal defect in 53 patients. *Ann Thorac Surg* 2006;**81**:1417–9.

120 Mishra YK, Khanna SN, Wasir H, *et al.* Port-access approach for cardiac surgical procedures: our experience in 776 patients. *Indian Heart J* 2005;**57**:688–93.

121 Schreiber C, Bleiziffer S, Kostolny M, *et al.* Minimally invasive midaxillary muscle sparing thoracotomy for atrial septal defect closure in prepubescent patients. *Ann Thorac Surg* 2005;**80**:673–6.

122 Shinkawa T, Yamagishi M, Shuntoh K, *et al.* Atrial septal defect repair through limited lateral thoracotomy in children. *Jpn J Thorac Cardiovasc Surg* 2006;**54**:469–71.

123 Yoshimura N, Yamaguchi M, Oshima Y, *et al.* Repair of atrial septal defect through a right posterolateral thoracotomy: a cosmetic approach for female patients. *Ann Thorac Surg* 2001;**72**:2103–5.

124 Casselman FP, Dom H, De Bruyne B, *et al.* Thoracoscopic ASD closure is a reliable supplement for percutaneous treatment. *Heart* 2005;**91**:791–4.

125 Bonaros N, Schachner T, Oehlinger A, *et al.* Robotically assisted totally endoscopic atrial septal defect repair: insights from operative times, learning curves, and clinical outcome. *Ann Thorac Surg* 2006;**82**:687–93.

126 Morgan JA, Thornton BA, Peacock JC, *et al.* Does robotic technology make minimally invasive cardiac surgery too expensive? A hospital cost analysis of robotic and conventional techniques. J Card Surg 2005;**20**:246–51.

127 Downing SW, Herzog WR Jr, McElroy MC, Gilbert TB. Feasibility of off-pump ASD closure using real-time 3-D echocardiography. *Heart Surg Forum* 2002;**5**:96–9.

128 Warinsirikul W, Sangchote S, Mokarapong P, *et al.* Closure of atrial septal defects without cardiopulmonary bypass: the sandwich operation. *J Thorac Cardiovasc Surg* 2001;**121**:1122–9.

129 Galal MO, Wobst A, Halees Z, *et al.*Peri-operative complications following surgical closure of atrial septal defect type II in 232 patients – a baseline study. *Eur Heart J* 1994;**15**:1381–4.

130 Cowen ME, Jeffrey RR, Drakeley MJ, *et al.* The results of surgery for atrial septal defect in patients aged fifty years and over. *Eur Heart J* 1990;**11**:29–34.

131 Fiore AC, Naunheim KS, Kessler KA, *et al.* Surgical closure of atrial septal defect in patients older than 50 years of age. *Arch Surg* 1988;**123**:965–7.

132 Magilligan DJ Jr, Lam CR, Lewis JW Jr, Davila JC. Late results of atrial septal defect repair in adults. *Arch Surg* 1978;**113**:1245–7.

133 Nasrallah AT, Hall RJ, Garcia E, *et al.* Surgical repair of atrial septal defect in patients over 60 years of age. Long term results. *Circulation* 1976;**53**:329–31.

134 Paolillo V, Dawkins KD, Miller GA. Atrial septal defect in patients over the age of 50. *Int J Cardiol* 1985;**9**:139–47.

135 Popelova J, Hlavacek K, Honek T, *et al.* Atrial septal defect in adults. *Can J Cardiol* 1996;**12**:983–8.

136 Shibata Y, Abe T, Kuribayashi R, *et al.* Surgical treatment of isolated secundum atrial septal defect in patients more than 50 years old. *Ann Thorac Surg* 1996;**62**:1096–9.

137 Horvath KA, Burke RP, Collins JJ Jr, Cohn LH. Surgical treatment of adult atrial septal defect: early and long-term results. *J Am Coll Cardiol* 1992;**20**:1156–9.

138 Jemielity M, Dyszkiewicz W, Paluszkiewicz L, *et al.* Do patients over 40 years of age benefit from surgical closure of atrial septal defects? *Heart* 2001;**85**:300–3.

139 Miyaji K, Furuse A, Tanaka O, *et al.* Surgical repair for atrial septal defect in patients over 70 years of age. *Jpn Heart J* 1997;**38**:677–84.

140 Actis Dato GM, Rinaudo P, Revelli A, *et al.* Atrial septal defect and pregnancy: a retrospective analysis of obstetrical outcome before and after surgical correction. *Minerva Cardioangiol* 1998;**46**:63–8.

141 Helber U, Baumann R, Seboldt H, *et al.* Atrial septal defect in adults: cardiopulmonary exercise capacity before and 4 months and 10 years after defect closure. *J Am Coll Cardiol* 1997;**29**:1345–50.

142 Kobayashi Y, Nakanishi N, Kosakai Y. Pre- and postoperative exercise capacity associated with hemodynamics in adult patients with atrial septal defect: a retrospective study. *Eur J Cardiothor Surg* 1997;**11**:1062–6.

143 Pfammatter JP, Zanolari M, Schibler A. Cardiopulmonary exercise parameters in children with atrial septal defect and increased pulmonary blood flow: short-term effects of defect closure. *Acta Paediatr* 2002;**91**:65–70.

144 Reybrouck T, Bisschop A, Dumoulin M, van der Hauwaert LG. Cardiorespiratory exercise capacity after surgical closure of atrial septal defect is influenced by the age at surgery. *Am Heart J* 1991;**122**:1073–8.

145 Brochu MC, Baril JF, Dore A, *et al.* Improvement in exercise capacity in asymptomatic and mildly symptomatic adults after atrial septal defect percutaneous closure. *Circulation* 2002;**106**:1821–6.

146 Liberthson RR, Boucher CA, Strauss HW, *et al.* Right ventricular function in adult atrial septal defect. Preoperative and postoperative assessment and clinical implications. *Am J Cardiol* 1981;**47**:56–60.

147 Maatouk F, Ben Farhat M, Betbout F, *et al.* Right ventricular dilatation and intraventricular septal motion after surgical closure of atrial septal defect. *Arch Mal Coeur Vaiss* 2001;**94**:204–10 (in French).

148 Meyer RA, Korfhagen JC, Covitz W, Kaplan S. Long-term follow-up study after closure of secundum atrial septal defect in children: an echocardiographic study. *Am J Cardiol* 1982;**50**:143–8.

149 Pearlman AS, Borer JS, Clark CE, *et al.* Abnormal right ventricular size and ventricular septal motion after atrial septal defect closure: etiology and functional significance. *Am J Cardiol* 1978;**41**:295–301.

150 Berbarie RF, Anwar A, Dockery WD, *et al.* Measurement of right ventricular volumes before and after atrial septal defect closure using multislice computed tomography. *Am J Cardiol* 2007;**99**:1458–61.

151 Eerola A, Pihkala JI, Boldt T, *et al.* Hemodynamic improvement is faster after percutaneous ASD closure than after surgery. *Catheter Cardiovasc Interv* 2007;**69**:432–41.

152 Giardini A, Donti A, Formigari R, *et al.* Determinants of cardiopulmonary functional improvement after transcatheter atrial septal defect closure in asymptomatic adults. *J Am Coll Cardiol* 2004;**43**:1886–91.

153 Pascotto M, Santoro G, Cerrato F, *et al.* Time-course of cardiac remodeling following transcatheter closure of atrial septal defect. *Int J Cardiol* 2006;**112**:348–52.

154 Santoro G, Pascotto M, Caputo S, *et al.* Similar cardiac remodelling after transcatheter atrial septal defect closure in children and young adults. *Heart* 2006;**92**:958–62.

155 Schussler JM, Anwar A, Phillips SD, *et al.* Effect on right ventricular volume of percutaneous Amplatzer closure of atrial septal defect in adults. *Am J Cardiol* 2005;**95**:993–5.

156 Thilén U, Persson S. Closure of atrial septal defect in the adult. Cardiac remodeling is an early event. *Int J Cardiol* 2006;**108**:370–5.

157 Kort HW, Balzer DT, Johnson MC. Resolution of right heart enlargement after closure of secundum atrial septal defect with transcatheter technique. *J Am Coll Cardiol* 2001;**38**:1528–32.

158 Cheung YF, Lun KS, Chau AK. Doppler tissue imaging analysis of ventricular function after surgical and transcatheter closure of atrial septal defect. *Am J Cardiol* 2004;**93**:375–8.

159 Di Salvo G, Drago M, Pacileo G, *et al.* Comparison of strain rate imaging for quantitative evaluation of regional left and right

ventricular function after surgical versus percutaneous closure of atrial septal defect. *Am J Cardiol* 2005;**96**:299–302.

160 Di Salvo G, Drago M, Pacileo G, *et al.* Atrial function after surgical and percutaneous closure of atrial septal defect: a strain rate imaging study. *J Am Soc Echocardiogr* 2005;**18**:930–3.

161 Salehian O, Horlick E, Schwerzmann M, *et al.* Improvements in cardiac form and function after transcatheter closure of secundum atrial septal defects. *J Am Coll Cardiol* 2005;**45**:499–504.

162 Dhillon R, Josen M, Henein M, Redington A. Transcatheter closure of atrial septal defect preserves right ventricular function. *Heart* 2002;**87**:461–5.

163 Beck W, Swan HJC, Burchell HB, Kirklin JW. Pulmonary vascular resistance after repair of atrial septal defects in patients with pulmonary hypertension. *Circulation* 1960;**22**:938–46.

164 Coles J, Sears G, Macdonald C. Atrial septal defect complicated by pulmonary hypertension – a long term follow-up. *Ann Surg* 1967;**166**:496–9.

165 Liddle HV, Meyer BW, Jones JC. The results of surgical correction of atrial septal defect complicated by pulmonary hypertension. *J Thorac Cardiovasc Surg* 1960;**39**:35–46.

166 Oelberg DA, Marcotte F, Kreisman H, *et al.* Evaluation of right ventricular systolic pressure during incremental exercise by Doppler echocardiography in adults with atrial septal defect. *Chest* 1998;**113**:1459–65.

167 Silversides CK, Siu SC, McLaughlin PR, *et al..* Symptomatic atrial arrhythmias and transcatheter closure of atrial septal defects in adult patients. *Heart* 2004;**90**:1194–8.

168 Bink-Boelkens MT, Meuzelaar KJ, Eygelaar A. Arrhythmias after repair of secundum atrial septal defect: the influence of surgical modification. *Am Heart J* 1988;**115**:629–33.

169 Karwot B, Bialkowski J, Szkutnik M, *et al.* Iatrogenic cardiac arrhythmias following transcatheter or surgical closure of atrial septal defect in children. *Kardiol Pol* 2005;**62**:35–43.

170 Berger F, Vogel M, Kramer A, *et al.* Incidence of atrial flutter/fibrillation in adults with atrial septal defect before and after surgery. *Ann Thorac Surg* 1999;**68**:75–8.

171 Giamberti A, Chessa M, Foresti S, *et al.* Combined atrial septal defect surgical closure and irrigated radiofrequency ablation in adult patients. *Ann Thorac Surg* 2006;**82**:1327–31.

172 Henglein D, Cauchemez B, Bloch G. Simultaneous surgical treatment of atrial septal defect and atrial flutter using a simple modification of the atrial incision. *Cardiol Young* 1999;**9**:197–9.

173 Kobayashi J, Yamamoto F, Nakano K, *et al.* Maze procedure for atrial fibrillation associated with atrial septal defect. *Circulation* 1998;**98**:II399–402.

174 Murakami M, Okada H, Nishida M, Hamano K. Right atrial separation effect for chronic atrial fibrillation with atrial septal defect: report of four cases. *Ann Thorac Cardiovasc Surg* 2006;**12**:210–2.

175 Chan KC, Godman MJ, Walsh K, *et al.* Transcatheter closure of atrial septal defect and interatrial communications with a new self expanding nitinol double disc device (Amplatzer septal occluder): multicentre UK experience. *Heart* 1999;**82**:300–6.

176 de Lezo JS, Medina A, Romero M, *et al.* Effectiveness of percutaneous device occlusion for atrial septal defect in adult patients with pulmonary hypertension. *Am Heart J* 2002;**144**:877–80.

177 Demkow M, Ruzyllo W, Konka M, *et al.* Transvenous closure of moderate and large secundum atrial septal defects in adults using the Amplatzer septal occluder. *Catheter Cardiovasc Interv* 2001;**52**:188–93.

178 Faella HJ, Sciegata AM, Alonso JL, Jmelnitsky L. ASD closure with the Amplatzer device. *J Interv Cardiol* 2003;**16**:393–7.

179 Fischer G, Stieh J, Uebing A, *et al.* Experience with transcatheter closure of secundum atrial septal defects using the Amplatzer septal occluder: a single centre study in 236 consecutive patients. *Heart* 2003;**89**:199–204.

180 Latson LA, Jones TK, Jacobson J, *et al.* Analysis of factors related to successful transcatheter closure of secundum atrial septal defects using the HELEX septal occluder. *Am Heart J* 2006;**151**:1129.e7–1129.e11.

181 Vincent RN, Raviele AA, Diehl HJ. Single-center experience with the HELEX septal occluder for closure of atrial septal defects in children. *J Interv Cardiol* 2003;**16**:79–82.

182 Mashman WE, King SB, Jacobs WC, Ballard WL. Two cases of late embolization of Amplatzer septal occluder devices to the pulmonary artery following closure of secundum atrial septal defects. *Catheter Cardiovasc Interv* 2005;**65**:588–92.

183 Hill SL, Berul CI, Patel HT, Rhodes J, *et al.* Early ECG abnormalities associated with transcatheter closure of atrial septal defects using the Amplatzer septal occluder. *J Interv Card Electrophysiol* 2000;**4**:469–74.

184 Krumsdorf U, Ostermayer S, Billinger K, *et al.* Incidence and clinical course of thrombus formation on atrial septal defect and patient foramen ovale closure devices in 1,000 consecutive patients. *J Am Coll Cardiol* 2004;**43**:302–9.

185 Fagan T, Dreher D, Cutright W, *et al.* Fracture of the Gore Helex septal occluder: associated factors and clinical outcomes. *Catheter Cardiovasc Interv* 2009;**73**:941–8.

186 Amin Z, Hijazi ZM, Bass JL, *et al.* Erosion of Amplatzer septal occluder device after closure of secundum atrial septal defects: review of registry of complications and recommendations to minimize future risk. *Catheter Cardiovasc Interv* 2004;**63**:496–502.

187 Pedra C, Pihkala J, Lee KJ, *et al.* Transcathter closure of atrial septal defects using the Cardioseal implant. *Heart* 2000;**84**:320–6.

188 Balasundaram RP, Anandaraja S, Juneja R, Choudhary SK. Infective endocarditis following implantation of Amplatzer atrial septal occluder. *Indian Heart J* 2005;**57**:167–9.

189 Bullock AM, Menahem S, Wilkinson JL. Infective endocarditis on an occluder closing an atrial septal defect. *Cardiol Young* 1999;**9**:65–7.

190 Giardini A, Donti A, Specchia S, *et al.* Long-term impact of transcatheter atrial septal defect closure in adults on cardiac function and exercise capacity. *Int J Cardiol* 2008;**124**:179–82.

191 Wu ET, Akagi T, Taniguchi M, *et al.* Differences in right and left ventricular remodeling after transcatheter closure of atrial septal defect among adults. *Catheter Cardiovasc Interv* 2007;**69**:866–71.

192 Eyskens B, Ganame J, Claus P, *et al.* Ultrasonic strain rate and strain imaging of the right ventricle in children before and after percutaneous closure of an atrial septal defect. *J Am Soc Echocardiogr* 2006;**19**:994–1000.

193 Pawelec-Wojtalik M, Wojtalik M, Mrowczynski W, *et al.* Comparison of cardiac function in children after surgical and

Amplatzer occluder closure of secundum atrial septal defects. *Eur J Cardiothorac Surg* 2006;**29**:89–92.

194 Jux C, Bertram H, Wohlsein P, *et al.* Interventional atrial septal defect closure using a totally bioresorbable occluder matrix: development and preclinical evaluation of the BioSTAR device. *J Am Coll Cardiol* 2006;**48**:161–9.

195 Mullen MJ, Hildick-Smith D, De Giovanni JV, *et al.* BioSTAR Evaluation Study (BEST): a prospective, multicenter, phase I clinical trial to evaluate the feasibility, efficacy, and safety of the BioSTAR bioabsorbable septal repair implant for the closure of atrial-level shunts. *Circulation* 2006;**114**:1962–7.

196 Ussia GP, Cammalleri V, Mulè M, *et al.* Percutaneous closure of patent foramen ovale with a bioabsobable occluder device: single-centre experience. *Catheter Cardiovasc Interv* 2009;**74**:607–14.

197 Hoehn R, Hesse C, Ince H, Peuster M. First experience with the BioSTAR device for various applications in pediatric patients with congenital heart disease. *Catheter Cardiovasc Interv* 2010;**75**:72–7.

22 Atrioventricular Septal Defects

Stuart Berger, Peter J. Bartz, David E. Saudek, John T. Hambrook & James S. Tweddell
Medical College of Wisconsin, Milwaukee, WI, USA

Introduction

Atrioventricular septal defects (AVSDs) are common and can be associated with morbidity and mortality in the fetus, neonates, and young infants. The anatomic defects relate to abnormalities in the embryologic development of the endocardial cushions including the atrioventricular valves, persistence of the atrial ostium primum, and associated ventricular septal openings.

Up to 17% of fetuses undergoing echocardiographic examination have a form of AVSD [1]. The fetal mortality associated with AVSDs can be shown by the much lower frequency of AVSDs diagnosed after birth, with most studies documenting an incidence of AVSDs in the 3–5% range [2,3].

AVSDs are strongly associated with genetic syndromes, such as Down syndrome. About 40% of children with Down syndrome have a congenital cardiac abnormality of which 40% have AVSDs. The association of syndromes with AVSDs suggests a very strong genetic influence, including the localization of these abnormalities to specific genes.

Finally, in general, the prognosis is excellent for most infants with AVSDs as surgical outcomes are outstanding. The good outcomes for infants with complete, balanced AVSDs implies early surgical intervention to avoid and prevent severe congestive heart failure or pulmonary vascular obstructive disease.

Pathologic anatomy

Currently, AVSD is the most widely used term to describe the spectrum of congenital heart malformations characterized by a common atrioventricular junction coexisting with deficient atrioventricular septation [4]. Many general and specific terms have been applied to this lesion, including endocardial cushion defect, atrioventricular canal defect, ostium primum defect, and common atrioventricular orifice. Terms to categorize AVSDs further have included partial, transitional, intermediate, and complete. Unfortunately, many of these terms can be interpreted as having a similar meaning or referring to a distinct entity, depending upon the individual users of the terms. For this reason, understanding and communicating about the anatomy are best achieved by describing the atrioventricular valve morphology and extent of atrial and ventricular septation.

In a normal heart, the tricuspid valve annulus is displaced apically with respect to the mitral valve annulus, so that separate left and right atrioventricular junctions result. In contrast, the morphological hallmark of AVSD is a common atrioventricular junction. In ASVD, the ventricular septum adjacent to the atrium is "scooped out." The lower attachment of the left atrioventricular valve annulus decreases the inlet length, as measured from the annulus to the left ventricle apex. Conversely, the outlet length measured from the left ventricular apex to the aortic valve is elongated (Figure 22.1) [5]. Thus, the aorta is not wedged between the mitral and tricuspid valves as in a normal heart (Figure 22.2). With the aorta "sprung" anterosuperiorly in AVSD, the left ventricular outflow tract is elongated and frequently narrowed, producing the so-called "gooseneck" deformity.

The leaflet morphology in AVSD bears little resemblance to the normal tricuspid and mitral valves. In AVSD, the valve guarding the common atrioventricular junction consists of five leaflets. Typically there is a left mural (or lateral) leaflet and a right mural leaflet that are positioned over the respective ventricles. Occasionally, a mural leaflet can be severely hypoplastic, which complicates achieving adequate surgical repair. The inferior (or posterior) bridging leaflet is

Figure 22.1 Left ventricular aspect of the septum in hearts with normal (a) and deficient (b) atrioventricular septation. (Reproduced from Anderson *et al.*, *Cardiol Young* 1991;1:290, with permission from Cambridge University Press.)
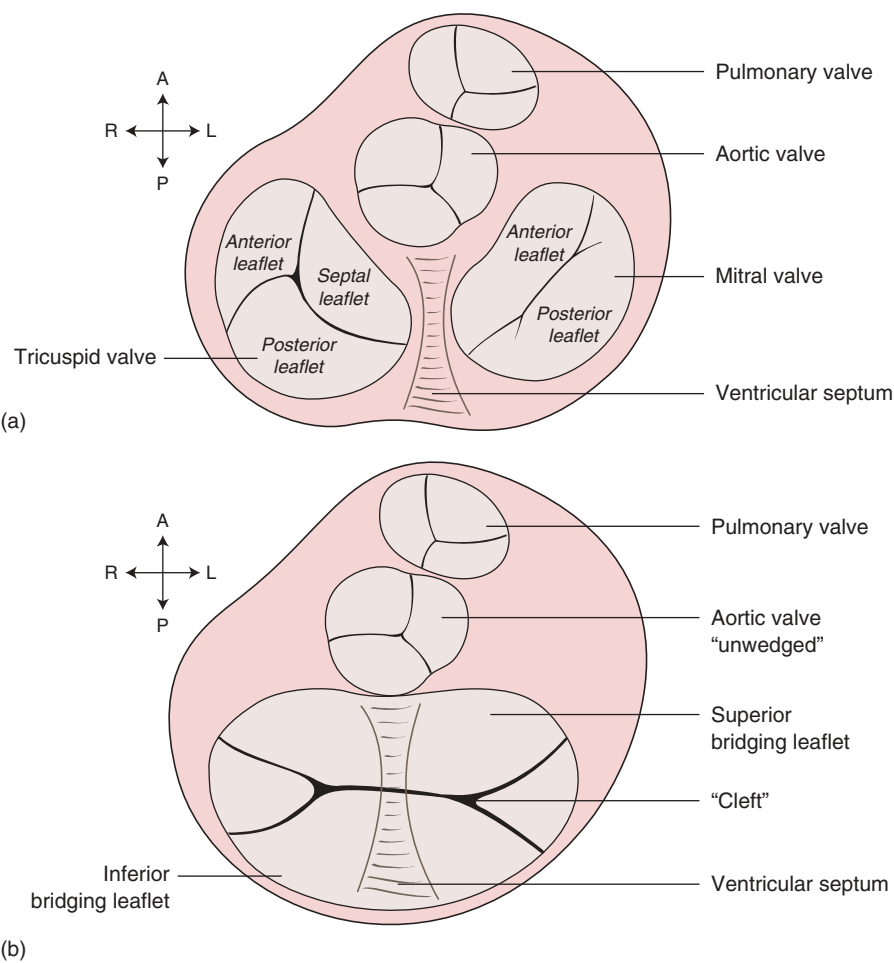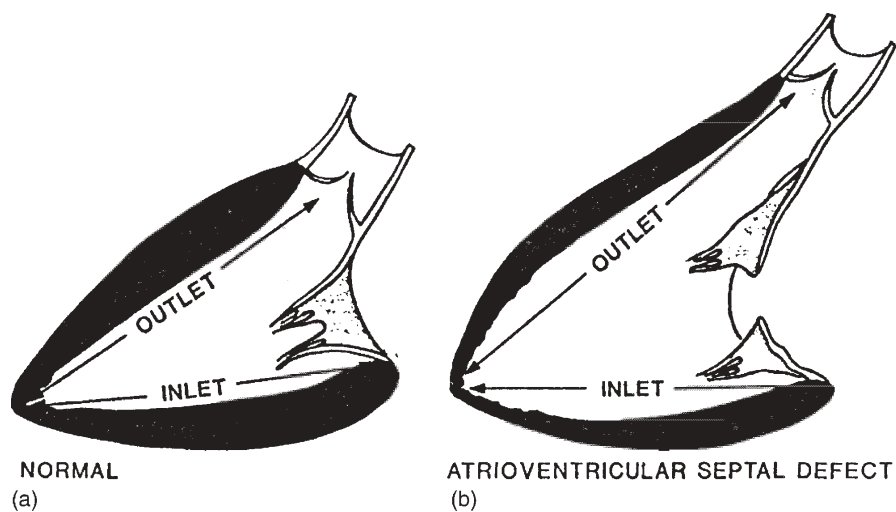
Figure 22.2 (a) Diagram depicting the relationship of the mitral and tricuspid valves to the aortic valve in a normal heart. The aortic valve sits wedged between the two atrioventricular valves. (b) The same view is depicted in this diagram of common atrioventricular septal defect. The superior and inferior bridging leaflets are demonstrated with the "cleft" where the two bridging leaflets come together at the ventricular septum. The aortic valve is unwedged anteriorly as a result of the superior bridging leaflet.

inferiorly positioned and crosses the ventricular septum with extensive chordal attachments to the crest of the septum. The superior (or anterior) bridging leaflet is positioned superiorly. The superior bridging leaflet can be considered variably divided, such as described by Rastelli *et al.* [6]. Alternatively, the superior portion of the valve can be considered to be composed of the superior bridging leaflet and the right anterosuperior (or accessory) leaflet, each of
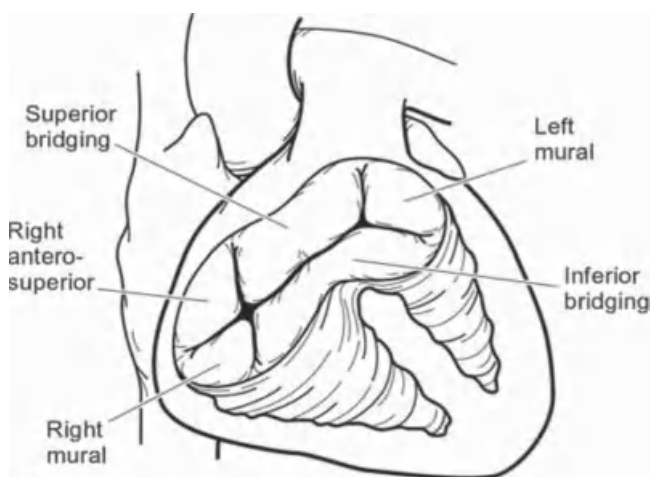
Figure 22.3 Arrangement of the atrioventricular valve leaflets in complete atrioventricular septal defect as seen from the apex looking towards the base.

variable size, resulting in the common valve being composed of five leaflets (Figure 22.3).

In a normal heart, the left-sided papillary muscles are obliquely situated in the posteromedial and anterolateral position. In AVSD, the left-sided papillary muscles are rotated to a superior and inferior position. The muscles are usually equal in size and support the commissures between the bridging leaflets and left mural leaflet. Other left atrioventricular valve abnormalities exist in ~10% of AVSDs. Most frequently, accessory mitral valve tissue connects the superior and inferior leaflets to create a double-orifice left atrioventricular valve. Less frequently, a single papillary muscle creates a parachute configuration. Such valve abnormalities may complicate surgical repair, with possible residual left atrioventricular valve regurgitation, stenosis, or both [7]. Two or three papillary muscles are found in the right ventricle, including a fairly consistent anterior and posterior papillary muscle and variably present and positioned medial papillary muscle.

In AVSD, the posterior position of the atrial and ventricular septal defects interfere with the development of the normal conduction pathways. The atrioventricular node is displaced posteroinferiorly from the apex of the triangle of Koch, the usual anatomic location [8]. The conduction system then courses posterior to the ventricular septal defect, and the left bundle is also displaced posteroinferiorly. This anatomic variation probably accounts for the typical electrocardiographic finding of left axis deviation because depolarization of the left bundle proceeds from right inferior to left superior. This course also has important implications for operative repair. In some hearts, both an anomalous anterolateral node and a "regular" posteroinferior node give rise to penetrating bundles and atrioventricular bundles to form a sling of conduction tissues. When AVSD is associated with atrial isomerism, dual atrioventricular nodes with conduction tissue sling are also found [9].

Partial AVSD

The differentiation of partial from complete AVSD is based largely on the common atrioventricular valve being divided by a bridge of tissue between the superior bridging leaflet and the inferior bridging leaflet, creating two separate orifices. Usually the bridging tissue adheres to the crest of the ventricular septum, allowing no ventricular level shunting. The atrial septal defect is frequently termed a primum defect and is anteroinferior to the fossa ovalis and immediately adjacent to the atrioventricular valve. The defect size varies, but is usually fairly large, allowing for significant atrial shunting. A patent foramen ovale or a secundum defect may coexist. Rarely, secundum and primum defects coalesce, producing, in effect, a common atrium.

Although the left atrioventricular valve is referred to as cleft, it may also be considered as failure of fusion of the superior and inferior bridging leaflets. Regurgitation occurs through this defect. Because the valvar defect can extend medially towards the ventricular septum, a regurgitant jet can be directed through the primum atrial septal defect, effectively passing from the left ventricle to the right atrium. Abnormalities of the right-sided atrioventricular valve can also occur. These include a "cleft" in the septal leaflet or even a gap at the commissure, resulting in valve incompetence. The term transitional or intermediate form of AVSD has been applied when there are two valve orifices and a variably sized ventricular septal defect.

Complete AVSD

In complete AVSD, there is both a large inlet ventricular septal defect with the characteristic "scooped" appearance of the ventricular septum and a primum atrial septal defect. The common atrioventricular valve has a single orifice spanning the ventricular septal defect. The superior and inferior leaflets are not connected by the bridge of tissue, as in partial AVSD.

As discussed previously, the common atrioventricular valve is generally described as having five leaflets: (1) left mural, (2) right mural, (3) right anterosuperior, (4) inferior bridging leaflet, and (5) superior bridging leaflet (Figure 22.3). Rastelli et al. [6] devised a widely used classification for complete AVSD based on superior bridging leaflet morphology and the resultant attachment to the ventricular septum (Table 22.1). In this classification, the superior bridging leaflet is considered to be divided or "cleft" without the existence of the right anterosuperior leaflet.

Unbalanced AVSD

In most patients with AVSD, the common atrioventricular valve is shared equally between the right and left ventricles,

Table 22.1 Rastelli classification of complete AVSD.

Type	Description
A	The superior bridging leaflet is divided into two relatively equal portions, both attached medially to the muscular septum. The membranous septum has formed, and the interventricular communication does not extend to the region adjacent to the aortic cusps
B	The superior bridging leaflet is divided into two relatively unequal portions, unattached to the septum, but both portions are attached medially to a papillary muscle in the right ventricle adjacent to the ventricular septum
C	The superior bridging leaflet is undivided and unattached to the septum, floating freely above it. The interventricular communication is complete under the common superior leaflet and extends to the region adjacent to the aortic cusps

Figure 22.4 (a) Diagram showing double-outlet right atrium with malalignment of the atrial septum towards the left atrium. (b) Diagram showing double-outlet left atrium with malalignment of the atrial septum towards the right atrium. (c) Diagram showing unbalanced common atrioventricular septal defect (AVSD) to the right with concomitant left ventricular hypoplasia. (d) Diagram showing unbalanced AVSD to the left with concomitant right ventricular hypoplasia. LA, left atrium; LV, left ventricle; RA, right atrium; RV, right ventricle.

creating a "balanced" defect. In the unbalanced form of AVSD, the relationship of the atrial or ventricular septum to the common atrioventricular valve is shifted either leftwards or rightwards with unequal sharing of the common valve orifice (Figure 22.4). With leftward shifting of the ventricular septum, the right ventricle is dominant and the left ventricle hypoplastic. Less commonly, the ventricular septum is shifted rightwards, creating left ventricular dominance and a hypoplastic right ventricle. Rarely, the atrial septum is unbalanced or malaligned, creating a double-outlet atrium. When the atrial septum is deviated leftwards, a double-outlet right atrium exists. Conversely, when the atrial septum is deviated rightwards, a double-outlet left atrium is created.

An unbalanced AV canal occurs in ~10% of patients with complete AV canal. Commonly, the ventricle receiving the smaller amount of blood flow is hypoplastic to some extent. In the extreme, one ventricle (usually the left) is severely hypoplastic and requires single ventricle palliation. With a mild hypoplasia, decisions between single-ventricle palliation and two-ventricle repair may be difficult. In a moderately unbalanced AV canal, ductal-dependent circulation, large VSD, and small ventricular volumes raise concern about the adequacy of the underdeveloped ventricle. A complete, unbalanced AV canal adds risk for patients undergoing the Norwood procedure.

Associated abnormalities

Atrioventricular septal defect and tetralogy of fallot

AVSD may be associated with tetralogy of Fallot. Surgical series report the association in 2.7–10% of atrioventricular septal repairs and 1–6.5% of tetralogy of Fallot repairs [10].

Trisomy 21 has been found in ~77% of patients with AVSD-TOF [11]. This combination of anomalies is not typically seen with heterotaxy syndrome, but the association of AVSD and double-outlet right ventricle commonly is [12].

In AVSD with tetralogy of Fallot, the inlet ventricular septal defect extends into the outlet septum and underneath the inferior bridging leaflet. Usually the atrioventricular valve morphology is Rastelli type C [11,13]. Significant atrioventricular valve regurgitation is not common [13]. The usual features of tetralogy of Fallot are seen. Rarely the pulmonary valve is atretic. The pulmonary arteries may be variably hypoplastic [10]. Details of this anatomy can be demonstrated echocardiographically.

Other associated defects

Almost any other form of congenital heart disease may be associated with complete AVSD, including abnormalities of venous connections, additional ASDs and VSDs, outflow
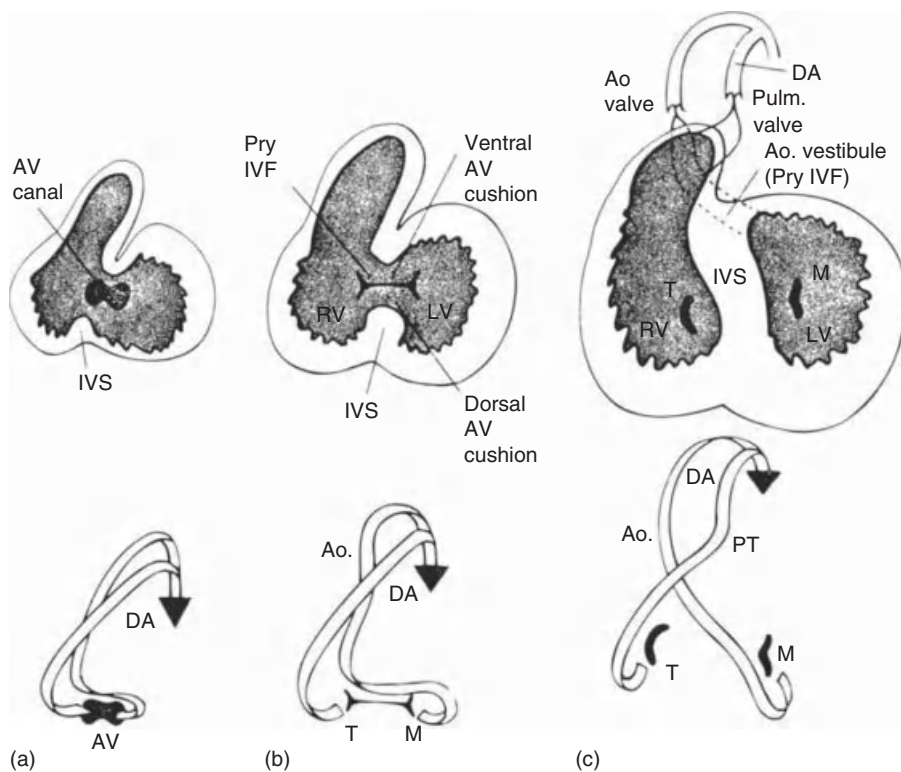
Figure 22.5 Sections through the heart at 4.5, 5 and 6 weeks of age. (a) The common atrioventricular canal has shifted to the midline. (b, c) Fusion of the endocardial cushions gives rise to the mitral and tricuspid orifices. The course of the circulation is noted in the figures in the lower row. Ao, aorta; ventral AV cushion, superior endocardial cushion; dorsal AV cushion, inferior endocardial cushion; DA, ductus arteriosus; IVS, intraventricular septum; M, mitral orifice; Pry IVF, primary intraventricular foramen; PT, pulmonary trunk; RV, right ventricle; T, tricuspid orifice.

tract obstruction of either ventricle, patent ductus arteriosus, and coarctation of the aorta. AVSD is common in patients with *heterotaxy syndrome* (see Chapter 50).

Embryology

During the fourth and fifth weeks of human embryo development, two swellings of mesenchymal tissue protrude from the superior and inferior portions of the atrioventricular junction of the primitive heart. These endocardial cushions fuse to form the supporting structure and precursor tissue for the atrioventricular valves. Following fusion of these endocardial cushions, cells overlying the future valve structures delaminate, differentiate and migrate to form mature valve structures by the sixth week. The embryologic events noted above are depicted in Figures 22.5 and 22.6.

AVSD forms from inadequate fusion of the endocardial cushions [14]. This process is guided and influenced by a number of undetermined pathways. Genetic influences on endocardial cushion development are an area of intense research focus. Because of the association between trisomy 21 and AVSD, a major genetic locus for AVSD would be suspected on chromosome 21, but linkage studies have not shown this. Linkage studies have pointed towards a mutation in CRELD1 for AVSD associated with trisomy 21 and also in isolation [15].

Hemodynamics

The hemodynamics of AVSD vary with the specific defect anatomy and physiology. Within the same anatomic subsets there may be differences in physiology.

An uncomplicated balanced AVSD typically has the physiology of a left-to-right shunt lesion influenced by the degree of atrioventricular (AV) valve regurgitation and the degree of pulmonary hypertension. The pulmonary artery pressure is at systemic level and if the resistance is not unduly elevated, the patient has left ventricular volume overload from the left-to-right ventricular level shunt. The left ventricular volume overload is accentuated by the AV valve regurgitation. Symptoms of heart failure occur as a result of both left ventricular volume overload and pulmonary overcirculation.

Patients with Down syndrome may develop elevated pulmonary vascular resistance early in infancy. As a result, heart failure may be attenuated or may not develop because of the limitation of left-to-right shunting. Surgical intervention early in infancy is warranted, even if symptoms of heart failure are not present, to prevent irreversible pulmonary hypertension.

In patients with a primum atrial septal defect and cleft mitral valve, the hemodynamics are typical of a large ASD. These findings include left-to-right shunt at the atrial
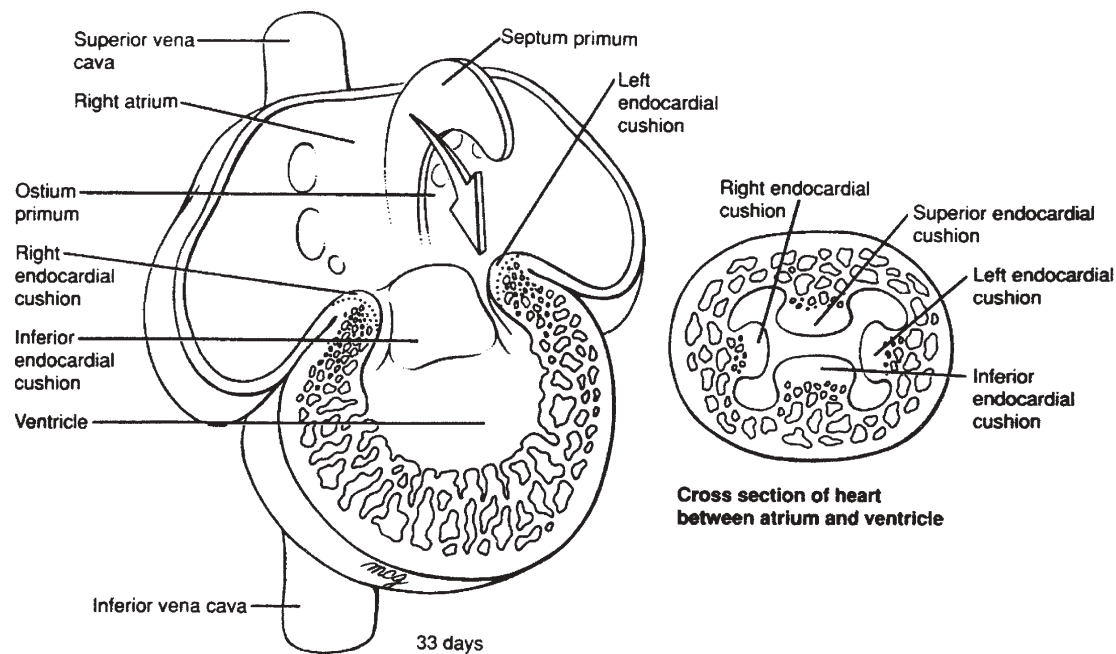
Figure 22.6 Embryo at 33 days of age showing inferior, right, and left endocardial cushions. The superior and inferior cushions have yet to fuse and divide the AV orifice in two. The right and left endocardial cushions contribute to AV valve formation.

level with accompanying right ventricular volume overload. Additionally, mitral regurgitation through the mitral valve cleft is associated with a varying degree of left ventricular volume overload. Despite these hemodynamics, this variant rarely results in significant symptoms in infancy or early childhood.

Patients with pulmonary outflow obstruction and AVSD present with a clinical picture of tetralogy of Fallot. Patients with Down syndrome are overly represented in this group. The degree of desaturation from diminished pulmonary blood flow varies and tends to progress.

The hemodynamics of the more complex forms of AVSD also vary. The left dominant form of AVSD presents like the patient with AVSD and tetralogy of Fallot described above. The right dominant form of AVSD presents with hypoplasia of the left ventricle and ascending aorta much like the infant with hypoplastic left heart syndrome. The AVSD variants associated with heterotaxy syndromes are influenced by the specific associated anatomic conditions.

Natural history

Survival with an unrepaired AVSD is extremely poor. About 60–80% of non-terminated pregnancies with AVSD are born live [16]. If left unrepaired after birth, survival at 6 months is 54%, at 12 months 35%, at 24 months 15%, and at 5 years 4% [17].

Many infants with unrepaired AVSD experience profound heart failure. Deaths before 24 months of age are primarily from severe congestive heart failure. Unfortunately, patients who do not die from heart failure at a young age have elevated pulmonary vascular resistance, which becomes irreversible if the defect remains unrepaired. As these patients age, pulmonary vascular resistance increases until they become cyanotic and eventually die from complications from pulmonary vascular disease. This process is seemingly accelerated in patients with Down syndrome, most likely as a result of accompanying airway, lung, and inherent pulmonary vascular issues. Hence surgical repair of complete AVSD should occur before 6 months of age, before the development of pulmonary vascular obstructive disease.

The development of pulmonary vascular disease in infants with complete AVSD is more severe than in those with an isolated VSD and is related to a cellular intimal proliferation that appears to develop earlier in life for unknown reasons. One possible factor is the obligatory left ventricular to right atrial shunt that delays or prevents the decrease in pulmonary vascular resistance. Because severe medial hypertrophy and intimal proliferation have been described as early as 6 months of life, intervention should occur in the first 6 months of life. If left untreated or unrecognized, or if the patient has arrived from a developing country without tertiary care, cardiac shunting may be minimal and right- and left-sided resistances are balanced. The time when this occurs varies. In later childhood and adolescence, it is not

uncommon for the shunt to reverse, with the patient becoming cyanotic and developing polycythemia, clubbing, and complications of fixed pulmonary vascular obstructive disease.

Finally, if there is associated pulmonary stenosis or atresia, the course and natural history (both treated and untreated) resemble tetralogy of Fallot. With an AVSD, the course parallels that of a single ventricle in both the treated and untreated forms.

History and physical examination

The history and physical examination vary depending on the specific anatomy and physiology of the endocardial cushion defect. Although the history and physical examination are targeted towards the cardiopulmonary systems, a general evaluation seeking information about an associated genetic condition should be performed.

Patients with an ostium primum AVSD are asymptomatic and do not develop symptoms of heart failure in childhood. Rarely, subtle respiratory symptoms and slow growth may occur with significant mitral regurgitation. The cardiac findings typically include an active right ventricle, a fixed, widely split second heart sound in the pulmonic area and a pulmonary ejection murmur, usually grade ≤3/6. With a large left-to-right atrial shunt, a grade 1–2/4 mid-diastolic flow rumble is heard at the mid-left sternal border from increased flow across the tricuspid valve. With a cleft in the anterior leaflet of the mitral valve and associated mitral regurgitation, a high-pitched, apical, pan-systolic murmur radiates to the left lower sternal border and axilla. If the regurgitant volume is large, an apical thrust and an apical mid-diastolic murmur are found.

In patients with complete AVSD, shunting occurs at both the atrial and ventricular level and is accompanied by variable severity of regurgitation of the common AV valve. Most patients develop symptoms in infancy, especially as the pulmonary vascular resistance decreases. Left ventricular volume overload results from the left-to-right shunt across the VSD and the mitral regurgitation [18]. Excess pulmonary blood flow and pulmonary hypertension at the systemic level are present. As a result, the typical symptoms include failure to thrive, frequent respiratory tract infections, and heart failure. If symptoms of heart failure are not present or resolve spontaneously, significant elevation of pulmonary vascular resistance is present.

On cardiac examination, typically the precordium is hyperactive, the second heart sound is narrowly split and P_2 is loud, and there may be an S_3 gallop. An apical holosystolic murmur is heard with mitral regurgitation and a more widely heard holosystolic murmur from the VSD. A mid-diastolic murmur is present at the left lower sternal border and apex from increased flow across the AV valves. Mild

cyanosis and a generalized diminution of pulses may be found. Decreased lower extremity pulses may indicate an associated coarctation of the aorta. Cyanosis associated with a loud, harsh pulmonic murmur suggests right ventricular outflow tract obstruction [19].

Electrocardiography

Related to the posteroinferior displacement of the AV node and left bundle [20], complete AVSDs have a "northwest axis," typically between –90° and –150° in the frontal plane. This is accompanied by left, right, or bi-ventricular hypertrophy reflecting the hemodynamics. A prolonged PR interval is common (see Figure 22.7). Patients with a primum ASD and cleft mitral valve also have a superior leftward axis, but not to the degree of a complete canal. Incomplete right bundle branch block (rSR′ in the right precordial leads), a widened or bifid P wave indicative of left atrial enlargement (dependent upon the degree of mitral valve regurgitation [21]), a tall P wave indicating right atrial enlargement, and electrocardiographic signs of right ventricular hypertrophy are typical.

Echocardiography

Transthoracic echocardiography
Transthoracic echocardiography is the primary tool for diagnosis and postoperative follow-up of AVSD. Important information can be obtained about both morphologic features of the defect and physiologic alterations that affect surgical planning. Initial evaluation should assess the AV valve morphology, atrial and ventricular septal defects, and relative ventricular size. Associated anomalies should be sought. Following repair, echocardiography is used to assess residual lesions.

Atrioventricular valve
The echocardiogram should differentiate between a partitioned or common AV valve orifice. This differentiation depends on the presence or absence of a tongue of tissue connecting the superior and inferior bridging leaflets that divides the valve into two separate orifices [22]. The subcostal and parasternal short axis views are useful for visualization of the AV valve orifice *en face*. Rotating the transducer 30–45° clockwise from the subcostal four-chamber view allows visualization of the AV valve *en face*. When the plane of sound is aligned with the fibrous annulus, the nature of the bridging tissue can be detected [23]. Although partial AVSD commonly lacks a VSD, the presence or absence of a VSD is not sufficient to differentiate complete from partial AV canal. Both partial AVSD with a large VSD and complete AVSD without a ventricular level shunt have been described [22].

Figure 22.7 12-lead ECG of a 3-month-old child depicting a sinus rhythm, northwest axis, and combined ventricular hypertrophy.

Rastelli *et al*. described division of the superior bridging leaflet in complete forms of AVSD, as described previously [24] (Figure 22.8). When the AV valve is viewed *en face* from the subcostal short-axis view, the division of the superior bridging leaflet and the status of septal attachments to the ventricular septum can be clearly seen [22,24,25]. Attachments of the superior bridging leaflet can also be demonstrated by sweeping superiorly from the apical four-chamber view [25].

The left ventricular papillary muscle configuration may affect surgical repair. Spacing of the papillary muscles can be clearly defined from the parasternal short-axis or subcostal short-axis views [26]. When the papillary muscles are closely spaced, the left mural leaflet may be small. A single left-sided papillary muscle results in absence of the left mural leaflet. Closure of the commissure between the superior and inferior bridging leaflets with a deficient left mural leaflet may result in left AV valve stenosis. Double-orifice left AV valve can be identified from both the parasternal and subcostal

short-axis views. Double-orifice left AV valve is more common in partial than complete AVSD, and the accessory orifice is more commonly associated with the posteromedial papillary muscle [27].

Atrioventricular valve regurgitation should be assessed with color Doppler. It is important to define the amount and location of regurgitation. Sweeps through the AV valve should be performed and the valve interrogated from orthogonal planes. Coaptation of leaflets may be complex and regurgitation may be underestimated from a single imaging plane.

Atrial and ventricular septal defects

The presence and size of atrial and ventricular septal defects should be determined. A primum atrial septal defect is characterized by deficient atrial septal tissue at the crux of the heart (Figure 22.9). These defects are typically well visualized from the apical and subcostal four-chamber views (Figure 22.10). Tilting posterior from the four-chamber view,
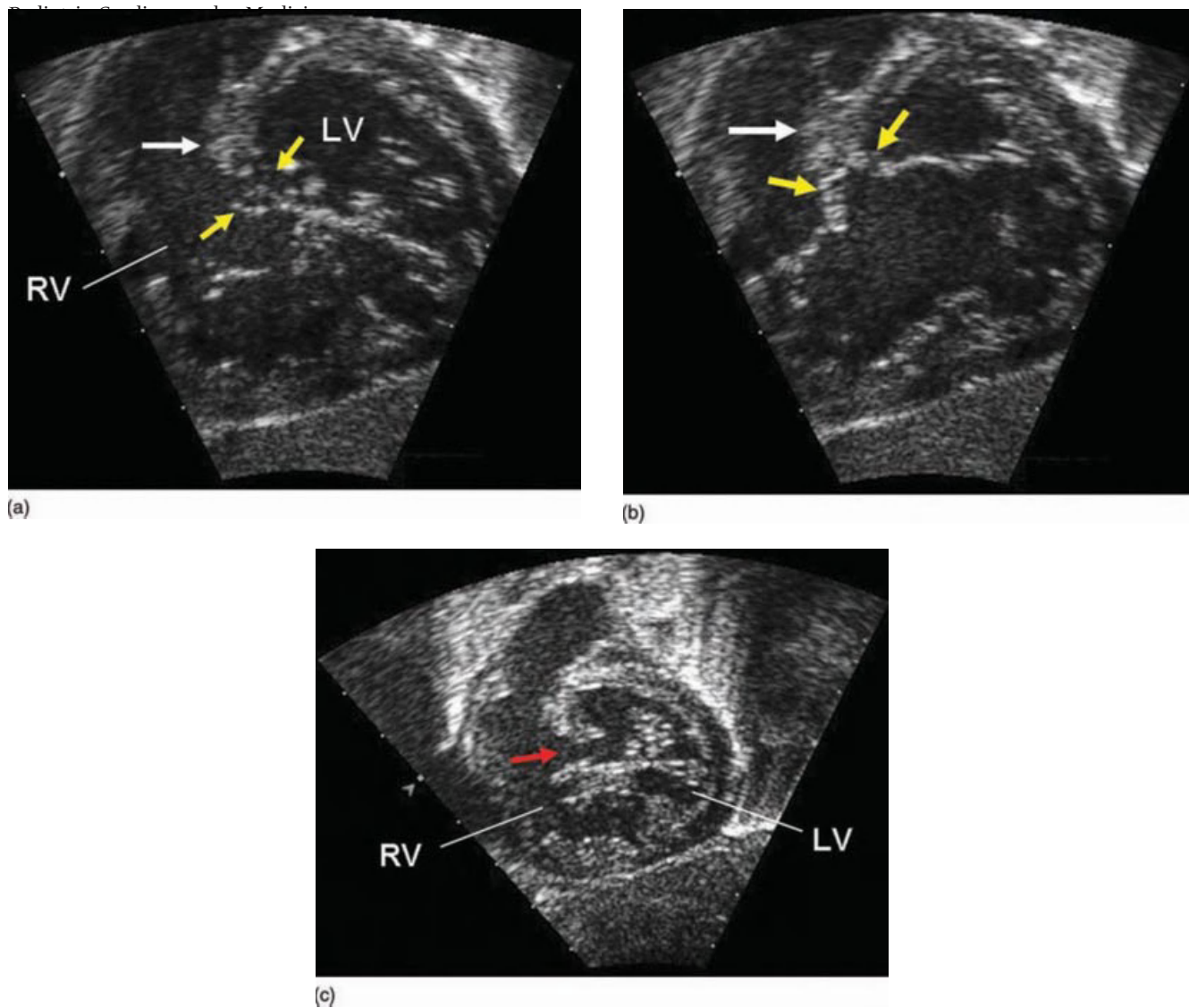
Figure 22.8 Subcostal imaging is helpful in determining the atrioventricular valve morphology. (a) During systole, the AV valve is closed. In Rastelli type A, attachments of the anterior bridging leaflet (yellow arrows) to the interventricular septum (white arrow) can be seen. (b) During diastole the valve is open and the anterior bridging leaflet is tented by the attachments to the ventricular septum. (c) With Rastelli type C, the anterior bridging leaflet is free floating without attachments to the interventricular septum (red arrow).
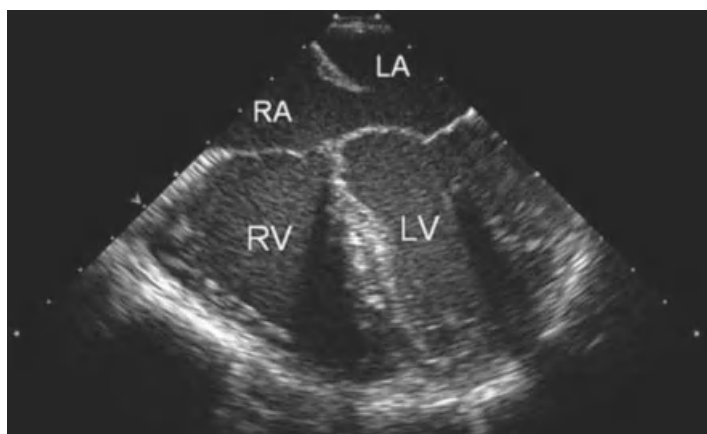
Figure 22.9 Transesophageal echocardiogram of a partial AV canal defect. The primum atrial septal defect is seen at the crux of the heart. The inlet ventricular septum is intact. Note that the left and right AV valves are at the same level, in contrast to the normal slight apical displacement of the tricuspid valve relative to the mitral valve. LA, left atrium; LV, left ventricle; RA, right atrium; RV, right ventricle.
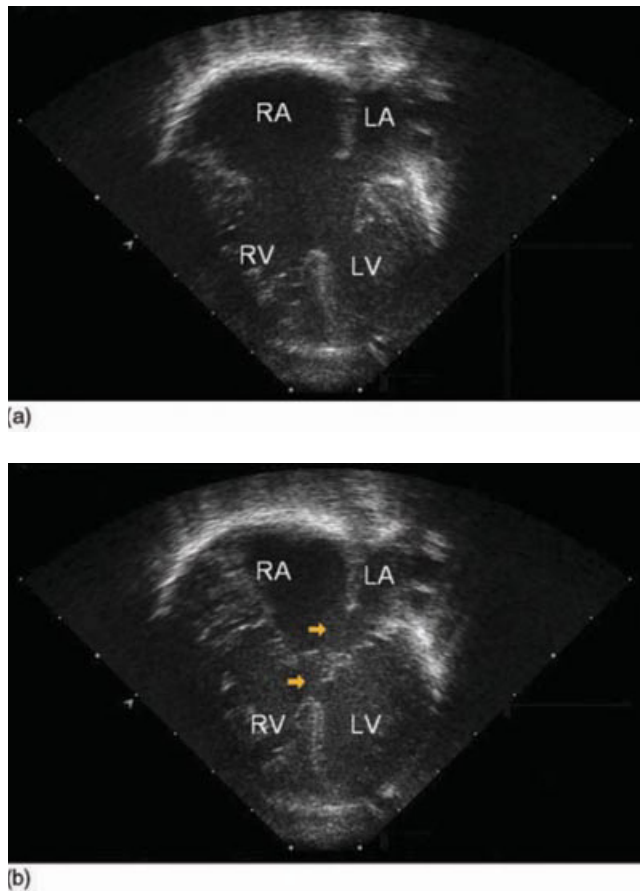
Figure 22.10 Apical four chamber view of a complete AV canal defect.
(a) The single atrioventricular valve opens into both ventricles during diastole.
The valve is mildly unbalanced to the right. (b) During systole the primum
atrial septal defect and inlet ventricular septal defects (arrows) are visualized.
LA, left atrium; LV, left ventricle; RA, right atrium; RV, right ventricle.

the imaging plane enters the coronary sinus, which may erroneously appear to be a primum ASD, particularly when the coronary sinus is dilated from receiving a left superior vena cava. Subcostal imaging may further delineate the size of the primum ASD. In an isolated primum ASD, the common AV valve is often divided (partial AVSD) and the bridging leaflets are adherent to the interventricular septum [25]. Additional ASDs should also be noted. Occasionally, the atrial septum is virtually absent, resulting in a common atrium. Rarely, the atrial septum is intact.

The inlet VSD is well visualized from the apical four-chamber view, and its size should be noted. Sweeping anteriorly from the four-chamber view may demonstrate outlet extension of the defect. From a subcostal short-axis view, a ventricular shunt may be demonstrated below the bridging leaflets. The inferior bridging leaflet often has dense attachments to the crest of the interventricular septum limiting shunting. Commonly, the shunt occurs beneath the superior bridging leaflet [22]. Extension of the defect into

the trabecular muscular septum or outlet septum should also be assessed. Additional muscular VSDs should be sought.

Ventricular size

Usually the atrioventricular valve is aligned equally over the ventricles. When the AVSD is unbalanced and there is a greater commitment of the atrioventricular valve to one ventricle, the ventricle receiving lesser inflow may be hypoplastic. The degree of hypoplasia varies from mildly but adequate to support systemic circulation to severely hypoplastic. The relative proportion of the atrioventricular valve inflow committed to each ventricle can be measured by planimetry of the valves *en face* [28]. Estimating left ventricular volume has also been performed when making decisions regarding suitability for two ventricle repair, although echocardiography underestimates left ventricular volumes in this setting [29].

Left ventricular outflow

In the normal heart, the aorta is wedged in the space anterior to the junction of the tricuspid and mitral valves. When the atrioventricular valves fail to divide, the aorta is unable to assume its usual wedged position and is displaced anteriorly, increasing the distance from the left ventricular apex to the aortic valve. This increased outflow length may contribute to late development of outflow tract obstruction. Additionally, left atrioventricular valve chordal attachments may cross the outflow tract, increasing the risk of obstruction [22]. A significant gradient is rarely found through the left ventricular outflow tract at the time of initial repair, but may develop later.

Associated lesions

A complete assessment of cardiac anatomy is important in all patients with AVSD to detect associated defects.

Left ventricular outflow tract obstruction may be caused by a number of mechanisms, and may be progressive [27]. Left ventricular outflow elongation often results in tunnel-like narrowing, although a gradient is not always present. Chordal attachments originating from the superior bridging leaflet of the left atrioventricular valve may cross the left ventricular outflow tract, resulting in obstruction that is more common with partial AVSD or Rastelli type A complete AVSD due to the dense chordal attachments to the crest of the septum [30]. A discrete fibromuscular ridge may cause obstruction, most commonly becoming apparent several years following initial repair [22]. Because left ventricular outflow tract obstruction often becomes apparent during late follow-up, serial assessment after repair is important [27].

Transesophageal echocardiogram

An intraoperative transesophageal echocardiogram helps guide surgical repair. Details of intracardiac anatomy can be confirmed, although in most patients transthoracic echocardiography clearly delineates the anatomy preoperatively.

Figure 22.11 Fetal four-chamber image of a complete AV canal defect in a patient with heterotaxy syndrome. There is a single common AV valve with large atrial and ventricular septal components to the AV canal. LA, left atrium; LV, left ventricle; RA, right atrium; RV, right ventricle.

The four-chamber view allows assessment of atrial and ventricular level shunts. The common atrioventricular valve can also be inspected from this view for morphology and regurgitation. The long-axis view is useful for assessing the left ventricular outflow tract. The AV valve can be viewed *en face* from the transgastric view. Any bridging tissue connecting the anterior and posterior bridging leaflets and also division of the superior bridging leaflet (Rastelli classification) can be seen from this view. Both left and right ventricular outflow tracts can also be interrogated from the transgastric view [31].

Fetal echocardiography

Complete AVSD is one of the more common lesions detected prenatally, but antenatal detection rates vary between centers [32] (Figure 22.11). Common reasons for referral for sub-specialty evaluation of fetuses with AVSD include abnormal four-chamber view, fetal bradycardia, hydrops, and concerns about trisomy 21 [33]. AVSD detected prenatally raises concerns about other abnormalities that may affect the prognosis. Heterotaxy syndrome, with or without complete heart block, and ventricular hypoplasia are commonly seen in the fetus diagnosed with AVSD [34]. These lesions are likely over-represented in fetal series because these more severe forms of atrioventricular septal defects are more easily detected during the obstetric screening. The relative risk of the fetus having an abnormal karyotype (trisomy 21 in particular, but also trisomy 13 and 18) is significantly increased with AVSD in the absence of heterotaxy syndrome [35]. Finding an AVSD in a fetus should prompt discussion about amniocentesis. Extracardiac anomalies have been reported in 15% of fetuses found to have AVSD [36].

Antenatal detection of AVSD provides the opportunity for counseling the family regarding the expected prenatal course, delivery plan, and postnatal outcome. The risk of hydrops or fetal demise in the fetus with complete AVSD is increased [36]. Risk factors *in utero* include development of complete heart block (often associated with heterotaxy syndrome) and significant AV valve regurgitation. Fetuses with left atrial isomerism appear to have a particularly poor prognosis [37]. Signs of significant fetal distress or concern about ductal-dependent lesions should prompt delivery at a center familiar with the evaluation and management of neonates with significant heart disease.

Radiography

The chest X-ray characteristics depend largely on the degree of pulmonary over-circulation and the amount of valvar regurgitation. With increased pulmonary blood flow, the chest X-ray demonstrates cardiomegaly, prominent pulmonary vasculature, and a large main pulmonary artery. With significant valvar regurgitation, the cardiac size is larger than expected for the amount of increased pulmonary vasculature.

Cardiac catheterization

Cardiac catheterization is rarely necessary for patients with AVSD, because. echocardiography delineates the anatomic and hemodynamic features so well. When echocardiography is unable to delineate complex associated anatomic abnormalities, cardiac magnetic resonance imaging (CMRI) may be useful. If the clinical information and echocardiographic findings cannot determine suitability for surgery because of concerns about elevated pulmonary vascular resistance (PVR), cardiac catheterization and measurement of PVR with acute pulmonary vasodilator testing may be useful. An elevation of PVR >10 units m^{-2}, in the absence of AV valve insufficiency, and despite provocative pulmonary vasodilator testing, is considered to deem the patient inoperable.

Cardiac magnetic resonance imaging

CMRI serves a complementary role to echocardiography in answering specific clinical issues, including quantification of right and left ventricular volume, function, pulmonary to systemic flow ratio, and valvar regurgitation. Details of intracardiac anatomy are also well demonstrated [38]. Volume measurements are typically performed in contiguous short-axis images through the ventricles from the apex to base of the heart using gradient echo cine imaging. The volumes of slices through the ventricles are summed, yielding

the ventricular volumes, which may be indexed to body surface area. Ventricular volume measurements at end-diastole and end-systole allow the calculation of the ejection fraction for both the left and right ventricles. Flow assessment can be used to quantify anterograde and retrograde flow through the atrioventricular valves. In the absence of an intra-cardiac shunt or significant semilunar valve regurgitation, comparison of stroke volumes from short-axis imaging can also be used to calculate valvar regurgitation. With borderline left ventricular size, ventricular volumes measured on CMRI can help with decisions about left ventricular adequacy. Left ventricular volume obtained by this method may underestimate the potential volume due to shifting of septal position towards the left ventricular cavity.

Medical management

In today's era of complete neonatal surgical repair, the preoperative management of AVSD involves managing pulmonary over-circulation until operation. Anticongestive medical therapy reduces preload, enhances cardiac contractility, reduces afterload, improves oxygen delivery, and enhances nutrition. Diuretic therapy is the mainstay of medical management. Other medications include digoxin and ACE inhibitors. Most infants with an AVSD have normal ventricular function, so there is little rationale for the use of digoxin. Ventricular volume overloading is the rationale for using ACE inhibitors, but data on its efficacy are lacking. Nutrition should be optimized. Medical management is maintained until surgical repair. Few data are available about the ideal size for surgical repair, with decisions varying between institutions. Excellent outcomes have been reported for repair of complete AVSD even in neonates. Pulmonary artery banding is rarely performed other than in premature or very sick infants or infants with complex anatomy.

After repair, patients typically require no more than routine follow-up. Medications are usually not needed after discharge from the hospital except for AV valve regurgitation when diuretics and/or afterload reduction may be necessary. Large residual septal defects are uncommon and would typically be addressed prior to hospital discharge.

Surgical repair of AVSD

The first successful repair of AVSD was reported by Lillehei and colleagues at the University of Minnesota in the mid-1950s [39,40]. They initially used cross-circulation for cardiopulmonary bypass and the complete AVSD was repaired by directly suturing the rim of the atrial septal defect (ASD) to the crest of the ventricular septal defect (VSD) [Editor's note – This patient is doing well and has not needed a reoperation in the 55 years since the operation. J.H.M.].

Within 2 years they transitioned to a heart–lung machine and along with other pioneering heart surgeons of 1950s, such as John Kirklin, Dwight McGoon and Denton Cooley, began to incorporate patch material into the repair of AVSD [41,42]. Mortality remained high in part because the patients were older and at risk for complications from elevated pulmonary vascular resistance. Improvements in the techniques of surgery and cardiopulmonary bypass paralleled the transition to earlier age at repair.

Operative techniques

Cardiopulmonary bypass is used for repair of AVSD. In general, mild to moderate hypothermia (25–32 °C), aortic cross-clamping, and cardioplegia are used. The conduction system is vulnerable along the inferior–posterior edge of the defect and the sutures are placed to the right side of the interventricular septum to avoid heart block (Figure 22.12) [43–45]. Regardless of the specific form of AVSD or the specific operative technique, the cleft in the left sided AV valve should be closed except when it would lead to stenosis. Following closure, valve competence is tested to identify important insufficiency [46], which is managed by commissuroplasty sutures (Figure 22.13) [47,48].

Transesophageal echocardiography is performed at the end of the operation to identify major residual lesions. Postoperatively, transesophageal echocardiography (TEE) can provide the surgeon with information about residual lesions that need to be addressed prior to sternal closure [31]. Important details of the postoperative TEE include residual atrial or ventricular level shunts, AV valve function, ventricular function, and outflow tract obstruction. Atrioventricular valves should be closely inspected for either regurgitation or stenosis. The degree of AV valve regurgitation seen on intraoperative TEE may not correspond to that on follow-up transthoracic echocardiography. Multiple variables, including level of sedation, inotropic support, ventricular function, and filling pressure, may lead to discrepancies in the assessment of AV valve function in the operating room and at follow-up [49]. Right ventricular pressure may be estimated by measuring the velocity of either tricuspid valve regurgitation or residual VSD gradient. If increased pulmonary vascular resistance is suspected, this information may help guide postoperative management.

Partial AVSD (Primum Atrial Septal Defect)

In this form of AVSD, the ventricular septal defect component is absent [50]. The morphology of the AV valve varies. In some, an annular fibrous ridge separates the left- and right-sided components of the AV valve. In others, the bridging leaflets of the common AV valve attach to the ventricular septum, obliterating any ventricular level communication but the fibrous separation between the left and right-sided components is indistinct. Patients with a partial AVSD are unlikely to have congestive heart failure unless there is
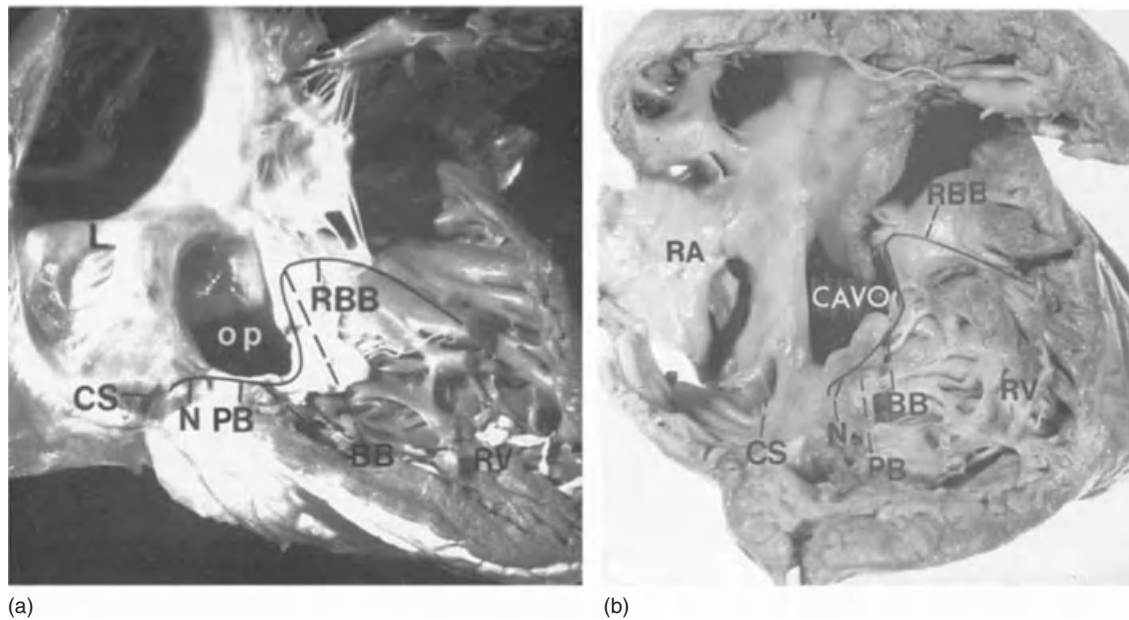
Figure 22.12 The conduction system in AVSD. (a) The conduction system in partial AVSD. Note the position of the atrioventricular node (N) in the atrium inferior to the coronary sinus ostium (CS) and the course of the penetrating bundle (PB) along the posterior inferior margin of the ASD. (b) The conduction system in complete AVSD. The atrioventricular node (N) is in the same position as in the partial AVSD. The course of the penetrating bundle (PB) is along the posterior inferior margin of the ventricular septal defect (CAVO). op, partial AVSD; L, limbus; BB, branching AV bundle; RA, right atrium; RBB, right bundle branch; RV, right ventricle. (Reproduced with permission from Ilbawi *et al*. [7].)
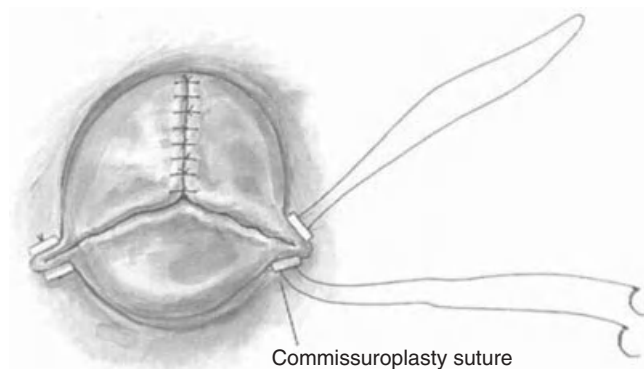
Figure 22.13 Achieving left AV valve competence is essential for successful repair of any form of AVSD. After closure of the cleft, which should be possible in most patients, the valve is assessed for competence and additional reparative procedures performed. In this example, commissuroplasty sutures are shown. (Reproduced with permission from Karl, *Semin Thorac Cardiovasc Surg* 1997;**9**:26–34.)

significant left AV valve insufficiency. It has been common to delay repair until preschool age, but surgery from 3 to 18 months of age is associated with a lower risk of residual left-sided AV valve regurgitation [51]. Repair includes closure of the left-sided AV valve cleft and patch closure of the defect (Figure 22.14) [44]. The conduction system in AVSD is exposed along the inferior end of the defect and care is taken to place sutures to the right side in this area [51]. Some place the coronary sinus ostium on the left side of the patch to decrease further conduction system injury.

Transitional and intermediate AVSD

Transitional and intermediate forms of AVSD have distinct left- and right-sided AV orifices, an ASD, and a VSD below the AV valves [50]. With a transitional AVSD, the ventricular component is restrictive and frequently at the level of the cleft. Repair includes closure of the cleft and suture closure of the VSD component by passing pledget-supported horizontal mattress sutures from the right side of the interventricular septum through the area of division of the common AV valve and then through the bottom of a separate pericardial or Gore-Tex patch. With a restrictive VSD, it is not necessary to repair in early infancy, but delay past 4 years of age is associated with worse long-term left-sided AV valve function [52]. The VSD can be nonrestrictive, associated with heart failure, and at risk for early development of pulmonary vascular disease [52]. Larger ventricular septal defects may require a separate VSD patch. The conduction system occupies the same position as with a complete AVSD.

Complete AVSD

Elective repair of AVSD is undertaken at between 2 and 4 months of age to avoid the development of elevated pulmonary vascular resistance. Currently there are three

Figure 22.14 Repair of partial AVSD.
(a) The cleft in the left-sided AV valve has been
closed and a patch is used to close the ASD.
(b) To minimize the risk of injury to the
atrioventricular node and His bundle the ASD
patch has been sewn in place, leaving the
coronary sinus on the left side of the patch.
(Reproduced with permission from Rastelli
et al. Mayo Clin Proc 1966;**41**:296–308.)

Publisher's Note:
Image not available
in the electronic edition

techniques used to repair AVSDs: the single-patch technique initially described by Maloney *et al.* in 1962 [53], the two-patch technique first reported by McGoon *et al.* at the Mayo Clinic in 1959 [42] and reintroduced by Trusler in Toronto in 1976 [54], and the modified one-patch technique originally described by Wilcox *et al.* in 1977 [55] and subsequently by Nicholson *et al.* in 1999 [56].

The one-patch technique

In this technique, the single AV valve is separated into left (mitral) and right (tricuspid) halves by incising the superior and inferior bridging leaflets back to the annulus. A single patch of pericardium, Dacron, or Gore-Tex, is sutured to the right side of the crest of the interventricular septum. The valve leaflets are then resuspended to this patch. The cleft in the left side of the valve is closed using interrupted sutures and then the atrial component of the defect is closed by suturing the upper portion of this patch to the native atrial septum using continuous suture.(Figure 22.15) The largest series of classic single-patch technique are summarized in Table 22.2. The classic one-patch technique provides excellent exposure of the interventricular septal crest and may decrease the risk of a residual VSD. This technique is well suited to repair of AVSD with tetralogy of Fallot because incising the anterior bridging leaflet provides excellent exposure to the outlet component of the VSD. Its suitability in neonates and very small infants is questionable because their valve tissue is very thin and flimsy. Division and reapproximation of the delicate valve tissue are difficult without producing insufficiency.

The two-patch repair

In this technique, the VSD component of the AVSD is repaired with a separate patch of either pericardium, Dacron, or Gore-Tex. This sickle-shaped shallow VSD patch is sutured to the right side of the interventricular septum. Sutures are then passed from the top of the VSD patch through the appropriate dividing line of the superior and inferior bridging

leaflets and then through the bottom of a separate ASD patch. The cleft in the left-sided AV valve is approximated with suture and the ASD is then closed by suturing the atrial patch to the edge of the defect. The two-patch technique is illustrated in Figure 22.16. The two patch repair preserves AV valve integrity. Most patients before surgery have a competent and non-stenotic common AV valve [57]. With the two-patch technique, the valve is not incised but rather the VSD patch is placed underneath the intact valve. A disadvantage of this approach is more difficult VSD exposure than in the classic one-patch technique. The two-patch repair of tetralogy of Fallot with AV canal is challenging because even after retracting the anterior bridging leaflet, exposure of the large outlet extension of the VSD is difficult. The two-patch technique may be better in neonates and small infants than the one-patch repair but the patch itself can distort the common AV valve and additional valvoplasty may be necessary to achieve competence. Experience with the two-patch repair is summarized in Table 22.3.

The modified one-patch technique

In this technique, a series of sutures are placed along the right side of the interventricular septum and then passed directly through the appropriate dividing line of the superior and inferior bridging leaflets of the common AV valve. These sutures are then passed through the bottom of a single patch, which is generally pericardium. The VSD is closed by suturing the leaflets of the common AV valve directly on to the crest of the interventricular septum. The atrial component of the defect is closed by approximating the edge of the patch to the remaining edge of the atrial septum (Figure 22.17). Valve integrity is maintained because no incisions are made in the common AV valve. The exposure of the VSD is less important because the technique does not require a separate VSD patch. It is suitable for neonates and small infants because there is minimal manipulation of the delicate leaflets. It is not suitable for repair of AVSD with tetralogy of Fallot or a large VSD. Direct approximation of the valve leaflets to the
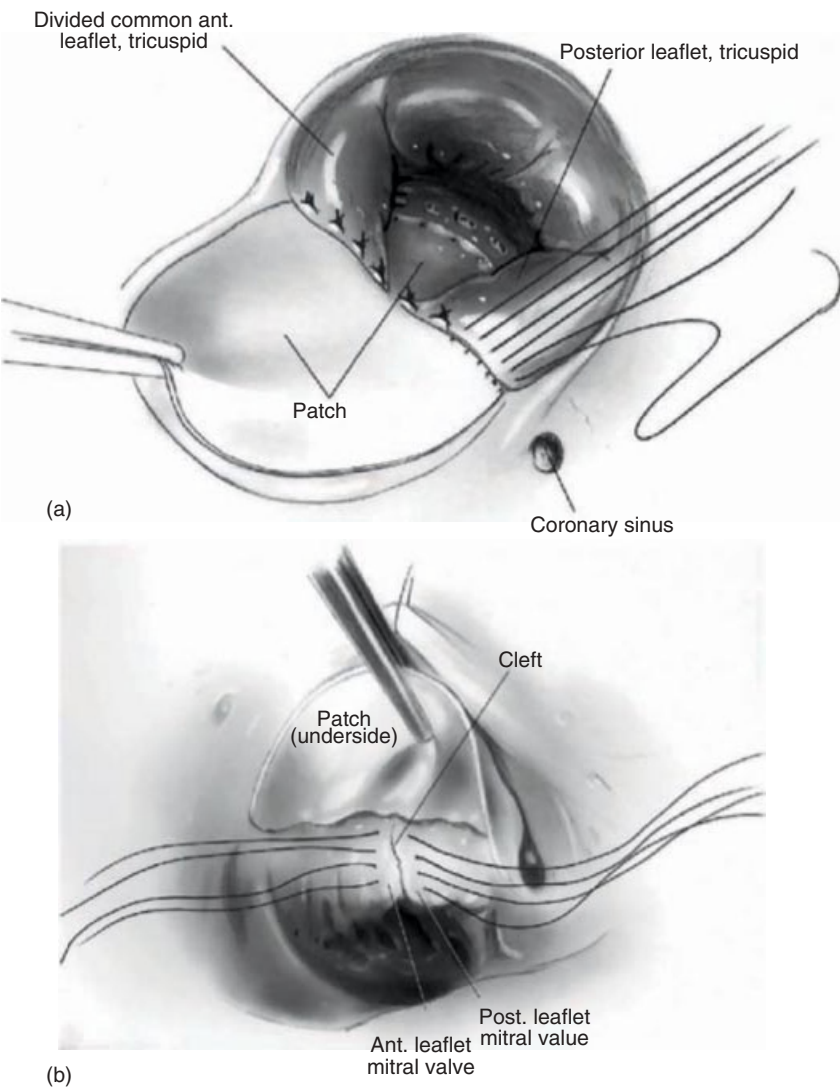
Figure 22.15 The one-patch repair. (a) A single patch is used to close both the ventricular and atrial components of the defect. The single patch has been sutured to the right side of the interventricular septum with interrupted sutures. The divided bridging leaflets have been reapproximated to the patch. (b) The left-sided AV valve cleft is approximated with interrupted suture. (Reproduced with permission from Smith *et al*. *Cardiol Young* 2006;**16**:437–54.)

Table 22.2 Results of one-patch repair.

Authors	Years	Patients	Average follow-up	Operative mortality (%)	Late mortality (%)	Mitral valve reoperation (%)	Heart block (%)
Reddy *et al*. [66]	1992–1997	72	24 months	1.3	1.3	3	0
Prifti *et al*. [67]	1990–2002	190	4 years	8.4	6.8	12	2.6
Crawford [47]	1995–2007	88	N/A	0	0	10	3.4

crest of the septum could predispose to left ventricular outflow tract obstruction. Polimenakos *et al*. reported the development of left ventricular outflow tract obstruction with modified one-patch repair, and with longer follow-up this complication may prove to be more common [58]. Outcomes of the modified one-patch technique are summarized in Table 22.4. In comparison with the tables summarizing the results of the two-patch and classic single-patch techniques, the series reporting outcomes of the modified single-patch technique are more recent, and mortality is lower and mitral valve reoperations are fewer because of the more recent era and shorter follow-up.

Publisher's Note:
Image not available
in the electronic edition

Figure 22.16 The two-patch repair. (a) The sickle-shaped shallow VSD patch has been sutured to the right side of the interventricular septum beneath the undivided common atrioventricular valve. (b) Sutures are then passed from the top of the VSD patch through the appropriate dividing line of the anterior and posterior bridging leaflets and then these same sutures are passed through the bottom of a separate ASD patch. (c) The left-sided AV cleft is approximated with interrupted suture and the remainder of the ASD closed. (Reproduced with permission from Rastelli *et al*. *Mayo Clin Proc* 1966;**41**:296–308.)

Table 22.3 Results of two-patch repair.

Authors	Years	Patients	Average follow-up	Operative mortality (%)	Late mortality (%)	Mitral valve reoperation (%)	Heart block (%)
Backer *et al*. [64]	1983–1994	115	2.4 years	6.0	2.6	6.9	3.5
Lacour-Gayet *et al*. [68]	1995–2006	110	N/A	3.6	1.8	6.3	2.7
Masuda *et al*. [69]	1981–1999	64	99 months	3.1	4.7	7.8	N/A
Ten Harkel *et al*. [70]	1990–2001	111	66 months	2.7	2.7	9.0	1.8
Fortuna *et al*. [71]	1995–2005	209	83% 1 year follow-up	2.9	1.4	7.2	1.0
Litwin *et al*. [72]	1988–2005	222	N/A	2.7	2.7	5.0	1.4
Suzuki *et al*. [73]	1997–2002	116	27 months	1.7	1.7	8.0	0
Bakhtiary *et al*. [74]	1999–2009	100	58 months	0	0	6.0	3.0

Special circumstances

Palliative procedures

Palliation with a pulmonary band is rarely used today but may be indicated in an infant with congestive heart failure and a contraindication to cardiopulmonary bypass such as intracranial hemorrhage or necrotizing enterocolitis. With tetralogy of Fallot and complete AVSD, the right ventricular outflow tract obstruction reduces pulmonary blood flow and heart failure. This initially amelierative effect on the pathophysiology may complicate subsequent repair. The decreased pulmonary blood flow results in less flow across the common atrioventricular valve and therefore a smaller common AV valve annulus and decreased biventricular volumes. [46] The smaller common AV valve area demands precise partitioning and the acceptable margin of error is decreased. Furthermore, the

smaller annulus limits annuloplasty techniques to deal with residual left AV valve regurgitation. Although excellent results with repair of tetralogy of Fallot and complete AVSD in infancy can be obtained, in a small cyanotic infant, systemic to pulmonary artery shunting or right ventricular outflow tract stenting provides suitable palliation and allows repair when the patient is larger and reparative techniques are more easily applied [59,60].

Double-orifice left av valve

Double-orifice left AV valve complicates 5% of AVSD [61]. Double-orifice left AV valve almost always consists of abnormal holes in essentially normal leaflets, rather than abnormal fibrous bridges or adhesions across commissures between leaflets [61]. The accessory orifice is not the result

of fusion or adhesion between leaflets. Therefore, division of the bridging tissue between the accessory orifice and the major orifice must be avoided as it will result in left AV valve regurgitation. Because the abnormal subvalvar apparatus with accessory papillary muscle and crossing chordae tendineae can result in inflow obstruction, limited cleft closure may be necessary to avoid stenosis of the reconstructed LAV valve. Avoiding division of the bridging leaflet tissue and selective partial cleft closure achieves results comparable to those for uncomplicated AVSD [62,63].

Postoperative status

In patients with coexistent AVSD and tetralogy of Fallot, recovery from surgical repair may be more complicated than with either anomaly alone. Residual right ventricular outflow tract obstruction or pulmonary insufficiency may exacerbate right AV valve insufficiency, increasing right ventricular work load [11]. Left AV valve insufficiency can increase pulmonary artery pressure, causing pulmonary insufficiency. Surgical results have improved, and excellent operative survival has been reported [13]. The need for late intervention for residual ventricular level shunting or left AV valve insufficiency is not unusual. In contrast to isolated complete AVSD, or partial AVSD, left ventricular outflow tract obstruction is rare [11]. Following repair of AVSD, residual lesions should be defined and followed serially. The most common reasons for reintervention are left AV valve insufficiency or left ventricular outflow tract obstruction [27]. Residual atrial and ventricular shunts should be sought.

AV valve function may be abnormal following repair. Left AV valve dysfunction is less well tolerated. Residual cleft between the superior and inferior bridging leaflets may result in residual left AV valve regurgitation. Two-dimensional imaging from the parasternal short-axis or subcostal sagittal view best demonstrates a residual cleft. Color Doppler may quantify and localize the regurgitation using orthogonal planes, as the regurgitant jet may have an irregular contour. Chamber dilation suggests significant regurgitation. The AV valves should also be interrogated for stenosis. Left AV valve stenosis should be considered with closely spaced papillary muscles, single papillary muscle, or double-orifice left AV valve. Continuous-wave Doppler from the apical four-chamber view can determine the mean gradient.

(a)   (b)

Figure 22.17 The modified one-patch repair. (a) Sutures are placed along the right side of the interventricular septum and then passed directly through the appropriate dividing line of the anterior and posterior bridging leaflets of the common AV valve. These same sutures are then passed through the bottom of a single patch, which is generally pericardium. (b) These interrupted sutures are then tied down and this closes the VSD by placing the leaflets of the common AV valve directly onto the crest of the interventricular septum. The left sided AV cleft is approximated with interrupted suture. The atrial component of the defect is then closed by approximating the edge of the patch to the remaining edge of the atrial septum (Reproduced with permission from Silverman et al. Int J Cardiol 1986;**13**:309–31.)

Summary and conclusions

A variety of operative techniques are used for repair of AVSD, and surgeons have reported excellent outcomes with all three approaches [54–75]. All of them achieve the goal of separating the VSD component, dividing the common AV valve into left- and right-sided components, and closing the ASD. In most patients, a durable left-sided AV valve is constructed with a low risk of late incompetence. The outcomes depend more on a surgeon's experience than the particular technique used. Indeed, most of the large series presented are dominated by a single surgeon author with a strong interest and experience in this lesion and whose experience over time is isolated to generally one technique.

Table 22.4 Results of "modified" one-patch repair.

Authors	Years	Patients	Average follow-up	Operative mortality (%)	Late mortality (%)	Mitral valve reoperation (%)	Heart block (%)
Wilcox et al. [55]	1992–1995	12	N/A	8.3	0	0	0
Nunn [75]	1983–2005	128	7.3 years	1.6	0	2.3	0
Jonas [48]	1997–2002	34	N/A	0	N/A	0	1
Backer et al. [65]	2001–2006	26	1.8 years	3.8	0	3.8	0

The dramatic improvements are likely due to many factors, but most importantly an earlier age at operation. The younger age of repair has generally eliminated the "pulmonary hypertensive crisis," previously a common postoperative occurrence. Transesophageal echocardiography has helped identify residual lesions, particularly mitral regurgitation, permitting early reintervention for significant left-sided AV valve regurgitation. Improvements in postoperative control of pulmonary hypertension have also contributed to improved results. Currently, a baby with AVSD is likely to have a successful early repair, an uncomplicated postoperative course, and a low likelihood of reintervention on the left-sided AV valve.

Prognosis after surgery

The outcomes after surgical repair of AVSD are excellent. Left AV valve regurgitation is the most common indication for reoperation, occurring in 5–15% of patients [74,76–80]. Typically, this is caused by incomplete closure of the zone of apposition between the inferior and superior bridging leaflets. Stenosis occurs less frequently, particularly when associated with parachute choral apparatus. Late left ventricular outflow tract obstruction necessitating intervention occurs in both forms of AVSDs, but is more frequent in partial AVSD.

References

1 Cook AC, Allan LD, Anderson RH, *et al*. AVSD in fetal life – a clinicopathologic correlation. *Cardiol Young* 1991;**1**:334–43.

2 Mitchell SC, Korones SB, Berendes HW. Congenital heart disease in 56,109 live births. Incidence and natural history. *Circulation* 1971;**43**:323–32.

3 Samanek M. Prevalence at birth, "natural risk" and survival with AVSD. *Cardiol Young* 1991;**1**:285–9.

4 Becker AE, Anderson RH. Atrioventricular septal defects: what's in a name? *J Thorac Cardiovasc Surg* 1982;**83**:461–9.

5 Penkoske PA, Neches WH, Anderson RH, Zuberbuhler JR. Further observations on the morphology of atrioventricular septal defects. *J Thorac Cardiovasc Surg* 1985;**90**:611–22.

6 Rastelli G, Kirklin JW, Titus JL. Anatomic observations on complete form of persistent common atrioventricular canal with special reference to atrioventricular valves. *Mayo Clin Proc* 1966;**41**:296–308.

7 Ilbawi MN, Idriss FS, DeLeon SY, *et al*. Unusual mitral valve abnormalities complicating surgical repair of endocardial cushion defects. *J Thorac Cardiovasc Surg* 1983;**85**:697–704.

8 Thiene G, Wenink AC, Frescura C, *et al*. Surgical anatomy and pathology of the conduction tissues in atrioventricular defects. *J Thorac Cardiovasc Surg* 1981;**82**:928–37.

9 Smith A, Siew YH, Anderson RH, *et al*. The diverse cardiac morphology seen in hearts with isomerism of the atrial appendages with reference to the disposition of the specialised conduction system. *Cardiol Young* 2006;**16**:437–54.

10 Karl TR. Atrioventricular septal defect with tetralogy of Fallot or double-outlet right ventricle: surgical considerations. *Semin Thorac Cardiovasc Surg* 1997;**9**:26–34.

11 Delius RE, Kumar RV, Elliott MJ, *et al*. Atrioventricular septal defect and tetralogy of Fallot: a 15-year experience. *Eur J Cardiothorac Surg* 1997;**12**:171–6.

12 Uretzky G, Puga FJ, Danielson GK, *et al*. Complete atrioventricular canal associated with tetralogy of Fallot. Morphologic and surgical considerations. *J Thorac Cardiovasc Surg* 1984;**87**:756–66.

13 Gatzoulis MA, Shore D, Yacoub M, Shinebourne EA. Complete atrioventricular septal defect with tetralogy of Fallot: diagnosis and management. *Br Heart J* 1994;**71**:579–83.

14 Wenink ACG, Zevallos JC. Developmental aspects of atrioventricular septal defects. *Int J Cardiol* 1988;**18**:65–78.

15 Joziasse IC, van de Smagt JJ, Smith K, *et al*. Genes in congenital heart disease: atrioventricular valve formation. *Basic Res Cardiol* 2008;**103**:216–27.

16 Huggon IC, Cook AC, Smeeton NC, *et al*. Atrioventricular septal defects diagnosed in fetal life: associated cardiac and extra-cardiac abnormalities and outcome. *J Am Coll Cardiol* 2000;**36**:593–601.

17 Delisle MF, Sandor GG, Tessier F, Farquharson DF. Outcome of fetuses diagnosed with atrioventricular septal defect. *Obstet Gynecol* 1999;**94**:763–7.

18 Feldt RH, Edwards WD, Hagler DJ, Puga FJ. Endocardial cushion defects. In: Moller JH, Neal WA, eds. *Fetal, Neonatal, and Infant Cardiac Disease*. Norwalk, CT: Appleton and Lange, 1990: 411–32.

19 Vick GW, Titus JL. Defects of the atrial septum including the atrioventricular canal. In: Garson A, Bricker JT, McNamara DG, eds. *The Science and Practice of Pediatric Cardiology*. Philadelphia: Lea and Feibiger, 1990: 1023–54.

20 Ih S, Fukuda K, Okada R, Saitoh S. Histopathological correlation between the QRS axis and disposition of the AV conduction system in common AV orifice and its related anomalies. *Jpn Circ J* 1983;**47**:1368–76.

21 Feldt RH, Porter CJ, Edwards WD, *et al*. Atrio-ventricular septal defects. In Emmanoulides GC, Allen HD, Riemenschneider TA, *et al*., eds. *Heart Disease in Infants, Children and Adolescent*s, 5th edn. Baltimore: Williams & Wilkins, 1995: 704–24.

22 Smallhorn JF. Cross-sectional echocardiographic assessment of atrioventricular septal defect: basic morphology and preoperative risk factors. *Echocardiography* 2001;**18**:415–32.

23 Minich LA, Snider AR, Bove EL, *et al*. Echocardiographic evaluation of atrioventricular orifice anatomy in children with atrioventricular septal defect. *J Am Coll Cardiol* 1992;**19**:149–53.

24 Rastelli G, Kirklin JW, Titus JL. Anatomic observations on complete form of persistent common atrioventricular canal with special reference to atrioventricular valves. *Mayo Clin Proc* 1966;**41**:296–308.

25 Silverman NH, Zuberbuhler JR, Anderson RH. Atrioventricular septal defects: cross-sectional echocardiographic and morphologic comparisons. *Int J Cardiol* 1986;**13**:309–31.

26 Chin AJ, Bierman FZ, Sanders SP, *et al*. Subxyphoid 2-dimensional echocardiographic identification of left ventricular papillary muscle anomalies in complete common atrioventricular canal. *Am J Cardiol* 1983;**51**:1695–9.

27 Sittiwangkul R, Ma RY, McCrindle BW, *et al*. Echocardiographic assessment of obstructive lesions in atrioventricular septal defects. *J Am Coll Cardiol* 2001;**38**:253–61.

28 Cohen MS, Jacobs ML, Weinberg PM, Rychik J. Morphometric analysis of unbalanced common atrioventricular canal using two-dimensional echocardiography. *J Am Coll Cardiol* 1996; **28**:1017–23.

29 Grosse-Wortmann L, Yun TJ, Al-Radi O, *et al*. Borderline hypoplasia of the left ventricle in neonates: insights for decision-making from functional assessment with magnetic resonance imaging. *J Thorac Cardiovasc Surg* 2008;**136**:1429–36.

30 Draulans-Noe HA, Wenink AC. Anterolateral muscle bundle of the left ventricle in atrioventricular septal defect: left ventricular outflow tract and subaortic stenosis. *Pediatr Cardiol* 1991;**12**:83–8.

31 Roberson DA, Muhiudeen IA, Silverman NH, *et al*. Intraoperative transesophageal echocardiography of atrioventricular septal defect. *J Am Coll Cardiol* 1991;**18**:537–45.

32 Bull C. Current and potential impact of fetal diagnosis on prevalence and spectrum of serious congenital heart disease at term in the UK. *Lancet* 1999;**354**:1242–7.

33 Delisle MF, Sandor GG, Tessier F, Farquharson DF. Outcome of fetuses diagnosed with atrioventricular septal defect. *Obstet Gynecol* 1999;**94**:763–7.

34 Fesslova V, Villa L, Nava S, *et al*. Spectrum and outcome of atrioventricular septal defect in fetal life. *Cardiol Young* 2002;**12**:18–26.

35 Langford K, Sharland G, Simpson J. Relative risk of abnormal karyotype in fetuses found to have an atrioventricular septal defect (AVSD) on fetal echocardiography. *Prenat Diagn* 2005;**25**:137–9.

36 Huggon IC, Cook AC, Smeeton NC, *et al*. Atrioventricular septal defects diagnosed in fetal life: associated cardiac and extra-cardiac abnormalities and outcome. *J Am Coll Cardiol* 2000;**36**:593–601.

37 Allan LD. Atrioventricular septal defect in the fetus. *Am J Obstet Gynecol* 1999;**181**:1250–3.

38 Parsons JM, Baker EJ, Anderson RH, *et al*. Morphological evaluation of atrioventricular septal defects by magnetic resonance imaging. *Br Heart J* 1990;**64**:138–45.

39 Lillehei CW, Cohen M, Warden HE, Varco RL. The direct-vision intracardiac correction of congenital anomalies by controlled cross circulation; results in thirty-two patients with ventricular septal defects, tetralogy of Fallot, and atrioventricularis communis defects. *Surgery* 1955;**38**:11–29.

40 Lillehei CW, Warden HE, Dewall RA, *et al*. Cardiopulmonary by-pass in surgical treatment of congenital or acquired cardiac disease; use in three hundred five patients. *Arch Surg* 1957;**75**:928–45.

41 Cooley DA. Results of surgical treatment of atrial septal defects. Particular consideration of low defects including ostium primum and atrioventricular canal. *Am J Cardiol* 1960;**6**:605–17.

42 McGoon DW, Dushane JW, Kirklin JW. The surgical treatment of endocardial cushion defects. *Surgery* 1959;**46**:185–96.

43 Ebels T, Elzenga N, Anderson RH. Atrioventricular septal defects. In: Anderson RH, Baker EJ, Redington A, *et al*., eds. *Paediatric Cardiology*. Philadelphia: Churchill Livingstone, 2010: 939–81.

44 Pacifico AD. Atrio-ventricular septal defects. In: Stark J, de Leval M, eds. *Surgery for Congenital Heart Defects*, 2nd edn. Philadelphia: Saunders, 1994: 373–89.

45 Bharati S, Lev ML, Kirklin JW. Operations in the right atrium. In: *Cardiac Surgery and the Conduction System*, 2nd edn. Mount Kisco, NY: Futura Publishing, 1992: 21–73.

46 Mitchell ME, Litwin SB, Tweddell JS. Complex atrioventricular canal. *Semin Thorac Cardiovasc Surg Pediatr Cardiol Surg Annu* 2007;32–41.

47 Crawford FA. Atrioventricular canal: single-patch technique. *Semin Thorac Cardiovasc Surg Pediatr Cardiol Surg Annu* 2007;11–20.

48 Jonas RA. Complete atrioventricular canal. In: Jonas RA, DiNardo J, Laussen PC, *et al*., eds. *Comprehensive Surgical Management of Congenital Heart Disease*. London: Arnold, 2004: 397–8.

49 Kim HK, Kim WH, Hwang SW, *et al*. Predictive value of intraoperative transesophageal echocardiography in complete atrioventricular septal defect. *Ann Thorac Surg* 2005;**80**:56–9.

50 Jacobs JP, Burke RP, Quintessenza JA, Mavroudis C. Congenital Heart Surgery Nomenclature and Database Project: atrioventricular canal defect. *Ann Thorac Surg* 2000;**69**(4 Suppl):S36–43.

51 Minich LL, Atz AM, Colan SD, *et al*. Partial and transitional atrioventricular septal defect outcomes. *Ann Thorac Surg* 2010;**89**:530–6.

52 Cetta F, Minich L, Edwards WD, *et al*. Atrioventricular septal defects. In: Allen HD, Driscoll DJ, Shaddy RE, Feltes TF, eds. *Moss and Adams' Heart Disease in Infants, Children, and Adolescents Including the Fetus and Young Adult*. Philadelphia: Lippincott Williams & Wilkins, 2008: 646–66.

53 Maloney JV Jr, Marable SA, Mulder DG. The surgical treatment of common atrioventricular canal. *J Thorac Cardiovasc Surg* 1962;**43**:84–96.

54 Trusler GA. Discussion of Mills NL, Ochsner IL, King TD: correction of type C complete atrioventricular canal. Surgical considerations. *J Thorac Cardiovasc Surg* 1976;**71**:20–8.

55 Wilcox BR, Jones DR, Frantz EG, *et al*. Anatomically sound, simplified approach to repair of "complete" atrioventricular septal defect. *Ann Thorac Surg* 1997;**64**:487–93;discussion 493–4.

56 Nicholson IA, Nunn GR, Sholler GF, *et al*. Simplified single patch technique for the repair of atrioventricular septal defect. *J Thorac Cardiovasc Surg* 1999;**118**:642–6.

57 Tweddell JS, Litwin SB, Berger S, *et al*. Twenty-year experience with repair of complete atrioventricular septal defects. *Ann Thorac Surg* 1996;**62**:419–24.

58 Polimenakos AC, Sathanandem, SK, Bharati S, *et al*. Depth of ventricular septal defect and impact on reoperation for left ventricular outflow obstruction after repair of complete atrioventricular septal defect: does double patch technique decrease the incidence of left ventricular outflow obstruction? Anatomical and clinical correlation. Presented at the 89th Annual Meeting of the American Association for Thoracic Surgery, Boston, MA, 11 May 2009.

59 Najm HK, Van Arsdell GS, Watzka S, *et al*. Primary repair is superior to initial palliation in children with atrioventricular septal defect and tetralogy of Fallot. *J Thorac Cardiovasc Surg* 1998;**116**:905–13.

60 McElhinney DB, Reddy VM, Silverman NH, *et al*. Atrioventricular septal defect with common valvar orifice and tetralogy of Fallot revisited: making a case for primary repair in infancy. *Cardiol Young* 1998;**8**:455–61.

61 Bano-Rodrigo A, Van Praagh S, Trowitzsch E, Van Praagh R. Double-orifice mitral valve: a study of 27 postmortem cases with developmental, diagnostic and surgical considerations. *Am J Cardiol* 1988;**61**:152–60.

62 Nakano T, Kado H, Shiokawa Y, Fukae K. Surgical results of double-orifice left atrioventricular valve associated with atrioventricular septal defects. *Ann Thorac Surg* 2002;**73**:69–75.

63 Lee CN, Danielson GK, Schaff HV, *et al*. Surgical treatment of double-orifice mitral valve in atrioventricular canal defects. Experience in 25 patients. *J Thorac Cardiovasc Surg* 1985; **90**:700–5.

64 Backer CL, Mavroudis C, Alboliras ET, Zales VR. Repair of complete atrioventricular canal defects: results with the two-patch technique. *Ann Thorac Surg* 1995;**60**:530–7.

65 Backer CL, Stewart RD, Bailliard F, *et al*. Complete atrioventricular canal: comparison of modified single-patch technique with two-patch technique. *Ann Thorac Surg* 2007;**84**:2038–46.

66 Reddy VM, McElhinney DB, Brook MM, *et al*. Atrioventricular valve function after single patch repair of complete atrioventricular septal defect in infancy: how early should repair be attempted? *J Thorac Cardiovasc Surg* 1998;**115**:1032–40.

67 Prifti E, Bonacchi M, Bernabei M, *et al*. Repair of complete atrioventricular septal defects in patients weighing less than 5 kg. *Ann Thorac Surg* 2004;**77**:1717–26.

68 Lacour-Gayet F, Campbell DN, Mitchell M, *et al*. Surgical repair of atrioventricular septal defect with common atrioventricular valve in early infancy. *Cardiol Young* 2006; **16**(Suppl 3):52–8.

69 Masuda M, Kado H, Tanoue Y, *et al*. Does Down syndrome affect the long-term results of complete atrioventricular septal defect when the defect is repaired during the first year of life? *Eur J Cardiothorac Surg* 2005;**27**:405–9.

70 Ten Harkel AD, Cromme-Dijkhuis AH, Heinerman BC, *et al*. Development of left atrioventricular valve regurgitation after correction of atrioventricular septal defect. *Ann Thorac Surg* 2005;**79**:607–12.

71 Fortuna RS, Ashburn DA, Carias de Oliveira N, *et al*. Atrioventricular septal defects: effect of bridging leaflet division on early valve function. *Ann Thorac Surg* 2004;**77**:895–902.

72 Litwin SB, Tweddell JS, Mitchell ME, Mussatto KA. The double patch repair for complete atrioventricularis communis. *Semin Thorac Cardiovasc Surg Pediatr Cardiol Surg Annu* 2007:21–7.

73 Suzuki T, Bove EL, Devaney EJ, *et al*. Results of definitive repair of complete atrioventricular septal defect in neonates and infants. *Ann Thorac Surg* 2008;**86**:596–602.

74 Bakhtiary F, Takacs J, Cho MY, *et al*. Long-term results after repair of complete atrioventricular septal defect with two-patch technique. *Ann Thorac Surg* 2010;**89**:1239–43.

75 Nunn GR. Atrioventricular canal: modified single patch technique. *Semin Thorac Cardiovasc Surg Pediatr Cardiol Surg Annu* 2007:28–31.

76 Alexi-Meskishvili V, Hetzer R, Dahnert I, *et al*. Results of left atrioventricular valve reconstruction after previous correction of atrioventricular septal defects. *Eur J Cardio-Thorac Surg* 1997;**12**:460–5.

77 El-Najdawi EK, Driscoll DJ, Puga FJ, *et al*. Operation for partial atrioventricular septal defect: a forty-year review. *J Thorac Cardiovasc Surg* 2000;**119**:880–9.

78 Permut LC, Mehta V. Late results and reoperation after repair of complete and partial atrioventricular canal defect. *Semin Thorac Cardiovasc Surg* 1997;**9**:44–54.

79 Stulak JM, Burkhart HM, Dearani JA, *et al*. Reoperations after repair of partial atrioventricular septal defect: a 45-year single-center experience. *Ann Thorac Surg* 2010;**89**:1352–9.

80 Malhotra SP, Lacour-Gayet F, Mitchell MB, *et al*. Reoperation for left atrioventricular valve regurgitation after atrioventricular septal defect repair. *Ann Thorac Surg* 2008;**86**:147–52.

23 Ventricular Septal Defect

Daniel J. Penny

Texas Children's Hospital and Baylor College of Medicine, Houston, TX, USA

Introduction and historical background

Anatomists and pathologists have documented defects in the ventricular septum for centuries. Defects associated with more major malformations have been described or referred to in numerous publications during the last 200 years – especially in association with right ventricular outflow tract obstruction (pulmonary stenosis or atresia) [1,2]. During the latter part of the nineteenth century, two widely different and notable publications drew attention to some of the clinical consequences of ventricular septal defect (VSD). First, the characteristic harsh and strikingly loud systolic murmur present in many affected patients was described, and the remarkable absence of symptoms experienced by such individuals was recognized [3]. Since this publication appeared, the term *maladie de Roger* has been widely used to imply a small asymptomatic VSD. The second was a report in 1897 by Eisenmenger, who described a patient who died at the age of 32 years, having suffered with cyanosis from early childhood [4]. At autopsy, he was found to have a ventricular septal defect with an overriding aorta and pulmonary arterial sclerosis. The development of cyanosis in adult life was attributed to the overriding aorta and so the defect described in this publication (large VSD with aortic override) came to be known as *Eisenmenger's anomaly*, and when cyanosis appeared in adolescence or adult life, the combination has been referred to as *Eisenmenger's complex* by Abbott. In the twentieth century, it was the detailed physiological assessments by Paul Wood [5] in the 1950s and the pathological studies of Heath and co-workers [6,7] which highlighted the role of the pulmonary vasculature in the development of cyanosis in this setting, the condition to which we now refer as *Eisenmenger syndrome*.

During the second half of the twentieth century, two schools of thought regarding the hemodynamic significance of a VSD emerged. The first was based on Roger's premise that most patients were asymptomatic and Eisenmenger's observations that unrepaired defects resulted in late cyanosis or death. Thus, until the 1970s, the strongly held view of many pediatric cardiologists was that most VSDs would if unrepaired, inevitably lead to pulmonary hypertension and the Eisenmenger syndrome [8]. More recent epidemiological studies, however, led to a very different, and more benign, view of most defects, suggesting that more than 70% are small and clinically asymptomatic and that a large proportion close spontaneously during infancy or early childhood [9,10]. This perspective is further supported by echocardiographic studies using color flow mapping, which have shown a high incidence of extremely small defects in the fetal and neonatal period or later in infancy. These are usually clinically silent and would in the past have gone undetected, often closing spontaneously in the first weeks or months of life [11,12].

Incidence and genetics

According to published population-based series, VSD accounts for up to 40% of congenital cardiac malformations. Of 4390 infants with congenital heart disease in the Baltimore–Washington Study, 1411 (32.1%) had VSD. Of these, 895 were reported to be perimembranous, 429 to be muscular, and 22 to be doubly committed [13]. A significant number of VSDs close spontaneously. According to Hoffman, ~85–95% of tiny muscular defects close spontaneously in the first year after birth and about 70% of small defects close during childhood [14]. Of the 10–25% of defects considered to be large, ~10–15% close spontaneously. The quoted incidence, or prevalence, of VSD within populations therefore varies according to the age of the population studied and to the method of diagnosis. Clinical studies of children born in

Bohemia [15] and Merseyside [16] demonstrated a prevalence of 2.56 and 2.74 per 1000 live births, respectively. More recent studies using echocardiography rather than clinical examination or postmortem have reported a higher prevalence. The true point prevalence of VSD at birth is higher still, as reported in a prospective echocardiographic study of 1053 prospective newborns, of whom 56 had a VSD at birth, (53.2 per 1000), but nearly 90% of these had closed within 10 months [17].

The genetic origins of VSD are complex and in most patients are probably multifactorial. Thus, an underlying genetic predisposition to CHD acts in synergy with other influences, including somatic mutations early in development, epigenetic factors, environmental influences, and purely stochastic effects to produce cardiac anomalies [18]. Family aggregation studies strongly suggest that genetic factors play an important role in the development of CHD, because the relative risk of having an affected child is increased when a first-degree relative also has a cardiac malformation [19]. The multifactorial origin of the majority of congenital cardiac defects, including VSD, is probably best supported by the observation that even identical twins display a relatively low concordance rate for congenital cardiovascular malformations, usually below 10% [20,21].

In some families, monogenic influences contribute to the pathogenesis of congenital cardiovascular malformations, including VSD [22]. The characterization of these has facilitated the identification of important components of the signaling pathways that regulate cardiac development and septation [23–25]. The roles of mutations in the T-box transcription factor gene *TBX5*, the zinc finger transcription factor gene *GATA4*, and the *NKX2.5* homeobox transcription factor in abnormal cardiac septation, have received particular attention. *GATA4* and *TBX5* are co-expressed in the heart and their interaction is critical for cardiac septation [26]. In addition to being expressed in the heart, *TBX5* is expressed in the upper limb buds and the eyes and the most often-reported mutation is associated with the autosomal dominant Holt–Oram syndrome [27,28], characterized by abnormalities of the forelimbs and also a number of cardiac abnormalities, including atrial septal defect, VSD, and tetralogy of Fallot. Recently, a *TBX5* polymorphism has been shown to be strongly associated with isolated VSD in a population of Chinese Han [29]. Recent reports have also identified *GATA4* sequence variants in familial septal defects (particularly atrial), although they have also been found in some patients with sporadic VSD [30–32].

Even in families with cardiac defects that have been linked to monogenetic mutations, pleiotropy and incomplete penetrance are typically seen.

Environmental influences, such as teratogens, including maternal alcohol and drugs, maternal infections, and untreated maternal metabolic illnesses have all been associated with VSD [33]. Lastly, many patients with VSD have no known predisposing risk factor, so that stochastic events or factors may play an important role in their development.

Embryology

The interventricular septum has distinct mesenchymal and muscular components [34]. The mesenchymal component faces the arterial valves and separates the ventricular inflow and outflow tracts, and appears to originate mainly from fusion of the conotruncal and atrioventricular endocardial cushions. The processes underlying the development of the muscular septum are less well defined, and at least two hypotheses have been proposed for this. Studies of human embryos [35,36] suggested that the muscular interventricular septum forms from the coalescence of the component of the ventricular wall that is interposed between the enlarging free walls of the developing right and left ventricles. Thus, as the ventricular cavities become deeper, the septum grows passively inwards. Observations, particularly in chick embryos, however, using *in vivo* labeling did not fully support this concept [37,38], and instead suggest that the muscular septum originates from a cluster of cells, the so-called "primitive interventricular septum" which grows actively towards the cushions of the AV canal [38].

Defects of the ventricular septum are likely to develop as a consequence of several factors. Failure of complete formation of the primary septum may contribute to trabecular defects, and many muscular defects in the trabecular septum likely result from excessive undermining beneath and between trabeculae, during formation of the trabecular part of the septum. Failure of fusion of the atrioventricular cushions, with each other or with the primary septum, may result in an inlet VSD, either in the context of an atrioventricular septal defect or as an isolated defect. Malalignment or poor development of the outlet cushions contributes to outlet defects, and finally, failure of complete closure of the area that forms the membranous septum leaves a perimembranous defect. Defects in this area are much larger than the normal membranous septum and are likely to result from incomplete development of one or other components of the muscular septum. This leaves a communication of such a substantial size that the normal mechanism for formation of the membranous septum is unable to effect complete closure.

Pathologic anatomy

VSD, in many respects, is considered to be one of the simpler congenital cardiac malformations, so it is ironic that there is still no universal consensus for its classification [39]. Some defects are completely surrounded by muscle (muscular
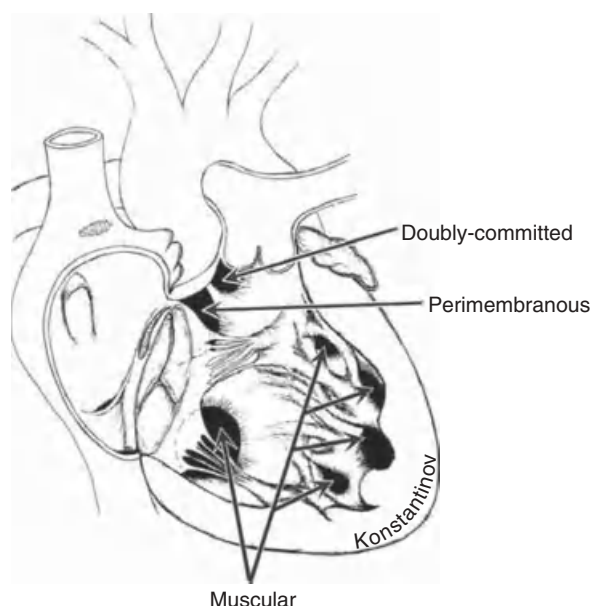
Figure 23.1 Cartoon demonstrating the position of ventricular septal defects from the right side of the ventricular septum. The positions of perimembranous, doubly committed, and muscular defects are shown.

defects) and classified according to their location within the muscular septum (inlet, apex or outlet). Defects at the margins of the muscular septum can be related to the hinge-points of the leaflets of the atrioventricular valves (perimembranous), those of the arterial valves (juxta-arterial), or both (Figure 23.1).

Muscular defects are located within the muscular septum. They are surrounded exclusively by muscular rims and, when viewed from the cavity of the right ventricle, may open into its inlet, its outlet, or its apex.

Perimembranous defects: the membranous septum is the smallest component of the ventricular septum, lying close to the central fibrous body. It delineates a small part of the left ventricle, immediately below the aortic valve, and is related to the commissure between its right coronary and noncoronary leaflets, and the part of the right ventricle adjacent to the septal commissure of the tricuspid valve. Defects in this area are termed *perimembranous VSDs*. They open into the right ventricle where the subpulmonary outflow tract turns superiorly relative to the atrioventricular junction, and are characterized by fibrous continuity between the leaflets of the tricuspid and the aortic valves, which form their postero-inferior margin. When a perimembranous VSD extends anterosuperiorly, it tends to lie in an immediately "subaortic" position, and may be referred to as a *subaortic VSD*. This type of defect usually excavates the outlet septum to a degree and may be called a *perimembranous outlet VSD*. When the aorta overrides such a defect, as in tetralogy of Fallot, the term *malalignment VSD* is some-

times applied. A perimembranous VSD may, alternatively, excavate the inlet septum (see inlet VSD) and then lie below the septal leaflet of the tricuspid valve, sometimes being associated with overriding or straddling of the tricuspid valve. A large perimembranous VSD may excavate into all three of the muscular parts of the septum, and this may be referred to as a *confluent defect.*

Part of the membranous septum separates the left ventricular outflow tract, adjacent to the commissure between the right and noncoronary leaflets of the aortic valve, from an area in the right atrium just above the annulus of the tricuspid valve, which is close to its septal commissure. This curious feature results from the fact that the anterior part of the annulus of the septal tricuspid leaflet is actually attached across the middle of the membranous septum, thus separating it into atrioventricular and interventricular components. Further posteriorly, behind the membranous septum, the annulus of the septal tricuspid leaflet is also attached at the inferior margin of the atrial septum, and is at a lower level than the mitral valve on the opposite side. This results in the characteristic offsetting of the septal leaflets of the mitral and tricuspid valves, readily seen on echocardiography in the four-chamber view. Such offsetting depends on an intact ventricular septum in this area, and a perimembranous VSD extending into the inlet septum (inlet perimembranous defect) is usually associated with loss of normal offsetting.

Gerbode defects refer to a spectrum of VSDs which are associated with a shunt directly from the left ventricle to the right atrium. This can occur with a VSD involving the atrioventricular component of the membranous septum, which allows direct communication between the left ventricle and the right atrium, a typical Gerbode VSD. There are other situations when a shunt from the left ventricle to the right atrium may occur through a VSD. Most commonly, the shunt through a perimembranous VSD that is directly related to the septal commissure of the tricuspid valve may flow through the commissure, from the left ventricle into the right atrium. Alternatively, there may be a defect in the septal leaflet at the area of the membranous septum, with lack of the normal annular attachment across the septum at this point, allowing the left ventricle to communicate with both the right atrium and the right ventricle.

Doubly committed and juxta-arterial defects are found in an area which in the normal heart constitutes a free-standing tube of muscular tissue – the muscular infundibulum – which supports the pulmonary valve. A defect in this region is characteristically associated with continuity between the aortic and pulmonary valves. Usually, these defects have a postero-inferior rim of muscle. If such defects extend into the perimembranous zone, then there is also fibrous continuity with the tricuspid valve, the so-called "doubly committed *and* juxta-arterial *and* perimembranous VSD."

Relation between conduction axis and ventricular septal defects

An understanding of the location of the cardiac conduction system is essential for a cardiac surgeon if damage to this pathway is to be avoided during surgical repair of VSD. The position of the cardiac conduction system in relation to VSDs is easily understood when the site of the defect is viewed in relation to anatomic landmarks. Those defects that directly abut the area of the membranous septum and central fibrous body (perimembranous defects) always have the conducting tissue at the posteroinferior margin of the VSD and related to the crest of the trabecular part of the ventricular septum. With an inlet perimembranous VSD, the atrioventricular node and His bundle are posteriorly displaced, and the bundle pursues a longer than normal course on the crest of the ventricular septum (as occurs with atrioventricular septal defects). With other types of perimembranous defects, the position of the His bundle tends to be more nearly normal, with a short course for the bundle before bifurcation immediately below the aortic valve on the left side of the crest of the trabecular septum.

The relationships between muscular VSDs and the atrioventricular conduction axis are more variable. Inlet defects lie consistently below and behind the conducting pathways. Trabecular defects usually open into the right ventricle anterior to the right bundle branch and into the left ventricle at a variable point, often with the radiations of the left bundle branch running around the anterior and the posterior margins of the defect. Most of these defects are distant from the bundle of His, although those that are close to the atrioventricular junction may have only a thin rim of muscle separating the defect from the bundle, and may therefore be vulnerable during repair. Outlet defects (muscular or doubly committed) are usually separated from the area of the membranous septum, although some may have only a slender muscle bar between the defect and the membranous septum. In most hearts with a doubly committed juxta-arterial defect, the conduction axis is protected by the muscular postero-inferior rim. However, in those juxta-arterial defects which extend into the perimembranous region, in which this muscular rim is deficient, the conduction axis will be contained within the postero-inferior rim of the defect, as occurs in other forms of perimembranous defect.

In general, perimembranous defects with their conducting system are likely to lie at the postero-inferior margin and are the most vulnerable to intraoperative damage. This is much less likely for muscular VSDs, as the bundle of His generally lies in the antero-superior rim of the defect with inlet defects and most commonly posterior to or inferior to most trabecular and outlet defects, and as such are less likely to be damaged.

Associated anomalies

In addition to existing in isolation, VSDs are present in a wide range of more complex cardiac malformations, including tetralogy of Fallot, tricuspid atresia, and transposition of the great arteries. These complex malformations are discussed elsewhere in this book. VSD is also commonly associated with atrial septal defect or persistent ductus arteriosus. In these settings, the clinical signs and symptoms are typically related to the VSD, rather than the other defects. On the other hand, when VSD is associated with aortic arch obstruction (coarctation or interruption), the clinical features related to arch obstruction usually predominate, particularly during the early neonatal period.

Association of VSDs with significant left ventricular outflow tract obstruction, either valvar or subvalvar aortic stenosis, may compound the clinical presentation, and add to the complexity of management. Other obstructive lesions of the left side of the heart, such as subaortic, mitral, or supramitral stenosis, may also coexist with VSD. The extent to which they aggravate the clinical symptoms depends on the severity of the associated obstruction.

By contrast, associated right ventricular outflow tract obstruction (valvar pulmonary stenosis or infundibular stenosis) may be well tolerated and often diminishes the effects of the VSD, especially if the septal defect is large. The development of increasing infundibular obstruction, which occurs in ~5% of patients with VSD, is probably related to progressive hypertrophy of anomalous muscle bundles in the right ventricle. Although different in its embryonic origins, this hypertrophy may progress during the first months of life, leading to tight infundibular stenosis, closely resembling that associated with tetralogy of Fallot.

Important but uncommon associated anomalies include those in which the mitral or the tricuspid valve overrides or straddles the VSD, because of malalignment between the atrial and the ventricular septums.

So-called aneurysms of the membranous septum are found in a high proportion of patients with a perimembranous defect, in which a fibrous sack around the right ventricular side of the VSD may partially occlude even a moderately large communication. These "aneurysms" are usually derived from tricuspid leaflet tissue, either of the septal leaflet or from accessory leaflet material, which becomes adherent to the rim of the VSD. The process of adhesion to the edge of the defect often progresses over months or years, leading to spontaneous diminution in size or closure in many patients.

Aortic valve prolapse may be found in patients with defects close to the aortic valve. This phenomenon is particularly characteristic of doubly committed defects, in which the prolapsing leaflet (the right coronary leaflet) may partially occlude the VSD, creating the impression clinically that the defect is small. Some perimembranous defects are associated

with prolapse of the noncoronary or the right coronary leaflet. Over time, if untreated, prolapse leads to progressively increasing aortic incompetence.

Pathophysiology

The key features that dictate the hemodynamic impact and clinical effects of a VSD are *the amount and direction of interventricular shunting*, *the degree of volume loading* to the cardiac chambers, and the presence of *secondary phenomena*, including prolapse or regurgitation of the aortic valve and obstruction to either the pulmonary or systemic outflow tract.

The amount of interventricular flow is determined first by the size of the defect and second by the relative resistances of the pulmonary and systemic vasculature. The amount of flow through a small, restrictive defect depends primarily on its size and, in the absence of other abnormalities, will usually be from the left to the right ventricle. The magnitude of flow through a larger nonrestrictive defect is determined by the relative resistances of the systemic and pulmonary vascular beds and may vary considerably during the clinical course and over time. Thus, with an elevated pulmonary vascular resistance during the early neonatal period, the magnitude of shunting, even through a very large defect, may be minimal. Consequently, many infants with an undiagnosed large VSD are discharged from the maternity hospital asymptomatic, with no appreciable murmur, only to develop an increase in the amount of left-to-right shunting and symptoms of pulmonary overcirculation as pulmonary vascular resistance falls during subsequent weeks. In a minority, the normal postnatal fall in pulmonary vascular resistance may be delayed or arrested, such that they never develop symptoms of excessive pulmonary blood flow and unfortunately only present later with signs of pulmonary vascular disease.

If a large VSD is unoperated, the pulmonary vascular bed remains exposed to a chronic elevation of pulmonary pressure and flow. These patients develop pulmonary vascular disease [40]. Pulmonary vascular resistance increases, reducing the amount of left-to-right shunting. Ultimately, as pulmonary vascular resistance increases further and exceeds systemic resistance, right-to-left interventricular shunting ensues, resulting in cyanosis and the so-called "Eisenmenger syndrome." The mechanisms for these changes are now well described. Characteristic histologic changes have been demonstrated in the pulmonary microvasculature with hypertrophy of the medial smooth muscle, migration of smooth muscle distally into normally nonmuscularized small vessels, deposition of interstitial elements within the media, migration of smooth muscle cells through a disrupted internal elastic lamina, and ultimately severe destruction of the normal vascular architecture and the so-called "plexiform

lesion" [41]. Studies in humans and animal models show that the endothelium plays a central role in the genesis of pulmonary vascular disease. Endothelial-derived vasoactive messengers whose synthesis is deranged in pulmonary vascular disease contribute both to the alterations in the function of vascular smooth muscle and to the structural changes characteristic of this condition [40,42,43] (see Chapter 5).

An increase in volume loading of the left atrium and ventricle typically results from the excessive pulmonary flow and, in turn, the increased pulmonary venous return associated with a moderate or large VSD. This volume loading dilates the left atrium and particularly the left ventricle. In response to the increase in wall stress, left ventricular hypertrophy may ensue. Significant longstanding pulmonary hypertension may result in right ventricular hypertrophy and dilation, which then predominate as a patient enters the terminal stages of severe Eisenmenger syndrome.

Secondary structural cardiac abnormalities may contribute significantly to the course of patients with VSD. Defects located near the aortic valve may be complicated by the later association with aortic valve prolapse. It appears that prolapse occurs secondary to the generation of Venturi forces in which the high-velocity jet across a restrictive VSD "sucks" the aortic leaflet into the defect [44]. Anatomic factors including a lack of structural support for the valvar leaflet (for example, in the setting of a doubly committed defect) or abnormal commissural suspension may also predispose particular patients to this complication. The type of VSD in which aortic prolapse occurs is usually the doubly committed subarterial ventricular septal defect, but a perimembranous defect may be involved if the VSD lies immediately adjacent to the aortic valve, without an intervening septal remnant. With a doubly committed defect, the right coronary sinus is involved; with a perimembranous defect, either the right or the noncoronary sinus is affected (or rarely both are). The consequence of aortic prolapse over time is the development of aortic regurgitation, which, if left untreated, may worsen the degree of left ventricular dilation.

The development of mid-cavity obstruction of the right ventricle due to hypertrophy of muscle bands creates the entity known as double-chambered right ventricle. This occurs in ~3%, according to the Joint Studies on the Natural History of Congenital Heart Disease [45,46], but may be higher [47]. The key pathophysiologic characteristic of this condition, which may represent accentuated septoparietal trabeculations [48], is the creation of a proximal "high-pressure" chamber and a distal "low-pressure" chamber within the cavity of the right ventricle. There is a well-recognized association between double-chambered right ventricle and membranous subaortic stenosis [49]. In a study of 21 patients with double-chambered right ventricle and VSD, the defect was perimembranous in 18, muscular in two and doubly committed in one. The defect was proximal to the muscle bundle in 13 and distal in eight

[50]. A right aortic arch [51] or a more horizontal pulmonary outflow tract [52] may be a risk factor for acquired right ventricular outflow tract obstruction.

Clinical features

Clinical history

Many infants with a VSD are asymptomatic at the time of presentation and come to notice when a murmur is detected on auscultation, either in the neonatal period or later. At least 75% of affected patients have a defect that is small with a hemodynamically insignificant left-to-right shunt, remain asymptomatic, and continue to feed and thrive normally. If careful assessment of such patients confirms that the shunt is small and that the heart is not subjected to significant volume loading, or associated anomalies of the outflow tracts or valvar dysfunction, there is little likelihood of symptoms developing, and the family may be reassured accordingly. Most infants with a larger VSD (except those in whom pulmonary resistance never falls) typically become symptomatic at between 2 and 6 weeks of age [53]. At this time, pulmonary resistance falls, and the increased pulmonary blood flow and venous return to the left atrium lead to the onset of pulmonary venous congestion with tachypnea, dyspnea, and feeding difficulties. The increased caloric demands resulting from the combination of high cardiac output and increased respiratory effort are further compounded by the difficulty in feeding. These infants typically fail to thrive.

Associated abnormalities may alter the clinical symptoms substantially. For instance, coexisting coarctation of the aorta usually leads to an earlier clinical presentation, often as the ductus closes in the first days of life. These infants typically present with dyspnea, poor feeding, and rapid progression to severe manifestations of systemic hypoperfusion and respiratory failure.

Physical examination

The typical murmur associated with VSD is described as a high-pitched murmur which usually occupies most, or all, of systole (pansystolic). In the early neonatal period, a small, restrictive defect may not always produce a typical murmur, and instead the murmur may be of medium frequency and occur in early to mid systole. The murmur generally becomes more characteristic over the next few weeks. There are usually few if any other abnormal findings on clinical examination of patients with a small defect. A thrill is present when the murmur is sufficiently loud. The murmur and thrill are usually most evident along the left sternal border, although the site of maximal intensity varies. An apical VSD may produce a murmur that is best heard toward the apex and may be mistaken for the murmur of mitral regurgitation.

With a larger VSD, the clinical findings are often different. In the early neonatal period and for several weeks, there may be no murmur or only a soft, nonspecific ejection murmur. As the shunt increases with gradual fall in pulmonary vascular resistance, the murmur becomes louder, often longer, and occupying more of systole. At the same time, with the increasing size of the left-to-right shunt, the heart becomes increasingly hyperdynamic. This is associated with a palpable systolic impulse at the left sternal edge due to the dilated and hypertensive right ventricle. At the apex, a mid-diastolic murmur due to high flow across the mitral valve becomes audible. With pulmonary hypertension, the pulmonic component of the second sound is accentuated. During this time, most infants become increasingly dyspneic and tachypneic and may manifest marked intercostal and subcostal retractions. Chronic dyspnea may result in the appearance of bilateral Harrison's sulci (horizontal depression across the lower thorax corresponding to insertion of diaphragm). These infants typically fail to thrive, falling away from their height and weight curves on a growth chart, and even occasionally from the curve of head circumference, and feed poorly, becoming sweaty on minimal exertion or on feeding.

Electrocardiographic features

The electrocardiogram (ECG) reflects the effect of the VSD on the cardiac chambers and pulmonary vasculature. With a small defect, the ECG may be normal. Left axis deviation occurs in a few patients and may reflect abnormal distribution of the left bundle branch [54]. Without other electrocardiographic abnormalities, it is usually of no sinister significance, but if partial or complete right bundle branch block coexists with a superior QRS axis, an atrioventricular septal defect or VSD of atrioventricular septal defect type should be excluded.

If the VSD is associated with a moderate or large shunt, the ECG manifests evidence of combined ventricular hypertrophy with increased left ventricular voltages along with prominent right ventricular forces or large combined voltages (R + S) in the mid-chest leads (V3, V4) (Katz–Wachtel phenomenon). Left atrial enlargement is also found in some patients. Left ventricular hypertrophy on voltage criteria may occur, especially in later childhood, usually indicating a significant shunt but nearly normal pulmonary resistance. Isolated right ventricular hypertrophy is a feature of infants with associated infundibular stenosis (similar to tetralogy of Fallot) or of patients with severe established pulmonary vascular disease (Eisenmenger's syndrome).

Chest X-ray

The chest radiograph reflects the hemodynamic disturbance associated with a VSD. Normal cardiac size and normally pulmonary vascular markings suggest only a minor left-to-right shunt and as such a hemodynamically unimportant defect.

(a)   (b)
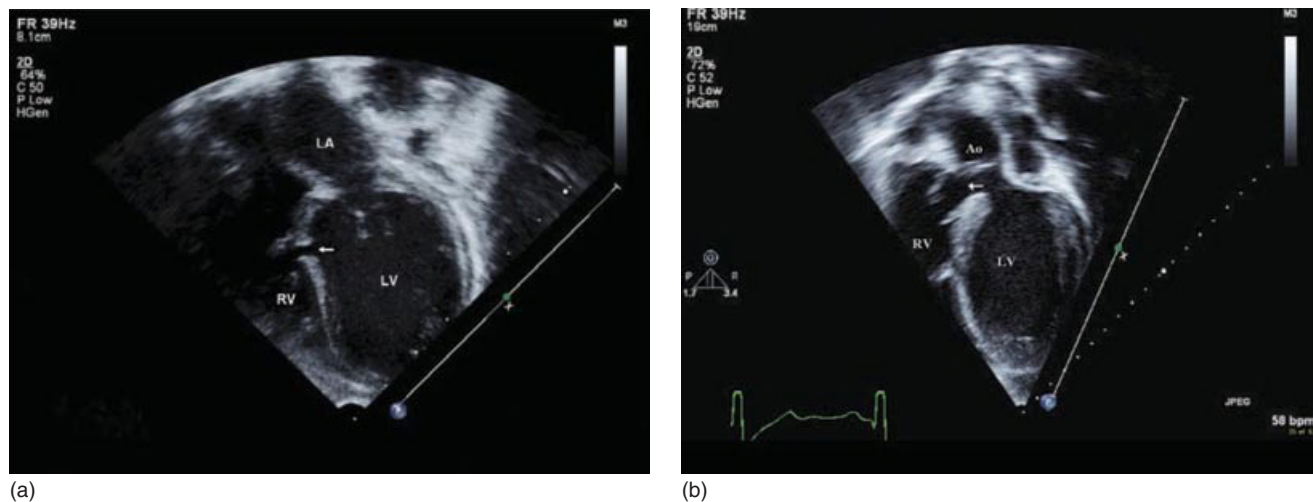
Figure 23.2 Echocardiograms from a patient with a muscular (a) and a perimembranous defect (b) taken from an apical and subcostal window. Ao, aorta; LA, left atrium; LV, left ventricle; RV, right ventricle

An increase in the transverse cardiac diameter usually indicates a significant shunt. The left ventricular apex is displaced laterally and inferiorly. The left atrium may be enlarged, producing flattening (upward displacement) of the left main bronchus and sometimes a double shadow over the right atrium. Increased pulmonary blood flow indicated by pulmonary arterial markings is evident as cross-sections of hilar vessels, which are distinctly larger than their accompanying bronchi. Prominent vessels are usually seen well out into the middle and upper zones of the lung, whereas such markings are seen only in the lower zones (particularly on the right side) in a normal chest radiograph. Hyperinflation is frequently seen in an infant with a large shunt and probably reflects altered airway resistance and compliance. Pulmonary congestion with interstitial edema may appear, and infective changes may be superimposed.

As pulmonary vascular obstructive disease develops, there may be a reduction in cardiac size toward normal, but the central pulmonary vascular markings become prominent and the peripheral pulmonary vascularity (beyond the hilar areas) become reduced ("pruned").

Echocardiography

A comprehensive echocardiogram is the mainstay of the diagnosis in most cardiac units. The goals of the echocardiographic examination, which would be part of a full segmental, sequential study, are to provide information about
• the location, size, and numbers of defects, whether they are restrictive and whether there are any indicators of their likelihood to close spontaneously
• the pulmonary-to-systemic flow ratio and the right ventricular systolic pressure

• the degree of volume loading of the left heart and left ventricular size
• the presence of aortic valvar prolapse, double-chambered right ventricle or straddling of an atrioventricular valve
• associated subpulmonary, or subaortic (with or without arch) obstruction.

The echocardiographer should be able to conceptualize the shape of the ventricular septum by integrating the multiple cross-sectional images to delineate the size of the defects and their relationship with surrounding structures. The newer technique of three-dimensional echocardiography may facilitate this integration [55,56].

The location of the defect can be determined from cross-sectional imaging. Depending on the location of the defect within the septum, this may be from subcostal, apical, or parasternal windows (Figure 23.2) (Videoclips 23.1 and 23.2). Small defects may only be detected on color Doppler, and finding one muscular defect should prompt the search for more, as these are commonly multiple. The parasternal short-axis projection is particularly important for demonstrating fibrous continuity between the tricuspid and aortic valves to distinguish a perimembranous defect from a muscular defect. This projection is also the best for demonstrating fibrous continuity between the aortic and pulmonary valves in a doubly committed defect, and for demonstrating a deviated outlet septum in defects with outlet extension.

VSDs are rarely circular and, in assessing the size of the defect, its dimensions should be examined in multiple projections. The cross-sectional area of the defect can be related to that of the aorta or to the body surface area [57]. In patients with a perimembranous VSD, it is worth noting whether the defect is related to aneurysmal tissue, which, with time, will tend to close it. This may be demonstrated using either a parasternal short-axis view or an apical four-chamber view. The apical projection is also used to

determine the degree of offsetting of the atrioventricular valves which will be deficient in patients with defects that extend into the inlet septum. Under these circumstances, it is particularly important to examine the morphology of the left atrioventricular valve to distinguish a ventricular septal defect with inlet extension from an atrioventricular septal defect, the latter characterized by a trifoliate left atrioventricular valve.

The accurate assessment of the pulmonary-to-systemic flow ratio by echocardiography would be welcomed by clinicians. It is theoretically possible to do this by examining the flow velocity profiles through the aortic and pulmonary valves, combined with an estimate of their cross-sectional areas. In general, however, the confidence limits around these estimates are wide and, as a result, they are rarely used routinely in clinical decision making. Continuous-wave Doppler interrogation of the flow velocity across a VSD, in the parasternal long- or short-axis projections, or sometimes a subcostal view, allows determination of the pressure drop across the defect. With a left-to-right shunt, higher velocities between left and right ventricles indicate a lower right ventricular systolic pressure. Where possible, this assessment should be combined with an examination of peak velocity of the tricuspid regurgitation jet, so that an estimate of right ventricular systolic pressure can be obtained and the relationship between the ventricular pressures can be clarified.

The degree of volume loading of the left atrium and ventricle can be assessed from parasternal windows and from M-mode measurement of the left ventricular dimensions on the short-axis projection. The left ventricular end-diastolic dimension is usually normalized to the body surface area and a Z-score derived.

In patients with VSD, associated aortic valve prolapse or regurgitation can be assessed using apical and parasternal projections. These views can also be used to detect obstruction within the cavity of the right ventricle (double-chambered right ventricle) or straddling of either the tricuspid or mitral valve. Where straddling exists, it is particularly important to measure the orifices of both atrioventricular valves.

Anterior deviation of the outlet septum may be associated with subpulmonary obstruction; whereas posterior deviation beneath the aortic valve may result in muscular subaortic stenosis (Videoclip 23.3) Parasternal short- and long-axis views can be used to confirm or exclude these important associations. In patients with posterior deviation of the outlet septum and subaortic obstruction, it is imperative to examine the aortic arch carefully, to exclude coexisting coarctation or interruption. With a large VSD, the velocity of flow across the aortic valve cannot provide an accurate estimate of the degree of its obstruction.

Intraoperative transesophageal echocardiography is widely used during surgical closure of VSD to locate defects, assess the surgical result, and detect residual defects. A recent study of 690 patients undergoing VSD closure revealed residual defects using transesophageal echocardiography in 260. Most were trivial, however, and closed spontaneously on follow-up. Reoperation was rarely needed [58]. Transesophageal echocardiography is considered essential by many operators in guiding transcatheter closure of VSDs.

Cardiac catheterization and angiography

Diagnostic cardiac catheterization is now rarely performed before VSD surgery, as echocardiography can provide accurate and detailed anatomic information. Nonetheless, there remain some patients for whom preoperative cardiac catheterization might be considered reasonable for both hemodynamic assessment and occasionally for additional profiling – particularly in those with multiple defects or associated abnormalities. Cardiac catheterization is occasionally performed to assess children in whom it is otherwise difficult to determine the severity of the hemodynamic disturbance. An example is an asymptomatic child with mild cardiomegaly and pulmonary plethora on chest X-ray, or with electrocardiographic changes. In this setting, cardiac catheterization helps decide whether it is safe to postpone an operation in the hope that the defect may become smaller or spontaneously close. Cardiac catheterization may also be indicated in patients with suspected pulmonary vascular disease, in order to decide about operability or for initiating medical therapy to manage this. Finally, cardiac catheterization may be therapeutic, with the intention of performing transcatheter closure of a defect (see below).

Hemodynamics

Hemodynamic measurements in a catheter study include oxygen saturations to assess the magnitude of the left-to-right shunt, or pulmonary-to-systemic flow ratio (Qp/Qs). Therefore, blood samples must be taken from the caval veins, a pulmonary vein (or left atrium, if it can be entered through a patent foramen or atrial septal defect), aorta, and pulmonary artery, including the main and branch pulmonary arteries.

Assessing pulmonary vascular resistance requires phasic and mean pressure measurements in the right atrium, left atrium (and pulmonary artery wedge pressure), main pulmonary artery, and aorta. In addition, phasic pressures in the left and right ventricles should be measured. Oxygen consumption should be measured in patients when calculating pulmonary resistance. Although assumed oxygen consumption values are commonly used, measured oxygen consumption in children may be very different from assumed values, resulting in significant errors in pulmonary resistance calculation [59].

In patients with elevated pulmonary vascular resistance, pulmonary vascular lability should be tested. In our laboratory, we do this by first ventilating the patient under conditions aimed at optimizing pulmonary vascular resistance–with 100% oxygen and 20 ppm of inhaled nitric oxide for at least 10 min, and then repeating the hemodynamic measurements. Decisions about suitability for repair with an elevated pulmonary resistance depend on the level of resting resistance, the evidence of lability or reversibility, and the patient's age. We consider that resistances $>8 \, U \, m^2$ $(mmHg \, l^{-1} \, min^{-1} \, m^{-2})$ under optimal conditions strongly indicate irreversible pulmonary vascular disease after the first year of life. Significant lability, with the level falling to $<6 \, U m^2$ in 100% oxygen, or with inhaled nitric oxide, and young age, however, are features that in otherwise borderline patients might favor operation.

Angiography

The anatomy and three-dimensional orientation of the ventricular septum and associated defects are complex. Thus, the effective angiographic demonstration of a VSD requires operators to have a detailed understanding of the anatomy of the ventricular septum in a normal heart and in a range of cardiac malformations. Using axial oblique views to profile the different parts of the ventricular septum accurately is now routine. The radiographic projection used must be aligned with the ventricular septum at the site of the defect, so that contrast medium passing across the defect is seen in profile. It is usually possible to identify the site or sites of VSDs with echocardiography before cardiac catheterization, thus making the choice of projection simpler.

Defects close to the membranous septum are best demonstrated by a left anterior oblique projection (40–45° from lateral) with moderate craniocaudal tilt (20°). This is not the conventional long-axial projection recommended for demonstrating a perimembranous VSD. The conventional projection (30° left anterior oblique with 15° craniocaudal tilt) is more useful for showing trabecular muscular, anterior muscular, or outlet muscular defects.

The so-called four-chamber view (16° left anterior oblique with 30° craniocaudal tilt) is used for profiling inlet defects and is particularly useful for demonstrating atrioventricular septal defects. A right anterior oblique projection is usually necessary to demonstrate doubly committed subarterial VSDs. When biplane angiography is used, the second plane produces a right oblique projection when the first plane is recorded in a long-axial, four-chamber, or intermediate projection. Thus, if an appropriate projection is obtained to exclude defects in the midmuscular, anterior muscular, outlet muscular, or perimembranous areas, the second projection will usually demonstrate a doubly committed subarterial defect.

The main requirement for angiography of a VSD is the need to identify multiple defects. Such defects can present a substantial challenge, both to the echocardiographer and to the cardiologist performing angiography. Multiple small muscular defects in the trabecular septum ("Swiss cheese" defects) are usually well demonstrated in a long-axial view. In some patients, however, several large defects are located at relatively distant sites within the septum. A moderate or large perimembranous defect may be accompanied by muscular defects at the apex or in the anterior muscular septum. Multiple axial oblique projections may be required to demonstrate all the defects adequately. A limiting factor, which may be difficult to surmount, is the equalization of ventricular pressures, so that shunting across the several defects may not be sufficient to outline each defect satisfactorily.

The angiographic study should always include attention to coexisting cardiovascular abnormalities that may require angiographic demonstration. Coexisting conditions, such as aortic coarctation or aortic regurgitation, may necessitate an aortogram, which will also help to confirm aortic valve prolapse and exclude an associated patent arterial duct. Right ventricular outflow obstruction or abnormalities of the pulmonary arteries, such as branch pulmonary artery stenosis, may necessitate a right ventricular angiogram or pulmonary arteriogram.

Other imaging modalities

Although comprehensive diagnostic information is provided by echocardiography in most patients, magnetic resonance imaging (MRI) may complete the diagnosis under some circumstances [60]. In an adult with a VSD, in whom echocardiographic imaging may be limited by suboptimal windows, MRI or computed tomography (CT) may improve the anatomic definition of the defect [61]. MRI and CT are useful adjunctive tools in the diagnosis of double-chambered right ventricle in an adult [62,63]. Associated extracardiac defects, such as aortic coarctation of the aorta or pulmonary artery stenosis, which may be difficult to demonstrate by echocardiography in older patients, can be demonstrated by these techniques. When the need for VSD closure is in question, MRI may provide an accurate assessment of the pulmonary-to-systemic flow ratio [64,65].

Management

Cardiac operation, generally by 3 months of age, is usually recommended for symptomatic infants with pulmonary hypertension, breathlessness, poor feeding, and failure to thrive. While awaiting surgery, improvement may result from low doses of diuretics with or without angiotensin-converting enzyme inhibitors. Digoxin is widely used, although we do not use it. The evidence base for these therapies is scanty. Blood pressure and renal function should be carefully monitored, because hypotension and renal failure are associated with medical therapy.

Frequently, patients with a VSD present with evidence of a volume-loaded left ventricle, from increased pulmonary flow, but without evidence of pulmonary hypertension. Many recommend surgical or transcatheter closure of these defects to avoid left ventricular dysfunction in the long term. In such patients without intervention over a follow-up period of 8 years, left ventricular end-diastolic dimension returned to normal levels in most [66]. The authors concluded that a conservative approach, with regular follow-up, might be appropriate for asymptomatic patients with a pressure-restrictive defects even with left ventricular dilation.

The outcome of asymptomatic patients without pulmonary hypertension or increased left ventricular volume loading treated conservatively is excellent. In patients with a VSD considered "not to require surgical closure during childhood" at mean age of 30 years, the mortality was zero, 94.6% remained symptom free and left ventricular size was normal or borderline in 99% [67]. The incidence of endocarditis was 1.8%.

Many small defects close or become smaller. One study of patients demonstrated that 68% of small or moderate muscular defects closed spontaneously, compared with 34% of perimembranous defects. Muscular defects closed spontaneously up to 88 months of age, but no perimembranous defect closed after the age of 62 months [68]. Muscular defects often close by ingrowth of muscle at the margins. Some perimembranous defects diminish in size, as discussed above. This process often produces a pouch of fibrous/leaflet tissue (aneurysm of the membranous septum), which can be seen by echocardiography or angiography, This is a favorable sign that spontaneous diminution in size or closure of the VSD is likely to occur.

Certain VSDs, however small, are unlikely to diminish in size or close spontaneously. These include defects in which semilunar leaflets of the aortic or pulmonary valve form the basal margin of the VSD, as occurs with many malalignment defects and doubly committed subarterial defects. Defects of the latter type may appear to be partially closed (and may be clinically small or trivial) by the distorted aortic sinus (usually the right coronary sinus) or semilunar leaflet tissue, which is entrapped in and partially occludes the septal defect.

A consensus has emerged regarding the management of patients with, or at risk of, aortic valve prolapse or regurgitation. We recommend that surgery not be delayed until the regurgitation becomes moderate or severe, as this will likely result in suboptimal repair and a higher likelihood of reoperation [69]. We recommend repair for patients with more than trivial aortic regurgitation. This recommendation applies particularly for patients with a juxta-arterial defect because of their high risk of aortic regurgitation and low rate of closing spontaneously.

Until recently, the treatment of patients with Eisenmenger syndrome was only supportive [70]. These patients should avoid dehydration and exposure to high altitudes, as this compounds the pre-existing hyperviscosity and arterial hypoxemia. Venesection to reduce the effects of polycythemia has been routine in many centers, but this may worsen exercise intolerance and iron deficiency and increase the risk of stroke [71]. Anticoagulation has been used in these patients, although the evidence is lacking about its application and the bleeding risk may be considerable [72]. Female patients must be made aware that pregnancy is associated with substantial maternal and fetal risk (see below).

The recognition of the contribution of endothelial dysfunction to the pathogenesis of Eisenmenger's syndrome has offered new therapeutic options and has revolutionized the pharmacological approach to their management [40]. Endothelial-based "advanced therapies" are being increasingly used to improve symptoms, quality of life, and survival in this condition. Two groups of pulmonary vasodilators are being used to treat patients with Eisenmenger's syndrome: inhibitors of the endothelial-derived vasoconstrictor endothelin-1, and drugs that enhance the nitric oxide–cyclic GMP pathway. The Breathe-5 study demonstrated that bosentan, an endothelin receptor antagonist, improved 6 min walk distances in a randomized placebo-controlled trial over 16 weeks [73] and this effect was continued in a subsequent open-label extension study [74,75]. Similarly, improvements in quality of life and functional capacity have been demonstrated in patients with Eisenmenger syndrome, in response to the oral phosphodiesterase-5 inhibitor sildenafil [76]. Advanced endothelial-based therapies enhance survival in these patients [77] (see Chapter 51).

These advances, combined with the observation that many patients with Eisenmenger syndrome respond to vasodilators in the catheterization laboratory [78], raise the possibility that aggressive treatment with endothelial-based therapies may make it possible to close a VSD in a previously inoperable patient. Despite favorable reports, systematic studies are lacking [79].

Surgery

Surgical closure is the mainstay of definitive treatment for an uncomplicated VSD. Surgery is performed through a midline sternotomy, generally with mild or moderately hypothermic cardiopulmonary bypass, with cardioplegic arrest. Bicaval cannulation allows direct visualization of the defect through the right atrium, facilitated by temporary detachment of the septal tricuspid valve leaflet [80]. The defect can be closed with a patch (generally autologous pericardium) or, if small, using interrupted or continuous sutures. Closure through one of the great arteries, particularly the pulmonary artery (a transpulmonary repair), is also fairly common. In patients with doubly committed defect with aortic regurgitation, a transaortic approach is used to close the defect and repair the aortic valve. Defects in the lower trabecular septum are sometimes approached through a short "fish-mouth" incision at the left ventricle apex. Closure through the right ventricle is rarely necessary. In

general, ventriculotomy is avoided as this increases the risk of ventricular dysfunction and arrhythmia.

The aim of surgical management is complete closure of the defect without damaging adjacent structures. The relationship between the conduction axis and the VSD is of particular importance. For muscular defects, the conduction axis is usually separated from the margin of the defect by a muscle bar, so that it is generally safe to place sutures around the margin of the defect without risk. For some muscular defects, however, this muscle bar might be fairly thin, placing the conduction axis at risk. The branching bundles of the conduction system can be close to the posterior and inferior margins of a perimembranous VSD. Suturing should be approached from the right ventricular side of the defect and away from its posteroinferior margin. Under some circumstances it might be possible to place very superficial sutures on the free margin of the defect [81]. Where a perimembranous defect is surrounded by fibrous tissue, it can usually be used to anchor the patch [81].

In patients previously considered inoperable due to elevated pulmonary vascular resistance, conventional patch closure can cause significant morbidity and mortality from intractable elevations in pulmonary arterial and right ventricular pressure, which result in right ventricular failure. A modified surgical technique with the creation of a "valved" patch which allows unidirectional right-to-left shunting across the residual shunt can be performed with low operative mortality [82]. The benefits of these methods over conventional closure have been questioned [83].

The postoperative course of most children after VSD closure is relatively uncomplicated, and mortality is exceedingly low. The postoperative period may be complicated by pulmonary hypertension – particularly in infants with very high preoperative pulmonary blood flow, with trisomy 21, or older infants with a large defect. Inhaled nitric oxide is commonly used to treat postoperative pulmonary hypertension [84], although there are few data supporting its use early after cardiac surgery [85]. Postoperative disturbances of rhythm affect a minority of patients early after surgery. A small proportion of patients require temporary pacing for postoperative atrioventricular conduction block. Failure to return to sinus rhythm within 7–10 days should prompt consideration of a permanent pacing system [86]. The long-term outlook for most children after surgery is excellent and quality of life is similar to that of age-matched controls. Behavioral and school performance problems may be increased in early childhood [87].

Banding of the pulmonary artery was previously performed as an initial palliative procedure to reduce pulmonary blood flow, particularly in small infants. This is now rarely performed except for patients with multiple or apical defects, in whom surgical access to the VSD(s) is difficult or impossible. There has been a recent trend to apply either absorbable or balloon-dilatable bands in patients with multiple muscular defects, possibly avoiding the necessity for band removal if the defects reduce in size or close spontaneously [88,89].

Transcatheter closure

Transcatheter techniques for VSD closure have been developed over the past decade. These are particularly useful for achieving closure of muscular defects which are difficult to access surgically. A variety of devices have been employed. Initially, double umbrellas, originally designed for closure of patent ductus arteriosus or atrial septal defects, were used [90,91]. More recently, specific septal occluders have been developed [92,93]. We always recommend the concomitant use of transesophageal echocardiography to guide the transcatheter closure. Right ventricular trabeculations can make crossing a muscular defect from its right ventricular side very challenging. Hence a double catheter technique is usually employed. A curved end-hole catheter is advanced through the defect from its left ventricular side via the femoral artery and aorta. A wire is passed through the catheter and the VSD to the right ventricle and pulmonary artery, where it is snared and exteriorized out of the internal jugular or femoral vein. This provides a stable "rail" along which a long delivery sheath can be advanced across the defect (Videoclip 23.4).

There has been considerable interest in transcatheter approaches for closure of perimembranous defects. Currently this approach is not used in most centers because of the unacceptable rate of post-procedure heart block associated with available devices (Figure 23.3). Of particular concern is that this risk does not appear to subside or decrease with time, with late-onset heart block being relatively prevalent [94,95]. It is possible that this approach may be reintroduced in the future as softer devices are developed.

Hybrid techniques

In smaller patients with muscular VSDs, in whom both transcatheter and standard surgical approaches are difficult, a hybrid technique combining surgery and transcatheter interventional methods has been introduced [96,97]. A sternotomy or a subxiphoid incision is performed. Under fluoroscopic and transesophageal guidance, the free wall of the right ventricle is punctured and a wire passed across the defect. An introducer sheath is passed over the wire with its tip placed in the left ventricle and the device is introduced through the sheath and deployed across the defect [96].

Long-term issues in treated and untreated adults

Exercise

Patients with a small defect and normal left ventricular function and pulmonary arterial pressure, without associated lesions, should have a normal exercise tolerance and
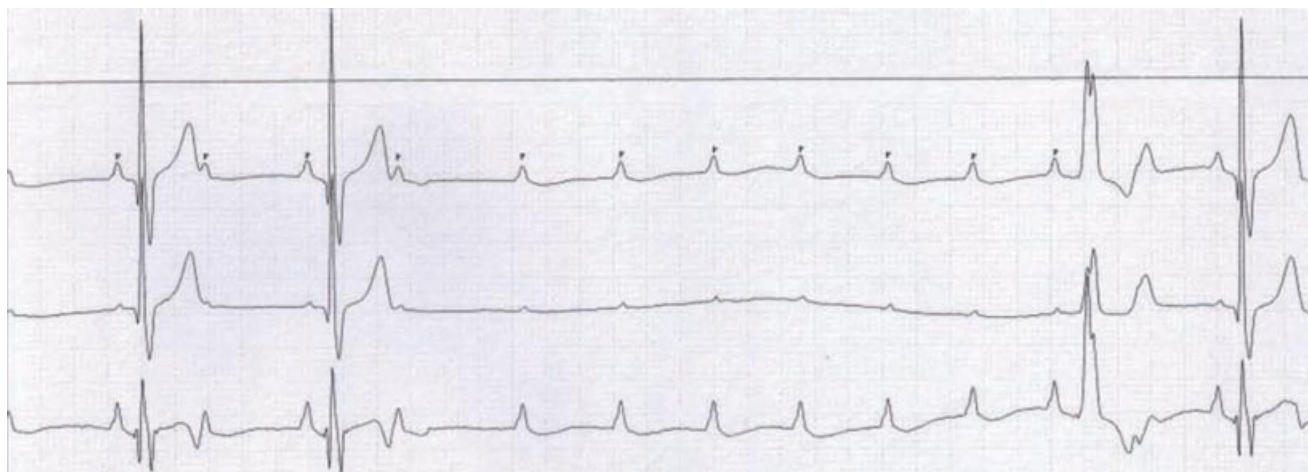
Figure 23.3 Ambulatory electrocardiogram from a patient who presented with new-onset syncope, 2 years after transcatheter closure of a perimembranous VSD, demonstrating complete heart block.

exercise restrictions are unnecessary. Patients with elevated pulmonary arterial pressure may have impaired exercise tolerance, and generally self-restrict their exercise levels. Exercise studies in adults showed that in those with Eisenmenger syndrome the peak levels of oxygen consumption were among the lowest of all patients. The relative reduction in peak oxygen consumption correlated with their long-term outcome [98].

Endocarditis

Traditionally, antibiotic prophylaxis was recommended to prevent procedure-associated endocarditis in patients with VSD. However, more recent evidence indicates that endocarditis is more likely to result from chronically poor oral hygiene. Moreover, there is very little evidence to support the efficacy of prophylactic antibiotics in patients with congenital heart disease. Recent guidelines for prophylaxis do not recommend that patients with a VSD receive antibiotic prophylaxis [99]. The primary prevention of dental infections, with careful daily dental hygiene and regular dental review, should be emphasized. Antibiotic prophylaxis for dental and other procedures is still recommended for 6 months after complete surgical or transcatheter closure of a VSD and indefinitely for a residual defect related to patch material which may inhibit endothelialization.

Pregnancy

Women with a small VSD and normal left ventricular function and pulmonary arterial pressures appear not to be at increased cardiovascular risk during pregnancy. Those with a moderate defect may experience symptoms related to increased pulmonary flow because of the increased circulatory volume during pregnancy. This may be compensated partially by the associated reduction in systemic vascular resistance. In women with Eisenmenger syndrome, pregnancy has an extremely high risk of maternal and fetal death and of premature delivery [100]. In one series of 17 ongoing pregnancies in 10 women with Eisenmenger syndrome, there was one maternal death, and in another patient there was severe maternal deterioration necessitating high-level intensive care. Four pregnancies resulted in spontaneous abortions, and there was one stillbirth. Ten of the 12 deliveries of live infants occurred prematurely [101]. As a result, women with Eisenmenger syndrome should be strongly counseled to avoid pregnancy and should be referred to a specialist for contraception advice [102]. Sterilization may be deemed appropriate for some, although this should be undertaken in a specialist center for the care of adults with congenital heart disease, as any surgical procedure requiring an anesthetic poses additional risk on these patients.

Acknowledgment

References

1 Farre JR. *Malformations of the Human Heart*. London: Hurst, Orme, Brown, 1814.
2 Fallot A. Contribution à l'anatomie pathologique de la maladie bleue (cyanose cardiaque). *Marseille Med* 1888;**25**:77.
3 Roger H. Recherches cliniques sur la communication congenitale des deux coeurs, par inocclusion du septum interventriculaire. *Bull Acad Med Paris* 1879;**8**:1074.
4 Eisenmenger V. Die angeborenen Defecte der Kammersscheidewand des Herzens. *Z Klin Med* 1897;**32**(Suppl):1–28.

5 Wood P, Magidson O, Wilson PA. Ventricular septal defect with a note on acyanotic Fallot's tetralogy. *Br Heart J* 1954;**16**:387–406.

6 Heath D, Edwards JE. The pathology of hypertensive pulmonary vascular disease: a description of six grades of structural changes in the pulmonary arteries with special reference to congenital cardiac septal defects. *Circulation* 1958;**18**:533–47.

7 Heath D, Helmholz HF Jr, Burchell HB, *et al.* Graded pulmonary vascular changes and hemodynamic findings in cases of atrial and ventricular septal defect and patent ductus arteriosus. *Circulation* 1958;**18**:1155–66.

8 Campbell M. Natural history of ventricular septal defect. *Br Heart J* 1971;**33**:246–57.

9 Dickinson DF, Arnold R, Wilkinson JL. Ventricular septal defect in children born in Liverpool 1960 to 1969. *Br Heart J* 1981;**46**:47–54.

10 Hoffman JIE, Christianson R. Congenital heart disease in a cohort of 19,502 births with long term follow up. *Am J Cardiol* 1978;**42**:641–7.

11 DeVore GR, Horenstein J, Siassi B, Platt LD. Fetal echocardiography. VII. Doppler color flow mapping: a new technique for the diagnosis of congenital heart disease. *Am J Obstet Gynecol* 1987;**156**:1054–64.

12 Lin MH, Wang NK, Hung KL, Shen CT. Spontaneous closure of ventricular septal defects in the first year of life. *J Formos Med Assoc* 2001;**100**:539–42.

13 Perry LW, Neill CA, Ferencz C, *et al.* Infants with congenital heart disease: the cases. In: Ferencz C, Rubin JD, Loffredo CA, Magee CA, eds. *Perspectives in Pediatric Cardiology. Vol. 4. Epidemiology of Congenital Heart Disease. The Baltimore–Washington Infant Study.* New York: Futura Publishing, 1997: 33–62.

14 Hoffman JIE. Incidence of congenital heart disease. 1. Postnatal incidence. *Pediatr Cardiol* 1995;**16**:103–13.

15 Šamánek M, Voříšková M. Congenital heart disease among 815569 children born between 1980 and 1990 and their 15-year survival: a prospective Bohemia survival study. *Pediatr Cardiol* 1999;**20**:411–17.

16 Jackson M, Walsh KP, Peart I, Arnold R. Epidemiology of congenital heart disease in Merseyside – 1978–1988. *Cardiol Young* 1996;**6**:281–90.

17 Roguin N, Du ZD, Barak M, Nasser N, *et al.* High prevalence of muscular ventricular septal defect in neonates. *J Am Coll Cardiol* 1995;**26**:1545–8.

18 Nora JJ. Multifactorial inheritance hypothesis for the etiology of congenital heart diseases. The genetic–environmental interaction. *Circulation* 1968;**38**:604–17.

19 Øyen N, Poulsen G, Boyd HA, *et al.* Recurrence of congenital heart defects in families. *Circulation* 2009;**120**:295–301.

20 Nora JJ, Gilliland JC, Sommerville RJ, McNamara DG. Congenital heart disease in twins. *N Engl J Med* 1967;**277**:568–71.

21 Newman TB. Etiology of ventricular septal defects: an epidemiologic approach. *Pediatrics* 1985;**76**:741–9.

22 Pierpont ME, Basson CT, Benson DW, *et al.* Genetic basis for congenital heart defects: current knowledge: a scientific statement from the American Heart Association Congenital Cardiac Defects Committee, Council on Cardiovascular Disease in the Young. *Circulation* 2007;**115**:3015–38.

23 Bruneau BG. The developmental genetics of congenital heart disease. *Nature* 2008;**451**:943–8.

24 Srivastava D, Olson EN. A genetic blueprint for cardiac development. *Nature* 2000;**407**:221–6.

25 Benson DW. Genetic origins of pediatric heart disease. *Pediatr Cardiol* 2010;**31**:422–9.

26 Maitra M, Schluterman MK, Nichols HA, *et al.* Interaction of GATA4 and GATA6 with TBX5 is critical for normal cardiac development. *Dev Biol* 2009;**326**:368–77.

27 Basson CT, Bachinsky DR, Lin RC, *et al.* Mutations in human TBX5 [corrected] cause limb and cardiac malformation in Holt–Oram syndrome. *Nat Genet* 1997;**15**:30–5.

28 Li QY, Newbury-Ecob RA, Terrett JA, *et al.* Holt–Oram syndrome is caused by mutations in TBX**5**: a member of the Brachyury (T) gene family. *Nat Genet* 1997;**15**:21–9.

29 Liu C-X, Shen A-D, Li X-F, *et al.* Association of TBX5 gene polymorphism with ventricular septal defect in the Chinese Han population. *Chin Med J* 2009;**122**:30–4.

30 Zhang W-M, Li X-F, Ma Z-Y, *et al.* GATA4 and NKX2.5 gene analysis in Chinese Uygur patients with congenital heart disease. *Chin Med J* 2009; **122**:416–9.

31 Zhang W, Li X, Shen A, *et al.* GATA4 mutations in 486 Chinese patients with congenital heart disease. *Eur J Med Genet* 2008;**51**:527–35.

32 Rajagopal SK, Ma Q, Obler D, *et al.* Spectrum of heart disease associated with murine and human GATA4 mutation. *J Mol Cell Cardiol* 2007;**43**:677–85.

33 Jenkins KJ, Correa A, Feinstein JA, *et al.* Noninherited risk factors and congenital cardiovascular defects: current knowledge: a scientific statement from The American Heart Association Council on Cardiovascular Disease in The Young. *Circulation* 2007;**115**:2995–3014.

34 Contreras-Ramos A, Sánchez-Gómez C, García-Romero HL, Cimarosti LO. Normal development of the muscular region of the interventricular septum – I. Significance of the ventricular trabeculations. *Anat Histol Embryol* 2008;**37**:344–51.

35 Grant PR. The embryology of ventricular flow pathways in man. *Circulation* 1962;**25**:756–79.

36 Goor AD, Edwards JE, Lillehei W. The development of the interventricular septum of the human heart: correlative morphogenetic study. *Chest* 1970;**58**:453–67.

37 de la Cruz MV, Quero-Jiménez M, Arteaga MM, Cayré R. Morphogenese du septum interventriculaire. *Coeur* 1982; **13**:442–8.

38 de la Cruz MV, Moreno-Rodriguez R. Embryological development of the apical trabeculated region of both ventricles. The contribution of the primitive interventricular septum in ventricular septation. In: de la Cruz MV, Markwald R, eds. *Living Morphogenesis of The Heart*. Basel: Birkhäuser, 1998: 120–30.

39 Anderson RH, Wilcox BR. The surgical anatomy of ventricular septal defect. *J Card Surg* 1992;**7**:17–35.

40 Beghetti M, Galiè N. Eisenmenger syndrome. A clinical perspective in a new therapeutic era of pulmonary arterial hypertension. *J Am Coll Cardiol* 2009;**53**:733–40.

41 Rondelel B, Naeije R. Pathophysiology of pulmonary arterial hypertension associated with congenital heart disease. In: Beghetti M, Barst RJ, Naeije R, Rubin LJ, eds. *Pulmonary Arterial Hypertension Related to Congenital Heart Disease*. Munich: Urban and Fischer, 2006: 19–36.

42 Oishi PE, Wiseman DA, Sharma S, *et al.* Progressive dysfunction of nitric oxide synthase in a lamb model of chronically increased pulmonary blood flow: a role for oxidative stress. *Am J Physiol Lung Cell Mol Physiol* 2008;**295**:L756–66.

43 Diller GP, van Eijl S, Okonko DO, *et al.* Circulating endothelial progenitor cells in patients with Eisenmenger syndrome and idiopathic pulmonary arterial hypertension. *Circulation* 2008;**117**:3020–30.

44 Tweddell JS, Pelech AN, Frommelt PC. Ventricular septal defect and aortic valve regurgitation: pathophysiology and indications for surgery. *Semin Thorac Cardiovasc Surg Pediatr Card Surg Annu* 2006;147–52.

45 Nadas AS. Report from the Joint Study on the Natural History of Congenital Heart Defects. *Circulation* 1977;**56**(2 Suppl I):1–87.

46 O'Fallon WM, Weidman WH. Long-term follow-up of congenital aortic stenosis, pulmonary stenosis and ventricular septal defect. Report from the Second Joint Study on the Natural History of Congenital Heart Defects. *Circulation* 1993;**87**(2 Suppl I):1–121.

47 Corone P, Doyon F, Gaudeau S, *et al.* Natural History of ventricular septal defect. A study involving 790 cases. *Circulation* 1977;**55**:908–15.

48 Alva C, Ho SY, Lincoln CR, *et al.* The nature of the obstructive muscular bundles in double-chambered right ventricle. *J Thorac Cardiovasc Surg* 1999;**117**:1180–9.

49 Vogel M, Smallhorn JF, Freedom RM, *et al.* An echocardiographic study of the association of ventricular septal defect and right ventricular muscle bundles with a fixed subaortic abnormality. *Am J Cardiol* 1988;**61**:857–60.

50 Hubail ZJ, Ramaciotti C. Spatial relationship between the ventricular septal defect and the anomalous muscle bundle in a double-chambered right ventricle. *Congenit Heart Dis*. 2007;**2**:421–3.

51 Varghese PJ, Allen JR, Rosenquist GC, Rowe RD. Natural history of ventricular septal defect with right-sided aortic arch. *Br Heart J* 1970;**32**:537–46.

52 Tyrrell MD, Kidd BSL, Keith JD. Diagnosis of tetralogy of Fallot in the acyanotic phase. *Circulation* 1970;**41**(Suppl III):113.

53 Rudolph AM. Circulatory adjustments after birth: effects on ventricular septal defect. *Br Heart J* 1971;**33**(Suppl):32–4.

54 Gumbiner CH, Gillette PC, Garson A. *Pediatric Cardiac Dysrhythmias.* New York: Grune & Stratton, 1981.

55 Mercer-Rosa L, Seliem MA, Fedec A, *et al.* Illustration of the additional value of real-time 3-dimensional echocardiography to conventional transthoracic and transesophageal 2-dimensional echocardiography in imaging muscular ventricular septal defects: does this have any impact on individual patient treatment? *J Am Soc Echocardiogr* 2008;**19**:1511–9.

56 Chen FL, Hsiung MC, Nanda N, Hsieh KS, Chou MC. Real time three-dimensional echocardiography in assessing ventricular septal defects: an echocardiographic–surgical correlative study. *Echocardiography* 2006;**23**:562–8.

57 Shirali GS, Smith EO, Geva T. Quantitation of echocardiographic predictors of outcome in infants with isolated ventricular septal defect. *Am Heart J* 1995;**130**:1228–35.

58 Hanna BM, El-Hewala AA, Gruber PJ, *et al.* Predictive value of intraoperative diagnosis of residual ventricular septal defects by transesophageal echocardiography. *Ann Thorac Surg* 2010;**89**:1233–7.

59 Li J, Bush A, Schulze-Neick I, *et al.* Measured versus estimated oxygen consumption in ventilated patients with congenital heart disease: the validity of predictive equations. *Crit Care Med* 2003;**31**:1235–40.

60 Vick GW. Recent advances in pediatric cardiovascular MRI. *Curr Opin Pediatr* 2003;**15**:454–62.

61 Kilner PJ, Geva T, Maemmerer H, *et al.* Recommendations for cardiovascular magnetic resonance in adults with congenital heart disease from the respective working groups of the European Society of Cardiology. *Eur Heart J* 2010;**31**:794–805.

62 Lascano ME, Schaad MS, Moodie DS, Murphy D Jr. Difficulty in diagnosing double-chambered right ventricle in adults. *Am J Cardiol* 2001;**88**:816–9.

63 Sarikouch S, Schaeffler R, Blanz U, *et al.* Adult congenital heart disease – double-chambered right ventricle. *Clin Res Cardiol* 2007;**96**:582–4.

64 Beerbaum P, Körperich H, Barth P, *et al.* Noninvasive quantification of left-to-right shunt in pediatric patients: phase-contrast cine magnetic resonance imaging compared with invasive oximetry. *Circulation* 2001;**103**:2476–82.

65 Körperich H, Gieseke J, Barth P, *et al.* Flow volume and shunt quantification in pediatric congenital heart disease by real-time magnetic resonance velocity mapping: a validation study. *Circulation* 2004;**109**:1987–93.

66 Kleinman CS, Tabibian M, Starc TJ, *et al.* Spontaneous regression of left ventricular dilation in children with restrictive ventricular septal defects. *J Pediatr* 2007;**150**:583–6.

67 Gabriel HM, Heger M, Innerhofer P, *et al.* Long-term outcome of patients with ventricular septal defect considered not to require surgical closure during childhood. *J Am Coll Cardiol* 2002;**39**:1066–71.

68 Turner SW, Hornung T, Hunter S. Closure of ventricular septal defects: a study of factors influencing spontaneous and surgical closure. *Cardiol Young* 2002;**12**:357–63.

69 Kostolny M, Schreiber C, von Arnim V, *et al.* Timing of repair in ventricular septal defect with aortic insufficiency. *Thorac Cardiovasc Surg* 2006;**54**:512–5.

70 Kumar RK, Sandoval J. Advanced pulmonary vascular disease: the Eisenmenger syndrome. *Cardiol Young* 2009;**19**:622–6.

71 Ammash N, Warnes CA. Cerebrovascular events in adult patients with cyanotic congenital heart disease. *J Am Coll Cardiol* 1996;**28**:768–72.

72 Galiè N, Manes A, Palazzini M, *et al.* Management of pulmonary arterial hypertension associated with congenital systemic-to-pulmonary shunts and Eisenmenger's syndrome. *Drugs* 2008;**68**:1049–66.

73 Galiè N, Beghetti M, Gatzoulis MA, *et al.* Bosentan therapy in patients with Eisenmenger syndrome: a multicenter, double-blind, randomized, placebo-controlled study. *Circulation* 2006;**114**:48–54.

74 Gatzoulis MA, Beghetti M, Galiè N, *et al.* Longer-term bosentan therapy improves functional capacity in Eisenmenger syndrome: results of the BREATHE-5 open-label extension study. *Int J Cardiol* 2008;**127**:27–32.

75 van Loon RLE, Hoendermis ES, Duffels MGJ, *et al.* Long-term effect of bosentan in adults versus children with pulmonary arterial hypertension associated with systemic-to-pulmonary shunt: does the beneficial effect persist? *Am Heart J* 2007;**154**:776–82.

76 Tay EL, Papaphylactou M, Diller GP, *et al.* Quality of life and functional capacity can be improved in patients with Eisenmenger syndrome with oral sildenafil therapy. *Int J Cardiol* 2010; in press.

77 Dimopoulos K, Inuzuka R, Goletto S, *et al.* Improved survival among patients with Eisenmenger syndrome receiving advanced therapy for pulmonary arterial hypertension. *Circulation* 2010;**121**:20–5.

78 Limsuwan A, Khosithseth A, Wanichkul S, Khowsathit P. Aerosolized iloprost for pulmonary vasoreactivity testing in children with long-standing pulmonary hypertension related to congenital heart disease. *Catheter Cardiovasc Interv* 2009;**73**:98–104.

79 Dimopoulos K, Peset A, Gatzoulis MA. Evaluating operability in adults with congenital heart disease and the role of pretreatment with targeted pulmonary arterial hypertension therapy. *Int J Cardiol* 2008;**129**:163–71.

80 Sasson L, Katz MG, Ezri T, *et al.* Indications for tricuspid valve detachment in closure of ventricular septal defect in children. *Ann Thorac Surg* 2006;**82**:958–63.

81 Van Doorn C, de Leval MR. Ventricular septal defect. In: Stark J, de Leval MR, Tsang VT, eds. *Surgery for Congenital Heart Defects.* Chichester: John Wiley & Sons, Ltd., 2006: 355–72.

82 Novick WM, Sandoval N, Lazorhysynets VV, *et al.* Flap valve double patch closure of ventricular septal defects in children with increased pulmonary vascular resistance. *Ann Thorac Surg* 2005;**79**:21–8.

83 Gan H-L, Zhang J-Q, Zhang Z-G, *et al.* The unidirectional valve patch provides no benefits to early and long-term survival in patients with ventricular septal defect and severe pulmonary artery hypertension. *J Thorac Cardiovasc Surg* 2010;**139**:950–5.

84 Russell IA, Zwass MS, Fineman JR, *et al.* The effects of inhaled nitric oxide on postoperative pulmonary hypertension in infants and children undergoing surgical repair of congenital heart disease. *Anesth Analg* 1998;**87**:46–51.

85 Bizzarro M, Gross I. Inhaled nitric oxide for the postoperative management of pulmonary hypertension in infants and children with congenital heart disease. *Cochrane Database Syst Rev* 2005;CD005055.

86 Villain E. Indications for pacing in patients with congenital heart disease. *Pacing Clin Electrophysiol.* 2008;**31**(Suppl I):S17–20.

87 Hövels-Gürich HH, Konrad K, Skorzenski D, *et al.* Long-term neurodevelopmental outcome and exercise capacity after corrective surgery for tetralogy of Fallot or ventricular septal defect in infancy. *Ann Thorac Surg* 2006;**81**:958–66.

88 Bonnet D, Patkaï J, Tamisier D, *et al.* A new strategy for the surgical treatment of aortic coarctation associated with ventricular septal defect in infants using an absorbable pulmonary artery band. *J Am Coll Cardiol* 1999;**34**:866–70.

89 Brown S, Boshoff D, Rega F, *et al.* Dilatable pulmonary artery banding in infants with low birth weight or complex congenital heart disease allows avoidance or postponement of subsequent surgery. *Eur J Cardiothorac Surg* 2010;**37**:296–301.

90 Rigby ML, Redington AN. Primary transcatheter umbrella closure of perimembranous ventricular septal defect. *Br Heart J* 1994;**72**:368–71.

91 Lock JE, Block PC, McKay RG, *et al.* Transcatheter closure of ventricular septal defects. *Circulation* 1988;**78**:361–8.

92 Thanopoulos BD, Tsaousis GS, Konstadopoulou GN, *et al.* Transcatheter closure of muscular ventricular septal defects with the Amplatzer ventricular septal defect occluder: initial clinical applications in children. *J Am Coll Cardiol* 1999;**33**:1395–9.

93 Tofeig M, Patel RG, Walsh KP. Transcatheter closure of a mid-muscular ventricular septal defect with an Amplatzer VSD occlusion device. *Heart* 1999;**81**:438–40.

94 Dumitrescu A, Lane GK, Wilkinson JL, *et al.* Trancatheter closure of perimembranous ventricular septal defect. *Heart* 2007;**93**:867.

95 Collins NJ, Benson L, Horlick E. Late complete heart block in an adult patient undergoing percutaneous ventricular septal defect closure. *J Invasive Cardiol* 2008;**20**:E200–3.

96 Bacha EA, Cao QL, Starr JP, *et al.* Perventricular device closure of muscular septal defects on the beating heart: technique and results. *J Thorac Cardiovasc Surg* 2003;**126**:1718–23.

97 Crossland DS, Wilkinson JL, Cochrane AD, *et al.* Initial results of primary device closure of large muscular ventricular septal defects in early infancy using perventricular access. *Catheter Cardiovasc Interv* 2008;**72**:386–91.

98 Diller G-P, Dimopoulos K, Okonko D, *et al.* Exercise intolerance in adult congenital heart disease: comparative severity, correlates, and prognostic implication. *Circulation* 2005;**112**:828–35.

99 Wilson W, Taubert KA, Gewitz M. Prevention of infective endocarditis: guidelines from the American Heart Association: a guideline from the American Heart Association Rheumatic Fever, Endocarditis, and Kawasaki Disease Committee, Council on Cardiovascular Disease in the Young, and the Council on Clinical Cardiology, Council on Cardiovascular Surgery and Anesthesia, and the Quality of Care and Outcomes Research Interdisciplinary Working Group. *Circulation* 2007;**116**:1736–54.

100 Bédard E, Dimopoulos K, Gatzoulis MA. Has there been any progress made on pregnancy outcomes among women with pulmonary arterial hypertension? *Eur Heart J* 2009;**30**:256–65.

101 Dranenkiene A, Opitz CF, Gumbiené L, *et al.* Pregnancy in patients with Eisenmenger's syndrome. Experiences from Vilnius 1967–2003. *Dtsch Med Wochenschr* 2004;**12** (Suppl 1):S35–9 (in German).

102 Silversides CK, Sermer M, Siu SC. Choosing the best contraceptive method for the adult with congenital heart disease. *Curr Cardiol Rep* 2009;**11**:298–305.

24

Aortopulmonary Shunts: Patent Ductus Arteriosus, Aortopulmonary Window, Aortic Origin of a Pulmonary Artery

Jie Shen[1] & D. Woodrow Benson[2]

[1]Shanghai Jiaotong University and Children's Hospital of Shanghai, Shanghai, China
[2]University of Cincinnati School of Medicine and Cincinnati's Children's Hospital Medical Center, Cincinnati, OH, USA

Anatomic connections between the aorta and the main or branch pulmonary artery usually cause aortopulmonary left-to-right shunts, although occasionally severe pulmonary arterial hypertension causes a right-to-left shunt. The connections from aorta to the main pulmonary artery are the patent ductus arteriosus (common) and the aortopulmonary window (rare). The connections between the aorta and a branch pulmonary artery are anomalous connection of one pulmonary artery to the aorta (rare) and multiple aortopulmonary collaterals; the latter is discussed in Chapter 41.

Patent ductus arteriosus

Introduction and historical background

The ductus arteriosus (DA) is a muscular artery connecting the left pulmonary artery to the aorta during intrauterine life. The DA is essential to the fetus, but normally it closes shortly after birth and is remodeled to form the ligamentum arteriosum. A defect in the closure mechanism leads to a clinical condition called patent ductus arteriosus (PDA). PDA usually occurs as an isolated cardiovascular malformation (CVM), but it may be associated with other CVMs. Based on distinctive auscultatory findings, PDA is easily diagnosed by physical examination; the precise diagnostic values of the physical findings may explain why PDA was one of the first congenital CVMs to be successfully treated by surgery over 70 years ago [1]. Although PDA occurring in preterm infants often closes spontaneously, immaturity of ductal closure mechanisms may lead to its persistence; some of these patients require PDA closure.

Epidemiology

Incidence

The incidence of PDA varies with gestational age and the age of subjects at the time of study. PDA incidence is ~1/2000 in term neonates, but ~8/1000 in premature infants, with the highest incidence in the youngest patients. The incidence in females is 2–3-fold higher than in males. PDA accounts for 5–10% of all CVMs [2].

Genetics

PDA typically has not been regarded as a genetic disorder because it most often occurs sporadically. Occasionally it is associated with cytogenetic abnormalities, for example, trisomy 21 and 4q-syndrome [3]. The idea that single genes can influence PDA has been demonstrated by a mouse model resulting from disruption of the prostaglandin E_2 receptor [4] and by rare syndromic forms of PDA, such as Char syndrome, an autosomal dominant disorder caused by mutations in the transcription factor TFAP2B, and familial thoracic aortic aneurysm with PDA due to mutations in MYH11 [3,5]. PDA recurrence risk is 1–5% [6], but family clustering of isolated PDA and PDA with bicuspid aortic valve has been reported [3]. In addition, Mani *et al.* [7] found a recurrence risk of 5% in a population with parental consanguinity and, using genome-wide linkage analysis, identified a locus on chromosome 12q24. Uncommon familial occurrence and infrequent association with genetic syndromes or cytogenetic abnormalities suggest that inheritance of PDA is complex.

Environmental factors

Prematurity increases the incidence of PDA, probably due to physiological factors related to prematurity, such as excess sensitivity to vasodilator prostaglandins and nitric oxide, decreased production of vasoconstrictor prostaglandins, response to inflammatory mediators, and relative resistance to local hypoxia–ischemia, rather than an inherent abnormality of the DA [8,9]. Hypoxia in newborns, and also altitude-related hypoxia, can also lead to failure of normal DA closure [10]. Maternal rubella infection during the first trimester of pregnancy is associated with a high incidence of PDA and peripheral pulmonary artery stenosis [11]. In congenital rubella syndrome, DA histopathology resembles that of a very immature ductus.

Embryology and development of DA

In normal cardiovascular development, the proximal portions of the sixth pair of embryonic aortic arches persist as the proximal branch pulmonary arteries, and the distal portion of the left sixth arch persists as the ductus arteriosus, connecting the left pulmonary artery with the left dorsal aorta. This arch transformation is complete by 8 weeks of human fetal life. In the past decade, our knowledge of the role of neural crest cells and the transcriptional networks that regulate smooth muscle development in the DA have provided new insights into patency and closure of the DA [12,13].

Pathophysiology

Normal postnatal closure of DA

In the fetus, the blood oxygen level is relatively low and the oxygen–hemoglobin dissociation curve is shifted to the left, enabling fetal blood to release oxygen in low-oxygen conditions. In addition, circulating prostaglandin levels are elevated. The placenta is the major site of prostaglandin production, whereas the fetal lung is the major site of prostaglandin degradation. As blood flow in fetal lungs is limited, the resulting high levels of prostaglandins in the fetus keep the DA open. After birth, prostaglandin synthesis is reduced due to separation from the placenta, and degradation is increased due to increased pulmonary blood flow [9,14]. The increased neonatal blood oxygen saturation associated with lung ventilation and elevated blood oxygen levels rapidly result in contraction of spiral and circular smooth muscle cells in the DA and thickening and shortening of the DA walls, leading to occlusion of the DA lumen. Usually, the DA is functionally closed within 12 h after birth. The nutrient blood vessels within the DA wall are then disrupted, and the cells undergo aseptic necrosis. Proliferating fibrous tissues then replace these cells, and the DA ultimately forms the ligamentum arteriosum. Thus, the combination of increased blood oxygen content and the decline of the prostaglandin levels that occur after birth are the main causes of postnatal DA closure [9,14]. In some premature infants, mechanisms other than prostaglandins appear to operate; these involve decreased expression of calcium and potassium channel genes, and also phosphodiesterase genes that modulate cAMP/cGMP signaling [15].

Anatomy of PDA

The DA lies between the pulmonary artery anteriorly and the descending aorta posteriorly. PDAs vary with regard to size, morphology, and orientation [16,17] (Figure 24.1). Usually, the PDA is vertical and is wider on the aortic side and narrower and cone-shaped on the pulmonary artery side. The opening on the aortic side may be dilated in a horn or funnel shape. The PDA can also connect from the right aortic arch to the right pulmonary artery or from the left subclavian artery to the left pulmonary artery.

For patients with congenital pulmonary artery atresia or severe pulmonary artery stenosis, the PDA tends to be very narrow and twisted. This causes the site at which it joins the aorta to shift towards the concave side of the aortic arch, most likely because the direction of blood flow in the DA is reversed from the aorta to the pulmonary artery. However, the structure of the PDA remains normal in these patients, and it can normally close after birth, thereby leading to a dramatic decline in pulmonary blood flow, exacerbating cyanosis [18]. Occasionally the PDA is right-sided or even bilateral.

Left-to-right shunting in the PDA

Normally, flow through the PDA is continuous because of the systolic and diastolic pressure gradients between the aorta and the pulmonary artery (left-to-right shunt). The arterial blood shunted from the aorta and the venous blood that comes from the right ventricle are mixed in the pulmonary artery, enter the pulmonary circulation, and then return to the left atrium and left ventricle. However, the size of the shunt and severity of symptoms vary between affected individuals, and are determined in part by the dimensions and morphology of PDA and pulmonary vascular resistance [19,20]. With a large shunt, left ventricular stroke volume is significantly increased. When the blood flow enters the aorta during systole, the systolic pressure in the aorta increases. During diastole, blood flow is shunted to the pulmonary artery, which has low resistance during diastole because the aortic valve is closed, thereby decreasing the diastolic pressure and widening the pulse pressure. As a result, these patients develop increased peripheral vascular pulsations, characterized by a rapidly rising and then rapidly decaying pulse (collapsing pulse) with an increased pulse pressure. The blood ejected from the left ventricle is partially diverted to the PDA and recirculates through the lungs to the left atrium. Therefore, blood volume must increase correspondingly to meet the requirements of the systemic circulation. Large shunts lead to left ventricular enlargement, elevated left ventricular end-diastolic pressure, and left atrial enlargement. The resulting pulmonary venous hypertension may cause pulmonary edema.
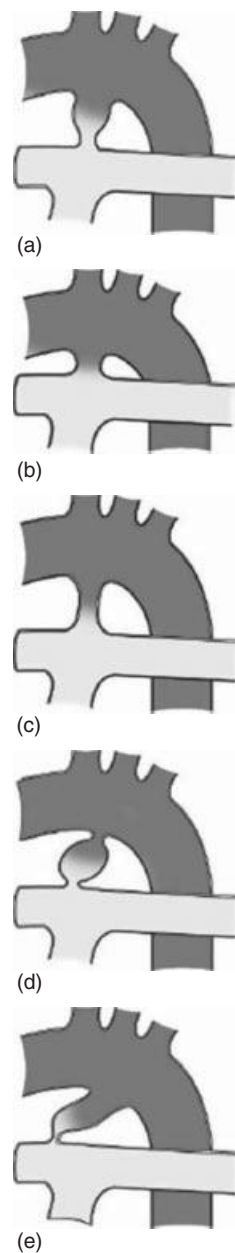
Figure 24.1 Diagrammatic representation of PDA configuration as demonstrated on the lateral angiogram as described by Krichenko *et al.* [16]. (a) A conical duct with well-defined aortic ampulla and constriction near the pulmonary artery end. (b) A large duct with window-like structure, which is very short in length. (c) A tubular duct without any constriction. (d) A complex duct with multiple constrictions. (e) An elongated duct with constriction remote from the edge of the trachea as viewed on lateral angiography. (Reproduced from Forsey JT, Elmasry OA, Martin RP. *Orphanet J Rare Dis* 2009;**4**:17, with permission from BioMed Central.)

Right-to-left shunting in the PDA

Flow from the pulmonary artery to aorta (right-to-left shunt) results in the non-oxygenated blood within the pulmonary artery being shunted to the descending aorta. This may result

in differential cyanosis. Right-to-left PDA shunting may occur in obstructed pulmonary venous return to left atrium, cor triatriatum, mitral stenosis, or elevated pulmonary vascular resistance [21]. When the pulmonary vascular resistance is suprasystemic, blood flow can be shunted from the pulmonary artery to the aorta via a PDA. When this occurs, pulmonary arterial blood flows into the descending aorta, causing differential cyanosis, in which cyanosis is present only in the lower half of the body and not the upper half [20].

If communication between the systemic and pulmonary circulation relies on the PDA alone, such as in complete transposition of the great arteries (TGA) without a septal communication, desaturated blood from the aorta is shunted into the pulmonary circulation via the PDA. If TGA is associated with coarctation of the aorta and a PDA, the lower body is perfused with saturated blood from the left ventricle. The upper extremities exhibit cyanosis, but because the lower body has high levels of oxygenated blood, it is not cyanotic [20].

Eisenmenger syndrome

All CVMs increasing the flow of blood to the lungs, or increasing transmission of pressure to the pulmonary artery, tend to develop pulmonary vascular disease. The likelihood and rate of development of vascular abnormalities are determined by several variables, including the amount of left-to-right shunting, the nature of the underlying defect, and the duration of exposure of the pulmonary vascular bed to increased flow and pressure. Exposure of the pulmonary circulation to increased blood flow impairs endothelially mediated relaxation and increases vasomotor tone, and produces intimal proliferation and fibrosis, and eventual obliteration of pulmonary arterioles and capillaries (see Chapters 5 and 51). As a result, pulmonary vascular resistance increases progressively. When pulmonary vascular resistance approaches and exceeds systemic vascular resistance, shunting reverses and becomes right-to-left [22].

Clinical manifestations

Clinical history

The clinical history varies from those who are completely asymptomatic to those with severe congestive heart failure or Eisenmenger syndrome. Many patients are referred for evaluation of an asymptomatic heart murmur. In others, PDA may be an incidental finding on echocardiogram. Parents of an infant with heart failure may report poor feeding and tachypnea. Although most patients with PDA compensate well even with a moderate left-to-right shunt and remain asymptomatic during childhood, many years of chronic volume overload may lead to symptoms of congestive heart failure in adulthood. In these adults, symptoms may begin with onset of atrial fibrillation resulting from chronic left atrial enlargement. Also in the adult, a previously well-tolerated PDA may become clinically significant when its effects are

combined with acquired lesions such as ischemic heart disease, essential hypertension, or calcific aortic stenosis.

Physical examination

The pulmonary artery pressure remains elevated for several days after birth, so the PDA shunt may be small with no audible murmur. When pulmonary vascular resistance decreases, left-to-right shunting occurs and loud murmurs may be audible. The hallmark physical finding is a continuous murmur, located at the upper left sternal border, referred to as a "machinery" murmur [3,23]. The murmur often radiates down the left side of the sternum and into the back, and a thrill may be palpable. Occasionally a diastolic rumble is audible at the cardiac apex in patients with moderate or large ductal shunts. With elevation of pulmonary artery pressure, the pulmonic component of the second heart sound is accentuated. If the shunt is moderate or large, the left ventricular impulse may be prominent, and the pulse pressure increased. The peripheral pulses may be prominent, bounding, or sometimes collapsing. In premature infants with a large shunt, arterial pulsation is felt in the thenar eminence and the digital arteries. The bounding pulses are due both to rapid run-off from aorta to pulmonary artery and also because increased distension of the aortic baroreceptors by the large stroke volume inhibits sympathetic vasoconstriction and causes increased peripheral run-off. This can be shown readily by Quincke's pulse, a pulsatile blanching of the nail bed when it is compressed slightly. Two points should be noted. First, with a large VSD, the left ventricle has to eject a large stroke volume rapidly, so that the aortic pressure rises quickly. Because, however, most of the stroke volume is ejected through the VSD into the right ventricle, the actual pulse pressure is not increased as it would be in a PDA with a similar stroke volume; this is sometimes called the small bounding pulse of a big VSD. Second, with severe congestive heart failure, the resultant sympathetic vasoconstriction reduces peripheral run-off, abolishes the typical bounding pulses, and confuses the diagnosis.

Except in older patients with congestive heart failure, rales are uncommon even with a large shunt.

The most characteristic sign of a PDA is a continuous murmur. Continuous does not mean that the murmur occurs during the whole of systole and diastole, but rather that the systolic murmur obscures the second heart sound and continues beyond it. No murmur is present during early systole or late diastole. A typical continuous murmur is usually easily heard and the systolic component is usually louder. During diastole, the only source of an audible murmur is the vibration of blood coming from PDA shunt. The diastolic pressure gradient is usually smaller than the systolic gradient; therefore, the shunt decreases, and the murmur becomes softer immediately following the second sound. The murmur is heard clearly in the first and second intercostal spaces at the left sternal border.

Patients with Eisenmenger syndrome are cyanotic and may have differential cyanosis (cyanosis and clubbing of the toes but not the fingers because the right-to-left ductal shunting is distal to the subclavian arteries). Cyanosis may be more profound when systemic vascular resistance is decreased, such as in hot weather or after exercise. There may be no murmur during systole or diastole, because shunting may be minimal. Auscultation may reveal a high-frequency diastolic decrescendo murmur indicative of pulmonary regurgitation, and/or a holosystolic murmur suggesting tricuspid valve regurgitation. The intensity of the pulmonic component of the second heart sound may be increased and its closure earlier, leading to a loud and single S2. Peripheral edema may be present late in the course of disease when right ventricular dysfunction is present.

If the PDA does not close promptly after birth, it may close later via a mechanism that has not been fully elucidated, called delayed closure of the DA [10,24]. However, once a patient has reached 3 months of age, the chance of spontaneous closure is low [25]. Others, however, believe that the incidence of spontaneous closure is appreciable [26,27], and the issue remains to be resolved. The natural disappearance of murmur can indicate spontaneous closure, but may also be caused by pulmonary hypertension due to progressive increase in pulmonary vascular resistance. The symptoms of PDA-induced pulmonary hypertension include exertional shortness of breath without other symptoms of heart failure. In severe pulmonary hypertension, dilation of pulmonary arteries may compress the recurrent laryngeal nerve, causing hoarseness.

Newborns may have no murmur, as their pulmonary artery pressure has not yet dropped. Infants may only have systolic murmurs as the pressure difference between the aorta and the pulmonary artery is not significant during diastole. If the shunt volume is large and pulmonary hypertension occurs in older children, the diastolic pressure in the pulmonary arteries increases significantly and is close to that of the aorta. This means that the diastolic component of the murmur disappears first. With the continued increase in pulmonary artery pressure, the systolic pressures of the pulmonary artery and aorta become more similar, causing the systolic component of the murmur to become softer and shorter and finally disappear. Patients with a large shunt can be identified by diastolic murmurs at the apex of the heart or even opening snaps of the relatively narrow mitral valve due to the large inflow of blood that occurs. To-and-fro murmurs can be heard in the anterior fontanelle in infant patients with a large shunt. This murmur is due to the excessive inflow of blood in the intracranial blood vessels during systole and the increased flow of blood returning to the low-resistance pulmonary arteries during diastole.

Electrocardiographic (ECG) features

The ECG changes observed in patients with PDA depend on the degree of volume overload of the left ventricle and the pressure overload of the right ventricle. Patients with a small PDA may have a completely normal ECG. Patients with moderate to large PDA may exhibit left ventricular hypertrophy and/or left atrial enlargement. The ECG may show enlargement of both ventricles when pulmonary artery pressure is elevated. Patients with Eisenmenger syndrome may exhibit right ventricular hypertrophy [28].

Chest X-ray

Heart size in PDA patients is directly related to the shunt volume. Infants with heart failure symptoms have enlarged hearts with a cardiothoracic ratio >0.6. In most asymptomatic patients, heart size is normal to mildly enlarged. The configuration of the heart shadow is usually normal; however, left atrial and left and right ventricular enlargement may be seen when the shunt is large, and a pulmonary artery bulge is present due to high pulmonary artery pressures. The ascending aorta is usually normal in infancy but may gradually dilate with enlargement of the aortic knob with patient growth. This may distinguish PDA from findings observed in other left-to-right shunts.

Infants usually have enlargement of both ventricles and the left atrium. All four chambers of the heart enlarge if the pulmonary artery pressure increases, the left-to-right shunt remains unchanged, and heart failure occurs. It is not a good sign if a previously seen enlarged cardiac silhouette decreases, as this means that the shunt has decreased because of pulmonary hypertension.

Echocardiography

The echocardiogram has emerged as the procedure of choice to confirm the diagnosis and to assess the functional significance of PDA (Figure 24.2). Combined with clinical information, the echocardiogram may be used to classify the PDA as silent, small, moderate, or large. The echocardiogram also identifies and assesses the presence of other CVMs, for example, ventricular septal defect (VSD) and/or aortopulmonary septal defect. M-mode echocardiography can detect enlargement of the left atrium and left ventricle caused by volume overload. When the PDA is small, chamber sizes are usually normal. Moderate or large PDA enlarges the left atrium and ventricle. Two-dimensional imaging reveals the geometry of the PDA, and color Doppler, a very sensitive modality, is frequently used to estimate the degree of ductal shunting. Even an extremely tiny (silent) PDA can be detected by a color flow signal entering the pulmonary artery near the origin of the left pulmonary artery. In patients with high pulmonary vascular resistance, the low velocity or right-to-left flow in the PDA may be difficult to demonstrate with color flow Doppler, even if the PDA is large. Echocardiographic findings such as septal flattening,
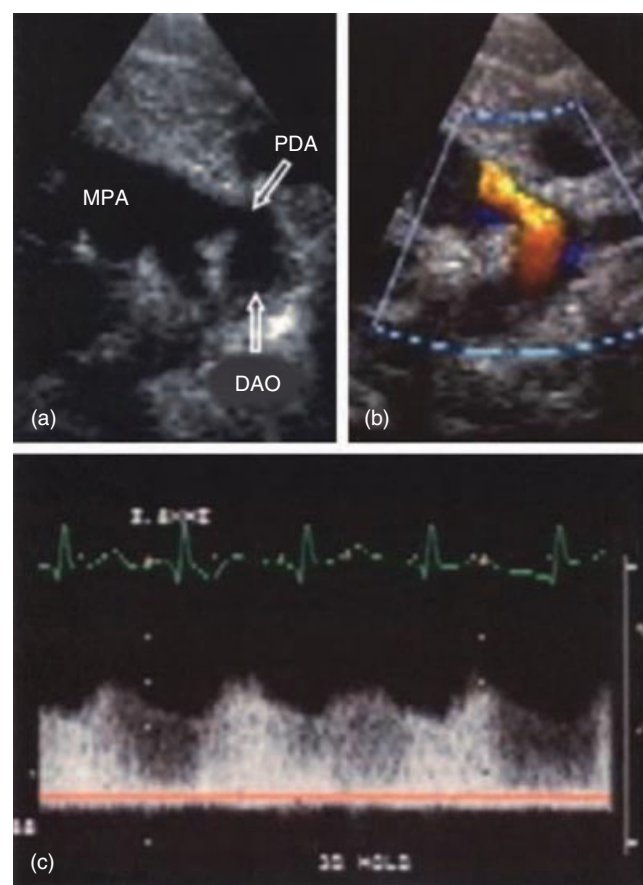
Figure 24.2 Echocardiographic study demonstrating PDA. (a) Two-dimensional image of a PDA as seen in a high parasternal shortaxis view. DAO, descending aorta; MPA, main pulmonary artery. (b) Color Doppler image in a similar view shows left-to-right shunting through the PDA. (c) Spectral Doppler profile of continuous left-to-right ductal flow. (Reproduced from Schneider DJ, Moore JW. *Circulation* 2006;**114**:1873–82, with permission from Wolters Kluwer Health.)

unexplained right ventricular hypertrophy, and high-velocity pulmonary regurgitation should prompt a thorough investigation for a PDA.

Cardiac catheterization and angiography

Typical PDA patients do not need diagnostic cardiac catheterization and angiography. However, therapeutic catheterization is currently the treatment of choice for PDA. Complete hemodynamic assessment before transcatheter closure is important in adults and in patients with elevated pulmonary artery pressure; assessment of pulmonary vascular resistance and its response to pharmacologic agents may help in determining the advisability of PDA closure. Assessing hemodynamics during transient occlusion with a balloon catheter may also provide information regarding the advisability of PDA closure. Angiography defines the anatomy of the ductus arteriosus; detailed assessment is essential before

transcatheter closure so that the proper device and device size can be chosen for the intervention [16,29].

Differential diagnosis

PDA is characterized by a continuous murmur. It is not difficult to detect in typical patients; however, there are other conditions that can result in murmurs that sound similar to that produced by PDA:

1 Ventricular septal defect (VSD) in infants. Heart failure caused by a large PDA is similar to that caused by VSD in infants. VSD generally only causes a systolic murmur, but mid-diastolic filling sounds due to increased transmitral flow are common when the shunt is large. The combination may be confused with a continuous murmur. Unless a patient has severe heart failure, a palpable pulse can be detected in the patient's peripheral arteries. Echocardiographic examination can easily differentiate these two conditions [3].

2 Aortic sinus (sinus of Valsalva) rupture into the right heart [30]. Aortic sinus rupture into the right atrium or ventricle can cause a continuous murmur. During the rupture, the patient may develop a sudden shock-like syndrome. The murmur, usually very prominent, is loudest in the precordial region. Again, ultrasound examination can distinguish these possibilities.

3 Arteriovenous fistula [31]. If a fistula is connected to veins near the coronary artery, intercostal artery, or internal thoracic artery, a continuous murmur, similar to that caused by a PDA, will be heard. However, the source of the sound is superficial and may seem to be generated outside the heart [31,32]. A continuous murmur from arteriovenous fistulas in the lungs can be heard in unusual places on the torso. If blood flow is large enough to generate audible murmurs, patients will have cyanosis. Other conditions, such as origination of pulmonary artery branch from the aorta [32,33] and branch pulmonary artery stenosis, can also generate continuous murmurs that mimic some aspects of PDA (see below).

4 Anomalies such as a VSD with aortic regurgitation and congenital absence of the pulmonary valve can also generate systolic and diastolic murmurs; however, the murmurs are to-and-fro, not continuous [34].

5 Total anomalous pulmonary venous connection [35]. Some types of anomalous pulmonary veins converge into the left innominate vein through the vertical vein. If there is no obstruction, a continuous murmur that is louder in diastole can be heard because there is a large amount of blood flow present and the vessels turn sharply. This condition can be differentiated from PDA by ECG, X-ray, and/or echocardiogram.

6 Venous murmur (venous hum). When blood returns to the subclavian vein from the jugular vein, a "woop, woop" sound may be auscultated in normal healthy children. This sound is affected by the turning of the head and neck, body position, and respiration. Compression of the jugular vein or having the patient lie down can cause the murmur to disappear.

7 Aortopulmonary septal defect (aortopulmonary window). See below.

Complications

Patients are usually diagnosed by the incidental finding of a heart murmur. Most patients have no complications, but complications may occur at any age.

Congestive heart failure

The decrease in pulmonary vascular resistance that occurs normally after birth, and the resultant increased shunt, can cause congestive heart failure, similar to a large VSD. The initial decompensation in heart function that occurs in these patients is due to pulmonary congestion induced by left ventricular failure. After a long time, because of the burden of continued volume overload, right ventricular failure also occurs, and can induce hepatomegaly and subcutaneous edema. When the DA is closed by interventional or surgical means, this complication can be reversed [36]. Older patients with long-standing volume overload of the left atrium and ventricle may develop atrial flutter and fibrillation.

Endocarditis

Prior to the availability of surgical and antibiotic therapy, endocarditis was the main cause of death of patients with a PDA [37]. Fortunately, endocarditis rarely leads to death in these patients in the modern era. If a pulmonic valve vegetation detaches and enters the pulmonary circulation, pneumonia-like symptoms will occur. Aggressive antibiotic therapy will be required for treatment until further surgical or interventional cardiology procedures are performed to close the PDA.

Pulmonary vascular lesions

Large DAs ultimately lead to obstructive pulmonary vascular disease. In a few rare instances of pulmonary hypertension, the pulmonary artery wall structure does not mature after birth and develop the typical characteristics that allow it to transform into a thin-walled structure with a wide lumen. These patients retain the fetal-type pulmonary artery characteristics, specifically a thick-walled pulmonary artery with a narrow lumen, leading to a right-to-left shunt and lower body cyanosis [16].

Treatment

Gross performed the first successful surgical ligation of PDA in 1938 [1]. Surgery has a very low mortality and offers definitive therapy and excellent long-term outcomes [38]. In adults, the PDA may be calcified and friable, and occasionally closure is best performed with cardiopulmonary bypass.

Interventional catheterization procedures are just as safe, and have become the most common method for PDA closure in recent years (Figure 24.3). Coils are used for a small PDA and an Amplatzer ductal occluder or similar device for a larger PDA. There is about a 10% procedural failure rate,
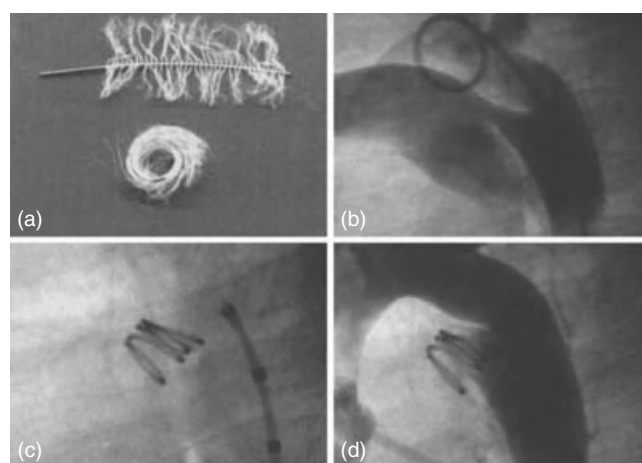
Figure 24.3 Gianturco coil occlusion of PDA. (a) Views of a Gianturco coil in its stretched out configuration (top) and in its natural coiled configuration (bottom). Note the attached Dacron fibers, which promote thrombosis, along its length. (b)–(d) Lateral angiograms demonstrating closure of a PDA with a single 0.038 in diameter Gianturco coil. (Reproduced from Schneider DJ, Moore JW. *Circulation* 2006;**114**:1873–82, with permission from Wolters Kluwer Health.)

and there are rare complications such as device embolization or hemolysis due to a high-velocity jet through a small residual PDA [39]. All patients should therefore receive treatment before they reach school age to maintain good health and to prevent complications.

In patients with pulmonary hypertension, the safety and risks of surgery or intervention must be assessed. Closure can be performed if cardiac catheterization examination shows that the patient's pulmonary vascular resistance responds to vasodilators, and is <10 Wood units m^{-2} body surface area, especially if <2 years of age. If there is little or no response to vasodilators, a balloon catheter can be inserted to occlude the PDA. If the pulmonary vascular resistance decreases following balloon insertion, then ductal closure can be undertaken. Another technique that can be utilized to assess pulmonary vascular responsiveness is tightening the PDA through a thoracotomy and observing the changes in pulmonary artery pressure to determine if ductal ligation will be safe and tolerated. Although some children have a slow initial reaction, their pulmonary artery pressure decreases day by day after PDA ligation. Some patients may have continued pulmonary hypertension even in this setting. Surgery should not be performed on patients with pulmonary vascular resistance >15 Wood units m^{-2} or differential cyanosis caused by right-to-left shunting [40,41].

Treatment of other congenital heart diseases associated with PDA

Patients with congenital heart diseases with left-to-right shunts, such as VSD and atrial septal defect, may also have PDA, which increases the size of their shunts. Therefore,

these lesions should be treated simultaneously, or in a staged operation. If a PDA is associated with other severe cardiovascular malformations, this shunt may be beneficial, and physicians should think carefully before closing the PDA. If patients have pulmonary atresia or aortic atresia, the pulmonary or systemic circulation depends upon a PDA so that blood can be transferred from one great artery to the other great artery. In these lesions, the PDA is a lifeline and should not be closed. Oxygenation should be considered carefully in these patients , because an increase in blood oxygen in newborns can promote the closure of PDA [42]. All measures that maintain DA patency are good for these patients. Drip infusions of prostaglandin E$_1$ can maintain the patency of the DA and provide infants with good preoperative conditions. Other anomalies where the DA should be kept open include tetralogy of Fallot, tricuspid atresia, coarctation of the aorta, and aorta arch interruption. In fact, a systemic–pulmonary artery shunt operation in patients with cyanotic congenital heart disease with decreased pulmonary blood flow is like a physiologically created PDA [43].

Treatment of PDA in premature infants

In premature babies, the DA does not close by the usual time after birth because the structures that close the DA are immature, and premature babies react weakly to the most important stimulation for DA closure, increases in blood oxygen levels after breathing is initiated. Furthermore, the smooth muscle layer of the pulmonary artery is not fully developed in premature babies, so the resistance is small and the shunt is large. Therefore, patients are prone to heart failure and even death [44]. Once the diagnosis is confirmed, if conservative medical treatment fails, closure should be performed immediately [45].

Even though the shunt in the PDA of premature babies is small, it can reduce the blood supply of the systemic circulation and lower systemic blood pressure. Therefore, it causes hypoperfusion in many organs, and produces clinical symptoms. The decreased blood supply to the brain and the widened pulse pressure in patients with PDA increase the risk of intracranial hemorrhage. Renal function may also be affected, as is the myocardium, especially the subendocardium, due to lack of an adequate blood supply. One cause of necrotizing enterocolitis in premature babies is thought to be intestinal ischemia; therefore, abdominal circumferences and gastric residual volumes should be measured before feeding premature babies with PDA. The mortality rate of these premature babies can be reduced if their DAs are closed early, and should be performed early for abdominal distension, increased gastric residuals volumes before feeding, bloody stool, diminished peristaltic sounds, and/or pneumatosis intestinalis [24,46].

Patients with anemia should be treated to increase their hematocrit to above 45%. The increase in the oxygen-carrying capacity of the blood can improve cardiac function. The fetal

oxygen–hemoglobin dissociation curve is shifted to the left, which is advantageous for oxygen uptake under low oxygen conditions but disadvantageous for oxygen release into tissues. Therefore, repeated transfusion of small amounts of adult blood can facilitate the release of oxygen from the blood release into the tissues. Electrolytes, glucose, and nutrition should be supplemented in a timely manner. If necessary, intravenous hyperalimentation can be used, and patients' intake of sodium and water should be controlled [47,48]. Generally, digitalis should not be used as it has little effect on premature babies.

The first choice of medication to close the DA is oral or intravenous indomethacin. This can inhibit the synthesis of prostaglandins, thereby promoting closure of the PDA. The best time to initiate this medication is within 10 days of birth. The typical initial dosage is $0.2\,mg\,kg^{-1}$, administered orally or intravenously. If an intravenous injection is used, the dosages vary according to age. If the medication is given within 48 h, the next two doses should be $0.1\,mg\,kg^{-1}$. Patients' urine output should also be observed. If their urine output decreases over 12–24 h, the medication should be delayed or stopped. If the murmur reappears, a second course of treatment should be given. The contraindications to medical therapy include decreased renal function (creatinine $>1.6\,mg\,dl^{-1}$ or blood urea nitrogen $>20\,mg\,dl^{-1}$), bleeding, shock, necrotizing enterocolitis, or evidence of myocardial ischemia on ECG. The most important side effect is renal; therefore, the dosage should be closely monitored. Anuria can happen if overly aggressive water restriction occurs while the medication is being administered; however, most incidents of low blood sodium and oliguria are transient, with no significant sequelae. If a patient's body weight is <1000 g and symptoms appear within 72 h after birth, treatment should be initiated immediately [49–52]. If medical therapy does not control heart failure symptoms after 48–72 h, surgical ligation should be performed.

Although there are good theoretical reasons for closing a large PDA in premature infants, and some anecdotal evidence of dramatic improvement in some of these infants, some authorities believe that there is as yet no evidence that closure is beneficial in reducing mortality, complications such as bronchopulmonary dysplasia, and the duration of intubation or hospital stay [53].

Aortopulmonary window

This is a rare anomaly involving absence of the septum between the ascending aorta and the main pulmonary artery but with two distinct semilunar valve rings.

Embryology
The anomaly is due to incomplete separation of the primitive truncus by the aortopulmonary septum.

Anatomy and pathology
As a rule the window is large, and round or oval. There are three anatomically distinct types. Type I is a proximal defect between the semilunar valve and pulmonary artery bifurcation, type II is a distal defect that is usually accompanied by an anomalous origin of the right pulmonary artery from aorta, and type III is a large defect seen in combination with type I and II defects [33,54,55]. PDA frequently coexists (~70%), and >50% of patients have associated anomalies. Aortic arch abnormalities are common, including type A and type B aortic arch interruption and coarctation of the aorta. Associated intracardiac abnormalities include tetralogy of Fallot and transposition of the great arteries [34,54–56].

Pathophysiology
Because the aortopulmonary communication is usually large, a large left-to-right shunt occurs when pulmonary vascular resistance decreases. Early congestive heart failure develops, and if the patient survives pulmonary vascular disease supervenes.

Natural history
If untreated, most of these patients die in infancy and few survive beyond 10 years of age [57].

Clinical features
Typically patients present early in life with heart failure with a nonspecific history. The physical findings resemble those of a PDA but the diastolic component of the murmur is often absent because of the high pulmonary arterial pressure. The murmur is often more retrosternal than under the left clavicle, and at times it resembles the murmur of an VSD rather than a PDA.

Electrocardiogram and chest X-ray
There are no distinguishing ECG or chest X-ray findings, although in older patients the ascending aorta is not enlarged, unlike a PDA.

Echocardiography
The anomaly is usually discovered during echocardiographic examination used for detecting other anomalies such as PDA and VSD.

Other imaging modalities such as MRI have been used.

Cardiac catheterization
This is needed only if pulmonary vascular reactivity needs to be assessed.

Management
Medical treatment is only supportive until closure can be performed. The defects are closed either through the aorta or pulmonary trunk, with an autologous tissue patch in the former and a synthetic patch in the latter [56,58–60]. The

occasional smaller defect can be closed by an occluder introduced via a cardiac catheter. Late results appear to be good in the absence of associated anomalies.

Anomalous pulmonary artery from aorta

In this rare anomaly, erroneously referred to as "hemitruncus," one branch pulmonary artery arises from the aorta.

Embryology

The proximal form (see below) is considered to be an anomaly of truncal septation or a migration defect of the sixth aortic arch. The distal form has been attributed to abnormal persistence of parts of the fifth or sixth aortic arches [32].

Pathological anatomy

An anomalous right is more common than an anomalous left pulmonary artery. Usually the right pulmonary artery arises from the posterior aspect of the ascending aorta just above the aortic valve, but it may arise more distally near the innominate artery. The anomalous pulmonary artery is wide, but may have a stenotic origin. About 50% have an associated PDA, and others are associated with tetralogy of Fallot, VSD, aortopulmonary window, coarctation of the aorta, or interrupted aortic arch [61–64].

If isolated, an anomalous left pulmonary artery almost always arises from a right aortic arch. More than 50%, however, are associated with tetralogy of Fallot and a left aortic arch.

Pathophysiology

This is identical with that of a large PDA, with the same risks of congestive heart failure or pulmonary vascular disease. Pressures in the anomalous artery are systemic. Some, especially with distal connections, may have ductus tissue that contracts and stenoses the orifice, and then pressures are low. The pressure in the normally connected pulmonary artery is usually systemic, probably because the total cardiac output has to pass through one lung. Pulmonary vascular disease begins early and can occur in both lungs unless one lung is protected by a stenosis at its origin.

Natural history

Most untreated patients die before 1 year of age from congestive heart failure [57].

Clinical features

These are similar to those of a PDA or aortopulmonary window, as are the ECG and chest X-ray. If the anomalous artery has a stenotic origin, pulmonary vascular markings may be decreased on that side. Definitive diagnosis is made by echocardiography, angiography, or other imaging modalities.

Cardiac catheterization may be needed to define the anatomy and assess pulmonary vascular resistance. In those with tetralogy of Fallot, the latter anomaly dominates the clinical features.

Management

Unless there is pulmonary vascular disease, the anomalous artery can be detached and reimplanted with or without an interposition graft. Mortality can be high, especially because of pulmonary hypertensive crises [62–64]. Hospital survivors usually have a benign long-term course, although occasionally the reconnected anastomosis may become too small from scarring or with growth and need replacement.

References

1 Kaemmerer H, Meisner H, Hess J, Perloff JK. Surgical treatment of patent ductus arteriosus: a new historical perspective. *Am J Cardiol* 2004;**94**:1153–4.

2 Hoffman JI, Kaplan S. The incidence of congenital heart disease. *J Am Coll Cardiol* 2002;**39**:1890–900.

3 Forsey JT, Elmasry OA, Martin RP. Patent arterial duct. *Orphanet J Rare Dis* 2009;**4**:17.

4 Nguyen M, Camenisch T, Snouwaert JN, et al. The prostaglandin receptor EP4 triggers remodelling of the cardiovascular system at birth. *Nature* 1997;**390**:78–81.

5 Gelb BD. Genetic basis of congenital heart disease. *Curr Opin Cardiol* 2004;**19**:110–5.

6 Nora JJ, Nora AH. Update on counseling the family with a first-degree relative with a congenital heart defect. *Am J Med Genet* 1988;**29**:137–42.

7 Mani A, Meraji SM, Houshyar R, et al. Finding genetic contributions to sporadic disease: a recessive locus at 12q24 commonly contributes to patent ductus arteriosus. *Proc Natl Acad Sci USA* 2002;**99**:15054–9.

8 Hammerman C. Patent ductus arteriosus. Clinical relevance of prostaglandins and prostaglandin inhibitors in PDA pathophysiology and treatment. *Clin Perinatol* 1995;**22**:457–79.

9 Hermes-DeSantis ER, Clyman RI. Patent ductus arteriosus: pathophysiology and management. *J Perinatol* 2006;**26**(Suppl 1): S14–8; discussion S22–3.

10 Penaloza D, Sime F, Ruiz L. Pulmonary hemodynamics in children living at high altitudes. *High Alt Med Biol* 2008;**9**:199–207.

11 Oster ME, Riehle-Colarusso T, Correa A. An update on cardiovascular malformations in congenital rubella syndrome. *Birth Defects Res A Clin Mol Teratol* 2010;**88**:1–8.

12 Huang J, Cheng L, Li J, et al. Myocardin regulates expression of contractile genes in smooth muscle cells and is required for closure of the ductus arteriosus in mice. *J Clin Invest* 2008;**118**:515–25.

13 Ivey KN, Sutcliffe D, Richardson J, et al. Transcriptional regulation during development of the ductus arteriosus. *Circ Res* 2008; **103**:388–95.

14 Clyman RI. Mechanisms regulating the ductus arteriosus. *Biol Neonate* 2006;**89**:330–5.

15 Waleh, N., Hodnick, R., et al. Patterns of gene expression in the ductus arteriosus are related to environmental and genetic

risk factors for persistent ductus patency. *Pediatr Res* 2010;**68**:292–7.

16 Krichenko A, Benson LN, Burrows P, *et al.* Angiographic classification of the isolated, persistently patent ductus arteriosus and implications for percutaneous catheter occlusion. *Am J Cardiol* 1989;**63**:877–80.

17 Bergwerff M, DeRuiter MC, Gittenberger-de Groot AC. Comparative anatomy and ontogeny of the ductus arteriosus, a vascular outsider. *Anat Embryol (Berl)* 1999;**200**:559–71.

18 Freedom RM, Wilson G, Trusler GA, *et al.* Pulmonary atresia and intact ventricular septum. *Scand J Thorac Cardiovasc Surg* 1983; **17**:1–28.

19 Driscoll DJ. Left-to-right shunt lesions. *Pediatr Clin North Am* 1999;**46**:355–68.

20 Kluckow M. Low systemic blood flow and pathophysiology of the preterm transitional circulation. *Early Hum Dev* 2005;**81**:429–37.

21 Haworth SG, Bull C. Physiology of congenital heart disease. *Arch Dis Child* 1993;**68**:707–11.

22 Kumar RK, Sandoval J. Advanced pulmonary vascular disease: the Eisenmenger syndrome. *Cardiol Young* 2009;**19**:622–6.

23 Schneider DJ, Moore JW. Patent ductus arteriosus. *Circulation* 2006;**114**:1873–82.

24 Laughon MM, Simmons MA, Bose CL. Patency of the ductus arteriosus in the premature infant: is it pathologic? Should it be treated? *Curr Opin Pediatr* 2004;**16**:146–51.

25 Arora R, Singh S, Dalra GS. Patent ductus arteriosus: catheter closure in the adult patient. *J Interv Cardiol* 2001;**14**:255–9.

26 Campbell M. Natural history of persistent ductus arteriosus. *Br Heart J* 1968;**30**:4–13.

27 Cosh JA. Patent ductus arteriosus. A follow-up study of 73 cases. *Br Heart J* 1957;**19**:13–22.

28 Mahoney LT. Acyanotic congenital heart disease. Atrial and ventricular septal defects, atrioventricular canal, patent ductus arteriosus, pulmonic stenosis. *Cardiol Clin* 1993;**11**:603–16.

29 Wang JK, Wu MH, Lin MT, *et al.* Transcatheter closure of moderate-to-large patent ductus arteriosus in infants using Amplatzer duct occluder. *Circ J* 2010;**74**:361–4.

30 Seto AH, Hermer A, Kern M. Sudden onset congestive heart failure with a continuous murmur: ruptured sinus of Valsalva aneurysm complicated by anomalous origin of the left coronary artery. *Cardiovasc Revasc Med* 2008;**9**:41–6.

31 Thiel R, Bircks W. Arteriovenous fistulas after median sternotomy – report of 2 cases and review of the literature. *Thorac Cardiovasc Surg* 1990;**38**:195–7.

32 Aru GM, English WP, Gaymes CH, Heath BJ. Origin of the left pulmonary artery from the aorta: embryologic considerations. *Ann Thorac Surg* 2001;**71**:1008–10.

33 Berry TE, Bharati S, Muster AJ, *et al.* Distal aortopulmonary septal defect, aortic origin of the right pulmonary artery, intact ventricular septum, patent ductus arteriosus and hypoplasia of the aortic isthmus: a newly recognized syndrome. *Am J Cardiol* 1982;**49**:108–16.

34 Miyabara S, Ando M, Yoshida K, *et al.* Absent aortic and pulmonary valves: investigation of three fetal cases with cystic hygroma and review of the literature. *Heart Vessels* 1994;**9**:49–55.

35 Stein P. Total anomalous pulmonary venous connection. *AORN J* 2007;**85**:509–20; quiz 521–4.

36 Saxena A. Optimal timing of surgery in common left-to-right shunts. *Indian J Pediatr* 1998;**65**:27–33.

37 Satoh T, Nishida N. Patent ductus arteriosus with infective endocarditis at age 92. Intern Med 2008;**47**:263–8.

38 Morris CD, Menashe VD. 25-year mortality after surgical repair of congenital heart defect in childhood. A population-based cohort study. *J Am Med Assoc* 1991;**266**:3447–52.

39 Magee AG, Huggon IC, Seed PT, *et al.* Transcatheter coil occlusion of the arterial duct; results of the European Registry. *Eur Heart J* 2001;**22**:1817–21.

40 Rao PS. Percutaneous closure of patent ductus arteriosus: state of the art. *J Invasive Cardiol* 2007;**19**:299–302.

41 Bose CL, Laughon MM. Patent ductus arteriosus: lack of evidence for common treatments. *Arch Dis Child Fetal Neonatal Ed* 2007;**92**:F498–502.

42 Alwi M. Management algorithm in pulmonary atresia with intact ventricular septum. *Catheter Cardiovasc Interv* 2006;**67**: 679–86.

43 Davies MJ, Dyamenahalli U, Leanage RR, Firmin RK. Total one-stage repair of aortopulmonary window and interrupted aortic arch in a neonate. *Pediatr Cardiol* 1996;**17**:122–4.

44 Sekar KC, Corff KE. Treatment of patent ductus arteriosus: indomethacin or ibuprofen? *J Perinatol* 2008;**28**(Suppl 1):S60–2.

45 Clyman RI, Chorne N. Patent ductus arteriosus: evidence for and against treatment. *J Pediatr* 2007;**150**:216–9.

46 DiMenna L, Laabs C, McCoskey L, Seals A. Management of the neonate with patent ductus arteriosus. *J Perinat Neonatal Nurs* 2006;**20**:333–40; quiz 341–2.

47 Simmer K, Rao SC. Early introduction of lipids to parenterally-fed preterm infants. *Cochrane Database Syst Rev* 2005;CD005256.

48 Berseth CL. Feeding strategies and necrotizing enterocolitis. *Curr Opin Pediatr* 2005;**17**:170–3.

49 Donze A, Smith JR, Bryowsky K. Safety and efficacy of ibuprofen versus indomethacin for the treatment of patent ductus arteriosus in the preterm infant: reviewing the evidence. *Neonatal Netw* 2007;**26**:187–95.

50 Herrera C, Holberton J, Davis P. Prolonged versus short course of indomethacin for the treatment of patent ductus arteriosus in preterm infants. *Cochrane Database Syst Rev* 2007;CD003480.

51 Thomas RL, Parker GC, Van Overmeire B, Aranda JV. A meta-analysis of ibuprofen versus indomethacin for closure of patent ductus arteriosus. *Eur J Pediatr* 2005;**164**:135–40.

52 Shah SS, Ohlsson A. Ibuprofen for the prevention of patent ductus arteriosus in preterm and/or low birth weight infants. *Cochrane Database Syst Rev* 2003;CD004213.

53 Benitz, WE Treatment of persistent patent ductus arteriosus in preterm infants: time to accept the null hypothesis? *J Perinatol* 2010;**30**:241–52.

54 Ho SY, Gerlis LM, Anderson C, *et al.* The morphology of aorto-pulmonary windows with regard to their classification and morphogenesis. *Cardiol Young* 1994;**4**:146–55.

55 Kutsche LM, Van Mierop LH. Anatomy and pathogenesis of aorticopulmonary septal defect. *Am J Cardiol* 1987;**59**:443–7.

56 Gangana CS, Malheiros AF, Alves EV, *et al.* Aortopulmonary window - impact of associated lesions on surgical results. *Arq Bras Cardiol* 2007;**88**:402–7.

57 Hoffman JIE. *The Natural and Unnatural History of Congenital Heart Disease.* Oxford: Wiley-Blackwell, 2009: 7–102.

58 Backer CL, Mavroudis C. Surgical management of aortopulmonary window: a 40-year experience. *Eur J Cardiothorac Surg* 2002;**21**:773–9.

59 Bagtharia RKR. Trivedi KR, Burkhart HM, *et al.* Outcomes for patients with an aortopulmonary window, and the impact of associated cardiovascular lesions. *Cardiol Young* 2004;**14**:473–80.

60 Mert M, Paker T, Akcevin A, *et al.* Diagnosis, management, and results of treatment for aortopulmonary window. *Cardiol Young* 2004;**14**:506–11.

61 Kutsche LM, Van Mierop LH. Anomalous origin of a pulmonary artery from the ascending aorta: associated anomalies and pathogenesis. *Am J Cardiol* 1988;**61**:850–6.

62 Abu-Sulaiman RM, Hashmi A, McCrindle BW, *et al.* Anomalous origin of one pulmonary artery from the ascending aorta: 36 years' experience from one centre. *Cardiol Young* 1998;**8**:449–54.

63 Nathan M, Rimmer D, Piercey G, *et al.* Early repair of hemitruncus: excellent early and late outcomes. *J Thorac Cardiovasc Surg* 2007;**133**:1329–35.

64 Prifti E, Bonacchi M, Murzi B, *et al.* Anomalous origin of the left pulmonary artery from the aorta. Our experience and literature review. *Heart Vessels* 2003;**18**:79–84.

25 Sinus of Valsalva Fistula

Alpay Çeliker & Seden Erten Çelik

Acıbadem University Medical Faculty, Acıbadem Maslak Hospital, Maslak, Istanbul, Turkey

Sinus of Valsalva aneurysm (SVA) is a rare cardiac anomaly first described by Hope in 1839 [1]. Lack of differentiation or fusion abnormality between the aortic media and aortic valve fibrous ring or failure of normal elastic tissue or abnormal development of bulbus cordis are the postulated mechanisms [2,3]. This weakened area may progress to aneurysm formation over time when subjected to high aortic pressure. Aneurysm progression at its apex may lead to rupture, causing shunting from the aorta to a cardiac chamber(s) [4,5].

Incidence and genetics

SVA may be congenital or acquired, comprises 0.1–3.5% of congenital heart defects (CHDs), and accounts for 0.14% of open heart operations for CHD [5]. The exact frequency of the SVA is unknown because they are often silent, although an autopsy study revealed 0.09% prevalence in the general population [6]. It is seldom familial.

Pathologic anatomy

Congenital SVA usually involves the right sinus (65–85%) of Valsalva, and less frequently the noncoronary sinus (10–30%) and left coronary sinus (1–5%) [4,5]. The most common associated cardiac anomalies are ventricular septal defect and aortic regurgitation, but associated bicuspid aortic valve, subaortic membranous stenosis, aortic coarctation, atrial septal defect, patent ductus arteriosus, and tetralogy of Fallot have been described [4,7,8]. Diagnosis in infancy is rare [9]. SVA is typically a single defect [10]. There is a male preponderance with a ratio of 4:1. SVA is less frequent in Western than Eastern countries [11], and the associated VSD

is supracristal, also more common in Eastern countries [12]. Occasionally, giant aneurysms 5–10 cm in diameter occur.

Acquired SVAs are rare compared with congenital forms. They may be caused by degeneration of the aortic wall from cystic medial necrosis, infections, or trauma [13,14]. The rounded and symmetrical shapes of the acquired aneurysms differ from the congenital form of the disease. SVA also differs from the diffusely dilated aortic sinuses characteristic of patients with Marfan and Ehlers–Danlos syndrome [15,16]. SVA also occurs in patients with Takayasu arteritis and Behçet syndrome [17,18]. Acquired aneurysms frequently occur after infective endocarditis and tend to extend superiorly. Left aortic sinus aneurysm is generally involved with acquired causes. Rupture of acquired SVA is usually extracardiac [15].

Natural history and clinical features

SVA is usually diagnosed by the third or fourth decade, most often secondary to complications [5]. Before rupture, most patients are asymptomatic, and the aneurysm remains undetected, although palpitations, fatigue, effort dyspnea, angina, swallowing problems, and dizziness may be presenting symptoms. Syncope may occur secondary to left or right ventricular outflow tract obstruction. Several reports describe rhythm problems, symptoms of myocardial ischemia from coronary artery compression by the SVA, or atrioventricular block secondary to pressure of SVA on the AV node or His–Purkinje system. Stroke occurs infrequently from a thromboembolic event in large aneurysms with thrombus formation [19,20]. Aortic regurgitation may be from prolapse of a cusp into a ventricular septal defect, distortion of the aortic valve ring, a bicuspid valve, or infective endocarditis.

Figure 25.1 Right coronary sinus to right ventricle fistula with two-dimensional (a) and color Doppler echocardiographic (b) views. Panel (a) in diastole, panel (b) in late diastole. The color shows regurgitant flow from the aorta into the aneurysm. An, aneurysm; Ao, aorta; LA, left atrium; LV, left ventricle; P LX, long axis; RV, right ventricle.
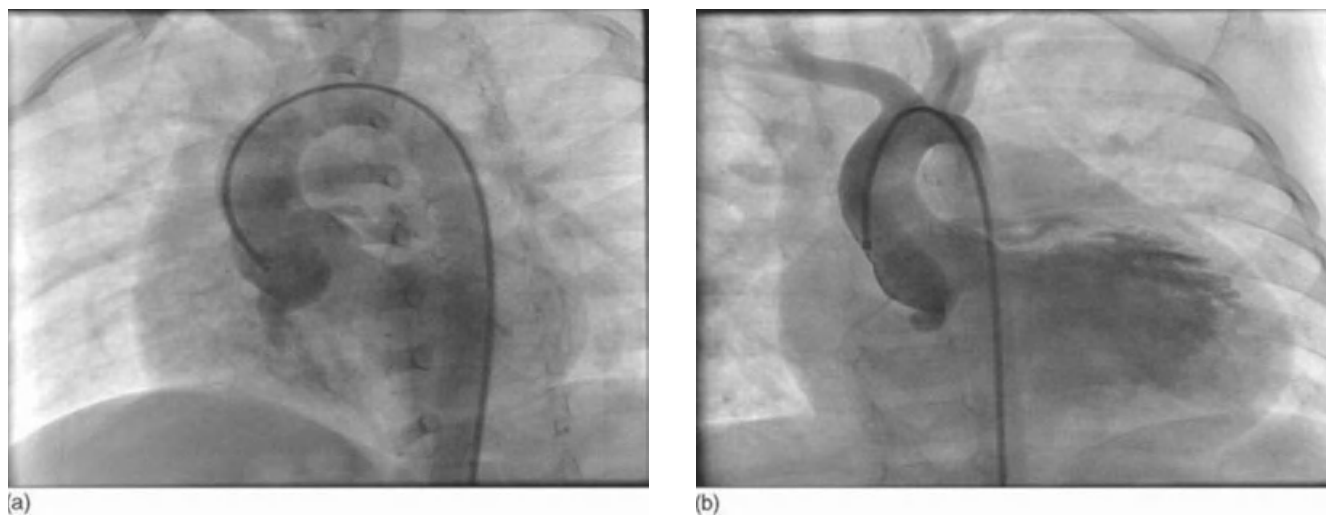
Figure 25.2 Aortic root angiogram showing right coronary sinus to right ventricle contrast filling via fistula (a) and severe aortic regurgitation (b). The patient has a subarterial-type ventricular septal defect.

SVA rupture typically occurs between 20 and 40 years of age [5] and is rare in infancy or childhood. The rupture occurs suddenly and may develop after heavy exercise, trauma, or during pregnancy. Right coronary sinus aneurysms usually rupture into the right ventricle, whereas aneurysms of the noncoronary sinus and left coronary sinus rupture into the right atrium and left atrium, respectively [5]. The interventricular septum is seldom affected by the rupture. The consequence of a rupture depends on the rupture speed, the rupture orifice size, and the chamber entered. The rupture may cause sudden deterioration, heart failure, acute cardiac tamponade, and death. There is left ventricular volume overload due to shunting through the aneurysmal tract. Ruptures with a small opening progress

insidiously, and patients become symptomatic only after months or years [21].

The first symptoms of rupture are acute chest or upper quadrant pain, followed by acute dyspnea or exercise intolerance. Progressive cough, dyspnea, edema, and oliguria are seen later after the acute rupture [5,21]. There are pulsatile peripheral pulses, a continuous murmur prominent in diastole, and a thrill at left or right sternal borders [22].

Laboratory investigations

The ECG may be normal or reveal evidence of biventricular hypertrophy. Findings secondary to myocardial ischemia or conduction problems may be seen in patients with compression

of coronary arteries or His–Purkinje system. Following rupture, the chest X-ray may show cardiomegaly and signs of pulmonary congestion [22]. Transthoracic echocardiography is very important for diagnosis and for demonstrating the extent of the aneurysm. The anatomic location of aneurysm, compressed cardiac structures, the rupture site, and associated abnormalities can be demonstrated by echocardiographic examination (Figure 25.1). The parasternal short-axis view is the most useful. Transesophageal echocardiography is mandatory in patients with SVA or where there is suspicion of aneurysm. Three-dimensional echocardiography may delineate the spatial relationships of complex abnormalities [23].

A computed tomographic scan is a very rapid diagnostic tool to obtain more data regarding the aneurysm size and location and site of rupture and also the coronary artery anatomy and its relation to the aneurysm [24]. Cardiac MRI examination may be used in patients for functional evaluation in a nonemergency setting [25]. Cardiac catheterization and angiography are needed some patients before surgery (Figure 25.2).

Management

Unrepaired SVA may cause death in months to years. The treatment for ruptured SVA is usually surgical. Early diagnosis may prevent endocarditis or further enlargement of the fistula, which might complicate surgical repair [5]. Depending on the SVA anatomy and related cardiac anomalies, primary or patch closure is the usual surgical approach. A combined approach through the involved chamber and aortic root is satisfactory. Patch closure of the aneurysm is preferred in most centers and gives excellent results, with a mortality of <5%. With severe distortion, aortic root replacement or the Ross procedure may be needed. Progressive aortic regurgitation is the crucial factor influencing prognosis [26–28], and aortic valve replacement may be required. The prognosis of small aneurysms is unclear and indications for operation in an asymptomatic patient with unruptured aneurysms are not defined. Progressive enlargement of the SVA on serial evaluation may be an indication.

Percutaneous closure of ruptured aneurysms has been reported [29,30]. Kerkar et al. [30] described successful results in 18 of 20 patients using an Amplatzer duct occluder. The results of this treatment modality, however, will have to be compared with surgery to evaluate its safety and efficacy.

References

1 Hope J. *A Treatise on the Diseases of the Heart and Great Vessels*, 3rd edn. London: J. Churchill & Sons, 1839.

2 Ring WS. Congenital heart surgery nomenclature and database project: aortic aneurysm, sinus of Valsalva aneurysm, and aortic dissection. *Ann Thorac Surg* 2000;**69**:S147–63.

3 Fishbein MC, Obma R, Roberts WC. Unruptured sinus of Valsalva aneurysm. *Am J Cardiol* 1975;**35**:918–22.

4 Taguchi K, Saski N, Matsura Y, et al. Surgical correction of aneurysms of the sinus of Valsalva: a report of forty-five consecutive patients including eight with total replacement of the aortic valve. *Am J Cardiol* 1969;**23**:180–91.

5 Takach TJ, Reul GJ, Duncan MJ, et al. Sinus of Valsalva aneurysm or fistula: management and outcome. *Ann Thorac Surg* 1999;**68**:1573–7.

6 Smith WA. Aneurysm of the sinus of Valsalva, with report of 2 cases. *J Am Med Assoc* 1914;**62**:1878–80.

7 Sakakibara S, Konno S. Congenital aneurysm of the sinus of Valsalva associated with ventricular septal defect. *Am Heart J* 1968;**75**:595–603.

8 Burchell HB, Edwards JE. Aortic sinus aneurysm with communications with the right ventricle and associated ventricular septal defect. *Proc Staff Meet Mayo Clin* 1951;**26**:336–40.

9 Heiner DC, Hara M, White HJ. Cardioaortic fistulas and aneurysms of sinus of valsalva in infancy. *Pediatrics* 1961;**27**: 415–26.

10 Chamsi-Pasha H, Musgrove C, Morton R. Echocardiographic diagnosis of multiple congenital aneurysms of the sinus of Valsalva. *Br Heart J* 1988;**59**:724–6.

11 Wang ZJ, Zou CW, Li DC, et al. Surgical repair of sinus of Valsalva aneurysm in Asian patients. *Ann Thorac Surg* 2007;**84**:156–60.

12 Choudray SK, Bhan A, Sharma R, et al. Sinus of Valsalva aneurysms: 20 years experience. *J Card Surg* 1997;**12**:300–8.

13 Sobrinho JH, Silva MA, Fontes WF, et al. Syphilitic aneurysm communicating with an aortic sinus of Valsalva. A case report. *Arq Bras Cardiol* 1989;**52**:341–4.

14 Greiss I, Ugolini P, Joyal M, et al. Ruptured aneurysm of the left sinus of Valsalva discovered 41 years after a decelerational injury. *J Am Soc Echocardiogr* 2004;**17**:906–9.

15 Ott DA. Aneurysm of sinus of Valsalva. *Semin Thorac Cardiovasc Surg Pediatr Card Surg Annu* 2006:165–76.

16 Oka N, Aomi S, Tomioka H, et al. Surgical treatment of multiple aneurysms in a patient with Ehlers–Danlos syndrome. *J Thorac Cardiovasc Surg* 2001;**121**:1210–1.

17 Yoshikai M, Ohnishi H, Fumoto H, Furutachi A. Aneurysm of the right sinus of Valsalva after aortic valve replacement in Takayasu arteritis. *J Card Surg* 2007;**22**:162–4.

18 Lee S, Lee CY, Yoo KJ. Acute myocardial infarction due to an unruptured sinus of Valsalva aneurysm in a patient with Behçet's syndrome. *Yonsei Med J* 2007;**48**:883–5.

19 Heydorn WH, Nelson WP, Fitterer JD, et al. Congenital aneurysm of the sinus of Valsalva protruding into the left ventricle. Review of diagnosis and treatment of the unruptured aneurysm. *J Thorac Cardiovasc Surg* 1976;**71**:839–45.

20 Channer KS, Hutter JA, George M. Unruptured aneurysm of the sinus of Valsalva presenting with ventricular tachycardia. *Eur Heart J* 1988;**9**:186–90.

21 Zhao G, Seng J, Yan B, et al. Diagnosis and surgical treatment of ruptured aneurysm in sinus of Valsalva. *Chin Med J* 2003;**116**:1047–50.

22 Sakakibara S, Konno S. Congenital aneurysm of the sinus of Valsalva: a clinical study. *Am Heart J* 1962;**63**:708–19.

23 Mahle WT, Kreeger J, Silverman NH. Echocardiography of the aortopulmonary window, aorto-ventricular tunnels, and aneurysm of the sinuses of Valsalva. *Cardiol Young* 2010;**20**:100–6.

24 Shambrook JS, Chowdury R, Brown IW, *et al*. Cross-sectional imaging appearances of cardiac aneurysms. *Clin Cardiol* 2010;**65**:349–57.

25 Hoey ET, Kanagasingam A, Sivananthan MU. Sinus of Valsalva aneurysms: assessment with cardiovascular MRI. *AJR Am J Roentgenol* 2010;**194**:495–504.

26 De Bakey ME, Diethrich EB, Liddicoat JE, *et al*. Abnormalities of the sinuses of Valsalva. Experience with 35 patients. *J Thorac Cardiovasc Surg* 1967;**54**:312–32.

27 Harkness JR, Fitton TP, Barreiro CJ, *et al*. 32-year experience with surgical repair of sinus of valsalva aneurysms. *J Card Surg* 2005;**20**:198–204.

28 Van Son JA, Danielson GK, Schaff HV, *et al*. Long-term outcome of surgical repair of ruptured sinus of Valsalva aneurysm. *Circulation* 1994;**90**:II20–9.

29 Kumar P, Banerji A. Transcatheter closure of ruptured sinus of Valsalva aneurysm. *Catheter Cardiovasc Interv* 2010;**76**:774–6.

30 Kerkar PG, Lanjewar CP, Mishra N, *et al*. Transcatheter closure of ruptured sinus of Valsalva aneurysm using the Amplatzer duct occluder: immediate results and mid-term follow-up. *Eur Heart J* 2010;**31**:2881–7.

Systemic Arteriovenous Fistula

Ahmad I. Alomari

Children's Hospital Boston, Harvard Medical School, Boston, MA, USA

Introduction and background

The widely used classification of vascular anomalies was proposed by Mulliken and Glowacki in 1982 [1]. This classification, based upon clinical, histologic, histochemical, biochemical, and imaging features, divides vascular anomalies into two major categories: tumors and vascular malformations (Table 26.1). Vascular malformations are divided into two major types: the slow-flow (e.g., venous malformation, lymphatic malformation) and fast-flow malformations [namely, arteriovenous malformation (AVM) and arteriovenous fistula (AVF)].

An arteriovenous shunt implies direct communication between the arteries and veins without passing through a capillary bed. In AVFs, the shunt is a simple direct communication between an artery and a vein, whereas in AVMs, the shunt is via a complex network of feeding arteries and draining veins. This distinction has major clinical, prognostic, and therapeutic implications. This chapter focuses on the clinical, imaging, and management aspects of systemic arteriovenous fistulas excluding the heart and lungs (see chapters 46 and 48).

Incidence

Congenital AVFs are much less common than acquired AVFs, and are rarely seen even at specialized vascular anomalies centers. Congenital fast-flow lesions are the least common types of vascular malformations.

The distinction between different types of vascular malformation has often been unclear in the literature. For example, Knudson and Alden reviewed 156 infants (<6 months old) with high flow lesions, of whom 81 had lesions in the CNS, 61 in the liver, and 14 in the lung [2]. The incidence of heart failure was 48–67% with a very high mortality (43–64%). Many of the patients with liver "high-flow" lesions probably had liver hemangiomas (as evident by a mass) rather than a true AV shunt. In one review of patients with AVFs, only 10% of the AVFs were in the head and neck area and none were visceral AVFs [3]. Nevertheless, accumulated experience with these lesions suggests a different distribution, with cerebrofacial fast-flow lesions being more frequent than in other locations [4].

Acquired AVFs are usually iatrogenic, particularly after percutaneous or surgical vascular interventions. Of >13 000 femoral arterial accesses for cardiac catheterization, iatrogenic AVFs were found in 0.11% [5]. Risk factors are periprocedural anti-coagulation, hypertension, and female gender [6]. The incidence is also higher with complex procedures using larger vascular sheaths. Other examples of acquired AFVs are shunts placed for dialysis and those created between and axillary artery and vein to enhance pulmonary blood flow in a patient with a Glenn anastomosis. Other causes are iatrogenic (surgery, biopsy), trauma (war injuries, fractures and stab wounds) [7], infection, and tumors.

Etiology and genetics

Formation of the vascular network in the embryo primarily includes two distinct mechanisms: vasculogenesis and angiogenesis [8–10]. Vasculogenesis *in situ* concerns differentiation and growth of blood vessels from mesodermal-derived hemangioblasts giving rise to the heart and the first primitive vascular plexus, and angiogenesis remodels and expands this network [10]. Both the arterial and venous lineages arise from this common plexus with complex network of communications between them. Nevertheless,

Table 26.1 Classification of vascular anomalies (Reproduced with permission from Mulliken JB, Glowacki J. *Plast Reconstr Surg* 1982;**69**:412–22.)

Vascular anomalies	
Tumors	**Malformations**
A. Benign (hemangiomas):	Low flow:
1. Infantile hemangioma (IH)	1. Capillary malformation (CM)
2. Rapidly involuting congenital hemangioma (RICH)	2. Venous malformation (VM)
3. Non-involuting congenital hemangioma (NICH)	3. Lymphatic malformation (LM)
	High flow:
	Arteriovenous malformations (AVMs) and fistulas (AVFs)
B. Borderline malignant: kaposiform hemangioendothelioma (KHE)/tufted angioma (TA), epithelioid hemangioendothelioma	Combined and syndromic
C. Other rare tumors, e.g., angiosarcoma	

there is an essential and early developmental distinction between arteries and veins, later exaggerated by blood pressure [11]. Molecular differences between arterial and venous channels, which accompany or even contribute to functional and morphologic differences, begin before the establishment of the circulation with several genes specifying the arterial–venous distinction (e.g., ephrinB2, EphB4. Notch1, Notch4, Dll4, and Jagged1, NRP1, CXCR4, connexin-37, connexin-40, CD44, Bmx, and Alk1) [12,13].

Primitive fetal arteriovenous connections are eventually obliterated. Congenital AVFs likely result from persistent embryonic connections between the primordia of arteries and veins originating from a common mesenchymal tissue between the fourth and eighth weeks of embryonic life [14–16].

Congenital AFVs are typically solitary and sporadic (i.e., unassociated with syndromes or known genetic defects). Several complex and overgrowth syndromes are associated with fast-flow vascular anomalies. Examples include hereditary hemorrhagic telangiectasia (Osler–Weber–Rendu syndrome), CLOVES syndrome, PTEN hamartoma syndromes, and capillary malformation–arteriovenous malformation (CM–AVM). AVFs have also been reported in Noonan syndrome [17], Ehlers–Danlos syndrome [18,19], VACTERL association and fibromuscular dysplasia [20], and liver hemangioma [21], among others. Infantile hemangioma and rapidly involuting congenital hemangioma (RICH) are probably the most vascular pediatric tumors and can occasionally be associated with arteriovenous shunts. Hepatic RICH is typically a large, solitary mass and might be associated with various types of transhepatic vascular shunts and high-output heart failure [22].

Hereditary hemorrhagic telangiectasia (HHT), or Osler–Weber–Rendu syndrome, is an autosomal dominant disease characterized by epistaxis, mucocutaneous and gastrointestinal telangiectasia, and arteriovenous malformations in the lungs, CNS, and liver [23]. The two most common genetic mutations affect endoglin (ENG) (type 1) and ALK1 (type 2). HHT gene mutations lead to the development of abnormal vascular structures, which range from dilated microvessels to large AVFs [24]. The resulting disorganized cytoskeleton and failure to form cord-like structures are common characteristics of endothelial cells in HHT patients and disrupted abnormal angiogenesis [25].

Capillary malformation–arteriovenous malformation (CM–AVM) is an autosomal dominant disease caused by RASA1 gene mutation. Clinically, patients develop multiple capillary malformations without overgrowth [26]. Arteriovenous malformation occurs in about 12% of patients and may involve the CNS.

Bannayan–Riley–Ruvalcaba syndrome, caused by mutation in PTEN gene, is characterized by macrocephaly, lipomatosis, pigmented penile macules, vascular malformations, mental/developmental delay, Hashimoto's thyroiditis, and assorted tumors [27]. A spectrum of vascular anomalies, including paraspinal AVM, occur in >50% of these patients [28].

CLOVES syndrome (congenital lipomatous overgrowth, vascular malformations, epidermal nevi, and skeletal/scoliosis/spinal anomalies), recently described, is a complex overgrowth disorder of vessels [29,30]. Fast-flow spinal–paraspinal vascular lesions, including AVMs and AFVs, are frequently encountered in this syndrome and cause debilitating spinal myelopathy [29,31].

Arteriovenous fistula can also be associated with persistent embryonal vessels such as the primitive olfactory [32,33] and sciatic arteries [34].

Klippel–Trenaunay syndrome (KTS) and Parkes–Weber syndrome (PWS) are two overgrowth syndromes of the extremities with complex vascular anomalies. Although they may share some clinical features, they are separate clinical entities with different pathogenesis and natural history. The designation "Klippel–Trenaunay–Weber syndrome" for a patient is misleading. KTS is a rare limb overgrowth disorder with slow-flow vascular anomalies including capillary, venous, and lymphatic malformations. KTS is not associated with fast-flow lesions [35,36] and the reported association between KTS and AVMs (particularly in the spinal region) is erroneous [37]. PWS is characterized by hypervascular (fast-flow) anomalies and capillary malformation in an overgrown limb (Figure 26.1). The capillary stain is pink, multiple, and diffuse. The symptoms are related to distal ischemia and high-output heart failure. PWS is not simply KTS with an AVM, as posited in some references. Improper assessment of patients can lead to the wrong diagnosis, mistreatment, and misdirected research efforts [38].
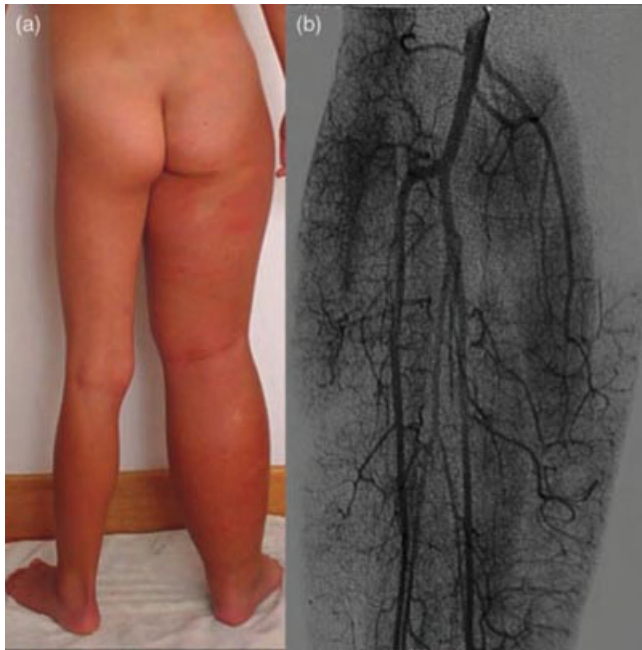
Figure 26.1 Parkes–Weber syndrome. (a) Diffuse faint capillary stain of the warmer hypertrophied right lower extremity. (b) The angiogram of the calf shows a diffuse increase in the arterial flow to the soft tissue with dense blush and no definite arteriovenous fistulas.

Pathologic anatomy

The two main types of fast-flow vascular malformations are AVMs and AVFs. Occasionally they are combined.. AVMs are abnormal communications between enlarged feeding arteries and draining veins via a smaller complex network of channels (nidus). AVFs are direct end-to-end communications between an artery and vein, and are classified as simple (supplied by one feeding artery) or complex (receiving blood supply from two or more feeding arteries) [39].

Based on the angioarchitectural pattern, arteriovenous shunts can be classified into three main categories: (1) arteriovenous (a few arterial feeders reaching a single draining vein which represents the initial venous compartment), (2) arteriolovenous (several small feeding arteries draining into a single vein which constitutes the initial venous compartment), and (3) arteriolovenulous (plexiform pattern of several small feeding arteries shunting into small corresponding small veins) [40]. The advantages of this classification are simplicity, accuracy, and the ability to predict the endovascular approach of treatment (arteriolovenulous lesions should be treated via the arterial route only, whereas arteriovenous and arteriolovenous shunt fistulas can be treated via transarterial or transvenous approaches). Although this classification was originally proposed for cerebral AVMs, it can be applied to other locations.

The histopathologic changes within the AVF pedicle include heterogeneity in vessel size and wall thickness, an increase in collagen deposition, splitting of the elastic lamina, multiple layers in the endothelium, and immature features of endothelial cells [41].

Pathophysiology

Shunting of arterial blood into a low-resistance draining vein causes several pathophysiologic changes. Both feeding artery and draining veins progressively dilate with increasing rate of left-to-right shunting. To compensate for the blood volume diverted via the shunt, both the blood volume and cardiac output increase. The sequential hemodynamic and structural changes resemble a large left-to-right shunt such as a PDA, including elevated arterial systolic pressure with normal/low diastolic pressure (widened pulse pressure), cardiomegaly (from enlargement of both ventricles), and high output failure [42]. Both fetal and postnatal AVFs are associated with persistent pulmonary hypertension (as are large AV shunts) with both functional and structural alteration of the pulmonary vasculature [43,44]. Following shunt closure, pulmonary hypertension subsided dramatically [45]. Significant AV shunting produces systemic vasoconstriction with decreased renal blood flow and activation of vasodilating systems [46–48].

Local hemodynamic and tissue disturbances can be attributed to the changes in the arterial and venous sides of the fistula. The capillary pressure is higher in tissue sharing the same feeding arterial pedicle as the AVF than in the draining vein. Blood preferentially flows away from the normal tissue, which eventually becomes chronically ischemic (steal phenomenon). The direct flow of arterial blood into the draining vein causes venous hypertension, which may become clinically evident particularly in the lower extremities.

Nicoladoni–Branham sign (bradycardia induced by temporary compression of large AVFs) is caused by arterial baroreceptor activation, which leads to decreased sympathetic nerve traffic, and increased arterial baroreflex sensitivity decreases heart rate [49].

Anatomic locations of AVFS

AV shunts have a predilection for the cerebrofacial region. Intracranial AV shunts are far more common than extracranial lesions, followed in frequency by the limbs, trunk, and viscera. Specific types and anatomic locations of AVFs are discussed below.

Intracranial AVFs
Intracranial fast-flow shunts can be broadly categorized as pial (parenchymal) and dural. They can be classified according to the angioarchitecture and the developmental etiology [50], and divided into single (AVM or AVF), multiple non-familial (metameric or nonmetameric), and multiple familial (systemic and nonsystemic).

Intracranial dural AVFs are shunts between the dural arteries and dural veins and sinuses. Although intracranial fistulas are

Table 26.2 Cognard classification of dural AVFs (Reproduced with permission from Alvarez H, Garcia Monaco R, Rodesch G, *et al. Neuroimaging Clin N Am* 2007;**17**:189–206.)

Type	Drainage
I	Normal anterograde flow into a dural sinus
IIa	Drainage into a sinus with retrograde flow
IIb	Drainage into a sinus with retrograde cortical flow
III	Drainage into cortical veins
IV	Drainage into ectatic cortical vein

typically considered to be congenital in children (e.g., vein of Galen aneurysmal malformation), dural AVFs in adults are typically acquired [50]. Several classifications [such as proposed by Cognard] (Table 26.2) and subclassifications of these lesions have been proposed, based primarily on their venous drainage [51,52], although a recent modified classification was based on the natural history of the disease and the risk of intracerebral hemorrhage or nonhemorrhagic neurologic deficits [53]. The venous drainage of dural AVFs is also responsible for the clinical presentations, including hemorrhage, progressive neurologic deficit, and intractable tinnitus. Leptomeningeal or cortical venous drainage is associated with a worse clinical presentation and requires prompt management [54].

The arterial supply of dural AVFs varies but is typically from branches of the external carotid artery, such as the middle meningeal, accessory meningeal, internal maxillary, occipital, and ascending pharyngeal arteries. Pial supply is rare [50]. The venous drainage can be into any dural sinus.

Dural AVFs with minor symptoms and no retrograde flow in the sinus or cortical vein can be managed conservatively. Endovascular therapy is preferred for most dural AVFs, although certain locations warrant neurosurgical or combined techniques (Figure 26.2) [55].

Cerebral (Pial or Parenchymal) AVMs

These are shunts from branches of the internal carotid or vertebral arteries and usually affect the cerebral hemispheres, including cortical locations, deep nuclei, and corpus callosum. Although congenital, they present in adults with variable symptoms depending on the location of the AVM and other factors. Bleeding, neurologic deficits, seizures, and headaches are common presentations. The risk factors predicting subsequent hemorrhage with cerebral AVMs are young age, previous rupture, deep and infratentorial locations, exclusively deep venous drainage, and large size [56]. The approach to treatment of cerebral AVMs should be managed by an interdisciplinary team. Therapeutic modalities include embolization, surgery, and radiotherapy. A combination of these is often used. About 10–40% of patients are completely cured by embolization.
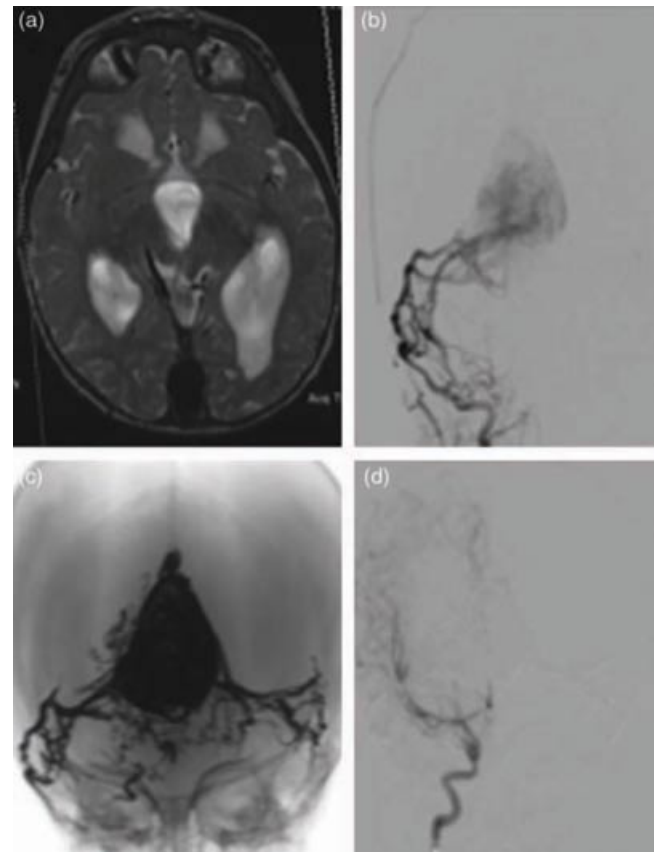
Figure 26.2 Dural AVF. (a) Axial T2 MR image of the brain depicting the dilated torcula herophili and intracranial, orbital, and scalp vessels. External carotid angiography demonstrated the fistulas to the dilated torcular herophili (b) which was successfully embolized utilizing microcoils and Onyx (ethylene–vinyl alcohol copolymer) (ev3 Neurovascular, Irvine, CA, USA), as shown in (c) and (d).

Vein of Galen Aneurysmal Malformations (VGAMs)

VGAMs are fistulous communications between the choroidal and quadrigeminal arteries and the embryonic median prosencephalic vein (the precursor of vein of Galen) [57]; the use of "vein of Galen" to refer to these malformations is a misnomer. Although rare, VGAMs represent approximately one-third of the infantile cerebral vascular anomalies [58].

Two main angioarchitectural types of VGAM are recognized: choroidal and mural [59]. The arterial supply of VGAMs is typically complex. In the choroidal type, multiple arteries (e.g., choroidal, subforniceal, pericallosal, thalamoperforating) fistulate into the anterior end of the vein, whereas the mural type has an AVF located in the inferolateral wall of the draining vein [60].

The clinical presentation depends on the patient's age: neonates typically present with high-output cardiac and respiratory difficulty, infants and older children with hydrocephalus, mental retardation, seizures and headache [58–66].
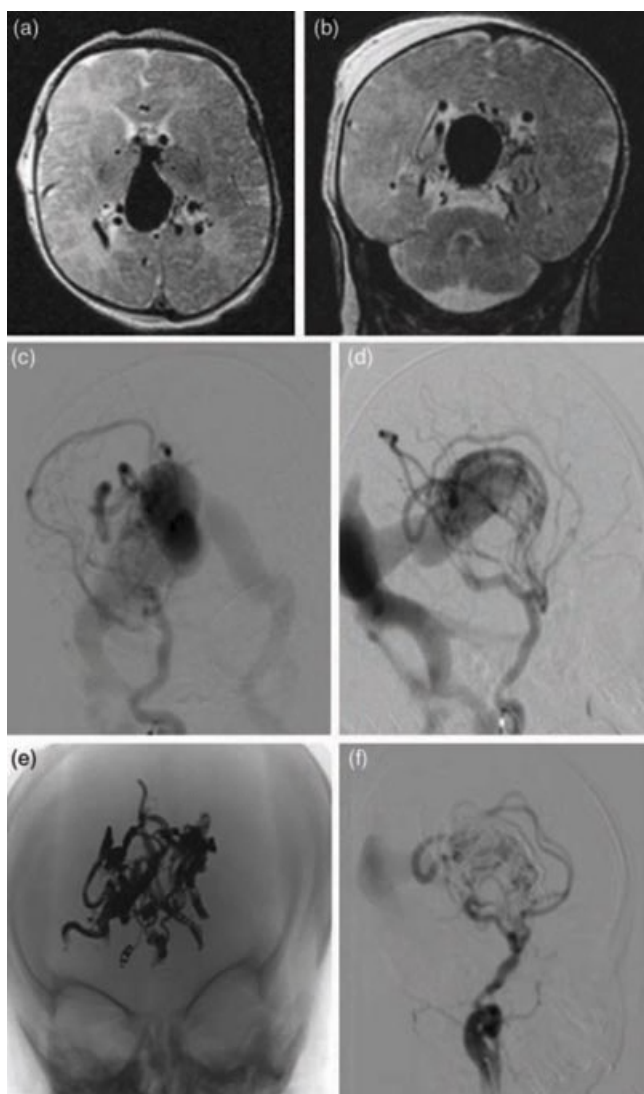
Figure 26.3 Vein of Galen aneurysmal malformation. Axial (a) and coronal (b) T2 MR images of the brain show the aneurysmally dilated median prosencephalic vein (the precursor of vein of Galen) with numerous surrounding flow voids representing arterial feeders. Internal carotid angiography in the frontal (c) and lateral (d) projections demonstrates numerous fistulas via small branches. Note the persistence of the limbic arch. Successfully transarterial embolization with Onyx was performed [frontal projection (e)] with excellent control of the malformation (f).

The optimal treatment of VGAMs is endovascular therapy at a tertiary care center with a multidisciplinary team experienced in these challenging malformations (Figure 26.3) [60]. Patients who may benefit from the endovascular treatment must be carefully selected using a systematic evaluation protocol performed within an optimal therapeutic window. The objective of therapy is normal development in a child without neurologic deficit [66].

Embolization of VGAMs via the arterial approach is widely used, but both transvenous and direct injection into the

confluence of dural sinuses have also been described [58], although the latter was associated with higher mortality. The percutaneous transvenous approach is sometimes used to treat complex, multipedicular VGAMs [58].

The outcome of embolization treatment of VGAMs at a tertiary center of 317 patients, of whom 233 were treated with transarterial embolization, revealed that 23 children (10.6%) died despite or because of the embolization; 143 of 193 surviving patients (74%) were neurologically normal, 30 (15.6%) were moderately retarded, and 20 (10.4%) were severely retarded [66].

Spinal dural AVFs

These account for 80–85% of high-flow shunts [67]. Spinal shunts are classified into four main categories: type I, dural arteriovenous fistulas (AVFs); type II, intramedullary glomus AVMs; type III, juvenile or combined AVMs; and type IV, intradural perimedullary AVFs [68]. These lesions lead to progressive neurologic impairment such as sensory, motor, and sphincter dysfunction [69,70]. Dural AVFs can be successfully treated with endovascular or surgical therapy [71]. Due to the complex angioarchitecture of these AV shunts and the presence of adjacent vital areas, super-selective angiographic techniques are used for cerebral and spinal shunts to define the site of the shunt precisely without disturbing associated structures [72].

Cervicofacial AVFs: Carotid-jugular fistulas

These are likely to be between the external carotid (rather than the internal carotid) and the jugular vein. These rare lesions may present early after birth with heart failure [73] or during the first decade of life [74]. In older children and adults, these lesions may present with pain, pulsatile mass, tinnitus, cardiac failure, bleeding, or local regional ischemia [75–82]. External carotid artery ligation has no role in the current management of carotid–jugular fistulas [80]. Ligation proximal to the AV shunt is eventually bypassed by collateral feeders that are smaller and more complex than the original feeding arteries. It also eliminates future transarterial access to the lesion. Embolization is the preferred management of external carotid–jugular fistulas [75].

Vertebrovertebral AVFs

These are connections between the extracranial vertebral artery or one of its branches to the adjacent veins. Most of these fistulas are iatrogenic and may occlude spontaneously neighboring veins [83]. They also can be congenital or associated with fibromuscular dysplasia and neurofibromatosis [84,85]. Symptoms are from arterial steal, spinal venous hypertension, and compression causing neurologic deficits, hemorrhage, and cardiac failure in neonates and infants, A local bruit is often the first sign [83,86]. Embolization, alone or in combination with surgical repair, is feasible, safe, and highly effective, with low morbidity and mortality
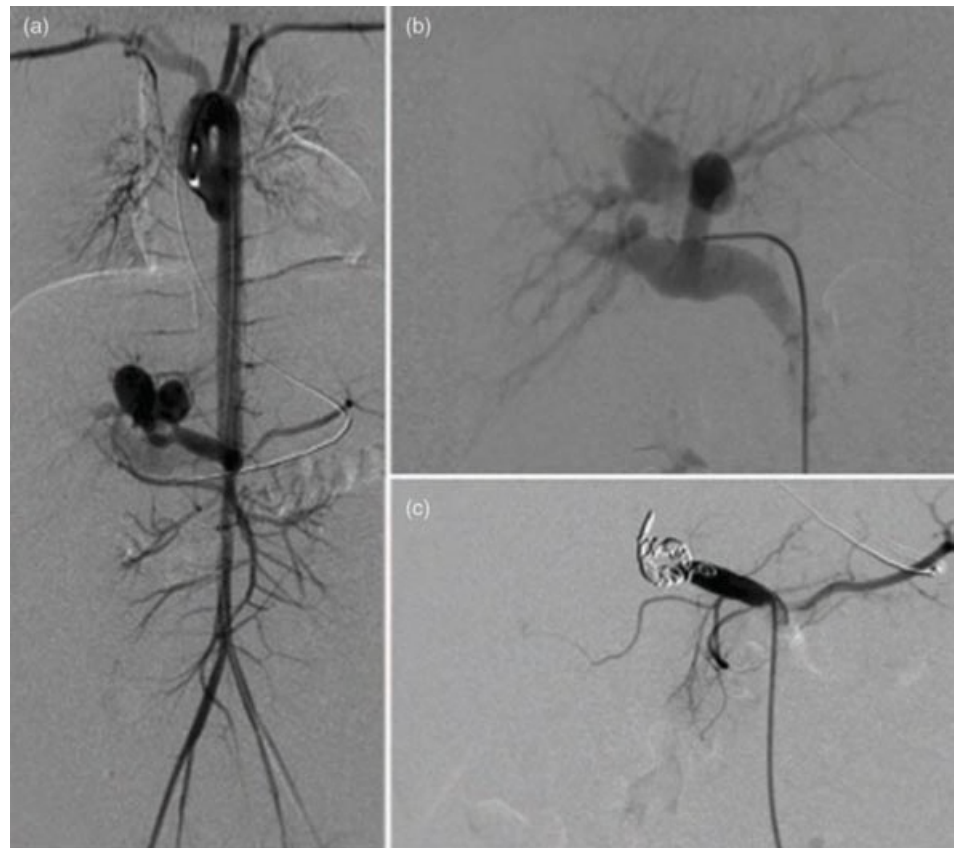
Figure 26.4 Simple arterioportal fistula. Aortography in the frontal (a) projection and selective injection (b) shows an enlarged hepatic artery with a fistula to an aneurysmal portion of the portal vein. (c) Angiographically and clinically successful occlusion of the fistula with coils.

[83,86]. Mandibular AVFs may present severe hemorrhage requiring urgent treatment [79–88].

Abdominal AVFs

Acquired renal AVFs are more common than congenital lesions and usually result from penetrating trauma, percutaneous biopsy, surgery, malignancy, or inflammation [89,90]. Spontaneous renal AVFs can be bilateral and often occur in females and on the right kidney. Significant morbidity with hypertension, hematuria, proteinuria, congestive heart failure, and rupture of the fistula may occur [91]. Renal AVF may present either in infancy [92] or later in life, particularly during pregnancy [93].

Treatment options include embolization [75], surgical ligation of the feeding artery [75], or total or partial nephrectomy [94–96]. Embolization should be the initial treatment because of its decreasing morbidity and increasing efficacy and the potential complications and loss of normal renal parenchyma from other treatment methods [96].

Arterioportal fistulas

Arterioportal fistulas can be either intra- or extrahepatic and either congenital or acquired (secondary to cirrhosis, tumors, trauma, rupture of hepatic artery aneurysm, and iatrogenic causes) [97–104]. Most congenital arterioportal shunts are sporadic. Rarely, these fistulas are associated with other disorders such as Down syndrome, hereditary hemorrhagic telangiectasia, Ehlers–Danlos syndrome, and biliary atresia [98,105–107]. Congenital arterioportal shunts present early in infancy, although symptoms may not present until childhood or adulthood. The signs and symptoms can be nonspecific, and include those of portal hypertension (ascites, malabsorption, gastrointestinal bleeding, and abdominal pain), bowel ischemia, and high-output cardiac failure [106,108,109].

The angioarchitecture of congenital arterioportal fistulas can be simple (end-to-side connection between an arterial feeder and the portal vein) (Figure 26.4) or complex with numerous small feeders from mesenteric (e.g., the hepatic, gastroduodenal, and superior mesenteric) and non-mesenteric (e.g., phrenic and internal mammary) arteries. Aortography typically depicts a dilated aorta proximal to the origin of the celiac artery and distal tapering. The portal vein is dilated or focally aneurysmal (portal varix) at the site of the fistula. The hepatic artery may have no or little supply to the liver parenchyma [98].

These lesions have been stratified into three major categories: type 1 is a small peripheral intrahepatic fistula (typically secondary to needle biopsy), type 2 is a large central fistula, and type 3 is a congenital lesion [110]. Type 1 usually

resolves spontaneously whereas type 2 and 3 cause portal hypertension and hepatic parenchymal changes and should be treated. Because portal hypertension develops, even asymptomatic arterioportal fistulas should be treated [110]. Embolization of congenital lesions allows definitive closure of most shunts, and surgical ligation is typically reserved for the rare failure of endovascular treatment [100,101,111,112]. Minimally invasive embolization techniques allow faster recovery, have fewer complications, and can be safely repeated [98]. Following embolization, the patient should be monitored for acute portal vein thrombosis, particularly if the portal vein is aneurysmally dilated. Liver transplantation may be considered in some patients in whom both embolization and surgical ligation of the fistulas fail [102,103].

The increased flow and pressure within the portal venous system from the arterioportal fistula may be decompressed via a patent ductus venosus. Acute presentation of arterioportal AVF with gastrointestinal bleeding could possibly be precipitated by spontaneous closure of the ductus venosus. Hence we believe that the ductus venosus should not be closed during the embolization treatment of the arterioportal AVF because, once obliterated, the ductus venosus spontaneously closes [98].

For acquired arterioportal fistulas, some authors consider surgical repair to be the procedure of choice for the extrahepatic type, whereas embolization is optimal for intrahepatic fistulas and for patients whose associated co-morbidity prohibits surgical treatment [110].

Portosystemic Fistulas (PSFs)

PSFs, although the shunt in a PSF connects two separate venous systems, have many similarities to AVFs. The normal pressure gradient between the portomesenteric and systemic veins always directs the flow toward the latter. PSFs divert portal and mesenteric venous blood into the systemic veins, via either intra- or extrahepatic channels, bypassing the liver. These rare shunts can be sporadic or associated with other disorders (e.g., Down syndrome, congenital heart disease, heterotaxy, Goldenhar syndrome, biliary atresia, mental retardation, and genitourinary malformations) [97,98,113]. Intrahepatic portosystemic shunts are connections between the portal vein and hepatic vein or IVC and can be divided into four main types: (1) single fistula between the right portal vein and the IVC, the most common form, (2) localized fistula within a hepatic segment, (3) fistula through a varix, and (4) multiple fistulas between peripheral portal and hepatic veins [114,115]. Extrahepatic portosystemic shunts were first described by Abernethy and later classified by Morgan and Superina into complete (type 1 or end-to-side) and partial (type 2 or side-to-side) portosystemic diversion, in addition to other less common forms [116,117]. In type I, the portal vein is believed to be absent; thus the mesenteric venous return is diverted into the IVC. Portosystemic fistulas should be differentiated from persistent ductus venosus-related rare hepatic metabolic disorders (e.g., neonatal hemochromatosis leading to hepatic failure, portal hypertension, and coagulopathy) in which closing the ductus venosus is contraindicated [118].

Symptomatic portosystemic shunts present with cardiopulmonary dysfunction, hepatic encephalopathy, metabolic abnormalities (hyperammonemia and galactosemia), coagulopathy, and failure to thrive [119–122]. There is an increased risk of developing hepatic tumors (such as focal nodular hyperplasia, nodular regenerative hyperplasia, adenoma, hepatoblastoma, and hepatocellular cancer) [123–126] and hepatopulmonary syndrome [127].

Children seem relatively less prone to develop hepatic encephalopathy. Nevertheless, some authors believe that a shunt ratio >60% should be corrected because of the risk of encephalopathy and liver dysfunction [98,121,122]. Some low-flow shunts regress spontaneously during infancy [98,119]. Both embolization and surgical banding have successfully obliterated these fistulas [98,119,123]. Closure of type 1 (complete) extrahepatic portosystemic shunts is contraindicated because the fistula is believed to be the sole drainage of the splanchnic venous system. For this rare subset of patients, liver transplantation has been successfully performed [128–133].

In a literature review of 91 reported patients with splenic AVFs, 44% were from a ruptured splenic artery aneurysm, 20% were congenital and 13% were sequelae of splenectomy [134].

Females are more commonly affected than males, and pregnancy and multiparity are considered predisposing conditions [135]. Splenic AVFs present with signs and symptoms of portal hypertension, including variceal gastrointestinal bleeding, ascites, abdominal pain, and bruit [136–140]. Post-traumatic splenic AVFs may spontaneously regress [141]. Because of the fistula's location, adhesions, and extensive portal collateral vessels, surgical repair of the fistula can be challenging [142]. As embolization is safe and efficacious [143–150], it should be the first line of management for these shunts.

Congenital uterine AV shunts are very rare and fed by extrauterine arterial branches [151]. Acquired lesions typically occur after pregnancy-related procedures, such as an abortion or Cesarean section [152]. The treatment of uterine AV shunts should consider the patient's future fertility. Thus, embolizing the uterine artery is indicated in patients who plan future pregnancies, whereas hysterectomy can be considered for recurrent bleeding after embolization in patients not planning future pregnancies [153,154].

AVFs of the extremities

The lower extremity is the most commonly affected site [22]. Besides trauma, iatrogenic causes are not uncommon and follow surgical and interventional procedures [5,6]. For instance, postcatheterization femoral artery AVFs are
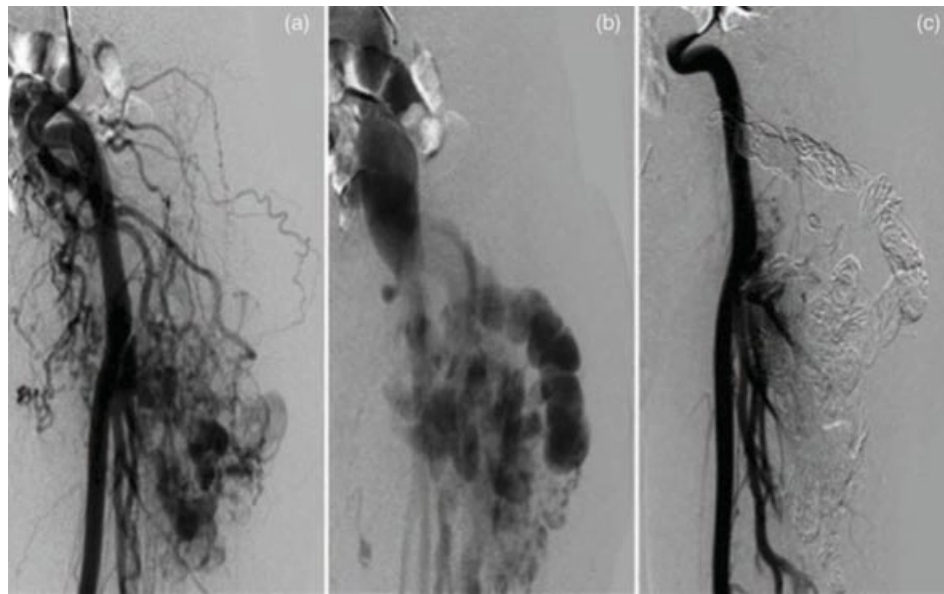
Figure 26.5 Extensive arteriovenous malformation of the left lower extremity and hemipelvis. The angioarchitecture as shown in the arterial phase (a) shows numerous dilated arteries from the internal iliac and profunda femoris arteries communicating directly with huge draining veins with some venous aneurysmal changes (b). Both fistulas and nidal types shunts are present. (c) The draining veins were embolized percutaneously with a marked reduction of the AV shunting.

frequently encountered at busy cardiac catheterization units. Nevertheless, they typically have a benign natural history and most (81%) resolve spontaneously [155,156]. Persistent femoral AVFs are typically repaired surgically.

Congenital AV shunts are typically complex with a nidal angioarchitecture supplied by numerous branches. The lesions typically affect the soft tissue component of the limb (Figures 26.1 and Figure 26.5), although some are centered within and around the bone. Extremity AV shunts can be extensive and have a large hemodynamic effect with potential high-output heart failure [157,158]. They present with diffuse, progressive overgrowth of the extremity (Figure 26.6). Distal to the shunt, signs of ischemia (e.g., skin atrophy, hair loss) become evident with time. In advanced disease, ischemia may also cause ulceration, bleeding, and pain [159–161]. Pain is the most common presenting symptom and hemorrhage is the rarest but most serious complication. Venous hypertension may cause marked cutaneous changes such as dark hyperpigmentation, skin thickening, and venous ulcers (Figure 26.7). Painful reddish violet cutaneous plaques (occasionally referred to as pseudo-Kaposi's sarcoma or Stewart–Bluefarb syndrome) may be associated with high-flow lesions of the extremities (Figure 26.7). The etiology of this phenomenon is not known, but possibly related to local venous flow disturbance [160,161].

Subclavian AVFs

Subclavian AVFs are exceedingly rare and may present in infancy with congestive heart failure, stridor, facial and neck swelling, and venous hypertension [162–165]. Popliteal AVFs

Figure 26.6 Arteriovenous malformation of the left foot with overgrowth.

Figure 26.7 (a) Sequelae of long-standing venous hypertension associated with AV shunt of the leg including swelling, hyperpigmentation, thickened, indurated leathery skin, and venous ulceration. (b) Early brownish–reddish macular changes in association with high-flow lesion of the foot (Stewart–Bluefarb syndrome).

are typically caused by trauma and have a high morbidity from high cardiac output and leg amputation [166–168].

Treatment of complex extremity AV shunts requires an interdisciplinary team [157,159], including interventional radiology, cardiology and plastic and orthopedic surgery.

Clinical features and natural history of AVFs

AVFs may present at birth or during childhood or adulthood. Occasionally, AVFs are diagnosed incidentally. The signs of AVFs depend primarily on the volume of blood shunted through the fistula (i.e., the number and size of the fistulas) and the anatomic location. Peculiar signs and symptoms can be specific to certain affected organs or areas.

Typically, in AVFs not located in a body cavity, the affected area is warm and overgrown with thrill or bruit. The overlying skin may demonstrate dilated veins, telangiectasia, capillary stain or, rarely, signs of ischemia. High-flow shunts may cause pain, bleeding, heart failure, ulceration, and tissue loss [169]. Associated tissue overgrowth can lead to disfigurement and compression of adjacent structures. Congenital shunts are a rare cause of congestive cardiac failure in newborns and, except for intracranial and intrahepatic AVFs, the onset of failure is usually later in life [170]. Neonates and young children may exhibit poor physical development and nonspecific symptoms of stress. For large AVFs, upon manual compression or temporary occlusion of the fistula (e.g., by an endoluminal balloon), the heart rate drops (Nicoladoni–Branham sign) [49].

Peripheral AVFs usually follow a progressive course with worsening symptoms. Increased blood flow over time leads to incorporation of more arterial feeders and draining veins, thickening and dilatation of the vessels, aneurysm formation, and weakening of the mucocutaneous coverage [169]. Chronic AVFs may be difficult to differentiate angiographically from nidal-type AVMs; this differentiation has important therapeutic implications [171].

Diagnostic imaging

Findings on plain radiographs are nonspecific and usually reflect secondary changes of the AV shunting. Chest radiographs may show cardiomegaly, increased fluid in the alveolar and septal walls, and pleural effusion (Figure 26.8). Soft tissue and bony overgrowth, altered opacity, atrophy, and opaque embolic agents can also be depicted on plain films. Other findings on plain radiographs include bone thinning and deformity, pathologic fractures, and enlarged vascular foramina of the long bones.

Compared with other vascular anomalies, destructive intraosseous changes are more commonly noted in the arterial or high-flow lesions, possibly related to altered skeletal growth from mechanical, physiologic, and developmental processes [172]. Ultrasonography with color Doppler interrogation is a simple and widely available diagnostic tool for the diagnosis of AVFs [173]. The main sonographic findings are dilated, tortuous feeding arteries and draining veins, lack of soft tissue mass, and thickening/overgrowth of the surrounding tissue. Arterialized veins may mimic arteries with low-resistance pulsatile flow (Figure 26.9). The distinction between vascular masses (e.g., infantile hemangioma) and AV shunts is critical, because their prognosis and treatment are different [175]. Aneurysmally dilated vessels

Figure 26.8 Chest radiograph. High-output heart failure secondary to a massive AV shunt. Note cardiomegaly, septal thickening, and small pleural effusions.

demonstrate turbulence of flow on both gray-scale and color Doppler images.

Computed tomography (CT) scanning provides less tissue contrast than MRI and is infrequently used for diagnosing soft tissue AVFs, but is invaluable for visualizing the bony changes. Both MR angiography (MRA) and CT angiography (CTA) can be used to depict the AVF's spatial anatomy and relations with the surrounding tissue (Figure 26.10).

Angiography is infrequently needed for the diagnosis of AVFs. Nevertheless, some chronic AVFs may mimic AVMs on clinical and sonographic examinations and must be differentiated. The typical angiographic features of infantile hemangiomas include a soft tissue mass with multiple, enlarged feeding arteries, well-circumscribed contrast blush in the tissue/capillary phase, and lack of immediate AV shunting. In addition, the closely packed proximal feeding arteries form an "equatorial" network at the periphery of the hemangioma, sending smaller feeding arteries into the lesion at right-angles to the peripheral vessels with large draining veins at the base of the mass [174].

Management

Management of arteriovenous fistulas is simpler than that of the nidus-type AVMs. The latter is one of the most challenging interventional procedures and requires extensive experience
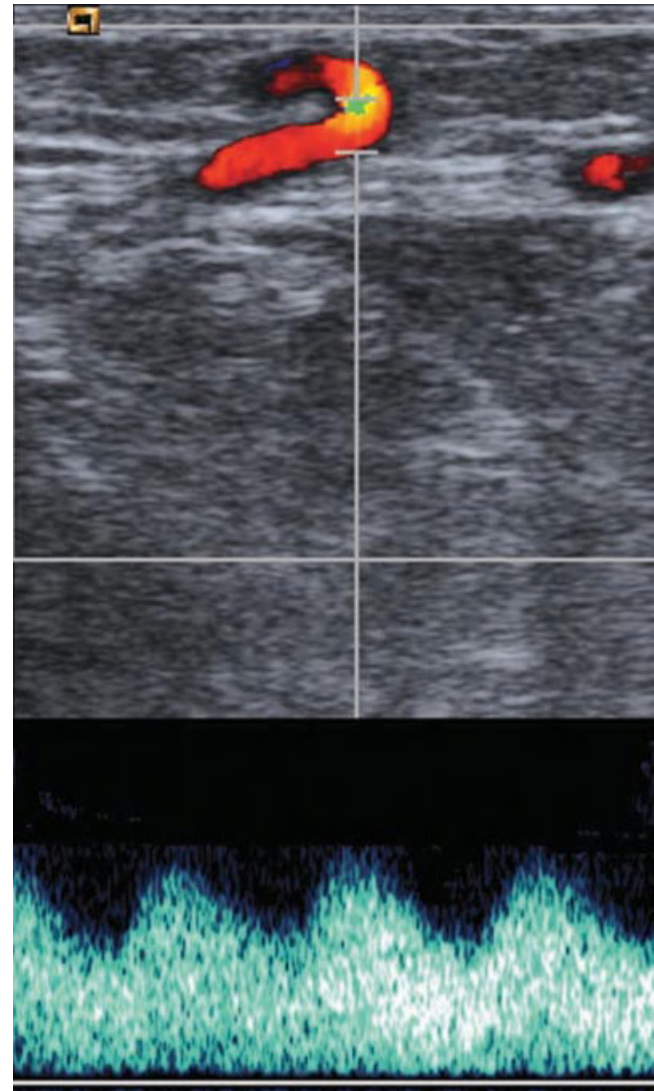
Figure 26.9 Ultrasound of an extensive AV shunt of the lower extremity. Note the abnormally superficial, tortuous arterial branch within the subcutaneous tissue. The spectral wave demonstrates a high diastolic component (low resistance pattern).

in performing superselective angiography using various types of embolic agents.

Proximal embolization of AV shunts by focal obliteration of a feeding vessel leaves some distal collateral flow. Proximal embolization is equivalent to proximal surgical ligation and should be avoided.

There are different approaches to close simple AVFs. The fistula can be closed transarterially or transvenously. Direct percutaneous access to some accessible fistulas sometimes offers a good alternative [175]. In some patients, a combination of accesses is warranted. Regardless of the approach, the fistula should be closed as close as technically possible to the direct communication between the artery and the vein.
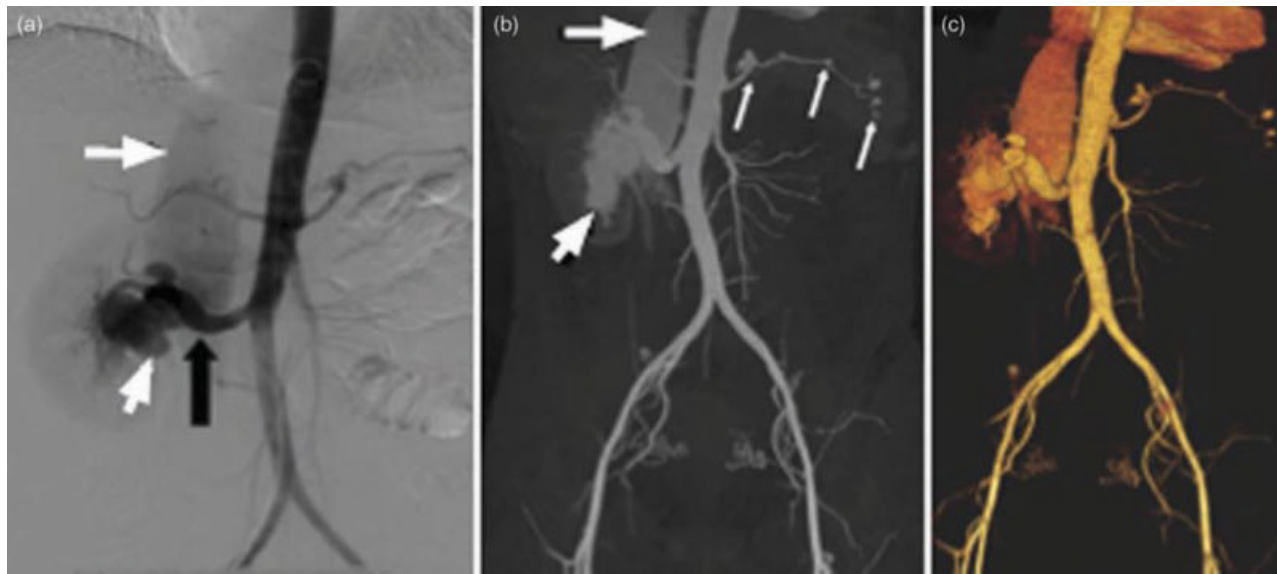
Figure 26.10 (a) Frontal abdominal aortogram of large renal AVF demonstrates the enlarged, single renal artery (large black arrow) with direct fistulas to the renal vein (lower white arrow) and dilated inferior vena cava (upper white arrow). Note the small aneurysm of the proximal segment of the splenic artery. (b) Coronal maximum intensity projections (MIP) and (c) volume rendering (VR) display of the AVF. The dilated draining renal artery, vein (lower thick arrow), dilated IVC (upper thick arrow) and multiple aneurysms of the splenic artery (thin white arrows) are clearly demonstrated in both techniques.

For complex AVFs with multiple feeding arteries and one dominant vein, obliterating the draining vein can achieve excellent control of the shunt without the need to embolize multiple or numerous feeding arteries.

Some AVFs, commonly arterioportal shunts, present with aneurysmal dilatation of the immediate segment of the draining vein, which can be large. These are treated by embolization transarterially without obliterating the venous aneurysm. There is a risk of post-embolization thrombosis of the venous aneurysm and, for some large aneurysms, post-embolization prophylactic anticoagulation is warranted. This is particularly important for arterioportal fistulas.

Sacrifice of the feeding artery is rarely needed for complex AVFs. The technique is still frequently used for caratico-cavernous fistulas and life-threatening cervicofacial hemorrhage from a carotid artery [176–180].

Proper management of AVFs requires an interdisciplinary group of interventional, surgical, and medical specialists.

Clinical and imaging follow-up is preferably performed or supervised by the individual who performed the procedure. Imaging studies should be simple and safe, particularly in children, and complex studies should be used only if essential. Minimizing the radiation in pediatric diagnosis and interventions can be achieved by standardizing workflow and encouraging team responsibility [181]. For instance, instead of repeating the angiographic or CT studies after embolizing a portovenous fistula, adequate diagnostic information can be obtained with ultrasonography.

References

1 Mulliken JB, Glowacki J. Hemangiomas and vascular malformations in infants and children: a classification based on endothelial characteristics. *Plast Reconstr Surg* 1982;**69**:412–22.

2 Knudson RP, Alden ER. Symptomatic arteriovenous malformation in infants less than 6 months of age. *Pediatrics* 1979;**64**:238–41.

3 Gomes M, Bernatz P. Arteriovenous fistula: a review and ten-year experience at the Mayo Clinic. *Mayo Clin Proc* 1970;**45**:81–102.

4 Mulliken JB, Fishman SJ, Burrows PE. Vascular anomalies. *Curr Probl Surg* 2000;**37**:517–84.

5 Kim D, Orron DE, Skillman JJ, *et al*. Role of superficial femoral artery puncture in the development of pseudoaneurysm and arteriovenous fistula complicating percutaneous transfemoral cardiac catheterization. *Cathet Cardiovasc Diagn* 1992;**25**:91–7.

6 Kelm M, Perings SM, Jax T, *et al*. Incidence and clinical outcome of iatrogenic femoral arteriovenous fistulas: implications for risk stratification and treatment. *J Am Coll Cardiol* 2002;**40**:291–7.

7 Linder F. Acquired arterio-venous fistulas. Report of 223 operated cases. *Ann Chir Gynaecol* 1985;**74**:1–5.

8 Patan S. Vasculogenesis and angiogenesis as mechanisms of vascular network formation, growth and remodeling. *J Neurooncol* 2000;**50**:1–15.

9 Glotzbach JP, Levi B, Wong VW, *et al*. The basic science of vascular biology: implications for the practicing surgeon. *Plast Reconstr Surg* 2010;**126**:1528–38.

10 Folkman J. Angiogenesis: an organizing principle for drug discovery? *Nat Rev Drug Discov* 2007;**6**:273–86.

11 Zhong TP, Childs S, Leu JP, Fishman MC. Gridlock signalling pathway fashions the first embryonic artery. *Nature* 2001; **414**:216–20.

12 Yamamizu K, Yamashita JK. Roles of cyclic adenosine monophosphate signaling in endothelial cell differentiation and arterial-venous specification during vascular development. *Circ J* 2011;**75**:253–60.

13 Rocha SF, Adams RH. Molecular differentiation and specialization of vascular beds. *Angiogenesis* 2009;**12**:139–47.

14 Sabin FR. Origin and development of the primitive vessels of the chick and of the pig. *Contrib Embryol Carnegie Inst* 1917;**6**:61–124.

15 Sabin FR. Preliminary note on the differentiation of angioblasts and the method by which they produce blood vessels, blood plasma, and red blood cells as seen in the living chick. *Anat Rec* 1917;**13**:199–204.

16 Young AE. Pathogenesis of the vascular malformations. In: Mulliken JB, Young. AE, eds. *Vascular Birthmarks*, 1st edn. Philadelphia: Saunders, 1988: 107–12.

17 Semizel E, Bostan OM, Saglam H. Bilateral multiple pulmonary arteriovenous fistulas and duplicated renal collecting system in a child with Noonan's syndrome. *Cardiol Young* 2007;**17**:229–31.

18 Lynch HT, Larsen AL, Wilson R, Magnuson CL. Ehlers–Danlos syndrome and "congenital" arteriovenous fistulae. A clinico-pathologic study of a family. *JAMA* 1965;**194**:1011–4.

19 Behjati S, Knight Y, Borgstein R, *et al*. A life-threatening complication of Ehlers–Danlos syndrome. *Br J Hosp Med (Lond)* 2009;**70**:360.

20 Alomari AK, Alomari AI. A rare association of fibromuscular dysplasia, renal agenesis, renal arteriovenous fistulae and vertebral anomalies: expanding the "V" in VACTERL association. *Am J Med Genet A* in press.

21 Christison-Lagay ER, Burrows PE, Alomari A, *et al*. Hepatic hemangiomas: subtype classification and development of a clinical practice algorithm and registry. *J Pediatr Surg* 2007;**42**:62–7.

22 Zenzen W, Perez-Atayde AR, Elisofon SA, *et al*. Hepatic failure in a rapidly involuting congenital hemangioma of the liver: failure of embolotherapy. *Pediatr Radiol* 2009;**39**:1118–23.

23 Shovlin CL, Letarte M. Hereditary haemorrhagic telangiectasia and pulmonary arteriovenous malformations: issues in clinical management and review of pathogenic mechanisms. *Thorax* 1999;**54**:714–29.

24 Govani FS, Shovlin CL. Hereditary haemorrhagic telangiectasia: a clinical and scientific review. *Eur J Hum Genet* 2009; **17**:860–71.

25 Fernandez-L A, Sanz-Rodriguez F, Zarrabeitia R, *et al*. Blood outgrowth endothelial cells from hereditary haemorrhagic telangiectasia patients reveal abnormalities compatible with vascular lesions. *Cardiovasc Res* 2005;**68**:235–48.

26 Eerola I, Boon LM, Mulliken JB, *et al*. Capillary malformation–arteriovenous malformation, a new clinical and genetic disorder caused by RASA1 mutations. *Am J Hum Genet* 2003;**73**:1240–9.

27 Marsh DJ, Kum JB, Lunetta KL, *et al*. PTEN mutation spectrum and genotype–phenotype correlations in Bannayan–Riley–Ruvalcaba syndrome suggest a single entity with Cowden syndrome. *Hum Mol Genet* 1999;**8**:1461–72.

28 Tan WH, Baris HN, Burrows PE, *et al*. The spectrum of vascular anomalies in patients with PTEN mutations: implications for diagnosis and management. *J Med Genet* 2007;**44**:594–602.

29 Alomari AI. Characterization of a distinct syndrome that associates complex truncal overgrowth, vascular, and acral anomalies: a descriptive study of 18 cases of CLOVES syndrome. *Clin Dysmorphol* 2009;**18**:1–7.

30 Sapp JC, Turner JT, van de Kamp JM, *et al*. Newly delineated syndrome of congenital lipomatous overgrowth, vascular malformations, and epidermal nevi (CLOVE syndrome) in seven patients. *Am J Med Genet A* 2007;**143**:2944–58.

31 Alomari AI, Chaudry G, Rodesch G, *et al*. Complex spinal–paraspinal fast-flow lesions in CLOVES syndrome: analysis of clinical and imaging findings in 6 patients. *AJNR Am J Neuroradiol* 2011 [Epub ahead of print].

32 Tsutsumi S, Shimizu Y, Nonaka Y, *et al*. Arteriovenous fistula arising from the persistent primitive olfactory artery with dual supply from the bilateral anterior ethmoidal arteries. *Neurol Med Chir (Tokyo)* 2009;**49**:407–9.

33 Moody RA, Poppen JL. Arteriovenous malformations. *J Neurosurg* 1970;**32**:503–11.

34 Madson DI, Wilkerson DK, Ciocca RG, Graham AM. Persistent sciatic artery in association with varicosities and limb length discrepancy: an unrecognized entity? *Am Surg* 1995;**61**:387–92.

35 Baskerville PA, Ackroyd JS, Browse NL. The etiology of the Klippel–Trenaunay syndrome. *Ann Surg* 1985;**202**:624–7.

36 Lindenauer SM. The Klippel–Trenaunay syndrome: varicosity, hypertrophy and hemangioma with no arteriovenous fistula. *Ann Surg* 1965;**162**:303–14.

37 Alomari AI, Orbach DB, Mulliken JB, *et al*. Klippel–Trenaunay syndrome and spinal arteriovenous malformations: an erroneous association. *AJNR Am J Neuroradiol* 2010;**31**:1608–12.

38 Cohen MM Jr. Klippel–Trenaunay syndrome. *Am J Med Genet* 2000;**93**:171–5.

39 De Cillis E, Burdi N, Bortone AS, *et al*. Endovascular treatment of pulmonary and cerebral arteriovenous malformations in patients affected by hereditary haemorrhagic teleangiectasia. *Curr Pharm Des* 2006;**12**:1243–8.

40 Houdart E, Gobin YP, Casasco A, *et al*. A proposed angiographic classification of intracranial arteriovenous fistulae and malformations. *Neuroradiology* 1993;**35**:381–5.

41 Tu J, Karunanayaka A, Windsor A, Stoodley MA. Comparison of an animal model of arteriovenous malformation with human arteriovenous malformation. *J Clin Neurosci* 2010; **17**:96–102.

42 Glaser R, Kramer RJ, Hamby RI, *et al*. Renal arteriovenous fistula masquerading as severe valvar heart disease. *Br Heart J* 1978;**40**:972–5.

43 Jouannic JM, Roussin R, Hislop AA, *et al*. Systemic arteriovenous fistula leads to pulmonary artery remodeling and abnormal vasoreactivity in the fetal lamb. *Am J Physiol Lung Cell Mol Physiol* 2003;**285**:L701–9.

44 Holden AM, Fyler DC, Shillito J Jr, Nadas AS. Congestive heart failure from intracranial arteriovenous fistula in infancy. Clinical and physiologic considerations in eight patients. *Pediatrics* 1972;**49**:30–9.

45 Hendenson L, Emery DJ, Phillipos EZ, *et al*. Persistent pulmonary hypertension of the newborn presenting as primary manifestation of intracranial arteriovenous malformation of the vein of Galen. *Am J Perinatol* 2000;**17**:405–10.

46 Dzau VJ. Renal and circulatory mechanisms in congestive heart failure. *Kidney Int* 1987;**31**:1402–15.

47 Dzau VJ, Colucci WS, Hollenberg NK, Williams GH. Relation of the renin–angiotensin–aldosterone system to clinical state in congestive heart failure. *Circulation* 1981;**63**:645–51.

48 Abassi ZA, Winaver J, Hoffman A. Large A-V fistula: pathophysiological consequences and therapeutic perspectives. *Curr Vasc Pharmacol* 2003;**1**:347–54.

49 Velez-Roa S, Neubauer J, Wissing M, *et al*. Acute arterio-venous fistula occlusion decreases sympathetic activity and improves baroreflex control in kidney transplanted patients. *Nephrol Dial Transplant* 2004;**19**:1606–12.

50 Berenstein A. Lasjaunias P, ter Brugge KG. Dural arteriovenous shunts. In: Berenstein A. Lasjaunias P, ter Brugge KG, eds. *Surgical Neuroangiography: Vol. 2.2: Clinical and Endovascular Treatment Aspects in Adults*, 2nd edn. Berlin: Springer, 2006: 566–607.

51 Borden JA, Wu JK, Shucart WA. A proposed classification for spinal and cranial dural arteriovenous fistulous malformations and implications for treatment. *J Neurosurg* 1995;**82**:166–79.

52 Cognard C, Gobin YP, Pierot L, *et al*. Cerebral dural arteriovenous fistulas: clinical and angiographic correlation with a revised classification of venous drainage. *Radiology* 1995;**194**:671–80.

53 Zipfel GJ, Shah MN, Refai D, *et al*. Cranial dural arteriovenous fistulas: modification of angiographic classification scales based on new natural history data. *Neurosurg Focus* 2009;**26**:E14.

54 Sarma D, ter Brugge K. Management of intracranial dural arteriovenous shunts in adults. *Eur J Radiol* 2003;**46**:206–20.

55 Lownie SP. Intracranial dural arteriovenous fistulas: endovascular therapy. *Neurosurg Clin N Am* 1994;**5**:449–58.

56 Hernesniemi JA, Dashti R, Juvela S, *et al*. Natural history of brain arteriovenous malformations: a long-term follow-up study of risk of hemorrhage in 238 patients. *Neurosurgery* 2008;**63**:823–9.

57 Raybaud CA, Strother CM, Hald JK. Aneurysms of the vein of Galen: embryonic considerations and anatomical features relating to the pathogenesis of the malformation. *Neuroradiology* 1989;**31**:109–28.

58 Casasco A, Lylyk P, Hodes JE, *et al*. Percutaneous transvenous catheterization and embolization of vein of Galen aneurysms. *Neurosurgery* 1991;**28**:260–6.

59 Alvarez H, Garcia Monaco R, Rodesch G, *et al*. Vein of Galen aneurysmal malformations. *Neuroimaging Clin N Am* 2007;**17**:189–206.

60 Gupta AK, Varma DR. Vein of Galen malformations: review. *Neurol India* 2004;**52**:43–53.

61 Li AH, Armstrong D, ter Brugge KG. Endovascular treatment of vein of Galen aneurysmal malformation: management strategy and 21-year experience in Toronto. *J Neurosurg Pediatr* 2011;**7**:3–10.

62 Gailloud P, O'Riordan DP, Burger I, *et al*. Diagnosis and management of vein of Galen aneurysmal malformations. *J Perinatol* 2005;**25**:542–51.

63 Rodesch G, Hui F, Alvarez H, *et al*. Prognosis of antenatally diagnosed vein of Galen aneurysmal malformations. *Childs Nerv Syst* 1994;**10**:79–83.

64 McSweeney N, Brew S, Bhate S, *et al*. Management and outcome of vein of Galen malformation. *Arch Dis Child* 2010;**95**:903–9.

65 Li AH, Armstrong D, ter Brugge KG. Endovascular treatment of vein of Galen aneurysmal malformation: management strategy and 21-year experience in Toronto. *J Neurosurg Pediatr* 2011; **7**:3–10.

66 Lasjaunias PL, Chng SM, Sachet M, *et al*. The management of vein of Galen aneurysmal malformations. *Neurosurgery* 2006;**59**(5 Suppl 3):S184–94.

67 Eskandar EN, Borges LF, Budzik RF Jr, *et al*. Spinal dural arteriovenous fistulas: experience with endovascular and surgical therapy. *J Neurosurg* 2002;**96**(Suppl 2):162–7.

68 da Costa L, Dehdashti AR, ter Brugge KG. Spinal cord vascular shunts: spinal cord vascular malformations and dural arteriovenous fistulas. *Neurosurg Focus* 2009;**26**:E6.

69 Kataoka H, Miyamoto S, Nagata I, *et al*. Venous congestion is a major cause of neurological deterioration in spinal arteriovenous malformations. *Neurosurgery* 2001;**48**:1224–30.

70 Spetzler RF, Detwiler PW, Riina HA, Porter RW. Modified classification of spinal cord vascular lesions. *J Neurosurg* 2002;**96**(Suppl 2):145–56.

71 Deshmukh VR, Chang S, Albuquerque FC, *et al*. Bilateral ethmoidal dural arteriovenous fistulae: a previously unreported entity: case report. *Neurosurgery* 2005;**57**(4):E809.

72 Tomlinson FH, Rüfenacht DA, Sundt TM Jr, *et al*. Arteriovenous fistulas of the brain and the spinal cord. *J Neurosurg* 1993;**79**:16–27.

73 Kuss JJ, Karli A, Fischbach M, *et al*. Congenital carotid to jugular aneurysm. *Arch Fr Pediatr* 1979;**36**:502–7.

74 Tekkok IH, Akkurt C, Suzer T, Ozcan OE. Congenital external carotid–jugular fistula: report of two cases and a review of the literature. *Neurosurgery* 1992;**30**:272–6.

75 Gobin YP, Garcia de la Fuente JA, Herbreteau D, *et al*. Endovascular treatment of external carotid-jugular fistulae in the parotid region. *Neurosurgery* 1993;**33**:812–6.

76 Berenstein A, Scott J, Choi IS, Persky M. Percutaneous embolization of arteriovenous fistulas of the external carotid artery. *AJNR Am J Neuroradiol* 1986;**7**:937–42.

77 Calbucci F, Scialfa C. Congenital arteriovenous malformations of the cervical region. *J Neurosurg* Sci 1977;**21**:211–20.

78 Coleman CC, Hopes JE. Congenital arteriovenous anomalies of the head and neck. *Plast Reconstr Surg* 1971;**47**:354–64.

79 Halbach VV, Higashida RT, Hieshima GB, Hardin GW. Arteriovenous fistula of the internal maxillary artery: treatment with transarterial embolization. *Radiology* 1988;**168**:443–5.

80 Merland JJ, Riche MC, Chiras J. Congenital arteriovenous malformations: long term therapeutic effects of arterial ligatures – a plea for their abandonment in favour of more recent procedures. *Ann Chir* 1980;**34**:389–95.

81 Prevot J, Babut JM. Congenital cervical jugulo-carotid fistula. *J Pediatr Surg* 1970;**5**:431–6.

82 Tekkok IH, Akkurt C, Suzer T, Ozcan OE. Congenital external carotid–jugular fistula: report of two cases and a review of the literature. *Neurosurgery* 1992;**30**:272–5.

83 Merland JJ, Reizine D, Riche MC, *et al*. Endovascular treatment of vertebral arteriovenous fistulas in twenty-two patients. *Ann Vasc Surg* 1986;**1**:73–8.

84 Cluzel P, Pierot L, Leung A, *et al*. Vertebral arteriovenous fistulae in neurofibromatosis: report of two cases and review of the literature. *Neuroradiology* 1994;**36**:321–5.

85 Bahar S, Chiras J, Carpena JP, *et al*. Spontaneous vertebro-vertebral arterio-venous fistula associated with fibromuscular dysplasia. *Neuroradiology* 1984;**26**:45–9.

86 Nakstad PH, Haakonsen M, Magnaes B, Hetland S. Combined endovascular and surgical treatment in vertebral arteriovenous fistula. A case report. *Acta Radiol* 1997;**38**:25–9.

87 Maurizi M, Fiumicelli A, Paludetti G, Simoncelli C. Arteriovenous fistula of the mandible: a review of the literature and report of a case. *Int J Pediatr Otorhinolaryngol* 1982;**4**:171–9.

88 Noreau G, Landry PP, Morais D. Arteriovenous malformation of the mandible: review of literature and case history. *J Can Dent Assoc* 2001;**67**:646–51.

89 Tarif N, Dunne PM, Parachuru PR, Bakir AA. Life-threatening hematuria from an arteriovenous fistula complicating an open renal biopsy. *Nephron* 1998;**80**:66–70.

90 Ullian ME, Molitoris BA. Bilateral congenital renal arteriovenous fistulas. *Clin Nephrol* 1987;**27**:293–7.

91 Smaldone MC, Stein RJ, Cho JS, Leng WW. Giant idiopathic renal arteriovenous fistula requiring urgent nephrectomy. *Urology* 2007;**69**:576.e1–3.

92 Macpherson RI, Fyfe D, Aaronson IA. Congenital renal arteriovenous malformations in infancy. The imaging features in two infants with hypertension. *Pediatr Radiol* 1991;**21**:108–10.

93 Korn TS, Thurston JM, Sherry CS, Kawalsky DL. High-output heart failure due to a renal arteriovenous fistula in a pregnant woman with suspected preeclampsia. *Mayo Clin Proc* 1998;**73**:888–92.

94 Zambrana AR, Martín FL, Blanco JZ, *et al*. Arteriovenous renal congenital fistula. *Actas Urol Esp* 2009;**33**:696–9 (in Spanish).

95 Yazaki T, Tomita M, Akimoto M, *et al*. Congenital renal arteriovenous fistula: case report, review of Japanese literature and description of non-radical treatment. *J Urol* 1976;**116**:415–8.

96 Crotty KL, Orihuela E, Warren MM. Recent advances in the diagnosis and treatment of renal arteriovenous malformations and fistulas. *J Urol* 1993;**150**:1355–9.

97 Gallego C, Miralles M, Marín C, *et al*. Congenital hepatic shunts. *Radiographics* 2004;**24**:755–72.

98 Golewale N, Paltiel HJ, Fishman SJ, Alomari AI. Portal vascular anomalies in Down syndrome: spectrum of clinical presentation and management approach. *J Pediatr Surg* 2010;**45**:1676–81.

99 Akahoshi T, Nishizaki T, Wakasugi K, *et al*. Portal–systemic encephalopathy due to a congenital extrahepatic portosystemic shunt: three cases and literature review. Hepatogastroenterology 2000;**47**:1113–6.

100 Altuntas B, Erden A, Karakurt C, *et al*. M. Severe portal hypertension due to congenital hepatoportal arteriovenous fistula associated with intrahepatic portal vein aneurysm. *J Clin Ultrasound* 1998;**26**:357–60.

101 Marchand V, Uflacker R, Baker SS, Baker RD. Congenital hepatic arterioportal fistula in a 3-year-old child. *J Pediatr Gastroenterol Nutr* 1999;**28**:435–41.

102 Hartung J, Chaoui R, Kalache K, *et al*. Prenatal diagnosis of intrahepatic communications of the umbilical vein with atypical arteries (A-V fistulae) in two cases of trisomy 21 using color Doppler ultrasound. *Ultrasound Obstet Gynecol* 2000;**16**:271–4.

103 Park JH, Cha SH, Han JK, Han MC. Intrahepatic portosystemic venous shunt. *AJR Am J Roentgenol* 1990;**155**:527–8.

104 Lumsden AB, Allen RC, Sreeram S, *et al*. Hepatic arterioportal fistula. *Am Surg* 1993;**59**:722–6.

105 D'Agostino D, Orsi M. Congenital hepatic arterioportal fistula. *J Pediatr Gastroenterol Nutr* 1999;**29**:487.

106 Burrows PE, Dubois J, Kassarjian A. Pediatric hepatic vascular anomalies. *Pediatr Radiol* 2001;**31**:533–45.

107 Alkim C, Sahin T, Oğuz P, *et al*. A case report of congenital intrahepatic arterioportal fistula. *Am J Gastroenterol* 1999;**94**:523–5.

108 Bakker J, Robben SG, Hazebroek FW, Meradji M. Congenital arterioportal fistula of the liver with reversal of flow in the superior mesenteric vein. *Pediatr Radiol* 1994;**24**:198–9.

109 Vauthey JN, Tomczak RJ, Helmberger T, *et al*. The arterioportal fistula syndrome: clinicopathologic features, diagnosis, and therapy. *Gastroenterology* 1997;**113**:1390–401.

110 Guzman EA, McCahill LE, Rogers FB. Arterioportal fistulas: introduction of a novel classification with therapeutic implications. *J Gastrointest Surg* 2006;**10**:543–50.

111 Li X, Li HC, Tang CW. Endovascular embolization for gastrointestinal bleeding caused by splenic arteriovenous fistula. Chin Med J (Engl) 2010;**123**:2616–8.

112 Agarwala S, Dutta H, Bhatnagar V, *et al*. Congenital hepatoportal arteriovenous fistula: report of a case. *Surg Today* 2000;**30**:268–71.

113 Saxena AK, Sodhi KS, Arora J, *et al*. Congenital intrahepatic portosystemic venous shunt in an infant with Down syndrome. *AJR Am J Roentgenol* 2004;**183**:1783–4.

114 Park JH, Cha SH, Han JK, Han MC. Intrahepatic portosystemic venous shunt. *AJR Am J Roentgenol* 1990;**155**:527–8.

115 Corness JA, McHugh K, Roebuck DJ, Taylor AM. The portal vein in children: radiological review of congenital anomalies and acquired abnormalities. *Pediatr Radiol* 2006;**36**:87–96.

116 Morgan G, Superina R. Congenital absence of the portal vein: two cases and a proposed classification system for portasystemic vascular anomalies. *J Pediatr Surg* 1994;**29**:1239–41.

117 Stringer MD. The clinical anatomy of congenital portosystemic venous shunts. *Clin Anat* 2008;**21**:147–57.

118 Tsai A, Paltiel HJ, Sena LM, *et al*. Neonatal hemochromatosis and patent ductus venosus: clinical course and diagnostic pitfalls. *Pediatr Radiol* 2009;**39**:823–7.

119 Gitzelmann R, Forster I, Willi UV. Hypergalactosaemia in a newborn: self-limiting intrahepatic portosystemic venous shunt. *Eur J Pediatr* 1997;**156**:719–22.

120 Akahoshi T, Nishizaki T, Wakasugi K, *et al*. Portal–systemic encephalopathy due to a congenital extrahepatic portosystemic shunt: three cases and literature review. *Hepatogastroenterology* 2000;**47**:1113–6.

121 Saxena AK, Sodhi KS, Arora J, *et al*. Congenital intrahepatic portosystemic venous shunt in an infant with Down syndrome. *AJR Am J Roentgenol* 2004;**183**:1783–4.

122 Kitagawa S, Gleason WA Jr, Northrup H, *et al*. Symptomatic hyperammonemia caused by a congenital portosystemic shunt. *J Pediatr* 1992;**121**:917–9.

123 Lee SA, Lee YS, Lee KS, Jeon GS. Congenital intrahepatic portosystemic venous shunt and liver mass in a child patient: successful endovascular treatment with an Amplatzer vascular plug (AVP). *Korean J Radiol* 2010;**11**:583–6.

124 Stringer MD. The clinical anatomy of congenital portosystemic venous shunts. *Clin Anat* 2008;**21**:147–57.

125 Kanamori Y, Hashizume K, Kitano Y, *et al*. Congenital extrahepatic portocaval shunt (Abernethy type 2), huge liver mass, and patent ductus arteriosus – a case report of its rare clinical presentation in a young girl. *J Pediatr Surg* 2003;**38**:E15.

126 Sawyer B, Dow C, Frank J, Lau E. Congenital portocaval shunt-associated liver lesions in a patient with cancer. *ANZ J Surg* 2008;**78**:613–4.

127 Alvarez AE, Ribeiro AF, Hessel G, *et al*. Abernethy malformation: one of the etiologies of hepatopulmonary syndrome. *Pediatr Pulmonol* 2002;**34**:391–4.

128 Charre L, Roggen F, Lemaire J, *et al*. Hematochezia and congenital extrahepatic portocaval shunt with absent portal

vein: successful treatment by liver transplantation. *Transplantation* 2004;**78**:1404–6.

129 Shinkai M, Ohhama Y, Nishi T, *et al*. Congenital absence of the portal vein and role of liver transplantation in children. *J Pediatr Surg* 2001;**36**:1026–31.

130 Howard ER, Davenport M. Congenital extrahepatic portocaval shunts. The Abernethy malformation. *J Pediatr Surg* 1997;**32**:494–7.

131 Barton JW III, Keller MS. Liver transplantation for hepatoblastoma in a child with congenital absence of the portal vein. *Pediatr Radiol* 1989;**20**:113–4.

132 Woodle ES, Thistlethwaite JR, Emond JC, *et al*. Successful hepatic transplantation in congenital absence of recipient portal vein. *Surgery* 1990;**107**:475–9.

133 Taoube KA, Alonso Calderon JL, Yandza T, *et al*. Congenital absence of portal vein in a girl with biliary atresia treated with liver transplant. *Cir Pediatr* 1999;**12**:38–40 (in Spanish).

134 Brothers TE, Stanley JC, Zelenock G. Splenic arteriovenous fistula. *Int Surg* 1995;**80**:189–94.

135 Vanhoenacker FM, Op de Beeck B, De Schepper AM, *et al*. Vascular disease of the spleen. *Semin Ultrasound CT MR* 2007;**28**:35–51.

136 Wenger JJ, Matter D, Dupeyron JP, *et al*. Arteriovenous fistula of the spleen revealed by ascites and profuse diarrhea. A case report including ultrasonography and arteriography findings. *J Radiol* 1981;**62**:321–5.

137 Schmidt JH, Howard RJ, Herrera MA, Hawkins IF. Splenic arteriovenous fistula with portal hypertension, ascites, and diarrhea. *South Med J* 1988;**81**:670–2.

138 Galler G, Yim A, Emond JC, *et al*. Splenic arteriovenous fistula. A rare lesion causing bleeding esophageal varices, ascites, and diarrhea. *Dig Dis Sci* 1996;**41**:816–9.

139 Hung CF, Tseng JH, Lui KW, *et al*. Intractable oesophageal variceal bleeding caused by splenic arteriovenous fistula: treatment by transcatheter arterial embolization. *Postgrad Med J* 1999;**75**:355–7.

140 Madsen MA, Frevert S, Madsen PL, Eiberg JP. Splenic arteriovenous fistula treated with percutaneous transarterial embolization. *Eur J Vasc Endovasc Surg* 2008;**36**:562–4.

141 Henry C, Dettloff L, Mhiri R, *et al*. Post-traumatic intrasplenic arteriovenous fistula in a child. Spontaneous regression. *J Radiol* 1998;**79**:271–3.

142 Li X, Li HC, Tang CW. Endovascular embolization for gastrointestinal bleeding caused by splenic arteriovenous fistula. *Chin Med J (Engl)* 2010;**123**:2616–8.

143 Oguz B, Cil B, Ekinci S, *et al*. Posttraumatic splenic pseudoaneurysm and arteriovenous fistula: diagnosis by computed tomography angiography and treatment by transcatheter embolization. *J Pediatr Surg* 2005;**40**:e43–6.

144 Maloo MK, Burrows PE, Shamberger RC. Traumatic splenic arteriovenous fistula: splenic conservation by embolization. *J Trauma* 1999;**47**:173–5.

145 Hagiwara A, Yukioka T, Ohta S, *et al*. Nonsurgical management of patients with blunt splenic injury: efficacy of transcatheter arterial embolization. *AJR Am J Roentgenol* 1996;**167**:159–66.

146 Madoff DC, Denys A, Wallace MJ, *et al*. Splenic arterial interventions: anatomy, indications, technical considerations, and potential complications. *Radiographics* 2005;**25**(Suppl 1): S191–211.

147 Gartside R, Gamelli RL. Splenic arteriovenous fistula. *J Trauma* 1987;**27**:671–3.

148 Kim D, Guthaner DF, Walter JF, Pyle R. Embolization of visceral arteriovenous fistulas with a modified steel wire technique. *AJR Am J Roentgenol* 1984;**142**:1215–8.

149 Rösch J, Dotter CT, Brown MJ. Selective arterial embolization. A new method for control of acute gastrointestinal bleeding. *Radiology* 1972;**102**:303–6.

150 Lin WC, Chen YF, Lin CH, *et al*. Emergent transcatheter arterial embolization in hemodynamically unstable patients with blunt splenic injury. *Acad Radiol* 2008;**15**:201–8.

151 Cura M, Martinez N, Cura A, *et al*. Arteriovenous malformations of the uterus. *Acta Radiol* 2009;**50**:823–9.

152 Yokomine D, Yoshinaga M, Baba Y, *et al*. Successful management of uterine arteriovenous malformation by ligation of feeding artery after unsuccessful uterine artery embolization. *J Obstet Gynaecol Res* 2009;**35**:183–8.

153 Kim TH, Lee HH. Presenting features of women with uterine arteriovenous malformations. *Fertil Steril* 2010;**94**:2330. e7–10.

154 Yokomine D, Yoshinaga M, Baba Y, *et al*. Successful management of uterine arteriovenous malformation by ligation of feeding artery after unsuccessful uterine artery embolization. *J Obstet Gynaecol Res* 2009;**35**:183–8.

155 Toursarkissian B, Allen BT, Petrinec D, *et al*. Spontaneous closure of selected iatrogenic pseudoaneurysms and arteriovenous fistulae. *J Vasc Surg* 1997;**25**:803–8.

156 Kiernan TJ, Ajani AE, Yan BP. Management of access site and systemic complications of percutaneous coronary and peripheral interventions. *J Invasive Cardiol* 2008;**20**:463–9.

157 Dickey KW, Pollak JS, Meier GH III, *et al*. Management of large high-flow arteriovenous malformations of the shoulder and upper extremity with transcatheter embolotherapy. *J Vasc Interv Radiol* 1995;**6**:765–73.

158 Rockman CB, Rosen RJ, Jacobowitz GR, *et al*. Transcatheter embolization of extremity vascular malformations: the long-term success of multiple interventions. *Ann Vasc Surg* 2003;**17**:417–23.

159 Burrows PE, Pap S. Vascular malformations of the upper limb: a review of 270 patients. *J Hand Surg Am* 1999;**24**:1019–35.

160 Alioua Z, Lamsyah H, Sbai M, *et al*. Pseudo-Kaposi's sarcoma secondary to superficial arteriovenous malformation: Stewart–Bluefarb syndrome. *Ann Dermatol Venereol* 2008;**135**:44–7.

161 Klode J, Kröger K, Grabbe S, Dissemond J. Ulcers associated with arteriovenous fistula within a Stewart–Bluefarb syndrome: arterial and/or venous therapy? *Vasa* 2007;**36**:134–7 (in German).

162 Tatum GH, Newman B, Ralphe JC. Neonatal congestive heart failure due to a subclavian artery to subclavian vein fistula diagnosed by noninvasive procedures. *Congenit Heart Dis* 2006;**1**:120–3.

163 Dogan R, Yilmaz M, Ozkutlu S, Elsharshari H. Congenital subclavian artery to subclavian vein fistula presenting with congestive heart failure in an infant. *Pediatr Cardiol* 2000;**21**:269–70.

164 Sapire DW, Lobe TE, Swischuk LE, *et al*. Subclavian-artery-to-innominate-vein fistula presenting with congestive failure in a newborn infant. *Pediatr Cardiol* 1983;**4**:155–7.

165 Dohlemann C, Hauser M, Nicolai T, Kreuzer E. Innominate artery enlargement in congenital arteriovenous fistula with

subsequent tracheal compression and stridor. *Pediatr Cardiol* 1995;**16**:287–90.

166 Ilijevski N, Radak D, Radević B, *et al*. Popliteal traumatic arteriovenous fistulas. *J Trauma* 2002;**52**:739–44.

167 Ilijevski NS, Nenezić DD, Sagić D, Radak D. Popliteal traumatic arteriovenous fistula. *Vascular* 2005;**13**:309–12.

168 Frykberg ER. Popliteal vascular injuries. *Surg Clin North Am* 2002;**82**:67–89.

169 Greene AK, Orbach DB. Management of arteriovenous malformations. *Clin Plast Surg* 2011;**38**:95–106.

170 Hofmann SR, Weise M, Nitzsche KI. An intrathoracic arteriovenous malformation discovered as an extremely uncommon reason of neonatal congestive cardiac failure. *Cardiol Young* 2009;**19**:530–3.

171 Lawdahl RB, Routh WD, Vitek JJ, *et al*. Chronic arteriovenous fistulas masquerading as arteriovenous malformations: diagnostic considerations and therapeutic implications. *Radiology* 1989;**170**:1011–5.

172 Boyd JB, Mulliken JB, Kaban LB, *et al*. Skeletal changes associated with vascular malformations. *Plast Reconstr Surg* 1984;**74**:789–97.

173 Paltiel HJ, Burrows PE, Kozakewich HPW, *et al*. Soft-tissue vascular anomalies: utility of US for diagnosis. *Radiology* 2000;**214**:747–54.

174 Burrows PE, Mulliken JB, Fellows KE, Strand RD. Childhood hemangiomas and vascular malformations: angiographic differentiation. *AJR Am J Roentgenol* 1983;**141**:483–8.

175 Inagawa S, Unno N, Yamashita S, *et al*. Laparotomized direct puncture for embolization of a retroperitoneal arteriovenous fistula. *Cardiovasc Interv Radiol* 2010;**33**:191–5.

176 Tjoumakaris SI, Jabbour PM, Rosenwasser RH. Neuro-endovascular management of carotid cavernous fistulas. *Neurosurg Clin N Am* 2009;**20**:447–52.

177 Ong CK, Lam DV, Ong MT, *et al*. Neuroapplication of Amplatzer vascular plug for therapeutic sacrifice of major craniocerebral arteries: an initial clinical experience. *Ann Acad Med Singapore* 2009;**38**:763–8.

178 Powitzky R, Vasan N, Krempl G, Medina J. Carotid blowout in patients with head and neck cancer. *Ann Otol Rhinol Laryngol* 2010;**119**:476–84.

179 Cohen J, Rad I. Current management of carotid blowout. *Curr Opin Otolaryngol Head Neck Surg* 2004;**12**:110–5.

180 Kim SH, Shin YS, Yoon PH, Kim DI. Emergency endovascular treatment of internal carotid artery injury during a transsphenoidal approach for a pituitary tumor – case report. *Yonsei Med J* 2002;**43**:119–22.

181 Sidhu M, Goske MJ, Connolly B, *et al*. Image gently, step lightly: promoting radiation safety in pediatric interventional radiology. *AJR Am J Roentgenol* 2010;**195**:W299–301.

27

Left Ventricular Inflow Obstruction: Pulmonary Vein Stenosis, Cor Triatriatum, Supravalvar Mitral Ring, Mitral Valve Stenosis

Walter H. Johnson, Jr & James K. Kirklin
University of Alabama at Birmingham, Birmingham, AL, USA

Introduction

In this chapter, obstructions to left heart inflow are considered in three broad categories: pulmonary vein obstruction, left atrial-level obstruction (cor triatriatum, and supravalvar mitral ring), and left ventricular (LV) inflow obstruction (mitral stenosis and hypoplasia). All have similar hemodynamic and clinical consequences: elevated pulmonary vascular resistance and limitation of left heart output, with signs and symptoms of heart failure, accompanied by pulmonary hypertension and/or edema [1] (Figure 27.1). Except for acquired mitral stenosis resulting from rheumatic fever, congenital forms of LV inflow obstruction are rare, with most occurring with other cardiac malformations. Isolated forms of LV inflow obstruction are very rare.

Left ventricular inflow obstructions are among the most challenging cardiovascular conditions to recognize, evaluate, and manage, and despite great advances in diagnosis and treatment, they remain very significant sources of morbidity and mortality for patients.

Pulmonary vein atresia, hypoplasia, and stenosis

Pulmonary vein stenosis (PVS) is rare, occurring more often (80%) with other severe cardiac malformations than as an isolated condition [2]. Congenital PVS has a reported incidence of 0.4% of congenital heart defects in an autopsy series [3] and with an incidence of 0.03% in children undergoing interventional procedures or surgery for congenital heart disease [4]. It has been estimated to occur in approximately two children per 100 000 [5].

Primary pulmonary vein atresia occurs in the setting of pulmonary agenesis [6] yet the term is most often used to describe the complete obliteration of an existing pulmonary vein following a period of progressive stenosis [7,8].

Pathophysiology
Obstruction to pulmonary venous return increases pulmonary vascular resistance, at a post-capillary level, with attendant pulmonary edema, pulmonary hypertension, and limited cardiac reserve. Infants who appear minimally symptomatic at rest may be unable to increase cardiac output appropriately during any increase in cardiac demand (such as occurs during feeding, or acute illness, particularly with fever) and may develop marked increase in symptoms.

Natural history
Although PVS and even obliteration have been reported with increasing frequency in adults, usually as an iatrogenic complication of radiofrequency ablation procedures for atrial arrhythmias, congenital forms have been recognized, very rarely, in adolescents and adults [9–13]. Otherwise, most congenital PVS is diagnosed in infancy, likely because of the progressive nature of the stenoses and the severe hemodynamic derangements that accompany it. However, neonatal PVS can present clinically as persistent pulmonary hypertension of the newborn (PPHN) [14,15]. The disease has been associated with high mortality [2,4] and is often refractory to medical, catheter [16], and surgical [17] interventions [18].

Embryology
The pulmonary veins and parenchymal tissue form from outpouchings of the embryonic foregut, whereas the heart forms from different precursor tissue. The concept of embryonic growth of the pulmonary veins towards the left atrium, with eventual incorporation of the veins into the left atrium, is
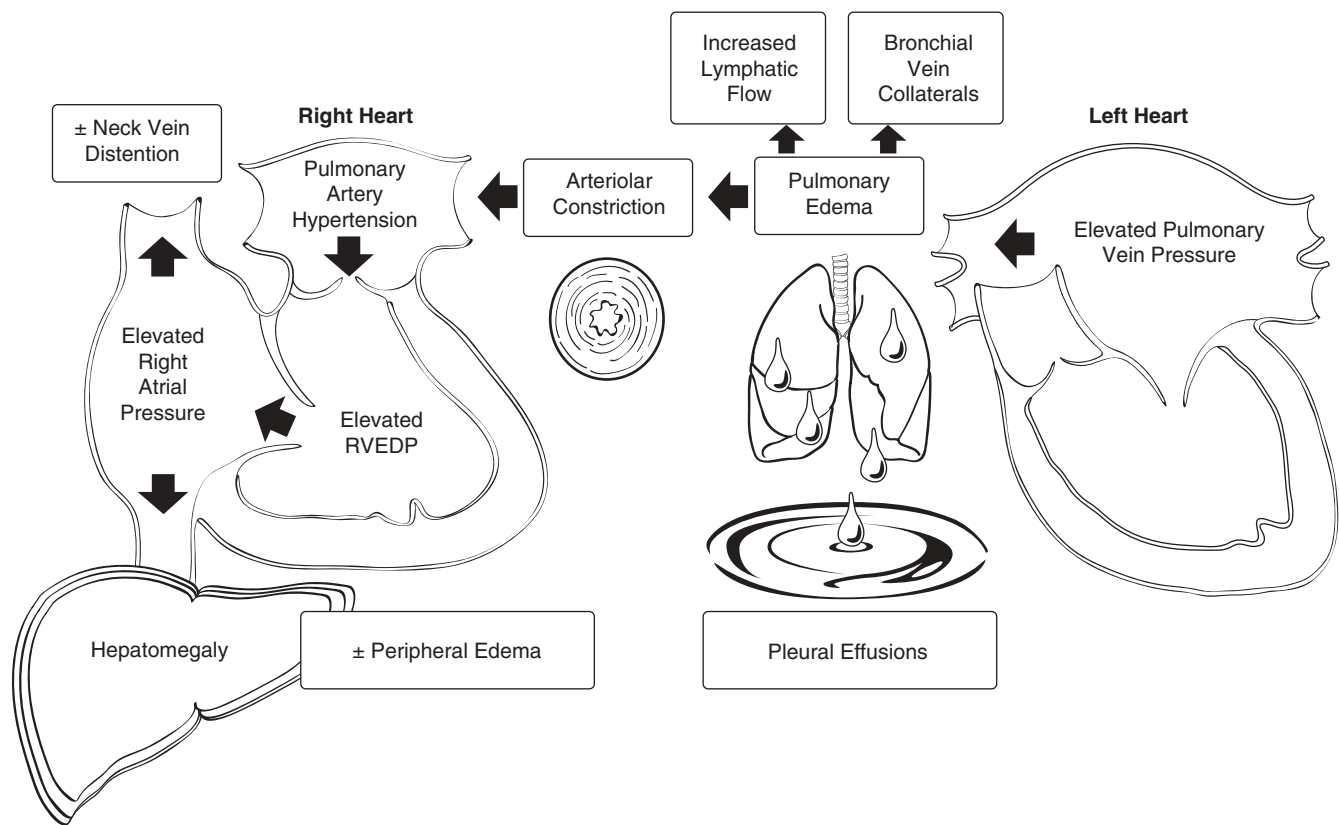
Figure 27.1 Pathophysiology of left ventricular inflow obstruction. Obstruction of pulmonary venous return at any level causes pulmonary venous hypertension. Pulmonary edema results in tachypnea in infants and dyspnea in older children and adults. If increased lymphatic flow is inadequate to compensate, pleural effusions may occur. Bronchial venous collaterals may develop and distend, leading to hemoptysis. Pulmonary arteriolar constriction results in pulmonary artery hypertension and elevated right heart pressures. Right heart failure may result in elevated systemic venous pressure, hepatomegaly in infants, and also jugular venous distension and peripheral edema in older children and adults. RVEDP, right ventricular end-diastolic pressure. (Adapted from Lucas RV Jr. Congenital causes of pulmonary venous obstruction. *Cardiovasc Clin* 1972;**4**:19–51.)

useful in understanding the postnatal pathologic anatomy, especially that of total and partial anomalous pulmonary venous return (see Chapter 34) and cor triatriatum, but is less able to account for pulmonary vein stenosis, particularly its progressive nature.

Pathologic anatomy and major associated anomalies

The causes of PVS, and especially the progressive nature of the disease, are not understood, although the rather constant but nonspecific histopathology has been well described for decades [3]. Many have referred to a localized collar of intimal fibrous thickening, usually at the venoatrial junction [3,19]. Distinctive gross pathology types have been described and classified [20], but may have less clinical prognostic significance than associated cardiac malformations. Various genetic syndromes (trisomy 21 being the most prevalent) have been observed in about one-third of patients in two series [2,5], but no characteristic genetic cause is known. Familial occurrence of PVS has been reported [21].

The histopathology of PVS is possibly due to abnormal proliferation of myofibroblasts, which has been demonstrated in the absence of fibrosis, inflammation, or thrombosis [22]. Although other myofibroblastic diseases have sometimes been treated with antiproliferative regimens, including chemotherapy and radiation, we are not aware of successful treatment of PVS in this way. As active proliferation of myofibroblasts has not been consistently demonstrated, cell proliferation may occur episodically, and subsequent intimal expansion by extracellular matrix and the resulting lumenal narrowing is an important factor in PVS [23].

Clinical features

Clinical history

The clinical diagnosis is challenging. The disease is often not recognized in early infancy, despite onset of symptoms, which are usually respiratory, and diagnosis may occur only after repeated diagnostic studies [5,14,24]. An association has been observed with prematurity [2] and many patients

have been diagnosed with bronchopulmonary dysplasia prior to definitive diagnosis with PVS [5].

Physical examination

Physical examination reflects nonspecific findings of pulmonary hypertension, including a loud second heart sound, and abnormal lung sounds from pulmonary edema. Tachypnea, even at rest, may be due to pulmonary edema or, in severe obstruction, to compensation for metabolic acidosis resulting from inadequate cardiac output. Tachycardia may reflect the limited filling of the left heart in severe obstruction. In this setting, an increase in heart rate is the only mechanism whereby cardiac output can increase as stroke volume is limited by the obstruction to venous return from the lungs.

Electrocardiographic features

The electrocardiogram shows progressive right ventricular hypertrophy/enlargement, and right atrial enlargement if pulmonary hypertension becomes severe. When PVS is accompanied by other cardiac malformations, the EKG findings characteristic for that lesion may predominate.

Chest X-ray

The radiograph classically shows a small heart, but increased pulmonary vascular markings, often with hyperinflation. The cardiac silhouette is small because of the small volume of blood returning to the heart from the lungs. Because PVS can be bilateral, unilateral, or even segmental, the X-ray may reflect nonhomogeneous vascular markings. Pulmonary edema and pleural effusions may be seen.

Echocardiography

Stenosis of the pulmonary veins can be among the most challenging diagnoses, especially as the obstruction may be progressive and early echocardiography may not detect obstruction. PVS is best demonstrated by Doppler as flow acceleration from the veins into the left atrium, rather than as narrowing of the vein lumen seen by two-dimensional echo.

In neonates, the problem is particularly acute, as right-to-left (pulmonary artery-to-aorta) flow via the ductus and right-to-left atrial level shunt via the foramen ovale result in limited flow across the stenoses, making flow acceleration impossible to detect, and because normal neonates may have transient flow acceleration via normal pulmonary veins [25].

Cardiac catheterization and angiography

Cardiac catheterization can be definitive, and allow precise imaging by selective contrast injection of affected pulmonary segments. Hemodynamic findings reflect the post-capillary nature of the obstruction, with pulmonary arterial capillary wedge pressures that are elevated, in the presence of pulmonary artery hypertension. Wedge injection of contrast has been used to demonstrate obstructed pulmonary veins (see Videoclip 27.1).

Direct measurement of elevated pressure via a catheter inserted into an individual pulmonary vein, along with a pressure gradient demonstrable on pullback, can be a dramatic demonstration of true stenosis. However, a large catheter in a small but normal vein can create a functional stenosis, a potential false positive.

Other imaging modalities

Magnetic resonance imaging (MRI) and computed tomography (CT) have been successfully used to diagnose obstruction and provide high-quality images of the veins and level of obstruction [26]. Images obtained have advantages over cineangiography but, as hemodynamic data and transcatheter intervention are limited or unavailable, these techniques often serve a complementary role with catheterization. Pulmonary perfusion scintigraphy can provide quantitative estimates of whole lung and lobar blood flow distribution but, like catheterization, results in some radiation exposure. MRI can provide segmental estimates of relative lung perfusion, and can be especially helpful in demonstrating improvement following interventions [27].

Management

Medical

Medical management is limited to supportive measures and nonspecific therapy for pulmonary hypertension, but without definitive and successful gradient relief the outcome is poor. Some infants with progressive PVS refractory to surgical and catheter treatment have undergone treatment with anti-inflammatory and antineoplastic drugs in the hope of attenuating the basic mechanism involved in the stenosis, but with little success.

Surgical

The prime surgical indication is significant symptomatic obstruction, especially with progression. The definitive treatment is to achieve gradient relief at the site of any and all obstructions and to restore as normal a pathway as possible for pulmonary venous return.

Surgical techniques have included patch enlargement with autologous left atrial appendage [28] and so-called "sutureless" techniques using an *in situ* pericardial patch to avoid anastomotic scarring at the site of stenosis reconstruction [29]. Unfortunately, restenosis and progression to obliteration in many children have necessitated multiple operations [17] and the long-term outcome remains poor in many patients.

Catheter-based therapies include balloon dilation or balloon dilation with stent placement [30], either in the catheterization laboratory or in the operating room at the time of surgery, as a "hybrid" procedure.

Long-term history of treated and untreated children and adults

Many have suggested that early intervention may possibly produce better outcomes, although this assertion remains unproven. When PVS progresses to obliteration, the conventional wisdom is that intervention must precede complete occlusion to salvage the lung segment involved. However, the nature of the disease appears highly pleomorphic, with some children responding favorably to a single operation, with no long-term sequelae or reobstruction, whereas others succumb to progressive and incessant obstruction, despite aggressive and repeated interventions.

Cor triatriatum

Literally meaning a "heart with three atria," the term usually refers to *cor triatriatum sinister* in which defective embryonic incorporation of the common pulmonary vein into the left atrium results in an "accessory" or proximal chamber between the pulmonary veins and the distal "true" left atrial chamber.

Incidence and genetics

Cor triatriatum is rare, reportedly found in 0.1–0.5% of congenital heart patients [31]. It can present at any age but most patients are affected in infancy [31–33]. Variable degrees of obstruction between the common pulmonary vein and the left atrium determine the degree of clinical severity.

Isolated forms of cor triatriatum are probably less common than cor triatriatum associated with other congenital heart malformations. Early series tended to be based on autopsy and showed a greater clinical association with ventricular septal defect, coarctation, atrioventricular canal, and tetralogy of Fallot, but later series observed less severe lesions, including atrial septal defect, partial anomalous pulmonary venous return, and persistent left superior vena cava [31,32,34].

Embryology

Cor triatriatum has been referred to as "stenosis of the common pulmonary vein," reflecting the idea that incomplete embryonic absorption of the coalesced pulmonary veins [the common pulmonary vein (CPV)] into the left atrium results in various degrees of obstruction, with the level of

connection between the CPV and the true left atrium determining the shape of the defect.

Pathology

There is a fibromembranous septum between the proximal common pulmonary vein and the left atrium, yet the shape of this barrier is variable, with tubular, hourglass, and membranous types having been described, and also with variable sized openings from the proximal to distal chambers [34]. The foramen ovale (or secundum atrial septal defect) is usually found between the right atrium and true left atrium, but sometimes is found between the proximal common pulmonary venous chamber and the right atrium [33,34] (Figure 27.2). The left atrial appendage communicates with the left atrial chamber.

Clinical features

Clinical findings resemble other forms of pulmonary venous obstruction. Dyspnea and other respiratory signs and symptoms predominate. Nonspecific physical findings, such as a loud second heart sound and tricuspid regurgitation murmur, reflect pulmonary venous and pulmonary arterial hypertension. Murmurs may be absent. Many are mistakenly diagnosed as chronic lung disease.

Electrocardiogram and chest X-ray

The electrocardiogram and chest radiograph are nonspecific. Right ventricular and right atrial enlargement and hypertrophy are present if the patient survives the neonatal period. Cardiomegaly, pulmonary edema, pleural effusions, and pulmonary artery enlargement may be seen. The dilated common pulmonary venous chamber may erroneously suggest left atrial enlargement, making radiographic differentiation from mitral stenosis impossible.

Echocardiography

Echocardiography provides the most likely diagnostic modality to identify the "membrane" between the pulmonary venous chamber and the true left atrium, and Doppler allows identification of the communication between the two chambers. The velocity and flow pattern by Doppler can be used to estimate the pressure gradient. Transesophageal, three-dimensional, and contrast echocardiography have all proved useful in the evaluation of cor triatriatum, particularly in adults [35–37].

Cardiac catheterization and angiography

Cardiac catheterization can confirm the diagnosis, but balloon dilation has not proved useful. Pulmonary artery and pulmonary capillary wedge pressures are elevated. When a patent foramen ovale or atrial septal defect is present, it
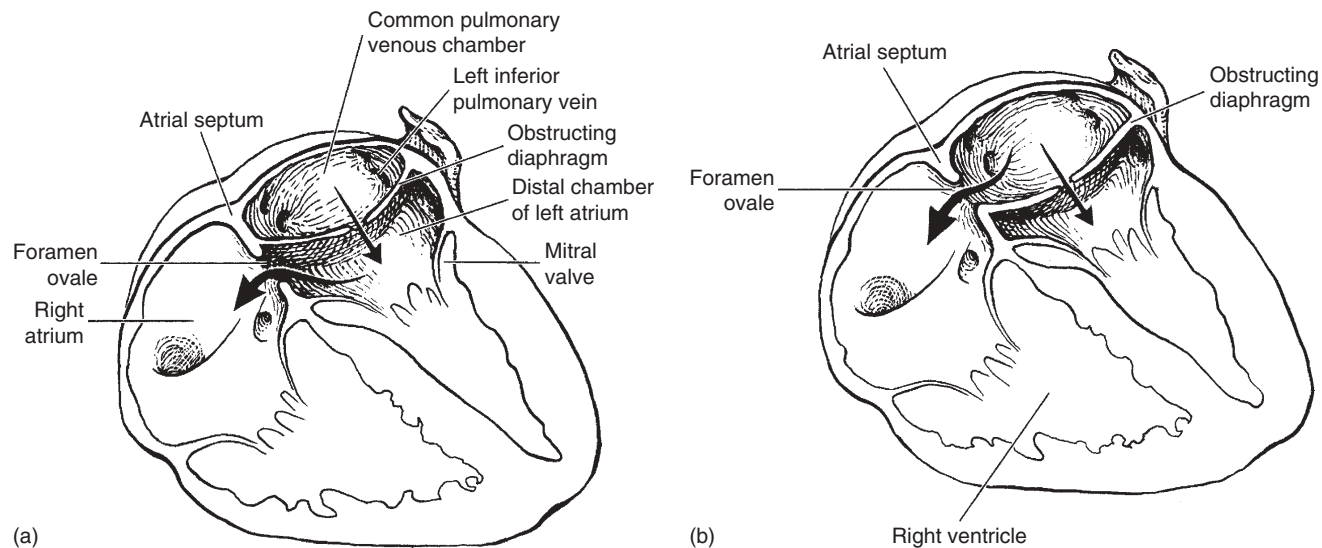
Figure 27.2 Morphology of cor triatriatum. (a) Cor triatriatum with patent foramen ovale below obstructing diaphragm. The common pulmonary venous chamber is separated from the atrial septum medially and immediately below the left inferior pulmonary vein laterally. The lateral attachment is also closely related to the mitral valve. The left atrial appendage is in the distal chamber. Clinical presentation is that of pulmonary venous obstruction (like mitral valve stenosis) when the hole in the diaphragm is small. The distal chamber communicates with the right atrium through the foramen ovale, but left-to-right shunt is small. (b) Cor triatriatum with patent foramen ovale above obstructing diaphragm, through which the common pulmonary venous chamber may communicate with the right atrium. Clinical presentation in this situation is that of a large left-to-right shunt or may mimic total anomalous pulmonary venous connection. (Reproduced with permission from Kouchoukas NT, Blackstone EH, Doty DB, *et al.*, *Kirklin/Barratt-Boyes Cardiac Surgery*, 3rd edn. Philadelphia: Churchill Livingstone Elsevier, 2003, Copyright Elsevier 2003.)

almost always communicates with the true left atrium, and a catheter advanced across the atrial septum can be used to demonstrate normal left atrial and left ventricular pressures. Occasionally, the proximal chamber can be entered with a catheter passed retrograde from the left atrium, revealing a pressure gradient. Angiography in the right ventricle or pulmonary arteries may demonstrate delayed transit through the pulmonary veins and allow imaging of the common pulmonary venous chamber proximal to the obstruction, yet there is a risk that pulmonary vascular tone may worsen.

Other imaging modalities

Magnetic resonance imaging and computed tomography can demonstrate the cor triatriatum, especially in adults presenting late [26]. These techniques have less fidelity and are often more subject to motion and heart rate artifact [38] in infants than echocardiography.

Surgical management

Surgical resection of the obstructing tissue is usually curative. Despite the reliability of two-dimensional echocardiography in establishing the diagnosis of cor triatriatum, considerable variability in the precise location of the membrane and adjacent structures mandates a general surgical approach that may require intraoperative modification.

The patent foramen ovale (or atrial septal defect) may lie above or below the membrane (Figure 27.2). A persistent left superior vena cava may be present, which may connect to the coronary sinus draining into the right atrium or directly to the upper left atrium (unroofed coronary sinus).

In neonates and small infants, continuous hypothermic cardiopulmonary bypass with preparations for brief periods of low flow perfusion or circulatory arrest is advisable to optimize exposure. In small patients, a right atrial approach is preferred. The foramen ovale (atrial septal defect) is enlarged by incising the atrial septum to provide access to the left atrium. Before excising the membrane, the surgeon must ascertain whether the proximal or distal chamber has been entered. The upper (proximal) chamber contains the pulmonary venous orifices and the lower (distal) chamber the mitral valve and left atrial appendage. The hole within the membrane is located and enlarged for visualization. While excising the membrane, care is taken to identify adjacent structures accurately, because the lateral attachment of the membrane is usually close to the orifice of the left inferior pulmonary vein and the mitral valve.

When the common pulmonary venous chamber is enlarged in older children and adults, a left atrial approach anterior to the right pulmonary veins may be convenient. Excision of the obstructing membrane begins at the

fenestration connecting the upper and lower chambers. Resection proceeds leftwards while accurately visualizing and preserving the mitral valve and left inferior pulmonary vein, and avoiding penetration of the left atrial free wall. The repair is completed with closure of the foramen ovale and atrial incision.

Results of surgical repair

Hospital deaths are uncommon after repair of isolated cor triatriatum, even in critically ill infants. Mortality following surgery for complex cor triatriatum is generally related to the risk of repairing the associated cardiac malformations.

Supravalvar mitral stenosis

Supravalvar mitral stenosing ring is a rare lesion consisting of a membranous disc situated just proximal to, and often in continuity with, the mitral valve leaflets. It may exist as an isolated lesion [39] but is more often described in association with other left heart obstructions [40], often mitral valve anomalies.

Incidence and genetics

The etiology of supravalvar mitral stenosis is unknown, but postoperative "acquired" and recurrent forms have been described [41], and some infants seem to develop and then have progressive lesions [42]. Therefore, deranged transmitral flow may lead to abnormal tissue growth, analogous to that considered to lead to fibromuscular subaortic stenosis [43].

Pathology

The pathology has been described in autopsy series [40]. The ring is supravalvar but often partially involves the mitral valve.

Pathophysiology

The pathophysiology resembles other left ventricular inflow obstructions, yet the hemodynamic effect of associated lesions, especially mitral valvar stenosis, typically predominates.

Clinical features

Clinical findings mimic mitral stenosis, or those of the hemodynamically most significant associated lesion. However, a supravalvar ring may be an unsuspected incidental finding by echocardiography, or at the time of surgery for other lesions.

Echocardiography, catheterization, angiography, and other imaging modalities

The diagnosis is most often made by echocardiography. Cineangiographic and CTA and MRI detection may be more

difficult, perhaps due to the proximity to the mitral valve itself, and due to the superior beat-to-beat resolution of two-dimensional echo.

Management

Catheter-based treatment (balloon dilation) is generally ineffective. If associated lesions potentially amenable to balloon dilation, such as mitral valvar stenosis, exist then balloon dilation is not considered advisable due to the supravalvar ring [44].

Surgical resection is usually indicated if the lesion is hemodynamically significant, yet not all patients have stenosis. The surgical observation that the ring is supravalvar proximal to the mural or posterior mitral valve leaflet, but intravalvar and attached to the opposing anterior mitral valve leaflet, means that careful resection must be performed to avoid damage to the anterior mitral leaflet [45].

Mitral Stenosis (MS) and mitral annular hypoplasia

Incidence and genetics

Acquired

Most mitral valve disease, both stenosis and insufficiency, is acquired as a result of rheumatic fever. Although rheumatic fever has become relatively rare in countries with advanced economies, the worldwide burden of patients with rheumatic valvar disease dwarfs that of congenital heart disease survivors (see Chapters 61 and 62).

Rheumatic MS accounts for almost all patients presenting in adulthood [46,47]. The typical pathology involves fibrous thickening and calcification of the leaflets, and fusion of the chordae [46].

Rare causes of "acquired" progressive childhood mitral valve thickening and dysfunction include storage diseases such as mucopolysaccharidoses, and endocrinopathy, such as hyperthyroidism, and genetic conditions, particularly Williams syndrome, yet in these conditions mitral regurgitation predominates and stenosis is usually not significant.

Congenital

The mitral valve and its tensor apparatus constitute one of the most complex functional units in the human body. Given that virtually any derangement of structure can lead to major impairments of function, many differing classification systems exist.

Congenital forms of MS are rare and often associated with other cardiac anomalies, including various forms of left heart hypoplasia. In an early surgical era, congenital MS comprised 0.017% of admissions to a tertiary children's hospital, yet 1.2% of autopsied congenital heart disease cases from the same center [48], likely reflecting the

increased lethality of the lesion relative to other congenital heart malformations.

Genetic factors are only now being elucidated [49], although family clustering of individuals with various and often discordant types of left heart lesions, including mitral valve abnormalities, have been reported [50–52].

Embryology

The atrioventricular valve and atrioventricular septum form from embryonic tissue, the endocardial cushions, and are the end result of a complex cascade of molecular and cellular events. Although the developmental morphometry is well described in embryos [53,54], the understanding of normal and abnormal differentiation of the endocardial cushions into septae and valves is incomplete.

Like other left heart lesions, MS may result in part from altered flow through the left heart. Although some lesions can be created experimentally by disrupting the normal flow in the developing heart, a genetic component is likely present also.

Pathologic anatomy and major associated anomalies

Several pathologic types are recognized, although pathologic descriptions, surgical classification, and functional correlation vary widely among authors [47,55–57].

Atresia and hypoplasia

Mitral atresia and hypoplasia are defining features of the relatively common hypoplastic left heart syndrome (HLHS) (see Chapters 38 and 39), with management limited to univentricular palliation. Rarer, less extreme, forms of MS, allowing for biventricular repair, are discussed here.

Parachute mitral valve

The most common anomaly resulting in congenital MS involves a single papillary muscle with chordal attachments to the leaflets that give the appearance of a person suspended beneath a parachute. The interchordal spaces are fewer and shorter than normal.

Mitral arcade

An arch-like fusion of the papillary muscles occurs, with shortened chordae and malformed leaflets.

Commissural fusion

Various forms of commissural fusion may result in incomplete opening of the valve, but it almost always accompanied by some degree of papillary muscle and chordal abnormality.

Double orifice mitral valve (also see chapter 28)

A double orifice mitral valve may exhibit two well-formed orifices and no stenosis or regurgitation, or various degrees of stenosis may be present. A short-axis parasternal
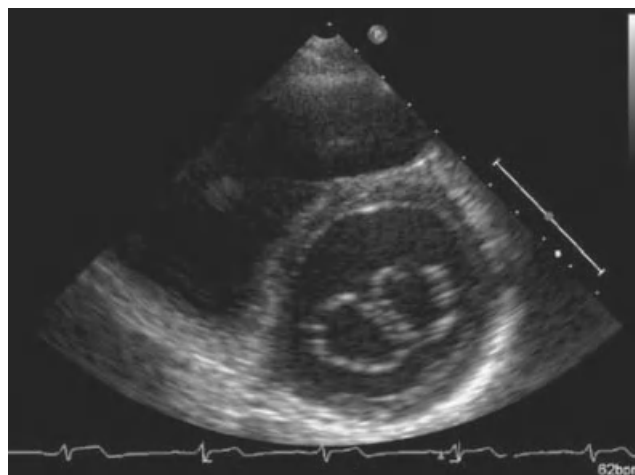
Figure 27.3 Double orifice mitral valve. Two-dimensional echocardiogram in parasternal short-axis view of the left ventricle at the level of the open mitral valve leaflets, showing the distinctive double orifice. In this patient, the finding was hemodynamically insignificant, as no stenosis or regurgitation was present.

echocardiogram view is characteristic (Figure 27.3) (see Videoclip 27.2), although it may be confused with cleft mitral valve.

Shone complex

As originally described, the complex comprised four anomalies: supravalvar stenosing ring, parachute mitral valve, subaortic stenosis, and coarctation of the aorta [40]. Most patients in the original report did not have each of the four lesions, yet the complex was speculated to result from deranged left heart flow interfering with normal development of proximal and distal structures, and the term "Shone" has come to refer loosely to multiple left heart inflow and outflow obstructions.

Other associated anomalies

Other anomalies, in addition to those seen in the Shone complex, include atrial and ventricular septal defects, double outlet right ventricle, and pulmonary stenosis [57]. In the neonate, atrial left-to-right shunt at the fossa ovalis (or atrial septal defect) and right-to-left shunt via the ductus arteriosus attenuates the hemodynamic effects of MS [58], but result, via the ductal level shunt, in arterial desaturation in the lower body.

Pathophysiology

As in other forms of left ventricular inflow obstruction, increased pulmonary venous pressure leads to pulmonary hypertension and attendant right heart failure. In MS, manifestations involving left atrial dilation may help differentiate MS from other forms such as pulmonary venous stenosis. Left atrial dilation, stretch, and progressive fibrosis are arrhythmogenic.

The degree of obstruction can be expressed quantitatively in various ways. For most cardiac obstructions, the pressure gradient is perhaps the most direct and commonly used parameter, but as the normal mitral valve has no gradient, and as the diastolic gradient in symptomatic MS is often deceptively small, and dependent on the transvalvar flow (equal to the cardiac output in patients without associated mitral regurgitation), a knowledge of the flow and the gradient can be combined to derive a cross-sectional orifice area [59]. This mitral valve area (MVA) can be calculated at catheterization [59] or by Doppler, using the continuity equation [60], or the area can be estimated directly from two-dimensional echocardiogram images of the open valve [61].

In adults, the normal mitral valve area is 4–5 cm^2. In adults with MS, symptoms do not usually occur if the MVA is >2.5 cm^2, but patients with mild stenosis (MVA >1.5 cm^2) may not have symptoms at rest yet typically develop dyspnea and other symptoms with any increase in cardiac output demand, such as during fever, anemia, exercise, or pregnancy, or if they develop atrial arrhythmia. Then, as cardiac output increases, the transmitral gradient increases exponentially [62], pulmonary venous and pulmonary artery hypertension increase, and ultimately, the expected increase in cardiac output will be blunted. Patients with moderate stenosis have an MVA 1.0–1.5 cm^2. An MVA <1.0 cm^2 is considered severe MS and patients may be symptomatic at rest [63].

The MVA may be indexed to body surface area (BSA), to compare values in children with the experience with adult MVA values. BSA, however, is not linear with age. In a series of children with severe congenital MS, the indexed MVA ranged from 0.44 to 2.1 cm^{2}m^{-2} with a mean of 1 cm^{2}m^{-2} [48]. This should not be confused with a similarly named and indexed value, commonly calculated by measuring the *annulus* echocardiographically [64], as it does not express *orifice* area, or include a factor for transmitral flow.

Natural history

The natural history of MS depends upon the etiology and severity, and whether the lesion is isolated or associated with other malformations, such as coarctation, which may predominate clinically.

In neonates with borderline or inadequate left ventricular size, MS is often lethal without surgery or transplant. Infants with less severe stenosis may escape detection and present at 1–2 years of age with pulmonary hypertension, often during an acute febrile respiratory illness. This reflects both their fragile cardiac output reserve and the propensity dramatically to increase further their already elevated pulmonary vascular resistance.

Mild forms of congenital MS may be well tolerated and produce no symptoms at rest, leading to delayed diagnosis in adulthood.

In longstanding MS, left atrial dilation may lead to atrial arrhythmias, such as atrial fibrillation. Embolic stroke is more likely due to the dilated atrium, even in the absence of atrial fibrillation.

Clinical features

Clinical history

Isolated MS in neonates may be well tolerated and asymptomatic, yet with age and growth, signs of tachypnea, poor feeding, and growth failure develop. Mitral stenosis is often clinically silent in the presence of other clinically evident lesions, such as coarctation or left ventricular outflow obstruction.

Physical examination

Classically, and in rheumatic disease, MS produces a mid-diastolic or proto-systolic murmur, which may be preceded by an opening snap occurring just after the second heart sound (S$_2$) and at the end of isovolumetric relaxation. An apical diastolic thrill may accompany the murmur. The opening snap and the mid-diastolic murmur, however, are rarely noted in congenital MS [58]. The first heart sound (S$_1$) is loud, presumably from delayed and therefore more forceful systolic mitral valve closure, unless the stenosis is very severe. A loud S$_1$ originating from the tricuspid valve may be a consequence of right ventricular hypertension.

Pulmonary hypertension leads to a loud S$_2$ and, rarely, the early diastolic murmur of pulmonary regurgitation (first described by Graham Steell in rheumatic mitral stenosis), and a holosystolic murmur of tricuspid regurgitation. However, differentiation of these right heart murmurs from the murmurs of associated aortic valve insufficiency and mitral regurgitation may be challenging.

Electrocardiogram

The electrocardiogram may reflect left atrial dilation, atrial arrhythmia, and pulmonary hypertension. It may be normal in mild mitral valve stenosis, or associated lesions, such as left ventricular outflow tract obstruction, may dominate.

Atrial dilation is manifest as broad, often biphasic, M-shaped P waves of "P-mitrale." This feature differentiates MS from most other congenital forms of left ventricular inflow obstruction.

In longstanding MS, atrial arrhythmias, often chronic, such as atrial fibrillation, develop.

Pulmonary hypertension manifests as varying degrees of right ventricular hypertrophy and right atrial enlargement.

Chest X-ray

The chest X-ray, as in other forms of left heart inflow obstruction, may reflect pulmonary hypertension, pulmonary edema, and pleural effusions, but the left atrial enlargement in MS helps to differentiate valvar from supravalvar and pulmonary venous forms. The lateral images typically show left atrial dilation as the posterior heart border projecting towards the vertebral bodies. In infants and children, this finding is generally more useful than features of left atrial

enlargement on the frontal images, such as elevation of the left main bronchus, and a double density. A redistribution of pulmonary blood flow to the upper lobes (cephalization) may be seen in some children, yet a generalized increase in pulmonary vascular markings may result from associated left-to-right shunt lesions [48].

Echocardiography

Echocardiography is usually the most valuable means of collecting data about the morphology and function of the mitral valve and in assessing associated lesions. Associated findings such as supravalvar mitral ring can be difficult to differentiate from pure valvar forms of MS.

Scoring of four variables, subvalvar thickening and leaflet mobility, thickening, and calcification, have been used to predict the efficacy of balloon dilation of rheumatic MS [65].

Mitral annular dimensions are usually measured by two-dimensional echo or angiographically, but because the valve annulus is best thought of as a saddle-shaped structure, simplified to that of an ellipse for the purposes of measurement, care must be taken to measure the valve with technique comparable to published normal values. The mitral valve diameter is often indexed to BSA and expressed as a Z statistic to represent the variance from the mean of normal patient values [66,67].

Doppler of the mitral valve diastolic signal allows estimation of the pressure gradient and derived values, including valve area, by the continuity equation technique [63]. The mitral valve peak gradient may be estimated from the Doppler peak velocity, but the mean gradient [68] is more commonly used; both values correlate well with catheterization-derived gradients. Mean mitral valve gradients in adults correlate clinically as follows: mild, <5 mmHg; moderate, 5–10 mmHg; and severe, >10 mmHg. [63] In a series of congenital MS, retrospective risk stratification by mean gradient at the initial infant echocardiogram ($\leq$2; 2–5.5; and $\geq$5.5 mmHg) based on longitudinal outcomes suggests that intervention or death is unlikely in the low-gradient group, very likely in the high-gradient group, and of intermediate risk with mid-range gradients [69].

A simpler echocardiographically derived value expressing only the annular, not orifice, area of the mitral valve has been used more commonly than the Gorlin calculation in infants to make decisions regarding suitability for biventricular repair versus single ventricle palliation (<4.75 cm^2 m^{-2} or <–2Z) [64,70,71]. This annular mitral valve area and the Gorlin hydraulic calculation of orifice MVA are different parameters and should not be compared with each other. (See Videoclip 27.3.)

Cardiac catheterization and angiography

Catheterization allows the collection of diagnostic data and therapeutic options (balloon dilation). The diagnostic role of catheterization and angiography has been largely replaced by echocardiography, although evaluating associated lesions and confirming mitral valve findings by catheterization remains common. Elevated pulmonary artery pressure and resistance are common. The pulmonary capillary wedge pressure is elevated, reflecting elevated left atrial pressure. Transatrial catheter puncture (Brockenbrough procedure) allows for direct measurement of the left atrial hypertension, and is ideally performed with simultaneous measurements of left ventricular pressure, allowing for instantaneous gradient measurements and calculation of valve area [59]. Without associated left heart obstructions, or mitral regurgitation, the left ventricular end diastolic pressure (LVEDP) is usually normal.

The left atrial injection, using axial angiography [72], demonstrates the level of obstruction, but does not usually offer a level of resolution comparable to echocardiography. Angiography, pulmonary arteriography in particular, may result in clinically adverse increases in pulmonary vascular resistance.

Other imaging modalities

Both CTA and MRI have been used to delineate mitral valvar stenosis, although these techniques generally offer better image and functional data in adolescent and adult patients with slower heart rates.

Management

Management options include symptomatic and palliative treatments, yet the ideal treatment, gradient relief of the stenosis, requires balloon dilation, surgical valvoplasty, or valve replacement.

There is no single criterion for seeking gradient relief. A variety of clinical factors (i.e., failure to thrive, dependence upon mechanical ventilation, etc.) and laboratory data (i.e., gradient, mitral valve area, degree of pulmonary hypertension, etc.) are considered, in addition to the potential to delay intervention until the child is larger.

Medical

Medical management of MS is limited to symptomatic treatment of right heart failure, including peripheral edema and pleural effusions. Pulmonary hypertension does not typically respond to medical treatment, but is often rapidly (within hours) reversible with effective gradient relief of MS.

Catheterization

Balloon dilation has been successful for rheumatic MS [73] and may be effective for congenital MS [74]; however, significant mitral regurgitation is a potentially severe complication in at least 25% of patients [44]. Balloon dilation is not effective for mitral valvar stenosis with associated supravalvar ring.

Surgical management

In congenital MS, the broad spectrum of mitral valve pathology, the large number of possible combinations of associated lesions, and the relative rarity of patients with the disease

make the comparison of surgical treatment outcomes difficult. Surgical options broadly involve repair versus replacement. Mortality and morbidity remain relatively high compared with many other malformations.

Associated conditions, such as coarctation and aortic stenosis (valvar and subvalvar), are often more easily remedied and with less risk. Closure of septal defects, such as ventricular septal defects, and patent ductus arteriosus may eliminate enough left heart volume overload to reduce the relative flow across the mitral valve and improve signs and symptoms, obviating or at least delaying the need for a direct intervention of MS.

Repair is generally considered preferable to and with better long-term outcomes than replacement, yet outcomes largely depend on the underlying anatomy and associated defects [75,76].

Although congenital MS can involve a single component of the mitral apparatus, usually multiple components are affected. In the absence of severe LV hypoplasia, the mitral valve annulus is usually not itself obstructive. Leaflet anomalies are common, with congenital absence of one or both commissures leading to a continuous sheet of leaflet tissue. Leaflet incisions can be made in the location of expected commissures, taking care to leave the created leaflet margins with adequate chordal support. The subvalvar apparatus may contribute to obstruction from short, fused chordae or, rarely, complete chordal absence with direct fusion of leaflet tissue on to the papillary muscles. Surgical maneuvers include splitting of fused chords and papillary muscles, creating new interchordal spaces, and cutting noncritical secondary chords that are tethering mitral leaflets. If annulus hypoplasia is severe, with a measured Z-value of less than –2, then repair is rarely feasible.

Because these reconstructive maneuvers may result in important mitral insufficiency, intraoperative evaluation with transesophageal echo (TEE) is essential. If TEE indicates important mitral regurgitation and elevated left atrial pressure after discontinuing cardiopulmonary bypass, mitral valve replacement is advisable.

Currently, mechanical mitral valve prostheses as small as 15 mm in diameter are available. If the annulus is too small to accept an available prosthesis, a portion of the prosthesis can be implanted in the supra-annular position, using an elliptical patch of Dacron to create a larger effective annulus size.

Valve replacement in children is problematic because a small prosthetic valve itself has some intrinsic impedance due to its support structures, long-term anticoagulation is necessary, and, most importantly, the prosthesis does not grow as the child grows. Surgically induced atrioventricular block is also an important complication. The risk and technical difficulty in a subsequent surgical revision to a larger prosthesis can be considerable. Early postoperative hemodynamics after supra-annular implantation often remain poor, despite the reduction in transvalvar gradient

[77]. Long-term data suggest that children who have an annular rather than supra-annular prosthesis have a better outcome [78]. The long-term outcome of children who require mitral valve replacement can be gratifying. Their care remains challenging [79] and the close monitoring of anticoagulation is critical.

Surgical management of rheumatic MS is often more efficacious relative to congenital forms, as patients usually present as older children or adults, and because the annulus is of normal size. Valvoplasty, annuloplasty, and valve replacement (particularly in patients with accompanying mitral regurgitation) are all effective and relatively low-risk options.

Long-term history of treated and untreated adults

Although congenital forms of all of the various types of pulmonary venous stenosis and left ventricular inflow obstructions have been reported to present in adult patients, these are usually minimally obstructive lesions with normal or near-normal hemodynamics.

The long-term outlook for adults with high-grade stenoses requiring intervention in childhood depends mostly on the effectiveness of the treatment in restoring the hemodynamics to normal. Pregnancy in women with mitral stenosis in particular can significantly alter the hemodynamics, because of both the increase in cardiac output and the decrease in the diastolic filling time associated with the increased heart rate [80].

References

1 Lucas RV Jr. Congenital causes of pulmonary venous obstruction. *Cardiovasc Clin* 1972;**4**:19–51.

2 Seale AN, Webber SA, Uemura H, *et al.* Pulmonary vein stenosis: the UK, Ireland and Sweden collaborative study. *Heart* 2009;**95**:1944–99.

3 Edwards JE. Congenital stenosis of pulmonary veins. Pathologic and developmental considerations. *Lab Invest* 1960;**9**:46–66.

4 Holt DB, Moller JH, Larson S, *et al.* Primary pulmonary vein stenosis. *Am J Cardiol* 2007;**99**:568–72.

5 Drossner DM, Kim DW, Maher KO, *et al.* Pulmonary vein stenosis: prematurity and associated conditions. *Pediatrics* 2008;**122**:e656–61.

6 Maltz DL, Nadas AS. Agenesis of the lung. Presentation of eight new cases and review of the literature. *Pediatrics* 1968;**42**:175–88.

7 Chakrabarti S, Mittal R, Gnanapragasam JP, *et al.* Acquired stenosis of normally connected pulmonary veins. *Cardiol Young* 2007;**17**:322–7.

8 McConnell ME, Pacifico AD, Johnson WH Jr, *et al.* Progressive pulmonary venous obstruction and pulmonary interstitial fibrosis associated with tetralogy of Fallot. *Pediatr Cardiol* 1994;**15**:95–9.

9 Kelly DJ, Brodison A, Millner RW, *et al.* Congenital pulmonary vein stenosis beyond childhood. *Int J Cardiol* 2008;**124**:e31–3.

10 Omasa M, Hasegawa S, Bando T, *et al.* A case of congenital pulmonary vein stenosis in an adult. *Respiration* 2004;**71**:92–4.

11 Tan CW, Munfakh N, Helmcke F, *et al.* Congenital bilateral pulmonary venous stenosis in an adult: diagnosis by echo-Doppler. *Catheter Cardiovasc Interv* 2000;**49**:328–30.

12 Saida Y, Eguchi N, Mori K, *et al.* Isolated pulmonary vein stenosis associated with full intrapulmonary compensation. *AJR Am J Roentgenol* 1999;**173**:961–2.

13 Rumoroso JR, Agredo J, Alcíbar J, *et al.* Congenital stenosis of pulmonary veins in the adult. *Rev Esp Cardiol* 1996;**49**:697–700 (in Spanish).

14 Massaro AN, Kanter JP, Scavo L, *et al.* Pulmonary vein stenosis diagnosed after failure to wean from extracorporeal membrane oxygenation. *Pediatr Cardiol* 2008;**29**:238–40.

15 Holcomb RG, Tyson RW, Ivy DD, *et al.* Congenital pulmonary venous stenosis presenting as persistent pulmonary hypertension of the newborn. *Pediatr Pulmonol* 1999;**28**:301–6.

16 Driscoll DJ, Hesslein PS, Mullins CE. Congenital stenosis of individual pulmonary veins: clinical spectrum and unsuccessful treatment by transvenous balloon dilation. *Am J Cardiol* 1982;**49**:1767–72.

17 van Son JA, Danielson GK, Puga FJ, *et al.* Repair of congenital and acquired pulmonary vein stenosis. *Ann Thorac Surg* 1995;**60**:144–50.

18 Devaney EJ, Chang AC, Ohye RG, *et al.* Management of congenital and acquired pulmonary vein stenosis. *Ann Thorac Surg* 2006;**81**:992–6.

19 Shone JD, Amplatz K, Anderson RC, *et al.* Congenital stenosis of individual pulmonary veins. *Circulation* 1962;**26**:574–81.

20 Herlong JR, Jaggers JJ, Ungerleider RM. Congenital Heart Surgery Nomenclature and Database Project: pulmonary venous anomalies. *Ann Thorac Surg* 2000;**69**:S56–69.

21 van de Laar I, Wessels M, Frohn-Mulder I, *et al.* First locus for primary pulmonary vein stenosis maps to chromosome 2q. *Eur Heart J* 2009;**30**:2485–92.

22 Sadr IM, Tan PE, Kieran MW, *et al.* Mechanism of pulmonary vein stenosis in infants with normally connected veins. *Am J Cardiol* 2000;**86**:577–9.

23 Riedlinger WF, Juraszek AL, Jenkins KJ, *et al.* Pulmonary vein stenosis: expression of receptor tyrosine kinases by lesional cells. *Cardiovasc Pathol* 2006;**15**:91–9.

24 Minich LL, Tani LY, Breinholt JP, *et al.* Complete follow-up echocardiograms are needed to detect stenosis of normally connecting pulmonary veins. *Echocardiography* 2001;**18**:589–92.

25 Agata Y, Hiraishi S, Oguchi K, *et al.* Changes in pulmonary venous flow pattern during early neonatal life. *Br Heart J* 1994;**71**:182–6.

26 Dillman JR, Yarram SG, Hernandez RJ. Imaging of pulmonary venous developmental anomalies. *AJR Am J Roentgenol* 2000;**192**:1272–85.

27 Prakash A, Powell AJ, Geva T. Multimodality noninvasive imaging for assessment of congenital heart disease. *Circ Cardiovasc Imaging* 2010;**3**:112–25.

28 Pacifico AD, Mandke NV, McGrath LB, *et al.* Repair of congenital pulmonary venous stenosis with living autologous atrial tissue. *J Thorac Cardiovasc Surg* 1985;**89**:604–9.

29 Lacour-Gayet F, Rey C, Planché C. Sténose des veines pulmonaires. Description d'une technique chirurgicale sans suture utilisant le péricarde *in situ*. *Arch Mal Coeur* 1996;**89**:633–6.

30 Mendelsohn AM, Bove EL, Lupinetti FM, *et al.* Intraoperative and percutaneous stenting of congenital pulmonary artery and vein stenosis. *Circulation*. 1993;**88**:II210–7.

31 Krasemann Z, Scheld HH, Tjan TD, *et al.* Cor triatriatum: short review of the literature upon ten new cases. *Herz* 2007; **32**:506–10.

32 Van Praagh R, Corsini I. Cor triatriatum: pathologic anatomy and a consideration of morphogenesis based on 13 postmortem cases and a study of normal development of the pulmonary vein and atrial septum in 83 human embryos. *Am Heart J* 1969;**78**: 379–405.

33 Niwayama G. Cor triatriatum. *Am Heart J* 1960;**59**:291–317.

34 Marín-García J, Tandon R, Lucas RV Jr, *et al.* Cor triatriatum: study of 20 cases. *Am J Cardiol* 1975;**35**:59–66.

35 Einav E, Perk G, Kronzon I. Three-dimensional transthoracic echocardiographic evaluation of cor triatriatum. *Eur J Echocardiogr* 2008;**9**:110–2.

36 Baweja G, Nanda NC, Kirklin JK. Definitive diagnosis of cor triatriatum with common atrium by three-dimensional transesophageal echocardiography in an adult. *Echocardiography* 2004;**21**:303–6.

37 Samal AK, Nanda NC, Thakur AC, *et al.* Three-dimensional echocardiographic reconstruction of atrial membranes. *Echocardiography* 1998;**15**:605–10.

38 Dillman JR, Hernandez RJ. Role of CT in the evaluation of congenital cardiovascular disease in children. *AJR Am J Roentgenol* 2009;**192**:1219–31.

39 Sethia B, Sullivan ID, Elliott MJ, *et al.* Congenital left ventricular inflow obstruction: is the outcome related to the site of the obstruction? *Eur J Cardiothorac Surg* 1988;**2**:312–7.

40 Shone JD, Sellers RD, Anderson RC, *et al.* The developmental complex of "parachute mitral valve," supravalvular ring of left atrium, subaortic stenosis, and coarctation of aorta. *Am J Cardiol* 1963;**11**:714–25.

41 Martin RP, Qureshi SA, Radley-Smith R. Acquired supravalvar membranous stenosis of the left atrioventricular valve. *Br Heart J* 1987;**58**:176–8.

42 Toscano A, Pasquini L, Iacobelli R, *et al.* Congenital supravalvar mitral ring: an underestimated anomaly. *J Thorac Cardiovasc Surg* 2009;**137**:538–42.

43 Tulloh RM, Bull C, Elliott MJ, *et al.* Supravalvar mitral stenosis: risk factors for recurrence or death after resection. *Br Heart J* 1995;**73**:164–8.

44 McElhinney DB, Sherwood MC, Keane JF, *et al.* Current management of severe congenital mitral stenosis: outcomes of transcatheter and surgical therapy in 108 infants and children. *Circulation* 2005;**112**:707–14.

45 Carpentier A, Brizard C. Congenital malformations of the mitral valve. In: Stark JF, de Leval MR, Tsang VT, eds. *Surgery for Congenital Heart Defects*, 3rd edn. Chichester: John Wiley & Sons, Ltd, 2006: 573–590.

46 Waller BF, Howard J, Fess S. Pathology of mitral valve stenosis and pure mitral regurgitation – Part I. *Clin Cardiol* 1994; **17**:330–6.

47 Roberts WC. Morphologic features of the normal and abnormal mitral valve. *Am J Cardiol* 1983;**51**:1005–28.

48 Collins-Nakai RL, Rosenthal A, Castaneda AR, *et al.* Congenital mitral stenosis. A review of 20 years' experience. *Circulation* 1977;**56**:1039–47.

49 Hinton RB, Martin LJ, Rame-Gowda S, *et al.* Hypoplastic left heart syndrome links to chromosomes 10q and 6q and is genetically related to bicuspid aortic valve. *J Am Coll Cardiol* 2009;**53**:1065–71.

50 Hinton RB Jr, Martin LJ, Tabangin ME, *et al.* Hypoplastic left heart syndrome is heritable. *J Am Coll Cardiol* 2007;**50**,1590–5.

51 Lewin MB, McBride KL, Pignatelli R, *et al.* Echocardiographic evaluation of asymptomatic parental and sibling cardiovascular anomalies associated with congenital left ventricular outflow tract lesions. *Pediatrics* 2004;**114**:691–6.

52 Cripe L, Andelfinger G, Martin LJ, *et al.* Bicuspid aortic valve is heritable. *J Am Coll Cardiol* 2004;**44**:138–43.

53 Oosthoek PW, Wenink AC, Vrolijk BC, *et al.* Development of the atrioventricular valve tension apparatus in the human heart. *Anat Embryol (Berl)* 1998;**198**:317–29.

54 Oosthoek PW, Wenink AC, Wisse LJ, *et al.* Development of the papillary muscles of the mitral valve: morphogenetic background of parachute-like asymmetric mitral valves and other mitral valve anomalies. *J Thorac Cardiovasc Surg* 1998;**116**:36–46.

55 Ruckman RN, Van Praagh R. Anatomic types of congenital mitral stenosis: report of 49 autopsy cases with consideration of diagnosis and surgical implications. *Am J Cardiol* 1978;**42**:592–601.

56 Glancy DL, Roberts WC. Congenital obstructive lesions involving the major pulmonary veins, left atrium, or mitral valve: a clinical, laboratory, and morphologic survey. *Cathet Cardiovasc Diagn* 1976;**2**:215–52.

57 Davachi F, Moller JH, Edwards JE. Diseases of the mitral valve in infancy. An anatomic analysis of 55 cases. *Circulation* 1971;**43**:565–79.

58 Ferencz C, Johnson AL, Wiglesworth FW. Congenital mitral stenosis. *Circulation* 1954;**9**:161–79.

59 Gorlin R, Gorlin SG. Hydraulic formula for calculation of the area of the stenotic mitral valve, other cardiac valves, and central circulatory shunts. I. *Am Heart J* 1951;**41**:1–29.

60 Nakatani S, Masuyama T, Kodama K, *et al.* Value and limitations of Doppler echocardiography in the quantification of stenotic mitral valve area: comparison of the pressure half-time and the continuity equation methods. *Circulation* 1988;**77**:78–85.

61 Wann LS, Weyman AE, Feigenbaum H, *et al.* Determination of mitral valve area by cross-sectional echocardiography. *Ann Intern Med* 1978;**88**:337–41.

62 Gorlin R. The mechanism of the signs and symptoms of mitral valve disease. *Br Heart J* 1954;**16**:375–80.

63 Bonow RO, Carabello BA, Chatterjee K, *et al.* Focused update incorporated into the ACC/AHA 2006 guidelines for the management of patients with valvular heart disease: a report of the American College of Cardiology/American Heart Association Task Force on Practice Guidelines (Writing Committee to Revise the 1998 Guidelines for the Management of Patients with Valvular Heart Disease). *Circulation* 2008;**118**: e523–661.

64 Colan SD, McElhinney DB, Crawford EC, *et al.* Validation and re-evaluation of a discriminant model predicting anatomic suitability for biventricular repair in neonates with aortic stenosis. *J Am Coll Cardiol* 2006;**47**:1858–65.

65 Wilkins GT, Weyman AE, Abascal VM, *et al.* Percutaneous balloon dilatation of the mitral valve: an analysis of echocardiographic variables related to outcome and the mechanism of dilatation. *Br Heart J* 1988;**60**:299–308.

66 Kouchoukas NT, Blackstone EH, Doty DB, *et al.* Anatomy, dimensions, and terminology. In *Kirklin/Barratt-Boyes Cardiac Surgery*, 3rd edn. Philadelphia: Churchill Livingstone Elsevier, 2003: 3–65.

67 Daubeney PE, Blackstone EH, Weintraub RG, *et al.* Relationship of the dimension of cardiac structures to body size: an echocardiographic study in normal infants and children. *Cardiol Young* 1999;**9**:402–10.

68 Hatle L, Brubakk A, Tromsdal A, *et al.* Noninvasive assessment of pressure drop in mitral stenosis by Doppler ultrasound. *Br Heart J* 1978;**40**:131–40.

69 Selamet Tierney ES, Graham DA, McElhinney DB, *et al.* Echocardiographic predictors of mitral stenosis-related death or intervention in infants. *Am Heart J* 2008;**156**:384–90.

70 Corno AF. Borderline left ventricle. *Eur J Cardiothorac Surg* 2005;**27**:67–73.

71 Rhodes LA, Colan SD, Perry SB, *et al.* Predictors of survival in neonates with critical aortic stenosis. *Circulation* 1991; **84**:2325–35.

72 Bargeron LM Jr, Elliott LP, Soto B, *et al.* Axial cineangiography in congenital heart disease. Section I. Concept, technical and anatomic considerations. *Circulation* 1977;**56**:1075–83.

73 Lock JE, Khalilullah M, Shrivastava S, *et al.* Percutaneous catheter commissurotomy in rheumatic mitral stenosis. *N Engl J Med* 1985;**313**:1515–8.

74 Moore P, Adatia I, Spevak PJ, *et al.* Severe congenital mitral stenosis in infants. *Circulation* 1994;**89**:2099–106.

75 Oppido G, Davies B, McMullan DM, *et al.* Surgical treatment of congenital mitral valve disease: midterm results of a repair-oriented policy. *J Thorac Cardiovasc Surg* 2008;**135**:1313–20.

76 Prifti E, Vanini V, Bonacchi M, *et al.* Repair of congenital malformations of the mitral valve: early and midterm results. *Ann Thorac Surg* 2002;**73**:614–21.

77 Selamet Tierney ES, Pigula FA, Berul CI, *et al.* Mitral valve replacement in infants and children 5 years of age or younger: evolution in practice and outcome over three decades with a focus on supra-annular prosthesis implantation. *J Thorac Cardiovasc Surg* 2008;**136**:954–61.

78 Adatia I, Moore PM, Jonas RA, *et al.* Clinical course and hemodynamic observations after supraannular mitral valve replacement in infants and children. *J Am Coll Cardiol* 1997;29:1089–94.

79 Beierlein W, Becker V, Yates R, *et al.* Long-term follow-up after mitral valve replacement in childhood: poor event-free survival in the young child. *Eur J Cardiothorac Surg* 2007;**31**:860–5.

80 Horstkotte D, Fassbender D, Piper C. Angeborene Herzfehler und erworbene Herzklappenfehler in der Schwangerschaft [Congenital heart disease and acquired valvular lesions in pregnancy]. *Herz* 2003;**28**:227–39.

28 Left Ventricular Inflow Regurgitation

Pierre-Emmanuel Séguéla, Bertrand Léobon & Philippe Acar

Toulouse University Hospital, Toulouse, France

Mitral regurgitation may occur as a component of a cardiac malformation, such as endocardial cushion defect, or as an independent abnormality, the latter as a congenital anomaly of the mitral valve mechanism or a component of a systemic disease such as Marfan syndrome or as a sequel of rheumatic fever or other rheumatic and connective tissue diseases (see Chapters 61, 62, 67 and 69).

Anatomy of the normal mitral valve

The mitral valve prevents backflow into the left atrium during ventricular systole. The mitral valvar complex comprises the annulus, the anterior and posterior leaflets, the chordae tendineae, and the papillary muscles. The valve is obliquely located in the heart and is closely related to the aortic valve.

Mitral annulus

The annulus is defined surgically as the level of visible transition between the left atrial myocardium and the whitish leaflet. It is considered as the fibrous hingeline of the valvar leaflets [1]. Due to fibrous continuity between the aortic valve and the anterior (or aortic) mitral leaflet, defining its exact limits is extremely difficult [2]. The annulus is either D-shaped or saddle-shaped [3] (Figure 28.1a), and decreases in size during systole [1].

Leaflets

The mitral leaflets are uninterrupted structures of variable shape and circumferential length. They are usually divided into anterior and posterior segments. Many authors have separated them into aortic (anterior) and mural (posterior) leaflets because of their connection with the aortic valve.

Unlike the tricuspid valve, the mitral valve leaflets are not attached to the ventricular septum. During systole, when the leaflets meet to close the ventricle, the line of coaptation looks like a smile.

A commissure is the meeting point between the anterior and posterior leaflets, and is located at each end of the closure line, that is, the anterolateral commissure and posteromedial commissure. According to Carpentier's classification [4], the free edge of the posterior leaflet is divided into three scallops: P1 (lateral), P2 (middle), and P3 (medial). The anterior leaflet is subdivided into the A1, A2, and A3 regions that oppose the scallops of the posterior leaflet (Figure 28.1b).

Tendinous cords

Chordae tendineae connect the leaflets to the papillary muscles. The cords have several shapes and are attached to the leaflets at various sites (Figure 28.2a). Thus, the marginal cords (attached to the free edge), rough zone cord (attached to the rough zone), and strut cord (attached to the basal portion of the posterior leaflet) have been identified [3].

Papillary muscles

The papillary muscles are usually organized as two groups of closely packed papillary muscles as opposed to two distinct muscles. These arise from the apical two-thirds of the left ventricular wall. The tendinous cords extend from their tips (Figure 28.2b). Papillary muscles are in anterolateral and posteromedial positions (Figure 28.3). The anterolateral (or superior) muscle is vascularized by an artery from the circumflex or anterior descending branch of the left coronary artery [1]. The posteromedial (or inferior) muscle is usually supplied by the right coronary artery.
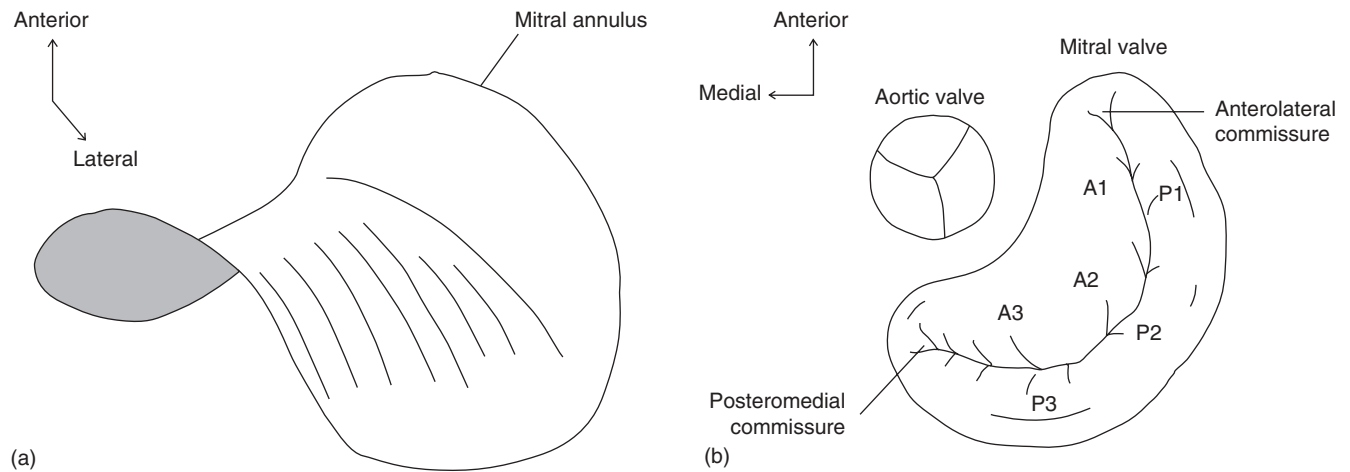
Figure 28.1 (a) Schematic representation of the saddle-shaped mitral annulus. (b) Schematic view of the mitral valve, seen from the ventricular side, showing its close relation with the aortic valve. In this plane, the mitral annulus is D-shaped. Leaflets are divided into three segments according to Carpentier's classification.
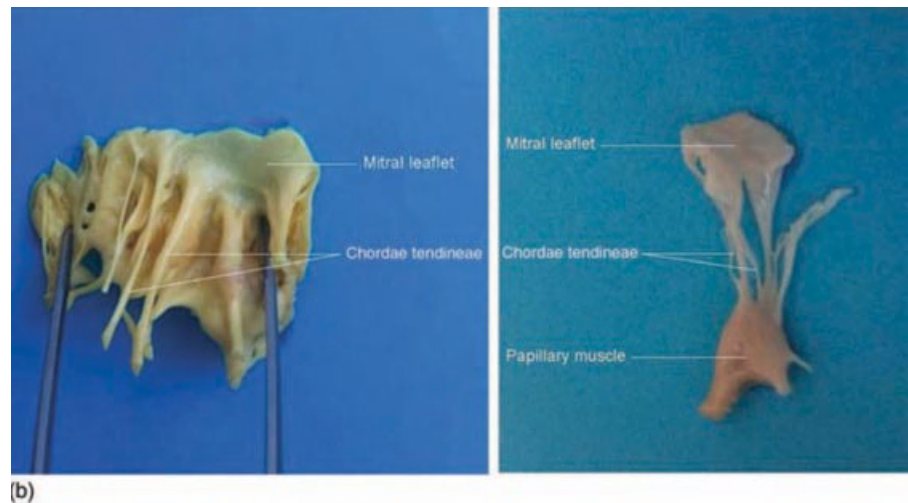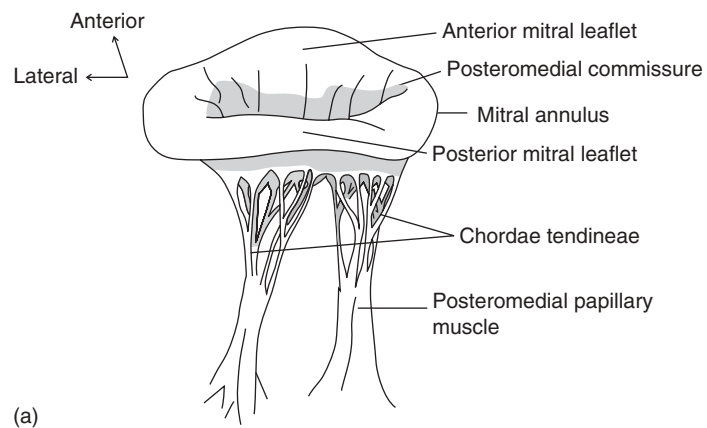
Figure 28.2 (a) Schematic view of the mitral valve complex. (b) Anatomic pieces showing the connection of chordae tendineae with the mitral valve leaflets.

Figure 28.3 Echocardiographic parasternal short-axis view showing the normal position of the papillary muscles. ALPM, anterolateral papillary muscle; LV, left ventricle; PMPM, posteromedial papillary muscle; RV, right ventricle.

Figure 28.4 Carpentier's functional classification of mitral regurgitation. Type I: leaflet motion is normal and mitral insufficiency is due to mitral annulus dilatation or valvar perforation (endocarditis). Type II: motion, of one or both leaflets, is excessive (mitral valve prolapse, chordal rupture). Type III: leaflet motion is restrictive.

Chronic compensated mitral regurgitation

When regurgitation is progressive, the left atrium dilates to accommodate the increase in volume and reduces the left atrial pressure. Eccentric cardiac hypertrophy allows left ventricular enlargement, and enables the forward stroke volume (the total stroke volume is increased) to be maintained The contractile function is normal and the ejection fraction is increased [6].

When mitral regurgitation is trivial or mild, patients are asymptomatic. A soft (grade 1–2/6), high-pitched holosystolic murmur with maximum intensity at the apex and radiation to the axilla is heard. Electrocardiography and chest radiography are usually normal.

When mitral regurgitation is moderate, fatigue, exercise limitation, and poor weight gain are common. The systolic murmur is louder (grade 3/6), maximum at the apex, and radiates to the axilla. A third heart sound and mid-diastolic murmur may be detected at the apex. The ECG shows left ventricular hypertrophy and left atrial enlargement. Cardiomegaly is noted on chest radiography and is proportional to the degree of regurgitation.

Chronic decompensated mitral regurgitation

In the decompensated phase, left ventricular contractile dysfunction (due to the lengthening of cardiac myocytes) reduces both total and forward stroke volume and increases the left ventricular filling pressure [5,6]. Ventricular dilatation aggravates mitral regurgitation as it increases the mitral annular diameter.

Signs of pulmonary edema are common. The apical pulse is displaced downwards to the left. In most instances, supraventricular tachyarrhythmias complicate chronic severe regurgitation.

According to Carpentier [7], three types of mitral valve dysfunction are observed. In this functional classification based on leaflet motion (Figure 28.4), etiology and valvar

Physiological and clinical presentation

Three hemodynamic forms are described: acute, chronic compensated, and chronic decompensated mitral regurgitation. Pulmonary hypertension (leading to pulmonary edema and congestive heart failure) may be observed in both acute and chronic decompensated phases.

Acute severe mitral regurgitation

In acute mitral regurgitation, filling of the left ventricle is increased because the pulmonary venous return volume is combined with the regurgitant volume. Despite the increase in total stroke volume, the major part is regurgitated into the left atrium and the forward volume is reduced. As a result, the end-diastolic pressure is increased. The elevated left atrial pressure, in a non-prepared left atrium (low compliance), causes pulmonary venous hypertension. The ventricular muscle function is normal [5].

Signs of congestive heart failure (orthopnea, dyspnea on exertion, fatigue) may occur. There is a short and unimpressive systolic murmur. A third heart sound is sometimes heard. The apical impulse is not displaced. Pulmonary congestion is found by chest radiography.

lesions have not been taken into account voluntarily in order to facilitate surgical management. Leaflet motion is described as normal (type I), excessive – prolapse (type II) or restrictive (type III). Complex mitral valve anomalies may include these three mechanisms to various degrees.

Anatomic malformations

Mitral valve prolapse

Mitral valve prolapse (MVP) occurs when the leaflets extend above the plane of the mitral annulus during ventricular systole [8]. The complications are endocarditis, sudden cardiac death, and severe mitral regurgitation. It is the most common cardiac valvar anomaly in developed countries. MVP is generally sporadic but is associated with disorders affecting the connective tissue, including Marfan and Ehler–Danlos syndromes, osteogenesis imperfecta, dominant cutis laxa, and pseudoxanthoma elasticum. The most common auscultatory observation is a mild systolic click heard at the cardiac apex and frequently associated with a late systolic murmur.

Previously, MVP was overestimated due to inconsistent echocardiographic definitions. New echocardiographic criteria have been established based on the understanding of the three-dimensional nonplanar shape of the mitral annulus. Since then, echocardiographic MVP has been defined as a single or bileaflet prolapse of 2 mm or more beyond the long-axis annular plane, with or without a thickening of leaflets [8]. Only prolapse shown in a parasternal long-axis view represents true MVP (Figure 28.5). Prolapse simply observed in a four-chamber view does not satisfy the diagnosis [9]. Classic prolapse is defined as a leaflet thickening exceeding 5 mm whereas a prolapse with a lesser degree of leaflet thickening is referred to as nonclassic.

In adults, the incidence of complications is proportional to the degree of leaflet thickening. Based on these criteria, the Framingham study, with its community-based population (as opposed to hospital-based populations in previous studies), revealed that 1.3% of the 3491 subjects had classic mitral valve prolapse and 1.1% had nonclassic mitral valve prolapse [10]. No difference was noted according to gender. MVP is uncommon before adolescence and its prevalence increases subsequently.

Causes

In adults, myxomatous degeneration is the most common etiology. Accumulation of proteoglycans and structural alterations of collagen are responsible for both leaflet thickening and redundancy, with interchordal hooding, chordal elongation, and annular dilatation [8]. Most myxomatous MVP are sporadic family-type instances and are described with mapped gene mutations.

Figure 28.5 Mitral valve prolapse. 2D echocardiography parasternal long-axis view. Leaflets are thickened and the superior displacement of the anterior leaflet exceeds 2 mm in a young patient with Marfan syndrome.

MVP may be secondary to distortion of the left ventricular geometry as in unrepaired atrial septal defect (right ventricular volume overloading and left ventricular size reduction). The mitral valve is normal histologically and the prolapse usually resolves postoperatively.

MVP is also observed in connective tissue disorders [8], especially in children. In Marfan syndrome, the percentage of MVP ranges from 40 to 91% [8,11]. In an adult population, however, fewer than 2% of patients with MVP have a related connective tissue disorder.

The Marfan syndrome is associated with mutations in fibrillin-1 on chromosome 15q21.1 and with mutations in TGF-β receptor 2 on chromosome 3p24.2-p25 [12]. Severe mitral valve disorders associated with the Marfan syndrome are generally observed in infants. As for adults, most complications are due to aortic aneurysm [13].

MVP most commonly involves both leaflets and is symmetrical (Figure 28.6), whereas it more frequently affects one leaflet (posterior) in myxomatous degeneration [11].

Management

Most patients with MVP have an excellent prognosis and are asymptomatic. Although mitral regurgitation is usually trivial or mild, long-term follow-up is recommended because the prolapse can progress slowly over the years. The most serious complication is severe mitral valve regurgitation, which is uncommon [14]. Patients with thickened valve leaflets, posterior leaflet prolapse, increased left ventricular dimensions, hypertension, and an increased body mass index are at high risk of developing severe mitral regurgitation. Vasodilator therapy is not recommended for treating asymptomatic patients with severe mitral regurgitation and a normal left ventricular function, as this may increase the
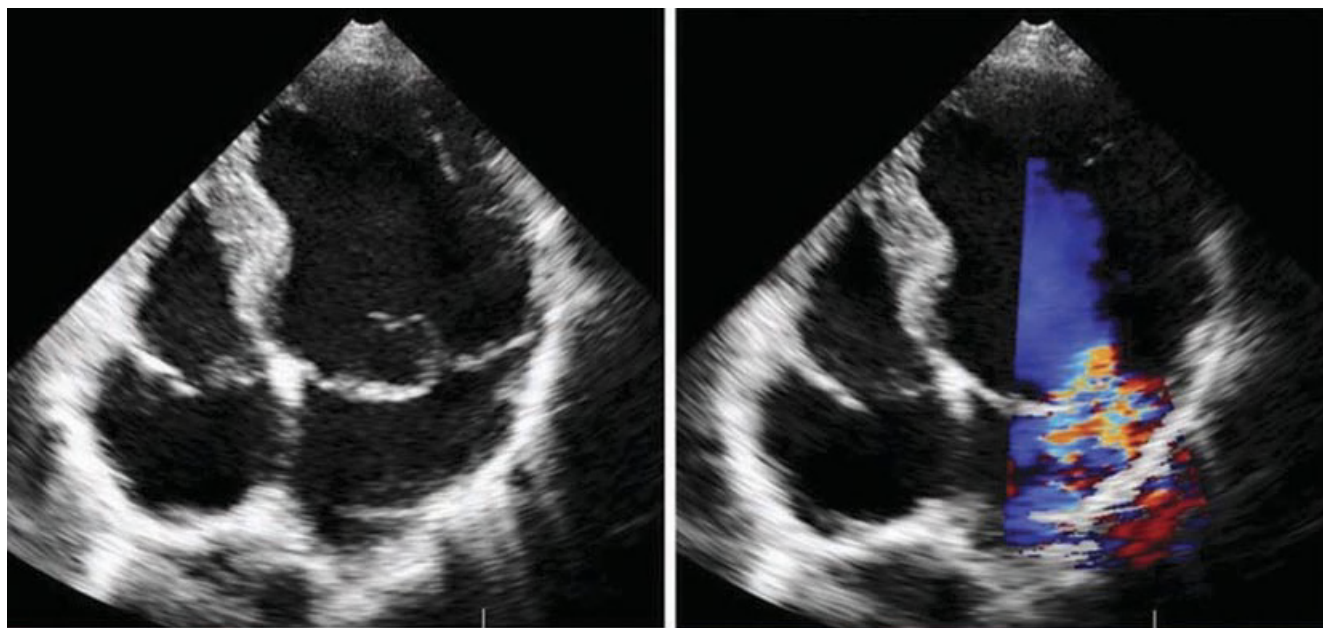
Figure 28.6 Mitral valve prolapse. Apical four-chamber view showing a bileaflet prolapse causing moderate mitral regurgitation in a child with Marfan syndrome.

risk of paradoxical worsening in mitral regurgitation [8]. Men aged >50 years are more likely to need valve surgery. Mitral valve repair, rather than replacement, is reserved for patients with symptomatic severe mitral regurgitation or ventricular enlargement or dysfunction in an asymptomatic patient.

The risk of endocarditis is higher for patients with MVP than for the general population, especially if the valve has thickened [8]. Antibiotic prophylaxis is not recommended according to the new ACC/AHA guidelines [15].

The incidence of sudden cardiac death is increased (twice as high as expected for the general population) in patients with MVP, but the mechanism is unknown [8,10,16].

MVP may confer a small risk of cerebrovascular events in older patients with advanced mitral regurgitation [8,16]. Prophylactic aspirin is sometimes used to prevent such events in patients with severe regurgitation.

Isolated cleft of the mitral valve

Although a cleft in the mitral valve can be present in either the anterior or posterior leaflet of the valve, it is usually in the anterior leaflet.

Isolated cleft of the anterior mitral valve leaflet (Figure 28.7)

This is rare with a pediatric incidence of 1/1340 [17]. The defect is a slit in the mid-portion of the anterior mitral leaflet, unassociated with an atrioventricular septal defect. It might be due to abnormal development of the embryological endocardial cushion tissue.

Isolated cleft of the anterior mitral valve leaflet is morphologically different from a cleft as observed in atrioentricular septal defect [17], even if some authors consider it as a forme fruste [18]. In isolated cleft of the anterior mitral valve leaflet, the mitral valve is supported by an annulus, which is separated from the right side of the heart by well-formed atrioventricular structures. In contrast, in atrioventricular septal defect, the valve ring is common to both atrioventricular valves. Furthermore, the isolated cleft points to the left ventricular outflow tract when the valve opens during diastole, whereas in atrioventricular septal defect, the cleft is directed towards the ventricular inlet septum [17].

A cleft anterior leaflet may also occur with a ventricular septal defect, coarctation of the aorta, transposition of the great arteries, double-outlet right ventricle, patent arterial duct, anomalous pulmonary venous connection, tricuspid atresia, and tetralogy of Fallot [19]. Chordal attachments may connect the edges of the cleft to the ventricular septum and subsequently create a subaortic obstruction [20].

Repair of isolated cleft of the anterior mitral valve leaflet associated with mitral regurgitation is preferred to replacement and usually consists in direct suture of the cleft [19,20]. Sometimes, an additional pericardial patch is used to close the cleft.
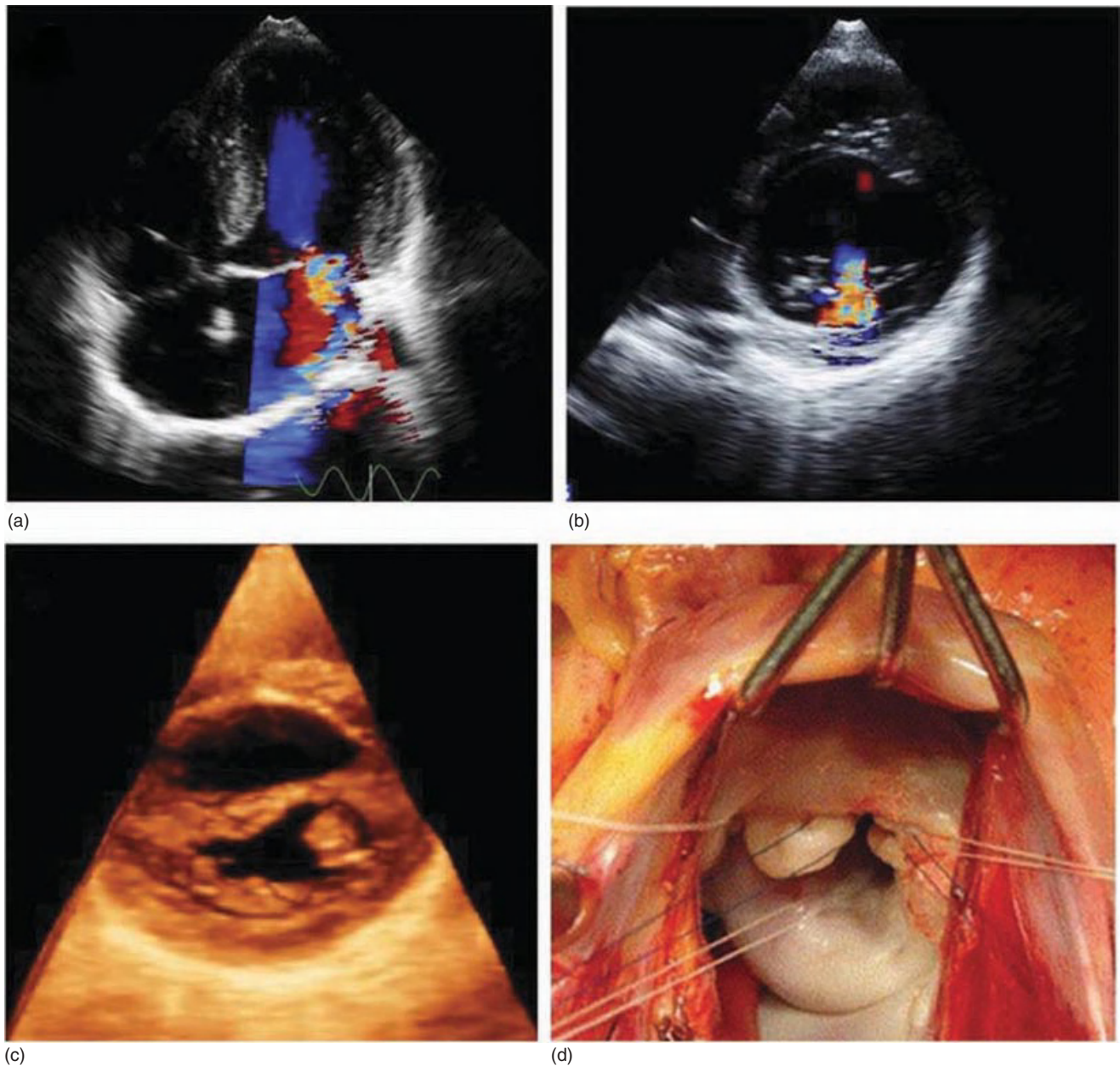
Figure 28.7 Isolated cleft of the anterior mitral valve leaflet. (a) 2D apical four-chamber color Doppler view. Mitral regurgitation is going through the anterior leaflet. (b) 2D parasternal short-axis color Doppler view showing the split anterior leaflet. (c) 3D left atrial view of the mitral valve providing a precise anatomic description of the cleft in order to define the ideal approach for surgical reconstruction. (d) Surgical view of the cleft.

Isolated cleft of the posterior mitral valve leaflet (Figure 28.8)

The predominant localization of the cleft is within scallop P2 [21], but it can occur at any segment of the posterior leaflet. The cleft may be isolated or associated with papillary muscle malrotation [22], accessory mitral valve leaflet [23], mitral valve prolapse [24], chordal rupture, and anterior leaflet cleft [25,26]. Mitral regurgitation is severe in 50% of clefts. Reconstruction of the mitral valve is the preferred management [27].

Double-orifice mitral valve

Double-orifice mitral valve (DOMV) is a rare anomaly characterized by a mitral valve with a single fibrous annulus and two orifices (Figure 28.9C). DOMV usually is associated with more complex cardiac anomalies [17], particularly
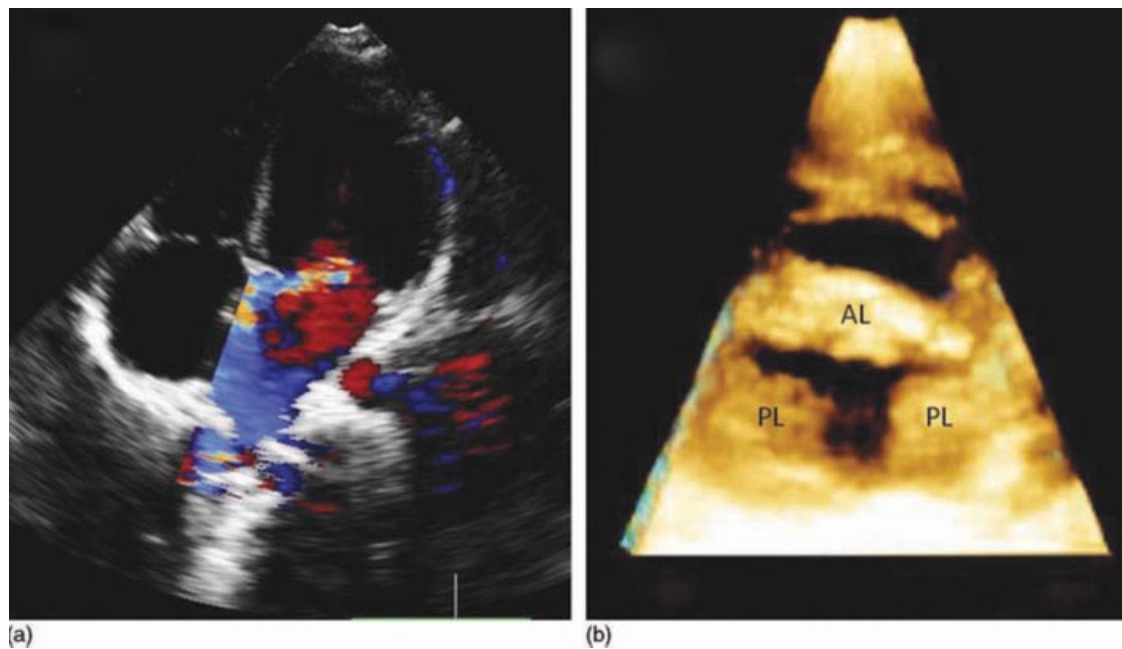
Figure 28.8 Isolated cleft of the posterior mitral valve leaflet. (a) 2D apical four-chamber view. The regurgitant jet is laterally directed and goes through the cleft. (b) 3D left ventricular view of the mitral valve. The posterior leaflet is divided into two equal parts by the cleft. AL, anterior leaflet; PL, posterior leaflet.
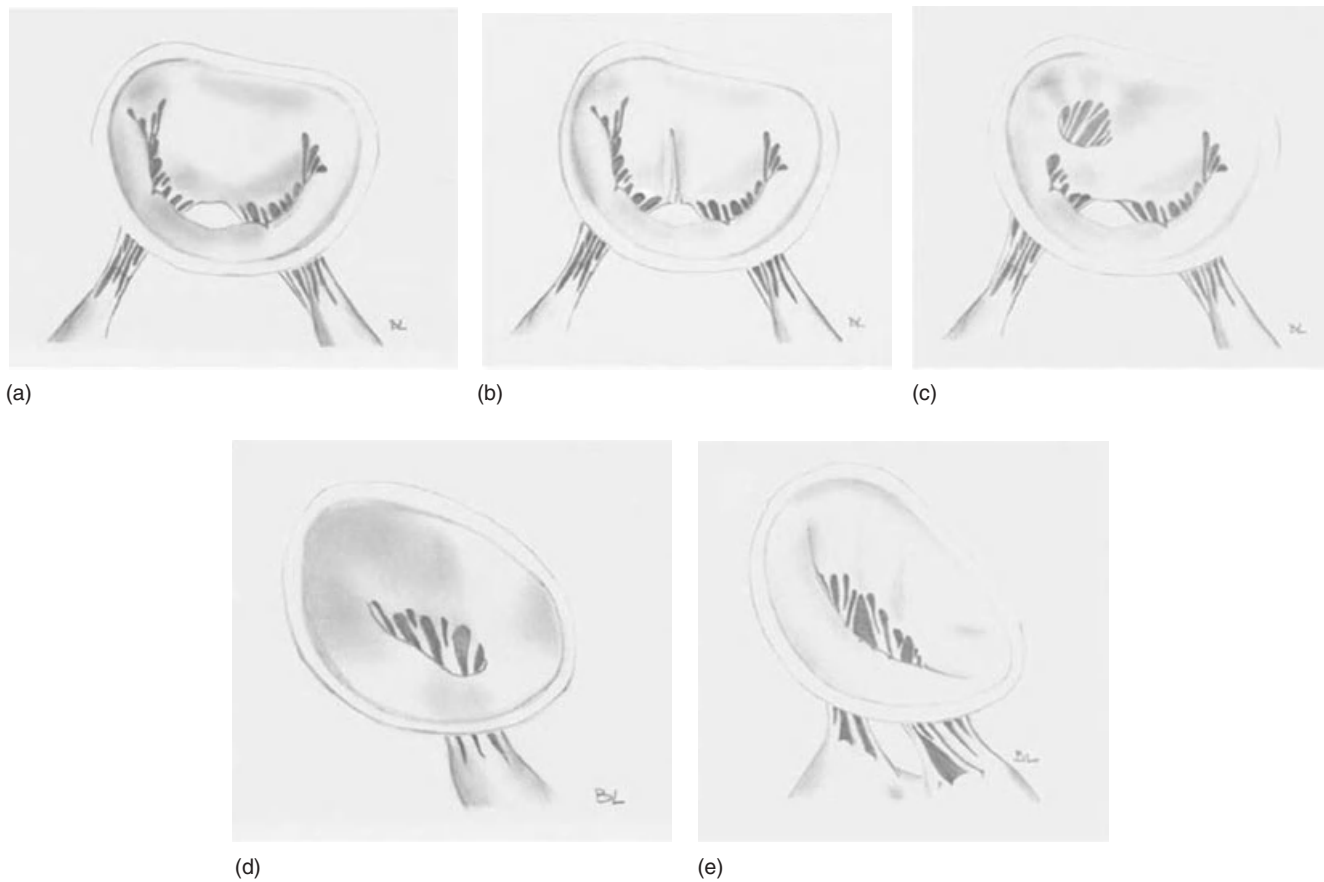
Figure 28.9 Surgical views of congenital mitral malformations causing mitral regurgitation. (a) Normal mitral valve. (b) Isolated cleft of the anterior mitral valve leaflet. (c) Double-orifice mitral valve (eccentric accessory orifice). (d) Parachute mitral valve. (e) Hammock mitral valve.
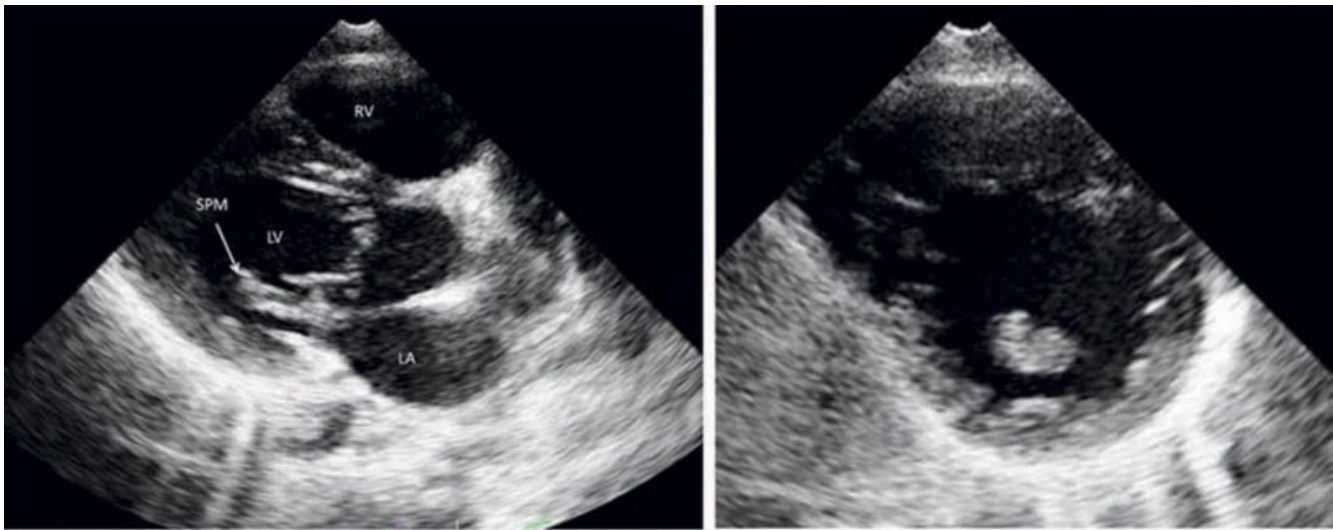
Figure 28.10 Parachute mitral valve. 2D echocardiography parasternal long- and short-axis views showing a single papillary muscle (SPM). LA, left atrium; LV, left ventricle; RV, right ventricle.

atrioventricular septal defect [28]. Thus, echocardiographic identification of DOMV is usually accidental because symptoms are not related solely to this anomaly. The mitral valve functions normally in 50% of patients [29]. Mitral regurgitation is the most frequent functional anomaly, but mitral stenosis, when either isolated or associated with regurgitation, is uncommon. According to the Baño-Rodrigo classification [29], DOMV almost always consists of abnormal holes in essentially normal leaflets, rather than abnormal fibrous bridges or adhesions between normal leaflets. Two types of DOMV are described: the eccentric hole with a small accessory orifice located at one of the commissures (85%) and the central hole with two equal-sized orifices (15%). The tensor apparatus of the mitral valve is always abnormal. Various malformations are observed such as a chordal ring, accessory papillary muscles, subdividing muscular ridge, parachute mitral valve, crossing chordae tendineae or central fibrous subdivision. DOMV is diagnosed and assessed through two- and three-dimensional echocardiography [30]. The management of DOMV is either continued observation or valve repair or replacement.

Parachute mitral valve

In an echocardiographic study of 13 400 subjects, parachute mitral valve was found in 0.17% [17]. Parachute mitral valve is characterized by the attachment of mitral chordae to a single or fused papillary muscle [17,31] (Figures 28.9d and 28.10). In a variant, parachute-like asymmetric mitral valve (PLAMV), there are two papillary muscles with one papillary muscle receiving most or all of the mitral chordae [31]. In this variant, the dominant papillary muscle is normal and the other is elongated and displaced towards the mitral annulus. Chordae tendineae are commonly attached

to the posteromedial papillary muscle in both parachute mitral valve and PLAMV. Oosthoek *et al.* [32] assumed that disruption of the development of papillary muscles occurs between the fifth and nineteenth weeks of gestation and causes their condensation into a single muscle. Mitral valve leaflets are thickened and their motion is usually restricted.

Doppler echocardiography shows significant mitral stenosis. Mitral regurgitation is less common but more progressive. Due to the left inflow obstruction, parachute mitral valve and PLAMV are associated with other obstructive lesions affecting the left heart [17,33], such as the supravalvar mitral ring, subaortic stenosis, and coarctation of the aorta. This combination produces either a complete or incomplete form of Shone's complex. The outcome is generally poor in patients with multilevel heart obstruction [31,33].

Hammock mitral valve

The hammock mitral valve is a very dysplastic valve without chordae and having the two papillary muscles directly fused with the leaflet tissue at the expected locations of the commissures (Figure 28.9e). This malformation causes mitral stenosis or regurgitation, or both. From the atrial side, it looks like a hammock. It may be difficult to distinguish parachute mitral valve and the hammock valve.

Anomalous mitral arcade

The mitral arcade is extremely rare and is characterized by thickened mitral leaflets with either shortened chordae or no chordae at all. The enlarged and elongated papillary muscles [34] are inserted directly into the leaflets by a typical fibrous tissue bridge acting as a single "muscle arcade" [35].

393

This fibrous continuity restricts valvar motion and limits coaptation of the leaflets. Mitral regurgitation progresses and may be associated with stenosis.

Mitral valve chordal rupture

Chordal rupture of the mitral valve is often associated with endocarditis, trauma, or acute rheumatic fever. Few examples of spontaneous rupture have been reported [36]. Common signs include acute pulmonary edema with severe mitral regurgitation. Echocardiography reveals a flail mitral valve leaflet with moderate to severe mitral regurgitation [37]. Both the left ventricle and atrium are normal in size. A linear structure moving around within the left heart chambers in a "whipping" manner is usually observed. Corrective surgery is required.

Submitral left ventricular aneurysm

Submitral left ventricular aneurysm occurs almost exclusively in young black African people. This anomaly is believed related to a congenital tissue weakness of the fibrous annulus at the connection point of the posterior mitral valve leaflet [38]. A submitral left ventricular aneurysm protrudes into the pericardial space either towards the floor of the left atrium or behind the left ventricle. Mitral regurgitation is caused by a limited leaflet motion and diminished coaptation due to distortion of the mitral annulus. Complications include calcification, thromboembolism, ventricular arrhythmia, compression of the left circumflex artery, and aneurysmal rupture into the left atrium. Surgical repair using either a transmitral or a transatrial approach is the best method to prevent the aneurysm. A meticulous description of the relationship existing between the aneurysm, the mitral valve, and the annulus is required for successful repair [39]. Echocardiography (transthoracic or transesophageal), MRI, and cardiac catheterization are usually used to define the anatomy.

Ebstein's malformation of the mitral valve

This exceptional anomaly is due to the downward displacement of the posterior leaflet of the mitral valve, which produces a functional atrialization of the proximal part of the left ventricle [40]. It causes a high mortality and occurs isolated or with another cardiac malformation.

Functional mitral regurgitation

Mitral regurgitation may occur with a normal mitral structure when the geometry of the valve is modified by another disease that increases left ventricular volume, including ventricular septal defect, patent ductus arteriosus, or dilated cardiomyopathy.

Dilated cardiomyopathy

Among cardiomyopathies, dilated cardiomyopathy is the most common in children with a high rate of mortality. It represents the main indication for the need for a heart transplantation in over 5-year-olds [41]. Mitral regurgitation is caused by dilatation of the annulus. Severe mitral regurgitation is an independent predictor of death [42]. Some authors have reported that mitral annuloplasty is sometimes efficient and may delay or replace the need for heart transplantation [43].

Ischemic mitral regurgitation

Abnormalities of the coronary arteries can cause myocardial ischemia leading to papillary muscle dysfunction (see Chapter 48). Regurgitation is due to disturbances of the posterior leaflet displacement, left ventricular dilatation, annular dilatation, and papillary muscle discoordination.

Congenital anomalies of the coronary system require prompt recognition and treatment because of the high lethal risk. Thus, an anomalous origin of the left coronary artery, congenital atresia of the left coronary artery, and coronary aneurysm (usually due to Kawasaki disease) must be meticulously detected. Cardiac catheterization or a CT scan may be particularly helpful in this context.

An anomalous origin of the left coronary artery from the pulmonary artery concerns one out of 300 000 live births [44]. After surgery, the majority of patients normalize mitral regurgitation. Regurgitation might sometimes persist or become worse. In this lesion the initial mitral insufficiency is due to a restrictive leaflet motion which itself is secondary to both the regional myocardial dysfunction and ischemia of the papillary muscle [45]. Due to myocardial desynchronyzation, chordae are elongated and cause a leaflet prolapse, which is the persistent mitral regurgitation mechanism. Direct coronary reimplantation is the preferred technique for repair in order to restore a two-coronary circulation system [46]. Associated mitral valve plasty seems to increase postoperative mortality and may not be required upon initial repair. Nevertheless, a few patients might need additional mitral valve repair for persistent severe mitral regurgitation [44].

Quantification of mitral regurgitation

Two-dimensional echocardiography

Left heart size and function

Two-dimensional echocardiography is used to assess the shortening and ejection fractions by measuring the left ventricular end-diastolic and end-systolic dimensions. Left ventricular volumes can be calculated using Simpson's method. Left ventricular size increases progressively in chronic mitral regurgitation. In contrast to adults, in children no validated values are available to determine the

Figure 28.11 PISA method. (a) Radius of the isovelocity area for an aliasing velocity of 30.8 cm s^{-1}. (b) Velocity–time integral of the mitral regurgitation jet.
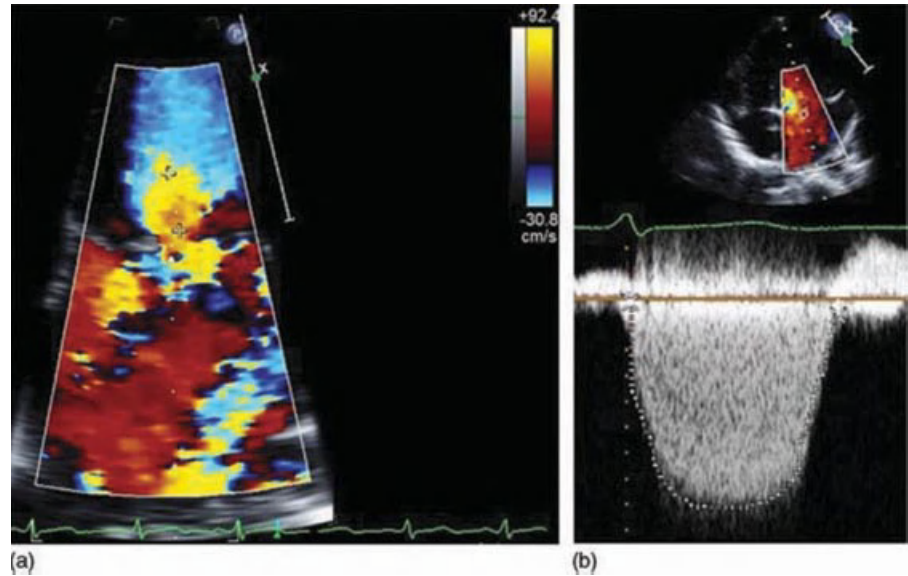
timing of surgery because the left ventricular size normally increases during childhood and depends on body weight. Nevertheless, changes in ventricular size and function must be serially monitored. A rapid increase in the end-systolic dimension reflecting the ability of the ventricle to eject the increased preload is reliable evidence of left ventricular pump failure. Measurements of left atrial volumes are also helpful for assessing the severity of mitral regurgitation.

Quantitative doppler method

The regurgitant volume is defined as the difference between the forward stroke volume across the mitral valve and the cardiac output at the aortic valve. It can be determined by using the pulsed Doppler technique and the following calculation:

$$MV = MSA \times VTI_M$$

$$AV = ASA \times VTI_{Ao}$$

$$RV = MV - AV$$

where MV = mitral stroke volume, MSA = mitral surface area, AV = aortic stroke volume, ASA = aortic surface area, RV = regurgitant volume, VTI_M = mitral velocity time integral of mitral inflow, and VTI_{Ao} = aortic velocity time integral.

The mitral annular diameter is calculated from an apical view and the aortic annular diameter from a parasternal long-axis view.

This method is applicable only in pure mitral regurgitation (with no associated aortic insufficiency). A small error in the diameter measurement leads to large variations of the annular area. Finally, this method assumes a circular geometry of the valve even though the mitral annulus is more D-shaped.

The regurgitant fraction (RF) is defined as

$$RF = \frac{RV}{MV}$$

Mitral regurgitation is classified as mild ($RF < 30\%$), moderate ($30 < RF < 49\%$) and severe ($RF \geq 50\%$).

The effective regurgitant orifice area is calculated by using the Doppler technique and the equation

$$OA = \frac{RV}{VTI_{MR}}$$

where ROA = regurgitant orifice area and VTI_{MR} = velocity time integral of the mitral regurgitation jet.

All of these values may also be more difficult to determine by two-dimensional volume analysis.

Proximal Isovelocity Surface Area (PISA) method (Figure 28.11)

The color Doppler technique is used to assess RV and ROA. Assuming that PISA is a hemisphere, RV and ROA are calculated with the following equations:

$$QMR = 2\pi r^2 \times VAL$$
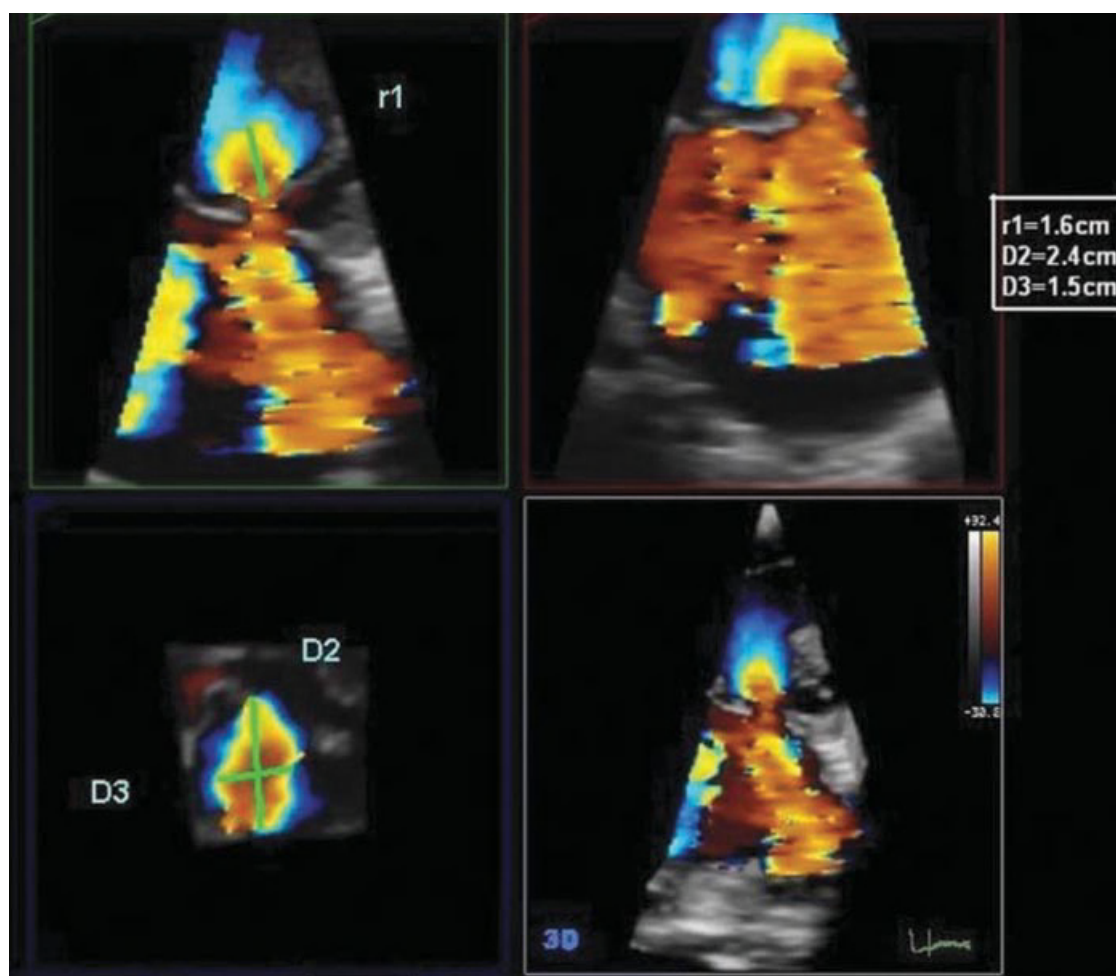
Figure 28.12 3D echographic PISA analysis. The isovelocity radius is measured in the longitudinal plane (r1) and the two diameters are measured in the transversal plane at the orifice level. The PISA shape is estimated according to these three measurements. (Reproduced with permission from Ziani *et al. Arch Cardiovasc Dis* 2009;**102**:185–91.)

$$ROA = \frac{Q_{MR}}{V_{MR}}$$

$$RV = ROA \times VTI_{MR}$$

where Q_{MR} = regurgitant flow rate, r = radius of the PISA, V_{AL} = aliasing velocity, ROA = regurgitant orifice area, V_{MR} = peak of regurgitant velocity, and VTI_{MR} = velocity time integral of the mitral regurgitation jet.

Three-dimensional echocardiography

Three-dimensional echocardiography assesses the severity of mitral regurgitation by determining the stroke volume or using the proximal isovelocity surface area (PISA method) [47]. Because the isovelocity surface is rarely hemispherical, regurgitation is frequently overestimated with the two-dimensional echocardiography PISA method. The isovelocity radius (measured in the longitudinal plane) and two diameters (measured in the transversal plane) are required to calculate the surface of the PISA (Figure 28.12). Thus, according to the mechanism, the PISA shape is described as hemispherical (20%), prolate hemispheroid (27%), oblate hemispheroid (47%), and hemiellipsoid (6%) (Figure 28.13).

Cardiovascular Magnetic Resonance (CMR)

CMR is a noninvasive technique that allows the accurate measurement of ventricular volumes. When quantification of mitral regurgitation is difficult by echocardiography, CMR may be particularly helpful. The regurgitant fraction, regurgitant volume, and direct planimetry of the anatomic regurgitant lesion are easily determined [48,49].
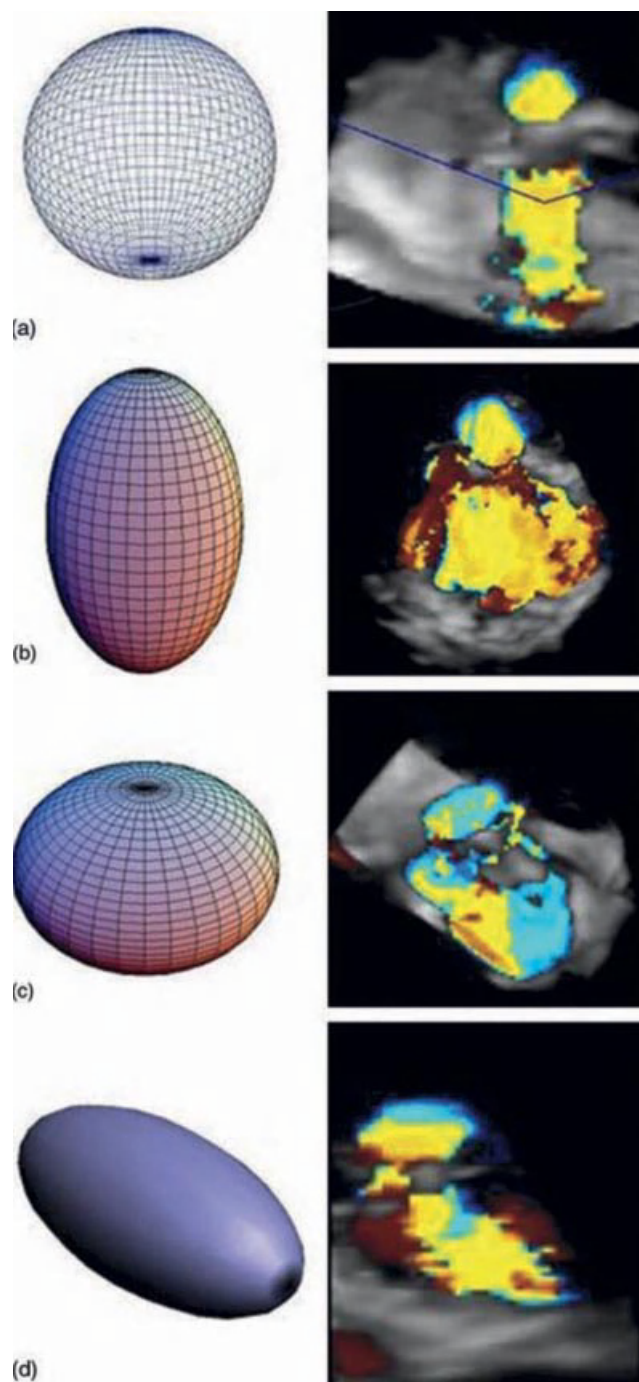
Figure 28.13 PISA geometries: mathematical model representations and their 3D visualization. (a) Hemispherical PISA shape. (b) Prolate hemispheroid PISA shape. (c) Oblate hemispheroid PISA shape. (d) Hemiellipsoid PISA shape. (Reproduced with permission from Ziani *et al*. *Arch Cardiovasc Dis* 2009;**102**:185–91.)

Surgical management

Because of the wide range of mitral anomalies and the frequent associated lesions, performing mitral valve surgery

on children is very delicate. When possible, mitral valve repair is preferred to replacement, because of the latter's mortality and morbidity. In children, bioprosthetic valves have early valve failure. Therefore, mitral valve replacement is performed with a mechanical prosthesis. Mitral valve replacement is complicated by the limited availability of adequate-sized prostheses for small children and the need for lifelong anticoagulation. In contrast, with repair, the subvalvar apparatus and ventricular geometry are maintained and left ventricular function is preserved. Significant predictors for poor freedom from reoperation and midterm survival are age <1 year, hammock mitral valve, and associated cardiac anomalies [50].

Mitral valve surgery is performed through a median sternotomy under cardiopulmonary bypass. According to the lesion, different techniques are used to repair the valve, as follows:

Annulus dilatation

Various annuloplasty techniques exist to treat a dilated annulus. The following are the most commonly performed. Strip materials, either autologous pericardium or Gore-Tex, are commonly used. There are several techniques:

- Posterior annuloplasty using strip or suture plication.
- The commissure plication principle (Kay–Wooler-type annuloplasty) consists in shortening the posterior annulus by a suture placation (Figure 28.14a). It is frequently used for small infants.
- Strip plication (Paneth-type annuloplasty) is used in children and adolescents. The posterior annulus is shortened with strip reinforcement (Figure 28.14b).
- Artificial ring annuloplasty is used for older children (Figure 28.14c).

Leaflet prolapse

Elongated chordae are either shortened or artificial chordae (Gore-Tex) are used.

Isolated cleft

The direct suture technique is the preferred method, although a pericardial patch is sometimes used to close the cleft.

Parachute valve

Following a careful commissurotomy, the papillary muscle is incised to divide it into two portions (Figure 28.14d).

Hammock valve

Splitting the papillary muscle is a difficult technique because the new papillary muscles must have a sufficient thickness to perform their function.

Chordal rupture

When prolapse of P2 of the posterior leaflet is caused by a chordal rupture, the flail segment is plicated towards the ventricle by a V-shaped suture line with stabilization of

(a)

(b) Pericardial strip

(c) Artificial ring

(d)
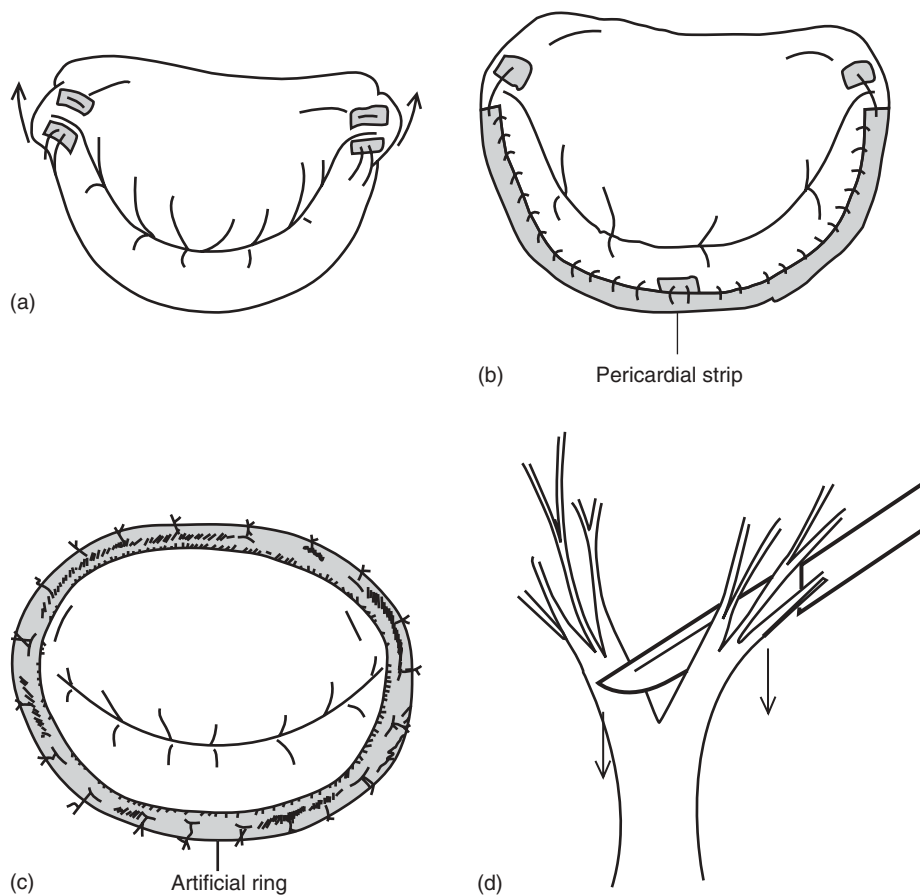
Figure 28.14 (a) Schematic representation of the posterior annuloplasty procedure using suture plication. (b) Schematic representation of the posterior annuloplasty procedure using strip plication. (c) Schematic representation of an artificial ring annuloplasty. (d) Incision of a single papillary muscle for a parachute mitral valve.
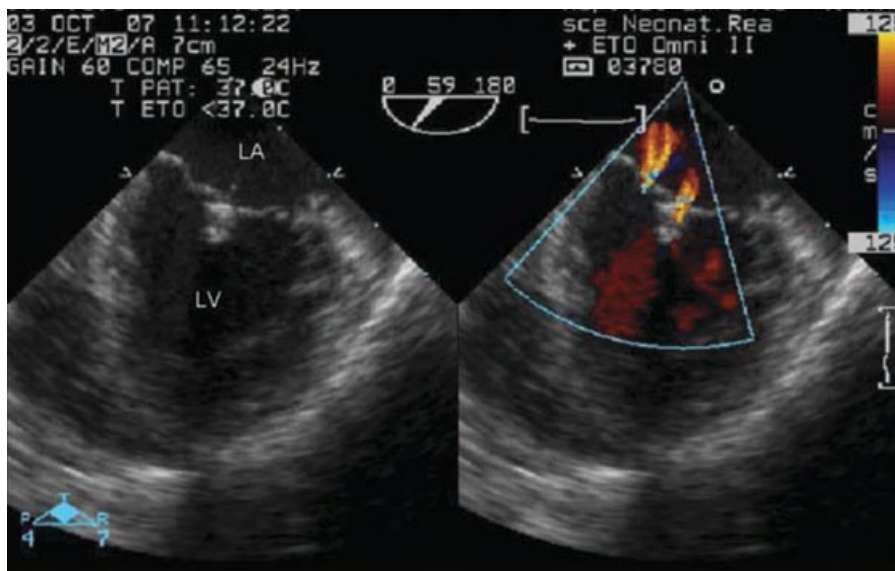
Figure 28.15 Perioperative transesophageal echocardiography images (two-chamber views) showing two residual mitral regurgitation jets after mitral valve repair in a child with isolated cleft of the anterior mitral valve leaflet. LA, left atrium; LV, left ventricle.

the posterior annulus by a strip such as for Gerbode-type annuloplasty.

Perioperative echocardiography allows an immediate functional evaluation of the mitral valve and may help the surgeon improve reconstruction (Figure 28.15).

Conclusion

In children, mitral regurgitation results from a number of anatomic variations, the most common being mitral valve

prolapse and isolated cleft of the anterior mitral valve leaflet. Echocardiography allows both quantification of mitral regurgitation and morphological analysis of the mitral valve apparatus. It should be used to assist the surgeon during operation. Surgery is often difficult and mitral valve repair is always preferred to mitral valve replacement.

References

1 Muresian H. The clinical anatomy of the mitral valve. *Clin Anat* 2009;**22**:85–98.

2 Kanani M, Moorman AF, Cook AC, *et al*. Development of the atrioventricular valves: clinicomorphological correlations. *Ann Thorac Surg* 2005;**79**:1797–804.

3 Ho SY. Anatomy of the mitral valve. *Heart* 2002;**88**(Suppl 4): iv5–10.

4 Carpentier A, Branchini B, Cour JC, *et al*. Congenital malformations of the mitral valve in children. Pathology and surgical treatment. *J Thorac Cardiovasc Surg* 1976;**72**:854–66.

5 O'Rourke RA, Crawford MH. Mitral valve regurgitation. *Curr Probl Cardiol* 1984;**9**:1–52.

6 Crawford MH, DiMarco JP, Paulus WJ, eds. *Cardiology*, 2nd edn. St Louis, MO: Mosby, 2003.

7 Carpentier A. Cardiac valve surgery – the "French correction." *J Thorac Cardiovasc Surg* 1983;**86**:323–37.

8 Hayek E, Gring CN, Griffin BP. Mitral valve prolapse. *Lancet* 2005;**365**:507–18.

9 Levine RA, Stathogiannis E, Newell JB, *et al*. Reconsideration of echocardiographic standards for mitral valve prolapse: lack of association between leaflet displacement isolated to the apical four chamber view and independent echocardiographic evidence of abnormality. *J Am Coll Cardiol* 1988;**11**:1010–9.

10 Freed LA, Levy D, Levine RA, *et al*. Prevalence and clinical outcome of mitral-valve prolapse. *N Engl J Med* 1999;**341**:1–7.

11 Taub CC, Stoler JM, Perez-Sanz T, *et al*. Mitral valve prolapse in Marfan syndrome: an old topic revisited. *Echocardiography* 2009;**26**:357–64.

12 Weyman AE, Scherrer-Crosbie M. Marfan syndrome and mitral valve prolapse. *J Clin Invest* 2004;**114**:1543–6.

13 Van Karnebeek CD, Naeff MS, Mulder BJ, *et al*. Natural history of cardiovascular manifestations in Marfan syndrome. *Arch Dis Child* 2001;**84**:129–37.

14 Freed LA, Benjamin EJ, Levy D, *et al*. Mitral valve prolapse in the general population: the benign nature of echocardiographic features in the Framingham Heart Study. *J Am Coll Cardiol* 2002;**40**:1298–304.

15 Nishimura RA, Carabello BA, Faxon DP, *et al*. ACC/AHA 2008 guideline update on valvular heart disease: focused update on infective endocarditis: a report of the American College of Cardiology/American Heart Association Task Force on Practice Guidelines: endorsed by the Society of Cardiovascular Anesthesiologists, Society for Cardiovascular Angiography and Interventions, and Society of Thoracic Surgeons. *Circulation* 2008;**118**:887–96.

16 St John Sutton M, Weyman AE. Mitral valve prolapse prevalence and complications: an ongoing dialogue. *Circulation* 2002 10;**106**:1305–7.

17 Sigfússon G, Ettedgui JA, Silverman NH, Anderson RH. Is a cleft in the anterior leaflet of an otherwise normal mitral valve an atrioventricular canal malformation? *J Am Coll Cardiol* 1995;**26**:508–15.

18 Van Praagh S, Porras D, Oppido G, *et al*. Cleft mitral valve without ostium primum defect: anatomic data and surgical considerations based on 41 cases. *Ann Thorac Surg* 2003;**75**:1752–62.

19 Tamura M, Menahem S, Brizard C. Clinical features and management of isolated cleft mitral valve in childhood. *J Am Coll Cardiol* 2000;**35**:764–70.

20 Abadir S, Fouilloux V, Metras D, *et al*. Isolated cleft of the mitral valve: distinctive features and surgical management. *Ann Thorac Surg* 2009;**88**:839–43.

21 Wyss CA, Enseleit F, van der Loo B, *et al*. Isolated cleft in the posterior mitral valve leaflet: a congenital form of mitral regurgitation. *Clin Cardiol* 2009;**32**:553–60.

22 Kent SM, Markwood TT, Vernalis MN, Tighe JF Jr. Cleft posterior mitral valve leaflet associated with counterclockwise papillary muscle malrotation. *J Am Soc Echocardiogr* 2001;**14**: 303–4.

23 Kanemoto N, Shiina Y, Goto Y, *et al*. A case of accessory mitral valve leaflet associated with solitary mitral cleft. *Clin Cardiol* 1992;**15**:699–701.

24 Izgi C, Feray H, Saltan Y, Kahraman R. Isolated cleft of the posterior mitral valve leaflet in a patient with Marfan syndrome. *Int J Cardiol* 2010;**145**(3):e102–4.

25 McDonald RW, Ott GY, Pantely GA. Cleft in the anterior and posterior leaflet of the mitral valve: a rare anomaly. *J Am Soc Echocardiogr* 1994;**7**:422–4.

26 Mohammadi S, Bergeron S, Voisine P, Desaulniers D. Mitral valve cleft in both anterior and posterior leaflet: an extremely rare anomaly. *Ann Thorac Surg* 2006;**82**:2287–9.

27 Amin A, Davis M, Auseon A. Isolated cleft posterior mitral valve leaflet: an uncommon cause of mitral regurgitation. *Eur J Echocardiogr* 2009;**10**:173–4.

28 Zalzstein E, Hamilton R, Zucker N, *et al*. Presentation, natural history, and outcome in children and adolescents with double orifice mitral valve. *Am J Cardiol* 2004;**93**:1067–9.

29 Baño-Rodrigo A, Van Praagh S, Trowitzsch E, Van Praagh R. Double-orifice mitral valve: a study of 27 postmortem cases with developmental, diagnostic and surgical considerations. *Am J Cardiol* 1988;**61**:152–60.

30 Anwar AM, McGhie JS, Meijboom FJ, Ten Cate FJ. Double orifice mitral valve by real-time three-dimensional echocardiography. *Eur J Echocardiogr* 2008;**9**:731–2.

31 Marino BS, Kruge LE, Cho CJ, *et al*. Parachute mitral valve: morphologic descriptors, associated lesions, and outcomes after biventricular repair. *J Thorac Cardiovasc Surg* 2009;**137**: 385–93.

32 Oosthoek PW, Wenink AC, Wisse LJ, Gittenberger-de Groot AC. Development of the papillary muscles of the mitral valve: morphogenetic background of parachute-like asymmetric mitral valves and other mitral valve anomalies. *J Thorac Cardiovasc Surg* 1998;**116**:36–46.

33 Schaverien MV, Freedom RM, McCrindle BW. Independent factors associated with outcomes of parachute mitral valve in 84 patients. *Circulation* 2004;**109**:2309–13.

34 Layman TE, Edwards JE. Anomalous mitral arcade. A type of congenital mitral insufficiency. *Circulation* 1967;**35**:389–95.

35 Espinola-Zavaleta N, Vargas-Barrón J, Keirns C, *et al*. Three-dimensional echocardiography in congenital malformations of the mitral valve. *J Am Soc Echocardiogr* 2002;**15**:468–72.

36 Baird CW, Constantinos C, Lansford E, Pigula FA. Mitral valve chordal rupture masquerades as endocarditis. *Pediatr Cardiol* 2007;**28**:297–9.

37 Snider AR, Serwer GA, Ritter SB, eds. *Echocardiography in Pediatric Heart Disease*, 2nd edn. St Louis, MO: Mosby, 1997.

38 Pektok E, Cikirikcioglu M, Didier D, Kalangos A. Submitral left ventricular aneurysm: a rare but challenging pathology to treat. *J Card Surg* 2008;**23**:533–5.

39 Müller H, Lerch R. Submitral left ventricular aneurysm presenting as a "strange" mitral valve prolapse. *Arch Cardiovasc Dis* 2009;**102**:157–8.

40 Jacob JL, da Silveira LC, Braile DM. Echocardiographic and angiographic diagnosis of Ebstein's anomaly of the mitral valve. *Br Heart J* 1991 ;**66**:379–80.

41 Alvarez JA, Wilkinson JD, Lipshultz SE. Outcome predictors for pediatric dilated cardiomyopathy: a systematic review. *Prog Pediatr Cardiol* 2007 1;**23**:25–32.

42 Azevedo VM, Santos MA, Albanesi Filho FM, *et al*. Outcome factors of idiopathic dilated cardiomyopathy in children - a long-term follow-up review. *Cardiol Young* 2007;**17**:175–84.

43 Walsh MA, Benson LN, Dipchand AI, *et al*. Surgical repair of the mitral valve in children with dilated cardiomyopathy and mitral regurgitation. *Ann Thorac Surg* 2008;**85**:2085–8.

44 Lange R, Vogt M, Hörer J, *et al*. Long-term results of repair of anomalous origin of the left coronary artery from the pulmonary artery. *Ann Thorac Surg* 2007;**83**:1463–71.

45 Blot-Souletie N, Paranon S, Acar P. Mitral regurgitation mechanism assessed by 2D and 3D echocardiography in a patient with an abnormal left coronary artery arising from the pulmonary artery. *Arch Cardiovasc Dis* 2008;**101**:585–7.

46 Huddleston CB, Balzer DT, Mendeloff EN. Repair of anomalous left main coronary artery arising from the pulmonary artery in infants: long-term impact on the mitral valve. *Ann Thorac Surg* 2001;**71**:1985–8; discussion 1988–9.

47 Ziani AB, Latcu DG, Abadir S, *et al*. Assessment of proximal iso-velocity surface area (PISA) shape using three-dimensional echocardiography in a paediatric population with mitral regurgitation or ventricular shunt. *Arch Cardiovasc Dis* 2009;**102**: 185–91.

48 Buchner S, Debl K, Poschenrieder F, *et al*. Cardiovascular magnetic resonance for direct assessment of anatomic regurgitant orifice in mitral regurgitation. *Circ Cardiovasc Imaging* 2008; **1**:148–55.

49 Cawley PJ, Otto CM. Valvular regurgitation: does cardiovascular magnetic resonance provide additional information compared to echocardiography? *Minerva Cardioangiol* 2009;**57**:521–35.

50 Prifti E, Vanini V, Bonacchi M, *et al*. Repair of congenital malformations of the mitral valve: early and midterm results. *Ann Thorac Surg* 2002;**73**:614–21.

29 Right Ventricular Inflow Obstruction

James H. Moller
University of Minnesota, Minneapolis, MN, USA

Right ventricular inflow obstruction is relatively uncommon, occurring in ~3% of children with a cardiac malformation. The two most frequent causes are tricuspid atresia and pulmonary atresia with intact ventricular septum, each accounting for ~1.4% of congenital heart disease. They are discussed in Chapters 35 and 40, respectively. This chapter reviews rare and unusual congenital and acquired conditions which obstruct blood flow into the right ventricle. Some are found predominately in neonates and others occur in older children and adolescents.

Neonatal period

In the neonatal period, right ventricular inflow obstruction is predominantly associated with either tricuspid atresia (Chapter 35) or pulmonary atresia with intact ventricular septum (Chapter 40). Other causes are very uncommon in this age group, but despite their rarity must be considered in the differential diagnosis because treatment and prognosis varies.

Cardiac malformations obstructing blood flow into the right ventricle have several common features that are well recognized in the two anomalies with an atretic valve, either tricuspid or pulmonary. Because of the obstruction, the right atrium is enlarged and usually the right ventricle is hypoplastic. An atrial right-to-left shunt occurs through a patent foramen ovale or atrial septal defect; the shunt is usually large (often 100%), so the neonate is intensely cyanotic. The pulmonary circulation is derived from flow through a ductus arteriosus while it remains patent. There is either no murmur or that of a patent ductus. The transverse diameter of the cardiac silhouette is enlarged primarily by the right atrial shadow to the right of the midline. The pulmonary arterial vascularity is decreased. Administration

of prostaglandin E_1 to maintain ductal patency benefits the neonate and allows time for accurate diagnosis and planning for treatment.

Three other conditions must be considered in the differential diagnosis of right ventricular inflow obstruction and distinguished from either tricuspid atresia or pulmonary atresia with intact ventricular septum.

Isolated hypoplastic right ventricle

In isolated hypoplastic right ventricle, the tricuspid valve is hypoplastic and its orifice narrowed by the small size of the tricuspid annulus, but the valve leaflets are diminutive but otherwise normal. This is distinct from congenital tricuspid stenosis, in which the valve orifice is narrowed by commissural fusion, forming a membrane-like structure with a small aperture [1]. Because of the hypoplasia, right ventricular volume is reduced and pulmonary blood flow limited. Right atrial pressure is elevated and a right-to-left shunt occurs through a patent foramen ovale or atrial septal defect. Usually the patients present in the neonatal period with intense cyanosis and tachypnea. There are no murmurs. The clinical picture resembles pulmonary atresia with intact ventricular septum.

Patients with milder degrees of hypoplasia are less cyanotic and relatively asymptomatic as newborns. Such patients do not need immediate treatment and can be followed until they are larger and older, even into adulthood. The ECG is not diagnostic, resembles that of pulmonary atresia with intact ventricular septum, and characteristically has a normal QRS axis, tall peaked P waves, and a small r wave in lead V1 and a prominent R wave in lead V6. The chest X-ray shows cardiomegaly and diminished pulmonary vascular markings. An echocardiogram helps to distinguish this condition from

pulmonary and tricuspid atresia and from Ebstein's malformation. On subcostal and apical cross-sectional views, there is an enlarged left ventricle and an adjacent small right ventricle. Although the diameter of the tricuspid annulus is reduced, the tricuspid and pulmonary valves appear normal. Doppler interrogation shows anterograde flow across both the valves. A right-to-left shunt is seen across the atrial septum and the size of the communication can be assessed. Cardiac catheterization and angiography are not needed for diagnosis or management decisions. Right atrial pressure may be elevated but right ventricular and pulmonary artery pressures are normal. It is one of the few anomalies with a right-to-left shunt and normal right ventricular systolic pressure.

Although the etiology is unknown, three families have been reported in which more than one sibling had this anomaly, and in one of these families more than one generation was affected [2]. Medd *et al.* [3] reported two infant siblings who died with this anomaly. We have cared for three siblings who presented in the newborn period with cyanosis [4–6]. Two died shortly after admission and the third following an aortopulmonary shunt. They were admitted over a 5 year period at a time when echocardiography was unavailable and the clinical diagnosis was pulmonary atresia with intact ventricular septum. An autopsy was preformed on each. Each component of the right ventricle was present but diminutive. The tricuspid valve was normal but the annulus was hypoplastic. Valproate administration to a pregnant woman has also been associated with this anomaly in a neonate [7].

Treatment has varied. Often the initial step is placement of an aortopulmonary shunt. Later, in some with only moderate hypoplasia, closure of the atrial defect by a device [8] or surgery [9] has been done, establishing a two-ventricle circulation. In those with more severe hypoplasia, cavopulmonary shunt procedures are performed.

Cor triatriatum dextrum

In the fetus, blood flow from the inferior vena cava is directed across the atrial septum by the inferior sinus venosus valve [10]. By 9–15 weeks, the valve differentiates into the eustachian (valve of the inferior vena cava) and thebesian valves (valve of the coronary sinus). If the inferior sinus venosus valve persists and extends towards the superior vena cava, the right atrium is divided into two parts, one receiving the systemic venous return and the other portion containing the tricuspid valve and the right atrial appendage [11,12]. The systemic venous return may be directed across the atrial septum through a perforation in the sinus venosus valve and some blood can reach the tricuspid valve. The quantity of blood presenting to the tricuspid valve and right ventricle is limited, so both of these structures can be hypoplastic. The clinical presentation is that of tricuspid or pulmonary atresia [12–15]. Echocardiography, particularly

from subcostal views [16], allows identification of the flow passing from the inferior vena cava towards the superior vena cava. The right-to-left shunt is found across the atrial septum. The size and characteristics of the tricuspid valve and size of the right ventricle can be assessed.

Once recognized, the anomaly can be treated by resection of the membrane dividing the right atrium.

A variant is persistence of the eustachian valve, which if large and redundant can obstruct the tricuspid valve. At times it may form a windsock that prolapses into the right ventricle. In patients with a large valve eustachian there may be an atrial right-to-left shunt and some right ventricular hypoplasia [17]. In another variant, a 20mm long narrow tube-like structure from the sinus venosus valve passed through the tricuspid valve and resembled a mass on an echocardiogram [18].

Cor triatriatum dextrum may not be recognized until an older age and the symptoms include ascites, weight loss and other signs of elevated venous pressure [19].

Rhabdomyoma

As indicated in Chapter 66, rhabdomyomas are the most common cardiac tumor in children overall and by far the most common in neonates. Associated with tuberous sclerosis in many (30–50%), they can arise in any cardiac chamber, but more frequently in the left side of the heart. Typically they arise in papillary muscles, from the ventricular septum, or in either atrium. In any location they are intramyocardial and not pedunculated. If large they obstruct flow through cardiac chambers. We have seen two neonates with a tumor that obstructed RV inflow arising in the right ventricle immediately below the tricuspid valve. Because of the obstruction, cyanosis occurred from an atrial septal defect. The tumors can be multiple and vary in size. They may be identified by echocardiography as a bright reflective mass(es). Although they may regress, they also can increase in size, becoming more obstructive. In cyanotic neonates the tumor can be resected with a risk of ~5%.

In two other conditions of neonates, a tumor-like mass can be present in the right atrium and prolapse through the tricuspid valve, causing obstruction. Premature infants weighing <1.5 kg are particularly prone to fungal infections because they are immunocompromised, require invasive therapy, such as indwelling catheters, and usually receive broad-spectrum antibiotics and occasionally steroids [20]. They can develop intracardiac fungal masses often attached to an indwelling catheter. We have seen them as large as 2 × 2cm, prolapsing through the tricuspid valve during diastole. Portions can embolize to the lung. The mass can be removed by cardiac surgery using inflow stasis [21].

Multiple small pinpoint cysts are commonly found on the atrial surfaces of atrioventricular valves at autopsy of infants up to 6 months of age. A cyanotic 4-month-old was found

with a large cyst shown by cineangiography to move freely though the tricuspid valve [22]. This angiogram also showed an atrial right-to-left shunt. At operation, the right atrium was filled by a large smooth bluish mass attached to septal leaflet by a thin 5 mm pedicle. The mass protruded into the right ventricle. It was found to be a unilocular cyst filled with blood and lined by endothelium.

Children and adolescents

Whereas much emphasis in this chapter has focused on neonates and infants, the lesions obstructing flow into the right ventricle can persist or appear in older children and adolescents. In these, the jugular venous pulse can be elevated, the liver enlarged, ascites present, and exudative enteropathy present. The patient may have mild cyanosis from an atrial right-to-left shunt as in older patients with a mildly hypoplastic right ventricle. The features resemble those of constrictive pericarditis (Chapter 59) or restrictive cardiomyopathy (Chapter 58).

Tricuspid stenosis (TS)

In tricuspid stenosis, abnormalities of each component of the valve can lead to obstruction. The tricuspid valve may be affected in rheumatic fever and develop changes associated with rheumatic heart disease. It is part of rheumatic multi-valvar disease, in which the mitral and aortic valves are also abnormal (see Chapter 62). The valve can become stenotic with fused commissures, thickened leaflets, and fixed stenotic orifice. Tricuspid stenosis of this cause is found predominantly in the developing world.

Congenital TS accounts for 0.3% of all congenital heart disease and usually coexists with other cardiac anomalies. Various types of deformity of leaflets (thickened, redundant), chordae (shortened, reduced interchordal spaces), commissures (fused) and annulus (narrowed), occurring alone or in combination, can narrow the tricuspid orifice [23,24]. The mortality is related to the age of the patient and underlying etiology. Tricuspid stenosis has been significantly reduced by balloon valvoplasty [25–27]. Rarely, TS is related to systemic lupus erythematosis or with endocarditis. Endocarditis on TV is relatively uncommon, even in i.v. drug users [28–30]. It can occur in children with a structurally normal heart. A large vegetation may obstruct the valve orifice.

Congenital polyvalvular disease

It was Bharati and Lev who gave the name congenital polyvalvular disease to a complex in which each of the cardiac valves is involved in a dysplastic process [31]. The leaflets are irregularly thickened, immobile, redundant, and often stenotic. The chordae are shortened, thickened, and nodular. There is an increase in spongiosa with degeneration and a lack of elastic tissue in the leaflets [32]. An increased amount of acid mucopolysaccharides is found in the valves. The condition has been found in trisomy 18 and trisomy 13–15 and is rare otherwise [33].

Tricuspid stenosis from interventional procedures

Tricuspid stenosis can follow interventional procedures. Reports have described the development of tricuspid stenosis years after placement of pacemaker leads through the tricuspid valve into the right ventricle [34–36]. The valvar change has been attributed to perforation of a cusp and to inflammation and fibrosis of the leaflets from a redundant pacemaker lead. It leads to elevated venous pressure and can result in ascites and can be treated by balloon valvoplasty. Severe tricuspid stenosis has also followed placement of an Amplatzer device for closing a perimembraneous ventricular septal defect in which the device caused adherence of the device to the septal leaflet [37].

Right atrial myxoma

These tumors can be found in patients as young as 3 years of age, but much more commonly in adolescents. Overall they are predominately found in adults, ~75% in females. As indicated in Chapter 66, atrial myxoma accounts for half of primary cardiac tumors. Up to 25% are found in the right atrium. In the right atrium they can reach twice the size of one in the left atrium before causing symptoms [38]. Usually originating from the atrial septum by way of a pedicle, they can protrude into the tricuspid orifice and cause obstruction. The patient experiences fatigue and peripheral edema and then progressive signs of right heart failure.

Portions of the tumor may embolize to the lungs, causing acute symptoms or the findings of pulmonary hypertension if the emboli are small, multiple, and recurrent. There may be constitutional symptoms of fever, joint pains, and weight loss, with laboratory findings of increased acute-phase reactants. The tumor is recognizable by echocardiography and can be resected with a small risk of recurrence.

Carcinoid syndrome

Carcinoid syndrome is characterized by diarrhea, flushing of the head and upper chest, and bronchospasm. It results from a carcinoid tumor often located in the appendix, but it can arise elsewhere in the gastrointestinal tract. The tumor may

metastasize and those which do to the liver are believed to cause carcinoid cardiac disease [39]. The cardiac lesions are thought to result from large amounts of circulating serotonin. The lesions are found predominantly on the ventricular surface of the tricuspid valve and the arterial surface of the pulmonary valve, the endocardial surfaces of the right ventricle, and the lining of the vena cava and pulmonary artery. Plaques of fibrous tissue form on the tricuspid valve, making it thick, rigid, and stenotic, and at times regurgitant. An echocardiogram shows valvar thickening. The youngest patient with carcinoid syndrome was 10 years old.

References

1 Svane S. Congential tricuspid stenosis: a report on six autopsied cases. *Scand Cardiovasc J* 1971;**5**:232–8.

2 Sackner MA, Robinson MJ, Jamieson WL, *et al*. Isolated right ventricular hypoplasia with atrial septal defect or patent foramen ovale. *Circulation* 1961;**24**:1388–402.

3 Medd WE, Neufeld HN, Weidman WH, Edwards JE. Isolated hypoplasia of the right ventricle and tricuspid valve in siblings. *Br Heart J* 1961;**23**:25–30.

4 Becker AE, Becker MJ, Moller JH, Edwards JE. Hypoplasia of right ventricle and tricuspid valve in three siblings. *Chest* 1971;**60**:273–7.

5 Davachi F, McLean RH, Moller JH, Edwards JE. Hypoplasia of the right venticle and tricuspid valve in siblings. *J Pediatr* 1967;**71**:869–74.

6 Raghib G, Amplatz K, Moller JH, *et al*. Hypoplasia of right ventricle and of tricuspid valve. *Am Heart J* 1965;**70**:806–12.

7 ten Berg K, van Oppen AC, Nikkels PG, *et al*. Complex cardiac defect with hypoplastic right ventricle in a fetus with valproate exposure. *Prenat Diagn* 2005;**25**:156–8.

8 Atiq M, Lai L, Lee KJ, Benson LN. Transcatheter closure of atrial septal defects in children with a hypoplastic right ventricle. *Catheter Cardiovasc Interv* 2005;**64**:112–6.

9 Nagel B, Beitzke A, Knez I, Koestenberger M. Biventricular repair despite hypoplastic tricuspid valve and right ventricle. *Clin Res Cardiol* 2009;**98**:283.

10 Hansing CE, Young WP, Rowe GC. Cor triatriatum dexter. Persistent right sinus venosus valve. *Am J Cardiol* 1972;**30**:559–64.

11 Trento A, Zuberbuhler JR, Anderson RH, *et al*. Divided right atrium (prominence of the eustachian and thebesian valves). *J Thorac Cardiovasc Surg* 1998;**96**:457–63.

12 Van Ledden-Klok M, de Mol A, Backx A. Asymptomatic divided right atrium in a newborn. *Cardiol Young* 2007;**17**:110.

13 Galli MA, Galletti L, Schena F, *et al*. A rare case of neonatal cyanosis due 'cor triatriatum dexter' and a review of the literature. *J Cardiovasc Med* 2009;**10**:535–8.

14 Barrea C, Rubay J, Wagner K, Ovaert C. Images in cardiovascular medicine: cor triatriatum dexter mimicking Ebstein disease. *Circulation* 2009;**120**:e86–8.

15 Basshour T, Kubanni S, Saalouke M, Cheng T. Persistent eustachian valve causing severe cyanosis in atrial septal defect with normal right heart pressures. *J Vasc Dis* 1983;**34**:79–83.

16 Burton DA, Chin A, Weinberg PM, Pigott JD. Identification of cor triatriaum dexter by two-dimensional echocardiogram. *Am J Cardiol* 1987;**60**:401–10.

17 Sehra R, Ensing G, Hurwitz R. Persistent eustachian valves in infants. Course and management in symptomatic patients. *Pediatr Cardiol* 1998;**19**:221–4.

18 Smith NM, Byard RW, Vigneswaran R, *et al*. Parachute-like sinus venosus remnant: echocardiographic and pathological appearance. *Pediatr Cardiol* 1993;**14**:82–5.

19 Alkhulaifi AM, Serref A, Planche C. Ascites and weight loss in a child:due to congenital division of the right atrium. *Cardiol Young* 1999;**9**:335–7.

20 Johnson DJ, Bass JL, Thompson TR, *et al*. *Candida* septicemia and right atrial mass secondary to umbilical vein catheterization. *Am J Dis Child* 1981;**135**:275–7.

21 Foker JE, Bass JL, Thompson T, *et al*. Management of intracardiac fungal masses in premature infants. *J Thorac Cardiovasc Surg* 1984;**87**:244–50.

22 Gallucci V, Stritoni G, Fasoli G, Thiene G. Giant blood cyst of tricuspid valve. Successful excison in an infant. *Br Heart J* 1976;**38**:990–2.

23 Medd WE, Kinmonth JB. Congenital tricuspid stenosis. A case treated by open operation. *Br Med J* 1962;**i**:598–600.

24 Dimich I, Goldflinger P, Steinfeld L, Lukban SB. Congenital tricuspid stenosis: case treated by heterograft replacement of the tricuspid valve. *Am J Cardiol* 1973;**31**:89–92.

25 Lokhandwala YY, Rajani RM, Dalvi BV, Kale PA. Successful balloon valvotomy in isolated tricuspid stenosis. *Cardiovasc Intervent Radiol* 1990;**13**:354–6.

26 Yeter E, Ozlem K, Kilic H, *et al*. Tricuspid balloon valvuloplasty to treat tricuspid stenosis. *J Heart Valve Dis* 2010;**19**:159–60.

27 Harle T, Kronberg K, Motz, Elsasser A. Balloon valvuloplasty of a tricuspid valve stenosis in double balloon technique. *Clin Res Cardiol* 2010;**99**:203–5.

28 Moraes NF, Santos CL, Mattos SS, *et al*. Tricuspid valve endocarditis in children. *Arq Bras Cardiol* 1992;**58**:375–7.

29 Goessler MC, Riggs TW, DeLeon S, Paul MH. Echocardiographic diagnosis of tricuspid valve endocarditis in a child with a normal heart. Special emphasis on surgical considerations. *Pediatr Cardiol* 1982;**2**:141–3.

30 Clifford CP, Eykyn SJ, Oakley CM. Staphylococcal tricuspid valve endocarditis in patients with structurally normal hearts and no evidence of narcotic abuse. *Q J Med* 1994;**87**:755–7.

31 Bharati S, Lev M. Congenital polyvalvular disease. Circulation 1973;**47**:575–86.

32 Bartram U, Bartelings MM, Kramer HH, Gittenberger-de Groot AC. Congenital polyvalvular disease: a review. *Pediatr Cardiol* 2001;**22**:93–101.

33 Balderston SM, Shaffer EM, Washington RL, Sondheimer HM. Congenital polyvalvular disease in trisomy 18. Echocardiographic diagnosis. *Pediatr Cardiol* 1990;**11**:138–42.

34 Hussain T, Knight WB, McLeod KA. Lead-induced tricuspid stenosis – successful management by balloon angioplasty. *Pacing Clin Electrophysiol* 2009;**32**:140–2.

35 Krishnan A, Moulick A, Sinha P, *et al*. Severe tricuspid valve stenosis secondary to pacemaker leads presenting as ascites and liver dysfunction: a complex problem requiring a multidisciplinary approach. *J Interv Card Elecrophysiol* 2009;**24**:71–5.

36 Uijlings R, Klun J, Salonsz R, *et al*. Pacemaker lead-induced severe tricuspid stenosis. *Circ Heart Fail* 2010;**3**:465–7.

37 Christiani LA, Bergman F, Tress JC, *et al*. Severe tricuspid stenosis during percutaneous occlusion of perimembranous ventricular septal defect with new Amplatzer device. *Congenit Heart Dis* 2006;**1**:239–43.

38 Kuralay E, Cingoz F, Gunay C, *et al*. Huge right atrial myxoma causing fixed tricuspid stenosis with constitutional symptoms. *J Card Surg* 2003;**18**:550–3.

39 Gustafsson BL, Hauso O, Drozdov J, *et al*. Carcinoid heart disease. *Int J Cardiol* 2008;**129**:318–24.

30 Left Ventricular Outflow Obstruction: Aortic Valve Stenosis, Subaortic Stenosis, Supravalvar Aortic Stenosis, and Bicuspid Aortic Valve

Colin McMahon

Our Lady's Children's Hospital, Crumlin, Dublin, Ireland

Introduction

Left ventricular outflow tract (LVOT) obstruction describes any obstruction to the egress of blood from the left ventricular cavity to the aorta. This may include one or more forms of obstruction, including subvalvar aortic stenosis (SAS), valvar aortic stenosis (AS), or supravalvar aortic stenosis (SVAS). SAS is unique as it is an acquired form of congenital heart disease whereas AS and SVAS obstruction tend to be congenital. The aortic valve morphology varies significantly in AS, although a bicuspid aortic valve (BAV) may exist with or without significant obstruction.

Incidence and genetics

The incidence of AS is reported as 0.4 per 1000, of SAS as 0.09 per 1000, and of SVAS as 0.05 per 1000 [1]. LVOT obstruction is not unique to humans. SAS is commonly encountered in Newfoundland puppies and similarly to humans tends to occur outside the neonatal period [2]. Genetic factors have been implicated in several forms of LVOT obstruction. BAV occurs in several families and is strongly associated with coarctation of the aorta [3]. Elastinopathies occur in both recognized syndromes such as Williams syndrome (chromosome 7q11.23 gene deletion) and familial non-Williams SVAS [4,5]. There are rare familial examples of SAS, but this is less common than familial SVAS [6].

Aortic valvar stenosis

Valvar AS accounts for 60–75% of LVOT obstruction. BAV is the most common congenital cardiac anomaly but may not come to attention until later in life when aortic valve dysfunction in the form of either stenosis or regurgitation ensues [7,8]. Valvar AS accounts for 3–6% of all cardiac defects [9]. There is a male to female ratio of 4:1. Recurrence risk is reported as 8% for mothers and 3.8% for fathers with AS [10]. Associated anomalies are recognized in 20% of patients and include coarctation of the aorta, interrupted aortic arch, ventricular septal defect and pulmonary stenosis.

Pathology

Valvar AS is associated with malformation in the aortic leaflet cusps and commissures. The valve develops by cavitation of three tubercles, two of which are positioned on the distal edge of truncal swellings involved in partitioning the primitive trunk and the third opposite to these [11]. Stenosis results from a failure of separation of the tubercles. The valvar leaflets are thickened with reduced excursion of the leaflets due to fusion of the commissures. There is a wide variation in the valve morphology, including unicuspid, bicuspid, tricuspid, or quadricuspid. There may be only a tiny aperture in critical stenosis. The most common pattern is a BAV with a single fused commissure and eccentric orifice. The deficient or absent commissure is intercoronary in the majority of bicuspid valves with right anterior and left posterior functional commissures. When the left

noncoronary or right noncoronary commissure is deficient, the commissures are left anterior and right posterior.

During systole, the limitation in valve opening often results in valve leaflet doming. The aortic annulus is hypoplastic in many patients. Critical neonatal AS results in severe left ventricular hypertension, left ventricular hypertrophy, and finally endothelial disruption represented as endocardial fibroelastosis (EFE) [12]. EFE occurs initially in the subendocardial region and rarely extends to the subepicardial region. In such patients, left ventricular filling is compromised, reducing atrial level shunting; consequently, right ventricular output through the ductus predominates, with resultant hypoplasia of the ascending aorta and aortic arch, left ventricle, and mitral valve. In older children, the left ventricular pressure loading results in left ventricular hypertrophy but not EFE.

Physiology

Valvar AS is characterized by a systolic pressure gradient between the left ventricle and aorta because of obstruction at the valve. LVOT gradient is a function of flow and annulus/aortic orifice size. This is not a linear relationship, however, and a doubling of blood flow has a squared result in gradient (increased by four). The Gorlin equation calculates the aortic valve area, AVA (cm^2 m^{-2}), as [13]

$$
\begin{aligned}
AVA \; &(\text{cm}^2 \, \text{m}^{-2}) \\
&= \frac{\text{flow / systolic - second (ml m}^{-2})}{44.5\sqrt{\text{mean gradient (mmHg)}}} \\
&= \frac{\text{stroke volume (ml m}^{-2}) \, / \, \text{systolic ejection time (s)}}{44.5\sqrt{\text{mean gradient (mmHg)}}}
\end{aligned}
$$

Severe aortic obstruction has an AVA of <0.5 cm^2 m^{-2}, moderate between 0.5 and 0.8 cm^2 m^{-2}, mild >0.8 cm^2 m^{-2}, and normal 2.0 cm^2 m^{-2}. Changes in preload or afterload systemic resistance may alter the true LVOT gradient, and simultaneous flow and pressure need to be measured to calculate LVOT obstruction accurately. Generally, a peak systolic pressure >60 mmHg and an aortic orifice <0.5 cm^2 m^{-2} constitute severe AS.

Hemodynamics

Valvar AS results in increased left ventricular systolic pressure, increased wall stress, and peak myocardial force. Wall stress increases as the left ventricular pressure increases but returns to normal in the setting of compensatory left ventricular hypertrophy (LVH). In older children, left ventricular function tends to be preserved or hyperdynamic, as a consequence of left ventricular hypertrophy and reduction in LV cavity size. Only in younger children or neonates is the development of left ventricular dysfunction typically encountered. End-systolic wall stress is inversely related to left ventricular function and hyperdynamic systolic function. In patients with AS, hyperfunction is a result of reduced end-systolic wall stress rather than increased myocardial contractility.

End-systolic wall stress is reduced because end-systolic wall thickness is increased, and end-systolic pressure is normal. At twice the normal cardiac output, increased cardiac output depends primarily on increase in heart rate and less so on increase in stroke volume. At higher exercise levels, there is a progressively higher stroke volume with a sharp increase in gradient, the change being proportional to the square of the increase in flow velocity. This reduces the filling time, which restricts coronary blood flow, particularly in the subendocardial region where flow is almost entirely diastolic. An estimate of potential coronary flow can be made from the area between the aortic and left ventricular diastolic pressures, the diastolic pressure time index (DPTI) [14]. The left ventricular oxygen requirement can be obtained from the area under the ventricular pressure curve during ejection, the systolic pressure time index (SPTI). In the absence of coronary disease, the DPTI/SPTI ratio allows a measure of the oxygen supply/demand ratio (see Chapter 4). Patients with an aortic valve area <0.7 cm^2 m^{-2} and a heart rate of 100 beats per minute have a DPTI × arterial oxygen content (g dl^{-1})/SPTI ratio <10, consistent with subendocardial ischemia [15]. With exercise-induced tachycardia, the diastolic filling time is reduced even more than the systolic ejection time, and myocardial oxygen delivery is decreased as systolic work is increasing.

Electrocardiographic ST depression appears consistently in left ventricular leads during exercise in patients with a resting LVOT catheter gradient of ~50 mmHg [16]. This level of obstruction can result in myocardial injury and subendocardial fibrosis, which may manifest as chest pain, syncope, arrhythmia, or sudden cardiac death. Ventricular arrhythmia is particularly a risk in a scarred dilated ventricle. Left ventricular baroreceptors may contribute to syncope in AS [17]. Any stimulus that elevates left ventricular systolic pressure may stimulate these receptors, resulting in vasodilatation that could reduce coronary flow. Left ventricular diastolic function may be impaired even when systolic function is well preserved [18]. As LVH progresses, elastic recoil and ventricular relaxation rate are reduced, so that passive chamber stiffness increases and active relaxation becomes impaired.

Natural history

The natural history of AS is related to the degree of LVOT obstruction. About 10% of patients presenting in childhood develop congestive heart failure in the first year of life, two-thirds in the first 2 months [19]. Patients with AS with hypoplastic left heart syndrome who are "duct dependent" experience circulatory collapse once ductal closure occurs

(see Chapter 38). Patients with borderline left ventricular dimensions may manage to maintain reasonable cardiac output, but at the cost of developing pulmonary venous and arterial hypertension later in life.

Patients with trivial AS may show minimal progression. Half of patients presenting with mild or moderate AS remain unchanged over one to two decades [20]. In a large natural history study of over 400 patients over 2 years of age, predicted survival in an age-matched normal population was 96%; 25-year survival of study patients was 92.5% for those with an initial catheter gradient <50 mmHg and 81% in those with a gradient ≥50 mmHg [21]. Sudden death from cardiac arrhythmia increases when the catheter-derived gradient exceeds 50 mmHg. An increase in severity occurred in 30–50% of patients with mild AS (gradient <40 mmHg) and 70–90% of patients with moderate AS (50–79 mmHg) [21,22].

History and physical examination

Persons with trivial to mild AS are asymptomatic and may present with a murmur. In patients with moderate to severe AS, symptoms may include exercise intolerance, chest pain, dyspnea, or syncope. Neonates with critical AS (including hypoplastic left heart syndrome) often present with circulatory collapse presenting with tachypnea, dyspnea, pallor, thready pulses, and acidosis. Failure to re-establish ductal patency promptly results in death secondary to acidosis, multiorgan failure, and arrhythmia.

Although a typical ejection murmur may be heard at birth with mild to moderate AS, the murmur is often minimal when obstruction is extreme and flow is low. Infants with mild or moderate AS have signs similar to those in older children. Beyond 1 year, most patients with mild AS (Doppler gradient 30–40 mmHg or catheter gradient 25–30 mmHg) have no cardiac symptoms, and 95% show normal growth and development [23]. Symptoms are rare in patients with moderate AS (Doppler gradients <70 mmHg or catheter gradients <55 mmHg), although as this level is approached a lack of competitive stamina is sometimes evident. Syncope occurred in 9% of patients with a catheter gradient >80 mmHg. In children, the typical signs of mild AS include normal venous pressure and a pulse that is normal or slightly jerky. There is a long ejection systolic murmur radiating to the suprasternal notch and usually associated with a thrill, and the second heart sound varies normally with respiration. As the severity of AS increases, the frequency of the murmur rises. With moderate obstruction, the A wave amplitude of the jugular venous pulse becomes more prominent over the years, resulting from impaired right heart filling from LVH. The signs most reliably related to moderate obstruction are not the intensity of the murmur but a reduction in pulse pressure and the respiratory variation in splitting of the second heart sound. A slowly rising pulse as a sign of severity is much less common in children than in adults.

Splitting of the second heart sound is narrowed as there is delayed valve closure due to prolonged left ventricular ejection interval. In some patients, splitting of the second sound may only be heard in expiration. An ejection click often present after the first heart sound is best appreciated in the fourth left intercostal space, apex, and lower left back. With increased stenosis, the click moves closer to the first heart sound. Aortic regurgitation (AR) is characterized by a diastolic descrescendo murmur. An Austin Flint murmur secondary to the regurgitant jet abutting the anterior leaflet of the mitral valve may be appreciated in mixed aortic valve disease.

Electrocardiography and exercise testing

A normal ECG does not exclude significant AS. LVH does not discriminate between the AS severity (Figure 30.1). However, LVH with a strain pattern usually indicates severe AS. Right ventricular dominance is usual regardless of the severity of AS in the early weeks of life, but left ventricular dominance and hypertrophy become manifest in three-quarters of older infants with important AS and normal left ventricular volume [24]. A sum of the voltages of the S wave in V_2 and the R wave in V_6 of 40 mm carries ~70% probability of LVH at any age. ST or T wave depression is virtually diagnostic of significant LVH.

Exercise stress testing adds further information regarding the severity of AS. There is some correlation between severity of AS and exercise duration, systolic blood pressure response, and ST segment depression with maximal exercise. ST depression >1 mm for more than 0.08 s after the J point has been reported to indicate a resting gradient >50 mmHg by catheter [25]. However, further studies showed a false-positive rate of up to 40% in patients with gradients of 30 mmHg [26]. Stress testing does not reliably indicate severity of AS.

Chest radiography

In infants with congestive heart failure secondary to AS, the chest radiograph demonstrates cardiomegaly with plethoric lung fields. In older children, the degree of pulmonary plethora is less significant. In critical neonatal AS, left-to-right shunting at the atrial level contributes to the pulmonary overcirculation. In older patients, poststenotic dilatation of the ascending aorta is a feature.

Echocardiography

Echocardiography is central in assessing AS and has supplanted the need for diagnostic cardiac catheterization. Standardized imaging planes include subcostal, apical parasternal, and suprasternal imaging planes.

Parasternal long-axis views allow evaluation of leaflet thickening and doming of the aortic valve in systole. Imaging in the parasternal short-axis plane usually allows visualization of leaflet anatomy, establishing the orientation of the

Figure 30.1 Electrocardiogram demonstrating criteria of left ventricular hypertrophy. Note the dominant R wave in lead V6 and the deep S wave in lead V1.
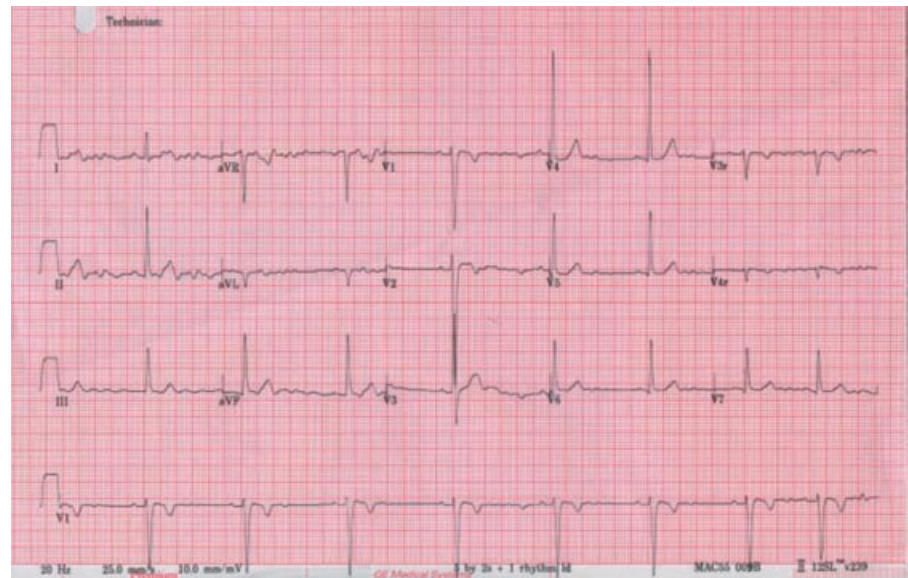
(a)
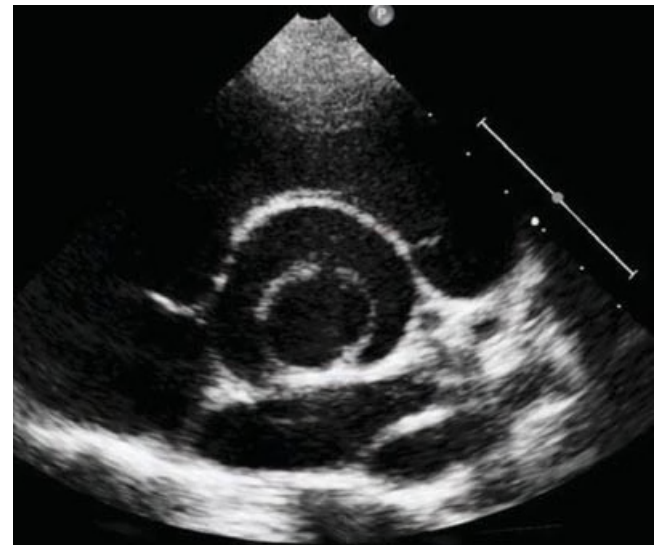
(b)

Figure 30.2 Two-dimensional echocardiograms in the parasternal short-axis plane demonstrating (a) a bicuspid aortic valve and (b) a unicommisural valve with dilated aortic root.

opening plane and allowing judgment of leaflet numbers and structure (Figure 30.2a). A valve that appears to be tricommissural in diastole (even though somewhat distorted) is frequently shown in systole to be essentially bicommissural but with a raphe in the fused leaflet. Some degree of fusion is also frequently shown at one of the two commissures; if marked, this can effectively produce a unicommissural valve (Figure 30.2b). Detailed two-dimensional and M-mode measurements are required to measure the aortic annulus and septal and free wall thickness and assess papillary muscle anatomy, left ventricular dimensions, and ventricular

function [27,28]. All values are compared with normal values. Assessment of the adequacy of the left ventricle and aortic arch, mitral valve, and aortic valve is particularly important in critical AS in the newborn. A highly echogenic endocardium suggests EFE, particularly with regional motion abnormalities.

Pulsed-wave, continuous-wave, and color Doppler interrogations assess the site and severity of obstruction and associated lesions [29,30]. Assessment can be based on the left ventricular aortic gradient with the modified Bernoulli equation [31] or the valve area according to the

continuity equation [32]. The reliability of the simplified Bernoulli equation [2]:

$$\text{pressure gradient} = 4 \times \text{peak velocity}^2$$

has been validated. The peak instantaneous gradient is generally significantly higher than the peak-to-peak gradient recorded at cardiac catheterization [33], due partly to sedation or damping in catheter systems, but mainly to the difference in the phase of the pressure pulses recorded. The peak instantaneous and mean gradient are higher in patients with higher pulse pressures, a finding which may be associated with a lesser degree of AS and increased by the presence of coexisting AR. There is no consistent correction factor to allow comparison between catheter peak-to-peak and echocardiographic-derived peak instantaneous calculations. On average, catheter-derived measurements are 80% of the echocardiographically derived gradient in patients with critical stenosis.

An echocardiographically acquired *mean* gradient correlates better with the catheter-derived figure [29]. With echo Doppler, valve area is derived from a direct application of the continuity equation:

$$\text{valve area} = A(\text{LVOT}) \times \frac{V(\text{LVOT})}{V(\text{AV})}$$

where A = area, LVOT = left ventricular outflow tract, V = mean velocity, and AV = aortic valve. Meticulous alignment of the Doppler signal is essential. Because the LVOT and aorta share the same ejection volume, measurement is valid in the presence of AR.

Cardiac MRI

Cardiac MRI can accurately define aortic valve morphology (Figure 30.3) and also provides accurate flow velocity and valve gradient data using velocity-encoded cine magnetic resonance imaging. This demonstrates good correlation with Doppler-derived gradients [34].

Cardiac catheterization

Catheterization is rarely required to define the severity of stenosis. It is indicated in severe AS or children with symptoms such as syncope, dizziness, or angina with a mild to moderate AS. Cardiac output is measured using the Fick methods or thermodilution. Left and right heart catheterization are performed. The left heart is accessed either anterograde with the transseptal puncture technique or in many centers retrograde via the femoral artery. The simultaneous recording of pressure in the left ventricle and ascending aorta is best to determine valve gradients, although a "pullback" of the catheter across the valve will also determine the gradient. The Gorlin equation is used to calculate valve area. This equation assumes that 100% of the pressure drop across
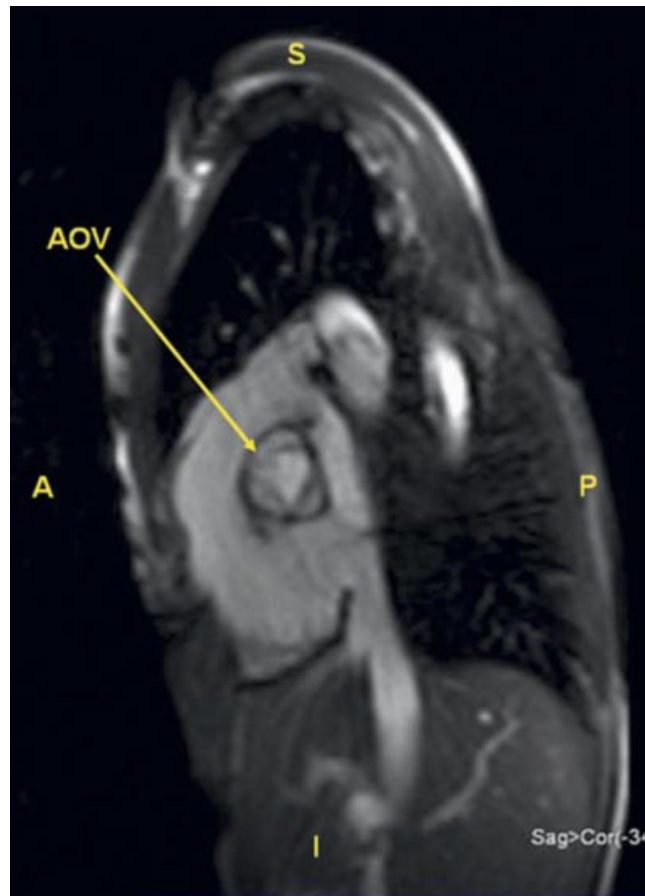
Figure 30.3 ECG-gated MRI cine bright blood with fast gradient echo image demonstrating trileaflet aortic valve in the short-axis view. AOV, aortic valve.

the aortic valve produces flow. Discrepancies have been noted between valve areas calculated from the Gorlin equation and actual measured areas, with questionable increases during exercise and questionable measurements at low flows [35–37]. An *in vitro* model showed that the estimate from the Gorlin equation of a known area increased directly with increase in flow, so that substantial errors are to be expected at both low and high flows [38]. At a critical point, small errors become important – an area of $0.6\,\text{cm}^2\,\text{m}^{-2}$ is on the margin of the severe range, and an area of $0.8\,\text{cm}^2\,\text{m}^{-2}$ is in the mild to moderate range. The Gorlin equation remains the basis for comparisons with other methods, but it is by no means a true "gold standard."

Gaining retrograde access to the left ventricle may be challenging in a severely stenotic valve and requires careful, delicate manipulation of the catheter. Left ventricular angiography allows visualization of the valve doming, tethering of leaflets, and the jet of AS. This is best performed using cranial tilt of the left anterior oblique view and straight

oblique views (usually about 60° left anterior oblique and 30° right anterior oblique) of the annulus.

After valve dilatation, the degree of AR should be assessed. A typical convention describes the AR as mild if opacification of the left ventricle does not equal that of the aorta, moderate if opacification is equalized after three cycles, and severe if it is equalized in less than three cycles [39]. The AR volume can be calculated by subtraction of net forward flow (calculated by the Fick method) from the total flow derived from angiography.

Comparison between catheter- and doppler-derived gradient

In adults, catheter peak-to-peak gradients averaged about 80% of Doppler peak instantaneous gradients with reasonable correlation but moderate scatter [40]. Interestingly, Doppler peak instantaneous gradients in these studies averaged only slightly above 80% of catheterization peak instantaneous gradients, primarily due to poor alignment of the Doppler signals in adult studies. Currie *et al.* showed an excellent correlation between simultaneous catheter and echocardiographic peak instantaneous gradients in children [41]. Assessments of mean gradients by echo Doppler and catheterization are much closer, catheter figures ranging from 2 to 4 mmHg higher on average than echo Doppler figures. Although more accurate, the mean gradients warranting intervention are less well established. For example, in an adult population judged to need operation because valve area was <0.75 cm², all patients had a mean gradient of >30 mmHg, and more than half >50 mmHg [42]. In children, by contrast, 11 patients with a mean gradient in the range 17–27 mmHg were judged to need operation [30]. A Doppler peak instantaneous gradient of 90–100 mmHg (equivalent to a peak-to-peak catheter gradient of >75 mmHg) or a valve area of 0.5 cm² m⁻² usually justifies early intervention. A Doppler peak instantaneous gradient of 70 mmHg (equivalent to a peak-to-peak gradient of ~55 mmHg) or an area <0.7 cm² m⁻² warrants intervention in the presence of symptoms or LVH with strain. Intervention may be judged appropriate in patients with a catheter or Doppler mean gradient of 30 mmHg, but a level of 50 mmHg is more common in older patients.

Treatment

Treatment is dictated by the severity of LVOT obstruction in addition to the size of the left heart structures and left ventricular volume. In the majority of children with mild AS there may be no indication for therapy. Treatment of AS can be described for children before and after 1 year of age and in the fetus. The UK National Institute for Health and Clinical Excellence (NICE) guidelines report increased risk of endocarditis in patients with valvar disease with either significant stenosis or regurgitation [43].

Fetal management of aortic valvar stenosis

Fetuses with AS have demonstrated progressive arrest of growth of the left ventricle, aortic valve, and mitral valve. This prompted the development of *in utero* interventional treatments in an attempt to alleviate LVOT gradient and allow potential biventricular repair. Kohl *et al.* reported the first series of 12 patients in which seven procedures were successful but only one fetus survived [44]. Other early reports demonstrated technical success but poor outcome [45]. A recent study of 70 fetuses with critical AS reported technical success in 74% with 17 patients reaching biventricular repair [46]. Nine pregnancies did not survive. Despite the investigators devising a multivariable threshold scoring system to define patients with poor prognosis, patient selection remains a challenge (see Chapter 16).

Management of infants younger than 1 year

Neonatal aortic stenosis

Infants presenting with critical AS or AS with the hypoplastic left heart syndrome or a borderline left ventricle represent the most seriously affected group. They may undergo acute cardiogenic collapse from ductal constriction or closure and loss of right ventricular systemic output. Immediate initiation of prostaglandin therapy is needed to re-establish cardiac output. Cardiorespiratory and inotropic support and mechanical ventilation are required. Balloon valvoplasty is the appropriate procedure in isolated AS. In neonates with a hypoplastic mitral valve and left ventricle, a single ventricle strategy is best adopted if parents agree. The most challenging group of patients is those with AS and a borderline left ventricle. Pursuing a biventricular approach in these infants may result in survival but at the cost of later pulmonary hypertension that may make cardiac transplantation impossible. Patients with severe AS and a small left ventricle and marked EFE may not respond well to valvoplasty and high left heart filling pressures may result in progressive pulmonary hypertension.

The aortic valve annulus, mitral annulus, and left ventricular volumes should be indexed to BSA and Z-scores derived. Additional features including non-apex forming left ventricle, hypoplastic mitral valve, EFE, infarction of papillary muscles, mitral regurgitation, and retrograde flow in the ascending aorta should be considered in the decision for biventricular repair [47,48]. Specific factors associated with a poor outcome include end-diastolic volume <20 ml m⁻², left ventricular inflow dimension (aortic annulus to apex) <25 mm, aortic annulus <5 mm, and mitral annulus <9 mm [49]. The Rhodes score was derived to predict likelihood of

good prognosis in neonates with aortic valve stenosis. This correctly predicted outcome in ~90% of patients, a discriminating score less than −0.35 predicting death:

$$score = 14.0(BSA) + 0.943(AOi) + 4.78(LAR) + 0.157(MVAi) - 12.03$$

where *BSA* is body surface area, *AOi* and *MVAi* are aortic sinus dimension and mitral valve area indexed to body surface area, respectively, and *LAR* is the ratio of the long axis of the left ventricle (from the plane of the mitral valve annulus to the apex of the ventricle) to the long axis of the heart (apical four-chamber view of the distance from the crux of the heart to the apical endocardium, either left or right ventricle, whichever forms the apex of the heart) [50].

If the score is below the critical level, a single ventricle palliation may be offered. There may be a higher risk of poor outcome in neonates with a borderline LV and significant LV mass in a single ventricle due to LV–RV interaction. Other crucial parameters in outcome are left ventricular function, rate, and potential for growth of left heart structures postoperatively. Colan *et al.* highlighted that minor errors in measurements of left-sided structures could result in an erroneous score [51].

Surgical intervention

Surgical valvotomy for isolated AS is less frequently required, given the improvements in interventional catheterization technology and techniques. Valvotomy is palliative and not curative. It may be indicated if the valve is unsuitable for balloon valvoplasty, cannot be crossed, or does not respond to dilatation. Valvotomy has excellent results with a low mortality among patients with normal ventricular function. Aortic commissurotomy can be performed with excellent alleviation of LVOT obstruction and minimal aortic valve regurgitation. When the surgeon attempts to abolish the valve gradient completely, moderate to severe AR may result. In one recent study of 36 patients after surgical valvotomy, 15 of whom had depressed left ventricular systolic function [52], there were no deaths among patients with normal left ventricular function but mortality increased to 47% among those with depressed left ventricular function. Several reports have demonstrated a good reduction in gradient with low mortality [53–58]. Aortic valve morphology has a significant impact on outcome. Commissurotomy resulting in trileaflet anatomy reduced mortality (0 versus 5%) and risk of reintervention (33 versus 92%), aortic reoperation (45 versus 92%) and aortic valve replacement (57 versus 100%) compared with patients with BAV [59]. Actuarial survival was 100% compared with 85% in favor of trileaflet valve morphology. A subgroup of children undergoing surgical valvotomy with restrictive left heart filling developed persistent pulmonary hypertension [60].
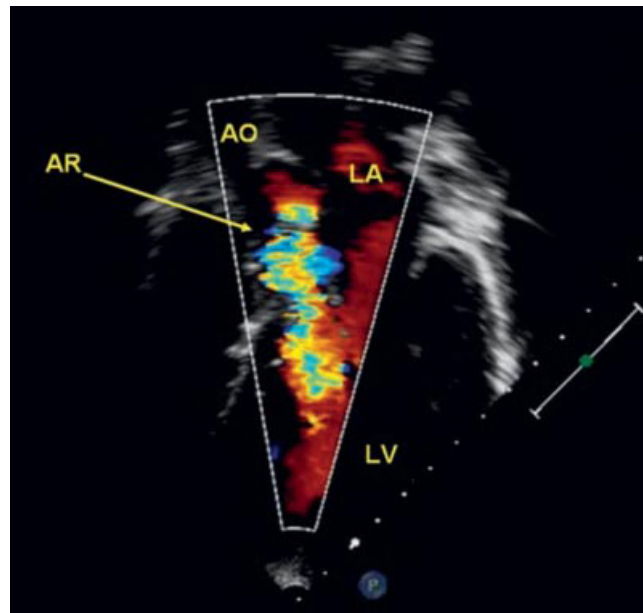
Figure 30.4 Two-dimensional echocardiogram using color Doppler imaging in the apical four-chamber view demonstrating severe aortic valve regurgitation. AO, aorta; AR, aortic valve regurgitation; LA, left atrium; LV, left ventricle.

Balloon valvoplasty

Balloon valvoplasty is recommended in most centers if the severity of AS exceeds 60 mmHg gradient with a normal cardiac output or an effective aortic orifice <0.5 cm^2 m^{-2}. Valvoplasty is also indicated in patients with LVH and strain or with symptoms at a lower gradient. In some centers, valvoplasty is undertaken with a gradient exceeding 50 mmHg. Valvoplasty is often undertaken in children with coexisting coarctation but not with other significant intracardiac lesions or the presence of mild or more severe aortic valve regurgitation.

Reports of valvoplasty in the 1980s demonstrated this to be an effective mode of treatment [61–63]. A balloon to annulus (BAR) ratio of 0.9–1.0 is advocated with many centers using a balloon diameter 1 mm less than the aortic annulus to avoid creating significant AR. Successful valvoplasty is considered to be a 60% reduction in peak-to-peak systolic echo gradient [64–67]. A recent study reviewed 1004 patients between 1 day and 18 years of age who underwent balloon aortic valvoplasty between 1985 and 2006 at 20 European centers [68]. The mean pressure gradient decreased from 65 (±24) to 26 (±16) mmHg and remained stable during a mean follow-up of 32 months. Newborns in the study had the most significant disease, with 60% manifesting impaired LV function predilatation. Complications occurred in 15% of newborns, 11% of infants, and 6% of older children. Freedom from intervention at 10 years was 50%. Severe AR may result from a tear of the valve cusp or raphe or valve detachment (Figure 30.4). Other complications from

valvoplasty include arrhythmia, bleeding, stroke, thrombosis, mitral valve injury, and rarely death. In the collaborative Valvuloplasty and Angioplasty of Congenital Anomalies (VACA) Registry, four of the five deaths among 204 patients occurred in infants younger than 1 month, as did all three life-threatening arrhythmias [69]. Loss of the femoral pulse may occur in 10% of children younger than 1 year of age [70]. Failed balloon valvoplasty, defined as residual gradient >60 mmHg or >50% of predilatation gradient, occurs in up to 30% patients. Factors in such patients include a dysplastic thickened valve, BAR ratio <0.9, age <3 months, and unrepaired coarctation. Balloon valvoplasty exacerbates AR in 20–70% of patients, 10% of which may be severe [71,72].

Technical aspects of balloon valvoplasty

Aortic valvoplasty may be performed via the femoral artery, carotid artery, or the umbilical artery. Outcomes are similar with either anterograde or retrograde approaches [64]. The femoral artery approach is often used in older children but the carotid approach may be required in neonates. The umbilical arterial approach has been used but it limits balloon manipulation. In older children, an anterograde approach can be used with a transseptal procedure and this is increasingly employed in neonates. Retrograde access can be achieved by placing an appropriately curved catheter above the aperture in the valve and advancing a small-gauge soft-tipped wire to the left ventricle. From an aortogram, the jet stream can be identified, which will aid entry into the left ventricle. Once entered, an extra-stiff wire with a soft tip can be curled in the left ventricle to maintain balloon stability.

The balloon should have a BAR ratio of 0.9–1.0. Firm control of the catheter shaft avoids displacement to either the left ventricle or aorta. Adenosine has been used in the past to produce temporary asystole and prevent valve tearing during valvoplasty [73]. Rapid ventricular pacing has also been used to stabilize balloon inflation [74]. Full dilatation should be maintained for about 4–5 s, and the balloon should be withdrawn to the aorta after dilation. Additional valvoplasty is not performed as it may exacerbate AR. A trivial increase in AR has been reported in 14% and moderate or severe AR in 4% of patients [75,76]. The risk of AR is greater in unicuspid valves. Permanent pulse loss occurred in 5–10% of patients, the risk being higher in infants. The use of low profile compliant balloons in adults achieves excellent alleviation of the aortic valve gradient with no mortality or worsening of AR [77]. Left bundle branch block, complete atrioventricular block, ventricular ectopics, and ventricular tachycardia have also been reported. Cardioversion or temporary pacing may occasionally be required. The mortality rate is 1%. The success rates of balloon aortic valvoplasty and surgical valvotomy are comparable [65,78].

Hybrid approach in children with borderline left ventricle

A hybrid approach may allow some children with a borderline left ventricle to achieve a biventricular repair. This approach includes ductal stenting, balloon atrial septostomy (± stent implant), and banding of the pulmonary arteries. This approach gives the left ventricle several months to adapt to lower pressure and normoglycemic conditions, and may allow the infant to bridge to a biventricular repair [19].

Management of children older than 1 year

Surgical intervention

The surgical mortality is less than 2% in this age group [61–63]. The commissures are incised judiciously to mobilize the fused leaflets and yet avoid AR. Patients >1 year of age have a better prognosis than younger children as the left ventricle is capable of sustaining cardiac output. Survival after surgical valvotomy is 95% at 5 years, 85% at 15 years, and 75% at 25 years [79]. Mild to moderate AR was reported in 10–28% of patients after valvotomy; AR may progress and be underestimated on clinical examination. In the Second Natural History Study, moderate or severe AR was diagnosed at follow-up of unoperated patients in 8% by clinical evaluation and 24% by echocardiography [80]. Among the operated patients, these figures were 12 and 30%, respectively. The need for reoperation begins 4–5 years after the first procedure, and up to 40% of patients require a second operation by 25 years [80].

Surgical intervention may include a Ross procedure, in which the pulmonary valve is placed within the aortic valve position and a biological valve replaces the native pulmonary valve. This procedure has the benefit of the valve growing as the child grows and avoids the need for anticoagulation. It tends to be favored in young children and older adults. It remains an option for younger adults. In a recent study of 487 patients who underwent the Ross procedure, survival was 82% at 16 years and hospital mortality 3.9% [81]. Freedom from reintervention was 82% and from autograft failure was 83%. Other studies have demonstrated similar freedom from valve reintervention of 95% at 8 years of follow-up [82]. A disadvantage of the Ross procedure is operating on both semilunar valves in a single valve disease. There have been several reports of neoaortic root dilatation, usually most dramatic in the first year, after which it levels off [83,84]. In a small group of patients, significant AR developed particularly when the Ross procedure was undertaken for AR [85,86]. The degree of AR is usually mild and remains relatively static. The need for further aortic valve replacement is 10% over 20 years. Additional postoperative complications include pulmonary homograft obstruction, usually amenable to balloon dilatation or percutaneous valve implantation.

Patients with combined AS and SAS may undergo a Ross–Konno procedure in which the subvalvar area is extensively reconstructed using an aortic ventriculoplasty.

Balloon valvoplasty

Balloon valvoplasty remains the treatment of choice in older children as it is less invasive and avoids cardiac bypass. Gradients on average are decreased from 70 mmHg or higher to 30 mmHg [69,87,88]. In the VACA study, 192 of 204 patients showed some benefit [69]. In patients in whom the BAR ratio is 0.9–1.0, there is minimal risk of valve damage and significant AR. Annulus size should be measured by echocardiography and aortography to ensure accurate measurement.

Prognosis

Long-term prognosis is worse in those presenting at a younger age with a significant obstruction or left ventricular dysfunction. Continued medical management helps preserve left ventricular function and minimize the risk of both sudden death and heart failure. Many patients will require future aortic valve replacement. Approximately 50% of patients avoided the need for aortic valve replacement at 10 years following balloon valvoplasty [68]. Long-term survival has been around 75% at 5 years, 60% at 10 years, and 40% at 15 years [89]. Although intervention in patients with aortic valve stenosis is often palliative, exercise capacity, NYHA status, and survival are generally good.

Percutaneous aortic valve replacement

Percutaneous aortic valve implantation (PAVI) is a procedure gaining popularity and becoming more widely used for the treatment of patients with severe AS at high risk for operation. Two devices are under evaluation, the CoreValve ReValving System and the Edwards SAPIEN valve [90]. Both devices are generally deployed retrogradely, mainly trans-femorally or via the subclavian artery, or, less commonly, transapically. Initial experience has been encouraging, with good short-term outcomes. Long-term data are lacking. Currently PAVI is advocated only for symptomatic high-risk older patients with AS. One series reported a reduction in peak LVOT gradient from 83.8 ± 23 to 12.6 ± 6 mmHg [91]. In a recent study of 30 adult patients (mean age 80 years) who underwent PAVI using the CoreValve ReValving System [92], implant was successful in 90% of patients with a reduction of peak from 76 ± 24 to 22 ± 7 mmHg at 30 days after device placement. Major adverse cardiovascular and cerebral events occurred in seven patients.

Subaortic stenosis

Subaortic stenosis (SAS) is a heterogeneous group of conditions that are either isolated in one-third of patients or associated with specific congenital cardiac lesions including atrioventricular septal defect, ventricular septal defect, coarctation, interrupted aortic arch, or double-chambered right ventricle [93–95]. It may develop after surgical repair of primum atrial septal defect [96]. SAS accounts for 15–20% of patients with LVOT obstruction and may be familial [97,98]. It is more common in males. In Shone syndrome, it is associated with a supravalvar mitral ring, parachute mitral valve, and coarctation of the aorta [99]. SAS is not a congenital lesion and typically develops after infancy [2,100].

Pathology

The most common forms of SAS include fibromuscular ridge, discrete membrane, and tunnel SAS. These may be combined, for example, a ridge with a discrete membrane. The membrane or ridge may extend to either the anterior leaflet of the mitral valve or the undersurface of the aortic valve leaflets. Histologically the ridge consists of irregularly oriented acellular dense collagen fibers, smooth muscle cell layer, elastic tissue, and abnormal myocytes with their own capillaries. There may be an intermediate group possessing some characteristics of ridge and membranous obstruction. Long narrow tunnel SAS can also occur in Shone syndrome. The degree of obstruction is SAS varies and may cause LVH. Some patients have an associated bicuspid aortic valve and a variable degree of AS. Over time, aortic valve function may be compromised by a systolic jet striking the aortic valve leaflets and in 40% of patients AR develops [101,102]. Aortic valve deformation may also result from extension of the ridge or membrane on to the aortic valve [103]. Feigl *et al.* described the involvement of at least one cusp of the aortic valve in 16 of 18 postmortem specimens and speculated that this is the mechanism of aortic valve damage and AR [104].

Pathogenesis

Although one fetus has been reported with SAS, the lesion develops after infancy and is recognized as an acquired condition [105]. The etiology is not fully known. An increased aortoseptal angle, increased mitral–aortic separation, and aortic override have been implicated in its development [106,107]. One study in patients with ventricular septal defect and coarctation reported an increased risk of SAS developing in patients with aortoseptal angle >135° or mitral–aortic separation >4 mm. The positive predictive value was 83% and the negative predictive value was 90% [107]. Another study demonstrated aberrant flow patterns by color Doppler flow in the LVOT proximal to the region of SAS, probably reflecting abnormal flow which would result in abnormal wall stress and endothelial proliferation [108].

Natural history

SAS tends to progress [109–111]. The median age of diagnosis is typically between 5 and 9 years [112,113]. Progression occurs in 75%, particularly in tunnel-type SAS and in patients younger at the time of diagnosis. The increase in

gradient across the LVOT may relate to an increase in thickness of the membrane or ridge or a narrowing of the LVOT tract in the tunnel-type obstruction [114]. This causes further septal and LVH that exacerbates the LVOT gradient. Detection of SAS has increased since the widespread availability of echocardiography and has resulted in its earlier diagnosis. Patients with coarctation, interrupted aortic arch type B, or double-chambered RV should be examined carefully because of an increased risk of SAS [115].

Over time, the SAS jet deforms the aortic valve and causes regurgitation. One study reported aortic regurgitation in 30% of patients at diagnosis, and this increased to 54% at a mean follow-up of 3.7 years [113]. Another study of 220 patients with SAS (109 of whom had SAS resection and 111 had no surgery) showed that risk factors for moderate to severe aortic regurgitation were older age at diagnosis, previous balloon or surgical aortic valvoplasty, and a longer follow-up period [102]. Excluding patients with previous surgical or balloon aortic valvoplasty, a higher maximal Doppler gradient was an independent risk factor for moderate to severe AR. Although there is an increased risk of bacterial endocarditis, the incidence is low.

Clinical findings

Many children with SAS are asymptomatic and have a short systolic murmur. As the SAS progresses to moderate or severe obstruction, symptoms may include fatigue, dyspnea, syncope, or rarely chest pain. Physical findings may include a prominent left ventricular impulse, and at the left lower to right upper sternal edge a long ejection systolic murmur radiating to the carotid arteries. The A2 component softens. In some patients with aortic regurgitation, a diastolic murmur can be detected. Differentiating SAS from valvar AS may be challenging. Typically, an ejection click is not heard except in those with a BAV and AS.

Chest radiography is typically normal. Unlike valvar AS, the ascending aorta is not prominent. The electrocardiogram may demonstrate left ventricular hypertrophy with strain in patients with severe LVOT obstruction. The electrocardiogram, however, may not detect progressive severe LVOT obstruction.

Echocardiography

Echocardiography is the diagnostic modality of choice. A thorough segmental analysis should be performed in all patients. Two-dimensional imaging is performed in standard views (Figure 30.5). Color Doppler and spectral Doppler interrogation of the LVOT complete the data set. The anatomic details of the LVOT and involvement of the aortic valve and mitral valve leaflets should be evaluated carefully. Doppler interrogation of the LVOT should start at the LV apex in the four-chamber view and the cursor moved across the LVOT to the ascending aorta to determine the peak instantaneous gradient. The severity of AR should be determined using the vena contracta diameter, aortic

Figure 30.5 Two-dimensional echocardiogram in the parasternal long-axis view during systole demonstrating discrete fibromuscular ridge (arrow) in the subaortic region. Aortic valve leaflets (thin arrows) lie against aortic wall. AOV, aortic valve; LA, left atrium; LV, left ventricle; SAS, subaortic stenosis.

annulus/vena contracta ratio, and the presence of retrograde flow in the descending aorta [102,116–118]. Typically, measurement of the aortoseptal angle and mitral aortic separation is not performed [107]. In older patients, transesophageal echocardiography may be required for accurate analysis of SAS [119].

Cardiac catheterization

Cardiac catheterization is rarely needed in patients with SAS. If transthoracic echocardiography cannot define the subaortic gradient or severity of AR, then transesophageal echocardiography usually provides this information. In patients with coexisting valvar AS and SAS, a gradient pullback will help to define the location of the gradient as being primarily at the valvar or subvalvar level. If a left ventriculogram is performed, the optimal angiographic views of the LVOT are biplane axial angiography and cranial angulation in either left anterior oblique or lateral projections. Aortic angiography quantifies the severity of AR. Balloon angioplasty of SAS can be carried out, but the results are mixed [120].

Management – surgical intervention

Surgical resection usually involves ridge or membrane excision or enucleation, with or without surgical myectomy [121–123]. It remains contentious whether myectomy is required and whether this reduces risk of recurrence [123,124]. Any membrane or ridge that has extended on to the undersurface of the mitral valve or aortic valve leaflets is carefully peeled from the valve [125]. There is a very low morbidity and mortality from isolated membrane or ridge resection. A myectomy may increase the risk of complete heart block. Recurrence has been reported in 7–25% of patients at a mean follow-up of 4–5 years [123–128].

Progressive AR may occur in patients with unoperated SAS. Children with mild SAS gradients often exhibit little progression of valve dysfunction [121]. In those with a higher gradient, AR may progress after surgical intervention [121,129]. Endocarditis is rare after surgical intervention [121]. Indications for operation in fixed SAS remain contentious. Because the incidence of residual stenosis is increased in patients with a high preoperative gradient [130], and AR is associated with more severe obstruction, some have advocated excision or enucleation with a catheter gradient of 25–30 mmHg or a mean Doppler-derived or catheter-measured gradient of 30 mmHg [130,131]. Others recommend operation when the gradient is higher, or when there is progression of obstruction or regurgitation, because some patients with a mild or moderate gradient remain stable for many years. Surgical resection is generally recommended when the Doppler-derived peak instantaneous gradient is >50 mmHg or when there is associated mild or greater AR. Serial echocardiography is required to evaluate progression of SAS and AR. A model exists to predict the progression of the SAS gradient [132].

Patients with tunnel-type SAS undergo a Konno procedure in which the LVOT is augmented by an aortoventriculoplasty or valve replacement [133,134]. There is a higher risk of complete heart block with the Konno procedure [135]. In some patients who require aortic valve replacement also, a Ross–Konno procedure is undertaken [136]. Progressive dilatation of the neoaortic root may occur in the Ross population, particularly in patients with mismatch between the sizes of native aortic and pulmonary valves [137].

Recurrence of SAS

Recurrence risks range from 7 to 25% [123–128]. In a study of 111 patients following successful surgical resection of SAS [125], predictors of reoperation in 16 patients (14%) were a distance of <6 mm between the aortic valve and the obstruction and a Doppler peak gradient ≥60 mmHg. If intraoperative variables are also considered, peeling of the membrane from the aortic valve or mitral valve at first operation, a distance of <6 mm between the SAS and the aortic valve, and a Doppler peak gradient ≥60 mmHg were associated with recurrence. Dodge-Khatami *et al.* studied 58 patients and found younger age at operation, complex defects, residual postoperative gradient, and an aberrant right subclavian artery increased recurrence in 19% of patients [127]. Myectomy in addition to membrane resection, even in simple lesions, did not reduce the risk of reoperation.

Supravalvar aortic stenosis

Supravalvar aortic stenosis (SVAS) accounts for 6% of LVOT obstruction [138]. There is a strong association with Williams–Beuren syndrome, an elastin gene mutation on chromosome 7q11.23 [139]. Features of the syndrome include a characteristic "elfin" facies, hypercalcemia, and developmental delay [140]. Half of SVAS occurs in patients with Williams syndrome. Familial SVAS has been described in an autosomal dominant pattern (25% of patients) [6]. A further 25% of patients have sporadic SVAS. SVAS has been reported in 37–73% of patients with Williams syndrome [141].

Pathology

The classic pattern of SVAS is an "hourglass" deformity of fibromuscular hypertrophy at the level of the sinotubular junction. The stenosis is a localized, hourglass deformity of the ascending aorta in 80% of patients and more diffuse in 20% [142]. The aortic wall at this level has a characteristic pathologic appearance involving all three layers with intimal hyperplasia, fibrosis, loss of the internal elastic lamina with indistinct intimal medial junctions, medial hypertrophy and dysplasia with distorted elastic fibers, and adventitial fibroelastosis [143].

One-quarter of patients have associated BAV [144]. As many as 60% of patients have coexisting branch pulmonary arterial stenosis which may extend into the distal branch pulmonary arteries and varies from mild to severe [145]. Other associations include renal artery stenosis, mitral valve stenosis/regurgitation, atrial and ventricular septal defect, PDA, and coarctation.

The coronary arteries may be obstructed at the ostial origin or the arterial wall may be involved by the medial hypertrophy, intimal fibrosis, and hyperplasia. This may cause myocardial ischemia or myocardial infarction.

Pathophysiology

The degree of obstruction correlates with the degree of left ventricular hypertension and LVH. Coronary arterial involvement produces myocardial subendocardial ischemia particularly when associated with significant LVH. The jet through the supravalvar narrowing often hugs the aortic wall (Coanda effect), with the right brachial artery pressure being greater than the left.

Natural history

Half of patients present at <5 years of age. This syndrome is rarely diagnosed initially in adulthood. Patients with Williams syndrome and severe generalized arteriopathy have a higher mortality than children without an underlying genetic condition. Peripheral pulmonary arterial stenosis may affect the course of patients with Williams syndrome. Those with extensive pulmonary arterial disease may be relatively asymptomatic and survive for a prolonged period, as even severe pulmonary arterial stenosis tends to improve over time [146,147]. Patients with suprasystemic RV pressure, however, have a poorer prognosis [148].

Echocardiography

Imaging from the parasternal and suprasternal windows identifies the pattern and site of obstruction. In patients with

(a)　　　　　　　　　　　　　　(b)
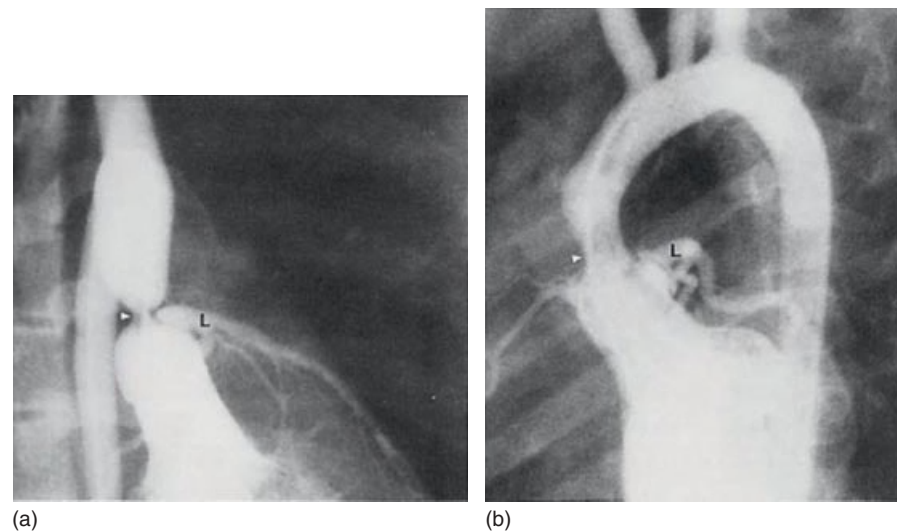
Figure 30.6 Frames from cineangiograms in two patients with supravalvar aortic stenosis and dilatation of aortic valve ring and sinuses. (a) Injection into left ventricle in right anterior oblique projection in a 15-year-old girl with severe stenosis (arrowhead) above the aortic valve. The diameter measured 15 mm compared with 26 mm across the aortic sinus. The left coronary artery (L) is dilated. (b) Left ventricular injection in left anterior oblique projection in a 7-year-old boy with moderate supravalvar stenosis (arrowhead), diameter 6 mm. The ascending aorta is mildly hypoplastic, diameter 12 mm. The aortic valve leaflets are thickened and domed, and adherence of the left leaflet obstructed flow into the dilated left coronary artery (L).

an hourglass deformity or diffuse hypoplasia of the ascending aorta, the diameter of the proximal ascending aorta is less than that of the aortic annulus. Careful imaging is required to detect coronary ostial abnormalities; intermittent coronary artery obstruction by tethered aortic valve leaflets may be difficult to diagnose. The aortic valve morphology and gradient across the LVOT are assessed. Serial obstruction (at the valve and supravalvar level) may result in an overestimation of the gradient, whereas the modified Bernoulli equation may underestimate the gradient when there is long-segment stenosis. Echocardiography may also identify branch pulmonary arterial stenosis and elevated right ventricular systolic pressure.

Cardiac catheterization

Catheterization may complement echocardiography. Cineangiograms demonstrate the extent and morphology of SVAS, involvement of the coronary arteries (Figure 30.6), and the degree of involvement of the branch pulmonary arteries. Pulmonary arterial stenosis may include discrete stenosis at the origin of the pulmonary arterial origins or diffuse branch pulmonary arterial stenosis [145,149].

Magnetic resonance imaging

MRI can assess the extent and severity of SVAS using black blood and gradient spin echo sequences. Phase contrast imaging can assess the velocity of blood flow through the area of obstruction. Additionally, quantification of left ventricular systolic function, LV mass, pulmonary arterial stenoses, and pulmonary arterial flow can be performed [150].

Management – surgical intervention

Surgical repair is the treatment of choice for SVAS, and balloon angioplasty has no role except for pulmonary arterial stenosis. Patients with symptoms, left ventricular strain pattern on electrocardiography or gradients >50 mmHg at cardiac catheterization or 75 mmHg at echocardiography require surgery. Patch angioplasty extends from above the area of stenosis down to the aortic sinuses [151,152]. There is a low mortality but reintervention may be required in up to 10–20% of patients for restenosis at the distal end of the patch. Patients with BAV may require valve replacement or the Ross procedure [153].

Bicuspid aortic valve

Bicuspid aortic valve (BAV) is the most common congenital cardiac anomaly [154] It usually occurs in isolation but is associated with coarctation of the aorta, interrupted aortic arch, ventricular septal defect and hypoplastic left heart syndrome [155–158]. There is a high incidence in Turner syndrome [159]. BAV may be familial, transmitted in an autosomal dominant fashion, or occur sporadically [160]. There is a male predominance of 2–4:1 which suggests an X-linked etiology. Mutations in the NOTCH1 gene (chromosome 9) may cause signal abnormalities which give rise to valvar calcification in addition to a bicuspid valve [161]. Downregulation of ubiquitin fusion degradation 1-like (UFDIL) gene on chromosome 22 has also been implicated [162]. Other genetic associations include 22q11 deletion,

ACTA2 gene mutation, and endothelium-derived nitric synthase expression [163,164].

Pathology

In BAV, the deficient or absent commissure is intercoronary in half of patients. The functional commissures are right anterior and left posterior, although the degree of obliquity may vary. When either the right noncoronary or the left noncoronary commissure is deficient, the commissures are left anterior and right posterior. In most patients, the combined leaflet is larger than the single leaflet. If a raphe cannot be identified, the valve is classified as indeterminate when the coronary arteries arise from separate sinuses.

Fewer than 10% of valves have equal sized cusps and two sinuses of Valsalva. Right and left coronary cusp fusion occurs in 80%, right and non-coronary cusps in 15%, and left and noncoronary cusps in 3% [165]. Echocardiographic studies have shown right–left fusion in 70% of cases and right–noncoronary fusion in 30% [166]. Usually the larger cusp has two sinuses and the nondominant cusp has a single sinus. The valve appears like a fish mouth because of partial valve opening. Unicuspid and quadricuspid valves are less common. Most BAV are non-stenotic but flow turbulence gives rise to a systolic murmur.

The aortic wall often demonstrates three distinctive histopathologic features: loss of vascular smooth muscular cells, fragmentation of elastic fibers, and increases in basophilic ground substances within cell-depleted areas of the ascending aorta media [167]. Patients with BAV demonstrate a reduction in fibrillin-1 relative to those with a trileaflet valve [168]. Fibrillin-1 is a glycoprotein which maintains the structural integrity of the wall and leaflets by tethering vascular smooth muscle cells to a matrix of collagen and elastin.

Incidence

Various studies have reported the incidence to be from 0.44 to 2.25% [169–171], the variability reflecting reporting based on patients with infective endocarditis or a predisposition to males. The incidence is probably closer to 1%, as found in a study of 293 bicuspid valves among 21 417 postmortem specimens [172].

Natural history

Typically, BAV thicken and calcify over the decades. Early signs of calcification become evident in the second to third decade of life and most patients in their sixth decade have calcified sclerotic valves. Progressive calcification results in valvar stenosis, but eventually AR may predominate. Valve deterioration may be accelerated in patients with right–noncoronary fusion compared with right–left fusion [16]. In children there is often little valve dysfunction and as the child develops into a young adult AR predominates. Older age is associated with increasing AS. Pachulski and Chan studied 51 patients from 21 to 67 years old, 31 of whom had a peak gradient <25 mmHg [173]. Over a mean follow-up of 21 months, 4/31 patients developed severe AS and 3/31 developed significant AR. Once older patients become symptomatic with congestive heart failure, the mean survival is 2 years [174]. Isolated AR tends to occur in a younger patient. This is better tolerated than AS, although in patients with significant AR left ventricular dilatation may result in progressive left ventricular dysfunction.

Aortic root dilatation

The diameters of the ascending aorta and aortic root are significantly dilated with BAV compared with a trileaflet valve. Dilatation of the root and ascending aorta was present in 56% of persons <30 years old and in 88% of those >80 years old [175]. The rate of growth of the ascending aorta ranges from 0.2 to 1.9 mm per year [176]. Larger aortas have a greater rate of growth and a high risk of rupture when the aortic diameter reaches 6 cm. For patients with aortic diameter >6 cm, the annual risk of rupture was 3.6%, dissection 3.7%, and aorta-related death 10.8% [177]. Serial review of these patients should include echocardiography, MRI or ECG-gated multidetector CT with three-dimensional reconstruction.

First-line medical therapy includes beta-blockers, but there is no evidence to suggest that ACE inhibitors, statins, or ACEII receptor blockers have a role [178,179]. Recent published criteria for surgical intervention include aortic diameter >4.5 cm when other clues indicate severe disease or if there is rapid dilatation of the aorta of >0.5 cm per year [180]. Surgical intervention is rarely needed in childhood.

Echocardiography

Two-dimensional echocardiography in the parasternal long and short axes allows detailed imaging of the valve. Pulse- and continuous-wave Doppler can quantify the LVOT gradient from the apical four-chamber and suprasternal views. Color Doppler imaging allows the determination of AR in the parasternal long- and short-axis views. The aortic valve morphology can be assessed in parasternal short-axis views and doming of the aortic valve can be visualized in parasternal long-axis views (Figure 30.7). Close attention to the pulmonary valve to assess the degree of regurgitation is important in assessing suitability for the Ross procedure.

Cardiac MRI

Black-blood double inversion–recovery fast spin-echo imaging of the ascending aorta can be performed in a sagittal plane to provide accurate aortic arch and root dimensions. Cine bright blood steady-state precession with fast gradient echo image demonstrates the systolic flow jet through the stenotic valve (Figure 30.8). Magnetic resonance angiography with three-dimensional reconstruction following gadolinium administration allows excellent delineation of the aortic arch [181].

CT imaging

Spiral CT angiography is generally used for routine arch evaluation. Where indicated, multidetector CT with three-dimensional reconstruction should be used with minimum radiation using ECG-gated imaging [182].

Figure 30.7 Two-dimensional echocardiogram in the parasternal long-axis view demonstrating prominent doming of bicuspid aortic valve.

Management – surgical intervention

In patients with significant AR, aortic homograft replacement, or Ross procedure are potential surgical interventions. Increasingly, older patients with other co-morbidities may be candidates for percutaneous CoreValve replacement for significant AS.

Surgical repair of BAV has become more popular recently in patients with isolated AR secondary to cusp disease, with or without aortic root disease. Boodhwani *et al.* reported 122 patients who underwent surgery for AR (43%), aortic root disease (14%), or both (43%) [183]. Raphe repair was performed by shaving (21%), resection with primary closure (60%), or pericardial patch (18%). Aortic annuloplasty was undertaken using sub-commissural annuloplasty, ascending aortic replacement, or aortic root replacement using a reimplantation or remodeling technique. At discharge, 93% of patients had either no or minimal aortic regurgitation and 7% grade 2 aortic regurgitation. Freedom from aortic valve reoperation was 94 and 83% at 5 and 8 years follow-up and freedom from aortic valve replacement was 96 and 92%, respectively.

In patients in whom aortic valve repair is not possible, prosthetic valve replacement is a successful option. A recent adult study of 1000 patients, mean age 70 years, who

(a)

(b)
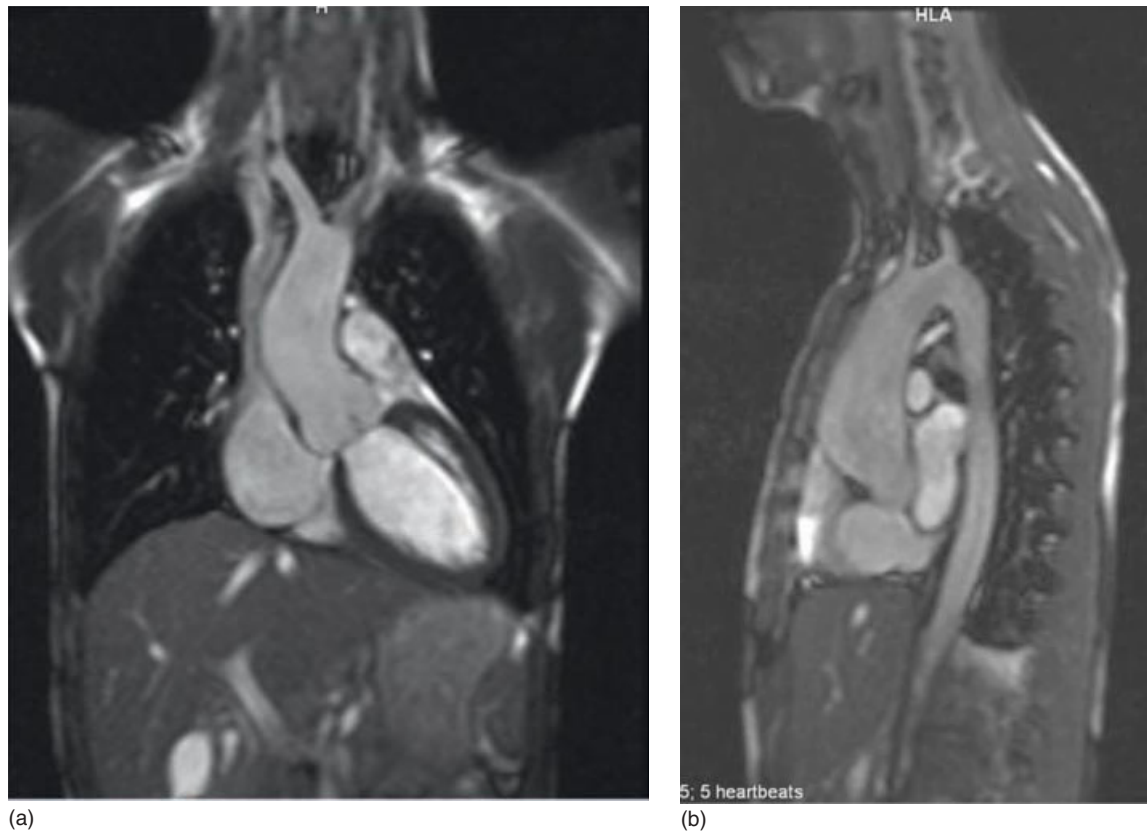
Figure 30.8 ECG gated cardiac MRI of an ascending aorta aneurysm with bicuspid aortic valve, cine bright blood steady-state precession with fast gradient echo image in the (a) coronal and (b) sagittal views.

underwent Carpentier–Edwards valve replacement, at a mean follow-up of 6 years reported surgical mortality of 7% with only 2.6% of patients requiring reoperation [184].

Endocarditis and bicuspid aortic valve

A recent study reported 50 adult patients with BAV developing endocarditis among 856 patients [185]. Patients with BAV were younger, had fewer co-morbidities, and had a higher risk of paravalvar abscess formation. Surgery was required in 72% of patients with BAV with a perioperative mortality of 8%. The UK NICE guidelines report that patients with aortic valve disease including stenosis or regurgitation have an increased risk of endocarditis [43].

References

1 Hoffman IE, Kaplan S. The incidence of congenital heart disease. *J Am Coll Cardiol* 2002;**39**:1890–900.

2 Freedom RM, Yoo SJ, Russell J, *et al*. Thoughts about fixed sub-aortic stenosis in man and dog. *Cardiol Young* 2005;**15**:186–205.

3 McBride KL, Pignatelli R, Lewin M, *et al*. Inheritance analysis of congenital left ventricular outflow tract obstruction malformations: segregation, multiplex relative risk, and heritability. *Am J Med Genet A* 2005;**134A**:180–6.

4 Lowery MC, Morris CA, Ewart A, *et al*. Strong correlation of elastin deletions, detected by FISH, with Williams syndrome: evaluation of 235 patients. *Am J Hum Genet* 1995;**57**:49–53.

5 Elcioglu N, Mackie-Ogilvie C, Daker M, *et al*. FISH analysis in patients with clinical diagnosis of Williams syndrome. *Acta Pediatr* 1998;**87**:48–53.

6 Ensing GJ, Schmidt MA, Hagler DJ, *et al*. Spectrum of findings in a family with nonsyndromic autosomal dominant supravalvar aortic stenosis: a Doppler echocardiographic study. *J Am Coll Cardiol* 1989;**13**:413–9.

7 Mahle WT, Sutherland JT, Frias PA. Outcome of bicuspid aortic valve in childhood. *J Pediatr* 2010;57: 445–9.

8 Roberts WC. Anatomically isolated aortic valvular disease: the case against it being of rheumatic origin. *Am J Med* 1970;**49**:151–9.

9 Freed MD. Aortic stenosis. In: Allen HD, Clark EB, Gutgesell HP, Driscoll DJ, eds. *Moss and Adams Heart Disease in Infants, Children and Adolescents*, 6th edn. Philadelphia: Lipincott, Williams & Wilkins, 2001: 970–87.

10 Driscoll DJ, Michels VV, Gersony WM, *et al*. Occurrence risk for congenital heart defects in relatives of patients with aortic stenosis, pulmonary stenosis, or ventricular septal defect. *Circulation* 1993;**87**:I114–20.

11 Freedom RM, Mawson JB, Yoo S-J, Benson LN. *Congenital Heart Disease: Textbook of Angiocardiography*, Armonk NY: Futura Publishing, 1997: 787–847.

12 Lofland GK, McCrindle BW, Williams WG, *et al*. Critical aortic stenosis in the neonate: a multi-institutional study of management, outcomes, and risk factors. Congenital Heart Surgeons Society. *J Thorac Cardiovasc Surg* 2001;**121**:10–27.

13 Teirstein P, Yeager M, Yock PG, *et al*. Doppler echocardiographic measurement of aortic valve area in aortic stenosis: a noninvasive application of the Gorlin formula. *J Am Coll Cardiol* 1986;**8**:1059–65.

14 Vincent WR, Buckberg GD, Hoffman JI. Left ventricular subendocardial ischemia in severe valvar and supravalvar aortic stenosis: a common mechanism. *Circulation* 1974;**49**:326–33.

15 Lewis AB, Heymann MA, Stanger P, *et al*. Evaluation of subendocardial ischemia in valvar aortic stenosis in children. *Circulation* 1974;**49**:978–84.

16 Kveselis DA, Rocchini AP, Rosenthal A, *et al*. Hemodynamic determinants of exercise-induced ST-segment depression in children with valvar aortic stenosis. *Am J Cardiol* 1985;**55**:1133–9.

17 Mark AL, Abboud FM, Schmid PG, *et al*. Reflex vascular responses to left ventricular outflow obstruction and activation of ventricular baroreceptors in dogs. *J Clin Invest* 1973;**52**:1147–53.

18 Villari B, Hess OM, Kaufmann P, *et al*. Effect of aortic valve stenosis (pressure overload) and regurgitation (volume overload) on left ventricular systolic and diastolic function. *Am J Cardiol* 1992;**69**:927–34.

19 Brown SC, Boschoff D, Eyskens B, *et al*. Hybrid approach as bridge to biventricular repair in a neonate with critical aortic stenosis and borderline left ventricle. *Eur J Cardiothorac Surg* 2009;**35**:1080–2.

20 Hossack KF, Neutze JM, Lowe JB, Barratt-Boyes BG. Congenital valvar aortic stenosis. Natural history and assessment for operation. *Br Heart J* 1980;**43**:561–73.

21 Keane JF, Driscoll DJ, Gersony WM, *et al*. Second natural history study of congenital heart defects. Results of treatment of patients with aortic valvar stenosis. *Circulation* 1993;**87**(Suppl 1):1–16.

22 Wagner HR, Ellison RC, Keane JF, *et al*. Clinical course in aortic stenosis. *Circulation* 1977;**56**:147–56.

23 Cohen LS, Friedman WF, Braunwald E. Natural history of mild congenital aortic stenosis elucidated by serial hemodynamic studies. *Am J Cardiol* 1972;**30**:1–5.

24 Hastreiter AR, Oshima, Miller RA. Congenital aortic stenosis syndrome in infancy. *Circulation* 1963;28:1084–95.

25 Driscoll DJ, Wolfe RR, Gersony WM, *et al*. Cardiorespiratory responses to exercise of patients with aortic stenosis, pulmonary stenosis and ventricular septal defect. *Circulation* 1993;**87** (Suppl I)I-102–13.

26 James FW, Schwartz DC, Kaplan S, *et al*. Exercise electrocardiogram, blood pressure, and working capacity in young patients with valvular or discrete subvalvular aortic stenosis. *Am J Cardiol* 1982;**50**:769–75.

27 Hatle L, Angelsen BA, Tromsdal A. Non-invasive assessment of aortic stenosis by Doppler ultrasound. *Br Heart J* 1980;**43**: 284–92.

28 Krabill KA, Ring WS, Foker JE, *et al*. Echocardiographic versus cardiac catheterization diagnosis of infants with congenital heart disease requiring cardiac surgery. *Am J Cardiol* 1987;**60**:351–4.

29 Beekman RH, Rocchini AP, Gillon JH, *et al*. Hemodynamic determinants of the peak systolic left ventricular–aortic pressure gradient in children with valvar aortic stenosis. *Am J Cardiol* 1992;**69**:813–5.

30 Bengur AR, Snider AR, Serwer GA, *et al*. Usefulness of the Doppler mean gradient in evaluation of children with aortic valve stenosis and comparison to gradient at catheterization. *Am J Cardiol* 1989;**64**:756–61.

31 Lima CO, Sahn DJ, Valdes-Cruz LM, *et al*. Prediction of the severity of left ventricular outflow tract obstruction by quantitative two-dimensional echocardiographic Doppler studies. *Circulation* 1983;**68**:348–54.

32 Skjaerpe T, Hegrenaes L, Hatle L. Noninvasive estimation of valve area in patients with aortic stenosis by Doppler ultrasound and two-dimensional echocardiography. *Circulation* 1985;**72**: 810–8.

33 Beekman RH, Rocchini AP, Gillon JH, *et al*. Hemodynamic determinants of the peak systolic left ventricular–aortic pressure gradient in children with valvar aortic stenosis. *Am J Cardiol* 1992;**69**:813–5.

34 Eichenberger AC, Jenni R, von Schulthess GK. Aortic valve pressure gradients in patients with aortic valve stenosis: quantitation with velocity encoded cine MR imaging. *AJR Am J Roentgenol* 1993;**160**:971–7.

35 Ubago JL, Figueroa A, Colman T, *et al*. Hemodynamic factors that affect calculated orifice areas in the mitral Hancock xenograft valve. *Circulation* 1980;**61**:388–94.

36 Bache RJ, Wang Y, Jorgensen CR. Hemodynamic effects of exercise in isolated valvular aortic stenosis. *Circulation* 1971;**44**:1003–13.

37 Richter HS. Mitral valve area: measurement soon after catheterization. *Circulation* 1963;**28**:451–4.

38 Cannon SR, Richards KL, Crawford M. Hydraulic estimation of stenotic orifice area: a correction of the Gorlin formula. *Circulation* 1985;**71**:1170–8.

39 Hunt D, Baxley WA, Kennedy JW, *et al*. Quantitative evaluation of cineaortography in the assessment of aortic regurgitation. *Am J Cardiol* 1973;**31**:696–700.

40 Otto CM, Pearlman AS, Comess KA, *et al*. Determination of the stenotic aortic valve area in adults using Doppler echocardiography. *J Am Coll Cardiol* 1986;**7**:509–17.

41 Currie PJ, Hagler DJ, Seward JB, *et al*. Instantaneous pressure gradient: a simultaneous Doppler and dual catheter correlative study. *J Am Coll Cardiol* 1986;**7**:800–6.

42 Yeager M, Yock PG, Popp RL. Comparison of Doppler-derived pressure gradient to that determined at cardiac catheterization in adults with aortic valve stenosis: implications for management. *Am J Cardiol* 1986;**57**:644–8.

43 Richey R, Wray D, Stokes T, Guideline Development Group. Prophylaxis against infective endocarditis: summary of NICE guidelines. *BMJ* 2008;**336**:770–1.

44 Kohl T, Sharland G, Allan LD, *et al*. World experience of percutaneous ultrasound-guided balloon valvuloplasty in human fetuses with severe aortic valve obstruction. *Am J Cardiol* 2000;**85**: 1230–3.

45 Wilkins-Haug LE, Tworetzky W, Benson CB, *et al*. Factors affecting technical success of fetal aortic valve dilation. *Ultrasound Obstet Gynecol* 2006;**28**:47–52.

46 McElhinney DB, Marshall AC, Wilkins-Haug LE, *et al*. Predictors of technical success and postnatal biventricular outcome after *in-utero* aortic valvuloplasty for aortic stenosis with evolving hypoplastic left heart syndrome. *Circulation* 2009;**120**: 1482–90.

47 Mocellin R, Sauer U, Simon B, *et al*. Reduced left ventricular size and endocardial fibroelastosis as correlates of mortality in newborns and young infants with severe aortic valve stenosis. *Pediatr Cardiol* 1983;**4**:265–72.

48 Pelech AN, Dyck JD, Trusler GA, *et al*. Critical aortic stenosis. Survival and management. *J Thorac Cardiovasc Surg* 1987;**94**: 510–7.

49 Parsons MK, Moreau GA, Graham TP Jr, *et al*. Echocardiographic estimation of critical left ventricular size in infants with isolated aortic valve stenosis. *J Am Coll Cardiol* 1991;**18**:1049–55.

50 Rhodes LA, Colan SD, Perry SB, *et al*. Predictors of survival in neonates with critical aortic stenosis. *Circulation* 1991;**84**: 2325–35.

51 Colan SD, McElhinney DB, Crawford EC, *et al*. Validation and re-evaluation of a discriminant model predicting anatomic suitability for a biventricular repair in neonates with aortic valve stenosis. *J Am Coll Cardiol* 2006;**47**:1858–65.

52 Agnoletti G, Raisky O, Boudjemline Y, *et al*. Neonatal surgical aortic commissurotomy: predictors of outcome and long-term results. *Ann Thorac Surg* 2006;**82**:1585–92.

53 Duncan K, Sullivan I, Robinson P, *et al*. Transventricular aortic valvotomy for critical aortic stenosis in infants. *J Thorac Cardiovasc Surg* 1987;**93**:546–50.

54 Kugler JD, Campbell E, Vargo TA, *et al*. Results of aortic valvotomy in infants with isolated aortic valvular stenosis. *J Thorac Cardiovasc Surg* 1987;**78**:553–8.

55 Leung MP, McKay R, Smith A, *et al*. Critical aortic stenosis in early infancy. Anatomic and echocardiographic substrates of successful open valvotomy. *J Thorac Cardiovasc Surg* 1991;**101**: 526–35.

56 Burch M, Redington AN, Carvalho JS, *et al*. Open valvotomy for critical aortic stenosis in infancy. *Br Heart J* 1990;**63**:37–40.

57 Gildein HP, Kleinert S, Weintraub RG, *et al*. Surgical commissurotomy of the aortic valve: outcome of open valvotomy in neonates with critical aortic stenosis. *Am Heart J* 1996;**131**: 754–9.

58 Karl TR, Sano S, Brawn WJ, *et al*. Critical aortic stenosis in the first month of life: surgical results in 26 infants. *Ann Thorac Surg* 1990;**50**:105–9.

59 Bhabra MS, Dhillon R, Bhudia S, *et al*. Surgical aortic valvotomy in infancy: impact of leaflet morphology on long-term outcomes. *Ann Thorac Surg* 2003;**76**:1412–6.

60 Burch M, Kaufman L, Archer N, *et al*. Persistent pulmonary hypertension late after neonatal aortic valvotomy: a consequence of an expanded surgical cohort. *Heart* 2004;**90**:918–20.

61 Meliones JN, Beekman RH, Rocchini AP, *et al*. Balloon valvuloplasty for recurrent aortic stenosis after surgical valvotomy in childhood: immediate and follow-up studies. *J Am Coll Cardiol* 1989;**13**:1106–10.

62 Sullivan ID, Wren C, Bain H, *et al*. Balloon dilatation of the aortic valve for congenital aortic valve stenosis in childhood. *Br Heart J* 1989;**61**:186–91.

64 Magee AG, Nykanen D, McCrindle BW, *et al*. Balloon dilation of severe aortic valve stenosis in the neonate comparison of antegrade and retrograde catheter approaches. *J Am Coll Cardiol* 1997;**30**:1061–6.

65 McCrindle BW, Blackstone EH, Williams WG, *et al*. Are outcomes of surgical versus transcatheter balloon valvotomy equivalent in neonatal critical aortic stenosis? *Circulation* 2001;**104**: I152–8.

66 Kuhn MA, Latson LA, Cheatham JP, *et al*. Management of pediatric patients with isolated valvar aortic stenosis by balloon aortic valvuloplasty. *Cathet Cardiovasc Diagn* 1996;**39**:55–61.

67 Rocchini AP, Beekman RH, Ben Shachar G, *et al*. Balloon aortic valvuloplasty: results of the Valvoplasty and Angioplasty of Congenital Anomalies Registry. *Am J Cardiol* 1990;**65**:784–9.

68 Ewert P, Bertram H, Breuer J, *et al*. Balloon valvuloplasty in the treatment of congenital aortic valve stenosis – a retrospective multicenter survey of more than 1000 patients. *Int J Cardiol* 2010;Epub ahead of print.

69 McCrindle BW. Independent predictors of immediate results of percutaneous balloon aortic valvotomy in children: Valvuloplasty and Angioplasty of Congenital Anomalies Registry (VACA) Investigators. *Am J Cardiol* 1996;**77**:286–93.

70 Reich O, Tax P, Marek J, *et al*. Long-term results of percutaneous balloon valvuloplasty of congenital aortic stenosis: independent predictors of outcome. *Heart* 2004;**90**:70–6.

71 Carminati M, Giusti S, Spadoni I, *et al*. Balloon aortic valvuloplasty in the first year of life. *J Interv Cardiol* 1995;**8**:759–66.

72 McElhinney DB, Lock JE, Keane JF, *et al*. Left heart growth, function and reintervention after balloon aortic valvuloplasty for neonatal aortic stenosis. *Circulation* 2005;**111**:451–8.

73 De Giovanni JV, Edgar RA, Cranston A. Adenosine induced transient cardiac standstill in catheter interventional procedures for congenital heart disease. *Heart* 1998;**80**:330–3.

74 Mehta C, Desai T, Shebani S, *et al*. Rapid ventricular pacing for catheter interventions in congenital aortic stenosis and coarctation: effectiveness, safety, and rate titration for optimal results. *J Interv Cardiol* 2010;**23**:7–13.

75 Sholler GF, Keane JF, Perry SB, *et al*. Balloon dilation of congenital aortic valve stenosis. Results and influence of technical and morphological features on outcome. *Circulation* 1988;**78**:351–60.

76 Lababidi Z, Wu JR, Walls JT. Percutaneous balloon aortic valvuloplasty: results in 23 patients. *Am J Cardiol* 1984;**53**:194–7.

77 Yamen E, Daniels DV, Van H, *et al*. Use of a low-profile, compliant balloon for percutaneous aortic valvuloplasty. *Catheter Cardiovasc Interv* 2010;**75**:794–8.

78 Cowley CG, Dietrich M, Mosca RS, *et al*. Balloon valvuloplasty versus transventricular dilation for neonatal critical aortic stenosis. *Am J Cardiol* 2001;**87**:I125–7, A10.

79 Keane JF, Bernhard WF, Nadas AS. Aortic stenosis surgery in infancy. *Circulation* 1975;**52**:1138–43.

80 Keane JF, Driscoll DJ, Gersony WM, *et al*. Second natural history study of congenital heart defects. Results of treatment of patients with aortic valvar stenosis. *Circulation* 1993;**87**(Suppl 1):1–16.

81 Elkins RC, Thompson DM, Lane MM, *et al*. Ross operation: 16-year experience. *J Thorac Cardiovasc Surg* 2008;**136**:623–30.

82 Sievers HH, Hanke T, Stierle U, *et al*. A critical reappraisal of the Ross operation: renaissance of the subcoronary implantation technique? *Circulation* 2008;**114**(1 Suppl):I504–11.

83 Solymar L, Sudow G, Holmgren D. Increase in size of the pulmonary autograft after the Ross operation in children: growth or dilation? *J Thorac Cardiovasc Surg* 2000;**119**:4–9.

84 Pasquali SK, Cohen MS, Shera D, *et al*. The relationship between neo-aortic root dilation, insufficiency, and reintervention following the Ross procedure in infants, children and young adults. *J Am Coll Cardiol* 2007;**49**:1806–12.

85 Luciani GB, Favaro A, Casali G, *et al*. Ross operation in the young: a ten year experience. *Ann Thorac Surg* 2005;**80**:2271–7.

86 Alsoufi B, Manlhiot C, Fadel B, *et al*. The Ross procedure in children: preoperative haemodynamic manifestation has signi-

ficant effect on late autograft re-operation. *Eur J Cardiothorac Surg* 2010;**38**: 547–55.

87 Sandhu SK, Silka MJ, Reller MD. Balloon aortic valvuloplasty for aortic stenosis in neonates, children and young adults. *J Interv Cardiol* 1995;**8**:477–86.

88 Knirsch W, Berger F, Harpes P, *et al*. Balloon valvuloplasty of aortic valve stenosis in childhood: early and medium term results. *Clin Res Cardiol*. 2008;**97**:587–93.

89 Kirklin JW, Barratt-Boyes BG. Congenital aortic stenosis. In: Kirklin JW, Barratt-Boyes BG, eds. *Cardiac Surgery*, 2nd edn. New York: Churchill Livingstone, 1993: 1195–237.

90 Layland JJ, Bell B, Mullany D, *et al*. Percutaneous management of aortic stenosis in high-risk patients. *Med J Aust* 2010; **192**:520–5.

91 Avanzas P, Muñoz-García AJ, Segura J, *et al*. Percutaneous implantation of the CoreValve self-expanding aortic valve prosthesis in patients with severe aortic stenosis: early experience in Spain. *Rev Esp Cardiol* 2010;**63**:141–8.

92 Baan J, Yong ZY, Koch KT. Percutaneous implantation of the CoreValve aortic valve prosthesis in patients at high risk or rejected for surgical valve replacement: clinical evaluation and feasibility of the procedure in the first 30 patients in the AMC-UvA. *Neth Heart J* 2010;**18**:18–24.

93 Silverman NH, Gerlis LM, Ho SY, *et al*. Fibrous obstruction within the left ventricular outflow tract associated with ventricular septal defect: a pathologic study. *J Am Coll Cardiol* 1995;**25**:475–81.

94 Marasini M, Zannini L, Ussia GP, *et al*. Discrete subaortic stenosis: incidence, morphology and surgical impact of associated subaortic anomalies. *Ann Thorac Surg* 2003;**75**:1763–8.

95 Reeder GS, Danielson GK, Seward JB, *et al*. Fixed subaortic stenosis in atrioventricular canal defect: a Doppler echocardiographic study. *J Am Coll Cardiol* 1992;**20**:386–94.

96 Taylor NC, Somerville J. Fixed subaortic stenosis after repair of ostium primum defects. *Br Heart J* 1981;**45**:689–97.

97 Richardson ME, Menahem S, Wilkinson JL. Familial fixed subaortic stenosis. *Int J Cardiol* 1991;**30**:351–3.

98. Fatimi SH, Ahmad U, Javed MA, *et al*. Familial membranous subaortic stenosis: review of familial inheritance patterns and a case report. *J Thorac Cardiovasc Surg* 2006;**132**:1484–6.

99 Shone JD, Sellers RD, Anderson RC, *et al*. The developmental complex of "parachute mitral valve," supravalvular ring of left atrium, subaortic stenosis, and coarctation of aorta. *Am J Cardiol* 1963;**11**:714–25.

100 Gersony WM. Natural history of subvalvar aortic stenosis: management implications. *J Am Coll Cardiol* 2001;**38**:843–5.

101 Sung C, Price EC, Cooley DA. Discrete subaortic stenosis in adults. *Am J Cardiol* 1978;**42**:283–90.

102 McMahon CJ, Gauvreau K, Edwards JC, *et al*. Risk factors for aortic valve dysfunction in children with discrete subvalvar aortic stenosis. *Am J Cardiol* 2004;**94**:459–64.

103 Kelly DT, Wulfsberg E, Rowe RD. Discrete subaortic stenosis. *Circulation* 1972;**46**:309–22.

104 Feigl A, Feigl D, Lucas RV Jr, Edwards JE. Involvement of the aortic valve cusps in discrete subaortic stenosis. *Pediatr Cardiol* 1984;**5**:185–9.

105 Yagel S, Weissman A, Rotstein Z, *et al*. Congenital heart defects: natural course and *in utero* development. *Circulation* 1997; **96**:550–5.

106 Rosenquist GC, Clark EB, McAllister HA, *et al*. Increased mitral–aortic separation in discrete subaortic stenosis. *Circulation* 1979;**60**:70–4.

107 Kleinert S, Geva T. Echocardiographic morphometry and geometry of the left ventricular outflow tract in fixed aortic stenosis. *J Am Coll Cardiol* 1993;**22**:1501–8.

108 Gewillig M, Daenen W, Dumoulin M, *et al*. Rheologic genesis of discrete subvalvular aortic stenosis: a Doppler echocardiographic study. *J Am Coll Cardiol* 1992;**19**:818–24.

109 Leichter DA, Sullivan I, Gersony WM. "Acquired" discrete subvalvar aortic stenosis: natural history and hemodynamics. *J Am Coll Cardiol* 1989;**14**:1539–44.

110 Choi J, Sullivan ID. Fixed subaortic stenosis: anatomical spectrum and nature of progression. *Br Heart J* 1991;**65**:280–6.

111 Oliver JM, Gonzalez A, Gallego P, *et al*. Discrete subaortic stenosis in adults: increased prevalence and slow rate of progression of the obstruction and aortic regurgitation. *J Am Coll Cardiol* 2001;**38**:835–42.

112 Frommelt MA, Snider AR, Bove EL, *et al*. Echocardiographic assessment of sub-valvular aortic stenosis before and after operation. *J Am Coll Cardiol* 1992;**19**:1018–23.

113 de Vries AG, Hess J, Witsenburg M, *et al*. Management of fixed subaortic stenosis: a retrospective study of 57 cases. *J Am Coll Cardiol* 1992;**19**:1013–7.

114 Freedom RM, Pelech A, Brand A, *et al*. The progressive nature of subaortic stenosis in congenital heart disease. *Int J Cardiol* 1985;**8**:137–48.

115 Baumstark A, Fellows KE, Rosenthal A. Combined double chamber right ventricle and subaortic stenosis. *Circulation* 1978;**57**:299–303.

116 Tribouilloy CM, Enriquez-Sarano M, Bailey KR, *et al*. Assessment of severity of aortic regurgitation using the width of the vena contracta: a clinical color Doppler imaging study. *Circulation* 2000;**102**:558–64.

117 Shiota T, Jones M, Agler DA, *et al*. New echocardiographic windows for quantitative determination of aortic regurgitation volume using color Doppler flow convergence and vena contracta. *Am J Cardiol* 1999;**83**:1064–8.

118 Tani LY, Minich LL, Day RW, *et al*. Doppler evaluation of aortic regurgitation in children. *Am J Cardiol* 1997;**80**:927–31.

119 Movsowitz C, Jacobs LE, Eisenberg S, *et al*. Discrete subaortic valvular stenosis: the clinical utility and limitations of transesophageal echocardiography. *Echocardiography* 1993; **10**:485–7.

120 Lababidi Z, Weinhaus L, Stoeckle H, *et al*. Transluminal balloon dilatation for discrete subaortic stenosis. *Am J Cardiol* 1987; **59**:423–5.

121 Rohlicek CV, del Pino SF, Hosking M, *et al*. Natural history and surgical outcomes for isolated discrete subaortic stenosis in children. *Heart* 1999;**82**:708–13.

122 Lupinetti FM, Pridjian AK, Callow LB, *et al*. Optimum treatment of discrete subaortic stenosis. *Ann Thorac Surg* 1992; **54**:467–70.

123 Parry AJ, Kovalchin JP, Suda K, *et al*. Resection of subaortic stenosis; can a more aggressive approach be justified? *Eur J Cardiothorac Surg* 1999;**15**:631–8.

124 Rayburn ST, Netherland DE, Heath BJ. Discrete membranous subaortic stenosis: improved results after resection and myectomy. *Ann Thorac Surg* 1997;**64**:105–9.

125 Geva A, McMahon CJ, Gauvreau K, *et al*. Risk factors for reoperation after repair of discrete subaortic stenosis in children. *J Am Coll Cardiol* 2007;**50**:1498–504.

126 Hirata Y, Chen JM, Quaegebeur JM, *et al*. The role of enucleation with or without septal myectomy for discrete subaortic stenosis. *J Thorac Cardiovasc Surg* 2009;**137**:1168–72.

127 Dodge-Khatami A, Schmid M, Rousson V, *et al*. Risk factors for reoperation after relief of congenital subaortic stenosis. *Eur J Cardiothorac Surg* 2008;**33**:885–9.

128 Brauner R, Laks H, Drinkwater DC Jr, *et al*. Benefits of early surgical repair in fixed subaortic stenosis. *J Am Coll Cardiol* 1997;**30**:1835–42.

129 Shem-Tov A, Schneewiess A, Motro M, *et al*. Clinical presentation and natural history of mild discrete subaortic stenosis. *Circulation* 1982;**66**:509–12.

130 Wright GB, Keane JF, Nadas AS, *et al*. Fixed subaortic stenosis in the young: medical and surgical course in 83 patients. *Am J Cardiol* 1983;**52**:830–5.

131 Coleman DM, Smallhorn JF, McCrindle BW, *et al*. Postoperative follow-up of fibromuscular subaortic stenosis. *J Am Coll Cardiol* 1994;**24**:1558–64.

132 Bezold LI, Smith EO, Kelly K, *et al*. Development and validation of an echocardiographic model for predicting progression to of discrete subaortic stenosis in children. *Am J Cardiol* 1998;**81**:314–20.

133 Jahangiri M, Nicholson IA, del Nido PJ, *et al*.Surgical management of complex and tunnel-like subaortic stenosis. *Eur J Cardiothorac Surg* 2000;**17**:637–42.

134 Vouhé PR, Ouaknine R, Poulain H, *et al*. Diffuse subaortic stenosis: modified Konno procedures with aortic valve preservation. *Eur J Cardiothorac Surg* 1993;**7**:132–6.

135 DeLeon SY, Ilbawi MN, Roberson DA, *et al*. Conal enlargement for diffuse subaortic stenosis. *J Thorac Cardiovasc Surg* 1991;**102**:814–20.

136 Hraska V, Krajci M, Haun C, *et al*. Ross and Ross–Konno procedure in children and adolescents: mid-term results. *Eur J Cardiothorac Surg* 2004;**25**:742–7.

137 Pasquali SK, Cohen MS, Shera D, *et al*. The relationship between neo-aortic root dilation, insufficiency, and reintervention following the Ross procedure in infants, children, and young adults. *J Am Coll Cardiol* 2007;**49**:1806–12.

138 Peterson TA, Todd DB, Edwards JE. Supravalvular aortic stenosis. *J Thorac Cardiovasc Surg* 1965;**50**:734–41.

139 Nickerson E, Greenberg F, Keating MT, *et al*. Deletions of the elastin gene at 7q11.23 occur in approximately 90% of patients with Williams syndrome. *Am J Hum Genet* 1995;**56**: 1156–61.

140 Williams JCP, Barratt-Boyes BG, Lowe JB. Supravalvular aortic stenosis. *Circulation* 1961;**24**:1311–8.

141 Zalzstein E, Moes CA, Musewe NN, *et al*. Spectrum of cardiovascular anomalies in Williams–Beuren syndrome. *Pediatr Cardiol* 1991;**12**:219–23.

142 Sharma BK, Fujiwara H, Hallman GL, *et al*. Supravalvar aortic stenosis: a 29-year review of surgical experience. *Ann Thorac Surg* 1991;**51**:1031–9.

143 van Son JA, Edwards WD, Danielson GK. Pathology of coronary arteries, myocardium, and great arteries in supravalvular aortic stenosis: report of five cases with implications for surgical treatment. *J Thorac Cardiovasc Surg* 1994;**108**:21–8.

144 Kitchiner D, Jackson M, Walsh K, *et al*. Prognosis of supravalve aortic stenosis in 81 patients in Liverpool (1960–1993). *Heart* 1996;**75**:396–402.

145 Geggel RL, Gauvreau K, Lock JE. Balloon dilation angioplasty of peripheral pulmonary stenosis associated with Williams syndrome. *Circulation* 2001;**103**:2165–70.

146 Giddins NG, Finley JP, Nanton MA, *et al*. The natural course of supravalvar aortic stenosis and peripheral pulmonary artery stenosis in Williams's syndrome. *Br Heart J* 1989;**62**:315–9.

147 Wren C, Oslizlok P, Bull C. Natural history of supravalvar aortic stenosis and pulmonary artery stenosis. *J Am Coll Cardiol* 1990;**15**:1625–30.

148 Stamm C, Friehs I, Moran AM, *et al*. Surgery for bilateral outflow tract obstruction in elastin arteriopathy. *J Thorac Cardiovasc Surg* 2006;**120**:755–63.

149 D'Orsogna L, Sandor GG, Culham JA, *et al*. Successful balloon angioplasty of peripheral pulmonary stenosis in Williams syndrome. *Am Heart J* 1987;**114**:647–8.

150 Sridharan S, Derrick G, Deanfield J, *et al*. Assessment of differential branch pulmonary blood flow: a comparative study of phase contrast magnetic resonance imaging and radionuclide lung perfusion imaging. *Heart* 2006;**92**:963–8.

151 Kaushal S, Backer CL, Patel S, *et al*. Midterm outcomes in supravalvular aortic stenosis demonstrate the superiority of multisinus aortoplasty. *Ann Thorac Surg* 2010;**89**:1371–7.

152 McElhinney DB, Petrossian E, Tworetzky W, *et al*. Issues and outcomes in the management of supravalvar aortic stenosis. *Ann Thorac Surg* 2000;**69**:562–7.

153 Hanke T, Charitos EI, Stierle U, *et al*. The Ross operation – a feasible and safe option in the setting of bicuspid aortic valve? *Eur J Cardiothorac Surg* 2010;**38**:333–9.

154 Basso C, Boschello M, Perrone C, *et al*. An echocardiographic survey of primary school children for bicuspid aortic valve. *Am J Cardiol* 2004;**93**:661–3.

155 Duran AC, Frescura C, Sans-Coma V, *et al*. Bicuspid aortic valves in hearts with other congenital heart disease. *J Heart Valve Dis* 1995;**4**:581–90.

156 Suzuki T, Nagai R, Kurihara Y, *et al*. Bicuspid aortic valve associated with a ventricular septal defect in an adult presenting with congestive heart failure: a rare observation. *Eur Heart J* 1994 **15**:402–3.

157 Aboulhosn J, Child JS. Left ventricular outflow obstruction: subaortic stenosis, bicuspid aortic valve, supravalvar aortic stenosis, and coarctation of the aorta. *Circulation* 2006;**114**:2412–22.

158 Dhoble A, Patel M, Shah I, *et al*. Cor triatriatum sinister with bicuspid aortic valve: a rare association. *Clin Cardiol* 2009;**32**:E88.

159 Mazzanti L, Cacciari E. Congenital heart disease in patients with Turner's syndrome. Italian Study Group for Turner Syndrome (ISGTS). *J Pediatr* 1998;**133**:688–92.

160 Cripe L, Andelfinger G, Martin LJ, *et al*. Bicuspid aortic valve is heritable. *J Am Coll Cardiol* 2004;**44**:138–43.

161 Garg V, Muth AN, Ransom JF, *et al*. Mutations in NOTCH1 cause aortic valve disease. *Nature* 2005;**437**:270–4.

162 Mohamed SA, Hanke T, Schuelter C, *et al*. Ubiquitin fusion degradation 1-like gene dysregulation in bicuspid aortic valve. *J Thorac Cardiovasc Surg* 2005;**130**:1531–6.

163 Guo DC, Pannu H, Tran-Fadulu V, *et al*. Mutations in smooth muscle alpha-actin (ACTA2) lead to thoracic aortic aneurysms and dissections. *Nat Genet* 2007;**39**:1488–93.

164 Lee TC, Zhao YD, Courtman DW, *et al*. Abnormal aortic valve development in mice lacking endothelial nitric oxide synthase. *Circulation* 2000;**101**:2345–8.

165 Sievers HH, Schmidtke C. A classification system for the bicuspid aortic valve from 304 surgical specimens. *J Thorac Cardiovasc Surg* 2007;**133**:1226–33.

166 Fernandes SM, Khairy P, Sanders S, *et al*. Bicuspid aortic valve morphology and interventions in the young. *J Am Coll Cardiol* 2007;**49**:2211–4.

167 Bonderman D, Gharehbaghi-Schnell E, Wollenek G, *et al*. Mechanisms underlying aortic dilatation in congenital aortic valve malformation. *Circulation* 1999;**99**:2138–43.

168 Fedak PWM, de Sa MPL, Verma S, *et al*. Vascular matrix remodeling in patients with bicuspid aortic valve malformations: implications for aortic dilatation. *J Thorac Cardiovasc Surg* 2003;**126**:797–805.

169 Osler W. The bicuspid condition of the aortic valves. *Trans Assoc Am Physicians* 1886;**1**:185–92.

170 Koletsky S. Congenital bicuspid aortic valve. *Arch Int Med* 1941;**67**:129–56.

171 Lewis T, Grant RT. Observations relating to subacute infective endocarditis. *Heart* 1923;**10**:21–99.

172 Larson EW, Edwards WD. Risk factors for aortic dissection: a necropsy study of 161 cases. *Am J Cardiol* 1984;**53**:849–55.

173 Pachulski RT, Chan KL. Progression of aortic valve dysfunction in 51 adult patients with congenital bicuspid aortic valve: assessment and follow-up by Doppler echocardiography. *Br Heart J* 1993;**69**:237–40.

174 Anderson MW. The clinical course of patients with calcific aortic stenosis. *Proc Staff Meet Mayo Clin* 1961;**36**:439–44.

175 Della Corte A, Bancone C, Quatro C, *et al*. Predictors of ascending aorta dilatation with bicuspid aortic valve: a wide spectrum of disease expression. *Eur J Cardiothorac Surg* 2007;**31**:397–404.

176 Holmes KW, Lehmann CU, Dalal D, *et al*. Progressive dilation of the ascending aorta in children with isolated bicuspid aortic valve. *Am J Cardiol* 2007;**99**:978–83.

177 Elefteriades JA. Natural history of thoracic aortic aneurysms: indications for surgery, and surgery versus nonsurgical risks. *Ann Thorac Surg* 2002;**74**:S1877–80.

178 Bonow RO, Carabello BA, Chatterjee K, *et al*. ACC/AHA 2006 guidelines for the management of patients with valvular heart disease. *J Am Coll Cardiol* 2006;**48**:e1–148.

179 Rossebo AB, Pedersen TR, Boman K, *et al*. Intensive lipid lowering with simvastatin and ezetimibe in aortic stenosis. *N Engl J Med* 2008;**359**:1343–56.

180 Tadros TM, Klein MD, Shapira OM. Ascending aortic dilatation associated with bicuspid aortic valve. *Circulation* 2009;**119**:880–90.

181 Hartnell GG. Imaging of aortic aneurysms and dissection: CT and MRI *J Thorac Imaging* 2001;**16**:35–46.

182 Woodard PK, Bhalla S, Javidan-Nejad C, *et al*. Non-coronary cardiac CT imaging. *Semin Ultrasound CT MR* 2006;**27**:56–75.

183 Boodhwani M, de Kerchove L, Glineur D, *et al*. Repair of regurgitant bicuspid aortic valves: a systematic approach. *J Thorac Cardiovasc Surg* 2010;**140**:276–84, e271.

184 McClure RS, Narayanasamy N, Wiegerinck E, *et al*. Late outcomes for aortic valve replacement with the Carpentier–Edwards pericardial bioprosthesis: up to 17-year follow-up in 1,000 patients. *Ann Thorac Surg* 2010;**89**:1410–6.

185 Tribouilloy C, Rusinaru D, Sorel C, *et al*. Clinical characteristics and outcome of infective endocarditis in adults with bicuspid aortic valves: a multicentre observational study. *Heart* 2010; **96**:1723–9.

31 Left Ventricular Outflow Regurgitation and Aortoventricular Tunnel

Vijaya Joshi[1] & Roxane McKay[2]
[1]University of Tennessee Health Science Center, Memphis, TN, USA
[2]Rochester, MN, USA

Introduction

In hearts with concordant ventriculoarterial connections, the left ventricular outflow extends from the area of fibrous continuity between aortic and mitral valves to the sinutubular junction between the ascending aorta and sinuses of Valsalva [1]. It thus encompasses portions of the left ventricular free wall, the muscular and membranous interventricular septums, the aortic valvar leaflets, arterial wall of the aortic sinuses, and the ostia of the coronary arteries. Although "left ventricular outflow obstruction" (see Chapter 30) is widely used to describe a variety of anomalies that impede blood flow through any portion of this area, from the left ventricle into the systemic circulation, its hemodynamic opposite, "left ventricular outflow regurgitation," is a less familiar concept. These are lesions which place a volume overload on the left ventricle, independent of a shunt, and cause the systemic blood pressure to approximate that in the left ventricle during diastole. The morphologic substrates for left ventricular outflow regurgitation include aortic, neo-aortic, and prosthetic valve disease, left ventricular aortoventricular tunnel, sinus of Valsalva fistula to the left ventricle (see Chapter 25), and coronary arterial fistula to the left ventricle (see Chapter 48). Although this chapter addresses only the first two and is limited to normally connected hearts, obstruction and regurgitation may also affect the left ventricular outflow of hearts with discordant, solitary or double-outlet ventriculoarterial connections.

Incidence

Regurgitant lesions of the left ventricular outflow tract are rare in children, yet encompass a wide spectrum of congenital and acquired pathology. They may be conveniently divided into those affecting primarily the valvar leaflets (Table 31.1) and those in which regurgitation results from disease of the supporting vascular wall, with or without leaflet involvement (Table 31.2).

Because it is the commonest congenital heart defect, affecting ~1% of the population, a two-leaflet aortic valve is probably the most common cause of aortic regurgitation. However, in the absence of balloon valvoplasty, only about 7% of children with a bicuspid valve develop aortic regurgitation of at least moderate severity [2], and this generally presents with some degree of obstruction after about 8 years of age. In infancy, the most common cause of left ventricular outflow regurgitation is aortoventricular tunnel [3].

Embryology

The leaflets and sinuses of the aortic valve derive from two embryologic components of the developing proximal outflow tract [4]: the septal endocardial cushion, with an ephemeral neural crest contribution, gives rise to the right and left coronary aortic sinuses and leaflets, while the noncoronary leaflet and sinus are formed from the rightward, inferior (aortic) intercalated cushion or "disc." Before this time, approximately Carnegie stages 18–20 in the human embryo, the septal and parietal cushions have fused progressively from the distal to the proximal outflow tract, dividing it into aortic and pulmonary trunks, with the so-called "dog-leg bend" indicating the ultimate site of sinutubular junctions. By mechanisms not yet fully understood but possibly related to changes in the extracellular matrix, myocardium that surrounds the developing valvar sinuses then regresses, leaving the right ventricular outflow supported by a free-standing muscular infundibulum, and the left communicating with the

Table 31.1 Valvar causes of aortic regurgitation and their genetic or immunologic associations[a].

Condition		Incidence	Association	Ref.
Congenital valvar malformations	One leaflet			
	Two leaflets	1% of population	NOTCH1	26,27
	Four leaflets	<0.008% at autopsy		28
	Five leaflets	3 reported patients		29
Trauma	Blunt chest injury			30
	Balloon valvoplasty			
	Atrial septal defect occluder	~1%		31
Metabolic storage disease	Gaucher disease type 3		D409H	32
	Mucopolysaccharide disorders			33
Nonsyndromic myxomatous valve dystrophy			Xq28	34
Skeletal dysplasia	Omani-type spondyloepiphyseal dysplasia		CHST3	35
Secondary to other cardiac malformations	Ventricular septal defect			
	Subaortic stenosis			
	Common arterial trunk			
	Aorto-left ventricular tunnel			
Inflammation	Rheumatic fever	10% of children with acute rheumatic fever		36
	Systemic lupus erythematosus	~13% of children with SLE		37
Infection	Endocarditis			
Postoperative	TGA – arterial switch operation	10–50%		38,39
	Damus–Kaye–Stansel procedure	~5%		40
	Ross operation (pulmonary autograft)	10–30%		41
Parental consanguinity				42
Drugs	Ecstasy			43
	Ergot alkaloids, serotonin uptake inhibitors, and ergot-derived dopamine agonists			44

[a]TGA, transposition of the great arteries; SLE, systemic lupus erythematosus.

extracardiac space. Coronary arteries grow through this muscular cuff before its disappearance, into what become the left and right aortic sinuses, when the leaflets and sinuses finally assume their respective tissue types.

The commonest type of bileaflet (or bicuspid) aortic valve is that in which the right and left coronary leaflets are fused, with both coronary arteries arising from the conjoined R–L sinus. This morphology is associated most often with coarctation of the aorta and aneurysms of the ascending aorta. In contrast, valves with fusion of the right and noncoronary aortic leaflets retain a coronary orifice in each sinus and tend to have more rapidly progressive stenosis and regurgitation. Observations in hamsters and mice [5] suggest that the former result from abnormal fusion of the septal cushions (or their contributions from the neural crest or second heart field), whereas the latter are produced by fusion of the septal cushion with an intercalated disc. Interestingly, fusion of the left and noncoronary aortic leaflets is exceedingly rare, and it is this commissure with its interleaflet triangle

that is virtually always conserved in the neonatal "unicusp" aortic valve [6]. Aorto-left ventricular tunnels are found in the tissue plane between the definitive aortic and pulmonary trunks, nearly always lie above the right or left aortic sinus, sometimes involve coronary arterial ostia, may be associated with bicuspid aortic or pulmonary valves, and usually communicate with the ventricle through the fibrous interleaflet triangle between left and right aortic leaflets, all of which support speculation that they too represent malformations of septal cushions, perhaps at an earlier stage of development [3].

Aortic regurgitation

Pathologic anatomy
Regurgitation through the aortic valve occurs whenever there is loss of coaptation between the leaflet free edges or a defect within the body of a leaflet. With inflammatory

Table 31.2 Vascular causes of aortic regurgitation.

Condition		Incidence	Association[a]	Ref.
Connective tissue disorders	Marfan syndrome		FBN1	45
	Loeys–Dietz syndromes		TGFBR1 or TGFBR2	46
	Ehlers–Danlos syndrome type IV		COL3A1	47,48
	Osteogenesis imperfecta	12% of affected patients		49
Vasculitis/inflammatory	Wiskott–Aldrich syndrome	4 per million live male births	X p11.22	50,51
	Takayasu's arteritis			52,53
	Behçet disease[b]			54
	Ankylosing spondylitis[b]/juvenile spondyloarthropathy[b]	8–10% of patients with B27-JA	HLA B-27	55,56
Drugs	Cocaine	25–36% of patients with dissection related to cocaine		57

[a]Association refers to genetic or molecular associations.
[b]Also affects leaflet tissue.

processes, such as rheumatic fever or autoimmune diseases, the leaflets become thickened with subsequent scarring that shortens their body and retracts the now bulky, rolled free edges from each other. This contrasts with regurgitation resulting from aneurysmal expansion of the aortic root, where, initially at least, normal, thin leaflets are stretched across an enlarged outflow, allowing central regurgitation.

In patients with ventricular septal defect and aortic regurgitation, one leaflet of the valve (usually the right coronary cusp) is poorly supported and "sucked" down into the defect by a Venturi effect, usually with elongation of the body of the cusp. Enlargement of the leaflet conserves coaptation, but eventually the prolapsed leaflet becomes thickened and retracted, resulting in valvar regurgitation. Subaortic stenosis may cause aortic regurgitation by two mechanisms: acceleration of an eccentric jet of blood through the fibrous ring damages the ventricular surface of the valve or, less frequently, the membrane extends up onto the ventricular aspect of a leaflet and restricts its mobility.

Congenitally malformed valves, generally with two leaflets, may have shortening of the leaflet free edge relative to the valve circumference. This results from abbreviated interleaflet triangles [6] and leaves insufficient tissue for effective coaptation. Alternatively, the conjoined leaflet, when larger and lacking in support by a normal interleaflet triangle, may prolapse into the ventricle and fail to oppose its opposite number. If the "raphe" of the fused leaflet is anchored to the wall of the aortic sinus by a thread of fibrous tissue, rupture of this structure allows sudden leaflet prolapse and produces acute regurgitation in a previously competent bicuspid valve.

Discrete holes in a leaflet are usually produced by infection, but are sometimes due to a wayward suture during ventricular septal defect closure, damage during surgical enlargement of a ventricular septal defect or resection of subaortic stenosis, and inappropriate resection of infundibular muscle during repair of tetralogy of Fallot. These latter complications tend to occur near the leaflet hinge points. In regurgitation following balloon valvoplasty or blunt chest trauma, it is usually the mid-portion of a leaflet that is ruptured completely from free edge to hinge point.

In all of the above, regurgitation through the valve causes turbulence and shear stress, producing further distortion of the leaflet tissue, which progressively intensifies valvar dysfunction.

Pathophysiology

Chronic aortic regurgitation subjects the left ventricle simultaneously to increased preload from the regurgitant volume, and to increased afterload from greater wall stress resulting both from increased end-diastolic volume and systolic hypertension when an enlarged stroke volume is not accommodated within the systemic vascular compliance. Early on, compensation at a molecular level by division of myocardial sarcomeres, combined with enlargement of myofibrils and myocytes, produces eccentric ventricular hypertrophy. This conserves the ratio of cavity radius-to-wall thickness and maintains normal wall stress and normal systolic function. With time, ventricular hypertrophy becomes insufficient to compensate for progressive cavity dilatation, resulting in impaired systolic function. Subsequently, elevation of end diastolic pressure transmits pressure back into the left atrium and pulmonary circulation, while reduction of coronary arterial flow occasionally compounds heart failure from aortic regurgitation with myocardial ischemia. Pathologic hypertrophy and dilatation, and also some degree of systolic dysfunction, are reversible,

however, if the left ventricular volume overload is relieved before contractility is impaired.

Acute aortic regurgitation, in contrast, subjects the left ventricle to a sudden volume overload for which the only compensatory mechanism is an increased heart rate. If inadequate to maintain cardiac output, left atrial and left ventricular end-diastolic pressures rise, leading to pulmonary edema and circulatory collapse (shock).

Systolic aortic regurgitation occurs in the rare combination of an incompetent aortic valve with a systemic blood pressure exceeding that of the left ventricle. It has been observed after the Damus–Kaye–Stansel procedure, with ventricular arrhythmias, and in patients on extracorporeal support. Although its pathologic significance is uncertain and probably variable, the phenomenon does reflect ineffective contraction of the underlying ventricle.

Natural history

Patients with acute aortic regurgitation generally become symptomatic with dyspnea and tachycardia within hours of its onset. Without intervention, the ventricle fails over several days, culminating in cardiac arrest and death. With infective endocarditis, less than one-third of patients who develop acute valvar regurgitation survive for 1 year. However, if the left ventricle was previously hypertrophied, as in balloon valvoplasty for critical aortic stenosis, acute regurgitation may be surprisingly well tolerated. Similarly, if the degree of regurgitation is not large, as in a limited cusp perforation, there may be time for ventricular adaptation to evolve to chronic aortic regurgitation.

Patients with chronic aortic regurgitation generally remain compensated with normal systolic ventricular function and no symptoms for many years or even decades. In adults [7], only ~3.5% per year experience deterioration of ventricular function in the absence of symptoms, and <6% per year develop either left ventricular dysfunction or symptoms. In contrast with obstruction of left ventricular outflow, the risk of sudden death is extremely low, <0.2% per year. The onset of impaired systolic ventricular function, however, portends clinical deterioration, with ~25% of such patients becoming symptomatic each year thereafter. Whereas >90% of patients survive 5 years after a diagnosis of *severe* aortic regurgitation, <10% are still alive at 10 years. Factors associated with death include severe left ventricular hypertrophy on the electrocardiogram, a cardiothoracic ratio of >0.6 on the chest X-ray, ventricular extrasystoles, and symptoms of heart failure.

Clinical features

Aortic regurgitation is usually associated with aortic valve stenosis, conal septal abnormalities, and ventricular septal defect. Thus, it is most commonly found during evaluation of (1) aortic root abnormalities, such as Marfan syndrome; (2) bicuspid aortic valve, often accompanied by a dilated aortic root; (3) rheumatic heart disease; or (4) endocarditis. Severe aortic regurgitation during early gestation is likely incompatible with fetal or neonatal viability [8]. In a child with a trileaflet aortic valve, rheumatic heart disease should be considered, especially with mitral valve regurgitation.

Children encountered in office practice rarely describe symptoms. The vital signs are notable for elevated systolic and decreased diastolic pressures. The patient is best examined sitting and leaning forward. On palpation, the apical impulse migrates towards the inferior lateral chest as the left ventricle enlarges. Auscultation discloses an early high-pitched diastolic decrescendo murmur along the mid-left sternal border. With increasing severity of regurgitation, the murmur becomes louder and longer, extending throughout diastole. The pulse pressure widens due to both an increased systolic stroke volume and also the retrograde diastolic runoff into the left ventricle. This abrupt upstroke and collapse are described as a "Corrigan's" or "water hammer" pulse. A high stoke volume may also produce a soft, systolic ejection murmur at the base of the heart from the increase ejection across the aortic outflow area. The Austin Flint murmur, heard at the apex as a rumbling diastolic sound, is attributed to fluttering of the mitral valve with severe regurgitation or to a posterior and laterally directed jet of regurgitation. Acute aortic regurgitation will not have these classic features if there is left ventricular decompensation, and then tachycardia and a third heart sound dominate the physical findings.

Echocardiography

Although cardiac magnetic resonance imaging (CMR) has become a standard for quantifying the severity of aortic regurgitation [9], in part because of inconsistency and lack of agreement by even experienced echocardiographers regarding the grading of moderate or severe regurgitation [10], most patients can be managed satisfactorily with echocardiography as the primary imaging tool. The left ventricular outflow tract is best assessed and measured in the parasternal long axis. The morphology of the aortic valve is scrutinized for leaflet motion, coaptation, and vegetations or leaflet perforation. A discrete subaortic membrane is seen best from the subcostal or apical projections, because this provides the most surface area for echo detection. Deformation of the right aortic sinus should raise the suspicion of an infundibular ventricular septal defect, which has been occluded by the aortic root. Diameters of the aortic valve annulus, aortic root, and the sinutubular junction are measured in early to mid-systole [11]. Although morphologically the subaortic region may be elliptical, a circle is assumed by measuring its maximum dimension. Dimensions of the left ventricle should also be quantified. Three-dimensional echocardiography can often provide excellent images of valve morphology, and also quantification of left ventricular volumes and ejection fraction. However, technical limitations still thwart its use in younger children.

Color flow Doppler localizes the region of regurgitation. The vena contracta (the smallest area of the jet of regurgitation, usually in or just below the valve plane) should be measured from at least the parasternal long- and short-axis views (Figure 31.1). It must be scrutinized from multiple projections. Continuous-wave Doppler measurement of the terminal aortic regurgitation velocity slope and the pressure half-time, useful especially for serial evaluation, are sensitive to alterations both in ventricular diastolic function and systemic vascular resistance. An increasing deceleration rate and a decreasing pressure half-time correlate with an increase in aortic regurgitation. A recently developed model employs a two-variable parasternal vena contracta-derived area divided by body surface area, and an abdominal aorta Doppler retrograde velocity–time integral divided by anterograde velocity–time integral to predict severity of regurgitation [12].

Cardiac catheterization and angiography

Cardiac catheterization and angiography are usually unnecessary in managing isolated aortic regurgitation but occasionally may be needed to document left ventricular end diastolic pressure or coronary artery anomalies. Angiography should be done with a pigtail catheter skillfully positioned in the ascending aorta, so as not to cause leaflet distortion. Long axial oblique and a companion right anterior oblique views will generally display the left ventricular outflow tract.

Other imaging modalities

If echocardiography imaging is suboptimal, CMR offers a robust alternative. Indeed, it has substantial advantages over both echocardiography and angiography for quantification of valve regurgitation, as it permits the quantification of both flow and ventricular volume. Cine CMR to image ventricular volume typically utilizes gradient recalled echo (GRE) or more commonly a steady-state free precession (SSFP). During image acquisition, the regurgitation is depicted as a dephasing intervoxel artifact retrograde into the ventricle. It is important to quantify both right and left ventricular volumes. If there is no other significant regurgitation or shunting, then left ventricular end systolic (LVESV) and diastolic volume (LVEDV) can be compared with right ventricular end systolic (RVESV) and diastolic volume (RVEDV). LV stroke volume – RV stroke volume then estimates the aortic regurgitation. Alternatively, phase contrast magnetic resonance (PCMR) maps flow velocity. The flow and velocity are measured through a slice placed immediately above the aortic root or, if possible, in the subvalvar plane. The resultant image shows the aorta as a circle. The estimated retrograde volume is divided by the prograde volume to derive a regurgitation fraction. The severity of aortic regurgitation, in adults, is arbitrarily graded by this regurgitant fraction: trivial <10%, mild 10–20%, moderate 21–39%, severe >40% [13]. A very similar scheme has been used in children [12].

Table 31.3 Grading severity of aortic regurgitation[a].

Method	Mild	Moderate	Severe
Diastolic murmur	≤Grade 1, short	Grade 2	≥Grade 2, long
Pulse pressure	Normal	↕	↕
LVEDD z score	<3	3–5	>5
Color flow Doppler central jet width	<25% of LVOT	25–64% of LVOT	≥65% of LVOT
PW Doppler descending aortic diastole flow	Brief, low velocity	Intermediate	Pandiastolic, high velocity
MR phase contrast or LV–RV SV calculation	<20%	21–39%	≥40%

[a]LVEDD, left ventricular end diastolic dimension; LVOT, left ventricular outflow tract; LV, left ventricle; RV, right ventricle; PW, pulse width; MR, magnetic resonance; SV, systolic volume.

Methods for grading aortic regurgitation are summarized in Table 31.3. However, it is always important for the physician to integrate the data from various sources into the proper context for managing an individual patient.

Management

Medical

In children with a dilated aortic root, slowing the rate of its progression would not only reduce complications and the need for surgery, but also preserve aortic valve function. Beta-blockers have disappointing efficacy in retarding root dilation in the Marfan syndrome [14], but angiotensin II blockade with, for example, losartan has demonstrated benefit in small cohorts [15].

Medical therapy for valvar aortic regurgitation should improve forward stroke volume, reduce the regurgitation, and preserve left ventricular function. There have been no large pediatric studies on this issue, however. Among 18 children with moderate-to-severe aortic regurgitation treated with angiotensin-converting enzyme (ACE) inhibitors for an average of 2.3 years, there were no significant effects on left ventricular dimensions or shortening fraction, but there was a small increase in the aortic regurgitation [16]. A study of patients treated with captopril, most of whom had rheumatic heart disease, showed favorable effects on left ventricular volume and aortic regurgitation over 1 year; but this cohort likely included subjects with spontaneous improvement [17]. The American College of Cardiology and American Heart Association Task Force report (concerned primarily with adult patients) recommends vasodilator therapy and especially noted the use of nifedipine [18]. However, in a well-designed controlled trial on adults, neither nifedipine

nor enalapril favorably changed left ventricular dimensions, aortic regurgitation volume, or timing of surgery [19]. Therefore, with normal ventricular systolic function and without root enlargement, no good evidence supports the use of any medicine.

Different types of athletic activity and physical work have varying effects on the heart. Aerobic exercise decreases systemic vascular resistance and thus decreases aortic regurgitation. High-intensity isometric work, such as power weight lifting, however, transiently increases blood pressure, systemic resistance, and therefore aortic regurgitation. This physiology mandates limitations on patients who do more than a modest amount of isometric work. Aortic root enlargement (at $z \geq 3.5$) alone warrants restriction from high intensity static work or sports with collision potential. Under medical supervision, athletes having mild or moderate aortic regurgitation *and* a left ventricle that is only mildly enlarged can participate in all competitive sports. After scrutiny of the cardiac rhythm and exercise testing, athletes with aortic regurgitation and moderate left ventricular enlargement can engage in moderate static and high dynamic competitive sports. Those with severe aortic regurgitation and more than moderate root enlargement should only participate in low-intensity sports. If there is root enlargement, greater than 45 mm (corresponding to a z value of about 5), activity should be limited to only low-intensity sports [20].

Surgical

Indications for surgery in aortic regurgitation are similar in pediatric and adult patients, although clinical judgment in children may be additionally influenced by associated cardiac or noncardiac malformations, patient size, and institutional experience. The indications are based on five parameters: symptoms, degree of aortic regurgitation, left ventricular systolic function, left ventricular dilatation, and degree of aortic dilatation. Symptoms, ventricular dysfunction (ejection fraction <50%), and ventricular enlargement (comparable to more than an adult end systolic diameter of 55 mm) each individually constitutes a class I or class IIa indication for operation. Referral for an operation is therefore an easy decision in a child with decreased physical work capacity, or symptoms from heart failure, angina, or ventricular arrhythmia.

When the degree of aortic regurgitation is severe and accompanied by either impaired systolic left ventricular function or severe left ventricular dilatation, operation is indicated even in the absence of symptoms. For regurgitation secondary to aortic root dilatation in connective tissue disorders, a diameter of 50 mm in patients with Marfan syndrome and 40 mm in those with Loeys–Deitz syndrome generally trigger surgery. This threshold may be lowered by unusually rapid progression of enlargement or a family history of complications.

As aortic regurgitation begins to increase from a mild or moderate degree, its serial quantification can provide insight and guidance for management. By echocardiography, increasing z-value for left ventricular end diastolic dimension, increasing ratio of aortic regurgitation vena contracta to left ventricular outflow tract and to body surface area, increasing retrograde flow velocity, or increasing relative descending aorta VTI ratio are used to time an operation. By magnetic resonance imaging, a regurgitant fraction of >40% leads to consideration of operation.

The goal of surgery is conservation or restoration of left ventricular function and removal of the risk of complications, but there is no perfect valve substitute with which to accomplish this. Hence all procedures on the left ventricular outflow tract should be regarded as palliative. Accordingly, valve reconstruction should be the first option, either as a valve-sparing root replacement [21] or by leaflet repair [22]. In the authors' personal, unpublished experience this proved possible in all of an unselected, consecutive series of 25 infants, children, and young adults operated for severe aortic regurgitation from a variety of causes (including two-leaflet valves). Operative and late death now approach zero, and long-term follow-up showed a 60% freedom from aortic valve replacement as long as 18 years after repair [22].

When conservation of the native valve is not possible (usually in acute endocarditis or at a reoperation), the two implants that offer a completely unobstructed, hemodynamically superior outflow are the aortic homograft and the pulmonary autograft (Ross operation). Early and late mortality for these procedures in patients with all types of aortic valve disease is ~1% today, and freedom from autograft reoperation at 15 years is 89% [23]. Moreover, the Ross procedure appears to confer a survival advantage over mechanical valve replacement (<4% versus 50% mortality), in patients <5 years of age (most of whom are operated on for aortic stenosis rather than regurgitation) [24]. Implantation of the pulmonary autograft in the subcoronary position is virtually always possible in patients with aortic regurgitation and may avoid late autograft dilatation, the commonest cause of autograft failure following the Ross operation.

Mechanical prosthetic valves, in theory and in contrast to the above, should have infinite durability and a lower rate of reoperation. Nevertheless, even when it is possible to implant an adult-sized valve, there remains a constant, late-phase risk of mortality and morbidity, from ingrowth of pannus, complications of anticoagulation, and infection [24]. Moreover, the necessity for anticoagulation places major life-style restrictions upon young patients, and when a mechanical valve fails (due to thrombosis, for example), it is often sudden and catastrophic.

A final option for larger children is a bioprosthetic prosthesis (pericardial or porcine). Although these valves have reduced durability in young patients (sometimes lasting less than 1 year and rarely >5 years) and, in smaller sizes,
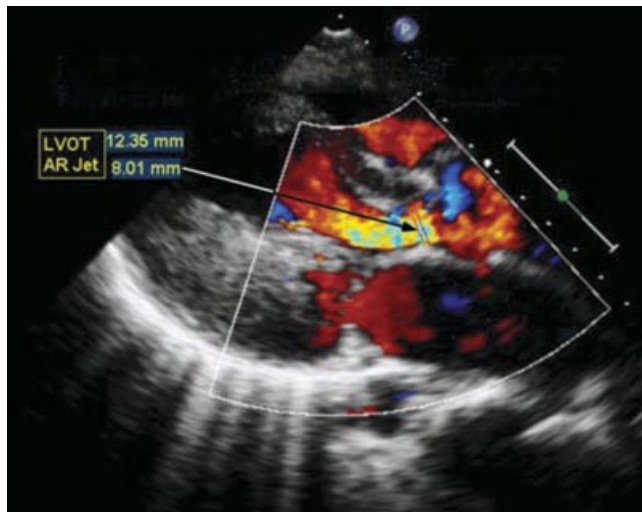
Figure 31.1 Aortic regurgitation. Color flow Doppler echocardiography of the left ventricular outflow tract in the parasternal long-axis view shows an 8 mm jet of aortic regurgitation (arrow), compared with a left ventricular outflow diameter of just over 12 mm.

may cause a significant gradient across the left ventricular outflow, they do not require anticoagulation and can be replaced with very low morbidity and mortality. As such, they may serve to transition a teenager or young adult through periods of participation in contact sports, noncompliance with drug therapy, or pregnancy, after which a mechanical prosthesis may become a more acceptable alternative.

Long-term history of treated and untreated adults

Provided they do not contract endocarditis, patients who reach adulthood with mild, stable aortic regurgitation from isolated valve disease generally enjoy a normal life span. When regurgitation is severe, however, systolic left ventricular function tends to deteriorate, usually producing symptoms, at a rate of ~5% of patients per year. Once symptomatic, deterioration accelerates to ~25% 5 year and 50% 10 year mortality among untreated adults. With heart failure, survival drops below 50% at 2 years. Restoring a competent valve improves ventricular function and prolongs life, both for patients who undergo operation as adults and those operated in childhood, although documentation of very long-term outcomes in the latter group is limited. Overall, there seems to be a constant rate of late reoperation among patients surviving into adulthood after aortic valve surgery. Depending upon a variety of factors, this ranges from ~1% to as much as 10% per year. When regurgitation is associated with other congenital heart malformations or is secondary to a systemic disease, those conditions usually determine overall clinical course and outcome.

Aortoventricular tunnel

Pathologic anatomy

Aortoventricular tunnel is a tubular, extracardiac structure connecting the ascending aorta above the sinutubular junction with the left ventricular outflow, usually through the interleaflet triangle between right and left coronary aortic valve leaflets (Figure 31.2) [3,58]. The most common variant of this rare anomaly lies above the right aortic sinus and passes through the tissue space between the aortic root and subpulmonary muscular infundibulum to reach the cavity of the left ventricle immediately below the hinge point of the aortic valve. Massive, diffuse enlargement of the ascending aorta is almost invariable. The size of both the aortic and ventricular openings of tunnels, and also the diameter of the tunnels themselves, are highly variable, ranging from a slit-like defect of a few millimeters to a structure >1 cm in diameter. Either the left or the right coronary artery may arise within a tunnel, or an ostium may be absent. Stenotic or atretic aortic and pulmonary valves are among the more frequently associated lesions, and tunnels have been observed in hearts with atrial septal defect, ventricular septal defect, or tricuspid atresia [3].

Pathophysiology

Despite the occasional occurrence of valve-like tissue within its walls, a tunnel affords unobstructed flow of blood from the left ventricle to the aorta during ventricular systole, and from the aorta into the ventricle throughout diastole. The volume-overloaded ventricle hypertrophies and dilates, and may suffer ischemia from inadequate coronary flow secondary to the large diastolic run-off. Because it is unsupported on its ventricular aspect, the right coronary leaflet tends to prolapse into the ventricle over time, compounding regurgitation through the tunnel with valvar regurgitation. A very large tunnel may displace the subpulmonary infundibulum and cause right ventricular outflow obstruction.

Natural history

In general, patients with aortoventricular tunnel develop symptomatic heart failure within the first year of life, if not during the neonatal period. The natural history, however, is difficult to characterize because of its variability and the rarity of the defect. Spontaneous closure of a very small tunnel, asymptomatic survival into adulthood, death *in utero*, and sudden death in infancy have all been described. Given the developmental basis of the anomaly and its ascending aortic enlargement, it would not be surprising if patients surviving into adulthood were eventually to manifest aortic aneurysms and dissections.
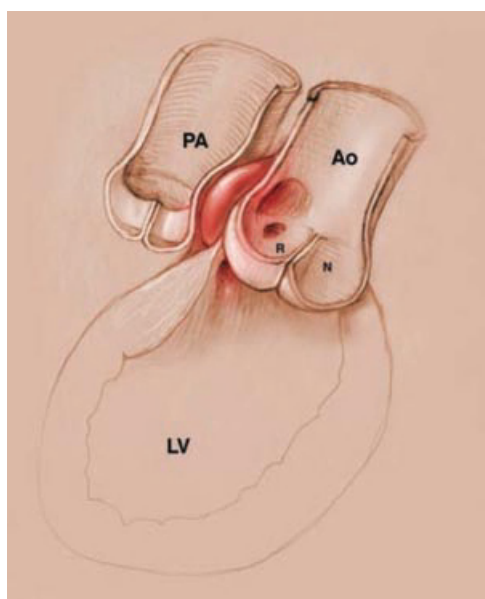
Figure 31.2 Aortoventricular tunnel. Schematic drawing of the most common type of tunnel, with an aortic orifice above the right sinus of Valsalva, and the ventricular opening in the fibrous interleaflet triangle between right and left coronary aortic leaflets. The potential for compression of the right ventricular outflow tract may be appreciated, although this usually occurs at a more proximal level than illustrated due to the position of the subpulmonary infundibulum. Ao, aorta; LV, left ventricle; N, non-coronary sinus of Valsalva; PA, pulmonary artery; R, right sinus of Valsalva.

Clinical features

The characteristic presentation of aortoventricular tunnel is a very loud "to-and-fro" murmur, heard over most of the precordium and accompanied by both systolic and diastolic thrills. Peripheral pulses are bounding, and a wide pulse pressure can be appreciated in older patients. The chest X-ray demonstrates cardiomegaly with dilatation of the ascending aorta, both of which may be out of proportion to the observed degree of heart failure. In some patients, the "bulge" of a very large tunnel may be seen along the left cardiac border. On the electrocardiogram, left ventricular hypertrophy with "strain" is usually found. On a fetal echocardiogram, hypertrophy and dilatation of the left ventricle with an enlarged aortic root and apparent aortic regurgitation are findings supporting a diagnosis of aortoventricular tunnel.

Echocardiography

Visualizing the tunnel beside the aortic root is done in a parasternal long-axis view, from which the tunnel can be followed to its aortic and ventricular ends. Using color-flow imaging, systolic and diastolic flow can be demonstrated in the tunnel. Associated valvar and coronary artery anomalies are not uncommon and should be characterized, and ventricular size and function quantified.
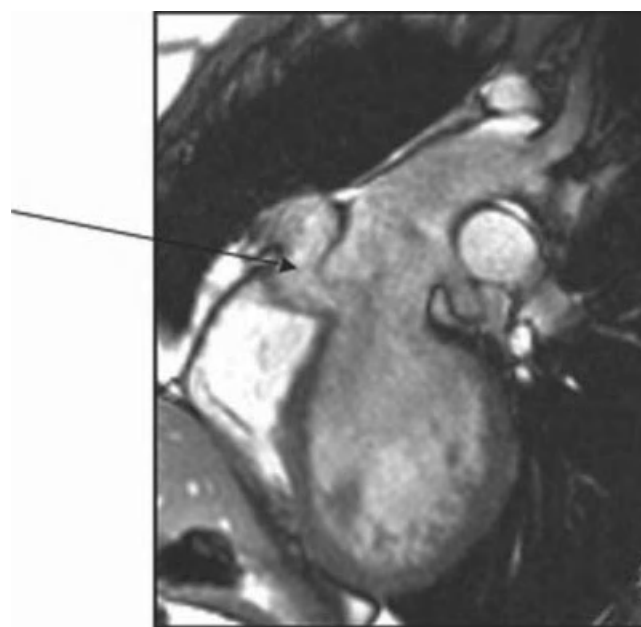
Figure 31.3 Aortoventricular tunnel. Single slice of a magnetic resonance angiogram using steady-state free precession imaging (FIESTA, GE Healthcare) to demonstrate the abnormal channel between the aorta and left ventricle (arrow) in a 13-year-old child. (Image provided by Dr Paul Julsrud and Dr Nandan S. Anavekar, Mayo Clinic, Rochester, MN, USA.)

Cardiac catheterization and angiography

Although an aortoventricular tunnel may be demonstrated by angiography, it is unnecessary for diagnosis. Cardiac catheterization is used to clarify coronary arterial anatomy and associated defects when these are not sufficiently elucidated by noninvasive imaging. Subpulmonary obstruction by the tunnel may cause increased right ventricular systolic pressure, but right heart hemodynamics are otherwise normal. There may be elevated left ventricular end diastolic pressure and widened aortic pulse pressure. When valvar aortic stenosis coexists, a gradient may or may not be found across the left ventricular outflow tract, as a large tunnel can obscure even atresia of the aortic valve.

Other imaging modalities

Both magnetic resonance imaging (Figure 31.3) and computed tomographic angiography offer elegant demonstrations of the complex anatomic relationships in this malformation. Their use, however, is generally more for follow-up of older or postoperative patients, as most patients are diagnosed and operated on in early infancy.

Management

Medical

Beyond resuscitation and stabilization for surgery, medical management offers little to these patients, most of whom will die from congestive heart failure without early repair.

Reversal of left ventricular dysfunction becomes progressively less likely after about 6 months of age, and distortion of the aortic valve superimposes aortic regurgitation, complicating later surgical intervention. The one exception is the exceedingly rare patient with a very small tunnel and good support of the aortic valve leaflets. As spontaneous closure of such a tunnel has been reported, observation is reasonable in this situation. However, if a tunnel is sufficiently large to require medical treatment of heart failure, it needs surgical repair.

Surgical

Most tunnels have been repaired using a pericardial patch, inserted through an aortotomy, to close the aortic end, and a prosthetic patch, inserted below the aortic valve through the opened tunnel itself, to close the ventricular end and support the valvar leaflet. When a coronary artery arises within the tunnel, it can be resected with a surrounding button of tunnel wall and reattached to the ascending aorta. Associated malformations are managed on their own merits, which may involve aortic or pulmonary valvotomy, aortic valve repair or replacement, aortic root replacement, or aortoventriculoplasty. Survival following primary repair of isolated aortoventricular tunnel now approaches 100%.

Long-term history of treated and untreated adults

Although they have not yet been followed to adulthood, patients in whom the tunnel was repaired before about 6 months of age have normalized left ventricular function on echocardiography and do not develop valvar aortic regurgitation during childhood. The ascending aorta remains enlarged, however, and in one patient showed myxomatous changes of connective tissue disease when a valve-sparing root replacement was later performed. Therefore, all patients need careful, life-long follow-up for this anomaly. Untreated adults are a very small population but have been reported. Most eventually develop aortic regurgitation and die of congestive heart failure, although occasional patients, for reasons not completely understood, remain asymptomatic [25].

Acknowledgments

References

1 Anderson RH, Freedom RM. Normal and abnormal structure of the ventriculo-arterial junctions. *Cardiol Young* 2005;**15** (Suppl. 1):3–16.

2 Mahle WT, Surtherland JL, Frias PA. Outcome of isolated bicuspid aortic valve in childhood. *J Pediatr* 2010;**157**:445–9.

3 McKay R, Anderson RH, Cook AC. The aorto-ventricular tunnels. *Cardiol Young* 2002;**12**:563–80.

4 Anderson RH, Webb S, Brown NA, *et al*. Development of the heart (3). Formation of the ventricular outflow tracts, arterial valves, and intrapericardial arterial trunks. *Heart* 2003;**89**:1110–8.

5 Fernández B, Durán AC, Fernández-Gallego R, *et al*. Bicuspid aortic valves with different spatial orientations of the leaflets are distinct etiological entities. *J Am Coll Cardiol* 2009;**54**:2312–8.

6 McKay R, Smith A, Leung MP, *et al*. Morphology of the ventriculoaortic junction in critical aortic stenosis. Implications for hemodynamic function and clinical management. *J Thorac Cardiovasc Surg* 1992;**104**:434–42.

7 Maganti K, Rigolin VH, Sarano ME, Bonoe RO. Valvular heart disease: diagnosis and management. *Mayo Clin Proc* 2010; **85**:483–500.

8 Bierman FZ, Yeh M-N, Swersky S, *et al*. Absence of the aortic valve: antenatal and postnatal two-dimensional and Doppler echocardiographic features. *J Am Coll Cardiol* 1984;**3**:833–7.

9 Weber OM, Higgins CB. MR evaluation of cardiovascular physiology in congenital heart disease: flow and function. *J Cardiovasc Magn Reson* 2006;**8**:607–17.

10 Kutty S, Whitehead KK, Natarajan S, *et al*. Qualitative echocardiographic assessment of aortic valve regurgitation with quantitative cardiac magnetic resonance: a comparative study. *Pediatr Cardiol* 2009;**30**:971–7.

11 Lopez L, Colan SD, Frommelt PC, *et al*. Recommendations for quantification methods during the performance of a pediatric echocardiogram: a report from the pediatric measurements writing group of the American Society of Echocardiography Pediatric and Congenital Heart Disease Council. *J Am Soc Echocardiogr* 2010;**23**:465–95.

12 Beroukhim R, Graham DA, Margossian R, *et al*. An echocardiographic model predicting severity of aortic regurgitation in congenital heart disease. *Circ Cardiovasc Imaging* 2010;**3**:542–9.

13 Biederman RW, Doyle M, Yamrozik J. *Cardiovascular MRI Tutorial: Lectures and Learning*. Philadelphia, PA: Lippincott Williams & Wilkins, 2008: 99.

14 Selamet Tierney ES, Feingold B, Printz BF, *et al*. Beta-blocker therapy does not alter the rate of aortic root dilation in pediatric patients with Marfan syndrome. *J Pediatr* 2007;**150**:77–82.

15 Brooke BS, Habashi JP, Judge DP, *et al*. Angiotensin II blockade and aortic-root dilation in Marfan's syndrome. *N Engl J Med* 2008;**358**:2787–95.

16 Gisler F, Knirsch W, Harpes P, Bauersfeld U. Effectiveness of angiotensin-converting enzyme inhibitors in pediatric patients with mid to severe aortic valve regurgitation. *Pediatr Cardiol* 2008;**29**:906–9.

17 Alehan D, Ozkutlu S. Beneficial effects of 1-year captopril therapy in children with chronic aortic regurgitation who have no symptoms. *Am Heart J* 1998;**135**:598–603.

18 Bonow RO, Carabello B, de Leon AC Jr, *et al*. ACC/AHA guidelines for the management of patients with valvular heart disease:executive summary. A report of the American College of Cardiology/American Heart Association Task Force on Practice Guidelines (Committee on Management of Patients With Valvular Heart Disease). *Circulation* 1998;**98**:1949–84.

19 Evangelista A, Tornos P, Sambola A, *et al*. Long-term vasodilator therapy in patients with severe aortic regurgitation. *N Engl J Med* 2005;**353**:1342–9.

20 Bonow RO, Cheitlin MD, Crawford MH, Douglas PS. 36th Bethesda Conference, Task Force 3: valvular heart disease *J Am Coll Cardiol* 2005;**45**:1334–40.

21 Badiu CC, Eichinger W, Bleiziffer S, *et al*. Should root replacement with aortic valve-sparing be offered to patients with bicuspid valves or severe aortic regurgitation? *Eur J Cardiothorac Surg* 2010;**38**:515–22.

22 Polimenakos AC, Sathanandam S, El Zein C, *et al*. Aortic cusp extension valvuloplasty with or without tricuspidization in children and adolescents: long-term results and freedom from aortic valve replacement. *J Thorac Cardiovasc Surg* 2010;**139**:933–41.

23 Brown JW, Ruzmetov M, Shahriari A, *et al*. Midterm results of Ross aortic valve replacement: a single-institution experience. *Ann Thorac Surg* 2009;**88**:601–8.

24 Alsoufi B, Al-Halees Z, Manlhiot C, *et al*. Mechanical valves versus the Ross procedure for aortic valve replacement in children: propensity-adjusted comparison of long-term outcomes. *J Thorac Cardiovasc Surg* 2009;**37**:362–70.

25 Kafka H, Chan KL, Leach AJ. Asymptomatic aortico-left ventricular tunnel in adulthood. *Am J Cardiol* 1989;**63**:1021–2.

26 Siu SC, Silversides CK. Bicuspid aortic valve disease. *J Am Coll Cardiol* 2010;**55**:2789–800.

27 Garg V. Molecular genetics of aortic valve disease. *Curr Opin Cardiol* 2006;**21**:180–4.

28 Coltharp WH, Warren ET, Heath BJ. Quadricuspid aortic valve with centrally fenestrated leaflets causing aortic insufficiency. *Texas Heart Inst J* 1988;**15**:187–8.

29 Wang S, Meng X, Zhang H, *et al*. Pentacuspid aortic valve with severe aortic regurgitation. *Ann Thorac Surg* 2010;**89**:2034–6.

30 Chi S, Blair C, Gonzales-Lavin L. Rupture of the normal aortic valve after blunt chest trauma. *Thorax* 1977;**32**:619–22.

31 Knepp MD, Rocchini AP, Lloyd TP, Aiyagari RM. Long-term follow up of secundum atrial septal defect closure with the Amplatzer septal occluder. *Congenit Heart Dis* 2010;**5**:32–7.

32 Cindik N, Ozcasy F, Süren D, *et al*. Gaucher disease with communicating hydrocephalus and cardiac involvement. *Clin Cardiol* 2010;**33**:E26–30.

33 Mohan UR, Hay AA, Cleary MA, *et al*. Cardiovascular changes in children with mucopolysaccharide disorders. *Acta Paediatr* 2002;**91**:799–804.

34 Trochu J-N, Kyndt F, Schott J-J, *et al*. Clinical characteristics of a familial inherited myxomatous valvular dystrophy mapped to Xq28. *J Am Coll Cardiol* 2000;**35**:1890–7.

35 Tuysuz B, Mizumoto S, Sugahara K, *et al*. Omani-type spondyloepiphyseal dysplasia with cardiac involvement caused by a missense mutation in CHST3. *Clin Genet* 2009;**75**:375–83.

36 Al Qurashi M. The pattern of acute rheumatic fever in children: experience at the Children's Hospital, Riyadh, Saudi Arabia. *J Saudi Heart Assoc* 2009;**21**:215–20.

37 Ahmed AM, El-Shamaa MF. Asymptomatic cardiac involvement in children with systemic lupus erythematosus. *J Med Sci* 2006;**6**:944–9.

38 Tobler D, Williams WG, Jegatheeswaran A, *et al*. Cardiac outcomes in young adult survivors of the arterial switch operation for transposition of the great arteries. *J Am Coll Cardiol* 2010;**56**:58–64.

39 Choi BS, Kwon BS, Kim GB, *et al*. Long-term outcomes after an arterial switch operation for simple complete transposition of the great arteries. *Korean Circ J* 2010;**40**:23–30.

40 Fujii Y, Kasahara S, Kotani Y, *et al*. Double-barrel Damus–Kaye–Stansel operation is better than end-to-side Damus–Kaye–Stansel operation for preserving the pulmonary valve function: the importance of preserving the shape of the pulmonary sinus. *J Thorac Cardiovasc Surg* 2010;**41**:193–9.

41 Brown JW, Ruzmetov M, Shahriari A, *et al*. Midterm results of Ross aortic valve replacement: a single-institution experience. *Ann Thorac Surg* 2009;**88**:601–8.

42 Nabulsi MM, Tamim H, Sabbagh M, *et al*. Parental consanguinity and congenital heart malformations in a developing country. *Am J Med Genet* 2003;**116A**:342–7.

43 Droogmans S, Cosyns B, D'haenen H, *et al*. Possible association between 3,4-methylenedioxymethamphetamine abuse and valvular heart disease. *Am J Cardiol* 2007;**100**:1442–5.

44 Smith SA, Waggoner AD, de las Fuentes L, Davilla-Roman VG. Role of serotoninergic pathways in drug-induced valvular heart disease and diagnostic features by echocardiography. *J Am Soc Echocardiogr* 2009;**22**:883–9.

45 Attias D, Stheneur C, Roy C, *et al*. Comparison of clinical presentations and outcomes between patients with TGFBR2 and FBN1 mutations in Marfan syndrome and related disorders. *Circulation* 2009;**120**:2541–9.

46 Loeys BL, Schwarze U, Holm T, *et al*. Aneurysm syndromes caused by mutations in the TGF-β receptor. *N Engl J Med* 2006;**355**:788–98.

47 Germain DP. Ehlers–Danlos syndrome type IV. *Orphanet J Rare Dis* 2007;**2**:32–40.

48 Wunderlich C, Schulze MR, Strasser RH. Severe aortic regurgitation in Ehlers–Danlos syndrome type IV. *Heart* 2005;**91**:126.

49 Hortop J, Tsipouras P, Hanley JA, *et al*. Cardiovascular involvement in osteogenesis imperfecta. *Circulation* 1986;**73**:54–61.

50 Ono M, Goerler H, Breymann T. Aneurysm of the aortic root in the setting of Wiskott–Aldrich syndrome. *Cardiol Young* 2009;**19**:212–5.

51 Johnston SL, Unsworth DJ, Dwight JF, Kennedy CTC. Wiskott–Aldrich syndrome, vasculitis and critical aortic dilatation. *Acta Paediatr* 2001;**90**:1346–8.

52 Berman DP, Lewis AB, Kung GC. Case report of a 2-year-old boy with Takayasu's arteritis: an atypical, severe presentation of a rare disease. *Pediatr Cardiol* 2010;**31**:1089–92.

53 Subramanyan R, Joy J, Balakrishnan KG. Natural history of aortoarteritis (Takayasu's disease). *Circulation* 1989;**80**:429–37.

54 Lee I, Park S, Hwang I, *et al*. Cardiac Behçet disease presenting as aortic valvulitis/aortitis or right heart inflammatory mass:a clinicopathologic study of 12 cases. *Am J Surg Pathol* 2008;**32**:390–8.

55 Huppertz HI, Voigt I, Müller-Scholden J, Sandhage K. Cardiac manifestations in patients with HLA B27-associated juvenile arthritis. *Pediatr Cardiol* 2000;**21**:141–7.

56 Stamato T, Laxer RM, DeFreitis C, *et al*. Prevalence of cardiac manifestations of juvenile ankylosing spondylitis. *Am J Cardiol* 1995;**75**:744–6.

57 Singh A, Khaja A, Alpert MA. Cocaine and aortic dissection. *Vasc Med* 2010;**15**:127–33.

58 McKay R. Aorto-ventricular tunnel. *Orphanet J Rare Dis* 2007;**2**:41.

32 Coarctation of the Aorta and Interrupted Aortic Arch

Eric Rosenthal

Evelina Children's Hospital, St Thomas' Hospital, London, UK

Coarctation of the aorta

Coarctation of the aorta is a narrowing of the aortic lumen at the origin of the descending aorta with obstruction to blood flow. First described by the anatomist Johann Meckel in 1750 and expanded upon by Paris in 1791, clinical recognition occurred from the early 1900s [1–3]. Coarctation is usually discovered in infancy, although adult presentation is more frequent (although not exclusively) in third-world populations. Coarctation occurs in 7% of live births with congenital heart disease [4]. The prevalence per 10 000 live births is significantly higher for white males (6.52) than for white females (3.17), but less common in black populations with no significant difference between the sexes (2.64 males and 1.69 females) [5].

Coarctation usually occurs sporadically, although occasionally more than one family member is affected [6]. There are also reports of monozygotic twins concordant for coarctation [7]. In girls with Turner's syndrome (46 XO), the incidence of coarctation is 10% [8,9].

Pathology and embryology

Pathology

The coarctation narrowing is in the thoracic aorta distal to the origin of the left subclavian artery and opposite the ductus arteriosus or ductal ligament [10]. The narrowing may be discrete but in some a more diffusely narrowed segment occurs. The literature divides coarctation into two common types, "preductal" or infantile and "postductal" or adult, and a third less common type, "juxtaductal" [11]. Clinically, however, juxtaductal is sufficiently descriptive, and the postductal position in adult coarctation is probably acquired during growth. The eccentric narrowing is formed by a posterior "ridge-like" infolding of the aortic wall medial layer containing a shelf of tissue that is ductal in origin and connected as a sling around the aorta to the ductus arteriosus [12,13]. Ductus smooth muscle extends into the aortic wall above and below the coarctation.

Intimal thickening is usually present. Beyond the obstruction, the aorta is often dilated (poststenotic dilatation), and the aortic wall demonstrates intimal proliferation and medial and elastic tissue disruption. Infective endarteritis may occur in this location as may aneurysm formation and dissection in later life [14]. The *posterior shelf* is the earliest echocardiographic marker of coarctation in the descending aorta in neonates even before a significant gradient develops. Hypoplasia of the aortic arch to varying extents is a common accompanying feature [15]. The origin of the left subclavian artery may be hypoplastic, and anomalous origin of the right subclavian artery below the coarctation occurs in >5% of patients [10]. Rarely, a coarctation is present in other locations, such as in the aortic arch before the left subclavian artery or in the descending thoracic or abdominal aorta [16]. Renal and mesenteric artery involvement frequently occurs, with abdominal coarctation found more commonly in girls [17].

The commonest associated cardiac anomaly is a bicuspid aortic valve, followed by a ventricular septal defect (isolated or multiple), aortic stenosis (valvar or subvalvar) and mitral valve anomalies (supravalvar ring, dysplasia of mitral leaflets, and "parachute" mitral valve). The combination of coarctation of the aorta, subaortic stenosis, and mitral stenosis is known as Shone syndrome [18]. Other cardiac lesions commonly associated with coarctation include double-outlet right ventricle, especially Taussig–Bing anomaly; tricuspid atresia, especially with d-transposition of the great arteries; d-transposition of the great arteries with an inlet ventricular septal defect and right ventricular hypoplasia; atrioventricular septal defect;

hypoplastic left heart syndrome; double-inlet left ventricle; and l-transposition of the great arteries. The arch is often hypoplastic with these complex defects. A bicuspid valve occurs in >50% of patients [19].

As a result of aortic obstruction, there is a progressive development of collateral blood flow around the coarctation segment, mainly from the subclavian artery and its branches through the internal mammary, intercostal, musculophrenic, transverse cervical, scapular, lateral thoracic, superior epigastric, and spinal arteries [4]. Dilatation of the left subclavian artery increases over time and the dilated and tortuous collateral arteries may erode the lower margins of the ribs in older children to produce "rib notching" on the chest X-ray. Berry aneurysms may develop in the circle of Willis due to the raised upper body blood pressure [20,21].

Embryology

The embryonic origin of coarctation is not completely defined and two competing theories prevail. The first considers coarctation as the result of an intrinsic defect in the media of the aortic wall. In mice, a deficiency of endothelin-1 has been associated with the development of tubular hypoplasia of the aortic arch, aberrant right subclavian artery, ventricular septal defect, abnormalities of the left ventricular outflow tract, and interrupted aortic arch [22]. An alternative theory is that abnormal fetal hemodynamics promote the development of coarctation [23]. The aortic isthmus between the left subclavian artery and the ductus arteriosus normally receives <10% of the combined ventricular output and is smaller in diameter than either the ascending or descending aorta in fetal life. Cardiac lesions that reduce left ventricular output may decrease blood flow through the aortic isthmus and lead to coarctation. Consistent with this hypothesis is the frequency of coarctation with a ventricular septal defect that is associated with posterior malalignment of the outlet septum and the fact that coarctation does not occur with pulmonary atresia. Similar considerations of fetal flow patterns apply to the higher incidence of a persistent left superior vena cava in coarctation patients [24]. The hemodynamic theory alone, however, does not explain the pathogenesis of isolated coarctation.

Pathophysiology

In fetal life, there is little effect of the coarctation, although when severe or with marked arch hypoplasia, the right ventricle and pulmonary artery are dilated early in gestation and the left ventricle and aorta are mall [25–27]. After birth, obstruction in the aortic arch elevates pressure and resistance in the upper extremity arteries and increases left ventricular work. Closure of the ductus postnatally increases acutely left ventricular afterload and left ventricular failure develops – often causing acute cardiovascular collapse. Decreased blood flow to the descending aorta leads to ischemia of abdominal organs and the lower extremities. Metabolic acidosis and renal failure ensue. Although closure of the ductus does not always lead to instantaneous collapse, with severe coarctation the elevated left ventricular afterload is eventually no longer tolerated and decompensation follows.

In infants with milder coarctation, the left ventricle adapts to the increased afterload, and overt heart failure does not always occur. Activation of the sympathetic nervous system initially increases the heart rate, myocardial contractility, and peripheral arteriolar constriction to maintain perfusion of the descending aorta and the abdominal organs. The left ventricular end-diastolic volume and pressure increase (Frank–Starling mechanism), and to a point sustain a nearly normal cardiac output. Subsequently, left ventricular hypertrophy enables the left ventricle to develop increased systolic pressure while maintaining a normal or nearly normal left ventricular wall stress [28]. The renin–angiotensin–aldosterone system is activated secondary to reduced renal perfusion, and raises systemic blood pressure, increasing perfusion to the lower body. Finally, as the child develops a collateral circulation, systemic arterial pressure and afterload decrease and blood supply to the abdominal organs and kidneys improves.

Associated cardiovascular lesions may aggravate the hemodynamic burden associated with coarctation. The increased systemic afterload increases both the amount of left-to-right shunting through atrial and ventricular septal defects and the amount of atrioventricular valve regurgitation in an atrioventricular septal defect. In coexisting aortic stenosis and coarctation, both left ventricular afterload and myocardial oxygen demand are further increased.

Natural history

Untreated coarctation of the aorta beyond infancy significantly decreases long-term survival, and death frequently occurs within the fourth to fifth decade of life [29,30]. Early postmortem studies showed that of those who survived the first 2 years of life, 25% died before age 20 years, >50% before 31 years, 75% before 43 years, and 90% before 55 years [31]. Causes of death with an unrepaired coarctation of the aorta include congestive heart failure (26%), aortic rupture (21%), bacterial endarteritis (18%), and intracranial hemorrhage (12%) [29,30]. Both intracranial hemorrhage and ruptured aorta also occurred in children and young adults without exceptionally high blood pressures [32]. The risk of endocarditis in unrepaired coarctation of the aorta was 1.3% per year before the surgical era and improvements in public health and dental hygiene [32].

History and physical examination

Clinical features depend on the age at presentation (Table 32.1). Despite the frequency with which coarctation is now suspected prenatally and routine childhood auscultation is performed, neonatal collapse and late detection in adolescence and adulthood still occur as in previous eras [33,34].

Table 32.1 Presenting features of coarctation.

Fetal life
Ventricular disproportion (right ventricle enlargement)
Great vessel disproportion (small transverse arch)
In association with other congenital heart disease
Nuchal thickening/chromosomal abnormality (Turner syndrome)

Neonates
Acute collapse with shock and acidosis
Heart failure
Systolic/continuous murmur radiating to back
Weak or impalpable femoral pulses
Upper limb hypertension

Infants
Heart failure and failure to thrive
Systolic/continuous murmur conducted to back
Weak or impalpable femoral pulses
Upper limb hypertension
Cardiomyopathy rarely

Children, adolescents, and adults
Systolic/continuous murmur conducted to back
Collateral murmurs over scapula
Weak or impalpable femoral pulses
Radio-femoral delay
Upper limb hypertension
Exercise intolerance
Claudication and leg fatigue
Cold feet
Cardiac arrest (left ventricular hypertrophy, and arrhythmia)
Hypertensive retinopathy/encephalopathy
Intracranial bleeding
Aortic dissection/rupture
Infective endocarditis

Neonates and infants

Neonates typically present with acute heart failure in the first 2–3 weeks of life shortly after duct closure when the compensatory mechanisms (see above) are inadequate. They are well at discharge from the hospital (the duct is still patent and femoral pulses are palpable) and present with a sudden onset of tachypnea and pallor. If not immediately diagnosed and correctly treated, shock, acidosis, and death can occur rapidly. A neonate presenting in shock from a critical coarctation (or aortic stenosis) is often erroneously diagnosed as septic or with a metabolic disorder, delaying appropriate management. Other infants with coarctation have a more insidious presentation with congestive heart failure. Typically, such infants have a history of dyspnea from shortly after birth and sweating with feeding, but failure to thrive brings them to medical attention. Rarely, an infant presents with an apparent dilated cardiomyopathy and a minimal gradient across the coarctation (due to low cardiac output), which can cause diagnostic difficulty.

Asymptomatic detection of a murmur during infancy is an occasional presentation.

Children, adolescents, and adults

Most individuals with coarctation are asymptomatic and the coarctation is detected when the arterial blood pressure is measured incidentally (e.g., for headache or nose bleeding). Reduced or absent femoral pulses (if looked for!) rapidly leads to the diagnosis. If symptoms are present, they are usually related to reduced blood supply to the lower extremities causing exercise-induced claudication (rare) or, even less commonly, complications of upper extremity hypertension (cerebral bleeding, aorta rupture) [35]. Endocarditis is now extremely rare.

Physical findings

The hallmarks of coarctation of the aorta are absent or diminished femoral pulses and hypertension in the upper extremities, together with a systolic murmur radiating to the back. Less commonly, the femoral pulses can be maintained by collateral flow, and upper limb hypertension in addition to the murmur is the clue [36]. Because the left subclavian artery is frequently involved with the coarctation segment or there is associated arch hypoplasia in some, the right arm is the preferred location for measuring upper extremity blood pressure in children.

Sometimes almost no blood pressure gradient or pulse difference will be found on physical examination:

1 In neonates with a patent ductus arteriosus, the right ventricle perfuses the lower part of the body at systemic pressure, eliminating a pressure difference between the arms and legs. Even when the pulmonary artery pressure falls, the duct ampulla may serve as a "bypass" around the developing coarctation.

2 Infants in severe heart failure, with poor left ventricular function, cannot maintain cardiac output and all extremity pulses are weak, so blood pressure differences may not be detectable.

3 In those with an aberrant right subclavian artery that arises below the coarctation, there is no difference in blood pressure between the right arm and lower extremities.

4 In a few adults, collateral size and flow are adequate to maintain similar pressures between the upper and lower extremities. Because of the long collateral pathway, however, there is usually a detectable delay between the right radial and the femoral pulses.

A prominent left ventricular heave may be present. A systolic thrill is uncommon and usually due to associated cardiovascular anomalies. The first heart sound is normal. A systolic ejection click is frequently present with a bicuspid aortic valve. The second heart sound is normal except in infants with congestive heart failure and pulmonary hypertension, when the second heart sound is narrowly split with increased intensity of the pulmonary

component. A grade 2–3/6 systolic ejection murmur is usually heard along the left sternal border and between the spine and the left subscapular region. Systolic murmurs may also be from aortic stenosis, mitral regurgitation, or a ventricular septal defect. In older children with an unrepaired coarctation, continuous murmurs, due to collateral blood flow, can be heard over the back and chest. Collateral pulsation may also be felt, especially over the scapular margins or under-side of the ribs. Enlarged tortuous retinal arteries may be seen on retinoscopy. Neonates with congestive heart failure usually have a gallop and significant hepatomegaly.

With abdominal coarctation, a loud murmur is heard in the abdomen and not the chest and is associated with more severe elevation in diastolic blood pressure. Collateral pulsations are usually absent.

Electrocardiogram

In the neonate or infant with congestive heart failure and coarctation of the aorta, right ventricular hypertrophy is usual [37], and reflects the *in utero* right ventricular dilatation and the postnatal pulmonary hypertension required to perfuse the descending aorta via the patent ductus arteriosus. T wave inversion may be present in the left precordial leads, but if significant left ventricular hypertrophy is present, there is likely to be coexisting severe aortic stenosis. By the second to third year of life, a pattern of left ventricular hypertrophy gradually emerges. Patients with isolated coarctation of the aorta may have a normal electrocardiogram even into adult life.

Chest film

In a neonate, the chest film shows cardiomegaly and increased pulmonary vascular markings (consistent with pulmonary edema). In an older child, the typical radiologic features of coarctation are a "3" sign consisting of the ascending aortic knob and the poststenotic dilatation that is usually present. After 5 years of age, rib notching may begin to be noted (Figure 32.1). The rib notching is most prominent on the lower margins of the upper ribs; if notching of the lower ribs is present, the diagnosis of an abdominal coarctation should be considered. More commonly, however, the chest X-ray appears normal.

Pseudocoarctation is a "kinking or buckling" of the aorta that results in an X-ray picture similar to coarctation of the aorta. In pseudocoarctation, unlike in coarctation, there is little or no obstruction to blood flow. Although pseudocoarctation is usually benign, in some patients dilatation and aneurysm formation develop just distal to the pseudocoarctation [38].

Echocardiographic features

Echocardiography has replaced cardiac catheterization as the primary diagnostic tool for coarctation of the aorta [39–42]. Associated lesions such as a patent arterial duct, ventricular

Figure 32.1 Chest X-ray showing rib notching (arrows) in unrepaired coarctation.

septal defect, aortic stenosis, and more complex congenital heart disease are all readily evaluated.

The hallmark finding in coarctation is a posterior shelf with narrowing of the descending aorta in the juxta-ductal position (Figure 32.2). It is associated with turbulent color flow and an increased velocity with diastolic extension of the systolic waveform and a double envelope. There is often left ventricular hypertrophy and dilatation in older patients. Aortic arch hypoplasia and aberrant origin of the subclavian artery should be sought. A bicuspid aortic valve is present in half of patients.

In neonates, the diagnosis is not always immediately apparent. When the ductus is patent and the ductal sling around the aorta has not contracted, the coarctation shelf may not be fully developed. Prominence of the anterior duct ampulla, which overlies the coarctation area in some views, should not be interpreted as a sign of coarctation. Although initially flow at ductal level may be right to left, this changes to left to right as the pulmonary resistance falls. As the ductus constricts, the coarctation begins to be unmasked, but may not be clearly apparent until complete closure of the ductus or indeed even some weeks later [24].

Fetal echocardiography

In fetal life, the coarctation is not easily identified due to lack of flow across the isthmus [the ascending and descending aorta are perfused by the left and right (via the ductus) ventricles, respectively, which have an identical pressure] and the arterial duct (with high flow) overlies the coarctation site [25–27]. Furthermore, constriction of the
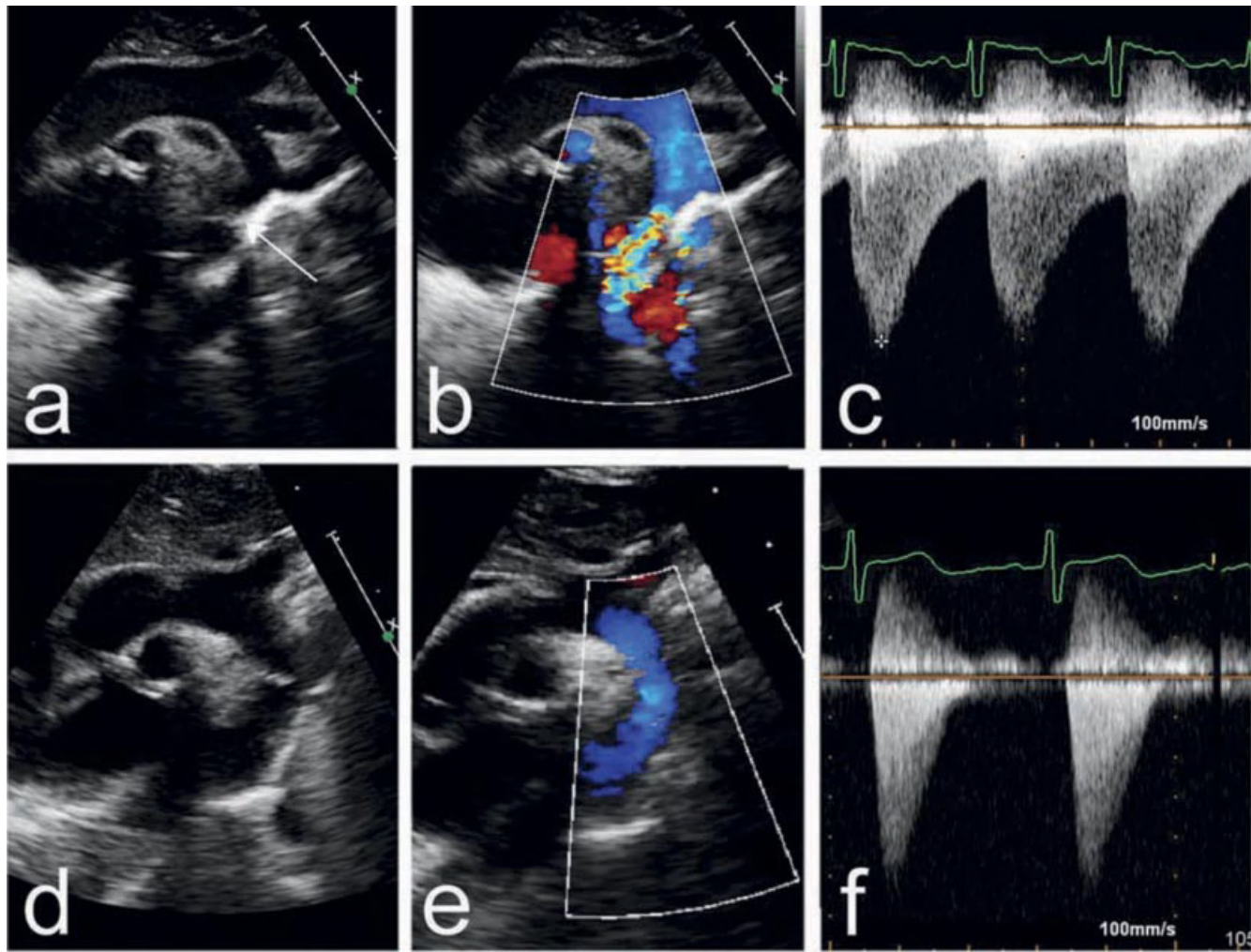
Figure 32.2 Echocardiogram in neonate showing coarctation shelf (arrow) in 2D (a) and the turbulent color jet (b). The continuous-wave Doppler trace shows continuous flow and a double envelope (c). After repair by end-to-end anastomosis, the arch is widely patent with echogenicity at the suture line (d) and laminar flow (e). The Doppler trace is now normal (f).

ductal sling around the aorta does not occur until after birth. The finding of right ventricular dilatation early during fetal life is a pointer towards coarctation development – especially when associated with additional transverse arch hypoplasia (Figure 32.3). Right ventricular dilatation in late gestation is common and without concomitant aortic arch hypoplasia is a much less specific sign of coarctation [25]. Antenatal detection is variable with a low rate in general obstetric units where great vessel assessment is not routine and mild ventricular disproportion may be ignored [41–43]. Even in dedicated fetal cardiology units there is a significant false-positive rate with more than two-thirds being normal at birth. Similarly, in those suspected to have a coarctation and a ventricular septal defect, two-thirds had only a ventricular septal defect postnatally [25,44]. When the disproportion between the ventricle and great vessels is marked, this may indicate progression to hypoplastic left heart syndrome, particularly if blood shunts left to right across the foramen ovale. Then continued evaluation is required until term.

Cardiac catheterization and angiography

With echocardiography and cross-sectional imaging with MRI, cardiac catheterization is no longer needed for anatomic assessment. It is performed primarily for interventional treatment. It retains a role in the hemodynamic assessment of mild or borderline coarctation or recoarctation associated with an increased Doppler gradient and mild hypertension.

Magnetic resonance imaging

Magnetic resonance imaging (MRI) with 3D reconstruction, supplemented by gadolinium contrast, has become the imaging modality of choice after clinical findings and
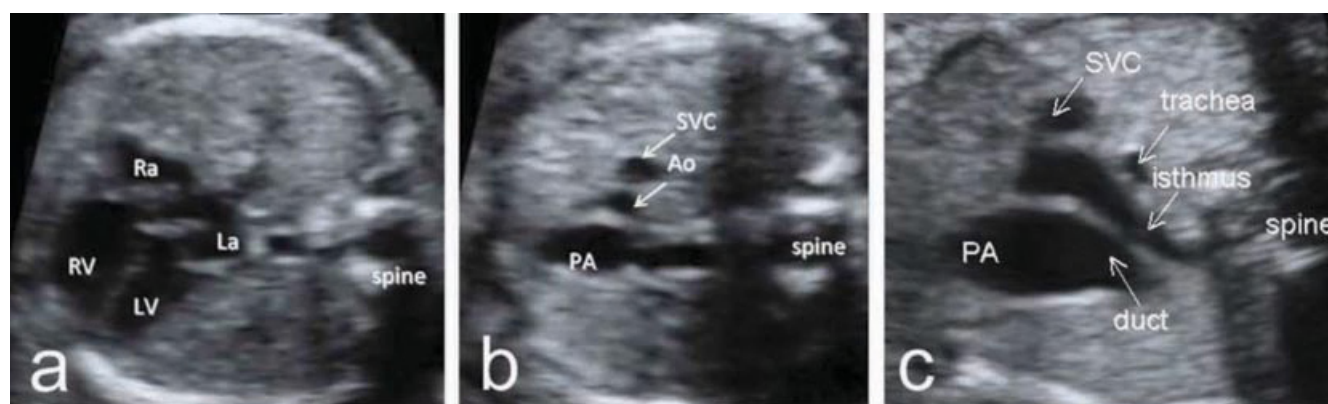
Figure 32.3 Fetal echocardiogram at 20 weeks' gestation showing right ventricular dilatation in early gestation (a). The aorta is smaller than the pulmonary artery in (b) and (c) and the isthmus is smaller than the duct in (c). An extended arch repair was performed a few days after birth. Ao, aorta; La, left atrium; LV, left ventricle; PA, pulmonary artery; RA, right atrium; RV, right ventricle; SVC, superior vena cava.
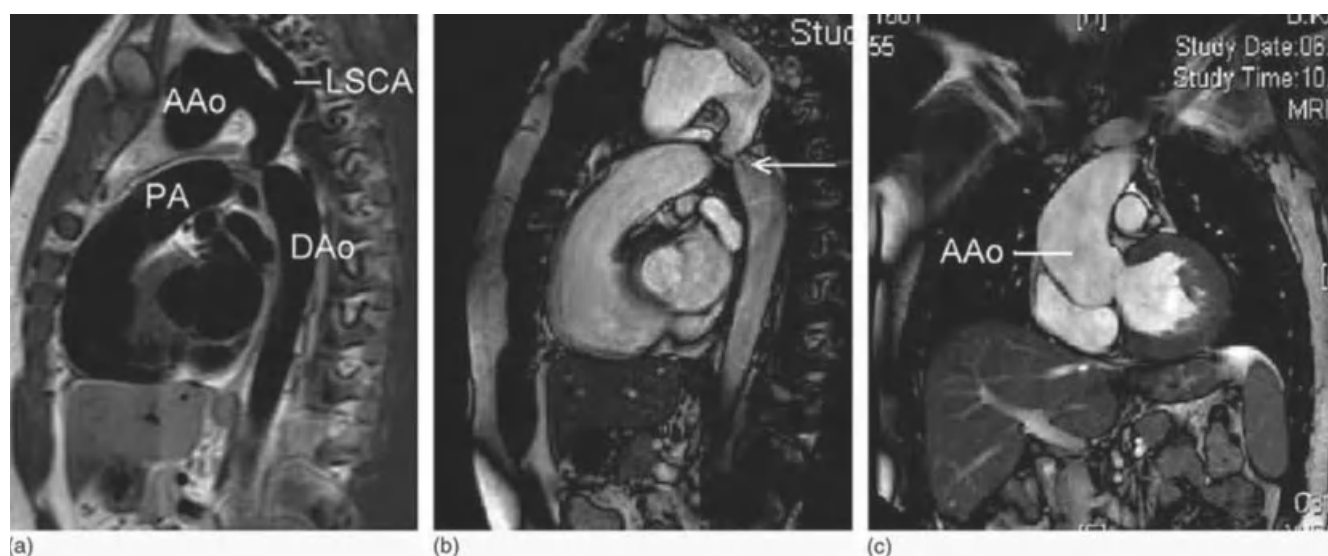
Figure 32.4 MRI scan in a 19-year-old asymptomatic male with an incidental blood pressure of 220/135. Black blood sequence in (a) shows a discrete coarctation beyond the left subclavian artery (LSCA). In (b) an SSFP sequence shows the coarctation with a jet of high turbulence (arrow). The ascending aorta (AAo) is dilated in (c). AAo, ascending aorta; DAo, descending aorta; LSCA, left subclavian artery; PA, pulmonary artery.

echocardiography have established the diagnosis. MRI gives unparalleled definition of the entire ascending and descending aorta and great vessels. Both the coarctation and hypoplasia of the aortic arch are clearly demonstrated and allow planning of interventional or surgical management. Demonstrating an aberrant subclavian artery is essential to planning the correct surgical approach. Following repair, MRI can demonstrate recurrent coarctation and aneurysm formation [45]. In addition, comprehensive assessment of aortic valve and left ventricular function are obtained during the same examination [46] (Figure 32.4). It has virtually supplanted diagnostic cardiac catheterization. It can diagnose pseudo-coarctation that has a fold in the medial aortic wall (inner curvature of the arch).

Management

Antenatal diagnosis

With suspicion of severe coarctation, the fetus should be delivered in a pediatric cardiology center so that a prostaglandin (PGE$_1$) infusion (5 ng kg^{-1} min^{-1}) can be commenced immediately. After echocardiographic confirmation of a posterior shelf at the coarctation site, prostaglandins are continued until elective surgical repair a few days later. When the findings are less convincing, the fetus is delivered and observed closely without prostaglandins while the duct closes. Regular monitoring of the four-limb blood pressure and femoral pulses and daily or alternate daily echocardiograms are performed until it is clear whether

a coarctation is developing. After ductus closure, those without a coarctation are allowed home but should be reviewed again in 4–6 weeks and finally at 6 months because of the occasional late detection of coarctation in the antenatally suspected cohort [25].

Early postnatal presentation

Neonates presenting with cardiovascular collapse require full resuscitation (intubation, ventilation, inotropes, and correction of metabolic acidosis) before transfer and surgery Prostaglandin (PGE$_1$) infusion to reopen the ductus, initially 50–100 ng kg^{-1} min^{-1}, may be needed for some hours to re-establish ductal patency, then the dose is reduced gradually to 5–10 ng kg^{-1} min^{-1}. Reopening of the duct together with inotopic support improves the hemodynamic status and corrects the acidosis so that an operation can be performed with the neonate in an optimal condition. With complex associated lesions, such as transposition, the coarctation is repaired at the time of the corrective surgery. When a ventricular septal defect (VSD) is the only additional lesion, a varied approach is taken;. either repair of all lesions on cardiopulmonary bypass or coarctation repair and banding of the pulmonary artery for later repair or even coarctation repair alone, deferring VSD repair until clinically indicated (heart failure or pulmonary hypertension) [47–50].

Infantile presentation

In older infants in whom the diagnosis is established because of clinical findings, development of mild cardiac failure, and/or failure to thrive, elective surgery is undertaken shortly after the diagnosis has been established. Rarely, an infant presents with an apparent dilated cardiomyopathy and a low gradient across the coarctation (due to low cardiac output), which can cause diagnostic difficulty. Since 1980, the surgical mortality for simple coarctation has progressively declined and is significantly lower than medical management [51]. Surgical repair is now routinely performed in neonates and infants at the time of diagnosis [52].

Childhood, adolescent, and adult presentation

In children beyond the first year of life, adolescents, and adults, both catheter intervention and surgery are options – the choice often depending on the views of individual centers. In adolescents and adults, catheter intervention is more likely to be used than surgery.

There are rare individuals with a mild coarctation, a systolic arm–leg gradient <20 mmHg, normal arm blood pressure, and normal ventricular function in whom no intervention is necessary. They should be examined periodically because aortic obstruction can increase and local complications can occur.

Operative repair

The first successful repair of coarctation of the aorta using primary end-to-end anastomosis was reported in 1945 by Craaford and Nylin [53] and by Gross [54]; neonatal repair was reported in 1952 by Kirklin *et al.* [55].

Resection and end-to-end anastomoses

Resection with end-to-end anastomosis is classically performed through a left posterior lateral thoracotomy (Figure 32.5). Extensive mobilization of the aorta from the left subclavian artery past the ductus arteriosus to the descending aorta is required. The ductus is divided and ligated. Sacrifice of dilated collateral intercostal arteries is often necessary for exposure. Adequate repair requires excision of the entire coarctation segment and the creation of a tension-free anastomosis. Early repairs using silk suture in a continuous running fashion were associated with a high incidence of restenosis [56]. Most surgeons advocate a continuous suture posteriorly and an interrupted layer anteriorly [57,58]. This operation theoretically removes all abnormal ductal and coarctation tissue and avoids the use of prosthetic material. When a tension-free anastomosis is impossible, an alternative method of repair may be required.

Prosthetic patch aortoplasty

The prosthetic patch aortoplasty was introduced in 1957 (Figure 32.5) [59]. A longitudinal incision is made in the aorta, the coarctation shelf is excised, and an elliptical patch of either Dacron or polytetrafluoroethylene is sutured to the aortotomy edges. This technique avoids extensive dissection and a prolonged operating time. Because of the late development of aneurysms on the posterior aortic wall opposite the patch, especially when Dacron was used [60–63], patching is now used only in selected circumstances.

Aneurysm formation has been attributed to excision of the posterior coarctation membrane weakening the posterior aortic wall or altered hemodynamics arising from the difference in tensile strength between the prosthetic patch and the posterior aortic wall [60–65].

Subclavian flap aortoplasty

Subclavian flap aortoplasty, introduced in 1966, is used extensively in infants and small children (Figure 32.5) [66]. The left subclavian artery is mobilized and divided and used to patch over an incision across the coarctation. The procedure is simple, avoids extensive aortic dissection and prosthetic patch material, and allows for growth. Disadvantages include complications from sacrificing the major vascular supply to the left arm [67,68], development of aneurysms [69,70], and recurrences from inadequate resection of ductal tissue [71]. It is currently less favored, although some centers continue with the technique [72].
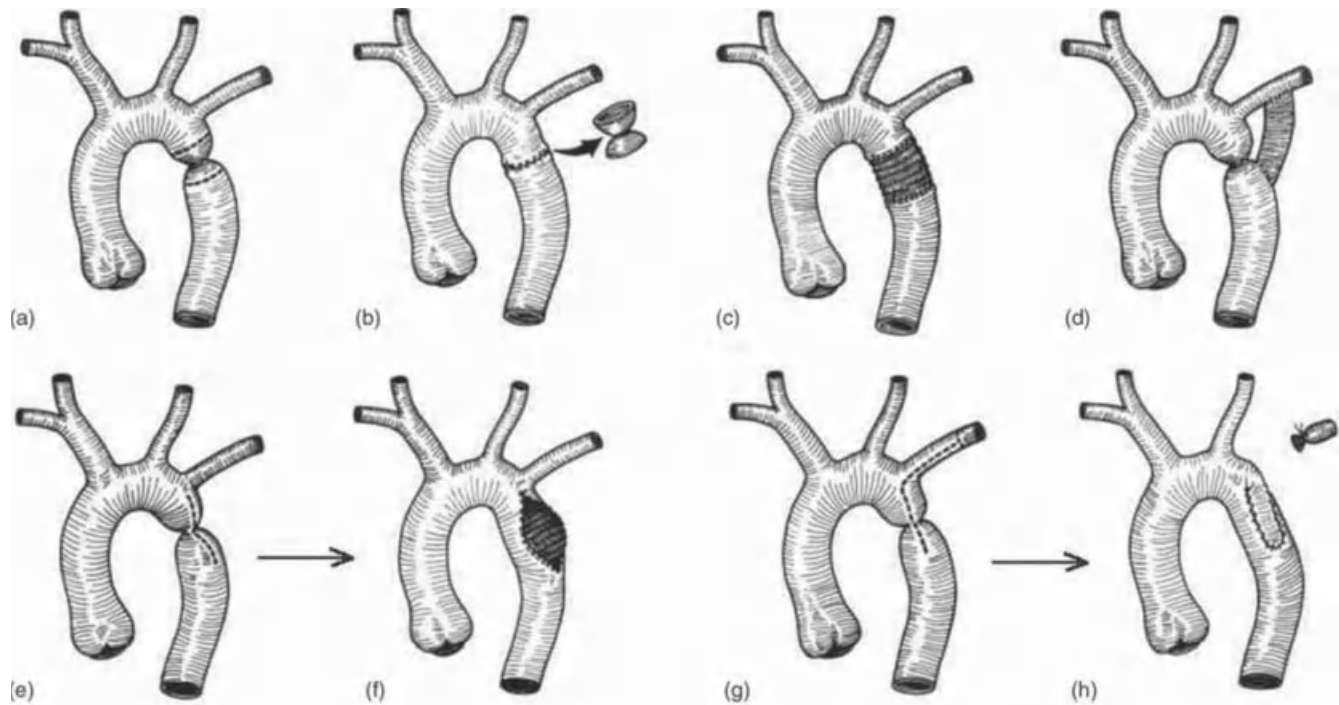
Figure 32.5 Diagrams of coarctation (a) repair using an end-to end anastomosis (b), interposition graft (c), subclavian to descending aorta conduit (d), Dacron patch repair (e, f), and subclavian flap repair (g, h).

Interposition grafts

A prosthetic or homograft interposition graft, first described in 1960, is currently used only for either older individuals with an associated aneurysm or recoarctation when end-to-end anastomosis cannot be accomplished (Figure 32.5) [73]. Disadvantages include predisposition to infection, aneurysm formation, and their lack of growth potential. In other patients, a subclavian artery (or carotid artery after a previous subclavian flap repair) to descending aorta graft is placed. Ascending to descending aorta bypass grafts can be used for repair of complex coarctation and aortic arch abnormalities – usually after prior surgery [74].

Extended end-to-end anastomosis

Extended end-to-end repair was introduced in the mid-1980s to correct both the coarctation and associated aortic arch hypoplasia [75–77]. After resecting the coarctation, an incision is made on the inferior surface of the arch and the distal aorta is then brought up and sutured to this incision (Figure 32.6). Temporary occlusion of the left subclavian artery and/or left carotid artery and part of the right innominate artery may be needed. The most obvious advantages are excising potentially abnormal aortic tissue and, by extending the incision across the isthmus and transverse aortic arch, correcting the transverse arch hypoplasia [78]. Recoarctation rates are as low as 3–6% after neonatal repair [79–82]. Disadvantages are similar
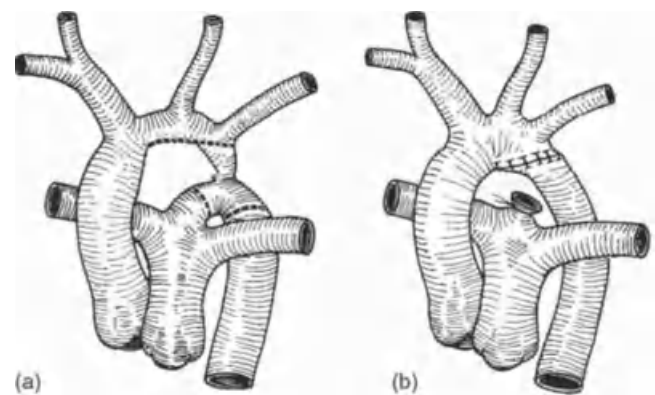
Figure 32.6 Diagram of coarctation and hypoplastic arch (a) repair using an extended end-to end anastomosis (b).

to those of end-to-end repair: extensive dissection and sacrificing of collateral arteries. A tension-free anastomosis is necessary, and occasionally is achieved by sacrificing the left (and even right) subclavian artery. There is a risk of tracheal and left bronchus compression. Extended end-to-end anastomosis is now the preferred technique for most infants. Its use for routine extended arch repair when the transverse arch is mildly hypoplastic, however, has been questioned, as adequate treatment of the coarctation site alone results in rapid remodeling of the hypoplastic arch in

many infants [83,84]. Failure to perform an extended arch repair when the arch is hypoplastic, however, leads to a significant incidence of arch obstruction despite "successful coarctation repair," and may lead to repeat surgery via a sternotomy and bypass approach [85]. In infants with a severely hypoplastic arch and in those needing intracardiac repair of associated lesions, repair is performed on cardiopulmonary bypass.

Early complications after surgical repair

Major operative complications include hemorrhage, paradoxical hypertension, stroke, paraplegia, and damage to adjacent structures. Bleeding is an early postoperative complication related to the extent of the dissection, a coagulopathy, and excessive tension along the suture line, and is worsened by paradoxical hypertension. Turner syndrome is associated with an increased incidence of hemorrhage because of abnormal tissue fragility [86]. Currently, surgical repair is performed with a low mortality even in neonates.

Paradoxical hypertension occurs after transection of the aorta and damage to sympathetic nerves [87,88]. During the initial phase of hypertension, the sympathetic nervous system is activated with a marked increase in systemic catecholamine secretion. The catecholamine hyperactivity activates the renin–angiotensin–aldosterone system, ultimately leading to sustained hypertension and fluid retention. If untreated, the hypertension can result in post-coarctation syndrome (severe abdominal pain, distention, and tenderness, and also fever) [89]. Acute inflammatory changes in the mesenteric arteries (possibly due to over-distention of these thin-walled arteries previously exposed to a low blood pressure) cause intestinal ischemia, necrosis, and death. Paradoxical hypertension can be either prevented if β-blockers are administered before surgery [90], or treated early postoperatively by the intravenous administration of β-blockers, converting enzyme inhibitors, or nitroprusside. The incidence is very low in neonates and infants [91].

Stroke and paraplegia are rare postoperative complications. Prolonged or excessive cross-clamping of cerebral vessels may cause ischemia, but is uncommon now. In the few who need repair with cardiopulmonary bypass, the risk may be higher. Paraplegia occurs in 0.4% of patients [92]. Predisposing factors include inadequate collaterals, anomalous origin of the right subclavian artery, and prolonged distal hypotension, but surprisingly neither sacrificing intercostal arteries nor aortic cross-clamp time was related [93]. To prevent spinal cord paraplegia, most surgeons try to maintain distal aortic pressure >50mmHg. If pharmacologic measures are ineffective in preventing distal hypotension, a temporary shunt or femoral bypass with a distal pump oxygenator is used [94]. Paraplegia is more of a concern for repeat surgery involving extensive dissection when the collaterals have diminished and the risk may be as high as 2.6% [95]. Paraplegia sometimes occurs weeks after surgery and may

respond to spinal decompression [95]. Undertaking late and complicated repeat surgery with cardiopulmonary bypass and deep circulatory arrest or with left heart bypass through a lateral thoracotomy has been proposed to reduce morbidity and allow full repair [96–98]. Ascending to descending aorta bypass grafts may reduce the risk of paraplegia by avoiding a repeat left thoracotomy [74,99].

Adjacent structure damage can involve injury to the phrenic nerve, resulting in diaphragmatic paralysis, injury to the recurrent laryngeal nerve affecting the vocal chords, damage to the sympathetic trunk, resulting in Horner's syndrome, and, rarely, the development of chylothorax due to injury of the thoracic duct.

Mortality for coarctation repair even in the neonatal period and infancy is low. because of adequate preoperative stabilization and improved anesthesia, surgery, and intensive care [100]. In early series mortality rates were >30%, but are now ~3% [52,101,102]. Primary coarctation repair in adults carries a higher risk. The aorta above and below the coarctation is atheromatous and friable, and there are often large, thin-walled intercostal aneurysms.

Catheter intervention

Percutaneous balloon angioplasty to avoid the risks of coarctation surgery or repeat surgery for recoarctation dates back to 1979, when Sos *et al.* demonstrated successful balloon dilatation of aortic coarctation in postmortem neonates [103]. Shortly thereafter, balloon dilatation was performed clinically, and in many centers it became the procedure of choice [104–108]. Stent implantation was first reported in 1991 and is becoming preferred to balloon dilatation, particularly with the development of covered stents in the early 2000s [109–111].

Balloon dilatation

Balloon dilatation acts by stretching and tearing the thickened intimal coarctation shelf and adjacent media layers, but tears in the adjacent "normal" aortic wall also occur, perhaps reflecting an inherent aortic weakness in coarctation [112,113]. Limiting damage to the coarctation shelf is not always possible and adventitial extension can lead to acute rupture, dissection, and aneurysm formation. For recoarctation, with added external support from previous scarring, it rapidly became the treatment of choice [114–118]. Acute rupture and dissection are rare, but aneurysms can develop later [119,120].

Safety is improved by avoiding overdilatation of the coarctation segment. In general, the balloon size should not be greater than either the aorta proximal to the coarctation (isthmus) or at the level of the diaphragm. After initial enthusiasm, balloon dilatation is now generally avoided in the first 6–12 months of life because of a high incidence of recoarctation (postulated to be due to elastic ductal tissue stretching and recoiling without sufficient tearing of the
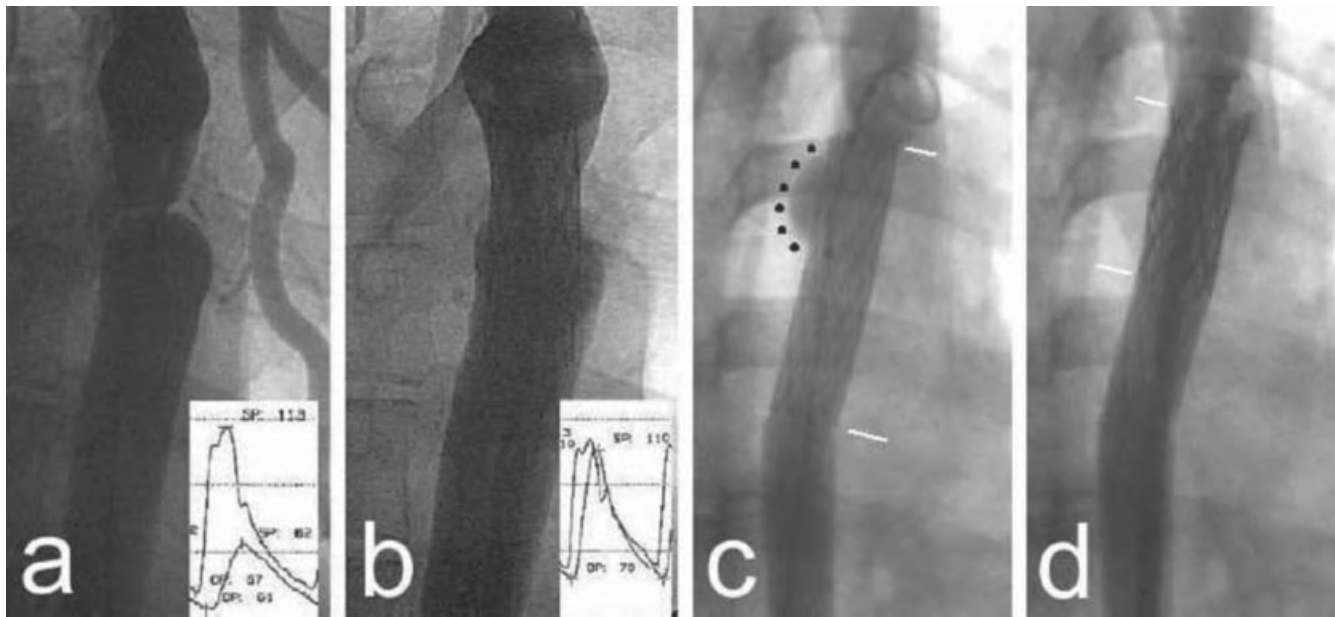
Figure 32.7 Coarctation (a) treated with a bare metal stent implantation in (b) abolishing the gradient. In another patient (c) an aneurysm (black dots) develops following bare metal stenting (white lines indicate length of stent) and is treated with a covered stent inside the first stent (white lines indicate length of second stent). Videoclips 32.1 and 32.2 demonstrate the acute effect on collateral flow of the patient in Figure 32.7a and b. (Reproduced from Eric Rosenthal, *Heart*, 2005; 91(11): 1495–1502, with permission from BMJ Publishing Group Ltd.)

coarctation shelf) and femoral artery damage [121]. The development of stenting has virtually restricted balloon dilatation to children weighing <25 kg [123,124].

Stent implantation

Stent implantation overcomes the natural recoil of elastic tissues after balloon dilatation and leads to greater relief of obstruction without excessive dilatation. The stent struts also splint any smaller tears against the aortic wall, preventing progressive dissection and aneurysm formation. Mild coarctation is less amenable to balloon dilatation and large balloons are needed to overcome the natural recoil with a risk of aortic tearing. Stent implantation allows mild coarctation to be easily treated, albeit with a small risk of stent migration [123]. Nevertheless, over-dilatation of a tight coarctation has caused aneurysm formation and rupture [124,125]. To prevent this, submaximal dilatation during the first procedure, allowing a period for healing, and further dilatation at a second procedure can be employed [126]. This strategy produces excellent results and stent implantation rapidly began to replace balloon dilatation (Figure 32.7 a and b; Videoclips 32.1 and 32.2). When aortic valve or root replacement or coronary bypass grafting is needed, presurgical stenting of the coarctation removes the need to dissect the coarctation area or to recover from cardiopulmonary bypass in the face of an aortic obstruction [127]. Stent implantation is also used for aortic arch hypoplasia either at the time of coarctation stenting or after prior successful treatment of the original coarctation [128].

For delivery of a stent large enough to open the aorta to adult size, the size of the delivery sheath in the femoral artery precludes use in most children weighing <25 kg [129,130]. In older children, the stents can be redilated after growth. [131]. Stents have been implanted in smaller children and even in neonates when surgical risks are considered to be too high [132,133]. The longer-term outcome of these "rescue" procedures is unknown.

Covered stent implantation

Covered stents were initially developed to treat acute dissection and aneurysm formation after aggressive stent implantation. A polyurethane sleeve attached to the outside of the stent sealed any tears from distension by the blood pressure. It subsequently found a role for primary implantation in tight coarctation in place of bare metal stents (Figure 32.7c and d). The disadvantages include the need for larger femoral artery sheaths to advance the covered stent, and a risk of occluding arch vessels when stenting the transverse arch. These stents are also used to seal existing aneurysms occurring either spontaneously or after surgical repair or catheter intervention. For more extensive aneurysm formation and dissection of the aorta longer than 25 mm, vascular stent-grafts, mounted on 22–24F delivery systems which require femoral or iliac exposure are used [134,135].

Early complications after catheter intervention

Early complications after catheter intervention are uncommon and include hemorrhage, femoral artery damage,

cerebrovascular accidents, and dissection and rupture. When performed after the first year of life, morbidity and mortality are lower than with surgery.

Regarding *femoral artery damage*, occlusion immediately after the procedure due to spasm and thrombosis responds to a heparin bolus and/or infusion for a few hours. If signs of occlusion persist, thrombolysis is usually effective. Less commonly, a dissection flap causes obstruction and surgical reconstruction of the puncture site is needed. Pseudo-aneurysm formation from inadequate compression after sheath removal can be treated by local thrombin injection and compression. Surgery is not needed. Acute rupture or avulsion of a femoral or iliac artery from a large sheath is extremely rare but requires emergency vascular repair. The leak can be occluded temporarily by a balloon inserted from the opposite femoral artery. With modern low-profile balloon catheters and femoral sheaths, the complications are reduced, although for stent implantation larger sheaths are still required.

Cerebrovascular accidents are rare and usually relate to inadequate heparinization and failure to de-air and flush the long sheath. The long guide-wire may also be a source of emboli.

Acute dissection and rupture are very rare and potentially life-threatening complications requiring immediate action. Initially a period of balloon tamponade allows volume replacement and then placement of a long covered stent. If this fails, then open surgery is performed.

This complication can occur when dilating a native coarctation without surrounding surgical scarring or after intervention for recoarctation [120,136]. Stent implantation with less aggressive dilatation has reduced but not abolished the occurrence [111,126]. *Stent migration* can be managed by capturing the stent on the balloon (or a larger balloon) and re-inflating to oppose the stent more closely to the aortic wall. If it is not possible to reposition the stent in the coarctation, it is expanded in an adjacent segment of the descending aorta or aortic arch and a new stent is implanted into the coarctation. Migration of a covered stent is a greater concern if it blocks either the arch or abdominal vessels and requires surgical removal.

Paraplegia has not been reported after catheter intervention. It occurs infrequently with stent-graft placement for extensive atheromatous dissection [135].

Surgery or catheter intervention – which to use?

The effectiveness of coarctation repair has evolved as each new technical approach has been introduced and refined. There are no sizeable randomized trials and few comparative series, and we are limited by retrospective analysis. In most centers, repair in the first year of life is performed through a left thoracotomy with either an end-to-end anastomosis or an extended arch repair when the arch is hypoplastic. In children beyond the first year of life, surgery or balloon dilatation are

common approaches depending on the views of individual centers, and in adolescents and adults catheter intervention with stent implantation is increasingly being used. A choice between the two approaches is not without controversy [111,137–144]. The difficulty in making a direct comparison is confounded by the concept that two catherizations may be better than one thoracotomy. Recurrence of the coarctation after surgery is invariably treated by catheter intervention and this is less controversial! [74,99,145].

Long-term outcome

Although coarctation of the aorta appears to be a simple, correctable lesion with operative repair in neonates or by catheter intervention in older patients, ongoing issues persist [146].

In 1987, the first large long-term series of 226 survivors of coarctation surgery with 15–30 years of follow-up reported a late mortality of 12% and hypertension in 68% (despite normal blood pressure after surgery) [147]. An even larger series of patients operated on from 1946 to 1981 revealed significant morbidity and mortality in the 571 survivors with a median follow-up of 20 years. Deaths due to coronary artery disease, sudden death, heart failure, cerebrovascular accidents, and ruptured aortic aneurysm occurred in 15% at a mean age of 38 years and were associated with systolic hypertension. Additional surgery was required in 11% and hypertension required treatment in 25%. Operations before the age of 9 years resulted in the best long-term survival [148]. A longer-term study of 254 survivors followed for 24–53 years revealed a cardiovascular mortality of 18% at a mean age of 34 years after surgery due to coronary artery disease and re-operation. Hypertension was present in 35%. [149].

Currently, the acute results from repair in infancy show a low mortality and morbidity. Coupled with the benefits of catheter intervention for recoarctation, the long-term results should be better than in the early series. Until this evidence emerges, however, a patient with a treated coarctation should be considered palliated rather than cured [19,150].

Long-term surveillance is required to monitor for:
- recoarctation
- persistent or developing hypertension with attendant cardiovascular complications
- aortic aneurysm formation
- aortic valve disease progression with ascending aorta dilatation and the risk of dissection.

Recoarctation

Recoarctation may follow surgical or catheter intervention, but the relative incidence is difficult to assess. Partly this is due to definitions. Previously, recoarctation was diagnosed when heart failure or hypertension was severe enough to mandate repeat intervention. Milder "recoarctation" with minimally elevated blood pressure might not have been categorized as such. The designation of recoarctation as an arm to leg blood pressure gradient of 20 mmHg *and*

hypertension has recently been changed to a 30 mmHg gradient *and* hypertension [151,152]. Obstructions at arch level with a "perfect" result at the coarctation site have been labeled as recoarctation by some but not others. When stent implantation deliberately underdilated the coarctation to stage the treatment, some (often surgeons!) classified this as recoarctation [126]. In reviewing the literature, the distinction between an inadequate initial repair with immediate "recoarctation" and true late occurrence of recoarctation is not always evident. Even more difficult has been the interpretation of gradients that develop with exercise in patients with normal blood pressure and gradients less than 20–30 mmHg at rest. It is unclear whether this reflects recoarctation or results from differential responses of the peripheral vasculature in the upper and lower body segments that persist despite correction [153,154].

For patients younger than 3 months treated between 1985 and 1990, freedom from recoarctation after 4 years was 57% after subclavian flap repair, 77% after end-to-end anastomosis, and 83% after extended end-to-end anastomosis [155]. Following changes to the technique of end-to-end repair and with the development of the extended end-to-end repair, recoarctation rates are now <10% after neonatal repair [79–82].

It is difficult to compare angioplasty with surgical correction of coarctation, as the technique has been evolving since the mid-1980s and there are no large randomized studies. The recoarctation rate in children under 1 year of age is high, with rates up to 31–50% [122,156]. For children older than 1 year, the recurrence rates after balloon dilatation are much lower [157]. In 102 patients followed up to 10 years after balloon dilatation for native coarctation, immediate success was achieved in 93 patients, of whom 21 (22%) required a repeat intervention. Most of these were younger than 7 months – for those children older than 7 months, the incidence of recoarctation was only 10% [158].

A randomized study of 36 children aged 3–10 years, of whom 20 underwent balloon dilatation and 16 surgical repair of native coarctation, showed no statistical difference in the incidence of recoarctation [159]. Late follow-up of 21 of these patients, an average of 10 years after intervention, showed no difference in the blood pressure, gradients, or reintervention rate, although the aneurysm rate was higher after balloon dilatation [160]. A nonrandomized study of 46 children showed a low recoarctation rate with both procedures (<7%) and no aneurysms in either [161]. Another nonrandomized retrospective study of 80 patients found a reintervention rate of 32% in the catheter intervention group (some had stenting) and 0% in the surgical group [162].

Management of recoarctation

Before 1983, reoperation was the accepted treatment for recoarctation. Repeat surgery, however, did not always abolish the residual obstruction, mortality was 3–33%, and significant morbidity included spinal cord damage and cerebrovascular

events [117,163–166]. Balloon dilatation rapidly became the method of choice for recoarctation after surgical repair [167]. Recoarctation after balloon dilatation could be treated with either repeat dilatation or surgery. Surgery is not compromised by the previous balloon dilatation, although when collaterals have regressed femoral bypass or extra-anatomic repair are performed to prevent paraplegia [74,99,145]. Since the introduction of stent implantation (and covered stent implantation), recoarctation after previous balloon dilatation is more likely to be treated by catheter intervention. Small aneurysms that previously might have been treated surgically rather than by catheter intervention can now be addressed at the same time with a covered stent [111,168].

Aneurysm formation

Aneurysms may occur spontaneously in coarctation, particularly if it is untreated for many years. They also occur after any type of coarctation surgery, but most often with Dacron patch repair. and after balloon dilatation and stent implantation. The incidence is low after covered stent implantation, which is also used to treat aneurysms [111,168]. Because of varying definitions of aneurysms and the lack of randomized studies, their incidence is unknown. Many surgical and balloon dilatation series report no aneurysm formation but the incidence rises with the duration of follow-up [14,169–175].

A 16% incidence of ascending or descending aortic wall complications causing death or requiring a surgical or catheter intervention was reported in 235 adults (182 surgical repair, 28 catheter intervention, and 26 untreated) [175]. Ascending aortic complications were three times more frequent than in those in the descending aorta (coarctation site). Age or type of repair did not predict aortic wall complications, but age at the time of follow-up and a bicuspid aortic valve were predictive. Importantly, even untreated patients with a mild coarctation had a 15% incidence in aortic wall complications. A smaller study of 124 adults after coarctation repair revealed a bicuspid aortic valve in 62%, and 28% required an aortic valve intervention. Ascending aorta dilatation >4.0 cm was present in 28% [176]. Bicuspid aortic valve is an independent risk factor for ascending aorta dilatation [177]. Presumably, minor increases in systemic blood pressure and/or a transverse arch or coarctation site gradient may accentuate the ascending aorta dilatation in coarctation patients with a bicuspid aortic valve.

Hypertension

Treatment of coarctation, whether by catheter or surgery, usually results in a rapid fall in upper limb blood pressure. In the longer term, however, numerous series report hypertension requiring medication in about one-third of patients. Hypertension contributes to the high mortality seen in the long-term studies of patients operated on many years previously. Although recoarctation is an obvious cause of ongoing hypertension, it is not the only factor [178,179].

Often a degree of transverse arch hypoplasia that did not warrant surgery in early life appears on MRI scanning later to be more significant and is associated with hypertension and increase in left ventricular mass [180,181]. Acceptance of gradients of 5–25 mmHg across the aortic arch or coarctation site may also be responsible for the incidence of hypertension [182]. In earlier years, a "perfect" result was less important than survival without major morbidity, and so recoarctation was defined by what was achievable. The long-term results of the extended end-to-end repair should address these issues. A counter argument is that the repair site, even if wide enough, cannot distend during exercise or acts as an obstruction to the arterial wave form, thus causing a gradient [183]. The incidence of hypertension may relate to the age of repair. Thus, either the early renal hypoperfusion prior to correction has "reset" the renin–angiotensin–aldosterone system or the upper limb hypertension has "reset" the aortic baroreceptors permanently [184,185]. Even early repair is accompanied by hypertension and increased arterial stiffness [186–188].

Ambulatory blood pressure should be obtained from the right arm so that the effects of the hypoplastic arch and left subclavian involvement in the coarctation or its repair do not falsely lower the blood pressure reading. Blood pressure measurements during exercise have been used to assess the repair state and blood pressure response. The significance of an exaggerated response in a patient with normal or minimally elevated blood pressure is unclear [189,190].

Coronary artery disease

Coronary artery disease seems accelerated in postoperative coarctation patients with early cardiac death observed [147–149,191]. Accelerated atheroma of the internal mammary arteries has been observed [192]. Although the etiology of this accelerated atherosclerotic heart disease is unknown, a number of factors probably play a role, including hypertension, residual mild obstruction, aortic valve disease, peripheral vasculature abnormalities, and the coronary microcirculation [154]. After coarctation repair, in the arm but not the leg, resistance is elevated and has a reduced hyperemic response [154,193,194]. The pulsatility of the poststenotic aorta, which is severely impaired prior to repair, does not return to normal, and the degree of impairment may correlate with the age at surgery [195]. The intima–media thickness in the precoarctation segment (carotid artery) remains greater than in the postcoarctation segment (femoral artery) after repair [196]. More recently, abnormal long-axis ventricular function and subendocardial ischemia in patients with a "good" repair have been found [197,198].

Future directions

Advances in prenatal detection should allow more accurate prediction of coarctation postnatally and avoid the risk of acute cardiovascular collapse in undiagnosed neonates. Pulse oximetry in the nursery also detects some patients not otherwise suspected of this diagnosis. Longer-term follow-up of current neonatal repair will reveal the likelihood of cure without ongoing hypertension and the risk of other cardiovascular complications. Fundamental issues such as the cause (and effect) of aortic elastic impairment and abnormal vascular reactivity need to be addressed [153,154]. Newer stents that are biodegradable may encourage implantation in small children [199], and lower profile delivery systems will reduce the risk of vascular access complications.

Interrupted aortic arch

Interrupted aortic arch differs from coarctation of the aorta in that continuity between the ascending and descending aorta is absent. When a fibrous cord is present across the interruption, the anomaly is called aortic arch atresia, but it has identical clinical presentation. In arch atresia with fibrous continuity at the level of the coarctation, the clinical presentation resembles severe coarctation because of collateral development. In some infants, a severe coarctation may progress to acquired atresia. Interrupted aortic arch is a rare anomaly that accounts for <1.5% of all congenital heart disease [200].

Pathology and embryology

Celoria and Patton [201] classified interrupted aortic arch into three types according to site of the interruption: A, distal to the left subclavian artery; B, between the left subclavian artery and the left common carotid artery; and C, between the left common carotid and innominate arteries (Figure 32.8). Types A and B have been subdivided into A2 and B2 when the right subclavian artery arises anomalously from the descending aorta. The most common type is B, and C is the rarest [201–203]. Interruption is invariably associated with other intracardiac anomalies, the commonest being a ventricular septal defect. In a series of 105 patients [202], a ventricular septal defect was present in 98, and the only coexisting malformation in 58. The ventricular septal defect is usually a perimembranous or muscular outlet with varying degrees of posterior deviation of the outlet septum that can cause subaortic obstruction, but doubly committed defects also occur [204]. Other coexisting anomalies include aortopulmonary window, double-outlet right ventricle, ventriculoarterial discordance, congenitally corrected transposition, and Shone syndrome. There are no reports associating interruption with pulmonary atresia. The most common extracardiac association is DiGeorge syndrome, due to microdeletion in the long arm of chromosome 22 [205], occurring in up to 44% of patients with type B interruption.

The most widely accepted theory on the embryologic basis of interrupted aortic arch is that the posteriorly deviated malaligned outlet septum alters fetal hemodynamics so that
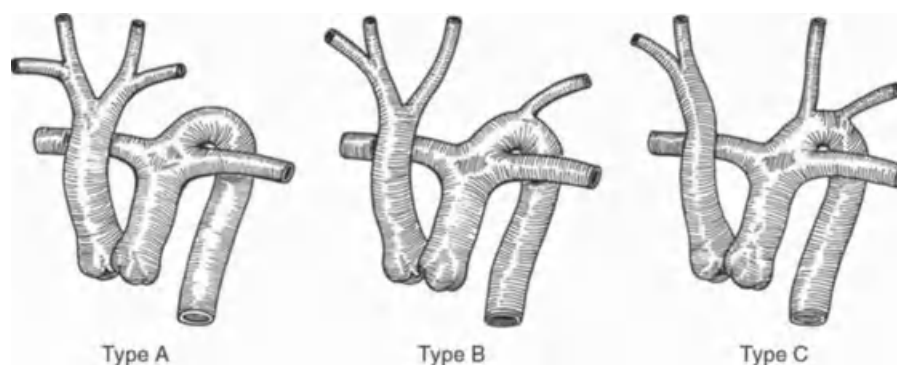
Figure 32.8 Anatomic classification of interrupted aortic arch.

reduced aortic flow hampers development of the aortic arch. Thus, the magnitude of blood flow through the fetal arch is critically important to both its enlargement and its evolution [206,207]. The rare patient of Pillsbury *et al.* [208], without any intracardiac malformations, however, suggests that morphogenic factors in addition to anterograde aortic blood flow are involved.

Pathophysiology

At birth, blood flow to the descending aorta depends on a patent ductus arteriosus. When the ductus closes, perfusion to the lower part of the body and kidneys becomes inadequate, renal function becomes impaired, urine output diminishes, and severe metabolic acidosis leads to hemodynamic collapse. If the ductus remains patent, then as the pulmonary resistance falls, pulmonary blood flow increases at the expense of reduced systemic perfusion. This is accompanied by left ventricular volume overload and acidosis that leads to progressive biventricular failure. Without treatment of interrupted aortic arch, the median age of death is 4–10 days [200]. Long-term survival is only possible with persistent patency of the ductus arteriosus and the development of pulmonary vascular disease from the increased right ventricular systolic pressure needed to perfuse the lower body.

History and physical examination

Patients with interrupted aortic arch often present with severe symptoms soon after birth – most with severe congestive heart failure during the first 2 weeks of life [200].

The physical findings depend on the size of the ductus arteriosus, the pulmonary vascular resistance, and the type of intracardiac malformations. The neonate is tachypneic with retractions, tachycardia, and hepatomegaly, and usually has rales. Precordial activity is always increased, and the second sound is accentuated. A systolic murmur is heard along the left sternal border due to increased pulmonary blood flow. A mid-diastolic rumble over the mitral valve from excessive pulmonary blood flow may also be heard. A gallop rhythm is usually present and an ejection click if the aortic valve is bicuspid.

Femoral pulses are usually weak, and there is almost always a blood pressure difference between upper and lower extremities. The difference in pulse character can be helpful in differentiating the type of interrupted aortic arch. In type C interruption, absent femoral and left carotid and brachial pulses and a normal right carotid and brachial pulse are found; type B interruption may have absent left brachial and femoral pulses, yet normal right and left carotid pulses; type A is similar to coarctation with only absent femoral pulses. If the right subclavian artery arises aberrantly from the descending aorta, the right carotid pulse is strong and the right brachial pulse weak. When the ductus is widely patent, there is little difference in upper and lower extremity pulses and blood pressures. With severe hemodynamic collapse, differences in pulses are often not apparent until resuscitation has improved the cardiac output.

In individuals who have normally related great arteries, differential cyanosis between the upper and lower parts of the body may be noted (a pink head and blue abdomen), but this is usually not striking because of massive intracardiac left-to-right shunting. In patients with double-outlet right ventricle or d-transposition, the upper part of the body may be cyanotic whereas the lower part of the body is acyanotic, resulting in reversed differential cyanosis. Although these differences in oxygen saturation may not be detected by physical examination alone, they can frequently be detected by pulse oximetry. In the rare natural survivors, finger clubbing is present in the cyanotic segment.

Electrocardiogram and chest film

The electrocardiogram is not diagnostic and its pattern depends on associated anomalies; there are usually right-axis deviation and right ventricular hypertrophy. The chest film is also not diagnostic, showing cardiomegaly and increased pulmonary vascular markings. Absence of a thymus shadow may suggest an associated 22q deletion.

Echocardiographic features

The site of interruption can be visualized from suprasternal arch views [209,210]. In interrupted aortic arch, type B, the
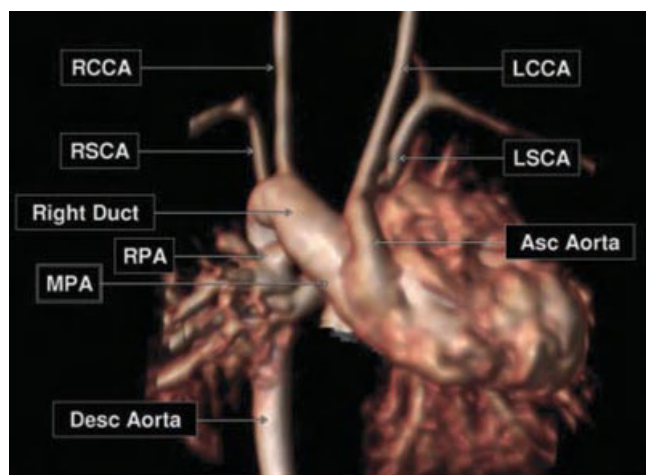
Figure 32.9 MRI scan to clarify the anatomy in a neonate with a right arch and interruption between the carotid arteries which was not clear on echocardiography. This is exquisitely demonstrated in Videoclip 32.3. Asc Aorta, ascending aorta; Desc Aorta, descending aorta; LCCA, left common carotid artery; LSCA, left subclavian artery; MPA, main pulmonary artery; RCCA, right common carotid artery; RPA, right pulmonary artery; RSCA, right subclavian artery.

ascending aorta is smaller than usual and can be seen to terminate in the left carotid artery, and the ductus arteriosus continues into the descending aorta which is large (Videoclip 32.3). There is no evidence of an aortic arch linking the ascending and descending portions of the aorta. Flow to the left subclavian artery is retrograde from the descending aorta. If there is an anomalous right subclavian artery, this too can be seen.

The apical and parasternal views can delineate the margins of the ventricular septal defect and its relationship to the great arteries and other intracardiac anomalies. Evidence of or potential for left ventricular outflow tract obstruction, which occurs in >50% of these children, is assessed. Useful preoperative echocardiographic predictors of left ventricular outflow tract obstruction include the cross-sectional area of the left ventricular outflow tract, an aortic valve annulus <4.5 mm and a Z score <−5 [211,212]. Type B interruptions have a higher incidence of outflow tract obstruction than type A, as does an aberrant right subclavian artery.

Cardiac catheterization and angiography

Cardiac catheterization has been supplanted by echocardiography. When the exact arch anatomy remains unclear, then tomographic cardiac CT or MRI are more frequently used than angiography to clarify the anatomy (Figure 32.9; Videoclip 32.3) [213]. Angiography is rarely needed for defining anatomic features that have not been clearly resolved by other imaging techniques. It has a role for intervention after surgical repair.

Medical management

When diagnosed prenatally, the neonate should be delivered at a cardiac center and commenced on a prostaglandin E_1 infusion (5 ng kg^{-1} min^{-1}) to maintain ductal patency until corrective surgery. In those who present in shock or heart failure, urgent stabilization, including mechanical ventilation, inotrope therapy, and prostaglandin infusion, is required. Higher doses of prostaglandin (50–100 ng kg^{-1} min^{-1}) are needed for some hours to re-establish ductal patency in these neonates. Once the hemodynamics have stabilized and the acidosis is resolved, surgery is performed. A high inspired concentration of oxygen is avoided as it may reduce the pulmonary vascular resistance and by increasing pulmonary blood flow reduce systemic perfusion and worsen the acidosis. Calcium levels should be measured because of the high incidence of DiGeorge syndrome and *irradiated blood should be used for transfusion*.

Surgical management

The first successful repair of interruption was in 1955 by Merrill *et al.* [214], who divided the ductus and performed an end-to-side anastomosis between the ascending and descending aorta in a 3½-year-old child. Two ventricular septal defects were subsequently closed 4 years later.

Re-establishment of continuity between the ascending and descending aorta is ideally performed without a prosthetic conduit. Although effective at relieving the aortic obstruction, conduits require replacement with growth of the child and increase morbidity and mortality from reoperating in a heavily scarred area [215]. Currently, a direct anastomosis is performed if possible [216]. This requires meticulous dissection to mobilize the proximal and distal ends of the aorta for a tension-free anastomosis and removal of all ductal tissue. Frequently, the left subclavian artery is ligated and divided for this purpose. When there is an anomalous right subclavian artery originating from the descending aorta, this too may need sacrificing. It is then impossible to measure an upper limb blood pressure. The recurrent laryngeal and phrenic nerves on the left can be damaged, and the spinal cord may be at risk during clamping of the descending aorta after the ductus is ligated and excised. The left main bronchus may be compressed by the newly constructed arch and may require subsequent surgical aortopexy [217,218]. Narrowing at the repair site responds well to balloon dilatation (and may be repeated with growth), but reoperation is needed in some [216,219,220]. Repeat surgical options include patch enlargement, extra-anatomic bypass, and subclavian or carotid turn-down procedures.

The approach to correcting the intracardiac anomalies has evolved since the first repairs when palliation for the intracardiac anomalies was invariable (Figure 32.10). The change to primary repair is well illustrated by Menahem *et al.* [220]. From 1979 through 1984, 15/17 infants underwent a two-stage repair with initial reconstruction of the arch and pulmonary artery banding with a surgical mortality of 65%. From 1984 through 1988, 22/29 had a single-stage repair with a mortality of 13%. Although single-stage repair is now routine, an individualized approach may be needed – for
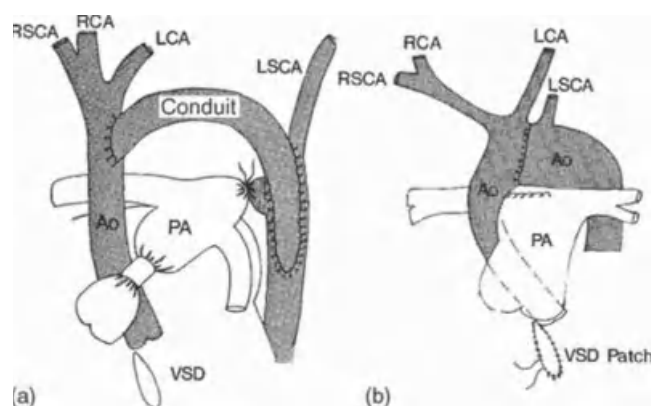
Figure 32.10 Diagram of interruption repair with interposition graft and pulmonary artery banding and duct ligation (a) and complete one-stage repair with a direct arch anastomosis and ventricular septal defect closure (b). LCA, left carotid artery; LSCA, left subclavian artery; PA, pulmonary artery; RCA, right carotid artery; RSCA, right subclavian artery; VSD, ventricular septal defect.

example, in low birth weight or premature neonates, staged repair is still more commonly used [220–225].

During single-stage repair, the most challenging aspect is managing left ventricular outflow tract obstruction [226,227]. Although complete repair including a subaortic myotomy/ myectomy is ideal, leaving a residual mild subaortic obstruction may be better than damaging the aortic valve by too extensive a dissection. Other approaches include the following: (1) Ross–Konno procedure –aortic root replacement with a pulmonary autograft combined with incision into the outlet septum and a pulmonary homograft placed in the right ventricular outflow tract [228,229]; (2) patching the ventricular septal defect to create a double-outlet left ventricle, aortopulmonary anastomosis, and conduit from right ventricle to pulmonary artery [230]; (3) resecting part of the outlet septum from a right atrial approach with patch closure of the enlarged ventricular septal defect to widen the subaortic area [231]; (4) placing the ventricular septal defect patch on the left side of the septum to deflect the outlet septum anteriorly and away from the subaortic area without resecting the outlet septum [223]; and (5) abandoning repair of the left ventricular outflow tract in favor of transplantation [232] or the Norwood procedure [233].

Currently, in patients with interruption and more complex intracardiac anomalies, for example, truncus arteriosus or double-outlet right ventricle, a biventricular repair is undertaken during the neonatal period, although the results are not as favorable. In a series of 50 neonates with interruption and truncus arteriosus who underwent predominantly one-stage repair, the survival at 6 months was 44% and at 10 years 31% [234]. Even in the setting of interruption and aortic valve atresia, single-stage repair is possible by repairing the arch and performing a Damus–Kaye–Stansel procedure [235].

When interruption is associated with a functional single ventricle, subaortic obstruction can be addressed by a Damus–

Kaye–Stansel procedure or the Norwood procedure. If outflow obstruction resection is required, it is ideally performed without a ventriculotomy to preserve ventricular function for a future single-ventricle repair. Good results have also been achieved with initial pulmonary artery banding followed by the Damus–Kaye–Stansel procedure [236].

Long-term outcome

Regardless of the type of repair, a high incidence of recurrent arch narrowing, left ventricular outflow obstruction, and bronchial compression are reported. The largest prospective study reported 472 neonates with interrupted arch and ventricular septal defect [237]. In this multi-institutional study, neonates were enrolled from 1987 to 1997. Nineteen died before repair from complications of prematurity and poor cardiac function. Of those who underwent surgery, the survival was 67% at 16 years, with 28% undergoing a second procedure. (The same group reported a 63% survival at 4 years when only 183 neonates had been enrolled [224].) In the subgroup who also underwent a left ventricular outflow tract procedure, survival was 63% at 16 years, with 28% undergoing a second procedure. A second arch procedure was performed in 109 patients, 52 by catheter intervention. Although direct anastomosis resulted in a lower mortality than with PTFE patch augmentation of the arch, the need for reintervention was similar. The risk factors for death and for left ventricular outflow tract procedure were low birth weight, younger age at repair, female gender, type B interruption, and major associated cardiac anomalies. The predicted mortality for an "ideal patient" – male, 3.5 kg, ventricular septal defect closed at the time of repair without PTFE augmentation of the arch and no other cardiac anomalies, was 7% at 16 years [237].

Other series have reported better results, but are much smaller with selected patient populations, retrospective, and often with shorter lengths of follow-up [215]. Although the mortality rates from surgery for this condition have improved, concerns remain about the neurodevelopmental outcomes [238]. Selective cerebral perfusion has improved mortality rates but not reduced neurodevelopmental disability [239]. Whereas the duration of deep hypothermic circulatory arrest correlates with worse developmental indices, as do chromosomal abnormalities, presentation with circulatory collapse and acidosis may also contribute.

Future directions

Improved surgical techniques are needed to minimize cerebral dysfunction during repair and correction of left ventricular outflow obstruction. Better prenatal diagnosis should prevent preoperative cardiovascular and neurological compromise.

Acknowledgments

References

1 Beekman R, Rocchini A. Coarctation of the aorta and interruption of the aortic arch. In: Moller J, Neal W, eds. *Fetal, Neonatal, and Infant Cardiac Disease*. Norwalk, CT: Appleton & Lange, 1990: 497–521.

2 Paris M. Rétrècissement considerable de l'aorte pectorale observé à l'Hotel Dieu de Paris. *J Chir Desault* 1791;**ii**:107.

3 Lewis T. Material relating to coarctation of the adult type. *Br Heart J* 1933;**16**:205–61.

4 Blankl H. Coarctation of the aorta. In: Blankl H, ed. *Congenital Malformations of the Heart and Great Vessels: Synopsis of Pathology, Embryology, and Natural History*. Baltimore: Urban & Schwarzenberg, 1977: 45.

5 Storch T, Mannick E. Epidemiology of congenital heart disease in Louisiana: an association between race and sex and the prevalence of specific cardiac malformations. *Teratology* 1992;**46**:271–6.

6 Beekman R, Robinow M. Coarctation of the aorta inherited as an autosomal dominant trait. *Am J Cardiol* 1985;**56**:818–9.

7 Sehested J. Coarctation of the aorta in monozygotic twins. *Br Heart J* 1982;**47**:619–20.

8 Ravelo H, Stephenson LW, Freidman S. Coarctation resection in children with Turner's syndrome. *J Thorac Cardiovasc Surg* 1980;**80**:427–30.

9 Gotzsche C-O, Krag-Olsen B, Nielsen J, *et al*. Prevalence of cardiovascular malformations and association with karyotypes in Turner's syndrome. *Arch Dis Child* 1994;**71**:433–6.

10 Edwards J, Christensen N, Clagett O. Pathologic considerations in coarctation of the aorta. *Mayo Clin Proc* 1948;**23**:324–32.

11 Becker AE, Becker MJ, Edwards JE. Anomalies associated with coarctation of aorta. Particular reference to infancy. *Circulation* 1970;**41**:1067–75.

12 Ho SY, Anderson RH. Coarctation, tubular hypoplasia, and the ductus arteriosus. Histological study of 35 specimens. *Br Heart J* 1979;**41**:268–74.

13 Russell G, Berry P, Watterson K. Patterns of ductal tissue in coarctation in the first three months of life. *J Thorac Cardiovasc Surg* 1991;**102**:596–601.

14 von Kodolitsch Y, Aydin MA, Koschyk DH, *et al*. Predictors of aneurysmal formation after surgical correction of aortic coarctation. *J Am Coll Cardiol* 2002;**39**:617–24.

15 Morrow WR, Huhta JC, Murphy DJ Jr, McNamara DG. Quantitative morphology of the aortic arch in neonatal coarctation. *J Am Coll Cardiol* 1986;**8**:616–20.

16 Poulias GE, Polemis L, Skoutas B, *et al*. Coarctation of the aorta of unusual morphology. *J Cardiovasc Surg (Torino)* 1984;**25**:211–5.

17 Graham M, Zelenock G, Erlandson E, Stanley J. Abdominal aortic coarctation and segmental hypoplasia. *Surgery* 1979; **86**:519–29.

18 Shone J, Sellers R, Anderson R. The developmental complex of "parachute mitral valve," supravalvar ring of left atrium, subaortic stenosis and coarctation of the aorta. *Am J Cardiol* 1963;**11**:714–25.

19 Rosenthal E. Coarctation of the aorta from fetus to adult: curable condition or life long disease process? *Heart* 2005;**91**: 1495–502.

20 Hodes H, Steinfeld L, Blumenthal S. Congenital cerebral aneurysms and coarctation of the aorta. *Arch Paediatr* 1959;**76**:28–43.

21 Serizawa T, Satoh A, Miyata A, *et al*. Ruptured cerebral aneurysm associated with coarctation of the aorta – report of two cases. *Neurol Med Chir (Tokyo)* 1992;**32**:342–5.

22 Kurihara Y, Kurihara H, Oda H, *et al*. Aortic arch malformations and ventricular septal defect in mice deficient in endothelin-1. *J Clin Invest* 1995;**96**:293–300.

23 Rudolph A, Heymann M, Spitznas U. Hemodynamic considerations in the development of narrowing of the aorta. *Am J Cardiol* 1972;**30**:514–25.

24 Head CEG, Jowett VC, Sharland GK, Simpson JM. Timing of presentation and postnatal outcome of infants suspected of having coarctation of the aorta during fetal life. *Heart* 2005;**91**:1070–4.

25 Allan LD, Chita SK, Anderson RH, *et al*. Coarctation of the aorta in prenatal life: an echocardiographic, anatomical, and functional study. *Br Heart J* 1988;**59**:356–60.

26 Sharland GK, Chan KY, Allan LD. Coarctation of the aorta: difficulties in prenatal diagnosis. *Br Heart J* 1994;**71**:70–5.

27 Hornberger L, Sahn D, Kleinman C, *et al*. Antenatal diagnosis of coarctation of the aorta: a multicenter experience. *J Am Coll Cardiol* 1994;**23**:417–23.

28 Graham T, Lewis B, Jarmakani M. Left ventricular volume and mass quantification in children with left ventricular pressure overload. *Circulation* 1970;**41**:203–12.

29 Abbott ME. Statistical study and historical retrospect of 200 recorded cases, with autopsy, of stenosis or obliteration of the descending arch in subjects above the age of two years. *Am Heart J* 1928;**3**:392–421, 574–618.

30 Reifenstein GH, Levine SA, Gross RE. Coarctation of the aorta: a review of 104 autopsied cases of the 'adult-type', 2 years of age or older. *Am Heart J* 1947;**33**:146–68.

31 Campbell M. Natural history of coarctation of the aorta. *Br Heart J* 1970;**32**:633–40.

32 Campbell M, Baylis J. The course and prognosis of coarctation of the aorta. *Br Heart J* 1956;**18**:475–95.

33 Strafford M, Griffiths S, Gersony W. Coarctation of the aorta: a study in delayed detection. *Pediatrics* 1982;**69**:159–63.

34 Wren C, Reinhardt Z, Khawaja K. Twenty-year trends in diagnosis of life-threatening neonatal cardiovascular malformations. *Arch Dis Child Fetal Neonatal Ed* 2008;**93**:F33–5.

35 Mehwald PS, Dittrich S, Grohmann J, *et al*. Coarctation of the aorta presenting as cerebral hemorrhage. *J Pediatr* 2005; **146**:293.

36 Ing F, Starc T, Griffiths S, Gersony W. Early diagnosis of coarctation of the aorta in children: a continuing dilemma. *Pediatrics* 1996;**98**:378–82.

37 Sinha S, Kardatzke M, Cole R, Paul M. Coarctation of the aorta in infancy. *Circulation* 1969;**40**:385–98.

38 Perloff J. Coarctation of the aorta. In: Perloff J, ed. *The Clinical Recognition of Congenital Heart Disease*. Philadelphia: Saunders, 1978: 126–53.

39 Smallhorn J, Huhta J, Adams P. Cross-sectional echocardiographic assessment of coarctation in the sick neonate and infant. *Br Heart J* 1983;**50**:349–61.

40 Huhta J, Gutgesell H, Latson L, Huffines F. Two-dimensional echocardiographic assessment of the aorta in infants and children with congenital heart disease. *Circulation* 1984;**70**:417–24.

41 Simpson I, Sahn D, Valdes-Cruz L. Color Doppler flow mapping in patients with coarctation of the aorta: new observations and improved evaluations with color flow diameter and proximal

acceleration as predictors of severity. *Circulation* 1988; **77**:736–44.

42 Carvalho J, Remington A, Shinebourne E. Continuous wave Doppler echocardiography and coarctation of the aorta: gradients and flow pattern in the assessment of severity. *Br Heart J* 1990;**64**:133–7.

43 Franklin O, Burch M, Manning N, *et al*. Prenatal diagnosis of coarctation of the aorta improves survival and reduces morbidity. *Heart* 2002;**87**:67–9.

44 Matsui H, Mellander M, Roughton M, *et al*. Morphological and physiological predictors of fetal aortic coarctation. *Circulation* 2008;**118**:1793–801.

45 Therrien J, Thorne SA, Wright A, *et al*. Repaired coarctation: a 'cost effective' approach to identify complications in adults. *J Am Coll Cardiol* 2000;**35**:997–1002.

46 Rosenthal E, Bell A. Optimal imaging after coarctation stenting. *Heart* 2010;**96**:1169–71.

47 Alsoufi B, Cai S, Coles JG, *et al*. Outcomes of different surgical strategies in the treatment of neonates with aortic coarctation and associated ventricular septal defects. *Ann Thorac Surg* 2007;**84**:1331–7.

48 Kanter KR. Management of infants with coarctation and ventricular septal defect. *Semin Thorac Cardiovasc Surg* 2007; **19**:264–8.

49 Walters HL III, Ionan CE, Thomas RL, Delius RE. Single-stage versus 2-stage repair of coarctation of the aorta with ventricular septal defect. *J Thorac Cardiovasc Surg* 2008;**135**:754–61.

50 Talwar S, Choudhary SK, Airan B. Single-stage versus 2-stage repair of coarctation of the aorta with ventricular septal defect. *J Thorac Cardiovasc Surg* 2008;**136**:1390–1.

51 Fyler D, Buckley L, Hellenbrand W. Report of the New England Regional Infant Cardiac Program. *Pediatrics* 1980;**65**:375–461.

52 Fesseha AK, Eidem BW, Dibardino DJ, *et al*. Neonates with aortic coarctation and cardiogenic shock: presentation and outcomes. *Ann Thorac Surg* 2005;**79**:1650–5.

53 Crafoord C, Nylin G. Congenital coarctation of the aorta and its surgical treatment. *J Thorac Surg* 1945;**14**:347–61.

54 Gross R. Surgical correction for coarctation of the aorta. *Surgery* 1945;**18**:673–8.

55 Kirklin J, Burchell H, Pugh D, *et al*. Surgical treatment of coarctation of the aorta in a ten week old infant: report of a case. *Circulation* 1952;**6**:411–4.

56 Kappetein A, Zwinderman A, Bogers A, *et al*. More than thirty-five years of coarctation repair. An unexpected high relapse rate. *J Thorac Cardiovasc Surg* 1994;**107**:87–95.

57 Messmer B, Minale C, Muhler E. Surgical correction of coarctation in early infancy: does surgical technique influence the results? *Ann Thorac Surg* 1991;**52**:594–600.

58 Arenas J, Myers J, Gleason M, *et al*. End-to-end repair of aortic coarctation using absorbable polydioxanone suture. *Ann Thorac Surg* 1991;**51**:413–7.

59 Vosschulte K. Surgical correction of coarctation of the aorta by an "isthmus-plastic" operation. *Thorax* 1961;**16**:338–45.

60 DeSanto A, Bills R, King H. Pathogenesis of aneurysm formation opposite prosthetic patches used for coarctation repair. *J Thorac Cardiovasc Surg* 1987;**94**:720–3.

61 Heikkinen L, Sariola H, Salo J, *et al*. Morphological and histopathological aspects of aneurysms after patch aortoplasty for coarctation. *Ann Thorac Surg* 1990;**50**:946–8.

62 Bromberg B, Beekman RH, Rocchini A, *et al*. Aortic aneurysm after patch aortoplasty repair of coarctation: a prospective analysis of prevalence, screening tests and risks. *J Am Coll Cardiol* 1989;**14**:734–41.

63 Parks WJ, Ngo TD, Plauth WH, *et al*. Incidence of aneurysm formation after Dacron patch aortoplasty repair for coarctation of the aorta: long-term results and assessment utilizing magnetic resonance angiography with three-dimensional surface rendering. *J Am Coll Cardiol*. 1995;**26**:266–71.

64 Rheuban K, Gutgesell H, Carpenter M, Jedeiken R. Aortic aneurysm after patch angioplasty for aortic isthmic coarctation in childhood. *Am J Cardiol* 1986;**58**:178–80.

65 McGiffin D, McGiffin P, Galbraith A, Cross R. Aortic wall stress profile after repair of coarctation of the aorta: is it related to subsequent true aneurysm formation? *J Thorac Cardiovasc Surg* 1992;**104**:924–31.

66 Waldhausen JA, Nahrwold DL. Repair of coarctation of the aorta with a subclavian flap. *J Thorac Cardiovasc Surg* 1966;**51**:532–3.

67 Todd PJ, Dangerfield PH, Hamilton DI, Wilkinson JL. Late effects on the left upper limb of subclavian flap aortoplasty. *J Thorac Cardiovasc Surg* 1983;**85**:678–81.

68 Van Son J, Van Asten W, Van Lier H, *et al*. Detrimental sequelae on the hemodynamics of the upper left limb after subclavian flap angioplasty in infancy. *Circulation* 1990;**81**:996–1004.

69 Martin M, Beekman R, Rocchini A, *et al*. Aortic aneurysms after subclavian angioplasty repair of coarctation of the aorta. *Am J Cardiol* 1988;**61**:951–3.

70 Kino K, Sano S, Sugawara E, *et al*. Late aneurysm after subclavian flap aortoplasty for coarctation of the aorta. *Ann Thorac Surg* 1996;**61**:1262–4.

71 Beekman R, Rocchini A, Behrendt D, *et al*. Long-term outcome for repair of coarctation in infancy: subclavian angioplasty does not reduce the need for reoperation. *J Am Coll Cardiol* 1986;**8**:1406–11.

72 Barreiro CJ, Ellison TA, Williams JA, *et al*. Subclavian flap aortoplasty: still a safe, reproducible, and effective treatment for infant coarctation. *Eur J Cardiothorac Surg* 2007;**31**:649–53.

73 Morris G, Cooley D, DeBakey M, Crawford R. Coarctation of the aorta with particular emphasis upon improved technique of surgical repair. *J Thorac Cardiovasc Surg* 1960;**40**:705–12.

74 Schoenhoff FS, Berdat PA, Pavlovic M, *et al*. Off-pump extra-anatomic aortic bypass for the treatment of complex aortic coarctation and hypoplastic aortic arch. *Ann Thorac Surg* 2008;**85**: 460–4.

75 Lansman S, Shapiro A, Schiller M, *et al*. Extended aortic arch anastomoses for repair of coarctation in infancy. *Circulation* 1986;**74**:136–41.

76 Zannini L, Lecompte Y, Galli R. Aortic coarctation with arch hypoplasia: a new surgical technique. *G Ital Cardiol* 1985; **15**:1045–8.

77 Elliott M. Coarctation of the aorta with arch hypoplasia: improvements on a new technique. *Ann Thorac Surg* 1987;**44**:321–3.

78 Elgamal M-A, McKenzie ED, Fraser CD. Aortic arch advancement: the optimal one-stage approach for surgical management of neonatal coarctation with arch hypoplasia. *Ann Thorac Surg* 2002;**73**:1267–73.

79 Younoszai AK, Reddy VM, Hanley FL, Brook MM. Intermediate term follow-up of the end-to-side aortic anastomosis for coarctation of the aorta. *Ann Thorac Surg* 2002;**74**:1631–4.

80 Wood AE, Javadpour H, Duff D, *et al.* Is extended arch aorto-plasty the operation of choice for infant aortic coarctation? Results of 15 years' experience in 181 patients. *Ann Thorac Surg* 2004;**77**:1353–8.

81 Thomson JDR, Mulpur A, Guerrero R, *et al.* Outcome after extended arch repair for aortic coarctation. *Heart* 2006;**92**:90–4.

82 Kaushal S, Backer CL, Patel JN, *et al.* Coarctation of the aorta: midterm outcomes of resection with extended end-to-end anastomosis. *Ann Thorac Surg* 2009;**88**:1932–8.

83 Brouwer MHJ, Cromme-Dijkhuis AH, Ebels T, Eijgelaar A. Growth of the hypoplastic aortic arch after simple coarctation resection and end-to-end anastomosis. *J Thorac Cardiovasc Surg* 1992;**104**:426–33.

84 Kiraly L, Környei L, Mogyorossy G, Szatmari A. Hypoplastic aortic arch in newborns rapidly adapts to post-coarctectomy circulatory conditions. *Heart* 2005;**91**:233–4.

85 DiBardino DJ, Heinle JS, Kung GC, *et al.* Anatomic reconstruction for recurrent aortic obstruction in infants and children. *Ann Thorac Surg* 2004;**78**:926–32.

86 Brandt B, Heintz S, Rose E. Repair of coarctation of the aorta in children with Turner's syndrome. *Pediatr Cardiol* 1984;**5**:175–7.

87 Rocchini A, Rosenthal A, Barger A, *et al.* Pathogenesis of paradoxical hypertension after coarctation resection. *Circulation* 1976;**54**:382–7.

88 Choy M, Rocchini A, Beekman R, *et al.* Paradoxical hypertension after repair of coarctation of the aorta in children: balloon angioplasty versus surgical repair. *Circulation* 1987;**75**:1186–91.

89 Sealy W, Harris J, Young W. Paradoxical hypertension following resection of coarctation of the aorta. *Surgery* 1957;**42**:135–47.

90 Gidding S, Rocchini A, Beekman R, *et al.* Therapeutic effect of propanolol on paradoxical hypertension after repair of coarctation. *N Engl J Med* 1985;**312**:1224–8.

91 Tabbutt S, Nicolson SC, Dominguez TE, *et al.* Perioperative course in 118 infants and children undergoing coarctation repair via a thoracotomy: a prospective, multicenter experience. *J Thorac Cardiovasc Surg* 2008;**136**:1229–36.

92 Brewer L, Fosberg R, Mulder G. Spinal cord complications following surgery for coarctation of the aorta. *J Thorac Cardiovasc Surg* 1972;**64**:368–81.

93 Moreno N, de Campo T, Kaiser G. Technical and pharmacologic management of distal hypotension during repair of coarctation of the aorta. *J Thorac Cardiovasc Surg* 1980;**80**:182–6.

94 Keen G. Spinal cord damage and operations for coarctation of the aorta: etiology, practice and prospects. *Thorax* 1987;**42**:11–8.

95 Peters P, Brennan JW, Hughes CF, *et al.* Late quadriplegia after adult coarctation repair. *Ann Thorac Surg* 2003;**75**:268–70.

96 Wong CH, Watson B, Smith J, *et al.* The use of left heart bypass in adult and recurrent coarctation repair. *Eur J Cardiothorac Surg* 2001;**20**:1199–201.

97 Rokkas CK, Murphy SF, Kouchoukos NT. Aortic coarctation in the adult: management of complications and coexisting arterial abnormalities with hypothermic cardiopulmonary bypass and circulatory arrest. *J Thorac Cardiovasc Surg* 2002;**124**:155–61.

98 Gudbjartsson T, Mathur M, Mihaljevic T, *et al.* Hypothermic circulatory arrest for the surgical treatment of complicated adult coarctation of the aorta. *J Am Coll Cardiol* 2003;**41**:849–51.

99 Levy Praschker BG, Mordant P, Barreda E, *et al.* Long-term results of ascending aorta–abdominal aorta extra-anatomic bypass for recoarctation. *Eur J Cardiothorac Surg* 2008;**34**:805–9.

100 Fesseha AK, Eidem BW, Dibardino DJ, *et al.*, Neonates with aortic coarctation and cardiogenic shock: presentation and outcomes. *Ann Thorac Surg* 2005;**79**:1650–5.

101 Wright GE, Nowak CA, Goldberg CS, *et al.* Extended resection and end-to-end anastomosis for aortic coarctation in infants: results of a tailored surgical approach. *Ann Thorac Surg* 2005;**80**:1453–9.

102 Hager A, Schreiber C, Nutzl S, Hess J. Mortality and restenosis rate of surgical coarctation repair in infancy: a study of 191 patients. *Cardiology* 2008;**112**:36–41.

103 Sos T, Sniderman K, Rettek-Sos B, *et al.* Percutaneous transluminal dilatation of coarctation of thoracic aorta post mortem. *Lancet* 1979;**ii**:970–1.

104 Singer MI, Rowen M, Dorsy TJ. Transluminal aortic balloon angioplasty for coarctation of the aorta in the newborn. *Am Heart J* 1982;**103**:131–2.

105 Lock J, Bass J, Amplatz K, *et al.* Balloon dilatation angioplasty of aortic coarctations in infants and children. *Circulation* 1983;**68**:109–16.

106 Lababidi Z, Daskalopoulos D, Stoeckle H. Transluminal balloon coarctation angioplasty: experience with 27 patients. *Am J Cardiol* 1984;**54**:1288–91.

107 Allen HD, Marx G, Ovitt T, Goldberg S. Balloon dilatation angioplasty for coarctation of the aorta. *Am J Cardiol* 1986;**57**:828–32.

108 Tynan M, Finley J, Fontes V, *et al.* Balloon angioplasty for the treatment of native coarctation: results of Valvuloplasty and Angioplasty of Congenital Anomalies Registry. *Am J Cardiol* 1990;**65**:790–2.

109 O'Laughlin MP, Perry SB, Lock JE, Mullins CE. Use of endovascular stents in congenital heart disease. *Circulation* 1991;**83**:1923–39.

110 Hijazi ZM. Catheter intervention for adult aortic coarctation: be very careful! *Catheter Cardiovasc Interv* 2003;**59**:536–7.

111 Tzifa A, Ewert P, Brzezinska-Rajszys G, *et al.* Covered Cheatham-platinum stents for aortic coarctation: early and intermediate-term results. *J Am Coll Cardiol* 2006;**47**:1457–63.

112 Lock J, Niemi T, Burke B, *et al.* Transcutaneous angioplasty of experimental aortic coarctation. *Circulation* 1982;**66**:1280–6.

113 Isner JM, Donaldson RF, Fulton D. Cystic medial necrosis in coarctation of the aorta. *Circulation* 1987;**75**:689–95.

114 Kan J, White R, Mitchell S, *et al.* Treatment of restenosis of coarctation by percutaneous transluminal angioplasty. *Circulation* 1983;**68**:1087–94.

115 Hellebrand WE, Allen HD, Golinko RJ, *et al.* Balloon angioplasty for aortic recoarctation: results of the Valvuloplasty and Angioplasty of Congenital Anomalies Registry. *Am J Cardiol* 1990;**65**:793–7.

116 Beekman R, Rocchini A, Behrendt D, Rosenthal A. Reoperation for coarctation of the aorta. *Am J Cardiol* 1981;**48**:1108–14.

117 Pollack P, Freed M, Castenada A, Norwood W. Reoperation for isthmic coarctation of the aorta: follow-up of 26 patients. *Am J Cardiol* 1983;**51**:1690–4.

118 Maheshwari S, Bruckheimer E, Fahey JT, *et al.* Balloon angioplasty of postsurgical recoarctation in infants: the risk of restenosis and long term follow-up. *J Am Coll Cardiol* 2000;**35**:209–13.

119 Balaji S, Oommen R, Rees P G. Fatal aortic rupture during balloon dilatation of recoarctation. *Br Heart J*, 1991;**65**:100–1.

120 Joyce D, McGrath L. Pseudo-aneurysm formation following balloon angioplasty for recurrent coarctation of the aorta. *Cathet Cardiovasc Diagn* 1990;**20**:133–5.

121 Redington AN, Booth P, Shore DF, Rigby ML. Primary balloon dilatation of coarctation of the aorta in neonates. *Br Heart J* 1990;**64**:277–81.

122 Suarez de Lezo J, Pan M, Romero M, *et al*. Immediate and follow-up findings after stent treatment for severe coarctation of aorta. *Am J Cardiol* 1999;**83**:400–6.

123 Marshall AC, Perry SB, Keane JF, Lock JE. Early results and medium-term follow-up of stent implantation for mild residual or recurrent aortic coarctation. *Am Heart J* 2000;**139**:1054–60.

124 Magee AG, Brzezinska-Rajszys G, Qureshi SA, *et al*. Stent implantation for aortic coarctation and recoarctation. *Heart* 1999;**82**:600–6.

125 Varma C, Benson LN, Butany J, McLaughlin PR. Aortic dissection after stent dilatation for coarctation of the aorta: a case report and literature review. *Catheter Cardiovasc Interv* 2003;**59**:528–35.

126 Forbes TJ, Garekar S, Amin Z, *et al*. Procedural results and acute complications in stenting native and recurrent coarctation of the aorta in patients over 4 years of age: a multiinstitutional study. *Catheter Cardiovasc Interv* 2007;**70**:276–85.

127 Magee AG, Blauth CI, Qureshi SA. Interventional and surgical management of aortic stenosis and coarctation. *Ann Thorac Surg* 2001;**71**:713–5.

128 Holzer RJ, Chisolm JL, Hill SL, Cheatham JP. Stenting complex aortic arch obstructions. *Catheter Cardiovasc Interv* 2008;**71**:375–82.

129 Mohan UR, Danon S, Levi D, *et al*. Stent implantation for coarctation of the aorta in children <30 kg. *JACC Cardiovasc Interv* 2009;**2**:877–83.

130 Rao PS. Stents in the management of aortic coarctation in young children. *J Am Coll Cardiol Interv*, 2009;**2**:884–886.

131 Duke C, Rosenthal E, Qureshi SA. The efficacy and safety of stent redilatation in congenital heart disease. *Heart* 2003;**89**:905–12.

132 Fink C, Peuster M, Hausdorf G. Endovascular stenting as an emergency treatment for neonatal coarctation. C*ardiol Young* 2000;**10**:644–6.

133 Bentham J, Shettihalli N, Orchard E, *et al*. Endovascular stent placement is an acceptable alternative to reoperation in selected infants with residual or recurrent aortic arch obstruction. *Cathet Cardiovasc Interv* 2010;**76**:852–9.

134 Ince H, Petzsch M, Rehders T, *et al*. Percutaneous endovascular repair of aneurysm after previous coarctation surgery. *Circulation* 2003;**108**:2967–70.

135 Mitchell RS, Miller DC, Dake MD, *et al*. Thoracic aortic aneurysm repair with an endovascular stent graft: the "first generation." *Ann Thorac Surg* 1999;**67**:1971–4.

136 Rao PS. Should balloon angioplasty be used instead of surgery for native aortic coarctation? *Br Heart J* 1995;**74**:578–9.

137 Hanley FL. The various therapeutic approaches to aortic coarctation: is it fair to compare? *J Am Coll Cardiol* 1996;**27**:471–2.

138 Sakopoulos AG, Hahn TL, Turrentine M, Brown JW. Recurrent aortic coarctation: is surgical repair still the gold standard? *J Thorac Cardiovasc Surg* 1998;**116**:560–5.

139 Gibbs JL. Treatment options for coarctation of the aorta. *Heart* 2000;**84**:11–3.

140 Rosenthal E. Stent implantation for aortic coarctation: the treatment of choice in adults? *J Am Coll Cardiol* 2001;**38**:1524–7.

141 Mullen MJ. Coarctation of the aorta in adults: do we need surgeons? *Heart* 2003;**89**:3–5.

142 Marshall AC, Lock JE. Leaving Neverland: a randomized trial for coarctation shows pediatric interventional cardiology is growing up. *Circulation* 2005;**111**:3347–8.

143 Karl TR. Surgery is the best treatment for primary coarctation in the majority of cases. *J Cardiovasc Med* 2007;**8**:50–6.

144 Brown JW, Ruzmetov M, Hoyer MH, *et al*. Recurrent coarctation: is surgical repair of recurrent coarctation of the aorta safe and effective? *Ann Thorac Surg* 2009;**88**:1923–30.

145 Schoenhoff FS, Berdat PA, Pavlovic M, *et al*. Off-pump extra-anatomic aortic bypass for the treatment of complex aortic coarctation and hypoplastic aortic arch. *Ann Thorac Surg* 2008;**85**:460–4.

146 Marx GR. "Repaired" aortic coarctation in adults: not a "simple" congenital heart defect. *J Am Coll Cardiol* 2000;**35**:1003–6.

147 Presbitero P, Demarie D, Villani M, *et al*. Long term results (15–30 years) of surgical repair of aortic coarctation. *Br Heart J* 1987;**57**:462–7.

148 Cohen M, Fuster V, Steele PM, *et al*. Coarctation of the aorta. Long-term follow-up and prediction of outcome after surgical correction. *Circulation* 1989;**80**:840–5.

149 Toro-Salazar OH, Steinberger J, Thomas W, *et al*. Long-term follow-up of patients after coarctation of the aorta repair. *Am J Cardiol* 2002;**89**:541–7.

150 Swan L, Kraidly M, Vonder Muhll I, *et al*. Surveillance of cardiovascular risk in the normotensive patient with repaired aortic coarctation. *Int J Cardiol* 2010;**139**:283–8.

151 Therrien J, Warnes C, Daliento L, *et al*. Canadian Cardiovascular Society Consensus Conference 2001 update: recommendations for the management of adults with congenital heart disease. Part III. *Can J Cardiol* 2001;**17**:1135–58.

152 Deanfield J, Thaulow E, Warnes C, *et al*. Management of grown up congenital heart disease. *Eur Heart J* 2003;**24**:1035–84.

153 Vogt M, Kühn A, Baumgartner D, *et al*. Impaired elastic properties of the ascending aorta in newborns before and early after successful coarctation repair: proof of a systemic vascular disease of the prestenotic arteries? *Circulation* 2005;**111**:3269–73.

154 Gardiner HM, Celermajer DS, Sorensen KE, *et al*. Arterial reactivity is significantly impaired in normotensive young adults after successful repair of aortic coarctation in childhood. *Circulation* 1994;**89**:1745–50.

155 Van Heurn L, Wong C, Spiegelhalter D, *et al*. Surgical treatment of aortic coarctation in infants younger than three months: 1985 to 1990. Success of extended end-to-end arch aortoplasty. *J Thorac Cardiovasc Surg* 1994;**107**:74–85.

156 Rao P, Mohinder K, Galal O, Wilson A. Follow-up results of balloon angioplasty of native coarctation in neonates and infants. *Am Heart J* 1990;**120**:1310–4.

157 Mendelsohn A, Lloyd T, Crowley D, *et al*. Late follow-up of balloon angioplasty in children with a native coarctation of the aorta. *Am J Cardiol* 1994;**74**:696–700.

158 Fletcher S, Nihill M, Grifka R, *et al*. Balloon angioplasty of native coarctation of the aorta: midterm follow-up and prognostic factors. *J Am Coll Cardiol* 1995;**25**:730–4.

159 Shaddy RE, Boucek MM, Sturtevant JE, *et al*. Comparison of angioplasty and surgery for unoperated coarctation of the aorta. *Circulation* 1993;**87**:793–9.

160 Cowley CG, Orsmond GS, Feola P, *et al*. Long-term, randomized comparison of balloon angioplasty and surgery for native coarctation of the aorta in childhood. *Circulation* 2005;**111**:3453–6.

161 Walhout RJ, Lekkerkerker JC, Oron GH, *et al*. Comparison of surgical repair with balloon angioplasty for native coarctation in patients from 3 months to 16 years of age. *Eur J Cardiothorac Surg* 2004;**25**:722–7.

162 Rodes-Cabau J, Miro J, Dancea A, *et al*. Comparison of surgical and transcatheter treatment for native coarctation of the aorta in patients > or = 1 year old. The Quebec Native Coarctation of the Aorta study. *Am Heart J* 2007;**154**:186–92.

163 Cerilli J, Lauridsen P. Reoperation for coarctation of the aorta. *Acta Chir Scand* 1965;**129**:391–4.

164 Kirklin J, Barratt-Boyes B. Coarctation of the aorta and aortic arch interruption. In: Kirklin J, Barratt-Boyes B, eds. *Cardiac Surgery: Morphology, Diagnostic Criteria, Natural History, Techniques, Results and Indications*. New York: John Wiley & Sons, Inc., 1986: 1030.

165 Rosenthal E, Qureshi SA, Tynan M. Stent implantation for aortic recoarctation. *Am Heart J* 1995;**129**:1220–1.

166 Hellenbrand W, Allen H, Golinko R, *et al*. Balloon angioplasty for aortic recoarctation: results of Valvuloplasty and Angioplasty of Congenital Anomalies Registry. *Am J Cardiol* 1990;**65**:793–7.

167 Minich LL, Beekman RH III, Rocchini AP, *et al*. Surgical repair is safe and effective after unsuccessful balloon angioplasty of native coarctation of the aorta. *J Am Coll Cardiol* 1992;**19**:389–93.

168 Chakrabarti S, Kenny D, Morgan G, *et al*. Balloon expandable stent implantation for native and recurrent coarctation of the aorta: prospective computed tomography assessment of stent integrity, aneurysm formation and stenosis relief. *Heart* 2010;**96**:1212–6.

169 Rao PS, Galal O, Smith PA, Wilson AD. Five to nine year follow-up results of balloon angioplasty of native coarctation in infants and children. *J Am Coll Cardiol* 1996;**27**:462–70.

170 Fawzy ME, Fathala A, Osman A, *et al*. Twenty-two years of follow-up results of balloon angioplasty for discreet native coarctation of the aorta in adolescents and adults. *Am Heart J* 2008;**156**:910–7.

171 Walhout RJ, Suttorp MJ, Mackaij GJ, *et al*. Long-term outcome after balloon angioplasty of coarctation of the aorta in adolescents and adults: is aneurysm formation an issue? *Cathet Cardiovasc Interv* 2009;**73**:549–56.

172 Knyshov GV, Sitar LL, Glagola MD, *et al*. Aortic aneurysms at the site of the repair of coarctation of the aorta: a review of 48 patients. *Ann Thorac Surg* 1996;**61**:935–9.

173 Fujita T, Fukushima N, Taketani S, *et al*. Late true aneurysm after bypass grafting for long aortic coarctation. *Ann Thorac Surg* 1996;**62**:1511–3.

174 Kino K, Sano S, Sugawara E, *et al*. Late aneurysm after subclavian flap aortoplasty for coarctation of the aorta. *Ann Thorac Surg* 1996;**61**:1262–4.

175 Oliver JM, Gallego P, Gonzalez A, *et al*. Risk factors for aortic complications in adults with coarctation of the aorta. *J Am Coll Cardiol* 2004;**44**:1641–7.

176 Roos-Hesselink JW, Schölzel BE, Heijdra RJ, *et al*. Aortic valve and aortic arch pathology after coarctation repair. *Heart* 2003;**89**:1074–7.

177 Warnes CA. Bicuspid aortic valve and coarctation: two villains part of a diffuse problem. *Heart* 2003;**89**:965–6.

178 Eicken A, Pensl U, Sebening W, *et al*. The fate of systemic blood pressure in patients after effectively stented coarctation. *Eur Heart J* 2006;**27**:1100–5.

179 Hager A, Kanz S, Kaemmerer H, *et al*. Coarctation long-term assessment (COALA): significance of arterial hypertension in a cohort of 404 patients up to 27 years after surgical repair of isolated coarctation of the aorta, even in the absence of restenosis and prosthetic material. *J Thorac Cardiovasc Surg* 2007;**134**:738–45.

180 Ou P, Bonnet D, Auriacombe L, *et al*. Late systemic hypertension and aortic arch geometry after successful repair of coarctation of the aorta. *Eur Heart J* 2004;**25**:1853–9.

181 Ou P, Celermajer DS, Raisky O, *et al*. Angular (Gothic) aortic arch leads to enhanced systolic wave reflection, central aortic stiffness, and increased left ventricular mass late after aortic coarctation repair: evaluation with magnetic resonance flow mapping. *J Thorac Cardiovasc Surg* 2008;**135**:62–8.

182 Vriend J, Zwinderman A, de Groot E, *et al*. Predictive value of mild, residual descending aortic narrowing for blood pressure and vascular damage in patients after repair of aortic coarctation. *Eur Heart J* 2005;**26**:84–90.

183 Chen SSM, Donald AE, Storry C, *et al*. Impact of aortic stenting on peripheral vascular function and daytime systolic blood pressure in adult coarctation. *Heart* 2008;**94**:919–24.

184 Beekman RH, Katz BP, Moorehead-Steffens C, *et al*. Altered baroreceptor function in children with systolic hypertension after coarctation repair. *Am J Cardiol*. 1983;**52**:112–7.

185 Johnson D, Perrault H, Vobecky SJ, *et al*. Resetting of the cardiopulmonary baroreflex 10 years after surgical repair of coarctation of the aorta. *Heart* 2001;**85**:318–25.

186 Seirafi PA, Warner KG, Geggel RL, *et al*. Repair of coarctation of the aorta during infancy minimizes the risk of late hypertension. *Ann Thorac Surg* 1998;**66**:1378–82.

187 O'Sullivan JJ, Derrick G, Darnell R. Prevalence of hypertension in children after early repair of coarctation of the aorta: a cohort study using casual and 24-hour blood pressure measurement. *Heart* 2002;**88**:163–6.

188 Kenny D, Polson JW, Martin RP, *et al*. Surgical approach for aortic coarctation influences arterial compliance and blood pressure control. *Ann Thorac Surg* 2010;**90**:600–4.

189 Swan L, Goyal S, Hsia C, *et al*. Exercise systolic blood pressures are of questionable value in the assessment of the adult with a previous coarctation repair. *Heart* 2003;**89**:189–92.

190 Markham LW, Knecht SK, Daniels SR, *et al*. Development of exercise-induced arm–leg blood pressure gradient and abnormal arterial compliance in patients with repaired coarctation of the aorta. *Am J Cardiol* 2004;**94**:1200–2.

191 Stewart A, Ahmed R, Travill C, Newman C. Coarctation of the aorta life and health 20–44 years after surgical repair. *Br Heart J* 1993;**69**:65–70.

192 Chen R, Reul G, Cooley D. Severe internal mammary artery athero-sclerosis after correction of coarctation of the aorta. *Ann Thorac Surg* 1995;**59**:1228–30.

193 de Divitiis M, Pilla C, Kattenhorn M, *et al*. Vascular dysfunction after repair of coarctation of the aorta: impact of early surgery. *Circulation* 2001;**104**(Suppl I):I-165–70.

194 Brili S, Dernellis J, Aggeli C, *et al*. Aortic elastic properties in patients with repaired coarctation of aorta. *Am J Cardiol* 1998;**82**:1140–3.

195 Pfammatter J-P, Berdat P, Carrel T. Impaired poststenotic aortic pulsatility after hemodynamically ideal coarctation repair in children. *Pediatr Cardiol* 2004;**25**:495–9.

196 Vriend JJW, De Groot E, Kastelein JJP, Mulder BJM. Carotid and femoral B-mode ultrasound intima–media thickness measurements in adult post-coarctectomy patients. *Int Angiol* 2004;**23**:41–6.

197 Lam YY, Kaya MG, Li W, *et al*. Effect of chronic afterload increase on left ventricular myocardial function in patients with congenital left sided obstructive lesions. *Am J Cardiol* 2007;**99**:1582–7.

198 Cook SC, Ferketich AK, Raman SV. Myocardial ischemia in asymptomatic adults with repaired aortic coarctation. *Int J Cardiol* 2009;**133**:95–101.

199 Schranz D, Zartner P, Michel-Behnke I, Akinturk H. Bio-absorbable metal stents for percutaneous treatment of critical recoarctation of the aorta in a newborn. *Cathet Cardiovasc Interv* 2006;**67**:671–3.

200 Collins-Nakai R, Dick M, Parisi-Buckley L, *et al*. Interrupted aortic arch in infancy. *J Pediatr* 1976;**88**:959–62.

201 Celoria G, Patton R. Congenital absence of the aortic arch. *Am Heart J* 1959;**58**:407–13.

202 Moller J, Edwards J. Interruption of aortic arch. Anatomic patterns and associated cardiac malformations. *Am J Roentgenol* 1965;**95**:557–72.

203 Van Praagh R, Bernhard W, Rosenthal A, *et al*. Interrupted aortic arch surgical treatment. *Am J Cardiol* 1971;**27**:200–11.

204 Freedom RM, Bain HH, Esplugas E, *et al*. Ventricular septal defect in interruption of aortic arch. *Am J Cardiol* 1977;**39**:572–82.

205 Momma K, Kondo C, Matsuoka R, Takao A. Cardiac anomalies associated with a chromosome 22q11 deletion in patients with conotruncal anomaly face syndrome. *Am J Cardiol* 1996; **78**:591–5.

206 Congdon E, Wang H. The mechanical processes concerned in the formation of the differing types of aortic arches of the chick and the divergent early development of the pulmonary arches. *Am J Anat* 1926;**37**:499–520.

207 Jaffee O. The development of the arterial outflow tract in the duck embryo heart. *Anat Rec* 1967;**158**:35–42.

208 Pillsbury R, Lower R, Shumway N. Atresia of the aortic arch. *Circulation* 1964;**30**:749–54.

209 Snider AR, Silverman N. Suprasternal notch echocardiography: a two-dimensional technique for evaluation of congenital heart disease. *Circulation* 1981;**63**:165–73.

210 Smallhorn J, Anderson R, Macartney F. Cross-sectional echocardiographic recognition of interruption of aortic arch between left carotid and subclavian arteries. *Br Heart J* 1982;**48**:229–35.

211 Geva T, Hornberger L, Sanders S, *et al*. Echocardiographic predictors of left ventricular outflow tract obstruction after repair of interrupted aortic arch. *J Am Coll Cardiol* 1993;**22**:1953–60.

212 Salem MM, Starnes VA, Wells WJ, *et al*. Predictors of left ventricular outflow obstruction following single-stage repair of interrupted aortic arch and ventricular septal defect. *Am J Cardiol* 2000;**86**:1044–7.

213 Roche KJ, Krinsky G, Lee VS, *et al*. Interrupted aortic arch: diagnosis with gadolinium-enhanced 3D MRA. *J Comput Assist Tomogr* 1999;**23**:197–202.

214 Merrill D, Webster C, Samson P. Congenital absence of the aortic isthmus. *J Thorac Cardiovasc Surg* 1957;**33**:311–20.

215 Hussein A, Iyengar AJ, Jones B, *et al*. Twenty-three years of single-stage end-to-side anastomosis repair of interrupted aortic arches. *J Thorac Cardiovasc Surg* 2010;**139**:942–9.

216 Morales DLS, Scully PT, Braud BE, *et al*. Interrupted aortic arch repair: aortic arch advancement without a patch minimizes arch reinterventions. *Ann Thorac Surg* 2006;**82**:1577–83.

217 Sell JE, Jonas RA, Mayer JE, *et al*. The results of a surgical program for interrupted aortic arch. *J Thorac Cardiovasc Surg* 1988;**96**:864–77.

218 Sakai T, Miki S, Ueda Y, *et al*. Left main bronchus compression after aortic reconstruction for interruption of aortic arch. *Eur J Cardiothorac Surg* 2005;**9**:667–9.

219 Brown JW, Ruzmetov M, Okada Y, *et al*. Truncus arteriosus repair: outcomes, risk factors, reoperation and management. *Eur J Cardiothorac Surg* 2001;**20**:221–7.

220 Menahem S, Rahayoe A, Brawn W, Mee R. Interrupted aortic arch in infancy: a 10-year experience. *Pediatr Cardiol* 1992;**13**:214–21.

221 Jacobs M, Chin A, Rychik J, *et al*. Interrupted aortic arch. Impact of subaortic stenosis on management and outcome. *Circulation* 1995;**92**(Suppl):II-128–31.

222 Sandhu S, Beekman R, Mosca R, Bove E. Single-stage repair of aortic arch obstruction and associated intracardiac defects in the neonate. *Am J Cardiol* 1995;**75**:370–3.

223 Luciani G, Ackerman R, Chang A, *et al*. One-stage repair of interrupted aortic arch, ventricular septal defect and subaortic obstruction in the neonate: a novel approach. *J Thorac Cardiovasc Surg* 1996;**111**:348–58.

224 Jonas R, Quaegebeur J, Kirklin J, *et al*. Outcomes in patients with interrupted aortic arch and ventricular septal defect. A multi- institutional study. Congenital Heart Surgeons Society. *J Thorac Cardiovasc Surg* 1994;**107**:1099–109.

225 Flint JD, Gentles TL, MacCormick J, *et al*. Outcomes using predominantly single-stage approach to interrupted aortic arch and associated defects. *Ann Thorac Surg*, 2010; **89**:564–9.

226 Mishra PK. Management strategies for interrupted aortic arch with associated anomalies. *Eur J Cardiothorac Surg* 2009; **35**:569–76.

227 Gersony W. Ventricular septal defect and left sided obstructive lesions in infants. *Curr Opin Pediatr* 1994;**6**:596–9.

228 Starnes V, Luciani G, Wells W, *et al*. Aortic root replacement with the pulmonary autograft in children with complex left heart obstruction. *Ann Thorac Surg* 1996;**62**:442–8.

229 Reddy V, Rajasinghe H, Teitel D, *et al*. Aortoventriculoplasty with the pulmonary autograft: the "Ross–Konno" procedure. *J Thorac Cardiovasc Surg* 1996;**111**:158–65.

230 Serraf A, Lacour-Gayet F, Robotin M, *et al*. Repair of interrupted aortic arch: a ten-year experience. *J Thorac Cardiovasc Surg* 1996;**112**:1150–60.

231 Bove E, Minich L, Pridjian A, *et al*. The management of severe subaortic stenosis, ventricular septal defect, and aortic arch obstruction in the neonate. *J Thorac Cardiovasc Surg* 1993;**105**:289–95.

232 Razzouk A, Chinnock R, Gundry S, *et al*. Transplantation as a primary treatment for hypoplastic left heart syndrome: intermediate-term results. *Ann Thorac Surg* 1996;**62**:1–7.

233 Jacobs M, Rychik J, Murphy J, *et al*. Results of Norwood's operation for lesions other than hypoplastic left heart syndrome. *J Thorac Cardiovasc Surg* 1995;**110**:1555–61.

234 Konstantinov IE, Karamlou T, Blackstone EH, *et al*. Truncus arteriosus associated with interrupted aortic arch in 50 neonates: a Congenital Heart Surgeons Society study. *Ann Thorac Surg* 2006;**81**:214–22.

235 Gruber PJ, Fuller S, Cleaver KM, *et al*. Early results of single-stage biventricular repair of severe aortic hypoplasia or atresia with ventricular septal defect and normal left ventricle. *J Thorac Cardiovasc Surg* 2006;**132**:260–3.

236 Rodefeld MD, Ruzmetov M, Schamberger MS, *et al*. Staged surgical repair of functional single ventricle in infants with unobstructed pulmonary blood flow. *Eur J Cardiothorac Surg* 2005;**27**:949–55.

237 McCrindle BW, Tchervenkov CI, Konstantinov IE, *et al*. Risk factors associated with mortality and interventions in 472 neonates with interrupted aortic arch: a Congenital Heart Surgeons Society study. *J Thorac Cardiovasc Surg* 2005;**129**:343–50.

238 Joynt CA, Robertson CMT, Cheung P-Y, *et al*.; Western Canadian Complex Pediatric Therapies Follow-up Group. Two-year neurodevelopmental outcomes of infants undergoing neonatal cardiac surgery for interrupted aortic arch: a descriptive analysis. *J Thorac Cardiovasc Surg* 2009;**138**:924–32.

239 Tlaskal T, Vojtovic P, Reich O, *et al*. Improved results after the primary repair of interrupted aortic arch: impact of a new management protocol with isolated cerebral perfusion. *Eur J Cardiothorac Surg* 2010;**38**:52–8.

33 Right Ventricular Outflow Tract Obstruction

Philipp C. Lurz[1], Ingo Daehnert[1] & Philipp Bonhoeffer[2]

[1]University of Leipzig – Heart Center, Leipzig, Germany
[2]Great Ormond Street Hospital for Children, London, UK

Right ventricular outflow tract obstruction may occur within the ventricle, at the valve itself, or in the pulmonary arteries. The obstruction may be solitary or occur at multiple levels. As an isolated lesion, pulmonic stenosis accounts for ~10% of cardiac malformations. In association with other lesions, the incidence may be as high as 25–30% of congenital heart disease.

Valvar pulmonic stenosis

Incidence and genetics

This is a common lesion that may occur sporadically or recur in families (>3% of siblings also have pulmonic stenosis) [1]. It may occur in the Noonan syndrome, the LEOPARD syndrome, or neurofibromatosis [2,3].

Embryology

The pathologic process has been ascribed to an abnormality in the development of the distal bulbus cordis [4]. The exact cause is unclear.

Pathology

Pulmonic stenosis may occur in a tricuspid, bicuspid, or dysplastic pulmonic valve. Usually, there are three cusps with fusion of the commissures. As a result, the valve becomes dome shaped and projects into the pulmonary trunk [5]. The stenotic valve orifice is usually central, but is occasionally eccentric. The valve cusps are usually thin, but can be thickened and even calcified.

As a result of the obstruction, generalized right ventricular hypertrophy occurs. This may be more marked in the infundibular region, where dynamic obstruction may develop. The right atrium may become dilated if the stenosis is severe and compliance of the right ventricle decreased.

The wall of the right atrium may thicken, and the foramen ovale dilate.

The pulmonary artery shows post-stenotic dilatation, which may extend into one of the branches and is almost always present after infancy. The left pulmonary artery is usually dilated as the "jet" through the stenotic orifice is directed towards the left pulmonary artery. There is no correlation between severity of the obstruction and the degree of post-stenotic dilatation. Although post-stenotic dilatation may occur in a dysplastic valve, its incidence is lower than in patients with classic pulmonic stenosis.

An important pathologic subgroup (having clinical and therapeutic implications) is that of the dysplastic valve, with an incidence in Noonan syndrome of ~60%. This valve consists of three thickened, immobile cusps with little, if any, commissural fusion. The cusps are composed of disorganized myxomatous tissue. The valve annulus is usually narrow, and the supravalvar area of the pulmonary trunk is also hypoplastic.

Pathophysiology

Regardless of the features of the pulmonary valve, the physiologic effects depend on the degree of stenosis. As the valve orifice diminishes, right systolic ventricular pressure increases (roughly as a squared function) to maintain the cardiac output. Right ventricular hypertrophy develops in proportion to the right ventricular systolic pressure. The ventricular trabeculations are increased. In severe stenoses, the right ventricular cavity is decreased in size.

Rarely in severe stenosis with suprasystemic right ventricular systolic pressure and especially if it is long-standing, myocardial ischemia may occur and lead to myocardial fibrosis and eventually congestive cardiac failure [6]. Rudolph has made a significant contribution to our understanding of fetal and neonatal factors contributing to the physiology in

such patients [7]. An essential difference in the response of the very young to afterload is hyperplasia in addition to hypertrophy of myocardial fibers. In the neonatal response to afterload, the number of capillaries is increased. This provides the capacity to produce extremely high systolic ventricular pressures. The stroke volume is usually maintained by the hypertrophied muscle although, after a period of sustained elevated pressure, cardiac failure may occur if the ventricle dilates. Cardiac output is usually maintained.

Pulmonary blood flow is decreased and cyanosis is present when right-to-left shunting occurs at the atrial level in association with right ventricular fibrosis (and decreased compliance), right ventricular failure, or decreased size of the right ventricle (due to hypertrophy, which also causes decreased compliance). Hypoplasia of the right ventricle, a separate entity, may simulate the last condition [8]. There is a continuum between severe neonatal pulmonary stenosis and pulmonary atresia with intact ventricular septum.

Clinical features

Clinical history

Neonates with critical stenosis may be in congestive heart failure or cyanotic from a right-to-left atrial shunt. In the first days of life, the gradient increases as pulmonary vascular resistance decreases. Symptoms may be mild provided that the arterial duct is patent and rapid deterioration may occur with duct closure.

Beyond the neonatal period, most patients are asymptomatic, even with severe stenosis. Currently, most patients undergo treatment to relieve the stenosis before symptoms appear (certainly those beyond the neonatal period). In infancy, symptoms are rare, but can include dyspnea and fatigue on effort. Even in severe stenosis, marked symptoms are unusual because the right ventricle maintains cardiac output for long periods before decompensation. Rarely, chest pain, syncope, and even sudden death may occur during exercise in patients with severe stenosis.

Cyanosis is rare in childhood but possibly occurs in adults as right ventricular compliance decreases and shunting occurs through a patent foramen ovale.

In nonsyndromic patients, intelligence is usually normal.

Physical examination

Growth and development are usually normal, regardless of the degree of the stenosis. Facial and other features may be specific in the Noonan syndrome [2,3], the LEOPARD syndrome, and neurofibromatosis. In the first two conditions, there are triangular facies, ptosis, and hypertelorism. In those with the Noonan and LEOPARD syndromes, both growth and development may be subnormal (often below the 10th percentile).

Cardiac findings depend on the severity of the obstruction. Signs of congestive cardiac failure are usually present only in severe stenosis during infancy. The peripheral pulse and systemic blood pressure are normal. The jugular venous pulse may be altered in severe stenosis, with a prominent *a* wave. A right ventricular heave may be found, depending on the degree of right ventricular hypertrophy. A systolic thrill at the second and third left intercostal spaces is common; it does not parallel severity of the lesion and is often present in mild to moderate stenosis.

Auscultation is particularly accurate in predicting the severity of the lesion, probably more so than in any other congenital lesion [9,10]. The first heart sound is usually normal. An early ejection systolic click is a typical and often identifying feature of classic pulmonic valvar stenosis. The ejection sound is heard with mild or moderate stenosis. It does not occur in subvalvar or supravalvar stenosis and is absent in patients with severe stenosis or a dysplastic valve. The click becomes louder during expiration and softer in inspiration. In expiration, the right atrial contractile force decreases so that the pulmonary valve is in a relatively closed position when the right ventricle contracts; therefore, its systolic excursion is increased, and the ejection sound is louder.

A systolic ejection murmur is heard best at the upper left sternal border. It may be transmitted throughout the precordium and importantly to the left upper back. In general, louder murmurs indicate more severe stenosis, but the distinction is imperfect.

The length and timing of the peak of the murmur vary with the severity of stenosis, which obviously determines the length of contraction. In patients with mild stenosis, the murmur is relatively short, and the peak does not occur beyond mid-systole. In moderate stenosis, the peak occurs later, and the murmur may end at or slightly beyond the aortic component of the second heart sound. With severe stenosis, the peak occurs even later in systole, and the murmur ends beyond the aortic component of the second sound. With increasing severity of stenosis, the frequency of the murmur also increases because the velocity of flow through the narrow orifice is increased.

The degree of splitting of the second heart sound varies with severity. In mild stenosis, the split is normal, and the pulmonic component is clearly audible. The degree of splitting increases with increasing severity and the pulmonic component becomes softer in severe stenosis so that the duration of the split may be 0.12–0.14 s and the pulmonic component soft or inaudible. In addition, if it is audible, the split may be almost unchanging because of a fixed right ventricular volume. A fourth heart sound may be heard in patients with severe stenosis. In infants with severe stenosis, an additional systolic murmur that increases with inspiration, indicating tricuspid insufficiency, may be audible.

Electrocardiographic features

The electrocardiographic changes are right atrial enlargement, right-axis deviation, and right ventricular hypertrophy [11]. In mild valvar stenosis, the electrocardiogram is often
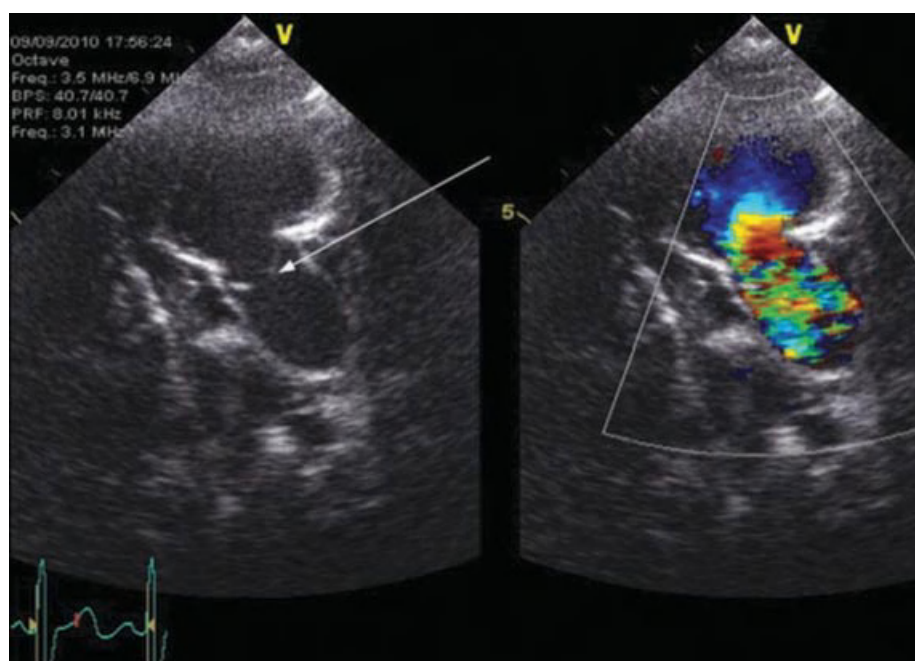
Figure 33.1 Typical 2D and color Doppler image of isolated valvar pulmonary stenosis in a modified parasternal long-axis view. The right ventricular outflow tract is not stenotic. Arrow points to doming valve.

normal, with only mild right-axis deviation and often an rSR′ or rR′ pattern in lead V1. In moderate stenosis, the electrocardiogram is abnormal in >90% of patients. Right-axis deviation may be present (usually between 90 and 30° mean frontal axis). On occasion, right atrial enlargement is found. An rR′ or RS complex is usually present in lead V1. In severe stenosis, the P wave is abnormal. The mean frontal axis varies from +100 to +170°. In lead V1, a pure R wave or RS or QR pattern may be present. The T waves may remain negative but often become upright in severe stenosis. An R wave above 30 mV in lead V1 correlates with severe stenosis. Although the electrocardiogram may be normal in aortic stenosis, even if severe, this is extremely rare in pulmonic stenosis.

In patients with a dysplastic valve (usually those with Noonan's syndrome), the electrocardiogram is atypical with a left anterior hemiblock pattern and counterclockwise QRS frontal plane loop. The mean frontal QRS axis is superiorly directed, and deep S waves are present in the precordium, regardless of the level of systolic pressure in the right ventricle. With associated hypertrophic cardiomyopathy, left ventricular hypertrophy may be present.

Arrhythmias are rare in pulmonic stenosis. Supraventricular arrhythmia may occur in an untreated patient with severe stenosis, and ventricular arrhythmias may occur in the older untreated patients, especially during exercise.

Chest X-ray
Radiographic features are much less reliable than physical findings and electrocardiographic features in assessing the severity of the lesion. Cardiac size is usually normal. Post-stenotic dilatation of the main and often the left pulmonary

artery is present and produces a prominent pulmonary artery segment on the posteroanterior chest radiograph. The prominence of the pulmonary artery does not correlate with the degree of stenosis, and although dysplastic valves may have little or no post-stenotic dilatation, this is certainly not a general rule [12]. It is not uncommon for a normal adolescent to be referred for evaluation of possible congenital heart disease because of a prominent pulmonary artery segment on the chest radiograph.

Echocardiography
The abnormal pulmonary valve can be visualized on a parasternal short-axis view at the level of the great arteries. The valve may also be evaluated from a subxiphoid short-axis view (Figure 33.1, Videoclips 33.1 and 33.2). The valve domes during systole, appearing as a convex line of varying thickness at the pulmonary annulus. The pulmonary trunk is dilated (post-stenotic dilatation). Color Doppler imaging shows the direction of the jet through the valve, and continuous-wave Doppler imaging allows assessment of the severity of the stenosis. The peak instantaneous systolic gradient across the valve may be calculated by the simplified Bernoulli equation ($\Delta P = 4 \times V_{max}^2$). A gradient ≤40 mmHg is considered mild, 40–70 mmHg is considered moderate, and >70 mmHg is severe. The right ventricular systolic pressure is increased according to the severity of the pulmonic stenosis. The severity of stenosis may be assessed qualitatively by the degree of thickening of the right ventricular wall or by the presence or absence of systolic flattening of the intraventricular septum on a short-axis view. However, flattening of the septum appears even when the systolic pressure in the

right ventricle is less than systemic. Due to increased wall stress of the RV free wall, there is prolonged right ventricular shortening as compared with left ventricular shortening, causing the septum to bow leftwards in late right ventricular systole, which coincidences with early left ventricular diastole/filling. If there is tricuspid regurgitation, the right ventricular systolic pressure may be assessed quantitatively by applying the simplified Bernoulli equation to the regurgitation jet. The right ventricular systolic pressure equals the peak systolic gradient of this jet in addition to the right atrial pressure (usually 5–10 mmHg). This pressure may be compared with the systemic blood pressure measured by the blood pressure cuff.

In neonates there might be a patent arterial duct with left-to-right shunt.

In infants with severe valvar pulmonic stenosis, a right-to-left shunt across the foramen ovale may be demonstrated by color Doppler or contrast-enhanced echocardiography. In these infants, some hypoplasia of the right ventricular cavity may be present, and this decreases the compliance of the ventricle and enhances the right-to-left shunt. Bowing of the atrial septum from right to left may be seen with a right-to-left shunt at the atrial level because of the increased right atrial pressure. In a dysplastic pulmonary valve, the leaflets are markedly thickened and move poorly, and there may be hypoplasia of the pulmonary valve annulus and narrowing of the pulmonary trunk.

Cardiac catheterization

Cardiac catheterization is principally performed for balloon valvoplasty. In most patients, oxygen saturation data do not demonstrate an intracardiac shunt, although the combination of pulmonic stenosis and a secundum atrial septal defect is common. In patients with severe obstruction and associated intracardiac communication, a right-to-left shunt through a foramen ovale may be detected.

The severity of the stenosis is determined by the peak systolic pressure gradient across the pulmonary valve and the systolic pressure ratio of the right ventricle to the aorta or the left ventricle. Carefully obtained withdrawal pressure tracings from the pulmonary artery to the right ventricle provide information concerning the site and severity of the stenosis.

When the resting right ventricular systolic pressure is <50 mmHg or the gradient is <30 mmHg, the stenosis is characterized as mild. In moderate valvar pulmonic stenosis, the right ventricular systolic pressure may equal that of the aorta or the gradient may be 30–50 mmHg. In severe obstruction, the resting right ventricular pressure is suprasystemic, and the gradient is >50 mmHg (the gradients measured at catheterization are usually less than those measured by Doppler echocardiography.) The pulmonary valve area may be calculated the Gorlin equation and is normally about 2 cm² m⁻². Because cardiac output is usually normal, even in severe stenosis, the valve area is only rarely calculated. The most important hemodynamic factor that influences the systolic pressure gradient is the heart rate.

The end-diastolic pressure in the right ventricle may be normal, but when there is severe obstruction or right ventricular dysfunction, it may be elevated. Tall right atrial *a* waves are usually present in severe pulmonic stenosis, particularly when there is only a small interatrial communication. Tall right atrial *v* waves are present when moderately severe tricuspid insufficiency is associated. In severe stenosis, the pulsatility of the pulmonary artery pressure tracing is absent. Associated infundibular stenosis may be present, especially in severe stenosis, and may be suspected from the withdrawal pressure tracing.

Angiography

Right ventriculograms in the PA and lateral projections with a 25° cranial tilt provide information about the right ventricular size and function, any associated infundibular stenosis, and the pulmonary valve (Videoclip 33.3).

The right ventricular size is usually normal, although there can be moderate to severe right ventricular hypoplasia, especially in neonates. The typical stenotic valve is thickened and domes during systole. The annulus is usually normal but may be hypoplastic in neonates or infants and in those with severe valvar pulmonic stenosis. Post-stenotic dilatation of the pulmonary trunk and left pulmonary artery is usually seen. In a dysplastic valve, the leaflets are thickened and relatively immobile. The main pulmonary artery and the annulus may be moderately hypoplastic. There may be post-stenotic dilatation of the pulmonary trunk, although this is less marked than in classic valvar stenosis.

In patients with severe valvar pulmonic stenosis, diffuse narrowing of the right ventricular outflow tract due to hypertrophy may be seen during middle to late systole, but this narrowing disappears during diastole.

Other imaging modalities

Magnetic resonance imaging (MRI) represents an important noninvasive imaging tool apart from echocardiography. Although in neonates the spatial resolution is an important limitation of this technique, its role is increasing, especially in adults. The static, three-dimensional anatomic features of the RVOT can easily be appreciated on MRI. Further, cine images give dynamic information on the function of the RVOT; for instance, they can nicely demonstrate any dynamic muscular RVOT obstruction. MRI also offers a quantitative analysis of pulmonary regurgitation in those patients who develop pulmonary insufficiency after surgical or interventional treatment. Most importantly, MRI represents the most valid technique to determine right ventricular size, function, and wall thickness and thereby facilitate the assessment of pathophysiology in the presence of RVOT dysfunction.

If MRI is contraindicated, cardiac computed tomography (CT) can be used for the three- dimensional assessment of the anatomy, and three-dimensional reconstruction of the RVOT throughout the cardiac cycle ("four-dimensional imaging") is possible. These images help in planning interventional strategies in these patients. Nevertheless, echocardiography represents the most important and easily accessible noninvasive imaging technique in the setting of RVOT obstruction.

Management

Patients with mild valvar pulmonic stenosis do not require intervention. They should be treated as normal children and not restricted from physical activity [13–15]. An indication for treatment in infants, children, and adolescents, with or without symptoms, is a transvalvar gradient >40 mmHg in the absence of fixed subpulmonary obstruction or additional lesions that need operative interventions. Most patients are asymptomatic, even with severe obstruction. The successful relief of obstruction improves clinical outcome. Severe valvar pulmonic stenosis leads to symptoms and signs of right-sided heart failure, especially in long-standing obstruction in adults [16–20].

Neonates

In contrast to older infants and children, critical pulmonic stenosis in neonates requires emergency treatment to prevent death [21–23].

Initially, infusion of prostaglandin E_1 or E_2 should be commenced as early as possible to maintain ductal patency until definitive treatment is available. Treatment, when necessary, consists of balloon valvoplasty, which gives excellent results. Surgical valvotomy is limited to patients with more complex lesions or those with dysplastic valves in whom balloon dilation has failed.

Successful dilatation occurs in >95% of neonates [24–40]. In some neonates, the smaller and noncompliant right ventricle may be inadequate for maintaining normal pulmonary blood flow. Prolonged prostaglandin infusion gives time for the right ventricular compliance to improve after regression of its hypertrophy. If slow recovery is to be expected, prostaglandin is not tolerated or if cyanosis persists (oxygen saturation <80%) after 3 weeks of prostaglandin infusion, ductal stenting or a systemic-to-pulmonary artery shunt should be considered.

Complications are more common in neonates than in older patients, with a mortality rate of 3%, major complications 3.5%, and minor complications 15% [24–34,41]. On longer follow-up, about 10–15% of patients need reintervention, either repeated balloon dilatation or surgery for either infundibular stenosis or a dysplastic valve. Morphologic follow-up studies have confirmed that the valve matures from its dysplastic appearance, and the annulus and right ventricular cavity grow [39]. The results compare favorably with operation [40]. Hence we currently consider balloon valvoplasty to be the treatment of choice in neonates with isolated critical valvar pulmonic stenosis, regardless of mild right ventricular hypoplasia or valve morphology.

Infants

Asymptomatic infants with severe valvar pulmonic stenosis should be treated electively, usually around the age of 9–12 months. Balloon valvoplasty may be performed earlier if the lesion is extremely severe. The rationale for intervention has included relief of symptoms, prevention of secondary changes in the right ventricle and pulmonary artery, and prevention of progression to more severe obstruction. Successful relief of obstruction is associated with an improved clinical outcome [16–20].

Balloon valvoplasty

After hemodynamic measurements of the right ventricle/aortic pressure ratio and the transvalvar gradient, accurate measurements of the diameter of the valve annulus are obtained from AP and lateral angiocardiograms. A guidewire of appropriate stiffness is positioned in a distal pulmonary artery. With the wire carefully fixed in place, the balloon dilatation catheter is advanced over the wire until the valve lies exactly half way along the length of the balloon. When a single balloon is used, the balloon diameter should be ~20% larger than the diameter of the pulmonary valve annulus. The balloon is inflated until the waist is abolished and not beyond its prescribed pressure. The balloon is then rapidly deflated, with the entire cycle of inflation and deflation taking no more than 10–15 s. The inflation–deflation process is repeated with the balloon repositioned slightly forwards or backwards between each inflation if the waist could not be abolished or the balloon position was not stable during inflation (Figure 33.2, Videoclip 33.4).

For a larger valve annulus, a double-balloon technique was developed. For this technique, a second exchange wire for a second balloon can be used. Alternatively, a multi-track balloon catheter allows for the advancement of two balloons over the same wire. When two balloons are used, the combined diameters of the two balloons should be at least 1.6–1.8 times the diameter of the valve annulus. The two balloons are inflated and deflated simultaneously. Although double-balloon dilatations are rarely required, several added advantages immediately become apparent for large patients. The two balloons inflate and deflate faster than a single larger balloon. This, coupled with the persistent "lumen" through the valve between the two inflated balloons, results in much less effect on the systemic arterial pressure at maximal inflation than with a single balloon. Even in a smaller valve, the relatively smooth contour of the two much lower profile balloons results in less trauma to the vessels at the site of introduction. Because of these advantages, the double-balloon technique has been adapted for most pulmonary valve
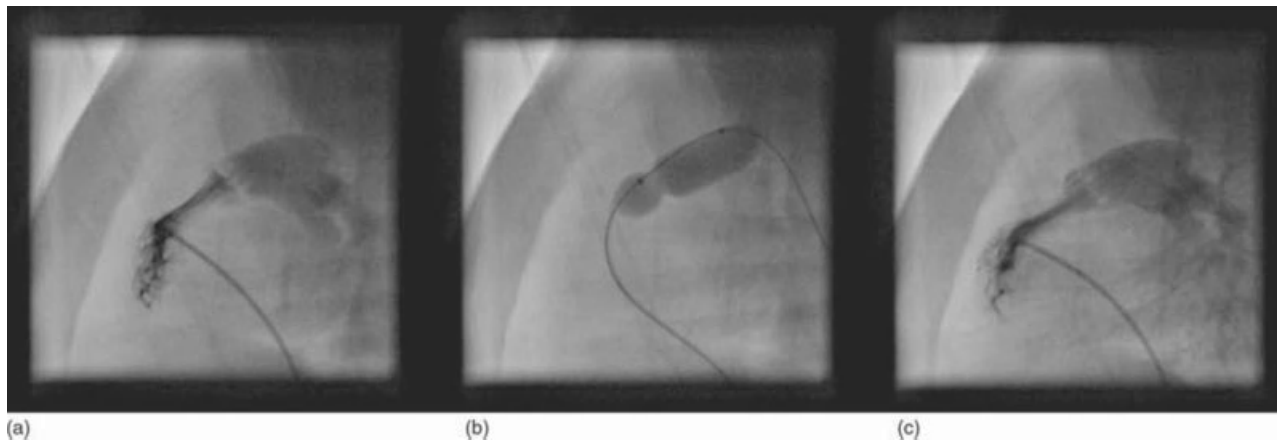
Figure 33.2 Lateral right ventricular angiograms (LAO 90°) of an infant with valvar pulmonary stenosis undergoing balloon dilation. (a) Before the intervention with a thick, doming valve and post-stenotic dilation of the main stem pulmonary artery. (b) The dilating balloon with a tight waist at the level of the stenosis. With higher pressure the waist disappears. (c) Typical result with a good central opening of the valve and a narrow right ventricular outflow tract ("reactive infundibular stenosis") which is due to right ventricular hypertrophy and will diminish over time.

dilatations in adult patients, even if a single adequate-sized balloon is available.

The goal of the pulmonary valve dilatation is to relieve outflow tract obstruction with residual gradient as low as possible. Often, the gradient across the valve can be reduced to <10–15 mmHg. However, particularly in patients with more severe stenosis, there may be dynamic subvalvar right ventricular outflow tract obstruction. Once the valvar obstruction is relieved, the subvalvar gradient becomes manifest, and angiographically the subvalvar area narrows markedly. This reaction was recognized long ago by the surgeons as the "suicide right ventricle" after operative relief of severe valvar stenosis. Fortunately, in the catheterization laboratory, without the trauma of operation and cardiopulmonary bypass, this is a nonfatal reaction, and the stenosis regresses with time if the valvar stenosis has been adequately relieved.

Some severely dysplastic pulmonary valves cannot be dilated adequately. Unless there are extreme degrees of these echocardiographic and angiocardiographic features, the valve may be mildly dysplastic and possible to dilate. An attempt should be made to dilate these valves when significant stenosis is present.

The safety and efficacy of balloon valvoplasty of a stenotic pulmonary valve in infants, children, adolescents, and adults have been confirmed by numerous studies [42–72]. Acute and long-term results are excellent, with reduction of valve gradient in most patients to a hemodynamically insignificant level. In comparison with valvotomy, balloon valvoplasty provides equivalent long-term gradient relief with only trivial to mild pulmonary insufficiency during follow-up in most patients [41,48,49–66].

Follow-up data for 533 patients from 22 institutions up to 7 years after an initial balloon valvoplasty [73] demonstrated that 23% of patients had a suboptimal outcome because of either a residual peak systolic gradient ≥36 mmHg or need for further treatment of pulmonic stenosis by repeated balloon pulmonary valvoplasty or surgical valvotomy. Significant independent predictors of suboptimal long-term outcome are an earlier year of the initial valvoplasty, a small valve hinge point diameter, and a higher immediate residual gradient. A small ratio of balloon-to-valve hinge point diameter significantly predicted suboptimal outcome for patients with valves morphologically classified as either typical or complex (primarily post-surgical valvotomy) but not for patients with dysplastic or combined morphologic features (dysplasia with commissural fusion). The patient's age, Noonan's syndrome or associated cardiac lesions, pre-balloon valvoplasty gradient, and use of the double-balloon technique did not independently predict follow-up outcome [61]. Other investigators [74] found that intervention in patients with a systolic gradient between 40 and 60 mmHg achieved a lower long-term gradient and fewer late symptoms.

Results of balloon pulmonary valvoplasty for patients with a dysplastic pulmonary valve vary and depend on the relative contribution to the degree of obstruction made by the thickened and immobile leaflets, the nodular tissue in the leaflet, the sinuses, and the commissural fusion, all of which may form a continuum with typical pulmonic stenosis. Because the degree of valve fusion is difficult to define, in the absence of a hypoplastic annulus (<75% of that predicted for age and body surface area), and perhaps the finding of a dilated pulmonary trunk, balloon valvoplasty should be attempted [41,48,75–80]. Although undersized balloons may be associated with a poor acute result, the use of oversized balloons increases the risk of valve disruption, outflow tract damage, and vascular complications [81]. Unsuccessful results were generally due to an inability to cross the valve, especially in neonates.

The experience in adults confirms the technical simplicity and hemodynamic improvement seen in the pediatric age groups [21,82–92].

Surgical valvotomy

Surgical valvotomy should be limited to patients with more complex lesions or those in whom balloon dilation is contraindicated or failed (severe dysplastic valves).

Surgical valvotomy may be performed by an open or closed technique, although almost all are performed under direct vision [22]. The approach is through the pulmonary artery, and valvotomy is performed. With a dysplastic pulmonary valve, the same approach is used. Balloon valvoplasty is attempted; should this fail because of either the thickened leaflets or the supravalvar stenosis, operative treatment is necessary. Valvotomy alone does not usually suffice, and valvectomy, partial or total, may be necessary. Enlargement of the annulus and patch enlargement of the pulmonary trunk may also be necessary.

The results of the surgical valvotomy on nondysplastic valves are excellent. Mortality is minimal.

After an operation, some pulmonary insufficiency may be present. This is usually minor and clinically insignificant and only rarely needs valve replacement. Associated infundibular hypertrophy, which occurs in severe stenosis and is probably secondary or functional, poses a special situation. Occasionally, infundibular obstruction does not regress after valvotomy, or the obstruction increases postoperatively. Death has been reported from the so-called suicidal right ventricle. Significant subvalvar obstruction recurring immediately after valvotomy may require treatment with a β-blocker. If there is no response, resection may be necessary. In most patients, however, the secondary obstruction decreases and resolves with time.

Natural history and long-term history of treated and untreated adults

The Natural History Study produced important information on the natural history of patients with valvar pulmonic stenosis [15,18]. In mild pulmonic valvar stenosis (defined as a gradient <30–35 mmHg), no intervention is indicated and long-term outcome is excellent in almost all patients. Exercise tolerance is normal or only mildly reduced [93]. Further, in postoperative patients with mild stenosis, reoperation is rarely necessary.

Patients with pressure gradients <25 mmHg did not experience an increase in gradient with time. If the gradient was >50 mmHg, valvotomy was deemed necessary. The management of patients with a gradient between 40 and 49 mmHg was controversial. There were 22 deaths, 19 in the surgically managed patients and three in the medically managed patients [15]. In the medical group, two of the three deaths were noncardiac and the third death was a result of ventricular fibrillation during catheterization. In the surgical group, 12 of 19 patients died of cardiac-related causes, including eight perioperative deaths. Morbidity after admission to the study was uncommon but was significant in individual patients, related to conditions such as bacterial endocarditis, brain abscess, syncope, congestive cardiac failure, stroke, and pacemaker implantation.

Apart from residual stenosis, both surgical valvotomy and balloon valvoplasty can induce relevant pulmonary regurgitation acutely or during follow-up. The incidence of severe pulmonary regurgitation long after balloon valvoplasty has been reported to be >15% [94].

Chronic severe pulmonary regurgitation late after surgical repair of tetralogy of Fallot is related to impaired exercise performance, right ventricular dilatation, and/or dysfunction and increased risk for arrhythmia [95–97]. However, the effect of long-standing, isolated pulmonary insufficiency on morbidity and mortality remains unknown. Accordingly, the indications and timing for pulmonary valve replacement in isolated severe pulmonary regurgitation are controversial.

Importantly, the currently used valved conduits (homografts, Hancock conduits, etc.) for pulmonary valve replacement all exhibit a limited lifespan, which ranges from 10 to 15 years [98–104]. Because of this limited life span, patient management strategies have been based on delaying surgical intervention for as long as possible (so that number of open-heart surgeries performed on any individual patient is kept to a minimum) but not beyond a theoretical point when RV dysfunction and functional impairment might be irreversible. Finding the right parameter to detect the point of no return in right ventricular volume overload has been described as the Holy Grail of pediatric cardiology [105], particularly for adults with congenitally malformed hearts, emphasizing the complexity of this issue.

With advanced cardiac magnetic resonance imaging, efforts have been made to establish volume thresholds as predictors for outcome after conduit placement. Cut-off points for end-systolic and end-diastolic right ventricular volumes have been reported [106–108] The end point in these studies was normalization of right ventricular volumes after correcting pulmonary regurgitation, with or without surgical remodeling of the right ventricular outflow tract. However, the effect of the timing of pulmonary valve replacement on RV function, exercise performance, and in particular long-term survival and risk for arrhythmia remains undefined.

Currently, we recommend pulmonary valve replacement for the following if this impairment cannot be explained adequately by extracardiac factors: symptomatic pulmonary regurgitation; moderate to severe right ventricular dilatation with a right ventricular volume of >150 ml m^{-2}; right ventricle to left ventricle end-diastolic volume ratio of >1.5; moderate to severe right systolic dysfunction; progressive tricuspid regurgitation; or significantly impaired exercise capacity (<65% of predicted maximal oxygen consumption on cardiopulmonary exercise testing).

Peripheral pulmonary artery stenosis

Incidence and Genetics

Peripheral pulmonary artery stenosis (PPAS) accounts for >3% of all congenital heart defects. PPAS may be sporadic or familial. It may be an isolated lesion (40%) or combined with other cardiac lesions (60%), such as valvar pulmonic stenosis, atrial septal defect, ventricular septal defect, and patent ductus arteriosus; about 20% of patients with tetralogy of Fallot have associated PPAS. Other complex-associated lesions include mitral obstruction and transposition of the great arteries. Another important association is with supravalvar aortic stenosis [109], classically present in the Williams syndrome and also as the central feature of a developmental complex that includes supravalvar stenosis of the aorta and pulmonary trunk, dysplasia of valves, and stenosis of ostia of coronary arteries and branches of the aortic arch [110]. In this complex, histologic examination of the aorta and major pulmonary arteries showed two patterns that may alternate from segment to segment in a given patient. One pattern is of a mosaic orientation of medial elements, and the other is of thickening of the media that appears to have an excess number of units of elastic and intervening layers. Syndromes that have PPAS as an important feature also include the rubella, Alagille, Keutel [111], cutis laxa, Noonan, and Ehlers–Danlos syndromes and familial supravalvar aortic stenosis.

Specific genetic abnormalities have been described for several syndromes associated with isolated PPAS. In Williams syndrome, a genetic deletion within chromosome 7 has been identified, which results in abnormal elastin production [112]. Further, a deletion in chromosome 20 is linked with the Alagille syndrome [113].

Embryology

Although probably multifactorial, the exact pathogenesis of PPAS remains unclear. In contrast, teratogenic agents such as the rubella virus are believed to affect directly the pulmonary artery tree.

Pathology

Functional or *physiologic* PPAS is relatively common in both premature and full-term neonates. The stenosis, evidenced by the typical murmur and a small gradient (echo Doppler), is mild. With time, these arteries grow, and the murmur disappears within a few months and almost invariably is gone by the first birthday.

PPAS may occur at a single site or, more commonly, at multiple sites of obstruction. The stenosis may be present at any level above the pulmonary valve and may involve one or many pulmonary artery branches. In a simplified classification [114], four types of obstruction were described: (i) stenosis of the pulmonary trunk; (ii) bifurcation stenosis extending into the right or left pulmonary arteries (or both); (iii) multiple peripheral pulmonary artery stenoses; and (iv) stenoses of both the pulmonary trunk and peripheral arteries.

PPAS also follows post-surgical aortopulmonary shunt placement. Insertion of the shunt into either the left or right pulmonary artery can lead to distortion and upward pulling of the pulmonary branches during somatic growth, resulting in significant obstruction.

Sometimes, closure of the ductus arteriosus leads to isolated stenosis of the left (or. in the presence of ductal or aortic arch anomalies. right) pulmonary artery. This lesion is called "pulmonary coarctation."

Pathophysiology

The pathophysiology and hemodynamics resemble valvar pulmonic stenosis. Proximal to the obstruction, the systolic pressure is elevated, and distally it is normal or low. Therefore, depending on the degree of obstruction, the right ventricular systolic pressure is elevated, as is the pressure in the pulmonary artery proximal to the obstruction. The diastolic pressure is often low and equal in the pulmonary artery both proximal and distal to the obstruction. Hence pressure tracing in the proximal pulmonary artery resembles the right ventricular pressure contour, although the diastolic pressure is not zero.

The pathophysiologic consequences of increased right ventricular afterload have been described above.

Another consequence of PPAS is unequal pulmonary perfusion. With several severely obstructed regions, non-stenotic areas experience high flow and/or high pressure and may develop pulmonary vascular disease. On the other hand, proximally obstructed vessels often remain small and "underdeveloped."

Clinical features

Clinical history

In general, PPAS is a more severe disease than isolated pulmonary stenosis. The patient's general appearance is either normal or that of an associated syndrome involved with possible typical facial features of the Noonan, rubella, Williams, or Alagille syndromes. Growth and development are normal in most patients or possibly delayed in the syndromes. Most patients are asymptomatic. With severe obstruction, fatigue or dyspnea on exertion is usually present. Signs of congestive cardiac failure are rare.

Physical examination

Decreased compliance of the right ventricle may be associated with a right-to-left shunt at the atrial level and cyanosis. In mild to moderate stenosis, no thrills or heaves are palpable; with severe obstruction, a right ventricular heave may be palpable.

The first heart sound is normal. The second sound is split, the width intensifying with the increasing severity of the

stenosis. No ejection click is present. Typically, the murmur is absent or soft over the precordium. It is heard below both clavicles. Of particular importance is the wide distribution of the murmur over the back and axillae; this is a major clinical clue pointing to the diagnosis. With multiple PPAS or an associated left-to-right shunt, a continuous murmur may be present and widely distributed over the precordium, back, and axillae. Its intensity varies with the degree of stenosis.

Electrocardiography

The electrocardiographic features are similar to those of valvar pulmonic stenosis. They vary from normal to those of severe right ventricular hypertrophy and even "strain" pattern.

Chest X-ray

Pulmonary vasculature is usually normal regardless of severity, although decreased vasculature may occur in severe stenosis. The main pulmonary artery segment is not prominent (as opposed to valvar stenosis). In severe unilateral stenosis, a difference in vasculature may be seen between the two lungs. Often with marked differences of stenosis in the two lungs, no significant differences in vasculature may be evident.

Echocardiography

Narrowing of the pulmonary artery branches may be present in either diffuse or discrete forms. The proximal right and left pulmonary arteries may be imaged from the suprasternal, high parasternal short-axis, or subxiphoid view. Flow into the narrow pulmonary artery branches is anterograde throughout the cardiac cycle, and this causes a characteristic systolic–diastolic high-velocity flow on Doppler study. The systolic Doppler gradient across a long obstruction is unreliable, but the severity of the narrowing may be assessed by the right ventricular systolic pressure.

Cardiac catheterization

Cardiac catheterization is important to confirm the diagnosis of PPAS and may be an important therapeutic modality for balloon angioplasty and endovascular stent implantation. The indications for cardiac catheterization are symptoms or noninvasive evidence of right ventricular hypertension (greater than two-thirds of systemic pressure), echocardiographic or X-ray findings of asymmetric pulmonary perfusion, and assessment after surgical repair (e.g., after repair of tetralogy of Fallot or the Fontan operation).

Carefully obtained withdrawal pressure tracings from the distal branches demonstrate systolic pressure gradients across the narrowest segment of the arteries. Systolic pressure gradients >10 mmHg are considered abnormal. With unilateral stenosis, a pressure gradient is usually present across the narrowed segment, but the proximal pulmonary artery pressure is normal. Sometimes, pressure is also elevated in the contralateral pulmonary artery. The pressure tracing proximal to the obstruction has a contour similar to that of the right ventricle in length and time up to the dicrotic notch; it also has a wide pulse pressure that becomes more pronounced with increasing severity of the obstruction. In unilateral or partial PPS, the pressure gradient is often lower than anatomically expected because there is increased flow to the nonobstructed regions with decreased flow to the contralateral lung.

Angiography

Selective angiography is important to define the location, extent, and distribution of the lesions in each pulmonary artery. The right pulmonary artery is best seen in an AP view and the left pulmonary artery in a left anterior oblique view with cranial angulation. Demonstrating stenosis in the main pulmonary artery and the origin of both left and right pulmonary arteries requires cranial angulation. Aortography should be performed to exclude frequently associated systemic arterial stenoses.

Other imaging modalities

MRI represents the most accurate and reproducible imaging technique for assessing right ventricular size, function and wall thickness. MR contrast agent (gadolinium)-enhanced three-dimensional angiography provides a noninvasive technique for visualizing the pulmonary artery tree. The sensitivity and specificity for assessing PPAS of the proximal and up to the third to fourth generation pulmonary arteries have been shown to be ~100%. Further, repeated accurate measurements of PPA dimensions are possible with this technique. There are, however, some limitations to visualizing the distal pulmonary vasculature; intravascular stents can significantly reduce the diagnostic performance of MRI in patients with PPAS.

Lung perfusion scintigraphy had been a useful noninvasive method for accurately determining relative pulmonary blood flows, allowing the clinician to plan and follow up transcatheter interventions in the pulmonary arteries [115–118]. However, "washout" effects from additional blood supply to the lung can make flow quantification inaccurate. Currently, MRI represents the gold standard for assessing differential blood flow to the lungs as derived by flow calculation in the branch pulmonary arteries.

Especially in patients with multiple previous stenting of the pulmonary tree, CT imaging is preferred. Similarly to MRI, contrast-enhanced CT provides excellent imaging of the proximal and distal pulmonary vasculature. For assessing hemodynamic relevance, however, catheterization remains the gold standard.

Management

Mild or moderate unilateral or bilateral PPAS does not usually require treatment. The indications for treating severe PPAS include cardiovascular symptoms, such as exercise intolerance, dyspnea, cyanosis, and signs of right-sided heart

failure; near-systemic (or higher) right ventricular pressure; markedly decreased flow to affected lung segments; hypertension in the unobstructed pulmonary artery; and documented stenosis in distal pulmonary arteries not easily accessible as a surgical prelude to definitive repair of a coexisting cardiac anomaly [117,118].

An operation performed to relieve pulmonary artery stenosis directly is difficult and often ineffective in relieving obstruction, with a success rate of ~30% [119–121]. In the surgical approach, a pericardial or Dacron ellipsoid patch is used to widen the lumen of the vessel. Furthermore, the surgical approach is confined to a small group of patients with well-localized stenosis of the pulmonary trunk or bifurcation of the origins of the main branch pulmonary arteries. The intraparenchymal pulmonary arteries are surgically inaccessible. For patients with multiple PPS or hypoplastic pulmonary arteries, there is no surgical alternative; therefore, interventional options such as balloon angioplasty and endovascular stent placement have been developed.

Successful angioplasty results in longitudinal or oblique intimal tears, medial disruption, and, in some patients, transmedial tears, with organization of intramural hemorrhage and scar formation as the mode of healing [122,123]. Pseudoendothelialization is complete in 3–6 weeks; areas of mural thinning within the scar may predispose to aneurysm formation. After angioplasty, perivascular fibrosis may reinforce the outer vessel wall, but several months must pass to allow complete tissue granulation and healing of transmedial tears induced by catheter intervention [123,124].

Balloon dilatation is usually well tolerated and should be considered an initial form of intervention, at least for postoperative stenosis. Acute technical success is judged by the modified criteria of the Boston group [117], and includes at least two of the following criteria: an increase in vessel diameter of >50% of the predilatation diameter, an increase of >20% in the relative blood flow to the affected lung, and a decrease to <60% of the systolic right ventricular/aortic pressure ratio. Balloon angioplasty for PPS has been effective according to these criteria in 50–60% of patients [117,118]. Restenosis occurs in 15–20% of patients and a long-term favorable result is achieved in 35–50% of patients [118,125] by the following criteria: resolution of the stenosis and avoidance of surgical intervention; optimization of future surgical intervention, judged by one of two standards: (1) pulmonary artery anatomy or pressure suitable for surgical repair in patients with pulmonary artery anatomy or pressure that was previously considered a contraindication for surgical repair or (2) obviating the need for surgical intervention in the areas of balloon angioplasty during the succeeding surgical repairs and reduction of the systolic right ventricular/aortic pressure ratio to <60% [126,127].

Significant complications may follow percutaneous balloon angioplasty of PPAS [124–128]. These complications include a mortality rate of ~1–2%, usually from exsanguination from a ruptured pulmonary artery during dilatation. Other complications include hemoptysis, transient pulmonary edema, thrombosed iliac veins, pulmonary artery aneurysm, cyanosis, and hypotension. Late death may also occur from aneurysm rupture.

Even after a technically successful procedure, these patients require careful serial evaluation and may need repeat cardiac catheterization to evaluate accurately the mid- and long-term results of the angioplasty procedure. Patients who develop aneurysms should be observed even more closely because the prognosis of these aneurysms remains unknown.

Importantly, although intuitively suggested, the clinical benefit of balloon dilatation of native PPS cannot yet formally be demonstrated.

Endovascular stents

The incidence of recurrent narrowing after balloon angioplasty (~17%) could be related to the elastic recoil of the pulmonary artery wall. The efficacy of endovascular stents to relieve such obstructions and the safety of implantation have been demonstrated with a success rate of >96% [129–132]. Excellent long-term results have been reported [133,134]. If obstructions are near to the bifurcation or side branches, simultaneous implantation of stents is recommended [133]. Sometimes resistant stenoses remain or develop within or adjacent to the stents following implantation, which can be treated effectively with ultra-high-pressure balloons [135] (Figure 33.3).

Major complications are few but include death from pulmonary artery embolism, vascular rupture, pulmonary bleeding, and embolization of incorrectly placed stents [136–139]. Compression of coronary arteries may also occur and must be excluded by simultaneous test-balloon dilation and coronary angiography [140]. Bronchial compression has been described [141].

Minor complications include occlusion of side branches, [136,139], longitudinal break of the stent during redilatation, acute thrombosis of the pulmonary artery distal to the stent that resolves after thrombolytic therapy, and balloon rupture during expansion [130].

Natural history and long-term history of treated and untreated adults

In PPAS in association with other cardiac defects, such as Williams and Noonan syndrome or tetralogy of Fallot, the long-term history is determined by the severity of the cardiac and extracardiac manifestation of the disease. In patients with mild to moderate PPAS, the degree of obstruction often remains stable or even reduces with growth. In severe PPAS and failure of stenting or surgery, prognosis, however, can be poor. Right ventricular failure due to chronic pressure overload can be observed as a terminal event. Untreated isolated PPAS in adults is rare, but has to be excluded in the presence

Figure 33.3 Pre- and post-interventional bilateral angiograms [(a) and (c) LAO 20°, cranial 20°; (b) and (d) LAO 90°] of a 20-year-old female with severe residual left pulmonary artery stenosis following multiple operative and percutaneous pulmonary valve implantation. Panels (a) and (b) show the stenosis distal to the bifurcation with contrast injection through a pigtail catheter in the left pulmonary artery. Panels (c) and (d) show the result of stent implantation with guidewire and balloon catheter still in place. Contrast is administered through a long delivery sheath with the tip just proximal to the stent-mounted pulmonary xenograft valve.
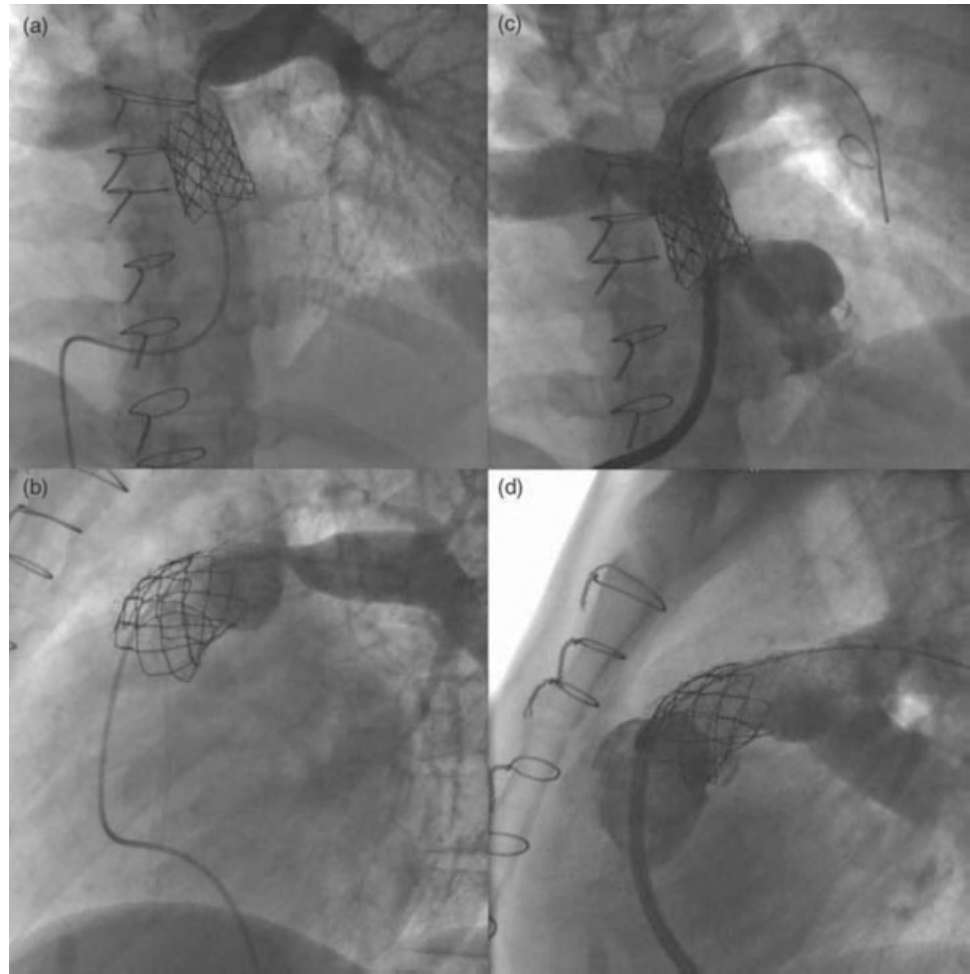
of a long-standing murmur since childhood. Long-term results of effectively treated supravalvar or peripheral stenosis are usually good [134]. Large stents positioned in an extra-anatomic, especially retrosternal, position may suffer from fatigue of the material, leading to compression or breaking [142].

Subvalvar stenosis

Two main types of obstruction may occur within the right ventricle: isolated infundibular stenosis and anomalous muscle bundles.

Isolated infundibular stenosis
This rare condition consists of narrowing of the infundibulum. The narrowing is either muscular or fibromuscular.

Physiology
The hemodynamics resemble those of other right-sided obstructions with a gradient within the right ventricle, causing hypertrophy of the proximal chamber. Clinically, the general features are similar to valvar stenosis. The features of right ventricular hypertrophy depend on the severity of obstruction. A systolic ejection murmur is heard along the left sternal border or in the pulmonary area. In severe stenosis, cyanosis develops from a right-to-left shunt at the atrial level.

The absence of an ejection click and the often lower position of the murmur help in differentiation from valvar stenosis. The murmur is often harsher than in valvar stenosis. The second sound is usually narrowly split. The electrocardiogram is nondiagnostic and varies with the degree of right ventricular hypertrophy. The chest radiograph shows normal cardiac size. The main pulmonary artery is not dilated; the pulmonary vasculature is usually normal. The apex may be elevated in severe stenosis.

Echocardiography
An infundibular subpulmonic obstruction may be present permanently or transiently after relief of valvar pulmonic stenosis. Normally, the tunnel-like obstructed subvalvar region is easy to recognize, but sometimes the entire right ventricular outflow tract must be visualized with 2D and color Doppler to find a discrete stenosis which is more typical for
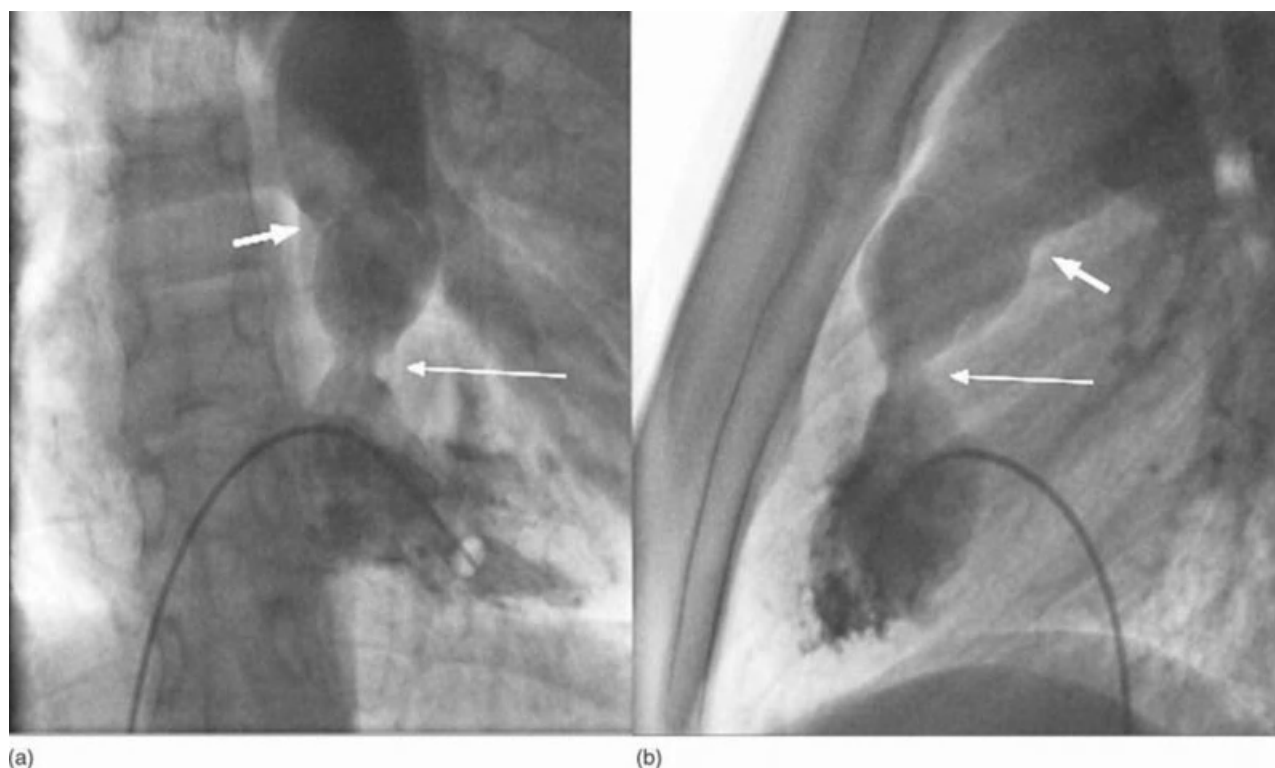
Figure 33.4 Bilateral angiograms [(a) RAO 0°; (b) LAO 90°] of a 23-year-old patient with circumscribed muscular stenosis of the right ventricular outflow tract forming the so-called double-chambered right ventricle. The long, thin arrow points to the anomalous muscle bundle and the short, thick arrow to the position of the pulmonary valve.

the double-chambered right ventricle (see below). A characteristic Doppler jet with a concave downstroke is indicative of dynamic subvalvar narrowing. When a fixed obstruction is present, the jet has a regular, convex downstroke.

Natural history
The degree of obstruction tends to increase with age.

Treatment
Definitive treatment is surgical, which has good results. In dynamic stenosis, β-blockers can temporarily reduce the gradient and thereby allow for postponement of surgery.

Anomalous muscle bundles
The other form of stenosis within the right ventricle is anomalous muscle bundles.

Physiology
In this condition, muscle bundles divide the ventricle into two chambers (hence the synonym *double-chambered right ventricle*) [143] (Figure 33.4). The muscle bundles pass from the septal wall close to the base of the anterior papillary muscle to the anterior wall of the right ventricle. A ventricular septal defect is present in most patients, although in some patients the muscle bundles may functionally close the septal defect. In

addition, a discrete membranous subaortic membrane completes a triad of commonly associated pathologic findings.

Right ventricular obstruction often progresses. Clinically, the patients are usually asymptomatic. The position of the ventricular septal defect may occasionally affect the clinical picture. If the septal defect is situated above the muscle bundles, a left-to-right shunt may predominate and even lead to heart failure. However, right-to-left shunting may be present only occasionally when the septal defect is below the muscle bundles.

The most striking clinical feature is a long, usually harsh, ejection systolic murmur heard along the left sternal border, possibly radiating to the pulmonary area. A thrill is often present. The heart sounds are usually normal. A systolic click is not present. The electrocardiogram shows different degrees of right ventricular hypertrophy, depending on the severity of the obstruction. The radiographic features are nonspecific.

Echocardiography
On echocardiography, the muscle bundle may be well imaged from a subxiphoid short-axis or a right anterior oblique view, which can be obtained by counterclockwise rotation of the transducer. The severity of the obstruction may be assessed by continuous-wave Doppler imaging.

Cardiac catheterization

Usually no evidence of shunt is found. On occasion, left-to-right or right-to-left shunting may be present. A pressure gradient is measured by catheter withdrawal.

Angiocardiography

The muscle bundles are characteristically demonstrated by filling defects in the right ventricle. The left-to-right or right-to-left shunt may also be demonstrated.

Treatment

When indicated by the severity of the gradient, treatment is surgical with removal of the muscle bundles. A characteristic dimple on the right ventricular free wall is the surgical landmark of the muscle bundle attachment. The associated ventricular septal defect is closed, and the subaortic membrane is excised.

Rare causes of right ventricular outflow tract obstruction

Rare causes of right ventricular obstruction include:
- pouch-like structures in the right ventricle, such as the "windsock" lesion
- tumors in the right ventricle – rhabdomyoma
- prolapse of right aortic cusp through a ventricular septal defect
- sinus of Valsalva aneurysm, which may prolapse into the right ventricular outflow region [144].

References

1 Driscoll DJ, Michels VJ, Gersony WM, Hayes CT. Occurrence risk for congenital heart defect in relatives of patients with aortic stenosis, pulmonary stenosis or ventricular septal defect. *Circulation* 1993;**87**(Suppl 1):114–20.

2 Noonan JA. Hypertelorism with Turner phenotype. A new syndrome with associated congenital heart disease. *Am J Dis Child* 1968;**116**:373–80.

3 Koretzky ED, Moller JH, Korns ME, *et al.* Congenital pulmonary stenosis resulting from dysplasia of the valve. *Circulation* 1969;**40**:43–53.

4 Campbell M. Factors in the aetiology of pulmonary stenosis. *Br Heart J* 1962;**24**:625–32.

5 Edwards JE. Congenital malformations of the heart and great vessels. In: Gould SE, ed. *Pathology of the Heart*. Springfield, IL: Charles C. Thomas, 1960: 391–7.

6 Franciosi RA, Blanc WA. Myocardial infarct in infants and children. I. A necropsy study in infants and children. *J Pediatr* 1968;**73**:309–19.

7 Rudolph AM. *Congenital Diseases of the Heart*. Chicago: Year Book, 1974.

8 Raghib G, Amplatz K, Moller JH, *et al.* Hypoplasia of right ventricle and of tricuspid valve. *Am Heart J* 1968;**70**:806–12.

9 Leatham A, Weitzman D. Auscultatory and phonocardiographic signs of pulmonic stenosis. *Br Heart J* 1957;**19**:303–17.

10 Vogelpoel L, Schrire V. Auscultatory and phonocardiographic assessment of pulmonary stenosis with intact ventricular septum. *Circulation* 1960;**22**:55–72.

11 Bassingthwaighte JB, TW, Dushane JW, Wood EH, Burchell HB. The electrocardiographic and hemodynamic findings in pulmonary stenosis with intact ventricular septum. *Circulation* 1963;**28**:893–905.

12 Schneeweiss A, Shem-tov A, Blieden LC, *et al.* Diagnostic angiographic criteria in dysplastic stenotic pulmonary valve. *Am Heart J* 1983;**106**:761–2.

13 Driscoll DF, Wolfe RR, Gersony WM, Hayes CJ. Cardiorespiratory response to exercise of patients with aortic stenosis, pulmonary stenosis and ventricular septal defect. *Circulation* 1993;**87**(Suppl I):102–13.

14 Wennevold A, Jacobsen JR. Natural history of valvular pulmonary stenosis in children below the age of two years. Long-term follow-up with serial heart catheterization. *Eur J Cardiol* 1978;**83**:371–8.

15 Hayes CJ, Gersony WM, Driscoll DJ. Second natural history study of congenital heart defects. Results of treatment of patients with pulmonary valvar stenosis. *Circulation* 1993;**87**(Suppl I):28–37.

16 Mody MR. The natural history of uncomplicated valvular pulmonic stenosis. *Am Heart J* 1975;**90**:317–21.

17 Tinker J, Howitt G, Markman P, Wade EG. The natural history of isolated pulmonary stenosis. *Br Heart J* 1965;**27**:151–60.

18 Nugent EW, Freedom RM, Nora JJ, *et al.* Clinical course in pulmonary stenosis. *Circulation* 1977;**56**(Suppl I):38–47.

19 Johnson LW, Grossman W, Dalen JE, Dexter L. Pulmonic stenosis in the adult. Long-term follow-up results. *N Engl J Med* 1972;**287**:1159–63.

20 Engle MA, Ito T, Goldberg HP. The fate of the patient with pulmonic stenosis. *Circulation* 1964;**30**:554–61.

21 Shrivastava S, Kumar K, Dev V, *et al.* Pulmonary balloon valvotomy for severe valvular pulmonic stenosis with congestive heart failure beyond infancy. *Cathet Cardiovasc Diagn* 1993;**28**:137–41.

22 Gersony WM, Bernard WF, Nadas AS, Gross RE. Diagnosis and surgical treatment of infants with critical pulmonary outflow obstruction. Study of thirty-four infants with pulmonary stenosis or atresia, and intact ventricular septum. *Circulation* 1967;**35**:767–76.

23 Freed MD, Rosenthal A, Bernhard WF, *et al.* Critical pulmonary stenosis with a diminutive right ventricle in neonates. *Circulation* 1973;**48**:875–81.

24 Zeevi B, Keane JF, Fellows KE, Lock JE. Balloon dilation of critical pulmonary stenosis in the first week of life. *J Am Coll Cardiol* 1988;**11**:821–4.

25 Caspi J, Coles J, Benson L, *et al.* Management of neonatal critical pulmonary stenosis in the balloon valvotomy era. *Ann Thorac Surg* 1990;**49**:273–8.

26 Ali Khan MA, al-Yousef S, Huhta JC, *et al.* Critical pulmonary valve stenosis in patients less than 1 year of age. Treatment with percutaneous gradational balloon pulmonary valvuloplasty. *Am Heart J* 1989;**117**:1008–14.

27 Ladusans EJ, Qureshi SA, Parson JM, *et al.* Balloon dilation of critical stenosis of the pulmonary valve in neonates. *Br Heart J* 1990;**64**:362–7.

28 Gournay V, Piechaud JF, Delogu A, et al. Balloon valvotomy for critical stenosis or atresia of pulmonary valve in newborns. J Am Coll Cardiol 1995;**26**:1725–31.

29 Santoro G, Formigari R, Di Carlo D, et al. Midterm outcome after pulmonary balloon valvuloplasty in patients younger than one year of age. Am J Cardiol 1995;**75**:637–9.

30 Fedderly RT, Lloyd TR, Mendelsohn AM, Beekman RH. Determinants of successful balloon valvotomy in infants with critical pulmonary stenosis or membranous pulmonary atresia with intact ventricular septum. J Am Coll Cardiol 1995;**25**:460–5.

31 Talsma M, Wittenburg M, Rohmer J, Hess J. Determinants for outcome of balloon valvuloplasty for severe pulmonary stenosis in neonates and infants up to six months of age. Am J Cardiol 1997;**71**:1246–8.

32 Colli AM, Perry SB, Lock JE, Keane JF. Balloon dilation of critical pulmonary stenosis in the first month of life. Cathet Cardiovasc Diagn 1995;**34**:23–8.

33 Gildein HP, Kleinert S, Goh TH, Wilkinson JL. Treatment of critical pulmonary valve stenosis by balloon dilatation in the neonate. Am Heart J 1996;**131**:1007–11.

34 Rao PS. Balloon valvuloplasty in the neonate with critical pulmonary stenosis (Editorial). J Am Coll Cardiol 1996;**27**:479–80.

35 Burzynski JB, Kveselis DA, Byrum CJ, et al. Modified technique for balloon valvuloplasty of critical pulmonary stenosis in the newborn. J Am Coll Cardiol 1993;**22**:1944–7.

36 Weber HS, Cyran SE, Gleason MM, et al. Critical pulmonary valve stenosis in the neonate. A technique to facilitate balloon dilation. Am J Cardiol 1994;**73**:310–2.

37 Latson L, Cheatham J, Froemming S, Kugler J. Transductal guidewire "rail" for balloon valvuloplasty in neonates with isolated critical pulmonary valve stenosis or atresia. Am J Cardiol 1994;**73**:713–4.

38 Zellers TM, Moake L, Wright J. Use of the Terumo SP catheter system for crossing the pulmonary valve in infants with critical pulmonary valve stenosis. Am J Cardiol 1995;**76**:1082–4.

39 Tabatabaei H, Boutin C, Nykanen DG, et al. Morphologic and hemodynamic consequences after percutaneous balloon valvotomy for neonatal pulmonary stenosis. Medium-term follow-up. J Am Coll Cardiol 1996;**27**:473–6.

40 Hanley FL, Sade RM, Freedom RM, et al. Outcomes in critically ill neonates with pulmonary stenosis and intact ventricular septum. A multi-institutional study. J Am Coll Cardiol 1993; **22**:183–92.

41 Stanger P, Cassidy SC, Girod DA, et al. Balloon pulmonary valvuloplasty. Results of the Valvuloplasty and Angioplasty of Congenital Anomalies Registry. Am J Cardiol 1990;**65**:775–83.

42 Lock JE, Keane JF, Fellows KE. Diagnostic and Interventional Catheterization in Congenital Heart Disease. Boston: Martinus Nijhoff, 1987.

43 Rao PS, Sideris EB. Transcatheter closure of patent ductus arteriosus: state of the art. J Invas Cardiol 1996;**8**:278–88.

44 Benson LN, Smallhorn JS, Freedom RM, et al. Pulmonary valve morphology after balloon dilatation of pulmonary valve stenosis. Cathet Cardiovasc Diagn 1985;**11**:161–6.

45 Lababidi Z, Wu JR. Percutaneous balloon pulmonary valvuloplasty. Am J Cardiol 1983;**52**:560–2.

46 Walls JT, Lababidi Z, Curtis JJ, Silver D. Assessment of percutaneous balloon pulmonary and aortic valvuloplasty. J Thorac Cardiovasc Surg 1984;**88**:352–6.

47 Kan JS, White RI, Mitchel SE, et al. Percutaneous transluminal balloon valvuloplasty for pulmonary valve stenosis. Circulation 1984;**69**:554–60.

48 McCrindle B, Kan SJ. Long-term results after balloon pulmonary valvuloplasty. Circulation 1991;**83**:1915–22.

49 O'Connor BK, Beekman RH, Lindauer A, Rocchini A. Intermediate-term outcome after pulmonary balloon valvuloplasty. Comparison with a matched surgical control group. J Am Coll Cardiol 1992;**20**:169–73.

50 Witsenburg M, Talsma M, Rohmer J, Hess J. Balloon valvuloplasty for valvular pulmonary stenosis in children over 6 months of age. Initial results and long-term follow up. Eur Heart J 1993;**14**:1657–60.

51 Elliott JM, Tuzcu EM. Recent developments in balloon valvuloplasty techniques. Curr Opin Cardiol 1995;**10**:128–34.

52 Ettedgui JA, Ho SY, Tynan M, et al. The pathology of balloon pulmonary valvoplasty. Int J Cardiol 1987;**16**:285–93.

53 Lau KW, Hung JS. Controversies in percutaneous balloon pulmonary valvuloplasty: timing, patient selection and technique. J Heart Valve Dis 1993;**2**:321–5.

54 Ali Khan MA, al-Yousef S, Moore JW, Sawyer W. Results of repeat percutaneous balloon valvuloplasty for pulmonary valvar stenosis. Am Heart J 1990;**120**:878–81.

55 Rao PS. Balloon pulmonary valvuloplasty. A review. Clin Cardiol 1989;**12**:55–74.

56 Miller GA. Balloon valvuloplasty and angioplasty in congenital heart disease. Br Heart J 1985;**54**:285–9.

57 Sullivan ID, Robinson PJ, Macartney FJ, et al. Percutaneous balloon valvuloplasty for pulmonary valve stenosis in infants and children. Br Heart J 1985;**54**:435–41.

58 Hwang B, Chen LY, Lu JH, Meng CC. A quantitative analysis of the structure of right ventricle–pulmonary artery junction for balloon pulmonary valvuloplasty in children. Angiology 1995; **46**:383–91.

59 Jaing TL, Hwang B, Lu JH, et al. Percutaneous balloon valvuloplasty in severe pulmonary valvular stenosis. Angiology 1995; **46**:503–9.

60 Medina A, Bethencourt A, Olalla E, et al. Intraoperative balloon valvuloplasty in pulmonary valve stenosis. Cardiovasc Intervent Radiol 1989;**12**:199–201.

61 Melgares R, Prieto JA, Azpitarte J. Success determining factors in percutaneous transluminal balloon valvuloplasty of pulmonary valve stenosis. Eur Heart J 1991;**12**:15–23.

62 Cazzaniga M, Vagnola O, Aldayl O, et al. Balloon pulmonary valvuloplasty in infants. A quantitative analysis of pulmonary valve-anulus-trunk structure. J Am Coll Cardiol 1992;**20**:345–9.

63 Fedderly RT, Beekman RH III. Balloon valvuloplasty for pulmonary valve stenosis. J Intervent Cardiol 1995;**8**:451–61.

64 Rao PS. Balloon pulmonary valvuloplasty for isolated pulmonic stenosis. In: Rao PS, ed. Transcatheter Therapy in Pediatric Cardiology. New York: Wiley-Liss, 1993: **59**.

65 Burrows PE, Benson LN, Smallhorn JF, et al. Angiographic features associated with percutaneous balloon valvotomy for pulmonary valve stenosis. Cardiovasc Intervent Radiol 1988;**11**:111–6.

66 Masura J, Burch M, Deanfield JE, Sullivan ID. Five-year follow-up after balloon pulmonary valvuloplasty. J Am Coll Cardiol 1993;**21**:132–6.

67 Schmaltz AA, Bein G, Gravinghoff L, et al. Balloon valvuloplasty of pulmonary stenosis in infants and children – co-operative

study of the German Society of Pediatric Cardiology. *Eur Heart J* 1989;**10**:967–71.

68 Rocchini AP, Kveselis DA, Crowley D, *et al*. Percutaneous balloon valvuloplasty for treatment of congenital pulmonary valvular stenosis in children. *J Am Coll Cardiol* 1984;**3**:1005–12.

69 Tynan M, Baker EJ, Rohmer J, *et al*. Percutaneous balloon pulmonary valvuloplasty. *Br Heart J* 1985;**53**:520–4.

70 Rao PS, Fawzy ME, Solymar L, Mardini MK. Long-term results of balloon pulmonary valvuloplasty of valvar pulmonic stenosis. *Am Heart J* 1988;**115**:1291–8.

71 Mullins CE, Ludomirsky A, O'Laughlin MP, *et al*. Balloon valvuloplasty for pulmonic valve stenosis – two-year follow-up: hemodynamic and Doppler evaluation. *Cathet Cardiovasc Diagn* 1988;**14**:76–81.

72 Fontes VF, Sousa EMR, Esteves CA, *et al*. Pulmonary valvoplasty – experience of 100 cases. *Int J Cardiol* 1988;**21**:335–42.

73 McCrindle BW. Independent predictors of long-term results after balloon pulmonary valvuloplasty. Valvuloplasty and Angioplasty of Congenital Anomalies (VACA) Registry investigators. *Circulation* 1994;**89**:1751–9.

74 Mendelson AM, Banerjee A, Meyer RA, Schwarz DC. Predictors of successful pulmonary balloon valvuloplasty. 10-year experience. *Cathet Cardiovasc Diagn* 1996;**39**:236–43.

75 Musewe NN, Robertson MA, Benson LN, *et al*. The dysplastic pulmonary valve. Echographic features and results of balloon dilatation. *Br Heart J* 1987;**57**:364–70.

76 Ballerini L, Mullins CE, Cifarelli A, *et al*. Percutaneous balloon valvuloplasty of pulmonary valve stenosis, dysplasia, and residual stenosis after surgical valvotomy for pulmonary atresia with intact ventricular septum. Long-term results. *Cathet Cardiovasc Diagn* 1990;**19**:165–9.

77 David SW, Goussous YM, Harbi N, *et al*. Management of typical and dysplastic pulmonic stenosis, uncomplicated or associated with complex intracardiac defects, in juveniles and adults. Use of percutaneous balloon pulmonary valvuloplasty with eight-month hemodynamic follow-up. *Cathet Cardiovasc Diagn* 1993;**12**:105–12.

78 Rao PS. Balloon dilatation in infants and children with dysplastic pulmonary valves. Short-term and intermediate-term results. *Am Heart J* 1988;**116**:1168–73.

79 Marantz PM, Huhta JC, Mullins CE, *et al*. Results of balloon valvuloplasty in typical and dysplastic pulmonary valve stenosis. Doppler and echocardiographic follow-up. *J Am Coll Cardiol* 1988;**12**:476–9.

80 DiSessa TG, Alpert BS, Chase NA, *et al*. Balloon valvuloplasty in children with dysplastic pulmonary valves. *Am J Cardiol* 1987; **66**:405–7.

81 Ring JC, Kulik TJ, Burke BA, Lock JE. Morphologic changes induced by dilation of the pulmonary valve anulus with overlarge balloons in normal newborn lambs. *Am J Cardiol* 1985; **55**:210–4.

82 Parsons JM, Ladusans EJ, Qureshi SA. Growth of the pulmonary artery after neonatal balloon dilatation of the right ventricular outflow tract in an infant with the tetralogy of Fallot and atrioventricular septal defect. *Br Heart J* 1989;**62**:65–8.

83 Battistessa SA, Robles A, Jackson M, *et al*. Operative findings after percutaneous pulmonary balloon dilatation of the right ventricular outflow tract in tetralogy of Fallot. *Br Heart J* 1990;**64**:321–4.

84 Sluysmans T, Neven B, Rubay J, *et al*. Early balloon dilatation of the pulmonary valve in infants with tetralogy of Fallot. Risks and benefits. *Circulation* 1995;**91**:1506–11.

85 Stumper O, Piechaud JF, Bonhoeffer P, *et al*. Pulmonary balloon valvuloplasty in the palliation of complex cyanotic congenital heart disease. *Heart* 1996;**76**:363–6.

86 Kreutzer J, Perry SB, Jonas RA, *et al*. Tetralogy of Fallot with diminutive pulmonary arteries. Preoperative pulmonary valve dilation and transcatheter rehabilitation of pulmonary arteries. *J Am Coll Cardiol* 1996;**27**:1741–7.

87 Kaul UA, Singh B, Tyagi S, *et al*. Long-term results after balloon pulmonary valvuloplasty in adults. *Am Heart J* 1993; **126**:1152–5.

88 Lau KWE, Hung JS, Wu JJ, *et al*. Pulmonary valvuloplasty in adults using the Inoue balloon catheter. *Cathet Cardiovasc Diagn* 1993;**29**:99–104.

89 Fawzy ME, Mercer EN, Dunn B. Late results of pulmonary balloon valvuloplasty in adults using double balloon techniques. *J Intervent Cardiol* 1988;**1**:35–42.

90 Sherman W, Hershman R, Alexopoulos D, *et al*. Pulmonic balloon valvuloplasty in adults. *Am Heart J* 1990;**119**:186–90.

91 Herrmann HC, Hill JA, Krol J, *et al*. Effectiveness of percutaneous balloon valvuloplasty in adults with pulmonic valve stenosis. *Am J Cardiol* 1991;**68**:1111–3.

92 Chen CR, Cheng TO, Huang T, *et al*. Percutaneous balloon valvuloplasty for pulmonic stenosis in adolescents and adults. *N Engl J Med* 1996;**335**:21–5.

93 Krabill KA, Wang Y, Einzig S, *et al*. Rest and exercise hemodynamics in pulmonary stenosis. comparison of children and adults. *Am J Cardiol* 1985;**56**:360–5.

94 Harrild DM, Powell AJ, Tran TX, *et al*. Long-term pulmonary regurgitation following balloon valvuloplasty for pulmonary stenosis: risk factors and relationship to exercise capacity and ventricular volume and function. *J Am Coll Cardiol*. 2009; **55**:1041–7.

95 Frigiola A, Redington AN, Cullen S, *et al*. Pulmonary regurgitation is an important determinant of right ventricular contractile dysfunction in patients with surgically repaired tetralogy of Fallot. *Circulation* 2004;**110**(Suppl 11):153–7.

96 Carvalho JS, Shinebourne EA, Busst C, *et al*. Exercise capacity after complete repair of tetralogy of Fallot. deleterious effects of residual pulmonary regurgitation. *Br Heart J* 2004;**67**:4703.

97 Gatzoulis MA, Balaji S, Webber SA, *et al*. Risk factors for arrhythmia and sudden cardiac death late after repair of tetralogy of Fallot: a multicentre study. *Lancet* 2000;**356**:975–81.

98 Boethig D, Thies WR, Hecker H, *et al*. Mid term course after pediatric right ventricular outflow tract reconstruction: a comparison of homografts, porcine xenografts and Contegras. *Eur J Cardiothorac Surg* 2005;**27**:58–66.

99 Mohammadi S, Belli E, Martinovic I, *et al*. Surgery for right ventricle to pulmonary artery conduit obstruction. risk factors for further reoperation. *Eur J Cardiothorac Surg* 2005;**28**:217–22.

100 Brown JW, Ruzmetov M, Rodefeld MD, *et al*. Right ventricular outflow tract reconstruction with an allograft conduit in non-Ross patients: risk factors for allograft dysfunction and failure. *Ann Thorac Surg* 2005;**80**:655–63.

101 Powell AJ, Lock JE, Keane JF, *et al*. Prolongation of RV–PA conduit life span by percutaneous stent implantation. Intermediate-term results. *Circulation* 1995;**92**: 3282–8.

102 Rastan AJ, Walther T, Daehnert I, *et al*. Bovine jugular vein conduit for right ventricular outflow tract reconstruction: evaluation of risk factors for mid-term outcome. *Ann Thorac Surg* 2006;**82**:1308–15.

103 Stark J, Bull C, Stajevic M, *et al*. Fate of subpulmonary homograft conduits: determinants of late homograft failure. *J Thorac Cardiovasc Surg* 1998;**115**:506–14.

104 Tweddell JS, Pelech AN, Frommelt PC, *et al*. Factors affecting longevity of homograft valves used in right ventricular outflow tract reconstruction for congenital heart disease. *Circulation* 2000;**102**(19 Suppl 3):III130–5.

105 Mertens L. Deciphering the mystery of the leaky pulmonary valve in a new era of interventional cardiology. *Eur Heart J* 2007;**28**:1793–4.

106 Oosterhof T, van Straten A, Vliegen HW, *et al*. Preoperative thresholds for pulmonary valve replacement in patients with corrected tetralogy of Fallot using cardiovascular magnetic resonance. *Circulation* 2007;**116**:545–51.

107 Buechel ER, Dave HH, Kellenberger CJ, *et al*. Remodelling of the right ventricle after early pulmonary valve replacement in children with repaired tetralogy of Fallot. assessment by cardiovascular magnetic resonance. *Eur Heart J* 2005;**26**:2721–7.

108 Therrien J, Provost Y, Merchant N, *et al*. Optimal timing for pulmonary valve replacement in adults after tetralogy of Fallot repair. *Am J Cardiol* 2005;**95**:779–82.

109 Bourassa MG, Campeau L. Combined supravalvar aortic and pulmonic stenosis. *Circulation* 1963;**28**:572–81.

110 Blieden LC, Lucas RV Jr, Miller JB, *et al*. A developmental complex including supravalvar stenosis of the aorta and pulmonary trunk. *Circulation* 1974;**49**:585–90.

111 Cormode EJ, Dawson M, Lowry RB. Keutel syndrome: clinical report and literature review. *Am J Med Genet* 1986;**24**:289–94.

112 Nickerson E, Greenberg F, Keating MT, *et al*. Deletions of the elastin gene at 7q11.23 occur in approximately 90% of patients with Williams syndrome. *Am J Hum Genet* 1995;**56**:1156–61.

113 Oda T, Elkahloun AG, Pike BL, *et al*. Mutations in the human Jagged1 gene are responsible for Alagille syndrome. *Nat Genet* 1997;**16**:235–42.

114 Gay BB, Franch RH, Shuford WH, Rogers JV. The roentgenologic features of simple and multiple coarctations of the pulmonary artery and its branches. *AJR Am J Roentgenol* 1963;**90**:599–613.

115 Raju BL, Sakowitz M, Golfarm R, *et al*. Lung-scan abnormality in pulmonary artery branch stenosis. *J Nucl Med* 1980;**21**:495–6.

116 Tamir A, Melloul M, Berant M, *et al*. Lung perfusion scans in patients with congenital heart defects. *J Am Coll Cardiol* 1992;**19**:383–8.

117 Rothman A, Perry JB, Keane JF, Lock JE. Early results and follow-up of balloon angioplasty for branch pulmonary artery stenosis. *J Am Coll Cardiol* 1990;**15**:1109–17.

118 Hosking MCK, Thomaidis A, Hamilton R, *et al*. Clinical impact of balloon angioplasty for branch pulmonary artery stenosis. *Am J Cardiol* 1992;**69**:1467–70.

119 Cohn LH, Sanders JH Jr, Collins JJ Jr. Surgical treatment of congenital unilateral pulmonary arterial stenosis with contralateral pulmonary hypertension. *Am J Cardiol* 1976;**38**:257–60.

120 McGoon DC, Kincaid OW. Stenosis of branch of the pulmonary arteries. Surgical repairs. *Med Clin North Am* 1976;**48**:257–63.

121 Gill CC, Moodie DS, McGoon DC. Staged surgical management of pulmonary atresia with diminutive pulmonary arteries. *J Thorac Cardiovasc Surg* 1977;**73**:436–42.

122 Lock JE, Niemi T, Einzig S, *et al*. Transvenous angioplasty of experimental branch pulmonary artery stenosis in newborn lambs. *Circulation* 1981;**64**:886–93.

123 Edwards BS, Lucas RV, Lock JE, Edwards JE. Morphologic changes in the pulmonary arteries after percutaneous balloon angioplasty for pulmonary arterial stenosis. *Circulation* 1985;**71**:195–201.

124 Fellows KE, Radke W, Keane JE. Acute complications of catheter therapy for congenital heart disease. *Am J Cardiol* 1987;**60**:679–83.

125 Kan JS, Marvin WJ, Bass JL, *et al*. Balloon angioplasty–branch pulmonary artery stenosis. Results from the Valvuloplasty and Angioplasty of Congenital Anomalies Registry. *Am J Cardiol* 1990;**65**:798–801.

126 Zeevi B, Berant M, Blieden LC. Midterm clinical impact versus procedural success of balloon angioplasty for pulmonary artery stenosis. *Pediatr Cardiol* 1997;**18**:101–6.

127 Fuster V, McGoon DC, Kennedy MA, *et al*. Long term evaluation (12–22 years) of open heart surgery for tetralogy of Fallot. *Am J Cardiol* 1980;**46**:635–42.

128 Saxena A, Fong W, Ogilvie BC, Keeton BR. Use of balloon dilatation to treat supravalvar pulmonary stenosis developing after anatomical correction for complete transposition. *Br Heart J* 1990;**64**:151–5.

129 Mullins CE, O'Laughlin MP, Dick M III, *et al*. Implantation of balloon-expandable intravascular grafts by catheterization in pulmonary arteries and systemic veins. *Circulation* 1988;**77**:188–99.

130 O'Laughlin MP, Perry SB, Lock JE, Mullins CE. Use of endovascular stents in congenital heart disease. *Circulation* 1991;**83**:1923–39.

131 Benson LN, Hamilton F, Dasmahaptra H, *et al*. Percutaneous implantation of a balloon-expandable endoprosthesis for pulmonary artery stenosis: an experimental study. *J Am Coll Cardiol* 1991;**18**:1303–8.

132 Mendelsohn AM, Bove EL, Lupinetti FM, *et al*. Intraoperative and percutaneous stenting of congenital pulmonary artery and vein stenosis. *Circulation* 1993;**88** (Suppl II):210–7.

133 Stapleton GE, Hamzeh R, Mullins CE, *et al*. Simultaneous stent implantation to treat bifurcation stenoses in the pulmonary arteries. Initial results and long-term follow up. *Cathet Cardiovasc Interv* 2009;**73**:557–63.

134 Law MA, Shamszad P, Nugent AW, *et al*. Pulmonary artery stents: long-term follow-up. *Cathet Cardiovasc Interv* 2010;**75**:757–64.

135 Maglione J, Bergersen L, Lock JE, McElhinney DB. Ultra-high-pressure balloon angioplasty for treatment of resistant stenoses within or adjacent to previously implanted pulmonary arterial stents. *Circ Cardiovasc Interv* 2009;**2**:52–8.

136 Fogelman R, Nykanen D, Smallhorn JF, *et al*. Endovascular stents in the pulmonary circulation. Clinical impact on management of medium-term follow-up. *Circulation* 1995;**92**:881–5.

137 Hatai Y, Nykanen D, Williams WG, *et al*. The clinical impact of percutaneous balloon expandable endovascular stents in the management of early postoperative vascular obstruction. *Cardiol Young* 1996;**6**:48–53.

138 Moore JW, Spicer RL, Perry JC, *et al*. Percutaneous use of stents to correct pulmonary artery stenosis in young children after cavopulmonary anastomosis. *Am Heart J* 1995;**130**:1245–9.

139 Hijazi ZM, Al-Fadzey F, Geggel RL, *et al*. Stent implantation for relief of pulmonary artery stenosis. immediate and short-term results. *Cathet Cardiovasc Diagn* 1996;**36**:16–23.

140 Gewillig M, Brown S. Coronary compression caused by stenting a right pulmonary artery conduit. *Cathet Cardiovasc Interv* 2009; **74**:144–7.

141 Moszura T, Mazurek-Kula A, Dryzek P, Sysa A. Bronchial compression as adverse effect of left pulmonary artery stenting in a patient with hypoplastic left heart syndrome. *Pediatr Cardiol* 2010;**31**:530–3.

142 Tomita H, Yazaki S, Echigo S, *et al*. Late distortion of the original Palmaz stent implanted in postoperative lesions associated with congenital heart disease. *Cathet Cardiovasc Interv* 2005; **65**:301–5.

143 Rowland TW, Rosenthal A, Castaneda AR. Double-chamber right ventricle: experience with 17 cases. *Am Heart J* 1975; **89**:445–62.

144 Chesler E, Korns ME, Edwards JE. Anomalies of the tricuspid valve, including pouches, resembling aneurysms of the membranous ventricular septum. *Am J Cardiol* 1968;**21**:661–8.

34 Total Anomalous Pulmonary Venous Connection

**Shiv Kumar Choudhary, Sachin Talwar &
Sivasubramanian Ramakrishnan**
All India Institute of Medical Sciences, New Delhi, India

Introduction

Anomalous pulmonary venous connections are rare congenital anomalies that can be either total or partial. Total anomalous pulmonary venous connection (TAPVC) encompasses anomalies in which the pulmonary veins are connected to the systemic venous circulation through persistent splanchnic connections. In partial anomalous pulmonary venous connection (PAPVC), only some of the pulmonary veins drain into the systemic venous system.

Historical background, incidence, and genetics

TAPVC was first described in 1798 by Wilson [1]. Friedlowsky (1868) first described an isolated supracardiac TAPVC [2]. Kirklin and Burroughs performed the first surgical repair under cardiopulmonary bypass in 1956 [3].

TAPVC is rare, representing 1.5–2% of all congenital cardiovascular abnormalities [4]. In a population-based registry, TAPVC represented 1.5% of all congenital cardiovascular malformations and had a prevalence of 6.8/100 000 live births [5]. The genetic basis for TAPVC is not understood. Most instances are sporadic, although there are a few reports of TAPVC recurring among siblings, father and two children, and twins [6,7]. TAPVC is rare in other genetic syndromes or chromosomal anomalies. Lead and pesticide exposure during pregnancy may be related to TAPVC [5]. Pesticide exposure and family clustering are related, suggesting that there could be a genetic predisposition to pesticide related injury.

Embryology

During early development of the lungs, blood drains to the splanchnic plexus, which in turn connects to the paired common cardinal and umbilicovitelline veins. The right common cardinal vein evolves into the right horn of the sinus venosus that ultimately develops into the right superior vena cava and the azygos vein. The left common cardinal vein evolves into the left horn of the sinus venosus, which ultimately develops into the left superior vena cava and the coronary sinus. The umbilicovitelline system becomes the inferior vena cava, ductus venosus, and portal vein.

During early development, the pulmonary venous plexus is not in direct communication with the left atrium, but retains connections to the right superior vena cava, left superior vena cava, and portal system. At 27–29 days' gestation, an endothelial out-pouching occurs from the posterior superior left atrial wall and represents the primitive (common) pulmonary vein that connects with the pulmonary venous plexus by 30 days' gestation. The tributaries to the common pulmonary vein form a common chamber which progressively incorporates into the posterior wall of the primitive left atrium. The pulmonary venous part of the splanchnic plexus gradually loses its connection with the cardinal and umbilicovitelline veins.

Most forms of TAPVC result when the common pulmonary vein fails to develop or fails to connect with the pulmonary venous plexus. This leads to the persistence of one or more earlier venous connections. Connection to the right common cardinal vein results in TAPVC to the left vertical vein/innominate vein or to the right superior vena cava. Persistence of connection to the left common cardinal vein

results in TAPVC to the coronary sinus, and persistent connection to the umbilicovitelline vein leads to infracardiac TAPVC. Failure of the septum primum to form normally, or abnormal septation of the sinus venosus, can lead to direct connection of the pulmonary veins to the right atrium.

Pathologic anatomy and major associated anomalies

The affected heart of all forms of TAPVC has in common dilatation and hypertrophy of the right ventricle and right atrium, dilatation of the pulmonary artery, a normal-sized left ventricle, and reduced left atrial size and volume. The specific findings depend on the type of TAPVC. The pulmonary veins usually form a confluence, also known as a common chamber, directly behind the left atrium. An anomalous channel termed the vertical vein connects the pulmonary venous confluence to the systemic venous system.

The classification proposed by Darling and colleagues [8] is widely followed and consists of four types: supracardiac, cardiac, infracardiac, and mixed. TAPVC can further be classified by the presence or absence of obstruction. The potential sites of connection of various forms of TAPVC are given in Table 34.1.

A supracardiac connection is present in ~55% of patients with TAPVC. Classically, the pulmonary vein confluence drains superiorly into the innominate vein via a left-sided ascending vertical vein. The common chamber is behind the left atrium and the vertical vein passes anteriorly, usually anterior to left pulmonary artery and left main bronchus, but sometimes between them. Rarely, the vertical

vein may drain directly to right or left superior vena cava, or azygos vein. Anomalous connection to the right superior vena cava is often associated with complex cardiac malformations [9].

A cardiac connection occurs in ~30% of patients with TAPVC. The pulmonary venous confluence drains into the coronary sinus near the AV groove. The coronary sinus ostium is enlarged, but is normally placed. Rarely, the pulmonary venous confluence may connect directly by a short channel into the posterior aspect of the right atrium, usually near the midatrial septum, or individual pulmonary veins may connect directly into the right atrium.

Approximately 13% of patients with TAPVC have an infracardiac connection. A vertical vein from the pulmonary vein confluence descends anterior to the esophagus and traverses the diaphragm through the esophageal hiatus. Most commonly it drains into the portal venous system. Rarely, it drains into the ductus venosus, hepatic veins, or the inferior vena cava.

Finally, a mixed type of TAPVC occurs in ~ 2–5% of patients and can involve any or all components of the previous three types. Most commonly, the left pulmonary veins connect via a left vertical vein into the left innominate vein and the right pulmonary veins drain directly into the right atrium or coronary sinus.

Obstruction is uniformly present in the infracardiac type because the pulmonary venous blood must pass through the sinusoids of the liver, and may worsen due to constriction or closure of ductus venosus. The obstruction may also occur as the descending vein travels through the diaphragm or at its junction with the portal vein system. Obstruction, considered rare in the cardiac type, has been underestimated and may occur in 22% of patients [10] when a very short, narrow channel connects the horizontally placed pulmonary veins to the coronary sinus. In supracardiac TAPVC, obstruction can be either intrinsic or extrinsic: obstruction most commonly occurs from compression of the ascending vertical vein between the left main stem bronchus posteriorly and left pulmonary artery anteriorly, but rarely intrinsic anatomic narrowing occurs at the pulmonary vein confluence and vertical vein, or at the insertion of the vertical vein into the innominate vein. In all forms of TAPVC, narrowing of individual pulmonary vein(s) can also produce varying degrees of obstruction.

A patent foramen ovale or an atrial septal defect is always present and considered a part of the TAPVC complex. A patent ductus arteriosus (PDA) is usually found in neonates presenting with TAPVC. TAPVC occurs alone in two-thirds of patients and occurs as part of a group of heart defects (e.g., heterotaxy syndromes) in approximately one-third of patients. Asplenia or right isomerism is characterized by two atrial chambers of right atrial morphology. TAPVC is a common feature in right isomerism as these hearts lack a morphological left atrium and coronary sinus.

Table 34.1 Classification of TAPVC according to the site of anomalous connection.

TAPVC	Site
Supracardiac TAPVC	Left brachiocephalic (innominate) vein[a]
	Right superior vena cava
	Azygos vein
	Left superior vena cava
	Hemiazygos vein
Cardiac TAPVC	Coronary sinus[a]
	Right atrium
Infracardiac TAPVC	Portal venous system[a]
	Splenic vein
	Splenic, superior mesenteric vein confluence
	Ductus venosus
	Hepatic veins
	Inferior vena cava

[a]Commonest sites of drainage.

Pathophysiology

The physiologic consequence of TAPVC in fetal life is negligible as only a small amount of blood normally flows through the lungs. When the neonatal lungs expand, pulmonary flow increases markedly, but because of the anomalous connection in all patients with TAPVC, the systemic blood flow depends on a right-to-left shunt through an atrial septal defect or patent foramen ovale. Venous obstruction and size of the atrial septal defect are the critical determinants of the size of the morphological left atrium and coronary sinus, and hemodynamics and clinical presentation.

Obstructed TAPVC increases the pulmonary venous pressure, and usually presents with pulmonary edema in neonates. Increase in pulmonary lymphatic flow, recruitment of pulmonary-bronchial venous anastomoses, and reflex pulmonary vasoconstriction ensue as compensatory mechanisms. All these changes increase pulmonary artery and right ventricular pressures. Right ventricular compliance decreases and consequently pulmonary blood flow diminishes. Because flow across an atrial septal defect is determined by the relative compliance of the pulmonary and systemic circulations, right-to-left shunting across the atrial septum increases, causing marked hypoxemia. Progressive hypoxia leads to acidosis, shock, and multiorgan dysfunction. Thus, obstructed TAPVC in a neonate is characterized by pulmonary edema, pulmonary hypertension, reduced pulmonary blood flow, and intense cyanosis.

The size of the atrial septal defect determines the systemic blood flow. In a few patients, the atrial septal defect or foramen ovale is small. Neonates with a restrictive atrial septal defect present early. During fetal life, the flow across the foramen ovale is only mildly increased in TAPVC. Hence 70–80% of patients with isolated TAPVC have only a patent foramen ovale at birth. As pulmonary blood flow increases after birth, pulmonary venous return also increases. Rapid growth in the first few weeks increases the demand for systemic output that a relatively restrictive foramen ovale is unable to accommodate. Hence right atrial, pulmonary venous, and pulmonary arterial pressures increase, producing systemic and pulmonary venous congestion. There is a large increase in pulmonary blood flow with a reduced systemic blood flow.

In unobstructed TAPVC, the oxygenated pulmonary venous drainage mixes with systemic venous drainage. Hence saturations are the same or nearly the same in the right and left cardiac chambers beyond the point of admixture. With a nonrestrictive atrial septal defect, the relative pulmonary and systemic blood flows depend on the relative compliances of the ventricles. Normally, a low pulmonary vascular resistance is associated with a compliant right ventricle and the pulmonary blood flow is significantly increased.

Hence mild cyanosis exists with increased pulmonary blood flow, and significant enlargement of the right atrium, right ventricle, and pulmonary artery. Conversely, the left atrium and left ventricle are small. Pulmonary artery hypertension develops in obstructed TAPVC and also in longstanding unobstructed TAPVC. With an increase in pulmonary vascular resistance, the right ventricle hypertrophies and become less compliant. The pulmonary arterial blood flow decreases and cyanosis increases. Severe pulmonary artery hypertension leading to Eisenmenger syndrome may also develop in a minority [11].

Natural history

With obstruction, the lifespan is brief. Pulmonary edema and right ventricular failure ensue within days to weeks of birth. Most infants die in the first few days or weeks of life and survival for up to 3–4 months is exceptional [12]. The natural history is unfavorable even in patients with unobstructed TAPVC, most of whom die within 3–6 months of birth; 75–90% of symptomatic infants do not reach 1 year of life. Heart failure and infections are the major causes of mortality. The minority who present after the first year of life invariably have a low pulmonary vascular resistance and a nonrestrictive atrial septal defect.

Clinical features

Patients with TAPVC with pulmonary venous obstruction often present in the early neonatal period, whereas patients with unobstructed TAPVC may present later; the majority present in infancy. The sex distribution is equal in supracardiac TAPVC, in contrast to the female preponderance in atrial septal defect. A strong male preponderance (3:1) is observed in infra-diaphragmatic TAPVC [13]. Cyanosis and respiratory distress are marked in symptomatic neonates with obstructed TAPVC. Pulmonary edema and shock may occur. In infra-diaphragmatic TAPVC, feeding may exacerbate symptoms due to worsening obstruction at the esophageal hiatus or an increase in intra-abdominal pressure. With a restrictive atrial septal defect, symptoms of heart failure and mild cyanosis on crying start in the first month of life and worsen progressively. Cyanosis is mild in unobstructed TAPVC and may escape clinical attention. Infants often present with tachypnea, feeding difficulties, diaphoresis, and failure to thrive. Pulmonary infections worsen the clinical course and are especially common in developing countries. Exceptional adult survivors may present like an atrial septal defect but with a dusky appearance.

In neonates and infants, physical signs are limited and are not easily appreciable owing to respiratory distress. In infants with obstructed TAPVC, signs of pulmonary hypertension

predominate. The second sound is loud and often single or closely split, and flow murmurs are usually not apparent. A soft, short, mid-systolic murmur in the pulmonary area may be the only murmur. A pulsatile liver may indicate restrictive communication at the atrial septal level.

The physical signs of unobstructed TAPVC generally resemble those of an atrial septal defect except that they begin earlier. Cardiac failure occurs in most patients before 6 months of age. There is right ventricular volume overload evident on physical examination. The tricuspid component of the first heart sound is loud and the second heart sound is widely and fixedly split. A right ventricular third heart sound is heard in most patients. A fourth heart sound may be heard in older patients. An ejection systolic murmur in the pulmonary area and a tricuspid diastolic flow murmur are frequent. Increased flow across the vertical vein, innominate vein, and superior vena cava can lead to a continuous murmur along the upper left sternal border, but is uncommon. Unlike a physiological venous hum, this murmur is not louder during diastole, and does not change with posture. As the pulmonary vascular resistance increases, the flow murmurs are attenuated. The second heart sound split narrows or disappears with a loud pulmonary component. A pulmonary ejection click and murmurs of tricuspid regurgitation and pulmonary regurgitation (Graham Steell murmur) may appear.

Chest X-ray

In neonates with obstructed TAPVC, chest radiographs reveal a normal heart size with a scattered, reticular, nodular, ground-glass pattern fanning out from the hilum (Figure 34.1). Meconium aspiration and hyaline membrane disease are important differential diagnoses for such an X-ray.

In unobstructed TAPVC, there is cardiomegaly with enlargement of the right atrium, right ventricle, and pulmonary artery. Radiological evidence of increased pulmonary blood flow becomes more apparent with increasing age. Enlargement of the anomalous channels results in distinct radiological signs, but these signs take time to develop. In supracardiac TAPVC, a "figure-of-eight" or "snowman" appearance is found (Figure 34.2). The upper part is formed by the dilated left vertical vein, innominate vein, and right superior vena cava. The dilated right ventricle and atrium form the lower portion.

Electrocardiogram

The ECG of a neonate with obstructed TAPVC shows right ventricular hypertrophy, mostly with a qR complex in right chest leads. Right atrial enlargement is infrequent. The electrocardiogram in unobstructed TAPVC resembles that of an ostium secundum atrial septal defect in most patients. The ECG usually shows right axis deviation and right atrial and ventricular enlargement with an incomplete right bundle branch block pattern.
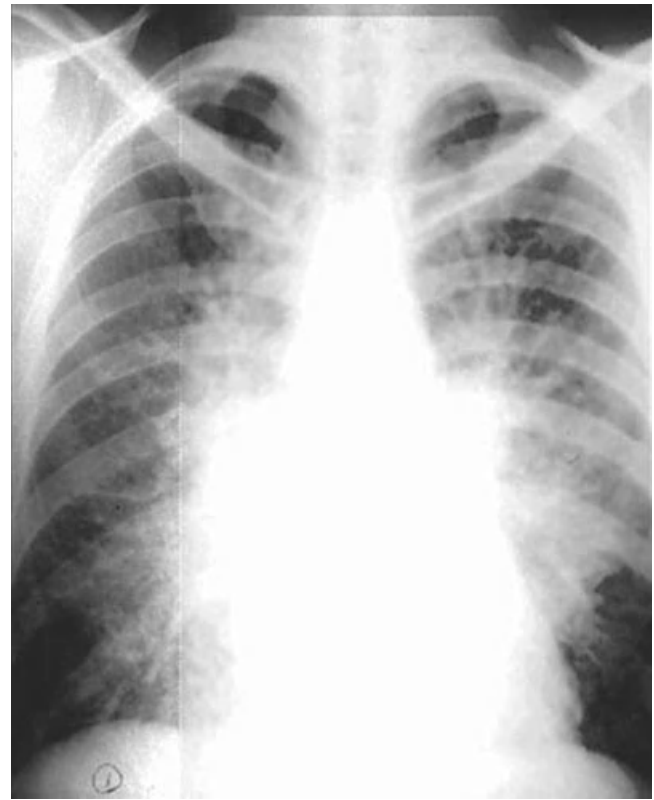
Figure 34.1 Chest X-ray showing scattered, reticular, nodular, ground-glass pattern fanning out from the hilum and relatively small heart characteristic of obstructed TAPVC.
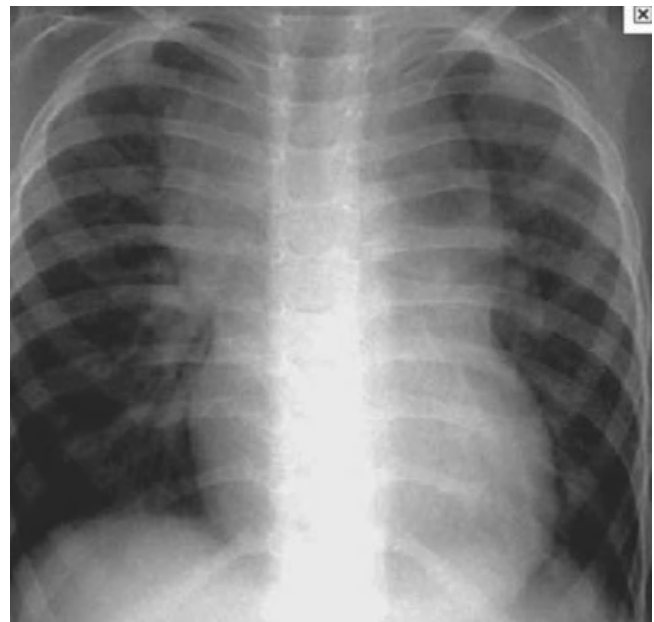
Figure 34.2 Chest X-ray showing snowman appearance, cardiomegaly, and increased pulmonary blood flow. The upper part of this "figure-of-8" appearance is due to dilated left vertical vein, innominate vein, and right superior vena cava. Dilated right ventricle and atrium form the lower portion.
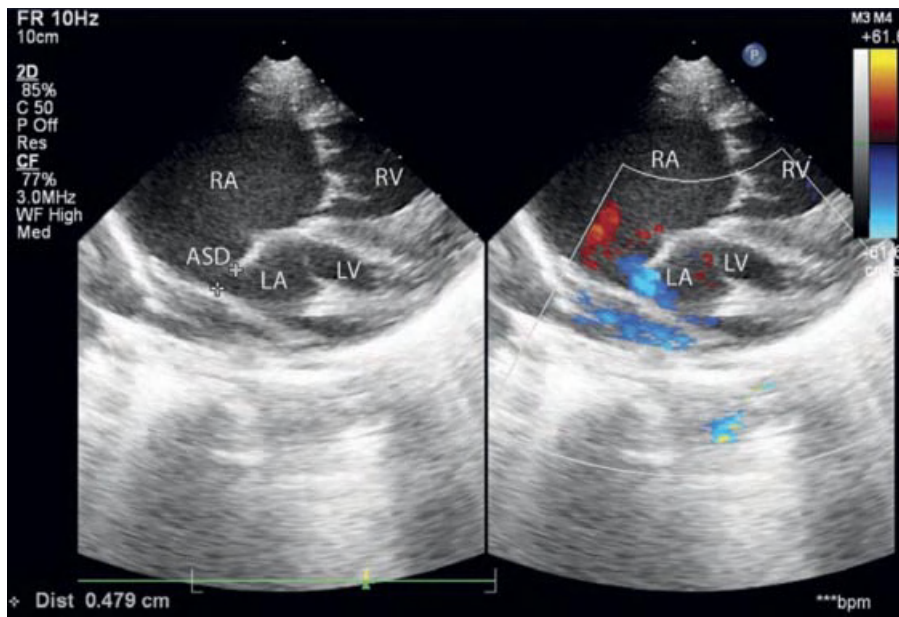
(a)
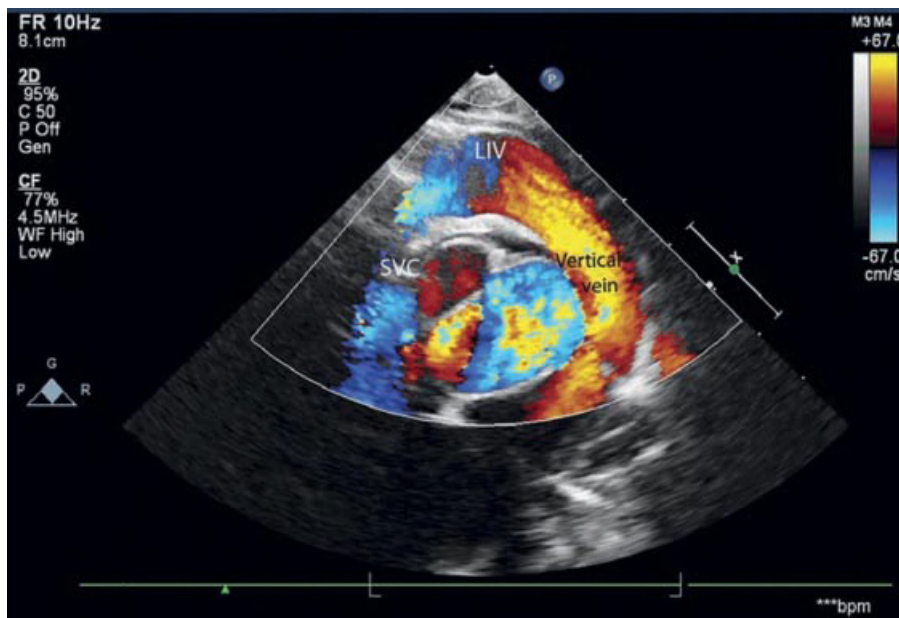
(b)

Figure 34.3 Echocardiographic images of a typical supracardiac TAPVC. (a) Modified subcostal view showing a nonrestrictive atrial septal defect with right-to-left flow across the defect. RA, right atrium; LA, left atrium; RV, right ventricle; LV, left ventricle; ASD, atrial septal defect.(b) Suprasternal view showing a left-sided ascending vertical vein draining into the left innominate vein (LIV) and to the right superior vena cava (SVC).

Echocardiography

Echocardiography is usually diagnostic and can identify associated abnormalities. Right atrial and right ventricular enlargement with a smaller than normal left atrium and left ventricle are evident. The interatrial septum and interventricular septum bulge to the left and there is para-doxical ventricular septal motion. Inability to demonstrate any pulmonary veins connected to the left atrium is the initial clue. Subcostal long- and short-axis views show the size of the atrial septal defect with right-to-left shunting across it (Figure 34.3a). A restrictive atrial septal defect is

associated with a right-to-left shunt with a continuous Doppler signal. The pulmonary venous confluence is easily identified as an echo free, non-pulsatile space posterior to the left atrium. Individual pulmonary veins and their con-fluences are best identified in apical, parasternal, and suprasternal views.

The size of the individual pulmonary veins is an impor-tant independent predictor of survival in TAPVC [14]. The size of and flow patterns across the superior vena cava, cor-onary sinus, and inferior vena cava give clues to the site of drainage. Commonly, the suprasternal view (crab's view)

shows an ascending vertical vein draining into the left innominate vein (Figure 34.3b). Modifications of this view identify all the various forms of supracardiac sites of drainage. Apical four-chamber and subcostal views best identify cardiac TAPVC. Rarely, there may be more than one portal of entry into the coronary sinus and a persistent left superior vena cava [15]. The subcostal view identifies a descending vein entering ductus venosus or portal veins with increased flow across the sinusoids of liver in infradiaphragmatic TAPVC. The descending vertical vein is commonly located between the inferior vena cava on the right and the descending aorta on the left. The flow in this anomalous channel is characterized by venous-type flow away from the heart. A pulmonary venous flow velocity $>2\,\mathrm{m\,s^{-1}}$ identifies obstruction [16]. Commonly, the venous channel dilates proximal to the obstruction and there is no phasic variation in flow pattern. The size of the individual pulmonary veins, the size and location of the pulmonary venous confluence, and the course of the vertical vein must be ascertained before surgery.

Fetal diagnosis

Because the fetal blood flow through the anomalous connections is limited, TAPVC may be difficult to diagnose. All forms of TAPVC have right ventricle volume overload, an enlarged right atrium, and a leftward bowing of the interatrial septum. TAPVC should be suspected when no pulmonary veins can be seen entering the left atrium on the short-axis scan. The common pulmonary channel may be identified behind the left atrium, with the pulmonary veins draining into it. The channel may be followed to the site of its connection [17].

Cardiac catheterization

Cardiac catheterization is rarely performed these days for diagnosis of TAPVC. Current indications are atrial septostomy or balloon dilation to relieve venous obstruction, or assessment of pulmonary vasoreactivity in older infants or children suspected of severe pulmonary hypertension. Occasionally it is used to identify complex mixed pulmonary venous connections. The saturations are usually similar in all the cardiac chambers, the pulmonary artery, and the aorta, but exceptions due to selective streaming are not uncommon [18,19]. Angiograms after right and left pulmonary artery injection with venous phase follow-through identify the site of connection. A direct injection into the vertical vein or individual pulmonary vein is usually unsatisfactory in the absence of obstruction because excess flow does not allow retrograde filling of the pulmonary vein. With obstruction, excellent visualization is possible, but the injection should be made by hand and done quickly because the pulmonary venous pressure may rise to dangerous levels with a catheter across an obstruction in a neonate. Some cardiologists advise against such an injection for this reason.

Atrial septostomy offers short- and intermediate-term palliation in selected patients [20]. Atrial septostomy may be technically challenging, especially in cardiac forms of TAPVC, due to a small left atrium without pulmonary venous connections. Echocardiographic guidance is often helpful. Blade septostomy or static balloon dilatation may be needed in older patients. The success of a septostomy in TAPVC is indicated by a drop in pulmonary artery pressure, an increase in systemic pressure, and a drop in systemic saturation [21]. Atrial septostomy in a patient with a restricted atrial septal defect increases cardiac output and relieves systemic and pulmonary venous congestion. These favorable hemodynamics lead to clinical stabilization, and help in optimizing the timing of surgery.

Balloon dilatation or stent placement is occasionally performed to relieve obstruction in sick neonates presenting with obstructed TAPVC [22,23]. Palliative stenting can be potentially life-saving in sick neonates and may aid preoperative stabilization.

Other imaging modalities

A computed tomography (CT) angiogram can identify the varied patterns of pulmonary venous connection in TAPVC. One study showed CT angiograms to be more sensitive than echocardiography for the accurate diagnosis of TAPVC [24]. CT angiography clearly establishes the course of the abnormal vessel into the systemic venous system (Figure 34.4) [25]. It is especially useful in mixed and unusual forms of TAPVC.

Magnetic resonance imaging (MRI) identifies the various sites of connection, and the site and severity of obstruction. In one study, the combination of axial and coronal MRI visualized 96% of the individual anomalous pulmonary veins and all the common pulmonary veins [26]. MRI is especially useful in complex heterotaxy syndromes associated with TAPVC and postoperative patients with residual pulmonary vein stenosis.

Management

Medical management is only supportive in managing TAPVC, and only intended to stabilize the patient before surgery. Preoperative stabilization includes correcting acidosis and hypotension, fluid management, and mechanical ventilation. Prostaglandin is occasionally helpful in keeping ductus venosus open in infra-diaphragmatic TAPVC, but in other forms it is harmful [27].

Surgery for TAPVC is aimed at achieving unobstructed pulmonary venous drainage to the left atrium. The clinical condition of the patient will usually decide the timing of surgery. In general, the diagnosis of TAPVC of any type is an indication to proceed with early surgery. An emergency operation is required in neonates with obstructed forms of TAPVC.
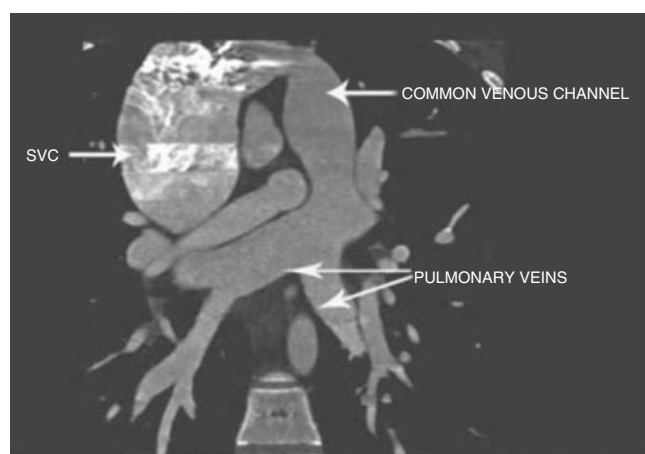
(a)
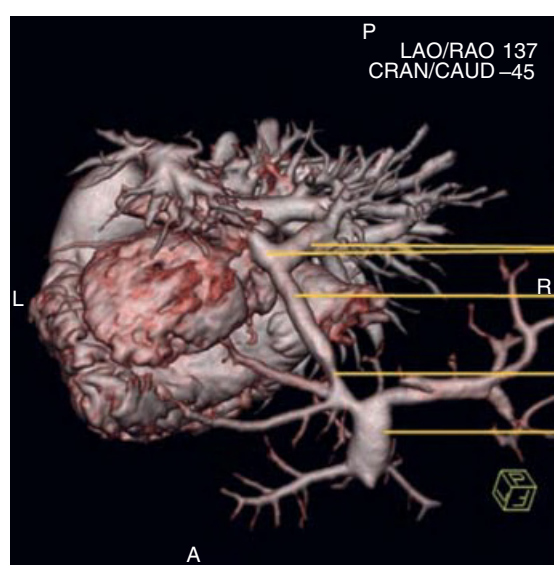
(b)

Right & Left side Pulmonary Veins

Common Chamber

Stenosis in the Descending vertical Vein

Main Portal Vein

Figure 34.4 CT angiograms. (a) Coronal oblique multiplanar reconstruction (MPR) image shows the confluence of the pulmonary veins into a common channel, which in turn drains into the SVC. (Reproduced from Shaheen F, Gojwari TA, Andrabi M, Sofi S, Singh M, *Indian J Radiol Imaging* 2009;**19**:54–6, an open access publication.) (b) 3D reconstruction showing infracardiac TAPVC. All the pulmonary veins form a narrow, long, common chamber draining into the portal vein through a long descending vertical vein that has narrowing at the lower margin. A, anterior; L, left; P, posterior; R, right; SVC, superior vena cava.

Surgical technique

The surgical approach to all anatomic forms of TAPVC is via a median sternotomy. In patients with the cardiac type of TAPVC, a pericardial patch is often harvested and treated with 0.6% glutaraldehyde for 5–10 min. This will be used subsequently in the repair. Purse string sutures are placed on the aorta and the right atrial appendage. After adequate systemic heparinization, cardiopulmonary bypass (CPB) is established and core cooling commenced.

Supracardiac TAPVC

The vertical vein is dissected and ligated, taking care to preserve the left phrenic nerve. A variety of surgical approaches have been used to establish a communication between the pulmonary venous chamber and the pulmonary venous

atrium. These include the following: (a) In Muller's closed approach, the pulmonary venous confluence is directly anastomosed to the left atrial appendage without using CPB. (b) In Cooley's trans-atrial approach, the right atrium is opened and the interatrial septum is incised. Following this, corresponding incisions are made in the posterior wall of the left atrium and the common pulmonary venous chamber and an anastomosis is fashioned between the two, with subsequent closure of the atrial septal defect and the right atrium. (c) In Schumaker and King's transverse biatrial approach, an incision is made in the right atrium inferior to the right atrial appendage. This incision is carried posteriorly through the foramen ovale and into the posterior wall of the left atrium. The common pulmonary venous is then incised and an anastomosis is made between the left atrium and the common chamber. (d) In Tucker's superior approach, the common pulmonary venous chamber is exposed through the
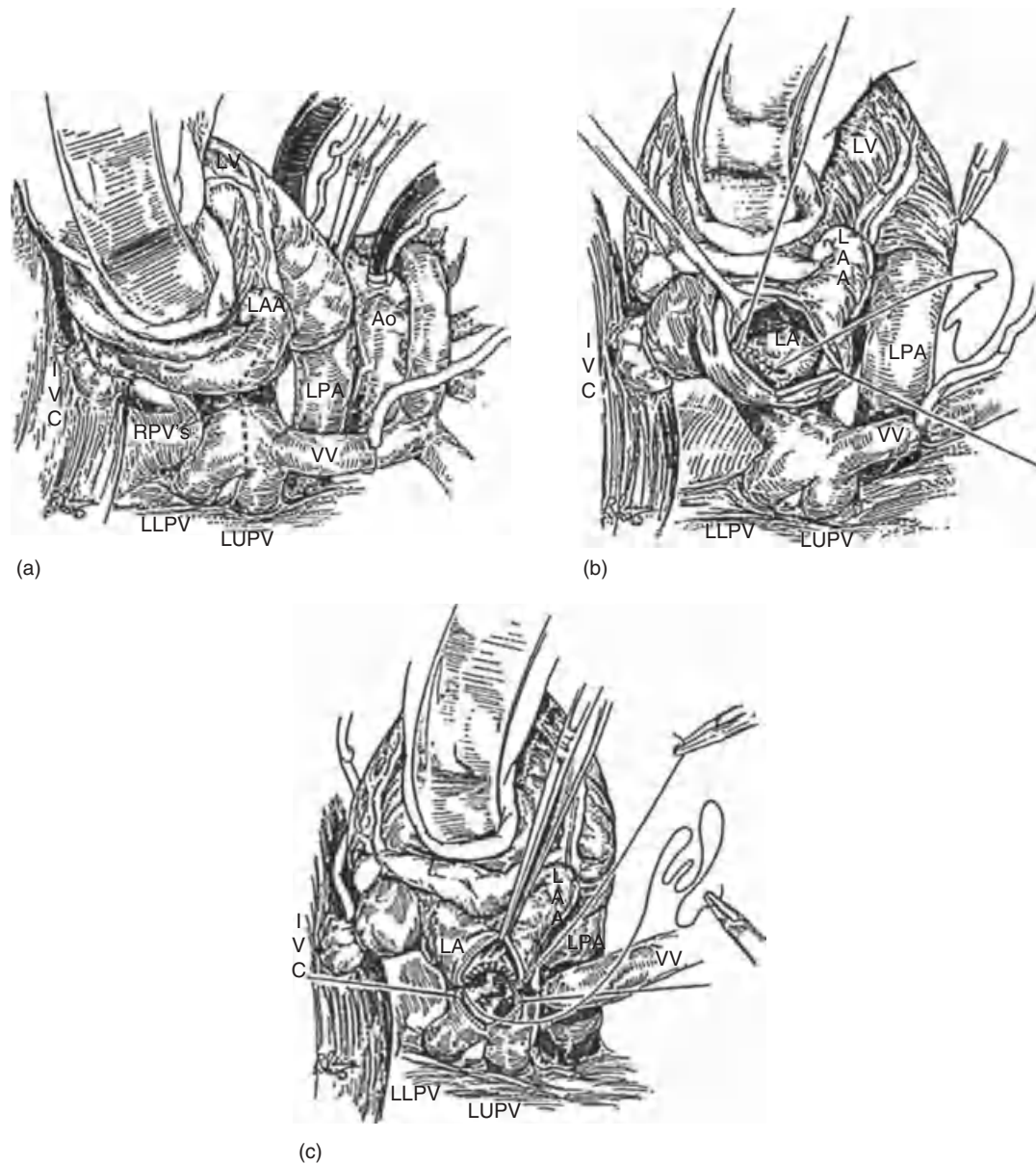
Figure 34.5 (a) Operative exposure from the left side of the operating table for a patient with type I (supracardiac) TAPVC during continuous cardiopulmonary bypass and cold blood cardioplegic arrest. The heart is retracted to the right and superiorly out of the pericardial cavity to expose the confluence of the pulmonary veins and the vertical vein. The vertical vein is controlled with a snugger that can be enforced during the anastomosis. The dotted lines represent proposed incisions of the confluence of the pulmonary veins and the left atrium, respectively, for the intended side-to-side anastomosis. (b) Once retrocardiac exposure is established, the vertical vein is controlled with the snugger, and a left atrial incision is performed from the base of the left atrial appendage centrally towards the interatrial septum corresponding to the confluence of the right upper and lower pulmonary veins. The patent foramen ovale is immediately encountered toward the inferoposterior portion of the left atrium and is closed with the running suture technique. (c) Side-to-side confluence of the pulmonary veins to the left atrial anastomosis is then performed in segments as the heart is lowered symmetrically into the pericardial cavity. To achieve this, care is taken to alternate small sections of the suture line reconstruction between the superior and inferior borders. In our technique, the right pleura is completely opened and the heart is dropped into the right pleural cavity as described in the text. Ao, aorta; IVC, inferior vena cava; LA, left atrium; LAA, left atrial appendage; LLPV, left lower pulmonary vein; LPA, left pulmonary artery; LUPV, left upper pulmonary vein; RPV, right pulmonary vein; VV, vertical vein. (Reproduced from Mavroudis C, Backer CL. *Operat Tech Thorac Cardiovasc Surg* 2001;**6**:12–23, with permission from Elsevier.)

transverse sinus of the pericardium after retracting the aorta to the left and the superior vena cava to the right. Transverse incisions are then made in the common chamber and the left atrium followed by anastomosis between the two. (e) In

Kirklin's right lateral approach, the posterior pericardial attachments of the heart are divided and the atria and vena cavae are retracted anteriorly and to the left. The common chamber is then exposed from within the pericardium and,
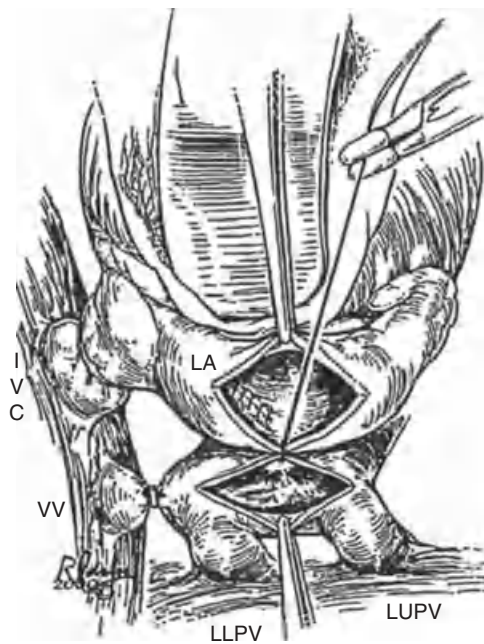
Figure 34.6 When type III TAPVC is encountered, the orientation of the side-to-side anastomosis should be tailored to accommodate a "best lie" configuration. This drawing shows the vertical incision in the confluence of the pulmonary veins and a corresponding incision in the left atrium, which produces the most favorable anatomic and geometric union for unrestricted flow. The anastomosis is started at the far center of the pulmonary vein confluence and left atrium as shown. Note that the inferior vertical vein is ligated and the patent foramen ovale is closed. IVC, inferior vena cava; LA, left atrium; LLPV, left lower pulmonary vein; LUPV, left upper pulmonary vein; VV, vertical vein. (Reproduced from Mavroudis C, Backer CL. *Operat Tech Thorac Cardiovasc Surg* 2001;**6**:12–23, with permission from Elsevier.)

after making corresponding transverse incisions on the common chamber and the left atrium, an anastomosis is made between the two.(f) In Ebert's posterior approach, the heart is lifted cephalad and to the right to expose the common pulmonary venous chamber, followed by incision of the chamber and the left atrium and anastomosis between the two (Figure 34.5).

At our institution, we prefer a modified posterior approach [28] (Figure 34.5). The anastomosis between the pulmonary venous chamber and the left atrium should be as large as possible and purse stringing of the suture line should be avoided.

In patients in whom the pulmonary venous confluence drains into the superior vena cava (SVC), the pulmonary venous drainage may be baffled across the atrial septal defect into the left atrium via a right atrial incision.

Cardiac TAPVC

This is approached via the right atrium. In patients with a coronary sinus type of TAPVC, the coronary sinus is unroofed by cutting back its ostium towards the ASD, and closed using a pericardial or PTFE patch. Thus the pulmonary venous return drains via the coronary sinus into the left atrium. TAPVC directly to the right atrium is repaired by using the previously harvested pericardium to create a baffle to direct the pulmonary venous return through the atrial septal defect to the left atrium.

Infracardiac TAPVC

The vertical vein is dissected to the level of the diaphragm and is ligated or divided (Figure 34.6). Care must be taken that the corresponding incisions in the pulmonary venous chamber and the left atrium are vertical and in cephalad direction, so that the resulting anastomosis is wide and unobstructed (Figure 34.6).

Mixed TAPVC

Principles of repair similar to those described above apply for the confluence of the three veins, with management of the fourth vein depending upon its size. If it is large enough, it can be re-anastomosed to the left atrial appendage or directed into the left atrium via the ASD if it is draining into the superior vena cava. However, if the vein is small and stenosis of the anastomosis is anticipated in the long term, we prefer to leave it alone and accept a small left-to-right shunt that may range between 1.02 and 1.82 [29]. Other forms of mixed TAPVC are more complex, in which two veins from either side drain to different sites. In these, repair has to be tailored to the individual anatomy, avoiding pulmonary venous obstruction.

Postoperative management

The postoperative course of many patients, in particular neonates with obstruction, tends to be prolonged. Meticulous attention to mechanical ventilatory support is required to prevent pulmonary hypertensive crises.

Immediate postoperative complications include low cardiac output, bleeding, pulmonary hypertensive crises, and bradyarrhythmias (after repair of coronary sinus type of TAPVC). Pulmonary hypertensive crisis is particularly common after repair of obstructed TAPVC. Its prevention consists in avoiding hypercarbia, acidosis, and hypoxemia and using minimal endotracheal suction. Crises are managed by hyperventilation, correcting acidosis, sedation, and paralysis, and by using pulmonary vasodilators such as sodium nitroprusside, nitroglycerin, milrinone, dobutamine, or inhaled nitric oxide. ECMO support may be needed if there is profound hypoxemia and acidosis. Delayed problems include pulmonary venous obstructive disease and arrhythmias.

Outcomes

The outcomes for patients undoing surgery for TAPVC have improved. Operative mortality was ~10–30% in the 1970s and 1980s. Currently it ranges from 5 to 9% in

patients undergoing TAPVC repair in the setting of normal biventricular physiology [30]. Independent risk factors for early mortality are preoperative pulmonary venous obstruction, univentricular heart, associated chromosomal or noncardiac syndromes, poor preoperative condition, severe pulmonary arterial hypertension, small pulmonary veins, and severe pulmonary hypertensive crisis after operation [30].

The long-term outcome for patients following repair of TAPVC early in infancy continues to be good, and more than 90% patients are in NYHA class I. Actuarial survival rates of up to 88% at 18 years have been reported [4]. In these patients, the pulmonary artery pressure and cardiac index often return to normal. In our own experience of TAPVC repair in a developing country, the actuarial survival was 73% at 9 years of follow-up [31].

Postoperative pulmonary vein stenosis occurs in 5–15% patients following repair of TAPVC [32–35]. This can be either anastomotic site stenosis or stenosis of individual pulmonary veins. Pathologically there may be an anastomotic fibrous stricture, discrete stenosis of the pulmonary venous ostia, or diffuse sclerosis of the pulmonary veins. The obstruction usually occurs in children 6–12 months after surgery and is identified by high-velocity turbulent flow exceeding $2\,\mathrm{m\,s^{-1}}$ across the vein or the site of anastomosis [36].

Most of the management options for recurrent pulmonary vein stenosis provide only temporary relief, and repeated interventions are required [33–35]. Nonoperative management consists of balloon dilatation with or without stenting, with steroids or chemotherapy to minimize the fibrosis. Recurrence is common. Surgical methods are equally unsatisfactory, and consist of patch enlargement using pericardium, native atrium, or PTFE. Ostial endarterectomy of intimal hyperplasia is another option. If the anastomosis is narrowed, consideration must be given to revising the common pulmonary vein to left atrium anastomosis. "Sutureless *in situ* pericardial repair" has also been proposed to enlarge the pulmonary veins and create a neo-atrium [37]. In this technique, the left atrium is disconnected from the pulmonary veins and the obstructed pulmonary veins are completely laid open. The opened left atrium is then sutured to the pericardium *in situ* so that suture placement into the pulmonary veins is completely avoided. Recent reports have focused on this as the primary method of repair to prevent pulmonary venous obstruction [38]. Long-term follow-up of the methods is not available.

References

1 Wilson J. A description of a very unusual formation of the human heart. *Philos Trans R Soc Lond* 1798;**88**:36.

2 Brody H. Drainage of the pulmonary veins into the right-side of the heart. *Arch Pathol* 1942;**33**:221–40.

3 Cooley DA, Ochsner A Jr. Correction of total anaomalous pulmonary venous drainage. *Surgery* 1957;**42**:1014–21.

4 Michielon G, DiDonato RM, Pasquini L, *et al.* Total anomalous pulmonary venous connection: long-term appraisal with evolving technical solutions. *Eur J Cardiothorac Surg* 2002;**22**: 184–91.

5 Correa-Villaseñor A, Ferencz C, Boughman JA, Neill CA. Total anomalous pulmonary venous return: familial and environmental factors. The Baltimore–Washington Infant Study Group. *Teratology* 1991;**44**:415–28.

6 Raisher BD, Dowton SB, Grant JW. Father and two children with total anomalous pulmonary venous connections. *Am J Med Genet* 1991;**40**:105–6.

7 Solymar L, Sabel KG, Zetterqvist P. Total anomalous pulmonary venous connection in siblings. Report on three families. *Acta Paediatr Scand* 1987;**76**:124–7.

8 Craig JM, Darling RC, Rothney WB. Total pulmonary venous drainage into the right side of the heart; report of 17 autopsied cases not associated with other major cardiovascular anomalies. *Lab Invest* 1957;**6**:44–64.

9 Stanger P, Rudolph AM, Edwards JE. Cardiac malpositions: an overview based on study of sixty-five necropsy specimens. *Circulation* 1977;**56**:159–72.

10 Jonas RA, Smolinsky A, Mayer JE, Castaneda AR. Obstructed pulmonary venous drainage with total anomalous pulmonary venous connection to the coronary sinus. *Am J Cardiol* 1987;**59**:431–5.

11 Levy AM, Naeye RL, Tabakin BS, Hanson JS. Far-advanced intimal proliferation and severe pulmonary hypertension secondary to total anomalous pulmonary venous drainage. *Am J Cardiol* 1965;**16**:280–5.

12 Duff DF, Nihill MR, McNamara DG. Infradiaphragmatic total anomalous pulmonary venous return. Review of clinical and pathological findings and results of operation in 28 cases. *Br Heart J* 1977;**39**:619–26.

13 Lucas RV Jr, Adams P Jr, Anderson RC, *et al.* Total anomalous pulmonary venous connection to the portal venous system: a cause of pulmonary venous obstruction. *Am J Roentgenol Radium Ther Nucl Med* 1961;**86**:561–75.

14 Jenkins KJ, Sanders SP, Orav EJ, *et al.* Individual pulmonary vein size and survival in infants with totally anomalous pulmonary venous connection. *J Am Coll Cardiol* 1993;**22**:201–6.

15 Tomar M, Radhakrishnan S, Iyer KS, Shrivastava S. Rare variants of total anomalous pulmonary venous connection to coronary sinus-echocardiographic recognition and surgical correction. *Indian Heart J* 2008;**60**:266–70.

16 Vick GW III, Murphy DJ Jr, Ludomirsky A, *et al.* Pulmonary venous and systemic ventricular inflow obstruction in patients with congenital heart disease: detection by combined two-dimensional and Doppler echocardiography. *J Am Coll Cardiol* 1987;**9**:580–7.

17 Allan LD, Sharland GK. The echocardiographic diagnosis of totally anomalous pulmonary venous connection in the fetus. *Heart* 2001;**85**:433–7.

18 Gathman GE, Nadas AS. Total anomalous pulmonary venous connection: clinical and physiologic observations of 75 pediatric patients. *Circulation* 1970;**42**:143–54.

19 el-Said G, Mullins CE, McNamara DG. Management of total anomalous pulmonary venous return. *Circulation* 1972;**45**:1240–50.

20 Ward KE, Mullins CE, Huhta JC, *et al.* Restrictive interatrial communication in total anomalous pulmonary venous connection. *Am J Cardiol* 1986;**57**:1131–6.

21 Mullins CE, el-Said GM, Neches WH, *et al.* Balloon atrial septostomy for total anomalous pulmonary venous return. *Br Heart J* 1973;**35**:752–7.

22 Ramakrishnan S, Kothari SS. Preoperative balloon dilatation of obstructed total anomalous pulmonary venous connection in a neonate. *Catheter Cardiovasc Interv* 2004;**61**:128–30.

23 Kyser JP, Bengur AR, Siwik ES. Preoperative palliation of newborn obstructed total anomalous pulmonary venous connection by endovascular stent placement. *Catheter Cardiovasc Interv* 2006;**67**:473–6.

24 Oh KH, Choo KS, Lim SJ, *et al.* Multidetector CT evaluation of total anomalous pulmonary venous connections: comparison with echocardiography. *Pediatr Radiol* 2009;**39**:950–4.

25 Shaheen F, Gojwari TA, Andrabi M, Sofi S, Singh M. 64-slice CT imaging in a case of total anomalous pulmonary venous circulation. *Indian J Radiol Imaging* 2009;**19**:54–6.

26 Choe YH, Lee HJ, Kim HS, *et al.* MRI of total anomalous pulmonary venous connections. *J Comput Assist Tomogr* 1994;**18**:243–9.

27 Bullaboy CA, Johnson DH, Azar H, Jennings RB Jr. Total anomalous pulmonary venous connection to portal system: a new therapeutic role for prostaglandin E1? *Pediatr Cardiol* 1984;**5**:115–6.

28 Bhan A, Sharma R, Iyer KS, *et al.* Improved exposure for TAPVC repair by posterior approach. *Ann Thorac Surg* 1996;**62**:1888.

29 Imoto Y, Kado H, Asou T, *et al.* Mixed type of total anomalous pulmonary venous connection. *Ann Thorac Surg* 1998;**66**:1394–7.

30 Kirshbom PM, Jaggers J, Ungerleider RM. In: Mavroudis C, Backer CL, eds. *Pediatric Cardiac Surgery*, 3rd edn. St Louis: Mosby, 2003: 612–24.

31 Choudhary SK, Bhan A, Sharma R. Repair of total anomalous pulmonary venous connection in infancy: experience from a developing country. *Ann Thorac Surg* 1999;**68**:155–9.

32 Bando K, Turrentine MW, Ensing GJ, *et al.* Surgical management of total anomalous pulmonary venous connection. Thirty-year trends. *Circulation* 1996;**94**(9 Suppl), II12–6.

33 Emmel M, Sreeram N. Total Anomalous pulmonary vein connection: diagnosis, management, and outcome. *Curr Treat Options Cardiovasc Med* 2004;**6**:423–9.

34 Caldarone CA, Najm HK, Kadletz M, *et al.* Relentless pulmonary vein stenosis after repair of total anomalous pulmonary venous drainage. *Ann Thorac Surg* 1998;**66**:1514–20.

35 Lacour-Gayet F, Zoghbi J, Serraf AE, *et al.* Surgical management of progressive pulmonary venous obstruction after repair of total anomalous pulmonary venous connection. *J Thorac Cardiovasc Surg* 1999;**117**:679–87.

36 Smallhorn JF, Burrows P, Wilson G, *et al.* Two-dimensional and pulsed Doppler echocardiography in the postoperative evaluation of total anomalous pulmonary venous connection. *Circulation* 1987;**76**:298–305.

37 Lacour-Gayet F, Rey C, Planché C. Pulmonary vein stenosis. Description of a sutureless surgical procedure using the pericardium *in situ*. *Arch Mal Coeur Vaiss* 1996;**90**:639–43 (in French).

38 Suarez MR, Panos AL, Salerno TA, *et al.* Modified "sutureless" anastomosis for primary repair of supracardiac total anomalous pulmonary venous connection. *J Cardiac Surg* 2009;**24**: 564–66.

35 Tricuspid Atresia

P. Syamasundar Rao

University of Texas at Houston Medical School, Houston, TX, USA

Introduction

Tricuspid atresia is a cyanotic cardiac malformation defined as congenital absence or agenesis of the morphologic tricuspid valve [1,2]. It is the third most common cyanotic cardiac anomaly and is the most common cause of cyanosis with left ventricular hypertrophy. The first patient with tricuspid atresia was described by Kreysig in 1817 [3], although the 1812 report by the Editors of *London Medical Review* [3] appears to fit the description of tricuspid atresia but without use of the specific term. Some authors [4,5] stated that tricuspid atresia was first described by Kühne in 1906 or Holmes in 1824, but a thorough review by Rashkind [3] suggests that this is not so.

Nomenclature

There has been a debate about terminology: tricuspid atresia, univentricular heart, or univentricular atrioventricular connection [6]. On the basis of evidence and arguments presented by Bharati and co-workers [7–9], Wenink and Ottenkamp [10], Gessner [11], and Rao [6,12], tricuspid atresia is the correct and logical term to describe this well-characterized pathologic and clinical entity [6] and is used in this chapter.

Incidence

Estimates of the incidence of tricuspid atresia based on autopsy and clinical series are 2.9% and 1.4% of cardiac malformations, respectively [13]. Assuming a prevalence of congenital heart disease of 0.8% of live births, tricuspid atresia occurs in approximately one in 10 000 live births [13]. A slight male preponderance has been suggested [4,14], but detailed analysis when gender is known [13] did not indicate a gender preponderance. However, male preponderance (66% versus 34%) was found in tricuspid atresia patients with coexisting transposition of the great arteries (types II and III) [13]. No difference in either geographic prevalence or racial background for tricuspid atresia has been described [13], although geographic differences in relative prevalence for aortic coarctation and stenosis have been found.

Embryology

The atrioventricular valves develop shortly after the atrioventricular canal divides. The tricuspid valve leaflets develop from several structures. The septal leaflet of the tricuspid valve mostly develops from the inferior and superior endocardial cushions. The anterior and posterior tricuspid valve leaflets develop by undermining of a skirt of ventricular muscle tissue. The process of undermining extends until the atrioventricular valve junction is reached. The muscle tissue undergoes resorption, producing normal-appearing valve leaflets and chordae tendineae [15–17]. Whether a muscular type of tricuspid atresia develops or well-formed but fused tricuspid–valve leaflets develop depends on the stage of development when the embryologic aberration takes place [12,17,18]. The classic muscular form of tricuspid atresia develops if the embryologic insult occurs early in gestation, and fused valve leaflets occur if the embryologic abnormality occurs slightly later than this in gestation. If the valve fusion is incomplete, stenosis of the tricuspid valve develops.

The pathologic, clinical, and electrocardiographic features of tricuspid stenosis and atresia are similar [19]. Consequently, the facts that isolated congenital tricuspid stenosis belongs

(see Chapter 29) to the group of tricuspid atresia defects and that their embryologic developments are similar are no surprise. Thus, the tricuspid valve stenosis, tricuspid atresia with well-formed but fused valve leaflets, and the muscular type of tricuspid atresia represent a spectrum of morphologic abnormalities [12,17,18].

Classification

Tricuspid atresia has been classified on the basis of valve morphology [20], radiographic appearance of pulmonary vascular markings [21]. and associated cardiac anomalies [22–24].

Classification based on valve morphology

Van Praagh et al. [20] proposed a classification based on morphology of the atretic tricuspid valve, and this was modified and expanded by that group and others [25]. The most common type is the muscular variety, characterized by a dimple or a localized fibrous thickening in the floor of the right atrium at the expected site of the tricuspid valve (Figure 35.1). The muscular type constitutes 89% of all tricuspid atresia (Table 35.1). Other types, namely membranous, valvar, Ebstein, atrioventricular septal defect, and unguarded with muscular shelf, account for the remaining 11% (Table 35.1) [7,15,20,25–31]. Pathologic, echocardiographic, and angiographic examples of the rare anatomic types can be found in previous publications [25,32].

Classification based on radiographic pulmonary vascular markings

Astley et al. [21] classified tricuspid atresia on the basis of pulmonary vascular markings on the chest radiograph: group A, decreased pulmonary vascular markings; and group B,

increased pulmonary vascular markings. To this Dick et al. [4] added a third group: group C, transition from increased to decreased pulmonary vascular markings. This categorization
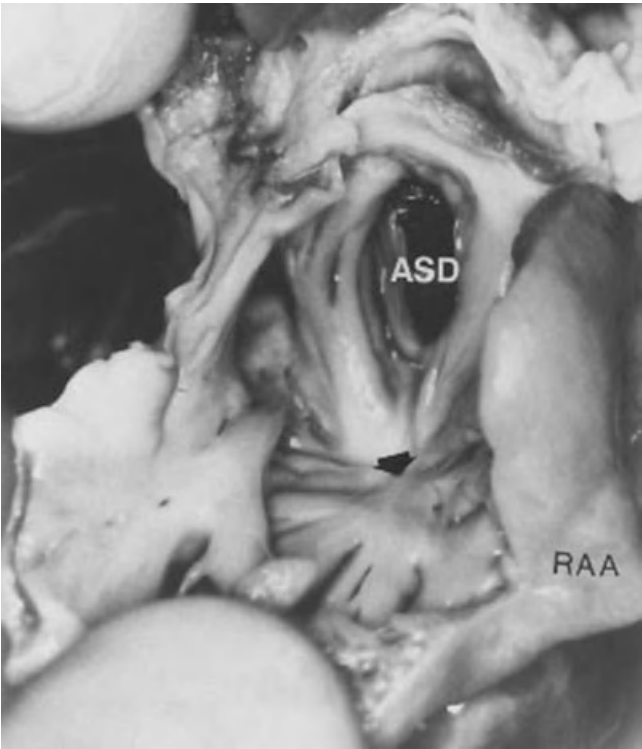
Figure 35.1 Muscular type of tricuspid atresia; the right atrium is opened by cutting through the right atrial appendage (RAA). There is a dimple (arrow) in the floor of the right atrium with muscle fibers radiating around it. Atrial septal defect (ASD) is shown. (Reproduced from Rao et al., *Am Heart J* 1991;**122**:829–35, with permission of Mosby/Elsevier.)

Table 35.1 Prevalence of types of tricuspid atresia based on valve morphology.

Authors	Year	Total N[a]	Muscular	Membranous	Valvar	Ebstein	AV[a] septal defect	Unguarded with muscular shelf
Van Praagh et al.	1971	38	32	3	0	3	0	0
Rao et al.	1973	38	37	0	0	1	0	0
Bharati et al.	1976	172	157	12	0	3	0	0
Anderson et al.	1977	83[b]	76	4	1	2	0	0
Weinberg	1980	33	25	4	2	2	0	0
Ando et al.	1980	29	20	8	0	1	0	0
Ottenkamp et al.	1984	34[b]	29	4	0	1	0	0
Scalia et al.	1984	76[b]	68	0	3	1	0	4
Rao	1987	28	27	0	0	0	1	0
Total (%)		531	471 (89)	35 (6.6)	6 (1)	14 (2.6)	1 (0.2)	4 (0.6)

[a]N, total number of patients; AV, atrioventricular.
[b]Number of patients who are common to these three studies cannot be ascertained.
Percentages in parentheses
Adapted with permission from Rao PS. *Tricuspid Atresia*, 2nd edn. Mount Kisco, NY: Futura Publishing, 1992:59–79.

Table 35.2 A unified classification of tricuspid atresia.

Type I	Normally related great arteries
Type II	d-Transposition of the great arteries
Type III	Malpositions of the great arteries other than d-transposition
Subtype 1	l-Transposition of the great arteries
Subtype 2	Double-outlet right ventricle
Subtype 3	Double-outlet left ventricle
Subtype 4	d-Malposition of the great arteries (anatomically corrected malposition)
Subtype 5	l-Malposition of the great arteries (anatomically corrected malposition)
Type IV	Persistent truncus arteriosus
Each type and subtype are divided:	
Subgroup a	Pulmonary atresia
Subgroup b	Pulmonary stenosis or hypoplasia
Subgroup c	Normal pulmonary arteries (no pulmonary stenosis)

Reproduced from Rao *Am Heart J* 1980;**99**:799–804, with permission of Mosby/Elsevier.

Table 35.3 Associated cardiac anomalies in tricuspid atresia

Anomalies that form the basis of classification
d-Transposition of the great arteries
l-Transposition of the great arteries
Double-outlet right ventricle
Double-outlet left ventricle
Other malpositions of the great arteries
Truncus arteriosus

Anomalies that may need attention before or at the time of palliative or total surgical correction
Absent pulmonary valve
Aneurysm of the atrial septum
Anomalous origin of the coronary arteries from the pulmonary artery
Anomalous origin of the left subclavian artery
Anomalous origin of the right subclavian artery
Aortopulmonary fistula
Coarctation of the aorta
Common atrium
Cor triatriatum dexter
Coronary sinus septal defect
Double aortic arch
Double-outlet left atrium
Hemitruncus
Hypoplastic ascending aorta and aortic atresia
Ostium primum atrial septal defect
Parchment right ventricle
Patent ductus arteriosus
Persistent left superior vena cava
Right aortic arch
Subaortic stenosis
Total anomalous pulmonary venous connection
Tubular hypoplasia of the aortic arch
Valvar aortic stenosis
Others
Juxtaposition of the atrial appendages
Anomalous entry of coronary sinus into the left atrium

Reproduced with permission from Rao PS, Covitz W, Chopra PS. *Tricuspid Atresia*, 2nd edn. Mount Kisco, NY: Futura Publishing, 1992: 297–320.

has clinical value, although more precise noninvasive definition of the defect complex by echo Doppler studies and pulse oximetry is readily available.

Classification based on associated defects

The interrelationship of the great arteries, used by Kühne [22] in 1906 as a basis for classification, was expanded later by Edwards and Burchell [23] and popularized by Keith *et al*. [24]. A variety of other classifications have been proposed, reviewed elsewhere [1,25]. To include all variations of great artery anatomy and to maintain uniformity of subgrouping, the present author proposed a comprehensive yet unified classification [1] that is listed in Table 35.2. The primary grouping is based on great artery relationships: type I, normally related great arteries; type II, d-transposition of great arteries; type III, other malpositions of great arteries, which are subdivided into subtypes 1–5 (Table 35.2); and type IV, persistent truncus arteriosus. The major types and subtypes are divided further into subgroup a, pulmonary atresia; subgroup b, pulmonary stenosis or hypoplasia; and subgroup c, normal pulmonary arteries (no pulmonary stenosis). The status of the ventricular septum and the other associated malformations (Table 35.3) [33] should then be stated for each heart.

This unified classification considers all variations in great artery anatomy described thus far, can be expanded if new great artery positional abnormalities are described, and maintains uniformity in subgroups but preserves the basic principles of previous classifications [22–24] If one wants to follow the terminology of congenital heart disease proposed by Van Praagh [34], the remaining cardiac segment subsets (i.e., visceroatrial situs and ventricular loop) could be added, and each heart is described by the notations {S,D,S}, {S,D,D}, and {S,D,L} as shown in the schematic drawing depicted in Figure 35.2.

Pathologic anatomy

The pathology of this lesion is best described by reviewing variations in the morphology of the atretic tricuspid valve. In the most common muscular type (Figure 35.1), no valve material can be identified by either gross or microscopic
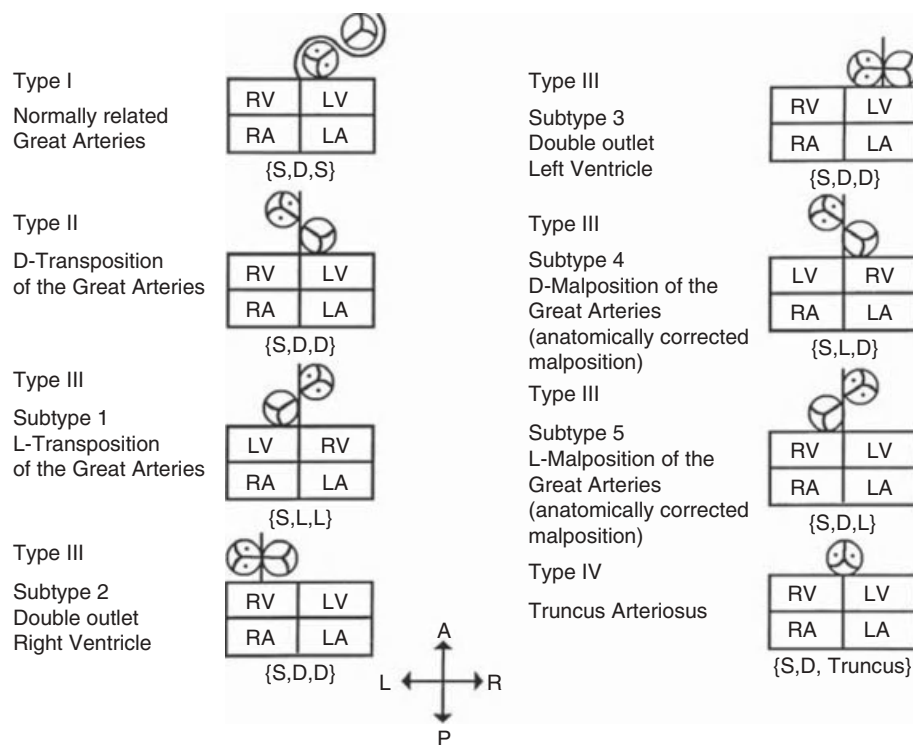
Figure 35.2 Representation of segmental subsets of tricuspid atresia with the heart in the left side of the chest. Only commonly described types are depicted. Each type can occur with dextrocardia and atrial inversion. Both double-outlet right ventricle and double-outlet left ventricle can occur with {S, D, L} and {S, L, L}. A, anterior; {–,D,–}, d-loop; {–,–,D}, d-transposition; {–, L, –}, l-loop; {–, –, L}, l-transposition; LA, left atrium; LV, left ventricle; P, posterior; R, right; RA, right atrium; RV, right ventricle; {S, –, –}, situs solitus; {–, –, S}, solitus normal great arteries. (Reproduced with permission from Rao PS. *Tricuspid Atresia*, 2nd edn. Mount Kisco, NY: Futura Publishing, 1992:59–79.)

examination [24]. Other types are described elsewhere [25,32]. In the membranous type, the atrioventricular portion of the membranous septum forms the floor of the right atrium at the expected location of the tricuspid valve [7,15,20]. An unusually high incidence of absent pulmonary valve leaflets occurs with this type of tricuspid atresia [25]. In the valvar type, the minute valve cusps are fused [24,27,28]. The Ebstein type, with fusion of the tricuspid valve leaflets (which had been displaced downwards and plastered on to the right ventricular wall), is rare [7,20,26]. In the atrioventricular septal defect type, the valve leaflet of the common atrioventricular valve seals off the only entrance into the right ventricle [31,35] The final form, in which the right atrioventricular junction is unguarded but the inlet component of the morphologic right ventricle is separated from its outlet by a muscular shelf [30], is also rare.

The right atrium is usually enlarged and its wall is thick and hypertrophied. The interatrial communication, necessary for survival, is usually a stretched patent foramen ovale, sometimes it is an ostium secundum atrial septal defect, and occasionally an ostium primum atrial septal defect. Rarely, the interatrial communication is obstructive and may form an aneurysm of the fossa ovalis. The left atrium may be enlarged, especially if the pulmonary blood flow is increased. The mitral valve is morphologically normal; the mitral orifice is large and occasionally incompetent. The left ventricle is clearly a morphologic left ventricle with only occasional abnormalities [7]; however, it is enlarged and hypertrophied. In contrast, the right ventricle is small and hypoplastic; even the largest of the right ventricles, seen in patients with a large ventricular septal defect (VSD) or transposition of the great arteries, is smaller than normal. Right ventricular size is determined by the anatomic type of tricuspid atresia. In patients with pulmonary atresia and normally related great arteries, the right ventricle may be extremely small and escape detection. However, in most patients, it is a true right ventricle [7,8], consisting of a sharply demarcated infundibulum with septal and parietal bands and a trabeculated sinus portion that communicates with the left ventricle through a VSD. The inflow region of the right ventricle, by definition, is absent, although papillary muscles may occasionally be present.

The relative position of the great vessels varies, as described in the classification section. Most have either normally related great arteries (type I) or d-transposed great arteries

(type II), but a few have other positional anomalies of the great arteries (type III) or truncus arteriosus (type IV).

Pulmonary outflow tract obstruction is common in type I tricuspid atresia. The pulmonary valve may be atretic (subgroup a), and either a patent ductus arteriosus or aortopulmonary collateral vessels supply the lungs. A stenotic pulmonary outflow tract (subgroup b) is more common. The stenosis is either subvalvar or valvar in patients with transposition of the great arteries, whereas in patients with normally related great arteries, obstruction occurs at the VSD level [36–42]. In a few patients, subvalvar pulmonary stenosis, a narrow outflow tract of the hypoplastic right ventricle, and rarely valvar pulmonary stenosis may be responsible for the pulmonary outflow obstruction. A normal pulmonary outflow tract (subgroup c) without stenosis may be present, although less commonly than those with obstruction. The ascending aorta is normal or enlarged.

The VSD may be large, small, or nonexistent, or multiple VSDs may be present. The VSD may be conoventricular or perimembranous (located inferior to the septal band), conal septal malalignment (located between the anterosuperior and posteroinferior limbs of the septal band), muscular (located inferiorly compared with the two previous types), or of the atrioventricular canal type [43] Muscular VSDs are the most common [36,37]. Most VSDs are restrictive, producing subpulmonic stenosis in patients with normally related great arteries and mimicking subaortic obstruction in patients with transposed great arteries [36–42].

About 30% of tricuspid atresia patients have associated anomalies (Table 30.3). Significant among these are persistent left superior vena cava and aortic coarctation, the latter more frequent in type II patients.

Pathophysiology

Prenatal circulation

In tricuspid atresia, both vena caval streams are shunted across the foramen ovale into the left atrium and left ventricle. Therefore, the arterial PO_2 is the same in all parts of the body. Whether a higher PO_2 in blood passing to lungs influences the pulmonary arteriolar smooth muscle development is not known [44]. The lower than normal PO_2 to the brain and upper part of the body does not seem to impair development, at least as observed clinically.

The pulmonary blood flow in type I (normally related great arteries) patients with intact ventricular septum or pulmonary atresia (type Ia) and type II (transposition of the great arteries) patients with pulmonary atresia (type IIa) must be supplied entirely through the ductus arteriosus. Because the ductus carries only the pulmonary blood flow (from left to right), representing 8–10% of combined

ventricular output in contrast to 66% (from right to left) in the normal fetus [44], the ductus arteriosus is smaller than normal. This fact and the acute angulation of the ductus from its aortic origin because of reversal of direction of ductal flow may render the ductus less responsive to the usual postnatal stimuli [44].

In type I patients with VSD, the amount of blood flow from the left ventricle through the VSD into the right ventricle, pulmonary artery, and ductus arteriosus compared with the quantity of blood flow retrograde from the aorta through the ductus arteriosus varies with size of the VSD. The larger the VSD, the greater is the amount of anterograde ductal flow.

In type I patients with either a small or no VSD, most of the left ventricular blood is ejected via the aorta to the entire body and the placenta. Thus, the aortic isthmus carries a larger proportion of ventricular output than normal; this presumably explains the rarity of coarctation of the aorta in tricuspid atresia without transposition of the great arteries. In type II (transposition) without significant pulmonary stenosis, because the VSD is usually smaller than the pulmonary valve annulus [45], a larger proportion of blood traverses the pulmonary artery and ductus arteriosus anterograde. Therefore, the isthmic blood flow is less, thus accounting for the high incidence of coarctation of the aorta and aortic arch anomalies in patients with tricuspid atresia and transposition [44,45].

Postnatal circulation

An obligatory right-to-left shunt occurs at the atrial level in most types and subtypes (exception: type III, subtypes 1 and 4; see Table 35.2) of tricuspid atresia. Consequently, the systemic and coronary venous blood mixes with pulmonary venous blood in the left atrium. This mixed pulmonary, coronary, and systemic venous blood enters the left ventricle. In type III, subtypes 1 and 4, because of ventricular inversion, the occluded morphologic tricuspid valve is left-sided and the pathophysiology is that of mitral atresia with left-to-right shunting of pulmonary venous blood.

In type I (normally related great arteries) patients with a VSD, a ventricular left-to-right shunt occurs, thus perfusing the lungs. If the ventricular septum is intact, the pulmonary circulation comes from a patent ductus arteriosus or through bronchopulmonary or persistent aortopulmonary collateral vessels. The aortic blood flow comes directly from the left ventricle.

In type II (with d-transposition of the great arteries), the pulmonary circulation is directly supplied from the left ventricle. The systemic circulation is supplied through the VSD and the right ventricle. In other type III and type IV patients, the systemic and pulmonary blood flows are determined by the size of the VSD and other associated anomalies.

Other physiologic principles

Arterial desaturation

Because of complete admixture of the systemic, coronary, and pulmonary venous returns in the left atrium and left ventricle, systemic arterial desaturation is always present. The oxygen saturation is proportional to the magnitude of the pulmonary blood flow [45,46]. The pulmonary-to-systemic blood flow ratio (Qp/Qs), which represents the pulmonary blood flow, has a curvilinear relationship with the arterial oxygen saturation. A Qp/Qs of 1.5–2.5 appears to produce an adequate oxygen saturation [46].

Pulmonary blood flow

The magnitude of pulmonary blood flow is the major determinant of clinical features in tricuspid atresia. An infant with markedly decreased pulmonary blood flow presents early in the neonatal period with severe cyanosis, hypoxemia, and acidosis. An infant with markedly increased pulmonary flow has minimal cyanosis but usually presents with signs of heart failure. Patients with decreased pulmonary flow usually belong to type I (normally related great arteries), and those with increased pulmonary blood flow are usually type II (transposition of the great arteries) and occasionally type Ic.

The quantity of pulmonary blood flow depends on the degree of obstruction to the pulmonary outflow tract and patency of the ductus arteriosus. The pulmonary outflow obstruction is either valvar or subvalvar in type II patients and valvar, subvalvar, or at VSD level in type I patients. In the present author's experience, the obstruction has been found most commonly at the VSD level [36–40]. If the VSD is large and nonrestrictive and the pulmonary valve not stenotic, the pulmonary flow is inversely proportional to the pulmonary-to-systemic vascular resistance ratio; the lower this ratio, the higher is the pulmonary flow.

Left ventricular volume overloading

Because the entire systemic, coronary, and pulmonary circulations are supplied by the left ventricle, greater than normal volume is ejected. This volume overloading is further increased if Qp/Qs is increased either because of minimal obstruction to pulmonary blood flow or a large surgical shunt, and may lead to heart failure. Normal left ventricular function is critical for a successful Fontan-type procedure. Left ventricular function tends to decrease with increasing age, Qp/Qs, and arterial desaturation [47–49].

Size of the interatrial communication

The interatrial communication is usually a patent foramen ovale. Because the entire systemic venous return must pass through the patent foramen ovale, it is not surprising to find interatrial obstruction, although this is clinically significant in only a few patients with tricuspid atresia [4]. Right-to-left shunt occurs in late atrial diastole with augmentation during atrial systole (*a* wave) [50]. A mean atrial pressure gradient >5 mmHg is usually associated with interatrial obstruction. Tall *a* waves in the right atrial pressure trace also indicate interatrial obstruction.

Natural history

With growth and development, several changes occur in patients with tricuspid atresia. The natural history of individual defects followed by that of the entire defect complex will be reviewed.

Patent ductus arteriosus

Closure of the ductus arteriosus in the early neonatal period may result in severe hypoxemia.

Interatrial communication

The size of the interatrial communication may diminish either in absolute terms or relative to the volume of the systemic venous return and cause systemic venous congestion, as alluded to above. Atrial septostomy may be required.

Ventricular septal defect

A VSD is necessary to maintain adequate intracardiac shunting essential for survival of the patient; these types of VSDs are physiologically advantageous VSDs [37–40]. Intermittent functional [40] and complete or partial anatomic [36–39, 41,42,51] closure of the VSD has been reported. Intermittent functional closure of a VSD is likely to produce cyanotic spells in tricuspid atresia. The causes of such functional closure are not clearly delineated but are likely to be similar to those suspected in tetralogy of Fallot [40,51]. Complete or partial anatomic closure in type I patients produces progressive cyanosis, increasing polycythemia, or disappearance of the heart murmur, requiring an operation earlier than planned [36,37,51]. In type II patients, partial closure of the VSD results in subaortic, systemic outflow obstruction; such obstruction may cause severe left ventricular hypertrophy which may contraindicate Fontan correction. Complete VSD closures have not been reported in these patients.

The prevalence of VSD closure in tricuspid atresia is difficult to estimate. The best estimates, based on the present author's data [36,37,51] and those of Sauer and Hall [42], are 38–44%, similar to that of spontaneous closure of an isolated VSD [52,53]. The ages at which the VSD closures take place vary, starting before 1 year and up to 20 years, with a median of 1.3 years [51]. Thus, a higher proportion of VSD closure occurs in early life, as has been found with an isolated VSD. Several mechanisms of closure have been observed, the most common being progressive muscular
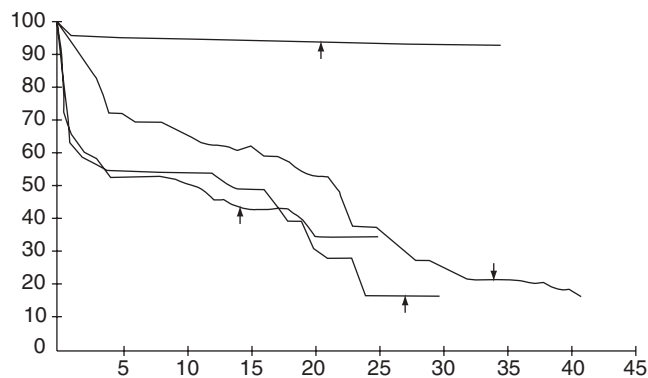
Figure 35.3 Actuarial survival curves from three series compiled by Dick and Rosenthal [55] show a high initial mortality in the first year of life, a plateau between the first year and the middle of the second decade of life, and a second bout of mortality from the middle of the second decade onward, presumably related to impaired left ventricular function. (Reproduced with permission from Rao PS. *Tricuspid Atresia*, 2nd edn. Mount Kisco, NY: Futura Publishing, 1992:59–79.)

encroachment of the margins of VSD with subsequent fibrosis and covering by endocardial proliferation. The factors initiating closure of VSD are unknown. There is a great natural tendency for a VSD to close spontaneously, whether it is isolated or a part of a more complex cardiac anomaly [38,51,54]. The reason for this tendency remains unclear.

Defect complex
Actuarial survival curves from three early clinical series [4,14,55] are shown in Figure 35.3. High mortality is seen in the first year of life. This may be related to hypoxemia, heart failure, surgical intervention, and/or a combination thereof. There is a plateau between the first year through the middle of second decade. A second bout of mortality occurs from the middle of the second decade onwards, presumably related to impaired left ventricular function.

Clinical features

Clinical history and physical examination
Nearly half of the patients with tricuspid atresia present with symptoms on the first day of life, and 80% have symptoms by 1 month of age [4,55]. Two modes of clinical presentation are related to pulmonary blood flow: either decreased or increased.

Infants with pulmonary oligemia present with symptoms of hypoxemia within the first few days of life; the more severe the pulmonary oligemia, the earlier is the clinical presentation. These hypoxemic infants are cyanotic and develop hyperpnea and acidosis if the pulmonary blood flow is markedly decreased. Most are type Ib. Patients with associated pulmonary atresia (subgroup a), irrespective of

the major type, also present with early cyanosis, especially as the ductus begins to close. Hypoxic spells are uncommon in a neonate, although they can occur later in infancy. Physical examination reveals central cyanosis, tachypnea or hyperpnea, normal pulses, a prominent *a* wave in the jugular venous pulse (if there is significant interatrial obstruction), and no hepatomegaly. Presystolic hepatic pulsations may be felt if severe interatrial obstruction exists. The precordium is quiet, and no thrills are usually felt. The second heart sound is single. A soft holosystolic murmur suggestive of a VSD may be heard at the left lower or midsternal border. Diastole is clear. In patients with associated pulmonary atresia, murmurs are usually not present, except occasionally the continuous murmur of a patent ductus arteriosus. Signs of congestive heart failure are notably absent.

Infants with pulmonary plethora usually present with signs of heart failure within the first few weeks of life, although an occasional infant may present within the first week of life [56]. They are only minimally cyanotic but present with dyspnea, fatigue, difficulty in feeding, and perspiration. Recurrent respiratory tract infection and failure to thrive are other modes of presentation. Most of these patients are type IIc, although a small number may be of type Ic. The association of coarctation of the aorta with type II patients may result in early cardiac failure. Examination reveals tachypnea, tachycardia, decreased femoral pulses (with coarctation of the aorta but without a large patent ductus arteriosus), minimal cyanosis, prominent neck vein pulsations, and hepatomegaly. Prominent *a* waves in jugular veins or presystolic hepatic pulsations may be observed with interatrial obstruction. The precordial impulses are increased and hyperdynamic. The second heart sound may be either single or split. A loud holosystolic murmur of a VSD is usually heard at the left lower sternal border. A loud third sound or an apical mid-diastolic murmur is often heard. Signs of congestive cardiac failure are usually present.

Issues related to long-standing cyanosis, such as clubbing, polycythemia, relative anemia, cerebrovascular accident, brain abscess, coagulation problems, and hyperuricemia, are similar to those of other cyanotic cardiac malformations [57]. The risk for development of endocarditis resembles that observed in other cardiac abnormalities.

Patients with tricuspid atresia are particularly prone to atrial arrhythmias; atrial fibrillation is more common, occurring in older children and adolescents with long-standing cyanosis, systemic-to-pulmonary arterial shunt, and left ventricular volume overloading.

Electrocardiographic features
The electrocardiogram is virtually diagnostic of tricuspid atresia in the presence of cyanosis. The characteristic features are right atrial hypertrophy, an abnormal, superiorly oriented major QRS vector (so-called left-axis deviation) in the frontal

plane, left ventricular hypertrophy, and diminished right ventricular forces (Figure 35.4).

Right atrial hypertrophy, manifested by tall, peaked P waves exceeding 2.5 mm in amplitude, may be present in 75% of the patients with tricuspid atresia [58]. A double-peak, spike-
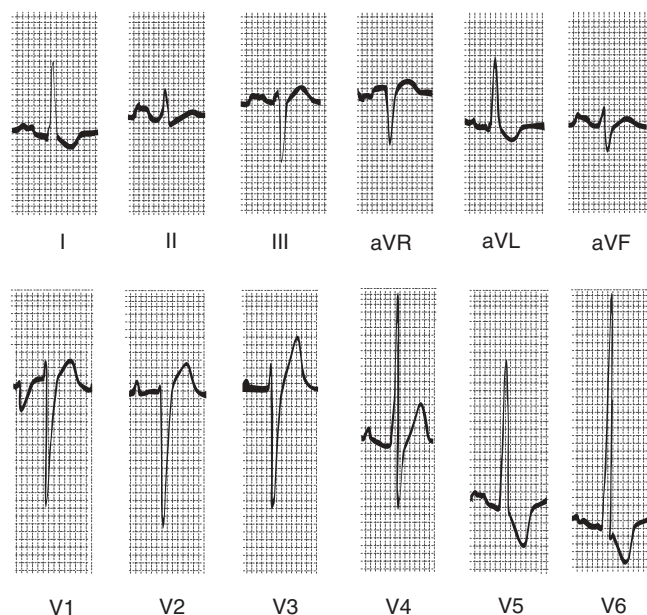
Figure 35.4 Electrocardiogram highly suggestive of tricuspid atresia: abnormal, superiorly oriented mean QRS vector in the frontal plane (−45°, left axis deviation), left ventricular hypertrophy and strain, and diminished anterior (R waves in leads V_1 and V_2) and rightward (S waves in leads V_5 and V_6) forces. Prominent P waves appear in several leads.

and-dome configuration of the P wave, referred to as P tricuspidale, may be present [58]. The first taller peak is contributed by the right atrial depolarization, and the second smaller peak is presumed to be from left atrial depolarization [59]. Regardless of the configuration, the P wave duration is prolonged, perhaps owing to right atrial enlargement.

An abnormal, superiorly oriented major QRS vector (ASV), more popularly called left-axis deviation, between 0 and −90° in the frontal plane, is present in most patients with tricuspid atresia (Figure 35.5). ASV is present in >80% of patients with type I anatomy (normally related great arteries), but <50% of patients with type II and type III anatomy show such a typical electrocardiographic pattern. Normal (0 to +90°) or right-axis deviation is present in a few patients, most of them with type II or type III anatomy. The mechanism of ASV has not been clearly delineated, but may include destructive lesions in the left anterior bundle, fibrosis of left bundle branch, abnormal distribution of the conduction system (unusually long right bundle branch and origin of left bundle branch close to the nodal–His bundle junction), small right ventricle, large left ventricle, and others [59]. Ventricular activation data from our group suggested that this characteristic QRS pattern in tricuspid atresia is produced by interaction of several factors, the most important being right-to-left phase asynchrony of ventricular activation, right-to-left ventricular disproportion, and the asymmetric distribution of the left ventricular mass favoring the superior wall [59,60].

Regardless of the frontal plane mean QRS vector, electrocardiographic left ventricular hypertrophy is present in most patients, manifested by S waves in right chest leads and R
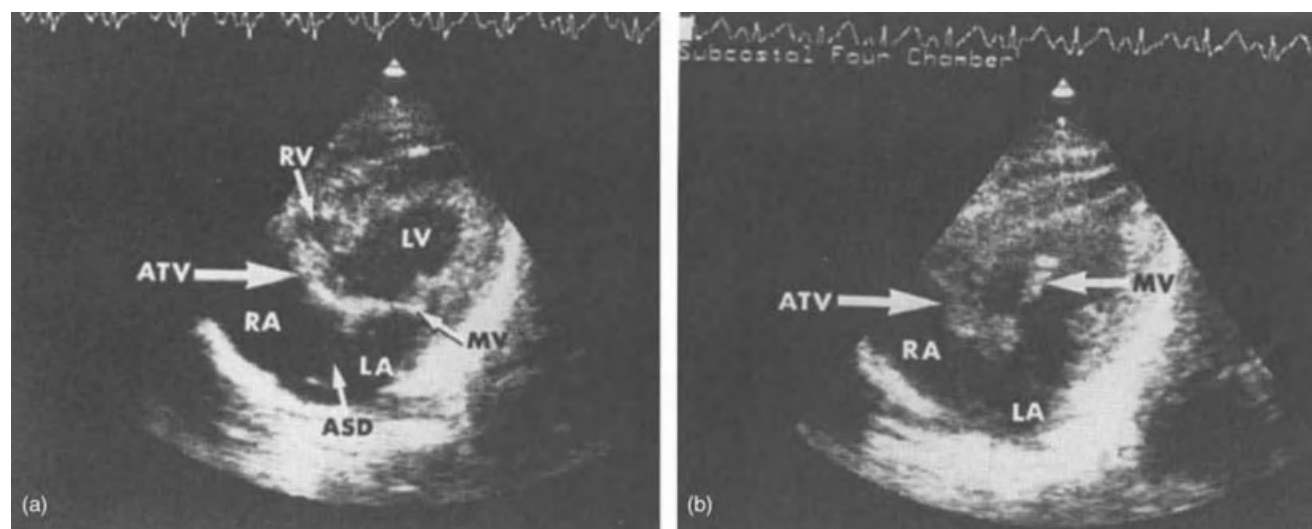
Figure 35.5 Subcostal four-chamber two-dimensional echocardiogram of a neonate with tricuspid atresia. (a) Enlarged left ventricle (LV), small right ventricle (RV), and a dense band of echoes (ATV) are shown at the site where the tricuspid valve echo should be. Atrial (ASD) and ventricular septal defects and the mitral valve (MV) are visualized. (b) Attachment of anterior leaflet of detectable atrioventricular valve to left side of atrial septum. LA, left atrium; RA, right atrium. (Reproduced from Rao *Fetal and Neonatal Cardiology*. Philadelphia, PA: Saunders, 1990: 525–40, with permission of W.B. Saunders/Elsevier.)

waves in left chest leads beyond the 95th percentile or by adult progression of the QRS in the chest leads in the neonates and infants. ST-T wave changes suggestive of left ventricular strain are present in half of patients [59]. Left ventricular hypertrophy is due to left ventricular volume overload and also lack of opposition to the left ventricular forces by the hypoplastic right ventricle. Biventricular hypertrophy may occasionally be present, and most of these patients have type II or type III anatomy with an adequately sized right ventricle [59]. Diminished R waves in right chest leads and S waves in left chest leads are related to right ventricular hypoplasia.

Electrocardiographic features of rare types of tricuspid atresia are reviewed elsewhere [59].

Chest X-ray

Radiographic features depend on the total pulmonary blood flow. In patients with decreased pulmonary flow (most infants fall into this category), cardiac size is either normal or mildly enlarged, whereas those with increased pulmonary blood flow have moderate to severe cardiomegaly. A variety of cardiac configurations have been described in the literature: "characteristic" tricuspid atresia appearance [61], *coeur en sabot* configuration [62], and egg-shaped [63], bell-shaped [64], and square [21] heart, but in the present author's and others' experience [63], no consistent pattern is diagnostic of tricuspid atresia. There may be concavity in the region of the pulmonary artery segment in patients with pulmonary oligemia and a small pulmonary artery. The right atrial shadow may be prominent.

A right aortic arch is present in 8% of patients with tricuspid atresia [63] and is less common than in tetralogy of Fallot (25%) and truncus arteriosus (40%). An unusual contour of the left cardiac border suggestive of l-transposition may be seen in association with or confused with tricuspid atresia [65].

The greatest use of the chest radiograph is its ability to categorize neonates into those with decreased pulmonary vascular markings and those with increased pulmonary vascular markings. Often, this is all that is necessary to make a correct diagnosis once a history, physical examination, and electrocardiogram have been obtained [65].

Echocardiography

M-mode echocardiographic features include an enlarged left atrium (usually proportional to the magnitude of pulmonary blood flow), a dilated left ventricle with normal or decreased left ventricular shortening fraction, a large mitral valve in continuity with the posterior semilunar valve, and a small right ventricle [65,66]. The pulmonary valve may or may not be recorded. The tricuspid valve is conspicuously absent [65].

Two-dimensional echocardiography, apart from showing an enlarged right atrium, left atrium, and left ventricle and a small right ventricle, demonstrates the atretic tricuspid valve directly. In the most common muscular type, a dense band of echoes is seen at the site where the tricuspid valve should be [65,67], and the anterior leaflet of the detectable atrioventricular valve is attached to the left side of the interatrial septum (Figure 35.5). The anatomy is best demonstrated in the apical and subcostal four-chamber views. A persistent left superior vena cava, when present, can usually be identified emptying into the coronary sinus, as can the entries of the superior and inferior venae cavae into the right atrium. Atrial and ventricular septal defects can also be demonstrated. Semilunar valves can be identified as pulmonary or aortic by following the great vessel until the bifurcation of the pulmonary artery or arch of the aorta is seen; this will identify associated transposition of the great arteries. Coarctation of the aorta, often present in type II patients, may be shown in the suprasternal notch view.

Contrast echocardiography with two-dimensional imaging clearly demonstrates sequential opacification of the right atrium, the left atrium, the left ventricle, and then the right ventricle, although this is not necessary for diagnosis.

Doppler echocardiography is helpful in demonstrating shunts and the degree of pulmonary stenosis. Right-to-left shunting across the atrial septum can be visualized by placing the pulsed Doppler sample volume on either side of the atrial defect and by color flow mapping. Most right-to-left shunting occurs during atrial systole. Left-to-right shunting, although transient, can be demonstrated by Doppler study during atrial diastole, secondary to instantaneous pressure differences across the atrial septum [50]. High-flow velocity across the VSD can be demonstrated in type Ib tricuspid atresia; the higher the velocity, the smaller is the defect. Color-guided continuous-wave Doppler, with use of the modified Bernoulli equation, is useful in quantitating the left-to-right ventricular pressure difference, thereby estimating the size of the VSD. Interrogating the right ventricular outflow tract may demonstrate subvalvar or valvar pulmonary stenosis. Careful interrogation of Doppler velocities across the VSD in type II patients identifies subaortic (at the VSD level) obstruction. Similarly, Doppler evaluation of the descending aorta is useful in demonstrating aortic coarctation.

M-mode, two-dimensional, Doppler (pulsed, continuous-wave, and color), and, when indicated, contrast echocardiography are useful in delineating most anatomic and physiologic issues related to tricuspid atresia.

Cardiac catheterization and angiography

The diagnosis of tricuspid atresia based on clinical, electrocardiographic, and echocardiographic features is relatively simple, and cardiac catheterization with selective cineangiography rarely, if ever, is essential for the diagnosis [46]. Cardiac catheterization should be performed only if sufficient

Table 35.4 Choussat criteria.

Normal vena caval connections
Normal right atrial volume
Mean pulmonary artery pressure ≤15 mmHg
Pulmonary vascular resistance ≤4 Wood units m^{-2}
Pulmonary artery to aortic root diameter ratio ≥0.75
Normal left ventricular function
Competent mitral valve
Undistorted pulmonary arteries

data needed for management are unavailable from echo Doppler and other noninvasive studies. Catheterization is generally recommended before operative correction to provide the surgeon with accurate anatomic detail. Specific information on the pulmonary artery anatomy, size, and pressures and left ventricular function is necessary before a Fontan-type procedure. Assessment of Choussat's hemodynamic and angiographic parameters [68] (Table 35.4) should be undertaken, although exceptions to some criteria can be made.

Catheter insertion and course

A percutaneous femoral venous route is used for catheterization [46,69]. The right ventricle cannot be directly entered from the right atrium because of atresia of the tricuspid valve, but the catheter can easily be advanced into the left atrium across the patent foramen ovale and from there into the left ventricle through the mitral valve. With the availability of balloon-tipped catheters and a variety of guidewires, it is usually possible to catheterize the right ventricle (through the VSD), pulmonary artery, and aorta. However, in a sick neonate, the procedure may be terminated after left ventricular angiography because further manipulation of the catheter may produce an arrhythmia or precipitate a hypercyanotic spell. In infants with clinical evidence of aortic coarctation (type II patients), retrograde femoral arterial catheterization may be necessary if left ventricular angiography does not clearly define the problem.

Oxygen saturations

Systemic venous oxygen saturation is decreased in proportion to systemic arterial desaturation and severity of congestive heart failure. Because of obligatory right-to-left shunting across the patent foramen ovale, a left-to-right shunt is ordinarily not detected. An increase in right atrial oxygen saturation, however, may be attributed to transient reversal of flow secondary to instantaneous pressure differences between the atria [50].

The pulmonary venous oxygen saturations are usually normal, with a lower left atrial oxygen saturation reflecting the atrial right-to-left shunt. Left ventricular oxygen saturation is also diminished and represents better admixture than that in the left atrium. The oxygen saturations in the left atrium, left ventricle, right ventricle, pulmonary artery, and aorta are similar. Systemic arterial desaturation is always present, the extent of oxygen desaturation being a function of the pulmonary-to-systemic flow ratio (Qp/Qs).

The vena caval, left atrial, and left ventricular oxygen saturations are generally lower in type I than in type II patients, presumably related to a greater preponderance of pulmonary oligemia in type I patients [46].

Pressures

The mean right atrial pressure is mildly increased, similar to or slightly higher than that in the left atrium. The right atrial a waves are prominent. A mean atrial pressure difference greater than 5 mmHg and giant a wave in the right atrial pressure trace indicate interatrial obstruction. When the left ventricular end-diastolic pressure is markedly elevated, lack of pressure difference across the atrial septum does not exclude interatrial obstruction [46].

Mean left atrial and left ventricular end-diastolic pressures are usually normal but increase with an elevated Qp/Qs and decreased left ventricular function. The left atrial v waves are lower than a waves in patients with decreased pulmonary blood flow. As the pulmonary flow increases, the v waves become taller.

The left ventricular peak systolic pressure is usually normal but may be elevated with aortic coarctation or subaortic stenosis. Aortic peak systolic pressure is normal unless there is associated aortic coarctation. Aortic diastolic pressure may be low because of diastolic runoff, secondary to an operatively placed aortopulmonary shunt. In a type II (transposition) patient, careful pressure pullback across the aortic and subaortic region should be performed. A peak pressure gradient between the ventricles indicates subaortic obstruction secondary to a small VSD [36,37].

The right ventricular peak systolic pressure is usually proportional to the size of the VSD in type I patients; the larger the VSD, the higher is the pressure. The pressure is occasionally high in the presence of a small VSD associated with right ventricular outflow tract stenosis. The right ventricular systolic pressure is at systemic level in type II patients.

Every attempt should be made to catheterize the pulmonary artery [46] because of the importance of measuring pulmonary artery pressure [68] in evaluating tricuspid atresia patients for corrective operation. When all methods fail, pulmonary venous wedge pressure should be measured to estimate the pulmonary artery pressure [70]. The pulmonary artery pressures are usually normal in type I patients, although they may be high in type Ic patients with a large VSD. In type II patients with transposition, the pulmonary artery pressure depends on the degree of subvalvar and
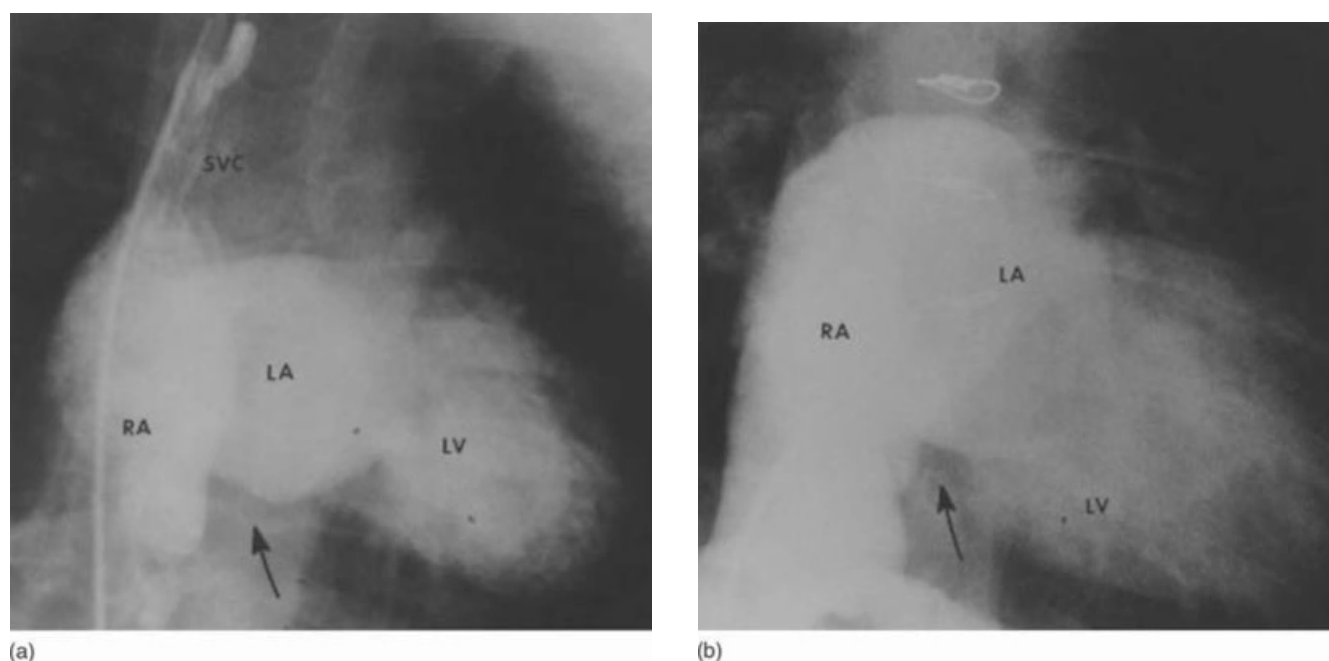
Figure 35.6 Cineangiograms from (a) superior vena cava (SVC) and (b) right atrium (RA) in frontal projection from two patients. There is sequential opacification of the left atrium (LA) and left ventricle (LV) without opacification of the right ventricle. The nonopacified right ventricular "window" (arrows) is formed by the RA on the right, the LA superiorly, and the LV on the left. This is a classic appearance of the muscular variety of tricuspid atresia. (Reproduced from Rao *Atlas of Heart Diseases*, Vol XII. Philadelphia, PA: Current Medicine, 1997: 14.1–14, with permission of Current Medicine/Springer.)

valvar pulmonary stenosis or the effectiveness of an operatively placed pulmonary artery band.

Calculated variables

Pulmonary and systemic blood flows, vascular resistances, and shunts may be calculated by the Fick principle, with either assumed or measured oxygen consumption. The principles and methods of calculation are detailed elsewhere [44,46] (see Chapter 10). The Qp/Qs ratio and pulmonary vascular resistance are the most important. The Qp/Qs ratio is diminished in type I and type II patients with pulmonary atresia and in type Ib patients with a small VSD. It may be markedly increased in type I patients with a large VSD (type Ic) and most type II patients.

Because of pulmonary outflow tract obstruction, pulmonary vascular resistance is normal in most patients with tricuspid atresia. In type Ic patients with a large VSD, type IIc patients without pulmonary stenosis, and patients with a large systemic–pulmonary artery shunt, the pulmonary resistance may be elevated.

Another calculated variable, described by Mair *et al*. [71], the preoperative catheterization index, recognizes the importance of pulmonary vascular resistance and left ventricular diastolic function. This index may be calculated as Rp + [LVEDP/(PI+SI)] where Rp is pulmonary vascular resistance (units m^{-2}), *LVEDP* is left ventricular end-diastolic pressure (mmHg), and *PI* and *SI* are pulmonary and systemic flow indices, respectively (l min^{-1} m^{-2}).

An index of ≤4 is associated with lower early and total mortality after a Fontan operation than is an index >4. This is a useful index, although with some limitations [71].

Angiography

The absence of direct anatomic continuity between the right atrium and the morphologic right ventricle is the hallmark of the angiographic features of tricuspid atresia. Selective superior vena caval or right atrial angiograms reveal successive opacification of the left atrium and left ventricle without immediate opacification of the right ventricle (Figure 35.6); this "typical sequence of tricuspid atresia" is considered characteristic. The negative shadow between the right atrium and left ventricle, named the right ventricular window, corresponds to failure of early filling of the right ventricle (Figure 35.6). These features are best demonstrated in the posteroanterior view. The size and location of the atrial septal defect are optimally shown in hepatoclavicular or lateral views and may produce the so-called onionskin or waterfall appearance (Figure 35.7) if the atrial septum is obstructive.

Reflux of the contrast material into the venae cavae and hepatic veins is seen normally after right atrial angiography. Dense opacification of the coronary sinus (Figure 35.8) suggests interatrial obstruction. The size of the right atrium and the location and size of the right atrial appendage should also be evaluated. For example, left-sided
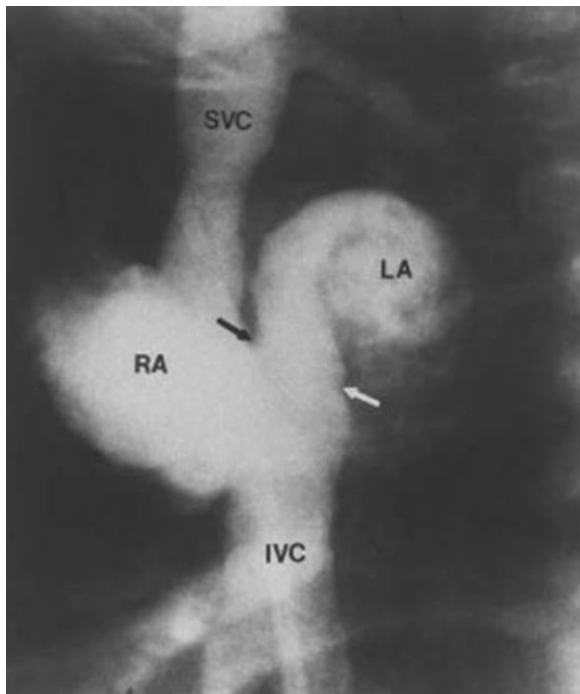
Figure 35.7 Selective superior vena caval (SVC) angiogram in a four-chamber (hepatoclavicular) projection reveals no opacification of the right ventricle and typical, onionskin appearance of the interatrial communication (arrows). Contrast material streams into the roof of the left atrium (LA). IVC, inferior vena cava; RA, right atrium. (Reproduced with permission from Schwartz and Rao *Tricuspid Atresia*, 2nd edn. Mount Kisco, NY: Futura Publishing, 1992: 223–46.)
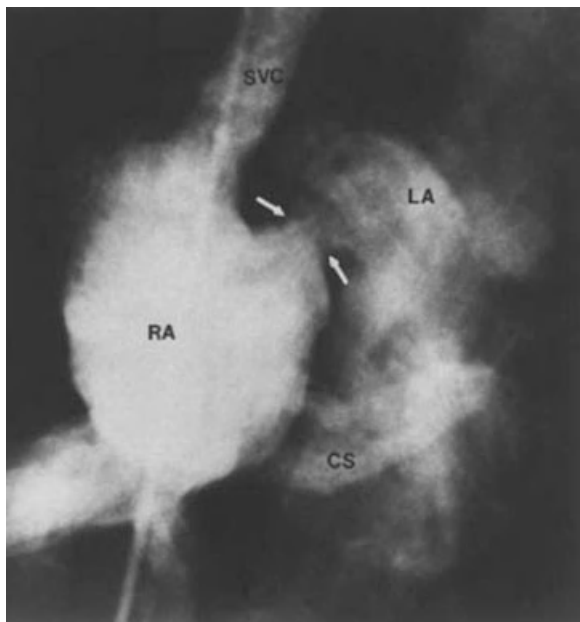
Figure 35.8 Selective superior vena caval (SVC) injection in four-chamber projection (hepatoclavicular) shows tricuspid atresia and filling of the left atrium (LA) through a restrictive atrial septal defect (arrows). There is retrograde filling of the coronary sinus (CS). RA, right atrium. (Reproduced with permission from Schwartz and Rao *Tricuspid Atresia*, 2nd edn. Mount Kisco, NY: Futura Publishing, 1992: 223–46.)
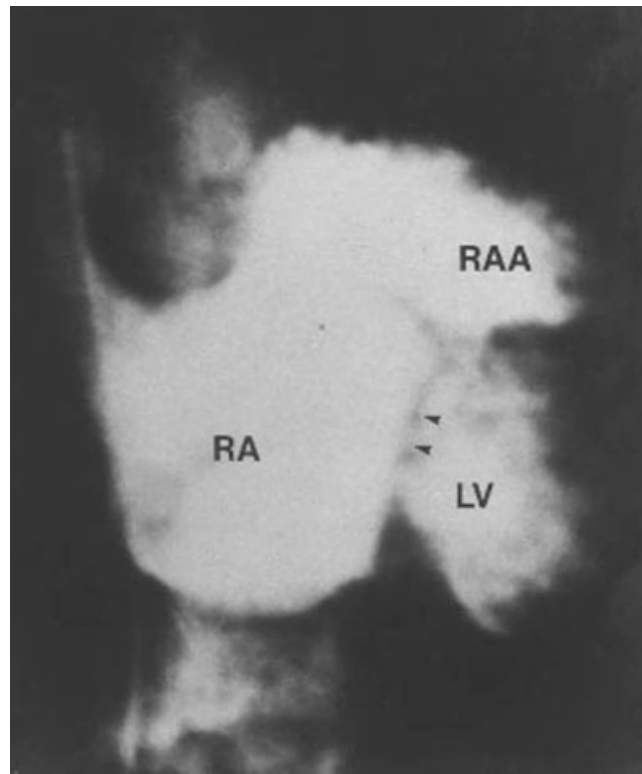
Figure 35.9 Selective superior vena caval injection in the right anterior oblique projection shows the right atrial appendage (RAA) juxtaposed leftwards. There is an imperforate tricuspid valve (arrowheads). LV, left ventricle; RA, right atrium. (Reproduced with permission from Schwartz and Rao *Tricuspid Atresia*, 2nd edn. Mount Kisco, NY: Futura Publishing, 1992: 223–46.)

juxtaposition of the atrial appendages (Figure 35.9) occurs more frequently in tricuspid atresia, especially when associated with transposition of the great arteries. Finally, different morphologic types of atretic tricuspid valves may be recognized [25,32,72].

Once tricuspid atresia is demonstrated, it is important to define the ventricular anatomy, type and size of the interventricular communication, ventriculoarterial connections, pulmonary artery anatomy, and associated abnormalities. Left innominate vein angiography to demonstrate a persistent left superior vena cava and bridging innominate vein, should also be performed; such information is useful in considering bidirectional Glenn and Fontan operations.

Selective left ventricular angiography reveals finely trabeculated, morphologically left ventricular anatomy. The origin and relative positions of the great arteries (Figures 35.10 and 35.11), the size and location of the VSDs, any mitral regurgitation, and the size of the right ventricle can be demonstrated. The present author initially performs left ventricular angiography in frontal and lateral views. Angiography is performed in additional views, such as left anterior oblique, hepatoclavicular, or long axial oblique,
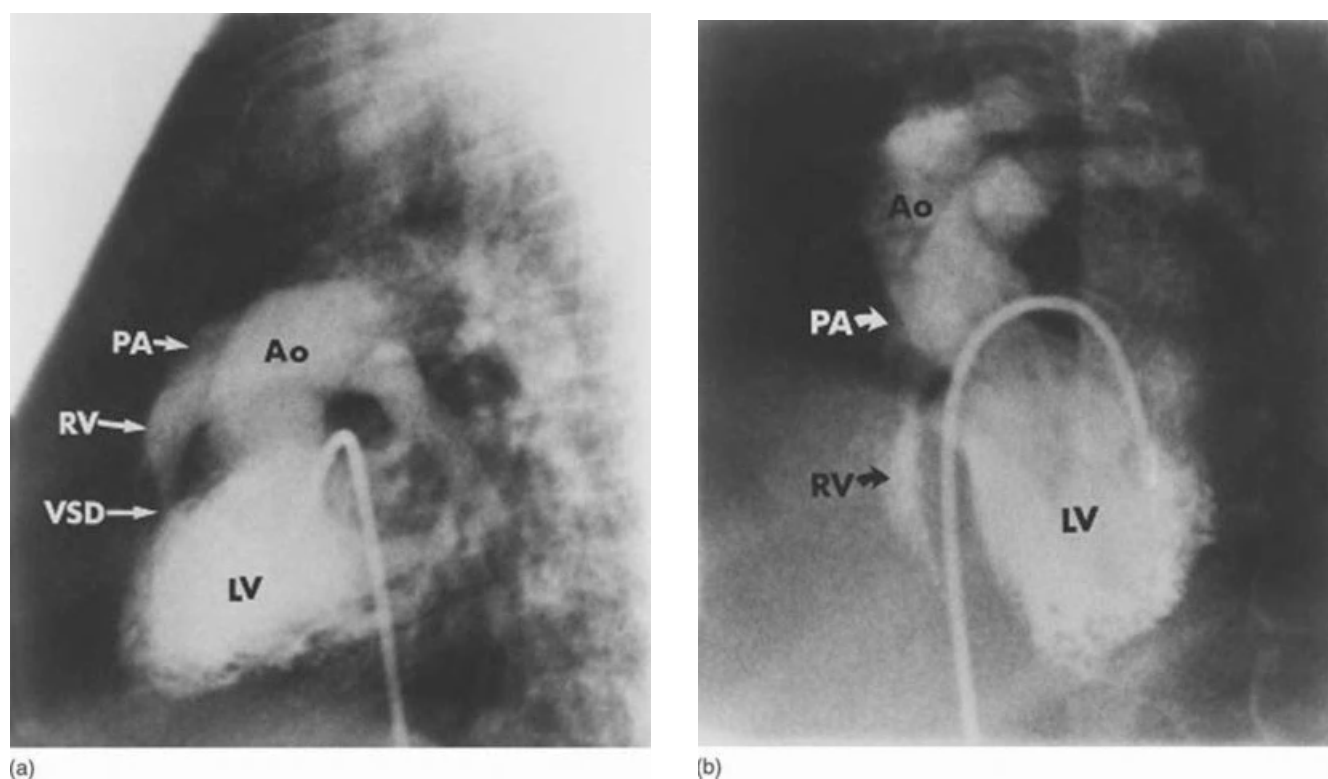
Figure 35.10 Selective left ventricular (LV) cineangiograms in lateral (a) and four-chamber (b) views demonstrate normal position of aorta (Ao) and pulmonary artery (PA). Ventricular septal defect (VSD) is seen with visualization of right ventricle (RV). (Reproduced from Rao, P.S., in Long, W.A. (ed.), *Fetal and Neonatal Cardiology*, 1990, p. 541, with permission of W.B. Saunders/Elsevier.)
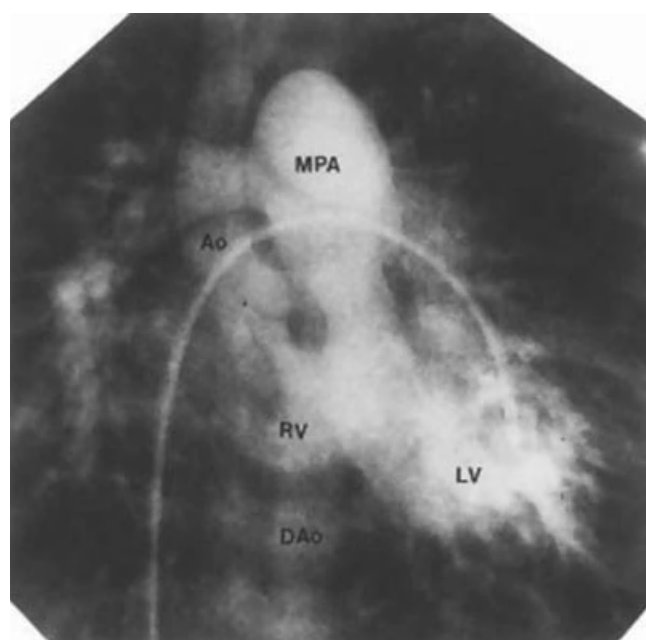
Figure 35.11 Selective left ventriculogram in frontal view in infant with type II tricuspid atresia shows transposition of the great arteries. Ao, aorta; DAo, descending aorta; LV, left ventricle; MPA, main pulmonary artery; RV, right ventricle. (Reproduced with permission from Schwartz and Rao *Tricuspid Atresia*, 2nd edn. Mount Kisco, NY: Futura Publishing, 1992: 223–46.)

depending on the structures that need greater definition. Special attention should be paid in evaluating subaortic obstruction at the VSD level in patients with transposition [36·37]. Quantitative measurements of the size and function of the left ventricle [47–49] should also be undertaken. Selective injections into the right ventricle, aorta, and pulmonary artery provide greater definition of these structures. Particular attention should be paid to define sources of pulmonary blood flow and pulmonary artery anatomy. Selective angiography with the catheter positioned proximal to or in the previously created shunts is also useful in evaluating the pulmonary arteries and, of course, the shunt itself.

Other laboratory studies

Pulse oximetry is readily available in an outpatient setting for noninvasive measurement of oxygen saturation. Hemoglobin level and hematocrit along with red blood indices should be routinely obtained to assess the degree of polycythemia and hypoxemia and to identify relative iron deficiency anemia [57]. Computed tomography (CT) and magnetic resonance imaging (MRI) are useful in defining issues not clearly defined by echocardiography.

Differential diagnosis

Differential diagnosis differs with the mode of presentation (Table 35.5).

Decreased pulmonary blood flow

Causes of cyanosis with decreased pulmonary blood flow are listed in Table 35.5. The electrocardiogram is most useful in the differential diagnosis [73]. Echocardiography and cineangiography may occasionally be necessary for confirming the diagnosis, especially in complex defects.

Increased pulmonary blood flow

The differential diagnostic considerations are also listed in Table 35.5. Although the characteristic electrocardiographic pattern (abnormal, superior vector, or left-axis deviation) of tricuspid atresia is helpful, it is not always present in tricuspid atresia with transposition. Furthermore, some of the conditions listed in Table 35.5 also have a similar displacement of the mean frontal plane vector. Often, echocardiograms and angiocardiograms are necessary for final diagnosis.

Management

Physiologically "corrective" operations for tricuspid atresia [74,75] and their modifications are usually performed in patients older than 2 years. Most patients present with

---

Table 35.5 Differential diagnosis of tricuspid atresia in the neonate.

Decreased pulmonary blood flow
Tetralogy of Fallot including pulmonary atresia with ventricular septal defect
Pulmonary atresia or severe stenosis with intact ventricular septum
Tricuspid atresia
Complex cardiac anomalies with severe pulmonary stenosis or atresia including d-transposition with ventricular septal defect; l-transposition with ventricular septal defect; single ventricle, double-outlet right ventricle, and asplenia syndrome

Increased pulmonary blood flow
d-Transposition of the great arteries with large ventricular septal defect
Coarctation of the aorta with ventricular septal defect
Multiple left-to-right shunts (ventricular septal defect, common atrioventricular canal, and patent ductus arteriosus)
Single ventricle, double-outlet right ventricle, and other complex cardiac defects without pulmonic stenosis
Total anomalous pulmonary venous connection without obstruction
Hypoplastic left heart syndrome
Truncus arteriosus

Adapted from Rao *Fetal and Neonatal Cardiology.* Philadelphia, PA: Saunders, 1990: 525–40, with permission of W.B. Saunders/Elsevier.

---

symptoms as neonates and should be effectively palliated to enable them to reach the age at which correction can be undertaken. The objective of the management plan, apart from providing symptomatic relief and increased survival rate, should be to preserve, protect, and restore structure (good-sized and undistorted pulmonary arteries) and function (normal pulmonary artery pressure and preserved left ventricular function) to normal such that a corrective procedure can be performed later.

Medical management at the time of presentation

In infants with low arterial PO_2 and oxygen saturation and with ductus-dependent pulmonary blood flow, the ductus should be kept open by intravenous administration of prostaglandin E_1 (PGE_1) [76] (see Chapter 17). The ductal dilatation increases pulmonary blood flow, thereby improving oxygenation and reversing the metabolic acidosis so that further diagnostic studies and other interventions can be performed with relative safety.

An occasional infant with signs of congestive heart failure (more common in type II patients) should be treated with routine anticongestive measures. Patients with associated severe coarctation of the aorta may also be helped with PGE_1 infusion; this time, the ductal dilatation improves systemic perfusion. This is followed by relief of aortic obstruction by operation or balloon angioplasty [77].

Palliative treatment of specific physiologic abnormalities

The type of palliation undertaken depends largely on the hemodynamic abnormality produced by the basic lesion and associated cardiac anomalies. These may be broadly grouped [33] into decreased pulmonary blood flow, increased pulmonary blood flow, and intracardiac obstruction.

Decreased pulmonary blood flow

Systemic–pulmonary artery shunts are most commonly used in palliating pulmonary oligemia. Since the description of subclavian artery to ipsilateral pulmonary artery anastomosis in 1945 by Blalock and Taussig [78], several other types of procedures have been devised to improve pulmonary blood flow. Modified Blalock–Taussig shunt with a Gore-Tex graft interposed between the subclavian artery and the ipsilateral pulmonary artery [79] is most commonly utilized, although distortion of the pulmonary artery sometimes created by the shunt may be a problem later.

Enlarging the VSD or resecting the right ventricular outflow tract stenosis has been recommended by Annecchino *et al.* [80] to augment the pulmonary blood flow. This ingenious approach attacks the site of obstruction rather than bypassing it. However, it requires cardiopulmonary bypass and may be unnecessary in neonates [33]. Stenting the arterial duct is not currently an initial therapeutic choice because of limited experience [81]. Rarely, the predominant

obstruction may be at the pulmonary valve level and, in such patients, balloon pulmonary valvoplasty [82] may augment pulmonary blood flow.

Despite the availability of many palliative procedures to increase pulmonary blood flow, some produce complications that prevent a successful Fontan–Kreutzer procedure subsequently. The Blalock–Taussig anastomosis or one of its modified versions is the preferred procedure with the least number of long-term complications, but at the same time it preserves suitable anatomy for subsequent corrective procedures and therefore is recommended as the procedure of choice for palliation of tricuspid atresia patients with decreased pulmonary blood flow.

Increased pulmonary blood flow

Infants with a moderate increase in pulmonary blood flow may not have significant symptoms and are less cyanotic than the pulmonary oligemic patients. Markedly increased pulmonary blood flow as in type Ic and type IIc patients, however, can produce congestive heart failure.

In type I patients, aggressive anticongestive measures should be promptly instituted. Natural history studies indicate that the VSD becomes smaller, and patients with pulmonary plethora will, in due course, develop pulmonary oligemia and require a palliative shunt. Right ventricular outflow tract obstruction may also develop, resulting in decreased pulmonary blood flow. Therefore, pulmonary artery banding should not be performed initially in this group of patients. If optimal anticongestive therapy does not relieve symptoms after a time [33], pulmonary artery banding should be considered. In those without a pulmonary artery band, careful follow-up with periodic assessment of pulmonary artery pressure and timely intervention are necessary to prevent pulmonary vascular obstructive disease.

Pulmonary artery bands with absorbable material have been used for palliation in such infants [83]. The absorbable polydioxanone band decreases pulmonary artery pressure by restricting the pulmonary blood flow, and initially helps abate symptoms of heart failure. As the VSD spontaneously closes, the pulmonary artery band is resorbed and does not produce the severe pulmonary oligemia that might have been associated with a conventional nonabsorbable band. Although this is an ingenious approach, it is likely to help only a limited number of patients [84].

In type II patients, banding of the pulmonary artery should be performed once the infant is stabilized with anticongestive therapy. If there is associated coarctation of the aorta, or aortic arch interruption or hypoplasia, adequate relief of the aortic obstruction should be provided concurrently with pulmonary artery banding, and a patent ductus arteriosus should be ligated. The importance of PGE_1 administration in the control of congestive heart failure has already been alluded to.

Intracardiac obstruction

Intracardiac obstruction can occur at two different levels: patent foramen ovale and VSD.

Interatrial obstruction

The interatrial defect should be large enough to accommodate the egress of the entire systemic venous return. A mean atrial pressure difference of 5 mmHg or more with prominent *a* waves (15–20 mmHg) in the right atrium is generally considered to represent obstruction of the interatrial septum [33]. It may be necessary to relieve the obstruction by balloon atrial septostomy [85]; if that is unsuccessful, by blade atrial septostomy [86,87] and rarely by surgical atrial septostomy. Significant interatrial obstruction requiring atrial septostomy in the neonate is unusual, although this can be a significant problem later in infancy [36,87].

Interventricular obstruction

Spontaneous closure of the VSD can occur, causing severe pulmonary oligemia in type I patients and subaortic obstruction in type II patients. Functional and anatomic closures have been reported in patients with normally related great arteries [37,40]. In functional closure, cyanotic spells similar to those in tetralogy of Fallot [40] may occur, and the management is similar, namely, knee–chest position, humidified oxygen, and morphine sulfate (0.1 mg kg^{-1}). If the spells are not averted, β-blockers (propranolol or esmolol) or intravenous vasopressors (methoxamine or phenylephrine) may be given to increase systolic blood pressure by 10–20%. Correction of metabolic acidosis or anemia, if present, should also be considered. If there is no improvement, immediate operative palliation may be necessary. If the infant improves, correction by a Fontan-type procedure or palliation by a systemic–pulmonary artery shunt or a bidirectional Glenn operation may be performed subsequently.

In partial or complete anatomic closure of the VSD, pulmonary oligemia with consequent hypoxemia and polycythemia ensues. Augmentation of the pulmonary blood flow is indicated and can be accomplished by several methods (see earlier). If the age and size of the patient or cardiac anatomy and hemodynamics are unsuitable for performing a modified Fontan or bidirectional Glenn operation, a systemic–pulmonary artery shunt, such as modified (Gore-Tex) Blalock–Taussig procedure [79], should be undertaken. A classic Glenn procedure should not be performed because if the VSD closes completely, the left pulmonary artery will be without flow, which may result in thrombosis or underdevelopment of the left pulmonary artery. In addition, long-term complications of the Glenn operation [51], particularly development of pulmonary arteriovenous fistulas, are of concern. Central aortopulmonary shunts should be avoided because they tend to raise pulmonary artery pressure and resistance and kink or distort the pulmonary arteries. Thus, a Blalock–Taussig type of

shunt [classic or modified (Gore-Tex) Blalock–Taussig] or a bidirectional Glenn procedure is preferable. In the present author's view, in younger infants a Blalock–Taussig shunt is to be preferred; in older infants and children, a bidirectional Glenn procedure preparatory to a modified Fontan operation is recommended.

Partial spontaneous closure of the VSD in type II patients causes subaortic obstruction [36,37,51], which should be relieved or bypassed in case the resultant left ventricular hypertrophy poses increased risk at the time of the Fontan procedure [88]. The obstruction must be tackled at the time of either a bidirectional Glenn or a modified Fontan operation. Resection of the conal muscular septum [89,90], thus enlarging the VSD, is a direct approach, although concern for development of heart block and spontaneous closure of the surgically produced VSD remains [51]. Alternatively, the VSD, right ventricle, and aortic valve may be bypassed by anastomosis of the proximal stump of the divided pulmonary artery to the ascending aorta (Damus–Kaye–Stansel) at the time of bidirectional Glenn (or Fontan) operation. Limited data are available about the superiority of one method over the other.

Medical management after a palliative operation

Problems encountered with tricuspid atresia patients are similar to those in other cyanotic cardiac malformations. Appropriate monitoring for and treatment of relative anemia, polycythemia, coagulopathy, and hyperuricemia should be undertaken. Hyperuricemia, gout, and uric acid nephropathy can develop in adolescents and adults with long-standing cyanosis and polycythemia and should be prevented by timely palliative or corrective operative therapy. If prevention is not feasible, periodic measurement of uric acid levels and treatment with allopurinol (if the uric acid level is >8 mg per 100 ml) may have to be instituted. The risks for developing a cerebrovascular accident or brain abscess are similar to those with other cyanotic anomalies, and appropriate consultation and treatment are indicated. Antibiotic prophylaxis before any bacteremia-producing procedures or surgery is indicated, as is routine immunization plus consideration for palivizumab (for prevention of RSV infection in infancy), polyvalent pneumococcal vaccine, or influenza vaccine.

Physiologic corrective surgery

Since the original descriptions by Fontan and Baudet [74] and Kreutzer et al. [75] of physiologically corrective operations for tricuspid atresia, many modifications of these procedures have been suggested [91,92]. The Fontan operation was based on the concept of using the right atrium as a pump. As originally described, it consists of superior vena cava–right pulmonary artery (Glenn) shunt, anastomosis of the proximal end of the divided right pulmonary artery to the right atrium directly or by means of an aortic homograft, closure of the atrial defect,

insertion of a pulmonary valve homograft into the inferior vena caval orifice, and ligation of the main pulmonary artery, thus bypassing the right ventricle completely [74]. Kreutzer's concept was that the right atrium may not function as a pump and that the left ventricle is the only suction pump in the system. His original operation consisted of direct anastomosis of the right atrial appendage with the pulmonary artery or through a pulmonary homograft. The atrial septal defect was not closed and neither a Glenn procedure nor prosthetic valve insertion into the inferior vena cava was performed [75].

Initially the approach was a classic Glenn anastomosis or a valve at the inferior vena cava–right atrial junction [91,92]. A bidirectional Glenn procedure followed by direct atriopulmonary anastomosis (without a valved conduit) has becme the standard procedure for most tricuspid atresia patients.

Bidirectional glenn procedure

In the bidirectional Glenn procedure [93–95], the upper end of the divided superior vena cava is anastomosed end-to-side to the superior aspect of the undivided right pulmonary artery, thus diverting the superior vena caval blood into both right and left pulmonary arteries [93–96]. There are hemodynamic advantages associated with the bidirectional Glenn procedure, including improved effective pulmonary flow, reduced total pulmonary flow, and less left ventricular volume overloading. When both right and left superior venae cavae are present, bilateral bidirectional Glenn shunting should be performed, especially if the bridging innominate vein is absent or small.

Total cavopulmonary diversion

On the basis of hydrodynamic studies, de Leval et al. [97] concluded that the right atrium has no efficient pump function; pulsations in the nonvalved circulation generate turbulence with a consequent decrease in net flow, and energy losses occur in the nonpulsatile chambers, corners, and obstructions. They devised and performed total cavopulmonary diversion in which bidirectional Glenn procedure was performed, and the inferior vena caval blood is directed through an intra-atrial tunnel into the cardiac end of the superior vena cava, which in turn is connected to the undersurface of the right pulmonary artery. The advantages of this procedure are technical simplicity, maintenance of low right atrial and coronary sinus pressure, and reduction in risk of formation of atrial thrombus. Experimental studies by Sharma et al. [98] suggested that complete or minimal offset between the orifices of the superior vena caval connection may decrease energy losses.

Extracardiac conduit

Diversion of the inferior vena caval blood into the pulmonary artery via an extracardiac conduit [99] was conceived as an alternative to the lateral tunnel in surgical completion of the Fontan procedure.

Staged fontan procedure

Performing a bidirectional Glenn procedure initially followed later by diversion of the inferior vena caval blood into the pulmonary artery [100,101] is the norm instead of performing all Fontan connections at the same time. Staging appears to decrease overall mortality, presumably related to improving the ventricular function by avoiding/correcting afterload mismatch associated with a one-stage Fontan procedure [101].

Fenestrated fontan

The criteria (Table 35.4) outlined by Choussat *et al.* [68] have been modified or exceeded by many groups of workers. These factors, when abnormal, make a Fontan–Kreutzer operation a high-risk procedure. They should be identified at the time of preoperative evaluation. They include elevated mean pulmonary artery pressure >18 mmHg or resistance >4 Wood units m^{-2}), distorted or small (McGoon ratio of 1.8 or less) pulmonary arteries, poor left ventricular function (end-diastolic pressure >12 mmHg), significant mitral regurgitation, subaortic obstruction, and severe left ventricular hypertrophy. With one or more of these risk factors, physiologically corrective procedures of the Fontan type may carry significant risk. In such high-risk Fontan–Kreutzer patients, leaving open a small atrial septal defect to allow decompression of the right atrium in the immediate postoperative period with a plan to close the defect later has been used by some workers [102–104]. The atrial defect is closed by a preplaced suture [102,103] or by transcatheter techniques [104]. Significant improvement in postoperative pleural effusions, systemic venous congestion, and higher cardiac index and possibly shorter hospitalization have been the beneficial effects of the fenestration, but at the expense of systemic arterial hypoxemia.

Operations that divide the pulmonary and systemic venous returns (Fontan–Kreutzer) are feasible for most patients with tricuspid atresia. The age (and weight) of the patient and anatomic and physiologic substrate determine the type of surgery. In neonates and young infants (3–6 months), a modified Blalock–Taussig shunt is the procedure of choice. Between 3 (or 6) months and 1 year of age, a bidirectional Glenn procedure is the procedure of choice. Between 1 and 2 years of age, a bidirectional Glenn procedure is used unless there is a contraindication. Beyond 2 years of age, total cavopulmonary anastomosis with or without fenestration, depending on the risk factors, may be performed. However, even at this age, staged cavopulmonary connection (initially bidirectional Glenn and then an extracardiac conduit diversion of inferior vena caval blood into the pulmonary artery) is recommended.

Preoperative catheter evaluation to define the pulmonary artery pressure and anatomy and to exclude a persistent left superior vena cava (because it may divert blood away from the pulmonary arteries) prior to bidirectional Glenn surgery should be undertaken. At the time of bidirectional Glenn procedure, stenoses, if any, of the pulmonary artery should be repaired. Issues related to subaortic obstruction and mitral valve regurgitation should also be addressed. Immediately prior to Fontan conversion, cardiac catheterization should be performed to ensure normal anatomy and pressure of the pulmonary artery and normal left ventricular end-diastolic pressure. At the same time, aortopulmonary collaterals should be evaluated by means of selective subclavian artery and descending thoracic aortic angiography. Any collateral vessels should be occluded with coils or devices, as appropriate. In patients with transposition of the great arteries, early pulmonary artery banding, treatment of aortic coarctation, and relieving or bypassing subaortic obstruction should also be incorporated into the treatment plan.

Catheter interventions

A number of catheter interventional procedures are useful in managing tricuspid atresia patients:

1 During the neonatal period, obstruction at the level of the atrial septum may be treated with conventional Rashkind balloon atrial septostomy [85]. In infants and children, the interatrial septum may be too thick to be torn with balloon septostomy; therefore, Park blade septostomy should precede the Rashkind procedure [86,87].

2 The obstruction to pulmonary blood flow is at the ventricular septal defect (VSD) level or in the subpulmonary region in most patients. In a rare patient, the obstruction is at the pulmonary valve, and then balloon pulmonary valvoplasty may improve pulmonary blood flow and oxygen saturation [82]

3 If progressive hypoxemia develops after a prior Blalock–Taussig shunt and is secondary to shunt stenosis, balloon dilatation [105] or stent implantation [106] may improve oxygen saturation. If the patient is of sufficient size and age to undergo a bidirectional Glenn procedure, this should be performed instead of catheter intervention to enlarge the narrowed Blalock–Taussig shunt.

4 If severe aortic coarctation is present, particularly in patients with tricuspid atresia type II, balloon angioplasty may relieve aortic obstruction and achieve better control of congestive heart failure [107,108]

5 If significant branch pulmonary artery stenosis is present either before bidirectional Glenn and Fontan conversion surgery or after a Fontan procedure, balloon angioplasty or placement of intravascular stents [109,110] is recommended.

6 Aortopulmonary collateral vessels develop. Before the final Fontan conversion, these vessels should be occluded in the catheterization laboratory, usually with Gianturco coils. This reduces reduces left ventricular volume overloading [111,112].

7 After a Fontan procedure, some patients may develop recurrent pleural effusion, liver dysfunction, plastic bronchitis, or protein-losing enteropathy. In these patients,

obstructive lesions in the Fontan circuit, if any, should be addressed by balloon angioplasty or stent. If the problem persists, creation of an atrial fenestration to produce right-to-left shunt may be beneficial [113]. In such situations, puncture of the atrial septum by using a Brockenbrough technique followed by static balloon atrial septal dilatation [114] or stent implantation may be helpful.

8 Patients who undergo a fenestrated Fontan operation or who have a residual atrial defect despite correction may have clinically significant right-to-left shunting causing severe hypoxemia. These residual atrial defects may be closed by using transcatheter techniques [115–118].

9 Some patients may develop systemic venous-to-pulmonary venous collateral vessels following Fontan operation, causing arterial desaturation. These vessels should be defined and closed by coils, plugs, or devices, depending on the size, location, and accessibility [111,112,119,120].

10 *Emerging therapies*. Two-stage cavopulmonary connection is currently recommended for achieving Fontan circulation. Konertz et al. proposed a staged surgical-catheter approach [121]. Initially, a modified hemi-Fontan surgery is performed which is later completed by a transcatheter method [121, 122]. This approach attempts to reduce the total number of operations. The modified hemi-Fontan operation consists of the usual bidirectional Glenn procedure. In addition, the lower end of the divided superior vena cava is anastomosed to the undersurface of the right pulmonary artery. The superior vena cava is then banded around a 16-gauge catheter with 6–0 Prolene suture slightly above the cavoatrial junction. A lateral tunnel with a Gore-Tex baffle is created to divert the inferior vena caval blood towards the superior vena cava. The baffle is then fenestrated with 3–5 five mm wide holes. Thus, the first stage achieves a physiologic bidirectional Glenn circulation. At the time of the transcatheter stage, the superior vena caval constriction is balloon dilated and fenestrations are closed with devices or by implantation of a covered stent. These procedures have been performed in a limited number of patients [121–124], and preliminary data suggest that the usual post-Fontan complications, such as pleural effusion and ascites, have not occurred with this approach. Examination of the results of larger experience and longer term follow-up and the ready availability of covered stents are necessary for routine application of this innovative approach.

Follow-up after corrective operation

Close follow-up after correction is indicated. Some patients need continued inotropic and diuretic therapy. Afterload reduction with an angiotensin-converting enzyme inhibitor is generally recommended to augment left ventricular output with consequent improvement in pulmonary flow, although controlled studies substantiating this principle have not been undertaken. Because of the potential for development of thrombi in the right atrium, anticoagulants are routinely
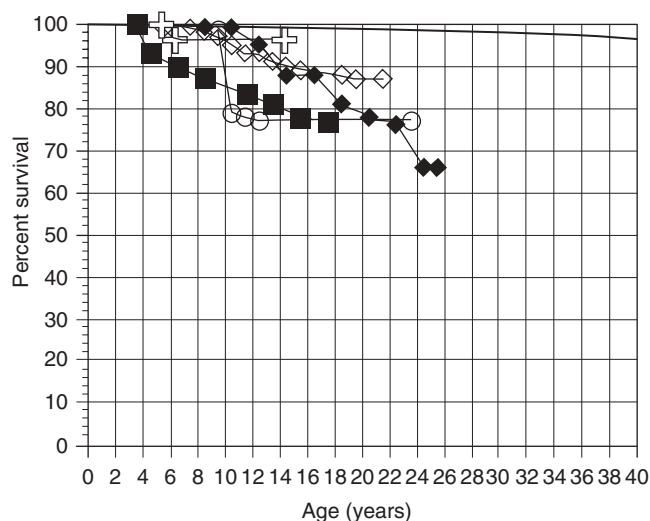
Figure 35.12 Actuarial survival after a Fontan operation. The three upper curves are from the Mayo Clinic, the most recent series (plus symbols) from 1988–97, and the oldest series (solid triangles) from 1973–80. The two lower curves are from Toronto Sick Children's Hospital (solid squares) for operations done between 1971 and 1999, and from Bordeaux (open circles) for operations done between 1968 and 1982. The later the series began, the better the results. Over 75% survive >10 years after operation. (Reproduced from Hoffman JIE, *The Natural and Unnatural History of Congenital Heart Disease*, 2009, with permission of Wiley-Blackwell.)

used by most cardiologists. The present author recommends platelet-inhibiting doses of aspirin; others advocate warfarin anticoagulation.

Most patients do well after operation (Figure 35.12) [125]. However, several problems have been observed after corrective surgery: arrhythmia, obstructed pulmonary outflow pathways, persistent shunts, and systemic venous congestion including protein-losing enteropathy. Supraventricular arrhythmias (atrial flutter or fibrillation, paroxysmal supraventricular tachycardia) are common and should be treated with appropriate pharmacologic therapy. In a patient without adequate control, electrophysiologic study and surgical or transcatheter ablation may be indicated [126]. Revision of the Fontan pathway to a cavopulmonary connection with elimination of the enlarged right atrium has been considered an alternative solution. Sick sinus node syndrome and atrioventricular block occur in some children and may require pacemaker therapy. Ventricular arrhythmia is less frequent.

Symptoms and signs indicative of obstruction to Fontan pathways should be promptly investigated. Poor echocardiography windows make noninvasive evaluation difficult, and catheterization and angiography may be necessary. Obstructive lesions, if identified, should be treated with balloon angioplasty, stenting, or even surgery, as indicated.

A persistent shunt may be secondary to intentional fenestration of the atrial septum or a residual atrial septal defect. If significant hypoxemia is present, the residual shunt

should be closed, preferably by a transcatheter device [115,118]. Test occlusion of the defect is advisable to ensure that adequate cardiac output is maintained after occlusion.

Recurrent pleural effusion, liver dysfunction, and protein-losing enteropathy have occurred in a small number of patients. Protein-losing enteropathy has a high mortality (75%) [113,127]. The cause of protein-losing enteropathy is unknown, but appears to be related to loss of protein in the bowel by lymphatic distention secondary to increased systemic venous pressure, although this can occur in patients with reasonably "normal" pressures for the Fontan procedure. Symptoms usually appear 6 months after the Fontan–Kreutzer procedure or later, and include diarrhea, edema, ascites, and pleural effusion. Significant hypoalbuminemia and increased α_1-antitrypsin in the stool are present. Evidence for obstruction of the Fontan–Kreutzer pathway must be scrutinized and, if found, relieved [113]. A medium-chain triglyceride diet and parenteral albumin supplementation may be supportive. Some workers have used prednisone [128], with favorable effect, although the experience with this mode of therapy is limited. So, too, is experience with regular high molecular weight heparin, low molecular weight heparin, an elementary diet, calcium replacement, somatostatin, high-dose spironolactone, sildenafil, and resection of localized intestinal lymphangiectasia (if demonstrated), all with variable success. Because protein-losing enteropathy appears to be a fatal complication of the Fontan procedure, aggressive management is suggested. In these patients with so called "failed Fontan," after excluding and addressing obstructions and residual shunts apart from other conventional treatment, consider (1) reducing right atrial pressure by creating an atrial septal defect (Brockenbrough's puncture plus static dilatation of the atrial septum114), (2) right atrial and left ventricular (atrioventricular sequential) pacing [129,130], (3) converting an atrioventricular Fontan procedure to total cavopulmonary anastomosis [131,132], and/or (4) cardiac transplantation [133,134]. However, most patients do well after the Fontan–Kreutzer procedure.

Long-term history of treated and untreated adults

Although tricuspid atresia patients usually present in infancy and only 10–20% of untreated patients may survive their first birthday [4,55], improvements in early identification, neonatal care, noninvasive diagnoses, anesthesia, neonatal cardiac surgery, and normalization of pulmonary blood flow by PGE_1 infusion and aortopulmonary shunt in patients with decreased pulmonary blood flow and by banding of the pulmonary artery in patients with pulmonary plethora has improved the survival. The potential for improved prognosis exists, and therefore each patient with tricuspid atresia should be offered aggressive medical and operative therapy. The advantages of the Fontan–Kreutzer procedure [125], namely decreasing or eliminating hypoxemia and normalizing ventricular volume overloading, have further improved childhood survival. Consequently, a substantial number of

patients reach adulthood. Some of them do well, but others develop an arrhythmia (atrial flutter or fibrillation, paroxysmal supraventricular tachycardia), obstructed Fontan pathways, branch pulmonary artery stenosis, thromboembolism, persistent right-to-left shunts (Fontan fenestrations or atrial septal defects), systemic venous-to-pulmonary venous collateral vessels and protein-losing enteropathy. Detailed evaluation of these problems and appropriate treatment are mandatory to prolong survival and maintain quality of life. This is usually accomplished by a team approach in an Adult Congenital Heart Disease Clinic.

References

1 Rao PS. A unified classification for tricuspid atresia. *Am Heart J* 1980;**99**:799–804.

2 Rao PS. Terminology: tricuspid atresia or univentricular heart? In: Rao PS, ed. *Tricuspid Atresia*. Mount Kisco, NY: Futura Publishing, 1982: 3–6.

3 Rashkind WJ. Tricuspid atresia: a historical review. *Pediatr Cardiol* 1982;**2**:85–8.

4 Dick M, Fyler DC, Nadas AS. Tricuspid atresia: clinical course in 101 patients. *Am J Cardiol* 1975;**36**:327–37.

5 Rosenthal A, Dick M II. Tricuspid atresia. In: Adams FH, Emmanouilides GC, eds. *Moss' Heart Disease in Infants, Children, and Adolescents*, 3rd edn. Baltimore: Williams & Wilkins, 1983: 271.

6 Rao PS. Is the term "tricuspid atresia" appropriate? (Editorial). *Am J Cardiol* 1990;**66**:1251–4.

7 Bharati S, McAllister HA Jr, Tatooles CJ, *et al*. Anatomic variations in underdeveloped right ventricle related to tricuspid atresia and stenosis. *J Thorac Cardiovasc Surg* 1976;**72**:383–400.

8 Bharati S, Lev M. The concept of tricuspid atresia complex as distinct from that of the single ventricle complex. *Pediatr Cardiol* 1979;**1**:57–62.

9 Bharati S, Lev M. Reply. *Pediatr Cardiol* 1979;**1**:1656.

10 Wenink ACG, Ottenkamp J. Tricuspid atresia: microscopic findings in relation to "absence" of atrioventricular connection. *Int J Cardiol* 1987;**16**:57–73.

11 Gessner IH. Embryology of atrioventricular valve formation and embryogenesis of tricuspid atresia. In: Rao PS, ed. *Tricuspid Atresia*, 2nd edn. Mount Kisco, NY: Futura Publishing, 1992: 39–57.

12 Rao PS. Terminology: is tricuspid atresia the correct term to use? In: Rao PS, ed. *Tricuspid Atresia*, 2nd edn. Mount Kisco, NY: Futura Publishing, 1992: 3–15.

13 Rao PS. Demographic features of tricuspid atresia. In: Rao PS, ed. *Tricuspid Atresia*, 2nd edn. Mount Kisco, NY: Futura Publishing, 1992: 23–37.

14 Taussig HB, Keinonen R, Momberger N, *et al*. Long-time observations of the Blalock–Taussig operation. IV. Tricuspid atresia. *Johns Hopkins Med J* 1973;**132**:135–45.

15 Ando M, Santomi G, Takao A. Atresia of tricuspid and mitral orifice: anatomic spectrum and morphogenetic hypothesis. In: Van Praagh R, Takao A, eds. *Etiology and Morphogenesis of Congenital Heart Disease*. Mount Kisco, NY: Futura Publishing, 1980: 421–87.

16 Van Mierop LH, Gessner IH. Pathogenetic mechanisms in congenital cardiovascular malformations. *Prog Cardiovasc Dis* 1972; **15**:67–85.

17 Wilson AD, Rao PS. Embryology. In: Kambam J, ed. *Cardiac Anesthesia for Infants and Children*. St Louis, MO: Mosby, 1994: 3–9.

18 Rao PS. Tricuspid atresia. In: Long WA, ed. *Fetal and Neonatal Cardiology*. Philadelphia, PA: Saunders, 1990: 525–40.

19 Keefe JF, Wolk MJ, Levine HJ. Isolated tricuspid valvular stenosis. *Am J Cardiol* 1970;**25**:252–7.

20 Van Praagh R, Ando M, Dungan WT. Anatomic types of tricuspid atresia: clinical and developmental implications. *Circulation* 1971;**44**(Suppl II):115.

21 Astley R, Oldham JS, Parson C. Congenital tricuspid atresia. *Br Heart J* 1953;**15**:287–97.

22 Kühne M. Über zwei Falle kongenitaler Atresie des Ostium Venosum Dextrum. *Jahrb Kinderh* 1906;**63**:235–7.

23 Edwards JE, Burchell HB. Congenital tricuspid atresia: a classification. *Med Clin North Am* 1949;**33**:1117–23.

24 Keith JD, Rowe RD, Vlad P. Tricuspid atresia. In: *Heart Disease in Infancy and Childhood*. New York: Macmillan, 1958: 434–70.

25 Rao PS. Classification of tricuspid atresia. In: Rao PS, ed. *Tricuspid Atresia*, 2nd edn. Mount Kisco, NY: Futura Publishing, 1992: 59–79.

26 Rao PS, Jue KL, Isabel-Jones J, *et al.* Ebstein's malformation of the tricuspid valve with atresia: differentiation from isolated tricuspid atresia. *Am J Cardiol* 1973;**32**:1004–9.

27 Anderson RH, Wilkinson JL, Gerlis LM, *et al.* Atresia of the right atrioventricular orifice. *Br Heart J* 1977;**39**:414–28.

28 Weinberg PM. Anatomy of tricuspid atresia and its relevance to current forms of surgical therapy. *Ann Thorac Surg* 1980; **29**:306–11.

29 Ottenkamp J, Wenink AGG, Rohmer J, *et al.* Tricuspid atresia with overriding imperforate tricuspid membrane: an anatomic variant. *Int J Cardiol* 1984;**6**:599–613.

30 Scalia D, Russo P, Anderson RH, *et al.* The surgical anatomy of the heart with no direct communication between the right atrium and the ventricular mass – so called tricuspid atresia. *J Thorac Cardiovasc Surg* 1984;**87**:743–55.

31 Rao PS. Atrioventricular canal mimicking tricuspid atresia: echocardiographic and angiographic features. *Br Heart J* 1987; **58**:409–12.

32 Rao PS. Tricuspid atresia: anatomy, imaging, and natural history. In: Braunwald E, ed. *Atlas of Heart Diseases*, Vol XII. Philadelphia, PA: Current Medicine, 1997: 14.1–14.

33 Rao PS, Covitz W, Chopra PS. Principles of palliative management of patients with tricuspid atresia. In: Rao PS, ed. *Tricuspid Atresia*, 2nd edn. Mount Kisco, NY: Futura Publishing, 1992: 297–320.

34 Van Praagh R. Terminology of congenital heart disease: glossary and commentary. *Circulation* 1977;**56**:139–43.

35 Van Praagh R. Discussion after paper by Vlad P. Pulmonary atresia with intact ventricular septum. In: Barrett-Boyes BG, Neutze JM, Harris EA, eds. *Heart Disease in Infancy: Diagnosis and Surgical Treatment*. London: Churchill Livingstone, 1973: 236.

36 Rao PS. Natural history of the ventricular septal defect in tricuspid atresia and its surgical implications. *Br Heart J* 1977; **39**:276–88.

37 Rao PS. Further observations on the spontaneous closure of physiologically advantageous ventricular septal defects in tricuspid atresia: surgical implications. *Ann Thorac Surg* 1983;**35**:121–31.

38 Rao PS. Physiologically advantageous ventricular septal defects (Letter). *Pediatr Cardiol* 1983;**4**:59–62.

39 Rao PS, Sissman NJ. Spontaneous closure of physiologically advantageous ventricular septal defects. *Circulation* 1971; **43**:83–90.

40 Rao PS, Linde LM, Liebman J, *et al.* Functional closure of physiologically advantageous ventricular septal defects: observations in three cases with tricuspid atresia. *Am J Dis Child* 1974; **127**:36–40.

41 Gallaher ME, Fyler DC. Observations on the changing hemodynamics in tricuspid atresia without transposition of the great vessels. *Circulation* 1967;**35**:381–8.

42 Sauer U, Hall D. Spontaneous closure or critical decrease in size of the ventricular septal defect in tricuspid atresia with normally connected great arteries: surgical implications. *Herz* 1980;**5**:369–84.

43 Weinberg PM. Pathologic anatomy of tricuspid atresia. In: Rao PS, ed. *Tricuspid Atresia*. Mount Kisco, NY: Futura Publishing, 1982: 49–67.

44 Rudolph AM. Tricuspid atresia with hypoplastic right ventricle. In: *Congenital Disease of the Heart*. Chicago: Year Book, 1974: 429–61.

45 Marcano BA, Riemenschnieder TA, Ruttenburg HD, *et al.* Tricuspid atresia with increased pulmonary blood flow: an analysis of 13 cases. *Circulation* 1965;**40**:399–410.

46 Rao PS. Cardiac catheterization in tricuspid atresia. In: Rao PS, ed. *Tricuspid Atresia*. Mount Kisco, NY: Futura Publishing, 1982: 153–78.

47 LaCorte MA, Dick M, Scheer G, *et al.* Left ventricular function in tricuspid atresia. *Circulation* 1975;**52,**:996–1000.

48 Graham TP, Erath HJG Jr, Boucek RJ, *et al.* Left ventricular function in cyanotic congenital heart disease. *Am J Cardiol* 1980;**45**:1231–6.

49 Rao PS, Alpert BS, Covitz W. Left ventricular function in tricuspid atresia. In: Rao PS, ed. *Tricuspid Atresia*, 2nd edn. Mount Kisco, NY: Futura Publishing, 1992: 247–59.

50 Rao PS. Left-to-right shunting in tricuspid atresia. *Br Heart J* 1983;**49**:345–9.

51 Rao PS. Natural history of ventricular septal defects in tricuspid atresia. In: Rao PS, ed. *Tricuspid Atresia*, 2nd edn. Mount Kisco, NY: Futura Publishing, 1992: 261–93.

52 Bloomfield DK. The natural history of ventricular septal defects in patients surviving infancy. *Circulation* 1964;**29**:914–55.

53 Hoffman JIE, Rudolph AM. The natural history of ventricular septal defects in infancy. *Am J Cardiol* 1965;**16**:634–53.

54 Rao PS. Subaortic obstruction after pulmonary artery banding in patients with tricuspid atresia and double-inlet left ventricle and ventriculoarterial discordance (Letter). *J Am Coll Cardiol* 1991;**18**: 1585–6.

55 Dick M, Rosenthal A. The clinical profile of tricuspid atresia. In: Rao PS, ed. *Tricuspid Atresia*. Mount Kisco, NY: Futura Publishing, 1982: 83–111.

56 Rowe RD, Freedom RM, Mehrizi A, *et al. The Neonate with Congenital Heart Disease*, 2nd edn. *Major Problems in Clinical Pediatrics*, Vol 5. Philadelphia, PA: Saunders, 1981: 456–79.

57 Rao PS. Pathophysiologic consequences of cyanotic heart disease. *Indian J Pediatr* 1983;**50**:479–87.

58 Gamboa R, Gersony WM, Nadas AS. The electrocardiogram in tricuspid atresia and pulmonary atresia with intact ventricular septum. *Circulation* 1966;**34**:24–37.

59 Rao PS, Kulungara RJ, Boineau JP, *et al*. Electrovectorcardiographic features of tricuspid atresia. In: Rao PS, ed. *Tricuspid Atresia*, 2nd edn. Mount Kisco, NY: Futura Publishing, 1992: 141–64.

60 Kulungara RJ, Boineau JP, Moore HV, Rao PS. Ventricular activation and genesis of QRS in tricuspid atresia (Abstract). *Circulation* 1981;**64**:IV-225.

61 Taussig HB. The clinical and pathologic findings in congenital malformations of the heart due to defective development of the right ventricle associated with tricuspid atresia or hypoplasia. *Bull Hopkins Hosp* 1936;**59**:435–40.

62 Wittenborg MH, Neuhauser EBD, Sprunt WH. Roentgenographic findings of congenital tricuspid atresia with hypoplasia of the right ventricle. *Am J Roentgenol* 1951;**64**:712–9.

63 Vlad P. Tricuspid atresia. In: Keith JD, Rowe RD, Vlad P, eds. *Heart Disease in Infancy and Childhood*, 3rd edn. New York: Macmillan, 1977: 518–41.

64 Elster SK. Congenital atresia of pulmonary and tricuspid valves. *Am J Dis Child* 1950;**79**:692–701.

65 Covitz W, Rao PS. Noninvasive evaluation of patients with tricuspid atresia (roentgenography, echocardiography and nuclear angiography). In: Rao PS, ed. *Tricuspid Atresia*, 2nd edn. Mount Kisco, NY: Futura Publishing, 1992: 165–82.

66 Seward JB, Tajik AJ, Hagler DJ, *et al*. Echocardiographic spectrum of tricuspid atresia. *Mayo Clin Proc* 1978;**53**:100–12.

67 Beppu S, Nimura Y, Tamai M, *et al*. Two-dimensional echocardiography in the diagnosis of tricuspid atresia: differentiation from other hypoplastic right heart syndromes and common atrioventricular canal. *Br Heart J* 1978;**40**:1174–83.

68 Choussat A, Fontan F, Besse P, *et al*. Selection criteria for Fontan procedure. In: Anderson RH, Shinebourne EA, eds. *Paediatric Cardiology*. Edinburgh: Churchill Livingstone, 1978: 559–66.

69 Rao PS. The femoral route for cardiac catheterization of infants and children. *Chest* 1973;**63**:239–41.

70 Rao PS, Sissman NJ. The relationship of pulmonary venous wedge to pulmonary arterial pressures. *Circulation* 1971;**44**:565–94.

71 Mair DD, Hagler DJ, Puga FJ, *et al*. Fontan operation in 176 patients with tricuspid atresia: results and a proposed new index for patient selection. *Circulation* 1990;**82**(Suppl IV):164–9.

72 Schwartz DC, Rao PS. Angiography in tricuspid atresia. In: Rao PS, ed. *Tricuspid Atresia*, 2nd edn. Mount Kisco, NY: Futura Publishing, 1992: 223–46.

73 Rao PS. Management of the neonate with suspected serious heart disease. *King Faisal Specialist Hosp J* 1984;**4**:209–16.

74 Fontan F, Baudet E. Surgical repair of tricuspid atresia. *Thorax* 1971;**26**:240–8.

75 Kreutzer G, Bono H, Galindez E, *et al*. Una operacion para la correccion de la atresia tricuspidea. Presented at the Ninth Argentinean Congress of Cardiology, Buenos Aires, Argentina, 31 October–6 November 1971.

76 Freed MD, Heymann MA, Lewis AB, *et al*. Prostaglandin E₁ in the infants with ductus arteriosus dependent congenital heart disease: the US experience. *Circulation* 1981;**64**:899–905.

77 Rao PS, Thapar MK, Galal O, *et al*. Follow-up results of balloon angioplasty of native coarctation in neonates and infants. *Am Heart J* 1990;**120**:1310–4.

78 Blalock A, Taussig HB. The surgical treatment of malformations of the heart in which there is pulmonary stenosis or pulmonary atresia. *JAMA* 1945;**128**:189–92.

79 DeLeval M, McKay R, Jones M, *et al*. Modified Blalock–Taussig shunt: use of subclavian orifice as a flow regulator in prosthetic systemic-pulmonary artery shunts. *J Thorac Cardiovasc Surg* 1981;**18**:112–9.

80 Annecchino FP, Fontan F, Chauve A, *et al*. An operation for the correction of tricuspid atresia. *Ann Thorac Surg* 1979;**29**:317–21.

81 Gibbs JL, Rothman MT, Rees MR, *et al*. Stenting of arterial duct: a new approach to palliation of pulmonary atresia. *Br Heart J* 1992;**67**:240–5.

82 McCredie RM, Lee CL, Swinburn MJ, *et al*. Balloon dilatation pulmonary valvuloplasty in pulmonary stenosis. *Aust N Z J Med* 1986;**16**:20–3.

83 Bonnet D, Sidi D, Vouhe PR. Absorbable pulmonary artery banding in tricuspid atresia. *Ann Thorac Surg* 2001;**71**:360–1.

84 Rao PS. Absorbable pulmonary artery band in tricuspid atresia (Editorial). *Ann Thorac Surg* 2001;**71**:361–2.

85 Rashkind WJ, Waldhausen JA, Miller WW, *et al*. Palliative treatment of tricuspid atresia: combined balloon atrial septostomy and surgical alteration of pulmonary blood flow. *J Thorac Cardiovasc Surg* 1969;**57**:812–8.

86 Park SC, Neches WH, Zuberbuhler JR, *et al*. Clinical use of blade atrial septostomy. *Circulation* 1978;**58**:600–6.

87 Rao PS. Transcatheter blade atrial septostomy. *Cathet Cardiovasc Diagn* 1984;**10**:335–42.

88 Salim M, Muster AJ, Paul MH, *et al*. Relation between preoperative left ventricular muscle mass and outcome of the Fontan procedure in patients with tricuspid atresia. *J Am Coll Cardiol* 1989;**14**:750–5.

89 Ottenkamp J, Wenink ACG, Quaegebeur JM, *et al*. Tricuspid atresia: morphology of the outlet chamber with special emphasis on surgical implications. *J Thorac Cardiovasc Surg* 1985;**89**: 597–603.

90 Smolinsky A, Castaneda AR, Van Praagh R. Infundibular septal resection: surgical anatomy of the superior approach. *J Thorac Cardiovasc Surg* 1988;**95**:486–94.

91 Chopra PS, Rao PS. Corrective surgery for tricuspid atresia: which modifications of Fontan–Kreutzer procedure should be used? A review. *Am Heart J* 1992;**123**:758–67.

92 Rao PS, Chopra PS. Modifications of Fontan–Kreutzer procedure for tricuspid atresia: can a choice be made? In: Rao PS, ed. *Tricuspid Atresia*, 2nd edn. Mount Kisco, NY: Futura Publishing, 1992: 361–75.

93 Haller JA, Adkins JC, Worthington M, *et al*. Experimental studies on permanent bypass of the right heart. *Surgery* 1966;59: 1128–32.

94 Azzolina G, Eufrate S, Pensa P. Tricuspid atresia: experience in surgical management with a modified cavopulmonary anastomosis. *Thorax* 1972;**27**:111–5.

95 Hopkins RA, Armstrong SE, Serwer GA, *et al*. Physiologic rationale for a bidirectional cavopulmonary shunt: a versatile complement to the Fontan principle. *J Thorac Cardiovasc Surg* 1985;**90**:391–8.

96 Bridges ND, Jonas RA, Mayer JE, *et al*. Bidirectional cavopulmonary anastomosis as interim palliation for high-risk Fontan candidates: early results. *Circulation* 1990;**82**(Suppl IV): 170–6.

97 de Leval MR, Kilner P, Gewilling M, *et al*. Total cavopulmonary connection: a logical alternative to atriopulmonary connection

for complex Fontan operation. *J Thorac Cardiovasc Surg* 1988; **96**:682–95.

98 Sharma S, Goudy S, Walker P, *et al*. *In vitro* flow experiments for determination of optimal geometry of total cavopulmonary connection for surgical repair of children with functional single ventricle. *J Am Coll Cardiol* 1996;**27**:1264–9.

99 Marcelletti C, Corno A, Giannico S, Marino B. Inferior vena cava–pulmonary artery extracardiac conduit. A new form of right heart bypass. *J Thorac Cardiovasc Surg* 1990;**100**:313–4.

100 Pridjian AK, Mendelsohn AM, Lupinetti FM, *et al*. Usefulness of the bidirectional Glenn procedure as staged reconstruction for the functional single ventricle. *Am J Cardiol* 1993;**71**:959–62.

101 Tanoue Y, Sese A, Ueno Y, *et al*. Bidirectional Glenn procedure improves the mechanical efficiency of a total cavopulmonary connection in high-risk Fontan candidates. *Circulation* 2001;**103**: 2176–80.

102 Billingsley AM, Laks H, Boyce SM, *et al*. Definitive repair in some patients with pulmonary atresia with intact ventricular septum. *J Thorac Cardiovasc Surg* 1989;**97**:746–54.

103 Bridges ND, Lock JE, Castaneda AR. Baffle fenestration with subsequent transcatheter closure: modification of the Fontan operation for patients with increased risk. *Circulation* 1990;**82**: 1681–9.

104 Laks H, Pearl JM, Haas GS, *et al*. Partial Fontan advantages of an adjustable interatrial communication. *Ann Thorac Surg* 1991;**52**: 1084–94;discussion 1094–5.

105 Rao PS, Levy JM, Chopra PS. Balloon angioplasty of stenosed Blalock–Taussig anastomosis: role of balloon-on-a-wire in dilating occluded shunts. *Am Heart J* 1990;**120**:1173–8.

106 Rao PS. Role of interventional cardiology in the treatment of neonates: Part III. *Congenital Cardiol Today* 2008;**6**:1–10.

107 Rao PS. Current status of balloon angioplasty for neonatal and infant aortic coarctation. *Prog Pediatr Cardiol* 2001;**14**:35–44.

108 Rao PS. Role of interventional cardiology in neonates: Part II, Balloon angioplasty/valvuloplasty. *Neonatol Today* 2007;**2**:1–12.

109 Rao PS. Stents in the management of congenital heart disease in pediatric and adult patients. *Indian Heart J* 2001;**53**:714–30.

110 Rao PS, Balfour IC, Singh GK, *et al*. Bridge stents in the management of obstructive vascular lesions in children. *Am J Cardiol* 2001;**88**:699–702.

111 Siblini G, Rao PS. Coil embolization in the management of cardiac problems in children. *J Invasive Cardiol* 1996;**8**:332–340.

112 Rao PS. Transcatheter embolization of unwanted blood vessels in children. In: Rao PS, Kern MJ, eds. *Catheter Based Devices for Treatment of Noncoronary Cardiovascular Disease in Adults and Children*. Philadelphia, PA: Lippincott, Williams & Wilkins, 2003: 457–73.

113 Rao PS. Protein-losing enteropathy following the Fontan operation (Editorial). *J Invasive Cardiol* 2007;**19**:447–8.

114 Rao PS. Static balloon dilatation of the atrial septum (Editorial). *Am Heart J* 1993;**125**:1824–7.

115 Rao PS, Chandar JS, Sideris EB. Role of inverted buttoned device in transcatheter occlusion of atrial septal defect or patent foramen ovale with right-to-left shunting associated with complex congenital cardiac anomalies. *Am J Cardiol* 1997;**80**: 914–21.

116 Goff DA, Blume ED, Gauvreau K, *et al*. Clinical outcome of fenestrated Fontan patients after closure: the first 10 years. *Circulation* 2000;**102**:2094–9.

117 Boudjemline Y, Bonnet D, Sidi D, *et al*. Closure of extracardiac Fontan fenestration by using the Amplatzer duct occluder. *Arch Mal Coeur Vaiss* 2005;**98**:449–54.

118 Rothman A, Evans WN, Mayman GA. Percutaneous fenestration closure with problematic residual native atrial septum. *Catheter Cardiovasc Interv* 2005;**66**:286–90.

119 Sugiyama H, Yoo SJ, Williams W, *et al*. Characterization and treatment of systemic venous to pulmonary venous collaterals seen after the Fontan operation. *Cardiol Young* 2003;**13**: 424–30.

120 Tsounias E, Rao PS. Versatility of Amplatzer vascular plug in occlusion of different types of vascular channels. *Cathet Cardiovasc Interv* 2008;71:S24.

121 Konertz W, Schneider M, Herwig V, *et al*. Modified hemi-Fontan operation and subsequent nonsurgical Fontan completion. *J Thorac Cardiovasc Surg* 1995;**110**:865–7.

122 Hausdorf G, Schneider M, Konertz W. Surgical preconditioning and completion of total cavopulmonary connection by interventional cardiac catheterisation: a new concept. *Heart* 1996;**75**:403–9.

123 Sidiropoulos A, Ritter J, Schneider M, *et al*. Fontan modification for subsequent non-surgical Fontan completion. *Eur J Cardiothorac Surg* 1998;**13**:509–12;discussion 512–3.

124 Galantowicz M, Cheatham JP. Fontan completion without surgery. *Semin Thorac Cardiovasc Surg Pediatr Card Surg Annu* 2004;**7**:48–55.

125 Freedom RM, Gow R, Caspi J, *et al*. The Fontan procedure for patients with tricuspid atresia: long-term follow-up. In: Rao PS, ed. *Tricuspid Atresia*, 2nd edn. Mount Kisco, NY: Futura Publishing, 1992: 377–86.

126 Gandhi SK, Bromberg BI, Schuessler RB, *et al*. Characterization and surgical ablation of atrial flutter after classic Fontan repair in acute canine model. *Ann Thorac Surg* 1996;**61**:1666–78.

127 Hill DJ, Feldt RH, Porter C, *et al*. Protein losing enteropathy after Fontan operation: a preliminary report (Abstract). *Circulation* 1989;**80**(Suppl II):490.

128 Rothman A, Synder J. Protein-losing enteropathy following Fontan operation: resolution with prednisone therapy. *Am Heart J* 1991;**121**:618–9.

129 Lopez JA. Transvenous right atrial and left ventricular pacing after the Fontan operation: long-term hemodynamic and electrophysiologic benefit of early atrioventricular resynchronization. *Tex Heart Inst J* 2007;**34**:96–101.

130 Estner HL, Kolb C, Schmitt C, *et al*. Long-term transvenous AV-sequential pacing in a failing atriopulmonary Fontan patient. *Int J Cardiol* 2008;**127**:e93–5.

131 Marcelletti CF, Hanley FL, Mavroudis C, *et al*. Revision of previous Fontan connections to total extracardiac cavopulmonary anastomosis: a multicenter experience. *J Thorac Cardiovasc Surg* 2000;**119**:340–6.

132 Sheikh AM, Tang AT, Roman K, *et al*. The failing Fontan circulation: successful conversion of atriopulmonary connections. *J Thorac Cardiovasc Surg* 2004;**128**:60–6.

133 Gamba A, Merlo M, Fiocchi R, *et al*. Heart transplantation in patients with previous Fontan operations. *J Thorac Cardiovasc Surg* 2004;**127**:555–62.

134 Jayakumar KA, Addonizio LJ, Kichuk-Chrisant MR, *et al*. Cardiac transplantation after the Fontan or Glenn procedure. *J Am Coll Cardiol* 2004;**44**:2065–72.

36 Ebstein Anomaly of the Tricuspid Valve

David J. Driscoll & Joseph A. Dearani

Mayo Clinic, Rochester, MN, USA

Introduction and historical background

On 28 June 1864, a 19-year-old laborer was admitted to All-Saints Hospital in Breslau, Germany, with shortness of breath and palpitations since childhood. The patient died on 6 July 1864 and Wilhelm Ebstein (1836–1912) performed the autopsy [1]. Although Ebstein is credited with this first description of the anomaly that would bear his name, he also is credited with describing postinfectious uric acid kidney stones, acute leukemia, funnel chest, and the "Pel–Ebstein" fever of lymphoma. He also studied purine metabolism, grouped obesity, gout, and diabetes as inheritable metabolic diseases, and authored a book on the treatment of obesity with a low carbohydrate diet [2].

Before the 1970s, the surgical treatment of Ebstein anomaly was poorly defined. Indeed, Engle *et al.* cautioned that even cardiac catheterization of these patients was risky because the catheter might become entangled and entrapped in the delicate tricuspid valve apparatus or provoke a fatal arrhythmia [3]. This, of course, was before the development of cardiac defibrillators. In 1974, Watson reported the outcome of 505 patients with Ebstein anomaly [4]. There were 13 deaths from 363 cardiac catheterizations. The surgical mortality was 54%. For palliative operations the mortality was 64% and for valve replacement it was 45%. He concluded that "patients … are bad surgical risks. Operation cannot be advised in the hope that if they (patients) are no better, at least they will be no worse … Palliative operations are not helpful … they have no place in treatment and are probably contraindicated."

Despite these admonitions, surgical procedures were gradually developed to treat patients with Ebstein anomaly. In the 1950s, the Blalock–Taussig procedure was used. In 1958, Hunter and Lillehei attempted to reposition the septal and posterior tricuspid valve leaflets [5]. In 1963, Barnard and Schire replaced the tricuspid valve with a prosthesis. [6] In 1966, the Glenn anastomosis was used for some of these patients [7]. Hardy and Roe, in 1969, attempted to reconstruct the valve [8,9]. In 1972, Danielson *et al.* described a technique to reconstruct the valve as a monocusp [10], an operation adopted widely for many years. In 1988, Carpentier *et al.* reported an operation in which the tricuspid valve was repositioned to the normal level [11]. In 1991, Starnes *et al.* described a technique for dealing with the highly lethal form of Ebstein anomaly presenting in the neonate [12] using a single ventricle strategy. In 2007, da Silva *et al.* described the "cone procedure," a near anatomic repair, the early results of which are fairly promising [13].

Incidence

Ebstein anomaly is relatively rare. It constitutes <1% of cardiac malformations and occurs in one in 210 000 live births. It is noted in one in 1000 autopsies.

Embryology and pathologic anatomy

The embryologic basis of Ebstein anomaly is failure of the tricuspid valve leaflets, especially the septal leaflet, to delaminate from the ventricular muscle (Figure 36.1).

The anterior leaflet, albeit the most completely delaminated, is usually fairly large but also may have tethered attachments to the right ventricular free wall. Thus, the apparent orifice of the tricuspid valve is displaced into the right ventricle. The true orifice, however, is not displaced and the portion of the heart between the true and apparent orifice is the so-called "atrialized portion" of the right ventricle (Figure 36.2).
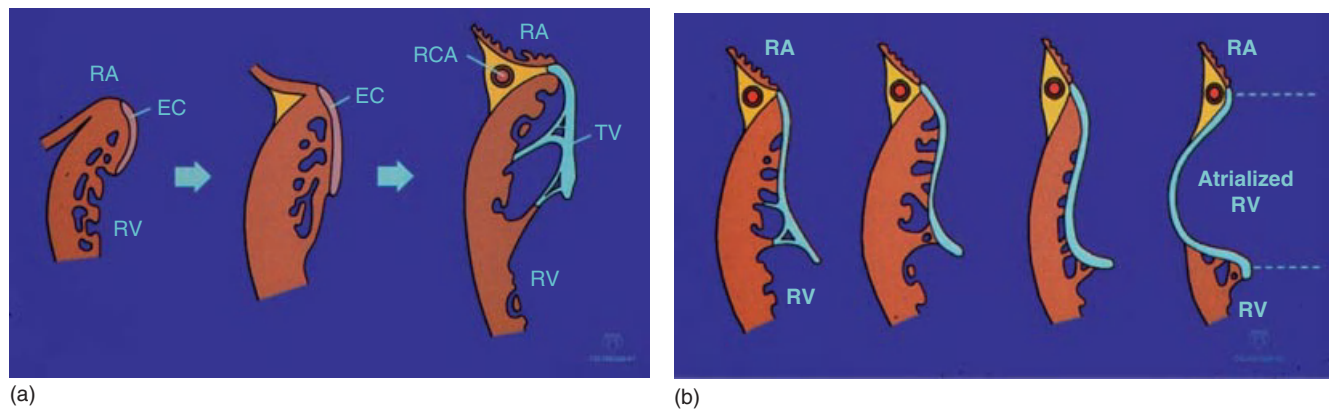
Figure 36.1 Artistic representation of (a) normal delamination of the tricuspid valve and (b) failure of delamination resulting in Ebstein anomaly. EC, endocardial cushion; RA, right atrium; RCA, right coronary artery; RV, right ventricle. TV, tricuspid valve.
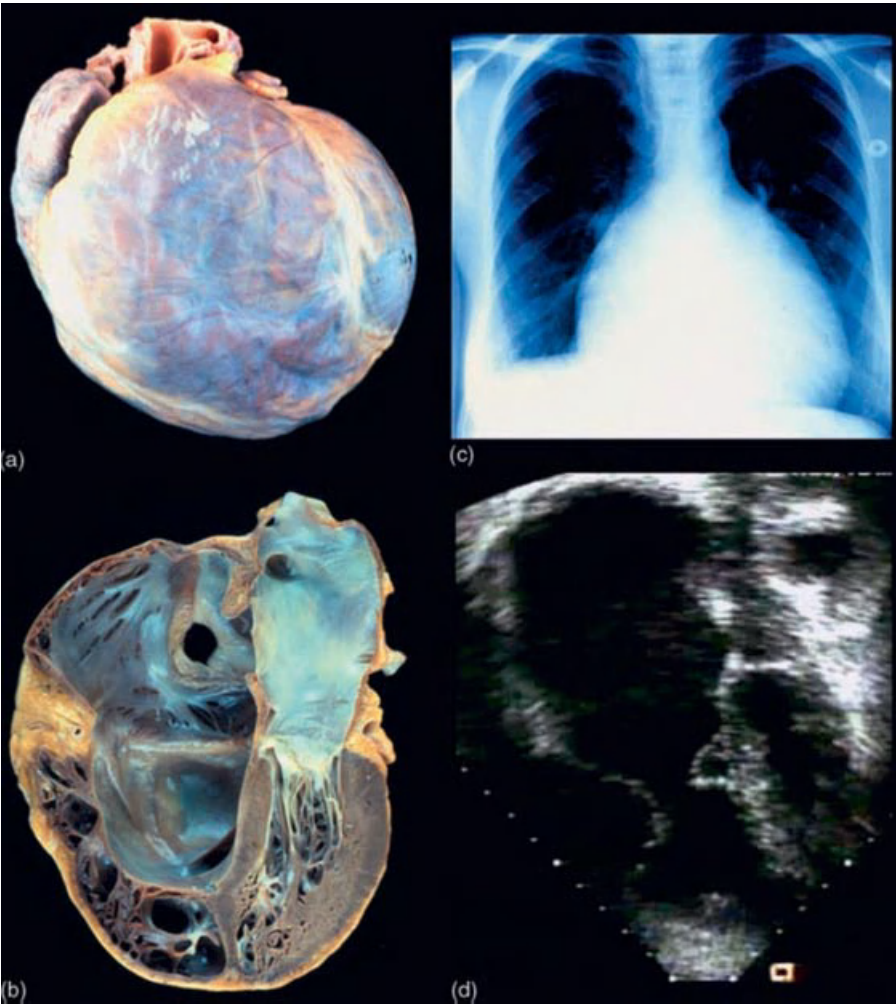
Figure 36.2 Composite of the typical features of Ebstein anomaly. (a) autopsy specimen demonstrating marked cardiomegaly and globular shaped heart. (b) a pathologic specimen prepared to demonstrate the downward displacement of the tricuspid valve, tethering of the anterior leaflet to the right ventricular wall and shift of the ventricular septum toward the left ventricle. (c) a typical radiograph of Ebstein anomaly. (d) Echocardiogram showing downward displacement of tricuspid valve and enlarged right atrium.

The abnormalities in Ebstein anomaly are not limited to the tricuspid valve. The right ventricle is always, to a greater or lesser extent, myopathic. In some patients, the left ventricle also may show fibrosis.

About 50–70% of patients have an atrial septal defect (ASD) or stretched patent foramen ovale (PFO), and 30% have an associated a right-sided accessory bypass tract or Wolff–Parkinson–White (WPW) syndrome.

Ebstein anomaly can be associated with pulmonary stenosis or pulmonary atresia. It may be difficult to determine if a patient with pulmonary atresia and intact ventricular septum (in which the tricuspid valve is usually dysplastic and always regurgitant) should be classified as "pulmonary atresia with intact ventricular septum" or as "Ebstein anomaly and pulmonary atresia." This distinction becomes important for planning surgical strategy and for measuring treatment outcomes. It may be reasonable to classify these patients as "pulmonary atresia with intact ventricular septum" if the right ventricle is smaller than normal and as Ebstein anomaly with pulmonary atresia if the right ventricle is larger than normal.

Pathophysiology

The pathophysiology depends on the degree of dysplasia of the tricuspid valve and of tricuspid valve regurgitation or rarely tricuspid valve stenosis. In addition, determinants of clinical severity include the severity of right ventricular myopathy and presence or absence of the following: an interatrial communication, degree of right ventricular outflow tract obstruction, degree of right or left ventricular dysfunction, or ventricular pre-excitation.

Patients with an intact atrial septum do not have a right-to-left shunt and their exercise tolerance is better than those with an ASD and a right-to-left shunt. Because of tricuspid regurgitation, pulmonary blood flow and hence cardiac output may be reduced, particularly during exercise. Also, with the downward displacement of the tricuspid valve and the atrialized portion of the right ventricle, anterograde blood flow may be impeded by the contraction of the atrialized portion of the right ventricle with an unguarded true tricuspid valve annulus.

Natural history

Without treatment, survival of patients with Ebstein anomaly is significantly less than normal [14] (Figure 36.3). Poorer survival occurs with major associated anomalies, and greater degrees of cyanosis, cardiomegaly, and echocardiographic severity [15–20].

Clinical features

History
The presentation and clinical course of patients with Ebstein anomaly vary, depending upon the severity of the malformation. At one end of the spectrum fetal death can occur, one of the more common reasons for demise among
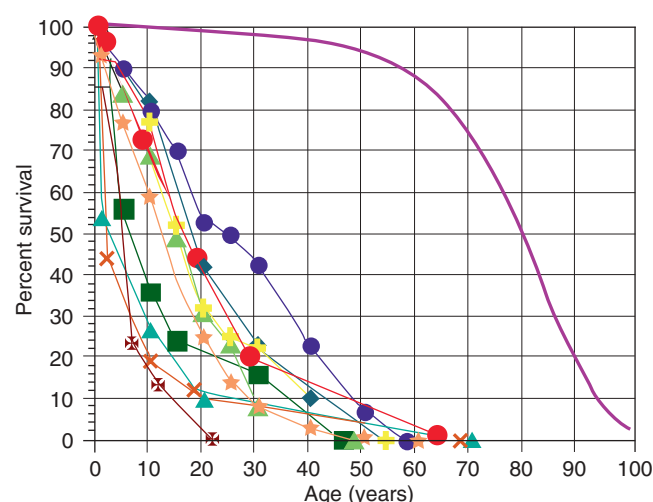
Figure 36.3 Composite survival curves of unoperated patients. (Courtesy of Dr. Julien Hoffman and reproduced from Hoffman, J., *The Natural and Unnatural History of Congenital Heart Disease*, Wiley-Blackwell, 2009, reproduced with permission of the publisher and the author.)

fetuses with a cardiac anomaly. At the other end of the spectrum, patients with mild forms of Ebstein anomaly can live a normal life span without medical or surgical intervention.

The classic presentation at birth is cyanosis and/or marked cardiomegaly. The cyanosis in neonates occurs from right-to-left shunting through a PFO or ASD, and is intensified by the high early postnatal pulmonary vascular resistance. Shunting can be so great and forward flow from the right ventricle so limited that the neonate, mistakenly, may be thought to have anatomic pulmonary valve atresia. In fact, there may be "functional" pulmonary atresia because of poor forward flow. Some have massive cardiomegaly with a cardiothoracic ratio that exceeds 85% on chest radiography. These infants have functionally small lungs and pulmonary vascular bed, and without reduction of heart size are unlikely to survive.

Beyond the newborn period, patients may present because of a murmur, fatigue, dyspnea, cyanosis, atrial arrhythmias, or cardiomegaly discovered serendipitously. Increasingly, the diagnosis of Ebstein anomaly is made prenatally using fetal ultrasound.

Physical examination
For patients with an ASD, cyanosis usually is apparent. Despite significant tricuspid regurgitation, because of the capacitance of the dilated right atrium the jugular venous pressure is usually normal. The cardiac impulse may be diffuse due to cardiomegaly and a volume overloaded right ventricle. Classically, patients with Ebstein anomaly have been described as having a "quadruple rhythm." This results from splitting of S_1 because of delay in the second component of S1, presumably because of the abnormal tricuspid valve apparatus. Splitting of S_2 is a result of right bundle branch
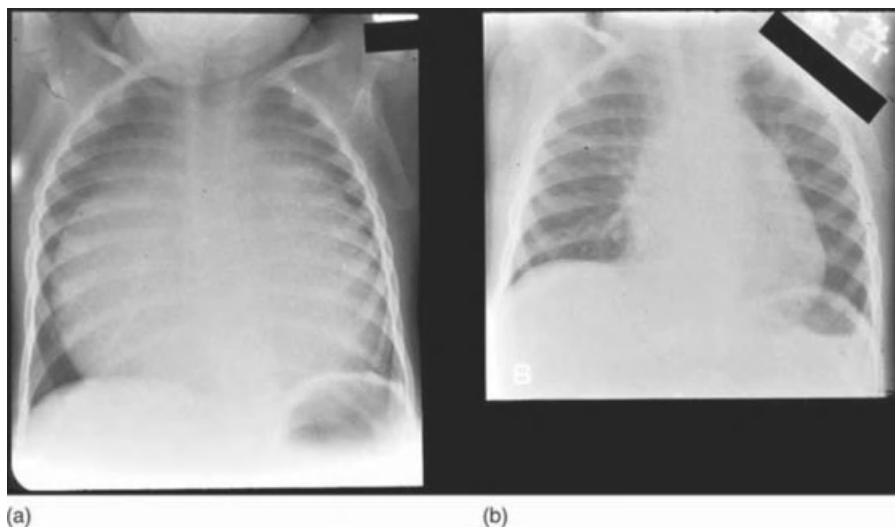
Figure 36.4 (a) Preoperative and (b) postoperative radiographs of a patient with Ebstein anomaly.

block. Usually there is a systolic murmur of tricuspid regurgitation. Rarely, if the valve is stenotic, a tricuspid diastolic murmur is present. In addition, there may be ventricular diastolic filling sounds. In our experience, these "classical" auscultatory findings are apparent in only ~50% of patients, possibly because the "classical" findings were described when only the most severe forms of Ebstein anomaly came to medical attention; now, with echocardiography, milder forms come to medical attention.

Patients with Ebstein anomaly may have a distinctive violaceous hue, particularly of the malar area and the upper arms, even without a right to left shunt and even after operation. The reason is unclear.

Electrocardiography

The classic finding in Ebstein anomaly is right atrial enlargement and right bundle branch block. Because 30% of patients with Ebstein anomaly have ventricular pre-excitation, these patients may have a short PR interval and a delta wave.

Chest radiography

Usually the chest radiogram shows cardiomegaly from enlargement of the right atrium and ventricle to an extent proportional to the severity of the lesion and the degree of tricuspid regurgitation (Figure 36.4). The pulmonary vasculature is diminished.

Echocardiography

Echocardiography (two-dimensional and, more recently, three-dimensional) is a mainstay in diagnosis [21,22] (Figure 36.5). The anatomy of the tricuspid valve can be delineated and associated anomalies, such as an ASD and right ventricular outflow tract obstruction, can be identified. Right atrial and right ventricular size and function can be estimated,

as can left ventricular function. The accuracy of measurement of both right and left ventricular function, however, is suboptimal because of the large size of the true and atrialized right ventricle, and the displacement of the ventricular septum towards the left ventricle (i.e., D-shaped left ventricle) by the enlarged right ventricle.

Two mathematical equations have been described to quantitate the severity of Ebstein anomaly. The first is the "displacement index," obtained by dividing the distance between the attachment of the septal leaflet of the tricuspid valve and the septal attachment of the mitral valve by the body surface area. A ratio of $\geq 0.8\,cm\,m^{-2}$ is considered diagnostic of Ebstein anomaly.

The second is the "Celermajer index," calculated by dividing the combined areas of the right atrium and atrialized portion of the right ventricle by the combined areas of the functional RV, LV, and LA [19,20]. It has been used as a marker of outcome in neonatal Ebstein anomaly. A value >1 portends a high mortality.

Echocardiography can provide detailed information about the anatomy of the tricuspid valve. In general, the four-chamber view is the most helpful because it demonstrates the degree of tethering between the tricuspid leaflets and the free wall of the right ventricle and the location of these attachments relative to the true tricuspid annulus and the right ventricular apex. It also provides information about the degree of displacement of the septal leaflet and the amount of septal leaflet present. Other valve features that echocardiography provides include the size of the anterior leaflet and the status of its leading edge (free versus tethered), and any direct muscular insertions into the leading edge of the anterior leaflet. Finally, echocardiography can define the nature of the regurgitant jet(s), that is, a single central jet of regurgitation as opposed to multiple origins of regurgitation or fenestrations of the leaflets [21,22]. When the functional

Figure 36.5 Normal four-chamber view of (a) a normal heart and (b) Ebstein anomaly. The downward displacement of the septal leaflet of the tricuspid valve (STL) is apparent, as is the "sail like" anterior leaflet. AML, anterior mitral leaflet, LV, left ventricle; RA, right atrium; RV, right ventricle. Arrows indicate separation of septal leaflets of mitral and tricuspid valves.
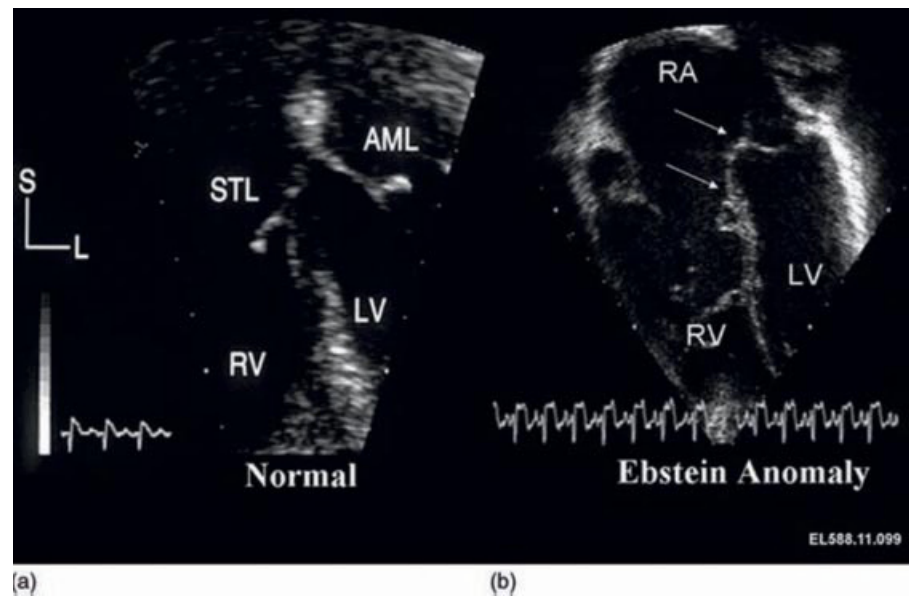
tricuspid orifice is markedly displaced towards the right ventricular outflow tract (i.e., tricuspid and pulmonary leaflet tissue noted in the short-axis view at the base of the heart), tricuspid valve repair can be difficult.

Magnetic resonance imaging

The utility of MRI in the management of Ebstein anomaly is undefined but, intuitively, may have an important role and is being used with increasing frequency. A major difficulty in determining the indications for operation and the short- and long-term results of treatment is the accuracy of measuring right ventricular size and function in this anomaly. Echocardiography has shortcomings in obtaining these measurements. An MRI might obviate these. Even with MRI, the "gold standard" for these measurements is unclear.

Cardiac catheterization

Cardiac catheterization is rarely necessary in a patient with Ebstein anomaly. Indications for cardiac catheterization include hemodynamic assessment in selected circumstances if a concomitant bidirectional cavopulmonary shunt is being considered, particularly if left ventricular function is depressed. It also may be necessary to exclude distortion of the pulmonary artery or pulmonary hypertension in patients in whom a systemic to pulmonary shunt had been placed previously. If anatomic pulmonary valve stenosis coexists, a balloon valvoplasty may be necessary.

Exercise testing

Patients with Ebstein anomaly have reduced exercise tolerance [23,24], the major determinant of which is right-to-left shunting in patients with an interatrial communication.

Other factors that may contribute to exercise intolerance are tricuspid valve regurgitation, reduced right or left ventricular function, and right ventricular outflow tract obstruction. After eliminating the right-to-left shunt, exercise tolerance improves significantly.

Intuitively, establishing a competent tricuspid valve should improve exercise tolerance. There are anecdotal examples to suggest that this is true, but no studies have sufficient statistical power to prove it.

Pregnancy and reproductive issues

We reported the outcome of pregnancy for 82 women who had an operation for Ebstein anomaly [25]. Before operation, 59 of these women had a total of 140 pregnancies, and after operation, 27 women had 62 pregnancies. There were no maternal deaths. The miscarriage rate before operation was 19% and after operation 33%. There were 232 liveborn children, 88 to fathers and 144 to mothers with Ebstein anomaly. Nine of the liveborn children (4%) were reported to have a cardiac abnormality including tricuspid atresia, atrial fibrillation, patent ductus arteriosus, "hole in heart" (that was surgically closed), Down syndrome with complete atrioventricular septal defect, an unspecified "valve problem," mitral valve prolapse, Ebstein anomaly, and ASD. Six were born to mothers and three to fathers with Ebstein anomaly.

Arrhythmias

Atrial arrhythmias are common in patients with Ebstein anomaly [26,27]. These can be associated with either ventricular pre-excitation (WPW syndrome) or dilated right atrium. Accessory conduction pathways should be identified and ablated during a preoperative electrophysiologic study.

Atrial arrhythmias secondary to dilated atria become less frequent after tricuspid valve repair/replacement and right reduction atrioplasty. The frequency of atrial arrhythmias, however, tends to increase again as time passes postoperatively. When paroxysmal or continuous atrial tachyarrhythmias occur preoperatively, a concomitant maze procedure should be performed at the time of operation. In selected patients, a prophylactic maze procedure can be considered at the time of operation.

Management, clinical course, and outcome

Treatment, clinical course, and outcome depend upon the severity of the deformity, age at presentation, and any associated anomalies.

Neonates with severe hypoxemia and extreme cardiomegaly are particularly challenging. Because of severe tricuspid valve regurgitation and elevated pulmonary vascular resistance, some neonates have "functional pulmonary atresia" without anatomic pulmonary atresia. They eventually respond to PGE_1. If there is anatomic pulmonary atresia or stenosis, a systemic to pulmonary shunt or a balloon pulmonary valvoplasty will be needed. Most require intubation and mechanical ventilation.

If pulmonary balloon valvoplasty is necessary and produces pulmonary valve regurgitation, the patient may demonstrate a "circular shunt." This consists of blood flowing from the aorta through the ductus arteriosus and then retrograde through the pulmonary valve to the right ventricle, retrograde through the tricuspid valve, then from the right to the left atrium, then through the left ventricle to the aorta, and finally back through the ductus. This volume of blood never participates in effective pulmonary blood flow or systemic perfusion. In these patients, some investigators have recommended discontinuing PGE_1, instituting nitric oxide inhalation, and passively allowing the ductus to close or actively closing it with indomethacin, a coil, a device, or operation [28].

Neonates who do not improve with these maneuvers may require an early operation. One option is the Knott–Craig repair of the tricuspid valve, which leads to a two-ventricle repair. This technique also includes a right reduction atrioplasty and, if possible, reduction (plication) of the size of the right ventricle [29] to allow space for the lungs. The second option is the Starnes procedure, leading to a one-ventricle repair. This technique involves placing a fenestrated patch over the tricuspid valve to exclude the right ventricle from the circulation, assuring that there is a large atrial septal defect, and performing a right reduction atrioplasty and a systemic to pulmonary artery shunt [12]. If the patient has an incompetent pulmonary valve, the pulmonary artery should be ligated. Sano et al. described a modified Starnes procedure in which the free wall of the right ventricle is resected and closed with a patch to reduce its size [30]. At a later date, these patients are considered for a modified Fontan procedure. The third option is neonatal cardiac transplantation. Transplantation rarely is required in the current era, but should be considered when there is significant left ventricular dysfunction.

Neonates without associated anomalies or extreme cardiomegaly who can be weaned from PGE_1 and/or nitric oxide and remain well can be considered for later operative repair when early mortality is substantially lower. Appropriate indications for operation must be defined because not all patients need an operation. The principle concept of operation is to provide the patient with a competent, nonstenotic tricuspid valve, eliminate right-to-left shunts, and reduce the size of the right atrium and, at times, the right ventricle. Some patients may require ablation or division of an accessory pathway, and others may require a maze procedure for atrial arrhythmias. The goal of reducing the volume overload of the right ventricle is to optimize right ventricular function and improve its longevity. Although establishing tricuspid competence by repair or replacement reduces right ventricular size after operation, there are no data to indicate that it improves right ventricular function. Indeed, because the RV is myopathic, this might not occur. In general, it is more desirable to repair than to replace the tricuspid valve, provided that a competent valve can be created.

There are several indications for operation:

1 Marked cardiomegaly or a progressively enlarging heart, because a C/T ratio >0.65–70 is associated with increased risk of sudden death and of operative death.

2 A right-to-left shunt because of the associated morbidity.

3 Declining left ventricular function because the operative mortality is higher with depressed left ventricular function. We have shown that left ventricular function usually improves after operation [31].

4 Other indications include right-sided heart failure, New York Heart Association (NYHA) class 3 or 4, progressive exercise intolerance, uncontrolled arrhythmias, and significant associated lesions such as ASD, VSD, or right ventricular outflow obstruction.

The technique for repairing the tricuspid valve has evolved over the past five decades. Many techniques have been described to repair Ebstein anomaly. Indeed, surgeons very experienced with repair of the tricuspid valve employ concepts from more than one type of repair technique to address the wide anatomic variability of the malformed valve.

Perhaps the technique used most frequently over the past 30 years has been monocusp reconstructions of either the "Danielson" type [10] or the "Carpentier" technique as described above [11]. Because of the great variability in the anatomy of the tricuspid valve with Ebstein anomaly, some valves are unrepairable and replacement is necessary. Early experience with the "cone" procedure, a near anatomic repair, suggests that this may be a superior technique with very few valves not amenable to repair [13]. Limited long-term outcome results are available for this relatively new operation. Relative contraindications to the cone repair

are age >50 years, moderate or severe pulmonary hypertension, left ventricular ejection fraction <30%, complete failure of delamination of the septal and inferior leaflets, and <50% delamination of the anterior leaflet, severe right ventricular enlargement, and severe dilatation of the true right ventricular annulus.

If the tricuspid valve cannot be repaired adequately, valve replacement is necessary. We prefer a porcine bioprosthetic valve that has proven fairly durable and avoids the need for long-term anticoagulation. A mechanical valve can be considered after failure of two bioprosthetic valves, and for patients who already are treated with warfarin because of a mechanical valve in another position. Mechanical valves should be avoided when right ventricular function is poor (as often happens with Ebstein anomaly), because the discs may not open and close properly and are thus more susceptible to thrombosis even with adequate warfarin anticoagulation.

Currently, the potential role for the so-called "bidirectional Glenn" operation as an adjunct to valve repair/replacement in Ebstein anomaly is being explored [32,33]. Indications include severe right ventricular enlargement and/or dysfunction (RV ejection fraction <25%), displacement of the left ventricular septum (D-shaped left ventricle), preoperative arterial desaturation at rest or with exercise, a post-repair RA:LA pressure ratio of >1.5:1, and a small effective tricuspid orifice after tricuspid repair. A bidirectional Glenn procedure has the potential benefit to unload volume from the dysfunctional right ventricle and to improve preload of the left ventricle. The potential disadvantage of the bidirectional Glenn operation is that it limits venous access to the heart, complicating future pacemaker lead placements or electrophysiological studies. No recent studies have demonstrated the utility of the bidirectional Glenn operation is this setting. Leaving an atrial septal fenestration routinely or when there is right ventricular dysfunction has been described [13]. Our policy is to close an interatrial communication in each patient undergoing operation for Ebstein anomaly when operation is being performed beyond the neonatal period.

We reported the long-term outcome for 539 patients with Ebstein anomaly who had operation at the Mayo Clinic from 1 April 1972 to 1 January 2006 [34]. The mean age of the initial operation at our institution was 24 years (range 8 days to 79 years). A total of 143 patients (26.5%) had a prior cardiac procedure before coming to the Mayo Clinic. At the first operation, 182 patients had tricuspid valve repair and 337 had tricuspid valve replacement. The 30-day mortality was 5.9% for the entire cohort (2.7% after 2001). Late survival was 71.2% at 20 years and the 20-year survival and freedom from reoperation was 46% (Figure 36.6).

Risk factors for mortality or reoperation can be divided into those present before the operation and those found at the time of the operation. Most are indications of increased
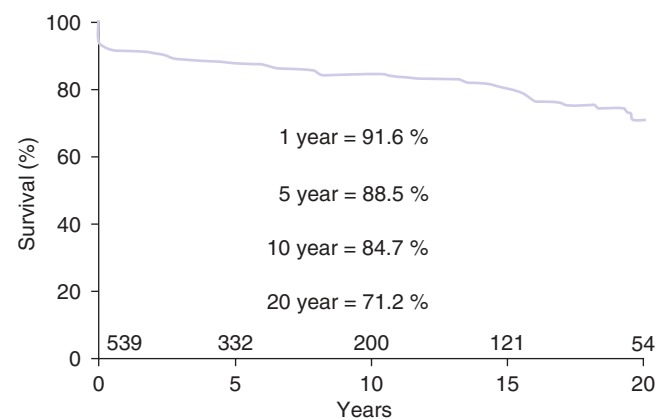
Figure 36.6 Kaplan Meier curve of over-all survival of 538 patients who had operation for Ebstein anomaly at the Mayo Clinic.

severity and many also predict longer operative procedures. Therefore, before operation the risk factors are a prior cardiac operation (especially a Glenn shunt), high hematocrit, larger C/T ratio on chest X-ray, right ventricular outflow tract obstruction, absence of sinus rhythm, moderate to severe right or left ventricular dysfunction systolic dysfunction, and mitral valve regurgitation judged marked enough to require operative repair. At the time of the operation, other important risk factors are the need for tricuspid valve replacement or a surgical procedure for arrythmia, and also the need for postoperative mechanical support or to reopen the chest in the ICU. Added risk factors are the absence of accessory pathways or sinus rhythm after surgery. The only unexpected risk factor was male gender.

We obtained follow-up medical survey information from 285 patients of 448 (64%) not known to be deceased at the time of the study [25]. At late follow-up (mean 6.9 years), 237 (83%) patients were in NYHA class I or II, 12% in class III, 4% in class IV, and 34% were taking no cardiac medication. A total of 103 patients (36%) reported an incident of atrial fibrillation or flutter, five patients (2%) reported having had endocarditis, and one patient (<1%) reported a stroke.

We assessed the effect of reduced left ventricular function on surgical outcome [31]. Of the 495 patients with preoperative echocardiographic assessment of LV function, 50 had moderate or greater LV systolic dysfunction. The tricuspid valve (TV) was repaired in 12 of these patients and replaced in 36 patients. One patient had a 1.5 ventricle repair and one patient had cardiac transplantation. There were five early deaths (10%). LV function after operation improved in all but four patients. and worsened in none. The 1-, 5-, and 10-year survivals were 86, 77, and 67%, respectively (Figure 36.7). Using univariate analysis, absence of sinus rhythm at dismissal ($p = 0.003$) was associated with greater overall mortality. For the entire cohort of 539 patients, LV
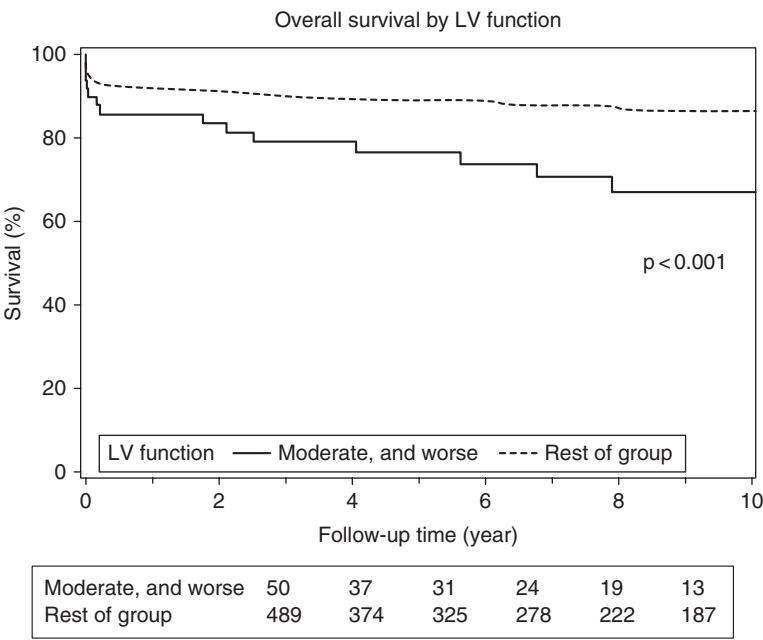
Figure 36.7 Comparison of survival for patients with significant reduction of left ventricular function with those with normal or mild reduction of left ventricular function.

Moderate, and worse	50	37	31	24	19	13
Rest of group		489	374	325	278	222	187

dysfunction, assessed echocardiographically, was independently predictive of late mortality (odds ratio 3.76, $p < 0.001$).

Tricuspid stenosis or insufficiency not associated with ebstein anomaly

Although relatively rare, Ebstein anomaly accounts for most congenital tricuspid valve dysfunction in children.

Pulmonary atresia with intact ventricular septum always is associated with tricuspid regurgitation and dysplasia of the tricuspid valve (see Chapter 40). The valve may have features reminiscent of Ebstein anomaly and, indeed, if the right ventricle is of near normal or normal size, distinguishing it from Ebstein anomaly with pulmonary atresia may be challenging. As noted above, this distinction becomes important for planning surgical strategy and for measuring treatment outcomes.

Transient tricuspid insufficiency of the newborn is associated with variable degrees of the neonatal stress such as perinatal asphyxia. It has been attributed to ischemic papillary muscle dysfunction, myocardial hypoxia associated with increased pulmonary vascular resistance, perinatal asphyxia, hypoxemia, and hypercarbia, and premature *in utero* constriction of the ductus [35–38]. These patients usually have respiratory distress and a holosystolic murmur of tricuspid regurgitation that frequently is confused with the murmur of a ventricular septal defect. Frequently, these infants are cyanotic because of right-to-left shunting across a PFO. In most instances, the tricuspid regurgitation resolves with time. Supportive therapy, mechanical ventilation and

using pulmonary vasodilators and inotropic support may be necessary in severely ill infants, and death can occur.

Congenital tricuspid valve dysplasia is a relatively rare cause of tricuspid stenosis and/or regurgitation. It can be confused with Ebstein anomaly. With proper attention to the echocardiographic features, however, this confusion should not occur. Ammash *et al.* reported 22 patients who were misdiagnosed as Ebstein anomaly [39]. The correct diagnoses were tricuspid dysplasia ($n = 9$), tricuspid prolapse ($n = 4$), traumatic tricuspid valve rupture ($n = 4$), tricuspid valve endocarditis ($n=1$), tricuspid annular dilation secondary to pulmonary regurgitation ($n = 1$), and right ventricular dysplasia ($n=3$). The management of tricuspid dysplasia depends upon the severity of the stenosis or regurgitation. Symptoms include fatigue, hepatic congestion, fluid retention, and atrial arrhythmias. Patients with tricuspid stenosis can develop protein-losing enteropathy. The indications for operations are the same as those for Ebstein anomaly.

References

1 Ebstein W. Ueber einen sehr seltenen Fall von Insufficienz der Valvula tricuspidalis, bedingt durch eine angeborene hochgradige Missbildung derselben. *Arch Anat Physiol* 1866;238–54.

2 Mann RJ, Lie JT. the life story of Wilhelm Ebstein (1836–1912) and his almost overlooked description of a congenital heart disease. *Mayo Clin Proc* 1979;**54**:197–204.

3 Engle M, Payne T, Bruins C, Taussig H. Ebstein's anomaly of the tricuspid valve: report of three cases and analysis of clinical syndrome. *Circulation* 1950;**1**:1246–60.

4 Watson H. Natural history of Ebstein's anomaly of the tricuspid valve in childhood and adolescence: an international cooperative study of 505 cases. *Br Heart J* 1974;**36**:417–27.

5 Hunter SW, Lillehei CW. Ebstein's malformation of the tricuspid valve: study of a case together with suggestion of a new form of surgical therapy. *Dis Chest* 1958;**33**:297–304.

6 Barnard C, Schire V. Surgical correction of Ebstein's malformation with prosthetic tricuspid valve. *Surgery* 1963;**54**:302–8.

7 Glenn W, Browne M, Whittemore R. Circulatory bypass of the right side of the heart: cava-pulmonary artery shunt – indications and results (a report of a collected series of 537 cases). In: Cassels DE, ed. *The Heart and Circulation in the Newborn and Infant*. New York: Grune & Stratton, 1966: 345–57.

8 Hardy KL, Roe BB. Ebstein's anomaly: further experience with definitive repair. *J Thorac Cardiovasc Surg* 1969;**58**:553–60.

9 Hardy KL, May IA, Webster CA, *et al*. Ebstein's anomaly: a functional concept and successful definitive repair. *J Thorac Cardiovasc Surg* 1964;**48**:927–40.

10 Danielson GK, Maloney JD, Devloo RE. Ebstein anomaly: surgical repair of Ebstein's anomaly. *Mayo Clin Proc* 1979;**54**:185–92.

11 Carpentier A, Chauvaud S, Macé L, *et al*. A new reconstructive operation for Ebstein's anomaly of the tricuspid valve. *J Thorac Cardiovasc Surg* 1998;**96**:92–101.

12 Starnes VA, Pitlick PT, Bernstein D, *et al*. Ebstein's anomaly appearing in the neonate: a new surgical approach. *J Thorac Cardiovasc Surg* 1991;**101**:1082–7.

13 da Silva JP, Baumgratz FJ, Fonseca L, *et al*. The cone reconstruction of the tricuspid valve in Ebstein's anomaly. The operation: early and midterm results. *J Thorac Cardiovasc Surg* 2007;**133**: 215–23.

14 Hoffman, JIE. *The Natural and Unnatural History of Congenital Heart Disease*. Oxford: Wiley-Blackwell, 2009.

15 Kumar AE, Fyler DC, Miettinen OS, Nadas AS. Ebstein's anomaly. Clinical profile and natural history. *Am J Cardiol* 1971;**28**:84–95.

16 Jaiswal PK, Balakrishnan KG, Saha A, *et al*. Clinical profile and natural history of Ebstein's anomaly of tricuspid valve. *Int J Cardiol* 1994;**46**:113–9.

17 Gentles TL, Calder AL, Clarkson PM, Neutze JM. Predictors of long-term survival with Ebstein's anomaly of the tricuspid valve. *Am J Cardiol* 1992;**69**:377–81.

18 Attie F, Rosas M, Rijlaarsdam M, *et al*. The adult patient with Ebstein anomaly. Outcome in 72 unoperated patients. *Medicine (Baltimore)* 2000;**79**:27–36.

19 Celermajer DS, Cullen S, Sullivan ID, *et al*. Outcome in neonates with Ebstein's anomaly. *J Am Coll Cardiol* 1992;**19**:1041–6.

20 Celermajer DS, Bull C, Till JA, *et al*. Ebstein's anomaly: presentation and outcome from fetus to adult. *J Am Coll Cardiol* 1994;**23**:170–6.

21 Oh J, Seward J, Tajik AJ. *The Echo Manual*, 3rd edn. Philadelphia: Wolters Kluwer–Lippincott, Williams & Wilkins, 2006.

22 Seward JB. Ebstein's anomaly: ultrasound imaging and hemodynamic evaluation. *Echocardiography* 1993;**10**:641–64.

23 Driscoll DJ, Mottram C, Danielson G. Spectrum of exercise intolerance in 45 patients with Ebstein's anomaly and observations on exercise tolerance in patients after surgical repair. *J Am Coll Cardiol*, 1988;**11**:831–6.

24 MacLellan-Tobert SG, Driscoll DJ, Mottram CD, *et al*. Exercise tolerance in patients with Ebstein's anomaly. *J Am Coll Cardiol* 1997;**29**:1615–22.

25 Brown ML, Dearani JA, Danielson GK, *et al*. Functional status after operation for Ebstein anomaly: the Mayo Clinic experience. *J Am Coll Cardiol* 2008;**52**:460–6.

26 Khositseth A, Danielson GK, Dearani JA, *et al*. Supraventricular tachyarrhythmias in Ebstein anomaly: management and outcome. *J Thorac Cardiovasc Surg* 2004;**128**:826–33.

27 Greason KL, Dearani JA, Theodoro DA, *et al*. Surgical management of atrial tachyarrhythmias associated with congenital cardiac anomalies: Mayo Clinic experience. *Semin Thorac Cardiovasc Surg Pediatr Card Surg Annu* 2003;**6**:59–71.

28 Wald R, Adatia I, van Arsdell G, Hornberger L. Relation of limiting ductal patency to survival in neonatal Ebstein's anomaly. *Am J Cardiol* 2005;**96**:851–6.

29 Knott-Craig CJ, Overholt ED, Ward KE, *et al*. Repair of Ebstein's anomaly in the symptomatic neonate: an evolution of technique with 7-year follow-up. *Ann Thorac Surg* 2002;**73**:1786–93.

30 Sano S, Ishino K, Kawada M, *et al*. Total right ventricular exclusion procedure: an operation for isolated congestive right ventricular failure. *J Thorac Cardiovasc Surg* 2002;**123**:640–7.

31 Brown ML, Dearani JA, Danielson GK, *et al*. Effect of operation for Ebstein anomaly on left ventricular function. *Am J Cardiol* 2008;**102**:1724–7.

32 Quinonez LG, Dearani JA, Puga FJ, *et al*. Results of the 1.5-ventricle repair for Ebstein anomaly and the failing right ventricle. *J Thorac Cardiovasc Surg* 2007;**133**:1303–10.

33 Malhotra S, Petrossian EV, Reddy M, *et al*. Selective right ventricular unloading and novel technical concepts in Ebstein's anomaly. *Ann Thorac Surg* 2009;**88**:1975–81.

34 Brown ML, Dearani JA, Danielson GK, *et al*. The outcomes of operations for 539 patients with Ebstein anomaly. *J Thorac Cardiovasc Surg* 2008;**135**:1120–36.

35 Bucciarelli RL, Nelson RM, Egan EA, *et al*. Transient tricuspid insufficiency of the newborn: a form of myocardial dysfunction in stressed newborns. *Pediatrics* 1977;**59**:330–7.

36 Nelson RM. Bucciarelli RL, Eitzman DV, *et al*. Serum creatine phosphokinase MB fraction in newborns with transient tricuspid insufficiency. *N Engl J Med* 1978;**298**:146–9.

37 Donnelly WH, Bucciarelli RL, Nelson RM. Ischemic papillary muscle necrosis in stressed newborn infants. *J Pediatr* 1980;**96**:295–300.

38 Setzer E, Ermocilla R, Tonkin I, *et al*. Papillary muscle necrosis in a neonatal autopsy population: Incidence and associated clinical manifestations. *J Pediatr* 1980;**96**:289–94.

39 Ammash N, Warnes C, Connolly H, *et al*. Mimics of Ebstein anomaly. *Am Heart J* 1997;**134**:508–13.

37 Anomalies of the Coronary Sinus

Shannon M. Mackey-Bojack[1] & James H. Moller[2]
[1]Jesse E. Edwards Registry of Cardiovascular Disease, United Hospital, St Paul, MN, USA
[2]University of Minnesota, Minneapolis, MN, USA

Introduction

Compared with the coronary arteries, far less attention is paid to the cardiac veins and coronary sinus. With advancements in interventional and surgical treatment for heart disease, interest in the anatomy of the coronary sinus and coronary sinus anomalies has increased. Failure to understand and identify coronary sinus anomalies may be associated with serious consequences during surgery or interventional procedures.

Embryology

In early development, paired symmetrical veins join to form the sinus venosus and drain into the common atrium. The three sets of veins include the vitelline, umbilical, and common cardinal veins, which drain into the atrium through right- and left-sided channels [1]. Simultaneously, as development continues, the atrial septum begins to form and the venous connections become incorporated into the right atrium. A remodeling process occurs, resulting in anastomoses between the right and left systemic veins with preferential flow of blood to the right side. The right-sided venous return enlarges, continues remodeling, and becomes incorporated into the right atrium [2]. With the formation of the anastomotic channels, the left-sided venous return decreases in size. During this process, the left sinus wall becomes incorporated into the left atrioventricular groove, forming the coronary sinus. This process has been described as a fold of the left sinus venosus, which migrates to connect with the right atrium, whereby the fold itself creates the floor between the left atrium and the coronary sinus [3]; however, it appears that this is not completely accurate and the left sinus venosus actually retains its own wall and is incorporated into the left atrioventricular groove [1,4]. The proximal and transverse portions of the left sinus venosus in the left atrioventricular groove become the coronary sinus and the distal left sinus venosus and left cardinal vein normally obliterate and become the ligament of Marshall [2].

Coronary sinus anomalies

There is a range of anomalies of the coronary sinus. Mantini *et al.* divided the defects into four categories: enlarged coronary sinus, absent coronary sinus, hypoplastic coronary sinus, and atresia of part of the coronary sinus [5]. The more commonly encountered anomalies are discussed below in further detail.

Persistent left superior vena cava

Failure to identify the uncommon anomalies of the coronary sinus can have serious consequences during cardiac surgery or interventional procedures. Formed from the left sinus venosus, it can retain connection with the left cardinal vein, creating a persistent left superior vena cava (PLSVC), which is the most common thoracic venous anomaly. PLSVC as an isolated anomaly, has a reported frequency of 0.3–0.5% in autopsy studies [6–8]. PLSVC is more common in congenital heart disease and may occur with any type of congenital cardiac anomaly [5]. The frequency of PLSVC associated with other cardiac anomalies ranges from 1.3 to 10% [5,8].

In most instances of PLSVC, the left-sided embryologic venous structures persist and connect to the coronary sinus, resulting in an enlarged ostium of the coronary sinus. Rarely, the LSVC connects directly to the left atrium. A right superior vena cava (RSVC) is usually present and the left innominate vein (bridging vein), connecting the RSVC and LSVC, may or may not be present [5].

(a)   (b)
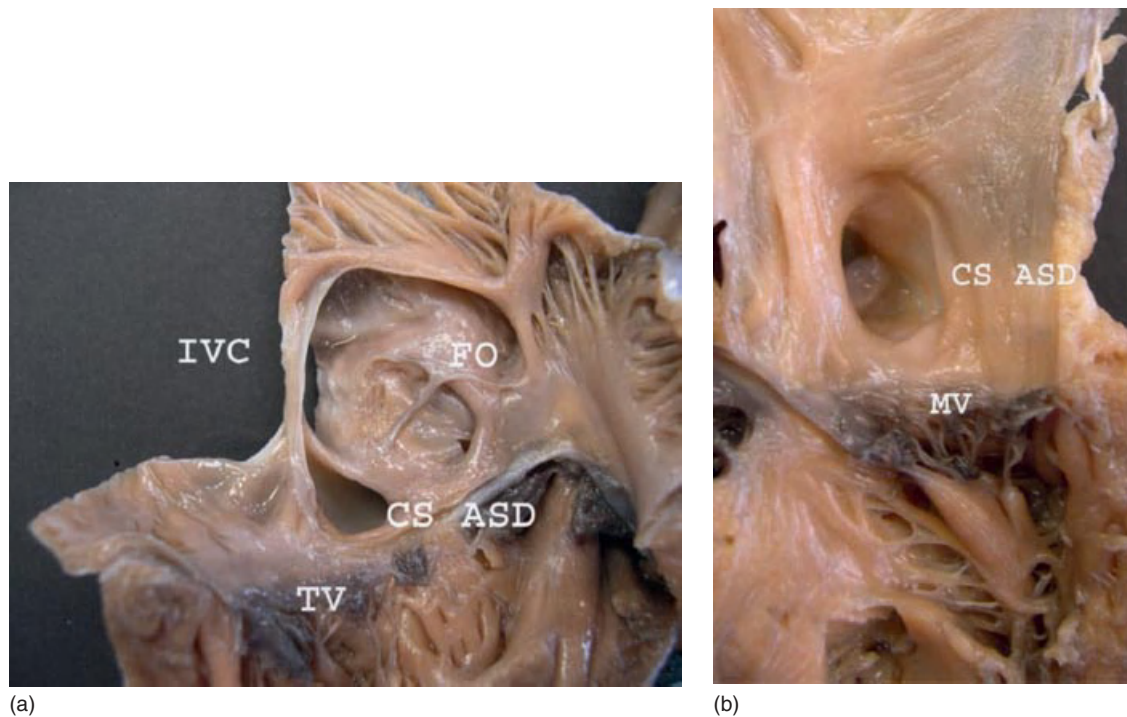
Figure 37.1 (a) Right atrial view of unroofed coronary sinus defect. The coronary sinus atrial septal defect (CS ASD) is at the posterior–inferior angle of the right atrium superior to the tricuspid valve (TV). The atrial septal defect is inferior to the fossa ovalis (FO) and inferior vena cava (IVC). (b) Left atrial view of unroofed coronary sinus defect. The CS ASD in the left atrium is superior to the posteromedial commissure of the mitral valve (MV).

The PLSVC is usually without clinical significance. It may be significant when associated with additional coronary sinus anomalies, such as unroofed coronary sinus or atresia of the coronary sinus, or when discovered during surgery while using retrograde cardioplegia or attempts at placement of pacemakers or defibrillators.

Unroofed coronary sinus

Unroofed coronary sinus consists of a range of anomalies associated with a defect in the wall between the coronary sinus and left atrium.

Complete unroofed coronary sinus, also referred to as Raghib syndrome, was first described in 1965 [3]. The syndrome is a combination of anomalies including PLSVC terminating in the left atrium, absent coronary sinus, and atrial septal defect in the posteroinferior angle of the atrial septum. Initially believed to be a result of failure of the left sinus venosus to migrate within the atriovenous fold to connect with the right atrium [3], it now appears that the anomaly results from failure in the formation of the wall between the coronary sinus and the left atrium [4]. As a result, the LSVC usually connects to the left atrium between the pulmonary veins posteriorly and the base of the left atrial appendage anteriorly [3]. These patients have the possibility of developing TIAs or brain abscess because of the right-to-left shunt (LSVC-LA). Notably, 80–90% of cases do not have a left innominate vein [3,9]. Since the coronary sinus is

absent, cardiac veins drain independently into the atria. From the right atrial aspect, the atrial septal defect is in the typical location of the coronary sinus ostium, posterior and inferior to the fossa ovalis, inferior and medial to the inferior vena cava, and superior to the septal leaflet of the tricuspid valve (Figure 37.1a). From the left atrial aspect, the defect is above the posteromedial commissure of the mitral valve (Figure 37.1b). Atrial septal tissue surrounds the defect anteriorly, superiorly, and inferiorly. The posterior left atrial wall forms the posterior boundary [3]. This condition may have an additional atrial septal defect, either at the fossa ovalis or within the endocardial cushions [9,10].

Variants

Within the range of unroofed coronary sinus is the partially unroofed or fenestrated coronary sinus defect. This condition is the result of a defect within the partially formed wall between the coronary sinus and the left atrium, resulting in a defect or fenestration between the coronary sinus and left atrium. This rare form of unroofed coronary sinus may be associated with a left-to-right shunt and may be clinically apparent. The clinical and diagnostic features resemble those of an atrial left-to-right shunt [11].

Echocardiography or MRI [12] may demonstrate the defect between the coronary sinus and left atrium. If there is a PLSVC, there may be a small right-to-left shunt into the left atrium [9]. Surgically, the defect is usually closed through

(a)   (b)
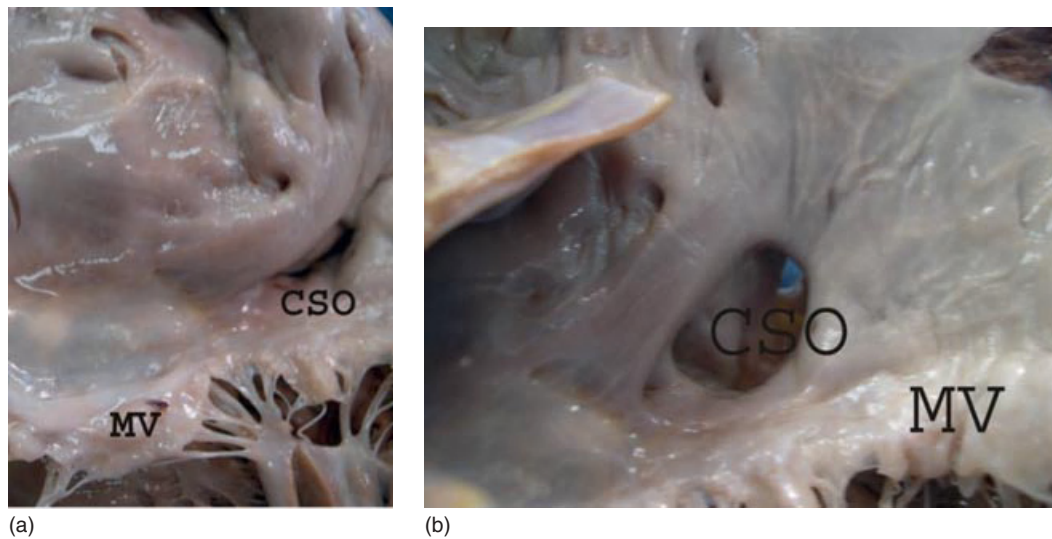
Figure 37.2 (a) Variant of unroofed coronary sinus defect with coronary sinus ostium (CSO) connecting directly to the left atrium superior to the posteromedial commissure of the mitral valve (MV). (b) Closer view of (a). The CSO connects directly to the left atrium above the MV.

the left atrium [13]. If there is no LSVC, the surgical correction is simply to close the coronary sinus ostium in the right atrium. The defect has reportedly been closed by a covered stent in an infant with cardiac failure due to a large left-to-right shunt [14]. This variant has also been associated with either right- or left-sided atrioventricular valve atresia or stenosis [9,10].

In another variant, the coronary sinus ostium opens directly into the left atrium and the distal segment is atretic. In this variant, the coronary sinus ostium is located in the posterior wall of the left atrium above the posteromedial commissure of the mitral valve and there is no right atrial component (Figure 37.2) [3,9]. This very rare variant often is not of clinical significance. It comes to cardiac surgeons' attention when they try to introduce retrograde cardioplegia during open-heart surgery and discover that there is not a coronary sinus ostium in the right atrium. It also is important to recognize this variant when attempting device placement, as the leads may enter the left atrium.

Atresia of coronary sinus

Atresia of the coronary sinus is rare and several variations exist. There may be atresia of the entire coronary sinus, a segment of the coronary sinus, or the coronary sinus ostium. If a segment is atretic, this results in a blind-ended pouch behind the left atrium. In some instances, a PLSVC coexists and the cardiac venous blood emptying into this segment travels retrograde via the LSVC to the left innominate vein, continuing to the right superior vena cava, with eventual drainage into the right atrium [15]. The terminal coronary sinus empties through the right atrial ostium and drains only a small percentage of the cardiac venous blood [16].
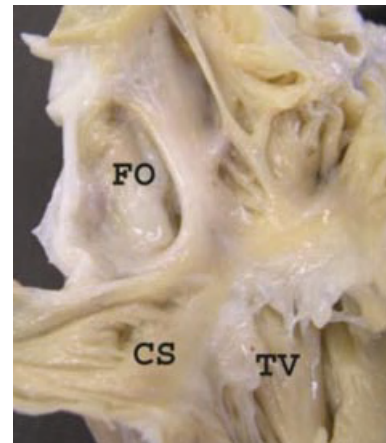
Figure 37.3 Right atrium with absent coronary sinus ostium. The typical location of the coronary sinus is labeled CS. There is no coronary sinus ostium in the right atrium. Tricuspid valve (TV) and fossa ovalis (FO) are normally formed.

There may be atresia of the coronary sinus ostium in the right atrium (Figure 37.3). The coronary sinus is present; however, it ends blindly behind the left atrium. Cardiac venous drainage is by retrograde flow via the PLSVC, to the left innominate vein, to the right superior vena cava, to the right atrium. Atresia of the right atrial coronary sinus ostium may be an isolated anomaly. It has also been reported with a variety of different types of cardiac anomalies. Atresia of the coronary sinus is often of little clinical significance; however, due to dependence of cardiac venous drainage via the PLSVC, care must be taken not to ligate the LSVC during surgery, which would result in myocardial congestion, distention, and ischemia [17,18].

(a)

(b)
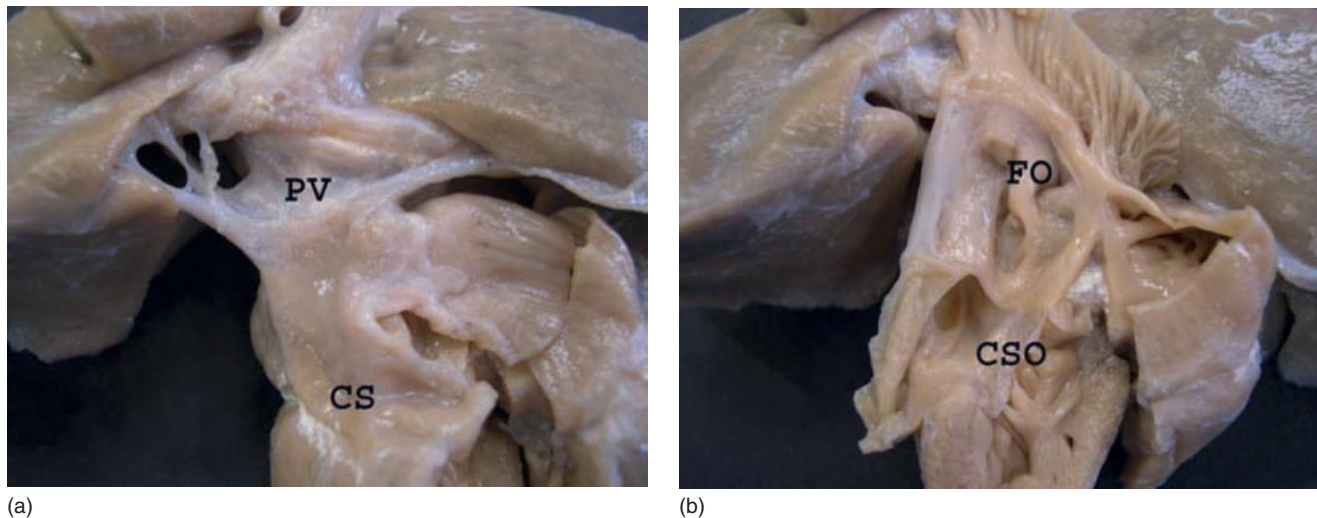
Figure 37.4 (a) External photograph of the heart and lungs demonstrating connection of the pulmonary veins (PV) with the coronary sinus (CS) in total anomalous pulmonary artery connection. (b) Right atrial view of same patient as in (a) demonstrating the dilated coronary sinus ostium (CSO) due to the total anomalous pulmonary venous connection to the coronary sinus. FO, fossa ovalis.

Absence of the coronary sinus is part of the complex cardiac malformations present in heterotaxia syndromes, particularly the asplenia syndrome. Common atrial components of asplenia are bilateral SVC, common atrium, and absence of the coronary sinus [5]. Malformations associated with asplenia syndrome are discussed in greater detail in Chapter 50.

Other abnormalities of the coronary sinus

Enlarged coronary sinus occurs with partial or total pulmonary venous connection. The pulmonary confluence which collects the pulmonary venous drainage connects to the coronary sinus with subsequent drainage into the right atrium (Figure 37.4) [5].

Other types of anomalous drainage to the coronary sinus include partial anomalous hepatic drainage to the coronary sinus and drainage of the inferior vena cava through the hemiazigous vein to a left superior vena cava to the coronary sinus [5].

References

1 Moorman AF, Brown N, Anderson RH. Embryology of the heart. In: Anderson RH, Baker EJ, Penny DJ, eds. *Paediatric Cardiology*, 3rd edn. Philadelphia: Churchill Livingstone/Elsevier, 2010: 37–55.

2 Kaushik N, Wessels A, Markwald RR, Keller BB. Molecular development of the heart. In: Fuster V, O'Rourke RA, Walsh RA, Poole-Wilson P, eds. *Hurst's The Heart, Manual of Cardiology*, 12th edn. New York, McGraw-Hill, 2007, http://www.accessmedicine.com/content.aspx?aID=3049316.

3 Raghib G, Ruttenberg HD, Anderson RC, *et al*. Termination of left superior vena cava in left atrium, atrial septal defect, and absence of coronary sinus. *Circulation* 1965;**31**:906–18.

4 Knauth A, McCarthy KP, Webb S, *et al*. Interatrial communication through the mouth of the coronary sinus. *Cardiol Young* 2002;**12**:364–72.

5 Mantini E, Grondin CM, Lillehei CW, *et al*. Congenital anomalies involving the coronary sinus. *Circulation* 1966;**33**:317–27.

6 Gonzalez-Juanatey C, Testa A, Vidan J, *et al*. Persistent left superior vena cava draining into the coronary sinus: report of 10 cases and literature review. *Clin Cardiol* 2004;**27**: 515–8.

7 Miraldi F, Carbone I, Ascarelli A, *et al*. Double superior vena cava: right connected to left atrium and left to coronary sinus. *Int J Cardiol* 2007;**131**:e78–80.

8 Vizzardi E, Fracassi F, Farina D, *et al*. Persistence of left superior vena cava, absence of coronary sinus and cerebral ictus. *Int J Cardiol* 2008;**126**:e39–41.

9 Kouchoukos NT, Blackstone EH, Doty DB, *et al*. Unroofed coronary sinus syndrome. In: Kouchoukos NT, Blackstone EH, Doty DB, *et al*., eds. *Kirklin/Barratt-Boyes Cardiac Surgery*, 3rd edn. Philadelphia: Churchill Livingstone/Elsevier, 2003: 790–9.

10 Amplatz K, Moller JH. Raghib syndrome and other coronary sinus anomalies allowing intracardiac shunts. In: Amplatz K, Moller JH, eds. *Radiology of Congenital Heart Disease*. St Louis, MO: Mosby, 1993: 339–44.

11 Ootaku Y, Yamaguchi M, Yoshima N, *et al*. Unroofed coronary sinus syndrome. Diagnosis, classification and surgical treatment. *J Thorac Cardiovasc Surg* 2003;**126**:1655–6.

12 Low SC, Oliveira GR, Maki JH. Magnetic resonance imaging of unroofed coronary sinus. *Heart* 2009;**95**:720.

13 Quaegebeur J, Kirklin JW, Pacifico AD, Bargeron LM Jr. Surgical experience with unroofed coronary sinus. *Ann Thorac Surg* 1979; **27**:418–25.

14 Torres A, Gersony WM, Hellenbrand W. Closure of unroofed coronary sinus with covered stent in a symptomatic infant. *Catheter Cardiovasc Interv* 2007;**70**:745–8.

15 Watson GH. Atresia of the coronary sinus orifice. *Pediatr Cardiol* 1985;**6**:99–101.

16 O'hAodha LT, Berg B, Jessurun J, *et al*. Localized atresia of the coronary sinus a short distance proximal to its ostium. *Cardiovasc Pathol* 2004;**13**:293–5.

17 Jha NK, Gogna A, Tan TH, *et al*. Atresia of coronary sinus ostium with retrograde drainage via persistent left superior vena cava. *Ann Thorac Surg* 2003;**76**:2091–2.

18 Fulton JO, Mas C, Brizard CP Karl TR. The surgical importance of coronary sinus orifice atresia. *Ann Thorac Surg* 1998;**66**:2112–9.

38   Hypoplastic Left Heart Syndrome

Robert B. Hinton & D. Woodrow Benson
Cincinnati Children's Hospital Medical Center, Cincinnati, OH, USA

Introduction

Although hypoplasia of the left ventricle resulting in single ventricle physiology is a cardinal feature of hypoplastic left heart syndrome (HLHS), the pathologic definition includes atresia or stenosis of both the aortic and mitral valves, and hypoplasia of the left ventricle and ascending aorta with intact ventricular septum and normally related great arteries. This definition excludes anatomic variations of left ventricular hypoplasia, including atrioventricular septal defect and double-outlet right ventricle that presumably have different causes. The diagnosis, treatment, and care of patients with HLHS have improved dramatically over the past 30 years. (Table 38.1).

Incidence and genetics

The prevalence of HLHS has been estimated as 0.06–1.20 (median 0.22) per 1000 live births [1]. This is consistent with findings from the larger epidemiologic studies, including the New England Regional Infant Care Program (NERICP) and the Baltimore–Washington Infant Study (BWIS), which place the prevalence at 0.16–0.27 per 1000 live births [2,3]. HLHS accounts for approximately 4–8% of all cardiovascular malformations (CVMs) [4]. Some fetal loss has been attributed to HLHS, but in general HLHS is viable *in utero*. HLHS is slightly more common in males; there is no ethnic or geographic association. Despite only one in 5000 live births resulting in HLHS and approximately 2000 infants born each year in the United States, the burden on society is substantial. The direct costs, medical morbidity, and utilization of a disproportionate share of pediatric cardiac resources make HLHS a central problem in pediatric cardiology [5,6].

Despite dramatic improvements in diagnosis, treatment, and prognosis, the cause of HLHS remains largely unknown. Recurrence risk provides significant evidence that HLHS has a genetic basis, but no genes have been identified. For a long time, HLHS was considered a rare, sporadic occurrence; however, Shokeir identified consanguineous families with multiple instances and proposed that HLHS was a recessive phenotype [7]. In a landmark paper, Brenner *et al.* identified a disproportionate number of first-degree relatives affected with bicuspid aortic valve (BAV) in families identified by an HLHS proband, further suggesting a genetic basis [8]. The heritability of HLHS has been estimated as 78–95% [9,10]. A large, family-based study in which all family members were screened with echocardiography for CVM identified a recurrence risk of 8% for HLHS and 22% for any CVM, including a 10-fold increase in BAV [10].

Analyses to date suggest HLHS is a complex trait, not following simple Mendelian inheritance; thus, a single gene mutation does not result in HLHS. There is substantial evidence supporting genetic heterogeneity. For example, HLHS is associated with genetic syndromes in ~10% of patients, most commonly Turner syndrome, trisomy 18, and Jacobsen syndrome [11,12]. Less common associations include Smith–Lemli–Opitz syndrome, VACTERL association, and Rubinstein–Taybi syndrome. There have been additional reports of HLHS in numerous other genetic syndromes; however, many of these reports equate left ventricular hypoplasia with HLHS (e.g.. Holt–Oram syndrome), and therefore may provide limited insight into the underlying genetic basis of HLHS. Interestingly, 25% of patients who do not have an identifiable genetic syndrome have noncardiac malformations, consistent with the idea that HLHS is a true syndrome [11]. Noncardiac anomalies include craniofacial, genitourinary (especially kidney), and central nervous system (CNS) abnormalities, and can be clinically significant in

Table 38.1 HLHS: historical landmarks.

Year	Landmark	Author
1849	Pathologic description	Canton
1952	Pathologic anatomy and classification scheme	Lev
1958	Entity named "hypoplastic left heart syndrome"	Noonan and Nadas
1970s	Genetic basis proposed	Shokeir
1980s	Surgical reconstructive palliation	Norwood
1980s	Epidemiology elucidated	BWIS
1989	Etiologic connection between HLHS and BAV proposed	Brenner
1990s	Specialized intensive care and anesthesia	Wessels
2000s	Fetal intervention	Tworetzky

the acute and chronic management of this patient population. Nearly half of all patients have CNS abnormalities, including microcephaly and evidence for preoperative white matter injury [13,14]. In addition, there is a disproportionate number of small for gestational age infants with HLHS and, in general, they have relatively low birth weights [15]. In a small number of patients, *NKX2.5* and *GJA1* mutations have been identified in HLHS probands [16,17]. Recently, two significant loci for HLHS and associated CVM have been identified on chromosomes 10q22 and 6q23 [18]. The clinical taxonomy is based on anatomy and physiology; however, as more is learned about the genetic basis of HLHS and other complex forms of CVM, this taxonomy will have to be reconciled with the emerging molecular taxonomy.

Embryology

HLHS pathology occurs in different cardiovascular tissue types, namely valve, muscle, and artery. Cardiac development for these tissues types spans primary cardiogenesis [19]. There are two hypotheses about the developmental origins of HLHS. First, in the context of reduced flow through the left-sided structures, as can happen with restriction of left ventricular outflow, for example aortic stenosis, or inflow obstruction, for example restriction of the foramen ovale, the left-sided structures fail to grow. Second, aberrant developmental programs selectively impair the left-sided structures (e.g., the aortic valve, the aorta, the left ventricular myocardium). Because aortic stenosis has been identified as part of the *in utero* natural history of HLHS in at least a subset of patients [20], a fetus may have a genetically based aortic valve malformation, which results in embryonic or fetal obstruction and subsequent growth failure of the remaining left-sided structures in the context of reduced blood flow. Given the severity of the phenotype, an early but viable insult would be expected. There are no animal models for

HLHS, although some models have recapitulated the left ventricular hypoplasia aspect of the phenotype. For example, in the chick embryo, ligation of the left atrial appendage results in reduced left atrial size and consequently left ventricular hypoplasia [21,22]. Notably, however, the aortic and mitral valves in this model are normal. The inability to induce this lesion in fetal animals combined with the striking absence of this phenotype in targeted mutagenesis mouse models of CVM further supports the idea that HLHS is a complex genetic phenotype [19,23].

Pathologic anatomy

HLHS was originally described in 1849 by Canton [24]. Lev was the first to describe the pathologic anatomy in a series of patients, and referred to the findings as "hypoplasia of the aortic tract complex" [25]. Noonan and Nadas described this constellation of findings as the "hypoplastic left heart syndrome" in 1958 [26]. Lev subsequently proposed a classification scheme based on valve morphology that continues to be in wide use. Based on these studies, four criteria are required for diagnosis (Table 38.2) and those that are diagnosed may be classified further by the status of the left-sided valves as either atretic or stenotic (aortic atresia, mitral atresia; aortic atresia, mitral stenosis; aortic stenosis, mitral stenosis) [27]. Of note, the hypothetical group aortic stenosis, mitral atresia does not occur. The surgical nomenclature defines HLHS broadly and prefers the term "hypoplastic left heart complex" to include numerous variants such as Shone anomaly [28]. This approach illustrates the heterogeneity of some of these findings, for example, left ventricular hypoplasia.

The anatomic features required to satisfy a diagnosis of HLHS include atresia or stenosis of the aortic and mitral valves and hypoplasia of the left ventricle and ascending aorta (Figure 38.1). Each of these findings has a continuum of severity, providing a breadth of subgroups. In addition,

Table 38.2 HLHS: diagnostic features and associated findings.

Feature	%
Diagnostic features	
Aortic valve atresia or stenosis	100
Mitral valve atresia or stenosis	100
Left ventricular hypoplasia	100
Hypoplasia of the ascending aorta	100
Associated findings	
Tricuspid valve abnormalities	40–65
Discrete coarctation of the aorta	20–65
Endocardial fibroelastosis	10–40
Intact/restrictive atrial septum	5–15
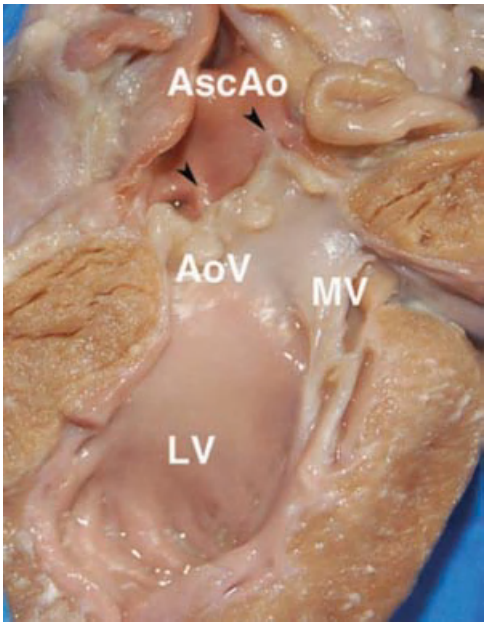
Figure 38.1 HLHS gross pathology showing longitudinal transection of the left-sided structures. There is hypoplasia of the aortic valve (AoV), mitral valve (MV), left ventricle (LV), and ascending aorta (AscAo). The aortic valve is bicuspid (arrowheads identify two commissures) and dysplastic.

there are features common to all patients. The left atrium is small. The right atrium, right ventricle, and pulmonary artery are enlarged. The morphologic right ventricle is hypertrophied and dilated, making the overall heart size large. A patent foramen ovale is present; in some infants, premature closure of the foramen ovale occurs *in utero*. Associated CVMs include discrete coarctation of the aorta (20–65%), tricuspid and pulmonary valve abnormalities (40–65%), and intact atrial septum (5–15%). The surprising finding of right-sided valve abnormalities has significant clinical implications and raises intriguing questions about the origin of HLHS. In some

patients, the myocardium appears normal, whereas in others there is endocardial fibroelastosis in 10–40%, subendocardial fibrosis, or left ventricle to coronary artery fistulae.

Pathophysiology

There is an obligatory left-to-right shunt at the atrial level, and in the right atrium oxygenated pulmonary venous blood mixes with the systemic venous return, and the mixed blood then flows into the right ventricle. From the right ventricle, the blood is delivered to both the pulmonary and systemic circulations. The brachiocephalic vessels and coronary arteries are perfused through retrograde flow from the ductus arteriosus into the transverse aortic arch and hypoplastic ascending aorta. These changes may be compatible with normal intrauterine growth or, in some instances, decreased somatic and head growth late in gestation.

After birth, transitional physiologic changes result in rapidly progressive hemodynamic disturbances that precipitate symptoms in the first week of life. There is a gradual decrease in pulmonary vascular resistance and spontaneous constriction of the ductus arteriosus. The gradual decrease in pulmonary vascular resistance in the first few days of life leads to a progressive increase in pulmonary blood flow, which in turn improves systemic arterial oxygen saturation but also diminishes systemic blood flow, lowers perfusion pressure, and causes volume overload of the right ventricle. The increased pulmonary blood flow is accompanied by pulmonary congestion and increased left atrial and pulmonary venous pressure. A restrictive interatrial communication, if present, further elevates left atrial pressure. Because the systemic and coronary circulations depend on flow through the ductus arteriosus, its constriction in the first few days of life leads to poor systemic perfusion, hypoxemia, and metabolic acidosis, eventually resulting in vascular shock and death. The coronary blood flow depends on the perfusion pressure in the aortic arch and the size of the ascending aorta. Various compensatory mechanisms, including redistribution of blood away from the less vital organs, such as the gastrointestinal tract, temporarily maintain nearly normal arterial pressure and coronary perfusion.

The pulmonary and systemic blood flows in infants with HLHS are determined by the ratio of the pulmonary to systemic vascular resistances. While the ductus arteriosus remains patent, most infants maintain a balance between the pulmonary and systemic resistances, resulting in adequate pulmonary and systemic perfusion. However, in some infants, excessive reduction of the pulmonary to systemic vascular resistance ratio leads to pulmonary overcirculation, with the development of congestive heart failure and diminished systemic perfusion. Less often, a higher pulmonary-to-systemic vascular resistance ratio leads to diminished pulmonary blood flow, as may occur when

pulmonary vascular resistance remains high in infants with persistent pulmonary hypertension or with an intact or restricted interatrial septum. The consequence is severe hypoxemia, progressive tissue hypoxia, metabolic acidosis, and death. The significance of the interaction between the pulmonary and systemic resistance in determining pulmonary and systemic blood flows and also systemic arterial oxygen saturation is crucial to understanding the clinical presentation of these infants and the pre- and postoperative management [29].

Clinical features

Clinical history

The circulatory hemodynamics in the fetus with HLHS appear adequate for normal development. At birth, the infant typically has normal Apgar scores without cardiovascular symptoms, and without the use of pulse oximetry may be sent home undiagnosed [30]. Symptoms usually appear within the first days of life. Clinical presentation in a neonate may occur in one of three ways: respiratory distress, shock, or cyanosis. Respiratory distress with tachypnea and mild cyanosis, the most common presentation, usually begins on the second or third day of life. Respiratory symptoms are due to the progressive increase in pulmonary blood flow and pulmonary congestion that result from the normal transitional decrease in pulmonary vascular resistance. The duskiness is due to mild hypoxemia. The second most frequent presentation, shock, occurs with precipitous constriction of the ductus arteriosus, resulting in low cardiac output as evidenced by hypotension, poor peripheral perfusion, and severe metabolic acidosis. Because this presentation may occur after neonatal discharge from the hospital, the arrival of the patient in an emergency department in vascular collapse is often mistaken for septic shock. The physical findings on examination are those of shock and severe cardiac failure; there is profound myocardial dysfunction, metabolic acidosis, and anuria. Seizures may also occur. The least common presentation is that of cyanosis, usually occurring shortly after birth on the first day of life. The cyanosis results from premature closure of the foramen ovale, inadequate atrial level shunting, or persistence of pulmonary artery hypertension of the newborn.

Physical examination

The incidence of small-for-gestational-age birth weights and microcephaly is increased. In addition, head size can be disproportionately small when indexed to somatic size. Physical examination reveals marked tachypnea and tachycardia. There is a right ventricular impulse at the xiphoid, and hepatomegaly. The peripheral pulses are diminished throughout, and there is poor capillary filling and mottling of the skin. Cyanosis is often not apparent because hypoxemia is

relatively mild and may be masked by simultaneous hyperbilirubinemia. Typically, a single second heart sound and gallop rhythm are heard. There is often a soft systolic ejection murmur audible at the bases and back bilaterally due to physiologic peripheral pulmonary stenosis accentuated by increased pulmonary blood flow. An additional regurgitant systolic murmur may be heard at the left lower sternal border if tricuspid regurgitation is present. An arterial blood gas obtained in room air usually has a PaO_2 of ~45–60 mmHg, with normal or moderately decreased $PaCO_2$ of 30–35 mmHg and low pH as a result of moderate metabolic acidosis. When the infant is breathing 100% oxygen, the PaO_2 may rise to ≥100 mmHg. Systemic arterial oxygen saturation measured by a pulse oximeter may be in the mid to high 80s or low 90s and is similar in all four extremities. With persistent poor perfusion and increasing metabolic acidosis, there may be associated hypoglycemia, hypocalcemia, and hyperkalemia and subsequently the development of disseminated intravascular coagulopathy.

Electrocardiographic features

The electrocardiogram soon after birth usually shows a dominant R wave in V_1 and a dominant S wave in V_6. This R/S reversal, rare in normal newborns, indicates left ventricular hypoplasia rather than pure right ventricular hypertrophy. Subsequent changes are related to left ventricular hypoplasia and right ventricular volume and pressure overload, and may include right atrial enlargement, right ventricular hypertrophy, and progressive diminution in left ventricular forces with absence of a Q wave in the left precordial leads and a pure R or QR in lead V_1. Right ventricular myocardial ischemic ST–T wave changes may appear. Conduction disturbances are rare.

Chest X-ray

The chest radiograph may be normal immediately after birth, but usually demonstrates cardiomegaly and increased pulmonary vascular markings on the first day of life. In infants with an intact or restricted interatrial communication, there is usually a pattern of pulmonary edema, and in those with persistent pulmonary hypertension the pulmonary vascular makings are diminished. While the infant is receiving prostaglandin E_1, progressive pulmonary edema and cardiomegaly are observed.

Echocardiography

Echocardiography is the gold standard for diagnosis, and currently >50% of patients are identified *in utero*. A prenatal diagnosis of HLHS may be made by fetal echocardiography as early as 16 weeks gestation after cardiogenesis. HLHS is typically identified during a screening obstetric ultrasound, often when there is a family history of congenital heart disease. Prenatal diagnosis has led to an improved ability to plan for care and

Figure 38.2 Echocardiographic findings of HLHS upon diagnosis. These show the following. (a) In the parasternal long axis view, aortic valve (AoV) atresia, left ventricular (LV) hypoplasia and mitral valve (MV) stenosis; in addition, there is mild endocardial fibroelastosis (EFE) along the ventricular septum in close proximity to the aortic valve and hypoplasia of the ascending aorta (AscAo). LA, left atrium. (b) In a modified suprasternal view, marked hypoplasia of the ascending aorta and retrograde flow in the descending (DescAo) and transverse (TAo) aorta. PDA, patent ductus arteriosus. (c) A discrete juxtaductal coarctation of the aorta (COA). (d) Thickened dysplastic tricuspid valve (TV) with abnormal chordal attachments (arrowhead). RA, right atrium; RV, right ventricle.
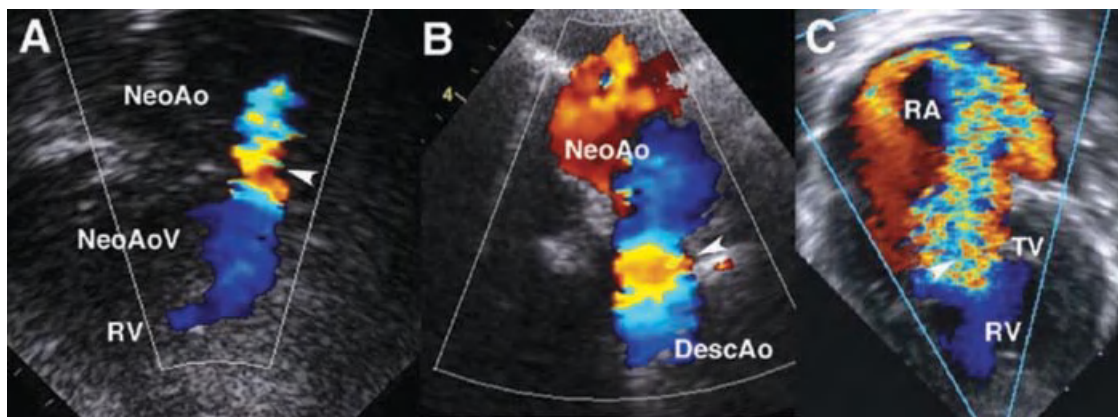
Figure 38.3 Interstage complications as identified by echocardiography include (a) neoartic (NeoAo) obstruction at the proximal aspect of the aortic patch (arrowhead), (b) residual or recurrent coarctation of the aorta (arrowhead), and (c) tricuspid regurgitation (arrowhead). DescAo, descending aorta; NeoAoV, neoaortic valve; RA, right atrium; RV, right ventricle; TV, tricuspid valve.

provide counseling to the family [31]. Longitudinal studies in the fetus have shown that aortic stenosis is part of the *in utero* natural history of HLHS. At mid-gestation, at the earliest stage imaging can be reliably obtained, a fetus that will have HLHS as a neonate may have obvious HLHS or isolated aortic stenosis, and severity of fetal aortic stenosis can be stratified based on physiologic parameters such as reverse flow in the transverse aorta. Interestingly, the left ventricular morphology progresses from ostensibly normal to dilated and dysfunctional and ultimately to hypoplastic during the second half of gestation.

A definitive diagnosis is made by two-dimensional and Doppler transthoracic echocardiography at birth (Figure 38.2). The characteristic echocardiographic features of HLHS include (1) atresia or stenosis of the aortic and mitral valves, (2) left ventricular hypoplasia, (3) hypoplasia of the ascending aorta and transverse arch with or without discrete coarctation, and (4) right ventricular enlargement. Once the diagnosis is established, special attention should be given to the interatrial communication, the ductus arteriosus, tricuspid valve morphology

and function, the distal aortic arch, and right ventricular function. Echocardiography is the primary tool to monitor patients between palliative stages. After stage I palliation, assessment of right ventricular and tricuspid valve function is critical, and also the adequacy of the interatrial communication, any functional abnormality of the pulmonary (neoaortic) valve, and presence of a left superior vena cava. If both a right and left superior vena cava are present, and there is no bridging innominate vein, a bilateral bidirectional caval–pulmonary connection may need to be established. Complications include recoarctation of the aorta at either the proximal or distal end of the anastomosis, and tricuspid regurgitation, either of which can result in ventricular failure (Figure 38.3).

In HLHS, the right ventricle functions as the systemic ventricle and is challenged by increased afterload and increased preload prior to stage 2 palliation. Myocardial ischemia, coronary abnormalities, and additional volume loading from tricuspid regurgitation may contribute to this

burden. A subset of patients with HLHS develop right ventricular failure and are at risk of increased morbidity. Systolic and diastolic function were assessed in children with HLHS to compare ventricular function following stage I palliative surgery with either an aortopulmonary shunt or a right ventricle to pulmonary artery shunt [32]. There were no early significant differences in right ventricular size, shape, or systolic and diastolic function between groups. Regardless of the type of stage I procedure, patients showed a decrease in both systolic and diastolic indices that persisted through stage II palliation months later [32]. Right ventricular mechanical dyssynchrony has been studied in children with HLHS using tissue Doppler imaging and strain derived from vector velocity imaging [33]. Right ventricular mechanical dyssynchrony was common and may contribute to ventricular dysfunction in some patients.

Cardiac catheterization, angiography, and other imaging modalities

Cardiac catheterization is rarely necessary for diagnosis. Angiography may be useful in the infant with critical aortic stenosis and a small but not diminutive left ventricle to assess the severity of left-sided obstruction or left ventricular hypoplasia if biventricular repair is contemplated. Interventional cardiac catheterization, with an atrial septostomy or blade septectomy, may be necessary for urgent relief of severe interatrial obstruction. Cardiac catheterization may be performed postoperatively to assess hemodynamics, patency of an aortopulmonary shunt, or other confounding anatomic features. Cardiac catheterization and angiography are essential for complete functional and anatomic assessment before stage II palliation (Glenn). Cardiac catheterization is done to assess stenoses, hypoplasia, or deformity of the pulmonary arteries, for direct or indirect measurement of pulmonary artery pressures, and to assess recurrent coarctation of the aorta and, if necessary, perform balloon dilatation of the aortic obstruction. Before stage III (Fontan), cardiac hemodynamic and angiographic studies are performed to determine pulmonary artery pressure, any possible deformity or obstruction of the pulmonary arteries, tricuspid valve competency, and right ventricular function. Major systemic venous collaterals that may be associated with obstruction of the cavopulmonary connection or large aortopulmonary collaterals, particularly from the internal mammary arteries, may require interventional therapy. The systemic venous collaterals may steal or direct blood away from the lungs. Aortopulmonary collaterals increase pulmonary blood flow and subsequent right ventricular volume overload and also pulmonary congestion. Large collaterals are occluded at the time of cardiac catheterization by metal coils or other devices.

Currently, there is a limited role for alternative imaging modalities. CT and MRI may be used to delineate preoperative associated CVM or elucidate complex postoperative anatomy. Ultimately, MRI may have a role in comprehensively and longitudinally evaluating right ventricular function.

Management

General considerations

The management of infants with HLHS varies significantly among physicians, institutions, and countries. If the diagnosis is made in the early prenatal period, termination of pregnancy may be an acceptable option for some families and is the preferred option in many European countries. Once the infant is born, some parents may elect to provide supportive care only. This decision is highly individualized and depends on the family, physician, and available services for care of these patients. Supportive care was much more prevalent in the United States previously than it is today. Options are discussed with the family and the recommendation, in the majority of centers, is staged palliative reconstructive surgery (Table 38.3). The ethical and economic dilemmas posed by HLHS infants are societal issues that require the cooperation of families, physicians, insurers, and various government institutions. The ethical issues raised in the management of these infants include the cost and potential benefits of treatment in an era of limited resources, potential distress and suffering of the infant and family associated with multiple major cardiac operations, and uncertain long-term prognosis.

Fetal management

Based on the observation that aortic stenosis is part of the natural history of HLHS, there has been enthusiasm for *in utero* balloon valvoplasty of the aortic valve in select patients who are predicted to evolve into HLHS. The fetal cardiology group at the Children's Hospital Boston has reported technical success in relieving aortic stenosis in second trimester fetuses, and in some patients preventing progression to HLHS [34]. Although this pertains only to a subset of HLHS, in most patients fetal severe aortic stenosis progresses to HLHS. The benefits of preserving a two-ventricle circulation balance the considerable risks of intervening during gestation, including fetal death and preterm labor (see Chapter 16).

Medical management

After establishing a diagnosis by echocardiography, the initial steps in managing an infant with HLHS include maintaining ductal patency by prostaglandin E_1 infusion and stabilizing hemodynamics before stage I palliation. Mechanical ventilation and inotropic support are required in some patients. Sedation is typically needed, and some patients benefit from increasing the hematocrit through blood transfusion. The focus of medical management is optimizing the balance

Table 38.3 HLHS: management options.

Prenatal
Pregnancy termination
Fetal intervention
Observation

Postnatal
Supportive care
Staged palliative reconstruction
Cardiac transplantation

Table 38.4 Risk factors for stage I palliation.

Associated genetic syndrome
Intact/restrictive atrial septum
Birth weight less than 2.5 kg
Aortic atresia, mitral stenosis subtype
Ascending aorta dimension <2 mm
Moderate plus tricuspid regurgitation
Prematurity (separate from weight)

between pulmonary (Qp) and systemic (Qs) blood flow, and the general goal is to reduce pulmonary blood flow and right ventricular volume load [35]. Estimating Qp/Qs can be done using the arterial saturation (SaO_2), systemic venous saturation (SvO_2), and pulmonary venous saturation ($SpvO_2$) as follows:

$$Qp/Qs = (SaO_2 - SvO_2)/(SpvO_2 - SaO_2)$$

Optimal oxygen delivery occurs when Qp/Qs = 1 and the arterial venous oxygen saturation difference is 25%. This occurs when SaO_2 = 75% and SvO_2 = 50%, assuming fully saturated $SpvO_2$. Although SvO_2 can vary, confounding interpretation of SaO_2, one strategy to promote patient stability is to use inspired carbon dioxide, which increases pulmonary vascular resistance and consequently increases systemic oxygen delivery [36]. Recently, near-infrared spectroscopy (NIRS) has been used to monitor somatic and cerebral tissue oxygenation and to provide an estimate of SvO_2 [37]. Stage I operative risk factors have been identified (Table 38.4).

Surgical management

HLHS is uniformly fatal without neonatal surgery. The introduction of prostaglandin E_1 to maintain patency of the ductus arteriosus in the 1970s prepared the way for surgical intervention, including staged reconstructive procedures and cardiac transplantation (Figure 38.4). The first successful reconstructive procedure, performed by Norwood *et al.* in 1983 [38], involved connecting the right ventricle to the

systemic circulation by the main pulmonary artery and restricting pulmonary blood flow by creating an aortopulmonary shunt. Stage I palliation may also proceed with a right ventricle to pulmonary artery shunt instead of an aortopulmonary shunt [39]. Alternatively, stage I palliation may be deferred by use of the Hybrid procedure [40]. A second or intermediate stage, modeled after the operation proposed by Glenn in 1958 [41], is subsequently performed, creating a superior vena cava to pulmonary artery connection and eliminating the shunt. In a third stage, the remaining systemic venous flow is connected to the pulmonary artery by the Fontan procedure, introduced in 1971 to treat tricuspid atresia [42]. There have been numerous modifications of each stage. Currently, the typical surgical course is stage I (Norwood) in the first week of life, stage II (Glenn) at 3–6 months, and stage III (Fontan) at around 2–4 years. The alternative operative procedure, cardiac transplantation, was first successfully performed by Bailey *et al.* in 1986, but is rarely used now due in part to limited donor availability [43].

Stage I palliation (Norwood)

The Norwood procedure is designed to (1) provide unobstructed systemic blood flow to the ascending aorta by dividing the main pulmonary artery and creating an anastomosis between the proximal main pulmonary artery trunk and the ascending aorta (patch augmentation is required to enlarge the ascending aorta and extend it beyond the coarctation); (2) provide pulmonary blood flow by creating an aortic-to-pulmonary artery anastomosis or aortopulmonary shunt (also known as a Blalock–Taussig shunt, typically a Gore-Tex 3.5 mm graft interposed between the right subclavian and right pulmonary arteries); (3) create a large interatrial communication by performing atrial septectomy. Alternatively, a right ventricle to pulmonary artery shunt can be used (also known as a Sano modification, typically a Gore-Tex 5–6 mm graft) instead of the aortopulmonary shunt to establish pulmonary blood flow (Figure 38.4a). This modification may be a particularly attractive option in a small infant. It has the hypothetical advantage that diastolic pressure and therefore coronary perfusion are maintained by eliminating diastolic run-off. Despite mixed results in initial studies, a recent multi-center, prospective clinical trial performed by the Pediatric Heart Network (www.pediatricheartnetwork.com) comparing the aortopulmonary shunt with the right ventricle to pulmonary artery shunt determined that there is improved early survival using the right ventricle to pulmonary artery shunt; however, the long-term effects of a right ventriculotomy in a single right ventricle heart remain unknown [44]. Recently, the so-called Hybrid approach to defer stage I palliation has been used. This innovative procedure combines expertise from cardiothoracic surgery and cardiac catheterization, and can be performed in the operating room or a Hybrid-ready catheterization suite. The procedure entails banding of the branch
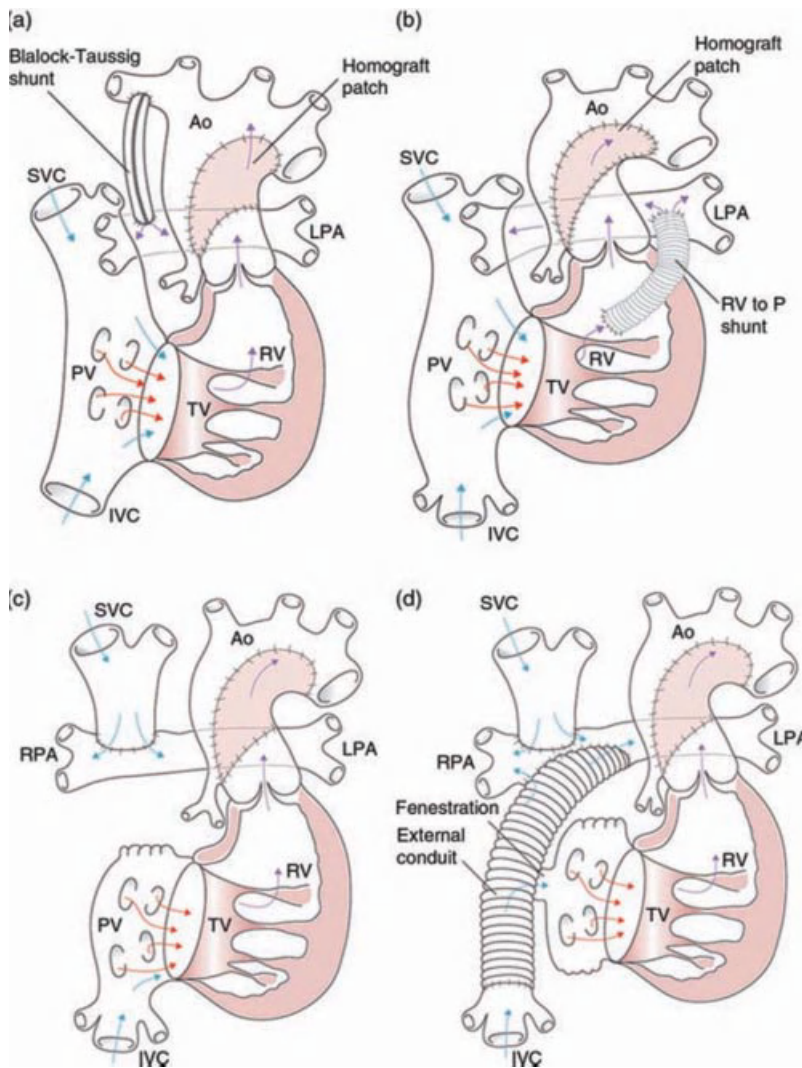
Figure 38.4 Staged reconstructive surgical palliation. HLHS patients generally undergo three operations: stage I (Norwood) may use either an aortopulmonary Blalock–Taussig shunt (a) or a right ventricle to pulmonary artery shunt (b), followed by stage II (Glenn) (c) and stage III (Fontan) (d). (Modified from Barron *et al*. *Lancet* 2009;**374**:551–64, with permission.)

pulmonary arteries, stenting of the patent ductus arteriosus, and balloon atrial septostomy [40]. This requires sternotomy without cardiopulmonary bypass, and bridges the patient to stage II palliation. Early results demonstrated that stage II palliation in these patients is far more complicated and carries a higher mortality; however, a few centers have reported early outcomes similar to stage I palliation. This strategy appears to be a good option for the high-risk patient, and trades a simpler initial operation for a more complex second operation that combines aspects of conventional stage I and stage II palliation. This trade may be advantageous in avoiding complex surgery in the neonate. It is unclear whether the Hybrid procedure will be established for routine use, but it is being used more frequently.

Stage II palliation (Glenn)

The second reconstructive operation is a bidirectional Glenn procedure, performed at ~3–6 months of age (Figure 38.4b). The superior vena caval blood flow is directed to the

pulmonary arteries, and the connection between the superior vena cava and right atrium is closed with the placement of a patch. At the same time, the aortopulmonary shunt is ligated. Systemic venous blood from the head and arms now perfuses the lungs to provide oxygenated blood, which then returns to the left atrium and through the atrial septal defect into the right atrium. After mixing with all the deoxygenated blood from the inferior vena cava, it is then pumped by the right ventricle into the aorta. The advantages of this operation are that it removes the right ventricular volume overload from the prior aortopulmonary shunt, tends to protect the pulmonary vascular bed from the development of pulmonary artery hypertension, and increases the diastolic systemic arterial blood pressure. Stage II palliation allows remodeling of right ventricular geometry, reducing stress while normalizing the mass-to-volume ratio of the chamber. It is also during this stage that other associated cardiac problems are corrected, such as tricuspid valve repair for tricuspid regurgitation, pulmonary angioplasty for any pulmonary

artery deformity or stenosis, and, if necessary, further enlargement of a restrictive interatrial defect.

Stage III palliation (Fontan)

The third stage of the physiologic repair is performed at ~2–4 years of age. It involves creating an inferior cavopulmonary connection with a separation between the oxygenated and deoxygenated blood in the right atrium so that blood from the inferior vena cava and also from the superior vena cava flows directly into the pulmonary arteries (Figure 38.4c). The conduit was initially intra-atrial, but recently extra-atrial tunnels have become popular. A small fenestration or connection between the conduit and right atrium is typically left to allow gradual accommodation for the increased venous flow, decompression of the conduit should systemic venous pressure rise excessively, and reduction in the frequency and severity of postoperative pleural effusions and other complications. The fenestration may diminish in size or close spontaneously with time, or it may be closed at cardiac catheterization.

Immediate postoperative management is designed to maintain adequate pulmonary blood flow by hyperoxygenation, hyperventilation, and the development of mild respiratory and metabolic alkalosis. Recently, more emphasis has been placed on adequacy of systemic blood flow, because pulmonary blood flow tends to be relatively constant, coming as it does through a conduit [45]. Systemic oxygen transport is monitored by measuring oxygen saturation in the fixed superior vena cava and manipulating systemic flows accordingly. The transpulmonary pressure gradient is monitored from a central venous line and a line placed in the "left" atrial chamber. An elevated transpulmonary gradient may indicate increased pulmonary vascular resistance or anatomic obstruction. Persistent postoperative pulmonary effusions may require prolonged pleural drainage and adequate fluid replacement therapy. Some patients will eventually need ligation of the thoracic duct or pleurodesis.

Postoperative management

Stage I palliation leads to hemodynamic parameters similar to those that existed preoperatively, with pulmonary blood flow and systemic blood flow closely related to the ratio of pulmonary-to-systemic vascular resistance. Residua following stage I palliation have been identified (Table 38.5). After stage I, there is right ventricular pressure overload, because the right ventricle functions as the systemic ventricle and there is continued volume overload from the aortopulmonary shunt. The pressure overload may be aggravated by such factors as residual coarctation and volume overload complicated by residual tricuspid regurgitation. If the aortopulmonary shunt is large, there may be a decrease in systemic blood flow and perfusion with low diastolic pressure, which may in turn lead to diminished coronary blood

Table 38.5 Residua following stage I palliation.
Hypoxemia
Congestive heart failure
Sudden unexplained death
Restrictive interatrial communication
Pulmonary artery hypoplasia
Right ventricular dysfunction
Tricuspid regurgitation
Coarctation of the aorta
Tracheobronchial obstruction

flow. In the immediate postoperative period, pulmonary vasoconstriction with moderate to severe hypoxemia is common and usually resolves with appropriate ventilatory support and maintenance of normal acid–base balance. Extracorporeal membrane oxygenation is occasionally used and is limited to patients with reversible myocardial dysfunction, an unexplained increase in pulmonary vascular resistance, or acute respiratory disease. Intravenous infusion of fentanyl or morphine is used for sedation and analgesia. Parenteral alimentation is started on the second postoperative day, particularly in those at risk for necrotizing enterocolitis. The importance of a well-trained staff and a designated pediatric cardiac intensive care unit cannot be overemphasized as essential for optimal outcome of infants with HLHS. In less seriously ill infants, early feedings are initiated by nasogastric tube and subsequently given orally. Feeding intolerance is common and needs to be treated aggressively.

Interstage monitoring programs vigilantly assess weight gain in addition to SaO_2 and improve survival [46]. A small dose of aspirin (20 mg per day) is administered as an anticoagulant. Angiotensin-converting enzyme inhibitors and diuretics are often started before discharge from the hospital to decrease right ventricular workload and improve pulmonary blood flow. Recently, a randomized clinical trial performed by the Pediatric Heart Network showed that angiotension-converting enzyme inhibitors are not recommended for empiric use [47].

Mortality during and after operation remains fairly high. The mortality is 10–20% in the first stage, 4–30% while awaiting stage II, 0–5% for second-stage surgery, 5–7% while awaiting the third stage, and under 10% for the third stage. As a result, current 10-year survival after all three stages is about 40–60%, although recent results appear to be better [48].

Long-term history of treated adults

There are significant long-term sequelae following stage III palliation for HLHS (Table 38.6). Because the systemic circulation depends on the right ventricle, maintaining normal

Table 38.6 Sequelae following stage III palliation.

Right ventricular dysfunction
Venovenous collaterals (right-to-left shunt)
Aortopulmonary collaterals (left-to-right shunt)
Protein-losing enteropathy
Bronchitis plastica
Tricuspid regurgitation
Rhythm disturbances
CNS abnormalities

right ventricular function is essential. Ischemia and hypertrophy of the right ventricle may in turn lead to fibrosis, which decreases myocardial function. Rhythm and conduction disturbances are often accompanied by symptoms and may be life-threatening. Atrial tachyarrhythmias and sick sinus syndrome increase in frequency with advancing age and require close monitoring, pharmacologic therapy, and not infrequently interventional or surgical therapy. Resistant atrial flutter may require conversion of a classic Fontan to a cavopulmonary tunnel or extracardiac conduit or performance of the maze procedure alone or combined with epicardial pacemaker implementation.

Protein-losing enteropathy develops in ~4–13% of patients who have had a Fontan procedure for univentricular heart and often presents with abdominal pain, diarrhea, or peripheral edema. It occurs on the average of approximately 3 years after the Fontan procedure with the development of albuminemia, malnutrition, and a compromised immune state. The loss of albumin depletes intravascular volume and, when coupled with a higher central venous pressure, predisposes the patients to thromboses and strokes. Protein-losing enteropathy in these patients is difficult to treat. Diet alone and periodic albumin replacement may be effective in mild or early enteropathy. Steroids may induce remission in some patients, but are often discontinued because of side effects. Subcutaneous heparin has been effective in many patients. Cardiac transplantation when necessary is also effective.

Neurodevelopmental abnormalities are one of the greatest long-term concerns in children with HLHS. There is both imaging and histopathologic evidence that brains from fetuses and newborns with HLHS are abnormal *before* surgery [14,49,50]. Reported associated congenital CNS malformations include agenesis of the corpus callosum, holoprosencephaly, microcephaly, Arnold–Chiari malformation, and immature cortical mantle. These abnormalities may predispose the patient to acquired CNS abnormalities, including periventricular leukomalacia, cerebral necrosis, intracranial hemorrhage, and cerebral ischemia or infarction. In addition, the compound effects of chronic cyanosis and multiple major operations requiring cardiopulmonary bypass in early childhood are known to predispose to developmental delay. Although most stage III survivors demonstrate normal intelligence and

communication skills, a significant proportion demonstrate cognitive, motor, and behavioral deficits in late childhood and adolescence that may adversely impact quality of life.

References

1 Hoffman JI, Kaplan S. The incidence of congenital heart disease. *J Am Coll Cardiol* 2002;**39**:1890–900.

2 Ferencz C, Rubin JD, McCarter RJ, , *et al*. Congenital heart disease: prevalence at livebirth. The Baltimore–Washington Infant Study. *Am J Epidemiol* 1985;**121**:31–6.

3 Report of the New England Regional Infant Cardiac Program. *Pediatrics* 1980;**65**(2 Pt 2):375–461.

4 Lloyd-Jones D, Adams RJ, Brown TM, *et al*. Heart disease and stroke statistics – 2010 update: a report from the American Heart Association. *Circulation* 2010;**121**:948–54.

5 Hospital stays, hospital charges, and in-hospital deaths among infants with selected birth defects – United States, 2003. *MMWR Morb Mortal Wkly Rep* 2007;**56**:25–9.

6 Burkhart HM, Dearani JA, Mair DD, *et al*. The modified Fontan procedure: early and late results in 132 adult patients. *J Thorac Cardiovasc Surg* 2003;**125**:1252–9.

7 Shokeir MH. Hypoplastic left heart. Evidence for possible autosomal recessive inheritance. *Birth Defects Orig Artic Ser* 1974;**10**:223–7.

8 Brenner JI, Berg KA, Schneider DS, *et al*. Cardiac malformations in relatives of infants with hypoplastic left-heart syndrome. *Am J Dis Child* 1989;**143**:1492–4.

9 McBride KL, Pignatelli R, Lewin M, *et al*. Inheritance analysis of congenital left ventricular outflow tract obstruction malformations: segregation, multiplex relative risk, and heritability. *Am J Med Genet A* 2005;**134**A:180–6.

10 Hinton RB, Martin LJ, Tabangin ME, *et al*. Hypoplastic left heart syndrome is heritable. *J Am Coll Cardiol* 2007;**50**:1590–5.

11 Natowicz M, Chatten J, Clancy R, *et al*. Genetic disorders and major extracardiac anomalies associated with the hypoplastic left heart syndrome. *Pediatrics* 1988;**82**:698–706.

12 Grossfeld PD, Mattina T, Lai Z, *et al*. The 11q terminal deletion disorder: a prospective study of 110 cases. *Am J Med Genet A* 2004;**129**A:51–61.

13 Wernovsky G. Current insights regarding neurological and developmental abnormalities in children and young adults with complex congenital cardiac disease. *Cardiol Young* 2006;**16**(Suppl 1):92–104.

14 Hinton RB, Andelfinger G, Sekar P, *et al*. Prenatal head growth and white matter injury in hypoplastic left heart syndrome. *Pediatr Res* 2008;**64**:364–9.

15 Rosenthal GL. Patterns of prenatal growth among infants with cardiovascular malformations: possible fetal hemodynamic effects. *Am J Epidemiol* 1996;**143**:505–13.

16 Dasgupta C, Martinez AM, Zuppan CW, *et al*. Identification of connexin43 (alpha1) gap junction gene mutations in patients with hypoplastic left heart syndrome by denaturing gradient gel electrophoresis (DGGE). *Mutat Res* 2001;**479**:173–86.

17 McElhinney DB, Geiger E, Blinder J, *et al*. NKX2.5 mutations in patients with congenital heart disease. *J Am Coll Cardiol* 2003;**42**:1650–5.

18 Hinton RB, Martin LJ, Rame-Gowda S, *et al*. Hypoplastic left heart syndrome links to chromosomes 10q and 6q and is genetically related to bicuspid aortic valve. *J Am Coll Cardiol* 2009;**53**:1065–71.

19 Bruneau BG. The developmental genetics of congenital heart disease. *Nature* 2008;**451**:943–8.

20 Hornberger LK, Sanders SP, Rein AJ, *et al*. Left heart obstructive lesions and left ventricular growth in the midtrimester fetus. A longitudinal study. *Circulation* 1995;**92**:1531–8.

21 Harh JY, Paul MH, Gallen WJ, *et al*. Experimental production of hypoplastic left heart syndrome in the chick embryo. *Am J Cardiol* 1973;**31**:51–6.

22 deAlmeida A, McQuinn T, Sedmera D. Increased ventricular preload is compensated by myocyte proliferation in normal and hypoplastic fetal chick left ventricle. *Circ Res* 2007;**10**:1363–70.

23 Fishman NH, Hof RB, Rudolph AM, Heymann MA. Models of congenital heart disease in fetal lambs. *Circulation* 1978;**58**:354–64.

24 Canton J. Congenital obliteration of the origin of the aorta. *Trans Pathol Soc London* 1849;**2**:38–9.

25 Lev M. Pathologic anatomy and interrelationship of hypoplasia of the aortic tract complexes. *Lab Invest* 1952;**1**:61–70.

26 Noonan JA, Nadas AS. The hypoplastic left heart syndrome; an analysis of 101 cases. *Pediatr Clin North Am* 1958;**5**:1029–56.

27 Bharati S, Lev M. The surgical anatomy of hypoplasia of aortic tract complex. *J Thorac Cardiovasc Surg* 1984;**88**:97–101.

28 Tchervenkov CI, Jacobs JP, Weinberg PM, Aiello VD, *et al*. The nomenclature, definition and classification of hypoplastic left heart syndrome. *Cardiol Young* 2006;**16**:339–68.

29 Rosenthal A. Physiology, diagnosis and clinical profile of the hypoplastic left heart syndrome. *Prog Pediatr Cardiol* 1996;**5**:19–27.

30 Chang RK, Gurvitz M, Rodriguez S. Missed diagnosis of critical congenital heart disease. *Arch Pediatr Adolesc Med* 2008;**162**:969–74.

31 Mahle WT, Clancy RR, McGaurn SP, *et al*. Impact of prenatal diagnosis on survival and early neurologic morbidity in neonates with the hypoplastic left heart syndrome. *Pediatrics* 2001;**107**:1277–82.

32 Frommelt PC, Sheridan DC, Mussatto KA, *et al*. Effect of shunt type on echocardiographic indices after initial palliations for hypoplastic left heart syndrome: Blalock–Taussig shunt versus right ventricle–pulmonary artery conduit. *J Am Soc Echocardiogr* 2007;**20**:1364–73.

33 Friedberg MK, Silverman NH, Dubin AM, Rosenthal DN. Right ventricular mechanical dyssynchrony in children with hypoplastic left heart syndrome. *J Am Soc Echocardiogr* 2007;**20**:1073–9.

34 Tworetzky W, Wilkins-Haug L, Jennings RW, *et al*. Balloon dilation of severe aortic stenosis in the fetus: potential for prevention of hypoplastic left heart syndrome: candidate selection, technique, and results of successful intervention. *Circulation* 2004;**110**:2125–31.

35 Barnea O, Austin EH, Richman B, Santamore WP. Balancing the circulation: theoretic optimization of pulmonary/systemic flow ratio in hypoplastic left heart syndrome. *J Am Coll Cardiol* 1994;**24**:1376–81.

36 Jobes DR, Nicolson SC, Steven JM, *et al*. Carbon dioxide prevents pulmonary overcirculation in hypoplastic left heart syndrome. *Ann Thorac Surg* 1992;**54**:150–1.

37 Hoffman GM, Stuth EA, Jaquiss RD, *et al*. Changes in cerebral and somatic oxygenation during stage 1 palliation of hypoplastic left heart syndrome using continuous regional cerebral perfusion. *J Thorac Cardiovasc Surg* 2004;**127**:223–33.

38 Norwood WI, Lang P, Hansen DD. Physiologic repair of aortic atresia–hypoplastic left heart syndrome. *N Engl J Med* 1983;**308**:23–6.

39 Sano S, Ishino K, Kawada M, *et al*. Right ventricle–pulmonary artery shunt in first-stage palliation of hypoplastic left heart syndrome. *J Thorac Cardiovasc Surg* 2003;**126**:504–9; discussion 509–10.

40 Galantowicz M, Cheatham JP. Lessons learned from the development of a new hybrid strategy for the management of hypoplastic left heart syndrome. *Pediatr Cardiol* 2005;**26**:190–9.

41 Glenn WW. Circulatory bypass of the right side of the heart. IV. Shunt between superior vena cava and distal right pulmonary artery; report of clinical application. *N Engl J Med* 1958;**259**:117–20.

42 Fontan F, Baudet E. Surgical repair of tricuspid atresia. *Thorax* 1971;**26**:240–8.

43 Bailey L, Concepcion W, Shattuck H, Huang L. Method of heart transplantation for treatment of hypoplastic left heart syndrome. *J Thorac Cardiovasc Surg* 1986;**92**:1–5.

44 Ohye RG, Sleeper LA, Mahony L, *et al*., for the Pediatric Heart Network Investigators. Outcomes of the Norwood procedure in infants randomized to a modified Blalock–Taussig versus right ventricle-to-pulmonary artery shunt. *N Engl J Med* 2010;**362**:1980–92.

45 Li J, Zhang G, McCrindle BW, *et al*. Profiles of hemodynamics and oxygen transport derived by using continuous measured oxygen consumption after the Norwood procedure. *J Thorac Cardiovasc Surg* 2007;**133**:441–8.

46 Ghanayem NS, Hoffman GM, Mussatto KA, *et al*. Home surveillance program prevents interstage mortality after the Norwood procedure. *J Thorac Cardiovasc Surg* 2003;**126**:1367–77.

47 Hsu DT, Zak V, Mahony L, *et al*. Enalapril in infants with single ventricle: results of a multicenter randomized trial. *Circulation* 2010;**122**:333–40.

48 Hoffman JIE. *The Natural and Unnatural History of Congenital Heart Disease*. Oxford: Wiley-Blackwell, 2009: 531–45.

49 Mahle WT, Tavani F, Zimmerman RA, *et al*. An MRI study of neurological injury before and after congenital heart surgery. *Circulation* 2002;**106**(Suppl 1):I109–14.

50 Dent CL, Spaeth JP, Jones BV, *et al*. Brain magnetic resonance imaging abnormalities after the Norwood procedure using regional cerebral perfusion. *J Thorac Cardiovasc Surg* 2006;**131**:190–7.

51 Barron DJ, Kilby MD, Davies B, *et al*. Hypoplastic left heart syndrome. *Lancet* 2009;**374**:551–64.

39

Univentricular Heart

Jacqueline Kreutzer[1], César Viegas[2], Eduardo A. Kreutzer[3] & Guillermo O. Kreutzer[2]

[1]University of Pittsburgh School of Medicine, Children's Hospital of Pittsburgh of UPMC, Pittsburgh, PA, USA
[2]Buenos Aires Children's Hospital and University of Buenos Aires Medical School, Buenos Aires, Argentina
[3]Hospital de Niños Pedro Elizalde and Centro Cardiovascular Infantil, Buenos Aires, Argentina

Introduction

The univentricular heart [1], single ventricle or "common" ventricle [2,3], accounts for ≤2% of congenital cardiac defects [4], predominating in males by a factor of 1.5–2 [2,5]. For many years, the definition of a univentricular heart has been disputed by various authors [1,3,6,7], differing in terminology and characterization criteria. In 1964, Van Praagh *et al.* [2] defined single ventricle as the absence of the sinus portion of a ventricular chamber, excluding tricuspid and mitral atresia. In contrast, Anderson *et al.* [1] and Shinebourne *et al.* [8], basing their definition on the anatomy of the atrioventricular valves [9] and the atrioventricular connections, rather than ventricular morphology *per se*, included hearts with one valve and >50% of the second valve, or >75% of a common atrioventricular valve, entering one ventricle [8–10]. Therefore, they included as univentricular hearts the single ventricle, the double-inlet ventricle with overriding atrioventricular valve of >50%, the unbalanced common atrioventricular canal [11], tricuspid atresia, and mitral atresia [8,9]. Because most of these hearts have two ventricles, although one is rudimentary or hypoplastic, single ventricle seemed an inappropriate term. Therefore, the term univentricular atrioventricular connection [12] was proposed when two atrioventricular valves (double inlet), one common atrioventricular valve (common inlet), and one single atrioventricular valve (single inlet) are connected completely or in their greater component to a certain ventricle (Figure 39.1). The second or additional ventricular chamber can be hypoplastic when it has an inlet portion (<50% of an atrioventricular valve or <25% of a common atrioventricular valve), including the overriding atrioventricular valves, or a rudimentary chamber in its absence. When the rudimentary chamber is superior, it is morphologically a right ventricle (thick trabecular component); when it is posteroinferior, it is morphologically a left ventricle (fine trabeculated component). The concept of single ventricle by Van Praagh *et al.* is based on morphology of the ventricle itself rather than surrounding structures and thus appears more scientifically sound. However, in clinical practice, the concept of single ventricle by Anderson *et al.* is often considered more practical and therefore is used more commonly.

A univentricular heart can be classified morphologically [13] as follows (Figures 39.1 and 39.2):
 I Single ventricle, with two subtypes
   A Single left ventricle, due to agenesis of the right ventricular inlet
   B Single right ventricle, due to agenesis of the left ventricular inlet
II Unbalanced ventricles with a dominant ventricular chamber, which can have either
   A Dominant left ventricle (hypoplastic right ventricular inlet) or
   B Dominant right ventricle (hypoplastic left ventricular inlet).
According to Anderson *et al.* [1], unbalanced ventricles have >1.5 atrioventricular valve rings or >75% of a common atrioventricular valve ring aligned to a dominant right or left ventricle; the other atrioventricular valve or portion of it is aligned with a hypoplastic right or left ventricle.

Embryology

Comparative morphologic studies [14] suggest that single ventricle in humans is not an evolutionary phylogenetic regression of the human heart towards the single ventricle present in amphibian, fish, and lower reptiles but rather
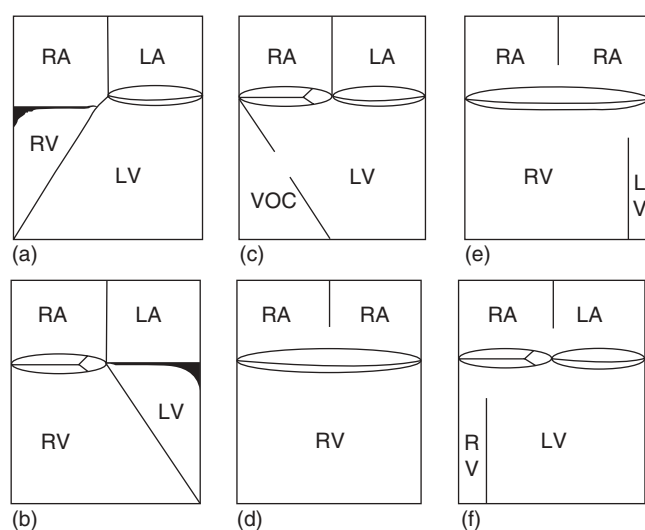
Figure 39.1 Schematic classification of univentricular atrioventricular connection. Atretic atrioventricular connection: tricuspid atresia (a) and mitral atresia (b). Single ventricle: single left ventricle IA with rudimentary bulboventricular outflow chamber in anterosuperior position (right ventricle) (c); single right ventricle with common atrioventricular valve and atrial dextroisomerism (d). Unbalanced ventricles: dominant right ventricle with hypoplasia of the left ventricle, common atrioventricular valve, and atrial dextroisomerism (e); dominant left ventricle with hypoplastic right ventricular inlet (f). RA, right atrium; LA, left atrium; LV, left ventricle; RV, right ventricle; VOC, ventricular outlet chamber.

results from defective cardiac ontogenesis. Once cardiac looping is complete, the internal structure of the heart still consists of a single convoluted tube including atria, ventricle, bulbus cordis, and truncus arteriosus. The morphologically left ventricle is known to be derived from the ventricle of the bulboventricular loop [14]. By Streeter's stages XI–XV, the atrioventricular canal of the embryo opens entirely into the left ventricle. Thus, common inlet and double-inlet left ventricle are potentially present in human development and may represent an arrest at this stage.

The morphologic aspects of the embryogenesis of single ventricle are still controversial [1,7,13,15]. According to Van Praagh et al. [13], in single left ventricle, there is agenesis of the right ventricular inlet; the right ventricle fails to evaginate from the ventricle of the bulboventricular loop, and the ventricular septum shifts toward the side of the absent right ventricle (anterior and to the right in a d-loop, anterior and to the left in an l-loop). As the ventricular septum moves beneath the infundibulum, it can create the picture of an infundibular outlet chamber. In a single or dominant right ventricle, the absent or poorly developed left ventricle shifts the ventricular septum posteriorly and to the left in a ventricular d-loop or posteriorly and to the right in an l-loop. In these anomalies, the location of the ventricular septum away from the infundibulum generally prevents the development of an infundibular outlet chamber.

Others have suggested that double-inlet left or right ventricle results from an abnormal shift of the atrioventricular canal septum by either growth failure or excessive rightward shift. Thus, some examples of straddling atrioventricular valve can be explained as a lesser degree of abnormal positioning of the atrioventricular canal relative to the ventricular chamber [1,7,15] (see Chapter 1).

Pathologic anatomy

An anatomico-clinical classification of univentricular hearts according to their atrioventricular connection is shown in Figure 39.2.

On the basis of a segmental approach to diagnosis [8,10], a pathologic study described 22 hearts with univentricular atrioventricular connection from a total of 196 congenital heart defects [16]; of the 22, six were single ventricles, six were unbalanced ventricles (four with dominant right ventricle and two with dominant left ventricle), five had classic tricuspid atresia, and five had mitral atresia.

Tricuspid atresia constitutes a typical anatomico-clinical entity among the hypoplastic right ventricles. Similarly, mitral atresia belongs to the hypoplastic left heart variants – although it may coexist with a large left ventricle. In both entities, the atrial septum is aligned normally to the interventricular septum at the level of the crux of the heart. This feature allows their echocardiographic characterization. Mitral and tricuspid atresia are not considered in this chapter (see Chapters 35 and 38). However, diagnostic and management approaches are shared by all these lesions.

Single ventricle, with double inlet or with common inlet

On the basis of a pathologic study of 60 hearts, single ventricle was classified by Van Praagh et al. [2] into four types (Figure 39.3):

• Type A, single morphologically left ventricle, characterized by numerous fine apical trabeculations, obliquely oriented. The papillary muscles originate from the ventricular free wall, into which two atrioventricular valves drain. An infundibular outlet chamber of superior position is separated from the ventricle by the bulboventricular septum and connected to it by the bulboventricular foramen.

• Type B, single morphologically right ventricle, characterized by thick, few, coarse, and straight apical trabeculations, with septal band and moderator band extending to the papillary muscle of the conus; the atria drain through one or two atrioventricular valves.

• Type C, common ventricle, with severe deficiency of the interventricular septum.

• Type D, undetermined ventricle (diagnosed as neither left nor right ventricle).
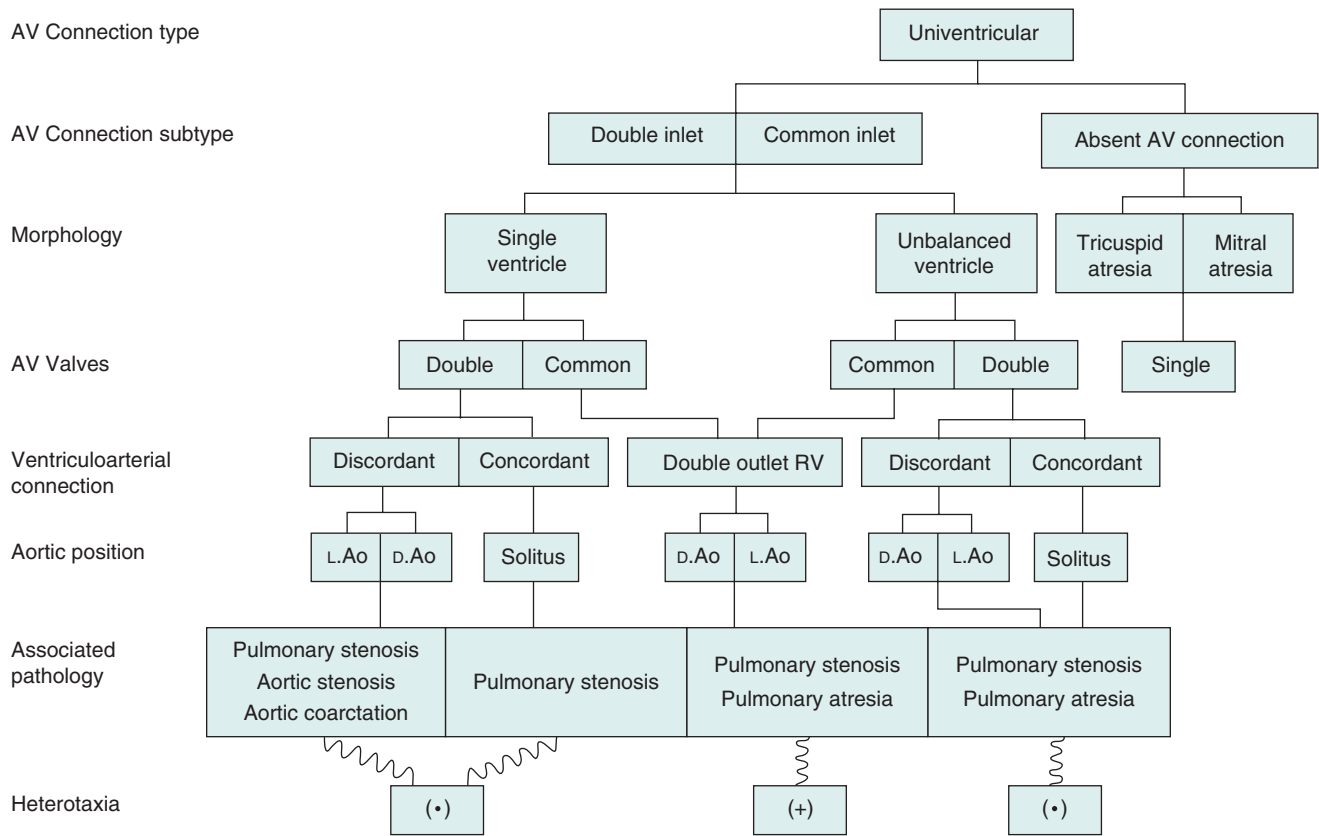
Figure 39.2 An anatomico-clinical classification of univentricular hearts according to their atrioventricular (AV) connection. Ao, aorta; RV, right ventricle.

With the segmental approach, single ventricle was classified according to its arterial relationships: I, normal or solitus; II, d-aorta anterior; III, l-aorta anterior; IV, l-aorta posterior (inversus). In addition, the ventricular loop was differentiated as dextro (d) or levo (l), according to the ventricular situs. The atrioventricular connections, the ventriculoarterial relationships (transposition, double outlet, or single outlet), and any obstruction at the pulmonary or aortic level were also determined.

The original type C [2] is not currently considered a form of single ventricle because of having two well-developed ventricles with absent or extremely hypoplastic interventricular septum [13]. Type D is considered to be a single right ventricle not adequately identified [13].

Single left ventricle
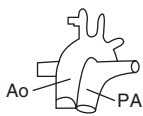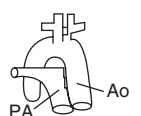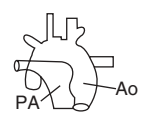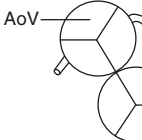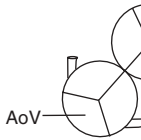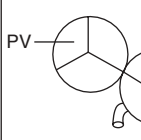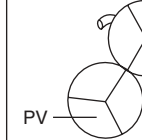
Single left ventricle (Figure 39.4) accounts for 80% of single ventricles [2,13,17], 90% of which have an infundibular outlet chamber and discordant ventriculoarterial connections (transposition). Ventricular l-loop with l-transposition and left outlet chamber occurs in 55% of patients; ventricular d-loop with d-transposition and right-sided infundibular outlet chamber is less common (35%) (Figure 39.4a). The remaining 10% have concordant ventriculoarterial connection
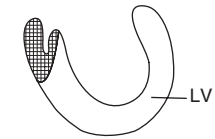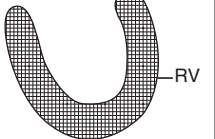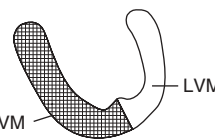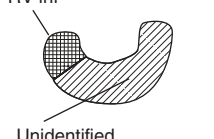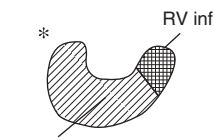
with right-sided infundibular outlet chamber and normally related great arteries (Holmes heart [18]).

The bulboventricular foramen is restrictive in 40% of the patients with discordant ventriculoarterial connection, causing subaortic stenosis, and in 90% of those with concordant ventriculoarterial connections (Holmes heart), causing subpulmonary stenosis. Coarctation of the aorta is associated in 15% of the patients with type IA and coexists with subaortic stenosis. Pulmonary stenosis or atresia occurs in 40% of patients.

There are usually two atrioventricular valves, right and left sided. The valve in contact with the bulboventricular septum is anatomically a tricuspid valve, and that related to the free wall of the ventricle without attachments to the septum is anatomically a mitral valve. Fibrous continuity commonly exists between the atrioventricular valves and the posterior semilunar valve. The atrioventricular valves appear "normal" in 70% of the patients but can be dysplastic with significant regurgitation (15%), more frequently of the left-sided valve. In 15% of patients, the atrioventricular valves are stenotic or even imperforate, particularly the right one.

When the infundibular outlet chamber is left sided and the ventriculoarterial connection is discordant (type IA III), the left coronary artery is usually dominant [17]. Close to its

Relationships between the great Arteries

Type	I	II	III	IV
SUP. R ←┼→ L INF. Anterior view	Normal Ao — PA	D-Transposition Ao — PA	L-Transposition PA — Ao	Inversus PA — Ao
POST. R ←┼→ L ANT. Superior view	AoV — PV	PV — AoV	PV — AoV	AoV — PV
Cases. no.(%)	9 (15%)	25 (42%)	26 (43%)	0

Ventricular Malformations

Type	A	B	C	D
Principal Malformation	Absence of RV Sinus	Absence of LV Sinus	Absent or Rudimentary Ventricular Septum	Absence of RV and LVSinuses and of Ventricular Septum
D–Loop RV(R) LV (L) Anterior view	RV Inf — LV	RV	RV inf RVM — LVM	RV inf Unidentified
L- Loop LV(R) RV (L) Anterior view	RV Inf LV	RV	LVM — RVM	RV inf Unidentified
Cases. no.(%)	47 (78%)	3 (5%)	4 (7%)	6 (10%)

✳ X – Loop, 2 cases with Dextrocardia. Since Ventricular Apex Posterior

✳ Dextrocardia
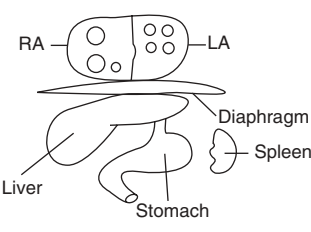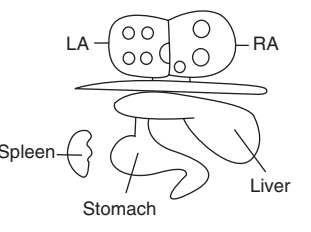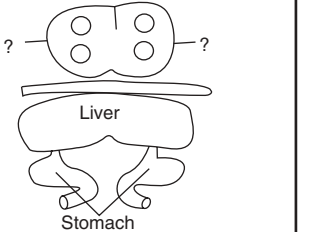
Situs of Viscera and Atria

Type	Solitus	Inversus	Heterotaxy
	(Ordinary, ie., Normal)	(Mirror image of Solitus)	(Uncertain situs with asplenia)
SUP. R ←┼→ L INF. Anterior view	RA — LA Diaphragm Spleen Liver Stomach	LA — RA Spleen Liver Stomach	? — ? Liver Stomach
Cases. no. (%)	50 (83%)	2 (3%)	8 (13%)

Figure 39.3 Classification of hearts with a single ventricle. Ao, aorta; AoV, aortic valve; Inf, infundibulum; LA, left atrium; LV, left ventricle; LVM, left ventricular mass; PA, pulmonary artery; PV, pulmonary valve; RA, right atrium; RV, right ventricle; RVM, right ventricular mass. (Reproduced with permission from Van Praagh R, Ongley P, Swan HJC. *Am J Cardiol* 1964;**13**:367–86.)
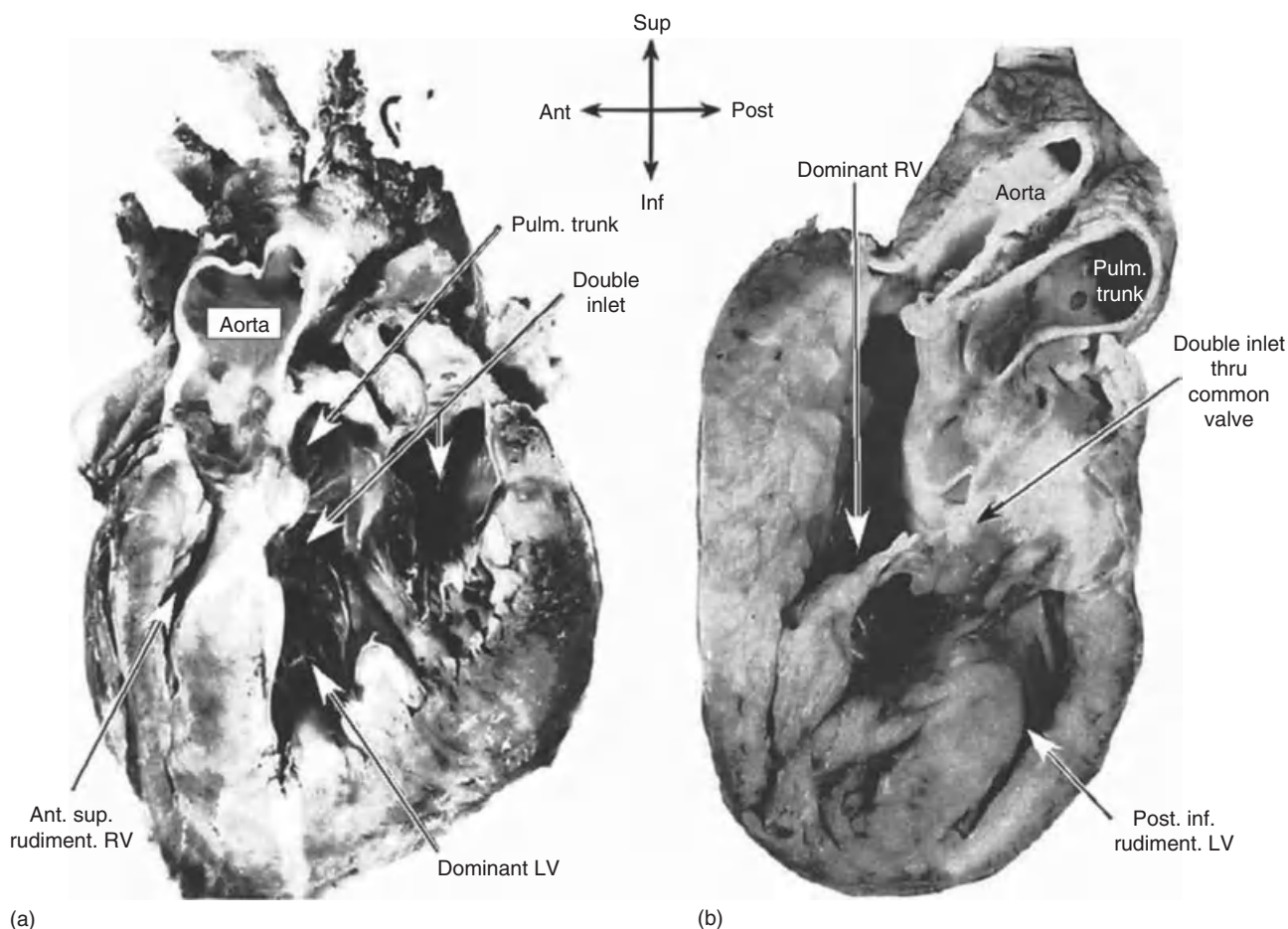
Figure 39.4 Arterial long-axis sections showing the anteroposterior position of the ventricular outlet chamber in single left ventricle IA (a) and the posteroinferior position of the hypoplastic left ventricle in unbalanced ventricles with dominant right ventricle IIB (b). Ant, anterior; Inf, inferior; LV, left ventricle; Post, posterior; RV, right ventricle; Sup, superior. (Reproduced from Barra Rossi *et al.*, *Rev Lat Cardiol Cir Cardiovasc Infant* 1986;**3**:171.)

origin in the posterior and leftward aortic cusp, the left coronary gives origin to a left delimiting artery that outlines the left bulboventricular septal groove. The right coronary originates in the right aortic sinus and runs in the right atrioventricular groove, giving origin to the right delimiting artery and two to six parallel delimiting arteries that cross the anterior surface of the heart, at the site of ventriculotomy for a ventricular septation procedure. When the infundibular chamber is right-sided and the ventriculoarterial connection is concordant, the delimiting arteries also course around the hypoplastic infundibular chamber.

In double-inlet single ventricle, the conduction system is characterized by an accessory atrioventricular anterolateral node [19,20] localized in the floor of the right atrium, at the acute anterolateral margin of the right atrioventricular ring. Through a nonbranching long bundle, it penetrates the ring, reaches the right parietal wall of the ventricle, and passes towards the rudimentary outlet chamber, following its right edge. If the infundibular outlet chamber is left sided, the bundle crosses the outflow tract of the main chamber

anteriorly towards the outlet chamber, immediately anterior and in proximity to the ring of the posterior great artery. If the outlet chamber is right sided, it crosses at the inferior and right edge of the bulboventricular foramen (Figure 39.5).

The location of the sinoatrial node depends on the atrial situs, which is solitus in most patients, rarely ambiguous, and inversus in 1% [21].

Single right ventricle

A single right ventricle is present in 20% of patients with single ventricles [2,13,22]. This includes examples of double-outlet single right ventricle with or without subaortic or bilateral conus, with anterior aorta (subaortic conus) or side-by-side great vessels.

More than 90% of the patients have associated pulmonary stenosis or atresia. Among other associated anomalies are common atrioventricular valve, ambiguous atrial situs [23,24], ostium primum atrial septal defect or common atrium, double-outlet right ventricle, anomalies of systemic venous return (interrupted inferior vena cava with azygos

(a)   Right sided rudimentary right ventricle

(b)   Left sided rudimentary right ventricle

(c)
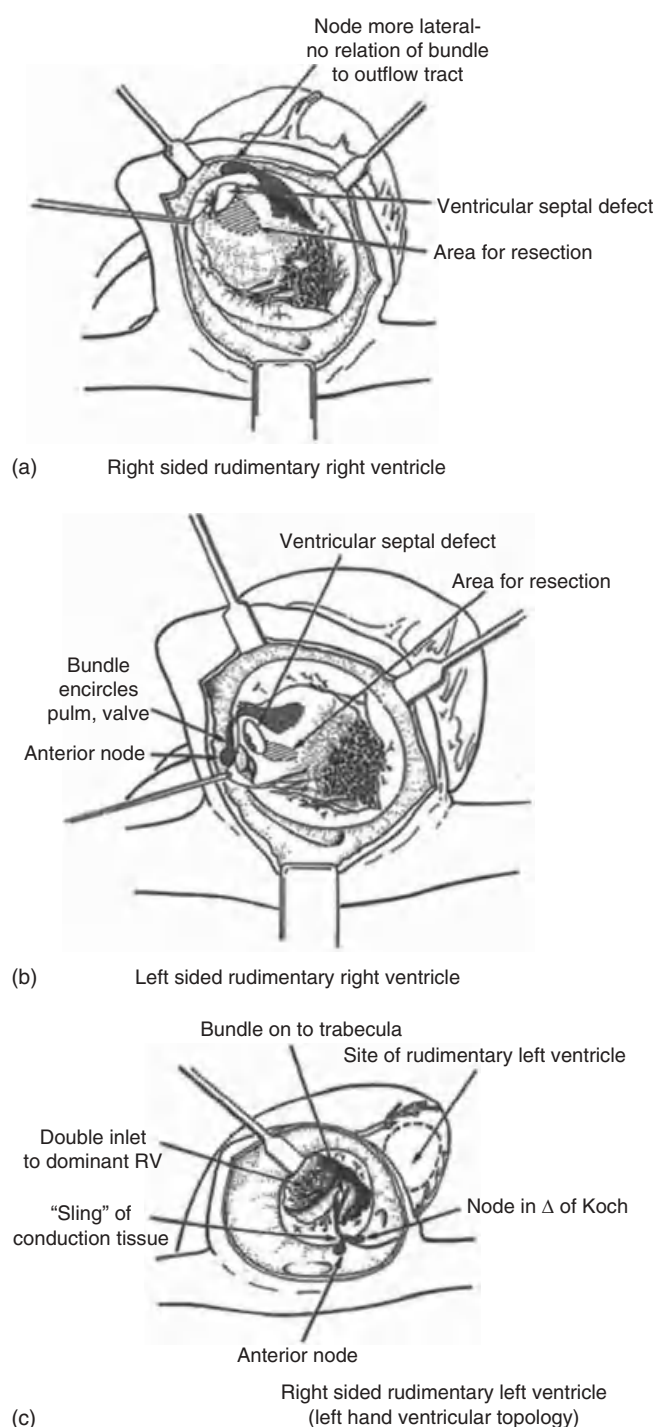
Figure 39.5 Diagrams illustrating the conduction system in single left ventricle with right and left ventricular outlet chamber (a, b) and in unbalanced ventricle with dominant left ventricle (c). (Parts (a) and (c) reproduced from Barra Rossi *et al.*, *Rev Lat Cardiol Cir Cardiovasc Infant* 1986;**3**:171.)

continuation in patients with polysplenia), inferior vena cava ipsilateral to the descending aorta (in patients with asplenia), double superior venae cavae, unroofed coronary sinus, and anomalous pulmonary venous connections of the extracardiac variety (asplenia) or at cardiac level (polysplenia) (see Figure 39.2) [24].

Unbalanced ventricles

We exclude in this chapter the overriding atrioventricular valves, when the overriding into the contralateral ventricle is <50% of an atrioventricular valve or <75% of a common atrioventricular valve [25], as these are considered as biventricular hearts. An unbalanced ventricle with either a dominant left ventricle [5](IIA) or a dominant right ventricle (IIB) (see Figures 39.1, 39.2, and 39.4) differs from a single ventricle [2,5] in that it has two ventricular inlet portions [26], resulting in an unbalanced biventricular heart, but with a univentricular atrioventricular connection. These are regarded as univentricular hearts. One ventricle is hypoplastic or secondary, and the other is dominant or major. There can be two atrioventricular valves, a common atrioventricular valve [27], or a single patent valve with an imperforate second atrioventricular valve, aligned to both ventricles, although predominantly to the dominant one.

Malalignment between the interventricular septum and the atrial septum, with an abnormal atrioventricular septal angle of 30–90° (normal 10°), has been described [28].

Among patients with unbalanced ventricles, 60% [5] have an unbalanced common atrioventricular valve [11] with either a dominant right ventricle (type IIB, 71%; see Figure 39.4b) or, less frequently, a dominant left ventricle (type IIA, 29%) [29]. They are commonly associated with heterotaxia, often asplenia syndrome, and a large ostium primum atrial septal defect or a common atrium [23,24], and other associated anomalies such as double-outlet right ventricle and pulmonary stenosis or atresia.

About 30% of patients with unbalanced ventricles have a dominant left ventricle (type IIA) with a conoventricular septal defect extending into the inlet septum. The atrioventricular valves are at the same level [5] with overriding of >50% of the tricuspid valve and insertion into an anomalous papillary muscle from the free wall of the left ventricle (Figure 39.6). The remaining 5–10% have a dominant right ventricle (type IIB) with overriding and straddling of the anterosuperior portion of the anterior leaflet of the mitral valve. The anterior mitral valve leaflet, commonly with a cleft, inserts on the anterior papillary muscle of the right ventricle through an anterior ventricular septal defect secondary to malalignment of the conal and anterior muscular septum.

When there are two atrioventricular valves, the ventriculo-arterial connection is discordant in 70% of patients [26] and occasionally associated with superoinferior ventricles. Double-outlet right ventricle occurs in a few patients. Rarely, the

(a)   Minimal

(b)   Moderate

(c)   Extreme
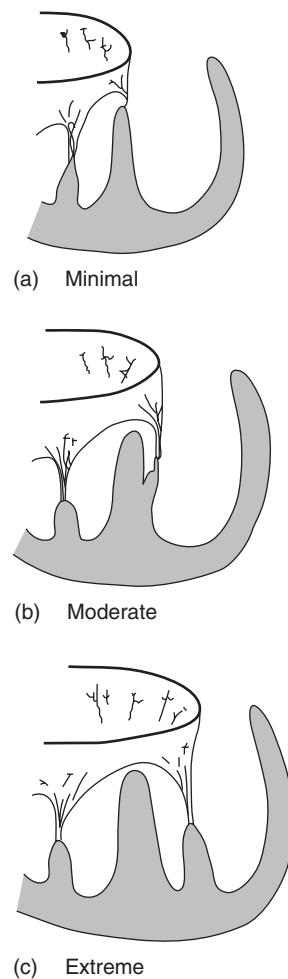
Figure 39.6 Illustration of the three grades of straddling of one atrioventricular valve. (Reproduced from Barra Rossi *et al.*, *Rev Lat Cardiol Cir Cardiovasc Infant* 1986;**3**:171.)

ventriculoarterial connection is concordant. In an unbalanced ventricle, the atrioventricular valves are commonly abnormal [5]. There may be a dysplastic tricuspid valve with insufficiency, a cleft or stenotic mitral valve, or a common atrioventricular valve. The last is common in patients with heterotaxia and unbalanced common atrioventricular valve into a dominant right ventricle [24–26,28,29].

Heterotaxia is common in patients with unbalanced ventricles (60%) and rare in patients with single ventricle (10%). When present, more commonly it is associated with a single right ventricle [5,24,29].

Hemodynamics

Hemodynamic patterns in patients with a univentricular heart [30–34] depend mostly on the presence or absence of obstruction to outflow into the aorta or pulmonary artery, the morphology and function of the single or dominant

ventricle, the type of atrioventricular connection, and the function of the atrioventricular valves.

Pulmonary blood flow

Patients without pulmonary stenosis [34] have increased pulmonary blood flow with a high Qp/Qs (≥3) and signs of congestive heart failure that appear during the first weeks of life. Systemic oxygen saturations approximate 90% without significant clinical cyanosis. When Qp/Qs approaches 2, they may present with mild cyanosis, with oxygen saturation approaching the mid-80s. These patients are generally well and compensated hemodynamically. Patients with moderate pulmonary stenosis and Qp/Qs approaching 1 have cyanosis with oxygen saturations of ~75–80%. When there is severe pulmonary stenosis and Qp/Qs is <1, their cyanosis may become extreme with saturations of 60–70% or less (Figures 39.7 and 39.8) Patients with coexisting pulmonary atresia present in the newborn period when the patent ductus closes spontaneously, as in other ductus-dependent lesions.

Ventricular and atrioventricular valve morphology

Although the effect of anatomy on function is not always predictable, when the single or dominant ventricle is anatomically a left ventricle, ventricular dysfunction is less common and tends to develop later. When the single or dominant ventricle is anatomically a right ventricle, however, it may perform adequately initially but with volume and pressure overload is more prone to evolve into a dilated myopathy because of mismatch between the ventricular mass and volume. This occurs commonly with progressive atrioventricular valve regurgitation. The clinical scenario resembles that in other patients with a systemic right ventricle, such as those with corrected transposition or transposition of the great arteries after the Senning or Mustard procedure. Abnormal and dysplastic atrioventricular valves can also be regurgitant, even without pressure or volume overload, and this may trigger early ventricular dysfunction.

Rarely, a stenotic or imperforate atrioventricular valve is associated with a restrictive atrial septal defect, causing pulmonary edema early in life and requiring emergency intervention to allow left atrial decompression and adequate mixing.

Systemic blood flow

In single left ventricle, obstruction to systemic blood flow is typically due to subaortic obstruction as a consequence of a progressive and relative decrease in the size of the bulboventricular foramen [31]. It can also occur acutely after a sudden decrease in preload and ventricular volume when a partial right-sided heart bypass operation is performed (bidirectional Glenn), in patients after pulmonary artery banding [32,35,36], or when preload normalizes in patients after total right-sided heart bypass operation [36]. Associated arch obstruction in patients with subaortic stenosis can be
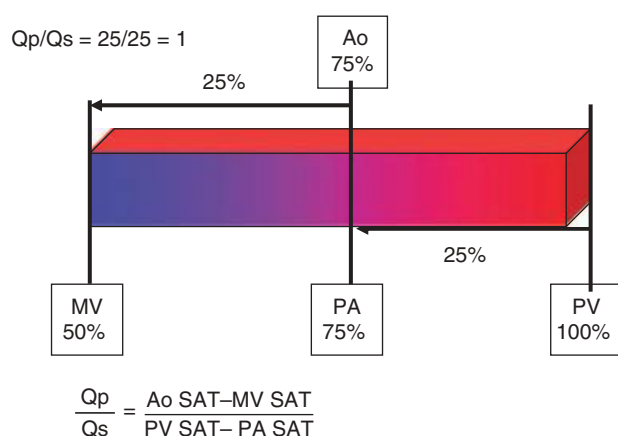
Figure 39.7 Hemodynamic graph indicating relationship between systemic (*Q*s) and pulmonary (*Q*p) blood flow in a hypothetical patient with single ventricle after initial neonatal palliation with an arterial oxygen saturation of 75%. In the absence of lung disease, a balanced *Q*p/*Q*s of 1 is likely present. AO, aortic oxygen saturation; MV, mixed venous or systemic venous oxygen saturation; PA, pulmonary artery oxygen saturation; PV, pulmonary vein oxygen saturation.
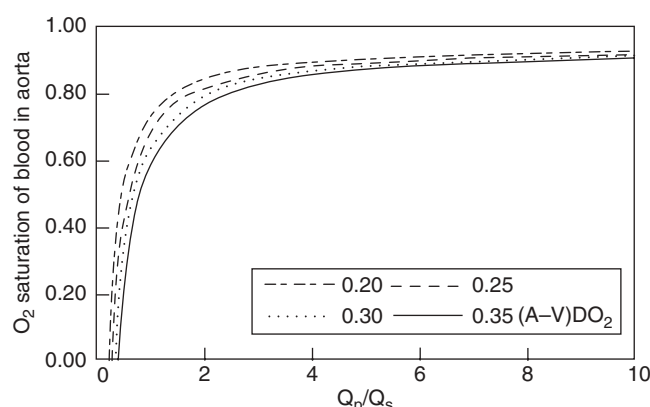
Figure 39.8 Demonstration of physiology of single ventricle with complete mixing showing an exponential increase in the pulmonary to systemic flow ratio associated with rising aortic oxygen saturation for any given arteriovenous gradient (A − V)DO$_2$. (Reproduced from Cardiac Surgery of the Neonate and Infant, Castaneda AR, Jonas RA, Mayer JE, Hanley FL. Chapter 5, P.80,1994 with permission from Elsevier.)

severe. If there is severe arch hypoplasia, patients are ductus dependent and present similarly to neonates with hypoplastic left heart syndrome.

Natural history

Most patients with single ventricle develop symptoms during the first weeks or months of life. Those with increased pulmonary blood flow show signs of congestive heart failure and pulmonary hypertension, whereas those with decreased pulmonary blood flow and pulmonary stenosis present with

cyanosis. Without treatment by operation, death occurs in infancy in 64% of these patients; more than half die during the neonatal period [37].

Patients with increased pulmonary blood flow [33] develop permanent pulmonary hypertensive vascular changes after the first year of life. This leads to a decrease in the *Q*p/*Q*s ratio and congestive heart failure, followed by progressive chronic cyanosis.

Among adult survivors without surgical intervention, 75% have pulmonary stenosis of moderate degree, and the remaining 25% have pulmonary hypertension with various levels of hypertensive pulmonary arteriopathy [38,39]. Most have congestive heart failure and are classified as New York Heart Association class II. They typically have a single left ventricle with two well-functioning atrioventricular valves, situs solitus, nonrestrictive subaortic bulboventricular foramen, and sinus rhythm. Complete heart block develops in 20% of these patients, requiring a pacemaker [39].

Progressive regurgitation of the atrioventricular valves is poorly tolerated in patients with univentricular heart, especially with a single or dominant right ventricle [35].

Single ventricle can be classified into types A and C, according to the presence or absence of a rudimentary outlet chamber [33,34]. Patients with type C have a poor prognosis, with 50% mortality by 4 years after diagnosis, compared with a 50% mortality at 14 years after diagnosis for patients with type A. The cause of death in patients with type A can be congestive heart failure, arrhythmia, or sudden death [39]. Patients with unbalanced ventricles have an even worse prognosis owing to the frequent association with heterotaxia [25], higher incidence and severity of their pulmonary stenosis, dominant right ventricle, and regurgitation of the atrioventricular valves that can lead to ventricular dysfunction [35].

History and physical examination

Pulmonary stenosis and limited pulmonary blood flow

Pulmonary stenosis occurs in 60% of the patients, who develop clinical manifestations similar to those of patients with tetralogy of Fallot with or without pulmonary atresia. Rarely, the pulmonary stenosis is mild, and the patient may be acyanotic.

In these patients, cyanosis tends to be moderate to severe; clubbing is evident in older patients. Patients rarely have thoracic deformities during infancy, but may later manifest scoliosis. The precordial activity is commonly normal, but patients with coexisting l-transposition may have a left superior parasternal lift. The peripheral pulses are usually normal, unless there is a coexisting coarctation of the aorta. There is a systolic ejection murmur, the intensity and duration of which correlate directly with the amount of pulmonary blood flow and inversely with the severity of the
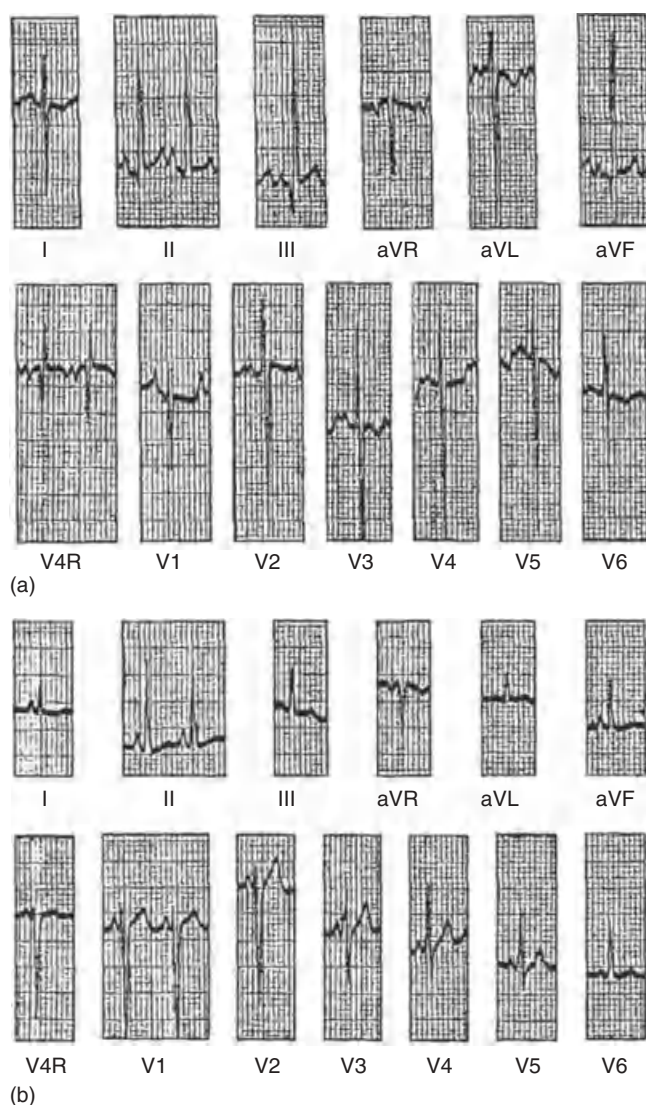
Figure 39.9 Electrocardiograms in patients with single left ventricle without pulmonary stenosis. (a) Type IA III, 28 days old, with QRS axis of 105° and counterclockwise loop, QR in V_4R, and no q waves in left precordial leads. (b) Type IA II, 45 days old, with QRS axis of 45°, rS in V_1, and R in V_6.

pulmonary stenosis and level of cyanosis. The absence of a systolic ejection murmur suggests severe pulmonary stenosis or atresia. A continuous murmur from a patent ductus arteriosus or a collateral may be heard in the pulmonary areas. The second heart sound is commonly loud, single (aortic component), and maximal at the upper left sternal border, particularly in patients with l-transposition.

Without pulmonary stenosis and increased pulmonary blood flow

About 40% of patients present similarly to those with an unrestrictive ventricular septal defect, increased pulmonary blood flow, and pulmonary hypertension. These patients develop congestive heart failure early in life with dyspnea, retractions, and poor weight gain. Cyanosis in infancy is minimal or absent. They more commonly have thoracic deformities and a hyperdynamic precordium. The second heart sound is loud and single. An S_3 gallop and a mitral mid-diastolic rumble can be heard in the apex. When a systolic thrill appears at the base and suprasternal notch, subaortic stenosis secondary to a restrictive bulboventricular foramen in types A III and A II should be suspected. On auscultation in such patients, there is a harsh, loud systolic ejection murmur at the base and midprecordium with radiation to the neck. A soft systolic ejection murmur in the midprecordium with radiation to the axilla and the back represents relative pulmonary stenosis. With coarctation of the aorta, the femoral pulses are diminished or absent.

More severe pulmonary edema and congestion than are accountable for by the amount of pulmonary blood flow or ventricular dysfunction suggest either severe stenosis or an imperforate left atrioventricular valve with restrictive atrial septal defect or anomalous pulmonary venous connections with obstruction, particularly in patients with asplenia.

Electrocardiography

Patients with single left ventricle, leftward bulboventricular outlet chamber, and ventricular l-loop (type IA III) have an inverted initial activation with q waves in the right precordial leads (qRS or qR in V_1) and no q waves in the left precordial leads (RS in V_6). Their QRS axis in the frontal plane is inferior and rightward, simulating left posterior hemiblock with clockwise loop [21] and qR in II, III, and aVF (Figure 39.9a). With time, complete atrioventricular block may develop [33]. Patients with single left ventricle with rightward outflow chamber and ventricular d-loop (types IA II or IA I) [40–42] have an electrocardiogram similar to tricuspid atresia, although generally without left anterior hemiblock. The precordial leads show an rS in V_1 and tall R waves in the left precordial leads consistent with left ventricular hypertrophy, with or without septal depolarization q waves (qR or R in V_6, due to abnormal initial activation directed anteriorly and to the left) (Figure 39.9b). In the frontal plane, the QRS axis is often in the left inferior quadrant.

Patients with single right ventricle (type IB) have signs of right ventricular hypertrophy (R, qR, or rsR'). The QRS axis is superior in the frontal plane with a counterclockwise loop. Rarely, the electrocardiogram may show rS waves in all the precordial leads. Patients with unbalanced ventricles commonly have a left anterior hemiblock pattern with signs of left ventricular hypertrophy when the left ventricle is dominant (type IIA). If there is a dominant right ventricle (IIB), the electrocardiogram most commonly shows right ventricular hypertrophy (Figure 39.10).
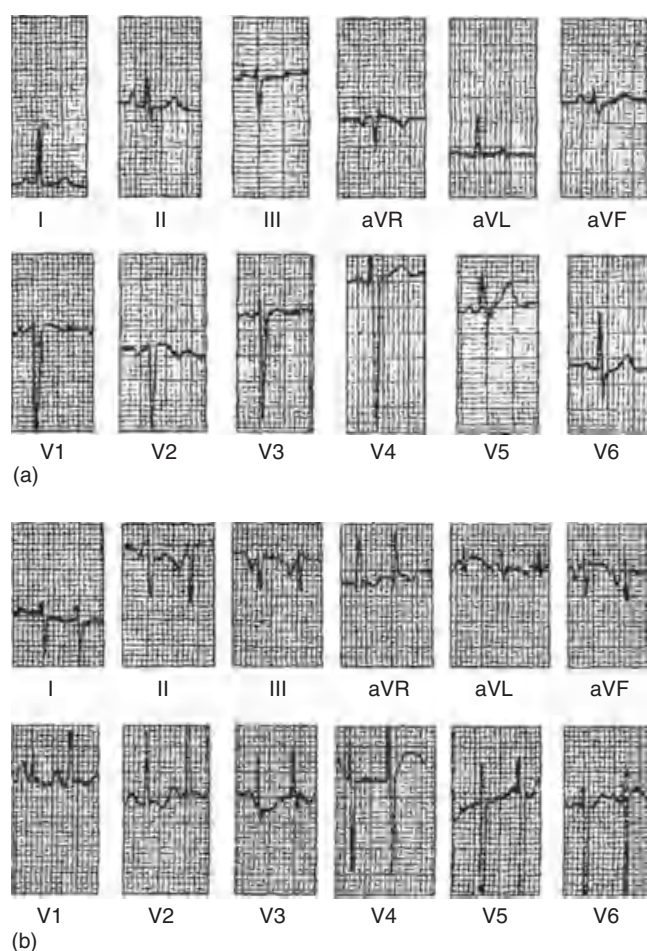
Figure 39.10 Electrocardiograms from patients with unbalanced ventricles. (a) Type IIA with pulmonary stenosis: left anterior hemiblock and absent right ventricular forces in a 2-year-old patient with a double-inlet dominant left ventricle. (b) Type IIB with pulmonary stenosis: low atrial rhythm, left anterior hemiblock, and right ventricular hypertrophy in a 1-month-old patient with polysplenia with interrupted inferior vena cava and common atrioventricular canal with a dominant right ventricle.

Patients with heterotaxia and asplenia syndrome or dextroisomerism can have two sinus nodes, and those with polysplenia or levoisomerism may lack a sinus node and have a low atrial rhythm. However, the sinus node coincides with the anatomic atrial situs in most patients with asplenia [29]. Congenital complete atrioventricular block in fetal life is associated with levoisomerism and a poor prognosis [43].

Imaging studies

Chest radiography

Patients can be characterized by chest radiography [4,44–46] as follows:

- patients with pulmonary stenosis, normal cardiac size, and diminished pulmonary vascular markings; or
- patients without pulmonary stenosis, severe cardiomegaly (cardiothoracic ratio >65%), and increased pulmonary arterial markings due to high flow or pulmonary venous congestion (pulmonary venocapillary hypertension secondary to congestive heart failure).

An atypical chest X-ray finding may be the first indication of a complex cardiac anomaly, such as a univentricular heart, in a patient who otherwise shows clinical signs of an unrestrictive ventricular septal defect or tetralogy of Fallot (Figure 39.11).

Patients with single ventricle typically have a cardiac silhouette with abnormal superior mediastinal densities, suggesting abnormal position and orientation of the great vessels [4,44–46]. Patients with normally related great arteries often show a "triad of densities" in the superior mediastinum which include in the frontal view ascending aorta, transverse aortic arch, proximal descending aorta, and pulmonary trunk [46]. The lack of an ascending aorta on the right and its presence on the left can indicate l-transposition (see Figure 39.11). A narrow superior mediastinum is commonly seen with d-transposition. The left cardiac border can appear abbreviated because of a bulge in the upper third from an inverted ventricular outlet chamber. A notch indicates the edge of the rudimentary outflow chamber located leftward and superiorly [46] A left anterior oblique projection demonstrating a hypoplastic right ventricle and enlargement of the left ventricle, supports a diagnosis of single left ventricle with outflow chamber.

An unbalanced complete atrioventricular canal can be suspected on chest radiography in patients with associated abdominal and cardiac malpositions, such as dextrocardia or mesocardia, suggesting heterotaxia. Dextroisomerism is more common in these patients and an unbalanced canal with dominant right ventricle with absent or hypoplastic left ventricle and double-outlet right ventricle is usually found.

Progressive cardiomegaly which develops in an older patient suggests the onset of dilated myopathy. Signs of pulmonary venous hypertension out of proportion to the amount of pulmonary blood flow can be observed with regurgitation or stenosis of the left atrioventricular valve with a restrictive atrial septal defect or anomalous pulmonary venous connection with obstruction, most likely in patients with asplenia.

Cardiovascular magnetic resonance (CMR)

CMR has become a powerful diagnostic tool [47], complementary to echocardiography, and it can replace diagnostic cardiac catheterization. It provides anatomic and functional information in addition to tissue characterization. It is considered the gold standard for evaluating ventricular volumes, mass, and ejection fraction [48,49]. The measurements can be made without assuming a certain geometric ventricular shape, which is highly advantageous
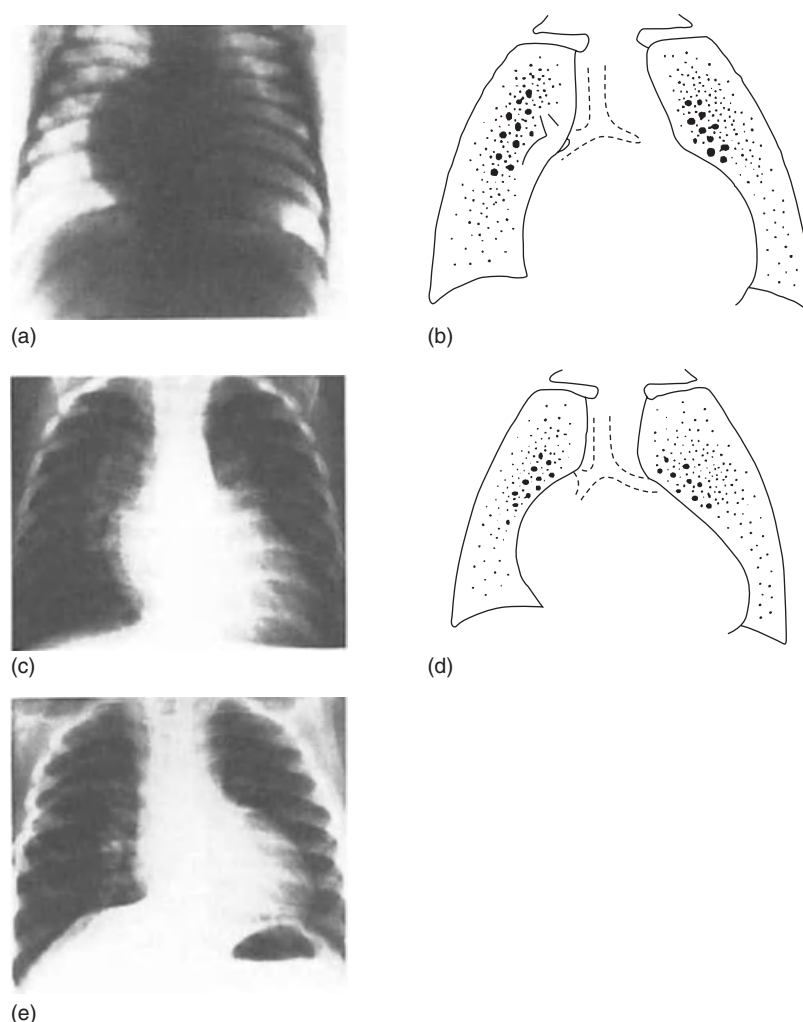
Figure 39.11 Chest radiographs and schematic X-ray drawings in patients with single ventricle. (a, b) Newborn with no pulmonary stenosis and congestive heart failure. (c, d) Infant with no pulmonary stenosis and congestive heart failure, d-transposition. (e) A 3-year-old child with pulmonary stenosis and l-transposition.

in patients with single ventricle as often ventricular shape is atypical. A limitation is that CMR cannot quantify pulmonary artery pressure or ventricular end diastolic pressure. In addition, particularly in young children, sedation or anesthesia is needed.

The protocol includes dark blood sequences (T1 and T2 weighted), bright blood sequences (cine-CMR or cine-loop), phase-contrast velocity mapping, gadolinium-enhanced 3D magnetic resonance volumetric angiography, 3D reconstruction (3D contrast MR angiography), and delayed enhancement (late gadolinium-enhanced CMR) for evaluating myocardial viability. Myocardial wall mechanics can be evaluated using tagging techniques [50].

The CMR evaluation in patients with single ventricle can be complex given the highly variable anatomic substrate (Figure 39.12). Prior to an operation, CMR can identify patient risk factors. Although many centers continue to perform elective cardiac catheterization in all patients before bidirectional Glenn and Fontan procedure, some only study

invasively those with risk factors [51] which have been identified by CMR.

In preparation for upcoming surgical staging, CMR allows the evaluation of chronic lung disease, heterotaxy, atrioventricular valve regurgitation, ventricular dysfunction, aortic regurgitation, pulmonary artery or vein stenosis or distortion, and systemic venous anomalies, all of which are considered high risk factors. Thus, CMR may indicate the need for a modified surgical procedure or an interventional cardiac catheterization [52]. The anatomic definition by CMR (Figure 39.13) confirms the underlying diagnosis, following the segmental analysis [52], especially focusing on the pulmonary vasculature to rule out hypoplasia, stenosis, compression, and distortion. The functional evaluation allows determination of ventricular volume, mass, and ejection fraction (Figure 39.14).

The development of veno–veno collaterals can be identified and systemic venous flow can be studied (Figures 39.15 and 39.16).
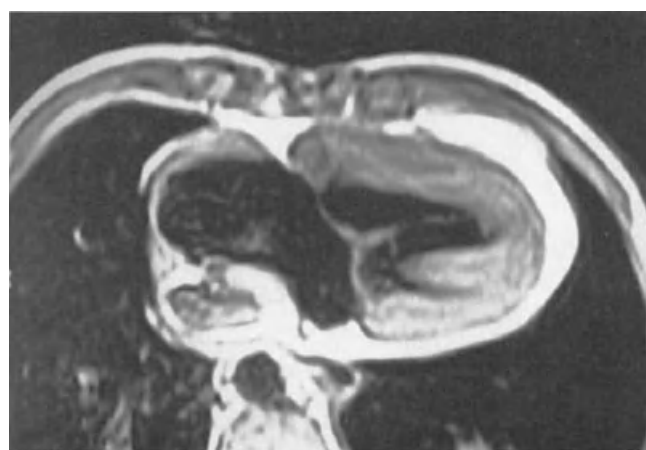
(a)
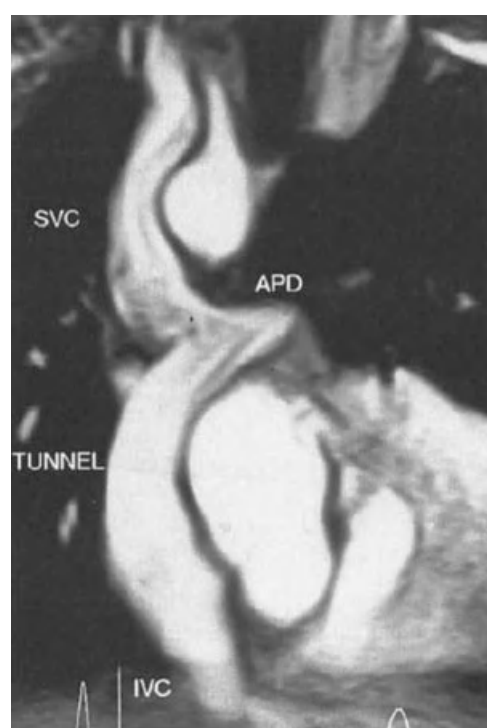
(b)

Figure 39.12 (a) Transverse image obtained by magnetic resonance in a patient with unbalanced ventricles (IIB) with a common atrioventricular canal and right ventricular dominance of >75% of the common atrioventricular valve aligned with the right ventricle. Note the hypoplastic posterior left ventricle. (b) Cine magnetic resonance imaging in a coronal plane of a total cavopulmonary anastomosis through a right-sided intra-atrial lateral tunnel showing widely patent anastomoses. Note direct anastomosis of the superior vena cava (SVC) to the right pulmonary artery (APD) and anastomosis of the inferior vena cava (IVC) to the right pulmonary artery through the intra-atrial tunnel (TUNNEL).

The position of the aorta or neoaorta relative to the sternum can be demonstrated, which is helpful prior to a repeat sternotomy (Figure 39.17).

Figure 39.13 Three-dimensional contrast MR angiography demonstrates interruption of the inferior vena cava with azygos continuation following bidirectional Glenn procedure or Kawashima. In a posterior view two arches are demonstrated (aortic and azygos).

Pleural or pericardial effusions can be quantified. Flow studies using phase-contrast velocity mapping allow one to evaluate flow dynamics in arteries and veins [53] and determine the relationship between both right and left pulmonary blood flow and also the Qp/Qs.

Following total right heart bypass or modified Fontan procedure, a similar protocol to that used post-Glenn is selected, incorporating some additional sequences and cuts [54].

In patients with an atriopulmonary anastomosis [55], the right atrial dimensions are assessed in addition to the usual pattern of slow flow (smoke-like) within the chamber (Figure 39.18), the presence of any thrombus (Figure 39.19), and anatomic features in addition to flow dynamics within the systemic veins and pulmonary arteries [56] and veins (Figures 39.20 and 39.21). Similarly, flow patterns and anatomy are addressed in patients with lateral tunnel Fontan or extracardiac conduits (Figures 39.22 and 39.23) [57,58]. A fenestration can be visualized and sized.

In assessing the distribution of pulmonary blood flow, lung scintigraphy has been traditionally considered the gold standard. However, its value in patients with single ventricle following surgical palliation can be limited, as the results are highly dependent on the site of injection (upper or lower extremity) and streaming flow patterns. Such limitations can be overcome with CMR, which allows determination of the relationship of right versus left pulmonary blood flow based on flow velocities. In addition, CMR allows quantification of aortopulmonary collateral flow via plane phase-contrast velocity mapping [59].

It is important to address ventricular function by CMR by determining myocardial fibrosis by delayed enhancement,
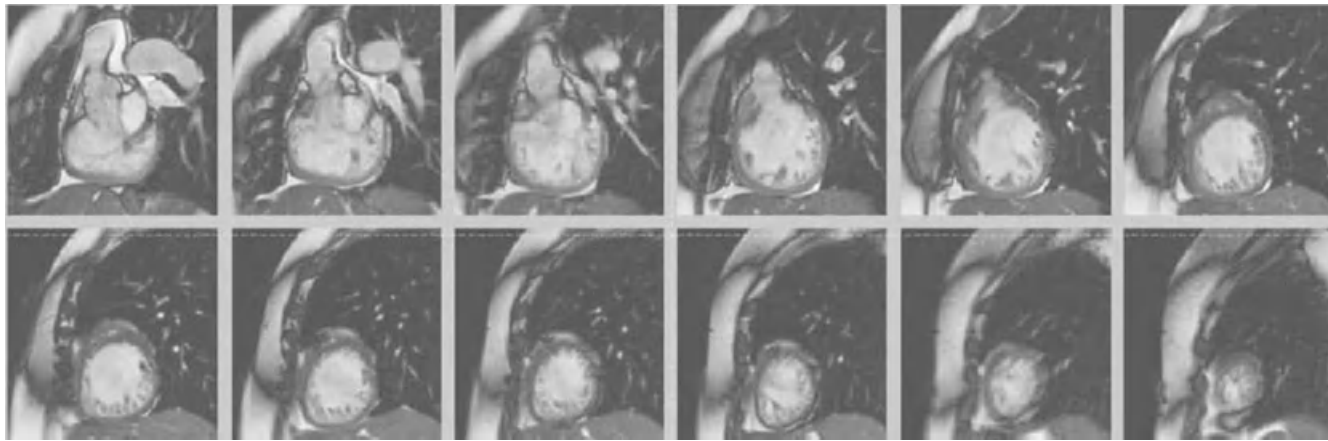
Figure 39.14 MR angiography in patient with single left ventricle after systemic to pulmonary artery shunt. Short-axis cuts from the ventricular apex to the base allow evaluation of ventricular volumes, ejection fraction, and ventricular mass.

(a)　　　　　　　　　　　　　　　　　(b)
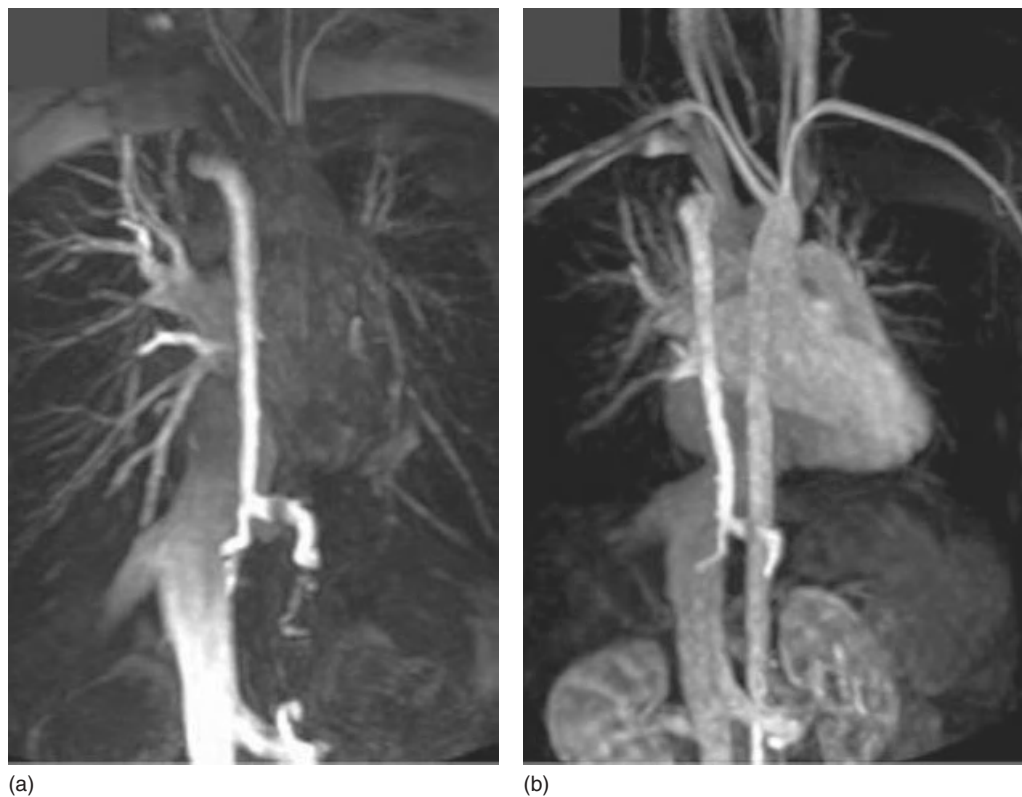
Figure 39.15 "Defunctionalized" bidirectional Glenn. (a) Real-time sequence following bolus of gadolinium. Through the azygos vein, which is recannalized, contrast travels to the inferior vena cava, instead of the pulmonary arteries. (b) 3D contrast MR angiography. Multiplanar 3D reformation using maximum intensity projection (MIP) of the 3D dataset. Note the enlarged azygos vein decompressing the bidirectional Glenn circuit.

as this information cannot be provided by any other diagnostic test with equivalent accuracy. CMR with the PAMM (spatial modulation of magnetization) technique [60,61] has allowed the study of right ventricular regional wall motion and strain analysis in patients at different stages of single ventricle surgical palliation. With this method, it is possible to compare ventricular mechanics in patients with a single ventricle with those in patients with a systemic right ventricle and to study ventriculo-ventricular interactions. In both groups, there were abnormalities in regional myocardial strain, twisting motion, and regional radial motion. In patients with a univentricular right heart, the lack of

Figure 39.16 3D contrast MR angiography, coronal cuts. Right single ventricle, with right pulsatile bidirectional Glenn, with wide open anastomosis (*). The left superior vena cava (LSVC), not seen prior to surgery, which enlarged to become a significant decompressing veno–veno collateral.

(a)

(b)

Figure 39.18 Cardiac MR cineangiogram performed in patient with l-transposition after atriopulmonary anastomosis. The coronal plane image (a) shows moderate to severe enlargement of the right atrium. Spin-echo T1 in axial plane (b) with isodense signal within the right atrium indicating slow flow. The anastomosis itself is wide open (APA). *, Superior vena cava; Ao, aorta; L, left pulmonary artery; R, right pulmonary artery.

Figure 39.17 Cardiac MRI image from a patient with heterotaxy, single left ventricle, interrupted inferior vena cava with azygos continuation. Spin-echo dark blood sequence. Axial cut at the level of the aortic valve showing the close relationship of the aorta to the sternum.

ventriculo-ventricular interaction determined by inferior wall paradoxical systolic wall motion is different from that observed in patients with a Senning operation, in whom paradoxical septal motion occurs.

The abnormalities in ventricular mechanics and geometry secondary to stress, strain, and regional twist in univentricular hearts with a right ventricular anatomy are similar to those in hearts with a left ventricular anatomy [57]. Such changes in ventricular mechanics generate a regional increase in oxygen consumption, which may play a role in the development of ventricular dysfunction.

(a)

(b)

(c)

(d)
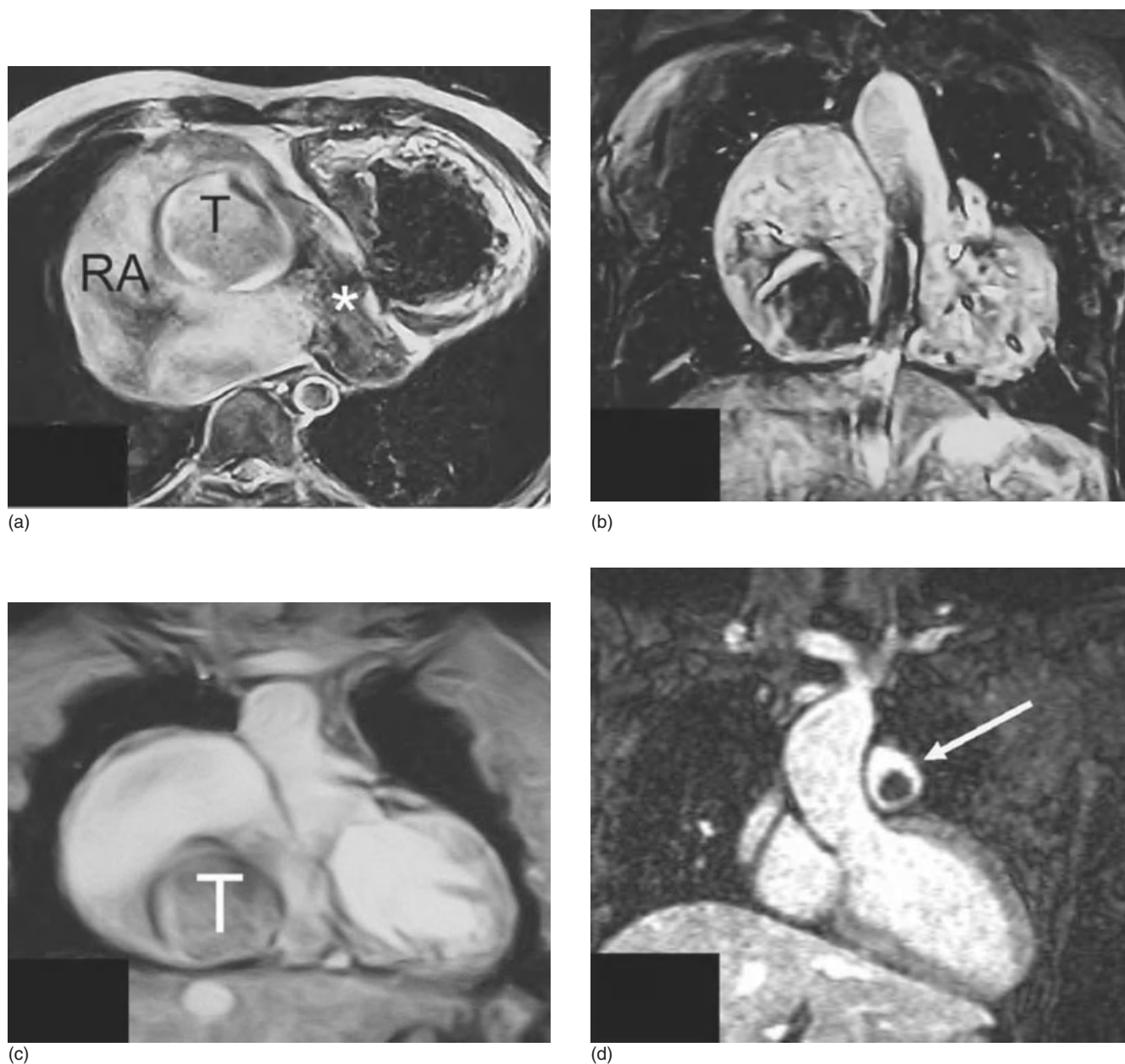
Figure 39.19 Single left ventricle, pulmonary atresia status post-atriopulmonary anastomosis. Spin-echo dark blood axial cut (a), with hyperintense signal in the right atrium (RA), due to slow flow demonstrates severe right atrial dilation with a round image consistent with intracavitary thrombus (T). Coronal cut spin-echo (b) with filling defect due to thrombus surrounded by slow flow with hyperintense signal. Coronal cut MR angiogram (c) shows ovoid thrombus (50 × 60 mm) surrounded by white blood. (d) Single left ventricle status post-extracardiac conduit. 3D contrast MR angiography demonstrates in coronal partition filling defect at main pulmonary artery stump consistent with thrombus (20 × 17.5 mm) which does not enhance with gadolinium (arrow). T, thrombus; *, coronary sinus.

Echocardiography

Two-dimensional echocardiography allows sequential determination of thoracoabdominal situs, atrioventricular and ventriculoarterial alignments and connections, morphology and function of the single ventricle or dominant ventricle and atrioventricular valves, position of the infundibular outlet chamber and size of the bulboventricular foramen, and associated cardiac defects.

The thoracoabdominal situs is determined from a subxiphoid window, in a transverse view at the level of the twelfth thoracic vertebral space, by analyzing the location of the inferior vena cava and the descending aorta relative to the spine. A second superior vena cava and communicating
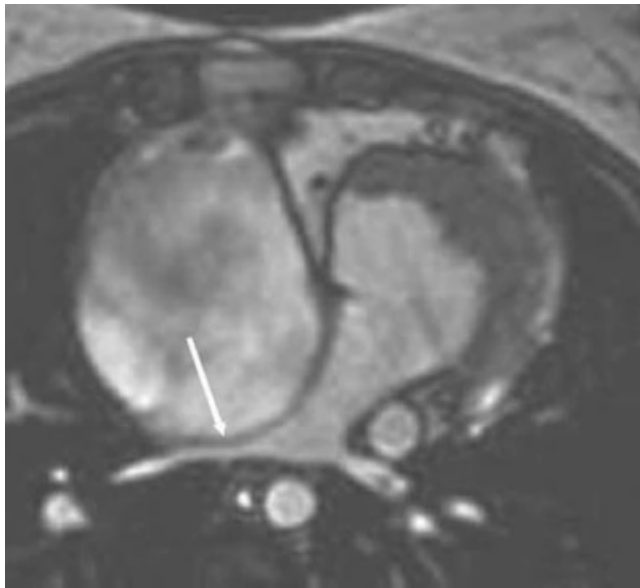
Figure 39.20 Following atriopulmonary anastomosis, a giant right atrium is documented with compression of the right upper pulmonary vein (RSPV) (arrow).

Figure 39.22 3D contrast MR angiographic reconstruction with surface rendering in a patient with single left ventricle with a history of bilateral bidirectional Glenn procedures followed by Fontan completion demonstrates stenosis at the distal anastomosis of the extracardiac conduit.

Figure 39.21 Inferior vena cava flow curves showing a biphasic pattern with a large systolic (S) and a small early diastolic peak (D), and retrograde flow in late diastole (A).

vein can be investigated from a high parasternal view. From an apical four-chamber view, scanning from posterior to anterior, the atrioventricular connection is demonstrated [5,62–66]. Patients with a single ventricle can have either two atrioventricular valves positioned at the same level (Figure 39.24) [5] or, rarely, one common atrioventricular valve aligned to the only ventricular chamber. In a short-axis

view, the morphologic aspects of each valve can be analyzed, including the number of leaflets and their attachments and relationship to each other (Figure 39.24). In addition, the position of the infundibular outlet chamber can be determined; it is always superior in patients with single left ventricle (Figure 39.24). The morphologic character of the ventricle can also be diagnosed by echocardiography, by finding either left ventricular thin trabeculations or right ventricular thick trabeculations and moderator band.

From parasternal long-axis, subxiphoid long-axis, and oblique views, the ventriculoarterial relationship is identified. Patients with single left ventricle most commonly have a posterior pulmonary artery and an anterior aorta arising from the infundibular outlet chamber (Figure 39.24). In patients with a Holmes heart, the pulmonary artery is anterior and aligned to the infundibular outlet chamber. The aorta is posterior, aligned to the single left ventricle, and has fibrous continuity with the atrioventricular valve.

From these projections, the size of the bulboventricular foramen is determined [64] by the ellipse formula, $\pi D_1 D_2/4\,\mathrm{m}^{-2}$, where D_1 and D_2 are the major and minor diameters of the ellipse. A measurement of $<2\,\mathrm{cm}^2\ \mathrm{m}^{-2}$ is consistent with a restrictive bulboventricular foramen. Although the gradient may be underestimated by continuous-wave Doppler study, color Doppler examination may localize the site of turbulent flow and the highest gradient. If the Doppler gradient is $>1.5\,\mathrm{m\ s}^{-1}$, the bulboventricular foramen is considered to be restrictive [64].

(a)

(b)
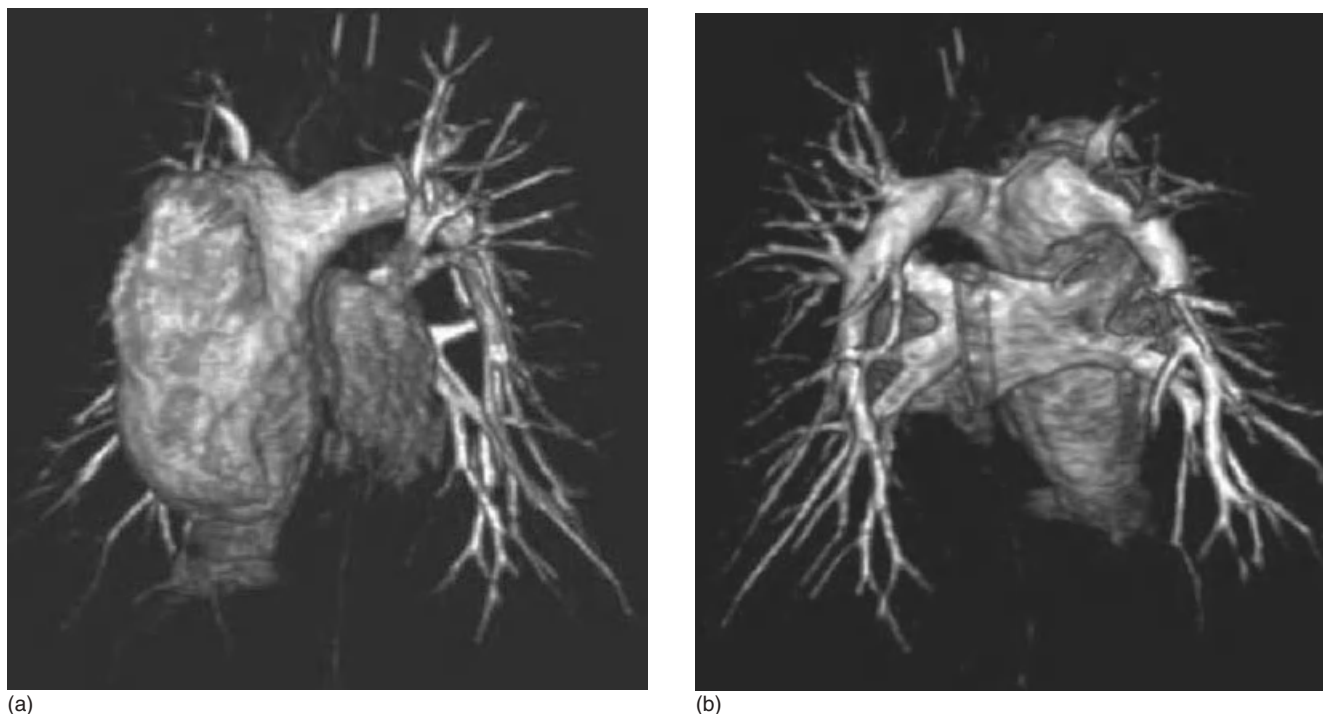
Figure 39.23 Anterior (a) and posterior (b) view of 3D contrast MR angiographic reconstruction with surface rendering in a patient with a history of atriopulmonary anastomosis. A markedly dilated right atrium is demonstrated with normal pulmonary artery branching pattern and development.

The morphologic features of the ventricular septal defect in patients with unbalanced ventricles and dominant left ventricle (type IIA) can be determined from an apical four-chamber view. Conoventricular septal defects extend to the inlet septum when there is additional malalignment of the ventricular septum to the atrial septum. In such patients, the atrioventricular valve and >50% of the second one or >75% of a common atrioventricular valve are aligned to the left ventricle (Figure 39.25). Patients with dominant right ventricle (type IIB) and common atrioventricular valve also have a primum atrial septal defect.

An unbalanced common atrioventricular canal is best diagnosed from an apical four-chamber view (Figure 39.25). From a parasternal short-axis view, a small component of the atrioventricular valve ring is identified aligned to a hypoplastic left ventricle. A double-outlet right ventricle can be diagnosed from a subxiphoid projection.

The maximal instantaneous gradients at aortic, subaortic, pulmonary, and subpulmonary levels are examined with continuous-wave Doppler study. The function of the atrioventricular valves is examined by color Doppler study.

The single ventricle differs from the normal left ventricle that resembles an ellipse. Hence it is not amenable to geometric assumptions and, therefore, functional assessment has been only qualitative and subjective. The myocardial performance index (MPI or Tei index) [67] is a Doppler-derived index of ventricular function that is independent of geometric constraint. It has been used for evaluating patients with single ventricle [68,69].

However, accurate assessment of ventricular function in single ventricle must rely on three-dimensional reconstruction, which can be done using two orthogonal views of the subcostal sagittal and coronal planes. This technique has been used to evaluate effects of resynchronization therapy with multisite pacing in univentricular hearts [70].

Transesophageal echocardiography

This is particularly indicated in patients with poor echocardiographic windows, or as part of the intraoperative and perioperative assessment Patients with single ventricle particularly benefit from this diagnostic tool when there is a need to rule out intracardiac thrombus prior to cardioversion or following a stroke or transient ischemic attack.

A high horizontal plane allows anatomic determination of the atrial appendages and atrioventricular connections. A transgastric short-axis view allows verification of the atrioventricular connections and gradients across the ventricular outflow tracts.

Catheterization and angiography

Diagnostic cardiac catheterization

Cardiac catheterization and angiography in patients with single ventricle [33,71–73] or unbalanced ventricles [74,75] provide anatomic and hemodynamic information

(a)

(b)

(c)
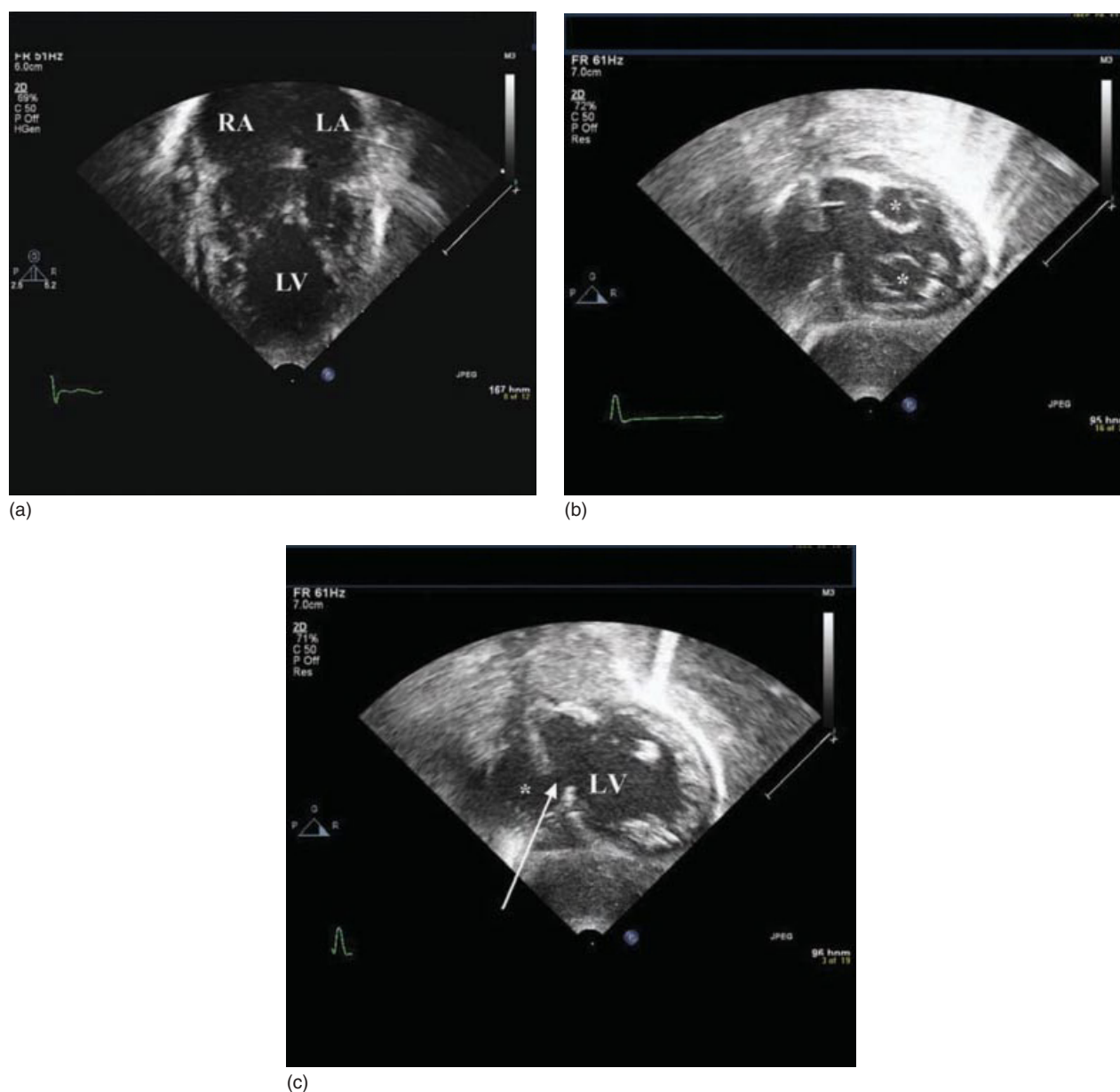
Figure 39.24 (a) Echocardiogram performed in a patient with {S,D,D} double-inlet left ventricle and d-malposed great arteries and subaortic infundibular outlet chamber. On apical four-chamber view, the two AV valves are demonstrated situated at the same level. (b) They can also be visualized opening "en-face" from subxyphoid view (*). (c) The anatomy of the bulboventricular foramen is demonstrated on subxyphoid view (arrow). There is a subaortic infundibular outlet chamber (*). LA, left atrium; LV, left ventricle; RA, right atrium.

necessary for management. Diagnostic anatomic data, which corroborate the results of noninvasive diagnostic tests, include the following:

1 Atrial situs.

2 Systemic venous connections (an additional superior vena cava, innominate vein, site of entry of the inferior vena cava and hepatic veins, interrupted inferior vena cava with azygos continuation).

3 Pulmonary venous connections.

4 Atrioventricular valves and connections [74]. These can be recognized by cineangiocardiography, through demonstration of anterograde flow through the atrioventricular valves during atrial injection or, more commonly, ventricular injection (unopacified blood). Valvar morphology can be determined by trapping of contrast material underneath the valve leaflet, by delineating the valve ring, or from the configuration of the closed valve after ventricular opacification or as a curved or lineal tangential defect if the valve is
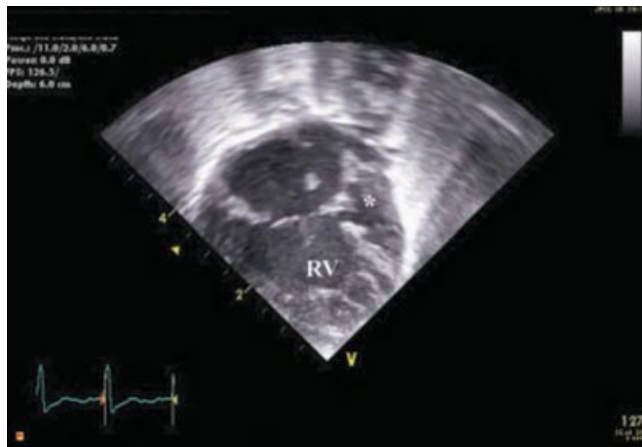
Figure 39.25 In apical four-chamber view the echcocardiogram demonstrates unbalanced common atrioventricular canal with dominant right ventricle (RV) and a hypoplastic left ventricle (*).

stenotic. A large valve annulus suggests either single or common atrioventricular valve, whereas when it is small, a hypoplastic or stenotic valve is likely. The relationship of the atrioventricular valves to the semilunar valves and degree of development of the conal septum (mitral to aortic continuity rules out subaortic conus) are delineated by a ventriculogram. A gooseneck deformity on a left ventriculogram is diagnostic of an atrioventricular septal defect [74].

5 Morphologic aspects of the single or dominant ventricle, infundibular outlet chamber, and hypoplastic rudimentary ventricle. A left ventriculogram in four-chamber view demonstrates the absence of the posterior ventricular septum in single left ventricle (type IA) (Figure 39.26) or a malaligned interventricular posterior septum in unbalanced ventricles with a dominant left ventricle (type IIA) (Figure 39.27).

6 Pulmonary or systemic obstruction (restrictive bulboventricular foramen, stenotic pulmonary or aortic valve).

7 Ventriculoarterial alignments and connections.

8 Anatomy of the pulmonary arteries (size of central pulmonary arteries, Nakata index [75] and McGoon ratio [76], arborization abnormalities and branch pulmonary artery stenosis, washing out of contrast medium by competing flow from aortopulmonary collaterals, pulmonary transit time, and arteriovenous fistulas).

9 Aortic arch anatomy, branching abnormalities, and any aortopulmonary collaterals.

10 Ventricular function (ejection fraction) and ventricular geometry (mass/volume relationship).

After any surgical procedure, a diagnostic cardiac catheterization is performed to rule out sequelae from prior operations, including acquired pulmonary artery stenosis at the site of previous shunt or pulmonary artery banding, pulmonary arteriovenous fistulas in patients with partial right ventricular bypass (classic Glenn, bidirectional Glenn, or Kawashima

operation) [77], cavocaval or cavoportal [78] decompressing venous collaterals after partial right-sided heart bypass, sources of right-to-left shunt after a total right-sided heart bypass through fenestration, interatrial communications [79], and baffle leaks or left-to-right shunts by aortopulmonary collaterals [80].

Before a second- or third-stage palliation, a complete hemodynamic study is performed. To obtain accurate and complete data, two pressure transducers must be used to record the transpulmonary gradient by simultaneous recording of pulmonary artery and pulmonary venous, left atrial, or ventricular end-diastolic pressures. Ideally, oxygen consumption should be measured and the patient should be in stable hemodynamic condition, preferably well sedated but breathing spontaneously, with normal arterial pH to avoid a falsely elevated estimated pulmonary vascular resistance. Oversedation should be avoided, given that retention of CO_2 and secondary respiratory acidosis increase the pulmonary vascular resistance, and airway obstruction leads to significant variability in intracardiac pressures. With the difficulties in achieving perfect sedation in some age groups, many authorities favor the use of general anesthesia, selecting drugs that minimally affect cardiovascular performance and performing the hemodynamic measurements at the time when the patient is relatively lightly anesthetized. Two sets of hemodynamic data should be collected and be consistent. Because major management decisions depend on the hemodynamic data, these should be collected with the utmost precision and accuracy. As a result, pulmonary arterial pressure, pulmonary vascular resistance, Qp/Qs ratio, and functional data evaluating ventricular mechanics (ventricular end-diastolic pressure, preload, and afterload) will be determined and/or calculated. A pulmonary vascular resistance <3 mmHg l^{-1} min^{-1} m^{-2} is required for successful surgical staging (see discussion about hematocrit and viscosity in Chapter 10).

With advances in noninvasive imaging, particularly CMR, some have adopted the practice of not performing routine cardiac catheterizations before surgical staging in patients who have a benign clinical course and no risk factors identified on echocardiography and CMR [51]. This approach remains controversial, as CMR does not provide complete hemodynamic data, often requires anesthesia, and not all cardiac centers have the necessary congenital cardiac CMR expertise to address accurately all potential risk factors for surgical staging.

Interventional cardiac catheterization

Patients with a univentricular heart may require a transcatheter intervention early in their course and before the initial surgical procedure if they have a restrictive atrial septal defect and left atrial outlet atresia or stenosis. Transcatheter creation of a new atrial septal defect with septostomy and balloon septoplasty may decompress the left
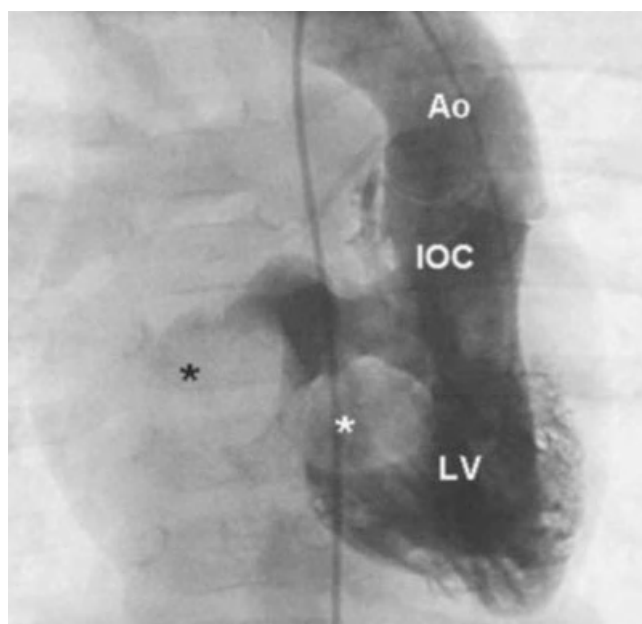
Figure 39.26 Left ventriculogram in the frontal plane demonstrating the anatomy of single double inlet left ventricle with L- transposition ({S,L,L} segmental combination) with acquired pulmonary atresia. Unopacified blood enters the left ventricle via two atrioventricular valves (*). There is a left sided subaortic infundibular outlet chamber (IOC). Ao, Aorta; LV, left ventricle; black asterix, right sided mitral valve; white asterix, left sided tricuspid valve.

Figure 39.27 Angiocardiogram in a patient with unbalanced common atrioventricular canal and dominant right ventricle. There is double-outlet right ventricle and a hypoplastic posteroinferior left ventricle. Lateral view.

atrium with significant improvement of hemodynamics, reduction in pulmonary venous congestion, and pulmonary vascular resistance. Patients with ductal-dependent lesions have been managed by stent placement in the ductus arteriosus [81]. This can be done to provide either an aortopulmonary shunt in patients with ductal-dependent pulmonary blood flow, or systemic blood flow in those with ductal-dependent systemic perfusion. Indeed, an accepted management option is to perform a *hybrid procedure* in patients with a single ventricle as an alternative to a Norwood procedure. Bilateral pulmonary artery banding and stent implantation in the patent ductus arteriosus are performed as a single procedure jointly by a surgeon and an interventional cardiologist. Some centers have pioneered this approach [81] and use it as a first-line therapy for neonates s with hypoplastic left heart syndrome and variants. Others use this approach only in high-risk patients (those who are born prematurely, with multiple congenital anomalies, significant ventricular dysfunction, or atrioventricular valve regurgitation, etc.).

Patients with severe pulmonary stenosis or atresia may have pulmonary arteries that are inadequate to allow future second- and third-stage surgical palliation. Transcatheter pulmonary artery rehabilitation through serial balloon dilatation procedures may be the only option for these patients to become candidates for either staged single ventricle palliation or heart transplantation.

If a source of potentially detrimental postoperative right-to-left or left-to-right shunting is identified during cardiac catheterization, transcatheter closure is indicated [82] to avoid excessive cyanosis or paradoxical embolus. Examples are a small, persistent, left superior vena cava draining to the coronary sinus (in the absence of coronary sinus ostia stenosis or atresia), other potential decompressing venous connections (particularly in patients with heterotaxia), and significant aortopulmonary collaterals.

Following the various stages of surgical intervention for single ventricle, interventional cardiac catheterization plays a key role in optimizing hemodynamics, particularly in symptomatic patients. Many abnormalities are amenable to transcatheter treatment (Table 39.1). Sometimes, emergency cardiac catheterization in the immediate postoperative period is needed in a severely compromised patient to create a new or augment a baffle fenestration [83], close a baffle leak, or dilate or stent a stenotic vessel.

Interventional catheterizations are also performed later postoperatively. Catheter interventions may be on either the primary defect or on a coexisting cardiac abnormality. Examples are coil embolization of a small, persistent, left superior vena cava or aortopulmonary collaterals [80,82], balloon dilatation of peripheral pulmonary artery stenosis, and rarely pulmonary valvotomy or balloon dilatation of a native coarctation in selected high-risk surgical patients. Interventions may be performed on postoperative

Table 39.1 "Abnormalities" in the total right-sided heart bypass circulation.

Type	Manifestation	Characteristics
Obstructions	Ventricular pressure overload	Cardiac: outflow tract obstruction, aortic valve stenosis
		Systemic arterial: arch obstructions, systemic hypertension
	Systemic venous pressure overload	Systemic venous: baffle stenosis
		Pulmonary arterial: branch pulmonary artery stenosis, high pulmonary vascular resistance
		Pulmonary venous: stenosis of pulmonary veins (intrinsic or extrinsic by compression)
Shunts	*Right-to-left shunt*	Cardiac: fenestration, interatrial communications, decompressing
	Cyanosis	veins to left atrium
		Systemic venous: decompressing venous collaterals
		Pulmonary atrial: arteriovenous malformations
	Left-to-right shunt	Cardiac: residual anterograde flow into main pulmonary artery,
	Ventricular volume overload	patch leak in atriopulmonary anastomosis with tricuspid valve patch
		Systemic arterial: aortopulmonary collaterals, residual patent ductus arteriosus or surgical grafts
Pump failure or dysfunction		Cardiomyopathy causing systolic or diastolic dysfunction, arrhythmias, atrioventricular valve insufficiency

abnormalities [82–85], such as branch pulmonary artery balloon dilatation or stent placement at a prior shunt insertion site, coil embolization of a patent aortopulmonary shunt and acquired aortopulmonary collaterals after prior thoracotomy, transcatheter closure of residual anterograde flow through the pulmonary valve, coil embolization of decompressing venous collaterals, transcatheter closure of fenestration or baffle leaks, and balloon dilatation of postoperative coarctation (Table 39.2; see also Table 39.1).

The role of interventional cardiac catheterization as adjunct to operation is clearly illustrated by transcatheter closure of a baffle fenestration after a total right-sided heart bypass procedure [84.85]. A complete hemodynamic study is performed, including test balloon occlusion of the fenestration, and if well tolerated (see Table 39.2), transcatheter closure is performed.

Management

In a normal biventricular circulation, the right ventricle allows an increase in the cardiac output with exercise without a rise in systemic venous and ventricular end-diastolic pressures [86]. Ventricular septation developed 165 million years ago, when the right ventricle appeared in reptiles and birds and allowed adaptation to air breathing, aerobic exercise, and flying [87]. Patients with univentricular circulation after total right heart bypass lack this important mechanism of adaptation to aerobic exercise.

In managing patients with univentricular hearts, the initial objective is to protect the pulmonary vasculature and

ventricular function, keep pulmonary artery pressures low, and allow adequate systemic oxygen saturation (≥80%). Early in life, this can be achieved at the original palliative surgery by a pulmonary artery banding or a Blalock–Taussig shunt (Table 39.3), according to the underlying anatomic substrate. Stent implantation of a ductus is an alternative to an aortopulmonary surgical shunt; the intermediate and long-term results are not well known [88].

Three different types of "corrective" operations have been proposed for these patients. Theoretically, ventricular septation [89] would be ideal, although it is possible only in rare anatomic types with two normal atrioventricular valves with adequate distribution of papillary muscles and attachments to allow partitioning. The technical difficulties and high early and late mortality have restricted ventricular septation to patients with both ideal anatomy and major risk factors that contraindicate a right-sided heart bypass procedure. Ventricular septation has been performed in patients with univentricular heart type IA III, normal atrioventricular valves, nonrestrictive bulboventricular foramen, no prior palliative operations, chronic cyanosis, and severe polycythemia. An additional requirement is a diastolic ventricular volume 250% larger than a normal left ventricle [89]. This procedure is also possible in patients with common ventricle (type C of Van Praagh *et al.* [2]) because there are two well-developed ventricles with a markedly deficient interventricular septum.

The most common surgical approach is staged surgical palliation by a partial (bidirectional Glenn procedure) or total (Fontan–Kreutzer procedure) right heart bypass operation.

Table 39.2 Suggested sequential steps for transcatheter fenestration closure.

Step	Procedure[a]
1	Determine RA or PA and AO saturations and pressures at baseline
2	Test balloon occlusion for 10 min
3	Determine RA or PA and AO saturations and pressures during balloon occlusion of the fenestration (after 10 min)
4	If RA pressure >16 mmHg and CI decreases to <2 l min^{-1} m^{-2}, the fenestration is left open. If RA pressure <16 mmHg and CI >2 l min^{-1} m^{-2}, the fenestration may be closed

[a]AO, aorta; CI, cardiac index; PA, pulmonary artery; RA, right atrium.

As a last option, some patients with univentricular heart may undergo cardiac transplantation, if unsuitable for staged surgical palliation or after a failed the surgical approach.

Surgical management

Initial palliative surgery

Neonates with coexisting severe pulmonary stenosis or pulmonary atresia who present with marked hypoxia (PO_2 < 30 mmHg) require prostaglandin E_1 to maintain ductal patency and increase blood flow to the pulmonary vasculature until a permanent source of pulmonary blood flow is established either surgically by an aortopulmonary shunt, or via a transcatheter approach with stenting of the ductus arteriosus. A modified Blalock–Taussig shunt with a Gore-Tex graft

positioned between a subclavian artery and the ipsilateral pulmonary artery is the most widely used type of shunt. Similarly, those with aortic arch hypoplasia or severe coarctation require prostaglandin infusion until arch reconstruction can be performed.

Neonates with increased pulmonary blood flow, elevated pulmonary artery pressures, and congestive cardiac failure need manipulation of the pulmonary vascular resistance to maintain an adequate preoperative Qp/Qs ratio, allowing sufficient systemic perfusion while limiting pulmonary blood flow [34,90]. This may be achieved either by use of a closed hood [91], to increase inspired PCO_2 and pulmonary vascular resistance, or by hypoventilation using mechanical ventilation, sedation, and paralysis. This can be achieved in some patients by a low inspired FiO_2 (<21%). Supplemental oxygen and hyperventilation should be avoided, as should any factor that could lower the pulmonary vascular resistance. Once patients are hemodynamically compensated, an initial palliative operation is performed (see Table 39.3). When pulmonary artery banding is indicated, this is achieved narrowing the pulmonary trunk to a luminal diameter of 21 mm + 1 mm kg^{-1} body weight [92]. By intraoperative pressure measurement, the distal pulmonary artery pressure should be ~50% of the systemic pressure. If the oxygen saturation drops to <80% or the patient develops bradycardia in the operating room, the band should be loosened. If the banding is unsuitable because of marked cyanosis (PO_2 <30 mmHg), persistent high pulmonary blood flow (oxygen saturation >85%, or high pulmonary venous flow velocity measured by echocardiography >0.7 m s^{-1} and transmitral flow E >1 m s^{-1}), a second procedure to revise the banding is indicated.

Table 39.3 Management algorithm for patients with univentricular heart.

Ductus dependent	Pulmonary obstruction	Systemic obstruction	Primary procedure	Secondary procedure	Final procedure
YES	YES	NO	BTS PDA stent	BDG BDG	
	NO	YES	Arch repair + PAB (#) Norwood Hybrid procedure	BDG Comprehensive stage II + BDG	Complete right heart bypass or Fontan
NO	YES	NO	< 3m – BTS or medical therapy if cyanosis not severe > 3m – BDG	BDG	
	NO	YES	Arch repair + PAB DKS/BTS	BDG	
		NO	PAB	BDG	

(#) if isolated aortic arch obstruction
BDG, bidirectional Glenn operation ; BTS, Blalock-Taussig shunt, usually of modified type; DKS, Damus-Stansel-Kaye operation; PAB, pulmonary arterial band; PDA, patent ductus arteriosus.
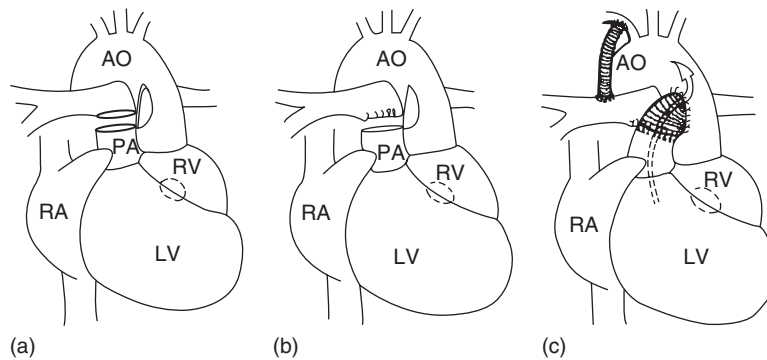
Figure 39.28 Damus–Kaye–Stansel anastomosis for single ventricle and subaortic stenosis. (a) The pulmonary artery (PA) is transected proximal to the bifurcation. An appropriately positioned and sized incision is made in the ascending aorta. (b) The distal end of the pulmonary artery is oversewn, and the proximal end of the pulmonary artery is anastomosed to the opening in the aorta. (c) An appropriately shaped hood (Dacron tube, pericardium, allograft, or Gore-Tex) is added to the anastomosis. AO, aorta; LV, left ventricle; RA, right atrium; RV, right ventricle. (Reproduced with permission from Park, *Pediatric Cardiology for Practitioners*, 3rd edn, Mosby, St. Louis, 1996, p. 234.)

Currently, the early operative mortality for the initial palliative procedures in neonates is <5%, but varies from 2.7 to 17%. according to the extent of procedures performed [90,93]. If an aortopulmonary shunt is performed after the neonatal period, the mortality is significantly lower than when aortic arch reconstruction or a Damus–Kaye–Stansel-type anastomosis is required.

After pulmonary artery banding, the reduction in the ventricular volume can decrease the size of the bulboventricular foramen, and subaortic stenosis may develop. This occurs in >73% of patients with coexisting transposition [94], for whom pulmonary artery banding should be avoided whenever there is a significant risk for development of subaortic stenosis.

In the intermediate and long-term follow-up of patients after the initial palliative procedure, ventricular dysfunction may become significant [95]. The increase in preload relative to the ventricular volumes at end-systole and end-diastole (2.5–3 times normal) reduces the long-axis/short-axis relationship (normal, 1.9:1).As a result, the ventricle becomes rounder, the end-systolic stress (afterload) increases, and ventricular function, mass/volume relationship, and ventricular contractility are reduced [95].

Second-stage palliative surgery: partial right-sided heart bypass (bidirectional Glenn procedure)

A partial right-sided heart bypass can be performed by a right cavopulmonary anastomosis, as proposed by Glenn [96] in 1958 and Bakulev and Kolesnikov [97] in 1959. Hopkins *et al.* [98] extended this concept in 1985 to a bidirectional cavopulmonary connection.

This operation can be performed with standby cardiopulmonary bypass, except when other intracardiac procedures are performed concomitantly, for example, atrioventricular valvoplasty, augmentation of the bulboventricular foramen,

Damus–Kaye–Stansel procedure (Figure 39.28), or branch pulmonary arterioplasty.

To optimize pulmonary blood flow distribution, the cavopulmonary anastomosis should be placed as centrally as possible. An end-to-side anastomosis is performed with readsorbable suture, interrupted in four quadrants. The azygos and or hemiazygos veins, when present, are always divided.

Pulsatility can be allowed by leaving anterograde flow across a restrictive open pulmonary outflow tract or a patent modified Blalock–Taussig shunt, predominantly perfusing the contralateral lung [99]. When anterograde flow is retained, a pulmonary artery band is adjusted over a 3 mm Hegar bougie to control the amount of pulmonary blood flow.

Pulmonary artery branch plasty can be performed with untreated autologous pericardium. In patients who require pulmonary arterioplasty, it is preferable to leave a source of pulsatility. To correct a restrictive bulboventricular foramen, a Damus–Kaye–Stansel procedure or a partial resection of the bulboventricular foramen may be performed (see Figure 39.28). Atrioventricular valve regurgitation is a difficult problem and is considered a significant risk factor, probably because of its association with ventricular dysfunction. When two atrioventricular valves are present, one of which is normal in size and function, closure of the regurgitant one may be considered, in association with resection of the atrial septum. A valve ring annuloplasty can be performed in the remaining atrioventricular valve to avoid its dilatation secondary to ventricular enlargement. If there is an insufficient single or common atrioventricular valve, an attempt at valvoplasty or even valve replacement may be undertaken. In patients with both right and left superior venae cavae without a significant communicating vein, cavopulmonary anastomosis should be performed bilaterally. Around 3 months of age, after cardiac catheterization and angiocardiography to identify risk factors for right-sided heart bypass (Table 39.4), a bidirectional cavopulmonary

Table 39.4 Risk factors for a total right-sided heart bypass operation: proposed incremental risk scale[a].

Risk factor	No incremental risk	Moderate increase in risk	High risk
Age (years)	<2[b]	<1.5	<1
Mean PA pressure (mmHg)	<15	15–18	≥18
McGoon index[c]	>2.4	1.8–2.4	<1.8
Pulmonary vascular resistance (PVR) (Wood units)	<2	2–3	>3
Transpulmonary gradient (mmHg)	<6	6–12	>12
Ventricular end-diastolic pressure (VEDP) (mmHg)	<10	10–14	>14
Ejection fraction	>60	45–60	<45
AV valve insufficiency	None or mild	Moderate	Severe
Heterotaxia	No heterotaxia	Polysplenia	Asplenia
History of PA banding	No PA banding	Yes	PA band associated with branch PA stenosis
Mayo Clinic index[d]	<2	2–4	>4
Nakata index[e]	>250	250–200	<200
PA stenosis	None	Mild to moderate	Severe
Restrictive BVF	No restriction	Mild (<30 mmHg)	Moderate to severe (>30 mmHg)
Left AV valve	Normal	Stenosis	Atresia valve

[a]AV, atrioventricular; BVF, bulboventricular foramen; PA, pulmonary artery.
[b]According to institutional preferences, this age may be variable. At the Buenos Aires Children's Hospital, the cutoff age between low and moderate risk is considered to be 4 years.
[c]McGoon index: [RPA (mm) + LPA (mm)]/descending aorta at the diaphragm (mm).
[d]Mayo Clinic index: [PVR (Wood units) + VEDP (mmHg)]/[Qp (l min^{-1} m^{-2}) + Qs (l min^{-1} m^{-2})].
[e]Nakata index: RPA + LPA (mm^2 m^{-2}).

anastomosis is performed. Severe high-risk factors, such as Nakata index <120 mm^2 m^{-2}, severe ventricular dysfunction, and severe peripheral pulmonary artery stenosis with distal hypoplasia, may contraindicate the operation.

After partial right-sided heart bypass, there is a more efficient pulmonary blood flow, as the Qp becomes effective blood flow (Qe), allowing adequate systemic oxygen saturation (80–85%) and a reduction in preload and atrial filling pressures [100]. An aortopulmonary shunt, which requires a Qp/Qs ratio >2 to keep oxygen saturation above 80%, is replaced by a hemodynamically advantageous system that allows adequate oxygen saturations, a Qp/Qs ratio of <1, without recirculation of blood [101], while reducing the ventricular volume load and preserving ventricular function [102,103]. Long-standing ventricular volume overload with an aortopulmonary shunt can lead to dilated myopathy and ventricular dysfunction [35,104], particularly with a single right ventricle and/or atrioventricular valve insufficiency. The change in ventricular geometry after a bidirectional Glenn anastomosis (decrease in ventricular volume and increase in the ventricular mass/volume ratio) results in an immediate 25% reduction in the area of the bulboventricular foramen [105]. This frequently produces subaortic stenosis

in patients with transposition [94]. Similarly, after a total right-sided heart bypass [105], the change in ventricular geometry causes a 40% reduction in the bulboventricular foramen size.

A bidirectional Glenn anastomosis is pulsatile with additional pulmonary blood flow from a shunt or anterograde flow across the pulmonary valve. In these situations, systemic oxygen saturation tends to be higher at the expense of increased ventricular volume and higher pulmonary artery pressures. A pulsatile bidirectional Glenn anastomosis is particularly indicated for patients with small or stenotic pulmonary arteries, in whom a simultaneous pulmonary arterioplasty is performed.

If there is significant atrioventricular valve regurgitation and depressed ventricular function, or if the intraoperative superior vena caval pressure is >14 mmHg, any source of pulsatility should be eliminated, The technique described by Kawashima *et al.* [106] can be employed in patients with heterotaxia, interrupted inferior vena cava, and azygos or hemiazygos continuation. After this operation, all systemic venous return, except from the hepatic veins, is directed to the pulmonary arteries. This should be considered a partial right-sided heart bypass operation, because the hepatic

venous flow is still excluded from the pulmonary circulation.

Lung perfusion scan

The distribution of pulmonary blood flow after a cavopulmonary connection is preferentially to the ipsilateral pulmonary artery [107,108]. On lung scintigraphy, with upper extremity intravenous isotope injection, both the pulsatile and nonpulsatile bidirectional Glenn procedures show dominant perfusion of the ipsilateral pulmonary artery, and this is reproduced during exercise. With time, this distribution could lead to relative hypoplasia of the contralateral pulmonary artery [109]. Other late complications after a bidirectional Glenn anastomosis include the development of pulmonary arteriovenous microfistulas [77,110] 50–100 μm in diameter, particularly in the lower lobes, which are the best-perfused areas. The absence of hepatic blood flowing into the pulmonary circulation has been postulated in their pathogenesis [77]. An additional source of pulmonary blood flow providing pulsatility in addition to blood flow that has passed through the liver may prevent the development of these fistulas. A larger volume of pulmonary blood flow and the pulsatility may also play a role in pulmonary arterial growth [102,111,112]. Therefore, some prefer a pulsatile bidirectional Glenn anastomosis [99] with a controlled source of pulmonary blood flow, maintaining the mean pulmonary artery pressure at <15 mmHg and the pulsatility amplitude at <5 mmHg higher than the mean pulmonary artery pressure.

Doppler flow dynamics

The echocardiographic evaluation of superior vena cava and pulmonary artery flow dynamics in a bidirectional Glenn procedure demonstrates [108,113] continuous laminar flow of low velocity (<0.5 m s^{-1}) (Figure 39.29). With an additional source of pulsatile flow, in the contralateral pulmonary artery there may be a low or moderate velocity (1 m s^{-1}), continuous flow (aortopulmonary shunt), or systolic flow (anterograde flow through the pulmonary valve). Doppler evaluation of the superior vena cava may identify (see Figure 39.29) continuous venous flow (hypopulsatile bidirectional Glenn), a reduction in the systolic flow (pulsatile bidirectional Glenn), or retrograde flow during systole (hyperpulsatile bidirectional Glenn) (Table 39.5).

Right-to-left shunts (venous collaterals, arteriovenous fistulas)

The increasing cyanosis in patients after a bidirectional Glenn procedure can be explained by the patient's growth, because the contribution of the head and neck vessels to the total cardiac output diminishes with time [114]. Other common sources of a right-to-left shunts such as decompressing venous collaterals [115,116], particularly in patients with a bidirectional Glenn anastomosis and an elevated pulmonary artery pressure, should be excluded. The incidence of decompressing venous collaterals ranges from 13% [110] to 75% [117].

Contrast echocardiography with fast injection of saline or dextrose solution (3–6 ml) in an upper extremity may show rapid filling of the pulmonary veins, suggesting pulmonary arteriovenous fistulas but decompressing venous collaterals to the pulmonary veins cannot be excluded by this finding. An abnormality in the upper extremity contrast echocardiogram occurs in 15% [117] to 60% [110] of these patients. Arteriovenous fistulas can be suspected from a typical radiographic reticular image in the lower lobes, which extends to the periphery. After a Kawashima operation [118], there is evidence of a right-to-left shunt with oxygen saturations of ~90% initially, with subsequent progressive cyanosis attributed to the development of pulmonary arteriovenous fistulas [80,110,118]. The progressive right-to-left shunt also results from decompressing venous collaterals, in particular with anomalous cavoportal connections [119], which become more prominent with time. In these patients, transcatheter embolization may be therapeutic.

The Doppler evaluation of the lower pulmonary venous flow during inspiration demonstrates continuous flow (>0.5 m s^{-1}) that decreases markedly in expiration (Figure 39.30), probably because of collapse of the microfistulas because of increased intrathoracic pressure. Diagnosis of pulmonary arteriovenous fistulas is confirmed by cardiac catheterization. Pulmonary angiograms demonstrate dilated terminal arteries, absent capillary phase, early pulmonary venous opacification, and dilated pulmonary veins. Oximetry reveals desaturation of the pulmonary veins that is not corrected with administration of oxygen. There are few therapeutic options for patients with pulmonary arteriovenous malformations. A brachial or axillary arteriovenous fistula can be performed to increase the pulmonary blood flow and allow blood from the liver to be incorporated in the pulmonary circulation [120,121]. Regression after liver transplantation in patients with liver disease [122] and after complete right-sided heart bypass [123] supports the hypothesis that pulmonary arteriovenous fistulas can be reversible with incorporation of hepatic blood flow.

Exercise capacity

Patients with partial right-sided heart bypass, whether pulsatile or not [124], have markedly depressed exercise capacity (48% of estimated functional capacity) directly related to the level of systemic desaturation [124]. The chronotropic response is normal, as it is in cyanotic congenital heart defects [125]. Exercise stress testing demonstrates that even with an adequate resting systemic saturation (>85%), marked desaturation (<70%) develops with exercise.
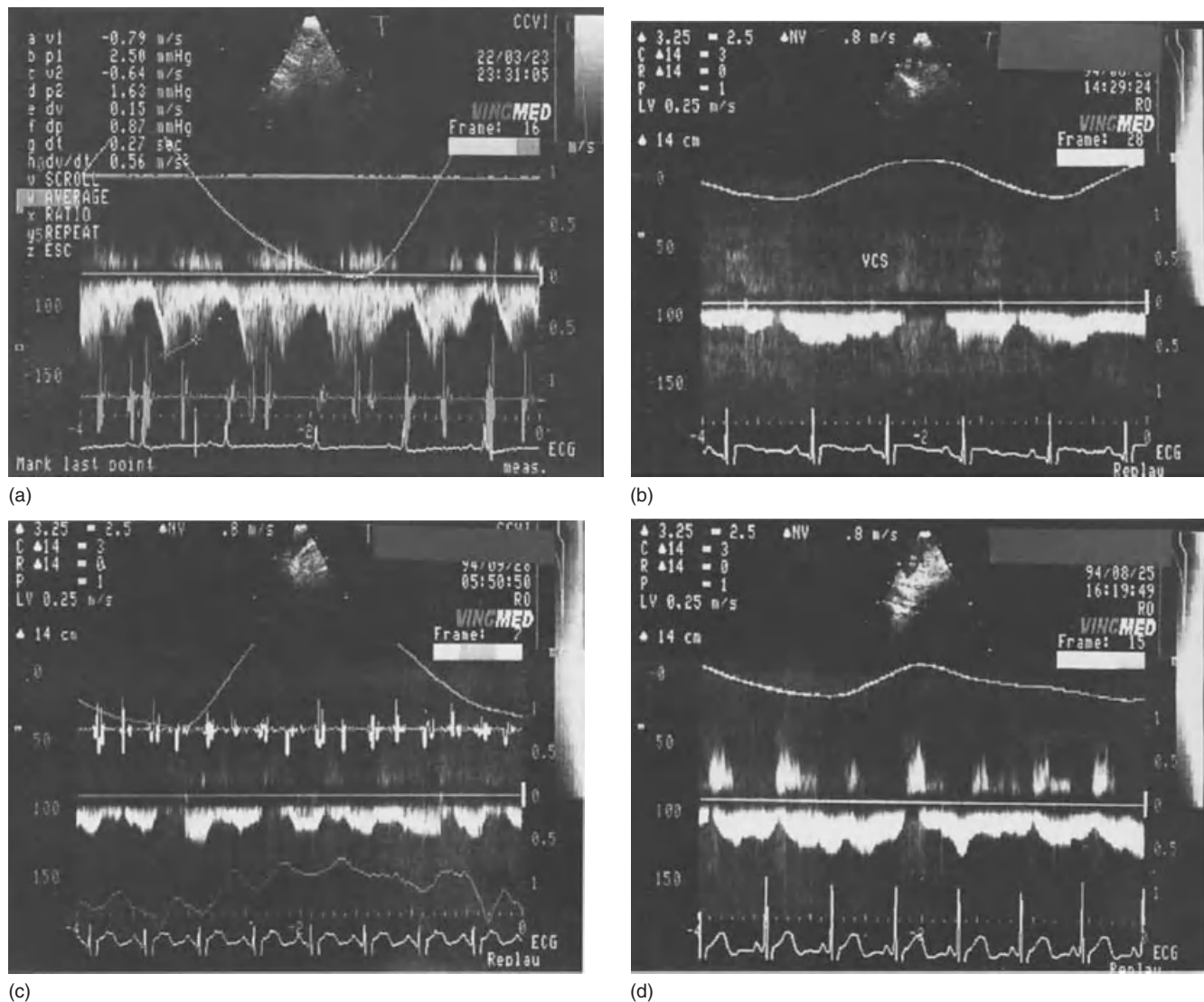
Figure 39.29 Two-dimensional Doppler flow dynamics in superior vena cava. (a) Normal, anterograde biphasic with increase at early inspiration. (b) Nonpulsatile bidirectional cavopulmonary anastomosis, with continuous flow and inspiratory increase in velocity. (c) Pulsatile bidirectional cavopulmonary anastomosis, anterograde flow with systolic slowing. (d) Hyperpulsatile bidirectional cavopulmonary anastomosis, with retrograde systolic flow in superior vena cava.

Definitive palliative surgery: total right heart bypass (Fontan–Kreutzer procedure)

A total or complete right heart bypass directs all systemic venous return into the pulmonary arteries in the absence of a ventricular pump. The operation was first performed by Fontan and Baudet in 1971 [126] for tricuspid atresia IB with the concept that the thickened atrium could be "ventricularized" [127]; they inserted inlet and outlet valves in the atrium. In the same year, and unaware of Fontan and Baudet's reported experience, we performed a total right-sided heart bypass in Argentina [128]. Even in that early experience, valves in the inferior or superior venae cavae

were avoided by our group. What is now known as a fenestrated Fontan procedure [85,129] was first performed in Argentina in 1971 by leaving a residual 6 mm atrial level communication to serve as a pop-off valve. We performed the atriopulmonary connection with a different hemodynamic concept to that of Fontan and Baudet, as we considered the right atrium to be a compliant chamber without any significant pump function and that the suction force of the system would be generated by the end-diastolic pressure of the systemic ventricle [130–132].

Multiple modifications of the initial Fontan procedure have been proposed and performed over time (Figure 39.31).

Table 39.5 Flow dynamics by transthoracic two-dimensional echo Doppler in bidirectional cavopulmonary connection.

Flow	Superior vena cava	Pulmonary artery (PA)
Nonpulsatile	Continuous $<0.5\,\mathrm{m\,s^{-1}}$ ↑ Inspiration	Continuous $<0.5\,\mathrm{m\,s^{-1}}$ ↑ Inspiration
Pulsatile	Continuous, decreasing in systole $<0.5\,\mathrm{m\,s^{-1}}$ ↑ Inspiration	Right PA: continuous, $<0.5\,\mathrm{m\,s^{-1}}$, ↑ inspiration Left PA: pulsatile, $>0.5\,\mathrm{m\,s^{-1}}$
Hyperpulsatile	Retrograde during systole Anterograde during diastole ↑ Inspiration	Right PA: continuous Left PA: hyperpulsatile, $>1\,\mathrm{m\,s^{-1}}$

Initially, as described above, the anterior atriopulmonary connections were performed, as reported by Fontan and Baudet [126], Kreutzer *et al.* [128], and Bjork *et al.* [133]. In 1978 the posterior atriopulmonary connection was introduced [55,134], but later improved surgical techniques were developed: the lateral tunnel by de Leval *et al.* [135], Jonas and Castaneda [136], and Puga *et al.* [137] and the extracardial conduit by Puga and co-workers in 1988 [138] and Marcelletti *et al.* in 1990 [139]. Both the lateral tunnel and extracardiac conduit are considered excellent surgical techniques. Although the extracardiac conduit has become the preferred approach at most centers, it remains controversial, and both approaches have excellent reported outcomes [140]. However, follow-up of the extracardiac conduit is shorter than for the lateral tunnel [130]. The lateral tunnel, which tends to produce more arrhythmias, is more often performed in small patients, given the growth potential of the surgical pathway. The extracardiac conduit has less tendency to produce arrhythmias because of the lack of atrial sutures and low-pressure exposure of the sinus node can be performed without an aortic cross-clamp, and for some, the fenestration may be closed without the need for an implantable device [141]. Indeed, at the Buenos Aires Children's Hospital, it is routine to close the fenestration before hospital discharge by adjusting a snare under local anesthesia [141].

Authorities differ about the optimum timing of this procedure. Following a partial right heart bypass, as the systemic oxygen saturation decreases below 80% or the hematocrit rises above 55%, completion to a total bypass (Fontan–Kreutzer procedure) should be considered, irrespective of age. Adults with a single ventricle can undergo total right heart bypass with low morbidity and mortality [142]. After a total bypass, even when performed on ideal patients, the clinical status may deteriorate with time, even with a normal Qp/Qs ratio of 1. This observation reinforces the concept that the procedure is indeed only palliative. The worrisome long-term complications that follow total right heart bypass operations make one reconsider the approach to timing of this palliative surgery.

The complications of pregnancy in patients after a total right heart bypass should be discussed preoperatively with female patients. Limited experience has demonstrated only 45% incidence of live births among 33 pregnancies [143]. The alternative of chronic cyanosis in a palliated partial right heart bypass circulation, however, is not a benign physiology for a pregnancy. A total right heart bypass normalizes oximetry, eliminates shunts, abolishes the risk of brain abscess, and establishes a series circulation but with only a single systemic ventricular pump.

In the long-term follow-up of patients with total right-sided heart bypass [144–154], poor results have been reported for patients with heterotaxia, low age at operation, weight <15 kg, elevated pulmonary artery pressure, atrioventricular valve dysfunction, and right atrial pressure >20 mmHg or left atrial pressure >10 mmHg in the early postoperative period [147,148,153].

Typically following cardiac catheterization and cineangiography or alternative noninvasive testing to determine risk factors for a total right heart bypass (Table 39.6; see also Table 39.4), patients undergo a total cavopulmonary anastomosis [101,135] with lateral intra-atrial tunnel, extracardiac conduit, or a cavoatriopulmonary anastomosis [155,156], each of which may or may not be fenestrated [84,129]. The cavoatriopulmonary modification protects the sinus node, allows low pressure in the coronary sinus [157], and permits homogeneous distribution of pulmonary blood flow, because it includes a mixing chamber similar to that in an atriopulmonary anastomosis [107]. The most common technique used currently in the United States is the fenestrated extracardiac conduit.

Associated cardiac malformations increase risk factors for a total right-sided heart bypass (see Table 39.4) and demand technical modifications.
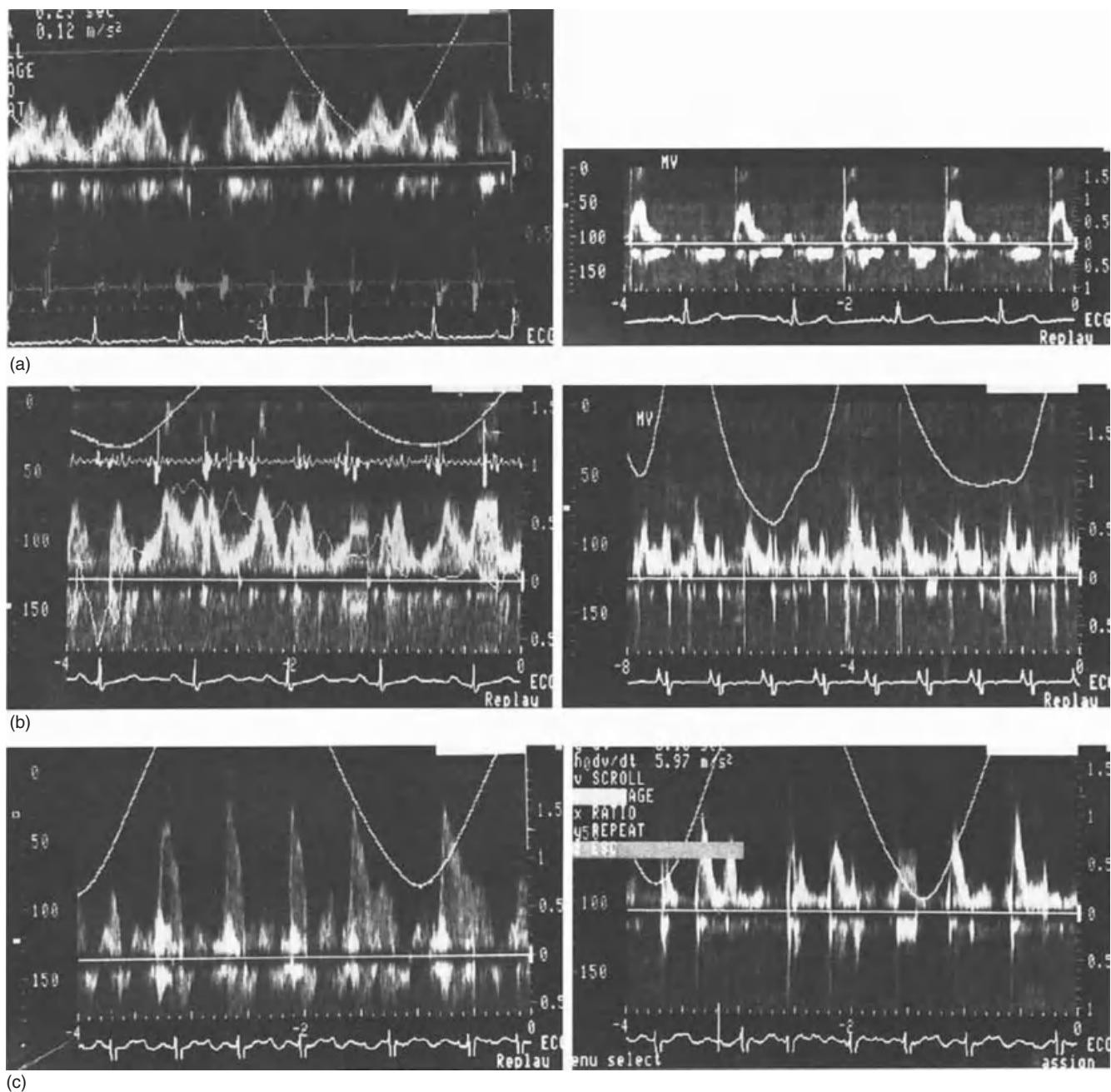
Figure 39.30 Flow dynamics by two-dimensional Doppler echocardiography at pulmonary veins (left) and mitral valve (right) in normal (a), atriopulmonary anastomosis (b), and late failure after atriopulmonary anastomosis (c). The pulmonary venous flow in (b) is triphasic anterograde (prodiastolic, telediastolic, and protosystolic), with increase in velocity during inspiration, the same as the transmitral flow. In (c), there are high velocities recorded in pulmonary veins (1.5 m s^{-1}) with a monophasic protodiastolic flow, differing from the transmitral flow velocity (0.7–1 m s^{-1}). Atrial flutter is present.

A staged approach for performing a total right heart bypass has allowed a significant reduction in morbidity [158] by avoiding a sudden change in ventricular geometry. After a total right-heart bypass performed without a prior staging partial bypass procedure, there is a 100% reduction in the ventricular chamber volume and an increase in both ventricular wall thickness and mass/volume ratio [159,160],

which leads to diastolic ventricular dysfunction early postoperatively [160].

An atriocavopulmonary anastomosis (central tunnel) (Figure 39.32) [155,156] with or without prosthetic material, is an alternative technique for performing a total right heart bypass. It is particularly useful in the conversion of atriopulmonary anastomosis by creating an intra-atrial
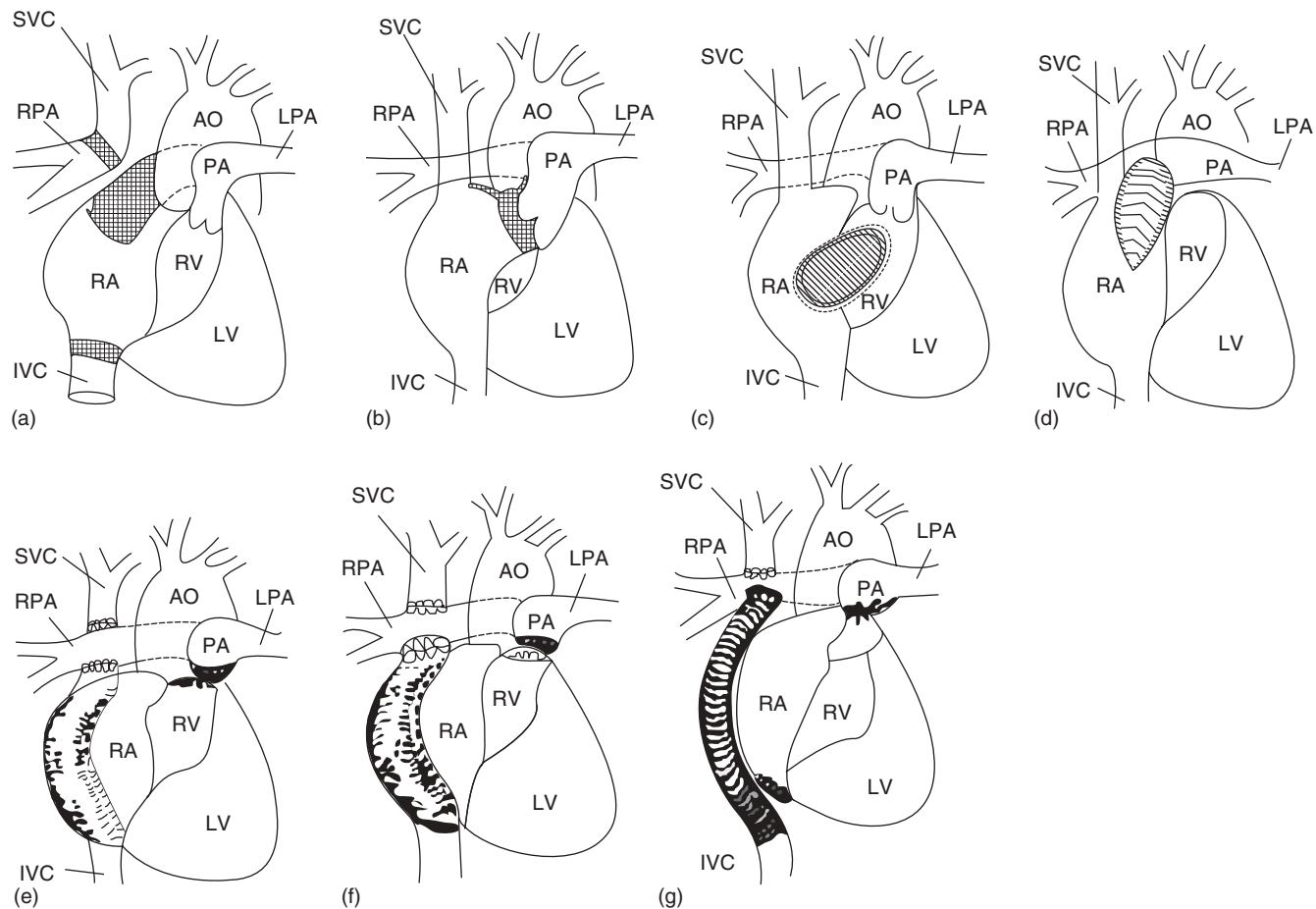
Figure 39.31 Modifications of the total right-sided heart bypass operation. (a) The original Fontan procedure [126]: an end-to-end anastomosis of the RPA to SVC, an end-to-end anastomosis of the right atrial appendage to the proximal end of the RPA by an aortic valved homograft, closure of atrial septal defect, insertion of a pulmonary valve homograft into the IVC, and ligation of the main pulmonary artery. (b) Total right-sided heart bypass [128]: anastomosis of right atrial appendage to the main pulmonary artery with its intact pulmonary valve (excised from the RV) after closing the atrial and ventricular defects. A Glenn operation was not performed, and no IVC valve was used. (c) Bjork *et al*. [133] anastomosed the right atrial appendage directly to the RV outflow tract if the pulmonary valve was normal, using a roof of pericardium to avoid a synthetic tube graft. (d) The posterior anastomosis of the RA to the PA [134]. (e, f) Separate anastomosis of the divided SVC to the RPA: insertion of an IVC to SVC intra-atrial baffle (total cavopulmonary connection) with (f) and without (e) fenestration. (g) Extracardiac conduit between the RPA and a bidirectional Glenn operation. AO, aorta; IVC, inferior vena cava; LPA, left pulmonary artery; LV, left ventricle; PA, pulmonary artery; RA, right atrium; RPA, right pulmonary artery; RV, right ventricle; SVC, superior vena cava. (Modified with permission from Park, *Pediatric Cardiology for Practitioners*, 3rd edn, Mosby, St. Louis, 1996, p. 217.)

tunnel. If made of autologous tissue, it is constructed using the patient's own atrial wall, reducing the size of the atrial chamber. The use of native atrial tissue may lead to increased incidence of arrhythmias long term, but allows for growth potential. In addition, a bidirectional cavopulmonary anastomosis is performed. The inferior vena cava is connected through this tunnel to the main pulmonary artery trunk and branches, similarly to performing an atriopulmonary anastomosis. The advantages of this central tunnel technique [156] are excluding the sinus node and coronary sinus from higher pressure [157], growth potential, absence of suture lines near the sinus node and nodal artery, avoiding prosthetic material, and theoretically favorable distribution of inferior

vena cava blood flow to both lungs. The extracardiac conduit technique [118] shares some advantages with the central tunnel technique, such as the absence of atrial suture lines, although it uses prosthetic material, lacks growth potential, and usually causes preferential distribution of inferior vena caval blood flow to the ipsilateral pulmonary artery, depending on the position of the anastomosis. The postoperative electrocardiogram in these patients shows small-amplitude P waves in the right precordial leads, suggesting low right atrial wall stress. The flow dynamics by Doppler evaluation demonstrate presystolic pulsatility in the inferior vena cava.

After atriopulmonary connection, late failures are common, [144], even in patients with ideal preoperative condition

Table 39.6 Choussat's criteria[a].

Age 4–15 years
Sinus rhythm
Normal drainage of caval veins
Normal volume of right atrium
Mean PA pressure ≤15 mmHg
Pulmonary resistance <4 U m^{-2}
Ratio PA/Ao ≥0.75
Normal ventricular function
No impairing effect of shunt

[a]PA, pulmonary artery; Ao, aorta.

according to the original Choussat's criteria (see Table 39.6) [150]. Experience has demonstrated that these criteria should be regarded as only a guide, because the absence of one or more of these factors should not be considered an absolute contraindication to surgery. It is no longer standard to use these criteria to determine candidacy for Fontan completion. Some patients with significant high-risk factors may still benefit from staged palliation even if considered as a bridge to cardiac transplantation.

Postoperative follow-up
As long-term follow-up data become available, more complications and side effects are identified associated with the procedure and specific techniques that have become outdated. The late results of all these procedures indicate that having a total right heart bypass operation has major long-term adverse consequences secondary to chronic venous hypertension. Limited follow-up data are available for patients with the more recent modifications. The mid-term results after extracardiac conduit are favorable, particularly regarding the incidence of atrial arrhythmias [152].

Exercise capacity
Patients with total right-sided heart bypass have mildly diminished functional capacity [124] to ~79% of estimated capacity as determined by ergometry. They have mild desaturation and subnormal chronotropic response [151–165]. Cardiac output does not increase normally [151–163], in part from both reduced pulmonary blood flow and impaired chronotropic and contractile responses to exercise [164]. Minute ventilation and the ventilatory equivalent for oxygen and carbon dioxide remain above normal [165]. In addition, arrhythmias are more frequent with exercise than at rest [161].

Lung perfusion scan
After total cavopulmonary anastomosis, preferential blood flow distribution to the lung ipsilateral to the cavopulmonary connection is commonly observed [107,108,166]. Certain technical modifications allow a more homogeneous distribu-

(a)   (b)

(c)   (d)
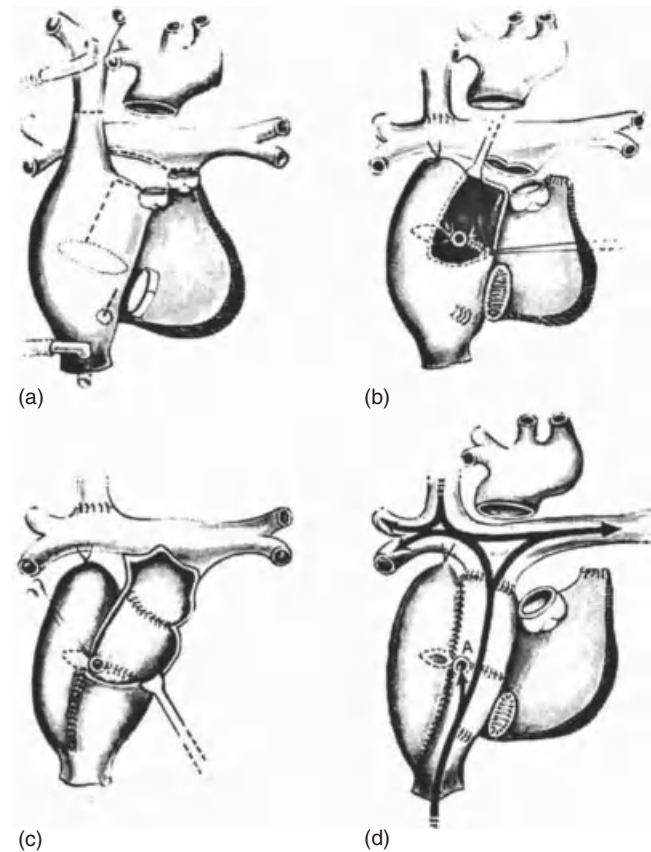
Figure 39.32 (a–d) Surgical technique for the central cavoatriopulmonary anastomosis with autologous material. (Reproduced with permission from Kreutzer *et al. J Card Surg* 1997;**12**:37–40.)

tion of blood flow that may have an effect on pulmonary arterial growth. Results can be difficult to interpret, however, as they vary according to the site of injection and streaming patterns, with the exception of the atriopulmonary anastomosis where there is a chamber of complete mixing.

Doppler flow dynamics
Hemodynamic failure after total right-sided heart bypass can be detected by Doppler echocardiographic analysis of flow dynamics (Table 39.7) [108].

Complications following total right heart bypass

Among the causes or manifestations of failure following a total right-sided heart bypass procedure are the following.

Increased transpulmonary pressure gradient
The flow dynamics after a total right-sided heart bypass depend on the pressure gradient between the right atrium and the left atrium, the transpulmonary gradient. This gradient should ideally not exceed 6 mmHg. Failure after a total right-sided heart

Table 39.7 Flow dynamics by transthoracic two-dimensional echo Doppler in atriopulmonary anastomosis[a].

Flow	"Normal" function	Dysfunctional
Inferior vena cava	Anterograde biphasic S/D $<0.5\,m\,s^{-1}$ ↑ Inspiration	Anterograde in inspiration Retrograde in expiration
Pulmonary artery	Anterograde biphasic S/D with PS exacerbation $0.5\,m\,s^{-1}$ ↑ Inspiration	Anterograde in inspiration $<0.5\,m\,s^{-1}$ Retrograde in expiration
Pulmonary veins	Anterograde biphasic D > S $<0.6\,m\,s^{-1}$ ↑ Inspiration	Anterograde diastolic $>1\,m\,s^{-1}$ ↑ Inspiration
Mitral valve	E > A $<0.6\,m\,s^{-1}$ ↑ Inspiration	Restrictive E $\geq 1\,m\,s^{-1}$ ↑ Inspiration Gradient VP – MV

[a]A, late diastolic filling; D, diastolic; E, early diastolic filling; MV, mitral valve; PS, presystolic; S, systolic; VP, pulmonary veins.

bypass may be secondary to a rise in the transpulmonary gradient with time. Various factors may contribute to this increase, such as deficient pulmonary arterial growth (Nakata index becoming smaller with time) [167,168] or chronic pulmonary micro- or macro-thromboembolism [169,170]. In these patients, oral anticoagulants should be routinely prescribed.

Giant right atrium

Another long-term complication after total right-sided heart bypass of the atriopulmonary anastomosis variety is the development of a giant right atrium. Commonly atrial arrhythmias and thromboembolic complications are associated, and the right pulmonary veins may be compressed by the posterior right atrial wall (Figure 39.20), which further increases the transpulmonary gradient. Patients benefit from conversion to a lateral tunnel connection [171,172] to increase their functional capacity and release compression of the right pulmonary veins.

Right-to-left shunts

In some patients, failure after a total right-sided heart bypass is characterized by cyanosis. Right-to-left shunting can result from a baffle leak, fenestration, and/or decompressing venous collaterals to pulmonary veins or to cardiac veins. Small interatrial communications can develop and cause cyanosis in the long-term follow-up, particularly in those with atriopulmonary connections [173]. To date, there have been no reports of pulmonary arteriovenous fistulas in patients with atriopulmonary connections or total cavopulmonary shunts with homogeneous distribution of hepatic venous blood flow to both lungs.

Thromboembolism

Patients with single ventricle variants following the Fontan procedure are at an increased risk for thrombosis, with significant morbidity and mortality. Those with atriopulmonary anastomosis can develop atrial flutter and chronic thromboembolism [169,170]. The incidence of thromboembolic complications (3.9%) seems to be independent of the type of connection for total right-sided heart bypass [169]. Systemic embolism can also follow a total right-sided heart bypass, particularly in those with a source of right-to-left shunting (fenestration).

There are anatomic predisposing factors, such as areas of blood flow stasis including in the central pulmonary arteries in patients with prior bilateral Glenn procedure [174], the main pulmonary artery surgical stump [175], a giant right atrium after atriopulmonary anastomosis, a prior Kawashima connection type, thrombogenic foreign material, arrhythmias, ventricular dysfunction, prolonged immobilization, and protein-losing enteropathy [176].

The prevalence of thrombosis following the Fontan procedure has ranged from 17 to 33% using transesophageal echocardiography [177–179]. Retrospective reviews report >15% risk for thrombosis and 1–7% risk for thrombosis-related events [176].

Patients with single ventricle variants may have intrinsic and acquired alterations in thrombophilic factors, which can predispose them to both bleeding and thrombosis [180–182]. Although these findings may explain the incidence of such complications, they have not altered practice guidelines, as typically extensive coagulation laboratory workups are not routinely performed prior to surgical staging.

Controversy continues about thrombosis prophylaxis in patients with single ventricle variants. Limited numbers of publications have addressed this issue. A retrospective observational study by Seipelt *et al.* [183] showed that patients taking either aspirin or warfarin had lower event rates than those without antithrombotic therapy. A study demonstrated that when using solely postoperative aspirin as antithrombotic agent, no thrombotic events occurred at mid-range follow-up (mean follow-up 40 months) [184]. Other studies have suggested that there may be no benefit to thromboprophylaxis [185,186].

In general, antiplatelet therapy with aspirin (3–5 mg kg^{-1} per day) has been recommended after Stage I palliation and also following bidirectional Glenn procedure. Many continue the use of antiplatelet therapy for long-term anticoagulation after Fontan procedure, although some advocate oral warfarin. Some elect a stronger anticoagulation regimen for 3–12 months after Fontan procedure and then continue with antiplatelet therapy alone. Which approach is the best management option with regard to risk–benefit is unknown. The ACC/AHA 2008 Guidelines for the management of adults with congenital heart disease [187] recommend the use of warfarin as a Class I recommendation (level of evidence C) for adult patients who after Fontan procedure have documented atrial shunt (all those fenestrated), atrial thrombus, atrial arrhythmias, or a thromboembolic event.

Arrhythmias

About 37% of patients with total cavopulmonary anastomosis have sinus node dysfunction [188,189]. This may occur from direct damage to the sinus node artery or to the node itself. Sinus node dysfunction can also occur after atriopulmonary connection (12%) and is particularly frequent after bidirectional Glenn or hemi-Fontan procedures [189].

Arrhythmias may occur in the early postoperative period, particularly in patients with high-risk factors and poor postoperative hemodynamics. Among these, atrial arrhythmias, junctional ectopic tachycardia, and even ventricular arrhythmias may develop [190]. Junctional ectopic tachycardia can occur in the immediate postoperative period after total right-sided heart bypass [191], particularly in patients younger than 3 years, and has a poor prognosis.

Supraventricular tachycardia seems to be less frequent in patients with total cavopulmonary connection than in those with atriopulmonary connection, although the follow-up periods are not comparable [191].

Protein-losing enteropathy

This serious complication of chronic venous hypertension occurs in >11% of the patients [148]. They present with hypoproteinemia, hypoalbuminemia, chronic edema, pleural effusions, ascites, pericardial effusions, and increase of fecal α_1-antitrypsin. Clearance of α_1-antitrypsin is currently the best method of evaluating protein-losing enteropathy.

Various management options have been considered for such patients, including steroid treatment, low molecular weight heparin, selective pulmonary vasodilator therapy, fenestration creation, heart transplantation, and Fontan takedown.

Plastic bronchitis

Another rare manifestation of failure after a total right-sided heart bypass has been chyloptysis and expectoration of bronchial casts, a rare, life-threatening complication of uncertain physiopathology [192,193]. However, procedures which decrease venous pressures may result in its resolution. In addition, cardiac transplantation is also generally therapeutic. The presentation is variable, typically during late follow-up, but may happen early. Manifestations include a chronic productive cough, which progresses to severe life-threatening airway obstruction. Patients cough bronchial casts that are acellular, made of mucin, fibers, and few mononuclear cells.

Liver disease

As more patients survive for many years after a single ventricle repair, the effects of long-term passive congestion of the liver are being reported. Apart from frequent disturbances of liver enzymes and clotting factors produced by the liver, established cardiac cirrhosis has been observed in 10–30% of patients, and hepatic adenoma and carcinoma have been reported [194–199]. There is some concern that these complications may develop more often with time, and evaluating the liver may need to be done more frequently.

General complications and management

Clinical failure after a total right-sided heart bypass is managed according to the specific hemodynamic abnormality or manifestation of failure. Anticongestive medications, afterload-reducing agents, and oral anticoagulants are widely used. Cardiac catheterization and potential transcatheter interventions should always be performed. Invasive evaluation of arrhythmias with possible ablation, in addition to medical management, may be beneficial [200]. Some patients improve after conversion from one form of total bypass to another with more favorable hemodynamics [172,201]. Other patients can only be either reverted to a partial right-sided heart bypass or referred for cardiac transplantation.

References

1 Anderson RH, Becker AE, Wilkinson JL, Gerlis LM. The morphogenesis of univentricular heart. *Br Heart J* 1976;**38**:558–72.

2 Van Praagh R, Ongley P, Swan HJC. Anatomic types of single or common ventricle in man. Morphologic and geometric aspects of 60 necropsied cases. *Am J Cardiol* 1964;**13**:367–86.

3 Lev M, Libertson RR, Kirkpatric KJ, *et al.* Single (primitive) ventricle. *Circulation* 1969;**39**:577–91.

4 Samanek M, Voriskova M. Congenital heart disease among 815,569 children born between 1980 and 1990 and their 15-year

survival: prospective Bohemia survival study. *Pediatr Cardiol* 1999;**20**:411–7.

5 Kidd BSL. Single ventricle. In: Keith J, Rowe R, Vlad P, eds. *Heart Disease in Infancy and Childhood*. London: Macmillan, 1978: 405–17.

6 De la Cruz MV, Miller VL. Double inlet left ventricle. Two pathological specimens with comments on the embryology and on its relation to single ventricle. *Circulation* 1968;**37**:249–60.

7 Muñoz Castellanos L, De la Cruz MV, Cieslinski A. Double-inlet right ventricle. Two pathological specimens with comments on embryology. *Br Heart J* 1973;**35**:292–7.

8 Shinebourne EA, Macartney FJ, Anderson RH. Sequential chamber localization – logical approach to diagnostics in congenital heart disease. *Br Heart J* 1976;**38**:327–40.

9 Anderson RH, Becker A, Freedom R, *et al*. Analysis of the atrioventricular junction – connections, relations and ventricular morphology. In: Godman MJ, ed. *Paediatric Cardiology*, Vol. 4. Edinburgh: Churchill Livingstone, 1981: 169–81.

10 Van Praagh R. The segmental approach to diagnosis in congenital heart disease. *Birth Defects Orig Artic Ser* 1972;**8**:4–23.

11 Bharati S, Lev M. The spectrum of common atrioventricular orifice (canal). *Am Heart J* 1973;**86**:553–61.

12 Anderson RH, Macartney FJ, Tynan M, *et al*. Univentricular atrioventricular connection, the single ventricle trap unsprung. *Pediatr Cardiol* 1983;**4**:273–80.

13 Van Praagh R, Plett JA, Van Praagh S. Single ventricle pathology, embryology, terminology and classification. *Hertz* 1979;**4**:113–50.

14 Lyons GE. Vertebrate heart development. *Curr Opin Genet Dev* 1996;**6**:454–46.

15 Van Mierop LHS. Embryology of the univentricular heart. *Hertz* 1979;**4**:78–85.

16 Viegas C, Kreutzer EA. Estudio anatomico de 196 corazones con cardiopatias congenitas aplicando el analisis segmentario secuencial. In: Kreutzer EA, ed. *Cardiología y Cirugía Cardiovascular Infantil*. Buenos Aires: Doyma Argentina, 1993: 152.

17 Keeton BR, Lie JT, McGoon DC, *et al*. Anatomy of coronary arteries in univentricular heart and its surgical implications. *Am J Cardiol* 1979;**43**:569–80.

18 Holmes AF. Case of malformation of the heart. *Trans Med Chir Soc Edinb* 1824;**1**:252–9.

19 Anderson RH, Arnold R, Thapar MK, *et al*. Cardiac specialized tissues in heart with an apparently single ventricular chamber (double inlet left ventricle). *Am J Cardiol* 1974;**33**:95–106.

20 Davies MJ, Anderson RH, Becker AE. Atrioventricular conduction tissues in congenital heart disease. In: Davies MJ, Anderson RH, Becker AE, eds. *The Conduction System of the Heart*. London: Butterworth-Heinemann, 1983: 135–45.

21 Van Praagh R, Van Praagh S, Vlad P, Keith JD. Diagnosis of the anatomic types of single or common ventricle. *Am J Cardiol* 1965;**15**:345–66.

22 Quero Jimenez M, Anderson RH, Tynan M, *et al*. Summation of anatomic patterns of atrioventricular and ventriculo-arterial connections. In: Godman MJ, ed. *Paediatric Cardiology*, Vol 4. Edinburgh: Churchill Livingstone, 1981: 211.

23 Van Mierop LHS, Gessner IH, Schiebler GL. Asplenia and polysplenia syndromes. *Birth Defects Orig Artic Ser* 1972;**8**(5):36–44.

24 Uemura H, Ho S, Devine W, Anderson RH. Analysis of visceral heterotaxy according to splenic status, appendage morphology or both. *Am J Cardiol* 1995;**76**:846–84.

25 Milo S, Ho SY, Macartney FJ, *et al*. Straddling and overriding atrio-ventricular valves: morphology and classification. *Am J Cardiol* 1979;**44**:1122–34.

26 Liberthson R, Paul M, Muster A, *et al*. Straddling and displaced atrioventricular orifices and valves with primitive ventricles. *Circulation* 1971;**43**:213–26.

27 Clapp SK, Perry BL, Farooki ZQ, *et al*. Surgical and medical results of complete atrioventricular canal: a ten year review. *Am J Cardiol* 1987;**59**:454–458.

28 Van Praagh R. The importance of ventriculoatrial malalignment in anomalies of the atrioventricular valves, illustrated by "mitral atresia" and congenital mitral stenosis with large left ventricle. In: Doyle EF, Engle MA, Gersony W, *et al.*, eds. *Paediatric Cardiology*. New York: Springer, 1986: 901–3.

29 Van Praagh S, Santini F, Sanders SP. Cardiac malpositions with special emphasis on visceral heterotaxy (asplenia and polysplenia syndromes). In: Fyler DC, ed. *Nadas' Pediatric Cardiology*. Philadelphia: Hanley & Belfus, 1992: 589–608.

30 Rahimtoola SH, Ongley P, Swan HJC. The hemodynamics of common (or single) ventricle. *Circulation* 1966;**34**:14–23.

31 Somerville J, Becu L, Ross D. Common ventricle with acquired subaortic obstruction. *Am J Cardiol* 1974;**34**:206–14.

32 Freedom RM, Sondheimer H, Dische R, Rowe RD. Development of "subaortic stenosis" after pulmonary arterial banding for common ventricle. *Am J Cardiol* 1977;**39**:78–83.

33 Ritter DG, Seward JB, Moodie D, *et al*. Univentricular heart (common ventricle): preoperative diagnosis, hemodynamic, angiocardiographic and echocardiographic features. *Hertz* 1979;**4**:198–205.

34 Wernovsky G, Chang AC, Wessel AL. Intensive care. In: Emmanouilides GC, Allen H, Riemenschneider TA, Gutgesell HP, eds. *Moss and Adams' Heart Disease in Infants, Children and Adolescents Including the Fetus and Young Adult*, 5th edn. Baltimore: Williams & Wilkins, 1995: 398–439.

35 Sano T, Ogawa M, Taniguchi K, *et al*. Assessment of ventricular contractile state and function in patients with univentricular heart. *Circulation* 1989;**79**:1247–56.

36 Rychik KJ, Jacobs M, Norwood W. Acute changes in left ventricular geometry after volume reduction operation. *Am Thorac Surg* 1995;**60**:1267–73.

37 Kidd BSL. Single ventricle. In: Keith JD, Rowe RD, Vlad P, eds. *Heart Disease in Infancy and Childhood*, 3rd edn. New York: Macmillan, 1978: 405–17.

38 Moodie DS, Ritter DG, Tajik AJ, *et al*. Long-term follow-up in the non-operated univentricular heart. *Am J Cardiol* 1984;**53**: 1124–8.

39 Ammash NM, Warnes CA. Survival into adulthood of patients with unoperated single ventricle. *Am J Cardiol* 1996;**77**:542–4.

40 Elliot LP, Ruttenberg HD, Elliot RS, Anderson RC. Vectorial analysis of the electrocardiogram in common ventricle. *Br Heart J* 1964;**26**:302–11.

41 Quero-Jiménez M, Casanova-Gómez M, Castro-Gussoni C, *et al*. Electrocardiographic finding in single ventricle and related conditions. *Am Heart J* 1973;**86**:449–61.

42 Guller B, Mair D, Ritter D, Smith R. Frank vectorcardiogram in common ventricle: correlation with anatomic findings. *Am Heart J* 1975;**90**:290–4.

43 Phoon CK, Villegas M, Ursell P, Silverman NH. Left atrial isomerism detected in fetal life. *Am J Cardiol* 1996;**77**:1083–8.

44 Carey L, Ruttenberg H. Roentgenographic features of common ventricle with inversion of the infundibulum. Corrected transposition with rudimentary left ventricle. *AJR Am J Roentgenol* 1964;**92**:652–68.

45 Elliot LP, Gedgadus E. The roentgenologic findings in common ventricle with transposition of the great vessels. *Radiology* 1964;**82**:850–65.

46 Elliot LP, Schiebler GH. *The X-Ray Diagnosis of Congenital Heart Disease in Infants, Children and Adults*. Springfield, IL: Charles C Thomas, 1979: 282–6.

47 Geva T, Kreutzer J. Diagnostic pathways for evaluation of congenital heart disease. In: Crawford MH, Demarco JP, Paulus WJ, eds. *Cardiology*, 2nd edn. London: Mosby International, 2004: 1239–60.

48 Sarwar A, Shapiro MD, Abbara S, Cury RC. Cardiac magnetic resonance imaging for the evaluation of ventricular function. *Semin Roentgenol* 2008;**43**:183–92.

49 Grothues F, Moon JC, Bellenger NG, *et al*. Interstudy reproducibility of right ventricular volumes, function, and mass with cardiovascular magnetic resonance. *Am Heart J* 2004;**147**:218–23.

50 Fogel MA, Gupta KB, Weinberg PM, Hoffman EA. Regional wall motion and strain analysis across stages of Fontan reconstruction by magnetic resonance tagging. *Am J Physiol* 1995;**269**:H1132–52.

51 Banka P, McElhinney DB, Bacha EA, *et al*. What is the clinical utility of routine cardiac catheterization before a Fontan operation? *Pediatr Cardiol*. 2010;**31**:977–85.

52 Prakash A, Khan MA, Hardy R, *et al*. A new diagnostic algorithm for assessment of patients with single ventricle before a Fontan operation. *J Thorac Cardiovasc Surg* 2009;**138**:917–23.

53 Yoo SJ, Kellenberger CJ, Román KS, *et al*. Magnetic resonance evaluation of pulmonary circulation in children. *Prog Pediatr Cardiol* 2006;**22**:211–23.

54 Fogel MA. Cardiac magnetic resonance of single ventricle. *J Cardiovasc Magn Reson* 2006;**8**:661–70.

55 Kreutzer GO, Vargas FJ, Schlichter AJ. Atriopulmonary anastomosis. *J Throrac Cardiovasc Surg* 1982;**83**:427–36.

56 Rebergen S, Ottenkamp J, Doornbos J, *et al*. Post-operative pulmonary flow dynamic after Fontan surgery: assessment with nuclear magnetic resonance velocity mapping. *J Am Coll Cardiol* 1993;**21**:123–31.

57 Klimes K, Abdul-Khaliq H, Ovroutski S, *et al*. Pulmonary and caval blood flow patterns in patients with intracardiac and extracardiac Fontan: a magnetic resonance study. *Clin Res Cardiol* 2007;**96**: 160–7.

58 Festa P, Ait Ali L, Bernabei M, De Marchi D. The role of magnetic resonance imaging in the evaluation of the functionally single ventricle before and after conversion to the Fontan circulation. *Cardiol Young* 2005;**15**(Suppl.3):51–6.

59 Whitehead KK, Gillespie MJ, Harris MA, *et al*. Noninvasive quantification of systemic-to-pulmonary collateral flow. *Circ Cardiovasc Imaging* 2009;**2**:405–11.

60 Fogel MA, Weinberg PM, Fellows KE, Hoffman EA. A study in ventricular–ventricular interaction. Single right ventricle compared with systemic right ventricles in a dual-chamber circulation. *Circulation* 1995;**92**:219–30.

61 Fogel MA, Gupta KB, Weinberg PM, Hoffman EA. Regional wall motion and strain analysis across stages of Fontan reconstruction by magnetic resonance tagging. *Am J Physiol* 1995;**269**:H1132–52.

62 Shiraishi H, Silverman NH. Echocardiographic spectrum of double inlet ventricle: evaluation of the interventricular communication. *J Am Coll Cardiol* 1990;**15**:1401–8.

63 Bevilacqua M, Sanders SP, Van Praagh S, *et al*. Double inlet single left ventricle: echocardiographic anatomy with emphasis on the morphology of the atrioventricular valves and ventricular septal defect. *J Am Coll Cardiol* 1991;**18**:559–68.

64 Matitau A, Geva T, Colan SD, *et al*. Bulboventricular foramen size in infants with double inlet left ventricle or tricuspid atresia with transposed great arteries: influence on initial palliative operation and rate of growth. *J Am Coll Cardiol* 1992;**19**:142–8.

65 Rigby ML, Anderson RH, Gibson D, *et al*. Two dimensional echocardiographic categorisation of the univentricular heart: ventricular morphology, type, and mode of atrioventricular connection. *Br Heart J* 1981;**46**:603–12.

66 Smallhorn JF, Tommasini G, Macartney FJ. Detection and assessment of straddling and overriding atrioventricular valves by two dimensional echocardiography. *Br Heart J* 1981; **46**:254–62.

67 Tei C. New non-invasive index for combined systolic and diastolic ventricular function. *J Cardiol* 1995;**26**:135–6.

68 Williams RV, Ritter S, Tani, LY, *et al*. Quantitative assessment of ventricular function in children with single ventricle using the Doppler myocardial performance index. *Am J Cardiol* 2000;**86**:1106–10.

69 Mahle WT, Coon PD, Wernovsky G, Rychik J. Quantitative echocardiographic assessment of the performance of the functionally single right ventricle after the Fontan operation. *Cardiol Young* 2001;**11**:399–406.

70 Bacha EA, Zimmerman FJ, Mor-Avi V, *et al*. Ventricular resynchronization by multisite pacing improves myocardial performance in the postoperative single ventricle patient. *Ann Thorac Surg* 2004; **78**:1678–83.

71 Soto B, Pacifico AD, Di Sciascio G. Univentricular heart: an angiographic study. *Am J Cardiol* 1982;**49**:787–94.

72 Soto B, Bertranou EG, Bream PR, *et al*. Angiographic study of univentricular heart of right ventricular type. *Circulation* 1979;**60**:1325–34.

73 Soto B, Ceballos R, Nath PH, *et al*. Overriding atrioventricular valves: an angiographic–anatomical correlate. *Int J Cardiol* 1985;**9**:323–39.

74 Ellis K. Angiocardiography in complex congenital heart disease: single ventricle, double-inlet, double outlet, and transposition. In: Davila JC, ed. *Second Henry Ford Hospital International Symposium on Cardiac Surgery*. Norwalk, CT: Appleton-Century-Crofts, 1977: 220–32.

75 Nakata S, Imai Y, Takanashi Y, *et al*. A new method for quantitative standardization of cross sectional areas of the pulmonary arteries in congenital heart disease with decreased pulmonary blood flow. *J Thorac Cardiovasc Surg* 1984;**88**:610–9.

76 Piehler MJ, Danielson GK, McGoon DC, *et al*. Management of pulmonary atresia with ventricular septal defect and hypoplastic pulmonary arteries. *J Thorac Cardiovasc Surg* 1980; **80**:552–67.

77 Srivastava D, Preminger T, Lock J, *et al*. Hepatic venous blood and the development of pulmonary arteriovenous malformations in congenital heart disease. *Circulation* 1995;**92**:1217–22.

78 Stumper O, Wright J, Sadiq M, De Giovani JV. Late systemic desaturation after total cavopulmonary shunt operations. *Br Heart J* 1995;**74**:282–6.

79 Hsu H, Nykanen D, Williams W, *et al*. Right to left interatrial communications after the modified Fontan procedure: identification and management with transcatheter occlusion. *Br Heart J* 1995;**74**:548–52.

80 Treidman JK, Bridges N, Mayer JE, Lock JE. Prevalence and risk factors for aortopulmonary collateral vessels after Fontan and bidirectional Glenn procedures. *J Am Coll Cardiol* 1993;**22**:207–15.

81 Galantowicz M, Cheatham JP. Lessons learnt from the development of a new hybrid strategy for the management of hypoplastic left heart syndrome. *Pediatr Cardiol* 2005;**26**:190–9.

82 Kreutzer J, Rome JJ. The role of cardiac catheterization during staged reconstruction. In: Rychik J, Wernovsky G, eds. *Hypoplastic Left Heart Syndrome*. Norwell, MA: Kluwer, 2002: 193–228.

83 Kreutzer J, Lock JE, Jonas RA, Keane JF. Transcatheter fenestration dilation and/or creation in postoperative Fontan patients. *Am J Cardiol* 1997;**79**:228–32.

84 Bridges ND, Lock JE, Castaneda AR. Baffle fenestration with subsequent transcatheter closure. *Circulation* 1990;**82**:1681–9.

85 Bridges ND, Lock JE, Mayer JE, *et al*. Cardiac catheterization and test occlusion of the interatrial communication after the fenestrated Fontan operation. *J Am Coll Cardiol* 1995;**25**:1712–7.

86 Furey S, Zieske H, Levy M. The essential function of the right ventricle. *Am Heart J* 1984;**107**:404–10.

87 Koshiba-Takeuchi K, Mori AD, Kaynak BL, *et al*. Reptilian heart development and molecular basis of cardiac chamber evolution. *Nature* 2009;**461**:95–8.

88 Schneider M, Zartner P, Sidiropoulos A, *et al*. Stent implantation of the arterial duct in newborns with duct-dependent circulation. *Eur Heart J* 1998;**19**:1401–9.

89 Imai Y, Hoshino S, Koh Y, *et al*. Ventricular septation procedure for univentricular connection of left ventricular type. *Semin Thorac Cardiovasc Surg* 1994;**6**:48–55.

90 Mayer JE. Initial management of the single ventricle patient. *Semin Thorac Cardiovasc Surg* 1994;**6**:2–7.

91 Kreutzer C, Kreutzer EA, Varon RF, *et al*. Preoperative management of congestive heart failure in neonates: the closed hood. *Int J Cardiol* 1997;**60**:139–42.

92 Trusler GA, Mustard WT. A method of banding the pulmonary artery for large isolated ventricular septal defect with and without transposition of the great arteries. *Ann Thorac Surg* 1972;**13**:351–5.

93 Welke KF, Shen I, Ungerleider RM. Current assessment of mortality rates in congenital cardiac surgery. *Ann Thorac Surg*. 2006;**82**:164–70; discussion 170–1.

94 Jensen RA, Williams RG, Laks H, *et al*. Usefulness of banding of the pulmonary trunk with single ventricle: physiology at risk for subaortic obstruction. *Am J Cardiol* 1996;**77**:1089–93.

95 Sluysmans T, Sanders S, Van der Velde M, *et al*. Natural history and patterns of recovery of contractile function in single left ventricle after Fontan operation. *Circulation* 1992;**86**:1753–61.

96 Glenn WWL. Circulatory bypass of the right heart. IV. Shunt between superior vena cava and distal right pulmonary artery: report of a clinical application. *N Engl J Med* 1958;**259**:117–20.

97 Bakulev AN, Kolesnikov SA. Anastomosis of superior vena cava and pulmonary artery in surgical treatment of certain congenital defects of the heart. *J Thorac Surg* 1959;**37**:693–702.

98 Hopkins RA, Armstrong BE, Serwer GA, *et al*. Physiological rationale for a bidirectional cavopulmonary shunt: a versatile complement to the Fontan principle. *J Thorac Cardiovasc Surg* 1985;**90**:391–8.

99 Kobayashi J, Matsuda H, Nakano S, *et al*. Hemodynamic effects of bidirectional cavopulmonary shunt with pulsatile pulmonary flow. *Circulation* 1991;**84**(Suppl III):219–25.

100 Salim MA, Case C, Sade RM, *et al*. Pulmonary/systemic flow ratio in children after cavopulmonary anastomosis. *J Am Coll Cardiol* 1995;**25**:735–8.

101 Jonas RA. Indications and timing for the bidirectional Glenn shunt versus the fenestrated Fontan circulation. *J Thorac Cardiovasc Surg* 1994;**108**:522–4.

102 Uemura H, Yagihara T, Kawashima Y, *et al*. Use of bidirectional Glenn procedure in the presence of forward flow from the ventricle to the pulmonary arteries. *Circulation* 1995;**92**(Suppl II):II-228–32.

103 Fogel M, Weinberg P, Chin AJ, *et al*. Late ventricular geometry and performance changes of functional single ventricle throughout staged Fontan reconstruction assessed by magnetic resonance imaging. *J Am Coll Cardiol* 1996;**28**: 212–21.

104 Kuroda O, Sano T, Matzuda H, *et al*. Analysis of the effects of the Blalock–Taussig shunt on ventricular function and prognosis in patient with single ventricle. *Circulation* 1987;**76**(Suppl III):III-24–8.

105 Donofrio MT, Jacobs ML, Norwood WI. Early changes in ventricular septal defect size in the single ventricle after volume unloading surgery. *J Am Coll Cardiol* 1995;**26**:1008–15.

106 Kawashima Y, Kitamura S, Matsuda H, *et al*. Total cavopulmonary shunt operations in complex cardiac anomalies. *J Thorac Cardiovasc Surg* 1984;**87**:74–81.

107 Kreutzer EA, Quilindro AH, Barber B, *et al*. Study of pulmonary perfusion using scintigraphy in total or partial bypass of the right ventricle at rest and with exertion. *J Am Coll Cardiol* 1995;**25**(Suppl A):305A.

108 Hager A, Fratz S, Schwager M, *et al*. Pulmonary blood flow patterns in patients with Fontan circulation. *Ann Thorac Surg* 2008;**85**:186–91.

109 Mendelsohn AM, Bove EL, Lupinetti FM, *et al*. Central pulmonary artery growth patterns after the bidirectional Glenn procedure. *J Thorac Cardiovasc Surg* 1994;**107**:1284–90.

110 Bernstein HS, Brook MM, Silverman NH, Bristow J. Development of pulmonary arteriovenous fistulae in children after cavopulmonary shunt. *Circulation* 1995;**92**(Suppl II):II-309–14.

111 Slavik Z, Salmon A, Daubeney P, *et al*. Do central pulmonary arteries grow following bidirectional superior cavopulmonary anastomosis? *J Am Coll Cardiol*. 1995;**25**(Suppl A):304A.

112 Miyaji K, Shimada M, Sekiguchi A, *et al*. Usefulness of pulsatile bidirectional cavopulmonary shunt in high-risk Fontan patients. *Ann Thorac Surg* 1996;**65**:845–50.

113 Salzer-Muhar V, Marx M, Ties M, *et al*. Doppler flow profiles in the right and left pulmonary artery in children with congenital heart disease and a bidirectional cavopulmonary shunt. *Pediatr Cardiol* 1994;**15**:302–7.

114 Gross G, Jonas R, Castaneda AR, *et al*. Maturational and hemodynamic factors predictive of increased cyanosis after bidirectional cavopulmonary anastomosis. *Am J Cardiol* 1994; **74**:705–9.

115 Kopf GH, Laks H, Stansel H, *et al*. Thirty year follow-up of superior vena cava pulmonary artery (Glenn) shunt. *J Thorac Cardiovasc Surg* 1990;**100**:662–70.

116 Magee AG, McCrindle BW, Mawson JL, *et al*. Systemic venous collaterals after the bidirectional cavopulmonary anastomosis: prevalence and predictions. *J Am Coll Cardiol* 1998;**32**:502–8.

117 Kreutzer EA, Narkizian G, Vazquez H, *et al*. Contrast echocardiography in bypassing of the right ventricle. *Ultrasound Med Biol* 1997;**23**(Suppl):S10A.

118 Kawashima Y, Matsuki O, Yagihara T, Matsuda H. Total cavopulmonary shunt operation. *Semin Thorac Cardiovasc Surg* 1994;**6**:17–20.

119 Stumper O, Wright JG, Sadig M, De Giovanni JV. Late systemic desaturation after total cavopulmonary shunt operations. *Br Heart J* 1995;**74**:282–6.

120 Mitchell IM, Goh DW, Abrams LD. Creation of brachial artery–basilic vein fistula: a supplement to the cavopulmonary shunt. *J Thorac Cardiovasc Surg* 1989;**98**:214–6.

121 Magee A, Sim E, Benson LN, *et al*. Augmentation of pulmonary blood flow with an axillary arteriovenous fistula after a cavopulmonary shunt. *J Thorac Cardiovasc Surg* 1996;**111**:176–80.

122 Lacroix J, Blanchard H, de Viele de Goyet J, *et al*. Reversal of cirrhosis-related pulmonary shunting in two children by orthotopic liver transplantation. *Transplantation* 1992;**53**:1135–8.

123 Knight WB, Mee RBB. A cure for pulmonary arteriovenous fistulas? *Ann Thorac Surg* 1995;**59**:999–1001.

124 Abella I, Torres I, Leveroni A, *et al*. Ergometría en el bypass total vs bypass parcial del ventrículo derecho. *Rev Argent Cardiol* 1996;**64**:517.

125 Sietsema KE, Cooper D, Perloff JK, *et al*. Dynamic of oxygen uptake during exercise in adults with cyanotic congenital heart disease. *Circulation* 1986;**73**:1137–44.

126 Fontan F, Baudet E. Surgical repair of tricuspid atresia. *Thorax* 1971;**26**:240–8.

127 Norwood WI. Our roots, our future. *World J Pediatr Congenit Heart Surg* 2010;**1**:127–31.

128 Kreutzer G, Galindez E, Bono H, *et al*. An operation for the correction of the tricuspid atresia. *J Thorac Cardiovasc Surg* 1973;**66**:613–21.

129 Billingsley AM, Laks H, Boyce SW, *et al*. Definitive repair in patients with pulmonary atresia and intact ventricular septum. *J Thorac Cardiovasc Surg* 1989;**97**:746–54.

130 Kreutzer GO, Schlichter AJ, Kreutzer C. The Fontan/Kreutzer procedure at 40: an operation for the correction of tricuspid atresia. *Semin Thorac Cardiovasc Surg Pediatr Card Surg Annu* 2010;**13**:84–90.

131 Jacobs ML. My back pages. *World J Pediatr Congenit Heart Surg* 2010;**1**:283–4.

132 Kreutzer GO. Letter to the Editor. Comment on "Our Roots, Our Future". *World J Pediatr Congenit Heart Surg* 2010;**1**:412.

133 Bjork VO, Olin CL, Bjarke BB, Thoren CA. Right atrial–right ventricular anastomosis for correction of tricuspid atresia. *J Thorac Cardiovasc Surg* 1979;**77**:452–8.

134 Kreutzer GO, Allaria A, Schlichter A, *et al*. A comparative long-term follow-up of the results of anterior and posterior approaches in bypassing the rudimentary right ventricle in patients with tricuspid atresia. *Int J Cardiol* 1988;**19**:167–79.

135 de Leval MR, Kliner P, Gewilling M, Bull C. Total cavopulmonary connection; a logical alternative to atriopulmonary connection for complex Fontan operations. Experimental studies and early clinical experience. *J Thorac Cardiovasc Surg* 1988;**96**:682–95.

136 Jonas RA, Castaneda AR. Modified Fontan procedure: atrial baffle and systemic venous to pulmonary artery anastomotic techniques. *J Card Surg* 1988;**3**:91–6.

137 Puga JF, Chiavarelli M, Hagler DJ. Modification of the Fontan operation applicable to patients with left atrioventricular valve atresia or single atrioventricular valve. *Circulation* 1987;**76**: 1153–60.

138 Humes RA, Feldt RH, Porter CJ, *et al*. The modified Fontan operation for asplenia and polysplenia syndromes. *J Thorac Cardiovasc Surg* 1988;**96**:212–8.

139 Marcelletti C, Corno A, Giannico S, Marino B. Inferior vena cava pulmonary artery extracardiac conduit: a new form of right heart bypass. *J Thorac Cardiovasc Surg* 1990;**100**: 228–32.

140 Fiore AC, Turrentine M, Rodefeld M, *et al*. Fontan operation: a comparison of lateral tunnel with extracardiac conduit. *Ann Thorac Surg* 2007;**83**: 622–30.

141 Kreutzer C, Schlichter AJ, Simón J, *et al*. A new method for reliable fenestration in extracardiac conduit. *Ann Thorac Surg* 2003;**75**:1657–9.

142 Gates RN, Laks H, Drinkwater DC Jr, *et al*. The Fontan procedure in adults. *Ann Thorac Surg* 1997;**63**:1085–90.

143 Canobbio MM, Mair DD, Van der Velde M, Koos BJ. Pregnancy outcomes after the Fontan repair. *J Am Coll Cardiol* 1996;**28**: 763–7.

144 Fontan F, Kirklin JW, Fernandez G, *et al*. Outcome after a "perfect" Fontan operation. *Circulation* 1990;**81**:1520–38.

145 Humes RA, Porter CJ, Mair D, *et al*. Intermediate follow-up and predicted survival after the modified Fontan procedure for tricuspid atresia and double-inlet ventricle. *Circulation* 1987;**76**(Suppl 3):67–71.

146 Driscoll DJ, Offord KP, Feldt RH, *et al*. Five to fifteen year follow-up after Fontan operation. *Circulation* 1992;**85**:469–96.

147 Mair DD, Hagler DJ, Julsrud PR, *et al*. Early and late results of the modified Fontan procedure for double-inlet left ventricle. The Mayo Clinic experience. *J Am Coll Cardiol* 1991;**18**:1727–32.

148 Feldt RH, Driscoll DJ, Offord KP, *et al*. Protein-losing enteropathy after the Fontan operation. *J Thorac Cardiovasc Surg* 1996;**112**:672–80.

149 Moore JW, Kirby WC, Madden W, Gaiber NS. Development of pulmonary arteriovenous malformations after modified Fontan operation. *J Thorac Cardiovasc Surg* 1989;**98**:1045–50.

150 Choussat A, Fontan F, Besse P, *et al*. Selection criteria for Fontan's procedure. In: Anderson RH, Shinebourne EA, eds. *Pediatric Cardiology 1977*. Edinburgh: Churchill Livingstone, 1978: 559–66.

151 Fontan F, Fernandez G, Costa F, *et al*. The size of the pulmonary arteries and the results of the Fontan operation. *J Thorac Cardiovasc Surg* 1989;**98**:711–9.

152 Amodeo A, Galletti L, Marianeschi S, *et al*. Extracardiac Fontan operation for complex cardiac anomalies. Seven years' experience. *J Thorac Cardiovasc Surg* 1997;**114**:1020–30.

153 Knott-Craig CJ, Danielson GK, Schaff HV, *et al*. The modified Fontan operation: an analysis of risk factors for early postoperative death or takedown in 702 consecutive patients from one institution. *J Thorac Cardiovasc Surg* 1995;**109**:1237–43.

154 Gentles TL, Mayer JE, Gauvreau K, *et al*. Fontan operation in five hundred consecutive patients: factors influencing early and late outcome. *J Thorac Cardiovasc Surg* 1997;**114**:376–91.

155 Uemura H, Yagihara T, Kawashima Y, *et al*. What factors affect ventricular performance after a Fontan-type operation? *J Thorac Cardiovasc Surg* 1995;**110**:405–15.

156 Kreutzer C, Schlichter AJ, Kreutzer GO. Cavoatriopulmonary anastomosis via a nonprosthetic medial tunnel. *J Card Surg* 1997;**12**:37–40.

157 Miura T, Hiramatsu T, Forbess JM, Mayer JE. Effects of elevated coronary sinus pressure on coronary blood flow and left ventricular function: implications after the Fontan operation. *Circulation* 1995;**92**(Suppl II):II-298–303.

158 Castaneda A. From Glenn to Fontan: a continuing evolution. *Circulation* 1992;**86**(Suppl II):II-80–4.

159 Mayer JE, Bridges N, Lock JE, *et al*. Factors associated with marked reduction in mortality for Fontan operations in patients with single ventricle. *J Thorac Cardiovasc Surg* 1992;**103**: 444–51.

160 Gewillig M, Daenen W, Aubert A, Van der Hauwaert L. Abolishment of chronic volume overload: implications for diastolic function of the systemic ventricle immediately after Fontan repair. *Circulation* 1992;**86**(Suppl):II-93–9.

161 Driscoll D, Danielson G, Puga F, *et al*. Exercise tolerance and cardiorespiratory response to exercise after the Fontan operation for tricuspid atresia or functional single ventricle. *J Am Coll Cardiol* 1986;**7**:1087–94.

162 Zellers T, Driscoll D, Mottram C, *et al*. Exercise tolerance and cardiorespiratory response to exercise before and after the Fontan operation. *Mayo Clin Proc* 1989;**64**:1489–97.

163 Schachar GB, Fuhrman B, Wang Y, *et al*. Rest and exercise dynamics after the Fontan procedure. *Circulation* 1982;**65**:1043–8.

164 Gewillig MH, Lundstrom UR, Bull C, *et al*. Exercise responses in patients with congenital heart disease after Fontan repair: patterns and determinants of performance. *J Am Coll Cardiol* 1990;**15**:1424–32.

165 Grant G, Mansell A, Garfano R, *et al*. Cardiorespiratory response to exercise after the Fontan procedure for tricuspid atresia. *Pediatr Res* 1988;**24**:1–5.

166 Lardo AC, Webber S, del Nido PJ, *et al*. Does the right lung receive preferential blood flow in Fontan repair? Comparison of total cavopulmonary and atriopulmonary connections: an *in vitro* study. *Circulation* 1995;**92**(Suppl I):I-579.

167 Siggfusson G, Webber S, Myers JL, *et al*. Growth of pulmonary arteries following Fontan operation: influence of age and type of connection. *Circulation* 1995;**92**(Suppl I):I-55.

168 Buheitel G, Hofbeck M, Tenbrink V, *et al*. Changes in pulmonary artery size before and after total cavopulmonary connection. *Heart* 1997;**78**:488–92.

169 Rosenthal DN, Friedman AH, Kleinman CH, *et al*. Thromboembolic complications after Fontan operations. *Circulation* 1995;**92** (Suppl II):II-287–93.

170 Day RW, Boyer RS, Tait VF, Ruttenberg HD. Factors associated with stroke following the Fontan procedure. *Pediatr Cardiol* 1995;**16**:270–5.

171 Brestcker M, Myers J, Cyran SE. Conversion of modified Fontan–Kreutzer connection to total cavopulmonary connection: result in improved exercise tolerance and quality of life. *Circulation* 1995;**92**(Suppl I):I-55.

172 Kreutzer J, Keane JF, Lock JE, *et al*. Conversion of modified Fontan procedure to lateral atrial tunnel cavopulmonary anastomosis. *J Thorac Cardiovasc Surg* 1996;**111**:1169–76.

173 Hsu H, Nykanen DG, Williams WG, *et al*. Right to left interatrial communications after the modified Fontan procedure: identification and management with transcatheter occlusion. *Br Heart J* 1995;**74**:548–52.

174 Iyer GK, Van Arsdell GS, Dicke FP, *et al*. Are bilateral superior vena cavae a risk factor for single ventricle palliation? *Ann Thorac Surg* 2000;**70**:711–6.

175 Yie K, Lee CH, Kim SJ. Thrombi in the main pulmonary artery stump after a Fontan operation. *Pediatr Cardiol* 2008;**29**:870–1.

176 Monagle P, Karl TR. Thromboembolic problems after the Fontan operation. *Semin Thorac Cardiovasc Surg Pediatr Card Surg Annu* 2002;**5**:36–47.

177 Fyfe DA, Kline CH, Sade RM, Gillette PC. Transesophageal echocardiography detects thrombus formation not identified by transthoracic echocardiography after the Fontan operation. *J Am Coll Cardiol* 1991;**18**:1733–7.

178 Kaulitz R, Ziemer G, Rauch R, *et al*. Prophylaxis of thromboembolic complications after the Fontan operation (total cavopulmonary anastomosis). *J Thorac Cardiovasc Surg* 2005;**129**:569–75.

179 Balling G, Vogt M, Kaemmerer H, *et al*. Intracardiac thrombus formation after the Fontan operation. *J Thorac Cardiovasc Surg* 2000;**119**:745–52.

180 Jahangiri M, Shore D, Kakkar V, *et al*. Coagulation factor abnormalities after the Fontan procedure and its modifications. *J Thorac Cardiovasc Surg* 1997;**113**:989–93.

181 Jahangiri M, Kreutzer J, Zurakowski D, *et al*. Evaluation of hemostatic and coagulation factor abnormalities in patients undergoing the Fontan operation. *J Thorac Cardiovasc Surg* 2000;**120**:778–82.

182 Odegard KC, McGowan FX Jr, DiNardo JA, *et al*. Coagulation abnormalities in patients with single-ventricle physiology precede the Fontan procedure. *J Thorac Cardiovasc Surg* 2002; **123**:459–65.

183 Seipelt RG, Franke A, Vazquez-Jimenez JF, *et al*. Thromboembolic complications after Fontan procedures. comparison of different therapeutic approaches. *Ann Thorac Surg* 2002;**74**:556–62.

184 Jacobs ML, Pourmoghadam KK, Geary EM, *et al*. Fontan's operation: is aspirin enough? Is coumadin too much? *Ann Thorac Surg* 2002;**73**:64–8.

185 Kaulitz R, Ziemer G, Rauch R, *et al*. Prophylaxis of thromboembolic complications after the Fontan operation (total cavopulmonary anastomosis). *J Thorac Cardiovasc Surg* 2005;**129**:569–75.

186 Cheung YF, Chay GW, Chiu CS, Cheng LC. Long-term anticoagulation therapy and thromboembolic complications after the Fontan procedure. *Int J Cardiol.* 2005;**102**:509–13.

187 Warnes CA, Williams RG, Bashore, TM *et al*. ACC/AHA 2008 Guidelines for the Management of Adults with Congenital Heart Disease. A Report of the American College of Cardiology/American Heart Association Task Force on Practice Guidelines (Writing Committee to Develop Guidelines on the Management of Adults With Congenital Heart Disease). *Circulation* 2008;**118**:e714–833.

188 Kavey RW, Gaum W, Byrum CJ, *et al*. Loss of sinus rhythm after total cavopulmonary connection. *Circulation* 1995;**92**(Suppl II):II-304–8.

189 Manning PB, Mayer JE, Wernovsky G, *et al*. Staged operation to Fontan increases the incidence of sinoatrial mode dysfunction. *J Thorac Cardiovasc Surg* 1996;**112**:833–9.

190 Gelatt M, Hamilton RM, McCrindle BW, *et al*. Risk factors for atrial tachyarrhythmias after the Fontan operation. *J Am Coll Cardiol* 1994;**24**:1735–41.

191 Cecchin F, Johnsrude CL, Perry JC, Friedman RA. Effect of age and surgical technique on symptomatic arrhythmias after the Fontan procedure. *Am J Cardiol* 1995;**76**:386–91.

192 Robotin MC, Edis BD, Weintraub RG, *et al*. Heart transplantation for chyloptysis after Fontan operation. *Ann Thorac Surg* 1995;**59**:1570–1.

193 Bowen A, Oudjhana K, Odagiri K, *et al.*, Plastic bronchitis. large, branching, mucoid bronchial casts in children. *AJR Am J Roentgenol* 1985;**144**:371–5.

194 Babaoglu K, Binnetoglu FK, Aydogan A, *et al*. Hepatic adenomatosis in a 7-year-old child treated earlier with a Fontan procedure. *Pediatr Cardiol* 2010;**31**:861–4.

195 Camposilvan S, Milanesi O, Stellin G, *et al*. Liver and cardiac function in the long term after Fontan operation. *Ann Thorac Surg* 2008;**86**:177–82.

196 Ghaferi AA, Hutchins GM. Progression of liver pathology in patients undergoing the Fontan procedure: Chronic passive congestion, cardiac cirrhosis, hepatic adenoma, and hepatocellular carcinoma. *J Thorac Cardiovasc Surg* 2005;**129**:1348–52.

197 Saliba T, Dorkhom S, O'Reilly EM, *et al*. Hepatocellular carcinoma in two patients with cardiac cirrhosis. *Eur J Gastroenterol Hepatol* 2010;**22**:889–91.

198 Shah H, Kuehl K, Sherker AH. Liver disease after the Fontan procedure: what the hepatologist needs to know. *J Clin Gastroenterol* 2010;**44**:428–31.

199 Wu FM, Ukomadu C, Odze RD, *et al*. Liver disease in the patient with Fontan circulation. *Congenit Heart Dis* 2011;**6**:190–201.

200 Treidman JK, Saul PS, Wendling SN, Walsh EP. Radiofrequency ablation of intraatrial reentrant tachycardia after surgical palliation of congenital heart disease. *Circulation* 1995;**91**:707–14.

201 Kao JM, Alejos JC, Grant PW, *et al*. Conversion of atriopulmonary to cavopulmonary anastomosis in management of late arrhythmias and atrial thrombosis. *Ann Thorac Surg* 1994;**58**:1510–4.

40 Pulmonary Atresia with Intact Ventricular Septum

Henry Chubb & Piers E. F. Daubeney

Royal Brompton Hospital, London, UK

Epidemiology and genetics

Pulmonary atresia with intact ventricular septum (PAIVS) is a relatively rare cardiac anomaly, accounting for ~3% of congenital heart disease, with an incidence of 7–8 per 100 000 live births. In the current era of fetal diagnosis (and in some countries the parental option for termination), the incidence has fallen to ~4.5 per 100 000 live births in the United Kingdom and Sweden [1–4]. There is no significant geographical variation and both sexes are equally affected. Several familial clusters of PAIVS have been noted [5–7], but most instances are sporadic with no genetic cause identified.

Pathogenesis

The pathogenesis of PAIVS is controversial [8]; developmentally, the disease is restricted to the right ventricle (RV), tricuspid valve (TV), and pulmonary valve (PV). Often critical pulmonary stenosis has progressed to pulmonary atresia *in utero* [2,9,10], but the etiology of the initial stenosis and subsequent atresia is incompletely understood.

More than one primary pathology may ultimately present with PAIVS [8]. There are those with a severely regurgitant TV, in whom the RV becomes severely dilated. Early in development the PV is patent, but acquired functional atresia develops because of reduced forward flow through the RV outflow tract from poor RV function and severe TR. The functional atresia progresses to anatomic atresia of the PV [11].

The remaining forms that present with a hypoplastic RV may be caused by two different pathologies. Histologic findings suggest that patients with large RV to coronary artery connections (RVCACs – see below) have a different intraventricular pathology compared with those without RVCACs. The latter are more likely to have significant endocardial fibroelastosis (EFE) [12,13]. The implication is that RVCACs may steal forward flow from the RV, thus reducing the anterograde flow across the PV, so that the RVCACs are thought to be part of the cause rather than the effect: there are reports of RVCACs forming even with severe TR [14]. In those without RVCACs, the EFE appears to be related to persistently high intraventricular pressure, and the atresia of the pulmonary valve appears to be the primary event.

Morphology

By definition, there is anatomic atresia of the pulmonary valve and an intact ventricular septum, although patients with a coexisting small restrictive muscular ventricular septal defect present in a very similar manner. The atrial situs is normal or solitus, with concordant atrioventricular and ventriculoarterial connections and a left-sided aortic arch in almost all patients [1,15,16], although PAIVS has been associated with congenitally corrected transposition of the great vessels [17–19].

In the majority of patients, the cardiac morphology can be classified within a spectrum as outlined in Table 40.1; the minority with a dilated right ventricle form a separate group.

Pulmonary valve

In 75% of patients, the atresia of the PV is membranous [1] (Figure 40.1). In the remaining 25% of patients. the atresia is muscular, with implications for catheter-based interventions.

Table 40.1 Spectrum of cardiac morphology in patients with pulmonary atresia and intact ventricular septum.

	Dilated RV	Mild RV hypoplasia	Moderate RV hypoplasia	Severe RV hypoplasia
RV morphology	Huge and thin-walled	Tripartite	"Bipartite"	"Unipartite"
Timing of closure of PV *in utero*	Any	Late	⇒	Early
Tricuspid valve	Large ($z > 0$)	Normal/small ($z = 0$ to -2)	Very small ($z = -2$ to -5)	Tiny ($z < -5$)
Angle of arterial duct	Obtuse/ acute	Obtuse	Obtuse/acute	Acute
RVCACs[a]	Not present	Not present/ mild	Mild/major	Major/ RVDCC[a]

[a]RVCAC, right ventricle to coronary artery connection; RVDCC, right ventricular-dependent coronary circulation.

Figure 40.1 Morphology of imperforate (asterisk) pulmonary valve with well-formed, but completely fused, commissures. (Reproduced with permission from Freedom RM, Mawson JB, Yoo SJ, Benson LN. *Congenital Heart Disease: Textbook of Angiocardiography*. Armonk, NY: Futura Publishing, 1997.)

In those with muscular atresia, the RV is usually small, with fibrous valve tissue above the level of the muscular obstruction. One patient was reported with an atretic RV infundibulum and a patent PV situated above it [20].

For those with membranous PV atresia, the PV morphology is of two distinct types. With a lower pressure RV (as with severe TR), prominent commissural ridges meet at the center of the thickened valve. In contrast, those with a higher pressure RV have less prominent commissural ridges and a smooth, thin, central portion of the valve [9,15]. The valve is usually tricuspid, although bicuspid variations have been described [21].

Tricuspid valve

The tricuspid valve (TV) is always abnormal [22]. The leaflets are often thickened, with short chordae tendineae and small papillary muscles, tethering the leaflets and reducing mobility. The TV annulus is usually small, and the largest population-based study of 182 patients found a mean tricuspid valve z-score of -5.2 (interquartile range -8.4 to -2.6) [1]. The z-scores calculated for the same valve vary depending on the z-score algorithm used and whether the normal data were derived from echocardiograms or postmortem specimens (Figure 40.2) [23–26]. Not all studies
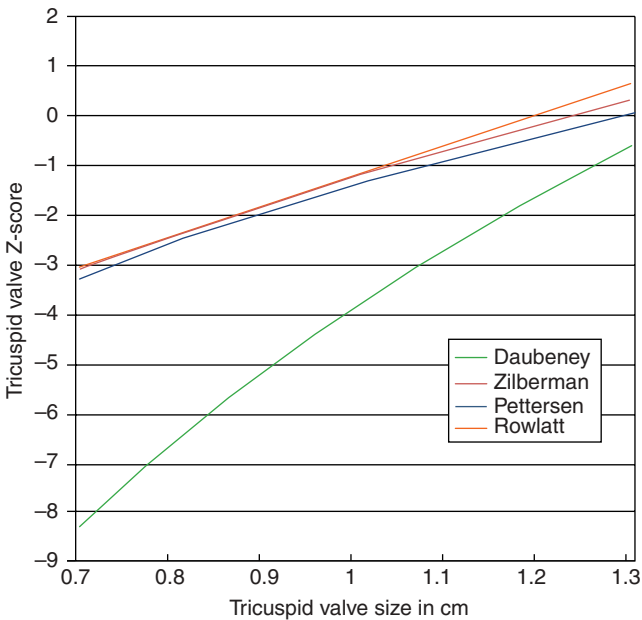
Figure 40.2 The z-score for the tricuspid valve (TV) annulus calculated from the most commonly used z-score algorithms in the literature [23–26]. The z-score is calculated for a neonate of typical body surface area (BSA) of 0.21 m². Note that the Rowlatt study [26], although widely used, is based on a postmortem series. The reason why Daubeney *et al.*'s data [23] have a steeper curve is the smaller spread of their normal data and hence smaller standard deviation.

Figure 40.3 Chest radiograph from a patient with pulmonary atresia and intact ventricular septum with severe tricuspid regurgitation.

report the algorithm used to calculate z-scores, so comparisons between studies should be interpreted with caution.

Patients with a significantly regurgitant TV have a poor prognosis. An Ebstein-type malformation of the tricuspid valve has been reported in 10% [1,27] to 37% [28] of patients, and an unguarded tricuspid orifice may occur [28–30]. The severe regurgitation can produce the so-called "wall-to-wall" heart [11] (Figure 40.3), with a near total absence of the myocardium and a paper-thin ventricular wall resembling Uhl's anomaly [31]. In this form of PAIVS, the pulmonary arteries are frequently hypoplastic [1].

Right ventricle

The RV morphology ranges from a severely hypoplastic and hypertrophied ventricle to a huge dilated thin-walled cavity. The RV has been described as tripartite (containing inlet, outlet, and apical components), bipartite (containing inlet and outlet components), or unipartite (inlet component only) (Figure 40.4). In reality, however, the three components are always present, but may not be identified because of intracavity muscle overgrowth. The occurrence of each type at birth is tripartite(59%), bipartite(34%), and unipartite(7%) [1].

The myocardium is generally abnormal. There is myocardial disarray with fibrosis and reduced numbers of myocytes, especially with the smaller RVs [32,33]. The moderator band and papillary muscles are often poorly

defined, and in ~25% there is significant endocardial fibroelastosis (EFE). EFE is rarely significant if there are RVCACs, but they may coexist [12,34]. Ventricular function may be further compromised by frank ischemia, infarction, and myocardial rupture, due to the abnormal coronary circulation in some (see below), and changes may involve left ventricular myocardium of the left ventricle by the time of birth [35].

Pulmonary arteries

The pulmonary arteries are usually normal in size and confluent. They are hypoplastic in about 9% of patients, particularly with significant RV dilatation. Rarely, the arteries are not confluent and supplied by separate ducts [36], or there may be aortopulmonary collaterals [1].

Arterial duct

When the RV is well formed, the arterial duct is usually normal and creates an obtuse angle at its junction with the distal aorta [1]. The more hypoplastic the RV, the more likely the duct is to be longer, more tortuous, and to join the aorta proximally and at an acute angle [1,2,9,37,38] (Figure 40.5). The earlier closure of the pulmonary valve in fetal life correlates with a more acute angle of ductal insertion into the aorta [9].

Coronary arteries

Abnormalities of the coronary circulation in PAIVS vary and can confuse the clinician. They are the most important determinants of long-term outcome [39]. The changes in the coronary circulation of a hypertensive right ventricle represent a continuum, ranging from clinically unimportant myocardial sinusoids, through right ventricular coronary connections (RVCACs), to a right ventricular-dependent coronary circulation (RVDCC) [27]. Some have attempted to grade these connections (Table 40.2).

Nomenclature varies, with the term "RV coronary artery connections" (RVCACs) used synonymously with "coronary artery fistulas" and even "myocardial sinusoids." The first two terms are generally held to be equivalent, but we concur with Freedom *et al.* that the use of the term "sinusoids" to describe these connections is incorrect [12]. Gittenberger-de Groot and co-workers have drawn a distinction between effectively blind-ending "myocardial sinusoids" that may connect to the myocardial capillary bed and "ventricular–coronary connections" that are direct communications with the coronary arteries (Figure 40.6a and b) [34,42,43]. Only
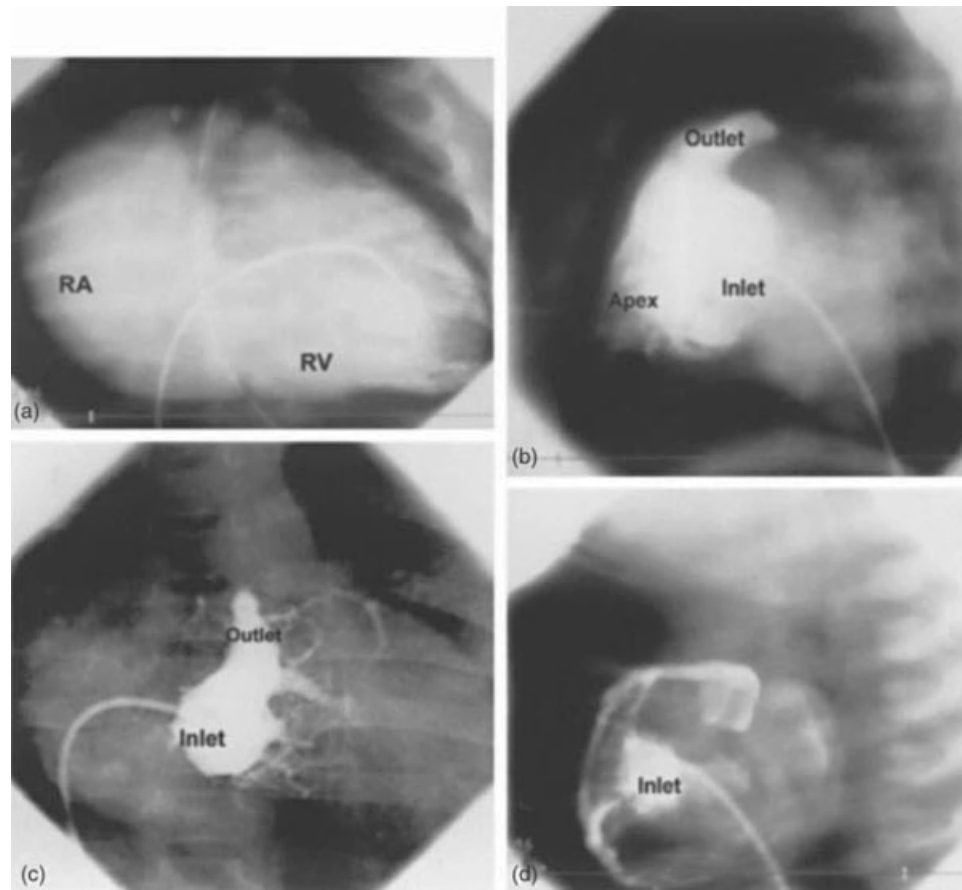
Figure 40.4 Spectrum of pathology in pulmonary atresia with intact ventricular septum. Right ventricular (RV) angiograms showing (a) dilated thin-walled RV and right atrium (RA) with severe tricuspid regurgitation and membranous pulmonary atresia (anteroposterior view); (b) so-called tripartite RV with membranous atresia (lateral view); (c) so-called bipartite RV with membranous atresia, with some RV-to-coronary fistulas (lateral view); (d) tiny so-called unipartite RV with muscular atresia and RV-to-coronary fistulas with retrograde filling of the aorta (lateral view). (Reproduced from Daubeney *et al. J Am Coll Cardiol* 2002;**39**:1670–9, with permission from the *Journal of the American College of Cardiology.*)
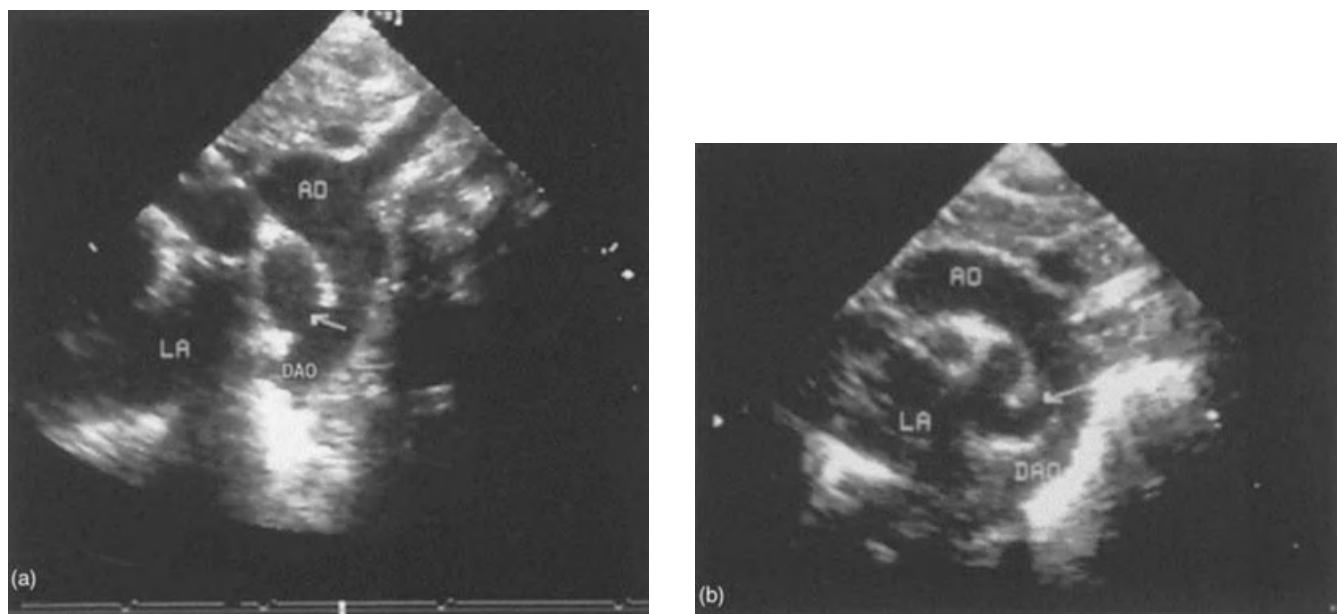
Figure 40.5 Ductal angle in pulmonary atresia with intact ventricular septum. (a) Echocardiogram showing normal obtuse angle of duct to descending aorta (>90°) in a patient with a tripartite RV and membranous pulmonary atresia. (b) abnormal acute angle duct (<90°) in a patient with "unipartite" RV and muscular pulmonary atresia. Ao, aorta; DAO, descending aorta; LA, left atrium. (Reproduced from Daubeney *et al. J Am Coll Cardiol* 2002;**39**:1670–9, with permission from the *Journal of the American College of Cardiology.*)

Table 40.2 Grading of connections.

Grade	RVCAC[a]	RVDCC[a]	Frequency (range) (%)[b]
0	Nil	No	46 (25–55)
1	Small and insignificant	No	18 (8–21)
2	Significant, filling the aortic root from RV injection	Possible	20 (18–23)
3	Associated with one interruption in a major coronary artery	Yes	10 (4–20)
4	Associated with interruptions in two major coronary arteries	Yes	5 (2–15)

[a]RVCAC, right ventricle to coronary artery connections; RVDCC, right ventricular-dependent coronary circulation.
[b]Frequency was calculated from review of a total of 511 patients, although exact definitions vary between observers [1,27,40,41].

in the latter would histologic abnormalities of the coronary system be expected to occur [12,34,44].

Typically, the RVCACs connect to branches of either the right coronary artery (RCA) or the left anterior descending artery (LAD). Reversed turbulent flow from the hypertensive RV disturbs the formation of the normal coronary vasculature. These effects range from mild intimal and medial thickening, with a normal-sized lumen, to complete loss of the normal arterial wall morphology, with replacement by fibrocellular tissue that causes severe stenosis or obliteration of the arterial lumen [12,34] (Figure 40.7). Macroscopically, stenoses and even interruption of the epicardial coronary arteries may develop, and occasionally the RVCACs become dilated and ectatic [1] (Figure 40.8). The affected coronary arteries are usually the proximal LAD and distal RCA [1,27,40] adjacent to the RV. Rarely, the circumflex artery is involved [1,14].

Right ventricular-dependent coronary circulation (RVDCC)

The most severe disruption of the native coronary arteries can cause an RVDCC. This occurs when the coronary artery blood supply depends upon maintaining systemic or suprasystemic RV pressures. An RVDCC is present when there is:

- coronary ostial atresia
- interruption of a single major coronary artery
- significant stenosis of a single major coronary artery
- markedly ectatic coronary artery connections sufficient to cause severe coronary steal if the RV were decompressed [1,12,45].
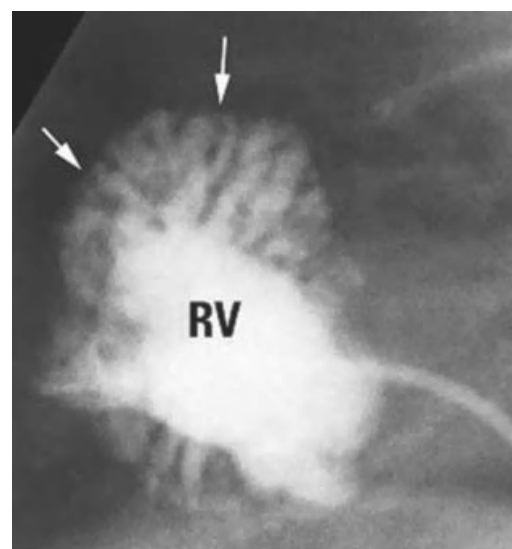
(a)
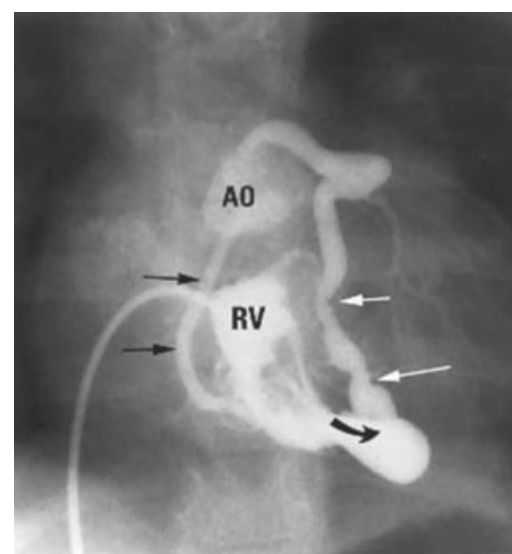
(b)

Figure 40.6 (a) The angiocardiographic appearance of spongy myocardium with extensive myocardial sinusoids (arrows) is demonstrated by this lateral right ventriculogram. (b) Ventriculocoronary connections between a diminutive right ventricle and both coronary arteries. Frontal right ventriculogram demonstrates opacification of both right and left coronary arteries. The curved black arrow notes the ventriculocoronary connection. The right coronary artery (black arrows) is also opacified and shows minimal luminal irregularities. The left anterior descending coronary artery shows multiple levels of stenosis (white arrows). AO, aorta; RV, right ventricle. (Reproduced with permission from Freedom *et al. Congenital Heart Disease: Textbook of Angiocardiography*. Armonk, NY: Futura Publishing, 1997, pp. 617–62.)

Some have more stringent criteria for defining RVDCC, requiring the involvement of two coronary arteries [40,46], but this seems excessive. Ultimately, the absence of an RVDCC in the presence of RVCACs can only be confirmed if decompression of the RV is tolerated by the coronary
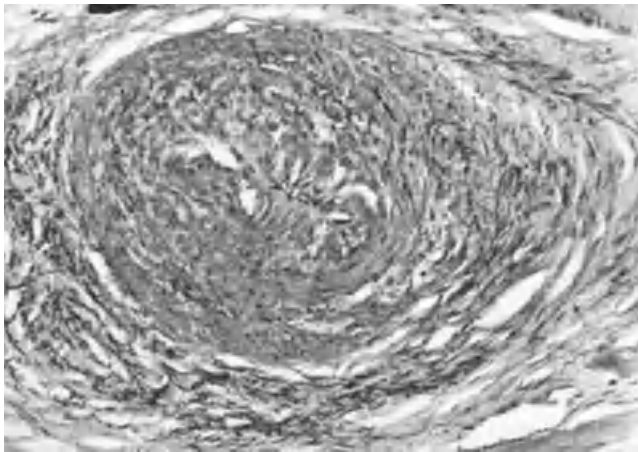
Figure 40.7 Cross-section of the anterior descending coronary artery demonstrates virtual luminal occlusion by myointimal hyperplasia in this neonate with, in retrospect, a right ventricular-dependent coronary circulation. (Reproduced with permission from Freedom *et al. Congenital Heart Disease: Textbook of Angiocardiography*. Armonk, NY: Futura Publishing, 1997, pp. 617–62.)
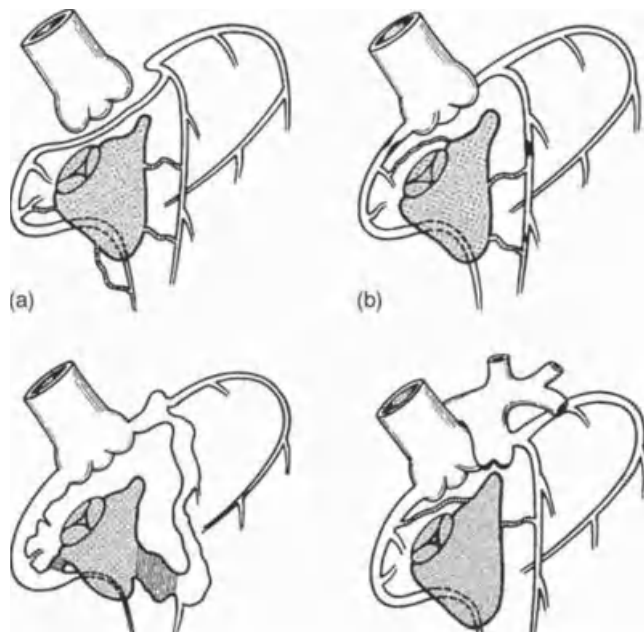
Figure 40.8 Various types of right ventricular-dependent coronary circulations in pulmonary atresia and intact ventricular septum. (a) Absent connections between coronary arteries and aorta; (b) multiple connections with proximal right coronary artery narrowing and left anterior descending interruption; (c) severe ectasia of both right and left coronary arteries with ventriculocoronary connections; (d) multiple ventriculocoronary connections with origin of left coronary artery from pulmonary artery. (Reproduced with permission from Freedom *et al. Congenital Heart Disease: Textbook of Angiocardiography*. Armonk, NY: Futura Publishing, 1997, pp. 617–62.)

circulation, and the intra-procedure ECG is a sensitive barometer of this measure [47].

The proportion of patients with an RVDCC varies between 7.6% [1] and 23% [8,12]. Once a diagnosis of RVDCC has

been established, the implications for the management are profound.

Left-sided structures

Although PAIVS is considered a pathologic condition of the right heart, it has important implications for left-sided heart development as a consequence of the disruption of the myocardium of the left ventricle and its coronary blood supply [35]. Additionally, the hypertensive RV may create a convex distortion of the LV septum, forming a subaortic bulge (Figure 40.9a–c). There is a relatively high proportion of coexisting LV and outflow tract abnormalities (8% in one population study [1]), aortic stenosis [48,49], and coarctation of the aorta [50,51].

Conduction system

The cardiac conduction system is generally normal [52], although Wolff–Parkinson–White syndrome has been reported [29,53].

Rare associated anomalies

Associated anomalies are rare and a large retrospective postmortem review found no significant associated extracardiac anomalies [54]. PAIVS has been associated with trisomy 21 [2], trisomy 18 [41,55], and 22q11 deletion [56].

Clinical presentation

Fetal diagnosis
PAIVS is increasingly being diagnosed in fetuses. The diagnosis is suspected from asymmetry on a four-chamber view, and features of critical pulmonary obstruction can be seen as early as 12 weeks' gestation [36]. Since an association with chromosomal or extracardiac abnormalities is rare, decisions regarding continuation of pregnancy are generally based on the malformation's severity. Gardiner *et al.* [10] formed a set of parameters that predict a final biventricular circulation with a sensitivity of 92% and a specificity of 100%, and other groups have reported similar results [57,58] (see Chapter 16). RVCACs can be detected *in utero* in some patients [10,44,59]. In the United Kingdom, the termination rate for antenatally diagnosed PAIVS was ~60% in the early 1990s [2].

When the pregnancy is continued, in a few centers *in utero* pulmonary valvoplasty is considered in selected patients (discussed later). At birth, appropriate plans can be put in

(a)

(b)

(c)
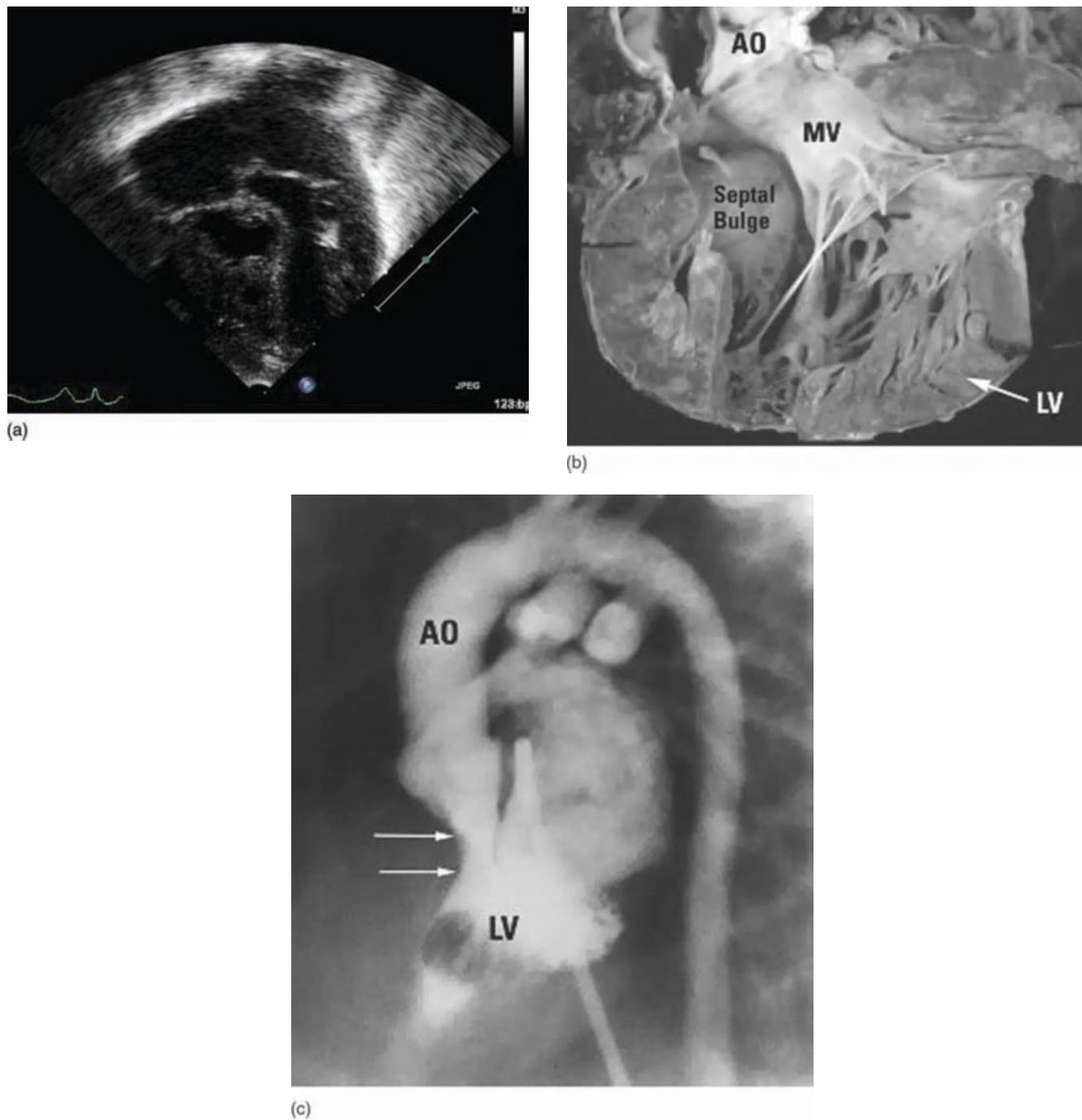
Figure 40.9 (a) Echocardiographic apical four-chamber view. A subaortic bulge is seen in this patient with a bipartite RV. (b) Convex septal bulge in a patient with a small and hypertensive RV. This septal bulge produces the substrate for LV outflow tract obstruction after volume-reducing surgery such as bidirectional cavopulmonary connection or a Fontan-type procedure. (c) Left long axial oblique left ventriculogram demonstrates the convex septal bulge (arrows) promoting dynamic left ventricular outflow tract obstruction. AO, aorta; LV, left ventricle; MV, mitral valve. (Parts (b) and (c) reproduced with permission from Freedom *et al. Congenital Heart Disease: Textbook of Angiocardiography.* Armonk, NY: Futura Publishing, 1997, pp. 617–62.)

place for a neonate with a duct-dependent lesion; the degree of hypoxia prior to intervention is generally much reduced in patients with an antenatal diagnosis, but so far there is no proven survival benefit [2,60].

History and examination

The initial presentation of an undiagnosed neonate with PAIVS is typically with cyanosis when the duct begins to close soon after birth, usually within the first 48 h. On

examination, the first heart sound is normal, the second heart sound single and soft, and there is no ejection click. A ductal murmur may be audible at the left upper sternal edge, or a soft blowing pansystolic murmur at the left lower sternal edge from tricuspid regurgitation. The peripheral pulses are generally good, unless the atrial septal defect is severely restrictive, with normal four-limb blood pressures and saturations low but equal in all extremities.

The presentation in neonates with severe tricuspid regurgitation is considerably different. The left side of the chest may be bulging, with a rocking precordium and systolic thrill, accompanying the loud pansystolic murmur. Heart failure is often conspicuous, with significant hepatomegaly. Respiratory distress or ventilatory difficulties may result from hypoplastic lungs.

Electrocardiogram and chest X-ray

The EKG in most neonates with PAIVS reflects the small right ventricle. The rhythm is generally normal sinus. The P waves are tall and peaked, reflecting right atrial hypertrophy. The mean frontal QRS axis is less rightward than in most neonates, between +30° and +90°. In the chest leads, there is a more adult-type pattern with an rS waveform in the right precordial leads (V4R and V1) and a pure R wave in the left precordial leads (V5 and V6). There may be markers of left ventricular hypertrophy, but EKG evidence of right ventricular hypertrophy is rare despite the RV muscle bulk. Occasionally, ST-T changes reflect myocardial ischemia.

The chest X-ray shows a relatively normal cardiothoracic ratio, except in those with a "wall-to-wall" heart. The right atrial border is prominent. The pulmonary vascular markings are diminished. The aortic arch is generally left sided.

Echocardiography

Echocardiography remains the most important imaging modality in the diagnosis of PAIVS. In such a heterogeneous condition, all morphologic features of the heart must be systematically evaluated to optimize management [61].

Atrial septal defect

The ASD is usually unrestrictive in a term neonate. The size and flow across the ASD should be defined. The right atrium is generally enlarged.

Tricuspid valve

The size of the tricuspid valve annulus should be measured from the four-chamber view in early diastole to allow comparison with published z-scores [23–25]. The anteroposterior diameter can be evaluated on a modified long-axis parasternal view, but it should not be used as a measurement for z-score calculation. The tricuspid valve is frequently dysplastic and small. With severe right ventricular

hypertrophy it may be difficult to evaluate the subvalvar apparatus. A short-axis sweep, from either a parasternal or subcostal view, should define the valve's morphology, particularly of the septal leaflet.

Right ventricle

The RV often looks smaller on echocardiography than its true size, as the intertrabecular spaces appear obliterated. Surrogate markers of RV size, such as TV annulus, are often used and have been well validated [62–64]. Some advocate RV length as a more accurate marker of RV size [61], although it may be difficult to define because of thick apical trabeculations. From a four-chamber and a modified oblique subcostal view, the inlet, apical, and infundibular portion of the RV can be assessed. This allows classification of the RV as "unipartite," "bipartite," or "tripartite." The RV systolic pressure is usually suprasystemic, and can be estimated from the velocity of the TR jet. There may occasionally be a small, insignificant muscular VSD, which is unmasked after RV decompression.

Pulmonary valve and branch pulmonary arteries

The size and morphology of the PV are generally evaluated from the short-axis parasternal view, and measurements for calculation of z-scores should be made from that position. It may be difficult to differentiate critical pulmonary stenosis from pulmonary atresia. The only clue about valve patency may be a few pixels of regurgitation on color flow evaluation. In patients with severe TR and poor RV function, particularly those with a "wall-to-wall" heart, differentiation of anatomic atresia from functional atresia of the PV may be difficult. Again, regurgitation is the most sensitive measure of patency of the PV.

The main pulmonary artery and branch pulmonary arteries are generally confluent and of good size. Rare anomalies should be excluded.

Coronary arteries

Significant RVCACs may be found on color Doppler evaluation. The Nyquist limit should be set low, ~40–60 cm s^{-1} [65], and at high sensitivity. Transmural color Doppler flow may be seen from RV cavity to coronary arteries during systole with reversed flow in diastole. The flow within RVCACs may be confused with flow within the deep trabeculations of the RV, but can be differentiated as the flow in the trabeculations should be towards the RV chamber in systole. The most useful view is a subcostal long-axis view, but four-chamber and short-axis parasternal views may also be helpful.

The origins of the coronary arteries at the aortic root should also be evaluated. z-Score algorithms are widely available for measurements of coronary arteries at significant positions, and an increased z-score ($> +2$) should arouse suspicion of RVCACs if not already identified (Figure 40.10).
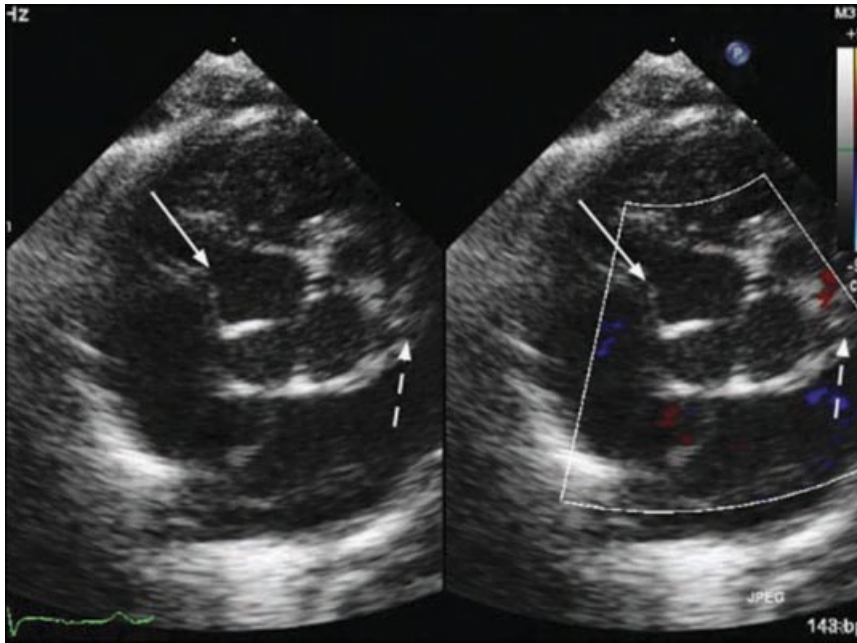
Figure 40.10 A large right coronary artery (solid arrows) arising from the aortic root should lead to a search for RVCACs. Left coronary artery shown by dotted arrows. (Courtesy Dr J. Simpson, Evelina Children's Hospital, London.)

Color and pulsed-wave Doppler evaluation of the coronary flow close to the coronary orifice should also be employed. Retrograde systolic or bidirectional flow suggests significant RVCACs [66,67].

Stenoses of the native epicardial coronary arteries are more difficult to identify, unless they occur in a region of the coronary artery that is well visualized. Occasionally, atresia of the coronary orifice may occur [68,69], and if a coronary orifice cannot be identified on transthoracic echocardiography this should be evaluated with another imaging modality.

Left heart structures

LV wall motion abnormalities should lead to a search for RVCACs, if not already identified [65]. The LV length and MV annulus should be measured to compare with the size of right heart structures, Aortic stenosis and coarctation should be excluded.

Diagnostic cardiac catheterization

The role of diagnostic catheterization in PAIVS has evolved. Catheter pulmonary valvotomy is now established as a common management technique for those with favorable anatomy and angiography is routinely performed during the procedure [70].

For those patients not undergoing catheter intervention, selective angiography remains the way to define the coronary anatomy. At some centers, all patients with PAIVS undergo cardiac catheterization [14,27]. Finding RVCACs alone does not contraindicate RV decompression of the right ventricle. Therefore, at other centers, diagnostic cardiac catheterization is reserved for those most likely to have an RVDCC. This includes patients with the smallest right ventricles; for those determined suitable for only a univentricular repair, it may be appropriate to perform the angiography later in these patients, before a bidirectional cavopulmonary anastomosis [36].

Angiography should include a RV angiogram, to define the form and function of the RV and the presence of RVCACs. Aortic root angiography should be performed in the same planes to establish the relationship of the RVCACs and the native epicardial coronary anatomy [71,72]. Angiograms require extensive experience in reviewing normal coronary anatomy and should be interpreted by the most experience operator available [27]. If a large RVCAC is identified but there is no retrograde flow into the aorta, dense opacification of the aortic root is required to rule out an interruption of the coronary artery [71–73].

Hemodynamic evaluation usually shows a right atrial pressure slightly higher than the left, and suprasystemic RV pressure.

Other imaging modalities

Computed tomography (CT) and magnetic resonance imaging (MRI) techniques have not been established in the routine evaluation of a neonate with PAIVS. Newer CT multidetector techniques, such as Flash spiral mode, can provide increasingly detailed coronary artery anatomy in neonates. They have not been validated, however, in the unusual anatomy that exists in PAIVS.

Table 40.3 Parameters suggested by investigators to determine treatment pathway[a].

Parameter[b]	Biventricular route	Borderline	Univentricular route
TV z-score [64]	>−2.5	−2.5 to −5	<−5
RV morphology [85]	Tripartite	Bipartite	Unipartite
RVDI [86]	>0.35	<0.35	<0.35 *and* muscular atresia
Presence of RV infundibulum [87]	Yes	Small and narrow	No
RVCACs	Nil/minor	Minor/major	RVDCC
Treatment at presentation	RF perforation or closed surgical valvotomy	RF perforation or surgical valvotomy/ RVOT patch *and consider* PDA stent/BTS	Palliative procedure – BTS ± BAS

[a]RVDI, RV development index {calculated as [RVEDV (%N) × TVD (%N) × RVOD (mm) × 10^{-5}]/BSA (m^2), where BSA, body surface area};%N, percentage of normal, RVEDV, RV end diastolic volume, RVOD, RV outflow diameter, TVD, TV diameter, RVCAC, RV to coronary artery connections; RVDCC, RV-dependent coronary circulation; RVOT, RV outflow tract; BTS, Blalock–Taussig shunt; BAS, balloon atrial septostomy.
[b]Note TV z-score is highly dependent upon z-score algorithm, and some investigators do not report which algorithm has been used.

MRI may play a future role in evaluating the hypoplastic RV, paralleling studies of the hypoplastic left heart. Currently, MRI is not used routinely to evaluate ventricular volumes and function of neonates.

Initial management

Fetal intervention

A fetal diagnosis of PAIVS is made in 30–70% of patients with PAIVS [60], depending upon the resources for fetal diagnosis. Fetal intervention is available in some centers, but the worldwide experience of *in utero* valvoplasty remains extremely small [74–77] (see Chapter 16). Limited evidence suggests that valvoplasty may improve RV growth *in utero* and the later chances of a biventricular outcome. Patients should be considered for the procedure only if they are at the severe end of the disease spectrum, likely to receive a univentricular repair without intervention and without significant RVCACs that would prevent RV decompression postnatally [10,74]. In 2006, the UK National Institute for Health and Clinical Excellence (NICE) issued guidelines on percutaneous fetal balloon valvoplasty [78], but noted that evidence is lacking for this procedure.

Treatment algorithms

At birth, the neonate has a duct-dependent pulmonary circulation. Therefore, the infant should be maintained on a prostaglandin E$_1$ infusion to maintain duct patency. In patients with severe RV hypoplasia and the greatest likelihood of possessing an RVDCC, good right-sided filling pressures and a high RV pressure must be maintained. Once the RVDCC is compromised, it is difficult to resuscitate these patients as extracorporeal membrane oxygenation (ECMO) generally reduces RV pressure, and cardiopulmonary resuscitation is also less effective than in most other neonates [79].

Once stabilized and evaluated, the best treatment pathway is selected on an individual basis according to RV and coronary anatomy. The management protocol for neonates remains controversial. Centers that achieve a balance of biventricular and univentricular pathways for patients generally have the best survival outcomes [80].

With the exception of those patients with an RVDCC or a severely regurgitant TV, it is becoming more widely accepted that most patients with membranous atresia and a tripartite and possibly bipartite ventricle should undergo RV decompression. [64,81]. This entails establishing forward flow through the RV, even if hypoplastic. There are several factors to be considered. First, the RV growth potential and regression of RVCACs following decompression are difficult to predict [1,62,81,82]. Second, LV function in a univentricular circulation is hampered by the adjacent hypertensive RV [83]. Third, in some patients, RVCACs progress postnatally to an RVDCC when the RV is not decompressed [1]. The risks of a more technically demanding procedure increase with the smallest RVs, and risk–benefit assessment must be individualized for each patient [84]. Table 40.3 illustrates the parameters suggested by various investigators to delineate the borderline heart anatomy.

Forward flow can be established by either catheter or surgical intervention. The RV of patients with borderline anatomy is often incapable of supplying the entire pulmonary circulation after creating forward flow. In these patients, the pulmonary blood flow can be augmented by one of three methods: continued prostaglandin E$_1$ infusion, stenting the arterial duct, or creating a systemic to pulmonary shunt. In those patients with the smallest RV, the atrial septal defect is often enlarged in the initial procedure [64]. The patient then requires careful evaluation at each follow-up as biventricular, one-and-a half ventricle, and univentricular outcomes all remain possible.

Catheter intervention

Transcatheter laser-assisted balloon pulmonary valve dilatation in pulmonary valve atresia was first described in 1991 [88]. Over the last two decades, significant progress has been made in terms of safety and technical limitations [89–96], and catheter pulmonary valvotomy now forms the mainstay of treatment for PAIVS in many centers for patients with favorable anatomy [8,36,97,98]. Results of the procedure are good, and may be better than in primary surgical intervention [97,99–103]. Comparison with surgical results is difficult, because patients selected for catheter valvotomy tend to have the most favorable anatomy [102].

Techniques for catheter perforation of the pulmonary valve include the use of mechanical force [104], laser energy, and radiofrequency energy (Figure 40.11a–e). The first two have been largely replaced by the last. The equipment required to produce radiofrequency energy is safer and more readily available than laser equipment, and is often already used in laboratories performing electrophysiologic procedures. Some use both arterial and venous access, with catheters "kissing" across the atretic pulmonary valve prior to perforation [70], whereas others use only venous access [105]. The greatest risk of the procedure is that the wire may burn through the pulmonary trunk, causing cardiac tamponade. Once the wire has been safely positioned across the atretic valve, a balloon is passed over the wire and the valve is dilated. Forward flow can be seen on subsequent RV angiography. The catheter technique is increasingly difficult with smaller patients and smaller RVs, and a hybrid procedure may be used in the highest risk patients. Direct access to the right ventricle is obtained via a small subxiphisternal incision and a transventricular sheath is placed to provide optimum position and stability for radiofrequency perforation of the valve [106,107].

At the end of the procedure, the arterial duct may be stented, if the pulmonary blood flow needs to be augmented for the first few months of life [90,108,109]. If such an approach is planned, the prostaglandin infusion should be stopped at the beginning of the catheter valvotomy to allow the duct to constrict and allow safe stent placement [70]. After opening the pulmonary valve, the RV becomes smaller, thus demonstrating the need for the stent [110]. The long-term results of this approach are unknown.

Surgical intervention

Operative management as the initial procedure has progressively become reserved for patients with the most severe forms of PAIVS, particularly at centers with the facility to perform catheter valvotomy. In patients in whom RV decompression is not contraindicated, a closed pulmonary valvotomy is performed or the right ventricular outflow tract (RVOT) is enlarged with a patch [47,62,65,80,81,84,85,98]. A Blalock–Taussig or central shunt is then created to supplement pulmonary blood flow in all patients except those with the most favorable anatomy. In patients assumed to follow a univentricular pathway, a balloon atrial septostomy is performed before creating the shunt [16,36].

Those who advocate a more aggressive approach towards achieving a biventricular repair also ligate the RVCACs in the initial procedure [65,81]. In this technique, the RVCACs are identified from preoperative echocardiography and angiography, and monitored in real time during the operation by both surface and transesophageal echocardiography. The RVCACs are trial occluded and the operators monitor for EKG and wall motion abnormalities. If the trial occlusion is well tolerated, the RVCAC is ligated. The aim is for patients with borderline RVDCC to progress to a biventricular circulation. In addition, this surgical procedure allows for tightening the ASD and encouraging forward flow through the TV and an increase in RV volume. Alternatively, those patients with significant RVCACs but without an RVDCC may undergo thromboexclusion of the RV [39,111], to protect the LV from the effects of a suprasystemic RV. From that point onwards, a univentricular outcome is mandated.

For patients with a proven RVDCC, the options are more limited. The RV cannot be decompressed, and the initial procedure is to create a systemic to pulmonary shunt [40,47]. Thereafter, the treatment pathway is towards a Fontan circulation, but thromboexclusion should not be performed [39].

The surgical treatment of those patients with severe tricuspid regurgitation is very different, and is similar to that for severe Ebstein's malformation. Rarely it is possible to repair the tricuspid valve, aiming for a biventricular repair. However, in most patients a univentricular outcome is pursued, and frequently a Starnes procedure [112] is appropriate. In this procedure, the tricuspid valve is closed with autologous pericardium and a 4 mm aortopulmonary shunt is placed.

Transplantation

The patients at the most severe end of the spectrum of RVDCC are those with aortocoronary atresia (Figure 40.12). This malformation is incompatible with life, with no survivors reported [47,68], except for one patient who had a direct collateral vessel from the descending thoracic aorta connecting with the coronary circulation [69]. These patients should be put forward for early transplantation if appropriate. Bridging the patients to transplant is difficult as they are not good candidates for ECMO: the right ventricle must remain filled and pressure loaded at all times. There is only a single report of a successful transplant performed for this pathology [113].

Late management and prognosis

The aim is to separate the pulmonary and systemic circulations, abolish cyanosis, and close systemic to pulmonary or pulmonary to systemic shunts. This may be achieved in a biventricular,
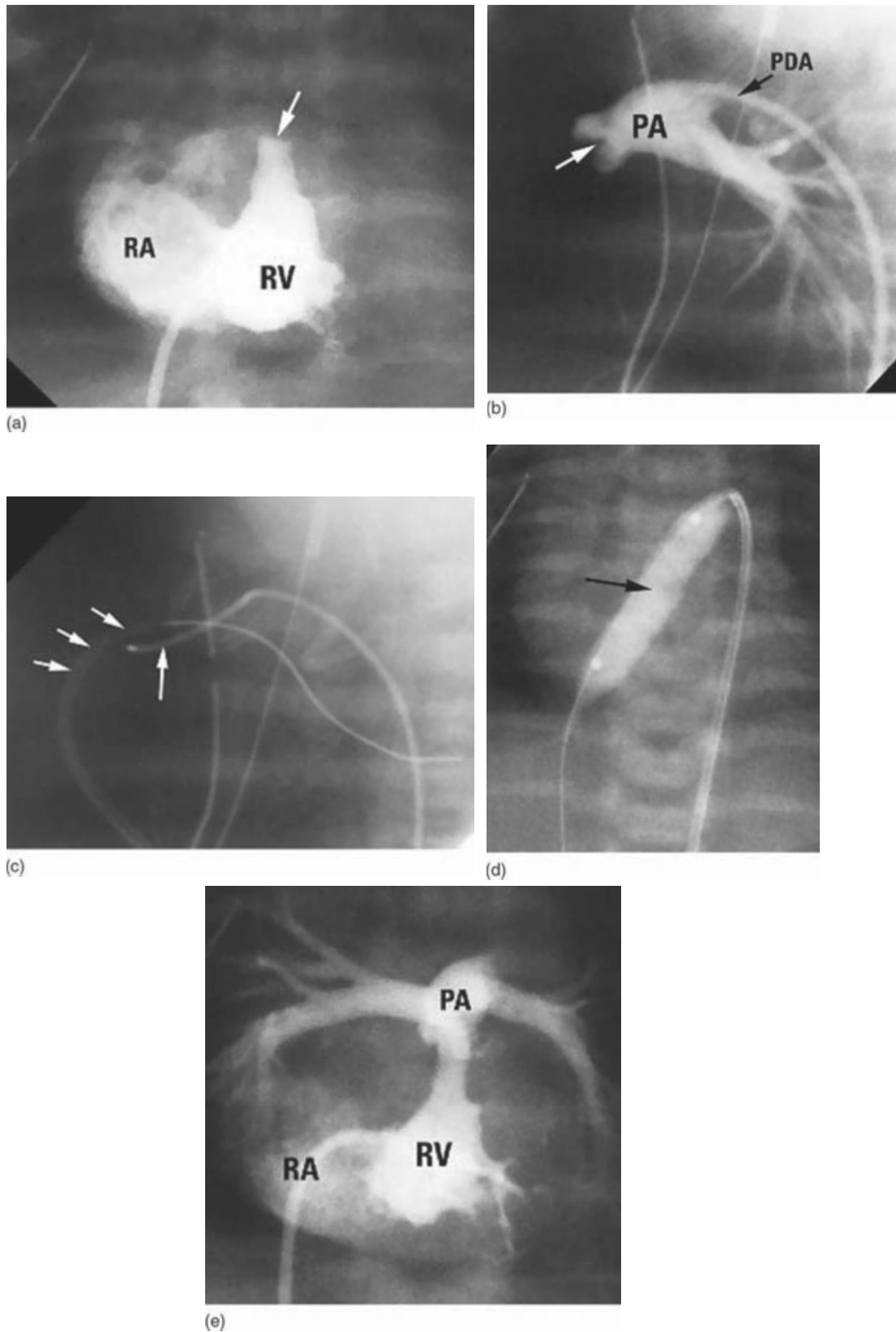
Figure 40.11 Catheter-based therapy for pulmonary atresia and intact ventricular septum using radiofrequency-assisted perforation of the atretic pulmonary valve. (a) Cranially tilted frontal right ventriculogram shows atresia (arrow) of the pulmonary valve. (b) Lateral pulmonary angiogram shows an imperforate pulmonary valve. (c) The Judkins right coronary artery catheter is introduced anterograde from the femoral vein to the right ventricular (RV) outlet (three arrows). After an application of radiofrequency energy to the atretic valve, a wire has been advanced into the pulmonary artery (PA). The pulmonary valve sinus has been marked by a wire introduced retrograde through the ductus arteriosus (single arrow). (d) The wire is advanced from the RV, through the PDA, and into the descending aorta to allow a balloon (black arrow) to be introduced across the perforated pulmonary valve for valvotomy. (e) After valvotomy, right ventricle–pulmonary artery continuity is clearly established with less tricuspid regurgitation. PDA, patent ductus arteriosus; RA, right atrium. (Reproduced with permission from Freedom *et al. Congenital Heart Disease: Textbook of Angiocardiography*. Armonk, NY: Futura Publishing, 1997, pp. 617–62.)

one-and-a-half ventricle or univentricular circulation. Where not possible, the circulation remains mixed [114].

Biventricular pathway

A single procedure is rarely sufficient, and further interventions are frequently required for eventual biventricular outcome [36,99,100].

- *Residual pulmonary stenosis:* Balloon dilatation should be considered for a gradient greater than 50 mmHg or symptoms of dyspnea or presyncope.
- *Cyanosis:* Residual cyanosis (saturations <90%) represents a residual atrial right-to-left shunt. Early postoperation (<3 months), it may be necessary to augment the pulmonary blood flow with a systemic to pulmonary shunt or stenting of the arterial duct if still patent. Later following operation (>1 year), it is necessary to decide if the RV can support the entire pulmonary blood flow. If the RV is capable, the ASD should be closed, either surgically or by device. Trial occlusion of the ASD reduces the risk of misjudging the RV potential. If the RV is small and restrictive but with good function, an RV overhaul, which enlarges the RV cavity, should be considered [115]. If the RV remains very small and has little prospect of supporting the entire pulmonary blood flow, a one-and-a-half ventricle pathway may be indicated (see below). MRI may help assess RV size and function.
- *Closure of shunts:* Systemic-to-pulmonary shunts and arterial duct stents may close spontaneously. If they remain patent

into childhood, they should be closed, usually by a catheter technique.

- *Late concerns:* The course resembles that of repaired tetralogy of Fallot. The pulmonary valve is frequently regurgitant, and may require replacement, either percutaneously or surgically. The dysplastic tricuspid valve may require repair.

Growth of the right ventricle

Evidence of RV growth in patients with a biventricular circulation is controversial. Growth implies that the z-scores of markers of RV size increase over time. Following surgical intervention, some groups have reported RV catch-up growth, particularly in those with the smallest RVs [63,82,116,117]. Follow-up studies of patients who have undergone catheter valvotomy have not shown convincing evidence of RV growth [100,118].

One-and-a-half ventricle pathway

In a one-and-a-half ventricle circulation, the superior vena cava drains directly to the pulmonary arteries via a bidirectional cavopulmonary anastomosis (CPA), while the inferior vena cava drains to the RV providing pulsatile blood flow to the lungs [119–122]. The atrial septal defect is closed. The cavopulmonary anastomosis is often combined with an RV overhaul procedure [115,121]. Although this approach provides some physiologic advantages, there is little evidence that long-term outcome in terms of exercise tolerance or freedom from arrhythmia is improved compared with a univentricular circulation [121,122].

Univentricular pathway

The Fontan circulation in patients with PAIVS is generally completed within the first 4 years of life. The complications of a univentricular circulation are the same as for other patients with a single ventricle circulation, and described in Chapter 39. Chronic low cardiac output and elevated systemic venous pressures create long-term concern about thrombotic events, arrhythmias, and protein-losing enteropathy [123].

There is a detrimental effect of the hypertensive RV adjacent to the LV [83] causing abnormal septal wall motion and convexity into the LV outflow tract resulting in subaortic obstruction [1,124]. Therefore, with a Fontan circulation RV thromboexclusion should be considered [39].

Right ventricular-dependent coronary circulation

Cardiopulmonary bypass (CPB) has a higher risk in patients with RVDCC because of the requirement to ensure adequate RV filling throughout the procedure [79]. With careful monitoring throughout CPB, the overall mortality is broadly comparable to that for other patients with PAIVS undergoing a Fontan procedure (19%) [47].
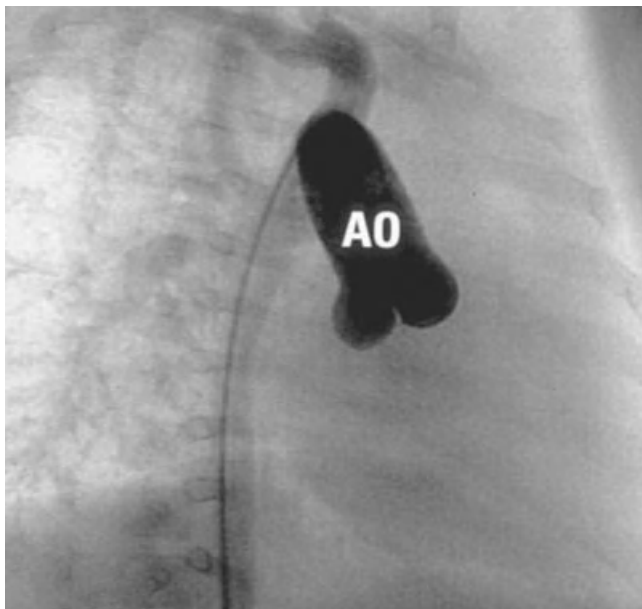
Figure 40.12 Retrograde aortogram shows dense opacification with atresia of the origins of both coronary arteries in a patient with pulmonary atresia with intact ventricular septum. AO, aorta. (Reproduced with permission from Freedom *et al. Cardiol Young* 2000;**10**:60–3.)

Table 40.4 Illustration of survival rates for children born with PAIVS reported in the largest long-term studies.

Study	No. of patients[a]	Median length of follow-up (years)	RVDCC (%)	Biventricular outcome (%)	Catheter valvotomy (%)	Survival at latest follow-up (%)
Daubeney et al. (2005) [16]	168	9	4.2	32	24	70
Ashburn et al. (2004) [80]	408	10.3	5	33	Nil	59
Ekman Joelsson et al. (2001) [4]	77	6	9[b]	41	Unknown	68
Hanley et al. (1993) [63]	171	4	9	32	0	64
Moller (2010) [125]	1039	1	Unknown	Unknown	14	80

[a]Number of patients includes only those put forward for intervention.
[b]Includes "significant RVCACs."

Prognosis

The prognosis for patients with PAIVS is difficult to compare across studies because of its heterogeneity and the wide range of approaches used by different institutions. Table 40.4 shows the cumulative experience of the largest multicenter and population-based studies: overall survival into adolescence is ~60–70%. Studies universally report excellent survival after the first year of life.

The overall quality of life for survivors with PAIVS has been found to be good, with no significant difference between a univentricular or biventricular circulation [126]. Exercise tolerance is universally decreased, and there is only a minor, if any, increase in exercise tolerance for those with biventricular compared with univentricular circulation [127,128].

Long-term concerns include tachyarrhythmia, but there are few data about patients with PAIVS in adulthood. Sudden death due to arrhythmia and atrial arrhythmias have been reported, but the overall incidence appears low [39,121,129]. As expected, the RV remains restrictive in later life [130]. Life-long surveillance is mandatory for all patients with PAIVS, but special care should be given to those with significant RVCACs and RVDCC, where evidence of progressive myocardial ischemia, LV dysfunction, and malignant ventricular arrhythmia should be sought [131,132].

Pregnancy

Successful pregnancies have been reported in women with PAIVS following biventricular repair [133]. Close supervision is required, preferably in an obstetric unit with expertise in the requirements of congenital heart disease patients.

References

1 Daubeney PEF, Delany DJ, Anderson RH, et al. Pulmonary atresia with intact ventricular septum: range of morphology in a population-based study. J Am Coll Cardiol 2002;**39**:1670–9.

2 Daubeney PE, Sharland GK, Cook AC, et al. Pulmonary atresia with intact ventricular septum: impact of fetal echocardiography on incidence at birth and postnatal outcome. UK and Eire Collaborative Study of Pulmonary Atresia with Intact Ventricular Septum. Circulation 1998;**98**:562–6.

3 Pradat P, Francannet C, Harris JA, Robert E. The epidemiology of cardiovascular defects. Part I: a study based on data from three large registries of congenital malformations. Pediatr Cardiol 2003;**24**:195–221.

4 Ekman Joelsson BM, Sunnegårdh J, Hanseus K, et al. The outcome of children born with pulmonary atresia and intact ventricular septum in Sweden from 1980 to 1999. Scand Cardiovasc J 2001;**35**:192–7.

5 Chitayat D, McIntosh N, Fouron J. Pulmonary atresia with intact ventricular septum and hypoplastic right heart in sibs: a single gene disorder? Am J Med Genet 1992;**42**:304–6.

6 De Stefano D, Li P, Xiang B, et al. Pulmonary atresia with intact ventricular septum (PA-IVS) in monozygotic twins. Am J Med Genet 2008;**146**A:525–8.

7 Grossfeld PD, Lucas VW, Sklansky MS, et al. Familial occurrence of pulmonary atresia with intact ventricular septum. Am J Med Genet A 1997;**72**:294–6.

8 Daubeney PEF. Pulmonary atresia with intact ventricular septum: The United Kingdom and Ireland Collaborative Study. DM Thesis, University of Oxford, 2007.

9 Allan LD, Cook A. Pulmonary atresia with intact ventricular septum in the fetus. Cardiol Young 1992;**2**:367–76.

10 Gardiner HM, Belmar C, Tulzer G, et al. Morphologic and functional predictors of eventual circulation in the fetus with pulmonary atresia or critical pulmonary stenosis with intact septum. J Am Coll Cardiol 2008;**51**:1299–308.

11 Freedom RM, Jaeggi E, Perrin D, et al. The "wall-to-wall" heart in the patient with pulmonary atresia and intact ventricular septum. Cardiol Young 2006;**16**:18–29.

12 Freedom RM, Anderson RH, Perrin D. The significance of ventriculo-coronary arterial connections in the setting of pulmonary atresia with an intact ventricular septum. *Cardiol Young* 2005;**15**:447–68.

13 Gittenberger-de Groot AC, Jongbloed MR, Wisse LJ, Poelmann RE. Pulmonary atresia with intact ventricular septum: second heart field derived myocardial and epicardial developmental clues. *Prog Pediat Cardiol* 2010;**29**:3–9.

14 Mair M, Julsrud M, Puga M, Danielson M. The Fontan procedure for pulmonary atresia with intact ventricular septum: operative and late results. *J Am Coll Cardiol* 1997;**29**:1359–64.

15 Zuberbuhler JR, Anderson RH. Morphological variations in pulmonary atresia with intact ventricular septum. *Br Heart J* 1979;**4**:281–8.

16 Daubeney PEF, Wang D, Delany DJ, *et al*. Pulmonary atresia with intact ventricular septum: predictors of early and medium-term outcome in a population-based study. *J Thorac Cardiovasc Surg* 2005;**130**:1071–8.

17 Shimizu T, Ando M, Takao A. Pulmonary atresia and intact ventricular septum and corrected transposition of the great arteries. *Br Heart J* 1981;**45**:471–4.

18 Steeg CN, Ellis K, Bransilver B, Gersony WM. Pulmonary atresia and intact ventricular septum complicating corrected transposition of the great vessels. *Am Heart J* 1971;**82**:382–6.

19 Knight C, Litovsky S, Pearce F, Faye-Petersen O. Pulmonary atresia with intact ventricular septum associated with congenitally corrected transposition. *Pediatr Cardiol* 2006;**27**:741–5.

20 Geva T, Van Praagh S, Van Praagh R. Thoracoabdominal ectopia cordis with isolated infundibular atresia. *Am J Cardiol* 1990;**66**:891–3.

21 Kutsche LM, Van Mierop L. Pulmonary atresia with and without ventricular septal defect: a different etiology and pathogenesis for the atresia in the 2 types? *Am J Cardiol* 1983;**51**:932–5.

22 Freedom RM, Dische MR, Rowe RD. The tricuspid valve in pulmonary atresia and intact ventricular septum: a morphological study of 60 cases. *Arch Pathol Lab Med* 1978;**102**:28–31.

23 Daubeney PE, Blackstone EH, Weintraub RG, *et al*. Relationship of the dimension of cardiac structures to body size: an echocardiographic study in normal infants and children. *Cardiol Young* 1999;**9**:402–10.

24 Pettersen MD, Du W, Skeens ME, Humes RA. Regression equations for calculation of z scores of cardiac structures in a large cohort of healthy infants, children, and adolescents: an echocardiographic study. *J Am Soc Echocardiogr* 2008;**21**:922–34.

25 Zilberman MV, Khoury PR, Kimball RT. Two-dimensional echocardiographic valve measurements in healthy children: gender-specific differences. *Pediatr Cardiol* 2005;**26**:356–60.

26 Rowlatt JF, Rimoldi JHA, Lev M. The quantitative anatomy of the normal child's heart. *Pediatr Clin North Am* 1963;**10**:499–588.

27 Calder AL, Peebles CR, Occleshaw CJ. The prevalence of coronary arterial abnormalities in pulmonary atresia with intact ventricular septum and their influence on surgical results. *Cardiol Young* 2007;**17**:387–96.

28 Anderson RH, Silverman NH, Zuberbuhler JR. Congenitally unguarded tricuspid orifice: its differentiation from Ebstein's malformation in association with pulmonary atresia and intact ventricular septum. *Pediatr Cardiol* 1990;**11**:86–90.

29 Magee AG, Rosenthal E, Bostock J, Gill J. Unguarded tricuspid orifice with pulmonary atresia: successful radiofrequency ablation of an accessory pathway in an infant. *Heart* 1998;**79**:101–3.

30 Takawira FF, Mitchell BJ, Du Plessis DJ. An unusual case of congenitally unguarded tricuspid valve orifice associated with pulmonary valve atresia and intact ventricular septum. *Echocardiography* 2010;**27**:202–4.

31 Uhl HS. A previously undescribed congenital malformation of the heart: almost total absence of the myocardium of the right ventricle. *Bull Johns Hopkins Hosp* 1952;**91**:197–209.

32 Daliento L, Scognamiglio R, Thiene G, *et al*. Morphologic and functional analysis of myocardial status in pulmonary atresia with intact ventricular septum: an angiographic, histologic and morphometric study. *Cardiol Young* 1992;**2**:361–6.

33 Bulkley BH, D'Amico B, Taylor AL. Extensive myocardial fiber disarray in aortic and pulmonary atresia. Relevance to hypertrophic cardiomyopathy. *Circulation* 1983;**67**:191–8.

34 Gittenberger-de Groot AC, Tennstedt C, Chaoui R, *et al*. Ventriculo coronary arterial communications (VCAC) and myocardial sinusoids in hearts with pulmonary atresia with intact ventricular septum: two different diseases. *Prog Pediatr Cardiol* 2001;**13**:157–64.

35 Akiba T, Becker AE. Disease of the left ventricle in pulmonary atresia with intact ventricular septum. The limiting factor for long-lasting successful surgical intervention? *J Thorac Cardiovasc Surg* 1994;**108**:1–8.

36 Shinebourne EA, Rigby ML, Carvalho JS. Pulmonary atresia with intact ventricular septum: from fetus to adult: congenital heart disease. *Heart* 2008;**94**:1350–7.

37 Marino B, Guccione P, Carotti A, *et al*. Ductus arteriosus in pulmonary atresia with and without ventricular septal defect. Anatomic and functional differences. *Scand J Thorac Cardiovasc Surg* 1992;**26**:93–6.

38 Santos MA, Azevedo VMP. Angiographic morphologic characteristics in pulmonary atresia with intact ventricular septum. *Arq Bras Cardiol* 2004;**82**:420–25.

39 Najm HK, Williams WG, Coles JG, *et al*. Pulmonary atresia with intact ventricular septum: results of the Fontan procedure. *Ann Thorac Surg* 1997;**63**:669–75.

40 Giglia TM, Mandell VS, Connor AR, *et al*. Diagnosis and management of right ventricle-dependent coronary circulation in pulmonary atresia with intact ventricular septum. *Circulation* 1992;**86**:1516.

41 Dyamenahalli U, McCrindle BW, McDonald C, *et al*. Pulmonary atresia with intact ventricular septum: management of, and outcomes for, a cohort of 210 consecutive patients. *Cardiol Young* 2004;**14**:299–308.

42 Gittenberger-de Groot AC, Sauer U, Bindl L, *et al*. Competition of coronary arteries and ventriculo-coronary arterial communications in pulmonary atresia with intact ventricular septum. *Int J Cardiol* 1988;**18**:243–58.

43 Gittenberger-de Groot AC, Eralp I, Lie-Venema H, *et al*. Development of the coronary vasculature and its implications for coronary abnormalities in general and specifically in pulmonary atresia without ventricular septal defect. *Acta Paediatr Suppl* 2004;**93**(446):13–9.

44 Sandor GG, Cook AC, Sharland GK, *et al*. Coronary arterial abnormalities in pulmonary atresia with intact ventricular septum diagnosed during fetal life. *Cardiol Young* 2006;**12**:436–44.

45 Jahangiri M, Zurakowski D, Bichell D, *et al*. Improved results with selective management in pulmonary atresia with intact ventricular septum. *J Thorac Cardiovasc Surg* 1999;**118**:1046–55.

46 Powell AJ, Mayer JE, Lang P, Lock JE. Outcome in infants with pulmonary atresia, intact ventricular septum, and right ventricle-dependent coronary circulation. *Am J Cardiol* 2000;**86**:1272.

47 Guleserian KJ, Armsby LB, Thiagarajan RR, *et al*. Natural history of pulmonary atresia with intact ventricular septum and right-ventricle-dependent coronary circulation managed by the single-ventricle approach. *Ann Thorac Surg* 2006;**81**:2250–7; discussion 2258.

48 Moral JP, Valero MB, Silva L. Pulmonary valve atresia with intact ventricular septum and severe aortic stenosis. *Pediatr Cardiol* 2004;**26**:117–8.

49 Kobayashi T, Momoi N, Fukuda Y, Suzuki H. Percutaneous balloon valvuloplasty of both pulmonary and aortic valves in a neonate with pulmonary atresia and critical aortic stenosis. *Pediatr Cardiol* 2005;**26**:839–42.

50 Shauq A, Gladman G, Ladusans EJ. Pulmonary atresia with intact ventricular septum associated with aortic coarctation. *Cardiol Young* 2009;**19**:522–3.

51 Mackie AS, Lang P, Powell AJ. Pulmonary atresia with intact ventricular septum coexisting with coarctation of the aorta. *Pediatr Cardiol* 2007;**28**:406–8.

52 Ansari A, Goltz D, McCarthy KP, *et al*. The conduction system in hearts with pulmonary atresia and intact ventricular septum. *Ann Thorac Surg* 2003;**75**:1502–5.

53 Yamagishi M, Kurosawa H, Hashimoto K, Nakamura Y. Pulmonary atresia with intact ventricular septum, antegrade coronary–right ventricular sinusoidal communication, and Wolff–Parkinson–White syndrome. *Jpn J Thorac Cardiovasc Surg* 2000;**48**:322–5.

54 Güçer S, Ince T, Kale G, *et al*. Noncardiac malformations in congenital heart disease: a retrospective analysis of 305 pediatric autopsies. *Turk J Pediatr* 2005;**47**:159–66.

55 Patel CR, Shah DM, Dahms BB. Prenatal diagnosis of a coronary fistula in a fetus with pulmonary atresia with intact ventricular septum and trisomy 18. *J Ultrasound Med* 1999;**18**:429–31.

56 Li C, Chudley AE, Soni R, Divekar A. Pulmonary atresia with intact ventricular septum and major aortopulmonary collaterals: association with deletion 22q11.2. *Pediatric Cardiol* 2003;**24**:585–7.

57 Salvin JW, McElhinney DB, Colan SD, *et al*. Fetal tricuspid valve size and growth as predictors of outcome in pulmonary atresia with intact ventricular septum. *Pediatrics* 2006;**118**:e415.

58 Roman KS, Fouron J, Nii M, *et al*. Determinants of outcome in fetal pulmonary valve stenosis or atresia with intact ventricular septum. *Am J Cardiol* 2007;**99**:699–703.

59 Emmel M, Bald R, Brockmeier K. Pulmonary atresia with intact ventricular septum and right coronary artery to right ventricle fistula detected *in utero*. *Heart* 2004;**90**:94.

60 Tzifa A, Barker C, Tibby SM, Simpson JM. Prenatal diagnosis of pulmonary atresia: impact on clinical presentation and early outcome. *Arch Dis Child Fetal Neonatal Ed* 2007;**92**:F199–203.

61 Drighil A, Aljufan M, Slimi A, *et al*. Echocardiographic determinants of successful balloon dilation in pulmonary atresia with intact ventricular septum. *Eur J Echocardiogr* 2009;**11**:172–5.

62 Yoshimura N, Yamaguchi M. Surgical strategy for pulmonary atresia with intact ventricular septum: initial management and definitive surgery. *Gen Thorac Cardiovasc Surg* 2009;**57**:338–46.

63 Hanley F, Sade R, Blackstone E, *et al*. Outcomes in neonatal pulmonary atresia with intact ventricular septum. A multiinstitutional study. *J Thorac Cardiovasc Surg* 1993;**105**:406–23.

64 Alwi M. Management algorithm in pulmonary atresia with intact ventricular septum. *Catheter Cardiovasc Interv* 2006;**67**:679–86.

65 Pyles LA, Berry JM, Steinberger J, Foker JE. Initial, intra-operative, and post-operative evaluation of children with pulmonary atresia with intact ventricular septum with emphasis on the coronary connections to the right ventricle. *Prog Pediatr Cardiol* 2010;**29**:25–34.

66 Foker JE, Setty SP, Berry J, *et al*. Treatment of right ventricle to coronary artery connections in infants with pulmonary atresia and intact ventricular septum. *J Thorac Cardiovasc Surg* 2008;**136**:749–56.

67 Garcia JA, Zellers TM, Weinstein EM, Mahony L. Usefulness of Doppler echocardiography in diagnosing right ventricular coronary arterial communications in patients with pulmonary atresia and intact ventricular septum and comparison with angiography. *Am J Cardiol* 1998;**81**:103–4.

68 Selamet SE, Hsu DT, Thaker HM, Gersony WM. Complete atresia of coronary ostia in pulmonary atresia and intact ventricular septum. *Pediatr Cardiol* 2004;**25**:67–9.

69 Freedom RM, Yoo SJ, Javois A. A most peculiar coronary circulation in a patient with pulmonary atresia and intact ventricular septum. *Cardiol Young* 2000;**10**:60–3.

70 Qureshi SA. Catheterization in neonates with pulmonary atresia with intact ventricular septum. *Catheter Cardiovasc Interv* 2006;**67**:924–31.

71 Burrows P, Freedom R, Benson L, *et al*. Coronary angiography of pulmonary atresia, hypoplastic right ventricle, and ventriculocoronary communications. *Am J Roentgenol* 1990;**154**:789–95.

72 Freedom RM, Mawson JB, Yoo SJ, Benson LN. *Congenital Heart Disease: Textbook of Angiocardiography*. Armonk, NY: Futura Publishing, 1997.

73 Law Y, Mawson J, Mikailian H, *et al*. Transatrial selective coronary arteriography in pulmonary atresia with intact ventricular septum. *Catheter Cardiovasc Diagn* 1998;**43**:174–6.

74 Tworetzky W, McElhinney DB, Marx GR, *et al*. In utero valvuloplasty for pulmonary atresia with hypoplastic right ventricle: techniques and outcomes. *Pediatrics* 2009;**124**:e510–8.

75 Tulzer G, Arzt W, Franklin RC, *et al*. Fetal pulmonary valvuloplasty for critical pulmonary stenosis or atresia with intact septum. *Lancet* 2002;**360**(9345):1567–8.

76 Galindo A, Gutierrez-Larraya F, Velasco J, de la Fuente P. Pulmonary balloon valvuloplasty in a fetus with critical pulmonary stenosis/atresia with intact ventricular septum and heart failure. *Fetal Diagn Ther* 2006;**21**:100–4.

77 Arzt W, Tulzer G, Aigner M, *et al*. Invasive intrauterine treatment of pulmonary atresia/intact ventricular septum with heart failure. *Ultrasound Obstet Gynecol* 2003;**21**:186–8.

78 NICE. *IPG176 Percutaneous Fetal balloon Valvuloplasty for Pulmonary Atresia with Intact Ventricular Septum – Guidance*. London: National Institute for Health and Clinical Excellence. Available from: http://guidance.nice.org.uk/IPG176/Guidance/pdf/English; last accessed 23 November 2010.

79 Walsh MA, Asoh K, Van Arsdell GS, Humpl T. Critical care outcomes in pulmonary atresia and intact ventricular septum undergoing single-ventricle palliation. *Cardiol Young* 2010;**20**:290–6.

80 Ashburn DA, Blackstone EH, Wells WJ, *et al*. Determinants of mortality and type of repair in neonates with pulmonary atresia and intact ventricular septum. *J Thorac Cardiovasc Surg* 2004;**127**:1000–7; discussion 1007–8.

81 Foker JE, Berry JM, Pyles LA. Treatment algorithm for pulmonary atresia with intact ventricular septum. *Prog Pediatr Cardiol* 2010;**29**:61–3.

82 Huang SC, Ishino K, Kasahara S, *et al*. The potential of disproportionate growth of tricuspid valve after decompression of the right ventricle in patients with pulmonary atresia and intact ventricular septa. *J Thorac Cardiovasc Surg* 2009;**138**:1160.

83 Tanoue Y, Kado H, Ushijima T, Tominaga R. Consequences of a hypertensive right ventricle on left ventricular performance of patients with pulmonary atresia and intact ventricular septum after right heart bypass surgery. *Prog Pediatr Cardiol* 2010;**29**:43–8.

84 Hannan RL, Zabinsky JA, Stanfill RM, *et al*. Midterm results for collaborative treatment of pulmonary atresia with intact ventricular septum. *Ann Thorac Surg* 2009;**87**:1227–33.

85 De Leval M, Bull C, Stark J, *et al*. Pulmonary atresia and intact ventricular septum: surgical management based on a revised classification. *Circulation* 1982;**66**:272.

86 Yoshimura N, Yamaguchi M, Ohashi H, *et al*. Pulmonary atresia with intact ventricular septum: strategy based on right ventricular morphology. *J Thorac Cardiovasc Surg* 2003;**126**:1417–26.

87 Pawade A, Capuani A, Penny DJ, *et al*. Pulmonary atresia with intact ventricular septum: surgical management based on right ventricular infundibulum. *J Cardiac Surg* 1993;**8**:371–83.

88 Qureshi SA, Rosenthal E, Tynan M, *et al*. Transcatheter laser-assisted balloon pulmonary valve dilation in pulmonic valve atresia. *Am J Cardiol* 1991;**67**:428–31.

89 Asnes JD, Fahey JT. Novel catheter positioning technique for atretic pulmonary valve perforation. *Cathet Cardiovasc Interv* 2008;**71**:850–2.

90 Gewillig M, Boshoff DE, Dens J, *et al*. Stenting the neonatal arterial duct in duct-dependent pulmonary circulation: new techniques, better results. *J Am Coll Cardiol* 2004;**43**:107–12.

91 Gibbs JL, Blackburn ME, Uzun O, *et al*. Laser valvotomy with balloon valvoplasty for pulmonary atresia with intact ventricular septum: five years' experience. *Heart* 1997;**77**:225–8.

92 Justo RN, Nykanen DG, Williams WG, *et al*. Transcatheter perforation of the right ventricular outflow tract as initial therapy for pulmonary valve atresia and intact ventricular septum in the newborn. *Cathet Cardiovasc Diagn* 1997;**40**:408–13.

93 Redington AN, Cullen S, Rigby ML. Laser or radiofrequency pulmonary valvotomy in neonates with pulmonary atresia and intact ventricular septum – description of a new method avoiding arterial catheterization. *Cardiol Young* 2008;**2**:387–90.

94 Rosenthal E, Qureshi SA, Chan KC, *et al*. Radiofrequency-assisted balloon dilatation in patients with pulmonary valve atresia and an intact ventricular septum. *Heart* 1993;**69**:347–51.

95 Rosenthal E, Qureshi SA, Kakadekar AP, *et al*. Technique of percutaneous laser-assisted valve dilatation for valvar atresia in congenital heart disease. *BMJ* 1993;**69**:556.

96 Rosenthal E, Qureshi SA, Tynan M. Percutaneous pulmonary valvotomy and arterial duct stenting in neonates with right ventricular hypoplasia. *Am J Cardiol* 1994;**74**:304–6.

97 Humpl T, Söderberg B, McCrindle BW, *et al*. Percutaneous balloon valvotomy in pulmonary atresia with intact ventricular septum: impact on patient care. *Circulation* 2003;**108**:826–32.

98 Mi YP, Chau AKT, Chiu CSW, *et al*. Evolution of the management approach for pulmonary atresia with intact ventricular septum. *Heart* 2005;**91**:657–63.

99 Agnoletti G, Piechaud JF, Bonhoeffer P, *et al*. Perforation of the atretic pulmonary valve. Long-term follow-up. *J Am Coll Cardiol* 2003;**41**:1399–403.

100 Marasini M, Gorrieri PF, Tuo G, *et al*. Long-term results of catheter-based treatment of pulmonary atresia and intact ventricular septum. *Heart* 2009;**95**:1520–4.

101 Wang JK, Wu MH, Chang CI, *et al*. Outcomes of transcatheter valvotomy in patients with pulmonary atresia and intact ventricular septum. *Am J Cardiol* 1999;**84**:1055–60.

102 Alwi M, Geetha K, Bilkis AA, *et al*. Pulmonary atresia with intact ventricular septum percutaneous radiofrequency-assisted valvotomy and balloon dilation versus surgical valvotomy and Blalock–Taussig shunt. *J Am Coll Cardiol* 2000;**35**:468–76.

103 NICE. *IPG095 Radiofrequency Valvotomy for Pulmonary Atresia – Guidance*. London: National Institute for Health and Clinical Excellence. Available from: http://guidance.nice.org.uk/IPG95/Guidance/pdf/English; last accessed 23 November 2010.

104 Latson LA. Nonsurgical treatment of a neonate with pulmonary atresia and intact ventricular septum by transcatheter puncture and balloon dilation of the atretic valve membrane. *Am J Cardiol* 1991;**68**:277–9.

105 Redington AN, Cullen S, Rigby ML. Laser or radiofrequency pulmonary valvotomy in neonates with pulmonary atresia and intact ventricular septum – Description of a new method avoiding arterial catheterization. *Cardiol Young* 1992;**2**:387–90.

106 Burke RP, Hannan RL, Zabinsky JA, *et al*. Hybrid ventricular decompression in pulmonary atresia with intact septum. *Ann Thorac Surg* 2009;**88**:688–9.

107 Lin M, Wei H, Fu Y, Jan S. A novel hybrid therapy for pulmonary atresia with intact ventricular septum. *Int J Cardiol* 2010;**144**:438–9.

108 Schneider M, Schranz D, Michel-Behnke I, Oelert H. Transcatheter radiofrequency perforation and stent implantation for palliation of pulmonary atresia in a 3060-g infant. *Cathet Cardiovasc Diagn* 1995;**34**:42–5.

109 Schneider M, Zartner P, Sidiropoulos A, *et al*. Stent implantation of the arterial duct in newborns with duct-dependent circulation. *Eur Heart J* 1998;**19**:1401.

110 Schmidt KG, Cloez JL, Silverman NH. Changes of right ventricular size and function and neonates after valvotomy for pulmonary atresia or pulmonary stenosis and intact venricular septum. *J Am Coll Cardiol* 1992;**19**:1032–7.

111 Yang J, Jun T, Park PW, *et al*. Exclusion of the non-functioning right ventricle in children with pulmonary atresia and intact ventricular septum. *Eur J Cardiothorac Surg* 2008;**33**:251–6.

112 Starnes VA, Pitlick PT, Bernstein D, *et al*. Ebstein's anomaly appearing in the neonate. A new surgical approach. *J Thorac Cardiovasc Surg* 1991;**101**:1082–7.

113 Wald RM, Juraszek AL, Pigula FA, Geva T. Echocardiographic diagnosis and management of bilateral coronary ostial atresia in a patient with pulmonary atresia and intact ventricular septum. *J Am Soc Echocardiogr* 2006;**19**:939.

114 Gatzoulis MA, Webb GD, Daubeney PEF. *Diagnosis and Management of Adult Congenital Heart Disease*, 2nd edn. Edinburgh: Churchill Livingstone, 2010.

115 Pawade A, Mee RBB, Karl T. Right ventricular overhaul: an intermediate step in the biventricular repair of pulmonary atresia with intact ventricular septum. *Cardiol Young* 1995;**5**:161–5.

116 Foker JE, Berry J, Setty SP, *et al*. Growth and function of hypoplastic right ventricles and tricuspid valves in infants with pulmonary atresia and intact ventricular septum. *Prog Pediatr Cardiol* 2010;**29**:49–54.

117 Hanséus K, Björkhem G, Lundström NR, Laurin S. Cross-sectional echocardiographic measurements of right ventricular size and growth in patients with pulmonary atresia and intact ventricular septum. *Pediatr Cardiol* 1991;**12**:135–42.

118 Ovaert C, Qureshi SA, Rosenthal E, *et al*. Growth of the right ventricle after successful transcatheter pulmonary valvotomy in neonates and infants with pulmonary atresia and intact ventricular septum. *J Thorac Cardiovasc Surg* 1998;**115**:1055–62.

119 Van Arsdell GS, Williams WG, Freedom RM. A practical approach to 1½ ventricle repairs. *Ann Thorac Surg* 1998;**66**:678–80.

120 Van Arsdell GS, Williams WG, Maser CM, *et al*. Superior vena cava to pulmonary artery anastomosis: an adjunct to biventricular repair. *J Thorac Cardiovasc Surg* 1996;**112**:1143–8; discussion 1148–9.

121 Numata S, Uemura H, Yagihara T, *et al*. Long-term functional results of the one and one half ventricular repair for the spectrum of patients with pulmonary atresia/stenosis with intact ventricular septum. *Eur J Cardiothorac Surg* 2003;**24**:516–20.

122 Chowdhury UK, Airan B, Talwar S, *et al*. One and one-half ventricle repair: results and concerns. *Ann Thorac Surg* 2005;**80**:2293–300.

123 Rychik J, Goldberg D, Dodds K. Long-term results and consequences of single ventricle palliation. *Prog Pediatr Cardiol* 2010;**29**:19–23.

124 Razzouk AJ, Freedom RM, Cohen AJ, *et al*. The recognition, identification of morphologic substrate, and treatment of subaortic stenosis after a Fontan operation. An analysis of twelve patients. *J Thorac Cardiovasc Surg* 1992;**104**: 938–44.

125 Moller JH. Operative and interventional procedures in 1039 neonates with pulmonary valvular atresia and intact ventricular septum: a multi-institutional study. *Prog Pediatr Cardiol* 2010;**29**:15–18.

126 Ekman-Joelsson B, Berntsson L, Sunnegårdh J. Quality of life in children with pulmonary atresia and intact ventricular septum. *Cardiol Young* 2004;**14**:615–21.

127 Sanghavi DM, Flanagan M, Powell AJ, *et al*. Determinants of exercise function following univentricular versus biventricular repair for pulmonary atresia/intact ventricular septum. *Am J Cardiol* 2006;**97**:1638–43.

128 Ekman-Joelsson B, Gustafsson P, Sunnegårdh J. Exercise performance after surgery for pulmonary atresia and intact ventricular septum. *Pediatr Cardiol* 2009;**30**:752–62.

129 Mishima A, Asano M, Sasaki S, *et al*. Long-term outcome for right heart function after biventricular repair of pulmonary atresia and intact ventricular septum. *Jpn J Thorac Cardiovasc Surg* 2000;**48**:145–52.

130 Liang X, Lam WWM, Cheung EWY, *et al*. Restrictive right ventricular physiology and right ventricular fibrosis as assessed by cardiac magnetic resonance and exercise capacity after biventricular repair of pulmonary atresia and intact ventricular septum. *Clin Cardiol* 2010;**33**:104–10.

131 Ekman-Joelsson BM, Berggren H, Boll AB, *et al*. Abnormalities in myocardial perfusion after surgical correction of pulmonary atresia with intact ventricular septum. *Cardiol Young* 2008;**18**:89–95.

132 Ekman-Joelsson B, Hanséus K, Söderberg B, *et al*. The long-term consequences of the coronary artery lesions in pulmonary atresia with intact ventricular septum. *Prog Pediatr Cardiol* 2010;**29**:35–42.

133 Drenthen W, Pieper PG, Roos-Hesselink JW, *et al*. Fertility, pregnancy, and delivery after biventricular repair for pulmonary atresia with an intact ventricular septum. *Am J Cardiol* 2006;**98**:259–61.

41

Tetralogy of Fallot and Pulmonary Atresia with Ventricular Septal Defect

Andrew Redington

University of Toronto and Hospital for Sick Children, Toronto, ON, Canada

Introduction

Tetralogy of Fallot is the commonest of the cyanotic congenital heart diseases and, in its simplest form, was one of the first to be successfully treated by palliative (the classical Blalock–Taussig shunt in 1945) and then open-heart surgery over 50 years ago. The survivors of these ground-breaking procedures are entering late middle life, and already there are more adults than children with the disease.

The term tetralogy of Fallot is often used as an umbrella diagnosis that includes those with abnormal ventriculo-arterial connections (tetralogy of Fallot with double-outlet right ventricle), and particular associated features (e.g., tetralogy of Fallot with pulmonary atresia, with and without major aortopulmonary collateral arteries, tetralogy of Fallot with absent pulmonary valve syndrome).

Anatomy

The fundamental abnormality that characterizes the disease is anterior and cephalad deviation of the outlet septum (Figure 41.1). The secondary effects of this singular abnormality are the creation of a ventricular septal defect (VSD), aortic override, and right ventricular outflow tract obstruction and hypertrophy [1–3].

Right ventricular outflow tract obstruction

The hallmark of the right ventricular outflow tract obstruction in tetralogy of Fallot is infundibular stenosis. This is due to many factors, the most important of which is the anterior cephalad deviation of the outlet septum [2]. Outlet obstruction is further aggravated by hypertrophy of the outlet septum, the anterior limb of the septomarginal trabeculation, and the septoparietal trabeculations. Indeed, in the absence of these coexisting abnormalities, the degree of outflow tract obstruction resulting from the malaligned outlet septum alone may be minimal or none, the intracardiac anatomy of the "Eisenmenger VSD" being almost indistinguishable from that of tetralogy of Fallot, except for the subpulmonary stenosis. [2]

The right ventricular outflow tract obstruction, however, is not limited to the infundibular region. In most patients, the pulmonary valve is stenotic, the pulmonary valve annulus itself can be hypoplastic, and supravalvar obstruction may be present at the level of the sinotubular ridge and extend to involve the pulmonary trunk. The branch pulmonary arteries can be diffusely small or may have focal areas of narrowing, most commonly at their origins, but also involving the lobar and segmental divisions. Obstruction is commonly in the proximal left pulmonary artery at the juxtaductal or juxtaligamental site. Delineating the sites of right ventricular outflow tract obstruction is important for planning repair.

Ventricular septal defect

The VSD in patients with tetralogy of Fallot is usually large and unrestrictive. In most patients, the VSD is perimembranous, with the central fibrous body forming the inferior border and the conduction system running adjacent. In approximately 20% of patients there is a muscular posteroinferior rim (Figure 41.1) [3]. Controversy remains as to whether tetralogy of Fallot can coexist with a doubly committed VSD. The hallmark of the doubly committed VSD is fibrous continuity of the leaflets of the aortic and pulmonary valves. This implies absence of the muscular outlet septum, which then clearly cannot be deviated anterior and cephalad. Nonetheless, there exists a group of children with identical anatomy and physiology to that of "classical" tetralogy, but who possess a

Figure 41.1 An anatomic specimen from tetralogy of Fallot. Note the hypertrophied outlet septum (OS), which is malaligned with respect to the rest of the septum. Consequently there is aortic override (AO), and right ventricular outflow tract obstruction with hypertrophied septoparietal trabeculations (SPT). Note that in this case there is a muscular postero-inferior rim (*) to the ventricular septal defect (VSD), separating the tricuspid valve (TV) leaflet from the aortic valve. Original image kindly supplied by Professor RH Anderson.
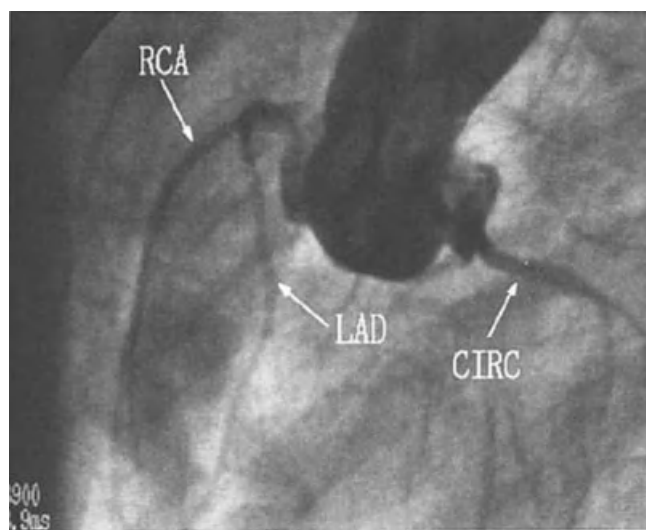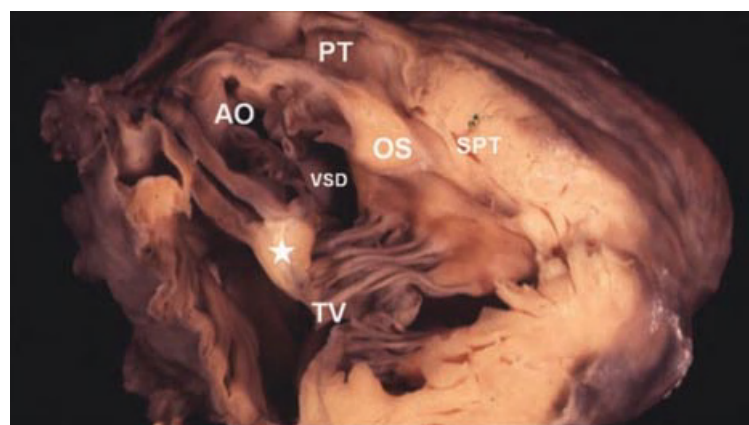
Figure 41.2 Aortogram in a long-axis oblique/cranial projection. The left anterior descending (LAD) coronary artery can be seen arising from the proximal right coronary artery (RCA) with a course that traverses the right ventricular outflow tract. CIRC, circumflex coronary artery.

doubly committed defect (sometimes described as the South American Tet, the Mexican Tet, the Asian Tet, etc.). As an accommodation, some suggest that the "fibrous component" of the outlet septum does indeed persist in these patients (a small ridge of fibrous tissue is often seen separating the semilunar valve leaflets), thus allowing the diagnosis of tetralogy.

Although most patients have a single large defect, additional muscular VSDs may be found.

Aortic override

The degree of aortic override varies considerably. It should be remembered that tetralogy of Fallot is a diagnosis, whereas double-outlet right ventricle defines a ventriculo-arterial connection, and the two may coexist. If the degree of override is >50%, then the designation of tetralogy of Fallot with double-outlet right ventricle may be made. This is sometimes, but not always, associated with a bilateral infundibulum

(associated muscular separation of the mitral and aortic valve leaflets). The latter is neither required for the definition of double-outlet connection (it may occur in the setting of a clearly dominant connection of the aorta to the left ventricle) nor excludes the diagnosis of tetralogy of Fallot.

Associated anatomic features

Several anatomic features frequently associated with tetralogy of Fallot can have considerable clinical and therapeutic implications. Atrial communications are fairly frequent and usually at the fossa ovalis as either a patent foramen ovale or more rarely a true secundum atrial septal defect. Approximately 25% of patients have a right-sided aortic arch that can alter the approach to a palliative shunt. Tetralogy of Fallot may coexist with atrioventricular septal defect (AVSD), and should be especially considered in children with Down syndrome. A primum component may not be present in these, and under such circumstances the clue to the presence of an AVSD is a trileaflet left atrioventricular valve on echocardiographic imaging. Straddling atrioventricular valve is a rare associated feature. Abnormalities of the coronary arteries, such as the left anterior descending coronary artery arising from the right coronary artery, occur in ~4% of patients (Figure 41.2). This anomaly is exceedingly important to recognize, as the left anterior descending coronary then crosses the right ventricular outflow tract, and failure to identify this vessel can result in its inadvertent transection during outflow tract repair. Occasionally, significant systemic-to-pulmonary collaterals are present even when the outflow tract is patent. This is commonly associated with discontinuous branch pulmonary arteries or bilaterally diminutive central pulmonary arteries.

Tetralogy of Fallot with absent pulmonary valve

Tetralogy of Fallot with absent pulmonary valve affects 2–10% of patients with intracardiac anatomy typical of tetralogy of Fallot, but characterized by the absence of a

functioning pulmonary valve [3]. The pulmonary annulus is usually small with vestigial pulmonary valve leaflets, resulting in some degree of stenosis and severe regurgitation. The anatomic hallmark of this lesion is aneurysmal dilatation of the main and branch pulmonary arteries, particularly the right, which may result in bronchial compression and airway compromise that can be life-threatening. The arterial duct and/or ligament is usually absent, and this feature has been implicated in the pathogenesis of the disease. The physiology varies considerably, but the early management depends primarily on the severity of the airway disease.

Tetralogy of Fallot with pulmonary atresia

This variant can be considered at the most severe end of the spectrum of tetralogy of Fallot, and occurs in 11–24%. The intracardiac anatomy is identical with that of classic tetralogy of Fallot with a large outlet VSD, an overriding aorta, normal or near-normal sized right and left ventricles, and normal atrioventricular valves. The outflow tract anatomy is variable, however, ranging from valvar atresia alone to muscular atresia beneath a usually small pulmonary trunk arising in the usual position, and to muscular atresia with absence of the pulmonary trunk (single-outlet connection) [3,4]. As a result, the pulmonary artery anatomy is much more variable. In the least complex form, the main pulmonary artery is supplied by the arterial duct. These patients are currently managed by complete repair in the early neonatal period. At the other end of the spectrum, the central pulmonary arteries are either absent or diminutive, and the segmental pulmonary blood flow is supplied by multiple aortopulmonary collateral arteries (MAPCAs). These MAPCAs arise usually from the descending thoracic aorta, but occasionally from the innominate or subclavian arteries or the upper part of the aortic arch; rarely they arise from the abdominal aorta. MAPCAs can supply multiple bronchopulmonary segments in either a unifocal manner or with a multifocal distribution of pulmonary blood flow to different segments by the central pulmonary arteries and the MAPCAs. Careful delineation of the segmental blood supply is required prior to surgical management. Although advanced imaging techniques (CT and MRI) are able to define the anatomy of the MAPCAs and central PAs, there remains an important role for cardiac catheterization and angiography, to define the nature of the segmental connections in the more complex patients.

Incidence

Tetralogy of Fallot occurs in 3–5/10 000 live births (see Chapter 19) and is among the three or four most common cardiac lesions requiring cardiac catheterization or operation

Table 41.1 Conditions associated with tetralogy of Fallot.

Trisomy 21 (Down)
Velocardiofacial (Shprintzen)
22q11 deletion or CATCH-22[a] syndrome
Goldenhars
Thrombocytopenia absent radius
CHARGE[b]
VATER[c]/VACTERL[d]
Fetal alcohol
Pierre Robin
Associated organ abnormalities
Include tracheoesophageal fistula, imperforate anus, hydrocephalus, omphalocele

[a]CATCH-22 = cardiac defects, abnormal facies, thymic hypoplasia, cleft palate, hypocalcemia, and abnormality of chromosome 22.
[b]CHARGE = coloboma, heart disease, atresia choanae, retarded growth and development, genital abnormalities, ear anomalies.
[c]VATER = vertebral defects, anal atresia, tracheoesophageal fistula, renal defects, and radial upper arm dysplasia.
[d]VACTERL = VATER + cardiac and limb anomalies.

in the first year of life [5–7]. It is slightly more common in males than females and is associated with chromosomal abnormalities in ~11% of patients, nonchromosomal syndrome complexes in ~8%, and problems of other major organs in ~16% (Table 41.1). A microdeletion of chromosome 22q11 may be present in 20–30% of patients with tetralogy of Fallot, with higher values if there is also pulmonary atresia [8–11]. This same chromosome is involved in DiGeorge syndrome and abnormalities considered previously such as the velocardiofacial syndrome (Shprintzen syndrome).

The recurrence risk for tetralogy of Fallot in families with one affected child is probably 2–5%. For mothers who have tetralogy of Fallot, the transmission risk for congenital heart disease in offspring is probably 5–10%; for fathers with tetralogy of Fallot, the transmission risk is ≤5 [12].

Natural history

Fallot's prediction [13] that ~75% of older cyanotic children would have tetralogy of Fallot was true before the advent of cardiac surgery. This lesion has the best untreated outcome of any cyanotic malformation, although the median age at death in different series has ranged from age 4 to 12 years [14,15]. Only ~10% of untreated patients live beyond 20 years [15–18], and they have neither pulmonary atresia nor absent pulmonary valves. Fewer than 5% survive to age 40 years [19]. Most long-term survivors had only mild cyanosis, although they are still at risk of many of the complications of

chronic cyanotic heart disease (see Chapter 52). In addition, ventricular tachycardia occurs with increasing frequency as they age [20].

About half of the patients with tetralogy of Fallot and absent pulmonary valve die before 1 year of age [3], mainly because of airway complications. The remainder continue to be mildly cyanotic for 5–20 years but die prematurely because of right ventricular failure caused by volume overload.

About half of the patients with tetralogy of Fallot and pulmonary atresia die before 1 year of age, and presentation with severe cyanosis and small MAPCAs is ominous [3,21]. The amount of pulmonary blood flow governs the outcome for the remainder, with some patients able to survive unoperated into adulthood.

Physical examination and clinical presentation

The clinical presentation of patients with tetralogy of Fallot depends primarily on the degree of right ventricular outflow tract obstruction. Presentation can range from a profoundly cyanotic newborn with ductus-dependent pulmonary circulation to an asymptomatic child with adequate pulmonary flow presenting with a murmur. Because of this wide spectrum of presentation, the physical findings vary widely. Relatively few are cyanotic at birth, but most become cyanotic by 3 months of age.

Inspection often reveals an apparently healthy infant or child, although major extracardiac anomalies, such as hypospadias, cleft lip and palate, pectus carinatum, and other bony abnormalities, can be seen [22]. Cyanosis is present to varying degrees and can be best appreciated in the mucous membranes or nail beds. The degree of cyanosis depends not only on the amount of right-to-left intracardiac shunting, but also on the hemoglobin concentration. To appreciate cyanosis, there must be approximately 3–5 g dl^{-1} of desaturated hemoglobin in arterial blood; this quantity is easier to achieve at higher hemoglobin concentrations. Therefore, the relatively erythrocytotic neonate may appear more cyanotic shortly after birth than at a few months of age during the period of normal postnatal physiologic anemia.

The level of cyanosis in a given individual also varies with activity and metabolic rate. Fever and exercise increase the level of cyanosis, both from the decreased systemic vascular resistance and from a resultant increase in right-to-left shunting, and also increased oxygen consumption by the tissues, with a resultant fall in mixed venous saturation.

Although rarely observed in "developed" countries, older children with unrepaired tetralogy of Fallot often squat. This position is thought to improve systemic saturation by increasing the systemic vascular resistance by kinking the large arterial vessels in the legs. The increased systemic resistance

shifts the biventricular output such that more blood flow enters the lungs across the pulmonary outflow obstruction, and forms the basis of the "knee–chest" positioning recommended for the early treatment of hypercyanotic spells in younger children.

Tetralogy spells or hypercyanotic spells are periods of severe cyanosis associated with hyperpnea, tachypnea, and agitation that can result in coma. They begin between 3 months and 2 years of age, and occur more commonly in the mornings, during the summer months, and during intercurrent illnesses. The episodes are usually self-limited and usually last 15–30 min, but they can be prolonged. The hypoxemia can be severe enough to alter mental status and even result in death. The physiologic basis for these episodes remains obscure, although a number of hypotheses have been proposed, including increased infundibular contractility or spasm, peripheral vasodilatation, hyperventilation, and stimulation of right ventricular mechanoreceptors [23]. The lack of a "sphincter-like" orientation of the muscles of the right ventricular outflow tract, and the occurrence of almost identical spells in the setting of a doubly committed VSD (and hence no infundibulum), make the popular characterization of "infundibular spasm" unlikely, and treatment is directed at modifying the SVR and mixed venous oxygen saturation, not the putative spasm. A child admitted with one of these spells should be diagnosed rapidly and clinically. Diagnostic investigations are not required. The combination of hyperpnea, deep cyanosis, and normal air entry into lung fields (thus excluding a foreign body in the airways) is pathognomonic. Some infants have minor spells with inconsolable irritability and only a slight increase in cyanosis. They are often erroneously diagnosed as having colic and, when severe, may even have been diagnosed as having seizures.

Clubbing of the fingers and toes develops in patients with chronic cyanosis. Although usually seen in older patients, it can develop in infancy. Clubbing resolves with restoration of normal systemic oxygen saturation after complete repair.

In a preoperative patient, the jugular venous pulsations are usually normal, although difficult to evaluate in infants. The right ventricle remains relatively compliant with normal or only mildly elevated diastolic pressures, and significant tricuspid regurgitation is uncommon. Thus the *a* and *v* waves in the jugular pulse are usually normal.

The peripheral pulses are usually normal, and accentuated pulses should suggest a large patent ductus arteriosus or significant aorticopulmonary collateral arteries. The precordial impulse can be normal, but usually a right ventricular parasternal lift can be appreciated. Hepatomegaly is unusual.

Auscultation reveals a normal first sound and a single second (aortic) sound that is loudest at the mid-left sternal border. With significant right ventricular outflow tract obstruction and low pulmonary arterial pressures, the pulmonary component of the second heart sound is usually

inaudible. Occasionally, if the outflow tract obstruction is not severe, splitting of the second heart sound can be appreciated. Third and fourth heart sounds are uncommon. An early systolic ejection click can be heard at the left mid-to-upper sternal border caused by the dilated ascending aorta and the increased systemic blood flow.

The murmur in patients with unrepaired tetralogy of Fallot is generated by the right ventricular outflow obstruction. The VSD is large and unrestrictive, and the right-to-left shunt does not produce a murmur. The murmur is classically described as a low-pitched, systolic crescendo/decrescendo ejection murmur best heard at the left mid-to-upper sternal border with radiation to the back. However, it is not uncommon for the murmur to resemble that of plateau quality, best heard at the left mid-to-lower sternal border. In these patients, one needs to rely on other physical findings such as cyanosis or a single second heart sound to suspect the diagnosis of tetralogy of Fallot. In an acyanotic neonate, the murmur caused by the left-to-right shunt across a small VSD is difficult to separate from the murmur of infundibular stenosis, and it is easy to misdiagnose the infant. The distinction can be made clinically in most infants; a neonate with tetralogy of Fallot will have a forceful right ventricular lift and usually a loud and single second heart sound.

Unlike pulmonary valve stenosis with an intact ventricular septum in which the intensity and length of the murmur increase with increasing obstruction, the murmur in tetralogy of Fallot diminishes with worsening obstruction. This is because the intensity of the murmur is related not only to the degree of obstruction, but also to the amount of flow across the obstruction. In tetralogy of Fallot, as the right ventricular outflow tract obstruction progresses, the right ventricular systolic output is preferentially shunted across the VSD and into the systemic circulation. The flow across the right ventricular outflow tract is reduced, resulting in a softer murmur. This phenomenon is best demonstrated by a tetralogy spell, during which the outflow obstruction can become so severe that the murmur becomes inaudible while the patient becomes progressively more cyanotic.

Diastolic murmurs are rarely heard in an unoperated patient with tetralogy of Fallot. A continuous murmur in the left infraclavicular region suggests a patent arterial duct. Very rarely a right-sided duct results in a continuous murmur in the right infraclavicular region. Continuous murmurs heard in the posterior lung fields raise concern about significant aorticopulmonary collaterals. An early diastolic murmur along the left sternal border is one of the hallmark findings in tetralogy of Fallot with absent pulmonary valve.

The physical examination in a postoperative patient depends on the type of procedure performed. Palliation with a systemic shunt produces a continuous murmur similar to a patent duct. Appreciation of this murmur in the immediate postoperative period may be difficult because of a ventilator or other competing noises. In this situation, auscultating with the bell of the stethoscope briefly applied to the end of the endotracheal tube often allows appreciation of the murmur because of the proximity of the shunt to the bronchi.

After complete repair of tetralogy of Fallot, a variety of physical findings can be found. On inspection, cyanosis should be absent and clubbing should resolve with time. If tricuspid regurgitation has developed, a prominent *v* wave can be appreciated in the jugular pulsations. Depending on the degree of pulmonary insufficiency and residual outflow tract obstruction, one can palpate a right ventricular parasternal lift. On auscultation, the first heart sound remains normal. The second heart sound frequently remains single. When, however, the pulmonary valve is partially or completely intact, or a valved conduit is used, the second heart sound can split normally with respiration or, if there is right bundle branch block, is widely split. It varies with respiration, but the split persists during expiration. Frequently, an ejection systolic murmur is present at the left mid-to-upper sternal border from mild residual right ventricular outflow obstruction. A louder ejection murmur should raise concern about more significant obstruction. During follow-up, long systolic ejection murmurs that are best appreciated at the left upper sternal border or in either the axilla or the back indicate branch pulmonary artery stenosis and usually warrant further investigation. A blowing, pansystolic murmur from a small residual VSD or tricuspid regurgitation may be heard at the left lower sternal border. A low-pitched delayed diastolic decrescendo murmur at the mid-left sternal border is common and results from pulmonary regurgitation caused by relief of the right ventricular outflow obstruction. This diastolic murmur should be differentiated from the high-pitched early diastolic decrescendo murmur at the left sternal border generated from aortic regurgitation. This latter murmur is not expected unless patients have had long-standing pulmonary atresia with a dilated aortic root, and it also warrants further evaluation. Most patients with satisfactory surgical results have soft systolic/diastolic to-and-fro murmurs of mild pulmonary stenosis and regurgitation along the mid-to-upper left sternal border.

Absent pulmonary valve

This is characterized by severe dilatation of the pulmonary arteries with mild pulmonary stenosis and severe pulmonary regurgitation. The dilated pulmonary arteries can compress the bronchi and result in life-threatening airway compromise as early as the immediate newborn period. Standard airway support, such as endotracheal intubation and mechanical ventilation, is sometimes only partially effective. Positioning the infant prone improves airway compromise by removing bronchial compression and can be life-saving.

Alternatively, if these infants do not have significant airway compromise, they are more apt to develop congestive

heart failure as their right ventricular outflow obstruction is less severe and left-to-right shunting with pulmonary overcirculation is possible. These infants may be intensely cyanotic at birth, but then after a few days, as pulmonary vascular resistance decreases and pulmonary blood flow increases, cyanosis is often mild or absent. On palpation, a prominent precordial impulse with a right ventricular lift is common, and a thrill may be present. Hepatomegaly can accompany other signs of congestive heart failure. On auscultation, the first heart sound is normal, and the second heart sound is single. Third or fourth sounds can be heard. There is a characteristic prominent systolic/diastolic to-and-fro murmur ("sawing wood" murmur) heard along the left sternal border. The murmur is often fairly loud. The systolic component is an ejection quality murmur generated by the pulmonary stenosis, and the diastolic component is a low-pitched decrescendo murmur generated from the severe pulmonary regurgitation.

Postoperatively, these patients may still have significant airway compromise. Depending on the type of repair, physical findings on cardiac examination often resemble those in other patients with tetralogy of Fallot.

Tetralogy of Fallot with pulmonary atresia

Auscultation reveals a single second heart sound and usually a continuous murmur from the arterial duct or MAPCAs. Occasionally, patients have no audible murmur, and, conversely, patients rarely can have loud continuous murmurs (predominantly over the back) and bounding pulses when pulmonary blood flow is unrestrictive and congestive heart failure can ensue.

Patients with a balanced degree of pulmonary flow and soft murmurs may escape detection in the neonatal period and be recognized only as their cyanosis becomes apparent, or physical examination becomes significant in terms of murmur or prominent precordial ventricular impulse.

Diagnosis

An acyanotic neonate with tetralogy of Fallot must be distinguished from an infant with a simple VSD (see earlier). If cyanotic, the infant needs to be distinguished from infants with other forms of cyanotic heart disease with pulmonic stenosis, including double-outlet right ventricle, transposition of the great arteries and a VSD, single ventricle, and tricuspid atresia with normally related great vessels. Each of these has distinctive echocardiographic features. Tricuspid atresia has a characteristic electrocardiogram, and all these entities are much less common than tetralogy of Fallot.

The diagnosis of tetralogy of Fallot is aided by electrocardiography and chest radiography. The electrocardiogram is

Figure 41.3 Posteroanterior radiograph showing the tetralogy of Fallot. The apex of the heart is elevated, resulting in a boot-shaped configuration (open arrows). The heart is not enlarged, and the pulmonary vasculature is at the lower limits of normal, suggesting a mild form of tetralogy of Fallot. There is displacement of the superior vena cava (arrows) by a right-sided aortic arch, which also displaces the esophagus towards the left (black arrow).

useful because it always shows right ventricular hypertrophy. In addition, right atrial enlargement and right-axis deviation are also usually present. Left-axis deviation should raise the possibility of an associated atrioventricular septal defect. Biventricular hypertrophy may be seen in patients who have so-called pink tetralogy with increased pulmonary blood flow. In a neonate, the first or only sign of right ventricular hypertrophy can be an upright T wave in lead Vi or V_4R after 3 days of age. As the child gets older, typical signs of right ventricular hypertrophy are present: right axis deviation, increased anterior (large R waves, or an rR' pattern or a QR pattern in V1) and rightward (large S in V6) forces, and upright T waves in V1.

The chest radiograph of the typical patient shows normal visceroatrial situs, a tilted-up apex, a concave main pulmonary artery segment, and normal to decreased pulmonary vascularity. The heart is usually not enlarged (see Figure 41.3). A right-sided aortic arch can be identified in ~25% of patients with tetralogy of Fallot.

Patients with tetralogy of Fallot and absent pulmonary valve usually have an enlarged heart and markedly enlarged main, right, and left pulmonary arteries. Frequently, lung hyperinflation and tracheobronchial compression occur (see Figure 41.4).

The electrocardiogram and chest radiograph in patients with co-existing pulmonary atresia are usually identical with those found in patients with simple tetralogy of Fallot.
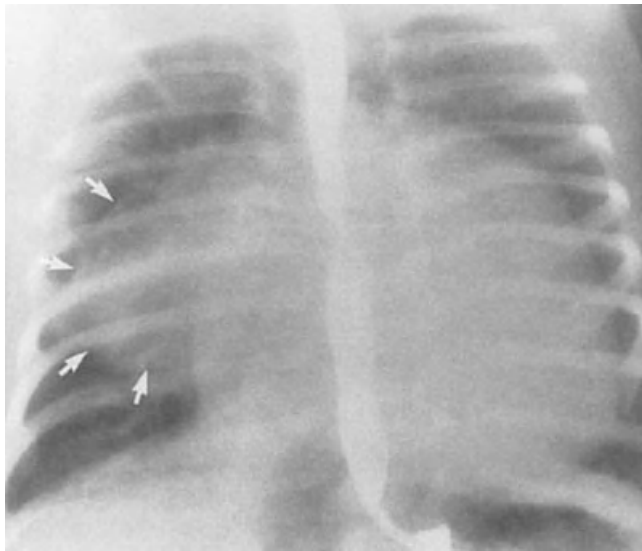
Figure 41.4 Posteroanterior radiograph of tetralogy of Fallot and absence of the pulmonary valve. Typically the right pulmonary artery shows massive dilatation (arrows). The heart is markedly enlarged because of the increased stroke volume of the right ventricle. Dilatation of the left pulmonary artery may occur but is much less common.

Figure 41.5 Echocardiogram showing a four-chamber image of a fetus with tetralogy of Fallot at 32 weeks' gestation, demonstrating large ventricular septal defect (arrow). LA, left atrium; LV, left ventricle; RA, right atrium; RV, right ventricle.

The rare patient with increased pulmonary blood flow caused by a large ductus or a large collateral can show an enlarged heart with increased vascularity and hyperinflated lung fields.

Echocardiography

Two-dimensional echocardiography and Doppler echocardiography usually completely define the diagnosis of tetralogy of Fallot, both prenatally and postnatally. Tetralogy of Fallot has been diagnosed as early as 14 weeks' gestation using transvaginal ultrasound.[24] This lesion, however, continues to evolve through mid and late gestation [25–28]. Serial studies of the embryo and fetus with tetralogy of Fallot are essential in preparing families for the postnatal course of these infants. Early in gestation, the large malalignment perimembranous VSD and aortic override can be seen. Anterior deviation of the outlet septum is also apparent. By mid-gestation, there is considerable variation in the size of the main pulmonary artery, ranging from normal to hypoplastic. The branch pulmonary arteries are usually of normal size. In the second half of pregnancy, patients with more severe forms of tetralogy of Fallot demonstrate abnormal growth of the main and branch pulmonary arteries, resulting in progressive hypoplasia, and even in loss of anterograde flow. The aorta may be normal or increased in size during mid-gestation, with an increased rate of growth compared with a normal fetus, resulting in the large ascending aorta characteristic of this lesion.

The likelihood of prenatal detection of tetralogy of Fallot during ultrasound screening depends on both the severity of the lesion and the experience of the ultrasonographer. Although the VSD should be seen in the four-chamber view during obstetric screening (Figure 41.5), this lesion has been missed during screening examinations that rely on this view alone. Visualization of the outflow tract views increases the likelihood of prenatal diagnosis of tetralogy of Fallot, although fetuses with a milder forms of this anomaly have relatively normal outflow tract views at mid-gestation. In large prenatal echocardiographic series using multiple imaging planes for comprehensive evaluation, tetralogy of Fallot is one of the more commonly diagnosed lesions, accounting for 4–28% of identified congenital cardiac anomalies. The subset of fetuses with tetralogy of Fallot with absent pulmonary valve are disproportionately represented in prenatal series, almost certainly because the dilated right ventricle and pulmonary arterial tree that characterize this lesion result in their more frequent identification.

During prenatal echocardiographic examination, the characteristic VSD can be demonstrated in the long-axis, sagittal, and four-chamber views. Doppler interrogation of the VSD should be included to rule out the rare restrictive VSD. Short-axis and sagittal views can be used to delineate the right ventricular outflow tract and main and branch pulmonary arteries. Although Doppler interrogation of the right ventricular outflow tract is important in assessing the severity of obstruction postnatally, flow velocities in the parallel fetal circulation are usually in the normal range [28,29]. Doppler interrogation and Doppler color flow mapping can, however, readily demonstrate the to-and-fro flow pattern
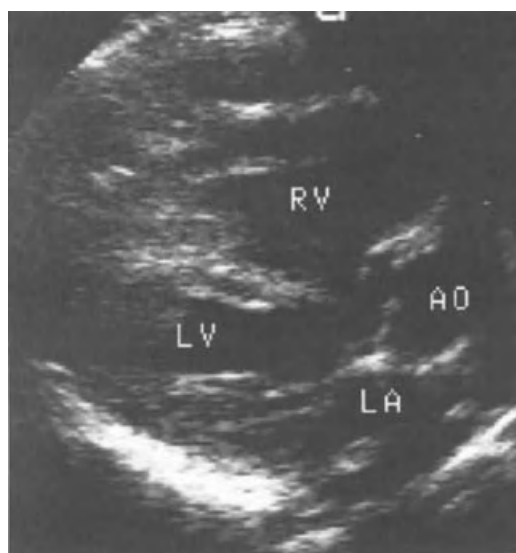
Figure 41.6 Echocardiogram showing a parasternal long-axis view of an infant with tetralogy of Fallot, demonstrating a large perimembranous ventricular septal defect, aortic override, and mitral/aortic valve fibrous continuity. AO, aorta; LA, left atrium; LV, left ventricle; RV, right ventricle.
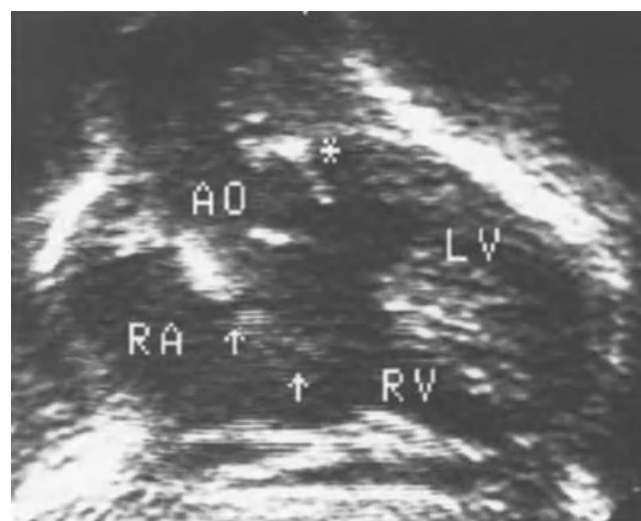
Figure 41.7 Echocardiogram showing a subcostal right oblique view in a neonate demonstrating large ventricular septal defect, overriding aorta, tricuspid/aortic valve fibrous continuity, and anterior deviation of the infundibular septum (*). Arrows identify tricuspid valve leaflet. AO, aorta; LV, left ventricle; RA, right atrium; RV, right ventricle.

seen in fetuses with absent pulmonary valve. Sagittal imaging also allows examination of the arterial duct and aortic arch. Fetuses with more severe right ventricular outflow tract obstruction have retrograde ductal flow *in utero* [25,30]. Other evidence of the severe right ventricular outflow tract obstruction includes significant hypoplasia of the main and branch pulmonary arteries and poor growth of the pulmonary arterial tree during the course of serial examinations.

As with all prenatal diagnoses of congenital heart disease, fetuses with tetralogy of Fallot should undergo assessment of fetal karyotype and comprehensive ultrasound examination to rule out extracardiac anomalies. Families should be counseled regarding the *in utero* evaluation of this lesion and the need for serial evaluations. All fetuses with the prenatal diagnosis of tetralogy for Fallot should be delivered at a tertiary care center with appropriate support staff for evaluating and managing these infants.

Postnatally, complete echocardiographic evaluation must include examination of all aspects of anatomy important to management. At most institutions, echocardiography is the primary method of evaluation before operation, with cardiac catheterization reserved for those patients with specific unresolved questions after echocardiographic examination. Elements of anatomy that must be assessed include the anatomic type and boundaries of the VSD, the presence or absence of multiple VSDs, the severity and level of right ventricular outflow tract obstruction, the anatomy of the pulmonary arteries, the anatomy of the aortic arch, the course of the coronary arterial tree, and the presence of associated abnormalities.

The large VSD present in this lesion can be imaged in multiple views. Its relationship to the aorta, the mitral valve, and the large VSD can be seen in the long-axis view (Figure 41.6). The relationship between the defect and the tricuspid valve can be seen in the parasternal short-axis view, in which the potential for extension as a doubly committed defect can also be assessed. The apical four-chamber view usually demonstrates the continuity among the tricuspid, aortic, and mitral valves and also allows assessment of the degree of aortic override. Caudal angulation of the transducer can be used to examine the degree of posterior extension of the defect.

The subcostal right oblique view is perhaps the most useful view to evaluate the VSD and outlet septum (Figure 41.7). Here, the relationship between the tricuspid and aortic valves in infants with a perimembranous defect is well seen. In the rare instances of obstruction of the VSD, the subcostal coronal view allows demonstration of the abnormal or accessory tricuspid valve tissue obstructing the defect and of possible attachments to the infundibular septum [31,32]. This abnormal tricuspid valve tissue can also be imaged in parasternal axis views.

The levels of right ventricular outflow tract obstruction are best assessed in the parasternal short-axis and subcostal views. The prominent septoparietal trabeculations can be seen intruding on the infundibular region in the subcostal coronal view. In the parasternal short-axis and subcostal sagittal views, the anterior and superior deviation of the infundibular septum can be appreciated, and the abnormal pulmonary valve can be seen (Figures 41.8 and 41.9). Measurements of the pulmonary valve annulus are important in predicting the need for transannular patch.

Pediatric Cardiovascular Medicine
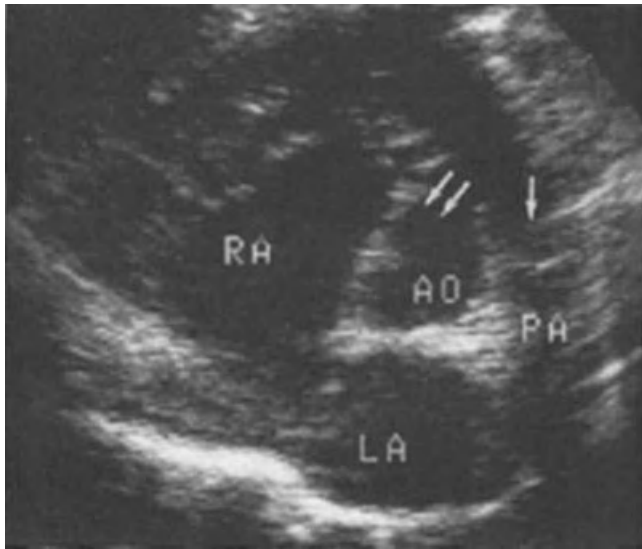
Figure 41.8 Echocardiogram showing a diastolic frame from parasternal short-axis view of a 3-week-old infant with tetralogy of Fallot. Tricuspid valve leaflets partially obscure ventricular septal defect (double arrows). Anterior deviation of the infundibular septum and small pulmonary annulus (single arrow) are demonstrated. AO, aorta; LA, left atrium; PA, pulmonary artery; RA, right atrium.
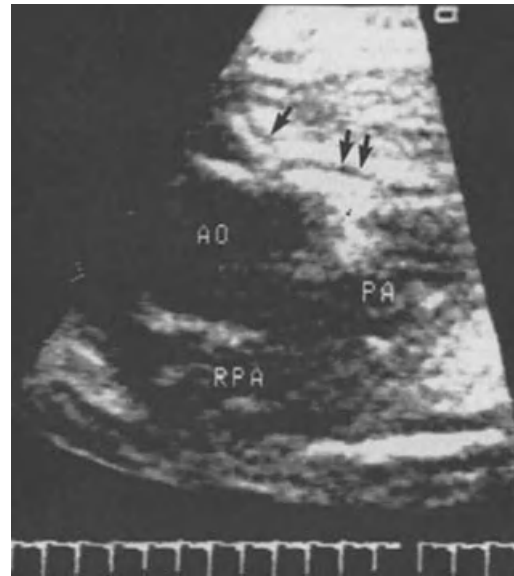
Figure 41.10 Echocardiogram showing a parasternal short-axis view with counter-clockwise rotation from a neonate with tetralogy of Fallot, demonstrating the right coronary artery (single arrow) originating from the right coronary orifice and giving rise to the left anterior descending coronary artery, which crosses the pulmonary outflow tract anteriorly (double arrows). AO, aorta; PA, pulmonary artery; RPA, right pulmonary artery.

Figure 41.9 Echocardiogram demonstrating a subcostal sagittal image from an infant with tetralogy of Fallot and a large ventricular septal defect (double arrows) with aortic override and anterior deviation of the infundibular septum (single arrow). AO, aorta; LA, left atrium; LV, left ventricle; PA, pulmonary artery; RV, right ventricle.

The parasternal short-axis view allows evaluation of the pulmonary artery confluence and proximal branch pulmonary arteries; the suprasternal short- and long-axis views also allow verification of the confluent nature of the pulmonary arteries

and visualization of the branch pulmonary arteries more distally. When the pulmonary arteries are not confluent, alternative sources of blood supply can be identified from these views. Assessment of the size and symmetry of the branch pulmonary arteries is important in both the decision regarding the appropriateness of primary repair and the need for patch augmentation of the proximal pulmonary arteries at the time of operation. Despite the multiple levels of right ventricular outflow tract obstruction and the elongated nature of the infundibular obstruction, predicted outflow tract gradients using the modified Bernoulli equation compare favorably with catheterization data [33], allowing verification of the usually low pulmonary arterial pressure.

These same views can be used to assess the right ventricular outflow tract in infants with tetralogy of Fallot and absent pulmonary valve. In these infants, the infundibular obstruction may not be as severe, although there is significant obstruction at the small pulmonary annulus and, in some patients, by dysplastic valvar tissue. There is marked dilatation of the proximal main and branch pulmonary arteries, and Doppler interrogation demonstrates the severe pulmonary insufficiency that characterizes this lesion.

Several groups have described the echocardiographic evaluation of coronary artery anatomy in this lesion [34–36]. Echocardiographic evaluation must demonstrate that no major coronary arteries cross the right ventricular outflow tract (Figure 41.10). The origin and course of the

left and right coronary arteries can be traced in multiple views, although the parasternal long- and short-axis views may be the most helpful. Any concerns regarding abnormal coronary anatomy should be verified angiographically.

Aortic arch anatomy can be demonstrated by echocardiography using suprasternal long- and short-axis views, first to determine the relationship between the trachea and the arch, and then to define the branching pattern. Doppler color flow mapping can be used to exclude a ductus arteriosus or prominent aortopulmonary collaterals.

Complete echocardiographic evaluation must also exclude associated anomalies important in planning the surgical approach. Two-dimensional imaging and color flow mapping in multiple planes must be used to identify an associated atrial septal defect and additional VSDs. Abnormalities of pulmonary and systemic venous connection must be delineated, and rare left-sided lesions, such as mitral valve abnormalities (e.g., straddling) and subaortic obstruction, must also be identified.

Postoperative studies must define residual septal defects and the degree and level of residual outflow tract obstruction. Care should be taken to examine the branch pulmonary arteries distally to identify branch stenosis at the sites of previous shunts or at the juxtaductal site (Figure 41.11). Many patients after transannular patch repair have significant pulmonary regurgitation, which can be assessed either comparing the width of the regurgitant jet to the annulus [37] or assessing the distal extent of the regurgitant jet from the annulus [38]. Although pulmonary regurgitation is generally well tolerated, assessment of right ventricular size and wall motion, and also tricuspid valve function, should be part of all postoperative echocardiographic studies.

Patients with coexisting pulmonary atresia and VSD have similar intracardiac anatomy to classic tetralogy of Fallot. In the absence of anterograde flow from the right ventricle to the pulmonary artery, careful echocardiographic study of the central pulmonary arteries is necessary. Echocardiographic study should define the intracardiac anatomy, evaluate ventricular function, valvar regurgitation, and coronary origins, define the status of central pulmonary arteries, measure the size of the main, right, and left pulmonary arteries, define the presence or absence of either a left- or right-sided ductus arteriosus, and define the site of origin and proximal distribution to right or left lungs of as many MAPCAs as possible. These studies can be difficult and time consuming, with the need for extensive color-flow mapping. A reasonable road map should be obtained before the necessary cardiac catheterization procedures. Intracardiac anatomy should be defined completely so that contrast media can be conserved at catheterization for comprehensive delineation of pulmonary artery origin, distribution, and anatomy.

(a)

(b)
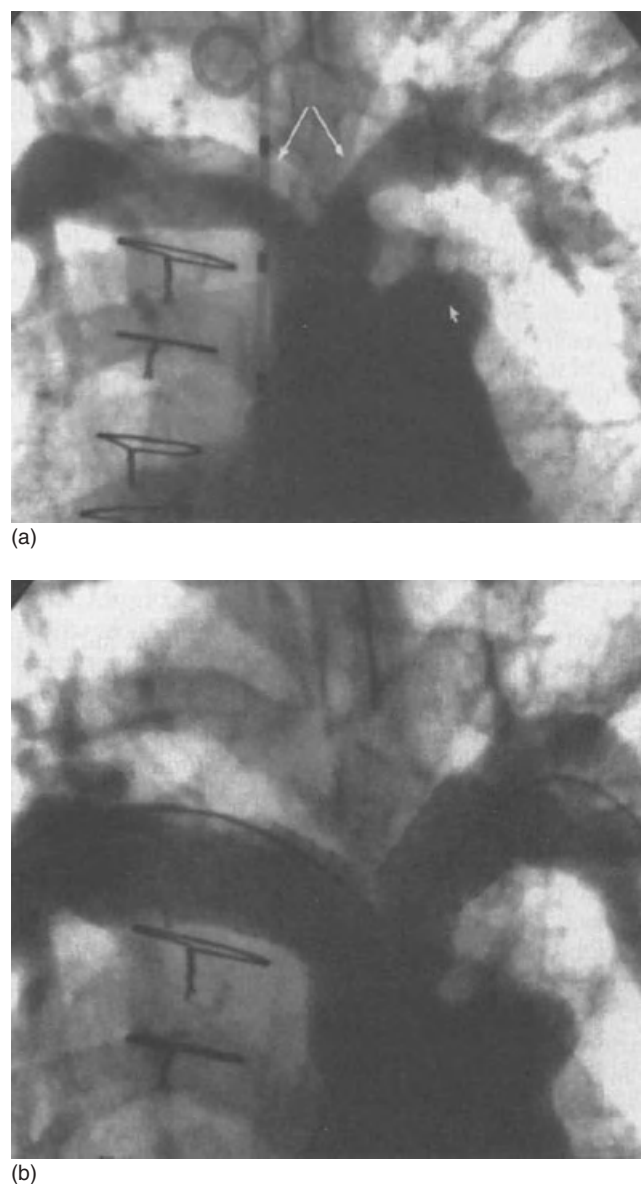
Figure 41.11 Two angiograms from a 22-year-old patient after complete repair in childhood with residual branch pulmonary artery stenosis and right ventricular hypertension. (a) The bilateral branch stenosis is well visualized (long arrows). A small diverticulum of the right ventricular outflow tract (short arrow) is demonstrated. (b) Angiography demonstrated relief of proximal pulmonary artery stenosis.

Computed tomography and magnetic resonance imaging

CT scanning is sometimes performed to delineate the anatomy and distribution of the central pulmonary arteries and MAPCAs in those with pulmonary atresia, but in general avoiding ionizing radiation is preferred. Consequently, MRI is more often chosen, particularly as full diagnostic studies can now be performed during postprandial sleep, or with sedation, even in young infants. In postoperative patients,
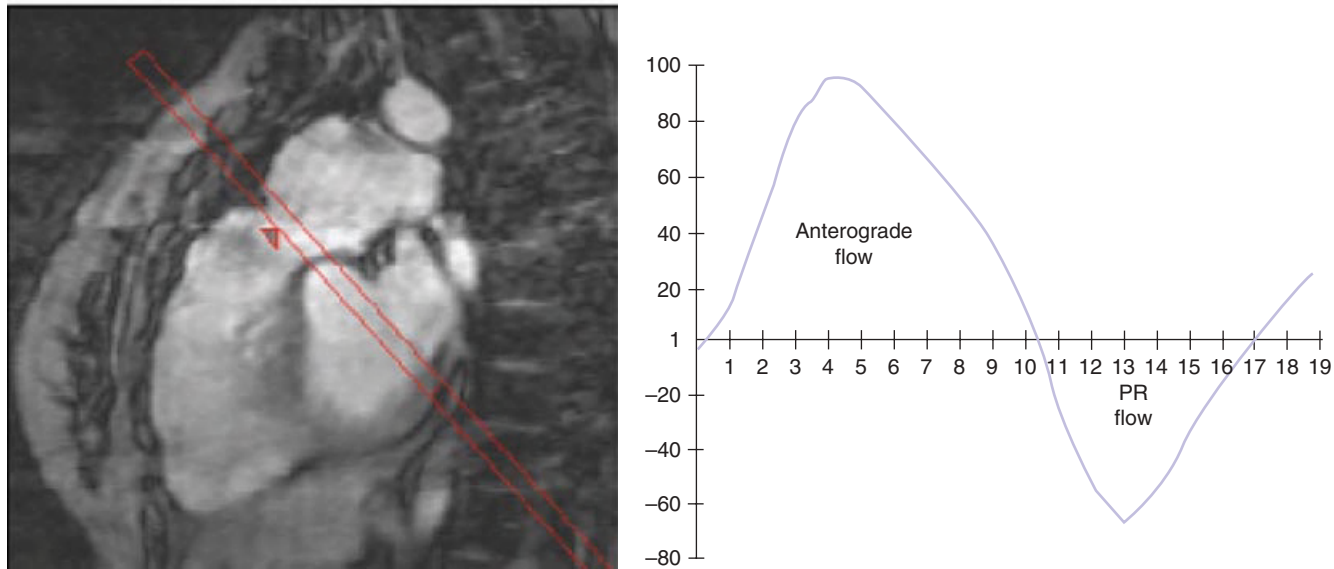
Figure 41.12 Magnetic resonance image of the right ventricle (left panel), with flow assessment in the right ventricular outflow tract (right panel). Note the anterograde and retrograde flow, the latter quantifiable as the volume of pulmonary regurgitation (PR).

MRI has become the mainstay of assessment of right ventricular function and volumes, particularly as they pertain to decision-making regarding the timing of pulmonary valve replacement. MRI allows the assessment of all aspects of cardiac and extracardiac anatomy, and the basics of RV function (Figure 41.12). Most importantly, it has become the gold standard for assessing pulmonary regurgitation, which, as discussed below, is one of the most important factors in late follow-up.

Medical management

The medical management of a patient with tetralogy of Fallot depends on the clinical presentation. A cyanotic neonate who is duct dependent should be stabilized with prostaglandin E_1 infusion.

In an asymptomatic infant with adequate pulmonary flow and systemic saturation, no initial therapy may be necessary. This infant can be followed as an outpatient with close attention to growth, symptoms, and systemic saturation. If the child develops significant cyanosis or reaches an appropriate size or age, repair can be performed electively. The development of tetralogy spells is an indication for early intervention.

Medical management of hypercyanotic spells is directed towards improving pulmonary blood flow and sustaining mixed venous oxygen saturations (reducing systemic oxygen consumption). Parents should be educated to comfort the child while placing him or her in the knee–chest position to increase systemic afterload and force more blood flow across the pulmonary outflow tract. In a hospital, the patient's airway and breathing should be assessed, the patient placed in the knee–chest position, and 100% oxygen given. Sedation with morphine sulfate ($0.1\,mg\,kg^{-1}$) can be given intravenously (i.v.), or intramuscularly (i.m.) should an intravenous line not be available. Acidosis may develop and should be treated with bicarbonate. An intravenous fluid bolus (5–$10\,ml\,kg^{-1}$) of saline or lactated Ringer's solution ensures adequate right ventricular filling. Should these measures fail, intravenous beta-blockade with propranolol or esmolol slows the heart rate and increases systemic vascular resistance, while decreasing catecholamine stimulation and contractility. Systemic afterload can be increased with alpha-agonists in an effort to force more blood flow through the right ventricular outflow tract. Phenylephrine (Neo-Synephrine) $0.02\,mg\,kg^{-1}$ i.v. or $0.1\,mg\,kg^{-1}$ i.m. is often more rapid and successful than other therapies [39]. Finally, should all measures fail, general anesthesia can reverse the episode or prepare the patient for an emergency aortopulmonary shunt if hypoxemia persists.

In patients with chronic hypoxemia, oral therapy with propranolol (0.5–$1\,mg\,kg^{-1}$ b.i.d.–q.i.d.) can improve oxygen saturations and reduce the risk of hypercyanotic spells. These patients are also at risk for thromboembolic complications, a risk that is highest in patients with coexisting iron deficiency anemia. Close monitoring of both hemoglobin concentration and hematocrit is necessary so mean corpuscular volume can be calculated. The hemoglobin should be approximately one-third of the hematocrit; if less, the patient has iron deficiency anemia. These patients should have an elevated hemoglobin at baseline, and a normal hemoglobin value

may actually represent a relative anemia. Iron deficiency anemia should be treated with supplemental iron.

Whether an infant or young child undergoes initial palliation or complete repair depends on the institution. In the past, the approach was to delay complete repair until later childhood. In the mid-1990s, successful complete repair in early infancy and even the immediate neonatal period was demonstrated, and most large units now reserve palliation (either surgical or by interventional catheterization [40–42]) for very small and/or premature infants, or those with additional abnormalities [43–45]. Elective primary repair is usually performed at 6–18 months of age.

Cardiac catheterization

Cardiac catheterization is now reserved for those with complex additional abnormalities, such as MAPCAs. The catheterization is most commonly performed from a femoral approach where both arterial and venous access is obtained. The left side of the heart can often be reached via an atrial communication so that most of the hemodynamic measurements can be performed with the venous catheter. Pressures and oxygen saturations should be obtained in the superior vena cava, both ventricles, both atria (if there is an atrial communication), and the aorta. If left atrial saturations are low, pulmonary venous saturations should be obtained. Systemic left and right ventricular systolic pressures should be expected, and any variation from this requires further investigation. Ventricular end-diastolic and atrial pressures are often normal or only mildly elevated. A wide systemic pulse pressure should suggest a patent arterial duct or large systemic to pulmonary artery collateral vessels. Saturation values usually demonstrate some right-to-left shunting, which can be at both the atrial and ventricular levels. Evidence of left-to-right shunting may also be found if the pulmonary arteries are entered. Whether to cross the right ventricular outflow tract in a patient who is being prepared for elective repair depends on the operator. The benefit is that pulmonary artery pressures and saturations can be obtained; pulmonary flow, pulmonary resistance, and left-to-right shunting can be calculated. Additionally, branch pulmonary artery stenosis may be further examined, although this may be difficult to assess in the presence of significant proximal obstruction. The benefits must be weighed against the risks, which include arrhythmia, perforation, and hypercyanotic spells, associated with attempts to cross the stenotic outflow tract.

Angiography should be guided by the anatomic questions to be answered. Biplane cineangiography is needed, and the angiograms that provide the most important information for a particular patient should be performed first. This ensures adequate contrast availability, should multiple angiograms of a particular structure be necessary.

With multiple levels of obstruction to pulmonary flow, including infundibular, valvar, supravalvar, and branch

pulmonary artery, an injection of contrast material into the right ventricle is often indicated (Figure 41.11). To visualize the branch pulmonary arteries and their bifurcation better, it is helpful to angle the anteroposterior (AP) camera about 30° cranially with a small amount of left anterior oblique (LAO) rotation. The cranial angulation prevents overlap of the outflow tract on to the pulmonary artery bifurcation. The LAO rotation of the camera improves evaluation of the proximal left pulmonary artery, which may be difficult to visualize in a straight AP projection. Keeping the lateral camera in a straight lateral (90° LAO) projection usually provides excellent imaging of the right ventricular outflow tract and allows evaluation of the infundibular, valvar, and supravalvar areas. Additionally, right-to-left shunting across the VSD may be seen in this view.

Evaluating the coronary arteries and aorta can often be accomplished with a single injection of contrast material into the ascending aorta. The catheter should be positioned close to the aortic valve to ensure adequate visualization of the coronary arteries. Camera positioning should be tailored to delineate the proximal coronary artery origins and distribution. A variety of camera angles have proven useful. Some have even advocated selective coronary angiography, although this has a risk in small infants and children. We have found that with the AP camera in 30° right anterior oblique (RAO) and the lateral camera in 70° LAO and 20° cranial (long axial oblique) positions, the injection usually delineates the coronary distribution adequately (see Figure 41.2). Should a particular view not demonstrate the coronary anatomy adequately, the operator should be prepared to try alternative views. The ascending aortic injection also provides information about the aortic arch (right- or left-sided), brachiocephalic vessels (distribution and size), and the ductus arteriosus and collateral vessels. Embolization of collateral vessels can be performed if deemed necessary.

An injection of contrast material into the left ventricle provides useful information about VSDs, degree of aortic override, and, if there is any significant left-to-right shunting, the right ventricular outflow tract obstruction. This is often best accomplished with the AP camera in a 30° RAO projection and the lateral camera in a long axial oblique projection.

Postoperative catheterization is usually reserved for patients with residual abnormalities, such as intracardiac shunting, right ventricular outflow tract obstruction, significant pulmonary regurgitation, or branch pulmonary artery stenosis. The goal may be purely diagnostic but is often therapeutic. The refinement of balloon angioplasty and percutaneous stenting techniques have proved invaluable in managing patients with residual obstruction that may be difficult or impossible to repair surgically (Figures 41.11 and 41.13).

Patients with pulmonary atresia and VSD present a difficult challenge for both diagnostic and interventional catheterization. Preoperative catheterization must attempt
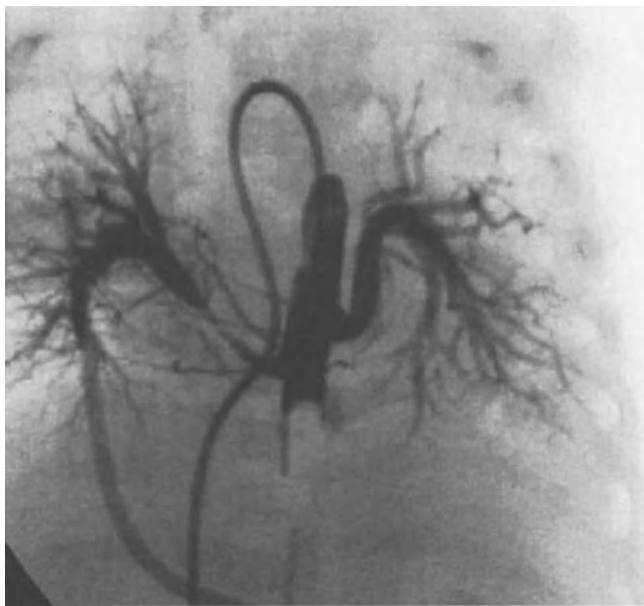
Figure 41.13 Balloon occlusion angiogram in the descending aorta. Berman's angiographic catheter has been passed from the right ventricle anterograde into the ascending aorta and positioned in the descending aorta. The balloon has been inflated to prevent runoff into the distal aorta during the injection. Dense opacification of the descending aorta with a large unobstructed collateral to the left lung and a severely stenotic collateral to the right lung can be seen.

Figure 41.14 Selective injection of a major aorticopulmonary collateral vessel. A 4 French right coronary catheter is engaged to the ostium of a single collateral vessel arising from the mid-thoracic aorta, and contrast agent is injected manually. Opacification of a well-developed lower left pulmonary artery is demonstrated. In addition, one can clearly see the seagull appearance of the extremely hypoplastic true or native pulmonary arteries (arrow).

to delineate all sources of pulmonary blood flow and identify the number of bronchopulmonary segments supplied by central pulmonary arteries and by MAPCAs. Ascertaining whether dual blood supply is present is also a goal, in addition to determining the severity of stenoses of central pulmonary arteries and MAPCAs. Various techniques to obtain these data include balloon occlusion aortography at various levels in the descending aorta (Figure 41.13), selective injection of MAPCAs or ductus (Figures 41.14 and 41.15), and pulmonary vein wedge angiography (Figure 41.16).

Postoperative catheterizations may be necessary to assess the patency of shunts or unifocalization procedures that have been performed, the growth of central pulmonary arteries, the distribution of flow to various bronchopulmonary segments, the presence of stenoses, and the presence of unifocal or dual blood supply from central pulmonary arteries and MAPCAs to various bronchopulmonary segments. Balloon dilatation of stenotic arteries and stenting of vessels are a major part of the reconstructive process for these patients. In addition, some patients need coil occlusion of redundant collaterals or MAPCAs to prevent pulmonary overcirculation.

Surgical repair

The report of the Blalock–Taussig (BT) shunt in 1945 opened the door to palliation of patients with tetralogy of Fallot by creating some type of aortopulmonary anastomosis [3] (see Chapter 14). A modification of this approach – anastomosis of the main pulmonary artery to the ascending aorta – is sometimes performed in patients with pulmonary atresia and MAPCAs in an attempt to grow diminutive but confluent pulmonary arteries.

The BT shunt provides excellent palliation, and it was not until 1954 that complete intracardiac repair, with closure of the VSD and relief of the right ventricular outflow obstruction, was demonstrated by Lillehei and colleagues [3]. Although fundamentally the technique has changed little, there have been many modifications. The VSD is now rarely closed via a ventriculotomy, with a transatrial approach now the method of choice. The extent of the ventricular incision has thus been markedly reduced and, when possible, avoided altogether in order to preserve infundibular and global right ventricular function. Similarly, the degree of resection of outflow tract muscle has diminished with experience. Formerly, cardiologists thought that residual obstruction was the root of all postoperative evils, but pulmonary regurgitation is now regarded as a much more frequent culprit. Consequently, transection of septoparietal trabeculations is preferred over removal, and preservation of the pulmonary valve has become more frequent. Indeed, often a small amount of residual obstruction will be tolerated, if a transannular patch can be avoided.

(a)

(b)

(c)
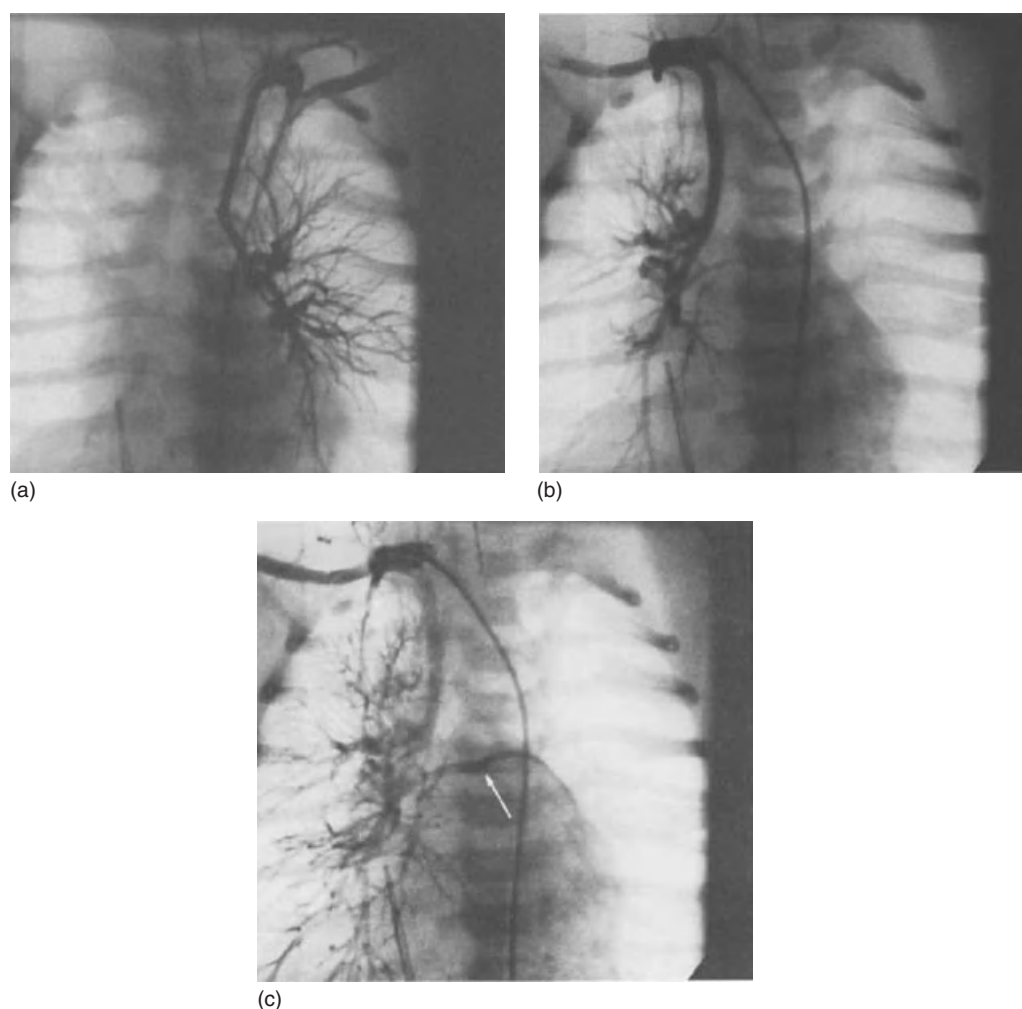
Figure 41.15 Collateral vessels arising from the brachiocephalic vessels. Selective manual injections are performed in the subclavian arteries. (a) A small but well-developed left pulmonary artery is supplied by a collateral from the left subclavian artery. (b) A well-developed right pulmonary artery is supplied by a collateral vessel arising from the right subclavian artery. (c) As the contrast agent passes further into the right pulmonary artery, the hypoplastic true or native pulmonary arteries can be seen with the typical seagull appearance (arrow).

One of the more important postoperative abnormalities is restrictive right ventricular physiology. Although much decreased in frequency since its original description in the mid-1990s [46–49], when present it predictably slows postoperative recovery, and can be associated with a markedly reduced cardiac output. As a result, it has become common to leave a patent foramen ovale to enhance systemic output from right-to-left atrial shunting in the early postoperative period.

The surgical approach to the patient with tetralogy of Fallot and absent pulmonary valve is less clear, particularly in the patient with significant respiratory compromise. Arguments have been made both for initial palliation to control the pulmonary blood flow and regurgitation and for initial complete repair. Most now favor early complete repair for symptomatic infants [3]. In essence, the surgeon closes the VSD, reconstructs the outflow tract, if necessary with a patch, and attempts to remove bronchial compression by plicating the aneurysmal pulmonary artery or even transecting and reimplanting the pulmonary artery in a more suitable position. Some surgeons implant a pulmonary valve.

Patients with tetralogy of Fallot and pulmonary atresia represent a more difficult surgical challenge [3]. Patients with good-sized central pulmonary arteries supplied by a ductus with distribution of normal or near-normal branching patterns to the majority of bronchopulmonary segments, and without significant MAPCAs, can follow a surgical algorithm similar to a standard tetralogy of Fallot patient. Unfortunately, a large number of patients have hypoplastic or absent central pulmonary arteries either with MAPCAs supplying the majority of bronchopulmonary segments alone or with a dual blood supply from MAPCAs and central pulmonary arteries. In these, a major goal of the initial operation has been to enlarge central pulmonary arteries by establishing continuity from the right ventricle to the main
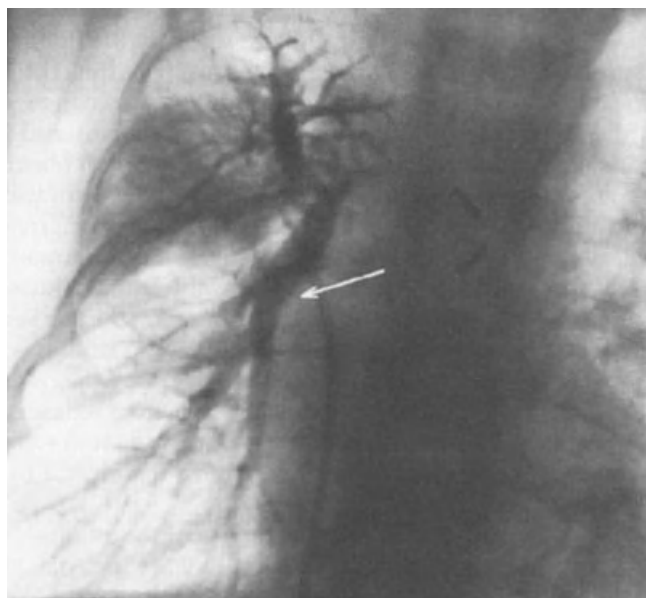
Figure 41.16 Pulmonary vein wedge angiogram. No arterial supply could be identified to the right lung in this child after an initial right unifocalization. A wedge catheter has been positioned in the right upper pulmonary vein. The balloon is inflated to occlude flow. Contrast agent is slowly injected retrograde into the capillary bed, followed rapidly with a saline flush. The right pulmonary artery (arrow) is easily seen and densely filled, indicating that it is patent but not being supplied with anterograde flow.

pulmonary artery or to the confluence of the right and left pulmonary arteries, or by implementing a central shunt to provide growth of these arteries, such that an eventual repair could be performed. When central pulmonary arteries provide blood flow to only a limited number of bronchopulmonary segments, however, unifocalization procedures must be performed so that central pulmonary arteries can be connected to the majority of the bronchopulmonary segments. This may require procedures in which shunts are performed to each lung with separate operations in which MAPCAs are divided from the aorta and connected together, with the shunt then providing all the blood flow to the ipsilateral lung. If possible, these unifocalized vessels are connected to a central right or left pulmonary artery. If no central pulmonary arteries are present, the eventual goal is to connect the unifocalized pulmonary arteries in the right and left hila using a central graft that can then be connected to the right ventricle with a valved or nonvalved conduit or homograft. Although this approach has been reported since the late 1980s, success has been variable, and many patients have not had enough growth of pulmonary arteries to undergo closure of the VSD [50–55].

Hanley and co-workers advocated early repair using extensive mobilization of MAPCAs and central pulmonary arteries with preferred time of operation from 3 to 6 months of age [56]. Small central arteries are enlarged considerably

with homograft material, and in most patients, connection is made to the right ventricle with a valved or nonvalved containing graft. If enough bronchopulmonary segments have been connected and the augmented pulmonary arteries appear to be of reasonable size, the VSD can be closed. These authors described a procedure for help with the decision about closure of the VSD. Immediately after pulmonary artery surgery, the heart–lung pump is used to direct a normal cardiac index through the lungs before the decision is made regarding VSD closure. If the pulmonary arterial pressure has not risen markedly during this procedure, the VSD is closed. With this procedure, the authors were able to achieve complete repair in most infants [57]. Although most units have adopted a similar approach, institutional preferences vary, as do results, and this remains a controversial area, with uncertain long-term results [58]. Furthermore, despite successful unifocalization and reparative procedures, these patients frequently have multiple stenoses in both the surgically created anastomoses and the native MAPCAs and pulmonary arteries. These patients require postoperative catheterization and frequently balloon dilatation or stent placement to achieve satisfactory right ventricular systolic pressure.

Postoperative problems and long-term outlook

Postoperative problems include both hemodynamic abnormalities and arrhythmias, which are listed in Table 41.2.

Residual VSD is uncommon with current surgical techniques. Echocardiography is fairly useful to detect left-to-right ventricular shunting but, in the presence of a surgical patch, estimating the size of the defect and the degree of shunting may be difficult.

Residual right ventricular outflow tract obstruction, valvar stenosis, annular stenosis, and supravalvar main pulmonary arterial obstruction can occur, particularly when transannular patching is avoided. The site and severity of obstruction can usually be determined echocardiographically, and balloon valvoplasty may be useful when there is valvar obstruction. If there is a moderate or severe residual supravalvar, annular, or infundibular stenosis, reoperation is usually required. Pulmonary artery branch stenosis is relatively common postoperatively and usually occurs in the left pulmonary artery at the site of prior ductal insertion, or at the site of a previous shunt. Fortunately, these conditions can now be treated with a high degree of success by using transcatheter balloon arterioplasty with or without the use of stents (see Figure 41.12).

Tricuspid regurgitation is relatively rare early after the repair, but increases with progressive right ventricular dilation and dysfunction. When operation is required for pulmonary valve replacement or correction of residual

Table 41.2 Postoperative problems.

Residual hemodynamic problems
Ventricular septal defect
Right ventricular outflow tract obstruction
Pulmonary valvar and/or annular stenosis
Supravalvar pulmonary artery stenosis
Pulmonary artery branch stenosis
Pulmonary regurgitation
Tricuspid regurgitation
Right ventricular dysfunction
Right ventricular outflow tract aneurysm
Left ventricular dysfunction
Pulmonary hypertension

Arrhythmia and conduction disturbances
Supraventricular tachycardia
Ventricular tachycardia
Complete heart block

outflow obstruction, tricuspid valve annuloplasty can be a useful adjunctive procedure.

Pulmonary regurgitation commonly accompanies tetralogy of Fallot repair because of the frequent need for transannular patching for adequate relief of right ventricular outflow tract obstruction. Pulmonary regurgitation is usually well tolerated when pulmonary arterial and right ventricular pressures are low. If any degree of pulmonary hypertension or pulmonary artery stenosis is present, pulmonary regurgitation is enhanced and right ventricular dilatation is accelerated. In the long term, pulmonary regurgitation is the single most important factor in the pathogenesis of symptomatic decline [1]. The natural history of isolated congenital pulmonary valve regurgitation has been reviewed. The development of cardiovascular symptoms increases with age, reaching 20% after 40 years and 48% after 50 years in patients without associated pulmonary stenosis, pulmonary hypertension, or a right ventriculotomy [59]. If right ventricular dysfunction develops in a high percentage of patients with an otherwise normal heart by age 50 years, postoperative patients with prominent pulmonary regurgitation almost certainly will have similar problems with increasing age.

Arrhythmias can be a significant postoperative problem. There has been a history of late sudden death in as many as 5% of patients on long-term follow-up [60–67]. This incidence appears to be declining with earlier age at operation. Patients who appear to be most at risk for ventricular tachyarrhythmia and sudden death have right ventricular dilatation, right ventricular dysfunction, right ventricular pressure overload, marked or rapidly developing QRS prolongation [68], and an older age at the time of repair. Both supraventricular tachycardia and ventricular tachycardia can occur. Because most patients have right bundle branch postoperatively, they have wide complex tachycardia, and it

may be difficult to differentiate between the two types of tachycardia. The "supraventricular" arrhythmia is usually atrial flutter or fibrillation. "SVT" will show a RBBB pattern but VT after tetralogy repair will nearly always have an LBBB pattern because of the right ventricular origin of the tachycardia.

Patients with documented arrhythmia associated with symptoms should undergo electrophysiologic studies and concurrent hemodynamic evaluation by electrophysiologists experienced in congenital heart disease. Supraventricular tachycardia and ventricular tachycardia may coexist. When either type of tachycardia is documented, radiofrequency ablation may be curative, or patients may be treated with an antitachycardia device. An alternative strategy, particularly if pulmonary valve replacement is contemplated, is for intraoperative mapping of the arrhythmia and cryoablation. This has proven particularly successful for those with ventricular tachycardia, where transcatheter ablation is less effective.

Infective endocarditis is rare after operation [69].

Exercise performance after tetralogy repair is less than normal, and the degree of impairment is usually directly related to the amount of pulmonary regurgitation [70–73]. Right ventricular dysfunction, as assessed by ventricular size and ejection fraction, has often been found in patients with more severe pulmonary insufficiency. Such patients also have a larger transannular patch and right ventriculotomy, factors that also depress ventricular function [74,75]. Pulmonary valve replacement usually decreases right ventricular size, increases ejection fraction, and improves exercise capacity [76–78]. However, right ventricular dysfunction [79] and chronotropic impairment of unknown origin [80] also contribute to diminished exercise tolerance.

The decision as to when to perform pulmonary valve replacement for pulmonary regurgitation is difficult. Patients with progressive right ventricular enlargement, particularly if associated with decreased exercise tolerance documented with exercise testing, clinical arrhythmia, or signs of right ventricular dysfunction should have the valve replaced, preferably when these signs or symptoms occur. Several groups have sought to define a threshold for right ventricular dilatation, above which reverse remodeling may not occur after valve replacement. Although far from resolved, most studies have found that a right ventricular end-diastolic volume of 150–170 ml m^{-2} or more makes recovery less likely, at least in adults [81,82]. There is usually a modest decrease in heart size after operation and often resolution of symptoms and ventricular ectopy. Several reports indicate favorable results with pulmonary valve replacement [76–78], with an earlier operation associated with better results.

Right ventricular aneurysms described after tetralogy repairs are usually not true aneurysms but simply prominent outflow patches that were too large to begin with. These patches are akinetic, can contribute to right ventricular

dysfunction, and should be resected and retailored when reoperation is required.

Transcatheter pulmonary valve replacement

Transcatheter valve replacement was first described by Andersen *et al*. in 1992 [83], but it failed to capture the imaginations of cardiologists or industry, perhaps because of a lack of importance attributed to pulmonary valve dysfunction at that time. However, in 2000, Bonhoeffer [84] described the use of a bovine jugular valve mounted in a stent, to reconstruct the right ventricular outflow tract in patients with stenosis and/or regurgitation. A dilated outflow tract makes transcatheter valve replacement infeasible for most patients, at least for the time being. Nonetheless, the introduction of the technique has been one of the most significant advances in the recent history of cardiology, spawning an explosion of methods for treating acquired and congenital valve diseases. For those with tetralogy of Fallot, this therapy is essentially restricted to those patients with a conduit between the right ventricle and pulmonary artery. Even so, the results have been very encouraging. Relief of stenosis and abolition of regurgitation can be expected in most, and these results seem to be sustained in the majority during the first 5 years after implantation. The technique has evolved during the decade since its original description by Bonhoeffer and colleagues [85], so the longer term outcomes of contemporary series remain to be seen. Furthermore, development of techniques to overcome the anatomic limitations in most of those without a conduit will likely change the face of, and indications for, pulmonary valve replacement in these patients (see also Chapters 10 and 33).

Most postoperative patients lead normal or near-normal lives. Patients who have excellent results with normal to near-normal heart size, and no residual significant hemodynamic lesions, can engage in high-level recreational and sports activities [86].

Long-term outcome after repair of tetralogy of Fallot has been reported to be very good for most patients, with actuarial survival reported as 86% after 32 years compared with an expected rate of 96% [87], 85% after 36 years [88], 84% after 20 years [89], and 84% after 15 years [90]. These survival rates are for some of the earliest patients receiving repair, and survival after successful early repair with more current techniques would be predicted to be even better.

References

1 Apitz C, Webb GD, Redington AN. Tetralogy of Fallot. *Lancet* 2009;**374**:1462–71.

2 Anderson RH, Weinberg PM. The clinical anatomy of tetralogy of Fallot. *Cardiol Young* 2005;**15**(Suppl 1):38–47.

3 Kouchoukas NT, Blackstone EH, Hanley FL, *et al*. Ventricular septal defect with pulmonary stenosis or atresia. In: Kouchoukas NT, Blackstone EH, Hanley FL, *et al*., eds. *Cardiac Surgery*, Vol. 1. Philadelphia: Churchill Livingstone, 2003: 946–1075.

4 Anderson RH, Devine WA, del Nido P. The surgical anatomy of tetralogy of Fallot with pulmonary atresia rather than pulmonary stenosis. *J Card Surg* 1991;**6**:41–58; discussion 58–49.

5 Fyler DC, Buckley LP, Hellenbrand WE, *et al*. Report of the New England Regional Cardiac Program. *Pediatrics* 1980; **65**(Suppl):375–461.

6 Mitchell SC, Korones SB, Berendes HW. Congenital heart disease in 56,109 births. Incidence and natural history. *Circulation* 1971;**43**:323–32.

7 Perry LW, Neill CA, Ferencz C, *et al*. Infants with congenital heart disease: the cases. In: Ferencz C, Rubin JD, Loffredo CA, Magee CH, eds. *Epidemiology of Congenital Heart Disease: The Baltimore–Washington Infant Heart Study in 1981–1989*. Mount Kisco, NY: Futura Publishing, 1993: 433–62.

8 Digilio MC, Marino B, Grazioli S, Agostino D, Giannotti A, Dallapiccola B. Comparison of occurrence of genetic syndromes in ventricular septal defect with pulmonic stenosis (classic tetralogy of Fallot) versus ventricular septal defect with pulmonic atresia. *Am J Cardiol* 1996;**77**:1375–6.

9 Gioli–Pereira L, Pereira AC, Bergara D, *et al*. Frequency of 22q11.2 microdeletion in sporadic non-syndromic tetralogy of Fallot cases. *Int J Cardiol* 2008;**126**:374–8.

10 Hofbeck M, Rauch A, Buheitel G, *et al*. Monosomy 22q11 in patients with pulmonary atresia, ventricular septal defect, and major aortopulmonary collateral arteries. *Heart* 1998;**79**: 180–5.

11 Khositseth A, Tocharoentanaphol C, Khowsathit P, Ruangdaraganon N. Chromosome 22q11 deletions in patients with conotruncal heart defects. *Pediatr Cardiol* 2005;**26**:570–3.

12 Whittemore R, Wells JA, Castelsague X. A second generation study of 427 probands with congenital heart disease and their 837 children. *J Am Coll Cardiol* 1994;**23**:1459–167.

13 Fallot E. Contribution à l'anatomie pathologique de la maladie bleu (cyanose cardiaque). *Marseilles Med* 1888;**25**:77–93.

14 Šamánek M. Children with congenital heart disease: probability of natural survival. *Pediatr Cardiol* 1992;**13**:152–8.

15 Hoffman JIE. Tetralogy of Fallot. In: Hoffman JIE, ed. *The Natural and Unnatural History of Congenital Heart Disease*. Oxford: Wiley-Blackwell, 2009: 415.

16 Rowe RD, Vlad P, Keith JD. Experiences with 180 cases of tetralogy of Fallot in infants and children. *Can Med Assoc J* 1955;**73**:23–30.

17 Rygg IH, Olesen K, Boesen I. The life history of tetralogy of Fallot. *Dan Med Bull* 1971;18(Suppl 2):25.

18 Child JS, Perloff JK. Natural survival patterns. A narrowing base. In: Perloff JK, Child JS, eds. *Congenital Heart Disease in Adults*. Philadelphia: Saunders, 1991: 21–59.

19 Bertranou EG, Blackstone.EH, Hazelrig JB, *et al*. Life expectancy without surgery in tetralogy of Fallot. *Am J Cardiol* 1978; **42**:458–66.

20 Deanfield JE, McKenna WJ, Presbitero P, *et al*. Ventricular arrhythmia in unrepaired tetralogy of Fallot: relation to age, timing of repair and haemodynamic status. *Br Heart J* 1984;**52**:77–81.

21 Hoffman JIE. Tetralogy of Fallot with pulmonary atresia. In: Hoffman, JIE, ed. *The Natural and Unnatural History of Congenital Heart Disease*. Oxford: Wiley-Blackwell, 2009: 438–49.

22 Kramer J, Majewska F, Trampisch HJ, *et al*. Malformation patterns in children with congenital heart disease. *Am J Dis Child* 1987;**141**:789–95.

23 Kothari SS. Mechanism of cyanotic spells in tetralogy of Fallot – the missing link? *Int J Cardiol* 1992;**37**:1–5.

24 Achiron R, Weissman A, Rotstein Z, *et al*. Transvaginal echocardiography examination of the fetal heart between 13 and 15 weeks' gestation in a low risk population. *J Ultrasound Med* 1994;**13**:783–9.

25 Pepas LP, Savis A, Jones A, *et al*. An echocardiographic study of tetralogy of Fallot in the fetus and infant. *Cardiol Young* 2003;**13**:240–7.

26 Rice M, McDonald RW, Reller MD. Progressive pulmonary stenosis in the fetus: two case reports. *Am J Perinatol* 1993;**10**:424–7.

27 Hornberger LK, Sanders SP, Sahn DJ, *et al. In utero* pulmonary artery and aortic growth and potential for progression of pulmonary outflow tract obstruction in tetralogy of Fallot. *J Am Coll Cardiol* 1995;**25**:739–45.

28 Shenker L, Reek KL, Marx GR, *et al*. Fetal cardiac Doppler flow studies in prenatal diagnosis of heart disease. *Am J Obstet Gynecol* 1988;**158**:1267–73.

29 Gembruch U, Weintraub Z, Bald R, *et al*. Flow analysis in the pulmonary trunk in fetuses with tetralogy of Fallot by color Doppler flow mapping: two case reports. *Eur J Obstet Gynecol Reprod Biol* 1996;**27**:481.

30 Berning RA, Silverman NH, Villegas M, *et al*. Reversed shunting across the ductus arteriosus or atrial septum in utero heralds severe congenital heart disease. *J Am Coll Cardiol* 1996;**27**: 481–6.

31 Musewe NN, Smallhorn JF, Moes CAF, *et al*. Echocardiographic evaluation of obstructive mechanism of tetralogy of Fallot with restrictive ventricular septal defect. *Am J Cardiol* 1988;**61**:664–8.

32 Flanagan MF, Foran RB, Van Praagh R, *et al*. Tetralogy of Fallot with obstruction of the ventricular septal defect. Spectrum of echocardiographic findings. *J Am Coll Cardiol* 1988;**11**:386–95.

33 Houston AB, Simpson IA, Sheldon CD, *et al*. Doppler ultrasound in the estimation of the severity of pulmonary infundibular stenosis in infants and children. *Br Heart J* 1986;**55**:381–4.

34 Berry JM, Einzig S, Krabill KA, Bass JL. Evaluation of coronary artery anatomy in patients with tetralogy of Fallot by two-dimensional echocardiography. *Circulation* 1988;**78**:149–56.

35 Caldwell RL, Ensing GJ. Coronary artery abnormalities in children. *J Am Soc Echocardiogr* 1989;**2**:259.

36 Jureidini SB, Appleton RS, Nouri S. Detection of coronary artery abnormalities in tetralogy of Fallot by two-dimensional echocardiography. *J Am Coll Cardiol* 1989;**14**:960–7.

37 Bigras JL, Boutin C, McCrindle BW, Rebeyka IM. Short term effect of monocuspid valves on pulmonary insufficiency and clinical outcome after surgical repair of tetralogy of Fallot. *J Thorac Cardiovasc Surg* 1996;**112**:33–7.

38 Joffe H, Georgakopoulos D, Celermajer DS, *et al*. Late ventricular arrhythmia is rare after early repair of tetralogy of Fallot. *J Am Coll Cardiol* 1994;**23**:1146–50.

39 Nudel DBM. A. Berman MA, Talner NS. Effects of acutely increasing systemic vascular resistance on oxygen tension in tetralogy of Fallot. *Pediatrics* 1976;**58**:248–51.

40 Kreutzer J, Perry SB, Jonas RA, *et al*. Tetralogy of Fallot with diminutive pulmonary arteries: preoperative pulmonary valve dilation and transcatheter rehabilitation of pulmonary arteries. *J Am Coll Cardiol* 1996;**27**:1741–7.

41 Sluysmans T, Neven B, Rubay J, *et al*. Early balloon dilatation of the pulmonary valve in infants with tetralogy of Fallot. Risks and benefits. *Circulation* 1995;**91**:1506–11.

42 Sreeram NA, Saleem M, Jackson M, *et al*. Results of balloon pulmonary valvuloplasty as a palliative procedure in tetralogy of Fallot. *J Am Coll Cardiol* 1991;**18**:159–65.

43 Reddy VM, Liddicoat JR, McElhinney DB, *et al*. Routine primary repair of tetralogy of Fallot in neonates and infants less than three months of age. *Ann Thorac Surg* 1995;**60**:S592–6.

44 Sousa Uva M, Chardigny C, Galetti L, *et al*. Surgery for tetralogy of Fallot at less than six months of age. Is palliation "old-fashioned"? *Eur J Cardiothorac Surg* 1995;**9**:453–9.

45 Hennein HA, Mosca RS, Urcelay G, *et al*. Intermediate results after complete repair of tetralogy of Fallot in neonates. *J Thorac Cardiovasc Surg* 1995;**109**:332–44.

46 Dodge-Khatami A, Tulevski, II, Hitchcock JF, *et al*. Neonatal complete correction of tetralogy of Fallot versus shunting and deferred repair: is the future of the right ventriculo-arterial junction at stake, and what of it? C*ardiol Young* 2001;**11**:484–90.

47 Cullen S, Shore D, Redington A. Characterization of right ventricular diastolic performance after complete repair of tetralogy of Fallot. Restrictive physiology predicts slow postoperative recovery. *Circulation* 1995;**91**:1782–9.

48 Rathore KS, Gupta N, Kapoor A, *et al*. Assessment of right ventricular diastolic function: does it predict post-operative course in tetralogy of Fallot. *Indian Heart J* 2004;**56**:220–4.

49 Sachdev MS, Bhagyavathy A, Varghese R, *et al*. Right ventricular diastolic function after repair of tetralogy of Fallot. *Pediatr Cardiol* 2006;**27**:250–5.

50 Sullivan ID, Wren C, Stark J, *et al*. Surgical unifocalization in pulmonary atresia and ventricular septal defect. A realistic goal? *Circulation* 1988;**78**(Suppl):III5.

51 Puga FJ, Leoni FE, Julsrud PR, Mair DD. Complete repair of pulmonary atresia, ventricular septal defect and severe peripheral arborization abnormalities of the central pulmonary arteries: experience with preliminary unifocalization procedures in 38 patients. *J Thorac Cardiovasc Surg* 1989;**98**:1018–28.

52 Sawatari K, Imai Y, Kurosawa H, *et al*. Staged operation for pulmonary atresia and ventricular septal defect with major aortopulmonary collateral arteries: new technique for complete unifocalization. *J Thorac Cardiovasc Surg* 1989;**98**:738–50.

53 Iyer KS, Mee RBB. Staged repair of pulmonary atresia with ventricular septal defect and major systemic to pulmonary artery collaterals. *Ann Thorac Surg* 1991;**51**:65–72.

54 Marelli AJ, Perloff JK, Child JS, Laks H. Pulmonary atresia with ventricular septal defect in adults. *Circulation* 1994;**89**:243–51.

55 Yagihara T, Yamamoto F, Nichigaki K, *et al*. Unifocalization for pulmonary atresia with ventricular septal defect and major aortopulmonary collateral arteries. *J Thorac Cardiovasc Surg* 1996;**112**:392–402.

56 Reddy VM, Liddicoat JR, Hanley FL. Midline one-stage complete unifocalization and repair of pulmonary atresia with ventricular septal defect and major aortopulmonary collaterals. *J Thorac Cardiovasc Surg* 1995;**109**:832–44.

57 Reddy VM, Petrossian E, McElhinney DB, *et al*. One stage complete unifocalization in infants: when should the ventricular septal defect be closed? *J Thorac Cardiovasc Surg* 1997;**113**:858–68.

58 Tchervenkov CI, Salasidis G, Cecere R, *et al*. One-stage midline unifocalization followed by complete repair for complex heart disease with major aortopulmonary collaterals. *J Thorac Cardiovasc Surg* 1997;**114**:727–37.

59 Shimazaki Y, Blackstone EH, Kirklin JW. The natural history of isolated congenital pulmonary valve incompetence. *Thorac Cardiovasc Surg* 1984;**32**:257–9.

60 Marin-Garcia J, Moller JH. Sudden death after operative repair of tetralogy of Fallot. *Br Heart J* 1977;**39**:1380–5.

61 Webb-Kavey RE, Blackmon MS, Sondheimer HM. Incidence and severity of chronic ventricular dysrhythmia after repair of tetralogy of Fallot. *Am Heart J* 1982;**103**:342–50.

62 Deanfield JE, Ho S-Y, Anderson RH, *et al*. Late sudden death after repair of tetralogy of Fallot: a clinicopathologic study. *Circulation* 1983;**67**:626–31.

63 Garson A Jr, Randall DC, Gillette DE, *et al*. Prevention of sudden death after repair of tetralogy of Fallot: treatment of ventricular arrhythmias. *J Am Coll Cardiol* 1985;**6**:221–7.

64 Zhao HZ, Miller G, Reitz BA, Shumway NE. Surgical repair of tetralogy of Fallot: long term follow-up with particular emphasis on late death and reoperation. *J Thorac Cardiovasc Surg* 1985;**89**:204–20.

65 Jonsson H, Ivert T, Lars-Ake B, Jonasson R. Late sudden deaths after repair of tetralogy of Fallot. *Scand J Thorac Cardiovasc Surg* 1995;**29**:131–9.

66 Dietl CA, Cazzaniga ME, Dubner SJ, *et al*. Life-threatening arrhythmias and RV dysfunction after surgical repair of tetralogy of Fallot. Comparison between transventricular and transatrial approaches. *Circulation* 1994;**90**(5 Pt 2):II7.

67 Khairy P, Aboulhosn J, Gurvitz MZ, *et al*. Arrhythmia burden in adults with surgically repaired tetralogy of Fallot: a multi-institutional study. *Circulation* 2010;**122**:868–75.

68 Gatzoulis MA, Till JA, Somerville J, Redington AN. Mechanoelectrical interaction in tetralogy of Fallot. *Circulation* 1995;**92**:231–7.

69 Morris CD, Reller MD, Menashe VD. Thirty-year incidence of infective endocarditis after surgery for congenital heart defect. *JAMA* 1998;**279**:599–603.

70 Wessel HV, Cunningham WJ, Paul MH, *et al*. Exercise performance in tetralogy of Fallot after intracardiac repair. *J Thorac Cardiovasc Surg* 1980;**80**:582–93.

71 Marx GR, Hicks RW, Allen HD, Goldberg SJ. Noninvasive assessment of hemodynamic responses to exercise in pulmonary regurgitation after operations to correct pulmonary outflow obstruction. *Am J Cardiol* 1988;**61**:595–601.

72 Rowe SA, Zahka KG, Manolio TA, *et al*. Lung function and pulmonary regurgitation limit exercise capacity in postoperative tetralogy of Fallot. *J Am Coll Cardiol* 1991;**17**:461–6.

73 Carvalho JS, Shinebourne EA, Buest C, *et al*. Exercise capacity after complete repair of tetralogy of Fallot: deleterious effects of residual pulmonary regurgitation. *Br Heart J* 1992;**67**:470–3.

74 Graham TP Jr, Cordell D, Atwood GF, *et al*. Right ventricular volume characteristics before and after palliative and reparative operation for tetralogy of Fallot. *Circulation* 1976;**54**:417–23.

75 Bove EL, Byrum CJ, Thomas FD, *et al*. The influence of pulmonary insufficiency in ventricular function following repair of tetralogy of Fallot. *Cardiovasc Surg* 1983;**85**:691.

76 Bove EL, Kavey RW, Byrum CJ, *et al*. Improved right ventricular function following late pulmonary valve replacement for residual pulmonary insufficiency or stenosis. *J Thorac Cardiovasc Surg* 1984;**90**:50–5.

77 Ilbawi MN, Idriss FS, DeLeon SG, *et al*. Long-term results of porcine valve insertion for pulmonary regurgitation following repair of tetralogy of Fallot. *Ann Thorac Surg* 1086;**41**:478–82.

78 Finck SJ, Puga FJ, Danielson EK. Pulmonary valve insertion during reoperation for tetralogy of Fallot. *Ann Thorac Surg* 1988;**45**:610–3.

79 Vetter HO, Reichart B, Seidel P, *et al*. Noninvasive assessment of right and left ventricular volumes 11 to 24 years after corrective surgery on patients with tetralogy of Fallot. *Eur J Cardiothorac Surg* 1990;**4**:24–8.

80 Perrault H, Drblik SP, Montigny M, *et al*. Comparison of cardiovascular adjustments to exercise in adolescents 8 to 15 years after correction of tetralogy of Fallot, ventricular septal defect, or atrial septal defect. *Am J Cardiol* 1989;**64**:213–7.

81 Therrien J, Provost Y, Merchant N, *et al*. Optimal timing for pulmonary valve replacement in adults after tetralogy of Fallot repair. *Am J Cardiol* 2005;**95**:779–82.

82 Oosterhof T, van Straten A, Vliegen HW, *et al*. Preoperative thresholds for pulmonary valve replacement in patients with corrected tetralogy of Fallot using cardiovascular magnetic resonance. *Circulation* 2007;**116**:545–51.

83 Andersen HR, Knudsen LL, Hasenkam JM. Transluminal implantation of artificial heart valves. Description of a new expandable aortic valve and initial results with implantation by catheter technique in closed chest pigs. *Eur Heart J* 1992;**13**:704–8.

84 Bonhoeffer P, Boudjemline Y, Saliba Z, *et al*. Percutaneous replacement of pulmonary valve in a right-ventricle to pulmonary-artery prosthetic conduit with valve dysfunction. *Lancet* 2000;**356**:1403–5.

85 Lurz P, Coats L, Khambadkone S, *et al*. Percutaneous pulmonary valve implantation: impact of evolving technology and learning curve on clinical outcome. *Circulation* 2008;**117**:1964–72.

86 Graham TP Jr, Bricker JT, James FW, Strong WB. 26th Bethesda Conference: recommendations for determining eligibility for competition in athletes with cardiovascular abnormalities. Task Force 1: Congenital Heart Disease. *J Am Coll Cardiol* 1994;**24**:867–73.

87 Murphy JG, Gersh BJ, Mair DD, *et al*. Long-term outcome in patients undergoing surgical repair of tetralogy of Fallot. *N Engl J Med* 1993;**329**:593–9.

88 Nollert G, Fischlein T, Bouterwek S, *et al*. Long-term survival in patients with repair of tetralogy of Fallot: 36-year follow-up of 490 survivors of the first year after surgical repair. *J Am Coll Cardiol* 1997;**30**:1374–83.

89 Jonsson H, Ivert T. Survival and clinical results up to 26 years after repair of tetralogy of Fallot. *Scand J Thorac Cardiovasc Surg* 1995;**29**:43–51.

90 Park I-S, Leachman RD, Cooley DA. Total correction of tetralogy of Fallot in adults: surgical results and long-term follow-up. *Tex Heart Inst J* 1987;**14**:160–9.

42 Complete Transposition of the Great Arteries

Daniel Sidi, Pascal Vouhé & Phalla Ou

Hôpital Necker – Enfants Malades, Université Paris V, Paris, France

Complete transposition of the great arteries (TGA) is a common and life-threatening cardiac malformation characterized by isolated ventriculo-arterial discordance. Neonatal survival depends on shunts between the two parallel circulations, mainly through the foramen ovale. Ductus arteriosus patency [natural or by prostaglandin E_1 (PGE_1) infusion] can also influence clinical tolerance but to a lesser extent and not always favorably.

About two-thirds of the neonates have no other cardiac abnormalities apart from a patent foramen ovale and a small patent ductus arteriosus. The remainder may have a ventricular septal defect, a large atrial septal defect, a large patent ductus arteriosus, or significant subpulmonic stenosis. The first group and those with only a small ventricular septal defect are often termed simple TGA. The rest are included in the group of complex TGA, which also includes those with pulmonic or tricuspid atresia and various types of double-outlet ventricles (see Chapter 44). Other terms that are used include dextro-TGA (d-TGA), aortopulmonary transposition, and transposition of the great vessels.

Key points

- Every cyanotic neonate without respiratory distress should be considered as possibly having TGA until two-dimensional echocardiography has shown a normal relationship between the great vessels and the ventricles.
- TGA is usually fatal soon after birth, and neonates can be saved by an early balloon atrioseptostomy (the Rashkind procedure).
- Prenatal diagnosis is possible. Deterioration soon after birth can be predicted from the size of the foramen ovale *in utero*, and delivery should be organized at a center where an early

Rashkind procedure can be performed with two-dimensional echocardiographic guidance in the delivery room.
- Atrial repair leaving the ventriculo-arterial discordance but adding atrioventricular discordance (the Mustard or Senning procedure) gives good immediate and midterm results but leads to frequent rhythm disturbances, and right ventricular failure may occur in the long term.
- Anatomic repair (arterial switch) gives excellent long-term results with a low perioperative mortality, but it can be performed only in a neonate while the left ventricle is still able to develop systemic pressures. Long-term follow-up is necessary to be sure that the fate of the great arteries and coronary arteries will allow a normal life.

Embryology and epidemiology

This lesion represents ~5% of congenital heart disease, occurring in ~1/3000 liveborn infants. TGA, especially simple TGA, has a marked male preponderance [1,2]. Extracardiac malformations or chromosome anomalies are uncommon [1,2]; in particular, there is no association with microdeletion of chromosome 22. The etiology is unknown, and the low recurrence rate in siblings and the low transmission rate to offspring [1,2] suggest that genetic effects play little role. Overt maternal diabetes has been associated with TGA [1,3].

The embryology is discussed in Chapter 1.

Pathologic anatomy

In TGA, the aorta rises from the right ventricle above an infundibulum, so that there has not been resorption of the subaortic conus. The pulmonary artery rises from the left

Figure 42.1 Pathology to show discordant ventriculo-arterial connections.

ventricle and is usually in continuity with the mitral valve, indicating complete resorption of the subpulmonic conus (Figure 42.1) (see Chapters 1 and 20). This means that TGA has a discordant ventriculo-arterial connection. The pulmonary artery rather than the aorta is situated in the center of the heart in continuity with both atrioventricular valves (see Chapter 44). The aorta is usually positioned anteriorly and to the right of the pulmonary artery (d-TGA), but can be in front of or beside the pulmonary artery; rarely, it can to the left of or posterior to the pulmonary artery, even though it is connected to the right ventricle.

The atria are normal, and there is almost always a patent foramen ovale, seldom a true secundum atrial septal defect. The ventricles are also normal, but the wedging of the pulmonary artery into the center of the heart produces a small central fibrous body and atrioventricular and membranous interventricular septa that are smaller than normal [4,5]. The ventricular septum, if intact, is relatively straight rather than sigmoid, so that the right and left ventricular outflow tracts are parallel. After 2 months of age, there is often functional subpulmonic obstruction from the ventricular septum bulging into the left ventricular outflow tract where it is apposed to the septal leaflet of the mitral valve [4–10]. A ridge of endocardial thickening may be found where the mitral valve edge contacts the septum. The obstruction usually disappears after an arterial switch repair but persists after an atrial baffle repair.

There may be minor anomalies of the mitral and tricuspid valves, but these are clinically important in <5% of patients with simple TGA [4,5,11].

The conduction system is normal except that the left bundle originates more distally than usual from the bundle of His and as a single cord rather than as a sheaf of fibers [12].

The coronary arterial anatomy is of great importance. The posterior commissure of the aortic valve is usually aligned with the anterior commissure of the pulmonary valve, and the coronary arteries arise from the posterior sinuses (never from the anterior sinus). The origin and distribution of the coronary arteries are important for a surgeon performing an arterial switch, because they have to be moved to the new aortic root. The right coronary artery is nearly always dominant. The left circumflex artery comes frequently (25%) from the right coronary artery (Figure 42.2). The two coronary ostia usually rise laterally from the two posterior sinuses, but they can rise in between the vessels from a single ostium or from two ostia near the posterior commissure; the latter pattern is often associated with an intramural left coronary artery (usually the left anterior descending). Multiple classifications have been used to describe the coronary arterial origin and distribution [11,13–15], the first and still most commonly used being the Yacoub classification [13] shown in Figure 42.2. The sinus node artery usually originates from the proximal right coronary artery and courses upward and to the right, being partly embedded in the upper part of the limbus of the atrial septum [11].

Although there is no structural abnormality of the cardiac chambers in complete TGA, the function and the mass of the right and left ventricles are normal only in the fetal and neonatal periods when both ventricles have similar afterloads. After birth, the right ventricle facing a systemic afterload grows more than the left ventricle because the latter supports the low pressure of the pulmonary circulation. Thus, after a few weeks, the left ventricle becomes unable to sustain a systemic pressure unless it is prepared for it by an artificial increased afterload (pulmonary arterial banding) that leads to preoperative hypertrophy.

In some patients, for unknown reasons, pulmonary vascular disease occurs. This complication is rare at <3 months of age [16–19], but it may develop in 25% of patients aged <1 year and in 15–67% of patients >12 months of age [11,16–19]. These pulmonary vascular changes are mild and do not cause profound pulmonary hypertension, but rarely (~1%) they may do so [17]. When pulmonary hypertension is significant, it does not react to oxygen or nitric oxide, and the small arteries histologically resemble classic pulmonary vascular disease, although sometimes numerous microthrombi are seen.
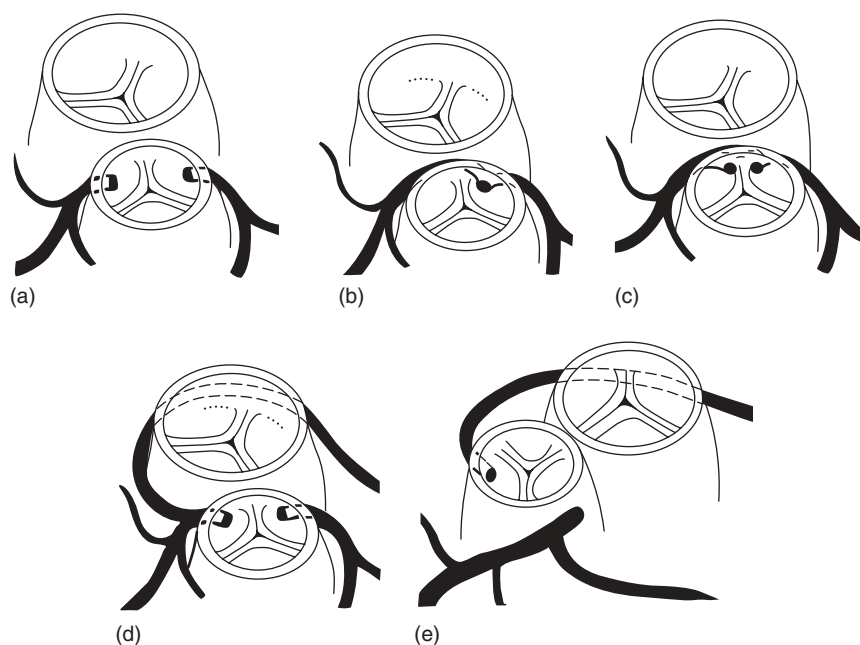
Figure 42.2 Yacoub classification of coronary arteries. (Reproduced with permission from Yacoub and Radley-Smith *Thorax* 1978;**33**:418–24.)

Hemodynamics and pathophysiology

The fetus

The fetus with TGA appears to have no disability. Because the pattern of streaming of the venous return is normal in these fetuses, the left ventricle receives much of its blood from the umbilical circulation (see Chapter 3), as in normal subjects, but then this blood, with an oxygen tension of about 24 mmHg, is distributed to the lungs and through the ductus arteriosus to the lower body (Figure 42.3). The heart and brain, on the other hand, receive blood with an oxygen tension of about 18 mmHg. There might possibly be greater flows through the lungs (less hypoxemia to cause vasoconstriction) and the heart and brain (autoregulation because of more hypoxemia). Whether these changes cause differences in vascular development of the organs is unknown.

Normal development of the cardiac chambers is expected in a fetus with TGA, because atrial and ductus communications equalize preload and afterload of the ventricles. The respective volumes and outputs of the two ventricles should be the same in a fetus with TGA as in a normal fetus with right ventricular output greater than left ventricular output. On the other hand, the sizes of the great arteries and of the foramen ovale that depend on the flow through them during fetal life are likely to be different (see Figure 42.3). Fetuses with TGA are likely to have a larger ascending and transverse aorta and a larger aortic isthmus because

of the higher right ventricular output, and the ductus arteriosus and the foramen ovale should be smaller because the higher pulmonary blood flow (due to a higher than normal PaO_2 in the pulmonary artery) decreases the amount of blood that passes through these structures during fetal life (see Figure 42.3). These factors may explain the rarity of coarctation of the aorta in simple TGA, and may also explain the devastating postnatal course due to inadequate shunting of blood between the two circulations in the absence of treatment.

There are increased number and size of pancreatic islet cells and an increased weight of the adrenal cortex; both of these findings resemble those found in infants of diabetic mothers.

The neonate

Without communications between systemic and pulmonary circulations, a neonate with TGA cannot survive more than a few minutes after the neonatal "placental–pulmonary switch." Because the two circulations are in parallel, blood oxygenated in the lungs returns exclusively to the lungs, whereas the desaturated systemic blood returns through the aorta to the systemic tissues. Survival is possible only through one or more communications that allow some oxygenated blood to cross from the left side of the heart or the pulmonary artery to the right side of the heart or the aorta and desaturated blood to cross back from the right side of the heart to the left side (Figure 42.4). Of necessity, the same
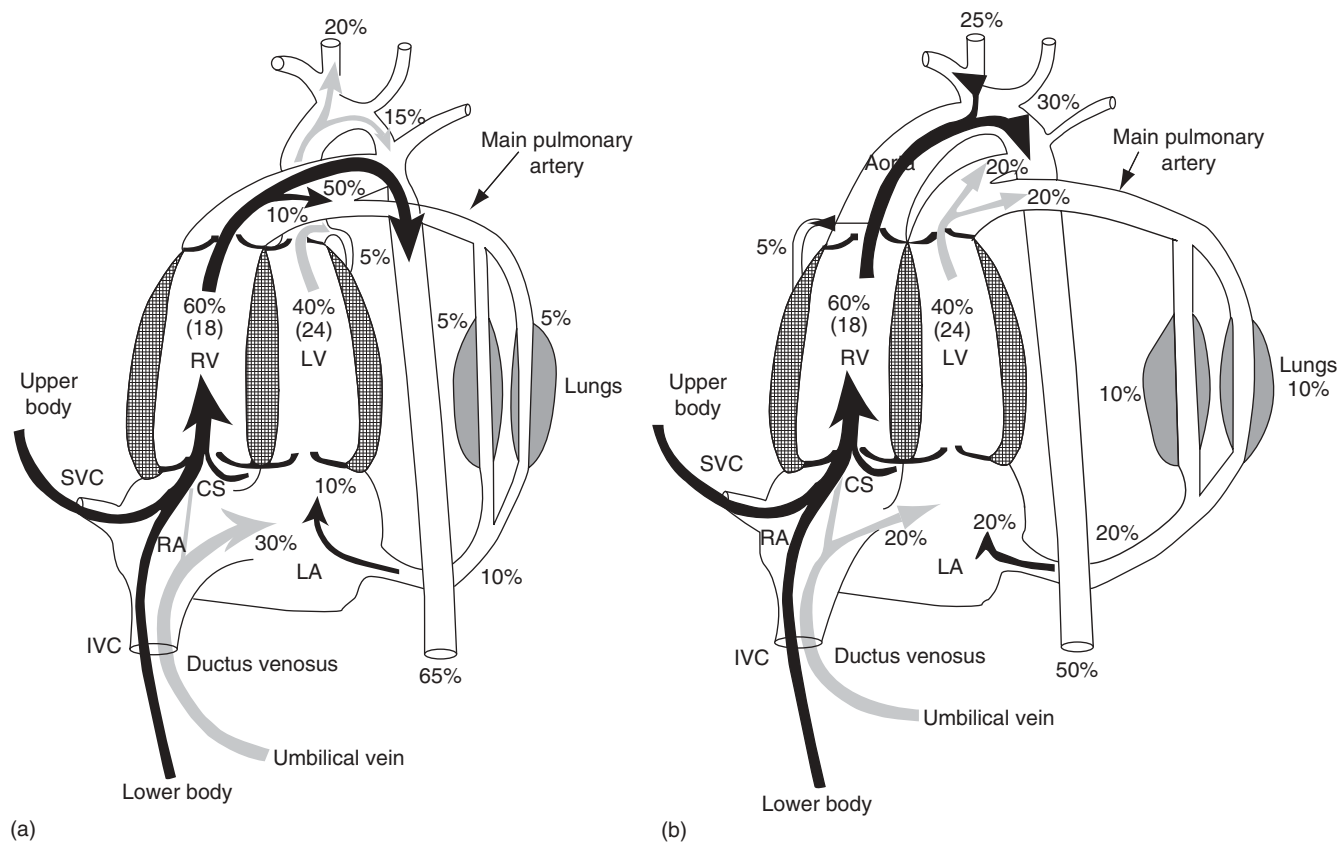
Figure 42.3 Fetal circulation in a normal subject (a) and one with TGA (b). The percentages shown are proportions of the combined ventricular output coming from each ventricle and being distributed to various regions of the body. The figures in parentheses in the ventricles are the oxygen tensions (mmHg). In (a), the desaturated blood returning from the lungs and body is shown by dark arrows. The better oxygenated blood returning from the umbilical vein is shown by the pale arrow, and it is distributed to the head, coronary arteries, and aortic isthmus, which is the narrowest part of the aortic arch. The lungs and descending aorta receive blood of intermediate saturation. In (b), note that in TGA, the aorta, main pulmonary artery, and aortic isthmus are wider than in the normal subject and that the foramen ovale and the ductus arteriosus are smaller. The distribution of well and poorly saturated blood differs from the normal. CS, coronary sinus; IVC, inferior vena cava; LA, left atrium; LV, left ventricle; RA, right atrium; RV, right ventricle; SVC, superior vena cava. (Courtesy of Dr David F. Teitel.)

amount of blood must cross in each direction; otherwise, one circulation would empty into the other. It is only this shunted blood that allows some oxygen uptake in the lungs and some oxygen transport to the tissues.

Initially, there may be bidirectional shunts through the ductus arteriosus and across the atrial septum. At birth, the ductus arteriosus is open, and aortic and pulmonary arterial pressures are similar. During systole, left ventricular ejection imparts enough kinetic energy to the blood that some oxygenated blood passes through the ductus arteriosus into the descending aorta. In diastole, aortic blood may enter the pulmonary artery with its lower vascular resistance. Then, with the rise in systemic vascular resistance that follows removal of the placenta and a decrease in pulmonary vascular resistance, pulmonary to aortic shunting ceases. The flap (Vieussens valve) of the foramen ovale (that is intended to close the atrial septum when the pressures become higher in the left compared

with the right atrium) usually crosses a foramen ovale distended by the increased pulmonary blood flow and allows a left-to-right atrial shunt; in addition, the rise in right atrial pressure due to the increased systemic vascular resistance helps to keep the valve of the foramen ovale open. In early ventricular diastole, blood shunts from right to left atrium because of the lower resistance to filling of the left ventricle [20]. In ventricular systole, blood shunts from left to right atrium because the left atrium has higher pressures and is less distensible. Respiration also influences atrial shunting because inspiration increases the caval venous return to the right atrium. These atrial shunts explain why most neonates with TGA do well at birth with an adequate flow through the ductus arteriosus from aorta to pulmonary artery (shunt of desaturated blood destined for the lungs) associated with a quantitatively equivalent left-to-right atrial flow of oxygenated blood destined for the body.
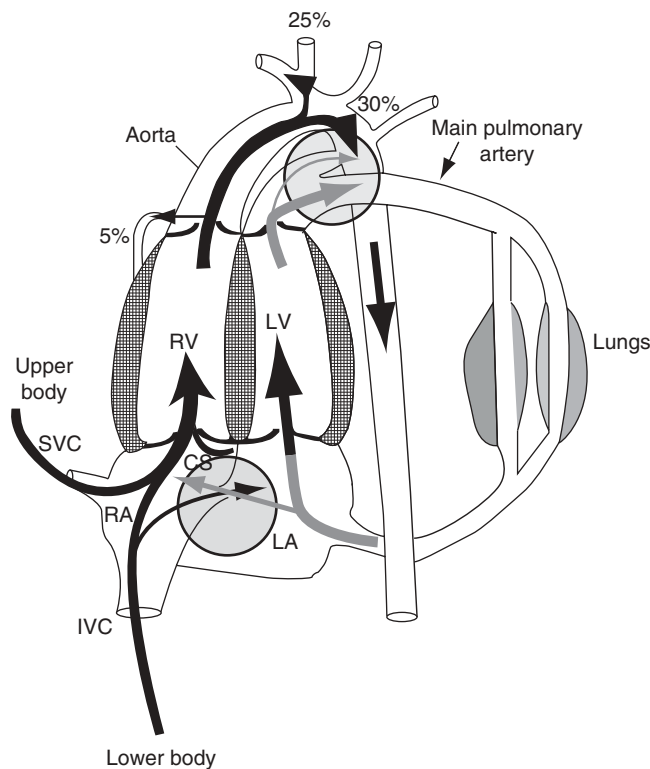
Figure 42.4 Diagram to show where shunts essential for survival (gray circles) after birth take place in simple TGA. It is possible for bidirectional shunting to occur through the ductus arteriosus, but the amounts are small. The least saturated blood is indicated by the darkest arrows, the best saturated blood by the lightest arrows. Intermediate saturations are suggested by intermediate shades of gray. CS, coronary sinus; IVC, inferior vena cava; LA, left atrium; LV, left ventricle; RA, right atrium; RV, right ventricle; SVC, superior vena cava.

The ductus arteriosus, smaller than normal in TGA, becomes progressively smaller soon after birth. When this happens, the neonate's survival depends on bidirectional shunting at the atrial level. If, however, the foramen ovale is too small or the flap is too large and closes the foramen ovale instead of crossing it, the atrial communication is absent or restrictive. These changes are poorly tolerated because the shunt is inadequate (severe hypoxemia); any shunting that occurs is possible only with a high left atrial pressure (due to increased pulmonary flow) and a resulting high capillary pressure that can cause pulmonary edema.

After the neonatal period, with adequate atrial shunting through a natural or post-Rashkind atrial communication, the hemodynamic status usually improves. There is an increased pulmonary blood flow ($Qp/Qs \approx 2$) and adequate shunting (about half of systemic flow) so that aortic saturation is ~70%, the pulmonary arterial saturation is ~85%, and mixed venous caval blood saturation is ~40%. With a normal decrease in pulmonary vascular resistance, pulmonary arterial pressure is low, and the pathophysiologic process resembles a simple atrial septal defect but with obligatory

cyanosis from blood going directly from the caval veins to the aorta. The major consequence of this fall in pulmonary arterial pressure is that the left ventricle in a neonate or infant behaves like a right ventricle in a normal circulation with an atrial septal defect. The left ventricle increases in size but loses wall thickness and perhaps forever the ability to develop a normal systemic pressure, and probably loses adequate coronary vascular bed growth.

Collateral circulation from the aorta to the pulmonary artery by bronchial arteries and from pulmonary veins to azygos vein can also play a role in the physiologic circulation in TGA. It can ensure some shunting in patients with closed foramen ovale, but the amount is insufficient to compensate for inadequate shunting at atrial and ductus levels. The collateral circulation complicates the evaluation of pulmonary blood flow and vascular resistance by the Fick method during catheterization because it alters the oxygen saturation proximally in the caval veins and distally in the pulmonary artery.

About half of the children with TGA have a greater than normal distribution of blood flow to the right lung, as shown by chest radiography, angiography, or radionuclide lung scans [21]. This effect is thought to be due to the abnormal rightward inclination of the main pulmonary artery towards the right pulmonary artery. This diversion probably does not have major physiologic effects, but it may explain associated hypoplasia of the left pulmonary arterial vessels and the occasional report of unilateral (always left-sided) pulmonary vein hypoplasia or stenosis [22,23].

Natural history

The natural history of untreated simple TGA is bleak; <5% survive more than 2 months [2,11,24]. Some with a large atrial septal defect may survive longer, but only 5–10% of them reach their first birthday. Death is usually from hypoxemia and acidosis, sometimes complicated by pulmonary edema.

Physical examination

These neonates are usually of normal birth weight, although reports of underweight and overweight exist, especially in the complex group [1]. They are initially well but may look dusky rather than overtly cyanotic. At this stage, pulses and breathing patterns are normal, as is activity. The heart is not enlarged and has the expected normal neonatal right ventricular lift. The first heart sound is normal. The second sound is usually single and heard with greatest intensity at the upper left sternal border because of the high position of the anterior aortic valve above the conus. A soft pulmonic closing sound is occasionally heard. No other sounds or clicks

are present. There may be no murmurs or only the soft murmur of a ductus arteriosus or a short midsystolic murmur along the midsternal border.

As hours or days pass, the ductus closes and shunting at ductus and atrial levels becomes inadequate. The neonate becomes deeply cyanotic, and this is usually equal in fingers and toes. Respiration becomes deep but without retractions, and there is usually no tachypnea unless there is acidosis. With the onset of severe acidosis, the baby's activity becomes reduced.

In older children who have not undergone surgical correction, there may be a soft ejection murmur along the upper left sternal border to indicate mild subpulmonic stenosis.

Electrocardiography

This shows merely the expected right ventricular dominance of the newborn term infant. After the first week, however, persistent upright T waves in the right precordial leads suggest abnormal right ventricular hypertrophy, as do decreased r waves in the left precordial leads. Should left forces be prominent (tall R waves in leads V_5 and V_6), some cause for a high left ventricular systolic pressure, such as pulmonary vascular disease or severe subpulmonic stenosis, should be sought.

Chest radiography

The pulmonary vascular markings are increased because pulmonary blood flow is usually increased. The heart is slightly enlarged, and the characteristic oval shape is due to absence of the pulmonary artery segment. As a rule, the thymus, although present, is notably small, so that the narrow mediastinal shadow gives an "egg on its side" or "apple on a string" appearance that is almost pathognomonic. The aortic arch is almost invariably left sided. The chest film may lack these diagnostic features immediately after birth. It is important not to exclude the diagnosis of TGA because of a nonspecific X-ray picture.

Echocardiography

In the fetus

TGA is well tolerated by the fetus, and the diagnosis can be made on two-dimensional echocardiography if the screening is not limited to the four-chamber view (that is normal in TGA) but includes the great vessels (see Chapter 8). It is crucial to check the size of the foramen ovale and the anatomy of the atrial flap to predict early closure of the atrial septum at birth and the need for an early Rashkind procedure.
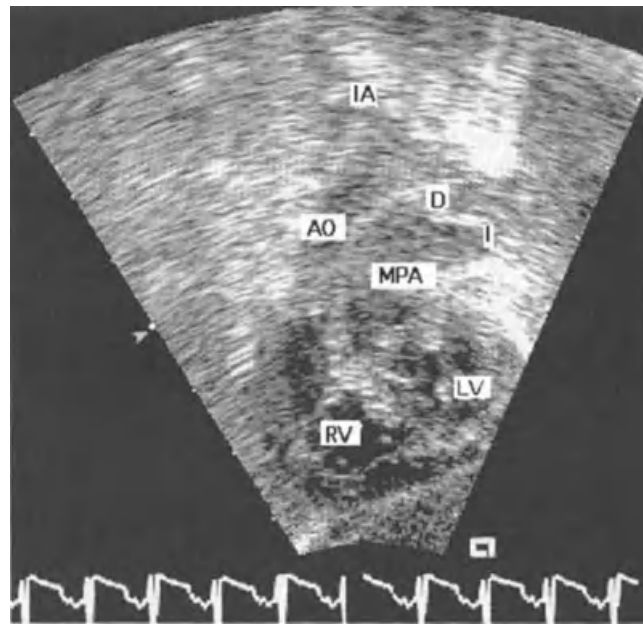
Figure 42.5 Echocardiogram, subcostal view, from a neonate with simple TGA. The left ventricle (LV) gives rise to the pulmonary artery (MPA), which divides into the left pulmonary artery (L) and ductus arteriosus (D). The right ventricle (RV) gives rise to the aorta (AO) from which the innominate artery (IA) originates. (Courtesy of Dr Norman H. Silverman.)

In the neonate

Two-dimensional echocardiography with Doppler interrogation is the major diagnostic method. It confirms the diagnosis by demonstrating a normal heart architecture but with two great vessels arising in parallel from the ventricles instead of crossing early after their origins (Figure 42.5). The anterior vessel that arises from the right ventricle above an infundibulum is the aorta because it is directed anteriorly and gives off the neck vessels, and the posterior vessel arising from the left ventricle in continuity with the mitral valve is a pulmonary artery because it is directed posteriorly and bifurcates or trifurcates into two branches and the ductus arteriosus. The two outflow tracts are parallel. On a transverse view, the aorta is usually anterior and to the right of the pulmonary artery, and there is usually good alignment between the commissures of the aorta and pulmonary artery with coronary arteries arising always from the posterior sinuses of the anterior vessel (Figure 42.6).

It is especially important to visualize the atrial septum (subxiphoid view) and the ductus view, as these are the sites of shunting in TGA. Although the need for the Rashkind procedure is primarily determined clinically, it should be performed early when the foramen ovale is obstructed by the flap as shown by a high Doppler velocity (>1 m s^{-1}) (unless arterial switch can be performed immediately). Conversely,

(a)   (b)
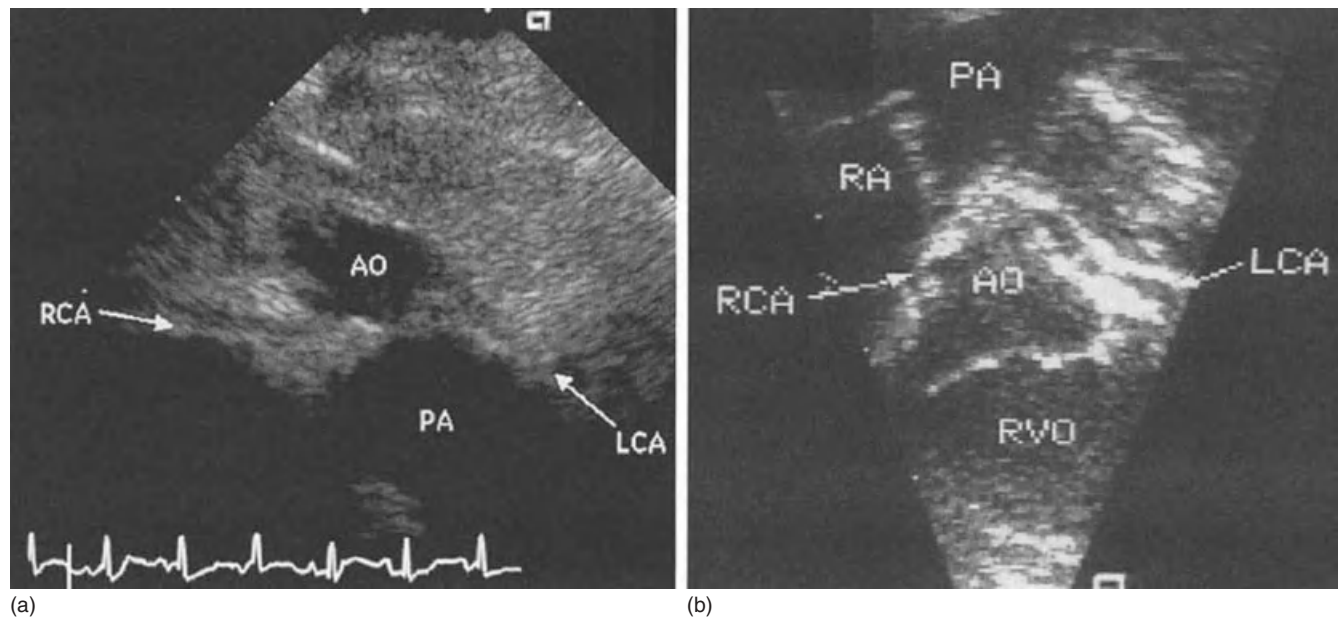
Figure 42.6 Echocardiograms showing the origin of the coronary arteries in TGA. (a) The left coronary (LCA) and right coronary (RCA) arteries arise from the facing aortic (AO) sinuses. PA, pulmonary artery. (b) Long intramural course of the LCA. RA, right atrium; RVO, right ventricular outflow tract. (Courtesy of Dr Norman H. Silverman.)

if the atrial communication is large and the patient is not doing well, echocardiography helps to find a reason for the symptoms (e.g., high pulmonary vascular resistance, or associated cardiovascular anomalies such as coarctation of the aorta or subpulmonic stenosis), and eventually indicate early surgery to obtain better oxygenation of the neonate and deal with high pulmonary vascular resistances.

It is particularly helpful to look at the atrial shunting. With an exclusive left-to-right atrial shunt, there must be another communication at the ventricular or the arterial level; if it is not at the ductal level, it must be elsewhere (ventricular septal defect or collateral circulation). If there is a bidirectional atrial level shunting, then no other significant communication is present and the ductus arteriosus is closed. If the ductus is widely patent and bidirectional atrial shunting is present, then the pulmonary vascular resistance is high.

Echocardiography helps to assess the hemodynamics by assessing the velocity of flow across the ductus arteriosus and foramen ovale and analyzing septal geometry. (Left ventricular deformation is related to the pressure difference between the ventricles.)

Finally, the coronary artery ostial origins and course should be examined. It is important to note an unfavorable distribution, for example, if one coronary artery passes between the great vessels and especially if it is intramural. However, because coronary artery transfer is always possible by a highly trained cardiac surgeon, it does not seem legitimate to use invasive techniques and deliver irradiation to the neonate to define precisely coronary anatomy.

Cardiac catheterization

Cardiac catheterization is useful only when a Rashkind procedure is indicated. Rarely is it used to look for associated abnormalities such as a trabecular ventricular septal defect, collateral circulation, abnormal coronary arteries, or a small aortic isthmus if a coarctation is suspected (this can also be looked at by MRI or CT scan).

The technique of cardiac catheterization is standard, except that special maneuvers are needed to enter the pulmonary artery from the left ventricle [24,25].

Calculating flows by the Fick method is inexact because it is difficult to have mixed pulmonary arterial saturation samples if the ductus is open and when there is bronchial circulation (common). Pulmonary arterial samples are taken proximal to the entry of the bronchial collaterals that contain desaturated blood, so that a true mixed pulmonary arterial blood sample cannot be obtained. If bronchial collateral blood flow is only 10% of total pulmonary blood flow, there could be a 40% overestimate of pulmonary blood flow [17]. Another complication is that the arteriovenous difference of oxygen saturation across the pulmonary vascular bed is usually small, so that a tiny measurement error is translated into a large error in estimating pulmonary blood flow. Comparison of pulmonary blood flows measured by angiographic and Fick techniques suggests that pulmonary flows as calculated by the Fick method are about twice the true flows [26]. This means that pulmonary blood flow is usually

overestimated, and pulmonary vascular resistance is underestimated. Nevertheless, in simple TGA, pulmonary blood flow is usually almost twice that in normal children, even without a large shunt.

Differential diagnosis

In a cyanotic neonate without respiratory distress, TGA must be the diagnosis until two-dimensional echocardiographic–Doppler examination shows a normal position of the great arteries. The differential diagnosis therefore concerns the distinction between simple and complex TGA in which a ventricular septal defect, an abnormality of the great vessels (pulmonary artery stenosis, coarctation of the aorta), an anomaly of the atrioventricular or semilunar valves, or an abnormality of size or function of the ventricles is present.

Three major diagnostic difficulties exist:

1 A muscular ventricular septal defect, especially at the apex, may be difficult to see on echocardiography. Such a ventricular septal defect should be sought when there is left ventricular hypertension unexplained by a widely patent ductus arteriosus or an exclusive left-to-right atrial shunt with a closed ductus arteriosus (see earlier).

2 An associated coarctation of the aorta when the ductus is open, especially if the right ventricle is smaller than the left ventricle and the pulmonary artery is much larger than the aorta. In this circumstance, it may be useful to stop PGE_1, so that the ductus arteriosus closes, and then evaluate the femoral pulses and the aortic isthmus. Catheterization may be needed to decide whether a coarctation repair should be done with an arterial switch.

3 Anatomic subpulmonic stenosis when an abnormal pulmonary arterial gradient cannot be explained by bulging of the ventricular septum. Particular attention should be paid to the mitral valve insertions on the septum or an abnormal pulmonary artery valve (bicuspid and/or dysplastic pulmonary valve).

Clinical course

Without an adequate atrial communication, death occurs early with metabolic acidosis. With an adequate atrial communication (natural or after a Rashkind procedure), the infant with TGA survives for years with only mild or moderate cyanosis. These patients are exposed to the complications of hypoxemia and polycythemia, mainly brain abscess or infarction (see Chapter 52) and progressive right ventricular failure. Some survive into adulthood, but most have problems by the age of 5 years (an age chosen in the 1960s and early 1970s for the Mustard operation). Progressive subpulmonic stenosis due to the bulge of the septum (displaced by the systemic right ventricle) under

Rashkind procedure
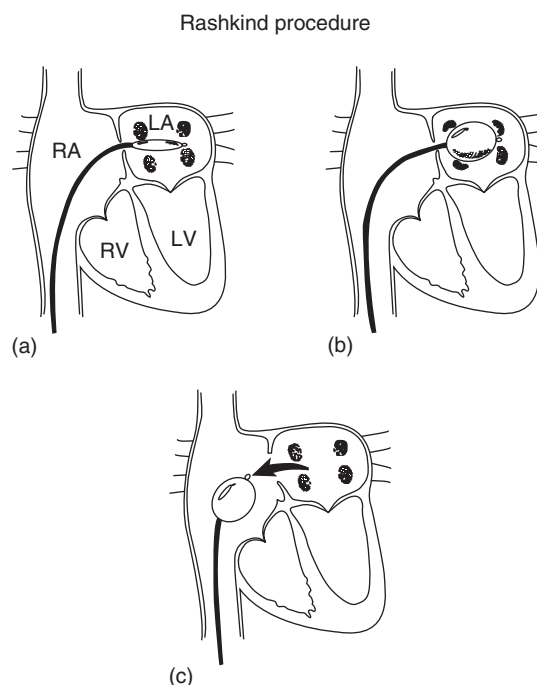
Figure 42.7 Diagram of Rashkind balloon atrial septostomy. (a) The catheter with the balloon deflated is passed from the right atrium (RA) through the foramen ovale into the left atrium (LA). (b) The balloon is inflated. (c) The inflated balloon is jerked back into the right atrium, tearing the atrial septum. RV, right ventricle; LV, left ventricle.

the pulmonary valve causes a systolic ejection murmur and left ventricular hypertrophy [6–10].

Medical management

Medical therapy at birth is based on balloon atrial septostomy (the Rashkind procedure) and maintaining or vasodilating the ductus arteriosus by PGE_1 infusion. These therapies have greatly improved the outcome of neonatal TGA.

When TGA is diagnosed prenatally, delivery should be carried out at a center where a Rashkind procedure can be performed safely and quickly (Figure 42.7; see Chapter 10 for details of the procedure). This can be done under two-dimensional echocardiographic guidance via the umbilical vein (through the ductus venosus) even in the delivery room.

If prenatal diagnosis was not made and severe hypoxemia occurs in the delivery room, PGE_1 should be infused and an emergency transfer organized to the nearest pediatric cardiology center that is able to perform the Rashkind procedure. Meanwhile, it may be useful to put an umbilical catheter into the heart in an attempt to push the flap and allow some atrial mixing before the Rashkind procedure or an emergency arterial switch.

PGE_1 infusion may be useful in the hypoxic neonate before the Rashkind procedure to allow some mixing and avoid

(sometimes, but not always) metabolic acidosis and death. It can also be useful after the Rashkind procedure to improve mixing (decrease hypoxemia) and increase pulmonary arterial and left ventricular pressure in preparation for an anatomic repair.

PGE_1 infusion has its drawbacks, however, because it can lead to apnea (with the need for artificial ventilation) and to pulmonary edema by the increase in pulmonary blood flow and pressure (especially if the foramen ovale is restrictive before or after a Rashkind procedure). This is why PGE_1 infusion should not be used routinely but reserved for neonates who do not tolerate hypoxemia. Rashkind procedure has also its drawbacks, even if it is done carefully with good equipment. A clot or air in the catheter may pass to the brain [27], and if the balloon is not kept in the left atrium it may damage the mitral valve. In addition, if the foramen ovale is small, the Rashkind procedure is only mildly efficient but can leave profound cyanosis. This is why, in a setting where surgery can be performed quickly, the Rashkind procedure is limited to real emergencies or when surgery has to be postponed for several days (infection, enterocolitis, or other).

Neonates with TGA are also at risk for hypoglycemia (they have pancreatic hyperplasia and increased insulin secretion) and necrotizing enterocolitis (the gut is perfused with a higher PaO_2 *in utero* than after birth). Therefore, these patients benefit from parenteral alimentation with high glucose concentrations for the first day of life and for 24h after a Rashkind procedure.

Surgical management

Surgery is the only solution for these patients. Their natural history is catastrophic in the short term unless the atrial septal defect is large, and even then they are exposed to serious neurologic and myocardial complications in the long term because of the chronic cyanosis.

There are two surgical options for treating TGA. The first is the anatomic option of correcting the ventriculo-arterial discordance by an arterial switch of the great vessels above the sinuses of Valsalva (Figure 42.8). Both arterial roots and semilunar valves have similar sizes, shapes, and histologic features, at least at birth. The coronary arteries that arise from the aortic sinuses of Valsalva need to be moved to the new aortic root to perfuse the myocardium at high pressure with fully oxygenated blood. Second is the "physiologic" option or atrial repair consisting of creating atrioventricular discordance (by intra-atrial rerouting) to correct the physiologic consequences of the ventriculo-arterial discordance (Figure 42.9).

In most pediatric cardiologic centers, anatomic repair is the choice in neonates. It restores the left ventricle to its normal systemic function and avoids extensive atrial surgery that is often responsible for subsequent rhythm disturbances.
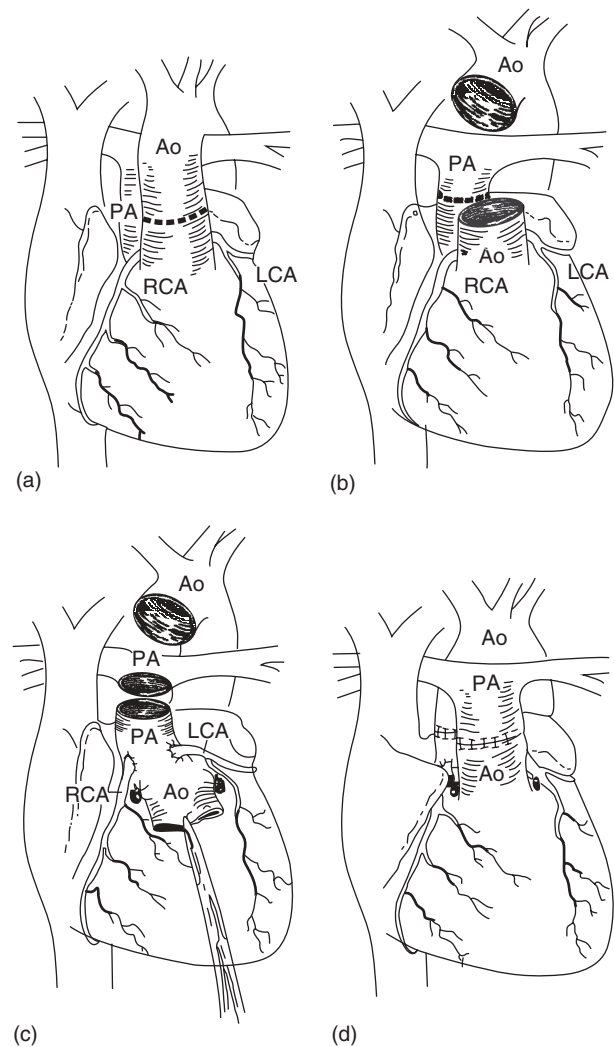
Figure 42.8 Diagram of arterial switch operation. (a) The anterior aorta is shown giving off the coronary arteries. The dashed line shows where the ascending aorta is transected. (b) The posterior pulmonary artery. The dashed line shows where the main pulmonary artery is transected. (c) The coronary arteries have been removed from the aorta and implanted into the old pulmonary root, now the neoaortic root. The holes left in the aorta are patched. (d) The distal pulmonary arteries are brought anteriorly after cutting the ligamentum arteriosum or the ductus arteriosus (Lecompte maneuver) and anastomosed to the old aortic root, now the neopulmonary arterial root. The pulmonary artery now receives blood from the right ventricle. The distal aorta has been anastomosed to the neoaortic root behind the pulmonary artery, and it receives blood from the left ventricle. Ao, aorta; LCA, left coronary artery; PA, pulmonary artery; RCA, right coronary artery.

The arterial switch remains challenging (see Figure 42.8), particularly because the transfer of the coronary arteries may sometimes be difficult.

The operation is performed with cardiopulmonary bypass. The ductus arteriosus is ligated and divided at the beginning

(a)

(b)

(c)
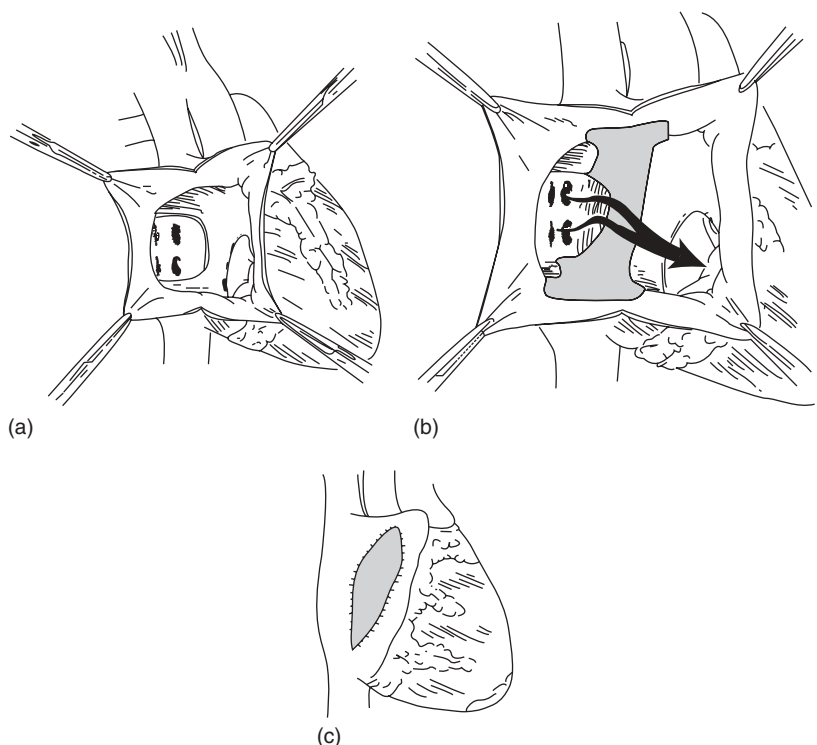
Figure 42.9 Diagram of atrial switch operation. (a) The right atrium has been opened. The four pulmonary veins and the tricuspid valve can be seen. (b) A patch made of pericardium (the Mustard procedure) or a displaced atrial septum (the Senning procedure) is shown in the shaded structure. It is placed to direct the drainage from the superior and inferior venae cavae through the mitral valve into the left ventricle, thence into the pulmonary artery (not shown, but posterior to the patch). At the same time, the patch directs the pulmonary venous return through the tricuspid valve into the right ventricle and thence into the aorta (arrow). This diagram does not show the precise anatomy of the patch. (c) The right atrium is closed with a patch to enlarge it and minimize the risk of obstruction to the pulmonary venous drainage.

of cardiopulmonary bypass. The aorta is cross-clamped and the heart is arrested with a cardioplegic solution infused into the aortic root. The aorta and the pulmonary trunk are transected above the semilunar valves. The coronary arteries are excised from the aortic root with a button of aortic wall and relocated on the native pulmonary root. The branch pulmonary arteries are dissected down to the pulmonary hila to gain sufficient length and allow a tension-free translocation of the pulmonary bifurcation anterior to the ascending aorta (Lecompte or "French" maneuver [28]). The native pulmonary root (now the neoaortic root arising from the left ventricle) is anastomosed to the ascending aorta. The defects created by the excision of the coronary arteries are covered with a patch of autologous pericardium. The native aortic root (now the neopulmonary root arising from the right ventricle) is anastomosed to the pulmonary artery.

The most difficult surgical step is the transfer of the coronary arteries with its inherent risk of coronary ischemia. Coronary transfer is usually easy in patients with "normal" coronary arteries (60–65% of neonates). In coronary patterns with arteries coursing either posterior or anterior to the great vessels (posterior and/or anterior loops – 30% of patients), there is an increased risk of kinking or elongation of the abnormal artery, but these potential problems can usually be overcome. In ~5% of neonates, the coronary arteries course between the great arteries; this is very often associated with an intramural course which may be stenotic. Coronary transfer is then always difficult; innovative and aggressive surgical techniques are necessary to avoid coronary ischemia.

The perioperative mortality, in experienced centers [29,30], is <5%; most deaths are due to ischemia from inadequate coronary artery transfer. Beyond the perioperative period, mortality and morbidity are extremely low [31]. Morbidity concerns the fate of three structures:

1 *The new pulmonary artery.* When the coronary arteries are removed from the aortic root, large buttons of aortic tissue are taken so as not to encroach on the coronary ostia. Large pericardial patches are used to fill the holes made by the harvesting of the coronary arteries. Following the Lecompte maneuver, the pulmonary trunk becomes anterior to the aorta and the pulmonary bifurcation may be elongated, leading to PA branch stenosis and asymmetrical PA blood distribution Thus, the previous aortic root (new pulmonary root) is the great artery that has had the most damage during the arterial switch operation [32]. Mild supravalvar pulmonary stenosis is the rule after an arterial switch (with systolic gradients of ~30 mmHg). Some patients, about 10% in our early experience, needed an operation during childhood to treat PA stenosis, but this is now fairly rare even with a 20 year follow-up, and it is unlikely to be a significant long-term problem. In the few patients with stenosis, percutaneous balloon dilatation of the stenotic pulmonary trunk has partially relieved the obstruction, but this procedure is successful in only one-third of patients. Stenting may improve the percutaneous results, but it is essential to check that the dilatation before the stenting does not compress the left coronary artery, which is usually close to the pulmonary trunk. If the artery is compressed, ST

Figure 42.10 Gothic arch. The ascending aorta is pushed posteriorly by the Lecompte maneuver so that is embraced by the pulmonary artery branches. Note the acute angulation of the aortic arch.

changes develop during dilatation. Before reoperation on the pulmonary trunk, we recommend a selective coronary angiogram to ascertain that no coronary arterial branches run in front of the pulmonary artery (commonly there is a right coronary artery in type E distribution). Pulmonary regurgitation is common after the switch operation, but it is usually mild and well tolerated by the right ventricle.

2 *The new aorta*. Dilatation of the new aortic root and minor leak of the new aortic valve is the rule after a neonatal switch operation. In our experience, it has nearly always been mild and well tolerated, and it has never required medical or surgical treatment during a 15 year follow-up. In patients from the late 1970s and early 1980s who had pulmonary artery banding before the arterial switch, aortic regurgitation can be moderate or even severe, and now after 30 years we recommend a Bentall operation in more patients because of LV or aortic root dilatation We have twice had to change the valves and the aortic root in such patients. However, dilatation of the aortic root and aortic regurgitation have a tendency to increase also in patients with neonatal switch, and this may lead in the long term to more aortic regurgitation and sinus of Valsalva dilatation. Reoperation may become necessary and involve, according to the lesions, aortic valve replacement, replacement of the ascending aorta with preservation of the valve (David operation), or combined replacement of the valve and ascending aorta (Bentall operation). The indications for these procedures are similar to those in other diseases, such as Marfan syndrome and bicuspid aortic valve. To date, the need for such reoperations has been extremely low. The

shape of the aorta is different after the Lecompte maneuver because the ascending aorta is pushed posteriorly which leads to a more angulated aortic arch. The so-called "gothic" arch (see Figure 42.10) is associated with enhanced reflection of the systolic pulse wave, dilatation of the ascending aorta, and aortic regurgitation [33]. The pathophysiologic mechanisms of the gothic arch have been well studied in post-coarctectomy patients with abnormal geometries of the aortic arch. Using MRI, we have demonstrated the direct impact of the acute angulated arch on the central aortic fluid and biomechanics. A gothic arch is associated with increased systolic wave reflection that leads to a systolic reflux in the ascending aorta, and also increased central aortic stiffness that contributes to the dilatation of the aortic root [34,35].

3 *The coronary arteries*. The major long-term concern after the arterial switch operation is left ventricular myocardial ischemia. Indeed, left ventricular coronary perfusion may be impaired by acquired lesions of the coronary arterial ostia resulting from surgical transfer, for example, stenosis or atresia by torsion or compression by the pulmonary artery or by fibrous tissue. This is the major cause of operative and early postoperative mortality and morbidity of the arterial switch procedure. Late coronary ostial stenosis or atresia is rare after an arterial switch, but most centers have not looked carefully at the fate of the coronary arteries after the switch. The assumption has been made that if clinical, electrocardiographic, or echocardiographic signs of ischemia did not develop after the operation and before discharge from the hospital, the coronary arteries were normal and would remain normal and grow normally. Coronary arterial damage, however, has been responsible for late deaths [31]. By performing selective coronary arterial angiograms in postoperative patients, we found coronary arterial anomalies in ~5% of patients who apparently had no evidence of postoperative ischemia [36,37]. Most had minor signs of ischemia on electrocardiography and echo-cardiography, but some showed no ischemia at all, even on a myocardial perfusion thallium scan. Selective coronary arterial angiograms disclosed coronary arterial stenosis or complete obstruction, almost always in the left coronary artery (except one in the right coronary artery), usually with adequate collateral circulation from the right coronary arterial bed. Patients in whom reversible ischemia could be demonstrated underwent reoperation. In most patients (even with obstructed arteries), normal coronary perfusion can be restored by surgical patch angioplasty of the stenosed/obstructed coronary artery. The patients who do not have ischemia are left with only one coronary artery; they may in the long term develop coronary arterial disease sooner and more often than will the normal population. Even without coronary artery stenosis, myocardial reserve may be impaired by inadequate position of the ostia for perfect diastolic filling, because of the high implantation of the coronary artery on the upper part of a dilated sinus of Valsalva, or by endothelial

damage from the operation (cannulation and cold blood flushing). In theory, there could be a constitutional inadequacy of the left ventricular coronary circulation because the right coronary artery is nearly always dominant in TGA, and the left circumflex or left anterior descending artery is frequently small. We do not have information on myocardial reserve in these patients, but positron emission tomographic scanning with dipyridamole (Persantine) in a few patients suggests that myocardial reserve may be decreased.

Despite these concerns, however, with a mean follow-up of >14 years, and more than 20 years for 300 patients, almost all these children after an arterial switch live a normal life, including participation in competitive sports.

Our patients are followed up yearly in the outpatient clinic with clinical history and examination, two-dimensional echocardiography–Doppler study, and an electrocardiogram; after 5 years of age, they have formal exercise testing. If ischemia is suspected, a coronary angiogram is indicated. We checked the coronary arteries systematically by a selective coronary angiogram by the age of 6 years, but we now perform a multislice CT scan and perform selective coronary angiogram only if the scan is abnormal. We have shown that 64-slice CT coronary angiography performs as well as invasive angiography for detecting significant coronary lesions (>30% reduction diameter) [38]. It allows direct visualization of the coronary artery lumen, and the course of the vessel in relation to the nearby major cardiovascular structures. CT also provides information about the underlying mechanism of coronary lesions, for example through stretching, compression, and/or kinking caused by the surrounding great arteries (see Figure 42.11). MRI is another modality that may be useful for follow-up imaging after arterial switch operation, particularly because it does not deliver X-radiation [39]. New-generation machines already offer promising results on cooperative children who can hold their breath during image acquisition. Our current policy is to perform a cardiac MRI in cooperative children for a complete and comprehensive anatomic and functional evaluation after the arterial switch. Coronary arteries and the great vessels are assessed on high-resolution 3D imaging with ECG- and respiratory-gated sequences (see Figure 42.12). Central aortic fluid dynamics and biomechanics of the ascending aorta are assessed on velocimetry mapping sequences. Myocardial perfusion and viability are also evaluated using first-pass perfusion and myocardial delayed enhancement, respectively. The long time required for the scan and the potential need for anesthesia are substantial drawbacks in small children. With a normal exercise test result and coronary angiogram, the children are allowed to participate in all sports, including competition.

Beyond the neonatal period

The arterial switch can be performed only in the neonatal period while the left ventricle is still competent to develop systemic pressures. Until recently, on the basis of echocar-

diographic characteristics of the thickness and shape of the left ventricle [40], the upper age limit for the arterial switch was set at 3–4 weeks. The belief was that if the left ventricle was much thinner than the right ventricle, and if the ventricular septum bulged into the lower pressure left ventricle, the left ventricle would be unable to support systemic arterial pressures and flows. However, some centers have observed that the arterial switch can be performed safely up to 8 weeks of age, whatever the shape of the left ventricle and the interventricular septum [41,42]. Beyond that age, only patients with a left ventricle having a high systolic pressure (because of an open ductus or subpulmonic stenosis) are good candidates.

For patients who do not meet these criteria, the arterial switch can be performed safely only if the left ventricle is prepared by an afterload challenge (usually pulmonary artery banding). If this causes severe hypoxemia, the patient may also need an aortopulmonary shunt. This two-stage surgery with a quick (~10 days) left ventricular preparation before the arterial switch has been successful in some centers [43]. It is not an easy procedure, however, and in our experience it has an increased mortality and morbidity. Furthermore, the left ventricular myocardium may have inadequate fiber quality and decreased coronary reserve; there is little evidence for growth of coronary arteries after the newborn period. Therefore, many centers (such as ours in Paris) perform an "atrial repair" rather than an arterial switch. Our current practice is to place a loose pulmonary band to maintain a degree of high pressure in the left ventricle; if the atrial switch is performed in infancy, the banding should become tighter as the child grows with subsequent increase in left ventricular pressure; the hope is to preserve septal geometry and tricuspid valve function and also to prepare the left ventricle for a late arterial switch.

Atrial repair: the Mustard and Senning operations

When the left ventricle has lost its systemic competence or when the surgical team has too high a mortality with the arterial switch, an atrial baffle repair can correct the physiologic abnormalities by rerouting the venous return. This is done by directing systemic venous drainage towards the mitral valve and pulmonary venous drainage toward the tricuspid valve by placing pericardial patches around the caval veins, as in the Mustard operation [44] introduced in 1964, or by moving the atrial septum in the Senning operation [45], described in 1959 but subsequently modified and made easier to perform in 1977 [46].

These operations can be performed at any age and have a low mortality. Most of the patients (80–90%) are doing well with a follow-up of >20 years [47]. There are, however, three major problems or theoretical concerns with this procedure.
1 The atrial channels can become obstructed, leading to caval or pulmonary venous hypertension. These uncommon complications can usually be treated or improved by
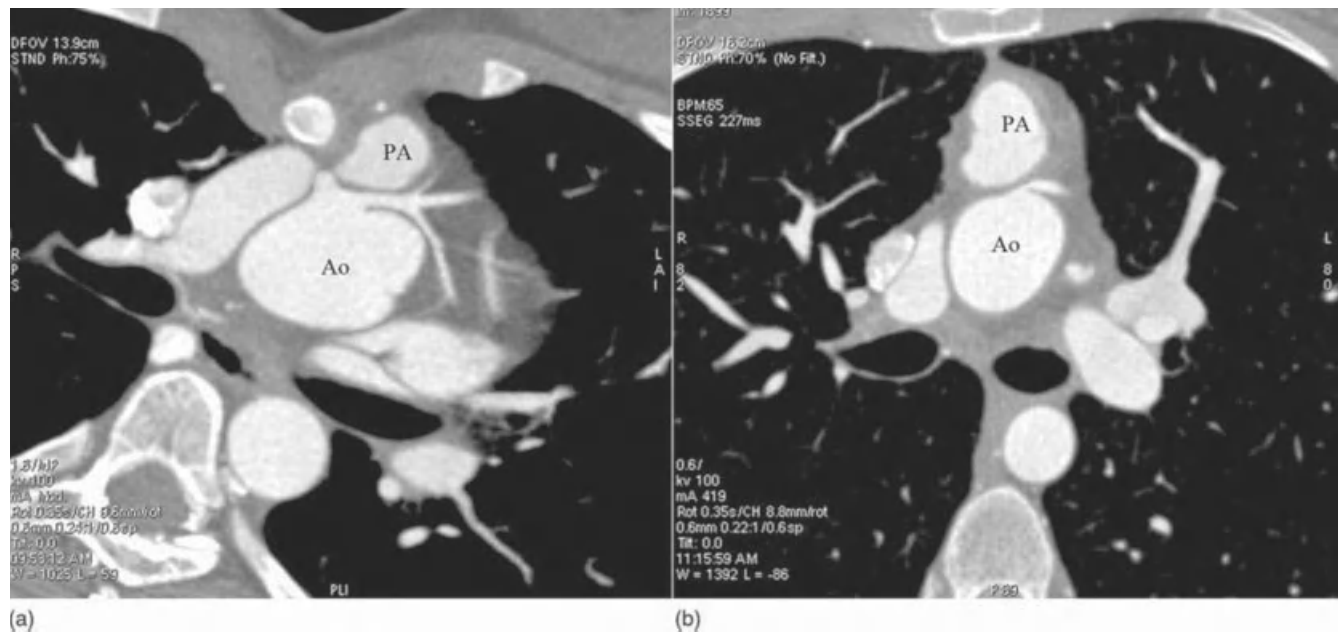
Figure 42.11 CT assessment of the coronary arteries and their relationship with the surrounding great arteries. (a) Note the anterior position of the reimplanted left ostium so that the left coronary artery has a course between the pulmonary artery (PA) and the aorta (Ao). There is a tight compression of the left ostium in (b).
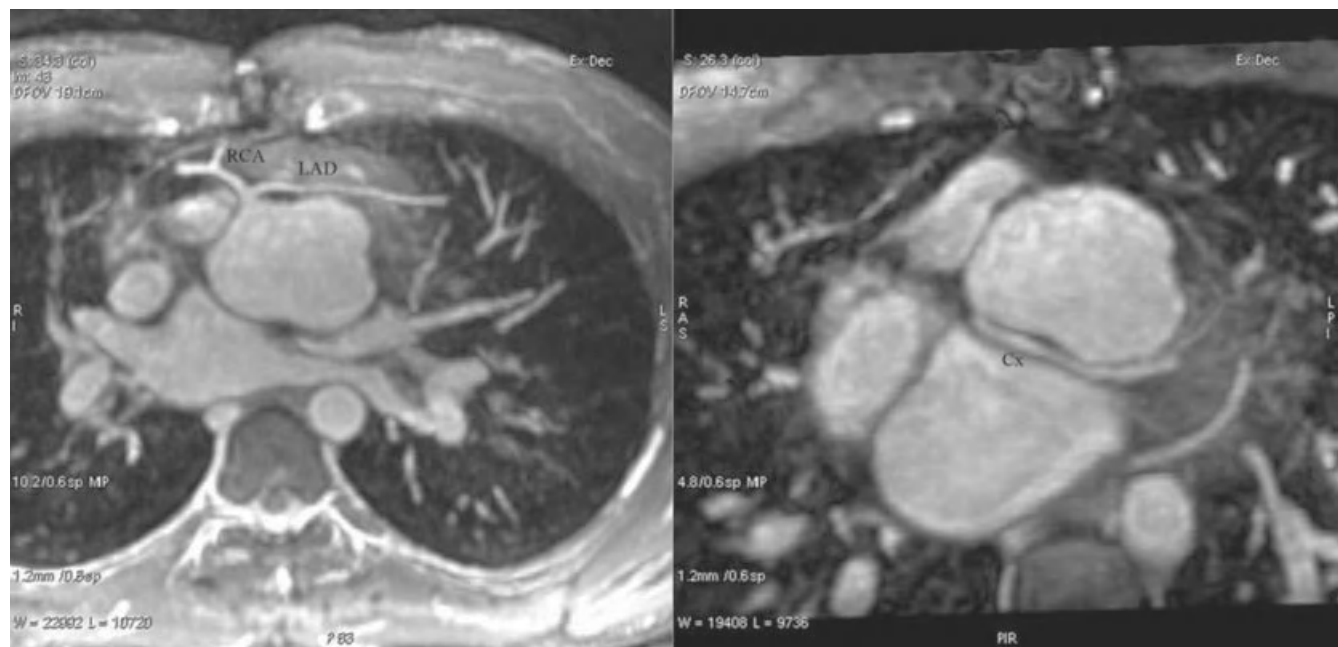
Figure 42.12 Cardiac MRI for the follow-up imaging of the reimplanted coronary arteries. The left ostium gives rise to both the left anterior descending artery (LAD) and the right coronary artery (RCA). The circumflex artery (Cx) rises from the right aortic sinus and has a long retro-aortic course.

interventional catheterization with dilatation and stents. They rarely require reoperation. When the stenosis is limited to the superior vena caval channel, there is usually an efficient rerouting of the blood by the azygos or hemiazygos veins towards the inferior vena cava. When the pulmonary venous channel is obstructed, the clinical picture resembles cor triatriatum or mitral stenosis with pulmonary edema and postcapillary hypertension. In some patients, this pulmonary arterial hypertension "prepared" the left ventricle for a late switch procedure.

2 The incidence of atrial dysrhythmias is high, probably because of damage to the sinus node or its artery, or the internodal tracts, during the operation. The dysrhythmias can be severe and difficult to treat, with a risk of sudden death even after pacemaker implantation. Abnormal sinus node dysfunction was reported first in 1972 [48]. Sinus node dysfunction progresses over time [49–51], and 10 years after operation only ~14% of these children remain in normal sinus rhythm [51]. The others have a tendency for bradycardia and junctional rhythm, sometimes with a restored sinus rhythm during exercise. These passive bradycardias are usually benign and rarely symptomatic, but 10–20% need a pacemaker. Dysrhythmias can also be "active" in these patients, with the appearance of ectopic atrial tachycardia, atrial flutter, or even atrial fibrillation [52]. A high proportion of these patients have inducible atrial flutter during electrophysiologic studies postoperatively [53], and many of these later develop spontaneous atrial flutter. On electrocardiographic examination, the atrial flutter is atypical, with rates often from 180–260 beats per minute, frequently with 1:1 atrioventricular conduction. The flutter waves are of low amplitude and may be difficult to see. In fact, any patient after an atrial baffle repair with a resting heart rate above 100 beats per minute should be checked carefully to exclude atrial flutter with 2:1 or 3:1 atrioventricular block. These active tachycardias or arrhythmias are dangerous for the patients and for right ventricular function. They can lead to serious myocardial or neurologic complications and even sudden death [54]. They are difficult to treat because they are associated with a weak or damaged sinus node, and antiarrhythmic drugs may be hazardous because of the risk of severe bradycardia. Therefore, treatment of these atrial tachycardias often requires pacemaker implantation.

3 The long-term function of a right ventricle and a tricuspid valve working at systemic pressure is uncertain [55]. Some of these patients develop heart failure after 10, 20, or 30 years. The example of patients with double discordance (corrected transposition) shows that the long-term failure of a systemic right ventricle is not a certainty (some patients can live to 70 years without heart failure). Most of those with an atrial baffle, however, will probably develop heart failure, perhaps in part owing to inadequate myocardial protection during surgery (especially in the early days of this repair) and in part owing to associated anomalies of rhythm and atrioventricular conduction.

When the right ventricle begins to dilate, the attachments of the tricuspid valve to the septum are pulled laterally, thereby inducing tricuspid regurgitation that increases the ventricular dilatation. A vicious circle is thus established. Furthermore, because the regurgitant blood enters the new pulmonary venous atrium, tricuspid regurgitation causes pulmonary venous hypertension and eventually pulmonary edema.

When right ventricular failure develops after a Senning or Mustard procedure, chronic dysrhythmia may be the mechanism. If right ventricular failure is present without dysrhythmia, nonspecific medical therapy with diuretics, converting enzyme inhibitors, and digoxin (with care for sinus node dysfunction) can be tried, but are seldom successful for long. The only possibility other than cardiac transplantation is conversion of the right ventricle into a subpulmonary ventricle by performing an arterial switch procedure and taking down the atrial baffle to reroute the venous returns to their original ventricles [56]. For this transformation, the left ventricle must be prepared for the arterial switch by an afterload challenge (pulmonary arterial banding).

This procedure of late preparation is different from the two-stage preparation done in the older infant with TGA and a low-pressure left ventricle. After a Mustard or Senning procedure, the heart has a circulation in series without hypoxemia, and the banding will directly affect only the left ventricle, although it may indirectly affect the preload of the right ventricle. The severe hypoxemia attendant on preparing the left ventricle in the infant with TGA is not a problem. The preparation of an older left ventricle cannot be obtained in few days, however, and it needs a long and uncertain process (several years in some patients) before achieving adequate left ventricular mass. Little information is available about the quality of the fibers and the coronary reserve. This situation is identical with the problem of treating a patient with double discordance or congenitally corrected transposition in whom the right ventricle is failing and the tricuspid valve regurgitating. The issues concern fundamental unanswered questions about postnatal ventricular growth and coronary artery angiogenesis.

Experience has shown, however, that pulmonary arterial banding changes the septal geometry in some patients, pushing the septum back towards the right ventricle, and improves both right ventricular and tricuspid valve function by decreasing tricuspid regurgitation. Often two or three banding adjustments may be needed to prepare the left ventricle during several years, while avoiding left ventricular failure. Hence it is crucial to evaluate right ventricular function in the follow-up of these patients and not wait for severe dysfunction and heart failure to develop before "retraining" a left ventricle.

References

1 Ferencz C, Loffredo CA, Correa-Villasenor A, Wilson PD. Malformations of the cardiac outflow tract. In: Ferencz C, Loffredo CA, Correa-Villasenor A, Wilson PD, eds. *Perspectives in Pediatric Cardiology, Vol. 5: Genetic and Environmental Risk Factors of Major Cardiovascular Malformations.* Armonk, NY: Futura Publications, 1997: 59–102.

2 Liebman J, Cullum L, Belloc NB. Natural history of transposition of the great arteries: anatomy and birth and death characteristics. *Circulation* 1969;**40**:237–62.

3 Burn J. The aetiology of congenital heart disease. In: Anderson RA, Baker EJ, Macartney FJ, *et al.*, eds. *Paediatric Cardiology*. London: Churchill Livingstone, 2002: 141–213.

4 Smith A, Wilkinson JL, Anderson RH, *et al*. Architecture of the ventricular mass and atrioventricular valves in complete transposition with intact ventricular septum compared with the normal. I. The left ventricle, mitral valve, and interventricular septum. *Pediatr Cardiol* 1986;**6**:253–7.

5 Smith A, Wilkinson JL, Anderson RH, *et al*. Architecture of the ventricular mass and atrioventricular valves in complete transposition with intact ventricular septum compared with the normal. II. The right ventricle and tricuspid valve. *Pediatr Cardiol* 1986;**6**:299–305.

6 Aziz KU, Paul MH, Idriss FS, *et al*. Clinical manifestations of dynamic left ventricular outflow tract stenosis in infants with d-transposition of the great arteries with intact ventricular septum. *Am J Cardiol* 1979;**44**:290–7.

7 Crupi G, Anderson RH, Ho SY, Lincoln C. Complete transposition of the great arteries with intact ventricular septum and left ventricular outflow tract obstruction. Surgical management and anatomical considerations. *J Thorac Cardiovasc Surg* 1979;**78**: 730–8.

8 Sansa M, Tonkin IL, Bargeron LM Jr, Elliott LP. Left ventricular outflow tract obstruction in transposition of the great arteries: an angiographic study of 74 cases. *Am J Cardiol* 1979;**44**:88–95.

9 Chiu I-S, Anderson RH, Macartney FJ, *et al*. Morphologic features of an intact ventricular septum susceptible to subpulmonary obstruction in complete transposition. *Am J Cardiol* 1984; **53**:1633–8.

10 Yacoub MH, Arensman FW, Keck E, Radley-Smith R. Fate of dynamic left ventricular outflow tract obstruction after anatomic correction of transposition of the great arteries. *Circulation* 1983;**68**(Suppl II):56–62.

11 Kirklin JW, Barratt-Boyes BG. Complete transposition of the great arteries. In: Kirklin JW, Barratt-Boyes BG, eds. *Cardiac Surgery*, 2nd edn. London, Churchill Livingstone, 1993: 1383–467.

12 Bharati S, Lev M. The conduction system in simple, regular (D), complete transposition with ventricular septal defect. *J Thorac Cardiovasc Surg* 1976;**72**:194–201.

13 Yacoub MH, Radley-Smith R. Anatomy of the coronary arteries in transposition of the great arteries and methods for their transfer in anatomical connection. *Thorax* 1978;**33**:418–24.

14 Gittenberger-de Groot AC, Sauer U, Oppenheimer-Dekker A, Quaegebeur J. Coronary arterial anatomy in transposition of the great arteries: a morphologic study. *Pediatr Cardiol* 1983;**4**(Suppl 1):15–24.

15 Mayer JE Jr, Sanders S, Jonas R, *et al*. Coronary artery pattern and outcome of arterial switch operation for transposition of the great arteries. *Circulation* 1990;**82**(Suppl IV):139–45.

16 Wagenvoort CA, Nauta J, van der Schaar PJ, *et al*. The pulmonary vasculature in complete transposition of the great arteries, judged from lung biopsies. *Circulation* 1968;**38**:746–54.

17 Lakier JL, Stanger P, Heymann MA, *et al*. Early onset of pulmonary vascular obstruction in patients with aortopulmonary transposition and intact ventricular septum. *Circulation* 1975;**51**:875–80.

18 Clarkson PM, Neutze JM, Wardill JC, Barrett-Boyes BG. The pulmonary vascular bed in patients with complete transposition of the great arteries. *Circulation* 1976;**53**:539–43.

19 Newfeld EA, Paul MH, Muster AJ, Idriss FS. Pulmonary vascular disease in transposition of the great vessels and intact ventricular septum. *Circulation* 1979;**59**:525–30.

20 Carr I. Timing of bidirectional atrial shunts in transposition of the great arteries and atrial septal defect. *Circulation* 1971;**44**(Suppl II):70.

21 Muster AJ, Paul MH, van Grondelle A, Conway JJ. Asymmetric distribution of the pulmonary blood flow between the right and left lungs in d-transposition of the great arteries. *Am J Cardiol* 1976;**38**:352–61.

22 Lock JE, Lucas RV Jr, Amplatz K, Bessinger FB Jr. Silent unilateral pulmonary venous obstruction: occurrence after surgical correction of transposition of the great arteries. *Chest* 1978;**73**:224–7.

23 Vogel M, Ash J, Rowe RD, *et al*. Congenital unilateral pulmonary vein stenosis complicating transposition of the great arteries. *Am J Cardiol* 1984;**54**:166–71.

24 Paul MH, Wernovsky G. Transposition of the great arteries. In: Emmanouilides GC, Allen HD, Riemenschneider TA, Gutgesell HP, eds. *Heart Disease in Infants, Children, and Adolescents Including the Fetus and Young Adult*. Baltimore: Williams & Wilkins, 1995: 1154–224.

25 Tynan M, Anderson RA. Complete transposition. In: Anderson RA, Baker EB, Macartney FJ, *et al.*, eds. *Paediatric Cardiology*. London: Churchill Livingstone, 2002: 1281–319.

26 Keane JF, Ellison RC, Rudd M, Nadas AS. Pulmonary blood flow and left ventricular volumes in transposition of the great arteries and intact ventricular septum. *Br Heart J* 1973;**35**:521–6.

27 McQuillen PS, Hamrick SE, Perez MJ, *et al*. Balloon atrial septostomy is associated with preoperative stroke in neonates with transposition of the great arteries. *Circulation* 2006;**113**(2):280–5.

28 Lecompte Y, Zannini L, Hazan E, *et al*. Anatomic correction of transposition of the great arteries: new technique without the use of a prosthetic conduit. *J Thorac Cardiovasc Surg* 1981;**82**:629–31.

29 Castaneda AR, Norwood WI, Jonas RA, *et al*. Transposition of the great arteries and intact ventricular septum: anatomical repair in the neonate. *Ann Thorac Surg* 1984;**38**:438–43.

30 Sidi D, Planché C, Kachaner J, *et al*. Anatomic correction of simple transposition of the great arteries in 50 neonates. *Circulation* 1987;**75**:429–35.

31 Tsuda E, Imatika M, Yagilhara T, *et al*. Late death after arterial switch operation for transposition of the great arteries. *Am Heart J* 1992;**124**:1551–7.

32 Paillole C, Sidi D, Kachaner J, *et al*. Fate of the pulmonary arteries after anatomic correction of simple transposition of the great arteries in newborn infants. *Circulation* 1988;**78**: 870–6.

33 Agnoletti G, Ou P, Celermajer DS, *et al*. Acute angulation of the aortic arch predisposes a patient to ascending aortic dilatation and aortic regurgitation late after the arterial switch operation for transposition of the great arteries. *J Thorac Cardiovasc Surg* 2008;**135**:568–72.

34 Ou P, Celermajer DS, Raisky O, *et al*. Angular (Gothic) aortic arch leads to enhanced systolic wave reflection, central aortic stiffness, and increased left ventricular mass late after aortic coarctation repair: evaluation with magnetic resonance flow mapping. *J Thorac Cardiovasc Surg* 2008;**135**:62–8.

35 Ou P, Celermajer DS, Mousseaux E, *et al*. Vascular remodeling after "successful" repair of coarctation: impact of aortic arch geometry. *J Am Coll Cardiol* 2007;**49**:883–90.

36 Bonhoeffer P, Bonnet D, Piechaud JF, *et al*. Coronary artery obstruction after the arterial switch operation for transposition of the great arteries in newborn. *J Am Coll Cardiol* 1997;**29**:202–6.

37 Bonnet D, Bonheoffer P, Piechaud JF, *et al*. Long term fate of the coronary arteries after arterial switch operation in newborns with transposition of the great arteries. *Heart* 1996;**76**:274–9.

38 Ou P, Celermajer DS, Marini D, *et al*. Safety and accuracy of 64-slice computed tomography coronary angiography in children after the arterial switch operation for transposition of the great arteries. *JACC Cardiovasc Imaging* 2008;**1**:331–9.

39 Taylor AM, Dymarkowski S, Hamaekers P, *et al*. MR coronary angiography and late-enhancement myocardial MR in children who underwent arterial switch surgery for transposition of great arteries. *Radiology* 2005;**234**:542–7.

40 Danford DA, Huhta JC, Gutgesell HP. Left ventricular wall stress and thickness in complete transposition of the great arteries. Implications for surgical intervention. *J Thorac Cardiovasc Surg* 1985;**89**:610–5.

41 Davis AM, Wilkinson JL, Karl TR, Mee RB. Transposition of the great arteries with intact ventricular septum. Arterial switch repair in patients 21 days of age or older. *J Thorac Cardiovasc Surg* 1993;**106**:111–5.

42 Foran JP, Sullivan ID, Elliott MJ, de Leval MR. Primary arterial switch operation for transposition of the great arteries with intact ventricular septum in infants older than 21 days. *J Am Coll Cardiol* 1998;**31**:883–9.

43 Boutin C, Wernovsky G, Sanders SP, *et al*. Rapid two-stage arterial switch operation. Evaluation of left ventricular systolic mechanics late after an acute pressure overload stimulus in infancy. *Circulation* 1994;**90**:1294–303.

44 Mustard WT. Successful two-stage correction of transposition of the great vessels. *Surgery* 1964;**55**:469–72,

45 Senning A. Surgical correction of transposition of the great vessels. *Surgery* 1959;**45**:966–80.

46 Quaegebeur JM, Rohmer J, Brom AG. Revival of the Senning operation in the treatment of transposition of the great arteries. Preliminary report on recent experience. *Thorax* 1977;**32**:517–24.

47 Williams WG, Trusler GA, Kirklin JW, *et al*. Early and late results of a protocol for simple transposition leading to an atrial (Mustard) repair. *J Thorac Cardiovasc Surg* 1988;**95**:717–26.

48 El-Said G, Rosenburg HS, Mullins CE, *et al*. Dysrhythmias after Mustard's operation for transposition of the great arteries. *Am J Cardiol* 1972;**30**:526–32.

49 Saalouke MG, Rios J, Perry LW, *et al*. Electrophysiologic studies after Mustard's operation. *Am J Cardiol* 1978;**41**:1104–9.

50 Flinn CJ, Wolff GSS, Dick M. Cardiac rhythm after the Mustard operation for transposition of the great arteries. *N Engl J Med* 1984;**310**:1635–8.

51 Hayes CJ, Gersony WM. Arrhythmias after the Mustard operation for transposition of the great arteries. *J Am Coll Cardiol* 1986;**7**:133–7.

52 Vetter VL, Tanner CS, Horowitz LN. Electrophysiologic consequences of the Mustard repair of d-transposition of the great arteries. *J Am Coll Cardiol* 1987;**10**:1265–73.

53 Vetter VL, Tanner CS, Horowitz LN. Inducible atrial flutter after the Mustard repair of complete transposition of the great arteries. *Am J Cardiol* 1988;**61**:428–35.

54 Garson A Jr, Bink-Boelkens M, Hesslein PS. Atrial flutter in the young: a collaborative study of 380 cases. *J Am Coll Cardiol* 1985;**6**:871–8.

55 Martin RP, Qureshi SA, Ettedgui JA, *et al*. An evaluation of right and left ventricular function after anatomical correction and intra-atrial repair for complete transposition of the great arteries. *Circulation* 1990;**82**:808–16.

56 Helvind MH, McCarthy JF, Imamura M. Ventriculo-arterial discordance: switching the morphologically left ventricle into the systemic circulation after 3 months of age. *Eur J Cardiothorac Surg* 1998;**14**:173–8.

43 Congenitally Corrected Transposition of the Great Arteries

Tim S. Hornung & A. Louise Calder

Auckland City Hospital, Auckland, New Zealand

Congenitally corrected transposition of the great arteries (CCTGA) is a rare cardiac anomaly characterized by combined atrioventricular and ventriculoarterial discordance. Other terms for this anomaly include physiologically corrected transposition of the great arteries, l-transposition, double discordance, and ventricular inversion. Congenitally corrected transposition is used preferentially because systemic venous blood is directed to the pulmonary arteries and pulmonary venous blood is directed to the aorta. This differentiates CCTGA from "complete transposition" (d-TGA) in which there is ventriculoarterial discordance but atrioventricular concordance.

Incidence

CCTGA represents approximately 0.5–1% of all congenital heart disease. In one series of 10 535 patients with congenital heart disease, 101 had corrected transposition [1]. Excluding patients with a univentricular atrioventricular connection reduced the prevalence to 0.57%. In another study of 4390 infants, there were 47 infants with CCTGA [2]. The anomaly is more common in males.

Embryology

CCTGA is due to failure of normal looping of the primitive heart tube. The heart tube has fixed proximal and distal attachments so its rapid growth necessitates looping of the tube. Looping is normally rightwards (D looping), but in CCTGA with situs solitus looping is leftwards (L looping). Therefore, the morphologic right ventricle is displaced leftwards and the morphologic left ventricle rightwards. The ventricles are in a more side-by-side relationship than the usual anteroposterior position. The atrioventricular valves loop with the respective ventricles, so the tricuspid valve connects to the morphologic right ventricle and the mitral valve to the morphologic left ventricle. After the looping process, truncus arteriosus development occurs. The conotruncal ridges divide the truncus into an aorta that connects to the left-sided ventricle and is displaced leftwards, anterior and superior, and a pulmonary artery that connects to the right-sided ventricle and is displaced more posteriorly and rightwards. The outflow tracts and great arteries are essentially parallel rather than crossing as in a normal heart.

Anatomy

There is usually normal connection of the systemic veins to the right atrium and the pulmonary veins to the left atrium. The right atrium connects via the mitral valve to the morphologic left ventricle, which supplies the pulmonary artery. The left atrium connects via the tricuspid valve to the morphologic right ventricle, which supplies the aorta via a subaortic infundibulum or conus. The cardiac connections are therefore:

systemic veins → right atrium → morphologic left ventricle → pulmonary artery

pulmonary veins → left atrium → morphologic right ventricle → aorta

An important anatomic implication is that the morphologic right ventricle supplies the systemic circulation.

The exact anatomic arrangement varies considerably (Table 43.1). The usual arrangement is situs solitus with L-looping of the ventricles and the aorta anterior and leftward of the pulmonary artery {S,L,L}, found in 19/22 of our postmortem subjects [3]. The aorta was anterior and

Table 43.1 Demographic data and segmental combinations in CCTGA with two ventricles, detailing individual and combined data from the series by Allwork *et al.* [7], Van Praagh *et al.* [11] and our own series in Auckland.

	Allwork *et al.*	Van Praagh *et al.*	Auckland	Total	Mean (%)
Number	38	33	22	93	
Age: median		3 years	8.9 years		
Age: range		40 h to 65 years	19 weeks' gestation to 48 years		
Gender: male/female ratio[a]		19/13 = 1.5	18/3 = 6		
Corrected TGA in situs solitus				86	92
CCTGA {S,L,L,}	31	31	19	81	87
CCTGA {S,L,D}	2	1	2	5	5
Corrected TGA in situs inversus					
CCTGA {I,D,D}	5	1	1	7	8

[a]One unknown in each series.

rightwards {S,L,D} in two subjects with situs solitus, both with criss-cross atrioventricular connections. The remaining subject (5%) had situs inversus with D-looping of the ventricles and aorta anterior and rightwards {I,D,D}.

In patients with situs solitus, the heart is frequently mesocardic but the apex remains leftwards in most: in our series, there was true mesocardia in one and dextrocardia in two others with situs solitus. Either ventricle may be hypoplastic, particularly the left-sided right ventricle. The anomaly may be associated with double-inlet ventricle or AV atresia [4].

Coronary artery anatomy

The coronary arteries are inverted (Figure 43.1). Thus, the morphologic left coronary artery (LCA) arises from the patient's right-sided sinus and the morphologically right coronary artery (RCA) from the left-sided sinus (Figure 43.1a and b). A variety of coronary arterial patterns is seen [4–7] (Figure 43.1). The two main coronary arteries may arise from the same sinus. The RCA may arise from the LCA and pass either anterior to the aorta (Figure 43.1c) or around and behind the pulmonary artery (Figure 43.1d). A variant of Figure 43.1d shown in Figure 43.1e is a separate right ventricular branch from the aorta. Another variation (Figure 43.1f) in a patient with pulmonary atresia and commisural malalignment had both coronary arteries arise from the same sinus. The single coronary artery may arise from either the right or left coronary sinus.

Anderson *et al.* pointed out the vulnerability of the coronary arteries in CCTGA with surgery [8], particularly the anterior descending artery running anterior to the pulmonary artery. Careful preoperative delineation of the coronary anatomy is particularly important before the double-switch operation.

Coronary venous anatomy

Coronary sinus anatomy varies and shows abnormalities in about 25% of patients. It usually drains normally into the right atrium. It may be absent with the coronary veins draining into the ipsilateral atrium, and in other patients some veins drain to one of the atria and others to the coronary sinus [9].

The coronary sinus could be assessed in 20 of our patients and was absent in five (25%). When the coronary sinus is absent, the coronary veins usually drain to the ipsilateral atria. In one of our patients, the coronary veins entered the right atrium via separate entrances. In Uemura *et al.*'s series with atrioventricular discordance (including double-outlet right ventricle) [9], all the left coronary veins drained directly to the right atrium in 20%, some directly to the right atrium and some to coronary sinus in 63%, and completely to coronary sinus in 17%. The right coronary veins all drained to coronary sinus in 87% and partially or totally directly to left atrium in 11%.

Conduction system

The anatomy of the conduction system is abnormal with the atrioventricular node because of the septal malalignment unable to connect to a penetrating atrioventricular conduction bundle. A second atrioventricular node positioned anteriorly gives rise to an elongated atrioventricular bundle [10].

Associated cardiac abnormalities

CCTGA without associated intracardiac abnormalities is rare. Coexisting lesions occur in >90% of patients, most frequently ventricular septal defect, left ventricular outflow tract
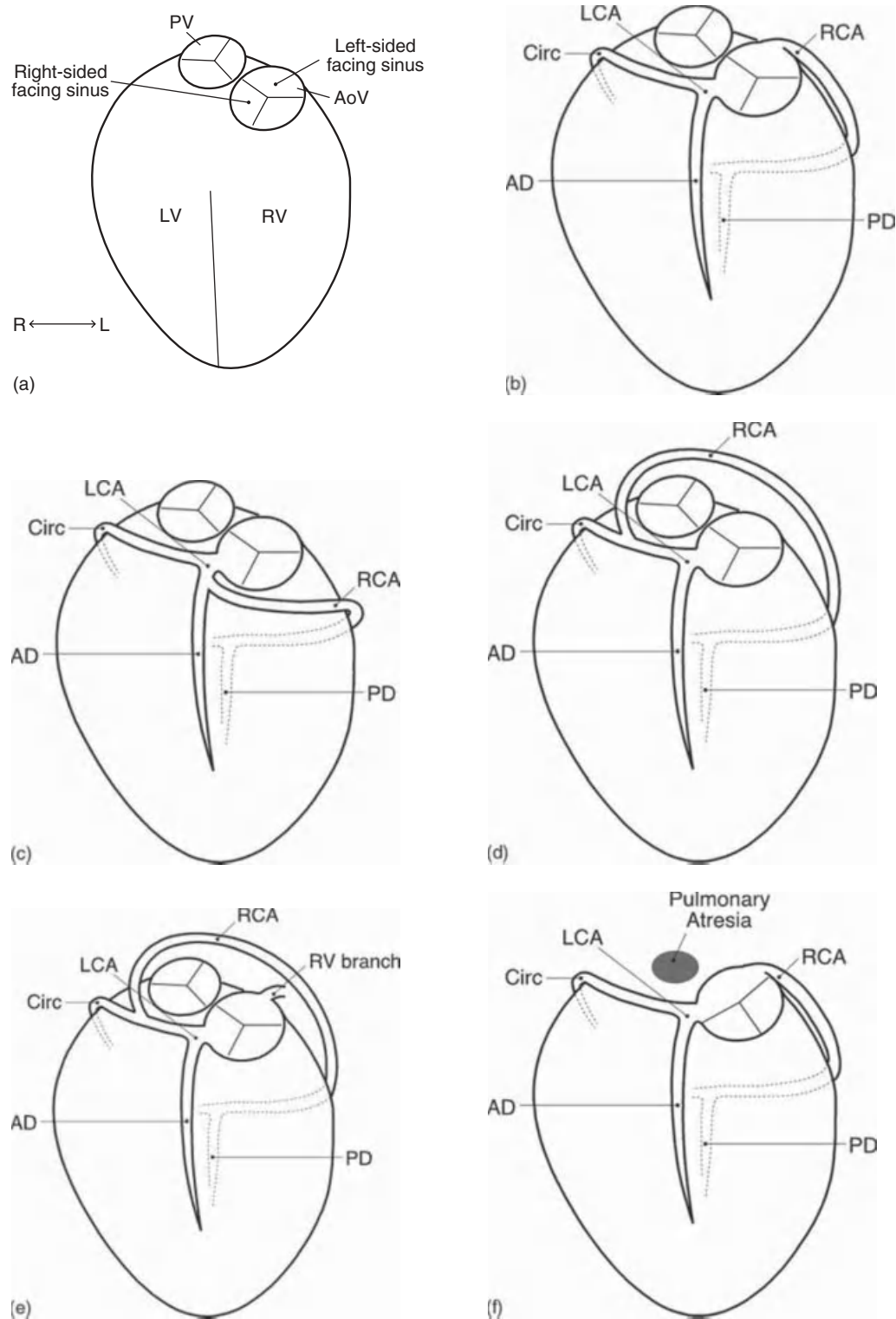
Figure 43.1 Coronary arterial patterns in CCTGA {S, L, L}. (a) A sketch of the morphological left ventricle (right-sided) and the morphological right ventricle (left-sided) viewed from the front, and the leftward, anterior aortic valve and the rightward, posterior pulmonary valve in a superior plane view. The coronary arteries usually arise from the right- and left-sided facing sinuses. (b) The usual coronary arterial pattern in CCTGA with the morphologic left coronary artery arising from the right-sided facing sinus. The anterior descending and circumflex coronary arteries arise from the left coronary artery. The morphologic right coronary artery arises from the left-sided facing sinus and passes around the atrioventricular groove adjacent to the right ventricle. (c–f) Single sinus origins of coronary arteries. In (c) the right coronary artery arises from the left anterior descending and then crosses anteriorly to the aorta to reach the atrioventricular groove. In (d) the right coronary artery arises from the left circumflex coronary artery and passes posteriorly to the great arteries to reach the atrioventricular groove. (e) is similar to (d) but with an additional branch to right ventricle arising from the left-sided coronary sinus. In (f), because of commissural malalignment, the coronary arteries do arise form the same sinus but on opposite sides. AD, anterior descending; AoV, aortic valve; Circ, circumflex; L, left; LCA, left coronary artery; LV, left ventricle; PV, pulmonary valve; PD, posterior descending. R, right; RCA, right coronary artery; RV, right ventricle.

Table 43.2 Associated anomalies in congenitally corrected TGA, detailing individual and combined data from the series by Allwork *et al.* [7], Van Praagh *et al.* [11] and our own series in Auckland.

	Allwork *et al.*	Van Praagh *et al.*	Auckland	Combined mean (%)
Number	38	33	22	
Ventricular septal defects	30 (78%)	25 (76%)	22 (100%)	85
Tricuspid valve anomalies	34 (89%)	30 (91%)	18 (82%)	87
Ebstein's anomaly	23 (61%)	20 (61%)	6 (27%)	50
TV stenosis or hypoplasia	5 (13%)	5 (15%)	1 (4%)	12
Straddling/overriding TV		6 (18%)	6 (27%)	22
Left ventricular outflow obstruction	20 (53%)	17 (52%)	13 (59%)	54
Pulmonary valve stenosis	14 (37%)	11 (33%)	7 (32%)[a]	34
Subpulmonary stenosis			9 (41%)[a]	
Pulmonary valve atresia	6 (16%)	6 (18%)	3 (14%)	16
Mitral valve anomalies				
Mitral regurgitation		5 (15%)	1 (4%)	10
Cleft mitral valve		5 (15%)	2 (9%)	12
Mitral stenosis		1 (3%)	0	1.8
Aortic outflow obstruction				
Aortic stenosis		4 (12%)	0	7
Aortic atresia		2 (6%)	0	3.6
Heterotaxy syndromes		1 polysplenia	2 asplenia	

[a]Six patients had both valvar and subvalvar stenosis.

obstruction, tricuspid valve abnormalities, and conduction abnormalities. All may occur in the same patient. Data from three postmortem series [7,11] with data from 93 patients are given in Table 43.2.

Ventricular septal defect

From the three combined series, a ventricular septal defect (VSD) was present in 84% of autopsies (Table 43.2); most clinical series have a similar high incidence. The defect is commonly a large perimembranous outflow (subpulmonary) defect and is thought to result from malalignment between the atrial and the ventricular septum. Other types of VSD have been described, including doubly committed subarterial (conal) (Figure 43.2a and b), muscular, and atrioventricular canal type Perimembranous defects may be partially obstructed by aneurysmal membranous septum tissue or overriding or straddling tricuspid valve tissue.

Left ventricular outflow obstruction

Left ventricular (pulmonary) outflow tract obstruction is also common, and in the three series was found in 53%, including 16% with pulmonary atresia (Table 43.2). The severity of the obstruction varies from mild stenosis to atresia. Obstruction occurs at the valvar or subvalvar level.

Subpulmonary stenosis may be from a fibromuscular membrane or tunnel-like hypoplasia. It may be related to an aneurysm of the membranous ventricular septum prolapsing into the left ventricular outflow tract because of the systemic pressure in the morphologic right ventricle (Figure 43.3) or from accessory mitral or tricuspid valve tissue or systolic anterior motion of the mitral valve.

Tricuspid valve abnormalities

The tricuspid valve is abnormal in most patients at autopsy, but not necessarily clinically relevant. The abnormality often involves dysplastic valve leaflets and/or Ebstein's anomaly (Figure 43.2c). The severity varies widely, with the worst being severe Ebstein's anomaly. In the three combined series, the tricuspid valve was abnormal in 87%, with Ebstein's anomaly in 50% (Table 43.2).

Mitral valve abnormalities

Mitral valve abnormalities are less frequent than those of the tricuspid valve (Table 43.2). Gerlis *et al.* reported mild abnormalities in the number of leaflets in 21% and of the tension apparatus in 21% in their autopsy series of 29 hearts [12]. Less common abnormalities present in 13% included dysplasia, common atrioventricular orifice, stenosis, and cleft valve.

(a)

(b)

(c)
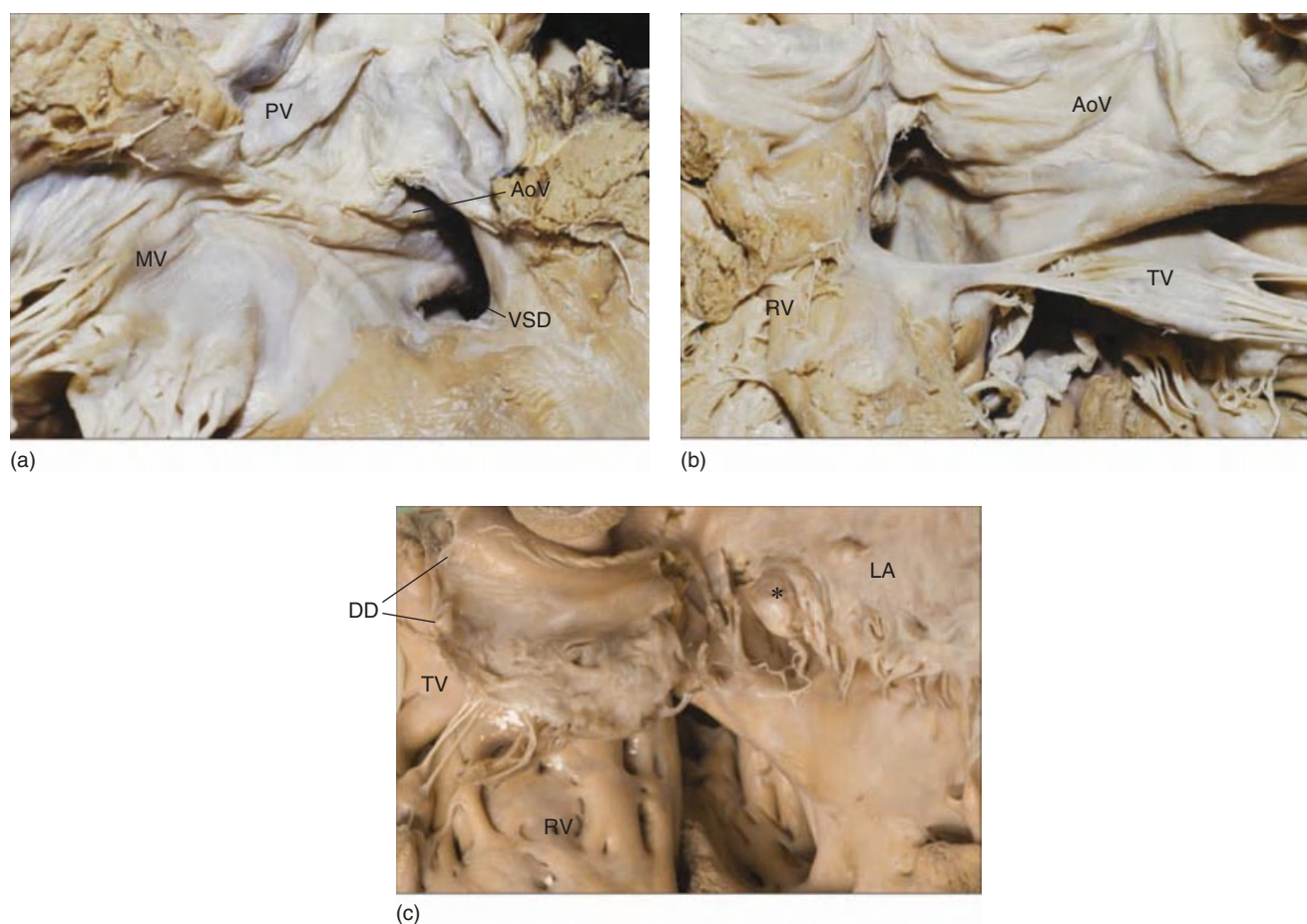
Figure 43.2 Ventricular septal defects in CCTGA. (a) and (b) from a 48-year-old man with a doubly committed (conal) type of VSD. (a) View from the left ventricle shows the VSD adjacent to both pulmonary and aortic valves. (b) A view of the VSD from the right ventricle with a deficient conal septum. (c) View from left atrium to right ventricle from a 10-year-old with a dysplastic (*) and mildly downwardly displaced (DD) left-sided tricuspid valve. AoV, aortic valve; LA, left atrium; MV, mitral valve; PV, pulmonary valve; RV, right ventricle; TV, tricuspid valve; VSD, ventricular septal defect.

Aortic valve abnormalities

Aortic valve abnormalities are uncommon (Table 43.2). Unusual extensions of the aortic valve sinuses inferiorly have been reported by McKay *et al.* [6]. The wall of the sinus in the enlarged areas was irregular with a lattice-like appearance.

Pathophysiology

In the patient with CCTGA without associated cardiac abnormalities, the prognosis is determined by progressive systolic dysfunction of the systemic right ventricle. Although there are macroscopic and microscopic structural differences between the morphologically left ventricle and right ventricle, the reasons for developing right ventricular dysfunction remain unknown. At a microvascular level, the coronary supply to the right ventricle differs from that of the left ventricle. Sestamibi myocardial perfusion scanning suggests that impaired myocardial perfusion and right ventricular myocardial fibrosis are frequent in this condition and associated with regional hypokinesis [13]. Recent attempts to confirm this finding using magnetic resonance delayed enhancement imaging have produced conflicting results [14,15]. Positron emission tomographic data have demonstrated that although resting myocardial blood flow to the systemic right ventricle does not differ from the systemic left ventricle in normal subjects, coronary flow reserve to the systemic right ventricle is substantially reduced (2.5 compared with 4.0) in the CCTGA group [16]. Thus, chronic low-grade coronary insufficiency may contribute to the progressive right ventricular dysfunction.

Tricuspid valve regurgitation frequently accompanies right ventricular dysfunction. The effect of tricuspid valve abnormalities may be greater in CCTGA because the right ventricle
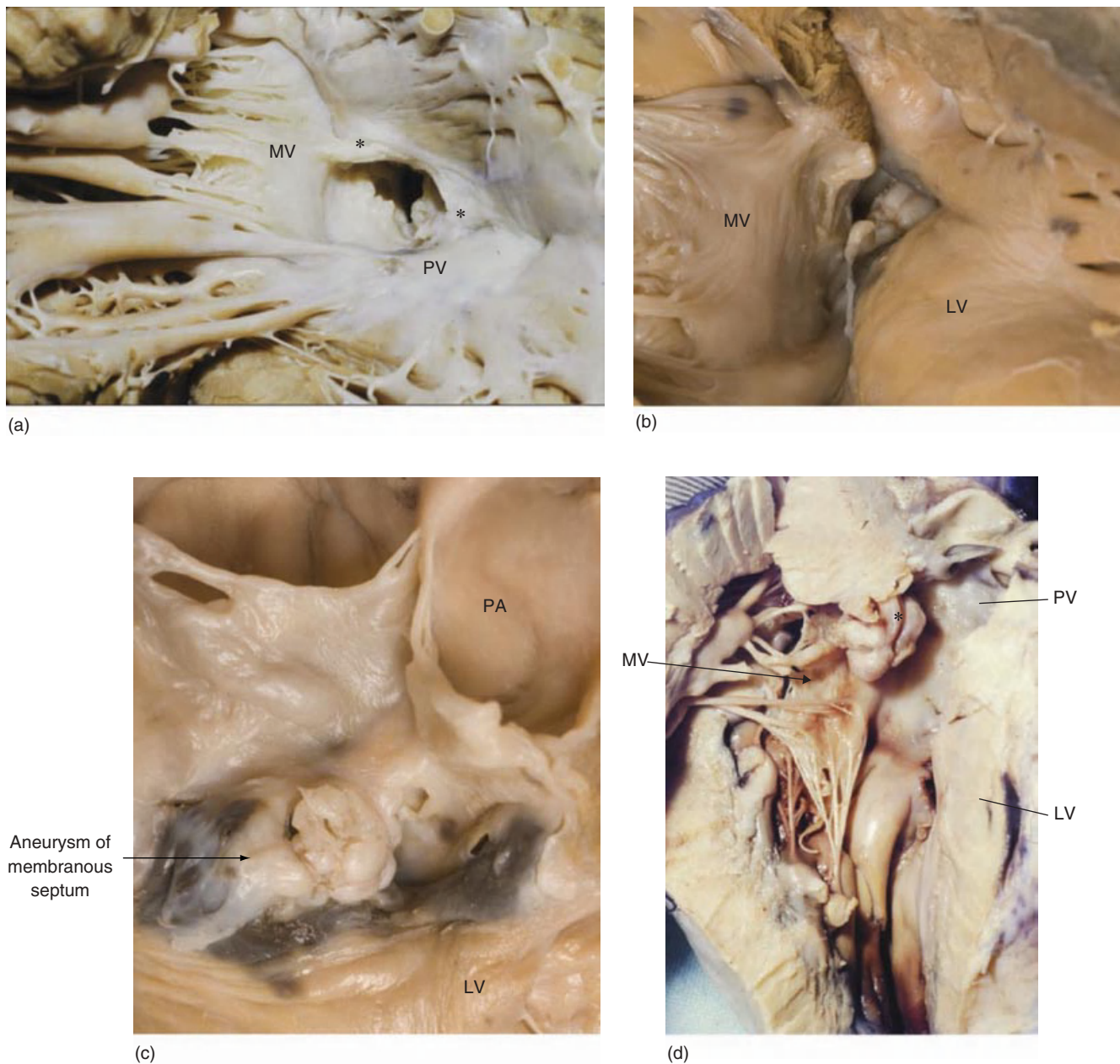
Figure 43.3 Left ventricular outflow tract obstruction in CCTGA. Views of left ventricular outflow obstruction produced by a postoperative remnant of a fibromuscular membrane between asterisks in (a), poor expansion and fibrous nodules in (b), aneurysm of the membranous septum bulging into the outflow in (c), and by accessory tissue (asterisk) attached to the mitral valve (MV) in (d). LV, left ventricle; MV, mitral valve; PA, pulmonary artery; PV, pulmonary valve.

is developing systemic pressure, therefore increasing the back-pressure on the tricuspid valve. The altered ventricular pressure relationship shifts the ventricular septum towards the left ventricle. This alters the geometry of the tricuspid annulus, which becomes more rounded than usual, and increases the likelihood that the tricuspid valve will become regurgitant. As the right ventricle fails and becomes more dilated, the associated tricuspid regurgitation worsens, adding to the right ventricular volume load.

Natural history

In a series of antenatal diagnoses from Guy's Hospital, when the pregnancy was continued, 19 of 23 babies survived to the end of pregnancy [17]. Postnatally the natural history of patients with CCTGA is largely dictated by right ventricular function and by the nature of associated lesions [18]. Patients with isolated CCTGA who have been diagnosed incidentally in

the fifth to seventh decades of life have been reported [19,20]. Although the right ventricle may supply the systemic circulation for decades, this appears to be the exception. Most patients develop progressive right ventricular dysfunction, sometimes as early as the first decade of life. A multinstitutional study of 182 adults with CCTGA showed that important systemic right ventricular dysfunction and congestive cardiac failure symptoms are common by the third decade of life and increase in frequency with advancing age, both in patients with and without associated lesions [21]. In this study, 25% of patients without associated lesions had clinical heart failure by age 45 years, compared with 67% of those with associated lesions. The study showed moderate or severe right ventricular dysfunction in 32% of patients without associated lesions and 56% of those with associated lesions. A single center review of 131 patients with CCTGA showed a survival rate of 75% at age 20 years, with a median age at death of 13 years [22].

Functional outcomes

In the muticenter study mentioned above [21], approximately 60% of patients with associated lesions were in Warnes–Sommerville functional class one, with most of the remainder being in class two. In patients without associated lesions, ~70% were in class one. Nevertheless, when measured objectively, most patients with CCTGA have impaired functional capacity. In a group of 41 adult patients [23], there was a markedly reduced maximal oxygen uptake of 22 ml kg^{-1} min^{-1} in the 19–29 years age group and 21 ml kg^{-1} min^{-1} in the 30–39 years age group (both were approximately half that of normal controls). In the 40–55 years age group, this dropped to 11 ml kg^{-1} min^{-1}, less than one-third of that of the healthy controls. Important causative factors include impaired ventricular function, limited chronotropic response to exercise, and abnormal lung function, particularly following cardiac surgery.

Electrophysiologic issues

Because of the abnormal anatomy of the atrioventricular node and the atrioventricular conduction bundle, patients with CCTGA have a 2% annual risk of developing complete heart block [24]. Careful follow-up with regular electrocardiograms and ambulatory electrocardiographic (Holter) monitoring should be performed to monitor cardiac conduction.

These patients have a high incidence of tachyarrhythmias [20,21,25], typically re-entry tachycardia due to either accessory atrioventricular pathways or a re-entry circuit between the two atrioventricular nodes [25]. In adult patients, the risk of atrial fibrillation increases and is related to ventricular dysfunction, atrioventricular valve regurgitation, and atrial dilatation.

Pregnancy

In a retrospective review of 60 pregnancies in 22 women with CCTGA over a 17 year period [26], 49 pregnancies resulted in live births. One woman had 12 pregnancies, of which 10 were successful; she had various complications, including congestive heart failure, endocarditis, and myocardial infarction. Only one of the 22 patients developed cardiac complications, congestive heart failure related to tricuspid valve regurgitation necessitating tricuspid valve replacement at 2 months postpartum. In another experience of 45 pregnancies in 19 patients, five had cardiac complications, including heart failure, worsening cyanosis, and cerebrovascular accident [27].

Although pregnancy may be well tolerated, detailed pre-pregnancy assessment should be performed. Women with functional class three or four, more than mild ventricular dysfunction, or significant tricuspid regurgitation should be counseled against pregnancy. Some data suggest that systemic right ventricular function may deteriorate, potentially irreversibly, during pregnancy. This concern should be discussed with patients [28]. During pre-pregnancy counseling, the uncertain maternal longevity in patients with CCTGA should be discussed.

Outpatient follow-up

Because of the concerns regarding the longer term outlook for patients with this diagnosis, all patients with CCTGA should be followed by a pediatric cardiologist or adult cardiologist with specific expertise in congenital heart disease. A follow-up interval of at least every 1–2 years is necessary. Because of the risk of progressive heart block, electrocardiography should be performed at each visit, with consideration of 24 h ambulatory electrocardiographic monitoring. Regular assessment of ventricular function is important. As cardiac magnetic resonance imaging (MRI) becomes more widely available, this should be performed at least every 3 years in patients without permanent pacemakers.

Clinical features

Clinical history

If not diagnosed antenatally, young children with CCTGA without associated lesions are likely to be asymptomatic. With an associated lesion, a murmur and/or symptoms of congestive cardiac failure are likely to be present. Older children and adults present with symptoms related to systemic right ventricular dysfunction. Cardiac conduction defects cause symptoms related to bradycardia. The diagnosis of isolated CCTGA is sometimes made in a previously asymptomatic adult patient in their sixth or seventh decade during investigation of a coronary event [19,20].

Physical examination

The pulse may be slow due to complete heart block. Palpation of the cardiac apex may reveal relative mesocardia or dextrocardia. A very loud single second heart sound due to the anterior positioning of the aorta is heard. With an associated lesion, a murmur is present. This may be a pan-systolic
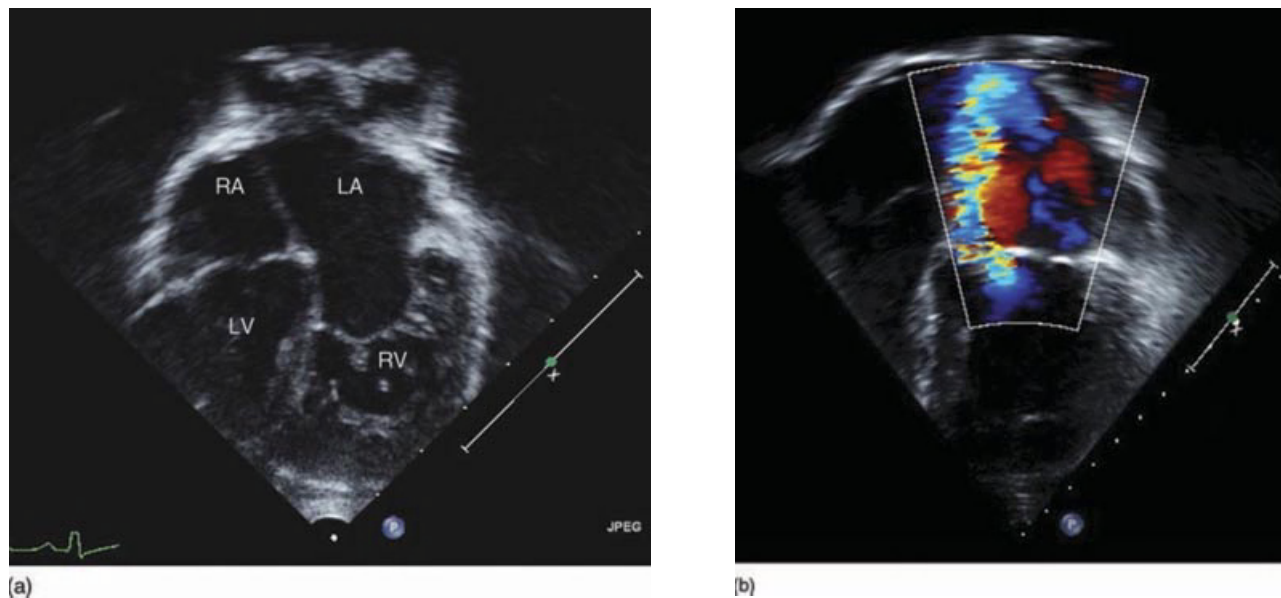
Figure 43.4 Echocardiographic images of CCTGA. (a) Apical four chamber view showing atrioventricular discordance with apical displacement of the tricuspid valve (Ebstein's anomaly). (b) Equivalent apical four chamber view with color Doppler showing regurgitation through the tricuspid valve. LA, left atrium; LV, left ventricle; RA, right atrium; RV, right ventricle.

murmur of a VSD or of tricuspid regurgitation, or may be an ejection systolic murmur of left ventricular outflow tract obstruction. With a large left-to-right ventricular level shunt, the infant shows signs of congestive cardiac failure with tachypnea, dyspnea, and hepatomegaly. Likewise, an older child or adult may develop signs of heart failure secondary to progressive systolic dysfunction of the systemic right ventricle.

Electrocardiographic features

The electrocardiogram is characteristic, at least in patients with situs solitus, with left-axis deviation and Q waves in the right but not the left precordial leads. Varying degrees of atrioventricular block may also be present and the combination of these two features strongly suggests the diagnosis of CCTGA.

Chest X-ray

There is a variable degree of mesocardia in some patients with CCTGA, and a minority have dextrocardia. The upper left heart border is straightened, representing the leftward position of the ascending aorta. The right pulmonary artery is often prominent because of the more medial position of the pulmonary trunk. Depending on associated lesions, there may be cardiomegaly, for example with a large VSD or significant tricuspid regurgitation.

Echocardiography

With increasing frequency, the diagnosis is made at antenatal echocardiography. Sharland *et al.* published a series of 34 antenatal diagnoses over a 10 year period [17]. In the fetal four-chamber echocardiographic view, the normal apical offsetting of the tricuspid valve is reversed, thus alerting the sonographer to the fact that the right atrium connects to a ventricle of left ventricular morphology. In a large VSD with inlet extension, especially with straddling or overriding of the tricuspid valve, the normal offsetting is not present.

Postnatally, echocardiography is the mainstay of diagnosis (Figure 43.4) A detailed sequential approach to the cardiac anatomy, starting with the visceral atrial situs and working through to the great arteries, must be used. The subcostal coronal view is very informative, allowing identification of venous, atrioventricular, and ventriculoarterial connections by sweeping through from posterior to anterior. In patients with CCTGA and situs solitus, the systemic veins connect to the right-sided atrium, which then connects via a mitral valve to a right-sided morphologically left ventricle. The mitral valve and left ventricle can be identified by the fine apical trabeculations, the smooth upper half of the ventricular septum, the basal offsetting of the septal hinge point of the atrioventricular valve, and the absence of septal insertions of the atrioventricular valve. The morphologic left ventricle connects to a bifurcating vessel (pulmonary artery), and there is mitral–pulmonary continuity.

On the left side, the pulmonary veins connect normally to the left atrium, but the left atrium connects via a tricuspid valve to the left-sided morphologic right ventricle. The tricuspid valve and right ventricle have characteristic features of heavy trabeculation of the ventricle apex, apical offsetting of the septal hinge point of the atrioventricular valve and septal insertions of the atrioventricular valve. The right ventricle connects to an arching vessel (aorta), which gives

rise to the coronary arteries. The aorta arises from a muscular infundibulum or conus. Therefore, there is tricuspid–aortic discontinuity.

In the parasternal short-axis view, the ventricles are essentially side-by-side and the septum is in an anteroposterior plane. The aortic and pulmonary valves are both seen en face in the short-axis view, due to the parallel arrangement of the great arterial origins. In most patients, the aorta is anterior and leftwards and the pulmonary artery posterior and rightwards. The coronary arterial anatomy is important and can usually be delineated by careful echocardiographic imaging, particularly using the parasternal short-axis view. The parasternal long-axis view is oriented more vertically than usual and, because of the anteroposterior orientation of the ventricular septum and side-by-side relationship of the ventricles, images may be obtained of only a single ventricle and outflow (either right ventricle and aorta, or left ventricle and pulmonary artery), which would not be possible when imaging a normal heart.

Associated lesions should be defined and the function of the systemic right ventricle and tricuspid valve assessed.

Cardiac catheterization and angiography

Prior to echocardiography, when cardiac catheterization was the major diagnostic method, the course of the catheters helped to reveal the abnormal relationships of the great arteries to the ventricles. Ventriculography demonstrated the ventricular "inversion" and the more vertical orientation of the ventricular septum. Occasionally, aortography may be necessary to delineate coronary anatomy, for example when the patient is being considered for a double-switch procedure, although cardiac computed tomography (CT) or MRI may provide this information noninvasively. Hemodynamic catheterization is usually necessary prior to considering the double-switch procedure, and to assess left ventricular retraining and adequacy of left ventricular pressure loading.

Other imaging modalities

Magnetic resonance imaging

Cardiac MRI has an increasing role in the quantitative assessment of systemic right ventricular function (Figure 43.5). Even MRI assessment of right ventricular function is challenging because of the complex shape of the right ventricle and the multiple coarse apical trabeculations and hypertrophy associated with systemic pressure functioning [29]. We use cardiac MRI as our primary method of tracking right ventricular size and function in patients without pacemakers, usually performing MRI approximately every 2–3 years in clinically stable patients.

Radionuclide ventriculography

In patients with a permanent pacemaker, MRI is not possible and echocardiography remains the primary imaging modality. In such patients, radionuclide ventriculography can assess the right ventricular function. This technique holds theoretical appeal for assessing the morphologic right ventricle because it is a blood pool technique which potentially solves the problems related to its shape and trabeculations. Radionuclide ventriculography, however, requires careful positioning and analysis, and should be performed by cardiologists trained in nuclear medicine or radiologists with expertise in the analysis of congenitally abnormal hearts. Radionuclear ventriculography of the systemic right ventricle correlates well with MRI in the related Mustard and Senning groups [30].

Medical management

Drug therapy

Data regarding the drug management of ventricular dysfunction of a systemic right ventricle are limited. In patients with symptomatic heart failure or moderate systemic right ventricular dysfunction, conventional left ventricular protection strategies are usually used. Angiotensin-converting enzyme (ACE) inhibitors and angiotensin receptor blockers have little or no benefit in postoperative Mustard and Senning patients, but the studies are small [31]. Beta-blocker use has not been studied in the CCTGA population, but there is some suggestion of benefit in Mustard and Senning patients [32].

Resynchronization therapy

Many CCTGA patients eventually require permanent pacing for complete heart block, with the ventricular lead being placed in the morphologic left ventricle. This may negatively affect the systemic right ventricle because of the resulting interventricular dyssynchrony. Resynchronization approaches to the systemic right ventricle have been used in patients with severe ventricular dysfunction, a coronary sinus lead being used to pace the right ventricle [33]. This approach has produced symptomatic improvement in some patients with class three to four symptoms.

Anatomic variations of the coronary sinus, mentioned above, have implications for placement of a coronary sinus lead to pace the right ventricle and would potentially make this approach impossible, necessitating a more invasive epicardial approach.

Surgical management

Conventional repair

Until recently, patients underwent repair of their associated lesions, for example VSD repair and/or insertion of a left ventricle to pulmonary artery conduit for pulmonary valve
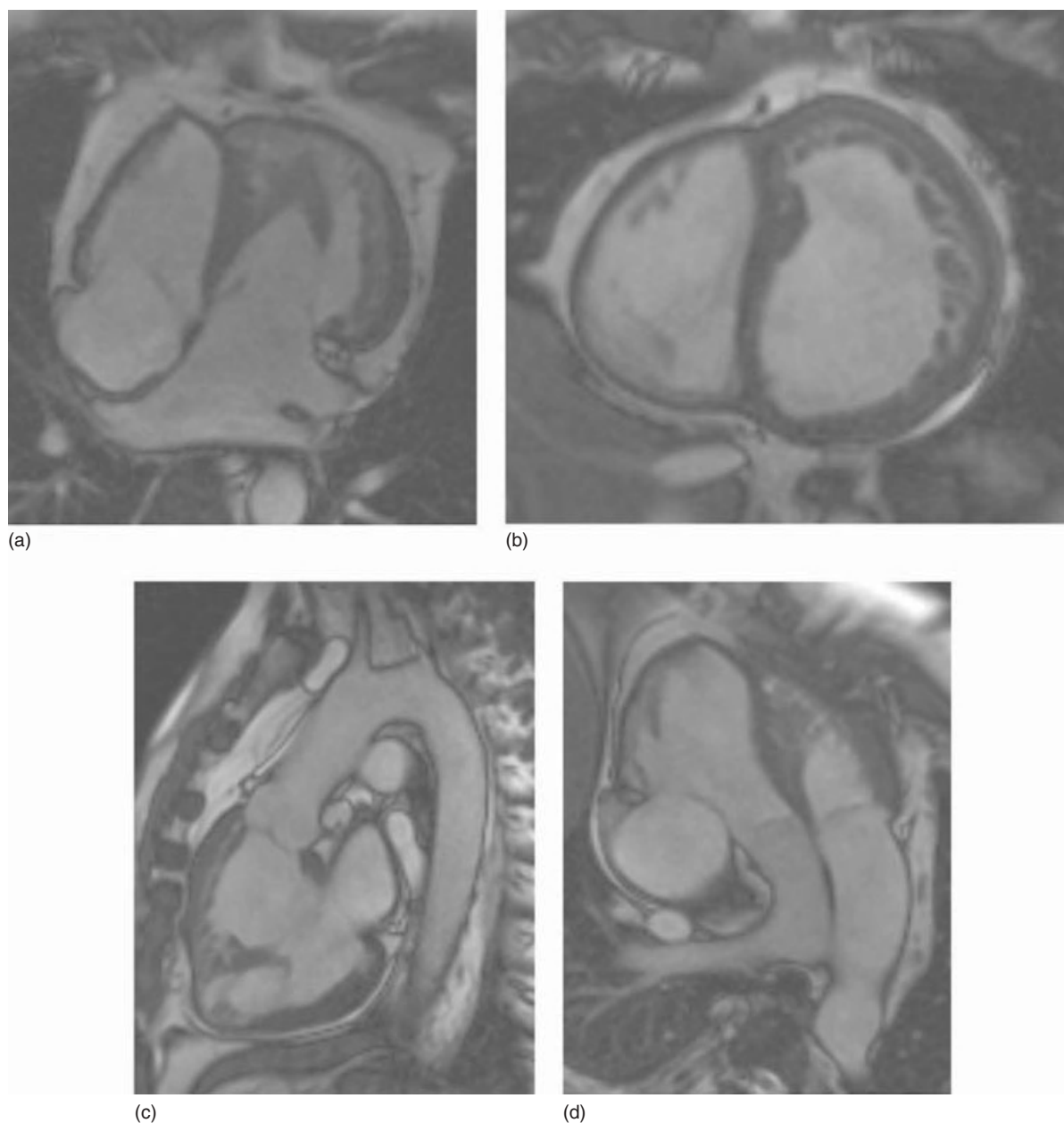
Figure 43.5 Magnetic resonance images of CCTGA. (a) Four-chamber image demonstrating atrioventricular discordance and mesocardia. The left atrium connects to a ventricle with heavy apical trabeculations and an apically displaced atrioventricular valve. (b) Short-axis image showing a hypertrophied, heavily trabeculated right ventricle on the right of the image and a thin-walled left ventricle on the left of the image. The septal position reflects the high-pressure right ventricle. (c) Long-axis view demonstrating the left atrium connecting to the right ventricle which supplies the aorta. (d) Image demonstrating the parallel course of the great arteries.

atresia or stenosis. After this repair, the right ventricle remained the systemic ventricle and the right ventricular dysfunction could be exacerbated by the negative myocardial effect of bypass surgery. Long-term results of this type of repair are disappointing: one group reported 52 patients with 15% operative mortality and a 10 year survival of 55% for patients with VSD and left ventricular outflow obstruction and 71%

for patients with VSD alone [34]. Another group reported 123 patients with a 10 year survival of 70% for VSD ± pulmonary stenosis or atresia [35]. Freedom from right ventricular dysfunction was ~40% at 15 years, with factors predicting right ventricular dysfunction being Ebstein's anomaly, tricuspid valve replacement, and postoperative complete heart block. Another group reported 127 patients (including nine

double-switch procedures) [36]. Operative mortality was 6%, 20 year survival was 48%, and the reoperation rate was 56%. Survival did not differ according to type of lesion.

Surgical management of systemic tricuspid valve regurgitation

Progressive tricuspid regurgitation is common and often associated with increasing right ventricular dysfunction. At the Mayo Clinic, 40 patients underwent tricuspid valve surgery, with valve replacement in 39 [37]. Preoperatively 68% were NYHA class three or four. Early mortality was 10%. With a median follow-up of 4.7 years (maximum 26 years), there were eight late deaths from congestive cardiac failure related to systemic right ventricular dysfunction. The 5 year survival was 78% and 10 year survival 68%. The surgery and preoperative right ventricular ejection fraction were correlated with survival. With right ventricular ejection fraction <44% the survival was 49% at 5 years and 20% at 10 years, whereas with right ventricular ejection fraction ≥44% the survival was 100%. The authors recommended that surgery for significant tricuspid regurgitation should be considered at the earliest sign of progressive right ventricular dysfunction. The Leiden group recently reported tricuspid valve surgery in 16 patients with a systemic right ventricle (including patients with d-TGA after the Mustard and Senning operations) [38]. Eight patients underwent repair and eight replacement. There was a trend towards decreased survival after valve repair compared with replacement and, after initial improvement in those undergoing repair, the regurgitation increased over the first postoperative year. This supports the impression that an approach of primary tricuspid valve replacement should be taken. Finally, pulmonary artery banding has been proposed as a definitive procedure to reset the position of the ventricular septum and improve tricuspid regurgitation in a systemic right ventricle [39].

Anatomic repair

Recent surgical approaches have focused on "anatomic" repair which returns the left ventricle to the systemic circulation and may improve long-term prognosis. These are major and technically challenging surgical procedures. Patients without left ventricular outflow obstruction and a pulmonary valve suitable to function as a neo-aortic valve may be operated using the double-switch procedure: this combines (1) the Senning atrial baffle procedure which redirects blood flow at atrial level and (2) the arterial switch procedure where the great arteries are transected and switched. Successful outcome depends on the left ventricle being adequately prepared to function at systemic arterial pressure. With a large VSD, the left ventricle has functioned at systemic pressure, but in the absence of associated lesions it has been functioning at normal pulmonary artery pressure. The low-pressure left ventricle can be "retrained" in younger children by pulmonary artery banding to increase left ventricular systolic pressure, although this approach has had mixed success. Patients with coexisting

VSD and left ventricular outflow obstruction can be approached using the Rastelli–Senning procedure. The Senning operation is combined with a Rastelli procedure which channels the left ventricular outflow across the VSD to the aorta and then places a right ventricle to pulmonary artery valved conduit.

Several series of double-switch and Rastelli–Senning procedures have reported a surgical mortality generally ranging from 0 to 10%. At the Cleveland Clinic, 46 patients underwent anatomic repair, with median age at surgery 28 months, the oldest patient being 16 years of age [40]. There were no hospital deaths and one late cardiac death during a median follow-up of 24 months. The Tokyo group published a series of 84 anatomic repairs with a 15 year survival of 75% for the double-switch and 80% for the Rastelli–Senning/Mustard procedure [41]. In another series of 54 patients, 7 year survival was 85% for the double-switch and 95% for the Rastelli–Senning procedure [42].

Left ventricular dysfunction is common after the double-switch procedure, being more frequent in those who required retraining [43]. The requirement for permanent pacing was a predictor for left ventricular dysfunction in one study of 44 patients [44].

Anatomic repair: patient selection

Most groups consider anatomic repair in patients requiring repair of associated defects when the left ventricle has been functioning at high systolic pressure. In patients without an associated lesion, subsystemic left ventricular pressure, and either right ventricular dysfunction or significant tricuspid regurgitation, retraining the left ventricle with pulmonary artery banding should be considered. Most centers would not recommend a double-switch procedure for such patients who have normal right ventricular and tricuspid valve function.

During childhood, the left ventricle has been successfully retrained using progressive pulmonary artery banding to increase left ventricular pressure load, promoting hypertrophy. Cardiac catheterization, echocardiography, and MRI can assess left ventricular pressure and wall thickness, mass, and function. In childhood a left ventricular systolic pressure at least 70–80% of systemic pressure and in adolescence a left ventricular systolic pressure closer to 100% of systemic pressure have been recommended to restore the left ventricle to the systemic circulation [40]. Others recommend a left ventricular mass: left ventricular volume ratio of >1.5 [45] or a normal left ventricular wall thickness and mass, using established echocardiographic or MRI values. During the banding process, the left ventricle must be monitored carefully. Development of left ventricular dysfunction is regarded as failure of left ventricular retraining. Age is one of the best predictors of failure of retraining, with most successfully retrained patients being <10 years of age. In a series of 23 patients considered candidates for a Senning plus arterial switch protocol [46], pulmonary artery banding was performed in 15 patients, in 11 for the sole purpose of

left ventricular retraining. The two oldest, aged 12 and 14 years, developed left ventricular failure necessitating band removal. Another banding patient following a double-switch procedure at age 7 years required heart transplantation for severe left ventricular failure with diastolic dysfunction.

The early results with the double-switch procedure have been promising, but long-term follow-up is uncertain.

References

1 Bjarke BB, Kidd BSL. Congenitally corrected transposition of the great arteries. A clinical study of 101 cases. *Acta Paediatr Scand* 1976;**65**:153–60.

2 Ferencz C, Rubin JD, McCarter RJ, *et al*. Congenital heart disease: prevalence at livebirth. The Baltimore–Washington Infant Study. *Am J Epidemiol* 1985;**121**:31–6.

3 Hornung TS, Calder L. Congenitally corrected transposition of the great arteries. *Heart* 2010;**96**:1154–61.

4 Van Praagh R. The segmental approach to diagnosis in congenital heart disease. *Birth Defects (Original Artic Ser)* 1972;**8**:4–23.

5 Ismat FA, Baldwin HS, Karl TR, *et al*. Coronary anatomy in congenitally corrected transposition of the great arteries. *Int J Cardiol* 2002;**86**:207–16.

6 McKay R, Anderson RH, Smith A. The coronary arteries in hearts with discordant atrioventricular connections. *J Thorac Cardiovasc Surg* 1996;**115**:988–97.

7 Allwork SP, Bentall HH, Becker AE, *et al*. Congenitally corrected transposition of the great arteries: morphologic study of 32 cases. *Am J Cardiol* 1976;**38**:908–23.

8 Anderson KR, McGoon DC, Lie JT. Vulnerability of coronary arteries in surgery for transposition of the great arteries. *J Thorac Cardiovasc Surg* 1978;**76**:135–9.

9 Uemura H, Anderson RH, Gerlis LM, *et al*. Surgical anatomy of the coronary circulation in hearts with discordant atrioventricular connections. *Eur J Cardiothorac Surg* 1996;**10**:194–200.

10 Anderson RH, Becker AE, Arnold R, *et al*. The conducting tissues in congenitally corrected transposition. *Circulation* 1974;**50**:911–23.

11 Van Praagh R, Papagiannis J, Grunenfelder J, *et al*. Pathologic anatomy of corrected transposition of the great arteries: medical and surgical implications. *Am Heart J* 1998;**135**:772–85.

12 Gerlis LM, Wilson N, Dickinson DF. Abnormalities of the mitral valve in congenitally corrected transposition (discordant atrioventricular and ventriculoarterial connections). *Br Heart J* 1986;**55**:475–9.

13 Hornung TS, Bernard EJ, Celermajer DS, *et al*. Right ventricular dysfunction in congenitally corrected transposition of the great arteries. *Am J Cardiol* 1999;**84**:1116–9.

14 Giardini A, Lovato L, Donti A, *et al*. Relation between right ventricular structural alterations and markers of adverse clinical outcome in adults with systemic right ventricle and either congenital complete (after Senning operation) or congenitally corrected transposition of the great arteries. *Am J Cardiol* 2006;**98**:1277–82.

15 Fratz S, Hauser M, Bengel FM, *et al*. Myocardial scars determined by delayed-enhancement magnetic resonance imaging and positron emission tomography are not common in right ventricles with systemic function in long-term follow up. *Heart* 2006;**92**:1673–7.

16 Hauser M, Bengel FM, Hager A, *et al*. Impaired myocardial blood flow and coronary flow reserve of the anatomical right systemic ventricle in patients with congenitally corrected transposition of the great arteries. *Heart* 2003;**89**:1231–5.

17 Sharland G, Tingay R, Jones A, *et al*. Atrioventricular and ventriculoarterial discordance (congenitally corrected transposition of the great arteries): echocardiographic features, associations, and outcome in 34 fetuses. *Heart* 2005;**91**:1453–8.

18 Paladini D, Volpe P, Marasini M, *et al*. Diagnosis, characterization and outcome of congenitally corrected transposition of the great arteries in the fetus: a multicenter series of 30 cases. *Ultrasound Obstet Gynecol* 2006;**27**:281–5.

19 Ikeda U, Furuse M, Suzuki O, *et al*. Long term survival in aged patients with corrected transposition of the great arteries. *Chest* 1992;**101**:1382–5.

20 Presbitero P, Somerville J, Rabajoli F, *et al*. Corrected transposition of the great arteries without associated defects in adult patients: clinical profile and follow-up. *Br Heart J* 1995;**74**:57–9.

21 Graham TP Jr, Bernard YD, Mellen BG, *et al*. Long-term outcome in congenitally corrected transposition of the great arteries: a multi-institutional study. *J Am Coll Cardiol* 2000;**36**:255–61.

22 Rutledge JM, Nihill MR, Fraser CD, *et al*. Outcome of 121 patients with congenitally corrected transposition of the great arteries. *Paediatr Cardiol* 2002;**23**:137–45.

23 Fredriksen PM, Chen A, Veldtman G, *et al*. Exercise capacity in adult patients with congenitally corrected transposition of the great arteries. *Heart* 2001;**85**:191–5.

24 Huhta JC, Maloney JD, Ritter DG, *et al*. Complete atrioventricular block in patients with atrioventricular discordance. *Circulation* 1983;**67**:1374–7.

25 Daliento L, Corrado D, Buja G, *et al*. Rhythm and conduction disturbances in isolated, congenitally corrected transposition of the great arteries. *Am J Cardiol* 1986;**58**:314–8.

26 Connolly HM, Grogan M, Warnes CA. Pregnancy among women with congenitally corrected transposition of the great arteries. *J Am Coll Cardiol* 1999;**33**:1692–5.

27 Therrien J, Barnes I, Somerville J. Outcome of pregnancy in patients with congenitally corrected transposition of the great arteries. *Am J Cardiol* 1999;**84**:820–4.

28 Guédès A, Mercier LA, Leduc L, *et al*. Impact of pregnancy on the systemic right ventricle after a Mustard operation for transposition of the great arteries. *J Am Coll Cardiol* 2004;**44**:433–7.

29 Winter MM, Bernink FJ, Groenink M, *et al*. Evaluating the systemic right ventricle by CMR: the importance of consistent and reproducible delineation of the cavity. *J Cardiovasc Magn Reson* 2008;**10**:40–7.

30 Hornung TS, Anagnostopoulos C, Bharadwaj P, *et al*. Comparison of equilibrium radionuclide ventriculography and cardiovascular magnetic resonance for assessing the systemic right ventricle after the Mustard or Senning procedures for complete transposition of the great arteries. *Am J Cardiol* 2003;**92**:640–3.

31 Dore A, Houde C, Chan KL, *et al*. Angiotensin receptor blockade and exercise capacity in adults with systemic right ventricles: a multicenter, randomized, placebo-controlled clinical trial. *Circulation* 2005;**112**:2411–6.

32 Josephson CB, Howlett JG, Jackson SD, *et al*. A case series of systemic right ventricular dysfunction post atrial switch for simple D-transposition of the great arteries: the impact of beta-blockade. *Can J Cardiol* 2006;**22**:769–72.

33 Jauvert G, Rousseau-Paziaud J, Villain E, *et al*. Effects of cardiac resynchronization therapy on echocardiographic indices, functional capacity, and clinical outcomes of patients with a systemic right ventricle. *Europace* 2009;**11**:184–90.

34 Termignon JL, Leca F, Vouhé PR, *et al*. "Classic" repair of congenitally corrected transposition and ventricular septal defect. *Ann Thorac Surg* 1996;**62**:199–206.

35 Hraska V, Duncan BW, Mayer JE Jr, *et al*. Long-term outcome of surgically treated patients with corrected transposition of the great arteries. *J Thorac Cardiovasc Surg* 2005;**129**:182–91.

36 Yeh T Jr, Connelly MS, Coles JG, *et al*. Atrioventricular discordance: results of repair in 127 patients. *J Thorac Cardiovasc Surg* 1999;**117**:1190–203.

37 Van Son JA, Danielson GK, Huhta JC, *et al*. Late results of systemic atrioventricular valve replacement in corrected transposition. *J Thorac Cardiovasc Surg* 1995;**109**:642–52.

38 Scherptong RW, Vliegen HW, Winter MM, *et al*. Tricuspid valve surgery in adults with a dysfunctional systemic right ventricle: repair or replace? *Circulation* 2009;**119**:1467–72.

39 Acar P, Sidi D, Bonnet D, *et al*. Maintaining tricuspid valve competence in double discordance: a challenge for the paediatric cardiologist. *Heart* 1998;**80**:424–5.

40 Duncan BW, Mee RB, Mesia CI, *et al*. Results of the double switch operation for congenitally corrected transposition of the great arteries. *Eur J Cardiothorac Surg* 2003;**24**:11–9.

41 Shin'oka T, Kurosawa H, Imai Y, *et al*. Outcomes of definitive surgical repair for congenitally corrected transposition of the great arteries or double outlet right ventricle with discordant atrioventricular connections: risk analyses in 189 patients. *J Thorac Cardiovasc Surg* 2007;**133**:1318–28.

42 Langley SM, Winlaw DS, Stumper O, *et al*. Midterm results after restoration of the morphologically left ventricle to the systemic circulation in patients with congenitally corrected transposition of the great arteries. *J Thorac Cardiovasc Surg* 2003;**125**:1229–41.

43 Quinn DW, McGuirk SP, Metha C, *et al*. The morphologic left ventricle that requires training by means of pulmonary artery banding before the double-switch procedure for congenitally corrected transposition of the great arteries is at risk of late dysfunction. *J Thorac Cardiovasc Surg* 2008;**135**:1137–44.

44 Bautista-Hernandez V, Marx GR, Gauvreau K, *et al*. Determinants of left ventricular dysfunction after anatomic repair of congenitally corrected transposition of the great arteries. *Ann Thorac Surg* 2006;**82**:2059–66.

45 Ly M, Belli E, Leobon B, *et al*. Results of the double switch operation for congenitally corrected transposition of the great arteries. *Eur J Cardiothorac Surg* 2009;**35**:879–83.

46. Devaney EJ, Charpie JR Ohye RG, Bove EL. Combined arterial switch and Senning operation for congenitally corrected transposition of the great arteries: patient selection and intermediate results. *J Thorac Cardiovasc Surg* 2003;**125**:500–7.

44 Transposition and Malposition of the Great Arteries with Ventricular Septal Defects

Daniel Sidi, Pascal Vouhé & Phalla Ou

Hôpital Necker – Enfants Malades, Université Paris V, Paris, France

Introduction: A new approach based on surgery

Conventionally, pediatric cardiology books have different chapters covering transposition of the great arteries with ventricular septal defects (VSDs) and double-outlet ventricles (especially double-outlet right ventricle). This is because the usual approach in pediatric cardiology is to classify malformations into subgroups according to their anatomy and hemodynamics and then apply the surgical technique appropriate for each subgroup. This approach, however, does not work well for this group of malformations because of their extreme anatomic polymorphism and because of the difficulty in defining surgically helpful subgroups based on classical definitions. In addition, there are controversies about the definitions of some malformations, for example, double-outlet right ventricle, that are based by some authors on embryology (the double infundibulum, regardless of the malposition of the vessels or the location of the VSDs), by others on anatomy (focusing on the malalignment between the vessels and the presumed septum), and by yet others on hemodynamic and surgical features depending on the position of the VSD relative to the great arteries.

Our group therefore decided to put these malformations together under the global appellation of either "malposition of the great arteries" or "abnormal ventriculoarterial connection with ventricular septal defect" and to base our approach in a nonconventional way on the different surgical options rather than on the different anatomic subgroups. We first describe the different surgical techniques and their anatomic and hemodynamic requirements, then look at the malformations to determine the best match between the repair and the malformation. We believe that each of these malformations deserves a "tailor-made" operation and not an operation "off the peg."

Key points

1 This group of lesions includes a large variety of malformations with different embryologic origins and different pathologic definitions but a common surgical approach.

2 The clinical presentation and surgical indications are based on the presence or absence of pulmonic stenosis and the position of the great arteries with respect to the VSD and the annuli of the atrioventricular valves.

3 Surgery is based on anatomic correction by constructing a tunnel between the left ventricle and the aorta (or the switched pulmonary artery) and reconstructing a right ventricle–pulmonary artery communication (or a communication to the switched aorta), if possible without prosthetic material. Despite the apparent complexity, with pertinent indications and when the VSD is perimembranous (below the infundibula of the great arteries) without added malformations of ventricular sizes or atrioventricular valves, the surgical results and the prognosis are good.

Epidemiology

These lesions represent ~5% of congenital malformations and ~20% of conotruncal malformations. Unlike tetralogy of Fallot, pulmonary atresia with VSD, and truncus arteriosus, these malformations are rarely (except in heterotaxia syndromes) associated with extracardiac malformations or chromosome abnormalities and have a low recurrence rate.

Embryology, pathology, and definitions

Cardiac malformations involving the ventriculoarterial connection are linked to the fate of the subarterial conus (infundibulum) during the later part of cardiac embryogenesis (see Chapter 1). Because conotruncal resorption participates not only in the spatial relationship between the aorta, the pulmonary artery, and the atrioventricular valves but also in the closure of the ventricular septum in the perimembranous and infundibular portion, the association of the three anomalies is frequent. The association results in an extreme polymorphism of malformations, however, because the three anomalies will not always combine in a consistent pattern. The VSD is usually in the perimembranous part of the septum just beneath the infundibulum of the great arteries (often persisting below both great arteries) and is often the consequence of malalignment between the infundibular septum and the rest of the ventricular septum (trabecular septum) [1–6]. This malalignment eventually produces sub-pulmonic stenosis when the infundibular septum is deviated towards the pulmonary artery (as in tetralogy of Fallot) [1,4,6] or subaortic stenosis when the infundibular septum is deviated towards the aorta (as in coarctation of the aorta or an interrupted aortic arch) [7]. As a result of the obstruction, the fetal growth of the corresponding great artery is impaired, producing a small aorta or pulmonary trunk (but with normal intrapulmonary branches).

The other major intracardiac consequence of a persistent conus is that it maintains the arterial orifice at a distance from the atrioventricular annulus and, depending on the length of the infundibulum, the great vessels arise near to or far from the atrioventricular valve annulus (Figure 44.1). In addition,

if there is an asymmetric infundibulum, the distances from the artery to the mitral valve and the tricuspid valve will differ.

To understand the wide spectrum of these malformations and why there are difficulties and debates about defining and classifying some of them (namely, the wide spectrum of the malformation called double-outlet right ventricle), it is necessary to describe the normal relationships between the great arteries and the ventricles and to realize that there is a large difference between concordance and alignment. The normal heart is characterized by an aorta that with the resorption of its infundibulum moves posteriorly into the center of the heart, in continuity with the annuli of the atrioventricular valves and the ventricular septum, whereas the pulmonary artery stays well above its persisting infundibulum in discontinuity with the atrioventricular valves (Figures 44.2 and 44.3). In addition, there is torsion
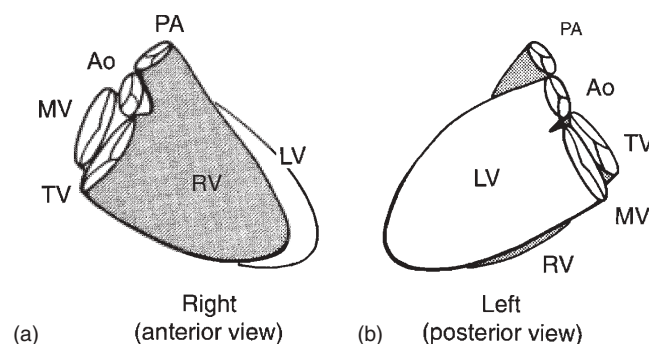
Figure 44.2 Diagram of normal heart to show aortic annulus in center of heart, closely associated with the annuli of the other three valves. (a) Right ventricular (RV) view. (b) Left ventricular (LV) view. o, aortic valve annulus; MV, mitral valve annulus; PA, pulmonic valve annulus; TV, tricuspid valve annulus.
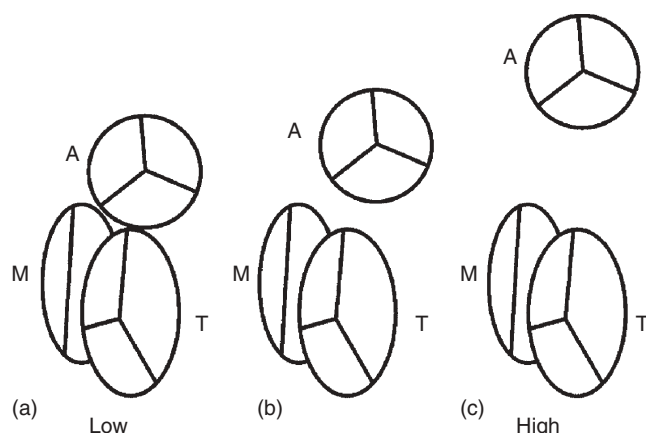
Figure 44.1 Diagram to show different relationships of the annulus of a great artery (A, shown by the upper circle with the triradius in it) to the mitral valve annulus (M) and the tricuspid valve annulus (T). (a) Close relationship. (b) The great artery annulus is further away, but its distances to both atrioventricular annuli are equal. (c) Not only is the great artery annulus far away, but also its distances from the mitral and tricuspid valve annuli are unequal.
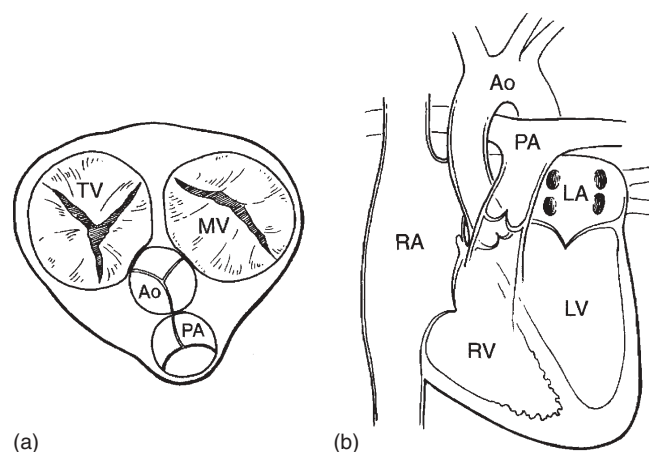
Figure 44.3 Diagram of normal heart to show continuity between the aortic valve annulus (Ao) and the annuli of the tricuspid valve (TV) and the mitral valve (MV). It also shows the discontinuity between the pulmonic valve annulus (PA) and the annuli of the tricuspid and mitral valves. Note that the pulmonary artery is anterior. (a) Cross-sectional view; (b) LA, left atrium; longitudinal section; LV, left ventricle; RA, right atrium; RV, right ventricle.

between the upper part of the heart (the origin of the great arteries) and its apical part (determined by the axis of the trabecular septum). This torsion explains why, in a normal heart, the aorta rises from the left ventricle but because of the twist appears to arise in line with the right ventricular outlet and the pulmonary artery from the right ventricle but above the left ventricle (Figure 44.4). Therefore, concordance does not match alignment even in the normal heart. When the septum is intact, however, concordance is evident, nobody pays attention to the "physiologic anatomic malalignment," and there is no controversy about the connections of a normal heart or the ventriculoarterial discordance of a complete transposition of the great arteries. When there is a large subarterial VSD, the question of connection and alignment is much more difficult to answer because the origin of the great artery depends on the supposed situation of the upper part of the ventricular septum (Figure 44.5).
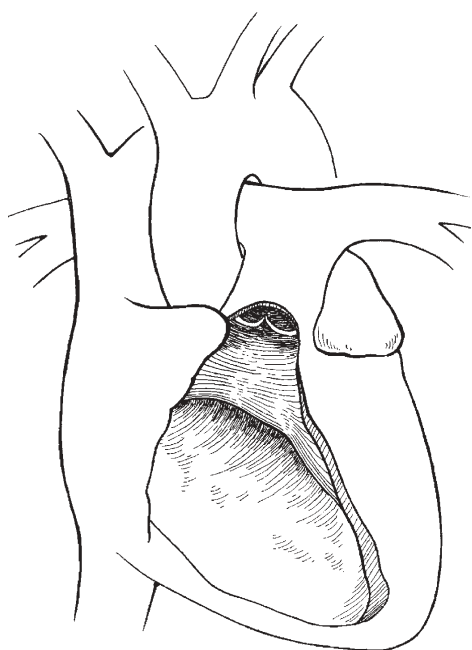
This is precisely the problem with double-outlet right ventricle, a congenital anomaly in which both great arteries arise wholly or principally from the right ventricle. This definition is clear only in theory. In reality, this definition leads to controversies when there is a large VSD beneath the infundibula of the great arteries.

Most pathologists insist on the alignment of the great arteries in relation to the ventricle; if more than half of the artery is over one ventricle, it is considered to arise from this ventricle, regardless of atrioventricular discontinuity (or subarterial conus) [4,8–10]. Because septal alignment is not physiologic, even in the normal heart, we believe that this definition is misleading, particularly when the two great arteries are above a VSD. Indeed, the origin of the vessel depends entirely on the way in which the VSD is closed at the upper edge of the septum, and this is not constant (see Figure 44.5). If the upper part of the septum is the conus between the aorta and the pulmonary artery, each artery arises from a different ventricle and there is no double-outlet right ventricle (Figure 44.5b). If the upper part of the septum is at the lateral edge of the conus, the two arteries arise from the right ventricle if the septum is at the left edge of the conus (double-outlet right ventricle) (Figure 44.5c). On the other hand, if the septum is at the right edge of the conus, the heart ends up with a double-outlet left ventricle (Figure 44.5a) [11]. In addition, what matters for the patient is not which part of the persisting infundibulum is really the upper septum, but what difficulty the surgeon has in closing the VSD in a correct position and allowing normal ventriculoarterial concordance or discordance without obstruction.

Figure 44.4 Diagram to show the normal spiral relationship of the aorta (Ao) and pulmonary artery (PA) to the right ventricle (RV).
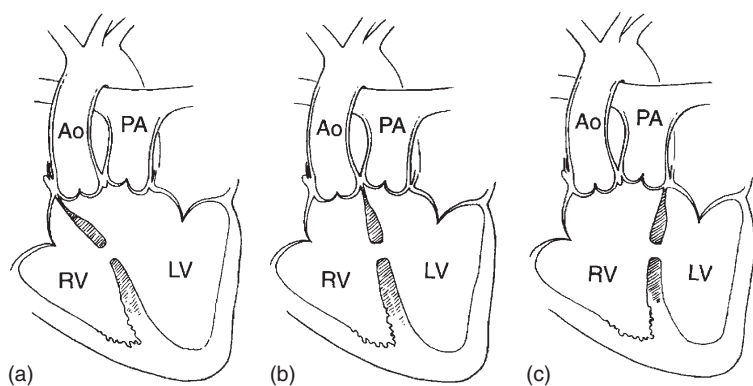
Figure 44.5 Diagram to show how the position of the infundibular septum determines whether there is a double-outlet left ventricle (a), a normal connection (b), or a double-outlet right ventricle (c). Ao, aorta; LV, left ventricle; PA, pulmonary artery; RV, right ventricle.
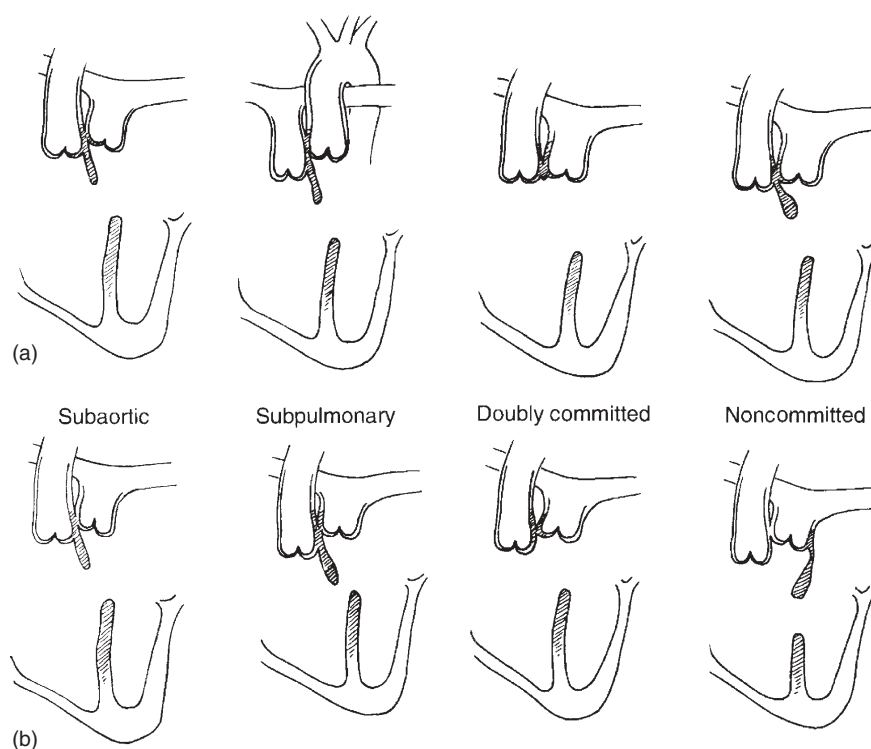
Figure 44.6 Diagram to show how the simple classification of Lev *et al*. [9] (a) becomes less useful once variations in the position of the infundibular septum occur (b).

Other pathologists require for the definition of double-outlet right ventricle a double infundibulum, regardless of the septal alignment [6]. This may have interesting embryologic or etiologic implications (in the chicken, various kinds of double-outlet right ventricle are created by stopping the embryologic process prematurely), but surgically speaking, it is not helpful or can even be misleading because the malformation is not completely identified by the conus abnormality alone. Some double-outlet right ventricles are nearly like a simple VSD despite a long subaortic infundibulum. Others with subpulmonary stenosis resemble a tetralogy of Fallot or a transposition of the great arteries with VSD with or without pulmonary stenosis. Some even resemble a more complex malformation such as a single ventricle if atrioventricular valve abnormalities, significant differences in ventricular cavity sizes, or even multiple VSDs are present.

This dilemma cannot be solved by the recommendation of Lev *et al*. [9] to identify double-outlet right ventricle by the position of the VSD relative to the great arteries: subaortic, subpulmonary, doubly committed, or noncommitted. The problem with this classification is that it is impossible to define clearly the extreme polymorphism of these malformations by this method alone because the polymorphism is determined by three independent variables (Figure 44.6). More important, there is no strict correlation between the commitment of the VSD to one or the other artery and the surgical options. Repair in many patients with double-outlet right ventricle and a subpulmonary VSD can be achieved by intraventricular rerouting, as for a subaortic

VSD, without an arterial switch or displacement of the pulmonary artery. Conversely, some subaortic VSDs may require other types of repair than just an intraventricular patch or a tunnel between the left ventricle and the aorta.

Double-outlet left ventricle is less controversial because this rare malformation is characterized almost always by complete resorption of the two infundibula, which brings the two great arteries into continuity with the atrioventricular valves above a large perimembranous VSD [11]. Pulmonic stenosis is usually present, there being a small annulus with a stenosed valve. The relation between the vessels and the atrioventricular valves and the presence or absence of pulmonic stenosis determine the best surgical strategy by the same rules as for any "malposition with a VSD."

Malposition of the great arteries can occur also in complex malformations such as atrioventricular canal or a large inlet VSD, particularly in heterotaxia syndromes.

The problem with any anatomic definition of these malpositions with VSD is that the malformation cannot be fully characterized by identifying the relationship between the great arteries alone, or the relation of the arteries with the atrioventricular valves alone, or the location of the VSD alone, because the three anomalies play independent roles. It is necessary to consider each of the three anatomic components, because they determine an infinite variety of anatomic malformations with different hemodynamics and surgical strategies. To summarize, under the conditions discussed in this chapter, if neither the clinician nor the surgeon is able to classify the individual patient into a single clear category, the

patients may receive a standardized but nonoptimal operation based on an incomplete anatomic description. Furthermore, the medical community cannot evaluate the results because it is difficult to know from the literature which anatomic lesion was operated on with each particular technique.

We think that the only way to achieve appropriate surgical decisions is not to classify subgroups of patients anatomically but to consider each patient with malposition and VSD as unique [12]. Then we need to determine whether the cardiac anatomy and hemodynamics fit with one of the possible anatomic repairs. If more than one surgical option exists for any given patient, one should choose the best and least risky procedure. It is therefore necessary for the pediatric cardiologist to know in detail the surgical requirements for the different operations. *Then the cardiologist checks by constructing mentally and on the echocardiography screen what the outflows of the two ventricles will be after repair*.

Surgical options and preoperative screening

Anatomic repair

We call anatomic repair a surgical procedure that allows the left ventricle to be connected to the aorta and the right ventricle to be connected to the pulmonary artery as directly as possible, preferably without a prosthetic conduit.

Before the different surgical options are described, it is necessary to remember certain important facts:

1 The infundibular septum can be removed with no risk of atrioventricular block if the VSD is perimembranous [8,13,14], even when there are tricuspid insertions on the septum.

2 The great arteries can be switched if there is no organic subpulmonic stenosis and if the pulmonary valve is normal, regardless of the coronary artery distribution (see Chapter 42).

3 The pulmonary artery can be connected to the right ventricle without a prosthetic conduit if the pulmonary artery branches are not fixed because of previous surgery (aortopulmonary shunts) [11,15–18]. This maneuver, however, sacrifices the pulmonary valve and therefore can be applied only if the pulmonary vascular resistance is low, pulmonary arteries are of adequate size without stenoses, and postcapillary hypertension (due to left ventricular or mitral valve dysfunction) is absent.

On the basis of these considerations, there are three fundamental types of anatomic repair (two ventricles and no tube).

Intraventricular repair

Intraventricular repair (IVR) consists of creating an intraventricular patch to direct the left ventricular blood towards the aortic orifice (Figure 44.7). The operation resembles simple closure of an isolated VSD, but if the aorta is far removed from the mitral valve, the operation requires a long intracardiac tunnel that passes posterior to the right ventricular outflow tract. The fundamental consideration is that the right ventricular outflow tract should not be obstructed by the tunnel, and this depends mainly on the position of the pulmonary artery in relation to the tricuspid valve. If the distance between the tricuspid valve and the pulmonary artery is long enough (equal to or greater than the distance to the aortic annulus), the left ventricular to aortic tunnel will not obstruct the right ventricular outflow tract regardless of the length of the tunnel (Figure 44.7a). If the distance from the pulmonary artery to the tricuspid valve is less than to the aortic annulus, either the pulmonary artery must be moved (Figure 44.7b) (see the later section on REV) or the tunnel must be constructed from the left ventricle to the pulmonary artery in association with a switch of the great arteries (Figure 44.7c) (see the next section on arterial switch).
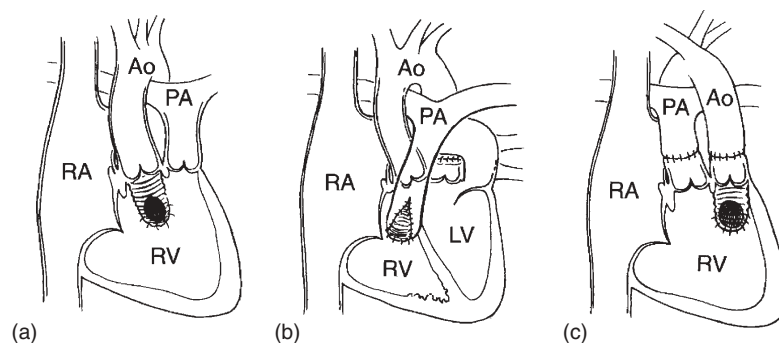
Figure 44.7 Diagram to show factors affecting the type of surgery for double-outlet right ventricle. (a) A long tunnel connects the left ventricle to the aorta without obstructing the outflow to the pulmonary artery. (b) If the tricuspid valve annulus is closer to the pulmonary artery than to the aortic annulus, the pulmonary artery can be removed and inserted into the anterior wall of the right ventricle in the REV operation. (c) Alternatively, the great arteries can be switched, and a tunnel connects the left ventricle to the pulmonary artery. Ao, aorta; LV, left ventricle; PA, pulmonary artery; RA, right atrium; RV, right ventricle.

To avoid left ventricular to aortic obstruction and to make this tunnel as short as possible (to avoid diminishing the size of the right ventricular cavity), the infundibular septum should be removed whenever it is in the way, that is, posterior to the aorta. If the VSD is perimembranous, there is no theoretical risk of atrioventricular block. If the tricuspid valve is inserted on the infundibular septum, the septum is not resected but mobilized posteriorly and reinserted on the patch. The only contraindication to this operation is insertion of the mitral valve on the infundibular septum.

Arterial switch with ventricular septal closure (IVR + Switch)

This operation consists in creating an intraventricular patch to direct the left ventricular blood towards the pulmonary artery, which will become an aorta after the arterial switch (Figure 44.7c). This is possible when the pulmonic valve is normal and there is no subpulmonic organic obstruction due to musculofibrous pulmonary valve tissue or mitral valve insertion in the subpulmonic region. As in IVR, the patch should not obstruct the future right ventricular outflow tract. In this respect, the same rules as for IVR are applied and the infundibular septum should be resected if it is anterior to the pulmonary artery (future aorta).

Intraventricular repair with reposition of the pulmonary artery on the right ventricle (Rastelli and REV)

Both operations have the same principles: creating an intraventricular tunnel to direct the left ventricular blood flow towards the aortic orifice and creating a new connection between the right ventricle and the pulmonary artery.

In the classical Rastelli operation [19], the left ventricle to aorta connection is achieved without resecting the conal septum and the right ventricle to pulmonary artery pathway is created using an extracardiac valved conduit. This procedure has major drawbacks: risk of subaortic stenosis, severe amputation of the right ventricular cavity, need for multiple reoperations for conduit obstruction, and high risk of endocarditis.

To obviate most of these problems, Lecompte and coworkers developed an operation called REV (réparation à l'étage ventriculaire) [17]. Compared with the Rastelli procedure, the REV operation presents two major modifications (Figure 44.7b). (1) The infundibular septum is always resected extensively (even if the VSD is large). This creates a short and straight intracardiac tunnel and reduces the risk of subaortic stenosis, reduces the amputation of the right ventricular cavity, and thus preserves right ventricular function, and finally improves left ventricular function by avoiding a large septal patch which may act as a diverticulum or even an aneurysm. (2) The pulmonary artery is translocated anterior to the aorta and reimplanted directly on the right ventricle; this reduces the need for multiple reoperations

(although the risk of developing RVOT obstruction is not completely avoided).

For all these reasons, in patients who need intraventricular repair with repositioning of the pulmonary artery, the REV operation is the procedure of choice, unless there are anatomic reasons (hypoplastic pulmonary arteries, elevated pulmonary arterial pressure) which demand a competent pulmonary valve.

Bex–Nikaidoh operation

The Bex–Nikaidoh procedure can be used when it is not possible to connect the left ventricle with one of the great arteries through the VSD [20,21]. This usually occurs when the VSD is not beneath the arteries (inlet or trabecular VSD), and may sometimes happen when there are abnormal insertions of the mitral valve on the infundibular septum.

The principle is to excise the aortic root with the subaortic conus from the right ventricle (as for the Ross operation) and to reimplant the aortic root on the left ventricular outflow tract (eventually after enlarging the conal septum, as for the Konno–Ross operation); this, of course, needs the concomitant transfer of the coronary arteries. The right ventricular outflow tract can be reconstructed using various techniques: with the native pulmonary valve when it is abnormal, using an extracardiac valved conduit, or by direct reimplantation (as for the REV procedure).

Nonanatomic repair

We consider a repair to be nonanatomic when the operation results in the right ventricle being located beneath the aorta or when each ventricle does not receive the correct venous return. We also need to differentiate between the one-ventricle repair (total cavopulmonary circulation equivalent to the repair of a single ventricle) and the "1½-ventricle repair," in which only part of the caval venous return (usually from the inferior vena cava) enters the right ventricle while the other part (usually from the superior vena cava) goes directly to the lungs (partial cavopulmonary anastomosis) [22,23].

A biventricular but nonanatomic repair can be achieved by leaving the right ventricle beneath the aorta in very special anatomy where the left ventricle or mitral valve is abnormal. The VSD is closed, allowing the creation of a nonstenotic right ventricle to aorta tunnel, and the left ventricle to pulmonary artery connection can be achieved with or without a tube depending on the anatomy. Sometimes it is necessary to add an atrial switch by a Mustard or Senning procedure in order to bring the oxygenated blood from the pulmonary veins to the subaortic right ventricle, as in double switch for corrected transposition when a Mustard or Senning procedure is necessary to bring oxygenated blood to the left ventricle.

If the ventricle is small, one can achieve the so-called "1½ ventricle repair" by adding to the repair a partial cavopulmonary circulation (usually performed as a palliative procedure first).

This type of surgery can leave the right ventricle beneath the aorta if it is the left ventricle or mitral valve that is not well developed or be more anatomic if the left ventricle can be put beneath the aorta when the right ventricle is too small.

Finally, sometimes the "best or the least worst" option is to abandon the idea of an intraventricular repair and plan for a single-ventricle strategy with a total cavopulmonary circulation. This option is often due to reduced left ventricle cavity size, straddling of the mitral valve, or multiple VSDs with more holes than septum.

Preoperative anatomic evaluation

Each patient must be regarded as unique, and all anatomic and hemodynamic aspects important to the operation must be investigated. The pediatric cardiologist must, like an architect, construct the tunnel mentally and use echocardiography to assess whether there is potential outflow tract obstruction after the anatomic repair (left ventricle to future aorta and right ventricle to future pulmonary artery). It is useful to perform the two-dimensional echocardiogram with the surgeon present to clarify particular anatomic details. Three-dimensional echocardiography and MRI will be particularly helpful in the future in this group of malformations [24]. The examination must evaluate the feasibility of an anatomic repair and, if it is possible, the feasibility of IVR. The echocardiographer must look carefully at the position of the VSD and search for multiple VSDs, especially at the apex; the relative position of the great arteries and above all their relation to the atrioventricular valves; the function and the insertions of the atrioventricular valves; and the size of the ventricles. MRI is very useful with relative hypoplasia of the RV in order to decide on the possibility of a two-ventricle repair, the help of a partial cavopulmonary circulation, or the need to accept a single-ventricle strategy. Quantitative assessment of ventricular volumes and function can be determined accurately based on the combination of a 3D data set and a high spatial and temporal resolution of the cardiac cavities regardless of their morphologies and without geometric assumptions. Independence from geometric assumption is especially important in this setting as the right ventricle may have an unusual shape. MRI is also a useful adjunct to echocardiography for a comprehensive assessment of the relationships of the great arteries with respect to each other, and also the relative positions of the great vessels with respect to the VSD and the atrioventricular valves.

Feasibility of an anatomic repair

Anatomic repair requires adequacy of both ventricles to assume their future workload. Therefore, both ventricles must be of adequate size and function; there is usually concern about the size of the left ventricle in malpositions with pulmonic stenosis (and reduced pulmonary venous return) and with the size of the right ventricle in malposition with coarctation of the aorta. Abnormal ventricular size or func-tion, however, also occurs with a restrictive VSD [25,26] or an inlet VSD with an overriding atrioventricular valve. We believe that the best index of ventricular size is the size of the atrioventricular valve annulus (in the absence of an overriding or straddling valve). An atrioventricular annulus size >2 SD below normal is a contraindication to anatomic repair. Assessment of ventricular function is based on ventricular contractility, knowing that the ventricle should be hyperkinetic if the afterload is low (increased pulmonary blood flow or atrioventricular valve regurgitation) or have adaptive hypertrophy secondary to valvar or subvalvar aortic obstruction or secondary to a restrictive VSD that functions like a subaortic stenosis if both great arteries originate from the right ventricle [25,26].

Both atrioventricular valves should be inspected carefully, not only for size and function but also for the subvalvar apparatus (chordae and papillary muscles), particularly any abnormal insertion on the subarterial infundibula. Tricuspid valve chordal attachments on the infundibular septum or even straddling it are not a contraindication because the valve can be repaired adequately and suffice for a low-pressure subpulmonic ventricle. Conversely, abnormal attachments of the mitral valve are usually a contraindication unless the valve is competent and the surgeon can avoid touching it during surgery without creating obstruction.

Multiple trabecular VSDs (Swiss cheese) or an inlet VSD may lead to serious complications.

A restrictive VSD can be a problem not only if it affects normal growth and function of the left ventricle (see earlier), but also if the VSD is not perimembranous. If it is not, any enlargement of the defect is dangerous for the conduction system (although anterior extension of the VSD is theoretically safe).

Finally, the afterload of both ventricles must be acceptable. We should pay particular attention to pulmonary arterial stenosis, especially after an aortopulmonary anastomosis, and to pulmonary hypertension. With pulmonic stenosis, the criteria are similar to those applied to tetralogy of Fallot. With pulmonary hypertension, assessing pulmonary vascular resistance is necessary, just as for a simple VSD with the added questions of operability and necessity for a patent pulmonary valve in the long term. It is these afterload factors that may justify cardiac catheterization.

Feasibility of an intraventricular repair

For this repair, the crucial point is to determine whether it is possible to construct a left ventricular to aortic tunnel between the tricuspid and pulmonic orifices. This is possible if the tricuspid to pulmonic distance is equal to or longer than the diameter of the aortic annulus. This is best seen on a subxiphoid right anterior view (Figure 44.8). If the pulmonary artery is above a well-developed infundibulum with a tricuspid to pulmonic distance greater than the aortic annulus, an IVR is possible regardless of the size of the aortic infundibulum. On the left anterior subxiphoid view (Figure 44.9),

Figure 44.8 Two-dimensional echocardiogram in subxiphoid view (oblique left anterior). This echocardiogram shows where a tunnel from the left ventricle (LV) to the aorta (Ao) would have to be for an intraventricular repair. PA, pulmonary artery; RV, right ventricle.

we can best see the infundibular septum that may need to be resected to construct a nonobstructed tunnel if the aorta is anterior (and the infundibular septum is posterior to the aorta) because it stands in the way from the posterior left ventricle to the anterior aorta. Conversely, when the aorta is posterior to the pulmonary artery, the infundibular septum is anterior to both the aorta and the left ventricular to aortic tunnel and may even constitute part of its wall.

If, however, the tricuspid to pulmonic distance is short (less than aortic annulus size), a simple IVR is not feasible. The choice is then between a tunnel from the left ventricle to the pulmonary artery in association with an arterial switch or a Bex–Nikaidoh operation and a tunnel from the left ventricle to the aorta with occlusion of the pulmonic orifice and direct right ventricle–pulmonary artery continuity (REV) or a right ventricle–pulmonary artery conduit (Rastelli).

Surgical classification

1 *Malposition that can be treated by IVR:* IVR is possible when the pulmonary artery annulus is far from the tricuspid valve annulus (see Figure 44.7a), regardless of the position of the aorta, as that determines only the length of the tunnel. If there is pulmonic or subpulmonic stenosis, the operation is
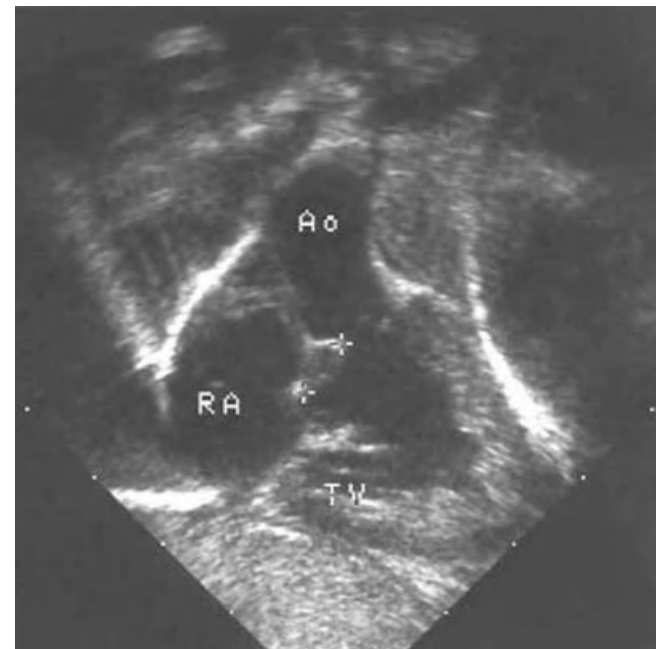
(a)
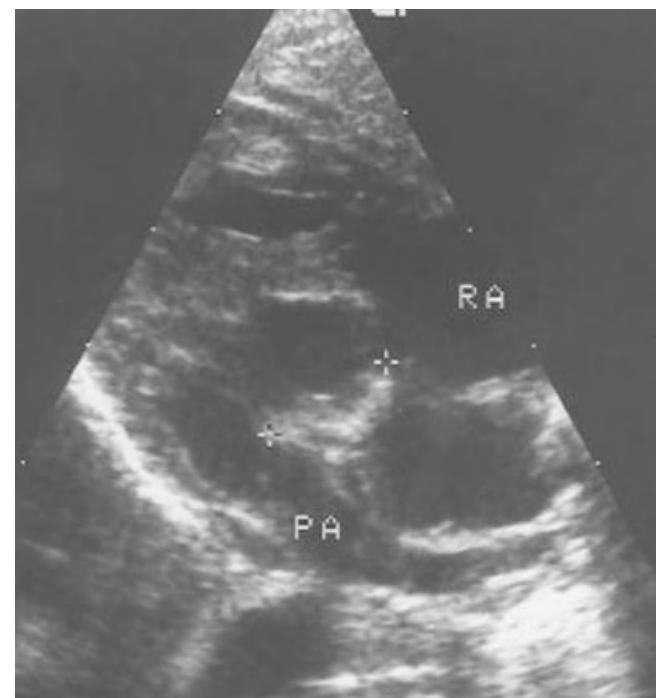
(b)

Figure 44.9 Two-dimensional echocardiograms in subxiphoid view (right anterior) of the same patient as in Figure 44.8. Because the distances from the tricuspid annulus to the aortic and pulmonary artery annuli cannot be seen in the same plane, two different views are needed. (a) The crosses show the distance between the tricuspid valve (TV) annulus and the annulus of the aorta (Ao). In this patient, the distance is 6.2 mm. (b) The crosses show the distance between the tricuspid valve annulus and the annulus of the pulmonary artery (PA). In this patient, the distance is 10.1 mm. Because the size of the subpulmonic conus is too short for an IVR, the appropriate correction would be a REV operation (see text). RA, right atrium.

similar to that for a tetralogy of Fallot with the same concerns about the coronary artery distribution (see Chapter 41).

2 *Malposition that can be treated by a tunnel from the left ventricle to the pulmonary artery in association with an arterial switch:* This operation is possible when there is no pulmonic or subpulmonic stenosis and when the aortic annulus is far from the tricuspid valve annulus. This distance allows a nonobstructive right ventricular outflow tract connection to the pulmonary artery (previous aorta) anterior to the left ventricular to aortic (previous pulmonary artery) tunnel (Figure 44.7c).

3 *Malposition that can be treated by a left ventricular to aortic tunnel in association with the displacement of the pulmonary artery (REV):* This operation can be done if there is a pulmonic stenosis (valvar or subvalvar) that contraindicates an arterial switch and when the pulmonary artery annulus is near the tricuspid annulus, which would lead to pulmonary artery obstruction by a left ventricular to aortic tunnel (Figure 44.7b). The pulmonary annulus and valves are sacrificed, and the junction between the right ventricle and the pulmonary artery is made either by a conduit (Rastelli operation) or better by the translocation of the pulmonary artery anteriorly on to the right ventricle (REV).

4 *Complex malpositions that cannot lead to a "simple" biventricular repair:* Biventricular repair usually cannot be performed when the VSD (inlet or trabecular) is not committed to a great artery because placing a tunnel from the left ventricle to one of the great arteries is difficult when both arise from the right ventricle. It can also be difficult to repair these malformations when there are anomalies of the ventricles or the atrioventricular valves or when the conal septum cannot be removed because of mitral attachments.

These complex malpositions need careful discussion before a decision is made between a palliative operation and corrective surgery with a high risk of atrioventricular block, atrioventricular valve replacement, or ventricular damage. Many of these complex situations can probably be solved using the Bex–Nikaidoh principle.

One interesting option in some patients is a 1½ ventricle repair (see earlier) when the right ventricle is too small initially or when it becomes too small after the left ventricular to aortic tunnel has been placed.

For clinical assessment, natural history, and pathophysiology, it is necessary to distinguish patients with and without pulmonary artery stenosis.

Malposition with ventricular septal defect without right ventricular outflow tract obstruction

Pathophysiology

The absence of right ventricular outflow tract obstruction leads (as in simple VSD) to pulmonary artery hypertension with increased pulmonary blood flow and a long-term risk of developing pulmonary vascular obstructive disease.

As in VSD, because the pulmonary vascular resistance decreases slowly after birth, pulmonary blood flow is not excessive in the neonatal period and heart failure does not occur unless there is aortic obstruction, usually associated with coarctation of the aorta [27].

Because of the malposition, some hypoxemia is present, depending on the relative position of the great arteries with respect to the ventricles and on the streaming patterns. Hypoxemia is never severe because of the increased pulmonary blood flow and adequate shunting through the VSD (right ventricle to pulmonary artery in systole and left to right ventricle in diastole).

Clinical findings, diagnosis, and management

In the fetus, malposition of the great arteries with a VSD is well tolerated. Diagnosis can be made on two-dimensional echocardiography if the screening includes exploration of the outlet septum and vessels and is not limited to the four-chamber view that can be normal.

In the neonate, there is usually mild cyanosis without respiratory distress and a systolic murmur (not constant) in an otherwise apparently healthy infant. If there is early heart failure, arterial pulses are usually diminished in the legs because of an associated coarctation of the aorta. After a few weeks, because of the increased pulmonary flow and left ventricular volume overload, congestive heart failure develops, manifested by dyspnea, liver enlargement, nutritional difficulties, and failure to gain weight. The clinical picture is that of a large VSD with mild cyanosis.

Chest radiography

The chest film shows cardiomegaly and increased lung vascularity. The thymus is present, and there is usually a left aortic arch.

Electrocardiography

The electrocardiogram shows right ventricular hypertrophy, sometimes with right axis deviation, depending on the location of the VSD and the course of the conduction pathways.

Echocardiography

Echocardiography confirms the diagnosis, demonstrating the VSD and the abnormal position of the great arteries. These have to be assessed independently. There is no correlation between the relative positions of the great arteries and the position of the VSD [17].

It evaluates pulmonary vascular resistance (if the patient is >3 months old) by evaluating left ventricular dimensions, looking at left ventricular dilatation as a sign of increased pulmonary blood flow and low pulmonary vascular resistance. It may be possible to estimate pulmonary artery

diastolic pressure from the velocity of a pulmonary artery regurgitant jet.

It indicates the likely type of surgery. It is crucial to analyze precisely the relationship of the aortic and pulmonary artery annuli to the atrioventricular valve annuli and also the size and position of the VSD. The two-dimensional echocardiographic subxiphoid view allows visualization of a tunnel between the left ventricle and one of the great arteries to see what it will look like (Figures 44.8 and 44.9). The examination also identifies any valvar attachment to the conal septum that would be removed at surgery.

Cardiac catheterization

Catheterization is usually not needed to define anatomic details except if there is a doubt on two-dimensional echocardiography about pulmonary artery branches or an associated trabecular VSD. Cardiac catheterization is useful for evaluating pulmonary vascular resistance in older children. In particular, it is the only way to assess the streaming patterns and to determine pulmonary artery oxygen saturation and therefore the arteriovenous difference in oxygen content that allows calculation of pulmonary vascular resistance. In the neonate, a streaming pattern with higher saturation in the pulmonary artery than in the aorta is a good indication for a Rashkind procedure that will probably improve aorta saturation without increasing pulmonary artery blood flow.

Natural history

Pulmonary vascular disease can develop as early as 3 months of age and be manifested by increased cyanosis and decreased congestive heart failure.

In some patients, the VSD becomes smaller and obstructs the left ventricular outflow if both vessels originate from the right ventricle, especially if there is no atrial septal defect. If there is a large atrial septal defect, there will be a rerouting of the blood and a progressive exclusion of the left ventricle from the circulation, so that the left ventricle will not grow properly.

Treatment and results

Medical treatment is nonspecific and intended to improve the circulation and stabilize the infant so that an operation can be performed soon. As in all patients with a VSD and heart failure, improvement can usually be obtained by diuretics, blood transfusion in anemic patients (to improve arterial oxygen content and decrease lung flow by increasing pulmonary vascular resistance through increased viscosity), vasodilators, and digoxin. If a neonate has cardiac failure, usually in association with coarctation of the aorta, prostaglandin E_1 (PGE_1) infusion, artificial ventilation, and inotropic support with dobutamine are helpful. If there is inadequate mixing or a high left atrial pressure, with increased flow and a functional gradient across the mitral valve, a Rashkind

atrioseptostomy is indicated to improve the clinical status (heart failure and cyanosis) before surgery.

Surgery is mandatory before 3 months of age to protect the lungs from developing pulmonary vascular disease.

Pulmonary artery banding may be indicated to protect the small pulmonary arteries, either if there is no straightforward anatomic repair or to wait until the infant is larger and healthier before undergoing an operation that may be difficult (e.g., if the tunnel will be long, if the tricuspid valve is attached to the infundibular septum, or if the right ventricle will be small after surgery). The banding is done by thoracotomy or sternotomy, improves congestive heart failure, but increases hypoxemia and may hinder an eventual arterial switch by dilating the pulmonary sinuses of Valsalva and altering the future aortic leaflets.

Corrective surgery with anatomic repair is usually possible (see the surgical classification earlier) either by a tunnel from the left ventricle to the aorta (IVR) if the pulmonary annulus is far enough from the tricuspid valve annulus or by a tunnel from the left ventricle to the pulmonary artery in association with an arterial switch if the aortic annulus is far from the tricuspid valve annulus.

With coarctation of the aorta, most surgical teams perform corrective surgery at once in the neonatal period rather than go through a coarctation repair and pulmonary artery banding as a first-stage procedure.

Hospital mortality for correction is ~10%, with excellent results. The patient needs an annual evaluation with two-dimensional echo Doppler examination to assess the left and right ventricular outflow tracts and the growth of the two great arteries. If an arterial switch has been performed, a coronary artery angiogram should be considered. Obstruction of the left ventricular–aortic junction is rare when the surgery has involved adequate removal of the conal septum. Usually, the heart grows in harmony, close to normal anatomy.

The long-term follow-up and results of IVR are similar to those for isolated VSD, because left ventricular-aortic obstructions are rare (none in the Lecompte series). When an arterial switch is added, complications of the switch procedure may be encountered (see Chapter 42) with common, but rarely severe, supravalvar pulmonic stenosis, common aortic dilatation with minimal (color Doppler) aortic regurgitation, and a few ischemic complications or potential complications due to the association of the coronary artery transfer with coronary ostial stenosis. When coarctation of the aorta is present, the follow-up should include the search for residual aortic obstruction and systemic hypertension at rest or during exercise. A scan or magnetic resonance imaging of the aorta may be useful to check the aortic isthmic anatomy after the aortoplasty.

When anatomic repair is not possible, the situation is similar to a single ventricle with pulmonary hypertension. It is imperative to protect the pulmonary arteries by

banding with the intention of later creating a cavopulmonary circulation.

Malposition with ventricular septal defect and pulmonic stenosis

Pathophysiology

The pathophysiologic features of this combination are similar to those in tetralogy of Fallot with more hypoxemia for the same degree of pulmonic stenosis because some of the oxygenated blood may return to the lungs as a result of streaming. There are usually no hypoxic spells because the subpulmonic stenosis is less muscular (especially if the vessels are transposed). The pulmonary artery branches are usually of normal size without proximal or distal stenosis.

If there is a higher saturation in the pulmonary artery than in the aorta, hypoxemia can be treated by creating an atrial septal defect by a Rashkind procedure (see Chapters 10 and 42).

Clinical findings, diagnosis, and management

In the fetus, malposition of the great arteries with VSD and pulmonic stenosis is well tolerated. The diagnosis can be made on two-dimensional echocardiography if the outlet septum and vessels are examined and the screening is not limited to the four-chamber view that can be normal.

In the neonate, cyanosis is present and is associated with a rough systolic ejection murmur in an otherwise apparently healthy infant. With severe pulmonic stenosis or even pulmonary atresia, cyanosis can be severe in the neonate, who may need early intervention with PGE_1 to maintain patency of the ductus arteriosus, followed by an early operation (usually a palliative shunt, but also a balloon dilatation). Cyanosis increases rapidly because of the increased oxygen consumption and decrease in pulmonary flow.

Chest radiography

The chest film shows normal cardiac size and variable lung vascularity. A thymus is present, and the aortic arch is usually left sided.

Electrocardiography

The electrocardiogram shows nonspecific right ventricular hypertrophy.

Echocardiography

It confirms the diagnosis, demonstrating the VSD, the abnormal position of the vessels, and the pulmonic stenosis.

It evaluates the degree and the type of the pulmonic stenosis, which is usually subvalvar and valvar and only rarely has anomalies of the pulmonary artery branches.

It helps establish the type of surgery. As explained before, it is crucial to analyze precisely the relationship of the aortic and pulmonary annuli with the atrioventricular valve annuli and also the size and position of the VSD. The two-dimensional echocardiographic subxiphoid view allows the physician to visualize the tunnel between the left ventricle and the aorta. The examination can also identify any valvar attachment to the conal septum that might need to be removed at surgery.

Cardiac catheterization

Catheterization is usually unnecessary unless a Rashkind procedure is indicated, except to assess pulmonary artery branches after a previous shunt or if there is a doubt on two-dimensional echocardiography, MRI, or CT scan about the pulmonary artery branches, associated trabecular VSD, or coronary artery disposition if there is to be a Fallot-type repair. Pressures in the pulmonary arteries (taken directly or through an occluded pulmonary vein) may also be useful in deciding about incorporating a valve in the right ventricle–pulmonary junction.

Natural history

Cyanosis increases, polycythemia occurs, and there will be increased collateral circulation from the aorta to the pulmonary arteries.

Treatment and results

If a neonate has severe hypoxemia, usually in association with pulmonic atresia or severe stenosis, PGE_1 infusion maintains ductal flow. A Rashkind procedure is often useful to improve the mixing of the blood.

Balloon dilatation may be useful if there is a valvar component to the pulmonic stenosis to avoid or delay an aortopulmonary anastomosis or defer corrective surgery. Balloon dilatation is especially effective when oxygen saturation is lower in the pulmonary artery than in the aorta (as in tetralogy of Fallot). This finding is common when the aorta is near the left ventricle, but it may occur even when the great arteries are transposed because of the streaming patterns due to the location (especially the angulation) of the infundibulum with respect to the outflow tracts of the ventricles.

Surgery

Aortopulmonary anastomosis can be performed to delay corrective surgery until the infant is larger and healthier. The anastomosis is usually carried out through a median sternotomy and although it improves hypoxemia, it may hinder later corrective surgery by distorting and fixing a pulmonary artery branch that will be difficult to mobilize for the REV.

Corrective surgery is usually possible by a tunnel from the left ventricle to the aorta, either by an IVR associated with removal of a right ventricular tract obstruction, as in a tetralogy of Fallot repair, or by mobilizing the pulmonary artery in an REV or Rastelli repair when the distance from the pulmonary

artery annulus to the tricuspid valve annulus is less than that to the aortic annulus. When the pulmonary artery is near the tricuspid valve annulus, the pulmonary artery is closed above the valve, and the distal pulmonary artery is mobilized and translocated on the right ventricle in an REV operation or connected to the right ventricle by a prosthetic tube in a Rastelli operation.

Most surgical teams try to wait for at least 6 months or for a patient's body weight to reach 6 kg before performing an REV operation, especially to avoid the risk of subaortic stenosis by inadequate resection of the conal septum, and to wait for several years for a Rastelli repair. They start with a Rashkind procedure and an aortopulmonary anastomosis or a balloon dilatation.

Mortality is ~10%, with excellent results. Annual follow-up is needed as in tetralogy of Fallot for IVR or REV and as in truncus arteriosus for a Rastelli procedure.

When indicated, a Bex–Nikaidoh procedure can be performed early in life. The late results are unknown, particularly the fate of the reconstructed right ventricular outflow tract. Nevertheless, over an average follow-up of 11 years, the results of this procedure were far better than those of the Rastelli procedure, albeit with some reoperations for right ventricular outflow tract obstruction [28].

References

1 Neufeld HN, DuShane JW, Edwards JE. Origin of both great vessels from the right ventricle. II. With pulmonary stenosis. *Circulation* 1961;**23**:603–12.

2 Neufeld HN, DuShane JW, Wood EH, *et al*. Origin of both great vessels from the right ventricle. I. Without pulmonary stenosis. *Circulation* 1961;**23**:399–412.

3 Neufeld HN, Lucas RV Jr, Lester RG, *et al*. Origin of both great vessels from the right ventricle without pulmonary stenosis. *Br Heart J* 1962;**24**:393–408.

4 Anderson RH, Wilkinson JL, Arnold R, *et al*. Morphogenesis of bulboventricular malformations. II. Observations on malformed hearts. *Br Heart J* 1974;**36**:948–70.

5 Sridaramont S, Feldt RH, Ritter DG, *et al*. Double-outlet right ventricle: hemodynamic and anatomic correlations. *Am J Cardiol* 1976;**38**:85–94.

6 Van Praagh S, Davidoff A, Chin A, *et al*. Double-outlet right ventricle: anatomic types and developmental implications based on a study of 101 cases. *Coeur* 1982;**12**:389–440.

7 Lev M, Rimoldi HJA, Eckner FAO, *et al*. The Taussig–Bing heart: qualitative and quantitative anatomy. *Arch Pathol* 1966; **81**:24–35.

8 Wilcox BR, Ho SY, Anderson RH, *et al*. Surgical anatomy of double-outlet right ventricle with situs solitus and atrioventricular concordance. *J Thorac Cardiovasc Surg* 1981;**82**:405–17.

9 Lev M, Bharati S, Meng L, *et al*. A concept of double-outlet right ventricle. *J Thorac Cardiovasc Surg* 1972;**64**:271–81.

10 Walters HL III, Mavroudis C, Tchervenkov CI, *et al*. Congenital Heart Surgery Nomenclature and Database Project: double outlet right ventricle. *Ann Thorac Surg* 2000;**69**:S249–63.

11 Hagler DJ, Edwards WD. Double-outlet left ventricle. In: Emmanouilides GC, Allen HD, Riemenschneider TA, Gutgesell HP, eds. *Heart Disease in Infants, Children and Adolescents: Including the Fetus and Young Adult*, 5th edn. Baltimore: Williams & Wilkins, 1995: 1270–8.

12 Lecompte Y, Batisse A, Di Carlo D. Double-outlet right ventricle: a surgical synthesis. *Adv Card Surg* 1993;**4**:109–36.

13 Kawashima Y, Fujita T, Miyamoto T, Manabe H. Intraventricular rerouting of blood for the correction of Taussig–Bing malformation. *J Thorac Cardiovasc Surg* 1971;**62**:825–9.

14 Bharati S, Lev M. The conduction system in double outlet right ventricle with subpulmonic ventricular septal defect and related hearts (the Taussig–Bing group). *Circulation* 1976;**54**:459–67.

15 Rubay J, Lecompte Y, Batisse A, *et al*. Anatomic repair of anomalies of ventriculo-arterial connection (REV). Results of a new technique in cases associated with pulmonary outflow tract obstruction. *Eur J Cardiothorac Surg* 1988;**2**:305–11.

16 Vouhé PR, Tamisier D, Leca F, *et al*. Transposition of the great arteries, ventricular septal defect, and pulmonary outflow tract obstruction: Rastelli or Lecompte procedure? *J Thorac Cardiovasc Surg* 1992;**103**:428–36.

17 Sakata R, Lecompte Y, Batisse A, *et al*. Anatomic repair of anomalies of ventriculoarterial connection associated with ventricular septal defect. I. Criteria of surgical decision. *J Thorac Cardiovasc Surg* 1988;**95**:90–5.

18 Kirklin JW, Barratt-Boyes BG. Double outlet right ventricle. In: Kirklin JW, Barratt-Boyes BG, eds. *Cardiac Surgery*, 2nd edn. New York: Churchill Livingstone, 1993: 1469–500.

19 Rastelli GC, Wallace RB, Ongley PA. Complete repair of transposition of the great arteries with pulmonary stenosis. A review and report of a case corrected by using a new surgical technique. *Circulation* 1969;**39**:83–95.

20 Bex JP, Lecompte Y, Baillot F, *et al*. Anatomical correction of transposition of the great arteries. *Ann Thorac Surg* 1980;**29**:86–8.

21 Nikaidoh H. Aortic translocation and biventricular outflow tract reconstruction. A new surgical repair for transposition of the great arteries associated with ventricular septal defect and pulmonary stenosis. *J Thorac Cardiovasc Surg* 1984;**88**:365–72.

22 Chowdhury UK, Airan B, Sharma R, *et al*. One and a half ventricle repair with pulsatile bidirectional Glenn: results and guidelines for patient selection. *Ann Thorac Surg* 2001;**71**:1995–2002.

23 Reddy VM, McElhinney DB, Silverman NH, *et al*. Partial biventricular repair for complex congenital heart defects: an intermediate option for complicated anatomy or functionally borderline right complex heart. *J Thorac Cardiovasc Surg* 1998; **116**:21–7.

24 Friedberg MK, Su X, Tworetzky W, *et al*. Validation of 3D echocardiographic assessment of left ventricular volumes, mass, and ejection fraction in neonates and infants with congenital heart disease: a comparison study with cardiac MRI. *Circ Cardiovasc Imaging* 2010;**3**:735–42.

25 Mason DT, Morrow AG, Elkins RC, Friedman WF. Origin of both great vessels from the right ventricle associated with severe obstruction to left ventricular outflow. *Am J Cardiol* 1969;**24**:118–24.

26 Lavoie R, Sestier F, Gilbert G, *et al.* Double outlet right ventricle with left ventricular outflow tract obstruction due to small ventricular septal defect. *Am Heart J* 1971;**82**:290–9.

27 Sondheimer HM, Freedom RM, Olley PM. Double outlet right ventricle: clinical spectrum and prognosis. *Am J Cardiol* 1977;**37**:709–14.

28 Yeh T Jr, Ramaciotti C, Leonard SR, *et al.* The aortic translocation (Nikaidoh) procedure: midterm results superior to the Rastelli procedure. *J Thorac Cardiovasc Surg* 2007;**133**:461–9.

45 Common Arterial Trunk (Truncus Arteriosus)

Albert P. Rocchini & Bryan H. Goldstein
University of Michigan Health System, Ann Arbor, MI, USA

Introduction, incidence, and genetics

Common arterial trunk, also called truncus arteriosus, is an anomaly in which the systemic, pulmonary, and coronary circulations each arise from a single vessel and valve at the base of the heart. First described by Wilson in 1798 [1], it was re-reported by Buchanan in 1864 [2]. It is uncommon, occurring in 0.086/1000 live births [3]. The most common genetic syndrome associated with truncus arteriosus is chromosome 22q11 deletion (DiGeorge syndrome). In a large prospective cohort of patients with conotruncal defects, the 22q11 deletion was found in 34.5% of patients with truncus [4].

Embryology

Van Mierop *et al.* [1] and Bartelings and Gittenberger-de Groot [5] described conal and aortopulmonary septation in great detail. Truncal swellings, similar to the endocardial cushions, develop and divide the truncal lumen into an aortic and pulmonary trunk. The left ventricular origin of the aorta and the right ventricular origin of the pulmonary artery result from fusion of the proximal portion of the truncal septum (derived from the truncal swellings) with the developing conal septum (derived from the conal swellings). Valve swellings develop from truncal tissue at the point of fusion between the truncal and conal septa. Excavation of these swellings leads to formation of the aortic and pulmonary valves. In the embryo of ~5–6 mm, the right and left primitive pulmonary arteries (from the sixth pair of aortic branchial arteries) are symmetrical structures with respect to the truncus arteriosus. However, this symmetrical arrangement is quickly lost, because the primitive right and left pulmonary arteries rotate clockwise, resulting in a relative shift of the primitive right and left pulmonary arteries towards the left. The primitive right pulmonary artery approaches the left and the neighboring parts of the walls fuse and then later the fused part is reabsorbed. Thus a short, undivided stem is formed and the primitive right pulmonary artery appears to originate from the left. The right dorsal aorta distal to the right subclavian artery and the distal part of the primitive right pulmonary artery disappear, and the left dorsal aorta and distal part of the primitive left pulmonary artery persist as the descending aorta and the ductus arteriosus. The result is that the embryonic pulmonary artery originates from the left side of the truncus and the paired fourth aortic arches shift rightwards. The roof of the aortic sac (a structure that lies distal to the conotruncus and gives rise to six bilaterally symmetric aortic arch arteries) invaginates to form an aortopulmonary septum that eventually fuses with the distal extent of the truncal septum. This results in the right and left pulmonary arteries originating from the pulmonary trunk and the aortic arches arising from the ascending aorta. The spiral course of the truncoaortic partition produces the normal intertwinement of the great arteries.

If the conotruncal or truncoaortic septation does not occur normally, various types of conal truncal anomalies may result [1]. If the conotruncal septum fails to develop, the pulmonary trunk has a left-sided origin from the undivided truncus arteriosus. In addition, either deficiency or absence of the conal septum produces a large ventricular septal defect. Because the valve swellings develop from truncal tissue at the point of fusion between the truncal and conal septa, failure of fusion results in deformities of the single truncal valve. If remnants of distal truncoaortic septation develop, the pulmonary arteries may arise together from a

short pulmonary trunk; otherwise, they arise separately from the truncal root.

Migration of neural crest tissue into both the developing cardiac tube and the developing truncal swellings plays a critical role in conal and aortopulmonary septation [6–9]. Preventing migration of neural crest tissue by administering teratogenic agents has been shown to produce conotruncal defects [10]. Finally, Thomas *et al.* demonstrated that mouse embryos lacking Rac1 (a small GTP-binding protein) in neural crest cells develop abnormal craniofacial development and a persistent truncus arteriosus [11]. Their data suggest that although Rac1 is not required for normal neural crest migration, during craniofacial and cardiac development Rac1 plays a critical cell-autonomous role in post-migratory neural crest cells by regulating the integrity of the craniofacial and pharyngeal mesenchyme.

Pathologic anatomy, anatomic classification, and major associated anomalies

Pathologic anatomy

The basic feature of truncus arteriosus is that one large trunk leaves the base of the heart and gives rise to the coronary arteries, aorta, and pulmonary arteries. The single semilunar valve is tricuspid in 69%, quadricuspid in 22%, bicuspid in 9%, and rarely either unicommissural or pentacuspid [12–15]. The truncal valve is always in fibrous continuity with the mitral valve, and when the septal band is not well developed it is also in fibrous continuity with the tricuspid valve. The truncal valve overrides the ventricular septum and faces downwards and slightly forwards. The valve is frequently thickened and also may have nodular dysplastic cusps, prolapse of unsupported cusps, and inequality of cusp size [12]. These abnormalities frequently result in some truncal regurgitation and rarely truncal stenosis.

A ventricular septal defect results from either absence or pronounced hypoplasia of the infundibular septum, and is almost always present and generally large. Very rarely the ventricular septal defect is small and restrictive or even absent [16].

Variations in coronary artery distribution and origin have important surgical implications. Usually there are two coronary arteries, the left arising above a left posterior cusp and the right arising above a right anterior cusp. Van Praagh and Van Praagh studied 57 specimens with truncus arteriosus [13]. In 29 they found abnormalities of the coronary ostia. Of these, one coronary artery arose totally or partially above the noncoronary sinus in 20, with 12 of these being the right coronary. However, in 49%, the coronary ostia are abnormal, the most frequent variant being either right (19%) or left (5%) coronary arteries arising from noncoronary cusps. Other coronary anomalies included the left anterior descending artery being small and displaced leftwards with a large conal branch

from the right, the posterior descending coronary artery arising from the left circumflex (27%), a single coronary artery, and two coronary ostia arising from the same truncal sinus. A high coronary ostial origin (above the sinotubular junction) is common in truncus. However, when the origin is at or slightly above a valve commissure, the ostium involved (frequently the left) may be functionally stenotic. Rarely, the left coronary artery originates from the pulmonary artery [17–19].

Anatomic classification

The variations in pulmonary artery anatomy, in large part, are the basis for the anatomic classification of truncus arteriosus. In 1949, Collett and Edwards proposed the first anatomic classification [14] They described five types:

Type I: A single pulmonary trunk and an ascending aorta arising from the common trunk.

Type II: The left and right pulmonary arteries arising closely together from the posterior or dorsal wall of the truncus.

Type III: Right, left, or both pulmonary arteries arising independently from either side of the truncus.

Type IV: No pulmonary arteries and apparent absence of the sixth arterial arch, the lung being supplied by way of bronchial arteries.

Type V: Aortopulmonary fenestration (AP window).

Currently, most cardiologists take issue with including Types IV and V as variants of truncus. Type IV is really pulmonary atresia with a ventricular septal defect and Type V is an aortopulmonary window.

Van Praagh and Van Praagh proposed a modified Collett and Edwards classification [13]. The Van Praagh classification originally was divided into Type A, those with a ventricular septal defect, and Type B, those without (only 2/57 specimens had no ventricular septal defect). In fact, Type B is probably not truncus, since both of these patients had two semilunar valves and therefore resemble a variety of aortopulmonary window. The Van Praagh Type A is subdivided into:

A1: Same as Collett and Edwards Type I.

A2: Same as Collett and Edwards Type II and III.

A3: Absence of one of the pulmonary artery branches, the respective lung being supplied by collaterals (incidence of 16%).

A4: Truncus with an interrupted aortic arch or severe coarctation and with a large persistent ductus arteriosus (incidence of 11–19%). The interruption of the aorta is almost always between the left carotid and left subclavian (Type B interruption). This lesion has a high incidence of DiGeorge syndrome [20].

The pulmonary arteries usually arise from the left posterolateral aspect of the truncus arteriosus. Frequently, the lesion

appears to be Type 1 when viewed from the front but Type 2 from the posterior aspect. The Van Praagh A3 probably represent patients in which one of the pulmonary arteries is either isolated or severely stenotic at its origin and initially supplied by a patent ductus; when the ductus closes, the pulmonary artery disappears. In a truncus, the absent pulmonary artery is most frequently on the side of the arch, whereas in tetralogy of Fallot, the absent pulmonary artery is frequently on the side opposite to the arch.

Associated anomalies

A right aortic arch with mirror-image brachiocephalic branching is associated more commonly with truncus arteriosus (~36%) than any other congenital cardiac malformation except pulmonary atresia with ventricular septal defect [13,15]. Patent ductus arteriosus is absent in approximately half the patients with truncus arteriosus, but when present remains patent postnatally in nearly two-thirds of patients [13]. A secundum atrial septal defect occurs in 9–20%, an aberrant subclavian artery in 4–10%, and a persistent left superior vena cava draining to the coronary sinus in 4–9%. Other rare associated anomalies include partial anomalous pulmonary venous connections, tricuspid atresia, mitral atresia, ventricular inversion, and asplenia complex [21–24]. Extracardiac anomalies occur in up to 30% of patients, and include skeletal deformities, hydroureter, bowel malrotation, and diaphragmatic hernia.

Pathophysiology

Physiologically, truncus arteriosus is an admixture type of cyanotic heart disease. The ventricular septal defect and single outlet result in nearly total mixing of blood from both ventricles. Sometimes the location of the pulmonary artery may permit preferential flow from the right ventricle into the pulmonary arteries and can result in a difference in oxygen saturation between pulmonary arteries and aorta of up to 10%. The clinical picture of individuals with truncus arteriosus is largely determined by the amount of pulmonary blood flow, which in turn depends on the pulmonary vascular resistance and/or narrowing of the pulmonary arteries. In most infants with truncus arteriosus, there is high pulmonary flow with low pulmonary resistance. This causes severe congestive heart failure and mild cyanosis (an oxygen saturation of 85%). Coexisting insufficiency of the truncal valve further aggravates the congestive failure. For those children who initially survive the initial high pulmonary blood flow without protection of the pulmonary vasculature, pulmonary vascular disease rapidly develops. As the pulmonary vascular resistance increases, pulmonary flow decreases and congestive heart failure gradually disappears, but cyanosis increases and the child ultimately develops Eisenmenger syndrome. Rarely, children are born with some pulmonary artery stenosis, but the stenosis is frequently segmental and only portions of the pulmonary

vascular bed are protected while the other unprotected regions develop aggressive vascular disease.

Natural history

Most infants with truncus present within the first few weeks of life with severe congestive heart failure. Because the pulmonary arteries are exposed to increased flow and pressure in both systole and diastole, congestive failure develops much earlier than in infants with just a ventricular level shunt. In the series of Calder et al., the median age of death was 5.5 weeks and 85% of untreated individuals died before 1 year of age [25]. Other contributors to early death include severe truncal regurgitation or stenosis and coronary artery abnormalities. In infants who survive the first year of life, congestive heart failure gradually improves as pulmonary vascular disease develops and they show better growth and exercise tolerance. By the end of the first decade, however, most of these children develop increasing cyanosis and the improved exercise tolerance begins to deteriorate. Survival into the third decade is extremely uncommon. Death results from hemoptysis, intrapulmonary thrombotic events, heart failure, and/or tachyarrhythmia.

Clinical features

Physical examination

The first heart sound is usually normal and the second sound is loud. In approximately half of the patients, the second sound may be narrowly split. Victorica et al. documented splitting of the second heart sound on phonocardiogram and speculated that the splitting was due either to the cusps not closing synchronously or to a duplicated sound set up by vibrations in the aorta [26]. A constant systolic ejection click is almost always heard. Most patients have a grade 2–3/6 systolic ejection murmur, although occasionally no murmur is heard. A mid-diastolic flow rumble is frequently heard at the apex. An early high-frequency diastolic decrescendo murmur, probably from truncal regurgitation, was heard in 36% of the patients reported by Calder et al. [25]. Rarely, a continuous murmur can be present.

Electrocardiogram

The electrocardiogram is not diagnostic and usually demonstrates right-axis deviation and biventricular hypertrophy (documented by large RS complexes in the mid-precordium).

Chest X-Ray

There is no typical X-ray for truncus arteriosus. In most instances, both the heart size and pulmonary vascularity are increased. In ~36% of patients, a right aortic arch is present;
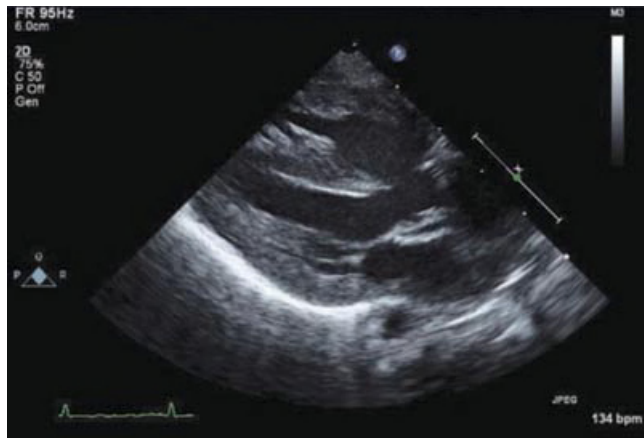
Figure 45.1 Two-dimensional echocardiographic image in the parasternal long-axis view demonstrates a large conoventricular septal defect in a neonate with truncus arteriosus. The differential diagnosis of this defect includes tetralogy of Fallot and pulmonary atresia with ventricular septal defect.

the combination of a right arch, cardiomegaly, and pulmonary plethora should make one suspect the diagnosis of truncus arteriosus.

Echocardiography

The diagnosis of truncus arteriosus may be made *in utero* with fetal echocardiography. A recent review of the fetal echocardiography database at the University of Michigan yielded 24 patients with prenatally diagnosed truncus arteriosus over 11 years. There were two *in utero* deaths (one spontaneous and one elective termination) and one fetus remains *in utero*. Of the 21 live births, 16 patients (76%) were correctly diagnosed with truncus arteriosus, and five patients (24%) were misdiagnosed (pulmonary atresia with intact ventricular septum and aortic atresia with ventricular septal defect accounted for the correct postnatal diagnoses). Despite vast improvements in ultrasound technology and referral rates to regional perinatal assessment centers, >50% of patients with truncus arteriosus do not receive a prenatal diagnosis [27].

Postnatally, transthoracic echocardiography is currently the standard diagnostic modality of choice. The differential diagnosis includes other conoventricular malformations, including tetralogy of Fallot and pulmonary atresia with ventricular septal defect (Figure 45.1), and also aortopulmonary window and anomalous origin of one pulmonary artery from the ascending aorta ("hemitruncus"). The subcostal coronal view demonstrates the overriding truncal root, posterolateral arising pulmonary artery, and large conoventricular septal defect (Figure 45.2). Truncal valve morphology may be assessed from both the subcostal sagittal and parasternal short-axis views. Truncal valve stenosis and regurgitation may be assessed quantitatively from the apical, suprasternal and parasternal views. A complete study

must evaluate the aortic arch for interruption, determine arch sidedness, examine the ventricular septum for additional defects, define coronary artery anatomy (including origin, branching and course), and visualize the branch pulmonary arteries. Imaging the pulmonary arteries from the subcostal coronal, parasternal short-axis, and suprasternal coronal views allows the determination of the anatomic type of common arterial trunk. Echocardiography may successfully distinguish patients with truncus arteriosus and normal aortic arch from those with interrupted aortic arch, and those with ascending aortic origin of one pulmonary artery ("hemitruncus").

Cardiac catheterization and angiography

Preoperative cardiac catheterization is now rarely undertaken in the neonate with truncus arteriosus. Catheterization may be indicated for angiography when precise anatomic detail, for example, exact pulmonary artery anatomy, is in question after echocardiography (Figure 45.3). With late diagnosis of truncus arteriosus (even if the child is only a couple of weeks old), catheterization may be performed to measure pulmonary vascular resistance and evaluate pulmonary vascular obstructive disease, which may develop fairly rapidly in this lesion [28]. Inhaled oxygen and nitric oxide may be used to measure pulmonary vasoreactivity and determine the appropriateness of surgical correction.

Because of streaming and the small arteriovenous difference in oxygen content across the pulmonary vascular bed, calculated pulmonary blood flow and vascular resistance can be greatly in error. At times, the clinical status (congestive heart failure and failure to thrive versus apparently normal wellbeing and growth) is a better indicator of the presence or absence of pulmonary vascular disease than the data derived from catheterization.

Other imaging modalities

Cardiac magnetic resonance imaging (cMRI) may be utilized in lieu of invasive catheterization when echocardiography fails to provide complete anatomic detail of the lesion. Further evaluation of the pulmonary arteries and delineation of the aortic arch in a complex interruption are the two most common (although still rare) indications for use of cMRI preoperatively (Figure 45.4).

Management

Medical

In patients with a fetal or early neonatal diagnosis, surgical repair is generally undertaken within days, after a brief period of intensive care medical management, consisting of general stabilization and treatment of pulmonary overcirculation. Patients with associated arch interruption require continuous prostaglandin infusion to maintain ductal patency.
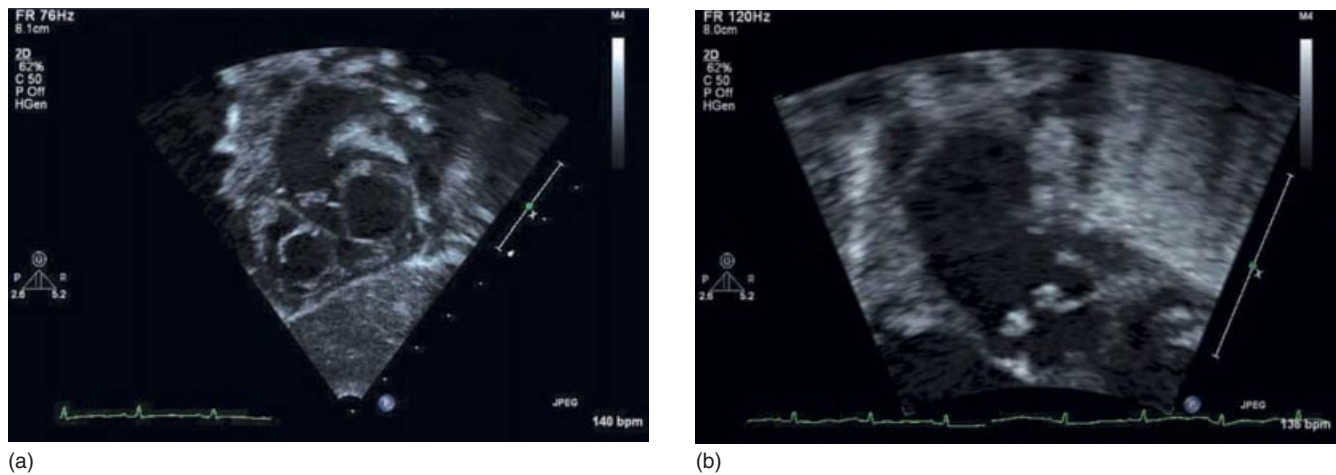
Figure 45.2 Two-dimensional echocardiographic images in the subcostal coronal view of a neonate with truncus arteriosus. These panels demonstrate a large conoventricular septal defect, common arterial trunk and posterior origin of the pulmonary artery (a) with a thickened, dysplastic truncal valve (b).
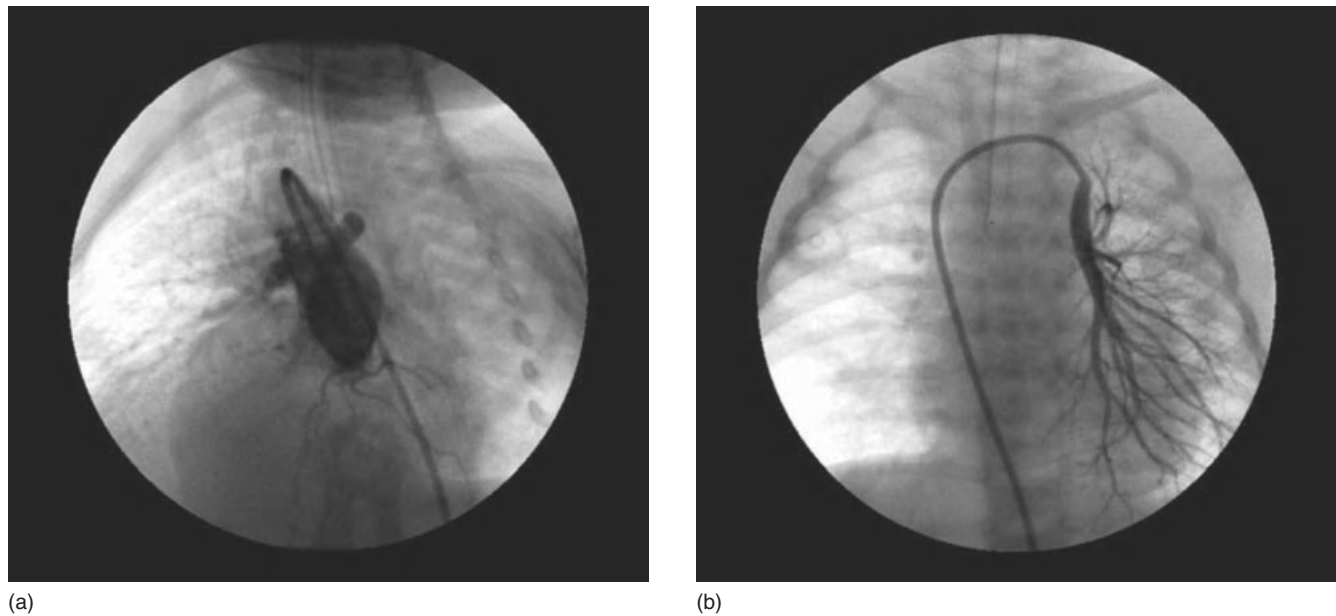
Figure 45.3 Angiocardiographic images in left anterior oblique (a) and anteroposterior (b) views in a neonate with truncus arteriosus and discontinuous pulmonary arteries. Panel (a) depicts the right pulmonary artery arising from the common trunk and (b) depicts the left pulmonary artery arising from the patent ductus arteriosus.

Infants diagnosed later than a few months of life may require catheterization for pulmonary vasoreactivity testing prior to surgical repair, if there is concern for early irreversible pulmonary vascular obstructive disease.

Surgical

Because most neonates develop heart failure, early development of pulmonary vascular obstructive disease is common [28], and surgical techniques and outcomes have improved markedly [29–32], complete repair of truncus arteriosus in the neonatal or early infant period is the standard of care. The modern approach of complete repair of truncus arteriosus in the neonatal or early infant period was pioneered in the 1970s by Ebert and co-workers [29]. A staged approach consisting of neonatal palliative pulmonary artery banding, followed by later complete repair, is no longer considered a primary strategy, given its tendency to cause severe anatomic abnormalities of the pulmonary arteries (ranging from stenosis to atresia) [33–36] and the residual risk of pulmonary vascular obstructive disease [36].

(a)   (b)
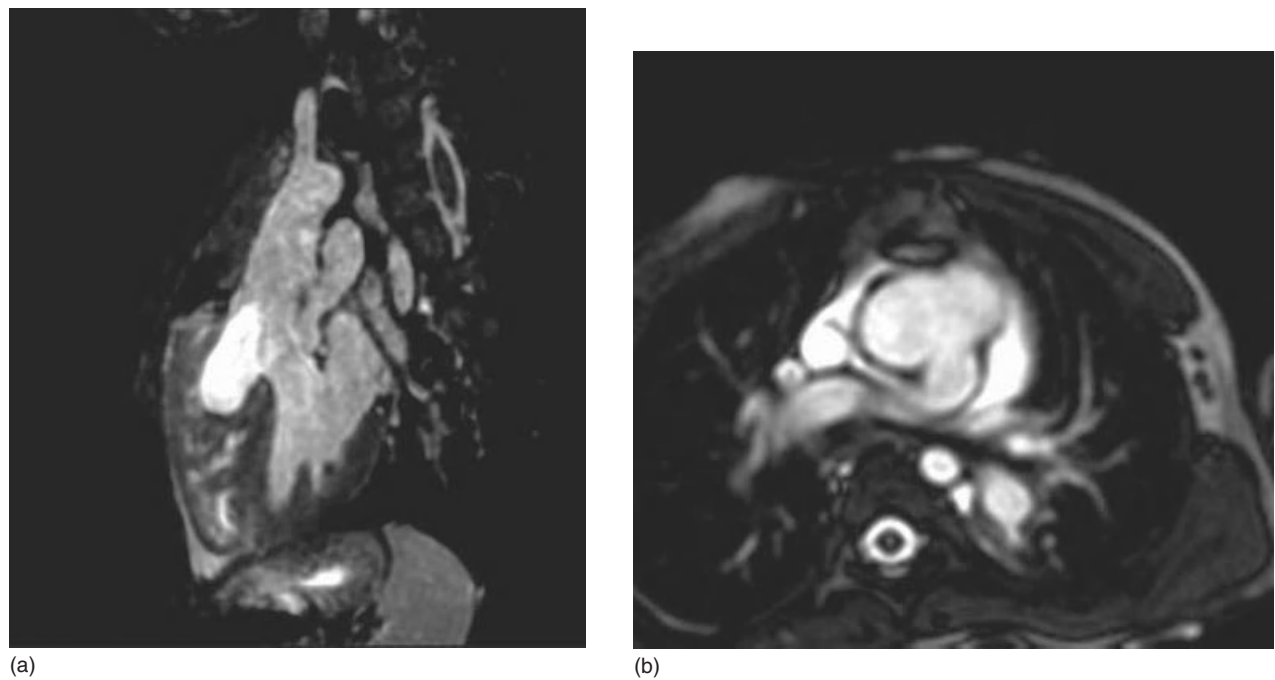
Figure 45.4 Steady-state free precession sequence cardiac magnetic resonance imaging in a 3-year-old child with unrepaired truncus arteriosus. The sagittal-oblique (a) and axial (b) planes demonstrate the large conoventricular septal defect, overriding truncal valve and posterior origin of the pulmonary arteries.
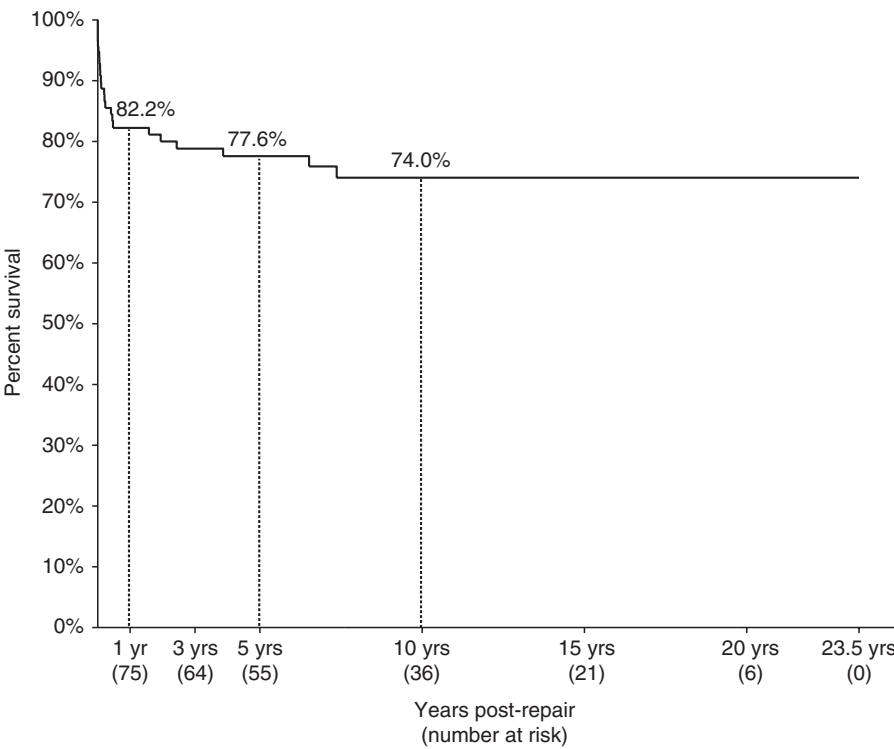
Figure 45.5 Overall survival after repair of truncus arteriosus at University of Michigan from 1985 to 2007. Numbers in parentheses on the x-axis are the number at risk.

Complete operative repair in the patient without associated lesions consists of ventricular septal defect closure, right ventricular outflow tract reconstruction (to the detached pulmonary arteries) using a valved conduit (typically valved, although some centers utilize a valveless conduit), and repair of the aortic wall deficiency (where the pulmonary arteries once arose). Aortic arch reconstruction (direct end-to-end anastomosis or patch augmentation) is performed for an interrupted aortic arch. Truncal valve repair or replacement at the time of initial repair is considered only in patients with severe truncal valve regurgitation. If necessary, valve repair is preferred as neonatal valve replacement options are severely limited.

Since the initial reports of early primary neonatal repair in the early 1990s by Bove *et al.* [30] and Hanley *et al.* [37], many centers have reported early and mid- to long-term results after neonatal/infant truncus repair [29,31,32,38–40]. Perioperative mortality ranges from 4 to 12.5% with 1-year survival of 84–92%. Commonly identified risk factors for early mortality include weight ≤2.5 kg, need for truncal valve repair or replacement at initial surgery, and, in some series, an interrupted aortic arch [29,41].

We recently completed a thorough review of operated truncus arteriosus patients at the University of Michigan from 1985 to 2007. A total of 113 neonates with truncus arteriosus underwent primary complete repair at a mean age of 19 days and a weight of 3.01 kg. Hospital survival was 87.6%, with no difference in hospital survival between patients with or without interrupted aortic arch. Neither weight nor age at time of repair was a risk factor for mortality. Major postoperative complications, including stroke, cardiac arrest, and need for tracheostomy or extracorporeal membrane oxygenator support, occurred in 21.2% of patients. Survival was 84.4% at 1 year and 77.6% at 5 years (Figure 45.5).

Long-term history of treated and untreated adults

Although survival into adulthood with unrepaired truncus arteriosus has been reported, early death is the norm. Approximately 70% of infants with unrepaired truncus arteriosus die in the first year of life, typically from heart failure [42]. For those surviving beyond the first few years of life, death usually occurs in late childhood or adolescence due to complications of pulmonary vascular obstructive disease, endocarditis, or, less commonly, heart failure. After age 3–4 years, repair is generally not undertaken because of severe, irreversible, pulmonary vascular obstructive disease.

Long-term management of repaired patients revolves, in large part, around the function of the truncal valve. Although mild truncal valve stenosis or regurgitation is generally well tolerated for years, more significant valvar disease (almost always regurgitation) may require intervention. A variety of valve repair techniques have been used [29,32,43]. In the University of Michigan experience, freedom from truncal valve intervention was 89% at 5 years and 84.6% at 10 years (Figure 45.6).
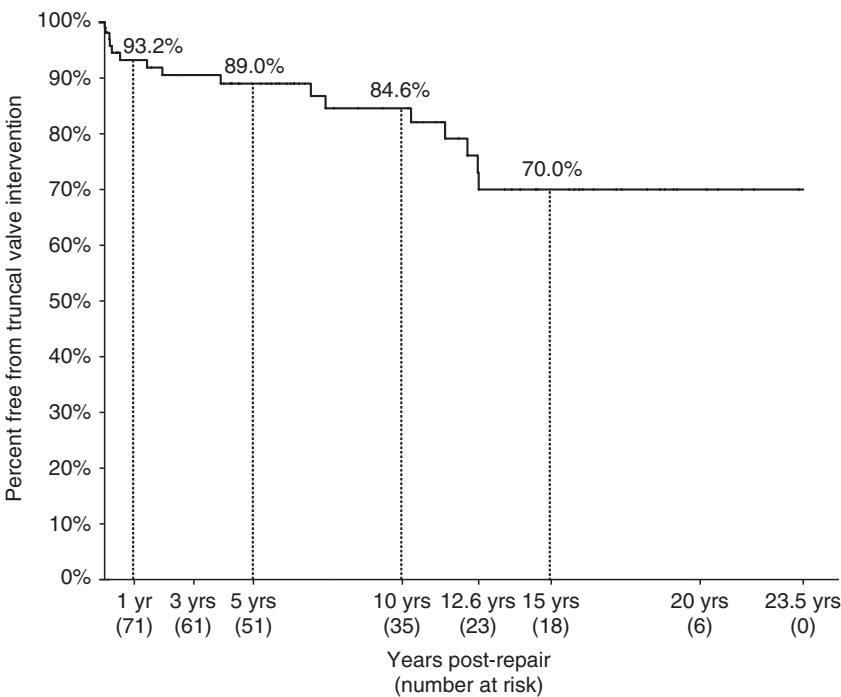
Figure 45.6 Freedom from truncal valve intervention after repair of truncus arteriosus at University of Michigan from 1985 to 2007. Numbers in parentheses on the *x*-axis are the number at risk.

The right ventricle to pulmonary artery conduit will become obstructed and require replacement in all patients. Percutaneous conduit balloon angioplasty and stent placement may delay conduit replacement [44,45]. Nevertheless, most patients will require at least one conduit replacement by the early teen years, if not much earlier. The more recent availability of a transcatheter pulmonary valve may further delay surgical conduit replacement by relieving obstruction and restoring functional pulmonary valve competence [46]. Although patients could once expect to undergo three or four or more operative conduit revisions in a lifetime, the availability of a transcatheter pulmonary valve may substantially reduce this surgical burden.

A single pulmonary artery has also been associated with an increased incidence of late death after repair of truncus arteriosus. In 1985, the Mayo Clinic reported their experience with 19 patients with a truncus arteriosus and a single pulmonary artery [47] who had corrective operations performed from 1969 to 1983. Compared with the 148 patients with truncus and two pulmonary arteries, patients with a single pulmonary artery had a similar operative mortality but a significantly high late mortality. In our series of 113 neonates repaired between 1985 and 2007, there was no patient with a single pulmonary artery.

Additional anatomic sequelae include pulmonary artery stenoses (typically proximal), recurrent aortic arch obstruction (in those who have undergone aortic arch reconstruction), and, less frequently, supravalvar aortic stenosis at the site of initial pulmonary artery connection. Many of these residual lesions can be managed successfully in the catheterization laboratory.

References

1 Van Mierop LH, Patterson DF, Schnarr WR. Pathogenesis of persistent truncus arteriosus in light of observations made in a dog embryo with the anomaly. *Am J Cardiol* 1978;**41**:755–62.

2 Buchanan A. Malformation of heart. Undivided truncus arteriosus. Heart otherwise double. *Trans Pathol Soc Lond* 1864;**15**:89.

3 Keith JD, Rowe RD, Vlad P. *Heart Disease in Infancy and Childhood*, 3d edn. New York: Macmillan, 1978.

4 Goldmuntz E, Clark BJ, Mitchell LE, *et al.* Frequency of 22q11 deletions in patients with conotruncal defects. *J Am Coll Cardiol* 1998;**32**:492–8.

5 Bartelings MM, Gittenberger-de Groot AC. Morphogenetic considerations on congenital malformations of the outflow tract. Part 2: Complete transposition of the great arteries and double outlet right ventricle. *Int J Cardiol* 1991;**33**:5–26.

6 Besson WT III, Kirby ML, Van Mierop LH, Teabeaut JR II. Effects of the size of lesions of the cardiac neural crest at various embryonic ages on incidence and type of cardiac defects. *Circulation* 1986;**73**;60–4.

7 Van Mierop LH, Kutsche LM. Cardiovascular anomalies in DiGeorge syndrome and importance of neural crest as a possible pathogenetic factor. *Am J Cardiol* 1986;**58**:133–7.

8 Nishibatake M, Kirby ML, Van Mierop LH. Pathogenesis of persistent truncus arteriosus and dextroposed aorta in the chick embryo after neural crest ablation. *Circulation* 1987;**75**:255–64.

9 Kirby ML. Plasticity and predetermination of mesencephalic and trunk neural crest transplanted into the region of the cardiac neural crest. *Dev Biol* 1989;**134**:402–12.

10 Tasaka H, Takenaka H, Okamoto N, *et al.* Abnormal development of cardiovascular systems in rat embryos treated with bisdiamine. *Teratology* 1991;**43**:191–200.

11 Thomas PS, Kim J, Nunez S, *et al.* Neural crest cell-specific deletion of Rac1 results in defective cell–matrix interactions and severe craniofacial and cardiovascular malformations. *Dev Biol* 2010 15;**340**:613–25.

12 Fuglestad SJ, Puga FJ, Danielson GK, Edwards WD. Surgical pathology of the truncal valve: a study of 12 cases. *Am J Cardiovasc Pathol* 1988;**2**:39–47.

13 Van Praagh R, Van Praagh S. The anatomy of common aorticopulmonary trunk (truncus arteriosus communis) and its embryologic implications. A study of 57 necropsy cases. *Am J Cardiol* 1965;**16**:406–25.

14 Collett RW, Edwards JE. Persistent truncus arteriosus;a classification according to anatomic types. *Surg Clin North Am* 1949;**29**:1245–70.

15 Crupi G, Macartney FJ, Anderson RH. Persistent truncus arteriosus. A study of 66 autopsy cases with special reference to definition and morphogenesis. *Am J Cardiol* 1977;**40**:569–78.

16 Rosenquist GC, Bharati S, McAllister HA, Lev M. Truncus arteriosus communis: truncal valve anomalies associated with small conal or truncal septal defects. *Am J Cardiol* 1976;**37**:410–2.

17 Shrivastava S, Edwards JE. Coronary arterial origin in persistent truncus arteriosus. *Circulation* 1977;**55**:551–4.

18 Anderson KR, McGoon DC, Lie JT. Surgical significance of the coronary arterial anatomy in truncus arteriosus communis. *Am J Cardiol* 1978;**41**:76–81.

19 de la Cruz MV, Cayre R, Angelini P, *et al.* Coronary arteries in truncus arteriosus. *Am J Cardiol* 1990;**66**:1482–6.

20 Radford DJ, Perkins L, Lachman R, Thong YH. Spectrum of Di George syndrome in patients with truncus arteriosus: expanded Di George syndrome. *Pediatr Cardiol* 1988;**9**:95–101.

21 Rao PS, Levy JM, Nikicicz E, Gilbert-Barness EF. Tricuspid atresia: association with persistent truncus arteriosus. *Am Heart J* 1991;**122**:829–35.

22 Rice MJ, Andrilenas K, Reller MD, McDonald RW. Truncus arteriosus associated with mitral atresia and a hypoplastic left ventricle. *Pediatr Cardiol* 1991;**12**:128–30.

23 Marino B, Ballerini L, Soro A. Ventricular inversion with truncus arteriosus. *Chest* 1990;**98**:239–41.

24 Gumbiner CH, McManus BM, Latson LA. Associated occurrence of persistent truncus arteriosus and asplenia. *Pediatr Cardiol* 1991;**12**:192–5.

25 Calder L, Van Praagh R, Van Praagh S, *et al.* Truncus arteriosus communis. Clinical, angiocardiographic, and pathologic findings in 100 patients. *Am Heart J* 1976;**92**:23–38.

26 Victorica BE, Gessner IH, Schiebler GL. Phonocardiographic findings in persistent truncus arteriosus. *Br Heart J* 1968;**30**:812–6.

27 Swanson TM, Selamet Tierney ES, Tworetzky W, *et al.* Truncus arteriosus: diagnostic accuracy, outcomes, and impact of prenatal diagnosis. *Pediatr Cardiol* 2009;**30**:256–61.

28 Juaneda E, Haworth SG. Pulmonary vascular disease in children with truncus arteriosus. *Am J Cardiol* 1984;**54**:1314–20.

29 Thompson LD, McElhinney DB, Reddy M, *et al.* Neonatal repair of truncus arteriosus: continuing improvement in outcomes. *Ann Thorac Surg* 2001;**72**:391–5.

30 Bove EL, Lupinetti FM, Pridjian AK, *et al.* Results of a policy of primary repair of truncus arteriosus in the neonate. *J Thorac Cardiovasc Surg* 1993;**105**:1057–65; discussion 1065–6.

31 Rajasinghe HA, McElhinney DB, Reddy VM, *et al.* Long-term follow-up of truncus arteriosus repaired in infancy: a twenty-year experience. *J Thorac Cardiovasc Surg* 1997;**113**:869–78; discussion 1078–9.

32 Rodefeld MD, Hanley FL. Neonatal truncus arteriosus repair: surgical techniques and clinical management. *Semin Thorac Cardiovasc Surg Pediatr Card Surg Annu* 2002;**5**:212–7.

33 Musumeci F, Piccoli GP, Dickinson DF, Hamilton DI. Surgical experience with persistent truncus arteriosus in symptomatic infants under 1 year of age. Report of 13 consecutive cases. *Br Heart J* 1981;**46**:179–85.

34 Singh AK, De Leval MR, Pincott JR, Stark J. Pulmonary artery banding for truncus arteriosus in the first year of life. *Circulation* 1976;**54**(6 Suppl):III17–9.

35 Oldham HN, Jr., Kakos GS, Jarmakani MM, Sabiston DC, Jr. Pulmonary artery banding in infants with complex congenital heart defects. *Ann Thorac Surg* 1972;**13**:342–50.

36 McFaul RC, Mair DD, Feldt RH, *et al.* Truncus arteriosus and previous pulmonary arterial banding: clinical and hemodynamic assessment. *Am J Cardiol* 1976;**38**:626–32.

37 Hanley FL, Heinemann MK, Jonas RA, *et al.* Repair of truncus arteriosus in the neonate. *J Thorac Cardiovasc Surg* 1993;**105**: 1047–56.

38 Reddy VM, Hanley F. Late results of repair of truncus arteriosus. *Semin Thorac Cardiovasc Surg Pediatr Card Surg Annu* 1998;**1**: 139–46.

39 Ullmann MV, Gorenflo M, Sebening C, *et al.* Long-term results after repair of truncus arteriosus communis in neonates and infants. *Thorac Cardiovasc Surg* 2003;**51**:175–9.

40 Tlaskal T, Chaloupecky V, Hucin B, *et al.* Long-term results after correction of persistent truncus arteriosus in 83 patients. *Eur J Cardiothorac Surg* 2010;37:1278–84.

41 Konstantinov IE, Karamlou T, Blackstone EH, *et al.* Truncus arteriosus associated with interrupted aortic arch in 50 neonates: a Congenital Heart Surgeons Society study. *Ann Thorac Surg* 2006; **81**:214–22.

42 Nadas AS, Fyler DC. *Pediatric Cardiology*, 3rd edn. Philadelphia: Saunders, 1972.

43 Mavroudis C, Backer CL. Surgical management of severe truncal insufficiency: experience with truncal valve remodeling techniques. *Ann Thorac Surg* 2001;**72**:396–400.

44 Powell AJ, Lock JE, Keane JF, Perry SB. Prolongation of RV–PA conduit life span by percutaneous stent implantation. Intermediate-term results. *Circulation* 1995;**92**:3282–8.

45 Peng LF, McElhinney DB, Nugent AW, *et al.* Endovascular stenting of obstructed right ventricle-to-pulmonary artery conduits: a 15-year experience. *Circulation* 2006;**113**:2598–605.

46 Zahn EM, Hellenbrand WE, Lock JE, McElhinney DB. Implantation of the melody transcatheter pulmonary valve in patients with a dysfunctional right ventricular outflow tract conduit early results from the U.S. Clinical trial. *J Am Coll Cardiol* 2009;**54**:1722–9.

47 Fyfe DA, Driscoll DJ, Di Donato RM, *et al.* Truncus arteriosus with single pulmonary artery: influence of pulmonary vascular obstructive disease on early and late operative results. *J Am Coll Cardiol*. 1985;**5**:1168–72.

46 Pulmonary Arteriovenous Malformations

Shivu Kaushik & James Gossage

Medical College of Georgia, Augusta, GA, USA

Introduction

Pulmonary arteriovenous malformations (PAVM) are abnormal communications between pulmonary arteries and veins. Although these lesions are uncommon, they are important in the differential diagnosis of common problems such as dyspnea, hemoptysis, hypoxemia, and pulmonary nodules. Churton, in 1897, reported the first description of PAVM [1]. Several terms have been used in the older literature to describe PAVM, including "pulmonary arteriovenous fistulas." We will use the term PAVM, currently the preferred scientific term. Specific literature with regard to PAVM in the pediatric population is sparse and there is considerable overlap with the adult population.

Incidence and genetics

PAVM are uncommon; the exact incidence in the pediatric population is unknown. Three reports, representing the collected Mayo Clinic experience, documented 194 patients of all ages with PAVM over 45 years, yielding an annual incidence of 4.3 patients per year at a large medical center [2–4]. PAVM are uncommonly identified in infancy and childhood, and gradually increase in incidence through the fifth and sixth decades of life. PAVM in the neonatal period are also extremely rare, with only 12 reports in the literature between 1975 and 2000 [5]. Giordano *et al.* [6] studied the incidence of PAVM in 19 children with genetically confirmed hereditary hemorrhagic telangiectasia (HHT). PAVM were detected in 10/19 patients using contrast echocardiography and computed tomography (CT) for an incidence of 53%. The authors noted that the incidence of PAVM in their pediatric population was similar to that in their adult population with HHT.

Much of the study regarding the genetics of PAVM has been done in the context of HHT. HHT is an autosomal dominant inherited disease, with variable inter- and intrafamilial expressivity and age-dependent penetrance [7]. Over 90% of affected subjects manifest signs or symptoms by the age of 40 years. Mutations in at least five genes can cause HHT. HHT1 is due to a mutation in the endoglin gene [8] whereas HHT2 is due to a mutation in the ACVRL1 gene [9]. PAVM are most common in patients with HHT1. In a large study in The Netherlands, PAVM large enough to warrant treatment were found in 32% of patients with HHT1 versus only 3% of patients with HHT2 [10]. Genetic testing of children in families with known HHT may assist in early screening for PAVM, even in those who are asymptomatic [11].

Etiology

There are no universally acceptable criteria for the classification of PAVM. Broadly, PAVM may be divided into congenital and acquired. HHT is the most common congenital etiology of PAVM, with at least 80% of congenital PAVM occurring in the context of HHT [12]. In our own experience, >95% of children with congenital PAVM ultimately have HHT. Although the PAVM in HHT are inherited, they are not always present at birth and, similarly to other clinical manifestations of HHT, the prevalence of PAVM is believed to increase with age.

An extremely rare congenital cause of PAVM is the Abernethy malformation, which arises from defects in vitelline vein formation [13]. In the Abernethy malformation, there is a shunt of venous blood from the intestines and spleen to the inferior vena cava without passing through the liver. It is postulated that there is no first pass metabolism of some unknown pulmonary vasodilator – resulting in a type

of hepatopulmonary syndrome (HPS). The Abernethy malformation syndrome is characterized clinically by radiographic findings of chronic liver disease combined with dilatation of subpleural pulmonary vessels resembling spider nevi, predominantly in the lower lobes of the lung [14,15].

Among the acquired causes of PAVM, one of the most commonly described is the HPS in children with juvenile cirrhosis and chronic liver disease. The prevalence of HPS in children with liver disease is 2–8% [16,17]. The hypoxemia that accompanies this syndrome is due to failure of the blood in the center of the dilated capillaries (15–100μm) to oxygenate completely due to an increased distance from alveolar gas. As in adults, there is no correlation between the severity of hepatic dysfunction and the severity of hepatopulmonary syndrome.

Another common cause of acquired PAVM in children follows surgery for congenital heart disease. PAVM are a well-established complication following the classic Glenn shunt [18], bidirectional cavopulmonary anastomosis (BCPA) [19], and total cavopulmonary shunt (TCPS) [20]. Post-surgical macroscopic PAVM occur most commonly in the right lower lobe and are due to focal exclusion of normal hepatic venous blood from the pulmonary arterial circulation [19,21,22]. Kim *et al.* [20] prospectively studied the prevalence of PAVM in 27 patients after bidirectional cavopulmonary shunt (BCPS) and in 10 patients after total cavopulmonary shunt (TCPS). PAVM was diagnosed if testing showed a shunt fraction >11% by lung perfusion scan, a positive contrast echocardiogram, or a positive pulmonary angiogram. They were further classified to have clinical or subclinical PAVM by the presence or absence of progressive oxygen desaturation by pulse oximetry plus aortic saturation of <80% at heart catheterization. All 10 patients with TCPS had PAVM, of which 50% were clinical. Interestingly, 70% of patients with BCPS had PAVM and all were subclinical. There was a combined mortality of 11% and a combined significant morbidity of 27% after 7 years of follow-up in untreated patients following these procedures [23].

Other rare acquired causes of PAVM more commonly described in adults include trauma, mitral stenosis, actinomycosis, Fanconi's syndrome, metastatic thyroid carcinoma, and schistosomiasis [24].

Embryology

Embryologic development of the vascular system occurs from the fifth to tenth week of intrauterine life, when a continuous differentiation of the vascular bed occurs, resulting in separate arterial and venous channels that are interconnected by capillaries. When a mistake or halt occurs in this process of vascular differentiation, malformations may appear at different sites, including the lungs, and with variable morphology depending on the stage of differentiation [25].

Anatomy and pathogenesis

PAVM are pathologically similar to AVM that occur elsewhere in the body. Two basic elements make up these malformations. The first element is thin-walled vascular channels, lined with a layer of endothelium [26]. The second element is the connective tissue stroma, which is usually scant with little or no connection to the surrounding lung tissue [26]. Occasionally the wall is thickened with fibrous tissue and elastic fibers. The malformation may have one of three typical appearances: (1) a large single sac, (2) a plexiform mass of dilated vascular channels, or (3) a dilated and often tortuous direct communication between an artery and a vein. Uncommonly there may be mural thrombi or mural calcifications associated with the PAVM [26].

Anatomically, PAVM are classified as diffuse or focal, and focal PAVM are further classified as simple or complex. About 80–90% of focal PAVM are simple in both adults and children, with all feeding arteries arising from a single subsegmental artery [27,28]. PAVM perfused by more than one subsegmental artery are defined as complex. Smaller (microvascular) telangiectasias are most commonly complex [29]. Although diffuse PAVM are uncommon in adults, they are seen in 29% of children presenting for treatment with transcatheter embolotherapy (TCE) [28]. About 95% of PAVM are supplied by pulmonary arteries and are usually drained by pulmonary veins, but may occasionally be fed by systemic arteries and/or drain directly into the left atrium or inferior vena cava. Macroscopically, the lesions may appear as a single sac, a plexiform mass of dilated vascular channels, or a dilated and direct anastomosis between artery and vein [29].

The pathogenesis of PAVM remains unknown. Proposed mechanisms include (a) a defect in terminal arterial loops which allows dilation of thin-walled capillary sacs; (b) incomplete resorption of the vascular septae that separate the arterial and venous plexuses during fetal development; (c) development of multiple small PAVM because of failure of capillary development during fetal development, followed by progressive dilation of favored limbs of smaller plexuses and formation of multiloculated sacs (ultimately, rupture of intervening vascular walls may result in formation of a single saccular PAVM); and (d) development of many small PAVM consisting of a single artery to vein connection without an intervening plexus [24].

The role of cytokines and various vascular growth factors in the development of PAVM is under intense investigation. Previous studies had shown serum vascular endothelial growth factor (VEGF) levels to be higher in adults with HHT than healthy controls. Giordano *et al.* [30] studied the correlation between growth factor levels and PAVM in 13 children with genetically proven HHT and age-matched controls. Although they found no difference in VEGF between children with HHT and controls, VEGF was significantly

higher in HHT children with PAVM than in those without PAVM. No difference was seen in transforming growth factor-β_1 levels. The authors suggested that the low levels of VEGF in children without PAVM may protect against PAVM, whereas the high levels in adults might be compensatory for the bleeding that occurs more commonly in adults.

Clinical features

Symptoms

Unlike the adult population, the specific clinical manifestations of PAVM in children have not been well studied. This is partly because symptoms of PAVM often develop between the fourth and sixth decades [24]. The later presentation of symptoms may be because PAVM generally tend to increase in size and rarely regress spontaneously. Features of PAVM that have been correlated with severity of symptoms in some studies have included HHT, the number of PAVM, size of the PAVM, and the magnitude of the shunt fraction [3,4,31,32]. Usually, a single PAVM <2 cm in diameter does not cause symptoms [4,33]. Patients with diffuse microvascular PAVM are always symptomatic [4,28].

Faughnan et al. [28] reported the first large series of children with PAVM and described their clinical presentation. From a database of 617 consecutive patients with PAVM treated by TCE at three HHT centers, they found 42 who were <18 years old. Some 86% of children were diagnosed to have HHT, 57% reported dyspnea on exertion or exercise intolerance, 7% reported previous hemoptysis (minor), and none had previous spontaneous hemothorax.

Epistaxis is the most common symptom of pediatric PAVM patients with HHT and has been reported in children as young as 4 years of age [34]. Bleeding from telangiectasias on the skin and gastrointestinal tract also occurs in HHT [24], but is uncommon in children. Other complaints described in the literature include chest pain, cough, platypnea (improvement in breathing with reclining), migraine headaches, tinnitus, dizziness, dysarthria, syncope, vertigo, and diplopia. Many of these symptoms are vague and may be related to hypoxemia, polycythemia, or cerebrovascular complications such as stroke [24]. The exact incidence of these symptoms as presenting complaints in children with PAVM is unknown.

Neurologic complications of PAVM (transient ischemic attack, MRI-detected stroke, and cerebral abscesses) occurred in 19% of children reported by Faughnan et al. [28]. Seven of the eight patients (88%) with previous neurologic complications were cyanotic [28].

Physical signs

Superficial telangiectasias attributable to underlying HHT are the most common – and frequently the only – physical finding in patients with PAVM. These lesions are macular but occasionally papular, round, 1–3 mm in diameter, ruby colored,
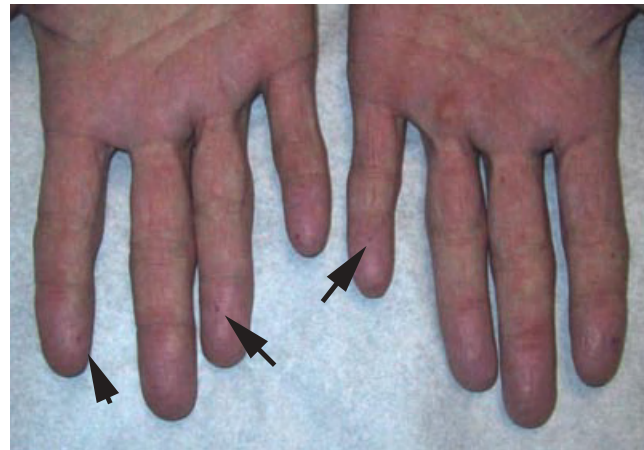
Figure 46.1 Multiple HHT-type telangiectasias on the fingers of an adult with HHT.

well demarcated from surrounding skin with few dendritic projections, and blanch easily with pressure (Figure 46.1). They are most commonly on the fingers, lips, nose, tongue, cheeks, and ears [7,24]. Although telangiectasias have been described in children as young as 1 year [35], their occurrence increases progressively with age. One study found a mean of nine telangiectasias in patients <20 years old, versus a mean of 56 in patients 20–40 years old [36]. In the study by Faughnan et al., cyanosis was seen in 60% and clubbing in 45% of patients requiring TCE [28]. Occasionally, a murmur or bruit may be heard over the site of the PAVM [24].

Chest X-ray

The classic roentgenographic appearance of a PAVM is that of a round or oval mass of uniform density, frequently lobulated but sharply defined, more commonly in the lower lobes, and ranging from 1 to 5 cm in diameter (Figure 46.2) [24]. Individual PAVM may show feeding vessels, with the artery radiating from the hilum and the vein deviating toward the left atrium (Figure 46.2) [3,4]. Cottin et al. [37] in a retrospective study found the sensitivity of chest radiography to be 70% for detecting treatable (amenable to embolization) PAVM in HHT patients. In some patients with complex malformations involving large segments of the lung, the only visible abnormality may be an increase in vascular markings or a hazy increase in opacity over the affected area [38]. Some individuals may show only evidence of a previous thoracotomy for PAVM excision [38].

Diagnosis

Shunt fraction

The fraction of cardiac output that shunts from right to left (shunt fraction, normal <5%) is elevated in 88–100% of selected patients with PAVM [24]. However, all studies thus

Figure 46.2 Screening chest radiograph in a 14-year-old girl with HHT complicated by recurrent epistaxis but no pulmonary complaints. A classic 2 cm PAVM sac is clearly seen in the left lower lung zone along with a feeding artery and draining vein (white arrows). Left-sided pulmonary angiography confirmed this PAVM along with six other smaller PAVMs which are not well seen on this radiograph.

Figure 46.3 Chest CT scan in an adult with HHT complicated by severe hypoxemia and strokes. A bilobed PAVM sac with a prominent associated vessel (long white arrow) is seen in the lateral right lower lobe. A second PAVM sac is seen in the posterior left lower lobe (short white arrow); a feeding artery and vein are visible in other cuts. A possible small PAVM is seen in the anterior left upper lobe (black arrow), but it is too small to characterize fully.

far have reported mainly adults and none have reported children exclusively. Shunt fraction is most accurately assessed by the oxygen method which involves measuring PaO_2 and SaO_2 after breathing 100% oxygen for 15–20 min [24]. A shunt fraction >5% by this method is considered abnormal and warrants consideration of PAVM in appropriate patients. However, this test is usually not performed in children as it requires arterial puncture. Other pitfalls such as technique (air leaks) and duration of oxygen breathing can affect the results [24], making this test ill-suited in children.

Contrast echocardiography

Transthoracic contrast echocardiography (TTCE) utilizes microscopic gas bubbles to visualize the right-to-left shunting characteristic of PAVM. The technique is performed by injecting 4–10 ml of saline that has been agitated with 0.1–1 ml of air into a peripheral vein while simultaneously imaging the atria with two-dimensional echocardiography. Intracardiac shunting is suggested when bubbles appear in the left atrium following a delay of less than or equal to two cardiac cycles after their appearance in the right atrium, whereas intrapulmonary shunting is suggested by a delay of three or more cycles [39–41]. Contrast enhancement may also localize to a draining pulmonary vein in a patient with PAVM [42]. There are no specific criteria about interpreting contrast echocardiography results in children, and studies in children [6] have utilized the standard criteria in adults. Transesophageal contrast echocardiography is more sensitive than transthoracic echocardiography for detecting

intrapulmonary shunt but is more invasive and typically unnecessary in asymptomatic patients [43].

In the largest study to date, van Gent *et al.* examined the prevalence of PAVM by TTCE and CT in 189 patients with genetically characterized HHT and 63 unaffected relatives [10]. TTCE was positive for intrapulmonary shunting in 85% of HHT1 and in 35% of HHT2 subjects. However, only 32% of HHT1 and 3% of HHT2 had treatable PAVM by CT examination. The negative predictive value for TTCE was 100%, making it an ideal screening tool for detecting PAVM. Although this study was performed mainly in adults, in our experience it is equally applicable to children.

One pitfall of contrast echocardiography is that it is positive in some patients with no visible PAVM on chest CT [37]. It also remains positive after TCE of PAVM in up to 90% of patients, even when no residual PAVM are seen on pulmonary angiography [44]. Such positive TTCE tests without visible PAVM are believed to represent microscopic PAVM causing genuine right-to-left shunting (with as yet unknown clinical significance), although a false-positive result cannot be excluded.

Computed tomography

A noncontrasted helical multidetector computed tomography (CT) scan of the chest with 1–2.5 mm reconstructions is now the method of choice for determining whether a PAVM is amenable to TCE. Using this technology, a PAVM typically shows one or more enlarged arteries feeding a serpiginous or lobulated mass, and one or more draining veins (Figure 46.3) [45]. Although contrast enhancement may be seen with central or larger PAVM, the characteristic

appearance on a thin-cut CT makes contrast unnecessary for most patients. Other vascular malformations, such as pulmonary varices, may be mistaken for PAVM, although the diagnosis may be corrected by checking for both afferent and efferent vessels of the putative PAVM [46,47]. In addition, nonspecific micro-nodules of uncertain significance are seen more commonly in children with HHT than in children without HHT [48]. The rare association of pulmonary hypertension with HHT may also be suspected by enlarged central pulmonary arteries and abnormalities in parenchymal attenuation [49].

Magnetic resonance imaging

Magnetic resonance imaging (MRI) of PAVM has not been studied as much as chest CT. With improving technology, however, there may be a role for its use in imaging of PAVM. Schneider *et al.* [50] screened 203 consecutive subjects (6–83 years old) with known HHT or their first-degree relatives using contrast-enhanced magnetic resonance angiography (CE-MRA). CE-MRA detected 124 PAVM in 56 patients. Direct comparison in 40 evaluable patients who subsequently underwent pulmonary angiography showed that only 79% of PAVM seen on CE-MRA were detected on pulmonary angiography. The authors concluded that CE-MRA is a sensitive screening tool for PAVM and potentially superior to pulmonary angiography.

The advantages of MRI lie in the true noninvasiveness of the examination, and also the ability to delineate PAVM angioarchitecture without ionizing radiation. The main limitations include expense, limited availability, breath-holding time exceeding 20s, respiratory motion artifact, need for sedation in children, and the need for highly specialized techniques for accurate interpretation.

Cardiac catheterization/pulmonary angiography

Pulmonary angiography has been the gold standard to determine the position and structure of abnormal vascular lesions in the lungs prior to treatment. Angiography is sensitive for detecting PAVM that are amenable to TCE, and when supplemented with hyperselective angiograms can accurately define the angioarchitecture of individual lesions [24]. Unfortunately, pulmonary angiography is cost, time, and radiation intensive, and therefore is impractical as a screening tool for patients with HHT. Radiation exposure is especially problematic in children. Minor and major complication rates ranging from 0.17 to 7% have been reported [51,52]. Therefore, pulmonary angiography is generally reserved for patients who have been determined by other screening techniques such as CT or CE-MRA to have PAVM large enough for TCE.

Diagnostic approach

The consensus guidelines for HHT recommend screening all adults with possible HHT for PAVM with TTCE, but do not specifically address the optimal method to screen children [11].

There is general agreement that children with HHT with cyanosis, clubbing, dyspnea, or possible neurologic complications of PAVM should undergo TTCE screening. In addition, our own approach involves supine and seated pulse oximetry in children <10 years old followed by TTCE in those with a resting saturation of <97% or in those who require an IV at the time of screening for other aspects of HHT (e.g., brain MRI). Children ≥10 years also receive TTCE. Children with a grade 2 or 3 shunt [41] or neurologic complications are referred for noncontrasted CT.

Management

Medical

In general, all PAVM with a feeding artery diameter of ≥2–3 mm should be treated [11]. The treatment of choice for PAVM in adults is transcatheter embolotherapy (TCE) because it avoids major surgery, prolonged periods of general anesthesia, and loss of pulmonary parenchyma. Data in children are, however, limited. Faughnan *et al.* retrospectively studied the outcome of TCE in 42 patients with a mean age of 12 years (range 4–18 years) [28]. TCE was performed for 172 focal PAVM and 35 diffuse regions (regional TCE) using standard embolic material: stainless-steel coils, platinum coils, detachable balloons, or a combination of these. The technical aspects of TCE were similar to those described in adults, except that general anesthesia or heavy sedation was frequently required in children. After TCE in patients with focal PAVM, oxygenation improved significantly. Acute complications included pleurisy after 24% of TCE sessions and deployment complications in <3% of sessions. Other rare complications included transient intraprocedural angina, perioral pain, intraprocedural leg pain, and transient brachial plexus injury caused by prolonged decubitus position. During long-term follow-up over a mean of 7 years, they found that 15% of PAVM reperfused in 45% of children, similar to the 10–15% reperfusion rate in adults [53]. The authors concluded that TCE has similar efficacy and safety in children and adults, and should be considered the treatment of choice in children. Although there are minimal data on the use of TCE to treat PAVM in the rare pediatric patient without HHT, there is no reason to expect that the results would be any different. In general, children should be referred to an HHT center of excellence for treatment of PAVM.

Surgery

With excellent safety and efficacy of TCE in children, there is little role for surgery in the management of PAVM in this age group [11]. This is because children may develop more PAVM or enlargement of small PAVM later in life, requiring repeat therapy. Rarely, surgery may be considered for complex PAVM not amenable to TCE, in patients with life-threatening

hemoptysis in hospitals without TCE expertise, or in patients with untreatable allergy to contrast material. Surgery may involve ligation or excision of the PAVM and carries the same risks of any similar thoracic surgical procedure. Successful video-assisted thoracoscopic resection of PAVM has been described in adults [54]. Lung transplantation has also been performed in patients with diffuse and bilateral PAVM not amenable to TCE [55,56].

Complications and long-term follow-up

The main aim of treating PAVM is to prevent serious complications. Neurologic complications are the most common and include strokes, transient ischemic attacks, cerebral abscess, migraine, and seizures. Less common but potentially life-threatening complications include hemothorax and hemoptysis. As mentioned previously, neurologic complications are less frequent in children than adults. However, serious complications are more common in cyanotic than acyanotic children [28].

Long-term follow-up is recommended following TCE. Although only 15% of PAVM develop reperfusion during follow-up, this occurs in almost half of children [28]. In the study by Faughnan *et al.* [28], follow-up was performed annually or biannually with helical CT of the chest. Our own practice is to follow the HHT consensus recommendations to repeat a noncontrasted CT scan at 6–12 months after TCE and then every 3 years thereafter [11], and also to follow the development of worsening hypoxemia or dyspnea. A significant increase in the size of PAVM warrants closer follow-up or repeat pulmonary angiography to detect continued or recurrent perfusion of the PAVM.

Finally, we recommend that patients with PAVM – even if only detectable on TTCE – be given antibiotic prophylaxis before dental and potentially bacteremic surgical procedures to the reduce risk of brain abscess [11]. Scuba diving should be avoided owing to the theoretically increased risk of air embolism, but snorkeling and flying are safe. When placing intravenous lines, care should be taken to avoid air embolism. Also, patients and their families should be educated about their diagnosis of PAVM and its clinical implications and complications.

References

1 Churton T. Multiple aneurysms of the pulmonary artery. *Br Med J* 1897;**1**:1223–5.

2 Swanson KL, Prakash UB, Stanson AW. Pulmonary arteriovenous fistulas: Mayo Clinic experience 1982–1997. *Mayo Clin Proc* 1999;**74**:671–80.

3 Dines DE, Arms RA, Bernatz PE, *et al.* Pulmonary arteriovenous fistulas. *Mayo Clin Proc* 1974;**49**:460–5.

4 Dines DE, Seward JB, Bernatz PE. Pulmonary arteriovenous fistulas. *Mayo Clin Proc* 1983;**58**:176–81.

5 Koppen S, Korver CR, Dalinghaus M, *et al.* Neonatal pulmonary arteriovenous malformation in hereditary haemorrhagic telangiectasia. *Arch Dis Child Fetal Neonatal Ed* 2002;**87**:F226–7.

6 Giordano P, Nigro A, Lenato GM, *et al.* Screening for children from families with Rendu–Osler–Weber disease: from geneticist to clinician. *J Thromb Haemost* 2006;**4**:1237–45.

7 Plauchu H, de Chadarevian JP, Bideau A, *et al.* Age-related clinical profile of herediatary telangiectasia in an epidemiologically recruited population. *Am J Med Genet* 1989;**32**:291–7.

8 McAllister KA, Grogg KM, Johnson DW, *et al.* Endoglin, a TGF-beta binding protein of endothelial cells, is the gene for hereditary haemorrhaghic telangiectasia type 1. *Nat Genet* 1994;**8**:345–51.

9 Berg JN, Gallione CJ, Stenzel TT, *et al.* The activin receptor-like kinase 1 gene: genomic structure and mutations in hereditary hemorrhagic telangiectasia type 2. *Am J Hum Genet* 1997;**61**:60–7.

10 van Gent MW, Post MC, Snijder RJ, *et al.* Real prevalence of pulmonary right-to-left shunt according to genotype in patients with hereditary hemorrhagic telangiectasia: transthoracic contrast echocardiography study. *Chest* 2010;**138**:833–9.

11 Faughnan ME, Palda V, Garcia-Tsao G, *et al.* International guidelines for the diagnosis and management of hereditary hemorrhagic telangiectasia. *J Med Genet* 2011;**48**:73–87.

12 Bayrak-Toydemir P, McDonald J, Markewitz B, *et al.* Genotype–phenotype correlation in hereditary hemorrhagic telangiectasia; mutations and manifestations. *Am J Med Genet A* 2006; **140**:463–70.

13 Alvarez AE, Ribeiro AF, Hessel G, *et al.* Abernethy malformation: one of the etiologies of hepatopulmonary syndrome. *Pediatr Pulmonol* 2002;**34**:391–4.

14 McAdams HP, Erasmus J, Crockett R, *et al.* The hepatopulmonary syndrome: radiologic findings in 10 patients. *AJR Am J Roentgenol* 1996;**166**:1379–85.

15 Engelke C, Schaefer-Prokop C, Schirg E, *et al.* High-resolution CT and CT angiography of peripheral pulmonary vascular disorders. *Radiographics* 2002;**22**:739–64 [erratum: *Radiographics* 2002;**22**:1516].

16 Barbé T, Losay J, Grimon G, *et al.* Pulmonary arteriovenous shunting in children with liver disease. *J Pediatr* 1995;**26**: 571–9.

17 Noli K, Solomon M, Golding F, *et al.* Prevalence of hepatopulmonary syndrome in children. *Pediatrics* 2008;**121**:e522–7.

18 Mathur M, Glenn WW. Long term evaluation of cavopulmonary artery anastamosis. *Surgery* 1973;**74**:899–916.

19 Bernstein HS, Brook MM, Silverman NH, *et al.* Development of pulmonary arteriovenous fistulae in children after cavopulmonary shunt. *Circulation* 1992;**92**(Suppl II):304–24.

20 Kim SJ, Bae EJ, Cho DJ, *et al.* Development of pulmonary arteriovenous fistulas after bidirectional cavopulmonary shunt. *Ann Thorac Surg* 2000;**70**:1918–22.

21 Lee J, Menkis AH, Rosenberg HC. Reversal of pulmonary arteriovenous malformation after diversion of anomalous hepatic drainage. *Ann Thorac Surg* 1998;**65**:848–9.

22 Srivastava D, Preniinger T, Lock JE, *et al.* Hepatic venous blood and the development of pulmonary arteriovenous malformations in congenital heart disease. *Circulation* 1995;**92**:1217–22.

23 Moore JW, Kirby WC, Madden WA, *et al.* Development of pulmonary arteriovenous malformations after modified Fontan operations. *J Thorac Cardiovasc Surg* 1989;**98**:1045–50.

24 Gossage JR, Kanj G. Pulmonary arteriovenous malformations: a state of the art review. *Am J Respir Crit Care Med* 1998;**158**:643–61.

25 Woolard HH. The development of the principal arterial stems in the forelimb of the pig. *Contemp Embryol* 1992;**14**:139.

26 Sloan RD, Cooley RN. Congenital pulmonary arteriovenous aneurysm. *Am J Roentgenol Radium Ther Nucl Med* 1953;**70**:183–210.

27 Pugash RA. Pulmonary arteriovenous malformations: overview and transcatheter embolotherapy. *Can Assoc Radiol J* 2001;**52**:92–102.

28 Faughnan ME, Thabet A, Mei-Zahav M, *et al.* Pulmonary arteriovenous malformations in children: outcomes of transcatheter embolotherapy. *J Pediatr* 2004;**145**:826–31.

29 Bosher LH Jr, Blake DA, Byrd BR. An analysis of the pathologic anatomy of pulmonary arteriovenous aneurysms with particular reference to the applicability of local excision. *Surgery* 1959;**45**:91–104.

30 Giordano P, Lenato GM, Pierucci P, *et al.* Effects of VEGF on phenotypic severity in children with hereditary hemorrhagic telangiectasia. *J Pediatr Hematol Oncol* 2009;**31**:577–82.

31 Stringer CJ, Stanley AL, Bates RC, *et al.* Pulmonary arteriovenous fistula. *Am J Surg* 1995;**89**:1054–80.

32 Haitjema TJ, Overtoom TT, Westermann CJ, *et al.* Embolisation of pulmonary arteriovenous malformations: results and follow up in 32 patients. *Thorax* 1959;**50**:719–23.

33 Hodgson CH, Burchell HB, Good CA, *et al.* Hereditary hemorrhagic telangiectasia and pulmonary arteriovenous fistula: survey of a large family. *N Engl J Med* 1959;**261**:625–36.

34 Folz BJ, Zoll B, Alfke H, *et al.* Manifestations of hereditary hemorrhaghic telangiectasia in children and adolescents. *Eur Arch Otorhinolaryngol* 2006;**263**:53–61.

35 Higgins CB, Wexler L. Clinical and angiographic features of pulmonary arteriovenous fistula in children. *Radiology* 1976;**119**:171–5.

36 Villada IB, Roume J, Raffestin B, *et al.* Assessment of an age-related threshold of mucocutaneous telangiectasia number for diagnosis of hereditary hemorrhagic telangiectasia: HHT Paris center experience in 165 relatives belonging to 80 genotyped families. 8th International HHT Scientific Conference. *Hematol Meet Rep* 2009;**3**:56.

37 Cottin V, Plauchu H, Bayle JY, *et al.* Pulmonary arteriovenous malformations in patients with hereditary hemorrhagic telangiectasia. *Am J Respir Crit Care Med* 2004;**169**:994–1000.

38 Cooley SC, Jackson JE. Pulmonary arteriovenous malformations. *Clin Radiol* 1998;**53**:396–404.

39 Barzilai B, Waggoner AD, Spessert C, *et al.* Two-dimensional contrast echocardiography in the detection and follow-up of congenital pulmonary arteriovenous malformations. *Am J Cardiol* 1991;**68**:1507–10.

40 Stewart MJ. Contrast echocardiography. *Heart* 2003;**89**:342–8.

41 Gossage JR. Role of contrast echocardiography in screening for pulmonary arteriovenous malformations in patients with hereditary hemorrhagic telangiectasia. *Chest* 2010;**138**:769–71.

42 Pick A, Deschamps C, Stanson AW. Pulmonary arteriovenous fistulae: presentation, diagnosis, and treatment. *World J Surg* 1999;**23**:1118–22.

43 Vedrinne JM, Duperret S, Bizollon T, *et al.* Comparison of trans-esophageal and transthoracic contrast echocardiography for detection of an intrapulmonary shunt in liver disease. *Chest* 1997;**111**:1236–40.

44 Lee WL, Graham AF, Pugash RA, *et al.* Contrast echocardiography remains positive after treatment of pulmonary arteriovenous malformations. *Chest* 2003;**123**:320–2.

45 Remy J, Remy-Jardin M, Wattinne, L *et al.* Pulmonary arteriovenous malformations: evaluation with CT of the chest before and after treatment. *Radiology* 1992;**182**:809–16.

46 Maillard JO, Cottin V, Etienne-Mastroïanni B, *et al.* Pulmonary varix mimicking pulmonary arteriovenous malformation in a patient with Turner syndrome. *Respiration* 2007;**74**:110–3.

47 Halbsguth A, Schulze W, Ungeheuer E, *et al.* Pitfall in the CT diagnosis of pulmonary arteriovenous malformation. *J Comput Assist Tomogr* 1983;**7**:710–2.

48 Manson D, Traubici J, Mei-Zahav M, *et al.* Pulmonary nodular opacities in children with hereditary hemorrhagic telangiectasia. *Pediatr Radiol* 2007;**37**:264–8.

49 Genereux GP. Computed tomography and the lung: review of anatomic and densitometric features with their clinical application. *J Can Assoc Radiol* 1985;**36**:88–102.

50 Schneider G, Uder M, Koehler M, *et al.* MR angiography for detection of pulmonary arteriovenous malformations in patients with hereditary hemorrhagic telangiectasia. *AJR Am J Roentgenol* 2008;**190**:892–901.

51 AbuRahma AF, Robinson PA, Boland JP, *et al.* Complications of arteriography in a recent series of 707 cases: factors affecting outcome. *Ann Vasc Surg* 1993;**7**:122–9.

52 Waugh JR, Sacharias N. Arteriographic complications in the DSA era. *Radiology* 1992;**182**:243–6.

53 Lee DW, White RI Jr, Egglin TK, *et al.* Embolotherapy of large pulmonary arteriovenous malformations. *Ann Thorac Surg* 1997;**64**:930–40.

54 Watanabe N, Munakata Y, Ogiwara M, *et al.* A case of pulmonary arteriovenous malformation in a patient with brain abscess successfully treated with video-assisted thoracoscopic resection. *Chest* 1995;**108**:1724–7.

55 Svetliza G, De la Canal A, Beveraggi E, *et al.* Lung transplantation in a patient with arteriovenous malformations. *J Heart Lung Transplant* 2002;**21**:506–8.

56 Reynaud-Gaubert M, Thomas P, Gaubert JY, *et al.* Pulmonary arteriovenous malformations: lung transplantation as a therapeutic option. *Eur Respir J* 1999;**14**:1425–8.

47 Vascular Rings

Kevin K. Whitehead & Paul M. Weinberg

The Children's Hospital of Philadelphia, University of Pennsylvania School of Medicine, Philadelphia, PA, USA

Introduction

Vascular rings are generally defined as complete encirclement of the trachea and esophagus by segments or atretic remnants of vascular tissue [1,2]. Although individually there are a confusing array of anatomic configurations, the etiology of all vascular rings can be thought of as occurring from two causes: incomplete regression of the distal fourth arch and dorsal aorta bilaterally or a ductus arteriosus contralateral to the side of the aortic arch, arising from the descending aorta or aberrant (retroesophageal) subclavian artery.

Incidence and genetics

The incidence of vascular rings in most surgical series represents ~1% of operations for congenital defects. Most vascular rings are secondary to either double aortic arch or right arch with aberrant left subclavian artery and diverticulum of Kommerell, which together account for ~90% of all vascular rings.

The genetics of vascular rings are ill-defined. Although they are occasionally associated with syndromes, most patients have no identified genetic abnormalities. The most commonly associated syndrome is 22q11 microdeletion [3]. There is also an increased incidence of vascular rings in patients with congenital heart disease, especially those with conotruncal abnormalities, such as tetralogy of Fallot, transposition of the great arteries, and truncus arteriosus.

Embryology

The embryology of the aortic arch is well described, with six bilateral primitive arches appearing and involuting sequentially, eventually forming the definitive arch, proximal head and neck vessels, and ductus arteriosus. Vascular rings are caused by changes in the regression of the various segments of the arch such that the trachea and esophagus are encircled by vascular tissue. (Figure 47.1) Normally, the dorsal aorta on one side (generally the right) regresses, leaving a single arch. If neither regresses or one only partially regresses, then a double aortic arch is formed. Similarly, an aberrant subclavian artery results from regression of the fourth aortic arch instead of the dorsal aorta. A diverticulum results when there is a ductus arising from the dorsal aorta on the side of the aberrant subclavian artery, such that all ductal flow must run through this region and dilate this dorsal aortic segment.

Pathologic anatomy and major associated anomalies

When addressing vascular rings, it is useful to classify them by the three fundamental mechanisms by which a vascular ring is formed: (1) double aortic arch with or without atresia of one arch, (2) duct from an aberrant subclavian artery on the opposite side of the arch, and (3) duct directly from the descending aorta on the side opposite the aortic arch.

Double aortic arch

The double aortic arch is the most common form of a vascular ring, accounting for about half of all surgical procedures in vascular rings. Usually both aortic arches are patent. The most common pattern is a right-dominant double arch, the right aortic arch being larger than the left arch (Figure 47.2). Less common is the dominant left arch, followed by both arches being relatively equal in size. Often one of the apparently equal arches narrows posteriorly near the connection with the descending aorta and may be better visualized by 3D modalities.
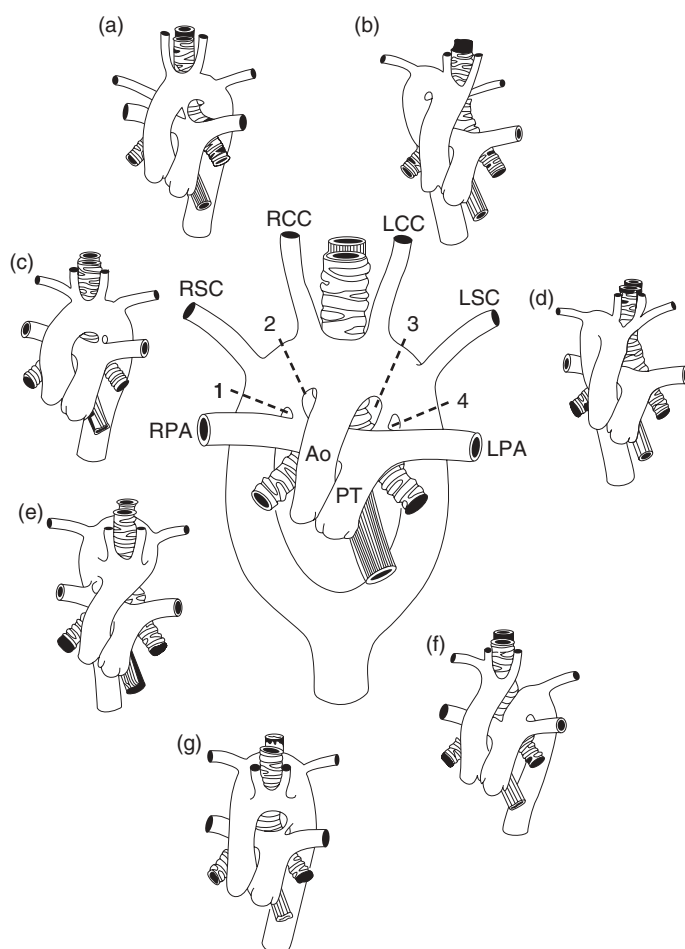
Figure 47.1 Hypothetical double aortic arch. During development, interruptions may occur at various sites (1 to 4), which give rise to different anatomic patterns of arch anatomy. If interruption occurs at site 1, a normal left aortic arch forms (c). If interruption occurs at site 4, a right aortic arch with mirror-image branching is formed (d). Interruptions at sites 2 and 3 form a left aortic arch with aberrant right subclavian artery (a) or a right aortic arch with aberrant left subclavian artery (b), respectively. If neither arch is interrupted, a double aortic arch with either right descending aorta (e) or left descending aorta (g) results. Two interruptions may occur in the hypothetical double aortic arch, giving rise to interruption of the aortic arch. One example is shown (f) in which the double arches were interrupted at sites 1 and 3, giving rise to interruption of the aorta distal to the left carotid artery. Ao, aorta; LCC, left common carotid artery; LPA, left pulmonary artery; LSC, left subclavian artery; PT, pulmonary trunk; RCC, right common carotid artery; RPA, right pulmonary artery; RSC, right subclavian artery.
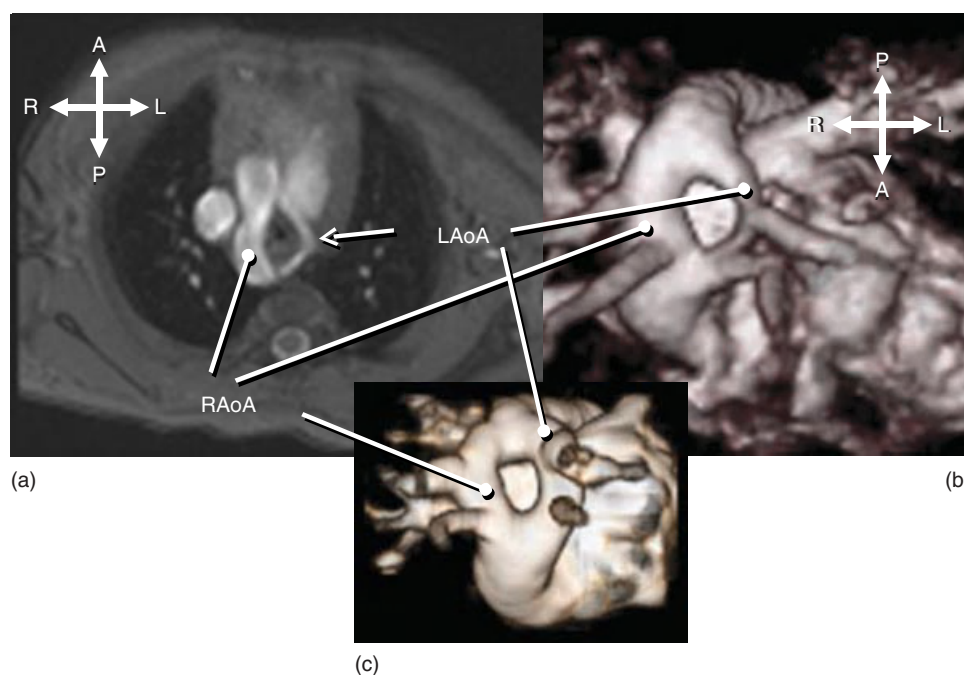
Figure 47.2 (a) Off-axis axial gradient echo image of a double aortic arch with a severely hypoplastic left arch (LAoA). (b) Volume rendered 3D reconstruction of the gadolinium magnetic resonance angiograph from the same patient, demonstrating the vascular ring. Note that the narrowest part of the arch is between the left carotid and the left subclavian arteries, but it can often occur distal to the left subclavian artery. This is difficult to discern with 2D imaging, but is fairly clear on the 3D volumetric rendering. This information is important in surgical planning. (c) 3D rendering of patient with double aortic arch and nearly equal arches. In these patients, flow measurements using magnetic resonance phase contrast velocity mapping can be useful in determining the dominant arch. RAoA, right aortic arch. Double-headed orientation arrows: A, anterior; L, left; P, posterior; R, right.
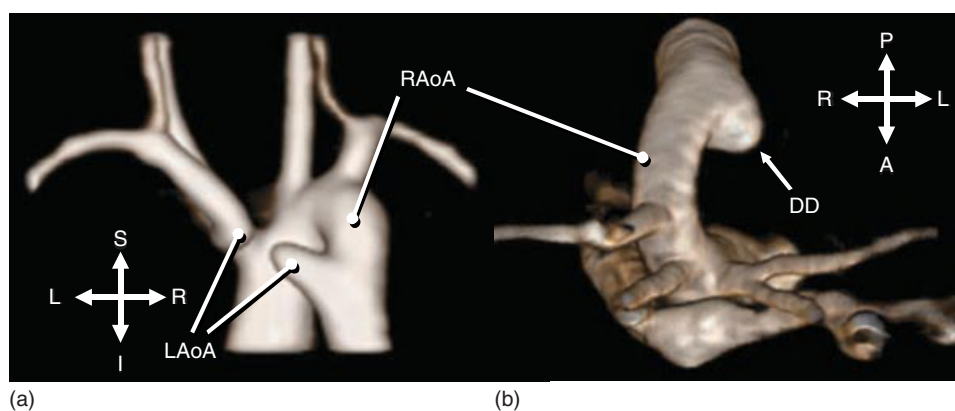
Figure 47.3 (a) Double aortic arch with atresia of the left arch (LAoA) distal to the left subclavian artery. Note that the distal left arch points towards the proximal left arch and note the dimple on the posterior aspect of the left subclavian artery. (b) Similar configuration of a right aortic arch (RAoA) and mirror image branching with a left ductus from the descending aorta. However, note the different configuration of the duct dimple (DD) and lack of significant posterior course of the left subclavian artery. Double-headed orientation arrows: as in Figure 47.2 plus I, inferior and S, superior.
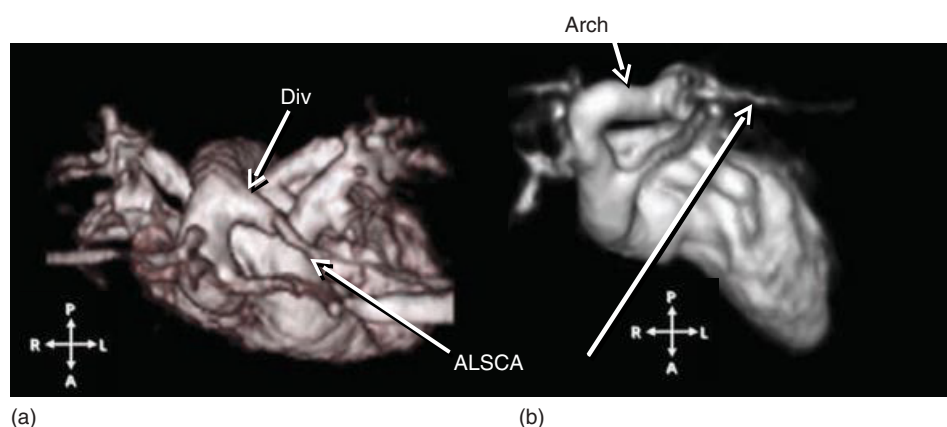
Figure 47.4 (a) Superior view of right aortic arch with an aberrant left subclavian artery (ALSCA) and diverticulum of Kommerell (Div). (b) Similar appearance of a cervical right aortic arch with a left descending aorta and ALSCA. Note that the subclavian artery does not pass behind the trachea. Instead, the aortic arch (Arch) itself crosses the midline and forms the posterior portion of the vascular ring. Double-headed orientation arrows: as in Figure 47.2.

Less commonly, a double aortic arch may be associated with atresia of the left arch. The atresia can be distal to the subclavian artery (Figure 47.3a, Video 47.1) or between the carotid and subclavian arteries. The former can appear similar to a contralateral ductus from the descending aorta (Figure 47.3b) and the latter can be difficult to distinguish from an aberrant subclavian artery with a diverticulum of Kommerell (Figure 47.4a). Clues that can distinguish an atretic arch from a ligamentum arteriosum include the posterior dimple on the subclavian or carotid artery, the extent of posterior course of the proximal head and neck vessels, and the orientation of the distal diverticulum or dimple.

Retroesophageal subclavian artery with diverticulum of Kommerell

The second most common type of vascular ring consists of a right aortic arch with an aberrant left subclavian artery with a diverticulum of Kommerell (Figures 47.4a and 47.5a). The diverticulum represents the pathway of fetal ductal flow across the proximal subclavian artery and implies a ligamentum arteriosum on the opposite side of the arch, completing the vascular ring. It is important to understand that the diverticulum extends behind the trachea and the caliber change will be on the side of the aberrant subclavian artery and opposite the arch. A subclavian artery without a duct has some tapering at its base but it is more gradual and does not extend to the level of the trachea (Figure 47.5c).

Although much less common, it is possible to have a diverticulum associated with a left arch and aberrant right subclavian artery (Figure 47.5b). In fact, the original diverticulum described by Kommerell was in the setting of a left aortic arch and aberrant right subclavian artery. Hence patients diagnosed with an aberrant right subclavian artery by echocardiography and with high clinical suspicion of a vascular ring clinically should generally undergo a magnetic resonance imaging (MRI) scan to rule out a vascular ring.
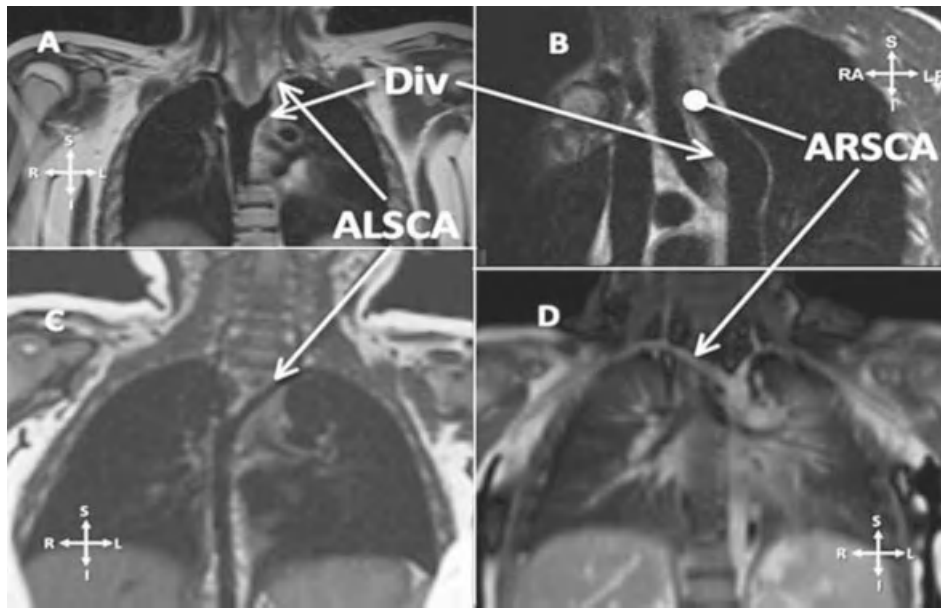
Figure 47.5 (a) Coronal dark blood view of right aortic arch with an aberrant left subclavian artery (ALSCA) and diverticulum of Kommerell (Div). (b) Off-axis coronal of rare left arch with aberrant right subclavian artery (ARSCA) and Div. (c) For comparison, right arch with ALSCA and no Div, which is not a vascular ring. (d) Bright blood image demonstrating an ARSCA without a Div. Note the gradual taper typical of an aberrant subclavian artery. Double-headed orientation arrows: as in Figure 47.3 plus RA, right anterior and LP, left posterior.

Duct from descending aorta, contralateral to side of aortic arch

A less common vascular ring comes involves a duct arising directly from the descending aorta on the opposite side of the aortic arch. This can be with either a thoracic descending aorta on the same or opposite side of the aortic arch. The most common in this category is a right aortic arch with a left thoracic descending aorta, also known as circumflex aortic arch, usually associated with a cervical arch (Figure 47.4b). Note that whereas nearly all descending aortas of right arches eventually cross over to the left by the level of the diaphragm, this circumflex arch refers to the fairly abrupt high crossing of the thoracic aorta superior to the level of the carina. A circumflex arch implies a left ductus or ligamentum or an atretic left arch. Similarly, a left aortic arch with a right descending aorta, again often with a cervical aortic arch, implies a right ductus or ligamentum creating a vascular ring. Note that although these forms of a vascular ring often also occur in the setting of an aberrant subclavian artery (Figure 47.4b), in this anomaly the aberrant subclavian artery is incidental and does not directly contribute to the ring. The subclavian artery does not cross the trachea or esophagus and therefore cannot contribute to symptoms. The posterior limb of the vascular ring is actually the crossing aortic arch.

Another form of vascular ring in this category is a right aortic arch with mirror image branching and a left ligamentum from the right-sided descending aorta (Figure 47.3b, Video 47.2). In this anomaly, the ligamentum actually forms the posterior limb of the vascular ring. As such, no diverticulum or posterior limb can be visualized. The only evidence will be a leftward-directed dimple on the descending aorta that represents the residual aortic ductal ampulla. A theoretical analog with a left aortic arch has not been described. Therefore, a left aortic arch with a left descending aorta is the only arch anatomy that can always be assumed to rule out a vascular ring.

Other arch anomalies

As discussed, a retroesophageal subclavian artery without a diverticulum is not a vascular ring and generally does not cause symptoms. However, some patients report varying degrees of dysphagia with only an aberrant subclavian artery and no other structural abnormalities. Furthermore, these patients have apparent relief from symptoms when the aberrant subclavian artery is either ligated or reimplanted. This finding is generally referred to as dysphagia lusoria. It most commonly occurs in adults in their fourth or fifth decade of life and is thought to be related to dilatation, calcification, and hardening of the subclavian artery. However, it has been reported in teenagers, and less commonly in infants and children. Esophageal manometry has been reported as helpful in confirming compression as the cause of symptoms in these patients [4].

Occasionally there can be significant vascular compression of the trachea in the absence of a vascular ring. However, these rarely reach clinical significance. These anomalies include compression between the ascending and descending aorta when they are in the same anterior–posterior plane, and compression by the innominate artery, often with

tracheomalacia. Innominate artery compression that needs relief can occur with extreme opisthotonus.

Another arch anomaly of note is that of a retroesophageal innominate artery because it is one of the rare instances when the branching pattern fails to identify arch sidedness. The first branch is on the same side as the aortic arch and can therefore make the identification of arch sidedness by the branching pattern (as done routinely in echocardiography) misleading. In a right aortic arch with an aberrant innominate artery, the first arch branch will be the right carotid artery (Video 47.3).

Natural history

The age and type of presentation are presumably in part secondary to the "tightness" of the ring. About 75% with a double aortic arch, 55% with a right aortic arch and aberrant left subclavian artery, and 95% with compression by an aberrant innominate artery [5] present in infancy with respiratory symptoms, including stridor, persistent cough, and frequent respiratory illnesses. Others can present in later childhood or even as teenagers and young adults with a history of respiratory symptoms that can mimic asthma or exercise-induced asthma. Some subjects remain asymptomatic throughout childhood and are occasionally diagnosed incidentally later in life. Because surgery is usually recommended for symptomatic vascular rings, the natural history of untreated symptomatic vascular rings has not been well studied.

The later the presentation, the more likely are gastrointestinal symptoms to be the prevailing symptoms. Vascular rings can present with significant dysphagia, occasionally with weight loss or failure to thrive. Choking or gagging on solid foods can result from interference with esophageal motility caused by vascular compression.

In adults, an aneurysmal origin of an aberrant subclavian artery can dissect or rupture.

Clinical features

History
The clinical history should be focused on the nature, severity, and timing of respiratory and gastrointestinal symptoms. Recurrent stridor and coughing in infants and children without concurrent infection are highly suspicious for a vascular ring. A history of refractory asthma, often with minimal or incomplete relief by bronchodilators and steroids, should raise the suspicion of a vascular ring. Older children may complain of wheezing or coughing with exercise or activity; they may carry the diagnosis of exercise-induced asthma. Dysphagia is a common presenting complaint in older patients. This is usually with solid foods, such as a piece of steak, that are not masticated completely. Occasionally, dysphagia can present in infants as choking or gagging on foods after solids are introduced into the diet, occasionally progressing to feeding refusal and failure to thrive.

Physical examination
The physical examination is often unremarkable. Stridor or wheezing may occur, but their absence does not rule out a vascular ring.

Electrocardiographic features
There are no characteristic findings in patients with vascular rings, because most have normal cardiac position and segmentation with structurally normal hearts. Any abnormalities are secondary to other associated structural heart disease.

Chest X-ray
A routine chest film may reveal a right-sided aortic knob or suggest a double aortic arch, but cannot definitively diagnose or exclude a vascular ring. Therefore, it should play little role in the routine workup of a suspected vascular ring. It may be useful in excluding other causes of respiratory symptoms.

Echocardiography
Because the air-filled trachea is often difficult to visualize on ultrasound, arch imaging tends to rely on defining the branching pattern of the aortic arch. A double aortic arch can be diagnosed by suprasternal sagittal imaging, defining two separate arches in different sagittal planes. A right aortic arch can be diagnosed if the first branch off the aortic arch goes to the left. If the first vessel does not branch, then an aberrant subclavian artery is suspected. However, it is often difficult to image directly posterior structures such as the subclavian artery, and defining the subclavian artery to determine whether there is a diverticulum is especially challenging. Furthermore, there are exceptions to these branching rules, including the rare aberrant innominate artery, in which the first branch off the arch is on the same side as the arch.

The reported degree of success in correctly identifying vascular rings by transthoracic echocardiography has ranged from one in six [6] to 100%.

Cardiac catheterization
Aortic angiography can certainly delineate aortic arch anatomy, and in the past has been the gold standard for the diagnosis of vascular rings. However, with better noninvasive tomographic and volumetric imaging methods now available, invasive angiography should no longer play a role in the routine diagnosis of vascular rings.

Other imaging modalities

Magnetic resonance imaging (MRI)

Because of their noninvasive nature and better ability to visualize 3D structures, tomographic and volumetric imaging methods are now the preferred technique in diagnosing vascular rings. Because it does not use ionizing radiation and has the ability to diagnose definitively all forms of vascular rings reliably, MRI is the preferred imaging modality for diagnosis.

Axial, bright blood images gated to end-diastole can be used effectively to visualize the branching pattern of the aorta. A second coronal stack, preferably turned slightly off-axis by multi-planar reformatting of the initial axial stack to align with the vessel of interest, is useful for identifying the caliber change of a diverticulum. If a vascular ring is identified, dark blood imaging aligned with the trachea can be performed to identify tracheal narrowing.

Volumetric imaging such as gadolinium angiography (or whole heart bright blood techniques if gadolinium is contraindicated) can allow the visualization of features difficult to see by planar imaging. These include identifying an aortic dimple where a ligamentum or atretic arch inserts, better visualization of a diverticulum, and visualizing the posterior portion of the two limbs of a double arch to determine which arch is smaller. The first two are important in diagnosis and the last is crucial information for the surgeon in planning which side to perform the thoracotomy. For this reason, high-resolution 3D magnetic resonance angiography should be performed routinely in the evaluation of a vascular ring. The only time when a vascular ring can be ruled out definitively by static axial imaging alone is a left aortic arch with normal branching and a left descending aorta.

Phase contrast velocity mapping can play a role in a double aortic arch with both arches nearly equal in size. Flow quantification in both arches distal to the origins of the subclavian arteries permits the determination of which arch carries the lesser flow.

Computed tomography (CT)

Chest CT can provide much of the same information as MRI, with the potential for decreased scan times and increased resolution. However, this comes at the cost of significant doses of ionizing radiation in a particularly vulnerable population.

Management

Medical

There is little role for medical management in vascular rings. Because airway symptoms are caused by a fixed obstruction, medications are ineffective. Older, asymptomatic individuals may be followed expectantly without intervention.

Surgical

Most recommend that all symptomatic young children diagnosed with vascular rings undergo surgical repair. Infants and toddlers have a very high likelihood of becoming progressively symptomatic, so even relatively minor symptoms should be considered for repair. Older children and adults with symptoms should also be referred electively for repair. However, incidental findings in older patients may be managed expectantly, with the understanding that future symptoms cannot be ruled out.

Surgical repair generally involves a thoracotomy on the side of the vascular structure that needs to be divided, either the opposite side of the arch or in a double arch, the side of the smaller or atretic arch. In the double aortic arch, the smaller arch is ligated and divided, generally at the narrowest segment, which is either between the carotid and subclavian arteries or distal to the subclavian artery. In a diverticulum, the ligamentum is simply ligated and divided [1]. Compression from an innominate artery can be treated by arteriopexy or transection and reimplantation.

Recovery is generally rapid and the primary postoperative issue is pain management. Some infants, however, require prolonged intubation for tracheal narrowing, and occasionally need reconstructive tracheal surgery. Transient pleural effusions are not uncommon. Rarely, recurrent chylous pleural effusions secondary to thoracic duct injury may require longer chest tube placement. The risk of recurrent laryngeal nerve injury should be minimal in the hands of an experienced surgeon.

In younger patients, division of the ring is almost always sufficient and relief of symptoms is rapid. Surgeons report dramatic relief of the vascular compression in the operating room. However, in older patients, long-standing compression and reduced tissue elasticity may make relief less dramatic. Some have advocated resecting the compressing diverticulum in this population [7] by reimplanting or ligating and sacrificing the subclavian artery. The ligation is generally well tolerated, but can put the patient at risk for a subclavian artery steal.

Long-term history

Children undergoing vascular ring division generally have long-term relief of symptoms. One series reported freedom from stridor in 19/20 in follow-up for 18 months [8] and another reported freedom from all symptoms in 47/48 patients with follow-up from 6 months to 14 years [9]. However, the latter study noted abnormal pulmonary function testing in 9/17 patients who consented to pulmonary function testing [8]. Others have reported that up to 40% of patients have long-term stridor, particularly those with younger age at repair [10].

References

1 Backer CL, Mavroudis C, Rigsby CK, Holinger LD. Trends in vascular ring surgery. *J Thorac Cardiovasc Surg* 2005;**129**:1339–47.

2 Berdon WE. Rings, slings, and other things: vascular compression of the infant trachea updated from the midcentury to the millennium – the legacy of Robert E. Gross, MD, and Edward B. D. Neuhauser, MD. *Radiology* 2000;**21**:624–32.

3 Momma K, Matsuoka R, Takao A. Aortic arch anomalies associated with chromosome 22q11 deletion (CATCH 22). *Pediatr Cardiol* 1999;**20**:97–102.

4 Klin B, Tauber Z, Peer A, *et al*. Dysphagia lusoria in children. *Eur J Vasc Endovasc Surg* 1996;**11**:504–6.

5 Hoffman JIE. Vascular rings and slings. In Hoffman JIE, ed. *The Natural and Unnatural History of Congenital Heart Disease*. Oxford: Wiley-Blackwell, 2009: 401–9.

6 van Son J, Julsrud P, Hagler D, *et al*. Imaging strategies for vascular rings. *Ann Thorac Surg* 1994;**57**:604–10.

7 Backer CL, Hillman N, Mavroudis C, Holinger LD. Resection of Kommerell's diverticulum and left subclavian artery transfer for recurrent symptoms after vascular ring division. *Eur J Cardiothorac Surg* 2002;**22**:64–9.

8 Turner A, Gavel G, Coutts J. Vascular rings – presentation, investigation and outcome. *Eur J Pediatr* 2005;**164**:266–70.

9 Marmon LM, Bye MR, Haas JM, *et al*. Vascular rings and slings: long-term follow-up of pulmonary function. *J Pediatr Surg* 1984;**19**:683–92.

10 Alsenaidi K, Gurofsky R, Karamlou T, *et al*. Management and outcomes of double aortic arch in 81 patients. *Pediatrics* 2006;**118**:e1336–41.

48 Coronary Arterial Abnormalities and Diseases

Julien I. E. Hoffman

University of California San Francisco, San Francisco, CA, USA

Classification

Anomalies of coronary arteries are classified as anomalies of origin from the aorta, of intrinsic anatomy and distribution, and of termination [1].

Incidence

Isolated coronary vascular anomalies (excluding innocuous variants) occurred in 0.3–1.3% of autopsies at all ages [2], 0.13–0.19% of pediatric autopsies [3], 0.3–1.5% of angiograms performed in adults [4–7], and 1.14% in echocardiograms of children [8]. In congenital heart disease, various coronary vascular anomalies that may be important only during surgery are common, and are described in their respective chapters.

Embryology

The primitive myocardium has sinusoids that develop into intramural vessels. These join a network of subepicardial vessels, which in turn join endothelial buds that emerge from the sinuses of Valsalva of both the aorta and main pulmonary artery [9]. The regulation of this organization is beginning to be explored [10].

Normal anatomy and variants

The right coronary artery (RCA) and left main coronary artery (LMCA) arise from the right and left sinuses of Valsalva (RSV, LSV), respectively, but sometimes are at or just above the supravalvar ridge. Their ostia are round or elliptical, and the arterial stems emerge approximately radially from the aorta [11]. The LMCA divides into the left anterior descending (LAD) and circumflex (LCx) branches, and the RCA gives off the conus branch and continues as the posterior descending artery to supply part of the posterior left ventricular wall (Figure 48.1a). About 35–50% of people have a separate conus branch coming from the RSV [7,12] (Figure 48.1b). About 1% of people have separate origins of the LCx and LAD arteries from the LSV [5–7,12–14] (Figure 48.1c). About 1% of coronary angiograms show a dual LAD, with a short proximal portion coming from the LCA and a longer portion arising from the RCA or RSV and taking a variable course to supply the distal part of the ventricles [15,16]. In 2% of angiograms, the origin of the LCx is acutely angulated where it arises from the LMCA [17]. None of these variants is clinically important unless it affects selective coronary artery catheterization, percutaneous transluminal coronary angioplasty (PTCA) or surgery.

There are excellent articles illustrating the anatomy of normal and abnormal coronary arteries as shown by magnetic resonance imaging (MRI) [18] and multidetector computed tomography (CT) [19].

Disorders of origin

Ectopic aortic origin of one or more coronary arteries

Origin of a coronary artery from the appropriate sinus of Valsalva with an abnormal orifice or intramural course

In some patients who died suddenly, and a few at operation, a coronary artery, usually the right, had a long intramural aortic course and emerged tangentially, making an angle of <45° to the aortic wall (Figure 48.1, inset). The ostium of the
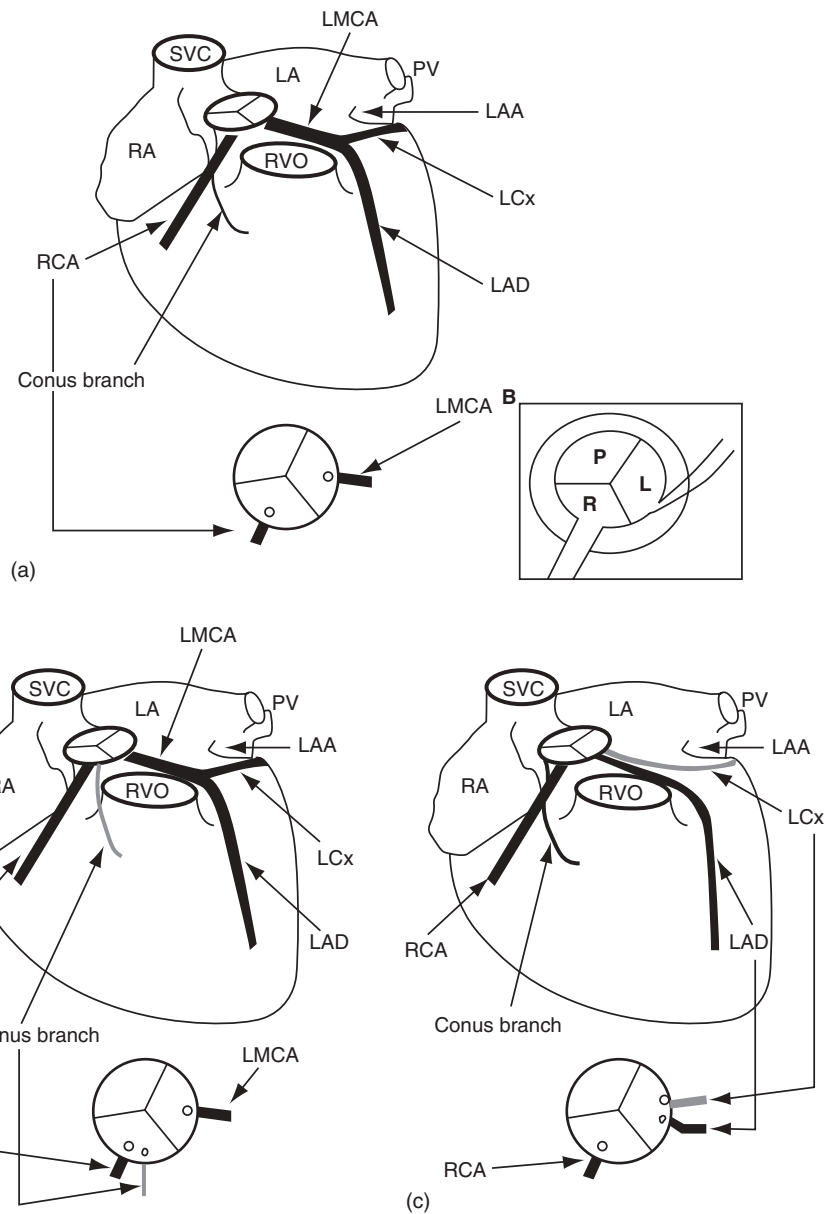
Figure 48.1 Normal and innocuous variations. (a) Normal main right and left coronary arteries, seen in an exploded frontal view (above) and diagrammatically from above (below). The inset shows a normal radially directed right coronary artery but an abnormal narrow, intramural LMCA emerging at an acute angle from the aortas. (b) Separate origin of conus branch of right coronary artery. (c) Separate origins of left circumflex and left anterior descending coronary arteries. The abnormal anatomy is shown in gray shading. L, left coronary sinus; LA, left atrium; LAA, left atrial appendage; LAD, left anterior descending coronary artery; LCx, left circumflex coronary artery; LMCA, left main coronary artery; P, posterior or non-coronary sinus; PV, pulmonary veins; R, right coronary sinus; RA, right atrium; RCA, right coronary artery; RVO, right ventricular outflow tract; SVC, superior vena cava.

artery was slit-like and partly covered by a valve-like ridge [11,20].Most of these patients were adults.

Abnormal origin of one coronary artery or a branch from the wrong sinus of Valsalva

Left main coronary artery from right sinus of Valsalva
This constitutes 1–12% of major coronary artery anomalies [4,5,14,21,22]. Four patterns are found [8,23,24]. In ~60%, the LMCA passes obliquely through the aortic wall and then between the aorta and the main pulmonary artery before bifurcating (interarterial course, Figures 48.2a and 48.3a). Its aortic origin may be slit-like and covered by a flap.

The intramural portion is elliptical with a diameter smaller than that of the extramural portion of the artery [25].The posterior or retro-aortic type occurs in 18%; a long LMCA passes behind the aorta and pulmonary artery before bifurcating (Figures 48.2b and 48.3b). In ~16% of these anomalous arteries [26], the LMCA passes intramyocardially through the ventricular septum along the floor of the right ventricular outflow tract (the septal type), and then reaches the surface before bifurcating (Figures 48.2c and 48.3c). The anterior type occurs in 8%; the LMCA runs on the anterior surface of the right ventricle almost like a normal conus branch, and bifurcates at about the mid septum (Figures 48.2d and 48.3d).

675
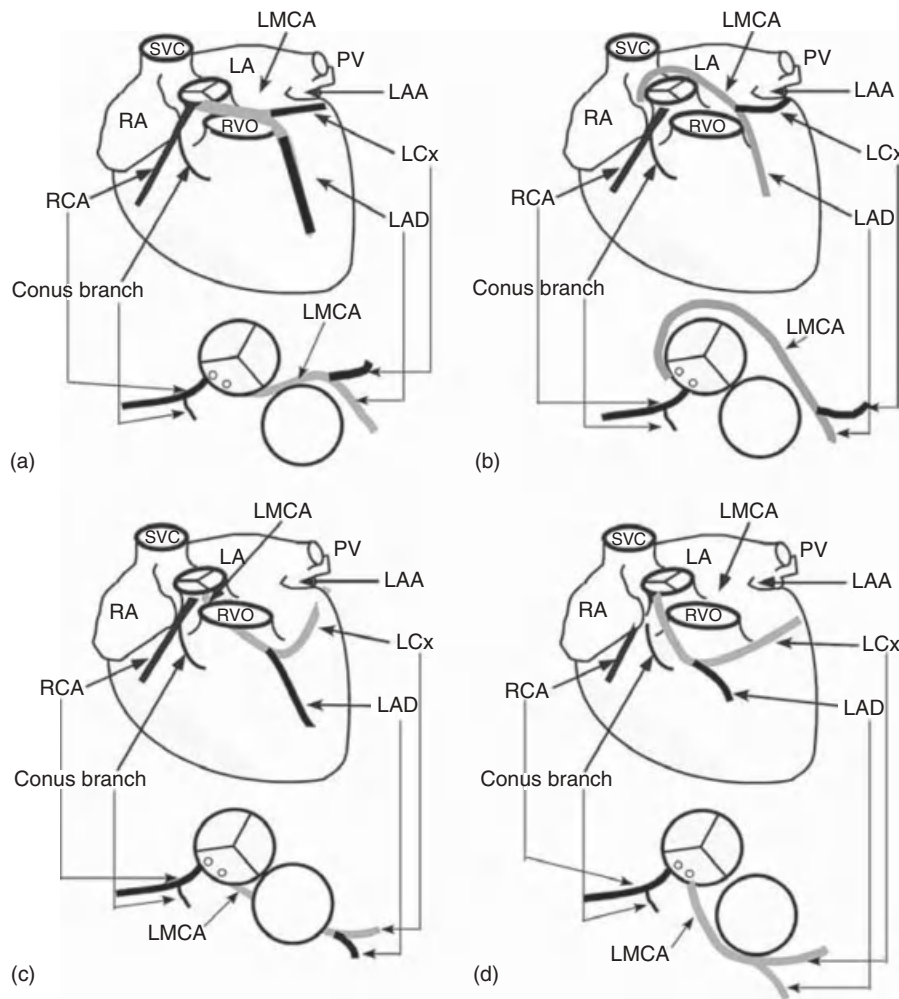
Figure 48.2 Left main coronary artery from right sinus of Valsalva. (a) Inter-arterial course; (b) posterior course; (c) intramural septal course; (d) anterior course. Abbreviations and views as in Figure 48.1. Abnormal anatomy shown in gray shading.

Right coronary artery from left sinus of Valsalva

This accounts for ~33% of all major coronary arterial anomalies [26]. The orifices of the RCA and LMCA are adjacent, and in 97% of patients the RCA passes between the aorta and the right ventricular outflow tract to reach the atrioventricular groove, after which it is distributed normally (Figures 48.4 and 48.5). The orifice can be slit-like and the proximal portion of the artery may be angulated [27–30].

Origin of left anterior descending, left circumflex, or both arteries from the right sinus of Valsalva or right coronary artery

An LCx coming from the RCA or RSV is common [26]. The LCx runs behind the aorta to the atrioventricular sulcus behind the atrioventricular valve rings (Figure 48.6a).

The LAD can originate in the RSV or the RCA. This anomaly is rare without congenital heart disease but is common in tetralogy of Fallot. The artery usually passes in front of the right ventricular outflow tract or through the interventricular septum. (Figure 48.6b).

Occasionally, both the LCx and the LAD arise by separate orifices from the RSV. These arteries take posterior and anterior courses, respectively, as described above.

Single coronary artery

These comprise 5–20% of major coronary arterial anomalies [26].

The best known of many classifications are those by Lipton *et al.* [31] and a variant by Shirani and Roberts [32]. There is a single ostium in the RSV or LSV; these are equally frequent. In type I, the single coronary artery (SCA) from the left ostium forms an LMCA that divides into LAD and LCx arteries, the latter continuing past the crux to form the RCA (type L1 of Lipton *et al.*, IB of Shirani and Roberts) (Figure 48.7a) or the SCA from the right ostium forms an RCA that is normally distributed, but the right posterior circumflex artery continues beyond the crux of the heart to

Figure 48.3 MRI sections and reconstruction of various courses of LCA coming from the right sinus of Valsalva. (a) Inter-arterial; (b) retroaortic (with stents in RCA); (c) transseptal passage of LAD, not LMCA; (d) anterior. Ao, aorta; LAD, left anterior descending; LM, left main coronary artery; PA, pulmonary artery; RCA, right coronary artery; RVOT, right ventricular outflow tract. (Reproduced from Patel *Semin Roentgenol* 2008;**43**:100–12, with permission from Elsevier.)
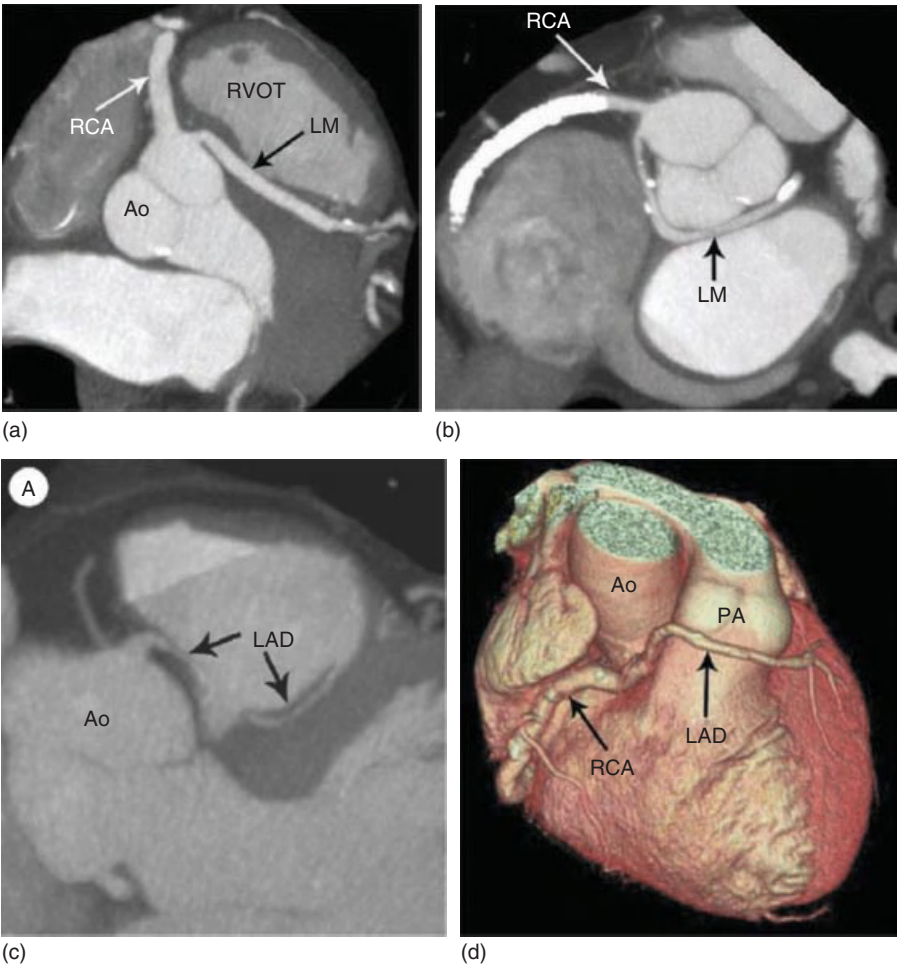
Figure 48.4 Right coronary artery from left sinus of Valsalva. Abbreviations and views as in Figure 48.1. Abnormal anatomy shown in gray shading.
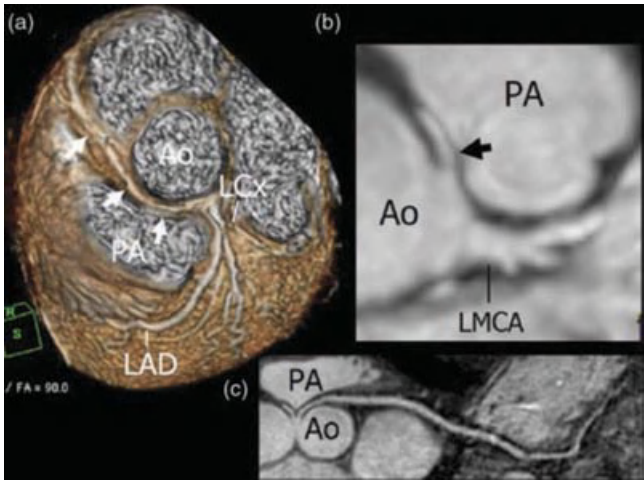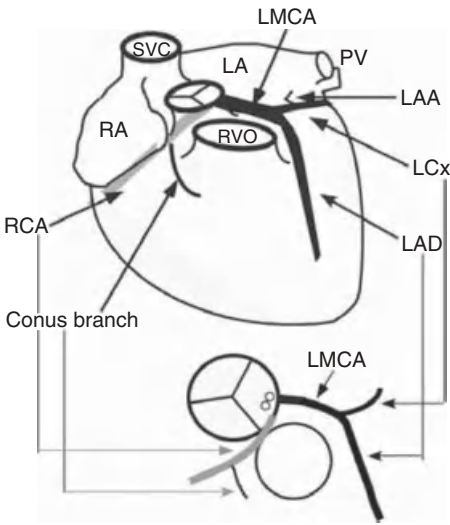
Figure 48.5 RCA (white arrows in (a), black arrow in (b)) from left sinus of Valsalva. Note acute angulation of RCA as it leaves the aorta. (a) surface view, (b) and (c) cross-sectional views. Right coronary artery (RCA) shown by arrows. (Reproduced from Sato *et al*. *Int J Cardiol* 2008;**127**:274–5, with permission from Elsevier.)

(a)

(b)
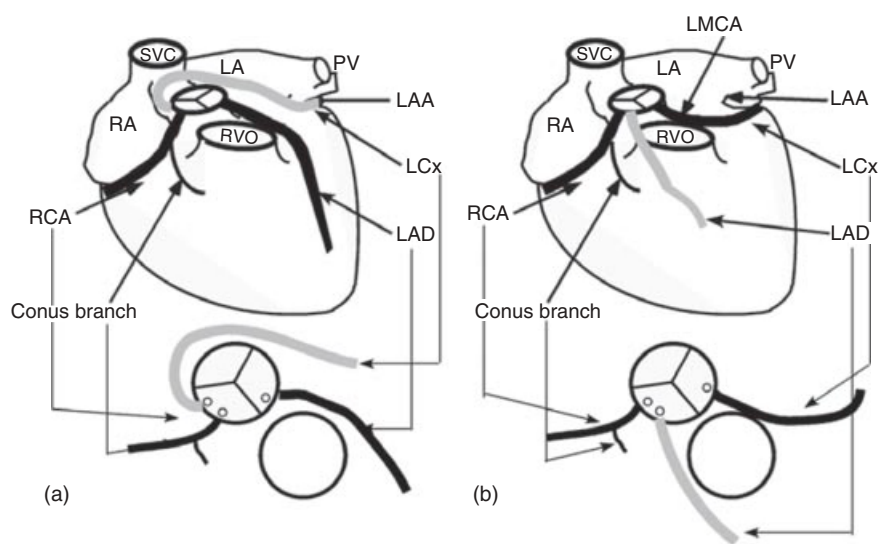
Figure 48.6 (a) LCx from right sinus of Valsalva; (b) LAD from right sinus of Valsalva.

(a)

(b)

(c)

(d)
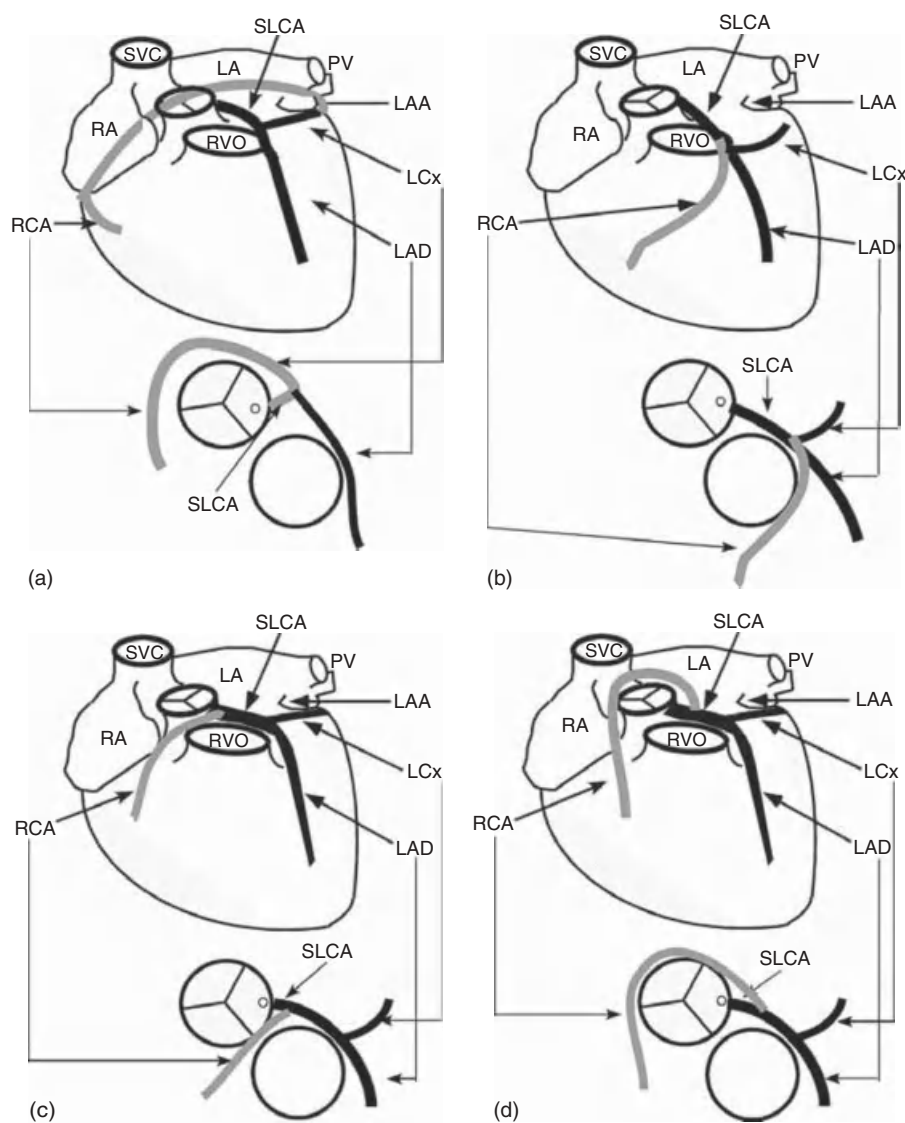
Figure 48.7 Single left coronary artery. (a) Type I. Right coronary artery as continuation of left coronary artery (L1 or IA); dashed outlines indicate passage in posterior atrioventricular groove. (b). Type II. Transverse right coronary artery with anterior course (L2a or IB1). (c) Type II. Transverse right coronary artery with inter-arterial course (L2b or IB2). (d) Type II. Transverse right coronary artery with posterior course (L2p or IB4). Abbreviations and views as in Figure 48.1. SLCA, single left coronary artery. Classifications with L by Lipton *et al.* [31] and classifications with I by Shirani and Roberts [32]. Abnormal course shown by gray shading.
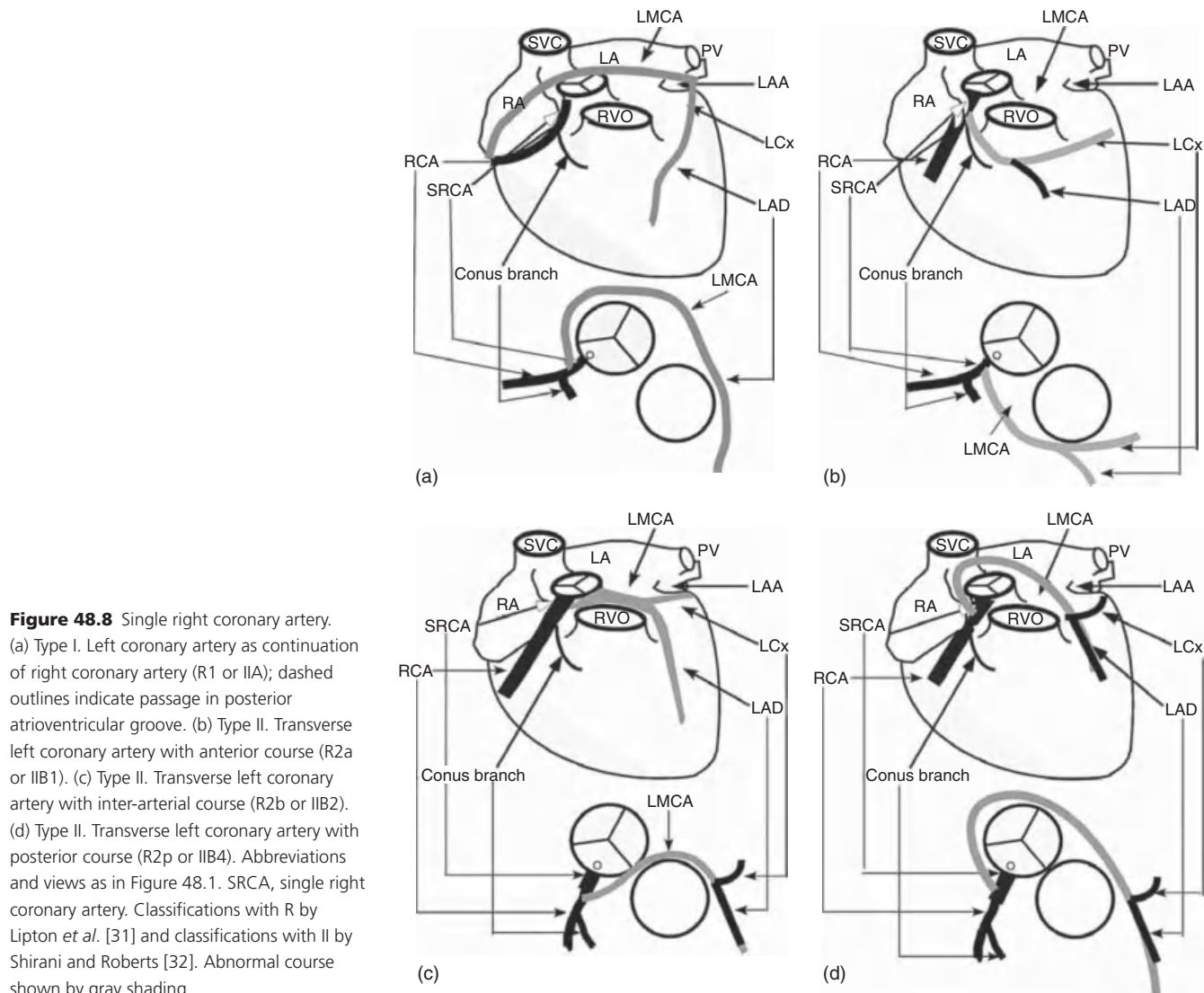
Figure 48.8 Single right coronary artery. (a) Type I. Left coronary artery as continuation of right coronary artery (R1 or IIA); dashed outlines indicate passage in posterior atrioventricular groove. (b) Type II. Transverse left coronary artery with anterior course (R2a or IIB1). (c) Type II. Transverse left coronary artery with inter-arterial course (R2b or IIB2). (d) Type II. Transverse left coronary artery with posterior course (R2p or IIB4). Abbreviations and views as in Figure 48.1. SRCA, single right coronary artery. Classifications with R by Lipton *et al.* [31] and classifications with II by Shirani and Roberts [32]. Abnormal course shown by gray shading.

form the LCx and LAD arteries (type R1 of Lipton *et al.*, IIA of Shirani and Roberts) (Figure 48.8a). Alternatively, the single artery branches early into typical right and left coronary arteries; each of these type II patterns is further subdivided according to whether the transverse branch passes anterior to the pulmonary artery (R2a and L2a, or IB1 and IIB1) (Figures 48.7b and 48.8b), between the great arteries (R2b and L2b, or IB2 and IIB2) (Figures 48.7c and 48.8c), posterior to the aorta (R2p and L2p, or IB4 and IIB4) (Figures 48.7d and 48.8d), or through the septum (IB3 and IIB3). Both classifications introduce added groups (three for Lipton *et al.*, groups IIC and IID for Shirani and Roberts) in which the branching patterns are uncommon. Type II variants are more common than type I variants. Type I variants are seen more often in single left coronary arteries, whereas type II variants occur slightly more often with single right coronary arteries.

Miscellaneous anomalies

Many uncommon variations of coronary arterial origins have been reported [26].

Associated anomalies

Most coronary anomalies are isolated but may be associated with other forms of congenital heart disease, particularly conotruncal abnormalities.

Pathology and pathophysiology

Some patients with a coronary arterial anomaly have a subendocardial scar from episodes of ischemia, or even a myocardial infarct. The suddenness of death, however, usually prevents infarction. Some patients had physiological hypertrophy of the left ventricle. Severe atherosclerosis may occur in a segment of the abnormal coronary artery, even in children, and is particularity frequent in the anomalous LCx

[4,21,33,34]. Occasionally, the initial few millimeters of artery run in the aortic wall or may be narrowed, or the whole anomalous artery is hypoplastic. Finally, the anomalous artery may arise tangentially from the aorta, and its ostium may be slit-like and partly covered by a valve-like flap.

Mechanisms of death

Sudden death is common, especially during exercise, almost certainly from myocardial ischemia that produces ventricular fibrillation or electromechanical dissociation. During strenuous exercise, blood flow and pressure increase and the left ventricular myocardium has an enormous demand for oxygen. The aortic root distends in systole, and any intramural anomalous artery may be compressed, or an artery running adjacent to the wall may be stretched or compressed. The ostial flap may occlude the inflow into the artery when maximal flow is needed, especially when blood pressure decreases rapidly post-exercise but skeletal muscle arterioles are still dilated [35,36]. Ischemia may cause acute ventricular dilatation with stimulation of cardiac sensory nerve endings that causes vasodepressor syncope. Why some patients have apparently identical anomalies but survive without ischemia until old age is unknown; there may be progressive obstruction to the orifice and first part of the artery with aging.

Natural history

Whereas ischemic pain usually leads to tests that reveal the diagnosis, the major concern with these anomalies is sudden death, a risk that varies with the precise anomaly.

The most dangerous anomaly is the LMCA arising from the RSV. Sudden death is rare <10 or >20 years of age, and is predominantly in those with intra-arterial passage (Table 48.1).

There were 228 patients with LCA from the RSV, of whom 175 had an interarterial course. Of these 175, 132 (75%) either died or had symptoms of ischemia, whereas the figure was 24/53 for all other courses combined. There were 109 deaths; 83(76%) were from the anomaly and the other 26 from other causes. Among the 83 deaths from the anomaly, 78/83 (94%) were from an interarterial course.

A similar literature search of patients with an interarterial course by Moustafa et al. [37] (almost certainly with overlap of patients) showed sudden death in 96/130 (74%) of these patients.

The issue is less clear for an RCA from the LSV. Once considered benign, there are now many reports of myocardial ischemia, infarction, deaths, and near deaths with this lesion [38]. Most deaths occur in teenagers or young adults, but seven neonates and infants died with this anomaly. There were 45 deaths in 83 patients (54%) due to the anomaly. Compared with anomalous LMCA, more deaths at <10 years of age occurred with anomalous RCA [26].

Table 48.1 Details of outcome with LCA from RSV.

Course	Due to anomaly		Not due to anomaly		Total
	Death	Symptoms	Death	Symptoms	
Interarterial	78	54	15	28	175
Other	5	19	11	18	53
Total	83	73	26	46	228

Based on data from the literature reported by Hoffman *The Natural and Unnatural History of Congenital Heart Disease.* Oxford: Wiley-Blackwell. 2009:384–400.
LCA, left coronary artery; RSV, right sinus of Valsalva.

Anomalous origin of the LCx is usually benign, except for a tendency for premature atherosclerosis [21], and it can be compressed if both aortic and mitral prosthetic fixation rings are implanted [39].

An anomalous LAD can cause ischemic symptoms, but rarely sudden death, in the absence of coronary atherosclerosis.

A single coronary artery usually produces no symptoms without severe atheroma (which is more serious with only one main artery supplying the whole heart), but a few premature deaths or infarctions have been reported [40,41].

Clinical features

Anomalous coronary arteries may be found during angiography for congenital heart disease or myocardial ischemia. As lesions causing primary problems, they are most often found in autopsies performed for sudden death. They may be detected by imaging studies of children and young adults presenting with syncope (especially with exercise), chest pain, arrhythmia, or other evidence of myocardial ischemia, including myocardial infarction. These symptoms usually come on during or just after strenuous exercise, and most victims have been athletes. There are no specific clinical findings.

Diagnosis and diagnostic studies

Any episode of syncope or severe chest pain during or after exercise requires intensive cardiac investigations, beginning with a standard clinical examination and an electrocardiogram to look for ventricular hypertrophy, arrhythmias, or prior infarction. A near maximum exercise test to evaluate blood pressure response and the electrocardiogram can be useful but has some risk; injecting a radioisotope at peak exercise might reveal ischemia. A normal exercise test, however, does not exclude a serious coronary artery anomaly, and exertional syncope or prolonged chest pain in a child or young adult warrants careful imaging studies.

Imaging studies

Echocardiography

An echocardiogram with Doppler interrogation should always be done to exclude intracardiac anomalies and hypertrophic cardiomyopathy. Arteries arising tangentially from the sinuses of Valsalva are readily detectable. Technically satisfactory transthoracic echocardiography has, however, sometimes failed to detect an anomalous coronary artery. In larger children and adults, transesophageal echocardiography has been more useful [42].

Aortic and coronary angiography

Failure to recognize an anomalous coronary arterial origin or branching pattern can lead to misdiagnosis of branch occlusion when selective coronary arteriography is done or a sinus of Valsalva shows no coronary ostium during an angiogram. In addition, an anomalous artery can be injured during an operation performed near the aortic and pulmonary arterial roots, particularly if the anomalous artery was buried in muscle or concealed in scar tissue.

Good descriptions of the cineangiographic features have been published for the various types of course taken by an LMCA arising from the right aortic sinus [43], other anomalies [44], and single coronary arteries [31].

Other imaging studies

Ultrafast CT or MRI has been used successfully [18,19,45,46]. MRI has excellent sensitivity and specificity for detecting these anomalies [47,48]. The sensitivity and specificity of axial CT have not been evaluated.

Treatment

Treatment is advisable for a known sinister anomaly with symptoms indicating myocardial ischemia, and is advisable for symptoms even without ischemia [49,50]. With a more benign anomaly, or no symptoms, provocative testing with exercise, pacing, dobutamine, or ergonovine might determine if the patient is at risk.

Coronary arterial bypass graft is inadvisable in younger patients because of doubts about graft longevity and the risk of competitive flow. No long-term follow-up has been described. The alternative is to remove tissue flaps that are covering the orifice, and revise the intramural aortic course of the artery. If the intramural artery runs distal to the commissure, unroofing the artery along its length creates a long orifice without obstruction [37,51,52]. If, however, the intramural artery is below the commissure, unroofing requires detaching and then replacing the commissure, risking aortic regurgitation. The surgeon may then unroof the distal part of the intramural anomalous artery up to the commissure and suture the edges to the aorta, creating a neo-orifice, and then obliterate the proximal part of the artery [52]. Both procedures eliminate stenosis at the orifice and the acute angulation of the first part of the artery. With

no intramural course, the surgeon reimplants the coronary artery into the correct sinus.

With these procedures, the portion of the LMCA between the aorta and pulmonary artery is not rerouted, suggesting that intra-arterial compression is not a major factor in producing ischemia. Occasionally there is a single coronary artery ostium that does not permit any of the above procedures to be done. In these patients, the pulmonary artery has been transected and translocated in such a way as to open up the space between the aorta and the pulmonary artery [52]. Perhaps opening the space reduces the angulation that may contribute to ischemia.

Because the obstruction may be from a narrowed intramural passage as well as acute angulation as the artery leaves the aorta, stenting of the initial portion of the artery may relieve the obstruction [25]. This is unproven.

After surgery, there has usually been relief of symptoms, and few late postoperative deaths are reported [49,53]. Exercise tolerance and quality of life are excellent [54].

In older patients with atherosclerotic occlusion of the anomalous artery, PTCA or stenting has been used. Relieving a stenosis in an anomalous artery, however, does not mean that angulation or narrowing at its origin may not cause problems later.

Absence or atresia of both main coronary arteries

Complete absence of both main coronary arteries is rare, occurring most often in pulmonary or aortic atresia with a small hypertrophied ventricle, suprasystemic pressures, and sinusoids supplying distal coronary arteries.

Atresia or stenosis of the coronary arterial origin

Pathological anatomy

Stenosis or atresia of the ostium or first few millimeters of the LMCA has been reported in ~60 patients. The LMCA is connected by a fibrous cord to a dimple in the LSV, but its distal branches are normal and supplied by multiple collaterals from the RCA [55,56]. Atresia of the RCA is rare [57,58]. Atresia may be associated with supravalvar aortic stenosis, but whether atresia is primary or secondary is not known.

A few patients had ostial stenosis, but whether this was congenital or acquired is unknown. Rarely, the coronary arteries are hypoplastic and may cause death in young adults.

Pathophysiology

With stenosis or atresia of the LMCA, the anterolateral portion of the left ventricular free wall is ischemic and dysfunctional, either reducing stroke volume or increasing left ventricular diastolic volume. Stress intensifies ischemia, and may elicit it even if it is absent at rest.

Clinical presentation

Patients present from 3 months to 60 years of age, most being <20 years of age. Younger patients present with congestive heart failure, and older patients present with angina pectoris or myocardial infarction. Sudden death, sometimes with exercise, is rare. Occasionally there are no symptoms. Signs of anterolateral ischemia or infarction of the left ventricle make one suspect anomalous origin of the left coronary artery from the pulmonary artery that is much more common than atresia.

Diagnosis

This diagnosis can be made when echocardiography or cineangiography fails to show the LMCA arising from the aorta, and when attempts made to catheterize the LMCA from the aorta fail. The distinction between atresia and anomalous origin of the LMCA from the pulmonary artery is that with atresia no flow enters the pulmonary artery from the LMCA as determined by echocardiography–Doppler or cineangiography studies; in particular, failure to fill the anomalous LMCA during a pulmonary angiogram favors the diagnosis of atresia.

Similarly to an atretic LMCA, a single RCA shows a large RCA and no left main coronary artery arising from the aorta or pulmonary artery. However, by angiography the atretic coronary artery anomaly shows collaterals from the RCA entering large major branches of the LCA, whereas in a single right coronary artery, blood flows through progressively smaller arteries as it passes towards the periphery [56].

Treatment

Several reports have described successful coronary artery bypass grafting, with a saphenous vein [59] or an internal mammary artery [55,56,59].

Ectopic origin of one or both coronary arteries from the main or peripheral pulmonary arteries

All coronary arteries from pulmonary trunk

Rarely, both main coronary arteries, or a single coronary artery, arise from the pulmonary trunk; by 1986 only 25 such anomalies had been described. Unless there is a cardiac lesion causing pulmonary hypertension, these children usually do not survive infancy, and even with other lesions survivors are rare [60–62].

Left main coronary artery from the pulmonary trunk

This anomaly, termed ALCAPA (anomalous left coronary artery from pulmonary artery) occurs in 6.5–15.3 per million live births. The first report relating clinical and autopsy findings in a 3-month-old boy was by Bland *et al*. [63], and the anomaly is often called the Bland–White–Garland syndrome. The history of the diagnosis and treatment of this lesion has been described [64].

Pathological anatomy

The RCA is greatly dilated and large superficial collaterals are seen. The LMCA enters the pulmonary artery, usually the left pulmonary sinus but occasionally a branch. Rarely, it is attached to the non-facing sinus [65]. It is usually only 2–5 mm long before it branches. The connection between the LMCA and pulmonary trunk may be narrow or even stenotic. Occasionally the initial portion of the LMCA is intramural.

In infancy, the left ventricle and atrium are dilated and hypertrophied. The anterolateral papillary muscle is atrophic and scarred, and its chordae may be shortened. Sometimes the posterior papillary muscle is similarly affected [13,60].

There may be diffuse endocardial fibroelastosis of the left ventricle, and the anterior mitral valve leaflet is often thickened. The anterolateral left ventricular wall and apex are thinned and scarred from infarction, and there are often mural thrombi. A biopsy of the affected left ventricular free wall at surgery in five patients showed that 51 ± 32% of the wall was fibrotic, and that the remaining muscle fibers, although viable, showed a paucity of contractile fibers [66].

In adults, the LCA is thin walled, resembling a vein. The heart is usually enlarged, but less than in infants, and there is usually no endocardial fibroelastosis. However, there is usually scarring and calcification of the anterolateral papillary muscle, and occasionally even of the adjacent left ventricle [14,67].

Associated lesions

ALCAPA has occasionally been associated with patent ductus arteriosus, ventricular septal defect, tetralogy of Fallot, or coarctation of the aorta [60]. If there is pulmonary hypertension, as with a large ventricular septal defect, left ventricular perfusion may be adequate, but closure of the defect with a fall in pulmonary arterial pressure may be catastrophic [68].

Pathophysiology

In fetal life this anomaly is innocuous. Pressures and oxygen saturations are similar in aorta and pulmonary artery, myocardial perfusion is presumably normal, and there is no stimulus to collateral formation. After birth, however, the left ventricle, with its huge demand for oxygen, is perfused with desaturated blood at low pressures. Collateral vessels between the normal right and abnormal LMCA enlarge, and so does the RCA.(Figure 48.9).

This collateral flow is of little use because most of the collateral flow that enters the left coronary arterial system tends to pass into the pulmonary artery rather than into
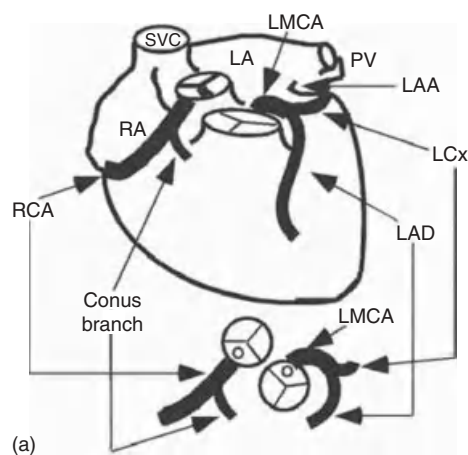
Figure 48.9 Left main coronary artery from pulmonary artery. (a) In fetus. (b) In neonate. The light gray apical region indicates the ischemic region. (c) In older infant. The slightly darker gray apical region indicates worsening ischemia, and the very dark central area is the infarct. The gray vessels joining left anterior descending and right coronary arteries are collaterals. The pale gray arrows indicate the direction and approximate magnitude of collateral blood flow and its distribution. The open arrows indicate the direction and approximate quantity of flow in the proximal and distal left coronary artery.
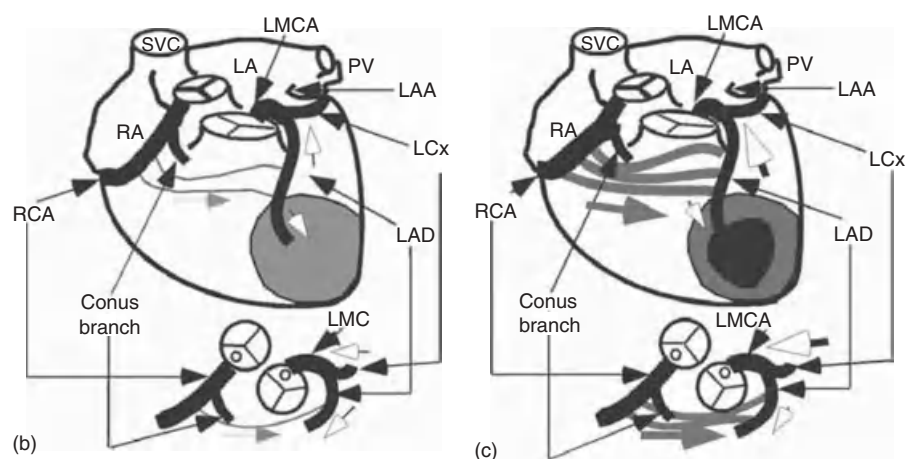
the high resistance myocardial blood vessels (Figure 48.9), as first demonstrated by Sabiston *et al.* [69]. The amount of left to right shunting is small relative to cardiac output, but large relative to coronary flow. Initially, left ventricular myocardial vessels dilate to reduce their resistance and increase flow, but when coronary vascular reserve becomes exhausted, myocardial ischemia ensues. At first, ischemia is transient and occurs only with exertion such as feeding or crying, but further increases in myocardial oxygen demand lead to infarction of the anterolateral left ventricular free wall. This causes congestive heart failure, often made worse by mitral regurgitation secondary to a dilated mitral valve ring or infarction of the anterior papillary muscle [70–72].

In some patients, the connection of the LMCA to the pulmonary artery is restrictive, no steal occurs, and all the collateral flow perfuses the free wall of the left ventricle. These patients may include many of the 15% of patients with these anomalies in whom myocardial blood flow is adequate to sustain myocardial function at rest or even during exercise, and who reach adult life [60,73]. Prolonged

survival is more likely in patients with a dominant right coronary system [73,74].

Natural history
About 87% of children born with this rare anomaly present in infancy, and if untreated 65–85% die before 1 year of age from intractable congestive heart failure, usually >2 months of age [26,60,74,75]. A few improve spontaneously. Others never have symptoms, perhaps because they have extensive collaterals or a restrictive opening between the origin of the left coronary artery and the pulmonary trunk. Nevertheless, even they are at high risk of sudden death [74,76], especially during exercise. Some present as adults with angina of effort or myocardial infarction [67,77,78], arrhythmias [78], or left ventricular dysfunction or even congestive heart failure associated with mitral regurgitation [79,80]. Operation markedly improves function. Whether an operation is required for an adult with this anomaly but no evidence of ischemia at rest or on exercise is unknown. The course without treatment is presented in Figure 48.11.

| I | II | III | aVR | aVL | aVF |

| V$_4$R | V$_1$ | V$_2$ | V$_3$ | V$_4$ | V$_5$ | V$_6$ |
| | (N/2) | (N/2) | (N/2) | (N/2) | | |
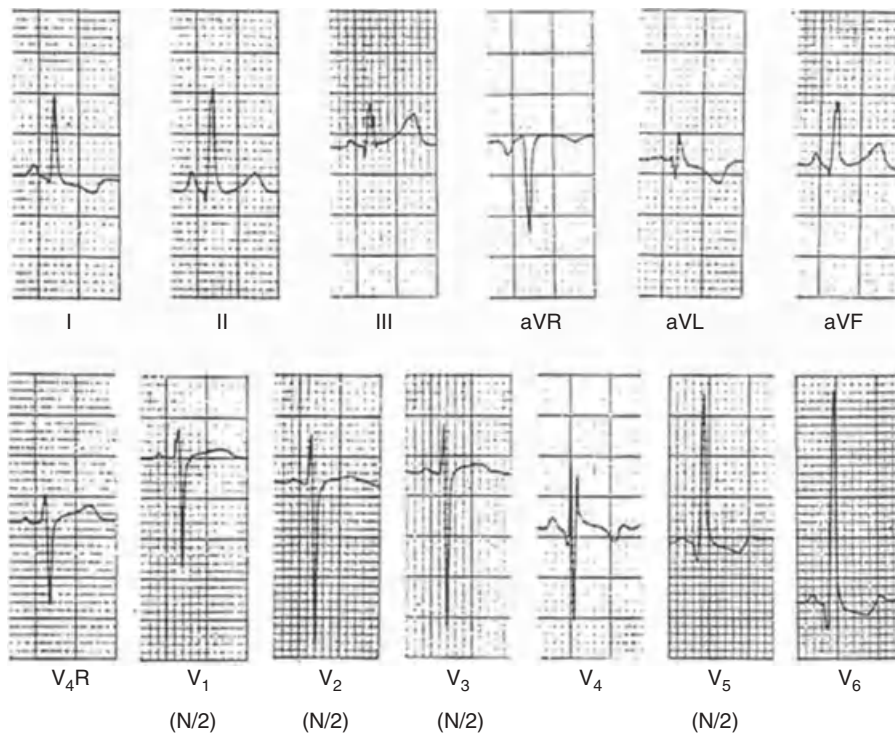
Figure 48.10 Electrocardiogram in ALCAPA. Note abnormal q waves in leads V5 and V6, and also abnormal R wave progression in the precordial leads.

Clinical findings

In infancy, the description by Bland *et al.* [63] still pertains. They wrote:

> Nothing remarkable was noted about the patient until the tenth week; while nursing from the bottle, the onset of an unusual group of symptoms occurred which consisted of paroxysmal attacks of acute discomfort precipitated by the exertion of nursing. The infant appeared at first to be in obvious distress, as indicated by short expiratory grunts, followed immediately by marked pallor and cold sweat with a general appearance of severe shock. Occasionally, with unusually severe attacks, there appeared to be a transient loss of consciousness. The eructation of gas at times seemed to relieve the discomfort and to shorten the duration of the attack which usually lasted from 5 to 10 minutes, and following which the infant might proceed to nurse without difficulty and remain free of symptoms for several days. … It seems probable that in this infant the curious attacks of paroxysmal discomfort … were those of angina pectoris. If this is true, it represents the earliest age at which this condition has been recorded.

Some infants present with signs and symptoms of congestive heart failure. A few children have severe difficulties in infancy and then gradually become asymptomatic. Rarely, this anomaly causes sudden death in infancy. Older children and adults may be entirely asymptomatic, or have dyspnea, syncope, ventricular arrhythmias, or angina pectoris on effort. Sudden death after exertion has been common

[74,76]. Typical myocardial infarctions or congestive heart failure are rare in adults.

On physical examination, there may be signs of congestive heart failure. In infants, the heart is usually enlarged, predominantly the left ventricle. There may be right ventricular enlargement and loud pulmonic closure if left ventricular failure has caused pulmonary hypertension. The first heart sound may be soft or absent (if there is mitral regurgitation), and apical gallop rhythms are common. There may be no murmurs, or the murmur of mitral regurgitation, or at times a soft continuous murmur at the upper left sternal border that resembles the murmur of a coronary arteriovenous fistula or a small patent ductus arteriosus.

Electrocardiography

By the time the infant presents for diagnosis, there is usually an anterolateral infarct, with abnormal q waves (≥ 3 mm deep and ≥ 30 ms duration [81]) in leads I, aVl, and precordial leads V4–V6 (Figure 48.10). There may also be abnormal R waves or abnormal R wave progression through the mid to left precordial leads. Although this pattern occurs in myocardial infarcts from other causes, or in cardiomyopathies, if found, the diagnosis of ALPACA should be considered and evaluated by other means. Even in asymptomatic adults, the resting electrocardiogram is abnormal, and abnormal ischemic responses occur with exercise [67].

Radiological findings

There is marked cardiomegaly, predominantly of the left atrium and ventricle, and pulmonary edema. These features are similar to those of cardiomyopathy, with which this anomaly is often confused.

Thallium uptake can show reduced uptake in the anterolateral ischemic region, but this finding has occurred in some patients with cardiomyopathies [82].

Echocardiography

The abnormal attachment of the origin of the LMCA must be sought in more than one view to avoid problems from lateral drop out. Doppler interrogation shows flow passing from the coronary artery to the pulmonary trunk, so that even if the attachment of coronary artery to great artery is uncertain, the direction of flow is diagnostic. The transverse sinus of the pericardium should not be confused with a normal left coronary artery. False negatives are rare, but one has been described [83]. The echocardiogram also shows the very large RCA and the enlarged collateral arteries. The size and function of the cardiac chambers, particularly the left ventricle, regional left ventricular wall motion abnormalities, and mitral regurgitation are shown. There may be increased echogenicity of the papillary muscle and adjacent endocardium due to fibrosis and fibroelastosis.

Cardiac catheterization

This is used only if echocardiography is not definitive; it may cause death due to arrhythmias. An unnecessary cardiac catheterization however is better than missing a potentially treatable anomaly.

Symptomatic infants have a low cardiac output, high filling pressures, and usually some elevation of pulmonary artery pressures. In asymptomatic older patients, cardiac output is usually normal, but left ventricular end-diastolic pressure may be increased. There may be a left to right shunt at the pulmonary arterial level, but as the amount of shunting may be small its absence does not exclude the diagnosis of ALCAPA. Angiography reveals the dilated left ventricle and atrium with dysfunction of the anterolateral left ventricular free wall, and any mitral regurgitation. Aortic root angiography shows the dilated RCA and, if there are large collaterals, shows filling of the LCA and passage of contrast material from the LMCA to the main pulmonary artery. Main pulmonary arterial angiography often shows reflux of contrast medium into the origin of the LMCA. This anomaly has to be distinguished from the very rare anomaly of an atretic LMCA (see above).

Treatment

Initially, ligating the origin of the LCA was performed to prevent the steal [69]. Most children benefit from this procedure, especially if they have extensive coronary to pulmonary arterial shunting, but late sudden death can occur [67,84–86]. Ligation is performed off cardiopulmonary bypass and is quick, but the circulation cannot be supported if ventricular fibrillation occurs.

Ligating the origin of the left coronary artery and reconstituting flow through it with a subclavian arterial or saphenous venous graft has also been successful [87,88], although clotting or stenosis of the graft has occurred. Late obliterative changes in saphenous vein grafts have occurred [87] and are dangerous, because by ~3 years after successful saphenous vein grafting for this anomaly there is usually a marked reduction of collaterals from the right coronary artery [89,90]. Possibly internal thoracic artery grafts would have longer survival.

Currently, recommendations are to reimplant the origin of the LMCA into the aorta (with a button of pulmonary artery around the origin) [91,92], or create an aortopulmonary window and then fashion a tunnel that directs the blood from the aorta to the left coronary ostium [93–95]. There have been few reports of occlusion of these nongrafted connections, and a short, wide connection is not likely to become occluded. Sometimes the tunnel procedure causes supravalvar pulmonic stenosis, and may need reoperation [96]. The longer the follow-up period, the more the two-artery approach seems better than ligation or bypass grafting [85,97–101].

Occasionally the orifice of the LMCA is far from the aorta, as for example attachment to the non-facing sinus. Then either the LMCA must be connected to the aorta by an interposition graft or a variety of flaps [102–104], tunneled through to the aorta, or else connected by some other technique [65].

The mortality of surgery in the very sick infant is up to 20%, often because of ventricular fibrillation occurring before the sternotomy [105], so some surgeons recommend the less desirable but safer simple ligation procedures (with or without cardiopulmonary bypass) for the sickest infants [105]. Recent reports indicate that satisfactory results are obtained in good centers with even the sickest infants [72,98], although postoperative support with left ventricular assist device (LVAD) or extracorporeal membrane oxygenation (ECMO) might be needed [106,107].

Late results after operation are good, even in adults. The heart becomes smaller, congestive heart failure abates, mitral regurgitation regresses, and left ventricular shortening fraction improves [72,78,84,95,98–102,108]. Symptoms disappear, and exercise tolerance is either normal or slightly reduced [109]. In one study, coronary flow reserve was slightly reduced [109]. The region of hypoperfusion shown by radionuclide scans may disappear or become smaller [107], suggesting that some ischemic tissue was hibernating. Because of the improvement in mitral regurgitation, mitral valve repair is not usually performed during the initial operation [70,72, 92,102,107]; it might, however, be required later [72].

Right main coronary artery from pulmonary trunk

This anomaly (termed ARCAPA) is rare, with ~100 patients reported.

Pathological anatomy

The RCA is attached to the pulmonary trunk, usually the anterior facing sinus, and receives many dilated collateral arteries from the LMCA. Myocardial infarction is rare, and the only grossly abnormal findings are increased size of the LMCA and thinning of the wall of the RCA. The RCA is usually free from atheroma, but its origin may be stenotic.

Associated lesions

This anomaly may be associated with aortopulmonary window, ventricular septal defect, tetralogy of Fallot, and a few other lesions [26,110]. As expected, older patients have fewer of these associated lesions.

Pathophysiology

This is similar to ALCAPA, with collaterals from the LMCA supplying the RCA, and retrograde flow from the RCA into the pulmonary artery. Because of the steal from the LCA, ischemic dysfunction of the left ventricle may occur. Coronary flow reserve is reduced. [111]

Natural history

This is a more benign lesion than ALCAPA (Figure 48.11). Sudden or early deaths are unusual, and only 10% present before 1 year of age [26]; 50% are diagnosed >20 years of age, the oldest being 90 years old [26]. About half of the patients are asymptomatic, but late-onset syncope or cardiac arrest can occur. The proportion of asymptomatic patients decreases with age.

Clinical findings

Most patients are asymptomatic, especially if young. Syncope, cardiac arrest, sudden death, angina pectoris (due to coronary steal), dyspnea, and congestive heart failure have been described [14,110]. The youngest patient reported was 2 months old [110]. There may be a continuous murmur at the left sternal border.

Electrocardiogram

This may be normal, show ischemic changes with exercise, or show signs of left ventricular ischemia at rest.

Echocardiography

This shows the anomalous connection of the RCA to the pulmonary artery, and high-velocity retrograde flow from the RCA into the pulmonary artery. There may be left ventricular dilatation, reduced ejection fraction, and wall motion abnormalities in the most severely affected patients.

Cardiac catheterization and angiography

These are usually unnecessary, but confirm the echocardiographic findings. The Qp/Qs ratio is seldom much elevated, but the proportion of cardiac output due to coronary flow is increased [111].
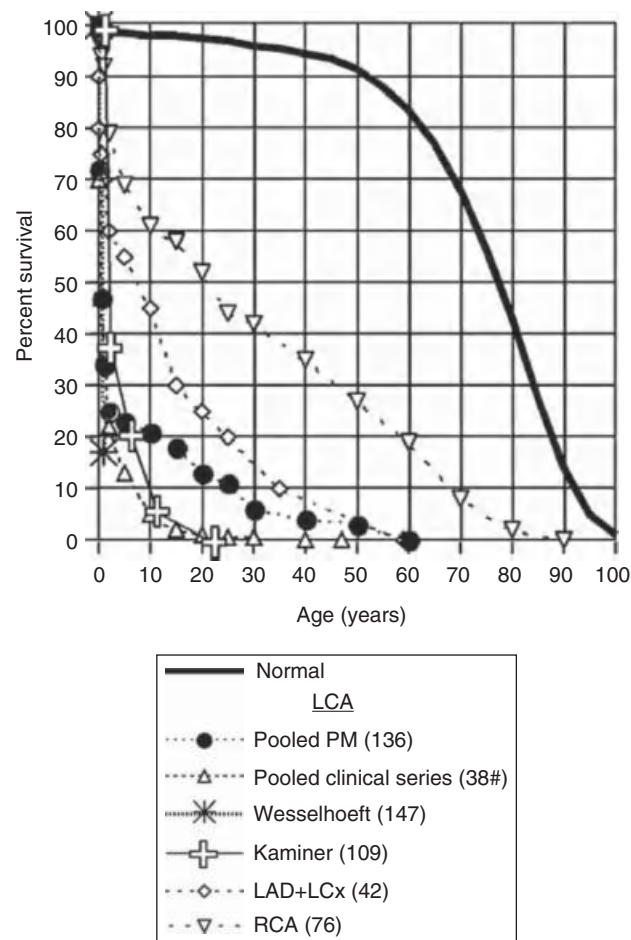
Figure 48.11 Natural history (survival) in various forms of coronary artery connection to the pulmonary artery.

Treatment

Most patients are asymptomatic, and there is no way of determining which are at risk of sudden death. Some patients managed conservatively have done well. Nevertheless, most cardiologists recommend operation, especially for symptoms or objective evidence of myocardial ischemia. The RCA is reimplanted into the aortic root [112,113].

Left anterior descending or left circumflex coronary artery from pulmonary trunk

These anomalous attachments are rare; ~20 of each have been described [114,115].

Pathological anatomy

The anomalous artery is attached to the main pulmonary trunk, but often an anomalous LCx is attached to a branch pulmonary artery. Left ventricular pathology is similar to that seen in ALCAPA, but usually less extensive.

Pathophysiology

This is similar to that described for ALPACA, with similar dependence of left ventricular wall flow on pulmonary arterial pressure and the adequacy of collateral formation from the normally attached coronary arteries.

Natural history

This is better than that for ALCAPA (Figure 48.11). Apart from a 7-month-old child who died with an anterior myocardial infarct, all the others have been from 7 to 55 years old. Seven had angina pectoris, one an anterior myocardial infarct, and one had mitral regurgitation from papillary muscle dysfunction. One 9-year-old child died suddenly. Congestive heart failure is uncommon.

Clinical features

Most patients had exertional dyspnea, chest discomfort, or frank angina of effort, but many were asymptomatic and detected by chance. Precordial murmurs were common, but there were no specific physical findings.

Electrocardiogram

Most patients had electrocardiographic evidence of ischemia at rest or after exercise, with the site of ischemia depending on the involved artery.

Cardiac imaging

X-rays were normal in about half of the patients and showed mild cardiomegaly in the rest. MRI done in a few patents was diagnostic. Thallium studies with exercise may reveal silent ischemia.

Cardiac catheterization and angiocardiography

These studies are usually unnecessary if the other imaging tests are adequate.

Management

Surgical treatment is recommended even in asymptomatic patients because of the risk of late ischemia. The best choice is reimplanting the anomalous artery into the aorta, but there may not be enough length for this to be done without tension. The alternatives are to ligate the artery, connect it to the aorta with an interposition graft, or ligate the proximal portion and perform a coronary bypass graft to the distal portion [14,115].

Disorders of structure or distribution

The coronary arteries can be involved in many forms of generalized systemic disease, for example, Kawasaki disease (Chapter 63), systemic lupus erythematosus (Chapter 69), and infantile polyarteritis nodosa (Chapter 69). These will not be discussed further here, but certain other abnormalities will.

Calcific arteriopathy of infancy

Fewer than 100 patients have been reported [116].

Pathology

This disease affects mainly the muscular arteries: coronary arteries in 90% of patients, and renal, pancreatic, and splenic arteries in 50%. The internal elastic lamina fragments, and then calcification begins there and extends to the media, where large calcium clumps form and destroy the muscle. Intimal connective tissue proliferation occurs and eventually occludes the lumen [117]. We do not know if there is a single etiology or several different processes with common end results [118]. The disease is unrelated to chronic renal disease, hypervitaminosis D, hyperparathyroidism, and HIV infection, or trisomies 13–15 and 17–18, all of which can show arterial calcification. An inherited genetic disease associated with elastin formation has been suggested because several sets of siblings with the disease have been described [119]. Arterial thromboses may occur, but spare the cerebral arteries [117].

Clinical features

The patients present in congestive heart failure by about 2 months of age, and may have signs of myocardial ischemia and infarction; less often, they have renal failure and hypertension [117,120]. Diagnosis is made by palpating hardened superficial arteries in the neck and limbs, finding calcified arteries on X-ray [121,122], and sometimes by ophthalmoscopy. Most infants die before 6 months of age, but some improve spontaneously [117,122,123]. Diphosphonates have been used therapeutically but their effectiveness has not been proved [119,124].

Myocardial infarction

Myocardial infarction in the fetus or neonate is rare [125,126].

Etiology

Many infarcts are probably due to intrauterine emboli from umbilical, hepatic, or renal veins [125,126], some to coronary arteriopathy [117], a few to severe intrauterine hypoxia and stress, and a few to coagulopathies, but most to unknown causes. Some unusual causes are the antiphospholipid syndrome; collagen vascular diseases, especially systemic lupus erythematosus; takotsubo cardiomyopathy after severe emotional distress; Kounis syndrome (allergic anaphylactoid angina) [127]; hyperlipoproteinemia; and Kawasaki syndrome (see Chapter 63). Occasionally, they occur from postnatal paradoxical embolism, or embolism from material extruded from cardiac catheters, particularly after several changes of guide wires [128]. The risk of coronary embolism may be particularly high in children with cyanotic heart disease. If there is an infarct, it is essential to exclude an anomalous coronary artery arising from the pulmonary artery.

Table 48.2 Etiologies of coronary arterial aneurysms.

1. Congenital
2. Atherosclerotic
3. Inflammatory and infectious causes:
   a. Kawasaki syndrome
   b. Syphilis
   c. Mycotic
   d. Infective endocarditis
4. Trauma, including PTCA
5. Connective tissue disorders:
   a. Marfan syndrome
   b. Ehlers–Danlos syndrome
6. Vasculitides:
   a. Takayasu arteritis
   b. Polyarteritis nodosa
   c. Scleroderma
   d. Systemic lupus erythematosus
7. Miscellaneous: Osler–Rendu–Weber disease, metastatic tumor

Modified from Smith *et al. Cathet Cardiovasc Diagn* 1984;**10**:583–91.

Diagnostic features

The children present with angina pectoris and often have congestive heart failure or shock. Electrocardiography shows evidence of infarction, and echocardiography demonstrates the left ventricular dysfunction. Thallium studies confirm regional ischemia. Because of its rarity, most children with myocardial infarction come to cardiac catheterization and angiography.

Treatment

Pediatric cardiologists see myocardial infarction so rarely that they should consult an adult cardiologist about the use of thrombolytic agents.

Coronary aneurysms

These have been found in 1–5% of coronary angiograms, the difference depending in part on the definition of an aneurysm; the usual definition is a localized dilatation with diameter >50% of the adjacent segments or the patient's largest coronary artery [129,130]. Possible causes are listed in Table 48.2.

The most common cause in children is Kawasaki syndrome (see Chapter 63), and in adults aneurysms are associated with coronary atherosclerosis. All other causes are rare. Aneurysms are usually found while investigating other problems. Occasionally, they appear on X-ray because of calcification. They are shown well by imaging techniques, usually echocardiography or angiography, but better details are often seen with MRI or CT.

Apart from problems pertaining to the underlying disease, aneurysms may thrombose and cause either coronary stenosis or distal coronary embolism, with resulting myocardial ischemia or infarction. Rupture is rare [132]. Treatment ranges from nothing to antiplatelet medication, thrombolytic agents for acute thrombosis, coronary bypass grafting for occlusive disease, and even excision of the aneurysm [132].

Myocardial bridges

The large epicardial coronary arteries are superficial, with only their terminal branches penetrating the muscle, but in 40–50% of people, part of an epicardial artery dips beneath the epicardial muscle (the muscle bridge) for several millimeters [133,134]. These bridges are probably present at birth. Most are over the LAD, predominantly its proximal half [134,135]. In ~75%, the LAD runs in the interventricular groove and may be covered by a few superficial bridging muscle fibers; in 25%, the LAD deviates towards the right ventricle and runs deep in the ventricular septum, where it is crossed by a bundle of muscle extending from the right ventricular apex to the septal muscle [135]. Most bridges are not functionally important, particularly if they are superficial. There are, however, reports of myocardial ischemia [135], infarction [136], or even death [137] associated with them, and of relief of ischemia after myotomy. Symptoms may occur if the bridge is abnormally long or deep, especially if the RCA is small [138].

During coronary angiography, a portion of the coronary artery appears to be narrowed in systole but widely patent in diastole [133,135].

Because myocardial bridges are so common and do not necessarily indicate present or future coronary arterial disease, the decision about myotomy to relieve anginal symptoms depends on demonstrating ischemia, based on lactate production in the regional vein, electrocardiographic changes, or deficient thallium uptake. Ischemia more likely occurs with long, thick bridges that compress the artery and relax unusually slowly so that diastolic filling beyond the bridge is impaired. Disappearance of symptoms and signs of ischemia may follow myotomy. Some patients obtain relief from anti-anginal therapy with β-adrenergic blockade. Myocardial bridges causing ischemia are rare in children; they are more common in children with ventricular hypertrophy, particularly hypertrophic cardiomyopathy [139,140].

Coronary atherosclerosis and atheromatosis

This is one of the major epidemic diseases of the developed world. Although precursors of coronary atherosclerosis appear in early childhood (see Chapter 65), the full-blown disease is rare in childhood. The most common causes of severe coronary arteriosclerosis in children are secondary to Kawasaki disease and to homozygous familial hypercholesterolemia; heterozygotes for familial hypercholesterolemia are also at risk. Children who have had heart transplants

are at risk for diffuse coronary artery vasculopathy as a manifestation of rejection. Other causes include the rare Hutchinson–Gilford syndrome (progeria).

Disorders of termination: fistulas between coronary arteries and cardiac chambers, venous vessels, or pulmonary arteries

A normally originating coronary artery may have a precapillary connection with the atria or ventricles (coronary–cameral fistula) or the coronary sinus, superior vena cava, or pulmonary artery (coronary–arteriovenous fistula). These anomalies constitute 0.2–0.4% of all congenital cardiac anomalies [60,141], with similar incidences in males and females. They are observed in 0.08–0.18% of routine coronary angiograms in adults, and make up 8–13% of the congenital coronary arterial anomalies observed in these studies [4,5].

Embryology

Persistence of wide intertrabecular spaces in the primitive myocardium could lead to coronary–cameral fistulas [142]. On the other hand, fistulas from coronary arteries to pulmonary or bronchial arteries, or the very common tiny communications between the coronary arteries and the pericardial, diaphragmatic, or mediastinal arteries [12] or even the superior vena cava, are probably communications between the primitive coronary arteries and the mediastinal plexus of vessels.

Anatomy and pathology

About 55–60% of the fistulas arise from the right coronary artery and ~5% arise from more than one coronary artery [143]. About 90% drain into the lesser circulation [60,141,143]: the right ventricle in 40%, the right atrium or venae cavae in 22%, and pulmonary artery in 30%. About 1.4% enter the coronary sinus, 5.5% enter the left ventricle, and 1.5% enter the left atrium [143]. Occasionally a complex fistula drains into several sites. The pulmonary artery is a favored site of entry of small fistulas, and most bilateral fistulas enter the pulmonary artery [144].

The fistulous coronary artery may be very small, particularly if it arises from the distal part of the artery [145], or may be dilated up to 40 mm in diameter and tortuous, with variations of diameter along its length. Sometimes there are bundles of small vessels rather than one large fistula. The fistula enters the affected chamber by one or several openings; occasionally plexiform lesions are seen. Saccular aneurysmal dilatation of the fistula can be seen, and these aneurysms are thin walled and often gigantic; some of the largest measured 14 × 12 × 11, 15 × 15 × 10, 8 × 10 × 22, and 17 × 23 × 14 cm. All these giant aneurysms were described in patients over 50 years of age [143].

Associated anomalies

Other congenital cardiac lesions can coexist [60,146], but most coronary artery fistulas are isolated. Connections between myocardial sinusoids and coronary arteries in pulmonary atresia with an intact ventricular septum carry blood into, not away from, the coronary arteries.

Pathophysiology

Small fistulas have no hemodynamic effect. A large fistula, however, causes a left-to-right shunt great enough to cause congestive heart failure. When a fistula enters the low-pressure lesser circulation, the shunt is continuous in systole and diastole. When it enters the left ventricle, the shunt is exclusively diastolic. A significant run-off through the fistula may reduce flow through more distal arteries, and cause a coronary steal and myocardial ischemia [147,148].

Natural history

Fistulas may be detected at any age from birth to the ninth decade [143]. Under 1 year of age, and particularly under 1 month of age, most patients are symptomatic. From 1 to 20 years of age, most are asymptomatic and detected by either a prominent murmur or an echocardiogram done for another diagnosis. After 20 years of age, ~75% of these patients are symptomatic. Asymptomatic coronary fistulas are uncommon in adults.

Because huge aneurysms are found only after 50 years of age, the lesion may progress, at least in some patients. However, very small fistulas, usually between a coronary artery and the pulmonary artery, may never increase in size or cause hemodynamic problems. Fistulas may, however, develop infective endocarditis [143], which usually occurs only in large fistulas. Spontaneous closure of fistulas has been described in >40 patients [143], possibly due to infection in some. Most closed at <15 years of age, and in several series of patients, spontaneous closure occurred in ~13%. Larger fistulas may cause congestive heart failure, dyspnea, fatigue, angina pectoris due to a coronary steal or to accelerated atherosclerosis, or rarely myocardial infarction. They rarely rupture [60,149], which is surprising in view of the massive aneurysmal dilatation of these thin-walled fistulas. Thrombotic occlusion has caused acute myocardial infarction, but rarely in children [26].

Clinical features

History

Those with small fistulas are asymptomatic, but the shunt can be so large that congestive heart failure occurs [60]. Symptoms are rare before 20 years of age [150], but in young adults, atrial fibrillation, fatigue, exertional dyspnea, or ischemic chest pain may appear, and myocardial infarction has been reported [150]. Angina pectoris is rare in children

but present in 80% of these patients >50 years of age [151], due to either coronary atherosclerosis or a coronary steal. About 10% of these patients present with infective endocarditis, even in children [146,152,153].

Physical findings

The cardinal finding is a continuous murmur resembling that of a patent ductus arteriosus but often sounding unusually superficial. The murmur is usually heard best at the mid left or right sternal border, or even the lower sternal border, but may be heard at the upper left sternal border, particularly if the fistula enters the pulmonary artery. The murmur often is louder in mid-diastole than mid-systole when the fistula enters the right ventricle. There may be a thrill, but not if the fistula enters the posterior part of the heart. Continuous murmurs are not heard when the fistula drains into the left ventricle, and fistulas can be silent. Other features include signs of a large left-to-right shunt, congestive heart failure, and occasionally an accentuated pulmonary valve closure.

Electrocardiography

The electrocardiogram is normal with small shunts, shows evidence of chamber enlargement and hypertrophy with large shunts, and occasionally shows evidence of myocardial ischemia.

Radiology

The heart may be normal, or affected chambers are enlarged with increased pulmonary vascular markings due to a large left-to-right shunt. Occasionally, an unusual soft tissue shadow seen on a heart border indicates the tortuous dilated fistula.

Nuclear medicine studies may indicate regional myocardial ischemia, but cannot exclude coronary atheroma as the cause. MRI [154,155] or multidetector CT [156] define these fistulas well.

Echocardiography

Echocardiography with Doppler studies shows the dilated parent artery and the fistula, including its entry into the chamber or vessel. Transesophageal echocardiography has been valuable in large patients [157]. Wall motion abnormalities on exercise indicate myocardial ischemia, but not its cause.

Cardiac catheterization and angiography

Although echocardiography, MRI, and multidetector CT scanning make the diagnosis, cardiac catheterization and angiography are often needed to show fine details of fistula drainage. Because many fistulas are closed by interventional methods, cardiac catheterization is a necessary preliminary procedure.

Treatment

Two comprehensive reviews should be consulted [145,158].

All patients with symptoms probably should have definitive treatment [158], although some older patients with mild angina pectoris have been managed successfully conservatively, with or without with β-blockers. A large fistula, however, should be closed to prevent infective endocarditis, congestive heart failure, myocardial ischemia or infarction, or the occasional rupture. With increasing age, symptoms increase, as do the complications of surgery; the complication rate was 23% >20 years of age and 1.5% for younger patients [151].

Until recently, closure was surgical. The fistula must be ligated near its origin and also near its entrance to the cardiac chamber where there may be multiple entries. Distal ligation alone may be followed by re-establishment of the fistula by collaterals that bypass the site of ligation. Proximal ligation risks ischemia in the territory supplied by normal branches of the fistulous artery. Although surgery can usually be performed without cardiopulmonary bypass, it is often necessary to open the cardiac chamber to find and ligate the points of entry. The risks of surgery are not negligible in older patients: myocardial ischemia or infarction, thrombosis of the parent coronary artery, rupture of the fistula, and ventricular fibrillation have been reported [60]. Surgical mortality, however, is <1% even in older and sicker patients or those with associated cardiac disease.

The long-term results of surgery are excellent, with 95% of the patients being asymptomatic; residual shunts or recanalization are rare, as is death associated directly with the fistula.

Because >90% of these fistulas enter the right side of the circulation, they are candidates for closure by interventional catheterization without risking systemic embolization [159–162]. Devices used include various types of coils and plugs. Occasionally, small or multiple fistulas are closed by microembolization with 300–500 μm diameter poly(vinyl alcohol) foam particles [163] or rapidly solidifying glues (cyanoacrylates) or plastics [164]. In some patients, a covered stent allowed closure of fistulous side branches without compromising flow to the more distal myocardium [165,166].

During the procedure, the operator usually occludes the fistula with a balloon for up to 10 min to make sure that occlusion does not produce ischemia. If it does, then an individual decision to proceed or not must based on the need for closure and the magnitude of the ischemia.

As compared with surgical closure, device closure has a slightly higher incidence of residual shunts, but this incidence is still <10%. Thrombosis of the fistula extending into the normal artery and causing an infarct occasionally occurs. Recanalization after device closure has not been described, but reconstitution of the fistula from small, previously undetected branches can occur. The proximal part of the fistula may remain dilated, especially in older patients.

There is little guidance for treatment of small fistulas in asymptomatic patients. Many of the small coronary to pulmonary artery fistulas cause no symptoms and may not enlarge. These do not have to be closed, but ought to be followed at least annually to determine if they are enlarging. Even if they do not enlarge, there is a risk of infective endocarditis, although this is rare in childhood. It seems reasonable to observe them for several years because some small fistulas may close spontaneously. However, Latson [158] recommended closure of all fistulas that were still clinically apparent after 3–5 years of age.

References

1 Angelini P, Velasco JA, Flamm S. Coronary anomalies: incidence, pathophysiology, and clinical relevance. *Circulation* 2002; **105**:2449–54.

2 Alexander RW, Griffith GC. Anomalies of the coronary arteries and their clinical significance. *Circulation* 1956;**14**:800–5.

3 Lipsett J, Cohle SD, Berry PJ, *et al*. Anomalous coronary arteries: a multicenter pediatric autopsy study. *Pediatr Pathol* 1994; **14**:287–300.

4 Wilkins CE, Betancourt B, Mathur VS, *et al*. Coronary artery anomalies: a review of more than 10,000 patients from the Clayton Cardiovascular Laboratories. *Texas Heart Inst J* 1988;**15**:166–73.

5 Yamanaka O, Hobbs RE. Coronary artery anomalies in 126,595 patients undergoing coronary arteriography. *Cathet Cardiovasc Diagn* 1990;**21**:28–40.

6 Barriales Villa R, Moris C, Lopez Muniz A, *et al*. Adult congenital anomalies of the coronary arteries described over 31 years of angiographic studies in the Asturias Principality: main angiographic and clinical characteristics. *Rev Esp Cardiol* 2001;**54**:269–81 (in Spanish).

7 Harikrishnan S, Jacob SP, Tharakan J, *et al*. Congenital coronary anomalies of origin and distribution in adults: a coronary arteriographic study. *Indian Heart J* 2002;**54**:271–5.

8 Lytrivi ID, Wong AH, Ko HH, *et al*. Echocardiographic diagnosis of clinically silent congenital coronary artery anomalies. *Int J Cardiol* 2008;**126**:386–93.

9 Dettman RW, Denetclaw W Jr, Ordahl CP, Bristow J. Common epicardial origin of coronary vascular smooth muscle, perivascular fibroblasts, and intermyocardial fibroblasts in the avian heart. *Dev Biol* 1998;**193**:169–81.

10 Tomanek RJ, Hansen HK, Dedkov EI. Vascular patterning of the quail coronary system during development. *Anat Rec A Discov Mol Cell Evol Biol* 2006;**288**:989–99.

11 Virmani R, Chun PKC, Goldstein RE, *et al*. Acute takeoffs of the coronary arteries along the aortic wall and congenital ostial valve-like ridges: association with sudden death. *J Am Coll Cardiol* 1984;**3**:766–71.

12 Baroldi G, Scomazzoni G. *Coronary Circulation in the Normal and the Pathologic Heart*. Washington, DC: Office of the Surgeon General, 1967.

13 Vlodaver Z, Neufeld HN, Edwards JE. *Coronary Artery Variations in the Normal Heart and in Congenital Heart Disease*. New York: Academic Press, 1975.

14 Roberts WC. Major anomalies of coronary arterial origin seen in adulthood. *Am Heart J* 1986;**111**:941–63.

15 Spindola-Franco H, Grose R, Solomon N. Dual left anterior descending coronary artery: angiographic description of important variants and surgical implications. *Am Heart J* 1983;**105**:445–55.

16 Agarwal PP, Kazerooni EA. Dual left anterior descending coronary artery: CT findings. *AJR Am J Roentgenol* 2008;**191**:1698–701.

17 Angelini P, Trfujillo A, Sawaya F, Lee V-V. "Acute takeoff" of the circumflex artery. *Tex Heart Inst J* 2008;**35**:28–31.

18 Patel S. Normal and anomalous anatomy of the coronary arteries. *Semin Roentgenol* 2008;**43**:100–12.

19 Kim SY, Seo JB, Do KH, *et al*. Coronary artery anomalies: classification and ECG-gated multi-detector row CT findings with angiographic correlation. *Radiographics* 2006;**26**:317–33; discussion 333–4.

20 Basso C, Frescura C, Corrado D, *et al*. Congenital heart disease and sudden death in the young. *Hum Pathol* 1995;**26**:1065–72.

21 Click RL, Holmes DR Jr, Vlietstra RE, *et al*. Anomalous coronary arteries: location, degree of atherosclerosis and effect on survival – a report from the Coronary Artery Surgery Study. *J Am Coll Cardiol* 1989;**13**:531–7.

22 Barriales Villa R, Diaz Molina B, Arias Castano JC, *et al*. Myocardial ischemia caused by an anomalous circumflex coronary artery. *Rev Esp Cardiol* 2002;**55**:200–2 (in Spanish).

23 Kragel AH, Roberts WC. Anomalous origin of either the right or left main coronary artery from the aorta with subsequent coursing between aorta and pulmonary trunk: analysis of 32 necropsy cases. *Am J Cardiol* 1988;**62**:771–7.

24 Roberts WC, Shirani J. The four subtypes of anomalous origin of the left main coronary artery from the right aortic sinus (or from the right coronary artery). *Am J Cardiol* 1992;**70**:119–21.

25 Hariharan R, Kacere RD, Angelini P. Can stent-angioplasty be a valid alternative to surgery when revascularization is indicated for anomalous origination of a coronary artery from the opposite sinus? *Tex Heart Inst J* 2002 29:308–13.

26 Hoffman JIE. Abnormal origins of the coronary arteries from the aortic root. In: Hoffman JIE, ed. *The Natural and Unnatural History of Congenital Heart Disease*. Oxford: Wiley-Blackwell. 2009: 384–400.

27 Chu E, Cheitlin MD. Diagnostic considerations in patients with suspected coronary artery anomalies. *Am Heart J* 1993; **126**:1427–38.

28 Rinaldi RG, Carballido J, Giles R, *et al*. Right coronary artery with anomalous origin and slit ostium. *Ann Thorac Surg* 1994; **58**:829–32.

29 Roberts WC, Siegel RJ, Zipes DP. Origin of the right coronary artery from the left sinus of valsalva and its functional consequences: analysis of 10 necropsy patients. *Am J Cardiol* 1982;**49**:863–8.

30 Sato Y, Matsumoto N, Komatsu S, *et al*. Anomalous origin of the right coronary artery: depiction at whole-heart coronary magnetic resonance angiography. *Int J Cardiol* 2008;**127**:274–5.

31 Lipton MJ, Barry WH, Obrez I, *et al*. Isolated single coronary artery: diagnosis, angiographic classification, and clinical significance. *Radiology* 1979;**130**:39–47.

32 Shirani J, Roberts WC. Solitary coronary ostium in the aorta in the absence of other major congenital cardiovascular anomalies. *J Am Coll Cardiol* 1993;**21**:137–43.

33 Ueyama K, Ramchandani M, Beall AC Jr, Jones JW. Diagnosis and operation for anomalous circumflex coronary artery. *Ann Thorac Surg* 1997;**63**:377–81.

34 Samarendra P, Kumari S, Hafeez M, *et al*. Anomalous circumflex coronary artery: benign or predisposed to selective atherosclerosis. *Angiology* 2001;**52**:521–6.

35 Angelini P, Walmsley RP, Libreros A, Ott DA. Symptomatic anomalous origination of the left coronary artery from the opposite sinus of Valsalva. Clinical presentations, diagnosis, and surgical repair. *Tex Heart Inst J* 2006;**33**:171–9.

36 Angelini P, Flamm SD. Newer concepts for imaging anomalous aortic origin of the coronary arteries in adults. *Catheter Cardiovasc Interv* 2007;**69**:942–54.

37 Moustafa SE, Zehr K, Mookadam M, *et al*. Anomalous interarterial left coronary artery: an evidence based systematic overview. *Int J Cardiol* 2008;**126**:13–20.

38 Taylor AJ, Byers JP, Cheitlin MD, Virmani R. Anomalous right or left coronary artery from the contralateral coronary sinus: "high-risk" abnormalities in the initial coronary artery course and heterogeneous clinical outcomes. *Am Heart J* 1997;**133**:428–35.

39 Roberts WC, Morrow AG. Compression of anomalous left circumflex coronary arteries by prosthetic valve fixation rings. *J Thorac Cardiovasc Surg* 1969;**57**:834–8.

40 Sharbaugh AH, White RS. Single coronary artery. Analysis of the anatomic variation, clinical importance, and report of five cases. *JAMA* 1974;**230**:243–6.

41 Liberthson RR, Zaman L, Weyman A, *et al*. Aberrant origin of the left coronary artery from the proximal right coronary artery: diagnostic features and pre- and postoperative course. *Clin Cardiol* 1982;**5**:377–81.

42 Fernandes F, Alam M, Smith S, Khaja F. The role of transesophageal echocardiography in identifying anomalous coronary arteries. *Circulation* 1993;**88**:2532–40.

43 Ishikawa T, Brandt PWT. Anomalous origin of the left main coronary artery from the right anterior aortic sinus: angiographic definition of anomalous course. *Am J Cardiol* 1985;**55**:770–6.

44 Serota H, Barth CW III, Seuc CA, *et al*. Rapid identification of the course of anomalous coronary arteries in adults: the "dot and eye" method. *Am J Cardiol* 1990;**65**:891–8.

45 Patel KB, Gupta H, Nath H, *et al*. Origin of all three major coronary arteries from the right sinus of Valsalva: clinical, angiographic, and magnetic resonance imaging findings and incidence in a select referral population. *Catheter Cardiovasc Interv* 2007;**69**:711–8.

46 Gharib AM, Ho VB, Rosing DR, *et al*. Coronary artery anomalies and variants: technical feasibility of assessment with coronary MR angiography at 3 T. *Radiology* 2008;**247**:220–7.

47 McConnell MV, Ganz P, Selwyn AP, *et al*. Identification of anomalous coronary arteries and their anatomic course by magnetic resonance coronary angiography. *Circulation* 1995;**92**:3158–62.

48 Post JC, van Rossum AC, Bronzwaer JG, *et al*. Magnetic resonance angiography of anomalous coronary arteries. A new gold standard for delineating the proximal course? *Circulation* 1995;**92**:3163–71.

49 Davies JE, Burkhart HM, Dearani JA, *et al*. Surgical management of anomalous aortic origin of a coronary artery. *Ann Thorac Surg* 2009;**88**:844–7; discussion 847–8.

50 Brothers J, Carter C, McBride M, *et al*. Anomalous left coronary artery origin from the opposite sinus of Valsalva: evidence of intermittent ischemia. *J Thorac Cardiovasc Surg* 2010;**140**:e27–9.

51 Erez E, Tam VK, Doublin NA, Stakes J. Anomalous coronary artery with aortic origin and course between the great arteries: improved diagnosis, anatomic findings, and surgical treatment. *Ann Thorac Surg* 2006;**82**:973–7.

52 Gulati R, Reddy VM, Culbertson C, *et al*. Surgical management of coronary artery arising from the wrong coronary sinus, using standard and novel approaches. *J Thorac Cardiovasc Surg* 2007;**134**:1171–8.

53 elZein C, Hanhan Z, Massad M, *et al*. Surgical repair of anomalous coronary arteries arising from the opposite sinus of Valsalva in infants and children. *J Card Surg* 2009;**24**:466–9.

54 Brothers JA, McBride MG, Marino BS, *et al*. Exercise performance and quality of life following surgical repair of anomalous aortic origin of a coronary artery in the pediatric population. *J Thorac Cardiovasc Surg* 2009;**137**:380–4.

55 Gay F, Vouhe P, Lecompte Y, *et al*. Atresia of the left coronary ostium. Repair in a 2-month-old infant. *Arch Mal Coeur Vaiss* 1989;**82**:807–10 (in French).

56 Bedogni F, Castellani A, La Vecchia L, *et al*. Atresia of the left main coronary artery: clinical recognition and surgical treatment. *Cathet Cardiovasc Diagn* 1992;**25**:35–41.

57 Gol MK, Ozatik MA, Kunt A, *et al*. Coronary artery anomalies in adult patients. *Med Sci Monit* 2002;**8**:CR636–41.

58 Karadag B, Ayan F, Ismailoglu Z, *et al*. An extraordinary cause of ischemic chest pain in a young man: congenital ostial atresia of the right coronary artery. *J Cardiol* 2009;**54**:335–8.

59 Gebauer R, Cerny S, Vojtovic P, Tax P. Congenital atresia of the left coronary artery – myocardial revascularization in two children. *Interact Cardiovasc Thorac Surg* 2008;**7**:1174–5.

60 Neufeld HN, Schneeweiss A. *Coronary Artery Disease in Infants and Children*. Philadelphia: Lea & Febiger, 1983.

61 Heifetz SA, Robinowitz M, Mueller KH, Virmani R. Total anomalous origin of the coronary arteries from the pulmonary artery. *Pediatr Cardiol* 1986;**7**:11–8.

62 Urcelay GE, Iannettoni MD, Ludomirsky A, *et al*. Origin of both coronary arteries from the pulmonary artery. *Circulation* 1994;**90**:2379–84.

63 Bland EE, White PD, Garland J. Congenital anomalies of the coronary arteries: report of an unusual case associated with cardiac hypertrophy. *Am Heart J* 1933;**8**:787–801.

64 Cowles RA, Berdon WE. Bland–White–Garland syndrome of anomalous left coronary artery arising from the pulmonary artery (ALCAPA): a historical review. *Pediatr Radiol* 2007;**37**:890–5.

65 Sodian R, Rassoullian D, Beiras-Fernandez A, *et al*. ALCAPA with the ectopic orifice at the non-facing sinus: successful anatomic repair by creation of an autologous extrapulmonary tunnel. *Tex Heart Inst J* 2008;**35**:32–5.

66 Shivalkar B, Borgers M, Daenen W, *et al*. ALCAPA syndrome: an example of chronic myocardial hypoperfusion? *J Am Coll Cardiol* 1994;**23**:772–8.

67 Moodie DS, Fyfe D, Gill CC, *et al*. Anomalous origin of the left coronary artery from the pulmonary artery (Bland–White–Garland syndrome) in adult patients: long-term follow-up after surgery. *Am Heart J* 1983;**106**:381–8.

68 Rao BN, Lucas RV Jr, Edwards JE. Anomalous origin of the left coronary artery from the right pulmonary artery associated with ventricular septal defect. *Chest* 1970;**58**:616–20.

69 Sabiston DC Jr, Neill CA, Taussig HB. The direction of blood flow in anomalous left coronary artery arising from the pulmonary artery. *Circulation* 1960;**22**:591–7.

70 Brown JW, Ruzmetov M, Parent JJ, *et al*. Does the degree of preoperative mitral regurgitation predict survival or the need for mitral valve repair or replacement in patients with anomalous origin of the left coronary artery from the pulmonary artery? *J Thorac Cardiovasc Surg* 2008;**136**:743–8.

71 Walsh MA, Duff D, Oslizlok P, *et al*. A review of 15-year experience with anomalous origin of the left coronary artery. *Ir J Med Sci* 2008;**177**:127–30.

72 Ben Ali W, Metton O, Roubertie F, *et al*. Anomalous origin of the left coronary artery from the pulmonary artery: late results with special attention to the mitral valve. *Eur J Cardiothorac Surg* 2009;**36**:244–8; discussion 248–9.

73 Pena E, Nguyen ET, Merchant N, Dennie G. ALCAPA syndrome: not just a pediatric disease. *Radiographics* 2009;**29**:553–65.

74 Wesselhoeft H, Fawcett JS, Johnson AL. Anomalous origin of the left coronary artery from the pulmonary trunk. Its clinical spectrum, pathology, and pathophysiology, based on a review of 140 cases with seven further cases. *Circulation* 1968;**38**:403–25.

75 Keith JD. Anomalous origin of the left coronary artery from the pulmonary artery. *Br Heart J* 1959;**21**:149–61.

76 George JM, Knowlan DM. Anomalous origin of the left coronary artery from the pulmonary artery in an adult. *N Engl J Med* 1959;**261**:993–8.

77 Wilson CL, Dlabal PW, Holeyfield RW, *et al*. Anomalous origin of left coronary artery from pulmonary artery. Case report and review of literature concerning teen-agers and adults. *J Thorac Cardiovasc Surg* 1977;**73**:887–93.

78 Alexi-Meskishvili V, Berger F, Weng Y, *et al*. Anomalous origin of the left coronary artery from the pulmonary artery in adults. *J Card Surg* 1995;**10**:309–15.

79 Driscoll DJ, Edwards WD. Sudden unexpected death in children and adolescents. *J Am Coll Cardiol* 1985;**5**(Suppl B):118B–21B.

80 Kang WC, Chung WJ, Choi CH, *et al*. A rare case of anomalous left coronary artery from the pulmonary artery (ALCAPA) presenting congestive heart failure in an adult. *Int J Cardiol* 2007;**115**:e63–7.

81 Johnsrude CL, Perry JC, Cecchin F, *et al*. Differentiating anomalous left main coronary artery originating from the pulmonary artery in infants from myocarditis and dilated cardiomyopathy by electrocardiogram. *Am J Cardiol* 1995;**75**:71–4.

82 Gutgesell HP, Pinsky WW, DePuey EG. Thallium-201 myocardial perfusion imaging in infants and children, value in distinguishing anomalous left coronary artery from congestive cardiomyopathy. *Circulation* 1980;**61**:596–9.

83 Breuer J, Barth H, Steil E, *et al*. Anomalous origin of the left coronary artery from the pulmonary artery. Variability of clinical aspects, echocardiography and angiography findings. *Monatsschr Kinderheilkd* 1992;**140**:346–53 (in German).

84 Shrivastava S, Casteneda AR, Moller JH. Anomalous left coronary artery from pulmonary trunk. Long-term follow-up after ligation. *J Thorac Cardiovasc Surg* 1978;**76**:130–4.

85 Wilson CL, Dlabal PW, McGuire SA. Surgical treatment of anomalous left coronary artery from pulmonary artery: follow-up in teenagers and adults. *Am Heart J* 1979;**98**:440–6.

86 Backer CL, Stout MJ, Zales VR, *et al*. Anomalous origin of the left coronary artery. A twenty-year review of surgical management. *J Thorac Cardiovasc Surg* 1992;**103**:1049–57; discussion 1057–8.

87 el-Said GM, Ruzyllo W, Williams RL, *et al*. Early and late result of saphenous vein graft for anomalous origin of left coronary artery from pulmonary artery. *Circulation* 1973;**48**:III2–6.

88 Stephenson LW, Edmunds LH Jr, Friedman S, *et al*. Subclavian–left coronary artery anastomosis (Meyer operation) for anomalous origin of the left coronary artery from the pulmonary artery. *Circulation* 1981;**64**:II130–3.

89 Moodie DS, Gill C, Loop FD, Sheldon WC. Anomalous left main coronary artery originating from the right sinus of Valsalva: pathophysiology, angiographic definition, and surgical approaches. *J Thorac Cardiovasc Surg* 1980;**80**:198–205.

90 Donaldson RM, Raphael MJ, Yacoub MH, Ross DN. Hemodynamically significant anomalies of the coronary arteries. Surgical aspects. *Thorac Cardiovasc Surg* 1982;**30**:7–13.

91 Backer CL, Hillman N, Dodge-Khatami A, Mavroudis C. Anomalous origin of the left coronary artery from the pulmonary artery: successful surgical strategy without assist devices. *Semin Thorac Cardiovasc Surg Pediatr Card Surg Annu* 2000;**3**:165–72.

92 Lange R, Vogt M, Horer J, Cleuziou J, *et al*. Long-term results of repair of anomalous origin of the left coronary artery from the pulmonary artery. *Ann Thorac Surg* 2007;**83**:1463–71.

93 Hamilton DI, Ghosh PK, Donnelly RJ. An operation for anomalous origin of left coronary artery. *Br Heart J* 1979;**41**:121–4.

94 Takeuchi S, Imamura H, Katsumoto K, *et al*. New surgical method for repair of anomalous left coronary artery from pulmonary artery. *J Thorac Cardiovasc Surg* 1979;**78**:7–11.

95 Arciniegas E, Farooki ZQ, Hakimi M, Green EW. Management of anomalous left coronary artery from the pulmonary artery. *Circulation* 1980;**62**:I180–9.

96 Lenzi AW, Solarewicz L, Ferreira WS, *et al*. Analysis of the Takeuchi procedure for the treatment of anomalous origin of the left coronary artery from the pulmonary artery. *Arq Bras Cardiol* 2008;**90**:167–71.

97 Vouhe PR, Tamisier D, Sidi D, *et al*. Anomalous left coronary artery from the pulmonary artery: results of isolated aortic reimplantation. *Ann Thorac Surg* 1992;**54**:621–6; discussion 627.

98 Dua R, Smith JA, Wilkinson JL, *et al*. Long-term follow-up after two coronary repair of anomalous left coronary artery from the pulmonary artery. *J Card Surg* 1993;**8**:384–90.

99 Wollenek G, Domanig E, Salzer-Muhar U, *et al*. Anomalous origin of the left coronary artery: a review of surgical management in 13 patients. *J Cardiovasc Surg (Torino)* 1993;**34**:399–405.

100 Alexi-Meskishvili V, Hetzer R, Weng Y, *et al*. Anomalous origin of the left coronary artery from the pulmonary artery. Early results with direct aortic reimplantation. *J Thorac Cardiovasc Surg* 1994;**108**:354–62.

101 Turley K, Szarnicki RJ, Flachsbart KD, *et al*. Aortic implantation is possible in all cases of anomalous origin of the left coronary artery from the pulmonary artery. *Ann Thorac Surg* 1995;**60**:84–9.

102 Alsoufi B, Sallehuddin A, Bulbul Z, *et al*. Surgical strategy to establish a dual-coronary system for the management of anomalous left coronary artery origin from the pulmonary artery. *Ann Thorac Surg* 2008;**86**:170–6.

103 Chowdhury UK, Kothari SS, Patel CD, *et al.* An alternative technique for transfer of anomalous left coronary artery from the pulmonary trunk in children and adults using autogenous aortic and pulmonary arterial flaps. *Cardiol Young* 2008; **18**:165–76.

104 Muneer Amanullah M, Rostron AJ, Leslie Hamilton JR, *et al.* Towards an anatomically correct repair for anomalous left coronary artery arising from the pulmonary trunk. *Cardiol Young* 2008;**18**:372–8.

105 Kirklin JW, Barratt-Boyes BG. Congenital anomalies of the coronary arteries. In: Kirklin JW, Barratt-Boyes BG, eds. *Cardiac Surgery*, 2nd edn. New York: John Wiley & Sons, Inc., 1993: 1167–93.

106 Alexi-Meskishvili V, Hetzer R, Weng Y, *et al.* Successful extracorporeal circulatory support after aortic reimplantation of anomalous left coronary artery. *Eur J Cardiothorac Surg* 1994;**8**:533–6.

107 Dodge-Khatami A, Mavroudis C, Backer CL. Anomalous origin of the left coronary artery from the pulmonary artery: collective review of surgical therapy. *Ann Thorac Surg* 2002; **74**:946–55.

108 Chiu HH, Wang JK, Chen CA, *et al.* Resolution of pathologic Q wave, left ventricular dysfunction and mitral regurgitation after dual coronary repair of the anomalous origin of the left coronary artery from the pulmonary artery. *Eur J Pediatr* 2008;**167**:1277–82.

109 Singh TP, Di Carli MF, Sullivan NM, *et al.* Myocardial flow reserve in long-term survivors of repair of anomalous left coronary artery from pulmonary artery. *J Am Coll Cardiol* 1998; **31**:437–43.

110 Vairo U, Marino B, De Simone G, Marcelletti C. Early congestive heart failure due to origin of the right coronary artery from the pulmonary artery. *Chest* 1992;**102**:1610–2.

111 Radke PW, Messmer BJ, Haager PK, Klues HG. Anomalous origin of the right coronary artery: preoperative and postoperative hemodynamics. *Ann Thorac Surg* 1998;**66**:1444–9.

112 Capuano C, Sesana M, Capuano F, *et al.* Right coronary artery arising from the pulmonary trunk. *Cardiovasc Revasc Med* 2007;**8**:76–9.

113 Kajihara N, Asou T, Takeda Y, Kosaka Y. Surgical treatment of an infant with myocardial ischemia due to an anomalous origin of the right coronary artery from the main pulmonary artery: report of a case. *Surg Today* 2009;**39**:969–71.

114 Roberts WC, Robinowitz M. Anomalous origin of the left anterior descending coronary artery from the pulmonary trunk with origin of the right and left circumflex coronary arteries from the aorta. *Am J Cardiol* 1984;**54**:1381–3.

115 Fu M, Hung JS, Yeh SJ, Chang CH. Reversal of silent myocardial ischemia by surgery for isolated anomalous origin of the left anterior descending coronary artery from the pulmonary artery. *Am Heart J* 1992;**124**:1369–71.

116 Stolte M, Jurowich B. Arteriopathia calcificans infantum. *Basic Res Cardiol* 1975;**70**:305–25.

117 Marrott PK, Newcombe KD, Becroft DM, Friedlander DH. Idiopathic infantile arterial calcification with survival to adult life. *Pediatr Cardiol* 1984;**5**:119–22.

118 MacMahon HE, Dickinson PC. Occlusive fibroelastosis of coronary arteries in the newborn. *Circulation* 1967;**35**:3–9.

119 Meradji M, de Villeneuve VH, Huber J, *et al.* Idiopathic infantile arterial calcification in siblings: radiologic diagnosis and successful treatment. *J Pediatr* 1978;**92**:401–5.

120 Gleason MM, Weber HS, Cyran SE, *et al.* Idiopathic infantile arterial calcinosis: intermediate-term survival and cardiac sequelae. *Am Heart J* 1994;**127**:691–5.

121 Witzleben CL. Idiopathic infantile arterial calcification – a misnomer? *Am J Cardiol* 1970;**26**:305–9.

122 Sholler GF, Yu JS, Dale PM, *et al.* Generalised arterial calcification of infancy: three case reports, including spontaneous regression with long-term survival. *J Pediatr* 1984;**1105**: 257–60.

123 Lussier-Lazaroff J, Fletcher BD. Idiopathic infantile arterial calcification: roentgen diagnosis of a rare cause of coronary artery occlusion. *Pediatr Radiol* 1973;**1**:224–8.

124 Thiaville A, Smets A, Clercx A, Perlmutter N. Idiopathic infantile arterial calcification: a surviving patient with renal artery stenosis. *Pediatr Radiol* 1994;**24**:506–8.

125 Kilbride H, Way GL, Mersenstein GB, Winfield JM. Myocardial infarction in the neonate with normal heart and coronary arteries. *Am J Dis Child* 1980;**134**:759–62.

126 Bernstein D, Finkbeiner WE, Soifer S, Teitel D. Perinatal myocardial infarction: a case report and review of the literature. *Pediatr Cardiol* 1986;**6**:313–7.

127 Biteker M, Duran NE, Biteker FS, Civan HA, *et al.* Allergic myocardial infarction in childhood: Kounis syndrome. *Eur J Pediatr* 2010;**169**:27–9.

128 Klys HS, Salmon AP, De Giovanni JV. Paradoxical embolisation of a catheter fragment to a coronary artery in an infant with congenital heart disease. *Br Heart J* 1991;**66**:320–1.

129 Seabra-Gomez R, Somerville J, Ross DN, *et al.*. Congenital coronary artery aneurysms. *Br Heart J* 1974;**36**:329–35.

130 Robinson FC. Aneurysms of the coronary arteries. *Am Heart J* 1985;**109**:129–35.

131 Smith MD, Cowley MJ, Vetrovec GW. Aneurysms of the left main coronary artery: a report of three cases and review of the literature. *Cathet Cardiovasc Diagn* 1984;**10**:583–91.

132 Burns CA, Cowley MJ, Wechsler AS, Wetrovec GW. Coronary aneurysms: a case report and review. *Cathet Cardiovasc Diagn* 1992;**27**:106–12.

133 Angelini P, Trivellato M, Donis J, Leachman RL. Myocardial bridges: a review. *Prog Cardiovasc Res* 1983;**26**:75–88.

134 Acuna LE, Aristeguieta LM, Tellez SB. Morphological description and clinical implications of myocardial bridges: an anatomical study in Colombians. *Arq Bras Cardiol* 2009;**92**:256–62.

135 Ferreira AG Jr, Trotter SE, König B Jr, *et al.* Myocardial bridges: morphological and functional aspects. *Br Heart J* 1991;**66**: 364–7.

136 Bestetti RB, Costa RS, Zucolotto S, Olivara JSM. Fatal outcome associated with autopsy proven myocardial bridging of the left anterior descending coronary artery. *Eur Heart J* 1989;**10**: 573–6.

137 Chiappa E, Vineis C. Sudden death during a game of soccer in a young adolescent with a myocardial muscle bridge. *G Ital Cardiol* 1993;**23**:473–7 (in Italian).

138 Morales AR, Romanelli R, Tate LG, *et al.* Intramural left anterior descending coronary artery: significance of the depth of the muscular tunnel. *Hum Pathol* 1993;**24**:693–701.

139 Bakir I, Riza Karaci A, Altin F, *et al*. Supracoronary myotomy for myocardial bridges in the setting of hypertrophic cardiomyopathy: off-pump experience. *J Cardiovasc Surg (Torino)* 2008;**49**:549–53.

140 Basso C, Thiene G, Mackey-Bojack S, *et al*. Myocardial bridging, a frequent component of the hypertrophic cardiomyopathy phenotype, lacks systematic association with sudden cardiac death. *Eur Heart J* 2009;**30**:1627–34.

141 McNamara JJ, Gross RE. Congenital coronary artery fistula. *Surgery* 1969;**65**:59–69.

142 Edwards JE. Anomalous coronary arteries with special reference to arteriovenous-like communications. *Circulation* 1958; **17**:1001–6.

143 Hoffman JIE. Coronary arterial fistula. In: Hoffman JIE, ed. *The Natural and Unnatural History of Congenital Heart Disease*. Oxford: Wiley-Blackwell, 2009: 111–20.

144 Baim DS, Kline H, Silverman JF. Bilateral coronary artery-pulmonary artery fistulas. Report of five cases and review of the literature. *Circulation* 1982;**65**:810–5.

145 Qureshi SA. Coronary arterial fistulas. *Orphanet J Rare Dis* 2006;**1**:51.

146 Ogden JA, Stansel HC. Coronary arterial fistulas terminating in the coronary venous system. *J Thorac Cardiovasc Surg* 1972; **63**:172–82.

147 Guo H, You B, Lee JD. Dilated cardiomyopathy caused by a coronary-pulmonary fistula treated successfully with coil embolization. *Circ J* 2006;**70**:1223–5.

148 Murphy BP, Gilbert T. Case report: coronary steal secondary to a left main coronary artery–pulmonary artery fistula only manifest after coronary artery bypass surgery. *Int J Cardiol* 2009;**137**:e47–8.

149 Kimura S, Miyamoto K, Ueno Y. Cardiac tamponade due to spontaneous rupture of large coronary artery aneurysm. *Asian Cardiovasc Thorac Ann* 2006;**14**:422–4.

150 Liberthson RR, Sagar K, Berkoben JP, *et al*. Congenital coronary arteriovenous fistula: report of 13 patients, review of the literature and delineation of management. *Circulation* 1979;**59**:849–54.

151 Effler DB, Sheldon WC, Turner JJ, Groves LK. Coronary arteriovenous fistulas: diagnosis and surgical management. Report of fifteen cases. *Surgery* 1967;**61**:41–50.

152 Daniel TM, Graham TP, Sabiston DC Jr. Coronary artery-right ventricular fistula with congestive heart failure. Surgical correction in the neonatal period. *Surgery* 1970;**67**:985–94.

153 Vlodaver Z, Neufeld HN, Edwards JE. Anomalous communication of a coronary artery with a cardiac chamber or major thoracic vessel. In: Vlodaver Z, Neufeld HN, Edwards JE, eds. *Coronary Arterial Variations in the Normal Heart and in Congenital Heart Disease*. New York: Academic Press, 1975: 43–77.

154 Parga JR, Ikari NM, Bustamante LN, *et al*. Case report: MRI evaluation of congenital coronary artery fistulae. *Br J Radiol* 2004;**77**:508–11.

155 Rathi VK, Mikolich B, Patel M, *et al*. Coronary artery fistula; non-invasive diagnosis by cardiovascular magnetic resonance imaging. *J Cardiovasc Magn Reson* 2005;**7**:723–5.

156 Versaci F, Del Giudice C, Sperandio M, *et al*. A case of coronary artery fistula visualized by 64-slice multidetector CT. *Nat Clin Pract* 2009;**6**:57–60.

157 Ata Y, Turk T, Bicer M, *et al*. Coronary arteriovenous fistulas in the adults: natural history and management strategies. *J Cardiothorac Surg* 2009;**4**:62.

158 Latson LA. Coronary artery fistulas: how to manage them. *Catheter Cardiovasc Interv* 2007;**70**:110–6.

159 Cheung DL, Au WK, Cheung HH, *et al*. Coronary artery fistulas: long-term results of surgical correction. *Ann Thorac Surg* 2001;**71**:190–5.

160 Qureshi SA, Tynan M. Catheter closure of coronary artery fistulas. *J Interv Cardiol* 2001;**14**:299–307.

161 Alekyan BG, Podzolkov VP, Cardenas CE. Transcatheter coil embolization of coronary artery fistula. *Asian Cardiovasc Thorac Ann* 2002;**10**:47–52.

162 Armsby LR, Keane JF, Sherwood MC, *et al*. Management of coronary artery fistulae. Patient selection and results of trans-catheter closure. *J Am Coll Cardiol* 2002;**39**:1026–32.

163 Strunk BL, Hieshima GB, Shafton EP. Treatment of congenital coronary arteriovenous malformations with micro-particle embolization. *Cathet Cardiovasc Diagn* 1991;**22**:133–6.

164 Karagoz T, Celiker A, Cil B, Cekirge S. Transcatheter embolization of a coronary fistula originating from the left anterior descending artery by using *n*-butyl 2-cyanoacrylate. *Cardiovasc Interv Radiol* 2004;**27**:663–5.

165 Okamoto M, Makita Y, Fujii Y, *et al*. Successful coil embolization with assistance of coronary stenting in an adult patient with a huge coronary arterial-right atrial fistula. *Int Med (Tokyo, Japan)* 2006;**45**:865–70.

166 Kilic H, Akdemir R, Bicer A, Dogan M. Transcatheter closure of congenital coronary arterial fistulas in adults. *Coron Artery Dis* 2008;**19**:43–5.

49 Pulmonary Artery Sling

Christian Apitz[1], Christoph Döhlemann[2] & Jürgen Apitz[3]

[1]University Children's Hospital, Giessen, Germany
[2]Dr. von Haunersches Kinderspital, University of Munich, Munich, Germany
[3]University Children's Hospital, Tübingen, Germany

Introduction and historical background

Pulmonary arterial sling (PAS) is a congenital anomaly of the left pulmonary artery (LPA), where the LPA arises extrapericardially from the proximal portion of the right pulmonary artery (RPA), passes posteriorly over the right main bronchus, around the right side of the distal trachea, and then courses to the left lung between the distal trachea and the esophagus and anterior to the descending aorta to the left hilus (Figure 49.1). The ductus arteriosus (DA) or the ligamentum arteriosum (lig. art.) passes from the descending aorta along the left side of the trachea to the end of the main pulmonary artery (MPA) at the level of the bifurcation. Hence together the DA or lig. art with the LPA form a sling, compressing the distal trachea and the right or both main stem bronchi.

PAS was first reported 1897 by Glaevecke and Doehle [1]. The first successful operation for this anomaly was published 1954 by Potts *et al.* [2].

Incidence and genetics

PAS is rare. Within the 40 years from 1947 to 1987, only nine patients with PAS were described [3,4]. In the last 20 years, however, nearly 200 patients have been reported. The male-to-female ratio is about 1.5:1 [5,6]. One report of PAS in identical female twins is – as far as we know – the only report of familial occurrence of PAS [7]. Association of 22q11 deletion, trisomy 18 and Mowat–Wilson syndrome have been described in patients with PAS [8–10].

Embryology

The embryologic basis of PAS is unknown, but has been postulated to result from abnormal development of the proximal segments of the left sixth aortic arch [11], leading to the RPA (derived from right sixth aortic arch) vascularizing the undivided primitive lung. With separation of the primitive lung buds, a branch of the RPA passes to the left lung behind the tracheobronchial tree and becomes the LPA. The anterior segment makes no link to the developing vascular plexus of the left lung or else resorbs after the connection [11].

A partial left pulmonary artery sling is rare, with a normal LPA supplying the left upper lobe and an anomalous component arising from the RPA and crossing to the left, behind the airway, supplying the left lower lobe [12]. Airway obstruction also occurs in partial PAS.

Pathologic anatomy and major associated anomalies

The LPA and the ductus ligament form a vascular ring, which compresses the right main bronchus (RMB) and the distal trachea [7,11], leading to tracheomalacia [13–15]. In 30–70% of the patients, complete cartilaginous rings of the trachea can be found [5,13,15–18]; the tracheal cartilage is not "U" shaped with a dorsal pars membranacea, but there is a completely closed ring of the cartilage ("O" shape). As a result, the trachea cannot grow in relation to the child's growth. Increasing airway obstruction and dyspnea result.

Other frequent anatomic findings are the origin of the right pre-eparterial bronchus from the trachea (bronchus suis) or a bridging bronchus (BB), arising from the left main bronchus, crossing the mediastinum to the right, supplying the right middle and lower lobes of the right lung.

Two forms of PAS are generally distinguished: type IA and B and type IIA and B (Figure 49.2) [18]. In type IA, there is a basically normal bronchial branch pattern and the sling (LPA) passes posteriorly above the RMB and behind the
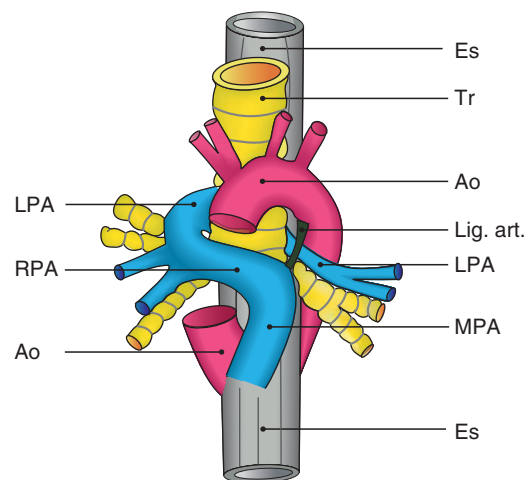
Figure 49.1 Demonstration of the abnormal course of the LPA between trachea (Tr) and esophagus (Es) in pulmonary arterial sling. Ao, aorta; lig. art., ligamentum arteriosum; LPA, left pulmonary artery; MPA, main pulmonary artery; RPA, right pulmonary artery.
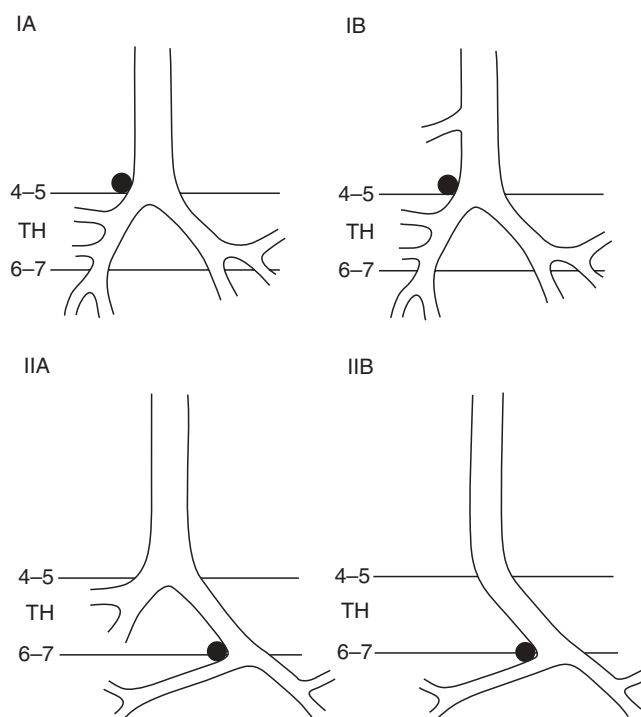
Figure 49.2 Tracheobronchial arborization disorders associated with sling left pulmonary artery (see text). The large black dot indicates the location of the sling relative to the tracheobronchial tree. (Modified from Baden W, Schaefer J, Kumpf M, *et al. Eur Respir J* 2008;**31**: 1125–31, with permission from the European Respiratory Society.)

carina or lower trachea. By imaging techniques the carina projects on vertebral level T4–T5 with normal tracheobronchial angles. Type IB resembles type IA, but there is a bronchus suis, the sling LPA passes to the left between the RMB and

bronchus suis and behind the carina or lower trachea, the carina projecting on T4–T5 as in type I A.

In type IIA and B, a BB has a horizontal course from the LMB to the right middle and lower lobe the origin of the BB from the LMB (pseudocarina) projects on vertebral level T6. In type IIA, there is a right tracheal bronchus (bronchus suis) for the upper lobe, projecting as a true carina on T4–T5. Type IIB resembles type IIA, but the right tracheal bronchus is absent and the right lung may be hypoplastic. The sling LPA passes above the BB and behind the LMB to the left. Patients with PAS type II regularly show tracheal and LMB stenosis and abnormal tracheal and left main bronchial cartilage rings [18].

Associated cardiovascular anomalies

Approximately half of patients have additional congenital heart defects: patent ductus arteriosus, atrial or ventricular septal defect, and persistent left superior vena cava. Rare associations are tetralogy of Fallot, atrioventricular septal defect, coarctation of the aorta, complete transposition, truncus arteriosus, scimitar syndrome, and single ventricle.

Miscellaneous associated non-cardiovascular anomalies

Occasionally, patients with imperforate anus and PAS have been reported, including the triad of imperforate anus, secundum ASD, and persistent left superior vena cava. Absent gall bladder was associated in four patients, one combined with an imperforate anus. Additional less frequent associations are with trisomy 21 and 18, Apert sydrome, Goldenhar syndrome, diaphragmatic hernia, and Hirschsprung's disease.

Pathophysiology

Tracheal and bronchial compression occur as the LPA passes posteriorly and caudally to the RMB and to the left behind the trachea. The course of the anomalous LPA to the right of the trachea deviates the lower trachea to the left, compressing the RMB and lower trachea. This causes airway obstruction that primarily affects the right lung, although compression of the lower trachea and left mainstem bronchus can result in bilateral obstruction. Compression caused by the sling produces obstructive emphysema, atelectasis of the right and left lungs, or both.

Natural history

Because pulmonary artery sling is rare, its natural history remains poorly defined. At least 65% have symptoms within the first year, and 85% by 10 years, but a few asymptomatic adults have been described.

Clinical features

Clinical history

If the trachea is nearly normal and not constricted, patients with PAS can be asymptomatic for a long time. More frequently, the sling is narrow and causes respiratory obstruction soon after birth with expiratory and/or inspiratory stridor and tachypnea leading to emergency intubation. Up to 90% of patients become symptomatic within the first year of life [5] with tachypnea, dyspnea, stridor, apnea, wheezing, and hypoxemic attacks with intermittent cyanosis [17]. Hypoplasia or compression and stenosis of the distal trachea or of RMB and LMB may lead to unequal aeration with obstructive emphysema of parts of the lungs, especially of the right upper lobe [19].

Physical examination

Significant findings on history and physical examination relate either to associated structural heart disease or to respiratory symptoms. In mild forms of PAS, history and physical examination findings are normal. Symptoms and signs of severe respiratory distress or stridor should raise suspicion for this diagnosis. Intercostal retractions may be evident. Prolonged expiratory phase of respiration may be heard.

Electrocardiographic features

There are no specific electrocardiographic features in patients with PAS.

Chest X-ray

The chest X-ray may show an overaeration with hyperexpansion of the right lung in 25–30% of patients and of the left lung in 4%, with displacement of the mediastinum and the distal trachea to the contralateral (mainly the left) side [4,5,16–18]. If displaced to the right side, hypoplasia or aplasia of the right lung has to be considered, as it may be associated with PAS. Dextrocardia with situs solitus also associated with PAS must be considered in the differential diagnosis. Viral or bacterial infections may lead to dystelectasis, atelectasis, or to lobar emphysema in ~28% of patients [20,21]. With more heavily penetrated X-rays taken in the AP projection, narrowing of the distal trachea from the right side and in the lateral view from behind can be seen in 77% of patients.

A horizontal course of the RMB and LMB ("inverted T-sign") and a lower than normal bifurcation on the vertebral level T5–T6 are typical radiographic signs of PAS (type II), but a classification based on the level of the carina is difficult because of different X-ray projections and different air contrast. The position and angles of the carina vary with respiratory cycle, diaphragm level and age.

Barium-filled esophagram

Barium-filled esophagram is the diagnostic procedure of choice and shows an anterior indentation of the esophagus at the level of the bifurcation of the trachea and the fifth dorsal vertebra (Figure 49.3) [20,22]. Anterior esophageal indentation is rare with any other type of vascular ring.

Echocardiography

Echocardiography demonstrates the absence of normal pulmonary artery bifurcation and the anomalous origin of the left pulmonary artery from the proximal right pulmonary artery [4,23,24], if there are satisfactory suprasternal, parasternal, or subcostal windows. Overaeration of the lungs, however, often makes echocardiography difficult. Antenatal detection of PAS has been reported by ultrasound, revealing an echogenic right lung from stenosis of RMB [25].

(a)   (b)
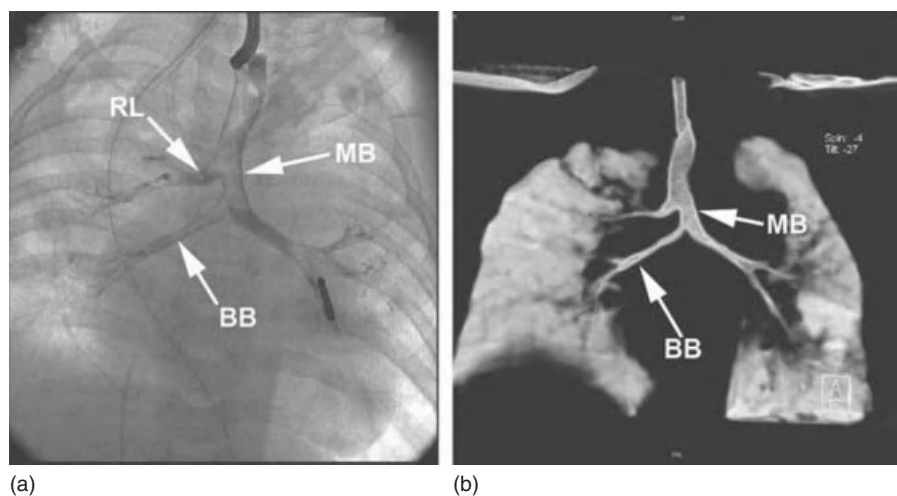
Figure 49.3 (a) Bronchography confirming a bridging bronchus (BB), originating after a short distance from the left main bronchus (MB). (b) Multidetector computed tomography showing the same BB. RL, right upper lobe. (Modified from Baden W, Schaefer J, Kumpf M, *et al. Eur Respir J* 2008;**31**:1125–31, with permission from the European Respiratory Society.)

Cardiac catheterization and angiography

Diagnosis of PAS can usually be established noninvasively. Pulmonary artery angiography can delineate anatomic details prior to surgical correction. Angiography permits diagnosis of variations of the blood supply into the left lung present in some patients. The PAS can be best detected in an anterior–posterior or left-anterior view with cranial angulation.

Other imaging modalities

Assessment of the trachea

Because of the high incidence of tracheal anomalies other than from simple compression by the sling, complete assessment of the trachea should be undertaken. This should include bronchoscopy and at least one other mode of imaging to delineate the severity and extent of tracheal stenosis. This may include computed tomographic scanning or magnetic resonance imaging.

Tracheobronchoscopy is important to exclude associated tracheobronchial anomalies, that is, a complete ring or stenosis of the trachea. In PAS, external dorsal compression of the trachea and compression with pulsations of the right main bronchus (RMB) can be seen. In addition, cartilaginous rings, stenosis of the trachea and the RMB, and abnormal branching of the bronchi can be detected (Figure 49.3). Tracheobronchography with water-soluble contrast is sometimes necessary for long-segment stenosis. Bronchography can produce spectacular imaging of tracheal stenoses but is generally reserved for children who are also undergoing angiography to define vascular anatomy, if unclear from echocardiography alone, or associated cardiac problems.

Multidetector computed tomography (MDCT) allows accurate quantitation of the tracheal luminal diameter and area at various levels and demonstrates complete rings. It is preferred by some centers because of the high quality of the images and short acquisition time, but the radiation dosage is not negligible [26].

With *magnetic resonance imaging* (MRI), the PAS can be diagnosed accurately (Figure 49.4) and noninvasively without radiation exposure [27,28]. MRI is considered the imaging technique of choice to diagnose PAS. However, MRI requires anesthesia, especially in newborns and infants, is expensive, and the acquisition is time consuming.

Differential diagnosis

Other forms of vascular rings, aortic arch anomalies, and respiratory disorders have to be excluded: bronchogenic cysts, lobar emphysema, which can occur even in patients with PAS and with coexisting congenital heart defects [29], and especially foreign body aspiration. Dextrocardia and mesocardia with underdevelopment of the right lung are associated with PAS [4]. Dextrocardia without PAS may also be associated with airway obstruction due to normally related, but deviated, great vessels [30].

Management

Medical

Medical care is only supportive until the patient can undergo operation. Hypoxemia and respiratory distress should be treated with supplemental oxygen and endotracheal intubation if indicated. Pneumonia should be treated with appropriate antibiotics, but respiratory tract infections may be difficult to clear completely before operation because of the difficulty in adequately clearing secretions. Infants without airway obstruction and with minimal symptoms may not require an operation, but this is an exception.

Surgical

Surgery is reserved for children with respiratory symptoms from the sling – the majority of children with PAS. In 1954, Potts and associates described an approach to a PAS through a left thoracotomy with division and translocation of the LPA anterior to the trachea and reimplantation [2]. Frequently, narrowing or occlusion of the LPA has been observed [2,13,31], especially if the LPA was small and hypoplastic or if the anastomosis was under stretch or kinked. The operative mortality has been reported to be as high as 50% [2,13,31,32].

In the early 1980s, repair by reimplantation of the left pulmonary artery was performed through a median sternotomy using cardiopulmonary bypass. None of the previous techniques had dealt directly with the frequently associated tracheal stenosis. Although primary repair of the tracheal anomaly had been suggested previously, it had not been attempted because of fear of early and late tracheal anastomotic problems in the infant. Improved cardiopulmonary bypass techniques, improved sutures, greater familiarity with microvascular techniques, and improved perioperative management strategies [33] have decreased the risk of tracheal anastomosis in infants [34]. Tracheal resection is currently considered an integral part of the repair when the sling is associated with significant localized tracheal stenosis [35–41]. Preoperative studies must identify the details of tracheal compression. Simple compression stenosis of the carinal region may be relieved by translocation of the left pulmonary artery. Localized anatomic stenosis of the trachea (generally associated with complete tracheal rings in this area) is best dealt with by tracheal resection and anterior translocation of the left pulmonary artery. Finally, diffuse and severe narrowing of the trachea related to complete tracheal rings may necessitate an extensive tracheoplasty procedure in addition to relocation of the left pulmonary artery [12,33–39]. Because of associated tracheomalacia, tracheal stenosis, and/or bronchial stenosis, postoperative symptoms of airway obstruction are common, but may resolve

(a)

(b)

(c)
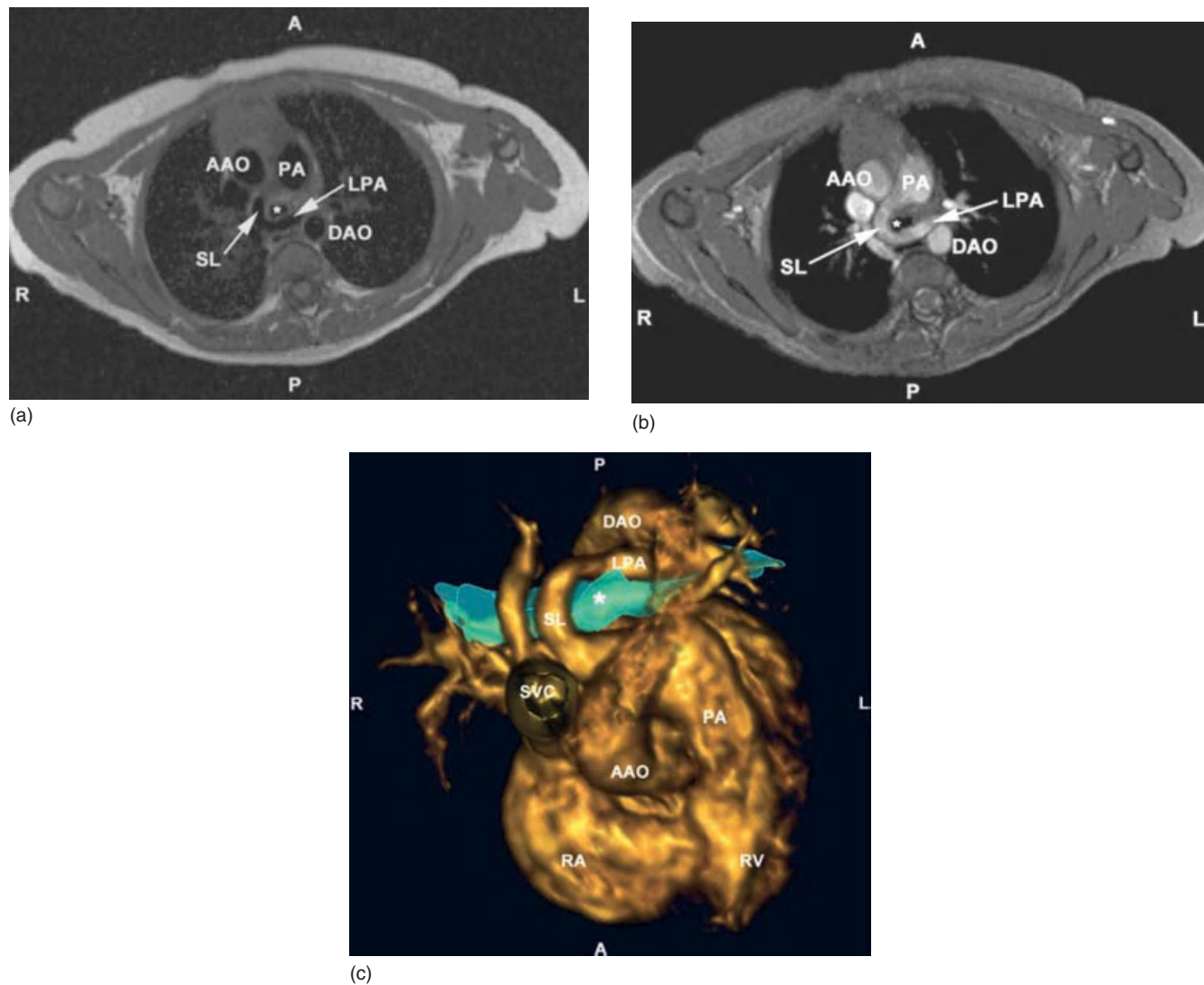
Figure 49.4 (a) Axial T1-weighted spin echo image showing a pulmonary artery sling. (b) Angulated MIP of the pulmonary artery sling (3D FISP MRA). (c) 3D volume-rendered model based on a 3D FISP MRA dataset. The tracheobronchial tree is colored blue. A, anterior; P, posterior; L, left; R, right; AAO, ascending aorta; DAO, descending aorta; LPA, left pulmonary artery; PA, pulmonary artery; RA, right atrium; RV, right ventricle; LPA, left pulmonary artery; SL, pulmonary artery sling; SVC, superior vena cava; asterisks, trachea. (Modified from Sieverding L, Klose U, Apitz J. *Pediatr Radiol* 1990;**20**:311–9, with permission from Springer.)

gradually with time. Left pulmonary artery stenosis may occur and can progress.

Long-term history of treated and untreated adults

Surgical survivors may be free of significant symptoms at long-term follow-up. Because many patients demonstrate some degree of persistent airway obstruction, they should be closely observed for both airway and pulmonary artery complications.

References

1 Glaevecke H, Doehle W. Über eine seltene angeborene Anomalie der Pulmonalarterie. *Münch Med Wochenschr* 1897;**34**:950–3.
2 Potts WL, Holinger PH, Rosenblum AH. Anomalous left pulmonary artery causing obstruction to the right main bronchus. *J Am Med Assoc* 1954;**155**:1409–11.
3 Backer CL, Ilbawi MN, Idriss FS, DeLeon SY. Vascular anomalies causing tracheosophageal compression. *J Thorac Cardiovasc Surg* 1989;**97**:725–31.
4 Döhlemann C, Mantel K, Vogl TJ, Nicolai T, *et al.* Pulmonary sling. *Eur J Pediatr* 1995;**154**:2–14.

5 Gikonyo BM, Jue KL, Edwards JE. Pulmonary vascular sling. *Pediatr Cardiol* 1989;**10**:81–9.

6 Jue KL, Raghib G, Amplatz K, *et al.* Anomalous origin of the left pulmonary artery from the right pulmonary artery. *Am J Roentgenol* 1965;**95**:598–610.

7 Westaby S, Dinwiddie R, Chrispin A, Stark J. Pulmonary artery sling in identical twins. *J Thorac Cardiovasc Surg* 1984;**32**:182–3.

8 Adam MP, Schelley S, Gallagher R, *et al.* Clinical features and management issues in Mowat–Wilson syndrome. *Am J Med Genet A* 2006;**140**:2730–41.

9 Jan SL, Tsai IC, Ho CL, *et al.* Pseudopulmonary artery sling in a 22q11 deletion newborn with tetralogy of Fallot and isolated left subclavian artery. *Echocardiography* 2008;**25**:931–3.

10 Derbent M, Saygili A, Tokel K, Baltaci V. Pulmonary artery sling in a case of trisomy 18. *Am J Med Genet* 2001;**101**:184–5.

11 Stewart JR, Kincaid OW, Edwards JE. *An Atlas of Vascular Rings and Related Malformations of the Aortic Arch System*. Springfield, IL: Charles C Thomas, 1964.

12 Tissot C, Darst JR, Kaza AK, *et al.* Partial left pulmonary artery sling associated with multiple ventricular septal defects. *J Thorac Cardiovasc Surg* 2008;**136**:1085–7.

13 Sade RM, Rosenthal A, Fellows K, Castaneda AR. Pulmonary artery sling *J Thorac Cardiovasc Surg* 1975;**69**:333–46.

14 Backer CL, Mavroudis C. Vascular rings and pulmonary artery sling. In: Mavroudis C, Backer CL, eds. *Pediatric Cardiac Surgery*, 2nd edn. St. Louis, MO: Mosby, 1984: 147–66.

15 Jonas RA, Spevak PJ, McGill T, Castaneda AR. Pulmonary artery sling: primary repair by tracheal resection in infancy. *J Thorac Cardiovasc Surg* 1989;**97**:548–50.

16 Berdon WE, Baker DH, Wung JT, *et al.* Complete cartilage ring tracheal stenosis associated with anomalous left pulmonary artery: the ring-sling complex. *Radiology* 1984;**152**:57–64.

17 Apitz J, Apitz C. Angeborene Anomalien der Lungengefäße. In: Apitz J, ed. *Pädiatrische Kardiologie*, 2nd edn. Darmstadt: Steinkopff, 2002: 315–40.

18 Wells TR, Gwinn JL, Landing BH, Stanley P. Reconsideration of the anatomy of sling left pulmonary artery. *J Pediatr Surg* 1988;**23**:892–8.

19 Clarkson PM, Ritter DG, *et al.* Aberrant left pulmonary artery. *Am J Dis Child* 1967;**113**:373–7.

20 Freedom RM, Benson LM, Smallhorn JF. *Neonatal Heart Disease*. Heidelberg: Springer, 1992: 746–9.

21 Spindola-Franco H, Fish BG. *Radiology of the Heart*. Heidelberg: Springer, 1985: 609–11.

22 Sprague PL, Kennedy JC. Anomalous left pulmonary artery with an unusual barium swallow. *Ped Radiol* 1976;**4**:188–92.

23 Gnanapragasam JP, Houston AB, Jamieson MP. Pulmonary artery sling. *Br Heart J* 1990;**63**:251–2.

24 Yeager SB, Chin AJ, Sanders SP. Two-dimensional echocardiographic diagnosis of pulmonary artery sling in infancy. *J Am Coll Cardiol* 1986;**7**:625–9.

25 Semple MG, Bricker L, Shaw BN, Pilling DW. Left pulmonary artery sling presenting as unilateral echogenic lung on 20-week detailed antenatal ultrasound examination. *Pediatr Radiol* 2003;**33**:567–9.

26 Baden W, Schaefer J, Kumpf M, *et al.* Comparison of imaging techniques in the diagnosis of bridging bronchus. *Eur Respir J* 2008;**31**:1125–31.

27 Sieverding L, Klose U, Apitz J. Morphological diagnosis of congenital and acquired heart disease by magnetic resonance imaging. *Pediatr Radiol* 1990;**20**:311–9.

28 Greil GF, Kramer U, Sieverding L, *et al.* Diagnosis of vascular rings and slings using an interleaved 3D double-slab FISP MR angiography technique. *Pediatr Radiol* 2005;**35**:396–401.

29 Apitz J, Richtering I, Wilutzky H. Über die Kombination des kongenitalen lobären Emphysems mit kongenitalen Angiokardiopathien. *Mschr Kinderheilkd* 1965;**113**:349–54.

30 Döhlemann C, Mantel K, Schneider K, *et al.* Deviated trachea in hypoplasia and aplasia of the right lung. *J Pediat Surg* 1990;**25**:290–3.

31 Vincent RN, Armstrong G, Dokler ML, Williams WH. Operative correction of subcarinal left pulmonary artery originating from the right pulmonary artery. *Am J Cardiol* 1989;**64**:687–88.

32 Mandell VS, Braverman RM. Vascular rings and slings. In: Fyler DC, ed. *Nadas' Pediatric Cardiology*. Philadelphia: Hanley & Belfuss, 1992: 724–6.

33 Tsai MH, Wong KS, Lien R, *et al.* Heliox as the rescue therapy for a neonate with congenital tracheal stenosis, pulmonary artery sling, and intracardiac anomalies. *Am J Perinatol* 2009;**26**:357–60.

34 Oshima Y, Yamaguchi M, Yoshimura N, *et al.* Management of pulmonary artery sling associated with tracheal stenosis. *Ann Thorac Surg* 2008;**86**:1334–8.

35 Loukanov TS, Sebening C, Springer W, *et al.* The evolution of the pulmonary arterial sling syndrome, with particular reference to the need for reoperations because of untreated tracheal stenosis. *Cardiol Young* 2009;**19**:446–50.

36 Ziemer G, Nagy Z. Anomalien der großen intrathorakalen Gefäße. In: Ziemer G, Haverich A, eds. *Herzchirurgie*, 3rd edn. Heidelberg: Springer, 2010: 549–51.

37 Beierlein W, Elliott MJ. Variations in the technique of slide tracheoplasty to repair complex forms of long-segment congenital tracheal stenoses. *Ann Thorac Surg* 2006;**82**:1540–2.

38 Jonas RA. *Comprehensive Surgical Management of Congenital Heart Disease*. London: Hodders Arnold, 2004.

39 Backer CL, Mavroudis C, Dunham ME, Holinger LD. Repair of congenital tracheal stenosis with a free tracheal autograft. *J Thorac Cardiovasc Surg* 1998;**115**:869–74.

40 Forsen JW Jr, Lusk RP, Huddleston CB. Costal cartilage tracheoplasty for congenital long-segment tracheal stenosis. *Arch Otolaryngol Head Neck Surg* 2002;**128**:1165–71.

41 Backer CL, Mavroudis C, *et al.* Tracheal surgery in children. *Eur J Cardiothorac Surg* 2001;**19**:777–84.

50 Abnormalities of Situs

Bruno Marino[1], Paolo Versacci[1], Paolo Guccione[2] & Adriano Carotti[2]

[1]"Sapienza" – University of Rome, Rome, Italy
[2]Bambino Gesù Children's Hospital, Rome, Italy

Introduction

Malposition of the heart is a nonspecific term used to indicate an abnormal position of the heart within or outside the thorax. It gives no specific information about cardiac structure, such as atrial situs, ventricular arrangement, or position of great arteries.

Levocardia indicates a left-sided heart and is the normal position of the heart in individuals with situs solitus; *dextrocardia* indicates a right-sided heart and is the normal position in individuals with situs inversus; *mesocardia* is the midline position of the heart in the thorax. *Ectopia cordis* is the malformation in which the heart is outside the thorax.

Cardiac position is genetically determined and is usually concordant with the ventricular loop; exceptionally, it is discordant.

The embryologic events that result in D-ventricular looping also usually result in levocardia, whereas events producing L-ventricular looping usually result in dextrocardia. When there is concordance between the visceroatrial situs and the position of the heart in the thorax (levocardia in a D-loop and dextrocardia in an L-loop), the pivoting of the ventricle has been complete. On the other hand, the pivoting of the heart is incomplete when discordance between the situs and the position of the heart occurs, resulting in malposition. With atrioventricular discordance, either in situs solitus or in situs inversus, the pivoting of the heart is more often incomplete, resulting in varying cardiac position (levocardia, dextrocardia, mesocardia). The same concept may be applied to patients with asplenia/right isomerism and polysplenia/left isomerism. However, because of ambiguous atrioventricular connections. these conditions preclude designated situs and therefore a concordant or discordant loop. It is not surprising to find a high prevalence of cardiac malposition in situs ambiguus.

The classification of cardiac malposition is difficult, and few discussions have been more controversial than those about the nomenclature of complex cardiac malformations [1–9]. Diagnosis is enhanced by a segmental approach to diagnosis [1,6,8,9] of patients with complex cardiac anomalies and in particular children with malposition of the heart. Because intracardiac anomalies frequently coexist in cardiac malpositions, segmental analysis is essential to understand and describe the cardiac anatomy. Three segments must be considered: (1) atrial situs, (2) ventricular position and connection to the atria, and (3) position of great arteries and connections to the ventricle.

Atrial situs

The first step to understanding the morphology of a heart is determining visceroatrial situs. The left–right orientation of the abdominal organs and of the hearts in vertebrates is a nonrandom and highly conserved phenomenon controlled by several genes [10–23].Visceroatrial situs refers to the relationship between the abdominal viscera and the cardiac atria. The three types of visceroatrial situs are *situs solitus* (normal), *situs inversus* (mirror image of normal), and *situs ambiguus* (similar anatomy of both atria).

Situs solitus

Visceroatrial situs solitus is the usual pattern present and frequently occurs with malformed hearts. In situs solitus, the major lobe of the liver, the inferior vena cava, and the anatomic right atrium are on the right side of the body, as is the trilobed lung and the eparterial bronchus. The stomach, the spleen, the descending aorta, and the anatomic left atrium are on the left side of the body, as is the bilobed lung and hyparterial bronchus.

In individuals with situs solitus, the heart is usually in the left hemithorax. Cardiac malposition in situs solitus includes dextrocardia and mesocardia.

Situs inversus

Situs inversus is the mirror image of situs solitus so that the major lobe of the liver, the inferior vena cava, and the anatomic right atrium are on the left side of the body, as is the trilobed lung and eparterial bronchus. The liver, descending aorta, anatomic left atrium, bilobed lung, and hyparterial bronchus are on the right side of the body.

The heart in situs inversus is in the right hemithorax (dextrocardia), but the cardiac mass may also be "malposed" to the left side.

Situs inversus may be associated with Kartagener syndrome, including bronchiectasis and primary ciliary dyskinesia [10–14].

Situs ambiguus

In any arrangement other than situs solitus or situs inversus, there is random orientation of different organs, a pattern defined as situs ambiguus or heterotaxy and some causative factors have been identified [24–40].

Situs ambiguus consists in all abnormalities of lateralization that show anomalous relationships and unpredictable anatomic relationships between major organs.

Altered left–right asymmetry is accompanied in >90% of instances by severe cardiac malformations and frequently with cardiac malposition, such as mesocardia or dextrocardia.

Other organs, such as the liver, spleen, and intestine, show abnormal morphology and position. In patients with heterotaxy, the genetic message of visceral asymmetry is completely or partially lost and morphologic symmetry of some organs, such as atrial appendages, bronchi, and lungs, is common This aspect prompted some authors to define these conditions as *atrial isomerism* or *isomerism* [33,34] *of the atrial appendages* [36,39,40]. Other investigators [35,37,38,41], although affirming the concept of isomerism as it relates to the heart, believe that it has never been biologically proved, is diagnostically difficult to assess, and is surgically irrelevant. Two forms of situs ambiguus, however, have been defined according to the status of the spleen and the morphology of the atrial appendages, bronchi, and lungs [30–32].

The first subtype of situs ambiguus is the *asplenia syndrome* with *right isomerism* of atrial appendages. In this type of heterotaxy, the spleen is absent (*asplenia*) and the atrial appendages, bronchi, and lungs tend to be mirror images of each other and to show the anatomic features of the right-sided structures (*right isomerism*) [33–40].

The second subtype of situs ambiguus is the *polysplenia syndrome* with *left isomerism* of atrial appendages. In this type of heterotaxy, two or more splenic masses (*polysplenia*) are present along the great curvature of the stomach on the right or the left side of the abdomen. The atrial appendages, bronchi, and lungs tend to be mirror images of each other and to show the anatomy of the left-sided structures (*left isomerism*) [30–35]. In these patients, there may be levocardia, dextrocardia, or mesocardia [42].

Genetics of situs ambiguus

The genetics of cardiac malformations and human situs abnormalities are a complex issue characterized by heterogeneity, gene–environment interaction, variable expression, and reduced penetrance [10–14]. Studies, including familial clustering, detailed descriptions of large series of patients and phenotype/genotype correlations, have improved our knowledge.

Human heterotaxy is usually sporadic, but many families have been described with horizontal recurrence (affected siblings born to unaffected parents), frequent twinning, and spontaneous abortion [10–14]. Consanguineous parents are not rare. This recurrence pattern is consistent with a maternal effect in a significant proportion of patients [28].

Situs ambiguus can be associated with a large number of genetic syndromes, including VACTERL, Alagille, Cantrell, Smith–Lemli–Opitz, oral–facial–digital, Ellis–van Creveld, Bardet–Biedl, Goldenhar, and del22q11.2 [10–15]. In addition, partial or complete trisomies and monosomies, balanced and unbalanced translocations, deletions, and inversions have all been described and show a possible location of genes involved in laterality development [10–14]. Situs ambiguus has also been associated with environmental exposures, such as retinoic acid, maternal diabetes, and first trimester cocaine use [13–26].

Studies of animal models, such as zebrafish, frog, chick, mouse, and shell, have increased our understanding the genetic mechanisms of left–right axis determination [10–25,28].

At present more than 80 genes involved in laterality defects have been detected in model organisms. Many of these genes have a conserved function in humans but relatively few mutations of these genes have been identified in children with situs ambiguus. These include NODAL [16], ZIC3 [20], LEFTYA [21], Criptic [22], ACVR2B [23], CRELD1 [24], and NKX2.5 [25].

The signaling cascade producing left–right asymmetry in humans remains unclear, but an early role of the Sonic Hedgehog gene has been established. Moreover, the NODAL gene encoding a TGFβ family transcription factor induces other genes as LEFTY1, LEFTY2, and PITX2 that are also expressed asymmetrically at the left side of Hensen's node [10–14]. At the level of the node, an asymmetric leftward flow of extraembryonic liquid caused by clockwise rotation of the cilia is involved in the early establishment of left–right asymmetry [10–14]. Mice with situs inversus consistently express NODAL gene in the right side of the node, the opposite side from normal.

Some mutations of genes involved in left–right asymmetry have been identified also in patients with situs solitus

and an isolated cardiac anomaly, such as transposition of great arteries [16,17]. Moreover, recent studies on familial recurrence [18], experimental teratology [19], and genetic mutations [16,17] suggest that isolated transposition of great arteries can be considered a laterality defect consisting only in an abnormality of spiralization of infundibula and great arteries. Nodal signaling, involved in left–right asymmetry and spiralization of great arteries in vertebrates [16], is a conserved gene causing also the normal and abnormal chirality of snail shells [27]. Therefore, these phenotypic and genetic similarities between spiralization of great arteries in vertebrates [16] and spiral pattern of snail shell [27] expand the phylogenetic development horizon of the human heart [28].

Along with the categorization of visceroatrial situs, cardiac malpositions can be classed in three types: with situs solitus, with situs inversus, and with situs ambiguus and heterotaxy.

Cardiac malposition with situs solitus

Dextrocardia

Dextrocardia is the most common type of malposition. Initially described by Fabricius in 1749 [43], dextrocardia simply means that the heart is predominantly in the right hemithorax. The incidence of dextrocardia is one in 12 000 births with a similar number of patients with situs solitus, situs inversus, and situs ambiguus [44]. Numerous classifications of dextrocardia have been proposed. Terms such as mirror-image dextrocardia, false dextrocardia, primary or secondary dextrocardia, dextroversion, and dextrorotation represent attempts to describe and categorize this condition [45,46]. In this chapter, we distinguish dextrocardia and dextroversion. Dextrocardia is the location of the heart in the right thorax with the apex pointing to the right (Figure 50.1), and it is usually due to anomalous pivoting of the ventricles [7]. Dextroversion is the location of the heart in the right thorax with the apex normally pointed towards the patient's left; it occurs in congenital or acquired lesions, such as diaphragmatic hernia or right lung hypoplasia, that push the heart to the right (Figure 50.2).

Dextrocardia with situs solitus

This is the most common type of dextrocardia in reported pathologic series. In dextrocardia but also in mesocardia, the incomplete pivoting of the ventricular septum determines a progressively narrower angle between the atrial and ventricular septa.

Dextrocardia with D-ventricular loop and normally related great arteries {S,D,S}

This is the second most frequent type of cardiac condition in dextrocardia; corrected transposition in situs solitus {S,L,L} is
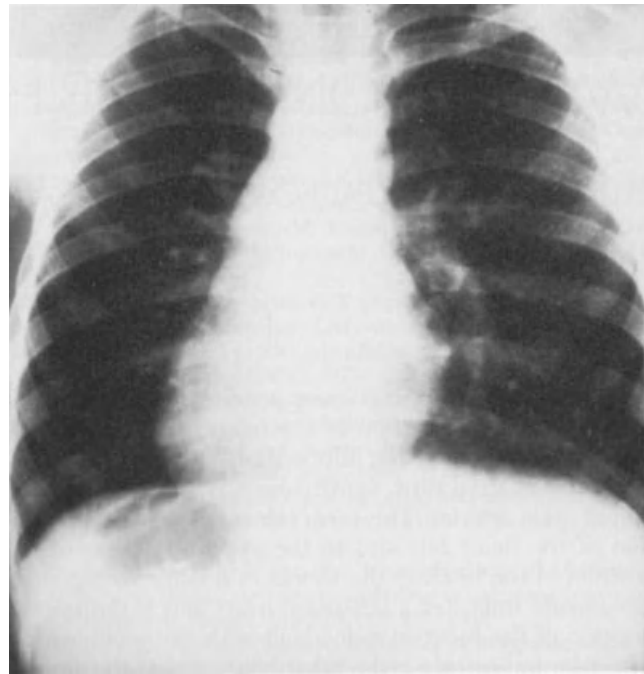
Figure 50.1 Dextrocardia, thoracic radiograph in posteroanterior projection. The heart is displaced in the right hemithorax with the apex towards the patient's right.

Figure 50.2 Dextroversion of the heart, thoracic radiograph in posteroanterior projection. The major part of the heart is displaced in the right hemithorax because of the enormous dilatation of the right atrium (Ebstein malformation). The apex of the heart is pointed towards the patient's left.

the most common. Several cardiac malformations have been described, in particular septal defects [3,47].

Dextrocardia with normal atrioventricular and ventriculoarterial relations {S,D,S} may be part of a syndrome usually with midline defects, as described by Cantrell *et al.* [48]. Five components are present: (1) midline epigastric abdominal
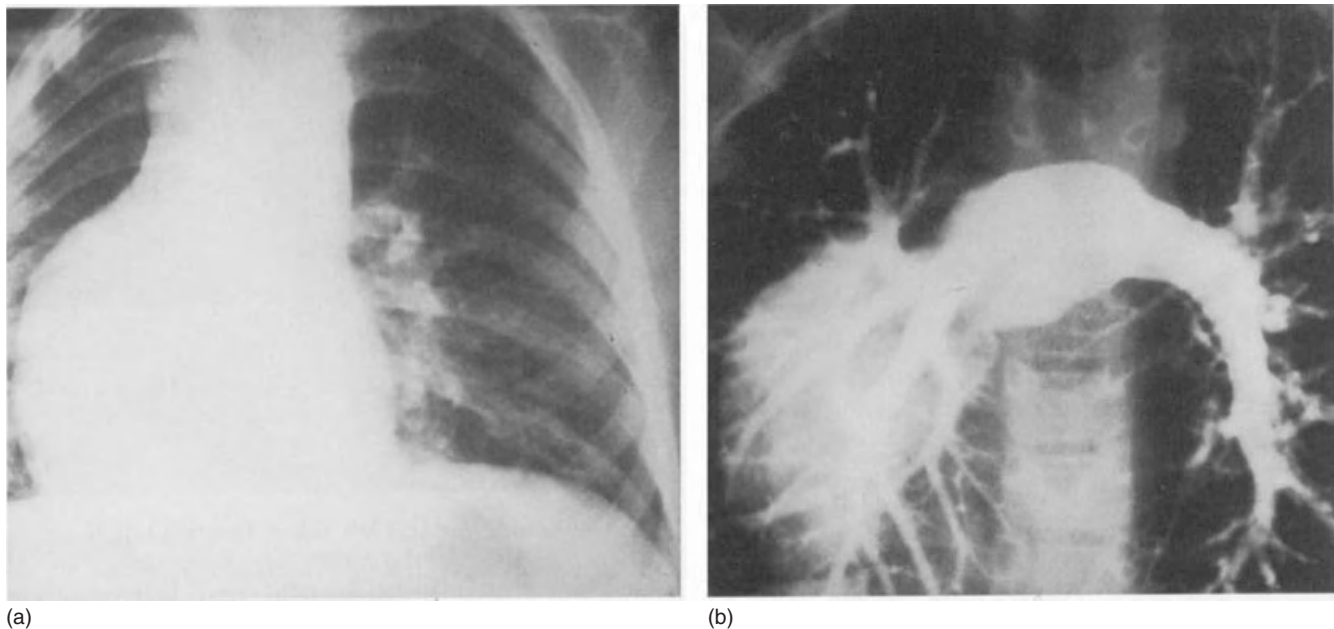
Figure 50.3 Dextroversion of the heart, scimitar syndrome. (a) Thoracic radiograph, heart in right hemithorax. The right hemithorax is smaller than the left because of the right lung hypoplasia. The right hemidiaphragm is elevated. (b) Pulmonary arteriogram shows hypoplastic vasculature in the right lung.

wall defect, often associated with herniation or omphalocele; (2) defect of the lower sternum; (3) deficiency of the anterior diaphragm; (4) defect of the diaphragmatic portion of the pericardium; and (5) diverticulum of the left or right ventricle with possible intracardiac thrombus [49]. A cardiac malformation often coexists, most frequently tetralogy of Fallot or ventricular septal defect. Although the presentation of Cantrell syndrome varies, one-stage repair of the cardiac defect is usually feasible [50].

Dextroversion of the heart

The malposition of a heart with atrioventricular and ventriculoarterial concordance {S,D,S} in the right thorax with the apex normally pointed towards the patient's left is defined as *dextroversion* (Figure 50.2). This mimic of dextrocardia is generally from a variety of anatomic or functional abnormalities of the lung, diaphragm, or thoracic cage.

These include right lung hypoplasia and dextroversion of the heart [51], usually associated with congenital lesions such as renal abnormalities (oligohydramnios), right bronchial tree abnormalities, deformity of the thoracic spine and rib cage, and left-sided diaphragmatic hernia. Diaphragmatic hernia is the most common cause of congenital dextroversion [51]. Hypoplastic left heart syndrome is commonly observed in fetuses with left diaphragmatic hernia. Fetal echocardiographic studies have shown that preferential streaming of the ductus venosus and inferior caval vein towards the right heart is associated with left heart underdevelopment with left-sided diaphragmatic hernia [51a]. This abnormal flow results from intrathoracic abdominal organ herniation and rightward displacement of the heart.

Acquired lesions resulting in dextroversion are left pneumothorax and pericardial or mediastinal tumor. *Scimitar syndrome* is one well-described anomaly [52] associated with dextroversion. It combines hypoplasia of the right lung, right pulmonary artery, and right bronchus; partial anomalous connection of the right pulmonary veins to the inferior vena cava; and anomalous arterial vessels arising from the descending aorta and directed to the right lung, often associated with bronchopulmonary sequestration (Figures 50.3 and 50.4).

Dextrocardia with D-ventricular loop and transposition of the great arteries {S,D,D}

Transposition of great arteries occurs frequently in dextrocardia (Figure 50.5). Complex forms of transposition of great arteries are more common in dextrocardia than in levocardia, with 75% having a ventricular septal defect and 75% left atrial appendage juxtaposition [47]. Dextrocardia is twice as common in transposition of great arteries with left atrial juxtaposition than in simple transposition of great arteries [53]. Dextrocardia in situs solitus reduces the size of the atrial free wall and may cause difficulties at surgery in creating an atrial baffle [54].

Dextrocardia with D-ventricular loop and L-malposition of the aorta {S,D,L}

Dextrocardia is frequent in this group of rare cardiac malformations that include double-outlet right ventricle with L-aorta and subaortic ventricular septal defect, anatomically corrected malposition of the great arteries, and double-outlet left ventricle.

705

(a)   (b)
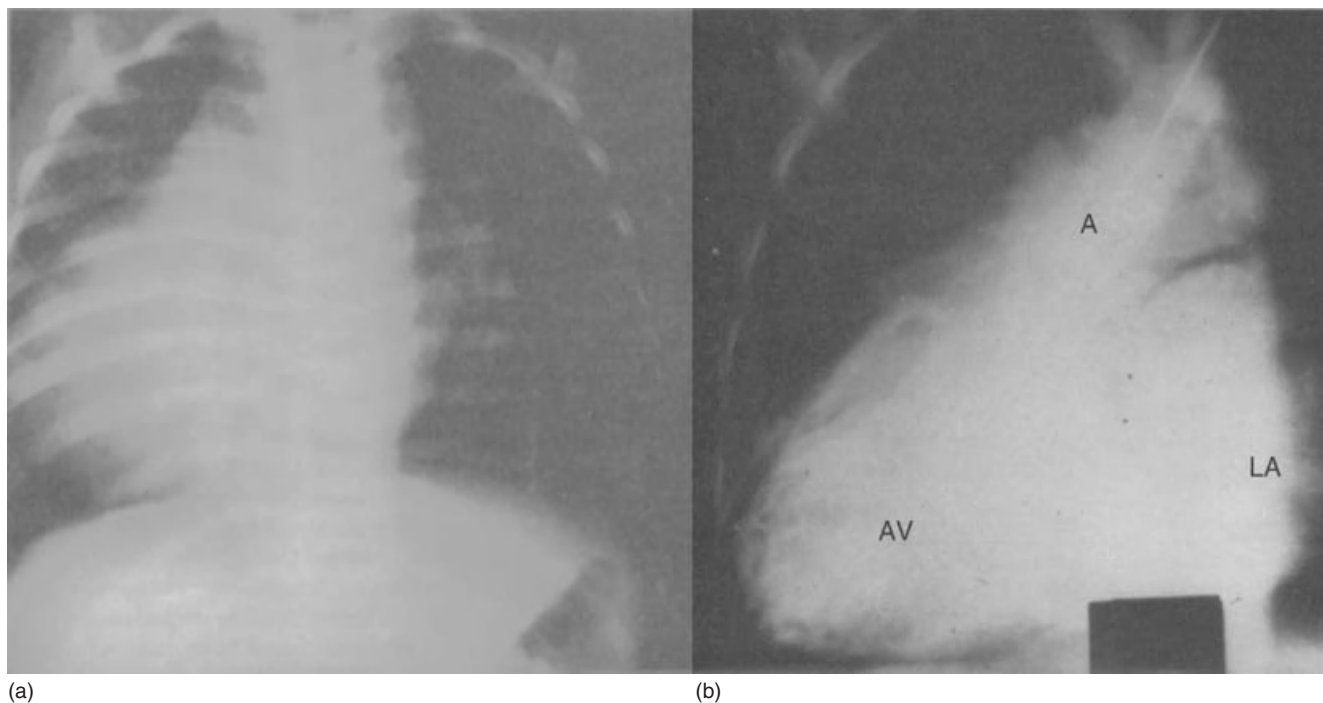
Figure 50.4 Dextroversion of situs solitus. (a) Heart in right hemithorax. (b) Injection in anterior ventricle (AV). Aorta (A) and left atrium (LA) are opacified. The descending aorta is on the left.
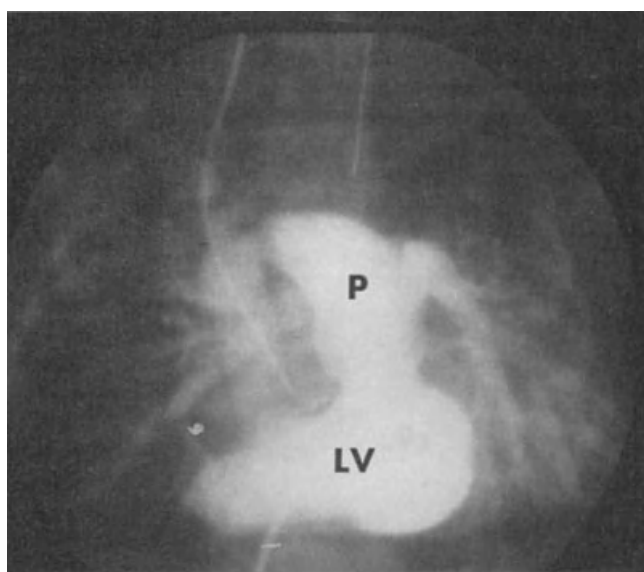
Figure 50.5 Left ventricular angiogram in a patient with dextrocardia and {S,D,D} and transposition of the great arteries. The pulmonary artery (P) originates from the left ventricle (LV).

A peculiar form of dextrocardia with {S,D,L} arrangement is represented by the crisscross heart [55]. In these patients, the right-sided right atrium is connected to the left-sided right ventricle, and the left-sided left atrium is connected to the right-sided left ventricle, so that the pathways of blood flowing through the atrioventricular valves cross each other. The great arteries are transposed, or both arise from the right ventricle with the aorta anterior and left-sided. In crisscross heart, the tricuspid valve and the right ventricle are always anterior and usually hypoplastic. The right ventricle frequently is superior so that crisscross heart and upstairs–downstairs ventricle (superoinferior ventricle) coexist [55] (Figure 50.6).

Dextrocardia with L-ventricular loop and transposition of the great arteries or double-outlet right ventricle {S,L,L}

This is characterized by discordant atrioventricular connection (L-ventricular loop) and discordant ventriculoarterial connection with anterior and left-sided aorta (L-aorta) (Figure 50.7). Thus, the anatomic features are those of congenitally corrected transposition. In double-outlet right ventricle with L-loop of the ventricles (atrioventricular discordance), both great arteries arise from the left-sided morphologic right ventricle. About 40% of patients with corrected transposition in situs solitus have dextrocardia [7,47]. Frequently, associated anomalies are found (Figure 50.8).

Corrected transposition of great arteries can be included in the group of cardiac defects due to anomalies of lateralization [18,56].

(a) (b)
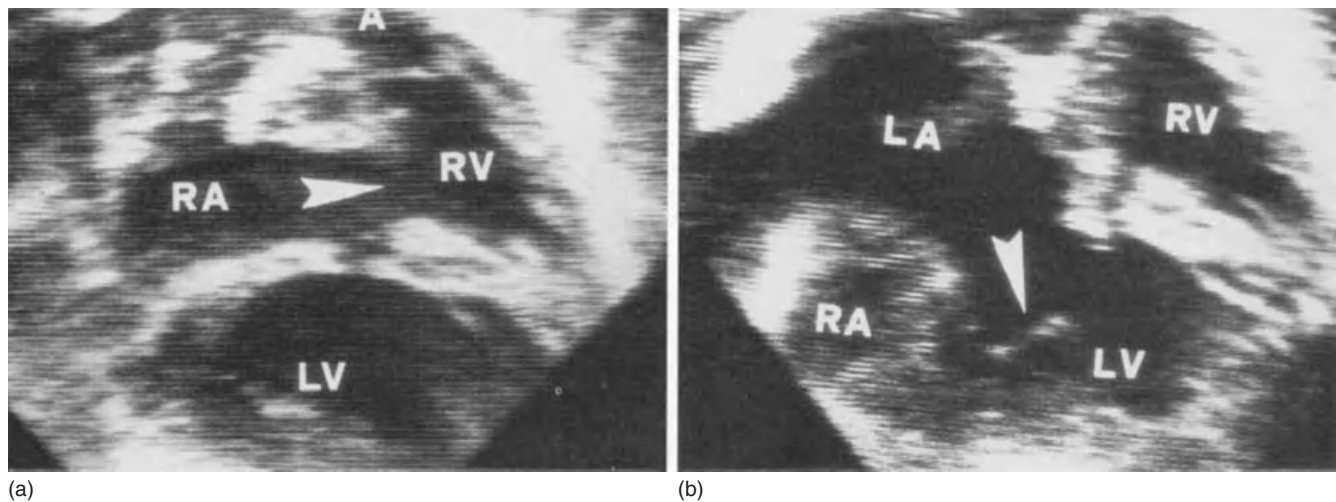
Figure 50.6 Two-dimensional echocardiography in an {S,D,L} crisscross heart. (a) The right atrium (RA) is connected (arrowhead) with the left-sided right ventricle (RV), which is anterosuperior and gives rise to the aorta (A). Note the horizontal position of the interventricular septum and the superoinferior position of the ventricles. The right ventricle is hypoplastic. (b) In a more posterior plane with respect to (a), the left atrium (LA) is connected (arrowhead) with the right-sided left ventricle (LV). Note the inferior position of the left ventricle compared with the right ventricle. (Reproduced with permission from Marino and Thieme, *Anatomia Ecocardiografia delle Cardiopatie Congenite*, USES Edizione Scientifiche, Florence, 1990, pp. 72–3.)

(a) (b)
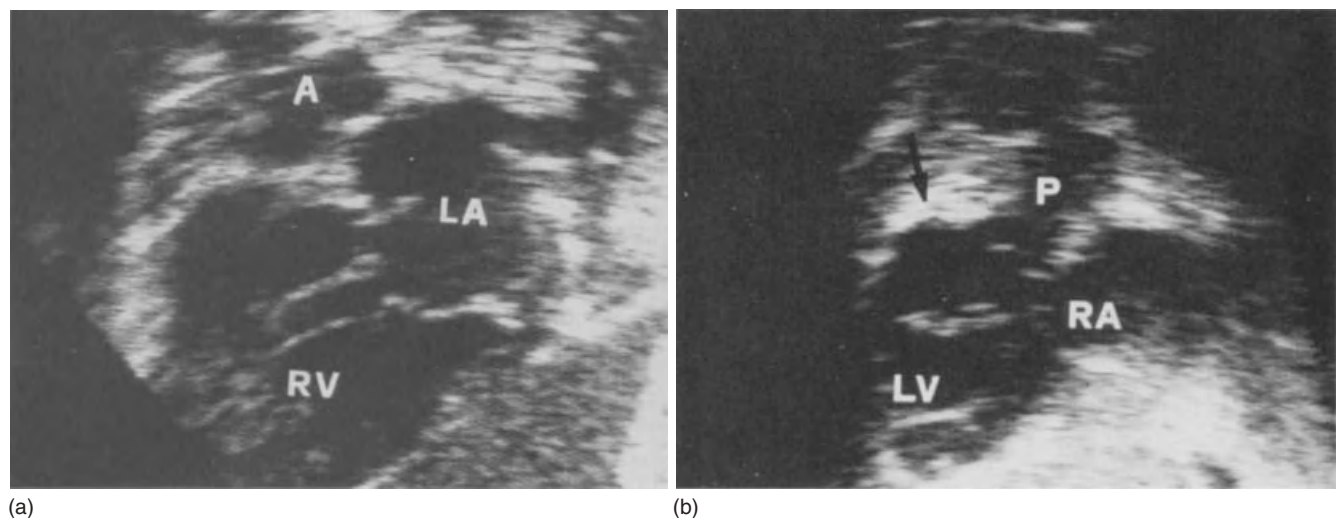
Figure 50.7 (a) Two-dimensional echocardiography in a patient with {S,L,L}, corrected transposition of great arteries, and dextrocardia. The left atrium (LA) is connected with the left-sided morphologic right ventricle (RV), which gives rise to the aorta (A) supported by a muscular infundibulum. (b) The right atrium (RA) is connected with the right-sided morphologic left ventricle (LV), which gives rise to the pulmonary artery (P). The arrow indicates the left ventricular outflow tract. (Reproduced with permission from Marino and Thieme, *Anatomia Ecocardiografia delle Cardiopatie Congenite*, USES Edizione Scientifiche, Florence, 1990, p. 60.)

Dextrocardia with L-ventricular loop and inverted related great arteries {S,L,I}

In hearts with situs solitus, atrioventricular discordance and ventriculoarterial concordance, and inverted related great arteries, dextrocardia is common [47]. This rare anomaly is associated with conotruncal anomalies, often tetralogy of Fallot. Atresia of the right superior vena cava with left superior vena cava connecting to the coronary sinus has been reported [57].

Cardiac malposition with situs inversus

Situs inversus with atrioventricular concordance (L-ventricular loop) shows dextrocardia as a frequent feature (Figure 50.9). An L-ventricular loop, "normal" in situs inversus, pivots the heart into the right hemithorax. In situs inversus and dextrocardia, there is alignment between the atrial and the ventricular septa, as in situs solitus and D-ventricular loop. Consequently, malposition of the heart in situs inversus should be defined as in patients with L-ventricular loop and levocardia.
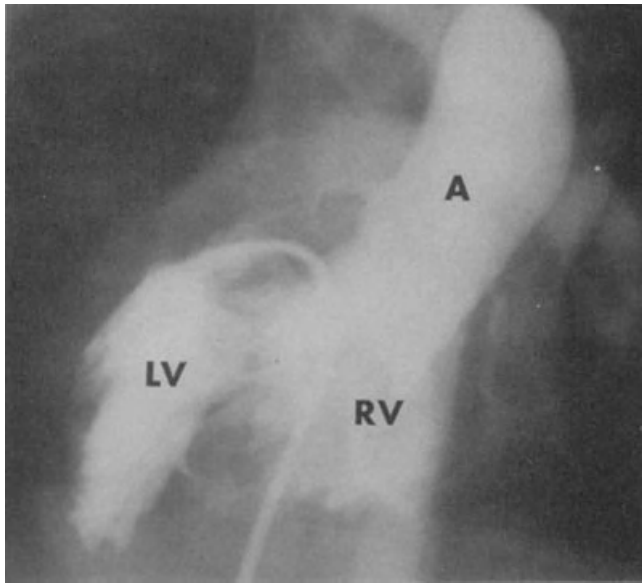
Figure 50.8 Left ventricular angiogram in a patient with {S,L,L} and double-outlet right ventricle (RV). The angiogram shows dextrocardia, situs solitus [the catheter is on the right side of the spine and the aorta (A) on the left], atrioventricular discordance [the morphologic left ventricle (LV) is on the right], and double outlet from the left-sided morphologic right ventricle.
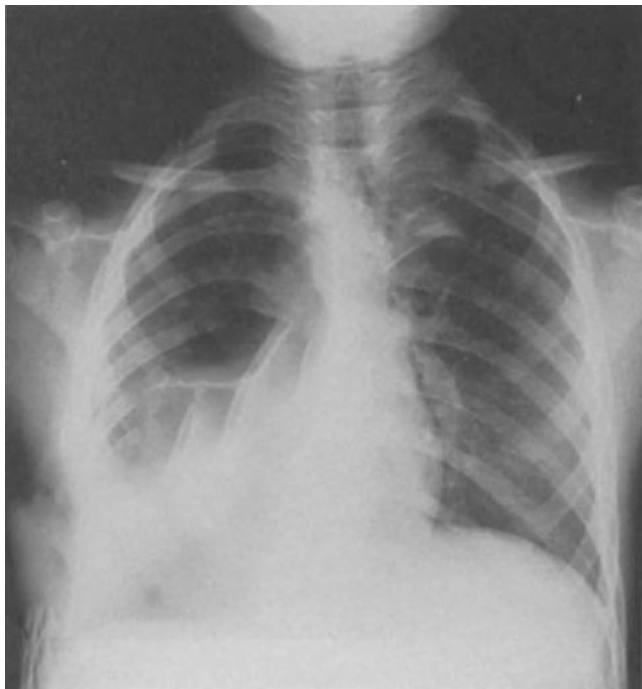
Figure 50.9 Posteroanterior chest radiograph in a patient with dextrocardia and atrial and visceral situs inversus. The liver shadow is in the left upper quadrant of the abdomen and the stomach bubble is on the right. The apex of the heart is pointed towards the patient's right.
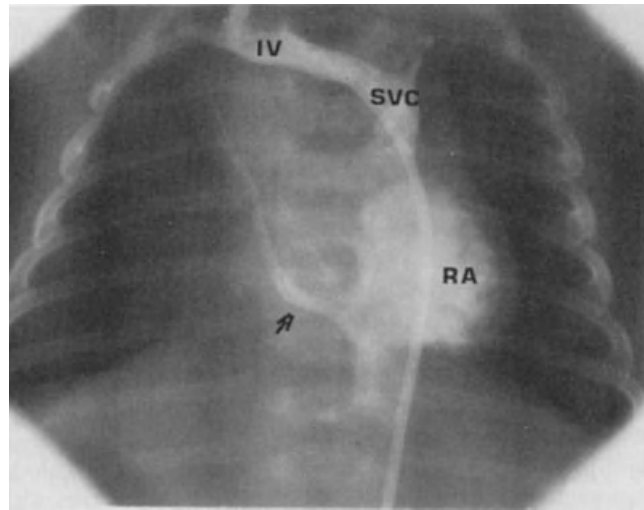
Figure 50.10 Angiogram in a patient with situs inversus and levocardia (so-called isolated levocardia). The angiogram demonstrates the innominate vein (IV) and the superior vena cava (SVC) (both on the left) connecting with the left-sided morphologic right atrium (RA). The coronary sinus (arrow) drains into the right atrium.

The expected position of a normal heart in situs inversus, that is, L-ventricular and inverted normal related great arteries (also called mirror-image dextrocardia), is in the right thorax. In contrast, situs inversus and levocardia (Figure 50.10), also called isolated levocardia, is almost always associated with cardiac defect. In publications on malposition of the heart in situs inversus, descriptions of the different positions of the heart in the thorax and the patterns of associated defects are usually included [45,46]. Therefore, we have included these conditions, for example, the normal dextrocardiac heart in situs inversus, although in fact they are not truly malpositions.

Dextrocardia

Dextrocardia with L-ventricular loop and inverted related great arteries {I,L,I}

This represents the normal heart in situs inversus. It is characterized by situs inversus (I), L-ventricular loop (L), and inverted, normally related great arteries (I). Because it might escape clinical detection when there are no associated malformations, its incidence is unknown. The commonly associated anomalies are ventricular septal defect, atrial septal defect, tetralogy of Fallot, double-outlet right ventricle, and pulmonary atresia with intact ventricular septum.

Kartagener syndrome

Kartagener first described a group of children and adults with situs inversus, chronic sinusitis, and airway disease [58]. This triad of symptoms with familial occurrence, known as Kartagener syndrome, appears to be due to ciliary dyskinesia and bronchiectasia [59,60]. Clinical studies indicate

that infertility was present in males as a result of sperm tail motility disorders [59]. Ciliary action is important in the embryogenesis, probably being one of the determinants of the situs [10,14]. Abnormal ciliary motility has been found in some patients with left isomerism [61].

Dextrocardia with L-ventricular loop and transposition of the great arteries {I,L,L}

In situs inversus, this is homologous with complete transposition of situs solitus {S,D,D}. Associated cardiac anomalies are frequent and include ventricular septal defect, hypoplastic left ventricle, and pulmonary stenosis with intact ventricular septum.

Dextrocardia with D-ventricular loop and transposition of the great arteries {I,D,D}

In situs inversus, this is homologous with corrected transposition in situs solitus {S,L,L} and occurs in 5–8% of patients with corrected transposition [62,63]. The segmental description of this anomaly is {I,D,D} and consists of situs inversus (I), atrioventricular discordance (ventricular D-loop), and ventriculoarterial discordance (D-transposition of the great arteries). The combination of atrioventricular and ventriculoarterial discordance allows a normal circulation. In 70% of patients, the heart is in the right thorax; in the remaining 30%, the heart is either mesocardia or levocardia. Associated anomalies are ventricular septal defect (60–100%) [62–66] and subvalvar and valvar pulmonary stenosis or pulmonary atresia (70–100%) [62–66]. Spontaneous or postoperative atrioventricular block appears less common than in patients with corrected transposition in situs solitus [65], perhaps from the more usual location of the conduction tissue [66].

Diagnostic features of malposition of the heart in situs solitus and inversus

On physical examination, the right and left hemithoraces should show symmetric excursion regardless of cardiac location. Reduced excursion of the right hemithorax may be evident in patients with dextroversion from right lung hypoplasia, as in scimitar syndrome, or in patients with diaphragmatic hernia; in these, on percussion, reduced movement of the right hemidiaphragm is noted.

The thoracic radiograph shows the position of the heart in the thorax and abdominal situs. The apex of the heart points downwards and to the left in the normal heart of levocardia, and downwards and to the right in dextrocardia (Figures 50.1, 50.2, and 50.9). In dextroversion, the heart is in the right hemithorax but the apex points towards the left, for example, left pneumothorax or diaphragmatic hernia. The situs can usually be determined by the position of the abdominal viscera. With few exceptions, the anatomic right atrium is almost always on the same side as the main liver

mass. An important radiologic guide to abdominal visceral situs is the gastric air bubble. The thoracic situs corresponds closely to atrial situs and may be determined by bronchial morphology, often evident on the standard or overpenetrated chest radiograph.

The electrocardiogram often allows determination of the situs and the position of the heart in the thorax. The P wave representing atrial activation is initiated from the SA node high in the right atrium. Hence, in situs solitus, the mean P wave vector in the frontal plane is ~+60, whereas in situs inversus it is +120, because the sinus node in the anatomic atrium is on the patient's left. The P wave on the horizontal plane proceeds posteroanteriorly in both types of situs but is towards the left (solitus) or right (inversus).

Using a segmental approach, echocardiography is the best tool for recognizing the cardiac situs and cardiac anatomy. The abdominal aorta and the inferior vena caval relationship, cardiac chamber morphology, their orientation in space, and their connections are easily recognizable by echocardiography, allowing a precise identification of the situs, atria, ventricular loop, and great artery relationship (see Chapter 8).

Magnetic resonance imaging (MRI) can improve the diagnostic accuracy for vascular and extracardiac structures in children and adolescents.

Cardiac catheterization and angiocardiography can be indicated in the preoperative physiologic assessment and in the evaluation of some anatomic details, such as the anatomy of the branch pulmonary arteries, the coronary artery circulation, or the venae cavae.

Surgical treatment of malposition of the heart in situs solitus and situs inversus

A variety of cardiac lesions can coexist in association with malpositioned hearts. The hearts can be divided into those amenable to univentricular palliation and those treatable with biventricular repair. Among the former are single ventricle or severely unbalanced ventricles, and apicocaval juxtaposition (dextrocardia with situs solitus or levocardia with situs inversus), which would be treated with a cava-to-pulmonary artery connection [67,68]. Among those suitable for biventricular repair are balanced biventricular hearts with atrioventricular and ventriculoarterial concordance or with either ventriculoarterial or double (atrioventricular and ventriculoarterial) discordance.

Coexisting atrioventricular and ventriculoarterial concordance is usually associated with a D-ventricular loop and associated anomalies that are amenable to total repair.

For anomalies of ventriculoarterial connection associated with ventricular septal defect and balanced ventricles with an intraventricular repair [69,70], a Rastelli-type [71] or a REV

procedure [72], or an arterial switch procedure (with the construction of a left ventricle-to-pulmonary orifice tunnel) [69,70], can be performed (see Chapters 42 and 44).

With combined atrioventricular and ventriculoarterial discordance and balanced ventricles, double-switch procedures can provide anatomic repair. Double discordance with left ventricular outflow tract obstruction (pulmonary or subpulmonary stenosis) can be treated by combined Senning/Mustard and Rastelli procedures [73,74], whereas patients with unrestricted pulmonary blood flow are best treated by combined atrial and arterial switch [75–77]. Double-switch procedures are usually feasible regardless of the cardiac malposition or atrial situs. Double-switch procedures in patients with situs inversus are more advantageous because of the D-loop arrangement of double discordance and have a lower incidence of atrioventricular conduction disturbances compared with an L-loop arrangement of this cardiac malformation in situs solitus [74].

Isolated ventriculoarterial or, sporadically, atrioventricular discordance can occur in malpositioned hearts. Arterial switch and atrial switch are the procedures of choice.

Biventricular repair has been suggested for crisscross heart [78], which is often associated with dextrocardia. A right ventricular volume >45% of normal and absence of straddling atrioventricular valves are the main requirements for a biventricular repair [79], although a one-and-a-half ventricular repair has been used in those with right ventricular hypoplasia [80].

Cardiac malposition with situs ambiguus

Heterotaxy remains an intriguing condition. The prevalence of these syndromes associated with heterotaxia is estimated to be 1–1.5 in 10 000 live births and accounts for ~3% of cardiac malformations [81–83] and for 30% of patients dying with cardiac malposition [84]. Asplenia/right isomerism is more common in males, whereas polysplenia/left isomerism has an equal gender preponderance [30]. These syndromes are usually sporadic, although several familial occurrences [10–14], in particular in children born of consanguineous parents, have been described [81–85]. Occasionally in the same family heterogeneous laterality defects including situs inversus, asplenia, and polysplenia are found [10–14,85].

Cardiac morphology

Extracardiac and cardiac anomalies are common to both asplenia/right isomerism and polysplenia/left isomerism syndromes, but there are also specific differences between them in the prevalence, anatomic types, and severity of cardiac malformations [86]:

1 The *abdominal organs* are abnormal in shape and position. The liver tends to be symmetric and to occupy a transverse position across the upper abdomen with both lobes showing a "right-like" shape [86,87]. The gallbladder may be absent or hypoplastic. Malrotation of the bowel and of the midgut loop is present [33] and may cause intestinal obstruction [30]. Adrenal and genitourinary tract anomalies have been described [32]. Extrahepatic biliary atresia leading to obstructive jaundice [88] has been found in polysplenia/left isomerism. The spleen is absent in asplenia/right isomerism and multiple in polysplenia/left isomerism, but its characteristics may be discordant with the type of isomerism of the atrial appendages [33,34]. Among extracardiac anomalies, midline defects are particularly frequent (about 40%) [89], and primary ciliary dyskinesia may be present [60].

2 The *thoracic organs* tend to be symmetric [30–33]. In patients with asplenia/right isomerism, the lungs are trilobed and have bilateral eparterial bronchi with the pulmonary artery coursing anterior to the main stem bronchus [32]. In patients with polysplenia/left isomerism, there are bilateral bilobed lungs and hyparterial bronchi; the pulmonary artery courses over and behind the main stem bronchus [30]. Pulmonary arteriovenous fistulas occur in patients with polysplenia/left isomerism [90]. In ~40% of children with asplenia/right isomerism and with polysplenia/left isomerism, cardiac malposition including mesocardia and dextrocardia is present.

3 *Systemic venous connections* are frequently anomalous [30,32,91,92]. In more than half of patients with heterotaxy, bilateral superior venae cavae connect to the respective atria and the innominate vein is absent. If a single superior vena cava is present, it is usually opposite to the cardiac apex. In most patients, the coronary sinus is absent. In patients with asplenia/right isomerism, the inferior vena cava and the abdominal aorta are ipsilateral and lie together on the right or left side of the spine (Figure 50.11). The inferior vena cava connects with the right or left side of the atria. In a few of these patients, the hepatic veins connect separately from the inferior vena cava (Figure 50.12). Interrupted inferior vena cava is extremely rare in patients with asplenia/right isomerism [38,93], but is present in >70% of patients with polysplenia/left isomerism. It connects into the azygos vein and terminates in either the left or right superior vena cava. The hepatic veins connect directly to the left or right side of the floor of the atria. Uncommonly, a small inferior vena cava persists on one side of the abdomen connecting to the atria, and an enlarged azygos vein connects to the superior vena cava on the opposite side. In other patients, the inferior vena cava ascends on one side of the abdomen and crosses to the opposite side at the level of the diaphragm to enter the azygos vein.

4 *Pulmonary venous connections* are often anomalous [29–32,38,40,91–94]. Over 80% of patients with asplenia/right isomerism have total anomalous pulmonary venous
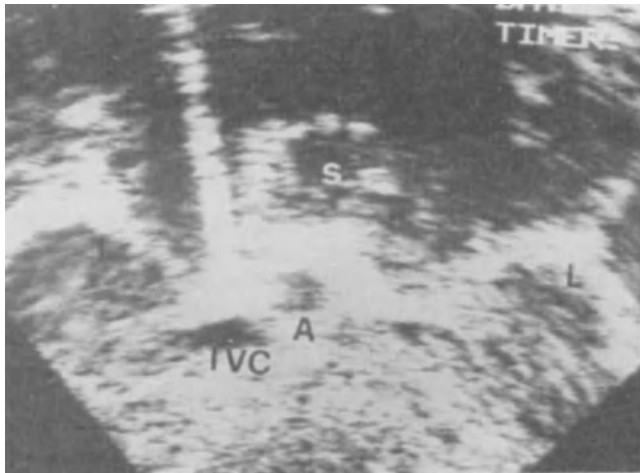
Figure 50.11 Two-dimensional echocardiography in abdominal short-axis view in a patient with asplenia/right isomerism. Note the ipsilateral position of the aorta (A) and the inferior vena cava (IVC) lying together on the right side of the spine (S). The liver (L) presents a symmetric transverse position. (Reproduced with permission from Marino and Thieme, *Anatomia Ecocardiografia delle Cardiopatie Congenite*, USES Edizione Scientifiche, Florence, 1990, p. 47.)
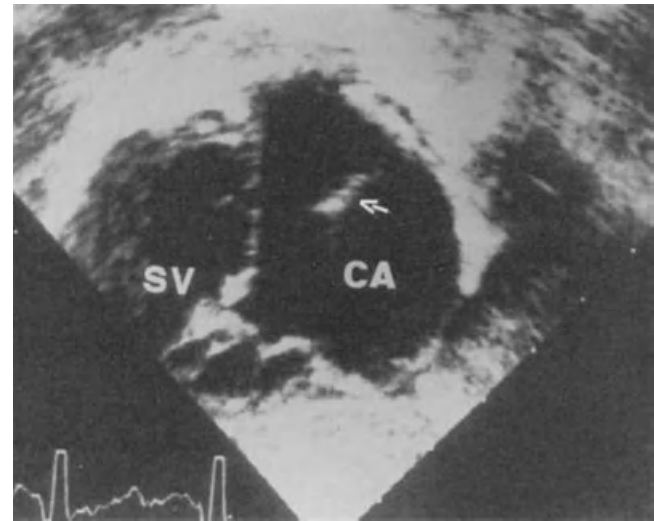
Figure 50.13 Two-dimensional echocardigraphy in subcostal view in a patient with asplenia/right isomerism and dextrocardia. In the common atrium (CA), a narrow band (arrow) crosses the midportion of the atria. SV, single ventricle. (Reproduced with permission from Marino and Thieme, *Anatomia Ecocardiografia delle Cardiopatie Congenite*, USES Edizione Scientifiche, Florence, 1990, p. 49.)
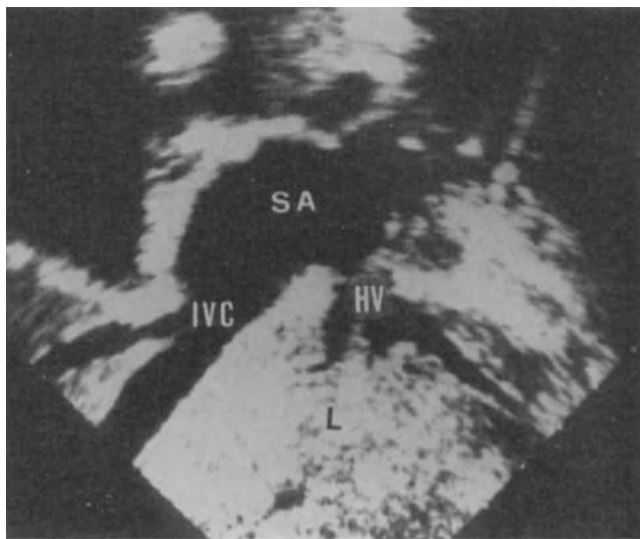
Figure 50.12 Two-dimensional echocardigraphy in subcostal view in a patient with asplenia/right isomerism shows the hepatic veins (HV) connected with the single atrium (SA) separately from the inferior vena cava (IVC). L, liver. (Reproduced with permission from Marino and Thieme, *Anatomia Ecocardiografia delle Cardiopatie Congenite*, USES Edizione Scientifiche, Florence, 1990, p. 48.)

connection (TAPVC) and in nearly half of these it is obstructed. TAPVC may be to either a supracardiac or an infradiaphragmatic location [38–40]. Significant hypoplasia of the pulmonary veins may coexist [95]. In polysplenia/left isomerism, the pulmonary veins connect to the atria, and TAPVC is rare. In 40% of these patients, the pulmonary

veins from each lung enter the posterior wall of the atria separately on opposite sides of midline, simulating a partial anomalous pulmonary venous connection [94].

5 *Anomalies at atrial level* and of the atrioventricular valves are frequent [29–32,38,40,91–94,96]. A common atrium with virtually absent atrial septum and bilateral sinus nodes are present in asplenia/right isomerism. The coronary sinus is usually absent. A narrow band, a remnant of the atrial septum, passes in an anteroposterior direction and crosses the midportion of the atria (Figure 50.13). Each atrial appendage shows a broad-based pyramidal morphology with pectinate muscles extending bilaterally round the atrioventricular junctions (right isomerism). In asplenia/right isomerism, the complete form of atrioventricular canal is the rule, with a common atrioventricular valve and left ventricular dominance. The morphology of the common atrioventricular valve differs from complete atrioventricular canal with situs solitus in showing a rudimentary common atrioventricular valve and reduced number of leaflets and papillary muscles which are short and hypoplastic [97]. Moreover, the inlet ventricular septum frequently shows severe hypoplasia, the ventricular septal defect is very large, and the atrioventricular canal is type C of Rastelli's classification [97]. Common atrium is also present in polysplenia/left isomerism (Figure 50.14), but the more frequent pattern is a large ostium primum atrial septal defect, a partial atrioventricular canal, and a cleft mitral valve. The septum primum is frequently displaced either leftwards or rightwards, depending on whether there is levocardia or dextrocardia, respectively. This displacement is responsible for the apparent partial anomalous
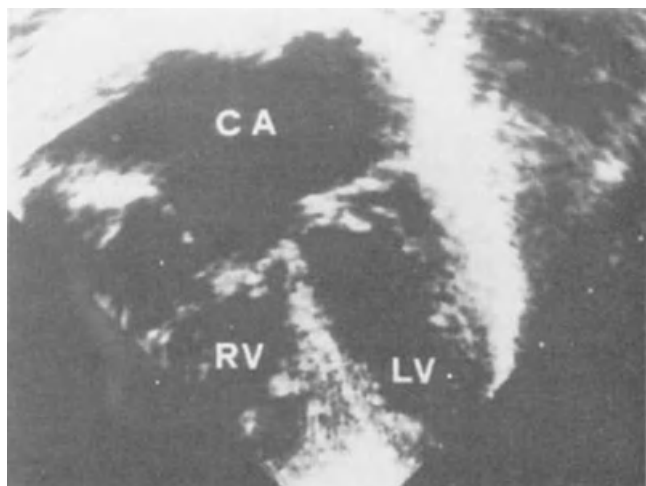
Figure 50.14 Two-dimensional echocardigraphy in subcostal four-chamber view in a patient with polysplenia/left isomerism shows common atrium (CA) with biventricular heart, D-loop of the ventricles, and intact ventricular separation. LV, left ventricle; RV, right ventricle. (Reproduced with permission from Marino and Thieme, *Anatomia Ecocardiografia delle Cardiopatie Congenite*, USES Edizione Scientifiche, Florence, 1990, p. 69.)

pulmonary venous connection [30,94]. Each atrial appendage is long and narrow, showing the features of a left appendage (left isomerism). This atrial anatomy is similar to that observed in patients with Ellis–van Creveld syndrome [98] and with other postaxial polydactyly syndromes [99].

6 *Anomalies at ventricular level* are also frequent [29–32, 38,40,91–94,100,101]. An L-loop of the ventricles occurs in ~40% of patients with both syndromes. A single ventricle of right ventricular type from malalignment of the atrioventricular canal with a hypoplastic left ventricle is the more frequent pattern, but single left ventricle and biventricular heart are also found. Ventricular septal defect in the setting of complete atrioventricular canal is constant in these children. In contrast, in polysplenia/left isomerism, a single ventricle is less frequent and the biventricular heart (with D- or L-loop ventricle) is common with intact ventricular septum in 20–30%.

7 *Conotruncal defects* and anomalies of the great arteries are usual [29–32,38,40,91–94,100–104]. The classic conotruncal pattern in asplenia/right isomerism occurring in most patients is double-outlet right ventricle with an anterior aorta associated with pulmonary stenosis or atresia, and hypoplasia of the infundibular septum. Transposition of great arteries is also present. Usually there is a bilateral muscular subarterial conus. With pulmonary atresia, the pulmonary arteries are usually confluent with ductus-dependent pulmonary circulation. In those with nonconfluent pulmonary arteries and bilateral ductus arteriosus (Figure 50.15), major aortopulmonary collateral arteries may be present [105]. A correlation between atresia of the

Figure 50.15 Angiocardiography with injection into the aorta in a patient with asplenia/right isomerism and pulmonary atresia. Bilateral ductus arteriosus supplies the right and left pulmonary arteries.

pulmonary valve and obstruction of the pulmonary venous connection [38,93,100,104] may explain the small size of the pulmonary veins [95]. Ventriculoarterial concordance with normally related great arteries is extremely rare [96]. Right-sided aortic arch with mirror-image branching of the brachiocephalic trunk may be present. In contrast, over 70% of children with polysplenia/left isomerism have concordant ventriculoarterial connection [92,101,106]. The great arteries are normally related in patients with D-loop ventricles, or inversely normally related (mirror image) with L-loop ventricles [101,106]. Double-outlet ventricle may be present with infundibular morphology of tetralogy of Fallot, whereas transposition of great arteries is rare. Obstruction of the pulmonary blood flow is present in ~30%, one-third with pulmonary atresia. Left-sided obstructions including mitral stenosis, hypoplastic left ventricle, aortic stenosis, and aortic coarctation are present in 25% of patients.

In summary, in patients with *asplenia/right isomerism*, the cardiac malformations are complex. The classic anatomy includes transverse liver; bilateral trilobed lungs and eparterial bronchi; levocardia, mesocardia or dextrocardia, bilateral superior venae cavae with absent coronary sinus, inferior vena cava coursing with the abdominal aorta on the same side of the spine connecting to the atria, extracardiac TAPVC (frequently obstructed), common atrium, right bilateral morphology of the atrial appendages, complete atrioventricular canal malaligned to a dominant right ventricle, D- or L-loop ventricle, transposition or double-outlet right ventricle with anterior aorta, and pulmonary stenosis or atresia (Figure 50.16).

In patients with *polysplenia/left isomerism*, the pattern of cardiac anomalies is less rudimentary, and they are less complex. The usual morphology includes transverse liver;
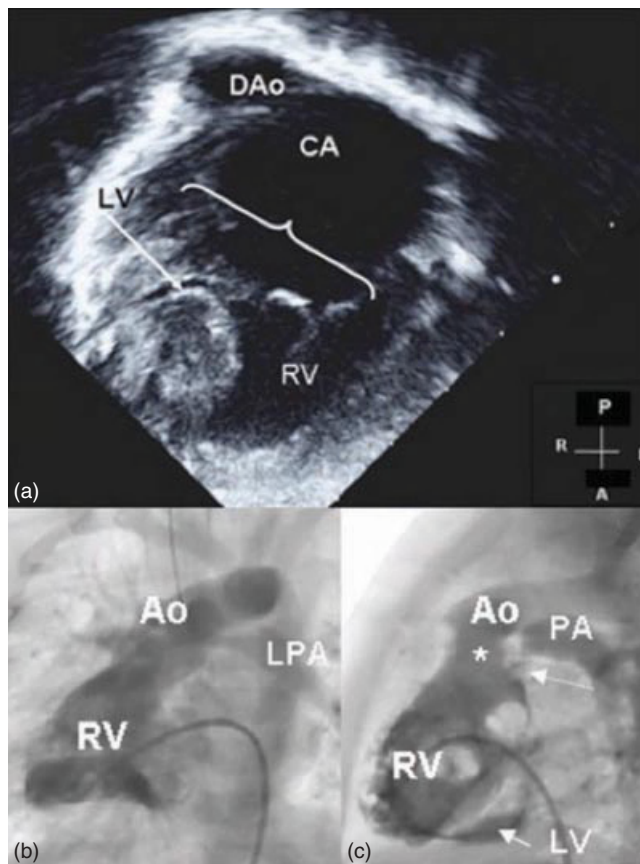
Figure 50.16 (a) Two-dimensional echocardiography in a patient with heterotaxy with asplenia/right isomerism. Complete atrioventricular canal with common atrium, dominant right ventricle and hypoplastic left ventricle. DAo, descending aorta; CA, common atrium; LV, left ventricle; RV, right ventricle. (b) Angiography, anteroposterior view. Note the dominant right ventricle and both great arteries arising from a single infundibulum connected with the right ventricle. RV, right ventricle; Ao, aorta; LPA, left pulmonary artery. (c) Angiography, lateral view. Note the dominant right ventricle, the hypoplastic left ventricle and both great arteries arising from a single infundibulum (*) connected with the right ventricle. The aorta is anterior and the stenotic pulmonary artery (arrow) is posterior. Ao, aorta; LV, left ventricle; PA, pulmonary artery; RV, right ventricle.

Figure 50.17 Magnetic resonance imaging (MRI) of systemic vein anomalies. (a) Multiplanar reconstruction (MPR) of angio-MRI. (b) Volume rendering (VR) of angio-MRI. Heterotaxy, azygos continuation of the inferior vena cava; RPA, right pulmonary artery.

bilateral bilobed lungs and hyparterial bronchi, levocardia, mesocardia, or dextrocardia, bilateral superior venae cavae, interruption of inferior vena cava with azygos continuation (Figure 50.17), pulmonary veins draining into the right and left posterior sides of the atria, common atrium or large ostium primum atrial septal defect, left bilateral morphology of the atrial appendages, partial atrioventricular canal, D- or L-loop ventricles with balanced or unbalanced ventricular masses, concordant ventriculoarterial connection, ventricular septal defect (frequent), pulmonary stenosis (possible), and systemic outflow tract obstruction (possible). Some crossover exists, however, with individuals presenting anatomic patterns of asplenia/right isomerism in the presence of polysplenia/left isomerism, and vice versa. Moreover, the heart may be completely normal in patients with polysplenia/left isomerism. An interesting subgroup of patients shows a hypoplastic or rudimentary spleen with many of the features of asplenia/right isomerism but sometimes presenting systemic obstruction [42].

Clinical features and diagnostic approach

Asplenia/right isomerism
The most frequent presentation is of a male neonate with intense cyanosis, respiratory distress, and systolic murmur or no murmur. A right-sided apical impulse, the heart sounds and murmur heard better over the right hemithorax, and the transverse lower hepatic margin are characteristic.

The electrocardiogram is generally abnormal. The P wave axis is directed inferiorly and to the right (90–105°) in patients with levocardia and to the left (75–90°) in those
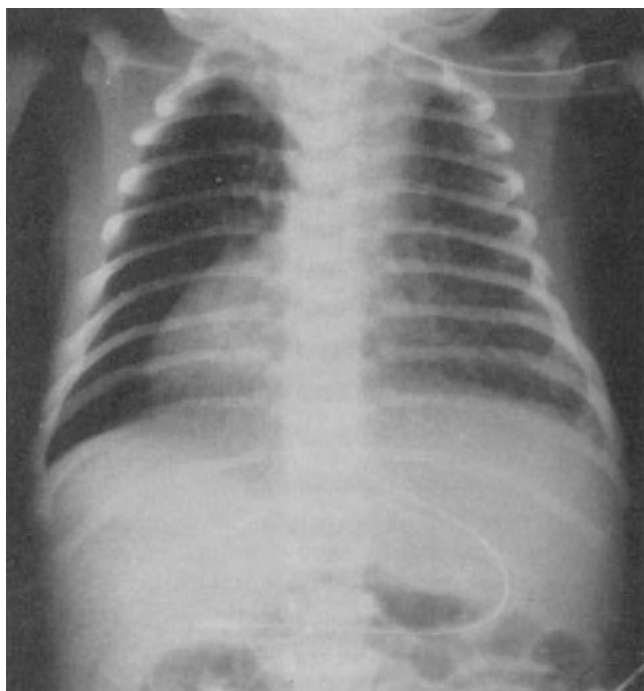
Figure 50.18 Chest radiograph in a patient with asplenia/right isomerism shows symmetric liver, dextrocardia, and reduced pulmonary blood flow.

Figure 50.19 Chest radiograph in a patient with asplenia/right isomerism shows symmetric liver and mesocardia.

with dextrocardia [107]. The frontal plane QRS axis is usually directed superiorly because of atrioventricular canal.

Clues to the diagnosis of asplenia/right isomerism are often present on the thoracic radiograph, which shows cardiac malposition frequently with mesocardia or dextrocardia and with the cardiac apex discordant with the position of the liver and the stomach. The lower hepatic margin lies horizontally across the upper abdomen. Cardiac size is normal. Pulmonary vascular markings are diminished from pulmonary stenosis or atresia (Figure 50.18) or show pulmonary edema from TAPVC obstruction (Figure 50.19). With tomography or high-kilovoltage radiographs, the bilateral eparterial bronchi may be visualized [108,109].

The diagnosis of asplenia syndrome and of the associated cardiac malformation can be established by two-dimensional echocardiography with color Doppler using the segmental approach [110–114]. With a short-axis subcostal view, the abdominal aorta and the inferior vena cava can be visualized on the same side of the spine (Figure 50.12); with a long-axis abdominal view with color Doppler, the infracardiac TAPVC can be imaged [115]. Furthermore, two-dimensional echocardiography cannot detect a spleen [116]. Isomerism of the atrial appendages is difficult to diagnose by echocardiography. Common atrium, complete atrioventricular canal [113], and single ventricle [112] are well imaged with echocardiography (Figure 50.13), and other details of intracardiac anatomy, including the conotruncal morphology, can be defined. Cardiac malposition (dextrocardia or mesocardia)

or horizontal liver on the chest radiograph (heterotaxy) and the echocardiographic recognition of common atrium, complete atrioventricular canal, single ventricle with anterior aorta, and pulmonary stenosis or atresia are the most precise diagnostic signs of asplenia/right isomerism.

Cine magnetic resonance imaging has improved morphologic diagnosis [117–119]. Because of anatomic complexity and the need for hemodynamic data, particularly of pulmonary vascular resistance, preoperative evaluation by cardiac catheterization and angiocardiography is still indicated in many children [93]. Angiocardiography is particularly useful to delineate the anatomy of pulmonary arteries and the pulmonary blood supply in patients with pulmonary atresia [102,104,120]. Moreover, angiocardiography reveals the site of pulmonary venous connection and the presence of pulmonary venous obstruction, although it might be masked by the pulmonary stenosis or atresia (Figure 50.20). Furthermore, angiocardiography in association with color Doppler echocardiography can quantify the degree of atrioventricular valve regurgitation that in neonates, but in particular in older children, can deeply influence the natural history [121–123].

Polysplenia/left isomerism

The clinical manifestations vary and usually appear later compared with asplenia/right isomerism because the pulmonary obstruction is less severe and the pulmonary veins are
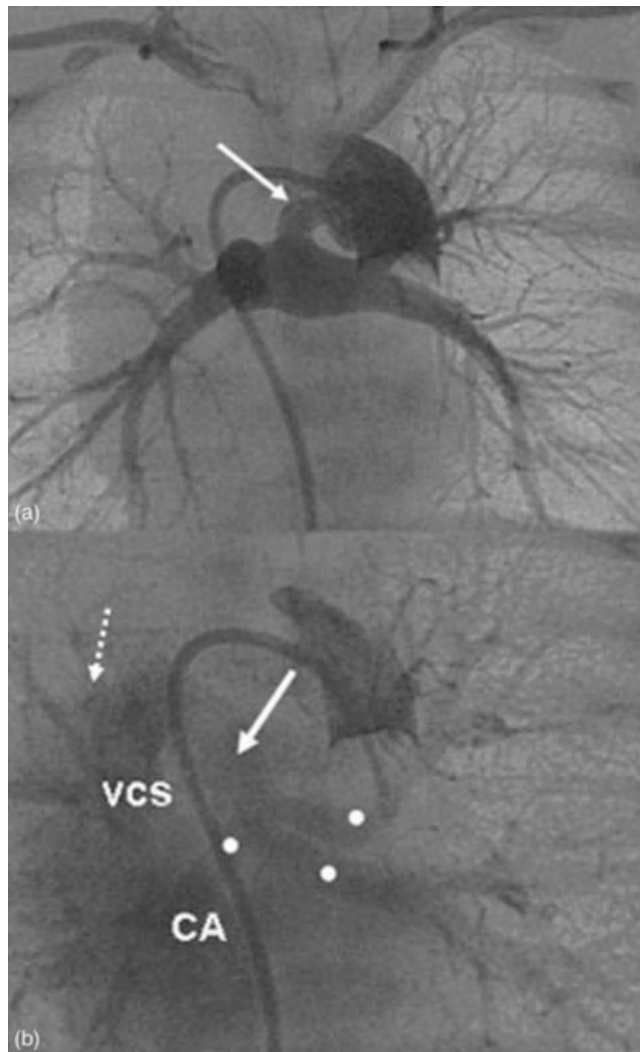
Figure 50.20 Heterotaxy syndrome, right isomerism, pulmonary atresia, ductus arteriosus, confluent pulmonary arteries and mixed pulmonary vein connection. Aortography in the frontal plane. (a) Right aortic arch. Opacification of the ductus arteriosus (white arrow) and of the right and pulmonary arteries. (b) Left pulmonary veins (white circles), right inferior pulmonary vein (solid white arrow) drain in a collector to the superior vena cava (VCS). Right superior pulmonary vein (dashed white arrow) drains separately in the superior vena cava.

Thoracic radiographs may suggest this syndrome, showing dextrocardia or mesocardia with discordance between the position of the heart and the liver and the stomach. Moreover, the absence of an inferior vena caval shadow on the lateral view and an enlarged azygos vein suggests polysplenia/left isomerism [127]. A high-kilovoltage chest radiograph may show a symmetric bronchial branching pattern characteristic of left pulmonary isomerism [108,109].

Echocardiography is the best tool for the noninvasive diagnosis of intracardiac malformations. Interruption of the inferior vena cava with azygos continuation and the pattern of pulmonary venous connection can be identified [110,111], as can malformations of atria, ventricles, and great arteries [101].

A cardiac malposition (dextrocardia or mesocardia) or horizontal liver on the chest radiograph and the echocardiographic recognition of azygos continuation, partial atrioventricular canal, biventricular heart or single ventricle, and normally aligned great arteries (concordant ventriculoarterial connections) are the best diagnostic signs of polysplenia/left isomerism.

Fetal echocardiography can reliably detect heterotaxy [128,129], but prenatal diagnosis seems not to improve neonatal survival [130]. During prenatal life, polysplenia/left isomerism is diagnosed more frequently but also spontaneous abortion occurs more frequently in fetuses with asplenia/right isomerism, probably due to the fetal heart block [129]. The spectrum of fetal cardiac defects in polysplenia/left isomerism seems more complex than found postnatally [131]. Moreover, echocardiography can identify the presence of multiple spleens [116].

Cardiac catheterization and angiocardiography are often required for definitive preoperative anatomic and functional assessment. Interruption of the inferior vena cava often requires a percutaneous approach from the neck to reach the heart directly and avoid the catheter loop in the azygos vein and superior vena cava [132]. A lateral view of a pulmonary arteriogram can demonstrate the superimposed branches of the pulmonary arteries arching posteriorly from the pulmonary trunk, because each has the characteristics of a left pulmonary artery [133].

Natural history

Asplenia/right isomerism

The natural history of asplenia/right isomerism is extremely poor [86], and death occurs in more than one-third of untreated neonates in the first week of life [134]. In a study among 191 patients, the mean age of death was 2.6 months [135]. Hypoxemia from cardiovascular abnormalities is the prominent cause of death, followed by sepsis secondary to the increased susceptibility to infections when spleen is absent [32,136–138].

not obstructed. Cyanosis is present only in children with pulmonic stenosis or atresia. Patients may be asymptomatic or show features of congestive heart failure.

The electrocardiogram shows distinctive features. Because the sinus node is a right atrial structure it may be absent, displaced, or hypoplastic [120]. A leftward and superiorly directed P wave axis and ectopic atrial rhythm are frequently present [107]. Even the QRS axis is superiorly directed because of the atrioventricular canal. Congenital complete atrioventricular block is occasionally present and may progress even in fetal life [124–126].

Polysplenia/left isomerism

The natural history of polysplenia/left isomerism is better than with asplenia/right isomerism [139–141]. Associated cardiac abnormalities are the main cause of death, followed by rhythm disturbances [92,125] and extrahepatic biliary atresia [140,141].

Medical management

Asplenia/right isomerism

Neonates usually develop severe cyanosis with hypoxemia and metabolic acidosis during the first hours of life from either pulmonary stenosis or atresia and/or obstructed TAPVC. Prostaglandin therapy may improve the oxygen saturation provided that the pulmonary venous system is unobstructed. Otherwise, prostaglandin therapy can unmask or increase the degree of pulmonary venous obstruction by increasing the total pulmonary blood flow [121,142,143]. Patients with infracardiac TAPVC should be operated on without delay. In the other neonates, the degree of pulmonary venous obstruction should be carefully evaluated under prostaglandin infusion [143] to provide the best indication for operation.

Because of the susceptibility to infection [136–138], aggressive perioperative antibiotic prophylaxis is important. Antibiotic prophylaxis against encapsulated bacteria with penicillin or amoxicillin is indicated daily. Immunization against pneumococcus is indicated at age 2 years.

Polysplenia/left isomerism

Few patients with polysplenia/left isomerism develop severe neonatal cyanosis because they do not usually have the obstructive lesions so typical of asplenia/right isomerism. If they do, prostaglandin therapy is required. If neonates become symptomatic soon after birth, it is from congestive heart failure and metabolic acidosis secondary to a combination of pulmonary overcirculation and systemic obstruction from severe aortic stenosis, coarctation, or hypoplastic left heart syndrome. Such patients should be managed appropriately [144,145]. Rarely, complete atrioventricular block is the main cause of neonatal symptoms [125]. Most patients become symptomatic some months after birth. Clinical manifestations differ according to the underlying lesions. Cyanosis is usually related to pulmonary outflow tract obstruction, even though it is occasionally associated with pulmonary arteriovenous fistulas [90]. On the other hand, heart failure is usually related to complete atrioventricular canal or isolated ventricular septal defect. Patients with common atrium or partial atrioventricular canal usually become symptomatic later in life, often in association with cardiac rhythm disturbances [146,147]. Biliary atresia can complicate the clinical status [88,140,141].

Surgical treatment of malposition of the heart in situs ambiguus

Single-ventricle repair

Asplenia/right isomerism

Almost all patients are unsuitable for biventricular repair. Such treatment, however, is often affected by pulmonary venous abnormalities, pulmonary outflow obstruction, and/or atrioventricular valve abnormalities [148].

TAPVC can be present in 90% of patients, with 30% having obstructed pulmonary veins. Both early and late mortality for the initial palliative procedure are high, especially in younger age and when TAPVC requires repair [121,122,149–151]. For this reason, in patients with confluent pulmonary arteries, without juxtaductal pulmonary stenosis, and unobstructed TAPVC, a simple initial palliation with a prosthetic shunt is preferred. This postpones pulmonary vein repair until after the first month of life and achieves a better chance of survival [134]. In all other neonates, a more extensive palliation with cardiopulmonary bypass must be performed, especially if pulmonary veins are obstructed. A systemic–pulmonary shunt should be performed in most neonates with patent, although stenotic, pulmonary inflow, to ensure an adequate pulmonary blood supply [149]. Pulmonary vein obstruction and pulmonary outflow obstruction are independent risk factors for earlier mortality. Recurrent pulmonary venous obstruction is common after TAPVC repair in patients with asplenia/right isomerism, and has been associated with the histologic evidence of abnormal development of the pulmonary vasculature, particularly in the veins, even without clinical evidence of pulmonary venous obstruction [150]. Primary sutureless repair of the pulmonary veins has a low incidence of postoperative pulmonary venous obstruction [152].

A major atrioventricular valve anomaly is present in >90% of patients and an independent risk factor for mortality. Common atrioventricular valve regurgitation occurs more frequently in heterotaxy than in other patients and may be amplified by a systemic-pulmonary shunt, especially in right univentricular hearts. Atrioventricular valve regurgitation requires thorough evaluation and aggressive surgical treatment, to be carried out preferably during staging towards Fontan operation [153].

More than 50% of patients with asplenia/right isomerism and single-ventricle physiology die before reaching the stage of Fontan operation. Both morbidity [154–156] and mortality (15–30% depending on the series) at Fontan are higher than those reported for nonisomeric patients [157–159], although dramatically lower than the preliminary experience of most groups. Preliminary reports described also an increased mortality after the Fontan operation in patients with asplenia/right isomerism, compared with patients with polysplenia/left isomerism, mainly due to a prevalence of

right ventricular morphology in asplenia/right isomerism, and the association with anomalous pulmonary venous connections. Such a difference is no longer described [159], and excellent long-term survival has been reported in patients with asplenia/right isomerism provided that anomalous and/or obstructive pulmonary venous return and atrioventricular valve regurgitation are treated aggressively, the Fontan repair is staged, a fenestration is used liberally, and the technique is carefully chosen to minimize the risk of pulmonary venous obstruction [159].

Fontan staging with a bidirectional cavopulmonary anastomosis has been proposed to reduce the risk of the Fontan operation [160]. A bidirectional cavopulmonary anastomosis can be constructed in patients with anomalous pulmonary venous connection with morbidity and mortality that are not different from those in patients with normal pulmonary venous connections [161]. Furthermore, early reduction of the ventricular volume load may be especially beneficial in patients with a common atrioventricular valve to prevent development of incompetence, which occurs more easily when the ventricular end-diastolic pressure is elevated and the atrioventricular valve annulus is dilated [162]. On the other hand, there is some controversy concerning the benefit of a bidirectional cavopulmonary anastomosis alone on an already regurgitant common atrioventricular valve, whose moderate to severe occurrence has been reported as a risk factor for mortality early postoperatively [163].

Modifications of surgical technique have played a crucial role in the improvement of results of surgery in patients with asplenia/right isomerism. A part from the extensive use of extracardiac tube grafts and conduit fenestration for safe direction of inferior vena cava and hepatic venous drainage to the pulmonary arteries [164,165], specific technical modifications have been described for separate drainage of hepatic veins [166], sometimes associated with apicocaval juxtaposition [67,68,167,168]. Such anatomic peculiarities need to be specifically addressed from a surgical point of view, taking into account the distance between inferior vena cava and hepatic veins and their reciprocal relationship with the spine, in order to construct an unobstructed pathway for blood diversion to the pulmonary arterial tree. Evolution of surgical techniques and careful attention to the specific anatomic patterns of the disease may play a crucial role in the improvement of survival of patients with asplenia/right isomerism [169].

Polysplenia/left isomerism

About 50–70% of patients with polysplenia/left isomerism have a cardiac anatomy that is unsuitable for biventricular repair and are consequently candidates for single-ventricle repair [141,170–172]. Initial palliation usually includes a systemic–pulmonary shunt (pulmonary obstruction), a Norwood-type procedure (hypoplastic left heart complex), or a pulmonary artery banding (unobstructed pulmonary

outflow). Pulmonary artery banding may be required at the time of coarctation repair, but may be needed also in patients without aortic outflow obstruction.

Single-ventricle physiology is an independent risk factor for increased mortality among patients with polysplenia/left isomerism. Additional extracardiac and cardiac factors independently affecting survival in patients with single-ventricle physiology, on a par with those with biventricular physiology, are biliary atresia, other gastrointestinal malformations, low birth weight, atrioventricular block, and coarctation of the aorta [141]. In contrast to asplenia/right isomerism, abnormal pulmonary venous connections are not associated with an increased risk, whereas fetal atrioventricular block and coarctation of the aorta are associated with poorer prognosis, the former in spite of pacing [173] and the latter due to its frequent association with aortic outflow obstruction and hypoplastic left ventricle [141].

Staging towards Fontan operation in patients with polysplenia/left isomerism and single-ventricle physiology is accomplished by the Kawashima operation [174], a bidirectional cavopulmonary anastomosis draining to the lungs almost the whole systemic venous return because of the azygos continuation of the inferior vena cava.

Early outcome of Kawashima operation, initially considered a sort of definitive palliation, is affected by an increased occurrence of pulmonary arteriovenous fistulas early postoperatively [90,175,176], due to the exclusion of the hepatic venous blood from the pulmonary circulation. From a theoretical viewpoint, an increased incidence of pulmonary arteriovenous malformations in patients with azygos continuation and bidirectional cavopulmonary anastomosis could be related to other factors, such as polysplenia/left isomerism [90,175–177] or a lesser extent of bronchial collateral flow related to a higher Qp/Qs ratio compared with bidirectional cavopulmonary anastomosis in the absence of azygos continuation. However, their complete regression after baffling the hepatic veins to the confluent pulmonary arteries [178–184] outlines the crucial role of a putative hepatic or splanchnic factor that prevents precapillary channels of the pulmonary circulation from dilating [185,186]. Pulmonary arteriovenous fistulas have been described as increasing early morbidity and mortality after a modified Fontan operation owing to severe arterial desaturation [187]. For this reason, patients with polysplenia/left isomerism who have undergone a Kawashima bidirectional cavopulmonary anastomosis should be strictly followed to assess the early onset of pulmonary arteriovenous fistulas by contrast echocardiography [188] and transcutaneous pulse oximetry and Fontan completion should be performed timely at a relatively short interval.

The mortality with Fontan operations in polysplenia/left isomerism has been reported to range from 0 to 30% [141,156,189], with an improvement over time [156], but with a mortality up to 50% for the extracardiac Fontan

operation. In fact, conduit interposition between the hepatic veins and the pulmonary circulation carries an increased susceptibility to thrombosis due to a genetic hypercoagulable condition of patients with interrupted inferior vena cava (i.e., factor XII deficiency or heterozygous presence of factor V Leiden mutation) [190] and a flow imbalance mechanism between the relatively low upward flow from the hepatic veins and the preponderant downward flow of the Kawashima bidirectional cavopulmonary anastomosis. Improved survival has recently been reported using a hepato-azygos connection, a sort of end-to-side anastomosis between hepatic veins and the nearby segment of the azygos vein, aimed at reproducing the normal anatomic pattern of the systemic venous system [182–184,191,192]. The optimal spatial arrangement provided by direct hepatoazygos connection obviates power dissipation associated with fluid collision [193] and avoids flow stagnation in the hepatic vein–pulmonary artery conduit in the case of conventional Fontan completion after the Kawashima operation [192].

Finally, close attention needs to be paid to atrioventricular valve function in patients with single-ventricle physiology and polysplenia/left isomerism on a par with those with asplenia/right isomerism. About 75% of initial patients receiving the Kawashima bidirectional cavopulmonary anastomosis were reported as receiving concomitant replacement of the incompetent common atrioventricular valve [174]. Furthermore, the degree of preoperative atrioventricular valve regurgitation was described as a significant risk factor for increased mortality rate in heterotaxy patients at the time of the Fontan operation [189]. Accurate evaluation and possible treatment of atrioventricular valve incompetence during staging are mandatory to improve the subsequent candidacy of such patients for the Fontan operation [153].

Despite the good results of the Fontan procedure quoted in recent studies of patients with polysplenia/left isomerism, the incidence of both early and late postoperative arrhythmia remains high, with freedom from late bradyarrhythmia and tachyarrhythmia at 78 and 70%, respectively [153]. Certainly, the extracardiac Fontan modification has led to a general reduction in arrhythmias, by effectively preserving sinus node function [194]. However, in spite of that, both early and late postoperative arrhythmias are more common in patients with heterotaxy syndrome. In particular, 87% of arrhythmias are bradyarrhythmia in patients with heterotaxy, and severe bradyarrhythmia requiring permanent pacemaker implantation is more common in those with polysplenia/left isomerism [172].

Biventricular repair

Asplenia/right isomerism

About 10% of patients with asplenia/right isomerism have a cardiac anatomy suitable for biventricular repair. Criteria [34,195,196] for biventricular repair in heterotaxy patients are the presence of two balanced ventricles of adequate volume and function, associated with septatable atrioventricular valves and venoatrial connections, although some complex associated lesions may still contraindicate biventricular repair even in the presence of favorable prerequisites [152,196,197]. Given the extent of the anatomic variability of these patients, there are no clear criteria to determine suitability for biventricular repair, and each case needs to be considered on an individual basis. Focusing on asplenia/right isomerism, sporadic cases and limited series of complex biventricular repair have been reported with overall satisfactory results and early and late survival [198] of >90% [199]. The most common anomalies are transposition complexes, complete atrioventricular canal defect, double-outlet right ventricle, and pulmonary artery and pulmonary vein anomalies [199–203]. The unfavorable factors noted for the Fontan strategy are also common for biventricular repair, including anomalous venoatrial connections often accompanied by obstruction of the pulmonary venous drainage and hypoplasia of the pulmonary arteries [157,204].

Literature reports indicate that atrioventricular valve regurgitation and, possibly, anomalous pulmonary venous connections do not place a heterotaxy patient at risk for mortality after biventricular repair (as opposed to the Fontan operation). Furthermore, although long-term morbidities, including arrhythmia and reoperation/reintervention, are equivalent to those of Fontan patients, biventricular repair provides better hemodynamics with lower systemic venous pressure than the Fontan procedure and good NYHA status [199]. For this reason, in selected circumstances with suitable morphologic features, biventricular repair should be considered for definitive repair in patients with asplenia/right atrial isomerism [198].

Polysplenia/left isomerism

In contrast to asplenia/right isomerism, biventricular atrioventricular connection has been reported to be present in up to 72% of patients with polysplenia/left isomerism, with two separate atrioventricular valves in 43% [202]. Not all of these patients are amenable to biventricular repair because of abnormalities of atrioventricular concordance or systemic and pulmonary venous connections [205]. However, in recent reports, surgeons have reported their ability to perform biventricular repair in 30–50% of patients presenting with left polysplenia/left isomerism [141,170–172].

Criteria to pursue biventricular repair do not differ from those described for asplenia/right isomerism. The frequent associated concordant ventriculoarterial connection [205,206] and normal outflow tracts [172] may further facilitate the feasibility of repair.

Biventricular repair in polysplenia/left isomerism includes different procedures, namely atrial partition associated with septation of a common atrioventricular valve and closure of a ventricular septal defect (complete atrioventricular canal

defect), suture of a mitral cleft (partial atrioventricular canal defect), ventricular septal defect closure (ventricular septal defect), and interventricular rerouting associated with right ventricular outflow tract reconstruction (tetralogy-type double-outlet right ventricle), depending on the coexisting conditions. Atrial partition may require septation with a straight patch, when systemic and pulmonary veins connect into either side of the atrium independently; intra-atrial rerouting with a tailored baffle, to separate the pulmonary veins from systemic veins; or atrial switch, when the pulmonary veins connect into the functional right atrium or more than two systemic veins connect into the functional left atrium [202]. Multiple lesions may coexist, requiring complex procedures as in the case of atrioventricular canal defect with common atrioventricular valve and double-outlet right ventricle [203].

Results of biventricular repair in polysplenia/left isomerism are excellent, leading to early survival >90–100% [172,199] and very good long-term outcome [171]. The presence of a common atrioventricular valve is a significant risk factor for morbidity leading to reoperation [207], but not for additional mortality. Arrhythmias are typical of polysplenia/left isomerism and may be unrelated to surgery. This can be due to absence, hypoplasia or abnormal location of the sinus node, or abnormalities of atrioventricular conduction system related to associated abnormalities of atrioventricular connection and ventricular architecture [208]. Some studies suggest that atrioventricular block is more common (7–39%) in patients with polysplenia/left isomerism and is four times more common in those with an associated atrioventricular canal defect [209]. Furthermore, progressive slowing of the atrial rhythm is also typical of polysplenia/left isomerism [147], even in the absence of intracardiac abnormalities [172]. However, the incidence of postoperative arrhythmia is significant in patients with polysplenia/left atrial isomerism [199] treated with biventricular repair compared with those undergoing single ventricle palliation [153,169], with an overall incidence of up to 50% [171]. Studies suggest that the types of atrial baffling, atrioventricular valve regurgitation, and systemic and pulmonary venous anomaly are not related to the occurrence of arrhythmia. However, tachyarrhythmia has been reported in association with older age at biventricular repair, whereas the need for right ventricular outflow tract procedures to relieve stenosis has been described in relationship to the development of bradyarrhythmias [199].

Mechanical assistance for malposition of the heart

Recent reports outline the peculiar usefulness of a ventricular assist device and extracorporeal membrane oxygenation in neonatal palliation of cardiac abnormalities associated with asplenia/right isomerism, especially when obstructed total anomalous pulmonary venous drainage coexists [152]. In fact, a ventricular assist device and extracorporeal membrane oxygenation may be used to support the myocardium through a pulmonary hypertensive crisis and can be discontinued after stabilization of pulmonary reactivity.

On the other hand, scattered reports in the literature describe specifically left ventricular assist device implantation as bridge to recovery [210] or in heart transplantation [211] patients with abnormalities of the situs, without particular technical differences compared with patients with situs solitus. However, patients receiving mechanical assist device implantation may become sensitized to a wide variety of leukocyte antigens [212–217] and, therefore, require thorough evaluation and treatment, whenever required, before and after heart transplantation is performed [218,219].

Cardiac transplantation for malposition of the heart

Neonatal cardiac transplantation has been advocated as a primary therapy for some forms of complex cardiac anomalies, such as those associated with asplenia/right isomerism [220,221]. Apart from the general shortage of adequate donors for small recipients, there is general agreement to reserve cardiac transplantation for patients with asplenia/right isomerism, mainly already palliated up to the stage of bidirectional cavopulmonary anastomosis [222], with uncorrectable atrioventricular valve incompetence associated with severe ventricular dysfunction. From this viewpoint, asplenia/right isomerism does not differ from polysplenia/left isomerism or from other cardiac malformations with single-ventricle physiology [223] with/without abnormalities of the situs.

Focusing on particular problems associated with orthotopic heart transplantation in patients with complex cardiac anomalies and abnormalities of the situs, they are mainly related to the position within the recipient's chest of the systemic venous return and to the previous surgery performed.

In fact, when examining the anatomy of cardiac structures for heart transplantation regardless of the situs, the left atrium is a midline structure that receives the right and left pulmonary veins, the pulmonary artery is a midline structure at some point, and the aorta is usually anterior and to the right of the pulmonary artery, regardless of whether it originates normally or is transposed [224]. Abnormalities of the situs, therefore, are mainly characterized by variations up to complete reversal of the anatomic position of the systemic venous return and require particular modification of the surgical technique to deal with them. Several reports have described technical modification of

the standard transplantation technique for patients with situs inversus, reported as being a serious technical challenge due to the complete reversal of the anatomic position of the systemic venous return [224–234]. Reconstruction of the mirror-image systemic venous pathway is generally performed using autologous tissues or prosthetic conduits [224,229,232], and the donor heart is seated in a somewhat clockwise-rotated position with the apex tipped frontwards [133,230] or completely within the recipient's pericardium in dextrocardia [234], according to the technique used. In the subset of patients with heterotaxia, pediatric cardiac transplantation has been reported [223,226,234–236], with a few in patients with situs ambiguus [237,238]. The operative technique in such patients can be complicated by the position of the heart, the abnormalities of systemic and pulmonary venous connections [223,225,235,236,239,240], and the relationship between the great vessels [241,242].

The surgically demanding effects of preliminary palliative procedures on the pulmonary arterial tree and chest adhesions [224,227,236,240] are a less important aspect related to previous surgical procedures. The major problem with heart transplantation in patients who have already undergone previous cardiac operations is the potential development of HLA-directed antibodies allowing allosensitization. In particular, patients who received homograft implantation, blood/platelet transfusions, and/or mechanical assist device implantation may become sensitized to a wide variety of leukocyte antigens [243]. They represent a heart transplant population at high risk of hyperacute rejection and require specific consideration and both pretransplant and postoperative immuno-treatment options [218,219].

Early results of pediatric cardiac transplantation for cardiac malformations showed in the past a significantly increased early mortality compared with idiopathic cardiomyopathy [244,245] because of major operative procedure-related complications. However, increasing proportions of positive results with cardiac transplantation in children with cardiac malformations have progressively been described despite multiple previous cardiac operations [223,224,236,240,246,247]. Under such circumstances, abnormalities of situs do not show a negative impact on both early and late results compared with series of patients undergoing heart transplant for congenital cardiac defects in situs solitus or dilated cardiomyopathy [224,228–230,235,238].

Nowadays, heart transplantation can be considered a safe and highly effective treatment for patients with complex congenital heart defects, irrespective of the situs [225]. In fact, according to the current literature, the outcome in patients with congenital heart disease does not differ from that in patients without such abnormalities [248–250].

Ectopia cordis

Classification

Ectopia cordis is the partial or complete location of the heart outside the thorax. This extremely rare condition occurs in 5.5–7.9 per million live births [251,252]. Anatomic and clinical similarities with Cantrell syndrome are evident [48–50]. Kanagasuntheran and Verzin [253] divided ectopia cordis into five types: cervical, thoracocervical, thoracic, thoracoabdominal, and abdominal. The cervical form was found only in malformed fetuses; the abdominal form is extremely rare, with only one patient described. Hence, for practical purposes, only two types of ectopia cordis need be considered: the thoracic and the thoracoabdominal forms.

The thoracic type is the classic form of ectopia cordis. In these patients, there is a cleft of the sternum that allows protrusion of the heart outside the thoracic cavity, absence of the parietal pericardium, cephalic orientation of the cardiac apex, epigastric omphalocele, diastasis recti, and small thoracic cavity. The thoracoabdominal form is a partial form of ectopia cordis that is characterized by partial absence or cleft of the lower sternum, defect of the parietal diaphragmatic pericardium, midline diaphragmatic defect resulting in free communication between the pericardium and abdominal cavity, and diastasis recti with partial displacement of the ventricular portion of the heart into epigastrium. Many types of cardiac malformations are associated with ectopia cordis: tetralogy of Fallot, ventricular septal defect, atrioventricular canal, common atrium, tricuspid atresia, pulmonary stenosis and atresia, and transposition of the great arteries. There are at least five instances of ectopia cordis without a cardiac anomaly [47].

Oligohydramnios due to amnion rupture causing compression of the heart during cardiogenesis has been hypothesized as a mechanism of both thoracic and thoracoabdominal ectopia cordis [254]. Despite this mechanical explanation, chromosome abnormalities [251,255,256] and associated anomalies such as cleft lip and palate, cranial anomalies, gastrointestinal and renal anomalies, and pulmonary hypoplasia have been identified in some affected patients [47,257,258].

Treatment

A dismal outcome is generally reported in patients with ectopia cordis [257–260], mainly because of associated extracardiac and cardiac anomalies [257,258]. The first successful operative treatment of thoracoabdominal ectopia cordis without cardiac and extracardiac anomalies was performed in 1888 by Lannelongue and reported 22 years later [261]. Major extracardiac problems in the treatment of ectopia cordis include external cardiac compression, lung hypoplasia, and large airway obstruction due to distorted vascular anatomy.

The prognosis is particularly poor in patients with the thoracic form of ectopia cordis. In these patients, even though the thoracic cavity may appear normal in size, the liver occupies much of the cavity and precludes placement of the heart in the thorax. Although the outcome for patients with thoracoabdominal ectopia cordis is considered more favorable than that for patients with the thoracic form, the mortality is still high in both groups. The outcome of a large group of children and infants with ectopia cordis and cardiac anomalies [262] shows that affected infants and children can survive beyond early infancy and undergo successful repair or definitive palliation of their cardiac anomaly.

Thoracopagus conjoined twins

The most common form of conjoined twins shows a fusion in the midportion of the body, and these children are called thoracopagus twins. These patients represent a rare type of cardiac malposition because the fusion involves the anterior chest region and the heart. Conjoined twins occur once in every 50 000 births. Female twins represent more than three-quarters of patients [263,264].

In thoracopagus twins, the livers are conjoined and the sternum is usually partially or totally absent (Figure 50.21). The pericardial and pleural cavities may be either separate or common to both children, and the cardiovascular fusion may be classified into three types [265]: common pericardium but separate hearts, fusion at atrial and ventricular levels, and fusion at atrial level only. Simple or, more frequently, complex cardiac malformations may coexist and may be discordant between the children.

Anomalies of visceroatrial situs are frequent in dicephalus (86%) and in thoracopagus twins (71%), occurring most frequently in the twin on the right side [265]. These laterality defects have been explained by the inhibition of the gene Sonic Hedgehog in the left side of the right twin due to the effect of Activin gene produced at the right side of the left twin [266].

Because anomalies of the visceroatrial situs and discordant atrioventricular and ventriculoarterial connections are frequent [267], the segmental approach to cardiac diagnosis [1,2,6,8] is mandatory in these patients. At atrial level, the most frequent anomalies are single atrium and large atrial septal defect. Venous channels interposed between the superior venae cavae and connecting the systemic venous drainages of the twins are frequent, as is partial or total anomalous pulmonary venous connection. At ventricular level, the most common anomalies are single ventricle and ventricular septal defect [268]; transposition of the great arteries and double-outlet right ventricle are the most common conotruncal defects. Pulmonary and aortic stenosis or atresia occur frequently, and one twin may show one of these conditions and the opposite twin the other [269].

The fetal diagnosis can be made by radiography [270]. Prenatal echocardiographic examination details the intracardiac anatomy [271].

At birth, the diagnosis of separate hearts can be suspected if one twin differs from the other in pulse rate and

(a)   (b)
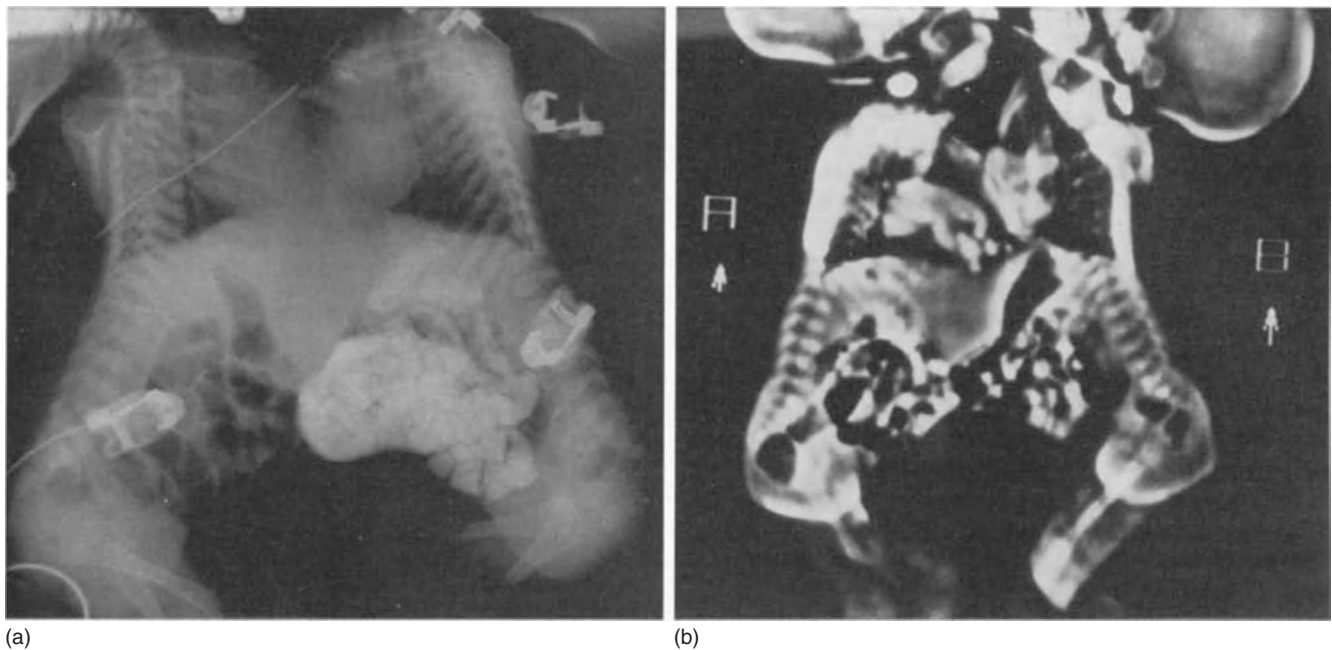
Figure 50.21 (a) Chest radiograph and (b) computed tomographic angiogram in thoracopagus twins. Note the conjoined livers and the fusion of the chests (twin A is right-sided and twin B is left-sided in the figure).

if they show separate QRS complexes on an electrocardiogram [270]. Echocardiography can diagnose the site and dimension of the heart fusion and the morphology of intracardiac anomalies [269]. Computed tomographic angiography [269,272] may also be useful for the diagnosis, but cardiac catheterization and angiocardiography, although technically difficult in these patients, are usually mandatory to assess the feasibility of separation [269,273]. Aortography and coronary angiography should be indicated to exclude fusion of the coronary vascular beds at ventricular level. Furthermore, the assessment of electromyocardial continuity should be considered in the preoperative work-up [274].

Separation of conjoined twins represents an operative challenge [275–283] and is best delayed until the infants are relatively mature (6–12 months of age). The assessment of the cardiovascular system is fundamental in planning the operative separation, but the evaluation of the liver, pancreaticobiliary tract, gastrointestinal tract, urinary tract, and central nervous system is also important. Therefore, the operative team must include many specialty consultants and surgeons. Moreover, the use of skin expanders and prosthetic mesh is mandatory to facilitate wound closure.

The ethical and legal problems of separation of conjoined twins are important aspects in medical and surgical treatment [282,283]. With conjoined hearts, the possibility of sacrificing one twin, allowing the other to lead a potentially normal life, comes into question [283]. The hospital's ethics committee is helpful in this respect, but obviously the parents always have the right to refuse surgical separation.

There are no reported long-term instances of separation of twins with conjoined ventricles (one patient survived for 3 months) [283] and there were few successes when the junction was at atrial level [276,277].

References

1 Van Praagh R, Van Praagh S, Vlad P, *et al*. Anatomic types of congenital dextrocardia. Diagnostic and embryologic implications. *Am J Cardiol* 1964;**13**:510–31.

2 Van Praagh R, Van Praagh S, Vlad P, *et al*. Diagnosis of anatomic types of congenital dextrocardia. *Am J Cardiol* 1965;**15**:234–47.

3 Lev M, Liberthson RR, Eckner FA, Arcilla RA. Pathologic anatomy of dextrocardia and its clinical implications. *Circulation* 1968;**37**:979–99.

4 Anselmi G, Munoz S, Blanco P, *et al*. Systematization and clinical study of dextroversion, mirror-image dextrocardia and laevoversion. *Br Heart J* 1972;**34**:1085–98.

5 Squarcia U, Ritter DG, Kincaid OW. Dextrocardia: angiocardiographic study and classification. *Am J Cardiol* 1973;**32**:965–77.

6 Shinebourne EA, Macartney FI, Anderson RH. Sequential chamber localization: the logical approach to diagnosis in congenital heart disease. *Br Heart J* 1976;**38**:327–40.

7 Stanger P, Rudolph AM, Edwards JE. Cardiac malpositions: an overview based on study of 65 necropsy specimens. *Circulation* 1977;**56**:159–72.

8 Van Praagh R. Terminology of congenital heart disease. Glossary and commentary. *Circulation* 1977;**56**:139–43.

9 De la Cruz MV, Nadal-Ginard B. Rules for the diagnosis of visceral situs, truncoconal morphologies, and ventricular inversions. *Am Heart J* 1972;**84**:19–32.

10 Casey B. Genetics of human situs abnormalities. *Am J Med Genet* 2001;**101**:356–8.

11 Maclean K, Dunwoodie SL. Breaking symmetry: a clinical overview of left–right patterning. *Clin Genet* 2006;**65**:441–57.

12 Ramsdell AF. Left–right asymmetry and congenital cardiac defects: getting to the heart of the matter in vertebrate left–right axis determination. *Dev Biol* 2005;**288**:1–20.

13 Levin M. Left–right asymmetry in embryonic development: a comprehensive review. *Mech Dev* 2005;**122**:3–25.

14 Zhu L, Belmont JW, Ware SM. Genetics of human heterotaxias. *Eur J Hum Genet* 2006;**14**:17–25.

15 Marino B, Digilio MC, Giannotti A, *et al*. Heterotaxia syndromes and 22q11 deletion. *J Med Genet* 1996;**33**:1052–4.

16 Goldmuntz E, Bamford R, Karkera JD, *et al*. CFC1 mutations in patients with transposition of the great arteries and double-outlet right ventricle. *Am J Hum Genet* 2002;**70**:776–80.

17 De Luca A, Sarkozy A, Consoli F, *et al*. Familial transposition of the great arteries caused by multiple mutations in laterality genes. *Heart* 2010;**96**:673–7.

18 Digilio MC, Casey B, Toscano A, *et al*. Complete transposition of the great arteries: patterns of congenital heart disease in familial recurrence. *Circulation* 2001;**104**:2809–14.

19 Cipollone D, Amati F, Carsetti R, *et al*. A multiple retinoic acid antagonist induces conotruncal anomalies, including transposition of the great arteries, in mice. *Cardiovasc Pathol* 2006;**15**:194–202.

20 Gebbia M, Ferrero GB, Pilia G, *et al*. X-linked situs abnormalities result from mutations in ZIC3. *Nat Genet* 1997;**17**:305–8.

21 Kosaki K, Bassi MT, Kosaki R, *et al*. Characterization and mutation analysis of human LEFTY A and LEFTY B, homologues of murine genes implicated in left–right axis development. *Am J Hum Genet* 1999;**64**:712–21.

22 Bamford RN, Roessler E, Burdine RD, *et al*. Loss-of-function mutations in the EGF-CFC gene CFC1 are associated with human left–right laterality defects. *Nat Genet* 2000;**26**:365–9.

23 Kosaki R, Gebbia M, Kosaki K, *et al*. Left–right axis malformations associated with mutations in ACVR2B, the gene for human activin receptor type IIB. *Am J Med Genet* 1999;**82**:70–6.

24 Robinson SW, Morris CD, Goldmuntz E, *et al*. Missense mutations in CRELD1 are associated with cardiac atrioventricular septal defects. *Am J Hum Genet* 2003;**72**:1047–52.

25 Watanabe Y, Benson DW, Yano S, *et al*. Two novel frameshift mutations in NKX2.5 result in novel features including visceral inversus and sinus venosus type ASD. *J Med Genet* 2002;**39**:807–11.

26 Kuehl KS, Loffredo C. Risk factors for heart disease associated with abnormal sidedness. *Teratology* 2002;**66**:242–8.

27 Grande C, Patel NH. Nodal signalling is involved in left–right asymmetry in snails. *Nature* 2009;**457**:1007–11.

28 Oliverio M, Digilio MC, Versacci P, *et al*. Shells and heart: are human laterality and chirality of snails controlled by the same maternal genes? *Am J Med Genet A* 2010;**52A**:2419–25.

29 Ivemark B. Implication of agenesis of the spleen on the patho-genesis of cono-truncus anomalies in childhood. *Acta Paediatr Scand* 1955;**44**(Suppl 1):590–2.

30 Moller JH, Nakib A, Anderson RC, Edwards JE. Congenital cardiac disease associated with polysplenia: a developmental complex of bilateral "left-sideness." *Circulation* 1967;**36**:789–99.

31 Van Mierop LH, Gessner IH, Schiebler GL. Asplenia and poly-splenia syndrome. *Birth Defects* 1972;**3**:74.

32 Rose V, Izukawa T, Moes CA. Syndromes of asplenia and poly-splenia. A review of cardiac and non-cardiac malformations in 60 cases with special reference to diagnosis and prognosis. *Br Heart J* 1975;**37**:840–52.

33 Macartney FJ, Zuberbuhler JR, Anderson RH. Morphological considerations pertaining to recognition of atrial isomerism. Consequences for sequential chamber localisation. *Br Heart J* 1980;**44**:657–67.

34 Sapire DW, Yen Ho S, Anderson RH, Rigby ML. Diagnosis and significance of atrial isomerism. *Am J Cardiol* 1986;**58**:342–8.

35 Van Praagh R, Van Praagh S. Atrial isomerism on the heterotaxy syndromes with asplenia, or polysplenia, or normally formed spleen: an erroneous concept. *Am J Cardiol* 1990;**66**:1504–6.

36 Sharma S, Devine W, Anderson RH, Zuberbuhler JR. The determination of atrial arrangement by examination of appen-dage morphology in 1842 heart specimens. *Br Heart J* 1998;**60**:227–31.

37 Phoon CK, Neill CA. Asplenia syndrome: insight into embry-ology through an analysis of cardiac and extracardiac anomalies. *Am J Cardiol* 1994;**73**:581–7.

38 Rubino M, Van Praagh S, Kadoba K, *et al.* Systemic and pulmo-nary venous connections in visceral heterotaxy with asplenia. *J Thorac Cardiovasc Surg* 1995;**110**:641–50.

39 Uemura H, Yen Ho S, Devine WA, Anderson RH. Analysis of visceral heterotaxy according to splenic status, appendage mor-phology, or both. *Am J Cardiol* 1995;**76**:846–9.

40 Uemura H, Yen Ho S, Devine WA, *et al.* Atrial appendages in venoatrial connections in hearts from patients with visceral heterotaxy. *Ann Thorac Surg* 1995;**60**:561–9.

41 Geva T, Vick GW III, Wendt RE, Rokey R. Diagnosis of hetero-taxy syndrome. *Circulation* 1995;**91**:907–8.

42 Frescura C, Marino B, Bosman C, Thiene G. Sindromi asplenica e polisplenica: malformazioni cardiovascolari ed interpretazioni embriogenetiche. In: *Progressi in Cardiologia Pediatrica*. Trieste: LINT, 1981: 123.

43 Cleveland M. Situs inversus viscerum: anatomic study. *Arch Surg* 1926;**13**:343–68.

44 Bohun CM, Potts JE, Casey BM, *et al.* A population-based study of cardiac malformations and outcomes associated with dextro-cardia. *Am J Cardiol* 2007;**100**:305–9.

45 Nadas AS, Fyler DC. Dextrocardias. In: Nadas AS, Fyler DC, eds. *Pediatric Cardiology*. Philadelphia: Saunders, 1972: 657–61.

46 Friedberg CK. Dextrocardia. In: Friedberg CK, ed. *Disease of the Heart*. Philadelphia: Saunders, 1966: 1284–7.

47 Van Praagh R, Weinberg PM, Smith SD, *et al.* Malpositions of the heart. In: Adams FH, Emmanouilides GC, Riemenschneider TA, eds. *Heart Disease in Infants, Children, and Adolescents*, 4th edn. Baltimore: Williams & Wilkins, 1989: 530–59.

48 Cantrell JR, Haller JA, Ravitch MM. A syndrome of congenital defects involving the abdominal wall, sternum, diaphragm, peri-cardium and heart. *Surg Gynecol Obstet* 1958;**107**:602–14.

49 D'Anastasio R, Di Silvestro G, Versacci P, *et al.* The heart of Santa Rosa. *Lancet* 2010;**375**:2168.

50 Borges AJ, Hazebroek FW, Hess J. Left and right diverticula, ventricular septal defect and ectopia cordis in a patient with Cantrell's syndrome. *Eur J Cardiothorac Surg* 1993;**7**:334–5.

51 Husain AN, Hessel RG. Neonatal pulmonary hypoplasia: an autopsy study of 25 cases. *Pediatr Pathol* 1993;**13**:475–84.

51a Stressig R, Fimmers R, Eising K, *et al.* Preferential streaming of the ductus venosus and inferior vena cava towards the right heart is associated with left heart underdevelopment in human fetuses with left-sided diaphragmatic hernia. *Heart* 2010;**96**:1564–8.

52 Neill CA, Ferencz C, Sabiston DC, Sheldon H. The familial occurrence of hypoplastic right lung with systemic arterial sup-ply and venous drainage: "scimitar syndrome." *Johns Hopkins Med J* 1960;**107**:1–21.

53 Van Praagh S, O'Sullivan J, Brili S, Van Praagh R. Juxtaposition of the morphologically right atrial appendage in solitus and inversus atria: a study of 35 postmortem cases. *Am Heart J* 1996;**132**:382–90.

54 Wood AE, Freedom RM, Williams WG, Trusler GA: The Mustard procedure in transposition of the great arteries associated with juxtaposition of the atrial appendage with or without dextro-cardia. *J Thorac Cardiovasc Surg* 1983;**85**:451–6.

55 Marino B, Sanders S, Pasquini L, *et al.* Two-dimensional echo-cardiographic anatomy in criss-cross heart. *Am J Cardiol* 1986;**58**:325–33.

56 Piacentini G, Digilio MC, Capolino R, *et al.* Familial recurrence of heart defects in subjects with congenitally corrected transpo-sition of the great arteries. *Am J Med Genet A* 2005;**137**:176–80.

57 Pasquini L, Sanders SP, Parness IA, *et al.* Echocardiographic and anatomic findings in atrioventricular discordance and ventricu-loarterial concordance. *Am J Cardiol* 1988;**62**:1256–62.

58 Kartagener M. Zur Pathogenese der Bronchiektasian: Bronchi-ektasian bei Situs Viscerum Inversus. *Beitr Klin Tuberk* 1933; **83**:489.

59 Eliasson R, Mossberg B, Cammer P. The immotile cilia syn-drome. A congenital abnormality as an etiologic factor in chronic airway infection and male sterility. *N Engl J Med* 1977;**297**:1–8.

60 Kennedy MP, Omran H, Leigh MW, *et al.* Congenital heart disease and other heterotaxic defects in a large cohort of patients with primary ciliary dyskinesia. *Circulation* 2007;**115**:2814–21.

61 Shidlow DV, Katz SM, Turtz MG. Polysplenia and Kartagener syndromes in a sibship: association with abnormal respiratory cilia. *J Pediatr* 1982;**100**:401–3.

62 McGrath LB, Kirklin JW, Blackstone EH, *et al.* Death and other events after cardiac repair of discordant atrioventricular connec-tion. *J Thorac Cardiovasc Surg* 1985;**90**:711–28.

63 Attie F, Cerda J, Richheimer R, *et al.* Congenitally corrected transposition with mirror image atrial arrangement. *Int J Cardiol* 1987;**14**:169–75.

64 Di Donato RM, Wernovsky G, Jonas R, *et al.* Corrected transpo-sition in situs inversus. Biventricular repair of cardiac anoma-lies. *Circulation* 1991;**84**(Suppl III):III193–9.

65 Huhta JC, Maloney JD, Ritter DJ, *et al.* Complete atrioventric-ular block in patients with atrioventricular discordance. *Circulation* 1983;**67**:1374–7.

66 Thiene G, Nava A, Rossi L. The conduction system in corrected transposition with situs inversus. *Eur J Cardiol* 1977;**6**:57–70.

67 Kitayama H, Oku H, Matsumoto T, Onoe M. Total cavopulmonary connection using a pedicled pericardial conduit for a patient with apicocaval juxtaposition. *Ann Thorac Surg* 2001;**72**:1393–4.

68 Kawahira Y, Nishigaki K, Ueno T. Extracardiac Fontan procedure bridging the vertebra for apico-caval juxtaposition. *Ann Thorac Surg* 2006;**82**:350–2.

69 Sakata R, Lecompte Y, Batisse A, *et al*. Anatomic repair of anomalies of ventriculoarterial connection associated with ventricular septal defect: criteria of surgical decision. *J Thorac Cardiovasc Surg* 1988;**95**:90–5.

70 Borromée L, Lecompte T, Batisse A, *et al*. Anatomic repair of anomalies of ventriculoarterial connection associated with ventricular septal defect: clinical results in 50 patients with pulmonary outflow obstruction. *J Thorac Cardiovasc Surg* 1988;**95**:96–102.

71 Rastelli GC. A new approach to "anatomic" repair of transposition of the great arteries. *Mayo Clin Proc* 1969;**44**:1–12.

72 Lecompte Y, Neveux JY, Leca F, *et al*. Reconstruction of the pulmonary outflow tract without prosthetic conduit. *J Thorac Cardiovasc Surg* 1982;**84**:727–33.

73 Ilbawi MN, DeLeon SY, Backer CL, *et al*. An alternative approach to the surgical management of physiologically corrected transposition with ventricular septal defect and pulmonary stenosis or atresia. *J Thorac Cardiovasc Surg* 1990;**100**:410–5.

74 Di Donato RM, Troconis CJ, Marino B, *et al*. Combined Mustard and Rastelli operations: an alternative approach for repair of associated anomalies in congenitally corrected transposition in situs inversus {I,D,D}. *J Thorac Cardiovasc Surg* 1992;**104**:1246–8.

75 Yamagashi Y, Imai Y, Hoshino S, *et al*. Anatomic correction of atrioventricular discordance. *J Thorac Cardiovasc Surg* 1993;**105**:1067–76.

76 Yagihara T, Kishimoto H, Isobe F, *et al*. Double switch operation in cardiac anomalies with atrioventricular and ventriculoarterial discordance. *J Thorac Cardiovasc Surg* 1994;**107**:351–8.

77 Imai Y, Sawatari K, Hoshino S, *et al*. Ventricular function after repair in patients with atrioventricular discordance. *J Thorac Cardiovasc Surg* 1994;**107**:1272–83.

78 Sato K, Ohara S, Tsukaguchi I, *et al*. A criss-cross heart with concordant atrioventricular connections. *Circulation* 1978;**57**:396–400.

79 Ohtakae S, Shimazaki Y, Kawata H, *et al*. Surgical management of criss-cross heart in association with complex cardiac anomalies. *Cardiol Young* 1993;**3**(Suppl 1):58.

80 Muster AJ, Zales VR, Ilbawi MN, *et al*. Biventricular repair of hypoplastic right ventricle assisted by pulsatile bidirectional cavopulmonary anastomosis. *J Thorac Cardiovasc Surg* 1993;**105**:112–9.

81 Lin AE, Ticho BS, Houde K, *et al*. Heterotaxy: associated conditions and hospital-based prevalence in newborns. *Genet Med* 2000;**2**,157–72.

82 Gatrad AR, Read AP, Watson GH: Consanguinity and complex cardiac anomalies with situs ambiguus. *Arch Dis Child* 1984;**59**:242–5.

83 Ferencz C, Rubin JD, McCarter RJ, *et al*. Congenital heart disease: prevalence at livebirth. The Baltimore–Washington Infant Study. *Am J Epidemiol* 1985;**121**:31–6.

84 Van Praagh R, Weinberg PM, Matsuoka R, Van Praagh S. Malpositions of the heart. In: Adams FH, Emmanouilides GC, eds. *Moss' Heart Disease in Infants, Children, and Adolescents*, 3rd edn. Baltimore: Williams & Wilkins, 1983: 422–58.

85 Niikawa N, Koshaka S, Mizumoto M, *et al*. Familial clustering of situs inversus totalis and asplenia and polysplenia syndromes. *Am J Med Genet* 1983;**16**:43–7.

86 Freedom RM, Jaeggi ET, Lim JS, *et al*. Hearts with isomerism of the right atrial appendages – one of the worst forms of disease in 2005. *Cardiol Young* 2005;**15**:554–67.

87 Randall PA, Moller JH, Amplatz K. The spleen and congenital heart disease. *Am J Roentgenol* 1973;**119**:551–9.

88 Carmi R, Magee CA, Neill CA, Karrer FM. Extrahepatic biliary atresia and associated anomalies: etiologic heterogeneity suggested by distinctive patterns of associations. *Am J Med Genet* 1993;**45**:683–93.

89 Ticho BS, Goldstein AM, Van Praagh R. Extracardiac anomalies in the heterotaxy syndromes with focus on anomalies of midline-associated structures. *Am J Cardiol* 2000;**85**:729–34.

90 Amodeo A, Di Donato R, Carotti A, *et al*. Pulmonary arteriovenous fistulas and polysplenia syndrome. *J Thorac Cardiovasc Surg* 1994;**107**:1378–9.

91 Ruttenberg HD, Neufeld HN, Lucas RV Jr, *et al*. Syndrome of congenital heart disease with asplenia. Distinction from other forms of congenital cyanotic cardiac disease. *Am J Cardiol* 1964;**13**:387–406.

92 Peoples WM, Moller JH, Edwards JE. Polysplenia: a review of 146 cases. *Pediatr Cardiol* 1983;**4**:129–38.

93 Marino B, Pasquini L. Systemic and venous connection in asplenia syndrome. *J Thorac Cardiovasc Surg* 1996;**111**:1109.

94 Van Praagh S, Carrera ME, Sanders S, *et al*. Partial or total direct pulmonary venous drainage to right atrium due to malposition of septum primum. *Chest* 1995;**107**:1488–98.

95 Kawahira Y, Kishimoto H, Kawata H, *et al*. New indicator for the Fontan operation: diameters of the pulmonary veins in patients with univentricular heart. *J Card Surg,*1999;**14**:259–65.

96 Lababidi Z, Stoeckle H, Hopeman A, *et al*. Congenital asplenia with bilateral right-sidedness and normally related great arteries. Case report. *Mo Med* 1972;**69**:742–5.

97 Francalanci P, Marino B, Boldrini R, *et al*. Morphology of the atrioventricular valve in asplenia syndrome: a peculiar type of atrioventricular canal defect. *Cardiovasc Pathol* 1996;**5**:145–51.

98 Digilio MC, Marino B, Giannotti A, Dallapiccola B. Single atrium, atrioventricular canal/postaxial hexodactyly indicating Ellis–van Creveld syndrome. *Hum Genet* 1995;**96**:251–3.

99 Digilio MC, Marino B, Giannotti A, *et al*. Specific congenital heart defects in RSH/Smith–Lemli–Opitz syndrome: postulated involvement of the sonic hedgehog pathway in syndromes with postaxial polydactyly or heterotaxia. *Birth Defects Res A Clin Mol Teratol* 2003;**67**:149–53.

100 Vairo U, Marino B, Parretti di Iulio D, *et al*. Isomerismo atriale destro con atresia polmonare: caratteristiche angiocardiografiche e modelli di circolazione polmonare. *G Ital Cardiol* 1991;**21**(Suppl 2):P3.

101 Vairo U, Marino B, Parretti di Iulio D, *et al*. Morfologia ventricolo-infundibolare nell'eterotassia viscerale con isomerismo sinistro. Studio eco-angiocardiografico. *G Ital Cardiol* 1991;**21**:969–74.

102 Marino B, Calabrò R, Gagliardi MG, *et al*. Patterns of pulmonary arterial anatomy and blood supply in complex congenital heart disease with pulmonary atresia. *J Thorac Cardiovasc Surg* 1987;**94**:518–20.

103 Formigari R, Vairo U, de Zorzi A, *et al*. Prevalence of bilateral ductus arteriosus in patients with pulmonic valve atresia and asplenia syndrome. *Am J Cardiol* 1992;**70**:1219–20.

104 Vitiello R, Moller JH, Marino B, *et al*. Pulmonary circulation in pulmonary atresia associated with the asplenia cardiac syndrome. *J Am Coll Cardiol* 1992;**20**:363–5.

105 Hsu JY, Wang JK, Lin MT, *et al*. Clinical implications of major aortopulmonary collateral arteries in patients with right isomerism. *Ann Thorac Surg* 2006;**82**:153–7.

106 Marino B, Capolino R, Digilio MC, *et al*. Transposition of the great arteries in asplenia and polysplenia phenotypes. *Am J Med Genet* 2002;**110**:292–4.

107 Blieden LC, Moller JH. Analysis of the P wave in congenital cardiac malformations associated with splenic anomalies. *Am Heart J* 1973;**85**:439–44.

108 Partridge JB, Scott O, Deverall PB, Macartney FJ. Visualization and measurement of the main bronchi by tomography as an objective indicator of thoracic situs in congenital heart disease. *Circulation* 1975;**51**:188–96.

109 Deanfield JE, Leanage R, Stroobant J, *et al*. Use of high kilovoltage filtered beam radiographs for detection of bronchial situs in infants and young children. *Br Heart J* 1980;**44**:577–83.

110 Hutha JC, Smallhorn JF, Macartney FJ. Two-dimensional echocardiographic diagnosis of situs. *Br Heart J* 1982;**48**:97–108.

111 Hutha JC, Hagler DJ, Seward JB, *et al*. Two-dimensional echocardiographic assessment of cardiac malposition. *Am J Cardiol* 1982;**50**:1351–60.

112 Smallhorn JS, Tommasini G, Macartney FJ. Two-dimensional echocardiographic assessment of common atrioventricular valves in univentricular hearts. *Br Heart J* 1981;**46**:30–4.

113 Arisawa J, Morimoto S, Ikezoe J, *et al*. Cross sectional echocardiographic anatomy of common atrioventricular valve in atrial isomerism. *Br Heart J* 1989;**62**:291–7.

114 Silverman NH, de Araujo LML. An echocardiographic method for the diagnosis of cardiac situs and malpositions. *Echocardiography* 1987;**4**:35–57.

115 Van Der Velte ME, Parness IA, Colan SD, *et al*. Two-dimensional echocardiography in the pre- and postoperative management of totally anomalous pulmonary venous connection. *J Am Coll Cardiol* 1991;**18**:1746–51.

116 O'Leary PW, Seward JB, Hagler DJ, Tajik J. Echocardiographic documentation of splenic anatomy in complex congenital heart disease. *Am J Cardiol* 1991;**68**:1536–8.

117 Geva T, Wesley V III, Wendt RE, Rokey R. Role of spin echo and cine magnetic resonance imaging in presurgical planning of heterotaxy syndrome. Comparison with echocardiography and catheterization. *Circulation* 1994;**90**:348–56.

118 Niwa K, Uchishiba M, Aotsuka H, *et al*. Magnetic resonance imaging of heterotaxia in infants. *J Am Coll Cardiol* 1994;**23**:177–83.

119 Chen SJ, Li YW, Wang JK, *et al*. Usefulness of electron beam computed tomography in children with heterotaxy syndrome. *Am J Cardiol* 1998;**81**:188–94.

120 Marino B, Vairo U, Marcelletti C, Calabrò R. Morphology of ductus arteriosus and of the pulmonary arteries in patients with pulmonary atresia and complex congenital heart disease. *Chest* 1990;**97**:766.

121 Di Donato R, di Carlo D, Squitieri C, *et al*. Palliation of cardiac malformations associated with right isomerism (asplenia syndrome) in infancy. *Ann Thorac Surg* 1987;**44**:35–9.

122 DeLeon SY, Gidding SS, Ilbawi MN, *et al*. Surgical management of infants with complex cardiac anomalies associated with reduced pulmonary blood flow and total anomalous pulmonary venous drainage. *Ann Thorac Surg* 1987;**43**:207–11.

123 Culbertson CB, George BL, Day RW, *et al*. Factors influencing survival of patients with heterotaxy syndrome undergoing the Fontan procedure. *J Am Coll Cardiol* 1992;**20**:678–84.

124 Dickinson DF, Wilkinson JL, Anderson KR, *et al*. The cardiac conduction system in situs ambiguus. *Circulation* 1979;**59**: 879–85.

125 Garcia OL, Mehta AV, Pickoff AS, *et al*. Left isomerism and complete atrioventricular block: a report of six cases. *Am J Cardiol* 1981;**48**:1103–7.

126 Swaminathan S, Parthiban A. Progressive fetal atrioventricular block in heterotaxy syndrome. *Cardiol Young* 2007;**17**:432–4.

127 Heller RM, Dorst JP, James AE, Rowe RD. A useful sign in the recognition of azygos continuation of the inferior vena cava. *Radiology* 1971;**101**:519–22.

128 Berg C, Geipel A, Smrcek J, *et al*. Prenatal diagnosis of cardiosplenic syndromes: a 10-year experience. *Ultrasound Obstet Gynecol* 2003;**22**:451–9.

129 Lim JS, McCrindle BW, Smallhorn JF, *et al*. Clinical features, management, and outcome of children with fetal and postnatal diagnoses of isomerism syndromes. *Circulation* 2005; **112**:2454–61.

130 Cohen MS, Schultz AH, Tian ZY, *et al*. Heterotaxy syndrome with functional single ventricle: does prenatal diagnosis improve survival? *Ann Thorac Surg* 2006;**82**:1629–36.

131 Phoon CK, Villegas MD, Ursell PC, Silverman NH. Left atrial isomerism detected in fetal life. *Am J Cardiol* 1996;**77**:1083–8.

132 Guccione P, Gagliardi MG, Bevilacqua M, *et al*. Cardiac catheterization through the internal jugular vein in pediatric patients. An alternative to the usual femoral vein access. *Chest* 1992;**101**:1512–4.

133 Moller JH. Malposition of the heart. In: Moller JH, Neal WA, eds. *Fetal, Neonatal and Infant Cardiac Disease*. Norwalk, CT: Appleton & Lange, 1990: 755–74.

134 Sadiq M, Stümper O, De Giovanni JV, *et al*. Management and outcome of infants and children with right isomerism. *Heart* 1996;**75**:314–9.

135 Phoon CK, Neill CA. Asplenia syndrome – risk factors for early unfavorable outcome. *Am J Cardiol* 1994;**73**:1235–7.

136 Waldman JD, Rosenthal A, Smith AL, *et al*. Sepsis and congenital asplenia. *J Pediatr* 1977;**90**:555–9.

137 Overturf GD, American Academy of Pediatrics, Committee on Infectious Diseases. Technical report: prevention of pneumococcal infections, including the use of pneumococcal conjugate and polysaccharide vaccines and antibiotic prophylaxis. *Pediatrics* 2000;**106**:367–76.

138 Wu MH, Wang JK, Lue HC. Sudden death in patients with right isomerism (asplenism) after palliation. *J Pediatr* 2002;**140**:93–6.

139 Gilljam T, McCrindle BW, Smallhorn JF, *et al*. Outcomes of left atrial isomerism over a 28-year period at a single institution. *J Am Coll Cardiol* 2000;**36**:908–16.

140 Chandra RS. Biliary atresia and other structural anomalies in the congenital polysplenia syndrome. *J Pediatr* 1974;**85**:649–55.

141 Dimmick JE, Bove KE, McAdams AJ. Extrahepatic biliary atresia and the polysplenia syndrome. *J Pediatr* 1975;**86**:644–5.

142 Gersony WM. Obstruction to pulmonary venous return obscured by decreased pulmonary blood flow. *Chest* 1973;**64**:283.

143 Freedom RM, Olley PM, Coceani F, Rowe RD. The prostaglandin challenge: test to unmask obstructed total pulmonary venous connections in asplenia syndrome. *Br Heart J* 1978;**40**:91–4.

144 Norwood WI. Hypoplastic left heart syndrome. *Cardiol Clin* 1989;**7**:377–85.

145 Jobes DR, Nicolson SC, Steven JM, *et al*. Carbon dioxide prevents pulmonary overcirculation in hypoplastic left heart syndrome. *Ann Thorac Surg* 1992;**54**:150–1.

146 Wren C, Macartney FJ, Deanfield JE. Cardiac rhythm in atrial isomerism. *Am J Cardiol* 1987;**59**:1156–8.

147 Momma K, Takao A, Shibata T. Characteristics and natural history of abnormal atrial rhythms in left isomerism. *Am J Cardiol* 1990;**65**:231–6.

148 Hashmi A, Abu-Sulaiman R, McCrindle BW, *et al*. Management and outcomes of right atrial isomerism: a 26-year experience. *J Am Coll Cardiol* 1998;**31**:1120–6.

149 Heinemann MK, Hanley FL, Van Praagh S, *et al*. Total anomalous pulmonary venous drainage in newborns with visceral heterotaxy. *Ann Thorac Surg* 1994;**57**:88–91.

150 Gaynor JW, Collins MH, Rychik J, *et al*. Long-term outcome of infants with single ventricle and total anomalous pulmonary venous connection. *J Thorac Cardiovasc Surg* 1999;**117**:506–14.

151 Caldarone CA, Najm HK, Kadletz M, *et al*. Surgical management of total anomalous pulmonary venous drainage: impact of coexisting cardiac anomalies. *Ann Thorac Surg* 1998;**66**:1521–6.

152 Yun TJ, Al-Radi OO, Adatia I, *et al*. Contemporary management of right atrial isomerism: effect of evolving therapeutic strategies. *J Thorac Cardiovasc Surg* 2006;**131**:1108–13.

153 Stamm C, Friehs I, Duebener LF, *et al*. Improving results of the modified Fontan operation in patients with heterotaxy syndrome. *Ann Thorac Surg* 2002;**74**:1967–78.

154 Gardiner HM, Dhillon R, Bull C, *et al*. Prospective study of the incidence and determinants of arrhythmia after total cavopulmonary connection. *Circulation* 1996;**94**(Suppl II):II-17–21.

155 Durongpisitkul K, Porter CJ, Cetta F, *et al*. Predictors of early- and late-onset supraventricular tachyarrhythmias after Fontan operation. *Circulation* 1998;**98**:1099–107.

156 Shirai LK, Rosenthal DN, Reitz BA, *et al*. Arrhythmias and thrombembolic complications after the extracardiac Fontan operation. *J Thorac Cardiovasc Surg* 1998;**115**:499–505.

157 Humes RA, Feldt RH, Porter CJ, *et al*. The modified Fontan operation for asplenia and polysplenia syndromes. *J Thorac Cardiovasc Surg* 1988;**96**:212–8.

158 Michielon G, Gharagozloo F, Julsrud PR, *et al*. Modified Fontan operation in the presence of anomalies of systemic and pulmonary venous connection. *Circulation* 1993;**88**(Suppl II):II-141–8.

159 Cetta F, Feldt RH, O'Leary PW, *et al*. Improved early morbidity and mortality after Fontan operation: the Mayo Clinic experience, 1987 to 1992. *J Am Coll Cardiol* 1996;**28**:480–6.

160 Di Donato RM, Amodeo A, di Carlo DD, *et al*. Staged Fontan operation for complex cardiac anomalies with subaortic obstruction. *J Thorac Cardiovasc Surg* 1993;**105**:398–404.

161 McElhinney DB, Reddy VM, Moore P, *et al*. Bidirectional cavopulmonary shunt in patients with anomalies of systemic and pulmonary venous drainage. *Ann Thorac Surg* 1997;**63**:1676–84.

162 Kuroda O, Sano T, Matsuda H, *et al*. Analysis of the effects of the Blalock–Taussig shunt on ventricular function and the prognosis in patients with single ventricle. *Circulation* 1987;**76**(Suppl III)III-24–8.

163 Albanese SB, Carotti A, Di Donato RM, *et al*. Bidirectional cavopulmonary anastomosis in patients under two years of age. *J Thorac Cardiovasc Surg* 1992;**104**:904–9.

164 Marcelletti C, Corno A, Giannico S, *et al*. Inferior vena cava–pulmonary artery extracardiac conduit: a new form of right heart bypass. *J Thorac Cardiovasc Surg* 1990;**100**:228–32.

165 Azakie A, Merklinger SL, Williams WG, *et al*. Improving outcomes of the Fontan operation in children with atrial isomerism and heterotaxy syndromes. *Ann Thorac Surg* 2001;**72**:1636–40.

166 Nakata T, Fujimoto Y, Hirose K, *et al*. Fontan completion in patients with atrial isomerism and separate hepatic venous drainage. *Eur J Cardiothorac Surg* 2010;**37**:1264–70.

167 Uchida T, Uemura H, Yagihara T, *et al*. Pulmonary venous obstruction after total cavopulmonary connection in heterotaxy. *Ann Thorac Surg* 2002;**73**:273–4.

168 Naito Y, Aoki M, Matsuo K, *et al*. Intracardiac Fontan procedure for heterotaxy syndrome with complex systemic and pulmonary venous anomalies. *Eur J Cardiothorac Surg* 2010;**37**:197–203.

169 Kim SJ, Kim WH, Lim HG, *et al*. Improving results of the Fontan procedure in patients with heterotaxy syndrome. *Ann Thorac Surg* 2006;**82**:1245–51.

170 Sinzobahamvya N, Arenz C, Brecher AM, *et al*. Atrial isomerism: a surgical experience. *Cardiovasc Surg* 1999;**7**:436–42.

171 Ichikawa H, Sawa Y, Fukushima N, *et al*. Late assessment after biventricular repair for isomerism heart. *Ann Thorac Surg* 2005;**80**:50–5.

172 Vodiskar J, Clur SA, Hruda J, *et al*. Left atrial isomerism: biventricular repair. *Eur J Cardiothorac Surg* 2010;**37**:1259–63.

173 Garcia OL, Mehta AV, Pickoff AS, *et al*. Left atrial isomerism and complete atrioventricular block: a report of six cases. *Am J Cardiol* 1981;**48**:1103–7.

174 Kawashima Y, Kitamura S, Matsuda H, *et al*. Total cavopulmonary shunt operation in complex cardiac anomalies. A new operation. *J Thorac Cardiovasc Surg* 1984;**87**:74–81.

175 Matsuda H, Kawashima Y, Hirose H, *et al*. Evaluation of total cavopulmonary shunt operation for single ventricle with common atrioventricular valve and left isomerism. *Am J Cardiol* 1986;**58**:180–2.

176 Cloutier A, Ash JM, Smallhorn JF, *et al*. Abnormal distribution of pulmonary blood flow after the Glenn shunt or Fontan procedure: risk of development of arteriovenous fistulae. *Circulation* 1985;**72**:471–9.

177 Papagiannis J, Kanter RJ, Effman EL, *et al*. Polysplenia with pulmonary arteriovenous malformations. *Pediatr Cardiol* 1993;**14**:127–9.

178 Knight WB, Mee RBB. A cure for pulmonary arteriovenous fistulas? *Ann Thorac Surg* 1995;**59**:999–1001.

179 Shah MJ, Rychik J, Fogel MA, *et al*. Pulmonary AV malformations after superior cavopulmonary connection: resolution after inclusion of hepatic veins in the pulmonary circulation. *Ann Thorac Surg* 1997;**63**:960–3.

180 Lee J, Menkis AH, Rosenberg HC. Reversal of pulmonary arteriovenous malformation after diversion of anomalous hepatic drainage. *Ann Thorac Surg* 1998;**65**:848–9.

181 Agnoletti G, Borghi A, Annecchino FP, *et al.* Regression of pulmonary fistulas in congenital heart disease after redirection of hepatic venous flow to the lungs. *Ann Thorac Surg* 2001;**72**:909–11.

182 Baskett RJF, Ross DB, Warren AE, *et al.* Hepatic vein to the azygous vein anastomosis for pulmonary arteriovenous fistulae. *Ann Thorac Surg* 1999;**68**:232–3.

183 Steinberg J, Alfieris GM, Brandt B III, *et al.* New approach to the surgical management of pulmonary arteriovenous malformations after cavopulmonary anastomosis. *Ann Thorac Surg* 2003;**75**:1640–2.

184 Lopez FE, van den Heuvel F, Pieper PG, *et al.* Off-pump connection of the hepatic to the azygos vein through a lateral thoracotomy for relief of arterio-venous fistulas after a Kawashima procedure. *Cardiol Young* 2008;**18**:311–5.

185 Silverman A, Cooper MD, Moller JH, *et al.* Syndrome of cyanosis, digital clubbing, and hepatic disease in siblings. *J Pediatr* 1968;**72**:70–80.

186 Krowka MJ, Cortese DA. Hepatopulmonary syndrome: an evolving perspective in the era of liver transplantation. *Hepatology* 1990;**11**:138–42.

187 Mazzera E, Corno A, Picardo S, *et al.* Bidirectional cavopulmonary shunts: clinical applications as staged or definitive palliation. *Ann Thorac Surg* 1989;**97**:779–84.

188 Bernstein HS, Brook MM, Silverman NH, *et al.* Development of pulmonary arteriovenous fistulae in children after cavopulmonary shunt. *Circulation* 1995;**92**(Suppl II):II-309–14.

189 Culbertson CB, George BL, Day RW, *et al.* Factors influencing survival of patients with heterotaxy syndrome undergoing the Fontan procedure. *J Am Coll Cardiol* 1992;**20**:678–84.

190 Mouton WG, Zehnder T. Deep vein thrombosis in azygos continuation. *Eur J Vasc Endovasc Surg* 2003;**25**:90–2.

191 Kaneko Y, Murakami A, Miyamoto T, *et al.* Hepatic vein-to-azygos vein connection in a patient with interrupted inferior vena cava. *Eur J Cardiothorac Surg* 2002;**21**:582–4.

192 Amodeo A, Grigioni M, Filippelli S, *et al.* Improved management of systemic venous anomalies in a single ventricle: new rationale. *J Thorac Cardiovasc Surg* 2009;**138**:1154–9.

193 Amodeo A, Grigioni M, Oppido G, *et al.* The beneficial vortex and best spatial arrangement in total extracardiac cavopulmonary connection. *J Thorac Cardiovasc Surg* 2002;**124**:471–8.

194 Bae EJ, Lee JY, Noh CI, *et al.* Sinus node dysfunction after Fontan modifications – influence of surgical method. *Int J Cardiol* 2003;**88**:285–91.

195 Marcelletti C, Di Donato R, Nijveld A, *et al.* Right and left isomerism: the cardiac surgeon's view. *Ann Thorac Surg* 1983;**35**:400–5.

196 Freedom RM, Van Arsdell GS. Biventricular hearts not amenable to biventricular repair. *Ann Thorac Surg* 1998;**66**:641–3.

197 Takeuchi K, McGowan FX Jr, Bacha EA, *et al.* Analysis of surgical outcome in complex double-outlet right ventricle with heterotaxy syndrome or complete atrioventricular canal defect. *Ann Thorac Surg* 2006;**82**:146–52.

198 Koh M, Yagihara T, Uemura H, *et al.* Biventricular repair for right atrial isomerism. *Ann Thorac Surg* 2006;**81**:1808–16.

199 Lim HG, Bacha EA, Marx GR, *et al.* Biventricular repair in patients with heterotaxy syndrome. *J Thorac Cardiovasc Surg* 2009;**137**:371–9.

200 Ando F, Shirotani H, Kawai J, *et al.* Successful total repair of complicated cardiac anomalies with asplenia syndrome. *J Thorac Cardiovasc Surg* 1976;**72**:33–8.

201 Pacifico AD, Fox LS, Kirklin JW, *et al.* Surgical treatment of atrial isomerism. In: Anderson RH, Macartney FJ, Shinebourne EA, Tynan M, eds. *Paediatric Cardiology*, Vol 5. Edinburgh: Churchill Livingstone, 1983: 223.

202 Hirooka K, Yagihara T, Kishimoto H, *et al.* Biventricular repair in cardiac isomerism. Report of seventeen cases. *J Thorac Cardiovasc Surg* 1995;**109**:530–5.

203 Devaney EJ, Lee T, Gelehrter S, *et al.* Biventricular repair of atrioventricular septal defect with common atrioventricular valve and double-outlet right ventricle. *Ann Thorac Surg* 2010;**89**:537–43.

204 Uemura H, Yagihara T, Kawashima Y, *et al.* What factors affect ventricular performance after a Fontan-type operation? *J Thorac Cardiovasc Surg* 1995;**110**:405–15.

205 Carotti A, Marino B, Oppido G, *et al.* Biventricular repair in patients with left isomerism. *J Thorac Cardiovasc Surg* 1995;**110**:1151–2.

206 Di Donato R, Marino B, Carotti A, *et al.* Biventricular repair in left atrial isomerism (polysplenia syndrome). *Circulation* 1989;**80**:II-363.

207 Hancock Freisen CL, Sherwood MC, Gauvreau K, *et al.* Intermediate outcomes of atrioventricular valvuloplasty in lateral tunnel Fontan patients. *J Heart Valve Dis* 2004;**13**:962–71.

208 Dickinson DF, Wilkinson JL, Anderson KR, *et al.* The cardiac conduction system in situs ambiguus. *Circulation* 1979;**59**:879–85.

209 Wren C, Macartney FJ, Deanfield JE. Cardiac rhythm in atrial isomerism. *Am J Cardiol* 1987;**59**:1156–8.

210 Southard RE, Nelson JC, Joyce DL, *et al.* Placement of a left ventricular assist device in a patient with dextrocardia. *J Heart Lung Transplant* 2005;**24**:338–9.

211 Musci M, Jurmann MJ, Drews T, *et al.* Implantation of a left ventricular assist device in situs inversus. *Ann Thorac Surg* 2002;**74**:586–8.

212 Stringham JC, Bull DA, Fuller TC, *et al.* Avoidance of cellular blood product transfusions in LVAD recipients does not prevent HLA allosensitization. *J Heart Lung Transplant* 1999;**18**:160–5.

213 Schuster M, Kocher AA, John R, *et al.* Allosensitization following left ventricular assist device (LVAD) implantation is dependent on CD40–CD40 ligand interactions. *J Heart Lung Transplant* 2001;**20**:211–2.

214 Schuster M, Kocher A, John R, *et al.* B-cell activation and allosensitization after left ventricular assist device implantation is due to T-cell activation and CD40 ligand expression. *Hum Immunol* 2002;**63**:211–20.

215 Itescu S, John R. Interactions between the recipient immune system and the left ventricular assist device surface: immunological and clinical implications. *Ann Thorac Surg* 2003;**75**(6 Suppl):S58–65.

216 Kirsch L, Timmermans T, Van Caenegem O, *et al.* Allosensitization in bridge to transplant Novacor left ventricular assist device patients: analysis of long-term outcomes with regard to acute rejection and chronic allograft vasculopathy. *Eur J Cardiothorac Surg* 2008;**34**:268–74.

217 Drakos SG, Kfoury AG, Kotter JR, *et al*. Prior human leukocyte antigen-allosensitization and left ventricular assist device type affect degree of post-implantation human leukocyte antigen-allosensitization. *J Heart Lung Transplant* 2009;**28**:838–42.

218 Holt DB, Lublin DM, Phelan DL, *et al*. Mortality and morbidity in pre-sensitized pediatric heart transplant recipients with a positive donor crossmatch utilizing peri-operative plasmapheresis and cytolytic therapy. *J Heart Lung Transplant* 2007;**26**:876–82.

219 Wright EJ, Fiser WP, Edens RE, *et al*. Cardiac transplant outcomes in pediatric patients with pre-formed anti-human leukocyte antigen antibodies and/or positive retrospective crossmatch. *J Heart Lung Transplant* 2007;**26**:1163–9.

220 Bailey LL, Assaad AN, Trimm RF, *et al*. Orthotopic transplantation during early infancy as therapy for incurable congenital heart disease. *Ann Surg* 1988;**208**:279–86.

221 Boucek MM, Mathius CM, Razzouk A, *et al*. Indications and contraindications for heart transplantation in infancy. *J Heart Lung Transplant* 1993;**12**:S154–8.

222 Turrentine MW, Kesler KA, Caldwell R, *et al*. Cardiac transplantation in infants and children. *Ann Thorac Surg* 1994;**57**:546–53.

223 Michielon G, Parisi F, Squitieri C, *et al*. Orthotopic heart transplantation for congenital heart disease: an alternative for high-risk Fontan candidates? *Circulation* 2003;**108**(Suppl II):II-140–9.

224 Doty DB, Renlund DG, Caputo GR, *et al*. Cardiac transplantation in situs inversus. *J Thorac Cardiovasc Surg* 1990;**99**:493–9.

225 Mayer JE, Perry S, O'Brien P, *et al*. Orthotopic heart transplantation for complex congenital heart disease. *J Thorac Cardiovasc Surg* 1990;**99**:484–91.

226 Cooper DK, Ye Y, Chaffin JS, Zuhdi N. A suggested technique for "orthotopic" heart transplantation in a patient with situs inversus. *Tex Heart Inst J* 1993;**20**:281–4.

227 Bailey LL. Heart transplantation techniques in complex congenital heart disease. *J Heart Lung Transplant* 1993;**12**:S168–75.

228 Michler RE, Sandhu AA. Novel approach for orthotopic heart transplantation in visceroatrial situs inversus. *Ann Thorac Surg* 1995;**60**:194–7.

229 Rubay JE, d'Udekem Y, Sluysmans T, *et al*. Orthotopic heart transplantation in situs inversus. *Ann Thorac Surg* 1995;**60**:460–2.

230 Vricella LA, Razzouk AJ, Gundry SR, *et al*. Heart transplantation in infants and children with situs inversus. *J Thorac Cardiovasc Surg* 1998;**116**:82–6.

231 Beiras-Fernandez A, Daebritz SH, Kaczmarek I, *et al*. Challenging venous reconstruction and heart transplantation in a patient with viscero-atrial situs inversus and complex congenital heart disease with Fontan circulation. *J Heart Lung Transplant* 2007;**26**:290–2.

232 Muñoz-Guijosa C, Ginel A, Montiel J, *et al*. Orthotopic heart transplantation in a patient with situs inversus, transposition of the great arteries and Mustard operation. *Eur J Cardiothorac Surg* 2008;**34**:219–21.

233 Chang YL, Wei J, Chang CY, *et al*. Cardiac transplantation in situs inversus: two cases reports. *Transplant Proc* 2008;**40**:2848–51.

234 Deuse T, Reitz BA. Heart transplantation in situs inversus totalis. *J Thorac Cardiovasc Surg* 2008;**139**:501–3.

235 Kanter KR, Vincent RN, Miller BE, *et al*. Heart transplantation in children who have undergone previous heart surgery: is it safe? *J Heart Lung Transplant* 1993;**12**:S218–24.

236 Vouhé PR, Tamisier D, Le Bidois J, *et al*. Pediatric cardiac transplantation for congenital heart defects: surgical considerations and results. *Ann Thorac Surg* 1993;**56**:1239–47.

237 Berdat PA, Mohacsi P, Althaus U, *et al*. Successful heart transplantation in a patient with Ivemark syndrome combined with situs inversus, single atrium and ventricle after total cavopulmonary connection. *Eur J Cardiothorac Surg* 1998;**14**:631–4.

238 Larsen RL, Eguchi JH, Mulla NF, *et al*. Usefulness of cardiac transplantation in children with visceral heterotaxy (asplenic and polysplenic syndromes and single right-sided spleen with levocardia) and comparison of results with cardiac transplantation in children with dilated cardiomyopathy. *Am J Cardiol* 2002;**89**:1275–9.

239 Razzouk AJ, Gundry SR, Chinnock RE, *et al*. Orthotopic transplantation for total anomalous pulmonary venous connection associated with complex congenital heart disease. *J Heart Lung Transplant* 1995;**14**:713–7.

240 Menkis AH, McKenzie FN, Novick RJ, *et al*. Expanding applicability of transplantation after multiple prior palliative procedures. *Ann Thorac Surg* 1991;**52**:722–6.

241 Reitz BA, Jamieson SW, Gaudiani VA, *et al*. Method for cardiac transplantation in corrected transposition. *J Cardiovasc Surg* 1982;**23**:293–6.

242 Harjula ALJ, Heikkilä LJ, Nieminen MS, *et al*. Heart transplantation in repaired transposition of the great arteries. *Ann Thorac Surg* 1988;**46**:611–4.

243 Girnita AL, Webber SA, Zeevi A. Anti-HLA alloantibodies in pediatric solid organ transplantation. *Pediatr Transplant* 2006;**10**:146–53.

244 Trento A, Griffith BP, Fricker FJ, *et al*. Lessons learned in pediatric heart transplantation. *Ann Thorac Surg* 1989;**48**:617–22.

245 Parness IA, Nadas AS. Cardiac transplantation in children. *Pediatr Rev* 1988;**10**:111–8.

246 Chartrand C, Guerin R, Kangah M, *et al*. Pediatric heart transplantation: surgical considerations for congenital heart diseases. *J Heart Transplant* 1990;**9**:608–17.

247 Merrill WH, Frist WH, Stewart JR, *et al*. Heart transplantation in children. *Ann Surg* 1991;**213**:393–400.

248 Shaffer KM, Denfield SW, Schowengerdt KO, *et al*. Cardiac transplantation for pediatric patients with inoperable congenital heart disease. *Tex Heart Inst J* 1998;**25**:57–63.

249 Lamour JM, Addonizio LJ, Galantowicz ME, *et al*. Outcome after orthotopic cardiac transplantation in adults with congenital heart disease. *Circulation* 1999;**100**(19 Suppl):II200–5.

250 Dionigi B, Razzouk AJ, Hasaniya NW, *et al*. Late outcomes of pediatric heart transplantation are independent of pre-transplant diagnosis and prior cardiac surgical intervention. *J Heart Lung Transplant* 2008;**27**:1090–5.

251 Khoury MJ, Cordero JF, Rasmussen S. Ectopia cordis, midline defects and chromosomal abnormalities: an epidemiologic perspective. *Am J Med Genet* 1988;**30**:811–7.

252 Carmi R, Boughman JA. Pentalogy of Cantrell and associated midline anomalies: a possible midline developmental field. *Am J Med Genet* 1992;**42**:90–5.

253 Kanagasuntheran R, Verzin JA. Ectopia cordis in man. *Thorax* 1962;**17**:159–67.

254 Torpin R. *Fetal Malformation Caused by Amnion Rupture During Gestation*. Springfield, IL: Charles C Thomas, 1968.

255 King CR. Ectopia cordis and chromosomal errors. *Pediatrics* 1980;**66**:328.

256 Soper SP, Roe LR, Hoyme HE, Clemmons JJW. Trisomy 18 with ectopia cordis, omphalocele and ventricular septal defect: case report. *Pediatr Pathol* 1986;**5**:481–3.

257 Shambererg RC, Welch KJ. Sternal defect. *Pediatr Surg* 1990;**5**:156–64.

258 Toyoma WM. Combined congenital defect of the anterior abdominal wall, sternum diaphragm, pericardium and heart: a case report and review of the syndrome. *Pediatrics* 1972;**50**:778–92.

259 Leca F, Thilbert M, Khoury W, *et al.* Extrathoracic heart (ectopia cordis): report of two cases and review of the literature. *Int J Cardiol* 1989;**22**:221–8.

260 Millhouse RF, Joos HA. Extrathoracic ectopia cordis: report of cases and review of the literature. *Am Heart J* 1959;**57**:470–6.

261 Lannelongue OM, in discussion of Kermisson EF. Volumineuse hernie sub-umbilicale avec ectopia cardiaque. *Bull Acc Med Paris* 1910;**63**:215–8.

262 Hornberger LK, Colan SD, Lock J, *et al.* Outcome of patients with ectopia cordis and significant intracardiac defect. *Circulation* 1996;**94**(Suppl):II-32–7.

263 Izukawa T, Kidd BS, Moes CA, *et al.* Assessment of the cardiovascular system in conjoined twins. *Am J Dis Child* 1978;**132**:19–24.

264 Gilbert-Barness E, Debich-Spicer D, Opitz JM. Conjoined twins: morphogenesis of the heart and a review. *Am J Med Genet A* 2003;**120A**:568–82.

265 Leachman RD, Latson JR, Kohler CM, *et al.* Cardiovascular evaluation of conjoined twins. *Birth Defects* 1967;**3**:52–65.

266 Levin M, Roberts DJ, Holmes LB, *et al.* Laterality defects in conjoined twins. *Nature* 1996;**384**:321.

267 Nichils BL, Blattner RJ, Rudolph AJ. General clinical management of thoracopagus twins. *Birth Defects* 1967;**3**:38.

268 Rossi MB, Burn J, Yen Ho S, *et al.* Conjoined twins, right atrial isomerism and sequential segmental analysis. *Br Heart J* 1987;**58**:518–24.

269 Gugliantini P, Marino B. Ecocardiografia, angio-TC e angiocardiografia per valutare la possibilità di separazione di gemelli siamesi. *Radiol Med* 1984;**88**:130–6.

270 Rudolph AJ, Michael JP, Nichols BL. Obstetric management of conjoined twins. *Birth Defects* 1975;**3**:28–37.

271 Sanders SP, Chin AJ, Parness IA, *et al.* Prenatal diagnosis of congenital heart defects in thoracoabdominally conjoined twins. *N Engl J Med* 1985;**313**:370–4.

272 Rossi P, Bordiuk JM, Golinko RJ. Angiographic evaluation of conjoined twins. *Ann Radiol* 1971;**14**:341–9.

273 Rossi P, Cozzi F, Iannaccone G. CT for assessing feasibility of separation of thoracopagus twins. *J Comput Assist Tomogr* 1981;**5**:574–6.

274 Wu MH, Lai YC, Lo HM, *et al.* Assessment of electromyocardial continuity in conjoined (thoracopagus) twins. *Am J Cardiol* 1992;**69**:830–2.

275 Simpson JS, Mustard WT, Moes CAF, *et al.* Emergency separation of thoracopagus twins (conjoined at thorax) in the newborn period: importance of careful preoperative cardiac evaluation. *Surgery* 1970;**67**:697–702.

276 Synhorst D, Matlak M, Roan Y. Separation of conjoined thoracopagus twins joined at the right atria. *Am J Cardiol* 1979;**43**:662–5.

277 McMahon CJ, Spencer R. Congenital heart defects in conjoined twins: outcome after surgical separation of thoracopagus. *Pediatr Cardiol* 2006;**27**:1–12.

278 Boles ET, Vassy LE. Thoraco-omphalopagus conjoined twins: successful surgical separation. *Surgery* 1979;**86**:485–92.

279 Cloutier R, Levasseur L, Copty M, Roy JP. The surgical separation of pygopagus twins. *J Pediatr Surg* 1979;**14**:554–6.

280 Hoshina H, Tanaba O, Obara H, Iwai S. Thoracopagus conjoined twins: management of anesthetic induction and postoperative chest wall defect. *Anesthesiology* 1987;**66**:424–6.

281 Roy M. Anesthesia for separation of conjoined twins. *Anesthesia* 1984;**39**:1225–8.

282 O'Neill JA, Holcomb GW, Schnaufer L, *et al.* Surgical experience with thirteen conjoined twins. *Ann Surg* 1988;**208**:299–312.

283 Annas GJ. Siamese twins: killing one to save the other. *Hastings Cent Rep* 1987;**17**:27–9.

51 Pediatric Pulmonary Hypertension

Cécile Tissot & Maurice Beghetti
The University Children's Hospital of Geneva, Geneva, Switzerland

Introduction

Pulmonary arterial hypertension (PAH) in children is a life-threatening disease characterized by progressive obliteration of the pulmonary vasculature leading to right heart failure and death if untreated. Prior to the current treatment era, PAH carried a poor prognosis and survival rate [1]. PAH in children may be idiopathic (IPAH) or associated with other diseases (APAH), more commonly with congenital heart disease (CHD). IPAH is diagnosed by excluding other diseases. The first description of PAH associated with CHD was made in 1897 by Victor Eisenmenger, who described the autopsy findings of a 32-year-old man with a large ventricular septal defect and pulmonary vascular disease (PVD). In 1958, Paul Wood's description of the Eisenmenger syndrome (ES) as pulmonary hypertension (PH) at the systemic level due to high pulmonary vascular resistance (PVR) with bidirectional or reversal of shunt is still relevant to our understanding today [2].

The prognosis of PAH has changed dramatically over the past decade since the introduction of new therapeutic agents and the off-label application of adult pulmonary hypertension (PH)-specific therapies to children [1,3–5]. Nevertheless, PH remains serious and extremely challenging to manage. The data in children are often limited by the small number of patients, and extrapolating from adults to children is not straightforward. The degree of pulmonary vasoconstriction relative to fixed pulmonary vascular obstruction is important in children in any form of PH and appropriate therapies must be carefully chosen according to the etiology and pulmonary vasoreactivity. In PAH associated with CHD, pulmonary vasoreactivity is very important in deciding whether the patient is a candidate for surgical repair or not. PAH still has no cure and the treatment aims at prolonging survival by improving quality of life, symptoms, exercise tolerance, and hemodynamics.

Definition and classification

PAH is defined as a mean pulmonary artery pressure (PAP) ≥25 mmHg at rest, with a normal pulmonary capillary wedge pressure (≤15 mmHg). Some authors also include an increased pulmonary vascular resistance index [≥3 Woods Units (WU) m^2] as part of the definition for PAH [6,7]. Exercise criteria have been deleted from the current definition, but some children show an abnormal vasoconstrictor response of the pulmonary vascular bed with increased PAP only with exercise at the early stage of the disease. Measurement of PAP during exercise, however, is extremely challenging in children. Compared with adults, children are thought to have a greater vasoreactive response to hypoventilation with a more pronounced oxygen desaturation [8].

A revision of the classification, including most of the forms of PH encountered in children, was proposed at Dana Point in 2008 (Table 51.1) [9]. A recent article reviewed the clinical presentation of children with PAH and outlined the difficulties of classifying pediatric PH according to this classification [10]. Category 1 includes idiopathic and familial PAH and also PAH related to or associated with various diseases, including CHD. The rationale for including PAH associated with CHD is that the histologies of category 1 PAH diseases are indistinguishable from each other, with the plexiform lesion being the cornerstone of severe pulmonary vascular disease (PVD). The plexiform lesions of patients with idiopathic or familial PAH contain monoclonal proliferating endothelial cells, whereas those of patients with associated PAH contain polyclonal endothelial cell proliferation [11]. The most common forms of associated PAH (APAH) in

Table 51.1 Revised classification of pulmonary hypertension from Dana Point 2008. (Reproduced from Simonneau G, *et al. J Am Coll Cardiol* 2009;**54**(1 Suppl):S43–54, with permission from Elsevier.)

1   Pulmonary arterial hypertension (PAH)
   1.1   Idiopathic PAH
   1.2   Heritable
      1.2.1   BMPR2
      1.2.2   ALK1, endoglin (with or without hereditary hemorrhagic telangiectasia)
      1.2.3   Unknown
   1.3   Drug and toxin induced
   1.4   Associated with
      1.4.1   Connective tissue diseases
      1.4.2   HIV infection
      1.4.3   Portal hypertension
      1.4.4   Congenital heart diseases
      1.4.5   Schistosomiasis
      1.4.6   Chronic hemolytic anemia
   1.5   Persistent pulmonary hypertension of the newborn
1'   Pulmonary veno-occlusive disease (PVOD) and/or pulmonary capillary hemangiomatosis (PCH)
2   Pulmonary hypertension owing to left heart disease
   2.1   Systolic dysfunction
   2.2   Diastolic dysfunction
   2.3   Valvar disease
3   Pulmonary hypertension owing to lung diseases and/or hypoxia
   3.1   Chronic obstructive pulmonary disease
   3.2   Interstitial lung disease
   3.3   Other pulmonary diseases with mixed restrictive and obstructive pattern
   3.4   Sleep-disordered breathing
   3.5   Alveolar hypoventilation disorders
   3.6   Chronic exposure to high altitude
   3.7   Developmental abnormalities
4   Chronic thromboembolic pulmonary hypertension (CTEPH)
5   Pulmonary hypertension with unclear multifactorial mechanisms
   5.1   Hematologic disorders: myeloproliferative disorders, splenectomy
   5.2   Systemic disorders: sarcoidosis, pulmonary Langerhans cell histiocytosis, lymphangioleiomyomatosis, neurofibromatosis, vasculitis
   5.3   Metabolic disorders: glycogen storage disease, Gaucher disease, thyroid disorders
   5.4   Others: tumoral obstruction, fibrosing mediastinitis, chronic renal failure on dialysis

children except CHD are related to chronic lung disease and hemoglobinopathies.

In the new Dana Point classification, venous PH has been renamed PH due to left heart disease and classified in category 2. It is divided into PH related to left ventricular (LV) systolic dysfunction, LV diastolic dysfunction, and left heart valvar disease. Except for restrictive cardiomyopathy, PH secondary to left ventricular diastolic dysfunction is rare in children and the most common causes of PH related to left heart disease

in children are left-sided CHD and cardiomyopathies. Nevertheless, with the emergence of childhood obesity, insulin resistance, systemic hypertension, and survivors of heart transplantation, PH due to diastolic dysfunction will become more frequent in children. The classification of PH does not address adequately the heterogeneity of PVD in children, particularly for two causes of pulmonary venous hypertension: pulmonary veno-occlusive disease (PVOD) is classified in category 1' and congenital pulmonary vein stenosis is not mentioned in this classification. It is still a matter of debate whether a specific pediatric classification should be developed.

Epidemiology and genetics

Data on pediatric epidemiology remain scarce and the exact incidence and prevalence of PH in children are not known. Although there are many registries of adult patients, registries of children with PH are less well established and powered [12–14]. PAH may be idiopathic or heritable with no underlying cause, or associated with a specific disease (associated PAH). Based on available data in children, the etiology of PH is probably more diverse than in adults, with PAH being much more common than pulmonary venous hypertension. In children, the predominant diagnoses are IPAH and PAH associated with CHD and shunt lesions [12]. ES is rarely seen now in developed countries because of early referral and surgical repair. Nevertheless, access to specialist care in developing countries is insufficient, and CHD remains the most common etiology of PAH worldwide [15]. Persistent pulmonary hypertension of the newborn (PPHN) is the most common cause of PH in the neonatal period. PH associated with chronic lung disease and hemoglobinopathies are less common and probably underreported causes of PH in infants and children. Two recent large registries will give important data about pediatric epidemiology in the near future.

PAH appears to be a disease of "predisposed" individuals in whom various stimuli may initiate the PVD process. A genetic trait may account for the variability in expression of different degrees of PH to similar stimuli. A genetic mutation of the bone morphogenetic protein receptor type 2 (BMPR2) on chromosome 2q33, a gene encoding a TGF-β receptor (the PPH1 gene), has been recognized in some patients with familial PAH (>50% of the patients) and IPAH (~20–25%), and in sporadic examples of PAH (26%) [16,17]. BMPR2 mutations are inherited as an autosomal dominant pattern with reduced penetrance and genetic anticipation. Often, the child is the first family member to present with severe disease, and evaluating first-degree relatives reveals milder forms of PAH. The genetics of PAH in children are still unclear but mutations of the BMPR2 gene seem to be involved in some patients [18,19], whereas other children may have a different genetic background [20]. More recently, a study by Rosenzweig *et al.* found that BMPR2 mutation positive

children appeared less likely to respond to acute vasodilator testing than BMPR2 mutation negative children [19]. Mutation in the BMPR2 gene is less common in PAH associated with CHD than in IPAH, but when present, it seems to have a profound impact on outcome.

Pathophysiology

Idiopathic PAH (IPAH)

PAH in adults and children shows many similarities but there are specific differences in children. PAH is a process of pulmonary vasoconstriction and proliferation and remodeling of the pulmonary vascular bed [21,22]. An imbalance in the biosynthesis of prostacyclin and thromboxane A2 [23,24] with increased thromboxane, endothelin, and serotonin and decreased prostacyclin and nitric oxide (NO) has been described [25]. In older children, intimal hyperplasia and occlusive changes and also plexiform lesions are found in the pulmonary arterioles [26]. In contrast to adults, children with IPAH have more pulmonary vascular medial hypertrophy, less intimal fibrosis, and fewer plexiform lesions [27,28]. This suggests that vasoconstriction leading to medial hypertrophy occurs early in the disease and may precede the development of fixed pulmonary vascular changes. This may explain severe acute pulmonary hypertensive crises occurring more often in response to pulmonary vasoconstrictor triggers in children than in adults.

PAH associated with CHD

Increased pulmonary artery pressure (PAP) and/or pulmonary blood flow (PBF) causes an increased pulmonary vascular resistance (PVR) related to active vasoconstriction and pathologic remodeling of the pulmonary circulation consisting of decreased luminal area of the pulmonary arteries ± a diminished number of vessels. This is reflected in the response to pulmonary vasodilatation with a decrease in PVR in patients with CHD [29,30]. Increased wall stress and endothelial shear stress serve as a growth stimulus and increased matrix protein synthesis responsible for the remodeling lesions [31]. In infants with CHD, vasoconstriction is predominant, but even in older children and adults the markedly increased PVR may remain reactive to pulmonary vasodilators. The normal physiologic response to increased flow is vasodilatation and decreased vascular resistance. The increased PVR associated with increased flow from CHD suggests resting vasoconstriction and/or pulmonary vascular remodeling [32].

The distinction between reversible and irreversible PVD and the ability to predict whether the PVR will decrease following surgical correction of CHD is crucial. Indeed, in patients with ES, closure of the pulmonary to systemic connection is associated with a worse clinical outcome than the natural history of the disease [2]. Patients with Eisenmenger syndrome may show a small degree of vasodilatation in response to pulmonary vasodilator testing, thus providing some rationale for therapy [33]. In children <2 years of age with mildly elevated PVR, PVR returns to normal after eliminating the shunt. In older patients with increased PAP and PVR, however, PVD may progress even after surgical correction. Medial hypertrophy is assumed to regress after removal of increased PAP and/or PBF [34].

Some variables have a major impact on the probability of reversal of PVD after surgical repair: the type of CHD, the age of the patient, and the level of PVR at the time of operation. Genetic and environmental factors are responsible for considerable individual variability of the pulmonary vasculature to CHD. The rapidity of evolution of pulmonary vascular remodeling towards irreversible lesions depends on whether the defect is associated with increased PAP, PBF, or both [35]. For patients with a mild increase in PBF, such as atrial septal defect (ASD), the risk of developing PVD is low in those <20 years of age [36]. With more pronounced increase in PBF, such as isolated ventricular septal defect (VSD), if closure is performed in the first 2 years of life, with a few exceptions an elevated PVR becomes normal. Favorable pulmonary vascular remodeling is even better when surgical closure is performed in the first year of life [37]. CHD with increases in both PAP and PBF evolves more rapidly towards severe PVD compared with those with increased PAP or PBF alone. Complex cardiac lesions with increased PAP and PBF together with high pulmonary arterial oxygen saturation (SaO_2), low systemic SaO_2, and polycythemia are at increased risk for the development of early PVD. For example, infants with unrepaired d-TGA and intact ventricular septum may have increased PBF but normal PAP after the early neonatal period and are at risk of developing increased PVR and PVD in the first year or two of life [38]. Infants with d-TGA and VSD or patent ductus arteriosus (PDA) develop early severe PVD in the first year of life, and some patients may develop PVD despite neonatal arterial switch operation [39]. Particular lesions prone to develop early PVD are common arterial trunk or aortic origin of a pulmonary artery [40]. For the latter, pulmonary vascular changes may occur even in the normally connected lung, emphasizing the role of other circulating vasoactive mediators.

PAH associated with hemoglobinopathies

Recently, several publications have reported an increased incidence of PH in children with hemolytic anemia, particularly sickle cell disease (SCD), but also thalassemia and spherocytosis. In a prospective study, Nelson *et al.* reported that 31% of children ≥10 years of age with SCD had evidence of pulmonary hypertension by Doppler echocardiography [41]. Factors associated with suspected PH were male sex and elevated reticulocyte count. In those patients, PH likely results from multiple factors, including high output state related to anemia, left ventricular diastolic dysfunction, and

thromboembolic disease due to hypercoagulability elevating PVR [42,43]. Moreover, intravascular hemolysis releases hemoglobin, which reacts and destroys nitric oxide [44].This reduced NO bioavailability stimulates an increase in endothelin-1, which further exacerbates PH [45].

PAH associated with chronic liver disease

Hepatopulmonary syndrome (HPS) and portopulmonary hypertension (PPHTN) are complications of portal hypertension [46]. HPS is defined as pulmonary arteriovenous malformations resulting in intrapulmonary vascular shunting, ventilation-perfusion mismatch, and chronic hypoxemia. There is vasodilatation of pulmonary arterioles and capillaries. In a study by Whitworth *et al.*, intrapulmonary vascular shunting was present in 19% of children with stable cirrhosis or extrahepatic portal hypertension [47]. PPHTN is defined as PH caused by a pulmonary arteriopathy in the presence of portal hypertension, with elevated PAP and PVR [48]. The origin is from several factors: hyperdynamic circulation, increased cardiac output, sheer stress injury to vascular walls, and imbalance of circulating vasoactive peptides, especially endothelin-1, and each has been implicated in the pathogenesis [49].The pathology of those two disorders is completely different with vasodilatation of arterioles and capillaries causing arteriovenous shunting in HPS and intimal fibrosis with endothelial and smooth muscle proliferation leading to increased PVR in PPHTN.

Persistent pulmonary hypertension of the newborn (PPHN)

PPHN is characterized by failure of the pulmonary circulation to achieve or sustain the normal drop in PVR following birth (see Chapter 17). There may be an abnormal transition to the extrauterine life with failure of the pulmonary vasculature to dilate. Strong experimental and clinical data support the role of impaired vascular endothelial growth factor (VEGF) signaling in the pathogenesis of two major clinical disorders of the developing lung circulation: PPHN and bronchopulmonary dysplasia (BPD). These disorders are each characterized by impaired vascular growth, structure, and reactivity, which are at least partly due to endothelial cell dysfunction [50,51]. Laboratory studies have identified the important role of NO–cGMP signaling in regulating the perinatal pulmonary circulation, leading to the development and application of inhaled NO therapy and cGMP-specific phosphodiesterase inhibitors (PDE) such as sildenafil [52,53].

Pulmonary capillary hemangiomatosis (PCH) and pulmonary veno-occlusive disease (PVOD)

PCH and PVOD are both characterized by precapillary PAH and are included in classification category 1. They are characterized by widespread vascular obstruction at either the alvelolar capillary bed (PCH) or the pulmonary venules

(PVOD). These disorders are difficult to diagnose and their treatments are different because pulmonary vasodilators may worsen the patient's status by inducing pulmonary edema [54]. Treatment of PCH and PVOD is frequently unsuccessful and requires lung transplantation.

PH associated with left heart diseases

Left heart diseases may increase pulmonary venous pressure and be responsible for pulmonary venous hypertension (or postcapillary PH). The initial pathophysiologic mechanism is a passive rise in PAP as downstream pressure increases to maintain left heart preload and cardiac output. The hemodynamic data in this setting show a normal transpulmonary gradient (<10 mmHg), a low PVR (<5 WU m^2) and a diastolic PAP equal to the left atrial pressure. Subsequent reflex vasoconstriction of the pulmonary arteries or veins, or both, leads to an increased transpulmonary gradient (>10 mmHg), increased PVR (>5 WU m^2) and diastolic PAP exceeds left atrial pressure. The patients usually respond to pulmonary vasodilators by a decrease in both the transpulmonary gradient and the PVR. Finally, the pulmonary arteries or veins have fixed vasoconstriction and are unresponsive to pulmonary vasodilators. The histopathology shows medial thickening of both pulmonary arteries and veins ("arterialization" of the pulmonary veins) [55]. Lymphangiectasia is seen in both longstanding venous PH and following *in utero* elevation of pulmonary venous pressure (pulmonary vein atresia, total anomalous pulmonary venous drainage, or hypoplasic left heart syndrome with intact atrial septum). Advanced lesions, such as cellular intimal proliferation or plexiform lesions, are not seen. PH regresses if the left heart obstruction or dysfunction is addressed early.

PAH associated with neonatal and chronic lung disease

Bronchopulmonary dysplasia (BPD) is a chronic lung disease in prematurely born or immature infants. BPD is predominantly defined as disruption of distal lung growth with abnormal growth of the alveoli and the pulmonary circulation. The number of small pulmonary arteries is reduced, leading to a reduced alveolar–capillary surface area and impaired gas exchange [56]. PH which presents early in the course of the disease contributes significantly to high morbidity and mortality of neonates with BPD [57]. Abnormalities of the pulmonary circulation in BPD include increased vascular tone and vasoreactivity, hypertensive remodeling, and decreased growth, leading to increased PVR with marked vasoconstrictor response to hypoxia [58]. The reduced vascular surface area implies that even a relatively minor increase in left-to-right shunting of blood through a patent foramen ovale (PFO) or patent ductus arteriosus (PDA) may induce a much greater injury to the lung vasculature than in normal infants. Early closure of shunt lesions should be performed prior to the development of progressive PH. Chronic

sildenafil therapy is well tolerated, safe, and effective for infants with PH related to chronic lung disease [52].

Congenital diaphragmatic hernia presents as PPHN. *In utero* lung growth is compromised by the intrathoracic position of the abdominal contents and leads to pulmonary vascular changes. A recent study by Keller *et al.* has shown that infants with congenital diaphragmatic hernia and poor outcome had higher plasma endothelin-1 (ET1) levels and severity of pulmonary hypertension than infants discharged on room air. The severity of pulmonary hypertension was associated with ET1 levels [59]. The two main factors determining long-term outcome are the degree of lung hypoplasia and the severity of the pulmonary vascular abnormalities [60].

Assessment

Clinical history and physical examination

Symptoms of PAH in children are frequently misleading and the diagnosis may be unrecognized for some time. A high degree of suspicion should be the rule, and PAH should be suspected in any child with undue shortness of breath, exercise intolerance, tiredness, or syncopal episodes. In children with congenital cardiac shunt lesions, feeding difficulties, poor weight gain, and recurrent respiratory tract infections are common signs of high PBF. Recurrent collapse of different lobes or segments of lung can be secondary to dilated proximal pulmonary arteries and airway compression. The signs and symptoms of heart failure usually improve as PVR increases and the patient may become asymptomatic until the shunt reverses and becomes obvious with arterial oxygen desaturation. In children with Eisenmenger syndrome, central cyanosis and digital clubbing are present. Patients with ES are at increased risk of hemoptysis in early adult life. In children with PAH, exercise intolerance is common and can be graded according to the WHO functional classification (Table 51.2).

The physical signs of PAH include a right ventricular lift, an accentuated and palpable second heart sound, and a pulmonary systolic ejection click secondary to a dilated pulmonary trunk. A high-pitched diastolic murmur of pulmonary insufficiency, a holosystolic murmur of tricuspid regurgitation, or gallop rhythm may be audible. The resting systemic arterial oxygen saturation should be normal in the absence of an intracardiac right-to-left shunt. Hepatomegaly with peripheral edema may be present in right heart failure. Even if associated PAH is rare in children except for CHD, all potential etiologies should be evaluated and treated (Table 51.3).

Electrocardiogram (ECG)

ECG findings include right ventricular hypertrophy and strain, right atrial enlargement, and right axis deviation (Figure 51.1). Atrial arrhythmias may be the presenting symptoms of PAH.

Table 51.2 World Health Organization (WHO) functional classification in PH.

Class I	• PH with no limitation of physical activity Ordinary physical activity does not cause undue dyspnea or fatigue, chest pain or near syncope
Class II	• PH with slight limitation of physical activity
	• Comfortable at rest
	• Ordinary physical activity causes undue dyspnea or fatigue, chest pain or near syncope
Class III	• PH resulting in marked limitation of physical activity
	• Comfortable at rest
	• Less than ordinary physical activity causes undue dyspnea or fatigue, chest pain or near syncope
Class IV	• PH with inability to carry out any physical activity without symptoms
	• Signs of right heart failure
	• Dyspnea and/or fatigue may be present even at rest
	• Discomfort is increased by any physical activity

Table 51.3 Pulmonary hypertension related to congenital heart diseases.

Left-to-right shunts	• Atrial septal defect (ASD)
	• Ventricular septal defect (VSD)
	• Atrioventricular septal defect (AVSD)
	• Patent ductus arteriosus (PDA)
	• Aortopulmonary window
Increased pulmonary venous pressure	• Cardiomyopathy
	• Coarctation of the aorta (CoA)
	• Hypoplastic left heart syndrome (HLHS)
	• Shone complex
	• Mitral stenosis (MS)
	• Supravalvar mitral ring
	• Cor triatriatum sinister
	• Pulmonary vein stenosis
	• Pulmonary veno-occlusive disease (PVOD)
	• Total or partial anomalous pulmonary venous connection (TAPVC/PAPVC)
Cyanotic heart lesions	• Transposition of the great arteries (TGA) with VSD
	• Common arterial trunk (CAT)
	• Tetralogy of Fallot (TOF) Univentricular heart with unobstructed pulmonary blood flow (with/without restrictive atrial septum)
Anomalies of the pulmonary artery	• Origin of a pulmonary artery from the aorta
	• Unilateral absence of a pulmonary artery
	• Scimitar syndrome
Shunt anastomosis	• Waterston anastomosis
	• Potts anastomosis
	• Blalock–Taussig anastomosis
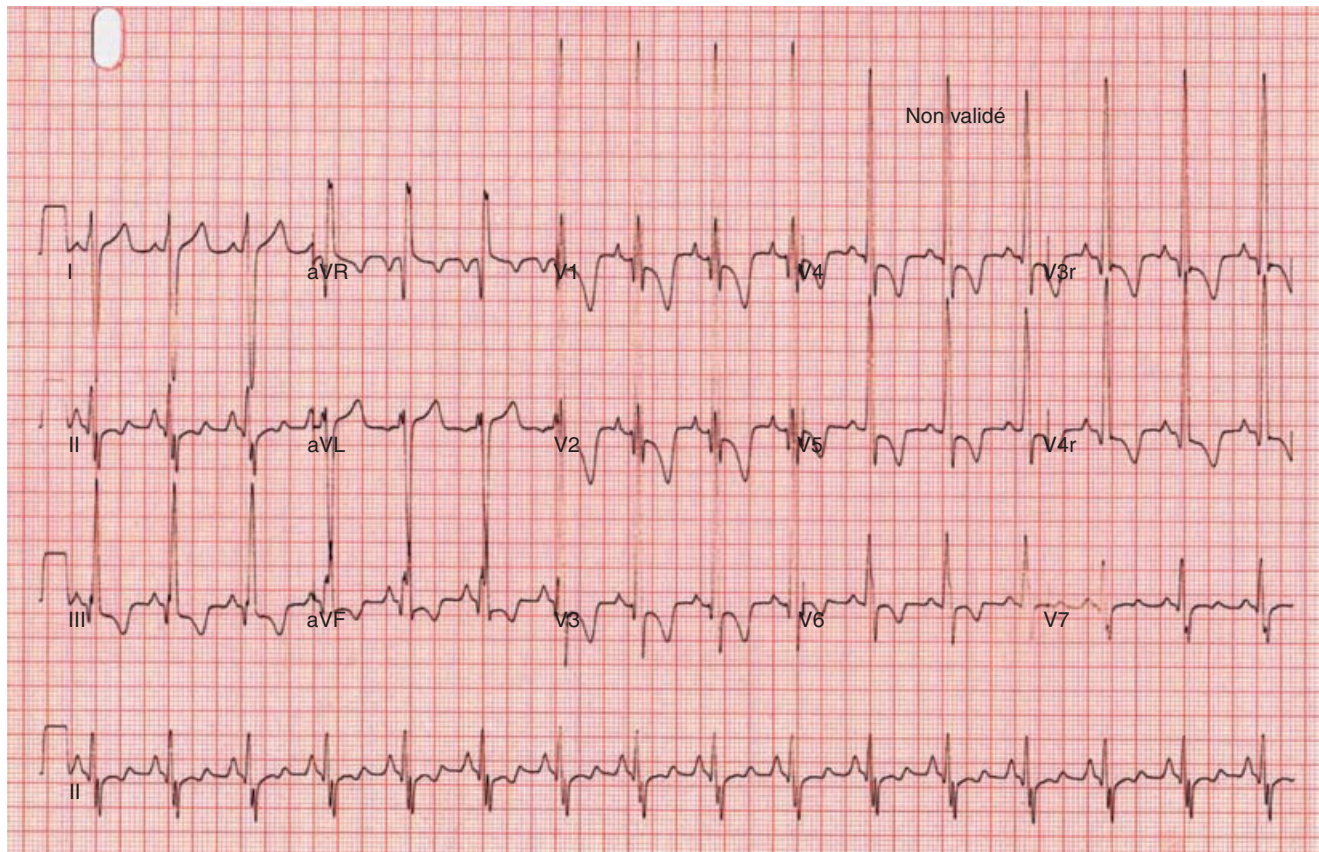
Figure 51.1 Electrocardiogram in a child with IPAH showing right ventricular hypertrophy and strain, right axis deviation, and incomplete right bundle branch block.

Chest X-ray

Chest X-ray findings in severe PAH are enlarged central pulmonary arteries and diminished peripheral pulmonary vascular markings (Figure 51.2a). Cardiomegaly is usual, secondary to right heart enlargement. In children with PAH related to congenital shunt lesions, the chest X-Ray is reassuringly plethoric when the PVR is sufficiently low to allow high PBF and will show dilatation of the proximal vessels with peripheral hypoperfusion in significant PAH. The chest X-ray in children with venous PH shows obvious pulmonary edema (Figure 51.2b).

Echocardiography

Although cardiac catheterization is necessary for disease confirmation and PAP measurement, echocardiography is a useful noninvasive tool for the diagnosis and follow-up of PAH. In the absence of pulmonary stenosis, echocardiography allows the estimation of the systolic PAP by measuring the peak systolic pressure gradient between the right ventricle and the right atrium using the TR jet and the modified Bernoulli equation ($\Delta P = v^2$, where ΔP is the pressure gradient and v the velocity) and by adding the estimated right atrial pressure (Figure 51.3a). One must be aware that using the TR jet velocity as an estimate of systolic PAP can over- or underestimate the PAP [61]. Echocardiography also allows the estimation of the end-diastolic and mean PAP from the pulmonary insufficiency (PI) flow velocity (Figure 51.3b). Good correlation has been demonstrated between echocardiographic and catheterization estimate of PAP. Echocardiography may reveal right heart dilatation and right ventricular hypertrophy and dilatation with bowing of the interventricular septum to the left (Videoclips 51.1 and 51.2). In children with a shunt lesion, the systolic PAP can also be estimated from the velocity through the shunt using the modified Bernoulli equation. In VSD or PDA, right-to-left shunt or low-velocity left-to-right shunt may suggest an elevated PAP.

Depending on the degree of PH, the interventricular septum may flatten only in systole (mild–moderate PH) or throughout the cardiac cycle (severe PH). The left ventricular eccentricity index (EI) is a measure of the interventricular septal shift towards the LV in end-diastole and is usually >1 in patients with PAH (Figure 51.3c). Marked septal shift can cause underfilling of the left ventricle with redistribution of LV filling from early to late diastole as a reflection of reduced LV compliance and diastolic dysfunction [62]. A pericardial

(a)   (b)
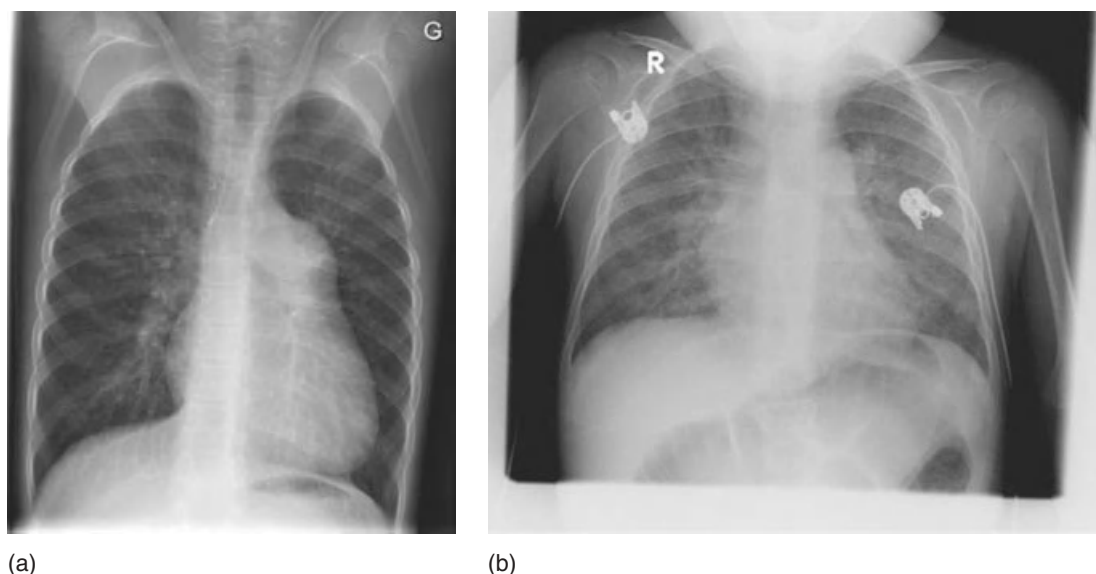
Figure 51.2 *Chest* X-ray (a) in a child with IPAH with enlarged central pulmonary arteries and peripheral hypoperfusion and (b) in a child with pulmonary veno-occlusive disease with obvious pulmonary edema secondary to pulmonary venous hypertension.

effusion is rare in children but is associated with an increased risk of poor outcome [63]. Right ventricular (RV) function can be assessed by echocardiography using the tricuspid annular plane systolic excursion (TAPSE) or the RV fractional area change (RVFAC). In adults with PAH, a TAPSE of <1.8 cm is associated with RV systolic dysfunction and a lower survival rate [64]. (Figure 51.3d). A RVFAC of ≤40% is considered abnormal, reflecting RV systolic dysfunction. A good correlation between RVFAC and EF by cardiac MRI, which represents the gold standard for evaluating RV systolic function, has been demonstrated. A reduced systolic velocity S' obtained by tissue Doppler imaging from the RV free wall at the tricuspid annulus also reflects RV systolic dysfunction.

Cardiac catheterization

Cardiac catheterization is necessary to exclude subtle CHD, such as pulmonary venous obstruction. PAH must be confirmed by catheterization, and pulmonary vasoreactivity testing should be performed, usually with inhaled nitric oxide (NO), but intravenous epoprostenol, adenosine, or inhaled iloprost may also be used [65,66]. Protocols for pulmonary vasodilator testing are center specific, but 20 ppm NO with or without increased oxygen concentration for 10 min usually achieves sufficient pulmonary vasodilatation. Acute responders should show a decrease of ≥10 mmHg in mean PAP with a mean PAP of ≤40 mmHg or a decrease in ≥20% in the mean PAP or PVR with an unchanged or increased cardiac output. It is uncertain if the same definition of vasoreactivity should be applied for adults and children with PAH. Recent data suggest that 7% of children with IPAH and 6% of those with APAH respond to acute vasodilator testing [12].

Cardiac catheterization in children with PAH related to CHD follows different rules and calculation of pulmonary and systemic blood flow and vascular resistance using the Fick principle with measured oxygen consumption is essential [67]. A baseline PVR index <6 WU m^2 with a pulmonary to systemic resistance ratio (PVR/SVR) of <0.3 indicates a favorable outcome following surgical repair. In children undergoing a Fontan operation, a mean PAP of >15 mmHg may be associated with both early and late mortality [68].

The measurement of the transpulmonary gradient (normal TPG <10 mmHg) is essential, particularly in patients with venous PH, and requires an accurate pulmonary capillary wedge pressure (PCWP) measurement. Wedge angiography is helpful in evaluating the severity of PVD (Videoclip 51.3). In patients with severe PAH and PVD, it shows decreased arborization, reduced background opacification and delayed venous filling. The pulmonary arteries may appear tortuous or have segmental dilatation and show abrupt tapering toward the periphery, characteristic of a high PVR [69]. Aortography should be performed at initial diagnosis to rule out aortopulmonary collaterals.

Exercise capacity

In children aged ≥7–8 years, exercise capacity can be assessed with a 6 min walking test (6-MW test). The 6-MW test remains the standard tool for testing exercise capacity in most clinical trials in adults with PAH [70], but is difficult to standardize in children, even though recent publications of reference values in healthy children are available [71–73]. The 6-MW test has not been validated in children with PAH. In older children, cardiopulmonary exercise testing to determine maximum oxygen consumption (VO_2), work rate, and
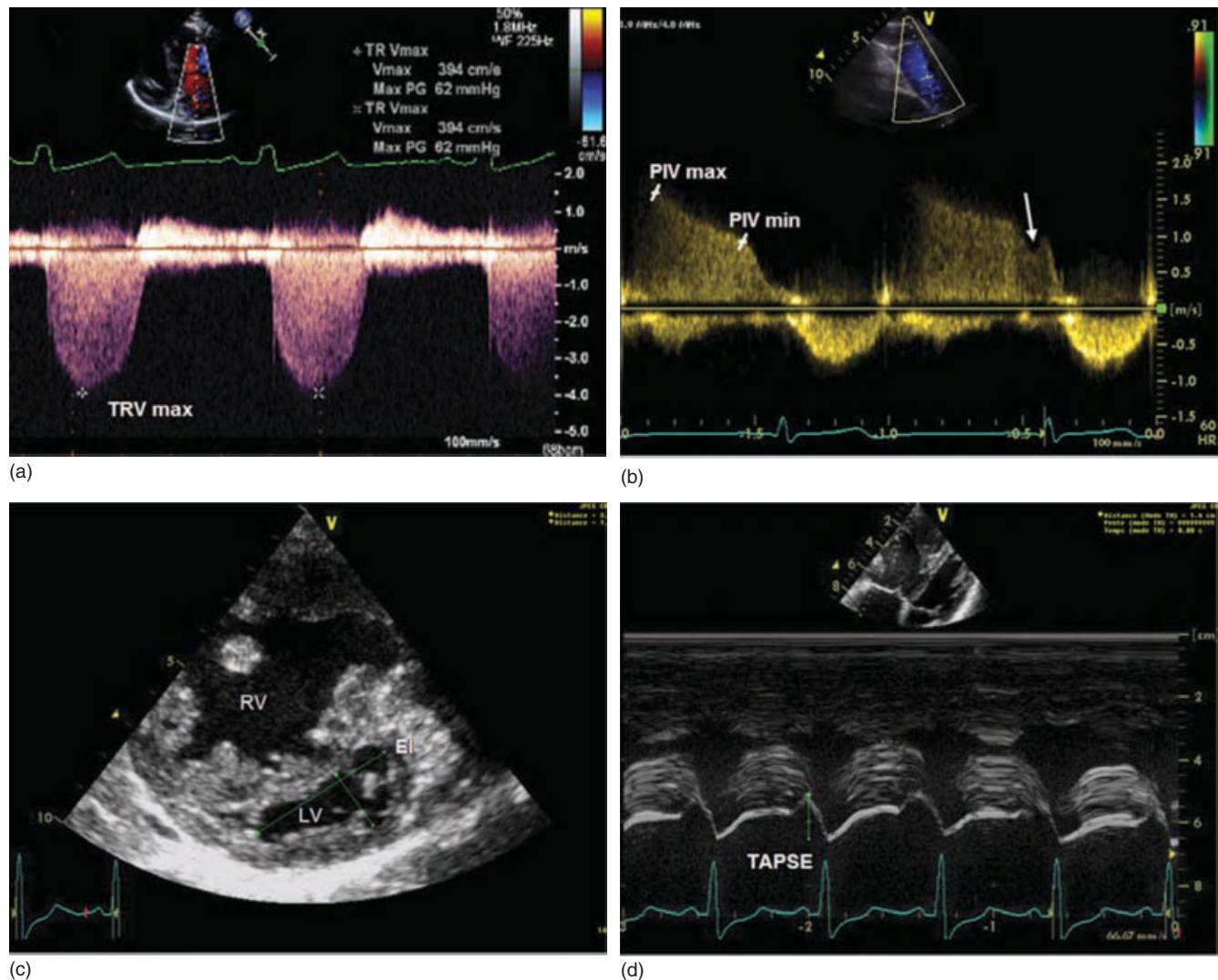
Figure 51.3 Doppler echocardiography with high-velocity tricuspid regurgitation (a) allowing for estimation of right ventricular systolic pressure ($RVSP = TRV_{max}^2 + RAP$), and with pulmonary insufficiency (b) allowing for estimation of end-diastolic pulmonary arterial pressure ($PAP\ diast = PIV_{min}^2 + RAP$) and mean pulmonary arterial pressure ($PAP\ mean = PIV_{max}^2$) using the modified Bernoulli equation. (c) 2D echocardiography in a patient with IPAH showing hypertensive and dilated right ventricle with septal shift towards the left ventricular and increased eccentricity index (EI > 1). (d) M-mode echocardiography in a patient with IPAH showing a decreased tricuspid plane systolic excursion (TAPSE <1.8 cm). PAP, pulmonary arterial pressure; PIVmax, maximal pulmonary insufficiency velocity; PIVmin, minimal pulmonary insufficiency velocity; RAP, right atrial pressure; RVSP, right ventricular systolic pressure; TRVmax, tricuspid regurgitation velocity max.

anaerobic threshold may be useful. Children with PH have significant impairment in aerobic capacity with decreased VO_2 compared with healthy controls [74]. Cardiopulmonary exercise testing can be performed safely in children with PH, with the exception of patients with severe limitation [75].

Cardiac magnetic resonance imaging (MRI)

Cardiac MRI is emerging as a potentially valuable tool for evaluating PH. The measurement of right ventricular volume, muscle mass, and left ventricular septal bowing, the calculation of stroke volume based on PBF, and delayed contrast enhancement suggestive of myocardial fibrosis may have a role in the serial follow-up of children with PH [76].

Nevertheless, cardiac MRI in young children necessitates anesthesia, which is an important consideration. Hence the risk of anesthesia must be carefully weighed against the benefit of additional information.

Brain natriuretic peptide (BNP)

BNP may be a useful tool to assess disease progression. Serial changes in BNP measurements correlate with the change in the functional status, hemodynamics, echocardiographic parameters, and outcome in children with PAH [77–79]. BNP correlates positively with functional status in children with PAH and a value >130 pg ml^{-1} is associated with increased risk of death or need for transplantation [78].

Furthermore, change in BNP over time correlates with change in hemodynamic and echocardiographic parameters in children with PAH. A BNP value >180 pg ml^{-1} predicts decreased survival [77].

Others

Serological studies (HIV, hepatitis) and blood screening for connective tissue diseases and coagulation disorders may help to discover potential causes of PAH. Ventilation–perfusion scan should be performed to exclude chronic thromboembolic disease, including patients with Eisenmenger syndrome because of their known increased incidence of thromboembolic events. An abdominal ultrasound scan should be performed to exclude portopulmonary hypertension. A high-resolution chest CT scan should also be performed before initiating pulmonary vasodilator therapy to exclude pulmonary capillary hemangiomatosis (PCH) or pulmonary veno-occlusive disease (PVOD) (Figure 51.4). Pulmonary function testing shows a mild restrictive pattern in about 20–50% of patients with IPAH and a mild reduction in the diffusion capacity in most of them [80]. Lung biopsy is rarely performed given its relatively high risk, but may be helpful, particularly in small children, to exclude certain diseases, such as PVOD, PCH, or alveolar capillary dysplasia. Those patients respond poorly to treatments currently available for PAH and need a definitive diagnosis for lung transplant listing [81]. In IPAH, the lung biopsy shows the classic features of medial hypertrophy, intimal fibrosis, microthrombi, and plexiform lesions.

Figure 51.5 summarizes the diagnostic algorithm recommended for pediatric patients with pulmonary hypertension.

A suggested work-up (with normal values) for pediatric pulmonary hypertension is presented in Table 51.4.

Figure 51.4 *Chest* CT scan in a patient with pulmonary veno-occlusive disease (PVOD) with diffuse typical infiltrate.
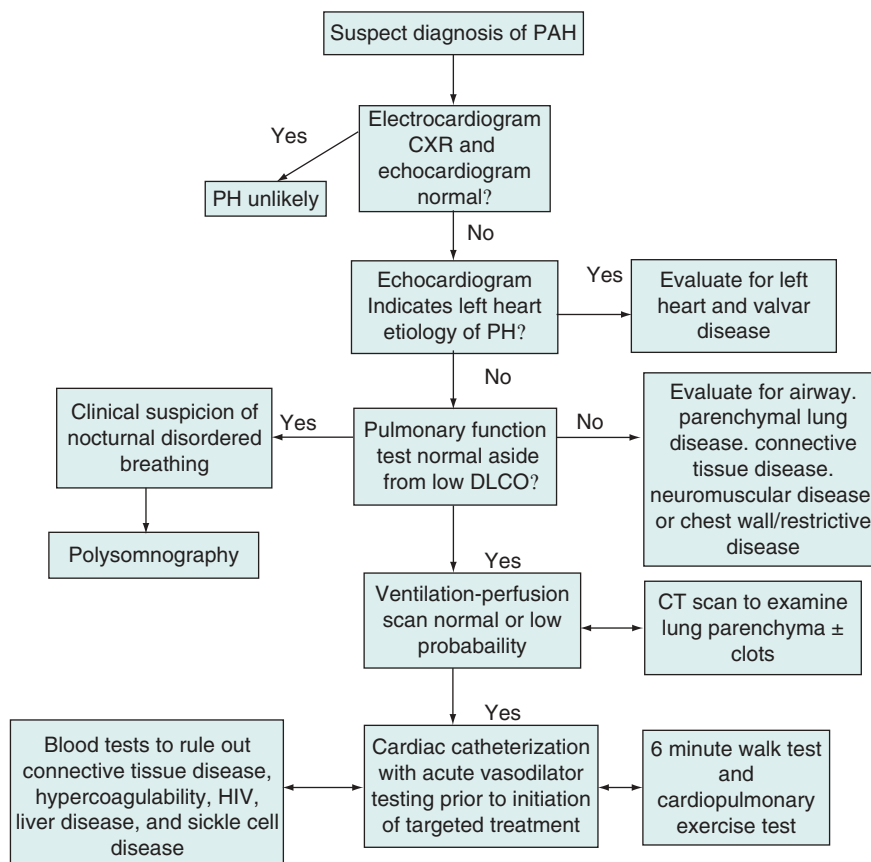
Figure 51.5 Schematic representation of the diagnostic work-up recommended in pediatric patients with PAH. (Reproduced from Rosenzweig EB, *et al., Prog Pediatr Cardiol*, *27*, pp. 7–11, Copyright (2009), with permission from Elsevier.)

Table 51.4 Pediatric pulmonary hypertension: suggested work-up (with abnormal values).

Chest radiograph	• Cardiomegaly
	• Enlarged central pulmonary arteries
	• Peripheral pulmonary hypoperfusion
Electrocardiogram	• Right atrial hypertrophy
	• Right ventricular hypertrophy and strain
	• Right axis deviation
	• ST segment changes
Echocardiography	• Right atrial dilatation
	• Right ventricular hypertrophy (free wall >0.5 cm) and dilatation
	• Decreased right ventricular function
	• Fractional area change (FAC) <40%
	• Tricuspid annular plane systolic excursion (TAPSE) <1.8 cm
	• Tissue Doppler S' <10 cm s^{-1}
	• Increased right heart filling pressure (IVC dilatation)
	• TR jet velocity >2.8 m s^{-1}
	• Flattening of the interventricular septum
	• Eccentricity index (EI) > 1
	• Myocardial performance index (MPI) >0.28 ± 0.04 s^{-1}
	• Pericardial effusion
Cardiac catheterization	• Mean pulmonary artery pressure (mPAP) >25 mmHg
	• Pulmonary vascular resistance index (PVRI) >3 WU m^2
	• PVR/SVR >0.3
	• Pulmonary capillary wedge pressure (PCWP) >15 mmHg
	• Right atrial pressure (RAP)
	• Pulmonary vasoreactivity testing (NO ± O_2)
	• Aorto-pulmonary collaterals and/or pulmonary arteriovenous malformations
Liver evaluation	• Liver function tests (ASAT, ALAT, γGT)
	• Abdominal ultrasound (portopulmonary hypertension)
Complete blood count (CBC)	• Anemia or erythrocytosis
	• Abnormal red blood cells
	• Thrombocytopenia
Urinalysis	• Proteinuria
Blood chemistry	• BNP >130 pg ml^{-1}
	• NT-proBNP
Serologies	• HIV
	• Hepatitis profile
Hypercoagulable evaluation	• Disseminated intravascular coagulation (DIC) screen
	• Factor V Leiden
	• Factor II, V, VII, VIII
	• Antithrombin III
	• Prothrombin mutation 22010
	• Protein C and S
	• Von Willebrand Ag
	• Von Willebrand sirtocetin cofactor
	• Anticardiolipin IgM and IgG
Electrophoresis	• Serum protein
	• Hemoglobin
Collagen vascular disease work-up	• Antinuclear antibody (ANA) with profile (DNA, Smith, RNP, SSA, SSB, centromere, SCL-70)
	• Rheumatoid factor (RF)
	• Erythrocyte sedimentation rate (ESR)
	• CH50 complement and components
Thyroid function tests	• TSH and free T4
Genetic	• BMPR2 testing
Lung evaluation	• Pulmonary function tests with DLCO and bronchodilator
	• Sleep study and pulse oximetry

Table 51.4 (cont'd)

Exercise capacity	• *Chest* CT scan • Ventilation/perfusion (V/Q) scan • Lung biopsy[a] • Six-minute walking test (walking distance and saturation) • Cardiopulmonary exercise test (VO$_{2\ max}$, work rate, and anaerobic threshold)

[a]Lung biopsy may be useful in infants with PAH to exclude pulmonary veno-occlusive disease (PVOD), pulmonary capillary hemangiomatosis (PCH). or alveolar capillary dysplasia.
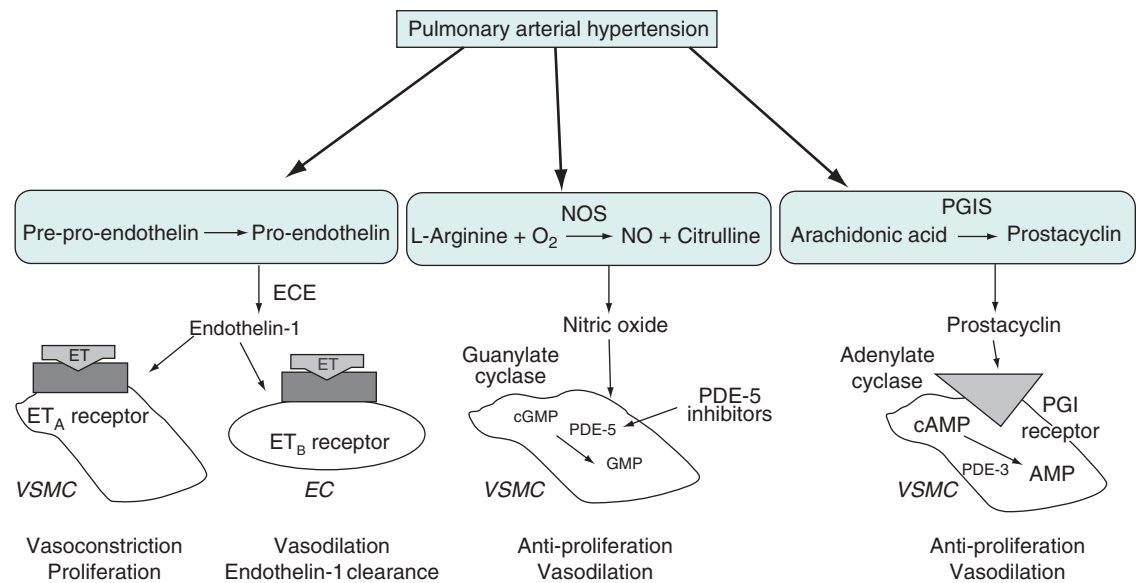
Figure 51.6 Schematic representation of the three pathways involved in the therapeutic approach of PAH. EC, endothelial cell; ECE, endothelin converting enzyme; ET, endothelin; NOS, nitric oxide synthase; PDE, phosphodiesterase type 5; PGI, prostacyclin; PGIS, prostacyclin synthase; VSMC, vascular smooth muscle cell.

Therapeutic approach to PAH

Evidence-based treatment recommendations for children with PAH do not exist, primarily because results from randomized clinical trials are lacking for pediatric patients. The aim of medical treatment is to dilate and reverse the abnormal remodeling of the pulmonary vascular bed and to restore endothelial function, by acting on the prostacyclin, endothelin, and nitric oxide (NO) pathways (Figure 51.6). In practice, the therapeutic algorithm developed for PAH in adults appears to guide treatment of children with PAH [6] (Figure 51.7). Nevertheless, there are some difficulties in applying adult criteria and dosage regimens to children.

The main determinant of treatment is the response to vasodilator testing at cardiac catheterization. Acute responders with IPAH can be treated initially with calcium channel blockers (CCBs). In children with PAH associated with CHD, acute responders are candidates for surgical repair with shunt closure. In nonresponders with right heart failure, the first-line treatment consists of continuous intravenous prostacyclin, whereas in the absence of right heart failure, other targeted therapies (endothelin receptor blockers, phosphodiesterase inhibitors, or prostacyclin analogs) may be tried first. Nonresponders have a very limited survival if not treated with targeted therapies [1,82]. Nonresponders with PAH associated with CHD are also candidates for targeted therapies. These therapies have not been approved for use in children with PAH, except for the pediatric formulation of bosentan, which has been recently approved in Europe [83].

Conventional medical therapy

Diuretic therapy may be necessary for children with heart failure, but should be initiated cautiously because children with PAH may be preload dependent to maintain an optimal cardiac output. Although the use of *digoxin* in PAH has not shown clear benefits in children, it is sometimes used for right ventricular failure or arrhythmias [84].
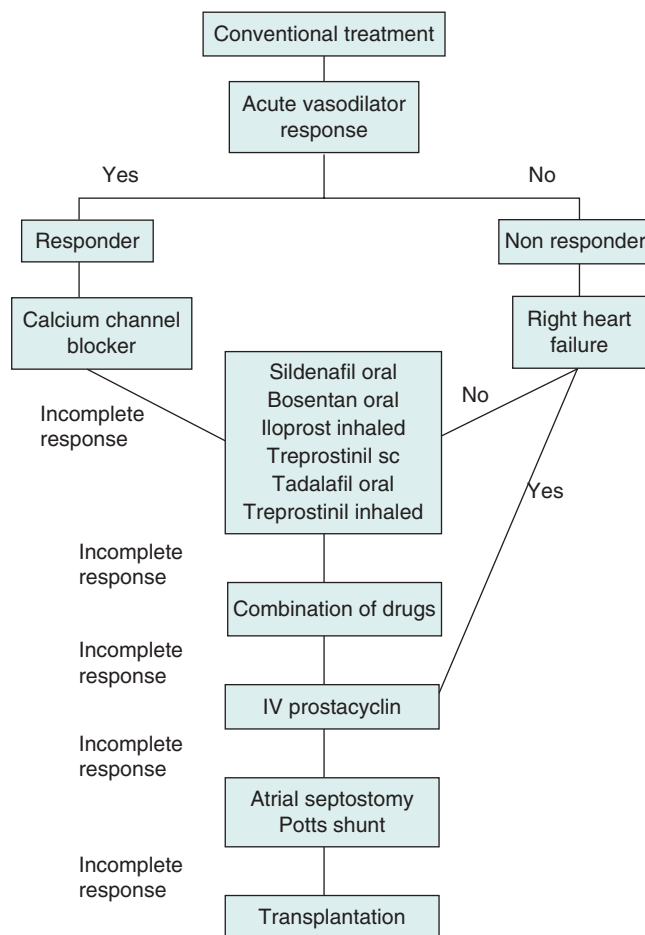
Figure 51.7 Therapeutic algorithm recommended for pediatric patients with PAH.

The benefits of chronic *anticoagulation* have not been widely studied in children with PAH, but may be beneficial in patients with low cardiac output leading to sluggish blood flow through the pulmonary arteries or in those with hypercoagulable states at risk of thrombosis in situ. The risk/benefit of anticoagulation should be weighed carefully, especially in small children prone to hemorrhagic complications. Low-dose warfarin is frequently used to target an INR of 1.5–2 [85]. In younger children, maintenance of an adequate anticoagulation level is frequently difficult and *antiplatelet* therapy with aspirin is sometimes used, even though data are unavailable for children with PAH. For teenagers requiring contraception, oral contraceptive agents without estrogen content are recommended to avoid the risk of thromboembolic events.

Enhanced inspired oxygen is usually not used as a mainstay of therapy in children with normal daytime saturations. Nevertheless, some children may show mild nocturnal hypoventilation and desaturation known to exacerbate PAH, which can be avoided using night-time supplemental

oxygen. Children with PAH should have oxygen supplement available at home for an emergency. They should receive supplemental oxygen during any respiratory tract infection associated with desaturation and also during air travel. For children with RV failure and resting hypoxemia secondary to increased oxygen extraction, chronic supplemental oxygen therapy may be considered. For children with PAH associated with CHD, enhanced inspired oxygen may be beneficial especially for those with hypoventilation or lung disease. Nevertheless, for those with right to left interatrial shunting, oxygen supplement does not usually improve oxygen saturation. A controlled study in patients with Eisenmenger syndrome showed no benefit in survival or level of hemoglobin [86].

Nitric oxide (NO) is a potent vasodilator with selective effect on pulmonary circulation. NO activates soluble guanylate cyclase in the pulmonary smooth muscle cells, increases cyclic GMP, and decreases intracellular calcium concentration, leading to smooth muscle relaxation and vasodilation. NO is useful in all forms of PH [87], and has been beneficial for treating postoperative pulmonary hypertensive "crisis" [88–90]. Rebound PH is problematic and may prolong postoperative NO administration in some patients [91]. The delivery system is a major limitation but chronic home administration of NO can be achieved in children using a pulsed nasal delivery system, which appears to have the same efficacy as the continuous delivery system [92].

Calcium channel blockers (CCBs) inhibit calcium influx into cardiac and smooth muscle cells, causing pulmonary vasodilation. Chronic calcium channel blockade is efficacious in patients who demonstrate an acute response to vasodilator testing. Recent data suggest that ~7% of children with PAH are "responders" and can be effectively treated with oral CCB [12]. In children with IPAH, Barst *et al.* showed that 5-year survival rates improved significantly in acute vasoreactive responders treated with CCBs compared with non-responders [1]. For acute responders treated with CCBs, survival at 1, 5, and 10 years was 97, 97, and 81%, respectively with a treatment success of 84, 68, and 47%, respectively, in IPAH [93].Careful follow-up is essential as some acute responders may become nonresponders with time [93]. Those patients usually deteriorate clinically and hemodynamically and should be switched to other targeted therapies. CCBs are usually not indicated in PAH associated with CHD [6]. Nevertheless, in patients with Eisenmenger syndrome complicating VSD, nifedipine has been shown to improve exercise tolerance and arterial oxygen saturation with exercise [94]. The long-term effect of nifedipine on PVR in children with PAH and CHD still needs to be determined [95]. The major side effect is systemic hypotension. The dosage for children is extrapolated from adult studies and the optimal dose for children still has to be determined.

Targeted therapies

Based on known mechanisms of action and the endothelial dysfunction, three classes of drugs are commonly used to treat children with PAH: prostacyclin analogs, endothelin receptor antagonists and phosphodiesterase inhibitors.

Prostacyclin analogs

Prostacyclin is a metabolite of arachidonic acid endogenously produced by the vascular endothelium. It is a potent pulmonary and systemic vasodilator with antiplatelet activity. Children with severe PAH show diminished NO and prostacyclin synthase expression in the pulmonary vasculature [25].

Epoprostenol, a prostacyclin analog mainly used by intravenous infusion, improves hemodynamics, quality of life, exercise capacity, and survival in adults and children with IPAH and APAH [1,4]. Barst *et al.* have shown improved survival in children treated with long-term IV epoprostenol, with a 4-year survival rate for treated children of 94% compared with 38% in untreated patients [1], and Yung *et al.* have reported a 10-year treatment success rate (freedom from death, transplantation, or atrioseptostomy) of 37% [93]. Epoprostenol lowers PAP and increases cardiac output and oxygen transport. In adults and children with PAH associated with CHD, epoprostenol decreases PVR, improves oxygen delivery, and increases exercise capacity, with a demonstrated effect on survival [96–98]. Tolerance may develop and most children need periodic dose escalation. The optimal dose of i.v. epoprostenol shows a significant patient variability, and should be titrated incrementally, with children usually needing relatively much higher doses than adults. Adverse effects are antiplatelet activity and systemic vasodilation. Diarrhea and jaw pain are common side effects. Epoprostenol has a short half-life (1–2 min), necessitating a continuous intravenous infusion with a permanent central venous catheter. Complications such as line sepsis, local infection, and catheter dislodgement are not unusual [99,100], and can be responsible for life-threatening rebound PAH. Recently, the use of specific closed hub systems has been described in children [101,102] Alternative routes of delivery are attractive but are not as efficacious.

Iloprost is an inhaled prostacyclin analog with a longer half-life. A recent review summarizes its use in pediatric PAH [103,104]. In children treated with iloprost, WHO functional class was improved in 35%, remained unchanged in 50%, and decreased in 15% [105]. Lower airway reactivity is a problem in some children, as is poor compliance with the need for frequent aerosol administrations (6–8 times daily). The short- and long-term efficacy of inhaled iloprost is still controversial [106]. In the critical care of CHD, inhaled iloprost is as efficacious as NO in lowering mean PVR and improves systemic oxygen saturation [107]. Nevertheless, clinical deterioration, side effects, and poor compliance could limit its chronic administration in children [105].

Treprostinil is a prostacyclin analog usually administered by continuous subcutaneous infusion, and is also FDA approved for intravenous and inhaled delivery in adults with PAH. Subcutaneous treprostinil improves exercise tolerance, clinical signs, symptoms, and hemodynamics in adult patients with PAH [108]. Discomfort at the infusion site is common and represents the major limiting factor. No change in exercise capacity was noted in children on changing from intravenous epoprostenol to intravenous treprostinil, but side effects were less [109]. The use of treprostinil in children can be considered for patients who have been on a stable dose of intravenous epoprostenol with clinical improvement. Treprostinil has been studied in inhaled and oral forms [110].

Beraprost is an oral prostacyclin analog, shown to improve hemodynamics and survival in patients with IPAH, including children [111]. Data in children are scarce and beraprost is not available in the United States or Europe but is used in Japan [112].

Endothelin receptor antagonists

Endothelin-1 is a potent vasoconstrictor peptide produced primarily by the endothelial cell. Endothelin-1 expression and plasma levels are increased in patients with PAH and correlate inversely with prognosis. The endothelins are a family of isopeptides consisting of ET-1, ET-2, and ET-3. ET-1 is a potent vasoactive peptide produced primarily in the vascular endothelial cell, but also may be produced by smooth muscle cells. Two receptor subtypes, ET_A and ET_B, mediate the activity of ET-1. ET_A and ET_B receptors on vascular smooth muscle mediate vasoconstriction, whereas ET_B receptors on endothelial cells cause release of NO and prostacyclin (PGI2), and act as clearance receptors for circulating ET-1.

Bosentan is an oral dual endothelin receptor antagonist acting on both ET_A and ET_B receptors [113]. A recent review summarizes its use in pediatric PAH [114]. In children with PAH, Barst *et al.* have demonstrated the beneficial effect of bosentan in lowering PAP and PVR [115]. In an open uncontrolled study in children with PAH, bosentan lowered mean PAP and PVR and improved WHO functional status and survival estimates at 1 and 2 years (98 and 91%, respectively) [116]. Nevertheless, in a study including both children and adults with PAH and a systemic-to-pulmonary shunting, bosentan therapy produced only short-term improvement in WHO functional class and 6-MW test [117]. The beneficial effect of bosentan declined progressively after 1 year, with a more pronounced decline in children, who tended to have more severe disease at baseline. In adults with ES, bosentan has been shown to decrease modestly both PAP and PVR [118] with an increased oxygen saturation at rest and a decreased level of hemoglobin [119]. Common side effects include dose-related hepatotoxicity, teratogenicity, and possibly male infertility [120]. Liver function tests

should be performed monthly. The safety of bosentan therapy in children with PAH has recently been reported by Beghetti *et al.* [120]. Elevated transaminase levels were reported in 2.7% of children compared with 7.8% of patients aged ≥12 years, and the overall discontinuation rate from bosentan was 14% in children compared with 28% in patients aged ≥12 years. In children with ES, bosentan is well tolerated and exercise capacity and hemodynamics improve without compromising peripheral oxygen saturation [118]. A specific pediatric formulation has recently been approved in Europe [83].

Sitaxsentan and *ambrisentan* are oral selective ET_A receptor antagonists with a long half-life. They block the vasoconstrictor effect of ET_A receptors while maintaining the vasodilator effect and clearance function of ET_B receptors. Sitaxsentan and ambrisentan have beneficial effects on exercise capacity and NYHA functional class in adult patients [121–123], but no data are available for children.

Phosphodiesterase inhibitors type 5 (PDE-5)

PDE-5 prevents the breakdown of cyclic GMP resulting in pulmonary vasodilatation. PDE-5 are acute pulmonary vasodilators as efficient as inhaled NO and potentiate pulmonary vasodilatation when used together with NO. They may be particularly beneficial where withdrawal of NO may lead to rebound PAH [124,125].

Sildenafil can be used orally or intravenously but is currently only available orally. Sildenafil has been approved for the treatment of WHO functional class II–IV PAH adult patients [126–128], but the data for children remain limited. In a pilot study of 14 children with PAH [129], oral sildenafil decreased PAP and PVR significantly and improved the mean 6-MW test, but a plateau was reached between 6 and 12 months. In a small study of children with IPAH and PH associated with CHD, sildenafil was well tolerated and safe, with improved oxyhemoglobin saturation and exercise capacity without significant side effects [130]. In children with PAH associated with chronic lung disease, sildenafil improved hemodynamics in 88% of patients, and was well tolerated and safe [52]. Moreover, PDI-5 appears to be highly expressed in the hypertrophied human right ventricle and acute inhibition with oral sildenafil has been shown to improve right ventricular contractility [131]. Side effects include systemic hypotension and penile erection. Preliminary safety and efficacy trials of oral sildenafil are under way in pediatric patients and results are to be expected soon. Intravenous sildenafil has been shown to potentiate the increase in cGMP in response to NO in children with increased PVR related to CHD or to postoperative state. Nevertheless, sildenafil infusion was associated with increased intra-pulmonary shunting and augmentation of hypoxemia related to V/Q mismatch in the postoperative patient [132,133]. In neonates with PPHN associated with congenital diaphragmatic hernia resistant to NO, oral sildenafil improved cardiac output by reducing PH [134]. In neonates with PPHN and an oxygenation index >15, continuous intravenous sildenafil was well tolerated and allowed acute and sustained improvements in oxygenation [135].

Tadalafil is also a selective PDE-5 with a longer duration of action. No data are available for children but tadalafil has been shown to improve oxygenation in an animal model of newborn PAH [136]. Tadalalfil was approved by the FDA in 2009 for adults with PAH. In adults with severe PAH, tadalafil has been used in addition to prostacyclin with some improvement [137].

Combination therapy

As for patients with heart failure, combination therapy is an attractive option to address simultaneously the multiple pathophysiologic pathways present in PAH. Acting on the three different pathways of PAH may be more efficacious than acting on a single one, by additive or synergistic effects. In adult patients with PAH, beginning combination therapy with epoprostenol and bosentan tended to show a greater improvement in hemodynamics compared with epoprostenol alone [138]. In a randomized placebo-controlled trial of initiating sildenafil or placebo at the same time as epoprostenol, the addition of sildenafil to long-term intravenous epoprostenol therapy improved exercise capacity, hemodynamic measurements, time to clinical worsening, and quality of life [139]. A therapeutic approach utilizing bosentan, sildenafil, and inhaled iloprost, by acting on the three pathways, improved survival and lowered the need for lung transplantation and for intravenous iloprost therapy in adult patients with severe PAH [140]. In a pediatric study by Ivy *et al.* [141], bosentan was successfully used in children on long-term epoprostenol therapy, and concomitant use of bosentan allowed for a decrease in epoprostenol dose. If the patient is started on intravenous epoprostenol before the availability of nonparenteral therapy, transition to oral or inhaled therapy for pulmonary arterial hypertension appears safe with efficacy maintained, but needs close follow-up [142].

Whether combination therapy should be used as a first step by simultaneous initiation of two or more drugs, or by addition of a second treatment to a previous therapy once insufficient, is unknown. More studies are needed to establish guidelines. Even if empiric combination of drugs is not uncommon in pediatric patients with PAH, there is a clear lack of studies in this area.

Atrioseptostomy

Atrioseptostomy is beneficial in patients with severe PAH and poor cardiac output, recurrent syncope, and/or intractable right heart failure refractory to vasodilator treatment. Right-to-left shunting through an interatrial defect allows maintenance of cardiac output but with increased hypoxemia. It alleviates signs of right heart failure

by decompressing the right heart [143,144]. Improvement of symptoms and an increase in survival have been reported, but this remains controversial. In a small series of 20 children deteriorating with severe PAH, atrioseptostomy improved symptoms and quality of life [143]. Patients with severe PAH, right heart failure, and markedly elevated PVR may not tolerate atrioseptostomy because of massive intracardiac right-to-left shunting and secondary severe hypoxemia.

Potts shunt

In patients with severe PAH, markedly elevated PVR, and right heart failure who do not tolerate an atrioseptostomy, creating a Potts shunt (anastomosis between the left pulmonary artery and the descending aorta) may decrease right ventricular afterload and improve right ventricular function [145,146]. Because of the high risk of the procedure, it should be reserved and used cautiously for the treatment of children with severe right heart failure resistant to other forms of therapy.

Transplantation

Lung or heart–lung transplantation remains the only available treatment for patients unresponsive to vasodilator treatment or with certain lesions such as pulmonary vascular obstructive lesions [147]. Its use is limited by the shortage of donors and the high incidence of bronchiolitis obliterans, which limits the long-term survival after lung transplantation [148] (see Chapter 70). Therefore, transplantation should be reserved for children with PAH which has progressed despite optimal medical therapy. Children should be listed for transplantation when their probability of 2-year survival without transplantation is ≤50% [149].

Future therapies [22,150]

Platelet-derived growth factor (PDGF) has been implicated in these processes. Altered PDGF signaling may be involved in the vascular remodeling observed in PAH [151] and a PDGF receptor antagonist such as *imatinib* or *sorafenib* could reverse pulmonary vascular disease [152,153]. Studies in animal models have suggested that Rho-kinase and NO synthase play important roles in the regulation of vasoconstrictor tone in physiologic and pathophysiologic states and that pulmonary hypertension can be reversed by agents that inhibit Rho-kinase, generate NO, or stimulate soluble guanylate cyclase [154]. Stimulating the *soluble guanylate cyclase*, a component of the nitric oxide receptor, by *BAY 63-2521* sensitizes the receptor to NO and may reverse right heart hypertrophy and structural lung vascular remodeling [155]. *Vasoactive intestinal polypeptide* (VIP) has a potent vasodilator effect on the pulmonary and systemic circulations and may exert an overall pulmonary vasodilatory effect in adults with PAH [156]. Rho-kinase has been shown to be involved in regulating baseline tone and in mediating pulmonary vasoconstrictor responses.

The 3-hydroxy-3-methylglutaryl-CoA (HMG-CoA) reductase inhibitor *simvastatin* inhibits Rho-kinase activity and attenuates and induces regression of chronic hypoxic pulmonary hypertension and reduces pulmonary artery pressure in animal models [157]. In a recent clinical trial in adult patients with PAH, simvastatin added to conventional therapy produced a small and transient early reduction in right ventricular mass and NT-proBNP levels in patients with PAH, but this was not sustained over 12 months [158]. In animal models of PAH, the Rho-kinase inhibitor *Y–27632* attenuated increases in pulmonary arterial pressures in response to vasoconstrictor agents [154]. *Serotonin* is a pulmonary vasoconstrictor and smooth muscle cell mitogen and is thought to be necessary for initiating the development and maintenance of pulmonary vascular remodeling. Complete reversal of PAH by *fluoxetine*, a 5-HT inhibitor, has been shown to reverse those lesions completely in an animal model of PAH [159]. These novel therapies are currently under active investigation either in animals or in preliminary studies in adults and may also be of interest for pediatric patients in the near future.

Management of PAH associated with CHD

Acute responders with PAH associated with congenital shunt lesions are considered candidates for surgical repair. Treatment for patients with CHD and nonreactive PAH (ES) is based on the same selective pulmonary vasodilators as in IPAH, even if data are limited [160,161].

Operability

Most PVD related to CHD may be prevented by correcting the defect at an early age, preventing permanent remodeling of the pulmonary vasculature and irreversible PVD. The window of opportunity for surgical correction and prevention of permanent PVD is wide and essentially lesion specific. Individual, environmental, and genetic susceptibilities also play a role; patients with Down syndrome are prone to early and fixed pulmonary vascular remodeling and have a more reactive pulmonary vascular bed in the postoperative period, being prone to pulmonary hypertensive "crisis." This may be related to the association of chronic upper airway obstruction responsible for alveolar hypoxia, hypercarbia, and acidosis with adverse effect on PVR.

Risk stratification of patients with PVD and CHD is important [67,68,162,163]. As previously mentioned under catheterization, a baseline PVR index <6 WU m^2 associated with a pulmonary to systemic resistance ratio of <0.3 without a vasoreactivity test is interpreted as indicating a favorable outcome following operations resulting in a biventricular circulation. Acute vasodilator challenge using oxygen/NO has been strongly encouraged if baseline PVR index is between 6 and 9 WU m^2 with a pulmonary to systemic

resistance ratio from ~0.3 to 0.5. Although there is no absolute consensus, operability with a favorable outcome is considered likely if the following criteria are met [163]:

- a decrease of 20% in the PVR index
- a decrease of ~20% in the ratio of pulmonary to systemic vascular resistance
- a final PVR index of <6 WU m^2
- a final ratio of pulmonary to systemic resistance of <0.3.

It remains unclear which preoperative pulmonary hemodynamic parameters correlate best with outcomes. Moreover, individual patient factors, such as type of cardiac lesion and genetic predisposition, influence the outcome but are incompletely understood. In children with a VSD, Neutze *et al.* found that those with PVR <8 WU m^2 who showed reactivity (decrease in PVR <7 WU m^2 after pulmonary vasodilatation with isoproterenol) had normal or modestly increased PVR after surgical repair [164]. In children with various types of CHD, Balzer *et al.* showed that a decrease in PVR of <5.3 WU m^2 and in PVR/SVR of <0.27 after pulmonary vasodilatation with 100% FIO$_2$ and inhaled NO was 97% sensitive for identifying patients with good outcome after repair [66].

It should be noted that the above criteria do not apply to patients with single ventricle physiology who are being assessed for a Fontan procedure. In those patients, obtaining accurate hemodynamic measurements can be even more difficult. Ideally, they should have PVR near normal and certainly ≤3 WU m^2. A mean pulmonary artery pressure of >15 mmHg has been associated with increased early and late mortality after the Fontan operation [68].

In general, ASD are repaired by 4–5 years, VSD during the first year of life, complete AVSD, and PDA by 6 months of age and *d*-TGA with VSD and common arterial trunk during the first few weeks of life. For neonates with a single ventricle physiology or complex CHD and unobstructed PBF (no pulmonary protection), the goal is to secure normal PAP with a pulmonary artery banding before proceeding to the cavopulmonary anastomosis.

Pulmonary artery banding

Placing a restrictive band on the main PA can reduce the PAP distal to the band and reverse pathologic pulmonary vascular remodeling [165,166]. Another alternative to PA banding is partial closure of the shunt, allowing for some degree of right-to-left shunting to prevent right heart failure. The use of a fenestrated VSD patch closure has been reported to be beneficial in children with high PVR [167,168].

Immediate postoperative care

In the immediate postoperative period, a child with PAH related to CHD is the most vulnerable. Postoperative pulmonary hypertensive "crisis" is characterized by acute and labile increase in PVR following cardiac surgery, related to heightened vascular reactivity secondary to vasospastic stimuli. Pulmonary hypertensive crisis leads to acute right heart failure, low cardiac output with systemic hypotension and myocardial ischemia, and may be lethal. Patients with extracardiac syndromes (particularly Down syndrome) seem to be at increased risk. In general, corrective surgery in the first 6 months of life decreases the risk of postoperative pulmonary hypertensive crisis, particularly for AVSD and VSD. For high-risk cardiac lesions, such as common arterial trunk or *d*-TGA, surgical repair should be performed at an earlier age [35]. Precipitating factors should be avoided, particularly stressful stimuli such as tracheal suction, pain, and anxiety, and also hypoxia, hypercapnia, acidosis, hyperthermia, or fluid overload. Adequate sedation, hyperventilation, and the use of sodium bicarbonate are useful in the immediate postoperative care of such patients [169].

In general, there is no clear level of PAP indicating the need for postoperative specific pulmonary vasodilator therapy. Patients with a mean PAP >25 mmHg or >50–60% of systemic pressure associated with signs of low cardiac output should be treated. Inhaled NO has become the accepted therapy because of its selective vasodilator effect on the pulmonary vascular bed. There is no optimal dosage but there is little benefit from doses >10–20 ppm [170]. Rebound PH is a common complication upon rapid withdrawal of NO [91] and can be minimized by slow weaning, particularly in the last 5 ppm, and adding oral sildenafil at 0.3–0.5 mg kg^{-1} [125].

Medical therapy

PVD related to CHD may be prevented by early diagnosis and correction. Once permanent pulmonary vascular remodeling is established and nonreactive to pulmonary vasodilator testing, therapy is supportive rather than designated to decrease PVR, even though patients with ES may show some improvement with targeted therapies.

Eisenmenger syndrome (ES)

ES represents the most advanced form of PAH associated with CHD. Treatment options for patients with ES were historically limited to palliative measures and heart–lung transplantation. Treatment most commonly involved the use of digoxin, diuretics, antiarrhythmics, and/or anticoagulants. None of these classes of drugs significantly modifies survival. The efficacy of calcium channel blockers in patients with ES is neither proven nor generally recommended, as their use can result in an acute decrease in systemic arterial pressure and increased right-to-left shunting, which may lead to syncope and sudden death. Patients with ES are at particular risk during cardiac and noncardiac surgery and anesthesia, and as a result of dehydration, chest infections, high altitude, and intravenous lines. They should also avoid strenuous exercise and competitive sports.

Nonoperable pre-Eisenmenger syndrome

These patients have a PVR considered too high for surgical repair but not at a level to diagnose ES. So far, the therapeutic approach for this group is to watch and wait. However, with the upcoming new targeted therapies use to treat PAH, the concept to treat and repair has emerged [171].

In PAH associated with CHD and a large shunt lesion, it is thought that the pressure and/or volume load on the pulmonary vascular bed leads to pulmonary vascular remodeling and lesions. By reducing PVR, the possibility arises that pretreatment with vasodilators can improve a patient's condition and an inoperable patient could be considered operable. Pretreatment may not always be efficacious, depending on the extent and severity of the lesions. Although pretreatment may reduce PVR, PAH could remain postoperatively, resulting in a worse prognosis. Moreover, the reversal of vascular remodeling and lesion formation with pretreatment, leading to an initial decrease in PVR, could actually result in an increase in pulmonary blood flow, re-establishing the propensity towards pulmonary vascular damage and lesions later.

Several reports have described pretreatment with prostacyclins or bosentan being used prior to CHD surgery to prepare borderline patients [172–175]. These reports suggest some benefit in improving hemodynamics and making conditions more favorable for repair. Nevertheless, most of these patients had simple CHD such as ASDs. A retrospective analysis of national registries of this type of data would be required to gain a complete picture.

Persistent pulmonary hypertension late after surgical repair [176]

Acute treatment and survival in the immediate postoperative period do not mean that PH resolves and the patient may present persistent PAH after successful repair. Literature on this subgroup of patients remains scarce, but the hemodynamics and prognosis appear very similar to those in idiopathic PAH [12]. This emphasizes the importance of accurate decision for operability, because survival may be better with a persistent shunt lesion and ES than with a closed shunt and RV failure [177].

Pulmonary hypertension and the Fontan circulation

The Fontan procedure (total cavopulmonary connection) results in a pulmonary circulation very different from physiological conditions, and a small increased in PAP has a profound effect on the passive pulmonary blood flow. As the child ages, PAP may increase and lead to failure of the Fontan circulation over time. For this reason, the idea of treating failing Fontan patients with a therapy that lowers PVR has emerged [178]. Therapies approved for PAH may, therefore, provide benefits in this patient population, but few data have been reported.

Inhaled NO is predominantly effective in patients with central venous pressure ≥15 mmHg and/or a transpulmonary pressure gradient (TPG) ≥8 mmHg [179]. In the early postoperative period, inhaled NO and milrinone are very effective in reducing the TPG [180,181]. The use of prostacyclins in the perioperative course of Fontan is seldom reported, but beraprost reduced mean PAP and PVR in preoperative Fontan candidates with mild elevation in PAP [182], and intravenous epoprostenol prevented the rebound effect after NO cessation in the early postoperative phase [183]. Treatment of late Fontan patients with inhaled NO reduced PVR but had no effect on cardiac index [184], whereas sildenafil improved exercise capacity and hemodynamic response to exercise [185]. The use of bosentan is anecdotal, but has improved functional class, symptoms, exercise capacity, and hemodynamic parameters in a child with plastic bronchitis following Fontan [186]. Given the important role of the pulmonary circulation in the Fontan physiology and the current lack of data, there is a need for clinical studies on the safety and efficacy of those potential therapies.

Outcome

Historically, PAH in children has had a poor prognosis, with a less than 1 year survival in untreated children [187].

For patients with IPAH who responded to calcium channel blockers, Yung *et al.* reported survivals at 1, 5, and 10 years of 97, 97, and 81%, respectively, with a treatment success (freedom from death, transplantation or atrioseptostomy) of 84%, 68%, and 47%, respectively; treatment success decreased significantly when acute responders became nonresponders [93]. For non-responders with IPAH treated with IV epoprostenol, survival at 1, 5, and 10 years was 94%, 81%, and 61%, respectively with a treatment success of 83%, 57%, and 37%, respectively. Since 1995, survival was even better for children with IPAH treated with intravenous epoprostenol with a survival rate of 97%, 97%, and 78% at 1, 5, and 10 years [93]. In children with severe IPAH treated with continuous prostacyclin, Barst *et al.* reported survival rates of 86.9, 72.4, and 63.3 at 1, 2, and 3-years, respectively [1], whereas Haworth and Hislop reported survival rates of 85.6, 79.9 and 71.9% at 1, 3 and 5 years, respectively, for those treated with a combination of intravenous epoprostenol and either bosentan or sildenafil, or both [12]. In APAH, survival rates were 92.3, 83.8 and 56.9% at 1, 3 and 5 years, respectively, with postoperative CHD-associated PAH having the worst outcome. Indeed, in a 5-year retrospective study of children with PAH in the United Kingdom, the subpopulation with postoperative CHD-associated PAH fared far worse than those with PAH associated with complex (unoperated) CHD and ES, and

almost one-quarter of these children died [12]. Children with ES had a greater cumulative survival time by 1.3 years, indicating that surgical repair is not necessarily always the best option.

Conclusion

Advances in the understanding of pulmonary vasculature have led to new therapeutic options and improved survival in children with PAH. In children with CHD, increased PBF is a potent stimulator to both active vasoconstriction and pathologic remodeling of the pulmonary vascular bed leading to increased PVR. With the exception of a few high-risk congenital cardiac malformations, irreversible PVD seldom occur in the first 1–2 years of age. Timely diagnosis is crucial as early surgical repair of congenital shunt lesions and earlier treatment of PAH leads to improved outcome. In children with PAH, an extensive work-up is necessary to determine the etiology, as the most successful strategy involves treatment of the underlying disorder. Initial evaluation includes acute vasodilator testing at cardiac catheterization, which determines initial and long-term therapy. Several novel therapeutic agents are under investigation and evolving clinical research should better define the role of new treatments for children with PAH. Moreover, improved delivery of medical and surgical care in underprivileged areas of the world should reduce PAH associated with CHD.

References

1 Barst RJ, Maislin G, Fishman AP. Vasodilator therapy for primary pulmonary hypertension in children. *Circulation* 1999;**99**:1197–208.

2 Wood P. The Eisenmenger syndrome or pulmonary hypertension with reversed central shunt. I. *Br Med J* 1958;**ii**:701–9.

3 McLaughlin VV, Archer SB, Badesch DB, *et al*. ACCF/AHA 2009 expert consensus document on pulmonary hypertension: a report of the American College of Cardiology Foundation Task Force on Expert Consensus Documents and the American Heart Association: developed in collaboration with the American College of Chest Physicians, American Thoracic Society, Inc., and the Pulmonary Hypertension Association. *Circulation* 2009;**119**:2250–94.

4 Barst RJ, Rubin LJ, McGoon MD, *et al*. Survival in primary pulmonary hypertension with long-term continuous intravenous prostacyclin. *Ann Intern Med* 1994;**121**:409–15.

5 Widlitz A, Barst RJ. Pulmonary arterial hypertension in children. *Eur Respir J* 2003;**21**:155–76.

6 Galie N, Hoeper MM, Humbert M, *et al*. Guidelines for the diagnosis and treatment of pulmonary hypertension: the Task Force for the Diagnosis and Treatment of Pulmonary Hypertension of the European Society of Cardiology (ESC) and the European Respiratory Society (ERS), endorsed by the International Society of Heart and Lung Transplantation (ISHLT). *Eur Heart J* 2009;**30**:2493–537.

7 Badesch DB, Champion HC, Sanchez MA, *et al*. Diagnosis and assessment of pulmonary arterial hypertension. *J Am Coll Cardiol* 2009;**54**(1 Suppl):S55–66.

8 Barst RJ. Pharmacologically induced pulmonary vasodilatation in children and young adults with primary pulmonary hypertension. *Chest* 1986;**89**:497–503.

9 Simonneau G, Robbins IM, Beghetti M, *et al*. Updated clinical classification of pulmonary hypertension. *J Am Coll Cardiol* 2009;**54**(1 Suppl):S43–54.

10 van Loon R, Roofhooft MT, van Osch-Gevers M, *et al*. Clinical characterization of pediatric pulmonary hypertension: complex presentation and diagnosis. *J Pediatr* 2009;**155**:176–82, e1.

11 Lee SD, Shroyer KR, Markham NE, *et al*. Monoclonal endothelial cell proliferation is present in primary but not secondary pulmonary hypertension. *J Clin Invest* 1998;**101**:927–34.

12 Haworth SG, Hislop AA. Treatment and survival in children with pulmonary arterial hypertension: the UK Pulmonary Hypertension Service for Children 2001–2006. *Heart* 2009;**95**:312–7.

13 Fasnacht MS, Tolsa JF, Beghetti M. The Swiss registry for pulmonary arterial hypertension: the paediatric experience. *Swiss Med Wkly* 2007;**137**:510–3.

14 Fraisse A, Jais X, Schleich JH, *et al*. Characteristics and prospective 2-year follow-up of children with pulmonary arterial hypertension in France. *Arch Cardiovasc Dis* 2010;**103**:66–74.

15 Butrous G, Ghofrani HA, Grimminger F. Pulmonary vascular disease in the developing world. *Circulation* 2008;**118**:1758–66.

16 Newman JH, Wheeler L, Lane KB, *et al*. Mutation in the gene for bone morphogenetic protein receptor II as a cause of primary pulmonary hypertension in a large kindred. *N Engl J Med* 2001;**345**:319–24.

17 Thomson JR, Machado RD, Pauciulo MW, *et al*. Sporadic primary pulmonary hypertension is associated with germline mutations of the gene encoding BMPR-II, a receptor member of the TGF-beta family. *J Med Genet* 2000;**37**:741–5.

18 Austin ED, Loyd JE, Phillips JA III. Genetics of pulmonary arterial hypertension. *Semin Respir Crit Care Med* 2009;**30**:386–98.

19 Rosenzweig EB, Morse JH, Knowles JA, *et al*. Clinical implications of determining BMPR2 mutation status in a large cohort of children and adults with pulmonary arterial hypertension. *J Heart Lung Transplant* 2008;**27**:668–74.

20 Willers ED, Newman JH, Loyd JE, *et al*. Serotonin transporter polymorphisms in familial and idiopathic pulmonary arterial hypertension. *Am J Respir Crit Care Med* 2006;**173**:798–802.

21 Haworth SG. Pulmonary vascular remodeling in neonatal pulmonary hypertension. State of the art. *Chest* 1988;**93**(3 Suppl):133S–8S.

22 Morrell NW, Adnot S, Archer SL, *et al*. Cellular and molecular basis of pulmonary arterial hypertension. *J Am Coll Cardiol* 2009;**54**(1 Suppl):S20–31.

23 Christman BW, McPherson CD, Newman JH, *et al*. An imbalance between the excretion of thromboxane and prostacyclin metabolites in pulmonary hypertension. *N Engl J Med* 1992;**327**:70–5.

24 Adatia I, Barrow SE, Stratton PD, *et al*. Thromboxane A2 and prostacyclin biosynthesis in children and adolescents with pulmonary vascular disease. *Circulation* 1993;**88**:2117–22.

25 Black SM, Kumar S, Wiseman D, *et al*. Pediatric pulmonary hypertension: roles of endothelin-1 and nitric oxide. *Clin Hemorheol Microcirc* 2007;**37**:111–20.

26 Haworth SG. Pathophysiological and metabolic manifestations of pulmonary vascular disease in children. *Herz* 1992; **17**:254–61.

27 Wagenvoort CA. The pathology of primary pulmonary hypertension. *J Pathol* 1970;**101**:Pi.

28 Allen KM, Haworth SG. Cytoskeletal features of immature pulmonary vascular smooth muscle cells: the influence of pulmonary hypertension on normal development. *J Pathol* 1989;**158** 311–7.

29 Shepherd JT, Wood EH. The role of vessel tone in pulmonary hypertension. *Circulation* 1959;**19**:641–5.

30 Swan H., Burchell HB, Wood EH. Effect of oxygen on pulmonary vascular resistance in patients with pulmonary hypertension associated with atrial septal defect. *Circulation* 1959;**20**:66–73.

31 Langille BL. Arterial remodeling: relation to hemodynamics. *Can J Physiol Pharmacol* 1996;**74**:834–41.

32 Auld PA, Gibbons JE, McGregor M.Vasomotor tone in the pulmonary vascular bed in patients with left-to-right shunts. *Br Heart J* 1963;**25**:257–61.

33 Budts W, Van Pelt N, Gillyns H, *et al*. Residual pulmonary vasoreactivity to inhaled nitric oxide in patients with severe obstructive pulmonary hypertension and Eisenmenger syndrome. *Heart* 2001;**86**:553–8.

34 Hoffman JIE, Rudolph AM, Heymann MA. Pulmonary vascular disease with congenital heart lesions: pathologic features and causes. *Circulation* 1981;**64**:873–7.

35 Haworth SG. Pulmonary vascular disease in different types of congenital heart disease. Implications for interpretation of lung biopsy findings in early childhood. *Br Heart J* 1984;**52**: 557–71.

36 Goetschmann S, Dibernardo S, Steinmann H, *et al*. Frequency of severe pulmonary hypertension complicating isoated atrial septal defect in infancy. *Am J Cardiol* 2008;**102**:340–2.

37 Yeager SB, Freed MD, Keane JF, *et al*. Primary surgical closure of ventricular septal defect in the first year of life: results in 128 infants. *J Am Coll Cardiol* 1984;**3**(5):1269–76.

38 Newfeld EA, Paul MH, Muster AJ, Idriss FS. Pulmonary vascular disease in transposition of the great vessels and intact ventricular septum. *Circulation* 1979;**59** 525–30.

39 Sreeram N, Petros A, Peart I, Arnold R. Progressive pulmonary hypertension after the arterial switch procedure. *Am J Cardiol* 1994;**7**:620–1.

40 Juaneda E, Haworth SG. Pulmonary vascular disease in children with truncus arteriosus. *Am J Cardiol* 1984;**54**:1314–20.

41 Nelson SC, Adada BB, McDonough EA, *et al*. High prevalence of pulmonary hypertension in children with sickle cell disease. *J Pediatr Hematol Oncol* 2007;**29**:334–7.

42 Sachdev V, Machado RF, Shizukuda Y, *et al*. Diastolic dysfunction is an independent risk factor for death in patients with sickle cell disease. *J Am Coll Cardiol* 2007;**49**:472–9.

43 Adedeji MO, Cespedes J, Allen K, *et al*. Pulmonary thrombotic arteriopathy in patients with sickle cell disease. *Arch Pathol Lab Med* 2001;**125**:1436–41.

44 Morris CR, Gladwin MT, Kato GJ. Nitric oxide and arginine dysregulation: a novel pathway to pulmonary hypertension in hemolytic disorders. *Curr Mol Med* 2008;**8**:620–32.

45 Villagra J, Shiva S, Hunter LA, *et al*. Platelet activation in patients with sickle disease, hemolysis-associated pulmonary hypertension, and nitric oxide scavenging by cell-free hemoglobin. *Blood* 2007;**110**:2166–72.

46 Law YM, Mack CL, Sokol RJ. Cardiopulmonary manifestations of portovenous shunts from congenital absence of the portal vein: pulmonary hypertension and pulmonary vascular dilatation. *Pediatr Transplant* 2010; Epub head of print.

47 Whitworth JR, Ivy DD, Gealla J, *et al*. Pulmonary vascular complications in asymptomatic children with portal hypertension. *J Pediatr Gastroenterol Nutr* 2009;**49**:607–12.

48 Hoeper MM, Krowka MJ, Strassburg CP. Portopulmonary hypertension and hepatopulmonary syndrome. *Lancet* 2004; **363**(9419):1461–8.

49 Ling Y, Zhang J, Luo B, *et al*. The role of endothelin-1 and the endothelin B receptor in the pathogenesis of hepatopulmonary syndrome in the rat. *Hepatology* 2004;**39**:1593–602.

50 Abman SH. Recent advances in the pathogenesis and treatment of persistent pulmonary hypertension of the newborn. *Neonatology* 2007;**91**:283–90.

51 Abman SH. Pulmonary hypertension in children: a historical overview. *Pediatr Crit Care Med*. 2010;**11**(Suppl):S4–9.

52 Mourani PM, Sontag MK, Ivy DD, Abram SH. Effects of long-term sildenafil treatment for pulmonary hypertension in infants with chronic lung disease. *J Pediatr* 2009;**154**:379–84.

53 Grover TR, Parker TA, Markham NE, Abman SH. rhVEGF treatment preserves pulmonary vascular reactivity and structure in an experimental model of pulmonary hypertension in fetal sheep. *Am J Physiol Lung Cell Mol Physiol* 2005;**289**(2):L315–21.

54 Humbert M, Tre SM, Capron F, *et al*. Pulmonary edema complicating continuous intravenous prostacyclin in pulmonary capillary hemangiomatosis. *Am J Respir Crit Care Med* 1998;**157** (5 Pt 1):1681–5.

55 Endo M, Yamaki S, Ohni M, Tabayashi K. Pulmonary vascular changes induced by congenital obstruction of pulmonary venous return. *Ann Thorac Surg* 2000;**69**:193–7.

56 Jobe AJ. The new BPD: an arrest of lung development. *Pediatr Res* 1999;**46**:641–3.

57 Khemani E, McElhinney DB, Rhein L, *et al*. Pulmonary artery hypertension in formerly premature infants with bronchopulmonary dysplasia: clinical features and outcomes in the surfactant era. *Pediatrics* 2007;**120**:1260–9.

58 Abman SH, Wolfe RE, Accusrso FJ, *et al*. Pulmonary vascular response to oxygen in infants with severe bronchopulmonary dysplasia. *Pediatrics* 1985;**75**:80–4.

59 Keller RL, Tacy TA, Hendriicks-Munoz K, *et al*. Congenital diaphragmatic hernia: endothelin-1, pulmonary hypertension and disease severity. *Am J Respir Crit Care Med*. 2010;**182**(4): 555–61.

60 Bohn D. Congenital diaphragmatic hernia. *Am J Respir Crit Care Med* 2002;**166**:911–5.

61 Fisher MR, Forifa PR, Chamera E, *et al*. Accuracy of Doppler echocardiography in the hemodynamic assessment of pulmonary hypertension. *Am J Respir Crit Care Med* 2009;**179**: 615–21.

62 Louie EK, Maron BJ. Hypertrophic cardiomyopathy with extreme increase in left ventricular wall thickness: functional and morphologic features and clinical significance. *J Am Coll Cardiol* 1986;**8**:57–65.

63 Raymond RJ, Hinderlier AL, Willis PW IV, *et al*. Echocardiographic predictors of adverse outcomes in primary pulmonary hypertension. *J Am Coll Cardiol* 2002;**39**:1214–9.

64 Forfia PR, Fisher MR, Mathai SG, *et al*. Tricuspid annular displacement predicts survival in pulmonary hypertension. *Am J Respir Crit Care Med* 2006;**174**:1034–41.

65 Berner M, Beghetti M, Spahr-Schopfer I, *et al*. Inhaled nitric oxide to test the vasodilator capacity of the pulmonary vascular bed in children with long-standing pulmonary hypertension and congenital heart disease. *Am J Cardiol* 1996;**77**:532–5.

66 Balzer DT, Kort HW, Day RD, *et al*. Inhaled nitric oxide as a preoperative test (INOP Test I): the INOP Test Study Group. *Circulation* 2002;**106**(Suppl 1):I76–81.

67 Lopes AA, O'Leary PW. Measurement, interpretation and use of hemodynamic parameters. *Cardiol Young* 2009;**19**(Suppl 1): 8–12.

68 Giglia TM, Humpl T. Preoperative pulmonary hemodynamics and assessment of operability: is there a pulmonary vascular resistance that precludes cardiac operation? *Pediatr Crit Care Med*. 2010;**11**(Suppl):S57–69.

69 Rabinovitch M, Keane JF, Fellows AR, *et al*. Quantitative analysis of the pulmonary wedge angiogram in congenital heart defects. Correlation with hemodynamic data and morphometric findings in lung biopsy tissue. *Circulation* 1981;**63**:152–64.

70 Miyamoto S, Nagaya N, Sahoh T, *et al*. Clinical correlates and prognostic significance of six-minute walk test in patients with primary pulmonary hypertension. Comparison with cardiopulmonary exercise testing. *Am J Respir Crit Care Med* 2000;**161**(2 Pt 1):487–92.

71 Li AM, Lin J, Au JT, *et al*. Standard reference for the six-minute-walk test in healthy children aged 7 to 16 years. *Am J Respir Crit Care Med* 2007;**176**:174–80.

72 Lammers AE, Hislop AA, Flynn Y, Haworth SG, The 6-minute walk test: normal values for children of 4–11 years of age. *Arch Dis Child* 2008;**93**:464–8.

73 Geiger R, Strasak A, Tremi B, *et al*. Six-minute walk test in children and adolescents. *J Pediatr* 2007;**150**:395–9, e1–2.

74 Yetman AT, Taylor AL, Doran A, Ivy DD. Utility of cardiopulmonary stress testing in assessing disease severity in children with pulmonary arterial hypertension. *Am J Cardiol* 2005;**95**:697–9.

75 Smith G, Reyes JT, Russell JL, Humpl T. Safety of maximal cardiopulmonary exercise testing in pediatric patients with pulmonary hypertension. *Chest* 2009;**135**:1209–14.

76 Kovacs G, Reiter G, Reiter U, *et al*. The emerging role of magnetic resonance imaging in the diagnosis and management of pulmonary hypertension. *Respiration* 2008;**76**:458–70.

77 Bernus A, Wagner BD, Accurso F, *et al*. Brain natriuretic peptide levels in managing pediatric patients with pulmonary arterial hypertension. *Chest* 2009;**135**:745–51.

78 Lammers AE, Hislop AA, Haworth SG. Prognostic value of B-type natriuretic peptide in children with pulmonary hypertension. Int J Cardiol 2008;**125**:21–6.

79 Van Albada ME, Loot FG, Fokkema R, *et al*. Biological serum markers in the management of pediatric pulmonary arterial hypertension. *Pediatr Res* 2008;**63**:321–7.

80 McGoon M, Gutterman D, Steen V, *et al*. Screening, early detection, and diagnosis of pulmonary arterial hypertension: ACCP evidence-based clinical practice guidelines. *Chest* 2004;**126**(1 Suppl):14S–34S.

81 Rabinovitch M, Haworth SG, Casteneda AR, *et al*. Lung biopsy in congenital heart disease: a morphometric approach to pulmonary vascular disease. *Circulation* 1978;**58**:1107–22.

82 Sandoval J, Bauerle O, Gomez A, *et al*. Primary pulmonary hypertension in children: clinical characterization and survival. *J Am Coll Cardiol* 1995;**25**:466–74.

83 Beghetti M, Haworth SG, Bonnet D, *et al*. Pharmacokinetic and clinical profile of a novel formulation of bosentan in children with pulmonary arterial hypertension: the FUTURE-1 study. *Br J Clin Pharmacol* 2009;**68**:948–55.

84 Rich S, Seidlitz M, Dodin E, *et al*. The short-term effects of digoxin in patients with right ventricular dysfunction from pulmonary hypertension. *Chest* 1998;**114**:787–92.

85 Frank H, Miczoch J, Huber K, *et al*. The effect of anticoagulant therapy in primary and anorectic drug-induced pulmonary hypertension. *Chest* 1997;**112**;714–21.

86 Sandoval J, Aguirre JS, Pulido T, *et al*. Nocturnal oxygen therapy in patients with the Eisenmenger syndrome. *Am J Respir Crit Care Med* 2001;**164**:1682–7.

87 Yung GL, Kriett J, Jamieson SW, *et al*. Outpatient inhaled nitric oxide in a patient with idiopathic pulmonary fibrosis: a bridge to lung transplantation. *J Heart Lung Transplant* 2001;**20**:1224–7.

88 Kulik TJ. Inhaled nitric oxide in the management of congenital heart disease. *Curr Opin Cardiol* 1996;**11**:75–80.

89 Wessel DL, Adatia J, Giglia TM, *et al*. Use of inhaled nitric oxide and acetylcholine in the evaluation of pulmonary hypertension and endothelial function after cardiopulmonary bypass. *Circulation* 1993;**88**:2128–38.

90 Wessel DL. Inhaled nitric oxide for the treatment of pulmonary hypertension before and after cardiopulmonary bypass. *Crit Care Med* 1993;**21**:S344–5.

91 Atz AM, Adatia I, Wessel DL. Rebound pulmonary hypertension after inhalation of nitric oxide. *Ann Thorac Surg* 1996; **62**:1759–64.

92 Ivy DD, Parker D, Doran A, *et al*. Acute hemodynamic effects and home therapy using a novel pulsed nasal nitric oxide delivery system in children and young adults with pulmonary hypertension. *Am J Cardiol* 2003;**92**;886–90.

93 Yung D, Widlitz AC, Rosenzweig EH, *et al*., Outcomes in children with idiopathic pulmonary arterial hypertension. *Circulation* 2004;**110**:660–5.

94 Wong CK, Yeung DWE, Lau CP, *et al*. Improvement of exercise capacity after nifedipine in patients with Eisenmenger syndrome complicating ventricular septal defect. *Clin Cardiol* 1991;**14** 957–61.

95 Wimmer M, Schlemmer M. Long-term hemodynamic effects of nifedipine on congenital heart disease with Eisenmenger's mechanism in children. *Cardiovasc Drugs Ther* 1992;**6**:183–6.

96 Barst RJ. Recent advances in the treatment of pediatric pulmonary artery hypertension. *Pediatr Clin North Am* 1999;**46**:331–45.

97 Rosenzweig EB, Kerstein D, Barst RJ. Long-term prostacyclin for pulmonary hypertension with associated congenital heart defects. *Circulation* 1999;**99**:1858–65.

98 Fernandes SM, Newburger JW, Lang P, *et al*. Usefulness of epoprostenol therapy in the severely ill adolescent/adult with Eisenmenger physiology. *Am J Cardiol* 2003;**91**:632–5.

99 Doran A, Harris S, Goetz B. Advances in prostanoid infusion therapy for pulmonary arterial hypertension. *J Infus Nurs* 2008;**31**:336–45.

100 Doran AK, Kaess H, Ivy DD, *et al*. Guidelines for the prevention of central venous catheter-related blood stream infections with prostanoid therapy for pulmonary arterial hypertension. *Int J Clin Pract Suppl* 2008;(160):5–9.

101 Dickinson MG, Scholvinge EH, Boonstra A, *et al*. Low complication rates with totally implantable access port use in epoprostenol treatment of pulmonary hypertension. *J Heart Lung Transplant* 2009;**28**:273–9.

102 Ivy DD, Calderbank M, Wagner BD, *et al*. Closed-hub systems with protected connections and the reduction of risk of catheter-related bloodstream infection in pediatric patients receiving intravenous prostanoid therapy for pulmonary hypertension. *Infect Control Hosp Epidemiol* 2009;**30**:823–9.

103 Hoeper MM, Schwarze M, Ehlerding S, *et al*. Long-term treatment of primary pulmonary hypertension with aerosolized iloprost, a prostacyclin analogue. *N Engl J Med* 2000;**342**(25)1866–70.

104 Tissot C, Beghetti M. Review of inhaled iloprost for the control of pulmonary artery hypertension in children. *Vasc Health Risk Manage* 2009;**5**:325–31.

105 Ivy DD, Doran AK, Smith KJ, *et al*. Short- and long-term effects of inhaled iloprost therapy in children with pulmonary arterial hypertension. *J Am Coll Cardiol* 2008;**51**:161–9.

106 Olschewski H, Simonneau G, Galie N, *et al*. Inhaled iloprost for severe pulmonary hypertension. *N Engl J Med* 2002;**347**:322–9.

107 Rimensberger PC, Spahr-Schopfer I, Berner M, *et al*. Inhaled nitric oxide versus aerosolized iloprost in secondary pulmonary hypertension in children with congenital heart disease: vasodilator capacity and cellular mechanisms. *Circulation* 2001;**103**:544–8.

108 Simonneau G, Barst RJ, Galie N, *et al*. Continuous subcutaneous infusion of treprostinil, a prostacyclin analogue, in patients with pulmonary arterial hypertension: a double-blind, randomized, placebo-controlled trial. *Am J Respir Crit Care Med* 2002;**165**:800–4.

109 Ivy DD, Claussen L, Doran A. Transition of stable pediatric patients with pulmonary arterial hypertension from intravenous epoprostenol to intravenous treprostinil. *Am J Cardiol* 2007;**99**:696–8.

110 Channick RN, Olschewski H, Seegar W, *et al*. Safety and efficacy of inhaled treprostinil as add-on therapy to bosentan in pulmonary arterial hypertension. *J Am Coll Cardiol* 2006;**48**:1433–7.

111 Galie N, Humbert M, Vachiery J-L, *et al*. Effects of beraprost sodium, an oral prostacyclin analogue, in patients with pulmonary arterial hypertension: a randomized, double-blind, placebo-controlled trial. *J Am Coll Cardiol* 2002;**39**:1496–502.

112 Saji T, Ozawa Y, Ishikita T, *et al*. Short-term hemodynamic effect of a new oral PGI2 analogue, beraprost, in primary and secondary pulmonary hypertension. *Am J Cardiol* 1996;**78**:244–7.

113 Rubin LJ, Roux S. Bosentan: a dual endothelin receptor antagonist. *Expert Opin Investig Drugs* 2002;**11**:991–1002.

114 Beghetti M. Bosentan in pediatric patients with pulmonary arterial hypertension. *Curr Vasc Pharmacol* 2009;**7**:225–33.

115 Barst RJ, Ivy DD, Dingemanse J, *et al*. Pharmacokinetics, safety, and efficacy of bosentan in pediatric patients with pulmonary arterial hypertension. *Clin Pharmacol Ther* 2003;**73**:372–82.

116 Rosenzweig EB, Ivy DD, Widlitz A, *et al*. Effects of long-term bosentan in children with pulmonary arterial hypertension. *J Am Coll Cardiol* 2005;**46**:697–704.

117 van Loon RL, Hoendermis ES, Duffles MGJ, *et al*. Long-term effect of bosentan in adults versus children with pulmonary arterial hypertension associated with systemic-to-pulmonary shunt: does the beneficial effect persist? *Am Heart J* 2007;**154**:776–82.

118 Galie N, Beghetti M, Gatzouilis MA, *et al*. Bosentan therapy in patients with Eisenmenger syndrome: a multicenter, double-blind, randomized, placebo-controlled study. *Circulation* 2006;**114**:48–54.

119 Kotlyar E, Sy R, Keogh AM, *et al*. Bosentan for the treatment of pulmonary arterial hypertension associated with congenital cardiac disease. *Cardiol Young* 2006;**16**:268–74.

120 Beghetti M, Hoeper MM, Kiely DG, *et al*. Safety experience with bosentan in 146 children 2–11 years old with pulmonary arterial hypertension: results from the European Postmarketing Surveillance program. *Pediatr Res* 2008;**64**:200–4.

121 Barst RJ. Sitaxsentan: a selective endothelin-A receptor antagonist, for the treatment of pulmonary arterial hypertension. *Expert Opin Pharmacother* 2007;**8**:95–109.

122 Galie N, Olsschwski H, Oudiz RJ, *et al*. Ambrisentan for the treatment of pulmonary arterial hypertension: results of the ambrisentan in pulmonary arterial hypertension, randomized, double-blind, placebo-controlled, multicenter, efficacy (ARIES) study 1 and 2. *Circulation* 2008;**117**:3010–9.

123 McGoon MD, Frost AF, Oudiz RJ, *et al*. Ambrisentan therapy in patients with pulmonary arterial hypertension who discontinued bosentan or sitaxsentan due to liver function test abnormalities. *Chest* 2009;**135**:122–9.

124 Atz AM, Wessel DL. Sildenafil ameliorates effects of inhaled nitric oxide withdrawal. *Anesthesiology* 1999;**91**:307–10.

125 Namachivayam P, Ulf T, Butt WW, *et al*. Sildenafil prevents rebound pulmonary hypertension after withdrawal of nitric oxide in children. *Am J Respir Crit Care Med* 2006;**174**:1042–7.

126 Galie N, Ghofrani HA, Torbicki A, *et al*. Sildenafil citrate therapy for pulmonary arterial hypertension. *N Engl J Med* 2005;**353**:2148–57.

127 Michelakis E, Tymchak W, Lien D, *et al*. Oral sildenafil is an effective and specific pulmonary vasodilator in patients with pulmonary arterial hypertension: comparison with inhaled nitric oxide. *Circulation* 2002;**105**:2398–403.

128 Michelakis ED, Tymchak W, Noga M, *et al*. Long-term treatment with oral sildenafil is safe and improves functional capacity and hemodynamics in patients with pulmonary arterial hypertension. *Circulation* 2003;**108**:2066–9.

129 Humpl T, Reyes JT, Holtby H, *et al*. Beneficial effect of oral sildenafil therapy on childhood pulmonary arterial hypertension: twelve-month clinical trial of a single-drug, open-label, pilot study. *Circulation* 2005;**111**:3274–80.

130 Karatza AA, Bush A, Magee AG. Safety and efficacy of sildenafil therapy in children with pulmonary hypertension. *Int J Cardiol* 2005;**100**:267–73.

131 Nagendran J, Archer SL, Soliman D, *et al*. Phosphodiesterase type 5 is highly expressed in the hypertrophied human right ventricle, and acute inhibition of phosphodiesterase type 5 improves contractility. *Circulation* 2007;**116**:238–48.

132 Schulze-Neick I, Hartenstein P, Li J, *et al*. Intravenous sildenafil is a potent pulmonary vasodilator in children with congenital heart disease. *Circulation* 2003;**108**(Suppl 1):II167–73.

133 Stocker C, Penny DJ, Brizard CP, *et al*. Intravenous sildenafil and inhaled nitric oxide: a randomised trial in infants after cardiac surgery. *Intensive Care Med* 2003;**29**:1996–2003.

134 Noori S, Frielich P, Wong P, *et al*. Cardiovascular effects of sildenafil in neonates and infants with congenital diaphragmatic hernia and pulmonary hypertension. *Neonatology* 2007;**91**: 92–100.

135 Steinhorn RH, Kinsella JP, Pierce C, *et al*. Intravenous sildenafil in the treatment of neonates with persistent pulmonary hypertension. *J Pediatr* 2009;**155**:841–7, e1.

136 Tessler RB, Zadinello M, Fiori H, *et al*. Tadalafil improves oxygenation in a model of newborn pulmonary hypertension. *Pediatr Crit Care Med* 2008;**9**:330–2.

137 Bendayan D, Shitrit D, Kramer MR. Combination therapy with prostacyclin and tadalafil for severe pulmonary arterial hypertension: a pilot study. *Respirology* 2008;**13**:916–8.

138 Humbert M, Sitbon O, Simonneau G. Treatment of pulmonary arterial hypertension. *N Engl J Med* 2004;**351**:1425–36.

139 Simonneau G, Rubin LJ, Galie N, *et al*. Addition of sildenafil to long-term intravenous epoprostenol therapy in patients with pulmonary arterial hypertension: a randomized trial. *Ann Intern Med* 2008;**149**:521–30.

140 Hoeper MM, Markevych I, Spiekeroetter E, *et al*. Goal-oriented treatment and combination therapy for pulmonary arterial hypertension. *Eur Respir J* 2005;**26**:858–63.

141 Ivy DD, Doran A, Claussen L, *et al*. Weaning and discontinuation of epoprostenol in children with idiopathic pulmonary arterial hypertension receiving concomitant bosentan. *Am J Cardiol* 2004;**93**:943–6.

142 Melnick L, Barst RJ, Rowan CA, *et al*. Effectiveness of transition from intravenous epoprostenol to oral/inhaled targeted pulmonary arterial hypertension therapy in pediatric idiopathic and familial pulmonary arterial hypertension. *Am J Cardiol*. **105**:1485–9.

143 Micheletti A, Hislop AA, Lammers A, *et al*. Role of atrial septostomy in the treatment of children with pulmonary arterial hypertension. *Heart* 2006;**92**:969–72.

144 Sandoval J, Gaspar J, Pulido T, *et al*. Graded balloon dilation atrial septostomy in severe primary pulmonary hypertension. A therapeutic alternative for patients nonresponsive to vasodilator treatment. *J Am Coll Cardiol* 1998;**32**:297–304.

145 Blanc J, Vouhe P, Bonnet D. Potts shunt in patients with pulmonary hypertension. *N Engl J Med* 2004;**350**:623.

146 Labombarda F, Maragnes P, Dupont-Chauvet P, Serraf A. Potts anastomosis for children with idiopathic pulmonary hypertension. *Pediatr Cardiol* 2009;**30**:1143–5.

147 Gaynor JW, Bridges ND, Clark BJ, Spray TL. Update on lung transplantation in children. *Curr Opin Pediatr* 1998;**10**:256–61.

148 Boucek MM, Aurora P, Edwards LB, *et al*. Registry of the International Society for Heart and Lung Transplantation: tenth official pediatric heart transplantation report – 2007. *J Heart Lung Transplant* 2007;**26**:796–807.

149 Rosenzweig EB, Widlitz AC, Barst RJ. Pulmonary arterial hypertension in children. *Pediatr Pulmonol* 2004;**38**:2–22.

150 Ghofrani HA, Barst RJ, Benza RL, *et al*. Future perspectives for the treatment of pulmonary arterial hypertension. *J Am Coll Cardiol* 2009;**54**:S108–17.

151 Ghofrani HA, SeegerW, Grimminger F. Imatinib for the treatment of pulmonary arterial hypertension. *N Engl J Med* 2005;**353**:1412–3.

152 Klein M, Schermuly RT, Ellinghaus PH, *et al*. Combined tyrosine and serine/threonine kinase inhibition by sorafenib prevents

153 Schermuly RT, Dony E, Gofrani HA, *et al*. Reversal of experimental pulmonary hypertension by PDGF inhibition. *J Clin Invest* 2005;**115**:2811–21.

154 Casey DB, Badejo AM, Dhaliwac JS, *et al*. Analysis of responses to the Rho-kinase inhibitor Y-27632 in the pulmonary and systemic vascular bed of the rat. *Am J Physiol Heart Circ Physiol* 2010;**299**:H184–92.

155 Grimminger F, Weimann R, Frey R, *et al*. First acute haemodynamic study of soluble guanylate cyclase stimulator riociguat in pulmonary hypertension. *Eur Respir J* 2009;**33**:785–92.

156 Rubinstein I. Human VIP-alpha: an emerging biologic response modifier to treat primary pulmonary hypertension. *Expert Rev Cardiovasc Ther* 2005;**3**:565–9.

157 Girgis RE, Mozammel S, Champion HC, *et al*. Regression of chronic hypoxic pulmonary hypertension by simvastatin. *Am J Physiol Lung Cell Mol Physiol* 2007;**292**:L1105–10.

158 Wilkins MR, Ali O, Bradlow W, *et al*. Simvastatin as a treatment for pulmonary hypertension trial. *Am J Respir Crit Care Med*. 2010;**181**:1106–13.

159 Guignabert C, Raffestin B, Benferhat R, *et al*. Serotonin transporter inhibition prevents and reverses monocrotaline-induced pulmonary hypertension in rats. *Circulation* 2005;**111**:2812–9.

160 Beghetti M, Galie N. Eisenmenger syndrome a clinical perspective in a new therapeutic era of pulmonary arterial hypertension. *J Am Coll Cardiol* 2009;**53**:733–40.

161 Beghetti M, Tissot C. Pulmonary arterial hypertension and congenital heart disease: targeted therapies and operability. *J Thorac Cardiovasc Surg* 2009;**138**:785–6; author reply 786.

162 Feinstein JA. Evaluation, risk stratification, and management of pulmonary hypertension in patients with congenital heart disease. *Semin Thorac Cardiovasc Surg Pediatr Card Surg Annu* 2009:106–11.

163 Viswanathan S, Kumar RK. Assessment of operability of congenital cardiac shunts with increased pulmonary vascular resistance. *Catheter Cardiovasc Interv* 2008;**71**:665–70.

164 Neutze JM, Ishikawa T, Clarkson PM, *et al*. Assessment and follow-up of patients with ventricular septal defect and elevated pulmonary vascular resistance. *Am J Cardiol* 1989;**63**:327–31.

165 Dammann JF Jr, McEachen JA, Thompson WM Jr, *et al*. The regression of pulmonary vascular disease after the creation of pulmonary stenosis. *J Thorac Cardiovasc Surg* 1961;**42**:722–34.

166 Wagenvoort CA, Wagenvoort N, Draulans-Noe Y. Reversibility of plexogenic pulmonary arteriopathy following banding of the pulmonary artery. *J Thorac Cardiovasc Surg* 1984;**87**:876–86.

167 Novick WM, Gurbuz AT, Watson DC, *et al*. Double patch closure of ventricular septal defect with increased pulmonary vascular resistance. *Ann Thorac Surg* 1998;**66**:1533–8.

168 Novick WM, Sandoval N, Lazorhysynets VV, *et al*. Flap valve double patch closure of ventricular septal defects in children with increased pulmonary vascular resistance. *Ann Thorac Surg* 2005;**79**:21–8; discussion 21–8.

169 Adatia I, Beghetti M. Early postoperative care of patients with pulmonary hypertension associated with congenital cardiac disease. *Cardiol Young* 2009;**19**:315–9.

170 Beghetti M, Habre W, Friedl B, Berner M. Continuous low dose inhaled nitric oxide for treatment of severe pulmonary

progression of experimental pulmonary hypertension and myocardial remodeling. *Circulation* 2008;**118**:2081–90.

hypertension after cardiac surgery in paediatric patients. *Br Heart J* 1995;**73**:65–8.

171 Dimopoulos K, Peset A, Gatzoulis MA. Evaluating operability in adults with congenital heart disease and the role of pretreatment with targeted pulmonary arterial hypertension therapy. *Int J Cardiol* 2008;**129**:163–71.

172 Yamauchi H, Yamaki S, Fujii M, *et al*. Atrial septal defect with borderline pulmonary vascular disease: surgery and long-term oral prostacyclin therapy for recalcitrant pulmonary hypertension. *Jpn J Thorac Cardiovasc Surg* 2004;**52**:213–6.

173 Eicken A, Balling G, Gilden HB, *et al*. Transcatheter closure of a non-restrictive patent ductus arteriosus with an Amplatzer muscular ventricular septal defect occluder. *Int J Cardiol* 2007;**117**:e40–2.

174 Schwerzmann M, Zafar M, McLaughlin PR, *et al*. Atrial septal defect closure in a patient with "irreversible" pulmonary hypertensive arteriopathy. *Int J Cardiol* 2006;**110**:104–7.

175 Hoetzenecker K, Ankersmit HJ, Bonderman D, *et al*. Atrial septal defect repair after a 10-month treatment with bosentan in a patient with severe pulmonary arterial hypertension: a case report. *J Thorac Cardiovasc Surg* 2009;**137**:760–1.

176 Beghetti M. Congenital heart disease and pulmonary hypertension. *Rev Port Cardiol* 2004;**23**:273–81.

177 Hopkins WE, Ochoa LL, Richardson GW, Trulock EB. Comparison of the hemodynamics and survival of adults with severe primary pulmonary hypertension or Eisenmenger syndrome. *J Heart Lung Transplant* 1996;**15**:100–5.

178 Beghetti M. Fontan and the pulmonary circulation: a potential role for new pulmonary hypertension therapies. *Heart* 2010;**96**:911–6.

179 Yoshimura N, Yamaguchi M, Oka S, *et al*. Inhaled nitric oxide therapy after Fontan-type operations. *Surg Today* 2005;**35**:31–5.

180 Cai J, Su Z, Shi Z, *et al*. Nitric oxide in conjunction with milrinone better stabilized pulmonary hemodynamics after Fontan procedure. *Artif Organs* 2008;**32**:864–9.

181 Cai J, Su Z, Shi Z, *et al*. Nitric oxide and milrinone: combined effect on pulmonary circulation after Fontan-type procedure: a prospective, randomized study. *Ann Thorac Surg* 2008;**86**:882–8; discussion 882–8.

182 Takahashi K, Mori Y, Yamamura H, *et al*. Effect of beraprost sodium on pulmonary vascular resistance in candidates for a Fontan procedure: a preliminary study. *Pediatr Int* 2003;**45**:671–5.

183 Miyaji K, Nagata N, Miyamoto T, Kitahori K. Combined therapy with inhaled nitric oxide and intravenous epoprostenol (prostacyclin) for critical pulmonary perfusion after the Fontan procedure. *J Thorac Cardiovasc Surg* 2003;**125**:437–9.

184 Bridges ND, Mayer JE Jr, Lock JE, *et al*. Effect of baffle fenestration on outcome of the modified Fontan operation. *Circulation* 1992;**86**:1762–9.

185 Giardini A, Balducci A, Specchia S, *et al*. Effect of sildenafil on haemodynamic response to exercise and exercise capacity in Fontan patients. *Eur Heart J* 2008;**29**:1681–7.

186 Apostolopoulou SC, Papagiannis J, Rammos S. Bosentan induces clinical, exercise and hemodynamic improvement in a pre-transplant patient with plastic bronchitis after Fontan operation. *J Heart Lung Transplant* 2005;**24**:1174–6.

187 Rosenzweig EB, Barst RJ. Pulmonary arterial hypertension in children: a medical update. *Curr Opin Pediatr* 2008;**20**:288–93.

52 Central Nervous System Complications

Jane W. Newburger

Harvard Medical School and Children's Hospital, Boston, MA, USA

Dramatic improvements in the survival of children with heart disease have been accompanied by the recognition that this population manifests a high prevalence of neurologic and developmental abnormalities, including mental retardation and lifelong language and learning problems [1]. The factors underlying central nervous system (CNS) morbidity in children with heart disease are complex, multifactorial, and probably cumulative. Such morbidities may be mediated by known genetic disorders (e.g., trisomy 21, chromosome 22q11 microdeletion). Developmental abnormalities for which a genetic origin is suspected are common in congenital heart disease (CHD) patients, in whom the prevalence of cerebral dysgenesis ranges from 10 to 29% in autopsy studies and varies with the underlying cardiac lesion [2–4]. Infants with hypoplastic left heart syndrome (HLHS) appear to be at particular risk for associated developmental cerebral abnormalities, ranging in severity from microdysgenesis to gross malformations such as holoprosencephaly [2]. Increasingly, abnormal fetal cerebral hemodynamics are suspected to play a role in adverse neurodevelopmental outcome of children with CHD [5].

Other neurologic abnormalities are acquired postnatally, either as sequelae of congenital heart disease itself or from its therapies. Neurologic complications of open heart surgery have received the greatest scrutiny, in part because CNS protection during cardiopulmonary bypass constitutes a modifiable risk factor. Brain injury among patients with CHD may be caused by pre- or postoperative hemodynamic instability and adverse events, severe chronic hypoxemia or congestive heart failure, episodes of arrhythmia or cardiac arrest, thromboembolic events unrelated to operation, poor nutritional status, and CNS infection.

Not surprisingly, given these risk factors, children with heart disease, compared with a normative sample, have significantly lower scores on IQ and achievement tests, delays in reaching motor milestones, higher frequencies of learning disabilities, use of special services, and speech, language, and behavioral abnormalities [6–14]. In general, outcomes after repair of simple lesions, such as atrial septal defect, are similar to those in the normal population [15], whereas developmental outcomes appear to be worse after biventricular repair of more complex lesions [14,16,17]. Importantly, adverse developmental outcome is most common among those with various forms of single ventricle [7,18,19]. For this reason, children with cardiac disease should undergo periodic neurodevelopmental screening and evaluation to facilitate prompt institution of interventions when needed.

Genetic factors

Wide variance in neurodevelopmental outcomes in CHD patients cannot be explained solely by intraoperative perfusion variables or other obvious risk factors. Hence the relationship of genetic factors to neurologic and developmental outcomes in CHD patients has been subject to increasing investigation.

Genetic factors causing congenital heart defects may also affect brain development. The association of cardiac defects and CNS impairment has long been described in patients with aneuploidy (e.g., trisomy 12, 18, and 21, Turner syndrome) and in chromosomal structural abnormalities, such as monosomy 22q11. The role of single-gene defects in causing CHD and neurodevelopmental impairment has been discovered more recently. For example, JAG1 encodes a ligand for the Notch intercellular signaling pathway, which is of tremendous importance in brain development [20–24]; mutations in JAG1 cause Alagille syndrome, which affects the heart, liver, kidney, and brain. Approximately 10% of

children with facial dysmorphism and multiple congenital anomalies in a series of 373 patients with a normal chromosome analysis had a chromosomal deletion and/or duplication by microarray [25]. More than three dozen genetic syndromes have been associated with single ventricle, a diagnosis particularly notable for its association with neurodevelopmental delays [26–30].

Children with CHD with a genetic or phenotypic syndrome fare worse and have a wider standard deviation in development scores than patients without such genetic abnormalities [31].

Fetal milieu

In some forms of CHD, the fetal circulation is associated with abnormalities of cerebral hemodynamics and brain metabolism. For example, in a fetus with HLHS, the brain is perfused retrograde through the ductus arteriosus. The association of microcephaly in HLVS with a smaller diameter of the ascending aorta suggests that inadequate cerebral perfusion may complement dysgenesis as a cause of abnormally small brain size at birth. Cerebral blood flow characteristics are also abnormal in mid-gestation fetuses with evolving HLHS, suggesting low cerebral vascular impedance [32]. Third-trimester fetuses with complex CHD have smaller gestational age- and weight-adjusted brain volume than normal fetuses and evidence of impaired neuroaxonal development and metabolism [32]. Thus, impaired cerebral perfusion and substrate delivery during fetal life may adversely affect the fetal brain. Furthermore, delayed or abnormal fetal brain development caused by perturbations in cerebral hemodynamics may increase the vulnerability of neonates with CHD to ischemia and reperfusion injury perioperatively [33].

Neonatal intracranial hemorrhage

Perhaps due to hemodynamic instability, the risk period for intraventricular–periventricular hemorrhage [34], characteristic of premature infants, appears to extend further into maturity in infants with a cardiac anomaly (see also Chapter 18). The diagnosis of intraventricular–periventricular hemorrhage in a neonate with CHD complicates operative planning. In these infants, the use of anticoagulants, the increase in fibrinolytic activity [35], and the variation in cerebral perfusion pressure during cardiopulmonary bypass may each predispose to extension of intraventricular–periventricular hemorrhage or hemorrhagic transformation of ischemic lesions. The timing and management of cardiac surgery in infants with intraventricular–periventricular hemorrhage attempt to balance the risks of extension of hemorrhage during a cardiac operation against those of

ischemia–reperfusion injury and further hemorrhagic extension during the persistent cardiorespiratory instability associated with an uncorrected cardiac malformation. The severity of the cardiac anomaly, the expected complexity of the operation, and the severity of the intracranial hemorrhage must be considered. Hemorrhage confined to the subependymal region should not delay operation. It is probably advisable to delay cardiopulmonary bypass for at least 1 week in infants with intraventricular hemorrhage, preferably longer in those with intraparenchymal hemorrhage.

The perioperative period

Acquired brain injury among patients with congenital cardiac anomalies has been well studied among those undergoing palliative and repairative cardiovascular surgery. Bypass-related sources of brain injury include hypoperfusion, macroemboli, and microemboli, both particulate and gaseous. The risk of brain injury related to cardiopulmonary bypass in infants and children may be influenced by many variables, including the duration of total support, the depth of hypothermia, the rate and duration of core cooling [36,37], the type of pH management chosen during core cooling (alpha-stat versus pH-stat) [17,38,39], the degree of hemodilution [40–42], the duration of total circulatory arrest [43–47], the type of oxygenator (bubble versus membrane), the use of arterial filtration, the use of regional cerebral perfusion [48], and other aspects of the biochemical milieu.

Pre- and postoperative risk factors interact with intraoperative vital organ support, with its "planned ischemia and reperfusion injury," in producing CNS injury. In particular, recent data have underscored the frequency and importance of preoperative neurologic state. Miller and colleagues showed that brain metabolism and microstructure, as measures of brain maturation, are abnormal in a high percentage of infants with CHD before they undergo cardiac surgery [33]. Indeed, the imaging findings are similar to those in premature infants. Licht and colleagues studied full-term infants with D-transposition of the great arteries and HLHS, demonstrating that brain maturation was delayed by ~1 month compared with a normative sample without CHD [49]. Thus these term infants had brains that were smaller and less mature prior to cardiac surgery, potentially predisposing to white matter injury. Furthermore, preoperative cerebral blood flow is reduced in neonates with CHD compared with normal infants [50]. In the preoperative period, more than half of infants with critical CHD have abnormalities on neurologic examination [51]. Abnormal preoperative neurological status is an important predictor of adverse longer term outcome in patients with CHD [12,52].

CNS damage may also be caused by early postoperative events, when cerebral vasoregulatory systems disrupted by

hypothermic circulatory arrest and bypass techniques may make the brain more vulnerable to hemodynamic fluxes, such as hypotension [53–56].

Neuropathologic studies of individuals who have undergone congenital heart surgery have demonstrated both diffuse cerebral injury, as might result from ischemia reperfusion injury related to hypoperfusion, and also focal infarctions from thromboembolic events. Among infants who died after reparative or palliative cardiovascular surgery, the most widespread and severe injury occurred in the cerebral white matter, where periventricular leukomalacia and diffuse white matter gliosis were evident [57]. Gray matter injury, however, was also detected. Autopsy series are subject to bias, however, because the most severely ill children are those who succumb.

Magnetic resonance imaging (MRI) has provided a "window" into the CNS in the perioperative period. Mahle and colleagues [58] conducted a prospective MRI study of infants with various types of CHD before and after surgical correction of their cardiac lesions. Periventricular leukomalacia was present in more than half of the subjects postoperatively, but white matter and gray matter injury were already present preoperatively in 15 and 8% of subjects, respectively. Neonates more likely demonstrate evidence of brain injury than infants older than 6 months of age at surgical correction [59]. Furthermore, preoperative magnetic resonance spectroscopy (MRS) showed that more than half of the children had elevated cerebral lactate peaks. In preoperative MRI studies, McConnell and colleagues [60] found enlargement of ventricles and subarachnoid spaces consistent with cerebral atrophy in one-third of their study sample. MR imaging performed on patients with CHD following surgery has revealed findings consistent with both gray matter and widely distributed white matter injury [61]. Taken in aggregate, documentation by MRI of brain abnormalities in children with CHD both before and after cardiac surgery suggest that the preoperative condition of the brain, and also perioperative course, contribute to long-term developmental outcome.

Postoperative delayed recovery of consciousness

Although hypoxic–ischemic reperfusion injury is often associated with postoperative delayed recovery of consciousness, postoperative hepatic or renal impairment resulting in accumulation of toxic metabolites or impaired metabolism or excretion of sedating drugs must be excluded. Prolonged use of neuromuscular blocking agents may delay the recovery of motor function [62–64] and, if severe, may mimic a state of impaired consciousness. As discussed later, a significant minority of infants develop postoperative seizures, which may recur serially and may be clinically silent [65].

A persistent depression of consciousness warrants consideration of occult seizures or a prolonged postictal state.

Postoperative seizures

Seizures are probably the most common neurologic complication of open heart surgery in infants and are clinically manifest in up to 15% of patients in the early postoperative period [65–67]. Prospective long-term video electroencephalographic monitoring has demonstrated a significantly higher incidence of electrographic seizure activity in this early postoperative period, frequently without typical behavioral seizure manifestations [65]. Postoperative seizures may have a number of possible etiologic factors; of greatest concern to long-term outcome are those resulting from hypoxic–ischemic reperfusion injury due to either generalized cerebral hypoperfusion or focal vasocclusive disease. More commonly, however, these early postoperative seizures remain cryptogenic and are often referred to as post-pump seizures. Although post-pump seizures are often assumed to be related to hypoxic–ischemic reperfusion injury, they differ in several respects from other forms of seizures. First, post-pump seizures typically occur later after injury than, for instance, those occurring after birth asphyxia. Whereas most asphyxial seizures have their onset within the first 12 h after birth, post-pump seizures are usually seen first during the second postoperative 24 h. Second, although post-pump seizures are associated with later neurologic and developmental dysfunction [68], they have a less devastating prognosis than asphyxial seizures, in which as many as 50% of infants are left with neurologic disability [69–71]. The delayed onset of post-pump seizures and their more favorable outcome may reflect the neuroprotective effective of hypothermia during cardiopulmonary bypass [72].

The prognosis of postoperative seizures varies with the underlying cause. A prospective study using continuous video electroencephalography demonstrated a significant association between post-pump seizures and worse neurologic and developmental outcome at ages 1 year [68] and 4 years [73]. None of these patients had developed epilepsy by age 4 years, however. Among infants whose seizures had a specific cause, long-term outcome is related to etiology. For instance, if seizures are a presenting symptom of cerebral dysgenesis, poor long-term outcome is nearly universal and subsequent epilepsy is common. If seizures result from a stroke, the risk of subsequent epilepsy ranges from 19 to 28% [74,75]. In these patients, the epilepsy risk relates to age at the time of stroke and the latency to first seizure after the stroke. In a neonate, the risk for subsequent epilepsy is low [76], whereas longer latency to first seizure is associated with greater incidence of epilepsy [75]. These features may guide decisions regarding duration of anticonvulsant therapy.

Movement disorders

Soon after the development of deep hypothermic cardiac surgery, striking movement disorders were reported [77–89]. Although the incidence in different series has ranged from 0.5% [90] to 19% [80], underdiagnosis and underreporting of these dyskinesias are such that the true incidence is unknown. Despite their relative rarity, these movement disorders are often dramatic, frequently intractable, and, if severe, associated with a substantial mortality. Although choreoathetosis is the most frequent form of dyskinesia complicating a cardiac operation, other movement disorders have been described, including oculogyric crises [91] and parkinsonism [92].

The appearance of postoperative movement disorders is typically preceded by a latency period of 2–7 days, during which neurologic recovery from operation appears uncomplicated. The dyskinesia is usually heralded by the subacute onset of delirium, with marked irritability, insomnia, confusion, and disorientation, followed shortly by abnormal involuntary movements. These movements begin in the distal extremities and orofacial muscles, progressing proximally to involve the girdle muscles and trunk; if severe, violent ballismic thrashing may develop. The abnormal movements are present during wakefulness, peak with distress, and resolve during sleep. In addition, an apraxia of oculomotor and oromotor function develops, with a loss of feeding and expressive language skills. A supranuclear ophthalmoplegia often appears, with a loss of voluntary gaze but sparing of reflex extraocular movements; these patients do not appear to look at parents or caretakers and show minimal facial signs of recognition, thereby arousing concerns about blindness. The onset of involuntary movements is usually followed by a period of deterioration lasting about 1 week, a plateau period of 1–2 weeks during which the movements remain relatively constant, and finally a recovery phase of more variable duration.

Diagnosis of postoperative hyperkinetic syndromes is clinical; to date, adjunctive neurodiagnostic tests have been useful primarily to exclude other disorders. Neuroimaging studies, including computed tomography (CT) and MRI, have shown nonspecific changes, most commonly diffuse cerebral atrophy. Focal abnormalities are rare [85–87,89]. Single-photon emission computed tomography (SPECT) functional brain imaging studies have shown a high incidence of both cortical and subcortical perfusion defects even in the absence of structural defects on CT and MRI [93]. Electroencephalographic studies are commonly normal or show diffuse slowing; ictal activity is not seen during these movements. Autopsy studies are limited and the neuropathologic findings are inconsistent [81,94], ranging from normal to extensive degrees of neuronal loss and gliosis, particularly focused in the external globus pallidus [94]. Typical features of infarction are characteristically absent.

The prognosis depends largely on their initial severity. Mild movement disorders tend to resolve within weeks to months, but more severe instances have an associated mortality approaching 40% and a high incidence of persistent neurodevelopmental deficits in survivors [89]. Only ~10% of survivors in the severe group demonstrate normal neurologic outcome [89]. Common residual deficits include generalized hypotonia, developmental delay, and expressive language impairment. However, these reports are anecdotal, and detailed long-term follow-up is lacking.

The mechanisms underlying these movement disorders after a cardiac operation remain elusive [95–97]. Despite the absence of a unifying mechanism, a number of risk factors have been identified. Children at particular risk include those with a cyanotic cardiac malformation, especially with systemic-to-pulmonary collaterals from the head and neck, age at operation older than 9 months, and excessively short cooling periods before attenuation of intraoperative blood flow. Some authors have suggested deep hypothermia itself as a cause [97]. Several reports have cited prolonged use of fentanyl and midazolam as a cause of postoperative dyskinesias. These drug-related dyskinesias tend to be relatively mild and to resolve during a period of weeks [98–100].

Cerebrovascular accident (stroke)

CHD is the most common condition associated with stroke in childhood, being present in 25–30% of affected patients [74,101,102]. Stroke of cardiac origin, that is, cardiogenic stroke, has three broad mechanisms. First, arterial emboli may be generated from an intracardiac source (cardioembolic stroke). Second, emboli may arise from a systemic venous or right-sided heart source and bypass the pulmonary circulation through a right-to-left shunt (paradoxical embolic stroke). Finally, cerebral venous thrombosis may result from a combination of central venous hypertension, venous stasis, and polycythemia. Risk factors for cardiogenic stroke include altered vascular surface, stasis, hypercoagulability, and paradoxical vascular pathways.

Open heart surgery presents multiple risk factors for stroke. During cardiopulmonary bypass, particulate and gaseous emboli originating from the cardiopulmonary bypass apparatus or operative field enter the systemic circulation directly [103–106]. Improvements in bypass circuits, particularly the switch from bubble to membrane oxygenators, have decreased the incidence of macroembolization; reduction in microembolic load is suggested by a smaller total ischemic area as assessed with retinal fluorescein angiography after use of membrane oxygenators compared with bubble oxygenators [107]. Although bypass-related cerebral injury in adults is related primarily to atheromatous emboli or fixed cerebrovascular stenoses, such injury in infants results most commonly from global hypoperfusion

during periods of decreased or arrested systemic blood flow. A further potential mechanism of intraoperative vascular injury may relate to the often marked inflammatory response triggered by the extensive and prolonged exposure between bypass blood and artificial surfaces [108–110]. These factors trigger complex cascades, including endothelium–leukocyte interactions [111–114]. Stroke in the early postoperative period may present with focal motor weakness and speech and visual dysfunction. Seizures are a particularly common presentation of stroke in young infants [74,115].

Patients with CHD are also at risk for stroke from factors outside the operating room. Cardiac catheterization poses a risk of both particulate and gaseous emboli, particularly in cyanotic patients who are at risk for paradoxical embolization. In patients with cardiomyopathy, cerebral emboli can arise from intracardiac thrombus. Similarly, embolic stroke may occur in patients with a left atrial clot who convert to normal sinus rhythm from atrial fibrillation, prompting the recommendation for either transesophageal echocardiography or anticoagulation before planned cardioversions. Vascular surfaces may promote thrombosis secondary to endothelial injury or prosthetic tissue, especially in an area of vascular stasis [59,116,117]. Patients with a left-sided prosthetic valve are at risk for thromboembolic complications. Those with left-sided infective endocarditis may have septic cerebral emboli and occasional intracranial mycotic aneurysms (see later). A number of risk factors for stroke converge in patients who have undergone the Fontan procedure. In a retrospective review of 645 patients after the Fontan operation, the incidence of stroke was reported to be 2.6% [59]. In the Pediatric Heart Network's cross-sectional study of Fontan patients, the incidence of stroke was 2% [118].

Stroke prevention may be regarded as primary (i.e., treatment of high-risk patients to prevent a first stroke) or secondary (i.e., aimed at preventing stroke recurrence) [119]. Most pediatric cardiologists use prophylactic anticoagulant therapy in children with a prosthetic heart valve and intracardiac thrombus identified by echocardiography. The need for stroke prophylaxis in individual patients should consider risk factors such as elevated right atrial pressure, intracardiac prosthetic material, and a right-to-left shunt in children requiring prolonged bedrest. Many pediatric cardiologists administer antithrombotic therapy, either aspirin or warfarin, indefinitely after Fontan surgery and in those with a dilated cardiomyopathy. Secondary stroke prophylaxis aims to balance the risk of recurrent embolism and that of hemorrhagic transformation of a bland cerebral infarction.

Headaches

Headaches in patients with a cardiac malformation commonly require evaluation. Acute severe headache should always raise the concern of a subarachnoid hemorrhage,

particularly in patients with a history of coarctation of the aorta. Patients with severe polycythemia experience more frequent headaches. Raised central venous pressure, as occurs after the Fontan procedure or the bidirectional Glenn procedure, may increase cerebral venous pressure, which by itself may be associated with headaches. Raised central venous pressure may also impair absorption of cerebrospinal fluid, resulting in communicating hydrocephalus [120] elevating intracranial pressure and causing headaches. Headache is the most common presenting feature in the otherwise often subtle clinical presentation of a brain abscess (see later).

Infectious endocarditis

Children with a cardiac anomaly are at increased risk for infectious endocarditis with its protean neurologic manifestations [121]. These include meningitis, brain abscess, seizures, and, most commonly, cerebrovascular injury. Despite modern antibiotic advances, approximately one-third of children with infectious endocarditis have neurologic complications, approximately half of which are embolic in origin [122]. Not only are cerebrovascular complications the most common form of neurologic injury in endocarditis, but they also have the highest mortality, reaching 80–90% with hemorrhage of mycotic aneurysms [123]. The high risk of hemorrhagic transformation of septic infarction or of direct subarachnoid hemorrhage through mycotic aneurysms contraindicates the use of anticoagulation in children with infectious endocarditis and cerebrovascular disease [124].

Brain abscess

Cyanotic cardiac malformations constitute the major predisposing factor for brain abscess [125], with an incidence ranging from 2 to 6% [126]. Conversely, CHD was present in almost half of childhood brain abscess cases in a single-center series [127]. Arterial oxygenation is inversely correlated with the incidence, morbidity, and mortality of brain abscess in CHD [126]. In cyanotic patients with polycythemia, periods of systemic illness and dehydration may critically disturb cerebral microvascular perfusion with subsequent localized areas of ischemia. Organisms bypassing the pulmonary filtration system may gain direct access to the brain, where they breach the disrupted blood–brain barrier, passing into necrotic areas to form focal septic cerebritis and, subsequently, an abscess.

In children with a cardiac anomaly, brain abscess is rare before the age of 2 years [128]. The clinical manifestations of brain abscess result from a combination of intracranial hypertension, focal neurologic injury, and sepsis. Headache is the predominant and usual presenting symptom [127]. The initial presentation is often subtle and the course

progresses slowly . Occasionally, the presentation may be abrupt, for example, a seizure. Headache, a common early symptom, is present in 50% of patients, and is often associated with vomiting, fever, and photophobia [127]. Personality changes and irritability occur early.

The diagnosis of brain abscess is best confirmed by MRI with gadolinium enhancement [129]. Contrast-enhanced CT scans are less sensitive, but can be obtained more quickly in emergency settings. A lumbar puncture should be obtained only after exclusion of a significant mass effect by brain imaging, and may show elevated protein but often only mild leukocytosis.

Brain abscess is usually managed by a combination of antibiotic therapy and surgical drainage (diagnostic and/or therapeutic) [129]. With or without surgery, high-dose antibiotic therapy should be administered for ≥6 weeks, with duration of therapy guided by clinical response and imaging studies. Two or more pathogens were isolated in cultures of 39% of patients in a recent series, and streptococcal species were the most common isolates in patients older than 1 month [127]. In immunosuppressed patients (e.g., after cardiac transplantation), pathogens can include lower virulence organisms and also fungi (e.g., *Aspergillus*) and parasites (e.g., *Toxoplasma*). Therapy should be guided by culture results, when they become available.

Although diagnostic and therapeutic advances have reduced the mortality of brain abscess [130], a minority of survivors return to their premorbid baseline function [127]. Epilepsy develops in as many as one-third of survivors, often after many years [127,131].

Future directions

Reparative infant cardiac surgery, with its necessity for the use of cardiopulmonary bypass techniques and ischemia–reperfusion injury, provides an unparalleled opportunity for prospective clinical trials of improved methods of cardiopulmonary bypass, neuroprotective pharmacologic agents, and postoperative interventions [132]. Standardization of the interpretation of existing neuroimaging techniques and the development of novel neuromonitoring modalities are needed to assess outcomes of new neuroprotective strategies. Finally, as CNS morbidity in cardiac children has moved to the forefront of outcomes research in pediatric cardiovascular disease, multi-center registries and trials should investigate the influence of genetic factors, including the host response to injury, and practice variation on neurodevelopmental outcomes.

References

1 Ferry PC. Neurologic sequelae of open-heart surgery in children. An "irritating question." *Am J Dis Child* 1990;**144**:369–73.

2 Glauser T, Rorke L, Weinberg P, Clancy R. Congenital brain anomalies associated with hypoplastic left heart syndrome. *Pediatrics* 1990;**85**:984–90.

3 Jones M. Anomalies of the brain and congenital heart disease: a study of 52 necropsy cases. *Pediatr Pathol* 1991;**11**:721–36.

4 Terplan K. Brain changes in newborns, infants and children with congenital heart disease in association with cardiac surgery. Additional observations. *J Neurosurg* 1976;**212**:225.

5 Limperopoulos C, Tworetzky W, McElhinney DB, *et al.* Brain volume and metabolism in fetuses with congenital heart disease: evaluation with quantitative magnetic resonance imaging and spectroscopy *Circulation* 2010;**121**:26–33.

6 Wernovsky G, Newburger J. Neurologic and developmental morbidity in children with complex congenital heart disease. *J Pediatr* 2003;**142**:6–8.

7 Mahle WT, Clancy RR, Moss EM, *et al.* Neurodevelopmental outcome and lifestyle assessment in school-aged and adolescent children with hypoplastic left heart syndrome. *Pediatrics* 2000;**105**:1082–9.

8 Mahle WT, Wernovsky G. Long-term developmental outcome of children with complex congenital heart disease. *Clin Perinatol* 2001;**28**:235–47.

9 Bellinger DC, Jonas RA, Rappaport LA, *et al.* Developmental and neurologic status of children after heart surgery with hypothermic circulatory arrest or low-flow cardiopulmonary bypass. *N Engl J Med* 1995;**332**:549–55.

10 Bellinger DC, Rappaport LA, Wypij D, *et al.*, for the Boston Circulatory Arrest Study Group. Patterns of developmental dysfunction after surgery during infancy to correct transposition of the great arteries. *J Dev Behav Ped* 1997;**18**:75–83.

11 Bellinger DC, Wypij D, Kuban K, *et al.* Developmental and neurologic status of children at four years of age after heart surgery with hypothermic circulatory arrest or low-flow cardiopulmonary bypass. *Circulation* 1999;**100**:526–32.

12 Limperopoulos C, Majnemer A, Shevell MI, *et al.* Predictors of developmental disabilities after open heart surgery in young children with congenital heart defects. *J Pediatr* 2002;**141**:51–8.

13 Limperopoulos C, Majnemer A, Shevell MI, *et al.* Functional limitations in young children with congenital heart defects after cardiac surgery. *Pediatrics* 2001;**108**:1325–31.

14 Forbess JM, Visconti KJ, Bellinger DC, *et al.* Neurodevelopmental outcomes after biventricular repair of congenital heart defects. *J Thorac Cardiovasc Surg* 2002;**123**:631–9.

15 Visconti KJ, Bichell DP, Jonas RA, *et al.* Developmental outcome after surgical versus interventional closure of secundum atrial septal defect in children. *Circulation* 1999;**100**(19:Suppl):Suppl-50.

16 Bellinger DC. Perspectives on incorporating human neurobehavioral end points in risk assessments. *Risk Anal* 2002;**22**:487–98.

17 Bellinger DC, Wypij D, du Plessis AJ, *et al.* Developmental and neurologic effects of alpha-stat versus pH-stat strategies for deep hypothermic cardiopulmonary bypass in infants. *J Thorac Cardiovasc Surg* 2001;**121**:374–83.

18 Wernovsky G, Stiles KM, Gauvreau K, *et al.* Cognitive development following the Fontan operation. *Circulation* 1995;**92**, I-121.

19 Williams DL, Gelijns AC, Moskowitz AJ, *et al.* Hypoplastic left heart syndrome: valuing the survival. *J Thorac Cardiovasc Surg* 2000;**119**(4:Pt 1):t-31.

20 Cohen JD, Perlstein WM, Braver TS, *et al.* Temporal dynamics of brain activation during a working memory task. *Nature* 1997;**386**:603–7.

21 Gaiano N, Fishell G. The role of notch in promoting glial and neural stem cell fates. *Annu Rev Neurosci* 2002;**25**:471–90.

22 Whitford KL, Dijkhuizen P, Polleux F, Ghosh A. Molecular control of cortical dendrite development. *Annu Rev Neurosci* 2002;**25**:127–49.

23 Pasini A, Wilkinson DG. Stabilizing the regionalisation of the developing vertebrate central nervous system. *Bioessays* 2002;**24**:427–38.

24 Brennan K, Gardner P. Notching up another pathway. *Bioessays* 2002;**24**:405–10.

25 Baris HN, Tan WH, Kimonis VE, Irons MB. Diagnostic utility of array-based comparative genomic hybridization in a clinical setting. *Am J Med Genet A* 2007;**143A**:2523–33.

26 Tabbutt S, Nord AS, Jarvik GP, *et al.* Neurodevelopmental outcomes after staged palliation for hypoplastic left heart syndrome. *Pediatrics* 2008;**121**:476–83.

27 Dorfman AT, Marino BS, Wernovsky G, *et al.* Critical heart disease in the neonate: presentation and outcome at a tertiary care center. *Pediatr Crit Care Med* 2008;**9**:193–202.

28 Stasik CN, Gelehrter S, Goldberg CS, *et al.* Current outcomes and risk factors for the Norwood procedure. *J Thorac Cardiovasc Surg* 2006;**131**:412–7.

29 Natowicz M, Chatten J, Clancy R, *et al.* Genetic disorders and major extracardiac anomalies associated with the hypoplastic left heart syndrome. *Pediatrics* 1988;**82**:698–706.

30 Schinzel AA. Cardiovascular defects associated with chromosomal aberrations and malformation syndromes. *Prog Med Genet* 1983;**5**:303–79.

31 Zeltser I, Jarvik GP, Bernbaum J, *et al.* Genetic factors are important determinants of neurodevelopmental outcome after repair of tetralogy of Fallot. *J Thorac Cardiovasc Surg* 2008;**135**:91–7.

32 McElhinney DB, Benson CB, Brown DW, *et al.* Cerebral blood flow characteristics and biometry in fetuses undergoing prenatal intervention for aortic stenosis with evolving hypoplastic left heart syndrome. *Ultrasound Med Biol* 2010;**36**:29–37.

33 Miller SP, McQuillen PS, Hamrick S, *et al.* Abnormal brain development in newborns with congenital heart disease. *N Engl J Med* 2007;**357**:1928–38.

34 Volpe JJ. Intracranial hemorrhage. In: *Neurology of the Newborn*, 3rd edn. Philadelphia: Saunders, 1994: 373–463.

35 Giuliani R, Szwarcer E, Aquino E, Palumbo G. Fibrin-dependent fibrinolytic activity during extracorporeal circulation. *Thromb Res* 1991;**61**:369–73.

36 Bellinger DC, Wernovsky G, Rappaport LA, *et al.* Cognitive development of children following early repair of transposition of the great arteries using deep hypothermic circulatory arrest. *Pediatrics* 1991;**87**:701–7.

37 Foster J, Burrows FA, Bissonnette B. Uneven cerebral cooling. Presented at the International Symposium on Neurohumoral Effects of Profound Hypothermia in Infant Heart Surgery, Royal Brompton National Heart and Lung Institute, 1993.

38 Jonas RA, Bellinger DC, Rappaport LA, *et al.* Relation of pH strategy and developmental outcome after hypothermic circulatory arrest. *J Thorac Cardiovasc Surg* 1993;**106**:362–8.

39 du Plessis AJ, Jonas RA, Wypij D, *et al.* Perioperative effects of alpha-stat versus pH-stat strategies for deep hypothermic cardiopulmonary bypass in infants. *J Thorac Cardiovasc Surg* 1997;**114**:991–1001.

40 duPlessis AJ. Higher hematocrit improves cerebral outcome after deep hypothermic circulatory arrest. *J Thorac Cardiovasc Surg* 1996;**112**:1610–21.

41 Shin'oka T, Shum-Tim D, Jonas RA, *et al.* Higher hematocrit improves cerebral outcome after deep hypothermic circulatory arrest. *J Thorac Cardiovasc Surg* 1996;**112**:1610–20.

42 Duebener LF, Sakamoto T, Hatsuoka S, *et al.* Effects of hematocrit on cerebral microcirculation and tissue oxygenation during deep hypothermic bypass. *Circulation* 2001;**104**(Suppl):I260–4.

43 Oates RK, Simpson JM, Turnbull JAB, Cartmill TB. The relationship between intelligence and duration of circulatory arrest with deep hypothermia. *J Thorac Cardiovasc Surg* 1995;**110**:786–92.

44 Fallon P, Aparicio JM, Elliott MJ, Kirkham FJ. Incidence of neurological complications of surgery for congenital heart disease. *Arch Dis Child* 1995;**72**:418–22.

45 Haneda K, Itoh T, Togo T, *et al.* Effects of cardiac surgery on intellectual function in infants and children. *Cardiovasc Surg* 1996;**4**:303–7.

46 Miller G, Tesman JR, Ramer JC, *et al.* Outcome after open-heart surgery in infants and children. *J Child Neurol* 1996;**11**:49–53.

47 Hovels-Gurich HH, Seghaye MC, Dabritz S, *et al.* Cognitive and motor development in preschool and school-aged children after neonatal arterial switch operation. *J Thorac Cardiovasc Surg* 1997;**114**:578–85.

48 Goldberg CS, Bove EL, Devaney EJ, *et al.* A randomized clinical trial of regional cerebral perfusion versus deep hypothermic circulatory arrest: outcomes for infants with functional single ventricle. *J Thorac Cardiovasc Surg* 2007;**133**:880–7.

49 Licht DJ, Shera DM, Clancy RR, *et al.* Brain maturation is delayed in infants with complex congenital heart defects. *J Thorac Cardiovasc Surg* 2009;**137**:529–36.

50 Licht DJ, Wang J, Silvestre DW, *et al.* Preoperative cerebral blood flow is diminished in neonates with severe congenital heart defects *J Thorac Cardiovasc Surg* 2004;**128**:841–9.

51 Limperopoulos C, Majnemer A, Shevell MI, *et al.* Neurologic status of newborns with congenital heart defects before open heart surgery. *Pediatrics* 1999;**103**:402–8.

52 Limperopoulos C, Majnemer A, Shevell MI, *et al.* Neurodevelopmental status of newborns and infants with congenital heart defects before and after open heart surgery. *J Pediatr* 2000;**137**:638–45.

53 Bassan H, Gauvreau K, Newburger JW, *et al.* Identification of pressure passive cerebral perfusion and its mediators after infant cardiac surgery. *Pediatr Res* 2005;**57**:35–41.

54 Greeley WJ, Ungerleider RM, Smith LR, Reves JG. The effects of deep hypothermic cardiopulmonary bypass and total circulatory arrest on cerebral blood flow in infants and children. *J Thorac Cardiovasc Surg* 1989;**97**:737–45.

55 Greeley WJ, Kern FH, Ungerleider RM, Boyd JL. The effect of hypothermic cardiopulmonary bypass and total circulatory arrest on cerebral metabolism in neonates, infants, and children. *J Thorac Cardiovasc Surg* 1991;**101**:783–94.

56 Lou H. The "lost autoregulation hypothesis" and brain lesions in the newborn – an update. *Brain Dev* 1988;**10**:143–6.

57 Kinney HC, Panigrahy A, Newburger JW, *et al.* Hypoxic–ischemic brain injury in infants with congenital heart disease dying after cardiac surgery. *Acta Neuropathol (Berl)* 2005;**110**:563–78.

58 Mahle WT, Tavani F, Zimmerman RA, *et al.* An MRI study of neurological injury before and after congenital heart surgery. *Circulation* 2002;**106**(Suppl 1):109–14.

59 du Plessis A, Chang A, Wessel D, *et al.* Cerebrovascular accidents following the Fontan procedure. *Pediatr Neurol* 1995;**12**: 230–236.

60 McConnell JR, Fleming WH, Chu WK, *et al.* Magnetic resonance imaging of the brain in infants and children before and after cardiac surgery. A prospective study. *Am J Dis Child* 1990;**144**:374–8.

61 Miller G, Mamourian AC, Tesman JR, *et al.* Long-term MRI changes in brain after pediatric open heart surgery. *Child Neuropsychol* 2001;**9**:390–7.

62 Gooch J, Suchyta M, Balbierz J, *et al.* Prolonged paralysis after treatment with neuromuscular junction blocking agents. *Crit Care Med* 1991;**19**:1125–31.

63 Partridge B, Abrams J, Bazemore C, *et al.* Prolonged neuro-muscular blockade after long-term infusion of vecuronium bromide in the intensive care unit. *Crit Care Med* 1990;**18**:1577–82.

64 Waitling S, Dasta J. Prolonged paralysis in intensive care unit patients after use of neuromuscular blocking agents: a review of the literature. *Crit Care Med* 1994;**22**:884–91.

65 Newburger JW, Jonas RA, Wernovsky G, *et al.* A comparison of the perioperative neurologic effects of hypothermic circulatory arrest versus low-flow cardiopulmonary bypass in infant heart surgery. *N Engl J Med* 1993;**329**:1057–64.

66 Ehyai A, Fenichel GM, Bender HW. Incidence and prognosis of seizures in infants after cardiac surgery with profound hypother-mia and circulatory arrest. *J Am Med Assoc* 1984;**252**:3165–7.

67 Miller G, Eggli K, Contant C, *et al.* Postoperative neurologic complications after open heart surgery on young infants. *Arch Pediatr Adolesc Med* 1995;**149**:764–8.

68 Bellinger DC, Wypij D, Kuban KCK, *et al.* Developmental and neurologic status of children at four years of age after heart surgery with hypothermic circulatory arrest or low-flow cardiopulmonary bypass. *N Engl J Med* 1995;**332**:549–5.

69 Andre M, Matisse N, Vert P. Prognosis of neonatal seizures. In: Wasterlain CG, Vert P, eds. *Neonatal Seizures*. New York: Raven Press, 1990: 27–39.

70 Bergman I, Painter MJ, Hirsch RP, *et al.* Outcome in neonates with convulsions treated in an intensive care unit. *Ann Neurol* 1983;**14**:642–7.

71 Volpe J. Neonatal seizures. In *Neurology of the Newborn*, 3rd edn. Philadelphia: Saunders, 1994: 172–207.

72 Dietrich W, Busto R, Alonso O, *et al.* Intraischemic but not postischemic brain hypothermia protects chronically following global forebrain ischemia in rats. *J Cerebr Blood Flow Metab* 1993;**13**:541–9.

73 Newburger JW, Wypij D, Kuban KCK, *et al.* Four year neurodevelopmental status: the Boston Circulatory Arrest Study. *Circulation* 1996;**94**:I-173.

74 Lanska M, Lanska D, Horwitz S, Aram D. Presentation, clinical course and outcome of childhood stroke. *Pediatr Neurol* 1991;**7**:333–41.

75 Yang J, Park Y, Hartlage P. Seizures associated with stroke in childhood. *Pediatr Neurol* 1995;**12**:136–8.

76 Levy S, Abroms I, Marshall P, *et al.* Seizures and cerebral infarction in the full-term newborn. *Ann Neurol* 1985;**17**:366–70.

77 Bergouignan M, Fontan F, Trarieux M. Syndromes choreiformes de l'enfant au decours d'interventions cardio-chirurgicales sous hypothermic profounde. *Rev Neurol* 1961;**105**:48–59.

78 Bjork V, Hultquist G. Contraindications to profound hypothermia in open-heart surgery. *J Thorac Cardiovasc Surg* 1962;**44**:1–13.

79 Barratt-Boyes BG. Choreoathetosis as a complication of cardiopulmonary bypass. *Ann Thorac Surg* 1990;**50**:693–4.

80 Brunberg JA, Doty DB, Reilly EL. Choreoathetosis in infants following cardiac surgery with deep hypothermic and circulatory arrest. *J Pediatr* 1974;**84**:232–8.

81 Chaves E, Scaltsas-Persson I. Severe choreoathetosis following congenital heart disease surgery. *Neurology* 1988;**38**(Suppl):284.

82 Curless R, Katz D, Perryman R, *et al.* Choreoathetosis after surgery for congenital heart disease. *J Pediatr* 1994;**124**:737–9.

83 DeLeon S, Ilbawa M, Arcilla R, *et al.* Choreoathetosis after deep hypothermia without circulatory arrest. *Ann Thorac Surg* 1990;**50**:714–9.

84 Donaldson D, Fullerton D, Gollub R, *et al.* Choreoathetosis in children after cardiac surgery. *Neurology* 1990;**40**:337 (abstract).

85 Huntley D, Al-Mateen M, Menkes J. Unusual dyskinesia complicating cardiopulmonary bypass surgery. *Dev Med Child Neurol* 1993;**35**:631–41.

86 Medlock M, Cruse R, Winek S, *et al.* A 10-year experience with postpump chorea. *Ann Neurol* 1993;**34**:820–6.

87 Robinson RO, Samuels M, Pohl KRE. Choreic syndrome after cardiac surgery. *Arch Dis Child* 1988;**63**:1466–9.

88 Wical B, Tomasi L. A distinctive neurologic syndrome after profound hypothermia. *Pediatr Neurol* 1990;**6**:202–5.

89 Wong PC, Barlow CF, Hickey PR, *et al.* Factors associated with choreoathetosis after cardiopulmonary bypass in children with congenital heart disease. *Circulation* 1992;**85**(Suppl 5):II118–26.

90 Gherpelli JL, Azeka E, Riso A, *et al.* Choreoathetosis after cardiac surgery with hypothermia and extracorporeal circulation. *Pediatr Neurol*. 1998;**19**(2):113–8.

91 Wessel D, duPlessis AJ. Choreoathetosis. In: Jonas RA, Newberger JW, Volpe JJ, eds. *Brain Injury and Pediatric Cardiac Surgery*. Boston: Butterworth-Heineman, 1995: 353–62.

92 Straussberg R, Shahar E, Gat R, Brand N. Delayed parkinsonism associated with hypotension in a child undergoing open-heart surgery. *Dev Med Child Neurol* 1993;**35**:1007–14.

93 du Plessis AJ, Treves S, Hickey P, *et al.* Regional cerebral perfusion abnormalities after cardiac operations. *J Thorac Cardiovasc Surg* 1994;**107**:1036–43.

94 Kupsky W, Drozd M, Barlow C. Selective injury of the globus pallidus in children with post-cardiac surgery choreic syndrome. *Dev Med Child Neurol* 1995;**37**:135–44.

95 Greenmyre T, Penney J, Young A, *et al.* Evidence for transient perinatal glutamatergic innervation of globus pallidus. *J Neurosci* 1987;**7**:1022–30.

96 Johnston M, Redmond J, Gillinov A, *et al.* Neuroprotective strategies in a model of selective neuronal necrosis from hypothermic circulatory arrest. In: Moskowitz M, Caplan L, eds. *Cerebrovascular Diseases*. Boston: Butterworth-Heinemann, 1995: 165–74.

97 Redmond J, Gillinov A, Zehr K, *et al.* Glutamate excitotoxicity: a mechanism of neurologic injury associated with hypothermic circulatory arrest. *J Thorac Cardiovasc Surg* 1994;**107**:776–86.

98 Bergman I, Steeves M, Burckart G, *et al.* Reversible neurologic abnormalities associated with prolonged intravenous midazolam and fentanyl administration. *J Pediatr* 1991;**119**:644–9.

99 Lane J, Tennison M, Lawless S, *et al.* Movement disorder after withdrawal of fentanyl infusion. *J Pediatr* 1991;**119**:649–51.

100 Petzinger G, Mayer SA, Przedborski S. Fentanyl-induced dyskinesias. *Mov Disord* 1995;**10**:679–80.

101 Riela A, Roach E. Etiology of stroke in children. *J Child Neurol* 1993;**8**:201–20.

102 Schoenberg B, Mellinger J, Schoenberg D. Cardiovascular disease in infants and children: a study of incidence, clinical features, and survival. *Neurology* 1978;**28**:763–8.

103 Boyajian R, Sobel D, DeLaria G, *et al.* Embolic stroke as a sequalae of cardiopulmonary bypass. *J Neuroimag* 1993;**3**:1–5.

104 Moody D, Bell M, Challa V, *et al.* Brain microemboli during cardiac surgery or aortography. *Ann Neurol* 1990;**28**:477–86.

105 Padayachee T, Parsons S, Theobold R, *et al.* The detection of microemboli in the middle cerebral artery during cardiopulmonary bypass: a transcranial Doppler ultrasound investigation using membrane and bubble oxygenators. *Ann Thorac Surg* 1987;**44**:298–302.

106 Solis R, Kennedy P, Beall A, *et al.* Cardiopulmonary bypass: microembolization and platelet aggregation. *Circulation* 1975;**52**:103–8.

107 Blauth C. Retinal fluorescein angiography in the assessment of microembolism during cardiopulmonary bypass. In: Smith P, Taylor K, eds. *Cardiac Surgery and the Brain*, 1st edn. London: Edward Arnold, 1993: 165–81.

108 Kirklin JK, Westaby S, Blackstone EH, *et al.* Complement and the damaging effects of cardiopulmonary bypass. *J Thorac Cardiovasc Surg* 1983;**86**:845–57.

109 Millar A, Armstrong L, van der Linden J, *et al.* Cytokine production and hemofiltration in children undergoing cardiopulmonary bypass. *Ann Thorac Surg* 1993;**56**:1499–502.

110 Steinberg J, Kapelanski D, Olson J, *et al.* Cytokine and complement levels in patients undergoing cardiopulmonary bypass. *J Thorac Cardiovasc Surg* 1993;**106**:1008–16.

111 del Zoppo G. Microvascular changes during cerebral ischemia and reperfusion. *Cerebrovasc Brain Metab Rev* 1994;**6**:47–96.

112 Elliott M, Finn A. Interaction between neutrophils and endothelium. *Ann Thorac Surg* 1993;**56**:1503–8.

113 Feuerstein G, Liu T, Barone F. Cytokines, inflammation, and brain injury. Role of tumor necrosis factor-α. *Cerebrovasc Brain Metab Rev* 1994;**6**:341–60.

114 Lucchesi B. Complement activation, neutrophils, and oxygen radicals in reperfusion injury. *Stroke* 1993;**24**:I41–7.

115 Clancy R, Malin S, Laraque D, *et al.* Focal motor seizures heralding stroke in full-term neonates. *Am J Dis Child* 1985;**139**:601–6.

116 Rosenthal D, Bulbul Z, Friedman A, *et al.* Thrombosis of the pulmonary artery stump after distal ligation. *J Thorac Cardiovasc Surg* 1995;**110**:1563–5.

117 Rosenthal D, Friedman A, Kleinman C, *et al.* Thromboembolic complications after Fontan operations. *Circulation* 1995;**92**:287–93.

118 McCrindle BW, Williams RV, Mitchell PD, *et al.* Relationship of patient and medical characteristics to health status in children and adolescents after the Fontan procedure. *Circulation* 2006;**113**:1123–9.

119 Anderson D. Cardioembolic stroke: primary and secondary prevention. *Postgrad Med* 1991;**90**:67–77.

120 Rosman P, Shands K. Hydrocephalus caused by increased intracranial venous pressure: a clinicopathological study. *Ann Neurol* 1978;**3**:445–50.

121 Ferrieri P, Gewitz MH, Gerber MA, *et al.* Unique features of infective endocarditis in childhood. *Pediatrics* 2002;**109**:931–43.

122 Saiman L, Prince A, Gersony W. Pediatric infective endocarditis in the modern era. *J Pediatr* 1993;**122**:847–53.

123 Jones H, Sieker R. Neurologic manifestations of infective endocarditis. *Brain* 1989;**122**:1295–315.

124 Pruitt A, Rubin R, Karchmer A, *et al.* Neurologic complications of bacterial endocarditis. *Medicine (Baltimore)* 1978;**57**:329–43.

125 Tyler HR, Clark DB. Cerebrovascular accidents in patients with congenital heart disease. *Arch Neurol Psychiatry* 1957;**77**:483–9.

126 Yang S-Y. Brain abscess associated with congenital heart disease. *Surg Neurol* 1989;**31**:129–32.

127 Goodkin HP, Harper MB, Pomeroy SL. Intracerebral abscess in children: historical trends at Children's Hospital Boston. *Pediatrics* 2004;**113**:1765–70.

128 Kagawa M, Takeshita M, Yato S, Kitamura K. Brain abscess in congenital heart disease. *J Neurosurg* 1983;**58**:913–7.

129 Southwick FS. Pathogenesis, clinical manifestations, and diagnosis of brain abscess. In: Basow DS, ed. *UptoDate*. Waltham, MA: UptoDate, 2010.

130 Dodge P, Pomeroy S. Parameningeal infections (including brain abscess, epidural abscess, subdural empyema). In: Feigin R, Cherry J, eds. *Textbook of Pediatric Infectious Diseases*, 3rd edn. Philadelphia: Saunders; 1992: 455–9.

131 Aebi C, Kaufmann F, Schaad U. Brain abscess in childhood: long-term experiences. *Eur J Pediatr* 1991;**150**:282–6.

132 Kaltman JR, Andropoulos DB, Checchia PA, *et al.* Report of the Pediatric Heart Network and National Heart, Lung, and Blood Institute orking group on the perioperative management of congenital heart disease. *Circulation* 2010;**121**:2766–72.

53 Adults with Congenital Heart Disease

Anji T. Yetman[1] & Gary D. Webb[2]
[1]Primary Children's Medical Center, University of Utah, Salt Lake City, UT, USA
[2]Cincinnati Children's Hospital Medical Center, Cincinnati, OH, USA

Over several decades, the life expectancy of individuals born with congenital heart disease (CHD) has increased substantially. Consequently, the population of adults with palliated and repaired CHD has grown, and many of these patients require lifelong subspecialized care. The practice of "Adult Congenital Cardiology" has emerged out of necessity to provide adequate care to these patients who require the expertise of both a pediatric cardiologist and an internist or adult cardiologist.

Demographics

With improved treatment for CHD, the number of patients >18 years of age with CHD has expanded rapidly. The long-term survival of infants born with CHD is ~85–95% [1,2]. Over 1 million adults in the United States have CHD, in addition to an estimated 3 million persons with bicuspid aortic valve [2].

These adults can be categorized by the complexity of their cardiac defect to determine the health burden of this patient cohort to develop and allocate healthcare resources properly. The 32nd Bethesda Conference [3] classified congenital cardiac defects in adults into those of mild, moderate, and high complexity and provided estimates of the prevalence of each (Table 53.1). Recommendations for ongoing care depend on the complexity of the patients' cardiac defect. More complex defects have an increased need for repeat surgical and interventional procedures in adulthood in addition to increased mortality. Such patients require closer surveillance. Although an internist may care adequately for those with relatively simple disease, patients with moderate or highly complex CHD require periodic or regular ongoing subspecialized care.

Transition and transfer of care

The number of adults with CHD who are currently receiving appropriate care in the United States reflects only a small proportion of the total number of patients [3]. Whereas children with CHD receive routine cardiac care, many patients are lost to care in the transition to adulthood. The reasons include lack of, or lack of access to, appropriate healthcare resources, failure to understand the need for lifelong cardiac care on the part of the patient or their pediatric healthcare providers, or the pediatric cardiologist's unawareness of acquired adult co-morbidities [4].

Transition

Transition of care is a process by which adolescents with CHD prepare to take responsibility for their health. This educational process should begin by early adolescence when these patients should receive ongoing, age-appropriate instruction regarding the items listed in Table 53.2. A checklist of age-appropriate topics can accompany each patient's chart, documenting that the topics have been adequately covered. Although such education may be the responsibility of the primary care physician, the pediatric cardiologist may be a better source of information. Education on these transitional issues may directly affect the patient's later cardiac morbidity and mortality [4], so all adolescents should receive adequate education before graduating from the pediatric cardiology clinic. Transitional education may be given by the pediatric cardiologist, clinical nurse specialists devoted to adolescent education, a formalized transition clinic within the pediatric cardiology practice, or through a combined pediatric cardiology–adolescent health facility. Historically, education on important lifestyle issues has not been performed well [4–6].

Table 53.1 Classification of congenital cardiac defects in adults.

Simple CHD	Moderate complex CHD	Severe complex CHD
Care by routine provider	*ACHD clinic visits at least every 2 years*	*ACHD clinic visits at least annually*
Aortic valve abnormalities	Aorto–left ventricular tunnel	Conduits – valved or nonvalved
Mitral valve abnormalities, except parachute and cleft	Anomalous pulmonary–venous connection	Double-outlet right ventricle
	Coarctation of aorta	Eisenmenger syndrome
Patent foramen ovale or small ASD	Ebstein's abnormality	All forms of single ventricle
Small VSD	Significant RVOT obstruction	Fontan
Mild pulmonary stenosis	PDA	Pulmonary atresia
Ligated or occluded PDA	Pulmonary regurgitation – moderate or severe	Pulmonary Vascular disease
Repaired ASD without residua	Sinus of Valsalva aneurysm	Transposition complexes
Repaired VSD without residua	Sinus venosus ASD	Truncus arteriosus
	Aortic stenosis – sub- or supravalvar	Atrioventricular or ventriculoarterial discordance
	VSD with outflow obstruction or valvar abnormalities	

Table 53.2 Educational topics to be covered prior to transfer.

Underlying cardiac diagnoses, preferably by way of pictorial illustration, in order to provide this information to other healthcare providers that they encounter
Importance of any residual cardiac lesions
The need for and rationale behind lifelong cardiac care
Instruction that congenital heart disease is markedly different to other forms of heart disease and that they must follow up with providers specializing in adult congenital heart disease.
Signs and symptoms of cardiac decompensation, where appropriate
The natural history of their disease, including need for eventual cardiac transplantation where appropriate
Insurability
Contraception counseling
Counseling regarding fertility, risks of pregnancy to mother and fetus, and the importance of a pregnancy plan
Career and vocational planning
Safety of recreational activities
Cardiovascular risk factors for ischemic heart disease
Physical fitness
Endocarditis

Young adults often leave a pediatric cardiology clinic without understanding their CHD, their long-term prognosis, or the effect of their disease on childbearing [4–6].

Transfer of care

Currently, >60% of adults with CHD after leaving a pediatric cardiac facility have a significant lapse in cardiac care (median 10 years, range 2–50 years) before establishing care at an adult facility [4]. Delayed transfer is associated with more adverse outcomes and often need for urgent cardiac intervention [4]. Many adults with CHD are cared for by adult cardiologists untrained in CHD, or pediatric cardiologists untrained in adult co-morbidities. Consequently, the patient does not receive the needed comprehensive medical care.

The ideal age to transfer a patient from the pediatric to an adult facility is unclear. Appropriately counseled patients with chronic illness usually can transition to an appropriately designed adult healthcare system when aged 17–19 years. At these ages, increasing maturity, better education, and improved confidence and social skills combine to improve patients' understanding of their condition, their participation in medical decision making, definition of health and life goals, recognition of changes in overall health, and ability to use the medical system successfully.

Although mortality rates associated with CHD have steadily improved, the improvement has primarily affected children [7]. Failure of appropriate transition and transfer is thought to decrease patient survival [4].

Establishing an ACHD service

Adults with congenital heart disease (ACHD) represent a unique clinical challenge. Although pediatric cardiologists understand their complex anatomy and physiology, the acquired co-morbidities of adulthood are often foreign to pediatricians. To address this challenge, regionalized ACHD centers are being developed. The minimal requirements for such a center have been established [3], recognizing that there is not a single optimal design.

Outpatient resources

An ACHD outpatient clinic may be in either a separate location within a children's hospital or an adult hospital. Both models are successful and depend upon the availability of skilled

personnel and high-quality diagnostic testing, including congenital cardiac echocardiography, congenital cardiac MRI and CT, and diagnostic and interventional catheterization.

Inpatient resources

Physicians knowledgeable about both CHD and adult cardiac and noncardiac co-morbidities must care for these patients. Because these patients often present with a variety of medical issues, they need, in addition to cardiologists trained in CHD, other medical and surgical subspecialty services to consult about their problems.

Unless instructed otherwise, patients typically utilize the emergency department affiliated with the location where they receive their outpatient care [8]. Emergency department providers, whether adult or pediatric, must be able to provide immediate medical care to these patients, who may present with problems unrelated to their underlying CHD [8,9]. Although they usually present with cardiovascular problems, such as arrhythmia, heart failure, syncope, aortic dissection, and endocarditis [9], they often need other subspecialty services [9].

Surgical resources

Although children with CHD who undergo an operation have it performed by a trained congenital cardiac surgeon, the same is not true for identical cardiac lesions in adults who often undergo an operation by a surgeon without specific training in congenital cardiac surgery [10]. The surgical results are not as good as for similar patients undergoing the same cardiac operation by a cardiac surgeon who devotes >75% of the time to congenital heart surgery [10]. Morbidity and mortality are often greater in adults than children with the same surgical procedure due to medical co-morbidities, acquired cardiac co-morbidities, or difficulty attaining vascular access for cannulation. Most CHD operations in adults are reoperations. The number of previous reoperations is a risk factor for adverse outcome, as is preoperative cyanosis or congestive heart failure, prolonged cardiopulmonary bypass time, and Fontan revision [11].

Patients with cyanotic CHD have an increased risk of adverse outcome with elective noncardiac surgery. Such operations should be performed in a facility with ACHD services and cardiac anesthesiology.

Preoperative imaging should assess the proximity of conduits or other cardiac structures to the posterior sternum. As vascular access may be required, we routinely assess the patency of the femoral vessels during preoperative MRI, catheterization, or preoperative ultrasound. Because of multiple preoperative co-morbidities, there is increased risk of postoperative morbidity, especially renal and liver dysfunction, endocrine disturbances, and gastrointestinal bleeding. Ready access to multiple medical and surgical adult subspecialties is required.

The ACHD team

The core group of care providers comprising an ACHD team includes a cardiologist with training in both CHD and internal medicine. This training may exist in one individual or by the combined expertise of two or more physicians. Guidelines for ACHD training have been published [12]. In addition to cardiologists trained in ACHD, the core team should include at least one nurse practitioner or physician assistant, at least two echocardiographers experienced and certified in congenital cardiac imaging, and affiliation with a cardiovascular surgical program experienced in operating on adults with CHD. The number of personnel must be adequate to provide both outpatient care and inpatient management.

Immediate access to a wide variety of medical and surgical consultants is required, especially heart failure/transplant services, genetics, pulmonary hypertension, cardiac anesthesia and intensive care, diagnostic and interventional cardiac catheterization, cardiac imaging, electrophysiology, gynecology, and high-risk obstetric/maternal fetal medicine.

Differences between the adult and the child with CHD

Arrhythmias

Ventricular and atrial arrhythmias are more frequent in adults with moderate and high complexity CHD lesions and may not respond well to medical therapy. In patients with tetralogy of Fallot, dextro-transposition of the great arteries (d-TGA) following atrial baffling procedures, and a Fontan connection, the risk of sudden death is significant. Residual hemodynamic lesions should be sought and treated as potential precipitants of arrhythmia. Implantable cardioverter defibrillator (ICD) therapy should be considered in a timely manner, although guidelines for its use are still poor. Predictors of sustained ventricular tachycardia (VT) or sudden death in this group of patients include impaired systemic ventricular systolic function and marked QRS prolongation [13].

Thrombosis

The risk of venous thromboembolism increases with age. Postoperative thromboprophylaxis following cardiac and noncardiac surgery is required in adolescents and adults who will not ambulate for some time. Routine medications associated with thromboses, such as oral contraceptives, should be discontinued during the perioperative period.

Cardiac management

Medical and surgical management guidelines may differ between adults and children having identical cardiac lesions. The natural history of specific cardiac defects differs at various ages, particularly as adults acquire co-morbidities that

affect progression of CHD. Changing operative procedures have produced adults with cardiac repairs, such as atrial baffles, which are no longer performed. Patients following an atrial switch require monitoring for atrial baffle leaks, baffle obstruction, and progressive sinus node dysfunction. Because of the differing natural history of cardiac lesions in adulthood, a comprehensive list of lesion-specific guidelines has been assembled to assist the clinician in the care of these often complex patients [14].

Contraception

Beginning in adolescence, women with CHD should be provided with accurate information about contraception and learn about the implications of their cardiac disease for pregnancy. Many young women do not receive such counseling before becoming sexually active [5,15,16]. Medical personnel with an understanding of the gyneco- logic issues that these women face should perform coun- seling; patients may be told by their cardiologist that pregnancy is contraindicated, when, in fact, it is not [16]. Instructing a patient not to become pregnant is not an effective form of birth control and more specific informa- tion should be provided. Which form of contraception is optimal for the patient depends partly upon the degree of maternal risk associated with pregnancy. Various forms of contraception are associated with different efficacy rates (Table 53.3) [17] and the patient should receive counseling about this.

Combination oral contraceptives

The "birth control pill" (OCP), a common contraceptive, contains estrogen and progesterone. Estrogen has prothrom- botic effects and increases the risk of intracardiac and venous thromboembolism (VTE) by increasing prothrombin and decreasing antithrombin III. Therefore, certain women with CHD should not receive this form of contraception (Table 53.4). Over the years, the dose of estrogen in oral contraceptives has decreased. Whereas first-generation estrogen doses started at 150μg, second-generation dosages decreased to 50μg, and current third-generation doses are now even lower, ranging from 20 to 35μg of ethinylestradiol (EE). The decrease in estrogen dose has led to a decrease in VTE, but current third-generation OCP users still have a risk of developing VTE which is 2–8 times greater than that of nonusers. Risk factors which further increase the risk of thrombosis include age >35 years, smoking, increased weight, and inherited thrombophilias.

Within the general population, women who are over- weight (BMI 25–30kg m⁻²) have an estimated age-adjusted odds ratio of VTE of 11.6 (95% CI: 7.5–18.1) when com- pared with healthy weight women. Women who are obese (BMI ≥30kg m⁻²) have an estimated age-adjusted odds ratio

Table 53.3 Contraceptive methods and their efficacy rates.

Contraceptive method	Annual efficacy rate (%) (typical/ perfect use)
Combined hormonal contraception:	
Oral pill	97/99
Vaginal ring	99.4
Transdermal patch	99.3/99.6
Progestin-only contraception:	
Progestin-only pill (mini-pill)	88/97
Progestin injection (Depo-Provera)	99.7
Progestin implants (Norplant/Implanon)	99.8
Intra-uterine device (Mirena)	99
Barrier methods:	
Male condom	88/97
Male condom with spermicide	99.9
Vaginal spermicide alone	79/94
Female condom	79/95
Vaginal sponge	91
Diaphragm	94
Sterilization	99.6

Table 53.4 Women with cardiac anomalies who should not receive combination hormonal contraception.

Eisenmenger syndrome
Mechanical cardiac valves
Severe systemic ventricular dysfunction
Previous thromboemboli
Intracardiac right-to-left shunting
Pulmonary arterial hypertension
Systemic arterial hypertension
Patients with an atrio-pulmonary Fontan anastomosis

of 23.78 (95% CI: 13.3–42.3) of developing VTE. When considering whether a patient is suitable to receive OCPs, all risk factors for thromboses should be considered [18,19].

If OCPs are not contraindicated but an increased poten- tial for thrombosis exists (atrial dilation with a history of atrial arrhythmias, moderately impaired systemic ventricu- lar function, ASD/PFO with DVT risk factors, nonfenes- trated lateral tunnel, or extracardiac conduit Fontan), a third-generation OCP with the lowest possible effective estrogen dose (20μg EE) should be recommended for women. Preparations containing 20 rather than 30μg of EE have been associated with reduced risk of VTE [18]. In addition, the type of progestogen should be considered, as the newer OCPs containing drospirenone have been associated with an increased risk of VTE when compared with those containing levonorgestrel [19].

Combination nonoral contraceptive hormones

Alternative forms of hormonal contraception include the transdermal patch and vaginal ring. Although these birth control methods are associated with improved compliance, there is no evidence to support a reduced risk of VTE. Hence they remain contraindicated in certain patient groups (Table 53.5).

Progesterone contraception

Progestin-only pills

A lack of consistent and correct use is a common cause of unintended pregnancy with progesterone-only pills [18,19]. In contrast to combined oral contraceptives, progestin-only pills require women to adhere more strictly to the time of day when they take their pills. This form of contraception is not contraindicated in any specific CHD, and is a suitable alternative to combination hormonal therapy in very compliant patients. The most common side effects include menstrual irregularities.

Contraceptive injections or subcutaneous implants

Both intramuscular and subcutaneous progesterone injections (depot medroxyprogesterone) have been approved by the FDA to prevent pregnancy, and in the United States are available under the name Depo-Provera. The perfect-use failure rate for intramuscular Depo-Provera in the first year is 0.3%, with a typical-use failure rate in the first year estimated to be ~3% [18,19]. The most common side effects include menstrual irregularities and weight gain [18]. The use of Depo-Provera is associated with a decrease in bone mineral density that is reversible over time upon cessation of use [20]. When contemplating the seriousness of this side effect, the magnitude of bone mineral density loss is comparable to that sustained during pregnancy and breast feeding [20].

An alternative form of nonoral progesterone-only contraception is the subdermal implant, Implanon. This $4 \times 2\,mm$ progesterone-containing rod is implanted subdermally under local anesthesia. The primary benefit is reliable contraception for up to 3 years after implantation. Local side effects are not uncommon and systemic side effects are similar to those described for Depo-Provera [21].

Intra-uterine devices

For nonpermanent birth control, the newer progesterone-eluting intra-uterine devices (Mirena) are reliable and favored in patients who should not receive oral contraceptives due to risk of thrombosis and in whom pregnancy is not desired or carries associated maternal risk. Although the device may be more easily placed in a woman with a prior pregnancy, nulliparity is not a contraindication. An experienced healthcare provider should insert the device.

Table 53.5 Cardiovascular medications and pregnancy.

Drug	Potential side effects	Risk[a]
Adenosine	None reported	C
Amiodarone	IUGR, prematurity, congenital goiter, hypo-/hyperthyroidism, prolonged QT	D
ACE inhibitors/ARB	Oligohydramnios, IUGR, prematurity, neonatal hypotension, renal failure, anemia, death, skull ossification defect, limb defects	D
β-Blockers:	Fetal bradycardia, IUGR, hypoglycemia	
Acebutolol		B
Labetalol		C
Metoprolol		C
Propranolol		C
Atenolol		D
Sotalol		B
Digoxin	None reported	C
Diltiazem	Major birth defects in small animals	C
Diuretics:		
Furosemide	↓ placental perfusion	C
Spironolactone	1 report of oral cleft	D
Thiazides	Congenital defects, ↓↑ electrolytes	D
Flecainide	Limited data	C
Hydralazine	None reported	C
Lidocaine	None reported	C
Nifedipine	Fetal distress due to maternal hypotension reported	C
Nitrates	Limited data	C
Nitroprusside	Limited data; potential thiocyanate fetal toxicity (avoid extended use)	C
Procainamide	Limited data; none reported	C
Verapamil	Limited data	C

[a]FDA classification: Category B: either animal reproduction studies have not demonstrated a fetal risk but there are no controlled studies in pregnant women, or animal reproduction studies have shown an adverse effect that was not confirmed in controlled studies in women. Category C: either studies in animals have revealed adverse effects on the fetus and there are no controlled studies in women, or studies in women and animals are not available. Drugs should be given only if potential benefits justify the potential risk to the fetus. Category D: there is positive evidence of human fetal risk, but the benefits from use in pregnant woman may be acceptable despite the risk. Category X: studies in animals or human beings have demonstrated fetal abnormalities. The risk of the use of the drug in pregnant women clearly outweighs any possible benefit. The drug is contraindicated in women who are or may become pregnant.

Contraception is effective for 5 years from implantation, and fertility may be readily restored upon earlier removal. Reported side effects are rare and include menstrual irregularities [18,19].

Barrier methods

To receive oral or injectable contraception, the patient typically requires a visit to a healthcare provider other than their cardiologist, and must be educated about the correct method of use of the contraceptive and its potential side effects. In contrast, a patient using over-the-counter barrier methods may not have any such instruction. A cardiologist who may be the only medical care provider caring for the patient should not assume that patients know how to use any particular form of contraception effectively.

Pregnancy

Pregnancy causes many physiologic alterations that significantly effect the cardiac status of women with CHD. Although many patients have been repaired before adulthood, residual defects may adversely affect maternal and/or fetal well-being. All women with CHD contemplating pregnancy should be seen in an ACHD clinic for pre-pregnancy counseling. Pregnancy counseling requires a multidisciplinary approach with close communication between maternal–fetal medicine specialists and ACHD providers. Women should be counseled about maternal and fetal risks of pregnancy, the effect of pregnancy on the natural history of their CHD, and the risk of CHD on their offspring. Many women may be receiving cardiac medications during pregnancy and their risks (Table 53.5) should be discussed [22].

Physiology of pregnancy, labor, and delivery

During pregnancy, circulating blood volume and cardiac output increase by 50%, usually peaking between 28 and 32 weeks' gestation. The increased blood volume is due more to increased plasma volume than red blood cell mass. The hemodilution reduces oxygen-carrying capacity. The augmented cardiac output comes from increased stroke volume early in pregnancy, aided by increased contractility, and later a smaller increase in heart rate, averaging 10–20 beats per minute. Because of the uterine circulation and endogenous hormones, systemic vascular resistance and diastolic blood pressure fall to a greater extent than pulmonary vascular resistance, possibly exacerbating an intracardiac right-to-left shunt. Inferior vena caval obstruction from a gravid uterus in a supine position can abruptly decrease cardiac preload and cause symptomatic hypotension, particularly in patients who are preload dependent. During the first stage of labor, contractions are associated with expulsion of 300–500 ml of blood into the general circulation. Women with right or left ventricular dilation and dysfunction may not tolerate this abruptly increased volume. Cardiac output rises by 2.5 l min^{-1}, partly due to anxiety and pain. During the second stage, pushing increases systemic vascular resistance. Cardiac output rises further. After delivery, venous return surges due to removal of IVC obstruction

Table 53.6 Factors associated with worsened maternal adverse outcome.

Prior congestive heart failure, TIA, stroke or arrhythmia
Baseline NYHA functional class ≥II
Baseline cyanosis
Mitral stenosis with MV area <2 cm^2
Aortic stenosis with aortic valve area <1.5 cm^2
Peak left ventricular outflow tract gradient >30 mmHg
Left ventricular ejection fraction <40%
Pulmonary hypertension
Symptomatic obstructive lesions (pulmonary stenosis, aortic stenosis, coarctation of the aorta)
Marfan syndrome with aortic diameter >42 mm
Severe pulmonary regurgitation
Depressed subpulmonary ventricular function

from the gravid uterus and autotransfusion from the contracted uterus. As intra-abdominal pressure falls dramatically, blood flow to the abdominal organs increases significantly and can lead to hypotension and cardiovascular collapse [23,24].

These hemodynamic changes are further accentuated by multiple pregnancy. Compared with a single pregnancy, in a multiple pregnancy maximum cardiac output is 20–30% higher, heart rate increases more by 20–30 beats per minute above baseline, and plasma volume increases by ~67% during pregnancy, in contrast to a 48% increase above baseline seen with singletons [23]. These marked changes need to be considered when counseling women regarding assisted methods of reproduction which are associated with a higher rate of multiple gestations.

Oxygen consumption is increased, as are minute ventilation, tidal volume, and functional residual capacity. The glomerular filtration rate (GFR) increases.

Pregnancy is also associated with a hypercoagulable state from relative decreases in protein S activity, stasis, and venous hypertension. Estrogens can interfere with collagen deposition within the media of the medium and large muscular arteries. Circulating elastase can break up the elastic lamellae and weaken the aortic media during pregnancy. Weakening of the arterial wall may in turn predispose to dissection with or without an underlying connective tissue disorder. Relaxin, an insulin-like growth factor hormone, is detectable in serum during pregnancy and causes a decrease in collagen synthesis, and may predispose to aortic dissection during pregnancy.

Adverse maternal and fetal outcomes

The physiological changes in pregnancy outlined above may be poorly tolerated in patients with certain types of CHD or other maternal risk factors (Table 53.6). Adverse cardiac outcomes include pulmonary edema, arrhythmias, CHF, and

Table 53.7 Maternal factors associated with fetal adverse outcome.

Smoking
Obesity
↑ NYHA class
Use of anticoagulation (warfarin or heparin)
Multiple gestations
Maternal cyanosis
Maternal left heart obstruction
Fontan physiology

thromboembolism. Adverse obstetric outcomes include pre-eclampsia, preterm labor, postpartum hemorrhage, and placental abruption. Couples should be counseled about maternal risk factors and risk factors for adverse fetal outcomes (Table 53.7) [22].

Pregnancy care plan

In coordination with specialists in maternal–fetal medicine, obstetrics, and anesthesia, the ACHD team should develop a plan for delivery. Multidisciplinary conferences prior to delivery are very helpful. The subjects discussed should include timing of delivery, the method of induction (if required), the mode of delivery (Cesarean section versus vaginal delivery versus vaginal delivery with an assisted second stage of labor), the need for and type of cardiovascular monitoring during labor and delivery, fluid management, medication management, and the type of anesthesia, and should be decided upon before the commencement of labor. A care plan should be documented and accompany the patient to the hospital to deal with changes in personnel or location of delivery.

Cesarean section is not necessarily indicated for CHD as it is associated with more deleterious effects on maternal hemodynamics than vaginal delivery. With moderate or high complexity cardiac lesions with sequelae, women may benefit from an assisted second stage of labor. This approach involves early placement of a dense epidural anesthesia followed by a passive second stage of labor without pushing and finally assisted delivery of the infant with forceps or vacuum extraction. Although associated with less hemodynamic alterations, this approach has a greater risk of local maternal injury [24].

Anticoagulation during pregnancy

Women requiring anticoagulation with coumadin or heparin present a challenging problem during pregnancy. Although pregnancy is feasible, they should receive pre-pregnancy counseling with discussion of treatment options and the maternal and fetal risks of warfarin and heparin therapies.

Warfarin crosses the placenta and has been associated with an increased incidence of spontaneous abortion, prematurity, and stillbirth. Warfarin can also cause bleeding in the fetus, and fetal cerebral hemorrhage can complicate labor and delivery, especially if forceps or vacuum extraction is necessary. Warfarin embryopathy (of nasal hypoplasia and/or stippled epiphyses and central nervous system abnormalities) has been described after *in utero* exposure during the first trimester with an incidence ranging from <5 to 67% [22,23]. Clinically significant embryopathy may not occur at doses ≤5 mg per day [26]. The drug is thought to be safe during the first 6 weeks of gestation, but embryopathy may occur if doses >5 mg are taken between 6 and 12 weeks of gestation. Women requiring long-term warfarin therapy who are attempting pregnancy should perform frequent pregnancy tests and, when pregnancy is achieved, switch to low molecular weight heparin (LMWH) therapy for the first trimester unless warfarin doses <5 mg are required. After the twelfth week, warfarin therapy can be restarted but must be discontinued and switched to a heparin several weeks before expected or scheduled delivery regardless of dose.

Unfractionated heparin does not cross the placenta or cause fetal bleeding or teratogenicity. However, in 12–24% of high-risk pregnant women there are maternal thromboembolic complications, including fatal valve thrombosis.

LMWH is associated with increased fetal wastage at rates similar to Coumadin. LMWH does not cross the placenta and fetal teratogenicity does not occur. Maternal thromboembolism and maternal death, however, are more frequent in women receiving LMWH therapy. Studies documenting increased thromboembolism, however, have been criticized because of inadequate heparin dosing and lack of meticulous monitoring. As pregnancy progresses and maternal weight gain occurs, the volume of distribution for LMWH changes. Plasma anti-Xa levels should be measured 4–6 h after the morning dose and the dose of LMWH adjusted to achieve an anti-Xa level of ~0.7–1.2 units ml^{-1}. LMWHs have been used successfully to treat pregnant patients with a mechanical heart valve, but their use remains controversial. An early warning issued by the manufacturer and the FDA in July 2001 describes safety concerns. In 2004, labeling approved by the FDA indicated specifically that the use of LMWH for thromboprophylaxis in pregnant women with mechanical prosthetic heart valves has not been studied adequately.

Aspirin at doses of <100 mg per day is considered safe during pregnancy. A recent meta-analysis found no increased risk of congenital anomalies by using aspirin in the first trimester [22].

Percutaneous and surgical intervention during pregnancy

Women with a hemodynamically significant cardiac lesion should have it addressed prior to conception. However, some pregnant women present with a hemodynamically significant cardiac lesion requiring percutaneous or surgical intervention. Non-emergency interventions are probably

best performed after embryogenesis but before the end of the second trimester (weeks 13–24). There is a trend toward fetal malformations in the first trimester, and to preterm delivery, maternal hemodynamic alterations, and mortality in the third [26]. Cardiac surgery during pregnancy carries a maternal mortality rate similar to that for nonpregnant women with a similar anomaly, but fetal mortality is 20–67%. Risk factors associated with maternal mortality in a cohort of 74 pregnant women undergoing cardiac surgery at a mean gestational age of 22 weeks included repeat sternotomy, emergency surgery, and higher NYHA class [26]. Fetal mortality was related not only to the factors associated with maternal mortality above, but also to anoxic time [26].

Acquired co-morbidities affecting care of the patient with CHD

Coronary artery disease

Adults with CHD have no different risk of coronary artery disease than the general population. Patients should be assessed for and receive counseling about modifiable cardiovascular risk factors of hyperlipidemia, hypertension, diabetes (type I or II), and smoking. Some exceptions are as follows:

1 *Cyanotic heart disease:* The coronary arteries in patients with long-standing cyanosis are atheroma free [27]. Such patients are hypocholesterolemic with a greater reduction in LDL cholesterol than HDL cholesterol. Chronic cyanosis is associated with reduced atherogenic intimal oxidized LDL cholesterol. In addition, upregulated nitric oxide, hyperbilirubinemia, and relatively low platelet counts are independent antiatherogenic factors [27].

2 *Coarctation of the aorta:* Coronary artery disease causes about one-third of deaths in adults with a repaired aortic coarctation. Following operation, these patients have persistent vascular dysfunction with impaired endothelial performance, decreased vascular distensibility, increased carotid intima/media thickness, and increased vascular levels of proinflammatory cytokines [28–31]. Myocardial reserve may be abnormal [32]. These vascular abnormalities are more marked in patients repaired at a later age [28–31], but also occur in normotensive children after repair without residual obstruction. Vascular abnormalities are present despite neonatal repair [28–31]. Although successful repair in childhood is often associated with normal resting blood pressure, exercise-induced hypertension is common and may be a risk factor for later coronary artery disease. The effect of aortic stent placement on vascular properties is unknown.

3 *Turner syndrome:* Mortality due to ischemic heart disease is increased as much as sevenfold in patients with Turner syndrome and may occur at a young age, irrespective of associated CHD. The higher incidence of obesity,

hyperlipidemia, hypertension, and diabetes in these patients likely plays a significant role. Life-long cardiac follow-up is required in this high-risk group of patients [33].

Within the general population, 10-year and lifetime risk calculators have been developed to assess the risk of developing cardiovascular disease based on known risk factors: [35]
- cigarette smoking
- hypertension (BP ≥140/90 or antihypertensive medication)
- low HDL cholesterol (HDL-C) (<40 mg dl^{-1})
- family history of premature CHD (in male first-degree relatives <55 years, in female first-degree relatives <65 years)
- age (men ≥45 years, women ≥55 years)
- with HDL-C ≥60 mg dl^{-1} counting as a "negative" risk factor, removing one risk factor from the total count.

All patients should be assessed for cardiovascular risk factors. Once these data have been obtained, they are entered into the "calculator" [33] that will provide a reliable estimate of risk in patients with two or more risk factors (other than LDL cholesterol) who do not have known coronary artery disease [34]. Although repaired coarctation of the aorta is a risk factor for coronary arterial disease, its weight in calculating risk is unknown, but it should be considered. Recommendations for lifestyle modification or initiation of medical therapy are determined by this calculated risk [35].

Obesity

Obesity has reached epidemic proportions in both children and adults. In adults, overweight and obesity are based on body mass index (BMI) calculations of 25–29.9 and ≥30 kg m^{-2}, respectively. Other indices with greater predictive value include waist circumference, waist-to-hip ratio and waist-to-height ratio [36]. Both general obesity and abdominal adiposity are associated with increased mortality in all patient groups, including those with CHD, placing them at greater cardiovascular risk due to pre-existing CHD or cardiac functional impairment. Obesity's deleterious effect on blood pressure, insulin resistance, and lipid profile is associated with endothelial dysfunction, right and left ventricular systolic and diastolic dysfunction, heart failure, left atrial dilation and atrial fibrillation, pulmonary hypertension, obstructive sleep apnea, and a generalized prothrombotic state [36]. Patients should be counseled from an early age about the importance of a healthy diet and routine aerobic exercise in order to avoid obesity and its attendant risks.

Sleep apnea

In part due to the obesity epidemic, obstructive sleep apnea (OSA) is diagnosed more frequently in adults with CHD. OSA appears to be related to several cardiovascular diseases: systemic or pulmonary hypertension, coronary artery disease (with severe OSA), atrial arrhythmias, and nocturnal bradyarrhythmias. Although isolated systemic hypertension, pulmonary hypertension, or coronary artery disease is not an indication for evaluating possible OSA, they should

prompt the physician to inquire about symptoms of OSA to determine if diagnostic evaluation is warranted [37–39].

Anemia

Anemia, common in patients with heart failure, affects functional capacity and survival [40]. The etiology of anemia is multifactorial, and related to impaired secretion of erythropoietin and neurohormonal activation. Anemia has a prevalence of 13–29% in adults with noncyanotic CHD [41,42]. Independent predictors of anemia include lower mean corpuscular volume (MCV), diuretic treatment, hyponatremia, warfarin treatment, and decreased renal function. Within a group of adults with CHD, anemia was associated with a threefold increased risk of death, even after adjustment for functional class, systemic ventricular function, and other established risk factors [41,42]. Evaluating anemia in adults with CHD should therefore be routine. Only 25% of anemic adults with CHD, however, have an abnormally low MCV. Initial evaluation of normocytic or microcytic anemia should include not only a CBC, but also serum ferritin and iron stores. Occult gastrointestinal blood loss should be sought when serum iron is decreased.

Liver disease

All patients who received blood or blood products prior to 1992 should be screened for hepatitis C. If the hepatitis C antibody screening test is positive, a confirmatory test should be performed. Normal transaminases do not exclude infection with hepatitis C. Most patients infected will develop chronic infection, and 80% develop cirrhosis over 20 years. Most patients will be asymptomatic [43]. Infected patients should be referred to a liver specialist.

Symptomatic liver dysfunction is seen most commonly in adults after a Fontan procedure. Cirrhosis, recognized with increasing frequency in these patients, results from chronic congestion [44]. Provided hepatic synthetic function remains intact, patients may benefit from Fontan revision or cardiac transplantation. If synthetic function is impaired, patients may be eligible for combined heart and liver transplantation [45]. Before either revision or transplantation, patients should be screened for esophageal varices, intestinal bleeding, and hepatocellular carcinoma. Routine screening for cirrhosis in adult Fontan patients has been adopted by many ACHD centers and includes serologic evaluation with measurement of platelet count, serum haptoglobin, α_2-macroglobulin, liver transaminases, protein, albumin, γ-GT, bilirubin, and α-fetoprotein. Further evaluation with ultrasound, CT imaging, or liver biopsy may be warranted.

Renal disease

Renal dysfunction is frequent in adults with CHD, especially cyanotic CHD, despite normal kidneys. Renal dysfunction is an independent predictor of adverse outcome following surgery in an adult with CHD. Nephrotoxic agents and volume depletion should be avoided. Adolescents and adults undergoing Fontan revision have had an acute decline in renal function postoperatively [46]. The need for dialysis should be anticipated, including preoperatively measuring GFR and creatinine. Younger age at initial Fontan procedure, higher preoperative blood pressure, and higher preoperative mixed venous saturation independently predicted better GFR at follow-up [46].

Comorbidities in patients with cyanotic CHD

Erythrocytosis

CHD patients with cyanosis typically have an elevated hematocrit level that increases blood viscosity, particularly with hematocrit >65%. Most have compensated erythrocytosis with stable hemoglobin that needs no management. Patients should avoid even mild dehydration and traveling to higher altitude. Historically, therapeutic phlebotomy was performed in these patients to decrease blood viscosity in the hope of eliminating the risk of stroke. This practice is no longer favored because it depletes iron and causes microcytosis, decreases oxygen carrying capacity and deformability of red blood cells, and increases stroke risk. Current indications for therapeutic phlebotomy include hemoglobin >20 g dl^{-1} and hematocrit >65% with symptoms of hyperviscosity and no evidence of dehydration [47,48]. At these extreme levels, patients may have headache and poor concentration. Removing 500 ml of blood with an equal volume replacement of dextrose or saline relieves symptoms. Before an elective operation, therapeutic phlebotomy may be beneficial to improve hemostasis. Evaluating iron deficiency with a peripheral blood smear, serum ferritin, and serum iron should be performed periodically in all patients with cyanotic CHD [47,48]. Patients should receive iron replacement if indicated.

Hemostasis

Hemostatic abnormalities occur in up to 20% of cyanotic patients. Thrombocytopenia and clotting factor deficiencies may combine to produce a bleeding tendency in these patients, most often epistaxis, gingival bleeding, menorrhagia, and pulmonary hemorrhage. Prophylactic anticoagulation is controversial be cause of increased risk of bleeding, but also increased risk of pulmonary artery thrombosis in patients with Eisenmenger syndrome [48,49].

Hyperuricemia

In chronic cyanosis, renal glomeruli are congested and eventually become sclerotic, reducing GFR, increasing creatinine, and causing proteinuria. Abnormal urate clearance is common, and in conjunction with an increased turnover of red blood cells from erythropoietic stimulation leads to

hyperuricemia (common) and gout (uncommon). Asymptomatic hyperuricemia is well tolerated and rarely requires treatment [48]. Initiating urate lowering therapy can provoke acute gout.

Gallstones

The increased breakdown of red blood cells in chronic cyanosis causes an increased risk of calcium bilirubinate gallstones. Operation is not recommended until patients become symptomatic.

The future

ACHD is a rapidly growing and relatively new medical specialty that has emerged to provide medical care to the ever-increasing number of adult survivors with CHD. The complex nature of these patients dictates that they receive their medical care from physicians with expertise in both adult medicine and pediatric cardiology.

References

1 Warnes C. The adult with congenital heart disease: born to be bad? *J Am Coll Cardiol* 2005;**46**:1–8.

2 Pillutla P, Shetty KD, Foster E. Mortality associated with adult congenital heart disease: trends in the US population from 1979 to 2005. *Am Heart J* 2009;**158**:874–9.

3 Warnes CA, Williams RG, Bashore TM, *et al*. ACC/AHA 2008 Guidelines for the Management of Adults With Congenital Heart Disease: a Report of the American College of Cardiology/American Heart Association Task Force on Practice Guidelines. *Circulation* 2008;**118**:e714–833.

4 Yeung E, Kay J, Roosevelt GE, *et al*. Lapse of care as a predictor for morbidity in adults with congenital heart disease. *Int J Cardiol* 2008;**125**:62–5.

5 Warnes CA. Pregnancy and contraception in congenital heart disease: what women are not told. *J Am Coll Cardiol* 2008;**52**:577–8.

6 Knauth A, Verstappen A, Reiss J, Webb GD. Transition and transfer from pediatric to adult care of the young adult with complex congenital heart disease. *Clin Cardiol* 2006;**24**:619–29.

7 Boneva RS, Botto LK, Moore CA, *et al*. Mortality associated with heart defects in the United States: trends and racial disparities, 1979–1997. *Circulation* 2001;**103**:2376–81.

8 McDonnell WM, Kokalas ID, Roosevelt GE, Yetman AT. Utilization of the pediatric emergency department by adults with chronic disorders of childhood. *Arch Pediatr Adolesc Med* 2010;**164**:572–6.

9 Kaemmerer H, Bauer U, Pensl U, *et al*. Management of emergencies in adults with congenital cardiac disease. *Am J Cardiol* 2008;**101**:521–5.

10 Karamlou T, Diggs BS, Person T, *et al*. National practice patterns for management of adult congenital heart disease. Operation by pediatric heart surgeons decreases in-hospital death. *Circulation* 2008;**118**:2345–52.

11 Giamberti A, Chessa M, Abella R, *et al*. Morbidity and mortality risk factors in adults with congenital heart disease undergoing cardiac reoperations. *Ann Thorac Surg* 2009;**88**:1284–9.

12 Williams RG, Pearson GD, Barst RJ, *et al*. Report of the National Heart, Blood and Lung Institute working group on research in adult congenital heart disease. *J Am Coll Cardiol*. 2006;**47**:701–7.

13 Schwerzmann M, Salehian O, Harris L, *et al*. Ventricular arrhythmias and sudden death in adults after a Mustard operation for transposition of the great arteries. *Eur Heart J* 2009;**30**:1873–9.

14 Warnes CA, Williams RG, Bashore TM, *et al*. ACC/AHA 2008 Guidelines for the Management of Adults With Congenital Heart Disease. A Report of the American College of Cardiology/American Heart Association Task Force on Practice Guidelines (Writing Committee to Develop Guidelines on the Management of Adults With Congenital Heart Disease). *J Am Coll Cardiol* 2008;**52**:1890–1947.

15 Rogers P, Mansour D, Mattinson A, O'Sullivan JJ. A collaborative clinic between contraception and sexual health services and an adult congenital heart disease clinic. *J Fam Plann Reprod Heath Care* 2007;**33**:17–21.

16 Reid GJ, Siu SC, McCrindle BW, *et al*. Sexual behavior and reproductive concerns among adolescents and young adults with congenital heart disease. *Int J Cardiol* 2008;**125**:332–8.

17 Canobbio MM, Perloff JK, Rapkin AJ. Gynecological health of females with congenital heart disease. *Int J Cardiol* 2005;**98**:379–87.

18 Shufelt C, Merz NB. Contraceptive hormone use and cardiovascular disease. *J Am Coll Cardiol* 2009;**53**:221–31.

19 Wu O. Oral contraceptives and venous thromboembolism: identifying the safest option. *Exp Rev Cardiovasc Ther* 2009;**7**:1513–6.

20 Guilbert ER, Brown JP, Kaunitz AM, *et al*. The use of depot-medroxyprogesterone acetate in contraception and its potential impact on skeletal health. *Contraception* 2009;**79**:167–77.

21 Pongsatha S, Ekmahachai M, Suntornlimsiri N, *et al*. Bone mineral density in women using the subdermal contraceptive implant Implanon for at least 2 years. *Int J Gynecol Obstet* 2010;**109**:223–5.

22 Newstead-Angel J, Gibson PS. Cardiac drug use in pregnancy: safety, effectiveness and obstetric implications. Exp Rev Cardiovasc Ther 2009;**7**:1569–80.

23 Eliseev O. *Cardiovascular Diseases and Pregnancy*. Berlin: Springer-Verlag, 1988.

24 Fernandes SM, Arendt KW, Landzberg MJ, *et al*. Pregnant women with congenital heart disease: cardiac, anesthetic and obstetrical implications. *Expert Rev Cardiovasc Ther* 2010;**8**:439–48.

25 Vitale N, De Feo M, De Santo LS, *et al*. Dose-dependent fetal complications of warfarin in pregnant women with mechanical heart valves. *J Am Coll Cardiol* 1999;**33**:1637–41.

26 Barth WH. Cardiac surgery in pregnancy. *Clin Obstet Gynecol* 2009;**52**:630–46.

27 Fyfe A, Perloff JK, Niwa K, *et al*. Cyanotic congenital heart disease and coronary artery atherogenesis. *Am J Cardiol* 2005;**96**:283–90.

28 Brili S, Tousoulis D, Antoniades C, *et al*. Evidence of vascular dysfunction in young patients with successfully repaired coarctation of aorta. *Atherosclerosis* 2005;**182**:97–103.

29 Toro-Salazar OH, Steinberger J, Thomas W, *et al*. Long-term followup of patients after coarctation of the aorta repair. *Am J Cardiol* 2002;**89**:541–7.

30 De Caro E, Spadoni I, Crepaz R, *et al*. Stenting of aortic coarctation and exercise-induced hypertension in the young. *Catheter Cardiovasc Interv* 2010;**75**:256–61.

31 Heger M, Willfort A, Neunteufl T, *et al*. Vascular dysfunction after coarctation repair is related to the age at surgery. *Int J Cardiol* 2005;**100**:335–6.

32 Cook SC, Ferketich AK, Raman SV. Myocardial ischemia in asymptomatic adults with repaired aortic coarctation. *Int J Cardiol* 2009;**133**:95–101.

33 Thomas J, Yetman AT. Management of cardiovascular disease in Turner syndrome. Expert Rev Cardiovasc Ther 2009;**7**:1631–41.

34 National Cholesterol Education Program. Risk Assessment Tool for Estimating 10-Year Risk of Developing Hard CHD (Myocardial Infarction and Coronary Death). http://hp2010.nhlbihin.net/atpiii/calculator.asp?usertype=prof (last accessed 3 March 2011).

35 National Cholesterol Education Program. Third Report of the National Cholesterol Education Program (NCEP) Expert Panel on Detection, Evaluation, and Treatment of High Blood Cholesterol in Adults (Adult Treatment Panel III). *Circulation* 2002;**106**:3143–421.

36 Lavie CJ, Milani RV, Ventura HO. Obesity and cardiovascular disease. *J Am Coll Cardiol* 2009;**53**:1925–32.

37 Young T, Finn L, Peppard PE, *et al*. Sleep disordered breathing and mortality: eighteen-year follow-up of the Wisconsin sleep cohort. *Sleep* 2008;**31**:1071–8.

38 Monahan K, Storfer-Isser A, Mehra R, *et al*. Triggering of nocturnal arrhythmias by sleep-disordered breathing events. *J Am Coll Cardiol* 2009;**54**:1797–804.

39 Kanagala R, Murali NS, Friedman PA, *et al*. Obstructive sleep apnea and the recurrence of atrial fibrillation. *Circulation* 2003;**107**:2589–94.

40 Go AS, Yang J, Ackerson LM, *et al*. Hemoglobin level, chronic kidney disease, and the risks of death and hospitalization in adults with chronic heart failure: the Anemia in Chronic Heart Failure: Outcomes and Resource Utilization (ANCHOR) Study. *Circulation* 2006;**113**:2713–23.

41 Dimopoulos K, Diller GP, Giannakoulas G, *et al*. Anemia in adults with congenital heart disease relates to adverse outcome. *J Am Coll Cardiol* 2009;**54**:2093–100.

42 Collins N, Piran S, Harrison J, *et al*. Prevalence and determinants of anemia in adults with complex congenital heart disease and ventricular dysfunction (subaortic right ventricle and single ventricle physiology). *Am J Cardiol* 2008;**102**:1–8.

43 Wang A, Book WM, McConnell M, *et al*. Prevalence of hepatitis C infection in adult patients who underwent congenital heart surgery prior to screening in 1992. *Am J Cardiol* 2007;**100**:1307–9.

44 Kiesewetter CH, Sheron N, Vettukattill JJ, *et al*. Hepatic changes in the failing Fontan circulation. *Heart* 2007;**93**:579–84.

45 Raichlin E, Daly RC, Rosen CB, *et al*. Combined heart and liver transplantation: a single center experience. *Transplantation* 2009;**88**:219–25.

46 Sammour F, Haw M, Paisey J, *et al*. Renal function in patients with a failed Fontan circuit undergoing cavopulmonary revision surgery. *Pediatr Cardiol* 2009;**30**:282–8.

47 Perloff JK, Rosove MH, Child JS, Wright GB. Adults with cyanotic congenital heart disease: hematologic management. *Ann Intern Med* 1988;**109**:406–13.

48 Galie N, Manes A, Palazzini M, *et al*. Management of pulmonary arterial hypertension associated with congenital systemic-to-pulmonary shunts and Eisenmenger's syndrome. *Drugs* 2008;**68**:1049–66.

49 Vongpatanasin W, Brickner ME, *et al*. The Eisenmenger syndrome in adults. *Ann Intern Med* 1998;**128**:745–55.

54 Quality of Life and Psychosocial Functioning in Adults with Congenital Heart Disease

Elisabeth M. W. J. Utens[1], Elisabeth H. M. van Rijen[2], Petra Opic[3] & Jolien W. Roos-Hesselink[3]

[1]Erasmus Medical Centre, Sophia Children's Hospital, Rotterdam, The Netherlands
[2]Erasmus University Rotterdam, Rotterdam, The Netherlands.
[3]Thoraxcentre, Erasmus Medical Centre, Rotterdam, The Netherlands

Introduction

The improved life expectancy of children with congenital heart disease (ConHD) has increased interest in their long-term quality of life, and stimulated studies into the psychosocial functioning of adults with ConHD [1–3]. The main question is whether quality of life and psychosocial functioning of adults with ConHD are comparable to those of their healthy peers from the general population. This chapter reviews briefly the outcomes of studies regarding

1 subjective health status and health-related quality of life
2 emotional functioning
3 other psychosocial aspect of living with congenital heart disease at adult age, such as
    a body image
    b feelings regarding the surgical scar
    c relational, psychosexual, and reproductive issues
    d living with an implantable cardioverter defibrillator (ICD).

Subjective health status and health-related quality of life

Although some studies have reported serious restrictions in subjective health status or health-related quality of life in adults with ConHD [4–9], other studies found that, apart from possible physical limitations, the perceived health of adult ConHD patients was comparable to or sometimes even better than that of the general population [10–15].

Table 54.1 indicates the main findings of studies conducted in this field, categorized according to subjective health status and health-related quality of life.

Long-term outcome of subjective health status

Several studies of adults with ConHD used the *Short Form Health Survey (SF-36)* [16], a self-report questionnaire for subjective health status [4,5,11,12,17–20]. The SF-36 assesses eight health concepts: limitations in physical activities due to health problems, limitations in social activities due to physical or emotional problems, limitations in usual role activities due to physical health problems, limitations in usual role activities due to emotional problems, bodily pain, general mental health, vitality, and general health perceptions.

Several other self-report instruments encompassing subjective health status have also been used in studies of adults with ConHD [6,8,10,13–15]. Other studies used the *Duke Health Profile* [19], shortened version of the *Quality of Life Questionnaire of the World Health Organization* (WHOQOL-BREF) [20], *Linear Analog Scale* (LAS), and the *Satisfaction with Life Scale* (SWLS) [21].

Long-term outcome of health-related quality of life

In contrast to the instruments above that assess subjective health status, the *TNO–AZL Quality of Life* instrument (TAAQOL) [22] measures health-related quality of life. Thus, the TAAQOL measures not only the patient's perception of

Table 54.1 Studies of subjective health status and health-related quality of life of adults with ConHD.

Study	Sample size (n)	Age range (years)	Instrument[a]	Rating of results (+/≈/−)[b]	Results
Subjective health status					
Saliba et al. [10]	67	17–49	Duke Health Profile	≈	ConHD sample reported physical, mental, social, general, and perceived health comparable to a reference group from the general population
Kamphuis et al. [4]	78	18–32	SF-36	−	ConHD sample reported more limitations in physical activities due to health problems, more limitations in usual role activities due to physical health problems, lower vitality, and lower general health perceptions compared with a reference group from the general population
Lane et al. [5]	276	16–85	SF-36	−	ConHD patients with inoperable conditions reported a lower subjective health status than the general population in all SF-36 domains
				−	ConHD patients deemed surgically cured also reported a lower subjective health status compared with the general population in nearly all SF-36 domains, except bodily pain
Simko and McGinnis [6]	124	18–59	SIP	−	ConHD sample reported poorer psychosocial and physical health compared with a matched control group
Jefferies et al. [75]	32	18–53	SF-36	−/≈	The rural ConHD sample reported poorer physical function and general health perceptions compared with a healthy rural cohort, but similar outcomes on nonphysical domains (e.g., emotional role, mental health)
Moons et al. [13]	89	20–27	LAS SWLS TAAQOL	+	Good/very good quality of life, general level of satisfaction with their life in Mustard or Senning patients
Simko and McGinnis [7]	124	Mean 26 (SD = 8.5)	SIP	−	ConHD sample, on average, experienced mild disability, especially on the psychosocial dimension (work, sleep, and rest). Patients with single ventricle physiology had poorer SIP outcomes than those with cyanotic anomalies
Immer et al. [17]	154	14–72	SF-36	≈	The total sample of ConHD patients showed normal reports of subjective health status, comparable to a matched control group
				−	A sub-sample of patients with complete AV canal defect reported more limitations in physical activities due to health problems and more limitations in usual role activities due to emotional problems
Daliento et al. [11]	54	Mean 32	SF-36	−	ConHD sample reported more limitations in physical activities due to health problems compared with a reference group from the general population
Rose et al. [8]	111	Mean 33	WHOQOL-BREF	−	ConHD sample reported more restrictions on physical health and to a lesser extent psychologic health compared with a reference group from the general population
Van Rijen et al. [12]	349	20–46	SF-36	−	ConHD sample reported more limitations in physical activities due to health problems compared with a reference group from the general population
				+	ConHD sample reported fewer limitations in social activities due to physical or emotional problems, fewer limitations in usual role activities due to emotional problems, and less bodily pain compared with a reference group from the general population

Study	N	Age range	Instrument	[b]	Findings
Moons et al. [14]	404	18–56	LAS	+	ConHD sample reported more favorable outcome compared with a matched control group of healthy peers
			SWLS	+	ConHD sample reported more favorable outcome compared with a matched control group of healthy peers
Bruto et al. [9]				−	Worse perceived health status
Moons et al. [15]	627	18–66	LAS	+	78% clustered into the good, 20% into the moderate, and 2% into the poor quality of life category
Loup et al. [76]c	345	15–37	SF-36	≈	Outcomes on both instruments comparable to the standard population, without a difference between diagnostic groups (ToF, TGA, and VSD). Frequent disease-specific social problems (e.g., with health insurance: 67%]
Vigl et al. [18]c	332 males	18–59	SF-12	?	Men with erectile dysfunction scored significantly poorer on both the physical and mental sum scale (SF-12) and on depression compared with males without erectile dysfunction (33% versus 3% depressive symptoms, respectively)

Subjective health status, health-related quality of life and exercise

Study	N	Age range	Instrument		Findings
Duffels et al. [77]c	58 (30 without, 28 with Down syndrome)	20–75	IIEF / SF-36		For patients without Down syndrome, Bosentan treatment resulted in longitudinal improvement (up to 18 months follow-up) on SF-36 scales role-physical limitations and vitality
Dua et al. [78]c	61	18–63	SF-12 / SWLS		A gentle graded exercise-training program improved quality of life, exercise capacity, and habitual physical activities in adult patients at all stages of ConHD
Gratz et al. [79]	564	14–73	SF-36		Despite several limitations at exercise, patients only reported reductions on the SF-36 regarding physical functioning and general health, and not psychosocial aspects. This was found in all diagnostic subgroups
Muller et al. [80]	57	8–52	SF 36 (>14 years)		Scores on SF-36 were fairly good, with lower scores on vitality, general health, and physical function

a BSI, Brief Symptom Inventory; BDI, Beck Depression Inventory; DPQ, Dutch Personality Questionnaire; DSM, Diagnostic and Statistical Manual; GHQ, General Health Questionnaire; HADS, Hospital and Anxiety Questionnaire; IMIQ, Implicit Models of Illness Questionnaire. NASSQ, Negative Affectivity Self-Statement Questionnaire; SCL-90-R, Symptom–Checklist-90-Revised; SCID-DSM-IV, Structured clinical interview for DSM-IV; STAI, State–Trait Anxiety Inventory; YASR, Young Adult Self-Report; YABCL, Young Adult Behavior Checklist;

b +, results of ConHD sample are more favorable than those of a normative group; ≈, results of ConHD sample are similar to those of a normative group; −, results of ConHD sample are less favorable than those of a normative group; ?, comparison with normative data not reported.

c Other instruments were also used in these studies; for details, see the original articles.

functioning, but also the patient's personal feelings regarding his/her functioning. The 12 domains of TAAQOL are gross motor functioning, fine motor functioning, pain, sleeping, cognitive functioning, social functioning, daily activities, sexual activity, vitality, happiness, depressive moods, and aggressiveness. It has been used in some studies with ConHD adults [22–24].

Summary of long-term outcomes of subjective health status and health-related quality of life

Several studies indicate that the health-related quality of life of adults with ConHD is favorable. When subjective health status and the physical aspects of health-related quality of life are assessed, however, scores of patient groups reflect limitations in physical health and emotional functioning. These limitations are not restricted to patients with the most severe diagnoses, but are also seen in patients with relatively mild ConHD.

For patients with limitations in physical functioning, monitored physical training might help those with poor physical condition to feel more secure about their bodily function.

Regarding limitations in emotional functioning, early screening and psychologic treatment for adult patients with ConHD are recommended.

Emotional functioning

Conflicting results about emotional functioning in adults with ConHD have been reported [3]. Negative outcomes predominate [25–31], but some favorable or neutral outcomes have been reported [32–36]. Cox *et al.* [34] even found a low prevalence of psychopathology in adults with ConHD, but used orthopedic patients as a reference group.

Differences in sample size, sample composition (including different diagnostic groups) and assessment procedures (questionnaires or diagnostic interviews used) make it difficult to compare the results from different studies.

Table 54.2 describes the characteristics and main results of studies of emotional functioning of adults with ConHD. The studies mostly included heterogeneous samples with various types of ConHD. The studies can be divided into

- comparisons with normative samples from the general population
- comparisons with somatic reference samples
- ratings of psychiatric diagnostic criteria
- experimental studies into the relationship between cognitive biases and emotional functioning in adults with ConHD.

Comparisons with normative samples from the general population

In studies comparing emotional functioning of adults with ConHD with normative samples, assessment instruments with different scopes have been used:

- psychopathologic symptoms
- emotional and behavioral problems
- personality traits.

Psychopathologic symptoms

ConHD patients may have a large variety and elevated levels of psychopathologic symptoms compared with normative samples [23,28]. Bromberg *et al.* [26] used the BSI to study a sample of ConHD patients with no apparent symptoms of depression or anxiety. In this apparent symptom-free sample, however, they also found psychopathologic emotional functioning.

Emotional and behavioral problems

Both Utens *et al.* [24] and Van Rijen *et al.* [27] found increased levels of emotional and behavioral problems in adult ConHD patients compared with normative groups. Both studies used the *Young Adult Self-Report* (YASR) [35], a self-report questionnaire with syndrome scales and two broad groupings of syndromes: internalizing problems (anxious, depressed, and withdrawn behavior, somatic symptoms) and externalizing problems (intrusive, delinquent, and aggressive behavior). Van der Rijken *et al.* [33] reported no differences on the YASR between a sample of adult ConHD patients and a normative sample. Balon *et al.* [36] used Ryff's psychologic wellbeing scale [37], and found no differences between patients with simple versus complex malformations. They did not clearly describe the level of psychologic wellbeing of the ConHD patients compared with normative data.

Personality traits

Two studies [30,31] used the *Dutch Personality Questionnaire (DPQ)* [38] and showed favorable outcomes in a cohort of ConHD patients on the personality traits of neuroticism, self-esteem, and hostility, compared with a normative samples. Possibly overcompensation and denial, which have been suggested for adults with ConHD [27,30], underlie the favorable outcomes regarding the personality traits, whereas the existence of concrete emotional and behavioral problems (as described above in the section Emotional and Behavioral Problems) is more difficult to deny.

Comparisons with somatic reference samples

Cox *et al.* [34] used the *Hospital Anxiety and Depression Scale* (HADS) [39] and the *General Health Questionnaire* (GHQ) [40], a more global self-report screening device for minor (non-psychotic) disorders. On both instruments, they found more favorable outcomes for the ConHD patient sample compared with a reference sample of orthopedic patients. These favorable findings might partly be explained by the relatively high prevalence of psychologic problems in the reference sample of orthopedic patients. Miatton *et al.* [41], however, pointed out that finding an appropriate comparison sample is challenging in studies about patients with ConHD.

Table 54.2 Studies into emotional functioning of adults with ConHD.

Authors	Sample size (n)	Age range (years)	Instrument	Rating of results (+/≈/−)[a]	Results
Comparisons with normative samples					
Psychopathologic symptoms					
Brandhagen et al. [23]	168	24–42	SCL-90-R	−	ConHD sample reported higher levels of obsessive compulsive thoughts, interpersonal sensitivity, depression, anxiety, hostility, phobic anxiety, paranoid ideation, and psychoticism compared with a normative sample
Bromberg et al. [26]	22	19–60	BSI (global symptom index, and anxiety and depression subscales)		27.3% of the ConHD sample reported pathologic emotional functioning
Geyer et al. [28]	361	14–45	BSI	−	ConHD sample reported higher levels of somatization, obsessive compulsive thoughts, interpersonal sensitivity, anxiety, hostility, and paranoid ideation compared with a normative sample
Emotional and behavioral functioning					
Utens et al. [24]	166	19–25	YASR	−	Proportions of ConHD patients scoring in the psychopathologic range were higher than those in the general population, which was mainly due to scores of 22–25-year-old-males
				−/+	ConHD patients reported more problems in only 2 out of 7 problem areas: more somatic complaints and more strange behavior and ideas (including obsessions and hallucinations) compared with a normative group
Van Rijen et al. [27]	251	20–32	YASR	−	Proportions of ConHD patients scoring in the psychopathologic range were higher than those in the general population
				−	ConHD patients reported more somatic complaints compared with a normative group
			YABCL	−	Proportions of ConHD patients scoring in the psychopathologic range were higher than those in the general population
				−	ConHD patients show more anxious or depressed behavior, withdrawn behavior, somatic complaints, thought problems, attention problems, intrusive behavior, and aggressive behavior compared with a normative group
Van der Rijken et al. [33]	48	18–27	YASR	≈	No differences in emotional and behavioral problems were found between a ConHD sample and normative sample
Balon et al. [36]	163	18–87	Ryff's scale	?	No differences in psychologic wellbeing (positive relations, autonomy, environmental mastery, personal growth, purpose in life, self-acceptance) between patients with simple versus complex malformations
Personality traits					
Utens et al. [30]	278	18–35	DPQ	+	ConHD patients reported fewer feelings of hostility and neuroticism and a higher self-esteem compared with a normative sample
Van Rijen et al. [31]	362	20–46	DPQ	+	ConHD patients reported fewer feelings of hostility and neuroticism and a higher self-esteem compared with a normative sample
Comparisons with somatic reference samples					
Cox et al. [34]	87	17–73	HADS	+	ConHD patients obtained more favorable scores compared with a reference group of orthopedic patients, with borderline significance
			GHQ	+	ConHD patients obtained more favorable scores compared with a reference group of orthopedic patients

Table 54.2 (cont'd)

Authors	Sample size (n)	Age range (years)	Instrument	Rating of results (+/≈/−)[a]	Results
Ratings of psychiatric diagnostic criteria					
Horner et al. [43]	29	26–56	Interview DSM-III-R criteria		4 out of 29 ConHD patients met the criteria for a major depressive disorder, and 5 out of 29 ConHD patients were diagnosed with panic disorder
Popelova et al. [25]	32	19–64	Zung's Questionnaire		Depression was found in 34% of the ConHD patients
Bromberg et al. [26]	22	19–60	Interview DSM-IV-criteria		27.3% of the ConHD sample met the criteria for a depressive episode and 9.1% met the criteria for a anxiety disorder
Kovacs et al. [29]	280	20–43	STAI BDI-II		34% (89/260): elevated anxiety symptoms (STAI) 12%: moderate/severe depressive symptoms (BDI-II)
	58		SCID-DSM-IV interview		50% (29/58) met criteria for a lifetime or mood anxiety disorder Perceived physical health status (SF-36) and social functioning: more predictive of depression and anxiety than medical variables
Experimental studies into the relationship between cognitive biases and emotional functioning					
Rietveld et al. [44][c]	82	17–77	NASSQ (negative thoughts) STAI SF-36		Compared with patients with few or moderate negative thoughts, patients with many negative thoughts scored worse on psychosocial adjustment and subjective health status, irrespective of severity of cardiac disease
Karsdorp et al. [45]	25 patients 24 healthy controls	21–64 19–55	STAI state/trait Perception of heart symptoms Physiology: heart and respiratory rate, blood pressure, arterial partial pressure of CO_2 outcomes	−	A combination of high trait anxiety and ConHD resulted in an increased perception of heart symptoms during a mental stress task (compared with healthy controls)
Karsdorp et al. [46]	26 patients 22 healthy controls	18–59 18–53	STAI state/trait		High anxious patients processed heart-related cues preattentively and in turn showed difficulty shifting attention away from heart-related sensations. The relation between ConHD and perceptual biases for heart symptoms was moderated by trait anxiety
Karsdorp et al. [47]	66 patients 50 healthy controls	18–56 19–53	Interpretation bias (IMIQ) STAI state/trait TAAQOL (e.g., daily functioning)	−	High trait anxious patients with ConHD who also display elevated levels of state anxiety exhibit the most pronounced negative interpretation for ambiguous heart-related sensations and in turn diminished daily functioning
Karsdorp et al. [48]	36 patients 44 healthy controls	19–54 18–54	STAI trait Perception of heart symptoms Physiology: heart and respiratory rate, arterial pressure of CO_2	≈	False heart rate feedback resulted in increased perception of heart symptoms in high trait anxious ConHD that could not be explained by simultaneous cardiac dysfunction

a–cSee footnotes to Table 54.1.

Ratings of psychiatric diagnostic criteria

Popelova *et al.* [25] used *Zung's questionnaire* [42], a self-rating instrument that focuses specifically on depression, and found depression in about one-third of a sample of cyanotic ConHD patients. In two studies [26,43], a structured interview was used to determine how many ConHD patients met the *DSM-III-R* or *DSM-IV* (*Diagnostic and Statistical Manual*) criteria of psychiatric illnesses, respectively. Both studies identified depressive and anxiety disorders in adults with ConHD. Kovacs *et al.* [29] used self-report questionnaires and the SCID–DSM-IV interview (semi-structured clinical interview) to assess the prevalence of mood and anxiety disorders among ConHD patients. They found that 50% of interviewed patients (29/58 patients) met diagnostic criteria for a current of past mood or anxiety disorder. These findings support those of Horner *et al.* [43] and Bromberg *et al.* [26], which showed psychiatric disorders in 28% (8/29 patients) and 35% (8/22 "well-adjusted" patients).

Experimental studies into the relationship between cognitive biases and emotional functioning

Rietveld *et al.* [44] tested the relationship between negative thoughts and adaptation to ConHD. Compared with patients with few or moderate negative thoughts, patients with many negative thoughts scored worse on psychosocial adjustment and subjective health status, irrespective of severity of cardiac disease. Karsdorp and colleagues [45,46]. suggested that high trait anxiety combined with chronic disease may produce stressful, negative experiences with disease and its symptoms. These experiences may be stored in cognitive memory structures, the so-called illness schemes. Perception of cues associated with these illness schemes can elicit processing biases toward disease-related sensations. Examples of such cognitive biases are a tendency to draw attention to disease-related sensations and interpreting ambiguous sensations as disease-related symptoms.

Karsdorp and colleagues [45–48] investigated biases to heart cues and symptoms in several studies by using experimental tasks (Table 54.2).

Summary of long-term outcome of emotional functioning

Emotional and behavioral functioning in adults with ConHD range from no difference from normative groups to positive or negative findings on personality traits. Most often, however, elevated levels of emotional and/or behavioral problems were detected, among which are internalized problems (anxiety, depression, interpersonal difficulties, or withdrawn behavior), externalized problems (hostility, intrusive and aggressive behavior), and even symptoms that may indicate psychotic disorders (see Table 54.1).

Several studies indicated that a combination of high trait anxiety and ConHD resulted in an increased perception of heart symptoms or negative interpretation of ambiguous heart-related sensations. These findings regarding cognitive, perceptual biases could not be explained by simultaneous cardiac dysfunction. Misperception of heart symptoms may unduly result in avoiding physical and social activities and/or unnecessary doctor visits [48]. Psychologic interventions, such as biofeedback training or interpretative bias training, may be beneficial in increasing the accuracy of interpreting heart beat perception and preventing anxiety.

Psychosocial aspects of living with congenital heart disease at adult age

Body image

The overt signs of ConHD (blue cyanotic color, surgical scars, or clubbed fingers) may have a negative influence on the patient's body image [3,49], and hamper adults with ConHD in their attempts to be considered "normal," "healthy," and "the same as others" [50–52]. Geyer *et al.* [53] found that the perception of body image was a stronger predictor for psychopathologic symptoms than limitations of activity and impaired cardiac performance in adult ConHD patients. They suggested that different underlying problems, such as perception of the body as deficient and injured in ConHD males and, to a lesser extent, lack of vitality in ConHD females, may be responsible for increased levels of psychopathology in adult ConHD patients.

Feelings regarding the surgical scar

ConHD adults may dislike or feel restricted by the scar [54,55] or try to conceal the scar by clothing or cosmetics [43,56,57]. Negative feelings regarding the surgical scar may adversely affect emotional and behavior problems [54]. Van Rijen *et al.* [54] found that 40.5% of female patients and 18.9% of male patients felt restricted by the scar. In a Canadian study [56] of 100 patients, 62% of the males and 53% of the females considered themselves disfigured by the scar.

Relational, psychosexual, and reproductive issues

Young adults with ConHD tend to live longer with their parents as compared with "normal" peers [30,57,58]. Favorable outcome regarding marital status has been reported in adults with ConHD [31,58–61], but others reported that patients with ConHD get married less often, or at a later age [57,62]. Offspring rates in adults with ConHD are lower than those in healthy peers [60–62]. Adults with ConHD seem to start families at a later age [31]. Gersony *et al.* [62], however, found no differences in offspring rates or marital status between male and female ConHD patients.

Young adults with ConHD were less sexually active than healthy peers [18,63,64]. Reid *et al.* [64] found that more young adult ConHD females than young adult ConHD males were sexually active, in line with rates of sexual behavior reported in chronically ill youth [65]. An alarming finding was that, among the sexually active patients, 36% of the young ConHD adults and 72% of the adolescent ConHD patients engaged in one or more types of potentially risky sexual behavior (i.e., two or more partners in the past 3 months, questionable birth control, using drugs or alcohol before sex at least sometimes) [64]. These findings underline the need for specific patient education. ConHD females report more sexual problems (not enjoying or being aroused during sex, being insecure) than ConHD males [66]. Vigl *et al.* [18] found that male ConHD patients under the age of 40 did engage less frequently in sexual relationships than peers from the general population. Fears before or during sexual intercourse were present in 9.9%, and also physical symptoms, such as dyspnea (9.0%), feelings of arrhythmia (9.0%), or chest pain (5.1%). About 10% obtained a score on the International Index of Erectile Function indicative of an erectile dysfunction (Table 54.2).

Young females with ConHD are often concerned about fertility, pregnancy, birth control, and genetic transmission [49,58,64]. They may be concerned about their physical ability to raise children. Inability to have children because of cardiac risks can negatively influence a woman's sense of identity and self-worth. Van Rijen *et al.* [31] reported that female patients can feel restricted by their ConHD in their choice of having children. Often, ConHD females are very poorly informed about reproductive matters [49,67], and receive poor or no advice about contraception or pregnancy risks [68], which results in uncertainties.

Living with implantable cardioverter defibrillator (ICD)

Few studies [69–73] have been performed on young patients living with an ICD.

Inappropriate shocks may cause fear of shocks and poor patient acceptance. In a national survey, Sears *et al.* [71] found that ~10–20% of 450 patients implanted with an ICD for <1 year reported difficulty with emotional adjustment to their ICD. ICD recipients receiving more shocks from their ICD, women and younger recipients, reported significantly more adjustment concerns, such as generalized fear, worry, fear of physical exertion, depression, and difficulties managing stress. In a study of 18 young recipients, Dubin *et al.* [72] found diminished social interactions, worry about exercise, problems during sexual activity, and body image concerns. In a study of nine young recipients, Vitale and Funk [73] found abnormal sleep patterns, fear of shock (firing of ICD), and concerns about dying.

In a recent review [69], anxiety was the most serious psychosocial reaction for young ICD patients, as in adult patients. Young ICD patients generally adjust well to life with an ICD, but for a sizeable minority of patients anxiety can be a serious problem.

Clinical implications

We can do better to help our patients adjust to living with ConHD, whether treated or not. The process starts with adequate explanations to parents and child about the anomaly and its likely consequences, both medical and psychosocial, and give them time to ask questions. Frequent repetition of the explanation may be needed, with changes appropriate to any major event. Written material and appropriate Internet references may be useful. Any limitations of physical functioning, as in sports, should be explained and specified and monitored physical training might help patients to feel more secure about their bodily function. Counseling about sexual behavior, fertility, and marriage should be provided early in adolescence by those with appropriate expertise.

Regarding limitations in emotional functioning, early screening and psychologic treatment for adult patients with ConHD are recommended. In our opinion, screening and treatment for psychopathology in adult patients with ConHD should be provided at an early stage, since at younger age these symptoms appear to be less persistent and better treatable [23]. Cardiologists should have the opportunity to refer patients with psychosocial problems to psychologists who specialize in this unique field, to enhance their emotional resilience and styles of coping [74].

References

1 Boneva RS, Botto, LD, Moore CA, *et al.* Mortality associated with congenital heart defects in the United States: trends and racial disparities, 1979–1997. *Circulation* 2001;**103**:2376–81.

2 Marelli AJ, Mackie AS, Ionescu-Ittu R, *et al.* Congenital heart disease in the general population: changing prevalence and age distribution. *Circulation* 2007;**115**:163–72.

3 Kovacs AH, Sears SF, Saidi AS. Biopsychosocial experiences of adults with congenital heart disease: review of the literature. *Am Heart J* 2005;**150**:193–201.

4 Kamphuis M, Ottenkamp J, Vliegen HW, *et al.* Health related quality of life and health status in adult survivors with previously operated complex congenital heart disease. *Heart* 2002; **87**:356–62.

5 Lane DA, Lip GYH, Millane TA. Quality of life in adults with congenital heart disease. *Heart* 2002;**88**:71–5.

6 Simko LC, McGinnis KA. Quality of life experienced by adults with congenital heart disease. *AACN Clin Issues* 2003;**14**:42–53.

7 Simko LC, McGinnis KA. What is the perceived quality of life of adults with congenital heart disease and does it differ by anomaly? *J Cardiovasc Nurs* 2005;**20**:206–14.

8 Rose M, Köhler K, Köhler F, *et al.* Determinants of the quality of life of patients with congenital heart disease. *Qual Life Res* 2005; **14**:35–43.

9 Bruto VC, Harrison DA, Fedak PW, *et al.* Determinants of health-related quality of life in adults with congenital heart disease. *Congenit Heart Dis* 2007;**2**:301–13.

10 Saliba Z, Butera G, Bonnet D, *et al.* Quality of life and perceived health status in surviving adults with univentricular heart. *Heart* 2001;**86**:69–73.

11 Daliento L , Mapelli D, Russo G, *et al.* Health related quality of life in adults with repaired tetralogy of Fallot: psychosocial and cognitive outcomes. *Heart* 2005;**91**:213–8.

12 Van Rijen EHM, Utens EMWJ, Roos-Hesselink JW, *et al.* Current subjective state of health, and longitudinal psychological wellbeing over a period of 10 years, in a cohort of adults with congenital cardiac disease. *Cardiol Young* 2005;**15**:168–75.

13 Moons P, De Bleser L, Budts W, *et al.* Health status, functional abilities, and quality of life after the Mustard or Senning operation. *Ann Thorac Surg* 2004;**77**:1359–65.

14 Moons P, Van Deyk K, De Bleser L, *et al.* Quality of life and health status in adults with congenital heart disease: a direct comparison with healthy counterparts. *Eur J Cardiovasc Prev Rehab* 2006;**13**:407–13.

15 Moons P, Van Deyk K, Marquet K, *et al.* Profile of adults with congenital heart disease having a good, moderate, or poor quality of life: a cluster analytic study. *Eur J Cardiovasc Nurs* 2009;**8**:151–7.

16 Ware JE, Sherbourne CD. The MOS 36-item short-form health survey (SF-36). Conceptual framework and item selection. *Med Care* 1992;**30**,473–83.

17 Immer FF, Althaus SM, Berdat PA, *et al.* Quality of life and specific problems after cardiac surgery in adolescents and adults with congenital heart disease. *Eur J Cardiovasc Prev Rehab* 2005;**12**:138–43.

18 Vigl M, Hager A, Bauer U, *et al.* Sexuality and subjective wellbeing in male patients with congenital heart disease. *Heart* 2009;**95**:1179–83.

19 Parkerson GR, Broadhead WE, Tse CK. The Duke health profile. A 17-item measure of health and dysfunction. *Med Care* 1990;**28**:1056–72.

20 The WHOQOL Group. Development of the World Health Organization WHOQOL-BREF quality of life assessment. *Psychol Med* 1998;**28**:551–8.

21 Diener E, Emmons RA, Larsen RJ, Griffin S. The satisfaction with life scale. *J Personality Assess* 1985;**49**:71–5.

22 Fekkes M, Kamphuis RP, Ottenkamp J, *et al.* Health-related quality of life in young adults with minor congenital heart disease. *Psychol Health* 2001;**16**:239–50.

23 Brandhagen DJ, Feldt RH, Williams DE. Long-term psychologic implications of congenital heart disease: a 25-year follow-up. *Mayo Clin Proc* 1991;**66**:474–9.

24 Utens EM, Versluis-Den Bieman HJ, Verhulst FC, *et al.* Psychopathology in young adults with congenital heart disease. Follow-up results. *Eur Heart J* 1998;**19**:647–51.

25 Popelova J, Slavik Z, Skovranek J. Are cyanosed adults with congenital cardiac malformations depressed? *Cardiol Young* 2001;**11**:379–84.

26 Bromberg JI, Beasley PJ, D'Angelo EJ, *et al.* Depression and anxiety in adults with congenital heart disease: a pilot study. *Heart Lung* 2003;**32**:105–10.

27 Van Rijen EHM, Utens EMWJ, Roos-Hesselink JW, *et al.* Longitudinal development of psychopathology in an adult congenital heart disease cohort. *Int J Cardiol* 2005;**99**:315–23.

28 Geyer S, Hessel A, Kempa A, *et al.* Psychological symptoms and body image in patients after surgery for congenital heart disease: comparisons between patients and general population samples. *Psychother Psych Med* 2006;**56**:425–31.

29 Kovacs AH, Saidi AS, Kuhl EA, *et al.* Depression and anxiety in adult congenital heart disease: predictors and prevalence. *Int J Cardiol* 2009;**37**:158–64.

30 Utens EMWJ, Verhulst FC, Erdman RAM, *et al.* Psychosocial functioning of young adults after surgical correction for congenital heart disease in childhood: a follow-up study. *J Psychosom Res* 1994;**38**:745–58.

31 Van Rijen EHM, Utens EMWJ, Roos-Hesselink JW, *et al.* Psychosocial functioning of the adult with congenital heart disease: a 20–33 years follow-up. *Eur Heart J* 2003;**24**:673–83.

32 Van Rijen EHM. Psychosocial aspects of congenital heart disease in adulthood. A longitudinal cohort study of 20–33 years follow-up. PhD thesis, Erasmus University Rotterdam, 2003.

33 Van der Rijken RE, Maassen BAM, Walk TM, *et al.* Outcome after surgical repair of congenital cardiac malformations at school age. *Cardiol Young* 2007;**17**:64–71.

34 Cox D, Lewis G, Stuart G, Murphy K. A cross-sectional study of the prevalence of psychopathology in adults with congenital heart disease. *J Psychosom Res* 2002;**52**:65–8.

35 Achenbach TM. *Manual for the Young Adult Self-Report and Young Adult Behavior Checklist.* Burlington, VT: University of Vermont, Department of Psychiatry, 1997.

36 Balon YE, Then KL, Rankin JA, Fung T. Looking beyond the biophysical realm to optimize health: results of a survey of psychological wellbeing in adults with congenital cardiac disease. *Cardiol Young* 2008;**18**:494–501.

37 Ryff CD. Happiness is everything, or is it? Explorations on the meaning of psychological wellbeing. *J Pers Soc Psychol* 1989;**57**:1069–81.

38 Luteijn F, Starren J, van Dijk H. *Manual for the Dutch Personality Questionnaire*, rev. edn. *Handleiding bij de NPV*, herziene uitgave. Lisse: Swets and Zeitlinger, 1985.

39 Zigmond AS, Snaith RP. The Hospital Anxiety and Depression Scale. *Acta Psychiatr Scand* 1983;**67**:361–70.

40 Goldberg D. Identifying psychiatric illness among general medical patients. *Br Med J* 1985;**291**:161–3.

41 Miatton M, De Wolf D, François K, *et al.* Neurocognitive consequences of surgically corrected congenital heart defects: a review. *Neuropsychol Rev* 2006;**16**:65–85.

42 Zung WWK. A self-rating depression scale. *Arch Gen Psychiatry* 1965;**12**:63–70.

43 Horner T, Liberthson R, Jellinek MS. Psychosocial profile of adults with complex congenital heart disease. *Mayo Clinic Proc* 2000;**75**:31–6.

44 Rietveld S, Mulder BJ, van Beest I, *et al.* Negative thoughts in adults with congenital heart disease. *Int J Cardiol* 2002;**6**:19–26.

45 Karsdorp PA, Kindt M, Rietveld S, *et al.* Stress-induced heart symptoms and perceptual biases in patients with congenital heart disease. *Int J Cardiol* 2007;**114**:352–7.

46 Karsdorp PA, Kindt M, Everaerd W, Mulder BJ. Preattentive processing of heart cues and the perception of heart symptoms in congenital heart disease. *Behav Res Ther* 2007;**45**:1893–902.

47 Karsdorp PA, Kindt M, Rietveld S, *et al.* Interpretation bias for heart sensations in congenital heart disease and its relation to quality of life. *Int J Behav Med* 2008;**15**:232–40.

48 Karsdorp PA, Kindt M, Rietveld S, *et al.* False heart rate feedback and the perception of heart symptoms in patients with congenital heart disease and anxiety. *Int J Behav Med* 2009;**16**:81–8.

49 Gantt LT. Growing up heartsick: the experiences of young women with congenital heart disease. *Health Care Women Int* 1992;**13**:241–8.

50 Tong EM, Sparacino PS, Messias DK, *et al.* Growing up with congenital heart disease: the dilemmas of adolescents and young adults. *Cardiol Young* 1998;**8**:287–9.

51 Claessens P, Moons P, de Casterlé BD, *et al.* What does it mean to live with a congenital heart disease? A qualitative study on the lived experiences of adult patients. *Eur J Cardiovasc Nurs* 2005;**4**:3–10.

52 Berghammer M, Dellborg M, Ekman I. Young adults experiences of living with congenital heart disease. *Int J Cardiol* 2006; **110**:340–7.

53 Geyer S, Norozi K, Zoege M, *et al.* Psychological symptoms in patients after surgery for congenital heart disease. *Cardiol Young* 2006;**16**:540–8.

54 Van Rijen EHM, Utens EMWJ, Roos-Hesselink JW, *et al.* Medical predictors for psychopathology in adults with operated congenital heart disease. *Eur Heart J* 2004;**25**:1605–13.

55 Crossland DS, Jackson SP, Lyall R, *et al.* Patient attitudes to sternotomy and thoracotomy scars. *Thorac Cardiovasc Surg* 2005;**53**:93–5.

56 Kańtoch MJ, Eustace J, Collins-Nakai RL, *et al.* The significance of cardiac surgery scars in adult patients with congenital heart disease. *Kardiol Pol* 2006;**64**:51–6.

57 Kokkonen J, Paavilainen T. Social adaptation of young adults with congenital heart disease. *Int J Cardiol* 1992;**36**:23–9.

58 Simko LC, McGinnis KA, Schembri, J. Educational needs of adults with congenital heart disease. *J Cardiovasc Nurs* 2006;**21**:85–94.

59 Ternestedt BM, Wall K, Oddsson H, *et al.* Quality of life 20 and 30 years after surgery in patients operated on for tetralogy of Fallot and for atrial septal defect. *Pediatr Cardiol* 2001; **22**:128–32.

60 Nieminen H, Sairanen H, Tikanoja T, *et al.* Long-term results of pediatric cardiac surgery in Finland: education, employment, marital status, and parenthood. *Pediatrics* 2003; **112**:1345–50.

61 Sairanen HI, Nieminen HP, Jokinen EV. Late results and quality of life after pediatric cardiac surgery in Finland: a population-based study of 6,461 patients with follow-up extending up to 45 years. *Semin Thorac Cardiovasc Surg Pediatr Card Surg Ann* 2005;**8**:168–72.

62 Gersony WM, Hayes CJ, Driscoll DJ, *et al.* Second natural history study of congenital heart defects. Quality of life of patients with aortic stenosis, pulmonary stenosis, or ventricular septal defect. *Circulation* 1993;**87**(2 Suppl):152–65.

63 Uzark K, VonBargen-Mazza P, Messiter E. Health education needs of adolescents with congenital heart disease. *J PediatrHealth Care* 1989;**3**:137–43.

64 Reid GJ, Siu SC, McCrindle BW, *et al.* Sexual behavior and reproductive concerns among adolescents and young adults with congenital heart disease. *Int J Cardiol* 2008;**125**:332–8.

65 Suris JC, Parera N. Sex, drugs and chronic illness: health behaviours among chronically ill youth. *Eur J Public Health* 2005;**15**:484–8.

66 Moons P, Van Deyk K, Marquet K, *et al.* Sexual functioning and congenital heart disease: something to worry about? *Int J Cardiol* 2007;**121**:30–5.

67 Hargrove A, Penny DJ, Sawyer SM. Sexual and reproductive health in young people with congenital heart disease: a systematic review of the literature. *Pediat Cardiol* 2005;**26**:805–11.

68 Rogers P, Mansour D, Mattinson A, O'Sullivan JJ. A collaborative clinic between contraception and sexual health services and an adult congenital heart disease clinic. *J Fam Plann Reprod Health Care* 2007;**33**:17–21.

69 Sears SF, St Amant JB, Zeigler V. Psychosocial considerations for children and young adolescents with implantable cardioverter defibrillators: an update. *Pacing Clin Electrophysiol* 2009;**32**:80–2.

70 Tomaske M, Bauersfeld U. Experience with implantable cardioverter–defibrillator therapy in grown-ups with congenital heart disease. *Pacing Clin Electrophysiol* 2008;**31**:35–7.

71 Sears SF Jr, Burns JL, Handberg E, *et al.* Young at heart: understanding the unique psychosocial adjustment of young implantable cardioverter defibrillator recipients. *Pacing Clin Electrophysiol* 2001;**24**:1113–7.

72 Dubin AM, Berul CI, Bevilacqua LM, *et al.* The use of implantable cardioverter–defibrillators in pediatric patients awaiting heart transplantation. *J Card Fail* 2003;**9**:375–9.

73 Vitale MB, Funk M. Quality of life in younger persons with an implantable cardioverter defibrillator. *Dimens Crit Care Nurs* 1995;**14**:100–11.

74 Van Rijen EH, Utens EMWJ, Roos-Hesselink J, *et al.* Styles of coping and social support in a cohort of adults with congenital heart disease. *Cardiol Young* 2004;**14**:122–30.

75 Jefferies JL, Noonan JA, Keller BB, *et al.* Quality of life and social outcomes in adults with congenital heart disease living in rural areas of Kentucky. *Am J Cardiol* 2004;**94**:263–6.

76 Loup O, von Weissenfluh C, Gahl B, *et al.* Quality of life of grown-up congenital heart disease patients after congenital cardiac surgery. *Eur J Cardiothorac Surg* 2009;**36**:105–11.

77 Duffels MG, Vis JC, van Loon RL, *et al.* Effect of bosentan on exercise capacity and quality of life in adults with pulmonary arterial hypertension associated with congenital heart disease with and without Down's syndrome. *Am J Cardiol* 2009; **103**:1309–15.

78 Dua JS, Cooper AR, Fox KR, Graham Stuart A. Exercise training in adults with congenital heart disease: feasibility and benefits. *Int J Cardiol* 2009;**138**:196–205.

79 Gratz A, Hess J, Hager A. Self-estimated physical functioning poorly predicts actual exercise capacity in adolescents and adults with congenital heart disease disease. *Eur Heart J* 2009;**30**:497–504.

80 Müller J, Christov F, Schreiber C, *et al.* Exercise capacity, quality of life, and daily activity in the long-term follow-up of patients with univentricular heart and total cavopulmonary connection. *Eur Heart J* 2009;**30**:2915–20.

Further reading

Beck AT, Steer RA, Brown GK. *Manual for the Beck Depression Inventory–II.* San Antonio, TX: The Psychological Corporation, 1996.

Bol Raap G, Meijboom F., Kappetein AP, *et al.* Long-term follow-up and quality of life after closure of ventricular septal defect in adults. *Eur J Cardiothorac Surg* 2007;**32**:215–9.

Damiano AM. *The Sickness Impact Profile User's Manual and Interpretation Guide*. Boston, MA: Medical Outcomes Trust, 1996.

Derogatis LR. *SCL-90-R, Administration, Scoring and Procedures Manual–II for the Revised Version and Other Instruments of the Psychopathology Rating Scale Series*. Towson, MD: Clinical Psychometric Research, 1992.

Derogatis LR, Melisaratos N. The Brief Symptom Inventory: an introductory report. *Psychol Med* 1983;**13**:595–605.

First MB, Spitzer RL, Gibbon M, Williams JBW. *Structured Clinical Interview for DSM-IV-TR Axis I Disorders, Research Version, Nonpatient Edition. (SCID-I/NP).* New York: Biometrics Research, New York State Psychiatric Institute, 2002.

Kamphuis M, Zwinderman KH, Vogels T, *et al.* A cardiac-specific health-related quality of life module for young adults with congenital heart disease: development and validation. *Qual Life Res* 2004;**13**:735–45.

Moons P, Van Deyk K, Dedroog D, *et al.* Prevalence of cardiovascular risk factors in adults with congenital heart disease. *Eur J Cardiovasc Prev Rehab* 2006;**13**:612–6.

Ronan KR, Kendall PC, Rowe R. Negative affectivity in children: development and validation of a self-statement questionnaire. *Cogn Ther Res* 1994;**18**:509–28.

Spielberger CD. *Manual for the State–Trait Anxiety Inventory STAI (Form Y).* Palo Alto, CA: Mind Garden, 1983.

Van Rijen EHM, Utens EMWJ. Psychological aspects of congenital heart disease in children. In: Wyszynski DF, Correa-Villasenor A and Graham TP, eds. *Congenital Heart Defects – From Origin to Treatment*. Oxford: Oxford University Press, 2010: 338–55.

Vigl M. Reproductive health in females with congenital heart disease. In: *Abstracts Book of AEPC Psychosocial Meeting, Bruges*, 27–29 February 2008: 30.

Cardiac Arrhythmias: Diagnosis and Management

George F. Van Hare[1] & Anne M. Dubin[2]
[1]Washington University and St Louis Children's Hospital, St Louis, MO, USA
[2]Stanford University, Palo Alto, CA, USA

General considerations

Basic cellular electrophysiology

The potential between the interior and the exterior of a myocardial cell is the transmembrane potential. In diastole the potential is −80 to −90 mV and is termed the resting potential. When the cell is stimulated, an action potential results (Figure 55.1). Rapid depolarization (phase 0) results from rapid sodium influx; the rapid return to near zero potential (phase 1) results from chloride influx. The less negative the transmembrane potential at the onset of depolarization, the slower the rate of depolarization (V_{max}) in phase 0; in turn, reduced V_{max} slows the velocity of propagation of the impulse through the fibers. Antiarrhythmic agents with class I activity (e.g., procainamide, flecainide) block sodium influx, reduce V_{max}, and therefore slow conduction. Phase 1 is followed by a plateau (phase 2) during which slow inward calcium and sodium currents are nearly balanced by potassium leaking out of the cell. Potassium conductance then increases, and potassium efflux causes the potential to become more negative rapidly (phase 3) until the resting membrane potential is reached. During phase 4, sodium is actively pumped out of the cell in exchange for potassium.

Once the action potential has begun, the cell is completely refractory to stimulation until it attains a transmembrane potential of about −55 mV in phase 3, and from this value until it reaches a resting potential of −85 mV in phase 4 the cell gradually regains excitability. Between complete refractoriness and complete responsiveness is the relative refractory period; in keeping with the relationship between V_{max} and transmembrane potential, a stimulus early in the refractory period produces a slow and poorly conducted action potential.

Prolongation of action potential duration and absolute and relative refractory periods occurs with slowing of the rate of depolarization, a long RR interval thus giving a longer refractory period of the next beat. Refractory periods are also prolonged by disease (myocarditis, ischemia) and by some antiarrhythmic drugs (ibutalide, sotalol).

Certain cells have a different pattern. The resting potential starts at about −80 mV but then automatically spontaneously and gradually becomes more positive. When the potential reaches a threshold of about −50 mV, the action potential begins spontaneously; hence these cells are called automatic cells and are said to have automaticity. Normally, only some cardiac muscle cells have automaticity; they may be found anywhere in the heart but are mainly in the SA node, the lower part of the AV node, muscle in the mitral and tricuspid valves, and the conduction system. The repetition rate at which groups of automatic cells depolarize depends mainly on the slope of spontaneous depolarization; the more rapid it is, the sooner the threshold is reached and the faster the heart rate. Catecholamines, vagal blockade, a raised temperature, lowered extracellular potassium or calcium, or a fall in tissue pH or oxygen tension accelerate diastolic depolarization rate and thus tend to increase heart rate. Vagal stimulation, β-adrenergic blockade, increased extracellular potassium, and drugs such as quinidine, procainamide, lidocaine, and phenytoin reduce the diastolic depolarization rate and thus reduce automaticity. The effect of these drugs in reducing automaticity makes them useful in treating many arrhythmias. Various automatic cells have different sensitivities for changes induced by these agents. Thus, phenytoin increases atrial diastolic depolarization but decreases ventricular diastolic depolarization, and lidocaine markedly affects ventricular automaticity but not atrial automaticity.

Transmembrane
potential

Phase 1:
Cl⁻ in

Phase 2:
Na^+, Cl^{2+} in
K^+ out

0 mV — Phase 0:
Na^+ in

Phase 3:
K^+ out

Phase 4:
Na^+ out,
K^+ in
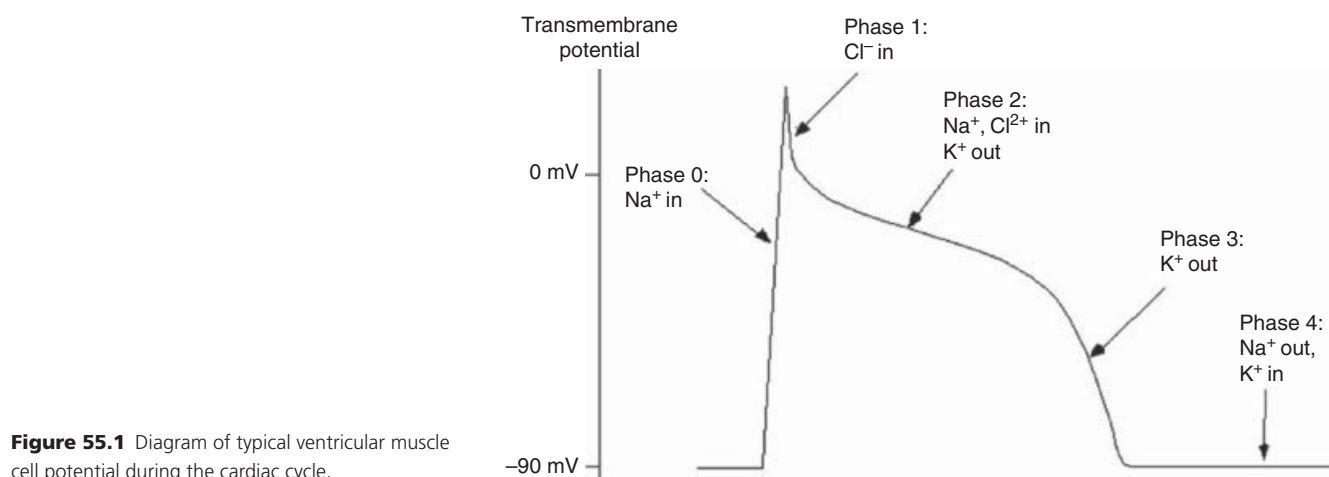
Figure 55.1 Diagram of typical ventricular muscle cell potential during the cardiac cycle.

−90 mV —

Normally the discharge rate is highest for automatic cells in the SA node, which is thus the usual pacemaker for the heart. Collections of automatic cells (latent pacemakers) lower in the conducting system have slower diastolic depolarization, the slowest being those in the ventricles. Normally these lower (or ectopic) pacemakers are discharged by impulses from the SA node before they can discharge spontaneously and, therefore, they are usually suppressed by impulses from above. The typical discharge rate of each pacemaker varies with age.

Most normal cardiac muscle and automatic cells show rapid depolarization and also conduct rapidly; hence they are known as fast-responding cells, but some cells show a slow response. Their transmembrane resting potential is only about −60 mV, depolarization is slow, as is conduction, and in phase 4 there is an after-depolarization that normally does not reach the threshold for initiating another action potential. Slow-responding cells are found normally in the SA and AV nodes and the AV valves. Ischemia, digitalis toxicity, excess potassium or catecholamines, or chronic dilatation can convert fast-responding cells into slow-responding cells. In these cells the rapid sodium influx of phase 1 is absent, and depolarization is achieved mainly by the slow inward calcium current and can be blocked by calcium channel blockers (verapamil, diltiazem).

The action potential of myocardial cells is controlled by channels that allow or hinder the influx or efflux of ions. The ion exchanges are more complex than shown in Figure 55.1, and a summary is given in Figure 55.2. Almost all the known mutations increase the intracellular positive ions, and most are associated with the long QT syndrome.

Cardiac arrhythmias (both fast and slow) result from abnormal impulse formation, abnormal impulse conduction, or a combination of the two. Abnormal automaticity occurs when ectopic pacemakers compete with the sinus node. Depression of sinus node automaticity may shift the origin of the cardiac impulse to other sites in the heart. Ectopic rhythms may be driven by sympathetic activity or other effects, such as ischemia or stretch. Triggered activity, a form of abnormal automaticity, results from a second depolarization that occurs either during repolarization (early after-depolarization) or after repolarization (delayed after-depolarization). Early after-depolarizations can be associated with hypoxia, ischemia, hypokalemia, cesium, catecholamines, and some antiarrhythmic drugs with proarrhythmic effects, such as the class I agents. Early after-depolarizations may be responsible for torsades de pointes, a type of ventricular tachycardia, especially when associated with antiarrhythmic agents [1].

Abnormal impulse conduction is another mechanism responsible for arrhythmias. Abnormal conduction occurs when it proceeds along abnormal pathways, as in pre-excitation, such as Wolff–Parkinson–White (WPW) syndrome and other re-entrant pathways, or when normal conduction is blocked, as in sinoatrial block or AV conduction block.

Mechanisms of tachycardias

Re-entrant versus automatic tachycardias

For a tachycardia to be termed re-entrant, three conditions must be met. First, an anatomically distinct re-entrant circuit must be present, allowing for the circular movement of excitation conduction. Second, an area of this potential re-entrant circuit must be subject to delay in conduction, or the circuit must be large enough to allow for recovery by the time the next re-entrant wave arrives. Third, unidirectional conduction block must occur, allowing subsequent reversed conduction in that segment.

The common *re-entrant* tachycardias in children include sinoatrial and intra-atrial re-entry, atrioventricular node
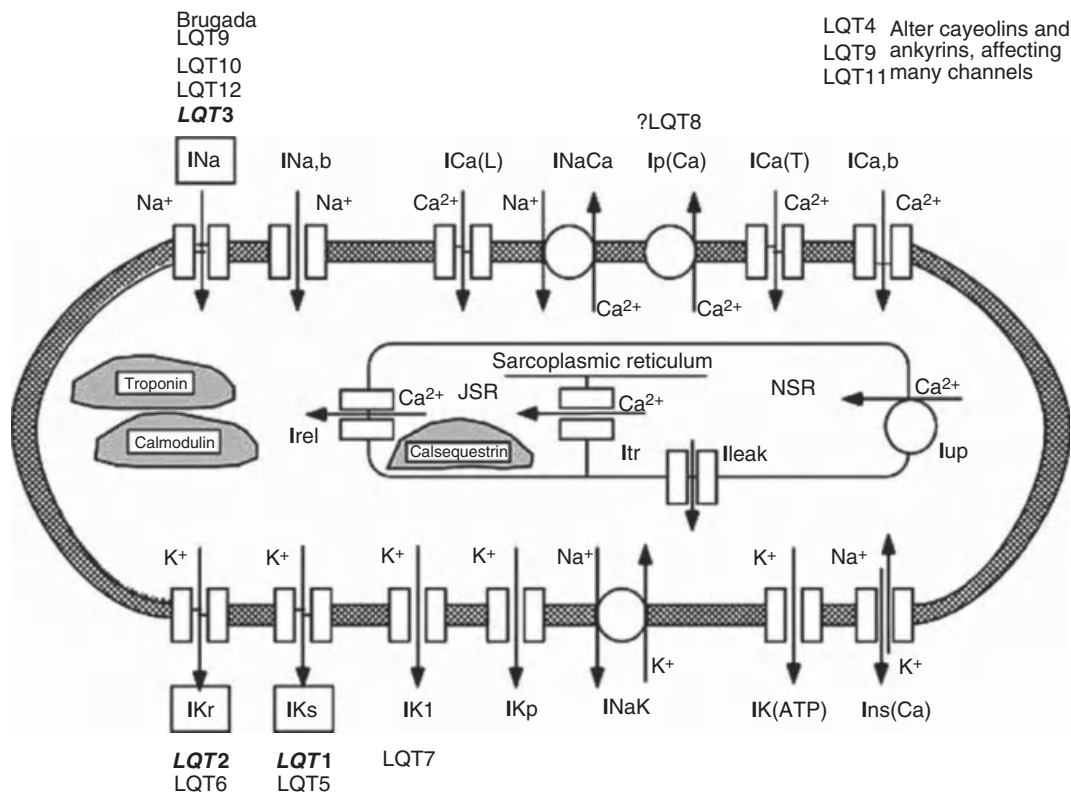
Figure 55.2 Diagram of cardiac muscle cell to show many of the known ion channels and some of the mutations that impair their function. Most of the mutations produce lengthening of the QT interval except for Brugada syndrome. The three major causes are shown in large bold italics, the less common defects in plain type. Some of the mutations affect caveolins and ankyrins, proteins that bind to and affect many different ion channels. (Modified with permission from an original diagram published by Viswanathan and Rudy, *Cardiovasc Res* 1999;**42**:530–42.)

re-entry, atrioventricular reciprocating tachycardia involving an accessory pathway, atrial flutter, the permanent form of junctional reciprocating tachycardia, and the re-entrant form of ventricular tachycardia. Tachycardias caused by increased *automaticity* include sinus tachycardia, atrial ectopic tachycardia, junctional ectopic tachycardia, and (automatic focus) ventricular tachycardia. Interestingly, atrial fibrillation was thought to be due mainly to complex multiple re-entrant circuits in the atrium, but now is understood to have its origin from very fast automatic foci in the pulmonary veins and elsewhere.

A major characteristic of the re-entrant tachycardias that allows differentiation from the automatic tachycardias is their tendency to start and stop suddenly. Premature atrial and ventricular contractions may initiate or terminate these rhythms, or they start during normal episodes of sinus bradycardia with junctional escape rhythm. Direct current cardioversion is generally successful in terminating re-entrant tachycardias but not automatic tachycardias [2].

Sinus tachycardia

Sinus tachycardia often masquerades as paroxysmal supraventricular tachycardia in children and is usually secondary to another problem; a careful search for such pro- blems should allow the diagnosis of sinus tachycardia (see Tables 55.1 and 55.2). For example, the gradual slowing of a narrow QRS tachycardia after an intravenous fluid bolus in a patient with dehydration provides strong evidence for sinus tachycardia and not other forms of paroxysmal supraventricular tachycardia. Causes of sinus tachycardia include high fever, pain, hypoxia, hyperthyroidism, seizures, chronotropic agents (isoproterenol or dobutamine), and sedation in paralyzed ventilated patients.

The criteria for *sinus tachycardia* include normal P-wave axis, a normal (not prolonged) PR interval, gradual onset and termination of the tachycardia and a heart rate below 250 beats per minute (bpm). Rates above 250 bpm rule out sinus tachycardia, whereas narrow complex tachycardias below 250 bpm are often, but not always, sinus tachycardia.

Sinus tachycardia must be ruled out, if possible, before antiarrhythmic therapy is instituted. This diagnosis may be fairly difficult in children because the P wave may be hidden in the preceding T wave. Several electrocardiographic leads should be carefully analyzed for deformation of the T wave by a P wave. Vagal maneuvers and other methods for converting supraventricular tachycardia do not terminate sinus tachycardia. Vagal maneuvers may briefly slow the rhythm, but because the underlying cause of sinus

Table 55.1 Common arrhythmias by patient age.

Age	Arrhythmia	Comment
Fetal	Sinus bradycardia (<100 bpm)	Fetal hypoxic stress
	Complete atrioventricular block (<60 bpm)	Isolated, or associated with maternal systemic lupus erythematosus or fetal congenital heart disease. May cause hydrops
	Sinus tachycardia (>180 bpm)	Maternal fever, drugs, fetal stress, anemia
	Supraventricular tachycardia (>200 bpm)	Causes hydrops if sustained
	Atrial flutter (280–450 bpm, conduction delay, 2:1)	Causes hydrops if sustained
	Ventricular tachycardia (>120 bpm)	Rare
		Causes hydrops if sustained
Neonate	Continuation of fetal arrhythmias	
	Sinus bradycardia	Associated with apnea of prematurity as primary event
Infant	Sinus tachycardia (<250 bpm)	Fever, anxiety, shock, dehydration, heart failure, pain
	Supraventricular tachycardia	Primary or sympathomimetic drug administration, fever, myocarditis, trauma
Older child and adolescent	Premature atrial beats	
	Premature ventricular beats	
	Paroxysmal atrial tachycardia	Thyrotoxicosis, idiopathic, atrial enlargement, mitral stenosis, sympathomimetic drugs
	Sinus bradycardia	Trained athlete, vasodepressor syncope
	Sinus tachycardia	As for infant (see above) plus drug abuse (cocaine, amphetamine)
	Various post-cardiac surgery arrhythmias	Surgical scars create lines of block

tachycardia is unaffected by such maneuvers, the rhythm resumes immediately. Therapy should be directed to the likely underlying causes. The response to such measures is likely to be diagnostic.

Accessory pathway tachycardia

An excellent example of a re-entrant supraventricular tachyarrhythmia is the reciprocating atrioventricular re-entrant tachycardia in patients with the WPW syndrome (Figure 55.3). In sinus rhythm, there is pre-excitation in patients with WPW, due to simultaneous conduction down the pathway and the node, forming a characteristic delta wave (Figure 55.4). A premature atrial contraction may block in the accessory pathway but be conducted down the atrioventricular node and the His-Purkinje system, but with significant delay in the atrioventricular node. Impulses arriving in the ventricle are then conducted retrograde via the accessory pathway back to the atrium. The conduction delay in the atrioventricular node allows the accessory pathway and atrium sufficient time to recover and thus establish sustained tachycardia. It is recognized by a characteristic narrow or normal QRS with P waves discernible on the early part of the T wave (Figure 55.5).

Patients with an accessory pathway but without the potential for anterograde conduction are classified as having concealed accessory pathways. A specific form of concealed accessory pathway, AV reciprocating tachycardia, also termed persistent junctional reciprocating tachycardia (PJRT), is mainly seen in children. It presents as a slow narrow QRS

tachycardia with abnormal P waves prior to each QRS. These P waves are characteristically inverted in leads II, III, and AVF (Figure 55.6). Because of the slow rate, the tachycardia may be relatively asymptomatic, but its tendency to be incessant means that it may lead to the development of tachycardia-induced cardiomyopathy [3]. Ventricular dysfunction from the incessant tachycardia may be seen when the patient presents and may be severe, particularly in infants. It generally resolves with successful treatment of the arrhythmia.

Atrioventricular node re-entry tachycardia

Atrioventricular node re-entry tachycardia (AVNRT) is the second common form of re-entrant supraventricular tachycardia. In this condition, so-called dual AV node pathways are demonstrable. Although the normal AV node has one "pathway" with a short conduction time, in AVNRT the AV node is functionally discontinuous with fast and slow AV node pathways. In AVNRT, a premature atrial contraction blocks the fast pathway, which generally has a long refractory period. Conduction proceeds down the slow pathway, producing a markedly prolonged PR interval. If conduction is slow enough, then adequate time is available for the fast pathway to recover and conduct the impulse retrograde, arriving back in the atrium and re-entering the slow pathway anterograde.

AVNRT is less common than accessory pathway tachycardia in younger children, and is rare in infants. It is more common, however, by young adulthood [4].

Table 55.2 Recognition of tachycardia with normal QRS duration.

Diagnosis	Electrocardiographic findings
Re-entrant tachycardias	
Atrial and sinoatrial re-entry	P waves present, precede next QRS complex
	Terminates with QRS rather than P wave
	Variable AV conduction possible AV block does not terminate atrial rhythm
	P wave axis may be superior or inferior, depending on origin
Atrial flutter	Sawtooth flutter waves
	AV block does not terminate atrial rhythm
	Atrial rate 300 in older children, up to 500 in newborns
Accessory pathway-mediated tachycardia (Wolff-Parkinson-White syndrome and concealed accessory pathway)	P waves follow QRS, typically on upstroke of T wave
	Superior or rightward P wave axis
	AV block always terminates tachycardia
	Typically terminates with P wave
	After termination, those with Wolff-Parkinson-White have pre-excitation
Persistent junctional reciprocating tachycardia	Incessant
	P waves precede QRS
	Inverted P waves in II, III, AVF
	AV block always terminates tachycardia
	May terminate with QRS or with P wave
	No pre-excitation after termination
Atrioventricular node re-entry	AV block usually terminates tachycardia
Atrial fibrillation	"Irregularly irregular," no two RR intervals exactly the same
	P waves difficult to see, or bizarre and chaotic
Increased automaticity	
Sinus tachycardia	Normal P wave axis
	P waves precede QRS
	Caused by extrinsic factor, e.g., heart failure, fever, anemia, catecholamine, or theophylline infusion
	Continues in presence of AV block
Atrial ectopic tachycardia	Incessant
	Abnormal P wave axis, which predicts location of focus
	P waves precede QRS
	Continues in presence of AV block
Junctional ectopic tachycardia	Capture beats with no fusion

Figure 55.3 Diagram of the re-entrant circuit in Wolff–Parkinson–White syndrome. Conduction proceeds normally down the normal conduction system, and then in a retrograde manner up the bundle of Kent (accessory pathway to the atrium), to re-enter the normal conduction system. (Reproduced from Van Hare GF. Circulation. In: Rudoph AM, Kamei RK, eds. *Rudoph's Fundamentals of Pediatrics*. Norwalk, CT: Appleton & Lange, 1994: 522.)

discernible P waves. Because of timing, the retrograde P waves are superimposed on the QRS complex (Figure 55.7). In young patients, however, the first part of the P wave may be observed just prior to the onset of the QRS complex. Other forms of AVNRT, such as atypical AVNRT with antero-grade fast pathway conduction and retrograde slow pathway conduction, are unusual in children.

Atrial ectopic tachycardia

Atrial ectopic tachycardia (AET) is a disorder of abnormal automaticity, due to a rapidly firing focus in the right or left atrium. The etiology is generally unknown, although in some patients it is related to myocarditis or dilated cardiomyopathy. Rarely, it is a manifestation of pulmonary disease. In children, it often presents as an asymptomatic incessant tachycardia, which, similarly to PRJT (discussed above), may lead eventually to tachycardia-induced cardi-omyopathy [5]. It is recognized as a narrow QRS tachycardia with a normal to somewhat prolonged PR interval, and abnormal P-wave morphology.

Atrial flutter

Atrial flutter is characterized by a rapid atrial rate of about 300 bpm in older children and adolescents and as high as 450–500 bpm in neonates. In the typical form, a sawtooth configuration of atrial waves (F waves) is seen best in leads II, III, and V$_1$, and there is variable AV block (Figure 55.8). After

These pathways can be detected by programmed stimulation in the electrophysiology laboratory, and may be suspected on electrocardiogram (ECG) inspection. On an ECG, there is a regular, narrow QRS tachycardia without
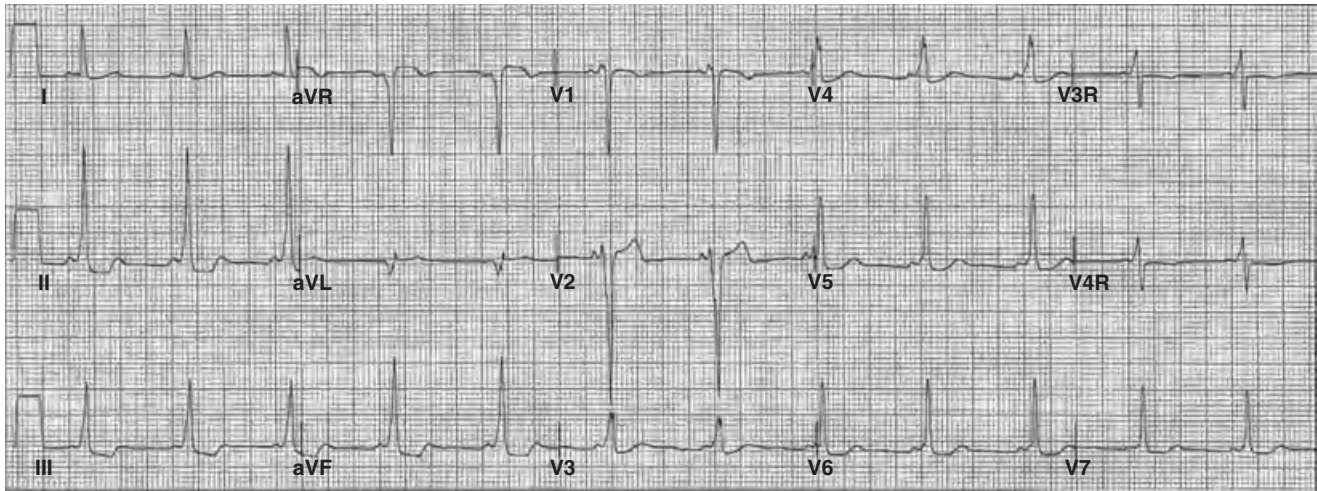
Figure 55.4 Electrocardiogram in a patient with Wolff–Parkinson–White syndrome. Note the short PR interval with a widened QRS.
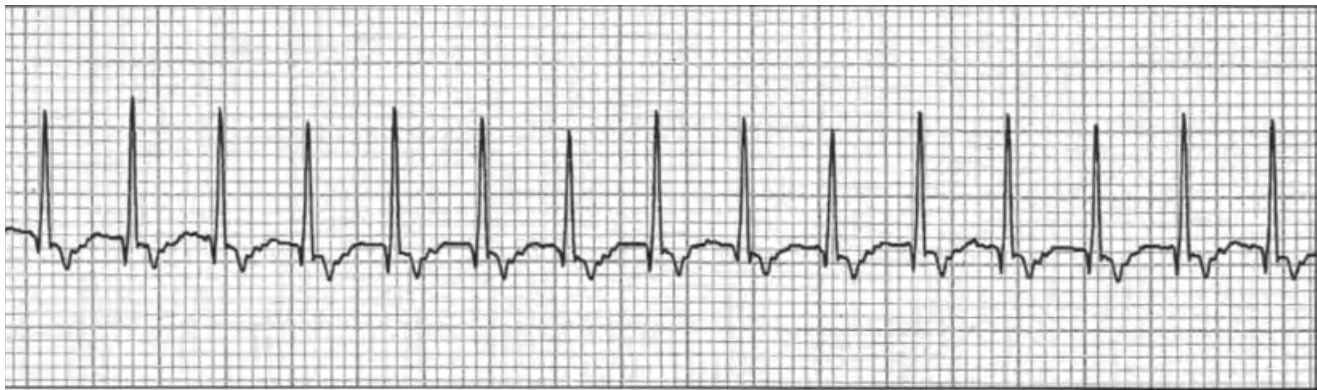
Figure 55.5 Lead II rhythm strip showing supraventricular tachycardia with clear P waves superimposed on the early part of the T wave. This is most consistent with accessory pathway tachycardia.

extensive atrial surgery, however, atrial flutter may be atypical without the usual sawtooth F waves. The ventricular rate may be regular or irregular; if regular, the ratio of atrial rate to ventricular rate can range from 2:1 (most frequent) to 8:1. With a reasonable ventricular rate, the arrhythmia is tolerated well for a long time, but with rapid ventricular responses, severe symptoms occur. Initial treatment should be with digoxin to increase the AV block and slow the ventricular rate; if this does not suffice, then propranolol, another β-blocker, or a calcium channel blocker (in older-aged children) can be added. Sometimes this treatment causes sinus rhythm to return, but if it does not, electrical cardioversion may be successful. Atrial flutter is rare in infants and children and is usually associated with structural heart disease, particularly with dilated atria. It sometimes occurs transiently in otherwise normal newborn infants. Because atrial flutter has been implicated in sudden death after a Mustard or Senning repair of transposition of the great

arteries, an aggressive approach to abolishing the arrhythmia has been recommended [6]. Interrupting the flutter circuit by catheter ablation or surgery is usually successful [7].

Atrial fibrillation

Atrial fibrillation is rare in children. It is characterized by disordered atrial activity. The ECG shows no P waves but instead has fine or coarse fibrillatory or f waves. The ventricular response is very irregular and usually rapid; generally it is difficult to find two exactly equal RR intervals. Treatment is initially with digoxin or other agents, such as diltiazem infusion, to decrease ventricular rate. If the atrium is enlarged, atrial fibrillation may be sustained. To restore sinus rhythm, antiarrhythmic agents, such as procainamide, sotalol, or ibutalide, may be employed, but cardioversion is generally more effective. To maintain sinus rhythm after it is restored, sotalol or amiodarone may be used. If the atrial fibrillation keeps recurring, the aim is to
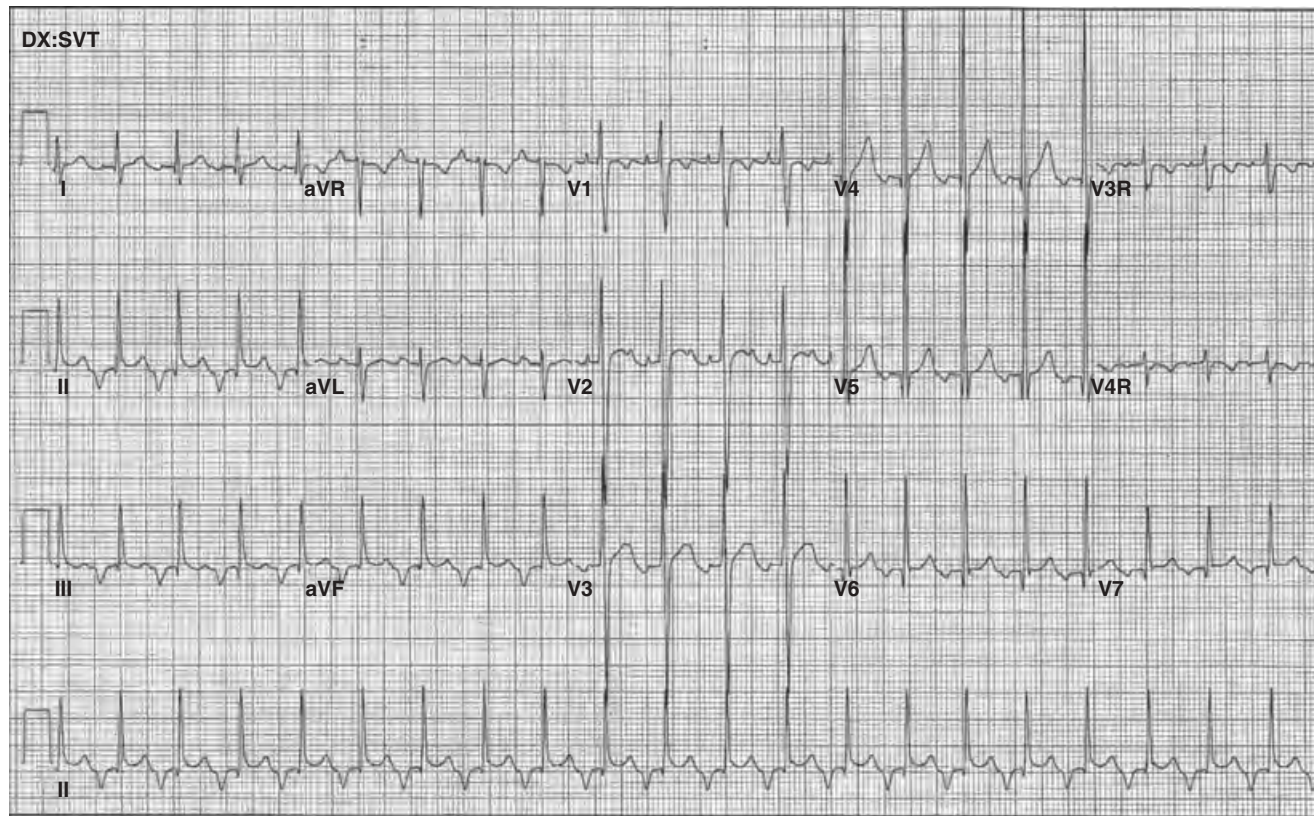
Figure 55.6 Persistent junctional reciprocating tachycardia (PJRT). Normal PR interval with inverted P waves in leads II, III, and AVF, and a relatively slow rate.
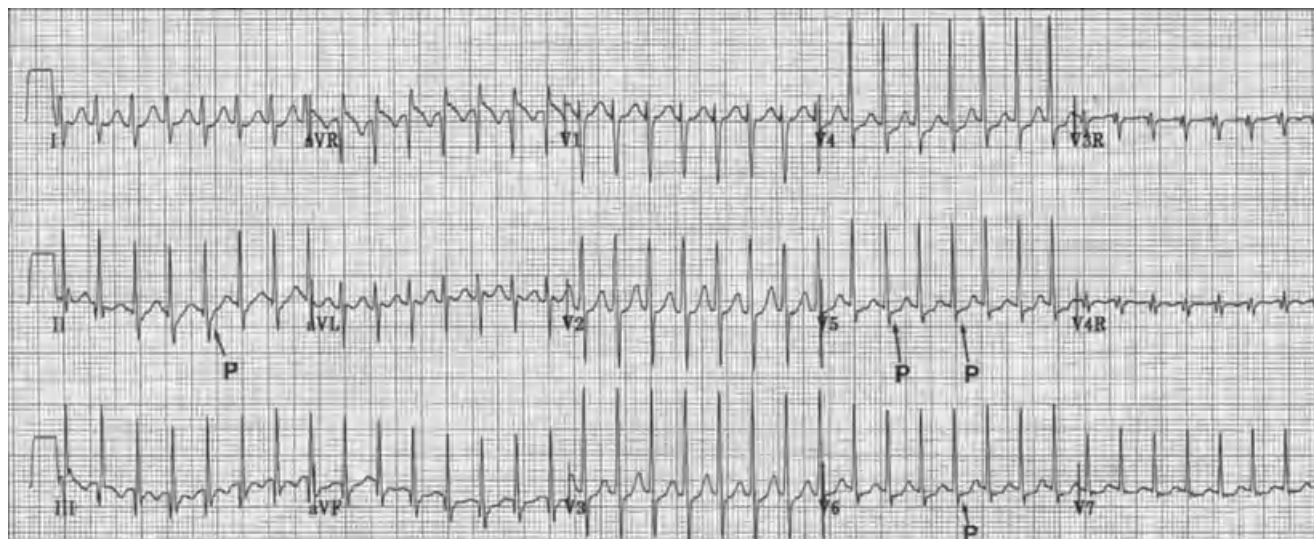
Figure 55.7 Atrioventricular node re-entry tachycardia (AVNRT). Lack of clearly discernible P waves, which are superimposed on the QRS. This can be barely appreciated on this tracing (arrows).

control the ventricular rate with digoxin; if ventricular rates still rise unduly with exercise, then propranolol or verapamil may be added. When atrial fibrillation occurs in the presence of an accessory pathway (WPW syndrome), conduction to the ventricle over the pathway may be dangerously rapid with wide QRS complexes. This is thought to be the mechanism of sudden death in this syndrome (Figure 55.9). Because digoxin may shorten the anterograde
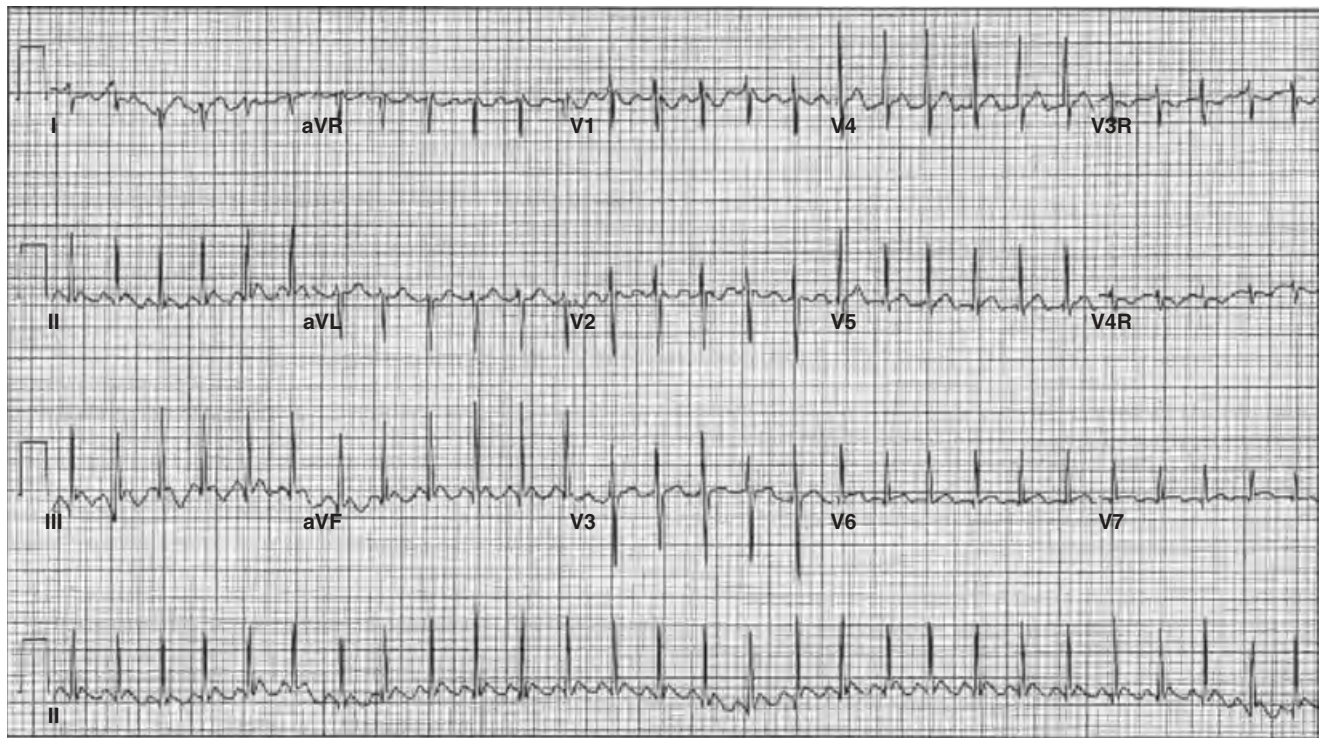
Figure 55.8 Atrial flutter with 2:1 atrioventricular conduction. The negative "F" waves are seen best in leads II, III, and AVF.
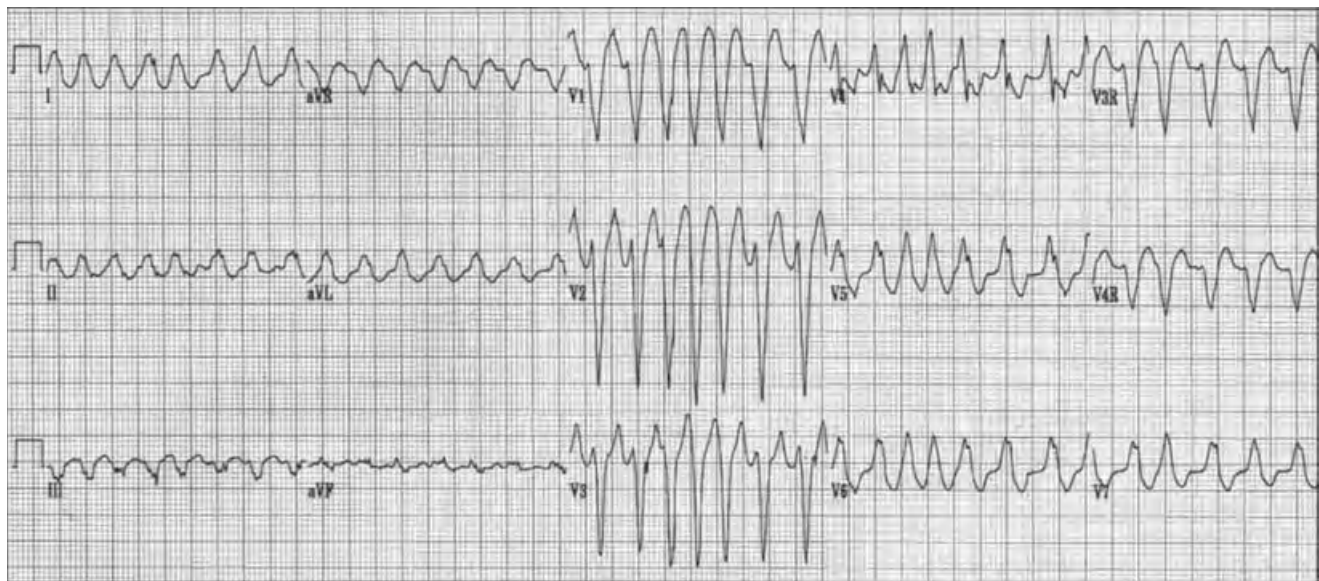
Figure 55.9 Atrial fibrillation in the presence of Wolff–Parkinson–White syndrome. Irregularly irregular ventricular rate and wide QRS complexes.

effective refractory period of the accessory pathway, allowing even faster ventricular rates, it is contraindicated for the acute and chronic treatment of patients of any age with the WPW syndrome, except when an electrophysiological study has documented that digoxin may be used safely [8].

Junctional ectopic tachycardia

An accelerated junctional pacemaker produces a ventricular rate that is faster than the underlying sinus rate. This rhythm occurs most often after surgery near the AV node (such as closure of ventricular septal defect), but there is a congenital form that is incessant and may lead to tachycardia-induced
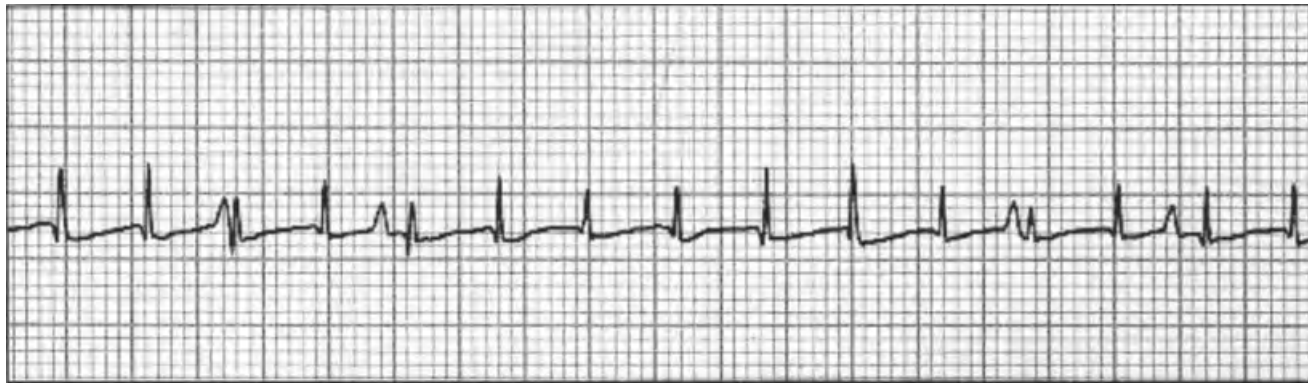
Figure 55.10 Junctional ectopic tachycardia (JET). Narrow QRS tachycardia with a slower atrial rate. QRS 5 demonstrates a shorter RR interval, due to sinus capture.
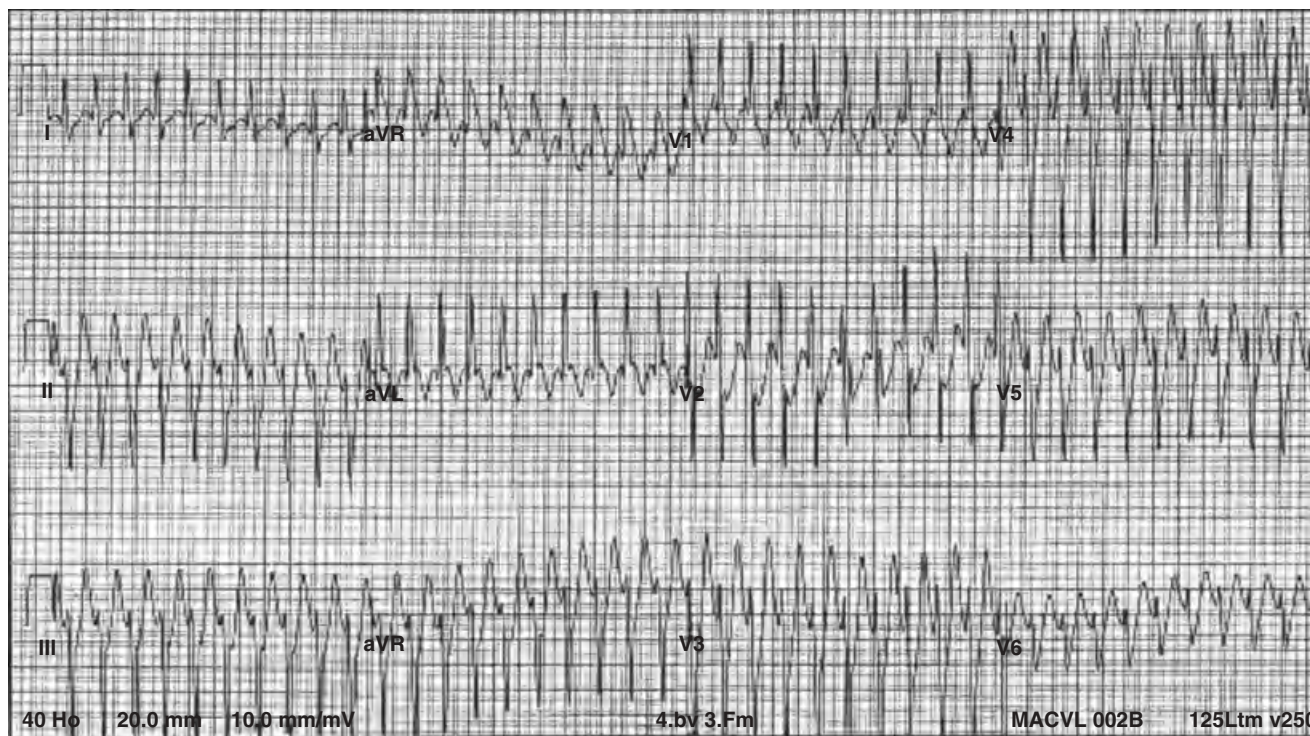
Figure 55.11 Ventricular tachycardia. In this tracing, there is no AV dissociation evident.

cardiomyopathy [9]. When an accelerated junctional focus is very fast, it is termed junctional ectopic tachycardia (JET). JET is recognized by narrow QRS tachycardia with AV dissociation (due to the slower sinus rate and lack of retrograde conduction). There may also be capture beats, in which a P wave occurs randomly at a time when anterograde conduction can occur, shortening the RR interval for one beat (Figure 55.10). In the postoperative period intravenous amiodarone is most often employed, along with atrial pacing to restore AV synchrony. Cooling the patient to around 34 °C may also be effective. In the congenital variety, the use of

β-blockers, flecainide, sotalol, and amiodarone has been reported. Catheter ablation is also effective, but with some risk of causing complete AV block [10,11].

Ventricular tachycardia

Ventricular tachycardia is defined as a series of three or more ventricular ectopic beats, often manifesting as a rapid tachycardia with wide QRS complexes (Figure 55.11). Although in children the QRS complex can be relatively narrow, its configuration always differs from the QRS in sinus rhythm. Often there is AV dissociation, with the P waves occurring

less often than QRS complexes; this may be seen by slight variations of the T waves caused by varying superimposition of P waves on them. In half of pediatric patients, there may be retrograde capture of the atria, particularly at slower ventricular rates; this results in a 1:1 relationship between atrial and ventricular contractions. The major differential diagnosis is from supraventricular tachycardia with aberrant conduction. Proof of the ventricular origin of the arrhythmia can be obtained if the QRS complexes resemble typical ventricular extrasystoles in previous ECGs or if ventricular fusion beats are seen.

Ventricular tachycardia may cause severe symptoms and, particularly in patients with structural heart disease, can lead to ventricular fibrillation. It should usually be treated as an emergency. Because most wide QRS tachycardias in children represent ventricular tachycardia, they should be treated as such unless one is certain of a supraventricular origin. Inappropriate treatment of ventricular tachycardia (with digoxin or verapamil, for example) may be fatal. Cardioversion is usually effective. If the patient is hemodynamically stable, amiodarone, lidocaine, or procainamide may be given intravenously. Future attacks may be prevented with propranolol, mexiletine, sotalol, flecainide, or amiodarone. Treatment decisions should always be made with a cardiology consultant. Occasionally, ventricular tachycardia occurs at a rate similar to a normal sinus rate, has a relatively narrow QRS complex, and is called ventricular accelerated rhythm. In the presence of an otherwise normal heart and without circulatory difficulties, it is benign [12]. It usually does not require treatment and, when seen in a newborn, episodes usually disappear within several weeks or months.

Ventricular fibrillation

Ventricular fibrillation produces a recording with no QRS complexes but just a wavy line. P waves can be present. There is no cardiac output, and cardiopulmonary resuscitation should be initiated immediately while preparations are made for electrical defibrillation.

Ventricular fibrillation is often the terminal event in many illnesses. It may follow hypoxemia, hyperkalemia, digitalis or quinidine intoxication, myocarditis, myocardial infarction, catecholamine infusions, anesthetics, and many drugs. It may be seen in patients with dilated cardiomyopathy. It is also a consequence of other arrhythmias, particularly ventricular tachycardia or multiple multiform ventricular ectopic beats.

Ventricular fibrillation may also occur in two other settings. Individuals with complete (third-degree) AV block have episodes of transient ventricular fibrillation that cause syncope (Adams–Stokes attacks) and indicate the need for an artificial pacemaker. Occasionally these attacks occur when the complete heart block is intermittent and is brought on by vagal or other stimuli. In the long QT syndrome, ventricular fibrillation also causes syncope and death. In this syndrome, the arrhythmia starts with an unusual form

of ventricular tachycardia called torsades de pointes; polymorphous QRS complexes seem to rotate around the isoelectric line. Several of these patients have died suddenly of fright or on hearing an unexpected loud noise. Nearly all of the congenital long QT syndromes are related to specific heritable abnormalities in cardiac potassium or sodium channels (Figure 55.2). Multiple specific genes coding for channels may be abnormal because of mutations or deletion, but a significant minority of patients with long QT syndrome have none of the known mutations. Treatment generally requires chronic β-adrenergic blockade. Some patients require an implantable cardioverter–defibrillator, particularly those with a history of aborted sudden death, or continued syncope despite appropriate β-blocker therapy, and or with the sodium-channel mutation (long QT 3) [13].

Mechanisms of bradycardia

Sinus bradycardia

Sinus bradycardia is recognized as a regular, slow atrial rate with normal P waves and 1:1 conduction. Causes include hypoxia, acidosis, increased intracranial pressure, abdominal distention, hypothyroidism, jaundice, and hypoglycemia. Agents such as digoxin, organophosphate pesticides, dexmedetomidine, and propranolol may cause sinus bradycardia. Mild heart rate slowing may also be due to increased vagal tone or cardiac conditioning in a trained athlete.

Atrioventricular block

Complete atrioventricular block may be congenital, surgically induced, or occur suddenly as a result of myocarditis or another infection, such as Lyme disease. It is recognized as atrioventricular dissociation, regular RR intervals, regular PP intervals, an atrial rate greater than the ventricular rate, and the absence of capture beats (Figure 55.12). Associated features of congenital AV block include maternal systemic lupus erythematosus (diagnosed or asymptomatic; anti-Ro antibody positive), whereas associated features of acquired heart block may include those of Lyme disease, Kearns-Sayre syndrome (mitochondrial inheritance, weakness, progressive external ophthalmoplegia, pigmentary retinal degeneration), or myotonic dystrophy (myotonia, weakness). There is an association with atrial septal defect and other congenital heart disease, due to mutations in the transcription factor Nkx 2.5 [14,15].

Second-degree AV block should be classified as Mobitz type 1 (Wenckebach) or Mobitz type 2. Wenckebach conduction is characterized by progressive PR interval prolongation followed by a blocked beat, followed by recovery of conduction (Figure 55.13). Type 2 block lacks this characteristic PR prolongation prior to block and subsequent shortening after the blocked beat. Type 1 generally has a better prognosis than type 2 and responds readily to medication.

Figure 55.12 Complete atrioventricular block. The atrial rate is higher than the ventricular rate and both atrial and ventricular rates are regular and not associated.

(a)
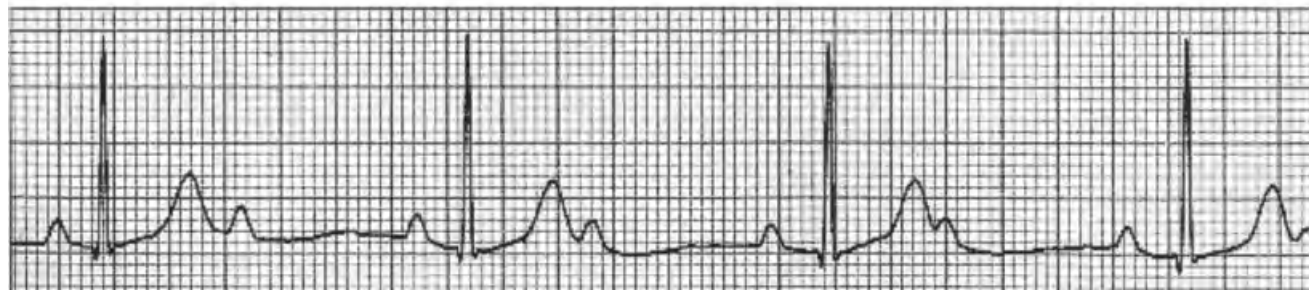
(b)

Figure 55.13 Second-degree AV block. On tracing (a), there is progressive PR prolongation followed by failure of conduction. On tracing (b), a 2:1 relationship is seen.

Other causes of bradycardia include (1) sinus exit block, in which sinus P waves intermittently disappear as impulses are blocked from leaving the region of the sinus node (rare in children), and (2) frequent premature atrial contractions occurring too early to be conducted to the ventricles. This slows the resulting ventricular rate (very common in infants).

Mechanisms of premature beats

Supraventricular premature contractions

Supraventricular premature contractions display narrow and early QRS complexes, but they occasionally are wide as a result of an associated bundle branch aberration. Those originating in the atrium [premature atrial contractions (PACs)]

should be recognizable by finding a premature P wave superimposed on and deforming the previous T wave. This sign may be subtle, and require examination of multiple ECG leads.

Ventricular premature complexes

Ventricular premature complexes (PVCs) are recognizable as wide, often bizarre, early beats, generally without preceding P waves. The differentiation between PVCs and aberrantly conducted supraventricular ectopic beats is sometimes difficult or impossible from a surface ECG. Although, traditionally, premature ventricular beats may be differentiated from supraventricular beats by a full compensatory pause, this sign is unreliable in children. The identification of fusion beats, in which a sinus beat occurs simultaneously with a premature beat, thus creating an intermediate morphology, is helpful and establishes the premature beat as ventricular in origin.

Clinical evaluation

General approach to evaluation

The starting point in the diagnostic evaluation of a cardiac arrhythmia is a careful history and physical examination and the recording of a baseline ECG (i.e., while the patient is not having the arrhythmia). In obtaining the patient's history, one is attempting to determine whether (1) the rhythm abnormality might be caused by a life-threatening problem; (2) the patient is experiencing episodes of tachycardia, premature beats, or bradycardia; (3) the symptoms are exercise related; and (4) there is structural cardiac disease. During the physical examination, structural heart disease can be identified and the cardiac rate and rhythm assessed. On the ECG, obvious evidence of a problem, such as a prolonged QT interval or the WPW syndrome, is sought. The QT interval varies with the heart rate. A corrected QTc interval may be determined by dividing the QT interval by the square root of the preceding RR interval. The normal QTc interval should be less than 0.44 s [16]. A life-threatening problem is suspected if episodes of palpitations are associated with near-syncope, syncope, severe chest pain, or aborted sudden death, or if there is a family history of the long QT syndrome or unexplained sudden death. Patients with a long QT interval are treated with β-adrenergic receptor blocking agents and avoidance of proarrhythmic drugs, which prolong the QT interval. Patients with normal QT intervals but who may have a life-threatening problem are referred for invasive electrophysiologic evaluation, to avoid delay in recording an episode and to initiate appropriate and early treatment of a dangerous arrhythmia.

Patients who do not have obvious evidence of a life-threatening arrhythmia are then differentiated by whether they are experiencing episodes of tachycardia or premature beats or bradycardia. Those with tachycardia proceed to a noninvasive evaluation (discussed later), with the goal of capturing an episode electrocardiographically for the purpose of diagnosis. An echocardiogram is obtained in those with evidence of structural heart disease. With electrocardiographic evidence of WPW syndrome, an echocardiogram is obtained, primarily to rule out associated Ebstein anomaly of the tricuspid valve or, rarely, hypertrophic cardiomyopathy. In patients with likely premature beats or bradycardia but no evidence of structural cardiac disease or an abnormal ECG, noninvasive evaluation is optional and based on symptom severity. If there is structural cardiac disease or an abnormal ECG (e.g., complete AV block), an echocardiogram is obtained, followed by a noninvasive evaluation. An invasive electrophysiologic study may be recommended, depending on the results of the noninvasive evaluation and the severity of the symptoms.

Noninvasive evaluation of the rhythm disturbance involves the use of a variety of diagnostic modalities short of an intracardiac electrophysiologic study. The goal is to capture an episode of the patient's symptom electrocardiographically. Patients whose symptoms are brought on by exercise are referred for exercise testing to attempt to reproduce the abnormal rhythm. If the exercise test is negative or the symptoms are unrelated to exercise, consideration of the frequency of symptoms leads to the use of either a Holter monitor, for those with daily symptoms, or transtelephonic incident recording, for those with less frequent symptoms. If incident recording is used, the correct mode for recording must be chosen. In general, if the episodes last <30 s, it is difficult for the patient or parent to locate the monitoring device, connect it, and make a recording before the symptom resolves. In such patients, a continuous memory-loop recorder is recommended. When a symptomatic episode is recorded, it is important to determine whether the symptom was in fact typical, because benign arrhythmias and sinus tachycardia may coexist with more serious conditions. Recording of multiple episodes increases the reliability of the diagnosis, particularly in patients who do not have a cardiac arrhythmia when they are symptomatic. The only definitive way to diagnose the cause of the palpitations is to record an ECG during the symptom. Nonetheless, information from the patient's history may help in diagnosing the problem and assessing the urgency of reaching a diagnosis.

Clinical history

The patient's description of the sensation is important. Sustained tachycardia is usually described as a "racing" heartbeat, whereas premature beats are usually described as skipping of a beat. For the latter symptom, the sensation of the heart stopping is likely caused by the pause that follows a premature beat. Abrupt onset of palpitations, with equally abrupt spontaneous termination, especially if paroxysmal, suggests supraventricular tachycardia and not sinus tachycardia. The duration and rate of the symptoms should be noted; for sustained fast rhythms, some assessment of likely rate may be obtained by asking the patient or parent to imitate the rhythm by tapping it out. Parents or patients may be taught to take the pulse during such episodes. Patients can usually tell whether the fast rhythm is regular or irregular. Fast rhythms, such as atrial fibrillation and often atrial flutter (with block), are irregular, whereas supraventricular tachycardia and ventricular tachycardia are usually regular.

Symptoms associated with palpitations give clues to the severity of the problem. The most ominous sign is syncope, defined as a sudden loss of consciousness with inability to maintain posture. Syncope occurs as a result of hemodynamic compromise caused by the arrhythmia (rapid supraventricular tachycardia, ventricular tachycardia, AV block). Patients with syncope associated with possible arrhythmia require full cardiac evaluation because of the possibility that future episodes may result in sudden death, depending on the underlying cardiac problem. Patients may complain of transient dizziness or lightheadedness, which suggests lesser hemodynamic compromise. Syncope is discussed in detail in Chapter 56.

Chest pain is occasionally reported but is often due to the strong, rapid heartbeat rather than to any coronary artery

abnormality. The sensation of the pulsations in the neck may signify atrioventricular nodal re-entrant tachycardia or ventricular tachycardia and is caused by contraction of the atria against closed atrioventricular valves, resulting in jugular venous regurgitation (cannon a waves).

Factors that elicit the symptom are important to note. For example, certain forms of ventricular tachycardia are elicited only by exercise [17]. These causes of arrhythmia may depend on sympathetic activity, and "stress" is frequently reported as an eliciting factor. Such patients may respond best to β-adrenergic receptor blocking agents.

Factors identified that terminate the episodes and the manner of termination also help in the diagnosis. Sustained fast heart rhythms that end suddenly are more likely re-entrant tachycardias, whereas those that slow gradually are more likely an automatic tachycardia. Termination by the Valsalva maneuver, gagging, or facial immersion in cold water suggests re-entrant supraventricular tachycardia, although atrial flutter may also terminate with these maneuvers.

The past medical history and review of systems are important, primarily for identifying structural cardiac disease and possible noncardiac causes of palpitations. The most important example of the latter is hyperthyroidism, which may manifest as sinus tachycardia or as atrial fibrillation. A history of deafness (some patients with prolonged QT syndrome), ocular disease (Kearns-Sayre syndrome: progressive ophthalmoplegia, pigmentary retinal degeneration, right bundle branch block or complete AV block), or muscle weakness (myotonic dystrophy: muscle weakness, myotonia, AV block) suggest specific underlying disorders.

Physical examination

Few specific physical findings aid in the diagnosis. Signs of structural cardiac disease are important because, if serious, patients tolerate arrhythmias poorly and are likely to have more complex and dangerous cardiac rhythms. Several specific cardiac abnormalities are strongly associated with arrhythmias. Patients with dilated cardiomyopathy often have a gallop rhythm or signs of heart failure and may have ventricular arrhythmias, including ventricular fibrillation. Those with hypertrophic cardiomyopathy have nonspecific ejection murmurs and an increased apical impulse; they are at risk for ventricular arrhythmias. Arrhythmias are often noted in patients with congenital heart disease both before and after corrective or palliative surgery. If one is fortunate enough to examine a patient in the midst of an episode, the rate, rhythm, blood pressure, and arterial and venous (cannon a jugular waves) pulsations should be noted.

Resting electrocardiogram

In all patients with symptoms suggesting a rhythm disturbance, a resting 15-lead ECG, obtained when the patient is asymptomatic, can indicate a specific diagnosis associated with arrhythmias, but unfortunately cannot exclude arrhythmias *per se.*

The PR interval normally increases with age [18]. Conduction time is shortened when an accessory pathway (WPW syndrome) bypasses the atrioventricular node. A long PR interval indicates prolonged conduction anywhere between the sinus node and the myocardium, but usually indicates atrioventricular node block. Diagnoses evident on a resting ECG include the WPW syndrome, the long QT syndrome, and conduction abnormalities, such as second-degree and third-degree atrioventricular block and premature beats. Nonspecific changes, such as T-wave abnormalities, may suggest a myocardial abnormality, and specific findings, such as left ventricular hypertrophy, may not provide a diagnosis but suggest hypertrophic cardiomyopathy.

Obviously, capturing the arrhythmia on an ECG is very helpful and expedites the diagnostic process.

The electrocardiographic diagnosis of the arrhythmia's mechanism is vital for determining the best treatment, particularly when antiarrhythmic medications are contemplated. Failure to document the tachycardia often leads to inappropriate treatment of patients with benign conditions, particularly sinus tachycardia and premature contractions.

Initially, the QRS duration and morphology during tachycardia are assessed as normal or increased. The "narrow" QRS tachycardias are usually caused by supraventricular tachycardia (Table 55.2). The "wide" QRS tachycardias may be caused by either ventricular tachycardia or supraventricular tachycardia with sustained aberration conduction or bundle branch block; in children, most wide complex tachycardias are ventricular tachycardias (Table 55.3).

Table 55.3 Recognition of tachycardia with prolonged QRS duration.

Diagnosis	Findings on electrocardiogram
Ventricular tachycardia	Often with AV dissociation Capture beats with narrower QRS than on other beats Fusion beats
Supraventricular tachycardia with pre-existing bundle branch block	QRS morphology similar to that in sinus rhythm QRS morphology is that of right or left bundle branch block
Supraventricular tachycardia with rate-dependent bundle branch block	QRS morphology usually similar to that of right or left bundle branch block Rare in small children Difficult to distinguish from ventricular tachycardia in children
Antidromic supraventricular tachycardia in Wolff-Parkinson-White syndrome	QRS morphology similar to pre-excited sinus rhythm, but wider Never with AV dissociation
Atrial fibrillation with Wolff-Parkinson-White syndrome	"Irregularly irregular" wide QRS tachycardia

Next, the relationship between P waves and QRS complexes is determined, if possible; this relationship is often diagnostic. For example, a narrow QRS tachycardia with atrioventricular dissociation and an atrial rate lower than the ventricular rate may be diagnosed as junctional ectopic tachycardia. For rhythms with a 1:1 relationship between P waves and QRS complexes, the relative timing of the respective waves is helpful. If P waves are close to the preceding QRS the diagnosis is likely to be AV reciprocating tachycardia; if close to the following QRS the diagnosis is likely to be either atrial tachycardia or persistent junctional reciprocating tachycardia; or if on top of QRS the diagnosis is likely to be AV node re-entry tachycardia. These characteristics help to differentiate between accessory pathway tachycardia, atrial tachycardia, and atrioventricular node re-entry. Although not completely reliable, an exact electrophysiologic diagnosis may be unnecessary for initial decisions concerning treatment.

Holter monitoring

Twenty-four-hour ambulatory monitoring (*Holter monitoring*) is commonly used to capture the rhythm abnormality on the ECG when symptoms occur. With Holter monitoring, the ECG is continuously recorded digitally (or on to magnetic tape) for 24h, capturing as many as three separate leads simultaneously, for later playback and analysis. The patient keeps a diary of events and symptoms. The Holter recording is examined at these times to determine the existing heart rhythm during the symptom. If symptoms occur daily, Holter monitoring is the most efficient method of diagnosis. It is particularly valuable in patients with frequent symptoms (many times per day) that are not clearly the result of an arrhythmia. In such patients, the recording of many symptom episodes that show no electrocardiographic abnormality provides strong and reassuring evidence against a dangerous cardiac arrhythmia. From the Holter recordings, additional information about cardiac conduction, average heart rates, response of sinus rates to normal daily exertion, and the prominence of atrial ectopy, or ventricular ectopy (premature beats), is obtained and may be useful diagnostically if an episode of palpitations is not captured.

Echocardiography

Echocardiography is helpful in diagnosing structural cardiac disease. Because many of the structural abnormalities (congenital heart disease, hypertrophic cardiomyopathy, rhabdomyoma, mitral valve prolapse) associated with arrhythmias are difficult to diagnose on physical examination and electrocardiography, certain patients require echocardiography. Patients with worrisome symptoms (syncope, chest pain, dyspnea, prolonged duration) and who may have life-threatening episodes of tachycardia should have an echocardiogram. In most patients with arrhythmias, the echocardiogram is normal.

Transtelephonic incident monitoring

When symptoms do not occur daily, Holter monitoring is inefficient, because several consecutive Holter recordings may be needed to capture a single episode or may not detect them. Transtelephonic incident recorders are small, battery-powered devices that the patient carries for 1 month or longer. When the symptom occurs, the patient makes a recording by placing the device on the chest or connecting it to wrist or chest electrodes. A single ECG lead is recorded into the device's memory for 60–120s. The patient then plays the recording back over the telephone to the clinician's office or monitoring center. The unit generates a series of signals that are decoded at the monitoring center into the ECG. For very transient symptoms, devices are available that are connected to the patient as with a Holter monitor and continuously record the heart rhythm in a memory loop. When a symptom is experienced, the patient presses a button, which causes the device to store an ECG for the 30–45s before and for a short period after the button was pushed.

For patients in whom the symptoms are very severe but very infrequent, and in whom standard loop recording has failed to capture an episode, implantable loop recorders are available [Reveal (Medtronic, Minneapolis, MN, USA), SJM Confirm (St. Jude Medical, St. Paul, MN, USA)]. These very small devices are implanted in the upper chest, like a pacemaker, and automatically capture arrhythmias. They can also be activated by the patient or a family member using a hand-held device. Stored electrograms are available for electronic downloading later [19,20].

Exercise testing

In some patients, an exercise test helps to elicit an episode of tachycardia or irregular heart rhythm and is a reasonable approach when symptoms are exercise related. The patient's ECG and blood pressure are monitored while the patient runs on a treadmill or rides a stationary bicycle (see Chapter 11). During the test, the work load is increased in discrete steps. The ECG is monitored during both exercise and recovery. Formal exercise testing, however, does not reproduce the type of exercise stress experienced by athletes, particularly the competitive stress. The failure to induce an arrhythmia with exercise testing does not exclude exercise-related arrhythmias.

Electrophysiology study

History of electrophysiology study

The His bundle was first recorded in 1969 and the technique was quickly adopted for use in children. In 1970, programmed stimulation techniques were incorporated with His bundle recordings and the electrophysiology study was developed [21–23]. This has become a powerful diagnostic tool and can be extremely helpful in determining arrhythmia risk and mechanism.

Principles and technical considerations

Education and family preparation are crucial when performing an invasive electrophysiology study. These studies are usually performed with conscious sedation or general anesthesia. In general, most patients who receive conscious sedation will receive a narcotic (such as fentanyl) and a benzodiazepine (midazolam). Midazolam is a good choice in electrophysiology studies because it lacks electrophysiologic effects [24]. A designated person monitors the patient's status and vital signs when using conscious sedation for EP studies. General anesthesia is being used more often as studies have become more complicated and smaller children are being studied. Propafol is a good anesthetic choice. Dexmedetomidine, commonly used as a sedation agent for cardiac catheterization, is not a good choice for electrophysiology studies, owing to its vagotonic effects [25].

Patients undergoing an EP study are usually positioned for a long procedure. The arms are positioned alongside the thorax to decrease brachial plexus injury. A full 12-lead ECG is placed. Oxygen saturation and blood pressure are continuously monitored. Defibrillation pads are routinely placed, to allow for rapid emergency defibrillation. Catheters are then inserted, usually via a femoral vein. Other approaches use the internal jugular vein or subclavian vein.

Catheter sizes come in a variety of sizes. Traditionally, 5 Fr catheters are used in young children and infants whereas 6 and 7 Fr catheters are used in older children and adolescents. The electrodes on this catheter vary in number and interval spacing. Most electrophysiology catheters are in a quadripolar configuration; however, 8, 10, and even 20 pole catheters are commonly used for mapping large areas.

Catheters are placed using fluoroscopy. Biplane fluoroscopy is helpful for precise catheter manipulation while mapping. Radiation exposure to the patient and staff must be carefully monitored and limited. The use of modern pulsed fluoroscopy with pulse rates of ≤ 7.5 pulsess^{-1} and proper shielding significantly decreases radiation exposure. Once catheters are in place, the tracings are displayed and recorded, usually in a bipolar manner. Most laboratories have an optical disk computer system which allows for recording and pacing of several signals simultaneously. This permits on-line measurements with a freeze-scope capability. The recording speed can be manipulated to allow for analysis of both tachycardias and bradycardias. A stimulator is also necessary to pace the heart at different cycle lengths.

Basic intracardiac study

Catheters are placed in four standard recording and stimulating positions within the heart: the right atrium, the right ventricular apex, the coronary sinus, and in the His bundle region. From these locations, electrograms can be recorded and the heart stimulated, allowing for the diagnosis of most arrhythmias. A variety of measurements and a formalized stimulation protocol are performed. Both surface ECG measurements and baseline measurements of the atrial–His (AH) and His–ventricular (HV) intervals are made. The AH interval may be prolonged in patients with AV nodal disease, receiving antiarrhythmic medications, or with increased vagal tone. HV interval prolongation usually reflects intrinsic His–Purkinje disease, or exposure to antiarrhythmic agents. A short HV is commonly present in patients with WPW syndrome.

EP testing usually consists of two basic pacing maneuvers performed in the atrium and ventricle. This first is rapid pacing at a set cycle length. This can determine AV block cycle length when performed in the atrium, and can occasionally elicit either atrial or ventricular arrhythmias. The other maneuver is programmed extrastimulation. An eight-beat drive train at a conventional cycle length is followed by premature stimuli. This sequence is repeated with the premature stimulus gradually shortened by 10 ms intervals until it fails either to conduct or to excite cardiac tissue. This interval indicates the effective refractory period for the site.

Although sinus node dysfunction is diagnosed by noninvasive testing and history, it can be formally evaluated by several pacing maneuvers. The two most common measurements are sinus node recovery time (SNRT) and sinoatrial conduction time (SACT). Sinus node recovery time measures the time for the sinus node to recover automaticity following overdrive suppression via atrial pacing. In a patient with a normal healthy sinus node it is short, but fairly prolonged (several seconds) in a patient with a diseased sinus node. Atrial pacing in the right atrium is performed for 30 s. The pacing is abruptly terminated, and the time for the sinus node to recover is then measured. This maneuver is repeated at faster pacing rates, and the maximum SNRT is recorded. The patient's concomitant sinus cycle length is then subtracted from the maximum SNRT to give a corrected sinus node recovery time (CSNRT). In children, CSNRT is usually <275 ms [26]. The SACT estimates conduction time through perinodal tissue. This is a measure of the time required for premature stimulus to penetrate into the SA node and reset the timing for the next normal sinus beat [27]. Single premature atrial contractions (PACS) are delivered either in sinus rhythm, or after an eight-beat drive train, and the coupling interval is made progressively shorter by 10 ms until atrial refractoriness is reached. The time from the paced beat to the next spontaneous beat is then measured (A2–A3). As the premature beat becomes more and more premature, the sinus node enters a "reset zone" where the extra beat penetrates the perinodal atrial tissue and resets the sinus node. At this point the A2–A3 reaches a plateau. Thus, during the reset zone, the A2–A3 represents three events, the conduction time of A2 into the sinus node, the spontaneous cycle length of the sinus node, and the conduction time out to the surrounding atrial muscle. Hence the SACT is calculated by subtracting the sinus cycle length from the A2–A3. The normal value for this is <200 ms [28].

The AV node and His–Purkinje system can also be examined during an EP study. The effective refractory period of the AV node is commonly measured. Dual AV nodal physiology can often be identified with atrial programmed stimulation, and is defined as an abrupt increase in the AH interval of 40–50 ms in response to a 10 ms decrease in S2 (a single induced premature beat). This can be a sign of AV nodal tachycardia. Occasionally in patients with His–Purkinje disease, block below the His bundle can be seen as two components – an S1 S2 This is usually considered a pathologic finding.

In a patient with SVT, an electrophysiology study serves several purposes. First, the SVT mechanism can be identified for a suitable target for ablation therapy (see below). If ablation cannot be performed, drug testing allows the prediction of a suitable anti-arrhythmic agent.

Second, SVT substrate can occasionally be identified by measuring the baseline intervals. In patients with WPW syndrome, a short HV interval diagnoses pre-excitation. The anterograde ventricular activation pattern can localize the accessory pathway in this situation, especially in patients with a left-sided pathway.

An atrial protocol is then performed, consisting of single premature stimuli that are shortened down to atrial refractoriness. This evaluates effective refractory periods, which can be very useful in patients with AVN re-entry tachycardia. Rapid atrial pacing can also be performed. These maneuvers can be repeated with an isoproterenol infusion to aid in inducing the arrhythmia. Finally, ventricular pacing can be performed to evaluate retrograde (VA) conduction and demonstrate eccentric atrial activation, suggesting an accessory pathway.

When ventricular tachycardia is suspected, programmed stimulation in the ventricle is often performed. The EP study can differentiate a wide complex SVT from VT, determine if a sustained VT can be elicited, and guide therapy, either ablative or medical. A ventricular protocol consists of pacing the ventricle with delivery of a single premature beat (S2) at several different cycle lengths. The S2 is progressively decreased by 10 ms increments until the effective refractory period of the local ventricular muscle is reached. Following this, double extra stimuli (S2, S3) and triple extra stimuli (S2, S3, S4) are delivered until the coupling intervals become too short to capture. This protocol is performed at two different ventricular locations, usually the right ventricular apex and right ventricular outflow tract. This is often repeated with the addition of a catecholamine, such as isoproterenol, to mimic stress/exercise.

Several responses to a ventricular protocol are commonly seen in a child. One is a short run (0–4 beats) of ventricular beats of the same morphology as the paced beats, which is commonly termed a repetitive ventricular response. This is likely due to bundle branch re-entry and is not believed to be a pathologic rhythm. Another is nonsustained ventricular tachycardia, defined as any ventricular arrhythmia which lasts from >4 beats to 30 s. If the arrhythmia lasts >30 s, or requires pacing or cardioversion for treatment, it is considered sustained ventricular tachycardia. These rhythms are further characterized as monomorphic, polymorphic, or ventricular fibrillation depending on QRS morphology and cycle length. These sustained rhythms are predictive of sudden death in children with congenital heart disease [29].

Advanced mapping techniques

Arrhythmia mapping has undergone major changes in the last decade. Several computer-based methods allow three-dimensional visualization of electrical and anatomic information. Complex arrhythmias in congenital heart disease can be mapped better with less fluoroscopy time. A noncontact mapping system uses electrical signals in the blood pool of a chamber to derive an inverse solution for the signals on the endocardial surface (EnSite, St Jude Medical) [30,31]. This system is particularly attractive in patients with nonsustained tachyarrhythmias or those with hemodynamically unstable rhythms. Electroanatomic mapping systems (CARTO, Biosense-Webster, Baldwin Park, CA, USA, and Nav-X, St. Jude Medical) use a set of magnets to identify catheter location and orientation in three-dimensional space [32]. Three-dimensional activation, propagation, and voltage maps can be constructed. Both systems currently allow integration of other imaging modalities, such as CT and intracardiac echocardiography, to their systems to allow for better anatomic visualization. One of their potential advantages is the ability to perform EP studies and ablations with less fluoroscopy, a major concern in a developing child [33].

Therapeutic EP interventions

An invasive "cure" for re-entrant SVT was first described in 1969 when Sealy *et al.* surgically ablated the aberrant pathway in a patient with WPW syndrome [34]. This began for many arrhythmias an era of invasive procedures which has progressed from open chest operations and uncontrolled higher energy direct current (DC) shocks through a catheter to routine controlled elective radiofrequency and cryoenergy catheter ablation in children [11,35–37]. At present many arrhythmias can either be cured or modified with the catheter techniques, including re-entrant rhythms, such as AVRT, AVNRT, atrial flutter, automatic atrial tachycardias, and ventricular tachycardias [38,39].

Either of two major energy sources is commonly utilized for destruction of myocardial tissue: radiofrequency and cryoenergy. Radiofrequency current heats tissue to destroy myocardial cells. Huang *et al.* attempted a closed-chest ablation of the AVN using catheter-delivered radiofrequency energy in 1987 [40]. This technique was quickly adopted, with reports of use for both AV node and pathway ablation appearing soon after [41]. The mechanism behind the cell destruction has been delineated [42,43]. Cell death results from protein denaturation and dehydration. Lesion size

grows exponentially with time. Temperature decreases hyperbolically with distance from the catheter tip [42]. Radiofrequency ablation quickly became the primary modality for therapeutic arrhythmia management.

Cryoablation has become established as an alternative for a subset of arrhythmic substrates. Cryoablation uses circulating nitrous oxide through the catheter tip to cool tissue to a temperature of –75 °C. Hypothermia causes myocardial cells to become more acidic, secondary to slower ion pump transportation, and slowing metabolism [44]. These effects are transient if the exposure to hypothermia is brief. However, with ice crystal formation, permanent tissue injury occurs. The ice crystals initially damage mitochondria and distort cellular membranes [45,46]. This is followed by hemorrhage and inflammation secondary to dehydration and ultimate necrosis of the cell [47,48]. Cryolesions tend to be well circumscribed with distinct borders and have less thrombogenic potential than do radiofrequency lesions [49]. This has led many centers to use cryoablation in patients with arrhythmogenic foci near the AV node. Successful cryoablation in the septal region has been reported with no episodes of incidental heart block [35,50].

Transesophageal study

Transesophageal pacing is useful in both diagnosis and therapy of a wide range of arrhythmias, particularly in the differentiation and therapy of supraventricular rhythms. It has been especially beneficial in small children because of its ease of use and relatively noninvasive nature.

History

Max Cremer was the first to record a transesophageal electrogram in 1906, when he persuaded a sword swallower to swallow an electrode under fluoroscopic guidance. In the 1960s, low-energy defibrillation of the atrium and emergency ventricular pacing were performed via the esophagus [51,52]. In the 1980s, esophageal pacing was reported as a therapeutic tool in AVNRT and atrial flutter [53–55]. This technology can predict the recurrence of SVT and drug efficacy in neonates with some success [56]. It is accepted for diagnosis and therapy in pediatric electrophysiology, especially in young infants where a more invasive electrophysiology study may be difficult.

Technical considerations

Adequate education and preparation of the patient and family are important before performing pediatric transesophageal pacing. Usually mild sedation is all that is required to maximize patient cooperation and comfort while performing a transesophageal study. Intravenous midazolam (0.05–0.1 mg kg^{-1}) and/or fentanyl (0.5–1.0 μg kg^{-1}) are often used. It is important to consider a sedation/pain strategy, as it is extremely difficult to perform a study in an uncooperative and anxious patient.

A transesophageal study can be performed in both inpatient and outpatient settings. A surface ECG and oxygen saturation monitoring should be used. A DC cardioverter–defibrillator should be present and personnel should be well versed in sedation monitoring and advanced life support.

Three major components are necessary for performing transesophageal pacing studies: the electrode catheter, the recording equipment, and the stimulator. There are several different models of transesophageal catheters, ranging in size from 4 to 10 Fr with differing interelectrode distances (2–30 mm) and differing number of electrodes (bipolar to hexapolar). Interelectrode distance has no significant effect on pacing thresholds regardless of age or size [57].

Placement of the catheter is similar to that of a nasogastric tube, and involves lubrication (lidocaine gel can be helpful). The catheter is placed through the nares and advanced through the posterior pharynx to the esophagus. Optimal catheter position is determined by patient height and can be facilitated by fluoroscopic visualization. Minor adjustment may be necessary to achieve the optimal pacing location. The catheter is then secured with tape to the patient's face.

A simple ECG machine can act as the recording equipment. A three-channel continuous recording ECG may be configured for two surface leads while the unipolar esophageal lead can be connected to one of the precordial leads (V1) This allows for comparison of the P waves on the surface leads with the esophageal electrograms. Recording during pacing can occur without recording of the atrial esophageal electrogram. Alternatively, a bipolar recording system may be used. The advantage of this system is that more reproducible and reliable electrograms can be produced. This system requires a preamplifier which can be set with a high-pass filter at 20 Hz.

The stimulator ideally should be able to deliver a pacing stimulus with a long pulse width (10–20 ms) and a high current (up to 50 mA). Pulse widths greater than the standard 2 ms used in intracardiac pacing are required to capture the atrium from inside the esophagus. Usually successful atrial pacing can be accomplished with a pulse width of 6–10 ms and a current of 10–15 mA [57,58]. Patient discomfort is often reported with currents >15 mA (at a constant pulse width of 10 ms) [57,58]. Successful pacing with minimal discomfort can be achieved in >90% of pediatric patients [53,54,59,60].

Pacing protocols are usually limited to atrial pacing for practical reasons. The protocols can include sinus node testing by measuring sinus node recovery times. AV conduction can be assessed with atrial overdrive pacing to measure AV block cycle length and determine AV nodal and atrial tissue refractory periods with premature atrial extrastimulation. SVT mechanisms can be identified by assessing means of inducibility, termination, and VA conduction. Drug therapy can be tested by SVT provocation before and after drug administration.

Complications of transesophageal pacing are rare and mostly minor [61]. Trauma to the mucosa from insertion of the catheter and discomfort are the most frequently reported. Rarely, inadvertent ventricular pacing can result in ventricular arrhythmias which may require cardioversion.

Emergency treatment

Tachycardia

Immediate treatment of patients with sustained symptomatic tachycardia starts with an assessment of the patient's hemodynamic status. Patients with signs of shock require immediate cardioversion, whatever the mechanism of tachycardia. Other modalities may be tried first in patients who are less symptomatic. Patients with a wide QRS during tachycardia should probably undergo electrical cardioversion because of the high likelihood that the rhythm is ventricular tachycardia. Intravenous lidocaine may be used alternatively, provided that the diagnosis of ventricular tachycardia is certain and the hemodynamic status is stable (Table 55.4). In uncertain diagnoses, intravenous procainamide may be effective in ventricular tachycardia and most forms of supraventricular tachycardia.

In patients with a normal QRS duration, maneuvers to increase vagal tone should used initially. Older children may be coached through a Valsalva maneuver or facial immersion in ice water, whereas younger children may have gagging induced, have rectal stimulation, or, more often, have an ice bag applied to the face. Although these measures often work, a time limit should be set so that the patient's hemodynamic status does not deteriorate during prolonged unsuccessful attempts. If maneuvers fail, the administration of adenosine intravenously is the preferred approach (Table 55.4) with continuous electrocardiographic monitoring in a room with a cardioverter-defibrillator available. Adenosine is given by very rapid intravenous injection at an initial dose of 0.05 mg kg^{-1}, and the ECG is observed for 10–15 s. If there is no effect, the dose is repeatedly doubled until a dose of 0.40 mg kg^{-1} is reached (maximum 24 mg in adolescents and adults). In patients with tachycardia involving the atrioventricular node (accessory pathway tachycardia, atrioventricular node re-entry), adenosine should terminate it by stopping atrioventricular conduction for 1–2 s. In patients with sinus or atrial tachycardia or atrial flutter, adenosine causes a short episode of atrioventricular block, and the underlying atrial rhythm is revealed on the continuous ECG recording. If the diagnosis is shown to be atrial tachycardia or flutter, patients >6 months old may receive intravenous verapamil. Those <6 months old should never receive verapamil; instead, they may undergo pace conversion using esophageal pacing or cardioversion, or may receive intravenous procainamide.

Many patients may not require long-term treatment if the episodes are not severely symptomatic and are either self-limited or easily converted with vagal maneuvers. If suppressive drug therapy is indicated, depending on the likely diagnosis, various medications may be used, including digoxin, β-blockers, verapamil, flecainide, sotalol, and amiodarone (Table 55.5). The last three agents are more potent

Table 55.4 Intravenous antiarrhythmic agents.

Agent	Dosage	Comments
Verapamil	0.1–0.2 mg kg^{-1} i.v., 5–10 mg maximum	Beware of hypotension Definitely contraindicated under 6 months of age, probably under 12 months of age Do *not* give with β-blockers
Esmolol	500 µg kg^{-1} over 1 min, then 50–250 µg kg^{-1} min^{-1} continuous infusion	Monitor pulse, blood pressure Contraindicated in those with asthma and those with congestive heart failure Do *not* give with verapamil
Procainamide	10–15 mg kg^{-1} i.v. over 30 min	May cause hypotension; continuous monitoring is essential Cardiology guidance is recommended
Digoxin	10 µg kg^{-1} i.v. as initial load Second dose in 6 h, third at 24 h	Do not use in hypokalemia or if digoxin toxicity is suspected
Lidocaine	1–2 µg kg^{-1} i.v. over 15 min	Continuous infusion 30–50 µg kg^{-1} min^{-1}
Phenylephrine	0.02 mg kg^{-1} i.v. slowly	Used for raising blood pressure and eliciting a baroreceptor vagal reflex
Adenosine	Starting i.v. dose: 0.05 mg kg^{-1}; double dose repeatedly until effect is seen, to maximum of 0.4 mg kg^{-1}	Contraindicated in pre-existing second- or third-degree AV block without pacemaker Use with caution in severe asthma; half-life is 10 s in serum

Table 55.5 Oral antiarrhythmic medications.

Agent	Dosage[a]	Comments
Propranolol	0.25–1 mg kg^{-1} p.o. every 6 h	Observe for wheezing and symptoms of hypoglycemia
Atenolol	0.5–2 mg kg^{-1} per day p.o. divided every 8 h	
Procainamide	50–100 mg kg^{-1} per day p.o. divided every 8 h	Monitor both procainamide and *N*-acetylprocainamide levels
Quinidine sulfate	30–60 mg kg^{-1} per day p.o. divided every 6 h	
Flecainide	50–200 mg m^{-2} per day p.o. divided every 12 h or 6.7–9.5 mg kg^{-1} per day divided every 8 h	Flecainide levels >1.0 mg ml^{-1} correlate with toxic effects
Mexiletine	1.4–5.1 mg kg^{-1} p.o. every 8 h	
Digoxin	10 mg kg^{-1} p.o. as initial load Second dose in 6 h, third in 24 h; reduce dosage in premature infants	Do not use in hypokalemia or if digoxin toxic reaction is suspected
Sotalol	2–8 mg kg^{-1} per day p.o. divided every 8 h	Torsades de pointes is likely with hypokalemia. Monitor ECG for QT prolongation
Amiodarone	5 mg kg^{-1} p.o. b.i.d. × 2 weeks, then 2.5 mg kg^{-1} p.o. b.i.d.	Monitor thyroid and pulmonary function

[a]b.i.d., twice per day; p.o., orally.

antiarrhythmic agents than the others and are associated with increased risk of side effects.

Intracardiac catheter ablation techniques during cardiac catheterization using radiofrequency energy are available for pediatric patients with nearly all forms of abnormal tachycardia and may be offered to ease life-threatening tachycardia. In older children this treatment may be used as an alternative to long-term medication therapy, or in younger children it may be used when medication fails to control the tachycardia.

Finally, in selected patients who are found to have life-threatening ventricular arrhythmias not amenable to ablation and not reliably prevented or controlled by medication, the use of implantable cardioverter–defibrillators may be appropriate. These devices are implanted in a procedure similar to that used for pacemaker implantation, and they detect and terminate dangerous ventricular arrhythmias either by rapid pacing or by the delivery of a high-voltage shock to the heart.

Bradycardia

The hemodynamic effect of a slow heart rate depends on the difference from the patient's usual heart rate. Sudden heart rate decreases may be poorly compensated by increases in stroke volume, particularly in those with limited cardiac function. Moderate sinus bradycardia in normal children rarely necessitates treatment. Underlying causes, such as hypothyroidism, should be corrected. Patients with third-degree AV block and those with severe sinus node dysfunction may require permanent artificial cardiac pacing. The occurrence of symptoms (over and above the symptom of palpitations) such as syncope, exercise intolerance, or dizziness prompts pacing. With severe sinus node dysfunc-

tion, pacing may be required if the patient is to be given antiarrhythmic agents to suppress episodes of tachycardia because of the danger that such medications will worsen sinus node dysfunction. Patients with persisting complete AV block as a result of cardiac surgery generally require pacing, even in the absence of symptoms. Prophylactic cardiac pacing may be recommended in completely asymptomatic patients with complete congenital AV block who are at greater risk for progressing to syncope or sudden death.

Therapy for specific tachyarrhythmias

Accessory pathway tachycardia (including Wolff-Parkinson-White syndrome)

Acute and chronic treatment can be directed at either the anterograde AV node conduction or the retrograde accessory pathway conduction. β-Blockers, digoxin, or calcium channel blockers affect the anterograde limb of the re-entrant circuit. The retrograde accessory pathway conduction is affected by procainamide or flecainide [62]. Long-term management depends on the severity of the problem and the frequency of the attacks. For children with rare, mildly symptomatic attacks of supraventricular tachycardia that are easily terminated, we advise no treatment at all. Infants and children with more frequent or symptomatic attacks are treated initially with β-blockers. Digoxin is used only if there is no evidence of pre-excitation in sinus rhythm. About one-third of adults with pre-excitation treated with digoxin have a shortening of the anterograde ERP of the accessory pathway, which could be dangerous if atrial fibrillation develops. Although atrial fibrillation is uncommon in infants and digoxin has been used for years to treat children with

pre-excitation, with few if any documented problems, some reports suggest the possibility of sudden death in infants treated with digoxin [63].

Transcatheter ablation of the accessory pathway is increasingly being used as first-line therapy in children. Its use in infants is still limited because of complications of perforation, AV block, and damage or occlusion of major coronary arteries. In addition, the natural history of accessory pathway tachycardia in infancy is favorable: 75–90% have spontaneous resolution of tachycardia by 12 months of age [64]. Ablation is reserved for patients with life-threatening, medically refractory tachycardias, as in those with PJRT and dramatically compromised left ventricular function.

Atrioventricular node re-entry tachycardia

Short-term treatment of AV node re-entrant tachycardia is directed at achieving a brief episode of AV block. Neonates might respond to vagal maneuvers or rectal stimulation. If vagal measures fail, the first choice of medication is intravenous adenosine. Other effective treatments include intravenous esmolol or digoxin, and esophageal or intracardiac atrial overdrive pacing is effective. Neonates with refractory AVNRT also respond to electrical synchronous cardioversion.

The natural history is unknown, but the condition may well disappear with time. Therefore, it is reasonable to treat such infants with antiarrhythmic medications for several years with the hope of avoiding transcatheter ablation.

Persistent junctional reciprocating tachycardia

Treatment of children with PJRT is challenging. In addition to the techniques and drugs used for children with WPW syndrome, amiodarone is often effective, and spontaneous resolution is occasionally observed [3].

Atrial flutter

Therapy is directed towards either converting the flutter to sinus rhythm or limiting the ventricular response. Vagal maneuvers can convert the rhythm. Digoxin, propranolol, or esmolol can slow the ventricular response and assist in converting the tachycardia.

Procainamide can convert the tachycardia, but may slow the atrial rate without converting the rhythm. If the faster atrial rate is associated with variable AV conduction, the slower rate can allow 1:1 AV conduction, paradoxically increasing the ventricular rate. For this reason, procainamide should be used only after a drug, such as digoxin, that limits AV conduction has been given.

If immediate tachycardia conversion is necessary, the first choice is esophageal atrial overdrive pacing. This method is effective, particularly in small children, and does not require anesthesia. In postoperative cardiac surgical patients, temporary atrial pacing wires can be used. If this method fails or is unavailable, electrical cardioversion with deep sedation or anesthesia will be effective.

For long-term treatment, the first choice is oral digoxin or propranolol. If this therapy fails, sotalol, is given three times per day [65]. Other choices are flecainide, two or three times per day, or propafenone, three times per day.

Atrial flutter in the newborn period often disappears within the first 6 months of life. Traditionally, such infants have been treated with digoxin for 1 year; after conversion they can probably be followed without medication.

Atrial ectopic tachycardia

Treatment of AET is difficult, and rate control may be the only achievable response to therapy. The atrial focus may be slowed by β-blockers, flecainide, or propafenone or by class III agents, such as sotalol and amiodarone. The goal of treatment is to protect against the subsequent development of tachycardia-induced cardiomyopathy. Intervention to cure the tachycardia, either by radiofrequency ablation or cryoablation, or by surgical cryoablation, should be performed at the earliest echocardiographic signs of reduced cardiac function [5].

Junctional ectopic tachycardia

The pharmacologic approach to AET can also be effective in treating JET. Although no agent is reliably effective in treating this arrhythmia, amiodarone is often effective. In selected patients, transcatheter ablation can eliminate the junctional focus. In very small infants, the proximity of the JET focus to the AV node increases the risk of causing complete AV block at the ablation. This risk is likely lower with cryoablation. Permanent pacemaker implantation is used in the sickest infants who have not responded to antiarrhythmic agents [10].

Postoperative JET is usually seen in infants with low cardiac output. JET could be caused by the poor cardiac output or could contribute to the hemodynamic compromise. Intravenous amiodarone is widely used for JET. Surface cooling can slow the junctional rate, allow effective AV sequential pacing, and restore AV synchrony, which often improves the cardiac output. Unlike congenital JET, postoperative JET is transient and resolves as the myocardium recovers [66].

Ventricular tachycardia

Pharmacologic suppression of ventricular tachycardia, when induced by catechol stimulation, includes the use of moderate to high doses of β-blocking medications. When unsuccessful, or when the ventricular tachycardia does not depend on catecholamine stimulation, class I agents, such as mexiletine, and flecainide can be used. Class III agents, such as sotalol and amiodarone, might also be effective. Infants with accelerated ventricular rhythm probably do not require treatment, because the tachycardia rate is not fast enough to produce hemodynamic compromise and the rhythms usually resolve by several months of age [12].

Premature beats

Premature beats of any kind without tachycardia rarely need treatment. Ventricular premature contractions may occasionally require treatment when

1 The contractions are multiform.

2 The contractions occur in couplets or in short runs of ventricular tachycardia.

3 The contractions follow a recently converted ventricular tachycardia.

4 The contractions exhibit the "R on T" phenomenon (i.e., they fall repeatedly on the early part of the T wave of the preceding beat).

Decisions concerning treatment of premature beats are difficult and should be made in consultation with a cardiologist. Possible inciting factors, such as drugs, hypoxia, and acidosis, should be corrected. If ventricular premature contractions require emergency treatment, the agent of choice is lidocaine, given by a continuous intravenous infusion. Bretylium has also been used to terminate ventricular tachycardia.

References

1 Lankipalli RS, Zhu T, Guo D, Yan GX. Mechanisms underlying arrhythmogenesis in long QT syndrome. *J Electrocardiol* 2005;**38** (4 Suppl):69–73.

2 Samson RA, Atkins DL. Tachyarrhythmias and defibrillation. *Pediatr Clin North Am* 2008;**55**:887–907.

3 Vaksmann G, D'Hoinne C, Lucet V, *et al.* Permanent junctional reciprocating tachycardia in children: a multicentre study on clinical profile and outcome. *Heart* 2006;**92**:101–4.

4 Porter MJ, Morton JB, Denman R, *et al.* Influence of age and gender on the mechanism of supraventricular tachycardia. *Heart Rhythm* 2004;**1**:393–6.

5 Salerno JC, Kertesz NJ, Friedman RA, Fenrich AL Jr. Clinical course of atrial ectopic tachycardia is age-dependent: results and treatment in children <3 or ≥3 years of age. *J Am Coll Cardiol* 2004;**43**:438–44.

6 Garson A Jr, Bink-Boelkens M, Hesslein PS, *et al.* Atrial flutter in the young: a collaborative study of 380 cases. *J Am Coll Cardiol* 1985;**6**:871–8.

7 Triedman JK, Alexander ME, Berul CI, *et al.* Electroanatomic mapping of entrained and exit zones in patients with repaired congenital heart disease and intra-atrial reentrant tachycardia. *Circulation* 2001;**103**:2060–5.

8 Perry JC, Garson A Jr. Diagnosis and treatment of arrhythmias. *Adv Pediatr* 1989;**36**:177–99.

9 Villain E, Vetter VL, Garcia JM, *et al.* Evolving concepts in the management of congenital junctional ectopic tachycardia. A multicenter study. *Circulation* 1990;**81**:1544–9.

10 Collins KK, Van Hare GF, Kertesz NJ, *et al.* Pediatric nonpostoperative junctional ectopic tachycardia medical management and interventional therapies. *J Am Coll Cardiol* 2009;**53**:690–7.

11 Van Hare GF, Velvis H, Langberg JJ. Successful transcatheter ablation of congenital junctional ectopic tachycardia in a ten-month-old infant using radiofrequency energy. *Pacing Clin Electrophysiol* 1990;**13**:730–5.

12 Levin MD, Stephens P, Tanel RE, *et al.* Ventricular tachycardia in infants with structurally normal heart: a benign disorder. *Cardiol Young* 2010;**20**:1–7.

13 Zareba W, Moss AJ. Long QT syndrome in children. *J Electrocardiol* 2001;**34**(Suppl):167–71.

14 Benson DW, Silberbach GM, Kavanaugh-McHugh A, *et al.* Mutations in the cardiac transcription factor NKX2.5 affect diverse cardiac developmental pathways. *J Clin Invest* 1999;**104**:1567–73.

15 Jay PY, Harris BS, Buerger A, *et al.* Function follows form: cardiac conduction system defects in Nkx2.5 mutation. *Anat Rec A Discov Mol Cell Evol Biol* 2004;**280**:966–72.

16 Garson A Jr. How to measure the QT interval – what is normal? *Am J Cardiol* 1993;**72**:14B–16B.

17 Tester DJ, Kopplin LJ, Will ML, Ackerman MJ. Spectrum and prevalence of cardiac ryanodine receptor (RyR2) mutations in a cohort of unrelated patients referred explicitly for long QT syndrome genetic testing. *Heart Rhythm* 2005;**2**:1099–105.

18 Davignon A, Rautaharju P, Barselle E, *et al.* Normal ECG standards for infants and children. *Pediatr Cardiol* 1979/80;**1**:123–34.

19 Frangini PA, Cecchin F, Jordao L, *et al.* How revealing are insertable loop recorders in pediatrics? *Pacing Clin Electrophysiol* 2008;**31**:338–43.

20 Sreeram N, Gass M, Apitz C, *et al.* The diagnostic yield from implantable loop recorders in children and young adults. *Clin Res Cardiol* 2008;**97**:327–33.

21 Denes P, Wu D, Dhingra R, *et al.* The effects of cycle length on cardiac refractory periods in man. *Circulation* 1974;**49**:32–41.

22 Roberts NK, Olley PM. His bundle recordings in children with normal hearts and congenital heart disease. *Circulation* 1972;**45**:295–9.

23 Scherlag BJ, Lau SH, Helfant RH, *et al.* Catheter technique for recording His bundle activity in man. *Circulation* 1969; **39**:13–8.

24 Yip AS, McGuire MA, Davis L, *et al.* Lack of effect of midazolam on inducibility of arrhythmias at electrophysiologic study. *Am J Cardiol* 1992;**70**:593–7.

25 Hammer GB, Drover DR, Cao H, *et al.* The effects of dexmedetomidine on cardiac electrophysiology in children. *Anesth Analg* 2008;**106**:79–83,

26 Yabek SM, Jarmakani JM, Roberts NK. Sinus node function in children. Factors influencing its evaluation. *Circulation* 1976;**53**:28–33.

27 Strauss HC, Saroff AL, Bigger JT Jr, Giardina EG. Premature atrial stimulation as a key to the understanding of sinoatrial conduction in man. Presentation of data and critical review of the literature. *Circulation* 1973;**47**:86–93.

28 Kugler JD, Gillette PC, Mullins CE, McNamara DG. Sinoatrial conduction in children: an index of sinoatrial node function. *Circulation* 1979;**59**:1266–76.

29 Alexander ME, Walsh EP, Saul JP, *et al.* Value of programmed ventricular stimulation in patients with congenital heart disease. *J Cardiovasc Electrophysiol* 1999;**10**:1033–44.

30 Schilling RJ, Peters NS, Davies DW. Noncontact mapping of cardiac arrhythmias. *J Electrocardiol* 1999;**32**(Suppl):13–5.

31 Schilling RJ, Peters NS, Davies DW. Simultaneous endocardial mapping in the human left ventricle using a noncontact catheter: comparison of contact and reconstructed electrograms during sinus rhythm. *Circulation* 1998;**98**:887–98.

32 Smeets JL, Ben-Haim SA, Rodriguez LM, *et al.* New method for nonfluoroscopic endocardial mapping in humans: accuracy assessment and first clinical results. *Circulation* 1998;**97**:2426–32.

33 Clark J, Bockoven JR, Lane J, *et al.* Use of three-dimensional catheter guidance and trans-esophageal echocardiography to eliminate fluoroscopy in catheter ablation of left-sided accessory pathways. *Pacing Clin Electrophysiol* 2008;**31**:283–9.

34 Sealy WC, Hattler BG Jr, Blumenschein SD, Cobb FR. Surgical treatment of Wolff–Parkinson–White syndrome. *Ann Thorac Surg* 1969;**8**:1–11.

35 Kirsh JA, Gross GJ, O'Connor S, Hamilton RM. Transcatheter cryoablation of tachyarrhythmias in children: initial experience from an international registry. *J Am Coll Cardiol* 2005;**45**:133–6.

36 Kugler JD. Radiofrequency catheter ablation for supraventricular tachycardia. Should it be used in infants and small children? *Circulation* 1994;**90**:639–41.

37 Kugler JD, Danford DA, Houston K, Felix G. Radiofrequency catheter ablation for paroxysmal supraventricular tachycardia in children and adolescents without structural heart disease. Pediatric EP Society, Radiofrequency Catheter Ablation Registry. *Am J Cardiol* 1997;**80**:1438–43.

38 Kugler JD, Danford DA, Deal BJ, *et al.* Radiofrequency catheter ablation for tachyarrhythmias in children and adolescents. The Pediatric Electrophysiology Society. *N Engl J Med* 1994;**330**:1481–7.

39 Van Hare GF, Lesh MD, Scheinman M, Langberg JJ. Percutaneous radiofrequency catheter ablation for supraventricular arrhythmias in children. *J Am Coll Cardiol* 1991;**17**:1613–20.

40 Huang SK, Bharati S, Graham AR, *et al.* Closed chest catheter desiccation of the atrioventricular junction using radiofrequency energy – a new method of catheter ablation. *J Am Coll Cardiol* 1987;**9**:349–58.

41 Borggrefe M, Budde T, Podczeck A, Breithardt G. High frequency alternating current ablation of an accessory pathway in humans. *J Am Coll Cardiol* 1987;**10**:576–82.

42 Haines DE, Verow AF. Observations on electrode–tissue interface temperature and effect on electrical impedance during radiofrequency ablation of ventricular myocardium. *Circulation* 1990;**82**:1034–8.

43 Haines DE, Watson DD. Tissue heating during radiofrequency catheter ablation: a thermodynamic model and observations in isolated perfused and superfused canine right ventricular free wall. *Pacing Clin Electrophysiol* 1989;**12**:962–76.

44 Baust J, Gage AA, Ma H, Zhang CM. Minimally invasive cryosurgery – technological advances. *Cryobiology* 1997;**34**:373–84.

45 Whittaker DK. Mechanisms of tissue destruction following cryosurgery. *Ann R Coll Surg Engl* 1984;**66**:313–8.

46 Iida S, Misaki T, Iwa T. The histological effects of cryocoagulation on the myocardium and coronary arteries. *Jpn J Surg* 1989;**19**:319–25.

47 Markovitz LJ, Frame LH, Josephson ME, Hargrove WC III. Cardiac cryolesions: factors affecting their size and a means of monitoring their formation. *Ann Thorac Surg* 1988;**46**:531–5.

48 Gill W, Fraser J, Carter DC. Repeated freeze–thaw cycles in cryosurgery. *Nature* 1968;**219**:410–3.

49 Khairy P, Chauvet P, Lehmann J, *et al.* Lower incidence of thrombus formation with cryoenergy versus radiofrequency catheter ablation. *Circulation* 2003;**107**:2045–50.

50 Drago F, De Santis A, Grutter G, Silvetti MS. Transvenous cryothermal catheter ablation of re-entry circuit located near the atrioventricular junction in pediatric patients: efficacy, safety, and midterm follow-up. *J Am Coll Cardiol* 2005;**45**: 1096–103.

51 Burack B, Furman S. Transesophageal cardiac pacing. *Am J Cardiol* 1969;**23**:469–72.

52 McNally EM, Meyer EC, Langendorf R. Elective countershock in unanesthetized patients with use of an esophageal electrode. *Circulation* 1966;**33**:124–7.

53 Benson DW Jr, Dunnigan A, Sterba R, Benditt DG. Atrial pacing from the esophagus in the diagnosis and management of tachycardia and palpitations. *J Pediatr* 1983;**102**:40–6.

54 Benson DW Jr, Dunnigan A, Benditt DG, *et al.* Transesophageal study of infant supraventricular tachycardia: electrophysiologic characteristics. *Am J Cardiol* 1983;**52**:1002–6.

55 Montoyo JV, Angel J, Valle V, Gausi C. Cardioversion of tachycardias by transesophageal atrial pacing. *Am J Cardiol* 1973;**32**:85–90.

56 Drago F, Silvetti MS, De Santis A, *et al.* Paroxysmal reciprocating supraventricular tachycardia in infants: electrophysiologically guided medical treatment and long-term evolution of the re-entry circuit. *Europace* 2008;**10**:629–35.

57 Benson DW Jr, Sanford M, Dunnigan A, Benditt DG. Transesophageal atrial pacing threshold: role of interelectrode spacing, pulse width and catheter insertion depth. *Am J Cardiol* 1984;**53**:63–7.

58 Dick M II, Campbell RM, Jenkins JM. Thresholds for transesophageal atrial pacing. *Cathet Cardiovasc Diagn* 1984;**10**:507–13.

59 Dick M II, Scott WA, Serwer GS, *et al.* Acute termination of supraventricular tachyarrhythmias in children by transesophageal atrial pacing. *Am J Cardiol* 1988;**61**:925–7.

60 Pongiglione G, Saul JP, Dunnigan A, *et al.* Role of transesophageal pacing in evaluation of palpitations in children and adolescents. *Am J Cardiol* 1988;**62**:566–70.

61 Benson DW Jr. Transesophageal electrocardiography and cardiac pacing: state of the art. *Circulation* 1987;**75**(4 Pt 2):III86–92.

62 Luedtke SA, Kuhn RJ, McCaffrey FM. Pharmacologic management of supraventricular tachycardias in children. Part 2: Atrial flutter, atrial fibrillation, and junctional and atrial ectopic tachycardia. *Ann Pharmacother* 1997;**31**:1347–59.

63 Deal BJ, Keane JF, Gillette PC, Garson A Jr. Wolff–Parkinson–White syndrome and supraventricular tachycardia during infancy: management and follow-up. *J Am Coll Cardiol* 1985;**5**:130–5.

64 Perry JC, Garson A Jr. Supraventricular tachycardia due to Wolff–Parkinson–White syndrome in children: early disappearance and late recurrence. *J Am Coll Cardiol* 1990; **16**:1215–20.

65 Saul JP, Ross B, Schaffer MS, *et al.* Pharmacokinetics and pharmacodynamics of sotalol in a pediatric population with supraventricular and ventricular tachyarrhythmia. *Clin Pharmacol Ther* 2001;**69**:145–57.

66 Walsh EP, Saul JP, Sholler GF, *et al.* Evaluation of a staged treatment protocol for rapid automatic junctional tachycardia after operation for congenital heart disease. *J Am Coll Cardiol* 1997;**29**:1046–53.

56 Syncope

John R. Phillips & Larry A. Rhodes

Robert C. Byrd Health Sciences Center, West Virginia University College of Medicine, Morgantown, WV, USA

Syncope, a transient loss of consciousness, is a common disorder affecting ~35% of the population at least once in their lives [1,2]. Symptoms often begin during adolescence and are recurrent [3], so that syncope is a common pediatric problem causing anxiety and concern for patients and parents alike. Vasovagal (neurocardiogenic) syncope is by far the most common cause of syncope in the community [4]. Syncope is best defined as a transient, self-limited loss of consciousness and postural control with a relatively rapid onset and recovery. More often than not, the syndrome is benign but may be a harbinger of complex medical problems, such as cardiac arrhythmias, structural heart disease, or neurologic disorders. In many circumstances, syncope may be the first symptom indicating those at risk for sudden cardiac death. Physicians must differentiate benign syncope from more life-threatening conditions. This chapter reviews the differential diagnosis of syncope in children and adolescents and concentrates on evaluating and treating vasovagal syncope.

Incidence and age at presentation

Several studies have attempted to identify the incidence and age at presentation of syncope. Syncope most often presents during adolescence with the age centered about 13 years [3]. In 1997, Driscoll *et al.* reported that patients seeking medical attention for syncope had an incidence rate of 125.8 per 100 000 with a peak age range between 15 and 19 years [5]. The incidence in girls (166.3 per 100 000) was higher than that in boys (92.9 per 100 000). A study of medical students under 22 years of age found a modal age of first syncope of 13–15 years [1]. Very few patients in either study were <7 years of age at onset of syncope. Lifetime prevalence of syncope has been reported to range from 7% [6] to 39% [1],

again with females affected more often than males. Studies of military personnel in early adulthood suggest a prevalence of 20–32% [7,8].

Causes of syncope

The brain requires an adequate supply of oxygen and glucose to function normally. Decreases in the steady supply of oxygen and glucose to the brain may lead to syncope or presyncope. The causes of syncope are numerous and can be categorized as circulatory, metabolic, or neuropsychologic (Table 56.1). Metabolic and neuropsychologic disorders that cause syncope are beyond the scope of this chapter. We concentrate on circulatory abnormalities leading to syncope.

Cardiac syncope

The mechanism of cardiac syncope is decreased cardiac output and, subsequently, blood flow to the brain. Cardiac syncope results from severe obstructive lesions, myocardial dysfunction, and arrhythmias. Obstructive lesions include severe aortic or pulmonary stenosis, obstructive hypertrophic cardiomyopathy, and pulmonary hypertension. Although rare, myocardial ischemia or infarction secondary to coronary artery anomalies, Kawasaki disease, and congenital or acquired cardiomyopathies may cause myocardial dysfunction and produce decreased cardiac output and cardiogenic syncope. Extreme tachycardia or bradycardia can decrease cardiac output and lower cerebral blood flow, causing syncope. Cardiac structure and function are often normal in young people with arrhythmias but congenital channelopathies, such as long QT syndrome and Brugada syndrome, predispose patients to malignant ventricular tachyarrhythmias. Conversely, severe bradycardia, as in congenital complete heart block and congenitally

Table 56.1 Causes of syncope.

Circulatory
Cardiac causes
  Obstructive lesions
    Aortic stenosis
    Pulmonic stenosis
    Hypertrophic cardiomyopathy
    Pulmonary hypertension
  Myocardial dysfunction and ischemia
    Coronary artery anomalies
    Kawasaki disease
    Congenital and acquired cardiomyopathy
  Arrhythmias
    Ventricular tachycardia (long QT syndrome, Brugada syndrome, arrhythmogenic right ventricular dysplasia, catecholamine-induced ventricular tachycardia)
    Supraventricular tachycardia (Wolff–Parkinson–White syndrome)
    Bradycardia (sick sinus syndrome, atrioventricular heart block, pacemaker malfunction)
Extracardiac causes
  Vasovagal syncope
  Orthostatic hypotension
  Situational (swallowing, micturition, defecation, cough)
  Failure of venous return (increased intrathoracic pressure, hypovolemia, hemorrhage)
  Cerebrovascular occlusive disease
  Subclavian steal

Metabolic
Hypoglycemia
Hyperventilation syndrome
Hypoxia
Acidosis

Neuropsychologic
Epilepsy
Brain tumors
Hysteria and anxiety disorders
Pseudoseizures
Migraine headaches

corrected transposition of the great arteries, may also decrease cardiac output.

Unlike vasovagal syncope, a cardiac cause of syncope should be considered particularly if syncope occurs with the patient recumbent, during exercise, or is associated with chest pain. Furthermore, a cardiac etiology should be considered if the patient has a history of repaired or unrepaired congenital heart disease or family history of sudden death. Pacemaker malfunction should be considered where appropriate.

Extracardiac syncope

Extracardiac causes of syncope include vasovagal syncope, orthostatic hypotension, situational syncope (after swallowing, urination, coughing, or defecation), carotid sinus hypersensi-

tivity, failure of venous return, and cerebrovascular occlusive disease including subclavian steal. Of all causes of syncope, vasovagal syncope, also called vasodepressor, neurocardiogenic, or common syncope, is by far the most common. It results from inappropriate output from the autonomic nervous system leading to symptomatic changes in blood pressure and heart rate. These changes typically occur while the patient is standing but may develop during emotional stress (e.g., speaking performances or standing at the altar), or after noxious stimuli such as phlebotomy or an unpleasant sight. A prodrome of dizziness is common. Others complain of an aura, such as flashing lights, changes in hearing (rushing sound), tunnel vision, or nausea. The blood pressure falls, the heart rate slows, and the subject becomes pale and loses consciousness. Injury from falling is rare. Repeated myoclonic jerks are common, and may lead to the misdiagnosis of epilepsy. True tonic–clonic seizures are rare if the patient is supine, and there is no incontinence.

Despite years of investigation, a complete understanding of the pathophysiology of vasovagal syncope remains elusive. Several mechanisms have been proposed. The first is that vasovagal syncope occurs as the result of an abnormal physiologic response to venous pooling in the lower extremities while standing. To understand this, consider the normal response to venous pooling in the legs. In a normal adult, ~500 ml of intravenous volume is displaced into the lower extremities during standing [9]. This is equivalent to ~10 ml per kilogram in a child [10]. With venous pooling, the central venous volume is decreased, as is left ventricular preload. The decreased ventricular filling reduces the stretching of mechanoreceptors in both atrial and ventricular tissues [5,9]. The resultant decreased signaling from the C fibers reflexly increases sympathetic tone and, subsequently, elevates heart rate and peripheral vascular resistance [11–13]. The atrial afferents are myelinated and arise from the junction of the vena cava and pulmonary veins within the atria [12]. They appear to be sensitive to central volume changes and insensitive to myocardial contractility [11,13]. The ventricular afferents are unmyelinated, slowly conducting C fibers sensitive to contractility and end-diastolic pressure [12]. With decreased stretching, there is less signaling from C fibers to the brain stem, leading to a reflex increase in sympathetic output [11–13].

In patients with vasovagal syncope, this reflex is abnormal. These patients experience a decrease in sympathetic tone and an increase in parasympathetic tone leading to hypotension and bradycardia [11]. The exact abnormality in the reflex is not fully understood. One proposed mechanism is that a decrease in left ventricular preload increases contractility, which then raises the intracavitary pressure. This pressure increase stimulates the left ventricular mechanoreceptors and in turn elevates parasympathetic tone [11]. The role of left ventricular mechanoreceptors in this reflex has been demonstrated in work by Oberg and Thoren [14]. They
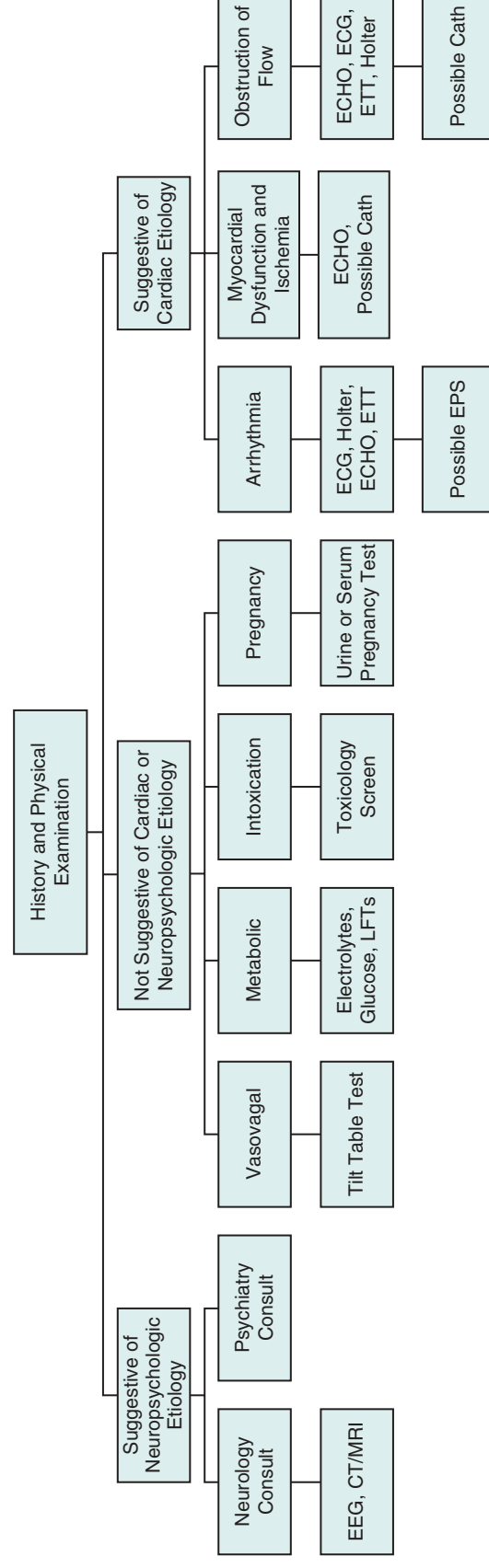
Figure 56.1 Scheme for the evaluation of the patient with syncope. Cath, catheterization; CT/MRI, computed tomography/magnetic resonance imaging; ECG, electrocardiography; ECHO, echocardiography; EEG, electroencephalography; EPS, electrophysiologic study; ETT, exercise tolerance testing; LFTs, liver function tests.

documented an initial decline followed by a marked increase in ventricular mechanoreceptor activity in cats subjected to experimental hemorrhage or occlusion of inferior vena cava blood flow leading to decreased ventricular filling [14]. They proposed that the underfilled left ventricle became distorted, activating the mechanoreceptors, which in turn fed back to the brain stem, causing a reflex withdrawal of sympathetic tone and an increase in parasympathetic tone [14]. Similar mechanisms may operate in the syncope that occurs in some patients with left or right ventricular outflow obstruction. A variation of this hypothesis suggests that there may be an initial increase in sympathetic tone contributing to this reflex. This is supported by the finding that patients with vasovagal syncope often have an increase in heart rate and arterial blood pressure immediately before syncopal episodes [15–17], in addition to increased levels of urinary catecholamines before the event [18].

The heart rate and blood pressure responses that accompany standing have also been evaluated in children [19]. In normal children, standing leads to an initial decrease in systolic and diastolic blood pressures followed by an increase in both pressures and an increase in heart rate. As the child continues to stand, the systolic blood pressure returns to baseline with the diastolic blood pressure and heart rate remaining elevated for as long as 2 min. In individuals susceptible to syncope, standing produces an exaggerated decrease in systolic and diastolic blood pressure and, in some, a paradoxical decrease in heart rate.

A second possible mechanism for vasovagal syncope may involve central triggers that lead to bradycardia and hypotension. Neurohormonal agents other than catecholamines may play an important role in leading to the depressor response in neurally mediated syncope. Increased levels of β-endorphin were found in patients with vasovagal syncope [20] and in hemorrhagic shock [21,22]. Evans *et al.* found that hypotension could be prevented in hemorrhagic shock by giving naloxone intracisternally [21]. Serotonin, a central mediator, may also play a role in vasovagal syncope. Animal studies have suggested that serotonin may lead to the depressor response in hemorrhage [23]. In a study by Abboud and Thames, intracerebrovascular serotonin induced hypotension and changes in renal sympathetic nerve activity and may have acted centrally to inhibit sympathetic activity [12].

Recently, implantable loop recorders (ILRs) have been placed in adults to establish the mechanism of vasovagal syncope. The International Study of Syncope of Uncertain Etiology (ISSUE) evaluated adult patients without structural heart disease or identifiable causes of syncope and negative or positive tilt-table testing with ILRs [24]. The most frequent finding was prolonged asystolic pauses preceded by progressive bradycardia recorded in 46% of tilt-negative patients and 62% of tilt-positive patients. Bradycardia without pauses was observed in 8 and 12% of patients, respectively. Another study of ILR showed that 69% of patients

had bradycardia during syncope [25]. These studies offer insight into the predominant cardiac rhythm during syncope but not an understanding of the pathophysiology of the bradycardia.

Evaluation of the patient with syncope (Figure 56.1)

History

Evaluating a child or adolescent with syncope begins with a thorough medical history that should include a precise, detailed account of the events surrounding the episode, including the type of activity engaged in prior to the episode. In particular, the occurrence of syncope during or immediately following exercise is a very important observation, as it strongly suggests a cardiac etiology. Important points include any prodromal symptoms, such as nausea, vomiting, palpitations, visual aura, auditory changes, or dizziness. A complete history may be difficult to obtain from a patient because of amnesia around the event. If so, efforts should be made to obtain eye-witness accounts. Helpful information includes an assessment of the patient's appearance, such as pallor or cyanosis before and during the event. An estimate of the duration of the syncopal episode is important. In general, vasovagal syncope is brief, in contrast to cardiac syncope. Abnormal movements, seizure activity, or abnormal posturing during the period of unconsciousness should be documented. The patient's mental status after an episode may help in developing a differential diagnosis. Other important historical data are illness around the time of the event, oral intake in the preceding 24 h, medications taken, and previous similar episodes.

A key element of the past medical history is a careful account of drugs that the patient may be using, including over-the-counter, recreational, and prescription medications. History of prior medical problems including cardiac and psychological illness should be obtained. A complete review of systems with special concentration on the cardiovascular and neurologic systems should be made. Finally, and perhaps most importantly, a detailed family history should also be elicited, particularly of congenital heart disease, arrhythmias, sudden death, and neurologic or psychologic disorders. In addition, specific questioning regarding hypertrophic cardiomyopathy, long QT syndrome, drowning, and pacemaker or defibrillator placement should be made. A social history is important in ascertaining the possibility of substance abuse, pregnancy, or factors leading to a conversion reaction.

Physical examination

A complete physical examination is performed. When examining the patient during and immediately after syncope, document heart rate, blood pressure, respiratory effort, and motor movements consistent with seizure activity. After a syncopal

event, evaluate blood pressure and heart rate with the patient supine and standing to exclude orthostatic hypotension or tachycardia. Signs of trauma or drug abuse are sought. Neurologic examination should be complete, including looking for papilledema or other signs of increased intracranial pressure. Cardiovascular examination includes palpation of the patient's pulses for rhythm and quality. A thorough auscultatory examination evaluates rhythm, characteristics of the heart sounds, and murmurs. This portion of the examination should be performed with the patient both sitting and supine, and with use of standing, squatting, and the Valsalva maneuver to enhance findings of mitral valve prolapse or hypertrophic cardiomyopathy. Particular attention should be given to the second heart sound to identify pulmonary hypertension.

Subclavian steal is an exception because it produces local cerebral ischemia with a normal cardiac output and blood pressure. The occurrence of syncope with arm exercise, especially in a patient with a Blalock–Taussig shunt, suggests this diagnosis. A blood pressure difference between the two arms is confirmatory.

Laboratory tests

Further testing is directed towards the patient's specific symptoms and physical examination findings. If a neurologic cause is being considered, a complete evaluation by a pediatric neurologist is indicated. If substance abuse or intoxication is suspected, a toxicology screen is performed. Other possible laboratory evaluations include serum electrolyte, blood urea nitrogen, creatinine, and glucose determinations as a screen for metabolic abnormalities. Serum or urine concentration of human chorionic gonadotropin β subunit can exclude pregnancy. Abnormal laboratory values of dehydration may not be found with the patient having a normal BUN, hemoglobin, or urine specific gravity.

A 12-lead electrocardiogram is reviewed for heart rate, rhythm, and conduction abnormalities, such as heart block and pre-excitation. PR, QRS, and corrected QT intervals should be measured. If syncope is associated with exercise, an exercise stress test may be performed, and the origin of the coronary arteries must be established by echocardiography or other imaging modality, to exclude a coronary artery anomaly. If an arrhythmia is suspected, 24 h ambulatory monitoring (Holter) or event monitoring (external or implanted) should be performed. A complete electrophysiologic study is considered if the Holter monitoring suggests an arrhythmia. In patients with a history of recurrent or atypical syncope, a tilt-table evaluation may be performed.

Tilt testing

Over the past decade, the use of tilt-table testing in evaluating patients with syncope has declined significantly, owing to inconsistency in tilt protocols and concerns about the sensitivity and specificity of the test. Protocol variations include the length of the study, the inclination of the table, the type of blood pressure monitoring (invasive versus noninvasive), the measurement of serum catecholamines, and the use of provocative medications, such as isoproterenol or epinephrine. Previously, the type of response to tilt testing was important in the management strategy. Determining the exact mechanism of noncardiac syncope may not be necessary to treat the patient successfully. Many cardiologists use tilt-table testing only for patients with a history inconsistent with a vasovagal mechanism or who have failed conventional therapy. It may help if a patient reports the same sensations as occurred before the syncopal event.

Treatment

This section discusses the treatment of children and adolescents with vasovagal syncope. Fortunately, most patients with vasovagal syncope require only lifestyle modification by increasing daily salt and fluid intake to treat their symptoms [26]. The remainder may need other measures, including dietary modification, physical training, medication and even pacemaker implantation. A recent review of current treatments by Kuriachan, Sheldon, and Platonov nicely outlined treatment effect, rated that effect, and summarized the evidence to substantiate their claims [27]. Their recommendations are outlined below.

Physical and lifestyle treatments

Increased salt and fluid

A 64 oz intake of noncaffeinated fluid per day and liberalizing dietary salt are primary therapy for vasovagal syncope. Up to 90% of adolescents with a previously positive tilt test who receive oral fluid therapy are free from recurrence [26]. Most patients with an initial positive tilt test have a negative repeat test after receiving increased fluid and salt supplements. The usual adult dose of salt tablets is 6–9 g per day. Side effects of salt tablets include stomach upset and bloating. Salt supplements are contraindicated in those with hypertension, renal dysfunction, or cardiac dysfunction. For those without contraindications to salt therapy, recommending salty foods, such as a bag of salted pretzels, may be sufficient.

Recommendation: In the absence of contraindications, liberalization of fluid and salt should be undertaken. This therapy is probably helpful with a moderate amount of evidence to support the claim [27].

Exercise training

Although exercise training acutely increases blood volume, there is limited evidence that shows improvement of syncope.

Recommendation: The benefits of exercise are well known and should be encouraged. The evidence in support a benefit of exercise in preventing syncope is weak [27].

Physical counterpressure maneuvers

Physical counterpressure maneuvers consist of isometric muscle contractions performed by presyncopal patients to prevent syncope. Leg crossing, pulling apart gripped hands, or squats are such maneuvers that increase cardiac output and arterial blood pressure while reducing peripheral resistance. Patients practicing these techniques decrease the number of subsequent syncopal episodes [28]. Although some patients have insufficient prodromal symptoms to perform counterpressure maneuvers, these maneuvers are easy to teach, without side effects, and free.

Recommendation: All patients should be taught these techniques to prevent syncope. Counterpressure techniques are probably helpful with good evidence to support the claim [27].

Tilt-test training

Because the reproducibility of tilt testing is inconsistent, researchers speculated that a training effect may be the cause [29]. To test the theory, patients were either tilted daily until tilt testing was negative or asked to stand against a wall at home for 30–60 min daily. Some studies demonstrated an encouraging effectiveness of the training with up to 82% freedom from recurrent syncope over 43 months. Other randomized trials, however, failed to corroborate these findings, and the compliance of long-term home training was brought into question.

Recommendation: Whether poor results are due to poor compliance or inefficacious therapy, orthostatic training in not currently recommended for routine use. Evidence suggests that it is probably unhelpful [27].

Pharmacological therapy

Fludrocortisone

Fludrocortisone is a mineralocorticoid steroid that stimulates the retention of sodium chloride and intravascular volume. Fludrocortisone prevented syncope in 90% of children and adolescents in one study [30]. With the use of salt, fludrocortisone, and increased fluid intake, significant changes in serum electrolyte concentrations, especially hypokalemia, may require monitoring and possible intervention. Hypertension and weight gain associated with the additional salt and fluid retention may result. This change in body weight may be secondary to normal growth of adolescence or related to increased fluid intake and retention, and may hinder successful treatment in this age group as they are sensitive to even minor increases in weight. More recently, a randomized, double-blinded, placebo-controlled study found that children receiving fludrocortisone were *more* symptomatic than children treated with placebo [31]. A randomized, controlled clinical trial is under way to evaluate the effectiveness of fludrocortisone in treating adults with syncope [32].

Recommendation: Fludrocortisone may be prescribed in frequently symptomatic patients but the effect is debatable and the evidence for its use is weak [27].

β-adrenergic blockers

A second treatment approach is β-adrenergic blockers. Theoretically, the negative inotropic effect of β-blockers may offset increased ventricular contractility seen as part of the abnormal reflex in vasovagal syncope or block the effect of circulating epinephrine, a possible central trigger of the abnormal vasovagal reflex. β-Blockers are well tolerated in children but must be used with caution in patients with reactive airway disease and depression. Side effects include depression, decrease in school performance, and fatigue.

Initially, the efficacy of β-blockers in preventing recurrent syncope in adults was encouraging, ranging from 71 to 100% [33–37]. Later, the results of five randomized clinical trials on the efficacy of β-blockers for the prevention of syncope were basically negative [38]. In 2006, a randomized, placebo-controlled, double-blinded trial assessing the usefulness of metoprolol in preventing syncope showed no benefit compared with placebo [39].

Recommendation: There is good evidence to show that the use of β-adrenergic blockers is probably unhelpful and they should not be used as first-line therapy [27].

Midodrine

α-Adrenergic agonists, such as midodrine, are another class of medications used to treat vasovagal syncope in young people. Decreased venous return to the heart while standing may be related to venodilatation and venous pooling. α-Adrenergic agents increase venous tone by direct sympathetic stimulation. Arterial vasoconstriction leads to increased systemic vascular resistance, blocking systemic hypotension [40]. These potential advantages have been verified in children and adults with vasovagal syncope. A randomized, open-label trial of children with at least three syncopal episodes per year showed a recurrence rate of 20% in those receiving midodrine compared with 80% in the control group [41]. A randomized crossover placebo-controlled study of midodrine reported a reduction in symptoms and positive tilt testing in adults receiving midodrine compared with the placebo group [38].

The use of midodrine in children and adults shows both short- and medium-term therapeutic success. The drug is well tolerated, with side effects including supine hypertension, nausea, scalp paresthesias, piloerection, and rash. The side effects are dose related and reversible. Midodrine is contraindicated in patients with hypertension or heart failure.

Recommendations: There is good evidence to show that midodrine is probably helpful in adult and pediatric patients with frequent syncope and should be used as a first-line therapy [27].

Selective serotonin uptake inhibitors (SSRIs)

The final class of medications prescribed in treating vasovagal syncope is the serotonin uptake inhibitors, including fluoxetine hydrochloride (Prozac) and sertraline hydrochloride (Zoloft). These agents have antidepressant properties and have been used in patients with vasovagal syncope refractory to conventional medications [42]. The abolition of the vasodepressor response by depletion or receptor blockade of serotonin has been well described in animal models of acute hemorrhage [22,43]. Although the exact mechanism of action of serotonin uptake inhibition in the treatment of vasovagal syncope is not fully understood, it is probably related to a similar decrease in the serotonin-mediated vasodepressor response. On the basis of findings in patients with clinical depression treated with fluoxetine hydrochloride in whom vasovagal syncope was alleviated, Grubb *et al.* studied the effects of sertraline hydrochloride therapy in pediatric patients with vasovagal syncope whose conventional therapy had failed [42]. A beneficial response to treatment with sertraline hydrochloride was found in 53% of the patients. Side effects included nausea, diarrhea, headache, and mild insomnia. A more recent randomized, placebo-controlled study reported equal effects between fluoxetine, propranolol, and placebo [44]. Therefore, the evidence suggesting that SSRIs are useful in the treatment of vasovagal syncope are mixed at best.

Recommendations: The evidence supporting the use of SSRIs in treating vasovagal syncope is debatable, with a moderate amount of evidence suggesting that SSRIs should not be used as initial treatment for vasovagal syncope [27].

Pacemaker therapy

A final therapeutic option is the use of cardiac pacing in patients with recurrent syncope. Pacing patients with vasovagal syncope is a class IIb indication as described by the American College of Cardiology/American Heart Association/Heart Rhythm Society 2008 guidelines [45]. The guidelines state: "Permanent pacing may be considered for significantly symptomatic vasovagal syncope associated with bradycardia documented spontaneously or at the time of tilt-table testing." The guidelines state that pacing is a class III indication and *not* indicated for "situational vasovagal syncope in which avoidance behavior is effective and preferred." Whether the subset of patients with vasovagal syncope associated with asystolic pauses would benefit from pacing remains unknown and is being studied [46]. It should be noted that even though pacing may prevent the bradycardia, it will have no effect on marked arteriolar vasodilatation caused by sympathetic inhibition.

Recommendation: Permanent pacemakers should not be used routinely to treat vasovagal syncope. The clinician may consider pacing in highly symptomatic patients failing drug therapy with documented asystole during syncope.

Conclusion

For the most part, particularly in children and adolescents, vasovagal syncope is benign and improves with time. First-line therapy is directed at liberalization of fluids and increased dietary salt. An intake of 64 oz of noncaffeinated fluid per day and increased salt intake were suggested [27]. The patient should be instructed that the goal of therapy is to keep the urine clear and avoid the sensation of thirst. Since syncope is common in the adolescent, a letter allowing the patient to carry a water bottle to school and allowing frequent restroom breaks is recommended to ensure compliance with the protocol. Counterpressure measures including leg crossing and squatting should be advised to all patients, particularly those with extended prodromal symptoms. For patients requiring pharmacologic management, midodrine is likely the most efficacious first-line therapy based on available evidence. Routine use of β-blockers, SSRIs, fludrocortisone, and pacemakers is discouraged. In patients with recurrent and refractory syncope or an atypical presentation and history, the clinician must consider those diagnoses that place the patient at increased risk for sudden cardiac death.

References

1 Ganzeboom KS, Colman N, Reitsma JB, *et al*. Prevalence and triggers of syncope in medical students. *Am J Cardiol* 2003;**91**:1006–8.

2 Ganzeboom KS, Mairuhu G, Reitsma J, *et al*. Lifetime cumulative incidence of syncope in the general population: a study of 549 Dutch subjects aged 35–60 years. *J Cardiovasc Electrophysiol* 2006;**17**:1172–6.

3 Sheldon RS, Sheldon AG, Connolly SJ, *et al*. Age of first faint in patients with vasovagal syncope. *J Cardiovasc Electrophysiol* 2006;**17**:49–54.

4 Van Dijk N, Boer KR, Colman N, *et al*. High diagnostic yield and accuracy of history, physical examination, and ECG in patients with transient loss of consciousness in FAST: the Fainting Assessment Study. *J Cardiovasc Electrophysiol* 2008;**19**:48–55.

5 Driscoll DJ, Jacobsen SJ, Porter CJ, *et al*. Syncope in children and adolescents. *J Am Coll Cardiol* 1997;**29**:1039–45.

6 Dermkasian G, Lamb LE. Syncope in a population of healthy young adults. *J Am Med Assoc* 1958;**168**:1200–7.

7 Lamb L, Green HC, Combs JJ, *et al*. Incidence of loss of consciousness in 1980 Air Force personnel. *Aerosp Med* 1960; **12**:973–88.

8 Murdoch BD. Loss of consciousness in healthy South African men: incidence, causes and relationship to EEG abnormality. *S Afr Med J* 1980;**57**:771–4.

9 Ibrahim MM, Tarazi RC, Dustan HG. Orthostatic hypotension: mechanisms and management. *Am Heart J* 1975;**90**:513–20.

10 Freed MD. Advances in the diagnosis and therapy of syncope and palpitations in children. *Curr Opin Pediatr* 1994;**6**:368–72.

11 Thoren P. Role of cardiac vagal C-fibers in cardiovascular control. *Rev Physiol Biochem Pharmacol* 1979;**86**:1–94.

12 Abboud FM, Thames MD. Interaction of cardiovascular reflexes in circulatory control. In: Shepherd JT, Abboud FM, eds. *Handbook of Physiology*. Bethesda, MD: American Physiological Society, 1983: 675–753.

13 Donald ED, Shepherd JT. Reflexes from the heart and lungs: physiological curiosities or important regulatory mechanisms. *Cardiovasc Res* 1978;**12**:449–69.

14 Oberg B, Thoren P. Increased activity in left ventricular receptors during hemorrhage or occlusion of caval veins in the cat: a possible cause of the vasovagal reaction. *Acta Physiol Scand* 1972; **85**:164–73.

15 Sra JS, Murthy V, Natale A, *et al*. Circulatory and catecholamine changes during head-up tilt in neurocardiogenic (vasovagal) syncope. *Am J Cardiol* 1994;**73**:33–7.

16 Graham DT, Kabler JD, Lunsford L Jr. Vasovagal fainting: a diphasic response. *Psychosom Med* 1961;**23**:493–507.

17 Glick G, Yu PN. Hemodynamic changes during spontaneous vasovagal reactions. *Am J Med* 1963;**34**:42–51.

18 Chosey JJ, Graham DT. Catecholamines in vasovagal fainting. *J Psychosom Res* 1965;**9**:189–94.

19 Dambrink J, Imholz B, Karemaker JM, *et al*. Circulatory adaptation to orthostatic stress in healthy 10–14-year-old children investigated in a general practice. *Clin Sci* 1991;**81**:51–8.

20 Perna GP, Ficola V, Salvatori MP, *et al*. Increase of plasma beta endorphins in vasodepressor syncope. *Am J Cardiol* 1990; **65**:929–30.

21 Evans RG, Ludbrook J, Potocnik SJ. Intracisternal naloxone and cardiac nerve blockade prevent vasodilatation during simulated haemorrhage in awake rabbits. *J Physiol (Lond)* 1989;**409**:1–14.

22 Rutter PC, Potocnik SJ, Ludbrook J. Sympathoadrenal mechanisms in cardiovascular responses to naloxone after hemorrhage in conscious rabbits. *Am J Physiol (Heart Circ Physiol)* 1987; **252**:H40–6.

23 Morgan DA, Thoren P, Wilczynski EA, *et al*. Serotonergic mechanisms mediate renal sympathoinhibition during severe hemorrhage in rats. *Am J Physiol (Heart Circ Physiol)* 1988;**255**: H496–502.

24 Moya A, Brignole M, Menozzi C, *et al*. Mechanism of syncope in patients with isolated syncope and in patients with tilt-positive syncope. *Circulation* 2001;**104**:1261–7.

25 Krahn AD, Klein GJ, Yee R, *et al*. Use of an extended monitoring strategy in patients with problematic syncope: Reveal Investigators. *Circulation* 1999;**99**:406–10.

26 Younoszai AK, Franklin WH, Chan DP, *et al*. Oral fluid therapy: a promising treatment for vasodepressor syncope. *Arch Pediatr Adolesc Med* 1998;**152**:165–8.

27 Kuriachan V, Sheldon RS, Platonov M. Evidence-based treatment for vasovagal syncope. *Heart Rhythm* 2008;**5**:1609–14.

28 van Dijk N, Quartieri F, Blanc JJ, *et al*. and the PC-Trial Investigators. Effectiveness of physical counterpressure maneuvers in preventing vasovagal syncope: the Physical Counterpressure Manoeuvres Trial (PC-Trial). *J Am Coll Cardiol* 2006;**48**:1652–7.

29 Ector H, Willems R, Heidbuchel H, *et al*. Repeated tilt testing in patients with tilt positive neurally mediated syncope. *Europace* 2005;**7**:628–33.

30 Grubb BP, Temesy-Arrnos P, Moore J, *et al*. The use of head upright tilt table testing in the evaluation and management of syncope in children and adolescents. *Pacing Clin Electrophysiol* 1992;**15**:742–8.

31 Salim MA, Di Sessa TG. Effectiveness of fludrocortisone and salt in preventing syncope recurrence in children: a double-blind, placebo-controlled, randomized trial. *J Am Coll Cardiol* 2005;**45**:484–8.

32 Raj SR, Rose S, Ritchie D, *et al*. and the POST II Investigators. The Second Prevention of Syncope Trial (POST II) – a randomized clinical trial of fludrocortisones for the prevention of neurally mediated syncope: rationale and study design. *Am Heart J* 2006;**151**:1186.e11–1186.e17.

33 Blanc JJ, Corbel C, Mansourati J, Genet L. Evaluation of beta-adrenergic blockade therapy in vasovagal syncope reproduced by head-up tilt test. *Arch Mal Coeur Vaiss* 1991;**84**:1453–7.

34 Muller G, Deal BJ, Strasburger JF, *et al*. Usefulness of metoprolol for unexplained syncope and positive response to tilt testing in young persons. *Am J Cardiol* 1993;**71**:592–5.

35 Leor J, Rotstein Z, Vered Z, *et al*. Absence of tachycardia during tilt test predicts failure of beta-blocker therapy in patients with neurocardiogenic syncope. *Am Heart J* 1994;**127**:1539–43.

36 Scott WA, Pongiglione G, Bromberg BJ, *et al*. Randomized comparison of atenolol and fludrocortisone acetate in the treatment of pediatric neurally mediated syncope. *Am J Cardiol* 1995;**76**:400–2.

37 Cox MM, Perlman BA, Mayor MR, *et al*. Acute and long-term beta-adrenergic blockade for patients with neurocardiogenic syncope. *J Am Coll Cardiol* 1995;**26**:1293–8.

38 Sheldon R, Morillo CA, Krahn A. Management of vasovagal syncope: 2004. *Expert Rev Cardiovas Ther* 2004;**2**:915–23.

39 Sheldon R, Connolly S, Rose S, *et al*. and the POST Investigators. Prevention of Syncope Trial (POST): a randomized, placebo-controlled study of metoprolol in the prevention of vasovagal syncope. *Circulation* 2006;**113**:1164–70.

40 Strieper MJ, Campbell RM. Efficacy of alpha-adrenergic agonist therapy for prevention of pediatric neurocardiogenic syncope. *J Am Coll Cardiol* 1993;**22**:594–7.

41 Zhang Q-Y, Du J-B, Tang C-S. The efficacy of midodrine hydrochloride in the treatment of children with vasovagal syncope. *J Pediatr* 2006;**149**:777–80.

42 Grubb BP, Samoil D, Kosinski D, *et al*. Use of sertraline hydrochloride in the treatment of refractory neurocardiogenic syncope in children and adolescents. *J Am Coll Cardiol* 1994;**24**:490–4.

43 Elam RF, Bergman F, Feverstein G. The use on anti-serotonergic agents for the treatment of acute hypovolemia in conscious mammals. *Am J Physiol (Heart Circ Physiol)* 1991;**260**,H305–18.

44 Theodorakis GN, Leftheriotis D, Livanis EG, *et al*. Fluoxetine vs. propranolol in the treatment of vasovagal syncope: a prospective, randomized, placebo-controlled study. *Europace* 2006;**8**:193–8.

45 Epstein AE, DiMarco JP, Ellenbogen KA, *et al*. ACC/AHA/HRS 2008 Guidelines for Device-Based Therapy of Cardiac Rhythm Abnormalities. *J Am Coll Cardiol* 2008;**51**,e1–62.

46 Brignole M. International Study on Syncope of Uncertain Etiology 3 (ISSUE 3): pacemaker therapy for patients with asystolic neurally-mediated syncope: rationale and study design. *Europace* 2007;**9**:25–30.

57 Cardiovascular Disease, Sudden Cardiac Death, and Preparticipation Screening in Young Competitive Athletes

Barry J. Maron

Minneapolis Heart Institute Foundation, Minneapolis, MN, USA

During the past several years, interest and concern have heightened considerably in the medical community and the lay public regarding the causes of sudden and unexpected death in young trained athletes [1–17]. The risks associated with participation in organized competitive sports are diverse and range from sudden collapse due to underlying (and unusually unsuspected) cardiovascular disease [8–23] to non-penetrating and often innocent appearing chest blows triggering ventricular fibrillation in the absence of structural cardiac disease [24–26]. Recognition that athletic field deaths may be due to a variety of detectable cardiovascular lesions has also stimulated intense interest in defining the most practical and effective strategy for preparticipation screening of largely high-school and college-aged [7–15,27–39] (but also professional) athletes [40], and also in the criteria for eligibility for and disqualification from competitive sports [3,11].

Definitions

A competitive athlete has been defined as one who participates in an organized team or individual sport requiring regular competition against others as a central component, places a high premium on excellence and achievement, and requires vigorous and intense training in a systematic fashion [41]. This definition can be regarded as somewhat arbitrary in that many individuals participate in "recreational" sports [42] in a truly competitive fashion.

Causes of sudden death in young athletes

Autopsy-based studies have documented the cardiovascular diseases responsible for sudden death in young competitive athletes [19–23]. These structural abnormalities are independent of the normal physiologic adaptations in cardiac dimensions evident or in many trained athletes, usually consisting of increased left ventricular end-diastolic cavity dimension, or occasionally mild wall thickening [43–46].

About 70% of sudden deaths in young athletes (aged <35 years) are due to a variety (more than 20) of primarily congenital cardiovascular diseases (Figures 57.1 and 57.2) [20–22]. Indeed, virtually any disease capable of causing sudden death in young people may potentially do so in young competitive athletes [5,6]. Although these conditions may be relatively common as causes of young athletes dying suddenly, each is uncommon within the general population [5,6].

Hypertrophic cardiomyopathy

In several autopsy-based studies, the single most common cardiac abnormality among the causes of sudden death in young athletes is hypertrophic cardiomyopathy (HCM) [19–22], usually without outflow obstruction under resting conditions [47–49], accounting for about one-third of such catastrophes (Figure 57.2).

HCM is a primary and familial cardiac malformation with heterogeneous clinical and morphologic expression, complex pathophysiology, and diverse natural history [47–49], for which >1000 mutations in 11 or more genes encoding proteins of the cardiac sarcomere have been reported [50]. HCM is the most common of the genetic heart diseases, occurring with phenotypic expression in about 1 in 500 of the general population [51].

Sudden death in HCM is most common in children and young adults, usually in previously asymptomatic individuals [48,49]; therefore, such catastrophes are often the first clinical manifestation of unsuspected disease. Although most patients die while they are sedentary or during mild exertion, an important proportion collapse during or just after vigorous physical activity [21]. This observation, and also the evidence that athletes with HCM usually have
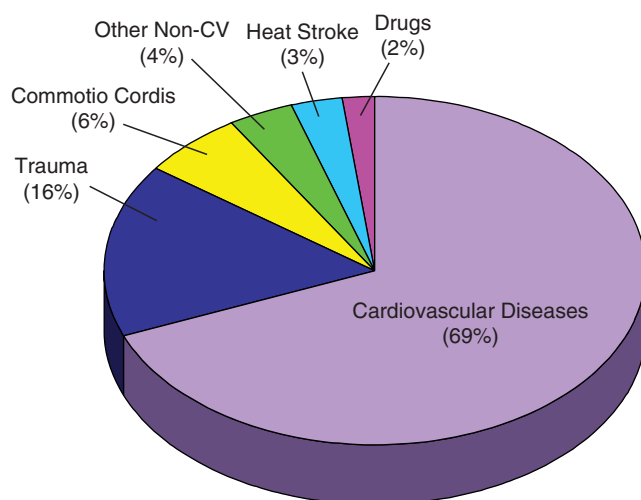
Figure 57.1 US National Registry for Sudden Death in 1866 Young Athletes [21]. Cardiovascular diseases are the predominant causes of sudden deaths in athletes, accounting for about 70%.
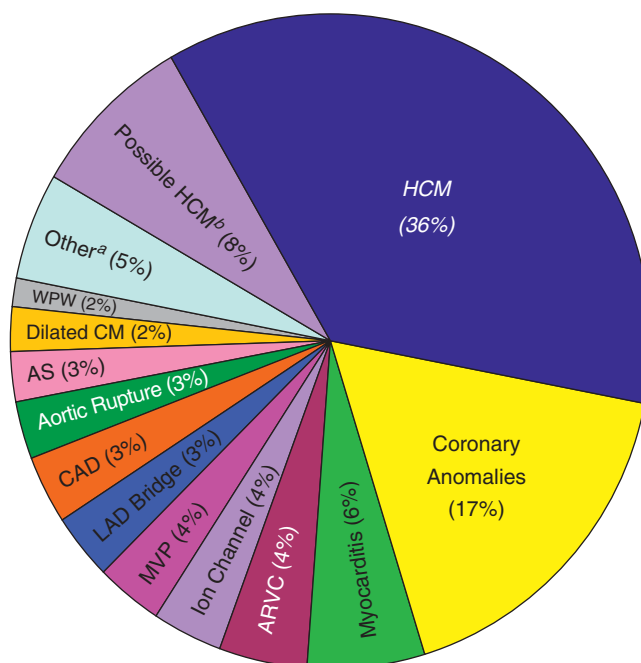
Figure 57.2 Cardiovascular causes of sudden death in young competitive athletes, with HCM the most common. [a]Includes congenital heart disease (n = 8); myocardial infarction (n = 6); Kawasaki disease or related conditions (n = 5); sickle cell trait (n = 5); sarcoidosis (n = 4); stroke (n = 3); cardiac tumor (n = 1); conduction system disease (n = 2); and miscellaneous (n = 2). [b]Regarded as possible (not definitive) evidence for HCM at autopsy with mildly increased LV wall thickness [18 (SD 4) mm] and heart weight [447 (SD 76) g]. Ao, aorta; ARVC, arrhythmogenic right ventricular cardiomyopathy; AS, aortic stenosis; CM, cardiomyopathy; CAD, atherosclerotic coronary artery disease; LAD, left anterior descending; MVP, mitral valve disease; WPW, Wolff–Parkinson–White.

events during training or competition [20–22], supports the view that intense physical activity represents a trigger for ventricular tachyarrhythmia-related sudden death, and disqualification of athletes with HCM from intense competitive sports is prudent [3,11] (Figure 57.3).

Clinical diagnosis of HCM is based on the most characteristic morphologic feature of the disease, namely asymmetric thickening of the left ventricular (LV) wall associated with a nondilated cavity in the absence of another cardiac or systemic disease capable of producing the magnitude of hypertrophy present (e.g., systemic hypertension or aortic stenosis) [48,49]. Although most HCM patients may demonstrate obstruction to LV outflow (at rest or with physiologic exercise), dynamic gradients are not required for diagnosis [52].

On the basis of echocardiographic, cardiovascular magnetic resonance (CMR), and necropsy analyses in large numbers of patients, the HCM disease spectrum is characterized by vast structural diversity with regard to the patterns and extent of LV hypertrophy [47,53]. Indeed, virtually all possible patterns of LV wall thickening have been reported in HCM, and no single phenotypic expression can be considered classic or typical of this disease. Nevertheless, the HCM phenotype is not invariably expressed as a greatly thickened LV, and a few genetically affected adults even have normal thicknesses (≤12 mm) [48–50].

Some young athletes with segmental hypertrophy of the anterior ventricular septum (wall thicknesses 13–15 mm), consistent with a relatively mild morphologic expression of HCM, may be difficult to distinguish from extreme expressions of physiologic LV hypertrophy, which represents an adaptation to systematic training (i.e., athlete's heart) [4,43–46]. In asymptomatic, trained athletes within this morphologic gray zone, the differential diagnosis between physiologic athlete's heart and HCM can often be resolved by clinical assessment and noninvasive testing (Figure 57.4).

Congenital coronary anomalies

Second in importance and frequency to HCM as a cause of athlete sudden death is a spectrum of congenital vascular malformations of the coronary arterial circulation (responsible for about 15–20% of young athlete deaths), the most common of which is anomalous left main coronary artery from the right (anterior) sinus of Valsalva, and less frequently anomalous right coronary from the left sinus [20–22,54]. Such coronary artery anomalies are difficult to detect clinically because they are not consistently associated with ECG abnormalities, or because the index of clinical suspicion is not sufficiently high. However, these anomalies are now recognized with increasing frequency due to penetration of CMR and CT angiography into clinical cardiovascular practice [55]. Such diagnostic considerations are particularly important since these malformations are rarely identified during life, but nevertheless are amenable to corrective surgery.
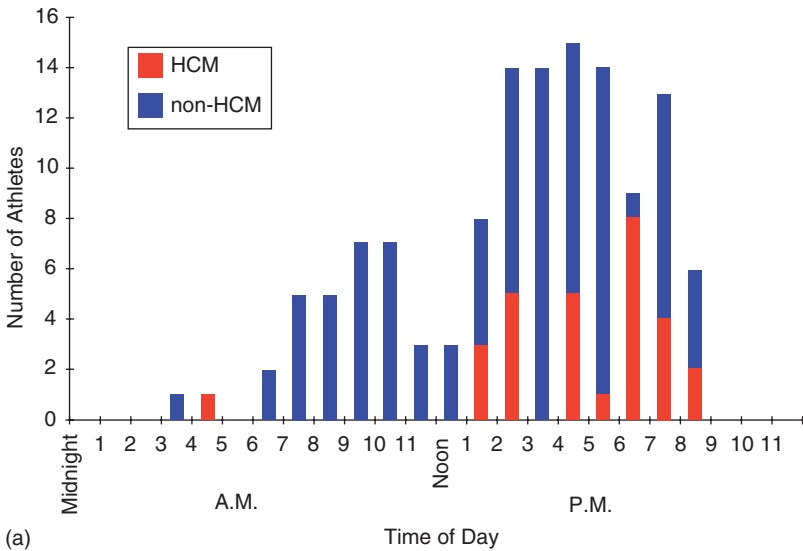
(a)
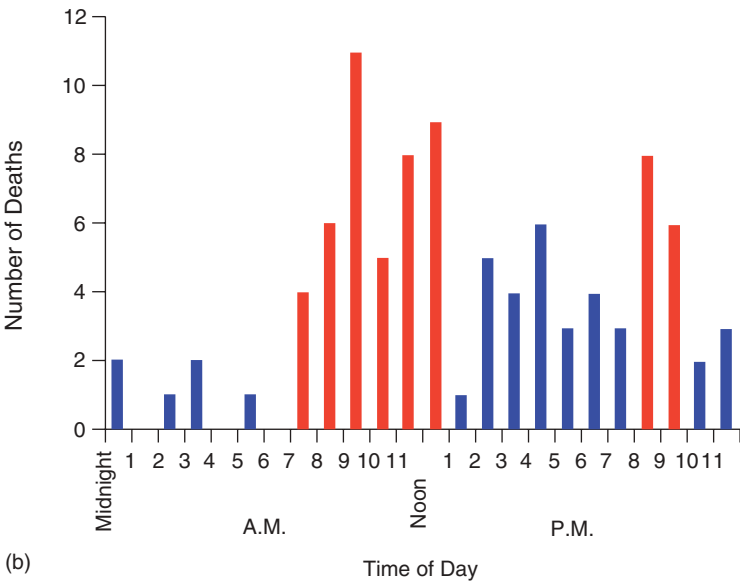
(b)

Figure 57.3 Hourly distribution of sudden cardiac deaths. (a) Histogram showing competitive athletes with either HCM (dark portion of bars) or a variety of other predominantly congenital cardiovascular malformations (light portion of bars). Time of death was predominantly in the late afternoon and early evening, corresponding largely to the time of training and competition. (b) In contrast, histogram for non-athlete HCM patients demonstrating a prominent early morning peak between 7 a.m. and 1 p.m. and a secondary peak in the early evening (most evident between 8 p.m. and 10 p.m.). (Reproduced from Maron *et al. JAMA* 1996;**276**:199–204, with permission from the American Medical Association.)

Other diseases

Less common causes of sudden death in young athletes are responsible for about 5% or less of athlete deaths and include myocarditis, dilated cardiomyopathy, aortic dissection and rupture due to Marfan syndrome, sarcoidosis, mitral valve prolapse, aortic valve stenosis, atherosclerotic coronary artery disease, long QT syndrome, and arrhythmogenic right ventricular cardiomyopathy/dysplasia (ARVC/D) [20–22] (Figure 57.2).

Of note, ARVC/D has been cited as the most common cause of sudden death in athletes in the Veneto region in northeastern Italy [56]. Although this disease is also a component of the US experience with athletic field deaths, its frequency is <5% in autopsy-based reports from the United States [19–22]. The explanation for such a discrepancy

between the United States and Italy remains incompletely resolved, although it is possible that the difference reflects a unique genetic substrate for ARVC/D in Italy. The relatively low frequency with which HCM is apparently responsible for sudden death in Italian athletes may however be due to the long-standing and systematic Italian national program for the cardiovascular assessment of competitive athletes [12,13,57]. which likely disqualifies disproportionate numbers of trained athletes with HCM, compared with ARVC/D (which is much more difficult to identify clinically).

On occasion, athletes may die suddenly without evidence of structural cardiovascular disease, even after careful gross and microscopic examination of the heart. In such instances (about 2% of autopsy cases) (Figure 57.1) [19–22], it may not be possible to exclude noncardiac factors (e.g., drug
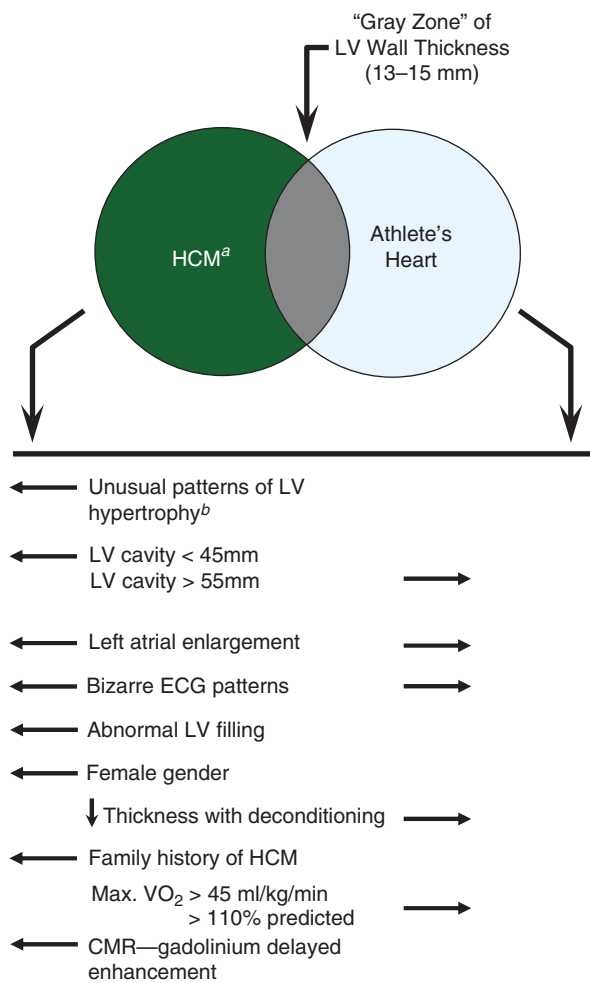
Figure 57.4 Clinical criteria used for differential diagnosis to distinguish hypertrophic cardiomyopathy (HCM) from physiologic athlete's heart when the left ventricular (LV) wall thickness is within the shaded gray zone of overlap (13–15 mm), consistent with both diagnoses. [a]Assumed to be the nonobstructive form of HCM because substantial mitral valve systolic anterior motion would confirm the diagnosis of HCM in an athlete. [b]May include a variety of abnormalities, including heterogeneous distribution of left ventricular hypertrophy (LVH) in which asymmetry is prominent, and adjacent regions may be of greatly different thicknesses, with sharp transitions evident between segments and areas of hypertrophy are non-contiguous, in addition to patterns in which the anterior ventricular septum is spared from the hypertrophic process and the region of predominant thickening may be in the posterior portion of the septum, or the anterolateral or posterior free wall, or left ventricular apex. ↓ = decreased; CMR, cardiovascular magnetic resonance; LV, left ventricular. (Adapted with permission from Maron et al. Circulation 1995;**91**:1596–601.)

Table 57.1 The 12-element American Heart Association recommendations for preparticipation cardiovascular screening of competitive athletes (Reproduced with permission from Maron BJ, Thompson PD, Ackerman MJ, et al. Circulation 2007;**115**:1643–55.).

Medical history[a]

Personal history

1. Exertional chest pain/discomfort
2. Unexplained syncope/near-syncope[b]
3. Excessive exertional and unexplained dyspnea/fatigue, associated with exercise
4. Prior recognition of a heart murmur
5. Elevated systemic blood pressure

Family history

6. Premature death (sudden and unexpected, or otherwise) before age 50 years due to heart disease in ≥1 relative
7. Disability from heart disease in a close relative <50 years of age
8. Specific knowledge of certain cardiac conditions in family members: hypertrophic or dilated cardiomyopathy, long-QT syndrome or other ion channelopathies, Marfan syndrome, or clinically important arrhythmias

Physical examination

9. Heart murmur[c]
10. Femoral pulses to exclude aortic coarctation
11. Physical stigmata of Marfan syndrome
12. Brachial artery blood pressure (sitting position)[d]

[a]Parental verification is recommended for high school and middle school athletes.
[b]Judged not to be neurocardiogenic (vasovagal).
[c]Auscultation should be performed in both supine and standing positions (or with Valsalva maneuver), specifically to identify murmurs of dynamic left ventricular outflow tract obstruction.
[d]Preferably taken in both arms.

abuse) as responsible for the catastrophe, or to determine whether careful inspection of the specialized conducting system and associated vasculature (which is not part of the standard medical examiner protocol) would have revealed occult but clinically relevant abnormalities. Some of these deaths may be due to primary ventricular tachyarrhythmias unassociated with cardiac structural abnormalities, such as Wolff–Parkinson–White syndrome or ion channelopathies such as long QT syndrome, possibly exercise-induced coronary spasm, or undetected segmental forms of ARVC/D.

Left anterior descending coronary artery tunneled within LV myocardium (i.e., "bridging") may constitute a potentially lethal anatomic variant in otherwise healthy young individuals during exertion [20–22,58]. Indeed, tunneled or bridged left anterior descending coronary artery completely surrounded by myocardium for at least a portion of its course (about 1–3 cm) was present in about 5% of the athlete field deaths in the US registry, in the absence of any other structural anomaly that could be assigned as the cause of death. On the other hand, bridged coronary arteries appear to play little role in promoting risk for sudden death in patients with HCM [58,59]. Also, the chronic ingestion of drugs (such as cocaine) may have adverse cardiovascular consequences, resulting in the clinicopathologic profiles of acute myocardial infarction and myocarditis [60].
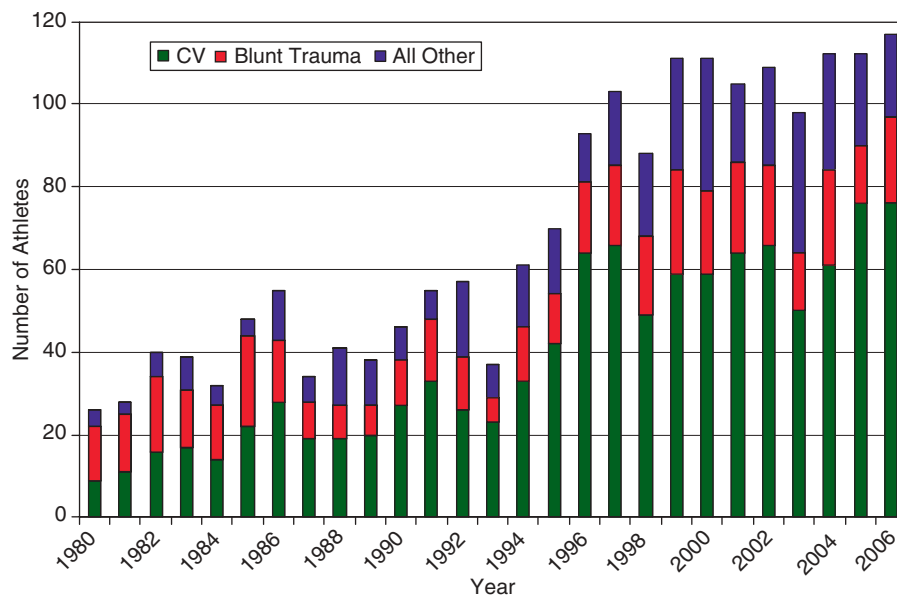
Figure 57.5 Number of cardiovascular, blunt trauma-related, or other sudden death events in 1866 US young competitive athletes, tabulated by year from the US National Registry. Other causes of these deaths include commotio cordis, heat stroke, illicit drugs, and pulmonary disease. (Reproduced with permission from Maron *et al*. *Circulation* 2009;**119**:1085–92.)

Prevalence and significance of the problem

Sudden unexpected death due to cardiovascular disease during competitive sports is rare in high-school students participating in organized interscholastic sports (i.e., about 1 per 220 000 participants per academic year or 1 per 70 000 participants during a 3-year high-school period [61]. In the large national US registry, the absolute number of cardiovascular sudden deaths in young athletes was relatively low with a rate of <100 per year [21] (Figure 57.5). Notably, the cardiovascular diseases responsible for sudden death in about one-third of these athletes would not likely be suspected or detected by screening (even with ECGs).

Somewhat higher estimates of the risk for sudden death have been reported for apparently healthy males, joggers, and marathon runners, usually due to atherosclerotic coronary artery disease [62,63]. Such estimates suggest that the intense and persistent public interest in these tragic events is perhaps disproportionate to their numerical significance in the general population. However, the emotional and social impact of athletic field catastrophes understandably remains high.

Despite its relatively low event rate, sudden death in young athletes continues to represent an important medical issue [1–3,5,6]. Indeed, it is an important responsibility of the medical community to create a fully informed public and also, when it is prudent and practical, to pursue early detection of the causes of catastrophic events in young athletes and initiate preventive measures. Because such events are uncommon relative to the vast numbers of athletes participating safely in sports, information about athlete field deaths should not raise undue anxiety among youthful athletes and their families and thereby inhibit participation in sports [7,8].

Demographics

On the basis of data assembled largely from broad-based US populations [19–22], a profile of young competitive athletes who die suddenly has emerged. Such athletes participate in a large number and variety of sports, the most frequent being basketball and football (about 70% combined), not only reflecting the high participation level in these popular team sports but also the intensity of competition. Most athletic field deaths occur in men (about 90%); the relative infrequency in women probably reflects a lower participation level, sometimes less intense levels of training, and the fact that some diseases most commonly accounting for sudden death in athletes may be recognized less frequently in women (e.g., HCM). Most athletes are of high-school age at the time of death (about 60%); however, not uncommonly, other sudden deaths have been reported in young athletes who have achieved collegiate or even professional levels of competition.

Most athletes who die suddenly, regardless of their particular underlying disease, have been free of symptoms and usually are not suspected of harboring a cardiovascular abnormality. Sudden collapse usually occurs with exercise, predominantly in the late afternoon and early evening hours, corresponding to peak periods of competition and training, particularly in organized team sports such as football and basketball (Figure 57.3). This observation for athletes with HCM contrasts sharply with prior reports in HCM patients who are not competitive athletes, for whom a bimodal pattern of circadian variability was evident, including a
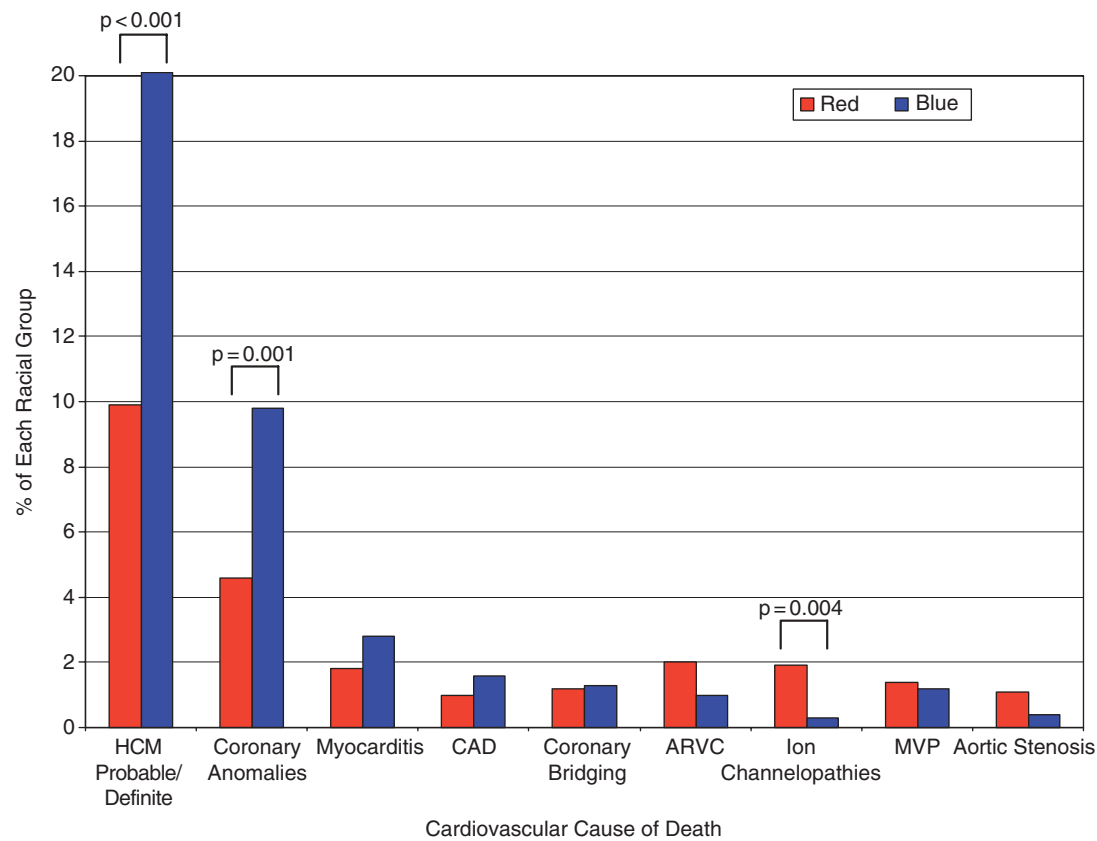
Figure 57.6 Cardiovascular deaths in athletes according to race. The data include 690/1866 total deaths that were proved to be due to cardiovascular causes and are shown with respect to the number of white and non-white athletes with each disease. ARVC, arrhythmogenic right ventricular cardiomyopathy; HCM, hypertrophic cardiomyopathy; CAD, coronary artery disease; MVP, mitral valve prolapse.

prominent early- to mid-morning peak, similar to that reported in patients with coronary artery disease and acute myocardial infarction or sudden death (Figure 57.3) [64].

Although most sudden deaths reported in competitive athletes have been in white men, a substantial proportion (>40%) were African-American athletes (Figure 57.6) [21,22]. This substantial occurrence of HCM-related sudden death in young black male athletes contrasts sharply with the infrequent identification of HCM in hospital-based populations. These data emphasize that it is less common for young African-American men to receive a cardiovascular diagnosis such as HCM (which requires echocardiography) than their white counterparts and, consequently, they are less likely to be disqualified from competition in accordance with the recommendations of the 36th Bethesda Conference [3] to reduce the risk for sudden death.

Mechanisms of SD and AEDs

Although the precise mechanism ultimately responsible for sudden death in young athletes depends on the particular disease state involved, in most victims (including athletes with HCM), cardiac arrest results from electrical instability and ventricular tachyarrhythmias. The most common exception is Marfan syndrome, in which death is usually due to ruptured aorta [19–22].

Automated external defibrillators (AEDs) represent an important and effective impetus to secondary prevention of sudden death in trained athletes with cardiovascular disease, and deserve greater dissemination, accessibility and penetration into the sports arena [65–70]. Several studies of early defibrillation using public access AEDs have demonstrated a survival benefit for out-of-hospital cardiac arrest [66,67,70]. The available AED literature suggests that the use of AEDs by trained or untrained bystanders and nontraditional responders produces survival rates of 40–75% when CPR is provided and defibrillation is rapid within 5 min of collapse. Particularly relevant is the recent study of Drezner *et al.* [70] surveying 1710 high schools with onsite AED programs; 2% of the high schools reported a sudden cardiac arrest either in student athletes, employers, or spectators, and 64% of these events had restoration of sinus rhythm and survival to hospital discharge, including athletes with cardiomyopathies, such as HCM and ARVC.
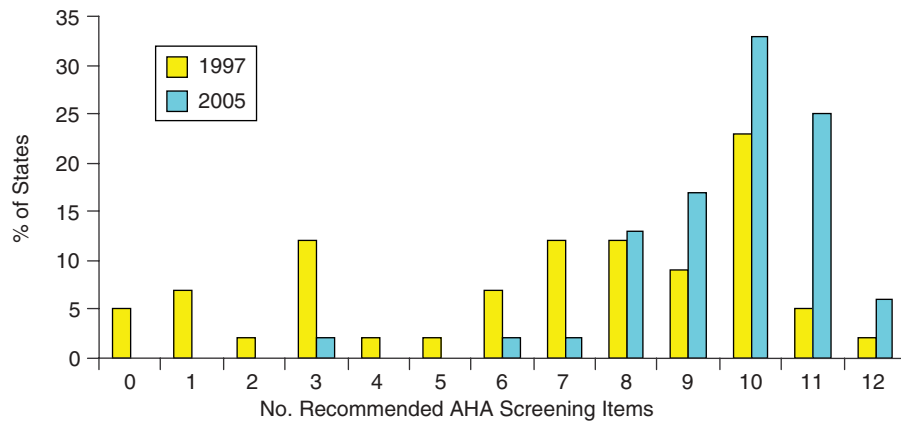
Figure 57.7 Comparison of state preparticipation screening questionnaire forms, 1997 versus 2005, for US high school athletes, analyzed with respect to American Heart Association recommendations. Screening forms could be assessed for 43 states in the 1997 and 48 states in 2005. (Reproduced from Glover *et al. Am J Cardiol* 2007;**100**:1709–12, with permission from Elsevier.)

Screening and preparticipation detection of cardiovascular abnormalities

General perspectives

The detection of pre-existing cardiovascular abnormalities with the potential for significant morbidity or sudden death is an important objective of the widespread practice of preparticipation screening of high-school and college-aged athletes (Figure 57.7). There is a general consensus within a benevolent society that a responsibility exists on the part of physicians to initiate prudent efforts to identify life-threatening diseases in athletes to minimize the cardiovascular risks associated with sport [1–3,5,7,8,11–13,71]. Screening recommendations are predicated on the probability that intense athletic training is likely to increase the risk for sudden cardiac death (or disease progression) in trained athletes with underlying structural heart disease, although it is currently not possible to quantify that risk with precision, or to know prospectively to which individual athletes these considerations will apply with certainty.

However, there are two major limitations to mass population screening for competitive athletes. First is the rarity of those lesions responsible for sudden cardiac death in young healthy people. The several largely congenital malformations most relevant to athletic screening (including HCM) [17,21] account for a combined prevalence of only about 0.3% or less within the general competitive athlete population [4,49,51]. The second consideration is the large reservoir of competitive athletes who are eligible for preparticipation screening, which in the United States is probably in the range of at least 10–15 million each year [8,21,28,31].

Customary practice and legal considerations

Two American Heart Association expert consensus panels [7,8] have recommended a standard, systematic preparticipation screening strategy to raise the suspicion (or detect) potentially lethal cardiovascular abnormalities with history and physical examination. However, no available screening design can detect all important lesions or affected athletes, and medical clearance for sports with history and physical examination does not necessarily imply the absence of cardiovascular disease [7,8]. US law enables the medical profession to establish the bounds of appropriate management of athletes by the physician [2,33,71]. Indeed, the medical standard is ultimately translated into the legal standard for malpractice purposes [2,33,71]. Although educational institutions and professional teams are required to use reasonable care in conducting their athletic programs, there currently is no clear legal precedent regarding their duty to conduct preparticipation screening of athletes for the purpose of detecting medically significant abnormalities. In the absence of binding requirements established by state law or athletic governing bodies, most institutions and teams at present rely on the team physician (or other medical personnel) to determine the appropriate medical screening procedures [33,71,72].

A physician who has medically cleared an athlete to participate in competitive sports is not necessarily legally liable for an injury or death caused by an undetected cardiovascular condition [71]. Malpractice liability for failure to discover a latent, asymptomatic cardiovascular condition requires proof that a physician deviated from customary or accepted medical practice in his or her specialty in performing the preparticipation screening of athletes and furthermore that the use of established diagnostic criteria and techniques would have disclosed that medical condition [72].

Some form of medical clearance by a physician or other trained healthcare worker, consisting of a history and physical examination, appears to be customary for most high-school and college athletes [71,72]. However, currently, there are no universally accepted standards for the screening of athletes in the United States, nor are there approved certification procedures for the healthcare professionals who perform such screening examinations [29,30,72]. Indeed, in

a number of states, non-physician healthcare workers are sanctioned to perform athletic screening examinations, including advanced nurse practitioners or physician assistants and even chiropractors. Standards may be mandated by state legislative action or rest with individual state high-school athletic associations or school districts. There is no agreement among the states, however, as to the precise format of preparticipation medical evaluations. Indeed, a small minority of states still have no standard history and physical forms to serve as a guide to the examiners of high school athletes, and in others the medical clearance forms have been criticized as generally inadequate when evaluated against the specific screening recommendations proposed by the 2007 American Heart Association consensus panel [8] (Table 57.1). However, over the last several years, largely in response to a highly visible critique [29], the history and physical examination forms have been improved substantially in many states [30], undoubtedly increasing the number of athletes diagnosed with cardiovascular disease (Figure 57.7). Nevertheless, it is not possible to ascertain with precision the extent to which such changes have enhanced identification of disease.

Expectations

Most of the lesions considered here as potentially responsible for sudden death in young athletes are challenging to detect by screening, even with echocardiography, ECG, or other noninvasive tests incorporated into the process, for example, congenital coronary anomalies, particularly anomalous origin of left main coronary artery from the right sinus of Valsalva. Despite its limitations, history and physical examination screening alone can be effective in raising suspicion of certain cardiovascular diseases such as HCM in some at-risk athletes [73]. Indeed, other genetic heart diseases, such as Marfan syndrome and ARVC/D, and also premature atherosclerotic coronary artery disease, can be suspected by family history or by prior transient symptoms. Physical examination may identify the stigmata of Marfan syndrome, mitral valve prolapse, or left ventricular outflow obstruction by a heart murmur (e.g., in aortic valvar stenosis and some patients with HCM), or systemic hypertension. Indeed, about 5% of the young patients referred to our center for HCM have been initially identified through preparticipation sports screening [73].

Electrocardiogram

The 12-lead ECG has been proposed as an effective alternative to echocardiography for population-based screening [9,10, 12–14,27,37,39,74,75]. Indeed, the ECG is abnormal in about 75–95% of patients with HCM [76–78] and is an effective tool for the detection of this disease in an Italian athlete population [12,18], and also will usually identify long QT syndrome. However, the ECG has low specificity as a screening test in athletic populations because of the high frequency of ECG alterations associated with the normal physiologic adaptations

to training ("athlete's heart") [4,7–9,15,31,36,38,79–81]. In mass preparticipation screening, about 10–20% of athletes examined have an ECG pattern that ultimately triggers echocardiographic study [4,7,8,13,15,28,31,44,81,82].

Finally, elite trained athletes not infrequently demonstrate distinctly abnormal ECG patterns indistinguishable from pathologic conditions, in the absence of structural heart disease [81,82]. These largely false-positive test results complicate efforts to use the 12-lead ECG as a primary screening tool in athletic populations [7,8,28,33,75,76,81–83], although occasionally they may be early markers of cardiomyopathies [16]. Notably, race also unavoidably impacts US screening specificity/sensitivity and reliability, as African-American athletes without heart disease may show distinctively abnormal ECG patterns [83] and thicker LV walls than white athletes [45]. Finally, even primary echocardiographic screening of athletes for HCM has resulted in a low yield of disease detection in the United States [32] and United Kingdom [17].

Screening strategies: US versus italian models

The preparticipation cardiovascular screening process of young trained athletes is time honored in the United States, Italy, and much of Europe, and generally conceded to be a desirable aspiration with potential benefits for public health [5,7–16,27,28,31,33,36,37,74,75,79,80,84]. However, controversy has emerged regarding the most effective strategy for examining large populations of competitive athletes [7,8,12–15,28,33,80,84]. At present, high school and college-aged athletes in the United States (and many other parts of the world) are screened by a personal and family medical history and physical examination performed by designated examiners with varying levels of cardiovascular training [7,8]. However, in Italy, a unique mandatory national preparticipation screening program has been employed for over 25 years, routinely consisting of a 12-lead ECG (in addition to history and physical examination) and administered by a select cadre of accredited sports medicine physicians dedicated to this process [13,28,57].

The Italian screening model with routine ECGs has achieved considerable visibility over the last several years and has been promoted as the standard by the European Society of Cardiology [13], the International Olympic Committee [27], and others [9,10,13,14,27,37,74]. In addition, studies from the Veneto region have documented identification of HCM in athletes [18] and most recently have reported a 90% decrease in athlete sudden deaths over the past 25 years which was attributed to the national screening program [12]. In contrast to the European zeal for mass screening with ECGs [12,13,27,37,84,85], the AHA consensus scientific panels have persistently discouraged such a program for the United States as impractical and possibly counterproductive, while alternatively supporting self-sustaining regional or local initiatives [7,8].
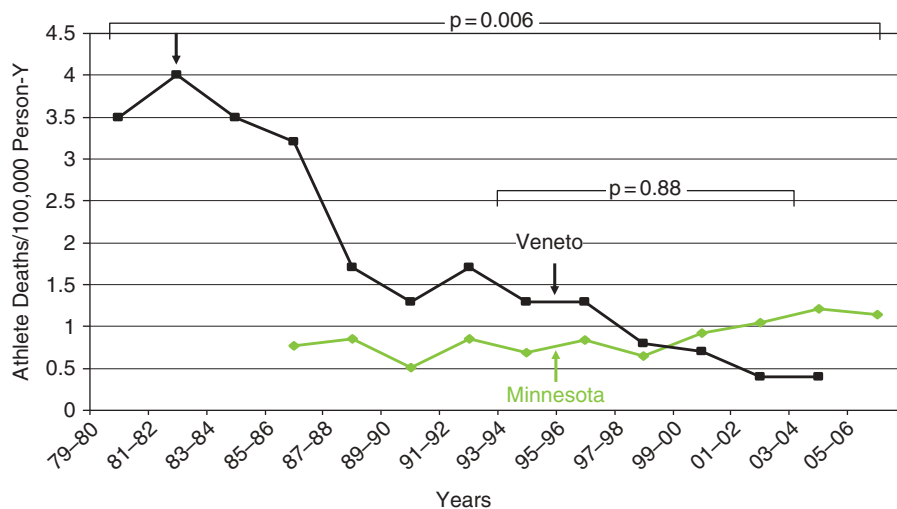
Figure 57.8 Plot comparing annual mortality in competitive athletes per 100 000 person-years in the Veneto region (Italy) and Minnesota (United States). Arrow denotes the beginning of the Italian national preparticipation screening program. (Reproduced from Maron *et al. Am J Cardiol* 2009;**104**:276–80, with permission from Elsevier.)

Obstacles in the United State to the Italian model of mandatory and routine athlete ECG screening include the lack of professional resources (without an established and dedicated group of sports medicine examiners, such as exists in Italy), and cost-efficacy considerations, in addition to the expected high proportion of false-negative (and particularly false-positive) results, which would create chaos for secondary testing. Furthermore, and perhaps most importantly, limiting systematic population screening to a select segment of the general youthful population would be regarded as both exclusionary and discriminatory. Therefore, US screening for cardiovascular disease would probably be acceptable ethically only if extended to the entire youthful population, involving up to about 30 million people annually, likely an impossible proposal.

Critics of the AHA position cite the Italian program and its apparent benefits, resulting in very low mortality rates in athletes over the most recent years, and implying that the US screening strategy (with only history and physical examination) could be responsible for an excess of cardiovascular deaths in athletes [33,84]. However, a comparison of published data from the Veneto region and from the United State (i.e., the demographically similar state of Minnesota) does not support this view [23]. Despite the different screening strategies employed (Veneto, history, physical examination and ECGs; Minnesota, history and physical examination alone), there was no significant difference evident in the incidence of athlete sudden deaths between Veneto and Minnesota over the most recent decade (Figure 57.8). In the period 1994–2004, when the two athlete populations could be compared directly in time, mortality rates were very low in both, relatively constant, and similar to that previously reported in US high school and college athletes [21,23,61], and were not significantly different in statistical terms. This observation supports data from other sources that cardiovascular sudden death in young athletes is in fact a low event rate (albeit tragic)

phenomenon [21,28,61]. Recognition of this principle is the basis for the decision not to screen competitive athletes systematically in Denmark [34,85].

Eligibility considerations for athletes with known cardiovascular disease

When a cardiovascular abnormality is identified in a competitive athlete, the following considerations arise: (a) the magnitude of risk for sudden cardiac death associated with continued participation in competitive sports; and (b) criteria to be implemented for determining whether individual athletes should be withdrawn temporarily or permanently from sports competition to reduce risk. Recommendations for athletic eligibility or disqualification are available in the 36th Bethesda Conference [3], and also in ESC guidelines [11], considering the severity of the cardiovascular abnormality and the nature of the sports training and competition. These recommendations are predicated on the principle that intense athletic training and competition increase the risk for sudden cardiac death (or disease progression) in trained athletes with clinically important underlying structural heart disease, although it is not possible at present to quantify that risk in precise terms.

References

1 Maron BJ. Sudden death in young athletes: lessons from the Hank Gathers affair. *N Engl J Med* 1993;**329**:55–7.

2 Maron BJ, Mitten MJ, Quandt EK, Zipes DP. Competitive athletes with cardiovascular disease – the case of Nicholas Knapp. *N Engl J Med* 1998;**339**:1632–5.

3 Maron BJ, Zipes DP. 36th Bethesda Conference: Eligibility Recommendations for Competitive Athletes with Cardiovascular Abnormalities. *J Am Coll Cardiol* 2005;**45**:1312–75.

4 Maron BJ, Pelliccia A. The heart of trained athletes: cardiac remodeling and the risks of sports including sudden death. *Circulation* 2006;**114**:1633–44.

5 Maron BJ. Sudden death in young athletes. *N Engl J Med* 2003;**349**:1064–75.

6 Maron BJ. Cardiovascular risks to young persons on the athletic field. *Ann Intern Med* 1998;**129**:379–86.

7 Maron BJ, Thompson PD, Puffer JC, *et al*. Cardiovascular preparticipation screening of competitive athletes: a statement for health professionals from the Sudden Death Committee (Clinical Cardiology) and Congenital Cardiac Defects Committee (Cardiovascular Diseases in the Young), American Heart Association. *Circulation* 1996;**94**:850–6.

8 Maron BJ, Thompson PD, Ackerman MJ, *et al*. Recommendations and considerations related to preparticipation screening for cardiovascular abnormalities in competitive athletes: update 2007. A Scientific Statement from the American Heart Association, Nutrition, Physical Activity, and Metabolism Council. *Circulation* 2007;**115**:1643–55.

9 Baggish AL, Hutter AM Jr, Wang F, *et al*. Addition of 12-lead electrocardiography to medical history and physical examination for cardiovascular screening in college athletes. A cross-sectional study. *Ann Intern Med* 2010;**152**:269–75.

10 Wheeler, MT, Heidenreich PA, Froelicher VF, *et al*. Cost-effectiveness of preparticipation screening for prevention of sudden cardiac death in young athletes. *Ann Intern Med* 2010;**152**:276–86.

11 Pelliccia A, Fagard, Bjornstad HH, *et al*. Recommendations for competitive sports participation in athletes with cardiovascular disease: a consensus document for the European Society of Cardiology. *Eur Heart J* 2005;**26**:1422–45.

12 Corrado D, Basso C, Pavei A, *et al*. Trends in sudden cardiovascular death in young competitive athletes after implementation of a preparticipation screening program. *JAMA* 2006;**296**:1593–601.

13 Corrado D, Pelliccia A, Bjørnstad HH, *et al*. Cardiovascular preparticipation screening of young competitive athletes for prevention of sudden death: proposal for a common European protocol. Consensus Statement of the Study Group of Sport Cardiology of the Working Group of Myocardial and Pericardial Diseases of the European Society of Cardiology. *Eur Heart J* 2005;**26**:510–24.

14 Myerburg RJ, Vetter LV. Electrocardiograms should be included in preparticipation screening of athletes. *Circulation* 2007;**116**:2616–26.

15 Chaitman BR. An electrocardiogram should not be included in routine preparticipation screening of young athletes. *Circulation* 2007;**116**:2610–4.

16 Pelliccia A, DiPaolo FM, Quattrini FM, *et al*. Outcomes in athletes with marked ECG repolarization abnormalities. *N Engl J Med* 2008;**358**:152–61.

17 Basavarajaiah S, Wilson M, Whyte G, *et al*. Prevalence of hypertrophic cardiomyopathy in highly trained athletes. Relevance to pre-participation screening. *J Am Coll Cardiol* 2008;**51**:1033–9.

18 Corrado D, Basso C, Schiaron M, Thiene G. Screening for hypertrophic cardiomyopathy in young athletes. *N Engl J Med* 1998;**339**:364–9.

19 Van Camp SP, Bloor CM, Mueller FO, *et al*. Nontraumatic sports death in high school and college athletes. *Med Sci Sports Exerc* 1995;**27**:641–7.

20 Maron BJ, Shirani J, Poliac LC, *et al*. Sudden death in young competitive athletes: clinical, demographic and pathological profiles. *JAMA* 1996;**276**:199–204.

21 Maron BJ, Doerer JJ, Haas TS, *et al*. Sudden deaths in young competitive athletes: analysis of 1,866 deaths in the U.S., 1980–2006. *Circulation* 2009;**119**:1085–92.

22 Maron BJ, Carney KP, Lever HM, *et al*. Relationship of race to sudden cardiac death in competitive athletes with hypertrophic cardiomyopathy. *J Am Coll Cardiol* 2003;**41**:974–80.

23 Maron BJ, Haas TS, Doerer JJ, *et al*. Comparison of U.S. and Italian experiences with sudden cardiac deaths in young competitive athletes and implications for preparticipation screening strategies. *Am J Cardiol* 2009;**104**:276–80.

24 Maron BJ, Gohman TE, Kyle SB, *et al*. Clinical profile and spectrum of commotio cordis. *JAMA* 2002;**287**:1142–6.

25 Maron BJ, Poliac L, Kaplan JA, Mueller FO. Blunt impact to the chest leading to sudden death from cardiac arrest during sports activities. *N Engl J Med* 1995;**333**:337–42.

26 Maron BJ, Estes NAM III. Commotio cordis. *N Engl J Med* 2010;**362**:917–27.

27 Bille K, Figueiras D, Schamasch P, *et al*. Sudden cardiac death in athletes: the Lausanne recommendations. *Eur J Cardiovasc Prev Rehabil* 2006;**13**:859–75.

28 Maron BJ. National electrocardiography screening for competitive athletes: feasible in the United States? (Editorial) *Ann Intern Med* 2010;**152**:324–6.

29 Glover DW, Maron BJ. Profile of preparticipation cardiovascular screening for high school athletes. *JAMA* 1998;**279**:1817–9.

30 Glover DW, Glover DW, Maron BJ. Evolution in the process of screening United States high school student-athletes for cardiovascular disease. *Am J Cardiol* 2007;**100**:1709–12.

31 Thompson PD, Levin BD. Protecting athletes from sudden cardiac death (Editorial). *JAMA* 2006;**296**:1648–50.

32 Lewis JF, Maron BJ, Diggs JA, *et al*. Preparticipation echocardiographic screening for cardiovascular disease in a large predominantly black population of collegiate athletes. *Am J Cardiol* 1989;**64**:1029–33.

33 Marek JC, Pelliccia A, Corrado D, Maron BJ. Electrocardiography and preparticipation screening of competitive high school athletes. *Ann Intern Med* 2010;**153**:131–3.

34 Maron BJ. Diversity of views from Europe on national preparticipation screening for competitive athletes. *Heart Rhythm* 2010;**7**:1372–3.

35 Maron BJ, Douglas PS, Graham TP, *et al*. Task Force 1: preparticipation screening and diagnosis of cardiovascular disease in athletes. 36th Bethesda Conference: Eligibility Recommendations for Competitive Athletes with Cardiovascular Abnormalities. *J Am Coll Cardiol* 2005;**45**:1322–6.

36 Lawless CE, Best TM. Electrocardiograms in athletes: interpretation and diagnostic accuracy. *Med Sci Sports Exerc* 2008;**40**:787–98.

37 Bessem B, Groot FP, Nieuwland W. The Lausanne recommendations: a Dutch experience. *Br J Sports Med* 2009;**43**:708–15.

38 Le VV, Wheeler MT, Mandic S, *et al*. Addition of the electrocardiogram to the preparticipation examination of college athletes. *Clin J Sport Med* 2010;**20**:98–105.

39 Ma JZ, Dai J, Sun B, *et al*. Cardiovascular pre-participation screening of young competitive athletes for prevention of sudden death in China. *J Sci Med Sport* 2007;**10**:227–33.

40 Harris KM, Sponsel A, Hutter AM Jr, Maron BJ. Cardiovascular screening practices of major North American professional sports teams. *Ann Intern Med* 2006;**145**:507–11.

41 Maron BJ, Zipes DP. Introduction. 36th Bethesda Conference: Eligibility Recommendations for Competitive Athletes with Cardiovascular Abnormalities – General Considerations. *J Am Coll Cardiol* 2005;**45**:1318–21.

42 Maron BJ, Chaitman B, Ackerman MJ, *et al*. American Heart Association Scientific Statement: Recommendations for Physical Activity and Recreational Sports Participation for Young Patients with Genetic Cardiovascular Diseases. *Circulation* 2004;**109**:2807–16.

43 Maron BJ, Pelliccia A, Spirito P. Cardiac disease in young trained athletes: insights into methods for distinguishing athlete's heart from structural heart disease with particular emphasis on hypertrophic cardiomyopathy. *Circulation* 1995;**91**:1596–601.

44 Maron BJ. Distinguishing hypertrophic cardiomyopathy from athlete's heart physiologic remodelling: clinical significance, diagnostic strategies and implications for preparticipation screening. *Br J Sports Med* 2009;**43**:649–56.

45 Basavarajaiah S, Boraita A, Whyte G, *et al*. Ethnic differences in left ventricular remodeling in highly-trained athletes. Relevance to differentiating physiologic left ventricular hypertrophy from hypertrophic cardiomyopathy. *J Am Coll Cardiol* 2008;**51**:2256–62.

46 Sharma S, Maron BJ, Whyte G, *et al*. Physiologic limits of left ventricular hypertrophy in elite junior athletes: relevance to differential diagnosis of athlete's heart and hypertrophic cardiomyopathy. *J Am Coll Cardiol* 2002;**40**:1431–6.

47 Klues HG, Schiffers A, Maron BJ. Phenotypic spectrum and patterns of left ventricular hypertrophy in hypertrophic cardiomyopathy: morphologic observation and significance as assessed by two-dimensional echocardiography in 600 patients. *J Am Coll Cardiol* 1995;**26**:1699–708.

48 Maron BJ. Hypertrophic cardiomyopathy: a systematic review. *JAMA* 2002;**287**:1308–20.

49 Maron BJ, McKenna WJ, Danielson GK, *et al*. American College of Cardiology/European Society of Cardiology Clinical Expert Consensus Document on Hypertrophic Cardiomyopathy. A Report of the American College of Cardiology Task Force on Clinical Expert Consensus Documents and the European Society of Cardiology Committee for Practice Guidelines Committee to Develop an Expert Consensus Document on Hypertrophic Cardiomyopathy. *J Am Coll Cardiol* 2003;**42**:1687–713.

50 Alcalai R, Seidman JG, Seidman CE. Genetic basis of hypertrophic cardiomyopathy from bench to the clinics. *J Cardiovasc Electrophysiol* 2008;**19**:104–10.

51 Maron BJ, Gardin JM, Flack JM, *et al*. Assessment of the prevalence of hypertrophic cardiomyopathy in a general population of young adults: echocardiographic analysis of 4111 subjects in the CARDIA study. *Circulation* 1995;**92**:785–9.

52 Maron MS, Olivotto I, Zenovich AG, *et al*. Hypertrophic cardiomyopathy is predominantly a disease of left ventricular outflow tract obstruction. *Circulation* 2006;**114**:2232–9.

53 Maron MS, Maron BJ, Harrigan C, *et al*. Hypertrophic cardiomyopathy phenotype revisited after 50 years with cardiovascular magnetic resonance. *J Am Coll Cardiol* 2009;**54**:220–8.

54 Basso C, Maron BJ, Corrado D, Thiene G. Clinical profile of congenital coronary artery anomalies with origin from the wrong aortic sinus leading to sudden death in young competitive athletes. *J Am Coll Cardiol* 2002;**35**:1493–501.

55 Knickelbine T, Lesser RJ, Brandenburg ER, *et al*. Identification of unexpected nonatherosclerotic cardiovascular disease with CT angiography. *J Am Coll Cardiol Img* 2009;**2**:1085–92.

56 Thiene G, Nava A, Corrado D, *et al*. Right ventricular cardiomyopathy and sudden death in young people. *N Engl J Med* 1988;**318**:129–33.

57 Pelliccia A, Maron BJ. Preparticipation cardiovascular evaluation of the competitive athlete: perspectives from the 30 year Italian experience. *Am J Cardiol* 1995;**75**:827–9.

58 Basso C, Thiene G, Mackey-Bojack S, *et al*. Myocardial bridging: a frequent component of the hypertrophic cardiomyopathy phenotype lacks systematic association with sudden cardiac death. *Eur Heart J* 2009;**30**:1627–34.

59 Maron BJ. Contemporary insights and strategies for risk stratification and prevention of sudden death in hypertrophic cardiomyopathy. *Circulation* 2010;**121**:445–56.

60 Kloner RA, Hale S, Alkekr K, Rezkalla S. The effects of acute and chronic cocaine use on the heart. *Circulation* 1992;**85**:407–19.

61 Maron BJ, Gohman TE, Aeppli D. Prevalence of sudden cardiac death during competitive sports activities in Minnesota high school athletes. *J Am Coll Cardiol* 1998;**32**:1881–4.

62 Maron BJ, Poliac LC, Roberts WO. Risk for sudden cardiac death associated with marathon running. *J Am Coll Cardiol* 1996;**28**:428–31.

63 Roberts WO, Maron BJ. Evidence for decreasing occurrence of sudden cardiac death associated with the marathon. *J Am Coll Cardiol* 2005;**46**:1373–4.

64 Maron BJ, Kogan J, Proschan MA, *et al*. Circadian variability in the occurrence of sudden cardiac death in patients with hypertrophic cardiomyopathy. *J Am Coll Cardiol* 1994;**23**:1405–9.

65 Estes NA III, Link MS, Cannon D, *et al*. Report of the NASPE policy conference on arrhythmias and the athlete. *J Cardiovasc Electrophysiol* 2001;**12**:1208–19.

66 Drezner JA, Courson RW, Roberts WO, *et al*.; Inter-Association Task Force. Inter-Association Task Force recommendations on emergency preparedness and management of sudden cardiac arrest in high school and college athletic programs: a consensus statement. *Heart Rhythm* 2007;**4**:549–65.

67 Drezner JA. Preparing for sudden cardiac arrest – the essential role of automated external defibrillators in athletic medicine: a critical review. *Br J Sports Med* 2009;**43**:702–7.

68 Rothmier JD, Drezner JA, Harmon KG. Automated external defibrillators in Washington State high schools. *Br J Sports Med* 2007;**41**:301–5.

69 Drezner JA, Rogers KJ, Zimmer RR, Sennett BJ. Use of automatied external defibrillators at NCAA Division I universities. *Med Sci Sports Exerc* 2005;**37**:1487–92.

70 Drezner JA, Rao AL, Heistand J, *et al*. Effectiveness of emergency response planning for sudden cardiac arrest in United States high schools with automated external defibrillators. *Circulation* 2009;**120**:518–25.

71 Mitten MJ, Maron BJ, Zipes DP. Task Force 12: legal aspects of the 36th Bethesda Conference Recommendations. 36th Bethesda Conference Eligibility Recommendations for Competitive Athletes with Cardiovascular Abnormalities. *J Am Coll Cardiol* 2005;**45**:1373–5.

72 Paterick TE, Paterick TJ, Fletcher GF, Maron BJ. Medical and legal issues impacting the cardiovascular evaluation of competitive athletes. *JAMA* 2005;**294**:3011–8.

73 Adabag AS, Kuskowski MA, Maron BJ. Determinants for clinical diagnosis of hypertrophic cardiomyopathy. *Am J Cardiol* 2006;**98**:1507–11.

74 Wilson MG, Basavarajaiah S, Whyte GP, *et al*. Efficacy of personal symptoms and family history questionnaires when screening for inherited cardiac pathologies: the role of electrocardiography. *Br J Sports Med* 2008;**42**:207–11.

75 Corrado D, Pelliccia A, Heidbuchel H, *et al*. Recommendations for interpretation of 12-lead electrocardiogram in the athlete. *Eur Heart J* 2010;**31**:243–59.

76 Montgomery JV, Harris KM, Casey SA, *et al*. Relation of electrocardiographic patterns to phenotypic expression and clinical outcome in hypertrophic cardiomyopathy. *J Am Coll Cardiol* 2005;**96**:270–5.

77 Maron BJ, Niimura H, Casey SA, *et al*. Development of left ventricular hypertrophy in adults with hypertrophic cardiomyopathy caused by cardiac myosin-binding protein C mutations. *J Am Coll Cardiol* 2001;**38**:315–21.

78 McLeod CL, Ackerman MJ, Nishimura RA, *et al*. Outcome of patients with hypertrophic cardiomyopathy and a normal electrocardiogram. *J Am Coll Cardiol* 2009;**54**:229–33.

79 Wren C. Screening for potentially fatal heart disease in children and teenagers. *Heart* 2009;**95**:2040–6.

80 Chaitman BR, Fromer M. Should ECG be required in young athletes? *Lancet* 2008;**371**:1489–90.

81 Culasso F, Di Paolo FM, Spataro A, *et al*. Clinical significance of abnormal electrocardiographic patterns in trained athletes. *Circulation* 2000;**102**:278–84.

82 Maron BJ, Bodison S, Wesley Y, *et al*. Results of screening a large group of intercollegiate competitive athletes for cardiovascular disease. *J Am Coll Cardiol* 1987;**10**:1214–21.

83 Magalski A, Maron BJ, Main ML, *et al*. Relation of race to electrocardiographic patterns in elite American football players. *J Am Coll Cardiol* 2008;**51**:2250–5.

84 Corrado D, Basso C, Schiavon M, *et al*. Preparticipation screening of young competitive athletes. *J Am Coll Cardiol* 2008;**52**: 1981–8.

85 Holst AG, Winkel BG, Theilade J, *et al*. Incidence and etiology of sports-related sudden cardiac death in Denmark – implications for preparticipation screening. *Heart Rhythm* 2010; **7**:1365–71.

Jeffrey A. Towbin
Cincinnati Children's Hospital, Cincinnati, OH, USA

Introduction

Cardiomyopathies are major causes of morbidity and mortality. The term was introduced in 1957 to identify a group of myocardial diseases not attributable to coronary artery disease [1]. The definition has since been modified and now refers to structural or functional abnormalities of the myocardium not secondary to hypertension, valvar or congenital heart disease, or pulmonary vascular disease. Over the past 20 years, our understanding of the major forms of cardiomyopathy has improved, largely from advances in genetics and genomics. Clinical understanding of childhood forms of cardiomyopathy has also improved by the longitudinal follow-up gained from the NIH–NHLBI-funded Pediatric Cardiomyopathy Registry (PCMR) [2–4]. New forms of cardiomyopathy have been described and classified, and further subdivided into genetic/inherited forms and acquired/noninherited forms [5]. Each form occurs in childhood, although ARVC (see below) is almost always identified in adolescents or young adults.

The five classified forms of cardiomyopathy are as follows [5]:

1 Dilated cardiomyopathy (DCM), previously called congestive cardiomyopathy, demonstrates left ventricular or biventricular dilation and depressed systolic function. Systolic dysfunction is a main clinical feature resulting in signs and symptoms of congestive heart failure.

2 Hypertrophic cardiomyopathy (HCM), formerly known as idiopathic hypertrophic subaortic stenosis, is characterized by left ventricular hypertrophy that may be asymmetric. Systolic function is usually preserved. Symptoms result from left ventricular outflow tract obstruction, diastolic dysfunction, or arrhythmias causing sudden death.

3 Restrictive cardiomyopathy (RCM) has impaired diastolic filling, but with generally normal ventricular dimensions and systolic function. It is recognized by markedly dilated atria,. Symptoms result from pulmonary and right-sided systemic venous congestion. Syncope may be a presenting feature.

4 Arrhythmogenic cardiomyopathy, formerly known as arrhythmogenic right ventricular dysplasia (ARVD) or arrhythmogenic right ventricular cardiomyopathy (ARVC), is a disease affecting both ventricles, with arrhythmias usually prominent. It is characterized by substantial fibrosis, with or without fatty replacement of the ventricular myocardium. Sudden death and heart failure are prominent.

5 Left ventricular noncompaction (LVNC), originally called spongy myocardium, is the newest classified form of cardiomyopathy [5], and is characterized by abnormal left ventricular trabeculations. It is clinically heterogeneous, taking on the features of other forms of cardiomyopathy or congenital heart disease. Important clinical features include heart failure, sudden death, and strokes.

Dilated cardiomyopathy

Dilated cardiomyopathy (DCM) is the most common form of cardiomyopathy, accounting for ~55% of patients [4–6]. In the United States, the mortality rate due to cardiomyopathy is >10 000 deaths annually, with DCM being the major contributor [6]. In 2009, the estimated cost of treating heart failure patients in the United States was >$39 billion [7].

Over the past 15 years, clinical features have been identified and multiple causative genes discovered. These genes appear to encode two major subgroups of proteins, cytoskeletal and sarcomeric proteins [8–11], and also sarcomeric genes encoding Z-disk proteins [12–15], ion channel

Table 58.1 Dilated cardiomyopathy (DCM) genetics.

CHR locus	Gene	Protein	Protein location
Xp21.2	DYS	Dystrophin	Cytoskeleton/SL
1q31-q42	PSEN2	Presenilin 2	Cytoskeletal
2q35	DES	Desmin	Cytoskeleton
5q33	SGCD	δ-Sarcoglycan	Cytoskeleton/SL
4q12		β-Sarcoglycan	Cytoskeleton/SL
10q22-q23	VCL	Metavinculin	Cytoskeleton
1q12	TNNI1	Cardiac troponin I	Sarcomere
19q13	TNNI3	Cardiac troponin I	Sarcomere
1q32	TNNT2	Cardiac troponin T	Sarcomere
3p21-p14	TNNC1	Cardiac troponin C	Sarcomere
11p11	MYBPC3	Myosin binding protein C	Sarcomere
14q12	MYH7	β-Myosin heavy chain	Sarcomere
15q14	ACTC	Cardiac actin	Sarcomere
15q22	TPM1	α-Tropomyosin	Sarcomere
2q31	TTN	Titin	Sarcomere
11p15.1	CSRP3	Muscle LIM protein	Z-disk
1q42-q43	ACTN2	α-Actinin 2	Z-disk
10p12	NEBL	Nebulette	Z-disk
17q12	TCAP	Telethonin	Z-disk
10q21.3	MYPN	Myopalladin	Z-disk
10q22.3–23.2	LBD3	ZASP	Z-disk
10q23.31	ANKRD1	CARP	Z-disk
1q21	LMNA	Lamin A/C	Nuclear membrane
10q25-q26	RBM20	RNA binding motif protein 20	Nuclear protein
Xq24	LAMP2	LAMP2	Lysosomal membrane
Xq28	G4.5	Tafazzin	Phospholipid
3p21	SCN5A	Cardiac sodium channel	Ion channel
6q22.1	PLN	Phospholamban	Calcium

homeostasis (sodium channel gene SCN5A and phospholamban) [16,17] and metabolic genes (G4.5/Tafazzin), and others [18] (Table 58.1).

Another form of DCM, viral myocarditis, has the clinical features of DCM including heart failure, arrhythmias, and conduction block [19]. The most common causes of myocarditis are viral, including the enteroviruses (coxsackie viruses and echovirus), adenoviruses, and parvovirus B19, among other cardiotropic viruses, and the predominant related virus appears to alternate every decade [20]. Viral myocarditis and DCM (genetic) seem to have similar disease mechanisms based on the proteins targeted.

Epidemiology and etiology

DCM is the most common form of cardiomyopathy in adults, with an annual incidence of 2–8/100 000 in the United States and Europe and an estimated prevalence of 36/100 000 population [21]. In adults with DCM and congestive heart failure, the most common causes are idiopathic (47%), myocarditis (12%), coronary artery disease (11%), and other identifiable causes (30%) [21]. In a study of 1426 children with DCM enrolled in the PCMR, the annual incidence of DCM in children <18 years old was 0.57/100 000 per year [4], was higher in boys than in girls (0.66 versus 0.47/100 000; $p < 0.001$), in blacks than in whites (0.98 versus 0.46/100 000; $p < 0.001$), and in infants than in children (4.40 versus 0.34 /100 000; $p < 0.001$). Most children (66%) had idiopathic disease. The most common known causes were myocarditis (46%) and neuromuscular disease (26%). The 1- and 5-year rates of death or transplantation were 31 and 46%, respectively. Independent risk factors of DCM for subsequent death or transplantation were older age, congestive heart failure, lower left ventricular fractional shortening, Z score, and cause of DCM ($p < 0.001$ for all). In two earlier studies of children of various ages with DCM, 2–15% had biopsy-proven myocarditis, whereas in 85–90% no cause was identified [22]. In 24 children <2 years old who presented with DCM, 45% had myocarditis, 25% had endocardial fibroelastosis, and the remainder had no identified cause [23]. Familial forms occur in 20–50% of patients with DCM [24–26].

Pathology

The chief morphologic feature is biventricular dilation; the atria are generally enlarged [27]. Mural thrombi may be present in the cardiac chambers. The heart is globular; the myocardium is pale and sometimes mottled. The endocardium is usually thin and translucent [28]; however, focal sclerosis may be seen. The heart weight is increased, indicating hypertrophy, and the coronary arteries are normal. Histologic features classically include myocyte hypertrophy and degeneration, with varying degrees of interstitial fibrosis [27,29]. Occasional small clusters of lymphocytes may be present [30]; if so, this disorder must be differentiated from myocarditis, in which the lymphocytes are associated with areas of myocyte damage and necrosis [31]. Electron microscopy shows nonspecific ultrastructural changes in the mitochondria, T tubules, and Z bands.

Pathophysiology

Depressed contractile function is shown by decreased shortening fraction, ejection fraction, and cardiac output. This decline in systolic function increases end-diastolic volume, end-diastolic pressure, and ventricular filling pressure [27]. To maintain an adequate cardiac output, the ventricles dilate and the myocardium hypertrophies. The dilation increases wall tension, thereby increasing oxygen consumption and decreasing myocardial efficiency. As cardiac output diminishes, renal blood flow decreases. As these features typically progress slowly, mild pulmonary edema and systemic venous congestion occur. In children with acute decompensation, significant pulmonary edema and systemic venous congestion occur. Neurohumoral mechanisms are increasingly activated, particularly the renin–angiotensin system and sympathetic nervous system. Activation of these systems contributes to peripheral vascular changes and the clinical picture of congestive heart failure (see chapter 70).

Ventricular myocardial fibrosis may occur and produce irritable foci causing ventricular arrhythmias [32,33] and contribute to systolic and diastolic dysfunction. The associated arrhythmias may occur from ion channel dysfunction.

Clinical presentation

If an adequate cardiac output cannot be maintained, signs and symptoms of congestive heart failure develop [4,5,8,32,34]. Initially these may be subtle with decreasing exercise tolerance and dyspnea with exertion. Infants may have tachypnea that is more pronounced with feeding, resulting in decreased oral intake and failure to thrive. Signs and symptoms may be unmasked by a superimposed infectious illness that causes further cardiac decompensation. Palpitations and syncope or near-syncope are reported in >13% of children [4,5,8,32,34]. Obtaining a thorough family history and echocardiograms from first-degree relatives is important to verify familial inheritance [24].

Figure 58.1 Chest film of a young child with dilated cardiomyopathy. The cardiac size is enlarged (cardiomegaly) with mildly congested lung markings.

Physical examination

A wide range of findings is found on physical examination [34–36]. Griffin *et al.* [37] reported that 70–80% of patients present with signs of congestive heart failure. Tachypnea and tachycardia are frequent. The skin appears pale. Cyanosis is uncommon unless circulatory collapse is imminent. Peripheral pulses are often weak with normal to low blood pressure and a narrow pulse pressure. The extremities may be cool with decreased peripheral perfusion.

Auscultation of the lungs may reveal diminished breath sounds posteriorly on the left if there is atelectasis from compression by an enlarged heart. Rales may occasionally be heard over an area with atelectasis, but otherwise they are rare in infants and small children even with pulmonary edema on chest radiography. Mild to marked intercostal retractions may be present.

The cardiac apical impulse is displaced laterally. The heart sounds may be muffled, and a prominent diastolic filling sound produces a gallop rhythm (S_3). Murmurs may be absent, but mitral regurgitation (due to a dilated mitral valve annulus or papillary muscle dysfunction) may be heard. Hepatomegaly is common. Other signs of systemic venous congestion include neck vein distention and peripheral edema, which are more common in an older child or young adult than in infants.

Diagnostic studies

Radiography

Chest films typically reveal cardiomegaly due to left atrial and left ventricular enlargement. Pulmonary venous congestion is often present and may progress to frank pulmonary edema (Figure 58.1). Atelectasis of the lower lobe of the left lung may occur because of compression of the left main stem bronchus by the dilated left atrium. Pleural effusions may be present.
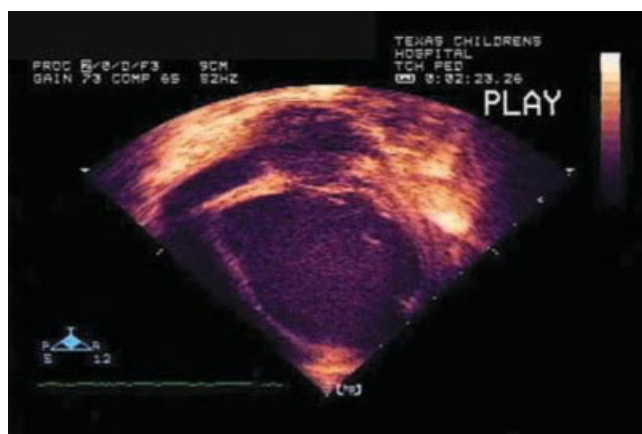
Figure 58.2 Echocardiogram of a child with dilated cardiomyopathy. This apical four-chamber view shows a dilated left ventricle with thin walls. In real time, left ventricular systolic function is depressed.

Electrocardiography and Holter monitoring

Most patients have sinus tachycardia. Nonspecific ST-T wave changes, left ventricular hypertrophy, right and left atrial enlargement, and right ventricular hypertrophy are common [32,34–36]. On Holter monitoring, one study [32] found arrhythmias in 46% of the children with DCM with atrial arrhythmias being more common than ventricular arrhythmias, but another study [36] found ventricular arrhythmias to be more common. The finding of fragmented QRS (fQRS) on 12-lead ECG, which represents myocardial conduction delays perhaps from myocardial scar, is a predictor of arrhythmic events in adults with ischemic and nonischemic heart disease [38]. Similar studies in children have not been reported.

Echocardiography

Echocardiographic features of DCM include dilation of the left ventricle (Figure 58.2) with systolic dysfunction represented by decreased shortening and ejection fractions [34]. Regional wall motion abnormalities may also be seen. In patients with DCM, the coronary artery origins should be identified to exclude anomalous left coronary artery arising from the pulmonary artery. Pericardial effusion may be present, and intracardiac thrombi also occur. Color and pulse Doppler echocardiography frequently demonstrate mitral regurgitation, which may be associated with a dilated left atrium. Decreased aortic flow velocity from diminished cardiac output and abnormal mitral inflow patterns due to diastolic dysfunction may be seen.

Cardiac catheterization and biopsy

Because DCM can be diagnosed by echocardiography, cardiac catheterization, angiography, and biopsy are sometimes deferred until the patient is stable or is being evaluated for transplantation [34]. Catheterization can be useful (1) to exclude anomalous left coronary artery as this is occasionally missed by echocardiography, (2) to predict etiology and prognosis if the biopsy shows myocarditis or metabolic abnormalities, or (3) to evaluate for cardiac transplantation, including measuring pulmonary vascular resistance. Hemodynamic measurements generally show elevated left ventricular end-diastolic, left atrial, and pulmonary capillary wedge pressures, a widened A–V oxygen difference, and usually diminished cardiac output. Angiography demonstrates left ventricular dilation and reduced ejection fraction, normal coronary artery origins, and mitral regurgitation.

Endomyocardial biopsy typically shows variable degrees of myocyte hypertrophy and fibrosis, without significant lymphocytic infiltrate [39–41]. Biopsies can detect myocarditis in addition to mitochondrial or infiltrative diseases, by either histologic examination or polymerase chain reaction (PCR). The findings may have a significant effect on prognosis and treatment [29–43].

Blood and urine studies

In infants and young children, other types of studies may help identify the etiology [4,8,10,18,34]. Examining urine for organic and amino acids, may be useful, particularly if 3-methylglutaconic aciduria is found (i.e., Barth syndrome) [8,18,34]. Blood studies for lactate, calcium, magnesium, carnitine/acylcarnitine, pyruvate, blood urea nitrogen, creatinine, and electrolyte determinations are useful diagnostically and for assessing metabolic function secondary to cardiac failure. In addition, B-type natriuretic protein (BNP), creatine kinase with isozymes (CK), and cardiac troponins have become increasingly useful in predicting disease course, risk stratification, and longitudinal follow-up of patients and family members [44–46]. Viral serology for myocarditis diagnosis has been questioned [47], with myocardial PCR now becoming standard [42]. Molecular analysis for the genetic basis of cardiomyopathies have also become standard [8,9,48–50].

Clinical genetics of dilated cardiomyopathy

Dilated cardiomyopathy was initially considered inherited in a small percentage of patients until Michels *et al.* [24] showed that ~20% of patients had family members screened by echocardiography who showed evidence of DCM. More recently, inherited familial DCM (FDCM) has been shown to occur in 30–50% of patients [49,51]. Autosomal dominant inheritance is the predominant pattern of transmission; X-linked, autosomal recessive, and mitochondrial inheritance are less common.

Molecular genetics of dilated cardiomyopathy

Progress in understanding the genetic etiology of FDCM was made in the early 1990s studying X-linked forms of DCM, and in the past decade studying autosomal dominant forms of DCM (Table 58.1). Three X-linked forms of DCM have been well characterized: X-linked cardiomyopathy (XLCM)

presenting in adolescence and young adults [52], Barth syndrome, most frequently identified in infancy [53], and Danon disease, which commonly presents with hypertrophic cardiomyopathy in boys, later becoming DCM and affecting female carriers with late-onset DCM [54].

X-linked cardiomyopathies

X-linked dilated cardiomyopathy (XLCM)

First described in 1987 by Berko and Swift [52] as DCM occurring in males in the teen years and early twenties and showing rapid progression from CHF to death due to VT/VF or transplantation, these patients are distinguished by elevated serum creatine kinase muscle isoforms (CK-MM). Female carriers develop mild to moderate DCM in the fifth decade and the disease is slowly progressive. Towbin *et al*. identified the disease-causing gene and characterized the functional defect [55]. The dystrophin gene was shown to be responsible for the clinical abnormalities by immunoblotting demonstrating severe reduction or absence of dystrophin protein in the hearts of these patients. The findings were confirmed [56] when a mutation in the muscle promoter and exon 1 of dystrophin was identified in another family with XLCM. Subsequently, multiple dystrophin mutations have been identified in these patients.

Dystrophin is a cytoskeletal protein that provides structural support to the myocyte by creating a lattice-like network to the sarcolemma [57]. In addition, dystrophin plays a major role in linking the sarcomeric contractile apparatus to the sarcolemma and extracellular matrix [57–60], and is involved in cell signaling, particularly through its interactions with nitric oxide synthase. The mutated dystrophin gene is also responsible for Duchenne and Becker muscular dystrophy (DMD/BMD) [61].These skeletal myopathies present early in life (DMD is diagnosed before age 12 years and BMD is seen in teenage males >16 years of age) and most patients develop DCM before the 25th birthday. In patients with DMD/BMD, CK-MM is elevated as in XLCM; in addition, female carriers develop disease late in life, similarly to XLCM. Furthermore, immunohistochemical analysis demonstrates reduced levels (or absence) of dystrophin, as in the hearts of patients with XLCM.

Murine models of dystrophin deficiency demonstrate disturbed muscle physiology based on membrane structural support abnormalities [62]. In addition to the dysfunction of dystrophin, mutations in dystrophin secondarily affect other proteins. At the amino-terminus (N-terminus), dystrophin binds to the sarcomeric protein actin, part of the thin filament of the contractile apparatus. At the carboxy-terminus (C-terminus), dystrophin interacts with α-dystroglycan, a dystrophin-associated membrane-bound protein involved in the function of the dystrophin-associated protein complex (DAPC), which includes β-dystroglycan, the sarcoglycan subcomplex (α-, β-, γ-, δ-, and ε-sarcoglycan), syntrophins,

and dystrobrevins [63–65]. In turn, this complex interacts with α$_2$-laminin and the extracellular matrix [66]. Like dystrophin, mutations in these genes lead to muscular dystrophies with or without cardiomyopathy, supporting the contention that this group of proteins is important to the normal function of the myocytes of the heart and skeletal muscles [66,67]. Mechanical stress [62] appears to play a significant role in the age onset-dependent dysfunction of these muscles. The information gained from the studies on XLCM, DMD, and BMD led us to hypothesize that DCM is a disease of the cytoskeleton/sarcolemma that affects the sarcomere [11], a "final common pathway" of DCM [68]. We suggested that dystrophin mutations play a role in idiopathic DCM in males, when we showed that 3/22 boys with DCM had dystrophin mutations and all were later found also to have elevated CK-MM [69]. In addition, eight families with DCM and possible X-linked inheritance were also screened and in three of the families dystrophin mutations were noted; CK-MM was elevated in all subjects carrying mutations [70]. Therapeutically, the efficacy of angiotensin-converting enzyme (ACE) inhibitor therapy and β-blockers has been shown [71,72]. Jefferies *et al*. [71] also suggested that age of onset and severity of DCM were associated with a specific mutation area: the 5′ area (encodes the N-terminus) of dystrophin, when mutated, leads to early onset DCM whereas the 3′ end (C-terminus) has later onset DCM. Whether this responds differently to therapy is unknown.

Barth syndrome

Initially described as X-linked cardioskeletal myopathy with abnormal mitochondria and neutropenia by Neustein *et al*. [73] and Barth *et al*. [53], this disorder typically presents in male infants as CHF associated with neutropenia (cyclic) and 3-methylglutaconic aciduria [74]. Mitochondrial dysfunction is noted on electron microscopy and electron transport chain biochemical analysis. Abnormalities in cardiolipin have also been noted [75]. These infants typically have echocardiographic evidence of left ventricular dysfunction with left ventricular dilation, endocardial fibroelastosis, or a dilated hypertrophic left ventricle. Some infants succumb from CHF/ sudden death VT/VF, or sepsis due to leukocyte dysfunction. Most children survive infancy and do well clinically, although DCM usually persists. Some require cardiac transplantation. Histopathologic evaluation typically demonstrates the features of DCM, although endocardial fibroelastosis may be prominent and the mitochondria are abnormal in shape and abundance.

The genetic basis of Barth syndrome was first described by Bione *et al*. [76], who cloned the disease-causing gene, G4.5. This gene encodes a novel protein called tafazzin (TAZ), whose gene product is an acyltransferase which when defective results in cardiolipin abnormalities [75]. Mutations in G4.5/TAZ result in a wide clinical spectrum, including classic DCM, hypertrophic DCM, endocardial fibroelastosis (EFE), and left ventricular noncompaction [18,77].

Autosomal dominant dilated cardiomyopathy

The most common form of inherited DCM is the autosomal dominant [8]. Patients present with either classic "pure" DCM or DCM associated with conduction system disease (CDDC). In the latter form, patients usually present in the third decade of life with mild conduction system disease that can progress to complete heart block over decades. DCM usually presents late in the course but is out of proportion to the degree of conduction system disease [78]. The echocardiographic and histologic findings in both subgroups are classic for DCM, although the conduction system may be fibrotic in patients with CDDC. In both groups of DCM patients, VT, VF, and torsades de pointes occur and may result in sudden death.

Genetic heterogeneity exists for autosomal dominant DCM with more than 15 genes identified for FDCM and for CDDC. The identified genes include those encoding cytoskeletal and sarcomeric proteins, although some ion channel genes and others have also been identified [8,9,79,80] (Table 58.1).

Mechanistically, cytoskeletal proteins (desmin, δ-sarcoglycan, metavinculin, MLP), are thought to cause defects of force transmission resulting in the DCM phenotype, and defects of force generation have been speculated to cause sarcomeric protein-induced DCM [81]. Purevjav *et al.* recently showed that the mutation in a gene may disrupt protein-binding partners and, depending on this interaction, differential phenotypes and severity occur [14].

Muscle is muscle: cardiomyopathy and skeletal myopathy genes overlap

Interestingly, nearly all of the genes identified for inherited DCM are also known to cause skeletal myopathy in humans and/or mouse models. Dystrophin mutations cause Duchenne and Becker muscular dystrophy whereas δ-sarcoglycan mutations cause limb girdle muscular dystrophy (LGMD2F). Lamin A/C causes autosomal dominant Emery–Dreifuss muscular dystrophy (EDMD) and LGMD1B and actin mutations are associated with nemaline myopathy. Desmin, G4.5/TAZ, α-dystrobrevin, Cypher/ZASP, MLP, α-actinin-2, titin, and δ-sarcoglycan mutations also have associated skeletal myopathy suggesting that cardiac and skeletal muscle function are interrelated. Possibly the skeletal muscle fatigue of patients with DCM may be due to primary skeletal muscle disease rather than cardiac dysfunction. Perhaps the function of these muscles has a "final common pathway" and both cardiologists and neurologists should consider evaluating both sets of muscles.

Further support for this concept comes from studies of animal models. Mutations in δ-sarcoglycan in hamsters cause cardiomyopathy whereas mutations in all sarcoglycan subcomplex genes in mice cause skeletal and cardiac muscle disease. Mutations in other DAPC genes and also dystrophin in murine models also consistently demonstrate abnormalities of skeletal and cardiac muscle function. Arber *et al.* [82]

produced a mouse deficient in muscle LIM protein (MLP), a structural protein that links the actin cytoskeleton to the contractile apparatus. The resultant mice develop severe DCM, CHF, and disruption of cardiac myocyte cytoskeletal architecture. Murine mutations in titin, cypher, α-dystrobrevin, desmin, and other proteins all demonstrate cardiac and skeletal muscle disease. Finally, the DCM that develops after viral myocarditis has a mechanism similar to the inherited forms [83]. Using coxsackievirus B3 (CVB3) infection of mice, the authors showed that the CVB3 genome encodes for a protease (enteroviral protease 2A) that cleaves dystrophin at its third hinge region, resulting in force transmission abnormalities and DCM. In addition, Xiong *et al.* [84] showed that abnormal dystrophin increases susceptibility to viral infection and resultant myocarditis. Interestingly, a similar dystrophin mutation that affects the first hinge region of dystrophin in patients with XLCM was previously reported by our laboratory, demonstrating a consistent mechanism of DCM development, abnormalities of the cytoskeleton/sarcolemma and sarcomere. Finally, we have shown that N-terminal dystrophin is reduced or absent in hearts of patients with all forms of DCM (ischemic, acquired, genetic, idiopathic) and that reduction of mechanical stress by use of left ventricular assist devices (LVADs) results in reverse remodeling of dystrophin and of the heart itself [85,86].

Differential diagnosis

The causes of DCM are varied (see Table 58.2) and the differential diagnosis depends on age. In infants and young children, DCM is typically more severe than in older children and adults and more frequently includes other systemic abnormalities.

Treatment

Targeted therapies based on mechanism in DCM

Once the mechanism(s) of disease have been identified and understood, targeted instead of symptom-based therapies can be considered and developed. To date, only a small number of successes have been defined. Because the "final common pathway" involved in DCM is the link between the sarcomere and sarcolemma, mechanical stress is a key secondary component to consider [11,68,80]. Reducing mechanical stress and stretch might favorably remodel the heart. In testing this hypothesis, LVAD therapy reduces LV size, myocyte hypertrophy, and fibrosis, ultimately improving systolic function and overall ventricular performance [85,86]. In a subset of patients, significant improvement of LV size and function led to removal of mechanical support and resumption of normal or near-normal cardiac function. This may also be a key mechanism in β-blocker and ACE inhibitor therapy in some patients. In addition, the recent discovery of the regulatory effects of the transforming growth

Table 58.2 Causes of dilated cardiomyopathy.

A. Familial dilated cardiomyopathy
Cardioskeletal myopathy, X-linked (Barth syndrome)
Familial idiopathic dilated cardiomyopathy
X-linked cardiomyopathy (XLCM)
Familial conduction defect with dilated cardiomyopathy
Arrhythmogenic right ventricular dysplasia
Left ventricular noncompaction

B. General system diseases
Systemic lupus erythematosus
Juvenile rheumatoid arthritis
Polyarteritis nodosa
Kawasaki disease

C. Tachyarrhythmias
Supraventricular tachycardia
Atrial flutter
Ventricular tachycardia

D. Infectious myocarditis
Viral
Bacterial
Fungal
Protozoal
Rickettsial
Spirochetal

E. Heredofamilial disorders
Muscular dystrophies/myopathies
Duchenne and Becker muscular dystrophies
Emery–Dreifuss muscular dystrophy
Myotonic dystrophy (Steinert)
Limb-girdle muscular dystrophy (Erb)
Autosomal recessive muscular dystrophy
Kugelberg–Welander spinal muscular atrophy
Nemaline myopathy
Myotubular (centronuclear) myopathy
Minicore–multicore myopathy

F. Mitochondrial syndromes
Kearns–Sayre
MELAS (mitochondrial encephalomyopathy, lactic acidosis, and stroke-like symptoms)
NADH–coenzyme Q reductase deficiency
MERRF (myoclonus epilepsy with ragged red fibers)

G. Congenital cardiovascular disease
Critical aortic stenosis of infancy
Anomalous left coronary artery
Ebstein anomaly
Postoperative congenital heart disease
Arteriovenous malformation

H. Sensitivity/toxic reactions
Sulfonamides
Penicillin
Anthracyclines
Chloramphenicol
Alcoholic cardiomyopathy
Hemochromatosis

I. Metabolic

J. Endocrine
Thyrotoxicosis
Hypothyroidism
Diabetic cardiomyopathy
Hypoglycemia
Pheochromocytoma
Neuroblastoma
Catecholamine cardiomyopathy
Hypocalcemia
Hypophosphatemia

K. Familial storage disease
Glycogen storage disease
Type IV (Andersen)
Type V (McArdle)
Type VI (Hers)
Mucopolysaccharidoses
Hurler syndrome (type I)
Sanfilippo syndrome (type III)
Morquio syndrome (type IV)
Maroteaux–Lamy syndrome (type VI)
Sphingolipidoses
Niemann–Pick disease
Farber disease
Gaucher disease
Tay–Sachs disease
G_{M1} gangliosidosis
Sandhoff disease (G_{M2})
Refsum disease

L. Nutritional
Kwashiorkor (protein deficiency)
Beriberi (thiamine deficiency)
Selenium deficiency
Carnitine deficiency
β-Ketolase deficiency
Hypertaurinuria
Acyl-CoA dehydrogenase deficiency
Propionicacidemia

M. Other
Hemolytic–uremic syndrome
Reye syndrome
Peripartum cardiomyopathy
Osteogenesis imperfecta

factor-β (TGF-β) pathway on the development of myocardial fibrosis and the inhibitory and protective effects of bone morphogenic protein-7 (BMP-7) on this pathway and the effects of TGF-β-induced fibrosis may offer an approach to therapy [87,88].

Other targeted therapies exist. Endocardial fibroelastosis (EFE) in infancy was shown to occur from intrauterine mumps virus infection [89]. The successful use of vaccinations has reduced the occurrence of mumps and the incidence of EFE subsequently dropped to essentially zero. Furthermore,

the key causes of HIV-related DCM are enteroviral and adenoviral infection of the heart, not HIV [90]. Coxsackievirus (an enterovirus), the most commonly identified viral genome in these hearts, cleaves dystrophin by the use of endogenous enteroviral protease 2A, leading to DCM [83,84]. Protease inhibitor use, a mainstay in HIV therapy, has limited the development of coxsackieviral myocarditis and hence reduced the incidence of heart disease in these patients.

Current medical therapy

If no identifiable and treatable cause of the DCM is found, therapy is supportive and consists of an anticongestive regimen, control of significant arrhythmias, and minimizing the risk of thromboembolic complications. Critically ill children frequently require intubation and mechanical ventilation. The mainstay of acute decompensated heart failure therapy is discussed in Chapter 70 [91–97]. The use of dobutamine and dopamine is limited because of the concept of mechanical stress relationship to disease worsening and its correlation with arrhythmia triggering. When used, dopamine is typically begun in renal doses to enhance renal perfusion and diuresis. Myocardial phosphodiesterase inhibitors, such as milrinone, are useful. In adults, reports of associated ventricular arrhythmias has tempered enthusiasm for this drug, but this complication has not been observed in childhood DCM. Nitroprusside can also be used for afterload reduction but may have a greater blood pressure effect in these at-risk patients and must therefore be used with caution. Correction of anemia is important [98]. For children, oral therapy is instituted as intravenous inotropic agents are weaned [91–93] (see chapter 70).

Arrhythmias are common in children with DCM [32,34]. Sometimes the only treatment required is medical management to improve cardiac function and normalize electrolyte imbalances. If significant arrhythmias persist, antiarrhythmic therapy is warranted [99]. Many antiarrhythmic drugs adversely affect ventricular function and may be proarrhythmic. For significant arrhythmias, amiodarone is effective and relatively safe in children. Temporary pacing of symptomatic bradyarrhythmias may be necessary during the acute phase of illness. Permanent pacing occasionally may be necessary. Elective pacing to optimize atrioventricular synchrony and ventricular filling remains investigational. implantable defibrillators (ICDs) are becoming the standard of care when systolic function is significantly depressed and life-threatening arrhythmias occur.

The utility of immunosuppressive agents in DCM, including steroids, cyclosporine, and azathioprine, remains unproven. Intracavitary thrombus formation and systemic embolization occur in young patients with DCM, and anticoagulation should be strongly considered [100]. If a thrombus is identified, patients are usually anticoagulated with heparin and then converted to warfarin. If a thrombus is not seen, antiplatelet drugs (aspirin, dipyridamole) may be useful in preventing thrombus formation.

In children with a metabolic cause of DCM, careful attention to biochemical derangement is important [4,8,10,34,101]. Correcting associated metabolic acidosis and diagnosing the underlying causes are paramount. Oral feeding should be reduced or discontinued until stabilization has occurred, with intravenous fluid and dextrose replacement used to provide energy and reduce the ongoing catabolic process, and total parenteral nutrition (TPN) used for nutrition.

Surgical

Despite maximum medical therapy, some patients continue to deteriorate [102]. Children with acute and severe decompensation may require mechanical circulatory support (MCS) therapy with a ventricular assist device (VAD), intra-aortic balloon counterpropulsion, or extracorporeal membrane oxygenation (ECMO) (see Chapter 14). In children, MCS commonly is a bridge to transplantation. It occasionally helps to remodel the heart favorably, allowing device removal. Typically, it is meant to stabilize children and reduce other end-organ damage while awaiting transplantation. Unlike in adults, where MCS may be used as "destination therapy," that approach is rarely considered in children. The other surgical approach is cardiac transplantation, which is used when children are unable to maintain functional stability and end-organ stability (see Chapter 70). The data on childhood transplantation have been stable for the past decade, with a median survival for infant transplant of 18.3 years and an adolescent transplant mean survival of 11.1 years [103].

Prognosis

In infants and children presenting with DCM, there are four possible outcomes [4,5,32,34]: complete resolution, improvement, death, and cardiac transplantation. Review of the available studies in children suggests that approximately one-third die, one-third improve but have some residual cardiac dysfunction, and one-third recover completely. In children, 1-year survival ranges from 63 to 70% and 5-year survival from 34 to 66%; 10–11-year survival is 50%. Mortality is highest during the first 1–2 years after presentation. Congestive heart failure is the most common cause of death, although sudden death also occurs. The time from presentation to ~6 months after diagnosis appears most critical in terms of defining outcome. In those who are going to recover or improve, signs of improvement are generally seen during the initial 6 months, although continued improvement may occur beyond 2 years. Most deaths occur in the first 6 months, with survival declining gradually thereafter. The persistence of congestive heart failure despite maximum medical therapy, and persistently low functional echocardiographic parameters on echocardiography, should prompt consideration of cardiac transplantation.

Myocarditis

Myocarditis is characterized by inflammatory infiltration of the myocardium associated with necrosis or degeneration of adjacent myocytes that differs from the ischemic damage associated with coronary artery disease [19,31,33]. The cause may be infectious, toxic, associated with connective tissue disorders, or other processes; the commonest cause is viral, but almost any organism can be the cause (see Table 58.3). Myocarditis is believed to be a significant cause of idiopathic DCM.

Epidemiology

Although epidemics have been reported, the disease is usually sporadic [4,10,19,20,33,34]. Over the years, different viruses have been dominant in a population and a shifting demographic of viral etiology occurs approximately every decade [20,43]. In the 1960s–1980s, the enteroviruses, particularly coxsackievirus B, were the most common causal agents, although the virus was rarely recovered from the heart. Coxsackievirus B is spread by the fecal–oral or airborne route and is most common in the spring and summer. Young children, particularly infants, are most commonly affected. In the 1990s, we showed that adenovirus was the most common cause of myocarditis in children during that decade [42,104]. Adenovirus infections occur sporadically throughout the year and in epidemics during winter, spring, and early summer. The outcomes for children with adenoviral myocarditis differed slightly from those for coxsackievirus, but in both instances most children improved. We were the first to show that parvovirus B19 was a significant cause of childhood myocarditis [105], and during 2000–2010 it became the predominant viral cause of myocarditis [20,42,106–108]. Parvovirus B19 infects the endothelium, unlike adenovirus and coxsackievirus, which both infect the cardiomyocyte [108]. Because of its attraction to the endothelium, parvovirus B19 inflames arteries, particularly the coronaries, leading to coronary insufficiency, myocardial injury, ischemia, and infarction. Currently, coxsackievirus is beginning to become more common again.

Clinical presentation

Children commonly present with signs and symptoms of congestive heart failure that may rapidly lead to cardiovascular collapse [10,19,109]. Infants usually are pale and clammy, irritable or somnolent, and have increasingly uncomfortable respiratory effort. On examination, they are tachypneic and tachycardic at rest. The cardiac examination demonstrates a gallop rhythm, and perhaps a mitral regurgitant murmur. The pulses are typically thready, and perfusion is poor. Commonly, there is moderate hepatomegaly. Rales are usually absent in small children. Older children generally present with breathlessness and signs of heart failure. Syncope may occur. Some children and adolescents present

Table 58.3 Infectious causes of myocarditis.

Viral
Adenovirus
Parvovirus B19
Enterovirus
Coxsackievirus A
Coxsackievirus B
Echovirus
Cytomegalovirus
Herpes simplex virus
Epstein–Barr virus
Mumps virus
Rubella virus
Rubeola virus
Influenza virus
Human immunodeficiency virus
Hepatitis C virus
Mycoplasma
Mycoplasma pneumoniae
Bacterial
Diphtheria
Meningococcal
Pneumococcal
Gonococcal
Fungal
Candidiasis
Aspergillosis
Protozoal
American trypanosomiasis (Chagas disease)
Toxoplasmosis
Spirochetal
Lyme disease
Rickettsial
Rocky Mountain spotted fever

with signs of ischemia, particularly in parvovirus B19 infections or fulminant myocarditis [107]. There may be a history of recent viral-type illness, although many have not been ill. Infectious contacts may not be known.

Diagnostic studies

Chest radiography

Cardiomegaly and pulmonary venous engorgement, with or without evidence of pneumonitis, are common. If the child improves, the chest radiograph becomes normal.

Electrocardiography

Classically, the surface electrocardiogram demonstrates low voltage of the QRS complexes in the limb leads (<5 mm total amplitude) with inverted T waves and absent or small Q waves

Table 58.4 Dallas criteria.

Type	Definition
General definition	Myocardial cell injury with degeneration or necrosis with inflammatory infiltrate not due to ischemia
Active myocarditis	Both myocyte degeneration or necrosis and definite cellular infiltrate with or without fibrosis
Borderline myocarditis	Definite cellular infiltrate without myocyte injury
Persistent myocarditis	Continued active myocarditis on repeated right ventricular endomyocardial biopsy
Resolving/resolved myocarditis	Diminished or absent infiltrate with evidence of connective tissue healing

Figure 58.3 Histologic appearance of lymphocytic myocarditis in this right ventricular endomyocardial biopsy specimen obtained from the child with new-onset heart failure. Note the lymphocytic inflammatory infiltrate and myocyte necrosis.

in leads V_5 and V_6. Sinus tachycardia is the rule, although bradycardia may be evident. Premature ventricular complexes and supraventricular tachycardia are the most common rhythm disturbances, although ventricular tachycardia, and complete atrioventricular block also occur [10,19,34,109–113].

Echocardiography
The echocardiogram demonstrates left ventricular dilation and depressed ventricular function. The atria (particularly the left atrium) may also appear mildly dilated. A pericardial effusion may be found. Doppler and color Doppler evaluation may demonstrate mitral regurgitation.

Cardiac catheterization and endomyocardial biopsy
Hemodynamic evaluation typically shows elevated ventricular end-diastolic pressures and reduced cardiac index [33,39]. Endomyocardial biopsy is used for histopathologic evaluation by light microscopy and electron microscopy, culture, and molecular analysis. Histopathologic analysis typically follows the Dallas criteria (Table 58.4), which rely on the amount of lymphocytic infiltrate, fibrosis, myocyte necrosis, and edema (Figure 58.3) [19]. Unfortunately, this approach is diagnostic in only 50% of patients [114–117]. Imaging approaches, including cardiac MRI, have replaced biopsies as the diagnostic modality in many patients and institutions. [117].

Viral culture and serology
Viral, bacterial, and fungal cultures are usually obtained from nasopharyngeal and stool specimens and also from the myocardium. Blood cultures are generally useless for viral diagnosis because the virus has usually cleared before clinical presentation [47]. If the culture is positive from a peripheral site, a presumptive etiologic diagnosis may be rendered but
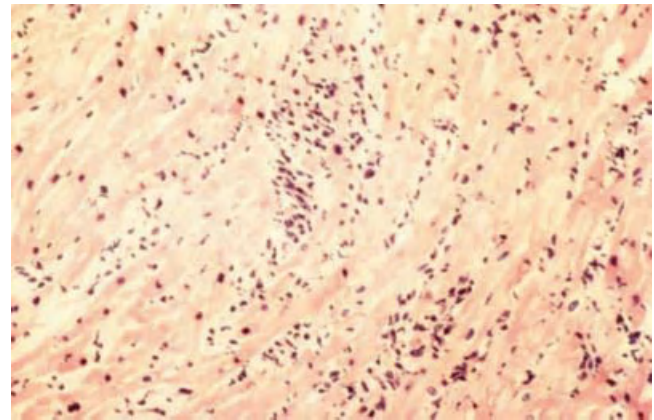
is commonly incorrect. Serologic identification requires a fourfold increase in antibody titers on serial analysis.

Molecular methods
In the 1980s, Bowles *et al.* [118] first described the use of *in situ* hybridization studies using probes designed for sequences of coxsackievirus to analyze myocardium. There were >50% hybridization-positive samples, suggesting that coxsackievirus was indeed a common cause of myocarditis. They also showed coxsackievirus probe hybridization in patients with idiopathic DCM and inferred that a previous subclinical infection caused the cardiomyopathy [118,119] Since the early 1990s, PCR has been used to analyze endomyocardial biopsy and autopsy specimens for viral sequences [120,121] This rapid amplification process is highly sensitive and has identified viral sequences in 30–50% of myocardial specimens studied over the past 20 years [19,20,33,42,43,89,90,104,105,117,120,121].

Therapy
Patients with myocarditis and acute decompensated heart failure require anticongestive therapy as described above. Therapy should be given intravenously and may include milrinone and diuretics. Intubation and mechanical ventilation may be necessary. VAD or ECMO support or intra-aortic balloon pump may be needed for circulatory support. In stable patients, oral therapy with afterload-reducing agents, such as captopril or enalapril, and diuretics are used. For persistent ventricular dysfunction, carvedilol or metoprolol are added. Therapy for treating the inflammatory response is controversial. Some centers advocate steroids and other centers use immunosuppressive agents such as cyclosporine or azathioprine [19,33,122–126]. Intravenous immunoglobulin (IVIG) has been used and appeared to have favorable results [19,33,43,117,127–129].

Future directions

Diagnosis

PCR analysis of myocardium is currently commercially available. Cardiac MRI with gadolinium late enhancement, applied in adults to diagnose myocarditis, is beginning to be used in children. Mechanical circulatory support is being used for a short-term bridge to recovery and appears useful in remodeling the heart.

Hypertrophic cardiomyopathy

Hypertrophic cardiomyopathy (HCM) is defined by its wall thickening [130–132] and is the most common cause of sudden death in young, healthy athletes [133–136]. It can cause heart failure [137–139] due to either diastolic factors or the development of systolic dysfunction, "burned out" HCM [137–138].

In children, the underlying etiologies of HCM and the variable age of onset differentiate the childhood form from the adult counterpart [8,101,131,139]. In infants, ventricular hypertrophy associated with systolic dysfunction is more the rule. Overlap disorders in which HCM coexists with atypical features are more common in children, further confounding the presentation, treatment, and outcome compared with adult disease.

Clinical aspects

HCM is a primary myocardial disorder with an autosomal dominant pattern of inheritance characterized by hypertrophy of the left (± right) ventricle with histological features of myocyte hypertrophy, myofibrillar disarray, and interstitial fibrosis [130–132,135,139]. HCM is one of the most common inherited cardiac disorders, with a prevalence in young adults of one in 500 [130,131]. HCM is also called hypertrophic obstructive cardiomyopathy (HOCM) and idiopathic subaortic stenosis (IHSS), names reflecting "classic" features of asymmetric septal hypertrophy and left ventricular outflow tract obstruction (Figure 58.4). This early disease description was based primarily on patients with severe symptoms seen in tertiary referral centers. Epidemiologic studies now suggest that a wide range of clinical manifestations, severity, and prognosis are present in the community. The first clinical description of HCM was in 1869 [140] and it was identified as a genetic disorder in the late 1950s. During the last 15 years, molecular genetic studies have given important insights into the pathogenesis of HCM and have provided a new perspective for the diagnosis and management of patients with this disorder [141,142].

Genetics of familial hypertrophic cardiomyopathy

The first gene for familial hypertrophic cardiomyopathy (FHC) was mapped to chromosome 14q11.2-q12 using genome-wide linkage analysis in a large Canadian family
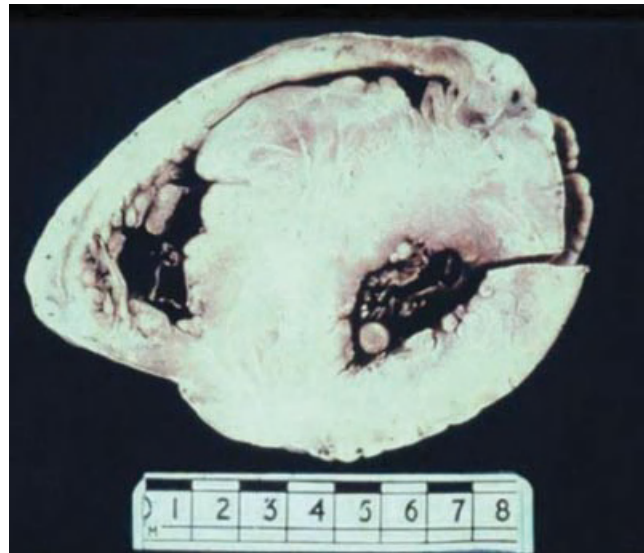
Figure 58.4 Gross pathology in hypertrophic cardiomyopathy. Note the very thick interventricular septum and small left ventricular cavity. The septum is significantly thicker than the free wall, consistent with asymmetric septal hypertrophy.

[143]. Soon afterwards, FHC locus heterogeneity was reported [144] and subsequently confirmed by mapping the second FHC locus to chromosome 1q3 and the third locus to chromosome 15q2 [145,146]. Since then, a large number of loci and genes have been identified with approximately 27 gene mutations reported to date.

Gene identification in familial hypertrophic cardiomyopathy

Most of the identified disease-causing genes code for proteins that are part of the sarcomere, the "final common pathway" of HCM [68]. The sarcomere is a complex structure with an exact stoichiometry and multiple sites of protein-protein interactions [141,147]. These include three myofilament proteins, the β-myosin heavy chain (β-MyHC), the ventricular myosin essential light chain 1 (MLC-1s/v), and the ventricular myosin regulatory light chain 2 (MLC-2s/v); four thin filament proteins, cardiac actin, cardiac troponin T (cTnT), cardiac troponin I (cTnl), and α-tropomyosin (α-TM); and one myosin-binding protein, the cardiac myosin binding protein C (cMyBP-C) [139,141,142,147]. Each protein is encoded by multigene families which exhibit tissue-specific, developmental, and physiologically regulated patterns of expression [148]. The giant protein titin [149] and its interactive Z-disc protein, muscle LIM protein (MLP), have also been identified [150], as have multiple other Z-disc-encoding genes including CARP, NEBL, and nexillin (NEXN) [14,151–153]. In addition, the gene located on chromosome 7q3 associated with HCM and Wolff–Parkinson–White (WPW) syndrome was identified as AMP kinase (AMPK), which may play a role in energy metabolism and

cause infiltration of a glycogen-like substance similar to Pompe disease [154–156]. This was further supported by identifying mutations in LAMP-2, the gene responsible for Danon disease [157–160].

Genotype–phenotype relations in familial hypertrophic cardiomyopathy

The pattern and extent of left ventricular hypertrophy in patients with HCM vary greatly even in first-degree relatives and a high incidence of sudden death is reported in selected families. Since the description of the first HCM-causing mutation, investigators have attempted to correlate genotypes with particular clinical phenotypic expressions. Stemming from earlier pedigree studies, specific missense mutations were associated with a markedly unfavorable prognosis whereas others had an uneventful natural history. These observations resulted in specific mutations being designated as either "malignant" or "benign." Several concepts have been published for mutations in the MYH7, TNNT2, and MYBPC3 genes. For MYH7, the prognosis for patients with different mutations varies. Watkins *et al.* [161 described mutations in MYH7 found in 12/25 families with HCM and concluded that the MYH7-R403Q mutation was associated with a significantly shorter life expectancy, and therefore considered a "malignant" mutation. In contrast, a noncharge change mutation (V606M) was associated with nearly normal survival and therefore was considered "benign." In 2003, Woo *et al.* analyzed mutations in functional domains in 15/70 MYH7-positive probands and concluded that there may be prognostically informative domains. [162]

Initial reports on the clinical expression from another common subtype of HCM with MYBPC mutations showed a slower progressive disease course, with later onset and milder disease characteristics [163–165]. Investigators in The Netherlands and South Africa discovered founder mutations in MYBPC3 with mild phenotypic expression present in >30% of their patients [166]. Certain genotype–phenotype correlations were attributed to TNNT2 (troponin T) mutant forms of HCM. Far less common than MYBPC or MYH7 forms, TNNT2 affects <5% of patients, is associated with less severe LV wall thickness, and has a higher incidence of premature sudden cardiac death [167–169]. Generally, patients who suddenly died had less hypertrophy and fibrosis, but more myocyte disarray, which may have provided the substrate for malignant arrhythmias [169].

These observations were made from studies of small cohorts involving larger families with penetrant disease expression whereas genotype–phenotype studies involving large cohorts of unrelated patients have indicated that great caution must be exercised when assigning particular prognostic significance to any particular mutation. [170–172]. Studies have demonstrated that the two most common forms of genetically mediated MYH7 and MYBPC3 are phenotypically indistinguishable [173].

Despite the inconsistent findings regarding outcomes based on genotype–phenotype correlations, several phenotype–genotype relationships have emerged. Recently, echocardiography-guided genetic testing has been explored [174]. Over two decades ago, Lever *et al.* noted a predominance of sigmoidal HCM among the elderly and suggested a strong age dependence with the various septal morphologies of HCM [175].They suggested a morphologic classification of septal morphology as reverse curve, sigmoidal, apical, and neutral contour HCM. Solomon *et al.* observed that patients with mutations in β-myosin heavy chain (MYH7) generally had reversed curvature septal contours (reverse curve HCM) [176].

Subsequently, a large genotype–phenotype analysis correlating the septal morphology with the underlying genotype was conducted in >400 unrelated patients, and demonstrated that sigmoidal HCM (47% of cohort) and reverse curve HCM (35% of cohort) represented the two most prevalent anatomic subtypes of HCM. They showed that the yield of genetic testing for myofilament HCM was 80% in reverse curve HCM, but only 10% in patients with sigmoidal HCM, and that septal contour was the strongest predictor of a positive HCM genetic test, regardless of age [174].

Therapy in hypertrophic cardiomyopathy

The mainstay of therapy in children with HCM has been pharmacologic approaches with β-blockers and calcium-channel blockers [177–182]. In small children, propranolol is our drug of choice due to ease of access, liquid formulation, and low side-effect profile. Therapy is monitored by heart rate response, with goal of ~80–100 beats per minute. Typically dosage ranges from 2 to 5 mg kg^{-1} per day divided three times daily. Verapamil has been used with good outcomes. In older children, we typically treat with atenolol; in those with excessive hypertrophy and severe outflow tract obstruction, we occasionally use combination therapy (β-blocker plus calcium-channel blocker), although this has risk. The risk:benefit ratio must be determined for each patient.

When standard pharmacologic therapy fails, there are limited options. In small children, myectomy is the only proven option, but has risks [183–186]. In older patients, pacing protocols have been used but are controversial [187–190]. In adults, alcohol septal ablation has been used, but this has not yet been adopted in children because of uncertainties regarding long-term outcome associated with creating an infarct in a young individual [191–195].

In patients with syncope, ventricular arrhythmias, or other presumed high-risk factors, ICD implantation should be considered [196–199]. In some patients, pacing is also necessary. Heart failure in HCM occurs from either diastolic or systolic dysfunction. In the latter, therapy is similar to that for DCM, including ACE inhibitor plus β-blocker therapy, with or without diuretic and digoxin [139,199,200]. Enalapril plus carvedilol is the most common ACE inhibitor–β-blocker combination used. With diastolic dysfunction, heart failure,

and preserved systolic function, combination therapy with ACE inhibitors and diuretics, with or without angiotensin II receptor blockers such as candesartan or losartan, is commonly used. In these patients, β-blockers, calcium-channel blockers, and pacing are also considered, along with surgical relief [139,199,200].

Finally, in children with metabolic or mitochondrial dysfunction underlying the HCM, metabolic therapies have occasionally been successful. Similarly to the therapy in DCM caused by these deficiencies, carnitine, coenzyme Q10, riboflavin, and thiamine may be considered [101,139].

Infiltrative forms of hypertrophic cardiomyopathy

A variety of disorders with apparent left ventricular hypertrophy and features of hypertrophic cardiomyopathy occur from infiltrative disorders. The classic infiltrative disease is Pompe disease, which typically presents in the first weeks of life [101,201]. Other infiltrative diseases, with later onset, have been identified, such as Fabry disease [202,203], Danon disease [157–160], and left ventricular hypertrophy due to mutations in AMP-activated protein kinase (AMP-K) encoded by the PRKAG2 gene [154–156,204]. These disorders, along with those caused by mitochondrial abnormalities and genetic dysmorphism syndromes, are caused by abnormalities not primarily affecting the sarcomere [205]. Therapy is similar to that for the sarcomeric form of the disease, unless systolic dysfunction occurs, when heart failure therapy should be instituted.

Pompe disease (Type II glycogen storage disease)

Genetic deficiency of acid α-1,4-glucosidase, an enzyme involved in the breakdown of glycogen to glucose, results in a wide clinical spectrum ranging from the rapidly fatal infantile onset to a slowly progressive adult-onset myopathy [101,201]. The infantile-onset form (Pompe disease) typically manifests during the first 5 months of life, and patients usually die before their second year of life unless they receive enzyme replacement therapy [206]. This rare inborn error of glycogen metabolism occurs in <1/100 000 births. Massive glycogen accumulation occurs, leading to an enlarged tongue, striking hepatomegaly, hypotonia with decreased deep tendon reflexes, and cardiomyopathy (usually HCM) with congestive heart failure. The glycogen accumulation can be noted histologically in the skeletal muscles, liver, and heart. The diagnosis may be suspected from the classic electrocardiogram (ECG) in which gigantic QRS voltages are notable, typically with a short PR interval [101,201]. The disease has autosomal recessive inheritance; the gene coding for the defective lysosomal enzyme resides at chromosome 17q23-q25 [101]. Prenatal diagnosis is possible by amniocentesis or chorionic villus sampling by assay of α-glucosidase. Enzyme therapy with Myozyme (alglucosidase alfa) is now possible and, in some patients, appears to reverse the cardiac phenotype [206].

Fabry disease

An X-linked recessive disorder with mild expression occasionally seen in carrier females is caused by deficiency of the enzyme α-galactosidase (α-Gal) and found in 1/40 000 people [203]. Deposits of glycosphingolipids in various tissues, particularly the kidneys and coronary arteries, cause the most important disease manifestations – renal failure and myocardial infarctions in young adult males. Fabry disease usually begins in adolescence with sensations of burning pain in the hands and feet [202,203] associated with fever, heat, cold, and exercise. With increasing age, multiple angiokeratoma become noticeable, especially around the umbilicus and genitalia. Corneal opacities are often noted. Progressive renal failure develops. CNS manifestations include seizures and headaches, and also hemiplegia associated with an increased risk of stroke. Primary cardiac manifestations in affected males are hypertrophic cardiomyopathy and mitral insufficiency. Diagnosis depends on echocardiography [203]. The left ventricular myocardium and mitral valve are regions of greatest storage of lipid material [203,206–208]. On electrocardiogram, the PR interval is usually short. Deposition of sphingolipids in the coronary arteries leads to myocardial ischemia and infarction. The disease-causing gene is localized to Xq22 and encodes the α-Gal gene [203,206–208]. Enzyme replacement therapy with recombinant human α-galactosidase A (algasidase) is promising but expensive.

Danon disease

Danon disease is an X-linked dominant disorder characterized by intracytoplasmic vacuoles containing autophagic material and glycogen in cardiac and skeletal muscle cells. The major manifestations relate to cardiomyopathy with or without conduction defect, WPW syndrome, skeletal myopathy, or mental retardation [54,157–160]. The abnormality affects lysosomal function due to mutations in the lysosomal associated membrane protein 2 (LAMP2). The clinical phenotypic expression of Danon disease varies. Charron *et al*. screened 50 patients with HCM for LAMP2 mutations and identified mutations in two patients with HCM and skeletal myopathy [159]. Both individuals presented as teenagers and other affected individuals in the family were identified as young as 7 years of age. WPW syndrome and high-voltage QRS complexes on electrocardiogram were notable along with elevated creatine kinase plasma levels. LV dilation and dysfunction occurred late with symptoms of heart failure. Atrial and ventricular arrhythmias and conduction disease were notable along with death during the twenties. Visual acuity abnormality from choriocapillary ocular atrophy is common. This disease appears under-recognized and may be a significant cause of heart failure and LVH in childhood [160].

AMP-activated protein kinase (AMP-K)

AMP-activated protein kinase (AMP-K), encoded by the γ2 regulatory subunit of the PRKAG2 gene on chromosome

7q31 [209], is an enzyme that has been thought to modulate glucose uptake and glycolysis [210,211] and regulate energy homoeostasis [204]. AMP-K is expressed in many tissues, including the heart and vasculature. It is activated in response to stresses that increase the cellular ratio of AMP to ATP caused either by inhibiting ATP production (i.e., anoxia or ischemia) or by accelerating ATP consumption (i.e., muscle contraction or fasting). In the heart, AMP-K activity increases during ischemia and functions to sustain ATP, cardiac function, and myocardial viability [204]. Dominant gene mutations have been identified [154,155] in patients with hypertrophic cardiomyopathy, WPW pre-excitation, and atrioventricular block. Blair *et al.* [155] argued that mutations in AMP-K resulted in HCM due to compromise of energy production and utilization, but Arad *et al.* [156] provided evidence that this disorder is a form of glycogen-storage disease. Cardiac pathology, however, differed from other forms of HCM in that there was pronounced vacuole formation in which glycogen-associated granules were noted and no myocyte or myofibrillar disarray was seen. The myocytes were enlarged and interstitial fibrosis was minimal. Utilizing a yeast system in which a similar enzyme is functional, Arad *et al.* introduced the same mutations found in the patients and showed that the enzyme activity is persistent (i.e., does not turn off), leading to glycogen accumulation. They confirmed these findings by developing a murine model which mimics the human disorder [156].

Energy-dependent forms of hypertrophic cardiomyopathy

Mitochondrial cardiomyopathies

The human mitochondrial genome is a small, circular DNA molecule that is maternally inherited. Mitochondrial DNA (mtDNA) encodes 13 of the 69 proteins required for oxidative metabolism, 22 transfer RNAs (tRNAs), and two ribosomal RNAs (rRNAs) required for their translation [212–214]. Because mtDNA has much less redundancy than the nuclear genome (in which essentially identical information is received from both parents), and tRNAs and rRNAs are present in multiple copies, the mitochondrial genome is an excellent target for mutations giving rise to human disease. Mitochondria enjoy a symbiotic relationship with the cell. These subcellular organelles depend on nucleocytoplasmic mechanisms for most structural components, but do contribute vital peptides that are central to cellular respiration. Mitochondria contain a permeable outer membrane and a highly restrictive inner membrane that guards the chemical microenvironment of the matrix compartment. Adaptive mechanisms exist for the passage of large and small molecules across the inner membrane. Translocases shuttle monocarboxylic acids, amino acids, acylcarnitine conjugates, small ions, and other metabolites in and out of the mitochondrial matrix. Energy is required for importing proteins into the mitochondria because the nuclear gene-synthesized mitochondrial proteins are precursor molecules that require presequence cleavage. The 13 mtDNA genes are located in the respiratory chain [212–214] and include seven complex I subunits (ND1, -2, -3, -4L, -4, -5, and -6), one complex III subunit (cytochrome *b*), three complex IV subunits (COI, -II, and -III), and two complex V subunits (ATPase 6 and 8). Coordination must exist between nuclear and mitochondrial genomes to permit assembly of the complex holoenzymes. Each cell contains numerous mitochondria and each mitochondrion contains multiple copies of mtDNA. This genetic material derives exclusively from the female gamete and any mutation must be passed from female parent to all progeny, male and female. The replicative segregation of mutant mtDNA copies within the cell determines whether this biological disadvantage is expressed. In most mitochondrial disorders, patients carry a mix of mutant and normal mitochondria, a condition known as heteroplasmy, with the proportions varying from tissue to tissue and from individual to individual within a pedigree in a manner correlating with severity of phenotype [212–215].

Mitochondrial diseases often produce disturbances of brain and muscle function, presumably because these two organs are so metabolically active, and therefore the metabolic demand is high during growth and development [213–216]. Cardiac disease is most commonly seen with respiratory chain defects [212]. Ragged red fibers are present in muscle biopsy specimens almost invariably when the molecular defect involves mtDNA (except in infants). These defects represent the genetics of ATP production. The diverse clinical syndromes associated with various respiratory chain complexes are thought to result from involvement of tissue-nonspecific (generalized) subunits in other cells, and the residual enzyme activity in affected tissues. The cardiac diseases associated with mitochondrial defects include both hypertrophic cardiomyopathy and dilated cardiomyopathy, and LV noncompaction [217].

Kearns–Sayre syndrome

This mitochondrial myopathy is characterized by ptosis, chronic progressive external ophthalmoplegia, abnormal retinal pigmentation, and cardiac conduction defects, in addition to DCM [212,218]. Approximately 20% of Kearns–Sayre syndrome patients have cardiac involvement and the majority have conduction defects causing progressive heart block [219]. These patients generally have large, heterogeneous deletions in the mitochondrial chromosome. Poulton *et al.* [220] showed germline deletions of mtDNA in a family with Kearns–Sayre syndrome with a deletion in muscle mtDNA and at low levels in blood that was identical with that found in the mother and sister. The probands, however, had more deleted DNA, correlating with more severe symptoms. Other mutations have also been described [214].
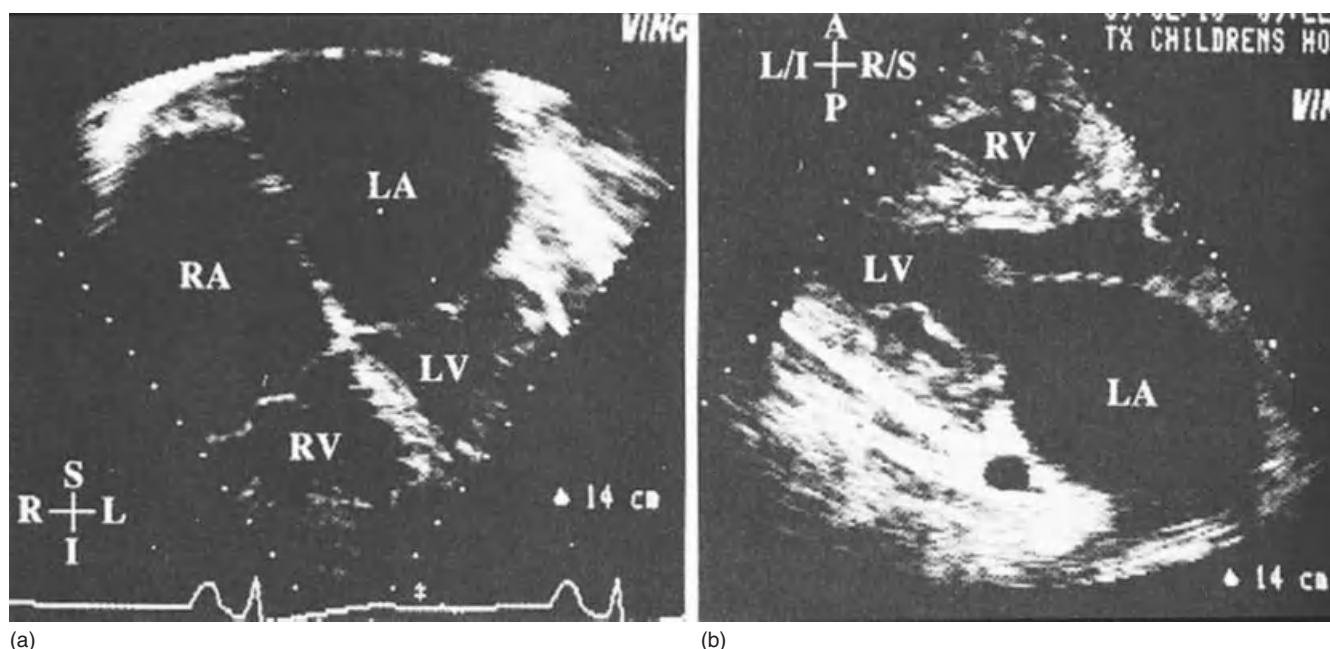
Figure 58.5 (a) Apical four-chamber echocardiographic view of a child with restrictive cardiomyopathy. Note the extremely dilated atria and normal-sized ventricles (which appear to be small because of the large atrial dimensions). The electrocardiographic strip at the bottom demonstrates a giant P wave as well. (b) Echocardiogram (parasternal long-axis view) in a child with restrictive cardiomyopathy. Note the giant left atrium and normal-sized left and right ventricles. LA, left atrium; LV, left ventricle; RA, right atrium; RV, right ventricle.

MERRF syndrome

This syndrome is characterized by myoclonic epilepsy with ragged red muscle fibers (MERRF) and is caused by a single nucleotide substitution in tRNA LYS that apparently interferes with mitochondrial translation [212,214,216,221]. This abnormality causes decline in ATP-generating capacity, with onset of disease that includes cardiomyopathy. Other reports outline various disease-causing mutations [222–224].

Restrictive cardiomyopathy

Restrictive cardiomyopathy (RCM) is a rare form of heart disease (<5% of cardiomyopathies in children) [225–228] characterized by "normal or decreased volume of both ventricles associated with biatrial enlargement, normal left ventricular wall thickness and atrioventricular valves, impaired ventricular filling with restrictive physiology, and normal (or near normal) systolic function" (Figure 58.5) [5].

Epidemiology

In children in the United States and Australia, RCM accounts for 2.5–5% of the diagnosed cardiomyopathies, with most having no specific identified cause [3,225–227,229]. In Australia, RCM accounted for 2.5% of the cardiomyopathies in children <10 years of age [229] and in the United States it accounted for 3% of the cardiomyopathies in patients <18 years of age. [3] The estimated annual incidence in children in the United States and Australia is 0.04/100 000 and 0.03/100 000, respectively [3,229].

Etiology and pathology

Multiple causes of RCM described in adults and children are listed in Table 58.5. The pathology and histology vary with the underlying disease process [230,231]. Histochemical stains show variable degrees of myocyte hypertrophy, interstitial fibrosis, and myocytolysis. Both sporadic and familial examples of RCM are reported. Worldwide, the most common etiology is endomyocardial fibrosis, which affects ~10 million people, most often children and adolescents [232,233]. Some inherited instances of RCM have autosomal dominant transmission, mostly caused by mutations in sarcomere-encoding genes such as troponin I, troponin T, β-myosin heavy chain, and actin [225,231]. RCM has also been associated with atrioventricular block and skeletal myopathy, and caused by mutations in desmin [225,231].

Clinical presentation and diagnostic evaluation

The common presenting symptoms in children with RCM include dyspnea that is frequently exacerbated by an intercurrent respiratory illness or "asthma," fatigue, exercise intolerance, syncope, and sudden death [225,230,234,235]. Abnormal findings on physical examination include hepatomegaly, ascites, elevated jugular venous pulse, a loud pulmonary component of the second heart sound (P2), and an S_3 or S_4 gallop. Chest radiography usually reveals

Table 58.5 Etiologies of restrictive cardiomyopathy.

Genetic	Mixed	Acquired
Sarcomeric mutations	Amyloidosis	Endomyocardial fibrosis
Troponin I	Endocardial fibroelastosis (EFE)	Myocarditis
Troponin T		Cardiac transplant
α-cardiac actin		*Pseudoxanthoma elasticum*
Myosin binding protein C		Diabetic cardiomyopathy
β-Myosin heavy chain		Sarcoidosis
Myosin light chain		Hemochromatosis
Non-sarcomeric mutations		Loffler syndrome
Desmin		Scleroderma
RSK2 (Coffin–Lowry)		Carcinoid
Lamin A/C (Emery–Dreifuss)		Metastatic cancers
Transthyretin (amyloidosis)		Radiation
		Drugs

cardiomegaly and pulmonary venous congestion (an indicator of poor prognosis). The electrocardiogram is abnormal in ~98% of patients [236]. The most common abnormalities are right and/or left atrial enlargement; however, ST segment depression and ST-T wave abnormalities are frequent (Figure 58.6). Right and/or left ventricular hypertrophy and conduction abnormalities may be present. Arrhythmias are found in ~15% of pediatric patients and include both atrial and ventricular tachyarrhythmias, including torsades de pointes and WPW syndrome, and various degrees of heart block. Symptomatic sinus bradycardia requiring pacing has also been reported [234].

The most striking finding on echocardiography is massive atrial dilation with normal AV valves.(Figure 58.5) [225]. In children, findings consistent with restrictive filling and increased left ventricular end diastolic pressure include elevated E/A ratios, short mitral deceleration times, increased pulmonary vein atrial reversal velocity and duration, and pulmonary vein atrial reversal duration greater than mitral A duration [237–239]. Some systolic dysfunction may be present and deteriorate with time [225,230,236,237]. Some concentric increase in septal and left ventricular posterior wall thickness is present in many patients otherwise fulfilling the criteria for RCM. The ventricular cavity sizes are usually normal.

Cardiac catheterization should be performed. It shows elevated left and/or right ventricular end diastolic pressures, and frequently pulmonary hypertension [225,237,239]. The pulmonary vasculature may remain reactive, but 40% of patients had elevated and nonreactive pulmonary vascular resistance when evaluated for cardiac transplantation [240]. The major hemodynamic problem in RCM is restricted ventricular filling. The diastolic pressure curve generally shows one of two patterns: (1) the pressure is elevated at the onset of diastole and rises further with ventricular filling; (2) a prominent *y* descent occurs in early diastole, followed by an abrupt rise during the rapid filling phase, producing the "square root" or "dip and plateau" pattern. The first pattern can also be seen in cardiac tamponade, and the second may be seen in constrictive pericarditis (see also Chapter 59). Elevated pulmonary artery pressure is common, and markedly elevated pulmonary vascular resistance can occur within 1–4 years of diagnosis. Endomyocardial biopsy reveals myofiber hypertrophy and mild to moderate interstitial fibrosis.

Treatment

Treatment of RCM is nonspecific and directed at alleviating symptoms. In general, medical therapy does not improve survival [234,236,237,240]. Diuretics are usually helpful in reducing pulmonary and systemic venous congestion. Because there is restriction on ventricular filling, care must be taken to avoid excessive reduction of preload. Afterload-reducing agents, calcium-channel blockers, and inotropic agents have not been beneficial Adrenergic agonists and phosphodiesterase inhibitors can improve left ventricular relaxation, but they are effective only in patients with concurrent systolic dysfunction. Chatterjee and Alpert [241] reported that in patients with RCM and severe heart failure, pharmacotherapy is ineffective and cardiac transplantation is the most effective therapy. Atrial thrombi or embolic events occur often, so anticoagulation or antiplatelet therapy appears warranted. ICD implantation has theoretical advantages but there are limited data to support its use. Transplantation remains the treatment of choice. Contemporary outcomes from transplantation far exceed the natural history of this disease, causing some groups to recommend listing for transplantation when the patient presents, even if asymptomatic. Progressive elevation of pulmonary vascular resistance should lead to early consideration of transplantation. Elevated pulmonary vascular resistance usually normalizes after transplantation.

Prognosis

The prognosis for children with RCM is poor [225,230, 234,236–240,242], with half dying or undergoing transplant within 3 years of diagnosis [225,230,234,236–240]. Sudden cardiac death is common [225,230,234,236–240], especially in those with signs and symptoms of ischemia, such as syncope and chest pain. Deaths from heart failure are the most common, with poor prognostic factors being cardiomegaly and pulmonary venous congestion on chest X-ray, age <5 years, thromboembolism, and elevated pulmonary vascular resistance [225,230, 234,236–240].
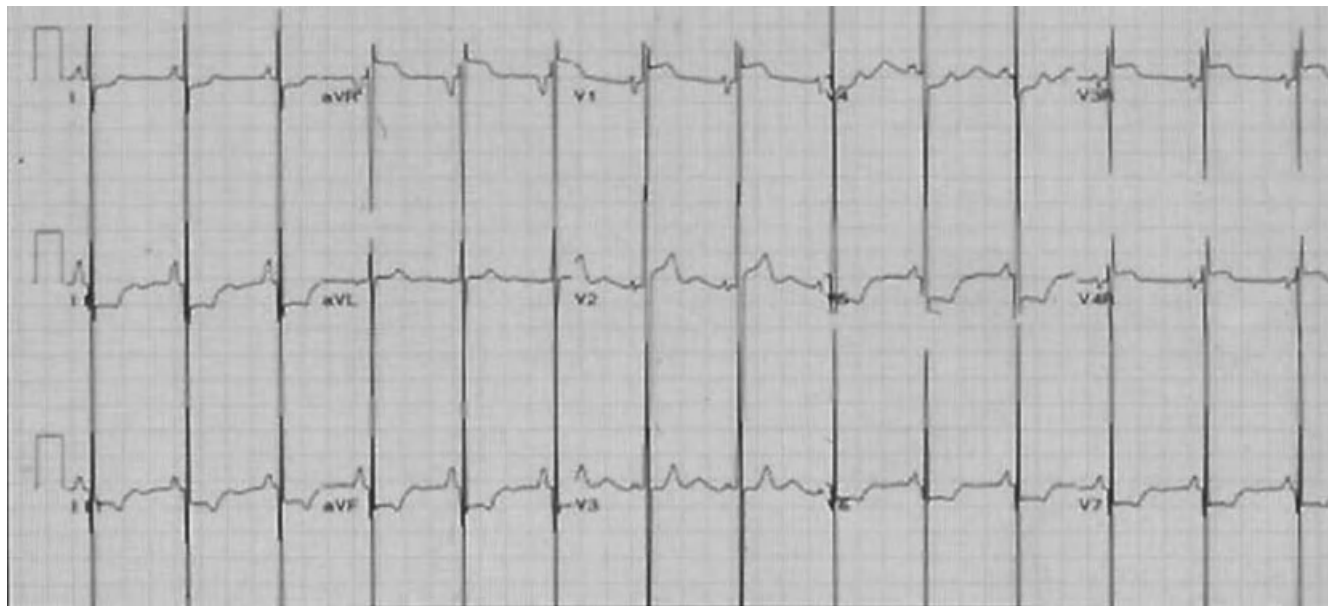
(a)

(b)

Figure 58.6 (a) This electrocardiogram demonstrates large P waves in addition to T-segment abnormalities consistent with ischemia. (b) Electrocardiographic strip demonstrating ventricular tachycardia. This occurred after the development of sinus tachycardia, which led to worsening ischemic abnormalities on electrocardiogram.

Arrhythmogenic cardiomyopathy

Arrhythmogenic right ventricular cardiomyopathy (ARVC), first reported in 1978 [243], has areas of fibrofatty replacement, inflammatory infiltrate, and fibrosis, predominantly in the right ventricular but also the left ventricular free wall. A spectrum of right ventricular involvement occurs. Classically, the patients present with syncope or palpitations secondary to ventricular tachycardia of left bundle branch block morphology, originating from the areas of fibrofatty replacement [244–246].

Pathology

Pathologically there is some right ventricular enlargement, frequently with aneurysms and thinning of the right ventricular free wall in the region of the infundibulum, apex, or inferior wall (known as the "triangle of dysplasia") associated with fibrosis with or without fatty replacement (Figure 58.7) [247,248]. These areas of replacement are white, thickened, and sclerotic on the endocardial surface. The left ventricle is also often affected. Histologic sections show a variable reduction in myofibrils and inflammation associated with interstitial infiltration by histiocytes and lymphocytes. The few remaining
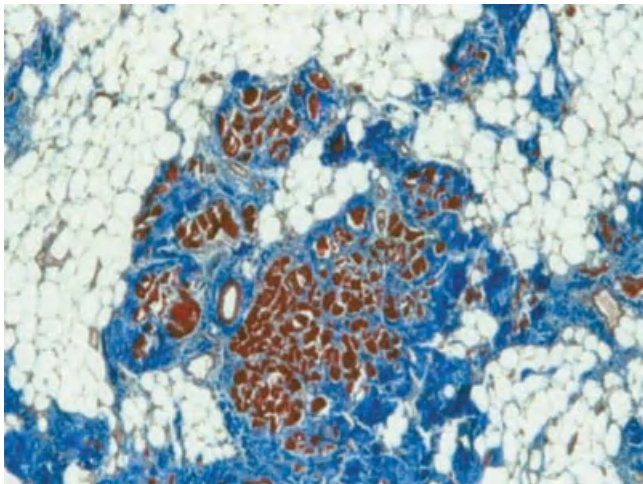
Figure 58.7 Histologic examination in arrhythmogenic right ventricular dysplasia shows fibrofatty infiltration within the right ventricular tissue. Note the fatty infiltration and the fibrous tissue surrounding the islands of cardiomyocytes.

Table 58.6 Arrhythmogenic RV cardiomyopathy genetics.

Locus name	Inheritance	Map position	Gene
ARVD1	AD	14q23	TGFB3
ARVD2	AD	1q42-q43	RyR2
ARVD3	AD	14q12	?
ARVD4	AD	2q32	?
ARVD5	AD	3p23	?
ARVD6	AD	10p12	?
ARVD7	AD	10p22	TMEM43
ARVD8	AD	6p24	Desmoplakin (DSP)
ARVD9	AD	12p11	Plakophilin-2 (PKP2)
ARVD10	AD	18q12	Desmocolin-2 (DSC2)
ARVD11	AD	18q12	Desmoglein-2 (DSG2)
Naxos	AR	17q21	Plakoglobin (JUP)
Carvajal	AR	6p24	Desmoplakin (DSP)

myofibrils are hypertrophied or show signs of degeneration. It is the fibrosis and fatty infiltration that are most characteristic of ARVC; all layers of the free wall are affected [246],

Prevalence

It is difficult to assess the prevalence of ARVC, because clinically evident right ventricular dysfunction is uncommon, and the reporting is based primarily on the arrhythmia and not right-sided failure. The estimates range from 1/1000 to 1/5000 population [249–251].

Etiology

Two etiologic factors for ARVC have been defined [252]. An inflammatory process, possibly infectious, has been implicated because infection with coxsackievirus B3 and adenovirus has been reported [253]. In susceptible individuals, a preceding viral infection could gradual destroy myocytes and cause fatty infiltration. Familial occurrence is recognized and genes encoding proteins of the desmosome or desmosome interacting proteins have been described.(Table 58.6) [252].

Clinical findings

The clinical picture seems to be independent of age [245,246,252]. The typical patient is male and in the third decade of life, but the ages range from the first year of life to the ninth decade. Athletic teens and 20–30-year-olds are the most at risk. Typically the patient presents abruptly with syncopal episodes, palpitations, or ventricular tachycardia, often associated with exercise. Sudden death may be the initial (and final) presentation. The physical examination is usually normal. When findings are abnormal, diastolic filling sounds are most frequent (20%), and prominence of the left anterior thorax occurs in <10%. An irregular rhythm is usually found on physical examination. Presentation with right ventricular failure occurs in <2% of patients [245,246,252–254].

Diagnostic studies

Chest radiography

The chest radiograph is normal in the absence of right ventricular failure. Although a cardiothoracic ratio of >50% occurs in many older patients, it is normal in children. Pulmonary vascular markings are usually normal.

Electrocardiography

The electrocardiogram is helpful [245,246,252]. It usually shows sinus rhythm, with frequent ventricular premature depolarizations of left bundle branch block morphology. The QRS, P wave, and T wave frontal plane axes are normal. Although precordial QRS morphology is normal, a pattern of incomplete right bundle branch block is seen in >30% of patients. The most striking and constant feature is the inversion of T waves in leads V_1–V_4. Whereas this sign is highly suggestive of ARVD in the adult, it may be normal in children <12 years old. Ventricular post-excitation waves, so-called epsilon waves, are found in the ST segments of the right precordial leads in 30% of adult patients. By increasing the gain or by using signal-averaging techniques, these potentials – which arise from areas with markedly delayed depolarization – can be made visible. Epsilon waves are considered a marker for risk of re-entry tachycardia. When present, ventricular tachycardia is characterized by a left bundle branch block morphology, a rate in the range 170–300 beats per minute (average 250), with a QRS axis that is normal to rightwards.

Noninvasive imaging

Noninvasive evaluation of ventricular morphology and function is helpful but may not detect all patients in childhood [255,256]. Cardiac MRI can visualize the anatomic abnormalities, myocardial fibrosis, and inflammation. Echocardiographic imaging can show right ventricular outpouching, diffuse dysfunction, or dilation. Global dysfunction and regional wall motion abnormalities may also be identified by radionuclide angiography [246,252,256].

Cardiac catheterization

If ARVC is suspected (e.g., ventricular tachycardia in a "normal heart") and not found on MRI or echocardiography, cardiac catheterization (especially with angiography) should be considered [245,252,257]. The pressures may be normal in each cardiac chamber. If abnormal, the most common finding is an elevated right atrial *a* wave, which in patients with severe right ventricular dysfunction may exceed the pulmonary artery diastolic pressure. A right ventriculogram usually shows dyskinesis and dilation in adults but less commonly in children. Children show segmental dilation with paradoxical motion of the outflow tract. The hallmark of the disease is systolic bulging of the right ventricular free wall. The "triangle of dysplasia" includes the anterior infundibulum, the right ventricular apex, and the diaphragmatic free wall. Hemodynamic and angiographic assessment of left ventricular function should also be done. Endomyocardial biopsy of the right ventricular septum should be performed, because classic pathologic changes are seen in >90% of patients [245,252,257]. Analysis of the biopsy should include histology with appropriate staining for fibrosis and adipose/lipid infiltration, PCR analysis for viral genome, and immunohistochemistry for desmosomal and gap junction proteins.

Electrophysiologic study

Invasive electrophysiologic investigation is usually not needed for diagnosis [257–259]. Atrial and atrioventricular node conduction times are often prolonged minimally and epsilon waves can be recorded in only half the patients. Electrophysiologic testing can confirm that the tachycardia originates in the right ventricle, map the location of initiation, and evaluate response to antiarrhythmic agents. An ICD can be implanted when appropriate during the electrophysiologic study [258].

Treatment

Treatment focuses on control of the arrhythmias [257–259]. Propranolol, sotalol, procainamide, disopyramide, and amiodarone have been effective in some patients. ICD implantation has become standard in adults but has been used only in symptomatic children [258].

Natural history

The natural history of ARVC requires further study [246,252,257,258]. Although sudden death occurred in ~5%
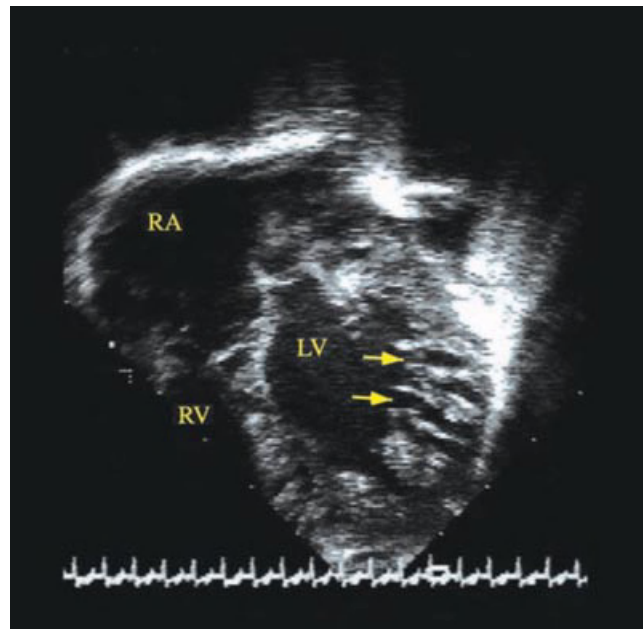
Figure 58.8 Echocardiogram of a child with left ventricular noncompaction. This apical three-chamber view shows an apparently thick left ventricle with small left ventricular chamber. Note the apical "fill in" and the strips of muscle (trabeculations) at the free wall with intertrabecular recesses between the trabeculations (arrows). RA, right atrium; RV, right ventricle; LV, left ventricle.

of the reported patients, most were either untreated or undiagnosed. Sudden death in childhood occurs, as does death from congestive failure, but it is uncommon. There is debate whether antiarrhythmic treatment will reduce the incidence of sudden death. The usual course appears to be one of slow deterioration of right ventricular function and reduction in the efficacy of antiarrhythmic treatment.

Overlap disorders

Left ventricular noncompaction

This disorder has been named spongy myocardium, fetal myocardium, and noncompaction of the left ventricular myocardium [77,260–262]. It may represent an arrest in the normal process of myocardial compaction, the final stage of myocardial morphogenesis. The result is persistence of multiple prominent ventricular trabeculations and deep intertrabecular recesses at the LV apex and at times the free wall and septum (Figure 58.8). This cardiomyopathy may be difficult to diagnose unless there is a high level of suspicion during echocardiographic evaluation. In fact, on careful review of echocardiograms and other clinical data, it appears that left ventricular noncompaction is relatively common in children and adults [8,77].

Left ventricular noncompaction (LVNC) is a clinically heterogeneous disorder that may present with multiple different
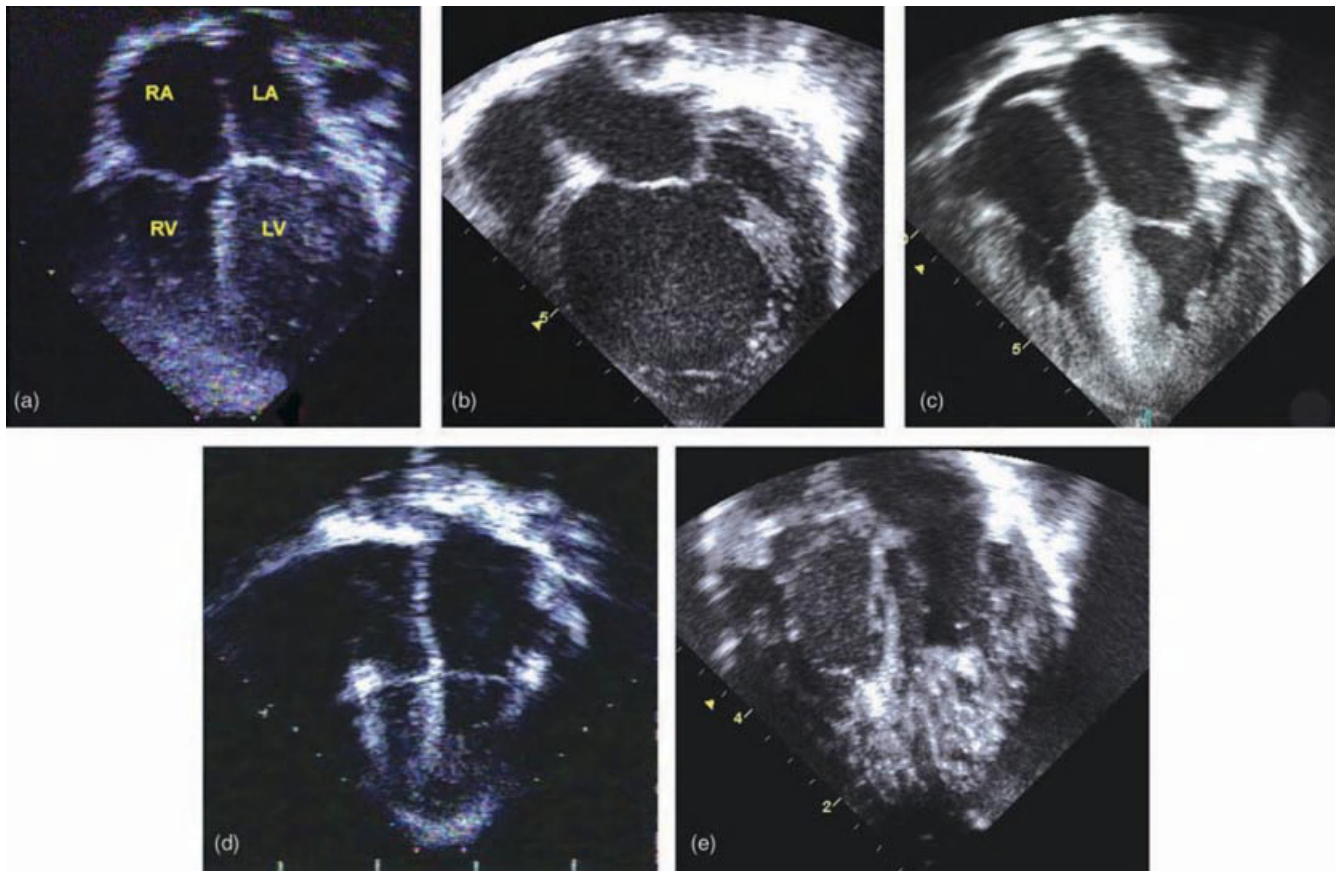
Figure 58.9 Echocardiograms of children with left ventricular noncompaction. These apical four-chamber views show the heterogeneous phenotypes that can occur in left ventricular noncompaction. (a) LV noncompaction associated with normal LV size, thickness, and function. Note the apical and free wall trabeculations in the LV. (b) LV noncompaction associated with a dilated LV and poor systolic function (DCM form of LVNC). Note the inappropriate apical and free wall thickening in this otherwise dilated LV. (c) LV noncompaction associated with a hypertrophic LV and hyperdynamic systolic function and diastolic dysfunction (HCM form of LVNC). Note the asymmetric septal hypertrophy with midseptal bulge, apical hypertrophy/trabeculations, and free wall trabeculations. (d) LV noncompaction associated with a dilated atria and normal LV size, thickness, and systolic function (RCM form of LVNC); (e) LV noncompaction associated biventricular trabeculations. The apex of both ventricles show hypertrophic "fill in" with trabeculations and the LV free wall is also heavily trabeculated, giving the appearance of a hypoplastic LV.
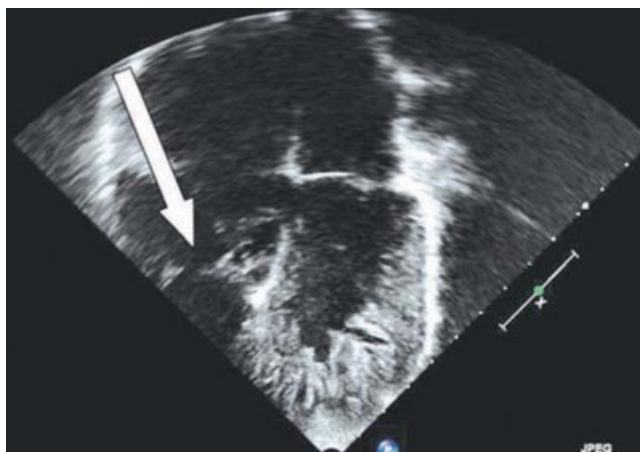
Figure 58.10 Echocardiograms of a child with left ventricular noncompaction associated with congenital heart disease. The associated CHD lesion in this case is Ebstein's anomaly; note the apically displaced tricuspid valve (arrow).

features (Figure 58.9) including the following [8,77, 263,264]:

1 LV noncompaction associated with normal LV size, thickness and function occurs in ~25% of LVNC. The patients are asymptomatic and features do not change.

2 LV noncompaction associated with a dilated LV and poor systolic function (DCM form of LVNC).

3 LV noncompaction associated with a hypertrophic LV and hyperdynamic systolic function and diastolic dysfunction (HCM form of LVNC).

4 LV noncompaction associated with a hypertrophic and dilated LV with systolic dysfunction (HDCM form of LVNC).

5 LV noncompaction associated with a dilated atria and normal LV size, thickness and systolic function (RCM form of LVNC).

6 LV noncompaction associated with congenital heart disease, commonly right-sided but with a variety of other lesions (Figure 58.10).

All leads ¼ standard
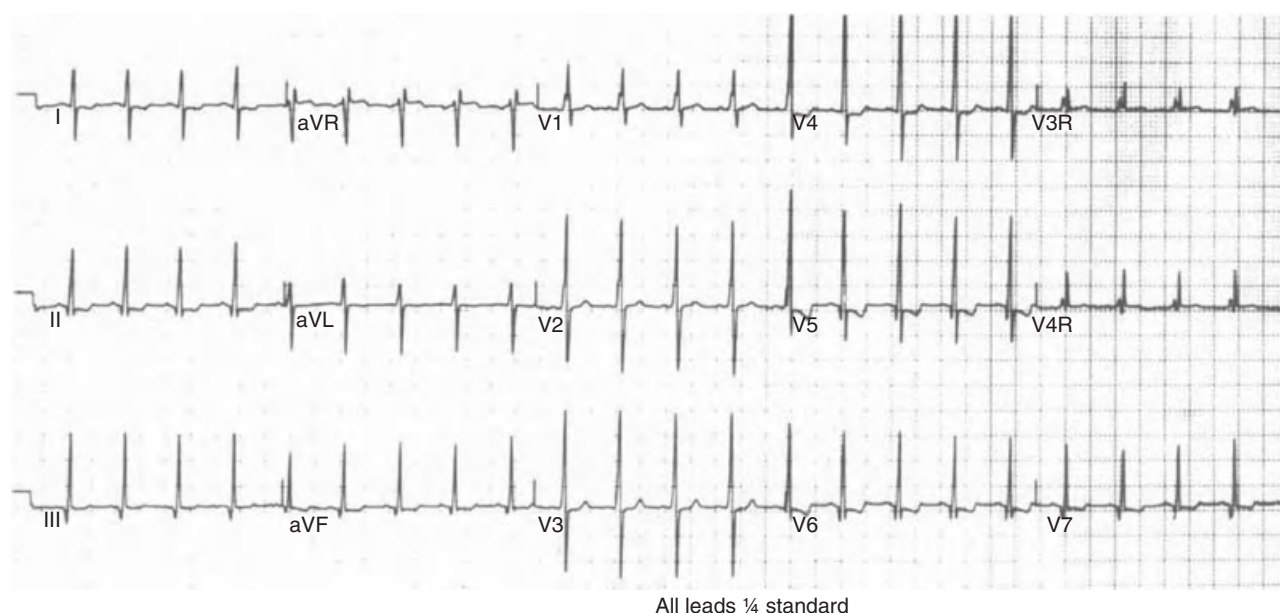
Figure 58.11 Electrocardiogram in a neonate with the dilated, hypertrophic form of left ventricular noncompaction. Note the extreme mid-precordial QRS complex voltages and the short PR interval. The voltages are set at one-quarter standard.

In the isolated form and that associated with congenital heart disease, metabolic derangements may be notable. [217,261]

Clinical features of left ventricular noncompaction

Towbin recently suggested that patients with a trabeculated left ventricle be subgrouped into phenotypes and that this subdivision is important in predicting outcome [264]. In approximately 25% of patients, the size, thickness, and function of the LV are normal, and these subjects, provided that they are arrhythmia free, appear to show a benign course. The other forms are dependent on the other features regarding outcomes. When LVNC coexists with another type of cardiomyopathy as defined above, many present in infancy with signs and symptoms of heart failure but others are identified later, even in adulthood. Pignatelli *et al.* [77] reported 36 children with a median age at presentation of 90 days (range 1 day–17 years). About 40% of these children presented with low cardiac output or congestive heart failure and only one child presented with syncope. Most of the other patients (42%) were asymptomatic, but had electrocardiographic or radiographic abnormalities. In an infant with LVNC, the ECG may show giant QRS complexes sometimes with pre-excitation (Figure 58.11). In addition, 14% of the 36 children had associated dysmorphic features and 19% of affected children had first-degree relatives with cardiomyopathy. The children who died each had a systemic disease and died in the first 3 months of life. Thromboembolic phenomena, including stroke, also occur in patients with LVNC [263]. Whether the disease in adults differs from that in children is unknown [265].

Genetics of left ventricular noncompaction

LVNC commonly has X-linked recessive or autosomal dominant inheritance [5,8,263,264]. In X-linked LVNC, female carriers do not develop frank clinical disease and their echocardiograms are normal. Consistent with X-linked inheritance, no male-to-male transmission of the disease occurs. In most patients with LVNC associated with CHD, autosomal dominant inheritance is seen in familial instances and less often in LVNC without CHD. When LVNC is associated with CHD, the CHD may be heterogeneous in families. In some of these, affected members may be identified with "minor" forms of CHD, which have spontaneously improved, whereas others have severe CHD. Penetrance may be reduced in some families and both autosomal dominant and X-linked inheritance have been described [263].

Molecular genetics of left ventricular noncompaction

A genetic cause of isolated LVNC was initially described by Bleyl *et al.* [18] when they identified mutations in the gene G4.5/TAZ in patients and carrier females. This gene, known as G4.5 or tafazzin (TAZ), encodes a novel protein family (tafazzins) with unclear function, and is also responsible for Barth syndrome (BTS) [76] and other forms of infantile cardiomyopathies [266,267]. BTS, a clinical association of myocardial dysfunction with a number of other features [53,73,74,268], was discussed above. It is an X-linked disorder and may be allelic to several phenotypically different disorders on Xq28 [269,270] such as LVNC and dilated cardiomyopathy. Congenital heart defects have not been associated with BTS or other G4.5-associated disease.

For autosomal dominant LVNC, multiple genes have been identified, including mutations in α-dystrophobrevin [271],

mutations in the Z-line protein encoding ZASP, located on chromosome 10q22 [12], mutations in sarcomere-encoding genes, mutations in β-myosin heavy chain (MYH7), α-cardiac actin (ACTC), and cardiac troponin T (TNNT2) [272], sarcomere-encoding genes and the cytoskeleton, and mutations in the sodium channel gene, SCN5A [273]. A cytoskeletal protein associated with LVNC is dystrophin in Duchenne and Becker muscular dystrophy [274]. Skeletal muscle biopsy has, in some patients, identified mitochondrial abnormalities, suggesting a nuclear import protein as the primary abnormality. Genetic testing can identify a disease-causing mutation in ~40% of these patients [275,276].

Therapy and outcome

The specific therapy [277–279] depends on the specific clinical and echocardiographic findings of the phenotypic subtype of LVNC [264], and these have been discussed above under the specific type of cardiomyopathy. In patients with forms of noncompaction with associated mitochondrial or metabolic dysfunction, some investigators add a "vitamin cocktail" to the cardiac therapy, with coenzyme Q10, carnitine, riboflavin, and thiamine commonly used alone or in combination [8,34,102,217,264].

In patients with associated congenital heart disease undergoing catheter intervention or surgical repair [280], the cardiac functional abnormalities must be understood, evidence of thrombi (which should be treated with anticoagulation) sought, cardiac rhythm disturbances addressed [264], and the metabolic status of the patient attended to.

References

1 Brigden W. Uncommon myocardial diseases. The noncoronary cardiomyopathies. *Lancet* 1957;**ii**:1179–84.

2 Grenier MA, Osganian SK, Cox GF, *et al*. Design and implementation of the North American Pediatric Cardiomyopathy Registry. *Am Heart J* 2000;**139**:S86–95.

3 Lipshultz SE, Sleeper LA, Towbin JA, *et al*. The incidence of pediatric cardiomyopathy in two regions of the United States. *N Engl J Med* 2003;**348**:1647–55.

4 Towbin JA, Lowe AM, Colan SD, *et al*. Incidence, causes and outcomes of dilated cardiomyopathy in children. *JAMA* 2006;**296**:1867–76.

5 Maron BJ, Towbin JA, Thiene G, *et al*. Contemporary definitions and classification of the cardiomyopathies: an American Heart Association Scientific Statement from the Council on Clinical Cardiology, Heart Failure and Transplantation Committee; Quality of Care and Outcomes Research and Functional Genomics and Translational Biology Interdisciplinary Working Groups; and Council on Epidemiology and Prevention. *Circulation* 2006;**113**:1807–16.

6 Abelman WH, Lorrell BH. The challenge of cardiomyopathy. *J Am Coll Cardiol* 1989;**13**:1219–39.

7 Lloyd-Jones D, Adams R, Carnethon M, *et al*. Heart disease and stroke statistics – 2009 update: a report from the American Heart Association Statistics Committee and Stroke Statistics Subcommittee. *Circulation* 2010;**119**:e21–181.

8 Towbin JA, Bowles NE. The failing heart. *Nature* 2002; **415**:227–33.

9 Fatkin D, Otway R, Richmond Z. Genetics of dilated cardiomyopathy. *Heart Fail Clin* 2010;**6**:129–40.

10 Hsu D, Canter CE. Dilated cardiomyopathy and heart failure in children. *Heart Fail Clin* 2010;**6**:415–32.

11 Towbin JA. The role of cytoskeletal proteins in cardiomyopathies. *Curr Opin Cell Biol* 1998;**10**:131–9.

12 Vatta M, Mohapatra B, Jimenez S, *et al*. Mutations in cypher/ZASP in patients with dilated cardiomyopathy and left ventricular non-compaction. *J Am Coll Cardiol* 2003;**42**;2014–27.

13 Mohapatra B, Jimenez S, Lin JH, *et al*. Mutations in the muscle LIM protein and α-actinin-2 genes in dilated cardiomyopathy and endocardial fibroelastosis. *Mol Genet Metab* 2003;**80**: 207–15.

14 Purevjav E, Varela J, Morgado M, *et al*. Nebulette mutations are associated with dilated cardiomyopathy and endocardial fibroelastosis. *J Am Coll Cardiol* 2010;**56**:1493–502.

15 Dubosc-Bidot L, Xu P, Charron P, *et al*. Mutations in the Z-disk protein myopaladin gene and idiopathic dilated cardiomyopathy. *Cardiovasc Res* 2008;**77**:118–25.

16 Olson TM, Michaels VV, Ballew JD, *et al*. Sodium channel mutations and susceptibility to heart failure and atrial fibrillation. *JAMA* 2005;**293**:447–54.

17 Schmitt JP, Kamisago M, Asahi M, *et al*. Dilated cardiomyopathy and heart failure caused by a mutation in phospholamban. *Science* 2003;**299**:1403–10.

18 Bleyl SB, Mumford BR, Thompson V, *et al*. Neonatal, lethal noncompaction of the left ventricular myocardium is allelic with Barth syndrome. *Am J Hum Genet* 1997;**61**:868–72.

19 Kuhl U, Schultheiss HP. Myocarditis in children. *Heart Fail Clin* 2010;**6**:483–96.

20 Breinholt JP, Moulik M, Dreyer WJ, *et al*. Viral epidemiologic shift in inflammatory heart disease: the increasing involvement of parvovirus B19 in the myocardium of pediatric heart transplant patients. *J Heart Lung Transplant* 2010;**29**:739–46.

21 Manolio TA, Baughman KL, Rodenheffer R, *et al*. Prevalence and etiology of idiopathic dilated cardiomyopathy (summary of a National Heart, Lung, and Blood Institute workshop). *Am J Cardiol* 1992;**69**:1458–66.

22 Wiles HB, McArthur PD, Taylor AB, *et al*. Prognostic features of children with idiopathic dilated cardiomyopathy. *Am J Cardiol* 1991;**68**:1372–6.

23 Matitiau A, Perez-Atayde A, Sanders SP, *et al*. Infantile dilated cardiomyopathy. Relation of outcome to left ventricular mechanics, hemodynamics, and histology at the time of presentation. *Circulation* 1994;**90**:1310–8.

24 Michels VV, Moll PP, Miller FA, *et al*. The frequency of familial dilated cardiomyopathy in a series of patients with idiopathic dilated cardiomyopathy. *N Engl J Med* 1992;**326**:77–82.

25 Keeling PJ, McKenna WJ. Clinical genetics of dilated cardiomyopathy. *Herz* 1994;**19**:91–6.

26 Taylor MRG, Carniel E, Mestroni L. Cardiomyopathy, familial dilated. *Orphanet J Rare Dis* 2006;**1**:27–35.

27 Gilbert EM, Bristow MR. Idiopathic dilated cardiomyopathy. In: Schlant RC, Alexander RW, eds. *Hurst's The Heart*, 8th edn. New York: McGraw-Hill, 1994: 1609.

28 Doshi R, Lodge KV. Idiopathic cardiomyopathy in infants. *Arch Dis Child* 1973;**48**:431–5.

29 Lewis AB, Neustein HB, Takahashi M, Lurie PR. Findings on endomyocardial biopsy in infants and children with dilated cardiomyopathy. *Am J Cardiol* 1985;**55**:143–5.

30 Tazelaar HD, Billingham ME. Leukocytic infiltrates in idiopathic dilated cardiomyopathy: a source of confusion with active myocarditis. *Am J Surg Pathol* 1986;**10**:405–12.

31 Aretz HT, Billingham ME, Edwards WD, *et al*. Myocarditis: a histopathologic definition and classification. *Am J Cardiovasc Pathol* 1987;**1**:3–14.

32 Friedman RA, Moak JP, Garson A Jr. Clinical course of idiopathic dilated cardiomyopathy in children. *J Am Coll Cardiol* 1991;**18**:152–6.

33 Cooper LT Jr. Myocarditis. *N Engl J Med* 2009;**360**:1526–38.

34 Jefferies JL, Towbin JA. Dilated cardiomyopathy. *Lancet* 2010;**375**:752–62.

35 Taliercio CP, Seward JB, Driscoll DJ, *et al*. Idiopathic dilated cardiomyopathy in the young: clinical profile and natural history. *J Am Coll Cardiol* 1985;**6**:1126–31.

36 Greenwood RD, Nadas AS, Fyler DC. The clinical course of primary myocardial disease in infants and children. *Am Heart J* 1976;**92**:549–60.

37 Griffin ML, Hernandez A, Martin TC, *et al*. Dilated cardiomyopathy in infants and children. *J Am Coll Cardiol* 1988;**11**:139–44.

38 Das MK, Maskoun W, Shen C, *et al*. Fragmented QRS on twelve-lead electrocardiogram predicts arrhythmic events in patients with ischemic and nonischemic cardiomyopathy. *Heart Rhythm* 2010;**7**:74–80.

39 Cooper LT, Baughman KL, Feldman AM, *et al*. The role of endomyocardial biopsy in the management of cardiovascular disease: a scientific statement from the American Heart Association, the American College of Cardiology, and the European Society of Cardiology. Endorsed by the Heart Failure Society of America and the Heart Failure Association of the European Society of Cardiology *Circulation* 2007;**116**:2216–33.

40 Veinot JP. Endomyocardial biopsy – when and how? *Cardiovasc Pathol* in press.

41 Veinot JP. Diagnostic endomyocardial biopsy: secondary myocardial diseases and other clinical indications – a review. *Can J Cardiol* 2002;**18**:287–96.

42 Bowles NE, Ni J, Kearney DL, *et al*. Detection of viruses in myocardial tissues by polymerase chain reaction: evidence of adenovirus as a common cause of myocarditis in children and adults. *J Am Coll Cardiol* 2003;**42**:466–72.

43 Moulik M, Breinholt JP, Dreyer WJ, *et al*. Viral endomyocardial infection is an independent predictor and potentially treatable risk factor for graft loss and coronary vasculopathy in pediatric cardiac transplant recipients. *J Am Coll Cardiol* 2010;**56**:582–92.

44 Kawahara C, Tsutamoto T, Nishiyama K, *et al*. Prognostic role of high-sensitivity cardiac troponin T in patients with nonischemic dilated cardiomyopathy. *Circ J* 2011;**75**:656–61.

45 Kim HN, Januzzi JL Jr. Biomarkers in the management of heart failure. *Curr Treat Options Cardiovasc Med* 2010;**12**:519–31.

46 Price JF, Thomas AK, Grenier M, *et al*. B-type natriuretic peptide predicts adverse cardiovascular events in pediatric outpatients with chronic left ventricular systolic dysfunction. *Circulation* 2006;**114**:1063–9.

47 Mahfoud F, Gartner B, Kindermann M, *et al*. Virus serology in patients with suspected myocarditis: utility or futility? *Eur Heart J* 2011;**32**:897–903.

48 Hershberger RE, Morales A, Sieggfried JD. Clinical and genetic issues in dilated cardiomyopathy. *Genet Med* 2010;**12**:655–67.

49 Hershberger RE, Lindfeld J, Mestroni L, *et al*. Genetic evaluation of cardiomyopathy – a Heart Failure Society of America practice guideline. *J Card Fail* 2009;**15**:83–97.

50 Towbin JA, Bowles KR, Bowles NE. Etiologies of cardiomyopathy and heart failure. *Nat Med* 1999;**5**:266–7.

51 Grunig E, Tasman JA, Kucherer H, *et al*. Frequency and phenotypes of familial dilated cardiomyopathy. *J Am Coll Cardiol* 1998;**31**:186–94.

52 Berko BA, Swift M. X-linked dilated cardiomyopathy. *N Engl J Med* 1987;**316**:1186–91.

53 Barth PG, Scholte HR, Berden JA, *et al*. An X-linked mitochondrial disease affecting cardiac muscle, skeletal muscle and neutrophil leucocytes. *J Neurol Sci* 1983;**62**:327–55.

54 Danon MJ, Oh SJ, DiMauro S, *et al*. Lysosomal glycogen storage disease with normal acid maltase. *Neurology* 1981;**31**:51–7.

55 Towbin JA, Hejtmancik JF, Brink P, *et al*. X-linked dilated cardiomyopathy (XLCM): molecular genetic evidence of linkage to the Duchenne muscular dystrophy gene at the Xp21 locus. *Circulation* 1993;**87**:1854–65.

56 Muntoni F, Cau M, Ganau A, *et al*. Brief report: deletion of the dystrophin muscle-specific promoter region associated with X-linked dilated cardiomyopathy. *N Engl J Med* 1993; **329**:921–5.

57 Cox GF, Kunkel LM. Dystrophies and heart disease. *Curr Opin Cardiol* 1997;**12**:329–43.

58 Hoffman EP, Brown RH, Kunkel LM. Dystrophin: the protein product of the Duchenne muscular dystrophy locus. *Cell* 1987;**51**:919–28.

59 Meng H, Leddy JJ, Frank J, *et al*. The association of cardiac dystrophin with myofibrils/z-discs regions in cardiac muscle suggests a novel role in the contractile apparatus. *J Biol Chem* 1996;**271**:12364–71.

60 Kaprielian RR, Stevenson S, Rothery SM, *et al*. Distinct patterns of dystrophin organization in myocyte sarcolemma and transverse tubules of normal and diseased human myocardium. *Circulation* 2000;**101**:2586–94.

61 Koenig M, Hoffman EP, Bertelson CJ, *et al*. Complete cloning of the Duchenne muscular dystrophy (DMD) cDNA and preliminary genomic organization of the DMD gene in normal and affected individuals. *Cell* 1987;**50**:509–17.

62 Petrof BJ, Shrager JB, Stedman HH, *et al*. Dystrophin protects the sarcolemma from stresses developed during muscle contraction. *Proc Natl Acad Sci USA* 1993;**90**:3710–4.

63 Campbell KP. Three muscular dystrophies: loss of cytoskeleton–extracellular matrix linkage. *Cell* 1995;**80**:675–9.

64 Klietsch R, Ervasti JM, Arnold W, *et al*. Dystrophin–glycoprotein complex and laminin colocalize to the sarcolemma and transverse tubules of cardiac muscle. *Circ Res* 1993;**72**:349–60.

65 Ozawa E, Yoshida M, Suzuki A, *et al*. Dystrophin-associated proteins in muscular dystrophy. *Hum Mol Genet* 1995;**4**:1711–6.

66 Emery AE. The muscular dystrophies. *Lancet* 2002;**359**:687–95.

67 Davies KE, Nowak KJ. Molecular mechanisms of muscular dystrophies: old and new players. *Nat Rev Mol Cell Biol* 2006; **7**:762–73.

68 Bowles NE, Bowles KR, Towbin JA. The "final common pathway" hypothesis and inherited cardiovascular disease: the role of cytoskeletal proteins in dilated cardiomyopathy. *Herz* 2000; **25**:168–75.

69 Feng J, Yan J, Buzin CH, *et al.* Mutations in the dystrophin gene are associated with sporadic dilated cardiomyopathy. *Mol Genet Metab* 2002;**77**:119–26.

70 Feng J, Yan J, Buzin CH, *et al.* Comprehensive mutation scanning of the dystrophin gene in patients with nonsyndromic X-linked dilated cardiomyopathy. *J Am Coll Cardiol* 2002;**40**:1120–4.

71 Jefferies JL, Eidem BW, Belmont JW, *et al.* Genetic predictors and remodeling of dilated cardiomyopathy in muscular dystrophy. *Circulation* 2005;**112**:2799–804.

72 Duboc D, Meune C, Lerebours G, *et al..* Effect of perindopril on the onset and progression of left ventricular dysfunction in Duchenne muscular dystrophy. *J Am Coll Cardiol* 2005;**45**:855–7.

73 Neustein HD, Lurie PR, Dahms B, Takahashi M. An X-linked recessive cardiomyopathy with abnormal mitochondria. *Pediatrics* 1979;**64**:24–9.

74 Kelley RI, Cheatham JP, Clark BJ, *et al.* X-linked dilated cardiomyopathy with neutropenia, growth retardation, and 3-methylglutaconic aciduria. *J Pediatr* 1991;**119**:738–47.

75 Schlame M, Towbin JA, Heerdt PM, *et al.* Deficiency of tetralinoleoyl-cardiolipin in Barth syndrome. *Ann Neurol* 2002;**51**:634–7.

76 Bione S, D'Adamo P, Maestrini E, *et al.* A novel X-linked gene, G4.5, is responsible for Barth syndrome. *Nat Genet* 1996;**12**:385–9.

77 Pignatelli RH, McMahon CJ, Dreyer WJ, *et al.* Clinical characterization of left ventricular noncompaction in children. A relatively common form of cardiomyopathy. *Circulation* 2003;**108**:2672–8.

78 Graber HL, Unverferth DV, Baker PB, *et al.* Evolution of hereditary cardiac conduction and muscle disorder: a study involving a family with 6 generations affected. *Circulation* 1986;**74**:21–35.

79 Karkkainen S, Peuhkurinen K. Genetics of dilated cardiomyopathy. *Ann Med* 2007;**32**:91–107.

80 Towbin JA, Bowles NE. Dilated cardiomyopathy: a tale of the cytoskeleton and beyond. *J Cardiovasc Electrophysiol* 2006;**17**:919–26.

81 Fatkin D, Graham RM. Molecular mechanisms of inherited cardiomyopathies. *Physiol Ref* 2002;**82**:945–80.

82 Arber S, Hunter JJ, Ross J Jr, *et al.* MLP-deficient mice exhibit a disruption of cardiac cytoarchitectural organization, dilated cardiomyopathy, and heart failure. *Cell* 1997;**88**:393–403.

83 Badorff C, Lee G-H, Lamphear BJ, *et al.* Enteroviral protease 2A cleaves dystrophin: evidence of cytoskeletal disruption in an acquired cardiomyopathy. *Nat Med* 1999;**5**:320–6.

84 Xiong D, Lee GH, Badorff C, *et al.* Dystrophin deficiency markedly increases enterovirus-induced cardiomyopathy: a genetic predisposition to viral heart disease. *Nat Med* 2002;**8**:872–7.

85 Vatta M, Stetson SJ, Perez-Verdra A, *et al.* Molecular remodeling of dystrophin in patients with end-stage cardiomyopathies and reversal for patients on assist device therapy. *Lancet* 2000;**359**:936–41.

86 Vatta M, Stetson SJ, Jimenez S, *et al.* Molecular normalization of dystrophin in the failing left and right ventricle of patients treated with either pulsatile or continuous flow-type ventricular assist devices. *J Am Coll Cardiol* 2004;**43**:811–7.

87 Towbin JA. Scarring in the heart – a reversible phenomenon? *N Engl J Med* 2007;**357**:1767–8.

88 Zeisberg EM, Tarnavski O, Zeisberg M, *et al.* Endothelial-to-mesenchymal transition contributes to cardiac fibrosis. *Nat Med* 2007;**13**:952–61.

89 Ni J, Bowles NE, Kim YH, *et al.* Viral infection of the myocardium in endocardial fibroelastosis. Molecular evidence for the role of mumps virus as an etiologic agent. *Circulation* 1997;**95**:133–9.

90 Bowles NE, Kearney DL, Ni J, *et al.* The detection of viral genomes by polymerase chain reaction in the myocardium of pediatric patients with advanced HIV disease. *J Am Coll Cardiol* 1999;**34**:857–65.

91 Joseph SM, Cedars AM, Ewald GA, *et al.* Acute decompensated heart failure: contemporary management. *Tex Heart Inst J* 2009;**36**:510–20.

92 Allen LA, Turer AT, Dewald T, *et al.* Continuous versus bolus dosing of furosemide for patients hospitalized for heart failure. *Am J Cardiol* 2010;**105**:1794–7.

93 Hsu DT, Canter CE. Dilated cardiomyopathy and heart failure in children. *Heart Fail Clin* 2010;**6**:415–432.

94 Penny DJ, Vick GW III. Novel therapies in childhood heart failure: today and tomorrow. *Heart Fail Clin* 2010;**6**:591–621.

95 Giglioli C, Landi D, Cecchi E, *et al.* Effects of ULTRAfiltration vs. DIureticS on clinical, biohumoral, and haemodynamic variables in patients with deCOmpensated heart failure: the ULTRADISCO study. *Eur J Heart Fail* 2011;**13**:337–46.

96 Price JF, Mott AR, Dickerson HA, *et al.* Worsening renal function in children hospitalized with decompensated heart failure: evidence for a pediatric cardiorenal syndrome? *Pediatr Crit Care Med* 2008;**9**:279–84.

97 Price JF, Goldstein SL. Cardiorenal syndrome in children with heart failure. *Curr Heart Fail Rep* 2009;**6**:191–8.

98 O'Meara E, de Denus S. Management of anemia and iron deficiency in heart failure. *Curr Treat Options Cardiovasc Med* 2010;**12**:532–48.

99 Stevenson WG, Ellison KE, Sweeney MO, *et al.* Management of arrhythmias in heart failure. *Cardiol Rev* 2002;**10**:8–14.

100 Pulerwitz T, Rabbani LE, Pinney SP. A rationale for the use of anticoagulation in heart failure management. *J Thromb Thrombolysis* 2004;**17**:87–93.

101 Towbin JA, Lipshultz SE. Genetics of neonatal cardiomyopathy. *Curr Opin Cardiol* 1999;**14**:250–62.

102 Jefferies JL, Price JF, Morales DL. Mechanical support in childhood heart failure. *Heart Fail Clin* 2010;**6**:559–73.

103 Kirk R, Edwards LB, Kucheryavaya AY, *et al.* The Registry of the International Society of Heart and Lung Transplantation: Thirteenth Official Heart Transplantation Report – 2010. *J Heart Lung Transplant* 2010;**29**:119–28.

104 Martin AB, Webber S, Fricker FJ, *et al.* Acute myocarditis. Rapid diagnosis by PCR in children. *Circulation* 1994; **90**:330–9.

105 Schowengerdt KO, Ni J, Denfield SW, *et al.* Association of parvovirus B19 genome in children with myocarditis and cardiac allograft rejection: diagnosis using the polymerase chain reaction. *Circulation* 1997;**96**:3549–54.

106 Bock CT, Klingel K, Kandolf R. Human parvovirus B19-associated myocarditis. *N Engl J Med* 2010;**362**:1248–9.

107 Dennert R. HJ Crijns, Heymans S. Acute viral myocarditis. *Eur Heart J* 2008;**29**:2073–82.

108 Mahrholdt H, Wagner A, Deluigi CC, *et al.* Presentation, patterns of myocardial damage, and clinical course of myocarditis. *Circulation* 2006;**114**:1581–90.

109 Friedman RA. Viral myocarditis in children. Current diagnosis and treatment. *Cardiol Rev* 1995;**3**:164–73.

110 Wiles HB, Gillette PC, Harley RA. Cardiomyopathy and myocarditis in children with ventricular ectopic rhythm. *J Am Coll Cardiol* 1992;**20**:359–62.

111 Friedman RA, Kearney DL, Moak JP. Persistence of ventricular arrhythmia after resolution of occult myocarditis in children and young adults. *J Am Coll Cardiol* 1994;**24**:780–3.

112 Lee KJ, McCrindle BW, Bohn DJ, *et al*. Clinical outcomes of acute myocarditis in childhood. *Heart* 1999;**82**:226–33.

113 Ichikawa R, Sumitomo N, Komori A, *et al*. The follow-up evaluation of electrocardiogram and arrhythmias in children with fulminant myocarditis. *Circ J* 2011;**75**:932–8.

114 Hauck AJ, Kearney DL, Edwards WD. Evaluation of postmortem endomyocardial biopsy specimens from 38 patients with lymphocytic myocarditis: implications for the role of sampling error. *Mayo Clin Proc* 1989;**64**:1235–45.

115 Chow LH, Radio SJ, Sears TD, McManus BM. Insensitivity of right ventricular endomyocardial biopsy in the diagnosis of myocarditis. *J Am Coll Cardiol* 1989;**14**:915–20.

116 JCS Joint Working Group. Guidelines for diagnosis and treatment of myocarditis (JCS 2009). *Circ J* 2011;**75**:734–43.

117 Blauwet LA, Cooper LT. Myocarditis. *Prog Cardiovasc Dis* 2010;**52**:274–88.

118 Bowles NE, Richardson PJ, Olsen EGJ, Archard LC. Detection of Coxsackie-B-virus specific RNA sequences in myocardial biopsy samples from patients with myocarditis and dilated cardiomyopathy. *Lancet* 1986;**327**:1120–3.

119 Bowles NE, Rose ML, Taylor P, *et al*. End-stage dilated cardiomyopathy: persistence of enterovirus DNA in myocardium at cardiac transplantation and lack of immune response. *Circulation* 1989;**80**:1128–36.

120 Jin O, Sole MJ, Butany JW, *et al*. Detection of enterovirus RNA in myocardial biopsies from patients with myocarditis and cardiomyopathy using gene amplification by polymerase chain reaction. *Circulation* 1990;**82**:8–16.

121 Griffin L, Kearney D, Ni J, *et al*. Analysis of formalin-fixed and frozen myocardial autopsy samples for viral genome in childhood myocarditis and dilated cardiomyopathy with endocardial fibroelastosis using polymerase chain reaction (PCR). *Cardiovasc Pathol* 1995;**4**:3–11.

122 Jones SR, Herskowitz A, Hutchins GM, Baughman KL. Effects of immunosuppressive therapy in biopsy-proved myocarditis and borderline myocarditis on left ventricular function. *Am J Cardiol* 1991;**68**:370–6.

123 Aziz KU, Patel N, Sadullah T, *et al*. Active myocarditis. Role of immunosuppression: a prospective randomised study. *Pediatr Cardiol* 2010;**20**:509–15.

124 Cooper LT. The heat is off: immunosuppression for myocarditis revisited. *Eur Heart J* 2009;**30**:1936–9.

125 Frustaci A, Russo MA, Chimanti C. Randomized study on the efficacy of immunosuppressive therapy in patients the virus-negative inflammatory cardiomyopathy: the TMIC study. *Eur Heart J* 2009;**30**:1995–2002.

126 Mason JW, O'Connell JB, Herskowitz A, *et al*. A clinical trial of immunosuppressive therapy for myocarditis. *N Engl J Med* 1995;**333**:269–75.

127 Drucker NA, Colan SD, Lewis AB, *et al*. Gamma-globulin treatment of acute myocarditis in the pediatric population. *Circulation* 1994;**89**:252–7.

128 Dennert R, Velthuis S, Schalla S, *et al*. Intravenous immunoglobulin therapy for patients with idiopathic cardiomyopathy and endomyocardial biopsy-proven high PVB19 viral load. *Antivir Ther* 2010;**15**:193–201.

129 Maisch B, Hufnagel G, Kolsch S, *et al*. Treatment of inflammatory cardiomyopathy and (peri)myocarditis with immunosuppression and i.v. immunoglobulins. *Herz* 2004;**29**:624–36.

130 Elliott P, McKenna WJ. Hypertrophic cardiomyopathy. *Lancet* 2004;**363**:188–9.

131 Colan SD, Lipshultz SE, Lowe AM, *et al*. Epidemiology and cause-specific outcome of hypertrophic cardiomyopathy in children: findings from the Pediatric Cardiomyopathy Registry. *Circulation* 2007;**115**:773–81.

132 McKenna WJ, Behr ER. Hypertrophic cardiomyopathy: management, risk stratification, and prevention of sudden death. *Heart* 2002;**87**:169–76.

133 Frenneaux MP. Assessing the risk of sudden cardiac death in a patient with hypertrophic cardiomyopathy. *Heart* 2004;**90**: 570–5.

134 Maron BJ, Carney KP, Lever HM, *et al*. Relationship of race to sudden cardiac death in competitive athletes with hypertrophic cardiomyopathy. *J Am Coll Cardiol* 2003;**41**:974–80.

135 Maron BJ. Hypertrophic cardiomyopathy and sudden death: new perspective on risk stratification and prevention with the implantable cardioverter-defibrillator. *Eur Heart J* 2000; **21**:1979–83.

136 Spirito P, Maron BJ, Bonow RO, Epstein SE. Occurrence and significance of progressive left ventricular wall thinning and relative cavity dilation in hypertrophic cardiomyopathy. *Am J Cardiol* 1987;**60**:123–39.

137 Aurigemma GP, Gaasch WH. Diastolic heart failure. *N Engl J Med* 2004;**351**:1097–105.

138 Gaasch WH, Zile MR. Left ventricular diastolic dysfunction and diastolic heart failure. *Annu Rev Med* 2004;**55**:373–94.

139 Towbin JA. Hypertrophic cardiomyopathy. *Pacing Clin Electrophysiol* 2009;**32**(Suppl 2):S23–31.

140 Vulpian A. Contribution à l'étude des rétrécissements de l'orifice ventriculo-aortique. *Arch Physiol* 1868;**3**:220–2.

141 Watkins H. Genetic clues to disease pathways in hypertrophic and dilated cardiomyopathies. *Circulation* 2003;**107**:1344–6.

142 Konno T, Chang S, Seidman JG, Seidman CE. Genetics of hypertrophic cardiomyopathy. *Curr Opin Cardiol* 2010;**25**: 205–9.

143 Jarcho JA, McKenna W, Pare JA, *et al*. Mapping a gene for familial hypertrophic cardiomyopathy to chromosome 14q1. *N Engl J Med* 1989;**321**:1372–8.

144 Solomon SD, Jarcho JA, McKenna WJ, *et al*. Familial hypertrophic cardiomyopathy is a genetically heterogeneous disease. *J Clin Invest* 1990;**86**:993–9.

145 Watkins H, MacRae C, Thierfelder L, *et al*. A disease locus for familial hypertrophic cardiomyopathy maps to chromosome 1q3. *Nat Genet* 1993;**3**:333–7.

146 Thierfelder L, MacRae C, Watkins H, *et al*. A familial hypertrophic cardiomyopathy locus maps to chromosome 15q2. *Proc Natl Acad Sci USA* 1993;**90**:6270–4.

147 Seidman JG, Seidman C. The genetic basis for cardiomyopathy from mutation identification to mechanistic paradigms. *Cell* 2001;**108**:557–67.

148 Schiaffino S, Reggiani C. Molecular diversity of myofibrillar proteins: gene regulation and functional significance. *Physiol Rev* 1996;**76**:371–423.

149 Satoh M, Takahashi M, Sakamoto T, *et al*. Structural analysis of the titin gene in hypertrophic cardiomyopathy: identification of a novel disease gene. *Biochem Biophys Res Commun* 1999;**2625**:411–7.

150 Geier C, Perrot A, Ozcelik C, *et al*. Mutations in the human muscle LIM protein gene in families with hypertrophic cardiomyopathy. *Circulation* 2003;**107**:1390–5.

151 Moulik M, Vatta M, Witt SH, *et al*. ANKRD1, the gene encoding cardiac ankyrin repeat protein, is a novel dilated cardiomyopathy gene. *J Am Coll Cardiol* 2009;**54**:325–33.

152 Arimura T, Bos JM, Sato A, *et al*. Cardiac ankyrin repeat protein gene (ANKRD1) mutations in hypertrophic cardiomyopathy. *J Am Coll Cardiol* 2009;**54**:334–42.

153 Wang H, Li Z, Wang J, *et al*. Mutations in NEXN, a Z-disc gene, are associated with hypertrophic cardiomyopathy. *Am J Hum Genet* 2010;**87**:687–93.

154 Gollob MH, Green MS, Tang AS, *et al*. Identification of a gene responsible for familial Wolff–Parkinson–White syndrome. *N Engl J Med* 2001;**344**:1823–31.

155 Blair E, Redwood C, Ashrafian H, *et al*. Mutations in the gamma(2) subunit of AMP-activated protein kinase cause familial hypertrophic cardiomyopathy: evidence for a central role of energy compromise in disease pathogenesis. *Hum Mol Genet* 2001;**10**:1215–20.

156 Arad M, Benson DW, Perez-Atayde AR, *et al*. Constitutively active AMP kinase mutations cause glycogen storage disease mimicking hypertrophic cardiomyopathy. *J Clin Invest* 2002;**107**:357–62.

157 Sugie K, Yamamoto A, Murayama K, *et al*. Clinicopathological features of genetically confirmed Danon disease. *Neurology* 2002;**58**:1773–8.

158 Nishino I, Fu J, Tanji K, *et al*. Primary LAMP-2 deficiency causes X-linked vascular cardiomyopathy and myopathy (Danon disease). *Nature* 2000;**406**:906–9.

159 Charron P, Villard E, Sebillon P, *et al*. Danon's disease as a cause of hypertrophic cardiomyopathy: a systematic survey. *Heart* 2004;**90**:842–6.

160 Yang Z, McMahon CJ, Smith LR, *et al*. Danon disease as a frequent cause of hypertrophic cardiomyopathy in children. *Circulation* 2005;**112**:1612–7.

161 Watkins H, Rosenzweig T, Hwang DS, *et al*. Characteristics and prognostic implications of myosin missense mutations in familial hypertrophic cardiomyopathy. *N Engl J Med* 1992;**326**:1108–14.

162 Woo A, Rakowski H, Liew JC, *et al*. Mutations of the beta myosin heavy chain gene in hypertrophic cardiomyopathy: critical functional sites determine prognosis. *Heart* 2003;**89**:1179–85.

163 Niimura H, Patton KK, McKenna WJ, *et al*. Sarcomere protein gene mutations in hypertrophic cardiomyopathy of the elderly. *Circulation* 2002;**105**:446–51.

164 Niimura H, Bachinski LL, Sangwatanaroj S, *et al*. Mutations in the gene for cardiac myosin-binding protein C and late-onset familial hypertrophic cardiomyopathy. *N Engl J Med* 1998;**338**:1248–57.

165 Charron P, Dubourg O, Desnos M, *et al*. Genotype–phenotype correlations in familial hypertrophic cardiomyopathy: a comparison between mutations in the cardiac protein-C and the beta-myosin heavy chain genes. *Eur Heart J* 1998;**19**:139–45.

166 Moolman-Smook JC, De Lange WJ, Bruwer EC, *et al*. The origins of hypertrophic cardiomyopathy-causing mutations in two South African subpopulations: a unique profile of both independent and founder events. *Am J Hum Genet* 1999;**65**:1308–20.

167 Moolman JC, Corfield VA, Posen B, *et al*. Sudden death due to troponin T mutations. *J Am Coll Cardiol* 1997;**29**:549–55.

168 Watkins H, Conner D, Thierfelder L, *et al*. Mutations in the cardiac myosin binding protein-C gene on chromosome 11 cause familial hypertrophic cardiomyopathy. *Nat Genet* 1995;**11**:434–7.

169 Varnava AM, Elliott PM, Baboonian C, *et al*. Hypertrophic cardiomyopathy: histopathological features of sudden death in cardiac troponin T disease. *Circulation* 2001;**104**:1380–4.

170 Ackerman MJ, Van Driest SL, Ommen SR, *et al*. Prevalence and age-dependence of malignant mutations in the beta-myosin heavy chain and troponin T gene in hypertrophic cardiomyopathy: a comprehensive outpatient perspective. *J Am Coll Cardiol* 2002;**39**:2042–8.

171 Van Driest SL, Maron BJ, Ackerman MJ. From malignant mutations to malignant domains: the continuing search for prognostic significance in the mutant genes causing hypertrophic cardiomyopathy. *Heart* 2004;**90**: 7–8.

172 Van Driest SL, Ackerman MJ, Ommen SR, *et al*. Prevalence and severity of "benign" mutations in the β-myosin heavy chain, cardiac troponin T, and α-tropomyosin genes in hypertrophic cardiomyopathy. *Circulation* 2002;**106**:3085–90.

173 Van Driest SL, Vasile VC, Ommen SR, *et al*. Myosin binding protein C mutations and compound heterozygosity in hypertrophic cardiomyopathy. *J Am Coll Cardiol* 2004;**44**:1903–10.

174 Binder J, Ommen SR, Gersh BJ, *et al*. Echocardiography-guided genetic testing in hypertrophic cardiomyopathy: septal morphological features predict the presence of myofilament mutations, *Mayo Clin Proc* 2006;**81**:459–67.

175 Lever HM, Karam RF, Currie PJ, Healy BP. Hypertrophic cardiomyopathy in the elderly: distinctions from the young based on cardiac shape. *Circulation* 1989;**79**:580–9.

176 Solomon SD, Wolff S, Watkins H, *et al*. Left ventricular hypertrophy and morphology in familial hypertrophic cardiomyopathy associated with mutations of the beta-myosin heavy chain gene. *J Am Coll Cardiol* 1993;**22**:498–505.

177 Doiuchi J, Hamada M, Ito T, Kokubu T. Comparative effects of calcium-channel blockers and beta-adrenergic blocker on early diastolic time intervals and A-wave ratio in patients with hypertrophic cardiomyopathy. *Clin Cardiol* 1987;**10**:26–30.

178 Ostman-Smith I. Hypertrophic cardiomyopathy in childhood and adolescence – strategies to prevent sudden death. *Fundam Clin Pharmacol* 2010;**24**:637–52.

179 Decker JA, Rossano JW, Smith EO, *et al*. Risk factors and mode of death in isolated hypertrophic cardiomyopathy in children. *J Am Coll Cardiol* 2009;**54**:250–4.

180 Colan SD, Lipshultz SE, Lowe AM, *et al*. Epidemiology and cause-specific outcome of hypertrophic cardiomyopathy in children: findings from the Pediatric Cardiomyopathy Registry. *Circulation* 2007;**115**:773–81.

181 Lorell BH. Use of calcium channel blockers in hypertrophic cardiomyopathy. *Am J Med* 1985;**78**:43–54.

182 Moran AM, Colan SD. Verapamil therapy in infants with hypertrophic cardiomyopathy. *Cardiol Young* 1998;**8**:310–9.

183 Nagueh SF, Ommen SR, Lakkis NM, *et al*. Comparison of ethanol septal reduction therapy with surgical myectomy for the treatment of hypertrophic obstructive cardiomyopathy. *J Am Coll Cardiol* 2001;**38**:1701–6.

184 Maron BJ, Dearani JA, Ommen SR, *et al*. The case for surgery in obstructive hypertrophic cardiomyopathy. *J Am Coll Cardiol* 2004;**44**:2043–53.

185 Woo A, Rakowski H. Does myectomy convey survival benefit in hypertrophic cardiomyopathy? *Heart Fail Clin* 2007;**3**:275–8.

186 Menon SC, Ackerman MJ, Ommen SR, *et al*. Impact of septal myectomy on left atrial volume and left ventricular diastolic filling patterns: an echocardiographic study of young patients with obstructive hypertrophic cardiomyopathy. *J Am Soc Echocardiogr* 2008;**2**:684–8.

187 O'Rourke RA. Cardiac pacing. An alternative treatment for selected patients with hypertrophic cardiomyopathy and adjunctive therapy for certain patients with dilated cardiomyopathy. *Circulation* 1999;**100**:786–8.

188 Maron BJ. Appraisal of dual-chamber pacing therapy in hypertrophic cardiomyopathy: too soon for a rush to judgment? *J Am Coll Cardiol* 1996;**27**:431–2.

189 Begley D, Mohiddin S, Fananapazir L. Dual chamber pacemaker therapy for mid-cavity obstructive hypertrophic cardiomyopathy. *Pacing Clin Electrophysiol* 2001;**24**:1639–44.

190 Galve E, Sambola A, Saldaña G, *et al*. Late benefits of dual-chamber pacing in obstructive hypertrophic cardiomyopathy: a 10-year follow-up study. *Heart* 2010;**96**:352–6.

191 Rigopoulos AG, Seggewiss H. A decade of percutaneous septal ablation in hypertrophic cardiomyopathy. *Circ J* 2010;**75**:28–37.

192 Chang SM, Lakkis NM, Franklin J, *et al*. Predictors of outcome after alcohol septal ablation therapy in patients with hypertrophic obstructive cardiomyopathy. *Circulation* 2004;**109**:824–7.

193 Nielsen CD, Killip D, Spencer WH III. Nonsurgical septal reduction therapy for hypertrophic obstructive cardiomyopathy: short-term results in 50 consecutive procedures. *Clin Cardiol* 2003;**26**:275–9.

194 Park TH, Lakkis NM, Middleton KJ, *et al*. Acute effect of nonsurgical septal reduction therapy on regional left ventricular asynchrony in patients with hypertrophic obstructive cardiomyopathy. *Circulation* 2002;**106**:412–5.

195 Hess OM, Sigwart U. New treatment strategies for hypertrophic obstructive cardiomyopathy. *J Am Coll Cardiol* 2004;**44**:2054–5.

196 Maron BJ. Hypertrophic cardiomyopathy and sudden death: new perspective on risk stratification and prevention with the implantable cardioverter-defibrillator. *Eur Heart J* 2000;**21**:1979–83.

197 Maron BJ. Risk stratification and role of implantable defibrillators for prevention of sudden death in patients with hypertrophic cardiomyopathy. *Circ J* 2010;**74**:2271–82.

198 Syska P, Przybylski A, Chojnowska L, *et al*. Implantable cardioverter-defibrillator in patients with hypertrophic cardiomyopathy: efficacy and complications of the therapy in long-term follow-up. *J Cardiovasc Electrophysiol* 2010;**2**:883–9.

199 Seggewiss H, Rigopoulos A. Management of hypertrophic cardiomyopathy in children. *Paediatr Drug*s 2003;**5**:663–72.

200 Aurigemma GP, Gaasch WH. Diastolic heart failure. *N Engl J Med* 2004;**351**:1097–105.

201 van der Ploeg AT, Reuser AJ. Pompe disease. *Lancet* 2008;**372**:1342–53.

202 Cable WJ, Kolodny EH, Adams RD. Fabry disease: impaired autonomic function. *Neurology* 1982;**32**:498–502.

203 O'Mahony C, Elliott P. Anderson–Fabry disease and the heart. *Prog Cardiovasc Dis* 2010;**52**:326–35.

204 Wong AK, Howie J, Petrie JR, Lang CC. AMP-activated protein kinase pathway: a potential therapeutic target in cardiometabolic disease. *Clin Sci (Lond)* 2009;**116**:607–20.

205 Gelb BD, Tartaglia M. RAS signaling pathway mutations and hypertrophic cardiomyopathy: getting into and out of the thick of it. *J Clin Invest* 2011;**121**:844–7.

206 Katzin LW, Amato AA. Pompe disease: a review of the current diagnosis and treatment recommendations in the era of enzyme replacement therapy. *J Clin Neuromuscul Dis* 2008;**9**:421–31.

207 Martins AM, D'Almeida V, Kyosen SO, *et al*. Guidelines to diagnosis and monitoring of Fabry disease and review of treatment experiences. *J Pediatr* 2009;**155**(4 Suppl):S19–31.

208 Zarate YA, Hopkin RJ. Fabry's disease. *Lancet* 2008;**372**:1427–35.

209 MacRae CA, Ghaisas N, Kass S, *et al*. Familial hypertrophic cardiomyopathy with Wolff–Parkinson–White syndrome maps to a locus on chromosome 7q3. *J Clin Invest* 1995;**96**:1216–20.

210 Cheung PC, Salt IP, Davies SP, *et al*. Characterization of AMP-activated protein kinase gamma-subunit isoforms and their role in AMP binding. *Biochem J* 2000;**346**:659–69.

211 Kemp BE, Mitchelhill KI, Stapleton D, *et al*. Dealing with energy demand: the AMP-activated protein kinase. *Trends Biochem Sci* 1999;**24**:22–5.

212 Yaplito-Lee J, Weintraub R, Jamsen K, *et al*. Cardiac manifestations in oxidative phosphorylation disorders of childhood. *J Pediatr* 2007;**150**:407–11.

213 Wallace DC. Bioenergetics and the epigenome: interface between the environment and genes in common diseases. *Dev Disabil Res Rev* 2010;**16**:114–9.

214 Wong LJ. Molecular genetics of mitochondrial disorders. *Dev Disabil Res Rev* 2010;**16**:154–62.

215 Poulton J, Chiaratti MR, Meirelles FV, *et al*. Transmission of mitochondrial DNA diseases and ways to prevent them. *PLoS Genet* 2010;**6**(8):e1001066.

216 DiMauro S. Pathogenesis and treatment of mitochondrial myopathies: recent advances. *Acta Myol* 2010;**29**:333–8.

217 Scaglia F, Towbin JA, Craigen WJ, *et al*. Clinical spectrum, morbidity, and mortality in 113 pediatric patients with mitochondrial disease. *Pediatrics* 2004;**114**:925–31.

218 Maceluch JA, Niedziela M. The clinical diagnosis and molecular genetics of Kearns–Sayre syndrome: a complex mitochondrial encephalomyopathy. *Pediatr Endocrinol Rev* 2006;**4**:117–37.

219 Channer KD, Channer JL, Campbell MJ, Rees JR. Cardiomyopathy in Kearns–Sayre syndrome. *Br Heart J* 1988;**59**:486–90.

220 Poulton J, Deadman ME, Ramacharan S, Gardiner RM. Germline deletions of mtDNA in mitochondrial myopathy. *Am J Hum Genet* 1991;**48**:649–53.

221 Shoffner JM, Lott MI, Lezza AM, *et al*. Myoclonic epilepsy and ragged-red fiber disease (MERRF) is associated with a mitochondrial DNA tRNA(Lys) mutation. *Cell* 1990;**61**:931–7.

222 Nakamura M, Nakano S, Goto Y, *et al*. A novel point mutation in the mitochondrial tRNA$^{Ser(UCN)}$ gene detected in a family with MERFF/MELAS overlap syndrome. *Biochem Biophys Res Commun* 1995;**214**:86–93.

223 Silvestri G, Moraes CT, Shanske S, *et al*. A new mtDNA mutation in the tRNA(Lys) gene associated with myoclonic epilepsy and ragged-red fibers (MERRF). *Am J Hum Genet* 1992; **51**:1213–7.

224 Fukuhara N. Clinicopathologic features of MERRF. *Muscle Nerve* 1995;**3**:590–4.

225 Denfield SW, Webber SA. Restrictive cardiomyopathy in childhood. *Heart Fail Clin* 2010;**6**:445–52.

226 Lewis AB. Clinical profile and outcome of restrictive cardiomyopathy in children. *Am Heart J* 1992;**123**:1589–93.

227 Denfield SW, Bricker JT, Gajarski R, *et al*. Restrictive cardiomyopathies in childhood: etiologies and natural history. *Tex Heart Inst J* 1997;**24**:38–44.

228 Cetta F, O'Leary PW, Seward JB, Driscoll DJ. Idiopathic restrictive cardiomyopathy in childhood: diagnostic features and clinical course. *Mayo Clin Proc* 1995;**70**:634–40.

229 Nugent AW, Daubeney P, Chondros P, *et al*. The epidemiology of childhood cardiomyopathy in Australia. *N Engl J Med* 2003;**348**:1639–46.

230 Russo LM, Webber SA. Idiopathic restrictive cardiomyopathy in children. Heart 2005;**91**:1199–202.

231 Sen-Chowdhry S, Syrris P, McKenna WJ. Genetics of restrictive cardiomyopathy. *Heart Fail Clin* 2010;**6**:179–86.

232 Mocumbi AO, Ferreira MB, Sidi D, *et al*. A population study of endomyocardial fibrosis in a rural area of Mozambique, *N Engl J Med* 2008;**359**:43–9.

233 Mocumbi AO, Yacoub S, Yacoub MH. Neglected tropical cardiomyopathies: II. *Heart* 2008;**94**:384–90.

234 Rivenes SM, Kearney DL, Smith EO, *et al*. Sudden death and cardiovascular collapse in children with restrictive cardiomyopathy. *Circulation* 2000;**102**:876–82.

235 Fitzpatrick AP, Shapiro LM, Rickards AF, *et al*. Familial restrictive cardiomyopathy with atrioventricular block and skeletal myopathy. *Br Heart J* 1990;**63**:114–8.

236 Denfield SW. Sudden death in children with restrictive cardiomyopathy. *Card Electrophysiol Rev* 2002;**6**:163–7.

237 Nihoyannopoulos P, Dawson D. Restrictive cardiomyopathies. *Eur J Echocardiogr* 2009;**10**:iii23–33.

238 Chen S, Balfour IC, Jureidini S. Clinical spectrum of restrictive cardiomyopathy in children. *J Heart Lung Transplant* 2001; **20**:90–2.

239 Neudorf U, Bolte A, Lang D, *et al*. Diagnostic findings and outcome in children with primary restrictive cardiomyopathy. *Cardiol Young* 1996;**6**:44–7.

240 Weller RJ, Weintraub R, Addonizo LJ, *et al*. Outcome of idiopathic restrictive cardiomyopathy in children, *Am J Cardiol* 2002;**90**:501–6.

241 Chatterjee K, Alpert J. Constrictive pericarditis and restrictive cardiomyopathy: similarities and differences. *Heart Fail Monit* 2003;**3**:118–26.

242 Chatterjee K. Diastolic ventricular failure: a clinician's approach. *ACC Curr J Rev* 1995;**4**(2):50–2.

243 Frank R, Fontaine G, Vedee J, *et al*. Electrocardiologie de quatre cas de dysplasie ventriculaire droite arythmogenique. *Arch Mal Coeur* 1978;**71**:963–72.

244 McKenna WJ, Thiene G, Nava A, *et al*. Diagnosis of arrhythmogenic right ventricular dysplasia/cardiomyopathy. Task Force of the Working Group Myocardial and Pericardial Disease of the European Society of Cardiology and of the Scientific Council on Cardiomyopathies of the International Society and Federation of Cardiology. *Br Heart J* 1994;**71**:215–8.

245 Marcus FI, McKenna WJ, Sherrill D, *et al*. Diagnosis of arrhythmogenic right ventricular cardiomyopathy/dysplasia: proposed modification of the Task Force Criteria. *Eur Heart J* 2010; **31**:806–14.

246 Ellinor PT, MacRae CA, Thierfelder L. Arrhythmogenic right ventricular cardiomyopathy. *Heart Fail Clin* 2010;**6**:161–77.

247 Marcus FI, Fontaine G, Guiraudon G, *et al*. Right ventriculardysplasia: a report of 24 adult cases. *Circulation* 1982; **65**:384–98.

248 Hasumi M, Sekiguchi M, Hiroe M, *et al*. Endomyocardial biopsy approach to patients with ventricular tachycardia with special reference to arrhythmogenic right ventricular dysplasia. *Jpn Circ J* 1987;**51**:242–9.

249 Peters S, Trümmel M, Meyners W. Prevalence of right ventricular dysplasia–cardiomyopathy in a non-referral hospital. *Int J Cardiol* 2004;**97**:499–501.

250 Thiene G, Basso C, Calabrese F, *et al*. Pathology and pathogenesis of arrhythmogenic right ventricular cardiomyopathy. *Herz* 2000;**25**:210–5.

251 Francés RJ. Arrhythmogenic right ventricular dysplasia/cardiomyopathy. A review and update. *Int J Cardiol* 2006;**110**: 279–87.

252 Sen-Chowdhry S, Morgan RD, Chambers JC, McKenna WJ. Arrhythmogenic cardiomyopathy: etiology, diagnosis, and treatment. *Annu Rev Med* 2010;**61**:233–53.

253 Bowles NE, Ni J, Marcus F, Towbin JA. The detection of cardiotropic viruses in the myocardium of patients with arrhythmogenic right ventricular dysplasia/cardiomyopathy. *J Am Coll Cardiol* 2002;**39**:892–5.

254 Herren T, Gerber PA, Duru F. Arrhythmogenic right ventricular cardiomyopathy/dysplasia: a not so rare "disease of the desmosome" with multiple clinical presentations. *Clin Res Cardiol* 2009;**98**:141–58.

255 Murphy DT, Shine SC, Cradock A, *et al*. Cardiac MRI in arrhythmogenic right ventricular cardiomyopathy. *AJR Am J Roentgenol* 2010;**194**:W299–306.

256 Campian ME, Verberne HJ, Hardziyenka M, *et al*. Assessment of inflammation in patients with arrhythmogenic right ventricular cardiomyopathy/dysplasia. *Eur J Nucl Med Mol Imaging* 2010;**37**:2079–85.

257 Marcus FI, Zareba W, Calkins H, *et al*. Arrhythmogenic right ventricular cardiomyopathy/dysplasia clinical presentation and diagnostic evaluation: results from the North American Multidisciplinary Study. *Heart Rhythm* 2009;**6**:984–92.

258 Komura M, Suzuki J, Adachi S, *et al*. Clinical course of arrhythmogenic right ventricular cardiomyopathy in the era of implantable cardioverter-defibrillators and radiofrequency catheter ablation. *Int Heart J* 2010;**51**:34–40.

259 Migliore F, Zorzi A, Silvano M, *et al*. Clinical management of arrhythmogenic right ventricular cardiomyopathy: an update. *Curr Pharm Des* 2010;**16**:2918–28.

260 Chin TK, Perloff JK, Williams RG, *et al*. Isolated noncompaction of left ventricular myocardium. A study of eight cases. *Circulation* 1990;**82**:507–13.

261 Stollberger C, Finsterer J, Blazek G. Left ventricular hypertrabeculation/noncompaction and association with additional cardiac abnormalities and neuromuscular disorders. *Am J Cardiol* 2002;**90**:899–902.

262 Stollberger C, Finsterer J. Left ventricular hypertrabeculation/noncompaction. *J Am Soc Echocardiogr* 2004;**17**:91–100.

263 Ichida F, Hamamichi Y, Miyawaki T, *et al*. Clinical features of isolated noncompaction of the ventricular myocardium: long-term clinical course, hemodynamic properties and genetic background. *J Am Coll Cardiol* 1999;**34**:233–40.

264 Towbin JA. Left ventricular noncompaction: a new form of heart failure. *Heart Fail Clin* 2010;**6**:453–69.

265 Sarma RJ, Chana A, Elkayam U. Left ventricular noncompaction. *Prog Cardiovasc Dis* 2010;**52**:264–73.

266 D'Adamo P, Fassone L, Gedeon A, *et al*. The X-linked gene G4.5 is responsible for different infantile dilated cardiomyopathies. *Am J Hum Genet* 1997;**61**:862–7.

267 Johnston J, Kelley RI, Fergenbaum A, *et al*. Mutation characterization and genotype–phenotype correlation in Barth syndrome. *Am J Hum Genet* 1997;**61**:1053–8.

268 Ino T, Sherwood WG, Cutz E, *et al*. Dilated cardiomyopathy with neutropenia, short stature, and abnormal carnitine metabolism. *J Pediatr* 1988;**113**:511–4.

269 Bolhuis PA, Hensels GW, Hulsebos TJM, *et al*. Mapping of the locus for X-linked cardioskeletal myopathy with neutropenia and abnormal mitochondria (Barth syndrome) to Xq28. *Am J Hum Genet* 1991;**48**:481–5.

270 Gedeon AK, Wilson MJ, Colley AC, *et al*. X-linked fatal infantile cardiomyopathy maps to Xq28 and is possibly allelic to Barth syndrome. *J Med Genet* 1995;**32**:383–8.

271 Ichida F, Tsubata S, Bowles KR, *et al*. Novel gene mutations in patients with left ventricular noncompaction or Barth syndrome. *Circulation* 2001;**103**:1256–63.

272 Klaassen S, Probst S, Oechslin E, *et al*. Mutations in sarcomere protein genes in left ventricular noncompaction. *Circulation* 2008;**117**:2893–901.

273 Shan L, Makita N, Xing Y, *et al*. SCN5A variants in Japanese patients with left ventricular noncompaction and arrhythmia. *Mol Genet Metab* 2008;**93**:468–74.

274 Finsterer J, Stöllberger C. Primary myopathies and the heart. *Scand Cardiovasc J* 2008;**42**:9–24.

275 Tang S, Batra A, Zhang Y, *et al*. Left ventricular noncompaction is associated with mutations in the mitochondrial genome. *Mitochondrion* 2010;**10**:350–7.

276 Hoedemaekers YM, Caliskan K, Michels M, *et al*. The importance of genetic counseling, DNA diagnostics, and cardiologic family screening in left ventricular noncompaction cardiomyopathy. *Circ Cardiovasc Genet* 2010;**3**:232–9.

277 Song ZZ. The treatment of noncompaction of ventricular myocardium. *Cardiovasc Ther* in press.

278 Fazio G, Corrado G, Zachara E, *et al*. Anticoagulant drugs in noncompaction: a mandatory therapy? *J Cardiovasc Med (Hagerstown)* 2008;**9**:1095–7.

279 Caliskan K, Szili-Torok T, Theuns DA, *et al*. Indications and outcome of implantable cardioverter-defibrillators for primary and secondary prophylaxis in patients with noncompaction cardiomyopathy. *J Cardiovasc Electrophysiol* in press.

280 Lake M, Lerakis S, Green J, *et al*. Ventricular noncompaction and associated cardiac anomalies. *Am J Med Sci* 2010;**340**:399–401.

59 Pericardial Diseases

Jonathan N. Johnson & Frank Cetta

Mayo Clinic College of Medicine, Mayo Clinic, Rochester, MN, USA

Introduction

Normal anatomy and physiology

The normal pericardium has two primary layers, the visceral pericardium and the parietal pericardium. The visceral pericardium, or epicardium, is a single serous layer covering the surface of the heart and proximal great vessels (Figure 59.1). The parietal pericardium has three layers, the innermost serous layer being continuous with the serous visceral pericardium. The space between the two serous layers is termed the pericardial space or cavity, and contains a small amount of serous fluid for lubrication (<20–30 ml in adults). The middle layer of the parietal pericardium is fibrous tissue and the outer layer is epicardial connective tissue, largely collagenous. The pericardium obtains its arterial blood supply from the internal mammary artery and descending aorta, and is innervated by the phrenic and vagus nerves. It is anchored within the thoracic cavity with attachments inferiorly to the diaphragm and a portion of the inferior vena cava, and posteriorly to the esophagus, aorta, pulmonary veins, and thoracic vertebrae [1].

The pericardium provides a mechanical barrier for the heart, protecting it from the spread of inflammatory, infectious, and neoplastic diseases from contiguous structures. The small amount of normal pericardial fluid allows free movement during the cardiac cycle. The pericardium limits acute distension of the heart, and therefore diastolic volume. It also allows diastolic coupling of the two ventricles, whereby filling pressure abnormalities of one ventricle affect the other. Slow accumulation of fluid within the pericardium is well tolerated by stretching and growth of the parietal pericardium, but rapid accumulation of even a small amount of fluid is typically poorly tolerated.

This chapter discusses the clinical features and etiology of acute pericarditis and associated pericardial effusion, congenital anomalies of the pericardium, and constrictive pericarditis.

Acute pericarditis

Clinical history

Children and adolescents with acute pericarditis of any etiology commonly present with precordial or substernal chest pain that is described as squeezing, sharp, or dull. It is typically worse when supine and the patient may refuse to lie down for the examination, preferring to sit upright and lean forward. The pain is worse with inspiration, coughing, and movement [2]. Younger children may present without typical chest pain symptoms. Respiratory distress is uncommon unless cardiac tamponade or pulmonary disease is present. Abdominal pain is rare, but can result from hepatic distension in patients with a fast-accumulating effusion and tamponade.

Physical examination

The pathognomonic physical finding of acute pericarditis is a friction rub, a high-frequency, scratching/sandpaper-like sound caused by friction between the inflamed pericardial surfaces. The rub is heard in systole and diastole, may be intermittent, and is best heard at the left sternal border or the apex. It is loudest when the heart is closest to the chest wall as when the patient leans forward, kneels, and/or inspires [2]. The absence of the rub does not exclude pericarditis, particularly with a large effusion, and then the heart sounds may be muffled. Fever, if present, is largely nonspecific.

Cardiac tamponade is compression of the heart from the fluid-filled pericardial cavity, restricting atrial and ventricular

Figure 59.1 Cadaveric heart specimen, showing the heart within the pericardial cavity (left) and the bilayered pericardium with the heart removed (right). (Courtesy of Dr. William D. Edwards, Division of Anatomic Pathology, Mayo Clinic, Rochester, MN, USA.)

filling and decreasing cardiac output [3]. Tamponade may result from either a sudden increase in pericardial volume or from gradual increases in pericardial volume beyond the point of potential pericardial distention. On physical examination, tamponade is characterized by Beck's triad of hypotension, distant heart sounds, and elevated central venous pressure with jugular venous distension [3]. Patients also have tachycardia, tachypnea, narrow pulse pressure, and pulsus paradoxus. Initially, cardiac output is maintained by increasing heart rate and ejection fraction. As the tamponade worsens and these mechanisms no longer maintain cardiac output, systemic vascular resistance increases to maintain blood pressure, narrowing pulse pressure and compromising systemic perfusion. Ultimately, coronary perfusion pressure falls, causing decreased myocardial function, decreased cardiac output, and hypotension [3].

Pulsus paradoxus in tamponade is an exaggerated decrease in blood pressure of >10 mmHg during inspiration. During normal inspiration, the systolic blood pressure decreases slightly because of increased capacity of the pulmonary venous bed and decreased intrathoracic pressure. With a significant pericardial effusion, the left ventricular diastolic volume and output are restricted by increased pericardial pressure, decreased pulmonary venous return, and shifting of the intraventricular septum to the left; consequently, blood pressure decreases to a greater extent in inspiration. (The paradox is that with inspiration in severe tamponade, the pulse may disappear but the cardiac impulse indicates a heart beat.) To measure pulsus paradoxus, the patient is placed supine. A blood pressure cuff is inflated until the radial pulse is no longer palpable. With slow release of cuff pressure, the initial Korotkoff sounds are listened for. With inspiration, the Korotkoff sounds disappear, particularly if pulsus paradoxus is present. Cuff pressure should be slowly released until the Korotkoff sounds are heard throughout the respiratory cycle. The pressure difference between when the auscultator hears the first Korotkoff sound and when it is heard on each heart beat is the pulsus. Normally, the pressure difference is ~5 mmHg during inspiration. If the pressure difference exceeds 10 mmHg, pulsus paradoxus is present.

Chest radiography

A normal heart size does not exclude pericarditis or pericardial effusion; tamponade can occur in patients with a "normal-sized" cardiac silhouette. With a large effusion, the cardiac silhouette commonly assumes a triangular or "water-bottle" shape, with normal pulmonary vascular markings (Figure 59.2). Chronic pericarditis may show pericardial calcifications (Figure 59.3). The chest radiograph may suggest a cause of pericarditis, with findings of bacterial pneumonia, tuberculosis, or neoplastic disease.

Electrocardiography

Electrocardiographic changes in pericarditis can be secondary to either direct inflammation of the epicardium, or pressure exerted on the epicardium by pericardial fluid. Acute pericarditis is the most frequent cause of ST segment elevation in children. Low QRS voltages can be seen in all leads with chronic pericarditis or a large pericardial effusion. Electrical alternans, a cyclical variation of the QRS amplitude, may occur secondary to the pendular motion of the heart with a large pericardial effusion (Figure 59.4).

Four stages of electrocardiogram (ECG) changes in pericarditis have been reported [4]. Stage 1 consists of ST segment elevation in the lateral leads (I, II, AVF, V4–V6), thought to be due to subepicardial myocarditis (Figure 59.5). A ratio of ST segment elevation (mm) to T-wave amplitude (mm) greater than 0.25 is predictive of pericarditis, and helps differentiate pericarditis from myocardial infarction [5]. Reciprocal ST depression occurs in leads AVR and V1. The T-waves remain normal, and PR depression can occur if atrial tissue is inflamed. In stage 2, the ST segment becomes isoelectric, and the amplitude of the T-wave diminishes. The PR segment becomes more depressed. In stage 3, the ST segment remains normal, but the T-waves become inverted in the lateral leads. Stage 4 shows normalization of the ECG, although some T-wave changes may persist.

Echocardiography

Echocardiography is the primary tool for diagnosis and monitoring pericardial effusions, which appear as an echo-free space adjacent to the heart [6] (Figure 59.4). Fibrinous strands may be noted in the pericardial space on two-dimensional imaging, and can be seen in postmortem specimens (Figure 59.6). Additionally, echocardiography helps detect other structural and myocardial causes of cardiomegaly. Pericardial effusions may be detected by fetal echocardiography, and are associated with hydrops fetalis [7].

With a supine patient, a small effusion is commonly seen posteriorly, and only be detectable in systole. A tiny pericardial
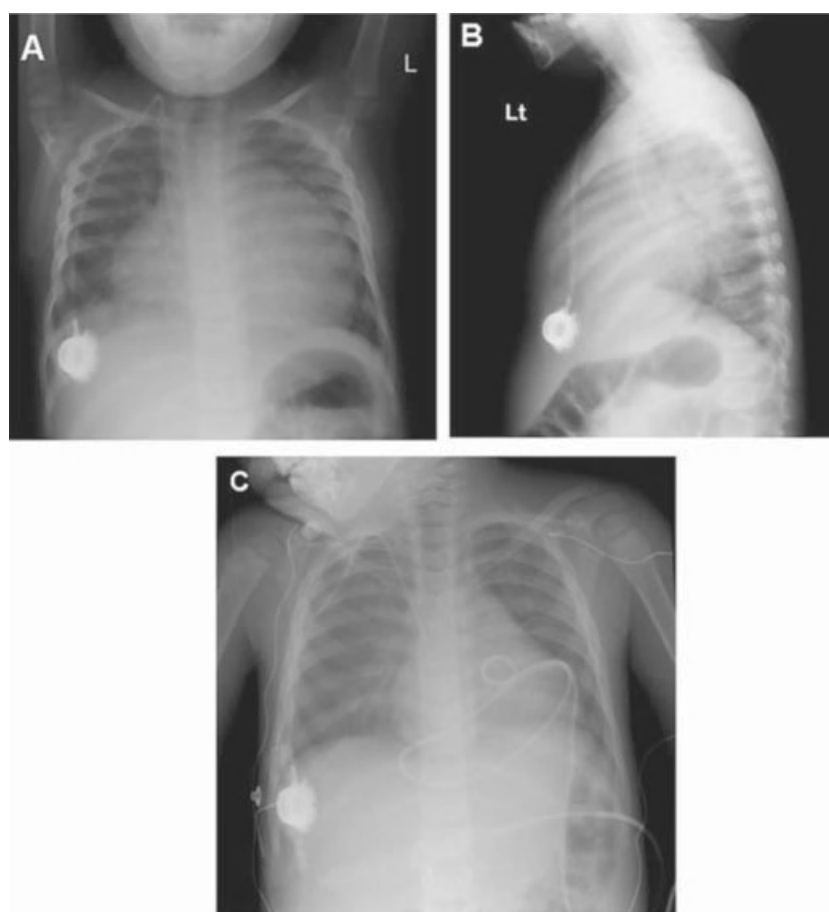
Figure 59.2 Chest radiogram of a 2-year-old female with immune deficiency after she presented with tachypnea, including the AP (a) and lateral (b) views. The patient required an emergency pericardiocentesis, after which (c) her cardiothymic silhouette had markedly decreased in size.
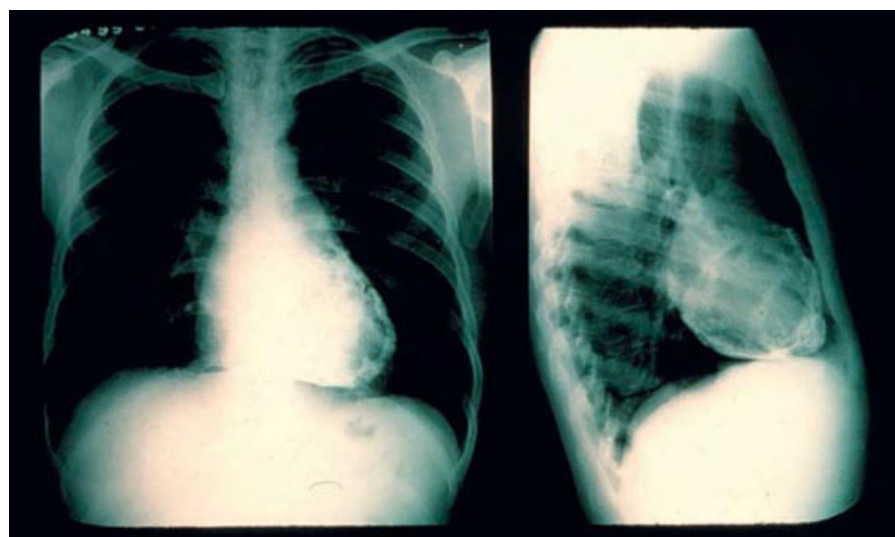
Figure 59.3 Chest radiogram of an adult patient with chronic pericarditis and resultant calcification of the pericardial space. (Courtesy of Dr. William D. Edwards, Division of Anatomic Pathology, Mayo Clinic, Rochester, MN, USA.)

space posteriorly in systole may be completely normal. In an adult, an effusion >25 ml is observed in both systole and diastole (Figure 59.7) [8]. With a larger effusion volume, fluid may be detected both anteriorly and posteriorly. In large effusions, the heart may swing to-and-fro within the pericardial cavity (Figure 59.4, Videoclips 59.1 and 59.2). This swinging motion may also be seen on M-mode echocardiography (Figure 59.8). The first sign of the hemodynamic impairment in tamponade is collapse of the right ventricular free wall in early to mid diastole (Figure 59.9) [8]. The right
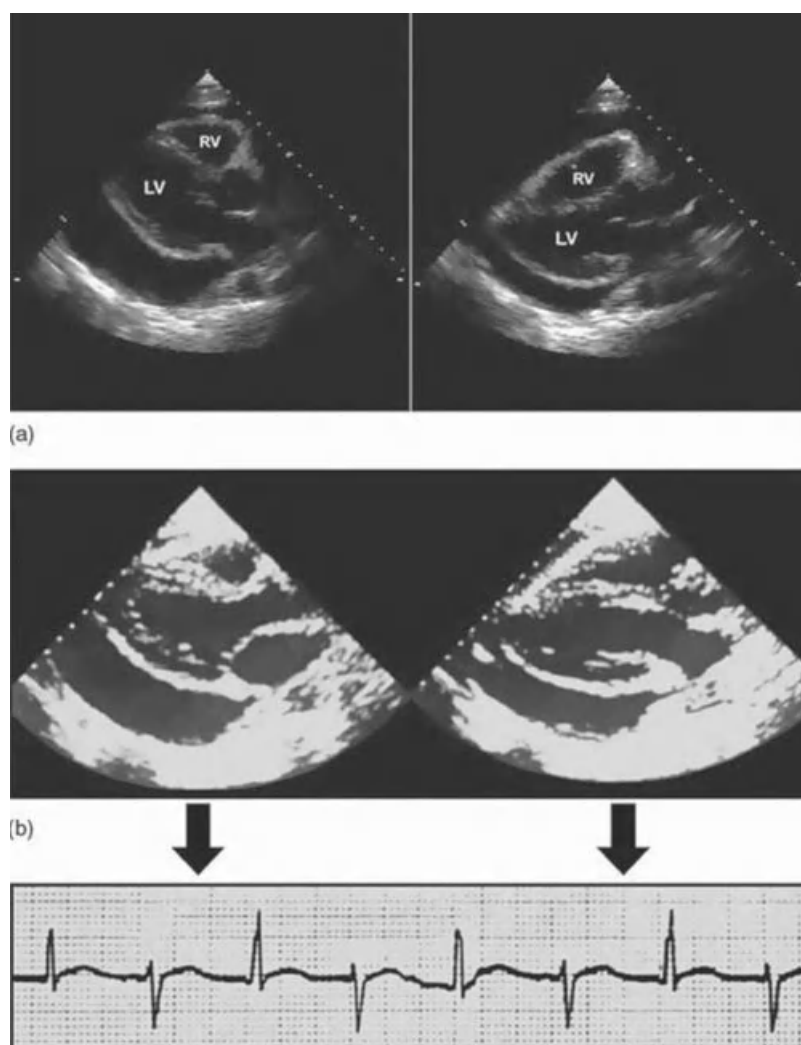
Figure 59.4 Parasternal long-axis echocardiographic views, demonstrating (a) a large effusion with swinging motion of the heart. This swinging motion may be an ominous sign of cardiac tamponade. (b) When the left ventricle is close to the sternum, the QRS voltage increases on the ECG, but it decreases when the left ventricle swings away from the surface, producing electrical alternans. ECG, electrocardiogram; LV, left ventricle; RV, right ventricle. (Adapted from Oh *et al.*, *The Echo Manual*, 2006, with permission from Lippincott Williams & Wilkins.)

atrium may invert in late diastole. The inferior vena cava may be dilated without normal inspiratory variation, and the ventricular septum may have abnormal motion described as a "bounce," where the septum shifts leftwards with right ventricular filling during inspiration. It then shifts back rightwards with expiration with the improved left ventricular filling.

Clues about etiology may be discovered. A clot in the pericardial space suggests hemopericardium. Air in the pericardium (pneumopericardium) can occur in patients with esophageal perforation. Adhesions or metastases may also be seen in the pericardial space.

Doppler echocardiography of the heart provides an excellent understanding of tamponade physiology (Figure 59.10). During inspiration, there is an exaggerated decrease in the mitral inflow velocity (E velocity) and velocity–time integral by an average of 35%, with a relatively increased atrial component (A velocity). Conversely, there is an exaggerated increase in tricuspid inflow velocity (tricuspid E velocity) and velocity–time integral by an average of 80% during inspiration [9]. The aortic and pulmonary outflow changes mirror those of their respective AV valves.

Cardiac catheterization

With large accumulations of pericardial fluid, diastolic pressures rise in all four chambers of the heart, and ultimately equalize. Right ventricular and pulmonary artery pressures may be elevated. Pulsus paradoxus can be seen on femoral artery and right atrial tracings [10]. The role of cardiac catheterization in differentiating between constrictive pericarditis and restrictive cardiomyopathy is discussed below.

Other imaging modalities

In assessing pericardial effusion, computed tomography (CT) and magnetic resonance imaging (MRI) may not add substantially to the evaluation. However, CT is helpful in evaluating constrictive pericarditis, as it can identify calcification, pericardial thickening, or other pericardial masses, including
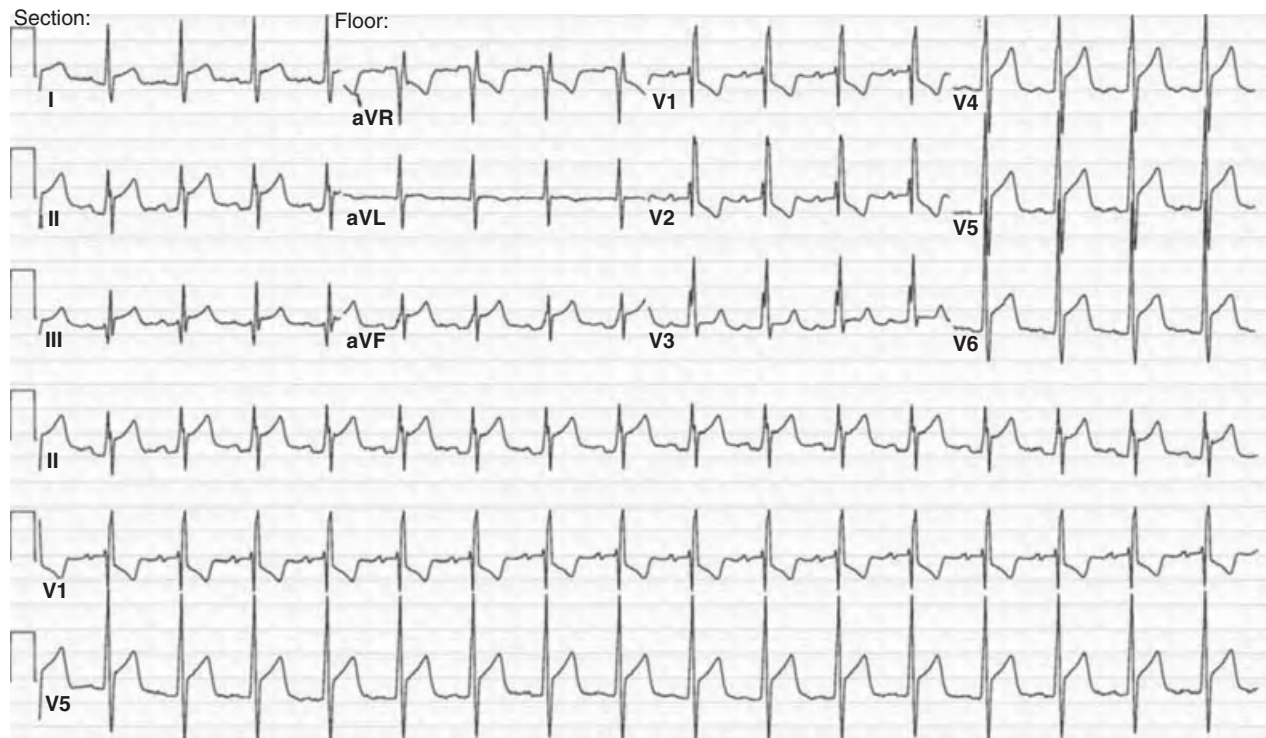
Figure 59.5 Electrocardiogram of a 17-year-old male several days after atrial septal defect repair. Note the diffuse ST segment changes including ST segment elevation in the lateral precordial leads.
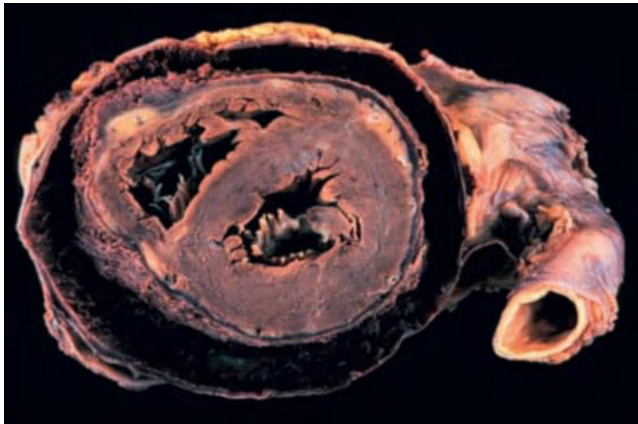
Figure 59.6 Cadaveric adult heart specimen, showing the heart within the pericardial space with a large effusion. Fibrinous stranding can be seen within the pericardial space. (Courtesy of Dr. William D. Edwards, Division of Anatomic Pathology, Mayo Clinic, Rochester, MN, USA.)
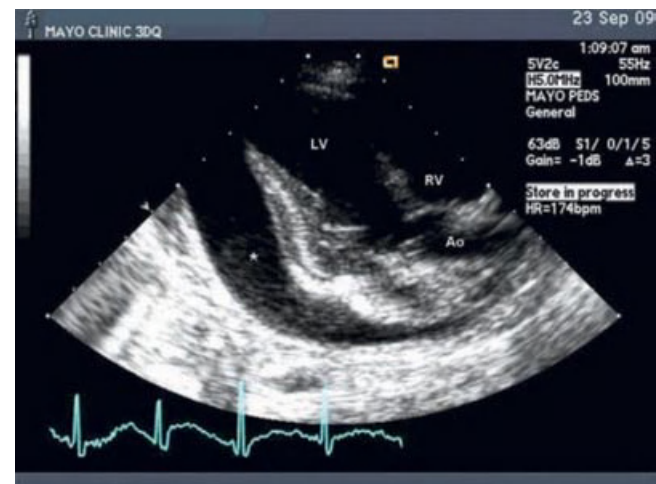
Figure 59.7 Parasternal long-axis echo image showing a large pericardial effusion (*). Ao, aorta; LV, left ventricle; RV, right ventricle.

neoplasias. Additionally, MRI and CT are valuable in evaluating pericardial cysts and absence of the pericardium [11].

Management of tamponade

If a child presents with cardiac tamponade, intravenous fluid should be given immediately to increase the diastolic filling pressure temporarily and provide stabilization. Medications that lower systemic pressure, including vasodilators and diuretics, should be avoided. Pericardiocentesis should be performed in patients with clinical tamponade (low cardiac output, hypotension, or pulsus paradoxus >10 mmHg), and in those with suspected bacterial pericarditis, immunocompromised hosts, or for diagnosis when the etiology of an effusion is unclear [12,13].

Pediatric Cardiovascular Medicine
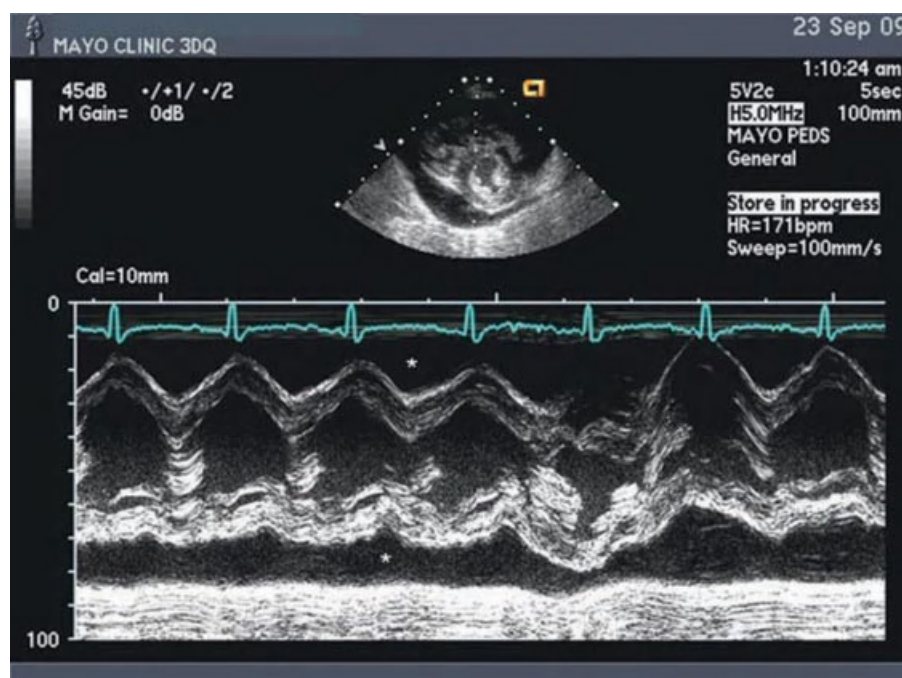
Figure 59.8 M-mode echo image showing a large pericardial effusion (*) anterior and posterior to the heart. Note the swinging motion of the heart evident in the M-mode signal.

Figure 59.9 Right ventricular collapse in early diastole in a patient with tamponade. Note that in the upper echo image in systole (a), the full four-chamber view is noted, and in the lower echo image in diastole (b), the right ventricular free wall is compressed (arrows).

Ideally, pericardiocentesis should be performed either in an intensive care unit, operating room, or cardiac catheterization laboratory. The patient should be placed in a 30° head-up position and be sedated, with continuous heart rate, blood pressure, and pulse oximetry measurements. The needle is introduced subxiphoid and advanced towards the left shoulder. Echocardiographic guidance allows for more accuracy, but is unnecessary in an emergency [13]. In most patients, a drainage catheter should be placed for at least 48 h due to the likelihood of recurrence of effusion [12]. Potential risks of the procedure include arrhythmias, myocardial puncture, coronary artery or vein laceration, hemopericardium and recurrent tamponade, pneumothorax, aortic or internal mammary artery injury, hepatic laceration, and death [13].

Aspirated pericardial fluid should be analyzed for cell count with differential, glucose and protein concentrations, Gram and acid-fast bacilli stains, bacterial, viral and fungal cultures, and microscopic analysis. Specific bacterial or viral-specific antigens may be assessed with polymerase chain reaction (PCR) studies and latex agglutination studies. A high triglyceride level is diagnostic for a chylopericardium. An adenosine deaminase activity level can be obtained if there is concern about tuberculous pericarditis [14].

Sometimes the purulent material may be too thick to drain, or may be loculated. Then, instead of attempting a repeat pericardiocentesis, an operation should be performed. The surgical approaches (thoracotomy, subxiphoid, and thorascopic) and the extent of pericardium removal (complete/partial pericardiectomy or pericardial window) vary, but all are effective [15].
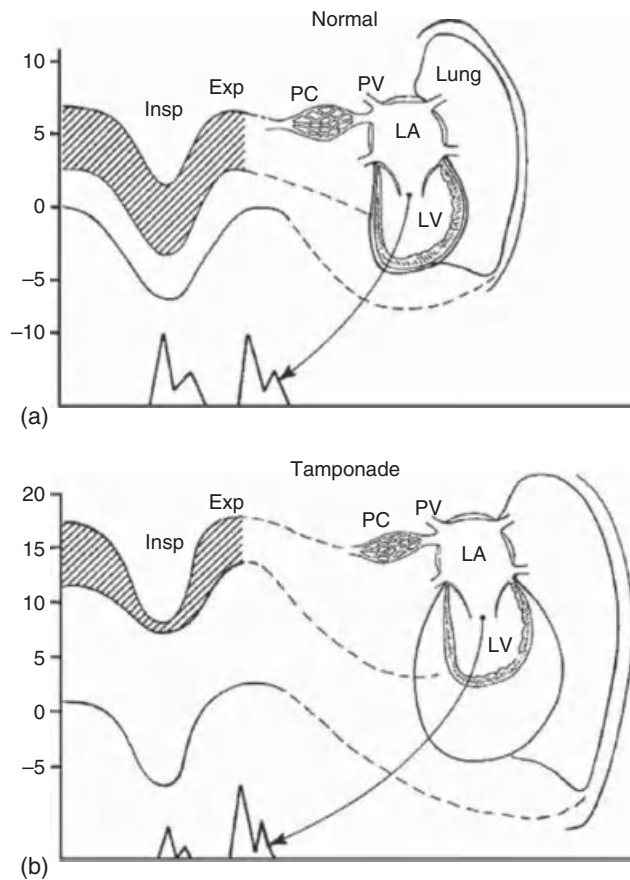
Figure 59.10 Diagram of intrathoracic and intracardiac pressure changes with respiration in (a) normal and (b) tamponade physiology. The shaded area indicates left ventricular filling pressure gradients (difference between pulmonary capillary wedge pressure and left ventricular diastolic pressure). At the bottom of each drawing is a schematic mitral inflow Doppler velocity profile. In tamponade, there is an inspiratory decrease in left ventricular filling because the pressure decrease in the pericardium and left ventricular cavity is smaller than the pressure drop in the pulmonary capillaries. Left ventricular filling is restored after expiration. LA, left atrium; LV, left ventricle; PC, pulmonary capillaries; PV, pulmonary vein. (Adapted with permission from Sharp, JT et al. Am J Med 1960;**29**:640–646.)

Etiology

Viral pericarditis

Viral pericarditis is the most common form of childhood pericarditis. Patients commonly present 10–14 days following an upper respiratory or gastrointestinal infection, with classic precordial chest pain and friction rub. Fever is typically present, and patients may complain of abdominal pain. Patients with viral pericarditis generally appear less toxic than those with bacterial pericarditis; however, concomitant myocarditis may worsen the clinical picture of a patient with a viral etiology. Tamponade is rare; however, patients should be monitored closely after initial diagnosis. The most common viral causes of pericarditis are listed in Table 59.1.

Table 59.1 Viral causes of pericarditis.

Enterovirus (primarily Coxsackie B)	Measles
Adenovirus	Cytomegalovirus (CMV)
Influenza virus (A and B)	Respiratory syncytial virus (RSV)
Rubella	Herpes simplex
Mumps	Hepatitis B
Epstein–Barr	HIV

Pericardial fluid is typically serous or serosanguineous, and shows a predominance of lymphocytes, although neutrophils are more common in early stages of pericarditis. Viral cultures can be obtained from pericardial fluid, nasopharynx, or stool, and PCR studies may assist in determining a specific viral cause. Coxsackievirus is the most frequently isolated virus in children with pericarditis, although numerous enteroviruses have been implicated (Table 59.1). [16].

Treatment is symptomatic, including bed rest and oral nonsteroidal anti-inflammatory drugs (NSAIDs). If anti-inflammatory agents are insufficient, steroidal therapy may be considered, but only if bacterial causes have been excluded. Resolution typically begins in days and is complete in <1 month. A few patients relapse and improve with retreatment. Constrictive pericarditis is a rare late sequela.

Bacterial pericarditis

Bacterial pericarditis, although less common, is serious and life-threatening. It occurs most commonly before 2 years of age [17]. Patients present with classic symptoms of precordial chest pain, friction rub, and muffled heart sounds, but often are in extremis, with decreased cardiac output. Markedly elevated fever is common and associated with dyspnea, tachypnea, and tachycardia out of proportion with the degree of fever. Often bacterial pericarditis results from a disseminated infection, either by a hematogenous route or by direct contact, most commonly from the lung. Septic arthritis, osteomyelitis, meningitis, or soft-tissue infection may also be the source [17,18].

The pericardial fluid shows a marked predominance of neutrophils, and cultures are typically positive for the causative organism. If antibiotics have been given before procuring a sample, latex agglutination studies of the pericardial fluid, serum, or urine may help diagnose the organism. *Staphylococcus aureus* is currently the most common bacterium isolated in bacterial pericarditis, accounting for half of these episodes [17], and is the most common cause of bacterial pericarditis occurring within 3 months of a cardiac operation. Anaerobic bacteria should be considered in children with an associated lung abscess, abdominal infection, or blunt chest trauma. Potential bacterial causes of pericarditis are listed in Table 59.2.

Antibiotic treatment alone is not sufficient for cure; all patients with evidence of bacterial pericarditis should

Table 59.2 Bacterial causes of pericarditis.

Staphylococcus aureus	Chlamydia psittaci
Haemophilus influenzae	Nocardia asteroides
Streptococcus pneumoniae	Brucella
Other Streptococcus species	Yersinia
Neisseria meningitidis	Salmonella
Neisseria gonorrhoeae	Actinomyces
Campylobacter fetus	Mycobacterium tuberculosis
Pseudomonas aeruginosa	Escherichia coli
Mycoplasma pneumoniae	Listeria monocytogenes
Mycoplasma hominis	Pasteurella multocida
Legionella	Klebsiella
Francisella tularensis	Anaerobes

undergo percutaneous or surgical drainage of the pericardial cavity. A surgically created window or pericardiectomy is necessary if the purulent pericardial fluid cannot be aspirated via pericardiocentesis [15]. Intrapericardial streptokinase may improve drainage [19]. Broad-spectrum antibiotics directed towards the most commonly affecting organisms, *Staphylococcus aureus* and *Haemophilus influenzae*, should be administered, and should include an intravenous penicillinase-resistant penicillin (nafcillin or oxacillin) or vancomycin in patients at risk for methicillin-resistant *S. aureus*, in addition to a third-generation cephalosporin (ceftriaxone, cefotaxime). An aminoglycoside can be added in immunocompromised patients. Specific therapy is designated once specific culture and sensitivity results are known. Most patients require 3–4 weeks of intravenous antibiotic treatment [19].

Survival in patients with bacterial pericarditis has improved considerably, and mortality is currently <10% [19,20]. Risk factors for a poor outcome include delay in diagnosis, failure to initiate early surgical intervention, inadequate drainage, myocardial involvement, tamponade, septicemia, younger age, and staphylococcal disease [19,20]. Constrictive pericarditis occurs rarely after recovery [18,19], most commonly following *S. aureus*, *H. influenzae*, or *Streptococcus pneumoniae* infection.

Tuberculous pericarditis

Once a common cause of pericarditis in the United States, *Mycobacterium tuberculosis* pericarditis now occurs primarily in developing countries. The onset is typically insidious, with weight loss, malaise, low-grade fever, night sweats, dyspnea, and chest pain. The presentation may also be subacute, complicated by pericardial tamponade. Tuberculous pericarditis often occurs secondary to miliary tuberculosis with direct extension or lymphatic spread into the pericardium. Hematogenous spread may occur without obvious pulmonary infiltrates.

Most patients have a positive Mantoux skin test. The pericardial fluid is typically serosanguinous or hemorrhagic, with a lymphocytic predominance. Acid-fast bacilli may be seen on auramine–rhodamine fluorescent-stained smears, but are present in <50% of patients [14]. Pericardial biopsy is useful and provides histologic confirmation of tuberculous infection. Elevated pericardial adenosine deaminase levels >50 U l⁻¹ may be diagnostic [14]. Mycobacterium cultures often take up to 6 weeks to grow, hence treatment must begin before culture confirmation of diagnosis. For pulmonary tuberculosis, PCR techniques, which have been developed, can make the diagnosis rapidly and with a high degree of sensitivity and specificity.

Multi-drug therapy is the mainstay of treatment, because of the risk of drug resistance. A regimen of rifampicin, isoniazid, pyrazinamide, and ethambutol for ≥2 months, followed by isoniazid and rifampicin for a further 4 months, is highly effective. A 1–2-month course of steroid therapy may be used to reduce inflammation and increase resorption of pericardial fluid. Tuberculosis is a common cause of chronic pericardial effusion. Tuberculous pericarditis is one of the leading causes of constrictive pericarditis worldwide [14]. Pericardiectomy may be difficult because of diffuse inflammatory and caseous material. Some surgeons delay pericardiectomy for at least 6–12 weeks, although this is controversial.

HIV and other infections

Pericardial effusions have been reported in 25% of children with HIV infection [21], but rarely cause tamponade. Pericardial fluid cultures are usually negative. Pericardial effusions commonly coexist with pleural effusions and ascites. Patients with a compromised immune system, including those with HIV, are at risk for fungal or parasitic pericarditis (Table 59.3). In the developing world, concurrent infection with HIV and tuberculosis is common, and HIV is a major risk factor for developing tuberculous pericarditis with effusion [14].

Other causes of pericardial effusion

Renal failure

Pericarditis is observed in 10% of patients with chronic renal failure [22]. The levels of creatinine and blood urea nitrogen (BUN) do not predict the likelihood of pericarditis. It occurs more commonly with concurrent systemic lupus erythematosus (SLE) or treatment with hydralazine for hypertension. Most effusions resolve with efficient dialysis [22]. Pericardial fluid is typically serous, but with heparinization may be bloody from pericardial hemorrhage that can result in tamponade. NSAIDs can be given for chest pain, but typically do not reduce effusion size. Pericardiocentesis should be performed for the usual indications. If dialysis fails to

Table 59.3 Other infectious causes of pericarditis.

Protozoal	*Toxoplasma gondii*
Parasitic	*Entamoeba histolytica, Echinococcus*
Spirochetal	Syphilis, leptospirosis
Rickettsial	Typhus, Q fever
Fungal	*Candida, Aspergillus, Blastomyces, Coccidioides, Histoplasma, Cryptococcus*

resolve the effusion, surgery may be indicated, particularly if constriction develops [22].

Kawasaki disease

During the acute phase of Kawasaki disease, one-third of patients have a pericardial effusion, but this typically resolves within 2 weeks and is unlikely to progress to tamponade [23].

Drug-induced pericarditis

A lupus-like drug reaction occurs in some patients treated with specific medications, most commonly hydralazine, isoniazid, procainamide, and phenytoin. Antinuclear antibodies are commonly elevated in these patients. Rarer causes are cyclosporine, methysergide, and chemotherapeutic agents such as cyclophosphamide, doxorubicin, and dactinomycin. Pericarditis occurs with the inflammatory reaction but rarely progresses to tamponade [24]. Treatment includes removal of offending medications and giving NSAIDs. Anticoagulants and thrombolytics may cause pericardial hemorrhage in an inflamed pericardial cavity, and lead to adhesions and eventual constriction. Hypersensitivity reactions to penicillin and cromolyn sodium have been associated with pericardial effusion [25,26].

Hypothyroidism

Pericardial effusion occurs in 80% of patients with myxedema, but rarely with mild hypothyroidism [27]. It is generally asymptomatic. Tamponade is rare because of the slow fluid accumulation [27]. Unlike others with a pericardial effusion, these patients are bradycardic. The pericardial fluid shows elevated protein and mucopolysaccharides [27]. With thyroid hormone replacement, the effusion resolves gradually.

Chylopericardium

Chylous pericardial effusion occurs following congenital heart surgery, especially with trauma to the thoracic duct or elevated central venous pressures [28]. Other causes are mediastinal masses obstructing lymphatic drainage, cystic hygromas, radiation therapy, and pancreatitis, or it may be idiopathic. There is often a concurrent chylous pleural effusion. The pericardial fluid is milky colored, having markedly elevated triglyceride and protein levels. Treatment includes a low-fat or medium-chain triglyceride diet, started after a period of parenteral nutrition without oral intake to allow resolution of the effusion. Treatment of the underlying cause should be applied, including therapy to lower the central venous pressure if this is causing the effusion. Persistent chylous effusions can be treated using thoracic duct ligation, or palliated with a pericardial window, pericardiectomy, or placement of a pericardio–peritoneal or pleuro–peritoneal shunt [28]. Intravenous octreotide has been used with some success in patients with chronic chylous pleural effusions [29].

Trauma

Blunt and penetrating cardiac trauma can cause a hemorrhagic pericardial effusion. The usual Beck's triad of symptoms rarely occurs. Echocardiography is diagnostic. Symptomatic trauma patients require emergency pericardiocentesis. Hemopericardium can also occur with placement or passage of catheters, pericardiocentesis, and placement of pacemaker leads. These types of pericardial trauma require an operation to identify and repair the rupture in the cardiac wall.

Neoplastic disease

Primary pericardial tumors are rare in children and include lymphoma, malignant teratoma, mesothelioma, and angiosarcoma. Metastatic tumors are more common and include Hodgkin disease, non-Hodgkin lymphoma, leukemia, neuroblastoma, Wilms tumor, and sarcomas of the soft tissue and bone [30].

Several non-malignant congenital intrapericardial lesions exist. These include pericardial cysts, extra-lobar pulmonary sequestrations, cystic lymphangioma, bronchogenic cysts, and pericardial teratomas [31,32]. Teratomas in particular can be large and cause hydrops fetalis. Surgical excision of these large tumors is typically curative [32].

Pericardial effusions may occur with a malignancy, independent of the primary tumor. This may be due to infectious causes, or secondary to metastatic invasion of pericardial lymphatics. Pericarditis can occur after treatment with certain chemotherapy agents. Pericardial involvement after chemotherapy is more common in patients receiving mediastinal irradiation. Pericardial fluid, if available, should be sent for cytologic analysis and culture.

Treatment regimens for Hodgkin disease and breast cancer have traditionally used mediastinal radiation. Up to 5% of patients who have received mediastinal irradiation develop pericarditis from 2 months to 2 years after the treatment, an effect that is dose related [5]. The pericarditis may be asymptomatic or lead to fulminant constrictive pericarditis. Most resolve with NSAIDs, but pericardiocentesis may be needed. Pericardiectomy or steroids may be required for recurrent effusions [33].

Postpericardiotomy syndrome

Postpericardiotomy syndrome is characterized by low-grade fever beyond the first week following intracardiac or pericardial surgery, although it may recur weeks to years later. Pericardial and pleural inflammation and effusions cause typical chest pain. Postpericardiotomy syndrome occurs as a single episode in up to 40% of patients following operation [34]. Children <2 years old, although rarely affected, show irritability, malaise, decreased appetite, and arthralgias. There is a friction rub, tachycardia, and fluid retention indicated by weight gain and hepatic congestion. Tamponade is rare, but must be considered and ruled out.

Postpericardiotomy syndrome is likely due to an autoimmune reaction. Similar pericardial effusions have been noted after blunt cardiac trauma, pacemaker lead placement, and in Dressler syndrome (postmyocardial infarction syndrome) [35]. Postpericardiotomy syndrome may occur after any cardiac surgery, but is more frequent after repair of tetralogy of Fallot, ventricular septal defect, and atrial septal defect [34]. It also occurs in half of children after cardiac transplantation [36]. Laboratory evaluation reveals nonspecific indicators of inflammation, including elevated erythrocyte sedimentation rate, C-reactive protein, and white blood cell count. Echocardiography may reveal an effusion that typically reaches maximum size by postoperative day 10 [34].

Postpericardiotomy syndrome is a benign, self-limited illness. Treatment consists of diuretics for fluid retention and anti-inflammatory medications, with pericardiocentesis performed for a symptomatic effusion [37]. Aspirin remains the primary anti-inflammatory medication, typically 30–75 mg kg^{-1} per day in four divided doses for 4–6 weeks, and then tapered. In patients with a large effusion or refractory to NSAIDs, prednisone (2 mg kg^{-1} per day, maximum dose 60 mg daily, for 1 week with a 3–4 week taper) can be effective. Although tamponade is rare, patients may require pericardiocentesis, and pericardiectomy in those with recurrent effusions [37].

Autoimmune and connective tissue diseases

Pericarditis and pericardial effusions occur in many autoimmune and connective tissue diseases. Approximately 25% of patients with systemic lupus erythematosus and 10% with juvenile rheumatoid arthritis develop pericarditis. Less common causes include dermatomyositis, periarteritis nodosa, mixed connective tissue disease, Wegener granulomatosis, Takayasu arteritis, inflammatory bowel disease, and spondyloarthropathies. Oral NSAIDs are effective treatment. Pericardiocentesis may be needed [38]. Short courses of steroids may also assist in resolving symptoms [39]. Pericarditis may develop in patients with acute rheumatic fever [40] (see Chapters 61 and 62).

Recurrent and chronic pericarditis

Recurrent pericarditis is intermittent pericardial inflammation due to relapsing of the underlying disease, or reaccumulation of pericardial fluid after discontinuing medical therapy [41]. It occurs most commonly with postpericardiotomy syndrome, juvenile rheumatoid arthritis, or systemic lupus erythematosus. Treatment includes NSAIDs, colchicine, and oral steroids. Patients improve with immune modulators including azathioprine and cyclophosphamide. Pericardiectomy may be performed for numerous recurrences.

Chronic pericarditis refers to symptoms lasting >3 months, typically with heart failure or systemic inflammatory disease (see above). Standard medical and surgical treatment is used for symptomatic patients [42]. Intravenous immunoglobulin has been used with encouraging results.

Congenital abnormalities of the pericardium

Absence of the pericardium

Complete or partial absence of the pericardium is rare, and usually identified incidentally at autopsy or surgery. Most patients with partial absence have a left-sided defect [43]. One-third of patients have an associated cardiac or pulmonary (sequestration, or bronchogenic cyst) anomaly. Although typically asymptomatic, patients may have nonspecific symptoms including chest pain, lightheadedness, or dyspnea. Sudden death due to herniation of the left atrium, left atrial appendage, or right atrium through the defect is rare [43]. Compression of a coronary artery and torsion of the great vessels may also occur.

Physical examination is nonspecific, but may demonstrate a leftward shift of the apical impulse. Chest radiography reveals leftward shift of the heart. Echocardiography will not delineate the exact diagnosis, but may show unusual scanning windows, cardiac hypermobility, and abnormal ventricular motion [44]. The entire heart is shifted to the left, and thus the right ventricular cavity appears enlarged from the standard parasternal windows [8]. CT and MRI are diagnostic because they can delineate the absence of pericardial tissue [11].

Treatment depends on symptoms and the defect's anatomy. In patients with herniation of atrial tissue, or a small defect where future herniation is possible, surgical repair is indicated [43]. The defect can be either closed or enlarged. Complete absence of the pericardium usually causes no symptoms and requires no treatment.

Pericardial cysts

These are congenital anomalies resulting from failure of fetal lacunae to coalesce into the pericardial coelom. Most patients are asymptomatic, and cysts are usually discovered
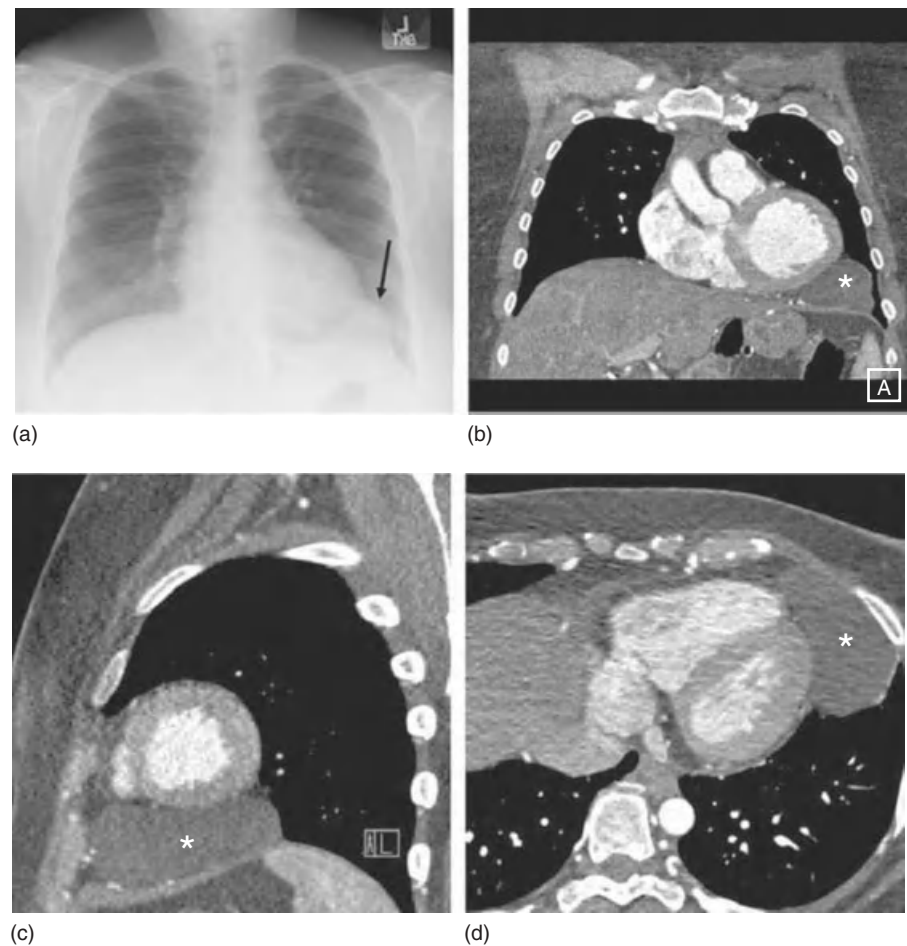
Figure 59.11 Chest radiography (a) and computed tomography scans (b–d) of a patient with a coarctation of the aorta and incidentally discovered pericardial cyst (arrow, *).

incidentally on chest radiography. They can occur anywhere on the pericardium, and can become infected or compress bronchi. Rarely, patients present with chest pain, dyspnea, or cough [45]. Due to the benign nature of the lesion, no treatment is indicated. Because they present as a thoracic mass, neoplasm or infection must be excluded. CT and MRI help confirm the diagnosis (Figure 59.11) [11]. On echocardiogram, they appear as echo-free spaces adjacent to the heart (Videoclip 59.3).

Constrictive pericarditis

Constrictive pericarditis is characterized by a thickened and fibrotic pericardium that restricts ventricular filling (Figure 59.12). Calcification of the pericardium occurs in only 25% of patients [8]. The constrictive process usually involves the entire pericardium, but focal constriction occurs. Constrictive pericarditis may develop without obvious cause or as the end-stage of any form of pericarditis [46]. In some patients with bacterial or viral pericarditis, a transient form of constriction has occurred with eventual resolution [47].
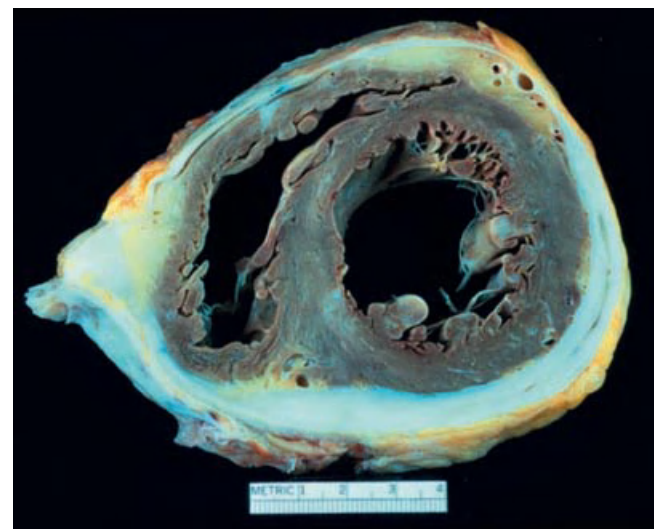
Figure 59.12 Severe constrictive pericarditis. Note the markedly thickened pericardium in this ventricular short-axis slice. (Courtesy of Dr. William D. Edwards, Division of Anatomic Pathology, Mayo Clinic, Rochester, MN, USA.)
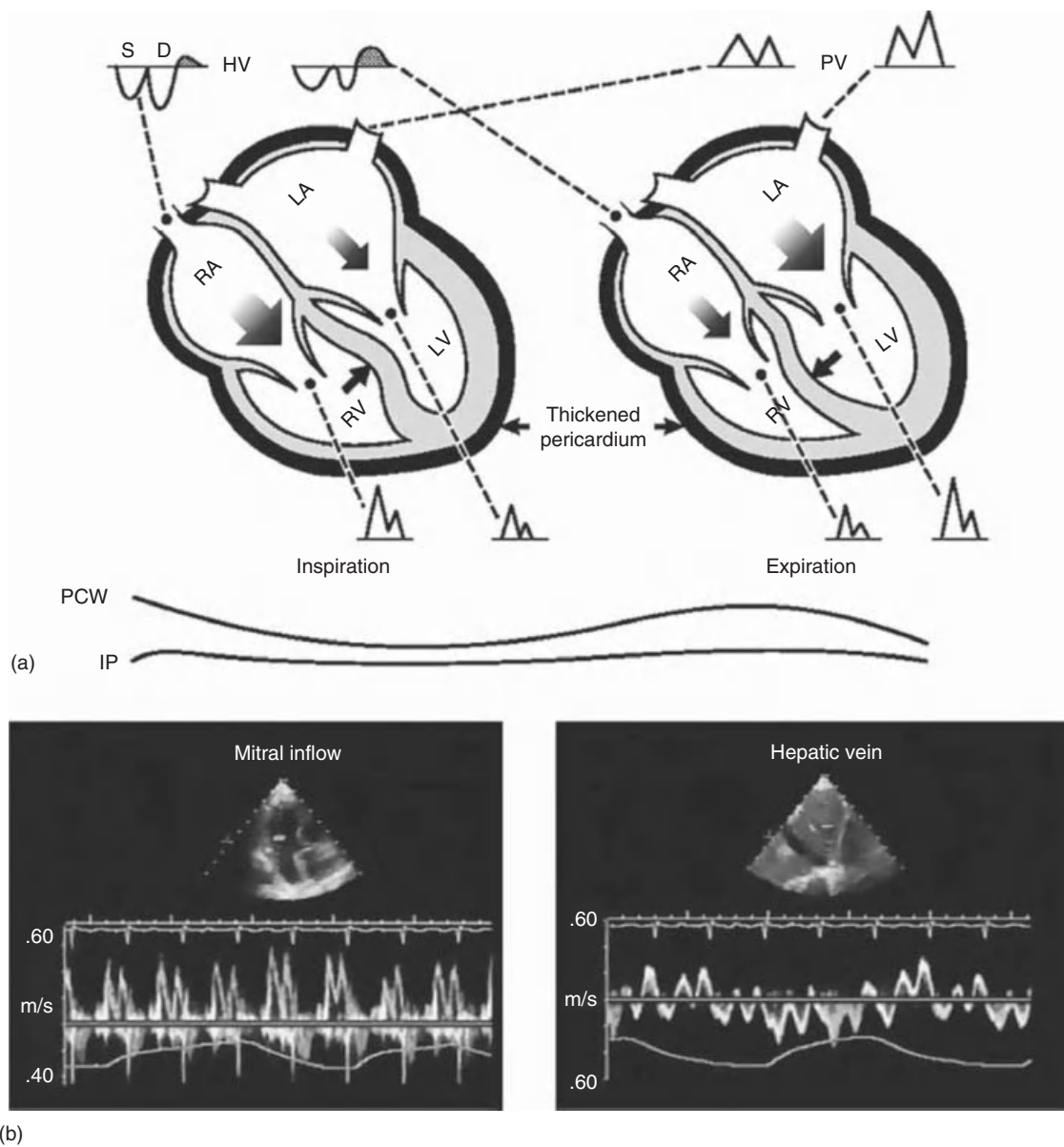
Figure 59.13 Hemodynamic filling patterns in constriction. (a) These diagrams illustrate a patient with constrictive pericarditis and (b) the corresponding Doppler echocardiographic patterns with inspiration and expiration. Bottom line on echocardiograms is a respiration trace, with inspiration shown by a rising line. Mitral inflow signals vary with respiration, with increased flow velocities on inspiration compared to expiration. Conversely, with inspiration, increased right ventricular filling causes hepatic vein diastolic forward flow to increase. In expiration, hepatic vein diastolic forward flow decreases, and significant flow reversals in diastole may be present. The width of the shaded arrows indicates relative flow. HV, hepatic vein; IP, intrapleural pressure; LA, left atrium; LV, left ventricle; PCW, pulmonary capillary wedge pressure; PV, pulmonary vein; RA, right atrium; RV, right ventricle. (Adapted from Oh *et al.*, *The Echo Manual*, with permission from Lippincott Williams & Wilkins.)

With constriction, ventricular systolic function generally remains normal, but diastolic expansion of the ventricles is limited. Early diastolic filling is normal, but mid and late diastolic filling are limited. Pulmonary wedge and central venous pressures are increased secondary to elevated filling pressures [48]. Patients complain of exercise intolerance, dyspnea, fatigue, weight gain, or syncope. Physical examination demonstrates hepatomegaly, splenomegaly, jugular venous distension, edema, or ascites.

During auscultation, one may hear a precordial knock, a diastolic filling sound corresponding to abrupt cessation of ventricular filling.

Chest radiography may be normal, or demonstrate pericardial calcification (~25%) (Figure 59.3). The electrocardiogram is nonspecific, but may show low-voltage QRS complexes and abnormal ST segments or T-waves. Echocardiography reveals paradoxical septal motion with a septal "bounce." Both vena cavae may be dilated. Doppler

500 ms

Figure 59.14 Catheterization tracing of a patient with constriction physiology. Note the equalization of LVEDP and RVEDP, creating the "square root sign" (**). Ao, Aorta; LV, left ventricle; RV, right ventricle. X axis is time, and Y axis is pressure in mmHg.
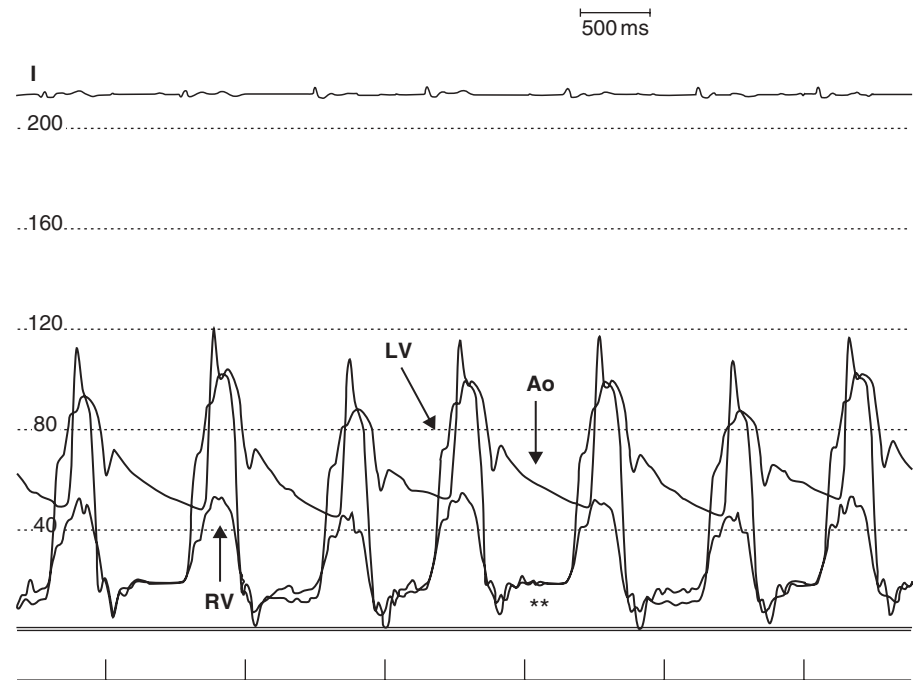
Table 59.4 Differentiating constrictive pericarditis and restrictive cardiomyopathy.

Finding[a]	Constriction	Restriction
Echo: septal "bounce"	Common	Typically absent
Echo: atrial size	Normal or mildly enlarged	Significantly enlarged
Echo: systolic function	Typically normal	Normal or mildly decreased
Echo: wall thickness	Normal	Normal or increased
Echo: Doppler changes with inspiration/expiration	Significant and common	Rarely occurs
CT: pericardial thickening	Common	Typically absent
Catherization: RVSP	<50 mmHg	>50 mmHg
Catherization: LVEDP – RVEDP	<4 mmHg	>4 mmHg
Catherization: wedge pressure – RA pressure	<4 mmHg	>4 mmHg
Catherization: RVEDP/RVSP	>0.33	<0.3
Catherization: systolic area index	>1.1	<1.1
History of cardiac surgery	Common	Uncommon

[a]RVSP, right ventricular systolic pressure; RVEDP, right ventricular end-diastolic pressure; LVEDP, left ventricular end-diastolic pressure; RA, right atrium.

echocardiography shows significant respiratory variation of both left- and right-sided flows (Figure 59.13) [49]. With inspiration, there is an exaggerated decrease in the mitral inflow velocity and an exaggerated increase in tricuspid inflow velocity (tricuspid E velocity) [49]. CT and MRI may reveal thickening and calcification of the pericardium [11]. Cardiac catheterization demonstrates equalization of left and right ventricular end-diastolic pressures, left and right atrial mean pressures, and mean pulmonary capillary wedge pressure. The "square root sign" may be noted, describing the early diastolic drop in pressure followed by a plateau phase, secondary to rapid early diasto-

lic filling with abrupt cessation (Figure 59.14). Definitive treatment is total pericardiectomy, which is safe and effective in children [42].

Differentiating constrictive pericarditis and restrictive cardiomyopathy

Restrictive cardiomyopathy is typically caused by an infiltrative process, including amyloidosis, hemochromatosis, endomyocardial fibrosis, and eosinophilic cardiomyopathy. It may be idiopathic [50]. Because it also is characterized by significantly abnormal diastolic function and preserved systolic function, differentiation from constrictive pericarditis is

(a)

(b)
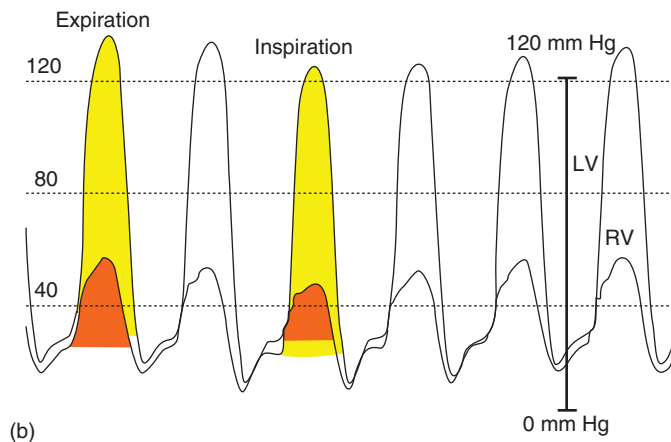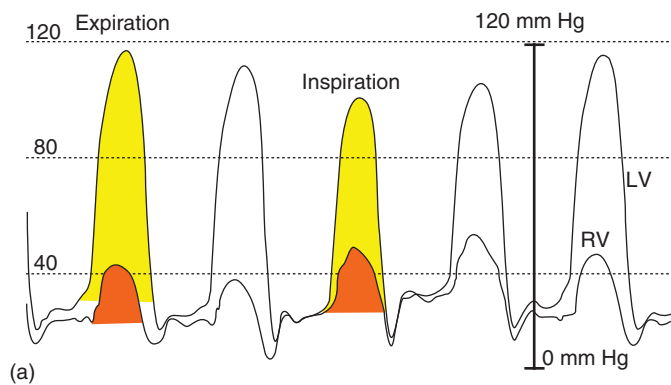
Figure 59.15 Catheterization tracings in constrictive physiology (a) and restrictive cardiomyopathy (b). Note that both patients have early rapid filling and elevation and end-equalization of the left ventricular (LV) and right ventricular (RV) pressures at end expiration. In constrictive pericarditis, there is an inspiratory increase in the area of the RV pressure curve (orange shaded area) compared with expiration. The area of the LV pressure curve (yellow shaded area) decreases during inspiration as compared with expiration. In restrictive cardiomyopathy, there is an inspiratory decrease in the area of the RV pressure curve (orange shaded area) as compared with expiration. The area of the LV pressure curve (yellow shaded area) is unchanged during inspiration as compared with expiration. (Adapted from Talreja et al. [48] with permission from Elsevier.)
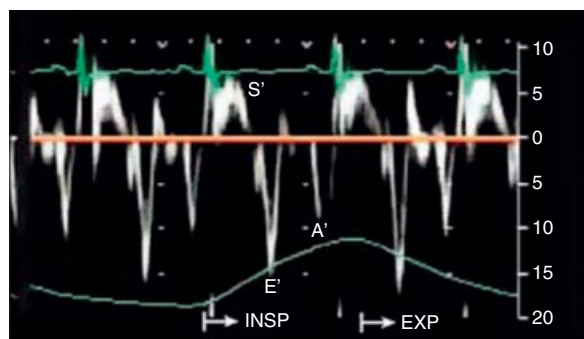
(a)
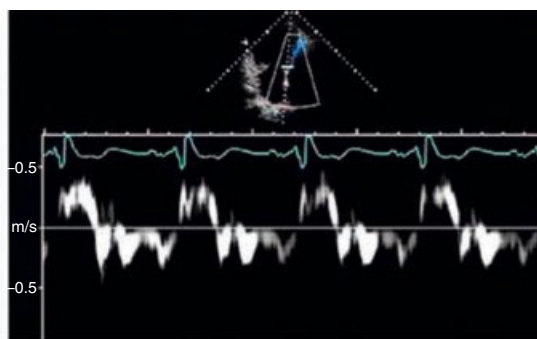
(b)
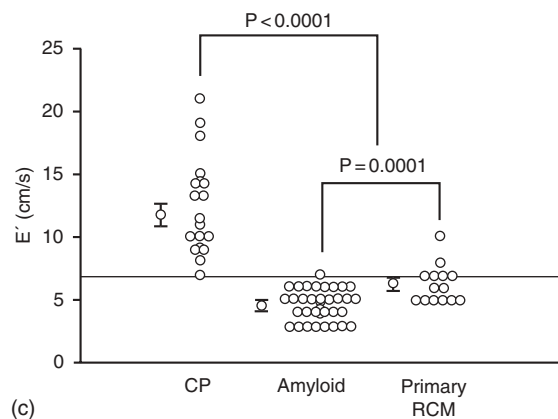
(c)

Figure 59.16 Tissue Doppler imaging of the septal mitral annulus in (a) constriction and (b) restriction. Note the relative normal or increased mitral septal annulus velocity (E′ velocity) in constriction, compared to the decreased E′ velocity seen in restriction. When comparing constriction with amyloidosis and restrictive cardiomyopathy in adults (c), there is a clear differentiation between the average E′ velocities. (Adapted with permission from Ha JW et al. *Am J Cardiol* 2004;**94**:316–19.)
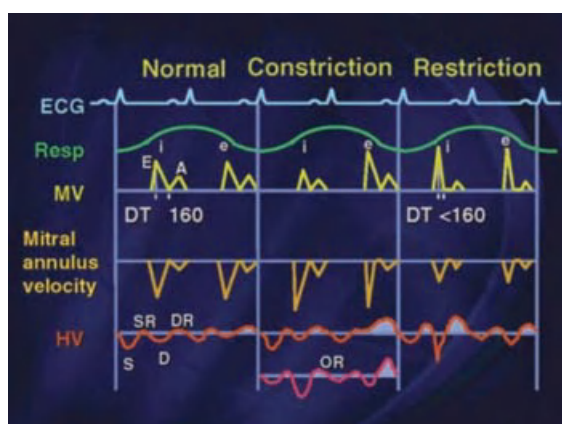
Figure 59.17 Diagram of Doppler velocities from mitral inflow (MV), mitral annulus velocity, and hepatic vein (HV) and the ECG and respirometer recordings indicating inspiration (i) and expiration (e). D, diastolic flow; DR,diastolic flow reversal; DT, deceleration time; S, systolic flow; SR,systolic flow reversal; blackened areas under curve, flow reversal. Typically, mitral inflow has respiratory variation, but not always. (Adapted from Oh *et al.*, *The Echo Manual*, 2006, with permission from Lippincott Williams & Wilkins.)

difficult [48]. Differentiation is important, as the definitive treatments for these disorders are disparate (pericardiectomy versus transplant). A list of potential differentiating factors is shown in Table 59.4.

A recently proposed catheterization-based method of differentiation involves calculating the *systolic area index*, defined as the ratio of the area under the right ventricular pressure curve to the area under the left ventricular pressure curve in inspiration versus expiration (Figure 59.15). A systolic area index value >1.1 was found to be 97% sensitive and 100% specific for diagnosing constrictive pericarditis [48]. This study was performed only in adults, and requires validation in children, who have different heart rate, respiratory rate, and filling pressures.

Echocardiographic differentiation between constrictive pericarditis and restrictive physiology includes those factors listed in Table 59.4. Visualization of the septal "bounce" is more common in constriction, whereas significant atrial enlargement is more common in restriction. Doppler velocities, including mitral inflow, tricuspid inflow, and pulmonary venous inflow, are affected by respiration in constriction. With inspiration, decreased left ventricular filling allows increased right ventricular filling, which causes hepatic vein diastolic forward flow to increase (Figure 59.13). In expiration, hepatic vein diastolic forward flow decreases, and significant flow reversals in diastole may occur. The use of a respirometer during the echocardiogram is critical in timing the flow patterns. Patients with restriction rarely present with such respiration-induced changes in Doppler velocities. Tissue Doppler imaging can also be helpful. The early diastolic septal mitral annulus velocity (E' velocity) tends to be higher in patients with constriction, often greater than $8\,cm\,s^{-1}$

(Figure 59.16). A reduced E' velocity is seen in restrictive cardiomyopathy, similar to other cardiomyopathies [8]. Figure 59.17 shows Doppler velocities from mitral inflow (MV), mitral annulus velocity, and hepatic vein (HV) and the ECG and respirometer recordings.

References

1 Spodick DH. Macrophysiology, microphysiology, and anatomy of the pericardium: a synopsis. *Am Heart J* 1992;**124**:1046–51.

2 Lange RA, Hillis LD. Clinical practice. Acute pericarditis. *N Engl J Med* 2004;**351**:2195–202.

3 Jacob S, Sebastian JC, Cherian PK, *et al.* Pericardial effusion impending tamponade: a look beyond Beck's triad. *Am J Emerg Med* 2009;**27**:216–9.

4 Spodick DH, The electrocardiogram in acute pericarditis. In: Spodick DH, ed. *Acute Pericarditis*. New York: Grune & Stratton, 1959: 17.

5 Maisch B, Seferovic PM, Ristic AD, *et al.* Guidelines on the diagnosis and management of pericardial diseases: executive summary; The Task Force on the Diagnosis and Management of Pericardial Diseases of the European Society of Cardiology. *Eur Heart J* 2004;**25**:587–610.

6 Pepi M, Muratori M. Echocardiography in the diagnosis and management of pericardial disease. *J Cardiovasc Med (Hagerstown)* 2006;**7**:533–44.

7 Slesnick TC, Ayres NA, Altman CA, *et al.* Characteristics and outcomes of fetuses with pericardial effusions. *Am J Cardiol* 2005;**96**:599–601.

8 Grogan M, Oh JK. Pericardial disorders. In: Eidem BW, Cetta F, O'Leary PW, eds. *Echocardiography in Pediatric and Adult Congenital Heart Disease*. Philadelphia: Lippincott Williams & Wilkins, 2010: 330–341.

9 Leeman DE, Levine MJ, Come PC. Doppler echocardiography in cardiac tamponade: exaggerated respiratory variation in transvalvular blood flow velocity integrals. *J Am Coll Cardiol* 1988;**11**:572–8.

10 Golinko RJ, Kaplan N, Rudolph AM. The mechanism of pulsus paradoxus during acute pericardial tamponade. *J Clin Invest* 1963;**42**:249–57.

11 Wang ZJ, Reddy GP, Gotway MB, *et al.* CT and MR imaging of pericardial disease. *Radiographics* 2003;**23**(Special Issue):S167–80.

12 Tsang TS, El-Najdawi EK, Seward JB, *et al.* Percutaneous echocardiographically guided pericardiocentesis in pediatric patients: evaluation of safety and efficacy. *J Am Soc Echocardiogr* 1998;**11**:1072–7.

13 Callahan JA, Seward JB, Nishimura RA, *et al.* Two-dimensional echocardiographically guided pericardiocentesis: experience in 117 consecutive patients. *Am J Cardiol* 1985;**55**:476–9.

14 Mayosi BM, Burgess LJ, Doubell AF. Tuberculous pericarditis. *Circulation* 2005;**112**:3608–16.

15 Piehler JM, Pluth JR, Schaff HV, *et al.* Surgical management of effusive pericardial disease. Influence of extent of pericardial resection on clinical course. *J Thorac Cardiovasc Surg* 1985;**90**:506–16.

16 Fujioka S, Koide H, Kitaura Y, *et al.* Molecular detection and differentiation of enteroviruses in endomyocardial biopsies and pericardial effusions from dilated cardiomyopathy and myocarditis. *Am Heart J* 1996;**131**:760–5.

17 Feldman WE. Bacterial etiology and mortality of purulent pericarditis in pediatric patients. Review of 162 cases. *Am J Dis Child* 1979;**133**:641–4.

18 Roodpeyma S, Sadeghian N. Acute pericarditis in childhood: a 10-year experience. *Pediatr Cardiol* 2000;**21**:363–7.

19 Pankuweit S, Ristic AD, Seferovic PM, Maisch B. Bacterial pericarditis: diagnosis and management. *Am J Cardiovasc Drugs* 2005;**5**:103–12.

20 Cakir O, Gurkan F, Balci AE, *et al*. Purulent pericarditis in childhood: ten years of experience. *J Pediatr Surg* 2002;**37**:1404–8.

21 Starc TJ, Lipshultz SE, Kaplan S, *et al*. Cardiac complications in children with human immunodeficiency virus infection. Pediatric Pulmonary and Cardiac Complications of Vertically Transmitted HIV Infection (P2C2 HIV) Study Group, National Heart, Lung, and Blood Institute. *Pediatrics* 1999;**104**:e14.

22 Renfrew R, Buselmeier TJ, Kjellstrand CM. Pericarditis and renal failure. *Annu Rev Med* 1980;**31**:345–60.

23 Newburger JW, Takahashi M, Gerber MA, *et al*. Diagnosis, treatment, and long-term management of Kawasaki disease: a statement for health professionals from the Committee on Rheumatic Fever, Endocarditis and Kawasaki Disease, Council on Cardiovascular Disease in the Young, American Heart Association. *Circulation* 2004;**110**:2747–71.

24 Rheuban KS. Pericarditis. *Curr Treat Options Cardiovasc Med* 2005;**7**:419–27.

25 Schoenwetter AH, Siber EN. Penicillin hypersensitivity, acute pericarditis, and eosinophilia. *JAMA* 1965;**191**:672–3.

26 Slater EE. Cardiac tamponade and peripheral eosinophilia in a patient receiving cromolyn sodium. *Chest* 1978;**73**:878–9.

27 Chou SL, Chern CH, How CK, *et al*. A rare case of massive pericardial effusion secondary to hypothyroidism. *J Emerg Med* 2005;**28**:293–6.

28 Campbell RM, Benson LN, Williams WW, Adatia I. Chylopericardium after cardiac operations in children. *Ann Thorac Surg* 2001;**72**:193–6.

29 Helin RD, Angeles ST, Bhat R. Octreotide therapy for chylothorax in infants and children: a brief review. *Pediatr Crit Care Med* 2006;**7**:576–9.

30 Lam KY, Dickens P, Chan AC. Tumors of the heart. A 20-year experience with a review of 12,485 consecutive autopsies. *Arch Pathol Lab Med* 1993;**117**:1027–31.

31 Snyder SN. Massive pericardial coelomic cyst. Diagnostic features and unusual presentation. *Chest* 1977;**71**:100–2.

32 Pratt JW, Cohen DM, Mutabagani KH, *et al*. Neonatal intrapericardial teratomas: clinical and surgical considerations. *Cardiol Young* 2000;**10**:27–31.

33 Lee PJ, Mallik R. Cardiovascular effects of radiation therapy: practical approach to radiation therapy-induced heart disease. *Cardiol Rev* 2005;**13**:80–6.

34 Clapp SK, Garson A Jr, Gutgesell HP, *et al*. Postoperative pericardial effusion and its relation to postpericardiotomy syndrome. *Pediatrics* 1980;**66**:585–8.

35 Dressler W. A post-myocardial infarction syndrome; preliminary report of a complication resembling idiopathic, recurrent, benign pericarditis. *JAMA* 1956;**160**:1379–83.

36 Cabalka AK, Rosenblatt HM, Towbin JA, *et al*. Postpericardiotomy syndrome in pediatric heart transplant recipients. Immunologic characteristics. *Tex Heart Inst J* 1995;**22**:170–6.

37 Engle MA, Zabriskie JB, Senterfit LB, Ebert PA. Postpericardiotomy syndrome. A new look at an old condition. *Mod Concepts Cardiovasc Dis* 1975;**44**:59–64.

38 Brigden W, Bywaters EG, Lessof MH, Ross IP. The heart in systemic lupus erythematosus. *Br Heart J* 1960;**22**:1–16.

39 Yancey CL, Doughty RA, Cohlan BA, Athreya BH. Pericarditis and cardiac tamponade in juvenile rheumatoid arthritis. *Pediatrics* 1981;**68**:369–73.

40 Persellin ST, Ramirez G, Moatamed F. Immunopathology of rheumatic pericarditis. *Arthritis Rheum* 1982;**25**:1054–8.

41 Shabetai R. Recurrent pericarditis: recent advances and remaining questions. *Circulation* 2005;**112**:1921–3.

42 Thompson JL, Burkhart HM, Dearani JA, *et al*. Pericardiectomy for pericarditis in the pediatric population. *Ann Thorac Surg* 2009;**88**:1546–50.

43 Gatzoulis MA, Munk MD, Merchant N, *et al*. Isolated congenital absence of the pericardium: clinical presentation, diagnosis, and management. *Ann Thorac Surg* 2000;**69**:1209–15.

44 Connolly HM, Click RL, Schattenberg TT, *et al*. Congenital absence of the pericardium: echocardiography as a diagnostic tool. *J Am Soc Echocardiogr* 1995;**8**:87–92.

45 Satur CM, Hsin MK, Dussek JE. Giant pericardial cysts. *Ann Thorac Surg* 1996;**61**:208–10.

46 Strauss AW, Santa-Maria M, Goldring D. Constrictive pericarditis in children. *Am J Dis Child* 1975;**129**:822–6.

47 Haley JH, Tajik AJ, Danielson GK, *et al*. Transient constrictive pericarditis: causes and natural history. *J Am Coll Cardiol* 2004;**43**:271–5.

48 Talreja DR, Nishimura RA, Oh JK, Holmes DR. Constrictive pericarditis in the modern era: novel criteria for diagnosis in the cardiac catheterization laboratory. *J Am Coll Cardiol* 2008;**51**:315–9.

49 Oh JK, Hatle LK, Seward JB, *et al*. Diagnostic role of Doppler echocardiography in constrictive pericarditis. *J Am Coll Cardiol* 1994;**23**:154–62.

50 Cetta F, O'Leary PW, Seward JB, Driscoll DJ. Idiopathic restrictive cardiomyopathy in childhood: diagnostic features and clinical course. *Mayo Clin Proc* 1995;**70**:634–40.

60 Infective Endocarditis

Michael H. Gewitz[1] & Kathryn A. Taubert[2]

[1]Maria Fareri Children's Hospital and New York Medical College, Valhalla, NY, USA
[2]University of Texas Southwestern Medical School, Dallas, TX, USA and World Heart Federation, Geneva, Switzerland

Introduction

The evaluation and management of the child with infective endocarditis (IE) continues to be a challenge for pediatric cardiologists and other providers of children's healthcare.

IE is an infection of the endothelial (endocardial) surface of the heart and involves valvar structures, mural endocardium, or great vessels. It can complicate intracardiac patches, prostheses, central catheters, surgically constructed shunts and conduits, and indwelling devices of various types. IE is caused not only by bacteria but also by fungi, rickettsiae, and viruses. With current antimicrobial and surgical therapies, mortality rates have been reduced to 10–20%, although morbidity and long-term sequelae are serious issues for many more. Even in the current era of advanced imaging technology, surgical treatment, and expanding antibiotic capabilities, IE remains a serious disease.

Epidemiology

In most developed countries, including the United States, IE has historically been seen most often in patients with an underlying structural cardiac abnormality [1]. Recently, however, new data have indicated an emerging trend towards an increasing proportion of children admitted to hospital for IE without pre-existing heart abnormalities [2]. Reported hospitalization rates for IE continue to vary widely but remain at approximately one in every 1300–2000 admissions annually [2]. Regardless of the specific hospitalization rate, the frequency of IE in children appears to have increased over the past several decades. Reasons for this increase include [1]

- improved survival among children with congenital heart disease at risk for IE, including increased numbers of operations
- increased use of prosthetic materials and indwelling devices
- changing neonatal and pediatric intensive care unit practices
- intravenous drug abuse in specific age groups (adolescents).

In contrast, whereas almost 50% of cases of IE in developed countries occurred in children with rheumatic heart disease (RHD) before the 1970s, the decline of RHD prevalence in those areas means that it is now relatively unusual for IE to be associated with RHD. In still developing countries, however, RHD remains an important underlying substrate for IE. Pooled data from 20 published series concerning specific congenital cardiac abnormalities associated with IE are shown in Table 60.1.

All ages can be affected, although it has been estimated that 50% of occurrences are in children ≥10 years of age. In particular, IE occurrence appears to be increasing at both ends of the age spectrum of childhood. Premature neonates are increasingly reported with right-sided IE, for example, and this is often associated with central catheters and longer-term indwelling arterial lines [1,3,4,6]. Older teens and young adults with postoperative congenital heart disease represent an additional emerging population for the development of IE, as treatment advances have increased life expectancy and vigor of lifestyle for patients with even the most complex cardiovascular abnormalities.

Pathogenesis

For IE to develop, two independent events are normally required: damage to an area of endothelium, and bacteremia caused by organisms with adherence capacity. Normal intact

Table 60.1 Underlying heart disease in children with infective endocarditis.

Disease	No. of patients[a]	Percentage of total
Congenital heart disease		
Acyanotic heart lesions		
Ventricular septal defect	194	21.8
Ventricular septal defect and other	18	2.0
Patent ductus arteriosus	25	2.8
Aortic stenosis	89	10.0
Subvalvar aortic stenosis	9	1.0
Coarctation of aorta	25	2.8
Pulmonary stenosis	21	2.4
Atrioventricular defect	16	1.8
Atrial septal defect	11	1.2
Mitral valve abnormality	16	1.8
Mitral valve prolapse	8	0.9
Cyanotic heart lesions		
Tetralogy of Fallot	143	16.0
Transposition of great vessels	35	3.9
Truncus arteriosus	8	0.9
Tricuspid atresia	9	1.0
Pulmonary atresia	8	0.9
Single ventricle	9	1.0
Other	79	8.9
Rheumatic heart disease	86	9.7
No heart disease	75	8.4

[a]Total 884 patients.

Source: Berkowitz, *Critical Heart Disease in Infants and Children*. St Louis, MO: Mosby-Year Book, 1995:961–86.

endothelium is not conducive to bacterial colonization. Endothelium is typically damaged by an abnormally high velocity jet stream that results in turbulent blood flow. A classic model developed by Rodbard [7] to delineate the hemodynamic mechanisms responsible for the development of endocarditis showed that endothelial damage and bacterial deposition can occur in a low-pressure area immediately distal to an obstruction. Examples of such physiology include coarctation of the aorta, regurgitant mitral or aortic valve, or ventricular septal defect. Thus, endothelium on the ventricular side of a regurgitant aortic valve would be damaged, and the right ventricular free wall (or right-sided heart valves) would be damaged from the jet created by a ventricular septal defect. Endothelium can also be damaged by direct trauma from intracardiac devices, such as an indwelling catheter, or from an intracardiac operation.

Trauma to the endothelium can induce thrombogenesis (deposition of fibrin and platelets), which leads to a sterile lesion known as *nonbacterial thrombotic endocarditis (NBTE)*.

This lesion is more receptive than normal undamaged endothelium to colonization by bacteria and serves as a nidus for subsequent infection. After bacteremia with an organism that can adhere to the NBTE, a vegetation forms. Certain bacteria are more likely than others to adhere and are also more able to avoid eradication by the host's defenses [8]. The adherence of streptococci may be related in part to the extracellular production of the polysaccharide dextran, which facilitates adherence [9]. The vegetation itself is composed of fibrin, platelets, red blood cells, white blood cells, and the microorganisms, which can grow to a concentration that is achievable in pure culture in a Petri dish.

Microbiology

Most instances of endocarditis are caused by a limited number of microorganisms. The most logical explanation relates to bacterial adherence. An *in vitro* study demonstrated that bacteria frequently responsible for endocarditis, such as viridans streptococci, readily adhere to canine or human cardiac valves, whereas Gram-negative organisms, which infrequently cause endocarditis, adhere poorly to valves [8].

In most series of endocarditis in children, Gram-positive cocci account for at least two-thirds of recoverable bacteria. Table 60.2 summarizes data from representative series outlining the organisms associated with IE in children [1]. Viridans streptococci were the largest group responsible for endocarditis in these specifically pediatric series. Staphylococci (*Staphylococcus aureus* and coagulase-negative staphylococci) were the second largest group. Gram-negative organisms less frequently cause endocarditis in children. Neonates, immunocompromised patients, and intravenous drug abusers, however, are at an increased risk for Gram-negative bacterial endocarditis. The slow-growing fastidious Gram-negative bacilli in the HACEK group (*Haemophilus*, *Actinobacillus*, *Cardiobacterium*, *Eikenella*, *Kingella*) can also cause endocarditis in children. They frequently affect damaged cardiac valves and often cause emboli. Other Gram-negative bacilli, such as *Neisseria gonorrhoeae*, can cause endocarditis presenting as an acute illness, affecting previously normal valves, and commonly resulting in valvar destruction. In intravenous drug abusers, the most commonly isolated organism is *S. aureus*. Other organisms include *Pseudomonas* and other Gram-negative bacilli and fungi (predominantly *Candida* species) [10].

In prosthetic valve endocarditis (PVE), the organisms differ according to whether endocarditis occurs within the first year after operation or later. Infection during the first year is primarily due to coagulase-negative staphylococci acquired during the operative procedure or nosocomially acquired [14]. *S. aureus*, Gram-negative bacilli, diphtheroids, and *Candida* species are also common causes of PVE during this period. The coagulase-negative staphylococci recovered

Table 60.2 Principal etiologic bacterial agents (%).

Organism	Series[a]		
	Johnson *et al.* [11]	Martin *et al.* [12]	Stockheim *et al.* [13]
	N = 149	*N* = 76	*N* = 111
Viridans group streptococci	43	38	32
Staphylococcus aureus	33	32	27
Coagulase-negative staphylococci	2	4	12
Streptococcus pneumoniae	3	4	7
HACEK	N/A	5	4
Enterococcus species	N/A	7	4
Culture-negative	6	7	5

[a]N/A, not applicable.

Source: Ferrieri *et al. Pediatrics* 2002;**109**:931–43.

within the first year of operation are frequently resistant to methicillin and all other β-lactams. In contrast, infection occurring more than 1 year after operation is caused by organisms similar to those present in native valve endocarditis [14].

Fungal endocarditis is relatively unusual in children and has a high morbidity and mortality even with intensive treatment [15–17]. It is difficult to diagnose and treat, and complications, especially embolization, are frequent [18]. The most frequently recovered fungal organism is *Candida albicans*; other organisms include *Aspergillus* species, *Torulopsis glabrata*, other *Candida* species, and other fungi [17,18]. Fungal endocarditis occurs in intravenous drug abusers and patients undergoing cardiac valve replacement, and also in immunocompromised patients and in neonates. In neonates, fungal endocarditis may be a complication of prolonged use of indwelling venous catheters, prolonged hyperalimentation, and broad-spectrum antibiotic use [19–21].

In the series in Table 60.2, ~5–7% of instances of endocarditis were culture-negative. There are many possible reasons for failure to recover organisms in apparent IE, particularly previous treatment with antibiotics [22]. However, when cultures are negative, physicians should carefully evaluate such patients for the possibility of other diseases (see the section on culture-negative endocarditis below).

Diagnosis

Criteria for the clinical diagnosis of IE have been developed over the years. In 1994, criteria were developed by Durack *et al.* [23] at Duke University. These so-called "Duke criteria" are listed in Table 60.3 and defined in Table 60.4. There are

Table 60.3 Duke criteria for diagnosis of infective endocarditis.

Definite infective endocarditis

Pathologic criteria

Microorganisms: demonstrated by culture or histology in a vegetation, or in a vegetation that has embolized, or in an intracardiac abscess, *or*

Pathologic lesions: vegetation or intracardiac abscess present, confirmed by histology showing active endocarditis

Clinical criteria, using specific definitions listed in Table 60.4

2 major criteria, *or*

1 major and 3 minor criteria, *or*

5 minor criteria

Possible infective endocarditis

Findings consistent with infective endocarditis that fall short of "definite" but not "rejected"

Rejected

Firm alternative diagnosis for manifestations of endocarditis, *or*

Resolution of manifestations of endocarditis, with antibiotic therapy for 4 days or less, *or*

No pathologic evidence of infective endocarditis at surgery or autopsy, after antibiotic therapy for 4 days or less

Reproduced with permission from Durack *et al. Am J Med* 1994;**96**:200–9.

two major criteria and six minor criteria. There are three diagnostic categories: definite, possible, and rejected. The clinical criteria can be used to establish a definitive diagnosis of IE when two major criteria, one major plus three minor criteria, or five minor criteria are met. The Duke criteria are effective in establishing a diagnosis of IE in both adults [24] and children [13].

Table 60.4 Definitions of terms used in the Duke criteria for the diagnosis of infective endocarditis[a].

Major criteria

1. Positive blood culture for IE
   - A. Typical microorganism consistent with IE from two separate blood cultures as noted below:
     - i. viridans streptococci[b], *Streptococcus bovis,* or HACEK group *or*
     - ii. community-acquired *Staphylococcus aureus* or enterococci, in the absence of a primary focus
   - B. Microorganisms consistent with IE from persistently positive blood cultures defined as
     - i. at least two positive cultures of blood samples drawn ≥12 h apart *or*
     - ii. all of three or a majority of four or more separate cultures of blood (with first and last sample drawn at least 1 h apart)
2. Evidence of endocardial involvement
   - A. Positive echocardiogram for IE defined as
     - i. oscillating intracardiac mass on valve or supporting structures, in the path of regurgitant jets, or on implanted material in the absence of an alternative anatomic explanation, *or*
     - ii. myocardial abscess, *or*
     - iii. new partial dehiscence of prosthetic valve
   - B. New valvar regurgitation (worsening or changing of pre-existing murmur not sufficient)

Minor criteria

1. Predisposition: predisposing heart condition or intravenous drug use
2. Fever: temperature ≥38.0 °C
3. Vascular phenomena: major arterial emboli, septic pulmonary infarcts, mycotic aneurysm, intracranial hemorrhage, conjunctival hemorrhages, and Janeway's lesions
4. Immunologic phenomena: glomerulonephritis, Osler's nodes, Roth's spots, and rheumatoid factor
5. Microbiologic evidence: positive blood culture but does not meet a major criterion as noted in Table 60.3[c] or serologic evidence of active infection with organism consistent with IE
6. Echocardiographic findings: consistent with IE but do not meet a major criterion above

[a]HACEK: *Haemophilus* species, *Actinobacillus actinomycetemcomitans*, *Cardiobacterium hominis*, *Eikenella* species, and *Kingella kingae*. IE, infective endocarditis.
[b]Includes nutritional variant strains.
[c]Excludes single positive cultures for coagulase-negative staphylococci and organisms that do not cause endocarditis.
Reproduced with permission from Durack *et al. Am J Med* 1994;**96**:200–9.

Clinical features

Symptoms of endocarditis usually arise within 2 weeks of the initiating bacteremia [25]. They are usually related to cardiac complications caused by the infection, persistent bacteremia, systemic embolization, or immunopathologic reactions by the patient. Endocarditis can mimic many disorders, including other infectious diseases, lymphoma, leukemia, and connective tissue diseases. Endocarditis should be part of the differential diagnosis in any patient with an underlying cardiac abnormality who has unexplained fever or who has another unusual illness that could be related to endocarditis.

Clinical findings in IE stem from the underlying principle disorders: microbial blood-borne infections, valvitis, immunologic responses, and peripheral embolic events.

Fever is the most common finding in patients with endocarditis, with the exception of neonates. Fever is frequently low grade, reaching a maximum temperature of 39 °C. In endocarditis caused by virulent bacteria such as *S. aureus*, however, there can be a spiking high fever. Other nonspecific symptoms include myalgia, arthralgia, anorexia, night sweats, headache, and malaise. Because initial symptoms are usually mild, the diagnosis of IE is often not made until 2–4 weeks after the infection starts. By this time, vegetations are well established and may be difficult to eradicate.

New or changing cardiac murmurs are usually heard in patients with valvar involvement but auscultatory findings in general depend on the specifics of the underlying heart disease and the location of the infection. Murmurs may not be heard at the initial examination. Frequent auscultation is essential because it may be difficult to recognize a new or changing murmur in a patient with a pre-existing cardiac abnormality and because vegetation pathology can be dynamic. Careful and frequent auscultation is necessary to assist not only with the diagnosis but also with the patient's medical or operative management. In some patients, notably those with complex cyanotic congenital heart disease post-systemic–pulmonary shunt creation, no change in murmur may be detected. A declining systemic saturation reflecting graft infection and/or pulmonary emboli may be the first apparent clinical sign.

The classic peripheral manifestations of endocarditis may be less frequent today than reported in the past and are often absent in endocarditis involving the tricuspid valve. *Petechiae* are the most common but least specific manifestations and are found on the palpebral conjunctiva, the buccal and palatal mucosa, and the extremities. *Splinter hemorrhages*, which resemble a splinter caught in the nail bed, are also a nonspecific finding in endocarditis. They are more helpful diagnostically if they are present in the proximal rather than the distal nail bed. *Osler's nodes* are small, tender, purple, subcutaneous nodules that develop in the digits and persist for hours or days. They are not pathognomonic and may be seen in other disorders, such as systemic lupus erythematosus and disseminated gonococcal infections. *Janeway's lesions* are small, erythematous or hemorrhagic, macular lesions on the palms and soles; unlike Osler's nodes, they are not tender. *Roth's spots* (also known as Litten's sign) are oval retinal hemorrhages with pale centers and are relatively rare.

Neurologic manifestations are found in ~20% of children with endocarditis [5]. They are associated with increased mortality and are more frequent in patients with *S. aureus* endocarditis. Neurologic complications include cerebral emboli, mycotic aneurysms, cerebritis, brain abscess, cerebral hemorrhage, and, less commonly, meningitis.

Embolic manifestations occur in some children with endocarditis, usually in association with infections that produce large, bulky vegetations. Clinically recognized emboli are found most commonly in the pulmonary or cerebral circulations. Endocarditis involving the left side of the heart often results in peripheral embolization, leading to ischemia, infarction, or mycotic aneurysms (aneurysms caused by growth of the organism in a vessel wall). Specific clinical findings depend on the localization of the emboli. Mycotic aneurysms may be silent but can rupture or thrombose weeks or months after IE has been cured. Embolization from the right side may be no less frequent, but such emboli are less easily appreciated clinically because of filtration by the lungs. Sometimes they cause an erroneous diagnosis of pneumonitis. Large, infected emboli may complicate endocarditis of the tricuspid valve, primarily in infants with IE secondary to indwelling catheters and in intravenous drug users. Embolic events are often an indication for surgical intervention. Table 60.5 reviews complications associated with the need for surgery.

Renal involvement occurs in some patients with endocarditis. Although overt renal dysfunction is usually secondary to hemodynamic changes, renal emboli may be asymptomatic or cause flank pain, may result in gross or microscopic hematuria, but rarely cause significant renal dysfunction. Renal insufficiency may also occur from immune complex glomerulonephritis, particularly in patients with endocarditis caused by less virulent bacteria, such as coagulase-negative staphylococci. Azotemia may result from immune complex nephritis, but it usually improves after appropriate antimicrobial therapy.

Table 60.5 Complications of IE indicating possible surgical therapy.

Related to vegetation
- Recurrent embolization despite antibiotics.
- Persistence of vegetation despite treatment.
- Anterior mitral leaflet lesion >10 mm in size.
- Increasing vegetation size on appropriate antibiotics.

Related to cardiac function.
- Acute severe mitral and/or aortic insufficiency with ventricular failure.
- Heart failure despite appropriate therapy.
- Valve rupture/perforation with chamber enlargement.

Extension of infection
- New heart block.
- Myocardial abscess proliferation on appropriate antibiotics.
- Valvar annulus abscess development.

Splenomegaly has been reported in 15–50% of patients with IE, but appears to be a less common finding in recent reports compared with earlier era case series.

In neonates, the clinical findings of IE may completely mimic other common syndromes such as septicemia or congestive heart failure from other etiologies [3,6]. Respiratory distress, hypothermia, tachycardia, hypotension, and new feeding difficulty may be the initial manifestations. A new murmur may, of course, follow; but often no murmur is present at all, especially in IE associated with indwelling central line infection. Peripheral emboli resulting in meningitis or osteomyelitis are not uncommon and neonates seem particularly prone to neurologic complications, including apnea and seizures.

Laboratory features

Blood cultures

A positive blood culture is a valuable aid in making the diagnosis of endocarditis. Although a positive blood culture in a child with an underlying or predisposing cardiac lesion does not necessarily indicate endocarditis, one must consider such a diagnosis. Blood cultures should be obtained in a child with a predisposition for endocarditis and persistent, unexplained fever.

It is impossible to specify the exact number of cultures that should be obtained in each situation. The collection of three sets of blood cultures during a 24 h period detects virtually all the usual organisms [26]. Once the etiologic agent has been identified, appropriate antimicrobial therapy can be begun. Sometimes making careful observations and obtaining more blood cultures before initiating antibiotic therapy are appropriate measures. In severely ill patients, three blood cultures should be obtained during a 1–2 h period and antibiotic therapy instituted. The counting of

days of recommended duration of therapy should begin on the first day on which blood cultures were negative when blood cultures were initially positive. At least two sets of blood cultures should be obtained every 24–48 h until bloodstream infection is cleared.

The bacteremia of endocarditis is often low grade and continuous [27]. Therefore, it is of no advantage to obtain blood cultures at any particular body temperature. Furthermore, the more blood that is collected, the better is the chance of growing the bacteria. At least 20 ml of blood is usually collected from an adult patient, but this may not possible in a small child, from whom as large a volume as is reasonable (preferably 3–5 ml) should be obtained. Either arterial or venous blood can be used, and samples should be drawn through venipuncture, not through an indwelling catheter. These samples should be taken after carefully sterilizing the venipuncture sites, as if for minor surgery. It is important to take blood from more than one site to reduce the risk of confusion by a skin contaminant. The microbiology laboratory should be consulted about the optimal volumes of blood and culture medium.

Culture-negative endocarditis

Culture-negative endocarditis refers to an individual with IE whose blood cultures are persistently negative. Blood cultures can be negative for a variety of reasons [28]. Previous antimicrobial therapy is a major cause of a negative blood culture [29]. Blood cultures should become positive after cessation of the antimicrobial therapy; they remain negative for a longer time after prolonged prior antibiotic treatment [27]. The antibiotic can be removed from the blood with the use of a resin device [26], if the laboratory is notified, in order to enhance microbial growth.

On occasion, a patient clinically suspected of having endocarditis may not have received antibiotics, yet still has a negative blood culture. True culture-negative endocarditis is uncommon. The data in Table 60.2 show that only 5–7% in three series had negative cultures. Many of these individuals eventually demonstrate subsequent proof of infection, either from culture of an infected embolus or from vegetations removed in the operating room or at necropsy. Some microorganisms capable of causing endocarditis are difficult to grow in culture with the use of standard laboratory techniques, and prolonged incubation, special media, or other special techniques are needed [22,26]. Consultation with a clinical microbiologist is invaluable in seeking unusual and fastidious organisms. Microorganisms reported to cause apparent culture-negative endocarditis include fastidious bacteria such as the nutritionally deficient streptococcus, fungi, HACEK organisms, *Coxiella burnetii*, and *Chlamydia* [22,30].

Other laboratory tests

A variety of other laboratory tests, although nonspecific, can help support the diagnosis of endocarditis. Acute-phase reactants (C-reactive protein and the erythrocyte sedimentation rate) are commonly elevated. Anemia is also common but may be missed if there was preceding polycythemia. It may be absent acutely but usually appears or worsens in long-standing infection. Leukocytosis is usually present, although it is not a prominent feature of fungal endocarditis. Rheumatoid factor is present in as many as half of individuals with endocarditis, especially if it is of long duration [27]. Circulating immune complexes (CICs), formed by an antibody–antigen interaction, are found in the sera of most patients with IE, especially in those whose illness is of longer duration [31,32]. CICs are associated with arthritis and acute or chronic glomerulonephritis. Levels of CICs usually fall with successful antibiotic treatment of IE and hence may be used to monitor therapy. Urinalysis may show proteinuria and macroscopic or microscopic hematuria.

Echocardiography

Many studies have confirmed the standard role of echocardiography in the diagnosis and management of endocarditis in adults [28,33] and children [5,34–48] with suspected IE. Two-dimensional echocardiography has a sensitivity in children of up to 80% [4,37–40]. Neither the sensitivity nor specificity of echocardiography is 100%, so that a normal echocardiogram does not exclude endocarditis. In fact, echocardiography may be more helpful in children with normal cardiac anatomy or with isolated valvar abnormalities than in children with very complex congenital anomalies [1]. The application of the Duke criteria for the diagnosis of IE in children has further demonstrated that in addition to a positive blood culture, echocardiography plays a major role in the diagnosis [13].

Transesophageal echocardiography (TEE) has been increasingly used in diagnosing endocarditis in adults, showing superior sensitivity for detecting vegetations compared with transthoracic echocardiography (TTE) [38,39]. In adult studies, TEE is able to detect smaller vegetations (1–1.5 mm) than is TTE (2 mm). Definitive studies of the usefulness of TEE in children with endocarditis have not been published, but standard practice now incorporates the use of TEE in children in whom TTE windows may be limited or in whom the diagnosis cannot be made using TTE but clinical suspicion remains high.

In addition to detecting vegetations (Videoclip 60.1), echocardiography is also useful for evaluating valvar and extravalvar complications of IE and for aiding in decision-making concerning the necessity for and timing of cardiac

operation (Table 60.5) (Videoclip 60.2). For more complete guidelines on the use of echocardiography in the diagnosis of IE, the reader is referred to the 1997 American College of Cardiology/American Heart Association Guidelines for the clinical use of echocardiography and its 2003 update [39,40].

Antimicrobial treatment

Eradicating infecting organisms in patients with endocarditis is the target of antibiotic therapy. A prolonged period of therapy (at least 2 weeks, often 4–6 weeks) is necessary for several reasons. Organisms are embedded within the fibrin–platelet matrix, which impedes the entry of host phagocytic cells into the vegetation, and they exist in high concentrations with relatively low rates of bacterial metabolism and cell division, which result in decreased susceptibility to antibiotics [41,42].

It is important to establish the microbiologic diagnosis before therapy is begun. This allows susceptibility testing and determination of minimal inhibitory concentration (MIC), the minimal concentration of antibiotic that inhibits growth *in vitro*. MIC determination helps in choosing the most appropriate antibiotic regimen. Treatment regimens outlined for viridans group streptococci, *Streptococcus bovis*, *Abiotrophia defectiva*, *Granulicatella* species, and *Gemella* species are subdivided into categories based on penicillin MIC data. Peak and trough serum levels should be monitored when potentially toxic antibiotics, such as vancomycin and aminoglycoside, are used. This ensures that levels are adequate and below the toxic range.

Bactericidal, rather than bacteriostatic, antibiotics should be chosen whenever possible to lessen the possibility of treatment failures or relapses. In treatment regimens where a combination of antibiotics is employed, it is important to administer the medications at or close to the same time in order to maximize the synergistic killing effect on the microbe [11,12,28–33,35–66]. Parenteral administration is recommended because of the need to achieve high serum levels of the antibiotics. In infants and small children, intravenous antibiotics are preferred over intramuscular agents because of small muscle mass. In addition, intramuscular injections can be painful. The use of heparin lock devices for intravenous therapy in older children allows them more mobility and activity. Outpatient treatment of endocarditis can be considered in selected patients after initial treatment in the hospital and after hemodynamic stability and the patient's (or parent's) compliance are confirmed. Outpatient therapy is now frequently used in adults [46], but it has been more sparingly recommended in children.

Blood cultures should be repeated often to assess the adequacy of the antibiotic regimen and to document the cessation of bacteremia. Bacteremia generally resolves within several days of beginning appropriate therapy. Patients with endocarditis require close follow-up. Obtaining follow-up blood cultures at 1 and 2 months after completing treatment is important, because most relapses occur during this period [28,47].

Cardiovascular surgery may be lifesaving in some patients with IE, but decisions for operative intervention must be individualized. Indications for operation include progressive cardiac failure, valvar obstruction, suppurative complications around or near an infected valve, fungal endocarditis, persistent bacteremia, and significant embolic events [28,66], especially when the aortic or mitral valve is involved. Medical management of progressive valvar damage and resulting cardiac failure can be deleterious. Operation should not be delayed solely because a full course of antibiotic therapy has not been completed or because a patient is seriously ill from complications of IE.

A detailed set of recommendations for antibiotic treatment of infective endocarditis has been produced by the American Heart Association [35] and the European Society of Cardiology [12]. Tables 60.6–60.8 are modeled after these guidelines. Antimicrobial treatment of endocarditis caused by the various Gram-positive organisms is detailed in the following sections.

Streptococcal and enterococcal endocarditis on native or prosthetic cardiac valves (Tables 60.6–60.8)

Streptococci are among the most common organisms causing IE in children [1,2]. Most of these organisms are viridans streptococci; the rest are *S. bovis* (nonenterococcal group D streptococci) or *Streptococcus pyogenes* (group A streptococci). Penicillin-susceptible streptococci have MIC to penicillin of ≤0.12 µg ml^{-1}. Treatment for native valve endocarditis caused by streptococci is given in Table 60.6. For patients who are able to take penicillin, 4-week therapeutic regimens with aqueous crystalline penicillin G or ceftriaxone have high cure rates.

A 2-week combined penicillin (or ceftriaxone) and aminoglycoside regimen has become increasingly popular for use in uncomplicated native valve IE, but is not recommended for patients who have had endocarditis for >3 months or for those who have extracardiac foci of infection, intracardiac abscesses, or mycotic aneurysm. It is also inappropriate for children at risk for adverse events caused by gentamicin therapy.

For patients allergic to β-lactam antibiotics, vancomycin therapy is recommended (Table 60.6). Each dose of this antibiotic should be infused during 1–2 h to reduce the risk of the histamine-release "red man" syndrome. Children "allergic" to penicillins, but without a clear-cut history of an anaphylactic reaction, may be candidates for penicillin desensitization.

Table 60.6 Therapy of native valve endocarditis caused by viridans group streptococci and *Streptococcus bovis*.

Regimen	Dosage[a] and route	Duration (weeks)	Comments
For patients with highly penicillin-susceptible strains (minimum inhibitory concentration ≤0.12 µg ml⁻¹)			
Aqueous crystalline penicillin G sodium *or*	Penicillin 200 000 U kg⁻¹ per 24 h i.v. in 4–6 equally divided doses (not to exceed 18 million U per 24 h)	4	Preferred in patients with impairment of 8th cranial nerve function or renal function
Ceftriaxone sodium	Ceftriaxone 100 mg kg⁻¹ per 24 h i.v./i.m. in 1 dose (not to exceed 2 g per 24 h)	4	
Aqueous crystalline penicillin G sodium *or*	Penicillin 200 000 U kg⁻¹ per 24 h i.v. in 4–6 equally divided doses (not to exceed 18 million U per 24 h)	2	2-week regimen not intended for patients with known cardiac or extracardiac abscess or for those with creatinine clearance of <20 ml min⁻¹, impaired 8th
Ceftriaxone sodium *plus*	2 ceftriaxone 100 mg kg⁻¹ per 24 h i.v./i.m. in 1 dose (not to exceed g per 24 h)	2	cranial nerve function, or *Abiotrophia*, *Granulicatella*, or *Gemella* spp. infection; gentamicin dosage should be adjusted to achieve peak serum concentration of 3–4 µg ml⁻¹ and trough serum concentration of <1 µg ml⁻¹ when 3 divided doses are used
Gentamicin sulfate[b]	3 mg kg⁻¹ per 24 h i.v./i.m. in 1 dose or 3 equally divided doses[c]	2	
Vancomycin hydrochloride[d]	40 mg kg⁻¹ per 24 h i.v. in 2–3 equally divided doses (not to exceed 2 g per 24 h unless concentrations in serum are inappropriately low)	4	Vancomycin therapy recommended only for patients unable to tolerate penicillin or ceftriaxone; vancomycin dosage should be adjusted to obtain peak (1 h after infusion completed) serum concentration of 30–45 µg ml⁻¹ and a trough concentration range of 10–15 µg ml⁻¹
For patients with strains relatively resistant to penicillin (minimum inhibitory concentration >0.12 to ≤0.5 µg ml⁻¹)			
Aqueous crystalline penicillin G sodium *or*	Penicillin 300 000 U per 24 h i.v. in 4–6 equally divided doses (not to exceed 24 million U per 24 h)	4	Patients with endocarditis caused by penicillin-resistant (MIC >0.5 µg ml⁻¹) strains should be treated with regimen recommended for enterococcal endocarditis
Ceftriaxone sodium *plus*	100 mg kg⁻¹ per 24 h i.v./i.m. in 1 dose (not to exceed 2 g per 24 h)	4	(see Table 60.4). Gentamicin dosage should be adjusted to achieve peak serum concentration of 3–4 µg ml⁻¹ and trough serum concentration of <1 µg ml⁻¹ when 3 divided doses are used
Gentamicin sulfate[b]	3 mg kg⁻¹ per 24 h i.v./i.m. in 1 dose or 3 equally divided doses[c]	2	
Vancomycin hydrochloride[d]	40 mg kg⁻¹ per 24 h i.v. in 2 or 3 equally divided doses (not to exceed 2 g per 24 h, unless serum concentrations are inappropriately low)	4	Vancomycin therapy recommended only for patients unable to tolerate penicillin or ceftriaxone therapy; vancomycin dosage should be adjusted to obtain peak (1 h after infusion completed) serum concentration of 30–45 µg ml⁻¹ and a trough concentration range of 10–15 µg ml⁻¹

[a]Dosages recommended are for patients with normal renal function.
[b]Other potentially nephrotoxic drugs (e.g., nonsteroidal anti-inflammatory drugs) should be used with caution in patients receiving gentamicin therapy.
[c]Data for once-daily dosing of aminoglycosides for children exist, but no data for treatment of IE exist.
[d]Vancomycin dosages should be infused during the course of at least 1 h to reduce risk of histamine-release "red man" syndrome.

On occasion, IE may be due to streptococci that are relatively resistant to penicillin (MIC >0.12 but ≤0.5 µg ml⁻¹). For these patients, the recommended treatment regimen is 4 weeks of penicillin or ceftriaxone combined with gentamicin for the first 2 weeks. For children who are allergic to β-lactams, vancomycin should be used.

Therapy for prosthetic valve/prosthetic material streptococcal endocarditis is given in Table 60.7. For penicillin-susceptible strains, 6 weeks of aqueous crystalline penicillin G or ceftriaxone with or without gentamicin for the first 2 weeks is recommended. The clinical benefit of gentamicin has not been formally shown, however (see the comments

Table 60.7 Therapy for endocarditis of prosthetic valves or other prosthetic material caused by viridans group streptococci and *Streptococcus bovis*.

Regimen	Dosage[a] and route	Duration (weeks)	Comments
Penicillin-susceptible strain (minimum inhibitory concentration ≤0.12 µg ml⁻¹)			
Aqueous crystalline penicillin G sodium *or*	300 000 U kg⁻¹ per 24 h i.v. in 4–6 equally divided doses (not to exceed 24 million U per 24 h)	6	Penicillin or ceftriaxone together with gentamicin has not demonstrated superior cure rates compared with monotherapy with penicillin or ceftriaxone for patients with highly susceptible strain.
Ceftriaxone *with or without*	100 mg kg⁻¹ i.v./i.m. once daily (not to exceed 2 g per 24 h)	6	Gentamicin dosage should be adjusted to achieve peak serum concentration of 3–4 µg ml⁻¹ and trough serum concentration of
Gentamicin sulfate[b]	3 mg kg⁻¹ per 24 h i.v./i.m. in 1 dose or 3 equally divided doses[c]	2	<1 µg ml⁻¹ when 3 divided doses are used; gentamicin therapy should not be administered to patients with creatinine clearance of <30 ml min⁻¹
Vancomycin hydrochloride[d]	40 mg kg⁻¹ per 24 h i.v. or in 2 or 3 equally divided doses (not to exceed 2 g per 24 h unless concentrations in serum are inappropriately low)	6	Vancomycin therapy recommended only for patients unable to tolerate penicillin or ceftriaxone; vancomycin dosage should be adjusted to obtain peak (1 h after infusion completed) serum concentration of 30–45 µg ml⁻¹ and a trough concentration range of 10–15 µg ml⁻¹
Penicillin relatively or fully resistant strain (minimum inhibitory concentration >0.12 µg ml⁻¹)			
Aqueous crystalline penicillin sodium *or*	300 000 U kg⁻¹ per 24 h i.v. in 4–6 equally divided doses (not to exceed 24 million U per 24 h)	6	See comments for penicillin, ceftriaxone and gentamicin above
Ceftriaxone *plus*	100 mg kg⁻¹ i.v./i.m. once daily (not to exceed 2 g per 24 h)	6	
Gentamicin sulfate[b]	3 mg kg⁻¹ per 24 h i.v./i.m. in 1 dose or 3 equally divided doses[c]	6	
Vancomycin hydrochloride[d]	40 mg kg⁻¹ per 24 h i.v. in 2 or 3 equally divided doses (not to exceed 2 g per 24 h unless concentrations in serum are inappropriately low)	6	See comments for vancomycin above

[a]Dosages recommended are for patients with normal renal function.
[b]Other potentially nephrotoxic drugs (e.g., nonsteroidal anti-inflammatory drugs) should be used with caution in patients receiving gentamicin therapy.
[c]Data for once-daily dosing of aminoglycosides for children exist, but no data for treatment of IE exist.
[d]Vancomycin dosages should be infused during the course of at least 1 h to reduce risk of histamine-release "red man" syndrome.

in the table). Vancomycin is recommended for patients unable to tolerate penicillin or ceftriaxone. For children with penicillin relatively or fully resistant strains, 6 weeks of gentamicin should be added to the 6 weeks of penicillin or ceftriaxone.

Enterococcal endocarditis is uncommon in children. Treatment (Table 60.8) is difficult because of the relative resistance of enterococci to penicillin, expanded-spectrum penicillins, and vancomycin and in view of their variable resistance to aminoglycosides [56,57]. The treatment regimen requires combination therapy of penicillin G or ampicillin with gentamicin for at least 4 and preferably 6 weeks [51,56]. For patients allergic to penicillins (but without a history of anaphylactic-type reaction), penicillin desensitization can be considered. If desensitization is not considered feasible, vancomycin plus gentamicin for 4–6 weeks is recommended. Nutritionally variant streptococci or streptococci with MIC >0.5 µg ml⁻¹ should be treated with the regimens listed for enterococci.

The above recommendations are for native valve enterococcal endocarditis. If the infection involves a *prosthetic* cardiac valve, 6 weeks of penicillin combined with gentamicin for at least the first 2 weeks is recommended [58]. If the infection is caused by "relatively penicillin-resistant" enterococci, penicillin treatment may be required for 8 weeks. A vancomycin plus gentamicin regimen is recommended for penicillin-allergic individuals who are not desensitized to penicillins.

Table 60.8 Therapy for native valve or prosthetic valve enterococcal endocarditis caused by strains susceptible to penicillin, gentamicin, and vancomycin.

Regimen	Dosage[a] and route	Duration (weeks)	Comments
Ampicillin sodium *or*	300 mg kg⁻¹ per 24 h i.v. in 4–6 equally divided doses (not to exceed 12 g per 24 h)	4–6	Native valve: 4-week therapy recommended for patients with symptoms of illness ≤3 months; 6-week therapy recommended for patients with symptoms >3 months
Aqueous crystalline penicillin G sodium *plus*	300 000 U kg⁻¹ per 24 h i.v. in 4–6 equally divided doses (not to exceed 30 × 10⁶ U per 24 h)	4–6	Prosthetic valve or other prosthetic cardiac material: minimum of 6 weeks of therapy recommended
Gentamicin sulfate[b]	3 mg kg⁻¹ per 24 h i.v./i.m. in 3 equally divided doses	4–6	
Vancomycin hydrochloride[c] *plus*	40 mg kg⁻¹ per 24 h i.v. in 2 or 3 equally divided doses	6	Vancomycin therapy recommended only for patients unable to tolerate penicillin or ampicillin. Adjust vancomycin to achieve 1 h serum concentration of 30–45 µg ml⁻¹ and trough concentration of 10–15 µg ml⁻¹
Gentamicin sulfate[b]	3 mg kg⁻¹ per 24 h i.v./i.m. in 3 equally divided doses	6	6 weeks of vancomycin therapy recommended because of decreased activity against enterococci

[a]Dosages recommended are for patients with normal renal function.
[b]Dosage of gentamicin should be adjusted to achieve peak serum concentration of 3–4 µg ml⁻¹ and a trough concentration of <1 µg ml⁻¹. Patients with a creatinine clearance of <50 ml min⁻¹ should be treated in consultation with an infectious diseases specialist.
[c]Vancomycin dosages should be infused during the course of at least 1 h to reduce risk of histamine-release "red man" syndrome.

Staphylococcal endocarditis on native or prosthetic valves or other prosthetic material (Table 60.9)

Staphylococcal endocarditis in children has become more prevalent in recent years [2,59] and *S. aureus* is the most common cause of IE in the developed world [67]. Staphylococci are coagulase positive (*S. aureus)* or coagulase negative (*S. epidermidis* and various other species). Most staphylococci are highly resistant to penicillin G and ampicillin because of production of of β-lactamases [59], one form of which is termed penicillinase. Staphylococci sensitive to penicillinase-resistant penicillins are termed oxacillin (or methicillin) susceptible. For oxacillin-susceptible strains of staphylococcal IE, in the absence of prosthetic materials antibiotic therapy must include a semisynthetic, penicillinase-resistant penicillin (nafcillin or oxacillin). The antibiotic should be administered intravenously for 6 weeks for complicated right-sided IE and for left-sided IE. A 2-week regimen can be used for uncomplicated right-sided IE and for left-sided IE. Gentamicin may be added for the first 3–5 days, although the clinical benefit of aminoglycosides has not been established. For patients who are penicillin allergic, cephalosporins are recommended as an alternative. Cephalosporins should not be used in patients with a history of an anaphylactic-type reaction to penicillin; rather, vancomycin should be used in these individuals.

Some coagulase-negative staphylococci and *S. aureus* strains are oxacillin resistant. Therefore, patients with IE associated with these organisms should not receive nafcillin, oxacillin, or a cephalosporin but should instead be treated for 6 weeks with vancomycin.

Staphylococcal endocarditis involving a prosthetic cardiac valve or other cardiac prosthetic material is most often, but not always, nosocomially acquired. Most infections involve methicillin-resistant organisms, especially if the endocarditis develops within 1 year of a cardiac operation [58]. Treatment requires a minimum of 6 weeks of vancomycin plus rifampin, with gentamicin for the first 2 weeks. If the bacteria are oxacillin susceptible, nafcillin or oxacillin can replace vancomycin. For further recommendations on the treatment of staphylococcal endocarditis involving intracardiac prosthetic material, the reader is referred to the American Heart Association guidelines [28,52].

Staphylococcal bacteremia in patients with indwelling venous catheters or lines may be treated for 10–14 days with appropriate antibiotics after removal of the catheter, provided that the patient is not severely ill and has no signs of organ involvement.

Gram-negative bacterial endocarditis

Gram-negative bacteria are an infrequent cause of endocarditis in children (see Table 60.2). The Gram-negative bacteria most commonly causing endocarditis in children are the HACEK group of fastidious coccobacilli (*Haemophilus parainfluenzae*, *Haemophilus aphrophilus*, *Actinobacillus actino-*

Table 60.9 Therapy for endocarditis caused by staphylococci.

Regimen	Dosage[a] and route	Duration (weeks)	Comments
In the absence of prosthetic materials			
Oxacillin-susceptible strains			
Nafcillin or oxacillin[b]	200 mg kg^{-1} per 24 h i.v. in 4–6 equally divided doses (not to exceed 12 g per 24 h)	6	For complicated right-sided IE and for left-sided IE; for uncomplicated right-sided IE, 2 weeks. It is optional to add gentamicin sulfate[†], 3 mg kg^{-1} per 24 h i.v./i.m. in 3 equally divided doses for 3–5 days; however, the clinical benefit of aminoglycosides has not been established. For penicillin-allergic (nonanaphylactoid type) patients, consider skin testing for oxacillin-susceptible staphylococci and questionable history of immediate-type hypersensitivity to penicillin
Cefazolin	100 mg kg^{-1} per 24 h i.v. in 3 equally divided doses (not to exceed 6 g per 24 h)	6	Cephalosporins should be avoided in patients with anaphylactoid-type hypersensitivity to β-lactams; vancomycin should be used in these cases. It is optional to add gentamicin sulfate[†], 3 mg kg^{-1} per 24 h i.v./i.m. in 3 equally divided doses for 3–5 days; however, the clinical benefit of aminoglycosides has not been established
Oxacillin-resistant strains			
Vancomycin[c]	40 mg kg^{-1} per 24 h i.v. in 2 or 3 equally divided doses	6	Adjust vancomycin dosage to achieve 1 h serum concentration of 30–45 μg ml^{-1} and trough concentration of 10–15 μg ml^{-1}.
In the presence of prosthetic valve or other prosthetic material			
Oxacillin-susceptible strains			
Nafcillin or oxacillin[b] plus	Nafcillin or oxacillin 200 mg kg^{-1} per 24 h i.v. in 4–6 equally divided doses (not to exceed 12 g per 24 h)	≥6	Vancomycin should be used in patients with immediate-type hypersensitivity reactions to β-lactam antibiotics; cefazolin may be substituted for nafcillin or oxacillin in patients with non-immediate-type hypersensitivity reactions to penicillins. Gentamicin dosage should be adjusted to achieve peak serum concentration of 3–4 μg ml^{-1} and trough serum concentration of <1 μg ml^{-1} when 3 divided doses are used; gentamicin therapy should not be administered to patients with creatinine clearance of <30 ml min^{-1}
Rifampin plus	20 mg kg^{-1} per 24 h i.v./p.o. in 3 equally divided doses (not to exceed 900 mg per 24 h)	≥6	
Gentamicin[d]	3 mg kg^{-1} per 24 h i.v./i.m. in 3 equally divided doses	2	
Oxacillin-resistant strains			
Vancomycin[c] plus	40 mg kg^{-1} per 24 h in 2 or 3 equally divided doses	≥6	Adjust vancomycin to achieve 1 h serum concentration of 30–45 μg ml^{-1} and trough concentration of 10–15 μg ml^{-1}. Gentamicin dosage should be adjusted to achieve peak serum concentration of 3–4 μg ml^{-1} and trough serum concentration of <1 μg ml^{-1} when 3 divided doses are used; gentamicin therapy should not be administered to patients with creatinine clearance of <30 ml min^{-1}
Rifampin plus	20 mg kg^{-1} per 24 h i.v./p.o. in 3 equally divided doses (not to exceed 900 mg per 24 h	≥6	
Gentamicin[d]	3 mg kg^{-1} per 24 h i.v./i.m. in 3 equally divided doses	2	

[a]Dosages recommended are for patients with normal renal function.
[b]Penicillin G 300 000 U kg^{-1} per 24 h i.v. in 4–6 equally divided doses (not to exceed 24 × 10^6 U per 24 h) may be used in place of nafcillin or oxacillin if strain is penicillin susceptible (minimum inhibitory concentration ≤0.1 μg ml^{-1}) and does not produce β-lactamase.
[c]Vancomycin dosages should be infused during course of at least 1 h to reduce risk of histamine-release "red man" syndrome.
[d]Gentamicin should be administered in close temporal proximity to vancomycin, nafcillin, or oxacillin dosing.

mycetemcomitans, *Cardiobacterium hominis*, *Eikenella corrodens*, and *Kingella kingae*). Recommended therapy for the HACEK group for both native valve and prosthetic valve (or other prosthetic material) IE is a 4-week course of ceftriaxone or ampicillin–sulbactam. In adults ciprofloxacin is an alternative for patients unable to tolerate ampicillin or cephalosporins but is generally not recommended for patients <18 years of age.

Other Gram-negative organisms, such as *Escherichia coli*, *Pseudomonas aeruginosa*, or *Serratia marcescens*, are occasionally noted. Most patients with these organisms are adolescent or

adult intravenous drug abusers, although a postoperative cardiac patient, an immunocompromised individual, or a neonate may occasionally have endocarditis with one of these organisms. Therapy must be individualized, guided by identification of the organism and antimicrobial susceptibility testing. Most experience has been with a broad-spectrum penicillin, such as ticarcillin, or a cephalosporin, such as cefotaxime or ceftazidime, combined with an aminoglycoside, such as gentamicin or amikacin [60]. At least 6 weeks of therapy is recommended. For specific treatment options, information is reviewed in the AHA guidelines [28] and those published by the ESC [66].

Gonococcal endocarditis can be treated successfully with high-dose penicillin, provided that the organism is penicillin susceptible. For penicillin-resistant organisms, an appropriate third-generation cephalosporin is recommended.

Fungal endocarditis

The prognosis in fungal endocarditis is poor and associated with high mortality and morbidity. Few patients survive when the entire treatment is only with antifungal agents. Valve replacement operation in conjunction with antifungal agents is usually required [16]. Operation is best performed after 10 days of medical therapy, but earlier if there are embolic phenomena or a deteriorating clinical picture.

Amphotericin B remains the first-line antifungal agent for medical therapy. A "test" dose of $0.1\,\text{mg}\,\text{kg}^{-1}$ of amphotericin B (maximum, 1 mg) is administered initially. If it is well tolerated, it is followed by a dose of $0.5\,\text{mg}\,\text{kg}^{-1}$ for 1 day and then 1 $\text{mg}\,\text{kg}^{-1}$ per day as the maintenance dose. The minimal duration of therapy should be 6–8 weeks. Renal function and serum potassium concentration should be carefully monitored.

Prosthetic valve endocarditis

Infection of a prosthetic cardiac valve occurs in 1–6% of all patients at some time during the lifespan of the prosthesis [66]. Antibiotic therapy for patients with an infected prosthetic cardiac valve or other prosthetic material must be appropriate for the specific infecting agent. Therapy is given for 6 weeks or longer. Treatment regimens for a prosthetic valve infected with streptococci, staphylococci, enterococci, or HACEK organisms are discussed in the preceding sections.

Prosthetic valve endocarditis caused by diphtheroids is best treated with penicillin and gentamicin, or with vancomycin for penicillin-allergic patients [61]. Duration of therapy should be 6 weeks.

Therapy for prosthetic valve endocarditis caused by Gram-negative bacilli must be based on the results of *in vitro* MIC tests and *in vitro* evaluation of antimicrobial synergy. Common regimens include a third-generation cephalosporin or a broad-spectrum penicillin with gentamicin for at least 6–8 weeks.

Experience with prosthetic valve endocarditis, derived mainly in adults, has emphasized that early replacement of the infected valve may lower the high mortality rate associated with such infections [14]. The timing of replacement of an infected prosthesis must be individualized. Some authorities recommend that most patients with staphylococcal or early-onset prosthetic valve endocarditis should undergo replacement of the infected prosthetic valve. Indications for cardiac operation during active infection of a prosthetic valve include moderate to severe heart failure, significant valvar obstruction, fungal endocarditis, persistent bacteremia despite appropriate antibiotics for 10–14 days, an unstable prosthesis, ruptured sinus of Valsalva or ventricular septum, and recurrent major emboli [14]. Less definite indications for surgery include a single major embolus, bacteriologic relapse after an appropriate course of therapy, echocardiographic demonstration of a large vegetation, and extension of infection to an annular abscess or myocardial abscess [14].

Culture-negative endocarditis

Blood culture-negative IE most commonly occurs as a result of prior administration of antibiotics before blood cultures were obtained. It can also occur because of infection with fastidious organisms or nonbacterial pathogens. Treatment of culture-negative IE is difficult. A variety of possible treatment regimens for native valve and early and late prosthetic valve IE are given by the AHA and ESC [28,66]. If blood cultures remain negative after careful workup and specialized laboratory techniques, patients with native valve endocarditis should be treated with a penicillinase-resistant penicillin (nafcillin or oxacillin) and gentamicin. Some experts recommend adding penicillin to this regimen [5]. If the infection involves a prosthetic cardiac valve, vancomycin should be added to the regimen [58]. For penicillin-allergic individuals, vancomycin and gentamicin should be used. Discontinuing the aminoglycoside after 2 weeks may be considered if there has been a substantial response to therapy. Treatment should be continued for 6 full weeks [66].

Prevention

Preventing endocarditis is desirable whenever possible. However, there has never been a prospective, controlled study in patients with underlying structural cardiac disease to determine definitively whether prophylactic antibiotics provide protection against the development of endocarditis during bacteremia-inducing procedures. Further, only a minority of instances of endocarditis (≤20%) have been attributable to an invasive procedure, and only about half of individuals who develop endocarditis have an underlying cardiac anomaly for which prophylaxis would have been given. Durack estimated that <500 instances of endocarditis per year in the United States could be prevented by use of a fully effective prophylactic regimen [62]. Nevertheless, for over 50 years antimicrobial prophylaxis regimens developed

Table 60.10 Comparison of recommendations from various groups.

AHA	ESC	NICE [65]
Patient groups for whom IE prophylaxis is recommended		

Cardiac conditions associated with the highest risk of adverse outcome from IE. This includes:
1. Prosthetic cardiac valve or prosthetic material used for cardiac valve repair
2. Previous infective endocarditis
3. Congenital heart disease (CHD), specifically:
  a. unrepaired cyanotic congenital heart disease, including those with palliative shunts and conduits
 	
  b. completely repaired CHD with prosthetic material or device either by surgery or catheter intervention during the first 6 months after the procedure
 	
  c. repaired CHD with residual defects at the site or adjacent to the site of a prosthetic patch or prosthetic device (which inhibit endothelialization)
4. Cardiac transplantation recipients who develop cardiac valvulopathy
	Cardiac conditions at highest risk of IE. This includes:
	1. Patients with a prosthetic valve or a prosthetic material used for cardiac valve repair
	2. Patients with previous IE
	3. Patients with congenital heart disease:
	  a. cyanotic congenital heart disease, without surgical repair, or with residual defects, palliative shunts, or conduits
	  b. congenital heart disease with complete repair with prosthetic material whether placed by surgery or by percutaneous technique, up to 6 months after the procedure
	  c. when a residual defect persists at the site of implantation of a prosthetic material or device by cardiac surgery or percutaneous technique
		No patient groups are recommended to receive routine IE prophylaxis

Types of medical/dental procedures for which prophylaxis is recommended for patient groups above		
All dental procedures and events that involve manipulation of gingival tissue or the periapical region of teeth or perforation of the oral mucosa. Does *not* include the following: 1. Routine anesthetic injections through uninfected tissue 2. Taking dental radiographs 3. Placement of removable prosthodontic or orthodontic appliances 4. Adjustment of orthodontic appliances 5. Placement of orthodontic brackets 6. Shedding of deciduous teeth and bleeding from trauma to the lips or oral mucosa	All dental procedures requiring manipulation of the gingival or periapical region of the teeth or perforation of the oral mucosa. Does *not* include the following: 1. Local anesthetic injections in uninfected tissue 2. Removal of sutures 3. Dental X-rays 4. Placement or adjustment of removable prosthodontic or orthodontic appliances or braces 5. Shedding of deciduous teeth or trauma to the lips and oral mucosa	Prophylaxis is not recommended for any procedure

AHA-American Heart Association.
ESC-European Society of Cardiology.
NICE-National Institute for Clinical Excellence.

by the American Heart Association were the accepted standard of practice in most countries. Recently, however, the world-wide view of the concept of prophylactic antibiotics has been dramatically changing. The absence of definitive data supporting their use, increasing reports of failure to prevent IE even when prophylactic regimens were scrupulously adhered to, and concerns about antibiotic overuse and anaphylactic reactions have driven revisions of the practice. Furthermore, not all situations in which bacteremia may occur are readily identifiable. Also, bacteremias occur spontaneously on a daily basis (chewing of food, teeth brushing) and cannot logically be prevented. In view of these issues, the British Society for Antimicrobial Chemotherapy issued markedly restrictive guidelines in 2006 which sharply limited the use of prophylactic antibiotics to prevent IE [63]. Amplifying this more restrictive approach, the AHA issued revised guidelines in 2007 which recommend limiting the use of prophylactic antibiotics to those in whom the risk of developing endocarditis was not only high but in whom, if infected, the morbidity and/or mortality likelihood would be

Table 60.11 Regimens for a dental procedure.

Situation	Agent	Regimen[a]
Oral	Amoxicillin	50 mg kg^{-1} (not to exceed 2 g)
Unable to take oral medication	Ampicillin	50 mg kg^{-1} i.m. or i.v. (not to exceed 2 g)
	or	
	Cefazolin or ceftriaxone	50 mg kg^{-1} i.m. or i.v. (not to exceed 1 g)
Allergic to penicillins	Cephalexin[b,c]	50 mg kg^{-1} (not to exceed 2 g)
or	or	
Ampicillin – oral	Clindamycin	20 mg kg^{-1} (not to exceed 600 mg)
	or	
	Azithromycin or clarithromycin	15 mg kg^{-1} (not to exceed 500 mg)
Allergic to penicillins	Cefazolin or ceftriaxone[b]	50 mg kg^{-1} i.m. or i.v. (not to exceed 1 g)
or	or	
Ampicillin and unable to take oral medication	Clindamycin phosphate	20 mg kg^{-1} i.m. or i.v. (not to exceed 600 mg)

[a]Single dose 30–60 min before procedure.
[b]Or other first- or second-generation oral cephalosporin in equivalent pediatric dosage.
[c]Cephalosporins should not be used in an individual with a history of anaphylaxis, antiedema, or urticaria with penicillins or ampicillin.

Table 60.12 Prophylaxis regimens for other procedures.

Procedure	Agent	Regimen[a]
Invasive respiratory tract procedure	Same as Table 60.11	Same as Table 60.11
Invasive respiratory tract procedure with known or suspected *S. aureus*	Anti-*Staph.* Penicillin	Same as above
	or	
	Cephalosporin	
	or	
	Vancomycin	20 mg kg^{-1} i.v. (not >1 g)
GI or GU procedure without known infection	No prophylaxis	–
GU tract procedure with known enterococcal urinary infection	Ampicillin	Same as above
	or	
	Amoxicillin	
	or	
	Vancomycin	20 mg kg^{-1} i.v. (not >1 g)

[a]Single dose 30–60 min before procedure.
Adapted with permission from Wilson *et al. Circulation* 2007;**116**:1736–54.

greatest [64]. This has greatly simplified the approach as a much smaller population of patients eligible for prophylaxis was in this statement (Table 60.10). In addition, the ESC issued similar guidelines in 2009 [66]. The AHA writing group also more sharply defined the procedures for which antibiotic prophylaxis was recommended (Table 60.10). Antibiotic regimens, however, were not considerably altered from previous statements (Tables 60.11 and 60.12), with an emphasis on oral amoxicillin remaining. It should be noted

that these guidelines have engendered controversy and that both the AHA and the British statements called for close follow-up and further study to determine the impact of these fairly radical changes. At least one prominent group, however, did not feel that the new recommendations went far enough and have called for eliminating all prophylactic regimens entirely [65]. Readers are advised to follow updated statements to be issued in the future as evidence develops to ascertain which direction is most closely in line with data

development. Table 60.10 compares the recommendations issued by these three prominent organizations.

Patients at risk for IE (or their parents) should be educated about endocarditis prevention. The importance of maintaining good oral health should be explained to all patients/parents. Children at risk for IE should establish and maintain the best possible oral health to reduce potential sources of bacteremia. Individuals with cyanosis often have spongy, friable gums [11], and optimal tooth care is especially important in them. Helpful educational materials are available from the American Dental Association (www.ada.org). Those in the highest risk categories should understand the need to take the prophylactic antibiotics. Finally, they should be made aware of symptoms (such as fever of unexplained origin) that could indicate IE and the importance of contacting the patient's physician.

The risk of IE may change after operative or other reparative procedures [34]. For example, successful closure of atrial septal defect, ventricular septal defect, or patent ductus arteriosus reduces the patient's long-term risk for development of endocarditis. Other procedures, such as palliative shunts and conduits, do not alter the patient's long-term risk for endocarditis. Still other procedures, such as replacement of a native cardiac valve with a prosthetic valve, actually put the patient in a higher risk category. Patients/parents should be reminded that a child's need for antibiotic prophylaxis could change as they go through treatment. Finally, as more data become available, subsequent revisions of antibiotic prophylaxis guidelines from authorities such as the AHA may alter a given patient's need to take these routine antibiotics.

Acknowledgment

References

1 Ferrieri P, Gewitz MH, Gerber MA, *et al.* Unique features of infective endocarditis in childhood. *Pediatrics* 2002;**109**:931–43.

2 Day MD, Gauvreau K, Shulman S, Newburger JW. Characteristics of children hospitalized with infective endocarditis. *Circulation* 2009;**119**:865–70.

3 Zakrewski T, Keith JD. Bacterial endocarditis in infants and children. *J Pediatr* 1965;**67**:1179–93.

4 Van Hare GF, Ben-Shachar G, Liebman J, *et al.* Infective endocarditis in infants and children during the past 10 years: a decade of change. *Am Heart J* 1984;**107**:1235–40.

5 Berkowitz FE. Infective endocarditis. In: Nichols DG, Cameron DE, Greeley WJ, *et al.*, eds. *Critical Heart Disease in Infants and Children*. St Louis, MO: Mosby-Year Book, 1995: 961–86.

6 Oelberg DC, Fisher DJ, Gross DM, *et al.* Endocarditis in high risk neonates. *Pediatrics* 1983;**71**:392–7.

7 Rodbard S. Blood velocity and endocarditis. *Circulation* 1963;**27**:18–28.

8 Gould K, Ramirez-Ronda CH, Holmes RK, Sanford JP. Adherence of bacteria to heart valves *in vitro*. *J Clin Invest* 1975;**56**:1364–70.

9 Scheld WM, Valone JA, Sande MA. Bacterial adherence in the pathogenesis of endocarditis: interaction of bacterial dextran, platelets, and fibrin. *J Clin Invest* 1978;**61**:1394–404.

10 Sande MA, Lee BL, Mills J, Chambers HF. Endocarditis in intravenous drug users. In: Kaye D, ed. *Infective Endocarditis*, 2nd edn. New York: Raven Press, 1992: 345–59.

11 Johnson DH, Rosenthal A, Nadas AS. A forty-year review of bacterial endocarditis in infancy and childhood. *Circulation* 1975;**51**:581–8.

12 Martin JM, Neches WH, Wald ER. Infective endocarditis: 35 years of experience at a children's hospital. *Clin Infect Dis* 1997;**24**:669–75.

13 Stockheim JA, Chadwick EG, Kessler S, *et al.* Are the Duke criteria superior to the Beth Israel criteria for the diagnosis of infective endocarditis in children? *Clin Infect Dis* 1998;**27**:1451–6.

14 Douglas JL, Cobbs CG. Prosthetic valve endocarditis. In Kaye D, ed. *Infective Endocarditis*, 2nd edn. New York: Raven Press, 1992: 375–96.

15 Seelig MS, Goldberg P, Kozinn PJ, Berger AR. Fungal endocarditis: patients at risk and their treatment. *Postgrad Med J* 1979;**55**:632–41.

16 Moyer DV, Edwards JE. Fungal endocarditis. In Kaye D, ed. *Infective Endocarditis*, 2nd edn. New York: Raven Press, 1992: 299–312.

17 Rubinstein E, Noreiga ER, Simberkoff MS, *et al.* Fungal endocarditis: analysis of twenty-four cases and review of the literature. *Medicine (Baltimore)* 1975;**54**:331–4.

18 Gulmen S, Anderson WR. *Candida* endocarditis with distal aortic embolization. *Minn Med* 1977;**60**:469–71.

19 Johnson DE, Base JL, Thompson TR, *et al. Candida* septicemia and a right atrial mass in infancy secondary to umbilical vein catheterization. *Am J Dis Child* 1981;**135**:275–7.

20 Dato VM, Dajani AS. Candidemia in children with central venous catheters: role of catheter removal and amphotericin B therapy. *Pediatr Infect Dis J* 1990;**9**:309–14.

21 Mayayo E, Moralejo J, Camps J, Guarro J. Fungal endocarditis in premature infants: case report and review. *Clin Infect Dis* 1996;**22**:366–8.

22 Van Scoy RE. Culture-negative endocarditis. *Mayo Clin Proc* 1982;**57**:149–54.

23 Durack DT, Lukes AS, Bright DK. New criteria for diagnosis of infective endocarditis: utilization of specific echocardiographic findings. *Am J Med* 1994;**96**:200–9.

24 Bayer AS, Ward JL, Ginzton LE, Shapiro SM. Evaluation of new clinical criteria for the diagnosis of infective endocarditis. *Am J Med* 1994;**96**:211–9.

25 Starkebaum M, Durack D, Beeson P. The "incubation period" of bacterial endocarditis. *Yale J Biol Med* 1977;**50**:49–58.

26 Raoult D, Caslta JP, Richet H, *et al.* Contribution of systemic serological testing in diagnosis of infective endocarditis. *J Clin Microbiol* 2005;**43**:5238–42.

27 Kaye KM, Kaye D. Laboratory findings including blood cultures. In Kaye D, ed. *Infective Endocarditis*, 2nd edn. New York: Raven Press, 1992: 117–124.

28 Baddour LM, Wilson WR, Bayer AS, *et al.* Infective endocarditis: diagnosis, antimicrobial therapy and management of complications: a statement for healthcare professionals from the Committee on Rheumatic Fever, Endocarditis, and Kawasaki disease, Council of Cardiovascular Disease in the Young, and the Councils on Clinical Cardiology, Stroke, and Cardiovascular. Surgery and Anesthesia, American Heart Association; endorsed by the Infectious Diseases Society of America. *Circulation* 2005;**111**:e394–434.

29 Hoen B, Selton-Suty C, Lacassin F, *et al.* Infective endocarditis in patients with negative blood cultures: analysis of 88 cases from a one-year nationwide survey in France. *Clin Infect Dis* 1995;**20**:501–6.

30 Roberts KB, Sidlak MJ. Satellite streptococci: a major cause of negative blood cultures in bacterial endocarditis? *JAMA* 1979;**241**:2293–4.

31 Bayer AS, Theofilopoulos AN, Eisenberg R, *et al.* Circulating immune complexes in infective endocarditis. *N Engl J Med* 1976;**295**:1500–5.

32 Kauffman RH, Thompson J, Valentijn RM, *et al.* The clinical implications and the pathogenetic significance of circulating immune complexes in infective endocarditis. *Am J Med* 1981;**71**:17–25.

33 Aragam JR, Weyman AE. Echocardiographic findings in infective endocarditis. In: Weyman AE, ed. *Principles and Practice of Echocardiography*, 2nd edn. Philadelphia: Lea & Febiger, 1994: 1178–97.

34 Saiman L, Prince A, Gersony WM. Pediatric infective endocarditis in the modern era. *J Pediatr* 1993;**122**:847–53.

35 Dillon T, Meyer RA, Korfhagen JC, *et al.* Management of infective endocarditis using echocardiography. *J Pediatr* 1980;**96**:552–8.

36 Kavey REW, Frank DM, Byrum CJ, *et al.* Two-dimensional echocardiographic assessment of infective endocarditis in children. *Am J Dis Child* 1983;**137**:851–6.

37 Bricker JT, Latson LA, Huhta JC, Gutgesell HP. Echocardiographic evaluation of infective endocarditis in children. *Clin Pediatr (Phila)* 1985;**24**:312–7.

38 Sable CA, Rome JJ, Martin GR, *et al.* Indications for echocardiography in the diagnosis of infective endocarditis in children. *Am J Cardiol* 1995;**75**:801–4.

39 Cheitlin MD, Alpert JS, Armstrong WF, *et al.* ACC/AHA Guidelines for the clinical application of echocardiography: a report of the American College of Cardiology/American Heart Association Task Force on Practice Guidelines (Committee on Clinical Application of Echocardiography). *Circulation* 1997;**95**:1686–744.

40 Cheitlin MD, Armstrong WF, Aurigemma, GP, *et al.* ACC/AHA/ASE 2003 Guideline update for the clinical application of echocardiography: a report of the American College of Cardiology/American Heart Association Task Force on Practical Guidelines (ACC/AHA/ASE Committee) to Update the 1997 Guidelines for the Clinical Application of Echocardiography. *Circulation* 2003;**108**:1146–62.

41 Durack DT, Beeson PB. Experimental bacterial endocarditis. I. Colonization of a sterile vegetation. *Br J Exp Pathol* 1972;**53**:44–9.

42 Durack DT, Beeson PB. Experimental bacterial endocarditis. II. Survival of bacteria in endocardial vegetations. *Br J Exp Pathol* 1972;**53**:50–3.

43 Baldassarre JS, Kaye D. Principles and overview of antibiotic therapy. In Kaye D, ed. *Infective Endocarditis*, 2nd edn. New York: Raven Press, 1992: 169–90.

44 Sande MA, Irvin RG. Penicillin–aminoglycoside synergy in experimental *Streptococcus viridans* endocarditis. *J Infect Dis* 1974;**129**:572–6.

45 Wolfe JC, Johnson WD Jr. Penicillin-sensitive streptococcal endocarditis: *in vitro* and clinical observations on penicillin–streptomycin therapy. *Ann Intern Med* 1974;**81**:178–81.

46 Tice AD, Rehm SJ, Dalovisio JR, *et al.* Practice guidelines for outpatient parenteral antimicrobial therapy. IDSA Guidelines. *Clin Infect Dis* 2004;**38**:1651–72.

47 Santoro J, Ingerman M. Response to therapy: relapses and reinfections. In Kaye D, ed. *Infective Endocarditis*, 2nd edn. New York: Raven Press, 1992: 423–33.

48 Douglas JL, Dismukes WE. Surgical therapy of infective endocarditis on natural valves. In Kaye D, ed. *Infective Endocarditis*, 2nd edn. New York: Raven Press, 1992: 397–411.

49 Citak M, Rees A, Mavroudis C. Surgical management of infective endocarditis in children. *Ann Thorac Surg* 1992;**54**:755–760.

50 Tolan RW Jr, Kleiman MB, Frank M, *et al.* Operative intervention in active endocarditis in children: report of a series of cases and review. *Clin Infect Dis* 1992;**14**:852–62.

51 Wilson W, Karchmer AW, Dajani AS, *et al.* Antibiotic treatment of adults with infective endocarditis due to streptococci, enterococci, staphylococci, and HACEK microorganisms. *JAMA* 1995;**274**:1706–13.

52 Karchmer AW, Moellering RC Jr, Maki DG, *et al.* Single-antibiotic therapy for streptococcal endocarditis. *JAMA* 1979;**241**:1801–6.

53 Francioli P, Etienne J, Hoigne R, *et al.* Treatment of streptococcal endocarditis with a single daily dose of ceftriaxone sodium for 4 weeks: efficacy and outpatient treatment feasibility. *JAMA* 1992;**267**:264–7.

54 Wilson WR, Thompson RL, Wilkowske CJ, *et al.* Short-term therapy for streptococcal infective endocarditis: combined intramuscular administration of penicillin and streptomycin. *JAMA* 1981;**245**:360–3.

55 Sande MA, Scheld WM. Combination antibiotic therapy of bacterial endocarditis. *Ann Intern Med* 1980;**92**:390–5.

56 Eliopoulos GM. Enterococcal endocarditis. In Kaye D, ed. *Infective Endocarditis*, 2nd edn. New York: Raven Press, 1992: 209–23.

57 Eliopoulos GM. Aminoglycoside resistant enterococcal endocarditis. *Med Clin North Am* 1993;**17**:117–33.

58 Karchmer AW, Gibbons GW. Infection of prosthetic heart valves and vascular grafts. In: Bisno AL, Waldvogel FA, eds. *Infections Associated with Indwelling Medical Devices*, 2nd edn. Washington, DC: American Society for Microbiology, 1994: 213–49.

59 Fowler VG Jr, Miro JM, Hoen B, *et al.*, ICE Investigators. *Staphylococcus aureus* endocarditis: a consequence of medical progress. *JAMA* 2005;**293**:3012–21.

60 Geraci JE, Wilson WR. Symposium on infective endocarditis. III. Endocarditis due to Gram-negative bacteria: report of 56 cases. *Mayo Clin Proc* 1982;**57**:145–8.

61 Pesanti EL, Smith IM. Infective endocarditis with negative blood cultures: an analysis of 52 cases. *Am J Med* 1979;**66**:43–50.

62 Durack DT. Prevention of infective endocarditis. *N Engl J Med* 1995;**332**:38–44.

63 Gould FK, Elliott TSJ, Foweraker J, *et al.* Guidelines for the prevention of endocarditis: report of the Working Party of the British Society for Antimicrobial Chemotherapy. *J Antimicrob Chemother* 2006;**57**:1035–42.

64 Wilson WR, Taubert KA, Gewitz MH, *et al.* Prevention of infective endocarditis: guidelines from the American Heart Association. *Circulation* 2007;**116**:1736–54.

65 Richey R, Wray D, Stokes T. Prophylaxis against infective endocarditis. Summary of the NICE (National Institute for Clinical Excellence) Guidance. *Br Med J* 2008;**336**:770–1.

66 Habib G, Hoen B, Tornos P, *et al.* Guidelines on the prevention, diagnosis, and treatment of infective endocarditis (new version 2009). The Task Force on the Prevention, Diagnosis and Treatment of Infective Endocarditis of the European Society of Cardiology (ESC). *Eur Heart J* 2009;**30**:2369–413.

67 Fowler VG, Moro JM, Hoen G, *et al.* ICE Investigators. *Staphylococcus aureus* endocarditis: a consequence of medical progress *JAMA* 2005;**293**:3012–21.

Further reading

American Heart Association. *1997 Heart and Stroke Statistical Update.* Dallas, TX: American Heart Association, 1997: 18.

Awadallah SM, Kavey R-EW, Byrum CJ, *et al.* The changing pattern of infective endocarditis in childhood. *Am J Cardiol* 1991;**68**:90–4.

Baltimore RS. Infective endocarditis in children. *Pediatr Infect Dis J* 1992;**11**:907–12.

Berkowitz FE, Dansky R. Infective endocarditis in black South African children: report of 10 cases with some unusual features. *Pediatr Infect Dis J* 1989;**8**:787–91.

Bhandari S, Kaul U, Shrivastava S, *et al.* Infective endocarditis in children. *Indian J Pediatr* 1984;**51**:529–32.

Blumenthal S, Griffiths SP, Morgan BC. Bacterial endocarditis in children with heart disease: a review based on the literature and experience with 58 cases. *Pediatrics* 1960;**26**:993–1017.

Dodo H, Child JS. Infective endocarditis in congenital heart disease. *Cardiol Clin* 1996;**14**:383–92.

Hugo-Hamman CT, de Moor MM, Human DG. Infective endocarditis in South African children. *J Trop Pediatr* 1989;**35**:154–8.

Johnson CM, Rhodes KH. Pediatric endocarditis. *Mayo Clin Proc* 1982;**57**:86–94.

Kramer HH, Bourgenis M, Liersch R, *et al.* Current clinical aspects of bacterial endocarditis in infancy, childhood, and adolescence. *Eur J Pediatr* 1983;**140**:253–9.

Millard DD, Shulman ST. The changing spectrum of neonatal endocarditis. *Clin Perinatol* 1988;**15**:587–608.

Moethilalh R, Coovadia HM. Infective endocarditis in thirteen children: a retrospective study (1974–1981). *Ann Trop Paediatr* 1982;**2**:57–62.

Noel GJ, O'Loughlin JE, Edelson PJ. Neonatal *Staphylococcus epidermidis* right-sided endocarditis: description of five catheterized infants. *Pediatrics* 1988;**82**:234–9.

Normand J, Bozio A, Etienne J, *et al.* Changing patterns and prognosis of infective endocarditis in childhood. *Eur Heart J* 1995;**16**(Suppl B):28–31.

Somers K, Patel AK, Steiner I, *et al.* Infective endocarditis: an African experience. *Br Heart J* 1972;**34**:1107–12.

61 Rheumatic Fever

Shaji C. Menon & Lloyd Y. Tani

University of Utah, Salt Lake City, UT, USA

Acute rheumatic fever (ARF) is a systemic inflammatory autoimmune disease secondary to infection with Lancefield group A β-hemolytic streptococci (*Streptococcus pyogenes*) [1]. In its acute stage, the disease is characterized by inflammation of several organ systems, including the heart, joints, brain, and skin, with the clinical manifestations of arthritis, carditis, chorea, erythema marginatum, and subcutaneous nodules [2]. Antibiotic treatment of and prophylaxis against streptococcal pharyngitis can prevent the occurrence and recurrence of ARF [3,4]. Long-term sequelae of the inflammation are minimal, with the exception of the heart, in which inflammation during the acute phase with subsequent fibrosis and scarring of the cardiac valves may lead to rheumatic heart disease (RHD) (see Chapter 62). Starting from the middle of the twentieth century, the incidences of ARF and RHD have significantly decreased in industrialized and developed countries [5], primarily as a result of vast improvements in living conditions among the populations. With a few notable exceptions, ARF and RHD are now largely diseases of developing countries and of underprivileged and indigenous populations of developed countries [6–18].

Epidemiology

According to reports published by the World Health Organization (WHO) in 2005, the prevalence of RHD worldwide is at least 15.6 million [6]. Every year, 280 000 new cases of RHD occur and 230 000 people die secondary to RHD [6]. The reported mortality rate for RHD varies from 0.5 per 100 000 population in Denmark to 8.2 per 100 000 population in China [19]. The true incidence and prevalence of RHD are thought to be significantly higher than these conservative estimates. Epidemiologic data from underdeveloped nations are incomplete or unavailable. The prevalence of RHD in children is highest in sub-Saharan Africa (5.7 per 1000) and in the indigenous populations of Australia and New Zealand (3.5 per 1000) and south central Asia (2.2 per 1000) [2,20–24]. The prevalence of RHD increases with age and peaks between 25 and 34 years [6]. In developed countries, the prevalence of RHD is estimated to be ~0.5 per 1000 [2].

ARF develops following group A β-hemolytic streptococcal infection of the upper respiratory tract. However, only 2–3% of patients with untreated streptococcal pharyngitis develop ARF. In populations where rheumatogenic group A streptococci are endemic, the lifetime cumulative incidence of ARF in exposed individuals has been estimated at 3–6% [13]. The age distribution of ARF incidence follows the incidence of streptococcal pharyngitis. ARF occurs most commonly in children between 5 and 14 years of age and is extremely rare in children <2 years old [25,26]. Only 5% of first episodes occur in children <5 years old [27]. The first episode of ARF usually occurs before adolescence and, in the absence of secondary prophylaxis, recurrences are common during adolescent and early adulthood years. Although reported, initial attacks of ARF are uncommon in adults [6]. Ethnic and racial differences in ARF and RHD burden are well documented [6–18,20]. In some developing countries, the incidence of ARF exceeds 50 per 100 000 children [6–18]. The highest reported rates are in the indigenous populations of Australia and New Zealand. In New Zealand, the incidence of ARF in school-age Maori and Pacific Islanders is 80–100 per 100 000, compared with an incidence of 10 per 100 000 in the non-indigenous population [28]. Even more striking are the rates as high as 245–351 per 100 000 reported in Australian aboriginal children [28]. These racial and ethnic differences in ARF and RHD persist even when corrected for socioeconomic status. In addition to this ethnic and racial predilection, there is also a familial predilection [1]. The
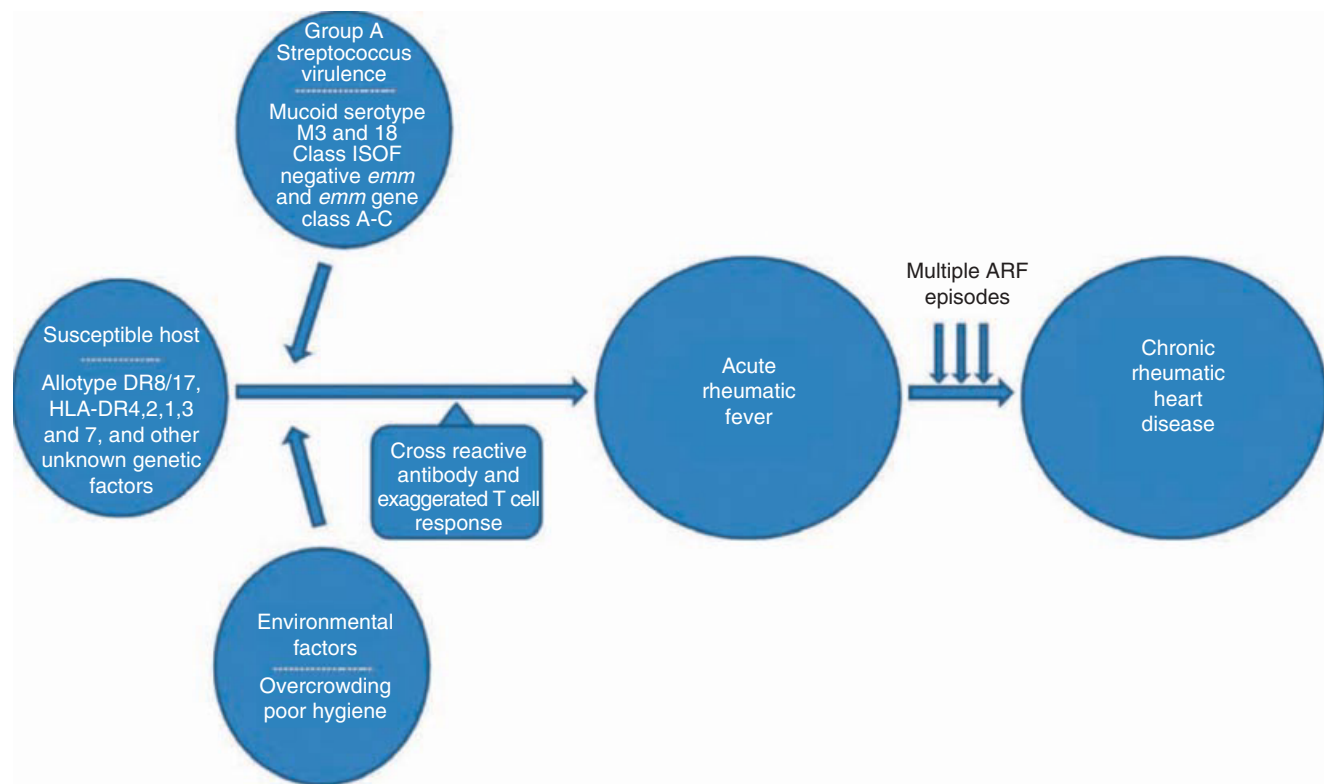
Figure 61.1 Pathogenic pathway for ARF and RHD. (Modified from Carapetis *et al. Lancet* 2005;**366**:155–68.)

likelihood of an individual developing ARF is five times higher if a family member has had ARF [1]. In a study of children raised separately from their parents in an Israeli kibbutz, the relative risk for development of ARF was 2.93 in children with a family history of RHD compared with those without a family history [29]. Furthermore, increased concordance in monozygotic twins compared with dizygotic twins has been reported [1,30]. The inheritance pattern is multifactorial and not simple Mendelian single-gene inheritance. Although no gender predisposition has been reported in most series, a female predominance of ARF and RHD has been reported in some studies [12]. The female predilection in these studies may be attributed to reduced access to health care for females in some populations.

Pathogenesis

There is irrefutable epidemiological evidence for an association between group A β-hemolytic streptococcal infections and ARF. ARF is the result of an exaggerated immune response in a susceptible individual to the cross-reactive group A streptococcal epitope [6]. The three key factors that determine the pathogenesis of ARF are (1) rheumatogenicity of group A streptococcus, (2) genetic susceptibility, and (3) host immune response [6] (Figure 61.1).

The organism

Streptococcus pyogenes (group A streptococcus) is a Gram-positive, β-hemolytic, non-motile, non-spore-forming coccus that occurs in chains or in pairs (Figure 61.2a) and is commonly found in the throat and on the skin. The prevalence of group A streptococcus carriage in an unselected, office-based adult population has been estimated at 5–12% [19,31,32]. Group A streptococcus may cause scarlet fever, impetigo, otitis media, sinusitis, or cellulitis, and is the most common cause of bacterial pharyngitis among children and adults [33]. Streptococcal pharyngitis occurs primarily among children 5–15 years of age [34].

The typical clinical and epidemiological features of group A streptococcal pharyngitis are shown in Table 61.1 [35]. Other more serious infections caused by group A streptococcus include necrotizing fasciitis, myositis, meningitis, and streptococcal toxic shock syndrome [36]. ARF and acute glomerulonephritis occur as immune-mediated post-streptococcal sequelae [36]. Group A streptococci produce a multitude of virulence factors and toxins, including M protein (impedes phagocytosis, binds immunoglobulins), adherence and colonization factors such as streptococcal fibronectin-binding protein 1 and lipoteichoic acid, hyaluronic acid capsule (inhibits phagocytosis by polymorphonuclear leukocytes and macrophages), and factors facilitating liquefaction of pus and spreading of infections
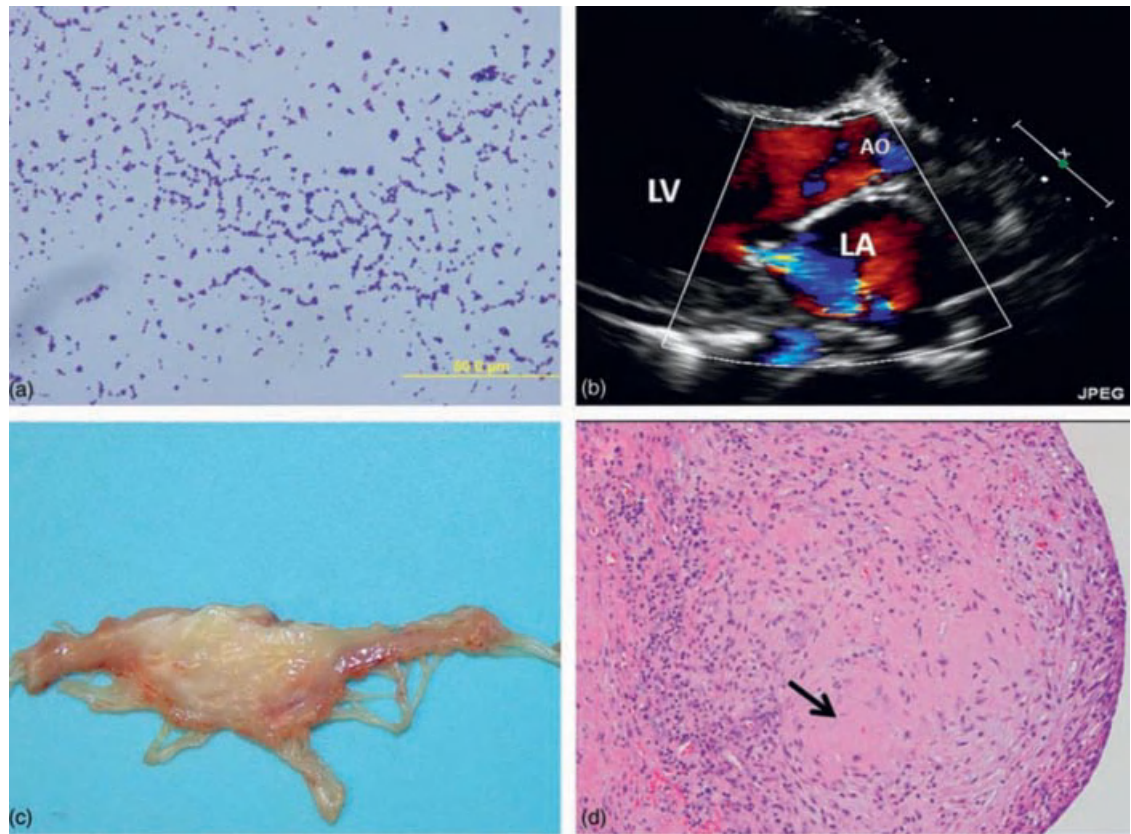
Figure 61.2 A 10-year-old boy presented with a 2-week history of fever, arthritis, breathlessness on exertion, and signs of heart failure. Throat swab culture was positive for group A streptococcus. (a) Grams stain of throat swab culture shows group A streptococcus in chains and pairs. (b) 2D echocardiogram, parasternal long-axis view shows posteriorly directed mitral valve regurgitation. The patient developed worsening heart failure secondary to mitral valvulitis requiring surgical intervention and mitral valve replacement. (c) Gross pathology specimen of resected mitral valve anterior leaflet shows thickened and edematous leaflet suggestive of acute rheumatic fever-associated valvulitis. (d) Microscopic images show signs of acute inflammation and foci of fibrinoid necrosis (arrow) with surrounding lymphohistiocytic infiltrate consistent with the patient's clinical history of acute rheumatic carditis. Following surgical replacement of the mitral valve, the patient's clinical condition improved and left ventricular function normalized. Ao, aorta; LA, left atrium; LV, left ventricle.

Table 61.1 Clinical and epidemiological features suggestive of group A streptococcal tonsillopharyngitis[a].

5–15 years of age
Presentation in winter or early spring (in temperate climates)
History of sick contact
Sudden-onset sore throat
Pain on swallowing
Fever
Scarlet fever rash
Headache
Nausea, vomiting, and abdominal pain
Tonsillopharyngeal erythema or exudate
Soft palate petechiae ("doughnut" lesions)
Red and swollen uvula
Tender, enlarged anterior cervical nodes

[a]Features suggestive of viral origin are coryza, cough, conjunctivitis, hoarseness, diarrhea, and characteristic exanthems or enanthems.

such as streptokinase, streptodornase (DNases A, B, C, and D), hyaluronidase, streptolysins, and streptococcal pyrogenic exotoxin B [37]. In addition to these factors, *S. pyogenes* possesses additional virulence factors. C5a peptidase (SCPA) inhibits the chemotactic signals by cleaving the complement component of C5a [37]. A protein antigen very closely associated with the M protein molecule of group A streptococci is called serum opacity factor (OF). OF opacifies mammalian serum by interacting with high-density lipoproteins and is antigenic and type specific [34]. OF is a potential vaccine candidate because it can evoke antibodies that protect against infections by OF-positive group A streptococci [38].

Rebecca Lancefield classified β hemolytic streptococci into 20 different groups (Lancefield groups) (A–H and K–V) based on the serologic reactivity of cell wall polysaccharide antigens [34]. The M protein is considered a major somatic virulence factor that binds the host fibrinogen and blocks the binding of complement to the underlying

peptidoglycan and inhibits phagocytosis [34]. M protein is a filamentous α-helical coiled macromolecule that is part of the cell membrane [34]. M protein is the major cause of antigenic shift and antigenic drift among group A streptococcus [39]. Based on M protein, about 120 different serotypes or genotypes of *S. pyogenes* have been identified [36]. Following an acute infection, type-specific antibodies against M protein confer immunity. Several epitopes of M protein cross-react with human myocardial and brain tissue. M serotypes 1, 3, 5, 6, 18, 19, and 24 may form mucoid colonies heavily encapsulated with antiphagocytic properties which have been associated with ARF, and are considered rheumatogenic [19,40–42]. In contrast, M serotypes 2, 49, 57, 59, 60, and 61 have been associated with pyoderma and glomerulonephritis, but not ARF [19]. Other reports have challenged this notion of higher rheumatogenic potential of specific M serotypes [19,43–45]. In many regions of the world with a high prevalence of ARF and RHD, rheumatogenic M serotypes are infrequently seen [44]. Furthermore, serotypes associated with skin infections have been associated with ARF [45]. In the Maori population of New Zealand, the classic rheumatogenic M-serotypes associated with pharyngitis are absent [44]. In the native Australian population with a high incidence of ARF, there is a low incidence of streptococcal pharyngitis and pharyngeal carriage, but a high incidence of pyoderma [46,47]. Although this suggests that other serotypes, possibly associated with streptococcal impetigo, may play a role in the pathogenesis of ARF in some patients, there is lack of conclusive evidence of streptococcal skin lesions leading to ARF.

Based on production of OF, the group A streptococcus can be classified into two antigenic groups, class I and II [48]. Class I strains are predominantly serum OF-negative and are associated with ARF, whereas class II strains are serum OF-positive and are associated with post-streptococcal glomerulonephritis [49]. Another means of classifying group A streptococcus is by M genotype; *emm* and *emm*-like genes on the group A streptococcus chromosome can be used to classify them into five groups, A–E [50]. Groups A–C are associated with pharyngitis and ARF, group D is associated with skin infections, and group E is known to cause infection at either site [50]. In highly endemic regions of the world, the streptococci identified from patients with ARF show evidence of significant genetic recombination, cross-trophism between skin and pharyngeal strains, and blurring of a distinction between rheumatogenic and non-rheumatogenic strains [51]. Another possible mechanism for pathogenicity of skin streptococcal strains in ARF includes immune priming of a host by repeated impetigo or pharyngeal colonization resulting in a subsequent exaggerated immune response. Horizontal transfer of genetic information between skin and throat strains of streptococci has also been documented [6].

Host factors

Only 2–3% of individuals with acute streptococcal pharyngitis develop RF, indicating the role of host susceptibility in the development of ARF [19]. Familial clustering and autosomal recessive inheritance of ARF have been reported [52,53]. The incidence of post-streptococcal pharyngitis associated recurrent ARF in individuals with a past history of ARF is as high as 65% compared with 2–3% in the general population [54]. Specific human leukocyte antigens (HLA-DR) class II alleles are associated with ARF [55]. The role of HLA-DR antigens in ARF susceptibility may be explained by their modulating role in the immune response [19,55]. HLA-DR alleles DR4, DR2, DR3, and DRw6 have been implicated as possible disease susceptibility alleles [56–60]. The presence of multiple predisposing HLA-DR alleles suggests that HLA predilection is not linked to one specific allele but is likely influenced by a gene near the HLA-DR locus. HLA-DR4 is present more frequently in Caucasians, DR2 in African-American populations, DR1 and DRw6 in South African populations, and HLA-DR3 in Indian populations [19,61]. Furthermore, there are HLA-specific predilections for different organ system involvement: HLA-A10 and HLA-DR11 with cardiac involvement and HLA-C2 in ARF without cardiac involvement. However, these susceptibility alleles vary in different populations [56–60]. Another susceptibility marker of ARF disease is a specific B-cell alloantigen,(D8/17) [62]. In one study, 95% of patients with a history of ARF carried the D8/17 antigen. In contrast, this antigen was found in 50% of first-degree relatives and only 4% of controls. This association between D8/17 and ARF has been found in different patient groups, including Australian aboriginal, North American, Caribbean, Israeli, Russian, Mexican, and Chilean populations [63]. The D8/17 antigen is thought to be a binding site for group A streptococcus on B cells. Although the D8/17 antibody may bind to the antigen on the B cells and cross-reacts with human cardiac, skeletal, and smooth muscle, and with streptococcal M protein, the precise role of the D8/17 antigen in ARF pathogenesis remains uncertain [64]. The D8/17 antigen was not highly prevalent in an Indian RHD population, which showed a higher incidence of monoclonal antibodies PG-12A, PG-13A, and PG-20A raised against B cells [65–67]. High concentrations of circulating mannose-binding lectin 72 and polymorphisms of transforming growth factor-β 173 and immunoglobulin genes have been associated with ARF [68,69].

Host immune response

Molecular mimicry between group A streptococcus antigens and human host tissue is believed to be the basis of an autoimmune response leading to the manifestations of ARF [70,71]. Structural and immunological similarities between α-helical cardiac proteins such as cardiac myosin, laminin,

and vimentin and group A streptococcus M protein, which is also α-helical, has been postulated as responsible for this molecular mimicry [72,73]. Laminin is an extracellular matrix protein present in the basement membrane of valves and around endothelium. This may explain the valvitis of ARF. T cells from rats immunized with group A streptococcus M protein and from RHD patients proliferate in response to both group A streptococcus M protein and cardiac myosin, but not to skeletal muscle myosin [57]. Human valve tissue also cross-reacts with streptococcus *N*-acetylglucosamine in the group A streptococcus carbohydrate. Normal cardiac cell turnover might expose self cardiac antigens, such as intracardiac myosin, to T cells. Subsequent exposure to group A streptococcus M protein that cross-reacts with cardiac myosin results in an exaggerated immune response from these T cells. The immune response is further emboldened by the high levels of cytokines in the human body resulting from streptococcal superantigens [74,75]. Apart from the initial antibody-mediated damage, T cell-mediated cellular immunity and macrophage infiltration are thought to result in long-term valvar fibrosis and dysfunction (chronic RHD).

Environmental factors

Disparity in the incidences of ARF and RHD between developing and developed nations indicates the key role that environmental factors play in the pathogenesis of disease. Poor living conditions, overcrowding, and limited access to health care are the most significant determinants of disease distribution [19]. In temperate climates, the incidence of streptococcal infections and ARF is higher in early fall, late winter, and early spring [19].

Pathology

Rheumatic fever is characterized by inflammation of the heart, skin, joints, and brain. Cardiac inflammation and its sequelae are responsible for the majority of immediate and long-term morbidity and mortality [19]. Acute RHD is a pancarditis, involving all three layers of the heart [19]. However, valvitis, rather than myocarditis or pericarditis, is the dominant factor responsible for the cardiac clinical manifestations, morbidity, and mortality associated with ARF [76–79]. Rheumatic carditis is almost always associated with mitral valvitis [19]. Unlike other myocarditides, significant myocyte necrosis and troponin elevation are rare. Cardiac manifestations are secondary to significant mitral and/or aortic valvar regurgitation and the resultant acute left heart volume overload (Figure 61.2b). The mitral valve is the primary target of endocardial involvement in ARF [80] (Figure 61.2c). Mitral annular dilatation and chordal elongation of the anterior leaflet of the mitral valve cause mitral regurgitation and, in the extreme, prolapse of the anterior leaflet with resultant mitral regurgitation directed posterolaterally

[80,81]. Dilatation of the left ventricle and restriction of posterior mitral leaflet mobility contribute to chronic MR in patients with RHD [82]. Mitral valvar involvement also includes valve edema and aggregation of fibrin and platelets forming small (1–3 mm) vegetations sometimes called "verrucae" along the closure lines of the leaflets [83,84]. The pathology of chronic RHD is described in Chapter 62.

The distribution of valvar involvement is variable. The mitral valve is most commonly involved, followed by aortic, tricuspid, and rarely pulmonary valve. Laminin in the valvar basement membrane and endothelium cross-reacts with sensitized T cells which may be responsible for initial valvitis [85]. However, cell-mediated immunity resulting in infiltration by macrophages and T cells is responsible for chronic valve injury [86,87]. Isolated pericarditis in the absence of valvitis is rare. Myocarditis may result in conduction system abnormalities. Endomyocardial biopsy studies in ARF have shown the absence of focal or diffuse myocytic necrosis and cellular infiltration of mononuclear lymphocytes, classic features of myocarditis as defined by Dallas Criteria [19]. There is usually focal perivascular mononuclear cell infiltration resulting in formation of the Aschoff body that is considered virtually pathognomonic of ARF [19]. An Aschoff body consists of a central area of fibrinoid collection surrounded by lymphocytes, histiocytes, and large basophilic cells (Figure 61.2d). Many of these cells have elongated nuclei with a distinctive chromatin pattern, sometimes called caterpillar or owl-eye nuclei. Cells containing these nuclei are called Anichkov's myocytes. These foci may be found in the pericardium, the myocardium, or the valves. Coronary arteritis has been described. As healing starts, Aschoff nodules and inflammatory cells disappear and fibroblastic proliferation occurs [88].

ARF-associated arthritis is characterized by a fibrinous and sterile effusion without erosion of the joint surfaces or pannus formation. Erythema marginatum is secondary to vasculitis and the subcutaneous nodules have histological features similar to Aschoff's nodules. Inflammation of the basal ganglia and caudate nuclei is responsible for Sydenham's chorea. The changes in the brain, joints, and skin usually resolve with time and do not result in long-term sequelae.

Clinical features and diagnosis

ARF shares many clinical features with other collagen vascular disorders. There is no single diagnostic test for ARF. The diagnosis is based on the Jones criteria, established in 1944 [89]. The criteria are divided into major and minor manifestations and in most patients the diagnosis requires evidence of a preceding group A streptococcal infection. The criteria have been revised and updated multiple times (Table 61.2) [90–93] with the aim of increasing the specificity of diagnosis following decreasing incidence of ARF in industrialized

Table 61.2 Updated Jones criteria (1992) for the diagnosis of a first episode of ARF [19][a].

Major manifestations	Minor manifestations	Supporting evidence of antecedent group A streptococcal infection
1. Carditis 2. Polyarthritis 3. Chorea 4. Erythema marginatum 5. Subcutaneous nodules	*Clinical* 1. Arthralgia 2. Fever *Laboratory* 1. Elevated acute-phase reactants: erythrocyte sedimentation rate or C-reactive protein 2. Prolonged P–R interval on electrocardiogram	1. Elevated or rising streptococcal antibody titer 2. Positive group A streptococcal throat culture or rapid streptococcal antigen test

[a]Two major or one major and two minor manifestations must be present, plus evidence of antecedent group A streptococcal infection are required for diagnosis of ARF. In patients with established RHD, recurrence of ARF requires two minor manifestations plus evidence of antecedent group A streptococcus infection. Chorea and indolent carditis do not require evidence of antecedent group A streptococcal infection.

nations [94]. In underdeveloped countries and indigenous populations of the developed countries, strict application of the updated Jones criteria may result in underdiagnosis of ARF. The WHO criteria (2002–2003) made the diagnostic criteria for recurrent ARF less stringent [19] to increase the sensitivity of diagnosis of recurrent ARF in regions of the world where the incidence is higher.

Based on the Jones criteria, two major or one major and two minor manifestations, plus evidence of antecedent group A streptococcus infection, are required for diagnosis of ARF [19]. Chorea and indolent carditis do not require evidence of antecedent group A streptococcus infection. It is important to remember that ARF is not ruled out if the Jones criteria are not met. This is similar to the atypical Kawasaki patient who subsequently develops coronary aneurysms. The WHO includes criteria (2002–2003) for diagnosing a recurrent episode of ARF:

1 In patients without established RHD: diagnose as if the first episode with Jones criteria.

2 In patients with established RHD: diagnosis requires two minor manifestations, plus evidence of antecedent group A streptococcus infection. Evidence of antecedent group A streptococcus infection as per Jones criteria, but with addition of recent scarlet fever [19].

Revision of some of criteria is being considered. In high-risk populations, the major features considered for revision to increase the sensitivity include joint manifestations, the diagnosis of carditis, and the definition of recurrent ARF. Monoarthritis or a polyarthralgia rather than the classic migratory polyarthritis are a presenting features in the indigenous New Zealand population. Furthermore, echocardiography is more sensitive than auscultation in detecting rheumatic valvitis, allowing detection of subclinical carditis.. The role of echocardiography in the diagnosis of ARF is still in question. Published guidelines from Australia (2005) and New Zealand (2006) accept subclinical carditis, monoarthritis, and polyarthralgia as major criteria [2,95].

Major manifestations

Arthritis

Arthritis is present in >75% of patients with ARF and is both the most common and earliest major manifestation [19]. It usually affects the large joints (knees and ankles followed by wrists and elbows) [19]. Joint involvement is more common in adolescents than adults [19]. An inverse correlation between the severity of arthritis and carditis has been reported [54]. Joint involvement ranges from arthralgia alone to severe arthritis characterized by pain, swelling, warmth, erythema, severe limitation of motion, and exquisite tenderness to pressure or motion. Patients with severe lower limb arthritis may be unable to walk ("pseudo-paralysis"). The hips and small joints of the hands and feet are occasionally affected. Involvement of shoulders and lumbosacral, cervical, sternoclavicular, and temporomandibular joints is rare. This is an asymmetric and migratory polyarthritis [19]. The arthritis in one joint can last for a few hours and then appear in another joint. A number of joints can be affected in succession, and the periods of involvement may overlap. In endemic areas, such as India and Australia, joint involvement may be less severe [96,97], perhaps from early self-treatment with anti-inflammatory agents. The arthritis of ARF is highly responsive to salicylates. If the arthritis persists for more than 48–72 h following

Table 61.3 Common differential diagnoses [19,157,166].

Diagnosis	Confirmatory test
Polyarthritis and fever	
Infectious	Synovial fluid and blood culture
Bacterial septic arthritis	Serology
Viral arthritis	Serology
Lyme disease	Blood culture
Bacterial endocarditis	Culture and serology
Reactive	
Enteric infection, Reiter syndrome	Culture
Inflammatory bowel disease	Clinical findings
Rheumatoid arthritis	Clinical findings and serology
Systemic lupus erythematosus	Clinical findings and serology
Chorea	
Seizures	Electroencephalogram (EEG) and altered consciousness
Familial chorea	Family history, MRI or CT scan
Cerebrovascular accidents	MRI and CT scan
Drug intoxication	Drug screen (phenytoin, metoclopramide, amitriptyline, fluphenazine)
Oral contraceptive-induced chorea	History
Pregnancy-induced chorea	History and pregnancy test
Wilson disease	Serum ceruloplasmin and urine copper
Hyperthyroidism	Thyroid function test
Hyperparathyroidism	Low serum calcium and high phosphorus
Erythema marginatum	
Sepsis	Blood culture
Drug reaction	History and drug screen
Glomerulonephritis	Urine microscopy and analysis
Juvenile rheumatoid arthritis	Clinical findings and serology
Lyme disease	Serology

initiation of salicylate therapy, the diagnosis of ARF should be reconsidered. Untreated, the arthritis of typically lasts for 2–3 weeks. If the joint is aspirated on suspicion of septic arthritis, the synovial fluid usually contains thousands of white blood cells, with a preponderance of polymorphonuclear leukocytes. Bacterial cultures are sterile [19]. The differential diagnosis for arthritis and other major criteria are shown in Table 61.3.

The term "post-streptococcal reactive arthritis" (PSRA) was first introduced in 1959 to describe arthritis occurring after an episode of group A streptococcal pharyngitis in the absence of other major criteria of ARF [98]. PSRA typically affects the small joints and is less responsive to anti-inflammatory agents [99]. There is no clear distinction between PSRA and ARF associated arthritis and some of these patients have developed full-blown ARF [99–101].

Although these patients have a lower risk of carditis, they should be observed for several months for evidence of cardiac involvement [101]. PSRA should be diagnosed with caution in populations with high risk of ARF. Antibiotic prophylaxis is recommended for 5 years in high-risk populations and for 1 year in low-risk populations [100,101]. If clinical evidence of carditis is not observed, the prophylaxis can be discontinued. If valvar disease is detected, the patient should be classified as ARF and continue secondary prophylaxis (discussed below).

Carditis

Although ARF is a systemic disease, the only manifestation leading to permanent damage is carditis. Carditis is the single most important prognostic factor in ARF [19]. RHD, a sequela of ARF, is the most common cause of acquired heart disease worldwide [19]. It accounts for 35–40% of cardiovascular disease-related hospital admissions, and is the predominant reason for cardiac surgery in developing countries. About 50% of patients with ARF have cardiac involvement [102]. The interval between arthritis and carditis rarely exceeds 7–10 days. The severity of cardiac involvement is variable, and the clinical diagnosis of carditis is based on the appearance of murmurs of mitral and/or aortic regurgitation, a pericardial friction rub, sometimes with radiographic cardiomegaly, and/or signs of heart failure [19]. Recurrent ARF with carditis is diagnosed by a new murmur, a change in a previous murmur [19], a new pericardial friction rub, or a radiographic increase in heart size [19]. Myocarditis without valvitis is unlikely to be of rheumatic origin [19].

Symptoms of carditis are related to the degree of valvar dysfunction and pericardial inflammation, and include shortness of breath, dyspnea on exertion, cough, paroxysmal nocturnal dyspnea, chest pain, and orthopnea. Myocarditis may result in disproportionate sinus tachycardia in a resting patient. Pericarditis is evident as distant heart sounds, a friction rub, and chest pain [19]. Low-voltage QRS complexes on ECG and cardiac enlargement on chest X-ray suggest a significant pericardial effusion. Pericarditis invariably occurs with concomitant left-sided valvar involvement. Both tamponade and subsequent constrictive pericarditis are very uncommon. A diagnosis of ARF should be reconsidered when pericarditis is present in the absence of valvar involvement. Uncommon presentations are arrhythmias and conduction system abnormalities. A prolonged PR interval (first-degree AV block) is a manifestation of myocarditis and a minor Jones criterion.

Inflammation of valve support structures along with changes in leaflets results in mitral valve dysfunction and regurgitation [81]. Isolated mitral valve involvement is seen in ~65% of patients, isolated aortic valve involvement in ~5%, and combined mitral and aortic valve involvement in ~30% of patients with carditis. The tricuspid and pulmonary valves are rarely involved. Characteristic murmurs of acute

mitral valvitis include the high-pitched, blowing, holosystolic, apical murmur of mitral regurgitation. In some patients, the murmur may be audible after positioning the patient in a left lateral decubitus position and auscultating over the apex with the patient at held expiration. With significant mitral regurgitation, a low-pitched, apical, mid-diastolic, flow murmur (Carey Coombs murmur) resulting from relative mitral stenosis can be heard. This murmur never occurs in isolation. Some authorities describe another mid-diastolic murmur that is isolated, not associated with cardiomegaly or mitral regurgitation, that is believed to be due to turbulence as blood flows over the mitral vegetations. Aortic regurgitation results in a high-pitched, decrescendo, diastolic murmur heard best at the mid-left sternal border. More subtle aortic regurgitant murmurs may be audible with the patient sitting up, leaning forward, with held expiration. Severe aortic regurgitation leads to bounding pulses due to aortic runoff. In chronic RHD, murmurs of mitral and aortic stenosis may be heard.

Echocardiography and ARF

Valvitis is the characteristic finding of the endocardial involvement in acute rheumatic carditis, with mitral regurgitation the most common abnormality. Echocardiographic findings of acute rheumatic mitral regurgitation include (1) annular dilatation, (2) chordal elongation/rupture, (3) leaflet prolapse, (4) coaptation defect, (5) nodules on valve tips with mild thickening of leaflets, and (6) left ventricular dilatation and subsequent dysfunction with significant valvar regurgitation [19,81,82]. Small nodules on the mitral valve leaflet found in >25% of patients with ARF disappear on follow-up [82]. Ventricular dilatation is usually not from myocardial dysfunction and systolic function indices are preserved. The ventricular function normalizes rapidly after surgical correction of significant valvar regurgitation [19].

Very mild valvar involvement may be subclinical and diagnosed solely by echocardiography in patients without a murmur [103–107]. Compared with the pre-echocardiography era, the auscultatory skills of medical professionals have declined. The clinical diagnosis of rheumatic carditis may not be made with confidence [106–108]. Mild valvar regurgitation is not always detected by routine clinical auscultation and may be missed even by expert clinicians [102,109]. In the Utah ARF outbreak, Doppler evidence of mitral regurgitation was demonstrated in 19% of ARF patients who were clinically considered to have either isolated arthritis or pure chorea [110]. Using WHO echocardiographic criteria, the prevalence of subclinical carditis is about 18% in patients with ARF without a murmur [111]. Although echocardiography has greater sensitivity than auscultation for assessing cardiac and valvar function, the role of echocardiography in identifying acute rheumatic carditis remains controversial [112]. Echocardiographic evidence of trivial amounts of valvar regurgitation is common in the normal population [113].

Physiological mitral regurgitation is present in 2.4–45% of individuals, aortic regurgitation in 0–33%, tricuspid regurgitation in 6.3–95%, and pulmonary regurgitation in 21.9–92% [19,114–116]. Echocardiographically detected physiologic mitral regurgitation is seen in 38–45% of healthy children with a normal heart, and may be even higher in febrile patients [113,117]. Physiologic valvar regurgitation must be distinguished from pathologic regurgitation by specific criteria. On echocardiography, mitral valvar regurgitation is considered pathologic if a mosaic color jet is visible in two imaging planes, is holosystolic by spectral Doppler, has a peak velocity >2.5 m s, and extends >1 cm beyond the plane of valve leaflets [19,105,118]. Similarly, aortic regurgitation is considered pathologic if it is visible in two planes, is holodiastolic, and extends >1 cm beyond the aortic valve leaflets [19,106]. "Physiologic" tricuspid and pulmonary regurgitation are much more common in the general population and in isolation cannot be considered a sign of rheumatic carditis. At present, the Jones criteria do not include subclinical carditis. The barriers for including echocardiographic criteria for diagnosis of ARF include (1) the long-term outcome of subclinical carditis is not well known, (2) difficulty in differentiating subclinical pathologic from physiological regurgitation, (3) limited availability of echocardiography in regions with a high incidence of ARF, and (4) risk of overdiagnosis of ARF in low-risk populations. Recent studies of RHD prevalence using echocardiography in India and Africa showed unexpectedly high rates of subclinical RHD (21–51 per 1000 school children) [119,120], perhaps from unrecognized subclinical carditis. Judicious use of echocardiography in high-risk populations may improve the sensitivity of ARF diagnosis and avoid misdiagnosis of ARF [19].

The recent Australian and New Zealand guidelines include echocardiographic subclinical carditis as a major criterion for ARF. All patients with suspected or definite ARF should have echocardiography to evaluate carditis [121–123]. The WHO recommends that silent indolent rheumatic carditis diagnosed by echocardiography should be managed as RHD until proven otherwise [19].

Sydenham's chorea (chorea minor, "St. Vitus Dance")

Sydenham's chorea, the third most common manifestation of ARF, occurs in 5–36% of patients [19,124] but rarely after 20 years of age. Chorea is a manifestation of involvement of the basal ganglia. The disease was first named by Thomas Sydenham in 1686 as "St. Vitus Dance" to differentiate it from then prevalent exorcism-associated dancing. The latent period between ARF and chorea is usually between 1 and 7 months and can be as long as 12 months [19]. Because of this long latency period, polyarthritis and chorea do not occur simultaneously and evidence of an antecedent streptococcal infection is often absent [19]. The clinical features of

chorea include emotional lability, personality change, muscular weakness, and uncoordinated, involuntary, abrupt, and purposeless movements. Other features of chorea include dysarthric speech, gait problems, and poor fine motor skills. The onset of chorea may be subtle and characterized by fretfulness, irritability, inattentiveness to schoolwork, and fidgety behavior. Chorea can be either unilateral or bilateral [125]. The manifestations are exacerbated by stress and they disappear or become less pronounced during sleep and with sedation. Hypotonia and abnormal movements result in lack of coordination, gait disturbances, and speech impairment, sometimes severely disturbing activities of daily living. Patients with chorea may manifest psychological and psychiatric issues such as depression, anxiety, personality changes, emotional lability, obsessive–compulsive disorder (OCD), tics, and attention deficit disorder. Clinical maneuvers to elicit features of chorea include (1) milkmaid's grip (contraction and relaxation of the hand muscles while squeezing the examiner's fingers), (2) wormian darting movements of the protruded tongue (bag of worms), (3) staccato and jerky speech, (4) "spoon" or "dish" appearance of the extended arms due to flexion of the wrist and hyperextension of the metacarpophalangeal joints, (5) pronation of one or both hands when raised above the head ("pronator sign"), and (6) worsening of handwriting or difficulty in buttoning and unbuttoning while testing for fine motor skills [19]. Patients with chorea gravidarum or chorea occurring with oral contraceptives may have a past history of Sydenham's chorea, suggesting enhanced susceptibility to chorea in some individuals [19]. Sydenham's chorea is usually self-limiting and resolves after a median duration of 15 weeks [19], ranging from 1 week to more than 2 years; it may recur [19]. The spectrum of post-streptococcal disease has expanded with the recognition of pediatric autoimmune neuropsychiatric disorders associated with streptococcal infection (PANDAS), which is characterized by OCD or a tic disorder with abrupt onset in childhood or exacerbations of symptoms temporally related to a preceding streptococcal infection [126,127]. Despite growing evidence of association between preceding streptococcal infection and OCD, its pathophysiologic implications remain controversial [127].

Erythema marginatum

Erythema marginatum is rare in ARF, occurring in 3–5% of patients [128], but some reports find it in >15% of ARF patients [19]. The variable incidence is possibly related to its transient nature. The rash is characterized by erythematous, serpiginous, macular, or papular lesions with a pale center (normal skin). The rash has been referred to as "smoke rings" [19]. The lesions are multiple, non-pruritic, non-painful, blanching, change in size and shape, and are often evanescent. They occur primarily on the trunk and proximal extremities but rarely on the face. They can be accentuated by warming the skin or friction. Erythema marginatum almost never occurs as the sole major manifestation, and is almost always associated with clinical, but not necessarily severe, carditis. Erythema marginatum occurs early in the ARF disease process and usually resolves quickly. It can persist or recur for months or even years after ARF has subsided [19].

Subcutaneous nodules

Subcutaneous nodules are uncommon, occurring in 2–3% of patients with ARF, but the incidence varies significantly in different populations and has been reported as >20% in some series [19,129]. These lesions are characterized by firm nodules approximately 0.5–2 cm in diameter along the extensor surfaces of tendons and on bony prominences. Sites of predilection include the extensor surfaces of the elbows, knees, and the wrists, the occiput, and the spinous processes of the thoracic and lumbar vertebrae. These nodules are non-tender and mobile with normal-appearing overlying skin and can be easily missed. They are not evanescent, usually persisting for a few days, ranging up to 1–2 weeks, rarely more than 1 month. Subcutaneous nodules almost never occur as the sole major manifestation, and most commonly occur with significant carditis [130].

Minor criteria and other manifestations

Fever and arthralgia are "minor" Jones criteria for the diagnosis of ARF. Although these two findings are the most common features of ARF, they lack specificity and are therefore classified as minor criteria. Fever is an almost universal manifestation of ARF and ranges from 101 to 104 °F (38.4 to 40.0 °C). The fever lacks a characteristic pattern. The fever may be low grade in children with mild carditis or patients may be afebrile at the time of presentation, especially in febrile patients who have received anti-inflammatory medication before a temperature is documented. Patients with chorea are usually afebrile. Arthralgia without objective signs of arthritis is common. Arthralgia usually involves larger joints, is often migratory in nature, and can range from mild discomfort to debilitating and severe pain. Arthralgia cannot be used as a minor criterion if arthritis is used as a major criterion.

An ECG should be performed in patients with suspected ARF. First-degree atrioventricular (AV) block is a minor Jones criterion [131]. First-degree AV block indicates more severe carditis, but is not associated with a greater likelihood of progression to RHD, and can be seen in more than one-third of patients with acute group A streptococcal infection in the absence of ARF [130,132]. With carditis, other ECG findings include sinus tachycardia, other conduction abnormalities, and arrhythmias. More severe conduction abnormalities can be seen [133,134].

Abdominal pain (typically periumbilical or epigastric) and epistaxis occur in ~5% of patients with ARF and may precede other manifestations [19,131]. They lack specificity and are not included in the Jones criteria.

Laboratory testing

No single laboratory test is diagnostic. Elevation of acute-phase reactants, such as C-reactive protein and erythrocyte sedimentation rate (ESR), is a minor Jones diagnostic criterion and is always present in the early phase of ARF. ESR is normal in patients with heart failure and increases as heart failure resolves [135]. Elevated acute-phase reactants can help distinguish between ARF and chronic and indolent RHD and also guide the duration of therapy.

A complete blood count (CBC) and peripheral smear may reveal leukocytosis with a predominance of polymorphonuclear leukocytes. Mild to moderate normocytic, normochromic anemia may be seen. The urine may contain protein, white cells, and red cells.

Radiographic studies may reveal cardiomegaly secondary to pericardial effusion or chamber enlargement in significant valvar regurgitation. Pulmonary edema may be evident in severe carditis and valvar regurgitation. Cardiac catheterization is rarely required in the management of ARF. Cardiac catheterization may be recommended in patients with chronic RHD who might benefit from balloon valvoplasty of a stenotic mitral valve or for coronary vascular evaluation prior to surgery in adults [136,137].

Documentation of a recent group A streptococcal infection is key. A throat culture or rapid streptococcal antigen test should be performed, but these tests are positive in only a minority of patients because of the latency period between pharyngitis and ARF. The gold standard for detecting *S. pyogenes* remains a throat swab culture, but 24–48 h are needed for growth of the bacteria and this may delay the initiation of antibiotics [19]. Rapid streptococcal tests based on carbohydrate cell-wall antigen detection have high specificity but the sensitivity varies with the type of test kit [19]. Furthermore, some patients are chronic carriers of streptococci. Measurement of streptococcal antibody titers is recommended to diagnose an antecedent infection [34]. An elevated or rising streptococcal antibody titer on a repeat test performed 3–4 weeks apart is considered evidence of an antecedent infection [19]. The serum titer of antistreptolysin O (ASO) is elevated in 80% or more of patients with ARF [138]. If the ASO titer is normal, an anti-DNase B titer can be measured. An elevated titer of at least one of these two tests is found in 90% of patients with a recent preceding group A streptococcal infection. ASO titers begin to rise at approximately 1 week and peak 3–6 weeks after the infection. Anti-DNase B titers begin to rise 1–2 weeks and peak 6–8 weeks after the infection. If both tests are initially normal, serial sampling may show a rising titer, providing evidence of an antecedent streptococcal infection. The cutoff for elevated streptococcal antibody titers varies with the test, patient's age, and geographic region. The titers are higher among school-age children than adults.

Treatment

All manifestations of ARF except carditis resolve spontaneously. Treatment of ARF can shorten the duration of inflammation. None of the treatment strategies, except for those preventing recurrences, alters the outcome of acute carditis and its sequelae. Many treatment strategies are not based on strong clinical evidence, but are driven by anecdotal experiences and institutional practices.

Treatment of group A streptococci

Antibiotics do not modify the acute course or long-term outcome of carditis, [138,139], but penicillin is given to eradicate any rheumatogenic group A streptococci remaining in the pharynx and to prevent its spread to close contacts [140,141]. Antibiotic therapy is warranted even if the throat cultures are negative (Table 61.4).

Treatment of arthritis

Fever, arthritis and arthralgia rapidly resolve with salicylate administration [142] which should be avoided until the diagnosis of ARF is confirmed [19]. The most widely used anti-inflammatory drugs are salicylates and corticosteroids. The usual dosage of salicylates is 80–100 mg kg^{-1} per day in children and 6–8 g per day in adults given in divided doses every 4–6 h. Salicylate levels should be measured, targeting a level of 20–30 mg dl^{-1} [19,143]. If gastrointestinal side effects are bothersome, a smaller dose can be given and gradually increased. Gastrointestinal prophylaxis may prevent salicylate-induced gastric mucosal damage and bleeding. Patients may develop gastrointestinal bleeding and signs of salicylism (e.g., headache, hyperpnea, tinnitus). After 2 weeks, the dosage may be gradually tapered and continued for an additional 4 weeks. In milder disease, 2 weeks of therapy may be sufficient and then aspirin can be stopped without tapering. The patient should be observed for "rebound" symptoms in the following 2 weeks. On cessation of anti-inflammatory therapy, the clinical and laboratory markers of acute inflammation may recur but usually resolve spontaneously. When the clinical rebound is significant, extending the course of salicylate therapy to 9–12 weeks may be effective. Influenza vaccine should be given to children receiving aspirin during the influenza season (autumn/winter). Other nonsteroidal anti-inflammatory agents, such as naproxen, have been used successfully in patients with arthritis, but have not been evaluated for carditis [19,143–145].

Treatment of carditis

In patients with symptomatic carditis, bed rest is recommended during the acute phase. This reduces the myocardial work load. Once the acute symptoms resolve, gradual mobilization is recommended [138]. Many patients with asymptomatic carditis are treated as outpatients with

Table 61.4 Primary prevention of acute rheumatic fever (ARF). Treatment of group A streptococcal tonsillopharyngitis.

Agent	Dosage	Mode	Duration
Benzathine penicillin G	600 000 units for ≤27 kg (60 lb) 1.2 million units for >27 kg or	Intramuscular	Single dose
Penicillin V (phenoxymethylpenicillin)	Children: 250 mg 2–3 times daily for ≤27 kg (60 lb); children >27 kg (60 lb). Adolescents and adults: 500 mg 2–3 times daily or	Orally	10 days
Amoxicillin	50 mg kg⁻¹ once daily (maximum 1 g)	Orally	10 days
For individuals allergic to penicillin			
Narrow-spectrum cephalosporin (cephalexin, cefadroxil)[a]	Variable or	Orally	10 days
Clindamycin	20 mg kg⁻¹ per day divided into three doses (maximum 1.8 g per day) or	Orally	10 days
Azithromycin	12 mg kg⁻¹ once daily (maximum 500 mg) or	Orally	5 days
Clarithromycin	15 mg kg⁻¹ per day divided into two doses (maximum 250 mg per dose)	Orally	10 days

[a] Avoid in type I hypersensitivity reaction to penicillin.
(Reproduced with permission from Gerber MA, Baltimore RS, Eaton CB, *et al. Circulation* 2009;**119**:1541–51.)

recommendations for rest during the acute phase and gradual mobilization as symptoms and acute inflammation resolve. There is no evidence that prolonged bed rest accelerates recovery. Anti-inflammatory doses of salicylates are recommended for patients with mild to moderate carditis. Some experts believe that corticosteroids should be used in treating severe carditis with associated cardiac failure because of their more potent anti-inflammatory effect [19,146,147]. Although neither salicylates nor corticosteroids change the long-term outcome of carditis, they are important in reducing inflammation [146–148]. Compared with aspirin, steroids result in more prompt resolution of inflammation, fever, and more rapid disappearance of existing murmurs and prevent the development of new murmurs [149–152].

Prednisone (or equivalent) at a dose of 2 mg kg⁻¹ in children or 40–60 mg per day in adults, may be used initially. After 2–3 weeks, steroids should be tapered slowly during an additional 3-week period [19]. If a rebound phenomenon (more common with corticosteroid use) is observed with tapering of corticosteroids, salicylates can be added for 4–6 weeks. Patients receiving corticosteroids should be monitored for side effects of gastrointestinal upset and bleeding, sodium and water retention, impaired glucose tolerance, and suppression of pituitary–adrenal axis. With fulminating carditis and profound heart failure, intravenous corticosteroids may be used. The duration of anti-inflammatory therapy is based upon the clinical response to therapy and acute-phase reactants becoming normal [19,143]. Progressive

heart failure is predominantly a result of acute valvar dysfunction. In severe, intractable heart failure, emergency valve replacement may be life-saving.

Treatment of Sydenham's chorea

Sydenham's chorea is self-resolving. Patients with mild manifestations can be managed with reassurance, rest, and avoidance of stressful environments. With severe symptoms affecting daily activities, treatments include phenobarbital, carbamazepine, diazepam, steroids, haloperidol, valproic acid, plasma exchange, and intravenous γ-globulin [153–155]. In a randomized double-blind study, adjunctive treatment with prednisone reduced the intensity and duration of acute Sydenham's chorea, but the effect on late recurrence is unknown [156]. Another study showed a reduction in severity of chorea with intravenous immunoglobulin (IVIG) therapy [19,157].

Prevention

Primary prevention

Improvement in living conditions and access to healthcare are keys to reducing the overall rate of ARF. Primary prophylaxis with antibiotics following tonsillopharyngitis caused by group A streptococcus started within 9 days of the onset of a sore throat prevents most subsequent ARF [19,158–160]. However, in more than two-thirds of patients with ARF,

Table 61.5 Treatment of acute rheumatic fever.

All patients
Treatment of group A streptococcal tonsillopharyngitis

Polyarthritis and fever
Acetaminophen and codeine until the diagnosis is established
Aspirin once diagnosis is confirmed
Naproxen can be used in patients without carditis
Influenza vaccine for children receiving aspirin during influenza season

Carditis
Anti-inflammatory treatment with aspirin for mild to moderate carditis
and corticosteroids for severe carditis

Table 61.6 Secondary prevention of rheumatic fever (prevention of recurrent attack) [19,101].

Agent	Dosage	Mode
Benzathine penicillin G	600 000 units for ≤ 27 kg (60 lb), 1.2 million units for >27 kg every 4 weeks[a] or	Intramuscular
Penicillin V (phenoxymethylpenicillin)	Children: 250 mg twice daily or	Orally
Sulfadiazine	0.5 g once daily for patients ≤ 27 kg (60 lb), 1.0 g once daily for patients >27 kg (60 lb)	Orally
For individuals allergic to penicillin and sulfadiazine		
Erythromycin ethylsuccinate	250 mg twice daily	Orally
	or	
Azalides	Variable	Orally

[a]In high-risk situations, administration every 3 weeks is justified and recommended.

Table 61.7 Duration of secondary prophylaxis [19,101].

Category	Duration after last attack
United States [101]	
Rheumatic fever with carditis and residual heart disease (persistent valvar disease[a])	10 years or until 40 years of age (whichever is longer), sometimes lifelong prophylaxis
Rheumatic fever with carditis but no residual heart disease (no valvular disease[a])	10 years or until 21 years of age (whichever is longer)
Rheumatic fever without carditis	5 years or until 21 years of age (whichever is longer)
World Health Organization [19]	
Patients without proven carditis	For 5 years after the last attack, or until 18 years of age (whichever is longer)
Patients with carditis (mild mitral regurgitation or healed carditis)	For 10 years after the last attack, or at least until 25 years of age (whichever is longer)
More severe valvar disease	Lifelong
After valve surgery	Lifelong

[a]Clinical or echocardiographic evidence.

---

there is no prior history of a sore throat, making primary prevention impossible [128]. The recommended antibiotic regimens for primary prevention or treatment of tonsillopharyngitis caused by group A streptococcus are listed in Table 61.4. No clinical isolate of group A β-hemolytic streptococcus (*S. pyogenes*) has been resistant to penicillin [19]. In a 1965 study of Navajo schoolchildren, patients with a culture-positive sore throat and carriers of group A streptococcus were treated with antibiotics The ARF incidence was reduced by 21%. This reduction was achieved at a cost of US$12 per child per year, or $65 000 per ARF patient prevented [161]. In contrast, a randomized study of school children in Auckland, New Zealand, found no reduction in ARF between treatment and no treatment groups. In addition to the lack of symptoms with pharyngitis, poor access to healthcare, inadequate microbiological testing facilities, poor availability of antibiotics, and the reluctance of some populations to seek medical services all limit the role of primary antibiotic prophylaxis in many high-risk populations.

Group A streptococcus vaccines are under development. A multivalent, M-serotype-specific vaccine is in phase II trials in North America. The lack of specific M serotype prevalence in high-risk regions and changing serotypes will limit its use [162]. Alternative vaccine production strategies using non M-type group A streptococcus protein or conserved regions of the M protein are under development.

Treatment of ARF is summarized in Table 61.5.

Secondary prevention

In patients with past history of ARF or RHD, long-term administration of antibiotics for the prevention of streptococcal pharyngitis and recurrent ARF is the only proven and cost-effective treatment. The greater the number of ARF recurrences, the higher is the likelihood of valvar damage and chronic RHD. Secondary prevention is the key to reducing RHD-associated morbidity and mortality worldwide, especially in ARF endemic regions. The recommended antibiotic regimens for secondary prophylaxis are listed in Table 61.6 [36]. Intramuscular benzathine penicillin G administered once every 3 weeks (every 4 weeks in low-risk areas or low-risk patients) is more effective than oral penicillin or sulfadiazine [19,163,164]. The serum levels of penicillin are less predictable with oral administration, even

in patients with good compliance [19]. The duration of secondary prophylaxis varies based on previous history and underlying heart disease and is listed in Table 61.7 [36]. Patient and family education, emphasizing the importance of adherence to secondary prophylaxis, is paramount to successful programs. Good follow-up, health education, central registries for case documentation and gathering epidemiological data, and continued research are important in worldwide reduction of ARF- and RHD-associated morbidity and mortality.

Long-term administration of antibiotics for the prevention of streptococcal pharyngitis and ARF in patients with a past history of ARF or RHD is the only proven strategy to prevent recurrence. Details of secondary prevention are presented in Chapter 62 and discussed in the literature [19,36,163,164].

Bacterial endocarditis prophylaxis

The American Heart Association (AHA) no longer recommends endocarditis prophylaxis for all patients with RHD [165]. Prophylaxis is recommended, however, for high-risk patients, including those with prosthetic valves, residual defects adjacent to prosthetic materials, and previous infective endocarditis (see Chapter 60). For patients in high-risk populations with RHD receiving chronic penicillin prophylaxis, the recommendations advise the use of a prophylactic agent other than penicillin because oral flora may have developed penicillin resistance [165].

References

1 Bryant PA, Robins-Browne R, Carapetis JR, Curtis N. Some of the people, some of the time. Susceptibility to acute rheumatic fever. *Circulation* 2009;**119**:742–53.

2 Steer AC, Carapetis JR. Acute rheumatic fever and rheumatic heart disease in indigenous populations. *Pediatr Clin North Am* 2009;**56**:1401–19.

3 Massell BF, Chute CG, Walker AM, Kurland GS. Penicillin and the marked decrease in morbidity and mortality from rheumatic fever in the United States. *N Engl J Med* 1988;**318**:280–6.

4 Markowitz M. Pioneers and modern ideas. Rheumatic fever – a half-century perspective. *Pediatrics* 1998;**102**:272–4; discussion 288–9.

5 Quinn RW. Comprehensive review of morbidity and mortality trends for rheumatic fever, streptococcal disease, and carlet fever: the decline of rheumatic fever. *Rev Infect Dis* 1989;**11**:928–53.

6 Carapetis JR, McDonald M, Wilson NJ. Acute rheumatic fever. *Lancet* 2005;**366**:155–68.

7 Padmavati S. Rheumatic fever and rheumatic heart disease in India at the turn of the century. *Indian Heart J* 2001;**53**:35–7.

8 Kechrid A, Kharrat H, Bousnina S, *et al*. Acute rheumatic fever in Tunisia. Serotypes of group A streptococci associated with rheumatic fever. *Adv Exp Med Biol* 1997;**418**:121–3.

9 Omar A. Pattern of acute rheumatic fever in a local teaching hospital. *Med J Malaysia* 1995;**50**:125–30.

10 Alves Meira ZM, de Castilho SR, Lins Barros MV, *et al*. Prevalence of rheumatic fever in children from a public high school in Belo Horizonte. *Arq Bras Cardiol* 1995;**65**:331–4 (in Portuguese).

11 Richmond P, Harris L. Rheumatic fever in the Kimberley region of Western Australia. *J Trop Pediatr* 1998;**44**:148–52.

12 Carapetis JR, Wolff DR, Currie BJ. Acute rheumatic fever and rheumatic heart disease in the top end of Australia's Northern Territory. *Med J Aust* 1996;**164**:146–9.

13 Carapetis JR, Currie BJ, Mathews JD. Cumulative incidence of rheumatic fever in an endemic region: a guide to the susceptibility of the population? *Epidemiol Infect* 2000;**124**:239–44.

14 Carapetis JR, Steer AC, Mulholland EK, Weber M. The global burden of group A streptococcal diseases. *Lancet Infect Dis* 2005;**5**:685–94.

15 Carapetis JR, Hardy M, Fakakovikaetau T, *et al*. High prevalence of rheumatic heart disease in Tongan school children, and evaluation of a screening protocol using portable echocardiography. *Nat Clin Pract Cardiovasc Med* 2008;**5**:411–7.

16 Carapetis JR, Currie BJ. Clinical epidemiology of rheumatic fever and rheumatic heart disease in tropical Australia. *Adv Exp Med Biol* 1997;**418**:233–6.

17 Carapetis JR, Currie BJ. Mortality due to acute rheumatic fever and rheumatic heart disease in the Northern Territory: a preventable cause of death in aboriginal people. *Aust N Z J Public Health* 1999;**23**:159–63.

18 Chun LT, Reddy DV, Yim GK, Yamamoto LG. Acute rheumatic fever in Hawaii: 1966 to 1988. *Hawaii Med J* 1992;**51**:206–11.

19 WHO. *Rheumatic Fever and Rheumatic Heart Disease: Report of a WHO Expert Consultation, Geneva, 29 October–1 November 2001*. Geneva: World Health Organization, 2004.

20 Neutze JM. Rheumatic fever and rheumatic heart disease in the western Pacific region. *N Z Med J* 1988;**101**:404–6.

21 Steer AC, Kado J, Wilson N, *et al*. High prevalence of rheumatic heart disease by clinical and echocardiographic screening among children in Fiji. *J Heart Valve Dis* 2009;**18**:327–35; discussion 336.

22 Steer AC, Kado J, Jenney AW, *et al*. Acute rheumatic fever and rheumatic heart disease in Fiji: prospective surveillance, 2005–2007. *Med J Aust* 2009;**190**:133–5.

23 Carapetis JR. Rheumatic heart disease in Asia. *Circulation* 2008;**118**:2748–53.

24 Jaine R, Baker M, Venugopal K. Epidemiology of acute rheumatic fever in New Zealand 1996–2005. *Paediatr Child Health* 2008;**44**:564–71.

25 Tani LY, Veasy LG, Minich LL, Shaddy RE. Rheumatic fever in children younger than 5 years: is the presentation different? *Pediatrics* 2003;**112**:1065–8.

26 Zaman MM, Rouf MA, Haque S, *et al*. Does rheumatic fever occur usually between the ages of 5 and 15 years? *Int J Cardiol* 1998;**66**:17–21.

27 Tani LY, Veasy LG, Minich LL, Shaddy RE. Rheumatic fever in children under 5 years. *Pediatrics* 2004;**114**:906.

28 Carapetis JR, Currie BJ. Group A streptococcus, pyoderma, and rheumatic fever. *Lancet* 1996;**347**:1271–2.

29 Davies AM, Lazarov E. Heredity, infection and chemoprophylaxis in rheumatic carditis: an epidemiological study of a communal settlement. *J Hyg (Lond)* 1960;**58**:263–76.

30 Denbow CE, Barton EN, Smikle MF. The prophylaxis of acute rheumatic fever in a pair of monozygotic twins. The public health implications. *West Indian Med J* 1999;**48**:242–3.

31 Ebell MH, Smith MA, Barry HC, *et al*. The rational clinical examination. Does this patient have strep throat? *JAMA* 2000;**284**:2912–8.

32 Shaikh N, Leonard E, Martin JM. Prevalence of streptococcal pharyngitis and streptococcal carriage in children: a meta-analysis. *Pediatrics* 2010;**126**:e557–64.

33 Bisno AL. Group A streptococcal infections and acute rheumatic fever. *N Engl J Med* 1991;**325**:783–93.

34 Bisno A, Stevens DL. *Streptococcus pyogenes*. In: Mandell G, Bennett JE, Raphael D, eds. *Mandell, Douglas, and Bennett's Principles and Practice of Infectious Diseases*, 7th edn. Philadelphia: Elsevier Churchill Livingstone, 2009, Chapter 198; electronic version.

35 Bisno AL, Gerber MA, Gwaltney JM Jr, *et al*. Practice guidelines for the diagnosis and management of group A streptococcal pharyngitis. Infectious Diseases Society of America. *Clin Infect Dis* 2002;**35**:113–25.

36 Martin JM, Green M. Group A streptococcus. *Semin Pediatr Infect Dis* 2006;**17**:140–8.

37 Stevens DL. The toxins of group A streptococcus, the flesh eating bacteria. *Immunol Invest* 1997;**26**:129–50.

38 Courtney HS, Hasty DL, Dale JB. Serum opacity factor (SOF) of *Streptococcus pyogenes* evokes antibodies that opsonize homologous and heterologous SOF-positive serotypes of group A streptococci. *Infect Immun* 2003;**71**:5097–103.

39 Musser JM, Hauser AR, Kim MH, *et al*. *Streptococcus pyogenes* causing toxic-shock-like syndrome and other invasive diseases: clonal diversity and pyrogenic exotoxin expression. *Proc Natl Acad Sci USA* 1991;**88**:2668–72.

40 Stollerman GH. Rheumatogenic group A streptococci and the return of rheumatic fever. *Adv Intern Med* 1990;**35**:1–25.

41 Stollerman GH. Rheumatogenic streptococci and autoimmunity. *Clin Immunol Immunopathol* 1991;**61**:131–42.

42 Veasy LG, Tani LY, Daly JA, *et al*. Temporal association of the appearance of mucoid strains of *Streptococcus pyogenes* with a continuing high incidence of rheumatic fever in Utah. *Pediatrics* 2004;**113**:e168–72.

43 Martin CR,. Rheumatogenic and nephritogenic group A streptococci. Myth or reality? An opening lecture. *Adv Exp Med Biol* 1997;**418**:21–7.

44 Martin DR, Voss LM, Walker SJ, Lennon D. Acute rheumatic fever in Auckland, New Zealand: spectrum of associated group A streptococci different from expected. *Pediatr Infect Dis J* 1994;**13**:264–9.

45 Pruksakorn S, Sittisombut N, Phornphutkul C, *et al*. Epidemiological analysis of non-M-typeable group A *Streptococcus* isolates from a Thai population in northern Thailand. *J Clin Microbiol* 2000;**38**:1250–4.

46 Gardiner DL, Sriprakash KS. Molecular epidemiology of impetiginous group A streptococcal infections in aboriginal communities of northern Australia. *J Clin Microbiol* 1996;**34**:1448–52.

47 Carapetis J, Gardiner D, Currie B, Mathews JD. Multiple strains of *Streptococcus pyogenes* in skin sores of aboriginal Australians. *J Clin Microbiol* 1995;**33**:1471–2.

48 Widdowson JP, Maxted WR, Pinney AM. An M-associated protein antigen (MAP) of group A streptococci. *J Hyg (Lond)* 1971;**69**:553–64.

49 Bessen DE, Veasy LG, Hill HR, *et al*. Serologic evidence for a class I group A streptococcal infection among rheumatic fever patients. *J Infect Dis* 1995;**172**:1608–11.

50 Bessen DE, Sotir CM, Readdy TL, Hollingshead SK. Genetic correlates of throat and skin isolates of group A streptococci. *J Infect Dis* 1996;**173**:896–900.

51 Bessen DE, Carapetis JR, Beall B, *et al*. Contrasting molecular epidemiology of group A streptococci causing tropical and non-tropical infections of the skin and throat. *J Infect Dis* 2000;**182**:1109–16.

52 Cheadle W. Various manifestations of the rheumatic state as exemplified in childhood and early life. *Lancet* 1889;**i**:821–32.

53 Wilson MG, Lubschez R, Schweitzer MD. The integration of genetic and epidemiological methods of analysis in rheumatic fever. *Science* 1943;**97**:335–6.

54 Feinstein AR, Wood HF, Spagnuolo M, *et al*. Rheumatic fever in children and adolescents. A long-term epidemiologic study of subsequent prophylaxis, streptococcal infections, and clinical sequelae. VII. Cardiac changes and sequelae. *Ann Intern Med* 1964;**60**(Suppl 5):87–123.

55 Sasazuki T, Kaneoka H, Nishimura Y, *et al*. An HLA-linked immune suppression gene in man. *J Exp Med* 1980;**152**:297s–313s.

56 Guedez Y, Kotby A, El-Demellawy M, *et al*. HLA class II associations with rheumatic heart disease are more evident and consistent among clinically homogeneous patients. *Circulation* 1999;**99**:2784–90.

57 Donadi EA, Smith AG, Louzada-Junior P, *et al*. HLA class I and class II profiles of patients presenting with Sydenham's chorea. *J Neurol* 2000;**247**:122–8.

58 Visentainer JE, Pereira FC, Dalalio MM, *et al*. Association of HLA-DR7 with rheumatic fever in the Brazilian population. *J Rheumatol* 2000;**27**:1518–20.

59 Simonini G, Porfirio B, Cimaz R, *et al*. Lack of association between the HLA-DRB1 locus and post-streptococcal reactive arthritis and acute rheumatic fever in Italian children. *Semin Arthritis Rheum* 2004;**34**:553–8.

60 Hernandez-Pacheco G, Aguilar-Garcia J, Flores-Dominguez C, *et al*. MHC class II alleles in Mexican patients with rheumatic heart disease. *Int J Cardiol* 2003;**92**:49–54.

61 Ayoub EM, Barrett DJ, Maclaren NK, Krischer JP. Association of class II human histocompatibility leukocyte antigens with rheumatic fever. *J Clin Invest* 1986;**77**:2019–26.

62 Khanna AK, Buskirk DR, Williams RC Jr, *et al*. Presence of a non-HLA B cell antigen in rheumatic fever patients and their families as defined by a monoclonal antibody. *J Clin Invest* 1989;**83**:1710–6.

63 Harel L, Zeharia A, Kodman Y, *et al*. Presence of the d8/17 B-cell marker in children with rheumatic fever in Israel. *Clin Genet* 2002;**61**:293–8.

64 Kemeny E, Husby G, Williams RC Jr, Zabriskie JB. Tissue distribution of antigen(s) defined by monoclonal antibody D8/17 reacting with B lymphocytes of patients with rheumatic heart disease. *Clin Immunol Immunopathol* 1994;**72**:35–43.

65 Taneja V, Mehra NK, Reddy KS, *et al*. HLA-DR/DQ antigens and reactivity to B cell alloantigen D8/17 in Indian patients with rheumatic heart disease. *Circulation* 1989;**80**:335–40.

66 Kumar D, Kaul P, Grover A, Ganguly NK. Distribution of cells bearing B-cell alloantigen(s) in North Indian rheumatic fever/rheumatic heart disease patients. *Mol Cell Biochem* 2001;**218**:21–6.

67 Kaur S, Kumar D, Grover A, *et al*. Ethnic differences in expression of susceptibility marker(s) in rheumatic fever/rheumatic heart disease patients. *Int J Cardiol* 1998;**64**:9–14.

68 Schafranski MD, Stier A, Nisihara R, Messias-Reason IJ. Significantly increased levels of mannose-binding lectin (MBL) in rheumatic heart disease: a beneficial role for MBL deficiency. *Clin Exp Immunol* 2004;**138**:521–5.

69 Chou HT, Chen CH, Tsai CH, Tsai FJ. Association between transforming growth factor-beta1 gene C-509T and T869C polymorphisms and rheumatic heart disease. *Am Heart J* 2004;**148**:181–6.

70 Guilherme L, Oshiro SE, Fae KC, *et al*. T-cell reactivity against streptococcal antigens in the periphery mirrors reactivity of heart-infiltrating T lymphocytes in rheumatic heart disease patients. *Infect Immun* 2001;**69**:5345–51.

71 Cunningham MW. Autoimmunity and molecular mimicry in the pathogenesis of post-streptococcal heart disease. *Front Biosci* 2003;**8**:s533–43.

72 Galvin JE, Hemric ME, Kosanke SD, *et al*. Induction of myocarditis and valvulitis in Lewis rats by different epitopes of cardiac myosin and its implications in rheumatic carditis. *Am J Pathol* 2002;**160**:297–306.

73 Lymbury RS, Olive C, Powell KA, *et al*. Induction of autoimmune valvulitis in Lewis rats following immunization with peptides from the conserved region of group A streptococcal M protein. *J Autoimmun* 2003;**20**:211–7.

74 Bhatnagar A, Grover A, Ganguly NK. Superantigen-induced T cell responses in acute rheumatic fever and chronic rheumatic heart disease patients. *Clin Exp Immunol* 1999;**116**:100–6.

75 Figueroa F, Gonzalez M, Carrion F, *et al*. Restriction in the usage of variable beta regions in T-cells infiltrating valvular tissue from rheumatic heart disease patients. *J Autoimmun* 2002;**19**:233–40.

76 Williams RV, Minich LL, Shaddy RE, *et al*. Evidence for lack of myocardial injury in children with acute rheumatic carditis. *Cardiol Young* 2002;**12**:519–23.

77 Kamblock J, Payot L, Iung B, *et al*. Does rheumatic myocarditis really exist? Systematic study with echocardiography and cardiac troponin I blood levels. *Eur Heart J* 2003;**24**:855–62.

78 Gentles TL, Colan SD, Wilson NJ, *et al*. Left ventricular mechanics during and after acute rheumatic fever: contractile dysfunction is closely related to valve regurgitation. *J Am Coll Cardiol* 2001;**37**:201–7.

79 Essop MR, Wisenbaugh T, Sareli P. Evidence against a myocardial factor as the cause of left ventricular dilatation in active rheumatic carditis. *J Am Coll Cardiol* 1993;**22**:826–9.

80 Atalay S, Ucar T, Ozcelik N, *et al*. Echocardiographic evaluation of mitral valve in patients with pure rheumatic mitral regurgitation. *Turk J Pediatr* 2007;**49**:148–53.

81 Marcus RH, Sareli P, Pocock WA, *et al*. Functional anatomy of severe mitral regurgitation in active rheumatic carditis. *Am J Cardiol* 1989;**63**:577–84.

82 Vasan RS, Shrivastava S, Vijayakumar M, *et al*. Echocardiographic evaluation of patients with acute rheumatic fever and rheumatic carditis. *Circulation* 1996;**94**:73–82.

83 Burchell HB, Edwards JE. Rheumatic mitral insufficiency. *Circulation* 1953;**7**:747–56.

84 Levy MJ, Edwards JE. Anatomy of mitral insufficiency. *Prog Cardiovasc Dis* 1962;**5**:119–44.

85 Galvin JE, Hemric ME, Ward K, Cunningham MW. Cytotoxic mAb from rheumatic carditis recognizes heart valves and laminin. *J Clin Invest* 2000;**106**:217–24.

86 Roberts S, Kosanke S, Terrence Dunn S, *et al*. Pathogenic mechanisms in rheumatic carditis: focus on valvular endothelium. *J Infect Dis* 2001;**183**:507–11.

87 Guilherme L, Kalil J. Rheumatic fever: from sore throat to autoimmune heart lesions. *Int Arch Allergy Immunol* 2004;**134**:56–64.

88 McKeown F. The pathology of rheumatic fever. *Ulster Med J* 1945;**14**:97–86.

89 Jones TD. The diagnosis of acute rheumatic fever. *JAMA* 1944;**126**:481–4.

90 Rutstein DD, Bauer W, Dorfman A, *et al*. Jones criteria (modified) for guidance in the diagnosis of rheumatic fever; report of the Committee on Standards and Criteria for Programs of Care. *Circulation* 1956;**13**:617–20.

91 Shulman ST, Amren DP, Bisno AL, *et al*. Prevention of bacterial endocarditis. A statement for health professionals by the Committee on Rheumatic Fever and Infective Endocarditis of the Council on Cardiovascular Disease in the Young. *Circulation* 1984;**70**:1123A–7A.

92 Special Writing Group of the Committee on Rheumatic Fever, Endocarditis, and Kawasaki Disease of the Council on Cardiovascular Disease in the Young of the American Heart Association. Guidelines for the diagnosis of rheumatic fever. Jones criteria, 1992 update. *JAMA* 1992;**268**:2069–73.

93 Ad Hoc Committee to Revise the Jones Criteria (Modified) of the Council on Rheumatic Fever and Congenital Heart Disease of the American Heart Association. Jones criteria (revised) for guidance in the diagnosis of rheumatic fever. *Circulation* 1965;**32**:664–8.

94 Shiffman RN. Guideline maintenance and revision. 50 years of the Jones criteria for diagnosis of rheumatic fever. *Arch Pediatr Adolesc Med* 1995;**149**:727–32.

95 Walsh W, Brown A, Carapetis J. The diagnosis and management of chronic rheumatic heart disease – an Australian guideline. *Heart Lung Circ* 2008;**17**:271–89.

96 Sanyal SK, Thapar MK, Ahmed SH, *et al*. The initial attack of acute rheumatic fever during childhood in north India; a prospective study of the clinical profile. *Circulation* 1974;**49**:7–12.

97 Carapetis JR, Currie BJ. Rheumatic fever in a high incidence population: the importance of monoarthritis and low grade fever. *Arch Dis Chil*d 2001;**85**:223–7.

98 Crea MA, Mortimer EA Jr. The nature of scarlatinal arthritis. *Pediatrics* 1959;**23**:879–84.

99 De Cunto CL, Giannini EH, Fink CW, *et al*.. Prognosis of children with poststreptococcal reactive arthritis. *Pediatr Infect Dis J* 1988;**7**:683–6.

100 Shulman ST, Ayoub EM. Poststreptococcal reactive arthritis. *Curr Opin Rheumatol* 2002;**14**:562–5.

101 Gerber MA, Baltimore RS, Eaton CB, *et al*. Prevention of rheumatic fever and diagnosis and treatment of acute streptococcal pharyngitis: a scientific statement from the American Heart Association Rheumatic Fever, Endocarditis, and Kawasaki Disease Committee of the Council on Cardiovascular Disease in the Young, the Interdisciplinary Council on Functional Genomics and Translational Biology, and the Interdisciplinary Council on Quality of Care and Outcomes Research, endorsed by the American Academy of Pediatrics. *Circulation* 2009;**119**:1541–51.

102 Narula J, Chandrasekhar Y, Rahimtoola S. Diagnosis of active rheumatic carditis. The echoes of change. *Circulation* 1999;**100**:1576–81.

103 Veasy LG. Time to take soundings in acute rheumatic fever. *Lancet* 2001;**357**:1994–5.

104 Narula J, Kaplan EL. Echocardiographic diagnosis of rheumatic fever. *Lancet* 2001;**358**:2000.

105 Wilson NJ, Neutze JM. Echocardiographic diagnosis of subclinical carditis in acute rheumatic fever. *Int J Cardiol* 1995;**50**:1–6.

106 Minich LL, Tani LY, Pagotto LT, *et al*. Doppler echocardiography distinguishes between physiologic and pathologic "silent" mitral regurgitation in patients with rheumatic fever. *Clin Cardiol* 1997;**20**:924–6.

107 Mota CC. Doppler echocardiographic assessment of subclinical valvitis in the diagnosis of acute rheumatic fever. *Cardiol Young* 2001;**11**:251–4.

108 Figueroa FE, Fernandez MS, Valdes P, *et al*. Prospective comparison of clinical and echocardiographic diagnosis of rheumatic carditis: long term follow up of patients with subclinical disease. *Heart* 2001;**85**:407–10.

109 Mangione S, Nieman LZ, Gracely E, Kaye D. The teaching and practice of cardiac auscultation during internal medicine and cardiology training. A nationwide survey. *Ann Intern Med* 1993;**119**:47–54.

110 Veasy LG, Wiedmeier SE, Orsmond GS, *et al*. Resurgence of acute rheumatic fever in the intermountain area of the United States. *N Engl J Med* 1987;**316**:421–7.

111 Tubridy-Clark M, Carapetis JR. Subclinical carditis in rheumatic fever: a systematic review. *Int J Cardiol* 2007;**119**:54–8.

112 Ozkutlu S, Ayabakan C, Saraclar M. Can subclinical valvitis detected by echocardiography be accepted as evidence of carditis in the diagnosis of acute rheumatic fever? *Cardiol Young* 2001;**11**:255–60.

113 Brand A, Dollberg S, Keren A. The prevalence of valvular regurgitation in children with structurally normal hearts: a color Doppler echocardiographic study. *Am Heart J* 1992;**123**:177–80.

114 Yoshida K, Yoshikawa J, Shakudo M, *et al*. Color Doppler evaluation of valvular regurgitation in normal subjects. *Circulation* 1988;**78**:840–7.

115 Shah PM. Quantitative assessment of mitral regurgitation. *J Am Coll Cardiol* 1989;**13**:591–3.

116 Kostucki W, Vandenbossche JL, Friart A, Englert M. Pulsed Doppler regurgitant flow patterns of normal valves. *Am J Cardiol* 1986;**58**:309–13.

117 Lembo NJ, Dell'Italia LJ, Crawford MH, *et al*. Mitral valve prolapse in patients with prior rheumatic fever. *Circulation* 1988;**77**:830–6.

118 Abernethy M, Bass N, Sharpe N, *et al*. Doppler echocardiography and the early diagnosis of carditis in acute rheumatic fever. *Aust N Z J Med* 1994;**24**:530–5.

119 Marijon E, Ou P, Celermajer DS, *et al*. Prevalence of rheumatic heart disease detected by echocardiographic screening. *N Engl J Med* 2007;**357**:470–6.

120 Bhaya M, Panwar S, Beniwal R, Panwar RB. High prevalence of rheumatic heart disease detected by echocardiography in school children. *Echocardiography* 2010;**27**:448–53.

121 Ramakrishnan S. Echocardiography in acute rheumatic fever. *Ann Pediatr Cardiol* 2009;**2**:61–4.

122 Carapetis JR, Brown A, Wilson NJ, Edwards KN. An Australian guideline for rheumatic fever and rheumatic heart disease: an abridged outline. *Med J Aust* 2007;**186**:581–6.

123 Atatoa-Carr P, Lennon D, Wilson N. Rheumatic fever diagnosis, management, and secondary prevention: A New Zealand guideline. *N Z Med J* 2008;**121**:59–69.

124 Bisino A. Noncardiac manifestations of rheumatic fever. In: Narula J, Virmani R, Reddy KS, Tandon R., eds. *Rheumatic Fever*. Washington, DC: American Registry of Pathology, 1994: 245–56.

125 Asherson RA, Derksen RH, Harris EN, *et al*. Chorea in systemic lupus erythematosus and "lupus-like" disease: association with antiphospholipid antibodies. *Semin Arthritis Rheum* 1987;**16**:253–9.

126 Swedo SE, Leonard HL, Garvey M, *et al*. Pediatric autoimmune neuropsychiatric disorders associated with streptococcal infections: clinical description of the first 50 cases. *Am J Psychiatry* 1998;**155**:264–71.

127 Moretti G, Pasquini M, Mandarelli G, *et al*. What every psychiatrist should know about PANDAS: a review. *Clin Pract Epidemiol Ment Health* 2008;**4**:13.

128 Veasy LG, Tani LY, Hill HR. Persistence of acute rheumatic fever in the intermountain area of the United States. *J Pediatr* 1994;**124**:9–16.

129 Rheumatic Fever Working Party of the Medical Research Council of Great Britain and Subcommittee of Principal Investigators of the American Council on Rheumatic Fever and Congenital Heart Disease, American Heart Association. The natural history of rheumatic fever and rheumatic heart disease. Ten-year report of a cooperative clinical trial of ACTH, cortisone, and aspirin. *Circulation* 1965;**32**:457–76.

130 Massell BF, Fyler DC, Roy SB. The clinical picture of rheumatic fever: diagnosis, immediate prognosis, course, and therapeutic implications. *Am J Cardiol* 1958;**1**:436–49.

131 Feinstein AR, Zagala JG, Spagnuolo M. The pattern of symptoms, pre-treatment interval, and prognosis of acute rheumatic fever. *Ann Intern Med* 1962;**57**:563–71.

132 Feinstein AR, Stern EK, Spagnuolo M. The prognosis of acute rheumatic fever. *Am Heart J* 1964;**68**:817–34.

133 Lenox CC, Zuberbuhler JR, Park SC, *et al*. Arrhythmias and Stokes–Adams attacks in acute rheumatic fever. *Pediatrics* 1978;**61**:599–603.

134 Zalzstein E, Maor R, Zucker N, Katz A. Advanced atrioventricular conduction block in acute rheumatic fever. *Cardiol Young* 2003;**13**:506–8.

135 Spagnuolo M, Feinstein AR. Congestive heart failure and rheumatic activity in young patients with rheumatic heart disease. *Pediatrics* 1964;**33**:653–60.

136 Bonow RO, Carabello B, de Leon AC Jr, *et al*. Guidelines for the management of patients with valvular heart disease: executive summary. A report of the American College of Cardiology/American Heart Association Task Force on Practice Guidelines (Committee on Management of Patients with Valvular Heart Disease). *Circulation* 1998;**98**:1949–84.

137 Krishnamoorthy KM, Tharakan JA. Balloon mitral valvulotomy in children aged < or = 12 years. *J Heart Valve Dis* 2003;**12**:461–8.

138 Wannamaker LW, Ayoub EM. Antibody titers in acute rheumatic fever. *Circulation* 1960;**21**:598–614.

139 Tompkins DG, Boxerbaum B, Liebman J. Long-term prognosis of rheumatic fever patients receiving regular intramuscular benzathine penicillin. *Circulation* 1972;**45**:543–51.

140 Mortimer EA Jr, Vaisman S, Vignau A, *et al*. The effect of penicillin on acute rheumatic fever and valvular heart disease. *N Engl J Med* 1959;**260**:101–12.

141 Carter ME, Bywaters EG, Thomas GT. Rheumatic fever treated with penicillin in bactericidal dosage for six weeks. Report of a small controlled trial. *Br Med J* 1962;**i**:965–7.

142 Illingworth RS, Lorber J, Holt KS, Rendle-Short J. Acute rheumatic fever in children; a comparison of six forms of treatment in 200 cases. *Lancet* 1957;**273**:653–9.

143 Thatai D, Turi ZG. Current guidelines for the treatment of patients with rheumatic fever. *Drugs* 1999;**57**:545–55.

144 Hashkes PJ, Tauber T, Somekh E, *et al.*; Pediatric Rheumatlogy Study Group of Israel. Naproxen as an alternative to aspirin for the treatment of arthritis of rheumatic fever: a randomized trial. *J Pediatr* 2003;**143**:399–401.

145 Uziel Y, Hashkes PJ, Kassem E, *et al*. The use of naproxen in the treatment of children with rheumatic fever. *J Pediatr* 2000;**137**:269–71.

146 Segal MS, Dulfano MJ. A comparison of short-term, intensive prednisone and acetylsalicylic acid therapy in the treatment of acute rheumatic fever. Combined Rheumatic Fever Study Group. *N Engl J Med* 1965;**272**:63–70.

147 Cilliers AM, Manyemba J, Saloojee H. Anti-inflammatory treatment for carditis in acute rheumatic fever. *Cochrane Database Syst Rev* 2003;CD003176.

148 Albert DA, Harel L, Karrison T. The treatment of rheumatic carditis: a review and meta-analysis. *Medicine (Baltimore)* 1995;**74**:1–12.

149 Rheumatic Fever Working Party of the Medical Research Council of Great Britain and the Subcommittee of Principal Investigators of the American Council on Rheumatic Fever and Congenital Heart Disease, American Heart Association. Treatment of acute rheumatic fever in children: a co-operative clinical trial of A.C.T.H., cortisone, and aspirin. *Br Med J* 1955;**i**:555–74.

150 Saxena A. Treatment of rheumatic carditis. *Indian J Pediatr* 2002;**69**:513–6.

151 Rothman PE. Treatment of rheumatic carditis. A critical evaluation. *Clin Pediatr (Phila)* 1965;**4**:619–25.

152 Markowitz M, Kuttner G. Treatment of acute rheumatic fever. *Am J Dis Child* 1962;**104**:313–20.

153 Pena J, Mora E, Cardozo J, *et al*. Comparison of the efficacy of carbamazepine, haloperidol and valproic acid in the treatment of children with Sydenham's chorea: clinical follow-up of 18 patients. *Arq Neuropsiquiatr* 2002;**60**:374–7.

154 Daoud AS, Zaki M, Shakir R, al-Saleh Q. Effectiveness of sodium valproate in the treatment of Sydenham's chorea. *Neurology* 1990;**40**:1140–1.

155 Genel F, Arslanoglu S, Uran N, Saylan B. Sydenham's chorea: clinical findings and comparison of the efficacies of sodium valproate and carbamazepine regimens. *Brain Dev* 2002;**24**:73–6.

156 Paz JA, Silva CA, Marques-Dias MJ. Randomized double-blind study with prednisone in Sydenham's chorea. *Pediatr Neurol* 2006;**34**:264–9.

157 Swedo SE. Sydenham's chorea. A model for childhood autoimmune neuropsychiatric disorders. *JAMA* 1994;**272**:1788–91.

158 Denny FW, Wannamaker LW, Brink WR, *et al*. Prevention of rheumatic fever; treatment of the preceding streptococcic infection. *J Am Med Assoc* 1950;**143**:151–3.

159 Catanzaro FJ, Rammelkamp CH Jr, Chamovitz R. Prevention of rheumatic fever by treatment of streptococcal infections. II. Factors responsible for failures. *N Engl J Med* 1958;**259**:53–7.

160 Robertson KA, Volmink JA, Mayosi BM. Antibiotics for the primary prevention of acute rheumatic fever: a meta-analysis. *BMC Cardiovasc Disord* 2005;**5**:11.

161 Coulehan JL, Baacke G, Welty TK, Goldtooth NL. Cost-benefit of a streptococcal surveillance program among Navajo Indians. *Public Health Rep* 1982;**97**:73–7.

162 Kotloff KL, Corretti M, Palmer K, *et al*. Safety and immunogenicity of a recombinant multivalent group a streptococcal vaccine in healthy adults: phase 1 trial. *JAMA* 2004;**292**:709–15.

163 Bonet A, Ferencz C, Markowitz M. A comparison of oral and intramuscular benzathine penicillin G for the prevention of streptococcal infections and recurrences of rheumatic fever. *Pediatrics* 1957;**19**:201–7.

164 Lue HC, Wu MH, Hsieh KH, *et al*. Rheumatic fever recurrences: controlled study of 3-week versus 4-week benzathine penicillin prevention programs. *J Pediatr* 1986;**108**:299–304.

165 Wilson W, Taubert KA, Gewitz M, *et al*. Prevention of infective endocarditis: guidelines from the American Heart Association: a guideline from the American Heart Association Rheumatic Fever, Endocarditis, and Kawasaki Disease Committee, Council on Cardiovascular Disease in the Young, and the Council on Clinical Cardiology, Council on Cardiovascular Surgery and Anesthesia, and the Quality of Care and Outcomes Research Interdisciplinary Working Group. *Circulation* 2007;**116**:1736–54.

166 Pinals RS. Polyarthritis and fever. *N Engl J Med* 1994;**330**:769–74.

62 Rheumatic Heart Disease

Raman Krishna Kumar

Amrita Institute of Medical Sciences and Research Center, Kerala, India

Introduction

Rheumatic heart disease (RHD) is the only long-term sequel of rheumatic fever (RF). Children with a scarred heart valve as a consequence of RHD are seldom seen in developed nations, but RF and RHD are significant public health problems in developing nations, where it selectively targets the underprivileged [1,2].

Before penicillin was introduced, the natural history of RF was characterized by initial episodes occurring in the very young, frequently associated with carditis, often severe [3,4], and recurrences were common. Advanced heart valve scarring with severe hemodynamic and clinical consequences, such as congestive heart failure, were common in the very young [2,5,6], often occurring several years after the first episode. After penicillin was introduced, the incidence and severity of acute RF declined sharply, as did recurrent episodes and RHD. The interval between acute RF and RHD increased progressively [3,4], as did the age of onset of clinically manifest RHD [2].

Where the disease is still rampant, the natural history of RF resembles that of the pre-penicillin era [1,2,5,6]. Juvenile rheumatic mitral valve stenosis is seen almost exclusively in regions with a high incidence of RF [2,6,7].

Epidemiology

Global trends

A few decades before penicillin was introduced, a sharp decline in acute RF and RHD occurred in all industrialized nations. Improving living standards, reduced overcrowding, better access to healthcare and more widespread use of antibiotics allowed prompt treatment of streptococcal infections and helped abort epidemics [1,2]. Industrialized nations now have an average annual RF incidence of <0.5 per 100 000 and RHD prevalence of <0.05 per 1000. The resurgence of RF in the United States during the mid-1980s and its persistence, however, suggest that additional factors also contribute to its occurrence [8]. Selected populations, such as Pacific Islanders, Maoris, and Australian Aborigines, continue to have an extremely high prevalence of RHD [9] that may not be altogether explained by living conditions and access to health care. (See Chapter 61).

In the developing world, RF and RHD continue unabated, reflecting the relatively poor living standards and availability of health care [1,2,7]. The prevalence of RHD in school-age children varies from 0.4 to 21 per 1000 children in developing countries [2,7,10–14], where 10–35% of cardiac admissions are for patients with RF and RHD. One in every 150 deaths in developing nations is estimated to be from RHD, with a total of >200 000 deaths per year [2]. RHD remains an obvious public health burden across the developing world.

Estimates of RHD prevalence

School surveys are often used [2]. In the worst affected regions, however, school enrollment rates are low and many affected children may not attend school [7]. Population-based registries can capture all age groups, but depend heavily on referral mechanisms. Hospital-based statistics have serious limitations because only the most seriously affected are represented.

Older surveys used cardiac auscultation to obtain estimates. More recent surveys used echocardiography to confirm the diagnosis when cardiac auscultation was abnormal (mostly audible murmurs) [15,16]. Congenital and nonrheumatic

heart valve disease can be incorrectly labeled as RHD in studies that use auscultation alone. Both strategies likely missed subclinical RHD [2].

Recent large population-based surveys used portable echocardiography. Marijon *et al.*, screening with echocardiography, suggested a very high prevalence of RHD in children from Cambodia and Mozambique. Most patients were clinically silent and no children with mitral stenosis were identified [17]. The natural history of clinically silent heart valve disease detected through echocardiography is unknown. It is unclear whether penicillin prophylaxis is warranted for these children, although most investigators recommend it.

Pathogenesis of rheumatic heart valve disease

Only heart valves are permanently damaged during an episode of RF. All other affected tissues typically heal without residua: pericarditis, chorea, and arthritis all resolve completely without constriction, long-term neurologic consequences, or joint disability, respectively. One of the mysteries of RF is the remarkable tendency for the disease to heal rather than to scar the tissues it affects, with the exception of cardiac valves. The following hypothesis appears most plausible.

Histopathologic findings indicate widespread diffuse collagen–vascular involvement during an acute episode of RF [18]. The immunologic findings suggest that RF predominantly damages the vascular endothelium and mesothelium. The adjacent subendothelial and submesothelial tissues are affected to a very limited depth [18]. The damaged endothelium is replaced by new endothelium within days after injury without significant scarring. The valves are structurally unfortunate in having a small core of connective tissue covered by two layers of endothelium.

The endothelium is initially damaged from a humoral immune response, resulting in VCAM-1 being expressed on the endothelium, followed by activation of cellular immune responses. As a result, CD4+ and CD8+ T lymphocytes and macrophages attach to the valvar endothelium and migrate to the connective tissue core, establishing an inflammatory response accompanied by neovascularization of the valve substance. The endothelium of the newly formed vessels may serve as a substrate for additional inflammation and perhaps set up a vicious cycle of inflammation, neovascularization, and further damage, resulting eventually in a permanently scarred valve [2,18].

Pathology of rheumatic heart valve disease

In autopsies of patients dying of RHD, the mitral valve was most commonly afflicted, either alone or together with the aortic (31.6%) and tricuspid valves (52.8%). Involvement of the tricuspid valve occurred in 38.4%. The extent and severity of the pathology was most marked in the mitral valve, followed by the aortic and tricuspid valves, respectively [19]. Pulmonary valve involvement is exceptional and almost always associated with the involvement of all the other valves. Mitral regurgitation is the commonest lesion encountered in adolescents and children [20].

Most of the gross pathologic features are well demonstrated by cross-sectional [two dimensional (2D)] and more recently, by three-dimensional (3D) echocardiography. Real-time 3D imaging allows an excellent understanding of mechanisms of most hemodynamic consequences of valvar pathology. Figures 62.1–62.5 serve to illustrate the pathology of the mitral valve defined by both 2D and 3D echocardiography (Table 62.1). Table 62.2 shows the echocardiographic correlations with the pathologic features of the aortic valve.

Clinical features of RHD

History and physical examination

A history of acute RF may be difficult to obtain in many patients with RHD [21]. Episodes of RF may be indistinguishable from other common childhood febrile conditions, especially in the absence of arthritis. Not all episodes of RF are severe enough to warrant medical attention [21]. A diagnosis of rheumatic carditis requires careful auscultation because murmurs can be subtle during the first episode of RF. Subcutaneous nodules are relatively uncommon and seldom clinically obvious, and must be searched for carefully at specific locations [22]. Erythema marginatum is also uncommon, often transient, and cannot be easily seen in dark-skinned individuals [23]. Rheumatic chorea often occurs late after the inciting streptococcal sore throat and is sometimes subtle [21].

The ability of family members to recall a history of RF depends on their socioeconomic and cultural background. In general, however, families of children with established RHD at a young age often recall the episode. In the worst affected, acute episodes of RF may evolve rapidly into established RHD with severe affliction of the cardiac valves after a very short quiescent interval [24].

The symptoms and physical signs (Table 62.3) of established RHD are related to the severity of the valve affliction and the individual lesions.

Mitral regurgitation

Mitral regurgitation (MR) is by far the commonest lesion seen in RHD. The inability to increase cardiac output during activity results in fatigue, the commonest symptom of significant MR. MR also causes palpitations because of a volume-loaded hyperdynamic left ventricle and tachycardia. Dyspnea is uncommon unless MR is severe, acute, or the left ventricular myocardium is failing. With a

View from above   **View from below**

(a)   (b)

(c)   (d)
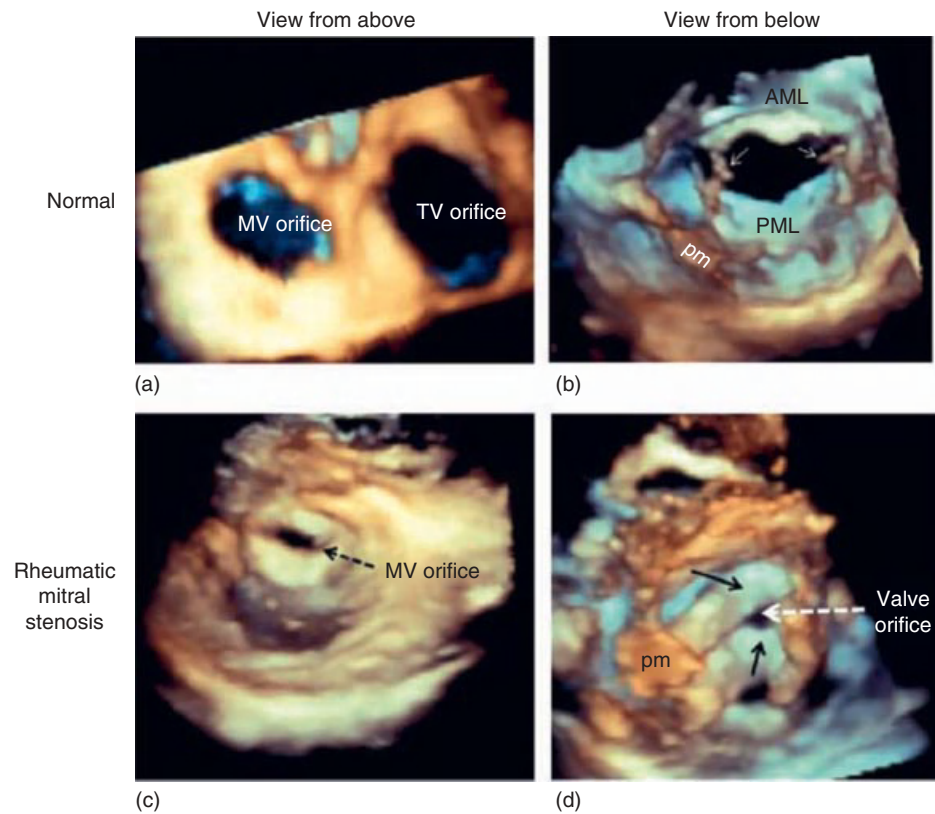
Figure 62.1 3D echocardiographic imaging in rheumatic mitral stenosis. All images were obtained through transthoracic echocardiography. Panels (a) and (c) show views from the atrial aspect, and (b) and (d) show views from the ventricular aspect. Diastolic frames from a normal mitral valve are shown in (a) and (b). Note that the mitral valve orifice is completely open in diastole and valve tissue is barely seen from the atrial aspect (b). Panels (c) and (d) show diastolic frames of the mitral valve from a 20-year-old patient with rheumatic mitral stenosis. Unlike in the normal valve, the mitral valve leaflet substance is seen from the atrial aspect during diastole. The solid arrows point towards the chordae tendinae of the tensor apparatus of the valve. Note the extensive thickening of the chordae that can no longer be distinguished from the papillary muscle (pm) unlike in the normal valve in (b). AML, anterior mitral leaflet; PML, posterior mitral leaflet; pm, papillary muscle; MV, mitral valve; TV, tricuspid valve.
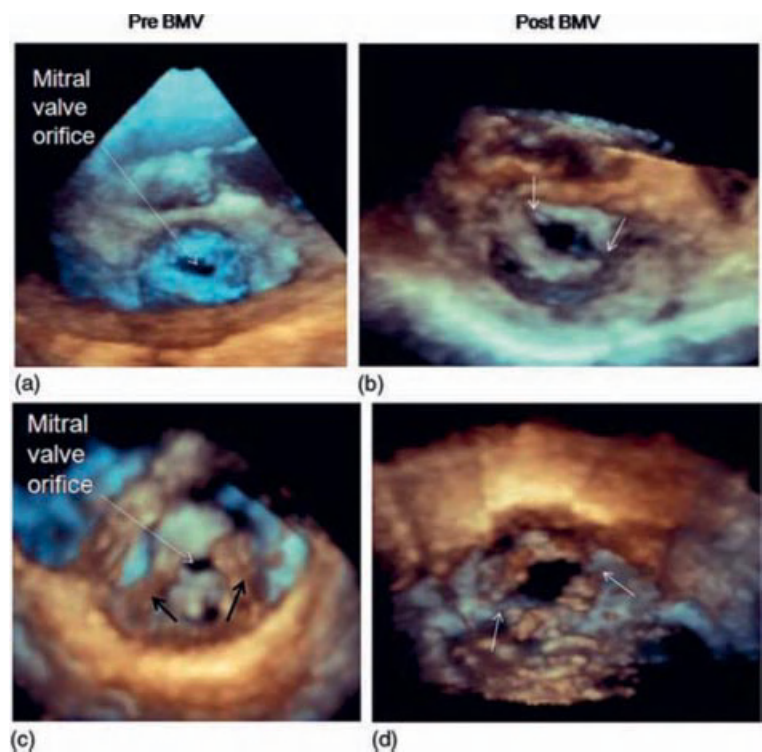
Figure 62.2 These 3D images were obtained from a patient with pure rheumatic mitral valve stenosis (a, c) before and after (b, d) balloon mitral valvotomy (BMV) with the Inoue balloon. Panels (a) and (b) show views from the atrial aspect and (c) and (d) show views from the ventricular aspect. All images were obtained during diastole. Note the thickened chordopapillary apparatus. These images demonstrate that the mechanism of benefit in BMV is through splitting along the commissures of the leaflets (white arrows). Leaflet movements continue to be restricted by the fibrosis in the chordopapillary apparatus (black arrows).

907
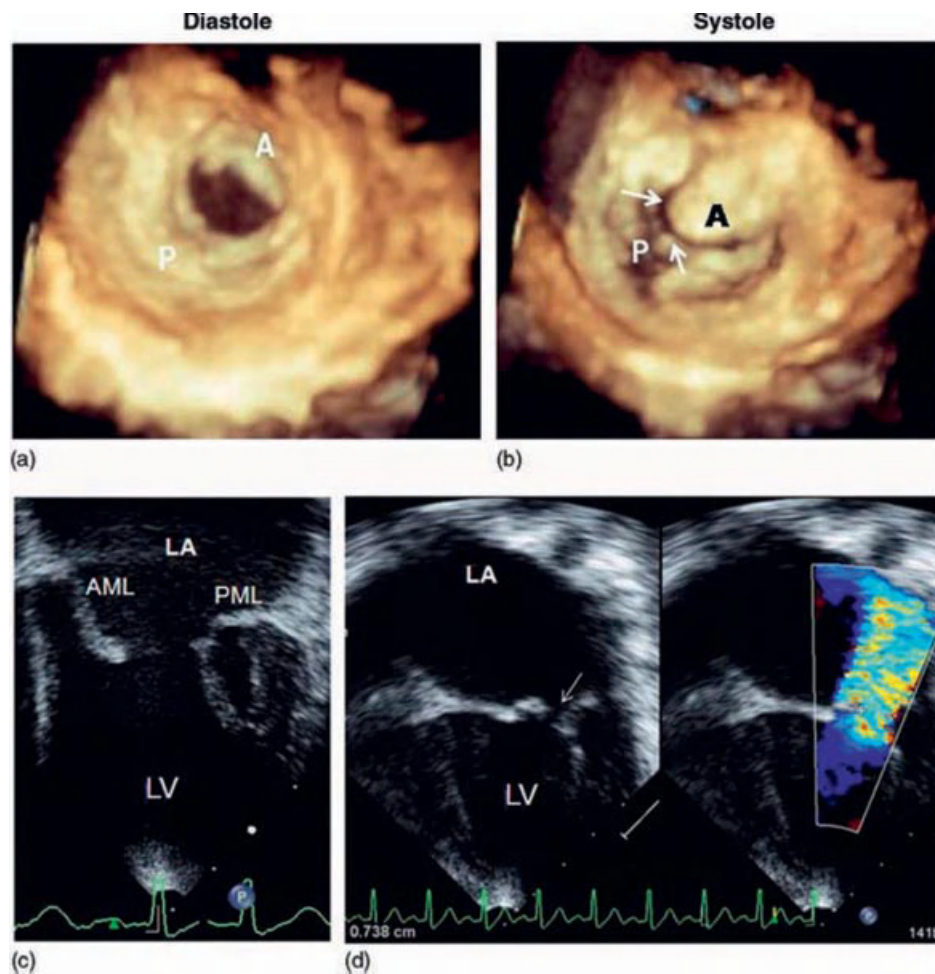
Figure 62.3 Rheumatic mitral valve disease with mitral stenosis and regurgitation. These frames are from a 10 year old child with rheumatic heart disease with severe affliction of the mitral valve. Although the predominant lesion is mitral regurgitation, there is also some mitral stenosis. 3D echocardiograms are shown in (a) and (b) and equivalent 2D frames obtained from apical four-chamber views in (c) and (d). The diastolic frame in the 3D image (a) shows the mitral valve from its left atrial aspect. Note that the leaflet substance is seen in diastole. The equivalent diastolic frame in 2D (c) shows several features of rheumatic affliction. The anterior mitral leaflet (AML) is thickened. The tip of the AML is oriented horizontally and does not point downwards, suggesting restriction of mobility of diastolic motion. The posterior mitral leaflet (PML) is also thickened and mobility is restricted to even a greater degree. The chordae tendinae beneath the PML are visibly thickened. During systole, the PML stays in a relatively fixed position. The free edge of the AML moves to a position above the optimal zone of coaptation between the two leaflets. The resultant regurgitation orifice is shown by white arrows in both the 3D and 2D frames. This orifice is typically crescentic and extends along the length of the AML. The resultant color Doppler jet is directed posteriorly and laterally. AML, anterior mitral leaflet; LA, left atrium; LV, left ventricle; PML, posterior mitral leaflet.

failing left ventricle, left ventricular diastolic pressure increases, left atrial and pulmonary venous pressures increase, and pulmonary congestion appears. Pulmonary arterial hypertension follows significant pulmonary venous hypertension. Some children with chronic severe MR can have disproportionately severe pulmonary arterial hypertension (PAH) from exaggerated vasoconstriction of the pulmonary arterioles [25]. Physical examination is considered in Table 62.3.

Acute marked MR causes severe symptoms in the initial stages, due to pulmonary venous hypertension causing pulmonary congestion. Over time, the left atrium dilates and becomes more compliant. The LV dilates, accommodates the extra volume, and the LV end diastolic pressure declines. A substantial reduction in dyspnea follows. This sequence is seen fairly frequently following an initial episode of RF with carditis and severe MR. Over time, symptomatic improvement occurs without a significant reduction in the degree of MR.

Mitral stenosis

In children, rheumatic mitral stenosis (MS) is less frequent than MR. The very early onset of juvenile MS, sometimes as early as 6 years [26], is largely confined to selected parts of the world where RHD is endemic with a very high prevalence [6,7].
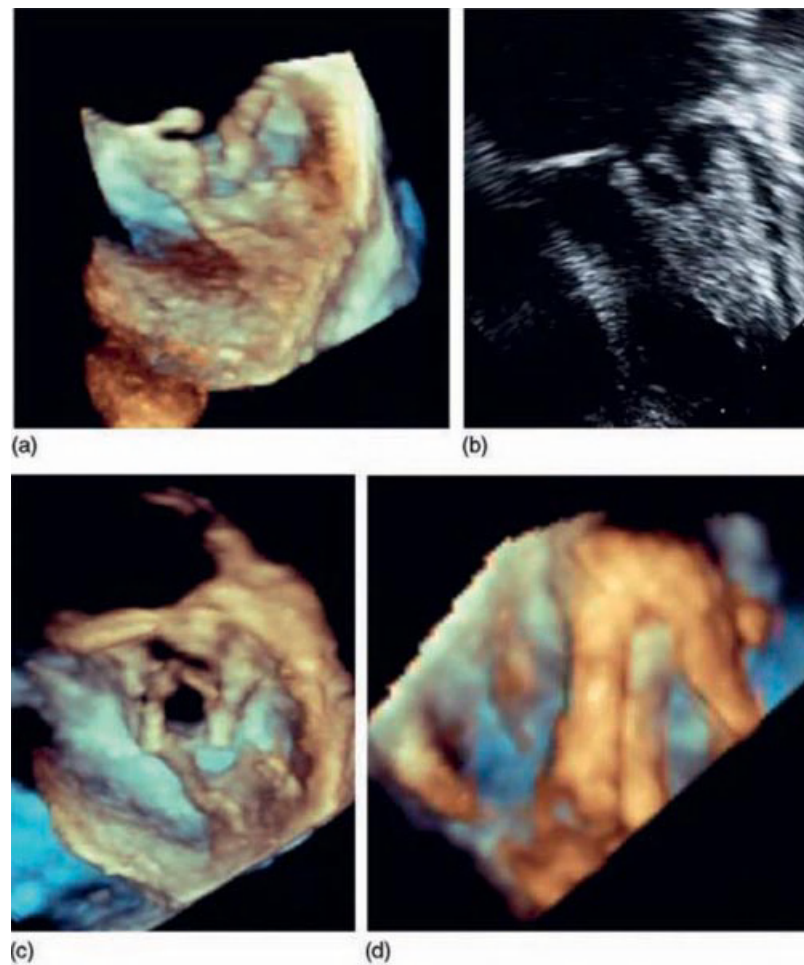
Figure 62.4 Pathology of the chordopapillary apparatus in juvenile RHD. Frames (a)–(c) were obtained from a 10-year-old child with a combination of mitral stenosis and regurgitation and (d) was obtained from a 20-year-old female with severe mitral stenosis documented at 12 years age with recurrence of symptoms after a "successful" balloon valvotomy 8 years previously. Note the diffuse fibrosis with fusion and shortening of the tendinous cords that can no longer be easily distinguished from the adjacent papillary muscle below and the valve leaflets above. Frame (d) was obtained through "virtual dissection" of the 3D image after removing the anterior wall of LV. This represents an extreme example of juvenile mitral valve stenosis that is not uncommon in regions where RHD is very prevalent.

Pulmonary venous hypertension and pulmonary congestion develop from elevated mean left atrial pressure. Dyspnea is, therefore, much commoner than in isolated MR. The severity of PAH varies, depending on the degree of "adaptive" pulmonary vasoconstriction. Thus, it is not unusual for children with severe (juvenile) MS and severe pulmonary venous and arterial hypertension to have no discomfort at rest in spite of extremely high pulmonary arterial and left atrial pressures. The severity of symptoms in MS is determined by the duration of diastolic filling. With tachycardia, diastole shortens to a greater extent than systole. Therefore, these children are exquisitely sensitive to tachycardia, whether from exercise, anxiety, or fever, and can deteriorate suddenly with these precipitating events. Physical examination is considered in Table 62.3.

Aortic regurgitation (AR)

The symptoms of AR are similar to those of MR. However, severe chronic AR may be tolerated very well for several years with no apparent limitation in exercise tolerance. Physical examination (Table 62.3) is characteristic and usually allows fairly accurate assessment of severity. The manifestations of aortic "run-off" are excellent indicators of severity of AR.

Tricuspid regurgitation

Tricuspid regurgitation (TR) typically results from elevated right ventricular pressure. There are no specific symptoms of TR. With the onset of TR, the dyspnea may be relieved to some extent in patients with MS. The patients may have a

(a)   (b)   (c)

(d)   Predominant AS, Systole   (e)   Predominant AS, Diastole   (f)   Predominant AR, Diastole
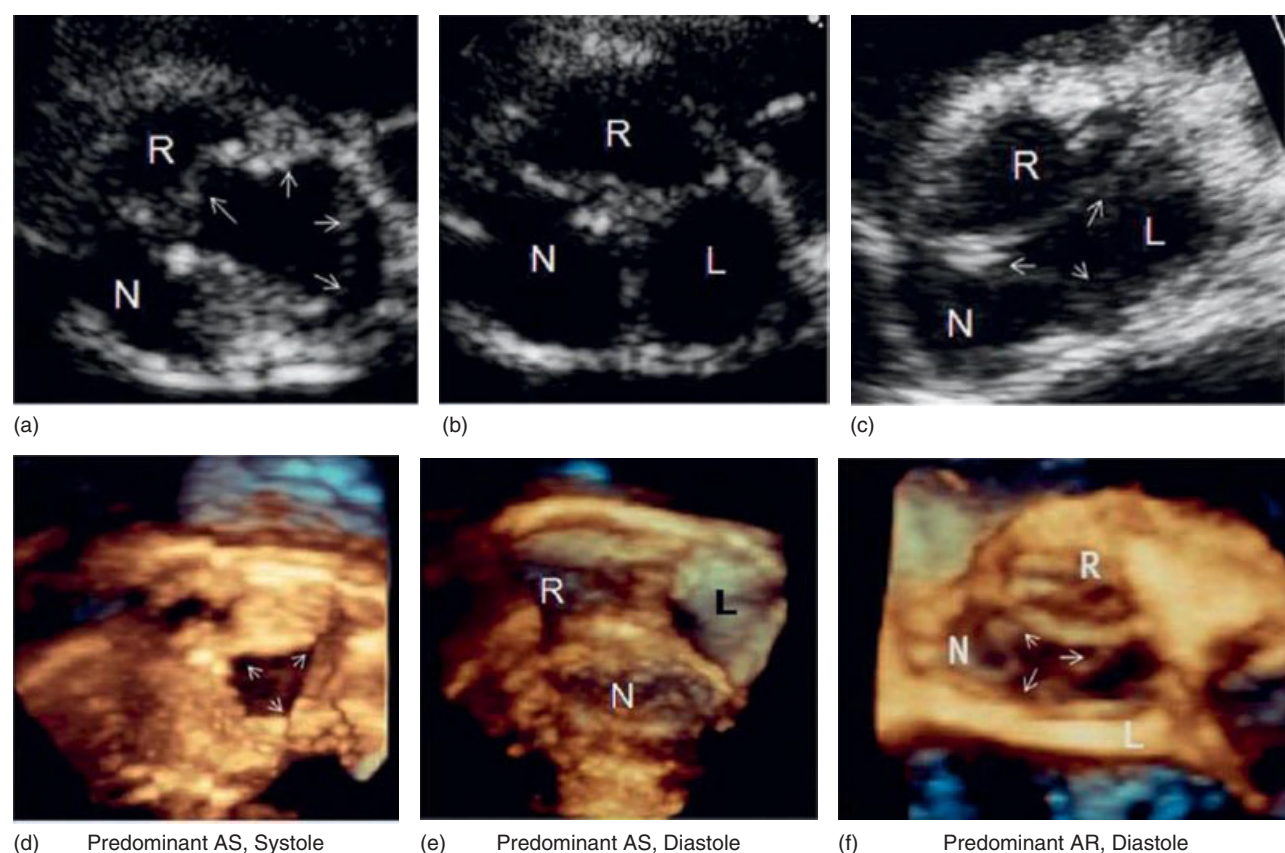
Figure 62.5 Aortic valve involvement in RHD. 2D echo frames of the aortic valve are shown in (a)–(c) and equivalent 3D frames in (d)–(f). Frames (a), (b), (d) and (e) are from a patient with predominant aortic stenosis (AS) and (c) and (f) from a patient with predominant aortic regurgitation (AR). The individual cusps are marked as R for right, L for left and N for noncoronary cusps. Note the thickening of the leaflet edges particularly in the central region where the three cusps come together. Aortic stenosis in this example (a, d) results from fusion of right–left and right non-coronary commissures; The resultant systolic orifice area is considerably reduced. The valve is largely competent in diastole (b, e). In the patient with AR (c, f), the valve closure is incomplete and the regurgitation orifice is seen during diastole. This results from shrinkage of the leaflet substance from extensive fibrosis. The thick leaflet margin is particularly evident along the free edge of the right coronary cusp.

Table 62.1 Pathology of rheumatic mitral valve disease and echocardiographic correlates.

Mitral valve	Pathology	Echocardiographic correlate
Anterior mitral leaflet (AML)	Thickening and restriction of leaflet mobility, especially at the edges, causing characteristic diastolic doming of the valve	Thickening (>3–4 mm) is identified on echocardiograms; diastolic doming is easily identified on 2D echocardiography
Posterior mitral leaflet (PML)	Fixed to a greater extent by the fibrotic and shortened tendinous chords	Fixed PML is very characteristic and a readily identifiable feature of chronic RHD irrespective of whether the dominant lesion is MS or MR
Commissures	Symmetric fusion of commissures of the mitral valve contributes substantially to mitral valve stenosis in most patients. This results in the characteristic "fish mouth" appearance	Commissural fusion is identified in the parasternal short-axis view during 2D echocardiography. The valve area of the stenotic valve is often calculated in this view along the free and fused margins of the leaflets
Tensor apparatus	Thickening and shortening of chords; extensive fibrosis involving the chords, papillary muscles, and the adjacent leaflets also contributes to mitral valve stenosis and accounts for residual stenosis after balloon dilation of the valve. Rupture of chords can occur during an episode of rheumatic fever, causing severe MR. Lengthening of the chords has also been described	The tensor apparatus of the mitral valve can be seen very well with both 2D and 3D echocardiography. Much of the reduced leaflet mobility is due to fibrosis and shortening of the tensor apparatus. Rupture of chords is identified by examining the free edge of the leaflets. Often the AML is involved

Table 62.2 Pathology of rheumatic aortic valve disease and echocardiographic correlates.

Aortic valve	Pathology	Echocardiographic correlate
Leaflet	Thickening especially at the edge, fibrosis, and shortening of the leaflet substance. Irregular thickening or nodularity is typical of RHD	Rolled up margins are identified on 2D echocardiography in the parasternal short-axis views. The reduction in valve substance reduces the zone of coaptation, causing incomplete closure and regurgitation
Commissures	Fusion can involve one or more commissures and causes reduced mobility	Doming of the aortic valve with aortic stenosis is due to commissural fusion

Table 62.3 Physical examination of the cardiovascular system in rheumatic heart disease.

Valve lesion	Mild	Moderate	Severe
Mitral stenosis	Normal S2, opening snap (OS) with wide A2–OS interval, relatively soft and late-onset mid-diastolic murmur often heard with the bell of the stethoscope. Murmur may be unmasked by exercise	S2 split normal but P2 is loud, A2–OS interval shortens, prominent mid-diastolic murmur with presystolic accentuation	Evidence of significant pulmonary hypertension, close splitting of S2, loud P2, short A2–OS interval, prominent mid-diastolic murmur with presystolic accentuation[a]
Mitral regurgitation	Normal apex, normal S2, no S3, blowing apical pan-systolic murmur, usually without a thrill, no flow murmurs. S1 merges with the murmur but may be loud and distinct with accompanying MS	Hyperdynamic apex, widely split S2, S3 may be present, prominent pan-systolic murmur	Cardiac enlargement, downward and outward displaced apex, hyperdynamic precordium, widely split S2 (early A2), P2 may be loud if pulmonary hypertension develops, S3 and frequently a mid-diastolic flow murmur without presystolic accentuation (unless associated with MS)
Aortic stenosis[b]	Normal carotid pulsations, no clinical evidence of left ventricular hypertrophy, relatively short ejection systolic murmur that peaks in early systole	Some delay in carotid upstroke may be appreciable, clinical evidence of LVH in the form of a sustained heave in the apical impulse. Prominent ejection systolic murmur, relatively longer duration peaking in mid-systole	Delayed carotid upstroke, clinical evidence of LVH, long ejection systolic murmur with delayed peaking
Aortic regurgitation	No peripheral signs of increased aortic run-off, normal pulse pressure, early diastolic murmur (EDM)	Wide pulse pressure (>50 mmHg), diastolic pressure usually >50 mmHg, hyperdynamic apical impulse, prominent EDM	Wide pulse pressure (>80 mmHg), diastolic pressure <50 mmHg, often as low as 0 mmHg (free AR), signs of increased aortic run-off are easily demonstrable, cardiac enlargement, hyperdynamic apical impulse, prominent EDM
Tricuspid regurgitation	Pan-systolic murmur of TR audible in the left lower parasternal region (may be heard only during inspiration)	Prominent TR murmur	Liver enlarged with systolic pulsations, elevated jugular venous pulsations (JVP) with prominent V waves, prominent murmur
Tricuspid stenosis (TS)	Mild and moderate TS are usually clinically silent	Elevated JVP with prominent a waves, prominent presystolic pulsations; the mid-diastolic murmur of TS may also be heard in the left lower sternal area	

[a]Rarely severe mitral stenosis may not be associated with a identifiable mid-diastolic murmur (silent MS); usually this is accompanied by severe pulmonary hypertension and gross right ventricular enlargement.
[b]Aortic stenosis (AS) is rarely seen in children with RHD. Isolated AS is exceptional. Some aortic regurgitation invariably accompanies AS and, typically, signs of AR are masked by AS.

history of pain in the right hypochondrium due to a congested liver, and fatigue due to a decrease in systemic output.

Aortic and tricuspid stenosis are rare in children with RHD. Isolated aortic valve involvement with dominant aortic stenosis is more likely to have a congenital basis.

Combined valve lesions

Combined lesions are frequent in RHD. Typically, MS and MR coexist, and their clinical features can be readily identified in most patients. Combinations of mitral, aortic, and tricuspid valve disease are common. The severity of each valve's involvement must be quantified to allow correct management decisions. For example, in a child with MS, if MR is moderate or severe and commissural in origin, balloon mitral valvoplasty is precluded. Similarly, in a patient undergoing mitral valve repair or replacement, the decision to replace the aortic valve is dictated by the severity of associated AR [27].

Chest X-ray

Left atrial and atrial appendage enlargement almost invariably accompany significant mitral valve disease. Right atrial enlargement is seen with PAH and tricuspid valve involvement. Left ventricular enlargement occurs with AR and MR. The lung fields show varying degrees of pulmonary venous congestion depending on the severity and duration of pulmonary venous hypertension (Figure 62.6).

Electrocardiogram

Left atrial enlargement and right ventricular hypertrophy are seen in pure or dominant MS (Figure 62.7). Left ventricular enlargement with volume overload from MR or AR is evident by Q waves in lateral chest leads. Atrial fibrillation is very unusual in children even with severe left atrial enlargement.

Echocardiography

Echocardiography is the most important investigation, and correlates well with pathology (Tables 62.1 and 62.2 and Figures 62.3, 62.8, and 62.9). Other specific features of RHD include simultaneous involvement of multiple valves, because the association of mitral and aortic valve pathology is infrequent in other conditions. The echocardiographic diagnosis may not be straightforward. Hence it helps to correlate the echocardiographic findings with the clinical context. The threshold for diagnosis of RHD is understandably lower in regions where RHD is very prevalent.

The severity of individual lesions can be defined with precision. Gradients across the affected valves can be determined and the severity of regurgitant lesions quantified (Figures 62.3, 62.8, and 62.9). The hemodynamic

Figure 62.6 Chest X-ray (posterior–anterior view) from an 8-year-old patient with juvenile mitral stenosis as a result of RHD. There is evidence of severe pulmonary venous hypertension in the form of prominent upper lobe pulmonary veins (cephalization), interstitial haze, and prominent inter-lobar fissures (arrow). Additionally, there is evidence of an enlarged left atrium (lifting up of the left bronchus) and left atrial appendage (straightening of the left heart border).

consequences of various lesions can be studied, including chamber enlargement, PAH, and ventricular function. Serial echocardiography often guides decisions regarding timing of operation. Important complications, such as infective endocarditis, can be recognized echocardiographically.

Echocardiographic criteria for rheumatic heart valve disease

A number of conditions must be distinguished from rheumatic valve disease. Specific criteria for rheumatic heart disease have been developed by an NIH working group (http://www3.niaid.nih.gov/topics/streptococcal/protocols.htm), and are listed below. Validation of these criteria by international long-term follow-up studies, particularly for patients with subtle or borderline findings, is in progress.

Echocardiographic evidence of *definite RHD* is *any* of:

1 A mitral regurgitant jet at least 2 cm from the coaptation point of the valve leaflets, seen in two planes and persisting throughout systole, *plus* thickened mitral valve leaflets and/or elbow or dog-leg deformity of the anterior mitral valve leaflet.

2 An aortic regurgitant jet at least 1 cm from the coaptation point of the valve leaflets, seen in two planes, *plus* thickened mitral valve leaflets and/or elbow or dog-leg deformity of the anterior mitral valve leaflet.
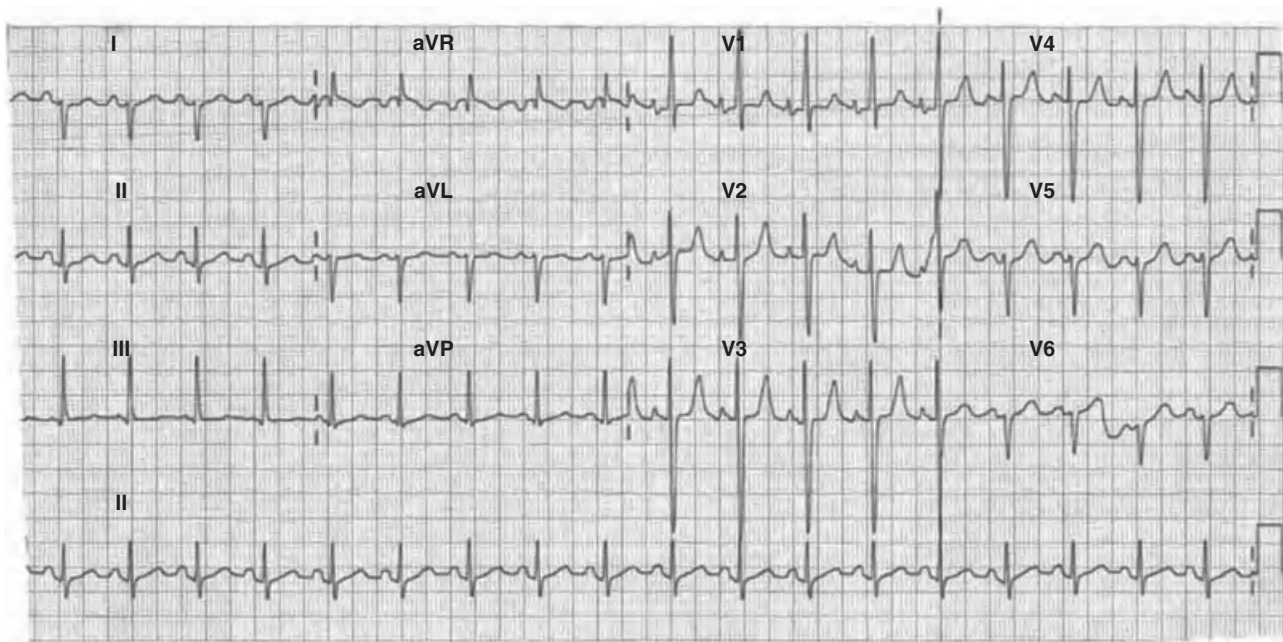
Figure 62.7 Electrocardiogram from an 8-year-old child with RHD and severe mitral stenosis. There is evidence of right ventricular hypertrophy in the form of rightward deviation of the QRS axis, prominent R waves in V1 and persistent S waves in V5 and V6. Additionally, there is evidence of left atrial enlargement in the form of prominent broad P waves in lead II.
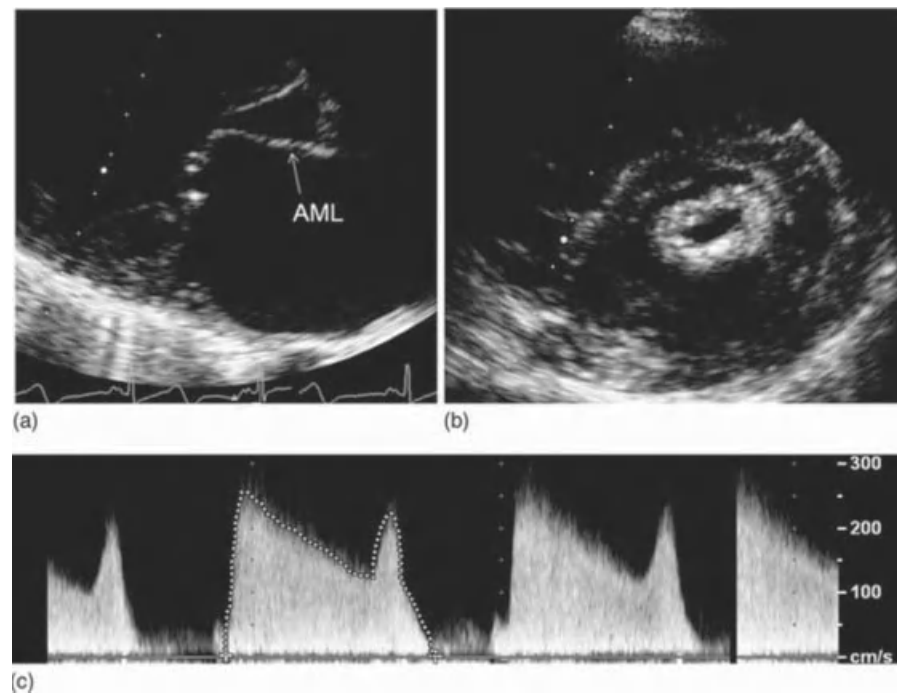
Figure 62.8 2D echocardiography for RHD and mitral stenosis. (a) A diastolic frame from the parasternal long axis view. The characteristic "dog-leg" or "elbow' deformity is shown in the anterior mitral valve leaflet (AML). The tips of the AML are thickened. The thick and shortened chordae attached to the posterior mitral leaflet are also shown in this frame. Frame (b) is a picture obtained from the parasternal short-axis view. This view captures the mitral valve orifice in mid-diastole and allows accurate estimation of the mitral valve area. This view is also very useful in planning balloon mitral valvotomy (BMV). In this patient, for instance, we can expect that the commissures would split favorably after BMV. Panel (c) is a Doppler tracing from the same patient showing the characteristic M-shaped flow acceleration across the stenotic valve that is seen in patients with MS and sinus rhythm. The second peak results from atrial contraction and is responsible for the presystolic accentuation of the mid-diastolic murmur.
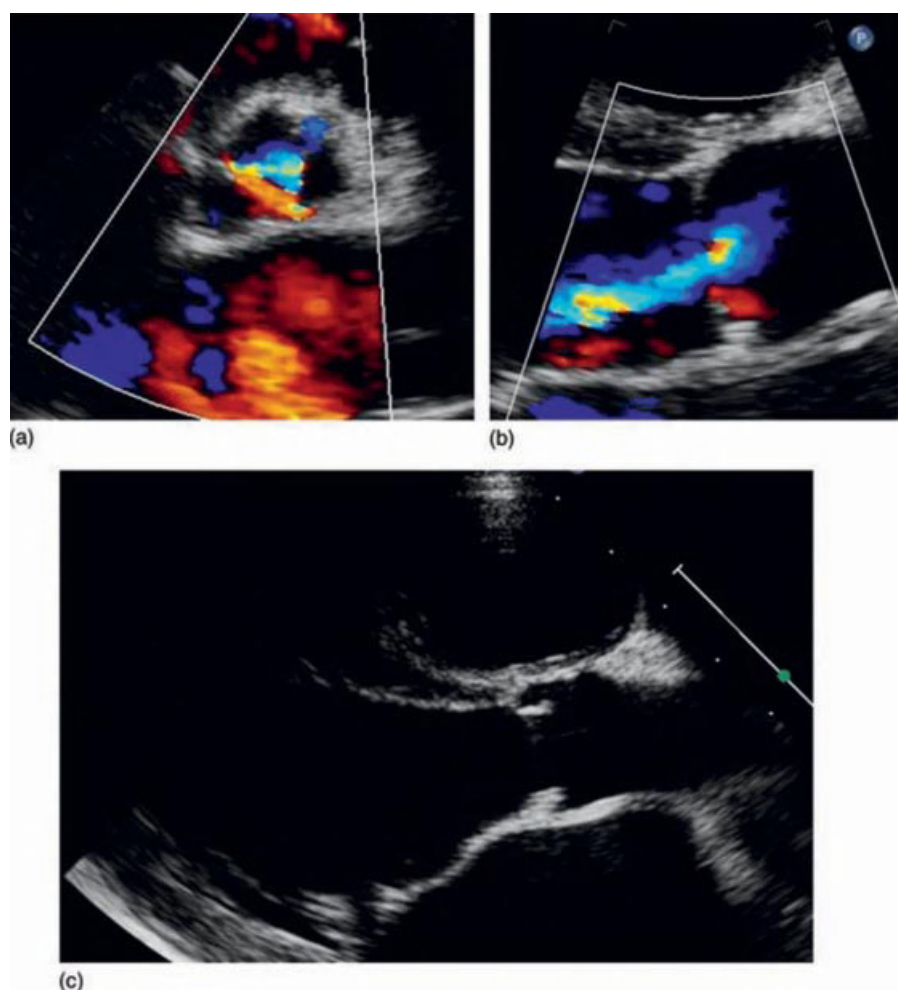
Figure 62.9 2D echocardiograms and color Doppler from a patient with RHD involving the aortic valve. The dominant lesion here is aortic regurgitation that is the result of fibrosis and shortening of the individual leaflet cusps. The jet is characteristically central (a, b). The thickened cusps are seen in the lower systolic frame (c) obtained in the parasternal short-axis view.

3 Any significant mitral stenosis (defined as flow acceleration across the mitral valve with a mean pressure gradient greater than 4 mmHg).

Echocardiographic evidence of *probable RHD* is *any* of:

1 Thickened mitral valve leaflets and/or elbow or dog-leg deformity of the anterior mitral valve leaflet regardless of the degree of mitral or aortic regurgitation.

2 A mitral regurgitant jet at least 2 cm from the coaptation point of the valve leaflets, seen in two planes and persisting throughout systole *without* thickened mitral valve leaflets and/or elbow or dog-leg deformity of the anterior mitral valve leaflet (in the setting of possible ARF, this may represent acute carditis, before valve leaflets have developed structural abnormalities).

3 An aortic regurgitant jet at least 1 cm from the coaptation point of the valve leaflets, seen in two planes *without* thickened mitral valve leaflets and/or elbow or dog-leg deformity of the anterior mitral valve leaflet.

Specific diagnostic challenges

Recurrence of RF in RHD

Detection of RF recurrence in a patient with pre-existing RHD is challenging. A diagnosis of carditis is difficult to establish unless by serial auscultation or echocardiography a new valve lesion is carefully documented. Other major diagnostic criteria may not be present in a recurrent episode. According to 2002–2003 WHO criteria, a diagnosis of recurrence of RF in RHD requires at least two minor manifestation of RF plus evidence of preceding group A streptococcal infection (in the form of elevated ASO titers or a positive throat swab for group A beta hemolytic streptococcus) [2].

Infective endocarditis

Infective endocarditis can complicate regurgitant lesions of the mitral or aortic valve resulting from RHD [28], but is

very uncommon in patients with pure mitral stenosis. In a large study of 1763 patients with RHD, the incidence of endocarditis was 2.3% over an average follow-up of 5.3 years [28]. The consequences of infective endocarditis are often devastating, and early diagnosis is vital before major valve damage occurs. Infective endocarditis must be considered in a patient with established RHD who has had a fever lasting more than 4–5 days. Distinguishing endocarditis from rheumatic fever recurrence is often challenging. Three or more blood cultures before giving antibiotics are mandatory. Other indicators of endocarditis, such as microscopic hematuria, leukocytosis, thrombocytopenia, and elevations in acute phase reactants have limited sensitivity and specificity. Echocardiography can identify vegetations on valves previously affected by RHD. Transesophageal echocardiography improves sensitivity substantially, especially in older children.

Complications and natural history

Pulmonary arterial Hypertension

PAH frequently complicates RHD and is a significant prognostic variable [29]. It is frequently associated both with severe MS and MR in children [26,29,30]. The PAH is due to passive transmission of left atrial and pulmonary venous hypertension, interstitial edema. and reactive pulmonary arteriolar vasoconstriction [31]. Following balloon mitral valvotomy, the component of the PAH attributable to passive transmission resolves immediately [30,31], while the reactive component resolves slowly over weeks to months.

Ventricular dysfunction

Left ventricular dysfunction is usually due to long-standing and severe mitral or aortic regurgitation. Combined severe MR and AR accentuate left ventricular enlargement and dysfunction that contribute to poor long-term outcomes following double valve replacement in children with RHD. Much of the dysfunction appears to result from chronic volume overload; available evidence does not support a substantial role for myocardial injury during episodes of rheumatic carditis [32]. The natural history of severe MR and AR is not well characterized in children and may differ from that in adults. Right ventricular dysfunction develops secondary to severe and long-standing PAH.

Infective endocarditis

Endocarditis must be suspected in the presence of persistent fever or sudden worsening of heart failure [25,28].

Dysrhythmias

Unlike in adults, atrial fibrillation is uncommon in children with RHD even with severe left atrial enlargement. Uncontrolled ventricular responses typically herald the onset of atrial fibrillation. The resultant tachycardia markedly worsens symptoms in patients with mitral stenosis.

Thromboembolism

Severe atrial dilation with resultant stasis of blood in the left atrium (often visible as spontaneous contrast in echocardiograms) promotes clot formation. Atrial fibrillation greatly increases the propensity for thrombosis. The left atrial appendage (LAA) is the most frequent site for clots that are often silent. However, there is a risk of dislodgement of an LAA clot if balloon mitral valvotomy is attempted. Therefore, transthoracic and, if needed, transesophageal echocardiography must be used to examine the LAA before balloon mitral valvotomy is contemplated.

Recurrence of rheumatic fever

Patients with established RHD are at a particularly high risk of recurrence of RF following an episode of streptococcal sore throat [33]. Recurrences are almost invariably associated with carditis. Many episodes of RF recurrences are not clinically obvious and this is reflected in the relatively liberal WHO criteria for diagnosis of recurrent RF in RHD [2].

Treatment of established rheumatic heart valve disease

Secondary prophylaxis to prevent recurrences of rheumatic fever

All patients with established RHD or one or more previous episodes of RF must receive regular penicillin. The success with secondary prophylaxis depends critically on patient education [2]. Benzathine penicillin injection (1.2 million units every 3–4 weeks, and 0.6 million units for children under 25 kg) is the most effective method. For high-prevalence regions, 3-weekly penicillin is recommended [2,34]. Compliance with benzathine penicillin injections has varied from 40 to 86% in reports from India [23,35]. Daily oral penicillin (250 mg penicillin V every 12 h) is an alternative. Compliance with oral penicillin is difficult to ensure because many doses may be missed inadvertently. Secondary prophylaxis is especially important in those who have not yet developed established RHD or those with mild disease. Patients with penicillin allergy may receive erythromycin (250 mg twice daily) or sulfonamides (1 g once daily; 0.5 g once daily for patients weighing 27 kg or under) [2,36].

Prophylaxis against infective endocarditis

Prophylaxis is no longer necessary unless there is a likelihood of a breach of oral mucosa, manipulation of either gingival tissue or the periapical region of teeth in presence of valve lesions that are at the highest risk of endocarditis [37]. Hence routine endocarditis prophylaxis is largely unnecessary for

pure mitral valve stenosis. High-risk lesions include prosthetic valve(s), AR, and MR [36,37]. Details of antibiotic prophylaxis are given in Chapter 60.

Drug therapy for heart failure: mitral stenosis

Diuretics, typically furosemide (frusemide), relieve symptoms of pulmonary congestion. Additionally, they often help to reduce the heart rate at rest and after exercise, and heart rate reduction translates into an increased diastolic filling period that helps reduce left atrial pressure. Digoxin, traditionally administered for this purpose, has been replaced by β-blockers because of their better efficacy and safety profile. β-Blockers may prevent acute worsening of symptoms and occurrence of pulmonary edema [38,39]. However, they do not appear consistently to improve exercise capacity in patients with MS who are in sinus rhythm [40]. β-Blocker alone or with a small dose of diuretic can be used in moderate MS while awaiting balloon mitral valvotomy or with a suboptimal result following the procedure [41]. Also see Chapter 27.

Regurgitant lesions

Diuretics are the mainstay when symptoms of pulmonary congestion accompany severe MR or AR. The role of systemic vasodilators, most commonly ACE inhibitors and calcium channel blockers, to reduce systemic afterload in isolated MR and AR is controversial [36]. Available data from adults do not support the role for systemic afterload reducing agents to delay development of LV dysfunction in MR. An important additional consideration in RHD is the presence of varying degrees of the mitral stenosis that accompanies MR. Also see Chapter 28.

For isolated severe AR, vasodilators are perhaps indicated for short-term therapy (until aortic valve surgery can be performed) in symptomatic patients, particularly with ventricular dysfunction [36]. In asymptomatic children with severe AR, there is no evidence that vasodilators can delay surgery. Also see Chapter 31.

Catheter-based management of mitral stenosis: balloon mitral valvotomy

Balloon mitral valvotomy (BMV), also known as percutaneous trans-septal mitral commissurotomy (PTMC), has largely replaced closed or open mitral commissurotomy for MS in children [41–43]. Improvement in mitral valve area following BMV or PTMC largely results from splitting of the fused commissures (Figure 62.2). The sub-valvar pathologic abnormalities of MS remain after BMV, so the mitral valve area does not normalize after BMV.

Among all available methods for BMV, the most popular is the Inoue balloon assembly that is specifically designed for the mitral valve. Catheter hardware and balloon assembly kits designed for adults are often adapted for pediatric use. Key adaptations include using the pediatric trans-septal needle and smaller balloons (24 mm) The initial step involves puncture of the inter-atrial septum with a Brockenbrough needle.

It is important to pay careful attention to the diameter of the balloon to avoid producing MR. The Inoue balloon can be inflated to a range of diameters based on the amount of fluid used for inflation. The average balloon diameter is determined by the height of the patient (the formula is 10 + height in cm/10); a child of 140 cm will typically require a 25 mm balloon). The mitral valve may not always yield at prescribed balloon diameters and oversizing by 1–2 mm may be needed to "split" the commissures. It is important to proceed carefully in a stepwise fashion with echocardiographic evaluation after each dilation to help minimize MR.

The pathologic features of the valve are important determinants of immediate and long-term outcome. Echocardiography can assess the variables that predict the results of BMV both in reduction in valve area and gradient and occurrence of significant MR (see Figure 62.8). These variables include the nature of commissural fusion, severity of subvalvar deformity, leaflet mobility, and calcification. Trivial MR via the central valve orifice does not worsen and may disappear following BMV. However, MR at the commissures may progress following BMV [43].

The immediate results of BMV in children are comparable to those in adults. In a series of 81 children with juvenile MS, Bahl *et al.* demonstrated an increase in valve area by $172 \pm 62\%$ (from a mean of 0.8 ± 0.4 to $2.2 \pm 0.5\,\text{cm}^2$) [44].

Long-term follow-up after BMV is mandatory because of the significant risk of restenosis with time. Restenosis is typically associated with significant residual MS (typically because of subvalvar pathology) following BMV. Repeat BMV is an option for restenosis and helps postpone mitral valve surgery.

Surgery for RHD

For significant MR, valve repair should be considered.. Excellent immediate and acceptable intermediate term outcomes follow valve repair of MR in RHD [45,46]. These reports could be subject to publication bias. The results of mitral valve repair in RHD are not as consistently reproducible as for MR associated with a myxomatous valve [47]. For the combination of MR and MS, it is particularly difficult to make management decisions.

There are major long-term concerns about operations in RHD. The inflammation in chronic RHD may continue well beyond the initial episode of RF and result in continuing injury to the mitral valve and tensor apparatus after "successful" repair [19]. There are several other challenges. Repeated operations are unrealistic in most environments where RHD is prevalent because of the expense involved with open-heart surgery. Furthermore, there are limitations to mitral valve replacement with a mechanical prosthetic valve in younger patients. Monitoring anticoagulation is particularly challenging in most parts of the developing world. Pregnancy imposes a substantial additional risk in

females. In the developing world, a number of factors, such as valve pathology, gender, age, resources, surgical expertise, and patient and family preferences, must be considered for mitral valve replacement in RHD.

There are no clear guidelines for the timing of mitral valve surgery (particularly replacement) in children. Standard guidelines for mitral valve surgery in adults do not apply to children. The natural history of chronic valve regurgitation appears to be very different in children and adults. Persistent symptoms, in spite of maximally tolerated medications, warrant consideration of surgery especially in the presence of pulmonary artery hypertension. For an asymptomatic child, evidence of ventricular dysfunction merits consideration for surgery. Rheumatic aortic valve disease is less suited for repair. Fortunately, it is not always necessary to operate on AR unless it is severe. There are isolated reports of good results following aortic valve repair for RHD [48,49]. The Ross operation is a poor option for RHD and the long-term durability of the pulmonary autograft is very limited in children with RHD [50]. Small children pose a significant challenge for aortic valve replacement. The aortic root often needs to be enlarged to fit the smallest available mechanical prosthesis and this requires technical expertise.

For patients with RHD with combined mitral and aortic valve disease, the threshold for replacing both valves is fairly high. because of expense, morbidity, and concerns regarding long-term anticoagulation. Many surgeons, therefore, choose to replace the more severely affected valve (typically the mitral valve) and to leave the less severely affected valve alone. Mild or moderate aortic valve disease does not progress rapidly over several years after mitral valve replacement for RHD [27].

Associated tricuspid valve disease can be repaired in most instances. Typically, annuloplasty of the dilated tricuspid valve annulus restores competence [51].

Prevention of RF and RHD – A public health perspective

RF and RHD continue to be important public health problems in the developing world [1,2,7,35]. The magnitude of the problem remains unrecognized in these regions and this obstructs planning public health strategies for disease prevention. Very few systematic surveys are available from rural populations which have a poor health care infrastructure, urban slums, or tribal colonies [35].

Penicillin prophylaxis, particularly secondary prophylaxis, remains the mainstay for prevention of RF and RHD [2]. Its importance should be stressed at institutional and governmental levels. Education about the disease is needed for health professionals and the public in these regions. Patients with established RHD and those who have had an episode of RF should receive targeted education on the importance of penicillin prophylaxis.

An effective vaccine against group A streptococcus (GAS) has the potential to reduce the RF–RHD disease burden, but many difficulties need to be overcome before an effective vaccine is available [35]. A number of questions remain about the usefulness of vaccines for streptococcal strains found in the developing world. There is also the practical issue of identifying the population at risk in the developing world, given the changing disease epidemiology. An effective vaccine cannot be seen as a magic bullet to control RHD, while disregarding the various interactive forces that contribute to disease occurrence. Any public health effort to control RF–RHD should adopt a comprehensive approach that includes all facets of disease prevention to achieve an enduring impact on the reduction of disease burden.

References

1 Kumar RK, Rammohan R, Narula J, Kaplan EL. Epidemiology of rheumatic fever. In: Narula J, Reddy KS, Tandon R, Virmani R, eds. *Rheumatic Fever*. Washington, DC: American Registry of Pathology Publications, 1999: 41–68.

2 WHO. *Rheumatic Fever and Rheumatic Heart Disease. Report of a WHO Expert Consultation*. Technical Report Series No. 923. Geneva: World Health Organization, 2004.

3 Feinstein AR, Di Massa R. Prognostic significance of valvular involvement in acute rheumatic fever. *N Engl J Med* 1959;**260**:1001–7.

4 Bland EF. Rheumatic fever: the way it was. *Circulation* 1987; **76**:1190–5.

5 Joswig BC, Glover MU, Handler JB, *et al.* Contrasting progression of mitral stenosis in Malayans, versus American-born Caucasians. *Am Heart J* 1982;**104**:1400–3.

6 Roy SB, Bhatia ML, Lazaro EJ, Ramalingaswami V. Juvenile mitral stenosis in India. *Lancet* 1963;**ii**:1193–5.

7 Sadiq M, Islam K, Abid R, *et al.* Prevalence of rheumatic heart disease in school children of urban Lahore. *Heart* 2009;**95**:353–7.

8 Veasy LG, Wiedmeier SE, Orsmond GS, *et al.* Resurgence of acute rheumatic fever in the intermountain area of the United States. *N Engl J Med* 1987;**316**:421–7.

9 Steer AC, Carapetis JR. Acute rheumatic fever and rheumatic heart disease in indigenous populations. *Pediatr Clin North Am* 2009;**56**:1401–19.

10 Padmavati S. Rheumatic fever and rheumatic heart disease in developing countries. *Bull WHO*, 1978;**56**:543–50.

11 Koshi G, Benjamin V, Cherian G. Rheumatic fever and rheumatic heart disease in rural South Indian children. *Bull WHO* 1981; **59**:599–603.

12 ICMR Task Force. *Community Control of Rheumatic Fever and Rheumatic Heart Disease. Report of ICMR Task Force Study*. Delhi: ICMR, 1994.

13 Jose VJ, Gomathi M. Declining prevalence of rheumatic heart disease in rural schoolchildren in India: 2001–2002. *Indian Heart J* 2003;**55**:158–60.

14 Arguedas A, Mohs E. Prevention of rheumatic fever in Costa Rica. *J Pediatr* 1992;**121**:569–72.

15 Thakur JS, Negi PC, Ahluwalia SK, Vaidya NK. Epidemiological survey of rheumatic heart disease among school children in

the Shimla Hills of northern India: prevalence and risk factors. *J Epidemiol Community Health* 1996;**50**:62–6.

16 Anabwani GM, Bonhoeffer P. Prevalence of heart disease in school children in rural Kenya using colour-flow echocardiograph. *East Afr Med J* 1996;**73**:215–7.

17 Marijon E, Ou P, Celermajer DS, *et al*. Prevalence of rheumatic heart disease detected by echocardiographic screening. *N Engl J Med* 2007;**356**:470–6.

18 Roberts S, Kosanke S, Dunn ST, *et al*. Pathogenic mechanisms in rheumatic carditis: focus on valvular endothelium. *J Infect Dis* 2001;**183**:507–11.

19 Chopra P, Bhatia ML. Chronic rheumatic heart disease in India: a reappraisal of pathologic changes. *J Heart Valve Dis* 1992;**1**:92–101.

20 Chockalingam A, Gnanavelu G, Elangovan S, Chockalingam V. Clinical spectrum of chronic rheumatic heart disease in India. *J Heart Valve Dis* 2003;**12**:577–81.

21 Bland EF. Chorea as a manifestation of rheumatic fever: a long-term perspective. *Trans Am Clin Climatol Assoc* 1961;**73**:209–13.

22 Singhi AK, Bobhate P, Kappanayil M. Acute rheumatic fever: subcutaneous nodules and carditis. *Circulation* 2010;**121**:946–7.

23 Ravisha MS, Tullu MS, Kamat JR. Rheumatic fever and rheumatic heart disease: clinical profile of 550 cases in India. *Arch Med Res* 2003;**34**:382–7.

24 Vasan RS, Selvaraj S. Natural history of rheumatic fever. In: Narula J, Reddy KS, Tandon R, Virmani R, eds. *Rheumatic Fever*. Washington, DC: American Registry of Pathology Publications, 1999: 347–58.

25 Srivastava S, Subramanyan K, Tandon R. Severity of rheumatic mitral regurgitation. *Indian J Paediatr* 1992;**59**:579–83.

26 Beg MH, Reyazuddin. Mitral stenosis in childhood and adolescence – a study of 45 cases and their surgical management. *Ann Trop Paediatr* 1989;**9**:98–101.

27 Namboodiri N, Remash K, Tharakan JA, *et al*. Natural history of aortic valve disease following intervention for rheumatic mitral valve disease. *J Heart Valve Dis* 2009;**18**:61–7.

28 Doyle EF, Spagnuolo M, Taranta A, *et al*. The risk of bacterial endocarditis during antirheumatic prophylaxis. *JAMA* 1967; **201**:807–12.

29 Sani MU, Karaye KM, Borodo MM. Prevalence and pattern of rheumatic heart disease in the Nigerian savannah: an echocardiographic study. *Cardiovasc J Afr* 2007;**18**:295–9.

30 Fawzy ME, Hassan W, Stefadouros M, *et al*. Prevalence and fate of severe pulmonary hypertension in 559 consecutive patients with severe rheumatic mitral stenosis undergoing mitral balloon valvotomy. *J Heart Valve Dis* 2004;**13**:942–7.

31 Dev V, Shrivastava S. Time course of changes in pulmonary vascular resistance on mechanism of regression of pulmonary artery hypertension after balloon mitral valvuloplasty. *Am J Cardiol* 1991;**67**:439–42.

32 Juneja R, Tandon R. Rheumatic carditis: a reappraisal. *Indian Heart J* 2004;**56**:252–5.

33 Feinstein AR. Recurrences of rheumatic fever. In: Narula J, Reddy KS, Tandon R, Virmani R, eds. *Rheumatic Fever*. Washington, DC: American Registry of Pathology Publications, 1999:339–46.

34 Lue HC, Wu MH, Hsieh KH, *et al*. Rheumatic fever recurrences: controlled study of 3-week versus 4-week benzathine penicillin prevention programs. *J Pediatr* 1986;**108**:299–304.

35 Kumar RK, Paul M, Francis PT. Rheumatic heart disease in India, are we ready to shift from secondary prophylaxis to vaccinating high risk children. *Curr Sci* 2009;**97**:397–404.

36 Bonow RO, Carabello BA, Chatterjee K, *et al* 2008 Focused update incorporated into the ACC/AHA2006 guidelines for the management of patients with valvular heart disease. A report of the American College of Cardiology/American Heart Association Task Force on Practice Guidelines (Writing Committee to Revise the 1998 Guidelines for the Management of Patients With Valvular Heart Disease) Endorsed by the Society of Cardiovascular Anesthesiologists, Society for Cardiovascular Angiography and Interventions, and Society of Thoracic Surgeons. *J Am Coll Cardiol* 2008;**52**:e1–142.

37 Gerber MA, Baltimore RS, Eaton CB, *et al*. Prevention of rheumatic fever and diagnosis and treatment of acute streptococcal pharyngitis: a scientific statement from the American Heart Association Rheumatic Fever, Endocarditis, and Kawasaki Disease Committee of the Council on Cardiovascular Disease in the Young, the Interdisciplinary Council on Functional Genomics and Translational Biology, and the Interdisciplinary Council on Quality of Care and Outcomes Research: endorsed by the American Academy of Pediatrics. *Circulation* 2009;**119**:1541–51.

38 Oakley CM. Beta blockers have important role in pulmonary oedema due to mitral stenosis. *BMJ* 1996;**312**:376.

39 Narasimhan C, Joseph G, Thomas CS. Propranolol for pulmonary oedema in mitral stenosis. *Int J Cardiol* 1994;**44**:178–9.

40 Monmeneu Menadas JV, Marín Ortuño F, Reyes Gomis F, *et al*. Beta-blockade and exercise capacity in patients with mitral stenosis in sinus rhythm. *J Heart Valve Dis* 2002;**11**:199–203.

41 Fawzy ME, Stefadouros MA, Hegazy H, *et al*. Long term clinical and echocardiographic results of mitral balloon valvotomy in children and adolescents *Heart* 2005;**91**:743–8.

42 Joseph PK, Bhat A, Francis B, Sivasankaran S. Percutaneous transvenous mitral commissurotomy using an Inoue balloon in children with rheumatic mitral stenosis. *Int J Cardiol* 1997;**62**:19–22.

43 Wilkins GT, Weyman AE, Abascal VM, *et al*. Percutaneous balloon dilatation of the mitral valve: an analysis of echocardiographic variables related to outcome and the mechanism of dilatation. *Br Heart J* 1988;**60**:299–308.

44 Bahl VK, Chandra S, Kothari SS, *et al*. Percutaneous transvenous mitral commissurotomy using Inoue catheter in juvenile rheumatic mitral stenosis. *Cathet Cardiovasc Diagn* 1994;Suppl 2:82–6.

45 Phan KP, Nguyen VP, Pham NV, *et al*. Mitral valve repair in children using Carpentier's techniques. *Semin Thorac Cardiovasc Surg Pediatr Card Surg Annu* 1999;**2**:111–20.

46 Talwar S, Rajesh MR, Subramanian A, *et al*. Mitral valve repair in children with rheumatic heart disease. *J Thorac Cardiovasc Surg* 2005;**129**:875–9.

47 Zakkar M, Amirak E, Chan KM, Punjabi PP. Rheumatic mitral valve disease: current surgical status. *Prog Cardiovasc Dis* 2009;**51**:478–81.

48 Tao L, Zeng XJ, Lim YP. Single cusp replacement for aortic regurgitation. *Ann Thorac Surg* 2008;**85**:946–8.

49 Reddy PK, Dharmapuram AK, Swain SK, *et al*. Valve repair in rheumatic heart disease in pediatric age group. *Asian Cardiovasc Thorac Ann* 2008;**16**:129–33.

50 Sampath Kumar A, Talwar S, Saxena A, Singh R. Ross procedure in rheumatic aortic valve disease. *Eur J Cardiothorac Surg* 2006;**29**:156–61.

51 Bernal JM, Pontón A, Diaz B, *et al*. Surgery for rheumatic tricuspid valve disease: a 30-year experience. *J Thorac Cardiovasc Surg* 2008;**136**:476–81.

63   Kawasaki Disease

Hirohisa Kato & Kenji Suda
Kurume University School of Medicine, Kurume, Japan

Kawasaki disease (KD) occurs in infants and children as an acute systemic vasculitis syndrome of unknown etiology; it mainly affects small- and medium-sized arteries, particularly the coronary arteries [1]. The cardiovascular problems in KD are related to coronary arterial lesions: aneurysm formation, thrombotic occlusion, progression to coronary artery disease, and premature atherosclerosis [2]. This disease was first described more than 40 years ago by Tomisaku Kawasaki in Japan [3,4]. Subsequently, it has been recognized throughout the world, and it is now a leading cause of acquired heart disease in children in North America and Japan.

History and background

When this disease was first described, it was considered benign and the prognosis good, because all acute symptoms disappeared within 2–3 weeks and the patient became well. Yamamoto and Kimura reported a patient with myocarditis [5], but coronary artery involvement went unrecognized. In 1970, the first nationwide survey in Japan demonstrated that 1.7% of the patients died from acute myocardial infarction (MI), and all four autopsies showed coronary arteritis accompanied by aneurysms and thrombotic occlusion. At that time, most pediatricians considered that KD was complicated by vasculitis only in small number of fatalities, because of the great contrast in prognosis between these rare fatalities and the large number of survivors who were asymptomatic.

In 1975, Kato *et al*. performed coronary angiography in 20 infants and children when their acute symptoms had disappeared. Of these, 12 showed multiple coronary aneurysms in both right and left coronary arteries, the first recognition that coronary aneurysms are present not only in fatalities

but also in asymptomatic survivors [1]. From the pathologic and coronary angiographic findings, KD was recognized as a systemic vasculitis syndrome of small- and medium-sized arteries in infants and young children.

In the past, KD may have been misdiagnosed as other diseases [6], such as scarlet fever [7], Izumi fever, measles, rheumatic fever [8], juvenile rheumatoid arthritis, drug hypersensitivity, Stevens–Johnson syndrome [9], and infantile polyarteritis [10], all now listed in the differential diagnosis of KD [11]. Landing and Larson reported identical pathologic findings in fatal KD and infantile polyarteritis, which was described only by autopsies [12]. Recent views are that infantile polyarteritis is the same as fatal KD, and that KD is a systemic vasculitis syndrome in infants and young children with a wide spectrum of clinical symptoms and disease severity.

Synonyms for Kawasaki disease include Kawasaki syndrome and (acute infantile) mucocutaneous lymph node syndrome (MCLS), now rarely used. The International Classification of Diseases (ICD-9) designates KD and mucocutaneous lymph node syndrome under rubric 446.1.

Epidemiology

The epidemiology in Japan, where KD is most prevalent, has been well documented [13]. The incidence has increased since 1968, and the number of patients affected now totals about 250 000. KD affects >10 000 children each year in Japan, and the incidence increased steadily to 216.9 per 100 000 children younger than 4 years by 2007–2008 [14]. The age distribution is from 1 month with a peak at 1 year; 50% of patients are younger than 2 years, and occurrence after 10 years of age is rare. Boys are affected more often than girls, with a ratio of 1.5:1.

KD is now widely prevalent in Asia, North America, South America, Europe, and Australia. Asians are more susceptible (5–10 times) than are white persons [15]. In countries with predominantly white populations, the incidence is ~15 per 100 000 children under 5 years of age [16]. There is a wide distribution, with no geographic difference between urban and rural areas or south and north. Seasonal variations are not distinct, but there are small peaks in winter–spring. The recurrence rate is about 3.3%, and 1–2% of siblings are affected, which is approximately 10 times the incidence in the general child population [17]. The increased incidence of KD among siblings and parents of patients, and racial differences, support a genetic predisposition. Time–space clustering and outbreaks in a community are recognized, but there is no evidence of person-to-person transmission. In 1979, 1982, and 1986, there were large nationwide outbreaks of KD in Japan, and occasional local clusters were recognized [18].

Pathology

On the basis of Hamashima's analyses of 37 KD autopsies, the Japanese Kawasaki Disease Research Committee reported the following pathomorphologic findings [19,20]. KD is an acute inflammatory disease with systemic vasculitis distinguishable from classic periarteritis nodosa of the Kussmaul–Maier type, a progressive and recurrent angiitis with marked fibrinoid necrosis but with rare pulmonary vasculitis. In contrast, KD is an acute inflammatory disease lasting about 7 weeks with rare and mild fibrinoid necrosis. Infantile polyarteritis nodosa (IPN) is indistinguishable from KD in many pathologic aspects [12,21], and clinical details of IPN are highly suggestive of KD.

The course of vasculitis can be classified into four stages according to the duration of illness:

1 *Stage 1 (1–2 weeks of illness):* Perivasculitis and vasculitis of the microvessels (arterioles, capillaries, and venules), small arteries, and veins; inflammation of intima, externa, and perivascular areas in the medium- and large-sized arteries; edema and inflammation with leukocytic and lymphocytic infiltration.

2 *Stage 2 (2–4 weeks of illness):* Less inflammation in the microvessels, small arteries, and veins than in stage 1; inflammatory changes of intima, media, externa, and perivascular areas in the medium-sized arteries with focal panvasculitis; aneurysms with thrombi and stenosis in the medium-sized arteries, especially in the coronary arteries. Panvasculitis is rarely seen in the large arteries. Edema (exudative stage), infiltration with monocytes or necrosis (infiltrative stage), and cellular granulation with increase of capillaries occur.

3 *Stage 3 (4–7 weeks of illness):* Subsidence of inflammation in the microvessels, small arteries, and veins and granulation in the medium-sized arteries.

4 *Stage 4 (>7 weeks of illness):* Scar formation and intimal thickening with aneurysms, thrombi, and stenosis in the medium-sized arteries (generally no acute inflammation in the vessels). These findings may persist until adult age and were observed in some autopsied patients who died more than 10 years after the illness.

KD is a systemic vasculitis syndrome which may involve many organs, such as myocardium (interstitial myocarditis with mild necrosis) [22] and the conduction system, and in other organs may cause pericarditis, endocarditis, cholecystitis, cholangitis, pancreatic ductitis, sialadenitis, meningitis, and lymphadenitis.

Etiology and pathogenesis

The etiology of KD remains unknown, despite extensive investigation. On the basis of clinical features and epidemiologic data, KD is now considered to be either of infectious origin with an unknown agent or an infection-triggered immune disorder. A variety of possible causative agents, such as bacteria, fungi, mycoplasma, rickettsiae, and viruses, have been proposed without confirmation. So far, two major hypotheses have been discussed in the past decade: the viral etiology and the superantigen or bacterial toxin theories.

KD has clinical similarities to scarlet fever and toxic shock syndrome, both of which are caused by toxin-producing bacteria. These toxins are superantigens capable of stimulating T cells carrying particular variable regions of the T cell receptor β-chain. A recent study on peripheral blood T cells in KD has shown that T cells expressing T cell receptor variable regions Vβ2 and Vβ8 were selectively expanded [23]. These observations suggest that KD may be caused by a toxin (superantigen)-producing microorganism, including viruses. Leung *et al.* suggested that the expansion of Vβ2+ T cells in most patients with KD may be caused by a new clone of toxic shock syndrome toxin-secreting *Staphylococcus aureus* or SPEB- or SPEC-producing group A streptococci by study of bacterial culture from patients with KD [24]. However, several other studies did not support this theory [25]. Yoshioka *et al.* reported that streptococcal pyogenic exotoxin (SPEC) induces activation and polyclonal expansion of Vβ2- and Vβ6.5-positive T cells, and that SPEC-induced activation of T cells may lead to the pathogenesis of KD [26]. Recently, Nagata *et al.* reported that several gut bacteria isolated from the jejunal mucosa produce superantigen and heat shock proteins that may have some role in the pathogenesis of KD [27].

Yersinia pseudotuberculosis appears to be one of the etiologic agents of KD [28], although only a small group of KD patients can be explained by this organism. *Propionibacterium acnes* isolated from the cervical lymph node of patients produced a cytotoxic protein-like bacterial exotoxin [29,30], but its etiologic role remains to be determined.

Epstein–Barr virus (EBV) induced clinical pictures mimicking those of KD on rare occasions [31] and 3/37

patients with chronic active EBV infection developed coronary lesions. However, epidemiologic, serologic, and virologic studies do not support EBV as a causative agent of KD. Rowley *et al.* reported that IgA plasma cells infiltrate the vascular wall and also other tissues such as myocardium, respiratory tract. kidney, and pancreas in acute KD. They suggested a mucosal portal of entry of a conventional antigen; however, no specific microbe has been proposed as the etiologic agent [32]. The possible association between a novel human corona virus (HcoV-NH) and KD has been reported, but further studies are necessary [33].

The acute phase of KD is associated with markedly increased production of inflammatory cytokines. tumor necrosis factor-alpha (TNFα), IL-1β and γ-IF induce activation antigens and adhesion molecules such as endothelial leukocyte adhesion molecule 1 and intercellular adhesion molecule 1 (ICAM-1) on endothelial cells, and TNFα and γ-IF caused endothelial injury in *in vitro* studies [34]. Leung *et al.* proposed a hypothesis that anti-endothelial antibodies cause endothelial injury in KD, based on the findings that circulating autoantibodies in KD were cytotoxic against human umbilical vein endothelial cells treated with TNFα, IL-1β or γ-IF [35]. Coronary artery endothelial cells in KD actually expressed activation antigens in a necropsy study [36]. Vascular endothelial growth factor (VEGF), monocyte chemotactic and activating factor (MCAF or MCP-1), and TNFα may have important roles in the pathogenesis of vasculitis [37–39].

The epidemiologic studies suggest a genetic predisposition for this disease. No single human leukocyte antigen (HLA) is common to most patients with KD. Recently, Onouchi *et al.* reported the important genetic role of the functional polymorphisms in the inosotol 1,4,5-triphosphate 3-kinase C gene in a network of gene single nucleotide polymorphisms [40].

Many hypotheses on the etiology and pathogenesis of KD have been proposed, but a host–microbial relationship specific to KD has not been identified. KD is widely scattered in the community, is self-limited, has multiorgan involvement, can recur, and has a tendency for epidemics every 3–4 years. These findings suggest that this disease may be caused in some susceptible children by a common infectious agent(s).

Clinical manifestations and diagnosis

The diagnosis of KD is made according to the diagnostic guidelines prepared by the Japan Kawasaki Disease Research Committee listed in Table 63.1 because of the absence of a specific laboratory test. These guidelines describe well the major symptoms and other significant clinical manifestations and laboratory findings. The principal diagnostic criteria of KD are persistent fever, conjunctival injection, changes in the mucosa of the oropharynx, changes in the peripheral extremities, erythematous rash, and cervical lymphadenop-

athy. At least five of the six principal features should be satisfied for a diagnosis of KD. However, some patients do not fulfill the classic criteria, and are diagnosed as having incomplete KD.

Fewer than four of the six principal symptoms indicate incomplete KD. Fever duration may be <5 days, particularly in those treated with γ-globulin within the first five febrile days. However, patients with four of these symptoms can be diagnosed when coronary abnormality is recognized by two-dimensional echocardiographic findings such as dilatation or non-uniformity of arterial lumen and brightness of the arterial wall. Incomplete KD is recognized in ~10% of all KD patients who have a higher incidence of coronary aneurysms (25%). Children <6 months or >7 years of age sometimes demonstrate atypical symptoms. Incomplete KD should be considered in children with unexplained fever for >4 days with three other principal symptoms. High CRP (>3 mg dl⁻¹), elevated ESR (>40 h⁻¹), thrombocytosis (>400 000), white blood cell count (>15 000), and erythema and induration at the site of previous vaccination of BCG (Bacillus Calmette–Guérin) are helpful findings for diagnosing incomplete KD. In children >7 years old, sometimes high fever and neck lymphadenopathy are initial symptoms for several days from the onset. Echocardiography should be considered in patients with suspected incomplete KD to check the coronary arterial wall brightness, ectasia, and lack of uniform diameter of the coronary artery. The American Heart Association Committee published guidelines for the management of patients with incomplete KD [41].

Cardiovascular spectrum and cardiac evaluation

Cardiovascular spectrum

The cardiovascular spectrum of 2450 patients with acute KD seen over the last 35 years in our Hospital is indicated in Table 63.2. Coronary aneurysms were diagnosed in 14%. Since γ-globulin treatment was introduced, the incidence of coronary aneurysms has declined to 8.3%. Coronary artery involvement is the most important lesion in KD; however, aneurysms in other arteries such as the axillary, iliac or renal arteries were observed in 1.0% of the patients. Valvar heart disease appeared in about 1.4% of the patients. MI occurred in 36 patients, with 12 deaths. Half of the fatalities did not demonstrate ischemic findings before the onset of MI [42].

In the earlier period most patients received aspirin only, but we introduced γ-globulin treatment from 1992, leading to a significant decline in the incidence of transient dilatation and aneurysm formation of coronary artery, systemic artery aneurysms, pericarditis, and myocarditis.

Although there are several scoring systems to identify high risk for coronary artery abnormalities or patients resistant to γ-globulin treatment who have a higher risk of coronary

Table 63.1 Diagnostic guidelines for Kawasaki disease.

Principal symptoms

1. Fever persisting for at least 5 days
2. Changes in peripheral extremities
   Initial stage: reddening of palms and soles, indurative edema
   Convalescent stage: membranous desquamation from fingertips
3. Polymorphous exanthema
4. Bilateral conjunctival congestion
5. Changes in lips and oral cavity: reddening of lips, strawberry tongue, diffuse injection of oral and pharyngeal mucosa
6. Acute nonpurulent cervical lymphadenopathy
   At least five of the principal symptoms should be satisfied for the diagnosis of Kawasaki disease to be made. However, patients with four of the principal symptoms can be diagnosed as having Kawasaki disease when coronary aneurysm is recognized by two-dimensional echocardiography or coronary angiography

Other significant symptoms or findings

The following symptoms and findings should be clinically considered:

1. Cardiovascular auscultation (heart murmur, gallop rhythm, distant heart sounds), electrocardiographic changes (prolonged PR-QT intervals, abnormal Q wave, low-voltage ST-T changes, arrhythmias), chest radiograph findings (cardiomegaly), two-dimensional echocardiographic findings (pericardial effusion, coronary aneurysms), aneurysm of peripheral arteries other than coronary (e.g., axillary), angina pectoris or MI
2. Gastrointestinal tract: diarrhea, vomiting, abdominal pain, hydrops of gallbladder, paralytic ileus, mild jaundice, slight increase in serum transaminase
3. Blood: leukocytosis with shift to the left, thrombocytosis, increased erythrocyte sedimentation rates, positive C-reactive protein, hypoalbuminemia, increased α_2-globulin, slight decrease in erythrocyte count and hemoglobin levels
4. Urine: proteinuria, increase in leukocytes in urine sediment
5. Skin: redness and crust at the site of Bacille Calmette–Guérin inoculation, small pustules, transverse furrows of the fingernails
6. Respiratory: cough, rhinorrhea, abnormal shadow on chest radiograph
7. Joint: pain, swelling
8. Neurologic: pleocytosis of mononuclear cells in cerebrospinal fluid, convulsion, unconsciousness, facial palsy, paralysis of the extremities

Remarks

1. For changes in peripheral extremities, the convalescent stage is considered important
2. Male-to-female ratio, 1.3–1.5; patients younger than 5 years of age, 80–85%; fatality rate, 0.3–0.5%
3. Recurrence rate, 2–3%; proportion of siblings, 1–2%

From *Diagnostic Guidelines of Kawasaki Disease*, 4th edn, Japan Kawasaki Disease Research Committee, Tokyo, 1984.

aneurysms [43,44], the Harada score, which was initially used to determine selection for IVIG treatment, is now often used to select patients with greater risk for coronary artery disease [45]. The patients who fulfill four of the following items may develop the coronary artery lesions: (1) white blood count >12 000 mm^{-3}, (2) platelet count <350 000 mm^{-3}, (3) CRP >3 mg dl^{-1}, (4) hematocrit <35%, (5) albumin <3.5 g dl^{-1}, (6) age ≤12 months, and (7) male gender.

Myocardial infarction and death

The main cause of death in KD is acute MI. A study of 104 fatalities in KD in Japan suggests that 56.7% of the patients died of acute MI and 18% died of congestive heart failure caused by ischemia. Five deaths were due to rupture of coronary aneurysms. In the 1970s the fatality rate in Japan was ~2%; however, by 2007–2008 it had declined markedly to 0.03%. We analyzed 195 KD patients with MI from the nation-wide survey in Japan [46]. MI usually occurred within 1 year

of illness, but late deaths several years after acute KD have increased recently. Death might occur at any time with obstructive lesions. Attacks of MI are relatively more frequent at night when the patient is sleeping or resting, with primary manifestations of shock symptoms, pallor, restlessness, vomiting, and abdominal pain. Chest pain was more frequently recognized in the survivors and in children >4 years of age. Asymptomatic MI was seen in 37%. Of the patients with MI, 22% died at the first attack; 16% of the survivors from the first attack had a second attack. The fatality rate was 63% in the second attack and 83% in the third attack. From coronary angiographic studies in the patients with MI, most of those who died had obstructions in the left main coronary artery or in both the right main coronary artery and the left anterior descending artery. In survivors, one-vessel obstruction, particularly in the right coronary artery, was frequently recognized.

Early recognition and treatment for acute MI are critical. Recurrence of MI is observed in ~20% of the patients who

Table 63.2 Cardiovascular spectrum: chronological changes (Kurume University: 1973–2007).

Lesion	1973–1990	1991–2007	Total
	Aspirin era $n = 1355$	γ-Globulin + aspirin era $n = 1095$	$n = 2450$
Coronary artery			
Transient dilatation	234/778 (30.1%)[a]	65/1095 (5.9%)	299/1873 (15.9%)
Coronary aneurysm	253/1355 (18.7%)[a]	91/1095 (8.3%)	344/2450 (14.0%)
Systemic artery aneurysm	20/1355 (1.5%)[a]	2/1095 (0.1%)	22/2450 (0.9%)
Valvar heart disease			
Mitral regurgitation	16/1355 (1.1%)	13/1095 (1.2%)	29/2450 (1.2%)
Aortic regurgitation	2/1355 (0.2%)	4/1095 (0.3%)	6/2450 (0.2%)
Pericarditis (pericardial effusion)	188/1019 (18.4%)[a]	63/1095 (5.7%)	251/2114 (11.8%)
Myocarditis	425/1355 (31.4%)[a]	193/1095 (17.6%)	618/2450 (25.2%)
Myocardial infarction	21/1355 (1.5%)	15/1095 (1.3%)	36/2450 (1.5%)
Fatalities	8/1355 (0.6%)	4/1095 (0.3%)	12/2450 (0.4%)

[a] $p < 0.005$.

have had a previous MI. Because the mortality of recurrent MI is high, careful management is needed for such patients. Patients with complications after MI, such as ventricular aneurysm, papillary muscle dysfunction, heart failure, severe arrhythmias, and post-infarction angina, are managed by medical and/or surgical approaches.

Systemic artery involvement

Coronary artery involvement is the most important lesion in KD, but aneurysms in other arteries were observed in 0.9% of patients [42].Our angiographic study of 22 patients with systemic artery aneurysms demonstrated aneurysms in axillary arteries (18), common iliac arteries (16), internal iliac arteries (12), renal artery (6), mesenteric arteries (2), and internal thoracic arteries (2). One patient had large common iliac artery aneurysms associated with dilatation of aorta. Although the prognosis of systemic artery aneurysms is generally favorable, renovascular hypertension may develop in a patient having a renal artery lesion, and intrathoracic arterial lesions may cause difficulty during coronary bypass surgery. There are some reports of digital gangrenous changes [47].

Valvar heart disease, myocarditis, and pericarditis

Valvar heart disease appears in ~1% of the patients, mostly mitral valve and rarely aortic. We demonstrated acute mitral regurgitation in 29/2450 patients (1.2%), half of which eventually disappeared after a few months to several years. The etiology of this condition may be valvitis or papillary muscle dysfunction caused by ischemia [48]. We had six

patients with aortic regurgitation (0.2%). Aortic regurgitation appeared after the acute or subacute stage of illness and progressed to severe regurgitation in several years in some patients [49]. Pericarditis or pericardial effusion appeared in 11.8% of the patients in the acute phase, was mostly subclinical, and disappeared within 1–2 weeks. Massive pericardial effusion or cardiac tamponade was rare. There have been no reports on progression of acute to chronic or constrictive pericarditis. Relatively mild myocarditis was observed in 25.2% of patients in the acute phase, especially in the first and second weeks of illness, regardless of coronary aneurysms. Gallop rhythm, distant heart sound, ST-T segment changes, and decreased voltage of R waves on ECG may suggest myocarditis. In many instances, cardiac enzyme levels such as creatine kinase did not change significantly. Cardiomegaly or decreased ejection fraction of the left ventricle caused by myocarditis was noted in some patients. It generally resolved, seldom developing into a chronic dysfunction or cardiomyopathy.

Echocardiography

The evaluation of the coronary artery lesions in KD in the acute stage of illness is important, even essential, and is usually done by two-dimensional echocardiography (2DE) for all patients and coronary angiography (CAG) for selected patients.

Serial 2DE studies are the most important and essential method to evaluate coronary aneurysms. The approach for 2DE in KD is well described in the Japan Kawasaki Disease Research Committee Report on Standardization of Diagnostic

Criteria and Reporting of Coronary Artery Lesions [50] and the Committee Report of the American Heart Association [51]. Coronary aneurysms are classified as small (<4 mm internal diameter in children <5 years old or >4 mm in children ≥5 years old), medium (5–8 mm) and giant or large (>8 mm) by the Japanese Research Committee. Recently, some reports have suggested that these criteria may underestimate the true incidence of coronary artery dilatation [52–54]. Mild dilatation or ectasia may be underestimated by these criteria, so the body surface area-adjusted coronary dimensions (Z-score) may evaluate the minimal changes of the coronary artery diameter more accurately [55]. If the serial 2DE studies reveal abnormal findings in a patient, coronary angiography may be indicated [56].

The evaluation of coronary artery morphology is particularly important in KD. The precordial short-axis segment is the standard approach for evaluating the left main coronary artery, the left anterior descending artery, and the right main coronary artery. The posterior descending artery can be evaluated by the apical four-chamber view. The middle segment of the right coronary artery is seen in the apical four-chamber view. From echocardiographic studies, it is evident that coronary artery dilatation appears at around 10 days of illness, and ~40% of patients reveal transient coronary artery dilatation in this period. However, two-thirds of these demonstrate transient dilatation and regression within 3–5 weeks from the onset of illness. This means that Kawasaki vasculitis may demonstrate various degrees of coronary artery dilatation from mild transient dilatation, small- or moderate-sized aneurysms, or giant aneurysms in more than half of the patients in the acute phase [57]. Aneurysms are classified as saccular if the axial and lateral diameters are nearly equal or as fusiform if symmetric dilatation with gradual proximal and distal tapering is seen. If the coronary artery diameter looks larger than normal without segmental dilatation, the coronary artery is considered ectatic. False-negative diagnoses were mainly due to isolated small peripheral coronary artery aneurysms, which appeared rarely. Follow-up echocardiography is essential to evaluate such findings to assess whether the ectatic changes are pathologic or normal. We routinely perform 2D echocardiography at the time of diagnosis, at around 8–10 days of illness when coronary dilatation may appear, at 2 weeks, and at 8 weeks after the onset of the disease.

Acute coronary thrombosis is also diagnosed by serial 2DE at the cardiac clinic. At that time, thrombolytic treatment by urokinase or t-PA is indicated [58]. Evaluating stenotic lesions of the coronary artery by 2DE is sometimes difficult, although by using a high-frequency transducer and careful examination it may be possible. The features of abnormal examinations are the loss of the uniformity of the lumen of arteries, irregularity of the arterial wall, and a dense echo in the coronary arterial wall.

Coronary angiography and heart catheterization

Selective coronary artery angiography (CAG) is the most accurate method for defining the severity of coronary arterial abnormalities in KD. We have used specially designed catheters (three types) for selective coronary angiography for infants, toddlers, and school children, with which coronary angiography can be performed safely and successfully [56]. The indications for CAG include abnormal 2DE findings, symptoms or signs of ischemia, audible valve regurgitation during auscultation, evidence of cardiac dysfunction, and the use of intracoronary thrombolytic treatment. If patients have severe coronary lesions, other systemic vascular involvement, such as the axillary, iliac, renal, or intrathoracic artery aneurysms, should be evaluated. Because the regression of coronary artery aneurysms and progression to stenotic lesions mostly occurred within 2 years from the onset of illness, repeat follow-up CAG is essential, especially in patients having coronary aneurysms [42]. The definition of regression of coronary aneurysms is that the follow-up CAG demonstrates completely normal findings with disappearance of aneurysms and even no irregular arterial wall in the whole coronary artery system. Regression can be diagnosed by CAG, but 2DE may miss some mild abnormal findings that subsequently progress to coronary artery disease. CAG is most important and essential for evaluating stenotic or obstructive lesions of the coronary artery or assessment of the collateral circulation (Figure 63.1).

The clinical feasibility of intravascular ultrasound imaging for coronary arteries has been reported in patients who had suffered from KD to assess the long-term pathology *in vivo* [59]. At the site of regressed aneurysms, there is marked thickening of the intima, as mentioned previously. The portion of the coronary artery with normal angiographic findings showed normal ultrasound findings except in the region near the regressed aneurysm, which showed mild intimal thickening. Positive remodeling (or compensatory remodeling) may contribute to maintaining the normal lumen although with mild intimal thickening [60].

Other noninvasive techniques

Magnetic resonance imaging (MRI) may evaluate aneurysms in the proximal coronary artery and the coronary flow profile [61–63]. MDCT (multi-detector-row computed tomography) is also available to evaluate coronary aneurysms, the wall morphology, and the tissue characterization of the coronary artery [64], but needs breath holding for several seconds; it may be useful for older children or adults.

Evaluating myocardial ischemia

Because the morbidity and mortality of this disease mostly depend on the extent of associated coronary artery disease, it is particularly important to assess accurately any myocardial ischemia during the follow-up. However, the available methods have some limitations for young children. 2DE can detect

Figure 63.1 Serial echocardiography and coronary angiography of giant coronary aneurysm and thrombus formation. (a, b) Two-dimensional echocardiography and coronary angiography at 1 month of illness demonstrated giant aneurysms in the left main trunk, the left anterior descending artery (LAD), and the circumflex artery (LCX). Ao, aorta; PA, pulmonary artery. (c, d) Ten months later, two-dimensional echocardiography demonstrated massive, dense abnormal echo in the left main trunk (arrows), which suggested massive thrombotic formation (T) in the coronary aneurysm. At that time, coronary angiography showed the decreased size and a severe obstruction of the coronary aneurysm. (Reproduced with kind permission from Springer Science+Business Media:Cardiovascular Medicine , Echocardiography of patient with myocardial infarction by thrombosis, 3rd ed, 2007, p 979–994, Willerson JT, Cohm JN, Wellens JJ, Holmes DR, Figure 41.3.)
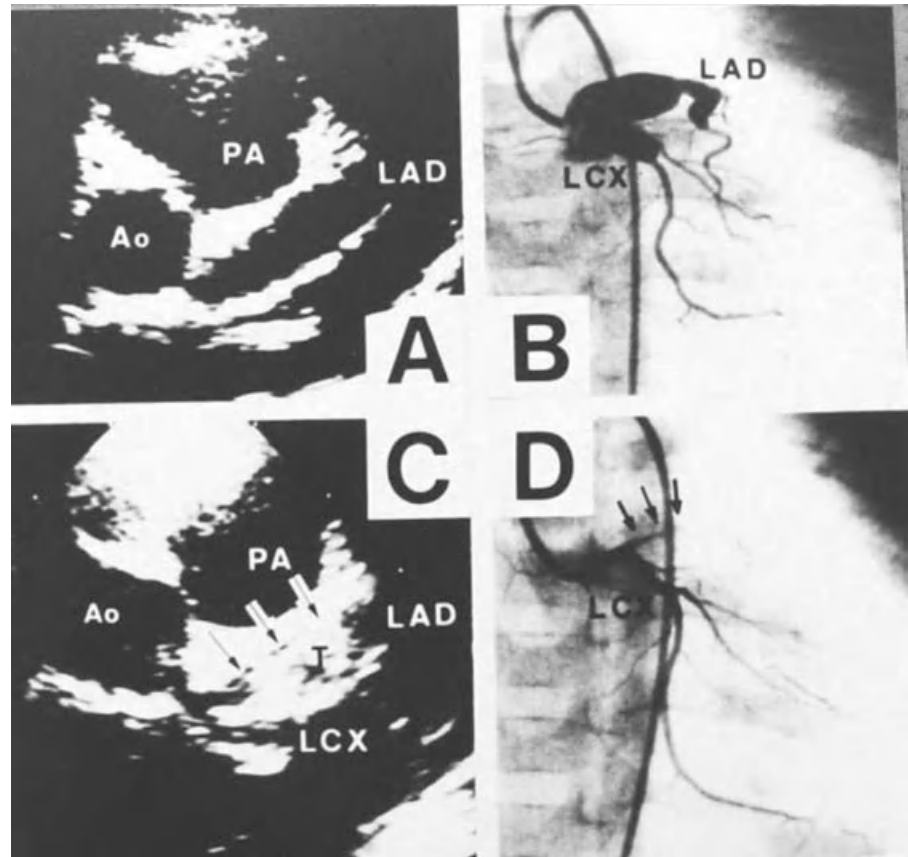
coronary aneurysms, but evaluating stenosis is not satisfactory. Similarly, the sensitivity of electrocardiography for detecting myocardial ischemia is inadequate. Coronary angiography is an accurate method to assess coronary artery involvement, but repeated evaluation is often difficult because of the invasive technique. Although an exercise stress test can detect myocardial ischemia and being noninvasive is easy to repeat, its sensitivity is not sufficient even in patients with significant coronary stenosis, and it is difficult to perform in young children. Myocardial single-photon emission computed tomography (SPECT) using pharmacologic stress (i.e., dipyridamole infusion) is considered the most accurate diagnostic method for identifying myocardial ischemia, especially in children in whom an exercise test cannot be performed [65]. Because pharmacologic stress SPECT provides quantitative analysis, the changes in severity of myocardial ischemia are detectable when serial studies are performed. Kamiya reported the sensitivity of detecting myocardial ischemia using various methods in patients having significant coronary stenosis (>75%) [66]. The most sensitive method was dipyridamole stress SPECT (85% sensitivity), whereas the sensitivity of a treadmill exercise test was <50%. Recently, many types of stress tests have been reported in children with KD, including nuclear perfusion scans with exercise [67], exercise echocardiography [68], stress echocardiography

using dobutamine [69], and contrast echocardiography with dipyridamole stress [70].

Long-term cardiovascular sequelae and natural history

Long-term consequences of coronary aneurysms and follow-up

The natural history or fate of coronary aneurysms is an important issue in KD [83]. We followed 594 consecutive patients with acute KD between 1973 and 1983 for 10–21 years [42]. In all patients, we evaluated the coronary lesions by coronary angiography just after the acute stage. A total of 146 patients (24.6%) were diagnosed as having coronary aneurysms. A second angiography, performed 1–2 years later in all 146 patients who previously had coronary aneurysms, demonstrated that 72(49.3%) had regression of the coronary aneurysms, suggesting that coronary aneurysm in KD shows a strong tendency for regression. None of the patients with regression of coronary aneurysms had cardiac symptoms in the long-term follow-up periods, and results of their ECGs, exercise stress test, thallium myocardial scintigraphy, and left ventricular function were all within normal limits. In contrast, by 10–21 years after the onset of
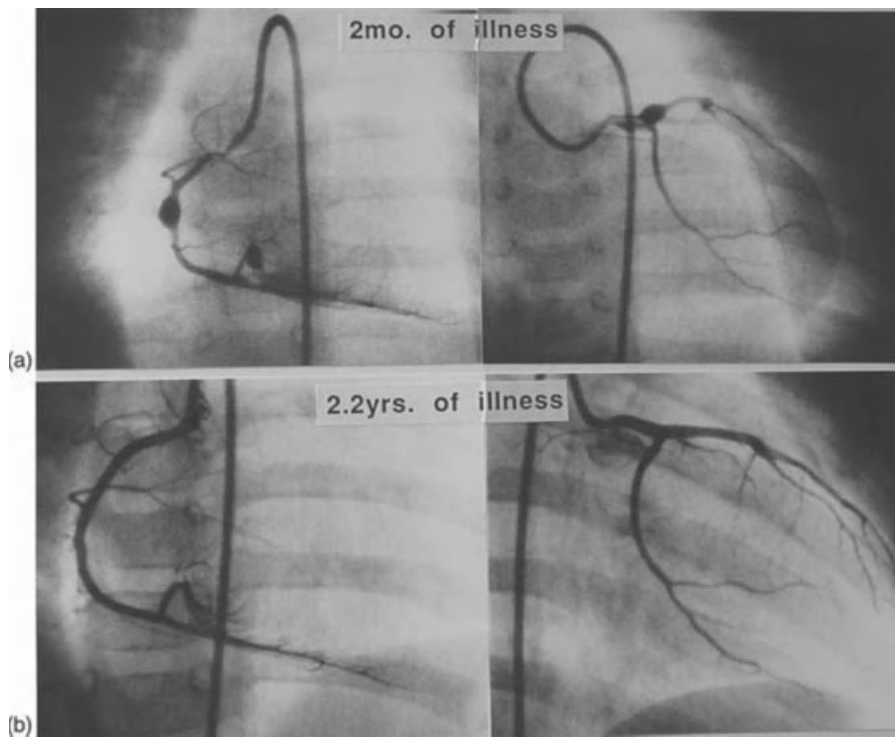
Figure 63.2 Regression of coronary aneurysms. (a) Eight-month-old boy with four coronary aneurysms in both right and left coronary arteries. (b) Two years later. Follow-up coronary angiography demonstrated regression of aneurysms, which included the disappearance of aneurysms and no irregular arterial wall in the entire coronary artery system.

the illness, stenosis in the coronary aneurysms had developed in 28 patients. Myocardial infarction occurred in 11 patients, with five deaths. From this study, we estimated that about 4% of patients with KD may develop ischemic heart disease.

When does this complication occur? We studied the time and incidence of regression or progression to obstructive lesions from the onset of KD using the Kaplan–Meier life table method. Regression of coronary aneurysms mostly occurred within 2 years from the onset of illness, whereas the obstructive lesions developed at 2 years and gradually increased over several years.

We investigated various factors that could affect the prognosis of coronary aneurysms [71]. The risk factors for coronary aneurysms developing into ischemic heart disease are aneurysmal diameter >8 mm, shape of large diffuse or saccular type, prolonged fever for >21 days, and age at onset >2 years. In the 26 patients with giant coronary aneurysms, stenotic lesions developed in 12, and no regression occurred in our follow-up study. Hence giant coronary aneurysms have a critical problem because they have a strong potential to develop ischemic heart disease. The incidence of giant coronary aneurysms was 17.8% in the patients with coronary aneurysms and 4.4% among all KD patients in our series (Figure 63.2).

The pathologic mechanism of regression of aneurysms is marked proliferation of intima with rich smooth muscle cells and well-regenerated endothelium without massive thrombus formation [72]. Hemodynamic forces may

regulate such arteries to maintain adequate lumina. It is uncertain whether intimal thickening eventually develops into obstructive lesions. However, from our 10–21 years' follow-up study, none of the patients who had regressed aneurysms developed ischemic heart disease. However, the regressed coronary aneurysms have intimal thickening and impaired endothelial function, so they should be carefully followed during adulthood to determine if they develop secondary atherosclerotic changes (Figure 63.3).

Kawasaki vasculitis may be an atherosclerotic risk factor

Pathology of the coronary artery in KD several years after onset demonstrates marked intimal proliferation and, in some patients, calcification, deposits of protein-like material and hyalinized degeneration in the thickened intima. An intravascular ultrasound study of the coronary artery after KD demonstrated marked thickening of the intima and calcification in the coronary aneurysms [59]. These findings are similar to arteriosclerotic lesions. Suzuki *et al.* reported the active expression of various growth factors in the coronary artery in the late phase of KD, suggesting that active vascular remodeling continues even several years after onset [73,74].

Concerning vascular function after KD, we studied the distensibility of the coronary arterial wall by intracoronary infusion of isosorbide dinitrate [75] and endothelial function by intracoronary infusion of acetylcholine [76,77]. Both vascular distensibility and endothelial function long after KD

Figure 63.3 Cardiovascular spectrum and natural history.
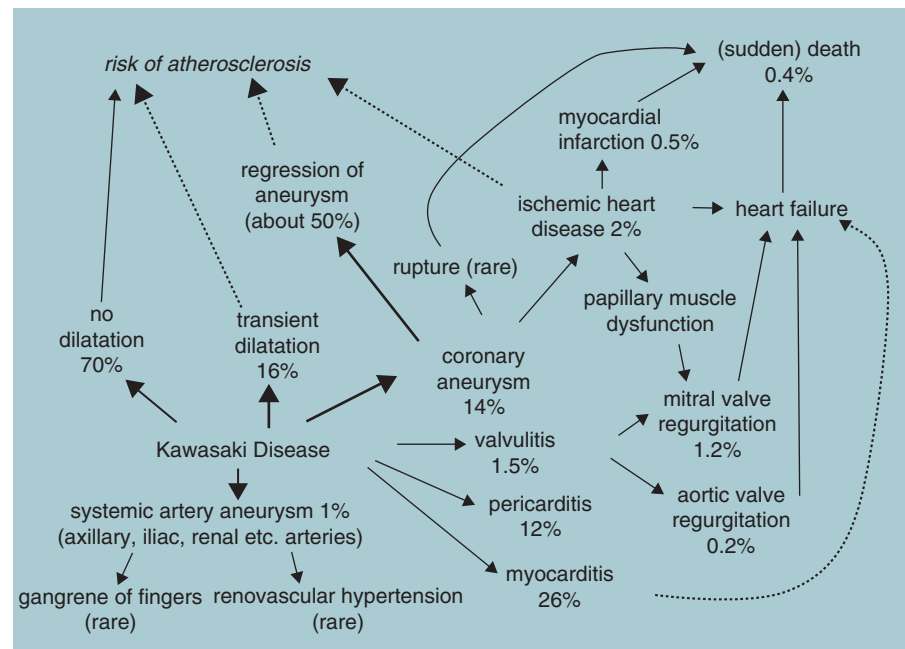
were impaired in the patients with coronary artery aneurysms, stenosis, and regressed aneurysms. Dhillon *et al.* [78] and Mitani *et al.* [79] also reported that endothelial dysfunction was observed even in the normal artery in KD. Pathology of the coronary artery in adults after KD demonstrated premature atherosclerotic changes [80]. Mitani *et al.* suggested that the high-sensitivity C-reactive protein was elevated in the late coronary sequelae in KD, and found dense calcium and necrotic core areas in the coronary arterial wall by a virtual histology-intravascular ultrasound study, which suggests the potential role of atherogenesis in the coronary artery in the long term after KD [81,82].

Adult coronary artery disease due to childhood kawasaki disease

It is now more than 40 years since the first description of KD as a new clinical entity, and many of the early KD children are now adults [83]. We surveyed major cardiovascular centers in Japan for such adults to investigate any coronary sequelae that might be due to their earlier KD, and reported 21 such patients and their cardiac conditions [84]. Most of these 21 patients were diagnosed as having fever of unknown origin, sepsis, or pneumonia, because they suffered from suspected KD before its first description in 1968. Most of the patients had ischemic symptoms, such as acute or old MI or angina pectoris, two or three decades after the onset of suspected KD. Some of the patients had mitral regurgitation or arrhythmias. Almost all had multiple coronary aneurysms with obstruction or stenosis and with severe calcification of the arteries. Coronary aneurysms of unknown etiology were also reported in 109 patients who had no suspected history

of KD. These patients were mostly free from ischemic symptoms but had abnormal Q waves on ECG or calcification of the coronary artery on chest X-ray. We suspect that some of these patients might have had childhood KD.

Our study suggested that some patients with coronary artery sequelae of KD have already developed young adult ischemic heart disease. A past history of KD in infancy or childhood is important, but this is sometimes unrecognized or was diagnosed as another disease. Abnormal Q waves or mitral regurgitation of unknown origin in younger adults is also important. Coronary angiographic findings are essential for diagnosis; there are multiple aneurysms frequently associated with calcification. Familial hypercholesteremia or collagen vascular disease should be excluded. After our publication [84], many reports of adult coronary artery disease probably due to childhood KD appeared and were reviewed by Burns and co-workers [85,86].

The issues concerning KD in adults include (1) the patients with coronary artery disease or valvar heart disease not diagnosed as having KD during childhood, (2) adults diagnosed as having KD during childhood without evaluating the coronary lesions during KD, (3) adults having persistent coronary artery lesions, and (4) adults who develop premature atherosclerosis after KD with various coronary risk factors. Those patients should be evaluated and followed by adult cardiologists. The coronary artery sequelae of KD may be an important cause of ischemic heart disease in young adults, particularly those under 40 years of age. Adult cardiologists should recognize this condition and include the sequelae of KD in the differential diagnosis of early-onset coronary artery disease in adults.

Treatment and management

Treatment in acute phase

After it became apparent that KD is not a benign self-limited disease, but can be fatal and result in significant long-term sequelae, especially coronary aneurysms, the target of the treatment of KD is to control inflammation as quickly as possible, especially within 10 days of illness, to prevent the development of coronary aneurysms.

Initial treatment

In 1979, Kato *et al.* [87] first compared the effectiveness of five different types of treatment protocols, (1) 30 mg kg^{-1} of aspirin, (2) aspirin and 2–3 mg kg^{-1} of prednisolone, (3) prednisolone alone, (4) prednisolone plus warfarin, and (5) antibiotics in the acute phase of KD, and found that aspirin was the most effective treatment (32/36, 89%) and steroid therapy was the least effective, with patients treated with prednisolone alone showing an incidence of coronary artery aneurysm of 65% (11/17). Based on this observation, oral aspirin has been one of the standard treatments in the acute phase of KD. In combination with intravenous γ-globulin infusion (IVGG), in Japan 30 mg kg^{-1} of aspirin in three doses is given and in the United States 80–100 mg kg^{-1} of aspirin in four doses is given during the febrile period. After being afebrile for 48–72 h, the dose of aspirin is reduced to 3–5 mg kg^{-1} and the aspirin is continued for 6–8 weeks after the onset of illness. Aspirin is thought to exert anti-inflammatory effects in high doses and anti-platelet effects in low doses. In patients with coronary aneurysms, aspirin should be continued indefinitely unless the patients show regression of coronary aneurysms.

Subsequently, Furusho *et al.* [88,89] reported that high-dose IVGG as a treatment for acute KD dramatically decreased the incidence of coronary aneurysms from 42 to 15%. Initially IVGG was given as 200 or 400 mg kg^{-1} for 4–5 consecutive days. However, several multi-institutional randomized controlled trials conducted in Japan [90–92] and the United States [93] revealed that the most effective regimen of this treatment includes a total of 1 or 2 g kg^{-1} of IVGG over 12–24 h together with medium- to high-dose aspirin. Interestingly, meta-analyses of these studies demonstrated a dose–response effect of IVGG [94,95], with higher doses given in a single infusion having a greater effect. The precise mechanisms by which IVGG produce such a striking anti-inflammatory effect and a marked reduction in the development of coronary abnormalities is still not clear.

Because most coronary artery dilation starts to occur at around 10 days of illness, initial treatment should be started within 7 days of illness to control inflammation and prevent the progression to coronary aneurysm.

Although current standard treatment using high-dose IVGG and oral aspirin is fairly effective, with an 80–90%

success rate, some patients are still resistant to initial treatment. To improve the effectiveness of initial treatment, additional steroid either as an intravenous prednisolone infusion or methylprednisolone pulse therapy was examined. Inoue *et al.* [96] reported the effectiveness of 2 mg kg^{-1} of intravenous prednisolone infusion in addition to 1 mg kg^{-1} of IVGG over 2 days plus aspirin, with tapering of oral prednisolone over 15 days. In their randomized controlled study, this regimen showed significantly fewer coronary artery aneurysms than with control treatment, 1 g kg^{-1} of IVGG over 2 days plus aspirin (2.2 versus 11.4%). However, drawbacks of this protocol included universal use of steroid and a rather long treatment period. Another trial with a dose of 30 mg kg^{-1} intravenous methylprednisolone infusion in addition to 2 g kg^{-1} of IVGG plus high-dose aspirin conducted in North America showed only a minimal beneficial effect [97].

Additional treatment

In patients resistant to initial treatment, many different types of treatment [98] are offered, such as another dose of IVGG alone or with addition of urinastatin, erastase inhibitor, steroid pulse therapy of 30 mg kg^{-1} of intravenous methylprednisolone infusion, inhibitor of TNFα [99–101], cyclosporine A [102], methotrexate [103], and plasma exchange [104].

Although failing as the initial treatment, pulse steroid therapy using methylprednisolone was revisited as the second or third treatment to reduce the cost of treatment in place of another dose of IVGG. As the second treatment, Furukawa *et al.* [105] reported comparable effectiveness (77 versus 63%) of pulse steroid therapy with the same incidence of coronary aneurysms (11 versus 11%) to the second dose of IVGG, although they were concerned about a tendency for fever to recur later in patients resistant to pulse steroid therapy, which could potentially delay the therapeutic decision-making process. As the third treatment, Hashino *et al.* [106] reported comparable effectiveness of pulse steroid therapy to the third dose of IVGG with shorter duration of fever. However, transient coronary dilation during pulse steroid therapy was observed, hence careful echocardiographic monitoring of the coronary artery is mandatory in this treatment. In addition, several adverse effects, such as hypertension, bradycardia, and hypothermia during this treatment, have to be checked [105,107].

To eradicate all the active cytokines, plasma exchange can be a definitive treatment in these diseases with cytokine storms. Indeed, plasma exchange is reported to be significantly effective treatment for patients resistant to IVGG [104]. However, the choice of the treatment depends on institutional accessibility and experience with this treatment.

Because serum levels of TNFα, a pro-inflammatory cytokine, increase markedly in patients with acute KD, with the highest levels observed in patients who developed coronary artery aneurysms [108,109], blockade of TNFα

might be effective in controlling inflammation. Recently, infliximab, a chimeric murine/human IgG1 monoclonal antibody that binds specifically to human TNFα, was given to patients with KD resistant to IVGG [100–102]. In the initial descriptive study, 13 of 16 patients who were resistant to initial IVGG responded to this drug, and a randomized controlled study is under way [102].

High-risk patients

Because we know that 15–20% of patients do not respond to the initial IVGG, it is reasonable to offer strengthened treatment for selected high-risk patients. Several risk scoring systems [43,44,110] have been developed in addition to Harada's scoring system [45]. Egami *et al.* reported a scoring system assigning 1 point for (1) infants less than 6 months old, (2) treatment ≤4 days of illness, (3) platelet count ≤30 × 10⁴ μl⁻¹, and (4) CRP ≥80 mg l⁻¹, and 2 points for (5) ALT ≥80 IU l⁻¹. A cut-off point of ≥3 with this prediction score identified patients with KD resistant to the initial IVGG with 78% sensitivity and 76% specificity [43]. Kobayashi *et al.* also reported a scoring system assigning 1 point for (1) age ≤12 months and (2) platelet count ≤30 × 10⁴ μl⁻¹, and 2 points for (3) sodium ≤133 mmol l⁻¹, (4) treatment ≤4 days of illness, (5) AST ≥100 IU l⁻¹, (6) % neutrophils ≥80%, and (7) CRP ≥100 mg l⁻¹. A cut-off point of ≥4 with this prediction score identified patients with KD resistant to the initial IVGG with 86% sensitivity and 67% specificity [44]. In addition, Sano *et al.* reported a simplified scoring system, in which patients with two of the three predictors (1) CRP ≥70 mg l⁻¹, (2) total bilirubin ≥0.9 mg dl⁻¹, and (3) AST ≥200 IU l⁻¹ could be resistant to the initial IVGG with 77% sensitivity and 86% specificity [110]. Although each of these risk-scoring systems may work well in selected institutions, multiple scoring or determination of percentage neutrophils can be cumbersome and the value of AST can be falsely elevated because of hemolysis frequently seen in small infants.

Based on these scoring systems to identify patients who would be resistant to the initial IVGG and carry a higher risk of coronary aneurysms, a combination of IVGG and pulse steroid therapy was offered to the selected patients as the initial treatment [111,112], although these studies could not prove effectiveness because of their retrospective nature [111] or small sample size [112]. Based on another scoring system [43], a randomized controlled trial of combination therapy consisting of 2 mg kg⁻¹ of intravenous prednisolone infusion, 2 g kg⁻¹ of IVGG, and 30 mg kg⁻¹ of aspirin in the acute phase with tapering of oral steroid is under way.

Treatment for patients with coronary aneurysms

In patients with coronary artery aneurysms, especially giant coronary aneurysms, anti-thrombotic treatment to prevent MI using continuous infusion of heparin should be considered in addition to aspirin, once the physician has recognized the development of coronary aneurysms. Care

must be taken to prevent insufficient anti-thrombosis because generally infants require a larger dose of heparin than do adults, namely 20–25 IU kg⁻¹ h⁻¹, to achieve the target level of anti-thrombotic effect, 60–85 s in activated pro-thrombin time. This anti-thrombotic treatment should be replaced by oral warfarin treatment and continued until the size of aneurysm decreases to medium or small without any sign of stenosis.

Even with the anti-thrombotic therapy, some patients may suffer from MI. In MI or impending MI in which thrombus is seen in coronary artery aneurysms, intracoronary thrombolysis using infusion of urokinase [58] or tissue plasminogen inhibitor [113] with or without coronary catheter intervention has been applied successfully.

Interestingly, a study suggested that abciximab, a platelet glycoprotein IIb/IIIa receptor inhibitor, may enhance regression of coronary artery aneurysms [114].

Management in late phase (Tables 63.3 and 63.4)

Long-term medical treatment for coronary aneurysms

Anti-thrombosis

In patients with small- to medium-sized coronary artery aneurysm, 3–5 mg kg⁻¹ of aspirin is given until regression of coronary artery aneurysm is confirmed. In patients with a giant coronary artery aneurysm, complete regression of the aneurysm cannot be expected, but rather development of thrombotic occlusion or stenosis adjacent to the aneurysm must be anticipated. Historically, warfarin plus aspirin was used to prevent acute MI with a high success rate. Sugahara *et al.* [115–117] reported a significantly lower incidence of MI in patients treated with warfarin plus aspirin compared with aspirin alone (5.2 versus 32.7%), with an MI-free rate of 95% at a mean follow-up of 7.7 years. The target strength of anti-thrombotic treatment using warfarin is set at 1.6–2.5 times the international normalized ratio of prothrombin time according to the revised guidelines of the Japanese Circulation Society. Warfarin is given even to infants with a giant coronary aneurysm despite the potential risk of developing bleeding complications, because there is a greater risk of thrombotic occlusion early after onset. In a multi-institutional study that enrolled 83 patients with giant coronary aneurysm treated with warfarin plus aspirin, Suda *et al.* [116] reported a 91% cardiac event-free rate at 10 years and an acceptably low hemorrhagic complication rate of 2.2% per patient-year.

Although other anti-platelet medications such as dipyridamole, flurbiprofen, and ticlopidine have been given in isolated regimens or in combination with aspirin or warfarin, there are few data concerning the effectiveness of these drugs. A recently approved anti-thrombotic agent, dabigatran etexilate (Pradaxa), that is safer and easier to control than warfarin may become available for children.

Table 63.3 Indications of treatment by classification of severity of coronary artery lesions.

Treatment[a]	Severity level[b]	Evidence level[c]
Anti-thrombotic drugs (aspirin, dipyridamole, ticropidine)	IV, V III I, II	Class I Class II Class III
Anticoagulant drugs (warfarin)	IV, V III I, II	Class I Class II Class III
Coronary vasodilators (Ca channel blockers, β-blockers, nitrates, etc.)	V IV I, II, III	Class I Class II Class III
Drug for heart failure (ACE inhibitors, angiotensin II receptor blockers, β-blockers)	V IV I, II, III	Class I Class II Class III
PCI	V (b) V (a) I, II, III, IV	Class I Class II Class III
CABG	V (b) V (a) I, II, III, IV	Class I Class II Class III

[a]ACE, angiotensin-converting enzyme; PCI, percutaneous coronary intervention; CABG, coronary artery bypass grafting.
[b]See Table 63.4.
[c]Evidence level:
Class I   Conditions for which there is general agreement that the treatment is useful and effective.
Class II   Conditions for which there is a divergence of opinion regarding the usefulness/efficacy of a treatment.
Class III   Conditions for which there is general agreement that the treatment is not useful/effective and may in some cases be harmful.
From *Guidelines for Diagnosis and Management of Cardiovascular Sequelae in Kawasaki Disease*, Japanese Circulation Society, Kyoto, 2008; http://www.j-circ.or.jp/english/activities/guidelines.html.

Revascularization therapy

Because increasing numbers of patients develop coronary stenosis adjacent to coronary aneurysms, catheter and surgical interventions to alleviate myocardial ischemia must be offered in a timely fashion [118,119]. There are three indications: patients presenting with clinical ischemic symptoms, patients presenting without clinical ischemic symptoms but having ischemic findings detected by several stress tests, and patients having no ischemic findings detected by any stress tests but with ≥75% of stenosis in the left anterior descending artery that can cause sudden cardiac death by its obstruction [118,119]. The selection of catheter or surgical intervention is determined by the same indications

as in adult coronary artery disease, where catheter intervention is not indicated in multiple coronary lesions, long segmental lesion, and coronary ostial lesions.

Based on the above indications, almost all types of catheter interventions for coronary artery disease have been offered in KD, such as balloon angioplasty [120,121], stent implantation [122,123], and rotational ablation [124–126]. Within 6 years after the onset of KD when coronary artery calcification is usually mild, coronary angioplasty is indicated. Special care must be taken to keep low inflation pressures of <8–10 atm to avoid the risk of new aneurysm formation [119].

Late after the onset of KD, catheter interventions must be chosen based on the degree of calcification and intimal growth, and intravascular ultrasound plays a pivotal role in evaluating vascular wall pathology [59]. With heavy circumferential calcification of the coronary wall, coronary rotational ablation, with as large a burr size as possible, is the choice of intervention to ensure long-term patency [125,126]. In addition to bare stents, covered [127] or drug-eluting stents [128] have been implanted in patients with KD, but the application of this procedure is limited because of the relatively larger equipment size and a risk of new coronary aneurysm formation and re-stenosis.

In patients who were unsuitable for catheter interventions, coronary artery bypass graft surgery has been offered with great success [129–131]. As a conduit vessel for bypass, an internal mammary artery is preferred to a saphenous vein graft because of its excellent patency and growth potential [132]. Age <12 years was once the limiting factor of patency of grafts, but this limitation has been overcome with technical innovation in addition to appropriate indications and timely catheter intervention [133–135].

Because re-stenosis at the site of catheter intervention or stenosis of anastomosis of the bypass graft has been reported, meticulous follow-up is mandatory [135]. In addition, although both catheter and surgical interventions are offered to relatively young patients with ischemic heart disease, sometimes it is still challenging and even risky for a small infant to undergo these interventions. Further development of equipment and techniques for these procedures is awaited.

In addition to catheter and surgical interventions, medical treatment to facilitate revascularization or neo-vascularization has been explored. Tateno *et al.* [136] reported the effectiveness of heparin–exercise therapy composed of twice-daily exercise with a bicycle ergometer plus heparin infusion in patients with totally occluded coronary arteries and stress-induced myocardial ischemia. After 10 days of this treatment, patients showed significant alleviation of myocardial ischemia as evaluated by dypyridamole-loading single photon emission computed tomography. Suda *et al.* [137] also reported the effectiveness of intermittent heparin infusion to alleviate myocardial ischemia in a small infant with multiple occluded coronary arteries.

Table **63.4** Summarized guidelines.

Severity level	Description	Pathophysiology	Diagnosis/clinical course	Treatment	Daily life/exercise management[a]
I	No dilatation	There is no evidence whether or not a history of Kawasaki disease is a factor associated with arteriosclerotic lesion	Follow up patients for 5 years. Evaluate at 30 days, 60 days, 6 months, 1 year, and 5 years after onset with ECG, echocardiography, and, if necessary, chest X-ray. It is desirable that patients be evaluated with exercise ECG at the final examination	Basically, no treatment is required during the remote phase.	No restriction is placed on daily life or exercise. Consult with parents (or patients) to determine further management. Lifetime prevention of lifestyle-related diseases is important. Junior and senior high school students should be educated on lifestyle-related diseases (blood lipid measurement, education on smoking cessation, and prevention of obesity)
II	Transient dilatation during the acute phase	During the acute phase, histopathologically vasculitis develops in the outer layer of the tunica media and then expands to the intima in coronary arteries. Echocardiography reveals diffuse dilatation of coronary arteries, but these changes subside within 30 days after onset		Patients with no coronary aneurysms after the acute phase may discontinue anti-platelet drugs such as aspirin	
III	Regression	In many patients regression may occur 1–2 years after onset, particularly in small- or medium-sized aneurysms. In the segment with regression, decrease in coronary diastolic function, abnormal function of vascular endothelium, and substantial intimal hyperplasia have been reported	Basically, follow patients annually with ECG, echocardiography, and chest X-ray up to entry into elementary school (age 6–7 years), and then with the same methods and exercise ECG in 4th grade (age 9–10 years), at entry into junior high school (age 12–13 years), and entry into senior high school (age 15–16 years). Follow patients who had coronary aneurysms with a large internal diameter during the acute phase with an appropriate combination of imaging techniques[b]		No restriction is placed on daily life or exercise. Follow the recommendations for Categories I and II
IV	Remaining coronary aneurysms	Aneurysms remaining during the convalescence phase or later are considered sequelae. Histopathologically, progression of inflammation leads to rupture of the internal elastic band, causing panangiitis. The internal and external elastic bands are broken into fragments and ruptured by arterial pressure to form aneurysms. Patients with giant aneurysms must be observed carefully for myocardial ischemia, since in such patients myocardial ischemia may develop even if no significant stenotic lesions are present	Patients must be followed with exercise ECG and an appropriate combination of imaging techniques[b]. It is desirable that patients who had coronary aneurysms with a large internal diameter during the acute phase be evaluated with stress myocardial scintigraphy every 2–5 years to monitor for progression to stenotic lesions	Continue treatment with anti-platelet agents such as aspirin. Anticoagulant therapy may be needed in patients with giant coronary aneurysms or thrombi in coronary aneurysms. CABG may be indicated for patients with giant coronary aneurysms not accompanied by significant stenotic lesions when myocardial ischemia has occurred	No restriction is placed on daily life or exercise except for those with giant aneurysms.

(continued)

Table 63.4 (cont'd).

Severity level	Description	Pathophysiology	Diagnosis/clinical course	Treatment	Daily life/exercise management[a]
V (a)	Coronary stenotic lesions (no findings of ischemia)	Thrombotic occlusion of medium-sizes or giant aneurysms may develop during the relatively early stage after onset. Sudden death may occur, although two-thirds of patients with occlusion are asymptomatic. Patients often show improvement of myocardial ischemia due to the development of recanalized vessels and collateral flow after occlusion. Development/progression of regional stenosis during the remote phase is more prevalent in the left than the right coronary artery. The segments with greatest prevalence are the proximal segment or the main trunk of the left anterior descending artery. The risk of progression to stenosis/ occlusion is higher in larger aneurysms.	Patients must be followed for life, and physicians must design the tailor-made management plan for individual patients. Follow-up examination must include exercise ECG and an appropriate combination of imaging techniques[b]. Although the schedule may differ among individuals, patients are generally evaluated every 3–6 months	Continue treatment with anti-platelet drugs such as aspirin. Use Ca channel blockers, nitrates, β-blockers, ACE inhibitors, and angiotensin receptor II blockers to prevent ischemic attacks and heart failure	No restriction is placed on daily life or exercise. For patients other than those with giant aneurysms. Explain the importance of drug treatment and ensure adherence, and also symptoms which may occur and actions to be taken when ischemia develops. Patients must be followed at least annually until regression of aneurysms is documented
V (b)	Coronary stenotic lesions (with findings of ischemia)	Stenosis may develop during long-term follow up		Follow the instructions for drug treatment in Category V (a). Consider CABG or appropriate PCI technique when exercise ECG or stress myocardial scintigraphy reveals ischemia	Exercise should be restricted. Categorize in "D" or higher category based on patient condition. School sports club activities should be "prohibited." Select the most appropriate category from "A" to "D" on the basis of findings of exercise testing and evaluation of severity of myocardial ischemia. Educate patients well about the importance of drug treatment

Anti-atherosclerosis

In addition to impaired vascular distensibility and endothelial function, dyslipidemia was reported in a cluster of patients with coronary artery aneurysms long after KD [138]. In fact, accelerated atherosclerosis expressed by thickened intima–media complex of the carotid artery and also increased stiffness was observed in patients with coronary artery aneurysms caused by KD [139,140]. Therefore, anti-atherosclerosis using statin or angiotensin receptor antagonists may be applied, as in adult patients with atherosclerosis. There is only one short-term study that showed the effectiveness of oral atorvastatin in patients with coronary aneurysms caused by KD as judged by improved endothelial function and decreased serum level of CRP in addition to a decrease in total and LDL-cholesterol [141]. Strategies to stop, delay, or even reverse early atherosclerosis seen in patients with a history of KD must be explored.

Prognosis

Since it is more than 40 years after the first description of this disease, the long-term prognosis of patients with a history of KD has been available for over 20 years. Based on a cohort of 6576 patients, Nakamura *et al.* [142] reported that the mortality rate among males with cardiac sequelae because of KD was significantly higher than in the general population, with a standardized mortality ratio of 2.55 (95% confidence interval 1.23–4.70). On the other hand, the mortality of females with cardiac sequelae and of both males and females without cardiac sequelae was not significantly elevated.

In terms of patients with giant coronary aneurysms who might have the worst prognosis, we have followed a cohort of 76 patients with giant coronary aneurysms caused by KD since 1972 [143]. The survival rate of these patients was acceptably high, being 88% at 30 years after onset. On the other hand, the cumulative cardiac intervention rate was also high, being 59% at 25 years, reflecting ongoing development of coronary stenosis that required appropriate cardiac interventions.

References

1 Kato H, Koike S, Yamamoto M, *et al.* Coronary aneurysms in infants and young children with acute febrile mucocutaneous lymph node syndrome. *J Pediatr* 1975;**86**:892–8.

2 Kato H, Akagi T, Sugimura T, *et al.* Kawasaki disease. *Coron Artery Dis* 1995;**6**:194–206.

3 Kawasaki T, Kosaki F, Okawa S. A new infantile acute febrile mucocutaneous lymph node syndrome prevailing in Japan. *Pediatrics* 1974;**54**:271–6.

4 Kawasaki T. Acute febrile mucocutaneous syndrome with lymphoid involvement with specific desquamation of the fingers and toes in children. *Jpn J Allergy* 1967;**16**:178–222.

5 Yamamoto T, Kimura J. A case report of acute febrile MCLS complicated with myocarditis. *Shonika Rinsho* 1968;**21**:336–9 (in Japanese).

6 Gee S. Aneurysms of the coronary arteries in a boy. *St Barth Hosp Rep London* 1871;**7**:148.

7 Atimson PM, Spector R. Scarlet fever, periarteritis nodosa, aneurysm of coronary artery with spontaneous rupture, hemopericardium. *Arch Pediatr* 1939;**56**:319–24.

8 Rae MV. Coronary aneurysms with thrombosis in rheumatic carditis. *Arch Pathol* 1937;**24**:369–76.

9 Fanney GC. Erythema multiforme exudativum, Stevens–Johnson syndrome. Cardiovascular and central nervous system involvement. *J Pediatr* 1949;**34**:195–205.

10 Munro-Faure H. Necrotizing arteritis of the coronary vessels in infancy: case report and review of the literature. *Pediatrics* 1959;**23**:914–26.

11 Shibuya N, Shibuya K, Kato H, Yanagisawa M. Kawasaki disease before Kawasaki at Tokyo University Hospital. *Pediatrics* 2002;**110**:e17.

12 Landing BH, Larson EJ. Are infantile periarteritis nodosa with coronary artery involvement and fetal mucocutaneous lymph node syndrome the same? Comparison of 20 patients from North America with patients from Hawaii and Japan. *Pediatrics* 1977;**59**:651–62.

13 Yanagawa H, Yashiro M, Nakamura T, *et al.* Results of twelve nationwide epidemiological incidence surveys of Kawasaki disease in Japan. *Arch Pediatr Adolesc Med* 1995;**149**:779–83.

14 Nakamura Y, Yashiro M, Uehara R, *et al.* Increasing incidence of Kawasaki disease in Japan. *Pediatr Int* 2008;**50**:287–90.

15 Nakamura Y, Yanagawa H. The worldwide epidemiology of Kawasaki disease. *Prog Pediatr Cardiol* 2004;**19**:99–108.

16 Holman RC, Curns AT, Belay ED, *et al.* Kawasaki syndrome: hospitalization in the U.S, 1997 and 2000. *Pediatrics* 2003;**112**:495–501.

17 Fujita Y, Nakamura Y, Sakata K, *et al.* Kawasaki disease in families. *Pediatrics* 1989;**84**:666–9.

18 Burns JC, Cayan DR, Tong G, *et al.* Seasonality and temporal clustering of Kawasaki syndrome. *Epidemiology* 2005;**16**:220–5.

19 Fujiwara H, Hamashima Y. Pathology of the heart in Kawasaki disease. *Pediatrics* 1978;**61**:100–7.

20 Naoe S, Shibuya K, Takahashi K, *et al.* Pathological observations concerning the cardiovascular lesions in Kawasaki disease. *Cardiol Young* 1991;**3**:212–20.

21 Kato H, Takahashi K. Kawasaki disease. In: Ball GV, Bridges SL, eds. *Vasculitis*, 2nd edn. London: Oxford University Press, 2008: 373–89.

22 Yutani C, Okano K, Kamiya T, *et al.* Histopathological study on right endomycardial biopsy of Kawasaki disease. *Br Heart J* 1980;**43**:589–92.

23 Abe J, Kotzin BL, Jujo K, *et al.* Selective expansion of T cells expressing T-cell receptor variable regions Vbeta2 and Vbeta8 in Kawasaki disease. *Proc Natl Acad Sci USA* 1982;**89**:4066–70.

24 Leung DYM, Meissner HC, Fulton DR, *et al.* Toxic shock syndrome toxin-secreting *Staphylococcus aureus* in Kawasaki syndrome. *Lancet* 1993;**342**:1385–8.

25 Sakaguchi M, Kato H, Nishiyori A, *et al.* Characterization of CD4+ T helper cells in patients with Kawasaki disease: preferential production of TNF-alpha by Vbeta2 and Vbeta8 CD4+ T helper cells. *Clin Exp Immunol* 1995;**99**:276–82.

26 Yoshioka T, Matsutani T, Toyosaki-Maeda T, *et al*. Relation of streptococcal pyrogenic exotoxin C as a causative superantigen for Kawasaki disease. *Pediatr Res* 2003;**53**:403–10.

27 Nagata S, Yamashiro Y, Ohisuka Y, *et al*. Heat shock protein and superantigenic properties of bacteria from the gastrointestinal tract of patients with Kawasaki disease. *Immunology* 2009;**128**:511–20.

28 Sato K, Ouichi K, Taki M. *Yersinia pseudotuberculosis* infection in children, resembling Izumi fever and Kawasaki syndrome. *Pediatr Infect Dis* J 1983;**2**:123–6.

29 Kato H, Fujimato T, Inoue O, *et al*. Variant strain of *Propionibacterium acnes*: a clue to the aetiology of Kawasaki disease. *Lancet* 1983;**ii**:1383–8.

30 Tomita S, Kato H, Fujimoto T, *et al*. Cytopathogenic protein in filtrates from cultures of *Propionibacterium acnes* isolated from patients with Kawasaki disease. *Br Med J* 1987;**295**:1229–32.

31 Kikuta H, Mizuno F, Osato T. Kawasaki disease and an unusual primary infection with Epstein–Barr virus. *Pediatrics* 1984;**73**:413–4.

32 Rowley AH, Shulman ST, Spike BT. Oligoclonal IgA response in the vascular wall in acute Kawasaki disease. *J Immunol* 2001;**166**:1334–43.

33 Esper F, Shapiro ED, Welbel C, *et al*. Association between a novel human coronavirus and Kawasaki disease. *J Infect Dis* 2005;**191**:499–502.

34 Furukawa S, Matsubara T, Jujoh K, *et al*. Peripheral blood monocyte/macrophages and serum tumor necrosis factor in Kawasaki disease. *Clin Immunol Immunopathol* 1988;**48**:247–51.

35 Leung DYM, Collins T, LaPierre LA, *et al*. Immunoglobulin M antibodies present in the acute phase of Kawasaki syndrome lyse cultured vascular endothelial cells stimulated by gamma interferon. *J Clin Invest* 1986;**77**:1428–35.

36 Terai M, Kohno Y, Nanba M, *et al*. Class II antigen expression in the coronary artery endothelium in Kawasaki disease. *Hum Pathol* 1990;**21**:231–4.

37 Yasukawa K, Terai M, Shulman ST, *et al*. Systemic production of vascular endothelial growth factor in fms-like tyrosine kinase-1 receptor in acute Kawasaki disease. *Circulation* 2002;**105**:766–9.

38 Furukawa S, Matsubara T, Umezawa Y, *et al*. Serum levels of p60 soluble tumor necrosis factor receptor during acute Kawasaki disease. *J Pediatr* 1994;**124**:721–5.

39 Lin CY, Lin CC, Hwang B, Chiang B. Serial changes of serum interleukin-6, interleukin-8, and tumor necrosis factor alpha among patients with Kawasaki disease. *J Pediatr* 1992;**121**:924–6.

40 Onouchi Y, Gunji T, Burns JC, *et al*. ITPKC functional polymorphism associated with Kawasaki disease susceptibility and formation of coronary artery aneurysms. *Nat Genet* 2008;**40**:35–42.

41 Newburger JW, Takahashi M, Gerber MA, *et al*. Diagnosis, treatment, and long-term management of Kawasaki disease. American Heart Association Scientific Statement. *Circulation* 2004;**110**:2747–71.

42 Kato H, Sugimura T, Akagi T, *et al*. Long-term consequences of Kawasaki disease: a 10-to-21-year follow-up study of 594 patients. *Circulation* 1996;**94**:1379–85.

43 Egami K, Muta H, Ishii M, *et al*. Prediction of resistance to IVIG treatment in patients with Kawasaki disease. *J Pediatr* 2006;**149**:237–40.

44 Kobayashi T, Inoue Y, Takeuchi K, *et al*. Prediction of IVIG unresponsiveness in patients with Kawasaki disease. *Circulation* 2006;**113**:2606–12.

45 Harada K. Intravenous gamma-globulin treatment in Kawasaki disease. *Acta Paediatr Jpn* 1991;**33**:805–10.

46 Kato H, Ichinose E, Kawasaki T. Myocardial infarction in Kawasaki disease: clinical analyses in 195 cases. *J Pediatr* 1986;**108**:923–7.

47 Tomita S, Chung K, Mas M, *et al*. Peripheral gangrene associated with Kawasaki disease. *Clin Infect Dis* 1992;**14**:121–6.

48 Akagi T, Kato H, Inoue O, *et al*. Valvular heart disease in Kawasaki syndrome: incidence and natural history. *Am Heart J* 1990;**120**:366–72.

49 Gidding SS, Shulman ST, Ilbawi M, *et al*. Mucocutaneous lymph node syndrome (Kawasaki disease): delayed aortic and mitral insufficiency secondary to valvulitis. *J Am Coll Cardiol* 1986;**7**:894–7.

50 Research Committee on Kawasaki Disease. *Report of Subcommittee on Standardization of Diagnostic Criteria and Reporting of Coronary Artery Lesions in Kawasaki Disease*. Tokyo: Japanese Ministry of Health and Welfare, 1984.

51 Dajani AS, Taubert KA, Takahashi M, *et al*. Guidelines for long-term management of patients with Kawasaki disease. Committee Report of Council on Cardiovascular Disease in the Young, American Heart Association. *Circulation* 1994;**89**:916–22.

52 de Zorzi A, Colan SD, Gauvreau K, *et al*. Coronary artery dimensions may be misclassified as normal in Kawasaki disease. *J Pediatr* 1998;**133**:254–8.

53 Kurotobi S, Nagai T, Kawakami N, *et al*. Coronary diameter in normal infants, children and patients with Kawasaki disease. *Pediatr Int* 2002;**44**:1–4.

54 Manlhiot C, Millar K, Golding F, McCrindle BW. Improved classification of coronary artery abnormalities based only on coronary artery z-scores after Kawasaki disease. *Pediatr Cardiol* 2010;**31**:242–9.

55 Crysal MA, Manliot C, Yeung RS, *et al*. Coronary artery dilatation after Kawasaki disease for children within the normal range. *Int J Cardiol* 2009;**16**:27–32.

56 Kato H, Ichinose E, Yoshioka F, *et al*. Fate of coronary aneurysms in Kawasaki disease: serial coronary angiography and long-term follow-up study. *Am J Cardiol* 1982;**49**:1758–66.

57 Kato H. Cardiovascular complications in Kawasaki disease: coronary artery lumen and long-term consequences. *Prog Pediatr Cardiol* 2004;**19**:137–45.

58 Kato H, Inoue O, Ichinose E, *et al*. Intracoronary thrombolytic therapy in Kawasaki disease: treatment and prevention of myocardial infarction. *Prog Clin Biol Res* 1987;**250**:445–54.

59 Sugimura T, Kato H, Inoue O, *et al*. Intravascular ultrasound of coronary arteries in children: assessment of the wall morphology and the lumen after Kawasaki disease. *Circulation* 1994;**89**:258–65.

60 Glagov S, Weinsenberg E, Kolettis G, *et al*. Compensatory enlargement of human coronary arteries. *N Engl J Med* 1987;**316**:1371–5.

61 Greil GF, Stuber M, Botnar RM, *et al*. Coronary magnetic resonance angiography in adolescent and young adults due to Kawasaki disease. *Circulation* 2002;**105**:908–11.

62 Takemura A, Suzuki A, Inaba R, *et al*. Utility of coronary MR angiography in children with Kawasaki disease. *AJR Am J Roentgenol* 2007;**188**:W534–9.

63 Greil GF, Seeger A, Miller S, *et al*. Coronary magnetic resonance angiography and vessel wall imaging in children with Kawasaki disease. *Pediatr Cardiol* 2007;**37**:666–73.

64 Frey EE, Matherne GP, Mahony LT, *et al*. Coronary artery aneurysms due to Kawasaki disease: diagnosis with ultrafast CT. *Radiology* 1998;**167**:725–6.

65 Fukuda T, Akagi T, Ishibashi M, *et al*. Noninvasive evaluation of myocardial ischemia in Kawasaki disease: comparison between dipyridamole stress thallium imaging and exercise stress testing. *Am Heart J* 1998;**135**:482–7.

66 Kamiya T. How to evaluate the myocardial ischemia in Kawasaki disease. In: Kato H, ed. *Kawasaki Disease*. Amsterdam: Elsevier, 1995: 447–50.

67 Kondo C, Hiroe M, Nakanishi T, Takao A. Detection of coronary artery stenosis in children with Kawasaki disease. *Circulation* 1989;**80**:615–24.

68 Pahl E, Sehgal R, Chrystof D, *et al*. Feasibility of exercise stress echocardiography for the follow-up of children with coronary involvement secondary to Kawasaki disease. *Circulation* 1995;**91**:122–8.

69 Noto N, Ayusawa M, Karasawa K, *et al*. Dobutamine stress echocardiography for detection of coronary artery stenosis in children with Kawasaki disease. *J Am Coll Cardiol* 1996; **27**:1251–6.

70 Ishii M, Himeno W, Sawa M, *et al*. Assessment of the ability of myocardial contrast echocardiography with harmonic power Doppler imaging to identify perfusion abnormalities in patients with Kawasaki disease at rest and during dipyridamole stress. *Pediatr Cardiol* 2002;**23**:192–9.

71 Ichinose E, Inoue O, Hiyoshi Y, *et al*. Fate of coronary aneurysms in Kawasaki disease: analysis of prognostic factors, In: Doyle EF, Engle MA, Gersony W, eds. *Pediatric Cardiology*. New York: Springer, 1986: 1099–101.

72 Sasaguri Y, Kato H. Regression of aneurysms in Kawasaki disease: a pathologic study. *J Pediatr* 1982;**100**:225–31.

73 Suzuki A, Miyagawa-Tomita S, Komatsu K, *et al*. Active remodeling of the coronary arterial lesions in the late phase of Kawasaki disease: immunohistochemical study. *Circulation* 2001;**101**:2935–41.

74 Suzuki A, Miyagawa-Tomita S, Komatsu K, *et al*. Immunohistochemical study of apparently intact coronary artery in a child after Kawasaki disease. *Pediatr Int* 2004;**46**:590–6.

75 Sugimura T, Kato H, Inoue O, *et al*. Vasodilatory response of the coronary arteries after Kawasaki disease: evaluation by intracoronary injection of isosorbide dinitrate. *J Pediatr* 1992;**121**:684–8.

76 Yamakawa R, Ishii M, Sugimura T, *et al*. Coronary endothelial dysfunction after Kawasaki disease: evaluation by intracoronary injection of acetylcholine. *J Am Coll Cardiol* 1998;**31**:1074–80.

77 Iemura M, Ishii M, Sugimura T, *et al*. Long term consequences of regressed coronary aneurysms after Kawasaki disease: vascular wall morphology and function. *Heart* 2000;**83**:307–11.

78 Dhillon R, Clarkson P, Donald AE, *et al*. Endothelial dysfunction late after Kawasaki disease. *Circulation* 1996;**94**:2103–6.

79 Mitani Y, Okuda Y, Shimpo H, *et al*. Impaired endothelial function in epicardial coronary arteries after Kawasaki disease. *Circulation* 1997;**96**:454–61.

80 Takahashi K, Oharaseki T, Naoe S. Pathological study of postcoronary arteritis in adolescents and young adults: with reference to the relationship between sequelae of Kawasaki disease and atherosclerosis. *Pediatr Cardiol* 2001;**22**:138–42.

81 Mitani Y, Sawada H, Hayakawa H, *et al*. Elevated levels of high-sensitivity C-reactive protein and serum amyloid-A late after Kawasaki disease: association between inflammation and late coronary sequelae in Kawasaki disease. *Circulation* 2005; **111**:38–43.

82 Mitani Y, Ohashi H, Sawada H, *et al. In vivo* plaque composition and morphology in coronary artery lesions in adolescents and young adults long after Kawasaki disease: a virtual histology–intravascular ultrasound study. *Circulation* 2009;**119**:2829–36.

83 Kato H. Long-term consequences of Kawasaki disease: pediatrics to adults. In: Kato H, ed. *Kawasaki Disease*. Amsterdam: Elsevier, 1996: 557–66.

84 Kato H, Inoue O, Kawasaki T, *et al*. Adult coronary artery disease probably due to childhood Kawasaki disease. *Lancet* 1992;**340**:1127–9.

85 McCrindle BW, Li JS, Minich SD, *et al*. Coronary artery involvement in children with Kawasaki disease: risk factors from analysis of serial normalized measurements. *Circulation* 2007;**116**: 174–9.

86 Gordon JB, Kahn AM, Burns JC. When children with Kawasaki disease grow up: myocardial and vascular complications in adulthood. *J Am Coll Cardiol* 2009;**54**:1911–20.

87 Kato H, Koike S, Yokoyama T. Kawasaki disease: effect of treatment on coronary artery involvement. *Pediatrics* 1979; **63**:175–9.

88 Furusho K, Sato K, Soeda T, *et al*. High-dose intravenous gammaglobulin for Kawasaki disease. *Lancet* 1983;**ii**:1359–60.

89 Furusho K, Kamiya T, Nakano H, *et al*. High-dose intravenous gammaglobulin for Kawasaki disease. *Lancet* 1984;**ii**:1055–8.

90 Furusho K, Kamiya T, Nakano H, *et al*. Japanese gamma globulin trials for Kawasaki disease. *Prog Clin Biol Res* 1987; **250**:425–32.

91 Furusho K, Kamiya T, Nakano H, *et al*. Intravenous gamma-globulin for Kawasaki disease. *Acta Paediatr Jpn* 1991;**33**: 799–804.

92 Morikawa Y, Ohashi Y, Harada K, *et al*. A multicenter, randomized, controlled trial of intravenous gamma globulin therapy in children with acute Kawasaki disease. *Acta Paediatr Jpn* 1994;**36**:347–54.

93 Newburger JW, Takahashi M, Beiser AS, *et al*. A single intravenous infusion of gamma globulin as compared with four infusions in the treatment of acute Kawasaki syndrome. *N Engl J Med* 1991;**324**:1633–9.

94 Durongpisitkul K, Gururaj VJ, Park JM, *et al*. The prevention of coronary artery aneurysm in Kawasaki disease: a meta-analysis on the efficacy of aspirin and immunoglobulin treatment. *Pediatrics* 1995;**96**:1057–61.

95 Mori M, Miyamae T, Imagawa T, *et al*. Meta-analysis of the results of intravenous gamma globulin treatment of coronary artery lesions in Kawasaki disease. *Mod Rheumatol* 2004; **14**:361–6.

96 Inoue Y, Okada Y, Shinohara M, *et al*. A multicenter prospective randomized trial of corticosteroids in primary therapy for Kawasaki disease: clinical course and coronary artery outcome. *J Pediatr* 2006;**149**:336–41.

97 Newburger JW, Sleeper LA, McCrindle BW, *et al.*; Pediatric Heart Network Investigators. Randomized trial of pulsed corticosteroid

therapy for primary treatment of Kawasaki disease. *N Engl J Med* 2007;**356**:663–75.

98 Uehara R, Yashiro M, Oki I, *et al*. Re-treatment regimens for acute stage of Kawasaki disease patients who failed to respond to initial intravenous immunoglobulin therapy: analysis from the 17th nationwide survey. *Pediatr Int* 2007;**49**:427–30.

99 Weiss JE, Eberhard BA, Chowdhury D, *et al*. Infliximab as a novel therapy for refractory Kawasaki disease. *J Rheumatol* 2004;**31**:808–10.

100 Burns JC, Mason WH, Hauger SB, *et al*. Infliximab treatment for refractory Kawasaki syndrome. *J Pediatr* 2005;**146**:662–7.

101 Burns JC, Best BM, Mejias A, *et al*. Infliximab treatment of intravenous immunoglobulin-resistant Kawasaki disease. *J Pediatr* 2008;**153**:833–8.

102 Raman V, Kim J, Sharkey A, *et al*. Response of refractory Kawasaki disease to pulse steroid and cyclosporin A therapy. *Pediatr Infect Dis J* 2001;**20**:635–7.

103 Ahn SY, Kim DS. Treatment of intravenous immunoglobulin resistant Kawasaki disease with methotrexate. *Scand J Rheumatol* 2005;**34**:136–9.

104 Mori M, Imagawa T, Katakura S, *et al*. Efficacy of plasma exchange therapy for Kawasaki disease intractable to intravenous gamma-globulin. *Mod Rheumatol* 2004;**14**:43–7.

105 Furukawa T, Kishiro M, Akimoto K, *et al*. Effects of steroid pulse therapy on immunoglobulin-resistant Kawasaki disease. *Arch Dis Child* 2008;**93**:142–6.

106 Hashino K, Ishii M, Iemura M, *et al*. Re-treatment for immune globulin-resistant Kawasaki disease: a comparative study of additional immune globulin and steroid pulse therapy. *Pediatr Int* 2001;**43**:211–7.

107 Miura M, Ohki H, Yoshiba S, *et al*. Adverse effects of methyl-prednisolone pulse therapy in refractory Kawasaki disease. *Arch Dis Child* 2005;**90**:1096–7.

108 Furukawa S, Matsubara T, Jujoh K, *et al*. Peripheral blood monocyte/macrophages and serum tumor necrosis factor in Kawasaki disease. *Clin Immunol Immunopathol* 1988;**48**:247–51.

109 Maury CP, Salo E, Pelkonen P. Elevated circulating tumor necrosis factor-alpha in patients with Kawasaki disease. *J Lab Clin Med* 1989;**113**:651–4.

110 Sano T, Kurotobi S, Matsuzaki K, *et al*. Prediction of non-responsiveness to standard high-dose gamma-globulin therapy in patients with acute Kawasaki disease before starting initial treatment. *Eur J Pediatr* 2007;**166**:131–7.

111 Okada K, Hara J, Maki I, *et al*.; Osaka Kawasaki Disease Study Group. Pulse methylprednisolone with gammaglobulin as an initial treatment for acute Kawasaki disease. *Eur J Pediatr* 2009;**168**:181–5.

112 Ogata S, Bando Y, Kimura S, *et al*. The strategy of immune globulin resistant Kawasaki disease: a comparative study of additional immune globulin and steroid pulse therapy. *J Cardiol* 2009;**53**:15–9.

113 Horigome H, Sekijima T, Miyamoto T. Successful thrombolysis with intracoronary administration of tissue plasminogen activator in an infant with Kawasaki disease. *Heart* 1997;**78**:517–8.

114 Williams RV, Wilke VM, Tani LY, *et al*. Does abciximab enhance regression of coronary aneurysms resulting from Kawasaki disease? *Pediatrics* 2002;**109**:e4.

115 Sugahara Y, Ishii M, Muta H, *et al*. Warfarin therapy for giant aneurysm prevents myocardial infarction in Kawasaki disease. *Pediatr Cardiol* 2008;**29**:398–401.

116 Suda K, Kudo Y, Higaki T, *et al*. Multicenter and retrospective case study of warfarin and aspirin combination therapy in patients with giant coronary aneurysms caused by Kawasaki disease. *Circ J* 2009;**73**:1319–23.

117 Onouchi Z, Hamaoka K, Sakata K, *et al*. Long-term changes in coronary artery aneurysms in patients with Kawasaki disease: comparison of therapeutic regimens. *Circ J* 2005;**69**:265–72.

118 Akagi T, Ogawa S, Ino T, *et al*. Catheter interventional treatment in Kawasaki disease: a report from the Japanese Pediatric Interventional Cardiology Investigation Group. *J Pediatr* 2000;**137**:181–6.

119 Ishii M, Ueno T, Akagi T, *et al*.; Research Committee of Ministry of Health, Labour and Welfare – "Study of treatment and long-term management in Kawasaki disease." Guidelines for catheter intervention in coronary artery lesion in Kawasaki disease. *Pediatr Int* 2001;**43**:558–62.

120 Ino T, Nishimoto K, Akimoto K, *et al*. Percutaneous transluminal coronary angioplasty for Kawasaki disease: a case report and literature review. *Pediatr Cardiol* 1991;**12**:33–5.

121 Ino T, Akimoto K, Ohkubo M, *et al*. Application of percutaneous transluminal coronary angioplasty to coronary arterial stenosis in Kawasaki disease. *Circulation* 1996;**93**:1709–15.

122 Ueno T, Kai H, Ikeda H, *et al*. Coronary stent deployment in a young adult with Kawasaki disease and recurrent myocardial infarction. *Clin Cardiol* 1999;**22**:147–9.

123 Iliadis EA, Duvernoy CS. Stent placement for coronary stenosis in Kawasaki disease: case report and literature review. *J Interv Cardiol* 2002;**15**:29–31.

124 Sugimura T, Yokoi H, Sato N, *et al*. Interventional treatment for children with severe coronary artery stenosis with calcification after long-term Kawasaki disease. *Circulation* 1997;**96**:3928–33.

125 Ishii M, Ueno T, Ikeda H, *et al*. Sequential follow-up results of catheter intervention for coronary artery lesions after Kawasaki disease: quantitative coronary artery angiography and intravascular ultrasound imaging study. *Circulation* 2002;**105**:3004–10.

126 Tsuda E, Miyazaki S, Yamada O, *et al*. Percutaneous transluminal coronary rotational atherectomy for localized stenosis caused by Kawasaki disease. *Pediatr Cardiol* 2006;**27**:447–53.

127 Waki K, Baba K. Transcatheter polytetrafluoroethylene-covered stent implantation in a giant coronary artery aneurysm of a child with Kawasaki disease – a potential novel treatment. *Catheter Cardiovasc Interv* 2006;**68**:74–7.

128 Li SS, Cheng BC, Lee SH. Images in cardiovascular medicine. Giant coronary aneurysm formation after sirolimus-eluting stent implantation in Kawasaki disease. *Circulation* 2005;**112**:e105–7.

129 Kitamura S, Kameda Y, Seki T, *et al*. Long-term outcome of myocardial revascularization in patients with Kawasaki coronary artery disease. A multicenter cooperative study. *J Thorac Cardiovasc Surg* 1994;**107**:663–73; discussion 673–4.

130 Tsuda E, Kitamura S; Cooperative Study Group of Japan. National survey of coronary artery bypass grafting for coronary stenosis caused by Kawasaki disease in Japan. *Circulation* 2004;**110**:II61–6.

131 Kitamura S, Tsuda E, Kobayashi J, *et al*. Twenty-five-year outcome of pediatric coronary artery bypass surgery for Kawasaki disease. *Circulation* 2009;**120**:60–8.

132 Kitamura S, Seki T, Kawachi K, *et al*. Excellent patency and growth potential of internal mammary artery grafts in pediatric coronary artery bypass surgery. New evidence for a "live" conduit. *Circulation* 1988;**78**:I129–39.

133 Tsuda E, Kitamura S, Kimura K, *et al*. Long-term patency of internal thoracic artery grafts for coronary artery stenosis due to Kawasaki disease: comparison of early with recent results in small children. *Am Heart J* 2007;**153**:995–1000.

134 Tsuda E, Fujita H, Yagihara T, *et al*. Competition between native flow and graft flow after coronary artery bypass grafting. Impact on indications for coronary artery bypass grafting for localized stenosis with giant aneurysms due to Kawasaki disease. *Pediatr Cardiol* 2008;**29**:266–70.

135 Miyazaki A, Tsuda E, Miyazaki S, *et al*. Percutaneous transluminal coronary angioplasty for anastomotic stenosis after coronary arterial bypass grafting in Kawasaki disease. *Cardiol Young* 2003;**13**:284–9.

136 Tateno S, Terai M, Niwa K, *et al*. Alleviation of myocardial ischemia after Kawasaki disease by heparin and exercise therapy. *Circulation* 2001;**103**:2591–7.

137 Suda K, Mastumoto M, Miyanishi S. Intermittent heparin infusion in children with ischemic heart disease caused by Kawasaki disease. *Int J Cardiol* 2009;**133**:417–9.

138 Cheung YF, Yung TC, Tam SC, *et al*. Novel and traditional cardiovascular risk factors in children after Kawasaki disease: implications for premature atherosclerosis. *J Am Coll Cardiol* 2004;**43**:120–4.

139 Cheung YF, Wong SJ, Ho MH. Relationship between carotid intima–media thickness and arterial stiffness in children after Kawasaki disease. *Arch Dis Child* 2007;**92**:43–7.

140 Noto N, Okada T, Karasawa K, *et al*. Age-related acceleration of endothelial dysfunction and subclinical atherosclerosis in subjects with coronary artery lesions after Kawasaki disease. *Pediatr Cardiol* 2009;**30**:262–8.

141 Huang SM, Weng KP, Chang JS, *et al*. Effects of statin therapy in children complicated with coronary arterial abnormality late after Kawasaki disease: a pilot study. *Circ J* 2008;**72**:1583–7.

142 Nakamura Y, Aso E, Yashiro M, *et al*. Mortality among persons with a history of Kawasaki disease in Japan: mortality among males with cardiac sequelae is significantly higher than that of the general population. *Circ J* 2008;**72**:134–8.

143 Suda K, Iemura M, Nishino H, *et al*. Long-term prognosis of patients with Kawasaki disease complicated by giant coronary aneurysms. A single-institution experience. *Circulation* 2011;**123**:1836–42.

64

Hypertension in Children and Adolescents

Bonita Falkner

Thomas Jefferson University, Philadelphia, PA, USA

Introduction

Hypertension may occur in any phase of childhood, from the newborn period through adolescence. There is a normal upward trend in blood pressure (BP) level throughout childhood that corresponds to normal growth and development. In children and adolescents, hypertension is defined as the BP level at the extreme of the normal distribution in healthy children. The diagnosis of hypertension requires BP measurements, systolic and/or diastolic, that are consistently ≥95th percentile for age, sex, and height [1]. With this statistical definition, the prevalence of hypertension is theoretically from 1 to 5%. More recent data, drawn from asymptomatic children and adolescents in primary care clinics [2] and in school screenings [3], indicate that the prevalence of hypertension is ~3.5%, with higher rates among obese adolescents. Therefore, hypertension is a very common chronic health issue in childhood. As measurement of BP in children during routine health care visits has become common practice, and as a result of the rising rates of childhood obesity, more children with hypertension are being identified. Because secondary causes of hypertension can be detected more frequently in hypertensive children, relative to adults, the approach to evaluating hypertension in the young differs from that of adults. High BP in the young is evaluated to determine whether the elevated BP is an early expression of primary hypertension or due to secondary hypertension. As in adults, severe untreated hypertension in children can have a poor outcome [4]. Children with primary (essential) hypertension commonly have the same risk factors for cardiovascular disease as adults, and can benefit from interventions to control the BP.

Definition of hypertension in childhood

Hypertension in adults is defined by the level of BP that predicts a heightened risk for subsequent cardiovascular or renal events. The risk for cardiovascular events increases as systolic BP rises above 120 mmHg [5], but hypertension continues to be defined as BP ≥140/90 mmHg, regardless of adult age or gender. In children, with the exception of extreme hypertension, long-term data which link a particular level of BP in childhood with subsequent cardiovascular events, such as stroke, heart failure, or kidney failure, are unavailable. In the absence of such data, hypertension is defined statistically. The combined results of several large epidemiologic studies that measured BP in healthy children [1,6] provide data from which the normal distribution of BP in children and adolescents in the United States has been established. An analysis of BP data from healthy children in Europe describes a very similar BP distribution pattern in childhood [7–9].

There is a consistent relationship of BP with body size in childhood. The BP level rises progressively with increasing age throughout childhood, and parallels the age-related increase in height. A gender difference in BP distribution emerges in adolescence and is concurrent with a gender difference in height. The definition of hypertension in children and adolescents is systolic and/or diastolic BP that, on repeated measurement, is ≥95th percentile for age, gender, and height [1]. The severity of hypertension is now staged: Stage 1 is systolic or diastolic BP that is between the 95th percentile and 5 mmHg above the 99th percentile, and Stage 2 is average systolic or diastolic BP that is >5 mmHg above the 99th percentile for age, gender, and height. In adults, a BP level between 120/80 and 139/89 mmHg is

designated prehypertension. Prehypertension in children is defined as systolic or diastolic BP between the 90th and 95th percentile for age, sex, and height. Because the BP level at the 90th percentile is >120/80 mmHg in some taller adolescents, a BP level >120/80 mmHg but <95th percentile is considered prehypertension in adolescents. Normal BP is systolic and diastolic BP <90th percentile for age, sex, and height. Table 64.1 provides the level of BP for the 50th, 90th, 95th, and 99th percentile for age and height percentile for boys, and Table 64.2 provides the same percentile levels for girls [1]. The 50th percentile for systolic and diastolic BP is provided to denote the midpoint of the BP distribution.

There are some limited data on normal levels of BP in newborns and very young infants [10–12]. In a large study on newborn infants that included a broad range of birth weights and gestational ages [12], at birth BP was directly related to both weight and gestational age. Daily BP measurements in healthy newborns, regardless of weight or gestational age at birth, demonstrate a rapid and consistent increase in BP during the first 5 days of life [11], reflecting the normal hemodynamic transition from intrauterine to extrauterine life. Subsequently, BP is directly related to body weight and age, in terms of gestation or post-conception age. The upper 95% confidence limit (CL) for a term infant (40 weeks post-conceptional age) is 90 mmHg for systolic blood pressure. Systolic BP levels >90 mmHg are considered hypertensive in a term infant, and by 4–6 weeks of age (44–46 weeks post-conception age) a systolic BP >100 mmHg represents hypertension.

Measurement of blood pressure in the young

Measurement of BP in children and adolescents should be performed in a standard method. In an office or clinic setting, the preferred method for BP measurement in children is auscultation with a cuff sphygmomanometer.

Correct BP measurement in children requires an appropriately sized BP cuff for the size of the child's upper arm [1]; the bladder width should be ~40% of the arm circumference midway between the olecranon and the acromion. This size of cuff bladder will usually cover 80–100% of the arm circumference. Most manufacturers of BP cuffs provide lines on the cuff that are useful in choosing the correct cuff size. The equipment necessary to measure BP in children 3 years of age through adolescence includes three pediatric cuffs of different sizes, and also a standard adult cuff, an oversized cuff, and a thigh cuff for leg BP measurements. The last two cuffs may be needed for obese adolescents.

Measurement of BP in children should be performed in a quiet and comfortable room after 3–5 min of rest. With the exception of acute illness, the BP should be measured with the child seated. The arm with the BP cuff should be supported at heart level. The child's feet should be on the floor while the BP is measured, rather than dangling from an examination table. Over-inflation of the cuff should be avoided because of discomfort, particularly in younger children. The BP should be measured and recorded at least twice.

Systolic BP is determined by the onset of the auscultated pulsation or first Korotkoff sound. The disappearance of Korotkoff sounds or fifth Korotkoff sound (K5) is the definition of diastolic pressure in adults. In children, particularly preadolescents, a difference of several millimeters of mercury is frequently present between the fourth Korotkoff sound, the muffling of Korotkoff sounds (K4), and K5 [13]. Normative BP data in children indicate that K5 can be used as the measure of diastolic BP in both children and adults [1].

The measured BP level in a child is interpreted by determining if the BP level is within the normal level (<90th percentile) or elevated for age (≥90th percentile). Precise interpretation requires plotting the BP on the pediatric BP tables according to the child's height percentile, age, and gender. Table 64.1 provides the systolic and diastolic BP levels for the 50th, 90th, 95th, and 99th percentile according to age (rows) and height percentile (columns) in boys. Table 64.2 provides the BP levels at each percentiles for age and height in girls. These tables can also be accessed at www.nhlbi.nih.gov/guidelines/hypertension/child_tbl.htm.

The child's height is measured and plotted on a standard growth curve. The height percentile is used in the tables, and the child's BP is compared with the BP level for the 90th, 95th, and 99th percentile at the child's age, gender, and height percentile. This process is cumbersome in a busy clinical setting. For practical purposes, BP measurements of 120/80 mmHg in adolescents and of 110/70 mmHg in children are considered "high-risk" BP in the young, and require a closer look at the BP tables.

An elevated BP level in a child or adolescent must be confirmed on repeated visits before confirming a diagnosis of hypertension or prehypertension. A more accurate characterization of an individual's BP level is an average of multiple BP measurements taken for weeks or months. A notable exception to this general guideline is if the child is symptomatic or has profoundly elevated BP. With their availability and convenience, automated devices for BP measurement are being used more frequently. Automated devices are acceptable for BP measurement in newborn and young infants in whom auscultation is difficult, and in intensive care units where frequent BP measurement is necessary. The reliability of these instruments in an ambulatory clinical setting is less clear because they need frequent calibration and established reference standards are lacking. When an elevated BP measurement is obtained using an automated device, the BP measurement should be repeated by auscultation to verify the measurements.

Table 64.1 Blood pressure (BP) levels for boys by age and height percentile.

Age (years)	BP percentile	Systolic BP (mmHg)							Diastolic BP (mmHg)						
		Percentile of height							Percentile of height						
		5th	10th	25th	50th	75th	90th	95th	5th	10th	25th	50th	75th	90th	95th
1	50th	80	81	83	85	87	88	89	34	35	36	37	38	39	39
	90th	94	95	97	99	100	102	103	49	50	51	52	53	53	54
	95th	98	99	101	103	104	106	106	54	54	55	56	57	58	58
	99th	105	106	108	110	112	113	114	61	62	63	64	65	66	66
2	50th	84	85	87	88	90	92	92	39	40	41	42	43	44	44
	90th	97	99	100	102	104	105	106	54	55	56	57	58	58	59
	95th	101	102	104	106	108	109	110	59	59	60	61	62	63	63
	99th	109	110	111	113	115	117	117	66	67	68	69	70	71	71
3	50th	86	87	89	91	93	94	95	44	44	45	46	47	48	48
	90th	100	101	103	105	107	108	109	59	59	60	61	62	63	63
	95th	104	105	107	109	110	112	113	63	63	64	65	66	67	67
	99th	111	112	114	116	118	119	120	71	71	72	73	74	75	75
4	50th	88	89	91	93	95	96	97	47	48	49	50	51	51	52
	90th	102	103	105	107	109	110	111	62	63	64	65	66	66	67
	95th	106	107	109	111	112	114	115	66	67	68	69	70	71	71
	99th	113	114	116	118	120	121	122	74	75	76	77	78	78	79
5	50th	90	91	93	95	96	98	98	50	51	52	53	54	55	55
	90th	104	105	106	108	110	111	112	65	66	67	68	69	69	70
	95th	108	109	110	112	114	115	116	69	70	71	72	73	74	74
	99th	115	116	118	120	121	123	123	77	78	79	80	81	81	82
6	50th	91	92	94	96	98	99	100	53	53	54	55	56	57	57
	90th	105	106	108	110	111	113	113	68	68	69	70	71	72	72
	95th	109	110	112	114	115	117	117	72	72	73	74	75	76	76
	99th	116	117	119	121	123	124	125	80	80	81	82	83	84	84
7	50th	92	94	95	97	99	100	101	55	55	56	57	58	59	59
	90th	106	107	109	111	113	114	115	70	70	71	72	73	74	74
	95th	110	111	113	115	117	118	119	74	74	75	76	77	78	78
	99th	117	118	120	122	124	125	126	82	82	83	84	85	86	86
8	50th	94	95	97	99	100	102	102	56	57	58	59	60	60	61
	90th	107	109	110	112	114	115	116	71	72	72	73	74	75	76
	95th	111	112	114	116	118	119	120	75	76	77	78	79	79	80
	99th	119	120	122	123	125	127	127	83	84	85	86	87	87	88
9	50th	95	96	98	100	102	103	104	57	58	59	60	61	61	62
	90th	109	110	112	114	115	117	118	72	73	74	75	76	76	77
	95th	113	114	116	118	119	121	121	76	77	78	79	80	81	81
	99th	120	121	123	125	127	128	129	84	85	86	87	88	88	89
10	50th	97	98	100	102	103	105	106	58	59	60	61	61	62	63
	90th	111	112	114	115	117	119	119	73	73	74	75	76	77	78
	95th	115	116	117	119	121	122	123	77	78	79	80	81	81	82
	99th	122	123	125	127	128	130	130	85	86	86	88	88	89	90
11	50th	99	100	102	104	105	107	107	59	59	60	61	62	63	63
	90th	113	114	115	117	119	120	121	74	74	75	76	77	78	78
	95th	117	118	119	121	123	124	125	78	78	79	80	81	82	82
	99th	124	125	127	129	130	132	132	86	86	87	88	89	90	90
12	50th	101	102	104	106	108	109	110	59	60	61	62	63	63	64
	90th	115	116	118	120	121	123	123	74	75	75	76	77	78	79
	95th	119	120	122	123	125	127	127	78	79	80	81	82	82	83
	99th	126	127	129	131	133	134	135	86	87	88	89	90	90	91

Table 64.1 (cont'd)

Age (years)	BP percentile	Systolic BP (mmHg)							Diastolic BP (mmHg)						
		Percentile of height							Percentile of height						
		5th	10th	25th	50th	75th	90th	95th	5th	10th	25th	50th	75th	90th	95th
13	50th	104	105	106	108	110	111	112	60	60	61	62	63	64	64
	90th	117	118	120	122	124	125	126	75	75	76	77	78	79	79
	95th	121	122	124	126	128	129	130	79	79	80	81	82	83	83
	99th	128	130	131	133	135	136	137	87	87	88	89	90	91	91
14	50th	106	107	109	111	113	114	115	60	61	62	63	64	65	65
	90th	120	121	123	125	126	128	128	75	76	77	78	79	79	80
	95th	124	125	127	128	130	132	132	80	80	81	82	83	84	84
	99th	131	132	134	136	138	139	140	87	88	89	90	91	92	92
15	50th	109	110	112	113	115	117	117	61	62	63	64	65	66	66
	90th	122	124	125	127	129	130	131	76	77	78	79	80	80	81
	95th	126	127	129	131	133	134	135	81	81	82	83	84	85	85
	99th	134	135	136	138	140	142	142	88	89	90	91	92	93	93
16	50th	111	112	114	116	118	119	120	63	63	64	65	66	67	67
	90th	125	126	128	130	131	133	134	78	78	79	80	81	82	82
	95th	129	130	132	134	135	137	137	82	83	83	84	85	86	87
	99th	136	137	139	141	143	144	145	90	90	91	92	93	94	94
17	50th	114	115	116	118	120	121	122	65	66	66	67	68	69	70
	90th	127	128	130	132	134	135	136	80	80	81	82	83	84	84
	95th	131	132	134	136	138	139	140	84	85	86	87	87	88	89
	99th	139	140	141	143	145	146	147	92	93	93	94	95	96	97

Reproduced from the National Guidelines on High Blood Pressure in Children and Adolescents NIH website www.nhlbi.nih.gov?guidelines/hypertension/child_tbl.htm

Ambulatory BP monitoring (ABPM) for 24h has become increasingly used in evaluating adults with hypertension, and is being applied to older children and adolescents. Some population standards for ambulatory BP values in children and adolescents are available [14] and this information can be helpful [15]. For example, ABPM can be used to identify white coat hypertension and masked hypertension. White coat hypertension is defined as average BP (systolic and diastolic BP) <95th percentile on ABPM despite BP measurements >95th percentile in a physician's office or other clinical setting. Masked hypertension is the reverse, with average systolic or diastolic BP >95th percentile on ABPM but with office or clinic BP measurements <95th percentile. ABPM is also useful in determining the need for and effectiveness of pharmacologic therapy. When ABPM is used in children or adolescents, the appropriate cuff size should be used.

Causes of hypertension in the young

Secondary hypertension
Secondary hypertension from underlying renal or endocrine disorders is found more frequently during childhood than in adults. Secondary hypertension is generally characterized by marked elevations in BP. Before the development of normative data on BP levels in children, BP was measured infrequently. When elevated BP was detected in children, the hypertension was, by current standards, fairly severe, and led to the belief that hypertension in children was *always* secondary. This concept has now changed, largely from a better understanding of normal levels of BP in the young and the practice of regularly measuring the BP in children as part of health assessment and maintenance.

The prevalence of secondary hypertension in the young varies according to the age and severity of hypertension. In a series of children, an identifiable secondary cause for hypertension was found in 90% of children <10 years of age, and only 10% were considered to have primary hypertension [16]. In another series including both children and adolescents with hypertension, an underlying cause of the hypertension was identified in 65% of the adolescents, with 35% thought to have primary hypertension [17].

The age of the child and severity of BP elevation are helpful in distinguishing secondary from primary hypertension. Children <12 years of age with sustained hypertension are more likely to have a secondary cause. The degree of hyperten-

Table 64.2 Blood pressure (BP) levels for girls by age and height percentile.

Age (years)	BP percentile	Systolic BP (mmHg)							Diastolic BP (mmHg)						
		Percentile of height							Percentile of height						
		5th	10th	25th	50th	75th	90th	95th	5th	10th	25th	50th	75th	90th	95th
1	50th	83	84	85	86	88	89	90	38	39	39	40	41	41	42
	90th	97	97	98	100	101	102	103	52	53	53	54	55	55	56
	95th	100	101	102	104	105	106	107	56	57	57	58	59	59	60
	99th	108	108	109	111	112	113	114	64	64	65	65	66	67	67
2	50th	85	85	87	88	89	91	91	43	44	44	45	46	46	47
	90th	98	99	100	101	103	104	105	57	58	58	59	60	61	61
	95th	102	103	104	105	107	108	109	61	62	62	63	64	65	65
	99th	109	110	111	112	114	115	116	69	69	70	70	71	72	72
3	50th	86	87	88	89	91	92	93	47	48	48	49	50	50	51
	90th	100	100	102	103	104	106	106	61	62	62	63	64	64	65
	95th	104	104	105	107	108	109	110	65	66	66	67	68	68	69
	99th	111	111	113	114	115	116	117	73	73	74	74	75	76	76
4	50th	88	88	90	91	92	94	94	50	50	51	52	52	53	54
	90th	101	102	103	104	106	107	108	64	64	65	66	67	67	68
	95th	105	106	107	108	110	111	112	68	68	69	70	71	71	72
	99th	112	113	114	115	117	118	119	76	76	76	77	78	79	79
5	50th	89	90	91	93	94	95	96	52	53	53	54	55	55	56
	90th	103	103	105	106	107	109	109	66	67	67	68	69	69	70
	95th	107	107	108	110	111	112	113	70	71	71	72	73	73	74
	99th	114	114	116	117	118	120	120	78	78	79	79	80	81	81
6	50th	91	92	93	94	96	97	98	54	54	55	56	56	57	58
	90th	104	105	106	108	109	110	111	68	68	69	70	70	71	72
	95th	108	109	110	111	113	114	115	72	72	73	74	74	75	76
	99th	115	116	117	119	120	121	122	80	80	80	81	82	83	83
7	50th	93	93	95	96	97	99	99	55	56	56	57	58	58	59
	90th	106	107	108	109	111	112	113	69	70	70	71	72	72	73
	95th	110	111	112	113	115	116	116	73	74	74	75	76	76	77
	99th	117	118	119	120	122	123	124	81	81	82	82	83	84	84
8	50th	95	95	96	98	99	100	101	57	57	57	58	59	60	60
	90th	108	109	110	111	113	114	114	71	71	71	72	73	74	74
	95th	112	112	114	115	116	118	118	75	75	75	76	77	78	78
	99th	119	120	121	122	123	125	125	82	82	83	83	84	85	86
9	50th	96	97	98	100	101	102	103	58	58	58	59	60	61	61
	90th	110	110	112	113	114	116	116	72	72	72	73	74	75	75
	95th	114	114	115	117	118	119	120	76	76	76	77	78	79	79
	99th	121	121	123	124	125	127	127	83	83	84	84	85	86	87
10	50th	98	99	100	102	103	104	105	59	59	59	60	61	62	62
	90th	112	112	114	115	116	118	118	73	73	73	74	75	76	76
	95th	116	116	117	119	120	121	122	77	77	77	78	79	80	80
	99th	123	123	125	126	127	129	129	84	84	85	86	86	87	88
11	50th	100	101	102	103	105	106	107	60	60	60	61	62	63	63
	90th	114	114	116	117	118	119	120	74	74	74	75	76	77	77
	95th	118	118	119	121	122	123	124	78	78	78	79	80	81	81
	99th	125	125	126	128	129	130	131	85	85	86	87	87	88	89
12	50th	102	103	104	105	107	108	109	61	61	61	62	63	64	64
	90th	116	116	117	119	120	121	122	75	75	75	76	77	78	78
	95th	119	120	121	123	124	125	126	79	79	79	80	81	82	82
	99th	127	127	128	130	131	132	133	86	86	87	88	88	89	90

Table 64.2 (cont'd)

Age (years)	BP percentile	Systolic BP (mmHg)							Diastolic BP (mmHg)						
		Percentile of height							Percentile of height						
		5th	10th	25th	50th	75th	90th	95th	5th	10th	25th	50th	75th	90th	95th
13	50th	104	105	106	107	109	110	110	62	62	62	63	64	65	65
	90th	117	118	119	121	122	123	124	76	76	76	77	78	79	79
	95th	121	122	123	124	126	127	128	80	80	80	81	82	83	83
	99th	128	129	130	132	133	134	135	87	87	88	89	89	90	91
14	50th	106	106	107	109	110	111	112	63	63	63	64	65	66	66
	90th	119	120	121	122	124	125	125	77	77	77	78	79	80	80
	95th	123	123	125	126	127	129	129	81	81	81	82	83	84	84
	99th	130	131	132	133	135	136	136	88	88	89	90	90	91	92
15	50th	107	108	109	110	111	113	113	64	64	64	65	66	67	67
	90th	120	121	122	123	125	126	127	78	78	78	79	80	81	81
	95th	124	125	126	127	129	130	131	82	82	82	83	84	85	85
	99th	131	132	133	134	136	137	138	89	89	90	91	91	92	93
16	50th	108	108	110	111	112	114	114	64	64	65	66	66	67	68
	90th	121	122	123	124	126	127	128	78	78	79	80	81	81	82
	95th	125	126	127	128	130	131	132	82	82	83	84	85	85	86
	99th	132	133	134	135	137	138	139	90	90	90	91	92	93	93
17	50th	108	109	110	111	113	114	115	64	65	65	66	67	67	68
	90th	122	122	123	125	126	127	128	78	79	79	80	81	81	82
	95th	125	126	127	129	130	131	132	82	83	83	84	85	85	86
	99th	133	133	134	136	137	138	139	90	90	91	91	92	93	93

Reproduced from the National Guidelines on High Blood Pressure in Children and Adolescents NIH website www.nhlbi.nih.gov?guidelines/hypertension/child_tbl.htm

sion is an important clue, as severe BP elevation in a young child is most likely due to an underlying abnormality. Children and adolescents with Stage 2 hypertension should be carefully evaluated for both possible cause of the hypertension and evidence of target organ damage. Although the list of conditions that can cause hypertension in the young is fairly long, the majority of the identifiable causes of hypertension in the young are related to renal disorders. Table 64.3 provides a list of underlying causes for chronic hypertension in the young, and the conditions associated with acute hypertension in the young.

Hypertension is uncommon in healthy newborn infants; however, certain conditions increase the risk for hypertension. Neonates with an umbilical artery catheter have heightened risk for thromboembolic events [18]. Low birth weight infants, with respiratory distress syndrome, who later develop bronchopulmonary dysplasia are at risk for hypertension. These infants frequently require chronic corticosteroid therapy with resulting sodium retention [19]. The most commonly identified causes of hypertension in newborn infants are renal artery thrombosis, renal artery stenosis, congenital renal malformations, patent ductus arteriosus, coarctation of the aorta, and bronchopulmonary dysplasia [20]. Infants who have been treated with the extracorporeal membrane oxygenation

procedure have also been observed to develop hypertension. In some critically ill newborn infants with hypertension, an underlying cause may not be identified. Regardless of whether a cause for the hypertension is determined, BP control and monitoring in these infants are important.

For children <10 years of age, the leading causes of secondary hypertension are renal parenchymal diseases, coarctation of the aorta, and renal artery stenosis. Coarctation of the aorta can be missed in infants and toddlers, and should be considered in an asymptomatic hypertensive child [21]. In later childhood, essential hypertension can also be detected. Causes of acute hypertension include post-infectious glomerulonephritis and hemolytic uremic syndrome. Some disorders, such as hemolytic uremic syndrome, may lead to permanent renal scarring that causes chronic hypertension.

Among hypertensive adolescents, primary (essential) hypertension occurs more frequently than secondary hypertension. The most frequent secondary causes of hypertension are renal parenchymal diseases, such as chronic pyelonephritis, and various types of chronic glomerulonephritis, such as focal segmental glomerulosclerosis, and IgA nephropathy. Adolescent behaviors that may contribute to high BP are illicit substance use, especially cocaine and amphetamine-related

Table 64.3 Secondary causes of hypertension.

Chronic hypertension

Renal	*Drugs*
Chronic glomerulonephritis	Corticosteroids
Interstitial nephritis	Alcohol
Collagen vascular diseases	Appetite suppressants
Reflux nephropathy	Anabolic steroids
Polycystic kidney disease	Oral contraceptives
Medullary cystic disease	Nicotine
Hydronephrosis	
Hypoplastic/dysplastic kidney	*Syndromes*
	Alport syndrome
Cardiac and vascular	Williams (renovascular lesions)
Coarctation of aorta	Turner (coarctation or renovascular)
Renal artery stenosis	Tuberous sclerosis (cystic renal)
Takayasu arteritis	Neurofibromatosis (renovascular)
	Adrenogenital syndromes
Endocrine	Liddle syndrome
Hyperthyroidism	
Pheochromocytoma	
Primary aldosteronism	

Acute hypertension

Renal	*Drugs*
Post infectious glomerulonephritis	Cocaine
Schönlein–Henoch purpura	Phencyclidine
Hemolytic uremic syndrome	Amphetamines
Acute tubular necrosis	Jimson weed
Vascular	*Miscellaneous*
Renal or renal vascular trauma	Burns
	Orthopedic surgery
Neurogenic	Urologic surgery
Increased intracranial pressure	
Guillain–Barré syndrome	

compounds. Other substances associated with high BP in adolescents include appetite suppressants (both prescription and over-the-counter remedies), oral contraceptives, excessive alcohol intake, and the use of anabolic steroids for body building [22].

Primary hypertension

Primary, or essential, hypertension classically has been considered a disorder of older adults. The concept that essential hypertension has its roots in childhood can be inferred from BP tracking data, which demonstrate that children with elevated BP continue to have elevated BPs as adults [1]. Risk factors associated with hypertension in adults, such as overweight and a positive family history of hypertension or cardiovascular disease, may be present in children with high BP. Although the combination of higher BP level for age and typical risk factors was thought to indicate risk for future hypertension, more recent reports indicate that this condition is more than just a risk for future problems. Using echocardiographic measures of cardiac mass adjusted for body size and appropriate childhood reference values for cardiac structure, left ventricular hypertrophy (LVH) has been reported in 30–40% of children and adolescents with hypertension [23,24]. Longitudinal data demonstrate a direct link between risk factors in childhood, including BP levels, with intermediate measures of target organ injury including greater intima–media thickness of carotid arteries [25] and vascular stiffness [26]. With this emerging evidence on the consequences of elevated BP in the young, primary hypertension in childhood can be considered the early phase of a chronic disease.

Primary hypertension in children and adolescents is associated with several clinical characteristics or associated risk factors. The degree of BP elevation is generally mild, ~95th percentile, and there is often considerable variability in BP over time. A consistent observation in children exhibiting mild essential hypertension is a positive history of hypertension in parents and/or grandparents [27,28].

Excess body weight has an effect on BP in both children and adults, and BP is higher in both overweight and obese children and adolescents [29,30]. Primary hypertension in childhood is frequently associated with obesity, which appears to be a contributory factor as even a modest reduction in excess adiposity is associated with a reduction in BP [31,32]. The cluster of mild BP elevation, a positive family history of hypertension, and obesity is a typical pattern in children and adolescents with essential hypertension [33].

The prevalence of childhood obesity has markedly increased both in the United States [34] and worldwide [35]. Data from the National Health and Nutrition Examination Survey (NHANES) indicate that as of 2004 the prevalence of obesity had increased to 17.4% among boys and to 17.8% among girls [36]. An analysis of two separate sets of data from NHANES demonstrates a statistically significant increase in childhood BP levels. The increase in BPs is largely due to the concurrent increase in obesity [37].

Among adult patients with cardiovascular disease, there is an overlap of hypertension, non-insulin-dependent diabetes mellitus, atherosclerosis, and obesity, a constellation described as the insulin-resistance syndrome or the metabolic syndrome [38]. The metabolic syndrome is clinically defined by a cluster of risk factors including abdominal obesity, abnormal glucose tolerance, dyslipidemia, and high BP. Adults with the metabolic syndrome are at increased risk for developing diabetes and cardiovascular events. Children also can exhibit characteristics of the metabolic syndrome [39]. The rates of metabolic syndrome among adolescents have increased in the past two decades, concurrent with the increases in rates of obesity and hypertension [40,41]. The characteristics of the metabolic syndrome are also congruent with the overweight child having a strong family history of hypertension or early heart disease. These children often have high BP [42]. Although these children are not at risk for immediate adverse effects of the higher than normal BP, they are at increased risk for premature cardiovascular disease.

Multiple factors, including both genetic and environmental factors, contribute to the origin, onset, and progression of primary hypertension. Barker *et al*. [43] proposed an alternative causative factor for primary hypertension based on historical data indicating an association of hypertension and ischemic heart disease in adult men who had low birth weights. They proposed that lower birth weight is a consequence of an altered or impaired intrauterine nutritional environment. Impaired fetal growth is indicative of alterations in organ growth which may affect organ function later in life [43,44]. Higher BP is the putative link between compromised intrauterine growth and the long-term risk for cardiovascular disease [43]. The low birth weight hypothesis is supported to some extent by experimental laboratory studies and population data [45]. However, the concept conflicts with the body of data in both childhood and adulthood, which consistently demonstrate a direct relationship between body weight and BP, and with data demonstrating BP tracking from childhood to young adulthood [46–48]. When reports on the association of birth weight with future BP are examined in a meta-analysis, the effect of birth weight on future BP is in the range of a 1–3 mmHg BP reduction for each 1 kg increase in birth weight [49]. Low birth weight appears to be linked with later overweight or obesity, and when the adolescent or adult weight is considered in analyses of population data, the birth weight effect is damped [50]. Although the population effect of low birth weight appears small, low birth weight can be another factor that increases risk for later obesity and high BP [51].

Evaluating hypertension in children and adolescents

A medical evaluation is needed for a child or adolescent with sustained hypertension, verified by repeated BP measurements ≥95th percentile. The extent of the diagnostic evaluation is determined by the suspected type of hypertension. When a secondary cause is considered, as in a young patient or one with severe hypertension, a more extensive evaluation may be necessary. On the other hand, if the elevated BP is more likely an early expression of primary hypertension, a few diagnostic screening studies may be sufficient. Currently, the recommendations for assessment of hypertension in children include evaluation for (1) an identifiable cause, (2) co-morbidity, and (3) target organ damage [1].

The medical history and physical examination are keys in determining whether the patient's presentation indicates primary hypertension or reflects a secondary, and potentially correctable, cause. Secondary causes should be suspected in any child who is hypertensive and is not growing normally, has a sudden onset of elevated BP, and has no positive family history of hypertension.

Another set of findings characterizes children and adolescents with essential (primary) hypertension: slight to mild elevations in BP, a strong family history of essential hypertension, elevated resting heart rate, variable BP readings upon repeated measurement, and obesity. If no other abnormalities are found on history or physical examination, these children require less extensive evaluation for an underlying disorder than those in whom secondary causes are suspected. Alternatively, the children with early expression of essential hypertension, particularly if obese, may have associated co-morbidities that include dyslipidemia, sleep apnea, and impaired fasting glucose.

Medical history
The family history of cardiovascular disease is very important. In both first- and second-degree relatives, the family history of hypertension, myocardial infarction, stroke, renal disease, diabetes, and obesity should be obtained. It can be relevant to the diagnosis in a hypertensive child if relatives had an onset at an early age of any of these conditions. A family history of genetically determined conditions that have hypertension as a component such as polycystic kidney disease and neurofibromatosis should be sought. Another familial disorder with hypertension is glucocorticoid-remediable aldosteronism, an autosomal dominant condition, which should be considered when multiple family members have early-onset hypertension associated with hypokalemia or stroke [52].

Past medical history can be pertinent. For example, with a history of urinary tract infections, there may be associated reflux nephropathy, renal scarring, and resultant hypertension. A history should be obtained of medications and over-the-counter products, including oral contraceptives and decongestants. Information should be obtained about health-related behaviors such as usual diet, amount of physical activity, and athletic participation. Other adverse adolescent lifestyles to consider are use of "street" drugs, smokeless tobacco, cigarettes, diet aids, ethanol, and anabolic steroids.

Physical examination
The child's general growth rate and growth pattern should be assessed, including weight gain or weight loss. Weight, height, and body mass index (BMI) should be plotted according to age and gender on the child growth charts. Growth abnormalities associated with hypertension can be seen with chronic renal disease, hyperthyroidism (causing primarily systolic hypertension), pheochromocytoma, adrenal disorders, or certain genetic abnormalities such as Turner syndrome.

To rule out coarctation of the aorta, the evaluation should include upper- and lower-extremity BP measurements taken with appropriately sized cuffs. Normally the leg BP levels are slightly higher than the arm BP levels. A child with coarctation will have systolic hypertension in an upper extremity, sometimes absent or decreased femoral pulses, and a BP

differential of >10 mmHg between the upper and lower extremities [21].

Other physical clues may suggest a secondary etiology for hypertension. Abnormal facies or dysmorphic features may suggest a syndrome associated with specific lesions causing hypertension. Examples are Turner and Williams syndromes, which have renovascular or cardiac lesions that cause hypertension. Renal vascular lesions may sometimes have an audible abdominal bruit detectable by auscultation of the abdomen. Skin lesions are sometimes the first manifestations of disorders such as tuberous sclerosis and systemic lupus erythematosus. Acanthosis nigricans in overweight children may be a sign of abnormal glucose tolerance, and can occur in children or adolescents with metabolic syndrome.

Diagnostic testing

When the history and physical examination provide clues for a specific underlying cause for the hypertension, testing should be directed to the area of clinical suspicion. In the absence of clues, however, underlying renal disease should be considered because chronic kidney disease is the most frequent cause of secondary hypertension in the pediatric population. The initial studies to screen for renal abnormalities include a urinalysis, electrolytes, creatinine, complete blood count, urine culture, and renal ultrasound. An evaluation for "co-morbidity" or other associated risk factors includes measurement of fasting plasma lipids for dyslipidemia, a sleep history to screen for sleep apnea, and if there is a positive family history of diabetes or acanthrosis nigricans on physical examination, additional testing of glucose tolerance may be indicated.

The other component of the evaluation includes assessing target organ injury. Target-organ injury provides a measure of chronicity and severity (characteristics sometimes difficult to ascertain from the history) and aid in deciding whether pharmacologic therapy should be instituted. Left ventricular hypertrophy (LVH) is an independent risk factor for cardiovascular morbidity and mortality in adults, and is considered to be the most prominent clinical evidence of target organ damage resulting from hypertension during childhood and adolescence [1]. Echocardiography is a sensitive means to detect and determine whether the child is developing LVH. Chest X-ray and electrocardiogram (ECG) are much less sensitive measures of LVH in children. In children, the echocardiographic measurements of left ventricular mass (LVM) should be indexed to height (in meters) to the power of 2.7 ($m^{2.7}$). Left ventricular mass index (LVMI, $LVM/m^{2.7}$) >51 g is a criterion for LVH in older children, adolescents and adults [1]. The proportion of hypertensive children and adolescents with this definition of LVH is small (<10%). However, when LVH is based on the LVM distribution in normal children, the prevalence of LVH in hypertensive children is higher. A cross-sectional study of 130 patients, ranging in age from 6 to 23 years, with persistent BP elevation >90th percentile for an average of 2 years reported that only 45% of the patients had a LVMI <90th percentile. Nineteen patients (14%) had an LVMI >99th percentile. Among those with LVMI >95th percentile, 17% had concentric hypertrophy and 30% had eccentric hypertrophy. When LVH was defined as LVMI ≥95th percentile, LVH was most frequent among overweight males [23]. Male gender and BMI also predicted LVMI in a recent report on children with high BP and chronic kidney disease[53].

Obesity may also contribute to the development of LVH in children with high BP. An analysis of longitudinal data from the Bogalusa Heart Study has shown that higher LVM in young adulthood is predicted by higher BP and adiposity in childhood [54].

Evidence for other sites of target organ damage in children with high BP is beginning to emerge. Data from a population study on healthy children show a significant association of higher BP with a reduced retinal diameter [55], so that an ophthalmologic examination can be helpful. Subtle changes in cognitive function among children with hypertension have been reported. These findings have been in measures of executive function such as problem solving and decision making [56,57]. There is also some evidence of increasing urinary albumin excretion, suggestive of possible renal injury, in children with high BP and other risk factors [58,59]. The clinical usefulness of other measures of target organ damage in evaluating individual pediatric patients requires additional investigation.

The remainder of the evaluation should be directed by specific findings on history, physical examination, and results of initial screening studies. An algorithm for evaluating hypertension in the young is provided in Figure 64.1. The algorithm indicates steps in evaluating and managing hypertension in children according to the severity of the hypertension, and the presence or absence of obesity.

Treatment of hypertension in children and adolescents

Health-related behavior changes in diet, physical activity, and weight control improve BP control in adults. Children may also benefit from these lifestyle changes. Children and adolescents with Stage 1 or mild elevation of BP, and without target organ damage, should begin treatment with non-pharmacologic interventions, including weight reduction or control (if overweight), exercise, and diet modifications. Children with secondary hypertension commonly require more intensive management, including treatment with antihypertensive medication [60].

Obesity is often associated with mild hypertension in childhood and weight reduction has benefit. Exercise training lowers BP in older children and adolescents [61] but,
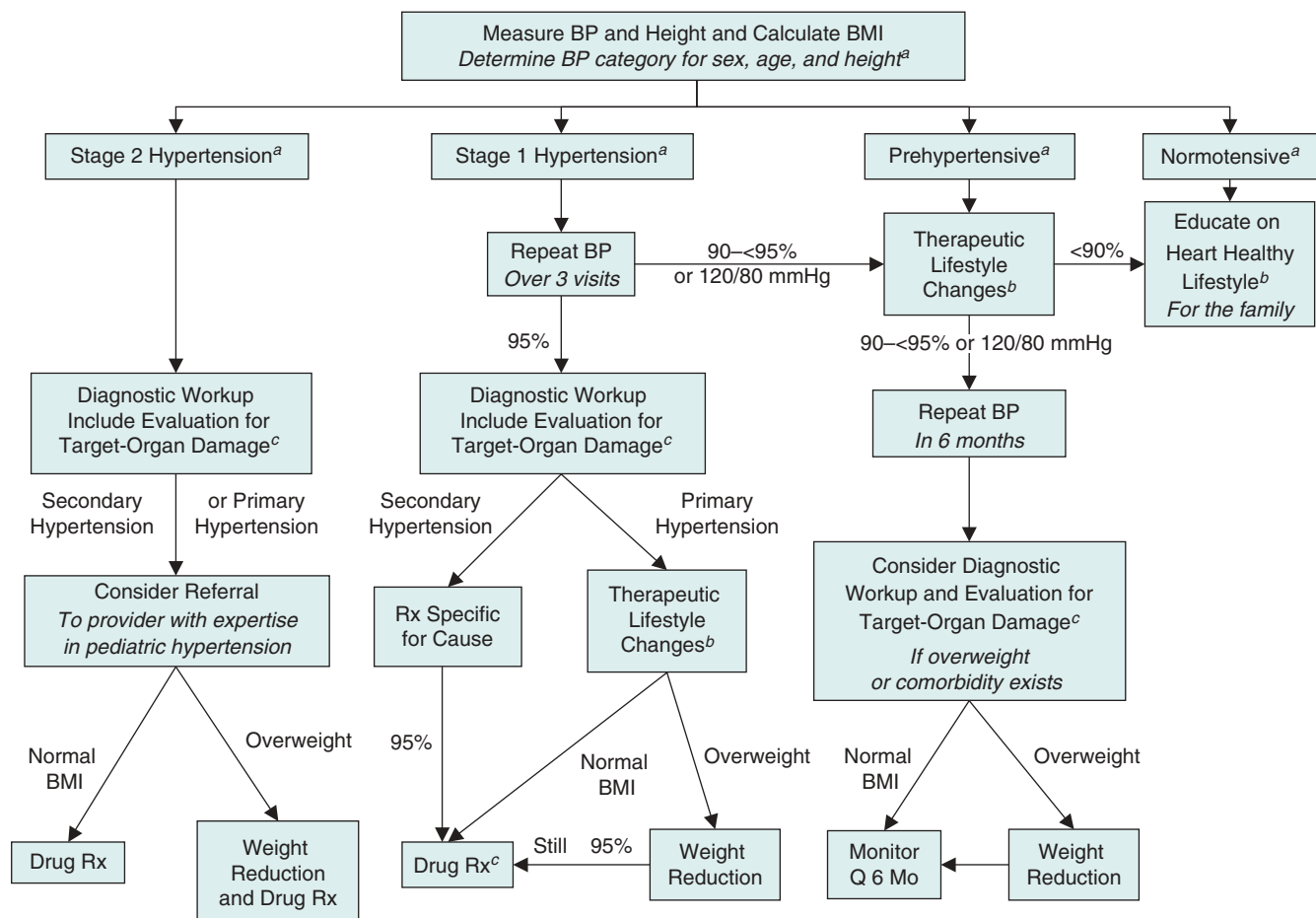
Figure 64.1 An algorithm is provided to guide the evaluation and management of prehypertension, Stage 1 hypertension, and Stage 2 hypertension. [a]See Tables 64.1 and 64.2 for blood pressure classification. [b]Diet modification and physical activity. [c]Children and adolescents with Stage 1 and Stage 2 hypertension should receive an echocardiogram to evaluate for target organ damage. Also consider in children with diabetes or other risk factors.

unless highly motivated, is difficult to sustain in both children and adults. Weight reduction can be extremely difficult to achieve and generally requires multiple strategies, including nutritional counseling, dietary education, emotional support, information about exercise, and family involvement. Power weight-lifting should be discouraged in hypertensive adolescents due to its potential to induce marked BP elevation. Participation in sports should be encouraged provided that BP is under reasonable control, regular monitoring of BP occurs, and a thorough examination has excluded cardiac abnormalities [22].

The guidelines for dietary modifications in the pediatric population are less clear than in adults. Information on the effects of salt on BP in children is not as definitive as in adults. A meta-analysis of 10 separate studies that investigated the effect of a change in sodium intake on BP in children found that a 54% reduction in sodium intake was associated with a 2.47 mmHg reduction in systolic BP [62,63]. Although the individual effect of lowering sodium intake on BP in children

appeared modest, the lifelong effect could be more substantial. Another effect of high dietary salt is thirst. In a study that compared sodium intake with the amount and type of beverage consumption in children, a high intake of sugary beverages was associated with high sodium intake [64]. There seems to be a subset of adolescents, particularly if obese, who demonstrate BP sensitivity to salt and also other risk factors for hypertension [65]. Because the usual dietary intake of sodium for most children and adolescents in the United States far exceeds nutrient requirements, it is reasonable to restrict sodium intake to <4 g day^{-1} by decreasing fast-food consumption and refraining from adding salt to cooked foods [1].

Current information on the effects of potassium, magnesium, and calcium intake on BP in children is even less definitive. The dietary intervention clinical trial Dietary Approaches to Stop Hypertension (DASH), conducted in adults with high BP, reported results that could be relevant to dietary management of children with high BP. In adults

Table 64.4 Antihypertensive drugs for outpatient management of hypertension in children 1–17 years old[a].

Class	Drug	Dose[b]	Dosing interval	Evidence[c]	FDA labeling[d]	Comments[e]
Angiotensin-converting enzyme (ACE) inhibitor	Benazepril	Initial: 0.2 mg kg⁻¹ day⁻¹ up to 10 mg day⁻¹ Maximum: 0.6 mg kg⁻¹ day⁻¹ up to 40 mg day⁻¹	q.d.	RCT	Yes	1. All ACE inhibitors are contraindicated in pregnancy – females of childbearing age should use reliable contraception
	Captopril	Initial: 0.3–0.5 mg kg⁻¹ per dose Maximum: 6 mg kg⁻¹ day⁻¹	t.i.d.	RCT, CS	No	2. Check serum potassium and creatinine periodically to monitor for hyperkalemia and azotemia
	Enalapril	Initial: 0.08 mg kg⁻¹ day⁻¹ up to 5 mg day⁻¹ Maximum: 0.6 mg kg⁻¹ day⁻¹ up to 40 mg day⁻¹	q.d.–b.i.d.	RCT	Yes	3. Cough and angioedema are reportedly less common with newer members of this class than with captopril
	Fosinopril	Children: >50 kg Initial: 5–10 mg day⁻¹ Maximum: 40 mg day⁻¹	q.d.	RCT	Yes	4. Benazepril, enalapril, and lisinopril labels contain information on the preparation of a suspension; captopril may also be compounded into a suspension
	Lisinopril	Initial: 0.07 mg kg⁻¹ day⁻¹ up to 5 mg day⁻¹ Maximum: 0.6 mg kg⁻¹ day⁻¹ up to 40 mg day⁻¹	q.d.	RCT	Yes	5. FDA approval for ACE inhibitors with pediatric labeling is limited to children ≥6 years of age and to children with creatinine clearance ≥30 ml min⁻¹ per 1.73 m²
	Quinapril	Initial: 5–10 mg day⁻¹ Maximum: 80 mg day⁻¹	q.d.	RCT, EO	No	
Angiotensin-receptor blocker	Irbesartan	6–12 years: 75–150 mg day⁻¹ ≥13 years: 150–300 mg day⁻¹	q.d.	CS	Yes	1. All ARBs are contraindicated in pregnancy – females of childbearing age should use reliable contraception
	Losartan	Initial: 0.7 mg kg⁻¹ day⁻¹ up to 50 mg day⁻¹ Maximum: 1.4 mg kg⁻¹ day⁻¹ up to 100 mg day⁻¹	q.d.	RCT	Yes	2. Check serum potassium, creatinine periodically to monitor for hyperkalemia and azotemia 3. Losartan label contains information on the preparation of a suspension 4. FDA approval for ARBs is limited to children ≥6 years of age and to children with creatinine clearance ≥30 ml min⁻¹ per 1.73 m²
α- and β-blocker	Labetalol	Initial: 1–3 mg kg⁻¹ day⁻¹ Maximum: 10–12 mg kg⁻¹ day⁻¹ up to 1200 mg day⁻¹	b.i.d.	CS, EO	No	1. Asthma and overt heart failure are contraindications 2. Heart rate is dose limiting 3. May impair athletic performance 4. Should not be used in insulin-dependent diabetics
β-Blocker	Atenolol	Initial: 0.5–1 mg kg⁻¹ day⁻¹ Maximum: 2 mg kg⁻¹ day⁻¹ up to 100 mg day⁻¹	q.d.–b.i.d.	CS	No	1. Non-cardioselective agents (propranolol) are contraindicated in asthma and heart failure
	Bisoprolol/HCTZ	Initial: 2.5/6.25 mg day⁻¹ Maximum: 10/6.25 mg day⁻¹	q.d.	RCT	No	2. Heart rate is dose limiting 3. May impair athletic performance
	Metoprolol	Initial: 1–2 mg kg⁻¹ day⁻¹ Maximum: 6 mg kg⁻¹ day⁻¹ up to 200 mg day⁻¹	b.i.d.	CS	No	4. Should not be used in insulin-dependent diabetics
	Propranolol	Initial: 1–2 mg kg⁻¹ day⁻¹ Maximum: 4 mg kg⁻¹ day⁻¹ up to 640 mg day⁻¹	b.i.d.–t.i.d.	RCT, EO	Yes	5. A sustained-release formulation of propranolol is available that is dosed once daily
Calcium channel blocker	Amlodipine	Children: 6–17 years 2.5–5 mg q.d.	q.d.	RCT	Yes	1. Amlodipine and isradipine can be compounded into stable extemporaneous suspensions
	Felodipine	Initial: 2.5 mg day⁻¹ Maximum: 10 mg day⁻¹	q.d.	RCT, EO	No	2. Felodipine and extended-release nifedipine tablets must be swallowed whole
	Isradipine	Initial: 0.15–0.2 mg kg⁻¹ day⁻¹ Maximum: 0.8 mg kg⁻¹ day⁻¹ up to 20 mg day⁻¹	t.i.d.–q.i.d.	CS, EO	No	3. Isradipine is available in both immediate-release and sustained-release formulations; the sustained release form is dosed q.d. or b.i.d.
	Extended-release nifedipine	Initial: 0.25–0.5 mg kg⁻¹ day⁻¹ Maximum: 3 mg kg⁻¹ day⁻¹ up to 120 mg day⁻¹	q.d.–b.i.d.	CS, EO	No	4. May cause tachycardia

Class	Drug	Dose	Frequency	Evidence[c]	FDA-approved pediatric labeling[d]	Comments[e]
Central α-agonist	Clonidine	Children: ≥12 years Initial: 0.2 mg day^{-1} Maximum: 2.4 mg day^{-1}	b.i.d.	EO	Yes	1. May cause dry mouth and/or sedation 2. Transdermal preparation also available 3. Sudden cessation of therapy can lead to severe rebound hypertension
Diuretic	HCTZ	Initial: 1 mg kg^{-1} day^{-1} Maximum: 3 mg kg^{-1} day^{-1} up to 50 mg day^{-1}	q.d.	EO	Yes	1. All patients treated with diuretics should have electrolytes monitored shortly after initiating therapy and periodically thereafter 2. Useful as add-on therapy in patients being treated with drugs from other drug classes 3. Potassium-sparing diuretics (spironolactone, triamterene, amiloride) may cause severe hyperkalemia, especially if given with ACE inhibitors or ARBs. 4. Furosemide is labeled only for treatment of edema but may be useful as add-on therapy in children with resistant hypertension, particularly in children with renal disease. 5. Chlorthalidone may precipitate azotemia in patients with renal diseases and should be used with caution in those with severe renal impairment
	Chlorthalidone	Initial: 0.3 mg kg^{-1} day^{-1} Maximum: 2 mg kg^{-1} day^{-1} up to 50 mg day^{-1}	q.d.	EO	No	
	Furosemide	Initial: 0.5–2.0 mg kg^{-1} per dose Maximum: 6 mg kg^{-1} day^{-1}	q.d.–b.i.d.	EO	No	
	Spironolactone	Initial: 1 mg kg^{-1} day^{-1} Maximum: 3.3 mg kg^{-1} day^{-1} up to 100 mg day^{-1}	q.d.–b.i.d.	EO	No	
	Triamterene	Initial: 1–2 mg kg^{-1} day^{-1} Maximum: 3–4 mg kg^{-1} day^{-1} up to 300 mg day^{-1}	b.i.d.	EO	No	
	Amiloride	Initial: 0.4–0.625 mg kg^{-1} day^{-1} Maximum: 20 mg day^{-1}	q.d.	EO	No	
Peripheral α-antagonist	Doxazosin	Initial: 1 mg day^{-1} Maximum: 4 mg day^{-1}	q.d.	EO	No	May cause hypotension and syncope, especially after first dose
	Prazosin	Initial: 0.05–0.1 mg kg^{-1} day^{-1} Maximum: 0.5 mg kg^{-1} day^{-1}	t.i.d.	EO	No	
	Terazosin	Initial: 1 mg day^{-1} Maximum: 20 mg day^{-1}	q.d.	EO	No	
Vasodilator	Hydralazine	Initial: 0.75 mg kg^{-1} day^{-1} Maximum: 7.5 mg kg^{-1} day^{-1} up to 200 mg day^{-1}	q.i.d.	EO	Yes	1. Tachycardia and fluid retention are common side effects 2. Hydralazine can cause a lupus-like syndrome in slow acetylators 3. Prolonged use of minoxidil can cause hypertrichosis 4. Minoxidil is usually reserved for patients with hypertension resistant to multiple drugs
	Minoxidil	Children: <12 years Initial: 0.2 mg kg^{-1} day^{-1} Maximum: 50 mg day^{-1} Children: ≥12 years Initial: 5 mg day^{-1} Maximum: 100 mg day^{-1}	q.d.–t.i.d.	CS, EO	Yes	

ACE, angiotensin-converting enzyme; ARB, angiotensin-receptor blocker; HCTZ, hydrochlorothiazide; q.d., once daily; b.i.d., twice daily; t.i.d., three times daily; q.i.d., four times daily.

[a]Includes drugs with prior pediatric experience or recently completed clinical trials.

[b]The maximum recommended adult dose should not be exceeded in routine clinical practice.

[c]Level of evidence upon which dosing recommendations are based (CS, case series; EO, expert opinion; RCT, randomized controlled trial).

[d]FDA-approved pediatric labeling information is available. Recommended doses for agents with FDA-approved pediatric labels are the doses contained in the approved labels. Even when pediatric labeling information is not available, the FDA-approved label should be consulted for additional safety information.

[e]Comments apply to all members of each drug class except where stated otherwise.

Table 64.5 Antihypertensive drugs for management of severe hypertension in children 1–17 years old.

Drug	Class	Dose[a]	Route	Comments
Most useful[b]				
Esmolol	β-Blocker	100–500 µg kg⁻¹ min⁻¹	i.v. infusion	Very short-acting – constant infusion preferred. May cause profound bradycardia. Produced modest reductions in BP in a pediatric clinical trial
Hydralazine	Vasodilator	0.2–0.6 mg kg⁻¹ per dose	i.v., i.m.	Should be given every 4 h when given i.v. bolus. Recommended dose is lower than FDA label
Labetalol	α- and β-blocker	Bolus: 0.2–1.0 mg kg⁻¹ per dose up to 40 mg per dose Infusion: 0.25–3.0 mg kg⁻¹ h⁻¹	i.v. bolus or infusion	Asthma and overt heart failure are relative contraindications
Nicardipine	Calcium channel blocker	1–3 µg kg⁻¹ min⁻¹	i.v. infusion	May cause reflex tachycardia
Sodium nitroprusside	Vasodilator	0.53–10 µg kg⁻¹ min⁻¹	i.v. infusion	Monitor cyanide levels with prolonged (>72 h) use or in renal failure; or co-administer with sodium thiosulfate
Occasionally useful[c]				
Clonidine	Central α-agonist	0.05–0.1 mg per dose, may be repeated up to 0.8 mg total dose	p.o.	Side effects include dry mouth and sedation
Enalaprilat	ACE inhibitor	0.05–0.1 mg kg⁻¹ per dose up to 1.25 mg per dose	i.v. bolus	May cause prolonged hypotension and acute renal failure, especially in neonates
Fenoldopam	Dopamine receptor agonist	0.2–0.8 µg kg⁻¹ min⁻¹	i.v. infusion	Produced modest reductions in BP in a pediatric clinical trial in patients aged up to 12 years
Isradipine	Calcium channel blocker	0.05–0.1 mg kg⁻¹ per dose	p.o.	Stable suspension can be compounded
Minoxidil	Vasodilator	0.1–0.2 mg kg⁻¹ per dose	p.o.	Most potent oral vasodilator; long-acting

ACE, angiotensin-converting enzyme; i.m., intramuscular; i.v., intravenous; p.o., oral.

[a]All dosing recommendations are based upon expert opinion or case series data except where noted otherwise.

[b]Useful for hypertensive emergencies and some hypertensive urgencies.

[c]Useful for hypertensive urgencies and some hypertensive emergencies.

with mild BP elevation (<160 mmHg systolic, 80–95 mmHg diastolic), a significant reduction in both systolic and diastolic BP occurred in subjects consuming a diet high in fruits, vegetables, and low-fat dairy products, compared with the subjects consuming the usual diet [66]. These results indicate a benefit for BP from diets that are high in multiple nutrients, including potassium, calcium, magnesium, and other vitamins. A similar approach may benefit children. A small study by Couch *et al.* [67] compared a DASH diet for children with standard nutrition counseling in 57 children with hypertension and prehypertension. A greater reduction in systolic BP occurred in the children assigned to the DASH diet compared with standard diet counseling. The results support recommendations for children that encourage optimal intakes of fruits, vegetables, fiber, and dairy products, with reductions in processed foods.

Pharmacologic therapy is indicated if non-pharmacologic approaches are unsuccessful, or when a child is symptomatic, has severe hypertension, or target organ damage. Children with diabetes mellitus or chronic kidney disease may benefit from additional renal protection with BP reduction.

For these children, it is reasonable to use pharmacologic therapy to lower BP to a level <90th percentile for age, sex, and height.

Most medications used for hypertension in adults can be used for children. Efficacy and long-term safety data are limited in children. The choice of antihypertensive medication should be individualized and depends upon the child's age, the etiology of the hypertension, the degree of BP elevation, adverse effects, and concomitant medical conditions. In most patients, therapy is begun with a single agent. The dose is titrated upwards slowly until the BP is controlled. usually defined as maintaining systolic and diastolic pressure <90th percentile. If BP control cannot be achieved using the maximum dose of a single agent, a second medication can be added or, alternatively, another agent from a different class selected. The more commonly used medications for chronic antihypertensive therapy in children are listed in Table 64.4 and those for use in acute, hypertensive emergencies in Table 64.5 [1].These tables can be accessed at www.nhlbi.nih.gov/guidelines/hypertension/child_tbl.htm. The dosing recommendations for children have been based mainly upon

practitioners' experience, not on large, multicenter trials. Some clinical trial work has been conducted on the medications that are already approved and prescribed for hypertension in adults. The results of these clinical trials, although still limited, provide some information on efficacy, safety, and dosing to guide pharmacologic therapy in children.

Beta-adrenergic blockers, such as propranolol, metoprolol, and atenolol, are good choices in some nonasthmatic children, but may not be well tolerated by athletes in whom exercise capacity could decrease. More frequently, first-line medications are either angiotensin-converting enzyme (ACE) inhibitors or calcium antagonists. ACE inhibitors rarely cause side effects (e.g., cough, rash, neutropenia) in children, are usually well tolerated, and many formulations have the advantage of once-a-day dosing. Not only are they effective in controlling BP, but they may also have beneficial effects on renal function, peripheral vasculature, and cardiac function. Importantly, children with diabetes and those with chronic kidney disease may be at special risk for progressive renal deterioration and may benefit from ACE inhibitors [68]. Because of their vasodilator effects on the efferent arteriole, ACE inhibitors can severely reduce glomerular filtration and should therefore be used with caution in patients with renal artery stenosis, a solitary kidney, or a transplanted kidney [69]. ACE inhibitors are contraindicated during pregnancy because of possible teratogenic effects upon the lungs, kidneys, and brain of the fetus [70], and so should be used with special caution in adolescent females who are or may become sexually active. Angiotensin receptor blockers (ARBs) also interact with the renin–angiotensin system and have benefits similar to ACE inhibitors. Experience is being developed in treating children with these agents.

Several calcium antagonists (or calcium channel blockers, CCBs) are being used in children. In children, CCBs can be either an initial therapy or the second or third medication when more than one drug is needed to control BP. As with most oral antihypertensive preparations, the appropriate dose for small children is often lower than the strength of available tablets. This makes determining the initial dose determinations challenging. When CCBs are needed for BP control in chronic hypertension, long-acting preparations are preferred, provided that the correct dosage preparation can be used.

Diuretics are generally recommended as initial drug therapy for uncomplicated hypertension in adults, based on a vast amount of clinical trial data. No such information is available to guide recommendations for the pharmacologic management of hypertension in children and adolescents. Unless there is clinical evidence of fluid retention in a hypertensive child, such as may occur when the elevated BP is related to chronic steroid use, diuretics are usually not preferred as the first step in drug treatment. Some hypertensive children, however, may achieve adequate BP control with a thiazide diuretic alone. Children receiving thiazide

diuretics may develop hypokalemia and require potassium supplements, which, for children, is extremely unpleasant and can lead to problems with adherence to the regimen. Although not favored as an initial drug to treat hypertension in children, low-dose diuretics can be very useful as a second or third drug in those children who require multiple drugs to achieve BP control.

References

1 National High Blood Pressure Education Program Working Group on High Blood Pressure in Children and Adolescents. The fourth report on the diagnosis, evaluation, and treatment of high blood pressure in children and adolescents. *Pediatrics* 2004;**114**(Suppl 2):555–76.

2 Hansen, M, PGunn PW, Kaelber DC. Underdiagnosis of hypertension in children and adolescents. *JAMA* 2007;**298**:874–9.

3 McNiece KL, Poffenbarger TS, Turner JL, *et al*. Prevalence of hypertension and pre-hypertension among adolescents. *J Pediatr* 2007;**150**:640–4, 644 e1.

4 Still JL, Cottom C. Severe hypertension in childhood. *Arch Dis Child* 1967;**42**:34–9.

5 Chobanian, AV, Bakris GL, Black HR, *et al*. Seventh Report of the Joint National Committee on Prevention, Detection, Evaluation, and Treatment of High Blood Pressure: the JNC 7 Report. *JAMA* 2003;**289**:2560–72.

6 National High Blood Pressure Education Program Working Group on Hypertension Control in Children and Adolescents. Update on the 1987 Task Force Report on High Blood Pressure in Children and Adolescents: a working group report from the National High Blood Pressure Education Program. *Pediatrics* 1996;**98**(4 Pt 1):649–58.

7 Menghetti E, Verdis R, Strambi M, *et al*. Blood pressure in childhood and adolescence: the Italian normal standards. Study Group on Hypertension of the Italian Society of Pediatrics. *J Hypertens* 1999;**17**:1363–72.

8 Pall D, Katona E, Fulessdi B, *et al*. Blood pressure distribution in a Hungarian adolescent population: comparison with normal values in the USA. *J Hypertens* 2003;**21**:41–7.

9 Lurbe E, Cifkova R, Cruickshank JK, *et al*. Management of high blood pressure in children and adolescents: recommendations of the European Society of Hypertension. *J Hypertens* 2009;**27**:1719–42.

10 Zinner SH, Rosner B, Oh W, Kass EH. Significance of blood pressure in infancy. Familial aggregation and predictive effect on later blood pressure. *Hypertension* 1985;**7**(3 Pt 1):411–6.

11 Hulman S, Edwards R, Chen YQ, *et al*. Blood pressure patterns in the first three days of life. *J Perinatol* 1991;**11**:231–4.

12 Zubrow AB, Hulman S, Kushner H, Falkner B. Determinants of blood pressure in infants admitted to neonatal intensive care units: a prospective multicenter study. Philadelphia Neonatal Blood Pressure Study Group. *J Perinatol* 1995;**15**:470–9.

13 Sinaiko AR, Gomez-Marin O, Prineas RJ. Diastolic fourth and fifth phase blood pressure in 10–15-year-old children. The Children and Adolescent Blood Pressure Program. *Am J Epidemiol* 1990;**132**:647–55.

14 Wuhl E, Witte K, Soergel M, *et al*. Distribution of 24-hour ambulatory blood pressure in children: normalized reference values and role of body dimensions. *J Hypertens* 2002;**20**:1995–2007.

15 Urbina E, Alpert B, Flynn J, *et al*. Ambulatory blood pressure monitoring in children and adolescents: recommendations for standard assessment: a scientific statement from the American Heart Association Atherosclerosis, Hypertension, and Obesity in Youth Committee of the Council on Cardiovascular Disease in the Young and the Council for High Blood Pressure Research. *Hypertension* 2008;**52**:433–51.

16 Hanna JD, Chan JC, Gill JR Jr. Hypertension and the kidney. *J Pediatr* 1991;**118**:327–40.

17 Arar MY, Hogg, RJ, Arant BS Jr, Seikaly MG. Etiology of sustained hypertension in children in the southwestern United States. *Pediatr Nephrol* 1994;**8**:186–9.

18 Vailas GN, Brouillette RT, Scott P, *et al*. Neonatal aortic thrombosis: recent experience. *J Pediatr* 1986;**109**:101–8.

19 Abman SH, Warady BA, Lum GM, Koops BL. Systemic hypertension in infants with bronchopulmonary dysplasia. *J Pediatr* 1984;**104**:928–31.

20 Task Force on Blood Pressure Control in Children. Report of the Second Task Force on Blood Pressure Control in Children – 1987. *Pediatrics* 1987;**79**:1–25.

21 Ing FF, Starc TJ, Griffiths SP, Gersony WM. Early diagnosis of coarctation of the aorta in children: a continuing dilemma. *Pediatrics* 1996;**98**:378–82.

22 American Academy of Pediatrics Committee on Sports Medicine and Fitness. Athletic participation by children and adolescents who have systemic hypertension. *Pediatrics* 1997;**99**:637–8.

23 Daniels SR, Loggie JM, Khoury P, Kimball TR. Left ventricular geometry and severe left ventricular hypertrophy in children and adolescents with essential hypertension. *Circulation* 1998;**97**:1907–11.

24 Sorof JM, Alexandrov AV, Cardwell G, Portman RJ. Carotid artery intimal–medial thickness and left ventricular hypertrophy in children with elevated blood pressure. *Pediatrics* 2003;**111**:61–6.

25 Raitakari OT, Juonala M, Kahonen M, *et al*. Cardioavascular risk factors in childhood and carotid artery intima–media thickness in adulthood. The Cardiovascular Risk in Young Finns Study. *JAMA* 2003;**290**:2277–83.

26 Li S, Chen W, Srinivasan SR, *et al*. Childhood cardiovascular risk factors and carotid vascular changes in adulthood: the Bogalusa Heart Study. *JAMA* 2003;**290**:2271–6.

27 Shear CL, Burke GL, Freedman DS, Berenson GS. Value of childhood blood pressure measurements and family history in predicting future blood pressure status: results from 8 years of follow-up in the Bogalusa Heart Study. *Pediatrics* 1986;**77**:862–9.

28 Munger RG, Prineas RJ, Gornez-Marin O. Persistent elevation of blood pressure among children with a family history of hypertension: the Minneapolis Children's Blood Pressure Study. *J Hypertens* 1988;**6**:647–53.

29 Falkner B, Gidding SS, Ramirez-Garcia G, *et al*. The relationship of body mass index and blood pressure in primary care pediatric patients. *J Pediatr* 2006;**148**:195–200.

30 Rosner B, Cook N, Portman R, *et al*. Blood pressure differences by ethnic group among United States children and adolescents. *Hypertension* 2009;**54**:502–8.

31 Rocchini AP, Katch V, Anderson J, *et al*. Blood pressure in obese adolescents: effect of weight loss. *Pediatrics* 1988;**82**:16–23.

32 Brownell KD, Kelman JD, Stunkard AJ. Treatment of obese children with and without their mothers: changes in weight and blood pressure. *Pediatrics* 1983;**71**:515–23.

33 Sinaiko AR. Hypertension in children. *N Engl J Med* 1996;**335**:1968–73.

34 Ogden CL, Flegal KM, Carroll MD, Johnson CL. Prevalence and trends in overweight among US children and adolescents 1999–2000. *JAMA* 2002;**288**:1728–32.

35 Wang Y, Lobstein T. Worldwide trends in childhood overweight and obesity. *Int J Pediatr Obes* 2006;**1**:11–25.

36 Li C, Ford ES, Mokdad AH, Cook S. Recent trends in waist circumference and waist–height ratio among US children and adolescents. *Pediatrics* 2006;**118**: e1390–8.

37 Muntner P, He J, Cutler JA, *et al*. Trends in blood pressure among children and adolescents. *JAMA* 2004;**291**:2107–13.

38 Reaven GM. Banting Lecture 1988. Role of insulin resistance in human disease. *Diabetes* 1988;**37**:1595–607.

39 Cruz ML, Huang TT, Johnson MS, *et al*. Insulin sensitivity and blood pressure in black and white children. *Hypertension* 2002;**40**:18–22.

40 Duncan GE, Li SM, Zhou XH. Prevalence and trends of a metabolic syndrome phenotype among U.S. adolescents 1999–2000. *Diabetes Care* 2004;**27**:2438–43.

41 Boyd GS, Koenigsberg J, Falkner B, *et al*. Effect of obesity and high blood pressure on plasma lipid levels in children and adolescents. *Pediatrics* 2005;**116**:442–6.

42 Sorof J, Daniels S. Obesity hypertension in children: a problem of epidemic proportions. *Hypertension* 2002;**40**:441–7.

43 Barker DJ, Osmond C, Golding J, *et al*. Growth *in utero*, blood pressure in childhood and adult life, and mortality from cardiovascular disease. *Br Med J* 1989;**298**:564–7.

44 Law CM, Shiell AW. Is blood pressure inversely related to birth weight? The strength of evidence from a systematic review of the literature. *J Hypertens* 1996;**14**:935–41.

45 Cruickshank JK, Mzayek F, Liu L, *et al*. Origins of the "black/white" difference in blood pressure: roles of birth weight, postnatal growth, early blood pressure, and adolescent body size: the Bogalusa Heart Study. *Circulation* 2005;**111**:1932–7.

46 Mahoney LT, Clarke WR, Burns TL, Lauer RM. Childhood predictors of high blood pressure. *Am J Hypertens* 1991;**4**:608S–10S.

47 Lauer RM, Clarke WR, Mahoney LT, Witt J. Childhood predictors for high adult blood pressure. The Muscatine Study. *Pediatr Clin North Am* 1993;**40**:23–40.

48 Falkner B, Hulman S, Kushner H. Birth weight versus childhood growth as determinants of adult blood pressure. *Hypertension*, 1998;**31**:145–50.

49 Gamborg M, Byberg L, Rasmussen F, *et al*. Birth weight and systolic blood pressure in adolescence and adulthood: meta-regression analysis of sex- and age-specific results from 20 Nordic studies. *Am J Epidemiol* 2007;**166**:634–45.

50 Falkner B, Hulman S, Kushner H. Effect of birth weight on blood pressure and body size in early adolescence. *Hypertension* 2004;**43**:203–7.

51 Nilsson PM, Lurbe E, Laurent S. The early life origins of vascular ageing and cardiovascular risk: the EVA syndrome. *J Hypertens* 2008;**26**:1049–57.

52 Rich GM, Ulick S, Cook S, *et al*. Glucocorticoid-remediable aldosteronism in a large kindred: clinical spectrum and diagnosis using a characteristic biochemical phenotype. *Ann Intern Med* 1992;**116**:813–20.

53 Matteucci MC, Wuhl E, Picca S, *et al*. Left ventricular geometry in children with mild to moderate chronic renal insufficiency. *J Am Soc Nephrol* 2006;**17**:218–26.

54 Urbina EM, Gidding SS, Bao W, *et al*. Effect of body size, ponderosity, and blood pressure on left ventricular growth in children and young adults in the Bogalusa Heart Study. *Circulation* 1995;**91**:2400–6.

55 Mitchell P, Cheung N, de Haseth K, *et al*. Blood pressure and retinal arteriolar narrowing in children. *Hypertension* 2007;**49**:1156–62.

56 Lande MB, Kaczorowski JM, Auinger P, *et al*. Elevated blood pressure and decreased cognitive function among school-age children and adolescents in the United States. *J Pediatr* 2003;**143**:720–4.

57 Lande MB, Adams H, Falkner B, *et al*. Parental assessments of internalizing and externalizing behavior and executive function in children with primary hypertension. *J Pediatr* 2009;**154**:207–12.

58 Assadi F. Effect of microalbuminuria lowering on regression of left ventricular hypertrophy in children and adolescents with essential hypertension. *Pediatr Cardiol* 2007;**28**:27–33.

59 Hanevold CD, Pollock JS, Harshfield GA. Racial differences in microalbumin excretion in healthy adolescents. *Hypertension* 2008;**51**:334–8.

60 Meyers K, Falkner B. Hypertension in children and adolescents: an approach to management of complex hypertension in pediatric patients. *Curr Hypertens Rep* 2009;**11**:315–22.

61 Hansen HS, Froberg K, Hyldebrandt N, Nielsen JR. A controlled study of eight months of physical training and reduction of blood pressure in children: the Odense Schoolchild Study. *Br Med J* 1991;**303**:682–5.

62 He FJ, MacGregor GA. Response to salt intake in children: increasing concerns? *Hypertension* 2007;**49**(2):e11.

63 He FJ, MacGregor GA. Importance of salt in determining blood pressure in children: meta-analysis of controlled trials. *Hypertension* 2006;**48**:861–9.

64 He FJ, Marrero NM, MacGregor GA. Salt intake is related to soft drink consumption in children and adolescents: a link to obesity? *Hypertension* 2008;**51**:629–34.

65 Rocchini AP, Key J, Bondie D, *et al*. The effect of weight loss on the sensitivity of blood pressure to sodium in obese adolescents. *N Engl J Med* 1989;**321**:580–5.

66 Appel LJ, Moore TJ, Obarzanek E, *et al*. A clinical trial of the effects of dietary patterns on blood pressure. DASH Collaborative Research Group. *N Engl J Med* 1997;**336**:1117–24.

67 Couch SC, Saelens BE, Levin L, *et al*. The efficacy of a clinic-based behavioral nutrition intervention emphasizing a DASH-type diet for adolescents with elevated blood pressure. *J Pediatr* 2008;**152**:494–501.

68 National High Blood Pressure Education Program Working Group. National High Blood Pressure Education Program Working Group report on hypertension in diabetes. *Hypertension* 1994;**23**:145–58; discussion 159–60.

69 Hricik DE. Dunn MJ. Angiotensin-converting enzyme inhibitor-induced renal failure: causes, consequences, and diagnostic uses. *J Am Soc Nephrol* 1990;**1**:845–58.

70 Pryde PG, Sedman AB, Nugent CE, Barr M Jr. Angiotensin-converting enzyme inhibitor fetopathy. *J Am Soc Nephrol* 1993;**3**:1575–82.

65 Cardiovascular Risk Factors: Obesity, Diabetes, and Lipids

William A. Neal, Collin John & Alia Rai

Robert C. Byrd Health Science Center, West Virginia University School of Medicine, Morgantown, WV, USA

Hyperlipidemia in children and adolescents remains a significant risk factor for cardiovascular disease (CVD) later in life, yet <2% of children have evidence of severe genetic dyslipidemia associated with premature coronary artery or cerebrovascular disease. These typically autosomal dominant familial hyperlipidemias are not preventable and may result in death in early to mid-adulthood if not diagnosed and treated appropriately. In this chapter, we briefly review the pathophysiology of the various lipid disorders, and discuss screening and individualized treatment guidelines applicable to children and adolescents.

It is the worldwide obesity epidemic, however, which confers the greatest risk to public health. Obesity was identified as a major risk factor for cardiovascular disease by the American Heart Association in 1998 [1]. The projection that one in four children alive today may develop type 2 diabetes secondary to chronic obesity is alarming [2]. In contrast to genetic dyslipidemia, obesity is preventable and must be addressed by a broad-based population approach involving all sectors of society. Although around one billion people are affected by malnutrition worldwide, and perhaps 1.5 million children die annually from severe undernutrition, many others are at risk because of qualitatively poor but energy-rich diets. The decrease in physical activity in many parts of the world further contributes to the obesity epidemic.

Healthcare providers have traditionally had a minimal impact on preventing and treating youth obesity. There are many reasons for this, but the unsustainable cost of disability related to obesity, £2 billion per year in the United Kingdom alone, calls for much greater emphasis on prevention as a major component of medical practice [3].

Epidemiology of childhood obesity

According to the National Health and Nutrition Examination Survey (NHANES) in 2007–2008, currently 16.9% of children and adolescents aged 2–19 years are obese, defined as a body mass index (BMI) >95th percentile for age and gender [4]. That obesity has reached epidemic proportions is evident by its marked increase in prevalence over the past several decades. Since 1976–1980, obesity has doubled from 5 to 10% among preschool children, tripled from 6.5 to 19.6% in children 6–11 years old, and increased nearly fourfold among adolescents, from 5 to 18.1% [4].

The rate of obesity in the United States varies significantly among regions. The prevalence is greatest in the southeastern United States, especially in rural Appalachia. The Coronary Artery Risk Detection in Appalachian Communities (CARDIAC) Project has documented an obesity rate of 17.7% among kindergarten students, 22.2% among 2nd graders, and 28.4% among 5th graders. Cultural attitudes, low population density, and poverty each contribute in disparate ways to obesity in this mostly white population [5].

Some racial/ethnic groups are affected more than others both in the United States and throughout the world. NHANES data from 2003–2004 showed a 24% prevalence of obesity among black girls and 22% among Mexican American boys [6]. Selected Pacific Islanders, such as Samoans, have obesity rates approaching 75% [7]. Childhood overweight and obesity in India rose from 16% in 2002 to 24% in 2006, and it is postulated that East Asians are more susceptible to the metabolic syndrome and diabetes than US Caucasians [8].

The recently established European Childhood Obesity Surveillance Initiative reports that 24% of 6–9-year-olds are overweight (>85th –94.9th percentile) or obese [9].

Weight status in China has increased significantly as a result of urbanization and globalization. Whereas only 5% of people living in the countryside are obese, in some cities the prevalence exceeds 20%. Access to fast-food restaurants and processed foods readily available in cities is considered a major contributing factor [10].

Genetic and prenatal determinants of body composition

The Barker hypothesis states that the greatest threat to adult health is a child of low birth weight who remains small during infancy, then rapidly gains weight thereafter [11]. The proposed mechanism, referred to as the "thrifty phenotype," is that less than optimal exposure to nutrients during intrauterine life causes the fetus to set its metabolic "thermostat" adversely so it is ill suited for the nutritional prosperity of postnatal life; this leads to excessive fat production rather than lean muscle mass [12]. In contrast to intrauterine nutritional deprivation, excessive maternal weight gain during pregnancy leads to large babies and higher BMI during adolescence and adulthood [13].

Barker's *early origins hypothesis* has evoked considerable controversy among epidemiologists. Critics argue that his theory detracts from the importance of behavioral issues as risk factors for premature heart disease. However, there is little doubt that genetic factors play an etiologic role in obesity [14]. Genes affecting leptin receptors have been identified in mouse models, and a number of candidate genes in humans have been associated with body fat and its distribution. The effect of nutrition on gene expression, epigenetics, is only now emerging as a mechanism by which our children and grandchildren's body composition is determined.

Smoking among pregnant women is increasing in developing countries and is associated with obesity among their offspring, presenting an opportunity for public health intervention [15].

Effect of obesity on cardiovascular disease

The strong relationship between obesity and hypertension is well established [16]. Long-standing hypertension may lead to renal failure and chronic congestive heart failure. Sympathetic nervous system activation secondary to obesity affects renal structure and function that in turn increase sodium adsorption and adversely affect renin–angiotensin regulation.

Childhood obesity confers a selective effect on lipoprotein and insulin metabolism. Its impact on low-density lipoprotein (LDL) cholesterol is modest whereas there is a strong inverse relationship with high-density lipoprotein (HDL) cholesterol levels. Compared with children of normal weight, obesity confers a twofold likelihood of increase in LDL cholesterol levels but a sevenfold likelihood of low HDL cholesterol levels. In obese individuals, low HDL cholesterol is often accompanied by elevated triglycerides and serum insulin. The constellation of obesity, hypertension, dyslipoproteinemia, hypercoaguability, and elevated insulin is characteristic of the metabolic syndrome, or *insulin resistance syndrome*. Whether insulin resistance is an independent risk factor for accelerated atherosclerosis is unknown, but its relationship to type 2 diabetes is established. The rise in childhood obesity has resulted in a concurrent rise in type 2 diabetes [17].

Approximately one-third of obese children and half of morbidly obese children are at great risk of developing type 2 diabetes. Body fat distribution is related to insulin resistance in that visceral fat is a greater metabolic determinant than skeletal fat [18].

Prevention, assessment, and treatment of childhood overweight and obesity

Body mass index (BMI), the ratio of weight in kilograms to the square of height in meters, is the most practical means of describing gender- and age-specific weight status. Obesity is defined as BMI >95th percentile, and overweight is defined as BMI between the 85th and 94.9th percentiles. BMI <5th percentile is considered "underweight" and BMI >99th percentile defines "morbid obesity." Because BMI normative values are unavailable for children <2 years of age, a weight for height value >95th percentile is used to categorize overweight in this age group (see addendum).

BMI levels correlate with body fat [19] and cardiovascular risk [20]. Because BMI percentiles are continuous, any given cut point is imperfect in distinguishing absolute risk. Muscular athletes, for example, often fall within the obese category because of tissue-dense lean muscle mass. More precise measures of body composition, such as dual-energy X-ray absorption (DEXA), are used in selected research studies. Waist circumference in children correlates with visceral adiposity and is a clinically useful adjunct to BMI as it is more likely reflects modest weight changes and lifestyle modification.

The Expert Committee Regarding the Prevention, Assessment, and Treatment of Child and Adolescent Overweight and Obesity recommends that clinicians avoid harsh use of the term "obese" during provider–patient encounters so as to minimize embarrassment or an inference of judgment. "Overweight" and "obese," however, are appropriately used in documentation of weight status and risk assessment in the patient's health record [21].

Figure 65.1 details recommended steps to prevent and treat overweight and obesity developed by the Expert
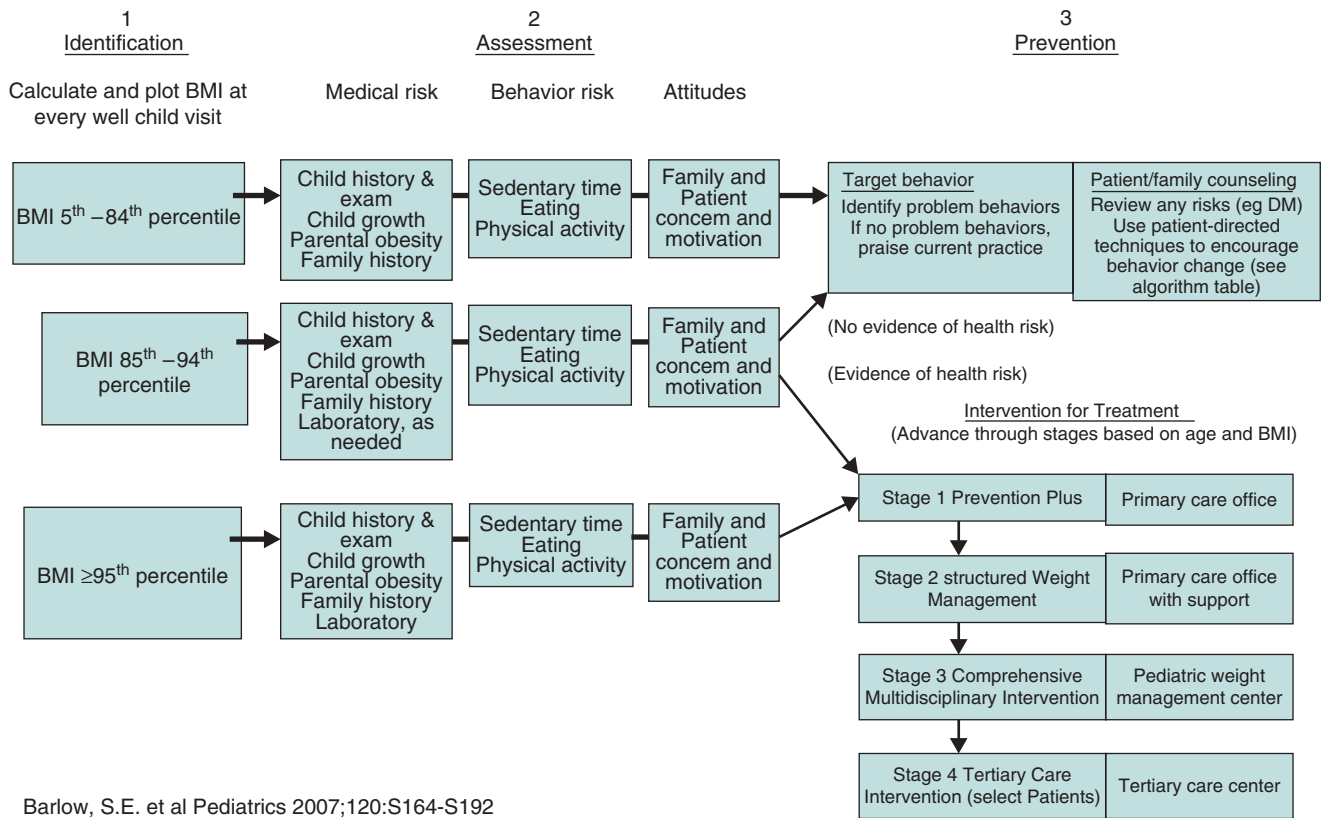
Figure 65.1 Universal assessment of obesity risks and steps for prevention and treatment. DM, diabetes mellitus. (Reproduced with permission from Barlow and Expert *Committee Pediatrics* 2007;**120**:S164–92, Copyright © 2007 by the American Academy of Pediatrics.)

Panel [21]. BMI should be calculated at every well child visit. Assessment includes medical risk, including growth, child and family history, parental obesity, and laboratory evaluation (glucose, insulin, hemoglobin A1-C, CRP, and fasting lipid profile) when BMI >95th percentile.

Behavior risk includes assessment of energy balance determined by quality of diet and the relative amounts of sedentary and physical activity. Family and patient concern about weight status and attendant risk, and also motivation to change, is of paramount importance. Effective behaviors for change include (1) limiting consumption of sweetened beverages; (2) limiting daily television and screen time to <2 h per day; (3) daily breakfast; (4) limited patronage of fast-food restaurants; (5) eating family meals together; and (6) food portion control. The child should undertake 60 min of moderate to vigorous physical activity daily [22]. Because smoking is a known cause of atherosclerosis (and also many other disorders), preventing smoking is an important part of treatment.

The technique of *motivational interviewing* includes reflective listening in a non-judgmental manner to elicit patient and parental concern and readiness to change [23]. Providing an opportunity for child–parent decisions about the actions for lifestyle changes is likely to be rewarding.

The chronic care model

Preventing childhood overweight and obesity requires a population approach. It is ideally suited to the theoretical and conceptual concepts of the *chronic care model* [24]. This model conceptualizes prevention and treatment in the context of health systems, including delivery system design, decision support, and clinical information systems; with self-management and support of the community. It connects a well-prepared practice team (the *medical home*) with an informed participatory patient. The application of this clinical model to preventing and treating obesity, regardless of the age of the patient, represents an ecological framework recommended by the Institute of Medicine [25]. It incorporates assets within the local community, such as dietetic, behavioral, and physical activity support, into the treatment paradigm. It relies on public policy to enhance the built environment, foster coordinated school wellness, conduct social marketing, and optimize public transportation.

Publicly available guides for practitioners and patients alike, such as the *We Can* program, are effective in promoting healthy weight management [26]. Quality improvement initiatives

implemented in school-based health centers have likewise improved the treatment of pediatric overweight [27].

Diabetes mellitus

Diabetes mellitus (DM) has long been recognized as a major risk factor for the development of coronary artery disease. The two major subgroups of DM are characterized by the ability to synthesize insulin. Type I DM is characterized by an absolute inability to synthesize insulin whereas Type II DM is characterized by insulin resistance. Although they result from contrasting mechanisms, both lead to elevated blood glucose, which in turn accelerates the development of various disorders, including coronary artery disease.

Type II diabetes mellitus

Type II DM is characterized by hyperglycemia resulting from a relative insulin resistance. Because insulin is produced, type II DM is referred to as non-insulin-dependent diabetes mellitus (NIDDM). Compared with type I DM, type II DM is a much greater public health problem because it is associated with obesity. This association theoretically gives a basis for prevention. Although typically thought of as adult onset DM, this term is antiquated and grossly inaccurate. As the worldwide pediatric obesity epidemic escalates, so does the incidence of type II DM among older children. Given the sporadic nature of screening children for type II DM worldwide, the true incidence and prevalence of type II DM Is difficult to estimate. In the United States, a retrospective study showed that the incidence of type II DM in children aged 10–19 years increased from 0.7/100 000 in 1982 to 7.2/100 000 in 1994 [28]. Similar trends have been found in studies in Japan, Argentina, and Thailand [29–31]. The prevalence of type II DM in the United States is estimated to be 18/100 000 individuals among non-Hispanic white youth 10–19 years old, with rates of 106/100 000 and 145/100 000 individuals in African-American and Navajo youth, respectively [32–34].

The diagnosis of type II DM can be made when a child meets one of the following four criteria [35]:
- a hemoglobin A1C >6.5%
- a fasting plasma glucose >126 mg dl^{-1}
- a 2 h plasma glucose >200 mg dl^{-1} following an oral glucose tolerance test
- a random plasma glucose >200 mg dl^{-1} in a child exhibiting classic signs and symptoms of hyperglycemia.

The American Diabetes Association also has developed criteria for individuals at risk for developing type II DM. These individuals are often referred to as having "impaired glucose tolerance" or "borderline diabetes." The criteria are:
- a fasting plasma glucose 100–125 mg dl^{-1}
- a 2 h plasma glucose 140–199 mg dl^{-1} following an oral glucose tolerance test
- a hemoglobin A1C 5.7–6.4%.

Treatment of type II DM focuses on lifestyle modification, with emphasis on healthy weight loss and monitoring of carbohydrate intake. In children, metformin is the only agent shown in a treatment study to reduce fasting plasma glucose levels compared with placebo without significant side effects [36]. Furthermore, in a recent study of obese adolescents with fasting hyperinsulinemia who did not meet criteria for type II DM, the addition of metformin to lifestyle modifications helped lower insulin levels and BMI, which could potentially prevent progression to type II DM [37].

Complications in type II DM are generally divided into two groups, microvascular and macrovascular. Microvascular complications occur in smaller arteries and the most commonly affected organs are the eyes, kidneys, and peripheral nerves. Macrovascular complications occur in larger arteries, notably the coronary arteries and peripheral arteries. In fact, the link between adult coronary artery disease and type II DM is so well established that both the American Diabetes Association and American Heart Association classify type II DM as a "coronary heart disease risk equivalent."

Type I diabetes mellitus

Type I DM (IDDM) is characterized by a lack of insulin production. It is commonly called childhood-onset or juvenile diabetes because the typical age of onset is childhood. There are various hypotheses about the etiology of this disease, including autoimmune, viral infection, and dietary. The incidence of type I DM in the United States is ~23.6/100 000 annually and the prevalence is about 200/100 000 [32]. The incidence of type I DM continues to increase worldwide for unknown reasons. In type I DM, treatment is focused on replacing insulin exogenously, with varying regimens and preparations of insulin available. Complications from type I DM are identical with those from type II DM.

Metabolic syndrome

"Metabolic syndrome," also termed "syndrome X" or "the deadly quartet," refers to adults with a constellation of specific cardiovascular disease risk factors. The World Health Organization first published criteria for this syndrome in 1998 [38], and subsequently other health organizations [39] have developed their own criteria to "diagnose" this condition. Although the criteria vary by the defining organization, the major unifying theme is that this syndrome is well recognized and established within the adult population. The major components include hypertension, central obesity, elevated fasting glucose, elevated triglycerides, and reduced HDL cholesterol.

There is no official definition of the metabolic syndrome in children and adolescents, despite the increasing prevalence of the specific components within this population. The use of a single set of cut points throughout all ages of childhood,

despite changing physiology, the lack of an accepted normal range for insulin across childhood, and the physiological insulin resistance in puberty, are just a few of the problems making it difficult to define metabolic syndrome in the pediatric population. The American Heart Association recently published a scientific statement about the metabolic syndrome in children [39].

Hyperlipidemia in children and adolescents

As demonstrated in the Bogalusa Heart Study and the Pathobiological Determinants of Atherosclerosis in Youth (PDAY) Study [40,41], the pathological changes of atherosclerosis begin in childhood, although clinical manifestations do not appear until middle age. In the Bogalusa study, autopsy findings on young people registered in the study showed early atherosclerotic lesions in the aorta and the coronary arteries that correlated with elevated LDL cholesterol, elevated blood pressure, and obesity, and were inversely related to HDL cholesterol levels [40].

The PDAY study also showed atherosclerotic changes in teenagers, and that the progression of the atherosclerotic changes can be delayed by reducing risk factors through lifestyle changes and medication [41]. Ideally, interventions should occur before clinical manifestations of CVD develop, hence the need to intervene in childhood.

Many years will be needed to establish scientifically a decreased CVD mortality in adults from risk factor modification in children. However, pathologic change in young people coupled with the evidence that modifying risk factors improves the atherosclerotic lesions persuades us that every effort should be made to identify and treat children at risk. Familial aggregation of premature CVD, generally defined as atherosclerotic disease before 55 years of age, suggests the likelihood of an abnormality of lipoprotein metabolism.

Lipoprotein metabolism

Because they are insoluble in water, lipids are transported by lipoprotein. Lipoprotein consists of a core of triglycerides and cholesteryl esters surrounded by phospholipids, cholesterol, and proteins, called apoproteins, which have multiple metabolic functions. The density of lipoproteins is inversely proportional to the ratio of lipid to protein. The lipoproteins found in serum include:
- low-density lipoprotein (LDL)
- high-density lipoprotein (HDL)
- very-low-density lipoprotein (VLDL)
- intermediate-density lipoprotein (IDL)
- chylomicrons.

Lipoproteins effect transport of fat either absorbed from the diet (exogenous pathway) or synthesized by the liver and adipose tissue (endogenous pathway). HDL metabolism is responsible for transport of excess cholesterol from peripheral tissues back to the liver for excretion as bile acids, a process called "reverse cholesterol transport."

Nongenetic, secondary causes of lipoprotein abnormality include endocrine disorders such as hypothyroidism and diabetes, nephrotic syndrome, obesity, alcoholism, and selected medications, such as thiazides, anabolic steroids, and beta-blockers.

Genetic dyslipidemias are categorized according to aberrations in specific lipoproteins: hypercholesterolemia, hypercholesterolemia with hypertriglyceridemia, hypertriglyceridemias, and disorders of HDL metabolism. Rare disorders of cholesterol metabolism are not discussed in this chapter [42].

Hypercholesterolemias

Polygenic
The most common cause of hypercholesterolemia is referred to as "polygenic" which affects about one in 30 individuals. It represents the interaction of multiple genes and environmental influences, such as a high-fat diet and sedentary activity. Elevation in LDL cholesterol is modest and generally controllable by adopting a healthy lifestyle.

Familial hypercholesterolemias (FH)
These monogenic autosomal co-dominant disorders are characterized by LDL receptor defects that lead to abnormal LDL uptake and metabolism. Nearly 800 mutations have been described, with patterns varying according to ethnic and racial groups. Severe mutations are associated with failure of synthesis of LDL receptors, whereas in others receptors are present but defective.

The homozygous form is rare, with a prevalence of 1/1 000 000. In affected individuals, the LDL cholesterol level ranges between 450 and 850 mg dl^{-1} and may exceed 1000 mg dl^{-1}. Multiple tendon and cutaneous xanthomas can be seen from a young age, and corneal arcus is also present. Atherosclerotic changes in the aortic root and the coronary arteries develop early, and can result in CVD by age 10 years. These individuals rarely survive to adulthood. Their response to cholesterol-lowering medication is not optimal. Hence LDL apheresis and liver transplantation have been used as therapeutic options.

Of greater importance is the heterozygous form of FH, with a prevalence of 1/500 worldwide, that can be treated effectively with cholesterol-lowering medications. Selected populations, such as Afrikaners, a group of French Canadians, and some Lebanese Christians, have been identified with "founder effect" mutations that result in frequencies >1/250.

The phenotypic expression of the disease is influenced modestly by environmental factors. CVD typically manifests between the ages of 30 and 50 years. Premenopausal women usually present later than men because of the protective effect of circulating estrogen.

A strong family history of premature heart disease affecting a parent, grandparent, and other first- and second-degree family members, in association with LDL cholesterol levels exceeding 190 mg dl^{-1}, should alert one to the probability of phenotypic expression of heterozygous FH. Genetic studies may confirm the diagnosis but are generally not performed clinically. When FH is suspected, other family members should be screened so that primary prevention can begin in those affected. As an autosomal dominant condition with nearly full penetrance, 50% of first-degree relatives and 25% of second-degree relatives would be expected to have the disease.

Familial defective ApoB-100 (FDB)

This autosomal dominant condition results in inefficient binding of LDL by the LDL receptor. Phenotypically, individuals resemble those with heterozygous FH. The prevalence is 1/700. Specialized laboratory testing can distinguish FDB from FH, but as treatment is identical, this is unnecessary.

Hypercholesterolemia with hypertriglyceridemia

Familial combined hyperlipidemia (FCH)

This autosomal dominant defect causes moderate elevation in both LDL cholesterol and triglycerides. Serum HDL may be decreased. The prevalence is ~1/150, and it is found in 10% of survivors of premature coronary artery disease. Premature atherosclerosis is not as prevalent in FCH as with FH. Typically, the LDL level is not as elevated as in heterozygous FH. Xanthomas are not present. Elevated apoB levels and increased small, dense LDL particles support the diagnosis.

Not infrequently, children and adults who fulfill criteria for a diagnosis of FCH also have visceral adiposity, hypertension, and hyperinsulinemia suggestive of the metabolic syndrome. Although criteria for the diagnosis of metabolic syndrome in children have not been developed, this constellation of findings indicates risk for type II DM.

Hypertriglyceridemias

Familial hypertriglyceridemia (FHTG)

This autosomal dominant condition is also called type IV hyperlipidemia according to the Frederickson classification system. It occurs in 1/500 of the population. It is caused by the production of abnormal VLDL due to a deficiency of lipoprotein lipase or apoprotein C-II. The triglyceride levels typically range from 200 to 1000 mg dl^{-1}, associated with a

Table 65.1 AHA recommended cut-off points for serum cholesterol levels in children aged 2–19 years.

Serum cholesterol	Acceptable	Borderline	High
Total cholesterol (mg dl^{-1})	<170	170–199	>200
LDL cholesterol (mg dl^{-1})	<110	110–129	>130

normal LDL and possibly low HDL. Although not highly associated with premature coronary vascular disease, it can result in pancreatitis. It generally does not become manifest until adulthood. To make the diagnosis, at least one other family member should have hypertriglyceridemia.

Disorders of HDL cholesterol

Primary hypoalphalipoproteinemia

Isolated low HDL may follow an autosomal dominant pattern, although often the family history is negative. HDL cholesterol levels are <10th percentile for gender and age. It is caused by increased catabolism of HDL and often a reduction in apoA-1 synthesis. The degree to which it may contribute to atherosclerosis is uncertain.

Hyperalphalipoproteinemia

This interesting but unusual condition is characterized by HDL levels >80 mg dl^{-1}. It appears to have a cardioprotective effect.

Lipoprotein patterns in children and adolescents

The AHA recommends the use of cut-off points for serum cholesterol levels in children between 2 and 19 years of age as shown in Table 65.1.

HDL cholesterol levels <40 mg dl^{-1} are a risk factor for heart disease. Triglyceride levels >150 mg dl^{-1} are abnormal and probably contribute to the development of atheromatous plaques, although not to the same extent as elevated LDL cholesterol.

Although the total cholesterol slowly rises until puberty, it transiently falls at that point from lowering of the HDL in males and of the LDL in females.

Screening and treatment for dyslipidemias

In 2008, the American Academy of Pediatrics (AAP) published recommendations for cholesterol screening and treatment in childhood [43]. They recommend a targeted

approach similar to that originally proposed by the National Cholesterol Education Program [44]. The recommendations are to screen selectively the following children:

1 children with a family history of dyslipidemia or premature coronary artery disease (which is defined as <55 years in men and 65 years in women)

2 children with an unknown family history, especially those with other risk factors such as obesity, hypertension, DM, or smoking.

Screening should occur between 2 and 10 years of age.

There is some rationale for universal blood cholesterol screening, especially in regions where the prevalence of heart disease and diabetes is well above average. A recent study of over 20 000 5th grade children who participated in a school-based blood cholesterol screening program found that one-third of the children who qualified for consideration of pharmacologic intervention (LDL >160 mg dl^{-1} plus other risk factors) would have been missed had selective screening criteria based on a positive family history been used [45].

Treatment guidelines

The AAP recommends a "two-pronged approach," which consists of a population focus and an individualized approach [43]. The population approach refers to the general recommendations for a healthy lifestyle appropriate for all children. The individualized approach targets children identified as being at increased risk for CVD because of a genetic dyslipidemia, obesity, hypertension, or DM.

Dietary modifications

Elevated LDL cholesterol is controlled best by a diet low in saturated fat and cholesterol. The AAP guidelines recommend that saturated fat should supply no more than 7% of the total caloric intake, and that no more than 200 mg of cholesterol should be consumed per day. Lifestyle modification alone is unlikely to lower blood cholesterol levels sufficiently to a safe range in children with severe genetic dyslipidemias.

An important dietary approach for both primary and secondary prevention of CVD considers the *type* of fats consumed. A diet with increased mono- and polyunsaturated fats and limited carbohydrate intake can decrease LDL and modestly increase HDL cholesterol.

Elevated triglycerides are controlled best by a diet with restricted carbohydrate and sugar intake.

Other nonpharmacologic approaches

Increased soluble fiber intake lowers LDL cholesterol levels. The AAP recommends a supplemental fiber dose of the child's age in years + 5 g per day, up to a maximum of 20 g [43].

Increased intake of plant sterols and stanols can decrease LDL cholesterol slightly, and may be found in some yogurt drinks and spreads.

Increased physical activity increases HDL and reduces LDL cholesterol and triglycerides. The AAP "5–2–1–0" plan recommends five fruits and vegetables daily, <2 h of "screen" time per day, at least 1 h of physical activity per day, and no sweetened drinks.

Omega-3 fatty acids can decrease triglycerides, and are well tolerated by children as a supplement. These fatty acids are present in oily cold-water fish (including salmon, sardines, mackerel, and tuna), eggs, milk, and some berries.

Pharmacologic intervention

The AAP guidelines have specific recommendations for children who should receive medication [43]. A child must be at least 8 years of age, and have failed to lower their cholesterol sufficiently after a suitable period of dietary restrictions. Pharmacologic treatment of children <8 years of age should be reserved for the rare child with homozygous FH and LDL cholesterol levels exceeding 500 mg dl^{-1}. For children with moderately severe heterozygous dyslipidemias, medication is recommended if:

- LDL cholesterol remains >190 mg dl^{-1}.
- LDL cholesterol remains >160 mg dl^{-1} and other risk factors are present, including positive family history of premature CVD, obesity, and/or hypertension.
- LDL cholesterol is >130 mg dl^{-1} in children with DM.

The goal of therapy is to decrease the LDL cholesterol to <130 mg dl^{-1}, or more ideally <110 mg dl^{-1}. There is no reason to lower LDL levels more as is recommended in high-risk adults.

Medications available include the following:

- *Bile acid-binding resins:* May lower the cholesterol by 10–20% below baseline and have the advantage of no systemic effects. However, the associated gastrointestinal discomfort and the fact that dosage forms are neither practical nor palatable for children limited their use.
- *Niacin:* Decreases both LDL cholesterol and triglycerides and also increases HDL cholesterol. The associated flushing, headaches, and elevations in hepatic enzymes prohibit its routine use in children. Niacin has been used selectively in children with marked hypertriglyceridemia at risk for acute pancreatitis, although dietary restriction of complex sugars and carbohydrates usually significantly lowers triglyceride levels.
- *HMG-CoA reductase inhibitors (statins):* These are extremely effective, cause a 20–50% decrease in LDL cholesterol, and reduce plaque inflammation. The rare side effects include liver enzyme elevation and rhabdomyolysis. Hepatic transaminases must be monitored regularly but they can be allowed to increase 2–3-fold before the medication needs to be discontinued. Children rarely report the muscle aches and cramps that adults note.
- *Cholesterol-absorption inhibitors (ezetimibe):* This relatively new class of medication is often useful in children with moderate elevation of LDL cholesterol not severe enough to

justify statins, or in combination with statins when there is severe hypercholesterolemia. They can decrease LDL by 20%. Side effects are few.

• *Fibric acid derivatives:* These are used in adults with for severe hypertriglyceridemia. This class of medication has very limited utility in children and may cause liver toxicity.

References

1 Eckel RH, Krauss RM. American Heart Association call to action: obesity as a major risk factor for coronary heart disease. AHA Nutrition Committee. *Circulation* 1998;**97**:2099–100.

2 Wang Y, Beydoun MA. The obesity epidemic in the United States – gender, age, socioeconomic, racial/ethnic, and geographic characteristics: a systematic review. www.cdc.gov/obesity/childhood/trends.html (last accessed 20 August 2010).

3 WHO/Europe. Facts and figures. http://www.who.int/en/what-we-do/health-topics/disease-prevention/nutrition/facts) (last accessed December 2010).

4 Division of Nutrition, Physical Activity and Obesity, National Center for Chronic Disease Prevention and Health Promotion. Prevalence of obesity among children and adolescents: United States, trends 1963–1965 through 2007–2008. http://www.cdc.gov/nchs/data/hestat.obesity child 07 08/obesity child 07 08. htm (last accessed August 2010).

5 Ice CL, Cottrell L, Neal W. Body-mass index as a surrogate measure of cardiovascular risk factor clustering in fifth-grade West Virginia children: results from the Coronary Artery Risk Detection in Appalachian Communities Project. *Int J Pediatr Obesity* 2009;**4**:316–24.

6 Ogden CL, Carroll MD, Curtin LR, *et al*. Prevalence of overweight and obesity in the United States, 1999–2004. *JAMA* 2006;**295**:1549–55.

7 Goel MS, McCarthy EP, Phillips RS, *et al*. Obesity among US immigrant subgroups by duration of residence. *JAMA* 2004;**292**;2860–7.

8 Bhardwaj S, Misra A, Khurana L, *et al*. Childhood obesity in Asian Indians: a burgeoning cause of insulin resistance, diabetes and subclinical inflammation. *Asia Pacific J Clin Nutr* 2008;**17**(SI):172–5.

9 WHO/Europe. European Childhood Obesity Surveillance Initiative (COSI). http://www.euro.who.int/en/what-w-d/health-topics/disease-prevention/nutrition/policy/ (last accessed December 2010).

10 Wu Y. Overweight and obesity in China. *BMJ* 2006;**333**:362–3.

11 Barker DJP. The fetal and infant origins of disease. *Eur J Clin Invest* 1995;**25**:457–63.

12 Guo SS, Huang C, Maynard LM, *et al*. Body mass index during childhood, adolescence and young adulthood in relation to adult overweight and adiposity: the Fels Longitudinal Study. *Int J Obes Relat Metab Discord* 2000;**24**:1628–35.

13 Oken E, Gillman MW. Fetal origins of obesity. *Obes Res* 2003;**11**:496–506.

14 Bouchard C, Perusse L. Genetic aspects of obesity. *Ann N Y Acad Sci* 1993;**699**:26–35.

15 Oken E, Huh SY, Taveras EM, *et al*. Association of maternal prenatal smoking with child adiposity and blood pressure. *Obes Res* 2005;**13**:2021–8.

16 Krauss RM, Winston M, Fletcher BJ, *et al*. Obesity impact on cardiovascular disease. *Circulation* 1998;**98**:1472–6.

17 Gregg EW, Cheng YJ, Cadwell BL, *et al*. Secular trends in cardiovascular disease risk factors according to body mass index in US adults. *JAMA* 2005;**293**:1868–74.

18 Fernandez JR, Redden DT, Pietrobelli A, Allison DB. Waist circumference percentiles in nationally representative samples of African-American, European-American, and Mexican-American children and adolescents. *J Pediatr* 2004;**145**:439–44.

19 Pietrobelli A, Faith MS, Allison DB, Gallagher D, *et al*. Body mass index as a measure of adiposity among children and adolescents: a validation study. *J Pediatr* 1998;**132**:204–10.

20 Freedman DS, Khan LK, Dietz WH, *et al*. Relationship of childhood obesity to coronary heart disease risk factors in adulthood: the Bogalusa Heart Study. *Pediatrics* 2001;**108**:712–8.

21 Barlow SE, Expert Committee. Expert Committee recommendations regarding the prevention, assessment, and treatment of child and adolescent overweight and obesity: summary report. *Pediatrics* 2007;**120**:S164–92.

22 Pate RR, Davis MG, Robinson TN, *et al*. Promoting physical activity in children and youth: AHA scientific statement. *Circulation* 2006;**114**:1214–24.

23 Resnicow K, Davis R, Rollnick S. Motivational interviewing for pediatric obesity: conceptual issues and evidence review. *J Am Diet Assoc* 2006;**106**:2024–33.

24 Logue E, Sutton K, Jarjoura D, Smucker W. Obesity management in primary care: assessment of readiness to change among 284 family practice patients. *J Am Board Fam Med* 2000;**13**:164–71.

25 Institute of Medicine. *The Future of the Public's Health in the 21st Century*. Washington, DC: National Academies Press, 2003.

26 National Heart, Lung, and Blood Intitute. We can! http://wecan.nhlbi.nih.gov (last accessed January 2011).

27 Oetzel KB, Scott AA, McGrath J. School-based health centers and obesity prevention: changing practice through quality improvement. *Pediatrics* 2009;**123**:S267–71.

28 Pinhas-Hamiel O, Dolan LM, Daniels SR, *et al*. Increased incidence of non-insulin-dependent diabetes mellitus among adolescents. *J Pediatr* 1996;**128**:608–15.

29 Pinhas-Hamiel O, Zeitler P. The global spread of type 2 diabetes mellitus in children and adolescents. *J Pediatr* 2005;**146**:693–700.

30 Urakami T, Kubota S, Nitadori Y, *et al*. Annual incidence and clinical characteristics of type 2 diabetes in children as detected by urine glucose screening in the Tokyo metropolitan area. *Diabetes Care* 2005;**28**:1876–81.

31 Likitmaskul S, Kiattisathavee P, Chaichanwatanakul K, *et al*. Increasing prevalence of type 2 diabetes mellitus in Thai children and adolescents associated with increasing prevalence of obesity. *J Pediatr Endocrinol Metab* 2003;**16**:71–7.

32 Bell RA, Mayer-Davis EJ, Beyer JW, *et al*. Diabetes in non-Hispanic white youth: prevalence, incidence, and clinical characteristics: the SEARCH for Diabetes in Youth Study. *Diabetes Care* 2009;**32**(Suppl 2):S102.

33 Dabelea D, DeGroat J, Sorrelman C, *et al*. Diabetes in Navajo youth: prevalence, incidence, and clinical characteristics: the SEARCH for Diabetes in Youth Study. *Diabetes Care* 2009;**32**(Suppl 2):S141.

34 Mayer-Davis EJ, Beyer J, Bell RA, *et al*. Diabetes in African American youth: prevalence, incidence, and clinical characteris-

tics: the SEARCH for Diabetes in Youth Study. *Diabetes Care* 2009;**32**(Suppl 2):S112.

35 American Diabetes Association. Diagnosis and classification of diabetes mellitus. *Diabetes Care* 2010;**33**(Suppl.1):S62–9.

36 Jones KL, Arslanian S, Peterokove VA, *et al*. Effect of metformin in pediatric patients with type 2 diabetes: a randomized controlled trial. *Diabetes Care* 2002;**25**:89–94.

37 Freemark M, Bursey D. The effects of metformin on body mass index and glucose tolerance in obese adolescents with fasting hyperinsulinemia and a family history of type 2 diabetes. *Pediatrics* 2001;**107**:E55.

38 World Health Organization. Definition, diagnosis and classification of diabetes mellitus and its complications: report of a WHO Consultation. Part 1: diagnosis and classification of diabetes mellitus. Geneva: World Health Organization, 1999. http://whqlibdoc.who.int/hq/1999/WHO_NCD_NCS_99.2.pdf (last accessed 30 December 2010).

39 Steinberger J, Daniels SR, Eckel RH, *et al*. Progress and challenges in metabolic syndrome in children and adolescents: a scientific statement from the American Heart Association Atherosclerosis, Hypertension, and Obesity in the Young Committee of the Council on Cardiovascular Disease in the Young, Council on Cardiovascular Nursing, and Council on Nutrition, Physical Activity, and Metabolism. *Circulation* 2009;**119**:628–47.

40 Berenson GS, Wattigney WA, Bao W, *et al*. Rationale to study the early natural history of heart disease: the Bogalusa Heart Study. *Am J Med Sci* 1995;**310**(Suppl 1):S22–8.

41 McGill HC Jr, McMahan CA, Gidding SS, *et al*. Preventing heart disease in the 21st century: implications of the Pathobiological Determinants of Atherosclerosis in Youth (PDAY) study. *Circulation* 2008;**177**:1216–27.

42 Neal WA. Disorders of lipotrotein metabolism and transport. In: Kliegman R, Behrman R, Nelson W, *et al*., eds. *Nelson's Textbook of Pediatrics*, 18th edn. Philadelphia: Saunders/Elsevier, 2006: 580–93.

43 Daniels SR, Greer FR. Lipid screening and cardiovascular health in childhood. *Pediatrics* 2008;**122**:198–208.

44 Expert Panel on Detection, Evaluation, and Treatment of High Blood Cholesterol in Adults. Executive Summary of the Third Report of the National Cholesterol Education Program (NCEP) Expert Panel on Detection, Evaluation, and Treatment of High Cholesterol in Adults (Adult Treatment Panel III). *JAMA* 2001;**285**:2486–97.

45 Ritchie SK, Murphy E, Ice C, *et al*. Universal versus targeted blood cholesterol screening among youth. *Pediatrics* 2010;**126**:260–5.

Addendum

Calculators and charts for BMI percentiles can be found at

http://apps.nccd.cdc.gov/dnpabmi/calculator.aspx
http://www.halls.md/body-mass-index/av.htm
http://kidshealth.org/misc/body_mass_index/P_bmi_chart.html
(all the above were accessed August 2011).

66 Cardiac Tumors

Saroja Bharati

Advocate Hope Children's Hospital, Advocate Christ Medical Center, Oak Lawn, IL; Rush University
Medical Center; Rosalind Franklin University of Medicine and Science, Chicago Medical School and
University of Illinois at Chicago, Chicago, IL, USA

Although cardiac tumors are rare in children, recent advances in various types of imaging techniques have made it possible to diagnose them fairly accurately. Today, most benign tumors are surgically removed with reasonable success [1–30].

The tumors usually seen in childhood are rhabdomyoma, fibroma, mesothelioma of the atrioventricular (AV) node, and sarcoma. Other types of tumors in children are myxoma, lipoma, papillary fibroelastoma, tumor of heterotopic tissue (teratoma), leiomyoma, granular cell tumor, mesothelioma, hemangioma, lymphangioma, melanoma, paraganglioma (pheochromocytoma), neurofibroma, neuroblastoma, neurinoma, lymphoma, and carcinoids.

Incidence

Primary cardiac tumors are extremely rare, with an incidence of 0.0017–0.28% in autopsy series. Approximately 75–80% of tumors of the heart and pericardium are benign. Among the benign tumors, atrial myxomas constitute 75%.

Genetics

Little is known about the cause of pediatric cardiac tumors. In the past two decades, however, a genetic etiology has been recognized for some tumors. Clinical genetic analysis has shown that Carney complex is transmitted as an autosomal dominant disorder and can manifest in a variety of tumors such as psammomatous melanotic schwannoma, pituitary adenoma, and testicular Sertoli cell tumors [31]. Molecular genetic studies have demonstrated that mutations in a subunit of protein kinase A and mutations in the MYH 8 gene that encodes prenatal myosin could be primary causes of the disorders that predisposes to cardiac tumorogenesis [31].

Likewise, tuberous sclerosis complex (TSC) is an autosomal dominant disorder that results from mutations in TSC1 or TSC2 genes and is associated with hamartoma formation in multiple organ systems [32].

Clinical manifestations

The clinical manifestations of cardiac tumors depend on the site, size, and characteristic pathological and histochemical features [3–30]. The tumor may remain asymptomatic and sudden death may be the first manifestation [24–26].

Tumors of the heart may produce hemodynamic effects, dysrhythmias, pericarditis, intracavity obstruction, embolism, mechanical hemolysis, and constitutional symptoms. Some tumors, such as carcinoids, may have biologic effects and with malignant tumors metastasis elsewhere in the body may be seen.

The hemodynamic effects include obstruction to the inflow or outflow tract of any chamber on the right or left side of the heart or intracavity obstruction at the level of the AV valves. Pulmonary hypertension may occur due to pulmonary emboli from the right heart, or due to pulmonary venous obstruction produced by left atrial or left ventricular outflow tract obstruction. Ascites may occur from right atrial obstruction. Various types of arrhythmias occur, such as atrial fibrillation, flutter, supraventricular tachycardia, pre-excitation, AV block, and repetitive ventricular tachycardia. The tumor may produce pericardial effusion and tamponade or may cause constrictive pericarditis. Emboli may pass to the brain or elsewhere in the systemic circulation. Depending on the site of the tumor, there may be left or right heart failure. The symptoms then include cardiac failure, general malaise, loss of weight, syncopal episodes, and pulmonary edema. Mechanical hemolysis and hemolytic

anemia may be produced by the tumor mass. In some patients the symptoms may resemble those of infective endocarditis with fever, signs of peripheral embolization, increase in sedimentation rate, and hyperglobulinemia. If the tumor is malignant, metastasis may occur in lungs, lymph nodes, mediastinum, liver, pancreas, spleen, kidneys, adrenals, bone, and brain.

Tumors of the pericardium

Pericardial tumors are less frequently seen than those within the heart and are very rare in children. The benign tumors are benign mesothelioma, miscellaneous pericardial celomic cysts, angiomas (hemangioma and lymphangioma), lipoma, leiomyoma, fibroma, neurofibroma, neuroblastoma, and neurinoma. The malignant tumors are rare and include various types of sarcomas and malignant mesothelioma [1,2,4,10–14].

Tumors of the heart

Rhabdomyoma

Rhabdomyoma is the most common primary cardiac tumor in infancy and childhood. It is rarely seen after the age of 15 years. It is usually associated with TSC complex, an autosomal dominant disorder resulting from mutations of TSC1 or TSC2 genes. It occurs with hamartoma formation in multiple organ systems. About 80% of the tumors present before the age of 1 year. The tumor is usually multiple but may be single. It is often in the walls of the right and left ventricle or the interventricular septum (Figure 66.1), but is rare in the atrial septum [1,5,7,10–15,32].

Microscopically, the tumor consists of vacuolated cells that look like spider cells and contain glycogen. On electron microscopy, glycogen is seen in the cytoplasm and in the mitochondria. The intercellular junctions resemble intercalated discs, desmosomes, and nexus.

The tumor may obstruct a coronary artery or affect the conduction system. It can also obstruct the tricuspid, pulmonary, mitral, or aortic valve, or the outflow tract of the right and left ventricle. Rarely, the tumor presents as fetal hydrops with AV block.

Although the obstructive phenomena may predominate in patients with outflow tract obstruction, they may also have varying types of arrhythmias, such as atrial fibrillation, flutter, supraventricular tachycardia, pre-excitation, AV block, and ventricular tachycardia. In general, the arrhythmias are abolished after surgical removal of the tumor. Rhabdomyomas are completely benign, with no metastasis, and most of them spontaneously regress either partially or completely.
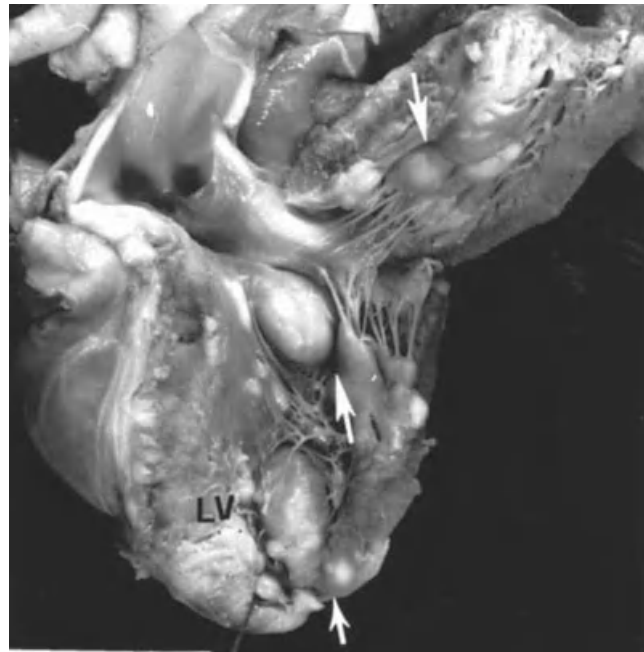
Figure 66.1 Multiple rhabdomyomas of the heart, left ventricular (LV) view. Arrows point to rhabdomyomas. (Reproduced from Bharati, S, Lev M. Cardiac tumors. In: Adams FH, Emmanouilides GC, Riemanschneider TA, eds. *Moss' Heart Disease in Infants, Children and Adolescents*, 4th edn. Baltimore, MD: Williams and Wilkins, 1989: 886–90, with permission from Wolters Kluwer.)

Fibroma

Fibroma is the second most common tumor in infancy. It is almost always solitary. The tumor occupies the septal or parietal wall of the left ventricle. Because it is not encapsulated, it intermingles with the myocardial cells of the wall of the ventricular mass. Despite this, it can often be shelled out at surgery and usually does not recur. The fibroma may compress the anterior descending coronary artery or affect the conduction system to varying degrees and cause AV block. The tumor may produce subaortic or subpulmonary obstruction or arrhythmias and may lead to sudden death [1–15].

Microscopically the tumor contains fibrous tissue, fibroblasts, fat cells, endothelial-lined spaces, and smooth muscle cells. It has also been called fibrous hamartoma [1,2,10,11].

Teratoma

Teratomas are extremely rare cardiac tumors. They contain derivatives of all three germ layers and may be associated with congenital heart disease [1–5,10–14]. They are usually extracardiac but intrapericardial. They may be attached to the right ventricular outflow tract and compress the heart and cause tamponade. Like all teratomas, intrapericardial teratoma has a malignant potential.

Myxoma

Although myxomas are rarely seen before the age of 15 years, they do occur in adolescence [10,11,17–24]. The

(a)   (b)
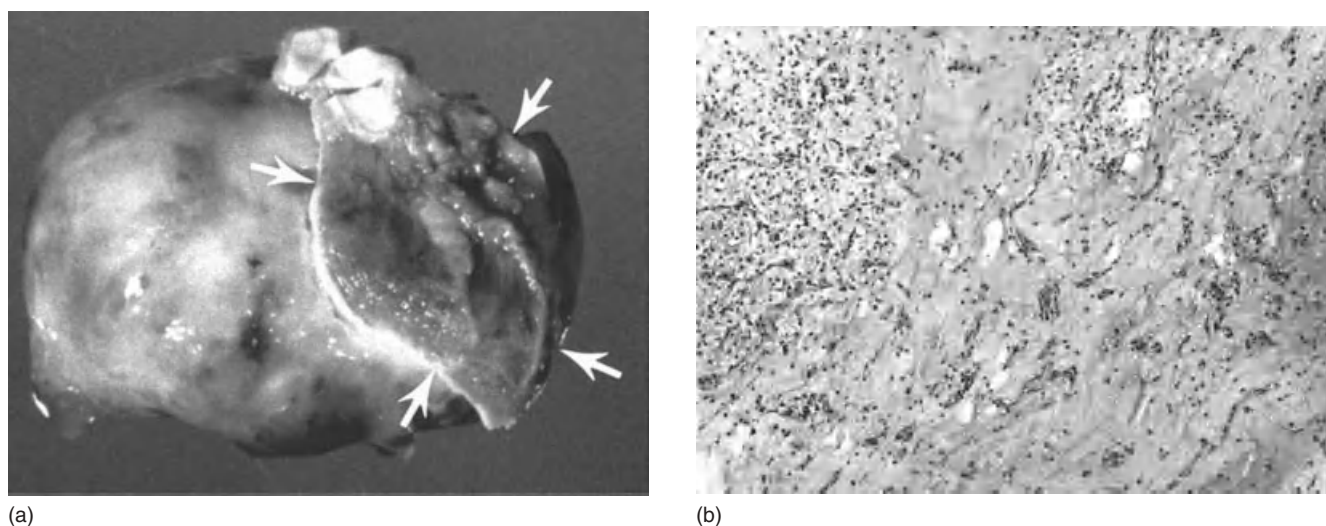
Figure 66.2 (a) Myxoma gross appearance. Arrows point to the region of attachment of tumor to atrial septum. (b) Myxoma. Hematoxylin–eosin stain, original magnification ×150. (Reproduced from Bharati, S, Lev M. Cardiac tumors. In: Adams FH, Emmanouilides GC, Riemanschneider TA, eds. *Moss' Heart Disease in Infants, Children and Adolescents*, 4th edn. Baltimore, MD: Williams and Wilkins, 1989: 886–90, with permission from Wolters Kluwer.)

tumor is usually in the left atrium and frequently in the right atrium. It is uncommon in the ventricles. Occasionally the tumor may be bilateral. When it occurs in the left atrium, it is usually near the fossa ovalis, but can occur in the parietal wall. In general, the tumor is attached to the atrial septum by a pedicle but it may be attached directly to the atrium. In one type the myxoma is transparent and in another it is a round or oval firm mass (Figure 66.2a).

Microscopically, it consists of plump endothelial cells associated with thin-walled capillaries and a large amount of amorphous matrix (Figure 66.2b). The myxoma cells are elongated and spindle shaped, with round or oval nuclei and a prominent nucleolus. Some cells are binucleated. The cells are arranged in syncytial groups and intimately associated with cleft-like, thin-walled capillaries. They have the combined features of smooth muscle cells and fibroblasts. On electron microscopy, a distinctive feature of myxoma cells is the presence of numerous cytoplasmic filaments. Calcification may occur. Large, thick-walled blood vessels are present in the pedicle. The predominant substance in the matrix is an acid mucopolysaccharide related to chondroitin C. The tumor also presents a variety of cell types: fibroblastic cells, macrophages, lymphocytes, plasma cells, mast cells, and mature and immature muscle cells. Gamma-Gandy bodies consisting of hemosiderin-laden macrocytes and degenerated collagen fibers encrusted with iron and calcium are also seen.

Most authors believe that the tumor originates from multipotential mesenchymal cells. Some believe that the myxoma is a true neoplasm and not an altered thrombus. A minority opinion still regards it is an organized mural thrombus, modified by mechanical forces.

Myxoma may embolize systemically or less commonly to one or both lungs. Occasionally, myxoma of the heart is associated with similar tumors in the choroid plexus, the left lateral ventricle of the brain, and the scapula. It is not known whether these constitute metastases or are related to embolization.

Clinically, the symptoms vary from obstruction of a valve to tumor embolus or systemic symptoms, or the patient may be asymptomatic. Myxomas often masquerade as mitral valve disease, connective tissue disorder, or infective endocarditis. Fever is common, and there may be weight loss, Reynaud's syndrome, polymyositis, hyperglobulinemia, and an elevated erythrocyte sedimentation rate. Some have attributed these findings to an increase in circulating interleukin-6 [24].

The mortality rate for surgical removal of cardiac myxoma is <5%. Recurrence may occur but is uncommon. Various types of arrhythmias, such as atrial flutter, fibrillation, junctional rhythm, sinus arrest, or complete AV block, may occur following surgical removal of the myxoma.

Cardiac myxomas are associated with various complexes [10,11,20–24,31]. One such complex consists of cardiac myxoma, multiple pigmented skin lesions (lentiginosis), myxoid fibroadenoma of the breast, skin myxomas, and primary pigmented nodular adrenocortical disease of the adrenal. A second, LAMB complex, consists of lentiginosis, atrial myxoma, mucocutaneous myxoma, and blue nevi. Another, NAME complex, consists of nevi, atrial myxoma, neurofibromatosis, and ephelides. Finally, Carney complex is a familial multiple neoplasia disorder consisting of cardiac myxoma, lentiginosis, primary pigmented nodular adrenocortical disease, bilateral myxoid fibroadenoma of the breast in the female, and testicular tumors in the male [(large cell calcifying Sertoli cell tumor and steroid-type tumor (Leydig cell)], with pituitary adenoma associated with acromegaly and giantism.
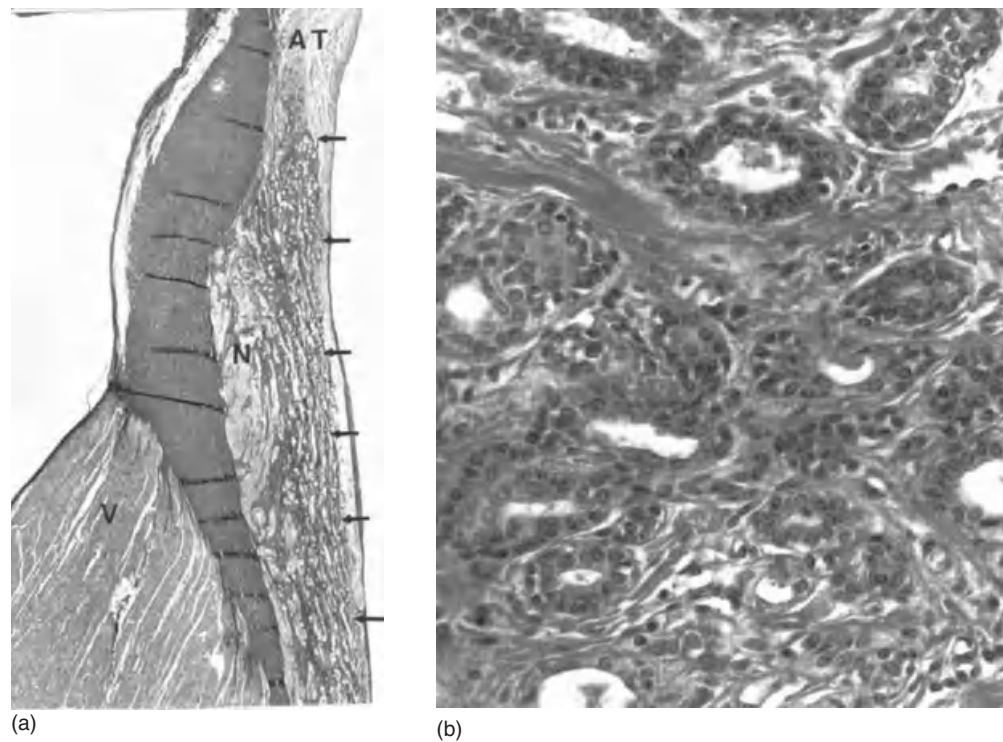
Figure 66.3 (a) Mesothelioma of the AV node in a 16-year-old young female who died suddenly 6 weeks following giving birth to a normal baby. AT, atrial septum; N, AV node; V, ventricular septum. Arrows point to mesothelioma replacing the AV node. Weigert-van Gieson stain, original magnification ×9.7. (b) Higher magnification of mesothelioma showing tubular formations of tumor. Hematoxylin–eosin stain, original magnification ×375. (Reproduced from Bharati S, Bicoff JP, Fridman JL, *et al. Arch Intern Med* 1976;**135**:224–8, with permission from the American Medical Association. Copyright © 1976 American Medical Association. All rights reserved.)

Papillary fibroelastoma

Although this is the second most common type of cardiac tumor, and the most common to affect endocardium and cardiac valves, it is rare in childhood. Any valve can be involved, most often aortic or mitral, then tricuspid, and least often the pulmonary valve. The fibroelastoma has a flower-like appearance with multiple elongated branching papillary fronds attached to the endocardium by a short pedicle [33]. Usually asymptomatic, it is a cause of systemic or pulmonary embolism; those on the aortic valve may cause myocardial infarction or sudden death. They are diagnosed by echocardiography, and can be removed surgically.

Other benign tumors

Several other benign tumors in the heart have been reported, including lipoma, hemangioma, granular cell tumor, and myoblastoma [1,2,10–14].

Mesothelioma of the AV node

This is a benign localized tumor of the AV node (Figure 66.3a) [10,25,26]. Although the tumor is rare, it may become evident clinically in adolescents. It usually produces complete heart block that may result in sudden death. The tumor affects the distal part of the atrial septum and the approaches to the AV node, and the AV node may be completely replaced by the tumor mass. It rarely extends to the AV bundle. Histologically it consists of cells arranged in masses or tubular form with no evidence of anaplasia (Figure 66.3b). In ultrastructure studies, it appears to be derived from mesothelial cells. About 50% of the reported patients are in younger age groups and more often in women.

Sarcoma

Primary cardiac sarcomas are rare in children but have been described in adolescence [1,2,5,10–14,28–30]. They are usually found in the atria, especially the right. Angiosarcoma is the most common type. The origin of these tumors in order of frequency is right atrium, left atrium, right ventricle, and left ventricle. These tumors are often associated with metastases to the lung, lymph nodes, mediastinum, liver, kidneys, adrenals, spleen, pancreas, brain, and bone. There are a number of types of sarcoma: angiosarcoma, rhabdomyosarcoma, leiomyosarcoma, spindle cell sarcoma, neurogenic sarcoma, osteosarcoma, undifferentiated sarcoma (Figure 66.4), fibrosarcoma, liposarcoma, fibromyxosarcoma, myxosarcoma, malignant melanoma,
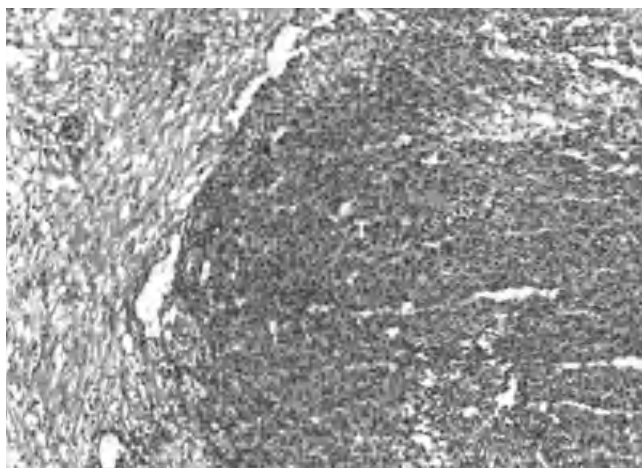
Figure 66.4 Sarcoma of atrial septum undifferentiated. Hematoxylin–eosin stain, original magnification ×120. T, tumor. (Reproduced from Bharati, S, Lev M. Cardiac tumors. In: Adams FH, Emmanouilides GC, Riemanschneider TA, eds. *Moss' Heart Disease in Infants, Children and Adolescents*, 4th edn. Baltimore, MD: Williams and Wilkins, 1989: 886–90, with permission from Wolters Kluwer.)
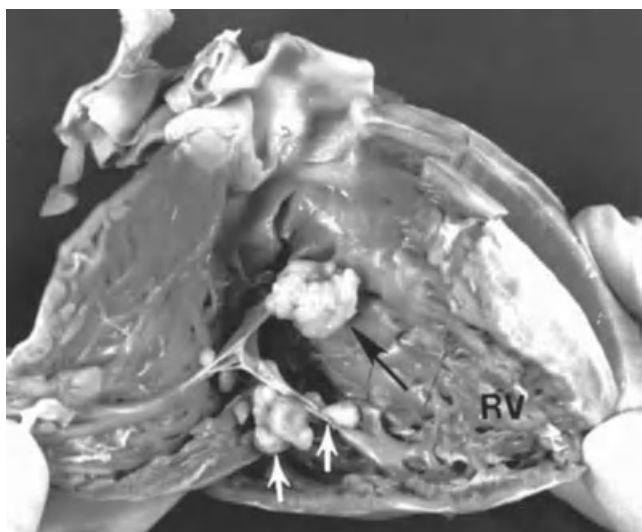
Figure 66.5 Metastases of an osteogenic sarcoma to the tricuspid valve in a 16-year-old girl. RV, right ventricle. Arrows point to the tumor on the tricuspid valve. (Reproduced from Bharati, S, Lev M. Cardiac tumors. In: Adams FH, Emmanouilides GC, Riemanschneider TA, eds. *Moss' Heart Disease in Infants, Children and Adolescents*, 4th edn. Baltimore, MD: Williams and Wilkins, 1989: 886–90, with permission from Wolters Kluwer.)

and mesenchymoma Among the lymphomas are reticulum sarcoma and lymphosarcoma.

Metastatases to the heart

In older people, metastatic tumors to the heart are twice as common as primary tumors. Carcinomas arising from breast, bronchi, kidneys, malignant melanoma, chondrosarcoma, malignant lymphoma, and leukemia may metastasize or spread to the heart. On the other hand, in children or adolescents, osteogenic sarcoma (Figure 66.5) [10,11] and chondrosarcoma are the most common causes of metastases to the heart.

References

1 McAllister HA Jr. Primary tumors of the heart and pericardium. *Pathol Ann*u 1979;**14**:325–55.

2 Smith C. Tumors of the heart. *Arch Pathol Lab Med* 1986;**110**:371–4.

3 Holley DG, Martin GR, Brenner JI, *et al.* Diagnosis and management of fetal cardiac tumors: a multicenter experience and review of published reports. *J Am Coll Cardiol* 1995;**26**:516–20.

4 Gunther T, Schreiber C, Noebauer C, *et al.* Treatment strategies for pediatric patients with primary cardiac and pericardial tumors: a 30-year review. *Pediatr Cardiol* 2008;**6**:1071–6.

5 Simpson L, Kumar SK, Okuno SH, *et al.* Malignant primary cardiac tumors: review of a single institution experience. *Cancer* 2008;**112**:2440–6.

6 Tatli S, Lipton MJ. CT for intracardiac thrombi and tumors. *Int J Cardiovasc Imaging* 2005;**21**:115–31.

7 Butany J, Nair V, Naseemuddin A, *et al.* Cardiac tumours: diagnosis and management. *Lancet Oncol* 2005;**6**:219–28.

8 O'Donnell DH, Abbara S, Chaithiraphan V, *et al.* Cardiac tumors: optimal cardiac MR sequences and spectrum of imaging appearances. *AJR Am J Roentgenol* 2009;**193**:377–87.

9 Riberi A, Gariboldi V, Grisoli D, Collart F. Cardiac tumors. *Rev Pneumol Clin* 2010;**66**:95–103.

10 Bharati, S, Lev M. Cardiac tumors. In: Adams FH, Emmanouilides GC, Riemanschneider TA, eds. *Moss' Heart Disease in Infants, Children and Adolescents*, 4th edn. Baltimore, MD: Williams and Wilkins, 1989: 886–90.

11 Bharati S, Lev M. Other complexes. In: *Pathology of Congenital Heart Disease. A Personal Experience with More than 6,300 Congenitally Malformed Hearts*. Armonk, NY: Futura Publishing, 1996: 1381–7.

12 Chan HSL, Sonley MJ, Moes CAF, *et al.* Primary and secondary tumors of childhood involving the heart, pericardium and great vessels: a report of 75 cases and review of the literature, *Cancer* 1985;**56**:825–36.

13 Uzun O, Wilson DG, Vujanic GM, *et al.* Cardiac tumours in children. *Orphanet J Rare Dis* 2007;**1**:2–11.

14 Van der Salm TJ. Unusual primary tumors of the heart. *Semin Thorac Cardiovasc Surg* 2000;**12**:89–100.

15 Pipitone S, Mongiovi M, Grillo R, *et al.* Cardiac rhabdomyoma in intrauterine life: clinical features and natural history. A case series and review of published reports. *Ital Heart J* 2002;**1**:48–52.

16 Chao AS, Chao A, Wang TH, *et al.* Outcome of antenatally diagnosed cardiac rhabdomyoma: case series and a meta-analysis. *Ultrasound Obstet Gynecol* 2008;**31**:289–95.

17 Coltart DJ, Billlingham ME, Popp RL, *et al.* Left atrial myxoma: diagnosis, treatment and cytological observations. *JAMA* 1975;**234**:950–3.

18 Chopra P, Sharma VK. Left atrial myxoma: a morphologic and histogenetic study. *Jpn Heart J* 1981;**22**:353–61.

19 Bateman TM, Gray RJ, Raymond MJ, *et al.* Arrhythmias and conduction disturbances following cardiac operation for the removal of the left atrial myxoma. *J Thorac Cardiovasc Surg* 1983;**87**:601–7.

20 Rhodes AR, Silverman RA, Harrist TJ, Perez-Atayde AR. Mucocutaneous lentigines, cardiomucocutaneous myxomas and multiple blue nevi: the LAMB syndrome. *J Am Acad Dermatol* 1984;**10**:72–82.

21 Carney JA, Gordon H, Carpenter PC, *et al.* The complex of myoxomas, and endocrine overactivity. *Medicine* 1985;**64**:270–83.

22 Landon G, Ordonez NG, Guardo JA. Cardiac myxomas, an immunohisochemical study using endothelial, histiocytic and smooth muscle cell markers. *Arch Pathol Lab Med* 1986;**110**:116–20.

23 Danoff A, Jormark S, Lorber D, Fleischer N. Adrenocortical micronodular dysplasia, cardiac myxomas, lentigines and spindle cell tumors: report of kindred. *Arch Intern Med* 1987;**147**:443–8.

24 Reynen, K. Cardiac myxomas. *N Engl J Med* 1995;**333**:1610–7.

25 Travers H. Congenital polycystic tumor of the atrioventricular node: possible familial occurrence and critical review of reported cases with special emphasis on histogenesis. *Hum Pathol* 1982;**13**:25–35.

26 Bharati S, Bicoff JP, Fridman JL, *et al.* Sudden death caused by benign tumor of the atrioventricular node. *Arch Intern Med* 1976;**135**:224–8.

27 Pinchot SN, Holen K, Sippel RS, Chen H. Carcinoid tumors. *Oncologist* 2008;**13**:1255–69.

28 Klima T, Milam JD, Bossart MI, Cooley DA. Rare primary sarcomas of the heart. *Arch Pathol Lab Med* 1986;**110**:1155–9.

29 Bear PA, Moodie DS. Malignant primary cardiac tumors: the Cleveland Clinic experience 1956 to 1986. *Chest* 1987;**92**:860–2.

30 Wakely RE. Angiosarcoma of the heart in an adolescent: a light and electron microscopic and immunohistochemical study. *Arch Pathol Lab Med* 1987;**111**:472–5.

31 Wilkes D, McDermott DA, Basson CT. Clinical phenotypes and molecular genetic mechanisms of Carney complex. *Lancet Oncol* 2005;**6**:501–8.

32 Oriova KA, Crino PB. The tuberous sclerosis complex. *Ann N Y Acad Sci* 2010;**1184**:87–105.

33 Gowda RM, Khan IA, Nair CK, *et al.* Cardiac papillary fibroelastoma: a comprehensive analysis of 725 cases. *Am Heart J* 2003;**146**:404–10.

67 Connective Tissue Disorders

Lut Van Laer & Bart Loeys
Center for Medical Genetics, Antwerp University Hospital,
University of Antwerp, Antwerp, Belgium

Introduction

"Connective tissue" refers to a complex structure composed of a cellular component (fibroblasts, smooth muscle cells) and the extracellular matrix. The extracellular matrix includes both structural proteins such as collagen, fibrillin, and fibronectin and ground substance such as proteoglycans. This matrix provides specific environmental signals to control cell morphology, migration, differentiation, proliferation, and metabolism. Together they form a network that provides resistance to mechanical forces while allowing diffusion of small molecules.

In the cardiovascular system, connective tissue is mostly present in the valves and vessel walls. The valves themselves (both atrioventricular valves and semilunar valves) are composed of different layers of connective tissue, covered with endothelial cells. As an example, the adult human aortic valve cusps are composed of about 10–15% of elastin and 45–55% of collagen. The composition of the extracellular matrix in blood vessels depends on the type and subtype of vessel, for example, elastic or muscular arteries, small, medium, or large veins. The larger arteries have proportionately more fibrillin and elastin, whereas the middle-sized arteries have more collagen in the medial layers.

Connective tissue disorders comprise a heterogeneous group of diseases, mostly affecting the ocular, skeletal, integument, and cardiovascular system. Common ocular findings include ectopia lentis, myopia, and corneal fragility. Frequent skeletal features include overgrowth leading to pectus deformities, scoliosis, disproportionate body measurements, joint laxity and contractures, osteoporosis, and fractures. The skin can be characterized by skin hyperlaxity, cutis laxa, easy bruising, smooth and velvety skin, and atrophic scarring. Cardiovascular findings include aortic and arterial aneurysms with tortuosity, valve insufficiency, patent ductus arteriosus, and atrial/ventricular septal defects.

In contrast to the skeletal dysplasias and osteogenesis imperfecta, which mainly affect the hard connective tissues, three groups of heritable disorders primarily affecting the soft connective tissues are discussed in this chapter, namely the heterogeneous group of Ehlers–Danlos syndromes, the aneurysm syndromes including Marfan and Loeys–Dietz syndrome, and the rare group of cutis laxa syndromes.

Ehlers–Danlos syndromes

Classification

The Ehlers–Danlos syndromes (EDS) comprise a clinically and genetically heterogeneous group of heritable disorders of which the principal clinical features are the result of varying degrees of tissue fragility of the skin, ligaments, blood vessels, and internal organs. The prevalence of EDS is estimated as ~1/5000 births, with no racial predisposition. However, this may be an underestimate as this group of diseases is not well known among clinicians. The first attempts to classify the EDS resulted in the Berlin Nosology in 1986, in which 10 subtypes were recognized [1]. Elucidating the molecular basis of several types of EDS resulted in refinement of this classification, which led to the 1997 Villefranche Nosology [2]. This classification recognizes six subtypes, based on clinical characteristics, mode of inheritance, and biochemical and molecular findings. The most frequent types of Ehlers–Danlos syndrome include the classic, hypermobility and vascular type, whereas the kyphoscoliosis, arthrochalasis, and dermatosparaxis types are very rare. During the past few years, it has become clear that this classification remains insufficient and that many patients present with overlapping

forms of EDS, which cannot unambiguously be classified into one of the six recognized subtypes. Recent insights into the molecular and biochemical basis of some EDS variants call for a refinement of the Villefranche classification, which will likely further improve appropriate diagnosis and counseling of affected families.

Clinical diagnosis

The main clinical characteristics of EDS present to varying degrees in each subtype of the syndrome, include joint hypermobility, skin hyperextensibility, delayed wound healing with atrophic scarring, easy bruising, and generalized fragility of the soft connective tissues.

Joint hyperlaxity is usually generalized but can vary tremendously in severity. Joint hypermobility is generally assessed using the Beighton scale. A score above five (out of nine) indicates joint hyperlaxity. However, joint hyperlaxity is present in ~10–20% of the normal population. Other common features in EDS include uni- or bilateral dislocation of the hip, club feet, and pes planum. During childhood, complications are usually limited to delayed motor development due to muscular hypotonia. From young adulthood on, subluxations and dislocations may occur, either spontaneously or after minimal trauma. All joints can be involved, but the most frequent ones include the costo-vertebral and costo-sternal joints, clavicles, shoulders, knee with patellar joint, and temporomandibular joints. Other problems related to joint hypermobility are joint effusions and premature osteoarthritis. Often adolescents start to suffer from chronic musculoskeletal pain, which is distinct from the acute pain associated with dislocations. The severity of the complaints is typically greater than expected based on physical and radiological examination, and the impact can be devastating, with disruption of sleep, work, physical activities, and social relations.

Skin hyperextensibility is characteristic for all EDS subtypes, except in the vascular type. In contrast to the skin in cutis laxa syndromes, the skin of EDS patients is hyperelastic, which means that it extends easily and snaps back after release. The skin is often very smooth and velvety to the touch. Wound healing is delayed, resulting in the formation of widened atrophic scars, so-called "cigarette-paper scars." These atrophic scars are typically located over knees, elbows, shins, forehead, and chin. In the vascular type, the skin is not hyperextensible, but rather thin and transparent, typically showing the venous pattern over the chest, abdomen, and extremities. Easy bruising is a common finding in patients with EDS and in small children it may even be the presenting symptom to the pediatrician. It manifests as spontaneous ecchymoses, frequently recurring in the same areas and causing a characteristic brownish discoloration of the skin, especially in exposed areas such as shins and knees. There is a tendency towards prolonged bleeding, for example, following brushing of the teeth, in spite of a normal coagulation status.

Other manifestations of generalized tissue fragility are observed in multiple organs and include cervical insufficiency, inguinal, umbilical, or other hernias, recurrent rectal prolapse in early childhood, and dehiscence of sutured incisions in skin or mucosa. Structural cardiac malformations are uncommon in most EDS types, but mitral valve prolapse and, less frequently, tricuspid valve prolapse may occur. The vascular type of EDS deserves special attention because this condition is associated with an increased risk of life-threatening complications and a decreased life expectancy.

Vascular Ehlers-Danlos syndrome

Vascular EDS (or the former type IV Ehlers–Danlos syndrome) is an autosomal dominant disorder caused by mutations in the gene encoding for type III collagen (COL3A1) (see Table 67.3). Clinical diagnosis can be confirmed biochemically by reduced type III collagen or identifying the causal COL3A1 gene after mutational analysis. In addition to the joint and skin problems, vascular EDS is clinically characterized by fragility of intestinal and genitourinary organs and vascular fragility leading to dissection or rupture of medium to large muscular arteries. Typically in vascular EDS, dissections often occur without preceding dilatation/aneurysm formation. In vascular EDS patients, complications in early childhood are rare. In the largest series reported so far, the average age at the time of a first complication was 23.5 years, with rupture of the gastrointestinal tract likely to occur at an earlier age than arterial rupture [3]. About half of the arterial complications in vascular EDS involved the thoracic or abdominal arteries and the rest were divided equally between the head, neck, and limbs. In vascular EDS, the reported incidence of fatal complications during or immediately after vascular surgery is around 45% [3]. It is very difficult to establish useful guidelines for cardiovascular imaging in vascular EDS because complications may occur unannounced and no specific treatment is available at present. Some authors advise not pursuing any additional investigation or surveillance, because a conservative approach will be adopted irrespectively and undue anxiety would be created. Others recommend noninvasive cardiovascular imaging with echocardiography and vascular computed tomography/magnetic resonance imaging (CT/MRI) [4].

Other rare variants of EDS

Although vascular ruptures are most typical for the vascular type of EDS, they can also occur in the rare kyphoscoliosis type of EDS. Features of classic EDS may be found in patients with other rare variants of EDS. For example, a subgroup of patients with the classic EDS phenotype has been observed who developed severe cardiac valvar problems, and in whom a complete deficiency of the proα2-chain of type I collagen has been identified. This autosomal recessive condition has been termed the "cardiac valvar subtype of

EDS" [5–7]. Classic EDS features were also observed in a number of children with non-glycine substitutions in the type I collagen triple helical domain [8]. Recent observations showed that this phenotype evolves to a vascular EDS-like phenotype in adult life, with increased risk for spontaneous arterial rupture [9].

Genetics/Inheritance

Most forms of EDS are autosomal dominant, although some more rare autosomal recessive forms occur. In the vascular form of EDS, every family has its own private mutation in the COL3A1 gene. Mutations most often affect the highly conserved glycine residues present at every third amino acid position in the helical domain of the type III collagen. About 50% of the COL3A1 mutations occur *de novo*, so the absence of a family history does not preclude this diagnosis.

Pathophysiology

Mutations of the COL3A1 gene typically result in a structural alteration of type III collagen that leads to intracellular storage and impaired secretion of collagen chains. A possible regulatory role for the type III collagen molecule has been suggested, although formal studies are still ongoing.

Marfan syndrome

Introduction

Over 100 years ago, the French pediatrician Antoine-Bernard Marfan described a 5-year-old girl, Gabrielle, with long slender digits, long bone overgrowth, and muscle hypoplasia [10]. Since then, clinical research has further delineated this condition and identified it as a systemic disorder of the connective tissue with severe manifestations in the cardio-vascular, ocular, and skeletal system demanding a multi-disciplinary approach for both diagnosis and management. Marfan syndrome (MFS) occurs worldwide with an incidence estimated up to 1/5000, affecting both sexes equally [11]. The disease demonstrates autosomal dominant inheritance with high penetrance and marked inter- and intrafamilial variability. MFS is caused by mutations in the FBN1 gene, encoding an important extracellular matrix protein, fibrillin-1.

Clinical characteristics

Long bone overgrowth contributes to the most striking observations in MFS, leading to disproportionately long limbs and anterior chest deformities due to rib overgrowth. Other major manifestations include arachnodactyly, elbow contractures, scoliosis or spondylolisthesis, protrusio acetabulae (detected by X-ray), and calcaneal displacement resulting in pes planus with hindfoot valgus. Arachnodactyly is often a subjective finding but requires the thumb sign (when the fully adducted thumb extends beyond the ulnar border of the palm) and wrist sign (when the distal phalanges of the thumb and fifth finger fully overlap when grasping the contralateral wrist). Patients may present with typical facial characteristics including downslanting palpebral fissures, enophthalmia, retrognathia, and a high arched palate with tooth crowding. Joint hypermobility may predispose to ligamentous injury, dislocations, chronic joint pain and premature arthrosis. Other troublesome locomotor symptoms include muscle hypoplasia and myalgia resulting in fatigue and spinal pain. These symptoms increase with age and affect up to 98% of adult patients [12]. MFS patients have been considered to have an increased number of fractures due to osteopenia, but this remains to be confirmed.

Ocular lens dislocation of any degree should promptly trigger further assessment for MFS. It occurs in about 50–67% of all patients. Final diagnosis of ectopia lentis can only be made by slit lamp examination. High myopia, retinal detachment, cataract, or glaucoma occur and may cause significant visual impairment or even blindness [13].

Although other systems may be severely impaired in MFS, cardiovascular pathology remains the leading cause of mortality and morbidity with aortic root dilatation, dissection, and rupture being life-threatening manifestations (see Table 67.3). The dilatation is generally greatest at the sinuses of Valsalva. Measurements should be normalized to body surface area and age [14]. Aortic root aneurysms occur in an age-dependent manner with high variability among individuals, prompting life-long follow-up. Although in severe disease the onset of dilatation occurs early in life, some individuals will never need aortic root replacement. The majority of fatal events associated with untreated MFS occur in early adult life. However, timely recognition and appropriate medical and surgical management of the disease increased the mean survival age to 72 years [15]. The improved life expectancy in MFS has revealed that patients are also prone to more distally occurring aortic manifestations, especially after aortic root replacement, requiring appropriate imaging [16]. Pulmonary artery diameters are significantly larger in MFS and may become apparent before aortic root dilatation, and so have potential diagnostic value, especially in children [17]. Two-thirds of patients have mitral valve dysfunction with most commonly valve prolapse, insufficiency and calcification often associated with myxomatous valve thickening [18]. In contrast, aortic valve insufficiency usually results from aortic root dilatation. At the extreme end of presentation, infants with neonatal MFS manifest severely impaired valve dysfunction leading to congestive heart failure, pulmonary hypertension, and even early death [19]. Primary progressive myocardial dysfunction is usually mild, but may be aggravated by β-adrenergic blockade or valve insufficiency [20].

Finally, some other organ systems are affected in Marfan patients. Dural ectasia is a frequent observation with a prevalence of up to 92% in Marfan patients, and may be detected in young children [21]. Unfortunately, many other

conditions, including neurofibromatosis and Loeys–Dietz and Ehlers–Danlos syndromes, manifest dural ectasia and its precise specificity and sensitivity are not established. Moreover, it requires specific imaging of the lumbosacral region with CT or MRI, reducing its accessibility. In some patients it causes discomfort such as low back pain, headaches, and irradiating leg pains [22].

Striae distensae independent of marked weight gain or pregnancy occur in up to two-thirds of all patients [23]. Recurrent inguinal or surgical hernias are common and need special attention. Pneumothorax and pulmonary emphysema and dysfunction, partly due to alveolar septation defects, represent rare but disabling manifestations. Restrictive lung disease may result from severe pectus deformities, but is rare in MFS. In view of the long bone overgrowth, pulmonary function should be normalized to sitting height rather than body surface area [24].

Diagnostic criteria

Diagnosis and management require a multidisciplinary approach by geneticists, cardiologists, orthopedic surgeons, and ophthalmologists with experience in this field [25]. The diagnosis of MFS has always relied on a set of international criteria, outlined by expert opinion. In 1996, the initial Berlin nosology was revised because of the risk of over-diagnosis and redefined as the Ghent nosology, a more stringent set of major and minor criteria [26]. These Ghent criteria have proven to work well because with improving molecular techniques, confirmation of the diagnosis is possible in >95% of patients [27]. However, concerns with the Ghent criteria are that some of the diagnostic manifestations have not been validated as thresholds (e.g., dural ectasia) and others necessitate cumbersome imaging studies. Moreover, in the absence of aortic dilatation, the diagnosis can be stigmatizing, hampering career aspirations and restricting life insurance opportunities. Following an international expert meeting, a revised Ghent nosology, in which aortic root aneurysm and ectopia lentis are cardinal features, is proposed [28] (Table 67.1). In the absence of any family history, the presence of these two manifestations is sufficient for the unequivocal diagnosis of MFS. In the absence of any of these two, the presence of bona fide FBN1 mutation or a combination of systemic features is required. For the latter, a new scoring system (Table 67.2) has been designed and validated. In this way, FBN1 testing is not mandatory but useful when available.

Pathophysiology

For a long time, the pathophysiology of MFS was entirely based on severely reduced and fragmented elastic fibers in affected tissues. This observation led to the hypothesis that structural deficiency of the fibrillin-1 protein was the most important player in the etiology of Marfan syndrome. Although this hypothesis offered an explanation for aortic

Table 67.1 Revised Ghent criteria for diagnosis of Marfan syndrome and related conditions[a].

With no family history:
1 Ao ($Z \geq 2$) AND EL = MFS[b]
2 Ao ($Z \geq 2$) AND FBN1 = MFS
3 Ao ($Z \geq 2$) AND Syst (≥7 pts) = MFS[b]
4 EL AND FBN1 with known Ao = MFS
   EL with or without Syst AND with an FBN1 not known with Ao or no FBN1= ELS
   Ao ($Z < 2$) AND Syst (≥5) without EL = MASS
   MVP AND Ao ($Z < 2$) AND Syst (<5) without EL = MVPS

With family history:
5 EL AND FH of MFS (as defined above) = MFS
6 Syst (≥7 pts) AND FH of MFS (as defined above) = MFS[b]
7 Ao ($Z \geq 2$ above 20 years old, $Z \geq 3$ below 20 years) + FH of MFS (as defined above) = MFS[b]

[a]Ao, aortic diameter at the sinuses of Valsalva above indicated Z-score or aortic root dissection; EL, ectopia lentis; ELS, ectopia lentis syndrome; FBN1, fibrillin–1 mutation; FBN1 with known Ao, FBN1 mutation that has been identified in an individual with aortic aneurysm; FBN1 not known with Ao, FBN1 mutation that has not previously been associated with aortic root aneurysm/dissection; MASS, myopia, mitral valve prolapse, aortic root dilatation, striae, skeletal findings, aortic aneurysm syndrome; Syst, systemic score (see Table 67.2); MFS, Marfan syndrome; MVPS, mitral valve prolapse syndrome; Z, Z-score.
[b]AND after TGFBR1/2, Caveat: without discriminating features of SGS, LDS or vasc. collagen biochemistry, COL3A1 testing if indicated, other conditions/genes will emerge with time, EDS (as defined in Table 67.3).

Table 67.2 Scoring of systemic features in Marfan syndrome.

- Wrist AND thumb sign – **3** (Wrist OR thumb sign – **1**)
- Pectus carinatum deformity – **2** (pectus excavatum or chest asymmetry – **1**)
- Hindfoot deformity – **2** (plain pes planus – **1**)
- Pneumothorax – **2**
- Dural ectasia – **2**
- Protrusio acetabuli – **2**
- Reduced US/LS AND increased arm/height AND no severe scoliosis – **1**
- Scoliosis or thoracolumbar kyphosis – **1**
- Reduced elbow extension – **1**
- Facial features (3/5) – **1** (dolichocephaly, enophtalmos, downslanting palpebral fissures, malar hypoplasia, retrognathia)
- Skin striae – **1**
- Myopia >3 diopters – **1**
- Mitral valve prolapse (all types) – **1**
Maximum total: **20** points; score ≥**7** indicates systemic involvement

pathology, it did not reconcile the observations of other clinical features such as long bone overgrowth, thickening of the cardiac valves, or muscle hypoplasia. The study of the fibrillin-1 mutant mouse that recapitulates the human

MFS has recently challenged this "mechanistic" view. Indeed, these mouse models have shown that structural fibrillin-1 deficiency leads to increased activation of the sequestered cytokine transforming growth factor beta (TGFβ) [29,30], which has a pivotal role in the development and maintenance of several tissues. Enhanced activation of the TGFβ pathway was shown to contribute to the development of emphysema, aortic aneurysms, and muscle hypoplasia seen in MFS. In murine models, these changes can be effectively blocked by the administration of TGFβ antibodies and an angiotensin receptor blocker, losartan [29,31,32].

Management

Cardiovascular follow-up should include serial evaluation with echocardiography or CT/MRI angiography when visibility of the aortic root and ascending aorta is limited [16]. The evaluation frequency should be tailored based upon aortic dimensions, the rate of aortic growth, and family history. β-Adrenergic blockade, titrated to physiological response, is a standard treatment to slow aortic growth mainly by virtue of its antihypertensive and negative inotropic effects [33]. If beta-blockade is contraindicated (asthma, Raynaud phenomenon, psoriasis, depression, fatigue), calcium antagonists or angiotensin-converting enzyme inhibitors may alternatively be used, although no randomized studies exist. Surgical repair of the aorta is indicated once the maximum diameter exceeds 5.0 cm in adults, when the rate of aortic growth exceeds >0.5–1.0 mm per year, or with significant aortic regurgitation. With proper aortic valve function, the preferred technique is the valve-sparing procedure, avoiding life-long anticoagulant therapy, especially in females in their fertile period. Although the superiority of this technique compared with the composite graft has not been established, the 10 year experience is very promising [34]. After surgical repair of the aortic root, imaging of the whole aorta is warranted for timely detection of aortic graft pseudo-aneurysms, more distally occurring aneurysms, and coronary artery aneurysms [25]. New therapeutic strategies, based upon the physiopathology in MFS, propose losartan as an anti-hypertensive agent attenuating TGFβ signaling. In mouse models, losartan has been shown to stop aortic growth and induces regression of emphysematous changes in the lung, even in adult life [32]. Currently ongoing randomized trials are focused on this new treatment possibility in MFS, which might also be beneficial in related conditions [31].

Orthopedic complications mainly involve anterior chest and vertebral column deformities that should be followed carefully, especially during and just after puberty. Because extreme pectus deformities have little impact on pulmonary function, surgery is considered a cosmetic issue.

Correction, preferably using the minimally invasive Nuss procedure, should not be done before the age of 11 years [35], as earlier intervention might lead to recurrent deformity due to continued rib growth. In contrast, severe (kypho)-scoliosis has major impact on quality of life, needing surgical stabilization, as bracing often remains inadequate [36]. Protrusio acetabulae is often asymptomatic in young adults, and the benefit of surgery is questioned [37]. Hormone therapy is indicated if predicted final height is unacceptable [38].

Diffraction anomalies due to lens subluxation, flat cornea, or myopia can easily be corrected by eyeglasses or contact lenses. Lens extraction for manifest ectopia lentis or cataract severely increases the pre-existing risk for retinal detachment and glaucoma with resultant significant visual impairment. Yearly examination by an experienced ophthalmologist in every Marfan patient is highly recommended.

Finally, lifestyle modifications may promote cardiovascular and psychosocial health and prevent or relieve many locomotor inconveniences, including arthrosis, fatigue, myalgia. and chronic joint pains. Patients should avoid competitive sports, straining, or isometric exercise, as these increase blood pressure and cause considerable dynamic stress on the aortic root. Additionally, contact sports should be avoided as these may precipitate aortic dissection [39]. Activity guidelines are available on the National Marfan Foundation website: http://www.marfan.org/.

Loeys–Dietz aortic aneurysm syndrome

Classification

A novel autosomal dominant aortic aneurysm syndrome characterized by the triad of hypertelorism, bifid uvula/cleft palate, and arterial tortuosity with ascending aortic aneurysm and dissection, caused by heterozygous loss-of-function mutations in the genes coding for the TGFβ receptors 1 or 2, TGFBR1 or TGFBR2, was recently described and designated "Loeys–Dietz syndrome" (LDS) [40]. Although some individuals show overlap with MFS, none satisfy diagnostic criteria. The main differences are the absence of significant long-bone overgrowth or lens dislocation, and many other discriminating findings can be present, including craniosynostosis, Chiari malformation, club feet, patent ductus arteriosus (PDA), and aneurysms/dissection throughout the arterial tree. In contrast to this typical presentation, referred to as LDS type 1, some patients show fewer craniofacial abnormalities but prominent skin and joint manifestations more reminiscent of EDS [41]. This phenotype, referred to as LDS type 2, is characterized by a velvety and translucent skin, easy bruising, widened atrophic scars, uterine rupture, severe peripartum bleedings, and arterial aneurysm/dissections throughout the arterial circulation.

Table 67.3 Differential diagnosis of aortic aneurysm syndromes[a,b].

	AD-CL	AR-CL	AR-CL	ATS	LDS	MFS	FTAAD	Vasc. EDS
Gene	ELN	FBLN-5	FBLN-4	SLC2A10	TGFBR1/TGFBR2	FBN1	ACTA2/MYH11	COL3A1
Inheritance	AD	AR	AR	AR	AD	AD	AD	AD
Arterial tortuosity	0	?	++	+++	++	0	0	0
Aortic/arterial aneurysm/dissection	+	0	++	++	+++	+++	+++	+++
Arterial stenosis	0	++	++	++	0	0	+	0
Cutis laxa/skin laxity	+++	+++	+	+	+/–	0	0	+
Emphysema	++	+++	+	0	0	+	0	0
Joint laxity	0	0	++	++	++	+	0	+
Contractures	0	0	0	+	+	+	0	0
Cleft palate/bifid uvula	0	0	0	+	++	0	0	0
Ectopia lentis	0	0	0	0	0	+++	0	0

[a]ACTA2, alpha2-actin; AD-CL, autosomal dominant cutis laxa; AR-CL, autosomal recessive cutis laxa; ATS, arterial tortuosity syndrome; COL, collagen; EDS vascular Ehlers–Danlos syndrome; ELN, elastin; FBLN, fibulin; FBN, fibrillin; FTAAD, familial thoracic aortic aneurysm dissection; LDS, Loeys–Dietz syndrome; MFS, Marfan syndrome; MYH11, myosin heavy chain 11. TGFBR, transforming growth factor beta receptor; Vasc.,.
[b]?, unknown; 0, absent; +, present; +/–, described but uncertain if associated.

Clinical characteristics

The Loeys–Dietz syndrome is characterized by four major groups of clinical findings: vascular dilatation and tortuosity, skeletal findings, facial dysmorphology, and skin symptoms.

In the cardiovascular system, dilatation of the aortic root, at the level of the sinuses of Valsalva, is the most important clinical finding (Table 67.3). At the time of diagnosis, about two-thirds of the patients already have an aneurysm of the aortic root, and virtually all LDS patients eventually develop dilatation of the aortic root [41,42]. Less frequently, and seldom isolated, aneurysms of the ascending and/or descending aorta are seen. The mean age at which aortic dilatation is established is in the teenage range. At the time of diagnosis, about one-fifth of the LDS patients already have an aortic dissection. Arterial tortuosity is seen in most individuals with a TGFBR1 or TGFBR2 mutation. Arterial tortuosity can be generalized but most commonly involves the head and neck vessels. Evaluation at baseline is best done with magnetic resonance angiography (MRA) or CT scan with 3D reconstruction. To identify all arterial aneurysms and arterial tortuosity throughout the arterial tree, it is mandatory to screen all vessels from head to pelvis. Approximately half of the individuals with LDS studied had an aneurysm distant from the aortic root that would not have been detected by echocardiography. Congenital heart diseases, such as a bicuspid aortic valve, an atrial septal defect, or a patent ductus arteriosus, are more frequently seen in LDS patients than in a normal population. Mitral valve prolapse and/or insufficiency is a recurrent finding in LDS patients, although less frequent than in MFS [43,44]. Recently, evidence was given that a TGFBR1 mutation in LDS can cause microvascular coronary artery dysplasia and subsequent cardiomyopathy [45].

Skeletal features in LDS show overlap with those of MFS: joint hyperlaxity, arachnodactyly, pectus deformity (pectus excavatum or carinatum), and scoliosis are frequently seen. In addition to the joint laxity, contractures of feet (talipes equinovarus) and fingers (camptodactyly) are common features in LDS [41,46–48]. Pes planus is often associated with inward rotation at the ankle. Dolichostenomelia (long limbs, leading to an increase in the arm span-to-height ratio and a decrease in the upper-to-lower segment ratio), as seen typically in MFS, is far less often described in LDS patients [41,46]. Other recurrent findings are cervical spine instability and spondylolisthesis [40,41,46]. The skeletal phenotype with respect to low bone mineral density and skeletal fragility is unclear. Approximately three-quarters of LDS patients have facial dysmorphologic features, and are therefore designated as patients with LDS type 1. Hypertelorism (wide-set eyes) and a cleft palate or a bifid uvula are major diagnostic characteristics of LDS [40,41]. Craniosynostosis is a recurrent feature. Most commonly the sagittal suture is prematurely closed (resulting in dolichocephaly), but the coronal suture (resulting in brachycephaly) and metopic suture (resulting in trigonocephaly) can also be involved. A bifid uvula (ranging in severity from a remarkable broad uvula, a uvula with raphe, to a clear split uvula) is the mildest form of a cleft palate. Other craniofacial findings are micro-retrognathia, blue sclerae, strabismus, and a high arched palate with dental crowding [42,49–51]. A correlation has been suggested between the severity and extent of craniofacial involvement (craniosynostosis, cleft

palate/abnormal uvula, and hypertelorism) and the age of first cardiovascular event [41]. Ectopia lentis, a cardinal clinical feature in MFS, is not seen in LDS [41]. In LDS type 2, there are no striking craniofacial features, although some patients have an isolated bifid uvula [41,52]. Some subtle facial features are observed: a tall, broad forehead, frontal bossing, a high anterior hair line, hypoplastic supraorbital margins, prominent upper central incisors in late childhood/adulthood, and an open-mouthed, myopathic face. Facies of adult LDS type 2 patients may also appear prematurely aged [52].

Skin findings include velvety, translucent skin with visible veins, and easy bruising [40,41,49]. Wound healing may be delayed, and scars appear dystrophic. Approximately 25% of LDS patients have these cutaneous features, and no craniofacial dysmorphology, and are designated as LDS type 2.

Importantly, the natural history of patients with TGFBR1/2 mutations is far more aggressive than in MFS or vascular EDS, with a mean age at death of 26.1 years. Aortic dissections occur in young childhood and/or at smaller aortic dimensions (<40 mm), and the incidence of pregnancy-related complications is high. However, these aneurysms are amenable to early and aggressive surgical intervention, a clear distinguishing feature from vascular EDS [17]. In congruence with the physiopathology in MFS, a paradoxically enhanced TGFβ signaling was demonstrated, opening perspectives on therapeutic intervention with losartan [15].

Management

Baseline evaluations are recommended to establish the extent of the disease. The aortic root must be measured by echocardiography. As approximately half of the individuals with LDS studied had an aneurysm distant from the aortic root that would have been missed by echocardiography, MRA or CT with 3D reconstruction from head to pelvis must be performed to detect arterial aneurysms throughout the arterial tree. Skeletal investigations should include an X-ray of the cervical spine to look for spine instability. Additional examinations for other manifestations of the disease (such as scoliosis or craniosynostosis) [53] can be guided based on physical examination. As there is no specific treatment for LDS, medical intervention should be focused on symptomatic treatment, prophylactic measures, and genetic counseling. Thorough follow-up of the cardiovascular situation, through echocardiography every 6 months and MRA/CT (frequency guided by initial baseline evaluation), is recommended [54]. As dissection occurs at smaller aortic diameters than observed in, for example, MFS, early and aggressive surgical intervention is a sensible approach [54]. Valve-sparing aortic root replacement using the reimplantation technique is the intervention of choice [55,56]. Because of the risk of patch pseudoaneurysm formation, the side branch technique for arch and visceral vessel reimplantation in arch and thoracoabdominal aortic repairs is advocated for patients with connective tissue disorders [57]. Open repair of descending thoracic and thoracoabdominal aneurysms should be the treatment of choice because the progressive aortic pathology is likely to result in late failures of endovascular repair as fixation zones continue to dilate [58]. Staged replacement of affected aortic segments is indicated, sometimes leading to replacement of the entire aorta [59]. Preventive, aggressive surgical reconstruction [60,61] is still controversial [62]. Beta-blocker therapy reduces hemodynamic stress. Angiotensin receptor blocker therapy may confer a long-term clinical benefit over beta-blocker therapy, similar to the beneficial role of angiotensin II blockade in patients with MFS [63]. Despite normal peripheral blood pressures, progression of aortic disease is seen in young individuals with LDS. Skeletal, craniofacial, and eye manifestations should be treated by a multidisciplinary team. Contact sports, isometric exercises, competitive sports, and activities that cause joint pain/injury should be avoided. Individuals should perform moderate physical activity.

Genetics

LDS is caused by heterozygous mutations in the TGFβ receptor 1 or 2 gene (TGFBR1 or TGFBR2), and is transmitted as an autosomal dominant trait. TGFBR1 is mapped on the long arm of chromosome 9, band 9q33–q34. The locus of TGFBR2 is situated on chromosome 3p22. No clinical difference can be made between patients with mutations in TGFBR1 and TGFBR2. About one-third of the mutations occur *de novo*.

Pathophysiology

Although the precise pathogenetic mechanism remains unclear, TGFβ signaling is enhanced in the presence of heterozygous mutations in TGFβR1 or TGFβR2 in LDS, as evidenced by increased nuclear accumulation of phosphorylated Smad2 (an intracellular mediator of TGFβ signaling) and increased output of TGFβ-responsive genes in aortic walls and aortic cell cultures derived from LDS patients. As in MFS, histology of the aortic wall in LDS patients shows disorganization of the elastic fibers in the aortic media, and increased collagen deposits, also suggestive of increased TGFβ signaling. LDS patients show predominantly medial degeneration of the diffuse type. This disturbance accounts for the propensity for arterial tears or dissections, typical for LDS syndrome.

Although until recently most studies have focused on the canonical TGFβ signaling, there is emerging evidence that non-canonical pathways such as the MAPKs (the mitogen-activated protein kinases) may have a role in aneurysm development. Recent studies observed in the aorta of fibrillin-1 deficient mice that TGFβ and angiotensin II -type 1 receptor (AT1R)-dependent activation of the extracellular-signal regulated kinases (ERK1 and ERK2) are involved in the pathogenesis of aneurysms, and further evidence for their importance was obtained from the abrogation of pathological aortic root growth after treatment with a specific ERK inhibitor [63a,63b].

Osteogenesis imperfecta

Historically, osteogenesis imperfecta (OI) has been viewed as an autosomal disorder of type I collagen, the major protein component in the extracellular matrix of bone. In the past several years, this paradigm of OI has undergone a major shift with the identification of several autosomal recessive forms. The autosomal dominant form is caused by mutations in the COL1A1 (chr 17) and COL1A2 (chr 7) coding for the alpha1 and alpha2 chain of type I collagen, respectively. Type I collagen is the major collagen in bone, which bears the brunt of the disease, but it occurs also in arterial walls and cardiac valves. [64–66]. There are four main autosomal dominant types:

I Normal stature, with bone fractures following minimal trauma, blue sclerae, and hearing loss (50% of families); tendency for decreased fractures with age. Dentinogenesis imperfecta is rare and distinguishes a subset.

II Due to *de novo* mutations, cause of intrauterine or neonatal death with gross bony and cartilaginous abnormalities. Counseling should take into account parental mosaicism.

III Very short stature and multiple fractures, leading to progressive deformity. Dentinogenesis imperfecta and hearing loss are common.

IV Milder form of type I, prominent tibial bowing.

Cardiac involvement is uncommon, and almost invariably affects the left side. Patients may have aortic root dilatation, but dissection and rupture are rare [67,68]. Aortic or mitral regurgitation may occur; mitral valve prolapse occurs, but probably not more frequently than in the normal population. Premature coronary artery disease occurs rarely.

For type V the genetic basis is unknown. In type V, the patients also have a triad of hypertrophic callus, dense metaphyseal bands, and ossification of the interosseus membranes of the forearm. Typical is the distinctive histology with irregular arrangements or a mesh-like appearance of the lamellae. Type VI is characterized by a fish-scale pattern of the lamellae and a decreased bone mineralization secondary to increased osteoid volume. Type VI is autosomal recessive and caused by mutation in the gene FKBP10, coding for FKBP65, a chaperone that participates in type I procollagen folding [69].

Types VII to IX are all severe or neonatally lethal recessive forms of OI. These forms are caused by defects of the collagen prolyl 3-hydroxylation complex [CRTAP coding for cartilage-associated protein, LEPRE-1 coding for the enzyme prolyl 3-hydroxylation (P3H1), and PPIB coding for cyclophylin B] [70–72]. Finally, two other recessive forms have recently been described with mutations in SERPINH1, which encodes the collagen chaperone HSP47 [73], and Osterix, a gene encoding a transcription factor SP7 [74].

Cutis laxa syndromes

Cutis laxa (CL) syndromes are a heterogeneous group of extremely rare connective tissue disorders characterized by an increased number of inelastic skin folds. Clinical classification is based on the mode of inheritance and systemic manifestations. Two major types of CL are important in the context of aortic aneurysm: autosomal dominant CL and type 1 autosomal recessive CL (see Table 67.3).

Autosomal dominant CL was historically considered to be a strictly dermal condition with generalized skin folds, but more recent reports mentioned pulmonary emphysema and aortic root dilatation with dissection in early adulthood [75]. The aortic pathology of these aneurysms was indistinguishable from what is seen in MFS. Mutations in the elastin (ELN) and fibulin 5 (FBLN5) genes have been associated with autosomal dominant CL.

Type 1 autosomal recessive CL is characterized by generalized cutis laxa and severe lung emphysema [76]. Arterial tortuosity with severe fragmentation of the elastic fibers is associated both in humans and mice. So far, genetic defects in patients with autosomal recessive CL are identified in the FBLN4, FBLN5, and LTBP4 genes [77–80].

Pseudoxanthoma elasticum

This rare autosomal recessive disorder of elastic tissue is associated with mutations in the ABCC6 gene on chromosome 16p3.1 [81]. The ABCC6 protein is a member of the ATP-binding transmembrane transporters but the substrate of this transporter is still unknown. There is fragmentation and calcification of elastic fibers [82,83]. The disease affects the skin that shows yellow papules and a crinkled appearance ("plucked chicken skin"). Retinal angiomatoid streaks develop and may interfere with vision. Arterial involvement is widespread and may result in gastrointestinal or other bleeding, renal vascular hypertension, intermittent claudication, or angina pectoris. Mitral valve prolapse is common [84,85]. Severe coronary arterial disease has been recorded in children as young as 8 years of age [86,87]. Restrictive cardiomyopathy has been described [88]. A few patients may have left ventricular hypertrophy, even in the absence of skin changes.

Related syndromic causes of aortic/arterial disease

Arterial Tortuosity Syndrome

Arterial tortuosity syndrome (ATS) is a rare autosomal recessive condition characterized by extensive and generalized tortuosity and aneurysms of the large and medium-sized

arteries, often resulting in death at young age (Table 67.3). Other typical features include stenosis of the pulmonary arteries, characteristic facial features including hypertelorism and bifid uvula, and several systemic connective tissue manifestations including pectus deformity, loose joints, and lax skin [89]. Loss of function of the facilitative glucose transporter GLUT10 (encoded by the SLC2A10 gene) underlies this peculiar phenotype [90]. Although it is surprising that a glucose transporter defect causes abnormal arterial patterning, additional studies indicated up-regulation of the TGFβ signaling pathway [90], consistent with the physiopathology in LDS and MFS.

Congenital contractural arachnodactyly

Congenital contractural arachnodactyly (CCA) or Beals syndrome is characterized by arachnodactyly and slender habitus in which arm span exceeds height. Most affected individuals have "crumpled" ears that present as a folded upper helix of the external ear and most have contractures of major joints (knees and ankles) at birth. The proximal interphalangeal joints also have flexion contractures, as do the toes. Hip contractures, adducted thumbs, and club foot may occur. Most affected individuals have muscular hypoplasia. Contractures usually improve with time. Kyphosis/scoliosis is present in about half of all affected individuals. Progressive enlargement of the ascending aorta at the sinuses of Valsalva has been reported, but there is no evidence that the aortic dilatation progresses to dissection or rupture [91]. FBN2, the gene encoding the extracellular matrix microfibril fibrillin-2, is the only gene known to be associated with CCA [92]. Inheritance is autosomal dominant.

Shprintzen–Goldberg syndrome (SGS)

Another differential diagnosis is Shprintzen–Goldberg syndrome (SGS), a rare craniosynostosis syndrome characterized by marfanoid skeletal features, craniofacial dysmorphism (exophthalmos, hypertelorism, downslanting palpebral fissures, maxillary and mandibular hypoplasia, high arched palate, and low-set ears), and developmental delay. Two SGS patients have been reported with TGFBR mutations; however, both patients were thought to have LDS based on aortic root aneurysm/arterial tortuosity and a bifid uvula or cleft palate [93]. Although SGS and LDS show extensive phenotypic overlap, most patients with SGS do not show vascular involvement. Other distinguishing features of LDS include bifid uvula, cleft palate, arterial tortuosity, and a low incidence of developmental delay.

Other syndromes with possible involvement of the aortic root

Turner syndrome (45,X0), Noonan syndrome (caused by PTPN11, KRAS, or SOS1 mutations), and autosomal dominant polycystic kidney disease (caused by PKD1 or PKD2 mutations) are associated with thoracic aortic aneurysm, but the precise

risk for dissection has not yet been determined. Regular evaluation of the aortic diameters is therefore recommended.

Related non-syndromic causes of aortic/arterial disease

Thoracic Aortic Aneurysm with Bicuspid Aortic Valve (TAA with BAV)

With a prevalence of 1–2%, bicuspid aortic valve (BAV) is one of the most common cardiac malformations of the general population and is found in up to 8% of patients with aortic dissection detected at postmortem examination. Importantly, the aortic dilatation often occurs above the sinuses of Valsalva, and CT or MRI is indicated if echocardiography does not allow good visualization of the ascending aorta. BAV is found in 9% of first-degree relatives of affected individuals, but accurate counseling is complicated by nonpenetrance. Increasing evidence indicates that both aberrant valve formation and aortic root dilatation are the consequences of a common underlying defect. Thus far, mutations have been identified in NOTCH1 and KCNJ2 genes in most patients with additional congenital cardiac malformations [94], but linkage analysis reveals genetic heterogeneity with loci identified on chromosomes 18q, 5q, and 13q [95].

Thoracic aortic aneurysm with patent ductus arteriosus (TAA with PDA)

Following genetic linkage analysis in two large families with a high incidence of TAA in conjunction with PDA, mutations were found in the MYH11 gene encoding the myosin heavy protein 11, a specific contractile protein of smooth muscle cells. The structural defect leads to lower aortic compliance, smooth muscle cell loss, and elastolysis, but the precise pathophysiology remains unclear [96].

Familial thoracic aortic aneurysm and dissection (FTAAD)

TAAD usually presents with no or minor systemic involvement. Importantly, aortic aneurysms in TAAD can also occur distally from the sinuses of Valsalva, warranting imaging of the entire aorta. Clinical presentation is extremely variable with regard to the age of onset and degree of progression of the dilatation. Genetic predisposition is an important etiologic factor because 20% of patients with TAAD have a positive history of familial TAAD (FTAAD) with predominantly autosomal dominant segregation with decreased penetrance.

In contrast to syndromic TAAD, the identification of genetic defects in nonsyndromic forms has only recently been started. Occasional FBN1 mutations have been identified in patients with TAAD, who often show limited skeletal marfanoid involvement and probably represent incomplete expression of the MFS. Genetic mapping studies

demonstrate large genetic heterogeneity with several loci identified so far. Some families are not linked to any of these loci so that other loci must exist. Therefore, it is not always possible to perform clinical diagnostic genetic testing for this syndrome. A first major locus mapped to 5q13–14 in 9/15 families with autosomal dominantly segregating FTAAD with reduced penetrance and 7/11 Finnish families in a subsequent study [97]. A second locus for familial aortic aneurysms, designated FAA1, mapped to 11q23–24 in a single, large family [98], characterized by a more diffuse vascular disease affecting the whole aorta in addition to middle-sized arteries. In the third locus predisposing to TAAD, TAAD2, mapped to 3p24–25 [99], TGFBR2 has been identified as the mutant gene. TGFBR2 mutations were found in 4/80 unrelated families with familial TAAD, making it a relatively rare cause of familial TAAD [100]. Although vascular disease in these families mainly involved the ascending aorta, widespread vascular involvement occurred and other connective tissue findings including pectus deformity and joint hypermobility were observed. It is unknown whether some members of these families had other features of LDS. Subsequently, TGFBR1 mutations were also identified in FTAA families [101]. Finally, mutations in the gene encoding ACTA2, another sarcomeric protein, were found responsible for up to 16% of familial aortic aneurysms. In these families, associated features included iris flocculi, livido reticularis, cerebral aneurysm, bicuspid aortic valves, and persistent ductus arteriosus [102,103].

Familial abdominal aortic dissecting aneurysm

Rupture of aortic aneurysms in adults beyond middle age, with a striking male predominance, is responsible for 1–2% of deaths in industrialized countries and has been attributed to atherosclerosis or hypertension. This attribution has had to be revised because familial aneurysms with a tendency to dissection have been described in the abdominal aorta [104,105]. Although these aortic aneurysms occur in about 1% of the population, patients with an aneurysm are 15 times more likely to have a relative with an aneurysm than is someone of the same age without an aneurysm [106,107]. The aorta shows cystic medial necrosis, sometimes with loss of elastic fibers, but microfibrillar fiber arrays have been normal. In some families, a deficiency of type III collagen was found [104,108]. Some patients have shown increases in serum and leukocyte elastolytic activity [109]. Although most of the dissection has occurred beyond middle age, deaths have occurred in children aged 10–15 years.

Should there be a family history of this disease, annual echocardiographic study of the aortic dimensions should be undertaken, as in MFS. Progressive dilatation of the aorta is a reason to consider surgical replacement of that segment.

There is an animal model of aneurysms in the blotchy mouse [110], which is known to have a deficiency of lysyl oxidase, an enzyme responsible for cross-linking elastin and collagen. Treatment with β-adrenergic blockade reduces the aneurysm formation.

References

1 Beighton P, De Paepe A, Danks D, *et al*. International Nosology of Heritable Disorders of Connective Tissue, Berlin, 1986. *Am J Med Genet* 1988;**29**:581–94.

2 Beighton P, De Paepe A, Steinmann B, *et al*. Ehlers–Danlos syndromes: revised nosology, Villefranche, 1997. Ehlers–Danlos National Foundation (USA) and Ehlers–Danlos Support Group (UK). *Am J Med Genet* 1998;**77**:31–7.

3 Pepin M, Schwarze U, Superti-Furga A, Byers PH. Clinical and genetic features of Ehlers–Danlos syndrome type IV, the vascular type. *N Engl J Med* 2000;**342**:673–80.

4 Oderich GS, Panneton JM, Bower TC, *et al*. The spectrum, management and clinical outcome of Ehlers–Danlos syndrome type IV: a 30-year experience. *J Vasc Surg* 2005;**42**:98–106.

5 Hata R, Kurata S, Shinkai H. Existence of malfunctioning proα2(I) collagen genes in a patient with a proα2(I)-chain-defective variant of Ehlers–Danlos syndrome. *Eur J Biochem* 1988;**174**:231–7.

6 Sasaki T, Arai K, Ono M, *et al*. Ehlers–Danlos syndrome. A variant characterized by the deficiency of proα2 chain of type I procollagen. *Arch Dermatol* 1987;**123**:76–9.

7 Schwarze U, Hata R, McKusick VA, *et al*. Rare autosomal recessive cardiac valvular form of Ehlers–Danlos syndrome results from mutations in the COL1A2 gene that activate the nonsense-mediated RNA decay pathway. *Am J Hum Genet* 2004;**74**:917–30.

8 Nuytinck L, Freund M, Lagae L, *et al*. Classical Ehlers–Danlos syndrome caused by a mutation in type I collagen. *Am J Hum Genet* 2000;**66**:1398–402.

9 Malfait F, Symoens S, De Backer J, *et al*. Three arginine to cysteine substitutions in the pro-alpha (I)-collagen chain cause Ehlers–Danlos syndrome with a propensity to arterial rupture in early adulthood. *Hum Mutat* 2007;**28**:387–95.

10 Marfan A. Un cas de déformation congénitale des quatres membres, plus prononcée aux extremités, caractérisée par l'allongement des os avec un certain degré d'amincissement. *Bull Mem Soc Med Hôp Paris* 1886;**13**:220–8.

11 Pyeritz R. Marfan syndrome and other disorders of fibrillin. In: Rimoin DL, Connor JM, Pyeritz RE, eds. *Emery and Rimoin's Principles and Practice of Medical Genetics*, 3rd edn. New York: Churchill Livingstone, 1997: 1027–66.

12 Grahame R, Pyeritz RE. The Marfan syndrome: joint and skin manifestations are prevalent and correlated. *Br J Rheumatol* 1995;**34**:126–31.

13 Maumenee IH. The eye in the Marfan syndrome. *Trans Am Ophthalmol Soc* 1981;**79**:684–733.

14 Roman MJ, Devereux RB, Kramer-Fox R, O'Loughlin J. Two-dimensional echocardiographic aortic root dimensions in normal children and adults. *Am J Cardiol* 1989;**64**:507–12.

15 Silverman DI, Burton KJ, Gray J, *et al*. Life expectancy in the Marfan syndrome. *Am J Cardiol* 1995;**75**:157–60.

16 Milewicz DM, Dietz HC, Miller DC. Treatment of aortic disease in patients with Marfan syndrome. *Circulation* 2005;**111**:e150–7.

17 De Backer J, Loeys B, Devos D, *et al*. A critical analysis of minor cardiovascular criteria in the diagnostic evaluation of patients with Marfan syndrome. *Genet Med* 2006;**8**:401–8.

18 Pyeritz RE, Wappel MA. Mitral valve dysfunction in the Marfan syndrome. Clinical and echocardiographic study of prevalence and natural history. *Am J Med* 1983;**74**:797–807.

19 Sisk HE, Zahka KG, Pyeritz RE. The Marfan syndrome in early childhood: analysis of 15 patients diagnosed at less than 4 years of age. *Am J Cardiol* 1983;**52**:353–8.

20 De Backer JF, Devos D, Segers P, *et al*. Primary impairment of left ventricular function in Marfan syndrome. *Int J Cardiol* 2006;**112**:353–8.

21 Fattori R, Nienaber CA, Descovich B, *et al*. Importance of dural ectasia in phenotypic assessment of Marfan's syndrome. *Lancet* 1999;**354**:910–3.

22 Foran JR, Pyeritz RE, Dietz HC, Sponseller PD. Characterization of the symptoms associated with dural ectasia in the Marfan patient. *Am J Med Genet* 2005;**134**:58–65.

23 Cohen PR, Schneiderman P. Clinical manifestations of the Marfan syndrome. *Int J Dermatol* 1989;**28**:291–9.

24 Streeten EA, Murphy EA, Pyeritz RE. Pulmonary function in the Marfan syndrome. *Chest* 1987;**91**:408–12.

25 Ades L. Guidelines for the diagnosis and management of Marfan syndrome. *Heart Lung Circ* 2007;**16**:28–30.

26 De Paepe A, Devereux RB, Dietz HC, *et al*. Revised diagnostic criteria for the Marfan syndrome. *Am J Med Genet* 1996;**62**:417–26.

27 Loeys B, De Backer J, Van Acker P, *et al*. Comprehensive molecular screening of the FBN1 gene favors locus homogeneity of classical Marfan syndrome. *Hum Mutat* 2004;**24**:140–6.

28 Loeys BL, Dietz HC, Braverman AC, *et al*. The revised Ghent nosology for the Marfan syndrome. *J Med Genet* 2010;**47**:476–85.

29 Neptune ER, Frischmeyer PA, Arking DE, *et al*. Dysregulation of TGF-beta activation contributes to pathogenesis in Marfan syndrome. *Nat Genet* 2003;**33**:407–11.

30 Pereira L, Andrikopoulos K, Tian J, *et al*. Targetting of the gene encoding fibrillin-1 recapitulates the vascular aspect of Marfan syndrome. *Nat Genet* 1997;**17**:218–22.

31 Cohn RD, van Erp C, Habashi JP, *et al*. Angiotensin II type 1 receptor blockade attenuates TGF-beta-induced failure of muscle regeneration in multiple myopathic states. *Nat Med* 2007;**13**:204–10.

32 Habashi JP, Judge DP, Holm TM, *et al*. Losartan, an AT1 antagonist, prevents aortic aneurysm in a mouse model of Marfan syndrome. *Science* 2006;**312**:117–21.

33 Shores J, Berger KR, Murphy EA, Pyeritz RE. Progression of aortic dilatation and the benefit of long-term beta-adrenergic blockade in Marfan's syndrome. *N Engl J Med* 1994;**330**:1335–41.

34 Kallenbach K, Baraki H, Khaladj N, *et al*. Aortic valve-sparing operation in Marfan syndrome: what do we know after a decade? *Ann Thorac Surg* 2007;**83**:S764–8; discussion S785–90.

35 Lawson ML, Mellins RB, Tabangin M, *et al*. Impact of pectus excavatum on pulmonary function before and after repair with the Nuss procedure. *J Pediatr Surg* 2005;**40**:174–80.

36 Jones KB, Erkula G, Sponseller PD, Dormans JP. Spine deformity correction in Marfan syndrome. *Spine* 2002;**27**:2003–12.

37 Giampietro PF, Raggio C, Davis JG. Marfan syndrome: orthopedic and genetic review. *Curr Opin Pediatr* 2002;**14**:35–41.

38 Knudtzon J, Aarskog D. Estrogen treatment of excessively tall girls with Marfan syndrome. *Acta Paediatr Scand* 1988;**77**:537–41.

39 Braverman AC. Exercise and the Marfan syndrome. *Med Sci Sports Exerc* 1998;**30**:S387–95.

40 Loeys BL, Chen J, Neptune ER, *et al*. A syndrome of altered cardiovascular, craniofacial, neurocognitive and skeletal development caused by mutations in TGFBR1 or TGFBR2. *Nat Genet* 2005;**37**:275–81.

41 Loeys BL, Schwarze U, Holm T, *et al*. Aneurysm syndromes caused by mutations in the TGF-beta receptor. *N Engl J Med* 2006;**355**:788–98.

42 Singh KK, Rommel K, Mishra A, *et al*. TGFBR1 and TGFBR2 mutations in patients with features of Marfan syndrome and Loeys–Dietz syndrome. *Hum Mutat* 2006;**27**:770–7.

43 Attias D, Stheneur C, Roy C, *et al*. Comparison of clinical presentations and outcomes between patients with TGFBR2 and FBN1 mutations in Marfan syndrome and related disorders. *Circulation* 2009;**120**:2541–9.

44 Taub CC, Stoler JM, Perez-Sanz T, *et al*. Mitral valve prolapse in Marfan syndrome: an old topic revisited. *Echocardiography* 2009;**26**:357–64.

45 Eckman PM, Hsich E, Rodriguez ER, *et al*. Impaired systolic function in Loeys–Dietz syndrome: a novel cardiomyopathy? *Circ Heart Fail* 2009;**2**:707–8.

46 Jamsheer A, Henggeler C, Wierzba J, *et al*. A new sporadic case of early-onset Loeys–Dietz syndrome due to the recurrent mutation p.R528C in the TGFBR2 gene substantiates interindividual clinical variability. *J Appl Genet* 2009;**50**:405–10.

47 Kirmani S, Tebben PJ, Lteif AN, *et al*. Germline TGF-beta receptor mutations and skeletal fragility: a report on two patients with Loeys–Dietz syndrome. *Am J Med Genet A* 2010;**152**A:1016–9.

48 Muramatsu Y, Kosho T, Magota M, *et al*. Progressive aortic root and pulmonary artery aneurysms in a neonate with Loeys–Dietz syndrome type 1B. *Am J Med Genet A* 2010;**152**A:417–21.

49 Aalberts JJ, van den Berg MP, Bergman JE, *et al*. The many faces of aggressive aortic pathology: Loeys–Dietz syndrome. *Neth Heart J* 2008;**16**:299–304.

50 Drera B, Ritelli M, Zoppi N, *et al*. Loeys–Dietz syndrome type I and type II: clinical findings and novel mutations in two Italian patients. *Orphanet J Rare Dis* 2009;**4**:24.

51 Yetman AT, Beroukhim RS, Ivy DD, Manchester D. Importance of the clinical recognition of Loeys–Dietz syndrome in the neonatal period. *Pediatrics* 2007;**119**:e1199–202.

52 Ades LC. Evolution of the face in Loeys–Dietz syndrome type II: longitudinal observations from infancy in seven cases. *Clin Dysmorphol* 2008;**17**:243–8.

53 Rodrigues VJ, Elsayed S, Loeys BL, *et al*. Neuroradiologic manifestations of Loeys–Dietz syndrome type 1. *Am J Neuroradiol* 2009;**30**:1614–9.

54 Williams JA, Loeys BL, Nwakanma LU, *et al*. Early surgical experience with Loeys–Dietz: a new syndrome of aggressive thoracic aortic aneurysm disease. *Ann Thorac Surg* 2007;**83**:S757–63; discussion S785–90.

55 David TE, Feindel CM, Webb GD, *et al*. Long-term results of aortic valve-sparing operations for aortic root aneurysm. *J Thorac Cardiovasc Surg* 2006;**132**:347–54.

56 Everitt MD, Pinto N, Hawkins JA, *et al*. Cardiovascular surgery in children with Marfan syndrome or Loeys–Dietz syndrome. *J Thorac Cardiovasc Surg* 2009;**137**:1327–32; discussion 1332–3.

57 Lemaire A, Nikolic I, Petersen T, *et al*. Nine-year single center experience with cervical mediastinoscopy: complications and false negative rate. *Ann Thorac Surg* 2006;**82**:1185–9; discussion 1189–90.

58 Williams ML, Wechsler SB, Hughes GC. Two-stage total aortic replacement for Loeys–Dietz syndrome. *J Card Surg* 2010;**25**:223–4.

59 Rankin JS, Braverman AC, Kouchoukos NT. Total aortic replacement in Loeys–Dietz syndrome. *Ann Thorac Surg* 2009;**87**:1949–51.

60 Augoustides JG, Andritsos M. Innovations in aortic disease: the ascending aorta and aortic arch. *J Cardiothorac Vasc Anesth* 2010;**24**:198–207.

61 Augoustides JG, Plappert T, Bavaria JE. Aortic decision-making in the Loeys–Dietz syndrome: aortic root aneurysm and a normal-caliber ascending aorta and aortic arch. *J Thorac Cardiovasc Surg* 2009;**138**:502–3.

62 Jayle C, Hajj-Chahine J, Corbi P. Aortic decision making in Loeys–Dietz syndrome. *J Thorac Cardiovasc Surg* 2010;**139**:1088–9; author reply 1089.

63 Matt P, Habashi J, Carrel T, *et al*. Recent advances in understanding Marfan syndrome: should we now treat surgical patients with losartan? *J Thorac Cardiovasc Surg* 2008;**135**:389–94.

63a Holm TM, Habashi JP, Doyle JJ, *et al*. Noncanonical TGFbeta signaling contributes to aortic aneurysm progression in Marfan syndrome mice. *Science* 2011;**332**:358–61.

63b Habashi JP, Doyle JJ, Holm TM, *et al*. Angiotensin II type 2 receptor signaling attenuates aortic aneurysm in mice through ERK antagonism. *Science* 2011;**332**:361–5.

64 Cole WG. The molecular pathology of osteogenesis imperfecta. *Clin Orthoped* 1997;**343**:235–48.

65 Kocher MS, Shapiro F. Osteogenesis imperfecta. *J Am Acad Orthoped Surg* 1998;**6**:225–36.

66 Bonita RE, Cohen IS, Berko BA. Valvular heart disease in osteogenesis imperfecta: presentation of a case and review of the literature. *Echocardiography* 2010;**27**:69–73.

67 Pyeritz RE, Levin LS. Aortic root dilatation and valvular dysfunction in osteogenesis imperfecta. *Circulation* 1981;**64**(Suppl IV):311.

68 Stein D, Kloster FE. Valvular heart disease in osteogenesis imperfecta. *Am Heart J* 1977;**94**:637–41.

69 Alanay Y, Avaygan H, Camacho N, *et al*. Mutations in the gene encoding the RER protein FKBP65 cause autosomal-recessive osteogenesis imperfecta. *Am J Hum Genet* 2010;**87**:572–3.

70 Morello R, Bertin TK, Chen Y, *et al*. CRTAP is required for prolyl 3-hydroxylation and mutations cause recessive osteogenesis imperfecta. *Cell* 2006;**127**:291–304.

71 Cabral WA, Chang W, Barnes AM, *et al*. Prolyl 3-hydroxylase 1 deficiency causes a recessive metabolic bone disorder resembling lethal/severe osteogenesis imperfecta. *Nat Genet* 2007;**39**:359–65.

72 van Dijk FS, Nesbitt IM, Zwikstra EH, *et al*. PPIB mutations cause severe osteogenesis imperfecta. *Am J Hum Genet* 2009;**85**:521–7.

73 Christiansen HE, Schwarze U, Pyott SM, *et al*. Homozygosity for a missense mutation in SERPINH1, which encodes the collagen chaperone protein HSP47, results in severe recessive osteogenesis imperfecta. *Am J Hum Genet* 2010;**86**:389–98.

74 Lapunzina P, Aglan M, Temtamy S, *et al*. Identification of a frameshift mutation in Osterix in a patient with recessive osteogenesis imperfecta. *Am J Hum Genet* 2010;**87**:110–4.

75 Szabo Z, Crepeau MW, Mitchell AL, *et al*. Aortic aneurysmal disease and cutis laxa caused by defects in the elastin gene. *J Med Genet* 2006;**43**:255–8.

76 Morava E, Guillard M, Lefeber DJ, Wevers RA. Autosomal recessive cutis laxa syndrome revisited. *Eur J Hum Genet* 2009;**17**:1099–110.

77 Hucthagowder V, Sausgruber N, Kim KH, *et al*. Fibulin-4: a novel gene for an autosomal recessive cutis laxa syndrome. *Am J Hum Genet* 2006;**78**:1075–80.

78 Loeys B, Van Maldergem L, Mortier G, *et al*. Homozygosity for a missense mutation in fibulin-5 (FBLN5) results in a severe form of cutis laxa. *Hum Mol Genet* 2002;**11**:2113–8.

79 Renard M, Holm T, Veith R, *et al*. Altered TGFbeta signaling and cardiovascular manifestations in patients with autosomal recessive cutis laxa type I caused by fibulin-4 deficiency. *Eur J Hum Genet* 2010;**18**:895–901.

80 Urban Z, Hucthagowder V, Schurmann N, *et al*. Mutations in LTBP4 cause a syndrome of impaired pulmonary, gastrointestinal, genitourinary, musculoskeletal, and dermal development. *Am J Hum Genet* 2009;**85**:593–605.

81 Struk B, Neldne KH, Rao VS, *et al*. Mapping of both autosomal recessive and dominant variants of pseudoxanthoma elasticum to chromosome 16p13.1. *Hum Mol Genet* 1997;**6**:1823–8.

82 Mendelsohn G, Bulkley BH, Hutchins GM. Cardiovascular manifestations of pseudoxanthoma elasticum. *Arch Pathol Lab Med* 1978;**102**:298–302.

83 Miki K, Yuri T, Takeda N, *et al*. An autopsy case of pseudoxanthoma elasticum: histochemical characteristics. *Med Mol Morphol* 2007;**40**:172–7.

84 Lebwohl MG, Distefano D, Prioleau PG, *et al*. Pseudoxanthoma elasticum and mitral-valve prolapse. *N Engl J Med* 1982;**307**:228–231.

85 Liberfarb R, Goldblatt A. Prevalence of mitral-valve prolapse in the Stickler syndrome. *Am J Med Genet* 1986;**24**:387–392.

86 Kevorkian JP, Masquet C, Kural-Menasche S, *et al*. New report of severe coronary artery disease in an eighteen-year-old girl with pseudoxanthoma elasticum. Case report and review of the literature. *Angiology* 1997;**48**:735–41.

87 Lebwohl M, Halperin J, Phelps RG. Brief report: occult pseudoxanthoma elasticum in patients with premature cardiovascular disease. *N Engl J Med* 1993;**329**:1237–9.

88 Challenor VF, Conway N, Monro JL. The surgical treatment of restrictive cardiomyopathy in pseudoxanthoma elasticum. *Br Heart J* 1988;**59**:266–9.

89 Callewaert BL, Willaert A, Kerstjens-Frederikse WS, *et al*. Arterial tortuosity syndrome: clinical and molecular findings in 12 newly identified families. *Hum Mutat* 2008;**29**:150–8.

90 Coucke PJ, Willaert A, Wessels MW, *et al*. Mutations in the facilitative glucose transporter GLUT10 alter angiogenesis and cause arterial tortuosity syndrome. *Nat Genet* 2006;**38**:452–7.

91 Callewaert BL, Loeys BL, Ficcadenti A, *et al*. Comprehensive clinical and molecular assessment of 32 probands with congenital contractural arachnodactyly: report of 14 novel mutations and review of the literature. *Hum Mutat* 2009;**30**:334–41.

92 Putnam EA, Zhang H, Ramirez F, Milewicz DM. Fibrillin-2 (FBN2) mutations result in the Marfan-like disorder, congenital contractural arachnodactyly. *Nat Genet* 1995;**11**:456–8.

93 Kosaki K, Takahashi D, Udaka T, *et al*. Molecular pathology of Shprintzen–Goldberg syndrome. *Am J Med Genet A* 2006;**140**: 104–8; author reply 109–10.

94 McKellar SH, Tester DJ, Yagubyan M, *et al*. Novel NOTCH1 mutations in patients with bicuspid aortic valve disease and thoracic aortic aneurysms. *J Thorac Cardiovasc Surg* 2007;**134**:290–6.

95 Martin LJ, Ramachandran V, Cripe LH, *et al*. Evidence in favor of linkage to human chromosomal regions 18q, 5q and 13q for bicuspid aortic valve and associated cardiovascular malformations. *Hum Genet* 2007;**121**:275–84.

96 Zhu L, Vranckx R, Khau Van Kien P, *et al*. Mutations in myosin heavy chain 11 cause a syndrome associating thoracic aortic aneurysm/aortic dissection and patent ductus arteriosus. *Nat Genet* 2006;**38**:343–9.

97 Guo D, Hasham S, Kuang SQ, *et al*. Familial thoracic aortic aneurysms and dissections: genetic heterogeneity with a major locus mapping to 5q13–14. *Circulation* 2001;**103**:2461–8.

98 Vaughan CJ, Casey M, He J, *et al*. Identification of a chromosome 11q23.2–q24 locus for familial aortic aneurysm disease, a genetically heterogeneous disorder. *Circulation* 2001;**103**:2469–75.

99 Collod G, Babron MC, Jondeau G, *et al*. A second locus for Marfan syndrome maps to chromosome 3p24.2–p25. *Nat Genet* 1994;**8**:264–8.

100 Pannu H, Fadulu VT, Chang J, *et al*. Mutations in transforming growth factor-beta receptor type II cause familial thoracic aortic aneurysms and dissections. *Circulation* 2005;**112**:513–20.

101 Tran-Fadulu VT, Pannu H, Kim DH, *et al*. Analysis of multigenerational families with thoracic aortic aneurysms and dissections due to TGFBR1 or TGFBR2 mutations. *J Med Genet* 2009;**46**:607–13.

102 Guo DC, Pannu H, Tran-Fadulu V, *et al*. Mutations in smooth muscle alpha-actin (ACTA2) lead to thoracic aortic aneurysms and dissections. *Nat Genet* 2007;**39**:1488–93.

103 Guo DC, Papke CL, Tran-Fadulu V, *et al*. Mutations in smooth muscle alpha-actin (ACTA2) cause coronary artery disease, stroke, and moyamoya disease, along with thoracic aortic disease. *Am J Hum Genet* 2009;**84**:617–27.

104 Kuivaniemi H, Tromp G, Prokop DJ. Genetic causes of aortic aneurysms. *J Am Soc Clin Invest* 1991;**88**:1441–4.

105 Kent KC, Zwolak RM, Egorova NN, *et al*. Analysis of risk factors for abdominal aortic aneurysm in a cohort of more than 3 million individuals. *J Vasc Surg* 2010;**52**:539–48.

106 Darling RC III, Brewster DC, Darling RC, *et al*. Are familial abdominal aortic aneurysms different? *J Vasc Surg* 1989;**10**: 39–43.

107 Kuivaniemi H, Shibamura H, Arthur C, *et al*. Familial abdominal aortic aneurysms: collection of 233 multiplex families. *J Vasc Surg* 2003;**37**:340–5.

108 van Keulen CJ, van de Akker E, Pais G, Rauwerda JA. The role of type III collagen in the development of familial abdominal aortic aneurysms. *Eur J Vasc Endovasc Surg* 1999;**18**:65–70.

109 Brophy CM, Tilson MD. New concepts in abdominal aortic aneurysm disease. *Resident Staff Physician* 1990;**36**:538–42.

110 Moursi MM, Beebe HG, Messina LM, *et al*. Inhibition of aortic aneurysm development in blotchy mice by beta adrenergic blockade independent of altered lysyl oxidase activity. *J Vasc Surg* 1995;**21**:792–9.

68

Cardiac Involvement in the Mucopolysaccharide Disorders

Elizabeth A. Braunlin

University of Minnesota, Minneapolis, MN, USA

Introduction

The mucopolysaccharidoses (MPSs) are a group of lethal inherited lysosomal storage diseases that result from the functional deficiency of specific enzymes. These enzymes degrade glycosaminoglycans (GAGs), compounds which are a significant component of the extracellular matrix in all tissues [1,2]. Each type of MPS is defined by the functional absence of a type-specific enzyme causing one or two characteristic GAGs and GAG-degradation products to accumulate (Table 68.1). The GAGs accumulate, generally as proteoglycans (protein-bound GAGs), and mirror their normal somatic occurrence. They account, in general, for the phenotypic differences between the various types of MPS (Table 68.2). Within each type of MPS, numerous distinctive gene mutations have been identified [3–8], which result in variations of the amount of functional enzyme present. These unique mutations partly explain differences in disease severity. The incidence of all types of MPS varies by country or region but is thought to occur in 1/25 000–1/52 000 births [9].

Diagnosis of MPS is established by finding excessive urinary excretion of disease-specific GAGs and the concomitant absence (or marked diminution) of the associated disease-specific enzyme activity within leukocytes [10]. Mutation analysis is usually performed to assess disease severity and prognosis.

The presentation of patients with MPS is highly variable, ranging from nonimmune fetal hydrops [11,12] and cardiomyopathy in infancy [13,14] to relatively asymptomatic adults [15]. The progressive deposition of GAGs in severe forms of MPS produces a classic phenotype that may include coarsening of facial features, growth retardation and bony abnormalities (dysostosis multiplex, short stature, lumbar gibbus, "claw" hands), hepatosplenomegaly, umbilical hernia, thickening and narrowing of airways with noisy breathing, and neurological abnormalities (mental retardation, blindness, deafness, increased intracranial pressure) [10]. Not all phenotypic features are present in each type of MPS, although bony abnormalities and facial dysmorphism are the most consistent features. In attenuated forms, clinical features may be easily overlooked [15].

Cardiac findings in the MPS disorders

Cardiac involvement is common in MPS [16–21], being responsible for >50% of reported deaths in untreated individuals [22]. Progressive deposition of GAGs may result in thickened cardiac valves (regurgitant and/or stenotic) (Figures 68.1 and 68.2), myocardial hypertrophy, cardiomyopathy, diffusely narrowed epicardial coronary arteries with myointimal proliferation (Figure 68.3), dilated aortic root (Figure 68.4) and thickened arterial blood vessels sometimes mimicking coarctation of the aorta. MPS types that accumulate dermatan-sulfated GAGs are most often associated with cardiac valve involvement [16]. Conduction delay and sudden death from complete heart block have been reported [23–25] and apical ventricular aneurysms may occur [26,27]. Congenital anomalies such as ventricular and atrial septal defects have been reported rarely [28,29]. MPS cardiac studies prior to 1975 [30] should be viewed with caution as they lacked supporting biochemical data to establish the specific type of MPS. Cardiac ultrasound studies have been reported for all the mucopolysaccharidoses [16–21]. The incidence of various MPS types within these studies not only reflects those in whom a diagnosis was made (often more severe) but also their country of origin [9,31–33].

Table 68.1 Categorization of the most common types of MPS disorders by common name, enzyme deficiency and accumulated GAG.

MPS subtype	Enzyme deficiency	Accumulated GAG
I (Hurler, Hurler-Scheie, Scheie)	α-L-iduronidase	HS, DS
II (Hunter)	Iduronate-2-sulfatase	HS, DS
III (Sanfilippo)		
A	Heparan sulfamidase	HS
B	N-acetyl-α-D-gluosaminidase	
C	Acetyl-CA-α-gluosaminidase N-acetyltransferase	
D	N-acetylglucosamine-6-sulfatase	
IV (Morquio)		
A	N-acetylgalactosamine-6-sulfatase	KS
B	β-galactosidase	CS, KS
VI (Maroteaux-Lamy)	N-acetylgalactosamine-4-sulfatase	DS
VII (Sly)	β-D-glucuronidase	CS, DS, HS

CS, chondroitin sulfate; DS, dermatan sulfate; HS, heparan sulfate; KS, keratan sulfate.

Table 68.2 Distribution of GAGs.

Type of GAG	Known site of distribution
Chondroitin sulfate (CS)	Cartilage, tendon, ligament, aorta
Dermatan sulfate (DS)	Skin, blood vessels, heart valves, lung interstitium
Heparan sulfate (HS)	Ubiquitous component of extracellular matrix (ECM), basement membrane of vasculature
Keratan sulfate (KS)	Cornea, cartilage, tendons

The cardiac evaluation of individuals with MPS may be difficult because of their lack of cooperation and noisy upper airway sounds that mask the cardiac tones. The absence of cardiac murmurs does not rule out cardiac valvar disease. Measurement of right upper and lower extremity blood pressures should be performed Twelve-lead ECG and two-dimensional cardiac ultrasound with Doppler provide important information about the severity of cardiac GAG accumulation.

The ECG can identify prolonged AV conduction and (rare) acute coronary insufficiency. Cardiac ultrasound is useful in determining chamber size, wall thickness, systolic function and cardiac valve thickening. Doppler interrogation can assess the severity of hemodynamics of cardiac valve abnormalities, estimate right ventricular systolic pressure and identify obstruction within the aorta.

Baseline ECG and cardiac ultrasound should be performed when the diagnosis is established and at regular intervals thereafter regardless of treatment [34,35]. Cardiac ultrasound cannot reliably diagnose coronary artery disease, and no other routinely used test can identify this diffuse myointimal thickening. Intracoronary ultrasound has been successfully used in other types of diffuse coronary myointimal disease, such as cardiac transplant vasculopathy [36] and Fabry disease [37], but currently it remains a research tool. Coronary artery thickening should be suspected in any MPS individual, so baseline troponin and BNP should be obtained, and optimal hemodynamic stability provided if anesthesia is required. Conventional medical management, including diuretics and angiotensin-converting enzyme inhibitors or angiotensin-receptor blockers, may be useful but enzyme replacement therapy has also successfully reversed heart failure in both infants and adults with MPS I [38,39]. Cardiac valve repair or replacement has been reported in all types of MPS [40–53] except MPS VII, the youngest currently being a 6-year-old child with MPS III who underwent mitral valvoplasty for severe mitral regurgitation [46].

MPS I (Hurler, Hurler–Scheie, Scheie syndromes)

MPS I, an autosomal recessive disorder, occurs from the functional absence of α-L-iduronidase, resulting in heparan- and dermatan-sulfated GAGs accumulating

(a)

Figure 68.2 Color flow Doppler modified four-chamber image of the left ventricle of a patient with MPS IV showing aortic regurgitation (arrows).
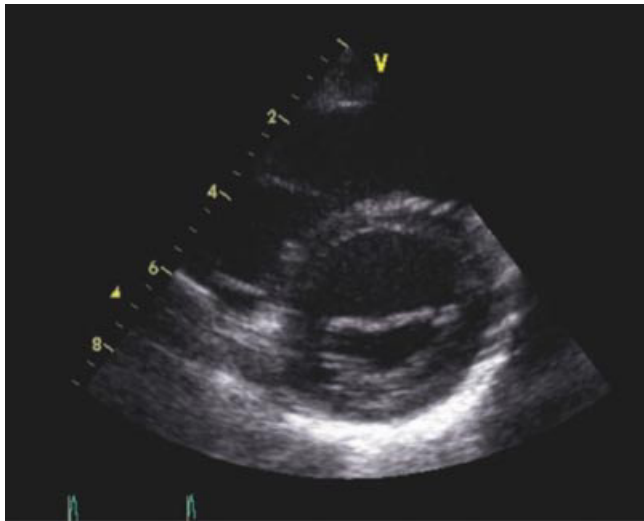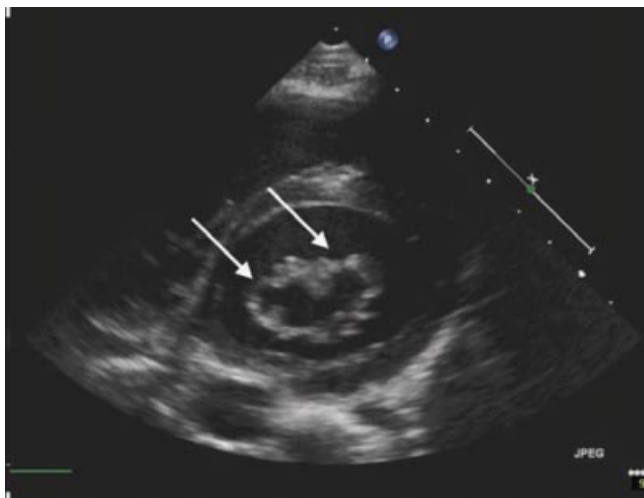
(b)

Figure 68.1 Two-dimensional cardiac ultrasound short axis views of (a) a normal mitral valve and (b) an MPS VI mitral valve. Note the increased thickness and irregularity of the MPS VI valve (arrows).
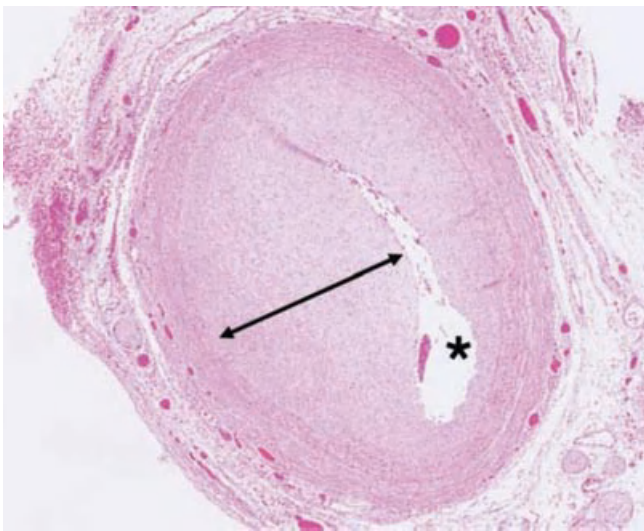
Figure 68.3 Left anterior descending coronary artery in a 14-month-old child with MPS I shortly after HSCT. Note myointimal proliferation (arrow) and slit-like coronary lumen (*).

within virtually all organs [1,2]. There are >100 reported mutations of the α-L-iduronidase gene on chromosome 4p16.3 [3,54], explaining the marked phenotypic variability. The incidence of MPS I varies widely by country, ranging from 1/26 000 births in the Irish traveler population of Northern Ireland [31] to about 1/100 000 births in Western Australia and the UK, with 75% of the births resulting in the severe form [9,55]. Currently the preferred terminology is to identify severe (Hurler syndrome) and attenuated (Hurler–Scheie, Scheie syndromes) forms of the disorder [35]. Our understanding of the correlation between disease severity and underlying genotype is incomplete because of the large number of mutations, many of which are "private" (occurring in a single pedigree). However, homozygosity for nonsense mutations such as W402X or Q70X (both of which are common within the US) is known to produce the severe phenotype [54]. Individuals with severe untreated MPS I die within the first decade of life from either cardiac or pulmonary causes, often suddenly, whereas those with untreated attenuated MPS I may live into early adulthood or even middle age [22,55,56].
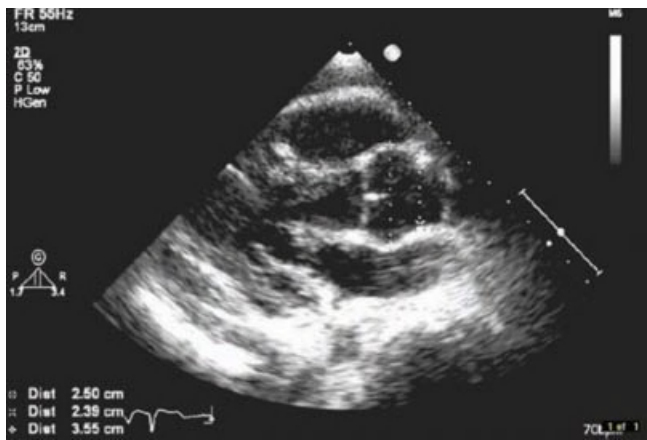
Figure 68.4 Two-dimensional cardiac ultrasound, long-axis view of the left ventricle and aorta in an adult with MPS I after HSCT, showing dilated aortic root (arrows).

Table 68.3 Systemic therapies available for the MPS disorders.

MPS type	Systemic therapy commonly offered
MPS I – severe (Hurler)	HSCT
MPS I – attenuated (Hurler–Scheie, Scheie)	ERT
MPS II – severe, attenuated (Hunter)	ERT
MPS III A–D (Sanfilippo)	(ERT)[a]
MPS IV (A, B) (Morquio)	(ERT)[a]
MPS VI (Maroteaux–Lamy)	ERT, HSCT[b]
MPS VII (Sly)	–

[a]ERTs (enzyme replacement therapies) for some subtypes of these MPS syndromes are currently under development (2011).
[b]HSCT (hematopoietic stem cell transplantation) is offered for failure of ERT.

Cardiac valve involvement (mitral and aortic) occurs in 80–100% in severe MPS I [16–20], often within the first year of life [57]. In attenuated MPS I, cardiac valve pathology may initially be less severe, but the valves become severely affected from progressive accumulation of GAGs [58]. Coronary artery stenosis or occlusion from GAG deposition within the myointima occurs within the first year of life in severe forms [59] and has been reported by late adolescence in attenuated MPS I [58]. The incidence and severity of coronary artery disease in untreated attenuated MPS I are unknown, but likely underestimated. Ventricular hypertrophy is common in MPS I; systolic ventricular function is usually normal, although a rare infant presents with dilated cardiomyopathy [38]. Progressive prolongation of atrioventricular conduction is uncommon but important.

Conventional cardiac surgical procedures have included mitral or combined mitral and aortic valve replacement [40–42] and repair of coarctation of the aorta in a 2-year-old after successful bone marrow transplantation [60].

Bone marrow or hematopoietic stem cell transplantation (HSCT) has been performed for over 30 years in infants and toddlers with severe MPS I (Table 68.3) [61]. The procedure has markedly increased the lifespan and arrested the associated neurological decline [62,63]. The HSCT procedure has a 10–15% early mortality [64], but after the peritransplant period (about 18 months), the risk of dying is exceptionally low [55]. Enzyme replacement therapy (ERT) has become available for MPS I but is generally not used as the sole therapy for severe forms of MPS I because it does not cross the blood–brain barrier [63]. With successful engraftment, cardiac hypertrophy regresses, ventricular function is preserved, and coronary artery obstruction appears arrested, or perhaps reversed [65,66]. The cardiac valves remain thickened and valve dysfunction may progress despite successful engraftment [65].

ERT has been approved for use in the USA since 2003 [67] for MPS I (laronidase, Aldurazyme). Phase III studies showed a significant improvement in pulmonary function tests and the 6 min walk for those participating in the company-sponsored trials. The cardiac effects of ERT in a small series [68] show preserved ventricular function and diminished ventricular hypertrophy, but cardiac valves remain thickened and dysfunctional. Reports detailing sudden death after 2 years of ERT with evidence of acute myocardial infarction underscore the importance of evaluating coronary artery status prior to treatment [69]. As experience with ERT has increased, studies in siblings with attenuated MPS and the same genetic mutation have shown that the clinical outcome of treatment begun soon after birth is significantly better than when treatment is delayed until 2–3 years of age [70]. A similar favorable outcome in MPS VI [71] has generated strong interest in newborn screening for the MPS disorders [72].

MPS II (Hunter syndrome – severe and attenuated)

MPS II, an X-linked disorder, occurs from the functional absence of iduronate-2-sulfatase and results in the systemic accumulation of heparan- and dermatan-sulfated GAGs [1,2]. More than 150 mutations of the iduronate-2-sulfatase gene on chromosome Xq28 have been reported [73]. MPS II is reported to occur in 1/320 000 births (1/165 000 male births) in Western Australia [9]. Hunter syndrome is divided into forms based upon the presence (severe) or absence (attenuated) of CNS involvement [73]. At present, genotype–phenotype correlation is imperfect in MPS II with the exception that the complete absence of functional enzyme

from either gene deletion or complex gene rearrangements results in the severe phenotype and the specific mutation c.1122C>T results in a mild phenotype [74]. Respiratory [73] or cardiac [75] causes account for most deaths in MPS II – within the second decade of life for severely affected and in adulthood for untreated attenuated disease [76].

Cardiac valve involvement is common in both severe and attenuated MPS II, occurring in 60–80% [16,77], with the mitral valve more often affected than the aortic. Coronary artery disease has unknown incidence but is found at postmortem examination, and likely under-reported clinically [75,27]. Ventricular hypertrophy is common and systolic ventricular function is usually normal. A large apical left ventricular aneurysm has been reported in a few patients [27]. Complete heart block and sudden death may occur from deposition of GAG within the conduction system [23].

HSCT has been performed in a small number of boys >3 years of age [78] and a 10-month-old infant [79] with MPS II. Despite successful engraftment, neurologic status continued to deteriorate in the severe form. Cardiac valve abnormalities stabilized after transplantation and neither cardiomyopathy nor myocardial infarction was reported in >17 years of follow-up [78].

Commercially available enzyme replacement for MPS II (idursulfase, Elaprase) became available in 2006 after significant improvements in pulmonary function testing and 6 min walk was demonstrated in nearly 100 individuals over a 3 year period [80]. There is sparse information on the effect of ERT upon the heart in MPS II. No change in cardiac valve findings was found in 10 adult men (>20 years of age) with clinically advanced MPS II who received ERT for 12 months [81]. Cardiac function was preserved in all but one individual with cardiomyopathy at baseline (EF of 27%) who deteriorated further (EF of 14%) during the study. As expected, LV mass was elevated at baseline and, although it decreased by 12.4% over 12 months, this was not statistically significant.

MPS III A, B, C, D (Sanfilippo syndrome)

MPS III, an autosomal recessive disorder, has four known subtypes – A, B, C and D – each resulting from the functional absence of a specific enzyme responsible for the degradation of heparan sulfate [1,2,82]. For each known subtype, the enzyme and its chromosome differ: MPS IIIA (heparan *N*-sulfatase, chromosome 17q25.3), MPS IIIB (*N*-acetylglucosaminidase, chromosome 17q21.1), MPS IIIC (acetyl-CoA glucosaminide *N*-acetyl transferase, chromosome 8p11.1), and MPS IIID (*N*-acetylglucosamine-6-sulfatase, chromosome 12q14). MPS III is the most common type of MPS, occurring in 1/58 000 births with subtypes MPS IIIA and IIIB the most frequent [9,82]. Both severe and attenuated forms of MPS III have been described from mutation analysis of

individuals with MPS IIIA, IIIB, and IIIC [83–85]. Life expectancy for severely affected individuals is between one and two decades [82], whereas those with attenuated disease may live into late adulthood [86]. Existing cardiac studies are reported without regard to subtype of MPS III.

Sanfilippo syndrome primarily affects the central nervous system and has been divided into three clinical phases [82]. The first phase is developmental delay beginning after 1–2 years of life. This is followed by progressive behavioral problems, mental deterioration, and ultimately dementia. In the third phase, neurological issues lessen while spasticity and motor difficulties, including swallowing problems, emerge and progress to death that is most often from pneumonia.

Cardiac disease has been considered uncommon in MPS III but this may be inaccurate. Cardiac ultrasound studies of large numbers of MPS III patients found morphologic and functional changes in >50–66% of mitral and 20–30% of aortic valves [16,18]. Multiple isolated reports [46,87–91] confirm that cardiac valve disease is common in MPS III. Diffuse coronary artery stenosis from myointimal proliferation has been reported from postmortem examination [89–91]. Fragmentation of collagen and the presence of GAG-laden cells have been found in the aorta and great vessels [91,92]. Ventricular hypertrophy is common and cardiomyopathy leading to cardiac transplantation may occur [16,86]. Successful mitral valvoplasty was performed in a 6-year-old child with MPS III [46].

HSCT has been performed in a few of these children, but the extent of neurologic benefit is unknown and the procedure remains investigational [63]. No cardiac follow-up after HSCT has been reported. No ERT therapy is currently available in MPS III. Genistein, a naturally occurring isoflavone that decreases synthesis of GAGs, appears to improve or stabilize neurocognitive function [93,94], but cardiac effects of genistein are unreported.

MPS IV (A, B) (Morquio syndrome)

MPS IV, an autosomal recessive disorder, has two known subtypes – A and B – each resulting from the functional absence of specific enzymes for the degradation of keratan sulfate [1,2]. The enzyme and its chromosome differ: MPS IV A (*N*-acetylgalactosamine-6-sulfate sulfatase, gene locus 16q24.3) and MPS IB B (β-galatosidase, gene locus 3p21.33) [2]. More than 150 mutations of the sulfatase gene have been identified [95], but mutation analysis of the β-galatosidase gene is more complex [96]. MPS IV is rare, ranging in incidence from 1/216 000 to 1/641 178 births [9], although it is the most common type of MPS found in Saudi Arabia [97]. MPS IV A is more common than MPS IV B. Life expectancy for severe forms of MPS IV is two to three decades whereas those with milder forms may live into the seventh

decade [95]. Individuals with MPS IV manifest skeletal abnormalities of dwarfism, pectus carinatum, and odontoid hypoplasia, the last sometimes responsible for paralysis and death. Quadriparesis has occurred as a consequence of perioperative atlanto-occipital subluxation. With rare exception, individuals with MPS IV have normal intelligence and mild facial dysmorphism.

Cardiac valvar disease is a prominent feature of MPS IV: isolated mitral valvar disease is uncommon but combined mitral and aortic valve abnormalities occur in 60–100% of those studied with MPS IV [16,98]. Coronary artery involvement with the classic features of MPS-type of myointimal proliferation occurred in a 15-year-old male [99] but not in a 48-year-old woman [100] with MPS IV. Biventricular hypertrophy and cardiomyopathy have been reported. Nonimmune fetal hydrops has been associated with MPS IV A [11,101]. Aortic valve replacement has been performed in adults with MPS IV [47,48]. Aortic valve replacement was required in an adult with MPS IV B 12 years after performance of the Ross procedure for aortic regurgitation [49].

Neither HSCT nor ERT has been reported in MPS IV and remains investigational [63].

MPS VI (Maroteaux–Lamy)

MPS VI, an autosomal recessive disorder, occurs from the functional absence of *N*-acetylgalactosamine-4-sulfatase (arylsulfatase B) and results in the systemic accumulation of dermatan-sulfated GAGs [1,2]. More than 100 mutations of the arylsulfatase gene on chromosome 5q11–q13 have been reported. [7]. The incidence of MPS VI varies widely by region from 1/43 261 births of Turkish immigrants living in Germany to 1/1 505 160 births in Sweden [102].A high prevalence of MPS VI in Brazil is attributed to an increase of one specific mutation, a finding referred to as the "founder effect." The clinical presentation of MPS VI has been divided into rapidly and slowly progressing subtypes and correlated with excretion of urinary GAG [103]. Urinary GAG levels of >200 μg mg⁻¹ creatinine are associated with a rapidly progressing phenotype manifested by small stature, impaired endurance, compromised pulmonary function, and reduced joint range of motion. The paucity of subjects over 20 years of age who excrete GAG levels >100 μg mg⁻¹ creatinine suggests that they do not commonly survive beyond age 20 years.

Cardiac valve disease occurs commonly in MPS VI [16,18,20] and generally involves both mitral and aortic valves, although the aortic valve may be less severely affected. Coronary artery disease has been reported in adults with MPS VI [50], but histopathologic evidence for MPS-type myointimal proliferation of epicardial coronary arteries is not available. In an adult with MPS VI and apical left ventricular aneurysm [26], the small coronary vessels were occluded by myointimal proliferation. Ventricular hypertrophy is common and congestive heart failure in infants has been reported [13,104]. Development of complete heart block requiring permanent pacemaker placement [24] and fibrosis of the conduction system [105] occur in MPS VI. Successful mitral [52], aortic [50], and combined aortic and mitral valve [51,53] replacement have been reported.

HSCT has improved myocardial function and relieved hypertrophy in a small series of individuals [106], but neither HSCT nor umbilical cord stem cell transplantation [107] reverse valve pathology. Cardiac findings after ERT (Naglazyme) in MPS VI have not been reported.

MPS VII (Sly syndrome)

MPS VII, an autosomal recessive disorder, occurs from the functional absence of β-glucuronidase and results in the systemic accumulation of dermatan-, heparan-, and chondroitin-sulfated GAGs [1,2]. Nearly 50 mutations of the β-glucuoronidase gene on gene locus 7q21.11 have been reported [108]. Sly syndrome is the rarest MPS disorder, calculated to be 1/345 000 births [33]. The clinical presentation is extremely variable, with dwarfism, dysostosis multiplex, and facial dysmorphology being common [109]. Nonimmune hydrops in fetuses with MPS VII occurs much more frequently than expected for such a rare disease [12,110–113].

The cardiac features are not well studied. Marked thickening and fibrosis of mitral and aortic valves with arterial stenoses from lysosomal storage material were found at autopsy from the first reported patient with MPS VII [114]. A 6-month-old child with MPS VII was found to have congestive heart failure from a thickened, prolapsing mitral valve with severe mitral regurgitation [115], and a 17-month-old child with MPS VII had dilated cardiomyopathy [116]. Sudden death has been reported in adults but without documentation for arrhythmia or atrioventricular block [117]. Diffuse hypoplasia of the thoraco-abdominal aorta occurred in a child with MPS VII and required a jump-graft for repair [118].

HSCT has been performed in a 12-year-old girl [119] with notable improvements in motor function but moderate aortic and mitral valve regurgitation remained unchanged despite successful engraftment. ERT is unavailable for MPS VII.

Conclusion

Glycosaminoglycans are ubiquitous substances that occur normally within the cardiac valves, the coronary arteries, the myocardium, and the great vessels. Cardiac valve thickening and dysfunction, coronary artery stenosis, ventricular hypertrophy, cardiomyopathy, and great vessel involvement occur from the genetic absence of lysosomal enzymes that catabolize GAGs. Awareness of potential for

progressive cardiac involvement in each MPS disorder is key to management. Conventional medical and surgical management has been useful but not curative in MPS. Systemic therapies such as HSCT and ERT preserve ventricular function, decrease ventricular hypertrophy, improve ventricular function, and arrest or reverse coronary artery disease, but do not appear to affect the cardiac valves. Systemic therapies within the first few weeks of life appear to prevent the development of cardiac pathology. The development of newborn screening for these uncommon, but devastating, diseases is an important next step.

References

1 Neufeld E, Muenzer J. *The Metabolic and Molecular Bases of Inherited Disease*. New York: McGraw-Hill, 2001: 3421–52.

2 NCBI. *Online Mendelian Inheritance of Man*, www.ncbi.nlm.nih.gov/omim.

3 Yogalingam G, Guo XH, Muller VJ, *et al*. Identification and molecular characterization of alpha-L-iduronidase mutations present in mucopolysaccharidosis type I patients undergoing enzyme replacement therapy. *Hum Mutat* 2004;**24**:199–207.

4 Froissart R, Da Silva IM, Maire I. Mucopolysaccharidosis type II: an update on mutation spectrum. *Acta Paediatr Suppl* 2007;**9**:71–7.

5 Yogalingam G, Hopwood JJ. Molecular genetics of mucopolysaccharidosis type IIIA and IIIB: diagnostic, clinical and biological implications. *Hum Mutat* 2001;**18**:264–81.

6 Tomatsu S, Montano AM, Nishioka T, *et al*. Mutation and polymorphism spectrum of the GALNS gene in mucopolysaccharidosis IVA (Morquio A). *Hum Mutat* 2005;**26**:500–12.

7 Karageorgos L, Brooks DA, Pollard A, *et al*. Mutation analysis of 105 mucopolysaccharidosis type VI patients. *Hum Mutat* 2007;**28**:897–903.

8 Tomatsu S, Montano AM, Dung VD, *et al*. Mutations and polymorphisms in GUSB gene in mucopolysaccharidosis VII. *Hum Mutat* 2009;**30**:511–9.

9 Nelson J, Crowhurst J, Carey B, Greed L. Incidence of the mucopolysaccharidoses in Western Australia. *Am J Med Genet* 2003;**123**A:310–3.

10 Muenzer J. The mucopolysaccharidoses: a heterogeneous group of disorders with variable pediatric presentations. *J Pediatr* 2004;**144**:S27–34.

11 Applegarth DA, Toone JR, Wilson RD, *et al*. Morquio disease presenting as hydrops fetalis and enzyme analysis of chorionic villus tissue in a subsequent pregnancy. *Pediatr Pathol* 1987;**7**:593–9.

12 Van Dorpe J, Moerman P, Pecceu A, *et al*. Non-immune hydrops fetalis caused by beta-glucuronidase deficiency (mucopolysaccharidosis VII): study of a family with 3 affected siblings. *Genet Counsel* 1996;**7**:105–12.

13 Miller G, Partridge A. Mucopolysaccharidosis type VI presenting in infancy with endocardial fibroelastosis and heart failure. *Pediatr Cardiol* 1983;**4**:62–3.

14 Nampoothiri S, Mahesh K, Hiran KR, Sunitha V. Sly disease: mucopolysaccharidosis type VII. *Indian Pediatr* 2008;**45**:859–61.

15 Brooks DA, Gibson GJ, Karageorgos L, *et al*. An index case for the attenuated end of the mucopolysaccharidosis type VI clinical spectrum. *Mol Genet Metab* 2005;**85**:236–8.

16 Dangel JH. Cardiovascular changes in children with mucopolysaccharide storage diseases and related disorders – clinical and echocardiographic findings in 64 patients. *Eur J Pediatr* 1998;**157**:534–8.

17 Gross DM, Williams JC, Caprioli C, *et al*. Echocardiographic abnormalities in the mucopolysaccharide storage diseases. *Am J Cardiol* 1988;**61**:170–6.

18 Wippermann C-F, Beck M, Schranz D, *et al*. Mitral and aortic regurgitation in 84 patients with mucopolysacchiardoses. *Eur J Pediatr* 1995;**154**:98–101.

19 Mohan UR, Hay AA, Cleary MA, *et al*. Cardiovascular changes in children with mucopolysaccharide disorders. *Acta Paediatr* 2002;**91**:799–804.

20 Lael GN, dePaula AC, Leone C, Kim CA. Echocardiographic study of paediatric patients with mucopolysaccharidosis. *Cardiol Young* 2010;**20**:254–61.

21 Fesslova V, Corti P, Sersale G, *et al*. The natural course and the impact of therapies of cardiac involvement in the mucopolysaccharidoses. *Cardiol Young* 2009;**19**:170–8.

22 Krovetz LJ, Lorincz AE, Schiebler GL. Cardiovascular manifestations of the Hurler syndrome. *Circulation* 1965;**31**:132–41.

23 Hishitani T, Wakita S, Isoda T, *et al*. Sudden death in Hunter syndrome caused by complete atrioventricular block. *J Pediatr* 2000;**136**:268–9.

24 Dilber E, Celiker A, Karagoz T, Kalkanoglu HS. Permanent transfemoral pacemaker implantation in a child with Maroteaux Lamy syndrome. *PACE* 2002;**25**:1784–5.

25 Misumi I, Chikazawa S, Ishitsu T, *et al*. Atrioventricular block and diastolic dysfunction in a patient with Sanfilippo C. *Intern Med* 2010;**49**:2313–6.

26 Oudit GY, Butany J, Williams WG, *et al*. Left ventricular aneurysm in a patient with mucopolysaccharidosis type VI (Maroteaux–Lamy syndrome): clinical and pathological correlation. *Cardiovasc Pathol* 2007;**16**:237–40.

27 Kettles DI, Sheppard M, Liebmann RD, Davidson C. Left ventricular aneurysm, aortic valve disease and coronary narrowing in a patient with Hunter's syndrome. *Cardiovasc Pathol* 2002;**11**: 94–6.

28 Kourouklis S, Chatzie D, Skafida M, *et al*. Outlet type on interventricular septal defect in SanFilippo type-B syndrome. *Int J Cardiol* 2007;**122**:e4–5.

29 Herranz Jordan B, Campo Sampedro F, Pedrola Guixe D, *et al*. Mucopolysaccharidosis type III A in a girl with atrial septal defect and paroxysmal supraventricular tachycardia. *Ann Esp Pediatr* 1990;**32**:85–7.

30 Schieken RM, Kerber RE, Ionasescu VV, Zellweger H. Cardiac manifestations of the mucopolysaccharidoses. *Circulation* 1975;**52**:700–5.

31 Murphy AM, Lambert D, Treacy EP, *et al*. Incidence and prevalence of mucopolysaccharidosis type I in the Irish republic. *Arch Dis Child* 2009;**94**:52–4.

32 Ozand PT, Gascon G, al Ageel A, *et al*. Prevalence of different types of lysosomal storage diseases in Saudi Arabia. *J Inherit Metab Dis* 1990;**13**:849–61.

33 Applegarth DA, Toone JR, Lowry RB. Incidence of inborn errors of metabolism in British Columbia, 1969–1996. *Pediatrics* 2000;**105**:1–6.

34 Giugliani R, Harmatz P, Wraith JE. Management guidelines for mucopolysaccharidosis VI. *Pediatrics* 2007;**120**:405–18.

35 Muenzer J, Wraith JE, Clarke LA, International Consensus Panel on Management and Treatment of Mucopolysaccharidosis I. Mucopolysaccharidosis I: management and treatment guidelines. *Pediatrics* 2009;**123**:19–29.

36 Tuzcu EM, Kapadia SR, Sachar R, *et al.* Intravascular ultrasound evidence of angiographically silent progression in coronary atherosclerosis predicts long-term morbidity and mortality after cardiac transplantation. *J Am Coll Cardiol* 2005;**45**:1538–42.

37 Kovarnik T, Mintz GS, Karetova D, *et al.* Intravascular ultrasound assessment of coronary artery involvement in Fabry disease. *J Inherit Metab Dis* 2008;**31**:753–60.

38 Hirth A, Berg A, Greve G. Successful treatment of severe heart failure in an infant with Hurler syndrome. *J Inherit Metab Dis* 2007;**30**:280.

39 Harada H, Uchiwa H, Nakamura M, *et al.* Laronidase replacement therapy improves myocardial function in mucopolysaccharidosis I. *Mol Genet Metab* 2011;in press.

40 Fischer RA, Lehr HA, Nixdorff U, Meyer J. Combined aortic and mitral stenosis in mucopolysaccharidosis type I-S (Ullrich–Scheie syndrome). *Heart* 1999;**81**:97–9.

41 Minakata K, Konishi Y, Matsumoto M, Miwa S. Surgical treatment for Scheie's syndrome (mucopolysaccharidosis type I-S). *Jpn Circ J* 1998;**62**:700–3.

42 Goksel OS, El H, Tireli E, Dayioglu E. Combined aortic and mitral valve replacement in a child with mucopolysaccharidosis type I: a case report. *J Heart Valve Dis* 2009;**18**:214–6.

43 Joly H, Auphin C, Motreff P, *et al.* Double aortic and mitral valve replacement in an 18 year old patient with Hunter's disease. *Arch Mal Coeur Vaiss* 2004;**97**:561–3.

44 Bhattacharya K, Givson SC, Pathi VL. Mitral valve replacement for mitral stenosis secondary to Hunter's syndrome. *Ann Thorac Surg* 2005;**80**:1911–2.

45 Antoniou T, Kirvassilis G, Tsourelis L, *et al.* Mitral valve replacement and Hunter syndrome: case report. *Heart Surg Forum* 2009;**12**:E54–6.

46 Muenzer J, Beekman RH, Profera LM, Bove EL. Severe mitral insufficiency in mucopolysaccharidosis type III-B (Sanfilippo syndrome). *Pediatr Cardiol* 1993;**14**:130–2.

47 Pagel PS, Almassi GH. Perioperative implications of Morquio syndrome in a 31-year old woman undergoing aortic valve replacement. *J Cardiothorac Vasc Anesth* 2009;**23**:855–7.

48 Nicolini F, Corradi D, Bosio S, Gherli T. Aortic valve replacement in a patient with Morquio syndrome. *Heart Surg Forum* 2008;**11**:E96–8.

49 Barry MO, Beardslee MA, Braverman AC. Morquio's syndrome: severe aortic regurgitation and late pulmonary autograft failure. *J Heart Valve Dis* 2006;**15**:839–42.

50 Wilson CS, Mankin HT, Pluth JR. Aortic stenosis and mucopolysaccharidosis. *Ann Intern Med* 1980;**92**:496–8.

51 Tan CTT, Schaff HV, Miller FA, *et al.* Valvular heart disease in four patients with Maroteaux–Lamy syndrome. *Circulation* 1992;**85**:188–95.

52 Marwick TH, Bastian B, Hughes CF, Bailey BP. Mitral stenosis in the Maroteaux–Lamy syndrome: a treatable cause of dyspnoea. *Postgrad Med J* 1992;**68**:287–8.

53 Hacida M, Nonoyama M, Bonkohara Y, *et al.* Combined aortic and mitral valve replacement in an adult with mucopolysaccharidosis (Maroteaux–Lamy syndrome). *Heart Vessels* 1996;**11**:215–7.

54 Terlato NJ, Cox GF. Can mucopolysaccharidosis type I disease severity be predicted based on a patient's genotype? A comprehensive review of the literature. *Genet Med* 2003;**5**:286–94.

55 Moore D, Connock MJ, Wraith JE, Lavery C. The prevalence of and survival in Mucopolysaccharidosis I: Hurler, Hurler–Scheie and Scheie syndromes in the UK. *Orphanet J Rare Dis* 2008;**3**:24.

56 Soliman OII, Timmermans RGM, Nemes A, *et al.* Cardiac abnormalities in adults with the attenuated form of mucopolysaccharidosis type I. *J Inherit Metab Dis* 2007;**30**:750–7.

57 Renteria VG, Ferrans VJ, Roberts WC. The heart in the Hurler syndrome: gross, histologic and ultrastructural observations in five necropsy cases. *Am J Cardiol* 1976;**38**:487–501.

58 Wassman ER, Johnson K, Shapiro LJ, *et al.* Postmortem findings in the Hurler–Scheie syndrome (mucopolysaccharidosis I-H/S). *Birth Defects Orig Artic Ser* 1982;**18**:13–8.

59 Brosius FC III, Roberts WC. Coronary artery disease in the Hurler syndrome: qualitative and quantitative analysis of the extent of coronary narrowing at necropsy in six children. *Am J Cardiol* 1981;**47**:649–53.

60 Braunlin EA, Krivit W, Burke BA, *et al.* Radiological case of the month. Coarctation of the aorta in Hurler syndrome. *Arch Pediatr Adolesc Med* 2000;**154**:841–2.

61 Hobbs JR, Hugh-Jones K, Barrett AJ, *et al.* Reversal of clinical features of Hurler's disease and biochemical improvement after treatment by bone-marrow transplantation. *Lancet* 1981;**ii**:709–12.

62 Peters C, Balthazor M, Shapiro EG, *et al.* Outcome of unrelated donor bone marrow transplantation in 40 children with Hurler syndrome. *Blood* 1996;**87**:4894–902.

63 Prasad VK, Kurtzberg J. Transplant outcomes in mucopolysaccharidoses. *Semin Hematol* 2010;**47**:59–69.

64 Boelens JJ, Wynn RF, O'Meara A, *et al.* Outcomes of hematopoietic stem cell transplantation for Hurler's syndrome in Europe: a risk factor analysis for graft failure. *Bone Marrow Transplant* 2007;**40**:225–33.

65 Braunlin EA, Stauffer NR, Peters CH, *et al.* Usefulness of bone marrow transplantation in the Hurler syndrome. *Am J Cardiol* 2003;**92**:882–6.

66 Braunlin EA, Rose AG, Hopwood JJ, *et al.* Coronary artery patency following long-term successful engraftment 14 years after bone marrow transplantation in the Hurler syndrome. *Am J Cardiol* 2001;**88**:1075–7.

67 Wraith JE, Hopwood JJ, Fuller M, *et al.* Laronidase treatment of mucopolysaccharidosis I. *BioDrugs* 2005;**19**:1–7.

68 Braunlin EA, Berry JM, Whitley CB. Cardiac findings after enzyme replacement therapy for mucopolysaccharidosis type I. *Am J Cardiol* 2006;**98**:416–8.

69 Lin HY, Lin SP, Chuang CK, *et al.* Mucopolysaccharidosis I under replacement therapy with laronidase – a mortality case with autopsy report. *J Inherit Metab Dis* 2005;**28**:1146–8.

70 Gabrielli O, Clarke LA, Bruni S, Coppa GV. Enzyme-replacement therapy in a 5-month-old boy with attenuated presymptomatic MPS I: 5-year follow-up. *Pediatrics* 2010;**125**:e183–7.

71 McGill JJ, Inwood AC, Coman DJ, *et al.* Enzyme replacement therapy for mucopolysaccharidosis VI from 8 weeks of age – a sibling control study. *Clin Genet* 2010;**77**:492–8.

72 Nakamura K, Hattori K, Endo F. Newborn screening for lysosomal storage disorders. *Am J Med Genet C Semin Med Genet* 2011;**157**:63–71.

73 Wraith JE, Scarpa M, Beck M, *et al*. Mucopolysaccharidosis type II (Hunter syndrome): a clinical review and recommendations for treatment in the era of enzyme replacement therapy. *Eur J Pediatr* 2008;**167**:267–77.

74 Muenzer J, Beck M, Eng CM, *et al*. Multidisciplinary management of Hunter syndrome. *Pediatrics* 2009;**1214**: e1228–39.

75 Young ID, Harper PS. Mild form of Hunter's syndrome: clinical delineation based on 31 cases. *Arch Dis Child* 1982;**57**:828–36.

76 Jones SA, Almassy Z, Beck M, *et al*. on behalf of the HOS Investigators. Mortality and cause of death in mucopolysaccharidosis type II – a historical review based on data from the Hunter Outcome Survey (HOS). *J Inherit Metab Dis* 2009;**32**:534–43.

77 Schwartz IV, Ribeiro MG, Mota JG, *et al*. A clinical study of 77 patients with mucopolysaccharidosis type II. *Acta Paediatr Suppl* 2007;**96**:63–70.

78 Guffon N, Bertrand Y, Forest I, *et al*. Bone marrow transplantation in children with Hunter syndrome: outcome after 7 to 17 years. *J Pediatr* 2009;**154**:733–7.

79 Mullen CA, Thompson JN, Richard LA, Chan KW. Unrelated umbilical cord blood transplantation in infancy for mucopolysaccharidosis type IIB (Hunter syndrome) complicated by autoimmune hemolytic anemia. *Bone Marrow Transplant* 2000; **25**:1093–7.

80 Muenzer J, Wraith JE, Beck M, *et al*. A phase II/III clinical study of enzyme replacement therapy with idursulfase in mucopolysaccharidosis II (Hunter syndrome). *Genet Med* 2006;**8**:465–73.

81 Okuyama T, Tanaka A, Suzuki Y, *et al*. Japan Elaprase® treatment (JET) study: idursulfase enzyme replacement therapy in adult patients with attenuated Hunter syndrome (mucopolysaccharidosis II, MPS II). *Mol Genet Metab* 2010;**99**:18–25.

82 Valstar MJ, Ruijter GJG, van Diggelen OP, *et al*. Sanfilippo syndrome: a mini-review. *J Inherit Metab Dis* 2008;**31**:240–52.

83 Valstar MJ, Neijs S, Bruggenwirth HT, *et al*. Mucopolysaccharidosis type IIIA: clinical spectrum and genotype-phenotype correlations. *Ann Neurol* 2010;**68**:876–87.

84 Valstar MJ, Bruggenwirth HT, Olmer R, *et al*. Mucopolysaccharidosis type IIIB may predominantly present with an attenuated clinical phenotype. *J Inherit Metab Dis* 2010;**33**:759–67.

85 Ruier GJ, Valstar MJ, van de Kamp JM, *et al*. Clinical and genetic spectrum of Sanfilippo type C (MPS IIIC) disease in The Netherlands. *Mol Genet Metab* 2008;**93**:104–11.

86 Van Hove JLK, Wevers RA, Van Cleemput J, *et al*. Late-onset visceral presentation with cardiomyopathy and without neurological symptoms of adult Sanfilippo A syndrome. *Am J Med Genet* 2003;**118**A:382–7.

87 Herd JK, Subramanian S, Robinson H. Type III mucopolysaccharidosis: report of a case with severe mitral valve involvement. *J Pediatr* 1973;**82**:101–3.

88 Cain H, Egner E, Kresse H. Mucopolysaccharidosis IIII A (Sanfilippo disease type A). Histochemical, electron microscopical and biochemical findings. *Beitr Pathol* 1977;**160**:58–72.

89 Kurihara M, Kumagai K, Yagishita S. Sanfilippo syndrome type C: a clinicopathological autopsy study of a long-term survivor. *Pediatr Neurol* 1996;**14**:317–21.

90 Shimamura K, Kakozaki H, Takahashi K, *et al*. Sanfilippo B syndrome. A case report. *Acta Pathol Jpn* 1976;**26**:739–64.

91 Danks DM, Campbell PE, Cartwright E, *et al*. The Sanfilippo syndrome: clinical, biochemical, radiological, haematological

and pathological features of nine cases. *Aust Paediatr J* 1972;**8**: 174–86.

92 Wittig C, Muller KM, Kresse H, *et al*. Morphological and biochemical findings in a case of mucopolysaccharidosis type III A (Sanfilippo's disease type A). *Beitr Pathol* 1975;**154**:324–8.

93 Wegrzyn G, Jakobkiewicz-Banecka J, Gabig-Ciminska H, *et al*. Genistein: a natural isoflavone with a potential for treatment of genetic diseases. *Biochem Soc Trans* 2010;**38**:695–701.

94 Piotrowska E, Jakobkiewicz-Banecka J, Maryniak A, *et al*. Two-year follow-up of Sanfilippo disease patients treated with a genistein-rich isoflavone extract: assessment of effects on cognitive functions and general status of patients. *Med Sci Monit* 2011;**17**:CR196–202.

95 Montano AM, Tomatsu S, Gottesman GS, *et al*. International Morquio A Registry: clinical manifestation and natural course of Morquio A disease. *J Inherit Metab Dis* 2007;**30**:165–74.

96 Hofer D, Paul K, Fantur K, *et al*. GM1 gangliosidosis and Morquio B disease: expression analysis of missense mutations affecting the catalytic site of acid β-galactosidase. *Hum Mutat* 2009;**30**:1214–21.

97 Ozand PT, Gascon G, Al Aqeel A, *et al*. Prevalence of different types of lysosomal storage diseases in Saudi Arabia. *J Inherit Metab Dis* 1990;**13**:849–61.

98 John RM, Hunter D, Swanton RH. Echocardiographic abnormalities in type IV mucopolysaccharidosis. *Arch Dis Child* 1990;**65**:746–9.

99 Factor SM, Biempica L, Goldfischer S. Coronary intimal sclerosis in Morquio's syndrome. *Virchows Arch A Pathol Anat Histol* 1978;**379**:1–10.

100 Ireland MA, Rowlands DB. Mucopolysaccharidosis type IV as a cause of mitral stenosis in an adult. *Br Heart J* 1981;**46**:113–5.

101 Beck M, Braun S, Coerdt W, *et al*. Fetal presentation of Morquio disease type A. *Prenat Diagn* 1992;**12**:1019–29.

102 Valayannopoulos V, Nicely H, Harmatz P, Turbeville S. Mucopolysaccharidosis VI. *Orphanet J Rare Dis* 2010;**12**:5.

103 Swiedler SJ, Beck M, Bajbouj M, *et al*. Threshold effect of urinary glycosaminoglycans and the walk test as indicators of disease progression in a survey of subjects with mucopolysaccharidosis VI (Maroteaux–Lamy syndrome). *Am J Med Genet A* 2005;**134**A:144–50.

104 Hayflick S, Rowe S, Kavanaugh-McHugh A, *et al*. Acute infantile cardiomyopathy as a presenting feature of mucopolysaccharidosis VI. *J Pediatr* 1992;**120**:269–72.

105 Keller C, Briner J, Schneider J, *et al*. Mukopolysaccharidose Typ VI-A (Morbus Maroteaux–Lamy): Korrelation der klinischen und pathologisch-anatomischen Befunde bei einem 27 jahrigen Patienten. *Helv Paediatr Acta* 1987;**42**:317–33.

106 Herskhovitz E, Young E, Rainer J, *et al*. Bone marrow transplantation for Maroteaux–Lamy syndrome (MPS VI): long-term follow-up. *J Inherit Metab Dis* 1999;**22**:50–62.

107 Lee V, Li CK, Shing MM, *et al*. Umbilical cord blood transplantation for Maroteaux–Lamy syndrome (mucopolysaccharidosis type VI). *Bone Marrow Transplant* 2000;**26**:455–8.

108 Tomatsu S, Montano AM, Dung VC, *et al*. Mutations and polymorphisms in GUSB gene in mucopolysaccharidoses VII (Sly syndrome). *Hum Mutat* 2009;**30**:511–9.

109 Schwartz I, Silva LR, Leistner S, *et al*. Mucopolysaccharidosis VII: clinical, biochemical and molecular investigation of a Brazilian family. *Clin Genet* 2003;**64**:172–5.

110 Lissens W, Dedobbeleer G, Foulon W, *et al*. Beta-glucuronidasae deficiency as a cause of prenatally diagnosed non-immune hydrops fetalis. *Prenat Diagn* 1991;**11**:405–10.

111 Kagie MJ, Kleijer WJ, Huijmans JGM, *et al*. Beta-glucuronidase deficiency as a cause of fetal hydrops. *Am J Med Genet* 1992;**42**:693–5.

112 Cheng Y, Verp MS, Knutel T, Hibbard JU. Mucopolysaccharidosis type VII as a cause of recurrent non-immune hydrops fetalis. *J Perinat Med* 2003;**31**:535–7.

113 Venkat-Raman N, Sebire NJ, Murphy KW. Recurrent fetal hydrops due to mucopolysaccharidoses type VII. *Fetal Diagn Ther* 2006;**21**:250–4.

114 Vogler C, Levy B, Kyle JW, *et al*. Mucopolysaccharidosis VII: postmortem biochemical and pathological findings in a young adult with beta-glucuronidase deficiency. *Mod Pathol* 1994; **7**:132–7.

115 Nampoothiri S, Kappanavil M, Hiran KR, Sunitha V. Sly disease: mucopolysaccharidosis type VII. *Indian Pediatr* 2008;**45**: 859–61.

116 Dickerman RD, Collie KO, Bruno CA Jr, Schneider SJ. Craniovertebral instability with spinal cord compression in a 17-month-old boy with Sly syndrome (mucopolysaccharidosis type VII): a surgical dilemma. *Spine* 2004;**29**:E92–4.

117 Storch S, Wittenstein B, Islam R, *et al*. Mutational analysis in longest known survivor of mucopolysaccharidosis type VII. *Hum Genet* 2003;**112**:190–4.

118 Honjo O, Ishino K, Kawada M, *et al*. Coarctation of the thoraco-abdominal aorta associated with mucopolysaccharidosis VII in a child. *Ann Thorac Surg* 2005;**80**:729–31.

119 Yamada Y, Kato K, Sukegawa K, *et al*. Treatment of MPS VII (Sly disease) by allogeneic BMT in a female with homozygous A619V mutation. *Bone Marrow Transplant* 1998;**21**:629–34.

69

Cardiovascular Manifestations of Pediatric Rheumatic Diseases

Bryce A. Binstadt

University of Minnesota, Minneapolis, MN, USA

Cardiovascular pathology can accompany most if not all rheumatic diseases due to pathogenic links between chronic inflammation and vascular endothelial injury. In the short term, cardiac involvement leads to greater morbidity and mortality in patients with pediatric rheumatic diseases. Perhaps more importantly, the onset of rheumatic diseases in children portends life-long exposure to vascular inflammation, a known risk factor for atherosclerotic coronary heart disease, as exemplified in adults with systemic lupus erythematosus (SLE) or rheumatoid arthritis [1,2].

This chapter discusses the cardiovascular complications of many childhood rheumatic diseases, including juvenile arthritis (including spondylitis), SLE, neonatal lupus, vasculitis, juvenile dermatomyositis, scleroderma, sarcoidosis, and Lyme disease. An additional section focuses on drug-induced lupus and also the cardiac side effects of certain immunosuppressive medications. Two key pediatric rheumatic diseases conspicuously absent from this chapter are discussed elsewhere in the book: rheumatic carditis (Chapters 61 and 62) and Kawasaki disease (Chapter 63). The diseases discussed in this chapter are depicted in Table 69.1, along with the most common sites of cardiac involvement.

Juvenile idiopathic arthritis

Juvenile idiopathic arthritis (JIA) is the current preferred term for what was known as juvenile rheumatoid arthritis (JRA) and juvenile chronic arthritis (JCA) [3]. JIA is defined as arthritis of unknown etiology that begins before the sixteenth birthday and persists for at least 6 weeks. The most recent classification scheme recognizes seven subtypes of JIA: systemic arthritis, oligoarthritis, polyarthritis (rheumatoid factor negative), polyarthritis (rheumatoid factor positive), psoriatic arthritis, enthesitis-related arthritis, and undifferentiated

arthritis (Table 69.1). Many pediatric rheumatologists continue to use the term "pauciarticular" arthritis rather than the newer "oligoarthritis." Cardiac involvement has been estimated to occur in 4.7–7.6% of patients with juvenile arthritis [4,5].

Systemic arthritis

Despite being the least common form of childhood arthritis, this is the subtype of JIA most often associated with cardiac involvement, and the only subtype for which cardiac involvement is a part of the diagnostic criteria. Systemic arthritis is characterized by arthritis in any number of joints, spiking fevers, and at least one of the following: a characteristic evanescent rash, lymph node enlargement, hepatomegaly and/or splenomegaly, or serositis (pericarditis or pleuritis).

Pericarditis, the most common cardiac manifestation in systemic arthritis, may occur at disease onset or with flares of disease. It can be asymptomatic or may cause dyspnea or chest pain. Findings can include tachycardia, a friction rub, and tachypnea. Electrocardiography or radiographs may provide clues to the diagnosis by showing T-wave abnormalities or cardiomegaly, but echocardiography is the standard diagnostic modality [6]. Pericardiectomy is sometimes required [7]. Progression to cardiac tamponade is rare but serious and may require urgent pericardiocentesis in addition to immunosuppressive therapy [8] (see Chapter 59).

Myocardial and endocardial involvement are much less common but are poor prognostic signs. Myocardial involvement may lead to cardiac dysfunction and death [4,5,9]. Aortic regurgitation has also been reported [10,11] and may require valve replacement [7].

During their initial presentation with fever, some patients have dilated coronary arteries [12], discovered typically when echocardiograms are performed to evaluate possible Kawasaki disease. The overlapping clinical features of systemic arthritis and Kawasaki disease may lead to diagnostic

Table 69.1 Pediatric rheumatic conditions affecting the heart. This table lists those diseases discussed in this chapter, with their most common anatomic sites of cardiac involvement depicted by shading. Black shading indicates common or well-recognized sites of involvement. Gray shading indicates less common sites of involvement. No shading indicates sites rarely involved.

Condition	Pericardium	Myocardium and conduction system	Valves	Coronary arteries	Other vessels
Juvenile idiopathic arthritis					
Systemic arthritis	●			○	○
Oligoarthritis/pauciarticular			●		
Polyarthritis (rheumatoid factor negative)			●		
Polyarthritis (Rheumatoid factor positive)			●		
Psoriatic arthritis			○		
Enthesitis-related arthritis			○		
Undifferentiated arthritis					
Systemic lupus erythematosus	●				○
Neonatal lupus		●			
Vasculitidies					
Kawasaki disease (Chapter 63)				●	
Wegener's granulomatosis	○	○	○	○	○
Churg–Strauss syndrome	○	○	○	○	○
Polyarteritis nodosa	○	○	○	○	○
Takayasu's arteritis				●	●
Cogan syndrome					
Behçet disease					
Juvenile dermatomyositis		○			
Systemic sclerosis	○	○	○	○	○
Sarcoidosis	○	○	○	○	○
Infectious/post-infectious					
Rheumatic fever (Chapters 61 and 62)			●		
Lyme disease		●			

confusion [13], and systemic arthritis should be considered in the differential diagnosis of patients who do not respond appropriately to therapy for Kawasaki disease.

Finally, patients with systemic arthritis are at risk for developing macrophage activation syndrome (MAS), a serious complication characterized by high fevers, hematologic cytopenias, and elevated liver enzymes, among other features [14]. Multi-organ failure may ensue, including, in the author's experience, profound yet reversible cardiac involvement in the form of asystole, requiring extracorporeal membrane oxygenation. Prompt recognition and aggressive treatment of MAS are essential.

The management of the cardiac manifestations of systemic arthritis depends on adequately controlling the systemic inflammatory state in close collaboration with a pediatric rheumatologist.

Polyarthritis and oligoarthritis

These forms of JIA are distinguished by the number of joints involved in the first 6 months of disease: <5 in oligoarthritis, and ≥5 in polyarthritis [3]. The rheumatoid factor positive variant of juvenile polyarthritis is indistinguishable from rheumatoid arthritis in adults. Cardiac involvement is rare among these children. Regurgitation of the aortic and/or mitral valves occurs and may require valve replacement surgery [15–17]. In addition, echocardiographic evaluation of JIA patients without cardiac symptoms can reveal systolic or diastolic dysfunction [18].

Adults with rheumatoid arthritis are at increased risk of coronary heart disease and sudden cardiac death [1]. This risk presumably extends to patients whose arthritis begins during childhood, and is hypothetically greater given their potentially longer duration of exposure to chronic inflammation. American Heart Association guidelines consider children with chronic inflammatory diseases, including JIA, at moderate risk for premature cardiovascular disease. These guidelines recommend careful identification and modification and/or treatment of traditional cardiovascular risk factors (fasting lipid profile, smoking history, family history of coronary artery disease, blood pressure, body mass index, fasting glucose, and physical activity history) and also optimal control of the arthritis [19].

Routine aerobic exercise should be encouraged for nearly all children with JIA.

Enthesitis-related arthritis

This subtype of JIA includes diseases traditionally considered under the heading "spondyloarthropathy," such as juvenile ankylosing spondylitis and HLA B27-associated juvenile arthritis. The term "enthesitis" refers to inflammation of the insertion sites of tendons or ligaments to bone. Additional features include involvement of the axial skeleton and sacroiliac joints, the HLA-B27 allele in many patients, a predominance of male patients (>6 years old), acute symptomatic anterior uveitis (red eye), and a family history of similar diseases including Reiter syndrome and inflammatory bowel disease [3].

Aortic regurgitation is the main cardiac concern in this group, but is much more common in adults than in children [20,21]. In one study of 36 patients with juvenile ankylosing spondylitis, none had cardiac symptoms, and only one had a murmur of aortic regurgitation. Three patients (8%) had mild aortic regurgitation and two had mild mitral regurgitation detected by echocardiogram [22]. In a separate study, aortic regurgitation was detected in 10% of 40 patents with HLA B27-associated juvenile arthritis [21]. Additional cardiac complications in adults with ankylosing spondylitis include conduction disturbances [23] and cardiomyopathy [20]. Baseline echocardiograms and electrocardiograms in these patients seem prudent even for asymptomatic patients [21], especially when transitioning from pediatric to adult care.

Psoriatic arthritis

Similarly to rheumatoid arthritis, adults with psoriasis or psoriatic arthritis are at increased risk for coronary heart disease and cerebrovascular accidents, thought to be related to chronic inflammation [24,25]. Therefore, children with psoriatic arthritis should be considered at moderate risk for premature cardiovascular disease and counseled accordingly (see the section Polyarthritis and Oligoarthritis above) [19].

Systemic lupus erythematosus

SLE is a multi-system autoantibody-associated disease that predominantly affects females. About 15% of SLE patients present during childhood, typically adolescence. SLE can affect nearly all tissues of the body. The numerous clinical and laboratory features of pediatric SLE are have recently been summarized [26]. In one large series of pediatric SLE, nearly half of the patients had cardiovascular involvement [27]. Raynaud's phenomenon is a common vascular manifestation of pediatric SLE, occurring in around one-fifth of patients, often at the time of diagnosis [26]. Raynaud's phenomenon may also indicate the presence of antiphospholipid antibodies, either primary or secondary to SLE [28].

Pericarditis is the only cardiac manifestation among the classification criteria for SLE, and occurs in 15–28.7% of pediatric patients [26,27,29,30]. It may occur with myocarditis, and rarely causes tamponade [30]. Anti-Ro (SS-A) and anti-La (SS-B) antibodies are detected more often in patients with cardiac involvement [30]. Pericardiectomy or creating a pericardial window might be necessary [7].

Isolated myocarditis occurs in 2–3% of pediatric SLE patients [26,30]. Cardiomegaly has been reported, however, in one-third of patients [27]. Furthermore, impaired myocardial perfusion was reported in five of 31(16%) children with SLE [31] and a similar percentage of patients have abnormalities of diastolic or systolic function [29,32]. Although myocardial involvement is often asymptomatic, congestive heart failure and arrhythmias may occur [27].

Valvar regurgitation has been reported in 20–36% of patients with pediatric SLE [29,32]. Non-infectious vegetations (Libman–Sacks endocarditis) are detected much less commonly [26], but can lead to microembolic cerebrovascular events and rarely valve regurgitation. Valve repair or replacement is the most common reason for cardiac surgery among patients with pediatric SLE [7].

Improved medical management of SLE has increased longevity, focusing attention on the long-term cardiovascular risks of SLE and its therapies [33]. Women with SLE 35–44 years of age have a 50-fold increase in incidence of myocardial infarction relative to healthy controls [34]. Younger patients are not spared; a recent literature review found 50 reports of acute myocardial infarction in SLE patients <36 years of age, including one in a 5-year-old child [35]. Patients with SLE have specific risk factors for the development of coronary artery disease, and chronic systemic inflammation alone seems to be a major driver of premature atherosclerosis [19,36,37]. The specific risk factors for premature coronary artery disease among pediatric patients with SLE include prothrombotic antiphospholipid antibodies (in 45% of patients [26]), nephritis resulting in nephrotic-range proteinuria [38] and hypertension [38,39], and dyslipidemia [40]. Corticosteroid therapy and physical inactivity (resulting from SLE disease activity) can lead to both hypertension and obesity, further increasing the risk of cardiovascular events. These concerns are detailed more extensively in a statement from the American Heart Association [19]. Children with SLE are at moderate risk for premature cardiovascular disease. As discussed in the section on juvenile arthritis, optimizing immunosuppressive and other medical management of the underlying disease and identifying and reducing traditional risk factor exposure are recommended [19]. It is reasonable for pediatric SLE patients to have echocardiograms periodically, paying particular attention to the pericardium, valves, and contractility. In addition to aggressively tailoring immunosuppressive therapy to control SLE disease activity, vigilance regarding the patient's antiphospholipid antibody status is necessary, and might include the use of

low-dose aspirin in patients without symptoms or more aggressive anticoagulation with heparin and then warfarin in patients with documented thrombotic events.

Neonatal lupus

Transplacental passage of anti-Ro (SS-A) and/or anti-La (SS-B) antibodies can cause neonatal lupus. The primary concern in affected infants is irreversible complete congenital heart block (CHB) due to antibody-mediated myocardial damage. The risk of congenital heart block among fetuses of women with anti-Ro antibodies is 2%, but this risk is increased 10-fold among women with a prior affected infant. Reversible rash occurs in 10–20% of infants, and hematologic and/or hepatic abnormalities in one-quarter; these aspects of the disease are transient. Congenital cardiac anomalies also seem more common in affected infants [41]. Mothers may be asymptomatic without evidence of SLE or a related disorder (Sjogren syndrome, mixed connective tissue disease), but up to half of them may develop symptoms subsequently [42].

The development of CHB can occur quickly during pregnancy and can lead to life-threatening cardiac dysfunction. Unfortunately, CHB, once identified, is not reversible. Efforts are therefore focused on early detection during pregnancy (via frequent echocardiograms and sonograms) and preventing the progression of heart block to cardiomyopathy by immunomodulatory agents, such as corticosteroids or intravenous immunoglobulin [43]. Involvement of a fetal–maternal medicine specialist is recommended. Prompt pacemaker implantation after delivery is often necessary [7]. Additional information regarding management is provided in Chapter 55.

Vasculitis

Vascular inflammation is the hallmark of several named diseases whose fundamental etiologies remain undefined (Table 69.2). The vasculitidies are classified according to the size and type of the vessels most often affected (Figure 69.1 and Table 69.2). Additional categorization criteria include primary vasculitis (not associated with another disease) versus vasculitis that occurs secondary to other rheumatic conditions (such as SLE, dermatomyositis, or JIA). The presence or absence of anti-neutrophil cytoplasmic antibodies (ANCAs) and the specific antigen against which those antibodies are directed also are used in classification (Table 69.2). The vasculitidies can affect virtually any organ system and, within the heart, any structure can be affected.

This section highlights the more common pediatric vasculitidies in which cardiac complications arise. Kawasaki disease, the most common childhood vasculitis associated with cardiac sequelae, is discussed in Chapter 63.

As a guiding principle, clinicians should recognize the potential for cardiac involvement in a child with any form of

Table 69.2 Major categories of noninfectious vasculitis[a].

Large-vessel vasculitis
Giant-cell arteritis
Takayasu's arteritis
Medium-sized vessel vasculitis
Polyarteritis nodosa
Kawasaki's disease
Primary granulomatous central nervous system vasculitis
Small-vessel vasculitis
ANCA-associated small-vessel vasculitis
Microscopic polyangiitis
Wegener's granulomatosis
Churg–Strauss syndrome
Drug-induced ANCA-associated vasculitis
Immune-complex small-vessel vasculitis
Henoch–Schönlein purpura
Cryoglobulinemic vasculitis
Lupus vasculitis
Rheumatoid vasculitis
Sjögren's syndrome vasculitis
Hypocomplementemic urticarial vasculitis
Behçet disease
Goodpasture syndrome
Serum-sickness vasculitis
Drug-induced immune-complex vasculitis
Infection-induced immune-complex vasculitis
Paraneoplastic small-vessel vasculitis
Lymphoproliferative neoplasm-induced vasculitis
Myeloproliferative neoplasm-induced vasculitis
Carcinoma-induced vasculitis
Inflammatory bowel disease vasculitis

[a]Vascular inflammation is categorized as either infectious vasculitis, which is caused by the direct invasion of vessel walls by pathogens (e.g., rickettsial organisms in Rocky Mountain spotted fever), or noninfectious vasculitis, which is not caused by the direct invasion of vessel walls by pathogens (although infections can indirectly induce noninfectious vasculitis, e.g., by generating pathogenic immune complexes). ANCA denotes antineutrophil cytoplasmic autoantibody.

(Reproduced with permission from Jennette JC, Falk RJ, *N Engl J Med* 1997;**337**:1512–23. Copyright © Massachusetts Medical Society. All rights reserved.)

vasculitis. Similarly, finding unexplained cardiac or vascular inflammatory disease should prompt a careful diagnostic search for systemic vasculitidies and consultation with a pediatric rheumatologist.

Wegener's granulomatosis

Wegener's granulomatosis, a necrotizing vasculitis, affects the paranasal sinuses, lungs, and kidneys and is usually associated with anti-proteinase 3 (anti-PR3) ANCA (c-ANCA). This uncommon disease in children can be severe. Cardiac complications include valvar disease, ischemic heart disease, and pericarditis [44–46]. Aggressive immunosuppression
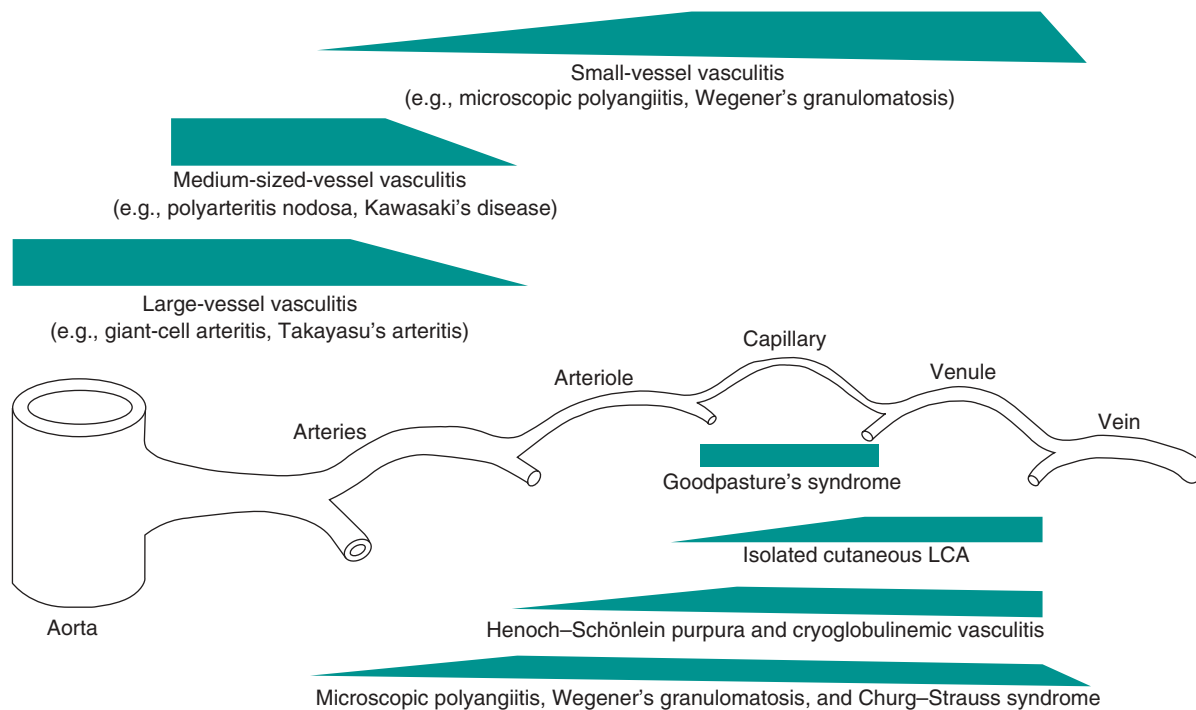
Figure 69.1 Preferred sites of vascular involvement by selected vasculitidies. The widths of the trapezoids indicate the frequencies of involvement of various portions of the vasculature. LCA denotes leukocytoclastic angiitis. (Reproduced with permission from Jennette JC, Falk RJ, *N Engl J Med* 1997;**337**:1512–23. Copyright © Massachusetts Medical Society. All rights reserved.)

with high-dose corticosteroids and cyclophosphamide is typically required to control the disease.

Churg–Strauss Syndrome (CSS)

CSS is an eosinophilic vasculitis that usually presents as severe asthma with peripheral blood eosinophilia. ANCAs are present in some patients and may be either anti-PR3 (c-ANCA) or anti-myeloperoxidase (anti-MPO, p-ANCA). Cardiac disease is a major cause of death in this disease. In a study of 49 adult patients, 22 had evidence of cardiac involvement with impaired left ventricular function (50%), valvar regurgitation (73%), pericardial effusions (41%), and endomyocarditis (59%). Patients with endomyocarditis had a more severe outcome, and two deaths due to severe cardiomyopathy and heart failure occurred [47]. Intriguingly, cardiac involvement was associated with the *absence* of ANCAs in this series [47]. Zwerina *et al.* compared 33 children with CSS with published series of adult CSS. The incidence of pericarditis was similar in both age groups (~25%), but cardiomyopathy occurred more commonly in children than in adults (42% versus 24%, $p = 0.04$) [48]. Six of the 33 children with CSS died, three from cardiac causes [48]. Aggressive immunosuppression is required, as with Wegener's granulomatosis.

Polyarteritis nodosa (PAN)

PAN is a necrotizing vasculitis predominantly affecting medium-sized arteries, including the coronary arteries. In adults, PAN may occur in conjunction with viral hepatitis, but in children PAN is typically idiopathic. A study of 15 children with PAN reported asymptomatic diminished left ventricular systolic function and mitral and/or tricuspid regurgitation as the most common cardiac complications [49]. Additional reported complications include pericarditis and myocardial infarction. Again, aggressive immunosuppression is indicated.

Takayasu's arteritis

Takayasu's arteritis, a giant cell arteritis, affects large arteries including the aorta and its main branches, including the coronary arteries. The affected arteries may be either stenotic or aneurysmal. Involvement of the base of the aorta may lead to aortic regurgitation. It affects any age group, but mainly teenage girls.

A high degree of clinical suspicion is necessary to make the diagnosis. Presenting symptoms may relate to peripheral vascular occlusion (e.g., syncope, dizziness, claudication), coronary artery narrowing (chest pain), headache (due to renal artery stenosis and hypertension), or abdominal pain due to mesenteric artery ischemia. Absence of pulses ("pulseless disease") is a crucial diagnostic sign, along with bruits or the murmur of aortic regurgitation [50]. Life-threatening complications may occur in children, including aortic dissection [51] and sudden cardiac arrest [52], sometimes as the presenting manifestation.

When Takayasu's arteritis is suspected, echocardiography is indicated in addition to extensive angiography (magnetic

resonance and/or conventional) to determine which vessels are affected.

Cogan syndrome

This rare vasculitis causes autoimmune eye disease (keratitis most commonly), sensorineural hearing loss, and large vessel vasculitis, particularly affecting the aorta, although other arteries can be involved. Surgical repair of aortic aneurysms in an adolescent has been reported [53].

Behçet disease

Behçet disease is a primary vasculitis that can affect both arteries and veins. Symptoms include recurrent oral ulceration, genital ulceration, uveitis, and dermatologic findings (e.g., erythema nodosum). Thrombosis, the main cardiovascular complication, can occur in superficial veins, the venous sinuses, pulmonary arteries, and even within the atria or ventricles [54,55]. Aneurysms of the great vessels occur in children, and may lead to myocardial infarction [54,56]. Arrhythmias may also arise [57]. Treatment with corticosteroids, colchicine, cyclophosphamide, or azathioprine and anticoagulation can be helpful [54].

Cardiac conditions mimicking vasculitis

Patients with cardiac myxomas may present with dermatologic findings similar to those seen in patients with vasculitis (e.g., petechiae, purpura, livedo reticular, ulcerations, digital necrosis) [58]. This rare condition should therefore be considered in the patient with suspected vasculitis.

Juvenile dermatomyositis

Children with dermatomyositis have proximal muscle weakness and characteristic dermatologic findings, including a heliotrope rash and Gottron's papules. In contrast to the adult form of the disease, juvenile dermatomyositis is rarely associated with malignancies. Aggressive immunosuppressive management is indicated, and can lead to complete resolution [59]. Although not formally considered under the rubric of vasculitis, the primary pathologic process is small vessel inflammation, including capillaries. Many other organ systems can be affected, including life-threatening gastrointestinal and pulmonary disease. Renal involvement is rare. Cardiac involvement occurs rarely in children and may reflect microvascular involvement. Reported cardiac complications include myocarditis, arrhythmias, and pericarditis [60,61].

Some authors have suggested that the nailfold capillary abnormalities, such as loop formation, tufting, and drop-out, that occur in this disease and others (systemic sclerosis, SLE, and the antiphospholipid antibody syndrome) might indicate systemic microvascular involvement, including those vessels perfusing the myocardium [62].

Systemic sclerosis (scleroderma)

Although rare in children, systemic sclerosis is a life-threatening disease whose mortality is often attributable to cardiac involvement [63–66]. The disease is characterized by fibrosis of skin and other organs, including the pericardium, myocardium, and pulmonary parenchyma. Raynaud's phenomenon is common, reflecting obstruction of the digital arteries. Similar vascular occlusion underlies the pathology in the affected internal organs. Thus, the disease has multiple pathogenic pathways, including autoimmune, fibrotic, and endothelial abnormalities. Importantly, some patients initially diagnosed with mixed connective tissue disease may progress over time to a disease course indistinguishable from systemic sclerosis.

Cardiac complications are numerous, including pericarditis, decreased myocardial perfusion in association with dilated cardiomyopathy, and rhythm abnormalities [63,64,67]. Pulmonary involvement is nearly universal, and can lead to significant pulmonary hypertension. Systemic hypertension also occurs due to renal involvement, and may be severe ("scleroderma renal crisis") [68].

Systemic sclerosis is perhaps the most challenging rheumatic disease to treat. Therapies directed against the autoimmune, fibrotic, and vascular aspects of the disease have been tried [69]. Traditionally, aggressive immunosuppressive therapy is used, including cyclophosphamide and other agents. Newer biologic immunosuppressive drugs, including anti-tumor necrosis factor (TNF) agents and B lymphocyte depleting therapy, have also been studied. For patients with severe disease, autologous stem cell transplantation has been attempted. Recently, attention has been focused on blocking growth factor signaling by using the tyrosine kinase inhibitor imatinib or antibodies directed against transforming growth factor β. Bosentan, an endothelin-1 receptor antagonist, has been used in patients with interstitial lung disease. Additionally, more standard vasodilators, including calcium channel blockers and angiotensin pathway inhibitors, are used. Angiotensin pathway inhibitors are effective and indicated for scleroderma renal crisis [68].

Sarcoidosis

This multisystem disease of unknown etiology is characterized by non-caseating granulomas in any tissue. Vascular involvement, including large vessel aneurysms, has been reported in children [30]. Cardiac sarcoidosis can affect any portion of the heart, including the pericardium, myocardium, valves, and conduction system. Cardiac presentations in childhood may be severe and fatal [70,71]. Immunosuppressive therapy is indicated, typically with corticosteroids as the initial agents.

Lyme disease

Infection with the spirochete *Borrelia burgdorferi* causes Lyme disease, characterized by rash (erythema migrans), arthritis, and cranial nerve palsies or frank meningitis. Lyme carditis can cause reversible complete atrioventricular block in children [72]. Such conduction abnormalities are uncommon in children with Lyme disease, both in the United States and Europe [73,74].

Patients with suspected Lyme disease should have a careful cardiac examination and an electrocardiogram. Likewise, Lyme disease should be considered in the differential diagnosis of a patient with unexplained heart block.

Side effects of pharmacologic agents

Rheumatic side effects of cardiovascular medications

Drug-induced lupus (DIL) may accompany certain cardiac medications, notably hydralazine and procainamide, particularly with higher doses. Patients typically develop cutaneous manifestations and/or pericardial disease. Nephritis is less common than in SLE. Antinuclear antibodies (ANAs) are usually but not always detected. If present, the ANAs usually recognize histone (anti-histone antibodies). Anti-double-stranded DNA antibodies are not common in DIL. Unfortunately, DIL may not resolve after discontinuation of the triggering agent [75].

Cardiovascular side effects of anti-rheumatic medications

Drug-induced lupus may also accompany sulfasalazine and other anti-rheumatic drugs (e.g., several of the biologic therapies), and also many other medications. The potential cardiac manifestations of DIL are numerous, including heart failure and tamponade [76]. Discontinuation of the potential inciting agent is indicated.

Corticosteroids, used widely to treat pediatric rheumatic diseases, can cause several cardiac complications, including hypertension, hyperlipidemia, and premature coronary atherosclerosis [19]. Decreasing the cumulative corticosteroid exposure for a child with a rheumatic disease is now easier, with the expanding arsenal of immunomodulatory agents.

TNF inhibitors are used in many rheumatic diseases, and may cause heart failure, a complication that seems more likely in elderly than in younger patients [77]. Additionally, vasculitis develops in some patients using these agents [78]. Discontinuation of the TNF inhibitor is indicated when such complications arise.

Tocilizumab, a monoclonal antibody directed against the interleukin 6 (IL6) receptor, is approved for use in adults with rheumatoid arthritis, and is being studied for use in children with systemic JIA [79]. In adult patients, tocilizumab use has been linked to lipid abnormalities and possibly myocardial infarction and cerebrovascular accidents [80].

Conclusion

Cardiovascular complications may arise in nearly any child with a rheumatic disease. This chapter has attempted to discuss those cardiac manifestations that are more common or more severe, and also those pediatric rheumatic diseases for which lifestyle modification or medical intervention during childhood may provide long-term cardiovascular benefit.

Three elements are critical for optimizing the clinical cardiovascular management of children with rheumatic diseases:
- a high clinical index of suspicion for cardiovascular involvement, with appropriate diagnostic evaluation
- aggressive immunosuppressive control of the rheumatic disease, with attention to the potential long-term cardiac complications of the disease and also its therapies
- close communication between the pediatric rheumatologist, pediatric cardiologist, and other subspecialists.

Acknowledgments

References

1 Maradit-Kremers H, Crowson CS, Nicola PJ, *et al*. Increased unrecognized coronary heart disease and sudden deaths in rheumatoid arthritis: a population-based cohort study. *Arthritis Rheum* 2005; **52**:402–11.

2 Manzi S, Meilahn EN, Rairie JE, *et al*. Age-specific incidence rates of myocardial infarction and angina in women with systemic lupus erythematosus: comparison with the Framingham Study. *Am J Epidemiol* 1997;**145**:408–15.

3 Petty RE, Southwood TR, Manners P, *et al*. International League of Associations for Rheumatology classification of juvenile idiopathic arthritis: second revision, Edmonton, 2001. *J Rheumatol* 2004; **31**:390–2.

4 Goldenberg J, Ferraz MB, Pessoa AP, *et al*. Symptomatic cardiac involvement in juvenile rheumatoid arthritis. *Int J Cardiol* 1992;**34**:57–62.

5 Svantesson H, Bjorkhem G, Elborgh R. Cardiac involvement in juvenile rheumatoid arthritis. A follow-up study. *Acta Paediatr Scand* 1983;**72**:345–50.

6 Brewer E Jr. Juvenile rheumatoid arthritis – cardiac involvement. *Arthritis Rheum* 1977;**20**:231–6.

7 Stingl C, Moller JH, Binstadt BA. Cardiac operations for North American children with rheumatic diseases: 1985–2005. *Pediatr Cardiol* 2010;**31**:66–73.

8 Yancey CL, Doughty RA, Cohlan BA, *et al*. Pericarditis and cardiac tamponade in juvenile rheumatoid arthritis. *Pediatrics* 1981;**68**:369–73.

9 Soylemezoglu O, Besbas N, Ozkutlu S, *et al*. Dilated cardiomyopathy in juvenile chronic arthritis. *Scand J Rheumatol* 1994; **23**:159–61.

10 Kramer PH, Imboden JB Jr, Waldman FM, *et al*. Severe aortic insufficiency in juvenile chronic arthritis. *Am J Med* 1983; **74**:1088–91.

11 Heyd J, Glaser J. Early occurrence of aortic valve regurgitation in a youth with systemic-onset juvenile rheumatoid arthritis. *Am J Med* 1990;**89**:123–4.

12 Binstadt BA, Levine JC, Nigrovic PA, *et al*. Coronary artery dilation among patients presenting with systemic-onset juvenile idiopathic arthritis. *Pediatrics* 2005;**116**:e89–93.

13 Komatsu H, Tateno A. Failure to distinguish systemic-onset juvenile idiopathic arthritis from incomplete Kawasaki disease in an infant. *J Paediatr Child Health* 2005;**43**:707–9.

14 Ravelli A, Magni-Manzoni S, Pistorio A, *et al*. Preliminary diagnostic guidelines for macrophage activation syndrome complicating systemic juvenile idiopathic arthritis. *J Pediatr* 2005;**146**:598–604.

15 Delgado EA, Petty RE, Malleson PN, *et al*. Aortic valve insufficiency and coronary artery narrowing in a child with polyarticular juvenile rheumatoid arthritis. *J Rheumatol* 1988;**15**:144–7.

16 Ozer S, Alehan D, Ozme S, *et al*. Mitral and aortic insufficiency in polyarticular juvenile rheumatoid arthritis. *Pediatr Cardiol* 1994;**15**:151–3.

17 Boris JR, Hollister JR, Tyson RW, *et al*. Severe aortic regurgitation with mechanical prosthetic valve replacement in pauciarticular juvenile rheumatoid arthritis. *J Rheumatol* 1998;**25**:1211–4.

18 Bharti BB, Kumar S, Kapoor A, *et al*. Assessment of left ventricular systolic and diastolic function in juvenile rheumatoid arthritis. *J Postgrad Med* 2004;**50**:262–5;discussion 266–7.

19 Kavey RE, Allada V, Daniels SR, *et al*. Cardiovascular risk reduction in high-risk pediatric patients: a scientific statement from the American Heart Association Expert Panel on Population and Prevention Science; the Councils on Cardiovascular Disease in the Young, Epidemiology and Prevention, Nutrition, Physical Activity and Metabolism, High Blood Pressure Research, Cardiovascular Nursing, and the Kidney in Heart Disease; and the Interdisciplinary Working Group on Quality of Care and Outcomes Research: endorsed by the American Academy of Pediatrics. *Circulation* 2006;**114**:2710–38.

20 Jimenez-Balderas FJ, Garcia-Rubi D, Perez-Hinojosa S, *et al*. Two-dimensional echo Doppler findings in juvenile and adult onset ankylosing spondylitis with long-term disease. *Angiology* 2001;**52**:543–8.

21 Huppertz H, Voigt I, Muller-Scholden J, *et al*. Cardiac manifestations in patients with HLA B27-associated juvenile arthritis. *Pediatr Cardiol* 2000;**21**:141–7.

22 Stamato T, Laxer RM, de Freitas C, *et al*. Prevalence of cardiac manifestations of juvenile ankylosing spondylitis. *Am J Cardiol* 1995;**75**:744–6.

23 Dik VK, Peters MJ, Dijkmans PA, *et al*. The relationship between disease-related characteristics and conduction disturbances in ankylosing spondylitis. *Scand J Rheumatol* 2010;**39**:38–41.

24 Gladman DD, Ang M, Su L, *et al*. Cardiovascular morbidity in psoriatic arthritis. *Ann Rheum Dis* 2009;**68**:1131–5.

25 Kimball AB, Guerin A, Latremouille-Viau D, *et al*. Coronary heart disease and stroke risk in patients with psoriasis: retrospective analysis. *Am J Med* 2010;**123**:350–7.

26 Hiraki LT, Benseler SM, Tyrrell PN, *et al*. Clinical and laboratory characteristics and long-term outcome of pediatric systemic lupus erythematosus: a longitudinal study. *J Pediatr* 2008; **152**:550–6.

27 Yeh TT, Yang YH, Lin YT, *et al*. Cardiopulmonary involvement in pediatric systemic lupus erythematosus: a twenty-year retrospective analysis. *J Microbiol Immunol Infect* 2007;**40**:525–31.

28 Nigrovic PA, Fuhlbrigge RC, Sundel RP. Raynaud's phenomenon in children: a retrospective review of 123 patients. *Pediatrics* 2003;**111**:715–21.

29 Al-Abbad AJ, Cabral DA, Sanatani S, *et al*. Echocardiography and pulmonary function testing in childhood onset systemic lupus erythematosus. *Lupus* 2001;**10**:32–7.

30 Oshiro AC, Derbes SJ, Stopa AR, *et al*. Anti-Ro/SS-A and anti-La/ SS-B antibodies associated with cardiac involvement in childhood systemic lupus erythematosus. *Ann Rheum Dis* 1997; **56**:272–4.

31 Gazarian M, Feldman BM, Benson LN, *et al*. Assessment of myocardial perfusion and function in childhood systemic lupus erythematosus. *J Pediatr* 1998;**132**:109–16.

32 Gunal N, Kara N, Akkok N, *et al*. Cardiac abnormalities in children with systemic lupus erythematosus. *Turk J Pediatr* 2003;**45**:301–5.

33 Stichweh D, Arce E, Pascual V. Update on pediatric systemic lupus erythematosus. *Curr Opin Rheumatol* 2004;**16**:577–87.

34 Esdaile JM, Abrahamowicz M, Grodzicky T, *et al*. Traditional Framingham risk factors fail to fully account for accelerated atherosclerosis in systemic lupus erythematosus. *Arthritis Rheum* 2001;**44**:2331–7.

35 Korkmaz C, Cansu DU, Kasifoglu T. Myocardial infarction in young patients (< or = 35 years of age) with systemic lupus erythematosus: a case report and clinical analysis of the literature. *Lupus* 2007;**16**:289–97.

36 Doria A, Iaccarino L, Sarzi-Puttini P, *et al*. Cardiac involvement in systemic lupus erythematosus. *Lupus* 2005;**14**:683–6.

37 Hashkes PJ, Wexler LF, Passo MH. Coronary artery disease in systemic lupus erythematosus: risk factors, assessment, and prevention. *J Clin Rheumatol* 1997;**3**:203–10.

38 Falaschi F, Ravelli A, Martignoni A, *et al*. Nephrotic-range proteinuria, the major risk factor for early atherosclerosis in juvenile-onset systemic lupus erythematosus. *Arthritis Rheum* 2000;**43**:1405–9.

39 Marini R, Costallat LT. Young age at onset, renal involvement, and arterial hypertension are of adverse prognostic significance in juvenile systemic lupus erythematosus. *Rev Rhum Engl Ed* 1999;**66**:303–309.

40 Ilowite NT, Samuel P, Ginzler E, *et al*. Dyslipoproteinemia in pediatric systemic lupus erythematosus. *Arthritis Rheum* 1988; **31**:859–63.

41 Eronen M, Siren MK, Ekblad H, *et al*. Short- and long-term outcome of children with congenital complete heart block diagnosed *in utero* or as a newborn. *Pediatrics* 2000;**106**:86–91.

42 Brucato A, Cimaz R, Caporali R, *et al*. Pregnancy outcomes in patients with autoimmune diseases and anti-Ro/SSA antibodies. *Clin Rev Allergy Immunol* 2011;**40**:27–41.

43 Buyon JP, Clancy RM, Friedman DM. Cardiac manifestations of neonatal lupus erythematosus: guidelines to management, integrating clues from the bench and bedside. *Nat Clin Pract Rheumatol* 2009;**5**:139–48.

44 Faurschou M, Mellemkjaer L, Sorensen IJ, *et al*. Increased morbidity from ischemic heart disease in patients with Wegener's granulomatosis. *Arthritis Rheum* 2009;**60**:1187–92.

45 Greidinger EL, Lemes V, Hellmann DB. Cardiac valve disease in Wegener's granulomatosis. *J Rheumatol* 1996;**23**:1485–7.

46 Rottem M, Fauci AS, Hallahan CW, *et al*. Wegener granulomatosis in children and adolescents: clinical presentation and outcome. *J Pediatr* 1993;**122**:26–31.

47 Neumann T, Manger B, Schmid M, *et al*. Cardiac involvement in Churg–Strauss syndrome: impact of endomyocarditis. *Medicine (Baltimore)* 2009;**88**:236–43.

48 Zwerina J, Eger G, Englbrecht M, *et al*. Churg–Strauss syndrome in childhood: a systematic literature review and clinical comparison with adult patients. *Semin Arthritis Rheum* 2009;**39**:108–15.

49 Gunal N, Kara N, Cakar N, *et al*. Cardiac involvement in childhood polyarteritis nodosa. *Int J Cardiol* 1997;**60**:257–62.

50 Ravelli A, Pedroni E, Perrone S, *et al*. Aortic valve regurgitation as the presenting sign of Takayasu arteritis. *Eur J Pediatr* 1999;**158**:281–3.

51 Civilibal M, Sever L, Numan F, *et al*. Dissection of the abdominal aorta in a child with Takayasu's arteritis. *Acta Radiol* 2008 **49**:101–4.

52 Basso C, Baracca E, Zonzin P, *et al*. Sudden cardiac arrest in a teenager as first manifestation of Takayasu's disease. *Int J Cardiol* 1994;**43**:87–9.

53 Su JW, Low AH, Tay KH, *et al*. Recurrent aortic aneurysms following thoracic aortic stent-graft repair in a patient with Cogan syndrome. *J Endovasc Ther* 2006;**13**:779–82.

54 Ozen S, Bilginer Y, Besbas N, *et al*. Behçet disease: treatment of vascular involvement in children. *Eur J Pediatr* 2010; **169**:427–30.

55 Vivante A, Bujanover Y, Jacobson J, *et al*. Intracardiac thrombus and pulmonary aneurysms in an adolescent with Behçet disease. *Rheumatol Int* 2009;**29**:575–7.

56 Zhuang J, Wang S, Zhang Z, *et al*. Acute myocardial infarction and ascending aortic aneurysm in a child with Behçet disease. *Turk J Pediatr* 2008;**50**:81–5.

57 Mirone L, Altomonte L, Ferlisi EM, *et al*. Behçet's disease and cardiac arrhythmia. *Clin Rheumatol* 1997;**16**:99–100.

58 Carlson JA, Chen KR. Cutaneous pseudovasculitis. *Am J Dermatopathol* 2007;**29**:44–55.

59 Kim S, El-Hallak M, Dedeoglu F, *et al*. Complete and sustained remission of juvenile dermatomyositis resulting from aggressive treatment. *Arthritis Rheum* 2009;**60**:1825–30.

60 Pereira RM, Lerner S, Maeda WT, *et al*. Pericardial tamponade in juvenile dermatomyositis. *Clin Cardiol* 1992;**15**:301–3.

61 Karaca NE, Aksu G, Yeniay BS, *et al*. Juvenile dermatomyositis with a rare and remarkable complication: sinus bradycardia. *Rheumatol Int* 2006;**27**:179–82.

62 Cutolo M, Sulli A, Secchi ME, *et al*. Nailfold capillaroscopy is useful for the diagnosis and follow-up of autoimmune rheumatic diseases. A future tool for the analysis of microvascular heart involvement? *Rheumatology (Oxford)* 2006;**45**(Suppl 4):iv43–6.

63 Quartier P, Bonnet D, Fournet JC, *et al*. Severe cardiac involvement in children with systemic sclerosis and myositis. *J Rheumatol* 2002;**29**:1767–73.

64 Martini G, Vittadello F, Kasapcopur O, *et al*. Factors affecting survival in juvenile systemic sclerosis. *Rheumatology (Oxford)* 2009;**48**:119–22.

65 Scalapino K, Arkachaisri T, Lucas M, *et al*. Childhood onset systemic sclerosis: classification, clinical and serologic features, and survival in comparison with adult onset disease. *J Rheumatol* 2006;**33**:1004–13.

66 Foeldvari I, Zhavania M, Birdi N, *et al*. Favourable outcome in 135 children with juvenile systemic sclerosis: results of a multinational survey. *Rheumatology (Oxford)* 2000;**39**:556–9.

67 Wozniak J, Dabrowski R, Luczak D, *et al*. Evaluation of heart rhythm variability and arrhythmia in children with systemic and localized scleroderma. *J Rheumatol* 2009 **36**:191–6.

68 Mouthon L, Bérezné A, Bussone G, *et al*. Scleroderma renal crisis: a rare but severe complication of systemic sclerosis. *Clin Rev Allergy Immunol*. 2011;**40**:84–91

69 Quillinan NP, Denton CP. Disease-modifying treatment in systemic sclerosis: current status. *Curr Opin Rheumatol* 2009;**21**: 636–41.

70 Burton DA, Kapur S, Shapiro SR, *et al*. Fulminant cardiac sarcoidosis in childhood. *Am J Cardiol* 1986;**58**:177–8.

71 Duke C, Rosenthal E. Sudden death caused by cardiac sarcoidosis in childhood. *J Cardiovasc Electrophysiol* 2002;**13**:939–42.

72 Silver E, Pass RH, Kaufman S, *et al*. Complete heart block due to Lyme carditis in two pediatric patients and a review of the literature. *Congenit Heart Dis* 2007;**2**:338–41.

73 Woolf PK, Lorsung EM, Edwards KS, *et al*. Electrocardiographic findings in children with Lyme disease. *Pediatr Emerg Care* 1991;**7**:334–6.

74 Mravljak M, Velnar T, Bricelj V, *et al*. Electrocardiographic findings in children with erythema migrans. *Wien Klin Wochenschr* 2006;**118**:691–5.

75 Dedeoglu F. Drug-induced autoimmunity. *Curr Opin Rheumatol* 2009;**21**:547–51.

76 Mor A, Pillinger MH, Wortmann RL, *et al*. Drug-induced arthritic and connective tissue disorders. *Semin Arthritis Rheum* 2008;**38**:249–64.

77 Curtis JR, Kramer JM, Martin C, *et al*. Heart failure among -younger rheumatoid arthritis and Crohn's patients exposed to TNF-alpha antagonists. *Rheumatology (Oxford)* 2007;**46**:1688–93.

78 Saint Marcoux B, De Bandt M. Vasculitides induced by TNFalpha antagonists: a study in 39 patients in France. *Joint Bone Spine* 2006;**73**:710–3.

79 Yokota S, Imagawa T, Mori M, *et al*. Efficacy and safety of tocilizumab in patients with systemic-onset juvenile idiopathic arthritis: a randomised, double-blind, placebo-controlled, withdrawal phase III trial. *Lancet* 2008;**371**:998–1006.

80 Storage SS, Agrawal H, Furst DE. Description of the efficacy and safety of three new biologics in the treatment of rheumatoid arthritis. *Korean J Intern Med* 2010;**25**:1–17.

70 Pediatric Heart Transplantation

Rebecca Ameduri[1] & Charles E. Canter[2]

[1]University of Minnesota School of Medicine, Minneapolis, MN, USA
[2]Washington University School of Medicine, St. Louis, MO, USA

Heart transplantation has become accepted in children for heart diseases associated with intractable heart failure unamenable to conventional medical or surgical therapy. Data from the registry of the International Society for Heart and Lung Transplantation (ISHLT) indicate that annually ~400 heart transplants have been performed in patients <18 years of age for the past 20 years [1]. This volume is ~10% of the total number of transplants reported to the ISHLT annually. Adults with congenital heart disease (CHD) now account for 2% of adult recipients [2]. Functional rehabilitation with no perceived activity limitations occurs in >90% of pediatric heart transplant recipients [1]. Adult survivors of pediatric heart transplantation have demonstrated a patient perception of physical and mental health similar to the general population [3].

One-quarter of pediatric heart transplants occur in infants <1 year of age, the remainder being split evenly between children 1–10 years of age and adolescents 11–18 years of age. CHD, both repaired and unrepaired, and cardiomyopathy are the most common diseases leading to heart transplantation in children (Figure 70.1) [1]. Infants are most likely transplanted for CHD. However, over the past 10 years, an increasing proportion of infant transplants have been for cardiomyopathies. Cardiomyopathies account for 50% of transplants in older children and nearly 67% of transplants in adolescents. As heart transplants have been performed for a number of years, it is not surprising that 6–7% of the heart transplants performed in older children and adolescents are for retransplantation.

Outcomes

Survival after pediatric heart transplantation has improved significantly over time and currently approaches 90% at 1 year and 77% at 5 years after transplantation (Figure 70.2)

[1]. The ISHLT registry calculates the graft half-life, the time when 50% of grafts are lost due to patient mortality or retransplantation, to be 18.4 years for infants, 14.7 years for older children, and 11.1 years for adolescents. Aside from the era effect, CHD, retransplantation, use of ventilator or dialysis at time of transplant, older recipient or donor age, sensitization to HLA antigens, higher serum creatinine, and lower heart transplant center volume are significant risk factors for 1 and 5 year mortality [1]. The increased mortality after heart transplantation associated with CHD is from an increased perioperative mortality, as outcomes are the same for patients transplanted for CHD and cardiomyopathy who survive at least 3 months after transplantation [4].

The most common causes of death after heart transplantation are rejection, transplant coronary artery disease, infection, primary graft failure (failure occurring in the first 30 days after operation) and chronic nonspecific graft failure (Figure 70.3) [1]. Primary graft failure is the most common cause of mortality in the first 30 days after transplantation, especially in infants [1,5]. Rejection, followed by infection, are the most common causes of death from 1 to 12 months after transplantation. Transplant coronary artery disease followed by nonspecific chronic graft failure are the most common causes of death >3 years after transplantation.

Mortality associated with heart transplantation really begins when the patient is listed for transplantation. Such "intent to treat" survival includes death while waiting for or after transplantation. Within the Pediatric Heart Transplant Study (PHTS) database, such "intent to treat" survival was 74% at 1 year, 66% at 5 years, and 59% at 10 years after listing for transplantation, with >50% of the 10-year mortality occurring in the first year after listing [6]. Competing risk analysis with the PHTS [7] demonstrates an overall decrease in the mortality with time while waiting in pediatric heart transplant candidates. In candidates listed for transplantation who required intravenous inotropes, mechanical ventilation,
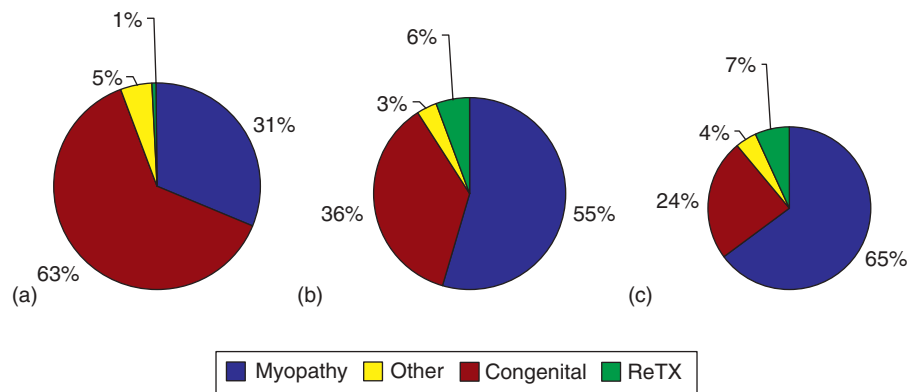
Figure 70.1 Distribution of diagnoses in heart transplant recipients by age, from ISHLT data [1] for recent era including transplants performed from January 1996 through June 2008. (a) Infant recipients <1 year of age; (b) child recipients aged 1–10 years; (c) adolescent recipients aged 11–17 years.
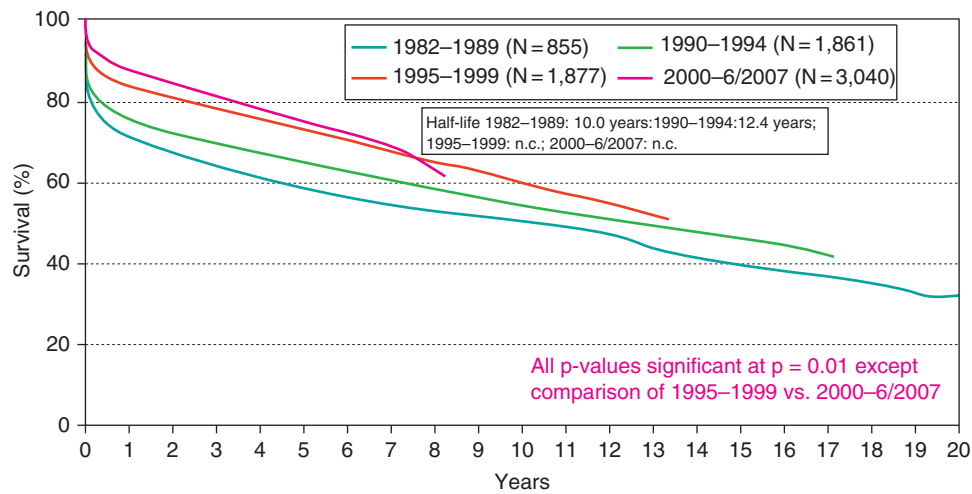
Figure 70.2 Survival after pediatric heart transplantation in the current era compared with earlier eras. (Reproduced with permission from Kirk R, Edwards LB, Aurora P, *et al. J Heart Lung Transplant* 2009;**28**:993–1006.)
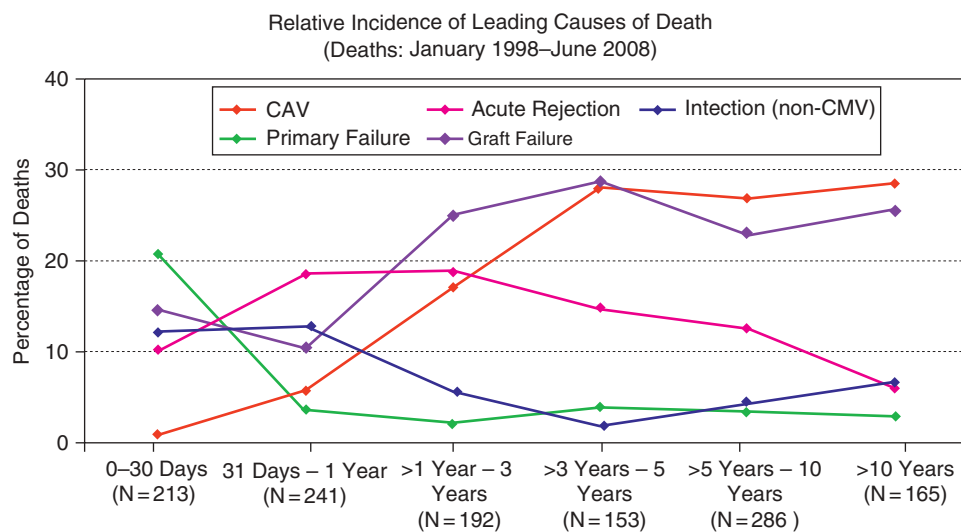
Figure 70.3 Etiology for cause of death after pediatric heart transplantation at various time periods after transplantation. (Reproduced with permission from Kirk R, Edwards LB, Aurora P, *et al. J Heart Lung Transplant* 2009;**28**:993–1006.)

or mechanical circulatory support, 19% died and 62% were transplanted within 6 months of the listing, as compared with 3% who died and 59% who were transplanted without needing such support. Within the United States Scientific Registry of Transplant Recipients (SRTR), multivariate risk factors for wait-list mortality in pediatric candidates include extracorporeal membrane oxygenator (ECMO) support, mechanical ventilation, dialysis support, CHD, and non-white race/ethnicity [8]. Patients listed on intravenous inotropic support have a 30 day wait-list mortality of 8% compared with an 18% 30 day mortality for patients listed on ventilatory support and a 38% 30 day mortality for patients listed on ECMO. Adolescent wait-list mortality has decreased by 50% over the last decade [9], likely reflecting the increased use of ventricular assist devices (VADs) as a bridge to transplant [10]. The recent availability of the Berlin Heart, which extends the ability for VAD support to children as small as 3.5 kg, may extend this benefit to younger children and infants [9,11].

Infants listed for heart transplantation face the single highest mortality waiting for heart transplantation of all children in the United States [12]. The absence of ABO isoagglutinins at birth has offered the successful [13] application of ABO-incompatible heart transplantation in infants with decreased wait-list mortality and post-transplant outcomes similar to ABO-compatible infant transplants [14]. Interestingly, ABO-incompatible heart transplant infants *do* develop antibodies to the incompatible blood group antigen in the allograft, suggesting some degree of immunologic tolerance. The proportion of infants listed for ABO-incompatible transplants has risen dramatically in recent years in the United States, especially in infants at the highest risk for wait-list mortality. This strategy has greatly increased the odds for transplantation for blood type O infant transplant candidates [15].

Indications/evaluation

A number of published consensus indications for pediatric heart transplantation have been published over the years [16,17], most recently in 2007 (Table 70.1) [7]. In general, the guidelines have included the following indications for cardiac transplantation in pediatric recipients:

- a need for ongoing intravenous inotropic, mechanical ventilatory or circulatory support
- complex CHD not amenable to conventional surgical repair or palliation or where the surgical procedure carried a higher short- and mid-term risk of mortality than transplantation
- progressive deterioration of ventricular function or functional status despite optimal medical care with digitalis, diuretics, angiotensin-converting enzyme inhibitors, and β-blockade
- postcardiac arrest malignant arrhythmia unresponsive to medical treatment, catheter ablation, or an automatic implantable defibrillator

- progressive pulmonary hypertension secondary to systemic ventricular failure or restrictive cardiomyopathy that could preclude transplantation at a later date
- growth failure secondary to severe congestive heart failure unresponsive to conventional medical treatment
- unacceptably poor quality of life secondary to heart failure
- progressive deterioration in functional status and/or presence of certain high-risk conditions following the Fontan procedure (i.e., protein-losing enteropathy, arrhythmias.

The literature about heart failure in adults supports the use of maximum oxygen consumption (VO_{2max}) to define severe heart failure and risk for 1 year mortality [18]. In general, VO_{2max} <14 ml kg^{-1} min^{-1} or <50% predicted VO_{2max} are accepted as indications for cardiac transplantation in adults [19–21]. It is difficult to apply this measurement in pediatrics because of the following: inability of young patients to perform exercise testing, baseline abnormal VO_{2max} in patients with complex CHD or cyanotic lesions even in the absence of heart failure, and the variability in VO_{2max} with different ages and sizes of patients [22–25]. For children and young adults, the use of percent predicted VO_{2max} may be a more accurate assessment of cardiac status. However, studies using exercise testing as a prognostic factor in pediatric heart disease have not been performed; therefore, exercise testing is not used as a sole criterion for defining heart failure in pediatrics.

Very few children with end-stage cardiac failure are unacceptable candidates for cardiac transplantation. The technical challenges of cardiac replacement in the presence of congenital or acquired abnormalities of body situs, pulmonary arteries, atria, and systemic and pulmonary venous return have been overcome with advanced surgical techniques. The exception is severe pulmonary arterial or venous hypoplasia [7,26]. The transplant evaluation is designed to identify the potential exclusion criteria of irreversible disease in the lungs, liver, kidney, or central nervous system, active infection, severe psychologic illness or psychosocial contraindications, or high titers of HLA antibodies that increase the risk of early rejection and graft failure (Table 70.2). Additionally, as increasing numbers of genetic etiologies for pediatric cardiomyopathy are identified [27], a genetic and/or metabolic evaluation becomes important.

There are few absolute contraindications to cardiac transplantation in children. Severe dysfunction of another organ that is not associated with low cardiac output typically excludes a patient from transplantation. HIV infection has been considered an absolute contraindication, although there are recent reports of successful cardiac transplantation in adults with HIV who are well controlled on antiretroviral therapy [28,29]. Active infection within 2 weeks before transplant also poses an increased risk of early mortality, and if possible transplant should be delayed until the infection is cleared or well controlled [1,30]. Active malignancy is a contraindication, and the cancer-free period required before cardiac transplantation depends on the type of malignancy and the opinion of the oncologist regarding likelihood

Table 70.1 American Heart Association guidelines for indications for heart transplantation for pediatric heart disease.

Cardiomyopathies and CHD in pediatric patients

Class 1:

- Heart transplantation is indicated as therapy for Stage D heart failure associated with systemic ventricular dysfunction in pediatric patients with cardiomyopathies or previous repaired or palliated CHD. Level of evidence B.
- Heart transplantation is indicated as therapy for Stage C heart failure associated with systemic ventricular dysfunction in pediatric patients with cardiomyopathies or previously repaired or palliated CHD when heart failure is associated with significant growth failure attributable to the heart disease. Level of evidence B.
- Heart transplantation is indicated as therapy for Stage C heart failure in pediatric heart disease with associated near sudden death and/or life-threatening arrhythmias untreatable with medications or and implantable defibrillator. Level of evidence C.
- Heart transplantation is indicated as therapy for Stage C heart failure in pediatric heart disease associated with reactive pulmonary hypertension and a potential risk of developing fixed, irreversible elevation of pulmonary vascular resistance which could preclude orthotopic heart transplantation in the future. Level of evidence C.
- In the presence of other indications for heart transplantation, heart transplantation is feasible in patients with pediatric heart disease and an elevated pulmonary vascular resistance index >6 Woods units m^{-2} and/or an transpulmonary pressure gradient >15 mmHg if administration of inotropic support and/or pulmonary vasodilators can decrease pulmonary vascular resistance to <6 Woods units m^{-2} and/or the transpulmonary gradient to <15 mmHg. Level of evidence B.

Class 2A:

- Heart transplantation is indicated as therapy for Stage C heart failure in pediatric heart disease associated with severe limitation of exercise and activity. If measurable, such patients would have peak maximum oxygen consumption <50% predicted for age and gender. Level of evidence C.
- Certain anatomic and physiologic conditions likely worsen the natural history of CHD in infant patients with a functional single ventricle, which can lead to use of heart transplantation as *primary* therapy. These conditions include:
    1. severe stenosis(es) or atresia in proximal coronary arteries
    2. moderate to severe stenosis and/or insufficiency of the atrioventricular and/or systemic semilunar valve(s)
    3. severe ventricular dysfunction.
    Level of evidence C
- Anatomic and physiologic conditions likely worsen the natural history of previously repaired or palliated CHD in pediatric patients which may lead to consideration for heart transplantation without severe systemic ventricular dysfunction:
    1. pulmonary hypertension and a potential risk of developing fixed, irreversible elevation of pulmonary vascular resistance which could preclude orthotopic heart transplantation in the future
    2. severe aortic or systemic A-V valve insufficiency not considered amenable to surgical correction
    3. severe arterial oxygen desaturation (cyanosis) not considered amenable to surgical correction
    4. persistent protein-losing enteropathy despite optimal medical–surgical therapy.
    Level of evidence C

Class 2B:

- The efficacy of heart transplantation as therapy for pediatric heart disease is not well established for patients with previous infection with hepatitis B, hepatitis C, or HIV infection. Level of evidence B.
- The efficacy of heart transplantation for pediatric heart disease is not well established for patients with a history of recent use of illicit drugs, tobacco, or alcohol abuse. Level of evidence B.
- The efficacy of heart transplantation for pediatric heart disease is not well established for patients with a history of psychological, behavior, or cognitive disorder; poor family support structures, or documented noncompliance with previous therapies that could interfere with successful performance of care regimens after transplantation. Level of evidence B.

Class 3:

- Heart transplantation for pediatric heart disease is not efficacious when heart disease is associated with severe, irreversible disease in other organ systems or when it is part of a severe, irreversible multi-systemic disease process. Multi-organ transplantation may be considered. Level of evidence C.
- Orthotopic heart transplantation for pediatric heart disease is not efficacious when heart disease is associated with severe, irreversible, fixed elevation of pulmonary vascular resistance. Level of evidence C.
- Heart transplantation is not feasible in the presence of severe hypoplasia of the central branch pulmonary arteries or pulmonary veins. Level of evidence C.
- The limited supply of pediatric donors, especially infant donors, makes heart transplantation not a feasible routine *primary* therapy for any specific congenital heart lesion. Level of evidence C.

Table 70.1 (cont'd).

Cardiac retransplantation in pediatric patients

Class 1:

- Retransplantation is indicated in children with abnormal ventricular function associated with Grade C or greater heart failure and at least moderate graft vasculopathy. Level of evidence B.

Class 2A:

- Retransplantation is indicated in children with normal ventricular function and at least moderate graft vasculopathy. Level of evidence B.

Class 2B:

- The efficacy of retransplantation is not well established when performed during the first 6 months following primary transplantation. Level of evidence B

Class 3:

- Retransplantation should not be performed during an episode of ongoing acute allograft rejection, even in the presence of graft vasculopathy. Level of evidence B.

Reproduced with permission from Canter CE, Shaddy RE, Bernstein D, *et al. Circulation* 2007;**115**:658–76.

Table 70.2 Basic evaluation protocol for evaluation for pediatric heart transplantation.

Cardiac catheterization

- Assess pulmonary vascular resistance and reactivity if needed
- Delineate complex anatomy (may need additional imaging with MRI/MRA or CT)

Exercise testing

- Obtain MVO_2 or 50% predicted VO_2 max

Assessment of end-organ function

- Evaluation of liver/kidney function
- Pulmonary function tests

HLA sensitization

- Panel reactive antibody

Psychosocial assessment

Financial

- Insurance and resource evaluation

Blood work

- Chemistry
  - Comprehensive panel
  - Electrolytes
  - BUN/creatinine
  - LFTs
  - Phosphorus
  - Total and direct bilirubin
  - Calcium and magnesium
  - Lipase and amylase if indicated
  - Triglycerides, cholesterol profile
  - Urinalysis (routine u/a, 24 h protein/creatinine)

Blood work (continued)

- Hematology
  - Complete blood count with differential
  - PT, PTT, INR
  - Fibrinogen
- Immunology
- HLA-tissue typing
- Panel reactive antibody
- Quantitative immunoglobulins if indicated
- Infectious disease
  - Viral testing
    - Cytomegalovirus
    - Epstein–Barr virus
    - Herpes simplex
    - HIV
    - Varicella
    - Toxoplasmosis
    - Hepatitis panel (A, B, C)
- Blood bank
  - Blood type X2
  - Blood group antibody screening

of cure or disease recurrence [31]. The post-transplant follow-up schedule is intensive, and patients must have the appropriate neuropsychiatric and social situation to allow for success [32–34].

End-stage cardiac disease is frequently associated with elevated pulmonary artery pressure and resistance. As most donor hearts have been exposed to only normal pulmonary pressures, pulmonary hypertension in the recipient may be

Table 70.3 United Network for Organ Sharing (UNOS) criteria for urgency status for pediatric heart transplant candidates in the United States [7,8].

A candidate listed as Status 1A meets at least one of the following criteria:
- Requires assistance with a ventilator
- Requires assistance with a mechanical device (i.e., ECMO, VAD)
- Requires assistance with a balloon pump
- Less than 6 months old with a congenital or acquired heart disease with reactive pulmonary hypertension >50% of systemic
- Requires infusion of high-dose inotropes (dobutamine/dopamine >7.5 µg kg^{-1} min^{-1} or milrinone >0.5 µg kg^{-1} min^{-1} or multiple inotropes)
- Candidate who does not meet other criteria but has life expectancy <14 days without transplant
- 1A exception

A candidate listed as Status 1B meets at least one of the following criteria:
- Requires infusion of low-dose single inotropes (e.g., dopamine or dobutamine ≤7.5 µg kg^{-1} min^{-1} or milrinone <0.5 µg kg^{-1} min^{-1})
- Less than 6 months old and does not meet the criteria for Status 1A
- Growth failure, i.e., <5% for weight and/or height, or loss of 1.5 standard deviations of expected growth
- 1B exception or variance

A candidate listed as Status 2 meets the following criteria:
- On oral medications
- Does not meet criteria for Status 1A or 1B

associated with acute right ventricular failure and death immediately after operation [35]. For this reason, a pulmonary vascular resistance of >6 Woods units m^{-2} or a transpulmonary gradient of >15 mmHg have been used as exclusion criteria in adults for cardiac transplantation and an indication for heart–lung transplantation. Experience with children suggests that pulmonary vascular reactivity is a more important indicator of suitability for transplantation [36,37]. One goal of pre-transplant cardiac catheterization is evaluation of the pulmonary vascular resistance (indexed to body surface area) and, if it is elevated, assessment of pulmonary vascular reactivity with vasodilators. Furthermore, intensive treatment of cardiac failure over weeks in a patient with an initial unfavorable pulmonary vascular resistance can lower the pulmonary resistance to an acceptable level. Most institutions consider a child suitable for cardiac transplantation alone if able to achieve pulmonary resistance <6 Woods units m^{-2} or a transpulmonary gradient <15 mmHg with pulmonary vasodilators.

Listing process/donor selection

In the United States, transplantation is controlled nationally through the United Network for Organ Sharing (UNOS) [7,8]. All patients are listed in an online database, and all donor offers and information are disseminated through the donor information system Donornet. Donors are matched to recipients based on ABO compatibility, age, size, wait-list status (Table 70.3), distance, and waiting time. Patients with the greatest need (status 1A) have priority. Organs are offered to local and regional recipients (500 mile radius from the donor hospital) first to minimize the ischemic time, which should ideally be kept <4 h. Some studies report, however, no difference in graft failure or mortality with ischemic times

as long as 6 h [38–41]. The available hearts for children come from brain dead donors, typically from motor vehicle crashes, head trauma, non-accidental head injury, drowning, or asphyxia. The mechanism of death may play a role in the function of the donor organ, and mild to moderate inotropic support in a potential donor does not necessarily make that heart unsuitable for transplantation [5,42,43].

An increasing number of recipients have preformed HLA antibodies, from exposures from prior cardiac operations that used homograft material (i.e., valves, aorta, pulmonary artery), blood product exposures, pregnancy, or mechanical circulatory support devices [44–46]. Patients with antibodies to multiple HLA antigens are at increased risk of acute rejection [1,44–49]. Matching a donor to a recipient with antibodies to the donor's HLA antigens can be performed using a virtual crossmatch [50] performed by matching the donor to a recipient who does not have preformed donor-specific antibody to the donor's HLA antigens. Some patients with a "+" virtual crossmatch will not have a positive complement-fixing tissue crossmatch as anti-HLA antibodies may have low plasma concentration or low avidity. Some centers have adopted plasmapheresis protocols and aggressive early immunosuppression to lower the antibody titers to perform heart transplant with a positive donor–recipient crossmatch [48,49]. Additionally, some investigators use pre-transplant plasmapheresis, intravenous immunoglobulin, or immunosuppression to lower antibody levels before transplant, with variable success [51,52].

Immunosuppression after transplantation

Cardiac transplantation is not a cure or a repair; it exchanges a fatal cardiac disease for a chronic disease. Lifelong immunosuppressant medications are required to prevent acute heart

Table 70.4 Medications used for initial and maintenance immunosuppression.

Drug (trade name)	Mechanism	Pediatric dosing	Goal levels	Comments
Steroids				
Methylprednisolone (Solu-Medrol)	Nonspecific immunosuppression	I.v.: Initial: 5–10 mg kg^{-1} before transplant 0.8 mg kg^{-1} day^{-1} divided every 6 h		
Prednisone	Nonspecific immunosuppression	Maintenance: 1 mg kg^{-1} day^{-1} divided every 6 h, then tapered over 6–12 months		
Calcineurin inhibitors				
Cyclosporine (Sandimmune)	CsA–cyclophilin complex inhibits T-cell activation	I.v.: Initial: 5–6 mg kg^{-1} day^{-1} starting 4–12 h before transplant Maintenance: 2–10 mg kg^{-1} day^{-1} divided twice daily Oral: Initial: 14–18 mg kg^{-1} day^{-1} starting 4–12 h before transplant Maintenance: 5–15 mg kg^{-1} day^{-1} divided every 12–24 h, then tapered	Initial: Trough level 250–350 ng ml^{-1} Maintenance: Trough level 100–300 ng ml^{-1}	Dose should be divided three times per day in infants
Cyclosporine (Neoral)	CsA–cyclophilin complex inhibits T-cell activation	2–6 mg kg^{-1} day^{-1} oral divided twice daily	Initial: Trough level 250–350 ng ml^{-1} Maintenance: Trough level 100–300 ng ml^{-1}	Dose should be divided three times per day in infants
Tacrolimus/FK-506 (Prograf)	Tacro–FKBP12 complex inhibits T-cell activation	0.05–0.1 mg kg^{-1} day^{-1} divided twice daily	Initial: Trough level 10–15 ng ml^{-1} Maintenance: Trough level 5–10 ng ml^{-1}	Dose should be divided three times per day in infants
Antiproliferative agents				
Azathioprine (Imuran)	Inhibition of cell proliferation	1–2 mg kg^{-1} day^{-1}	WBC count of 4000–12 000 ml^{-1}	
Mcyophenolate mofetil (Cellcept)	Selective inhibitor of B- and T-lymphocyte proliferation	Initial: 100–125 mg kg^{-1} day^{-1} Maintenance: 25–50 mg kg^{-1} day^{-1}	Maintenance: Trough level 3–7 ng ml^{-1}	

rejection. Multiple chronic immunosuppression protocols have been developed to prevent immunologic destruction of the transplanted organ. Some protocols use induction therapy to alter favorably the immune environment at the time of transplant and decrease the incidence of early rejection [53–57]. ISHLT data support the use of induction agents to decrease the risk of early rejection, although data regarding effects on survival or incidence of cardiac allograft vasculopathy are lacking. Currently, >60% of children receive cytolytic induction agents, including either polyclonal antibody preparations (thymoglobulin or ATGAM) or newer anti-cytokine receptor antibodies (basiliximab or daclizumab) [1]. The maintenance immunosuppression protocols in general use triple immunosuppression to minimize toxic side effects of the medications. The protocols include steroids, a calcineurin inhibitor [cyclosporine or tacrolimus (FK-506)], and an antiproliferative agent (azathioprine or mycophenolate mofetil) [1]. The degree of immunosuppression is greatest in the first months after transplantation; however, there is clinical practice support for establishing a steroid-free regimen in selected patients by 1 year post-transplant to minimize the risk of steroid-associated morbidity [58,59]. The calcineurin inhibitors, which block interleukin-2 secretion and subsequent T lymphocyte activation and proliferation, are the cornerstone of chronic immunosuppressive therapy. Currently, based on the most recent ISHLT report, ~50% of patients are on cyclosporine and 50% are on tacrolimus. There is also increasing use of the newer antiproliferative agent mycophenolate mofetil, with now >50% of recipients receiving this over azathioprine [1]. Table 70.4 reviews the common immunosuppression medications, typical pediatric dosing, and goal levels.

Rejection

The goal of immunosuppression is to prevent rejection of the donor heart. Rejection is an immune response to mismatched human leukocyte antigens on the recipient and donor cells.

The resultant inflammation is mediated through T-cell and humoral immune mechanisms, causing eventual necrosis of the heart tissue. Rejection is most common in the first 6 months after transplant, but remains a risk lifelong and is the most common cause of death in the first 5 years after transplant [1]. Data from the PHTS from 1993 to 2005 [60] (Figure 70.4) demonstrate that pediatric heart transplant recipients on average experience one episode of rejection in the first year after transplant, although many never have such an episode. The frequency of rejection in the first year after transplant has been decreasing recently, likely from changes in initial and chronic immunosuppression strategies [61]. Neonates and infants seem to be more immunotolerant to heart grafts and have a decreased incidence of rejection
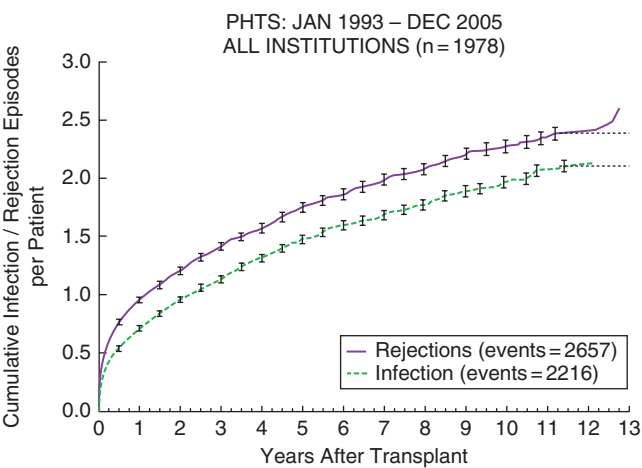
Figure 70.4 Cumulative episodes of rejection and infection in pediatric heart transplantation over time within the Pediatric Heart Transplant Study Database [60].

[1,62]. Preformed donor-specific antibody, especially when there is a positive donor–recipient crossmatch, is associated with an increased risk for rejection in the first 6 months after transplantation [48,49].

Pediatric heart transplant recipients continue to have late rejection episodes >1 year after transplantation (Figure 70.4). Approximately 25% of recipients have an episode of late rejection by 3 years after transplantation [63]. Late rejection occurs infrequently in infants [62]. Late rejection is a leading cause of mortality >1 year after transplantation [1] and increases the risk for developing transplant coronary disease [64]. Risk factors for late rejection include two or more episodes of rejection in the first year after transplant, older age, and black race. Late rejection is frequently attributed to patient non-compliance [65,66] with single-parent home, non-white race, and older age, especially adolescence identified as increasing the risk of medical non-compliance. The association of late rejection with black race is independent of age and socioeconomic circumstances, and is due to unfavorable genetic polymorphisms in black recipients [67].

Diagnosis

Endomyocardial biopsy is considered the "gold standard" for diagnosing T-cell associated or cellular rejection. Standardized grading systems have been formulated as outlined in Table 70.5, based on lymphocytic infiltrates and myocardial necrosis (Figure 70.5) [68]. Surveillance for rejection is most intense during the first 3 months after transplantation and gradually decreases to a 6 monthly schedule 18 months following transplantation. The relatively low rate of cellular rejection after the first 6–12 months post-transplantation has led some centers to eliminate surveillance endomyocardial biopsies after this time [59,69].

Table 70.5 International Society for Heart and Lung Transplantation cardiac biopsy grading scheme for the diagnosis of acute cellular rejection.

2004		1990	
Grade	**Description**	**Grade**	**Description**
Grade 0 R	No rejection	Grade 0	No rejection
Grade 1 R	Interstitial and/or perivascular infiltrate with up to one focus of myocyte damage	Grade 1, mild	
		A – focal	Focal perivascular and/or interstitial infiltrate without myocyte damage
		B – diffuse	Diffuse infiltrate without myocyte damage
		Grade 2, moderate(focal)	One focus of infiltrate associated with myocyte damage
Grade 2 R	Two or more foci of infiltrate with associated myocyte damage	Grade 3, moderate	
		A – focal	Multifocal infiltrate with myocyte damage
		B – diffuse	Diffuse infiltrate with myocyte damage
Grade 3 R	Diffuse infiltrate with multifocal myocyte damage ± edema, ± hemorrhage, ± vasculitis	Grade 4, severe	Diffuse, polymorphous infiltrate with extensive myocyte damage ± edema, ± hemorrhage, ± vasculitis

Reproduced with permission from Stewart S, Winters GL, Fishbein MC, *et al. J Heart Lung Transplant* 2005;**24**:1710–20.
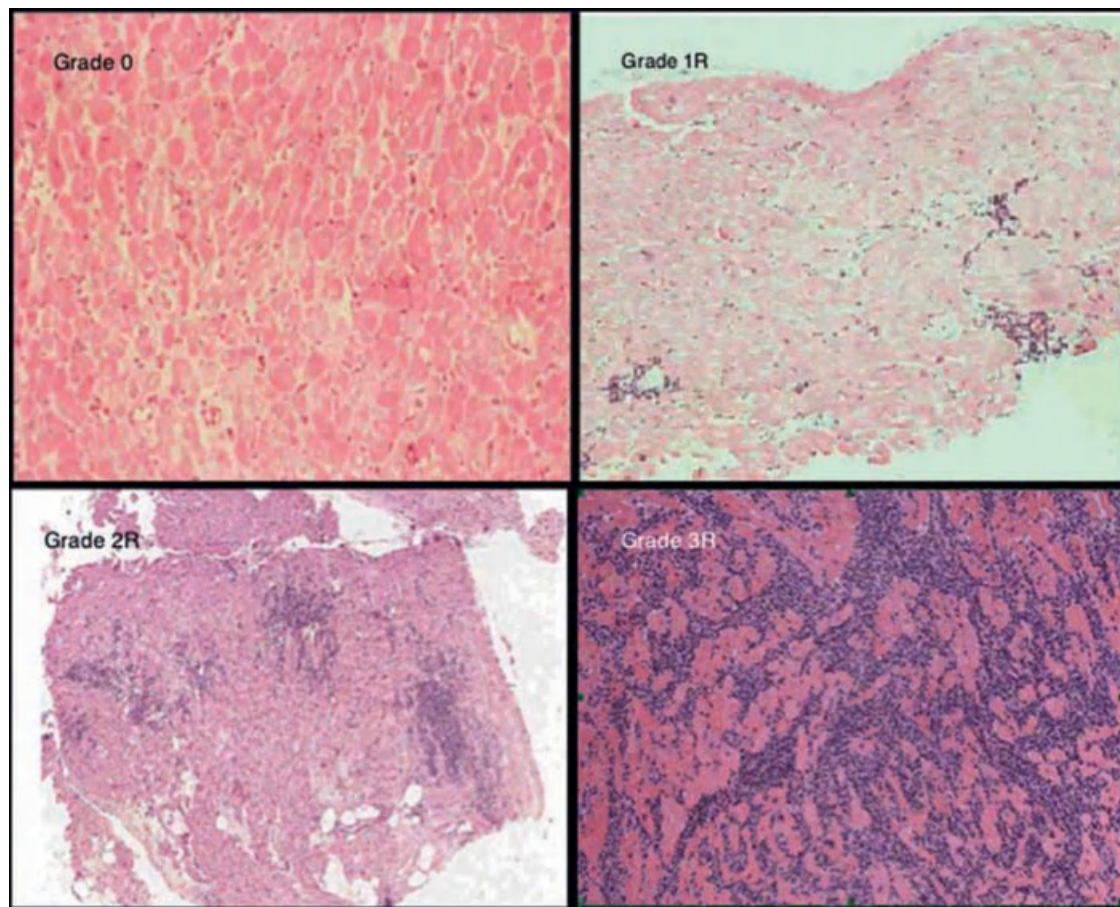
Figure 70.5 Representative histology of various endomyocardial biopsy grades of rejection by the revised ISHLT grading scheme. Grade 0, no rejection; Grade 1R, focal, perivascular lymphocytic infiltrates without myocyte damage; Grade 2R, multiple foci of damaging lymphocytic infiltrate with normal myocardium intervening; Grade 3R, diffuse damaging lymphocytic infiltrates with encroachment of myocytes and disruption of normal architecture.

In adults, gene-expression profiling from peripheral blood specimens in selected patients is equivalent to surveillance of rejection by endomyocardial biopsy [70], but extrapolating this strategy to pediatric patients remains untested.

Serial endomyocardial biopsies in children have many challenges because of patient size, lack of vascular access, and need for sedation/anesthesia, but can generally be performed with low risk in children of all sizes [71]. In children, rejection has been diagnosed much more frequently by a combination of clinical signs and symptoms and non-invasive testing than in adult recipients. Decreased appetite, afebrile "flu" symptoms, irritability, gallop rhythm, enlarged cardiac silhouette on a chest radiograph, and decreased QRS voltages on an electrocardiogram have been considered signs of rejection. In many centers, echocardiography has been utilized as the primary diagnostic modality for rejection in infants [72]. However, pediatric heart transplant centers are increasingly using endomyocardial biopsy over noninvasive methods to diagnose cellular rejection [61].

Humoral or antibody-mediated rejection is increasingly recognized as an important cause of morbidity and mortality in heart transplantation [73–76]. It is generally associated with varying degrees of left ventricular dysfunction and heart failure. In addition, anti-HLA antibodies specifically directed to donor HLA antigens are found in the serum [73]. Although "mixed" instances of cellular and antibody-mediated rejection may occur [76], specific histopathologic findings in antibody-mediated rejection include tissue edema and endothelial swelling and macrophage infiltration [73]. In addition, tissue immunofluorescence and histochemistry demonstrate endothelial deposition of immunoglobulin or complement fragments C4d or C3d in the endothelium and/or + CD 68 staining for intra-endothelial macrophages (Figure 70.6).

Treatment

Asymptomatic mild rejection (old ISHLT 1A or 1B, new ISHLT 1R) is often not treated because of the high rate of spontaneous resolution and the lack of association with long-term graft survival and transplant cardiac allograft vasculopathy [77]. Most centers, however, treat a patient with a biopsy showing moderate rejection (old ISHLT grade 3A or greater, new ISHLT 2R or greater) with intensified immunosuppression, typically
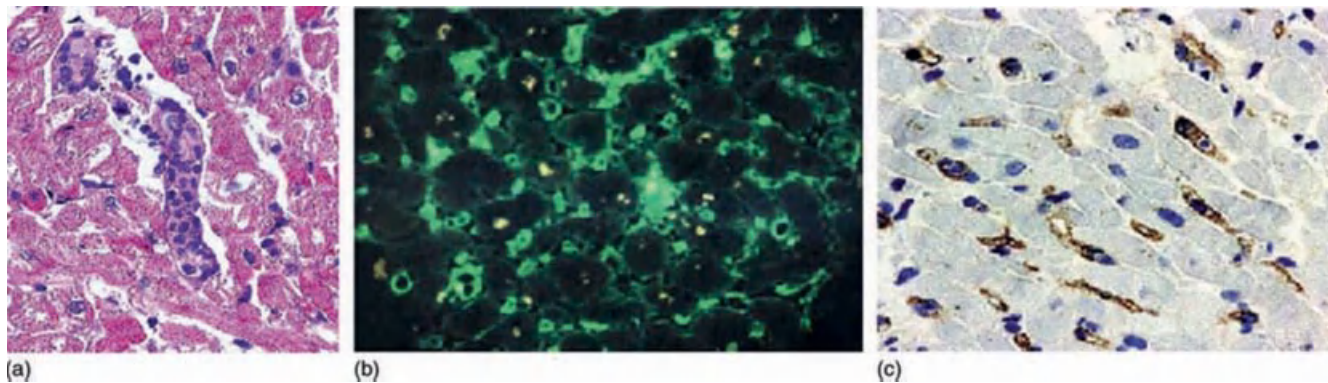
Figure 70.6 Representative pathology consistent with antibody-mediated rejection. (a) Endothelial cell swelling and intravascular infiltration of macrophages. (b) Capillary deposition of immunoglobulin G by immunofluorescence. (c) Capillary deposition of complement fragment C4d by immunoperoxidase staining.

high-dose intravenous or pulsed oral steroids [78,79]. Refractory rejection is defined as ongoing rejection after 2–3 consecutive episodes treated with steroids. Experience in both adults and children supports the use of anti-lymphocytic antibodies in treating steroid-resistant rejection [80,81]. Other options include changing calcineurin inhibitors from cyclosporine to tacrolimus or changing antiproliferative agents from azathioprine to mycophenolate mofetil [82–86]. In extreme refractory rejection, total lymphoid irradiation [87–89] or photopheresis [90] have been used.

Specific treatments for antibody-mediated rejection typically include the same regimens as used for cellular rejection. Additionally, circulating donor-specific antibodies can be removed with intravenous immunoglobulin, plasmapheresis, or both [91–93]. Specific therapies, including cyclophosphamide and rituximab, have been used to target B-cells, and protocols for these agents are being developed [94–97].

If rejection is associated with heart failure or cardiogenic shock, treatment typically involves global immunotherapy, including treating cellular and antibody-mediated rejection with steroids, anti-lymphocyte antibodies, plasmapheresis, and cyclophosphamide [98,99]. Although these regimens often resolve acute heart failure, long-term outcomes after rejection with hemodynamic compromise are poor, with a high risk of mortality from recurrent rejection, infection, or transplant coronary disease [100].

Infection

Infection, along with primary graft failure and rejection, is an important cause of death early after pediatric cardiac transplantation (Figure 70.3) [1,2]. Similarly to rejection, serious infections most likely occur in the first 3 months after transplantation when immunosuppression is greatest. The intensity of immunosuppression and the degree of illness in

a patient before transplantation increase the risk of serious infection after transplantation [101].

Pediatric cardiac transplant recipients average approximately one infection requiring hospitalization or treatment with intravenous medications in the first year after transplantation (Figure 70.4) [1,102].

The type of infection varies at different times after transplantation [103]. Within the first month after transplantation, infections are related either to the surgical wound from bacteria or yeast or to related infection in the recipient or donor organ. Herpes simplex may reactivate in a recipient in the first 2 weeks after transplant. From 1 to 6 months after transplantation, infections from immunomodulating viruses [notably cytomegalovirus (CMV)] and opportunistic fungal or protozoal infections predominate. Late transplant infections are generally community-based infections or a recurrence of opportunistic infections in patients who require repeated exposure to high-dose immunosuppression with rejection episodes. Infants appear to have more chronic and recurrent infections late after transplant than older recipients [104]. Prophylactic nystatin and trimethoprim–sulfamethoxazole are routinely given after heart transplantation to prevent fungal or protozoal infections.

CMV and EBV infections

Cytomegalovirus (CMV) infections commonly occur as a result of primary exogenous infection, donor–recipient transfer of the virus, or reactivation of infection in the recipient [102]. CMV infection generally occurs 2–12 weeks after transplantation and can be associated with pneumonitis and gastroenteritis. CMV infection may be a risk factor for developing transplant coronary disease [105], but an association between CMV infection and transplant coronary disease was not observed in a recent PHTS analysis [106]. CMV infection is frequently treated with oral valgancyclovir or intravenous ganacylovir. Treatment may be prophylactic or at the time of detection of infection with serial monitoring of CMV viral

load in the bloodstream. Studies have [107] and have not [106] found prophylaxis to be a superior strategy to prevent complications from CMV infection.

Epstein–Barr virus (EBV) infections may also occur in the first year after transplant from the same pathways as CMV infections. The importance of EBV, especially a primary EBV infection, in these children is its association with the development of post-transplant lymphoproliferative disease (PTLD) [108,109]. EBV viral load in blood is often monitored early after transplant for adjustment of immunosuppression in the presence of EBV infection.

Immunizations

Immunosuppressed patients should avoid live virus vaccines (e.g., oral polio, measles–mumps–rubella, varicella, nasal influenza) and killed virus or protein vaccines, such as diphtheria, pertussis, and tetanus [110]. Salk polio, hepatitis B, *Haemophilus influenzae* type b, and influenza vaccines should be given (Table 70.6). Varicella as a primary or reactivated infection can be treated with oral or intravenous acyclovir [111]. If possible, children should receive as many live virus vaccinations as are feasible prior to transplantation.

Transplant cardiac allograft vasculopathy

A year after transplantation, transplant cardiac allograft vasculopathy (CAV) becomes a leading cause of cardiac mortality and morbidity (Figure 70.3) [1]. Transplant CAV is a progressive, concentric myointimal proliferation that initially appears as intimal thickening and may lead to luminal occlusion. Transplant CAV involves the entire length of the vessel. In contrast, traditional atherosclerosis is usually characterized by focal lesions with asymmetric intimal proliferation in the proximal vessels. Unlike atherosclerosis, transplant CAV lesions rarely calcify and are unassociated with disruption of the internal elastic lamina. Transplant coronary disease may result from an immunologic injury to the coronary endothelial cells, leading to stimulation and proliferation of smooth muscle cells elaborating growth factors, cytokines, and extracellular matrix proteins and producing intimal proliferation, impaired vascular function, and luminal narrowing [112,113].

Manifestations and risk factors

Because of variability in the reinnervation of the transplanted heart, myocardial infarction with CAV is usually not associated with angina. The manifestations of transplant coronary artery disease range from unexplained chest or abdominal pain to left ventricular dysfunction or sudden death. For these reasons, cardiac transplantation protocols routinely include coronary angiography yearly or biannually. Angiographic findings include diffuse lesions, rapid pruning of vessels, distal obliteration of small tertiary vessels, and focal stenoses (Videoclip 70.1), but angiography

may underestimate the presence and severity of transplant CAV because of the diffuse nature of the disease [114]. Intravascular ultrasound is a much more sensitive invasive test to determine the presence of transplant CAV and often shows intimal proliferation in apparently normal vessels (Figure 70.7) [115,116]. Exercise or dobutamine stress echocardiography may be the best relatively noninvasive tests to make the diagnosis in children. A negative test strongly supports the absence of angiographic transplant CAV, and wall motion abnormalities (positive test) correlate with angiographically identifiable disease ~80% of the time [117–119].

In children, angiographic evidence of transplant coronary artery disease is present in 15–25% of recipients 5 years after transplantation [1,120]. In both angiographic and intravascular ultrasound studies, transplant CAV occurs less frequently at a given time after transplant in younger children (Figure 70.8) [1,115,120]. Older donor age and rejection episodes >1 year after transplantation [115,121] have also been identified as risk factors for pediatric transplant CAV diagnosed by angiography or intravascular ultrasound. CMV infection has [105] and has not [106] been related to pediatric transplant CAV. Other factors associated with transplant CAV include "explosive sudden cerebrovascular death in the donor" and factors associated with traditional atherosclerosis, such as hyperlipidemia, hypertension, and smoking [122].

Treatment

Once present, CAV typically progresses and is irreversible. Coronary angioplasty, stenting, or bypass surgery can be performed for focal lesions [123]. Additionally, statins are now being instituted early after transplantation to prevent the development of CAV, utilizing both their lipid lowering properties and inherent anti-inflammatory and immune-modulating effects [124,125]. Preliminary studies with pravastatin suggest that it may be able to reverse intimal proliferation and halt progression of CAV [126].

Mycophenolate mofetil as part of maintenance immunosuppression reduces intimal thickening after heart transplantation [127,128]. Evolving strategies for preventing vasculopathy include newer agents such as sirolimus (rapamycin) and everolimus. These medications have a different mechanism of immunosuppression than other agents, and also inhibit smooth muscle and endothelial cell proliferation. In adults, sirolimus may slow progression of established transplant CAV [129], and everolimus or sirolimus decrease the magnitude of coronary intimal thickening if used for maintenance immunosuppression after transplant [130,131].

Pediatric transplant CAV associated with luminal narrowings ≥50% is associated with an ~50% risk of graft loss within 2 years [120]. Retransplantation is probably the only definitive treatment for substantial transplant CAV and is associated with survival similar to primary transplantation [132,133].

Table 70.6 Suggested immunization schedules for pediatric solid organ recipients before and after transplantation.

Vaccine	Inactivated/live attenuated (I/LA)	Recommended before transplant[a]/strength of recommendation	Recommended after transplant/strength of recommendation	Monitor vaccine titers?	Quality of evidence
Influenza, injected	**I**	**Yes/A**	**Yes/A**	**No**	**II**
Hepatitis B	I	Yes/A	Yes[b]/B	Yes[b]	II
Hepatitis A	I	Yes/A	Yes/A	Yes	II
Pertussis	I	Yes/A	Yes/A	No	III
Diphtheria	I	Yes/A	Yes/A	No	II
Tetanus	I	Yes/A	Yes/A	No	II
Polio, inactivated	I	Yes/A	Yes/A	No	III
H. influenzae	I	Yes/A	Yes/A	Yes[c]	II
S. pneumoniae[d] (conjugated or polysaccharide vaccine)	I/I	Yes/A	Yes/A	Yes[c]	III
N. meningitidis[e]	I	Yes/A	Yes/A	No	III
Rabies[f]	I	Yes/A	Yes/B	No	III
Varicella	LA	Yes/A	No/D	Yes	II
Measles	LA	Yes/A	No/D	Yes	II
Mumps	LA	Yes/A	No/D	Yes	III
Rubella	LA	Yes/A	No/D	Yes	II
BCG[g]	LA	Yes/B	No/D	No	III
Smallpox[h]	LA	No/C	No/D	No	III
Anthrax	I	No/C	No/C	No	III

[a]Whenever possible, the complete complement of vaccines should be administered before transplantation. Vaccines noted to be safe for administration after transplantation may not be sufficiently immunogenic after transplantation. Some vaccines, such as pneumovax, should be repeated regularly (every 3–5 years) after transplantation.

[b]Routine vaccine schedule recommended prior to transplant and as early in the course of disease as possible; vaccine poorly immunogenic after transplantation, and accelerated schedules may be less immunogenic. Serial hepatitis B surface antibody titers should be assessed both before and after transplantation to assess ongoing immunity.

[c]Serologic assessment recommended if available.

[d]Children older than 5 years should receive 23-valent pneumococcal polysaccharide vaccine. Children younger than 2 years should receive conjugated pneumococcal vaccine (Prevnar). Those 2–5 years of age should receive pneumococcal vaccine.

[e]Certain patients (members of the military, travelers to high-risk areas, properdin deficient, terminal complement component deficient, those with functional or anatomic asplenia, college freshmen living on campus) are candidates for the meningococcal vaccine.

[f]Not routinely administered. Recommended for exposures, or potential exposures due to vocation or avocation.

[g]The indications for BCG administration in the United States are limited to instances in which exposure to tuberculosis is unavoidable and where measures to prevent its spread have failed or are not possible.

[h]Transplant recipients who are face-to-face contacts of a patient with smallpox should be vaccinated; vaccinia immune globulin may be administered concurrently if available. Those who are less intimate contacts should not be vaccinated.

Reproduced with permission from Guidelines for vaccination of solid organ transplant candidates and recipients. *Am J Transplant* 2004;**4**(Suppl 10):160–3.

Other medical morbidities

Cardiac

Transplanted hearts in infants and children grow proportionately as the child ages [134]. Transplanted hearts, denervated at the time of implantation, may attain partial reinnervation with time, but the heart rate response to exercise is usually blunted. As in adult recipients, most pediatric cardiac transplant recipients have a lower than normal exercise capacity [135,136]. Infant recipients have had normal exercise capacities [137]. Sequential cardiac catheterization studies have demonstrated hemodynamics consistent with diastolic dysfunction and restrictive physiology in long-term survivors of pediatric cardiac transplantation [138]. Moderate to severe tricuspid regurgitation occurs in many pediatric heart transplant recipients due to surgical technique, postoperative right ventricular dysfunction, and trauma from repetitive endomyocardial biopsies [139].

Figure 70.7 (a) Coronary angiogram of the left anterior descending artery. Arrow points to the area of intravascular ultrasound imaging shown to the right. (b) Intravascular ultrasound image demonstrates severe intimal thickening noted on the ultrasound (line) within an angiographically normal coronary segment.

(a)

(b)
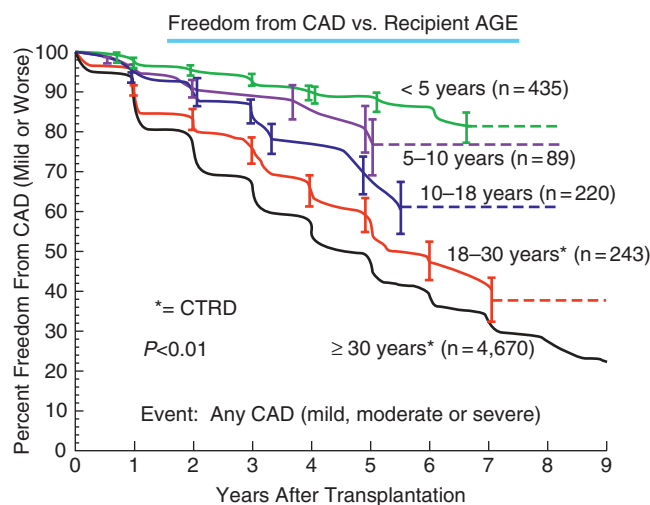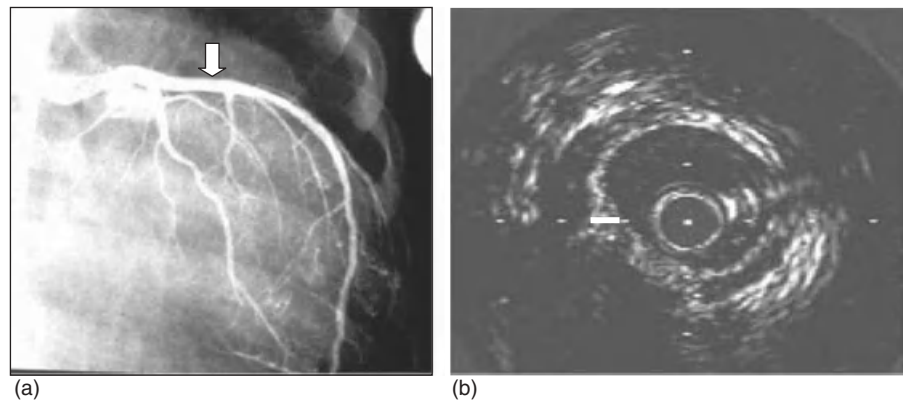
Figure 70.8 Influence of age at transplantation on the development of allograft vasculopathy within the Pediatric Heart Transplant Study and Cardiac Transplant Research Database. (Reproduced with permission from Pahl E, Naftel DC, Kuhn M, *et al. J Heart Lung Transplant* 2005;**24**:645–51.)

Arrhythmias are common. Significant bradycardia may occur immediately postoperation, usually improves, but may require permanent pacing. Right bundle branch block is typically present, most likely from injury to the right bundle with repeated endomyocardial biopsies. Isolated atrial or ventricular premature contractions, including nonsustained ventricular tachycardia, occur at a greater frequency than observed in normal hearts [140,141]. Supraventricular arrhythmias, including atrial flutter, ectopic atrial tachycardia, and atrioventricular reciprocating tachycardias, may occur in the first year after transplantation, with or without rejection [142–144]. Supraventricular tachycardias occurring late after transplantation are usually not associated with acute rejection, but more likely are a sign of transplant coronary arteriopathy.

Many medical problems can be attributed to side effects of immunosuppressive medications. Hypertension is common and associated with steroid and calcineruin inhibitor administration [1]. Children are at increasing risk for developing hypertension after transplant; the prevalence is ~50% at 1 year, 60% at 5 years, and >67% at 8 years after transplantation [145] (Table 70.7). Hypertension appears to occur more frequently with use of cyclosporine than with tacrolimus [146]. Calcium channel blockers are the most frequently used antihypertensive agents, but diuretics, angiotensin-converting enzyme inhibitors, β-blockers, and α-blockers have been used alone or in combination. Hyperlipidemia occurs in ~25% of pediatric heart transplant recipients [145] and may require therapy with statins.

Renal

Nephrotoxicity is frequently observed with calcineurin inhibitor therapy. Patients taking these agents typically demonstrate prerenal azotemia, with a level of blood urea nitrogen level disproportionately elevated compared with serum creatinine. Renal tubular acidosis, hyperuricemia, and hyperkalemia can also be observed. There may be reversible acute renal failure. Knowledge of the drugs that interact with cyclosporine and tacrolimus is important to avoid acute toxicity or underimmunosuppression. Drugs that inhibit the hepatic cytochrome-P450 system, such as ketaconazole, macrolide antibiotics, and calcium channel blockers, elevate calcineurin inhibitor levels whereas administration of anticonvulsants with calineurin inhibitors decreases their levels.

Long-term administration of calcineurin inhibitors in pediatric heart transplant recipients is associated with an increased risk for chronic kidney disease (Table 70.7). Less than 50% of pediatric thoracic transplant recipients have a normal glomerular filtration rate 1 year after transplantation, a level that declines to 14% 5 years after transplantation [147]. Overt renal dysfunction is present in ~6% of pediatric recipients 1 year after transplantation and increases to 10% by 8 years [145].

Neoplasms

Chronic immunosuppression is associated with an increased risk for developing neoplasms. The most common neoplasm observed after pediatric cardiac transplantation is lymphoproliferative disease (PTLD). It commonly occurs within the

Table 70.7 ISHLT registry data [1] on the proportion of patients with hypertension, renal dysfunction, hyperlipidemia, and diabetes at 1, 5, and 8 years after pediatric heart transplantation.

Outcome	Within 1 year	Within 5 years	Within 8 years
Hypertension	47.2% (*n* = 2428)	62.7% (*n* = 836)	68.3% (*n* = 325)
Renal dysfunction	5.8% (*n* = 2431)	9.9% (*n* = 862)	10.3% (*n* = 339)
Abnormal creatinine <2.5 mg dl^{-1}	3.9% (1.2%)[a]	8.2% (0.8%)[a]	7.7% (0.6%)[a]
Chronic dialysis	0.7%	0.6%	1.5%
Renal transplant	0.0%	0.2%	0.6%
Hyperlipidemia	10.8% (*n* = 2555)	25.1% (*n* = 902)	28.1% *n* = 356)
Diabetes	3.4% (*n* = 2436)	5.2% (*n* = 833)	4.0% (*n* = 323)

[a]Creatinine values in parentheses are >2.5 mg dl^{-1}.
Reproduced with permission from Boucek MM, Edwards LB, Keck BM, *et al. J Heart Lung Transplant* 2005;**24**:968–82.

first months after transplantation and is usually associated with either a primary or a reactivated EBV infection [108,109]. Approximately 5% of 5 year survivors and 8% of 10 year survivors develop PTLD [1]. Lymphoproliferative disease is a heterogeneous disorder ranging from a plasmacytic hyperplasia lacking oncogene and tumor suppressor gene alterations to an aggressive metastatic immunoblastic lymphoma, Burkitt's lymphoma, or multiple myeloma. It may present as an isolated disease process in the oropharyngeal nodes, lungs, or gastrointestinal tract or as a disseminated multisystem disease that can involve the central nervous system. The more benign forms of lymphoproliferative disease respond to reduction of immunosuppression; however, chemotherapy, anti-B cell monoclonal antibodies (rituximab), and radiation therapy, have been used to treat more malignant variants. Basal cell carcinomas, cervical carcinomas, and Kaposi's sarcoma have also been observed at higher frequency than in the general population.

Heart retransplantation

An increasing number of pediatric heart retransplant procedures have been performed over the last decade. Currently the ISHLT database reports ~40 of these procedures performed per year, comprising 6–7% of the heart transplantation performed in pediatric patients >1 year of age (Figure 70.1) [1]. Transplant coronary vasculopathy accounts for ~50% of retransplants, followed by graft failure and rejection [132]. Retransplantation performed >6 months after primary transplantation has a substantially higher survival that approaches the rate for primary transplants [132,133]. Current guidelines (Table 70.1) [5] state that cardiac retransplantation is indicated in patients with moderate–severe coronary vasculopathy, especially if associated with heart failure. Retransplantation within the first 6 months after transplantation or for acute rejection is discouraged.

Heart–lung and lung transplantation and pediatric cardiovascular disease

Primary pulmonary hypertension, CHD with pulmonary vascular disease, and pulmonary vein stenosis/veno-occlusive disease are the primary conditions leading to heart–lung and lung transplantation in children. The National Institutes of Health registry for primary pulmonary hypertension demonstrated an inverse correlation with duration of survival and magnitude of central venous pressure, pulmonary artery pressure, and pulmonary vascular resistance [148]. A smaller retrospective study demonstrated a similar relationship in pediatric patients with primary pulmonary hypertension or pulmonary vascular disease associated with CHD [149]. Pulmonary vasodilators, such as prostacyclin, sildenafil, and bosentan, have improved transplant-free survival in children with primary pulmonary hypertension [150] and patients with pulmonary vascular disease and CHD (Eisenmenger syndrome) [151]. Surgery and catheter interventional procedures may palliate pulmonary vein obstruction [152], but patients <18 months of age with associated pulmonary arterial hypertension and bilateral involvement often have progressive disease that can lead to early consideration for lung transplantation [153]. Adhesions from multiple prior thoracotomies can increase perioperative bleeding and be a relative contraindication to transplantation [154].

Heart–lung transplantation is currently reserved for co-existing heart lesions that are extensive or not easily repairable at the time of lung transplantation [154]. The ISHLT registry records <20 pediatric heart–lung transplants annually worldwide over the past decade. Pediatric heart–lung and lung transplantation have a similar higher mortality rate than cardiac transplantation, with a 12 month survival rate of 80–85% (Figure 70.9) [155]. Survival has improved recently with graft half-life
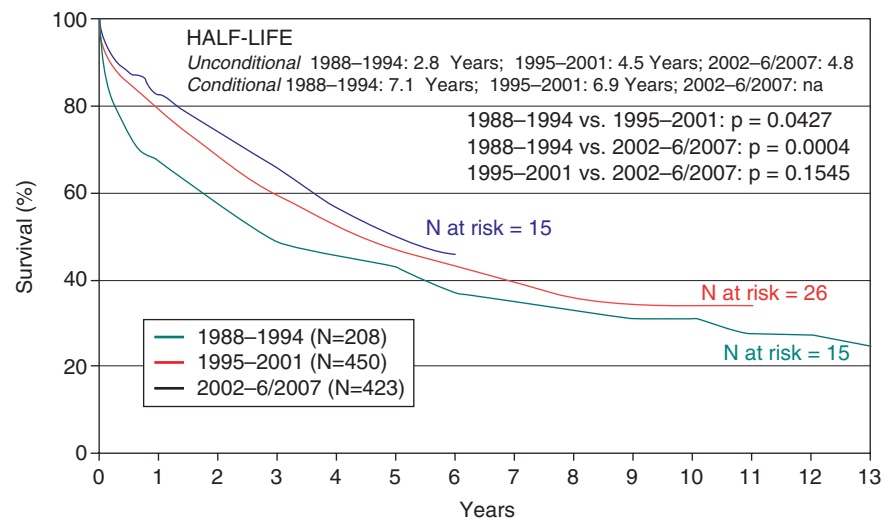
Figure 70.9 Kaplan–Meier survival curves for pediatric lung transplantation stratified by era from the ISHLT database. (Reproduced with permission from Boucek MM, Edwards LB, Keck BM, *et al. J Heart Lung Transplant* 2005;**24**:968–82.)

approaching 6 years. The need for ventilator support before transplantation is a risk factor for 1 and 5 year mortality.

The patterns of rejection and infection after lung transplantation resemble those observed after cardiac transplantation [156]. The transplanted lung, however, is more susceptible to infection because of its greater exposure to environmental pathogens. Bronchiolitis obliterans in pulmonary allografts is the counterpart to transplant coronary artery disease in cardiac allografts. Bronchiolitis obliterans can progress rapidly, leading to respiratory failure, or may stabilize after an acute decrease in lung function. In children, it has a prevalence of 25–30%, the prevalence increasing with longer follow-up [156,157]. The prevalence of bronchiolitis obliterans in heart–lung recipients equals or is greater than its prevalence in isolated lung transplant recipients [158,159]. The prevalence of transplant coronary artery disease, however, is less in heart–lung than heart transplant recipients [160].

References

1 Kirk R, Edwards LB, Aurora P, *et al*. Registry of the International Society for Heart and Lung Transplantation: Twelfth Official Pediatric Heart Transplantation Report – 2009. *J Heart Lung Transplant* 2009;**28**:993–1006.

2 Taylor DO, Stehlik J, Edwards LB, *et al*. Registry of the International Society for Heart and Lung Transplantation: Twenty-sixth Official Adult Heart Transplant Report – 2009. *J Heart Lung Transplant* 2009;**28**:1007–22.

3 Petroski RA, Grady KL, Rodgers S, *et al*. Quality of life in adult survivors greater than 10 years after pediatric heart transplantation. *J Heart Lung Transplant* 2009;**28**:661–6.

4 Lamour JM, Kanter KR, Naftel DC, *et al*. The effect of age, diagnosis, and previous surgery in children and adults undergoing heart transplantation for congenital heart disease. *J Am Coll Cardiol* 2009;**54**:160–5.

5 Canter C, Naftel D, Caldwell R, *et al*. Survival and risk factors for death after cardiac transplantation in infants. A multi-institutional study. The Pediatric Heart Transplant Study. *Circulation* 1997;**96**:227–31.

6 Morrow RW, Kirklin JK. Survival after pediatric heart transplantation. In: Canter CE, Kirklin JK, eds. *Pediatric Heart Transplantation. ISHLT Monograph Series*, Vol. 2, Philadelphia: Elsevier, 2007: 123–38.

7 Canter CE, Shaddy RE, Bernstein D, *et al*. Indications for heart transplantation in pediatric heart disease: a scientific statement from the American Heart Association Council on Cardiovascular Disease in the Young; the Councils on Clinical Cardiology, Cardiovascular Nursing, and Cardiovascular Surgery and Anesthesia; and the Quality of Care and Outcomes Research Interdisciplinary Working Group. *Circulation* 2007;**115**:658–76.

8 Almond CSD, Thiagarajan RR, Piercey GE, *et al*. Waiting list mortality among children listed for heart transplantation in the United States. *Circulation* 2009;**119**:717–27.

9 Johnson MR, Meyer KH, Haft J, *et al*. Heart transplantation in the United States, 1999–2008. *Am J Transplant* 2010;**10**(Pt 2):1035–46.

10 Blume ED, Naftel DC, Bastardi HJ, *et al*. Outcomes of children bridged to heart transplantation with ventricular assist devices: a multi-institutional study. *Circulation* 2006;**113**:2313–9.

11 Cassidy J, Haynes S, Kirk R, *et al*. Changing patterns of bridging to heart transplantation in children. *J Heart Lung Transplant* 2009;**28**:249–54.

12 Mah D, Singh TP, Thiagarajan RR, *et al*. Incidence and risk factors for mortality in infants awaiting heart transplantation in the USA. *J Heart Lung Transplant* 2009;**28**:1292–8.

13 West LJ, Pollock-Barziv SM, Dipchand AI, *et al*. ABO-incompatible heart transplantation in infants. *N Engl J Med* 2001;**344**:793–800.

14 West LJ, Karamlou T, Dipchand AI, *et al*. Impact on outcomes after listing and transplantation, of a strategy to accept ABO blood group-incompatible donor hearts for neonates and infants. *J Thorac Cardiovasc Surg* 2006;**131**:455–61.

15 Almond CS, Gauvreau K, Thiagarajan RR, *et al*. Impact of ABO-incompatible listing on wait-list outcomes among infants listed for heart transplantation in the United States. A propensity analysis. *Circulation* 2010;**121**:1926–33.

16 Costanzo MR, Augustine S, Bourge R, *et al*. Selection and treatment of candidates for heart transplantation. A statement for health professionals from the Committee on Heart Failure and Cardiac Transplantation of the Council on Clinical Cardiology, American Heart Association. *Circulation* 1995;**92**:3593–612.

17 Mudge GH, Goldstein S, Addonizio LJ, *et al*. 24th Bethesda Conference: Cardiac Transplantation. Task Force 3: Recipient guidelines/prioritization. *J Am Coll Cardiol* 1993;**22**:21–31.

18 Hunt SA, Baker DW, Chin MH, *et al*. ACC/AHA Guidelines for the Evaluation and Management of Chronic Heart Failure in the Adult: Executive Summary. A Report of the American College of Cardiology/American Heart Association Task Force on Practice Guidelines (Committee to Revise the 1995 Guidelines for the Evaluation and Management of Heart Failure): Developed in Collaboration with the International Society for Heart and Lung Transplantation; Endorsed by the Heart Failure Society of America. *Circulation* 2001;**104**:2996–3007.

19 O'Neill JO, Young JB, Pothier CE, *et al*. Peak oxygen consumption as a predictor of death in patients with heart failure receiving beta-blockers. *Circulation* 2005;**111**:2313–8.

20 Stelken AM, Younis LT, Jennison SH, *et al*. Prognostic value of cardiopulmonary exercise testing using percent achieved of predicted peak oxygen uptake for patients with ischemic and dilated cardiomyopathy. *J Am Coll Cardiol* 1996;**27**:345–52.

21 Aaronson KD, Mancini DM. Is percentage of predicted maximal exercise oxygen consumption a better predictor of survival than peak exercise oxygen consumption for patients with severe heart failure? *J Heart Lung Transplant* 1995;**14**:981–9.

22 Washington RL, van Gundy JC, Cohen C, *et al*. Normal aerobic and anaerobic exercise data for North American school-age children. *J Pediatr* 1988;**112**:223–33.

23 Fredriksen PM, Ingjer F, Nystad W, *et al*. A comparison of VO2(peak) between patients with congenital heart disease and healthy subjects, all aged 8–17 years. *Eur J Appl Physiol Occup Physiol* 1999;**80**:409–16.

24 Gewillig MH, Lundstrom UR, Bull C, *et al*. Exercise responses in patients with congenital heart disease after Fontan repair: patterns and determinants of performance. *J Am Coll Cardiol* 1990;**15**:1424–32.

25 Zellers TM, Driscoll DJ, Mottram CD, *et al*. Exercise tolerance and cardiorespiratory response to exercise before and after the Fontan operation. *Mayo Clin Proc* 1989;**64**:1489–97.

26 del Nido PJ, Bailey LL, Kirklin JK. Surgical techniques in pediatric heart transplantation. In: Canter CE, Kirklin JK, eds. *Pediatric Heart Transplantation. ISHLT Monograph Series*, Vol. 2. Philadelphia: Elsevier, 2007: 123–38.

27 Hershberger RE, Lindenfeld J, Mestroni L, *et al*. Genetic evaluation of cardiomyopathy – a Heart Failure Society of America practice guideline. *J Card Fail* 2009;**15**:83–97.

28 Calabrese LH, Albrecht M, Young J, *et al*. Successful cardiac transplantation in an HIV-1-infected patient with advanced disease. *N Engl J Med* 2003;**348**:2323–8.

29 Kuo PC, Stock PG. Transplantation in the HIV+ patient. *Am J Transplant* 2001;**1**:13–7.

30 Anguita M, Arizon JM, Valles F, *et al*. Results of heart transplantation in recipients with active infection. *J Heart Lung Transplant* 1993;**12**:808–9.

31 Goldstein DJ, Seldomridge JA, Addonizio L, *et al*. Orthotopic heart transplantation in patients with treated malignancies. *Am J Cardiol* 1995;**75**:968–71.

32 Cimato TR, Jessup M. Recipient selection in cardiac transplantation: contraindications and risk factors for mortality. *J Heart Lung Transplant* 2002;**21**:1161–73.

33 Shapiro PA, Williams DL, Foray AT, *et al*. Psychosocial evaluation and prediction of compliance problems and morbidity after heart transplantation. *Transplantation* 1995;**60**:1462–6.

34 Miller LW, Kubo SH, Young JB, *et al*. Report of the consensus conference on candidate selection for heart transplantation – 1993. *J Heart Lung Transplant* 1995;**14**:562–71.

35 Addonizio LJ, Gersony WM, Robbins RC, *et al*. Elevated pulmonary vascular resistance and cardiac transplantation. *Circulation* 1987;**76**:V52–5.

36 Kieler-Jensen N, Ricksten SE, Stenqvist O, *et al*. Inhaled nitric oxide in the evaluation of heart transplant candidates with elevated pulmonary vascular resistance. *J Heart Lung Transplant* 1994;**13**:366–75.

37 Gajarski RJ, Towbin JA, Bricker JT, *et al*. Intermediate follow-up of pediatric heart transplant recipients with elevated pulmonary vascular resistance index. *J Am Coll Cardiol* 1994;**23**:1682–7.

38 Morgan JA, John R, Park Y, *et al*. Successful outcome with extended allograft ischemic time in pediatric heart transplantation. *J Heart Lung Transplant* 2005;**24**:58–62.

39 Scheule AM, Zimmerman GJ, Johnston JK, *et al*. Duration of graft cold ischemia does not affect outcomes in pediatric heart transplant recipients. *Circulation* 2002;**106**:I163–7.

40 Mitchell MB, Campbell DN, Clarke DR, *et al*. Infant heart transplantation: improved intermediate results. *J Thorac Cardiovasc Surg* 1998;**116**:242–52.

41 Kawauchi M, Gundry SR, de Begona JA, *et al*. Prolonged preservation of human pediatric hearts for transplantation: correlation of ischemic time and subsequent function. *J Heart Lung Transplant* 1993;**12**:55–8.

42 Huang J, Trinkaus K, Huddleston CB, *et al*. Risk factors for primary graft failure after pediatric cardiac transplantation: importance of recipient and donor characteristics. *J Heart Lung Transplant* 2004;**23**:716–22.

43 Bailey LL, Gundry SR, Razzouk AJ, *et al*. Bless the babies: one hundred fifteen late survivors of heart transplantation during the first year of life. The Loma Linda University Pediatric Heart Transplant Group. *J Thorac Cardiovasc Surg* 1993;**105**:805–14; discussion 814–5.

44 Jacobs JP, Quintessenza JA, Boucek RJ, *et al*. Pediatric cardiac transplantation in children with high panel reactive antibody. *Ann Thorac Surg* 2004;**78**:1703–9.

45 Shaddy RE, Hawkins JA. Immunology and failure of valved allografts in children. *Ann Thorac Surg* 2002;**74**:1271–5.

46 Elkins RC, Lane MM, Capps SB, *et al*. Humoral immune response to allograft valve tissue pretreated with an antigen reduction process. *Semin Thorac Cardiovasc Surg* 2001;**13**:82–6.

47 Loh E, Bergin JD, Couper GS, *et al*. Role of panel-reactive antibody cross-reactivity in predicting survival after orthotopic heart transplantation. *J Heart Lung Transplant* 1994;**13**:194–201.

48 Pollock-BarZiv SM, den Hollander N, Ngan B-Y, *et al*. Pediatric heart transplantation in human leukocyte antigen sensitized patients:

evolving management and assessment of intermediate-term outcomes in a high-risk population. *Circulation* 2007;**116**:I172–8.

49 Holt DB, Lublin DM, Phelan DL, *et al*. Mortality and morbidity in pre-sensitized pediatric heart transplant recipients with a positive donor crossmatch utilizing peri-operative plasmapheresis and cytolytic therapy. *J Heart Lung Transplant* 2007;**26**:876–82.

50 Zangwill SD, Ellis TM, Zlotocha J, *et al*. The virtual crossmatch – a screening tool for sensitized pediatric heart transplant recipients. *Pediatr Transplant* 2005;**10**:38–41.

51 Itescu S, Burke E, Lietz K, *et al*. Intravenous pulse administration of cyclophosphamide is an effective and safe treatment for sensitized cardiac allograft recipients. *Circulation* 2002;**105**:1214–9.

52 Glotz D, Haymann JP, Sansonetti N, *et al*. Suppression of HLA-specific alloantibodies by high-dose intravenous immunoglobulins (IVIg). A potential tool for transplantation of immunized patients. *Transplantation* 1993;**56**:335–337.

53 Di Filippo S. Anti-IL-2 receptor antibody vs. polyclonal anti-lymphocyte antibody as induction therapy in pediatric transplantation. *Pediatr Transplant* 2005;**9**:373–80.

54 Chin C, Pittson S, Luikart H, *et al*. Induction therapy for pediatric and adult heart transplantation: comparison between OKT3 and daclizumab. *Transplantation* 2005;**80**:477–81.

55 Parisi F, Danesi H, Squitieri C, *et al*. Thymoglobuline use in pediatric heart transplantation. *J Heart Lung Transplant* 2003;**22**:591–3.

56 Di Filippo S, Boissonnat P, Sassolas F, *et al*. Rabbit antithymocyte globulin as induction immunotherapy in pediatric heart transplantation. *Transplantation* 2003;**75**:354–8.

57 Boucek RJ Jr, Naftel D, Boucek MM, *et al*. Induction immunotherapy in pediatric heart transplant recipients: a multicenter study. *J Heart Lung Transplant* 1999;**18**:460–9.

58 Canter CE, Moorhead S, Saffitz JE, *et al*. Steroid withdrawal in the pediatric heart transplant recipient initially treated with triple immunosuppression. *J Heart Lung Transplant* 1994;**13**:74–9; discussion 79–80.

59 Leonard HC, O'Sullivan JJ, Dark JH. Long-term follow-up of pediatric cardiac transplant recipients on a steroid-free regime: the role of endomyocardial biopsy. *J Heart Lung Transplant* 2000;**19**:469–72.

60 Pediatric Heart Transplant Study Group. *Pediatric Heart Transplant Study Annual Report, November 2006*. Birmingham, AL: Data Collection and Analysis Center, University of Alabama at Birmingham.

61 Gossett JG, Canter CE, Zheng J, *et al*. Decline in rejection in the first year after pediatric cardiac transplantation: a multi-institutional study. *J Heart Lung Transplant* 2010;**29**:625–32.

62 Ibrahim JE, Sweet SC, Flippin M, *et al*. Rejection is reduced in thoracic organ recipients when transplanted in the first year of life. *J Heart Lung Transplant* 2002;**21**:311–8.

63 Webber SA, Naftel DC, Parker J, *et al*. Late rejection more than 1 year after pediatric heart transplantation: risk factors and outcomes. *J Heart Lung Transplant* 2003;**22**:869–75.

64 Mulla NF, Johnston JK, Vander Dussen L, *et al*. Late rejection is a predictor of transplant coronary artery disease in children. *J Am Coll Cardiol* 2001;**37**:243–50.

65 Ringwald JM, Gidding SS, Crawford SE, *et al*. Nonadherence is associated with late rejection in pediatric heart transplant recipients. *J Pediatr* 2001;**139**:75–8.

66 Dobbels F, Van Damme-Lombaert R, Vanhaecke J, *et al*. Growing pains: non-adherence with the immunosuppressive regimen in adolescent transplant recipients. *Pediatr Transplant* 2005;**9**:381–90.

67 Girnita DM, Brooks MM, Webber SA, *et al*. Genetic polymorphisms impact the risks of acute rejection in pediatric heart transplantation: a multi-institutional study. *Transplantation* 2008;**85**:1632–9.

68 Stewart S, Winters GL, Fishbein MC, *et al*. Revision of the 1990 working formulation for the standardization of nomenclature in the diagnosis of heart rejection. *J Heart Lung Transplant* 2005;**24**:1710–20.

69 Kertesz NJ, Denfield SW, Kearney DL, *et al*. Usefulness of routine surveillance biopsies in children more than one year after orthotopic heart transplantation. *Am J Cardiol* 2001;**87**:667–8.

70 Pham MX, Teutenberg JJ, Kfoury AG, *et al*. Gene-expression profiling for rejection surveillance after cardiac transplantation. *N Engl J Med* 2010;**362**:1890–900.

71 Pophal SG, Sigfusson G, Booth KL, *et al*. Complications of endomyocardial biopsy in children. *J Am Coll Cardiol* 1999;**34**:2105–10.

72 Boucek MM, Mathis CM, Boucek RJ Jr, *et al*. Prospective evaluation of echocardiography for primary rejection surveillance after infant heart transplantation: comparison with endomyocardial biopsy. *J Heart Lung Transplant* 1994;**13**:66–73.

73 Reed EF, Demetris AJ, Hammond E, *et al*. Acute antibody-mediated rejection of cardiac transplants. *J Heart Lung Transplant* 2006;**25**:153–9.

74 Casarez TW, Perens G, Williams RJ, *et al*. Humoral rejection in pediatric orthotopic heart transplantation. *J Heart Lung Transplant* 2007;**26**:114–9.

75 Michaels PJ, Espejo ML, Kobashigawa J, *et al*. Humoral rejection in cardiac transplantation: risk factors, hemodynamic consequences and relationship to transplant coronary artery disease. *J Heart Lung Transplant* 2003;**22**:58–69.

76 Book WM, Kelly L, Gravanis MB. Fulminant mixed humoral and cellular rejection in a cardiac transplant recipient: a review of the histologic findings and literature. *J Heart Lung Transplant* 2003;**22**:604–7.

77 Kobashigawa JA, Patel JK. Immunosuppression for heart transplantation: where are we now? *Nat Clin Pract Cardiovasc Med* 2006;**3**:203–12.

78 Delgado DH, Luu L, Edwards J, *et al*. Should moderate acute rejection of a cardiac transplant graft be treated? *Clin Transplant* 2002;**16**:217–21.

79 Park MH, Starling RC, Ratliff NB, *et al*. Oral steroid pulse without taper for the treatment of asymptomatic moderate cardiac allograft rejection. *J Heart Lung Transplant* 1999;**18**:1224–7.

80 Ferraro P, Carrier M, White M, *et al*. Antithymocyte globulin and methotrexate therapy of severe or persistent cardiac allograft rejection. *Ann Thorac Surg* 1995;**60**:372–6.

81 Cantarovich M, Latter DA, Loertscher R. Treatment of steroid-resistant and recurrent acute cardiac transplant rejection with a short course of antibody therapy. *Clin Transplant* 1997;**11**:316–21.

82 Kobashigawa JA, Miller LW, Russell SD, *et al*. Tacrolimus with mycophenolate mofetil (MMF) or sirolimus vs. cyclosporine with MMF in cardiac transplant patients:1-year report. *Am J Transplant* 2006;**6**:1377–86.

83 De Bonis M, Reynolds L, Barros J, *et al*. Tacrolimus as a rescue immunosuppressant after heart transplantation. *Eur J Cardiothorac Surg* 2001;**19**:690–5.

84 Yamani MH, Starling RC, Pelegrin D, *et al*. Efficacy of tacrolimus in patients with steroid-resistant cardiac allograft cellular rejection. *J Heart Lung Transplant* 2000;**19**:337–42.

85 Mathieu P, Carrier M, White M, *et al*. Conversion of cyclosporine A to tacrolimus following heart transplantation. *Can J Cardiol* 1999;**15**:1229–32.

86 Boucek MM, Pietra B, Sondheimer H, *et al*. Anti-T-cell-antibody prophylaxis in children: success with a novel combination strategy of mycophenolate mofetil and antithymocyte serum. *Transplant Proc* 1997;**29**:16S–20S.

87 Chin C, Hunt S, Robbins R, *et al*. Long-term follow-up after total lymphoid irradiation in pediatric heart transplant recipients. *J Heart Lung Transplant* 2002;**21**:667–73.

88 Asano M, Gundry SR, Razzouk AJ, *et al*. Total lymphoid irradiation for refractory rejection in pediatric heart transplantation. *Ann Thorac Surg* 2002;**74**:1979–85.

89 Kirklin JK, George JF, McGiffin DC, *et al*. Total lymphoid irradiation: is there a role in pediatric heart transplantation? *J Heart Lung Transplant* 1993;**12**:S293–300.

90 Kirklin JK, Brown RN, Huang ST, *et al*. Rejection with hemodynamic compromise: objective evidence for the efficacy of photopheresis. *J Heart Lung Transplant* 2006;**25**:283–8.

91 Grauhan O, Knosalla C, Ewert R, *et al*. Plasmapheresis and cyclophosphamide in the treatment of humoral rejection after heart transplantation. *J Heart Lung Transplant* 2001;**20**:316–21.

92 Jordan SC, Quartel AW, Czer LS, *et al*. Posttransplant therapy using high-dose human immunoglobulin (intravenous gammaglobulin) to control acute humoral rejection in renal and cardiac allograft recipients and potential mechanism of action. *Transplantation* 1998;**66**:800–5.

93 Berglin E, Kjellstrom C, Mantovani V, *et al*. Plasmapheresis as a rescue therapy to resolve cardiac rejection with vasculitis and severe heart failure. A report of five cases. *Transplant Int* 1995;**8**:382–7.

94 Garrett HE Jr, Duvall-Seaman D, Helsley B, *et al*. Treatment of vascular rejection with rituximab in cardiac transplantation. *J Heart Lung Transplant* 2005;**24**:1337–42.

95 Baran DA, Lubitz S, Alvi S, *et al*. Refractory humoral cardiac allograft rejection successfully treated with a single dose of rituximab. *Transplant Proc* 2004;**36**:3164–6.

96 Aranda JM Jr, Scornik JC, Normann SJ, *et al*. Anti-CD20 monoclonal antibody (rituximab) therapy for acute cardiac humoral rejection: a case report. *Transplantation* 2002;**73**:907–10.

97 Zhu LP, Cupps TR, Whalen G, *et al*. Selective effects of cyclophosphamide therapy on activation, proliferation, and differentiation of human B cells. *J Clin Invest* 1987;**79**:1082–90.

98 McOmber D, Ibrahim J, Lublin DM, *et al*. Non-ischemic left ventricular dysfunction after pediatric cardiac transplantation: treatment with plasmapheresis and OKT3. *J Heart Lung Transplant* 2004;**23**:552–7.

99 Pahl E, Crawford SE, Cohn RA, *et al*. Reversal of severe late left ventricular failure after pediatric heart transplantation and possible role of plasmapheresis. *Am J Cardiol* 2000;**85**:735–9.

100 Pahl, E, Naftel DC, Canter CE, *et al*. Death after rejection with severe hemodynamic compromise in pediatric heart transplant recipients: a multi-institutional study. *J Heart Lung Transplant* 2001;**20**:279–87.

101 Renoult E, Butequ C, Lamarre V, *et al*. Infection risk in pediatric organ transplant recipients: is it increased with the new immunosuppresive agents? *Pediatr Transplant* 2005;**9**:470–9.

102 Schowengerdt KO, Naftel DC, Seib PM, *et al*. Infection after pediatric heart transplantation: results of a multi-institutional study. *J Heart Lung Transplant* 1997;**16**:1207–16.

103 Keough WL, Michaels MG. Infectious complications in pediatric solid organ transplantation. *Pediatr Clin North Am* 2003;**50**:1451–69.

104 Kulikowska A, Boslaugh S, Huddleston CB, *et al*. Infectious, malignant, and autoimmune complications in long term follow up of infant and older pediatric heart transplant recipients. *J Pediatr* 2008;**152**:671–7.

105 Hussain T, Burch M, Fenton MJ, *et al*. Positive pretransplantation cytomegalovirus serology is a risk factor for cardiac allograft vasculopathy in children. *Circulation* 2007;**115**:1798–805.

106 Mahle WT, Fourshee MT, Naftel DC, *et al*. Does cytomegalovirus serology impact outcome after pediatric heart transplantation? *J Heart Lung Transplant* 2009;**28**:1299–305.

107 Potena L, Grigioni F, Magnani G, *et al*. Prophylaxis versus preemptive anti-cytomegalovirus approach for prevention of allograft vasculopathy in heart transplant recipients. *J Heart Lung Transplant* 2009;**28**:461–7.

108 Webber SA, Naftel DC, Fricker FJ, *et al*. Lymphoproliferative disorders after paediatric heart transplantation: a multi-institutional study. *Lancet* 2006;**367**:233–9.

109 Manlhiot C, Pollock-BarZiv SM, Holmes C, *et al*. Post-transplant lymphoproliferative disorder in pediatric heart transplant recipients. *J Heart Lung Transplant* 2010;**29**:648–57.

110 Guidelines for vaccination of solid organ transplant candidates and recipients. *Am J Transplant* 2004;**4**(Suppl 10):160–3.

111 Pandya A, Wasfy S, Hébert D, *et al*. Varicella-zoster infection in pediatric solid-organ transplant recipients: a hospital-based study in the prevaricella vaccine era. *Pediatr Transplant* 2001;**5**:153–9.

112 Caforio ALP, Tona F, Belloni-Fortina A, *et al*. Immune and nonimmune predictors of cardiac allograft vasculopathy: multivariate risk factor analysis and role of immunosuppression. *Am J Transplant* 2004;**4**:962–70.

113 Rahmani M, Curz RP, Granville DJ, *et al*. Allograft vasculopathy versus athersclerosis. *Circ Res* 2006;**99**:801–15.

114 Kass M, Allan R, Haddad H. Diagnosis of graft coronary artery disease. *Curr Opin Cardiol* 2007;**22**:139–45.

115 Nicolas RT, Kort HW, Balzer DT, *et al*. Surveillance for transplant coronary artery disease in infant, child and adolescent heart transplant recipients: an intravascular ultrasound study. *J Heart Lung Transplant* 2006;**25**:921–7.

116 Kuhn MA, Jutzy KR, Deming DD, *et al*. The medium-term findings in coronary arteries by intravascular ultrasound in infants and children after heart transplantation. *J Am Coll Cardiol* 2000;**36**:250–4.

117 Larsen RL, Applegate PM, Dyar DA, *et al*. Dobutamine stress echocardiography for assessing coronary artery disease after transplantation in children. *J Am Coll Cardiol* 1998;**32**:515–20.

118 Pahl E, Crawford SE, Swenson JM, *et al*. Dobutamine stress echocardiography: experience in pediatric heart transplant recipients. *J Heart Lung Transplant* 1999;**18**:725–32.

119 Di Filippo S, Semiond B, Roriz R, *et al*. Non-invasive detection of coronary artery disease by dobutamine-stress echocardiography in children after heart transplantation. *J Heart Lung Transplant* 2003;**22**:876–82.

120 Pahl E, Naftel DC, Kuhn M, *et al*. The impact and outcome of transplant coronary artery disease in a pediatric population: a 9-year multi-institutional study. *J Heart Lung Transplant* 2005;**24**:645–51.

121 Mulla NF, Johnston JK, Dussen LV, *et al*. Late rejection is a predictor of transplant coronary artery disease in children. *J Am Coll Cardiol* 2001;**37**:243–50.

122 Pahl E, Caforio ALP, Kuhn MA. In: Canter CE, Kirklin JK, eds. *Pediatric Heart Transplantation. ISHLT Monograph Series*, Vol. 2. Philadelphia: Elsevier, 2007: 123–38.

123 Shaddy RE, Revenaugh JA, Orsmond GS, *et al*. Coronary interventional procedures in pediatric heart transplant recipients with cardiac allograft vasculopathy. *Am J Cardiol* 2000;**85**(11):1370–2.

124 Kobashigawa JA, Katznelson S, Laks H, *et al*. Effect of pravastatin on outcomes after cardiac transplantation. *N Engl J Med* 1995;**10**:621–7.

125 Wenke K, Meiser B, Thiery J, *et al*. Simvastatin reduces graft vessel disease and mortality after heart transplantation. *Circulation* 1997;**96**:1398–402.

126 Mahle ST, Vincent RN, Berg AM, *et al*. Pravastatin therapy is associated with reduction in coronary allograft vasculopathy in pediatric heart transplantation. *J Heart Lung Transplant* 2005;**24**:63–6.

127 Kobashigawa JA, Tobis JM, Mentzer RM, *et al*. Mycophenolate mofetil reduces intimal thickness after heart transplant: reanalysis of the multicenter trial. *Am J Transplant* 2006;**6**:993–7.

128 Kaczmarek I, Ertl B, Schmauss D, *et al*. Preventing cardiac allograft vasculopathy: long-term beneficial effects of mycophenolate mofetil. *J Heart Lung Transplant* 2006;**25**:550–6.

129 Mancini D, Pinney S, Burkhoff D, *et al*. Use of rapamycin slows progression of cardiac transplantation vasculopathy. *Circulation* 2003;**108**:48–53.

130 Eisen HJ, Tuzcu EM, Dorent R, *et al*. Everolimus for the prevention of allograft rejection and vasculopathy in cardiac-transplant recipients. *N Engl J Med* 2003;**349**:847–58.

131 Keough A, Richardson M, Ruygrok P, *et al*. Sirolimus in *de novo* heart transplant recipients reduces acute rejection and prevents coronary artery disease at 2 years. A randomized clinical trial. *Circulation* 2004;**110**:2694–700.

132 Mahle WT, Vincent RN, Kanter KR. Cardiac retransplantation in childhood: analysis of data from the United Network for Organ Sharing. *J Thorac Cardiovasc Surg* 2005;**130**:542–6.

133 Chin C, Naftel DC, Pahl E, *et al*. Cardiac retransplantation in pediatrics: a multi-institutional study. *J Heart Lung Transplant* 2006;**25**:1420–4.

134 Bernstein D, Kolla S, Miner M, *et al*. Cardiac growth after pediatric heart transplantation. *Circulation* 1992;**85**:1433–9.

135 Dipchand AI, Manlhiot C, Russell JL, *et al*. Exercise capacity improves with time in pediatric heart transplant recipients. *J Heart Lung Transplant* 2009;**28**:585–90.

136 Davis JA, McBride MG, Chrisant MRK, *et al*. Longitudinal assessment of cardiovascular exercise performance after pediatric heart transplantation. *J Heart Lung Transplant* 2006;**25**:626–33.

137 Abarbanell G, Mulla N, Chinnock R, *et al*. Exercise assessment in infants after cardiac transplantation. *J Heart Lung Transplant* 2004;**23**:1334–8.

138 Sigfusson F, Fricker FJ, Bernstein D, *et al*. Long-term survivors of pediatric heart transplantation. A multicenter report of sixty-eight children who have survived longer than 5 years. *J Pediatr* 1997;**130**:862–71.

139 Ben Sivarajan V, Chrisant MRK, Ittenbach RF, *et al*. Prevalence and risk factors for tricuspid valve regurgitation after pediatric heart transplantation. *J Heart Lung Transplant* 2008;**27**:494–50.

140 Jacquet L, Ziady G, Stein K, *et al*. Cardiac rhythm disturbances early after orthotopic heart transplantation: prevalence and clinical importance of the observed abnormalities. *J Am Coll Cardiol* 1990;**16**:832–7.

141 Scott CD, Dark JH, McComb JM. Arrhythmias after cardiac transplantation. *Am J Cardiol* 1992;**70**:1061–3.

142 Kertesz NJ, Towbin JA, Clunie S, *et al*. Long-term follow-up of arrhythmias in pediatric orthotopic heart transplant recipients: incidence and correlation with rejection. *J Heart Lung Transplant* 2003;**22**:889–93.

143 Collins KK, Thiagarajan RR, Chin C, *et al*. Atrial tachyarrhythmias and permanent pacing after pediatric heart transplantation. *J Heart Lung Transplant* 2003;**22**:1126–33.

144 LaPage MJ, Rhee EK, Canter CE. Tachyarrhythmias after pediatric heart transplantation. *J Heart Lung Transplant* 2010;**29**:273–7.

145 Boucek MM, Edwards LB, Keck BM, *et al*. Registry of the International Society for Heart and Lung Transplantation: the Official Pediatric Report, 2005. *J Heart Lung Transplant* 2005;**24**:968–82.

146 Taylor DO, Barr ML, Radovancevic B, *et al*. A randomized, multicenter comparison of tacrolimus and cyclosporine administration: decreased hyperlipidemia and hypertension with tacrolimus. *J Heart Lung Transplant* 1999;**18**: 336–45.

147 Pradhan M, Leonard MB, Bridges ND, *et al*. Decline in renal function following thoracic organ transplantation in children. *Am J Transplant* 2002;**2**:652–7.

148 D'Alonzo GE, Barst RJ, Ayres SM, *et al*. Survival in patients with primary pulmonary hypertension. *Ann Intern Med* 1991;**115**:343–9.

149 Clabby ML, Canter CE, Moller JH, Bridges ND. Hemodynamics and survival in children with pulmonary hypertension. *J Am Coll Cardiol* 1997;**30**:354–360.

150 Yung D, Widlitz AC, Rosenzweig EB, *et al*. Outcomes in children with idiopathic pulmonary arterial hypertension. *Circulation* 2004;**110**:660–5.

151 Dimopoulos K, Inuzuka R, Goletto S, *et al*. Improved survival among patients with Eisenmenger syndrome receiving advance therapy for pulmonary arterial hypertension. *Circulation* 2010;**121**:20–5.

152 Latson LA, Prieto LR. Congenital and acquired pulmonary vein stenosis. *Circulation* 2007;**115**:103–8.

153 Holt DB, Moller JH, Larson S, *et al*. Primary pulmonary vein stenosis. *Am J Cardiol* 2007;**99**:568–72.

154 Pigula FA, Gandhi SK, Ristich J, *et al*. Cardiopulmonary transplantation for congenital heart disease in the adult. *J Heart Lung Transplant* 2001;**20**:297–303.

155 Aurora P, Edwards LB, Christie JD, *et al*. Registry of the International Society for Heart and Lung Transplantation: Twelth Official Pediatric Lung and Heart/Lung Transplantation Report – 2009. *J Heart Lung Transplant* 2009;**28**:1023–30.

156 Sweet SC, Spray TL, Huddleston CB, *et al*. Pediatric lung transplantation at St. Louis Children's Hospital 1990–1995. *Am J Resp Crit Care Med* 1997;**155**:1027–35.

157 Armitage JM, Kurland G, Michaels M, *et al*. Critical issues in pediatric lung transplantation. *J Thorac Cardiovasc Surg* 1995;**109**:60–5.

158 Conte JV, Robbins RC, Reichenspurner H, *et al*. Pediatric heart–lung transplantation: intermediate-term results. *J Heart Lung Transplant* 1996;**15**:692–699.

159 Whitehead B, Rees P, Sorenson K, *et al*. Incidence of obliterative bronchiolitis after heart–lung transplantation in children. *J Heart Lung Transplant* 1994;**13**:903–8.

160 Lim TT, Botas J, Ross H, *et al*. Are heart–lung transplant recipients protected from developing transplant coronary artery disease? *Circulation* 1996;**94**:1573–7.

71　Cardiac Failure

**Beth D. Kaufman, Kimberly Y. Lin, Akash R. Patel,
Maryam Y. Naim, Maully J. Shah & Robert E. Shaddy**
The Children's Hospital of Philadelphia, Philadelphia, PA, USA

Pathophysiology

Heart failure is the clinical syndrome described below that results when, because of cardiac dysfunction, cardiac output does not meet the metabolic demands of the body. The etiologies of heart failure in children are diverse. In adults, coronary artery disease and hypertension are the major contributing factors of heart failure. Children most often present with heart failure because of congenital heart disease (CHD) with excessive volume loads (left-to-right shunts or valvar regurgitation) or excessive pressure loads (usually inflow or outflow tract obstruction), a cardiomyopathy, or extrinsic pressure on the heart as in a pericardial tamponade or constriction. Regardless of etiology, all heart failure syndromes are now thought of as a unified common pathway involving an index event, compensatory mechanisms, and secondary damage.

Our understanding of the pathophysiology of heart failure has grown in conjunction with an increased understanding of its cellular and neurohormonal mechanisms. Adrenergic nervous system activation, the renin–angiotensin–aldosterone system (RAAS), and left ventricular remodeling are the major maladaptive mechanisms. Adrenergic activation is a cornerstone of the neurohormonal response to heart failure. When cardiac output decreases, baroreceptors in the carotid sinus and aortic arch decrease their rate of firing, leading to increased sympathetic and decreased parasympathetic output. A short-term improvement in myocardial performance follows that is mediated by the β_1-adrenergic receptor, resulting in an increase in heart rate and ventricular contractility (thus augmenting cardiac output), and the α-adrenergic receptor, resulting in vasoconstriction (thus augmenting preload and blood pressure). In the long term, however, β-adrenergic stimulation is deleterious to

heart function. Norepinephrine causes direct myocyte toxicity, abnormal calcium handling, decreased macromolecular synthesis, and contractile dysfunction [1]. Adrenergic stimulation also increases myocardial oxygen demand at a time when oxygen delivery is limited.

The RAAS pathway is the other major limb of neurohormonal compensation that is activated in heart failure. In addition to direct β_2-adrenergic receptor stimulation by the adrenergic system at the juxtaglomerular level, renin secretion is also stimulated by decreased renal artery perfusion from low cardiac output and decreased salt delivery to the macula densa. Increased renin levels lead to the formation of angiotensin II, whose multiple effects include vasoconstriction, hypothalamic thirst stimulation, and aldosterone secretion via the adrenal cortex. Aldosterone, in turn, acts at the distal convoluted tubule of the kidney to promote sodium reabsorption and thus fluid retention. Again, although this compensatory increase in preload through angiotensin II and aldosterone is beneficial in the short term, chronic activation of this system promotes fluid overload in addition to a myriad of adverse cellular and genetic changes.

The chronic effect of neurohormonal activation includes myocyte toxicity leading to ventricular remodeling. The term remodeling refers to changes in chamber architecture; with respect to heart failure, a consensus statement defined cardiac remodeling as "genomic expression resulting in molecular, cellular, and interstitial changes that are manifested clinically as changes in size, shape, and function of the heart after cardiac injury" [2]. Elevated levels of bioactive molecules such as norepinephrine, endothelin, tumor necrosis factor, aldosterone, and angiotensin II all contribute to progressive left ventricular hypertrophy, enlargement, and cavity distortion. The development of left ventricular remodeling may subsequently cause a self-amplifying cycle of progressive

cardiac dysfunction, which may continue independent of adrenergic or RAAS activation [3].

The relationship of heart function to vascular stiffness, often referred to as ventricular-arterial (VA) or ventricular-vascular (VV) coupling, has spawned a great deal of interest in adult heart failure [4]. This has led to the recognition that the stiffening of the left ventricle is intimately related to stiffening of the large arteries; an increase in one often leads to an increase in the other. These changes have clear implications in the adult heart failure population, where increased vascular stiffness is seen with increasing age and also with co-morbidities such as hypertension, diabetes, and renal disease. With new and improved noninvasive methods, vascular stiffening has also been identified in multiple pediatric populations. The short- and long-term implications of such findings with respect to the development of heart failure in children, however, have not been clearly defined [5].

Differences in calcium homeostasis have been observed between mature and immature hearts [6]. In animal models and also human adults with heart failure, a decrease in sarcoplasmic reticulum Ca^{2+}-ATPase (SERCA2a) and an increase in Na^+–Ca^{2+} exchanger have been observed, potentially contributing to progressive myocyte contractile dysfunction [7,8]. We know that the $Na^{+-}Ca^{2+}$ exchanger activity is higher and that sarcoplasmic reticulum is relatively immature in neonates as compared with adults; this has implications on the effects of therapies that target calcium-dependent pathways in younger populations.

Despite the variation in underlying etiology and the cellular, inflammatory, genetic, anatomic, and neurohormonal processes that ensue, most heart failure in adults and children eventually follows a final common pathway of ventricular remodeling and systolic and/or diastolic dysfunction. Unraveling those underlying processes has provided multiple targets for intervention in this otherwise progressive disease.

Diagnosis and evaluation

Heart failure presenting during infancy or childhood is of diverse etiology and differs significantly from that of adults. Diagnostic evaluation begins with a thorough history. In infants and small children, feeding intolerance and failure to thrive can be symptoms of heart failure. Ischemic pain, although uncommon in children, can present as severe colic and irritability in an infant. Heart failure can also present with gastrointestinal and/or respiratory symptoms due to ventricular dysfunction and resultant systemic and/or pulmonary venous congestion and low cardiac output. A history of asthma and frequent wheezing may be from pulmonary venous congestion rather than primary reactive airway disease. These symptoms, initially thought to be secondary to an infection, ultimately are diagnosed as cardiac

in origin. Conversely, in some children, the stress of an infection, and its resultant increased cardiac output from fever or dehydration, result in symptoms of a previously subclinical cardiac abnormality. Seizures, syncope, or presyncopal episodes may be related to arrhythmias or underlying cardiomyopathies associated with heart failure. Children with structural CHD, either before and/or after surgical repair, may present with heart failure from volume overload and/or ventricular dysfunction. Symptoms of heart failure may begin suddenly or can develop gradually. For instance, a careful history may reveal that a child has gradually stopped playing sports now deemed "boring," when he or she is actually self-limiting due to the onset of symptomatic heart failure. A history of a recognizable syndrome or genetic diagnosis must be sought, and has been reported in 27% of pediatric cardiomyopathies [9]. Cardiac disease can be associated with a systemic syndrome, such as neuromuscular or metabolic diseases that may manifest as skeletal myopathy in addition to cardiomyopathy [10,11]. Exposures to known cardiac toxins such as anthracyclines received as cancer therapy, or iron overload related to frequent blood transfusions, should be identified. History should also include questions related to motor strength and clumsiness, frequent infections, other systemic medical problems, deafness, hypertension, and developmental delay.

A careful family history of at least three generations is an important part of the diagnostic evaluation of heart failure in children, as cardiomyopathies of genetic etiology can be transmitted within families via autosomal dominant, autosomal recessive, X-linked, or maternal (mitochondrial) transmission patterns. A familial cardiomyopathy is defined by at least two family members affected by cardiomyopathy, even those of different phenotypes [12]. Family history should also include sudden death, any form of cardiac disease, and muscular diseases.

Detailed careful physical examination must include:
• Assessment of the child's wellbeing, including respiratory rate and effort, color, pallor, edema, nutritional state, and activity level.
• Assessment of vital signs (including oxygen saturation) and four-extremity blood pressures.
• Examination of the extremities to assess perfusion, pulses, and edema.
• Palpation of the precordium for bulges, heaves, increased impulses and/or thrills.
• Palpation of the abdomen for hepatomegaly or masses.
• In older children, neck examination should be performed to look for jugular venous distention; the triad of hepatomegaly, edema, and increased jugular venous pressure are pathognomonic of right heart failure.
• Auscultation for abnormal heart tones, irregular rhythm, systolic or diastolic murmurs, gallops, clicks or rubs. A loud second heart sound suggests pulmonary hypertension. In infants, auscultation of the head and the liver should be

performed to exclude arteriovenous malformations of the brain or liver, respectively.

• Auscultation of the lungs to listen for crackles in older children that suggest either pulmonary edema or pneumonia. Crackles from heart failure are very rare in infants and small children and, if heard, point towards an infectious etiology.

Physical examination must also include other noncardiac features such as body habitus (cachexia), abnormal facial features associated with genetic syndromes such as coarse facial features of glycogen disorders, skeletal muscle tone to assess for hypotonia, pseudohypertrophy of calves, and/or organomegaly.

An electrocardiogram may help to identify evidence of ischemia such as Q waves in lateral leads I and AVL, often associated with an anomalous left coronary artery from the pulmonary artery (ALCAPA), particularly in infants, or other coronary abnormalities. Myocarditis is often associated with low voltage and/or diffuse ST segment abnormalities, whereas large voltages and severe hypertrophy on ECG may be associated with infiltrative processes such as Pompe disease or hypertrophic cardiomyopathy. Atrial enlargement may indicate restrictive physiology or severe atrioventricular valve regurgitation. Atrial and ventricular arrhythmias may be either a primary cause of heart failure or secondary to an underlying cardiomyopathy.

Heart failure in children is often first recognized by an abnormal chest radiograph with pulmonary edema and cardiomegaly, although acute processes, such as myocarditis, may often have a normal cardiac silhouette.

An echocardiogram is essential for evaluating a child with heart failure to assess ventricular function and structural abnormalities (see Chapter 8). Each cardiac valve and chamber, and the aortic arch, must be carefully assessed. In the presence of left ventricular systolic dysfunction, etiologies for the dysfunction, including coronary artery abnormalities, need to be actively sought. Both visualizing coronary origins and demonstrating normal flow patterns and also the absence of any secondary signs of coronary abnormalities such as discrepant size of the coronary arteries are essential for assessing an ischemic etiology. Coronary artery abnormalities may not be easily detected by an echocardiogram, and coronary angiography may be useful for diagnosis. Other structural causes of left ventricular dysfunction and heart failure, including left ventricular outflow tract obstruction and aortic arch abnormalities, including coarctation of the aorta, should be excluded by echocardiogram. Volume overload from a large left-to-right shunt such as ventricular septal defect, large patent ductus arteriosus, and aortopulmonary window can also be assessed. Heart failure with a structurally normal heart and normal or hyperdynamic left ventricular function suggests an arteriovenous malformation or a metabolic cause.

After structural heart defects have been excluded, the most common cause of heart failure from left ventricular dysfunction in a child is a primary cardiomyopathy. Cardiomyopathies are typically categorized by phenotype on echocardiogram, based on the size of the atrial and ventricular chambers (dilated, normal, or small), ventricular wall thickness (hypertrophied, normal, or thin), pattern of wall abnormalities (concentric or asymmetric), regional wall motion abnormalities, and nature of myocardium (trabeculated or not). Careful echocardiographic assessment of chamber sizes in addition to systolic and diastolic performance usually allows accurate classification of the cardiomyopathy type: dilated, hypertrophic, restrictive, or noncompaction (see Chapter 58). The degree of systolic and diastolic dysfunction can vary greatly over time and is best assessed by serial measurements of ventricular performance.

Laboratory blood tests can contribute to the diagnosis of a metabolic etiology of heart failure in children. Blood analyses should include amino acids, carnitine, acylcarnitine profile, lactate-to-pyruvate ratio, and ammonia. Urine should be screened for carnitine and organic acids. Troponin and creatine kinase (MB fraction) can detect myocyte damage in myocarditis, ischemia, or cardiomyopathy. Liver and renal function tests are important to assess degree of end-organ damage. Brain-type natriuretic peptide can help to diagnose ventricular wall stress and its change over time. When myocarditis is suspected, serum and respiratory specimens can be screened for viral genome using the polymerase chain reaction (PCR). Although almost any virus can cause myocarditis, the most common are adenovirus, enteroviruses, parvovirus, coxsackie, respiratory syncytial virus, influenza, and parainfluenza.

Genetic testing may be performed using commercially available molecular studies and screening panels for sarcomere gene mutations (common genetic etiologies of hypertrophic cardiomyopathy and dilated cardiomyopathy) and also syndrome-specific testing. Genetic counseling should be considered prior to performing tests.

Cardiac magnetic resonance imaging may help in evaluating heart failure secondary to dilated cardiomyopathy for many reasons, including the ability to provide information that may help distinguish myocarditis from other forms of cardiomyopathy [13]. Cardiac catheterization may be indicated to perform coronary angiography to diagnose coronary abnormalities such as ALCAPA, coronary ostial atresia, or thrombi which may be responsible for heart failure associated with left ventricular dysfunction. Assessing hemodynamics may also be important to determine the degree of dysfunction through measurement of intracardiac pressures and cardiac output. Cardiac endomyocardial biopsy for histology, electron microscopy, and viral PCR may be useful in patients with new onset heart failure to look for evidence of acute myocarditis [14]. Skeletal muscle biopsy for histology, electron microscopy, and mitochondrial respiratory chain analysis may help diagnose cardiomyopathy

associated with related peripheral myopathy. Consultation with specialists in metabolism, genetics, and/or neuromuscular abnormalities can be very useful for diagnostic evaluation when there is concern about an underlying related systemic disorder.

Medical management of chronic heart failure

Chronic heart failure in children is increasingly recognized. Now that operative mortality for CHD has decreased significantly, the number of children surviving surgical palliation has grown and has been accompanied by an increased incidence of ventricular dysfunction and heart failure. The features of heart failure from cardiomyopathy have been well described [15,16]. Although the evidence base for the management of chronic heart failure in adults is broad, there is a paucity of evidence for the treatment of chronic heart failure in children [17,18]. With few exceptions, the management strategies for treating chronic heart failure in children have been extrapolated from large multicenter randomized trials in adults. Current medical management consists of diuretics, angiotensin-converting enzyme (ACE) inhibitors, β-adrenergic receptor blockers (β-blockers), aldosterone antagonists, and digoxin. Although no randomized trials have ever proven that diuretics are beneficial for survival in treating chronic heart failure, they do provide significant symptomatic improvement in patients with heart failure and fluid overload. Potential adverse effects associated with diuretic use include stimulating the renin–angiotensin–aldosterone system (RAAS) and potentially deleterious renal effects. However, when fluid retention is part of the heart failure syndrome, diuretics are an essential part of management. ACE inhibitors improve symptoms and survival in adults with symptomatic heart failure and in adults with asymptomatic left ventricular dysfunction [19–21]. Five large multicenter randomized placebo-controlled trials of β-blockers have also shown that β-blockers with heart failure produce improvements in symptoms, survival, and left ventricular function with mild, moderate, and severe heart failure [22–26]. The aldosterone antagonists spironolactone and eplerenone also afford a significant survival benefit in selected adults with heart failure [27]. Although digoxin has been the mainstay of treatment of heart failure for decades, large randomized trials have demonstrated only a benefit in reducing symptoms, and not mortality, in adults with heart failure. More recently, there has been increasing evidence that lower serum concentrations of digoxin may be better than higher serum concentrations [28]. Finally, angiotensin receptor blockers (ARBs) are essentially equal in efficacy to ACE inhibitors in adults with heart failure, but are currently only recommended for use in patients with heart failure who are intolerant to ACE

inhibitors [17]. In addition to medical therapy of chronic heart failure, electrophysiologic interventions such as cardiac resynchronization therapy and implantable cardioverters/defibrillators also improve symptoms and survival. These modalities are discussed below.

The management of chronic heart failure in children differs from that of adults for many reasons, including:
• different etiologies of heart failure (ischemic, hypertensive, and diabetic in adults compared with nonischemic, nonhypertensive, and nondiabetic in children)
• different ventricular morphologies
• different responses to medications (pharmacokinetic and pharmacodynamic) and electrophysiologic interventions
• different end-organ responses to heart failure
• lower incidence of sudden cardiac death in pediatric heart failure than adult heart failure.

For children with systemic left ventricular dysfunction, it is reasonable to consider the management strategies recommended in adults: diuretics for fluid overload, ACE inhibitors for asymptomatic and symptomatic ventricular dysfunction (ARBs for those who are intolerant to ACE inhibitors), and β-blockers, aldosterone antagonists, and possibly digoxin for symptomatic ventricular dysfunction [18]. For patients with a systemic ventricle that is not a left ventricle, the rationale for using these medications is much less clear. Diuretics for fluid overload continue to be a mainstay of therapy for heart failure with fluid retention, regardless of ventricular morphology. Studies in children and adults with single or right systemic ventricular morphology have failed to show any benefit from ACE inhibitors or ARBs [29–31]. Data from the Pediatric Carvedilol Study suggest that there may be a differential response to β-blockers in children, depending on the morphology of the systemic ventricle: those with a systemic left ventricle tended to show improvement when treated with β-blockers, whereas those with a systemic ventricle that was not a left ventricle did not [32]. There are no data to support or refute the use of aldosterone antagonists in children with heart failure due to systemic ventricular dysfunction in morphologically abnormal ventricles, but there could be theoretical benefit to using these agents due to their beneficial effects on reducing sympathetic nervous system innervation and myocardial fibrosis [33]. Newer medications such as sildenafil may have beneficial effects on selected patients with heart failure, especially those with Fontan physiology, but further study is needed before making recommendations. Despite all of these relatively new treatment modalities, some data suggest that the outcomes for children with heart failure are no better than they were before the development of therapies such as ACE inhibitors and β-blockers [34]. For those patients who "fail" medical therapy, the only option is to proceed towards heart transplantation. Indications include severe, refractory heart failure, severely restricted activity and

quality of life, and significant growth failure due to heart failure [35] (see Chapter 70).

Electrophysiologic management

Electrical device therapy in patients with heart failure has demonstrated additional clinical benefit and has become a mainstay in adult practice [36]. Implantable cardioverter defibrillators (ICDs) have clear survival benefit over standard medical therapy, which has resulted in their use for both primary and secondary prevention of sudden death [36]. Conventional pacemaker therapy has been applied to manage co-morbid electrophysiologic conditions. More recently, cardiac resynchronization therapy (CRT) has improved ventricular performance and benefited survival [36]. The role of these interventions in the management of children with heart failure with and without CHD remains limited, however, and in certain instances unclear [18].

The rationale for the use of ICDs is the increased incidence of sudden death mediated by ventricular arrhythmias in patients with heart failure [37]. Based on numerous adult trials for both primary and secondary prevention [37–43], ICDs have significantly improved survival in patients with heart failure.

Currently, the 2008 guidelines from the American Heart Association (AHA), American College of Cardiology (ACC), and Heart Rhythm Society (HRS) for device-based therapy of cardiac rhythms abnormalities and 2006 guidelines from the AHA, ACC, and European Society of Cardiology for the management of patients with ventricular arrhythmias and the prevention of sudden cardiac death have been used to manage adults with heart failure [36,44]. Based on these guidelines, ICDs are recommended or should be considered in patients with heart failure who meet various combinations of the following criteria: presence or absence of ischemia, time from infarction, degree of cardiac dysfunction, presence or absence of syncope, sudden cardiac arrest, documented ventricular tachycardia or ventricular fibrillation, presence or absence of structural heart disease, type of cardiomyopathy, and/or family history of sudden death [36,44].

The data for using ICDs in children with heart failure are limited [18,45,46]. Some small studies involving a heterogeneous population of children with and without CHD have demonstrated the efficacy of ICDs in terminating arrhythmias and, by extrapolation, improving survival [47–59]. A single study by Dubin *et al.* evaluated the role of ICD therapy in pediatric patients with heart failure [60]. This study evaluated 28 patients with and without CHD awaiting heart transplantation who underwent ICD placement due to ventricular tachycardia/fibrillation, syncope, aborted sudden death, ventricular ectopy, and/or poor cardiac function. A total of 55 ICD discharges occurred in 17 patients, of which 47 (85%) were appropriate [60]. The small numbers and heterogeneity of patients in this and other studies prevent the generalization of these findings with ICDs. Although the ICD terminated arrhythmias, these ventricular arrhythmias might not have been hemodynamically significant and might have self-terminated without therapy. The survival benefit of ICD intervention in children with heart failure is unknown. In a recent multicenter study, the incidence of sudden death in children with heart failure awaiting transplantation was low, 1.3% [61]. Hence the lack of data and the low incidence of death have prompted a more conservative stance for the use of ICDs in children [18].

Based on AHA/ACC/HRS 2008 and ISHLT 2004 guidelines, ICD use in children with heart failure is limited to secondary prevention indications [18,36]. Patients with heart failure usually should have survived a previous cardiac arrest, have symptomatic ventricular tachycardia, and/or have recurrent syncope in the setting of heart failure to be considered for device therapy. The application of ICDs is further limited in pediatrics by technical aspects and issues related to long-term morbidity with device therapy. In particular, the need for generator changes and lead extraction, the higher incidence of lead failure, limited vascular access and venous occlusion, complexity of anatomy, changing patient size, type of device, and psychological issues including the effect of inappropriate shocks should be considered [46,62]. Ultimately, the use of ICDs in children with heart failure is more complex than in adults and should be individualized.

In children with heart failure, regardless of the presence or absence of CHD, electrophysiologic abnormalities may exist. These include symptomatic bradycardia, loss of atrioventricular synchrony, that is, high-grade atrioventricular block, and intra-atrial re-entrant tachycardia, that is, atrial flutter/fibrillation [63]. Based on the AHA/ACC/HRS 2008 guidelines, these patients should be considered for pacemaker device therapy [36].

Most children who require conventional ventricular pacing undergo right ventricular apex pacing. The effect of this pacing site on further progression of heart failure is unknown in children, but data suggest that it may contribute to adverse left ventricular remodeling and diminished function [64–68]. This is illustrated by reports in patients with complete atrioventricular block of right ventricular pacing-induced cardiac dysfunction that function improved after conversion to biventricular pacing [69–73]. Right ventricular apex pacing in adult patients with heart failure with or without atrioventricular block has increased the risk of heart failure [74,75]. This has prompted further investigation in adults into the benefits of conventional versus biventricular pacing [76]. The implications of this study and others could alter the way in which pacing therapy is delivered in children who require long-term pacing to prevent progression of heart failure [64].

The rationale for the cardiac resynchronization therapy is based on observations that electric intraventricular conduction delay, that is, bundle branch block, causes

mechanical intraventricular dyssynchrony that can impair the efficacy of ventricular contraction and reduce ejection fraction [77]. Re-establishing "normal" ventricular conduction and uniform ventricular contraction using biventricular pacemakers improves measures of cardiac function, quality of life, symptoms, functional status, and survival [78]. Additionally, CRT can reverse remodeling of the abnormal myocardium [79,80]. Adult trials including the recent MADIT-CRT trial have shown improved survival and reduced heart failure events over conventional or ICD-only therapy [41,78,81]. Based on these trials, the use of CRT has become the standard of care for some adults. Device therapy is recommended for patients with an ejection fraction <35%, a QRS duration on ECG >120 ms, and a New York Heart Association (NYHA) Class III or ambulatory Class IV. It can also be considered in patients with NYHA Class I or II status who meet other indications for pacing or placement of an ICD [36]. The guidelines are clear, but not all patients respond to therapy and the pre-procedure identification of CRT responders remains elusive.

The clinical efficacy of CRT has led to its consideration for children [63]. To date, CRT with biventricular and multisite pacing in both acute and short-term settings has been described in patients with and without CHD [44,45,55–67,71,72, 82–90]. The two largest multicenter observational studies, by Dubin *et al.* and Janousek *et al.*, reported the effect of CRT on 212 pediatric and CHD patients who received device therapy for various indications. Short-term results demonstrated improvements in functional class, symptoms, and/or ventricular performance by echocardiographic parameters [68–70,91,92]. Unfortunately information about long-term improvement, survival, and improvement of heart failure events cannot be generalized from these studies. Attempts to extrapolate from the adult experience may also be invalid because of differences in etiologies of cardiac dysfunction, the complexities of pre- and postoperative CHD, and differences in the pattern and degree of intraventricular conduction delay, namely predominately right bundle branch block in children compared with left bundle branch block in adults. Also, the type of CHD may preclude or limit the use of this modality because of technical aspects and concern for alterations in medical management [93]. Investigations into the echocardiographic diagnosis of mechanical dyssynchrony have not been reliably useful in adults but may be more important in pediatrics. Based on the available data, no guidelines have been proposed for use of CRT in children with heart failure with or without CHD. CRT should therefore be individualized until further evidence regarding its utility is available.

Acute decompensated heart failure

Acute decompensated heart failure (ADHF) can be defined as the gradual or rapid deterioration in heart failure signs and symptoms requiring urgent therapy. Regardless of the underlying precipitant cause, patients present with symptoms of systemic volume overload with congestion, which can include dyspnea, hepatomegaly, peripheral edema, ascites, symptoms of low cardiac output with poor peripheral perfusion, fatigue, and end-organ dysfunction. In a recent cohort of children presenting to an emergency department with ADHF, the most common symptoms were those related to the gastrointestinal system, including nausea, vomiting, abdominal pain, and diarrhea [94].

In neonates with critical structural CHD presenting with acute heart failure from narrowing of the ductus arteriosus, prostaglandin therapy is the definitive management strategy. These neonates often require additional inotropic support for the myocardium, and invariably require careful attention to balance systemic and pulmonary circulations, until operative management can occur.

Children with ADHF from other causes require aggressive and timely treatment. In general, there is a stepwise approach to management by initiating therapies aimed at decreasing symptoms of congestion and improving myocardial performance. A general approach to management of ADHF includes pharmacologic and nonpharmacologic therapies.

Diuretics are the mainstay of pharmacologic therapy in patients with symptoms of systemic volume overload. The most commonly used agents are loop diuretics (e.g., furosemide and bumetamide), that promote natriuresis and diuresis by their actions on the loop of Henle in the kidney. Their effect can be augmented with thiazide diuretics (e.g., chlorothiazide) that act on the distal tubule. The combination of thiazides that retain calcium and furosemide that increases its excretion may be beneficial for prolonged treatment. The adverse effects of diuretic therapy include renal dysfunction, electrolyte abnormalities, and symptomatic hypotension from a rapid reduction in intravascular volume. These rapid shifts occur less frequently when continuous infusions of loop diuretics are used, and there is some evidence that continuous infusions are more advantageous than bolus injections [95].

Inotropes are the most commonly used agents for improving myocardial performance in children with ADHF. However, no inotrope improves contractility without increasing myocardial oxygen consumption and intracellular calcium accumulation, both of which can lead to arrhythmias and cell death. Inotropic agents include the catecholamines dopamine, dobutamine, and epinephrine, and the phosphodiesterase inhibitor milrinone. Dopamine, dobutamine, and epinephrine increase contractility by stimulating β_1-adrenergic receptors. In a study of hypotensive preterm infants, short-term use of dopamine was more effective than dobutamine; however, there were no benefits in mid- to long-term treatments [96]. Epinephrine and milrinone are agents commonly used in treating postoperative low cardiac output syndrome (LCOS) in children. In the PRIMACORP

study of pediatric postoperative LCOS in children, the incidence of LCOS was reduced significantly with milrinone therapy [97]. However, in the OPTIME-CHF study in adults with an acute exacerbation of heart failure [98], milrinone showed no benefit over placebo, but did increase the incidence of hypotension and arrhythmias. To date, no randomized studies have tested intravenous milrinone therapy in children with ADHF.

Nitroglycerin and nitroprusside are the most commonly used vasodilators in ADHF; both drugs act by conversion to nitric oxide, causing vasodilation, and thereby decreasing afterload on the failing ventricle. Nitroglycerin is primarily a venodilator, and nitroprusside is also an arterial vasodilator. Both agents improve cardiac function after heart surgery in children [99]; however, nitroprusside may cause thiocyanate poisoning after prolonged administration, and continuous use of nitroglycerin has caused tolerance. Both agents can result in hypotension and need to be used cautiously in ADHF with low blood pressure.

Nesiritide is a recombinant form of B-type natriuretic peptide that has primarily vasodilatory and secondarily natriuretic effects. In the VMAC trial in adults with ADHF, nesiritide therapy showed improved short-term symptomatic relief and hemodynamic profile when compared with nitroglycerin [100]. In the ADHERE study of adults hospitalized with ADHF, therapy with either nesiritide or nitroglycerin was associated with a significantly lower in-hospital mortality than with milrinone and dobutamine [101]. Although preliminary studies in children with heart failure suggest that nesiritide may be well tolerated and improve diuresis [102], there is some concern about its use based on a meta-analysis in adults that showed increased morbidity and mortality from renal failure [103].

Levosimendan is a calcium-sensitizing agent with unique dual activity. It improves myocardial contractility by increasing cardiac troponin C calcium sensitivity, without increasing myocardial oxygen consumption. Additional peripheral and coronary vasodilatory effects are facilitated by potassium channel opening. In the initial LIDO trial in adults with cardiogenic shock, levosimendan was superior to dobutamine in reducing pulmonary capillary wedge pressure and decreased long-term mortality at 6 months compared with placebo [104]. In preliminary studies in children with ADHF, levosimendan decreased catecholamine requirements and improved myocardial performance [105]. The most recent study in adults (SURVIVE), however, showed no benefit of levosimendan over dobutamine in 180 day mortality [106].

Arginine vasopressin is elevated in heart failure. This hormone acts through vasopressin-1 (V_1) receptors on the vasculature causing vasoconstriction, and vasopressin-2 (V_2) receptors on the kidneys leading to free water retention. Vasopressin receptor antagonists have been studied as potential therapies for ADHF. Drugs include the V_2 receptor antagonist tolvaptan, which promotes salt-free diuresis ("aquaresis") by selectively binding to renal V_2 receptors, and conivaptan, which by dual antagonism for V_1 and V_2 receptors also has the potential to decrease systemic vascular resistance and improve myocardial performance. In the EVEREST trial of adults with heart failure, oral tolvaptan therapy resulted in symptomatic relief with no mortality benefit [107,108].

The endothelins are a group of peptides with potent vasoconstrictor properties that can worsen outcomes of acute heart failure. However, the intravenous endothelin receptor antagonist tezosentan did not improve symptoms or clinical outcomes in an adult trial of acute heart failure, and the trial was terminated early because of futility [109].

Children with decompensated heart failure benefit from intubation and mechanical ventilation that reduce both left ventricular afterload by decreasing aortic transmural pressure, and also oxygen consumption by decreasing respiratory muscle work. Intubation has some risk in children with heart failure. Some children are overly sensitive to the myocardial depressant effects of sedative medications used for intubation. Other children do not tolerate the increased afterload and/or decreased preload on the right ventricle from increased intrathoracic pressure following intubation and initiation of mechanical ventilation.

Mechanical circulatory support with venoarterial extracorporeal membrane oxygenation (VA-ECMO), ventricular assist devices (VADs), and intra-aortic balloon pumps (IABPs) can augment cardiac output and allow myocardial rest either as a bridge to recovery or transplant (see Chapter 14). VA-ECMO is used for myocardial support and oxygenation, and can be used in children with intracardiac shunts. In children with a structurally normal heart, the left ventricle must be decompressed with an atrial septectomy, septostomy, or with a left atrial vent. VADs include devices that assist the right or left ventricle, or both. These devices cannot be placed in children with an intracardiac shunt and do not support oxygenation. The Berlin Heart EXCOR system has been used to support infants and children with severe circulatory failure. In the largest published series of VAD support in children, 73 children were supported with the Berlin Heart for a mean support time of 36 days; 62% survived to transplantation or were weaned off support, and 51% were discharged home [110]. IABPs are most commonly used in adolescents with heart failure. These devices provide intra-aortic balloon counterpulsation that augments coronary perfusion and provides mechanical circulatory assistance in cardiogenic shock [111]; however, like VADs, they do not support oxygenation.

In children with CHD and acute postoperative heart failure with atrioventricular and inter-/intraventricular conduction delay, resynchronization with temporary epicardial pacing wires may be a useful adjunct therapy, and significantly improves hemodynamics [82].

An alternative nonpharmacologic intervention to diuretic therapy being studied in adults is veno-venous ultrafiltration, which has been shown to alleviate symptoms of congestion by removing isotonic fluid. In adults with weight gain due to fluid overload from ADHF, in the UNLOAD trial ultrafiltration resulted in a greater reduction in weight compared with loop diuretics and a lower re-hospitalization rate at 90 days [112].

The prognosis of ADHF in children depends on the etiology and end-organ function. Children with acute fulminant myocarditis in general have a good prognosis; however, the time for myocardial functional recovery can be prolonged [113,114]. Worsening end-organ function is a poor prognostic sign and can indicate a need for mechanical circulatory support. In one series of children with ADHF, worsening renal function was associated with prolonged hospitalization, in-hospital death, and the need for mechanical circulatory assistance [115]. Transplantation should be considered early if there is no evidence of recovery of myocardial function. In a study of 1091 children with dilated cardiomyopathy and heart failure who underwent heart transplant, survival at 10 years post-transplantation was 72% compared with a 64% survival with conventional treatment at 5 years [116] (see Chapter 70).

References

1 Mann DL, Kent RL, Parsons B, Cooper G. Adrenergic effects on the biology of the adult mammalian cardiocyte. *Circulation* 1992;**85**:790–804.

2 Cohn JN, Ferrari R, Sharpe N. Cardiac remodeling – concepts and clinical implications: a consensus paper from an international forum on cardiac remodeling. *J Am Coll Cardiol* 2000;**35**:569–82.

3 Mann DL. Mechanisms and models in heart failure: a combinatorial approach. *Circulation* 1999;**100**:999–1008.

4 Kass DA. Ventricular arterial stiffening: integrating the pathophysiology. *Hypertension* 2005;**46**:185–93.

5 Cheung YF. Arterial stiffness in the young: assessment, determinants, and implications. *Korean Circ J* 2010;**40**:153–62.

6 Mahony L. Regulation of intracellular calcium concentration in the developing heart. *Cardiovasc Res* 1996;**31**(Spec No):E61–7.

7 Reinecke H, Studer R, Vetter R, *et al*. Cardiac Na$^+$/Ca^{2+} exchange activity in patients with end-stage heart failure. *Cardiovasc Res* 1996;**31**:48–54.

8 Schillinger W, Lehnart SE, Prestle J, *et al*. Influence of SR Ca^{2+}-ATPase and Na$^+$–Ca^{2+}-exchanger on the force–frequency relation. *Basic Res Cardiol* 1998;**93**(Suppl 1):38–45.

9 Cox GF, Sleeper LA, Lowe AM, *et al*. Factors associated with establishing a causal diagnosis for children with cardiomyopathy. *Pediatrics* 2006;**118**:1519–31.

10 Goodwin FC, Muntoni F. Cardiac involvement in muscular dystrophies: molecular mechanisms. *Muscle Nerve* 2005;**32**:577–88.

11 Scaglia F, Towbin JA, Craigen WJ, *et al*. Clinical spectrum, morbidity, and mortality in 113 pediatric patients with mitochondrial disease. *Pediatrics* 2004;**114**:925–31.

12 Hershberger RE, Lindenfeld J, Mestroni L, *et al*. Genetic evaluation of cardiomyopathy – a Heart Failure Society of America practice guideline. *J Card Fail* 2009;**15**:83–97.

13 Friedrich MG, Sechtem U, Schulz-Menger J, *et al*. Cardiovascular magnetic resonance in myocarditis: a JACC White Paper. *J Am Coll Cardiol* 2009;**53**:1475–87.

14 Cooper LT, Baughman KL, Feldman AM, *et al*. The role of endomyocardial biopsy in the management of cardiovascular disease: a scientific statement from the American Heart Association, the American College of Cardiology, and the European Society of Cardiology. Endorsed by the Heart Failure Society of America and the Heart Failure Association of the European Society of Cardiology. *J Am Coll Cardiol* 2007;**50**:1914–31.

15 Towbin JA, Lowe AM, Colan SD, *et al*. Incidence, causes, and outcomes of dilated cardiomyopathy in children. *JAMA* 2006;**296**:1867–76.

16 Daubeney PE, Nugent AW, Chondros P, *et al*. Clinical features and outcomes of childhood dilated cardiomyopathy: results from a national population-based study. *Circulation* 2006;**114**:2671–8.

17 Hunt SA, Abraham WT, Chin MH, *et al*. ACC/AHA 2005 Guideline update for the diagnosis and management of chronic heart failure in the adult – summary article. A Report of the American College of Cardiology/American Heart Association Task Force on Practice Guidelines (Writing Committee to Update the 2001 Guidelines for the Evaluation and Management of Heart Failure). *J Am Coll Cardiol* 2005;**46**:1116–43.

18 Rosenthal D, Chrisant MR, Edens E, *et al*. International Society for Heart and Lung Transplantation: practice guidelines for management of heart failure in children. *J Heart Lung Transplant* 2004;**23**:1313–33.

19 CONSENSUS Trial Study Group. Effects of enalapril on mortality in severe congestive heart failure. Results of the Cooperative North Scandinavian Enalapril Survival Study (CONSENSUS). The CONSENSUS Trial Study Group. *N Engl J Med* 1987;**316**:1429–35.

20 Cohn JN, Johnson G, Ziesche S, *et al*. A comparison of enalapril with hydralazine–isosorbide dinitrate in the treatment of chronic congestive heart failure. *N Engl J Med* 1991;**325**:303–10.

21 SOLVD Investigators. Effect of enalapril on survival in patients with reduced left ventricular ejection fractions and congestive heart failure. The SOLVD Investigators. *N Engl J Med* 1991;**325**:293–302.

22 Bristow MR, Gilbert EM, Abraham WT, *et al*. Carvedilol produces dose-related improvements in left ventricular function and survival in subjects with chronic heart failure. MOCHA Investigators. *Circulation* 1996;**94**:2807–16.

23 Packer M, Colucci WS, Sackner-Bernstein JD, *et al*. Double-blind, placebo-controlled study of the effects of carvedilol in patients with moderate to severe heart failure. The PRECISE Trial. Prospective Randomized Evaluation of Carvedilol on Symptoms and Exercise. *Circulation* 1996;**94**:2793–9.

24 CIBIS-II Investigators and Committees. The Cardiac Insufficiency Bisoprolol Study II (CIBIS-II): a randomised trial. *Lancet* 1999;**353**:9–13.

25 MERIT-HF Study Group. Effect of metoprolol CR/XL in chronic heart failure: Metoprolol CR/XL Randomised Intervention Trial in Congestive Heart Failure (MERIT-HF). *Lancet* 1999;**353**:2001–7.

26 Packer M, Fowler MB, Roecker EB, *et al*. Effect of carvedilol on the morbidity of patients with severe chronic heart failure: results of the Carvedilol Prospective Randomized Cumulative Survival (COPERNICUS) study. *Circulation* 2002;**106**:2194–9.

27 Pitt B, Zannad F, Remme WJ, *et al*. The effect of spironolactone on morbidity and mortality in patients with severe heart failure. Randomized Aldactone Evaluation Study Investigators. *N Engl J Med* 1999;**341**:709–17.

28 Rathore SS, Curtis JP, Wang Y, *et al*. Association of serum digoxin concentration and outcomes in patients with heart failure. *JAMA* 2003;**289**:871–8.

29 Kouatli AA, Garcia JA, Zellers TM, *et al*. Enalapril does not enhance exercise capacity in patients after Fontan procedure. *Circulation* 1997;**96**:1507–12.

30 Hechter SJ, Fredriksen PM, Liu P, *et al*. Angiotensin-converting enzyme inhibitors in adults after the Mustard procedure. *Am J Cardiol* 2001;**87**:660–3, A11.

31 Dore A, Houde C, Chan KL, *et al*. Angiotensin receptor blockade and exercise capacity in adults with systemic right ventricles: a multicenter, randomized, placebo-controlled clinical trial. *Circulation* 2005;**112**:2411–6.

32 Shaddy RE, Boucek MM, Hsu DT, *et al*. Carvedilol for children and adolescents with heart failure: a randomized controlled trial. *JAMA* 2007;**298**:1171–9.

33 Ezekowitz JA, McAlister FA. Aldosterone blockade and left ventricular dysfunction: a systematic review of randomized clinical trials. *Eur Heart J* 2009;**30**:469–77.

34 Kantor PF, Abraham JR, Dipchand AI, *et al*. The impact of changing medical therapy on transplantation-free survival in pediatric dilated cardiomyopathy. *J Am Coll Cardiol* 2010;**55**:1377–84.

35 Canter CE, Shaddy RE, Bernstein D, *et al*. Indications for heart transplantation in pediatric heart disease: a scientific statement from the American Heart Association Council on Cardiovascular Disease in the Young; the Councils on Clinical Cardiology, Cardiovascular Nursing, and Cardiovascular Surgery and Anesthesia; and the Quality of Care and Outcomes Research Interdisciplinary Working Group. *Circulation* 2007;**115**:658–76.

36 Epstein AE, DiMarco JP, Ellenbogen KA, *et al*. ACC/AHA/HRS 2008 Guidelines for device-based therapy of cardiac rhythm abnormalities: a report of the American College of Cardiology/ American Heart Association Task Force on Practice Guidelines (Writing Committee to Revise the ACC/AHA/NASPE 2002 Guideline Update for Implantation of Cardiac Pacemakers and Antiarrhythmia Devices) developed in collaboration with the American Association for Thoracic Surgery and Society of Thoracic Surgeons. *J Am Coll Cardiol* 2008;**51**:e1–62.

37 Narang R, Cleland JG, Erhardt L, *et al*. Mode of death in chronic heart failure. A request and proposition for more accurate classification. *Eur Heart J* 1996;**17**:1390–403.

38 Domanski MJ, Sakseena S, Epstein AE, *et al*. Relative effectiveness of the implantable cardioverter–defibrillator and antiarrhythmic drugs in patients with varying degrees of left ventricular dysfunction who have survived malignant ventricular arrhythmias. AVID Investigators. Antiarrhythmics Versus Implantable Defibrillators. *J Am Coll Cardiol* 1999;**34**:1090–5.

39 Connolly SJ, Hallstrom AP, Cappato R, *et al*. Meta-analysis of the implantable cardioverter defibrillator secondary prevention trials. AVID, CASH and CIDS Studies. Antiarrhythmics vs Implantable Defibrillator Study. Cardiac Arrest Study Hamburg. Canadian Implantable Defibrillator Study. *Eur Heart J* 2000;**21**:2071–8.

40 Moss AJ, Fadl Y, Zareba W, *et al*. Survival benefit with an implanted defibrillator in relation to mortality risk in chronic coronary heart disease. *Am J Cardiol* 2001;**88**:516–20.

41 Bristow MR, Saxon LA, Boehmer J, *et al*. Cardiac-resynchronization therapy with or without an implantable defibrillator in advanced chronic heart failure. *N Engl J Med* 2004;**350**:2140–50.

42 Kadish A, Dyer A, Daubert JP, *et al*. Prophylactic defibrillator implantation in patients with nonischemic dilated cardiomyopathy. *N Engl J Med* 2004;**350**:2151–8.

43 Bardy GH, Lee KL, Mark DB, *et al*. Amiodarone or an implantable cardioverter–defibrillator for congestive heart failure. *N Engl J Med* 2005;**352**:225–37.

44 Zipes DP, Camm AJ, Borggrefe M, *et al*. ACC/AHA/ESC 2006 Guidelines for management of patients with ventricular arrhythmias and the prevention of sudden cardiac death: a report of the American College of Cardiology/American Heart Association Task Force and the European Society of Cardiology Committee for Practice Guidelines (Writing Committee to Develop Guidelines for Management of Patients with Ventricular Arrhythmias and the Prevention of Sudden Cardiac Death): developed in collaboration with the European Heart Rhythm Association and the Heart Rhythm Society. *Circulation* 2006;**114**:e385–484.

45 Silka MJ, Bar-Cohen Y. Pacemakers and implantable cardioverter–defibrillators in pediatric patients. *Heart Rhythm* 2006;**3**:1360–6.

46 Berul CI. Implantable cardioverter defibrillator criteria for primary and secondary prevention of pediatric sudden cardiac death. *Pacing Clin Electrophysiol* 2009;**32**(Suppl 2):S67–70.

47 Silka MJ, Kron J, Dunnigan A, Dick M II. Sudden cardiac death and the use of implantable cardioverter–defibrillators in pediatric patients. The Pediatric Electrophysiology Society. *Circulation* 1993;**87**:800–7.

48 Hamilton RM, Dorian P, Gow RM, Williams WG. Five-year experience with implantable defibrillators in children. *Am J Cardiol* 1996;**77**:524–6.

49 Groh WJ, Silka MJ, Oliver RP, *et al*. Use of implantable cardioverter–defibrillators in the congenital long QT syndrome. *Am J Cardiol* 1996;**78**:703–6.

50 Stefanelli CB, Bradley DJ, Leroy S, *et al*. Implantable cardioverter defibrillator therapy for life-threatening arrhythmias in young patients. *J Interv Card Electrophysiol* 2002;**6**:235–44.

51 Alexander ME, Cecchin F, Walsh EP, *et al*. Implications of congenital heart disease and pediatrics. *J Cardiovasc Electrophysiol* 2004;**15**:72–6.

52 Goel AK, Berger S, Pelech A, Dhala A. Implantable cardioverter defibrillator therapy in children with long QT syndrome. *Pediatr Cardiol* 2004;**25**:370–8.

53 Gradaus R, Wollmann C, Kobe J, *et al*. Potential benefit from implantable cardioverter–defibrillator therapy in children and young adolescents. *Heart* 2004;**90**:328–9.

54 Korte T, Koditz H, Niehaus M, *et al*. High incidence of appropriate and inappropriate ICD therapies in children and adolescents with implantable cardioverter defibrillator. *Pacing Clin Electrophysiol* 2004;**27**:924–32.

55 Werner B, Przybylski A, Kucinska B, *et al*. Implantable cardioverter–defibrillators in children. *Kardiol Pol* 2004;**60**:239–46.

56 Ten Harkel AD, Blom NA, Reimer AG, *et al*. Implantable cardioverter defibrillator implantation in children in The Netherlands. *Eur J Pediatr* 2005;**164**:436–41.

57 Apitz C, Gass M, Dornberger V, *et al*. The use of implantable cardioverter–defibrillators (ICD) in children and adolescents. *Klin Pädiatr* 2006;**218**:270–5 (in German).

58 Eicken A, Kolb C, Lange S, *et al*. Implantable cardioverter defibrillator (ICD) in children. *Int J Cardiol* 2006;**107**:30–5.

59 Berul CI, Van Hare GF, Kertesz NJ, *et al*. Results of a multicenter retrospective implantable cardioverter–defibrillator registry of pediatric and congenital heart disease patients. *J Am Coll Cardiol* 2008;**51**:1685–91.

60 Dubin AM, Berul CI, Bevilacqua LM, *et al*. The use of implantable cardioverter–defibrillators in pediatric patients awaiting heart transplantation. *J Card Fail* 2003;**9**:375–9.

61 Rhee EK, Canter CE, Basile S, *et al*. Sudden death prior to pediatric heart transplantation: would implantable defibrillators improve outcome? *J Heart Lung Transplant* 2007;**26**:447–52.

62 Shah MJ. Implantable cardioverter defibrillator-related complications in the pediatric population. *Pacing Clin Electrophysiol* 2009;**32**(Suppl 2):S71–4.

63 Hsu DT, Pearson GD. Heart failure in children. Part II: diagnosis, treatment, and future directions. *Circ Heart Fail* 2009;**2**:490–8.

64 Karpawich PP. Chronic right ventricular pacing and cardiac performance: the pediatric perspective. *Pacing Clin Electrophysiol* 2004;**27**:844–9.

65 Thambo JB, Bordachar P, Garrigue S, *et al*. Detrimental ventricular remodeling in patients with congenital complete heart block and chronic right ventricular apical pacing. *Circulation* 2004;**110**:3766–72.

66 Manolis AS. The deleterious consequences of right ventricular apical pacing: time to seek alternate site pacing. *Pacing Clin Electrophysiol* 2006;**29**:298–315.

67 Gebauer RA, Tomek V, Kubus P, *et al*. Differential effects of the site of permanent epicardial pacing on left ventricular synchrony and function in the young: implications for lead placement. *Europace* 2009;**11**:1654–9.

68 Gebauer RA, Tomek V, Salameh A, *et al*. Predictors of left ventricular remodelling and failure in right ventricular pacing in the young. *Eur Heart J* 2009;**30**:1097–104.

69 Taylor-Albert E, Reichlin M, Toews WH, *et al*. Delayed dilated cardiomyopathy as a manifestation of neonatal lupus: case reports, autoantibody analysis, and management. *Pediatrics* 1997;**99**:733–5.

70 Moak JP, Barron KS, Hougen TJ, *et al*. Congenital heart block: development of late-onset cardiomyopathy, a previously underappreciated sequela. *J Am Coll Cardiol* 2001;**37**:238–42.

71 Udink ten Cate FE, Breur JM, Cohen MI, *et al*. Dilated cardiomyopathy in isolated congenital complete atrioventricular block: early and long-term risk in children. *J Am Coll Cardiol* 2001;**37**:1129–34.

72 Moak JP, Hasbani K, Ramwell C, *et al*. Dilated cardiomyopathy following right ventricular pacing for AV block in young patients: resolution after upgrading to biventricular pacing systems. *J Cardiovasc Electrophysiol* 2006;**17**:1068–71.

73 Takabayashi S, Shimpo H, Mitani Y, Komada Y. Pediatric cardiac remodeling after cardiac resynchronization therapy. *Pediatr Cardiol* 2006;**27**:485–9.

74 Wilkoff BL, Cook JR, Epstein AE, *et al*. Dual-chamber pacing or ventricular backup pacing in patients with an implantable defibrillator: the Dual Chamber and VVI Implantable Defibrillator (DAVID) Trial. *JAMA* 2002;**288**:3115–23.

75 Sweeney MO, Hellkamp AS, Ellenbogen KA, *et al*. Adverse effect of ventricular pacing on heart failure and atrial fibrillation among patients with normal baseline QRS duration in a clinical trial of pacemaker therapy for sinus node dysfunction. *Circulation* 2003;**107**:2932–7.

76 Curtis AB, Adamson PB, Chung E, *et al*. Biventricular versus right ventricular pacing in patients with AV block (BLOCK HF): clinical study design and rationale. *J Cardiovasc Electrophysiol* 2007;**18**:965–71.

77 Spragg DD, Kass DA. Pathobiology of left ventricular dyssynchrony and resynchronization. *Prog Cardiovasc Dis* 2006;**49**:26–41.

78 McAlister FA, Ezekowitz J, Hooton N, *et al*. Cardiac resynchronization therapy for patients with left ventricular systolic dysfunction: a systematic review. *JAMA* 2007;**297**:2502–14.

79 Ghio S, Freemantle N, Scelsi L, *et al*. Long-term left ventricular reverse remodelling with cardiac resynchronization therapy: results from the CARE-HF trial. *Eur J Heart Fail* 2009;**11**:480–8.

80 St John Sutton M, Ghio S, Plappert T, *et al*. Cardiac resynchronization induces major structural and functional reverse remodeling in patients with New York Heart Association class I/II heart failure. *Circulation* 2009;**120**:1858–65.

81 Moss AJ, Hall WJ, Cannom DS, *et al*. Cardiac-resynchronization therapy for the prevention of heart-failure events. *N Engl J Med* 2009;**361**:1329–38.

82 Janousek J, Vojtovic P, Hucin B, *et al*. Resynchronization pacing is a useful adjunct to the management of acute heart failure after surgery for congenital heart defects. *Am J Cardiol* 2001;**88**:145–52.

83 Rodriguez-Cruz E, Karpawich PP, Lieberman RA, Tantengco MV. Biventricular pacing as alternative therapy for dilated cardiomyopathy associated with congenital heart disease. *Pacing Clin Electrophysiol* 2001;**24**:235–7.

84 Blom NA, Bax JJ, Ottenkamp J, Schalij MJ. Transvenous biventricular pacing in a child after congenital heart surgery as an alternative therapy for congestive heart failure. *J Cardiovasc Electrophysiol* 2003;**14**:1110–2.

85 Zimmerman FJ, Starr JP, Koenig PR, *et al*. Acute hemodynamic benefit of multisite ventricular pacing after congenital heart surgery. *Ann Thorac Surg* 2003;**75**:1775–80.

86 Strieper M, Karpawich P, Frias P, *et al*. Initial experience with cardiac resynchronization therapy for ventricular dysfunction in young patients with surgically operated congenital heart disease. *Am J Cardiol* 2004;**94**:1352–4.

87 Senzaki H, Kyo S, Matsumoto K, *et al*. Cardiac resynchronization therapy in a patient with single ventricle and intracardiac conduction delay. *J Thorac Cardiovasc Surg* 2004;**127**:287–8.

88 van Beek E, Backx A, Singh S. Cardiac resynchronization as therapy for congestive cardiac failure in children dependent on chronic cardiac pacing. *Cardiol Young* 2006;**16**:187–9.

89 Jones BO, Davis AM, Alison J, *et al*. Cardiac re-synchronization therapy in a child with severe anthracycline-induced congestive heart failure and normal QRS duration. *J Heart Lung Transplant* 2007;**26**:1333–5.

90 Sojak V, Mazic U, Cesen M, *et al*. Cardiac resynchronization therapy for the failing Fontan patient. *Ann Thorac Surg* 2008;**85**:2136–8.

91 Dubin AM, Janousek J, Rhee E, *et al*. Resynchronization therapy in pediatric and congenital heart disease patients: an international multicenter study. *J Am Coll Cardiol* 2005;**46**: 2277–83.

92 Janousek J, Gebauer RA, Abdul-Khaliq H, *et al*. Cardiac resynchronisation therapy in paediatric and congenital heart disease: differential effects in various anatomical and functional substrates. *Heart* 2009;**95**:1165–71.

93 Karpawich PP. Technical aspects of pacing in adult and pediatric congenital heart disease. *Pacing Clin Electrophysiol* 2008;**31**(Suppl 1):S28–31.

94 Macicek SM, Macias CG, Jefferies JL, *et al*. Acute heart failure syndromes in the pediatric emergency department. *Pediatrics* 2009;**124**:e898–904.

95 Salvador DR, Rey NR, Ramos GC, Punzalan FE. Continuous infusion versus bolus injection of loop diuretics in congestive heart failure. *Cochrane Database Syst Rev* 2004;CD003178.

96 Subhedar NV, Shaw NJ. Dopamine versus dobutamine for hypotensive preterm infants. *Cochrane Database Syst Rev* 2000;CD001242.

97 Hoffman TM, Wernovsky G, Atz AM, *et al*. Efficacy and safety of milrinone in preventing low cardiac output syndrome in infants and children after corrective surgery for congenital heart disease. *Circulation* 2003;**107**:996–1002.

98 Cuffe MS, Califf RM, Adams KF Jr, *et al*. Short-term intravenous milrinone for acute exacerbation of chronic heart failure: a randomized controlled trial. *JAMA* 2002;**287**:1541–7.

99 Artman M, Graham TP Jr. Guidelines for vasodilator therapy of congestive heart failure in infants and children. *Am Heart J* 1987;**113**:994–1005.

100 Publication Committee for the VMAC Investigators. Intravenous nesiritide vs nitroglycerin for treatment of decompensated congestive heart failure: a randomized controlled trial. *JAMA* 2002;**287**:1531–40.

101 Abraham WT, Adams KF, Fonarow GC, *et al*. In-hospital mortality in patients with acute decompensated heart failure requiring intravenous vasoactive medications: an analysis from the Acute Decompensated Heart Failure National Registry (ADHERE). *J Am Coll Cardiol* 2005;**46**:57–64.

102 Mahle WT, Cuadrado AR, Kirshbom PM, *et al*. Nesiritide in infants and children with congestive heart failure. *Pediatr Crit Care Med* 2005;**6**:543–6.

103 Sackner-Bernstein JD, Kowalski M, Fox M, Aaronson K. Short-term risk of death after treatment with nesiritide for decompensated heart failure: a pooled analysis of randomized controlled trials. *JAMA* 2005;**293**:1900–5.

104 Follath F, Cleland JG, Just H, *et al*. Efficacy and safety of intravenous levosimendan compared with dobutamine in severe low-output heart failure (the LIDO study): a randomised double-blind trial. *Lancet* 2002;**360**:196–202.

105 Namachivayam P, Crossland DS, Butt WW, Shekerdemian LS. Early experience with levosimendan in children with ventricular dysfunction. *Pediatr Crit Care Med* 2006;**7**:445–8.

106 Mebazaa A, Nieminen MS, Packer M, *et al*. Levosimendan vs dobutamine for patients with acute decompensated heart failure: the SURVIVE Randomized Trial. *JAMA* 2007;**297**:1883–91.

107 Gheorghiade M, Konstam MA, Burnett JC Jr, *et al*. Short-term clinical effects of tolvaptan, an oral vasopressin antagonist, in patients hospitalized for heart failure: the EVEREST Clinical Status Trials. *JAMA* 2007;**297**:1332–43.

108 Konstam MA, Gheorghiade M, Burnett JC Jr, *et al*. Effects of oral tolvaptan in patients hospitalized for worsening heart failure: the EVEREST Outcome Trial. *JAMA* 2007;**297**:1319–31.

109 McMurray JJ, Teerlink JR, Cotter G, *et al*. Effects of tezosentan on symptoms and clinical outcomes in patients with acute heart failure: the VERITAS randomized controlled trials. *JAMA* 2007;**298**:2009–19.

110 Stiller B, Lemmer J, Schubert S, *et al*. Management of pediatric patients after implantation of the Berlin Heart EXCOR ventricular assist device. *ASAIO J* 2006;**52**:497–500.

111 Boehmer JP, Popjes E. Cardiac failure: mechanical support strategies. *Crit Care Med* 2006;**34**(9 Suppl):S268–77.

112 Costanzo MR, Guglin ME, Saltzberg MT, *et al*. Ultrafiltration versus intravenous diuretics for patients hospitalized with acute decompensated heart failure. *J Am Coll Cardiol* 2007;**49**: 675–83.

113 O'Sullivan JJ, Roche SL, Crossland DS, *et al*. Recovery of heart function in children with acute severe heart failure. *Transplantation* 2008;**85**:975–9.

114 Amabile N, Fraisse A, Bouvenot J, *et al*. Outcome of acute fulminant myocarditis in children. *Heart* 2006;**92**:1269–73.

115 Price JF, Mott AR, Dickerson HA, *et al*. Worsening renal function in children hospitalized with decompensated heart failure: evidence for a pediatric cardiorenal syndrome? *Pediatr Crit Care Med* 2008;**9**:279–84.

116 Kirk R, Naftel D, Hoffman TM, *et al*. Outcome of pediatric patients with dilated cardiomyopathy listed for transplant: a multi-institutional study. *J Heart Lung Transplant* 2009;**28**:1322–8.

72 Pediatric Cardiology in the Tropics and Underdeveloped Countries

Andrea Beaton[1], Stephanie Lacey[2], Tom Mwambu[3], Charles Mondo[3], Peter Lwabi[3] & Craig Sable[1]

[1]Children's National Medical Center and George Washington University Medical School, Washington, DC, USA
[2]Wolfson Children's Hospital and University of Florida College of Medicine, Jacksonville, FL, USA
[3]Uganda Heart Institute, Mulago Hospital and Makerere University School of Medicine, Kampala, Uganda

Introduction

The burden of pediatric heart disease is significantly greater in underdeveloped than developed nations, even though it may not receive the same focus as more common problems such as AIDS, malaria, malnutrition, and trauma. The effect of cardiac disease in children is twofold. First, although the incidence of congenital heart disease (CHD) is the same as in developed countries, its impact is magnified by several factors. Although diagnostic capability exists (echocardiography), affordable treatment options are limited so that many children grow up with unrepaired anomalies not commonly encountered in developed countries. This is compounded by the very young mean age of the population (often below 20 years) and very high birth rate (2–3-fold higher than in the United States or Europe) [1]. Second, the incidence of acquired heart disease in children is much higher than in developed nations. This includes diseases that are endemic in almost all developing countries, most notably rheumatic heart disease, and problems that are regional, including endomyocardial fibrosis in East Africa and Chagas disease in Latin America. This chapter focuses on both congenital and acquired heart disease in children occurring in developing countries, drawing, in part, from the authors' personal experience in Uganda.

Burden of congenital heart disease

The incidence of CHD is relatively constant in most countries throughout the world, affecting ~1% of the population [2]. The incidence may be as high as 3%, however, in countries with high rates of consanguinity, and regional genetic and environmental factors may alter the distribution of congenital heart defects. Nearly half of children with CHD require intervention. In many developing countries, echocardiography is available for diagnosis, but not more advanced diagnostic or surgical care. Strikingly, the 4000 pediatric cardiology surgery units worldwide serve only 7% of the planet's children [3]. Even fewer pediatric cardiac catheterization laboratories are available. This discrepancy is most significant in sub-Saharan Africa. Recent estimates suggest that over 5.5 million children worldwide have potentially treatable (with a single staged intervention) CHD but do not have access to care [3]. Many of these children are very sick (with unrepaired ventricular septal defects and tetralogy of Fallot being the most prevalent) and it is a significant burden for their families to take care of them. Pollution and frequent respiratory infections likely increase pulmonary hypertension in patients with a left-to-right shunt and episodes of dehydration exacerbate cyanosis in patients with tetralogy of Fallot. These issues do not even include the numerous children with more complex conditions who die in infancy, often without cardiac diagnosis.

Several factors explain the huge discrepancy in care [4]. First and foremost, these countries, especially those in sub-Saharan Africa, are the most economically challenged in the world and the disparity is increasing; per capita aid has dropped by 40% in the last 10 years. As a result, there is often very poor health care infrastructure and limited health care education. Many countries face a huge burden of HIV/ AIDS, malnutrition, and very high infant (50–200 per 1000 live births) and maternal pre-/peripartum (3–11 per 1000 pregnancies) mortality. Unstable political systems and wars compound these problems.

Developing and maintaining a cardiac surgical program face many challenges [5,6]. Financing the necessary technology is often more expensive than in North America or Europe. Consumable products are especially hard to

acquire, and maintenance and repair of equipment are a huge challenge. Complete cardiovascular teams are difficult to maintain because the "brain drain" phenomenon is prevalent. Physicians, nurses, and other healthcare professionals (especially young people fresh out of training) are often offered attractive financial incentives to move abroad. Many of these personnel were sent abroad for a short period of time at hospital and/or government expense to receive training to improve local care. Some developed countries (e.g., the United Kingdom) have relatively strict regulations to prevent promoting the "brain drain" whereas others (e.g., the United States) have almost no rules against recruiting foreign trained medical personnel. Within most developing countries, private sector positions compete with government programs for the most highly qualified personnel. This is counterproductive to programs, such as cardiovascular surgery, that can only succeed if all local resources are pooled and care is performed at a single institution (usually the government/public hospital).

The levels of care for children with heart disease in need of cardiac intervention vary greatly between countries. Some countries offer open-heart surgery routinely whereas others have no or limited closed heart procedures (e.g., patent ductus ligation). Many programs have sufficient infrastructure to host visiting surgical teams for 1–2 week missions. Unfortunately, for most children, the only option is care abroad. The cost is almost always prohibitive relative to local income levels [5]. Even though many charitable organizations place children in established cardiac surgical centers throughout the world, only a small fraction of those in need receive care.

The only way to provide pediatric cardiac surgical care to this significant population of deserving children is to develop regional units that are sustainable. The cost of performing cardiac surgery in developing countries is often 10–20-fold less than it would be abroad. An argument can be made that the benefit (in terms of dollars spent per years of life saved) of performing open-heart surgery (at a cost of $4000–5000 per patient) compares favorably with vaccination and HIV treatment programs.

Coordination of several key individuals and organizations is required in order to create a sustainable cardiovascular surgery program in a developing country [1]. The intent is to build a partnership among cardiovascular specialists in all aspects of perioperative care, legal and financial advisors, nongovernmental and other international organizations invested in healthcare, and local cardiovascular specialists, governmental officials, and the private sector. The early stages of such a partnership will likely include caring for children abroad. In addition to the obvious benefit to the individual child and family, this effort can raise awareness and bring about important fund-raising opportunities.

Subsequently, a combination of relatively frequent medical missions by visiting teams of cardiologists, surgeons, and allied specialists focused on training local teams, training of key personnel abroad for short periods of time, international charitable support, and local governmental funding is critical for success. These missions must be coordinated and provide for a gradual increase in complexity, with local teams assuming more responsibility and performing their own operations between medical missions. The path and obstacles (as outlined above) to long-term sustainability must always be kept in mind. Visiting teams must create a safe and productive practice model but not recreate "first-world" practice that cannot be replicated when they leave. Additionally, "medical tourism," having individuals or teams visit without being part of a bigger picture with no eye towards sustainability, should be avoided.

Uganda case study

Uganda's population is 30 million, with a mean age that is the youngest on the planet. It is estimated that at least 5000 children in Uganda are candidates for single-stage "curative" open-heart surgery or catheterization [3]. Uganda has many favorable attributes that make it a candidate for establishing a sustainable open-heart surgery program. English being the official language, a relatively stable government, ease of travel to and from Uganda, and safety and modernization of the Ugandan capital and other cities make it attractive for international medical efforts.

Uganda had unmatched success, relative to other developing countries, in reducing the incidence of HIV infectivity in the 1990s because of a very aggressive mass publication education program [7,8]. In the first decade of this century Uganda was at the forefront of antiretroviral treatment, at first for pregnant woman and then for any HIV-infected patients. This success has led to multiple collaborations between medical and research institutions, NGOs, governmental healthcare agencies throughout the world, and the main teaching public hospital (Mulago Hospital) and medical school (Makerere University) over the last 20 years. The Uganda Heart Institute is a semi-private ward within Mulago Hospital, and its leadership reports directly to the Ugandan Minister of Health. High-quality pediatric echocardiography has existed for nearly a decade and two cardiovascular surgeons with extensive pediatric training in India are full-time staff members.

The senior author (C.S.) was invited in 2002 by the Ugandan Ambassador to the United States to visit Uganda, assess and collaborate with the local team (P.L. and T.M.), and attempt to provide care for Ugandan patients in the United States. The first mission in February 2003 involved one person (C.S.) and diagnostic echocardiograms were performed on 40 patients. Six children were subsequently cared for in Washington, DC. More importantly, a blueprint for long-term development of a sustainable cardiac surgical program was developed. Ongoing missions with the ultimate goal of building a sustainable heart surgery program include the following:

- diagnose children with heart disease
- teaching programs with focus on patient care, education, critical assessment of personnel, and equipment needs
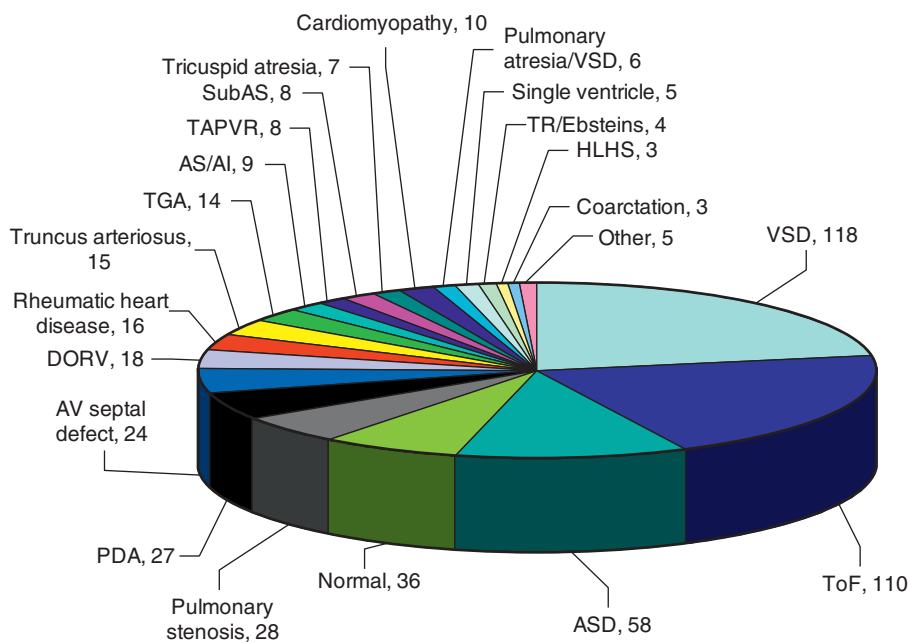
Figure 72.1 Distribution of diagnoses among Ugandan children referred for cardiac evaluation. AS/AI, aortic stenosis/aortic insufficiency; ASD, atrial septal defect; AV, atrioventricular; DORV, double-outlet right ventricle; HLHS, hypoplastic left heart syndrome; PDA, patent ductus arteriosus; Sub AS, subaortic stenosis; TAPVR, total anomalous pulmonary venous return; TGA, transposition of the great arteries; ToF, tetralogy of Fallot; TR/Ebstein's, tricuspid regurgitation/Ebstein's anomaly; VSD, ventricular septal defect.

- facilitate treatment of children abroad as needed
- facilitate donation of technology
- meet with hospital and government officials
- develop ongoing sustainable financial model
- build a consortium of key individuals and groups.

To date, 10 missions have been carried out; the last five included performing open-heart surgery. Key team members on every surgical trip have included cardiologists, cardiac surgeons, intensivists, anesthesiologists, perfusionists, scrub nurses, critical care nurses (at least four per trip), respiratory therapists, and biomedical engineers. High-level cardiology and intensive care trainees from the United States have also been part of the team and work side-by-side with their Ugandan counterparts. A number of cardiovascular programs have played a major role in this effort, including those from Children's National Medical Center in Washington, DC, Wolfson Children's Hospital in Jacksonville, FL, University of North Carolina in Chapel Hill, NC, and Great Ormond Street Hospital in London, UK.

Key charitable groups involved at the beginning of the project and still actively supporting the program include the Samaritan's Purse Children's Heart Project and Larry King Cardiac Foundation. Other charities with a significant role include Gift of Life International, Garth Brooks Teammates for Kids, Save a Child's Heart, and Health Volunteers Overseas. Several vendors and pharmaceutical companies have given significant in-kind donations, including Philips Medical, Medtronics, and Sanofi-Aventis. Many of these organizations have very generous charitable arms that have official application sites available on the Internet.

It was also very important early on to receive the support of key individuals in Uganda. Ugandan President Yoweri Museveni visited the team in 2007 on the occasion of the first open-heart surgery in Uganda. He pledged ongoing Ugandan governmental financial support for pediatric heart surgery at Mulago Hospital. The authors have met with Ugandan First Lady Janet Museveni on several occasions and also the United States Ambassador to Uganda and the Ugandan Ambassador to the United States. Each mission visit includes meetings with hospital leadership and members of the Ministry of Health. The first two Ugandan patients who received care in the United States were hosted by then Senate Majority Leader Dr Bill Frist, who had operated at Mulago Hospital in 2002.

In the first 8 years of the program, the frequency of trips averaged one every 9 months; Participation by additional medical teams will enable this to increase to one every 3 months. An average of 150 echocardiograms and 10 operations were performed during the last five five medical missions dating from March 2007. A number of patients have been seen on multiple visits. Echocardiography (both images and reports) and surgical data have been maintained since collaboration began. Rheumatic heart disease and cardiomyopathy are under-represented in the data acquired during medical missions. This is related to the difficulty in getting patients who need valve replacement accepted abroad or by initial visiting surgery teams because of the concern of compliance with warfarin anticoagulation regimens.

Complete data are available for 532 children cared for during the missions. The most common diagnoses (Figure 72.1) were ventricular septal defect ($n = 118$), tetralogy of Fallot ($n = 110$), atrial septal defect ($n = 58$), and pulmonary stenosis ($n = 28$). Of note, truncus arteriosus was more common ($n = 15$) and coarctation ($n = 3$) was less common than
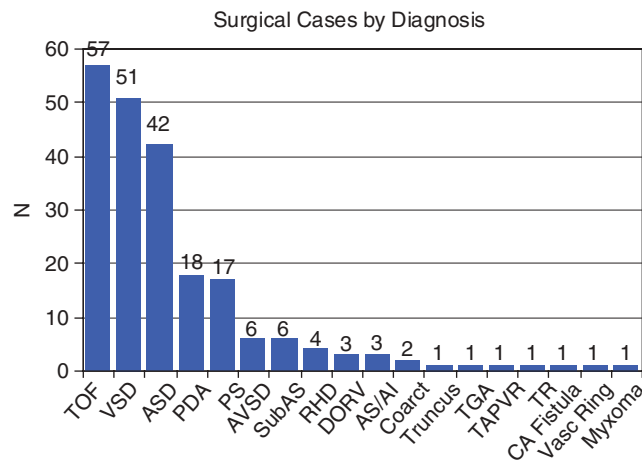
Figure 72.2 Diagnoses of Ugandan children undergoing cardiac surgery. Abbreviations as in Figure 72.1, and AVSD, atrioventricular septal defect; CA, coronary artery; Coarct, coarctation of the aorta; PS, pulmonary stenosis; RHD, rheumatic heart disease; Truncus, truncus arteriosus; Vasc, vascular.
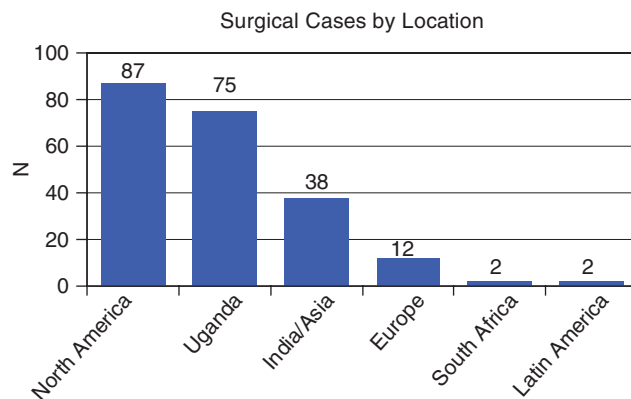
Figure 72.3 Location of surgery for Ugandan children.

Figure 72.4 Patients receiving treatment by diagnosis. Abbreviations as in Figures 72.1 and 72.2.

expected from known prevalence data. We speculate that there is incomplete blood pressure assessment for noncritical coarctation and early death without diagnosis for critical coarctation. Future studies of genetic and environmental factors contributing to the high number of truncus arteriosus patients are warranted.

The mean ages at diagnosis were 11 years for atrial septal defect, 3.5 years for ventricular septal defect and 6.4 years for tetralogy of Fallot; the distribution reflects the natural history of congenital heart disease not seen in developed nations. Survival into the second decade of life is frequent in tetralogy of Fallot. Some older children with ventricular septal defect may develop irreversible pulmonary vascular disease, but many are still likely operable. Medical management of cyanotic tetralogy of Fallot was primarily with propranolol. Medical management of congestive heart failure (ventricular septal defects and large atrial septal defects) was with digoxin and furosemide for most patients.

Many were also treated with captopril and/or carvedilol. β-Blockers were much more commonly used for left-to-right shunts than in developed nations. Only pills are available (digoxin 250 μg, furosemide 40 mg, and propranolol 40 mg). Pills are halved or quartered by the pharmacy operated by the Uganda Heart Institute. Most children aged under 1 year take one half or quarter pill once per day.

After the Idi Amin era, a cardiac surgical program was rebuilt in the 1980s by Dr Francis Omaswa. Before 2007, however, the only cardiac surgical procedures performed in Uganda were patent ductus ligation, pericardiectomy (often for tuberculosis), pacemaker insertion (either epicardially or transvenously with single-plane C-arm guidance), and for cardiac trauma. Ductus ligation was often performed in patients with a coexisting large membranous ventricular septal defect to decrease the ductal shunt, hoping to decrease left-sided volume sufficiently to improve symptoms and promote shrinkage of the ventricular septal defect. This was observed anecdotally in several patients.

Patients in our program began to receive care abroad in 2003 and the first open-heart surgical procedure in Uganda (atrial septal defect repair in an 11 year old) was performed in October 2007. The Ugandan team performed the first of five atrial septal defect repairs on its own in May 2009. To date, 216 patients have received cardiac repair in our program, including 75 in Uganda (55 open-heart patients). This includes patients with pulmonary stenosis or atrial septal defects treated abroad via interventional catheterization. The distribution of surgical patients by diagnosis and location is shown in Figures 72.2 and 72.3. The percentage of patients accepted for treatment by diagnosis is shown in Figure 72.4. The decision to accept a patient is determined by several factors, including urgency, risk, and finances. Because of financial support in North America it is more challenging to place surgical than interventional catheterization patients. Atrial septal defects, pulmonary stenosis, patent ductus, and subaortic stenosis have had the highest acceptance rate abroad. Ventricular septal defect patients between the ages

Open Heart Surgery in Africa
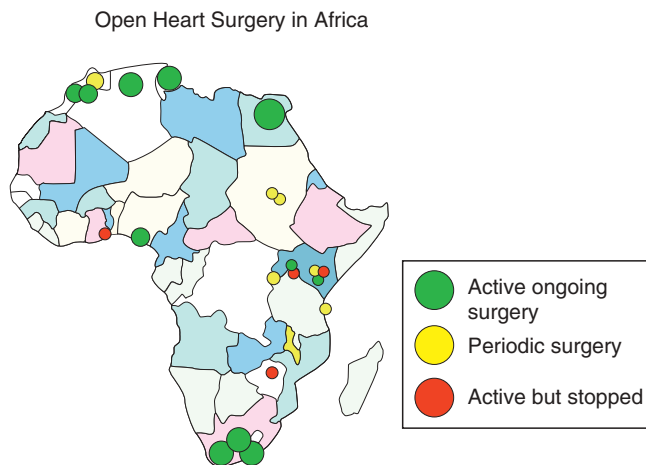
Figure 72.5 Location of open-heart surgery programs in Africa.

of 1 and 3 years had a very high acceptance rate, but infants and older children have not.

In the first 2 years, surgery in Uganda has focused on repair of atrial septal and ventricular septal defects in an effort to increase the local surgeons' skills. One tetralogy of Fallot repair, three subaortic stenosis resections, and one right atrial myxoma removal have also been performed in Uganda. In addition to Ugandan citizens, children from Kenya, Congo, and Sudan have come to Mulago Hospital for surgery because of the higher success rate than in their own countries. Very few programs are currently performing open-heart surgery in Africa (Figure 72.5).

Overall survival for the entire program is 98%; no patient operated on in Uganda has died. The diagnoses of the five children who died were ventricular septal defect (with pulmonary hypertension), tetralogy of Fallot, pulmonary stenosis/hypoplastic right ventricle, aortic stenosis/insufficiency, and rheumatic mitral regurgitation. Twenty children who did not receive surgery have died and others with more complex diagnoses have probably died without our knowledge.

The outpatient screening process is a key to the early success of this program. Patients undergo echocardiography on digital ultrasound units with storage on a digital echocardiography image and reporting system in Uganda (Xcelera, donated by Philips Medical, Andover, MA, USA) and in the United States. Patient data are compiled and stored in parallel, and easy access to all the data exists. This resulted in a database of over 500 children that can be reviewed together by Ugandan and visiting teams before the medical missions to optimize surgical planning and minimize diagnostic errors. Echocardiograms are repeated on all patients undergoing surgery at the beginning of the medical mission and reviewed with the entire team. Intraoperative transesophageal echocardiography (pediatric and adult omniplane) is available for all open-heart operations and performed by Ugandan cardiologists under the supervision of visiting echocardiographers. All demographic data, including family cell phone contact information, is kept by a local charity (Samaritan's Purse) and the Ugandan Heart Institute. As a result, the percentage of patients lost to follow-up or who do not show up for scheduled appointments is <5%. Follow-up care is also very good. Compliance is very high even though patients may travel significant distances, and Samaritan's Purse provides home assessment of each patient who has undergone surgery. Advancing telemedicine technology allows for communication and sharing of patient information on pre- and postoperative patients. The Ugandan team is participating in an international quality assurance initiative that also helps track postoperative patients.

The way forward to a sustainable open-heart surgical program will require the Ugandan team to be able to perform a wide variety of procedures, including repair of tetralogy of Fallot and rheumatic heart disease. Currently, skilled surgeons, anesthesiologists, perfusionists, scrub nurses, and cardiologists are in place. A modern cardiac bypass machine is operational and most of the other large equipment in the operating room is up-to-date. Monitors in the intensive care unit are state of the art. Three modern echocardiography systems are available with all sizes of transducers and digital storage capability. Most medicines are available, but not in the quantity or variety that those practicing in developed nations are used to.

Many obstacles remain to achieve long-term success. The intensive care unit is the weakest link in the current process. There are few skilled intensive care unit nurses and no critical care physicians; the surgeons provide all the postoperative care. Many additional nurses require training and remuneration is not sufficient to avoid losing nurses to local private hospitals or programs abroad. The frequency of operations is not sufficient to maintain nursing skills as less than one open-heart procedure is performed per week between our visits. As mission frequency increases, it will be important to adhere to consistent practice and education protocols.

The cost of disposable items remains a significant factor. Important examples include cartridges for blood gas machines and cardiac bypass circuits and oxygenators. Electric power is relatively stable and the operating room has a backup generator. Nonetheless, there are significant power surges that can affect the function of the operating room and intensive care unit. No cardiac catheterization is available; there is no Ugandan physician capable of performing catheterizations and the cost of maintaining a catheterization laboratory is prohibitive.

Ongoing funding is critical. The cost of an open-heart surgery procedure in Uganda from admission to discharge is ~$5000. Although this may be more than 10-fold less than in North America, the average Ugandan family income is 100-fold less. Only a small number of families can afford surgery; no public health insurance exists. Government

subsidization of the costs of surgery will be essential as the program moves forward. Growth of such a high profile program cannot be separated from politics; political stability is always tenuous.

Currently, we are in the second of a 5 year plan that we hope will include four medical missions per year each performing 10 operations, with Ugandan teams performing one open-heart operation per week between missions. The complexity of patients cared for will gradually increase. Ongoing teaching and training will occur on each mission and will be complemented by developing a telemedicine program and participating in an international quality initiative. Funding for a catheterization laboratory had been allocated and should move forward when the program is ready. Ultimately, the hope is that the Uganda Heart Institute will be a referral source for all of East Africa and this will help supplement the program financially.

Acquired heart disease

The prevalence of acquired heart disease is often much higher than that of congenital heart disease in children in developing countries. Rheumatic disease is the most common acquired disease throughout the world. It is estimated that ~16 million, the majority being children, have rheumatic heart disease worldwide; ~500 000 new patients are diagnosed and ~250 000 deaths occur each year [9]. The diagnosis and treatment of rheumatic heart disease is addressed in detail in Chapters 61 and 62. A brief discussion of the unique challenges and solutions to primary and secondary rheumatic fever prevention will be presented here. We will also discusses two other diseases affecting the heart and having a significant impact: endomyocardial fibrosis and Chagas disease. Over 100 million people are thought to be at risk for Chagas disease, with nearly one million affected [10]. Endomyocardial fibrosis affects nearly 20% of the population in endemic regions of Mozambique, with children bearing the brunt of the disease [1,11].

Rheumatic heart disease

In many developing countries, rheumatic fever/rheumatic heart disease (RF/RHD) is a common cause of cardiovascular morbidity and mortality that imposes a great burden on health care services for children. Unfortunately, most children are diagnosed late, after valve damage is already advanced. Many factors cause this unfortunate situation, including genetics, poor socio-economic conditions, and ignorance. Lack of prevention from inadequate diagnosis and treatment of streptococcal sore throat or rheumatic fever and failure to provide ongoing prophylaxis play an important role. This failure to provide preventive measures probably results from poor parental education and lack of adequate medical facilities and medical personnel. The long-term effect is that rheumatic heart disease is one of the commonest causes of admission with heart failure among children and young adults in developing countries. Because RF/RHD is a preventable disease, programs are needed that are aimed at educating the public about the disease, detecting affected individuals at an early stage, and encouraging the establishment of protective measures aimed at the most vulnerable age group, children 5–15 years old.

The A.S.A.P. model, coordinated by the Pan African Society of Cardiology (PASCAR) in collaboration with the World Health Federation, which arose following the Drakensberg Declaration by delegates at the 1st All Africa Workshop on Rheumatic Fever and Rheumatic Heart Disease in South Africa in October 2005, focuses on **A**wareness, **S**urveillance, **A**dvocacy, and **P**revention [12]. Increased awareness has been proven to reduce the incidence of RF/RHD. A 10 year educational study from two French–Caribbean Islands (1981–1991) started with widely distributed posters and pamphlets, television advertisements, and educational videos, and the reported instances of RF increased by 10–20% from baseline numbers. The increase was attributed to increased awareness. Furthermore, over the 10 years of study, RF declined on both islands by approximately 75% [13].

As stated in the 2001 WHO report on RF/RHD, collecting epidemiologic data is crucial for planning and implementing a national program for preventing and controlling RF and RHD [14]. Epidemiological data allow policymakers and practitioners to identify groups or locations that are most affected by RF/RHD in order to direct and concentrate control effort appropriately. The WHO STEPwise approach states that, in resource-constrained settings, collecting a small amount of accurate data is more valuable than large quantities of inaccurate data, or no data at all [14]. PASCAR has outlined a four-step approach for surveillance to be completed in order to maximize results: (1) creating and maintaining RF/RHD registries, (2) prospective RF incidence surveys, (3) cross-sectional RHD prevalence surveys, and (4) epidemiology of streptococcal throat and skin infections.

Effective methods of RF/RHD prevention have been available for over 50 years, yet the developing world has not succeeded in controlling the disease whereas the developed world has nearly eradicated it. The unfortunate side effect is de-emphasis of the disease toll on populations around the globe. Advocacy efforts to encourage increased public demand to give this disease priority will result from community awareness of the link between streptococcal sore throat and RF/RHD. This should lead to policy makers advocating government-based programs focusing on education and prevention strategies.

Preventing RF/RHD can be achieved through two discrete strategies, namely primary and secondary prevention. Primary prevention works by treating the preceding streptococcal infection with antibiotics. Secondary prevention is used after the initial RF attack to prevent the recurrence of

RF and progression of RHD. Both primary and secondary prevention are efficacious for preventing RF. Barriers making primary prevention difficult in the developing world include lack of awareness among the public and health care providers with regard to the link between RF and streptococcal infections, lack of policy for preventing RF based on use of antibiotics in the appropriate setting, and the high prevalence of subclinical group A streptococcal infection.

Endomyocardial fibrosis

Endomyocardial fibrosis (EMF) is the most common cause of restrictive cardiomyopathy globally. EMF is characterized by patchy fibrosis of the endocardial surface that leads to decreased compliance and restrictive physiology. Patients usually present late with signs of right and/or left heart failure and striking ascites with little or no peripheral edema. While the disease has been reported from around the globe, it clusters in the tropical and subtropical regions around the Equator. The populations in sub-Saharan Africa, in particular Uganda, are disproportionately affected.

The natural history, pathogenesis, and etiology of EMF remain poorly understood, despite its recognition for >60 years as a major cause of heart disease in these regions. EMF strikes its victims in the prime of life. Once symptoms develop, prognosis is very poor. There is considerable hemodynamic compromise and risk of sudden death. Surgical options are limited and medical therapy has little effect on symptoms or survival.

Incidence and epidemiology

The incidence and distribution of EMF are difficult to determine, in part because its victims reside disproportionately in regions that are poorly equipped to diagnose and treat cardiovascular disease. Before imaging technology became more widespread, diagnosis was often made on autopsy [15] or by clinical presentation alone [16]. Most cases of EMF appear within 15° of the Equator [17]. Roughly half come from sub-Saharan Africa, and almost one-quarter come from Uganda alone [18]. Within Uganda, EMF is one of the most common forms of heart disease, historically comprising 20% of patients referred for echocardiography [19]. Other significant clinical series have been reported from Nigeria [20,21], coastal Mozambique [22], Kerala State in India [23,24], Brazil [25], and the Ivory Coast [26].

Regional variations exist, even within endemic countries. High-prevalence areas tend to be low-lying, humid, and tropical. Residents of the coastal forests of Mozambique [16], the tropical forests in India's Kerala region [17], and Guangxi province in southern China [27] suffer high incidence of EMF, even though neighboring regions see few if any patients. Similarly large dichotomies appear elsewhere, usually between adjacent tropical regions of contrasting elevations; for example, Uganda has a strikingly large burden of EMF, whereas cooler, higher regions of Kenya and Rwanda/Burundi have little if any, and Brazil and Columbia report some patients, but Peru and Ecuador none.

Only one epidemiological study of EMF in an African population exists. Echocardiographic screening of 948 residents, aged 4–45 years, of the Inharrime district of Mozambique revealed a prevalence rate of 19.8%, much higher than previously suspected. These data suggest that the amount of mild subclinical disease may be grossly underestimated [28]. An increased prevalence was noted if a family member was affected: 24% among persons with one or more affected family members (95% CI, 20.6–27.4); 28.3% among those with two or more (95% CI, 23.4–33.2); and 38.3% among those with three or more (95% CI, 31.2–46.4). These results are corroborated by series in Uganda [29] and Zambia [30], which also showed an increased incidence among family members.

At least one country has also seen an ethnic predisposition. Even though Uganda features the world's highest incidence of EMF, the disease affects Rwandan and Burundian immigrants living in Uganda at a much higher rate than it does Rwandans, and Burundians living in their native countries and native Ugandans living in Uganda [31–33]. In Rwanda and Burundi themselves very few patients are reported. Autopsy data gathered at a Ugandan hospital from 1950 to 1965 showed 172 examples of EMF, 63% of which occurred in Rwandan immigrants, even though that population accounted for just 24% of total autopsies [34].

EMF strikes in the prime of life. Data from Uganda show a bimodal peak incidence: children between the ages of 8 and 10 years and young adults between the ages of 20 and 30 years and native Ugandans living in Uganda [33,34]. The childhood peak is equally distributed between the sexes, but females outnumber males 2:1 in the young adult peak [35,36]. In Nigeria, some studies reported that twice as many males are affected, although others showed no differences between the sexes [37].

Etiology

Many theories have attempted to explain EMF's unique pathology and regional distribution. Its tropical concentration suggests environmental or infectious causes. Some believe that it may part of a spectrum of eosinophilic carditis that includes Loffler endocarditis, but any link between eosinophils and EMF is inconsistent at best. No one theory has been proven and very few investigators have directly tested the proposed causes.

Investigators have examined geochemical and nutritional factors. In a case–control study in Uganda, markers of poverty independently predicted EMF [33]. These included farming, lack of shoes, a cassava-based diet, and a diet low in animal protein. Serotonin is the only potential cause that has been rigorously tested through prospective studies; however, EMF lesions could not be reproduced in animal models [38–40], nor did human EMF patients see a rise in their 5-HT levels after a plantain-rich diet [41]. High concentrations of soil

cerium or thorium [23], magnesium deficiency [42], and protein deficiency [43] have all been examined as possible etiologies of EMF, with inconclusive results.

The role of eosinophilia has been highly debated. Eosinophils contain major basic proteins, cationic protein, protein X, and other substances released during degranulation and thought to be toxic to the endo- and myocardium [44]. Histological and echocardiographic arguments often link EMF and Loffler endocarditis. A comparison of 30 patients with Loffler endocarditis and 32 patients with EMF from Uganda, Nigeria, and Brazil showed a final fibrotic stage in Loffler endocarditis identical with that of EMF [45]. Another study detected no echocardiographic difference between 47 EMF patients and 11 Loffler endocarditis patients [35].

Studies exploring an eosinophilia–EMF link, however, are inconsistent. Endomyocardial biopsies fail to demonstrate an eosinopilic myocarditis even early in the disease [29]. Some studies show no difference in eosinophil levels between patients with EMF and controls [46,47], and others show that EMF patients have higher peripheral eosinophilia than controls [48]. In a recent study, 60% of patients with echocardiographic evidence of EMF had at least mild peripheral eosinophilia when compared with 10% of controls (odds ratio 4.6) [18]. Bukhman *et al*. found that eosinophilia was an independent risk factor for EMF not attributable to parasitism. In addition, their data showed that the eosinophil morphology in EMF is unusual, with a tendency towards multilobular forms with evidence of degranulation [18]. Recent data from Nigeria may explain these discrepancies. Andy *et al*. found an inverse relationship between eosinophil levels and the duration of illness in EMF [49]. In their series, only 20% of patients who presented within 6 months of symptoms had normal eosinophil levels, whereas those with long-standing illness were rarely found to have peripheral eosinophilia. Rutakingirwa *et al*. suggested that this finding may represent a "hit-and-run" phenomenon, where EMF represents the end-stage of an acute eosinophilic injury [33].

Investigators have also sought a more direct connection between EMF and an infectious agent. In Nigeria, a seasonal pattern of acute disease appeared, peaking in the rainy season. This suggests that the mechanism may reside in a vector-mediated host [50]. Uganda's consistent predominance of disease in Rwanda/Burundi immigrants (since the 1960s) raises questions about geography and tribal origin. Some think that the key lies in altered exposure to malaria [18,51], a year-round threat in Uganda that only strikes seasonally, if at all, in Rwanda/Burundi. When compared with the local Ganda tribe, immigrants over the age of 15 years also have heavier spleens than the local Gandans [52], and are at higher risk of developing malarial hypersplenomegaly syndrome [53] (thought to be a hyperimmune response to repeated malarial exposure). In fact, in a series

of five Ugandan families (all Rwanda/Burundi immigrants) with nine instances of EMF, four patients had a history of malarial hypersplenomegaly syndrome [54].

Laboratory results also support the link between EMF, malaria, and a hyperimmune response. A histologic study of early-stage endomyocardial biopsy specimens found cardiac tissue swollen with mucopolysaccharides and endocardium covered in fibrin [55], suggesting a hypersensitivity trigger [56]. In addition, anti-heart antibodies are significantly more frequent (29 versus 3%) and significantly more intensely positive in EMF than in all other African heart diseases combined. The same study also showed a clear relationship between the frequency of anti-heart antibodies and the titer of malaria antibodies (1/200 malaria antibodies = 10% chance of anti-heart antibodies, 1/1600 malaria antibodies = 62% chance of anti-heart antibodies) [57].

Not everyone believes malaria to be EMF's inciting agent; the global distribution of *Plasmodium* does not match the global distribution of EMF. Immunological sensitization, an autoimmune reaction incited by exposure to a new highly immunogenic organism, might provide the common pathway. Many Europeans who have lived and worked in tropical Africa have developed EMF [58,59]. Some surely were exposed to malaria, but other foreign infectious agents were undoubtedly present also. In Nigeria, Brockington's group found almost 100% rates of filariasis (onchocerciasis) in 42 patients with angiographic findings of EMF [60], suggesting a second infectious agent as a potential immune trigger. In addition, Uganda's age/gender pattern fits with an autoimmune theory: a bimodal distribution with the peak after adolescence heavily in favor of women. Recent work has shown autoantibodies against myocardial proteins in EMF patients [61–63]. In one study, 54/56 EMF patients tested positive for IgG class anti-myocardial antibodies, a statistically significant increase from healthy controls [64].

Pathology and pathophysiology

EMF is characterized by patchy fibrosis of the endocardial surface of the inflow tract and the apex of one or both ventricles. There can be a striking amount of endomyocardial thickening – up to several millimeters – leading to reduced compliance and restrictive physiology. Progressive obliteration of the right ventricular cavity typically appears in right-sided involvement as the right ventricular apex draws toward the tricuspid valve. The tricuspid valve, the papillary muscles, and valve apparatus can also be fibrotic; this in turn may lead to tethering of valve leaflets and valvar regurgitation [45]. Left ventricular disease tends to affect the posterior mitral cusp and the chordae attached to this cusp, sparing the anterior mitral apparatus. The posterior cusp involvement can occur with or without apical involvement, and often features a well-defined "skip" of tissue demarcation between apical and valvar involvement [65]. Normally a well-defined cleavage plane divides the endocardium and

myocardium. This plane can be interrupted by strands of fibrous tissue that extend into the underlying myocardium, usually limited to the inner third of the muscle [66]. Thrombus, adherent to the involved ventricular endocardial surface, commonly appears in both right and left heart disease [34,67].

Histologically, the changes are very uniform, despite their variations in gross appearance. Endocardial fibrosis is divided into three zones. The most superficial, zone 1, is usually acellular and often hyalized. Any calcification appears in this layer. The intermediate zone 2 consists of loosely textured fibrous tissue, with occasional macrophages and lymphocytes, but only rarely neutrophils or eosinophils. Next to the myocardium is zone 3, a granulation tissue layer containing small blood vessels and a few chronic inflammatory cells [66].

Clinical course and outcomes

EMF's natural history is not well understood. Many patients recall an early stage of acute illness with symptoms such as urticaria, facial edema, fever, appetite loss, and general malaise [50]. At this point, patients appear ill and usually have a fever. Their physical examinations may reveal an enlarged and tender liver, peripheral edema, tachypnea, or tachycardia. This is when an acute carditis, with or without eosinophilia, likely occurs. Patients do not always present at this stage; when they do, the active carditis is often misdiagnosed or missed entirely. Signs of raised venous pressure, coupled with a third heart sound and tachycardia out of proportion to fever, should raise concern about the possibility of early disease. Even when active carditis is correctly diagnosed, it is difficult to know whether it will lead to EMF. Thus far no predictive tests exist.

Patients usually present in the late stages of disease, exhibiting finger and toe clubbing, failure to develop secondary sexual characteristics, growth retardation, and cachexia [61,68]. These late-stage victims tend to have a peculiar appearance: big, bright eyes with an icteric hue [69]. Patients with right-sided disease have signs of chronic systemic venous congestion, with elevated jugular venous distension, gross hepatomegaly, and congestive splenomegaly. Patients with left-sided disease often have significant pulmonary edema. Striking ascites with little or no peripheral edema is a puzzling part of the typical clinical presentation. The ascitic fluid is almost always exudative (75%), unlike the transudative ascites commonly seen with right ventricular failure. It is also associated with peritoneal fibrosis [70]. Significant ascites is a poor prognostic sign. Brazilian EMF patients with ascites were found to have higher mortality than those without (30% at 2 years versus 15% at 2 years, p = 0.002), plus lower New York Heart Association (NYHA) functional class scores, longer duration of illness, and high rates of atrial fibrillation [71].

Historically, EMF has had a very poor prognosis. Autopsy data collected between 1959 and 1969 in Uganda showed only a 2 year average survival after patients sought medical attention [15]. Later series show greater variability, with some patients having a rarer fulminant course, and most patients having a longer indolent period [50,56,72]. The 1970s saw the introduction of surgical resection. Since then, 10 year survival rates are as high as 68% for some patients [73], although the risk of perioperative mortality remains high [74,75]. Biventricular involvement, right ventricular fibrosis, and AV valve regurgitation all predicted increased early mortality in Brazilian EMF patients, regardless of whether patients received surgical intervention or medical management alone [72]. Other predictors of early mortality include hemoglobin <10 g dl^{-1}, cyanosis, embolic episodes, QRS duration >0.12 s, and short symptomatic history before hospital admission [56].

Diagnostic studies

Electrocardiogram
The electrocardiogram is nonspecific. The most common abnormalities are low-voltage QRS due to myocardial fibrosis, intraventricular conduction delays, right and/or left atrial enlargement, and atrioventricular blocks [76]. Atrial fibrillation can occur in one-third of patients [56].

Chest X-ray
The cardiac silhouette commonly exhibits significant enlargement of the involved atria. Right atrial enlargement seen with predominately right-sided EMF creates a cardiac silhouette resembling the African continent and has been dubbed the "Heart of Africa."

Echocardiography
Conventional transthoracic echocardiography correlates well with angiographic assessment [77]. Echocardiography accurately predicts the presence and distribution of fibrosis when compared with autopsy data [19]. The disease's hallmark is obliteration of the involved ventricular cavity, usually associated with a grossly dilated ipsilateral atrium and normal sized ventricle [78]. Figure 72.6 shows a patient with severe right atrial enlargement. In addition, patients with left- or right-sided involvement often exhibit thickening of the posterior left ventricular wall or anterior interventricular septum, respectively [79,80]. Additional findings include right ventricular outflow dilation, AV valve regurgitation, and a restrictive-type flow pattern. Pericardial effusion, often large, is present in up to 43% of patients [81].

In 2008, Yacoub and colleagues described a set of echocardiographic criteria designed to help study disease progression and understand its staging (Table 72.1). They based their criteria on advanced disease features and also early-stage pathologic features described in postmortem studies [11]. Six major and seven minor criteria comprise their classification system. Two major criteria, or one major and two minor criteria, signal a definite diagnosis. A total
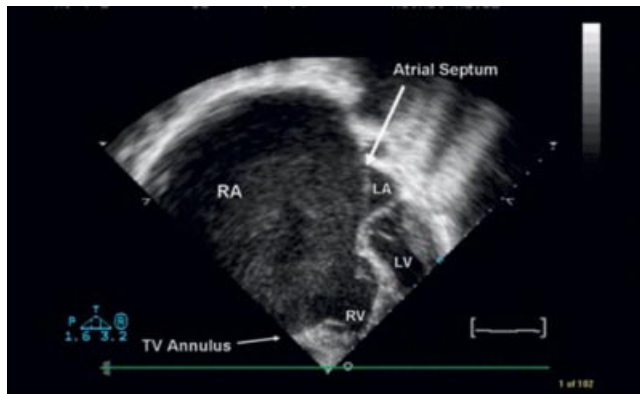
Figure 72.6 Apical four-chamber echocardiographic image of a patient with severe endomyocardial fibrosis of right ventricle. Right atrium is severely dilated, tricuspid valve does not coapt, and spontaneous contrast is seen in right heart. LA, left atrium; LV, left ventricle; RA, right atrium; RV, right ventricle; TV, tricuspid valve.

Table 72.1 Criteria for diagnosis of endomyocardial fibrosis

Criteria	Score
Major criteria	
Endomyocardial plaques >2 mm in thickness	2
Thin (<1 mm) endomyocardial patches affecting more than one ventricular wall	3
Obliteration of the right left ventricular apex	4
Thrombi or spontaneous contrast without severe ventricular dysfunction	4
Retraction of the right ventricular apex (right ventricular apical notch)	4
Atrioventricular valve dysfunction due to adhesion of the valve apparatus to the ventricular wall	1–4[a]
Minor criteria	
Thin endomyocardial patches localized to one ventricular wall	1
Restrictive flow pattern across mitral or tricuspid valves	2
Pulmonary valve diastolic opening	2
Diffuse thickening of the anterior mitral leaflet	1
Enlarged atrium with normal-sized ventricles	2
Movement of the interventricular septum and flat posterior wall	1
Enhanced density of the moderator or other intraventricular bands	1

[a]Depending on the severity of the regurgitation.

score <8 indicates mild EMF, 8–15 signals moderate disease, and >15 represents severe disease [28]. Although these criteria have not been validated across multiple studies, they provide the first formal criteria for the echocardiographic diagnosis and staging of EMF.

MRI

MRI is unnecessary for diagnosis, but characteristic findings are worth noting as MRI becomes more available. Patients with EMF have normal systolic function but delayed endocardial enhancement with no significant myocardial-delayed enhancement [82]. This finding is unique to EMF and amyloidosis, but whereas both display the classic findings of restrictive ventricular physiology (dilated atria, valvar regurgitation, and decreased diastolic function), only EMF shows a thrombotic mass extending into the ventricular cavity [83].

Management

Medical

No well-designed studies have examined EMF's responsiveness to medical management. If patients present early, with active myocarditis and with or without hypereosinophilia, corticosteroids and immunosuppression are probably beneficial. Formal guidelines for dosing and intervals of treatment, however, do not exist. Patients more often present during the disease's late stages, when caregivers can only attempt to relieve symptoms. As in other patients with diastolic dysfunction who do not tolerate tachycardia well, we assume that EMF patients may benefit from heart rate modulation through β-blockers or Ca^{2+} channel blockers. Diuretics provide symptomatic relief to patients with left-sided disease and pulmonary congestion, but have little effect on patients with right-sided disease. Paracentesis may provide relief from ascites, which can be massive, but frequent paracentesis leads to significant protein loss and fluid often reaccumulates quickly. In addition, a significant number of EMF patients suffer thromboembolic complications [84]. At a minimum, these patients should probably receive aspirin; clopidogrel or warfarin might also prove beneficial, although their safety and efficacy are limited in the resource-poor settings where the disease is endemic. In general, medical management alone does not seem to slow the disease progression, and leads to only minimal relief of symptoms.

Surgical

Endocardial decortication is the procedure of choice for surgical treatment of EMF. It is a basic procedure that has changed very little since its first description: surgeons remove diseased tissue by excavating along the well-defined cleavage plane between the fibrotic endocardium and the healthy myocardium [85]. In many patients, surgical advances have made it possible to perform valve-preserving surgery. Perioperative mortality is high, usually 15–20% [86–88]. In one very small study, where surgeons preserved all valves, the perioperative mortality was only 4.6% [89]. In one of the largest surgical series to date, Moraes *et al.* reported 83 EMF patients in Brazil, operated on between December 1977 and December 1997 [74]. Patients' ages ranged from 4 to 59 years, with a mean of 31 years. Thirty-seven (44.5%) had biventricular disease, 34 (41%) had isolated right ventricular

disease, and 12 (14.5%) had isolated left ventricular disease. All patients were in NYHA Class III or IV at time of surgery. Sixty-eight (81.9%) patients survived the operation. Follow-up ranged from 2 months to 17 years (mean 92 months). There were 15 late deaths, but only nine related to the underlying disease. Only 24 (45%) of the 53 surviving patients were found to be in NYHA Class I or II at last follow-up [74].

Surgical treatment is only palliative; it does not alter the disease's progression. Moreover, surgical mortality is high. Objectively, patients with left-sided disease have better late surgical outcomes than those with right-sided disease [90]. Cardiac transplantation has been successful and is available – if only rarely so – as a last resort.

Chagas disease

Chagas disease, also known as American trypanosomiasis, was first reported in 1909 by Carlos Chagas [91], but there is evidence for its existence long before that; Charles Darwin may have contracted Chagas disease [92]. Chagas disease is one of the world's most under-recognized epidemics.

Epidemiology

The greatest burden of Chagas disease is in Central and South America; the most endemic countries are Paraguay, Ecuador, Belize, and Honduras. Today, Chagas disease threatens 20% of the Latin American population (50% in the four countries listed above); >100 million people are at risk. Nearly 7.7 million people were infected in 2005 [10]. Several initiatives, including vector control and blood bank screening, have reduced the number of infected individuals by >50% over the last 20 years in endemic countries [93]. Between 1990 and 2006, there were significant decreases in the number of annual deaths (from 50 000 to 12 500) and new patients (from 700 000 to 40 000) [94]. Emigration of people from Latin America, however, has resulted in more widespread disease; over 300 000 individuals (most from Mexico) in the United States are estimated to be infected [95,96]. Spain is the second most common destination for Latin American emigrants with Chagas disease.

Pathophysiology

The causative agent of Chagas disease is the protozoan parasite *Trypanosoma cruzi* [10]. The disease is transmitted to humans and domestic and wild animals by blood-sucking triamotine bugs [97], also known as the "kissing bugs." Chagas disease can also be transmitted through blood transfusions (the risk is 10 –20% per unit of infected blood) or vertically from mother to infant. Maternal transmission rates vary from 1 to 5% [98]. Disease has also been reported from solid organ transplantation [99]. There are rare reports of contraction of Chagas disease by oral ingestion of contaminated food or drink [100]. The pathophysiology of Chagas disease is related to the parasite and immune system in both the acute and chronic phases [101].

Clinical course

Although the clinical manifestations of Chagas disease primarily affect adults, many are infected in childhood. The acute infective phase of *T. cruzi* usually lasts 4–8 weeks and is usually asymptomatic or shows as merely a brief febrile illness [102]. Occasionally, ECG changes, including sinus tachycardia, first degree atrioventricular block, low voltages, or T wave changes and/or cardiomegaly on chest X-ray are seen during the infectious phase [103]. If symptoms appear, it is usually after 1–2 weeks of exposure to triatomine bugs (longer after transfusion exposure). Treatment with benznidazole or other appropriate antiparasitic drugs cure the acute infection. Rarely (<5% of patients), death occurs in the acute phase secondary to acute myocarditis or meningoencephalitis. Acute symptoms resolve in 90% patients, even if untreated. Two-thirds of these individuals never develop clinically significant manifestation of Chagas disease; they have an indeterminate form of chronic Chagas disease, only having positive antibodies [10]. Reactivation can occur in immune compromised patients [104]. Approximately one-third of patients initially infected with *T. cruzi* 10–30 years after infection develop a determinant form of chronic Chagas disease characterized by a cardiac, digestive (megaesophagus or megacolon), or cardiodigestive form of the disease. The cardiodigestive form is most frequently marked by the development of megaesophagus before involvement of the heart and colon.

A slowly progressive incessant myocarditis develops in the cardiac form of chronic Chagas disease and ultimately leads to dilatation of all four chambers and impairment of ventricular contractility. An apical left ventricular aneurysm and other regional wall motion abnormalities are common early in the chronic phase [105]. Progressive myocyte death and fibrosis along with damage to the coronary microvasculature result in heart failure, ventricular arrhythmias, thromboembolism, and ultimately death [103]. Biventricular failure is the hallmark of late Chagas disease, with a predominance of right-sided symptoms (especially ascites and liver congestion) in the more advanced phases. Conversely, isolated left heart failure is present in the early phases. The conduction system is affected, resulting in bradycardia, atrioventricular block, and bifascicular block [106]. Premature ventricular beats and ventricular tachycardia are also common. Systemic, especially cerebral, and pulmonary emboli from mural ventricular thrombi are very common [107]. Sudden death is the most common cause of death (nearly two-thirds) in Chagas disease, especially in the earlier stages [108]. It is often due to ventricular tachyarrhythmias and can occur in otherwise asymptomatic patients. Chronic heart failure and embolic disease can also cause death [109].

Congenital Chagas disease

Neonatal Chagas disease may be apparent at birth or develop a few weeks after delivery [110]. Symptoms include hypotonia, fever, anemia, and hepatosplenomegaly. *In utero*

death secondary to placental infection can occur. A woman infected with *T. cruzi* can give birth to an infected infant during no, one, or multiple pregnancies at any stage of the disease. Neonatal diagnosis can be made by examining cord or infant blood. Testing for *T. cruzi* antibodies should be deferred until 9 months (when maternal antibodies are no longer present). Polymerase chain reaction (PCR) for *T. cruzi* DNA is available at some centers [111].

Diagnosis, prognosis, and treatment

Acute infection is diagnosed by detecting parasites in blood. In the chronic phase, two different serologic methods should be performed to detect IgG antibodies against *T. cruzi* [112]. PCR can be performed but is not widely available. Asymptomatic patients with positive antibodies should be monitored every 12–24 months with an ECG and for signs of gastrointestinal involvement. If cardiac involvement is suspected, more thorough evaluation including echocardiography and ambulatory 24h ECG monitoring should be carried out. Prognosis is variable in patients with cardiac disease and is worse in those with NYHA Class III or IV, ventricular tachycardia, and ventricular dysfunction. The 10 year mortality varies from 10 to >80% based on risk stratification scoring [113].

There are two goals of treatment, eradicating the parasite and treating symptoms. Anti-trypanosomal treatment, with benznidazole or nifurtimox, is recommended for anyone with acute, congenital, and reactivated infection, and for all children <18 years old with chronic disease [96]. Benznidazole is the safest and most effective; in children it should be given for 60 days (5–10 mg kg⁻¹ per day in two or three divided doses after meals). Drug treatment should be given to adults aged 19–50 years without advanced heart disease but has not been proven beneficial in older patients. Benznidazole and nifurtimox are contraindicated in pregnancy and in patients with advanced heart failure, severe hepatic or renal disease, and advanced megaesophagus. The BENEFIT trial questioned anti-trypanosomal therapy in adults with mild to moderate cardiac involvement [114].

Some data support the use of amiodarone for patients with Chagas disease with sustained ventricular tachycardia or the combination of nonsustained ventricular tachycardia and ventricular dysfunction [115]. Implantable defibrillators have been used in patients with refractory ventricular arrhythmias and resuscitated sudden death, despite data that show no protection from mortality in this population [116]. Standard treatment for heart failure is often used in patients with Chagas disease; however, the use of higher dosages is often warranted with right heart failure. There are no studies to date supporting the use of β-blockers. There should be a low threshold for using anticoagulation. Results for surgery, including cardiomyoplasty and partial left ventriculectomy, are poor and these procedures should not be offered. Conversely, results in transplant recipients for Chagas disease have been promising [117].

Disease prevention

In the past 30 years, significant progress has been made in preventing and controlling Chagas disease. This has resulted from measures such as rigorous screening of blood donors in endemic areas, aggressive use of insecticides in highly infective areas, and public education. A vaccine is not available, however, and the risk of resurgence of vector-borne disease continues in several Latin American countries. Furthermore, areas such as the United States and Spain are at increasing risk from non-vector transmission. Ongoing vigilant anti-parasitic treatment is important for all acutely and many chronically affected patients. Improved rapid diagnostic testing, both before and after treatment, and more ready access to benznidazole and nifurtimox (especially pediatric formulations) are needed [118].

References

1 Yacoub MH. Establishing pediatric cardiovascular services in the developing world: a wake-up call. *Circulation* 2007;**116**:1876–8.
2 Hoffman JIE, Kaplan S. The incidence of congenital heart disease. *J Am Coll Cardiol* 2002;**39**:1890–900.
3 Children's HeartLink. *Children's HeartLink Global Report.* http://www.childrensheartlink.org/report, 2007 (last accessed 7 January 2011).
4 Hewitson J, Brink J, Zilla P. The challenge of pediatric cardiac services in the developing world. *Semin Thorac Cardiovasc Surg* 2002;**14**:340–5.
5 Rao SG. Pediatric cardiac surgery in developing countries. *Pediatr Cardiol* 2007;**28**:144–8.
6 Larrazabal LA, Jenkins KJ, Gauvreau K, *et al*. Improvement in congenital heart surgery in a developing country: the Guatemalan experience. *Circulation* 2007;**116**:1882–7.
7 Kirby D. Changes in sexual behaviour leading to the decline in the prevalence of HIV in Uganda: confirmation from multiple sources of evidence. *Sex Transm Infect* 2008;**84**(Suppl 2):ii35–41.
8 Miiro G, Todd J, Mpendo J, *et al*. Reduced morbidity and mortality in the first year after initiating highly active anti-retroviral therapy (HAART) among Ugandan adults. *Trop Med Int Health* 2009;**14**:556–63.
9 Carapetis JR, Steer AC, Mulholland EK, Weber M. The global burden of group A streptococcal diseases. *Lancet Infect Dis* 2005;**5**:685–94.
10 Rassi A Jr, Rassi A, Marin-Neto JA. Chagas disease. *Lancet* 2010;**375**:1388–402.
11 Yacoub S, Kotit S, Mocumbi AO, Yacoub MH. Neglected diseases in cardiology: a call for urgent action. *Nat Clin Pract Cardiovasc Med* 2008;**5**:176–7.
12 Marijon E, Ou P, Celermajer DS, *et al*. Prevalence of rheumatic heart disease detected by echocardiographic screening. *N Engl J Med* 2007;**357**:470–6.
13 Bach JF, Chalons S, Forier E, *et al*. 10-year educational programme aimed at rheumatic fever in two French Caribbean islands. *Lancet* 1996;**347**:644–8.

14 Bonita R, de Courten M, Dwyer T, *et al*. *Surveillance of Risk Factors for Noncommunicable Diseases: the WHO STEPwise Approach*. Geneva: World Health Organization, 2001.

15 Davies JN. Endomyocardial fibrosis in Uganda. *East Afr Med J* 1948;**25**:10–6.

16 Acquatella H, Schiller NB, Puigbo JJ, *et al*. Value of two-dimensional echocardiography in endomyocardial disease with and without eosinophilia. A clinical and pathologic study. *Circulation* 1983;**67**:1219–26.

17 Hutt MS. Epidemiology aspects of endomyocardial fibrosis. *Postgrad Med J* 1983;**59**:142–6.

18 Bukhman G, Ziegler J, Parry E. Endomyocardial fibrosis: still a mystery after 60 years. *PLoS Negl Trop Dis* 2008;**2**:e97.

19 Freers J, Mayanja-Kizza H, Ziegler J, Rutakingirwa M. Echocardiographic diagnosis of heart disease in Uganda. *Trop Doct* 1996;**26**:125–8.

20 Brockington IF, Olsen EG. Eosinophilia and endomyocardial fibrosis. *Postgrad Med J* 1972;**48**:740–1.

21 Nwokolo C. Endomyocardial fibrosis and other obscure cardiopathies in eastern Nigeria. *West Afr Med J* 1955;**4**:103–16.

22 Ferreira B, Matsika-Claquin MD, Hausse-Mocumbi AO, *et al*. Geographic origin of endomyocardial fibrosis treated at the central hospital of Maputo (Mozambique) between 1987 and 1999. *Bull Soc Pathol Exot* 2002;**95**:276–9 (in French).

23 Kutty VR, Abraham S, Kartha CC. Geographical distribution of endomyocardial fibrosis in south Kerala. *Int J Epidemiol* 1996;**25**:1202–7.

24 Datta BN, Babu SK, Khattri HN, *et al*. Endomyocardial fibrosis in Chandigarh area, India. A study of nine autopsies. *Trop Geogr Med* 1977;**29**:346–52.

25 Guimaraes AC, Esteves JP, Filho AS, Macedo V. Clinical aspects of endomyocardial fibrosis in Bahia, Brazil. *Am Heart J* 1971;**81**:7–19.

26 Bertrand M, Renambot J, Chauvet J, *et al*. 14 cases of constrictive endocardial fibrosis or endomyocardial fibrosis. *Arch Mal Coeur Vaiss* 1975;**68**:625–35 (in French).

27 Yin R. Endomyocardial fibrosis in China. *Chin Med Sci J* 2000;**15**:55–60.

28 Mocumbi AO, Ferreira MB, Sidi D, Yacoub MH. A population study of endomyocardial fibrosis in a rural area of Mozambique. *N Engl J Med* 2008;**359**:43–9.

29 Patel AK, Ziegler JL, D'Arbela PG, Somers K. Familial cases of endomyocardial fibrosis in Uganda. *Br Med J* 1971;**4**:331–4.

30 Lowenthal MN. Endomyocardial fibrosis: familial and other cases from northern Zambia. *Med J Zambia* 1978;**12**:2–7.

31 Shaper AG, Coles RM. The tribal distribution of endomyocardial fibrosis in Uganda. *Br Heart J* 1965;**27**:121–7.

32 Hutt MS. Pathology of African cardiomyopathies. *Pathol Microbiol (Basel)* 1970;**35**:37–43.

33 Rutakingirwa M, Ziegler JL, Newton R, Freers J. Poverty and eosinophilia are risk factors for endomyocardial fibrosis (EMF) in Uganda. *Trop Med Int Health* 1999;**4**:229–35.

34 Shaper AG. Hutt MS, Coles RM. Necropsy study of endomyocardial fibrosis and rheumatic heart disease in Uganda 1950–1965. *Br Heart J* 1968;**30**:391–401.

35 Davies J, Spry CJ, Vijayaraghavan G, De Souza JA. A comparison of the clinical and cardiological features of endomyocardial disease in temperate and tropical regions. *Postgrad Med J* 1983;**59**:179–85.

36 Connor DH, Somers K, Hutt MS, *et al*. Endomyocardial fibrosis in Uganda (Davies' disease). 1. An epidemiologic, clinical, and pathologic study. *Am Heart J* 1967;**74**:687–709.

37 Falase AO. Endomyocardial fibrosis in Africa. *Postgrad Med J* 1983;**59**:170–8.

38 McKinney B, Crawford MA. Fibrosis in guinea pig heart produced by plantain diet. *Lancet* 1965;**ii**:880–2.

39 McKinney B. Studies on the experimental production of endomyocardial fibrosis and cardiomegaly of unknown origin by dietary means. *Am Heart J* 1975;**90**:206–14.

40 McKinney B. Endocardial changes produced in Patus monkeys by the ablation of cardiac lymphatics and the administration of a plantain diet. *Am Heart J* 1976;**91**:484–91.

41 Ojo GO. The pathogenesis of endomyocardial fibrosis: the question of 5-hydroxytryptamine. *Br Heart J* 1970;**32**:671–4.

42 Valiathan SM, Kartha CC. Endomyocardial fibrosis – the possible connexion with myocardial levels of magnesium and cerium. *Int J Cardiol* 1990;**28**:1–5.

43 Sezi CL. Effect of protein deficient cassava diet on *Cercopithecus aethiops* hearts and its possible role in the aetiology and pathogenesis of endomyocardial fibrosis in man. *East Afr Med J* 1996; **73**:S11–6.

44 Tai PC, Ackerman SJ, Spry CJ, *et al*. Deposits of eosinophil granule proteins in cardiac tissues of patients with eosinophilic endomyocardial disease. *Lancet* 1987;**i**:643–7.

45 Olsen EG. Pathological aspects of endomyocardial fibrosis. *Postgrad Med J* 1983;**59**:135–41.

46 Carlisle R, Ogunba EO, McFarlane H, *et al*. Immunoglobulins and antibody to *Loa loa* in Nigerians with endomyocardial fibrosis and other heart diseases. *Br Heart J* 1972;**34**:678–80.

47 Urhoghide GE, Falase AO. Degranulated eosinophils, eosinophil granule basic proteins and humoral factors in Nigerians with endomyocardial fibrosis. *Afr J Med Med Sci* 1987;**16**:133–9.

48 Freers J, Mayanja-Kizza H, Rutakingirwa M, Gerwing E. Endomyocardial fibrosis: why is there striking ascites with little or no peripheral oedema? *Lancet* 1996;**347**:197.

49 Andy JJ, Ogunowo PO, Akpan NA, *et al*. Helminth associated hypereosinophilia and tropical endomyocardial fibrosis (EMF) in Nigeria. *Acta Trop* 1998;**69**:127–40.

50 Parry EH, Abrahams DG. The natural history of endomyocardial fibrosis. *Q J Med* 1965;**34**:383–408.

51 Shaper AG. Cardiovascular disease in the tropics. II. Endomyocardial fibrosis. *Br Med J* 1972;**3**:743–6.

52 Shaper AG. Spleen weights in Uganda with reference to malaria, migration and idiopathic tropical splenomegaly. *Trans R Soc Trop Med Hyg* 1969;**63**:206–15.

53 Shaper AG. Immunological studies in a tropical environment. *East Afr Med J* 1968;**45**:219–28.

54 Patel AK, Ziegler JL, D'Arbela PG, Somers K. Familial cases of endomyocardial fibrosis in Uganda. *Br Med J* 1971;**4**:331–4.

55 van der Geld H, Peetoom F, Somers K, Kanyerezi BR. Immunohistological and serological studies in endomyocardial fibrosis. *Lancet* 1966;**ii**:1210–3.

56 Gupta PN, Valiathan MS, Balakrishnan KG, *et al*. Clinical course of endomyocardial fibrosis. *Br Heart J* 1989;**62**:450–4.

57 Shaper AG, Kaplan MH, Foster WD, *et al*. Immunological studies in endomyocardial fibrosis and other forms of heart disease in the tropics. *Lancet* 1967;**i**:598–600.

58 Brockington IF, Olsen EG, Goodwin JF. Endomyocardial fibrosis in Europeans resident in tropical Africa. *Lancet* 1967;**i**:583–8.

59 Gray IR. Endocardial fibrosis. *Br Heart J* 1951;**13**:387–96.

60 Ive FA, Willis AJ, Ikeme AC, Brockington IF. Endomyocardial fibrosis and filariasis. *Q J Med* 1967;**36**:495–516.

61 Jaiyesimi F, Salimonu LS, Antia AU. Serum immunoglobulins in children with cardiomyopathies. *Trans R Soc Trop Med Hyg* 1984;**78**:127–31.

62 Mathai A, Kartha CC, Balakrishnan KG. Serum immunoglobulins in patients with endomyocardial fibrosis. *Indian Heart J* 1986;**38**:470–2.

63 Vijayaraghavan G, Sadanandan S. Immunological phenomena in tropical endomyocardial fibrosis. *Indian Heart J* 1984;**36**:87–9.

64 Mocumbi AO, Latif N, Yacoub MH. Presence of circulating anti-myosin antibodies in endomyocardial fibrosis. *PLoS Negl Trop Dis* 2010;**4**:e661.

65 Davies JN. The ridge in endomyocardial fibrosis. *Lancet* 1968;**i**:631–2.

66 Davies JN, Ball JD. The pathology of endomyocardial fibrosis in Uganda. *Br Heart J* 1955;**17**:337–59.

67 Olsen EG. The pathology of cardiomyopathies. A critical analysis. *Am Heart J* 1979;**98**:385–92.

68 Bolarin DM, Andy JJ. Clinical feminization and serum testosterone levels in male patients with chronic African endomyocardial fibrosis. *Trop Geogr Med* 1982;**34**:309–12.

69 Marijon E, Ou P. What do we know about endomyocardial fibrosis in children of Africa? *Pediatr Cardiol* 2006;**27**:523–4.

70 Freers J, Masembe V, Schmauz R, Mayanja-Kizza H. Endomyocardial fibrosis syndrome in Uganda. *Lancet* 2000;**355**:1994–5.

71 Barretto AC, Mady C, Oliveira SA, *et al*. Clinical meaning of ascites in patients with endomyocardial fibrosis. *Arq Bras Cardiol* 2002;**78**:196–9.

72 Barretto AC, da Luz PL, de Oliveira SA, *et al*. Determinants of survival in endomyocardial fibrosis. *Circulation* 1989;**80**:I177–82.

73 Valiathan MS, Balakrishnan KG, Sankarkumar R, Kartha CC. Surgical treatment of endomyocardial fibrosis. *Ann Thorac Surg* 1987;**43**:68–73.

74 Moraes F, Lapa C, Hazin S, *et al*. Surgery for endomyocardial fibrosis revisited. *Eur J Cardiothorac Surg* 1999;**15**:309–12.

75 Schneider U, Jenni R, Turina J, *et al*. Long-term follow up of patients with endomyocardial fibrosis: effects of surgery. *Heart* 1998;**79**:362–7.

76 Hassan WM, Fawzy ME, Al Helaly S, *et al*. Pitfalls in diagnosis and clinical, echocardiographic, and hemodynamic findings in endomyocardial fibrosis: a 25-year experience. *Chest* 2005;**128**:3985–92.

77 Camara EJ, Guimaraes AC, Godinho AG. Evaluation of endomyocardial fibrosis by two-dimensional echocardiogram. Analysis of the severity and correlation with angiocardiography. *Arq Bras Cardiol* 1991;**57**:307–12 (in Portuguese).

78 Berensztein CS, Pineiro D, Marcotegui M, *et al*. Usefulness of echocardiography and Doppler echocardiography in endomyocardial fibrosis. *J Am Soc Echocardiogr* 2000;**13**:385–92.

79 Hernandez-Pieretti O. Echocardiographic diagnosis and evaluation of cardiomyopathies: idiopathic hypertrophic subaortic stenosis, Chagas' heart disease and endomyocardial fibrosis. *Postgrad Med J* 1977;**53**:533–6.

80 Davies J, Gibson DG, Foale R, *et al*. Echocardiographic features of eosinophilic endomyocardial disease. *Br Heart J* 1982;**48**:434–40.

81 Tello R, Cuan V, Abunde A, *et al*. Doppler echocardiography in endomyocardial fibrosis. *Arch Inst Cardiol Mex* 1994;**64**:251–5 (in Spanish).

82 Smedema JP, Winckels SK, Snoep G, *et al*. Tropical endomyocardial fibrosis (Davies' disease): case report demonstrating the role of magnetic resonance imaging. *Int J Cardiovasc Imaging* 2004;**20**:517–22.

83 Shapiro S, Pinney SP, Anyanwu AC, Garcia MJ. An atypical presentation of endomyocardial fibrosis diagnosed by cardiac MRI. *Circ Heart Fail* 2009;**2**:77–80.

84 Shaper AG, Wright DH. Intracardiac thrombosis and embolism in endomyocardial fibrosis in Uganda. *Br Heart J* 1963;**25**:502–8.

85 Lepley D Jr, Aris A, Korns ME, *et al*. Endomyocardial fibrosis. A surgical approach. *Ann Thorac Surg* 1974;**18**:626–33.

86 Moraes CR, Buffolo E, Victor E, *et al*. Endomyocardial fibrosis: report of 6 patients and review of the surgical literature. *Ann Thorac Surg* 1980;**29**:243–8.

87 Dubost C, Prigent C, Gerbaux A, *et al*. Surgical treatment of constrictive fibrous endocarditis. *J Thorac Cardiovasc Surg* 1981;**82**:585–91.

88 Metras D, Coulibaly AO, Ouattara K, *et al*. Endomyocardial fibrosis: early and late results of surgery in 20 patients. *J Thorac Cardiovasc Surg* 1982;**83**:52–64.

89 de Oliveira SA, Pereira Barreto AC, Mady C, *et al*. Surgical treatment of endomyocardial fibrosis: a new approach. *J Am Coll Cardiol* 1990;**16**:1246–51.

90 Metras D, Coulibaly AO, Ouattara K. The surgical treatment of endomyocardial fibrosis: results in 55 patients. *Circulation* 1985;**72**:II274–9.

91 Chagas C. Nova tripanozomiase humana. Estudos sobre a morfolojía e o ciclo evolutivo de *Schizotrypanum cruzi* n. gen., n. sp., ajente etiolójico de nova entidade morbida do homen. *Mem Inst Oswaldo Cruz* 1909;**1**:159–218.

92 Bernstein RE. Darwin's illness: Chagas' disease resurgens. *J R Soc Med* 1984;**77**:608–9.

93 Moncayo A. Chagas disease: current epidemiological trends after the interruption of vectorial and transfusional transmission in the Southern Cone countries. *Mem Inst Oswaldo Cruz* 2003;**98**:577–91.

94 Moncayo A, Silveira AC. Current epidemiological trends for Chagas disease in Latin America and future challenges in epidemiology, surveillance and health policy. *Mem Inst Oswaldo Cruz* 2009;**104**(Suppl 1):17–30.

95 Bern C, Montgomery SP. An estimate of the burden of Chagas disease in the United States. *Clin Infect Dis* 2009;**49**:e52–4.

96 Bern C, Montgomery SP, Herwaldt BL, *et al*. Evaluation and treatment of Chagas disease in the United States: a systematic review. *JAMA* 2007;**298**:2171–81.

97 Deane LM. Animal reservoirs of *Trypanosoma cruzi* in Brazil. *Rev Bras Malariol Doencas Trop* 1964;**16**:27–48.

98 Torrico F, Alonso-Vega C, Suarez E, *et al*. Maternal *Trypanosoma cruzi* infection, pregnancy outcome, morbidity, and mortality of congenitally infected and non-infected newborns in Bolivia. *Am J Trop Med Hyg* 2004;**70**:201–9.

99 Milei J, Guerri-Guttenberg RA, Grana DR, Storino R. Prognostic impact of Chagas disease in the United States. *Am Heart J* 2009;**157**:22–9.

100 Pereira KS, Schmidt FL, Guaraldo AM, *et al*. Chagas' disease as a foodborne illness. *J Food Prot* 2009;**72**:441–6.

101 Andrade ZA. Immunopathology of Chagas disease. *Mem Inst Oswaldo Cruz* 1999;**94**(Suppl 1):71–80.

102 WHO. *Control of Chagas Disease. Second Report of the WHO Expert Committee. Technical Report Series No 905*. Geneva, World Health Organization, 2002.

103 Rassi JA, Rassi A, Marin-Neto JA. Chagas heart disease: pathophysiologic mechanisms, prognostic factors and risk stratification. *Mem Inst Oswaldo Cruz* 2009;**104**(Suppl 1):152–8.

104 MoncayoA, Silveira AC. Current epidemiological trends for Chagas disease in Latin America and future challenges in epidemiology, surveillance and health policy. *Mem Inst Oswaldo Cruz* 2009;**104**(Suppl 1):17–30.

105 Acquatella H. Echocardiography in Chagas heart disease. *Circulation* 2007;**115**:1124–31.

106 RassiA Jr, Rassi A, Little WC. Chagas' heart disease. *Clin Cardiol* 2000;**23**:883–9.

107 Samuel J, Oliveira M, Correa de Araujo RR, *et al*. Cardiac thrombosis and thromboembolism in chronic Chagas' heart disease. *Am J Cardiol* 1983;**52**:147–51.

108 Rassi A Jr, Rassi SG, Rassi A. Sudden death in Chagas' disease. *Arq Bras Cardiol* 2001;**76**:75–96.

109 Rassi A Jr, Rassi A, Rassi SG. Predictors of mortality in chronic Chagas disease: a systematic review of observational studies. *Circulation* 2007;**115**:1101–8.

110 Freilij H, Altcheh J. Congenital Chagas' disease: diagnostic and clinical aspects. *Clin Infect Dis* 1995;**21**:551–5.

111 Mora MC, Sanchez NO, Marco D, *et al*. Early diagnosis of congenital *Trypanosoma cruzi* infection using PCR, hemoculture, and capillary concentration, as compared with delayed serology. *J Parasitol* 2005;**91**:1468–73.

112 Gomes YM, Lorena VM, Luquetti AO. Diagnosis of Chagas disease: what has been achieved? What remains to be done with regard to diagnosis and follow up studies? *Mem Inst Oswaldo Cruz* 2009;**104**(Suppl 1):115–21.

113 Rassi A Jr, Rassi A, Little WC, *et al*. Development and validation of a risk score for predicting death in Chagas' heart disease. *N Engl J Med* 2006;**355**:799–808.

114 Marin-Neto JA, Rassi A Jr, Morillo CA, *et al*. Rationale and design of a randomized placebo-controlled trial assessing the effects of etiologic treatment in Chagas' cardiomyopathy: the BENznidazole Evaluation For Interrupting Trypanosomiasis (BENEFIT). *Am Heart J* 2008;**156**:37–43.

115 Scanavacca MI, Sosa EA, Lee JH, *et al*. Empiric therapy with amiodarone in patients with chronic Chagas cardiomyopathy and sustained ventricular tachycardia. *Arq Bras Cardiol* 1990;**54**:367–71 (in Portuguese).

116 Cardinalli-Neto A, Bestetti RB, Cordeiro JA, Rodrigues VC. Predictors of all-cause mortality for patients with chronic Chagas' heart disease receiving implantable cardioverter defibrillator therapy. *J Cardiovasc Electrophysiol* 2007;**18**:1236–40.

117 Bocchi EA, Fiorelli A. The paradox of survival results after heart transplantation for cardiomyopathy caused by *Trypanosoma cruzi*. First Guidelines Group for Heart Transplantation of the Brazilian Society of Cardiology. *Ann Thorac Surg* 2001;**71**:1833–8.

118 Rassi A Jr, Dias JC, Marin-Neto JA, Rassi A. Challenges and opportunities for primary, secondary, and tertiary prevention of Chagas' disease. *Heart* 2009;**95**:524–34.

Index

Page numbers in *italics* denote figures, those in **bold** denote tables.

Index

Index

Index

Index

Index

Index

Index